dbmc

11th International Conference on
Durability of Building Materials and Components

Durability of Building Materials and Components 11

Globality and Locality in Durability

Proceedings CD of the Eleventh International Conference
on Durability of Building Materials and Components, 11dbmc

Istanbul, Turkey
11-14 May 2008

Editors:

A. Nil Türkeri
I.T.U. Faculty of Architecture
Özkan Şengül
I.T.U. Faculty of Civil Engineering

dbmc
11th International Conference on
Durability of Building Materials and Components

Full Proceedings CD
ISBN: 978-975-561-330-7

Published in book form as well:
Durability of Building Materials and Components 11: Proceedings of the Eleventh International Conference on Durability of Building Materials and Components
Complete in 4 volumes
ISBN: 978-975-561-325-3 (set number)

Correct citation: Türkeri, A. Nil and Şengül, Özkan *(Editors)* 2008. Durability of Building Materials and Components 11: *Globality and Locality in Durability.* CD-ROM.

dbmc

11th International Conference on
Durability of Building Materials and Components

The Conference wishes to acknowledge and warmly thank the following organizations and companies for sponsorship and generous support.

CORPORATE SPONSORS

PLATINUM SPONSOR

Dow Building Solutions

GOLD SPONSOR

Onduline groupe

Onduline AVRASYA A.Ş.

SILVER SPONSORS

TÇMB

TÜRKİYE ÇİMENTO MÜSTAHSİLLERİ BİRLİĞİ

ısı yalıtımı sanayicileri derneği XPS

TITAN WOOD

the pioneers of accoya the strength within

OTHER SPONSOR

TÜRK MÜHENDİS VE MİMAR ODALARI BİRLİĞİ
İNŞAAT MÜHENDİSLERİ ODASI
İ S T A N B U L Ş U B E S İ

Preface

This conference represents the 11th triennial in a series, in which the previous ten were held in Ottawa (1978), Gaithersburg (1981), Espoo (1984), Singapore (1987), Brighton (1990) Omiya (1993), Stockholm (1996), Vancouver (1999), Brisbane (2002) and Lyon (2005). The evolution of these works indicate that the notion of durability of materials and components is becoming more significant in society as public awareness of environmental issues combined with the requirement for economic sustainability is steadily rising, in part due to concerns for the future. In the context of buildings and constructed assets, with special reference to materials and components that constitute the structural system, building elements and mechanical services, such notions on sustainability inevitably have implications on life-cycle performance. Awareness that investment and design decisions affect the subsequent life-cycle phases of construction, occupancy and demolition is reflected in the increasing number of contributions touching on this aspect. Such awareness of the life cycle of buildings has brought about further advances in implementing sustainable design principles. For example, within the preliminary design phase, designers may now review the occupancy phase and the manner in which this may be extended through refurbishment to take advantage of the prescribed economic service life of building components. This has, in part, been possible through the development of tools, methods, approaches and techniques for life-cycle analysis and service life planning and prediction that have been the outcome of these many conferences over the past decades.

One of the more important prerequisites for a "satisfactory" building, one for which the maintenance and refurbishment costs are minimized whilst offering an acceptable minimum level of performance, is ensuring a durable external as well as internal fabric, for which the weakest component may perhaps dictate the overall degree of long-term performance of the building assembly or system. Hence appropriate choices in respect to the type of components selected at the component design and selection phase is a foremost consideration to avoid premature failure or the need to subsequently rectify design choices. Consideration should also me made to spatial design of the building; flexibility in design is highly useful as it may very well obviate the need for premature refurbishment of components and as well, help accommodate subsequent changes in building function. Appropriate choices of components for building projects of "sustainable design" may indeed require basic research, or the development of materials and components, prior to acquiring adequate specifications for performance-based and competitive products that also conform to the requirements for sustainable construction. But what of sustainable design practices in the context of design proposals that incorporate "durable" and "recyclable" products? Such approaches, using products perhaps requiring minimal repair and maintenance, are regarded as viable solutions that are in keeping with the basic notions of ecological waste management. However, there are still some conflicts to resolve regarding the implementation of such notions within a consumer-oriented society for which there is a tendency to use products of reduced service life. It is not well understood that products identified as having a long service life combined with a short ecological recovery life are deemed as most "sustainable". In this aspect, the current proceedings lend credence to the idea that the development of viable sustainable products and methods can only be based on knowledge of their durability, that is, their long-term performance, as is evident from the many contributions published in these proceedings.

dbmc
11th International Conference on
Durability of Building Materials and Components

The intent of this conference is to gather information on and provide a forum for review and discussion of the most recent theoretical, experimental and field research work completed in this domain. This process necessarily allows dissemination of the proceedings to, for example, public and private practitioners and institutions, but also, offers an opportunity to review the various research approaches that, in turn, helps determine the scope for further research. Hence the primary research themes on which the conference was based covered a wide range of areas including: Durability of Materials, Durability of Systems and Components in Buildings, Response of Building Elements to Environmental Loads, Service Life Prediction & Planning Methodologies, Risk Analysis Approaches, Durability and Sustainable Buildings, Building Maintenance and Pathology from materials to maintenance; significant contributions to the advancement of research in these fields are offered in the proceeding.

The proceeding will be of interest to researches, designers, civil engineers, and expert practitioners in building construction, as well as manufacturers and suppliers of construction materials, components and systems.

A. Nil Türkeri
Özkan Şengül
Editors, 11 DBMC
İstanbul, 2008

Conference Committees

Steering Committee

Jean-Luc Chevalier, *Chair*
Ralph Paroli
Christer Sjöström
Walter Rossiter
Michael Lacasse
Geert De Schutter

Members At Large

Stewart Burn
Michael Chew
Bruno Daniotti
Vasco De Freitas
Kribanandan G. Naidu
Per Jostein Hovde
Vanderley M. John
Chun-Qing Li
Kenji Motohashi
A. Nil Türkeri

Organising Committee

A. Nil Türkeri, *Chair*
M. Cem Altun
N. Murat Aygün
İkbal Çetiner
Kevser Coşkun
Ecem Edis
Caner Göçer
Hülya Kuş
Nilüfer Özyurt
Özkan Şengül
Aslıhan Tavil
Fatih Yazıcıoğlu
Hasan Yıldırım

Advisory Committee

Mehmet Ali Taşdemir, *Chair*
Zeynep Ahunbay
Yılmaz Akkaya
Feridun Çılı
Ahmet Ersen
Bilge Işık
Mustafa Karagüler
Alaattin Kanoğlu
Gül Koçlar Oral
Hulusi Özkul
Mete Tapan

dbmc
11th International Conference on
Durability of Building Materials and Components

Scientific Committee

Michael Lacasse, *Chair*
Yılmaz Akkaya
M. Cem Altun
Carmen Andrade
Enrico De Angelis
Nihal Arıoğlu
N. Murat Aygün
Luigia Binda
Eric Brandt
Christian Brischke
Jorge M C. Lopes De Brito
Jean-Luc Chevalier
Sergio Croce
İkbal Çetiner
Bruno Daniotti
Ahmet Ersen
Peter Flueler
Vasco Peixoto De Freitas
Kribanandan G. Naidu
Malcolm Hollis
Andreas Holm
Per Jostein Hovde
Bilge Işık
Vanderley M. John
Mustafa Karagüler
Hartwig Künzel
Hülya Kuş
Brian Kyle
Chun-Qing Li
Holger Merkel
Kenji Motohashi
Hulusi Özkul
Ralph Paroli
Walter Rossiter
Christer Sjöström
Özkan Şengül
Mehmet Ali Taşdemir
Aslıhan Tavil
Thiery Mickael
Wolfram Trinius
Christian R. Welzbacher

dbmc
11th International Conference on
Durability of Building Materials and Components

CONTENTS

Microstructural Assessment of the Interfacial Transition Zone in Granitic Concrete
Azimah Hussin, Colin Poole, Robert Fowell

Durability Problems of Macro Defect Free (MDF) Cements Prepared with Polyvinyl Alcohol Copolymers and Alumina Cements
Özgür Ekincioğlu, M. Hulusi Özkul, Leslie J. Struble

Discussing the Durability Assessment of Cement Mortars – a Contribution for a Prediction Model
Vasco Peixoto Freitas, Helena Corvacho, Ana Vaz Sá, Marisa Antunes Quintela

Carbonation in Concrete with High Fly Ash Content and Hydrated Lime
Juarez Hoppe Filho, Maria Alba Cincotto

Effect of Curing Age on the Durability of High-Volume Fly Ash Concrete
Nele De Belie, Stijn Lammertijn, Kathelijn Cox

Analysis of Rebar Cross Sectional Area Loss by Reinforced Concrete Corrosion
Angela Gaio Graeff, Luiz Carlos P. da Silva Filho

Durability of Metakaolin Based Cement Mortar to Chloride Attack under Wet – Dry and Freeze – Thaw Exposure
Shweta Goyal, Maneek Kumar, B. Bhattachargee

Alternative Reinforcement for Durable Reinforced Concrete Structures
Marijana Serdar, Irina Stipanović Oslaković, Dubravka Bjegović

Modeling of Time Depended Changes of Chloride Diffusion Coefficient
Irina Stipanović Oslaković, Marijana Serdar, Dubravka Bjegović, Dunja Mikulić

Prediction of Elastic Properties of Concrete Using the Virtual Cement and Concrete Testing Laboratory
Sinan T. Erdoğan, Edward J. Garboczi, Jeffrey W. Bullard

Chloride Ion Measurement for Cement-Based Materials
Ceki Halmen, David Trejo

Fungal Colonization on Fiber Cement Exposed to the Elements in a Tropical Climate
Márcia Aiko Shirakawa, Edson Yoshio Aihara, Cleber Marcos Ribeiro Dias, Christine Claire Gaylarde, Vanderley Moacyr John

Durability of the HPC Cured in Sulphate Environment
Rabah Chaid, Raoul Jauberthie, Mohamed Tahar Abadlia, Abderrahim Bali

Effects of Ternary Blended Binders on Chloride Diffusivity of Concrete
Özkan Şengül, Mehmet Ali Taşdemir

Durability and Mechanical Properties of Fiber Reinforced Cement Composites Exposed to High Temperatures
Eva Vejmelková, Jan Toman, Pavel Padevět, Petr Konvalinka, Robert Černý

Critical Evaluation of the Definition of "Sulfate-Resistance" a Focus on the Flexural Strength Performance of SR Cements
Pinar Akpinar, Ignasi Casanova

Implementation of Durability in the Design of Glass Fibre Reinforced Concrete Structures
Heidi Cuypers, Petra Van Itterbeeck, Tine Tysmans, Jan Wastiels

Permeability and Porosity as an Essential Factors in the Long-term Durability of Steel Fibres Reinforced Concrete
Beddar Miloud

Accelerated Weathering Effects on the Mechanical and Surface Properties of CFRP Composites
Saud Aldajah, Ashraf Biddah, Abd Alsattar Noureldin, Ammar Al-Omari

Monitoring Moisture Content in Autoclaved Aerated Concrete as a Mean to Achieve Higher Durability
Zbyšek Pavlík, Lukáš Fiala, Zbigniew Suchorab, Robert Černý

Durability Properties of High Performance Concrete Containing Alternative Silicate Binders
Eva Mňahončáková, Pavla Rovnaníková, Robert Černý

Multidisciplinary Collaborations for a Qualitative Systemization towards a Durable Structure
Shohre Shahnoori, Liek Voorbij

Concrete Crack Width under Combined Reinforcement Corrosion and Applied Loads
Chun-Qing Li, Shangtong Yang, T. K. Ho

Deterioration of Cement Hydrates Containing Mineral Admixtures Due to Sulfuric Acid Attack
Kenji Kawai, Akihiro Sako, Tomoya Ikuta, Takeo Ishida

Corrosion Resistance of GGBS Concrete
M. Hulusi Ozkul, Unal Anil Dogan, Ali Raif Saglam, Nazmiye Parlak

Durability of Autoclaved Aerated Concrete
Berit Straube, Peter Langer, Andreas Stumm

Prediction of Residual Stress due to Early Age Behaviour of Massive Concrete Structures: On Site Experiments and Macroscopic Modelling
Jihad Zreiki, Vincent Lamour, Mohend Chaouche, Micheline Moranville

Repair & Rehabilitation of Initially Cracked RCC Beams by CFRP
Liaqat. A. Qureshi, Imran A. Bukhari, Kamran A. Qureshi

Chloride Transport in Concrete Structures Exposed to Marine Environments Considering Time Dependent Characteristics
Ha-Won Song, Seung-Woo Pack, Ki Yong Ann

Improvement of Durability of RC Column by Transverse Prestressing
Yasuji Shinohara

Durability Properties of Geopolymer Mortars
David W. Law, Andi A. Adam, Tom K. Molyneaux, Indubhushan Patnaikuni

Concrete Mix Proportions with Ultra-High Electrical Resistivity
Mohammad Shekarchizadeh, Mohammad Tahersima, Amir Hajibabaee, Hamed Layssi

Non destructive Test Methods for Evaluation of Concrete: The Case Study of Punta Perotti (Italy)
Luprano Vincenza, Caretto Flavio, Labia Nicola, Ciniglio Gabriele, Tatì Angelo, Tundo Antonella, Pfister Valerio

Influence of Fibers Weight Fraction and Nature of Fibers on Thermal and Mechanical Properties of Vegetable Fibers/Cement Composites
Cristel Onésippe, Fernando Toro, Ketty Bilba, Silvio Delvasto, Marie-Ange Arsène

A Study on the Addition of Extra Water Which Affects the Durability Degradation of Concrete
Woo Young Je, Ryu Hwa Sung, Jung Sang Hwa, Chae Sung Tae

Behaviour of Four Repair Materials under Accelerated Testing of Carbonation and Chloride Penetration
Carmen Andrade, Unal Anil Dogan, Nuria Rebolledo, Isabel Martinez

Coarse Aggregate Mineralogy, Size and Water Content Influence on Concrete Permeability
C. Gonilho Pereira, J.P. Castro-Gomes, A. Pereira de Oliveira

Mechanical and Durability Properties of Concrete with Ground Waste Glass Sand
L. A. Pereira de Oliveira, J.P. Castro-Gomes, P. Santos

Durability Modelling of Behaviour of Different Concrete Types As Tunnel Lining Elements
Marijan Skazlic, Nenad Gucunski, Dubravka Bjegovic

Chloride Threshold Determination in Prestressing Steel Beams
C. Alonso, F.J. Recio, M. Sanchez, C. Andrade

Analysis of Reinforced Concrete Flexural Members Strengthened with Near-Surface Mounted CFRP
N. Chikh, G. Foret, B. Bousalem, S. Firas

Effect of Cement Type on the Resistance of Concrete against Rapid Chloride Permeability
Tolga Ilıca, Hasan Yıldırım, Özkan Şengül

Effects of Cement with Mineral Additive and without Mineral Additive on the Concrete Durability
Hasan Yıldırım, Özlem Yörük, Aslı Özbora

Effect of Fire on Microstructure and Mechanical Properties of Blended Cement Pastes Containing Metakaolin and Silica Fume
M. M. Morsy, S. S. Shebl, A. M Rashad

Easy Evaluation Method of Self-Compactability of Self-Compacting Concrete
Masanori Maruoka, Hiromi Fujiwara, Erika Ogura, Nobu Watanabe

On Durability of Fiber Reinforced Concrete
M.A. Aiello, E. Vasanelli, G.A. Plizzari

Effect of High Temperature on Mechanical and Microstructural Properties of Cement Mortar
Özge Andiç-Çakır, Oğuzhan Çopuroğlu, Kambiz Ramyar

Durability of Cement Mortars with Carbon Material Admixtures
Pedro Garcés, Juan Alcaide, Eva G. Alcocel, Emilio Zornoza, Luis G. Andión

Durability Properties of Polypropylene Fiber Reinforced Concrete
Hamed Layssi, Mehrdad Mahoutian, Mohammad Shekarchi

The Use of Maturity Method in Estimating Early Concrete Strength
Amr E. Salama, Gouda M. Ghanem, Sayed Mohamed Abd El-bakey, Esraa Emam Ali

Concrete for Durability at Marmaray Project
Serap Erdoğdu, Steen Lykke

Rebound and Composition of in-Situ Polypropylene Fibre-Reinforced Shotcrete
Atef Badr, Jeff Brooks

Mechanical Behaviour of GFRP-Confined Concrete after Exposure to Severe Conditions
Francesco Micelli, Maria Antonietta Aiello, Alfonso Maffezzoli, Rossella Modarelli

The Characteristics of Boron Modified Active Belite (BAB) Cement and its Utilization in Mass and Conventional Concrete
Aydın Sağlık, Oya Sümer, Ergin Tunç, M.Fatih Kocabeyler, Rahmi Sencer Çelik

Wood and Wood Components

The Efficiency Comparison of Polyester, Acid Catalyzed Lacquers and Nitrocellulose Lacquers on *Fagus Orientalis* Wood and Plywood
Saeed Keshani Langroodi, Mehrdad Sedghi, Davood Parsapajouh, Azad Henareh Khalyani

Modification of Wood with Si and B Compounds
S. Nami Kartal, Tsuyoshi Yoshimura, Yuji Imamura

The Old, Wooden Window, a Balance between Romantism and Performance
Ana-Maria Dabija

Hurricane Katrina: An Overview of Damage to Timber Structures
Anthony J. Lamanna, Brian Metrovich, Jeremy Martin

Wood as a Structural Material
N.Papatya Seçkin

Preparation Method and Service Condition Effects on The Performance and Durability of Epoxy Adhesives Used in Structural Timber Repairs
João Custódio, Helena Cruz, James Broughton

Durability of External Wood-Frame Door System, A Case Study
Fatih Yazıcıoğlu, Kevser Coşkun

Reduction of Water Absorption and Swelling of Fiberboard
Javad Torkaman

Attenuated Total Reflectance (ATR) Fourier Transform Infrared (FTIR) Radiation Studies of Wood Rot Decay and Mould Fungi Growth on Building Materials
Bjørn Petter Jelle, Idar Myklebost, Jonas Holme, Per Jostein Hovde, Tom-Nils Nilsen

Attenuated Total Reflectance (ATR) Fourier Transform Infrared (FTIR) Radiation Investigations of Natural and Accelerated Climate Aged Wood Substrates
Bjørn Petter Jelle, Petra Rüther, Per Jostein Hovde, Tom-Nils Nilsen

Performance-based Specification of Wooden Components
Christian Brischke, Andreas O. Rapp

Fire Resistance Performance Study on the Compartment Walls in Wood Platform Construction
Chun-Ta Tzeng, Hung-Chi Su, Pang-An Hsiao

Production of Dimensionally Stable and Decay Resistant Wood Components Based on Acetylation
Roger M. Rowell, Bert Kattenbroek, Peter Ratering, Ferry Bongers, Francesco Leicher, Hal Stebbins

Building Gaskets and Sealant Products

Development of an Automated Artificial Ageing Test Apparatus for Sealants and Comparison with Outdoor Exposure Testing
Hiroyuki Miyauchi, Yoshiaki Takemoto, Michael A. Lacasse, Kyoji Tanaka

Quantification of Effect of Dynamic Movement for Weatherability of Construction Sealants
Noriyoshi Enomoto, Kyoji Tanaka

Acrylic Foam Structural Glazing Tapes
Steve Austin, Uwe Manert

Non-Destructive Testing of Elastomeric Joint Sealants in Construction
Daniel N. Huff

Natural and Artificial Stone

The Sandstone Conundrum
Edward Gerns, Rachel Will

Visual Effects of Building Stone Texture
Jun Tsuchiya, Shoji Sunaga

The Perception of Small Scale Damage and Repairs of Natural Stone
Wido Quist, Rob van Hees, Silvia Naldin, Timo Nijland

Biofilm Effect and Microbiological Deterioration on the Material Surface
Sedat Kurugöl, Dilek Dilhan Hatipoğlu

Determination of Water and Nitrate Transport Properties of Sandstone Used in Historical Buildings
Zbyšek Pavlík, Lukáš Fiala, Milena Pavlíková, Robert Černý

The Correlation of Electric Emissions with Stress and Strain on Stressed Rock Samples
Ilias Stavrakas, Antonis Kyriazopoulos, Panayiotis Kyriazis, Konstantinos Ninos, Cimon Anastasiadis, Dimos Triantis

Freeze Thaw Susceptibility of Natural Stone – Characterization of the Mechanical Strength and Microstructure During Frost Cycling
T. Yates, A. Mauko

Surface Coatings and Paints

Outdoor Wall Painting Semi-Natural Test
Alberto Giacardi, Luigi Morra

Durability Evaluation of Newly Developed Water-Based Paint Systems for Buildings
Kenji Motohashi

Effect of Anti-Graffiti Coatings on The Drying Behaviour of Building Materials
Barbara Lubelli, Rob P.J. van Hees, Teun van de Weert

Durability of Surface Protection Systems in Harsh Marine Climates
Claus K. Larsen, Jan-Magnus Østvik

Polymer-based Building Materials and Composites

Long-term Performance of Extruded Polystyrene Thermal Insulation Products
Holger Merkel

Durability of Roof Underlays Exposed to Natural Climate
Birgitte Dela Stang, Erik Brandt, Morten Hjorslev Hansen

Polymer-based Building Materials: Effects of Quality on Durability
Esin Kasapoğlu

Service Life of Light Weight Bathrooms
Erik Brandt

Innovative Materials and Products for Durability

Properties of Concrete with Shredded Waste Tyres
Özer Dogan, Gülser Çelebi, Soofia Tahira Elias-Ozkan

Oriented Straw Cable Composites for Housing Applications
Seda Yeşilmen, Anthony J. Lamanna, Gerhard Piringer

Experimental Study of Geopolymer Concrete Resistance to Sulphuric Acid Attack
Robert Munn, Xiujiang Song, Marton Marosszeky

Roof Management Program for Multiple Roof Systems
Steven P. Bentz, Walter J. Rossiter, Jr.

Development of Test Method for Evaluating Root Resistance of Waterproofing Membrane
Kyoji Tanaka, Saori Ishihara, Soonju Pyo, Hiroyuki Miyauchi

Condensation Problems in Cool Roofs
Christian Bludau, Daniel Zirkelbach, Hartwig M. Künzel

Design of Mineral Fibre Durability Test Based on Hygrothermal Loads in Flat Roofs.
Daniel Zirkelbach, Hartwig M. Künzel, Christian Bludau

A Model for Determining Accelerated Ageing Cycles in Durability Research: A Case Study on Continuous Roofing
Maurizio Nicolella, Alba De Pascale

Durability of Clay Roofing Tiles under Salt Mist Atmosphere
Cláudio Cruz, M. Rosário Veiga, Victor M. Ferreira

Designing Replacement Roof Systems to Achieve Long Term Service Life: A Sustainable Solution
Thomas W. Hutchinson

The Specification and Selection of CE Marked Reinforced Bitumen Membranes for Low Sloped Roofs to Ensure Their Durability in the UK
Gerry Saunders

Wind Tunnel Tests of Various Mechanically Anchored Waterproofing Membranes
Hirokazu Ichikawa, Nobuo Kato, Hiroyuki Miyauchi, Kyoji Tanaka

Service Life (Model) for Bituminous Roofing
Erik Brandt, Tommy Bunch-Nielsen

Flexible Polyolefin Roofing Membranes: 15 Years of Field Experience
Hans-Rudolf Beer, Anthony Mayr

Performance of Silicone Water Repellent for FRC Corrugated Roof Tiles
Flávio L. Maranhão, David Selley, Cleber Dias, Kai Loh, Vanderley M. John

Effects of Wet and Dry Cycles on The Performance and Microstructure of Asbestos-free Fiber Cement
C. M. R. Dias, H. Savastano Jr., V. Agopyan, V. M. John

Polyolefin Roof Membranes on Site Durability Evaluation
Sergio Croce, Matteo Fiori

Facades and Curtain Walls

Materials Used in Transparent Facades: an Approach Towards Building Maintenance
Geísa Gaiger de Oliveira, Oliveira, Roberto de Oliveira, Cláudio Renato de Camargo Mello

Use of a Peltier Element to Increase Time of Wetness of Unglazed Solar Collector Specimens in a Natural Field Exposure Test
Bojan Stojanović, Jan Akander

Minimum Required Performance Level for Rendered Facades
Pedro Lima Gaspar, Jorge de Brito

Durability of Sandwich Panels
Çiğdem Çelik Tekin, Ülger Bulut

Experimental Programme to Assess ETICS Cladding Durability
Bruno Daniotti, Riccardo Paolini

Defacement of ETICS Cladding due to Hygrothermal Behaviour
Eva Barreira, Vasco Peixoto de Freitas

Durability of External Wall Insulation Systems with Extruded Polystyrene Insulation Boards
Durmuş Topçu, Holger Merkel

Durability of Repaired Concrete Facade Elements
Riccardo Nelva, Roberto Vancetti

Enhanced Service Life of Coated Wooden Facades
Per Jostein Hovde, Bjørn Jacobsen, Bjørn Petter Jelle, Erik Larnøy, Geir Vestøl

Study on the Relation Between Mockup Test and Lifecycle of Curtain Wall Construction - Case Study in Taiwan
Chih-Min Chi, Chun-Ta Tzeng

Preservation and Refurbishment of Historical Buildings

Decay Diagnosis of Goan Laterite Stone Monuments
Sutapa Das

Faults and Repairs in House of Bagheri: A Cultural Heritage Construction in Gorgan (North of Iran) – A Case Study
Mehrab Madhoshi, Javid Eimanian

Issues in the Identification and Monitoring of Historical Structures – Monuments
Yasemin Didem Aktaş, Ahmet Türer

The Durability of Materials and Treatments for the Operation on the External Curtains of the Historical Buildings
Rosa Caponetto, Giuseppe Luciano, Umberto Rodonò, Salvatore Secondo

Durability Properties of Innovative Plasters for Renovation of Historical Buildings
Radka Pernicová, Milena Pavlíková, Robert Černý

Decision Making about Cleaning Interventions on Marble Surfaces Using a Fuzzy Logic Approach
Antonia Moropoulou, Ekaterini T. Delegou, Myrto Konstandinidou, Chris Kiranoudis

The Assessment of Roof Drainage System of a Historical Turkish Bath: Sengul Hammam
Gülşen Dişli, Ayşe Tavukçuoğlu, Levent Tosun, Ermanno Grinzato

The Restoration and Upgrading of The 100 Year Old Victoria Institution: The Adaptive Reuse of a School into an Auditorium
Kribanandan Gurusamy Naidu

Classification of Restoration Mortars by Principal Component Analysis and Correlation between Their Properties and Synthesis
Antonia Moropoulou, Kyriaki Polikreti, Petros Moundoulas, Eleni Aggelakopoulou

Technological Features and Decay Processes of A “New” Building Type at the Beginning of XX Century
Fabio Fatiguso, Giambattista De Tommasi

RESPONSE OF BUILDING ELEMENTS TO ENVIRONMENTAL LOADS

Climate Loads on Buildings

Evaluation of Environmental Degradation Factors for Service Life Prediction
Johann Mc Duling, Emile Horak, Chris Cloete

Climatic Comparison to Analyse Different Degradation Levels in External Walls' Outdoor Exposure
Bruno Daniotti, Sonia Lupica Spagnolo

Climatic Data Analysis to Define Accelerated Ageing for Reference Service Life Evaluation
Bruno Daniotti, Sonia Lupica Spagnolo, Riccardo Paolini

Hail Impact Resistance of Building Materials - Testing, Evaluation and Classification
Peter Flüeler, Maja Stucki, Fabio Guastala, Thomas Egli

Prediction of Atmospheric Corrosion Rate Using an Artificial Neural Network
Gülşah Doğan, Emrah Gökaltun

Heat and Moisture Transfer in Buildings

Predicting The Initial Rate of Water Absorption in Clay Bricks
Mariarosa Raimondo, Michele Dondi, Davide Gardini, Guia Guarini

Simulating Water Leaks in External Walls to Check the Moisture Tolerance of Building Assemblies in Different Climates
Hartwig M. Künzel, Daniel Zirkelbach, Achilles Karagiozis, Andreas Holm, Klaus Sedlbauer

Daily Hygroscopic Inertia Classes: Application in a Design Method for the Prevention of Mould Growth in Buildings
Nuno M. M. Ramos, Vasco P. de Freitas

Modelling for Development of Wood Rot Decay with Simultaneous Heat and Moisture Transfer for Building Envelopes
Hiroaki Saito, Kiyoharu Fukuda, Takao Sawachi, Akira Oshima

Influence of Thermal Properties of Materials in Condensation and Microorganism Growth on Building Facades
Neide Matiko Nakata Sato, Marcia Aiko Shirakawa, Kai Loh, Vanderley Moacyr John

Development and Benchmarking of a New Hygrothermal Model
Fitsum Tariku, Kumar Kumaran, Paul Fazio

The Impact of the Indoor Climate on the Hygrothermal Behaviour and the Durability of External Components – Standard Boundary Conditions vs. Hygrothermal Indoor Climate Simulation
Andreas Holm, Hartwig M. Künzel, Klaus Sedlbauer

Influences of the Indoor Environment on Heat, Air and Moisture Conditions in the Building Component: Boundary Conditions Modeling
Paul Steskens, Carsten Rode, Hans Janssen

SERVICE LIFE PREDICTION AND PLANNING METHODOLOGIES, RISK ANALYSIS APPROACHES

Service Life Planning

Feedback System for Determination and Elimination the Effects of Durability Problems
Gamze Özkaptan Alptekin

Factor Method Application Using Factors' Grids
Bruno Daniotti, Sonia Lupica Spagnolo, Riccardo Paolini

Service Life Estimation using Reference Service Life Databases and Enhanced Factor Method
Bruno Daniotti, Sonia Lupica Spagnolo

French National Service Life Information Platform
Julien Hans, Julien Chorier, Jean-Luc Chevalier, Sonia Lupica

Quantification of Façade Defects Using Photogrammetry within the *BuildingsLife* System
Pedro Vaz Paulo, F. A. Branco, Jorge de Brito

Homes in Iceland--Flexibility and Service Life Fulfilment of Functional Needs
Björn Marteinsson

Information System and Interworking for a Durable Inheritance
Boulekbache Mazouz Hafida

Service Life of a Building in Environmental Assessment of Buildings
Appu Haapio, Pertti Viitaniemi

Whole Life Cycle Costing as a Decision Tool for Use in French Healthcare Facilities
Samer Sliteen, Orlando Catarina

Service Life Prediction Methods

Service Life Prediction Beyond the 'Factor Method'
Johann Mc Duling, Emile Horak, Chris Cloete

Evolution of Degradation and Decay in Performance of ETICS
Bruno Daniotti, Riccardo Paolini

A Multi-Performance Approach for Service Life Prediction
Aurélie Talon, Daniel Boissier, Julien Hans

Fuzzy Lifetime Prediction of RC Structures Subject to Chlorides
Giuseppe Carlo Marano, Giuseppe Quaranta, Sara Sgobba, Simona Sasso, Michele Notarnicola

Timber Structures Service Life Modelling
Jan-Willem van de Kuilen, Nadine Edi Montaruli

Probabilistic and Reliability Models

Performance-based Design for Anticorrosion of Reinforced Concretes under Air-borne Salt Attack
Kai-Lin Hsu

Application of the Reliability Theory to the Assessment of the Corrosion Risk due to Carbonation
Thiery Mickael, Crémona Christian

Durability Limit States of Concrete Structures: Probabilistic Modelling
Dita Matesová, Markéta Chromá, Břetislav Teplý

Development of a Simulation Tool for Insulated Glass Durability
Russell Pylkki, Michael Doll

Critical Considerations on the Assessment of the Durability (Serviceability) Limit State of Reinforced Concrete Structures
Rui Miguel Ferreira, Joost Gulikers

Development of Guides, Regulations and Standards

DURABILITY AND SUSTAINABLE BUILDINGS

Service Life and Sustainable Design Methods and Technologies

Life Cycle Analysis (LCA) and Sustainable and Durable Design

BUILDING MAINTENANCE AND PATHOLOGY

Pathology Surveys and Diagnostic Tools

Maintenance Planning and Procedure

Life Cycle Management System – A Planning Tool Supporting Long-Term Based Design and Maintenance Planning
Daniel Hallberg, Jan Akander, Bojan Stojanović, Mikael Kedbäck

Quantifying Maintainability Parameters for Vertical Transport System
Chew M.Y.L., Sutapa Das, Nur H.B. Sulaiman

Optimal Maintenance Plan by Minimizing Life-cycle Cost Including Deterioration Risk
Chien-Kuo Chiu, Takafumi Noguchi, Manabu Kanematsu, Hironori Nagai

Deterioration of Reinforced Concrete Buildings and Rehabilitation Process
Nilay Coşgun, E. Özlem Aydin

Service Life Prediction Tools for buildings' Design and Management
Bruno Daniotti, Sonia Lupica Spagnolo

FMECA and Management of Building Components
Aurélie Talon, Daniel Boissier, Julien Hans, Michael A. Lacasse, Julien Chorier

Condition Assessment of a 63-year Old Reinforced Concrete Structure Exposed to the North Sea
Robert E Melchers, Chun-Qing Li, Mark Davidson, Shangtong Yang

A GIS-Based Framework for the Evaluation of Building Façade Performance and Maintenance Prioritization
Brian Kyle, Michael A. Lacasse & Steven M. Cornick, Denis Richard, Khaled Abdulghani &Thibaut Hilly

A Methodology for Protection of Masonries against Rising Damp
Maria Karoglou, Antonia Moropoulou, Magdalyni K. Krokida, Dimitris K. Konstantopoulos, Vasilis Z. Maroulis

Optimization of the Building Maintenance Management Process Using A Markovian Model
Michael A. Lacasse, Brian Kyle, Aurélie Talon, Daniel Boissier, Thibaut Hilly, Khaled Abdulghani

A Structural Condition Assessment; Environmental Agents Versus Structural Failures - The Case of Ataturk Culture Center AKM, *Istanbul, Türkiye*
Kemal Çayırlı

Development of Autoclaxed Lightweight Concrete Outer Walls and its Freeze-Thaw Resistance

Taku Sanda [1]
Toshizi Mimori [2]
Takao Tairaku [3]

T 11

ABSTRACT

In order to build a house in Japan, one must consider that there are four seasons. Durable houses are necessary to create stable living conditions.Outer wall materials are directly affected by climatic change. The motivation for this type of research is that there is a significant demand for highly durable outer wall materials. In addition, because of the compulsory 10-year guarantee on houses, it is demanded that outer wall materials are made much lighter, high strength and more durable than ever before. Furthermore, due to diverse customer needs, the demand for materials that are distinctive has increased.

The focus of this research is to develop the autoclaved lightweight concrete outer walls with long-term stability, high-strength and high-durability and investigate its freeze-thaw resistance.The outer walls have dimensional stability by generation of 1.1nm tobermorite in the materials and high-strength by reduction of water to powder ratio of the materials and autoclaved curing.Since significant scaling or cracking deterioration did not observed on these high Strength Lightweight Concrete during sustained one-side freezing testing, it is estimated that these materials were resistant to freeze-thaw action with little risk of deterioration under normal use conditions. I propose to conduct research on how to decrease changes in measurements due to heat/cold, and dryness/moisture, and age- related deterioration caused by the ultraviolet ray, the heat and snow, and to develop materials which improve the long-term durability.

KEYWORDS

Autoclave curing, High-strength lightweight concrete, Dimensional stability, High durability, Freeze-thaw resistance

[1] Misawa Homes Institute of Research and Development Co., Ltd, Tokyo, Japan 1680071, Phone +81 3 3247 5647, Fax +81 3 5370 7324, Taku_Sanda@home.misawa.co.jp
[2] Kushiro National College of Technology, Hokkaido,Japan 0840916, Phone +81 154 57 7375, Fax +81 154 57 6252, mimo@archi.kushiro-ct.ac.jp
[3] Kushiro National College of Technology, Hokkaido,Japan 0840916, Phone +81 154 57 7372, Fax +81 154 57 6252, tairaku@itu.edu.tr

1 INTRODUCTION

In constructing housing in Japan, an important item to be considered is existence of four seasons. Surrounded with a variety of climates such as spring, summer, autumn and winter, housing with durability is required for people to spend stable and peaceful lives.

As the part of building, the materials that receive the strong impact of climate are outer walls. Therefore, long-term durability is required as their functions. In addition, the enactment of the "Law for the promotion of ensuring housing quality" and the "Housing quality warranty system" has enforced 10-year guarantee for housing. As a result, building materials have come to be required to have better qualities in terms of lightweight, high strength, high durability (freeze-thaw resistance), and dimensional stability [Saito *et al.* 2005]. Let's think about these four requirements for qualities for general housing materials (outer wall materials). For instance, ALC (autoclave-cured lightweight foam concrete) is excellent in lightweight, thermal insulation, flame resistance, and dimensional stability, and it is widely used as building materials.

However, since ALC has low compressive strength and high water absorption rate, it is very vulnerable against freezing deterioration depending on usage, which requires special precautions in using in cold regions. When ordinary concrete is used as outer walls, it has similar defects as ALC. Since ordinary cement has problems of shrinkage and considerable degree of heavyweight as outer wall panels, it troubles human hands in manual work.Then, this study aimed to develop outer wall materials with improved four performances such as lightweight, high strength, high durability (freeze-thaw resistance) and dimensional stability to satisfy the performances required for long-term durability as housing outer walls.Specifically, as a high-strength building material, calcium silicate hydrate, which was formed by mixing cement and siliceous material in low water-powder ratio, followed by autoclave processing, was considered. The low water-powder ratio was realized using a high-performance AE water-reducing admixture.

2 EXPERIMENTAL SCHEME

2.1 Materials Used

The materials used were ordinary Portland cement (3000 cm^2/g), silica sand (2700-3300 cm^2/g), lightweight aggregate (fly ashhollow material) for decreasing weight, and accelerated curing admixture (calcium aluminate : anhydrite = 1:1) for quickly hardening. Other materials used were aramid fiber for reinforcing panels, high-performance AE water-reducing admixture (polycarboxilate type), and foaming agent.

2.2 Material Compositions

The chemical components of main used materials are shown in Table 1, and the mixing ratio for mortar is shown in Table 2.

Table 1. Chemical components of main used materials (%).

	SiO_2	Al_2O_3	Fe_2O_3	CaO	SO_3	f-CaO
PC	21.64	5.08	2.93	64.53	1.95	0.4
SI	95.9	1.54	0.99	-	-	-
F	56.2	26.8	5.1	3.5	0.3	-
AC	3.5	54.5	1.3	36.5	-	-

PC: Portland cement, SI: Silica sand, F: Fly ash (type IV), AC: Accelerated curing admixture

Table 2. Mixing ratio for mortar (wt%).

W/P	PC	SI	LG	AC	fiber	Admix-ture
0.36 ~ 0.4	49.0	29.5	15.0	6.0	0.25	0.25

W/P: Water-powder ratio, LG: Lightweight aggregate, Admixtures:high-performance AE water-reducing admixture, foaming agent, and hydration modifier

2.3 Manufacturing Methods

2.3.1 Kneading

Admixtures (high-performance AE water-reducing admixture, foaming agent, and hydration modifier) and water for kneading are fed into an omni-mixer and agitated for 1min in order to generate foams. Next, powders such as cement and aggregates are fed, and the mixture is agitated for 1 min. Finally, the accelerated curing admixture, in the form of slurry made by mixing with part of water for kneading, is added, followed by agitating for 30sec for preparing mortar.

2.3.2 Curing

Manufactured mortar is cast into a mold form, and after maintaining at 40°C (ambient temperature) for 60 min, the product is demolded. By demolding at early stages due to the use of the accelerated curing admixture, manufacturing time can be shortened. Then, wet-air curing for pre-curing is applied at 40°C for 10 h, and autoclave curing (high-temperature high-pressure curing) is applied at 180°C and 10 atm for 8 h. Then, in preparation for coating as outer walls, forced drying is applied to reduce water content.

2.4 Evaluation on Compositions, Physical Properties and Durability

Using manufactured specimens, measurements of basic properties such as scanning electron microscope, absolute dry density, compressive strength, bending strength, as well as testing for freeze-thaw resistance are conducted. Meanwhile, when manual work at a site such as crusting board is supposed, it is necessary to set density at 1.0 or below. On the other hand, in order to prevent chipping and cracking during transfer after manufacturing, reasonable strength is necessary. Then, considering application at a site, the absolute dry density of specimens is set at 0.9 g/cm^3 and 0.95 g/cm^3 for evaluating durability performance.

2.4.1 Scanning Electron Microscope (SEM)

The crystalline morphology of tobermorite is observed with SEM

2.4.2 Compressive Strength Test and Bending Strength Test

Using an angular specimen of 4×4×16 cm, these tests are conducted following JIS R5201.

2.4.3 RILEM CIF Method Test [RILEM 2000]

In CIF test, predetermined curing is applied to a beam-shaped specimen of 10×10×20 cm, and the sides of the specimen was sealed with aluminum tapes with butyl rubber. Then, the lower surface is immersed in a temperature-controlled chamber at 20°C and 60% RH for 7 days to absorb water. Afterwards, using a CIF freeze-thaw test apparatus shown in Fig. 7, one-side freeze-thaw test, under lower- surface water-absorbing condition, is repeated at a rate of two cycles a day up to 100 cycles. The conditions are as follows; highest temperature at 20°C (keeping for 1 h), lowest temperature at –20°C (keeping 3 h), and temperature gradient at ±10 K/h. Measurement items are weight change, relative dynamic elastic coefficient, and peel-off quantity. In the peel-off quantity test, 3-minute ultrasonic cleaning is applied to the whole test apparatus after each measurement cycle, and the solution was filtrated. The peeled pieces are dried at 105°C for 24 h, and the weight is measured. The relative dynamic elastic coefficient is measured with a flexural oscillation method.

2.4.4 Measurement of Foam Structure [Hama *et al.* 2005]
Measurement of foam structure is conducted following ASTM C457 (linear traverse method), and air volume, average foam diameter, and foam interval coefficient are calculated.

2.4.5 In-water Freezing and in-Water Thawing Test
This test is conducted following JIS A1148 Method A (freeze and thaw test of concrete). A beam-shaped specimen of 10×10×40 cm is used. Before the test, the whole body of specimen is immersed in water for 48 h for absorbing water. Using a freeze and thaw test apparatus, the specimen is subjected to midair freezing at –18°C for 2.5 h and in-water thawing at +5°C for 1.5 h, and this cycle is repeated up to 300 cycles. Measurement items are weight change and relative dynamic elastic coefficient, and the latter is measured with a flexural oscillation method.

3 RESULTS AND DISCUSSIONS

3.1 Basic Physical Properties

Within four performances lightweight, high strength, high durability freeze-thaw resistance and dimension stability that satisfy required performances for long-term durability, dimension stability has already been described. Here, in order to reduce weight, by changing the addition quantity of a foaming agent, specimens with different slurry densities of mortar were prepared, and their physical properties were measured. For comparison, ALC of pre-form type (P-ALC) was measured.

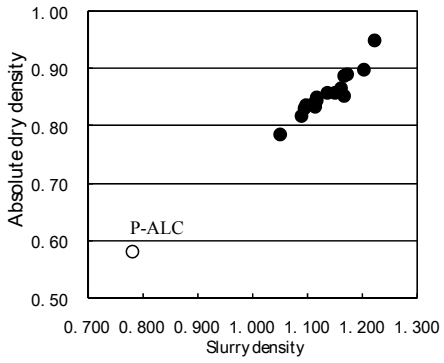

Fig. 1. Relations between mortal density and absolute dry density.

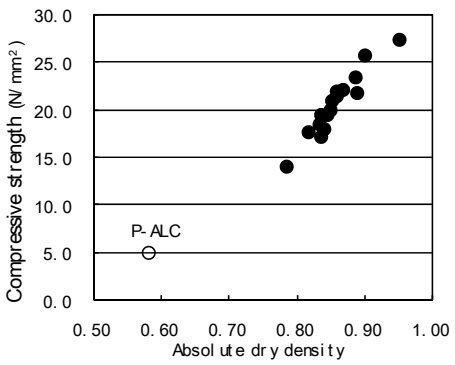

Fig. 2. Relations between absolute dry density and compressive strength.

In the relations between the mortar density after kneading and the density of a sample absolutely dried (drying at 105°C for 48 h) after autoclave curing, absolute dry density linearly increased as mortal density increased. From these relations, it is possible to estimate absolute dry density after autoclave curing from the figure when mortar is kneaded. In the relations between absolute dry density and compressive strength, compressive strength linearly increased as absolute density increased. When the absolute density of high-strength lightweight concrete was 0.9 and 0.95 g/cm^3, corresponding compressive strength was 25.7 and 27.4 N/mm^2. Due to the autoclave treatment, it was possible to obtain high-strength lightweight concrete with about threefold of relative strength compared with P-ALC.

3.2 CIF Test

Changes in relative dynamic elastic coefficient are shown in **Fig. 3**. Decrease in the relative dynamic elastic coefficient of the high-strength lightweight concretes was hardly seen, and the figure was 96% and 97%, respectively, at the end of 100 cycles. In comparison, the relative dynamic elastic coefficient of P-ALC tended to decrease immediately after the start of the freeze-thaw test, and it showed 78%

after the end of 100 cycles.Changes in peel-off quantity are shown in **Fig. 4**. The high-strength lightweight concretes showed minor scaling in the rang of 5 g, while P-ALC showed rapid scaling around after 20 cycles, recording 40 g of peel-off (ca. 10 mm as peel-off depth) when the test ended.

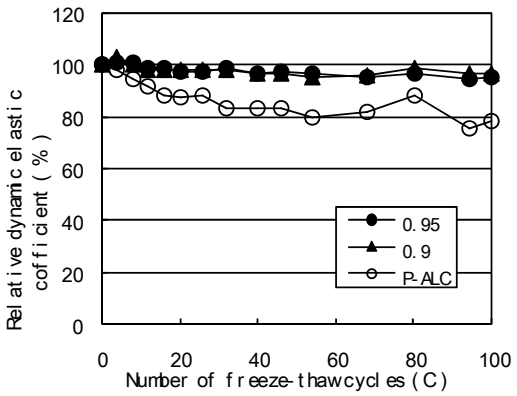

Fig. 3. Changes in relative dynamic elastic coefficient in CIF test.

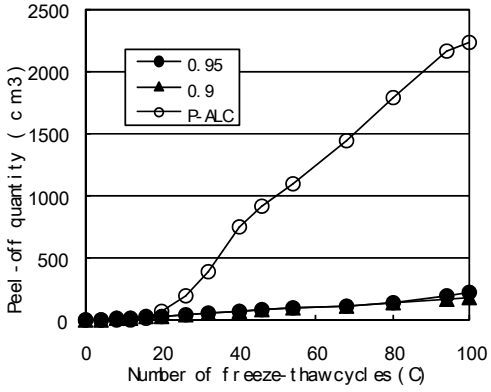

Fig. 4. Changes in peel-off quantity.

Changes in water absorption rate are shown in **Fig. 5**. The water absorption tendency of the high-strength lightweight concretes was similar to that of P-ALC. The water absorption rate after 40 cycles hardly showed an increase, keeping saturated conditions. P-ALC showed a little increase in water absorption during 7 days of lower-surface water absorption, and a remarkable increase during later freeze-thaw conditions.

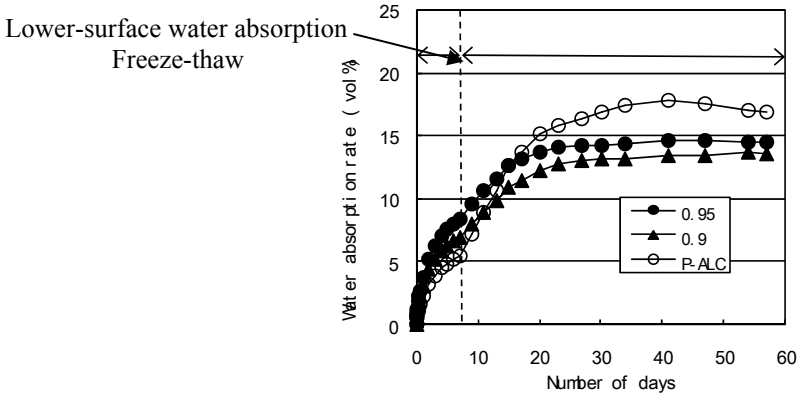

Fig. 5. Changes in water absorption rate in CIP test.

Since deterioration due to freeze-thaw has a close relation with absorption conditions, it is important to judge the possibility of reaching threshold water saturation degree (saturation degree within a limit not to cause deterioration) under supposed environment. Then, let's discuss deterioration from the viewpoints of changes in relative dynamic elastic coefficient in **Fig. 3** and changes in water absorption rate in **Fig. 5**. In P-ALC, relative dynamic elastic coefficient started to decrease immediately after freeze-thaw started. From this fact, it is suggested that deterioration started when water absorption rate reached 5.5 vol%, as the absorption rate when lower-surface water absorption ended, and successively water absorption accelerated due to damage of fine structure following the progress of deterioration. On the other hand, in the high-strength lightweight concretes, water absorption rate reached nearly saturated condition at 14 vol%, and yet deterioration was not recognized ever at this high water absorption rate. Although it is difficult to specify the threshold water saturation degree, the possibility of deterioration, such as strength decrease and collapse due to freeze-thaw action, seems be little under normal environment.

3.3 Measurement of Foam Structure

The relations between absolute dry density and air volume are shown in **Fig. 6**, the relations between absolute dry density and average foam diameter in **Fig. 7**, and the relations between absolute dry density and foam interval coefficient in **Fig. 8**. Although the air volume of the high-strength lightweight concretes varied in a wide range such as 25.0-38.3%, average foam diameter and foam interval coefficient little varied. In particular, foam interval coefficient was nearly 0.1 mm, showing very excellent foam structure against freeze-thaw damage compared with evaluation on ordinary concrete [Hama *et al.* 2005].

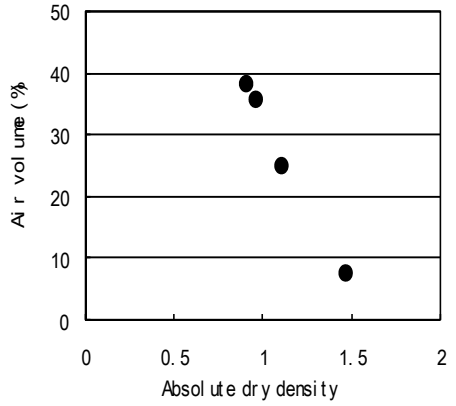

Fig. 6. Changes in absolute dry density and air volume.

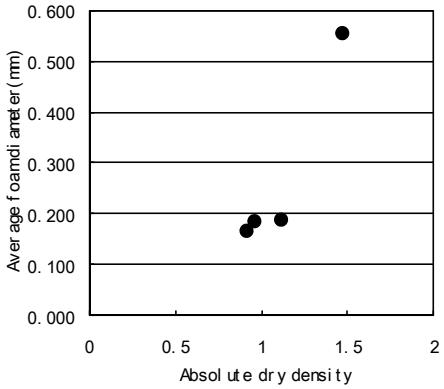

Fig. 7. Changes in absolute dry density and average foam diameter.

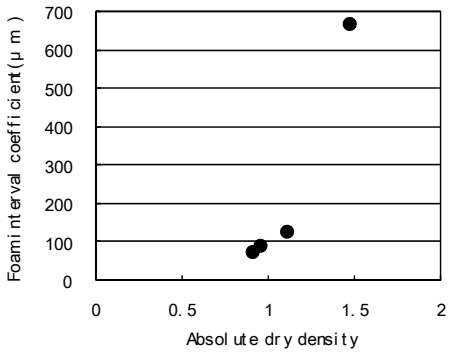

Fig. 8. Changes in absolute dry density and foam interval coefficient.

3.4 In-water Freeze and in-water thaw test

Changes in relative elastic coefficient are shown in **Fig. 9**. The high-strength lightweight concrete with a density of 0.95 g/cm^3 dropped its relative dynamic elastic coefficient to 80% or below during 90-120 cycles. With a density of 0.9 g/cm^3, decrease in relative dynamic elastic coefficient was suppressed, and it was kept over 80% even after 300 cycles. In comparison, P-ALC tended to show decrease in relative dynamic elastic coefficient immediately after the start of freeze-thaw, and it dropped to 68% during 30-60 cycles.

Changes in weight are shown in **Fig. 10**. The weight of any specimen tended to increase from the start of the test, and any of the high-strength lightweight concretes reached saturated conditions at 90 cycles. P-ALC was considered to have reached threshold water saturation degree due to water absorption before the start of freeze-thaw, and abrupt deterioration proceeded before 30 cycles from

the start of freeze-thaw, and water absorption seemed to have accelerated following the damage of fine structure.

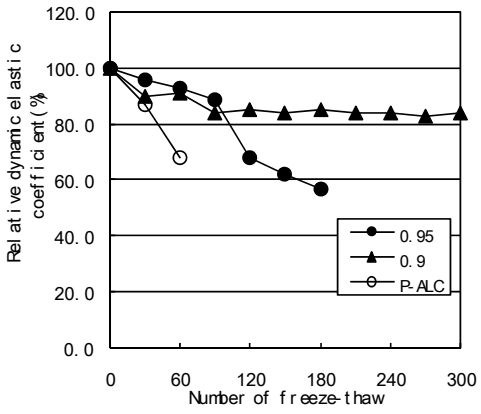

Fig. 9. Changes in relative dynamic elastic coefficient in in-water freeze and in-water thaw.

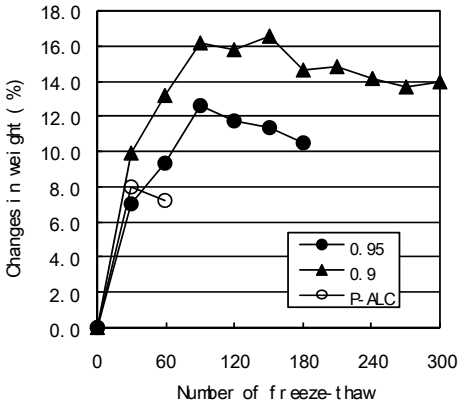

Fig 10. Changes in weight in in-water freeze and in-water thaw.

4 CONCLUSIONS

This study aimed to make full use of the advantages of ALC such as lightweight and dimension stability, and to further pursue high strength and high durability (freeze-thaw resistance). As a result, the following conclusions have been obtained on the high-strength lightweight concretes with absolute dry density of 0.9-0.95 g/cm^3.

(1) Using cement and siliceous materials as well as a high-performance AE water-reducing admixture, mortar with reduced water-powder ratio could be manufactured. By treating this mortar inside an autoclave, the high-strength lightweight concrete with high relative strength of approximately threefold of P-ALC could be obtained. The main constituent of hydration product of the high-strength lightweight concrete was calcium silicate hydrate.

(2) When manufacture efficiency as manufacturing conditions is considered, by using an accelerated curing admixture (calcium aluminate : anhydride = 1:1), demolding at 40°C for 60 min became possible. These conditions are advantageous as industrial production process.

(3) By mixing foams, lightweight product could be obtained and freeze-thaw resistance was improved, as in the case of ordinary concrete [Hama *et al.* 2005].

(4) Intense scaling as seen in P-ALC was not observed.

(5) Even in the severe test based on in-water freeze in-water thaw, the high-strength lightweight concrete with a density of 0.9 g/cm^3 retained 80% of relative dynamic elastic coefficient even after 300 cycles. Under normal use conditions, strength lowering and deterioration due to freeze damage will hardly occur.

ACKNOWLEDGEMENT

In performing this study, we received cooperation of Assoc. Prof. Hama, graduation thesis student Mr. Tomoya Sato, and fifth graders of Architecture Science Division, all at Kushiro National College of Technology. We would like express heartfelt gratitude to them.

REFERENCES

Saito, T., Sakai, E., Sanda, T., & Daimon, M. 2005, 'Effects of water-powder ratio on the hydrothermal reaction of Portland cement – α-quartz – water system', *Journal of the Society of Inorganic Materials Japan*, 12.

RILEM Recommendation, 2000, 'CIF Test – Capillary Suction, Internal Damage and Freeze-Thaw test; Reference method and alternative methods A&B' Materials & Structure, 34, pp. 515-525.

Hama, Y. et al. 2005, 'Study on the freeze-thaw resistance of autoclaved high-strength lightweight concrete' Technical papers of the annual meeting of Japan Concrete Institute, Vol. 27, No. 1, pp. 1375-1380.

Reinforcement of Cement Materials Using Date Palm Fibres for Use in Hot Dry Climates

Abdelouahed Kriker [1]
Abderrahim Bali [2]
Gérard Debicki [3]

T 11

ABSTRACT

This research integrates a global program, which is interested in the improvement of the performances of building materials in hot dry climate zones by the beneficiation of the local natural resources. The local resource used in this research is the male date palm surface fibre (MDPSF). This paper provides mechanical and physical properties of MDPSF, and flexural properties of MDPSF reinforced concrete. Regarding the mechanical performance of more common vegetable fibres, the MDPSF has average mechanical properties and a weak elasticity modulus.

The volume fraction and the length of fibres reinforcement were 2-3% and 15-60 mm respectively. The study revealed that increasing the length and percentage of fibre in reinforced concrete improves the post-crack flexural strength, but decreases the first crack.

The durability of MDPSF reinforced concrete was investigated according to its flexural properties and some scanning electron micrographs at the fibre-matrix interface zones. Two curing types were used: 1- In hot-dry climates, 2- Initially 14 days in water then in hot-dry climates. As a result, the durability of the SDPF reinforced concrete loosed in the first cure, but an improvement of its first crack strength is obtained with the second cure and appropriate cement.

KEYWORDS

Date palm, Fibre, Durability, Concrete, Flexural strength

[1] Laboratoire E.V.R.N.Z.A., Université de Ouargla Algérie, BP 511 Ouargla, Algérie 30000, Fax 00213 29 71 19 31, a_kriker@yahoo.fr
[2] Laboratoire L.C.E., Ecole Nationale Polytechnique BP 182 El-Harrah, Algérie 16200, balianl@yahoo.fr
[3] URGC INSA de Lyon, 34 Av. des Arts 69621 Villeurbanne cedex, France, Gérard.Debicki@insa-lyon.fr

1 INTRODUCTION

The date palm (*phoenix dactylifera)* is the one of the most cultivated palms around the world. It is commonly found in the Afro-Asiatic dry-band, which stretches from North Africa to the Middle East. It has a good tolerance to cold and dry-hot climates. Date palms have a fibrous structure, with four types of fibre: leaf fibres in the peduncle, bast fibres in the stem, wood fibres in the trunk and surface fibres around the trunk. Surface fibres were chosen in this study as it seemed most suitable for exploitation. After annually trimming operations, enormous quantities of palm fibre are thrown away, except on a smaller scale where it is used for artisan products.

The local natural resource, used in this study (surface date palm fibres) for reinforcement of concrete are from Ouargla which is situated in the south of Algeria, and where a part of the tests conducted in this study were completed. Oaurgla is characterized by a hot-dry climate during summer. Table 1 provides the average climatic data for Oaurgla, where it is evident that the temperature in the day is very high (up to 43°C), the daily amplitude between day and night regularly reaches about 18°C, and the humidity level stays very low. Furthermore, the site is located in a zone having an average wind velocity of 8 –16 km/h. In fact, most materials used for construction, especially concrete, are sensitive to and adapted with difficulty to hot-dry climatic conditions. Research [Soroka 1993; Kriker & Bali 1992] indicates that mechanical properties of conventional concrete, particularly the flexural strength, decrease with time under similar climatic conditions. In addition, previous work [Alekrish & Alsayed 1994] indicates that conventional concretes and mortars exhibit a high level of shrinkage and cracking in this type of environment.

According to the results of various research studies on more common vegetable fibres, [Swamy 1988; Cook 1980; Khenfer *et al.* 2000; Savastano & Agopyan 1999] the presence of natural fibres in concrete is beneficial for flexural properties. In addition, in a previous work [Kriker *et al.* 2005] it has been shown that firstly, the male date surface palm fibre (MDPSF) has the greatest tensile strength amongst the other types of date palm surface fibres. Secondly a direct exposure of MDPSF concrete to hot dry conditions reduces its mechanical performance.

The aim of this study is to investigate the flexural properties of concrete reinforced with male date palm surface fibres produced for use in a hot-dry climate. It also endeavours to examine the possibility of utilizing these local natural resources in local construction. In addition, the paper examines the effect of curing (wet, hot dry and mixed environment) on the durability of MDPSF reinforced concrete. The durability of MDPSF reinforced concrete at a later-age is evaluated by the variation of their flexural strengths and some scanning electron micrographs at fibre-concrete interfacial zones.

Table 1. Monthly mean climatic data for Ouargla, Algeria.

	June	July	Aug.	Sept.	Octo.	Nov.
T_{max} (°C)	39.8	43.2	42.2	37.6	30.7	23.6
T (°C)	31.5	34.3	33.6	29.8	23.4	16.6
T_{min} (°C)	23.2	25.3	25.0	22.0	16.0	9.6
RH (%)	28.5	24.4	26.4	34.4	47.6	56.5
WV (Km/h)	16.02	13.43	10.80	10.33	08.86	08.06

T: average temperature; T_{max}: maximum temperature; T_{min}: minimum temperature;
RH: relative humidity; WV: wind velocity

2 MATERIALS AND METHODS

2.1 Materials

The natural fibres used are from the surface of the male date palm. The male date palm surface fibres are naturally weaved, and are retrieved from the trunk in the form of a nearly rectangular mesh (length

300-500 mm, width 200-300 mm) formed with three superposing layers. It is easy to separate them into individual fibres when these are placed in water. Table 2 present the upper, lower, and mean physical properties of MDPSF as well as the coefficient of variation (CV). Regarding these results, the MDPSF has a porous structure capable of absorbing a great quantity of water.

Table 2. Physical properties of MDPSF [Kriker et al. 2005].

Property	Lower-upper	Mean-CV (%)
Diameter (mm)	0.1-0.8	0.45-54.43
Bulk density [kg/m^3]	512.21 -1088.81	900-17.64
Absolute Density [kg/m^3]	1300 - 1450	1383.33 - 5.52
Natural moisture content (%)	9.5-10.5	10-5.00
Water absorption after 5 min (%) under water	60.05 – 84.12	74 –14.02
Water absorption to saturation (%)	96.83 – 202.64	132.5 – 20.56

Table 3 provides the mechanical properties of MDPSF. Compared to the information obtained from literature on the mechanical performance of more common vegetable fibres [Savastano & Agopyan 1999; Tolêdo Filho *et al.* 2000; Bentur & Akers 1989], MDPSF have only average tensile strength and a lower elastic modulus.

Table 3. Mechanical properties of MDPSF [Kriker *et al.* 2005].

Condition	Natural			
Fibre type	Specimen's length (mm)	Tensile Strength (MPa)	Elongation (%)	Modulus of Elasticity (GPa)
MDPSF	100	170±40	16±3	4.74±2
	60	240±30	12±2	5.00±2
	20	290±20	11±2	5.25±3

Portland cement (CPA-CEM I 52.5) was used according to the NFP 15-301 standards, and having the following physical properties: Fineness = 385 m^2/kg; Initial Setting time = 200 min; and, σ_C at 28days = 50MPa. Table 4 gives the chemical properties of this cement.

Table 4. Chemical properties of used cement.

SiO_2	AL_2O_3	Fe_2O_3	MgO	CaO	Na_2O	SO_3	K_2O	Loss on ignition
20.29	4.60	2.98	1.66	65.24	0.30	2.70	0.99	2.80

Natural sand having a bulk density of 1660 kg/m^{3}and a maximum size of 5 mm was used in the mix formulation. As well, a natural aggregate having a bulk density of 1610 kg/m^{3}and aggregate minimum and maximum size of 5 and 10 mm respectively was used .

2.2 Specimen Fabrication

Concrete specimens with dimensions 70x70x280 mm were used for flexural strength. Table 5 gives the mix design proportions of concretes. For the mix design of the concrete without fibres (control formulation), the experimental method recommended by [Lesage 1974] and [Gorisse 1978] was used to obtain the optimum sand-aggregate ratio. For all mixes of concretes containing fibre, the mass of cement and sand was kept equal to that of concrete without fibres. The volume fraction of fibres in concrete was varied but the mass of fibres plus aggregates was maintained constant. With a

workability established according to the VB time equal to 20±5 s and slump equal to 70±10 mm, the water quantity was adjusted to adapt the mix with the given percentage of fibre content. The volume fraction of fibre was 2% and 3%. In fact, when the volume fraction of fibres increased, the demand for water also increased due to absorption of water by the fibres. For each mix, the fibre lengths were 15 and 60 mm. The variation of workability with fibre length was slight. A conventional horizontal axis Zyklos mixer was used to mix the concrete composites. The fibres used in the concretes were washed beforehand with tap water and dried in free air.

The production of composites was carried out as follows: in order to facilitate their separation, the fibres were initially immersed in 10% of the total volume of water required for 5 min,. At this stage, the rate of saturation of fibres was about 56%. The sand, aggregates, plus 30% of water were mixed for 30 s in a running mixer. Then, the fibres were added together with 30% of the water and mixed for 3 min. This was done slowly in order to obviate the possible clumping of fibres. After adding all the quantity of cement, the remaining water was added during the next 2.5 min.

In order to investigate the relation between volume fraction of fibre in the mix and the importance of the nominal fibre length, four types of fibre concretes were prepared in addition to concrete without fibre. The concretes were referenced by the following notation: N%-L, where N is the volume fraction and L is the length in mm of fibres. For example 2%-60 refers to volume fraction, N = 2% and fibre length, L = 60 mm. The filling of the moulds and the vibration using a vibrating table were carried out in accordance with standard NFP18-409.

2.3 Curing Conditions

The specimens were initially cured in the laboratory for 24 hours under normal climatic conditions: temperature, T = 20±2°C, and relative humidity, RH = 65±5%. After demoulding, they were cured until the test date in two types of environment. For the first type of environment (referenced: Curing 1), the test specimens were placed 28 days in water at 20±2°C followed by curing in a wet chamber at 20±2°C, with the RH = 100%. For the second type of environment (referenced: Curing 2), they were placed 14 days in water at 20±2°C followed by a hot dry room at 32±2°C and RH = 28±2%. The hot dry room was used to simulate the mean temperature and humidity of the environment of Ouargla (Table 1). The concrete specimens were tested at 28, and 180 days. Six replicate specimens were tested for each parameter setting.

Table 5. Mix design proportion.

Materials	Mix 1 (0%)	Mix 2 (2%)	Mix 3 (3%)
Cement (kg/m^3)	400	400	400
Aggregate (kg/m^3)	1000	982	973
Sand (kg/m^3)	750	750	750
Water (kg/m^3)	240	270	290
MDPSF (kg/m^3)	0	18	27

2.4 Test Methods

The mechanical properties (tensile strength, elongation and the modulus of elasticity) of fibres were determined in accordance with standards NF EN ISO 5079, under the following climatic conditions, T=20±2°C and RH = 65±2 %, and using an Instron universal testing machine equipped with a 250 N load-sensor and two LVTD displacement transducers at a cross-head speed of 0.5 mm/min.

Test data were digitally recorded and reduced using a numerical chain data acquisition system connected to a device that plotted the force-deformation curve. For each fibre length, tests were performed on thirty fibres.

The flexural strength properties were determined with an experimental set-up in accordance with standard NFP 18-409, using an Instron universal testing machine and a four-point test configuration, with 210 mm span and crosshead rate of 0.1 mm/min. The system was equipped with a load-sensor of 50 kN and two LVDT displacement transducers. These continuously recorded to a numerical data acquisition system, which made it possible to determine the deflection at the mid-span of the specimen as function of loading.

The flexural properties were evaluated using four parameters:

- The first crack strength (FCS) determined from the load at the first visible crack using equation (1).

$$FCS = 6M_0/bd^2 \quad (1)$$

Where M_0 is the failure moment of the test specimen at the first visible crack (P_0) and b and d are the width and depth of the specimen respectively. P_0 is the maximum load of the load-deflection- curve in the elastic range.

- The maximum post-crack flexural load (P_{max}) carried by the composite after the first crack.
The concrete was tested at the following ages: 28 and 180 days for flexural strength. Six specimens were used for each test.

3 RESULTS AND DISCUSSION

3.1 Flexural Properties

Table 6 provides the mean and the coefficient of variation (CV) of the first crack strength (FCS), the maximum post-crack flexural load (P_{max}), for concrete formulations cured under Curing 1, and 2 conditions. The results showed that, for both Curing 1 and 2 curing conditions and for each concrete type, the FCS continues to increase with age. However, when the length and the percentage of fibres increase the FCS decreases. Therefore, the 2%-15 fibre-concrete type presents the maximum FCS, which remained lower than that of the concrete without fibres. In addition the FSC of concrete cured in Curing 1 conditions is lower than that of concrete cured in Curing 2 conditions. This is due to the thermo activation brought about by this last cure. In fact, it has been noted in a previously completed work [Kriker & Bali 1992] that the Curing 2 conditions improved the FSC of conventional concrete.

The examination of toughness properties represented by the P_{max}, (Table 6), show that for each term (28 or 180 days) the P_{max}, increases with an increase in the length and percentage of fibres incorporated in the mix, with the maximum P_{max}, being obtained with the 3%-60 fibre-concrete type for both Curing 1 and 2 conditions. However, for each concrete type, the P_{max}, decreases with age; this is probably caused by the loss of tensile strength of fibres in an alkaline environment. It is noticed that the P_{max} of the concrete conserved in Curing 1 slightly exceeded those cured in Curing 2 conditions. The relatively losses of P_{max}, between 28-180 days of concrete cured in Curing 1 conditions are slightly lower than that of concrete cured in Curing 2 conditions. For example, for the concrete mix that yields the largest P_{max} (3%-60), the loss of P_{max} between 28-180 days for this mix is 32%. When comparing to literature results, about durability of more common vegetable fibre-concrete, according to flexural properties, it's can reveal that the MDPSF-concrete, conserved in Curing 1 or 2, has a low durability. That is probably due for the reasons already exposed in our former research [[Kriker et al; 2005], principally to the mediocre mechanical performance of MDPSF.

That can be explained by observations derived by Gram [1983], where it was revealed that the transport of hydration products from the matrix to the fibres was accelerated by a thermo activation process. Therefore, the durability of fibres in the concrete cured in Curing 2 conditions should be more greatly affected than those cured in Curing 1 conditions.

In addition, we compare the flexural properties (FSC, Pmax) of the concrete cured in Curing 2 conditions with those cured continuously in a hot, dry environment [Kriker *et al.* 2005]. One can see that cure in Curing 2 conditions has a beneficial effect on the flexural performance of fibre-concrete at early curing times (up to 28 days). However, for longer-term cure, the effect is only beneficial in respect to the FSC of the fibre-concrete.

The mean bending load-deflection of MDPSF-reinforced concretes at 180 days when cured in Curing 2 conditions is presented in Figure 1. At the beginning of the loading cycle, the behaviour is elastic up to the first crack strength (FCS) is attained. Beyond the first crack strength, the recorded deflection around 0.05 mm, the initiated crack had an unstable growth leading either to separation of the body into parts when there is no fibre, or to a macro-crack with a deflection around 0.5 mm, when the fibres could stop the crack growth. This crack instability could be connected with the elastic modulus of the MDPSF-fibre. After that, the load became nearly constant with increasing bending deflection.

Table 6. FCS and P_{max} for MDPSF-concretes as a function of time and type of cure.

	Concrete types (%-length of fibre)					
Flexural properties	Curing (Time d)	0%-0	2%-15	3%-15	2%-60	3%-60
FCS (CV) (MPa)(%)	C. 1(28)	7.6 (7)	6.5 (12)	5.50(15)	6.02(11)	5.34(13)
	" (180)	8.4 (6)	7.4 (9)	6.30(11)	6.82 (9)	6.21(13)
	C. 3 (28)	7.9 (7)	6.7 (5)	5.80 (6)	6.30 (5)	5.60 (7)
	" (180)	8.7 (3)	7.6 (4)	6.50 (4)	7.22 (6)	6.40 (3)
P_{max} (CV) (kN)(%)	C. 1(28)	--	0.80(19)	1.69(12)	1.18(11)	2.96 (3)
	" (180)		0.70(27)	1.40(11)	0.99(30)	2.02(19)
	C. 3 (28)		0.59(25)	1.50(26)	1.15(18)	2.23(20)
	" (180)		0.49(23)	1.20(12)	0.96(17)	1.50(13)

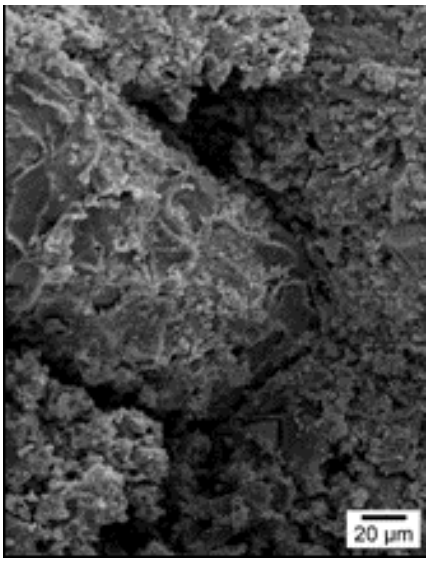

Fig. 1. Load-Deflection at 180 days in Curing 2

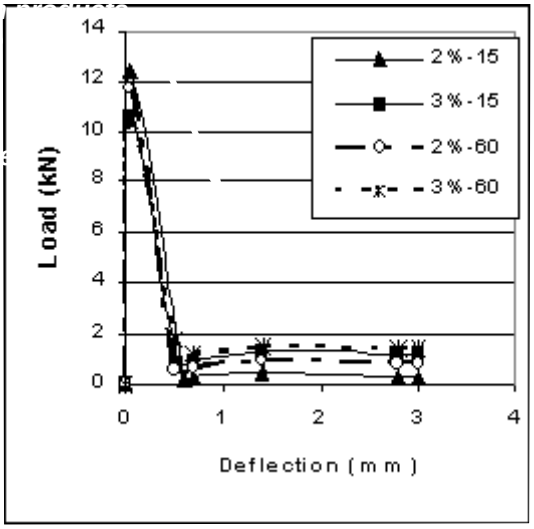

Fig. 2. Scanning electron micrograph at the fibre-matrix interface of MDPSF-concrete cured for 3 months in Curing 2 conditions.

To explain the fibres-matrix adhesion, Fig. 2 presents the scanning electron micrograph at the broken surface, at the fibre-matrix interface of some typical fibre-concrete conserved during three months respectively in Curing 2. Observing those microstructures of the fibre-matrix interface, it can be seen that the voids around the fibres of concretes is not large. In addition, Fig. 2 shows the uniform deposition of hydration products on all fibre surfaces. Those observations confirm the uniformed deposit of alkaline hydration products on surface of the fibre in Curing 2. Those also explain why the flexural properties of MDPSF-concrete after the first crack at long term in Curing 2, is slightly lower

than that in Curing 1. In fact, the durability of MDPSF was more affected by cement alkaline products in Curing 2 than that in Curing 1. That confirms also the findings of [Tolêdo Filho *et al.* 2000] and [Bentur & Akers 1989], regarding mineralization of vegetable fibres due to migration of hydration products, especially calcium hydroxide after natural wet ageing. Like shown it surface of fibre on Fig.3.

4 CONCLUSIONS

The Afro-Asiatic dry band is rich in date palm fibres that could also be utilized in local material construction products. However, when compared to the mechanical performance of more common vegetable fibres, the male date palm surface fibres (MDPSF) have average tensile strengths and lower elastic modulus.

Based on the results derived in this study, for all Curing 1 and 2 conditions and for each concrete type, the initial crack strength (FCS) continues to increase with cure age. However, for each cure period (28 or 180 days), the initial crack strength of the concrete without fibre is greater than those of the fibre-concretes.

The initial crack strength (FCS) of concretes cured in Curing 2 conditions (14-d in water at 20°C; hot dry room 32°C and RH = 28%) is slightly greater than that of fibre-concretes cured in Curing 1 conditions (28 days in water at 20°C; curing in wet chamber at 20°C and RH = 100%). This can be attributed to the thermo activation process and hence to the enhanced formation of hydration products of concretes cured in Curing 2 conditions. For those reasons, after the initial crack, the flexural properties (P_{max}) and the durability of the fibre-concretes cured in Curing 2 conditions were lower than that of those cast in Curing 1 conditions.

The Curing 2 cure condition has a beneficial effect on the early strength (28-day) performance of fibre-concretes in hot dry climate. However, over the longer-term the beneficial effect is only achieved in respect to the initial crack strength (FSC). Some other treatments of MDPSF and matrix are then necessary to improve their durability, especially after the first cracking. This will be investigated in a future paper.

REFERENCES

Alekrish, A.A. & Alsayed S.H., 1994, 'Shrinkage of fibre and reinforced fibre concrete beams in hot-dry climate', *Cem. & Concr. Compos.* **16**, pp. 299-307.

Bentur, A. & Akers, S.A.S. 1989, 'The microstructure and ageing of cellulose fibre reinforced cement composites cured in normal environment', *Int. J. Cem. Compos. Lightweight Concr.* **11**[2], pp. 99-109.

Cook, D.J. 1980, 'Concrete and cement composites reinforced with natural fibres', Proc. Symp. on Fibrous Concrete, April, Construction Press Ltd., Lancaster, UK, pp. 99-114.

Gorisse, F. 1978, '*Essais et contrôle des bétons'*, Ed. Eyrolles, Paris.

Gram, H.E. 1983, 'Durability of natural fibres in concrete', *Swedish Cem. and Concr. Resear.* Fo. 1 Stockholm, p. 255.

Khenfer, M.M., Bali, A. & Morlier, P. 2000, 'The effect of water and fibre length on the fracture resistance of cellulosic fibre cement', *Concr. Scien. Engin.* **2**, pp. 56-62.

Kriker, A. & Bali, A. 1992, 'Effect of types curing on the mechanical properties of El-Hadjar slag concrete', Proceedings of International Seminar on quality of concrete in hot climate, Univ. of Blida and CTC Sud, Algeria, pp.45-54.

Kriker, A., Debicki, G., Bali, A., Khenfer, M.M. & Chabannet, M., 2005, 'Mechanical properties of Date Palm Fibres and Concrete Reinforced with Date Palm fibres in Hot-Dry Climate', *Cem. & Concr. Compos* **27**, pp. 27-143.

Savastano Jr., H. & Agopyan, V. 1999, 'Transition zone studies of vegetable fibre-cement paste composites', *Cem. & Concr. Compos.* **21**[1], pp. 49-57.

Lesage, R. 1974, '*Etude expérimentale de la mise en place du béton frais*', Rapport de Recherche n° 37, Laboratoire Central des Ponts et Chaussés.

Soroka, I. 1993, '*Concrete in Hot Environments'*, First Ed., E & FN Spon, Oxford, UK.

Swamy, R.N. 1988, 'Natural Fibre reinforced cement and concrete', Ed. R.N. Swamy, *Concrete Technology and Design*, Vol. 5, Surrey Uni. Press, p. 200.

Tolêdo Filho, R.D., Scrivener, K., England, G.L. & Ghavami, K. 2000, 'Durability of alkali-sensitive sisal and coconut fibres in cement mortar composites', *Cem. & Concr. Compos.* **22**[6], pp. 27-143.

Cement Industry and Concrete Technology in Algeria: Current Practices and Future Challenges

Said Kenai [1]
Ahmed Attar [2]
Belkacem Menadi [3]

T 11

ABSTRACT

In this paper, the development of cement industry in Algeria, the production process and the types of cement produced are presented. A summary of ongoing research on cement replacement materials such as limestone, slag and natural pozzolana is given. The current field practices in concrete technology are discussed. Durability issues related to the local hot environment conditions, aggressive soils and underground water and site practices are highlighted. The lack of river sand is highlighted and the use of crushed sand with limestone fines as sand replacement in concrete is discussed. Statistical analysis of concrete quality on site is analysed showing variability of construction materials quality, poor workmanship and lack of proper quality control procedures. A number of ongoing challenges for concrete technology and cement industry are identified and recommendations are proposed suggesting a way forward.

KEYWORDS

Cement, Concrete, Quality control, Workmanship; Durability

[1] Civil Engineering Department University of Blida, PO Box 270, Blida, Algeria; Phone: (213) 770904482; Fax: (213) 25433939, sdkenai@yahoo.com
[2] Civil Engineering Department, University of Blida, P.O Box 270, Blida, Algeria; Phone: (213); Fax: (213) 25433939, ahmed_attar@yahoo.fr
[3] Civil Engineering Department, University of Blida, P.O Box 270, Blida, Algeria; Phone: (213); Fax: (213) 25433939, bmenadi@yahoo.com

1 INTRODUCTION

Algeria is facing a serious housing shortage which is estimated at more than one million units. Hence, it is undertaking a vast five year construction program including the construction of housing units, 1200 km of motorways, three new cities around the Algiers region and other basic infrastructure such as schools, universities and hospitals. This program has raised many challenges to the construction industry. Among the challenges are the availability of good quality local construction materials, quality control on site, and durability.

.

Algeria is situated in a high seismic zone and its climate is hot and dry in summer especially in the southern regions. Some regions in the south and the west are known of their aggressive underground water soils. In addition, most of the construction projects are located on the aggressive sea environment of Mediterranean coastal region which is 1200 km long. Concrete is the main construction material used in most of these projects and hence its durability could be affected if precautions are not taken in preparing specifications to withstand these harsh environments.

In this paper, a review of the cement and concrete industry in Algeria is given. Concrete durability issues are discussed and field practices reviewed. A number of ongoing challenges for concrete technology and cement industry are identified and some recommendations suggesting the way forward are proposed.

2 CEMENT INDUSTRY IN ALGERIA

The first cement plant in operation in Algeria was a small wet processing plant which dates back to 1901 with an annual production capacity of 50 000 tonnes/year which was later modernised. Until 1962, there were three cement plants with a total annual capacity as low as 800 000 tonnes and hence a consumption of about 80 kg per capita [Stiti, 1999]. Today, in 2008, there are fourteen (14) cement plants in operation producing more than 13 million tonnes annually and hence 400 kg per capita consumption as compared for example to 350 kg per capita produced in Germany [Cement International, 2005]. Up to 50% of the deliveries are in the form of bulk cement and the remaining portion in the form of bagged cement. All cement plants are now using the dry process. Most factories use natural gas as energy carrier. The two newest cement factories are now owned by the multinational company Lafarge, and all the remaining cement plants are state owned but with some shares held by different multinational companies. Table 1 provides a summary of the production capacity of all cement plants.

The cements manufactured in Algeria are Ordinary Portland Cement type CEMI, CEM II/A, CEMII/B with two strength classes: 32.5 and 42.5. In addition, sulphate resistant cement is produced in the Ain-Kebira plant and white cement is produced at a new cement plant located in Sig. The use of cement composites can decrease the production costs, the CO_2 emissions, eliminates the costs of dust disposal and reduces environmental pollution. Hence most cement plants are using limestone, natural pozzolana or slag in a proportion of 10 to 15% by weight of cement. Fly ashes and silica fume are not available but are imported for special projects. Table 2 gives typical chemical and mineralogical compositions of some of these cements.

3 CEMENT REPLACEMENT MATERIALS

Given the large supply of slag, natural pozzolana and limestone, most cement plants are using these materials as cement replacement materials. The chemical composition of Algerian slag, natural pozzolana and limestone are presented in Table 3. A summary of the undergoing research on these materials is given here.

3.1 Slag Cement

Slag is available in the MITTAL steel factory of El-Hadjar and is used either as aggregates in road construction or as cement replacement materials in some cement plants. The production of slag is estimated at about 0.3 Million tonnes/year. The reactivity of the Algerian slag is low and hence the optimum recommended level of cement replacement is about 30% by weight [Kenai & Amrane, 1996]. Local materials including slag were used to produce good self-compacting concrete. The addition of slag by substitution to cement was found very beneficial to fresh self-compacting concrete. An improvement of workability was observed up to 20% of slag content with an optimum content of 15%. Workability retention of about 60 minutes with 15% of slag content was obtained.

Table 1. Cement plants in Algeria, current production capacities and additions used.

N°	Cement plants	Production year	Current Production (tonnes/year)	Additions used
01	Meftah	1901	800 000	Limestone
02	Rais Hamidou	1914	300 000	Limestone
03	Zahana	1948	800 000	Limestone and natural pozzolana
04	Hadjar Soud	1973	600 000	Slag
05	Saida	1978	400 000	Natural pozzolana
06	Chelef	1978	1 200 000	Limestone and Natural pozzolana
07	Beni Saf	1979	800 000	Natural pozzolana
08	Hamma Bouziane	1982	700 000	Limestone and Slag
09	Sour-el-ghozlane	1983	1000 000	Limestone
10	Ain Touta	1987	1 000 000	Limestone and Natural pozzolana
11	Tebessa	1995	500 000	---
12	M'sila	2004	4000 000	Limestone and natural pozzolana
13	Sig	2007	---	----

Table 2. Typical chemical and mineralogical compositions of Algerian cements

Composition	Cement Type			
	A	B	C	D
Chemical				
SiO_2	21.53	21.50	20.32	20.92
CaO	66.87	65.52	64.34	61.74
MgO	1.08	1.05	0.56	1.58
Fe_2O_3	3.24	2.84	3.20	3.43
Al_2O_3	5.57	5.13	4.71	5.33
Loss on ignition	0.26	2.02	4.26	1.65
SO_3	1.09	1.53	1.26	1.83
Insoluble residue	0.06	1.60	1.14	1.35
Free CaO	0.30	0.39	0.21	2.17
C_2S	12.35	15.45	20.30	16
C_3S	65.33	56.58	50.59	56
C_3A	8.28	8.79	7.70	5.65
C_4AF	9.85	8.63	9.55	12

3.2 Natural Pozzolana

Natural pozzolana is being used for cement manufacture by at least six cement plants. These cement plants add usually about 15% of natural pozzolana cement replacement by weight. Natural pozzolana

have been widely used as a substitute for Portland cement in many applications because of their advantageous properties which include reduction in heat evolution, decreased permeability and increased chemical resistance. According to Ghrici et al [2006], binary and ternary cements with natural pozzolana have lower chloride permeability and lower sorptivity and hence better durability than ordinary cement or limestone cement (Figs.1& 2). However, natural pozzolana is often associated with shortcomings such as the need for moist-curing for longer periods of time and a reduction of strength at early ages and up to 28 days.

Table 3. Chemical and physical properties of slag, Natural pozzolana and limestone

Element	Slag	Natural Pozzolaan	Limestone
SiO_2	40.1	46.9	1.78
CaO	42.2	9.38	54.3
MgO	4.7	2.84	0.20
Al_2O_3	6.0	16.6	0.79
Fe_2O_3	2.0	9.37	0.34
SO_3	0.15	0.36	-
MnO	2.6	-	-
K_2O	1.2	-	-
Loss of Ignition	-	5.79	42.5

3.3 Limestone Cement

The strength development of mortar mixes containing varying amounts of limestone fines (LSF) is shown in Figure 3. In this experimental study, cement was partially replaced with 0, 5, 10, 15, 20, 25 and 30% of crushed limestone fines (LSF). The binder to cement and the water to binder ratios were maintained constant at 1:3 and 0.55 respectively. Compressive strength testing was conducted at 2, 7, 28 and 90 days of curing. The results showed that there is a decrease in strength with increasing amounts of LSF up to at least 30%, regardless of the age of curing.

All mortars, with and without LSF, show an increase in strength with the age of curing. This increase is mainly due to the evolution of the hydration of cement with time. No decrease in strength was observed with the age of curing for mortars containing LSF. At the age of 2 days, mortars with limestone fines (0, 5, 10, 15, 20, 25 and 30%) show comparable compressive strength to mortar without fines. This can be explained by the physical and chemical effect of limestone particles on the development of the mortar strength of cement. The improvement in compressive strength can be also attributed to the acceleration of the hydration of C_3S in particularly with finer limestone fines and the formation of carboaluminates [Kenai, 1997].

At the age of 28 days and 90 days, compressive strength decreases with the increase in the content of limestone fines. The replacement of cement by LSF beyond a content of 15% shows a noticeable decrease in compressive strength. This reduction in strength is due to the dilution effect.

4 CRUSHED SAND

Recently, there has been an increasing interest in using crushed sand from limestone quarries in concrete construction to overcome inherent deficiencies in river sand in particular regions of Algeria. Crushed limestone fine sand is a by-product of the quarry process and typically does not have a significant demand due to its high fines content that exceeds the standard allowable limit of 5%. The fines are particles whose diameters are less than 80 µm. For this reason, most of the fines at present are destined to landfill. In Algeria there is around 1010 aggregate quarries with a total annual production of 68 million tonnes of which about 47% goes to the building sector and 33% to roads and motorways. Around 15 millions tonnes of sand are produced in these quarries as a by-product

containing 8 to 25% of fines (i.e. < 80 µm), mainly used in road construction and usually sold at a lower price (about the third). The demand in sand is estimated at 25.1 million tonnes in which 16 millions for concrete for building construction and 9.1 millions for road construction [Kenai, 1999].

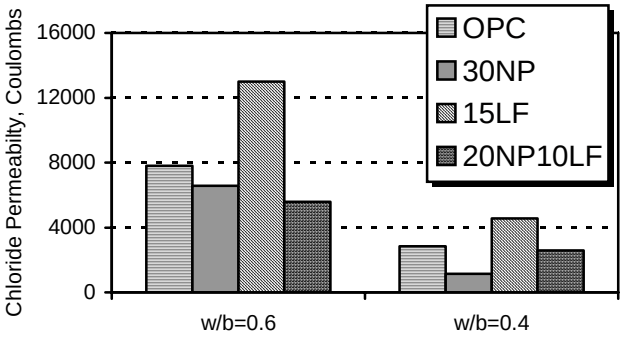

Figure 1. Chloride permeability of concrete at 28 days

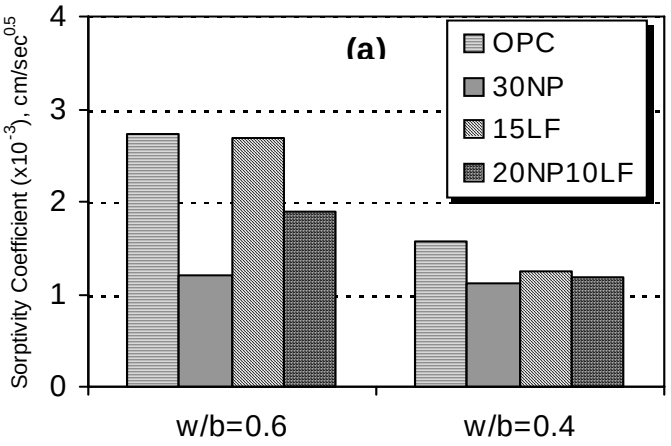

Figure 2. Sorptivity coefficients of concrete at 28 days.

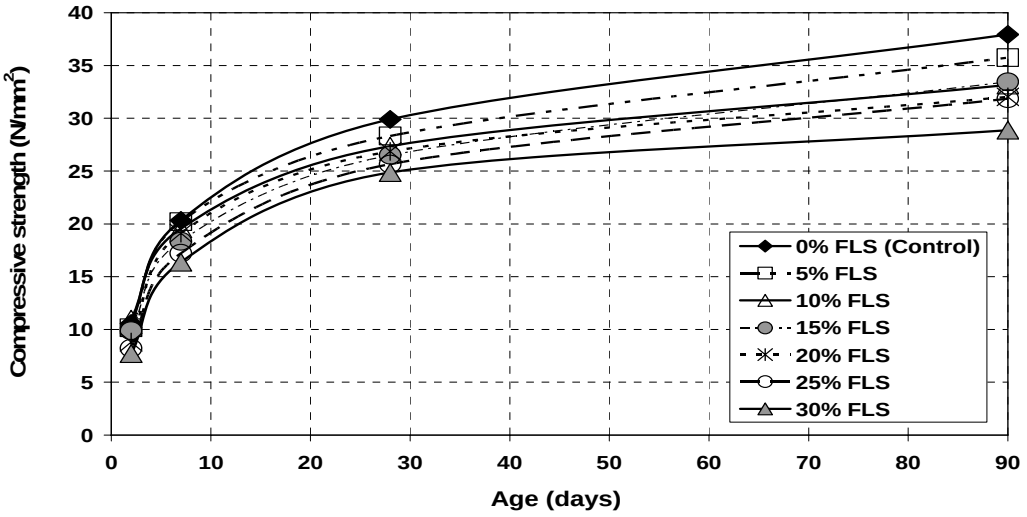

Figure 3. Strength development of mortars containing varying amounts of limestone fines.

Crushed sand is very abundant in limestone gravel quarries and its use could significantly decrease the materials cost of concrete, eliminate the dust disposal cost, reduces environmental pollutions and dilapidation of natural resources. Other countries such as Spain, France and Argentina also experienced similar shortage. For this reason, standards have increased the fines allowable limit in crushed sand. For example British standards (BS 882) allow up to 15% of fines in sand whereas ASTM C33 sets the limit to less than 7%. In addition, up to 35% of limestone fines are allowed in European cements according to EN197-1 (1996).

An experimental investigation was undertaken and showed that up to 15% of fines content in crushed sand could be used without adversely affecting concrete strength. Comparable water absorbed capillary were obtained for all concrete mixtures and higher values were observed in concretes with lower cement fineness when 15% of fines were used. The resistance to chloride-ion penetration and gas permeability decreased for all concrete mixtures with the inclusion of 15% limestone fines as sand replacement. The presence of 15% limestone fines as partial replacement of fine aggregate cause an increase in chloride ion penetration and gas permeability whereas reduces water permeability. The higher chloride-ion penetration and gas permeability of crushed sand concrete with 15% of limestone fines means that its use in structures exposed to marine environment should be limited [Menadi, 2008].

5 CONCRETE QUALITY ON SITE

The fast growing needs for buildings and structures has led to less quality control and the use of defective materials and hence produced much defective concrete. Statistical studies on building failures showed that the main causes of building failure and deterioration were design deficiencies, poor workmanship and low quality concrete [Kenai, 1999 & 2004]. Concrete compressive strength test results at the age of 28 days at 41 construction sites of more than 2300 test results during the period of 1987 to 1994 showed that 77% of the results were less than the required 25 MPa. The coefficient of variation was in about 60% of the sites more than 20% indicating a high variability of concrete strength and hence a lower degree of quality control on concrete mix design, concrete materials and concreting operations. The standard deviation varied from 2.8 to 6.0 MPa with more than 36% of the sites at more than 5 MPa. The analysis of the strength of cement in an Algerian plant during the period of 1989 to 1995 showed a higher variability of strength (coefficient of variation of 7.2% and a standard deviation of 3.7 MPa) compared to 3% and below 1.5 MPa respectively in Swedish cements [Fagerlund, 1994]. This showed that many aspects of basic good concreting practice need to be improved. The standard of quality control was unsatisfactory with poor workmanship by lack of supervision and lack of care resulting in honeycombing, lack of cover and bad finishes [Kenai & Bahar 2003].

It should be noted that data for concrete used in the construction of bridges showed lower variability, higher strength and better quality control because of the use of ready mixed concrete. The use of ready mixed concrete (RMC) could improve concrete quality on site and reduce irregularities observed. Strength irregularities are usually reduced with the use of RMC and hence cement consumption could also be reduced. In Sweden, there are more than 200 RMC factories with an annual production capacity of 3000 m^3. The spread of use of RMC has decreased cement consumption by 25 to 35% during the period of 1965 to 1985 [Fagerlund, 1994]. The variability in strength was low; standard deviation was 2.6 MPa to 3.5 MPa for a concrete class of 25 to 40 MPa. Cement consumption was only 210 kg/m^3 for 20 MPa concrete; 235 kg/m^3 for 25 MPa concrete and 265 kg/m^3 for 30 MPa concrete as compared to the Algerian average consumption of 350 kg/m^3 for 25 MPa concrete.

6 ALGERIAN RESEARCH NEEDS IN CEMENT AND CONCRETE

There are a lot of new challenges and research needs for the next two decades. The research priorities in cement and concrete are to be seen in the context of industrial and university perspectives and also national strategic perspectives:

- Emphasis should be given to local concrete making materials and durability and deterioration issues. There is a need to test the performance of the available materials and to find cheaper alternative materials.
- Replacing the river sand which is lacking by alternative sands such as dune, crushed or sea-dredged sands is important. National panels have been recently set up, by both the Ministry of Housing and the Ministry of Public Works, to look at these issues.
- Durability should address local conditions such as marine environment, hot dry climate and sulphate attack. The development of specifications and local design guidelines for easy use by designers and constructors to ensure long-term durability should also be addressed.
- The effect of local cement replacement materials such as limestone fines, natural pozzolana and metakaolin on the durability of concrete in different environments has to be investigated furthermore for the development of more durable materials with minimum maintenance costs. The development of ternary cement is also to be considered.
- The increased expenditure on repair and rehabilitation of concrete infrastructure and the ageing of some concrete structures has to be addressed by assessing existing concrete structures and developing suitable repair and strengthening techniques and materials.
- Development of equipment and non destructive techniques to monitor the rate of deterioration of concrete structures at an early stage is necessary. There is also a need to the use of modelling by neural networks and expert systems to predict the service life of both existing and new structures.
- The high strength, high elastic modulus and low density and high resistance to corrosion of carbon fibre relative to steel has a promising use for structural strengthening and the assessment of the performance of case studies under local aggressive environments at long term is needed.
- The development of high performance concrete and self compacting concrete using local materials is important.
- The development of environment friendly materials by using recycling demolition and construction waste and developing composite cements to reduce CO_2 emission which has a green house effect.
- Roller Compacted Concrete (RCC) has been used in three dams and there is a need to develop appropriate mix design, testing procedures and construction technique for RCC for use in pavements and dams.

These research needs are to be undertaken through industry and cooperation and exchange of staff. Universities should aim to develop suitable training skills and highly trained people in the field of concrete technology.

7 CONCLUSION

A review of the cement industry in Algeria has been undertaken. An emphasis was given on some ongoing research results on the performance of slag, natural pozzolana and limestone cements. Quality of concrete on site was discussed and the variability of strength and the lower quality of control on site highlighted. The Algerian needs in research on cement and concrete for the next two decades are identified in the context of industrial and university perspectives and also national strategic perspectives.

REFERENCES

Cement International, 2005, 'The cement industry in Germany', Cement International, Vol. 3, N° 3, pp. 36-44.

Fagerlund, G. 1994,'*Economical use of cement in concrete',* , Building issues, vol. 6, N°. 2, Lund University and Lund centre for Habitat studies, Sweden.

Ghrici, M.; Kenai, S.; Said Mansour, M. & Kadri, E. 2006, 'Some engineering properties of concrete containing natural pozzolana and silica fume', Journal of Asian Architecture and Building Engineering, vol. 5, N.2, pp.349-354.

Kenai, S & Amrane, A. 1996, 'Mechanical properties and permeability of slag in Algerian hot climate", *Proceedings of Fourth Int. Conf. on Concrete Technology in Developing Countries*, Gazimagusa, Turkey, pp. 138-148.

Kenai, S. 1997, 'Effect of limestone addition on cement and concrete', Proceedings of the seventh Arab structural engineering conference, Abu-Dhabi, UAE, Vol. 1, pp. 119-128.

Kenai, S. Laribi, A. & Berroubi, A. 1999 'Building failures and concrete construction problems in Algeria', *Proceedings of the international conference on infrastructure regeneration and rehabilitation* (Ed. Swamy, R.N), Sheffield, UK, pp. 1147-1156.

Kenai, S. & Bahar, R. 2003,'Evaluation and repair of Algiers new airport building', Journal of cement and concrete composites, vol. 25, pp. 633-641**.**

Kenai, S. 2004, *'Fabrication* et contrôle de qualité du béton dans un pays en développement et à climat chaud', In proceedings of *1er séminaire sur les technologies du béton, Le béton, perfection et incertitudes,* Algerian Cement Company (ACC), Algiers, Algeria, pp. 103-120.

Menadi, B., Kenai, S., Khartib, J. & Ait Mokhtar, K. 2008, 'Strength and durability of concrete incorporating crushed limestone sand' Accepted for publication in Construction and Building Materials.

Stiti, S. 1999, 'Le pari des cimentiers Algériens', Habitat & Construction, N° 5, Algiers, pp. 32-39.

Selection of the Mix Constituents to Produce a Highly Performing and Durable Concrete Material

Mohamed Chemrouk [1]

T 11

ABSTRACT

Concrete is a mixture of aggregate, cement and water. In Algeria in recent years, the negative effects of an excess of mixing water in concrete have been made clearly evident. A number of structures were found to be vulnerable following the collapses observed during the Boumerdes-Algiers earthquake in 2003. Following these events, there has been a singular interest for improving the structural properties of the concrete manufactured in Algeria, and the means necessary to achieve this with the use of local materials in a cost effective manner.

It is well known that high performance concrete requires a low water/cement ratio as compared to normal concrete. This reduction in the quantity of mixing water reduces micro structural voids in the concrete, making it both denser and more compact. The degree of compactness and density of the hardened mass, which is enhanced by the use of ultra-fine materials, reduces the permeability of concrete, and with it, risks from external chemical attacks. The loss in workability, resulting from the reduction in the mixing water, is compensated by the use of adequate superplasticisers compatible with the cement.

Indeed, it is possible to produce a high performance concrete in the shorter term (early strength requirement) as well as the longer term (durability) provided specific measures are taken in the selection of aggregates based on specifications for shape, size, strength, stiffness and mineralogy, in the choice of a potentially active cement, and in the preference for a reduced quantity of mixing water. This paper provides information on a method that produces concrete material having a 28-day compressive strength of 65 MPa based on locally available (region of Chlef in Algeria) ingredients. In the context of this work, high performance is used to mean concrete having strengths greater than 40MPa.

KEYWORDS

High performance concrete, Workability, Permeability, Compactness, Strength, Durability

[1] Faculty of Civil Engineering, University of Science & Technology Houari Boumediene, USTHB, Algiers, Algeria, Phone +213 21 247914, Fax +213 21 247224, mchemrouk@yahoo.fr

1 INTRODUCTION

Concrete is a material in perpetual evolution, starting from empiricism in its early uses to a more scientific rationalisation today. In the early days, its use as a construction material has been conditioned by security. And then, with time, durability of constructions made with this material became a second factor as important as the first, conditioning the use of such a material. The same 'durability' factor is strongly linked to the 'economy' factor which is, at our days, continuously improving. Indeed, the possibility of building safer for the longer term and with less cost is an equation with three variables and for which the solution is an approximate one, with its precision continuously improving as advances in material technology are achieved.

Concrete can be very performing at our days; compressive strengths well in excess of 80 MPa have been achieved throughout the world and the same concrete used in real structures [Malier 1992]. This was made possible by the reduction of micro structural voids in the material; such voids are often filled with water, in excess at the early age, which evaporates with time under climatic effects. The denseness of the concrete material, which is improved by the use of ultra-fine materials, improves impermeability and, hence, reduces the risks of chemical attacks by external agents on the concrete and steel.

The reduction of voids is due to the reduction of the quantity of mixing water, part of which hydrates the cement particles and the excess helps provide a workable fresh concrete. With the development of superplasticisers, it is possible to improve the workability of fresh concrete, hence compensate the loss of this rheological property and thus reduce the quantity of excess water to a strict minimum. For this to be achieved, it is advised to carefully study the constituents of the mix in order to minimise water absorption by the aggregates, and make the cement react totally and effectively with the mixing water; the activity of a given cement never attains 100%. Other properties of the aggregates are also important for achieving a highly performing concrete and will be further examined in subsequent sections of this paper.

The qualification of 'high performance' is, however, used in this paper with a relative meaning since a concrete material considered as ordinary in one practice may be considered as high performance in another practice. In this work, based in Algeria, a concrete material having a compressive strength of more than 40 MPa [Ansari, 2002] is considered a high performance material.

2 HISTORICAL EVOLUTION OF THE MATERIAL

Despite the fact that high performance concrete (HPC) is considered as a relatively new material, its development has been gradual through the years. With the continuous development of the material technology, the definition of 'performance' itself has evolved. Earlier on, the term “high strength” referred to a concrete of 30 MPa and more. Afterwards, it was possible to obtain a concrete with strengths between 40 MPa and 50 MPa in the laboratory.

At the end of the seventies, a concrete with a compressive strength of 60 MPa was industrially produced in some developed countries and the idea of 'high performance' was born with this type of concrete. From this point on, interest was placed on the mechanical behaviour of the material under load and its interaction with the environment. However, for years, concrete having strength in excess of 40 MPa was available only in few places, hence very rare. This explains why until very recently most of the national codes dealing with the design of reinforced concrete structures considered compressive strengths not exceeding 40 MPa. Nowadays, the latest versions of some of these design codes go up to 60 MPa where strengths in excess of 80 MPa have been achieved in some real structures.

3 SELECTION OF THE INGREDIENTS FOR THE DESIGN OF HPC

It is evident that, in the absence of a precise method for the formulation a HPC, it is not with any one type of aggregate, or any one type of cement or, indeed, with any given water reducer that such a material can be obtained. The work described here provides means to fabricate this material and consists in:
This work traces a way to help elaborating this material; it consists on:

- A rigorous choice of the mix constituents, reflecting qualitative aspects
- The proportioning of these constituents, reflecting quantitative aspects

Indeed, up to now, there has not been any 'miracle recipe' to obtain a high performance concrete.

3.1 Aggregates

The aggregates occupy about 70% of the concrete volume and, hence, have a direct influence on the material properties both at the fresh state and at the hardened state.

3.1.1 Fine Aggregate: Sand

The fine aggregate to be used for the confection of a HPC should have a fineness modulus higher than 2.8 . A fineness modulus smaller than 2.5 makes the concrete 'sticky' and difficult to compact and hence, less resistant. Moreover, fine aggregates with a smaller fineness modulus have a more important specific surface and this requires more water. A continuous grading gives a better results in the longer term. The sand particles should have a round shape or at least a cubic one and should not contain flat or elongated shapes. The specific surface would hence be reduced and this in turn will reduce the quantity of mixing water required. Irregular shapes require more water and should be avoided. Round shapes increase also the compactness of the material and with it the resistance and in the longer term the durability of the material.

3.1.2 Coarse Aggregate

The selection of coarse aggregate depends on many factors such as the particle shape and size, the strength, the stiffness and the mineralogy.

3.1.2.1 Shape and Size. Crushed aggregates have a rougher surface than natural gravel and develop a better bond with the cement paste and hence result in a better strength. The gain in compactness of round shaped gravel is overweighed by their poor bond with the cement paste. However, irregular shapes in the crushed aggregates may 'punch' the cement paste under the effect of external loads and also require more mixing water for the concrete to be workable in its fresh state. For a HPC to be achieved, the ideal aggregate should be a crushed one, with a clean surface, having a regular shape, hence a reduced angularity, containing less flat or elongated particles since these shapes are very weak in resisting cracking [Gutierrez & Canovas 1996, Hamrat & Chemrouk 2003] and require more water.

For the size of aggregate, it has been shown that [Hamrat 1994, Hamrat & Chemrouk 2003] for an optimum strength with a reduced water/cement (w/c) ratio and a higher quantity of cement, the maximum size of aggregate should be kept between 9.5 and 12.5 mm. Smaller size aggregates would induce less stress concentration at the cement paste around the aggregate. Moreover, a higher difference between the elastic modulus of the cement matrix and that of the aggregate would aggravate such stress concentration.

3.1.2.2 Mechanical Strength. To produce a high strength concrete, aggregate should not break or crush before the hardened cement paste. A stronger aggregate is necessary to achieve higher strengths for concrete [Iravani 2000, Chemrouk & Hamrat 2002]. Using weaker aggregate will induce failure planes through the aggregate that adds to those possible through the cement paste and through the bond between the aggregate and the cement paste.

3.1.2.3 Stiffness of Aggregate. Higher differences between the modulus of elasticity of aggregate and that of the hardened cement paste induces a stress concentration around the aggregate which can affect

negatively the bond between the two constituents of the hardened concrete. To reduce such an negative effect, the aggregate used in HPC should have an elastic modulus comparable to that of the hardened cement paste. This will minimise the differential deformation at the aggregate-cement paste interface, often a source of failure of concrete.

3.1.2.4 Mineralogy of Aggregates. The bond between the cement paste and the aggregate is the determinant factor for the development of higher strengths in concrete and hence the mineralogy of aggregate should be such that it would promote such bond. Some types of aggregates such as the calcareous ones react chemically with the cement paste and as a result the bond between the two constituents is improved. On the other hand, harmful reactions between the aggregate and the cement paste such as the alkali-granulate reaction, can take place resulting in cracking and deterioration of the concrete over the longer term, hence affecting its durability.

3.2 Cement

Portland cement is important for the production of HPC. To obtain a higher resistance, it is desirable to finely grind the clinker. This increases the proportion of hydrates in the hardened concrete and reduces the proportion of passive cement particles. However, the proportion of hydrates is conditioned by the quantity of water. The fineness of cement increases the degree of hydration and hence increases the strength of concrete. Finer cement results in a higher specific surface. However, an excess fineness causes the risk of an early set and a higher heat of hydration that in turn could induce thermal cracking, particularly for mass concrete. For a high performance concrete to be achieved, the specific surface of the cement should be in the order of 3500 cm^2/g to 4000cm^2/g.

Among the four essential chemical constituents of Portland cement (C_3S, C_2S, C_3A, C_4AF), tricalcium Aluminate (C_3A) is the first one to hydrate followed by the tricalcium silicate (C_3S), the principal factor in the development of higher strengths. The rapid hydration of C_3A results in early age strengths for concrete. However, such a rapid hydration causes an early stiffening of concrete and hence results in a loss in workability [Punkki et al. 1996 & [Hamrat 1994]. Consequently, for high performance concrete to be achieved, the cement should contain less C_3A and the proportions of this constituent are recommended to be well below 10% [Hamrat & Chemrouk 2003].

3.3 Superplasticisers

Water, evidently a key of concrete, fulfils two functions:

- Chemically, in that it contributes to the development of the hydration reaction.
- Physically, it provide flow to concrete.

An ideal concrete would be a material in which the quantity of water is only that portion strictly necessary for the hydration of the cement and which, at an early age, and precisely before the setting of the cement paste, fulfils the flow requirements for the concrete to be placed. However, the present types of cements can not produce such an ideal concrete since the hydration reaction starts immediately after adding mixing water, and hence well before the placing of concrete in the formwork. Completely eliminating the C_3A component on the cement directly in the production phase is very costly. This explains the practice of using a surplus of mixing water to facilitate the placing of concrete.

To reduce the quantity of water used, superplasticisers, which are products of organic chemistry, have been used. These dispersants have properties that can result in a sensible reduction of the quantity of mixing water used (up to 30%) by reducing the liquid trapped in the floccules of cement particles. The superplasticisers can keep the concrete workable sufficiently long to enable it to be properly placed in the formwork (up to 45 min) [Boulmelh 2002, Karouche 2001]. It is to be noted however, that cement rich in C_3A has difficulties in maintaining workable concrete even when using a higher proportion of the dispersants. This seems to be the case for Portland cement produced in Algeria for which the proportion of C_3A is higher than 10% [Hamrat & Chemrouk 2003].

Depending on the reactivity of the cement, the proportion of superplasticisers should vary between 1% and 3% by weight of cement used [Hamrat & Chemrouk 2003, Boulmelh 2002]; a very reactive cement needs more water for the concrete to be workable and consequently needs more dispersant liquid. An excess amount of superplasticisers can have a negative effect on concrete and bring about segregation, bleeding or delayed setting. It is recommended to use these superplasticisers [Malier 19992] in two portions, 1/3 of the quantity added with the mixing water and the remaining 2/3 added on site just before placing the concrete in the moulds or the formwork.

3.4 Mineral Additives (Ultra-Fines)

Ultra-fines are mineral additives having a smaller granularity than that of cement; they are often added to a concrete mix and play a double role :

- As an inert filler that, once incorporated in the mix, inserts itself between the cement particles, thereby reducing the quantity of water and in turn increasing the density of the cement paste.
- As an active agent, whereby these combine partially or totally with water or with some cement compounds such as the alkaline or lime. This reduces the risks of formation of swelling gels and the risks of alkali-granulate reaction which affects the durability of the material in the longer term.

Mineral additives which can be used with cement in a proportion not exceeding 30% are typically quarry products such as calcareous-based fillers and siliceous fillers, silica fume, fly ash and blast furnace slag. In addition, these mineral additives attenuate the heat of hydration and hence reduce the risks of higher differential temperature responsible for early cracking. They also moderate some of the negative effects which result from the use of superplasticisers, i.e., mineral additives reduce the risk of bleeding or segregation when superplasticisers are used.

4 APPLICATION: PRODUCTION OF HIGH PERFORMANCE CONCRETE WITH LOCAL INGREDIENTS

To produce a highly performing concrete from the point of view strength as well as for long term performance (durability), the quantity of water used in the mix should be reduced since a higher proportion will evaporate leaving voids that weaken the hardened concrete; the ideal being to reduce the quantity of mixing water to that strictly necessary for the hydration reaction. Such an ideal is, however, far from being achieved despite advances in materials technology.

As an application of the present study, this section consists of providing information on specifications for producing a high performance concrete using local materials common to the local construction industry in the region of Chlef situated in the central western part of Algeria. After a number of preliminary tests, a crushed calcareous aggregate with a maximum size of 15 mm was used. The aggregate particles were angular and elongated and hence could not allow for a higher reduction in the quantity of mixing water. Furthermore, subsequent compression tests revealed that these aggregate shapes resulted in failures through the aggregate particles themselves (inter-granular ruptures).

A river sand having a specific density of 2.65 and a fineness modulus of 2.9 was used in the mix. It is Malier [2002] suggests that a sand with a fineness modulus greater than 2.8 should be used for producing HPC since it requires less mixing water.

The cement used in producing the present HPC is that locally produced and is an ordinary Portland cement conforming to the Algerian Norm NA 442, which itself is an extract from the French Norms (AFNOR) namely NFP 15-302 and NFP 15-442. This cement, however, contains a higher proportion of tricalcium aluminate C_3A (more than 10%), a constituent which hydrates very rapidly causing an early stiffening of the fresh concrete and hence inducing a loss of workability. Indeed, the HPC

produced in the laboratory had difficulties to be workable for a sufficient time to allow for its transportation and use on site.

A liquid superplasticiser of the type "Meda-Fluid", locally produced, was used in a quantity of 2% by weight of cement. This superplasticiser was added to the mix aggregate-cement-water [Malier 1992]. The accidental and irregular shapes of the aggregate particles used in the mix formulation, in addition to cement containing a higher proportion of C_3A did not allow for a higher reduction of the quantity of mixing water. A water/cement ratio of 0.40 was used as compared to ratios between 0.6 and 0.7 for ordinary concrete which may have even more water considering the generally hot and dry climate of the region. The aggregate/cement ratio was 3.75.

Tests for compressive strength and indirect tensile strength were carried out on cylindrical concrete specimens (150x300 mm). All the concrete tests were undertaken at different ages (i.e., 1d, 3d, 7d, 14d, 28d, 56d) to allow monitoring of the strength gain with age. Each result represents the average of three specimen tested. Table 1 gives results obtained for the compression as well as the tensile splitting strengths. Figure 1 shows the strength gain in compression over time.

Table 1. Strength evolution for a High Performance Concrete having W/C=0.40 and A/C=3.75.

Age (days)	1	3	7	14	28	56
Compression (MPa)	20	27	40	52	60	64
Tension (MPa)	1.9	/	3.2	/	4.1	4.2

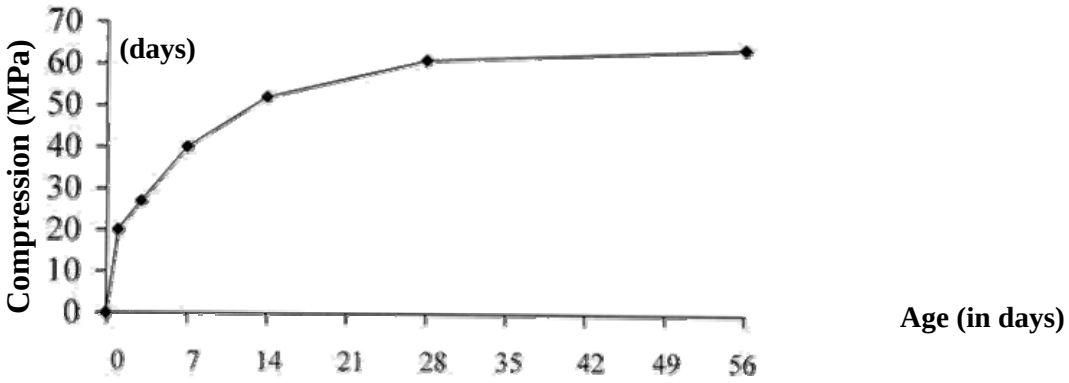

Figure 1. Strength gain with age for High Performance Concrete

The present work, as provided in Table1 and Fig.1, shows that concrete could be even more versatile, with compressive strengths more than twice that of ordinary concrete, leading to savings in materials as well as in overall cost. In this good quality dense and low permeability concrete, causes of deteriorations will be minimised and the material would become more durable at the longer term and hence fulfils the requirements of a sustainable built environment [Chemrouk & Attari 2003].

5 CONCLUSION

With societies increasingly focussing on sustainable development in our day to day life, building less expensively and targeting longer periods with consideration to reducing any negative environmental effects are indeed approaches that are gradually incorporated as part of the construction industry. In this sense, high performance concrete is gradually emerging as a defiant building material. However, formulating this building material is more complex than ordinary concrete owing to the addition of

supplementary parameters in the mix (superplasticisers – mineral additives) and to the qualitative aspect required. The cement paste and aggregate dominate quantitatively and qualitatively the formulation of high performance concrete. The former parameter is strongly related to the water/cement (W/C) ratio which varies between 0.6 and 0.7 for ordinary concrete.

For economical considerations and with the aim of producing a viable high performance concrete, the aggregate/cement ratio (A/C) should vary between 3 and 4 and that of the water/cement ratio should be below 0.4. The resulting loss of workability would be compensated by the use of an adequate superplasticisers. Without dispersants in the form of superplasticisers, concrete can not be of high performance since, with less mixing water, the fresh mix would be too stiff and hence difficult to fill in all the gaps in the formwork or moulds even when mechanical compaction is used, and particularly with cement containing a high proportion of C_3A.

With a careful selection of the mixing ingredients and taking advantage of the continuous advance in the materials technology, it is possible to produce concrete having strengths in the order of 60MPa to 80 MPa. With a more carefully studied selection of aggregate type, a lesser reactive Portland cement (containing less C_3A), the use of mineral additives such as silica fume, the addition of 3% of superplastisers compatible with cement, it is even possible to obtain strengths in excess of 80 MPa. With such strengths, the W/C ratio would vary between 0.3 and 0.25, depending on the type of aggregate used.

REFERENCES

Malier, I. 1992, '*Les Bétons à Haute Performance : Caractéristiques, Durabilité, et Applications'*, Presse de l'Ecole Nationale des Ponts et Chaussée, Paris.

Ansari, F. 2002, 'Stress-Strain Response and Failure Surface of High Strength Concrete Under Generalized State of Stress', Proc. of the International Congress: Challenges of Concrete Construction, Conference 1 : Innovations and Development in Concrete Constructions; Dundee, Scotland, 5-11 September 2002, pp 781 – 794.

Gutierrez, P.A.A and M. F. Canovas, M.F. 1984, 'High Performance Concrete: Requirements for Constituents Materials and Mix Proportioning', A.C.I *Materials Journal*, **93**(3), 233-241.

Hamrat, M. and Chemrouk, M. 2003, 'Béton à Haute Performance : Etude expérimentale sur la formulation', Proc. National Seminar on Civil Engineering, Oran (Algeria), January.

Hamrat, M. 1994, '*Béton à Haute Performance : Formulation et Propriétés Rhéologiques et Mécaniques'*, Msc thesis, Institut de Genie-Civil, Centre Universitaire de Chlef, Algeria.

Iravani, S. 1996, 'Mechanical Properties of High Performance Concrete', *A.C.1 Materials Journal*, **93** (5), 416-426.

Chemrouk, M. and Hamrat, M. 2002, 'High Performance Concrete – Experimental studies of the Material', Proc. of the International Congress: the Challenges of Concrete Construction, Conference 1 : Innovations and Development in Concrete Constructions; Dundee, Scotland, 5-11 September 2002, pp 869 – 877.

Punkki, J., Golaszewski, J. and Gjorv, O. 1996, 'Workability Loss of High Strength Concrete', *A.C.I Materials Journal*, **93** (5), 427-431.

M. Boulmelh, M. 2002, '*Formulation et propriétés d'un béton à haute performance à partir de matériaux locaux'*, Msc thesis, University of Science and Technology Houari Boumediene, Algiers.

Karouche, A. 2001, *'Béton à Haute Performance : Caractérisation du Matériau avec référence particulière aux déformations différées'*, Msc thesis, University of Science and Technology Houari Boumediene, Algiers.

Chemrouk, M. and Attari, N. 2003, 'Durability of concrete with particular reference to high performance concrete', Proc. of the International Symposium : Role of Concrete in Sustainable Development; Dundee, Scotland, 3-4 September 2003, pp 245 – 254.

Effects of Landfill Leachate on the Properties of Self-Levelling Cement Mortars

Francesco Colangelo [1]
Raffaele Cioffi [1]

T 11

ABSTRACT

In this work the behaviour of special mortars immersed into strongly aggressive solution is reported. The study is very useful to predict durability of a new typology of concretes, called self-compacting, which can be cast and compacted without external vibration and thus are especially suitable for building deep-laid poles and waterproofing separators. Specifically, five mixtures, one ordinary (reference) and four self-levelling, containing several mineral additions were prepared and tested. All the specimens prepared have been characterized before and after the immersion in municipal solid waste landfill fresh leachate (condition of maximum aggressiveness). Then, specimens have undergone compressive and flexural strength tests and determination of water absorption, capillary absorption and porosity. The results of analyses carried out on cured specimens, even if after relatively short exposure times (365 days), allow obtaining interesting information on durability requirements for concrete employed in confining landfills.

KEYWORDS

Landfills, Bulkheads, Durability, Leachate, Self-compacting concrete

[1] University of Naples Parthenope, Faculty of Engineering, Department of Technology, Naples 80143, Phone +39 081 5476732, Fax 081 5476777, raffaele.cioffiniparthenope.it, colangeloniparthenope.it

1 INTRODUCTION

The existence of uncontrolled landfills necessarily implies the requirement for safety actions. Due to the remarkable technical difficulties and the cost of such operations, the isolation of the contaminated site is often preferable in respect to the total removal of materials or to their reclamation in situ. The isolation action is carried out by a macro-encapsulation made by means of vertical waterproof (bulkheads) and horizontal deep (depth buffers) shields. The bulkheads must be notably impermeable in order to block the leachate of contaminants or rather to send them to interception and treatment points.

Containment and encapsulation must be thought as feasible technical solutions, in line with the present particular laws in force [Directive 1999/31/CE]. Such techniques can be used as emergency safety actions to reduce and/or limit contamination within a site reclamation which needs medium-long times. They can also be useful tool for cleaning, favouring the site check or avoiding unwanted spreading coming from the application of the techniques themselves.

The vertical waterproofing systems often have structural requirements linked to the site stability, thus their mechanical strength must be good and steady over time. In these cases concrete products in the form of cast in situ adjacent poles are normally used, because of their low cost, simplicity of the technique and quick execution. This work is part of a local project on the reclamation of uncontrolled landfills subject to landslides.

1.1 Background and Objectives

Once the isolation has been realized the possible contact with several aggressive substances for concrete (sulphates, chloride, etc), able to damage its functionality, must be considered.

The chemical analyses carried out on leachates coming from several landfills located in the Campania region of Italy have shown that to obtain efficient containment systems, it is necessary to use concretes protected with a suitable coatings. This, of course, is only possible for the pre-cast components and not for those casted in-situ. In the present work, self-compacting concrete (SCC) has been used to obtain high durable materials that resist the transfer of leachates. [Ouchi, M., & Okamura H. 1999, , Collepardi M. 2003, , Ambroise J. *et al.* 1999, www.britishsafetycouncil.co.uk /safetymanagement/news/vibration.htm].

This paper reports on a series of preliminary studies in which on Self-Levelling Mortar (SLM) have been considered as a containment and encapsulation medium. Following the physical and moisture transport characterization of specimens, these were then placed in a fresh solution of landfill leachate. This experimental method was used to simulate accelerated conditions as might be expected in real situations where the concrete would be in contact the soil mass saturated with landfill leachate. Specimen placed in the leachate solution for a period of 1-year following which further tests were used to characterise their relevant performance characteristics including compressive strength development, water absorption and capillary absorption.

2 EXPERIMENTAL

2.1 Materials

The basic constituens of the SLM mix included different proportion of the following materials: cement, blast furnace slag, silica fume, limestone power and fine aggregate. The cement used was CEM II/A-L 42,5 R conforming to European Standards EN-197/1, and manufactured by Italcementi (Salerno, Italy). The aggregate used was river sand 4-mm maximum size. The blast furnace slag (GBFS) was a granulated product ground to a Blaine fineness of about 4500 cm^2/g, with a particle

size ranging from 1-10 μm and with basicity coefficient [Kb=(CaO+$MgSO_4$)/(SiO_2+Al_2O_3)] equal to 1.08. The silica fume (SF) was a commercial material produced by ELKEM – Norway. Values for the chemical composition and specific surface area of all the above materials,including powdered limestone, are proviced in Table 1; L, SF and BFS refer respectively to limestone, silica fume and blast furnace slag.

The superplasticizer (SP) used was an acrylic-based product having 40% solid content and a specific gravity of 1.2 kg/dm^3. It was used in all the SLM mixtures and its amount was proportioned to ensure a constant workability. The water content of SP was considered during the mix-design phase. To enhance stability an inorganic Viscosity Modifying Agent (VMA) was also used in all SLM mixtures [Khayat K.H. & Guizzani Z. 1997, Rols S. *et al.* 1999].

Table 1. Chemical composition and specific surface area of the limestone cement, slag, silica fume and limestone powder.

Oxides (%)	CEM II	GBFS	SF	L
SiO_2	20.56	35.16	93.00	0.30
Fe_2O_3	3.21	1.40	0.70	-
Al_2O_3	4.88	10.76	0.80	0.10
CaO	60.93	41.91	0.20	55.10
MgO	1.62	7.68	0.60	0.50
Na_2O	-	0.11	0.60	-
K_2O	-	0.14	1.00	-
SO_3	2.78	1.92	-	-
TiO_2	-	0.32	-	-
L.O.I.	5.76	1.78	1.50	43.00
Specific surface area, cm^2/g	3970	4500	200000	4250

2.2 Mixtures Proportion

Four SLM mixtures were designed in addition to a conventional mortar (CM). A vibrating table was used to prepare specimens cast with CM. Table 2 shows mixture proportions for all the mortar specimens. In this table, the first part of the mixture code gives information on the mineral additions contained in the mortar, while the second part indicates the kind of mortar (SLM for Self-Levelling and CM for Conventional Mortar). The mixtures used presented similar proportions in terms of the aggregate to cement ratio.

Table 2. Mortar mixture proportions.

	Composition, g						
Mix code	Sand (mm)	CEM II	BS	SF	L	SP	VMA
CM	1956.3	525.0				7.9	
SLM	1883.2	591.0				5.5	2.4
L-SLM	1910.4	547.5			54.8	6.4	2.4
SF-SLM	1879.8	567.0		45.4		8.4	2.5
BS-SLM	1913.3	547.5	54.8			7.0	2.4

The water to cement ratio was kept constant at 0.5 for all the mixtures, moreover the water/ (cement + powder) ratio was similar for all SLMs. The total amount of binder (including cement, ground limestone, blast furnace slag and silica fume) was about 600 g.
For all mixtures 40 x 40 x 160 mm^3 specimens were prepared and cast. After casting the specimens were cured for 24 hours and then removed from the moulds and moist cured at 20 °C. After 28 days, test specimens were dipped in a leachate solution whereas the control specimens were stored in

laboratory conditions to be used as reference specimens. The volume ratio between the specimens and the aggressive solution was 0.33.

The main chemical characteristics of the leachate solution are reported in Table 3.
According to UNI EN 206-1, the leachate solution used is classified as a chemically strong corrosive agent. The exposure classes for concretes subject to chemical attack by natural soil, groundwater, sea water and waste water are assigned as follows: XA1-chemically weak corrosive ($SO4^{2-}$ concentration ≥ 200 and ≤ 600), XA2-chemically moderate corrosive ($SO4^{2-}$ concentration ≥ 600 and ≤ 3000) and XA3-chemically strong corrosive ($SO4^{2-}$ concentration ≥ 3000 and ≤ 6000).

Table 3. Chemical composition of leachate solution.

pH	8.2
Conducibility	18.06 mS
C.O.D.	1880 mg/l
Salinity	8768 mg/l
Sulphate	5169 mg/l
SiO_2	24.5 mg/l
Phosphate	58.2 mg/l
Fe	0.6 mg/l
Ni	<0.1 mg/l
Pb	<0.1 mg/l
Cu	<0.1 mg/l
Cr	<0.1 mg/l
Zn	<0.1 mg/l
Cd	<0.1 mg/l

2.3 Methods

In order to prepare all the mortar mixtures, a 3-dm^3 mixer was used. After mixing, fresh mortars were employed to determine the slump flow. The slump flow test measures the mean diameter of mortar spread after removal of the slump cone. A spread of at least 250-mm diameter is required for self-levelling mortars [Bignozzi M.C. *et al.* 2003]. All the mixtures prepared were characterized by slump flow values according to this limit and did not show any segregation phenomena.

Water and capillary absorption were also measured. Capillary absorption is described by the capillary absorption coefficient. It was measured following the procedure given in the Italian standard Normal - 11/85. Three specimens (40 x 40 x 160 mm^3) were used for each data point and dried to constant mass. Their water uptake was measured for 3 days. The mass of water absorbed per unit area is plotted as a function of the square root of time. The capillary absorption coefficient is the slope of this straight line.

Water absorption was determined by complete immersion of specimens in water at atmospheric pressure whereas the total porosity of the specimens was measured using a mercury intrusion porosimeter (Thermo Finnigan 140-240).

To evaluate the strength development, compressive tests were carried out after 7, 28, 90 and 365 days of curing in water. The specimens were kept covered with a wet cloth and a plastic sheet during the first 24 hours; after this period, they were cured in water until the test age. The specimens were dried in air for two hours prior to testing. Four prismatic specimens (40 x 40 x 160 mm^3) were broken for each data point. A 150 kN capacity compressive testing machine was used according to Italian Standard UNI EN 196-1.

Furthermore, another set of compressive tests were also carried out on mortars that had completed a 28-days water cure and thereafter had been immersed for 11 months in leachate solution. As well, following the long term contact with the aggressive solution the specimens were evaluated to determine changes in mass variations, the degreeof water absorption,porosity and coefficient of capillary absorption; the surface damages to the specimen were also observed and recorded.

3 RESULTS AND DISCUSSION

3.1 Compressive Strength Development

The compressive strength development up to one year's curing for all the mixtures is shown in Figure 1. The 365-day strengths obtained ranged from 60.6 to 82.1 MPa.

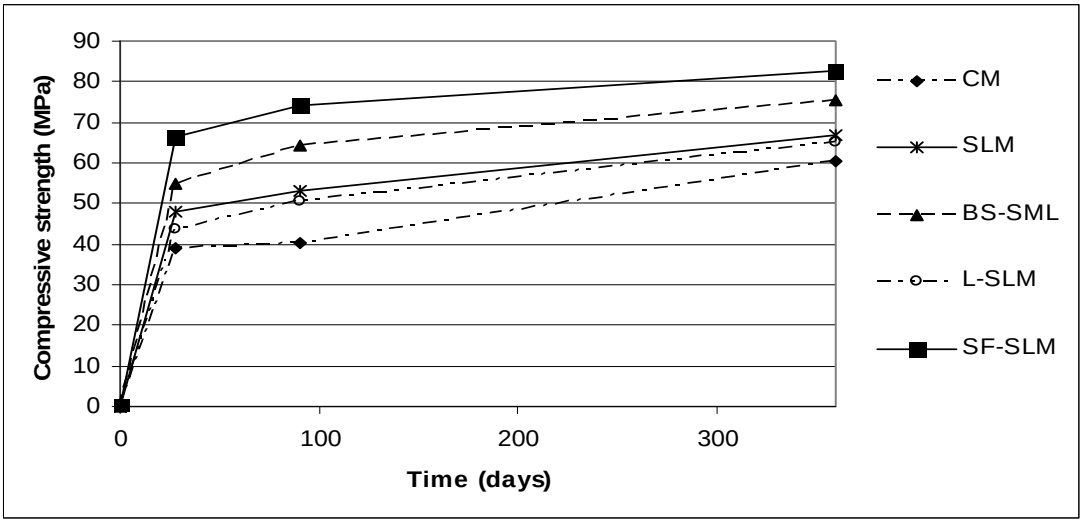

Figure 1. Compressive strength development with age, Mpa.

The maximum strength value was recorded for the SF-SLM mixture(Silica Fume-SLM), whereas the lowest was for the CM (Conventional Mortar) mix. The addition of silica fume gave higher compressive strength, at both early (7 days) and late ages, compared to other mineral additions. This is in agreement with the previously reported results by the authors in the case of SCC specimens [Colangelo *et al.* 2004]. However, as stated in literature, [Klug Y. & Holschemacher H. 2003] SLMs displayed a higher compressive strength than the conventional mortar mixes, regardless of the type of addtion used.

3.2 Durability

The values measured for the total porosity percentage of the specimens after 28-day water cure, are as follows: 11.74%, 10.85%, 5.61%, 10.70% and 6.17% for the mixtures CM, SLM, SF-SLM, L-SLM and BS-SLM, respectively . The lowest and the highest values observed in the case of SF-SLM and CM, respectively, are in agreement with the mechanical behaviour showed above. After 340-days of exposure to leachate a small reduction on total porosity has been observed for all mortars tested. Specifically, the values became 10.94%, 10.15%, 5.34%, 10.08% and 5,97% for the mixtures CM, SLM, SF-SLM, L-SLM and BS-SLM, respectively. The decrease in compressive strength after leachate immersion is shown in Figure 2.

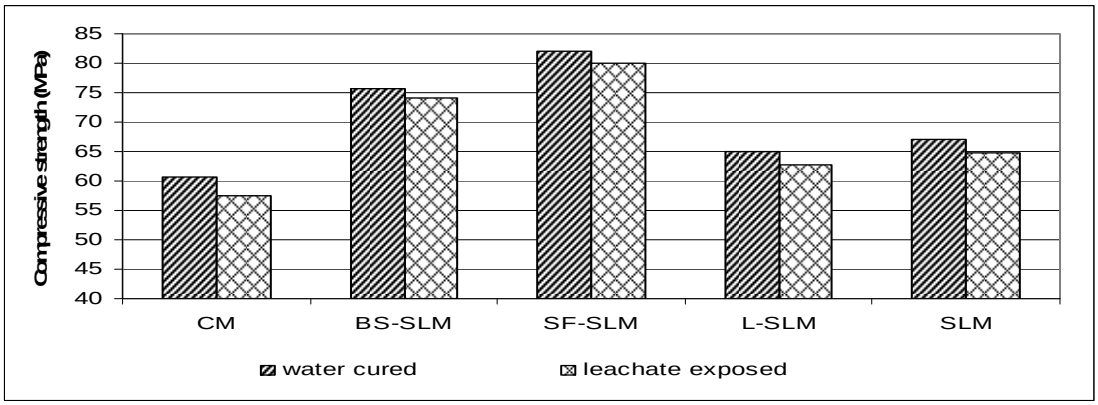

Figure 2. Compressive strength of mortars after water curing and leachate immersion, Mpa.

All the mixtures tested show a decrease of a few percentage points in terms of strength. In particular, the SLM mixtures shows a better result than the CM mixture, with decreases equal to 5.0%, 1.9%, 2.7%, 3.7% and 3.3% for mortars CM, BS-SLM, SF-SLM, L-SLM and SLM, respectively. There are no significant differences between the control (365-day water cure) and the exposed (28-day water cure and 11 months exposure to leachate) specimens in terms of water and capillary absorption and variation in unit mass as shown in Table 4 and in Figure 3, respectively.

Table 4. Water absorption and capillary absorption of mortars.

	CM	SLM	L-SLM	SF-SLM	BS-SLM
Capillary Absorption (water cured) - mg/cm^2· √s	0.51	0.48	0.41	0.31	0.35
Capillary Absorption (leachate exposed) - mg/cm^2·√s	0.55	0.51	0.43	0.32	0.36
Water Absorption (water cured) - %	1.71	1.74	1.47	1.11	1.14
Water Absorption (leachate exposed) - %	1.80	1.79	1.50	1.13	1.16

It can clearly be seen that the BS and SF SLM mixtures show a enhanced behaviour in comparison to the other mortar mixes given that the coefficient of capillary absorption and percentage of water absorption is respectively less than 0.36 mg/cm2• √s and 1.16%, even after leachate immersion.

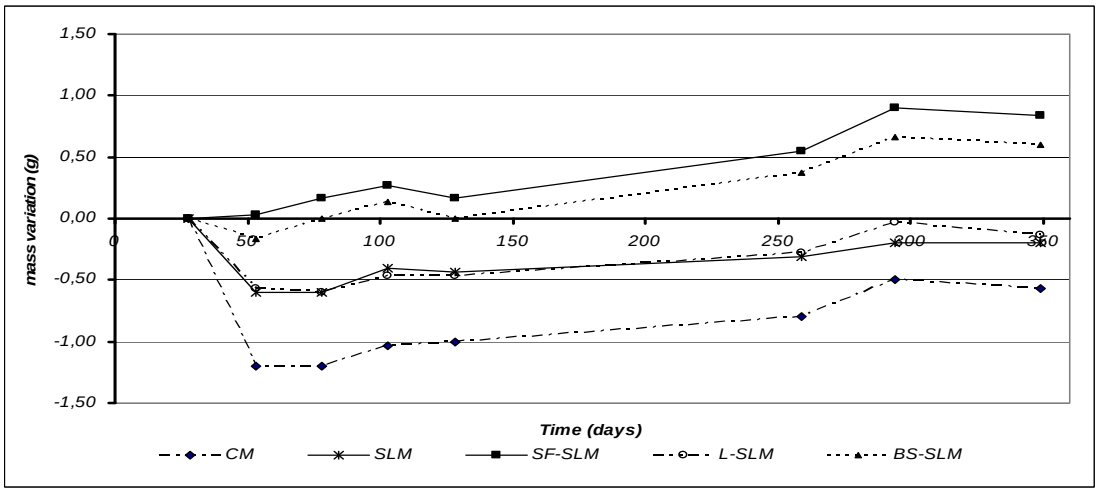

Figure 3. Mass variation of mortars at fixed times during leachate immersion, g.

The following pictures show the CM specimen (left) and SLM one (right) after 340-day to exposure to the leachate solution. It is possible to observe that there are no cracks in the specimen and the decay only involves the surface of the mortar.

Figure 4. CM specimen (left) and SLM one (right) after 340-day to exposure to the leachate solution.

4 CONCLUSIONS

The self levelling mortars investigated in this study show a good resistance to the presence of aggressive solutions,typical of leachates that emanate from municipal solid waste landfills. The use of these kinds of mortar mixtures, typically characterized by their high mechanical strength, make it possible to specify these mortars for the design of bulkheads used in landfills. In has been shown that, the attack by the leachate solution on the cement paste is only superficial and do not alter the physico-mechanical properties of the mortars. Moreover the use of mineral additivies can considerably improve the behaviour of the mortar mixtures when in contact with such type of leachates.

ACKNOWLEDGMENTS

The authors whish to thank the National Researche Programme PRIN 2006 for financial support of this work.

REFERENCES

Ambroise, J., Rols, S. & Pèra, J. 1999 'Self-Levelling Concrete- Design and Properties', *Concrete Science and Engineering*, 1, 140-147.

Bignozzi M.C., Franzoni, E. & Sandolini F. 2003 'Waste Materials employed in the manufacture of self-compacting mortars' Proc. of the 4th International Congress Added Value and Recycling of Industrial Waste, L'Aquila – Italy, pp. 24-27.

Colangelo, F., Marroccoli, M., Cioffi R. & Molfetta, M. 2004 'Influence of mineral additions on the properties of Self-Compacting Concrete', Proc. of the International Congress IMTCR, Lecce – Italy, pp. 153-161.

Collepardi, M. 2003, *New concrete*, Enco s.r.l., Spresiano, Italy.

D.Lgs.13/01/03 n. 36 - 1999/31/CE. Wastes landfilling.

Internet source,www.britishsafetycouncil.co.uk /safetymanagement/news/vibration.htm, assessed 29/04/2002.

Italian NORMAL – 11/85. Water absorption and capillary absorption of the mortars.

Khayat, K.H. & Guizzani, Z. 1997, 'Use of viscosity-modifying admixture to enhance stability of fluid concrete', *ACI Materials Journal*, 94 [4], 332-341.

Klug, Y. & Holschemacher, H. 2003, 'Comparison of the Hardened Properties of Self Compacting and Normal Vibrated Concrete', Proc. of 3rd International RILEM Symposium on Self-Compacting Concrete, Ed. O. Wallevik and I. Nielson, France, pp. 596-605.

Ouchi, M., & Okamura, H. 1999 'Self-compacting concrete development, Present and future' Proc. 1st Int. Symposium on Self-compacting Concrete, RILEM, Sweden, pp. 212-220.

Rols, S., Ambroise, J. & Pèra, J. 1999 'Effects of Different Viscosity Agents on the properties of Self-Levelling Concrete', *Cement and Concrete Research*, 29 [2], 261-266.

UNI EN 206-1 Concrete – Specification, performance,production and conformity.

UNI EN 196-1 Methods of testing cement – Determination of strength.

11DBMC International Conference on Durability of Building Materials and Components
ISTANBUL, Turkey 11-14 May 2008

Performances of Palm Oil Fuel Ash Cement Based Aerated Concrete in Acidic and Sulphate Environments

M.W.Hussin [1]
K.Abdullah [2]
F.Zakaria[3]

T 11

ABSTRACT

Malaysia as the world's largest exporter of palm oil has been facing problem in disposing palm oil fuel ash, a by-product of palm oil mill since many years ago. The discovery made by researchers of Universiti Teknologi Malaysia last century in revealing the potential of this waste as a partial cement replacement in normal concrete has stem more efforts towards studying the possibility of using it in lightweight concrete production. Currently, investigation conducted proved that this material also can be integrated as a partial cement replacement material producing lightweight concrete known as Palm oil fuel ash cement based aerated concrete which possess adequate strength with lower density than OPC aerated concrete. This paper illustrates the durability aspect of this new agro blended cement based aerated concrete in terms of resistance towards aggressive chemicals such as acid and sulphate. Aerated concrete cube consisting 20% palm oil fuel ash and control specimen with 100% OPC were cast and then subjected to water curing for 28 days before immersed in the hydrochloric solution prepared using 0.3% hydrochloric acid having 99% concentration. The pH of the solution was controlled to about 2 throughout the immersion period of 1800 hours. The durability performance of the cubes involved the measurement of weight loss at a different period of immersion in the solution. In order to study the performance of this material in sulphate environment, a set of control specimen and another one consisting the same proportion of POFA were prepared before water cured for 28 days. Sulphate resistance of the binders was evaluated by measuring the expansion of mortar bars after immersion in 10% sodium sulphate solution for the period of 6 months. Finding will be discussing the performance of POFA cement based aerated concrete in both acidic and sulphate environments.

KEYWORDS

Palm oil fuel ash, Partial cement replacement, POFA cement based aerated concrete, Acid resistance, Sulphate resistance

[1] Universiti Teknologi Malaysia, Faculty of Civil Engineering, 81310 UTM Skudai, Johor, Malaysia, Phone + 607-5531607 Fax 5531607, warid@utm.my
[2] Universiti Malaysia Pahang, Faculty of Civil & Environmental Engineering, Locked Bag 12, 25000 Kuantan, Pahang, Malaysia, khairunisa@ump.edu.my
[3] Universiti Teknologi Malaysia, Faculty of Civil & Environmental Engineering, Locked Bag 12, 25000 Kuantan, Pahang, Malaysia, Phone +609-5492297, Fax 609-5492299, fadhadli@ump.edu.my

1 INTRODUCTION

Concrete, the oldest manufactured construction material used in building work all around the world has occupied a unique place with its unquestionable application use in the construction industry. This construction material has been subjected to endless research throughout the century thus resulting in fruitful findings which successfully lead to creation of value added concrete materials fulfilling to customers requirement. The availability of high-tech telecommunication network system nowadays, has indubitably assist active knowledge dissemination specifically among researchers involved in concrete research area, resulting in sharing of fascinating ideas such as converting worthless industrial or agricultural by-product available to be partially cement or sand substitute constituent. Implementation of unique ideas has results in discovery of new type of environmental friendly concrete with lower cost than the existing concrete or able to offer more benefits than the original one.

In Malaysia, aerated concrete which began to capture the interest of local contractors due to its lightness and easier handling during building process has also subjected to innovation process. In early 21st century, Faculty of Civil Engineering from Universiti Teknologi Malaysia has become the pioneer in the country attempting to integrate waste material in gas concrete production which well known as aerated concrete. The study on utilization of waste as partial constituent in aerated concrete started off with Arreshvhina [2002] whom integrated slag, a industrial waste as cement replacement and then followed by Mat Yahaya [2003] whom partially substituted sand partially with agriculture ash. The current researcher, Abdullah [2006a] has incorporated palm oil fuel ash as partial cement replacement successfully producing POFA cement based aerated concrete possessing satisfying strength. This approach is one of the effort to make use of the palm oil fuel ash, a by-product of palm oil mill that is generated abundantly in increasing volume throughout the year since Malaysian palm oil industry continue to grow in order to meet the customers demand. This achievement will have the double advantage towards palm oil mill whereby development of this material could increase the palm oil industry earnings and also a means of disposing the waste.

Glancing through on the discovery of POFA as a alternative constituent for cement production, Hussin & Abdul Awal [1996] has successfully manage to incorporate palm oil fuel ash as partial cement replacement for normal concrete enhancing the strength and durability of the new modified material known as POFA concrete. Then, usage of this material was broaden to other types of concrete when Sata, Jaturapitakkul and Kiattikomol [2004] successfully integrated a very finely ground POFA as partial cement replacement to produce high-strength concrete. Succeeding the findings, Faculty of Civil Engineering again discovered that it is possible to add palm oil fuel ash up to 30% as partial cement replacement in a type of concrete categorized as lightweight concrete known as POFA cement based aerated concrete [Abdullah et.al 2006b]. Though, few properties of this material has been looked into [Abdullah et.al 2006a, Abdullah et.al, 2006c, Abdullah et.al, 2006d] but durability aspect of this material still silent and this issue will be discussed in this paper.

2 MATERIALS AND EXPERIMENTAL PROGRAMME

2.1 Materials

Materials used in this study consisted of ordinary Portland cement, fine sand, POFA, aluminium powder, superplasticizer and water. The fine sand was local river sand that has been oven dried at the temperature of 110ºC for 24 hours and then sieved before stored in airtight container. Aluminium powder which is a gas foaming agent and a powder form superplasticizer was also employed in all aerated concrete mixtures. The POFA used is a by-product obtained from burning the remaining of extracted palm oil fibers and shells from a palm oil mill owned by Yayasan Pembangunan Johor which is located in State of Johor. The collected ashes were dried in the oven at the temperature of 110ºC ± 5 for 24 hours to remove moisture in it before sieved and ground until 99% of the ashes passes 45µm sieve during wet sieve test. A single batch of ordinary Portland cement (OPC) classed ASTM Type 1

was used throughout the experiment. Both chemical compositions of the OPC and POFA used in this work are shown in Table 1.

Table 1. Chemical compositions of ordinary Portland cement and palm oil fuel ash.

Chemical Composition	*OPC (%)*	*POFA (%)*
Silicon Dioxide (SiO_2)	**28.2**	**53.82**
Aluminium Oxide (AL_2O_3)	**4.9**	**5.66**
Ferric Oxide (Fe_2O_3)	**2.5**	**4.54**
Calcium Oxide (CaO)	**50.4**	**4.24**
Magnesium Oxide (MgO)	**3.1**	**3.19**
Sodium Oxide (Na_2O)	**0.2**	**0.1**
Potassium Oxide (K_2O)	**0.4**	**4.47**
Sulphur Oxide (SO_3)	**2.3**	**2.25**
Phosporus Oxide (P_2O_2)	**<0.9**	**3.01**
Loss On Ignition (LOI)	**2.4**	**10.49**

2.2 Test For Acid Resistance

Aerated concrete cube specimens (70.6x70.6x70.6mm) having a mix proportion of 1:1 for cement and fine sand by weight with fixed amount of aluminium powder and superplasticizer were cast. Another set of specimen with ash was also prepared in a similar way where OPC was replaced, mass for mass, by 20% POFA. The water cement ratio for OPC aerated concrete mix for both mixes was adjusted in order to produce specimens which possess similar density as POFA cement based aerated concrete mix. Then, all specimens were demoulded after 24 hours before subjected to water curing for 28 days prior to immersing them into test solution as shown in Fig. 1. The durability performance of both OPC and POFA concretes were determined by measuring the loss of weights of the samples at different periods of immersion hydrochloric acid solution prepared using 0.3% hydrochloric acid having 99% concentration. The pH of the solution was controlled to about 2 throughout the immersion period of 1800 hours [Abdul Awal, 1998].

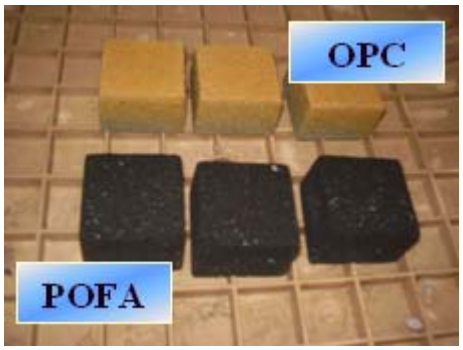

Figure 1. Specimens immersed in acid Hydrocloric solution.

2.3 Test For Sulphate Resistance

Data presented in this paper also include the durability performance of OPC aerated concrete acting as control and POFA cement based aerated concrete mortar bar immersed in 10% sodium sulphate solution. The procedure followed in conducting this test was in accordance with ASTM C1012-89. The design mix for OPC and POFA aerated concrete is similar to the design mix used for preparing cubes for acid test as mentioned above. Both samples either OPC or POFA were subjected to water curing for 28 days before immersed in the prepared sulphate solution. The performance of the specimens was evaluated in terms of expansion characteristic of mortar bars immersed in the sulphate

solution. Figure 2 illustrates few mortar bars ready to be measured for the expansion. Data reported in this paper were the averages of six measurements for both mortar bars and cubes.

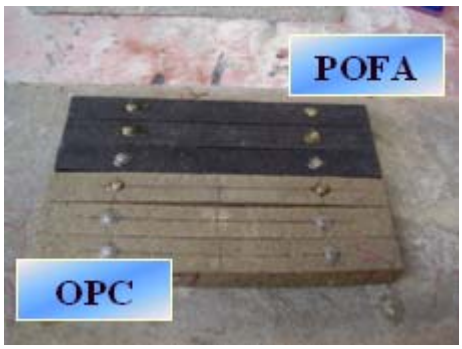

Figure 2. Mortar bar for Sulphate resistance test.

3 RESULTS AND DISCUSSION

3.1 Resistance to Acid Attack

The study on resistance to acid attack of aerated concrete cube specimens has been carried out by measuring the loss of weight of the samples continuously submerged in a 5% hydrochloric acid solution. Figure 3 reveals that aerated concrete with POFA exhibited better resistance towards the acid at all periods of immersion. Although both specimens begin to lose its weight as the period of immersion increased, percentage of weight loss for OPC cubes always higher than POFA specimen. In addition, the surface of OPC aerated concrete begins to soften and become loose. This fact has been highlighted by Zivica & Bajza [2001] whom mentioned that loss of mass is one of the signs of acidic attack, and crushing and dropping of material from concrete is one of the deterioration sign. By the end of the immersion period, OPC aerated concrete already loss 3.94% of its weight; POFA cement based aerated concrete on the other hand only loss 0.90%. It is interesting to note that surface of POFA cement based aerated concrete cube showed better surface condition than those with OPC aerated concrete in not only have considerable amount of surface softening but also faces loss of small particles on both surface and edges. Both visual observation and weight loss evidently analysis proves that POFA aerated concrete has higher resistance towards acid attack compared to control specimen.

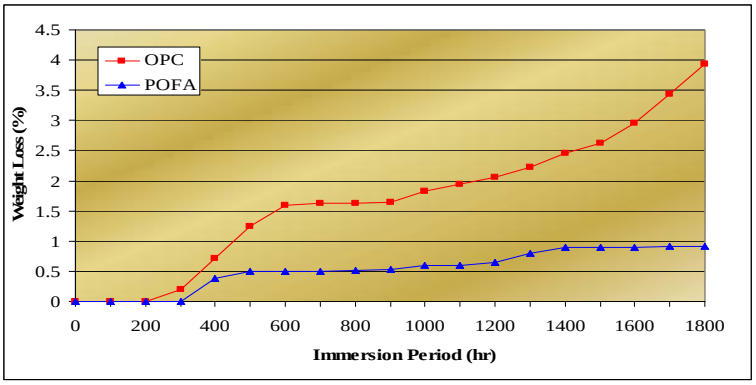

Figure 3. Comparative weight loss of OPC and POFA cement based aerated concrete specimens continuously immersed in Hydrocloric acid solution.

The better resistance of POFA specimen is expected not only because of the fact that POFA is being identified as a good pozzolanic material [Hussin & Abdul Awal, 1997] but also due to its low CaO content which is 4.24% in comparison to the high content of approximately 50% in OPC. Amount of

CaO presence in the binder material tend to play significant role in production of Calcium Hydroxide which is susceptible to acid attack finally leading to deterioration of hardened concrete material. This is because acid medium attacks mainly calcium hydroxide and then hydration products in cement matrix which leads to hydrolytic decomposition of hydration cement products followed by degradation of mechanical properties of cement based material [Zivica, 1999]. In addition, another researcher Mehta [1992] concludes that because of the higher content of CaO the hydration products of OPC contain about 25% CaOH which turns to be primarily responsible for the resistance of ordinary Portland cement exposed to acidic attack. As POFA contains a small amount of CaO, consequently the amount of CaOH would surely be less in the products of hydration.

3.2 Resistance to Sulphate Attack

Figure 4 shows the expansion patterns of POFA cement based aerated concrete and OPC specimen mortar bar throughout the immersion period in 10% Sulphate Solution. Basically, OPC aerated concrete bars had higher expansion value throughout the immersion period than that of POFA specimen bars. OPC mortar bar begin to exhibit significant expansion starting from 4th week when at the same time it was observed the development of crack at both end of the specimen. However, POFA specimen remains intact although there is slight expansion which is far lower than the control specimen. After 8 weeks of immersion period, it was noted that the expansion of OPC aerated concrete bar were 18.4 % having map cracks all over the specimens causing he mortar bars to disintegrate before measurement can be taken at the following week. On the other hand, POFA specimen bar expansion was as low as 1.92 % without any crack development on it. Elongation of OPC mortar bar compared to POFA specimen can be observed in Figure 5. It is justifiable for aerated concrete to exhibit significant expansion after four weeks exposed to Sulphate solution as compared to other types of concrete that been studied by Cao et.al [1997] and Abdul Awal [1998] that took more than 20 weeks for the specimens to exhibit similar pattern of failure as presented in this study. This is because aerated concrete which is a very porous material allows the sulphate solution to penetrate the internal structure of the material permitting fast response towards sulphate ion resulting in formation of cracks and elongation.

Discussing on the performance of OPC and POFA specimen, it is obvious POFA cement based aerated concrete mortar bar possess higher resistance towards Sulphate attack. Basically, the results obtained suggested that POFA as a partial cement replacement in aerated concrete could improve the sulfate resistance of this lightweight concrete. This is because according to Neville [1995] mortar or specimens having pozzolanic materials exhibit better chemical resistance that specimens with Portland cement due to the depletion of calcium hydroxide liberated during the hydration process, thereby reducing the amount of free calcium hydroxide for leaching and rendering the aluminium-beraing face inactive. Since POFA also a pozzolanic material, integrating it as partial cement replacement lead to reduction in the amount of C_3A, hence, all the aluminate bearing phases will accordingly be reduced. Basically, inclusion of POFA not only successfully reduce the amount of $Ca(OH)_2$ formed during the hydration of Portland Cement , which is susceptible to Sulphate attack but also the pozzolans presence reacted with the calcium hydroxide eventually reducing amount of $Ca(OH)_2$ that is susceptible to sulphate attack while at the same time producing a secondary calcium silicate hydrate (C-S-H).

Following that, the pozzolanic reactions contribute to space-filling process [Colak, 2003] whereby the secondary C-S-H formed were deposited in the pores making blended cement impermeable and therefore, the sulfate ions cannot easily penetrate through the concrete matrix which also become dense [Al-Amoudi, 2002]. Generally, addition of POFA not only decrease the amount of $Ca(OH)_2$ formed, but also contributed towards formation of concrete with lower permeability as a result of pozzolanic reaction that refines the pore structure and its capability to be filler because of its small particle size. This fact has been supported by Jaturapittakul et.al [2006] whom justified that use of POFA to replace Portland Cement not only decreases the $Ca(OH)_2$ content of hydrated cement but also serves as a filler and reduce voids between the aggregates and hydration products, leading to denser concrete.

On the other hand, OPC aerated concrete is susceptible to sulfate attacks due to its larger amount of $Ca(OH)_2$ and the condition of the pore structure which is bigger makes this highly permeable material possess lower resistance towards sulfate attack. The weakness of concrete consisting 100% OPC has been highlighted by Colak [2003] whom mentioned that the presence of Tricalcium Aluminate (C_3A) and Tetracalcium Aluminoferrite (C_4AF) contents in Portland Cement tend to react with sulfates to form ettringite which causes expansion and disintegration of the hardened Portland Cement pastes. As for the permeability aspect, Khatri and Sirivivatnon [1997] added that it is an important property that directly affects the durability of concrete against sulfate attack. This is because concrete with bigger pore structure due to existence of gaps among aggregates and hydrated product is more susceptible to penetration of sulfate because of its less permeable nature. In conclusion, it can be said that the lower amounts of calcium hydroxide in this agro blended cement based aerated concrete which also possess finer pore structure that reduce its permeability provides a considerable improvement in the durability of these composites towards sulphate attack.

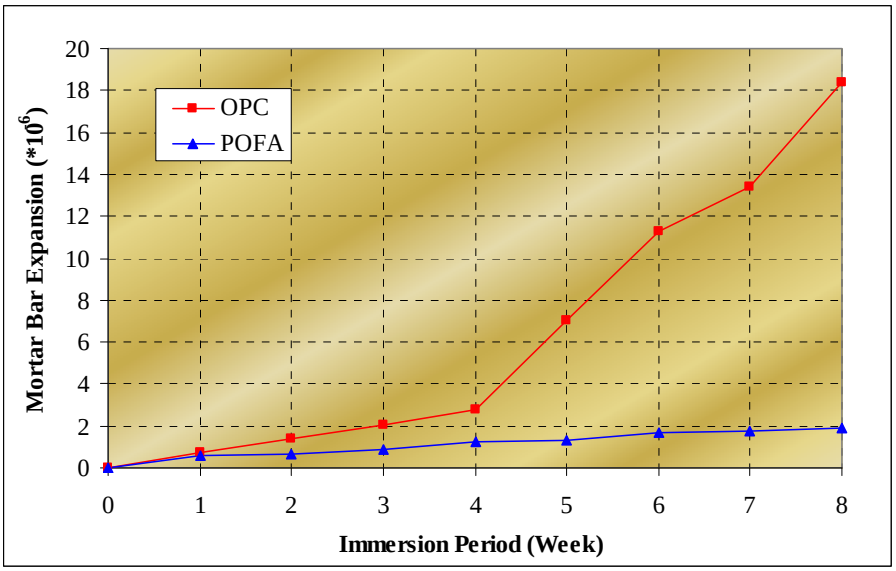

Figure 4. Expansion of OPC and POFA cement based aerated concrete mortar bar during the immersion period in 10% Sodium Sulphate solution.

Figure 5. OPC specimen expand more than POFA specimen.

3 CONCLUSION

The work presented in this paper indicates that both acid and sulphate resistance of aerated concrete improves with the integration of POFA as partial cement replacement material. Integration of POFA

which possess very low content of CaO is responsible to produce lower amount of Calcium Hydroxide which is susceptible to both acid and sulphate attack. Therefore, inclusion of POFA in aerated concrete not only able to reduce Calcium Hydroxide formed in the first place but also able to make use of the available $Ca(OH)_2$ during pozzolanic reaction thus successfully refine the pore structure of agro blended cement based aerated concrete eventually producing a more impermeable matrix as compared to specimen consisting 100% OPC aerated concrete. Conclusively, POFA cement based aerated concrete which consist POFA with lower amount of CaO play important role to make this material be superior in terms of acid and sulphate resistance as compared to OPC aerated concrete.

ACKNOWLEDGEMENTS

The authors would like to extend their gratitude to the entire management team of palm oil mill in Ladang Alaf owned by Yayasan Pembangunan Johor for the cooperation and support in providing the palm oil fuel ash samples. The contribution by the staff from Structure & Material Laboratory of Faculty of Civil Engineering, Universiti Teknologi Malaysia where the research was carried out is gratefully acknowledged. Financial support from the Construction Industry Development Board of Malaysia (CIDB) is greatly appreciated. The researcher also wishes to thank Universiti Malaysia Pahang for the provision of study leave.

REFERENCES

Abdul Awal, A.S.M. & Hussin, M.W. 1996, 'Properties of fresh and hardened concrete containing palm oil fuel ash' Proceedings Of The 3rd Asia-Pacific Conference On Structural Engineering And Construction, Johor Bahru, Malaysia, 17th -19th June 1996, pp. 359-367.

Abdul Awal, A.S.M. 1998, 'A study on strength and durability performances of concrete containing palm oil fuel ash', University Teknologi Malaysia: PhD Thesis

Abdullah, K., Hussin, M.W., Zakaria, F., Muhammad, R., and Abdul Hamid, Z. 2006a, 'POFA : a potential partial cement replacement material in aerated concrete' Proceedings of the 6th Asia-Pacific Structural Engineering & Construction Conference, Kuala Lumpur, Malaysia Sept 5-6 2006.

Abdullah, K., Hussin, M.W., Zakaria, F., and Abdul Hamid, Z. 2006c, 'Development in compressive strength of POFA cement based aerated concrete', Proceedings of the 1st International Conference On Technology Management, Putrajaya, Malaysia Dec 4-5.

Arreshvhina, N. 2002, 'Application of slag cement based aerated lightweight concrete in non-load bearing wall panels' Universiti Teknologi Malaysia. Master Thesis

Annual Book of ASTM Standards, 1989, 'Standard test method for length change of hydraulic-cement mortars exposed to a sulphate solution' American Society of Testing And Materials, Philadelphia, ASTM C1012-89.

Cao, H.T., Bucea, L., Ray, A. and Yozghatlian, S. 1997, 'The effect of cement composition and pH of environment on sulfate resistance of Portland cement and blended cements', *Cement And Concrete Composites*, [19], pp 161-171.

Colak, A. 2003, 'Characteristics of pastes from a Portland cement containing different amounts of natural pozzolan', *Cement And Concrete Research*, [33], pp 585-593.

Hussin, M.W. & Abdul Awal, A.S.M. 1996, 'Influence of palm oil fuel ash on strength and durability of concrete', Proceedings Of The 7th International Conference On Durability Of Building Materials And Components, Stockholm, E & FN Spon, London, Vol.1, pp 291 – 298.

Hussin, M.W. & Abdul Awal, A.S.M. 1997, 'Palm oil fuel ash – a potential pozzolanic material in concrete construction', *Journal of Ferrocement*, **27**[4], 321- 327.

Khatri, R.P. & Srivivatnon, V. 1997, 'Role of permeability in sulphate attack', *Cement Concrete Research*, **27**[8], 1179-1189.

Mat Yahaya, F. 2003, 'Pengaruh abu terbang kelapa sawit terhadap kekuatan mampatan dan ketahanlasakan konkrit berudara', Universiti Teknologi Malaysia. Master Thesis.

Mehta, P.K. 1992, 'Rice husk ash – a unique supplementary cementing material' in *Advances In Concrete Technology*, CANMET, Ottawa, pp 407-431.

Neville, A.M. 1995, *Properties of Concrete*, Addison Wesley Longman Limited, England.

Sata, V., Jaturapitakkul, C. & Kiattikomol, K. 2004, 'Utilization of palm oil fuel ash in high-strength concrete', *Journal Of Materials In Civil Engineering*, [16], 623-628.

Zivica, V. & Bajza, A. 2001, 'Acidic attack of cement based materials – a review. art 1. principle of acidic attack', *Construction and Building Materials*, [15], 331-340.

Zivica, V. 1999, 'Acidic attack of materials based on the novel use of silica fume in concrete', *Construction and Building Materials*, [13], 263-269.

Al-Amoudi, O.S.B. 2002, 'Attack on plain and blended cement exposed to aggressive sulfate environments', *Cement & Concrete Composites*, [24], 305-316.

11DBMC International Conference on Durability of Building Materials and Components
ISTANBUL, Turkey 11-14 May 2008

Effect of the Type of Supplementary Materials and Viscosity Enhancing Admixture on the Durability of Self-Compacting Concrete

Mohammed Sonebi [1]
Vincent O'Donoghue [2]
Gerard Keogh [3]

T 11

ABSTRACT

Self-compacting concrete (SCC) is designed to exhibit high deformability and moderate viscosity to maintain homogeneity and adequate stability. Any concrete should have high impermeability and low chloride diffusion to reduce the risk of corrosion and enhance service life. Permeability of concrete is influenced by the porosity and the interconnectivity of pores in the cement paste and the micro-cracks in concrete, especially at the interface of the paste-aggregate. The movements of gases, liquids and ions through concrete is important because of their interactions with concrete constituents including pore water which can alter the integrity of concrete directly and indirectly, leading to the deterioration of structures. In this study, the effect of supplementary materials such as limestone powder (LSP), pulverized fuel ash (PFA), ground granulated blastfurnace slag (GGBS) and viscosity enhancing admixture (VEA) on the durability of self-compacting concrete was investigated. All mixes were design for strength grade C40. The filling ability, passing ability and segregation were measured by slump flow, V-funnel, L-box and column segregation tests. The concrete compressive strength was also evaluated. The air permeability, water permeability, capillarity absorption, carbonation, and freeze-thaw were used to assess the durability of SCC and compared to traditional concretes. The results showed that SCC mixes using GGBS or PFA had improved transports properties, greater resistance to freeze-thaw and carbonation than the traditional concretes.

KEYWORDS

Air and water permeability, Sorptivity, Freeze-thaw, Carbonation

[1] Queen's University Belfast, School of Planning, Architecture, and Civil Eng., Belfast, UK, Phone +44 2890974013, Fax 44 2890663754, m.sonbei@qub.ac.uk
[2] Queen's University Belfast, School of Planning, Architecture, and Civil Eng., Belfast, UK, Phone +44 2890974013, Fax 44 2890663754, vodonoghue01@qub.ac.uk
[3] Queen's University Belfast, School of Planning, Architecture, and Civil Eng., Belfast, UK, Phone +44 2890974013, Fax 44 2890663754, gkeogh01@qub.ac.uk

1 INTRODUCTION

Self-compacting concrete (SCC) is considered to be one of the most rapidly emerging technologies in concrete. SCC is a material that meets a unique combination of performance and uniformity requirements that cannot always be achieved by using conventional constituents and usual construction practices [Sonebi & Bartos 2001, 2002, Sonebi et al. 2005]. The durability of concrete is mainly influenced by the transport of potentially aggressive substances. Majority of the influential properties of hardened concrete are related the quantity and characteristics of various types of pores in the cement paste and aggregate components of the concrete. The durability of concrete was assessed by measuring the permeation properties such as absorption, permeability. This described the movement of gases, liquids and ions through concrete, and it is important because of their interactions with the concrete materials and the pore water which can alter the integrity of concrete, leading to the deterioration and damage of structures. The carbonation and freeze-thaw of concrete are very important for reinforced concrete. This paper reports the results of the transport properties of SCC mixes by investigating the air and water permeability measured with Autoclam test, capillarity absorption, the freeze-thawing and carbonation resistance tested according to RILEM recommendations [CPC 18, TC 116].

2 MATERIALS, MIX PROPORTIONS, AND TEST METHODS

2.1 Materials and Mix Proportions

The SCC mixes investigated in this study were prepared with Portland cement (Class 42.5), either ground granulated blastfurnace slag (GGBS) or limestone powder (LSP) or pulverized fluel ash (PFA) added as the filler. The reference mixes were made with 100%C, 30%PFA, and 72%GGBS. The PFA was obtained from bituminous coal from a Northern Ireland power station. The limestone powder was produced from carboniferous limestone of very high purity and finer than cement. The limestone had grading of 99.8% < 125 μm and 83% < 5 μm.

A continuously graded crushed basalt aggregate with a nominal particle size of 5-20mm and a well-graded quartzite sand from Lough Neagh, with a fineness modulus of 1.95, were used. The typical relative densities of the coarse aggregate and sand were 2.9 and 2.72, and typical absorption values 1.2% and 1.18%, respectively. A copolymer-based superplasticiser (SP) was used. This had a solid content and specific gravity of 40% and 1.10, respectively. SP was used from 0.60% to 0.95% (by mass of binder). Diutan gum was supplied by Kelco-crete which is an anionic polysaccharide gum as used as viscosity enhancing admixture (VEA). It was used as powder at 0.05% (by mass of binder). No air entraining agent was used in the mixes. The mix proportions are summarised in Table 1.

2.2 Test Methods

The slump flow test, V-funnel and JRing and settlement segregation column were used to evaluate filling ability, passing ability and segregation of SCC [Bartos et al. 2002]. The resistance to segregation was measured by the column segregation test which consisted of a PVC column divided into three equal sections of 190-mm diameter and 170-mm height, held together with circular metal clamps. This was filled with concrete and left to rest for 15 min.

For the transport properties, the air and water permeability of concrete was measured on the preconditioned slabs (250 x 250 x 75 mm) using the Autoclam Permeability system. More details of the test procedure can be found in reference Basheer et al. [1992]. The capillary absorption test determines the rate of absorption of water through a concrete surface and was carried out on the moulded bottom face of two 100 mm cubes according to RILEM recommendations [TC 116] of determination of the capillary absorption of water in hardened concrete (TC 116). The cubes were preconditioned at 105 ± 5°C until constant weight (8-10 days). The uptake of water was measured through weight gain of the cubes at intervals of 10 min, 30 min, 1 hr, 2 hrs, 4 hrs and 24 hrs in contact

with water. The sorptivity (mm/√min) was determined for each mix as the slope of the capillary absorption vs. √Time.

Table 1. Mix proportions of all mixes.

(kg/m³)	*Traditional concrete*			*SCC*			
	TC-OPC Mix 1	*TC-PFA Mix 2*	*TC-GGBS Mix 3*	*SCC-PFA Mix4*	*SCC-LSP Mix 5*	*SCC-GGBS Mix 6*	*SCC-VEA Mix 7*
Cement	**350**	**280**	**129**	**340**	**290**	**180**	**365**
Limestone powder	---	---	---	---	**260**	---	---
PFA	---	**120**	---	**150**	---	---	---
GGBS	---	---	**301**	---	---	**270**	---
Total of binder	**350**	**400**	**430**	**490**	**550**	**450**	**365**
Sand (0-5 mm)	**872**	**834**	**883**	**968**	**992**	**1075**	**800**
C. A. (20 mm)	**1023**	**979**	**1036**	**730**	**730**	**800**	**1023**
SP (%)	---	---	**0.60**	**0.78**	**0.63**	**0.95**	**0.84**
VEA (0.05% mass of binder)	---	---	---	---	---	---	**0.18**
Water/powder ratio	**0.56**	**0.48**	**0.35**	**0.40**	**0.33**	**0.35**	**0.58**
Water/cement ratio	**0.56**	**0.69**	**1.16**	**0.58**	**0.63**	**0.86**	**0.58**
Binder/C. aggregate	**0.34**	**0.41**	**0.42**	**0.67**	**0.75**	**0.56**	**0.46**
Slump flow (mm)	**190***	**175***	**70***	**680**	**735**	**665**	**653**
T_{50} (s)	---	---	---	**2.24**	**0.85**	**4.95**	**0.92**
JRing (mm)	---	---	---	**480**	**568**	**568**	**670**
V-funnel (s)	---	---	---	**5.06**	**4.25**	**11.2**	**3.9**
Segregation ratio (%)	---	---	---	**0.80**	**0.94**	**0.94**	**0.88**
f'_c at 3 d (MPa)	**16.1**	**12.9**	**18.3**	**27.2**	**26.0**	**22.0**	**15.4**
f'_c at 7 d (MPa)	**20.6**	**20.1**	**27.2**	---	**28.7**	**32.8**	--
f'_c at 28 d (MPa)	**34.2**	**30.8**	**47.0**	**49.1**	**37.3**	**57.6**	**36.5**

* Slump (mm)

To determine carbonation rates, three cores 50mm Ø x 75mm deep were cut from each slab (250 x 250 x 75 mm). The slabs were cured in tank for three days then placed in sealed polythene bags and stored for 80 days. The cores were placed in accelerated carbonation chamber with relative humidity (65-70%) and temperature 20 ± 2ºC, and CO_2 =10%, for 6 weeks. The depth of carbonation was measured according to the procedure described in RILEM CPC-18. All specimens, after 6 weeks kept in accelerated carbonation chamber, were split and spread with phenolphthalein indicator. The mean value of carbonation depth of three cylinders was calculated. The RILEM test for freeze-thaw [Setzer et al. 1996], 100 mm diameter cylinders and 125 mm high was used. The curved surfaces were painted and sealed with an epoxy coating to prevent moisture movement from sides. The samples were placed in containers and immersed in 15mm of 3% salt solution for one week. The samples were then transferred to individual cylindrical containers for starting the test. A 5 mm depth of their samples was immersed in the test solution in individual containers. Each cycle of freezing and thawing was for 12 h. The scaled material from the test surface was collected, dried at 100°C for 24 h and weighed periodically during the test. This was continued for 100 cycles.

3 RESULTS AND DISCUSSION

3.1 Fresh and Hardened Properties

The results of slump, slump flow, JRing, V-funnel, segregation and compressive strength at 3 d, 7 d, and 28 d are given in Table 1. The required value of slump flow for all of the SCC mixes was achieved all up 650 mm. All the results of the T_{50}, V-funnel, J-Ring and segregation were considered to satisfy

the requirements from the European SCC guidelines [2005]. As expected, the development of the compressive strength was strongly affected by the W/B ratio and filler types. However, all mixes achieved the compressive strength required (Grade 40). The compressive strengths at 28 d were ranged between 30.8 to 57.6 MPa. The relatively faster strength development of SCC-LSP compared to TC-OPC, particularly at early ages, is believed to be mainly due to the inclusion of fine limestone powder, which may have an accelerating effect on C_3S hydration and early strengths. The SCC mixes containing GGBS, instead of limestone powder, had lower compressive strength at 3 days compared to 100% C, but developed higher strength at 28 days. This was due to the slower, but prolonged reaction (hydraulic and pozzolanic) between cement hydration products and GGBS, which contributes significantly to strength. It can be observed that SCC-PFA and SCC-GGBS resulted in a high compressive strength at 28 d compared to the corresponding mixes TC-PFA and TC-GGBS due to the higher binder contents and lower W/B in case of SCC-PFA (0.40 vs. 0.48).

3.2 Durability Performance

The results of air permeability and water permeability of all mixes are plotted in Fig. 1. All SCC mixes show lower air permeability compared with the traditional mixes and the GGBS-SCC mix had the lowest air permeability index (API) followed by PFA-SCC and LSP-SCC. VEA-SCC mix had slight higher air permeability than PFA-SCC and LSP-SCC mixes. It can be also noticed that TC-GGBS had lower air permeability than TC-OPC and TC-PFA mixes. The addition of GGBS, PFA and LSP improved the paste matrix (denser surface concrete) and improved the interfacial transition zone (ITZ) property where micro cracks mostly starts, with GGBS and PFA being more effective [Zhu, Bartos 2003, Sonebi & Ibrahim, 2007]. PFA reduces the number and the size of pores during the hydration process (increased degree of hydration) and LSP improves particle packing [Bosilijkov, 2003] reducing capillary porosity. The lack of pore filling effect/capability in SCC-VEA and higher W/B ratio, resulted in a higher capillary porosity and increased interconnection of pores but was lower than the TC-OPC and TC-PFA mixes

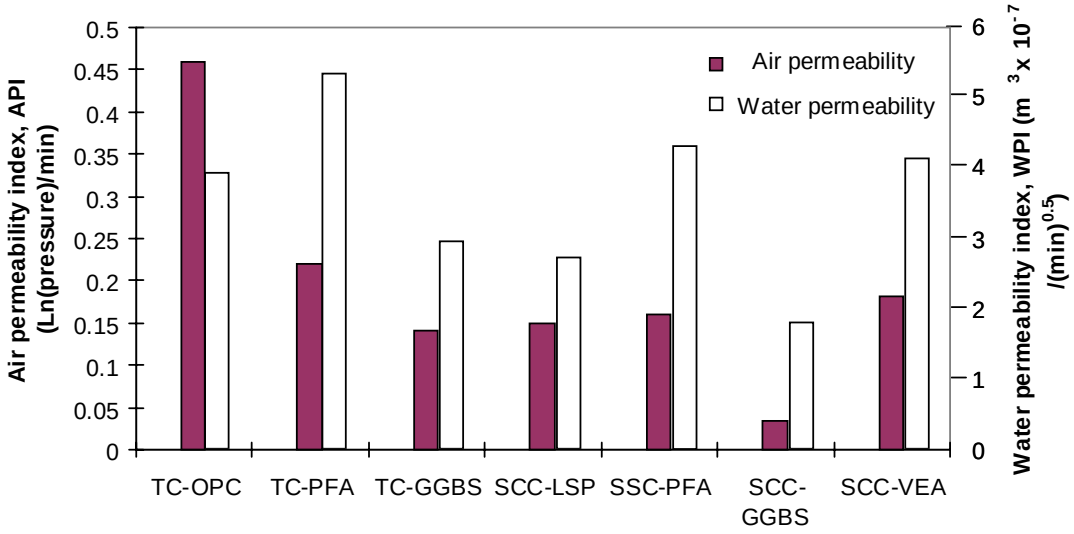

Figure 1. Variation of air and water permeability indexes (API & WPI) of all mixes.

The higher air permeability of TC-GGBS and TC-PFA compared to their corresponding SCC mixes could be due to the lack of homogeneity of TC-GGBS and TC-PFA as a result to the compaction process and their higher W/B ratio [Scrivener & Nemati 1996] and/or the lower binder to aggregate ratio (0.42 and 0.41 for TC vs. 0.56 and 0.67 for SCC) which means more poorer ITZ (more micro cracks within the concrete). The micro-cracks that occur in the ITZ are larger in width than most capillary cavities present in the cement paste matrix. These micro-cracks help to establish interconnections in the pore structure, increasing the permeability of the system. Higher coarse aggregate percentage also increases the bleed water trapping under the coarse aggregates which leads

to an increase in local w/c ratio (increase porosity) and increase permeability of the concrete [Basheer et al. 2005]. The protective quality index (Fig. 1) of SCC-GGBS was less than 0.1 which considered very good, and good for others SCC mixes (API < 0.5) [Basheer et al. 2005].

SCC-GGBS also had the lowest water permeability followed by SCC containing LSP, PFA and VEA, respectively. As in the air permeability test, the water permeability is affected by the amount and type of binder and W/B. The water permeability index (WPI) of SCC-GGBS was considered very good [Basheer et. al. 2005]. Similarly to air permeability test, TC-GGBS and TC-PFA mixes had higher water permeability compared to SCC-GGBS and SCC-PFA mixes which was caused by the compaction process, the higher W/B ratio of TC-PFA mix and most probably the lower binder to coarse aggregate ratio which contribute to capillary porosity and increase interconnection of pores.

The water permeability SCC-LSP and SCC-VMA was lower that that of TC-OPC. Tsivilis et al. [2003] suggested that, while air permeability was closely related with porosity, water permeability and sorptivity were more affected by the size and kind of pores which could explain the results. Further investigation of the microstructure and the surface quality is required to determine the pore size, distribution, and continuity more conclusively. It can be concluded that SCC incorporating GGBS or PFA led to a better water permeability which was due to the better interfacial zone and more refined pore structure of the paste matrix.

Fig. 2 presents the results of capillary absorption. It can be seen that SCC mix containing GGBS and PFA showed the lowest sorptivity value due to the pore filling effect of PFA's hydration products and refined structure of the cement matrix with GGBS. In the SCC-VEA the lack of pore filling ability by additional powder such as GGBS, or PFA or LSP, the higher W/B ratio and low binder/coarse aggregate ratio (0.46 vs. 0.56, 0.67 and 0.75) increased the porosity and led to the poorer ITZ area, which increased the interconnection of pores and therefore leading to higher sorptivity value. The SCC-LSP also had lower capillary absorption than SCC-VEA due to the improvement of packing density of concrete and having lower W/B ratio (0.33 vs. 0.58).

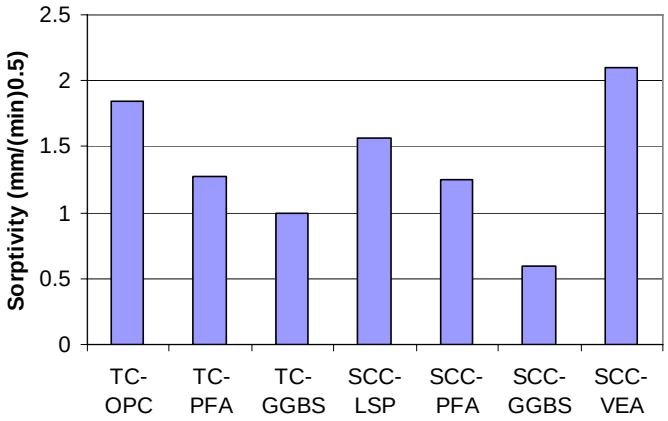

Figure 2. Variation of sorptivity of all mixes.

The carbonation depths of all SCC mixes are compared with the traditional concrete mixes as shown in Fig. 3. It can be observed that all SCC mixes exhibited lower carbonation depth, except SCC-VEA, compared to the traditional mixes. SCC mixes containing PFA and GGBS had the lowest carbonation depth due to the refined pore structure and more uniform interfacial transition zone (ITZ). SCC mix containing VEA exhibited high carbonation depth compared to SCC-LSP which they had similar compressive strength. Although VMA help to stabilize the components and control segregation, sedimentation and bleeding, the lack of pore filling effect/capability and higher W/B ratio results in a higher capillary porosity and increase interconnection of pores. Among SCC mixes tested in this study, having lower capillary absorption led to lower carbonation depth. This confirms other findings e.g. Audenaert and De Schutter [2007]. They reported that an increase in W/B, i.e. an increase in the

capillary absorption led to an increase in the carbonation depth of SCC. Anagnostopoulos et al. [2007] also reported that the improvement of carbonation of SCC is influenced by the W/B ratio, the composition and the amount of the binder system.

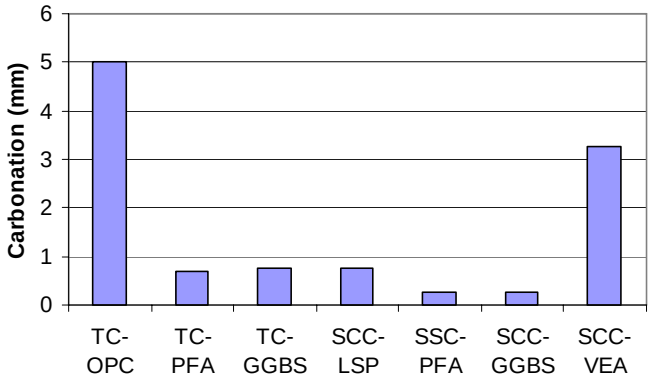

Figure 3. Variation of carbonation of all mixes.

Fig. 4 shows the variation of the freeze-thaw expressed as the cumulative scaling weight. The SCC-GGBS and SCC-PFA lasted through the 100 cycles of the test without being broken. The results indicated that SCC-GGBS and SCC-PFA mixes exhibited a greater resistance to freeze-thawing and sustained up 100 cycles compared to other SCC-VEA and SCC-LSP mixes which had higher weight losses at only 34 and 74 cycles, respectively. The cumulative scaling weights of SCC-GGBS and SCC-PFA after 100 cycles were only 26 g and 49 g, respectively. The SCC-LSP demonstrated better resistance than SCC-VEA. For example, it can be seen that for 200 g of lost of weight, SCC-LSP had resist until 36 cycles compared to 18 cycles for SCC-VEA. After 100 cycles, TC-GGBS had lost 3 times of weight compared to SCC-GGBS (81g vs. 26 g), and SCC-PFA lost only 50 g. SCC-PFA showed better resistance to freeze-thaw than TC-PFA. It can observed that SCC-LSP lost 300 g at 19 cycles of freeze-thaw compared to TC-OPC which it needed 42 cycles to loose similar amount of scaling. TC-PFA had performed well than TC-OPC.

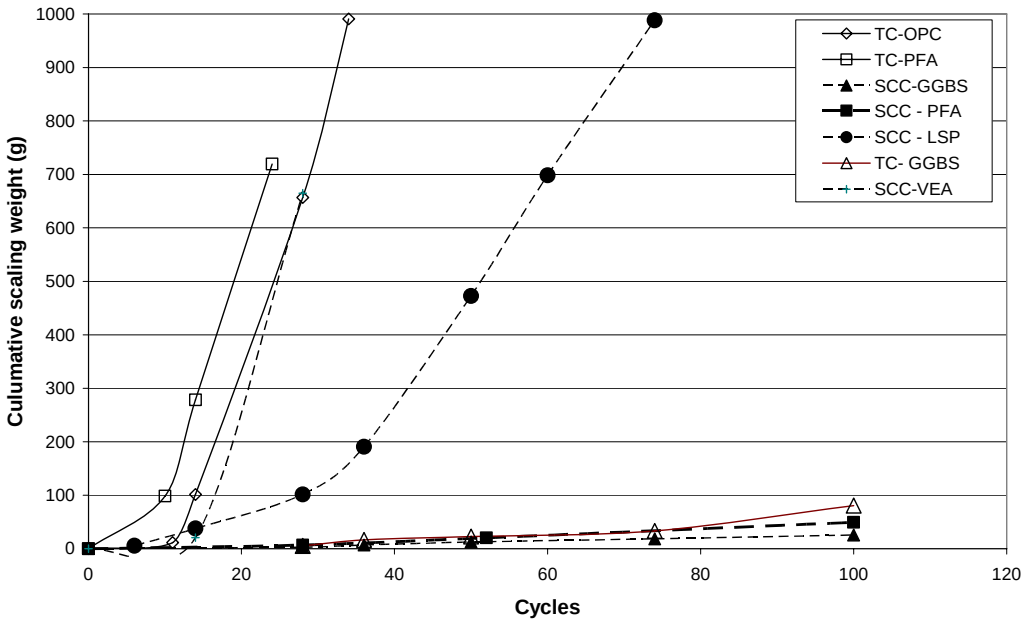

Figure 4. Variation of freeze-thaw of all mixes.

4 CONCLUSIONS

In this investigation, four SCC mixes have been investigated with three traditional concretes and the durability of these mixes was determined. The following conclusions can be drawn:

- The SCC mixes containing GGBS, PFA, LSP and VMA had lower air permeability compared to traditional mixes. For water permeability, SCC mix made with GGBS and LSP had the lowest water permeability compared to traditional concretes. SCC mixes containing GGBS exhibited better capillary absorption, but SCC-PFA demonstrated similar capillary absorption compared to TC-PFA. SCC-LSP indicated lower capillary absorption compared to TC-OPC. The highest capillary absorption was obtained with SCC-VEA.
- All SCC mixes except SCC-VEA demonstrated lower carbonation depth than the traditional concretes due to mostly to their lower W/B ratio and the type of binder which seems the main factors governing the carbonation.
- SCC-GGBS and SCC-PFA mixes showed the highest freeze-thaw resistance. However, SCC-LSP mix had better freeze-thaw resistance than SCC-VEA.
- Among the four SCC mixes, SCC mix made with VEA exhibited the highest air permeability, water permeability, capillary absorption, and the lowest resistance to freeze-thaw and carbonation. The SCC mix containing GGBS and PFA resulted in the best durability performance.

REFERENCES

Anagnostopoulos, N., Georgiadis, A.S. & Sideris, K.K., 2007, 'Carbonation of self-compacting concrete produced with different materials', Proc. of 5th Int. RILEM Symposium on self-compacting concrete, Vol. 2, Ghent, Belgium, pp.721-727.

Audenaert, K. & De Schutter, G., 2007, 'Water vapour diffusion through self-compacting concrete', Proc. of 5th Int. RILEM Symposium on self-compacting concrete, Vol. 2, Ghent, Belgium, pp. 683-688.

Bartos, P.J.M., Sonebi, M. & Tamimi, A., 2002, 'Workability and Rheology of Fresh Concrete: Compendium of Tests', Report of RILEM Technical Committee TC145 WSM – Workability of Special Concrete Mixes, RILEM Publications S.a.r.l, Paris, 156 p.

Bosilijkov. V.B., 2003, 'Self-compacting concrete mixes with poorly graded aggregate and high volume of limestone filler', *Cement and Concrete Research*, **33**(9), pp. 1275 – 1286.

Basheer, P.A.M., Long, A.E. & Montgomery, F.R., 1992, 'The Autoclam for measuring the surface absorption and permeability of concrete on site', Proc. CANMET/ACI Int. Conf. on advances in concrete technology, Ed. V.M. Malhotra, Athens, Greece, pp. 211-221.

Leemannn, A. & Hoffmann, C. 2005, 'Properties of self-compacting and conventional concrete – differences and similarities', *Magazine of Concrete Research,* **57**(6), pp. 315-319.

CPC18 'Measurement of hardened concrete carbonation depth', TC-14 CPC, *RILEM Technical Recommendations for the Testing and use of Construction Materials*, Taylor Francis ed., pp. 56-58.

European Guidelines for Self-compacting Concrete, Specification, Production and Use, 2005.

Setzer, M.J., Fagerlund, G. & Janssen, D.J. 1996, 'CDF test – Test method for the freeze-thaw resistance of concrete – tests with sodium chloride solution (CDF)' *Materials and Structures*, Vol 29, pp. 523 – 528.

Sonebi, M. & Ibrahim, R. 2007, 'Assessment of the durability of medium strength SCC from permeation properties', Proc. of 5th Int. RILEM Symposium on self-compacting concrete, Vol. 2, Ghent, Belgium, pp.677-682.

Sonebi, M. & Bartos, P.J.M., 2001, 'Performance of Reinforced Columns Cast with Self-Compacting Concrete', Proc. of the 5th CANMET/ACI Int. Conf. on Recent Advances in Concrete Technology, SP 200-25, Ed. Malhotra, V.M., Singapore, pp. 415-431.

Sonebi, M. & Bartos, P.M.J. 2002, 'Bond Behaviour and Pull-off Test of Self-Compacting Concrete', Proceedings of the International Symposium on Bond in Concrete – from Research to Standards, Budapest, Hungary, Ed. Balázs, G.L., Bartos, P.J.M., Cairns, J., Borosnyói, A. 20-22 Nov., pp. 511-519.

Sonebi, M., Grünewald, S. & Walraven, J. 2005, 'Effect of the Mixture Composition on Filling Ability and Passing Ability of Self-Consolidating Concrete', Proc. of the 2nd North American Conf. on Design and Use of Self-Consolidating Concrete and the fourth International RILEM Symposium on Self-Compacting Concrete in Chicago, Oct-Nov., pp. 737-743.

Tsivilis. S., Tsantilas. J., Kakali. G., Chaniotakis. E. & Sakellarious, A. 2003, 'The permeability of Portland limestone', *Cement and Concrete Research,* **33** [9], pp. 1465-1471.

Zhu, W., & Bartos, P.M.J. 2003, 'Permeation properties of self-compacting concrete', *Cement and Concrete Research,* **33** [6], pp. 921-926.

11DBMC International Conference on Durability of Building Materials and Components
ISTANBUL, Turkey 11-14 May 2008

Deterioration Mechanism of Reinforced Concrete Beam Corroded by Climate Environment and Galvanostatic Method

Yingshu Yuan [1]
Qing Wu [2]
Yongsheng Ji [2]
Surendra P. Shah [3]

T 11

ABSTRACT

Deterioration of reinforced concrete structures caused by corrosion of steel bars is a major problem in concrete structural durability. Normally, the Galvanostatic method is used for accelerating steel bar corrosion in concrete for laboratory testing. However, the corrosion distribution on the steel bar is different when the corrosion is induced between using Galvanostatic method and under natural climate environment. Recently, artificial climate environment has been used to induce corrosion in the laboratory. This method is becoming important in assessing the durability of concrete structures, because of the same electro-chemical corrosion process and similar corrosion distribution on the surface of the steel bar between natural and artificial climate environment. In this study, two groups of reinforced concrete beams were degraded as a result of the corrosion of steel bars under artificial climate environment and using Galvanostatic method respectively. The test results between the two groups show obvious differences on the structural behavior based on identical width of corrosion cracking. Because the electro-chemical corrosion processes in the beams between the two corrosion ways are different, the different corrosion processes lead to the different corrosion distribution. Further comparison studies on the mechanical behavior of corroded bar, the bond strength and the corrosion distribution on the surface of steel bar verified the analysis of the electro-chemical corrosion process.

KEYWORDS

Corrosion, Reinforcement, Concrete, Deterioration, Climate environment

[1] School of Civil Engineering, China University of Mining and Technology, Xuzhou, Jiangsu 221008, China, Phone +86 516 83884360, ysyuan@cumt.edu.cn
[2] School of Civil Engineering, China University of Mining and Technology, Xuzhou, Jiangsu 221008, China.
[3] Center for Advanced Cement-Based Materials, Northwestern University, Evanston, IL 60208, USA.

1 INTRODUCTION

Corrosion of steel reinforcement is one of the major causes inducing deterioration of reinforced concrete structures. Accelerated test technique of steel bar corrosion in concrete is significant for evaluating structural deterioration in laboratory. Galvanostatic method and artificial climate environment are used to accelerating steel bar corrosion in concrete. But two accelerated test techniques will lead to different corrosion distribution on the surface of the steel bar in concrete because of different corrosion process using the Galvanostatic method or under a natural environment. Different corrosion process will lead to different corrosion characteristics on the surface of the steel bar and different deterioration of the bond behavior between the corroded bar and concrete, and lead to different bearing capacity and ductility behavior of the structure.

In this research, the corrosion process and the differences of the structural behavior under climate environment and Galvanostatic method are studied. The purpose is to verify that the artificial climate environment will be an effective accelerated technique for the durability test instead of the Galvanostatic method. Identical reinforced concrete beams were corroded under the two accelerated corrosion techniques, and deterioration mechanism of corroded reinforced concrete beam was discussed.

2 EXPERIMENTAL INVESTIGATIONS

2.1 Reinforced Concrete Beams for Testing

The reinforced concrete beams employed for testing are divided into two groups. The first group (Group C) is corroded under an artificial climate environment; the second group (Group G) is corroded using the Galvanostatic method. The concrete composition, reinforcement and dimension of the test beams are identical in the groups. The structural behavior comparisons of the corroded beams are carried out under the same corrosion crack width caused by steel bar corrosion.

The dimensions of the test beams are b×h×l=100×160×1500mm, the concrete grade is C25, and the mix proportions by weight are C:S:A:W = 1:1.75:2.98:0.55. Normal Portland cement #32.5, river sand and coarse aggregate of crushed basalt stone with a maximum aggregate size of 16mm were used. The beam, shown in Fig.1, was simply supported with a span of 1.2m, and two concentration forces were applied on the span. The arrangement of reinforcement in the test beam is shown in Fig. 2, and the thickness of the concrete cover is 15mm. Three different corrosion-cracking widths were selected for the corrosion control and comparisons. The beams are loaded to failure after corrosion. The grouping of the specimens is shown in Table 1.

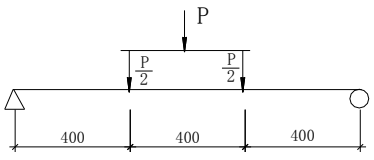

Figure 1. Arrangement of loading on the test beam

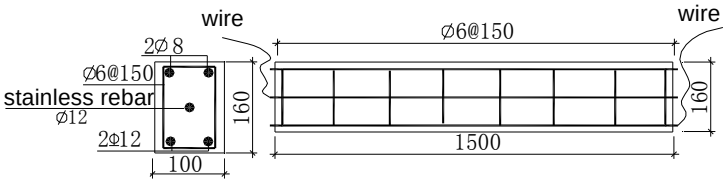

Figure 2. Arrangement of reinforcement

2.2 Artificial Climate Environment for Accelerating Corrosion

The corrosion process of the test beams under an artificial climate environment can be accelerated by way of high temperature, high humidity and repeated wetting-drying cycles. Corrosion of the test beams in this group was carried out in the artificial climate room controlled by a computer system. The artificial climate conditions in this testing were temperature T=40^{o}C, humidity RH=80%, and salt water (5% NaCl solution) spraying (1 hour) and infrared light shining (7hours) for wetting-drying cycle.

Table1. Comparisons of capacity and ductility of corroded beam.

Beam No.	Corrosion crack width mm	Yielding capacity P_y kN	Ultimate capacity P_u kN	Ductility f_y/f_u
Beam C-0	0.0	49.11 [1.00]	51.67 [1.00]	3.84[1.00]
Beam C-1	0.5	42.51 [0.86]	49.84 [0.96]	3.23[0.84]
Beam G-1	0.5	44.35 [0.90]	48.38 [0.94]	2.44[0.63]
Beam C-2	0.8	43.03 [0.87]	46.21 [0.89]	2.75[0.72]
Beam G-2	0.8	32.21 [0.66]	36.50 [0.71]	2.30[0.60]
Beam C-3	1.2	31.90 [0.65]	33.39 [0.64]	2.13[0.55]
Beam G-3	1.2	--	21.26 [0.41]	---

2.3 Galvanostatic Method for Accelerating Corrosion

The test beam is immersed in a solution of 5% NaCl for 7 days, and then direct electric current is impressed on the steel. The position of the corroding steel bar in concrete is higher than the level of the solution for avoiding the dissolution of oxidation products. The two bars (main tensile reinforcement in the beam) act as the anode and the stainless bar in the centre of the beam section acts as the cathode. The amount of corrosion and the current density can be estimated by Faraday's law based on the corrosion degree. A current of 1A (ampere) was applied in the corrosion process. During the corrosion process, the current density should be kept constant. The process was continued until the crack width achieved the desired value shown in Table 1.

3 STRUCTURAL BEHAVIORS OF CORRODED BEAMS

3.1 Capacity and Ductility

Fig.3 and Fig.4 show the comparisons of the structural behavior between non-corroded (no corrosion) beams and the corroded beams, and shows the comparisons of the structural behavior between the beams corroded under artificial climate environment (ACE) and using the Galvanostatic method (G method) based on the corrosion crack width 0.8mm or 1.2mm. The corresponding values of capacity and ductility are shown in Table 1.

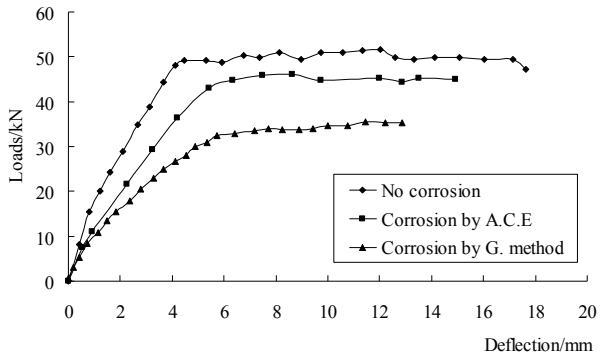

Figure 3. Comparisons of beam behavior under loading (Corrosion crack width 0.8mm)

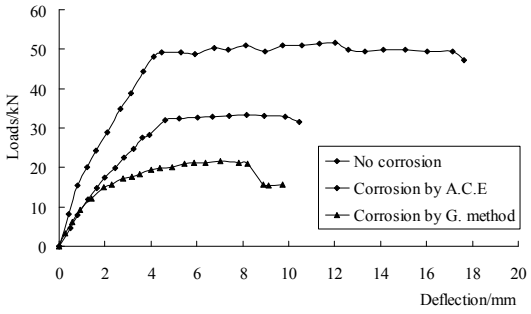

Figure 4. Comparisons of beam behavior under loading (Corrosion crack width 1.2mm)

In the Table 1, Group Beam C is corroded under artificial climate environment, Group Beam G is corroded using the Galvanostatic method; The value in **[--]** indicates ratio of the value of corroded beam and the value of no corrosion beam.

3.2 Failure mode of corroded beam

The corroded beams (Beam C-1, 2 and Beam G-1, 2) show similar failure mode. The mode shows that the tensile bar yielded first in the tension zone, and then underwent obvious plastic deformations of the bar, and finally, concrete crushed in the compression zone of the beam. This failure mode shows ductile characteristics.

When the corrosion crack width reaches 1.2mm, the comparison of failure modes between Beam C-3 and G-3 show a clear difference. Beam C-3 corroded under artificial climate environment still showed ductile failure characteristics. However, Beam G-3 corroded using the Galvanostatic method showed bond failure mode. This failure shown in Fig.5 is caused by bond failure of the main tension corroded bar.

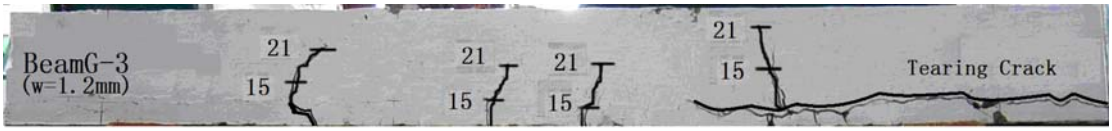

Fig. 5 Bond failure pattern

4 DETERIORATION MECHANISM OF CORRODED REINFORCED CONCRETE BEAM

4.1 Corrosion Characteristics on Surface of Steel Bar in Concrete

After the structural behavior testing, the samples for observing corrosion distribution were drilled from the beams. Figs. 6 and 7 show corrosion distribution along the surface of the steel bar under artificial climate environment and using the Galvanostatic method respectively. The corrosion shows nearly uniform distribution around the steel bar corroded using the Galvanostatic method, but the corrosion was found at the surface of the steel bar facing the concrete cover mainly under artificial climate environment.

Figure 6 Corrosion distributions under artificial climate environment

Figure 7 Corrosion distributions using the Galvanostatic method

4.2 Mechanical Behavior of Corroded Steel Bars

After the structural behavior testing, the beams were broken and the steel bars were cut and removed for testing. The mechanical behavior comparisons of the corroded bars based on the same corrosion crack width were carried out. Table 2 shows the comparison results. In the table, the nominal yield and ultimate strength are the measured tension force by the nominal section area of the steel bar. The toughness is the deformation near tension failure in the 100mm zone divided by 100mm .

The corrosion characteristic of the steel bar corroded using the Galvanostatic method is nearly uniform; the loss of the section area of the bar is main factor influencing the mechanics behavior. The pit corrosion characteristic is found on the surface of the steel bar corroded under artificial climate environment, the stress concentration of the steel bar under tension testing is main factor influencing the mechanics behavior.

Table 2. Comparisons of mechanics behavior of corroded bar.

Beam No.	Corrosion crack width mm	Nominal yield strength MPa	Nominal ultimate strength MPa	Toughness (%)
Beam C-0	0.0	373.3[1.00]	536.1[1.00]	27.5[1.00]
Beam C-1	0.5	337.9[0.91]	436.1[0.81]	22.3[0.81]
Beam G-1	0.5	340.2[0.91]	507.3[0.95]	24.2[0.88]
Beam C-2	0.8	326.4[0.87]	419.1[0.78]	18.4[0.67]
Beam G-2	0.8	306.7[0.82]	435.0[0.81]	21.5[0.78]
Beam C-3	1.2	279.5[0.75]	352.9[0.66]	16.7[0.60]
Beam G-3	1.2	273.3[0.73]	405.1[0.75]	19.8[0.72]

4.3 Deterioration of Bond Strength between Corroded Bar and Concrete

Fig.8 shows the bond strength under artificial climate environment is high than using the Galvanostatic method under the same corrosion crack width. The deterioration degree of the bond strength based on the same corrosion crack width is different between the two accelerated corrosion techniques due to the different corrosion distribution on the bar surface. The main reason is the corrosion shows on the surface of the steel bar facing the concrete cover only under artificial climate environment and shows nearly uniform distribution around the steel bar corroded using the Galvanostatic method. Therefore, the bond strength of the main tension bars in Beam C-3 was higher than that in Beam G-3, this is reason why results in different failure modes of the two beams.

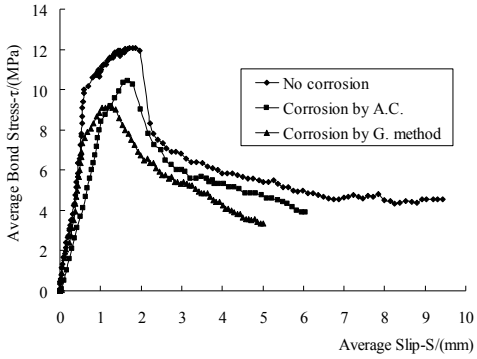

Figure 8. Comparisons of bond behavior (Corrosion crack width 0.8mm).

5 ELECTROCHEMICAL CORROSION PROCESS

5.1 Corrosion Process under Natural or Artificial Climate Environment

Chloride diffusion under natural or artificial environment is gradual processes proceeding from the concrete surface to the inside. The passivity of the steel bar facing the concrete cover is at first broken. Fig. 9 is a sketch of the corrosion process under natural or artificial environment, and shows that the anodes of electrochemical corrosion reaction is mainly located on the bar surface facing the concrete cover. Therefore, the corrosion distribution shown in Fig.6 mainly occurred on the surface of the steel bar facing the concrete cover under a natural or an artificial climate environment

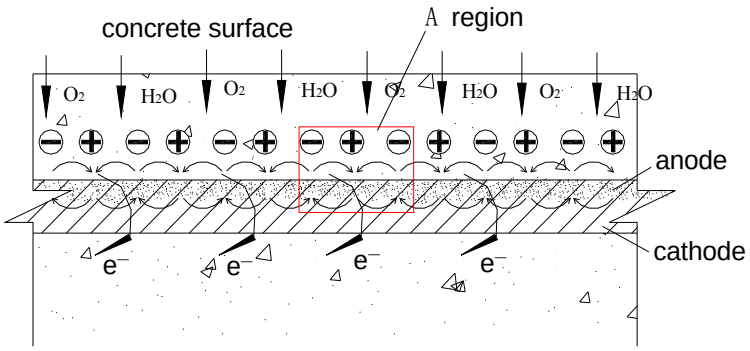

Fig 9. Corrosion process under natural or artificial climate environment.

5.2 Corrosion Process Using the Galvanostatic Method

Fig.10 shows the electrochemical process using the Galvanostatic method. In the reaction, the whole surface of the steel bar in concrete is the anode; the corrosion occurred almost entirely around the whole surface of steel. The corrosion characteristics shown in Fig.7 are almost uniform in distribution on the surface of the steel bar facing to and back of the concrete cover.

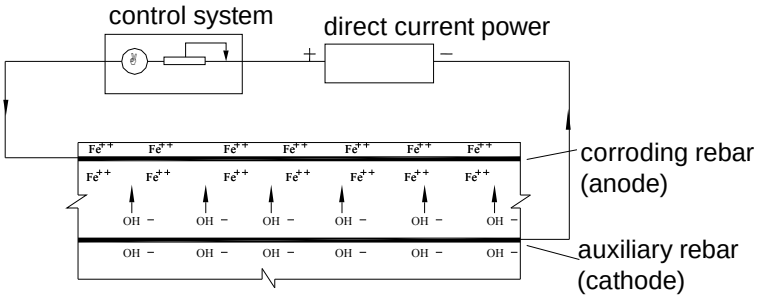

Fig 10. Corrosion process using the Galvanostatic method.

6 CONCLUSIONS

Based on the results of the experimental investigation using artificial climate environment and using the Galvanostatic method, the following conclusions are drawn:

(1) The steel bar in concrete can be corroded using the Galvanostatic method, but its electro-chemical corrosion process is different from the corrosion process under the artificial climate environment. The differences lead to different corrosion distribution on the surface of the steel bar. The corrosion mainly occurs on the surface of the steel bar on the side facing the concrete cover under artificial climate environment, however, the steel bar is corroded on the whole surface of the steel bar when using the Galvanostatic method.

(2) The corrosion of the main steel bar in the beam can reduce the bearing capacity and ductile characteristic, and can transfer the failure mode from under-reinforced beam failure to bond failure mode. Different corrosion characteristics on the surface of the steel bar, deterioration of the mechanics behavior of corroded bars and bond behavior of concrete and corroded bar are main reasons to cause the different structural behavior of the concrete beams corroded by two different methods of inducing corrosion.

(3) The corrosion process and corrosion characteristics of the steel bar under artificial climate environment are similar to that of corrosion under natural environment. Artificial climate environment as an accelerated laboratory test method is more representative than the Galvanostatic method.

ACKNOWLEDGEMENT

The authors would like to express their appreciation to the National Science Foundation of China. The research works belong to one part of the projects (50478100 and 50538070), which are supported by NSFC.

REFERENCE

Abdullah A. Almusallam, 2000, 'Effect of Degree of Corrosion on the Propereties of Reinforcing Steel Bars', *Construction and Building Materials*, 15, pp.361-368.

Chun Qing Li and Robert E. Melchers, 2005, 'Time-Dependent Risk Assessment of Structural Deterioration Caused by Reinforcement Corrosion', *ACI Structural Journal*, Vol.102, No.5, September-October, pp754-762.

Chun Qing Li, 2001, 'Initation of Chloride-Induced Reinforcement Corrosion in Concrete Structural Members-Experimentation', *ACI Structural Journal*, Vol.98, No.4, July-August, pp502-510.

CongqiFang， karin Lundgren, Liuguo Chen, Chaoying Zhu 2004, 'Corrosion Influence on Bond on Reinforced Concrete', *Cement and Concrete Research*, 34, pp. 2159-2167.

Ghassan Nounu, Zia-UL-Hasan Chaudhary, 1999, 'Reinforced concrete repairs in beams', *Construction and Building Materials*, 13, pp. 195-212.

Han-Seung Lee, Takafumi Noguchi, Fuminori Tomosawa, 2002, 'Evaluation of the Bond Properties between Concrete and Reinforcement as a Function of the Degree of Reinforcement Corrosion', *Cement and Concrete Research*, 32, pp.1313-1318.

Sanchun Yoon, Keijin Wang, W.Jason Weiss, and Surendra P. Shah, 2000, 'Interaction between Loading, Corrosion, and Serviceability of Reinforced Concrete', *ACI Material Journal*, Vol.97, No.6, November-December, pp.637-644.

Tamer A. EI Maaddawy and Khaled A. Soudki, 'Effectiveness of Impressed Current Technique to Simulate Corrosion of Steel Reinforcement in Concrete', *ASCE Journal of Materials in Civil Engineering*, Vol.15, No.1, January-February 2003, pp.41-47.

T. Uomoto, S. Misra, 1987, 'Deteriation of Concrete Beams and Columns Caused by Corrosion of Reinforcing Steel Bars', 4th International Conference on Durability of Building Materials & Components, Singapore.

W. Ahn, D.V.Reddy, 2001, 'Galvanostatic Testing for the Durability of Marine Concrete under Fatigue Loading', *Cement and Concrete Research*, 31, pp.343-349.

Yingshu Yuan, Guo Li, Dewen Jiang, 2003, 'Corrosion Rate of Rebar in Concrete', International Conference on Advances in Concrete and Struceures (ICACS), Sep. 17-19 2003, Xuzhou, China, pp. 388-373.

YuBun Auyeung, P. Balaguru, and Lan Chung, 2000, 'Bond Behavior of Corroded Reinforcement Bars', *ACI Materials Journal*, Vol. 97, No. 2, March-April, pp.214-220.

Y. Ballim, J.C. Rei, 2003, 'Reinforcement corrosion and the deflection of RC beams—an experimental critique of current test methods', *Cement and Concrete Composites*, 25, pp.625–632.

11DBMC International Conference on Durability of Building Materials and Components
ISTANBUL, Turkey 11-14 May 2008

Durability of Carbon and Stainless Steel Reinforced Concrete Members in Marine Environment

Toshihiko Yamamoto [1]
Toru Yamaji [2]
Seiji Mizuma [3]

T 11

ABSTRACT

This paper presents an experimental investigation of the carbon and stainless steel reinforced concrete beams in the marine environment exposed for five years. The corrosion resistance of carbon steels and alternative stainless steels under severe material, structural and environmental conditions was examined. Chloride was initially added to some specimens to examine the effect of internal chloride on the corrosion of steels. First, the specimens were subjected to loading and deformed to the limit displacement to examine the structural performance. The specimens had many cracks and the reinforcement yielded with scratches on the surfaces at the loading test. After that the specimens were exposed under seawater splash environment. In the exposure test an electric corrosion monitoring was conducted. The stainless steel reinforced concrete specimens with many cracks showed the outstanding durability in corrosion in the exposure test. Stainless steels were not affected by the internal and external chloride. The chloride content limit of the occurrence of corrosion for stainless steel is suggested from the test result to be more than 10 kg/m^3. In contrast, carbon steels were corroded heavily along with the cracks and lost the cross sectional area, especially in the outer lateral reinforcing bars. The monitoring was effective and in accordance with the test results. If use of the stainless steel for the structure of the marine under severe conditions is used with the monitoring system, it can become very effective.

KEYWORDS

Stainless steel, concrete, durability, chloride.

[1] Daido Institute of Technology, Department of Architecture, Nagoya, Japan 457-8532, Phone +81 52 612 5571, Fax 52 612 5953, yamamoto@daido-it.ac.jp
[2] Port and Airport Research Institute, Yokosuka, Japan, Phone +81 46 844 5010, Fax 46 841 8307, yamaji@pari.go.jp
[3] Daido Steel Co., Ltd. Kawasaki Plant, Kawasaki, Japan, Phone +81 44 266 3760, Fax 44 266 3768, D3525@so.daido.co.jp

1 INTRODUCTION

Although the life-time of concrete structures are expected to be long, the use of carbon steel does not always guarantee sufficient resistance to corrosion in severe environments. In spite of many experimental investigations of the corrosion of carbon steel have been done [Li et al. 2002, Paulsson-Tralla et al. 2002], its protection against steel corrosion has not yet been confirmed. To avoid corrosion, alternatively stainless steel can be used. Recently stainless steel reinforcements have been used in new construction and in repair work on existing structures to provide sufficient resistance to corrosion. Technical reports and standards on stainless steel have also been compiled [The Concrete Society 1998, ASTM 2001, BS 2001]. However, the information for designing and constructing stainless steel reinforced concrete structures is not sufficient. It is necessary to know the structural behaviors and corrosion resistance of stainless steel in concrete. In seismic zones, the post-yielding behaviors and the corrosion resistance of yielded stainless steel are important issues.

An experimental investigation was performed to examine the structural and durability performance of stainless steel reinforced concrete beams under severe loading and environmental conditions. First, a short-term loading test was conducted to examine the structural performance. Then, a long-term exposure test with the same short-term test specimens was conducted to examine the durability performance. Chloride was initially added to some specimens to examine the effect of internal chloride on the corrosion of steels. In the exposure test corrosion monitoring was conducted by an electrochemical investigation.

2 SPECIMENS AND MATERIALS

2.1 Specimens

The specimens are shown in Fig. 1 and Table 1. The specimens had a cross section of 180mm×300mm, 1750mm length, 1.74% flexural reinforcing ratio and 0.53% lateral reinforcing ratio. Stainless steel reinforcement was used for specimens S-1, S-2 and S-3. Carbon steel reinforcement was used for specimens N-4, N-5 and N-6. The specific concrete strength was 21 MPa for all specimens. The shear strength of the specimens was calculated by the Ohno-Arakawa equations [AIJ 1988] and exceeded the shear corresponding to the flexural strength [AIJ 1997]. In the concrete of specimens S-3 and N-6, chloride equivalent to 3.0 kg/m^3 of chlorine was added to examine the effect of internal chloride ions on steel corrosion. Two limit deformations for the loading test were set to produce different post-yielding situations of the specimens.

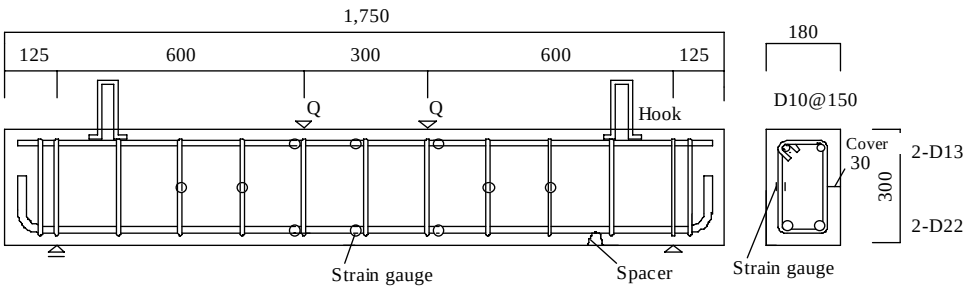

Figure 1. Specimen details (unit of length: mm)

2.2 Materials

The mix proportions and mechanical properties of concrete are shown in Tables 2. The concrete strength of the specimens was assumed to be the same as the test pieces taken at the time of casting.

Table 1. Specimens

Specimen	Reinforcement			Hoo	Pre-deflection*	Chloride
	Longitudinal	Lateral	Steel type		(mm)	(kg/ ^{3})
S-1	2-D22	D10@15	Stainless	Stainless	7.5(yield)	-
S-2	2-D22	D10@15	Stainless	Stainless	15.0(yield-crush)	-
S-3	2-D22	D10@15	Stainless	Stainless	15.0(yield-crush)	3.00
N-4	2-D22	D10@15	Carbon	Stainless	7.5(yield)	-
N-5	2-D22	D10@15	Carbon	Stainless	15.0(yield-crush)	-
N-6	2-D22	D10@15	Carbon	Stainless	15.0(yield-crush)	3.00

*yield: reinforcing bar, crush: concrete

Table 2. Mix proportions and mechanical properties of concrete.

Type	W/C	Cement	Water	Slump	Strength at 28 days		Young's modulus
					Tensile	Compressive	
	(%)	(kg/m^3)	(kg/m^3)	(mm)	(MPa)	(MPa)	(GPa)
Normal	61.2	292	178	180	2.89	24.4	21.3

Table 3. Chemical composition of stainless steel

Type	C	Si	Mn	P	S	Cu	Ni	Cr
	(%)	(%)	(%)	(%)	(%)	(%)	(%)	(%)
SUS304	0.05	0.34	1.33	0.34	0.26	-	8.11	18.39

Table 4. Mechanical properties of reinforcing steel

Type	Shape	Size	Yield Point	Tensile Strength	Elongation
		(mm)	(MPa)	(MPa)	(?)
SUS304	Deformed	22	365*	691	45.0
SUS304	Deformed	13	340*	532	45.7
SUS304	Deformed	10	395*	655	40.0
Carbon Steel	Deformed	22	370	562	22.0
Carbon Steel	Deformed	13	345	550	26.8
Carbon Steel	Deformed	10	367	573	-

*0.2% Proof Strength

and cured in a sealed condition. The strength of the concrete was 24.4MPa at the time of the loading test. Austenitic stainless steel SUS304 (Japanese Industrial Standard) was used. The chemical composition of the stainless steel is shown in Table 3. The mechanical properties of both reinforcing steels are shown in Table 4. Because stainless steels do not exhibit a well-defined yield point, the

proof strengths are determined as the stress at which the plastic strain equals 0.2% strain. The yield strengths of stainless steels and carbon steels are almost the same.

3 OUTLINE OF EXPOSURE TEST

3.1 Pre-Loaded Specimens

Before the exposure test the specimens were deformed under the load to certain limit deflections. The limit deflections at the centre of the specimens were 7.5mm (R=1/100) and 15.0mm (R=1/50), where R is the relative deflection angle between the specimen center and supports. They were assumed to be the deflections of the specimens at the fully yielded and ultimate strength, respectively. The concrete crack patterns of the specimens are shown in Fig. 2. Because the strengths of the stainless and carbon reinforcing bars were almost the same, the crack patterns were also about the same, except for the shrinkage cracks in N-6. The crack widths of the carbon steel reinforced specimens were relatively larger than those of the stainless steel reinforced specimens. The crack widths of specimens S-3 and N-6, which had the added chloride, were larger than those of specimens S-2 and N-5, which did not have chloride. The compressive side of the concrete of the 15.0mm deformed specimens crushed at the end of loading.

Table 5. Results of the loading test.

Specimen	Strength			Bar strain*			Maximum crack width	
	Calculated	Tested	Ratio	Longitudinal		Lateral	Front	Back
	cQ (kN)	eQ (kN)	eQ/cQ	Lower	Upper		(mm)	(mm)
S-1	99.5	105	1.05	y	e	e	0.55	0.60
S-2	99.5	110	1.10	y	e	e	1.20	1.20
S-3	99.5	103	1.03	y	y	e	1.50	3.00
N-4	101	103	1.02	y	y	e	1.50	1.00
N-5	101	104	1.03	y	y	e	2.50	2.50
N-6	101	98.9	0.98	y	y	e	2.00	3.00

*y: yield, e: elastic

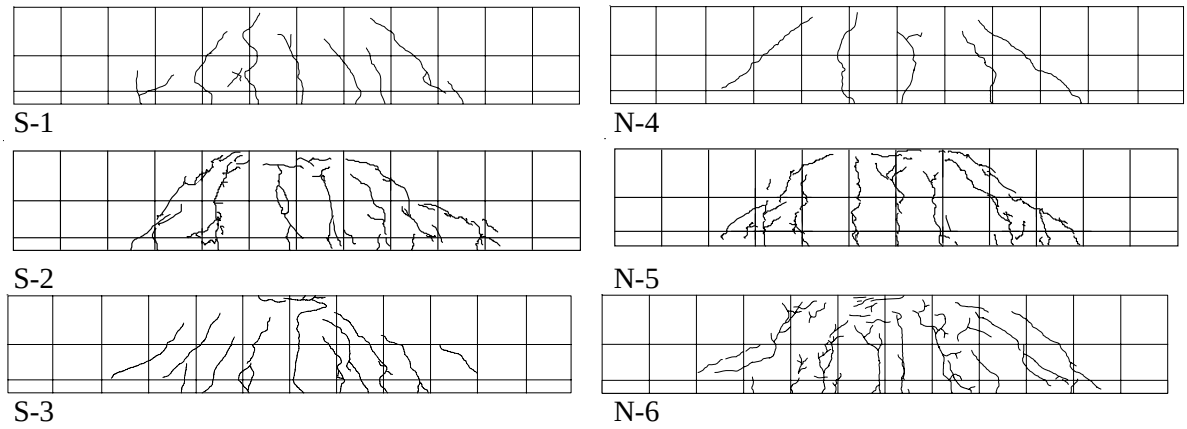

Figure 2. Crack patterns of the specimens

3.2 Test Procedures

The specimens were set on the exposure site in the Port and Airport Research Institute (Yokosuka, Japan) after pre-loading. The front face of each specimen was directed towards the sea. This test site was modeled as a splash zone in a marine environment. Seawater was splashed automatically by pumps twice a day for three hours, during the test. Visual observations and measurements of the half-cell potential were carried out periodically to investigate the corrosion of the stainless and carbon steel in the specimens. The measurement timing of the half-cell potential was three hours after the seawater splashing. The electrical connections to the steel bars in the concrete were made by a lead wire attached to the steel bars before the casting of the concrete. The reference electrode was a saturated KCl-Ag/AgCl electrode (SSE), which was placed on the concrete surface during the measurement. The probability of corrosion based on the half-cell potential is according to ASTM C876.

4 TEST RESULTS

4.1 Visual Observations and Steel Corrosion

The results of the visual observations and loss of steel cross sectional area are shown in Table 6. Three months after the exposure test, the iron rust was observed in the cracked regions of the carbon steel reinforced specimens. On the other hand no rust was observed in the stainless steel reinforced specimens. After the exposure test, specimens S-3 and N-6 (one year), S-2 and N-5 (three years) and S-1 and N-4 (five years) were broken apart to observe the corrosion condition. As time of the exposure became long, corrosion area and loss of the cross sectional area increased. No corrosion was observed in the stainless steels. The maximum loss of cross sectional area of the carbon steels increased with increase in the exposure duration. The maximum loss of the cross sectional area of the lateral bars of specimen N-4 was about one third.

Photo 1. shows the steels taken out from the inside of specimens S-2 and N-5. The carbon steels in the specimens were corroded heavily, especially in the center portion of the specimen. Figure 3 shows the corrosion area of the carbon steels of specimens N-4 and N-5. Due to the cracking, the longitudinal main bars corroded along the length. On the contrary, the longitudinal bars of the compression side only corroded near the center portion in specimen N-5 which concrete had crushed.

Table 6. Results of visual observation and steel corrosion

Specimen	Content Chloride	Exposure duration (year)	First rust (year)	Corrosion area*		Loss of cross sectional area**		
				D22 (%)	D13 (%)	D22 (%)	D13 (%)	D10 (%)
S-1	-	5.1	-	0	0	0	0	0
S-2	-	3.1	-	0	0	0	0	0
S-3	○	1.1	-	0	0	0	0	0
N-4	-	5.1	0.25	46	5	9	17	31
N-5	-	3.1	0.25	36	20	7	11	20
N-6	○	1.1	0.25	17	-	-	-	-

* Average ** Maximum

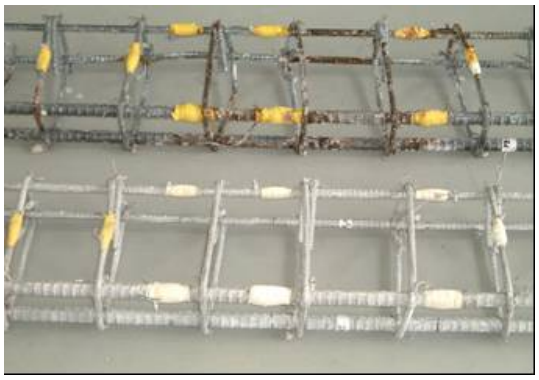

Photo 1. Steels taken out from specimens N-5 and S-2.

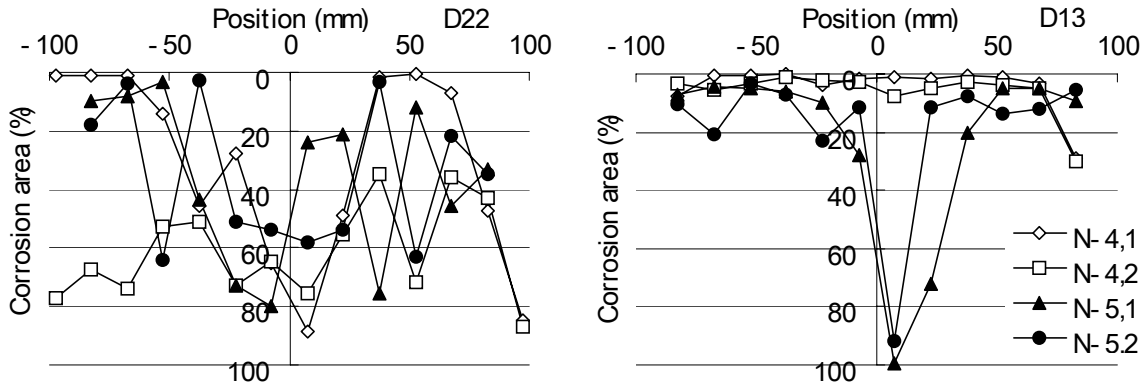

Figure 3. Corrosion area of the carbon steels

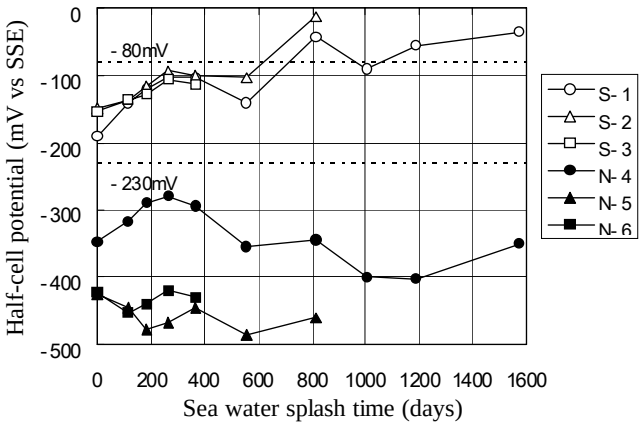

Figure 4. Changes in the half-cell potentials

4.2 Half-Cell Potentials

The changes in the half-cell potentials during the exposure test are shown in Fig. 4. These were measured in the center of the concrete specimens. The potentials of the carbon steel were more negative than –230 mV during the exposure test. The potentials of specimen N-4 which had deformed smaller deflection were more positive than those of specimens N5 and N6 with larger crack widths. The potentials of all the stainless steel reinforced specimens were more positive than the –230 mV measured during the exposure test. The half-cell potentials showed the same tendency as corrosion. Based on these results, the half-cell potentials are supposed to be useful for predicting the occurrence of steel corrosion.

4.3 Chloride Content

Concrete samples were extracted from the un-cracked part of specimen S-1 (upper and lower sides). The whole chloride content was measured by a constant-current titration way based on JCI-SC4 and is shown in Fig. 5. The chloride content was 5.0-7.0 kg/m^3 at the laterl reinforcing steel surface and 2.0-5.0 kg/m^3 at longitudinal main upper and lower reinforcing steel surface. The chloride content of each point exceeded the threshold of occurrence of corrosion (1.2kg/m^3) according to the JSCE standard specification [JSCE 2002].

The chloride content distribution of the cracked section around the reinforcing steel (crack width 0.70mm, central part of specimen S-1) was measured by EPMA (Electron Prove Micro Analyzer) and is shown in Fig. 6. The chloride content was about 10kg/m^3 except for the crack neighborhood and it was relatively high compared with that of the un-cracked concrete part. The corrosion of the carbon steel specimens was caused by this high chloride content. On the other hand, the stainless steel specimens did not corrode during the test. This result suggests that the chloride content limit of the occurrence of corrosion for stainless steel is more than 10kg/m^3.

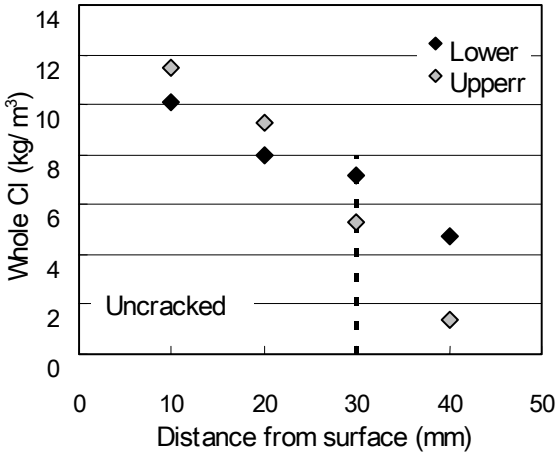

Figure 5. Chloride content of un-cracked concrete section (S-1 after five-year of exposure).

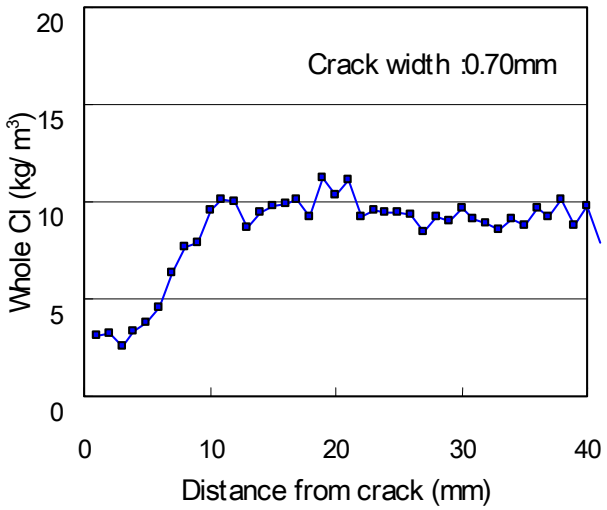

Figure 6. Chloride content of cracked concrete section by EPMA (S-1 after five-year of exposure).

5 CONCLUSIONS

Based on the loading and exposure tests conducted in this study, the following conclusions are derived.

1. The chloride content (whole chloride) of the un-cracked concrete section was 5.0-7.0 kg/m^3 at the lateral reinforcing bar surface. The chloride content of the cracked section near the longitudinal main bars varied from 3.0 to 10.0 kg/m^3.
2. The carbon steel corroded heavily due to high chloride content especially in the cracked and crushed section.
3. The stainless steel reinforced concrete specimens showed excellent durability in the exposure test. The chloride content limit of the occurrence of corrosion for stainless steel is suggested from the test result to be more than 10kg/m^3.
4. Electrochemical measurement of the reinforcing bars was effective and its results were in accordance with the visual test and broken apart results.

REFERENCES

AIJ, 1988, *Standard for Structural Calcu-lation of Reinforced Concrete Structures*, Architectural Institute of Japan, 167-176.

AIJ, 1997, *Design Guidelines for Earth-quake Resistant Reinforced Concrete Buildings Based on Inelastic Displacement Concept*, Architectural Institute of Japan, 440 pp.

ASTM A 955/A 955M-01, 2001, *Standard Specification for De-formed and Plain Stainless Bars for Concrete Reinforce-ment*, 6 pp.

BS 6744:2001, 2001, *Stainless steel bars for reinforcement of and use in concrete – Requirements and test method*, 24 pp.

JSCE, 2002, *Standard Specification for Concrete Structures-Materials and Construction: Materials and Construction*, Japan Society of Civil Engineers, 24-28.

Li C. Q., 2002, 'Initiation of Chloride-Induced Reinforcement Cor-rosion in Concrete Structural Members –Prediction, *ACI Structural Journal*, Vol.99, No.2, 133-141.

Paulsson-Tralla J. & Silfwerbrand J., 2002, 'Estimation of Chlo-ride Ingress in Uncracked and Cracked Concrete Using Measured Surface Concentrations, *ACI Structural Journal*, Vol.99, No.1, 27-36.

The Concrete Society, 1998, *Guidance on the Use of Stainless Steel Reinforcement*, The Technical Report No.51, 57 pp.

11DBMC International Conference on Durability of Building Materials and Components
ISTANBUL, Turkey 11-14 May 2008

Long-Term Preserving Effect on Aggregate-Recovery-Type Completely Recyclable Concrete

Masaki Tamura [1]
Yoshinori Kitsutaka [2]

T 11

ABSTRACT

Japan's urban areas dense with structures have reached a stage at which demolished concrete is socially required to be recycled as concrete materials for the sake of sustainable preserving of urban structures in the present. Originally, concrete which has conditions in complete recycling allows repeated recycling similarly to steel and aluminum. " Aggregate-Recovery-Type Completely Recyclable Concrete", which proposed in this study, is designed to reduce the adhesion between aggregate and the matrix to an extent that does not adversely affect the mechanical properties of concrete by modifying the aggregate surfaces beforehand, thereby facilitating recovery of original aggregate. In order to re-collect high quality recycled aggregates with ease from demolished concrete, the concrete can be made with surface coated virgin aggregate. The coating agent can be expected to have the effect of decreasing adhesive strength between aggregate and paste, but not to the extent that mechanical properties of the concrete deteriorate much. In the related studies before, it had been already explained the fundamental properties and the modifying effectiveness of the prototype aggregate-recovery type concrete, so this study was highlighted the long-term underwater preserving effects of the concrete properties, which was relatively evaluated between the specimens of 28 days and 5 years. The compressive strength, elastic modulus, changes of strain, poisson's ratio, qualities of recoverd aggregate and so on were experimentally investigated by comparison with surface modifyng of aggregates and ages of concrete. As the results, the propeties of long-term preserving concrete were adequately filled with correspondence to material ages, the surface modifying effectiveness were fully maintained, and finally it would be expected to recover the high-quality recycled aggregate with ease under the long term preserving. This enables concrete to be recycled in a fully closed system expecting the reduced waste disposal of natural resources toward the future.

KEYWORDS

Long-term preserving, aggregate recoverbility, recyclable concrete, closed system.

[1] Kogakuin University, Department of Architecture, Design in Architecture and Urbanism, 1-24-2 Nishishinjyuku, Shinjyuku, Tokyo, Japan, Phone +81 3 3342 1211, Fax +81 3 3340 0149, masaki-t@ecomp.metro-u.ac.jp
[2] Tokyo Metropolitan University, Department of Architecture, Urban Environment and Science Engineering, 1-1 Minamiosawa Hachioji, Japan, Phone +81 426 77 1111, Fax +81 426 77 2793, kitsu@comp.metro-u.ac.jp

1 INTRODUCTION

Japan's urban areas dense with structures have reached a stage at which demolished concrete is socially required to be recycled as concrete materials for the sake of sustainable preserving of urban structures [Tamura *et al*,2005]. The use of recycled aggregate concrete for structures was standardized as Japan Industrial Standard(JIS) in 2007, improving the social condition for making a step forward from conventional recycling systems [Pietersen, H.G. *et al*,1999] based solely on cascade recycling of concrete lumps for road bottoming. This trend points to level-cycling of concrete, in which concrete turns into concrete again, on the road to achieving Completely Recyclable Concrete [Tomosawa *et al*,1986] (Fig. 1).

In the process of studying Cement-Recovery-Type Completely Recyclable Concrete(CRC) shown in the figure, the authors have already materialized actual structures that can be entirely recycled into cement materials when they are demolished[Tamura *et al*,2004]. Our ongoing study intends to develop concrete from which aggregate can be readily recovered. Also, design concepts involving environmental benefits from concrete structures during their service lives, such as for planting concrete, have now reached a stage of practical use as shown in the Table 1. The production of concrete structures integrating these technologies is currently being attempted.

Under such social circumstances in Japan, the authors have investigated the possibilities of fully developing the aggregate boundary stripping effect, while ensuring certain mechanical performances intended at the design stage, of Aggregate-Recovery-Type CRC to be recycled as aggregate when demolished [Tamura *et al*,2001]. In this study, such possibilities are explored in regard to concrete preserved for a long time based on the results of previous studies, thereby investigating the technical development necessary for preserving activities to be carried out for sustainable concrete structures.

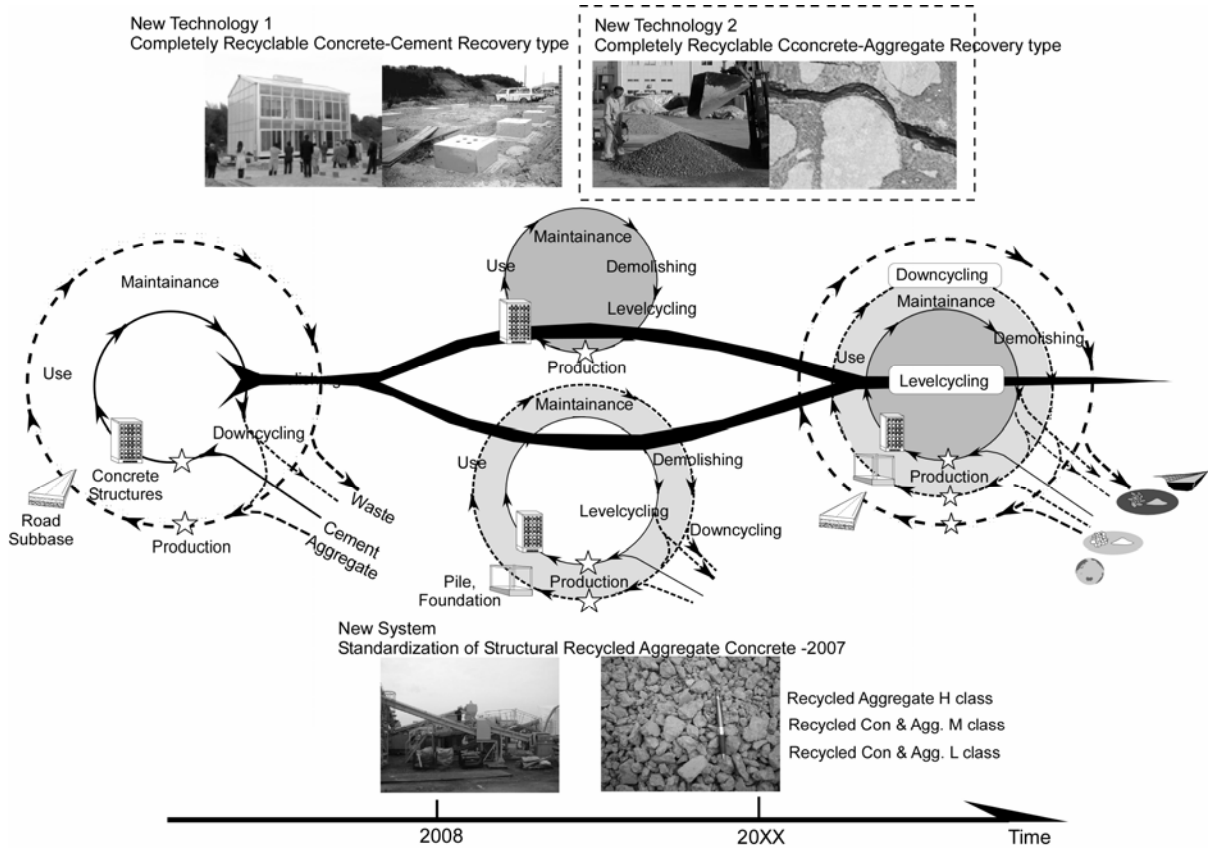

Figure 1. Sustainable concrete structure's material flow toward the future in Japan.

Table 1. The definition of Environment-harmonized concrete.

Environment-harmonized concrete refers to:

Concrete designed to improve and enhance over time the specific environments[*1] for all people involved [*2] while ensuring its basic performances[*3].

Notes

*1:Environments surrounding the whole activities related to concrete structures including the atmosphere, water, substances, flora, fauna, humans, and interrelationships among them. These include various scales of space from the global environment to local environments.

*2:All of the parties involved, such as builders including designers, constructors, and maintaining bodies, as well as users including the owner.

*3:Basic performances directly related to human physiology and safety, such as structural safety, durability, and usability.

2 AGGREGATE-RECOVERY-TYPE COMPLETELY RECYCLABLE CONCRETE

In order to circulate the entire amount of concrete in a closed system, concrete structures to be the sources of aggregate will become necessary in addition to those to be the sources of cement. “Aggregate-recovery-type CRC” is another type of concrete permitting complete recycling. It is designed to reduce the adhesion between aggregate and the matrix to an extent that does not adversely affect the mechanical properties of concrete by modifying the aggregate surfaces beforehand, thereby facilitating recovery of original aggregate. The adhesion of crushed stone with the matrix is generally stronger than that of gravel. Crushed stone therefore provides higher strength but comes with more cement paste when recovered. Also, gravel as a natural resource is being depleted. In consideration of both aspects of quality assurance and global environment protection, crushed stone is more suitable than gravel as the aggregate for surface modification.

Experiments were carried out to verify the aggregate-recoverability as described below: Table 2 gives the aggregate surface modification methods employed to easily recover original aggregate from concrete. Table 3 gives the properties of concrete components. Concrete types are listed in Table 4, while the items of experiment are given in Table 5. Three types of coarse aggregates with different particle shapes were treated chemically and physically to facilitate recovery from concrete. Chemical treatment involved inhibition of cement hydrate formation on the aggregate-paste interfaces. Physical treatment involved smoothing of minute irregularities on the aggregate surfaces to reduce mechanical friction by forming a membrane on the aggregate-paste interfaces. Surface-modified aggregate was prepared by uniformly spraying a modifier on the saturated-surface-dry aggregate, air-drying it, and then repeating the process three more times. As given in Table 4, 9 types of specimens were fabricated. The mechanical properties were measured at an age of 28 days[Noguchi and Tamura,2001] and 5 years. Finally, recycled aggregate was produced by simple crushing to grasp the recovery ratio and evaluate the quality of recycled aggregate.

Table 2. Surface modification treatments for original aggregate.

a) Chemical treatment

The principal ingredient of the coating agent is mineral oil emulsion. The agent hydrolyzes in alkali conditions of fresh concrete, forming acidic matter and indissoluble amalgam on the surface of the aggregate. The surface coating results in decreased amounts of cement hydrate, and leads to decreased adhesive strength between aggregate and paste matrix, allowing easy recovery of the original aggregate.

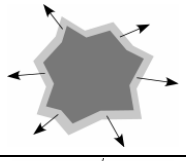

b) Physical treatment

The coating agent is a water-soluble synthetic resin emulsion, which is applied in process of abrasion, and which is chemically stable in fresh concrete. The uneven surfaces of virgin aggregate become smoother, the shape of the aggregate being roughly maintained. This has the effect of decreasing adhesive strength between aggregate and paste matrix.

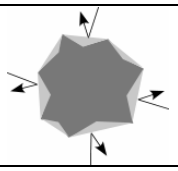

Table 3. Properties of concrete components.

Aggregate	Symbol	Type of Aggregate	Density (g/cm^3)	Water Absorption (%)	Weight of Unit Volume(kg/l)	Solid Volume for Shape Determination (%)
Fine	S	Crushed sandstone	2.62	1.71	1.44	55.8
Coarse	L	Crushed limestone	2.71	0.24	1.68	60.7
	S	Crushed sandstone	2.66	0.80	1.59	60.2
	G	River gravel	2.60	1.34	1.71	65.7

Note) Other materials: Normal Portland Cement (Density: 3.15 (g/cm^3)), Silica fume and High-range AE water reducer

Table 4. Standard mix proportions of concrete

Mark	W/B	Unit weight (kg/m^3)				
		Water	Cement	Silica fume	Fine aggregate	Course aggregate
L-series	0.28	185	613	42	621	938
S-series					629	912
G-series					525	991

Note) Each series are constituted of 3 kinds by the chemical, the physical and no treatment. The mark B notes C+SF, Mass volume of course aggregate is 0.57-0.58 m^3/m^3

Table 5. Test items and methods.

Target	Contents
Concrete	Fresh properties(Air volume, Slump) by JIS A 1128 and 1150
	Compressive strength at 28days and 5years by JIS A 1108
	Young's modulus at 28days and 5years by JIS A 1149
	Longitudinal strain, Transverse strain, Volumetric strain and Poisson's Ratio at 5years
Recycled aggregate	Recovered ratio of original aggregate
	Exfoliated ratio of original aggregate

Table 6. Experiment factors and levels.

Factor	Levels
W/C	High strength(0.3)
Fine aggregate	S
Coarse aggregate	L, S, G
Improvement method	No treatment (n), Chemical treatment (c), Physical treatment (p)
Material ages	Standard (28days), Long term (5years)

2.1 Mechanical Properties of Concrete

Figure 2 and 3 show the measured compressive strength and elastic modulus of aggregate-recovery-type CRC at two material ages of the standard 28days and long-term preserved 5 years. The compressive strength of concrete made with surface-modified aggregate decreased regardless of the material ages. As for the specimens of the standard 28 days, series G with round gravel exhibited about 10% lower compressive strength than concrete made using untreated aggregate, indicating the relatively low effect of surface modification. On the other hand, Series L and S using angular crushed stone exhibited about 25% lower compressive strengths, indicating the significant effect of surface modification. Nevertheless, the compressive strength values of specimens containing surface-modified crushed stone were evidently higher than those of specimens containing surface-modified gravel. Mechanical interlocking between the aggregate and the matrix resulting from particle shapes evidently affects the strength. A similar tendency was observed in the elastic modulus. Moreover, it would be so

significant points that these mechanical tendencies were appeared almost equal as the long-term preserved specimens.
When a surface modifier is applied, the difference in the effect of particle shapes on the mechanical properties had confirmed to be widened [Tamura *et al*,2001]. The dependence of the surface-modifying effect on the water-cement ratio was also confirmed, with high strength mortar exhibiting greater strength reduction due to surface modification after long-term preserving. This may be because the increased strength of the matrix, together with the essential strength of aggregate, causes the crack-propagation zone to be predominantly formed in the weak portions at aggregate-matrix boundaries, leading to failure at a lower stress.

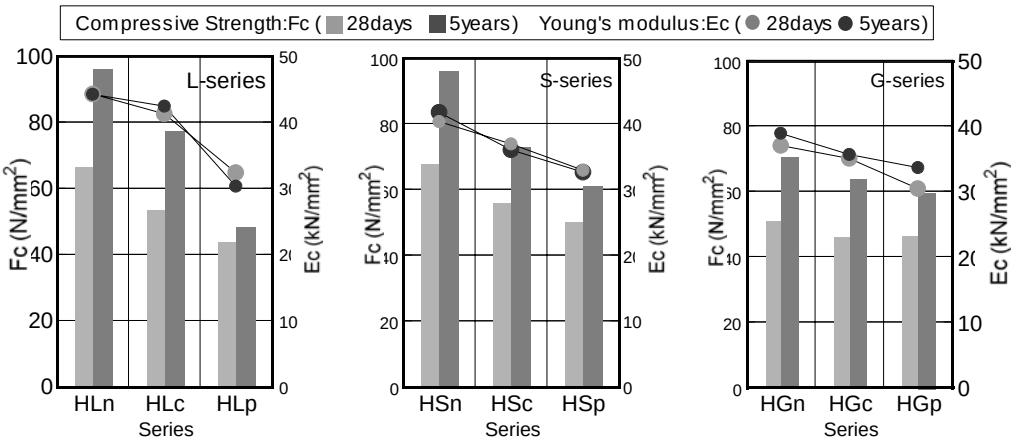

Figure 2. Relationship between Compressive strength(Fc) and young's modulus(Ec).

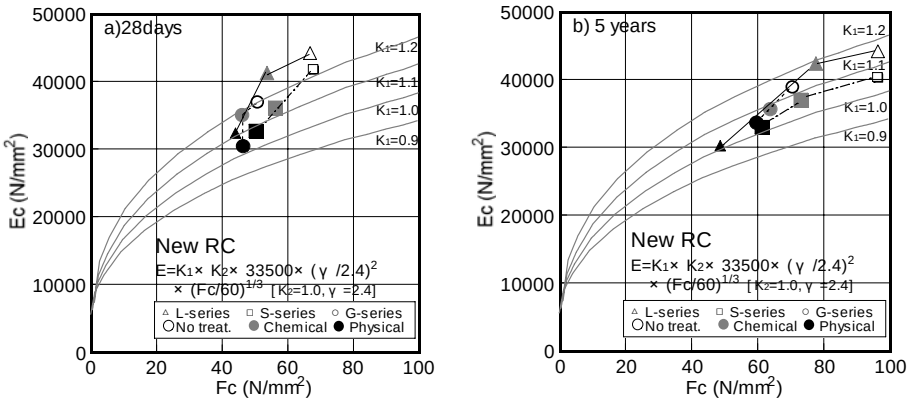

Figure 3. Relationship between Compressive strength(Fc) and young's modulus(Ec) of New RC equation.

2.2 Strain Properties of Long-Term Preserved Concrete

Figure 4 shows the Poisson's ratios related to the longitudinal strain and compressive strength, respectively. Figure 5 shows the strain distribution of concrete by each type of modification treatment. This section deals with concrete made using limestone aggregate in consideration of Japan's future aggregate availability.

Figures 4 reveal that Poisson's ratio of concrete with surface-treated aggregate increases with a strain of around 70% of the maximum strain of concrete with untreated aggregate, leading to an expansion phenomenon as Poisson's ratio exceeds 0.5. The compressive strength significantly decreases to around 75% and 50% with chemical and physical treatments, respectively. It can be said that deformation properties that are characteristic of modification and explicable by Poisson's ratio are present under compressive stress. On the other hand, these properties represent the aggregate surface stripping effect

being retained, which can be regarded as basic information for efficiently developing the confining effect of reinforcement.

The strain distribution shown in Fig. 5 includes the volumetric strain that expresses the volumetric changes of the entire substance in addition to the longitudinal and transverse strains. When focusing on a rectangular solid part of a homogeneous body, the volumetric strain expressed by Eq.(1) generally holds on the assumption that the strains in all directions are equal. By observing the volumetric strain, the point at which an unstable failure condition begins can be recognized. At this point, cracks on the aggregate boundaries predominate, connecting one another into major cracks in the process in which Poisson's ratio departs from around 0.2 and the stress conditions turn to expansion, with the volumetric strain turning to negative. When aggregate is untreated a), the volumetric strain does not turn to expansion until immediately before failure due to the effect of chemical bonding on the boundaries, which is characteristic of crushed limestone. Though this poses no problem in regard to the mechanical properties of concrete, such a concrete is prone to brittle failure, resulting in a low possibility of recovering aggregate. On the other hand, when aggregate is treated [b] and c]], the crack onset point, at which the volumetric strain turns to expansion due to the boundary stripping effect, is clearly recognized, indicating the occurrence and progress of internal cracks. This suggests a possibility of avoiding brittle failure characteristic of high strength concrete. In such a case, the development of a crack deflection effect, with which cracks are deflected along the aggregate boundaries, is also inferred, suggesting the retention of properties beneficial for increasing the aggregate recoverability even under compressive stress.

$$\varepsilon = 3(1-2\upsilon)\sigma/E \quad (1)$$

where υ *: Poisson's ratio*

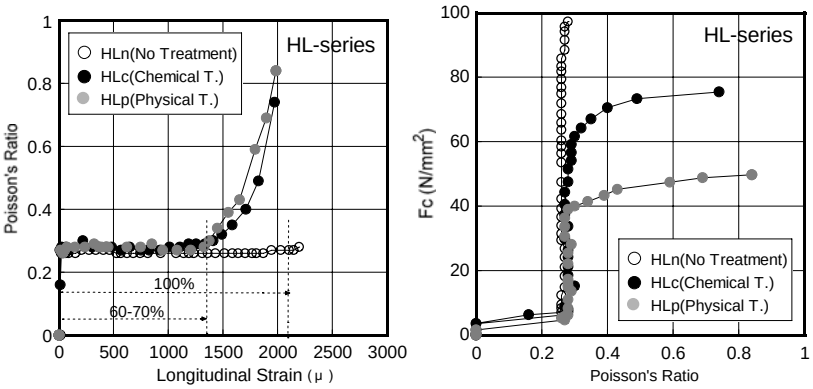

Figure 4. Poisson's ratios related to the longitudinal strain and compressive strength.

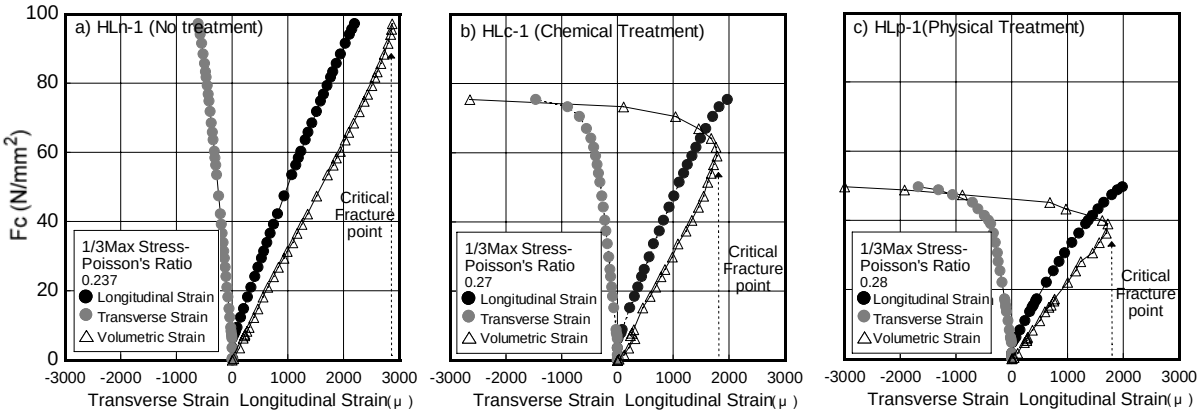

Figure 5. The strain distribution of concrete by each type of modification treatment.

2.3 Paste-Exfoliating Properties of Aggregate

The properties of cracked surfaces of concrete with aggregate surfaces modified to facilitate aggregate recovery were investigated to study the paste-exfoliating effect of surface modification.
Specimens were the same as those used in the experiment for mechanical properties. Binarized images of two-dimensional photographs of ruptured surfaces were also used to calculate the areas of stripped aggregate surface and cracked aggregate surface by image analysis to quantify the paste-exfoliating effect using Eq.(2). Figure 6 shows a binarized image distinguishing the mortar phase from aggregate phase of a cracked surface. Figure 7 shows the ratio of the area of stripped aggregate to the total ruptured surface.

$$R = Sp/(Sc+Sp) \times 100 \quad (2)$$

where R : Ratio of aggregate exfoliating (%)

Sp : Area ratio of stripped aggregate (%)

Sc : Area ratio of splitted aggregate (%)

When surface-modified aggregate is used, the ratio of aggregate exfoliating was greater than the case of untreated aggregate. This tendency was more evident with angular aggregate. In other words, both chemical and physical surface treatment of crushed stone aggregate led to less cracking through aggregate particles and more split along the aggregate-matrix boundaries than in the case of untreated crushed stone. This phenomenon was not observed in the case of concrete containing gravel. Accordingly, surface modification of aggregate was found to cause cracking to detour to weak boundaries between aggregate and the matrix, suggesting the possibility of easy separation of aggregate from the matrix.

These results of experiments indicate that the effect of aggregate surface modification is maximized when coarse aggregate having a low solid percentage to judge the particle shape, such as crushed stone, is used in a matrix having a high strength. Such a concrete, which normally poses a difficulty in recovering high-quality recycled aggregate, is expected to contribute to the increase in the aggregate recovery ratio and quality of recycled aggregate by surface modification treatment of aggregate.

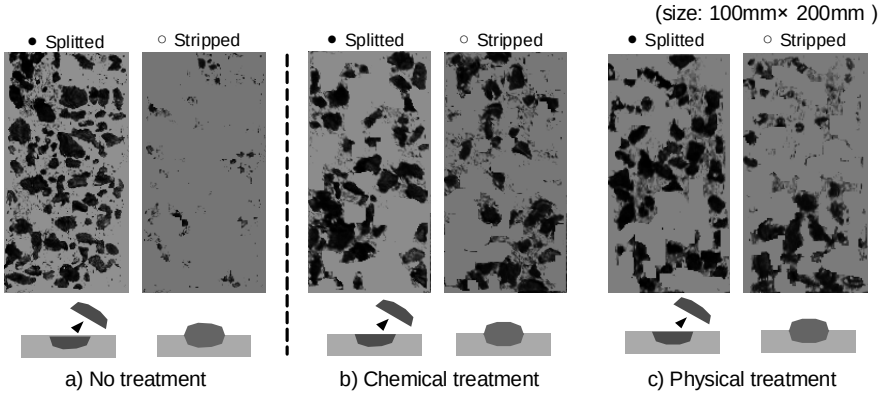

Figure 6. Image on the side of cracked concrete of Long-term-preserving CRC.

2.4 Recovery of Original Aggregate from Demolished Concrete

The same concrete as that used in the mechanical property tests was subjected to aggregate-recovery tests. Concrete was crushed in a two-phase process. The primary crushing was carried out using an improved jaw crusher having a mechanism that scrubs aggregate particles. The entire amount of the crushed aggregate was charged into a ball mill and subjected to scrubbing (secondary crushing) for a specified length of time. Recycled coarse aggregate 5-20 mm in diameter was sifted out of the

produced recycled aggregate to measure the density and water absorption. The percentage by mass of the original aggregate in the total recycled coarse aggregate was defined as the aggregate recovery ratio, and the value was determined.

Figure 7 shows the original aggregate recovery ratio of each concrete. The aggregate recovery ratio of concrete containing crushed stone was increased by aggregate surface modification regardless of the strength. The effect of chemical treatment was particularly evident. On the other hand, the effect of aggregate surface treatment was less evident in concrete containing round aggregate. No appreciable difference was observed between the aggregate recovery ratios of treated and untreated gravels in high strength concrete. Similar results were obtained for the density and water absorption of recycled aggregate. Improved quality of recycled coarse aggregate was confirmed when the aggregate was surface-treated.

In order to improve the resource conservability of aggregate in concrete, it is effective to use surface-treated aggregate. Though such a concrete generally tends to exhibit slightly low mechanical properties in the plastic zone, such as compressive strength, the separation of aggregate from the matrix can have a favorable effect from the standpoint of fracture mechanics in some cases. For instance, fracture of concrete can be made ductile by detours of cracking towards the aggregate-matrix boundaries in the case of certain aggregate types and water-cement ratios [Tamura *et al*,2001]. The surface treatment realizes recovery of high quality recycled aggregate with little adhering paste from demolished concrete by a simple crushing technique.

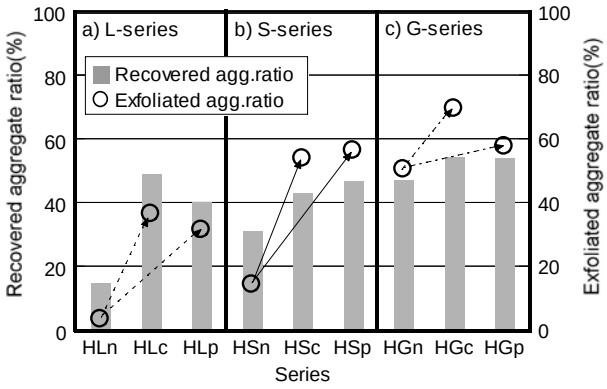

Figure 7. Area ratio of aggregate on the side of cracked concrete.

3 CONCLUDING REMARKS

Through the research and development for concrete recycling and investigation of the difficulties and problems of recycling practice for a long time, the authors learned that the above-mentioned two methods are vital for recycling to hold in Japan.
Efforts for closed-loop recycling have also begun in the fields of glass, gypsum board, and other construction materials. This trend will prevail in all fields in the future, eventually leading to a society in which materials recyclable in closed loops or disposable in a nature-friendly form expel those that are not, as in the case of chlorofluorocarbons driven out of the market.

ACKNOWLEDGMENTS

The authors express their gratitude to the TOSTEM scholarship foundation, the young encouragement scholarship of Tokyo Metropolitan University and Mr. Minoru Takahira (Past undergraduate student of Tokyo Metropolitan University) for their a part of support.

REFERENCES

Tamura, M., Noguchi, T. & Tomosawa, F. 2005, 'Environmental Aspects of Concrete Structures in Sustainable Society', 10DBMC International Conférence On Durability of Building Materials and Components, Lyon, 17-20.

Pietersen, H.G. & Hendriks, C.F. 1999, 'Toward Large Scale Application of Recycled Aggregate in the Construction Industry, European Research and Developments', Proceedings of the Fourth International Conference on Eco materials, Gifu, 217-221.

Tomosawa, F. & Noguchi, T. 1996. 'Towards Completely Recyclable Concrete', *Integrated Design and Environmental Issues in Concrete Technology*, E & FN SPON, 263-272.

Tamura, M., Tomosawa, F. & Noguchi, T. 2004, 'Cementitious-Waste-Free-Type Completely Recyclable Concrete', RILEM International Symposium on Environment-Conscious Materials and Systems for Sustainable Development ECM2004, 61-72.

Tamura, M., Tomosawa, F. Noguchi, T. & Kitsutaka, Y. 2001, 'Concrete Design toward Complete Recycling', Proceedings of fib international Symposium, Concrete and Environment, Berlin,Vol.1.

Testing of Concrete Specimens by Means of Non-Linear Ultrasonic Spectroscopy

Marta Korenska [1]
Michal Matysik [2]
Lubos Pazdera [3]
Monika Manychova [4]

T 11

ABSTRACT

On the basis of non-linear effect studies, new diagnostic and defectoscopic methods have been designed, which are based on the elastic wave non-linear spectroscopy. The non-linear acoustic spectroscopy brings new prospects into the acoustic non-destructive testing of material degradation. Poor material homogeneity and, in some cases, shape complexity of some units used in the building industry, are heavily restricting the applicability of "classical" ultrasonic methods. These linear acoustic methods focus on the energy of waves, which are reflected by structural defects, variations of the wave propagation velocity or changes in the wave amplitude. However, none of these "linear" wave characteristics is as sensitive to the structure defects as the specimen non-linear response. In this way, non-linear methods thus open new horizons in non-destructive ultrasonic testing, providing undreamed-of sensitivities, application speeds and easy interpretation. One of the fields in which a wide application range of non-linear acoustic spectroscopy methods can be expected is civil engineering. It is predicted that these advanced techniques can contribute a great deal to the improvement and refinement of the defectoscopic and testing methods in the building industry practice. The present paper deals with analyzing one of the non-linear acoustic defectoscopic methods from the viewpoint of its application to the concrete specimen structural integrity evaluation. Both intact specimens and specimens subject to various kinds of stress have been tested. The effect of structural defects on the elastic wave propagation has been studied.

KEYWORDS

Non destructive testing, non linear ultrassonic spectroscopy, concrete, structural integrity.

[1] Brno University of Technology, Faculty of Civil Engineering, Department of Physics, Zizkova 17, 602 00 Brno, Czech, Phone +420541147657, Fax +420541147666, korenska.m@fce.vutbr.cz
[2] Brno University of Technology, Faculty of Civil Engineering, Department of Physics, Zizkova 17, 602 00 Brno, Czech, Phone +420541147664, Fax +420541147666, matysik.m@fce.vutbr.cz
[3] Brno University of Technology, Faculty of Civil Engineering, Department of Physics, Zizkova 17, 602 00 Brno, Czech, Phone +420541147657, Fax +420541147666, pazdera.l@fce.vutbr.cz
[4] Brno University of Technology, Faculty of Civil Engineering, Department of Building Structures, Veveri 95, 602 00 Brno, Czech, Phone +420541147431, manychova.m@fce.vutbr.cz

1 INTRODUCTION

Thanks to the stormy development of concrete and reinforced concrete buildings taking place in the last century, the condition of concrete and reinforced concrete became a hot topic in the last decade. Concrete proved to be a durable construction material in the past, however, concrete structures often experienced degradation after years of service. Rehabilitation techniques have been developed in foreign countries for several decades showing a rapid development in general. However, the absence of an acceptable, relatively fast and cheap monitoring method, which would be capable of detecting structure faults at an early stage, thus making a simple and cost-effective maintenance possible, is still persisting [Maceck 2003].

Filling this gap, acoustic testing methods, rank among the most promising methods of building element and structure diagnostics. Non-linear ultrasonic spectroscopy methods are opening new horizons in the non-destructive acoustic testing of material degradation.

2 NON-LINEAR ULTRASONIC SPECTROSCOPY

On the basis of non-linear effect studies, new diagnostic and defectoscopic methods have been designed, which are based on the elastic wave non-linear spectroscopy. Existing linear acoustic methods focus on the energy of waves reflected at structural defects, analyzing the reflected wave energy, wave velocity or amplitude variations. It is to be emphasized, however, that none of these linear wave characteristics is as sensitive to the structural defect occurrence as the non-linear response of the material.

Recently, various papers are being published on the theoretical or experimental verification of different methods in some application areas. One may state that, on the one hand, and, regarding the topic complexity, the requirements for newly developed special instrumentation and a high potential application diversity, the research and development of the respective methods, the required instrumentation and, last but not least, practical applications of these methods, is still in its infancy. On the other hand, most published papers as well as our experience show these methods to be highly promising for both the defectoscopy and the material testing purposes in the near future.

One of the fields in which a wide application range of non-linear acoustic spectroscopy methods may be expected to take place is civil engineering. Poor homogeneity of materials and in some cases also intricate shape of the specimens, restrict heavily the applicability of the classical ultrasonic methods. Precisely these non-linear acoustic defectoscopy methods are less susceptible to the mentioned restrictions and one may expect them to contribute a great deal to further improvement of the defectoscopy and material testing in civil engineering.

2.1 Non-Linear Spectroscopic Methods

Non-resonance methods are used to study suppressed resonance specimens. These methods analyse the effect of non-linearities on acoustic signals propagating through them. These methods can again be split into two groups:

- measurements using a single harmonic ultrasonic signal (a single frequency f_1)
- measurements using multiple harmonic ultrasonic signals (usually, two frequencies f_1, f_2).

We pay attention to single harmonic ultrasonic signal measurement method which was used in experimental part. In this case, where a single exciting frequency f_1 is used (Fig. 1), the non-linearity gives rise to other harmonic signals, whose frequencies f_v obey the Fourier series formulas:

$$f_v = n f_1 \quad | \; n = 0, 1, 2, \ldots \infty \tag{1}$$

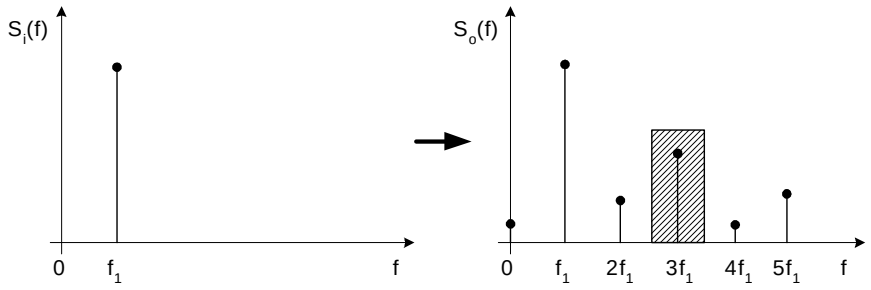

Figure 1. Frequency spectrum of a non-linear medium response

In general, these frequency component amplitudes are falling when the harmonic order natural number, *n*, is increasing. If the non-linearity effect is not entirely symmetrical, there can arise low-amplitude second and higher even-numbered harmonic components, whose amplitudes may be much lower than those of the odd-numbered ones. Among these emerging components, the third harmonic is the most distinctive one [Hajek and Sikula 2004]. Therefore, its amplitude is being evaluated most frequently.

2.2 Measuring Apparatus

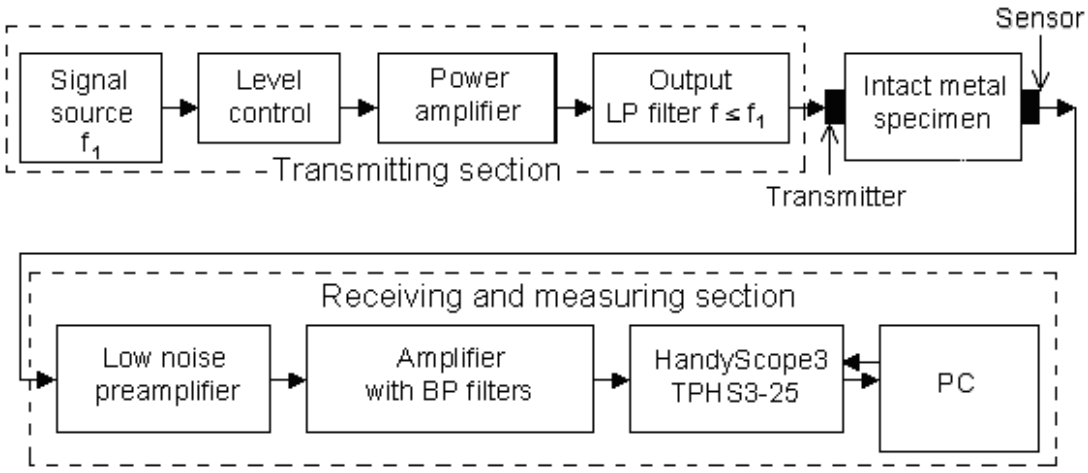

Figure 2. Block diagram of the measuring apparatus

Receiving section consists of piezoceramics sensor, low noise preamplifier with classical or differential input connector, amplifier with band - pass filters. These output signal are used for final evaluating. The starting measures were realized by normal spectral analyser in our case oscilloscope HandyScope3 TPHS3-25.

For the recorded data to be interpreted properly, each of the measuring instruments must meet following criteria [Prevorovsky and Abeele 2004]:

- High linearity of all instruments (generators, amplifiers, sensor, transmitter,…).
- High resolution in the frequency domain.
- High dynamic range (90 to 130 dB).
- Highly efficient filtration of detected signals (fundamental frequency suppression).
- Frequency range 10 kHz to 10 MHz.
- Optimized sensor and transmitter location.

A program package to control the measuring process and the data processing and evaluation makes an indispensable tool.

3 EXPERIMENT

3.1 Intact Concrete Specimens

In the first stage of the experiment, we tried to find out whether the high inhomogeneity of the material gives rise or does not give rise to non-linear phenomena. Two groups of specimen denoted A, B, featuring the same concrete mix charge. Each group comprised 10 specimens of dimensions 150 mm × 150 mm × 150 mm, the A group specimen having been aerated, the B group ones, non-aerated.

3.1.1 Measurement Results

Fig. 3 shows the results obtained from A-group specimens. It shows the frequency spectrum of the A3 specimen response to the harmonic ultrasonic excitation at a frequency of 29 kHz, as captured by K33 sensor. First five harmonic frequencies appear to be emphasized, their amplitudes decreasing with the serial number *n*. Similar results have been obtained from B-group specimens, as is seen in Fig. 4, showing the frequency spectrum of B4 specimen. Comparison of the diagrams show that aerated specimen of the A-group suppress the higher harmonic frequencies more intensely, which is apparently due to the air pores in the specimen structure. All of the specimens tested showed the same amplitude decreasing trend for the harmonic frequency increasing order.

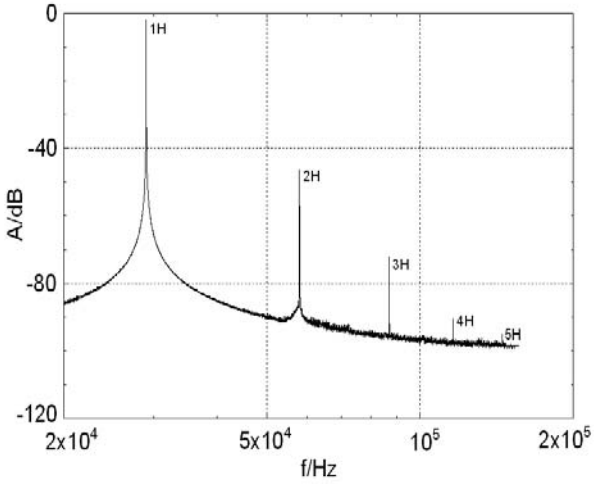

Figure 3. Frequency spectrum of A3 specimen.

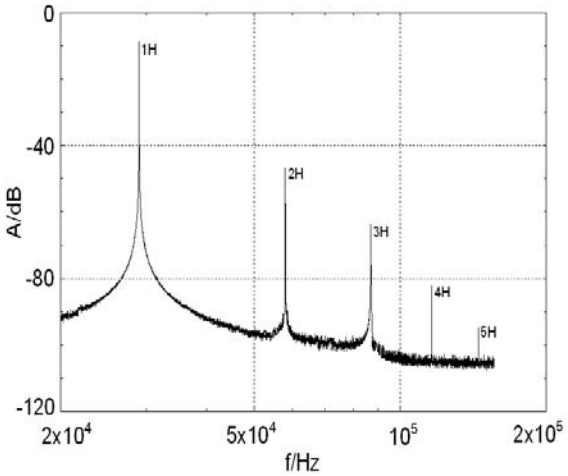

Figure 4. Frequency spectrum of B4 specimen.

3.2 Freeze-Thaw Cycle Degraded Concrete Specimens

In the second stage, we studied the concrete specimen structure having been stressed by thermal shocks. The concrete specimens were stressed by recurrent freeze-thaw cycles. Measurements were realized after 25 and 50 freeze-thaw cycles.

3.2.1 Measurement Results

The curve shown in Fig. 5 shows the A2 specimen's pre-degradation frequency spectrum. Its shape features a gradual amplitude drop, without any non-linear effects. The transfer characteristic, Fig. 6, which corresponds to the same specimen having been subjected to 25 freeze-thaw cycles, does show a non-linearity. It is becoming evident from a distinct drop of the fourth harmonic's amplitude (4H), which is exceeded by the fifth harmonic's amplitude (5H). The frequency spectrum shown in Fig. 7, corresponding to the specimen having undergone 50 freeze-thaw cycles, shows non-linearities, too. In this case, they consist in a drop of the third harmonic's amplitude and an increase of the fourth harmonic (4H). Fig. 8 shows the high harmonics' amplitudes relative to the first harmonic's amplitude for A2 specimen.

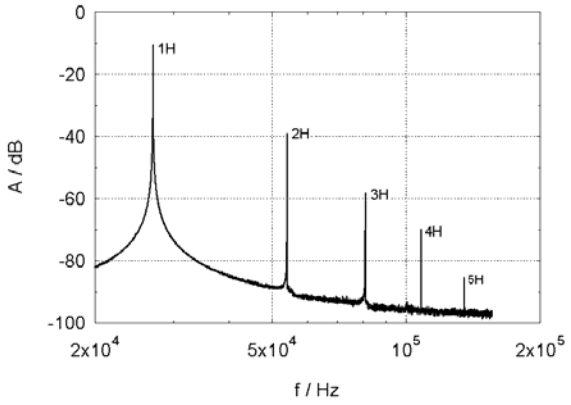

Figure 5. A2 specimen prior to degradation.

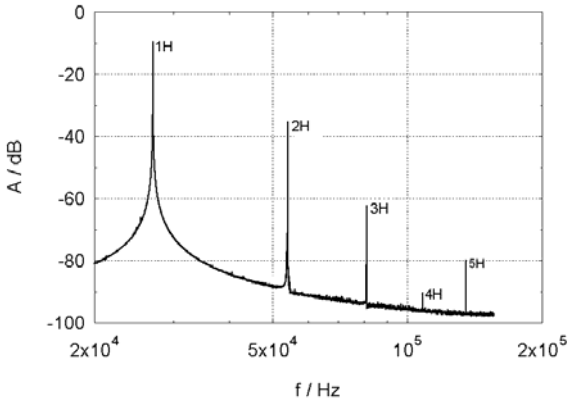

Figure 6. A2 specimen after 25 cycles.

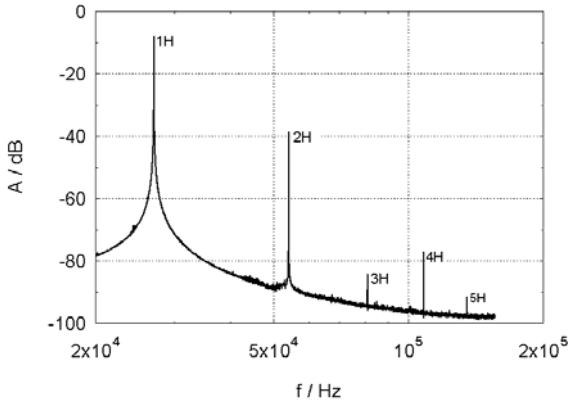

Figure 7. A2 specimen after 50 cycles.

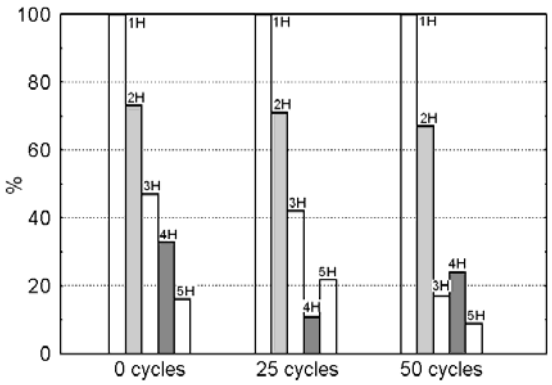

Figure 8. Relative amplitude values.

3.3 Polymer-Fibre-Filled Concrete Specimens

Finally, we tested concrete specimens of dimensions 100 mm x 100 mm x 400 mm which had been filled with polymer fibres. The specimens were examined for flexural tensile strength in a two-weigh pressing machine. The load test was terminated as soon as visible cracks appeared. These cracks closed again after the strain had been taken off. In the case of TP7 specimen a visible crack remained after the specimen had been relieved. The transmitter and sensor configuration is shown in Fig. 9.

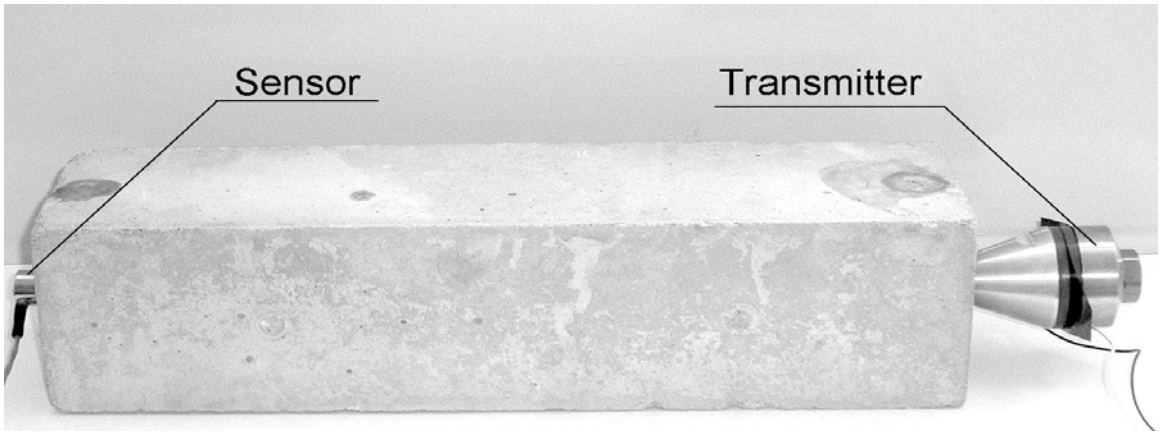

Figure 9. Location of the exciter and the sensor on the specimen under test.

3.3.1 Measurement Results

Pre-test measurements of TP7 specimen are shown in Fig. 10. The shape of the frequency spectrum corresponds to that of intact specimen and higher harmonic amplitudes are decreasing with their serial number. Fig. 11 shows the frequency spectrum of the same specimen after load test has been carried out in the pressing machine. When compared with Fig. 10, the response function shows the higher harmonic frequencies to have lower amplitudes. The fifth harmonic has disappeared entirely which is probably due to the structure-degradation-induced higher attenuation. Another change consists in emphasizing the second harmonic's amplitude with respect to the first harmonic as well as the third and fourth harmonic.

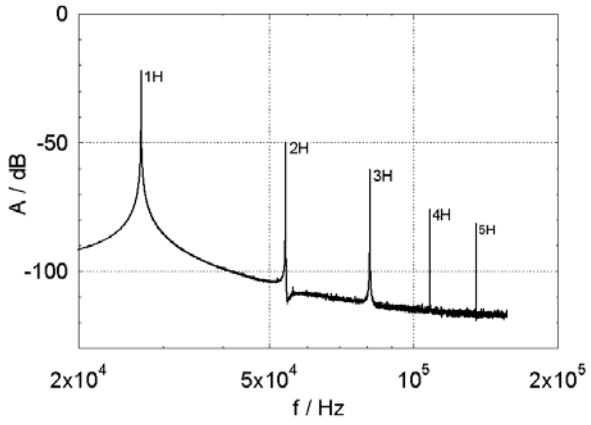

Figure 10. Pre-test frequency spectrum of TP7 specimen

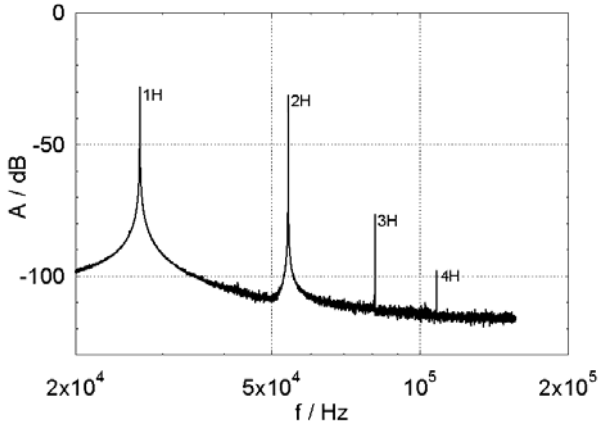

Figure 11. Frequency spectrum of TP7 specimen after load test

4 CONCLUSION

This paper presents our first results of concrete specimen structure testing by means of non-linear ultrasonic spectroscopy using a single exciting harmonic frequency.

To interpret properly the measuring results, the transfer function of the whole measuring set-up must be determined and all measuring instruments must comply with high quality standards. It is therefore essential to minimize any harmonic distortion in the signal pick-up and amplification path by eliminating any spurious signals ($3\,f_1$ parasitic signal, noise) from the measuring apparatus stages. It is to be noted that a perfect mechanical coupling must be ensured between the exciter and the specimen and, further, between the specimen and the pick-up element during the experiment setup process.

Our measurements show that the effect of a material inhomogeneity is very low in the case of non-linear ultrasonic spectroscopy, its non-linear effect being substantially lower than in the case of common defects.

Furthermore, it has been proved that structure defects, which are due to the freeze-thaw cycles as well as mechanical strain, give rise to non-linear effects.

In conclusion, it is to be emphasized that a perfect mechanical coupling must be ensured between the exciter and the specimen and, further, between the specimen and the pick-up element during the experiment setup process.

ACKNOWLEDGMENTS

This research is supported by GA ČR 103/06/1711 and MSM 0021630511 projects.

REFERENCES

Hajek, K. & Sikula, J. 2003, 'Testing of Low-Current Contacts Quality and Reliability by Using Third Harmonic Distortion', Proc. 45th- IEEE Holm Conference, Washington, September 2003, p. 211-213.

Převorovský, Z. & Van Den Abeele, K.E. 2004,'Calibration Samples for Use in Nonlinear Ultrasonic Spectroscopy' Proc. 34th International Conference and NDT Technique Exposition Defektoskopie 2004, November 3-5, Špindlerův Mlýn, Czech Republic, 347 - 349.

Macecek, M. 2003, 'Ultrasonic Concrete Testing', Defektoskopie 2003, 33rd International Conference, November 19-21, 2003, Ostrava, Czech Republic, 117-132.

11DBMC International Conference on Durability of Building Materials and Components
ISTANBUL, Turkey 11-14 May 2008

A Tool for Strength Durability Modelling of Glass Fibre Reinforced Concrete

Petra Van Itterbeeck [1]
Heidi Cuypers [1]
Phil Purnell [2]
Jan Wastiels [1]

T 11

ABSTRACT

Concrete composites with high ductility can be obtained by reinforcing cement pastes or mortars with fibres. When a glass fibre textile reinforcement is used in a cementitious matrix, the load bearing capacity of the concrete can be enhanced in such a way that steel reinforcement can be omitted. However, even today these concrete composites are subject to degradation of their mechanical properties with ageing, especially in a wet environment. Loss of tensile strength is the most important manifestations of this ageing. Over the years many researchers have tried to model the strength durability. Several models will be presented and discussed within the scope of this paper. Generally the prediction of the service life of GRC composites in various climates is essentially performed with an accelerated ageing technique. Immersion in water for various periods of time and at various temperatures going from 20°C to 80°C is the most commonly used accelerating environment. The changes in the mechanical properties induced by such an exposure are then assessed. These tests are widely used to evaluate and predict the long term durability. It is however not clear how many accelerating temperatures and time/temperature points are needed to achieve a reliable prediction taking into account the strength prediction model used, the number of specimens utilized to obtain the avaraged time/temperature points and the scatter inherently present on the tested specimens. Therefore it is the aim of this paper to present a theoretical procedure which allows the reader to establish how large the uncertainty is on a long-term real life prediction taking into account all parameters elaborated above.

KEYWORDS

Strength durability, GRC, Durability modelling

[1] Vrije Universiteit Brussel, Faculty of Engineering, Mechanics of Materials and Constructions (MeMC), 1050 Brussels, Belgium, Phone +32 2 629 28 98, Fax +32 2 629 29 28, petra.van.itterbeeck@vub.ac.be
[2] University of Warwick, School of Engineering, Coventry CV4 7AL, United Kingdom, Phone +44 (0)24765 28392, pp@eng.warwick.ac.uk

1 INTRODUCTION

By reinforcing cement pastes with fibres, composites with improved ductility can be obtained. Moreover, when using a glass fibre textile reinforcement in cement the mechanical properties of the composite can also be improved in such a manner that it becomes a very suitable material for the production of thin elements with variable shapes. Unfortunately, these concrete composites are subject to degradation of their mechanical properties with ageing (Litherland *et al.* [1981], Purnell *et al.* [2001], Orlowsky [2005]), especially in wet environments. The most important manifestation of this ageing is the loss of tensile strength. Many have tried to determine the mechanisms which govern this ageing in order to further improve the strength durability. Following main mechanisms were identified: (1) chemical attack of the fibre, (2) growth of hydration products, (3) static fatigue. Improved materials have been developped of which the durability now needs to be predicted to enable the use in for instance structural applications.

The aim of this paper is to provide a helpful tool for researchers when faced with durability testing of Glass fibre Reinforced Concretes (GRC). Following questions will be treated: (1) which predictive models are available, (2) how is durability testing performed and (3) how many experiments need to be performed within an accelerated ageing testing program (how many accelerated ageing temperatures and data points within each temperature series) for a reliable prediction. To achieve this goal, first of all an overview will be given of the in literature available strength durability models and durability test programs for GRCs. In the second and main part of this paper a method will be presented to evaluate the sensitivity of the different strength durability models towards scatter on the measurements. This method will enable the reader to select a testing program that will provide a trusthworthy prediction of the strength durability. For illustrative purposes this method will be used on one of the models and the results will be discussed in some detail.

2 STRENGTH DURABILITY MODELS FOR GRCs

2.1 Background on the Different Strength Durability Models

Recent durability studies on GRCs (Purnell *et al.* [2001], Orlowsky [2005], Cuypers *et al.* [2006] and Cuypers and Orlowsky [2007]) assume a certain physical background is responsible for the strength losses recorded. They state that the failure stress will decrease with time due to the growth of flaws (nano-defects) inherently present on the surface of the glass fibres. The bulk failure stress of the glass fibres can then be calculated as a function of the flaw size and geometry of the largest flaw present in the fibre and this with the help of classical elastic fracture mechanics:

$$\sigma_t = \frac{K_{IC}}{A \cdot \sqrt{\pi \cdot a}} \tag{1}$$

Where: σ_t is the bulk tensile strength at time t (*in MPa*)
K_{IC} is the critical stress intensity factor (Mode I) (*in* $Nm^{-3/2}$)
A is a shape factor (*dimensionless*)
a is the flaw size at time t (*in nm*)

If one assumes that the critical stress intensity factor and the shape factor are invariable with time, the following general expression for the residual strength (S) can be constructed with the help of Equation 1:

$$S = \frac{\sigma_t}{\sigma_{t=0}} = \frac{1}{\sqrt{1 + \frac{X}{a_0}}} \quad \text{with:} \quad a = a_0 + X \tag{2}$$

Where: a_0 is the initial flaw size (*in nm*)
X is the flaw growth over a time span t (*in nm*)

σ_t is the failure strength at time t (*in MPa*)
$\sigma_{t=0}$ is the initial failure strength (*in MPa*)
S is the residual strength (*dimensionless*)

The presence of moisture and pH have been recognised by several authors as accelerating factors for this flaw growth. Starting from the basic assumptions described above, several models were constructed over the years. In this paper four of these models will be referred to as: (1) the kinetic model, (2) the diffusion model, (3) the non-linear model and (4) the combined model. The essential difference between these models is the general expression assumed for the rate of flaw growth.

2.1.1 The Kinetic Model

Some researchers (Purnell *et al.* [2001]) state that the growth of a flaw can be written as a linear function of the ageing time t:

$$\frac{dX}{dt} = k_1 \tag{3}$$

Where: k_1 is a temperature dependant rate coefficient (*in nm/day*)

This however is only valid when one assumes that the reaction between the glass and the environment is solely controlled by the reaction kinetics.

2.1.2 The Diffusion Model

Some researchers (Cuypers *et al*. [2006], Orlowsky [2005]) stated that the flaw growth decreases with time. This slowing down of the reaction and consequent decrease in strength loss rate might be the direct result of reaction products covering the surface of the fibres with time and/or of a bottle neck effect (the confined space within the growing flaw could possibly in combination with a deposition of reaction products within this flaw itself also limit the further reaction rate). Some researchers stated that the chemical reaction will be diffusion-controlled from the start Cuypers et al [2006]. In that particular case the flaw size growth can be expressed with the help of Fick's law of diffusion as follows:

$$\frac{dX}{dt} = \frac{k_2}{X} \tag{4}$$

Where: k_2 is a temperature dependant rate coefficient (*in nm/day²*)

2.1.3 The non-linear model

Other researchers (Cuypers and Orlowsky [2007]) suggested a non-linear progression of the flaw depth due to for instance a varying Zr content along the section of the fibres or a varying flaw shape with time. This assumption resulted in Equation (5), enabling the user to model the slowing down as well as the acceleration of a chemical reaction.

$$a = a_0 + (k_3 \cdot t)^n \tag{5}$$

Where: k_3 is a temperature dependant rate coefficient (*in* $(nm^{1/n})/day$)

This formula can be rewritten in a similar form as presented in equations (3) and (4). This will then result in the following expression for the rate of flaw growth:

$$\frac{dX}{dt} = n \cdot k_3^{\,n} \cdot t^{n-1} \tag{6}$$

2.1.4 The Combined Model

Some researchers (Orlowsky [2005]) state that the rate of degradation is initially determined by kinetics and becomes diffusion controlled in a later stage. In this particular case, following expressions for the rate of flaw size growth can be used.

$$\frac{dX}{dt} = \frac{1}{\frac{1}{k_4} + \frac{X}{k_5}} \tag{7}$$

Where: k_4 is a temperature dependant rate coefficient (*in nm/day*)
k_5 is a temperature dependant rate coefficient (*in nm/day²*)

2.2 The Rate Coefficients and Their Dependance on Temperature

Durability studies available in literature (Litherland *et al.* [1981], Purnell *et al.* [2001], Cuypers *et al.* [2006], Orlowsky [2005]) postulate that for classical cementitious mixtures (with Portland cement) one chemical reaction is responsible for the strength loss at all temperatures in the range of 20-80°C and that an Arrhenius type relationship exists between the rate of this chemical reaction and the temperature at which the test was carried out.

$$k_i = k_{0,i} \cdot e^{-\frac{E_{A,i}}{R \cdot T}} \tag{8}$$

Where: k_i rate coefficient of the chemical reaction i (*dimensions depend on the model used*)
$k_{0,i}$ reference rate coefficient of the chemical reaction i (*dimensions depend on the model used*)
$E_{A,i}$ activation energy of the chemical reaction i (*in KJ mol^{-1}*)
T temperature at which the test is performed (*in K*)
R gas constant (*in J mol^{-1} K^{-1}*)

Implementing this assumption back into the durability models presented above implies that each of the temperature dependant rate coefficients (k_1, k_2, k_3, k_4 and k_5) should present an Arrhenius type relationship in function of the temperature. Each of these temperature dependant rate coefficients can thus be written as function of two model paramaters (an activation energy $E_{A,i}$ and a reference rate coefficient $k_{0,i}$) which themselves are solely function of the material combination under study.

3 STRENGTH PREDICTIONS

3.1 Introduction

When faced with GRCs durability remains an important issue and should therefore already be taken into consideration during the design stage. Instead of testing specimens in real climatic conditions, specimens are stored in well controlled lab conditions. Specimens are immersed in hot water at temperatures ranging from 20°C-80°C for various periods of time. It was found over the years that this approach provides a good means for accelerating the degradation process and this without altering the processes which take place. When the experimental data is gathered an inverse method can then be used for the determination of the rate coefficients of the different models at each testing temperature (see section 2). First starting values are allocated to each of the rate coefficients. The rate coefficients are altered in a second step and the modelled strength predictions are compared with the experimental results through the Sum of Squares method (SS). The rate coefficients corresponding to the lowest value of the Sum of Squares are then retained. With those rate coefficients the Arrhenius assumption can be checked and the model parameters (activation energy and reference rate, see section 2.2) are determined for the model under study. In a final stage, the in the previous step determined model parameters are used for a strength prediction over the life time of the material. The strength loss occurring over an established period in a certain climate can be defined by for instance assuming that over the life time of the material an average temperature of the climate will occur in combination with a relative humidity of 100%. This method is a widely adopted approach for strength predictions. It is however not clear how significant the influence of the scatter of the measurements is on the strength predictions. Therefore, in the following section a sensitivity study will be presented which will enable the user to establish how large the error is on his or her predictions.

3.2 Sensitivity Study of the Strength Predictions

Experimental series of GRC tests generaly exhibit a large scatter. Coefficients of Variation (CV) of around 15% and above are not exceptional. A vast majority of the authors working on GRC materials also use only a limited amount of specimens per test series: series with 3 to 5 specimens are commonly used. The combination of a large scatter, a limited amount of specimens per temperature/time point, a small amount of tested accelerated ageing temperature/time points and a limited number of temperatures might greatly influence the strength predictions effectued on the basis of these experimental results. Therefore it is the aim of this paper to evaluate the influence of these parameters on the strength predictions. In order to achieve this goal a theoretical investigation was carried out. Two main parts can be distinguished in this study. First of all (see Fig. 1) for each group of number of temperatures and number of time/temperature points (at several times within a temperature serie) the number of possible combinations is determined (e.g. in the case of 3 temperatures and 4 time/temperature points being used: (1) 35 temperature combinations can be constructed with the 7 temperatures given in Fig. 1, (2) 210 time combinations can be obtained using the 10 time possibilities given in Fig. 1, (3) in total 7350 experimental combinations are thus possible with 3 temperatures and 4 data points from the range shown in Fig. 1).

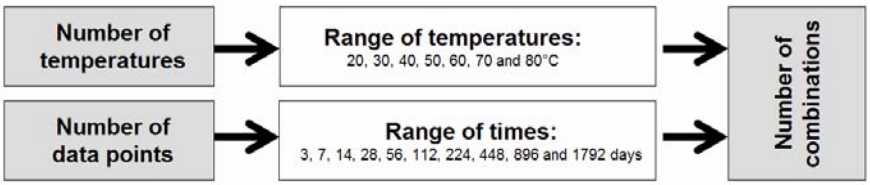

Figure 1. Scheme used to determine the number of combinations under study.

In the second part of the theoretical study the sensitivity to scatter will be determined for each of the possible "virtual" experimental combinations determined in the previous step. The 4 steps which have to be completed to achieve this goal are illustred in Fig. 2. First theoretical curves can be constructed (see step 0 in Fig. 2). The model parameters used in this paper to construct these theoretical curves are typical for traditional Portland cement mixtures (see e.g. Van Itterbeeck *et al.* [2007] and Cuypers *et al.* [2006]). In step 1 (see Fig. 2) the time/temperature time/temperature points of these theoretical curves will be shifted taking into account possible scatter on the results. For instance if 5 specimens are used per time/temperature time/temperature point, 5 values are determined at random but taking into account the probability distribution present on the results. For the distribution function, the scatter present on the reference specimens is taken as a reference. One could argue that scatter might evolve with ageing, but for a first calculation, using the scatter present on the reference specimens is more than adequate. Once all the data points have been shifted - taking into account the scatter present on the results in step 2 - the rate coefficients can be determined again with the same inverse method as the one discussed in section 3.1. From these rate coefficients the model parameters (activation energy and reference rate) can then be determined. Subsequently the residual strength after for instance 10 years of Belgian outdoor weathering can then be determined (e.g. for Belgium an average temperature of 11°C can be used). The procedure shown in Fig. 2 is now repeated 50 times for each simulated combination. Comparing the average residual strength after X years of outdoor exposure (S^{V}_{Xyears}) with the initial assumed theoretical residual strength (S^{T}_{Xyears}) will give an order of magnitude for the error on the prediction.

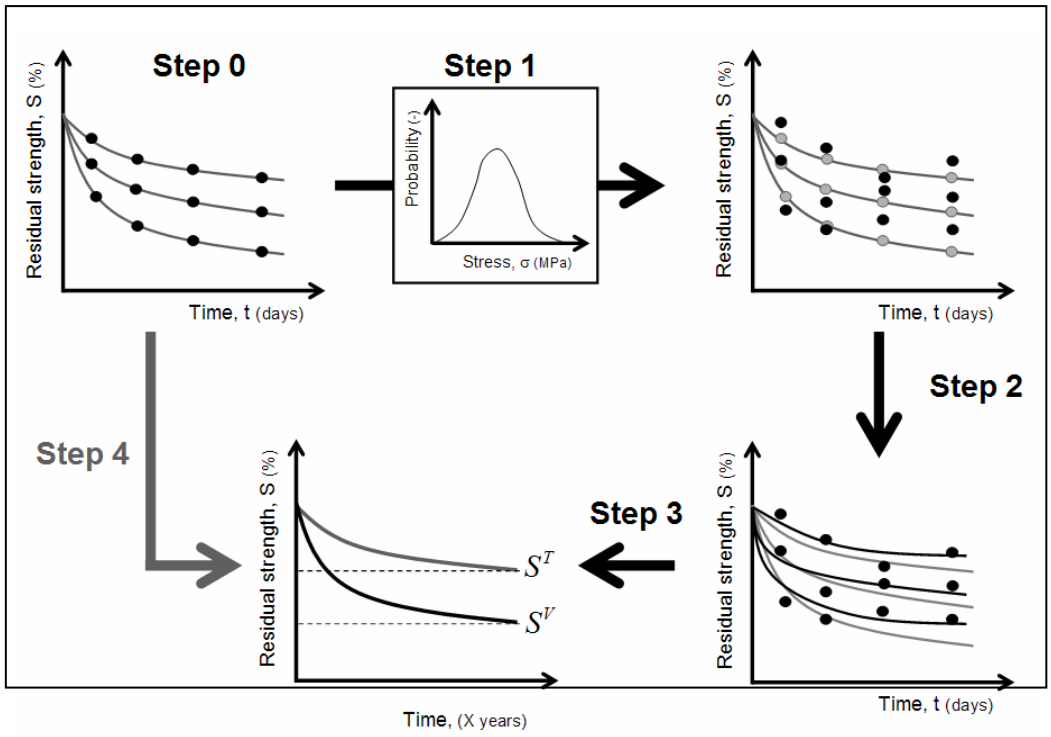

Figure 2. Scheme used for the sensitivity study

3.3 Sensitivity Study Performed on the Kinetic Model

The approach elaborated in the previous section was now adopted to check the sensitivity of the Kinetic model to scatter on the measurements. For part one of the calculations the same premises were used. The same range of temperatures and times were thus used as presented in Fig. 1. For part 2, 10 specimens were used with a CV of +/- 7% (own experiments on SIC specimens showed a Weibull distribution, the distribution parameters were taken from literature (Van Itterbeeck *et al.* [2007])). As starting/theoretical values for the model parameters for the Kinetic model the following were chosen: 82 kJ/mol for the activation energy and 8,84 nm day^{-1} for the reference rate. These values were obtained through the fitting of results from literature (Litherland *et al.* [1981]) on a large set of SIC specimens. For the determination of the residual strength, an exposure to 10 years of Belgian outdoor weathering was assumed (average annual temp of 11°C).

With the above mentioned input for each "virtual" experimental combination the residual strength due to scatter on the measurements was calculated 50 times and the average "virtual" experimental residual strength was determined. For each combination of number of temperatures and number of time/temperature point (within each temperature series) this resulted in a similar graph as presented in Fig. 3a. The results depicted in Fig. 3a show the results for all possible combinations with 3 temperatures and 4 time/temperature points when 10 specimens are used with a CV of +/- 7% (210x35=7350 combinations see section 3.2). The points represent the average of the 50 simulated values (7350 points). Through these points a 5^{th} degree polynomial was fitted in the X and in the Y direction. From this figure it can be clearly seen that some experimental test schemes should better be avoided. Using only high temperatures and longer periods of time most likely results in large underestimations of the residual strength. The graph also shows that if a mix of high and low temperatures is used the average residual strength predicted usually approximates the theoretical predicted residual strength, which is equal to 0,53 in this specific case. It should however be empasized that this graph only gives the average of the residual strength of 50 simulations, one should also consider the standard deviation on this average value since this might be quite high.

The results depicted in fig. 3a were summarized in fig. 3b into 2 points A and B, which are respectively representing the maximum and minimum values within fig. 3a. This procedure was repeated for several combinations (with 3 temperatures and different amounts of time/temperature datapoints) and these results are also summarized in fig. 3b. It can be clearly seen from this Figure that large underestimations can be obtained when only a limited number of time/temperatures points are under consideration and this even when a large number of specimens (10) per time/temperature "virtual" experimental value and a low CV (+/- 7%) are being used. It should be emphasized that the results presented in Fig. 3a and 3b were constructed based on the fact that the Kinetic model represents the real bahaviour of the flaw growth. The conclusions taken for this case are thus not necessarely similar for all possible material combinations.

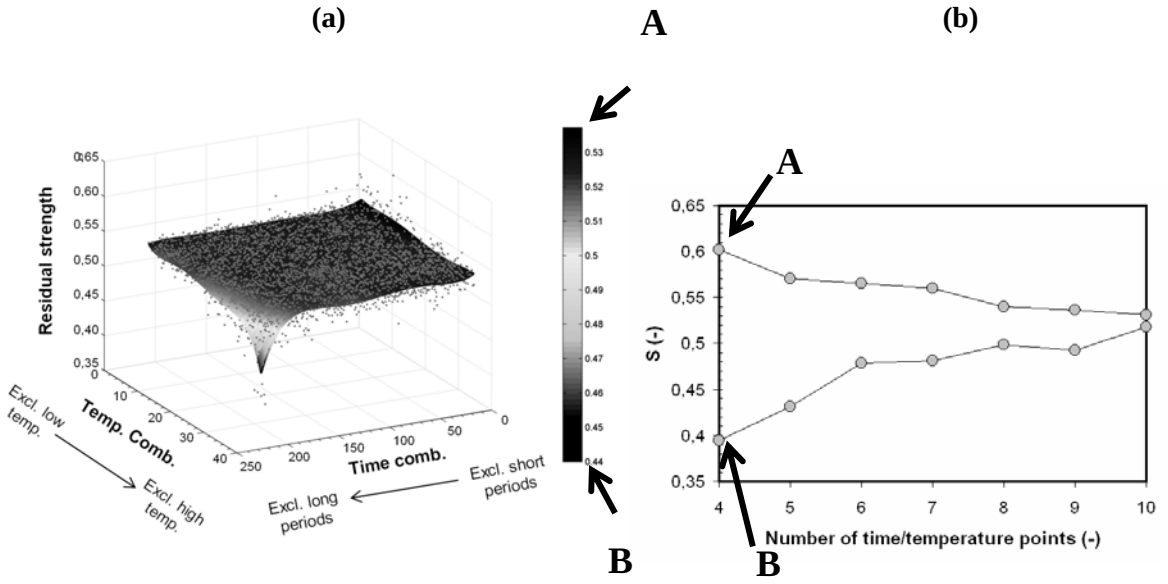

Figure 3. Results of the sensitivity study for the Kinetic model: (a) when 3 temperatures and 4 time/temperature points (within each temperature series) are being used (b) for all temperature and time combinations.

4 CONCLUSIONS

Over the years different strength durability models for GRCs have been developed. The four models presented and discussed within the scope of this paper are all based on a similar physical background, that the growth of flaws in the fibres due to chemical attack is responsible for the reduction in strength. All of these models also require a similar approach for the calibration. Specimens are immersed in hot water at temperatures ranging from 20°C-80°C for various periods of time and the residual strength is assessed after this exposure. Through an inverse method the rate coefficients of the models can be determined and the model parameters can be obtained. With these model parameters a strength prediction can be performed. In this paper a methodology was developed which enables the user to determine the uncertainty on his/her prediction as function of the number of acceleration temperatures and time/temperature points used, number of specimens which constitute the average values of each of the time/temperature points and the scatter inherently present on the tested specimens. Some preliminary results for the Kinetic model presented within the scope of this paper indicate that for this specific model some acceleration schemes are to be avoided (exclusively high temperatures in combination with exclusively high exposure times) since they can result in large underestimations of the strength. Large underestimations are also obtained when only a limited number of time/temperatures points are used and this even when a large number of specimens (10) and a low Coefficient of Variation (+/- 7%) are assumed. It should be emphasized once again that the results presented within the scope of section 3.3 were constructed based on the fact that the Kinetic model

represents the real bahaviour of the flaw growth. This is not necessarely the case for all possible material combinations. Therefore it is also necessary to perform this study on the other strength durability models.

ACKNOWLEDGMENTS

Funding by the Flemish Fund for Scientific Research (FWO) under the contract FWOAL320 is gratefully acknowledged. Funding by the Flemish Fund for Scientific Research (FWO) of the post-doctoral research of the co-author H. Cuypers is also gratefully acknowledged. Funding by the Flemish Fund for Scientific Research (FWO) for a long stay abroad at the University of Warwick of the first author is gratefully acknowledged (FWO reference V4.074.07).

REFERENCES

Cuypers, H. & Orlowsky, J. 2007, 'Ageing of composites, Chapter 5: Chemical Ageing mechanisms of glass fibre reinforced concrete", ed. R. Martin, Woodhead Publishing (In press)

Cuypers, H., Van Itterbeeck, P. & Wastiels, J. 2006, 'The effect of durability on the design of self-bearing sandwich panels with cementitious composite faces', Proc. Brittle Matrix Composites 8 (BMC 8), Warsaw, Poland, 23-25 October 2006.

Litherland, K.L., Oakley, D.R. & Proctor, B.A. 1981, 'The use of accelerated ageing procedures to predict the long term strength of GRC composites', *Cement and Concrete research*, **11**, 455-466.

Orlowsky, J. 2005, 'Zur Dauerhaftigkeit von Ar-Glabewehrung in Textilbeton', PhD thesis, RWTH-Aachen, Germany

Purnell, P., Short, N.R. & Page, C.L. 2001, 'A static fatigue model for the durability of glass fibre reinforced cement', *Journal of Materials Science*, **36**[22], 5385-5390.

Van Itterbeeck, P., Cuypers, H., Orlowsky, J. & Wastiels, J. 2007, 'Evaluation of the Strand In Cement (SIC) test for GRCs with improved durability', *Materials and structures* (in press)

The Sand Concrete: A Very Little Cracked Material

A. Benaissa [1]
A. Boutaleb [2]
S.E. Boudraa [3]
S. Malab [4]

T 11

ABSTRACT

The observation of hardened sand concrete fragments under the sweeping electronic microscope (SEM) makes it possible to describe the material as being little fissuring with a good overall homogeneity and a good bond between cement paste and sand grains. This small fissuring character is confirmed by the very uniform kinetics of drying between the peripheral face and the heart of a test-tube. Indeed this uniformity of drying involves small hydrous gradients and thus low tensile stresses on the surface and consequently a low density of cracking. The evolution of the shrinkage deformation according to the rate of drying shows a perfect linearity thus proving the absence of notable cracks.

KEYWORDS

Sand concrete, Porosity, Cracking, Desiccation, Rate of drying

[1] University of Science and Technology, Civil Eng. Faculty, BP 1505 El M'nouer Oran, Algéria, Tél/Fax +213 41 583063, mobile +213 61203808, dzbenaissa@yahoo.fr
[2] Ecole Normale Supérieur de l'Enseignement Technique, BP 1523 El M'nouer Oran, Algéria, Tél/Fax +213 41 514347, aboutalebdz@yahoo.fr
[3] Ecole Normale Supérieur de l'Enseignement Technique, BP 1523 El M'nouer Oran, Algéria, Tél/Fax +213 41 514347, mobile +213 62331294, sboudraa@yahoo.fr
[4] University of Science and Technology, Civil Eng. Faculty, BP 1505 El M'nouer Oran, Algéria, Tél/Fax +213 41 583063, s_malab@yahoo.fr

1 INTRODUCTION

The sand concrete is a material made from sand, cement, water and natural or industrial fillers. In a country like Algeria of more than two million km^2 with a very vast desert occupying most of the surface, the transport cost prices of stones or aggregates on hundreds of kilometres, can be very high. However precisely the Algerian south is very rich in sand of various grading as well as natural fines (Laghouat, Ouargla, etc.)

This new material can consequently replace the traditional concrete for economic reasons which we have just seen but also for specific qualities. Indeed its good workability implies a cheaper installation energy, its small granularity authorizes its use in the strongly armed structures and its beautiful surface aspect makes it possible to do without traditional rough-casting from where a certain profit out of cement, water, labour and painting.

The sand concrete, because of its appreciable resistances, 12 to 60 MPa, makes its use in manufacturing filler blocks (bricks, breeze blocks, hollow tiles, etc…) completely possible and preferable to ordinary concrete. The road field can also constitute a privileged place of the use of this material as well as the recoveries in ground work. The other interest of this material for a country as Algeria is the use of industrial fillers (phosphogypsum, glass and metal fibres, etc…) to increase the compactness of the sand concrete. The absorption of these industrial wastes is not only of economic interest but ecological interest as well.

In France, sand concrete finds its origins in the "agglomerated concrete" made by F. Coignet in the third quarter of nineteenth century. This material then consisted of sand, cement, lime and water. The retaining wall in Passy and the Coignet house in Saint-Denis, constitute the first applications of this technique which one also finds in the realization of the Port-Saïd tower in Egypt (height: 52 m) and a bridge in New York, as described in C.E.B.T.P.[1986].

The first granular correction attempts remain the prerogative of F Coignet which, for the needs of realization of certain parts of the Vanne aqueduct built between 1869 and 1872, mixed traditional fine sand with sand not used at that time because it was considered to be unsuitable for Construction.

In reality, according to Chauvin [1987], this technique was developed since decades in the ex-USSR, as testified by the achievements of the port of Kaliningrad at the beginning of last century and the bridge of Chernavski. This technique was taken again later, at the end of Second World War, by Professor Rebinder who allowed the use of this material in many fields (roadways, runways, filler blocks, architectural walls, floors, concrete slabs, etc…).

Indeed under the impulsion of this academician, the Soviet carried out certain technological tests on the sand concretes while being based in their work, in particular, on the parameters of aggregate grading, fineness of binders, reducers of water and the modes of vibration. Thereafter, this material fell in disuse because of the great mechanical resistances obtained by the use of large aggregates, but the shortage of coarse alluvial aggregates and the availability of large sand layers pushed to study a made cement and sand material to replace the ordinary concrete in certain fields (bricks, breeze blocks, hollow tiles, little requested structures, etc…).

The project "SABLOCRETE" (association for the promotion and the development of the sand concrete) tends, amongst other things, to optimize the exploitation of the sand layers, in fact rationalizing the use of sand and aggregates.

To date, the major concern as regards research on the sand concrete was directed towards the formulation of this one in order to obtain a good workability and good mechanical performances. Nevertheless a better approach of the material implies the knowledge of the microstructure, in particular the character with respect to cracking, object of this study.

2 TESTING CONCRETE

2.1 Composition

The component materials of our concrete as well as the fractions of each one of them are presented in [Table 1].

Table 1. Composition of the sand concrete (for 1 m^3)

Elements	*Sand: rolled-siliceous (Kg)*	*CPJ-CEM II /A-42,5 (Kg)*	*Calcareous filler (Kg)*	*Super plasticizer (l)*	*Water (l)*
Sand concrete	*1500*	*350*	*200*	*7*	*190*

2.2 Mechanical Characteristics

The compression test was carried out in accordance with French standard NFP 18-406. The tensile test was carried out in accordance with the French standard NFP18-400. The measurement of the elastic modulus was made by an extensometer equipped with cylinder and control in accordance with the test process project L.P.C-Oct. 89. The values of various measurements are consigned in [Table 2]; each value is the average of three measurements.

Table 2. Mechanical characteristics of sand concrete.

stresses	*Age (days)*				
	03	*07*	*14*	*28*	*90*
Compressive strength (MPa)	*11*	*17*	*21,5*	*23,6*	*28,8*
Tensile strength (MPa)	*1,24*	*1,97*	*2,24*	*2,36*	*2,53*
E (MPa)	*17000*	*19700*	*-*	*23000*	*23000*

2.3 Principle of Formulation

The sand concrete, unlike the mortars, uses a cement factor close to the ordinary concretes (300 to 400 Kg/m3). What distinguishes the sand concrete from the ordinary one resides primarily in the use of aggregates of low diameter ($\phi \leq 5$ mm), an addition of coarse aggregates is however possible but in a mass ratio G/S lower than 1. The different cement factors were possible because of the filling of sand vacuums by a limestone filler (0/80 µm), this has as a positive consequence in increasing compactness by the creation of a continuous granular extent. The fillers used, in general, are of limestone nature thanks to their great reactivity with the hydrates. The great specific surface obtained by the use of a high fraction of fine particles requires a significant wetting from where the utility of a water reducer, with an aim of increasing the performances and attenuating the differed deformations.

3 STUDY OF CRACKING

3.1 Studies with the SEM

The observations carried out with the **SEM** are represented by the figures 1 to 6 which show that the sand concrete is an amorphous and homogeneous material. The interface paste-aggregate 'Fig.6' does not have a particular texture and the bond is good. We do not notice notable cracks apart small faults visible 'Fig.6' in the vicinity of the interfaces which could result from shocks because the sample analyzed has a volume of 1 cm^3 and is obtained by shock fragmentation of a test-tube. The cracking of traditional concrete is due to gradients of traction related to non uniform drying which is at the origin of hydrous gradients. If our material is little or not fissuring, it implies that the hydrous gradients are negligible, this means that the drying of a test-tube is uniform and this is what we propose to check.

Some aspects of the hardened cement paste

Figure 1. Dense paste rather homogenous (X1200)

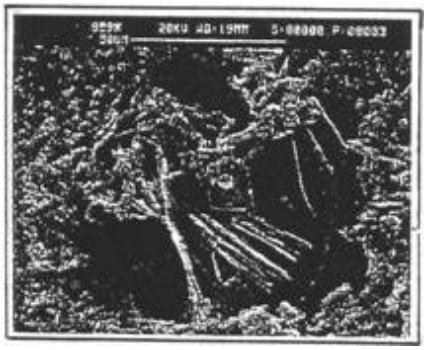

Figure 2. Particular structuring of the hydrated products inside a pore (X 859)

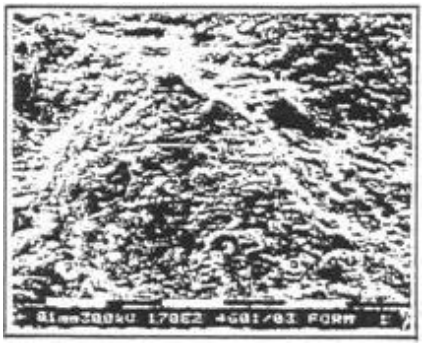

Figure 3. Good bond – no cracks – homogeneous paste (X1050)

Figure 4. General aspects of the p.c.d. (x 1250)

Figure 5. Hydrated products inside a pore (X 156)

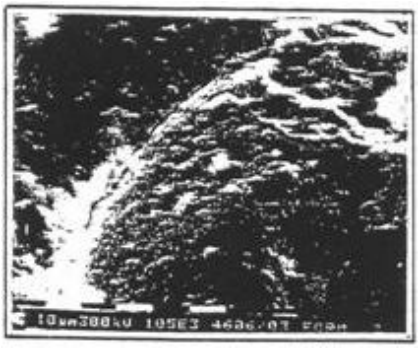

Figure 6. Separation of a tangled up aggregate (Exceptional phenomenon) (X 1050)

3.2 Study of the Kinetics of Drying

A sand concrete test-tube whose faces were made tight thus undergoing a radial drying was analyzed with the bench gamma. The diagram of the study of this test-tube is represented below [Fig.7]. This method, based on the absorption of gamma rays, makes it possible to follow the evolution of the loss of density according to the radius and the age. In this test, the cylindrical test-tube is posed on a plate which can move vertically and is crossed by a collimated beam of gamma rays which one measures the rate of absorption. The position of the test-tube makes it possible to determine, by differences with initial measurements, the variation of the average density of a crown.

The bench used not being equipped with a plate allowing rotation with the test-tube and thus a sweeping of the ring; measurements were made in several points whose average was used as value for the crown. The vertical displacement of the plate authorizes obtaining the distribution of these values along the diameter [Fig 8].

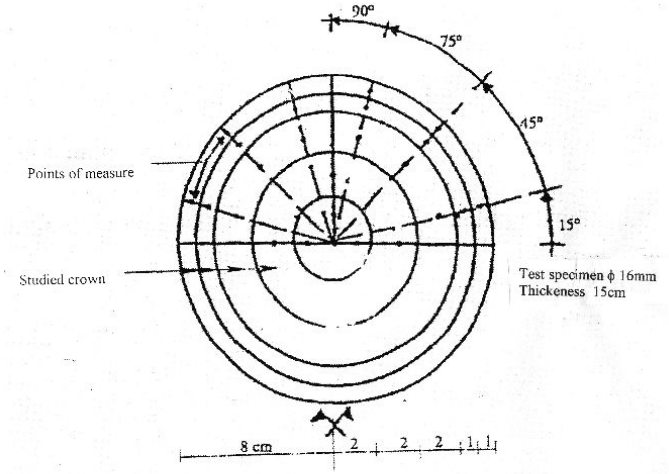

Figure 7. Diagram of the gammametric study

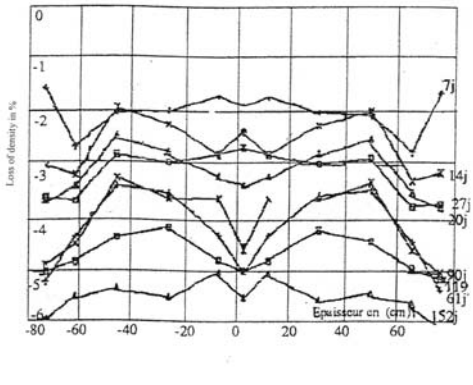

Figure 8. Evolution of the loss of density in function of thickness and age of the sand concrete.

Contrary to the traditional concretes where drying affects only one peripheral crown of a few mm thickness during the first months, the sand concrete test-tube is affected by a drying extremely fast and uniform, indeed the heart undergoes drying from the fifth day after the dismantling, which is operated at 48 hours and the amplitude of variation of density in the heart at the end of 20 days represent more than 80% of that measured at peripheral during the same period. One can think consequently, that the gradients of constraint on the surface are not very significant and density of cracking which results from this is weak. Homogeneity of the sand concrete confirmed by observations with the MEB doesn't explain by itself such behaviour.

The recourse to the porosimetry with mercury prove extremely instructive in similar case, this is why fragments of hardened sand concrete were analyzed. The results obtained being appreciably the same (other evidence of the homogeneity of the concrete), only one of the histograms of the pores is represented [Fig. 9].

The structure of the sand concrete is of monomodal type with a single peak being at the vicinity of 250 A around where are located more than 90% of the pores of the complex. These pores are thus of type "micro", whereas in traditional concrete, hardened cement paste present two peaks.

A first peak corresponds to the pores of small diameters and is located in the space going from 50 to 100 A according to water/cement ratio. The second peak corresponds to the pores of large diameters (600 to 1300 A) of the "macro" type; this last peak l is strongly influenced by water/cement ratio.

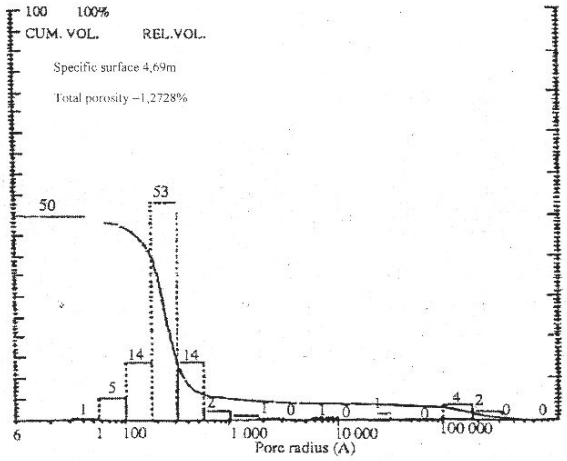

Figure 9. Porosimetry with mercury of the sand concrete.

It is undoubtedly this particular porosimetry of the sand concrete which explains the behaviour with drying. The bimodal structure of the ordinary concrete acts likes a water retention factor in the body of the test-tube, whereas the monomodal structure seems to support on the contrary evaporation. The large pores present in the ordinary concrete act according to us like barrier and are opposed to water evaporation of the micro pores. Such as for example by increasing pressure in the small pores, making any water expulsion difficult. It is not here question of a theory, but of an attempt to explain a phenomenon difficult to interpret, because it is difficult to reason on the scale of infinitely small.

The other explanation would come from the fact that the water of the ordinary concrete pores passes by two successive phases, an accelerated macro diffusion because of the large diameters (peak of the porosimetric curve in the vicinity of 10^3 A) followed by an evaporation of the micro pores clearly more slowed down. This deceleration is to be connected to smallness of pores which have an average diameter of 10^2 A, that is to say 10 times the thickness of one water molecule only, which makes difficult the expulsion of water. Moreover, absorption powers of water in these micro pores must be significant because of the reduced volume of the pores.

In the sand concrete, the main part of the pores (approximately 90%) have an average diameter of 250 A which is 25 times the thickness of the molecule supporting a uniform drying and especially not constrained, from where the fast and plain kinetics forms highlighted previously.

In corollary, according to Benaissa et al. [1992], we advance that the uniformity of drying and the homogeneity of the sand concrete, are the determining factors of the absence of cracks. This state explains, at least partially, the desiccation shrinkage of the sand concrete more significant than that of the ordinary concrete.

Let us note in addition that the weak dispersion of the compressive strengths and measurements of moduli of elasticity, respectively 1.2% and 2.2%, confirms the homogeneous character of the concrete. The moduli of elasticity of the sand concrete are lower than those of the ordinary concrete from where a greater deformability and thus a less cracking.

3. 3 Shrinkage According to the Rate of Drying

The existing linearity between the shrinkage and the rate of drying shows well that the shrinkage is an increasing function of evaporable water. The first measurement being made at 7 days, it is normal to consider that before this age, there is a non nil desiccation shrinkage, which is in addition highlighted by the line (intersection with the axis of the deformations), the other very remarkable information is that the aspect of the line remains rather regular (the experimental points are very close to the line),

whereas one could have expected a break of slope because of possible cracks appearing beyond a certain degree of drying as very precisely stipulated by Abiar [1986] but it is not the case. This regularity translates a likely absence of cracking, while being superimposed on the effect of the evaporation of water, to cause a deformation more slowed down than evaporation, at least in a second phase appearing after the first stage where there is linearity between the variation of the deformation and the rate of drying [Fig 10].

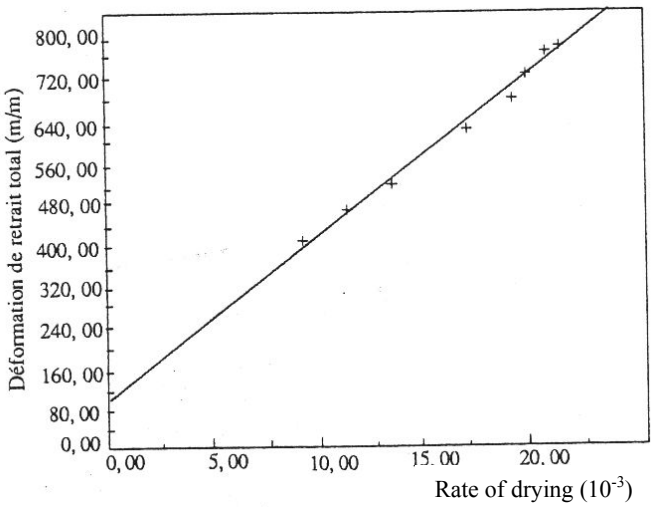

Figure 10. Total shrinkage according to the rate of drying sand concrete

4 CONCLUSIONS

It was shown that the sand concrete is a homogeneous material and of monomodal structure whereas the ordinary concrete is of bimodal type. The fine porosimetry of the sand concrete is at the origin of the nature of the drying which is uniform contrary to the traditional concrete where it is not uniform. This particular kinetics of the desiccation of the sand concrete, explains the not fissuring character of the material. The absence of large inclusions in the matrix is an additional factor which attenuates the risk of cracking.

This not fissuring character, opens to the sand concrete great hopes of use in very varied fields in particular in sub work thanks to its very fine granularity and thus an energy of installation much less expensive than traditional concretes. The use of this material in projected form is to be considered in the rehabilitation of the worn water collectors

REFERENCES

C.E.B.T.P. 1986, '*Rapport de synthèse des connaissances du béton de sable'*. N° 52 G 119, Décembre.

Chauvin, J.J. 1987, '*Laboratoire Régional des Ponts et Chaussées de Bordeaux'*, rapport interne, Béton de Sable, Réf. FAER 1.30.24.5 et 1.30.24.6, Janvier.

Benaissa, A., Morlier, P. Viguier, C. & Chauvin, J.J.1992 'Cinétique de dessiccation et retrait du béton de sable', *Annales de l'ITBTP*, n° 504 - Juin.

Abiar, G. 1986, '*Cinétique de dessiccation et de déformation différée du béton'*. Thèse de l'E.N.P.C. Octobre.

Flexural Behavior of Steel-Concrete Composite Girders Strengthened via Fiber Reinforced Plastic FRP

Abdul Qader Melhem [1]

T 11

ABSTRACT

Many of bridge and building elements are in the need of continuous maintenance, repair, and strengthening because of the severe environmental conditions and heavy unpredicted moving loads. This paper elucidates in details theoretically and experimentally how to broaden the structural capacities of steel-concrete composite girders implementing fiber reinforced polymers FRP materials and high strength concrete HSC. Theoretical formulas derived and designing equations put forward in order to improve flexural capacities of steel-concrete composite girder models. Failure modes of those composite models will be discussed also. The experimental composite models are employed to verify the accuracy of the theoretical results. The first model is the steel beam alone, the second model is the steel-concrete composite model assembles of reinforced concrete slab connected by means of studs to the top of steel beam while the third composite model is the second composite model but fabricated with FRP plate to the bottom surface of the steel beam. The simple composite models have the same span length, steel beam section, yield and ultimate strength of steel beam and FRP thickness. High strength concrete has been utilized to improve durability. The models had been exposed to two concentrated loads increased gradually up to failure.

KEYWORDS

Composite beam, Elastic-plastic, Ultimate moment, Strengthening, Durability, Fiber reinforced polymers

[1] University of Aleppo, Civil Engrg. Faculty, Aleppo, Syria 00963, Phone +963 933 589 634, Fax +963 212 264 432, aqmelhem@scs-net.org

1 INTRODUCTION

With increasing harsh environmental conditions (creep, cracking, de-lamination, wear, and/or effects of foreign object damage …etc) along with unpredictable live loads on highway bridges and other vital structures, there is growing tendency to boost up the structural capacity of the composite components rather than replacing them according to the cost-effective standard. In recent years, there has been a renewed emphasis on improving durability and increasing service life of structures. The value of the concrete is defined in terms of maturity, permeability, air-void structure quantification, sulfate resistance, chloride penetration, strength, and in situ performance [David and Meyerhof 1958].

Strengthening of existing steel-concrete composite structures is becoming a major concern for the industries due to age, steady increase in the applied loads, environmental effects, lack of adequate maintenance … etc. The advent of fiber reinforced polymers FRP has been explored as new materials for strengthening of existing structures. These innovative materials are characterized by their high strength to weight ratio and environmental and fatigue sturdiness. It has been employed successfully in the reinforced concrete structures at least for the last thirty years, but until recently has been utilized momentarily in the composite structures. In fact, the FRP plates, laminates or sheets can be epoxy bonded to the tension face of the composite members to enhance their strength and stiffness.

An earlier study conducted, at the University of South Florida, using CFRP in the repair of steel-concrete composite bridges [Sen and Liby 1994]. Other researchers have investigated the possibility of strengthening steel beams with CFRP plates [Mertz and Gillespie 1996]. The effectiveness of using FRP to increase the stiffness of steel–concrete composite beams also has been demonstrated experimentally [Tavakkolizadeh and Saadatmanesh 2003 and Al-Saidy et al 2004]. Using of externally bonded high modulus carbon fibre reinforced polymer (HM CFRP) materials to strengthen steel bridges and structures has been proposed along with guidelines and installation techniques based on the best practice reported in the literature and the extensive practical experience in bonding of composite materials [Schnerch et al 2007].

2 BASIC ASSUMPTIONS AND OBJECTIVES

The impending failure manners for a steel-concrete composite beam strengthened with FRP materials are: rupture of the FRP plate, de-bonding of the FRP plate, and crushing of the compression concrete due to loading , environmental conditions or both. There are other failure modes such as, buckling of the compression flange and shear failure of the web. To prevent de-bonding of the FRP plate, it is important to give a ruling for the actual state of stress near the end of the plate. The main objectives of this research are:

- To strengthen previously damaged or distressed steel-concrete composite members making use of FRP plates.
- To build up a procedure that could be used for strengthening of existing steel-concrete composite members, using FRP plates, subjected to up-normal loads or to severe atmospheric conditions.
- To design steel-concrete composite members making use of FRP plates for architectural purpose, such as: reducing the height, weight, etc.

3 STRESSES OWING TO ENVIRONENTAL CIRCUMSTANCES

These stresses are by reason of creep, shrinkage, relative temperature differences, difference between thermal expansion of concrete and steel, and concrete growth. During a sudden rise in temperature, the steel beam and probably the FRP become warmer than that the connected concrete slab because of quicker temperature stabilization of steel. This kind of temperature differential creates an additional strain of $1x(10)^{-4}$ which should be considered in the design. The net combination effect of creep, shrinkage, and temperature differential between cold concrete and warmer steel is shown in Fig.

1.a.The effect of difference between thermal expansion of concrete and steel is shown in Fig. 1.b. Concrete growth causes stresses in composite section similar to that produced by differences in thermal expansion coefficients of steel and concrete. Concrete growth may be due to physical causes such as; freezing-thawing, wetting-drying, heating-cooling, etc. The chemical cause are due to certain cement-aggregate combinations.

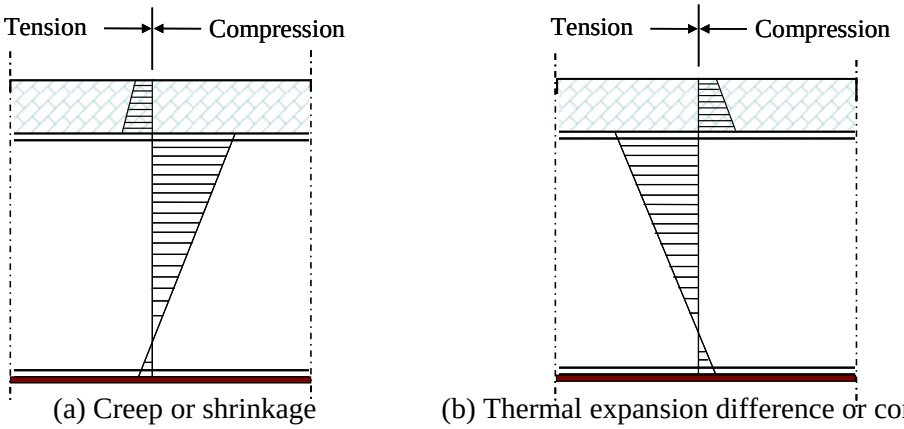

(a) Creep or shrinkage (b) Thermal expansion difference or concrete growth

Figure 1. Stresses due to Environmental conditions.

4 FULL PLASTIC BENDING

When the applied moment becomes greater than that moment which generates first yield of farthest fibers, portions of the composite section will keep hold of a constant yield stress, at strains which go beyond the elastic limit. Progressive straining and yielding of the material will then take place until complete plasticization of the section. At this bound no additional moment can be developed, thus a full plastic moment is reached. At this stage, the plastic neutral axis may be located in the concrete slab, steel top flange, or steel web.

The failure load with shoring is almost the same as that developed when no shoring is used. This is because of redistribution of stresses in the steel beam, which has little effect on the final plastic moment capacity of the beam. The amount of longitudinal shear which must be taken in to account should include that produced by the dead loads (if shoring is used), live loads, creep, shrinkage, temperature difference, and any difference between the thermal coefficients of expansion of slab and steel beam. From previous numerous tests, it has been shown that if shear connectors are properly designed, composite beam failure is due to only ultimate compressive stress in the concrete slab or full plasticity in the steel beam, or both combination.

4.1 Neutral Axis in the Concrete Slab (Fig. 2a):

If: $0.85\, f_c^{'} A_c > A_s F_y + A_{frp}\, f_{y,frp}$, the plastic neutral axis is located within the concrete slab. The plastic neutral axis location and ultimate moment are given by these equations:

$$a_{T1} = \frac{A_s F_y + A_{frp}\, f_{y,frp}}{0.85\, f_c^{'} b_e} \qquad (1)$$

$$M_u = 0.85\, f_c^{'} b_e\, a_{T1} [d + t_c - d_T - 0.5\, a_{T1}] + T_{frp}\, (d_T + 0.5\, t_{frp}) \qquad (2)$$

Where,

$T_s = A_s F_y$, $T_{frp} = A_{frp}\, f_{,frp}$

$$d_T = (1/A_s)[A_{bf}\, (0.5 t_{bf}) + A_w\, (t_{bf} + \frac{d_w}{2}) + A_{tf}\, (t_{bf} + d_w + \frac{t_{tf}}{2})]$$

When the section is symmetric: $d_T = d/2$

A_s = Area of steel section = (A_{bf} + A_w + A_{tf})

A_{frp} = b_{frp} t_{frp} = Area of FRP plate

F_y = Yield stress limit of steel beam, f_{frp} = Ultimate tensile strength of the FRP material

Other terms are shown in Fig. 2

4.3 Neutral Axis in the Steel Section (Fig. 2b, 2c**):**

If: $0.85\, f_c^{'} A_c < F_y A_s + A_{frp} f_{y,frp}$, the plastic neutral axis is located in the steel section.

1. If: $F_y A_{tf} > C^T$, the plastic neutral axis is in the top flange of the steel section.

Where,

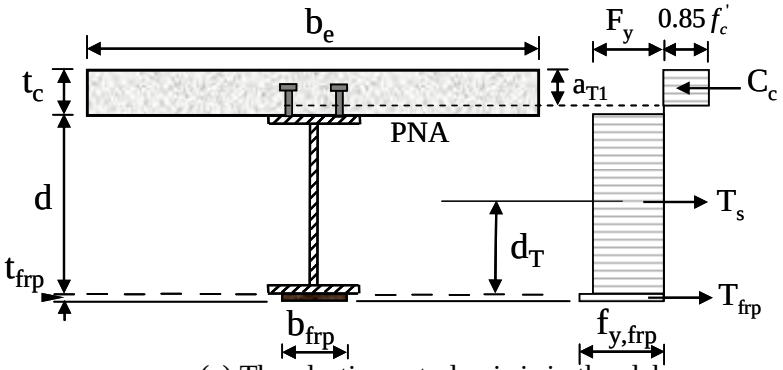

(a) The plastic neutral axis is in the slab.

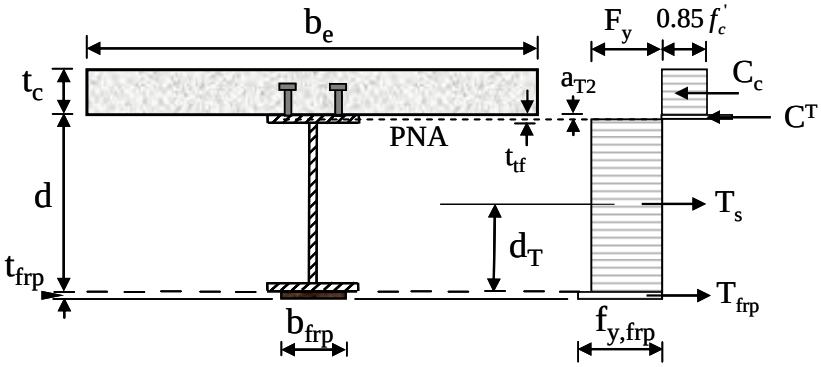

(b) The plastic neutral axis is in the top steel flange.

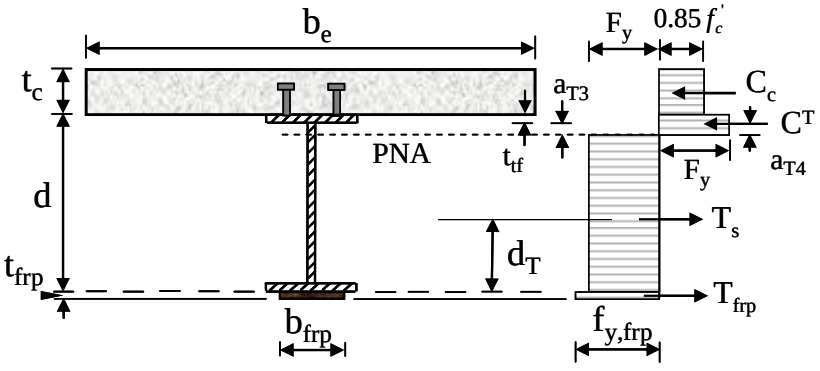

(c) The plastic neutral axis is in the web of steel section.

Figure 2. Plastic analysis of steel-concrete composite model.

$$C^T = 0.5\, [(F_y A_s + A_{frp} f_{y,frp}) - 0.85\, f_c^{'} A_c] \qquad (3)$$

The location of neutral axis and ultimate bending moment are given by these equations:

$$a_{T2} = \frac{C^T}{F_y\, b_{tf}} \tag{4}$$

$$M_u = 0.85\, f_c^{'} b_e\, t_c\, [d + 0.5t_c - d_T] + C^T(d - d_T - 0.5\, a_{T2}) + T_{frp}\, (d_T + 0.5\, t_{frp}) \tag{5}$$

$$d_T = (1/A_{s1})[A_{bf}\, (0.5t_{bf}) + A_w\, (t_{bf} + \frac{d_w}{2}) + b_{tf}\, (t_{tf} - a_{T2})\, (t_{bf} + d_w + \frac{t_{tf} - a_{T2}}{2})]$$

$$A_{s1} = A_{bf} + A_w + b_{tf}\, (t_{tf} - a_{T2})$$

2. If: $F_y\, A_{tf} < C^T$, the plastic neutral axis is in the web of the steel section.

The location of neutral axis and ultimate bending moment are given by these equations:

$$a_{T3} = \frac{C^T - A_{tf} F_y}{F_y\, t_w} \tag{6}$$

$$M_u = 0.85\, f_c^{'} b_e\, t_c\, [d + 0.5t_c - d_T] + C^T[d - (t_{tf} + a_{T3}) + a_{T4} - d_T] + T_{frp}\, (d_T + 0.5\, t_{frp}) \tag{7}$$

$$d_T = (1/A_{s2})[A_{bf}\, (0.5t_{bf}) + t_w\, (d_w - a_{T3})\, (t_{bf} + \frac{d_w - a_{T3}}{2})]$$

$$A_{s2} = A_{bf} + t_w\, (d_w - a_{T3})$$

5 SPECIMEN DETAILS

A steel-concrete composite girder model has been reproduced and reworked again in more specifics [Sen, et al, 2001] using high strength concrete (HSC) to boost up the durability. This is another way to heighten service life through designing, specifying, and building structures using (HSC). The American Concrete Institute has previously defined (HSC) as concrete with a compressive strength greater than 41 MPa (6000 Psi).

The aim of the test is to evaluate the viability of using FRP plates for improving the strength of steel-concrete composite girder models. Table 1 present material properties of the models. Figure 3 shows cross section of the model. The simple model was subjected to two concentrated loads as been show. The loads were applied through two 710 mm transverse stiffened spreader beams welded to a 1220 mm long longitudinal stiffened beam. The loads were two uniform transverse line loads spaced 1220 mm apart, transferred equally to the two spreader beams.

Table 1. Properties of Materials.

Concrete		*Steel*		*FRP*	
Compressive Strength, MPa	43.6	Yield strength, Mpa	370	Tensile Strength, MPa	1840
Elastic Modulus, MPa	13800	Elastic Modulus, Mpa	198300	Elastic Modulus, MPa	114000
Peak strain	0.00197	Poisson's ratio	0.31	Failure Strain	1.6 %
Failure strain	0.00380			Poisson's ratio	0.34

The cross section consists of a 710 mm reinforced concrete slab width, 114 mm thickness attached to a W 8 x 24 steel section via 36 stud shear connectors. The studs were spaced at; @ 127.6 mm for the shear spans and @ 254 mm for the distance between concentrated loads. The FRP plate length was 3650 mm, bonded to the bottom steel surface using epoxy adhesive. Table 1 presents mechanical properties of the model materials. The first phase of the experimental program was testing W 8 x 24 steel section under two concentrating loads. The second phase of the experimental program was the steel-concrete composite girder model had been loaded beyond yield stress limit of its bottom tension flange, which is 0.55 F_y , according to the AASHTO Bridge Specifications.

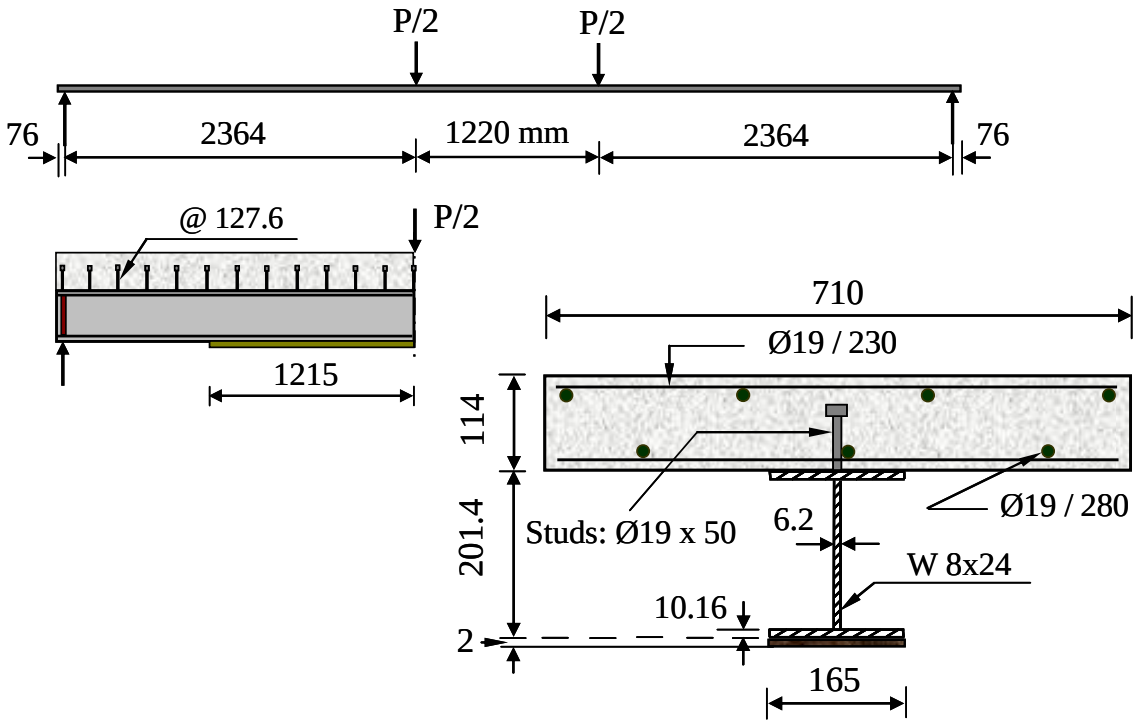

Figure 3. The experimental composite girder model.

As a result of this loading, higher than yield stress limit of tension flange, there was permanent deformation prior to strengthening by means of FRP plate. The third phase of the experimental program was the deformed steel-concrete composite girder model had been strengthened with 2 mm thick, 165 mm width and 3650 mm length epoxy adhesive. After the adhesive cured for 48 h, the ends of FRP plate were bolted to resist the peeling stresses. The same loading scheme had been used for testing the repaired model. The test was stopped when no extra load could be applied and the deflection exceeded the 100 mm limit. No adhesive failure had been observed. Table 2 presents elastic model properties. These properties have been calculated using AASHTO Bridge Specifications.

Table 2. Elastic properties of the sections.

Beam	y_{bot} *(mm)*	y_{top} *(mm)*	I_{com} (cm^4)	S_{bot} (cm^3)	S_{top} (cm^3)
Composite beam	216.8	98.6	13177.11	607.77	1336.28
Composite beam with FRP	216.5	101.0	14072.48	650.15	1393.73

The deflection at midspan is calculated by this equation:

$$\Delta_{L/2} = \frac{(P/2)}{6EI_{tr}}\left(\frac{a}{L}\right)(L^3)\left[\frac{3}{4}-\left(\frac{a}{L}\right)^2\right] \approx \frac{1}{51}\frac{PL^3}{EI_{tr}} \qquad (8)$$

The strains at the top and bottom of the steel-concrete composite section are given by these equations:

$$\varepsilon_c = \frac{P\,a\,y_{top}}{2EI_{tr}} \text{ and } \varepsilon_s = \frac{P\,a\,y_{bot}}{2EI_{tr}} \qquad (9)$$

Where,

L = Span length between supports, equal to 5948 mm

a = Shear span, the distance between support and first load which is equal to 2364 mm

a/L = Shear span ratio is equal to 0.3974

E = Modulus of elasticity of the homogeneous section

I_{tr} = Moment of inertia of composite section

P = Applied load

y_{top} and y_{bot} = Distances from neutral axis to the top and bottom of the steel-concrete composite section

Table 3 presents summary of the theoretical and experimental studies. Figure 4 shows three load-displacement curves; the top one is for the composite girder strengthened with FRP plate, the middle is for the composite girder without FRP plate and the lower curve is for the steel section alone.

Table 3. Summery of outcomes.

Beam	a_{T1} *(mm)*	P_{elast} *(KN)*		P_{ult} *(KN)*	
		Thoe.	*Exp..*	*Thoe.*	*Exp.*
Composite beam	53.8	125	130	225	249
Composite beam with FRP	87.3	131	150	325	271

These curves outline the phases of the experimental program. The curve for repaired or strengthened composite beam is gaining more strength in the post – yield region as been shown. The simulating service damage load for un-strengthened composite beam was 186 KN, while the ultimate load for strengthened composite beam was 271, a strength gain of 46 %. On the other hand, the predicted ultimate load for unstrengthened composite beam was 249 KN while the ultimate load for strengthened composite beam 271 KN, a strength gain of 8.8 %. This low value is attributed to the fact that the FRP plate has a lower elastic modulus than that of steel; 198300 MPa versus 114000 MPa. So, the stresses in FRP plate were less than those stresses in the bottom steel flange prior to yielding.

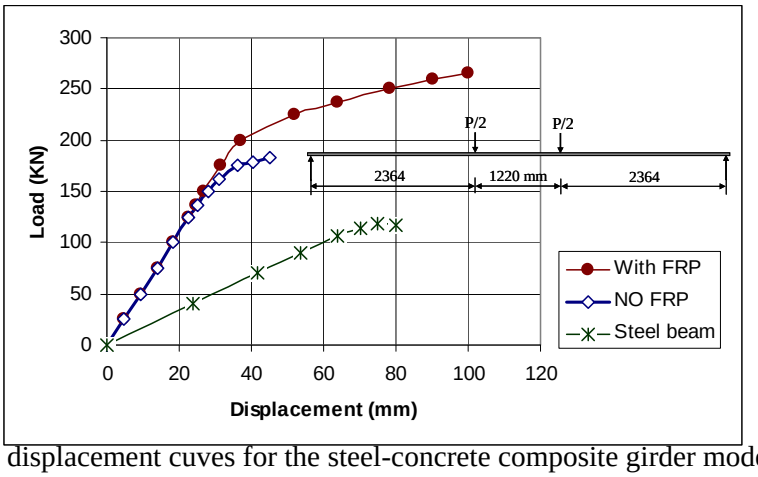

Figure 4. Load displacement cuves for the steel-concrete composite girder models.

6 DESIGNING EQUATIONS

Designing equations have focused on the case where the neutral axis is within the slab **(**Fig. 2a**)**. The Majority of steel-concrete composite girders full under this category. The designing equations may be summarized as followings (Eq. 1 and Eq. 2):

$$q_{frp}^2 + 2\left[q_s - \frac{d}{t_c} - 1\right] q_{frp} + 2\left\{\left[0.5q_s - \left(\frac{d - d_T}{t_c}\right) - 1\right] q_s + \frac{M_u}{0.85 f_c' b_e t_c^2}\right\} = 0 \qquad (10)$$

$$q_{frp} = \frac{-b \pm \sqrt{b^2 - 4ac}}{2a}$$

Where: a = 1 , b = $2\left[q_s - \frac{d}{t_c} - 1\right]$, c = $2\left\{\left[0.5\, q_s - \frac{d - d_T}{t_c} - 1\right] q_s + \frac{M_u}{0.85 f_c' b_e t_c^2}\right\}$

$$q_{frp} = \frac{A_{frp}}{A_c} \frac{f_{frp}}{0.85 f_c'} \text{ and } q_s = \frac{A_s}{A_c} \frac{F_y}{0.85 f_c'}$$

7 CONCLUSIONS

- The presence of FRP plate increases the stiffness of the steel-concrete composite model provided that adequate anchorage of the FRP plate to the bottom steel flange. Therefore, the composite beams strengthened with FRP plates using HSC can be utilized effectively in durability practice.

- A ductile failure mechanism comes about for the repaired or strengthened composite model with FRP reinforcement accompanied with considerable deformation, provided that shear connectors are properly designed against heavier loads and environmental conditions.

- The deformed or distressed sections can be strengthened successfully via FRP plates a substantial strength gain was attained.

- In addition to increases in ultimate load, the elastic region of the un-strengthened composite beam was significantly extended in the repaired composite beam. This provides a valuable marginal safety factor.

- The designed equations can be employed for selection of the area fraction of FRP plate needed to upgrade existing bridges superstructures, provided that ultimate bending moment is available.

REFERENCES

David, R., & Meyerhof, G.G., 1958, 'Composite Construction of Bridges Using Steel and Concrete', *The Engineering Journal, May*, Canad, 41-47.

Sen, R. & Liby, L., 1994, 'Repair of steel composite bridge sections using carbon fiber reinforced plastic laminates', *Rep. No. FDOT-510616, Florida Department of Transportation.*

Mertz, D. & Gillespie, J., 1996, 'Rehabilitation of Steel Bridge Girders Through the Application of Advanced Composite Materials', *Transportation Research Board, National Research Council.*

Tavakkolizadeh, M. & Saadatmanesh, H., 2003, 'Strengthening of Steel-Concrete Composite Girders Using Carbon Fibre Reinforced Polymers Sheets', *Journal of Structural Engineering, Vol. 129, No. 1*, 30–40.

Al-Saidy, A. H., Klaiber, F. W. & Wipf, T. J., 2004, 'Repair of Steel Composite Beams with Carbon Fiber-Reinforced Polymer Plates', *Journal of Composites for Construction ASCE, Vol. 8, no. 2, April,* 1001–1010.

Schnerch, D., Dawood, M., Rizkalla S. & Sumner, E., 2007, 'Proposed design guidelines for strengthening of steel bridges with FRP materials', *Construction and Building Materials 21,* 163–172.
Sen, R., Liby, L. and Mullins, G., 2001, 'Strengthening Steel bridge Sections using CFRP Laminates', *Composites: Part B 32*, pp 309-322.

11DBMC International Conference on Durability of Building Materials and Components
ISTANBUL, Turkey 11-14 May 2008

Corrosion Detection of Embedded Steel in Concrete

Mohammad Ismail [1]
Rosly Abdul Rahman [1]
Erica Dina [1]

T 11

ABSTRACT

Corrosion of reinforcement is a worldwide problem. It can occur either by carbonation or chloride attack. If the electrochemical process of corrosion can be detected at an earlier stage, some preventive measures can be arranged. The aim of this research is to look at the possibility of using modified fibre optic sensor to detect and monitor the corrosion process of reinforcing steel. The corrosion process was monitored by an unclad plastic optical fibre sensor which is attached to the steel bar. A fibre optic silicon pin detector was used with light source to detect the spectrum of the light. The light spectrum change in intensity due to corrosion product developed on the bar surface becomes thicker as the corrosion progressed. Three types of samples (concrete prisms) with steel bars inserted at the centre have been prepared for this research. One sample was immersed in 10% Sodium Chloride (NaCl) solution and another in 40% NaCl to speed up the corrosion process. Reference sample was immersed in distilled water. The data of corrosion process was collected for a period of 45 days. Replicate samples were prepared and subjected to similar exposure conditions, but the corrosion progress was monitored using half cell kit. The result shows that the potential value of the control sample outgoing light from the optical fibre was about constant at 10500 mV. However for sample immersed in solutions containing 10% and 40% NaCl, the potential value reduced to less than 6000 mV. The intensity value decreases slowly with the progress of corrosion. Similar pattern were also observed by half cell measurements.

KEYWORDS

Fibre Optic Sensor, Corrosion of Reinforcement, Chloride, Durability

[1] Universiti Teknologi Malaysia, Faculty of Civil Engineering, 81310 Skudai, Johor Bahru, Johor, MALAYSIA, Phone 607 5531688, Fax 607 5566157, mohammad@utm.my

1 INTRODUCTION

Corrosion of reinforcement is a worldwide problem that affects durability and integrity of reinforced concrete structures. Corrosion of reinforcement primarily occurs because of carbonation process which reduces the alkalinity of concrete or due to chloride ions which attack the passive layer on the reinforcement [Broomfield 1997, Elsener *et al*. 1999]. Repairing deteriorated reinforced concrete structures at an advanced stage is very costly and time consuming. It is more advantageous if corrosion can be detected at an earlier stage so that some preventive measures can be carried out. The fibre optic sensors monitoring technology were developed to describe the unique marriage of materials in structural engineering. Although this structurally integrated sensing system could monitor the state of a structure's stability and durability but in order to improve the quality control of these structures, it is necessary to develop a good sensor that has the capability to continuously identify the actual changes in the activities leading to corrosion, both at fresh and hardened states.

Fibre optic sensors have demonstrated the ability to take some of the key structural evaluation and performance measurements as described by [Huston and Fuhr 1995]. Fibre optic sensors are similar to electrical sensors in that the fibre optic sensors use light as both the sensing and information transduction medium. However, while electrical sensors operate by modifying the voltage, current, frequency, or phase of an electrical signal the fibre optic sensors operate by modifying the intensity, fast frequency (wavelength), slow frequency (time-modulated intensity), polarisation, phase, and coherence [Huston *et al*. 1999].

The applications of fibre optic sensors in engineering components and systems have been tested in several laboratories and installed in different structures. The laboratory results have been quite promising, showing potentials for further improvements [Eric 1995 and Siaw *et al*. 2002]. The majority of the field installations are currently of the study or demonstration type. Mendez *et al*. [1990] first suggested the use of embedded fibre optic sensors to measure physical properties in concrete. They found that the alkaline nature of concrete could damage the silicon in glass, but the damage can be avoided by jacketing the glass fibre with plastic buffers.

Huston and Fuhr [1992] and [Fuhr *et al*.1993] also used fibre optic sensors in reinforced concrete. Their studies involved embedding optical fibres of various types inside small reinforced concrete cubes (100 mm x 100 mm x 100 mm). The initial tests focused on whether or not optical fibres could survive the concrete environment and curing process. Escobar *et al*. [1992] used bonded fibre optic strain gauges on concrete beams. Maher and Nawy [1993] reported the successful use of fibre optic bragg grating strain gauges in laboratory concrete beam test. The use of fibre optic sensor to determine the physical properties of concrete such as cracking, stress-strain, and temperature has been well developed by [Huston and Fuhr 1995]. This paper highlighted a development of sensor that can monitor corrosion process by modifying a fibre optic.

2 MATERIALS AND TEST PROCEDURES

The properties of specimens used in this experiment are; 1:2:4 concrete prism size 50 mm x 50 mm x 100 mm. 0.6 water/cement (W/C) ratio, and 2% NaCl by weight of cement added to the mix. A 6 mm diameter mild steel rod, cleaned with sandpaper was immersed in nitric acid until the steel is silvery in colour. Fibre optic was cut into pieces of 300 mm length. About 40 mm at the middle of the fibre was unclad. The unclad plastic optical fibre was finally tied to the steel rod and embedded in the concrete prism as shown in Fig. 1.

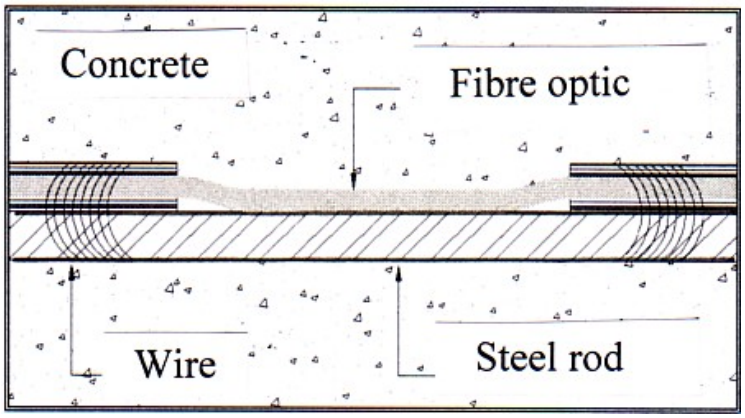

Figure 1. Fibre optic sensor attached to reinforcement.

The glass rod was used to protect the plastic optical fibre from the NaCl solution. The prisms were then immersed in the NaCl solution to speed up the corrosion process. The samples are as shown in Fig. 2.

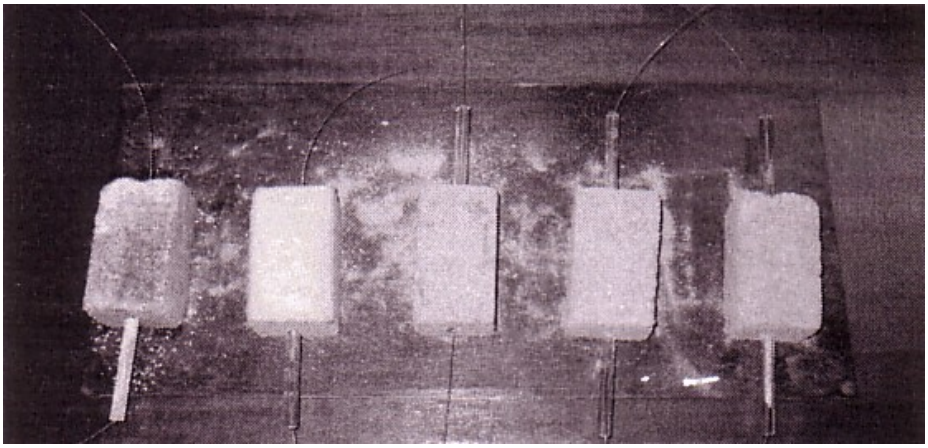

Figure 2. Samples of reinforced concrete prisms.

A specimen was immersed to each of the 10% and 40% NaCl solutions. A HeNe laser was later used to ensure that the cladding was properly removed. The experimental setup is shown in Fig. 3.

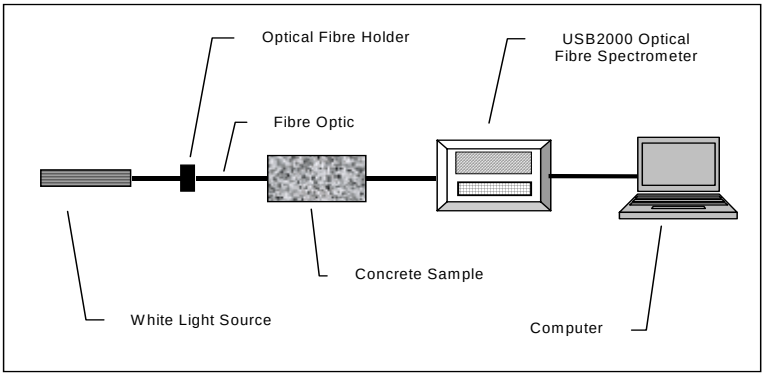

Figure 3. The illustration of experimental setup.

The intensity of the outgoing white light was recorded using Silicon pin detector and the spectra obtained before and during the corrosion process were also recorded.

When corrosion of the reinforcement occurred, it is reflected by transmission of light through the unclad portion of the plastic optical fibre. The light signals from the fibre were then recorded at intervals of 24 hours. This process continued for a period of 45 days.

3 RESULTS AND DISCUSSION

Figure 4 shows the corrosion curve recorded by the unclad plastic optical fibre corrosion sensor of the controlled sample (sample A). The reinforcing steel was not corroded after 45 days. The curve shows that the output voltage is always stable throughout the 45-day period. The voltage for non-corroded reinforcement steel rod fluctuated between 9500 and 10500 mV. Similar observation was also recorded from half cell measurement where the potential stable was around -100 mV. There was no pattern to suggest the occurrence of corrosion.

Observations on sample B which was immersed in 10% NaCl solution for 45 days are shown in Fig. 5. From the figure, the output voltage starts to decrease after day-20. The voltage then drops slowly from 10337 mV to 6110 mV on day-45. The reduction in the output voltage was believed to be attributed to the accumulation and change in colour on the surface of the reinforcing steel. This corrosion product disturbed the light travel along the fibre hence the reduction in the voltage. This observation is also recorded from the half cell results, where the reading drops from -105 mV to -201 mV on day-45. This is an important observation on reinforcement corrosion.

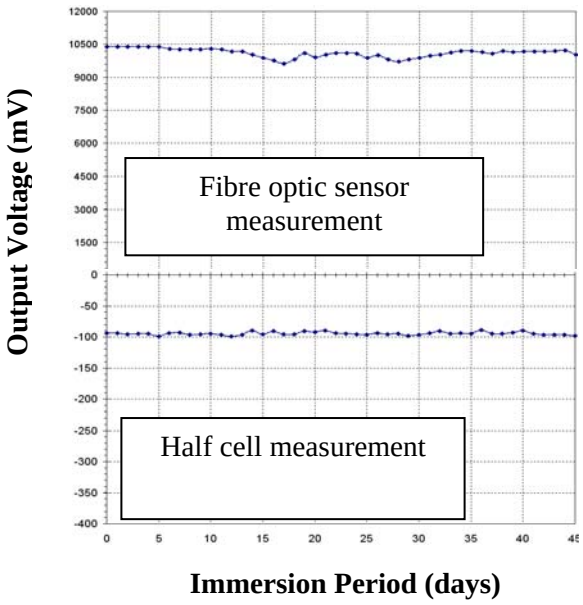

Figure 4. Curve of output voltage Vs Exposure period for controlled sample.

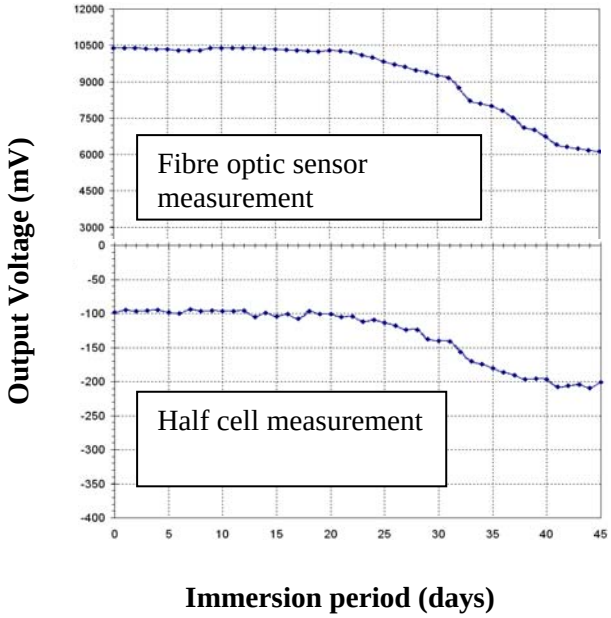

Figure 5. Curve of output voltage Vs exposure period for sample immersed in 10% NaCl.

Figure 6 shows the curve of voltage output due to sample C that was immersed in 40% NaCl solution for 45 days. The voltage curve of this sample drops slowly up to day-20. After day-20 the drop was quite rapid.

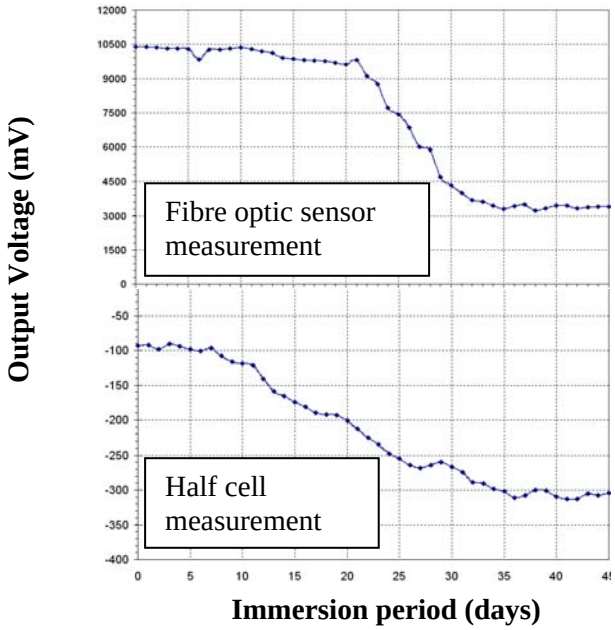

Figure 6. Curve of output voltage Vs exposure period for sample immersed in 40% NaCl.

The pattern showed by the voltage curves proved that, the unclad plastic optical fibre corrosion sensor was capable of observing early corrosion process. This finding is similar to what was found by [Siaw *et al*. 2002] who work on Y-shape fibre bundle and also by [Mohammad *et al*. 2005] in observing corrosion process of reinforcing bar. From the above observation, the application of optical fibre for monitoring the process of corrosion in concrete is very reasonable and promising. Photos of the condition of reinforcement in the three samples after the experiment are shown in Figs. 7, 8 and 9.

Figure 7. Condition of reinforcement in controlled sample after 45 days exposure period.

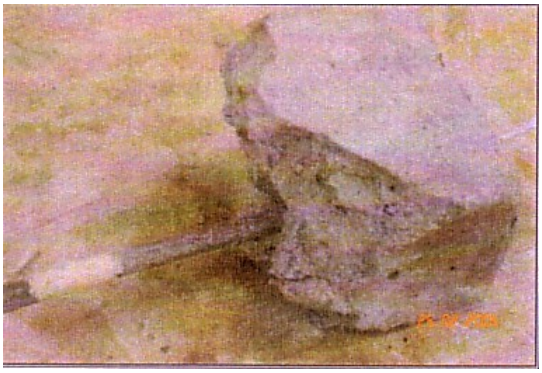

Figure 8. Condition of reinforcement in 10% NaCl solution after 45 days exposure period.

Figure 9. Condition of reinforcement in 40% NaCl solution after 45 days exposure period.

4 CONCLUSIONS

From this study, it is observed that the application of optical fibre sensor to monitor the corrosion process of reinforced concrete structures was encouraging. The changes of white light spectrum intensity tell us about the corrosion intensity of reinforcing steel in concrete.

The following conclusions may be drawn:

i. The unclad plastic optical fibre corrosion sensor can be used as a corrosion monitoring sensor by attaching it to the reinforcement surface.
ii. This type of investigation is very appropriate because the plastic optical fibre can be attached directly to the reinforcement surface.
iii. The transmitted optical power going through the plastic optical fibre decreases dramatically with the severity of corrosion in reinforced concrete.

ACKNOLEDGEMENTS

The author gratefully acknowledges the support for this research from Ministry of Science and Technology Malaysia, Research Management Centre UTM, and Technicians, Faculty of Civil Engineering and Faculty of Science, Universiti Teknologi Malaysia.

REFERENCES

Broomfield, J.P. 1997, 'Corrosion of steel in concrete: Understanding, Investigation and Repair', E & FN SPON, UK.

Elsener, B., Buchler, M., Stalder, F., and Bohni, H. 1999, 'Migrating corrosion inhibitor blend for reinforced concrete, Part 1—Prevention of Corrosion, Corrosion', Houston, **55**(12): 1155-1167.

Eric, U. 1995, 'Fibre optic smart structures technology', In Eric U. (ed.) Fibre Optic Smart Structures, John Wiley and Son, New York.

Escobar, P., Gusmeroli, V., and Martineeli, M. 1992, 'Fibre–optic interferometric sensors for concrete structures', SPIE, Vol. 1777.

Fuhr, P.L., Huston, D.R, Ambrose, T.A., and Snyder, S. 1993, 'Stress monitoring of concrete using embedded optical fibre sensors', ASCE Journal of Structural Engineering, **119**(7): 2263-2269

Huston, D.R, and Fuhr, P L. 1992, 'Fibre optic monitoring of concrete structures', SPIE, Vol. 1798.

Huston, D.R, and Fuhr, P.L. 1995, 'Fibre optic smart civil structures', In Eric U. (ed.) Fibre Optic Smart Structures, Wiley - Interscience.

Huston, D.R., Fuhr, P.L., Eric Udd. and Inaudi, D. 1999, 'Fibre Optic Sensors for Evaluation and Monitoring of Civil Structures', SPIE, Vol. 3860.

Maher, M. H. & Nawy, E.G, 1993, 'Evaluation of fibre optic bragg grating strain in high strength concrete beams'. In Ansari, F. (ed.) Applications of Fibre Optic Sensor in Engineering Mechanic, ASCE Journal of Structural Engineering, **119**(1): 120-133.

Mendez, A, Morse, T.F., and Mendez, F. 1990, 'Application of Embedded Optical Fibre Sensors in Reinforced Concrete Bridges and Structures', SPIE, Vol. 1170.

Siaw W. S., Mohammad Ismail, Madzlan Aziz and Rosly Abd Rahman 2002, 'Y-shape optical fibre bundle in monitoring corrosion', Jurnal Kejuruteraan Awam, **14**(2): 47-59.

Mohammad Ismail, Erica Dina, Rosly Abdul Rahman and Sabirin Ikhsan 2005, 'Observation of Corrosion Process of Reinforcing Steel', Jurnal Kejuruteraan Awam **17**(1): 13-22

11DBMC International Conference on Durability of Building Materials and Components
ISTANBUL, Turkey 11-14 May 2008

Fracture Toughness of Hybrid Fiber Reinforced High Strength Concrete under High Temperature

Kazuo Watanabe [1]
Takashi Horiguchi [2]
Kasunori Shimura [3]

T 11

ABSTRACT

Various fibers (i.e. polypropylene, steel, etc.) were added to concrete with the purpose of reducing its deterioration rate due to fire. From experimental studies, it was understood that high strength concrete frequently causes explosive spalling under high temperature environment, compared with normal strength concrete.

In order to prevent explosive spalling on high strength concrete, addition of organic fiber was found to be able to provide a good effect. However, on the other hand, concrete structure with organic fiber encountered significant degradation after high temperature heating. Therefore, improvement by hybrid fiber including organic fiber and steel fiber was suggested.

In this research, material testing of the fiber reinforced high strength concrete and the test regarding fracture energy of these types of concrete was performed. In addition, the tensile softening curve was back-calculated with the poly-liner approximation method.

Physical properties and fracture energy were evaluated under a heating stage (i.e. hot test) as well as a cooling stage (i.e. residual test). The experimental results verified the tenacity effect by the hybrid fiber on high strength concrete under high temperature environment.

KEYWORDS

Bending strength, Explosive spalling, Fire resistance, Fracture toughness, High strength concrete, High temperature, Hybrid fiber reinforcement, Residual strength

[1] Hokkaido University, Graduate School of Eng., Sapporo, Japan, Phone +81 011 7066180,kazuo-be@eng.hokudai.ac.jp
[2] Hokkaido University, Graduate School of Eng., Sapporo, Japan, Phone +81 011 7066180, horiguti@eng.hokudai.ac.jp
[3] Hokkaido University, Graduate School of Eng., Sapporo, Japan, Phone +81 011 7066180, shimura@eng.hokudai.ac.jp

1 INTRODUCTION

Recently, long tunnels are constructed with high strength concrete and have become an important means of traffic infrastructure worldwide. But, damage due to fire accident inside the tunnel occurs in some cases. As a consequence of the damage for the fire in the tunnel, concrete strength decreases. In terms of high strength concrete, there is a characteristic deterioration due to the explosive spalling phenomenon. With respect to structural collapse mechanism, this will cause secondary damage that must be considered as an important problem. In addition to a recent tunnel structure, secondary tunnel linings are often uninstalled due to the aspect of economical efficiency. With this trend increasing, improvement in fire resistance of primary concrete tunnel linings is required. However, research that deals with fracture behavior of high strength concrete under high temperature condition, comparing to normal strength concrete is still limited [C.V. Nielsen *et al*.2003]. Topics on this issue are still open to be investigated. Therefore, detailed examination regarding fire resistance of high strength concrete is needed worldwide.

In this research, polypropylene (PP) fiber is utilized to prevent the explosive spalling [S.L. Suhaendi *et al*.[2006]], while steel fiber is expected to retain the remaining strength of the concrete. Deterioration behavior of fiber reinforced high strength concrete (FRHSC) exposed to high temperature is examined from the viewpoint of fracture mechanics. This experimental study compares fire resistance of two kinds of FRHSC that utilized various fibers inside HSC mixture. Evaluation of fracture toughness is back-calculated using the poly-liner approximation method [Y. Kitsutaka, 1997].

2 EXPERIMENTAL PROGRAM

2.1 Fibers, Materials, Specimens, and Experimental Conditions

Mix proportion of concrete is shown in Table 1. All series of concrete were casted using ordinary Portland cement, river sand, and crushed stone. Specific gravity of river sand is 2.70, and specific gravity of crushed stone is 2.65 (maximum nominal size of 20 mm). Some parameters of mix proportion were kept constant: W/C = 0.3, sand to aggregate ratio (s/a) = 50%, and water content = 170 kg/m^3. A polycarboxylate-based superplasticizer, air entraining agent, and bubble cutter agent were used to attain desired workability and air content of fresh concrete. Specimens were mixed using a double-axes mixer. All specimens were prisms of 100×100×400mm.

Table 1. Mixture Proportion.

Series	W/C (%)	s/a (%)	Fiber volume (%)			W (kg/m^3)	Air (%)	SP[*1] (%×c)	AE[*2] (%×c)	BC[*3] (%×c)
			Polypro-pylene	Steel (S13)	Steel (30)					
Plain	30	50	-	-	-	170	6	0.8	0.012	-
PP			0.1	-	-			1.2	0.006	0.001
HY1			0.1	-	0.5			1.35	0.008	0.001
HY2			0.1	0.1	0.4			1.4	0.008	0.001

[*1]SP:super plasticizer [*2]AE: air entraining agent [*3]BC: bubble cutter

Polypropylene and two-steel fibers having 18 , 160 and 600-micron effective diameter were used in this experimental study. All of fibers came in bundles that were well dispersed inside the concrete mixture. Properties of fibers are shown in Table 2.

After casting, the specimens were demoulded after 24 hours, and then cured under lime-saturated water at temperature of 20±2℃ for 28 days. The notch with a thickness of 5 mm and a depth of 30

mm was made in the center section of all specimens making use of concrete cutter. Some specimens were heated using electric furnace and heating device. Both heating rates were set at 10℃/min with the maximum temperature kept at 200, 400, and 600℃ for 2 hours. In the case of residual test, heated specimens were let to cool inside the furnace until its temperature coincided with room temperature to prevent cracks upon cooling.

Table 2. Properties of Fibers.

	Polypropylene	Steel (S13)	Steel (S30)
Diameter (mm)	0.018	0.16	0.6
Length (mm)	6	13	30
Shape	Filament	Straight	Indent
Density (gr/cm^3)	0.9	7.8	7.8
T_{melt} (℃)	160-170	1370	1370
$T_{vaporize}$ (℃)	341	-	-

2.2 Experimental Device and Evaluation Method of Fracture Energy

With a designated loading span of 300 mm, the fracture energy test was executed under load control using a servo jack testing machine. The beam specimen was arranged on some rollers under both fulcrums to let it move freely in horizontal direction.

In the case of fracture energy test, loading rate was set at 0.1 mm/min. The fracture energy test was conducted in accordance with a JCI (Japan Concrete Institute) test method [JCI-S-002-2003]. During the fracture energy test, load (P), crack mouth opening displacement (CMOD), and load point displacement (LPD) were measured. The loading device and measurement points layout are shown in Figure 1.

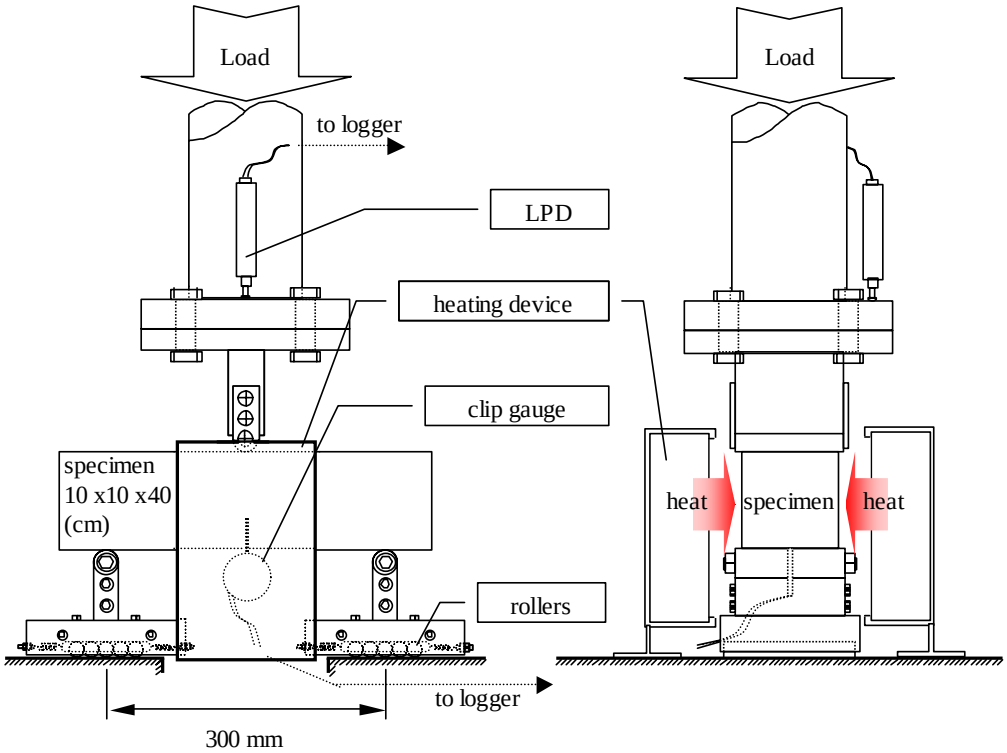

Figure 1. The Fracture Toughness Test Equipment (with Heating Device of Hot Test).

Fracture energy of specimen was calculated as follows:

$$G_F = \left(0.75W_0 + W_1\right)/A_{lig}$$

$$W_1 = 0.75\left(S/L \cdot m_1 + 2m_2\right)g \cdot CMOD_c$$

(1)

where;

G_F :Fracture energy (N/mm)

W_0 :Area under Load-CMOD curve before specimen breaking (N·mm)

W_1 :Weight of the specimen and the work from loading jig forms (N·mm)

A_{lig} :Area of ligament (b·h)

m_1 :Weight of specimen (kg)

S :Loading span (mm)

m_2 :Weight of jig appearing in a specimen (kg)

$CMOD_c$: (mm)

3 RESULTS AND DISCUSSION

3.1 Bending Strength under Hot Test and Residual Test

Bending strength was evaluated both under the heating stage (hot test) and cooling stage (residual test). Bending strength ratio with relation to heating temperatures is shown in Figure 2 and Figure 3.

It is found that inclusion of fiber into concrete will guarantee the residual bending strength, as shown in Figure 2. In addition, in the case of residual test, increase in strength can be noticed at 200. This phenomenon is widly recognized as “dry strength (Austrocknungsfestigkeit)” of Czernin [W. Czernin 1977]. On the other hand, in the case of hot test, the bending strength ratio shows quite different trend, as shown in Figure 3. The bending strength ratio decreases quickly at 200℃ and then stays almost constant up to 600.

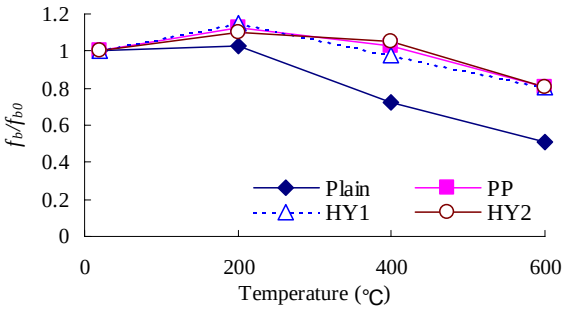

Figure 2. Bending Strength Ratio (Residual Test).

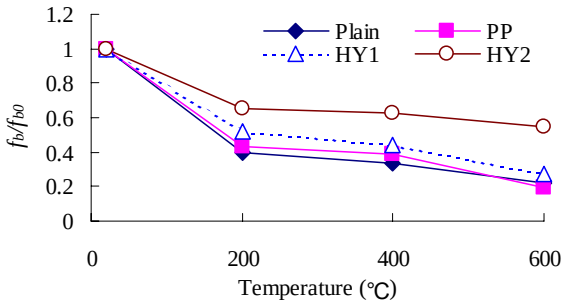

Figure 3. Bending Strength Ratio (Hot Test).

3.2 Fracture Toughness Test Results (Load - CMOD Curve)

Load - CMOD curve is given in Figure 4 (residual test) and Figure 5 (hot test) showing one representative result from the experimental tests. The maximum load decreases with increasing heating temperature.

From Figure 4 and Figure 5, it was verified that CMOD at maximum load becomes larger with relation to the increase in heating temperature. With the increase in heating temperature, stiffness decreases, as shown in both Figures. In each heating temperature of both tests, the load decrease of Plain and PP is considerable after the peak. However, not breaking either after the peak is due to steel fiber reinforcement. Especially, HY2 verified that continues to support the large load, in comparison with Plain and PP.

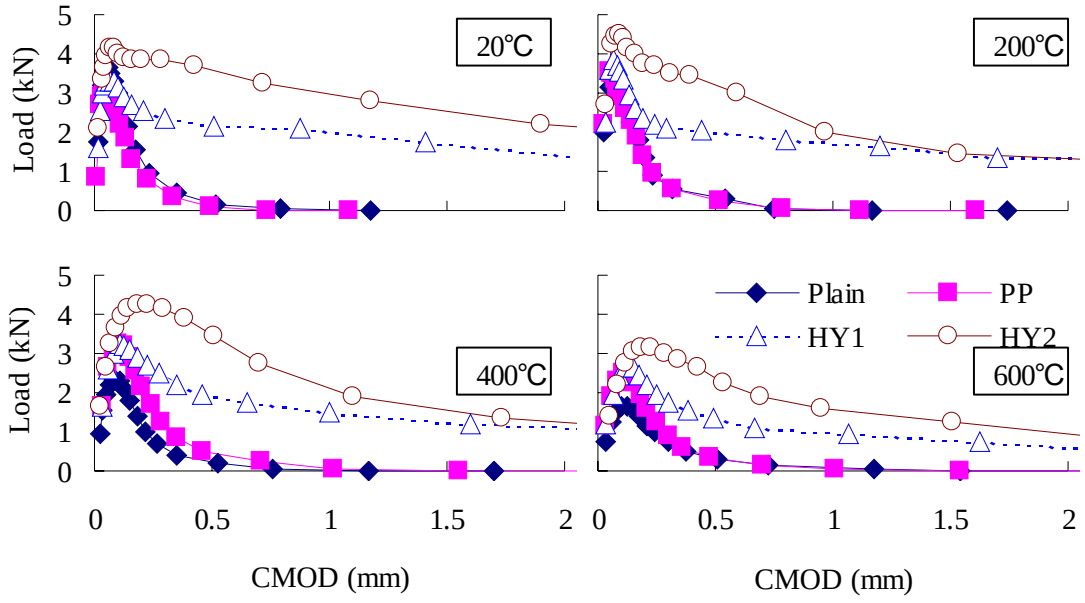

Figure 4. Load–CMOD Curve at 20℃, 200℃, 400℃, and 600℃ (Residual Test).

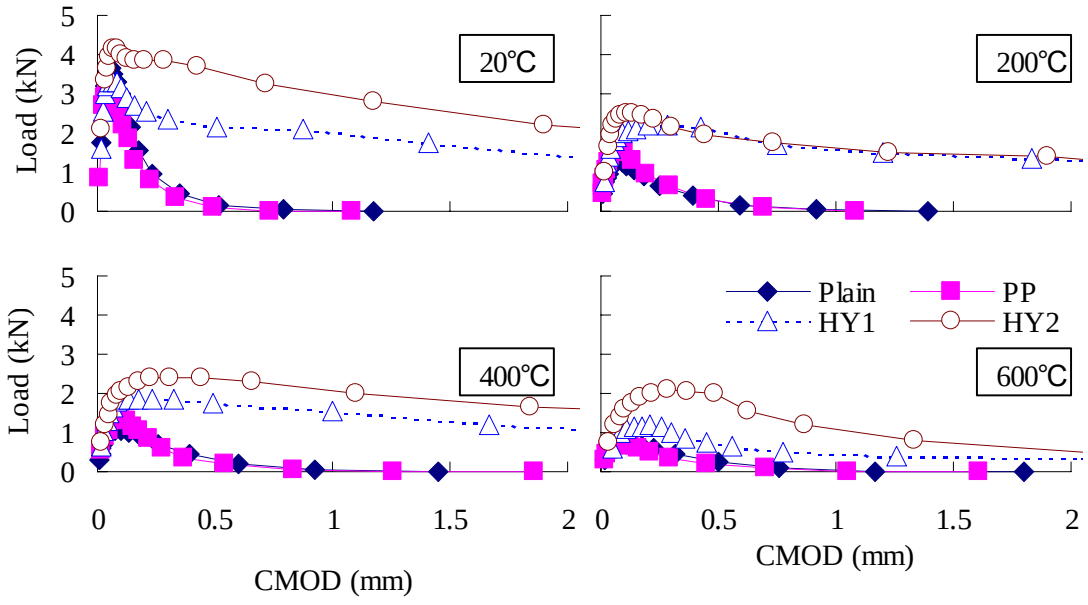

Figure 5. Load–CMOD Curve at 20℃, 200℃, 400℃, and 600℃ (Hot Test).

On the other hand, it is found that the strength decrease of PP under high temperature is small in comparison with that of Plain. Plain and PP destructive behavior almost same. With the polypropylene fiber of 6mm length, it has not contributed to the pulling out efficiency of the fiber before and after heating.

In both tests, the specimens including steel fibers didn't show rapid descending behavior after maximum load. Previous tendency becomes high with the increase in heating temperature. However, in the case of hot test, sudden decrease after maximum load is not observed. The reason of this finding should be investigated further.

3.3 Fracture Toughness Test Results (Fracture Energy)

Fracture energy was calculated from Formula (1). The relationship between fracture energy and heating temperatures is shown in Figure 6. As shown in the figure, large difference of fracture energy between the Plain/PP series and the HY series was observed. As for the fracture toughness of the HY series, it was found that the fracture energy decreased with the increase in heating temperature.

Especially, when it is exposed to high temperature above 200℃, fracture energy of concrete decreases suddenly and converted to fail in a brittle manner. This phenomenon is thought to be affected by the fiber due to the fact that under hot environment polypropylene fiber melts and disappears.

For both tests, it could be found that the fracture energy of concrete that includes steel fiber exceeds the one of Plain and PP series at any heating temperature. Therefore, it was confirmed that the mixture of the steel fiber improves fracture toughness. But, this result should be verified for other mixture proportions.

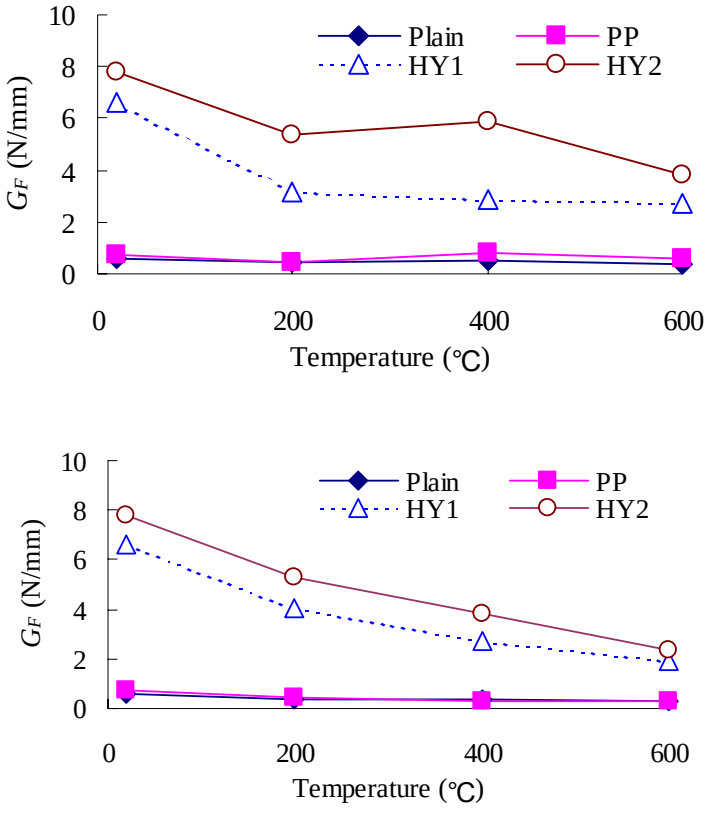

Figure 6. Relatives Fracture Energy Under Residual Test (upper) and Hot Test (bottom).

4 CONCLUSIONS

Quite remarkable difference was observed from the strength quality of HFRHSC due to heating test method, hot test and residual test. Especially, at the time of hot heating above 200℃, sudden decrease of maximum load was verified in the case of hot test. But, the mechanism of deterioration behavior for each mix proportion was not excessively verified. Therefore, bending the concrete with hybrid fiber reinforcement that has large initial strength is found to be effective.

For specimens including steel fiber, the maximum load does not drop suddenly in hot test. It was verified from the Load-CMOD curve that it only caused gradual decrease.

As for mixing the steel fiber which combines long and short fibers into the concrete (HY2), the effect is larger than single use (HY1).

In hot test, hybrid fiber reinforcement in high strength concrete mixture is very effective to prevent brittle fracture. It is verified that this type of reinforcement is very effective with the favor of fracture energy test.

REFERENCES

Nielsen C.V. & Bicanic N. 2003, 'Residual Fracture Energy of High-Performance and Normal Concrete Subject to High Temperatures', *Material and Structures*, Vol. 36, pp. 515-521.

RILEM Draft Recommendation 1985, 'Determination of Fracture Energy of Mortar and Concrete by Means of Three Point Bending Tests on Notched Beams', *Material and Structures*, Vol. 18, No. 106, pp. 285-290.

Lie, T.T. & Kodur, V.K.R. 1996, 'Thermal and Mechanical Properties of Steel Fiber Reinforced Concrete at Elevated Temperatures', *Canadian Jornal of Civil Engineering*, Vol. 23, pp. 511-517.

Suhaendi, S.L. & Horiguchi, T. 2006, 'Effect of short fibers on residual permeability and mechanical properties of hybrid fiber reinforced high strength concrete after heat exposition', *Cement and Concrete Research*, Vol. 36, September, No.9, pp. 1672-1678.

Suhaendi, S.L., Suto, M. & Horiguchi, T. 2006, 'Optimization of polypropylene fibers for high strength concrete under high temperature condition', Proceedings of the 10th East Asia Pacific Conference on Structural Engineering and Construction, Vol. 6, pp. 467-472.

Suhaendi, S.L., Shimura, K. & Horiguchi, T. 2006, 'Non-destructive test of heated fiber reinforced high strength concrete', *Proceedings of the Japan Concrete Institute*, JCI, Vol. 28, No.1, pp. 407-412.

Kitsutaka, Y. 1997, 'Fracture Parameters by Poly-linear Tension Softening Analysis', *Journal of Engineering Mechanics*, ASCE, Vol. 123, No. 5, pp. 444-450.

Japan Concrete Institute Research Committees: *Method of test for load-displacement curve of fiber reinforcement concrete by use of notch beam*, JCI-S-002-2003.

Czernin, W. 1977, '*Zementchemie für Bauingenieure*', 3. neubearb. Aufl., Bauverlag, Wiesbaden.

11DBMC International Conference on Durability of Building Materials and Components
ISTANBUL, Turkey 11-14 May 2008

MICROSTRUCTURAL ASSESSMENT OF THE INTERFACIAL TRANSITION ZONE IN GRANITIC CONCRETE

Azimah Hussin [1]
Colin Poole [2]
Robert Fowell [3]

T11

ABSTRACT

The exploitation of granitic aggregate in concrete fabrication is quite common in the construction industry throughout the world. The vast majority of studies have agreed that the mechanical performance of the concrete is strongly related with the characteristics of the aggregates. Thus, the characteristics of aggregates are also one of important variables affecting the concrete microstructure including the development of interfacial transition zone (ITZ). As the weakest link, the ITZ is also well known as the medium in which the transmission of stresses between aggregate and the matrix occurs. However in granitic concrete, most previous experiments have claimed that the siliceous aggregate is chemically inert and plays very little role in the occurrence of the ITZ in concrete. A significant amount of research is now being undertaken in evaluating the effects of granitic aggregate in the development of the ITZ microstructure. This study describes possible differences in the microstructural nature of the ITZ in concrete containing three different types of granitic aggregate. The ITZ microstructure has been investigated in a petrographic manner with the application of backscattered SEM analysis.

Keywords: Granitic aggregate; Interfacial zone; Microstructure

[1] Programme Geology, Faculty Science and Technology, National University of Malaysia (UKM), 43600, Bangi, Selangor, Malaysia, Phone +06 03 89215496, Fax +06 03 89215490, azie6371@yahoo.com
[2] Institute of Particle Science & Engineering, School of Process, Environmental and Material Engineering, Houldsworth building, Clarendon Road, University of Leeds, Leeds LS2 9JT, UK, Phone +44 (0) 113 343 2798, Fax +44 (0) 113 343 2405, c.poole@leeds.ac.uk
[3] Institute of Particle Science & Engineering, School of Process, Environmental and Material Engineering, Houldsworth building, Clarendon Road, University of Leeds, Leeds LS2 9JT, Phone +44 (0)113 343 2803, Fax +44 (0)113 246 7310, r.j.fowell@leeds.ac.uk

1 INTRODUCTION

Modern concrete is a three phase, complex composite material consisting of aggregate particles and cement linked together by an interfacial transition zone (ITZ). Amongst these three phases, the ITZ is known to be the weakest link, influencing both the mechanical properties and the durability of the concrete [Scrivener and Pratt, 1986; Struble, 1988; and Stankowski et al., 1990]. Durability and strength are two major properties that establish the performance of a good concrete. Without these, the concrete is more susceptible to premature failure. Since the ITZ was first identified as one of the factors associated with strength and durability [Thomas and Floyd, 1963] its characterisation has been a crucial parameter in concrete technology. Many researchers have conducted various microstructure tests to evaluate variations in the ITZ. One of the first was Jacques Farran, the pioneer researcher who observed the behaviour of the aggregate-cement paste interface [Scrivener et al., 1988]. He suggested that this aggregate-cement interfacial zone exhibits specific changes in mineralogy and microstructure. Later work by Mindness and Young [1981] confirmed the ITZ as a zone of weakness, both in terms of mechanical properties and durability.

Aggregate occupies 75-80% of the volume of concrete and can, therefore, be considered to have a significant influence on the performance of the ITZ system [Mindness and Young, 1981]. Although rock aggregate is a basic geological product, there is an enormous array of coarse aggregates available for use in concrete making. As a consequence, the most viable sources for a particular use of concrete must have specific characteristics which are often dependent upon the fundamental features of the parent rock or the operations used in their production. This means that the understanding of aggregate characteristics requires a profound knowledge of the rock properties and the variation in these properties. In fact, research shows that coarse aggregate plays a considerable role in determining the strength, stability, workability and durability of concrete [Jamkar and Rao, 2004].
Since the late 1990s, the discussion on aggregate function in the ITZ of concrete has been given greater priority. Among the influential authors on the subject are Tasong et al. [1998], Irvine [1999] and Elsharief et al. [2003]. Their works have examined the development of the ITZ from the viewpoint of the crushed aggregate properties and their findings have provided evidence that aggregates are not inert, as previously supposed. Their results reveal that aggregates are, in fact, chemically active and the interfacial bond strength is controlled by factors such as aggregate structure, aggregate strength and the chemical interaction with cement. In fact, it is now believed that the traditional mineralogical and geochemical behaviour of aggregate sources is responsible for the wide variation of the ITZ in concrete.
The objective of this paper is to present the effects of granitic aggregate in the development of the ITZ microstructure. The methodology and test results of the investigation into the microstructural nature of the ITZ in concrete containing three different types of granitic aggregate are presented and discussed.

2 EXPERIMENTAL INVESTIGATIONS

Three sources of crushed granitic aggregate were used as normal weight coarse aggregate in this study. These three sources consisted of;

i) Shap granite from the Lake District,UK.
ii) Mountsorrel granite from Leicestershire,UK.
iii) Johor granite from Johor, Malaysia

Normal strength concrete specimens (28day nominal strength of 40MPa) with a water binder ratio of 0.5 were prepared using the above granitic aggregate. Polished thin sections of each concrete have been used to obtain results on the microstructure features of the ITZ. Briefly, thin section were sliced from bulk

concrete by low-speed precise diamond-bladed saws using non-aqueous lubricants and all the sections were coated with platinum-paladium film.
The investigations described in this section attempt to address the influence of granitic aggregate type on the microstructure of the ITZ from the normal strength concrete. This study has investigated the characteristics of the ITZ microstructure in a petrographic manner, but as the normal polarizing microscope is unsuitable for this, so investigations proceeded with the application of SEM techniques.
Using SEM observations, the study has attempted to best describe any possible differences in the nature of the ITZ. Analysis was carried on polished sections and the backscattered mode of SEM (Phillips XL 30 environmental scanning electron microscope) analysis was performed randomly on each selected aggregate. The images were taken at x200 and x500 magnification and over 60 images of different ITZs and curing ages were analysed to differentiate the composition. Higher magnifications were used to view the specific morphology occurring in the ITZ.

3 RESULTS AND DISCUSSION

Throughout the BSE imaging analysis, the ITZ specimens containing different type of granitic aggregate displayed considerable heterogeneity in their microstructure. Figure 1 illustrates a typical microstructure found in most analysed images (in this case, one day old Johor granite ITZ). The common constituents in this region are comparatively easy to distinguish, as they show significant microstructural differences.
In all of the present ITZ sections examined, the polymineralic nature appears as its original microstructure outline. The main deposition phase is quite distinct. CH has already been well developed and has a light grey colour appearance, while the dark grey C-S-H is mainly deposited around the aggregate. Other constituents include anhydrous cement grains, pores with dark spot marks and other minor hydration products of needle shaped ettringite(AFt).

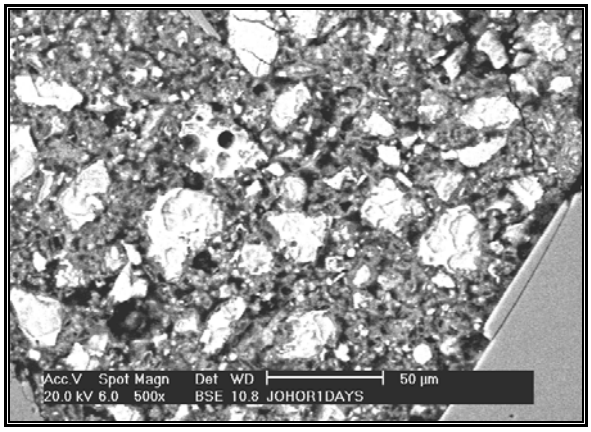

Figure 1. Typical BSE image of the ITZ prepared from one day old concrete containing Johor granite.

After 1 day curing period, the microstructure of the ITZ in each sample (shown in Figure 2) showed a lower degree of hydration and significantly showed a “sheaf of wheat” morphology. Unhydrated cement grains and porosity are common features seen in most samples and masses of CH were also observed throughout the ITZ. In all granitic specimens, higher magnification helped to identify well crystallised CH grains (Figure 3).

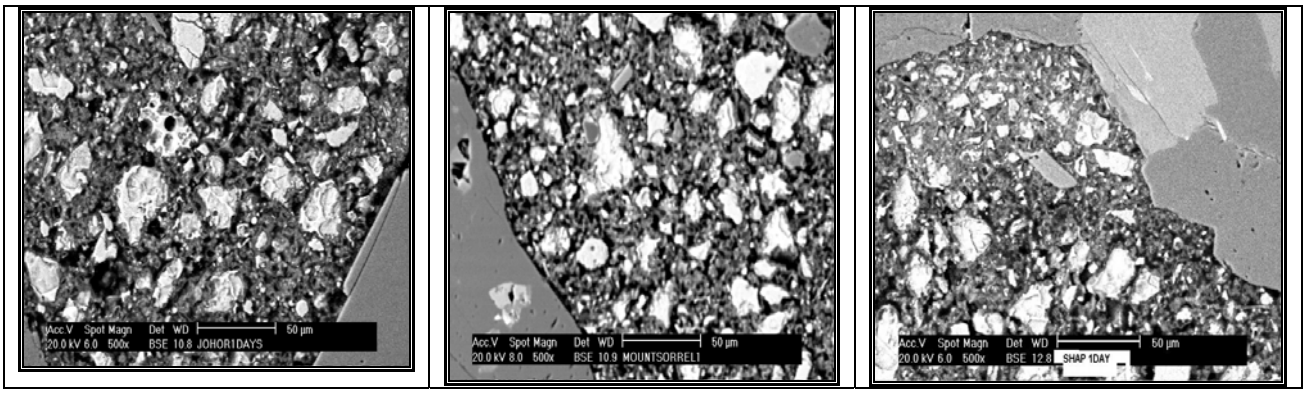

Figure 2. General microstructure of the ITZ and bulk phase of concrete for different types of aggregates after 1 day curing period.

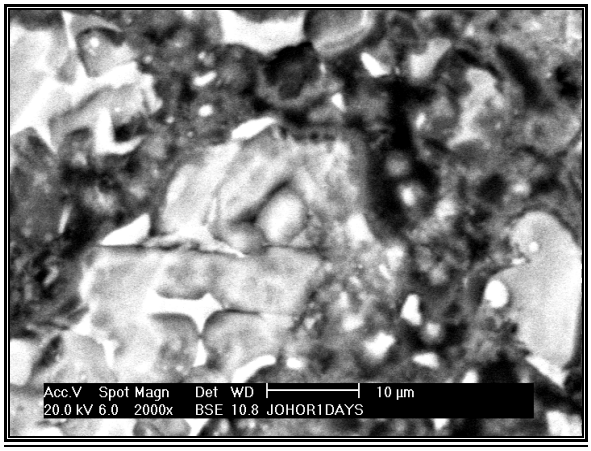

Figure 3. Higher magnification of BSE image for the ITZ of Johor granite concrete after 24 hours curing period. C-S-H is still badly crystallized, but calcium hydroxide show well developed hexagonal plates.

However, it was not possible to indentify any ettringite crystals in any of the samples. These results agree with the suggestion by Scrivener and Taylor [1993], that at this early stage of hydration, ettringite is still embedded within the C-S-H product. The "sheaf of wheat" morphology in ITZ refers to a structure which tends to branch in a radial fashion. According to Zampini et al. [1997] the "sheaf of wheat" morphology is an early formed C-S-H product but structurally similar to CH. These morphology resulting from the reaction of the silica species and the calcium ions. BSE images studies reveal that this kind of morphology is very obvious in granitic ITZ. Apparently, the more numerous 'sheaf of wheat" morphology in the granitic specimens in this study may have related to Wiliamson [1968] statement: the silicate rich particles provides and facilitates the nucleation of C-S-H with branching morphology.

With the progress of hydration continued to 28days, the ITZ became denser and abundant C-S-H was growing. Figure 4 illustrates the general microstructure of the ITZ for each aggregate type after the completion of 28 days curing. At longer age, the porosity has been greatly reduced and the ITZ becomes more amorphous. Although the hydration process was not yet completed, these observation indicate that the ITZ microstructure of each sample, especially with granitic aggregates, appear denser and less porous after 28 days and the acceleration effect of the curing period on the microstructure is more apparent, with hydrated grains such as AFt, CH and C-S-H being well formed in the ITZ region.

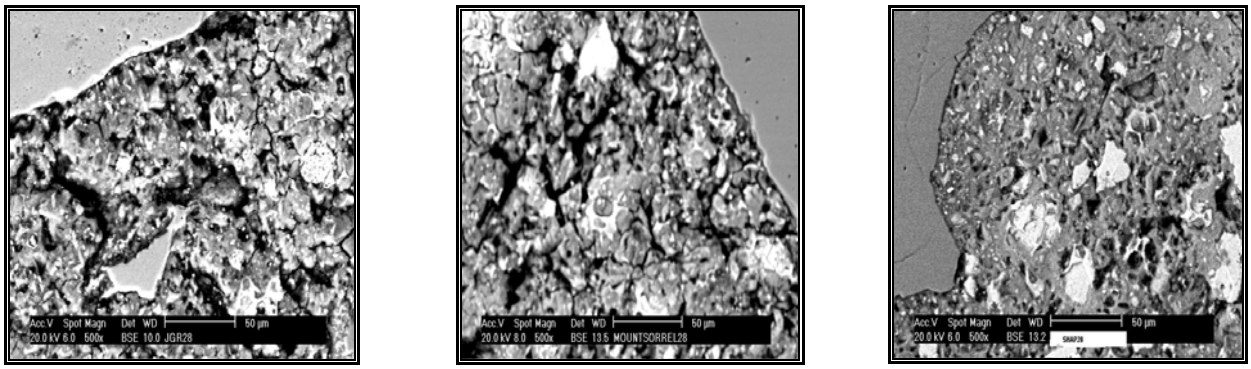

Figure 4. BSE images of the ITZ and bulk phase of concrete prepared from different types of granitic aggregates after 28 days curing period.

SEM observation suggests that the granitic ITZs appear to have, in general, lower porosity and a finer pore structure. The observations also reveal that among the three types of concretes prepared, the Johor granite concrete had the densest appearance. Although a number of 10µm or larger size pores were present in the ITZ, the total volume of pores was obviously much lower than in the other samples. Hardly any granular-like hydrates, and flake-like crystals could be found. The EDAX pattern of the hydrates indicates that it consisted mainly of C-S-H. All of those observations support the assumption that the ITZ microstructure is affected by the mechanism of formation [Scrivener and Pratt, 1996]. For instance, in the fresh granitic concrete, a water film normally will form around the aggregates due to wetting and bleeding effects. Poon et al, [2004]. observed that the local W/C ratio at the ITZ can be twice than that in the bulk paste. As hydration progresses, the water-filled space near the aggregate is gradually replaced by an increasing amount of hydrates.

In the granitic samples, it is probable that there was denser packing of cement particles adjacent to the aggregates, due to the role of the aggregate grain composition. This situation agrees with the hypothesis given by Livingston et al. [1999] and Richard et al. [1999]. They pointed out that the proportions of each type of mineral present in the aggregate produced variations in interface development. In this study, all three types of granitic aggregate had a large proportion of feldspar, including Ca-rich plagioclase and Na-rich albite.

A relatively dense ITZ was obtained in the Shap granite concrete (see Figure 5). The mechanism here could be that the granitic aggregate had a low initial moisture content which lowered the initial W/C ratio in the ITZ at the early hydration stage. Newly formed hydrates then gradually filled the region, and these processes effectively improved the interfacial bond between aggregate and cement.

Furthermore, the variations in hydrate concentration in the ITZ for each specimen in this study appear to support previous work by Maso [1980] and Breton et al. [1993]. In all ITZ specimens three distinct zones could be identified:

- the region located at adjacent to aggregates surface (within 0-15µm), which is rich with CH.
- the region situated between 15-50µm which contained less CH but more C-S-H,
- the region >50µm, which has a similar appearance to normal strength concrete and, in this study, is therefore considered as the bulk phase.

The microstructure of the bulk phase (the region>50µm) in every specimen is generally compact and tends to be more amorphous than crystallized. Based on EDAX analysis, this phase was essentially

composed of more C-S-H. Pores and entrapped air voids were also visible in most samples with a size range of 10-100µm. As well as C-S-H, some massive crystals of CH were also observed in the bulk phase.

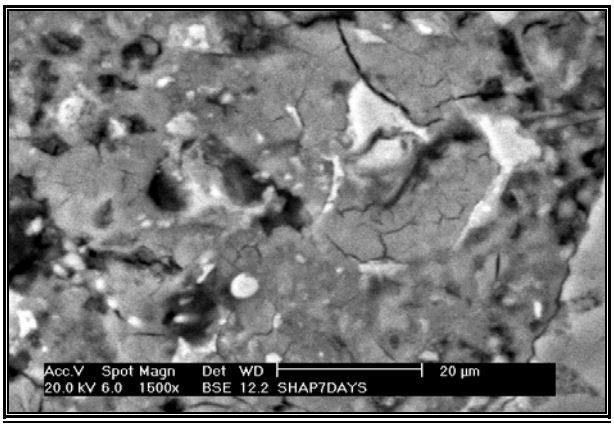

Figure 5: View of higher magnification of the ITZ of Shap granite. The dense looking textural appearance is a result of the growth of hydrate crystal.

4 CONCLUDING REMARKS

Based on observations, the following conclusions can be drawn:

- Normal strength concretes made with crushed granitic aggregates display variation in ITZ properties with excellent behavior
- After 1 day curing, many of the unhydrated cement particles and a few of the products of initial hydration, such as C-S-H and CH, exist in the area about 0-20µm from the edge of the aggregate, with C-S-H appearing as a mesh shape.
- After 28 days curing, more hydration product develops.
- In the range 0-50µm of the ITZ, the porosity changes as the curing age increases. After 1 day, the area of the pores is at its highest, and the pores are distributed uniformly in a large lump. After 28days, more hydration product exists and fills most of the pores, thus the pores are reduced and a denser structure results
- Microstructural observations clearly show that there is an increased frequency of porous patches in the ITZ. This frequency increases towards the interface.

REFERENCES

Elsharief A., Cohen M.D. and Olek J. ,2003, 'Influence of aggregate size, water cement ratio and age on the microstructure of the interfacial transition zone', *Cement and Concrete Research*, 33.1837-1849.

Irvine H., 1999, 'Characterising the influence of northern Irish aggregate on the properties of high stregth concrete' *PhD Thesis*, The Queen University of Belfast.

Jamkar S.S. and Rao C.B.K. , 2004, 'Index of aggregate particle shape and texture of course aggregate as a parameter for concrete mix proportioning', *Cement and Concrete Research*, 34. 2021-2027.

Livingston R.A., Manghnani M. and Prasad M. , 1999, 'Characterisation of Portland cement concrete microstructure using the scanning acoustic microscope', *Cement and Concrete Reseach*, 29. 287-291.

Maso J.C. , 1980, 'The bond between aggregate and hydrated cement paste', *7th International Congress on Chemistry of Cement, Paris*, 3/1-3/9.

Mindness S. and Young F.J. ,1981, *Concrete*, Prentice-Hall Inc. New Jersey.

Poon C.S., Shui Z.H. and Lam L. ,2004, 'Effect of microstructure of ITZ on compressive strength of concrete prepared with recyled aggregates', *Construction and Building Materials*, 18. 461-468.

Richard A.L., Manghnani M., and Prasad M. , 1999, ' Characterisation of Portland cement concrete microstructure using the scanning acoustic microscope', *Cement and Concrete Research*, 29.287-291.

Scrivener K.L. and Pratt P.L., 1986, 'Preliminary study of the microstructure of the cement/sand bond in mortar', *8th International Congress on the Chemistry of Cement*. Rio de Geneiro, Brazil. 466.

Scrivener K.L. and Pratt P.L., 1996, 'Characterisation of interfacial microstructure', *Interfacial Transition Zone in Concrete*, Maso J.C. ed. E and FN Spon, London. 3-17.

Scrivener K.L. and Taylor H.F.W., 1993, 'Delayed ettringite formation: A microstructural and microanalytical study', *Adv. Cementitious Reseach*, 5(20). 139-146.

Scrivener K.L., Bentur A. and Pratt P.L., 1988, 'Quantitative characterisations of the transition zone in high stregth concrete', *Advances in Cement Research*, 1. 230-237.

Struble L., 1988, 'Microstruture and the fracture at the cement paste aggregate interface', *Materials Reseach Society Symposium Proceedings*, 114(11-20).

Tasong W.A., Cripps J.C. and Lynsdale C.J. , 1998, 'Aggregate-cement chemical interactions', *Cement and Concrete Research*, 28(7) 1037-1048.

Thomas T.C. and Floyd O. , 1963, 'Tensile bond strength between aggregate and cement paste or mortar', *Proceeding of ACI*, 60.

Williamson R.B., 1968, 'Constitutional supersaturation in Portland cement solidified by hydration', *Journal of Crystal Growth*, 34.787-794.

Zampini D.,Jennings H.M. and Shah S.P. , 1995, 'Characterization of the paste-aggregate interfacial transition zone surface roughness and its relationship to the fracture toughness of concrete', *Journal of Material Science*. 30. 3149-3154.

11DBMC International Conference on Durability of Building Materials and Components
ISTANBUL, Turkey 11-14 May 2008

Frost Resistance of Pervious Concrete with Different Freezing and Thawing Tests

Takuro Nakamura [1]
Takashi Horiguchi [2]
Kazunori Shimura [3]

T 11

ABSTRACT

Pervious concrete has large continuous voids of 20-30 % by volume, and has some particular properties (i.e. high-permeability, purification, vegetation, etc). Pervious concrete is attractive as new environmental material and has begun to be applied for the river bank protection and road pavement in Japan. The object of this study is to investigate the frost resistance of pervious concrete as environmental materials. This investigation attempts to address this concern by comparing 3 kinds of specified freezing and thawing tests methods (ASTM C 666 procedure A, B methods and RILEM CIF). RILEM CIF test is different from ASTM C 666 method in water absorption, rate of cooling, length of freezing and thawing period, and number of freezing and thawing cycles. Test result of ASTM C 666 procedure A method, which is widely used for evaluating the frost resistance of concrete, showed extremely low durability of pervious concrete. Because of the low strength and the high porosity due to large void structure, frost resistance of pervious concrete seems to be lower than that of conventional concrete. However, result of RILEM CIF test showed adequate frost resistance. From these test results, it is found that difference of freezing and thawing test has influence on the evaluation of frost resistance. In addition, this study has conducted in situ exposure test for 5 years. Some pervious concrete blocks have been applied for river bank protection of Hokkaido Naie river in Japan, which resembles 70-80 cycles of freezing and thawing action annualy. Frost damage of these blocks by ultrasonic velocity measurement were evalutated to be in a slight degree. From these tests, a total of 350-400 cycles of natural freezing and thawing action showed a similar damage trend as RILEM CIF test and a significant difference with ASTM C 666 procedure A method is observed.

KEYWORDS

Pervious concrete, Frost resistance, ASTM C666, RILEM CIF, Exposure test

[1] Hokkaido University, Civil Engrg. Faculty, Sapporo, Japan, Phone +81-11-706-6180, takuroh@eng.hokudai.ac.jp
[2] Hokkaido University, Civil Engrg. Faculty, Sapporo, Japan, Phone +81-11-706-6179, horiguti@eng.hokudai.ac.jp
[3] Hokkaido University, Civil Engrg. Faculty, Sapporo, Japan, Phone +81-11-706-6180, shimura@eng.hokudai.ac.jp

1 INTRODUCTION

In recent years, necessity of the environmental materials for sustanable development is increasing over the world, and pervious concrete has been proposed to be used as such material. The characteristic of pervious concrete has a large continuous void strcure, which accounts for about 20-30 % of the whole volume. Pervious concrete can have a high permeability (about 1.0 cm/sec) and is generally applied for road pavement. This type of concrete, which has large void structure, came from "No-Fines Concrete". According to Malhotra, No-fines concrete had been used in Europe and the United Kingdom since 1930s for building of single story and multistory. In recent Japan, this type of concrete is sometimes called as "Porous concrete", and has begun to gain attention as a promising environmental material. The idea is that the large continuous void structure can give pervious concrete the ability of high permeability, purification, and vegetation. Pervious concrete has begun to be applied for the protection of river dam and further to road pavement.

It is necessary to confirm the frost resistance when pervious concrete is used in cold region. Many reports investigated the environmental functions of pervious concrete [JSCE, 2002]. However, there are few reports of the frost resistance. Frost resistance of pervious concrete has been investigated by several freezing and thawing tests method [M. Sugiyama, 2002 ; Obi and Taguchi, 2004]. The results were not clearly in agreement with in situ exposure condition. Therefore frost resistance of pervious concrete should be evaluated by an specified freezing and thawing test methods. This study attempts to address this concerns by comparing the test result of RILEM CIF test method ("RILEM Recommendation TC176-IDC"), and that of ASTM C666 procedure A and procedure B methods ("Standard Test Method for Resistance of Concrete to Rapid Freezing and Thawing").

It is necessary to conduct in situ exposure test as well as some laboratry tests. This investigation compared the result of in situ exposure test at Hokkaido Naie River in Japan with that of laboratory freezing and thawing tests.

The results of this study provide additional evidence to support the need in obtaining a viable freezing and thawing method and applicable to pervious concrete as environmental material.

2 MATERIALS AND MIXTURE PROPORTION

The mixture proportion in this study is shown in Table 1. The test specimen consisted of 3 types. Design values for the void ratio is set to 20%. Water cement ratio are set to about 23.5 % and 24 %. The matrix constituents of pervious concrete consisted of ordinarily portland cement (C), fine aggregate (S), coarse aggregate (G6 or G7), tap water (W) and some chemical admixtures. Particle size of G6 is 5-13 mm with specific gravity of 2.63. Particle size of G7 of 2.5-5 mm with specific gravity is 2.62. For NR6, a high viscosity agent was added. All specimen contained air-entraining and high-range water-reducing admixture (SP).

Table1. Mixture proportion.

	Void	W/C	Unit content (kg/m^3)						
	(%)	(%)	W	C	S	G6	G7	Ad	SP
NR6	20	24	99	413		1550		8.3	3.1
PG6	20	23.5	80	340	106	1503			3.4
PG7	20	23.5	80	340	172		1431		3.4

3 EXPERIMENTAL PROCEDURES

3.1 Freezing and Thawing Test

The frost resistance of pervious concrete was determined using the specifications of ASTM C 666 procedure A method and procedure B method ("Standard Test Method for Resistance of Concrete to Rapid Freezing and Thawing"), and RILEM CIF test ("RILEM Recommendation TC176-IDC"). Some of important details of three procedures are given in Table 2. As shown in this table, ASTM C 666 is a more severe testing method than CIF test in relation to rate of cooling, length of freezing and thawing period, and number of cycles. A brief description of each test method is provided in the next paragraphs.

Table 2. Test details of ASTM C 666 and RILEM CIF tests methods.

	ASTM C 666 test (procedure A)	ASTM C 666 test (procedure B)	RILEM CIF test
Number of cycles (test period)	300 6 cycles/day (50 days)	300 6 cycles/day (50 days)	56 2 cycles/day (28 days)
Freezing period Lowest temperature	2.75 hr -17.8 C	2.75 hr -17.8 C	7 hr -20 C
Cooling rate	14.4 deg C/hr	14.4 deg C/hr	10 deg C/hr
Thawing period Highest temperature	1 hr 4.4 C	1 hr 4.4 C	5 hr 20 C
Water absorption condition	Entire surfaces	Entire surfaces (only thawing phase)	Only 1 test surface
Evaluation method	Fundamental transverse frequency	Fundamental transverse frequency	Ultrasonic pulse velocity

3.1.1. ASTM C 666 Tests (Procedure A and Procedure B)

Specimens were presoaked in water for 24 hr before starting of freezing and thawing test. For Procedure A, each specimen is completely surrounded by not less than 1 mm nor more than 3 mm of water at all times while it is being subjected to freezing and thawing cycles. For Procedure B, each specimen is completely surrounded by air during the freezing phase of the cycle and by water during the thawing phase. Freezing and thawing test continued on each specimen until it has been subjected to 300 cycles or until it is impossible to measure fundamental transverse frequency. In this test methods, relative dynamic modulus of elasticity is used to evaluate frost damage.

3.1.2 RILEM CIF Test

Specimens were placed in the test containers on 10 mm high spacers with the tested surface underneath. Subsequently, the test liquid was filled into the container to a height of 15 mm. Pre-saturation of test liquid by capillary suction was conducted for 7 days at a temperature of 20 deg C before starting freezing and thawing test. During capillary suction, the liquid level was checked and adjusted. To evaluate frost damage, ultrasonic pulse velocity (UPV) was measured. The transducers were mounted on the sides of the container so that the transit path axis should be parallel and 35mm from the test surface.

3.2 In Situ Exposure Test

Pervious concrete blocks for river protection were exposed at Hokkaido Naie-river in Japan, which has severe environment of freezing and thawing action. The freezing and thawing cycles of this site is about 70 - 80 cycles in a year. The blocks were similar mixture of NR6 in Table 1. To evaluate frost damage, ultrasonic pulse velocity had been measured for 5 years. Consequently a total of 350-400 freezing and thawing cycles were considered to be occured during the investigartion.

4 RESULT AND DISCUSSION

4.1 Frost Resistance with ASTM C 666 Test Procedure A Method

Relative dynamic modulus of elasticity conducted by ASTM C666 procedure A method is shown in Figure 1. As shown in this figure, relative dynamic modulus of elasticity of PG6 and PG7 decreased to about 50 % and 80 % with the same freezing and thawing cycles. Relative dynamic modulus of elasticity of NR6 decreased sharply and specimens of NR6 failed before 30 freezing and thawing cycles. From these results, pervious concrete failed at early freezing and thawing cycles. It showed extremely low durability of pervious concrete with regards to ASTM C666 procedure A method. Because of the low strength and the high porosity, the frost resistance of pervious concrete seems to be lower than that of conventional concrete. In other words, this type of test method seems to bring the pervious concrete in significant disadvantage.

The frost resistance of NR6 was lower than that of PG6 and PG7. One of major differences between NR6 and PG6 is without/with fine aggregate. This indicated that addition of fine aggregate improves the frost resistance. As can be seen on PG7 and PG6 in this figure, the resistance to freezing and thawing improved with a decrease in the particle size of coarse aggregate. Figure 2 shows the typical fracture patterns of NR6 conducted by ASTM C666 procedure A method. The failure of specimen could be attributed to the formation and rapid propagation of large cracks. These cracks originated from stress of ice formation that occured in large continuous voids (greater than 1 mm in diameter). As particle size of coarse aggregate is large, large continuous void size grows larger. Therefore frost resistance of PG6 and NR6 were lower than that of PG7.

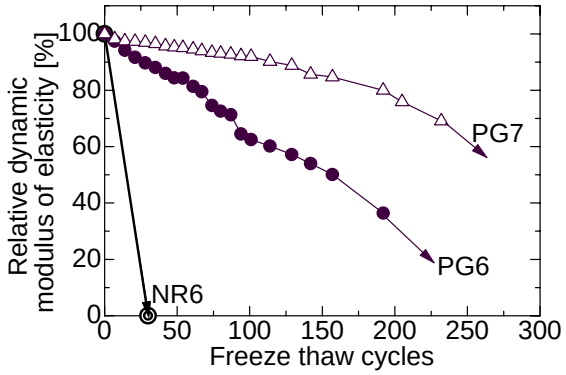

Figure 1. Relative dynamic modulus of elasticity (ASTM C666 procedure A).

Figure 2. Typical fracture patterns after ASTM C666 test procedure A (NR6).

4.2 Frost Resistance with ASTM C 666 Test Procedure B Method

Figure 3 shows relative dynamic modulus of elasticity under ASTM C666 procedure B method. As shown in this figure, relative dynamic modulus of elasticity decreased to about 80 % gradually with additional cycles of freezing and thawing. Comparing with procedure A method, the influence of different particle size and usage of fine aggregate can not be confirmed. Most specimens showed similar decreasing tendency.

Figure 4 shows typical fracture patterns of NR6 by ASTM C666 procedure B. The corner of specimen dropped out with fracture patterns shown in Figure 4, making impossible to measure the fundamental transverse frequency. This phenomenon originated from frost damage of a slight cement paste matrix of pervious concrete. As micro crack developed in cement paste matrix, more water could enter the specimens and freeze, thus further accelerating the rate of crack propagation and eventually leading to spalling and crumbling on the corner of specimen.

4.3 Frost Resistance by RILEM CIF Test

Relative ultrasonic pulse velocity under RILEM CIF test is shown in Figure 5. The result of RILEM CIF test was different from that of ASTM C 666 procedure A and B methods. Relative ultrasonic pulse velocity remained on the same level with additional cycles of freezing and thawing. Therefore deterioration at all specimens of this study was evaluated as a slight frost damage.

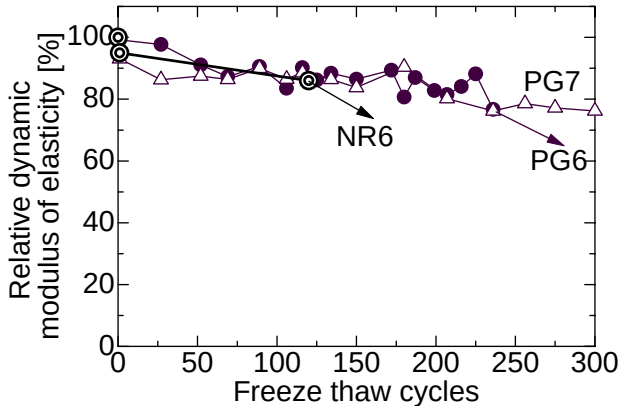

Figure 3. Relative dynamic modulus of elasticity (ASTM C666 procedure B).

Figure 4. Typical fracture patterns after ASTM C666 test procedure B (NR6).

Figure 6 shows a typical fracture patterns after RILEM CIF. In addition, after finishing freezing and thawing test (56 cycles), a little scaling of cement paste without coarse aggregate was found,.and deterioration on tested surface was a slight degree.

The main objective of this investigation is to compare ASTM C 666 procedure A method, procedure B method and RILEM CIF test. Frost resistance of pervious concrete seems to be lower than that of conventional concrete. From the result of ASTM C 666 procedure A method in this study, frost resistance of pervious concrete was evaluated to have a low durability with agrees well with previous research. However, results of RILEM CIF test showed pervious concrete has adequate frost resistance without causing severe scaling and spalling. From these results, the difference of freezing and thawing tests influenced the evaluation of frost resistance on pervious concrete.

4.4 In Situ Exposure Test

Figure 7 presents the change of relative ultrasonic pulse velocity in Naie River blocks for 5 years. Total of 6 blocks (No 1, 2, 3, 9, 13, 24) were measured. As shown in this figure, the ultrasonic pulse velocity for 5 years showed almost a constant valve. The relative ultrasonic pulse velocity of all blocks showed higher than 90 %. These results was found to be that there is no significant frost damage. In addition, the blocks surface seemed to show no deterioration, without spalling nor large crack.

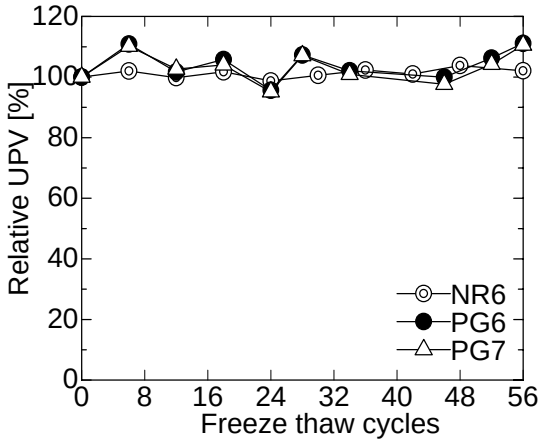

Figure 5. Relative ultrasonic pulse velocity under RILEM CIF

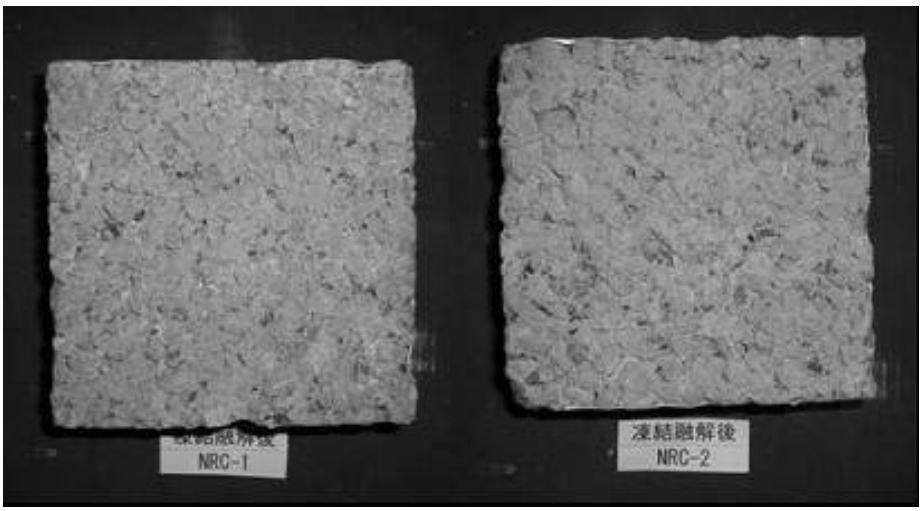

Figure 6. Typical fracture patterns after RILEM CIF (NR6)

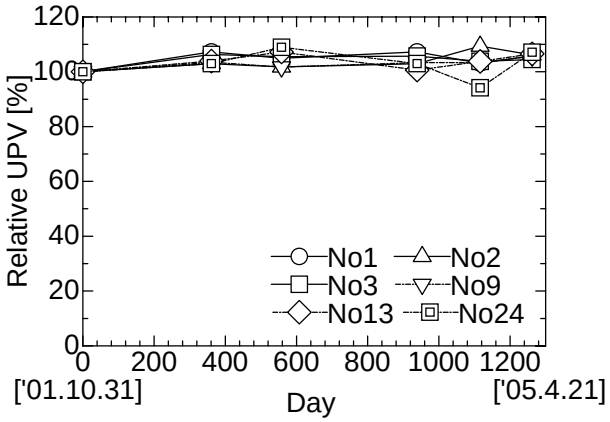

Figure 7 Relative ultrasonic pulse velocity in Naie River blocks.

As already mentioned, more than 70 cycles of freezing and thawing per year were affected to the concrete in situ exposure test. This indicates that more than 350 cycles of freezing and thawing action during the whole 5 years doesn't correlate with the result of ASTM C 666 procedure A method but it shows better correlation with the one of procedure B method and RILEM CIF test.

5 CONCLUSION

Based on the results of shis study, the following conclusions can be drawn:

1. By ASTM C666 procedure A method, relative dynamic modulus of elasticity decreased rapidly and the failure of specimen was attributed to the formation and rapid propagation of large crack. These cracks originated from stress of ice formation which occured in large continuous voids. Frost resistance of pervious concrete may be improved by using small particle size (G7) and fine aggregate in this investigation.

2. By ASTM C666 procedure B method, relative dynamic modulus of elasticity decreased to about 80 % gradually with additional freezing and thawing cycles. This phenomenon originated from frost damage of a slight cement paste matrix of pervious concrete in rapid freezing and thawing actions. The severe fracture patterns observed on ASTM C666 procedure A method did not occured.

3. By RILEM CIF, all specimens showed no clear declination of relative ultrasonic velocity. After freezing and thawing test, surface damage with large cracks was not found. Similar specimens tested in the rapid freezing and thawing environment of ASTM C 666 displayed a far greater degree of frost damage. This phenomenon seemed to originate from the cooling rate and large void strcture which is a characteristic of pervious conrete.

4. The result of in situ exposure test showed little frost damage for five years. The change in relative ultrasonic velocity indicated that freezing and thawing action of in situ exposure test didn't correlate with that of ASTM C 666 procedure A method, but showed better correlation with procedure B method and RILEM CIF test. Total of 350-400 cycles of natural freezing and thawing action showed a similar trend as RILEM CIF test but a significant difference with ASTM C 666 procedure A method.

5. The resistance of pervious concrete to freezing and thawing seems to be considered to be lower than conventional concrete. It is because porous concrete has continuous void structure into which water can permeate during freezing and thawing. However, it is found that the pervious concrete has adequate frost resistance by results of RILEM CIF and in situ exposure test.

REFERENCES

Malhotora, V.M. 1976, 'No-Fines Concrete-Its Properties and Applications', *ACI JOURNAL*, November, pp.628-644.

'The concrete structure of the waterside', *Concrete engineering series* 45, Japan Society of Civil Engineerings, pp.36-38, 2002 (Japan).

Sugiyama, M. 2002, 'The evaluation of the freez-thaw resistance of porous concrete carried out using different test methods', Frost Resistance of Concrete, Proceedings of the International RILEM Workshop, RILEM Proceedings Pro24, April, pp.311-316, Essen, Germany.

Miroru Obi, Fumio Taguchi, 2004 '*Study on Mix Proportions of Porous concrete with Freeze-thaw Resistance*', Monthly report of Hokkaido civil research institute, No.612, pp.37-47,(Japan).

American Society for Testing Materials 1989, 'Resistance of concrete to Rapid Freezing and Thawing', (ASTM C 666), *Annual book of ASTM standards*, V, 4.02, Philadelphia, pp.312-317.

RILEM Recommendation TC176-IDC, Material and Structures, Vol.34, pp.515-525, 2001.

Durability Problems of Macro Defect Free (MDF) Cements Prepared with Polyvinyl Alcohol Copolymers and Alumina Cements

Özgür Ekincioğlu [1]
M. Hulusi Özkul [2]
Leslie J. Struble [3]

T 11

ABSTRACT

Macro-Defect Free (MDF) Cements, which are cement-polymer composites, have been developed by Birchall et al at the early 1980's in order to increase the strength of cement based materials. MDF cements can be produced by adding small amounts of polymer and water into the cement. In addition, high shear and hot press should be applied to the mixture during production in order to get high flexural strengths. Achievement of very high flexural strengths is the most important advantage of this material and more than 200 MPa flexural strengths can be easily obtained while ordinary cement paste has only 5-10 MPa flexural strength. The highest strengths are obtained by using calcium alumina cements (CAC) and polyvinyl alcohol acetate (PVAc) copolymers. In spite of their excellent flexural strengths, MDF cements have serious durability problems under the effect of water. In this study, durability problems of MDF cements were investigated. In the first part of the study, the effect of hydrolysis degree of PVAc on MDF cements was investigated. The influence of alumina cement type on MDF properties is the subject of second part. Biaxial flexural strength tests were applied on the specimens after storing in both dry and humid conditions. Purpose of these tests was finding the most suitable PVAc and CAC type with respect to both mechanical and durability properties.

KEYWORDS

Cement, Polymer, PVAc, MDF, Composite

[1] Istanbul Technical University, Civil Engrg. Faculty, Istanbul, Turkey 34469, Phone +90 212 2853768, Fax 212 2856587, ekincioglu@itu.edu.tr
[2] Istanbul Technical University, Civil Engrg. Faculty, Istanbul, Turkey 34469, Phone +90 212 2853762, Fax 212 2856587, hozkul@ins.itu.edu.tr
[3] University of Illinois at Urbana-Champaign, Dept. of Civil and Environmental Engineering, Urbana-Champaign, USA 61801, Phone +1 217 3332544, Fax +1 217 2658040, lstruble@uiuc.edu

1 INTRODUCTION

Macro-Defect Free (MDF) cements, which are cement-polymer composites, had been developed and patented by Birchall et al. [1982, 1983] in London in order to increase the strength of cement based materials by decreasing large voids. Birchall et all produced a new composite material by adding a small amount of polymer and water into the cement. This composite has very high flexural strengths and it is the most important feature of this material. The MDF cement specimens produced by Birchall et. al. had reached 177 MPa of flexural strength while some other researchers [Russell 1991, Desai 1990 ve Desai 1992] achieved around 300 MPa flexural strengths, which are nearly equal to the strength of steels and it was a very important breakthrough when compared with ordinary cement paste which has only 5-10 MPa flexural strength.

MDF cements can be prepared by using cement, polymer and water. Birchall et al. used 60-70 % cement, 1-15 % polymer and less than 25 % water at the production of MDF cements. A proper water soluble polymer is necessary for the production of MDF cements. However, some researchers [Pushpalal et al. 1987] have proposed alcohol soluble polymers for this purpose in recent years. A calendering machine has been used in order to decrease large voids by applying shear forces like in rubber industry, after mixing the ingredients in a planetary mixer. Cement, PVAc and water blended in a planetary mixer until obtaining a crumble mix. Then, this mixture passed through between steel roller mills repeatedly until obtaining it in a sheet form. This sheet is cut into desired dimensions and pressed under moderate temperature and pressure.

Birchall et all attributed the high flexural strengths to the elimination of macro voids during the production process and named this material as macro defect free cement but further studies [Rodger 1985, Popoola 1991] showed that it is not the only reason which causes of such high flexural strengths. Crosslinking reactions between polymer and cement, and also the pressing the material after production at moderate temperature and pressure are playing important roles in achievement of high strengths. Reactions of PVA with hydrated calcium alumina cement were described by Rodger et al [Rodger 1985] and they proposed that the behavior of the polymer is more complex than being an inert rheological aid. They studied the evidence of polymer-cement interactions provided by calorimetry, solution chemistry and infrared spectroscopy. When water is added into the cement and partially hydrolyzed polyvinyl acetate mixture, the rising pH causes the hydrolysis of the acetate groups, leaving polyvinyl alcohol in solution with acetate ions, which subsequently react with calcium ions to form calcium acetate. Then, the metal ions in the solution crosslink with the polyvinyl alcohol chains; which makes the polymer matrix rubbery and thus allows the physical processing to continue as the cement-polymer mix attains a plasticine like consistency. The polymer will also coordinate with metal ions on the surface of the cement grains producing a cohesive matrix which links the anhydrous particles. This reaction scheme can be seen on Fig. 1.

Although, this composite has very high flexural strength it has a very important disadvantage. Their flexural strength decreases when they are stored in water and this water sensitivity is the main problem for using this material in commercial applications. Therefore most of the researches about MDF cements are focused on their water sensitivity. Some researchers [Russell 1991, Desai 1992, Atkinson and Walsh 1986, Lewis and Boyer 1995, Pushpalal et al. 1997, Mojumdar et al. 2004, Chowhurry 2004] made some improvements, but none of them seems acceptable enough for this purpose.

Different cement and polymer types were tested for the production of MDF cements. According to Santos [1997] and Sinclair [1985] MDF cements, produced with ordinary portland cement and polyacrylamide, are less sensitive against water comparing with the calcium alumina cement (CAC)-polyvinyl alcohol-acetate (PVAc) MDF systems; however, the highest flexural strengths were always obtained with CAC-PVAc copolymers. Therefore, researches about MDF cements mostly concentrated on CAC-PVAc systems.

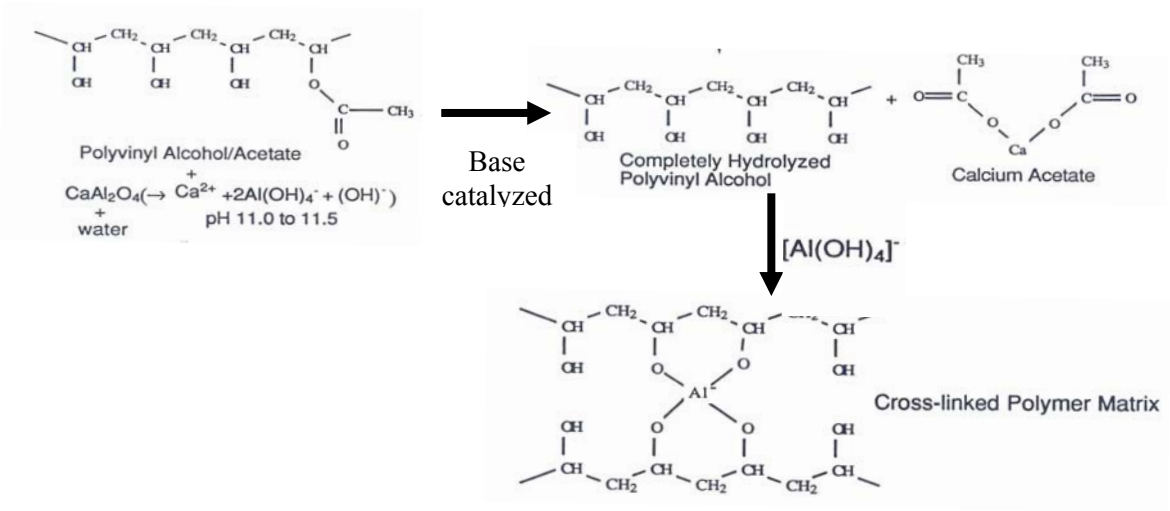

Figure 1. Schematic representation of the CAC with PVA in the presence of water [Desai 1992].

In order to understand the reasons behind the strength loss of MDF cements in contact with water, the properties of polymer and cement and their interaction should be examined. Durability problems of macro defect free cements were investigated in 2 different steps in this study. In first step, PVAc polymers with different hydrolysis degrees were used at the production of MDF cements. In second step, the type of alumina cements used were changed. Thus, effect of hydrolysis degrees of PVAc copolymers and the type of Alumina cements on the durability of MDF cements were investigated. Purpose of this study is finding the most suitable PVAc and alumina cement type for the production of MDF cements.

2 EXPERIMENTAL STUDY

2.1 Materials

2.1.1 Polyvinyl alcohol acetate (PVAc)

Polyvinyl acetate can be produced by the polymerization processes of monomer vinyl acetate, which is reacted with NaOH and methanol in order to obtain polyvinyl alcohol, but this reaction should be controlled and when it is terminated some acetate groups may remain on the polymer. Then, the copolymer of poly (vinyl alcohol) and poly (vinyl acetate), called poly (vinyl alcohol-*co*-vinyl acetate), is the most widely used polymer at the production of MDF, and shows different characteristics, such as alcohol groups are hydrophilic while acetate groups are hydrophobic. So when the copolymer is put in water, it turns into a ball. The alcohol repeated units are on the outer side of this ball, while the acetate groups are on the inner side of the ball [http://pslc.ws].

Table 1. Effect of degree of polymerization (DP) and degree of hydrolysis (DH) on the properties of PVAc [www.poval.jp].

	Polymerization degree		Hydrolysis degree	
	High 1700-2400	Low 500-600	High 98-99	Low 87-89
Solubility	↓	↑	↓	↑
viscosity of aqueous solution	↑	↓	↑	↓
Film strength	↑	↓	↑	↓
Moisture absorption property	↓	↑	↓	↑

The properties of PVAc are mostly determined by their polymerization and hydrolysis degrees. PVAc, which has high degree of hydrolysis, show less moisture absorption according to Table 1, but a previous attempt [Santos 1997] in order to produce MDF with high hydrolysis degree polymers were unsuccesfull, due to their low solubility at room temperature. However, they can be made more soluble by heating up to 80 ^{0}C (Figure 2).

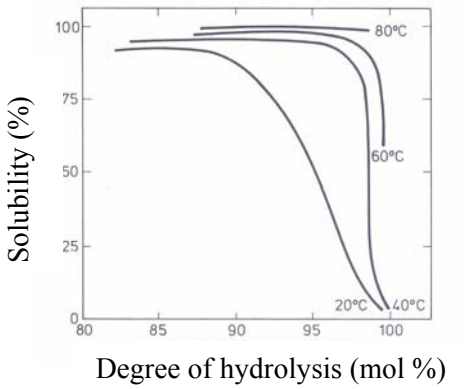

Figure 2. Effect of temperature on the solubility and degree of hydrolysis of PVAc [Finch 1992].

2.1.2 Calcium Alumina Cements (CAC)

Calcium alumina cements (CAC) are mostly preferred to portland cements or other types of cements at the production of MDF, because MDFs produced with CACs have higher flexural strengths than other cement types. It is considered that strong crosslinking reactions take place between Al ions and polymer chains in MDF [Rodger 1985, Popoola 1991, Bonapasta 2000]. Although, mostly the alumina cements which have 70 % Al_2O_3 content were preferred for the production of MDF cements [Birchall et al. 1983, Russell 1991, Desai 1990, Desai, 1992], there is not enough study about investigating the effect of Al_2O_3 content on the moisture sensitivity of MDF cements.

2.2 Production of MDF Cements with Different PVAc's

MDF cements were produced with 7 different type of PVAc in first step. Their hydrolysis degrees were changing between % 79.6 to % 99.1. Properties of PVAc copolymers, which have different degree of hydrolysis can be seen in Table 2. Only N300 type PVAc was fully hydrolyzed while KH17 and GH20R were partially hydrolyzed. Other types were modified with some other groups like carboxyl or acetoacetyl in order to make them more soluble even at room temperature (Table 2).

Table 2. Properties of PVAc's used at the production of MDF.

Product Name	Hydrolysis (mol, %)	pH	Feature
KH17	79.6	5.5	Partially Hydrolyzed
GH 20R	87.1	5.5	Partially Hydrolyzed
Z 320	92.7	4.7	Acetoacetylated
T 330	96.0	7.0	Carboxylated
Z 410	97.9	4.9	Acetoacetylated
N 300	98.4	5.9	Fully Hydrolyzed
Z 100	99.1	5.0	Acetoacetylated

High alumina cement, which has 70 % Al_2O_3 and 29,2 % CaO in composition, was used in this study. Small amounts of water between 11-20 % of cement weight and small amount of glycerol (less than 1 %) were added in to the mixture for plasticizing. MDF specimens were prepared in 3 different ways, and coded as -1, -2 or -3 depending on the method used, as shown in Table 3. These methods can be summarized as follows:

1st method: Conventional production method, optimized by Russell [1991] for PVAc and HAC.
2nd method: Similar with first method. Only difference is preheating the polymer up to 70-90 ^{0}C before adding into the mixture in order to increase the solubility.
3rd method: Similar with first method. Only difference is adding adipyl hydrazide crosslinking agent into to the mixture. Because Z type PVAcs are also known with their high crosslinking capacity when they used with Aldehydes or Amines.

Table 3. Compositions of the mixtures prepared with different PVAcs.

Mixtures	KH17 1	KH17 2	GH20 1	GH20 2	Z320 1	Z320 2	Z320 3	Z410 1	Z410 2	Z410 3	Z100 1	Z100 2	Z100 3
Wat./cem.	0.11	0.11	0.13	0.13	0.15	0.15	0.15	0.20	0.20	0.20	0.15	0.13	0.15
Poly./cem.	0.07	0.07	0.07	0.07	0.07	0.07	0.07	0.07	0.07	0.07	0.07	0.07	0.07

2.3 Production of MDF Cements with Different CACs

In the second step, MDF cements were produced with 4 different types of calcium alumina cements. Their alumina contents were changing between 42 to 79 % and they were coded according to alumina contents. Compositions of cements which were provided by the producer can be seen in Table 4.

Table 4. Compositions of calcium alumina cements used at the production of MDF cements.

Cement Type	Alumina % (Al_2O_3)	Calcium Oxide % (CaO)	Ferric Oxide % (Fe_2O_3)	Silica (SiO_2)
CAC 42	42.29	35.05	14.05	4.52
CAC 49	48.86	34.89	7.16	5.56
CAC 70	70.0	29.2	-	-
CAC 79	78.95	19.57	-	-

PVAc copolymer which has a 79.6 % hydrolysis degree and 5.5 pH ratio was used in all compositions. It was the most widely used PVAc in literature at the production of MDF cement and also it is confirmed that it is the less sensitivite PVAc against water in the previous part of this study. Small amounts of glycerol, which is 10% of PVAc by weight, were also added in to the mixtures. Water/cement ratio was changing between 0.09 and 0.19 while the polymer/cement ratio was kept constant at 0.07. Twenty five different batches were prepared in order to produce MDF cements, which differ in their water contents. These mixtures can be seen in Table 5. Eight circular specimens were cut with diamond saw from each sheet and stored in dessicator or water.

2.4 Biaxial Flexural Strength Tests

All specimens, produced with one of the above methods, separated into two groups. Half of the specimens were stored in desiccator while the other half were in water for 7 days in order to see the effect of water on flexural strength. Then, the biaxial flexural strength test was applied at the ages of 7 days according to ASTM F-394. An Instron model universal testing machine equipped with a 1 kN load cell was used to test the specimens with a cross-head speed of 0.5 mm/min. Dry strength means the flexural strengths of specimens stored in desiccators while wet strength is the strength of specimens stored in water.

2.4.1 Effect of Different PVAcs on the Durability of MDF Cements

MDF cements were successfully produced with 5 of 7 different hydrolyzed PVAcs, except those with fully hydrolyzed PVAc (N300) or carboxylated PVAc (T 330). All mixtures were affected from moisture in different rates between 45 % and 80 % depending on PVAc type. However, the PVAc at the lowest hydrolysis degree (79,6 %) gave the lower strength loss (45 %). Increasing the degree of hydrolysis of PVAc increased the strength loss of MDF specimens, which were stored in water. Preheatiıng the polymer before mixing (specimens coded with -2) sightly increased the flexural

strengths except KH17-2 with respect to conventional production method (coded with -1). All results can be seen in Figure 3.

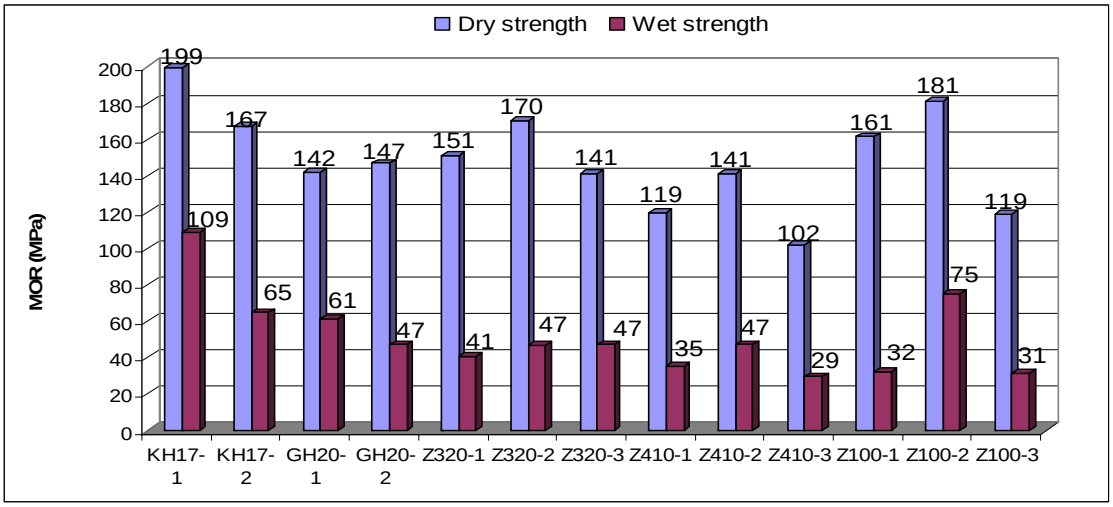

Figure 3. Biaxial flexural strength test results of MDF cements produced with different PVAc's.

2.4.2 Effect of Different Calcium Alumina Cements on the Durability of MDF Cements
MDF cements were successfully produced with all 4 different types of Alumina cements. It was impossible to obtain MDF sheets only with 2 out of 25 batches (49-7 and 79-4) due to the lack of coherence at low w/c ratios. Biaxial flexural strength results and standart deviations as well as coefficient of variations for each batch were calculated and given in Table 5. The highest biaxial flexural strength was obtained as 257 MPa on CAC 70 composite, which was prepared by a cement with 70% Al_2O_3 content and at a water/cement ratio of 0.15. The lowest biaxial flexural strength was 70 MPa and belongs to the CAC 79 composite, which was prepared with 79% Al_2O_3 content cement at water/cement ratio of 0.19. For high level of Al_2O_3 (79%), the production of MDF becomes harder than those with low Al_2O_3 content.

Strength loss is plotted against Al_2O_3 content of alumina cements in Fig. 4. It seems that changing Al_2O_3 content from 42 to 70 % slightly changed the results, but a sharp decrease in strength loss is observed when Al_2O_3 content is 79 %. Composites produced with CAC 79 cement have the smallest flexural strengths and highest strength loss which may be due to the high content of alumina in this cement (79 %). However, all composites produced with all types of alumina cements are sensitive to water and show strength loss after 7 days water storage in varying extents.

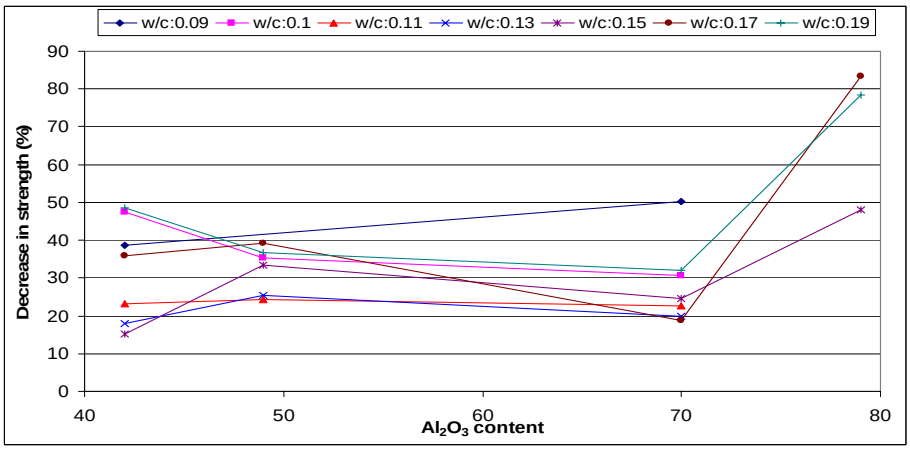

Figure 4. Strength loss versus Al_2O_3 content.

Table 5. Biaxial flexural strength test results of MDF cements produced with different CACs.

Cement type	Mixtures	w/c	Dry Strength (MPa)			Wet Strength (MPa)		
			f_c	σ	V %	f_c	σ	V %
CAC 42	42-1	0.19	169	30	18	87	5	6
CAC 42	42-2	0.17	194	14	7	124	8	7
CAC 42	42-3	0.15	206	18	9	175	25	14
CAC 42	42-4	0.13	220	19	9	180	18	10
CAC 42	42-5	0.11	233	17	7	179	29	17
CAC 42	42-6	0.10	235	25	11	124	27	22
CAC 42	42-7	0.09	206	19	9	126	27	21
CAC 49	49-1	0.19	205	13	6	130	12	9
CAC 49	49-2	0.17	178	8	5	108	6	6
CAC 49	49-3	0.15	213	17	8	142	4	3
CAC 49	49-4	0.13	216	16	7	161	30	18
CAC 49	49-5	0.11	238	12	5	180	46	27
CAC 49	49-6	0.10	221	21	10	143	21	14
CAC 49	49-7	0.09	-	-	-	-	-	-
CAC 70	70-1	0.19	187	11	6	127	16	13
CAC 70	70-2	0.17	209	26	13	170	45	27
CAC 70	70-3	0.15	257	8	3	193	21	11
CAC 70	70-4	0.13	248	7	3	199	15	8
CAC 70	70-5	0.11	248	19	8	191	36	19
CAC 70	70-6	0.10	243	22	9	169	34	20
CAC 70	70-7	0.09	174	26	15	87	19	22
CAC 79	79-1	0.19	70	18	26	15	3	22
CAC 79	79-2	0.17	105	6	6	17	6	33
CAC 79	79-3	0.15	85	5	6	44	1	2
CAC 79	79-4	0.13	-	-	-	-	-	-

3 CONCLUSIONS

- MDF cements can be successfully produced with 5 out of 7 different hydrolyzed PVAc's, sometimes with modified procedures.
- MDF cements could not be produced with fully hydrolyzed PVAc or carboxylated PVAc.
- All specimens showed moisture sensitivity. However, the PVAc at the lowest hydrolysis degree (79,6 %) gave the lowest strength loss. Increasing degree of hydrolysis of PVAc's increased the strength loss of MDF specimens which were stored in water.
- Preheating the polymer before mixing (specimens coded with -2) slightly increased the flexural strengths, except KH17-2 with respect to conventional production method (coded with -1)
- MDF cements can be successfully produced with 4 different type of alumina cements.
- Flexural strengths of all specimens decreased between 15 and 83 % after storing in water for 7 days.
- The highest biaxial flexural strength was obtained as 257 MPa on CAC 70 composite, which was prepared by a cement with 70% Al_2O_3 content and at a water/cement ratio of 0.15.
- The lowest biaxial flexural strength was 70 MPa and belongs to the CAC 79 composite which was prepared with 79% Al_2O_3 content cement at water/cement ratio of 0.19.
- It seems that there is an optimum alumina content between 42-70 % for minimum strength loss in water.
- For high level of Al_2O_3 (79%), the production of MDF becomes harder and the level of strength drops while strength loss in water increases comparing with other cements.

ACKNOWLEDGMENTS

The authors would like to thank The Scientific & Technological Research Council of Turkey (TÜBİTAK) for providing scholarship for the first author at the University of Illinois at Urbana-Champaign.

REFERENCES

American Society For Testing And Materials, "ASTM F 394– 78 (Reapproved 1996) Standard Test Method for Biaxial Flexure Strength (Modulus of Rupture) of Ceramic Substrates", 1996.

Atkinson A. W. and Walsh A. T. 1986, 'Treatment of cementitious products**',** *Europan patent number GB2168692.*

Birchall, J. D, Howard, A. J., Kendall, K. 1982, 'Flexural strength and porosity of cements', *Nature* **vol 289**, 388-390.

Birchall, J. D, Howard, A. J., Kendall, K., Raistrick, J. H. 1983, 'Cement composition and product', *United States Patent No: 4,410,366.*

Bonapasta, AA, Buda, F, Colombet, P. 2000, 'Cross-Linking of Poly(Vinyl Alcohol) Chains by Al Ions in Macro-Defect-Free Cements: A Theoritical study', *Chem. Mater.,* **12**, 738-743.

Chowdhury B. 2004, **'**Investigations into the role of activated carbon in a moisture-blocking cement formulation', *Journal of Thermal Analysis and Calorimetry*, **Vol 78,** 215–226.

Desai, P. G. 1992, 'Cement Polymer Interactions in Macro-Defect-Free Composites', *M. S. Thesis,* University of Illinois.

Desai, R. A. 1990, 'An Investigation Into The Moisture Resistance Of Macro-Defect-Free Composites', *M. S. Thesis,* University of Illinois

Finch, C.A. 1992, *Polyvinyl Alcohol Developments,* John Wiley&Sons Limited, pp.5.
http://pslc.ws/macrog/pva.htm

Lewis J. A. ve Boyer M. A. 1995, 'Effects of an organotitanate cross-linking additive on the processing and properties of macro-defect-free cement', *J. of Advanced Cement Based Materials*, **Vol. 2,** 2–7.

Mojumdar S. C., Chowdhury B., Varshney K.G. and Mazanec K. 2004, 'Synthesis, moisture resistance, thermal, chemical and SEM analysis of macro-defect-free (MDF) cements', *Journal of Thermal Analysis and Calorimetry*, **Vol 78,** 135-144.

Popoola, O.O., Kriven, W.M., Young J.F. 1991, 'Microstructural and Microchemical Characterization of a Calcium Aluminate-Polymer Composite (MDF Cement)', *Journal of American Ceramic Society,* **74**(8), p. 1928-1933.

Pushpalal G.K.D., Kobayashi T., Hasegawa M. 1997, **'**High alumina cement-phenol resin composite: water resistivity and effect of post hydration of unreacted cement on durability', *Cement and Concrete Research,* **Vol 27**, No 9, 1393–1405.

Rodger, S, A., Brooks. S. A., Sinclair, W., Groves, G., W., Double, D.D. 1985, 'High strength cement pastes-Part 2: Reactions during setting', *Journal of Materials Science,* **20**, 2853-2860.

Russell, P.P. 1991, 'Processing Studies Of Macro-Defect Free Cement and Investigation of Chemical Modifiers To Improve The Water Resistance of the Composite', *M. S. Thesis,* University of Illinois,.

Santos, Rosemar Sant'Anna dos 1997, 'Materiais Cimentosos Isentos de Macro Defeitos Utilizando Álcool Polivinílico (PVA) e Silicato de Sódio: Influência da Massa Molar Média e do Grau Hidrólise do Polímero' Universidade Estadual De Campinas.

Sinclair, W., Groves, G., W. 1985, 'High strength cement pastes-Part 1:Microstructures', *Journal of Materials Science,* **20**, 2846-2852.

www.poval.jp/english/poval/tec_info/ti_01.html

11DBMC International Conference on Durability of Building Materials and Components
ISTANBUL, Turkey 11-14 May 2008

Discussing the Durability Assessment of Cement Mortars – a Contribution for a Prediction Model

Vasco Peixoto Freitas [1]
Helena Corvacho [2]
Ana Vaz Sá [3]
Marisa Antunes Quintela [4]

T 11

ABSTRACT

The aim of this paper is to present a discussion on the assessment of the durability of industrial cement mortars, based on two experimental research works carried out at the Building Physics Laboratory, Faculty of Engineering, University of Porto, Portugal.

The service life prediction of any construction material is not an easy task. The researchers must choose between several different approaches, which one with its advantages and its limitations.

While in real buildings, with in-use conditions, the material or component is subject to changeable actions in an environment where the great majority of the degradation agents is not controllable by man, in laboratory, we can choose to expose the material to artificial and controlled conditions, using chambers of accelerated ageing. The main difficulty of this last type of tests consists in the interpretation of the results, in what concerns their correspondence to real time. Researchers on durability have been discussing this problem since a long time: how to get a valuable correlation between the results of accelerated ageing tests and the one issued from natural exposure? In this paper, a discussion on this subject is presented based on the above mentioned studies, concerning the performance over time of two different types of industrial cement mortars exposed to accelerated ageing tests and also to natural ageing. The main advances and the main difficulties in implementing a service life prediction model will be identified. Finally, suitable strategies are discussed for the future development of this approach.

KEYWORDS

Durability, Performance, Accelerated ageing tests, Aatural ageing, Prediction model

[1] Building Physics Laboratory (LFC), Faculty of Engineering, University of Porto, Portugal (FEUP), vpfreita@fe.up.pt
[2] Building Physics Laboratory (LFC), Faculty of Engineering, University of Porto, Portugal (FEUP), corvacho@fe.up.pt
[3] Building Physics Laboratory (LFC), Faculty of Engineering, University of Porto, Portugal (FEUP), vaz.sa@fe.up.pt
[4] Building Physics Laboratory (LFC), Faculty of Engineering, University of Porto, Portugal (FEUP), marisa@fe.up.pt

1 INTRODUCTION

The objective of any service life prediction of a material, system or component integrated into a building is to evaluate its ability to satisfactorily perform its operations throughout the service life of the building or throughout the period considered reasonable for its replacement or repair. The definition of a model of service life prediction and its application are imperative, through this being able to evaluate the reliability of the defined model. The two experimental studies that are presented here use the same model of service life prediction applied to two types of different mortar, but lead to results whose interpretation differs. Therefore, a reflection is presented on the factors that could influence the service life prediction, on the structure of the model and on the possibility of its generalized application.

2 SERVICE LIFE PREDICTION

2.1 Service Life Prediction Model Adopted by LFC - FEUP

Two experimental studies carried out in the Building Physics Laboratory of the Faculty of Engineering of the University of Porto, Portugal were based on the general methodology proposed by ISO 15686-1 standard and lead to the proposal of the model that we are presenting. Tests campaigns were carried out for accelerated ageing and natural ageing stations were simultaneously set up where the materials were exposed to the external environment.

In this way, according to the diagram in figure 1, when in possession of the test results, referring to accelerated ageing and to natural ageing, given that the type of degradation resulting from either one or the other test is seen to be similar, it is possible to interpret these results and develop a model of service life prediction of the products and systems being studied through the establishment of a correlation between the number of cycles of artificial ageing and the real time of natural ageing (Figure 1).

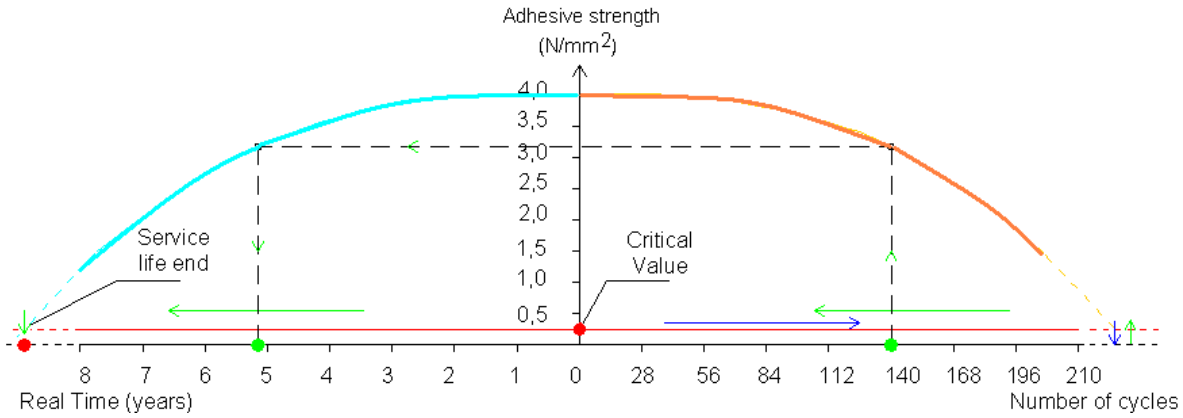

Figure 1. Correlation between the number of accelerated artificial ageing cycles and real time natural exposure – Prediction Model.

Knowing the degradation curve of a given characteristic (as an example, the figure 1 considers the adhesive strength between the mortar and its substrate) it will be possible to establish a correspondence between the number of accelerated artificial ageing cycles and the number of years in real time.

2.2 Critical Analysis of the Difficulties Associated to the Chosen Model

The model presupposes the identification of a degradation curve as a function of time, obtained in accelerated ageing tests. This procurement can be met with several difficulties. Firstly, the most

relevant agents of degradation for the material being studied have to be rigorously identified and the effects of action variation on these agents. For this identification, the performances of the preliminary tests become important. Secondly, performance characteristics to be evaluated must be selected, opting for those that are shown to be critical for durability. This choice is very important and could be based, on the one hand, on the results of the preliminary tests and, on the other hand, on the historical pathologies normally associated with the material to be evaluated. If the identified degradative agents or the selected performance characteristics were not the most adequate, the tests could be shown to be inconclusive and the model would not be able to be applied.

With the adequate performance characteristics chosen and the necessary artificial accelerated ageing tests performed, an other problem could still arise: the results obtained for different stages of ageing do not reveal any definable tendency, making it impossible to draw a degradation curve. In this case, the hypothesis that there are other aspects that are more relevant to ageing of the material or system in study becomes plausible: the agents of degradation being considered may not be very relevant for the variation of the characteristic being tested as it is overall dependent on, for example, the execution, on the interaction between different elements of the construction (interfaces), on the type of in-use conditions, etc. In this case, the application of the model as presented becomes unviable.

It can also be observed that the model assumes the occurrence of a degradation curve that is continuous in time and does not consider the interventions hypothesis along this timeline that restitute or improve a given performance characteristic, which could obviously take place in reality. However, the objective of the model is to obtain a prediction of a reference value for the service life. With this value determined, it will then be possible to take into account the effects of modifying factors related to the various aspects present in the life cycle of each system or material, with these factors being related to the design, the execution, the use, the specific environments to which they will be exposed, maintenance measures, etc.

Regarding the service life prediction starting from a specific number of tests in a natural ageing scheme, it will be as easy as the ease of gauging the deterioration observed and its comparison with the results of the accelerated ageing tests. In this way, for products or systems with a history of applications, it will also be possible to complement the information with a study of its record with respect to pathologies and the repair measures, being able to more easily evaluate the significance of the observed deterioration in the early stages of the experimental installation. In addition to this, the tests on service conditions, performed at construction sites of different ages, could substitute or complement the tests made on the experimental installations of natural ageing, as long as it is possible to retrieve results in a sufficient number to be statistically significant and as long as there is information about the type of products applied, the date of application and the conditions to which they have been subject over the years.

3 EXPERIMENTAL STUDIES

3.1 Brief Description of the Studied Systems

3.1.1 Cementitious Adhesive in Bonded Ceramic Coverings of External Walls

In the first study (Sá, Ana V., 2005), the durability of cementitious adhesive in bonded ceramic coverings is evaluated. This kind of covering has a long tradition in Portuguese construction. It continues, in modern times, to be widely used, both for its aesthetic aspect as well as because an increased durability is expected of it along with a satisfying functional performance. Added to this is the relative ease of cleaning and maintenance.

The system under study is basically composed of three essential elements: the substrate, the bonding material (in this case, the cementitious adhesive) and the ceramic tile. The evaluation of durability of

one of the elements must take into account, by necessity, the durability of the system and the compatibilities between the different elements.

The substrate for the ceramic coverings is defined as a function of the nature of its constituent materials. In the present study, only concrete walls or brick walls covered with extremely hardened mortar were considered. The designation of cementitious adhesive applies to a hydraulic adhesive mortar with a cement base, with aggregates (fine granulometry) and additives that improve water retention, plasticity and adherence.

The ceramic tiles are thin plates made from clay and/or other organic raw materials and are generally utilized as coverings of walls and floors. They are, usually, formed by extrusion or pressing at room temperature but can also be molded by other processes. Next they are dried and finally cooked at a temperature appropriate for obtaining the required characteristics.

3.1.2 One-Coat Rendering Mortar for External Use

In the second study (Quintela, M. A., 2006), the performance of a one-coat rendering mortar made up of an industrial mortar applied at a single layer is evaluated. This type of covering is normally applied by projection and is classified as an impermeable covering, contributing to the overall sealing of the wall and simultaneously carrying out the functions of finishing and decoration, dispensing the need for painting.

3.2 Performance Indicators Evaluated and Criteria for Durability

In the evaluation of the durability of the **adherent ceramic covering system**, the criterion selected for its characterization was the value of the adhesive strength to its substrate. It was considered that this characteristic would be the most important one for the service life prediction of the system. The set critical value was that of 0,3 N/mm^2.

Over a period of time, adhesion tests were performed in order to evaluate the adhesive strength, at different moments of the accelerated ageing process, with the aim of characterizing its influence on the performance of the cementitious adhesive.

Regarding the **one-coat rendering mortar**, in general we can say that in order to effectively contribute to the satisfaction of the functional requirements of the walls, the following characteristics must be maintained: good adhesion to the substrate surface; good waterproofing ability, thereby being unlikely to crack and having low capillarity; increased permeability to water vapor; adequate aesthetic aspect and preservation of its decorative properties through adequate maintenance.

Therefore, given the requirements to meet, the following characteristics were evaluated, also in several different stages of ageing: coefficient of water absorption by capillarity; permeability to liquid water, adhesion to the substrate and aspect characteristics like superficial cracking and coloring. However, in order to compare the results obtained in the two studies and discuss their implications, we present, for this second product, only the results obtained for the value of the adhesive strength. In this case, 0,3 N/mm^2 was considered as the recommended value, with 0,2 N/mm^2 being set as the minimum admissible value.

Of the various mechanisms and agents of degradation responsible for the ageing of the study systems, those of hygrothermic character are considered, namely: variation in temperature; variation in relative humidity; incidence of solar radiation and precipitation. These actions will have a determining role in the ageing of the exterior coverings. Therefore we submitted specimens of the two systems under analysis to accelerated ageing cycles.

The cycles performed in the study of **cementitious adhesive** consist of the exposure of the specimens to extreme conditions of usage, with harsh variations in temperature, relative humidity and radiation in

such a way as to provoke the rapid degradation of the system of covering, figure 2 portrays the cycle utilized.

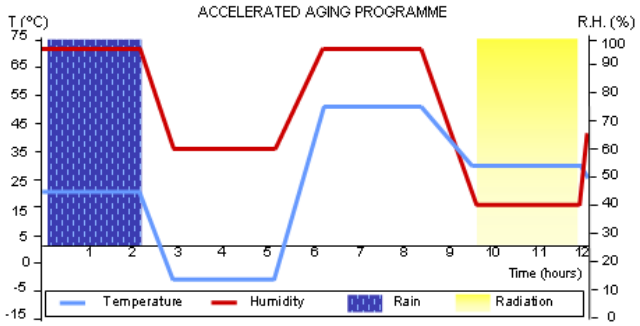

Figure 2. Complete cycle – 12 hours.

In the study of the **one-coat rendering mortar**, brick models covered with this mortar were submitted to three different processes of ageing: the combination of Cycles A; Cycle B and Cycle C. The combination of cycles A corresponds to an adaptation of the process of ageing referenced in the European Standard 1015-21 of 2002 and consists of the association of cycles of heating/freezing and of humidification/freezing, separated by a time of rest in the laboratory atmosphere, Table 1 portrays this combination.

Table 1. Cycles combination A

Cycle A1 heating/freezing				*Standard environment (laboratory environment)*				*Cycle A2 humidification/freezing*		
T	RH	D		T	RH	D		T	RH	D
60ºC	n.c.	8 h						Immersion in water		8 h
20ºC	65 %	½ h	+	20ºC	65 %	48 h	+	20ºC	65 %	½ h
-15ºC	n.c.	15 h						-15ºC	n.c.	15 h
20ºC	65 %	½ h						20ºC	65 %	½ h

T: temperature [ºC]; RH: Relative Humidity [%]; D: duration of the established conditions [h]; n.c.: Relative Humidity non-controlled

The second ageing process, which can be observed in figure 3, consists of the repetition of a cycle (Cycle B) that involves the variation of the conditions of temperature and relative humidity for 24 hours, determined through the analysis of the records of recent years obtained by the meteorology stations of LFC, taking into account, for the definition of the temperature variation, the heating of the surfaces exposed to solar radiation.

Finally, Cycle C consists of the variation of conditions of temperature and relative humidity, associated with the effects of rain (spraying with water) and of solar radiation (Xenon arc lamp), having a duration base of 12 hours. This cycle has the same configuration as the one adopted for the study of cementitious adhesive. These conditions were achieved using a chamber specialized for this type of testing.

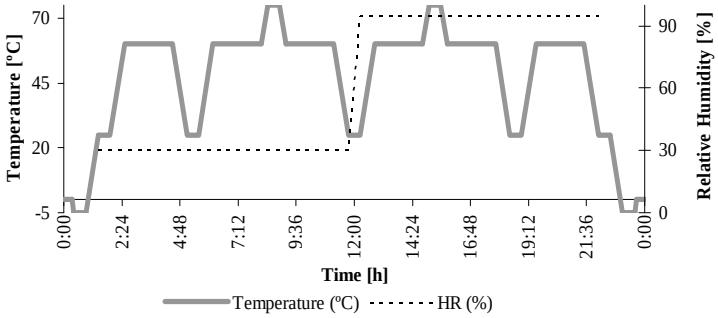

Figure 3. Cycle B.

Simultaneously, stations were set up for **natural ageing** consisting, in the first case, of a wall covered with different ceramic tiles and, in the second case, of a wall covered with different types of one-coat mortar, both exposed to the external environment. Similarly to that performed in the laboratory, adhesion tests were performed on these walls, in order to determine the time period.

3.3 Experimental results

As regards the durability of **cementitious adhesive**, the graphic in figure 4 presents the variation in the adhesive strength as a function of the number of ageing cycles to which the specimens designated as PE0, PE1 and PE3 had been subjected. In these three specimens cementitious adhesive of type C2 [EN 12004] was used along with three different types of ceramic tiles. There is a very clear decreasing tendency and it can be predicted that, independent of the type of ceramic tile used, in the set of tests performed on the specimens with class C2 cementitious adhesive, 140 cycles would be sufficient to drop below the critical adhesive strength value of 0,30 N/mm^2 and thereby reach the service life term of the product.

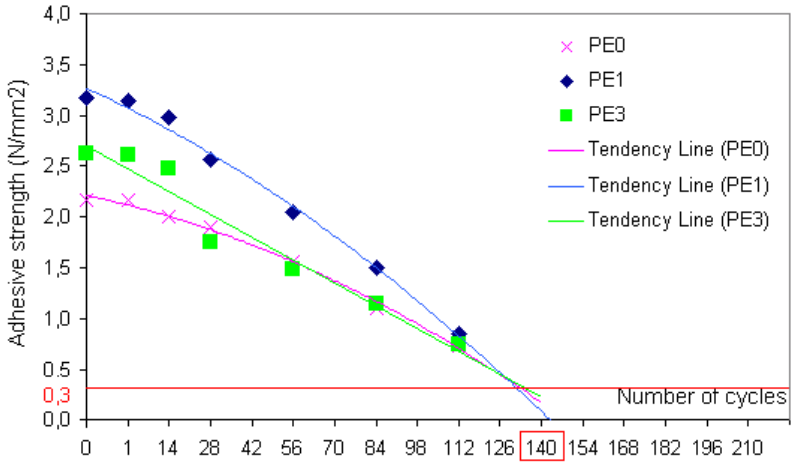

Figure 4. Service life term prediction for C2 cementitious adhesive

Regarding the tests performed on the wall of the natural ageing station, given the little time of exposure that passed by until the performance of the first tests, it was only intended to demonstrate the methodology to follow to establish the correlation between the results obtained from accelerated ageing and those obtained with natural ageing.

As regards the durability of the **one-coat rendering mortar**, figure 5 displays the variation in the adhesive strength of the single layer covering, applied with 1 or 2 cm of thickness, on the brick models submitted to the accelerated ageing cycles.

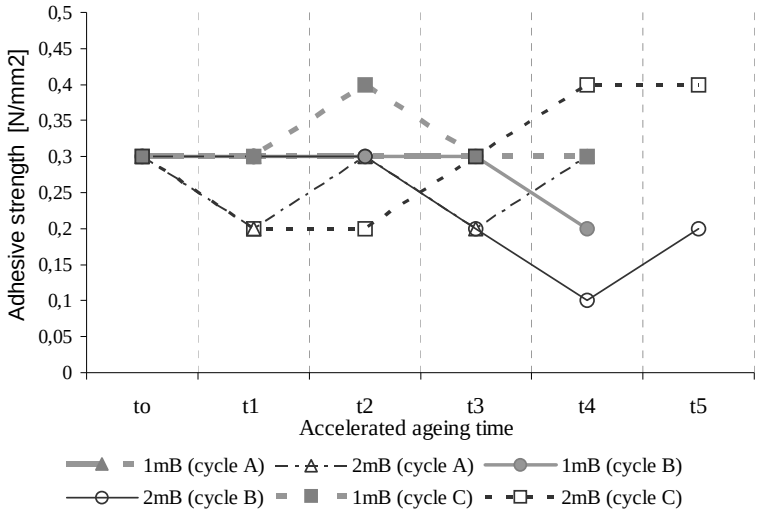

Figure 5. Evolution of the adhesive strength in the models submitted to the three ageing processes. Specimens with 1 cm and 2 cm of covering.

In figure 5 we can observe a random variation in the performance of the one-coat rendering mortar in terms of adhesion to the substrate, being impossible to identify any tendency for any one of the ageing processes. At the natural ageing station, two series of in-situ adhesion tests were performed. Between the first series of tests and the second series of tests a tendency of diminished adhesion to the substrate surface was observed. However, the observed tendency doesn't allow us to come to a conclusion because the time that had passed since the execution of the wall was still too short.

4 CONSIDERATIONS REGARDING THE APPLICABILITY OF THE MODEL IN THE EVALUATION OF MORTAR DURABILITY

4.1 Main Problems

As regards the **cementitious adhesive** applied in a system of adherent ceramic covering, once it is possible to obtain a degradation curve in the accelerated ageing tests, to be able to reliably apply the model, it becomes necessary to only perform the tests in the natural ageing station, for defined time periods (every six months, for example) in order to be able to establish a relationship between the short term tests and the long term tests. However, in this case, it is in the long term testing that we encountered the most difficulties. For products with a reduced application experience or for new products, it becomes more difficult to avoid the necessity of waiting for a relatively long time for the long term tests in the experimental installation, if we intend to quantify its service life period in absolute terms, we do not have performance data for these products in service conditions that serve to gauge the significance of the tests in which they were obtained.

As regards to the cementitious adhesive, it will be possible to collect the performance data for in-service conditions, although total characterization would not always be easy in terms of historical application and utilization. For this case study, we are convinced that in a relatively short time, it will be possible to completely apply a prediction model.

In the case of the **one-coat rendering mortar** the characteristic that was considered to be significant for the definition of its durability, adhesion to the substrate, presented a behavior that significantly varied with time, unable to result in a degradation curve. The evaluation of the situation led us to the conclusion that there are several exogenous factors that significantly affect the performance. In this case, the application conditions are determinant, as well as the roll of the interfaces between layers. This fact made the application of the adopted prediction model unviable in this case.

4.2 Future Strategies

For the development and the future application of the prediction model to different systems and materials, campaigns of accelerated ageing tests must be taken into consideration accompanied by natural ageing tests and the systematic collection of data from existing buildings. For the adopted strategies to be actually efficient, a rigorous identification of the relevant characteristics to be tested (those that are seen to be critical to durability) is very important and also the performance of previous tests for the gauging of the expected variations and for the identification of the most influential agents.

After a service life prediction has been obtained for specified conditions, where we would be able to have the service life as a reference point, it becomes necessary to evaluate the influence of the specific conditions of each real situation. For this, for example, the factorial method proposed in the ISO standard 15686-1 or other equivalent method could be adopted. The method takes into account, for each situation in the project, the conditioning factors of an estimated service life. They are: the intrinsic quality of the material or system; the quality of the design; the quality of the execution; the environmental, interior and exterior characteristics; the type of use and the level of maintenance.

5 CONCLUSION

In this paper, a model of service life prediction of a material or system of construction based on accelerated artificial ageing tests and on natural ageing tests was presented. Its application was discussed and the main difficulties identified.

In general, we can say that the proposed model can be adopted as long as it is possible to identify a degradation curve as a function of time. The dispersion of the results determined by the influence of factors such as the execution characteristics and the role of the interfaces between the layers led to its adoption being unviable.

REFERENCES

European Committee for Standardization (CEN), 2001, '*Adhesives for tiles – Definitions and specifications*'. EN 12004.

European Committee for Standardization (CEN), 2002, '*Methods of test for mortar for masonry – Part 21: Determination of the compatibility of one-coat rendering mortars with substrates*'. EN 1015-21'.

International Organization for Standardization (ISO), 2001, '*Buildings and constructed assets – Service Life Planning — Part 1: General principles'*. ISO 15686-1'.

Quintela, Marisa A. 2006, '*Durabilidade de Revestimentos Exteriores de Parede em Reboco Monocamada*' (Durability of One-coat rendering mortar for external use), Ms. Sc. Thesis, 177p, Faculty of Engineering of the University of Porto, Portugal.

Sá, Ana V. 2005, '*Durabilidade de Cimentos-Cola em Revestimentos Cerâmicos Aderentes a Fachadas*' (Durability of Cementitious Adhesive in Ceramic Adherent Coverings of Walls), Ms. Sc. Thesis, 148p, Faculty of Engineering of the University of Porto, Portugal.

Carbonation in Concrete with High Fly Ash Content and Hydrated Lime

Juarez Hoppe Filho [1]
Maria Alba Cincotto [2]

T 11

ABSTRACT

Substituting a portion of the cement with fly ash when producing concrete reduces the cost per cubic meter and contributes to sustainable development practices.

Pozzolanic activity is the interaction of fly ash with calcium hydroxide which, forms secondary silicate and aluminate hydrates that reduce the alkalinity of the concrete and the content of portlandite. This causes spreading of the carbonation front, which is undesirable for reinforced concrete. For the purpose of increasing the calcium hydroxide due to the substitution of cement and that consumed by pozzolanic activity, 20% of hydrated lime was added to the concrete and 50% of the high early strength portland cement (HESC) replaced with fly ash.

To achieve compressive strengths of 55 MPa at 91 days, concretes with HESC, HESC + fly ash and HESC + fly ash + hydrated lime were cast with different water/cementitious material ratios. The specimens were then submitted to accelerated carbonation (5% CO_2 and 75% R.H.) for 20 weeks.

The hydrated composition and degree of carbonation were determined by thermogravimetry. The results show that the addition of hydrated lime is efficient in producing a partial reposition of portlandite and accelerates pozzolanic activity. There was identical carbonation in concretes with cement + fly ash, with or without hydrated lime, the spread of the carbonation front was higher in these concretes than the reference concrete.

KEYWORDS

Fly ash, Hydrated lime, Concrete, Carbonation

[1] University of São Paulo, Department of Civil Engineering Construction, São Paulo, Brazil, Phone +55 11 3091-5459, juarez.hoppe@poli.usp.br
[2] University of São Paulo, Department of Civil Engineering Construction, São Paulo, Brazil, Phone +55 11 3091-5792, maria.cincotto@poli.usp.br

1 INTRODUCTION

Substituting high early strength cement (HESC) for fly ash, in concrete, changes the microstructure of the hydrated paste, affecting durability. Normally, these modifications improve performance in the hardened state, although, there is an increase in carbonation. [Papadakis 2000, Mira *et al.* 2002].

The pozzolanic activity of fly ash consumes the calcium hydroxide that results from cement hydration, forming hydraulic compounds [Massazza 1998]. The lower portlandite content increases the neutralization rate of the pore solution by carbon dioxide action. As a result, the reduction in alkalinity takes less time to reach the vicinity of the steel, making the reinforced concrete with high fly ash content more susceptible to corrosion [Papadakis 2000].

Sustainable development aims to increase the amount of pozzolan used in clinker substitution [Papadakis 2000, Mira *et al.* 2002], which reduces the portlandite content in hydrate cementitious material [Taylor 1997, Zhang *et al.* 2000, Sakai *et al.* 2005]. Adding hydrated lime minimizes this disadvantage by partially re-establishing the amount of calcium hydroxide.

The hydrated lime in concrete containing fly ash stimulates pozzolanic activity [Mira *et al.* 2002]. The immediate availability of lime in solution increases the precipitation of hydrates in relation to similar concretes, without the addition of lime [Biernacki *et al.* 2001, Saeki & Monteiro 2005].

Carbonation results from the diffusion of carbon dioxide throughout the covercrete, which it dissolves in aqueous pore solution by neutralizing the alkalinity due to ions OH^-, Ca^{+2}, Na^+ and K^+, forming calcium carbonate [Taylor 1997]. The consumption of portlandite decreases the pH-value, inducing a higher solubility of the other hydrated compounds, which partially reestablishes the alkalinity resulting in more carbonation of C-S-H and aluminate phases [Houst & Wittmann 2002, Thiery *et al.* 2007]. To avoid degradation of C-S-H, which is the most responsible for compressive strength, adding hydrated lime to concrete with pozzolan is proposed which, will increase the amount of portlandite available for carbonation.

The carbonation that occurs in concrete with HESC performs differently in relation to concrete containing pozzolan, which consumes portlandite [Thiery *et al*. 2007]. Adding hydrated lime changes the kinetics of the cement's hydration and pozzolanic activity, affecting carbonation [Mira *et al.* 2002]. Therefore, the aim is to evaluate what efficiency a 20% addition in hydrated lime, of the cementitious materials by weight (50% portland cement + 50% fly ash), may have on the accelerated carbonation of concretes which have reached 55 MPa at 91 days.

2 EXPERIMENTAL PROCEDURES

2.1 Materials

High early strength cement (HESC), in accordance with Brazilian standard ABNT NBR 5733 (ASTM C 150), low-calcium fly ash and calcium hydrated lime were used. The specific gravity, measured by helium picnometry, and Blaine/BET specific surface area of each material, are in Table 1.

Table 1. Physical properties of the materials.

Materials	Specific gravity (g/dm^3)	Specific surface area	
		Blaine (m^2/kg)	BET (m^2/g)
Cement (HESC)	**3.02**	**514**	**1.50**
Fly ash	**2.38**	**678**	**3.63**
Hydrated lime	**2.26**	**1597**	**9.40**

The chemical composition of cement (HESC) and low-calcium fly ash determined by X-ray fluorescence is in Table 2:

Table 2. Chemical composition of the materials.

Materials	SiO_2	Al_2O_3	Fe_2O_3	CaO	MgO	SO_3	L.O.I.
Cement (HESC)	**17.1%**	**3.7%**	**3.1%**	**64.8%**	**0.7%**	**4.6%**	**4.1%**
Fly ash	**63.6%**	**25.1%**	**2.7%**	**4.0%**	**1.0%**	**0.3%**	**2.0%**

The hydrated lime included 60% calcium hydroxide and 32% calcium carbonate residue of raw material, determined by thermogravimetry using a NETZSCH STA 409 PG. The coarse aggregate consisted of crushed and washed granite using the fraction between 19.0 and 6.3 mm. Quartz sand, washed and sieved in 4.8 mm mesh, served as fine aggregate. The admixture used in this study was a water-reducing MBT Glenium 51, the chemical base of which is modified polycarboxylic ether.

2.2 Concrete Mix Proportion

The mix proportions are in Table 3. The cement used was 50% in mass replaced by low-calcium fly ash. To re-establish the portlandite consumed by pozzolanic activity, 20% hydrated lime (by weight) was added to the cementitious materials (portland cement + fly ash).
To achieve the 55 MPa compressive strength of the 91-day-old reference concrete, concretes containing fly ash must have the water/cementitious material ratio decreased. This leads to an increase in the consumption of binding materials. However, as 50% of the mass is composed of fly ash, there is a reduction in the amount of cement utilized, by weight.

Table 3. Concrete mix proportion.

Abbreviation	w/cm	Portland Cement	Fly Ash	Hydrated Lime	Fine Aggregate	Coarse Aggregate	Water	Admixture
	(kg/kg)	**(kg/m^3)**	**(kg/m^3)**	**(kg/m^3)**	**(kg/m^3)**	**(kg/m^3)**	**(kg/m^3)**	**(kg/m^3)**
HESC	**0.52**	**304**	**---**	**---**	**872**	**1088**	**157.9**	**0.60**
HESC + Fly ash	**0.42**	**189**	**189**	**---**	**758**	**1088**	**158.2**	**1.05**
HESC + Fly ash + Hydrated lime	**0.43**	**179**	**179**	**72**	**743**	**1054**	**152.2**	**2.25**

slump – 85 ± 10 mm

The specimens (ϕ10 x 20 cm) tested for compressive strength cured in the wet chamber at 23ºC ± 2ºC and 95% relative humidity for 91 days.

The samples analyzed for accelerated carbonation were extracted from 15 x 15 x 60 cm beams and cured in the wet chamber at 23ºC ± 2ºC and 95% relative humidity for 28 days, Fig. 1.

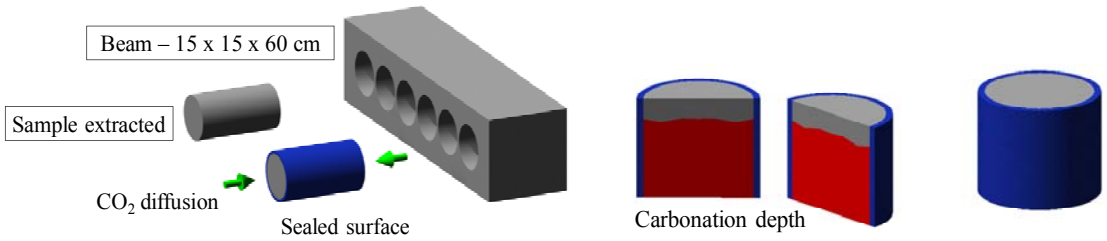

Figure 1. Schematic representation of the samples used in the accelerated carbonation test.

2.3 Accelerated Carbonation Test

The extracted samples (ϕ8 x 15 cm) were pre-conditioned in accordance with RILEM TC-116 PCD [1999] before undergoing the accelerated carbonation test. The pre-conditioning phase occurred for 63

days, until the extracted samples were 91 days-old. Subsequently, the accelerated carbonation test lasted for 20 weeks in a chamber with 5% CO_2 volumetric concentration, 75% relative humidity, and 20ºC ± 1ºC. One sample remained vacuum-sealed to be the non-carbonated reference concrete.
After 4; 8; 12; 16 and 20 weeks, samples were removed from the chamber, split into two halves and the carbonation depth measured by spraying a phenolphthalein solution on the freshly broken concrete surfaces, in accordance with RILEM CPC-18 [1988].

2.4 Chemically Bound Water and Portlandite Content

Preparation of Samples: After the accelerated carbonation test, thin sample slices were taken from the carbonated region of all the concretes. Thin sample slices were also cut from the non-carbonated concretes. From these samples, the coarse aggregate was removed and the mortars submitted to thermogravimetry analysis. These analytical samples were frozen in liquid nitrogen, stored at –30ºC and D-dried.

Thermogravimetry analysis: the dried mortar samples were ground to 150 – 75 □m and the fraction analyzed by thermogravimetry using a NETZSCH STA 409 PG, in a nitrogen atmosphere. The heating rate was 10ºC/minute, applied from 30ºC to 1000ºC. The mass losses were all corrected to non-volatile base [Taylor 1997]. Deconvolution of the calcium carbonate peak (DTG) was determined with the NETZSCH Peak Separation program.

3 TEST RESULTS

3.1 Compressive Strength

Table 4 shows the compressive strength of concretes at 91 days. In the reference concrete, the BET specific surface area available for hydrates precipitation was 1.50m^2/g. This area represents the cement particle surface gradually covered by hydrates. Concrete containing cement + fly ash had 2.56m^2/g. This larger area speeds up the dissolution/precipitation of cement, increasing the degree of hydration by heterogeneous nucleation [Lawrence *et al*. 2003]. The addition of hydrated lime increased the area for crystals growth up to 3.71 m^2/g.

Table 4. Compressive strengths of concretes at 91 days.

Abbreviation	Compressive strenth (MPa)
HESC	**54,7 ± 1,4**
HESC + Fly ash	**54,5 ± 1,6**
HESC + Fly ash + Hydrated lime	**54,9 ± 1,6**

Increases in the compressive strength of concretes with fly ash result mostly from the chemical (pozzolanic activity) and physical effect produced by the extra nucleation sites. The greater degree of cement hydration in concretes containing fly ash, results in Van der Waals forces that are more intensive. In Table 5, concretes with fly ash have lower quantities of chemically bound water as C-S-H and AFt/AFm phases than the reference concrete. Conclusion, the compressive strength of concrete containing fly ash does not depend only on the chemical effects (cement hydration and pozzolanic activity). The physical effect contributes heavily to the compressive strength when pozzolan replaces a portion of the cement.

3.2 Carbonation Depth

Fig. 2 (A) gives the results of carbonation depths, as determined by spraying phenolphthalein solution. The carbonation depth in the reference (HESC) concrete was approximately half of that in concretes with fly ash. When hydrated lime was added, the carbonation depth did not significantly decrease in relation to concrete produced with cement + fly ash, without the addition of lime.

Carbonation is not entirely limited to the areas indicated by the phenolphthalein solution [Chang & Chen 2006, Thiery *et al.* 2007]. Nonetheless, the carbonation coefficient for the area with a pH ≤ 9 may be calculated using the colorimetric test results and used to adequately compare differing concretes.

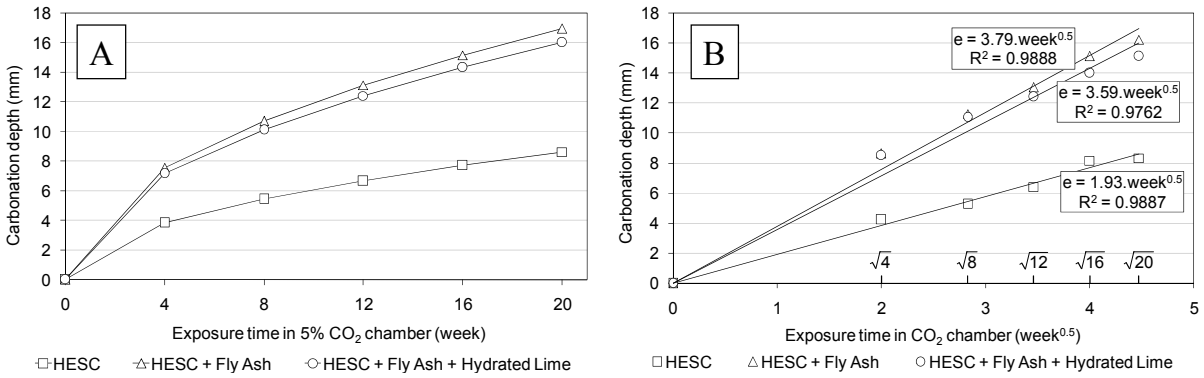

Figure 2. Carbonation depth of concretes in accelerated condition for 20 weeks.

Calculation of the carbonation coefficient was achieved by plotting the carbonation depth against the square root of time, as shown in Fig 2 (B). The angular coefficient of the linear equation represents the carbonation coefficient of the concrete. The reference concrete, with HESC, has a coefficient of 1.9 mm/week$^{0.5}$. The carbonation coefficients of concretes with fly ash, with or without hydrated lime, are very similar, 3.6 mm/week$^{0.5}$ and 3.8 mm/week$^{0.5}$, respectively.

3.3 Chemically bound water and portlandite content

Fig. 3 shows the mass loss (TG) and mass loss rate (DTG) for the reference concrete, carbonated, and non-carbonated. The difference between curves represents the accelerated carbonation effects in hydrates (C-S-H + aluminates + magnesium compounds) and portlandite in relation to the non-carbonated concrete.

Mass loss between 30ºC and 390ºC is due to the decomposition of C-S-H and aluminates (AFt and AFm phases). Calcium hydroxide decomposes between 390ºC and 480ºC and, calcium carbonate above 480ºC.

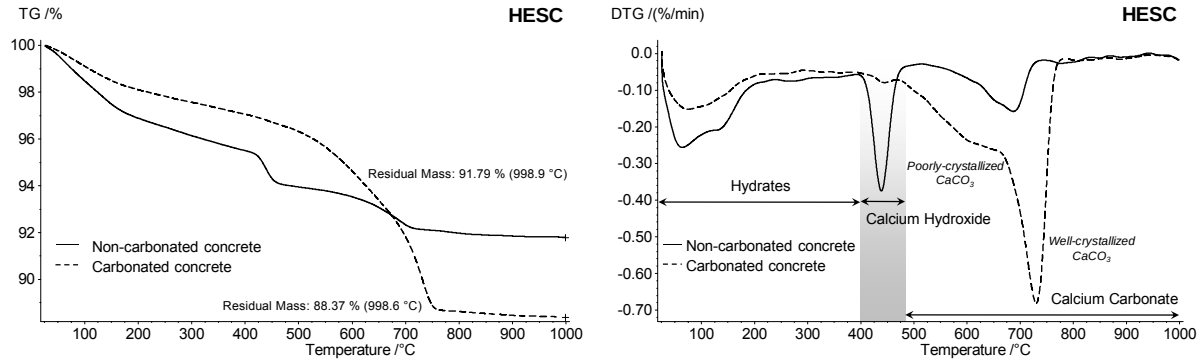

Figure 3. TG/DTG of HESC concrete, carbonated and non-carbonated (20 weeks).

X-ray diffraction (Fig. 4) showed there was some remaining portlandite in the carbonated zone of the reference concrete while in concretes containing fly ash, with or without hydrated lime, there was none. This residual portlandite in the carbonated zone is due to the formation of a $CaCO_3$ coating around the $Ca(OH)_2$ crystals, reducing their solubility in pore solution [Thiery *et al.* 2007]. Vaterite appeared in the reference concrete but not in concretes containing fly ash.

Calcium carbonate formed during accelerated carbonation results in well-crystallized $CaCO_3$ (calcite) and poorly crystallized $CaCO_3$ (vaterite and/or aragonite). In stable form (calcite), the decomposition of crystals occurs at higher temperatures than in meta-stable phases. Fig. 5 displays the mass loss rate (DTG) for all concretes above 480ºC. Deconvolution of DTG curves results in two main reactions of decomposition.

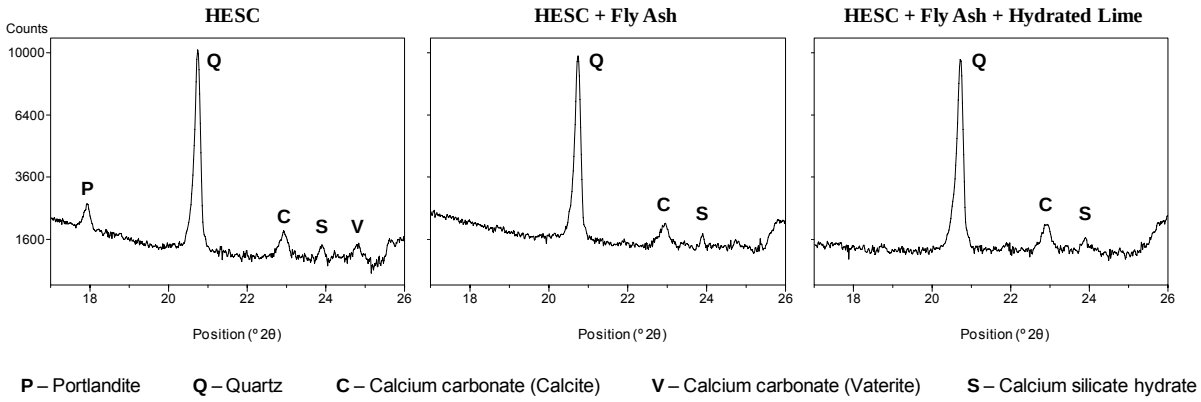

Figure 4. X-ray diffraction of concretes after accelerated carbonation.

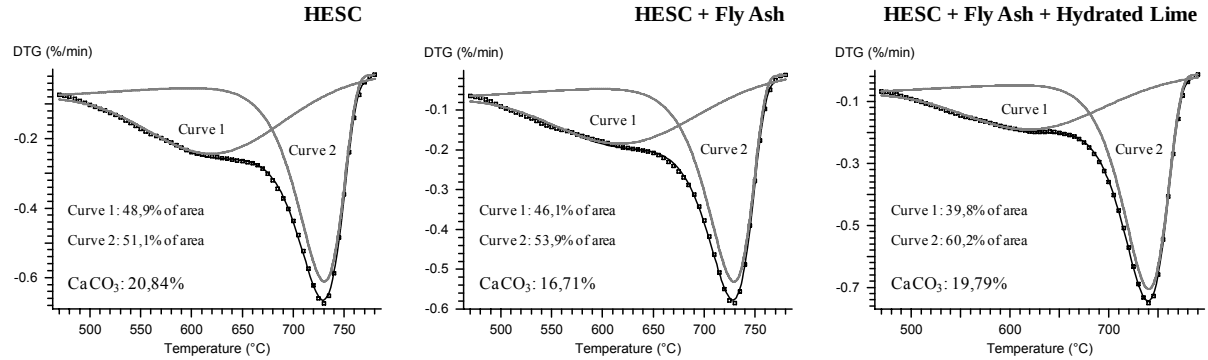

Figure 5. Deconvolution of DTG curves in calcium carbonate decomposition zone.

The first reaction (curve 1) represents vaterite/aragonite and calcite in a less crystalline state of decomposition. Curve 2 indicates well-crystallized calcite decomposition. Each concrete in the study presented these two reactions. However, when hydrated lime was added to concrete with fly ash, the amount of well-crystallized calcite became higher than in the other concretes because lime has well-crystallized calcium carbonate in its composition.

The mass loss data of all carbonated and non-carbonated concretes is in Table 5. The addition of hydrated lime in concrete with cement and fly ash increased the remaining amount of calcium hydroxide. With the addition of hydrated lime, the quantity of portlandite increased to 66% of that found in the reference concrete. Without the addition of hydrated lime, the portlandite content remained at 46%.

In concrete containing cement + fly ash, the total theoretical amount of calcium hydroxide produced was 4.24%, and the remaining portlandite content was 3.12%. Pozzolanic activity consumed 1.12%. With the addition of hydrated lime the theoretical amount rose to 7.65%, the portlandite remaining was 4.48% and the portlandite consumed was 3.17%. Thus, adding hydrated lime speeds up the pozzolanic activity, which consumes greater quantities of portlandite and consequently forms more hydraulic compounds.

Carbonation consumes the portlandite and provokes decomposition of the hydrated compounds to form calcium carbonate. After carbonation, the chemically bound water, in the form of C-S-H and AFt/AFm phases, is lower than in non-carbonated concretes, Table 6.

Table 5. Mass losses, on the same ignited mass, of carbonated and non-carbonated concretes.

Concrete	Chemically bound water (%)	Calcium Hydroxide (%)		Calcium Carbonate (%)		Loss on Ignition (%)
	C-S-H Aluminates	Water	$Ca(OH)_2$*	CO_2	$CaCO_3$#	
HESC – NC (*non-carbonated*)	**4.78**	**1.66**	**6.82**	**2.43**	**5.52**	**8.87**
HESC – C (*carbonated*)	**3.27**	**---**	**---**	**9.18**	**20.84**	**13.1**
HESC + Fly Ash – NC	**2.99**	**0.76**	**3.12**	**2.28**	**5.18**	**6.03**
HESC + Fly Ash – C	**2.45**	**---**	**---**	**7.36**	**16.71**	**10.29**
HESC + Fly Ash + Hydrated Lime – NC	**2.81**	**1.09**	**4.48**	**1.85**	**4.20**	**5.75**
HESC + Fly Ash + Hydrated Lime – C	**2.37**	**---**	**---**	**8.72**	**19.79**	**11.68**

* $Ca(OH)_2$ = % chemically bound water as portlandite x [$Ca(OH)_2$ molecular mass / H_2O molecular mass]
\# $CaCO_3$ = % carbon dioxide x [$CaCO_3$ molecular mass / CO_2 molecular mass]

Table 6 shows the amount of calcium oxide bound as portlandite and calcium carbonate, in non-carbonated concrete, and the amount bound as calcium carbonate in carbonated concrete, using the data in Table 5.

Table 6. Calcium oxide as portlandite and calcite in non-carbonated and carbonated concretes and calcium oxide from hydrates to form calcium carbonate in carbonated concrete.

Concrete	Calcium Hydroxide (%)		Calcium Carbonate (%)		CaO Total (%) (as portlandite and calcium carbonate)	CaO from Hydrates (%)
	$Ca(OH)_2$	CaO*	$CaCO_3$	CaO#		
HESC – NC (*non-carbonated*)	**6.82**	**5.16**	**5.52**	**3.09**	**8.25**	**3.42**
HESC – C (*carbonated*)	**---**	**---**	**20.84**	**11.67**	**11.67**	
HESC + Fly Ash – NC	**3.12**	**2.36**	**5.18**	**2.90**	**5.26**	**4.10**
HESC + Fly Ash – C	**---**	**---**	**16.71**	**9.36**	**9.36**	
HESC + Fly Ash + Hydrated Lime – NC	**4.48**	**3.39**	**4.20**	**2.35**	**5.74**	**5.34**
HESC + Fly Ash + Hydrated Lime – C	**---**	**---**	**19.79**	**11.08**	**11.08**	

* CaO = % calcium hydroxide x [CaO molecular mass / $Ca(OH)_2$ molecular mass]
\# CaO = % calcium carbonate x [CaO molecular mass / $CaCO_3$ molecular mass]

The total amount of calcium oxide calculated from the calcium hydroxide and calcium carbonate in non-carbonated concretes is insufficient to produce the amount of calcium carbonate measured in the carbonated concrete, as shown in Table 6. Therefore, the difference represents the amount of calcium oxide resulting from the decomposition of hydrates (decalcification), which forms calcium carbonate [Kobayashi *et al*. 1994].

The amount of calcium oxide resulting from the decomposition of hydrates and consumed by carbonation reactions was higher in concretes containing fly ash than in the reference concrete. The addition of hydrated lime increases this consumption. Therefore, the lower alkaline reserve in concretes containing fly ash, with or without hydrated lime, results in a higher degradation of the C-S-H and AFt/AFm phases than for the reference concrete, when submitted to the accelerated carbonation test.

4 CONCLUSIONS

This work leads to the following considerations:

The carbonation depth in concrete containing a high amount of fly ash, measured in accelerated test for 20 weeks after 91 days of casting, was approximately two times higher than reference concrete with high early strength cement.

The addition of hydrated lime increases the amount of portlandite remaining in concrete with cement + fly ash. However, the percentage of portlandite is not a determinant factor for slowing down the spread of the alkaline interface in concrete containing high amounts of fly ash when they were cast for the same compressive strength.

Carbonation decreases the amount of chemically bound water in C-S-H and AFt/AFm phases. The decomposition of these compounds, measured by thermogravimetry, was more evident in the reference concrete, with high early strength cement than concrete containing fly ash, with or without hydrated lime.

ACKNOWLEDGEMENTS

The authors wish to acknowledge the financial support provided by Fundação de Amparo à Pesquisa do Estado de São Paulo – FAPESP.

REFERENCES

Biernacki, J. J., Williams, P. J. & Stutzman, P. E. 2001, 'Kinetics of reaction of calcium hydroxide and fly ash', *ACI Materials Journal*, Vol. 98, July – August, Nº 4, p. 340 – 349.

Chang, C. F. & Chen, J. W. 2006, 'The experimental investigation of concrete carbonation depth'. *Cement and Concrete Research*, Vol. 36, September, Issue 9, p. 1760 – 1767.

Houst, Y.F. & Wittmann, F.H. 2002, 'Depth profiles of carbonates formed during natural carbonation'. *Cement and Concrete Research*, Vol. 32, December, Issue 12, p. 1923 – 1930.

Kobayashi, K.; Suzuki, K. & Uno, Y. 1994, 'Carbonation of concrete structures and decomposition of C-S-H'. *Cement and Concrete Research*, Vol. 24, Issue 1, p. 55 – 61.

Lawrence, P., Cyr, M.; Ringot, E. 2003, 'Mineral admixture in mortars. Effect of inert materials on short-term hydration'. *Cement and Concrete Research*, Vol. 33, December, Issue 12, p. 1939 – 1947.

Massazza, F. 1998, 'Pozzolana and pozzolanic cements'. In: *Lea´s chemistry of cement and concrete*. Edited by Peter C. Hewlett. Fourth Edition.

Mira, P., Papadakis, V.G. & Tsimas, S. 2002, 'Effect of lime putty addition on structural and durability properties of concrete'. *Cement and Concrete Research*, Vol. 32, May, Issue 5, p. 683 – 689.

Papadakis, V.G. 2000, 'Effect of supplementary cementing materials on concrete resistance against carbonation and chloride ingress'. *Cement and Concrete Research*, Vol. 30, February, Issue 2, p. 291 – 299.

Rilem 1999, 'Permeability of concrete as a criterion of its durability. Rilem TC 116-PCD: recommendation'. *Materials and Structures Journal*, Vol. 32, April, Number 3, p. 174 – 179.

Rilem 1988, 'Measurements of hardened concrete carbonation depth. Rilem CPC-18: recommendation'. *Materials and Structures Journal*, Vol. 21, November, Number 6, p. 453 – 455.

Saeki, T. & Monteiro, P.J.M. 2005, 'A model to predict the amount of calcium hydroxide in concrete containing mineral admixture'. *Cement and Concrete Research*, Vol. 35, Oktober, Issue 10, p. 1914 – 1921.

Sakai, E., Miyahara, S., Ohsawa, S., Lee, S. H. & Daimon, M. 2005, 'Hydration of fly ash cement'. *Cement and Concrete Research*, Vol. 35, June, Issue 6, p. 1135 – 1140.

Taylor, H. F. W. 1997, '*Cement chemistry'*. Thomas Telford Publishing, London.

Thiery, M., Villain, G., Dangla, P. & Platret, G. 2007, 'Investigation of the carbonation front shape on cementitious materials: effects of the chemical kinetics'. *Cement and Concrete Research*, Vol. 37, July, Issue 7, p. 1047 – 1058.

Zhang, Y. M., Sun, W. & Yan, H. D. 2000, 'Hydration of high-volume fly ash cement pastes'. *Cement & Concrete Composites*, Vol. 22, December, Issue 6, p. 445 – 452.

11DBMC International Conference on Durability of Building Materials and Components
ISTANBUL, Turkey 11-14 May 2008

Effect of Curing Age on the Durability of High-Volume Fly Ash Concrete

Nele De Belie [1]
Stijn Lammertijn [1]
Kathelijn Cox [1]

T 11

ABSTRACT

High volume fly ash (HVFA) concrete is one of the "green" alternatives developed to reduce the energy consumption and CO_2 emission related to the cement production. The pozzolanic reaction of fly ash is a retarded process compared to the cement hydration. As a result, the strength, microstructure development and consequently also the durability behavior of fly ash mixtures will be strongly influenced by age. After all, durability is, to a large extent, determined by the possibility for aggressive substances to penetrate into the concrete, and the latter is in turn determined by the porosity and transport properties of the concrete.

This paper describes the results of tests on 4 fly ash mixtures, each with a different fly ash replacement level namely 0, 35, 50 and 67%, but with the same water-to-cementitious materials ratio. The experiments were executed at the age of 1, 3 and 6 months. Permeable porosity and gas permeability increased with increasing fly ash content. A reduction in porosity was noticed between 1 and 3 months for the fly ash mixtures due to the pozzolanic reaction. The carbonation depth was considerably higher for the 50 and 67 % fly ash mixtures at all ages compared to the ordinary Portland cement concrete. Carbonation appeared to have a negative effect on gas permeability, especially for the 50 and 67 % mixtures.

KEYWORDS

Fly ash, durability, porosity, carbonation, permeability.

1 Magnel Laboratory for Concrete Research, Ghent University, Technologiepark Zwijnaarde 904, 9052 Ghent, Belgium, Phone +32 9 264 55 22, Fax +32 9 264 58 45, nele.debelie@ugent.be

1 INTRODUCTION

The production of portland cement consumes a great deal of energy and yearly produces a considerable amount of CO_2. By replacing cement in concrete by fly ash (FA), which is a by-product of the combustion of pulverized coal, the environmental impact of the concrete production can be reduced [Malhotra & Mehta 2005]. Concrete with a fly ash replacement level above 50% is called high-volume fly ash concrete (HVFA concrete). Fly ash is a pozzolanic material which has to be activated by the hydration products coming from the hydration of portland cement. The replacement of a large quantity of cement by fly ash has an important influence on the composition, the microstructure and the properties of fresh and hardened concrete. Therefore the durability characteristics of high-volume fly ash (HVFA) concrete are different from those of ordinary Portland cement (OPC) concrete. In this article, carbonation is investigated, which plays a major role in the resistance of the concrete to corrosion of the embedded steel. Gas permeability – strongly influenced by porosity – is a determining factor in this mechanism and is therefore studied as well. Also the influence of carbonation on porosity and gas permeability is tested.

2 LITERATURE REVIEW

2.1 Permeable Porosity

Potentially harmful substances penetrate into the concrete through connected pores. Factors influencing the permeable or 'open' porosity therefore automatically have an impact on durability. Several authors mention 2 important effects through which a lower porosity could be obtained in HVFA concrete compared to OPC concrete [Malhotra & Mehta 2005, Bilodeau *et al.* 1994, Berry *et al.* 1994, Kosmatka *et al.* 2002]: (1) Fly ash improves concrete workability; therefore a lower water - cementitious materials ratio (W/CM) can be used with increasing fly ash content; (2) due to the pozzolanic reaction, additional hydration products are formed which fill the pores and produce a denser structure. According to Papadakis *et al.* [1992] a higher fly ash replacement level in concrete with a constant W/CM leads to a higher porosity and an increasing percentage of large pores. Khan [2003] performed experiments on concrete with a FA/CM level between 0 and 40 % and W/CM between 0.27 and 0.50. According to Khan fly ash replacement has little influence on the porosity. Only for very low W/CM ratios the porosity decreased with increasing fly ash level.

2.2 Gas Permeability

Gas permeability gives an indication of the difficulty for harmful substances such as CO_2 to penetrate into the concrete. It is strongly related to the open porosity and the distribution of the pores. Abbas *et al.* [1999] mention that the coefficient of gas permeability varies with the pressure gradient because of the change from laminar to molecular flow. They also state that the permeability is strongly dependent on the degree of saturation of the concrete. Moisture in the pores forms a barrier for the gas molecules, as a result of which their penetration is hindered. Because most authors are convinced that a lower porosity is possible in HVFA concrete, also a lower gas permeability should be possible. Tests executed by Kosmatka *et al.* [2002] and McCarthy & Dhir [2005] confirmed this. Following their conclusions on porosity Papadakis *et al.*[1992] found that for a constant W/CM ratio the gas permeability increased with increasing fly ash content, while Khan [2003] concluded the opposite.

2.3 Carbonation

There are two determining factors concerning carbonation [Jiang *et al.* 2000] :

- the lower the gas permeability, the slower the CO_2 diffusion and the lower the carbonation rate.
- the more $Ca(OH)_2$ is available, the more CO_2 molecules can react, which leads to a slower ingress of CO_2. In the pozzolanic reaction of fly ash $Ca(OH)_2$ is consumed. Therefore less carbonatable material is available in HVFA concrete.

Papadakis *et al.* [1992] noticed a higher carbonation depth with increasing fly ash content for concrete with a constant W/CM ratio, because of the higher permeability and lower amount of carbonatable material. Jiang *et al.* [2000] found conflicting results in literature, but generally it seemed that the carbonation depth increased with increasing fly ash content, which was confirmed by their own research (fly ash replacements of 0, 55 and 70 % but decreasing W/CM with increasing fly ash content). They are convinced though that HVFA concrete with appropriate mixture proportions could match the resistance to carbonation of OPC concrete. They experienced that not all fly ash in HVFA concrete had reacted as a result of an insufficient amount of $Ca(OH)_2$. They concluded that the effective W/CM ratio, W/CM*, which takes into account the amount of cementitious materials that effectively can be hydrated, is the most important parameter concerning porosity and that the amount of cement C is the most important one for the amount of carbonatable material. Tange Jepsen *et al.* [2001] found that a 40% fly ash mixture with W/CM = 0.4 carbonates considerable faster than other "green" concrete due to the consumption of $Ca(OH)_2$ in the pozzolanic reaction.

2.4 Influence of Carbonation on Porosity and Gas Permeability

$CaCO_3$ formed in the carbonation process has a very low solvability and therefore will precipitate in the pores as a result of which in general a denser structure will be obtained. The effect of carbonation on the concrete structure is nevertheless not the same for all types of concrete. Ngala & Page [1997] executed tests on OPC concrete and a 30% fly ash concrete with different W/CM ratios to investigate the influence of carbonation on porosity and gas permeability. The total porosity was reduced for all mixtures after they were fully carbonated. The capillary porosity on the other hand seemed to increase slightly for the OPC concrete, but increased significantly (± 140%) for the fly ash concrete. Ngala & Page attribute the reduction in total porosity to filling of the gel pores with $CaCO_3$. The increase in capillary porosity can be explained by the formation of silica gel as a result of the decomposition of CSH gel during CO_2 exposure, causing a "pore size redistribution". The higher increase in capillary porosity for the fly ash concrete compared to the OPC concrete can be explained by the higher amount of CSH gel as a result of the pozzolanic reaction. Ngala & Page also found that carbonation has a large influence on gas permeability, especially for fly ash concrete, where the gas permeability increased with a factor 10.

3 EXPERIMENTAL DETAILS

3.1 Materials

Four different mixtures were made: a reference mixture (REF) with 100% portland cement and three fly ash mixtures (FA) with 35, 50 or 67 % of the portland cement replaced by fly ash. A portland cement CEM I 52.5, complying with EN 197-1 (2000), was used and a class F (according to ASTM standards) fly ash with a low calcium oxide content (1.96%). All mixtures had a total amount of CM (cement + fly ash) of 400 kg/m³ and were made with a W/CM of 0.4. A superplasticizer, based on carboxylic acid, was added to obtain a decent workability and an air entraining agent was used to obtain an air content of about 4% and a good freeze-thaw resistance. The mixture proportions are given in Table 1.

3.2 Experimental Procedures

All durability tests - except gas permeability - were performed at the age of 1, 3 and 6 months; gas permeability was only examined after 3 months of curing. During this period the specimens were stored in a climate chamber with a relative humidity above 90% and temperature around 20 °C.

Table 1. Concrete mixture proportions.

	REF	FA35	FA50	FA67
sand 0/4 [kg/m³]	686.4	667.8	659.8	651.9
aggregate 2/8 [kg/m³]	450.5	437.2	431.9	426.6
aggregate 8/16 [kg/m³]	694.3	678.4	667.8	659.8
CEM I 52.5N [kg/m³]	400	260	200	132
water [kg/m³]	160	160	160	160
fly ash [kg/m³]	0	140	200	268
air entraining agent [ml/m³]	270	350	400	400
superplasticizer [ml/m³]	1080	486	473	342
W/CM [-]	0.4	0.4	0.4	0.4

3.2.1 Permeable Porosity

A vacuum saturation technique, as described in the Belgian standard NBN B05-201 (1976), is used to determine the open porosity. For each mixture 3 cylindrical specimens (diameter = 100 mm, thickness = 50 mm) were taken out of a 150 mm cube. The specimens were dried in a ventilated oven at 45 °C to constant mass, then vacuum saturated and weighed. The procedure was repeated after drying at 105 °C. This allows to get a rough estimation of the capillary and gel porosity of the concrete [Audenaert & De Schutter 2007].

3.2.2 Gas Permeability

An oxygen permeation test was executed as described in RILEM TC 116-PCD [1999]. For each mixture three cylindrical specimens with a diameter of 150 mm and a thickness of 50 mm were taken out of a 400 x 400 x 100 mm slab. After 3 months of curing the specimens were dried at a temperature of 60° C until the mass loss in 24 hours was below 0.1% (approximately 10 days). The gas permeability was measured using a “cembureau” permeameter. Tests were performed under a pressure of 2, 3 and 4 bar. The apparent oxygen permeability coefficient was calculated using equation (1):

$$K = \frac{2.P_a.Q.L.\eta}{A.(P^2 - P_a^2)} \quad (1)$$

where P_a = the atmospheric pressure (Pa), Q = volume flow rate of the fluid (m^3/s), L= thickness of the specimen (m), η = dynamic viscosity of the fluid (for oxygen at 20°C equal to 2.2 x 10^{-5} $N.s/m^2$), A = cross-sectional area of the specimen (m^2), P = absolute inlet pressure (Pa).

3.2.3 Carbonation

For each mixture 4 cubes (100 mm) were cast and placed in a room with 10% CO_2 (20 °C, 60% RH) to obtain an accelerated carbonation. Five of the six surfaces of the cubes were coated to ensure unidirectional CO_2-ingress. At 1, 3, 6, 10, 14, and 18 weeks the carbonation depth was measured on 3 cubes by removing a 10 mm thick slice from the cubes perpendicular to the exposed side and spraying with phenolphthalein. The slices of the remaining cubes (only for 3 months curing period) were used for thermogravimetric analysis (TGA) to estimate the content of $Ca(OH)_2$. The 10 mm near to the exposed surface was removed from the slice, crushed and sieved. The powder was heated in Argon atmosphere to 1100 °C at a rate of 10 °C/min, which leads to the decomposition of $Ca(OH)_2$ around 450 °C. The mass loss caused by $Ca(OH)_2$ decomposition was corrected with the loss of chemically bound water in the interval considered.

3.2.4 Influence of Carbonation on Porosity and Gas Permeability

The samples were made in the same manner as for normal tests. However, before accelerated carbonation they were coated and sealed with plastic in a way that CO_2 could only enter at one side. Tests were performed after 0, 6 and 14 weeks of exposure to 10% CO_2.

4 RESULTS AND DISCUSSION

4.1 Permeable porosity

In Fig. 1 the average values and standard deviations on individual measurements are shown for capillary permeable porosity (CPP) and total permeable porosity (TPP) respectively. The gel porosity (GP) can be calculated as the difference between total and capillary porosity. The initial capillary porosity at 1 month of age increases with increasing fly ash content due to the actual increase in W/C ratio and is approximately equal for FA50 and FA67. The initial gel porosity decreases with increasing fly ash content. The CPP hardly changes for the reference mixture after 1 month of curing. The fly ash mixtures however show a substantial reduction in CPP between 1 and 3 months of curing as a result of pore filling with additional hydration products from the pozzolanic reaction. The reduction is more pronounced for FA50 than it is for FA35, but is lower for FA67 than for FA50. A possible explanation is that the amount of fly ash which reacts is lower for FA67 than for FA50 because of the lower clinker content, resulting in a shortage of $Ca(OH)_2$. Between 3 and 6 months the CPP hardly decreases for all mixtures. In fact, a small increase is noticed for FA67. This can be the result of a starting carbonation (see further). Fig. 1 shows that the TPP decreases between 1 and 3 months for all mixtures, even for the reference. Apparently the further hydration of portland cement in the reference mixture fills the gel pores, but not the capillary pores. For FA50 and FA67 there is an increase in GP, inferior to the decrease in CPP, between 1 and 3 months of age. This illustrates the transformation of capillary pores into gel pores in time, also called pore refinement. Between 3 and 6 months a slight increase in TPP is noticed for FA35 and FA50, while the GP hardly changes. The TPP and GP of FA67 decrease, which is possibly caused by starting carbonation. The results from this research are contradictory to Khan's [2003] but similar to those of Papadakis *et al.* [1992]: an increasing porosity with increasing fly ash replacement for a constant W/CM ratio.

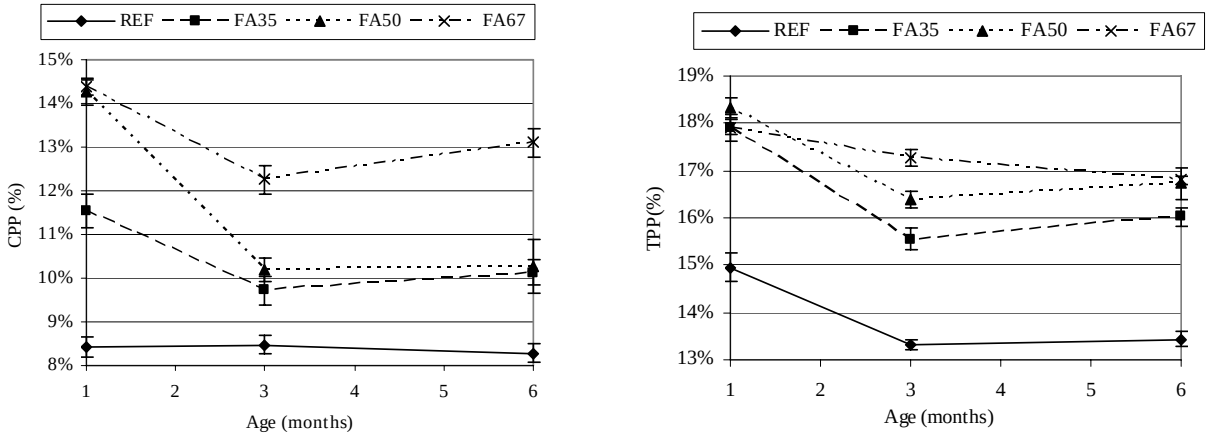

Figure 1. Capillary permeable porosity, CPP (left) and total permeable porosity, TPP (right) at different ages, including standard deviation on individual measurements.

4.2 Gas Permeability

The results of the permeation test at the age of 3 months are shown in Fig. 2. The decrease of K with increasing applied pressure is in accordance with RILEM TC 116-PCD [1999]. The gas permeability at all pressures is lower for FA35 than for REF, in spite of the higher capillary porosity for FA35. Nevertheless, generally the gas permeability seems to increase with increasing capillary porosity. Just as with porosity, the test results for gas permeability are in general contradictory to Khan's [2003] but similar to those of Papadakis *et al.* [1992]: an increasing gas permeability with increasing fly ash replacement for a constant W/CM ratio.

4.3 Carbonation

The carbonation depths after accelerated carbonation tests, starting at 1, 3 and 6 months of age, could be expressed at each age as:

$$x = A\sqrt{t} \quad (2)$$

where x = carbonation depth (mm), A = carbonation coefficient (mm/week$^{0.5}$) and t = time of exposure (weeks). The carbonation coefficients for each mixture are presented in Fig. 2. The more open structure and lower amount of carbonatable material for HVFA concrete has a substantial negative effect on the resistance to carbonation. The carbonation coefficient decreases with increasing age for all fly ash mixtures. This means that the positive effect of the decreasing porosity at later age is more significant than the negative effect of the decreasing amount of $Ca(OH)_2$ because of the ongoing pozzolanic reaction. As with the capillary porosity, the decrease is most pronounced for FA50. The results show that the carbonation coefficient strongly increases between FA50 and FA67, which indicates that it will not be easy to make mixtures with a good resistance to carbonation if more than 50% of the cement is replaced by fly ash.

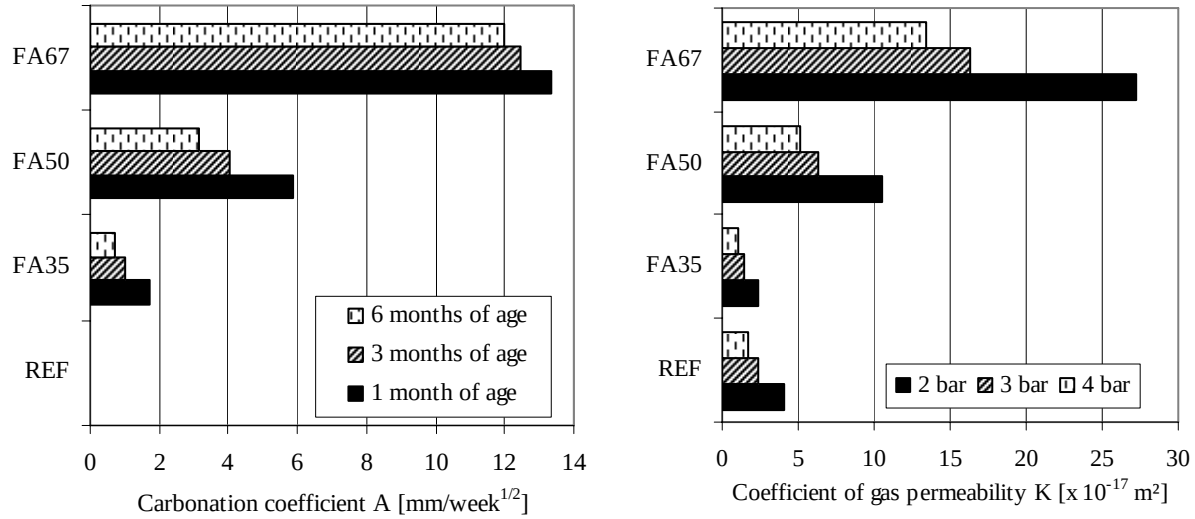

Figure 2. Coefficient of gas permeability K after 3 months of curing for several applied pressures (left) and carbonation coefficient A at different ages (right).

4.4 Thermogravimetric Analysis (TGA)

At all exposure times the amount of $Ca(OH)_2$ decreased with increasing fly ash replacement level, due to the lower amount of portland cement and the consumption of $Ca(OH)_2$ in the pozzolanic reaction. For all mixtures a substantial part of the $Ca(OH)_2$ in the outer concrete zone was consumed in the carbonation process after 1 week of exposure. After 3 weeks all $Ca(OH)_2$ in the outer 10 mm of the 67% mixture had reacted. For FA50 no $Ca(OH)_2$ was left after 10 to 18 weeks. During the test period there was always $Ca(OH)_2$ left in the reference and 35% mixtures.

4.5 Influence of carbonation on porosity and gas permeability

Tests were performed at 0, 6 and 14 weeks of exposure of 3 month old samples to 10% CO_2. Only the samples for FA67 were completely carbonated after 14 weeks, while for REF en FA35 hardly any carbonation could be measured. Therefore it is more correct to speak about influence of exposure to CO_2 than about influence of carbonation on porosity and gas permeability.

4.5.1 Porosity

Fig. 3 presents the results for the CPP and TPP. Despite the fact that for the reference mixture no carbonation could be measured using phenolphthalein (on thin sections carbonation was visible), the capillary porosity decreases significantly after 6 weeks of exposure. For FA35 and FA50 the CPP also decreases because of the exposure to CO_2, while for FA67 there is a slight increase. The TPP remains equal for REF, but decreases for all fly ash mixtures. So globally it can be said that carbonation doesn't seem to have a big negative effect on the porosity of concrete. These results for the reference mixture are contradictory to the ones from Ngala & Page [1997], who say that in (fully carbonated) OPC concrete the total porosity decreases and the capillary porosity stays approximately equal.

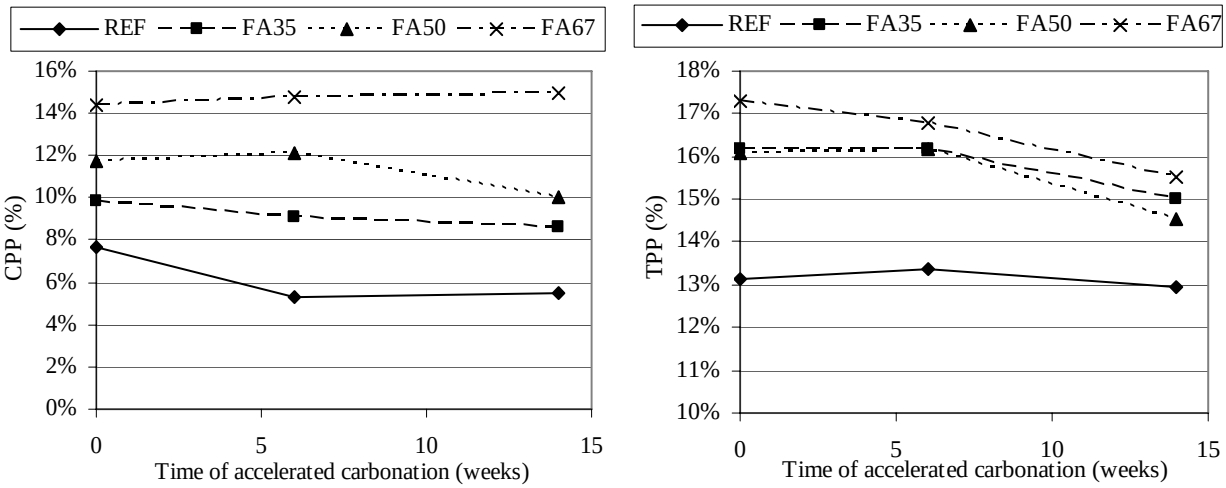

Figure 3. Change in capillary permeable porosity, CPP (left) and total permeable porosity, TPP (right) during accelerated carbonation

4.5.2 Gas permeability

The influence of carbonation on gas permeability is shown in Fig. 4 for an applied pressure of 3 bar. For all mixtures the gas permeability increases with increasing carbonation. For REF and FA35 the increase is limited, but for FA50 and FA67 the gas permeability increases considerably: after 14 weeks of exposure with a factor 2.6 for FA50 and 3.6 for FA67. This will of course have a negative influence on the resistance of the concrete to corrosion. Not only the carbonation rate will increase, but also the penetration of O_2 – necessary for corrosion – will become more easy.

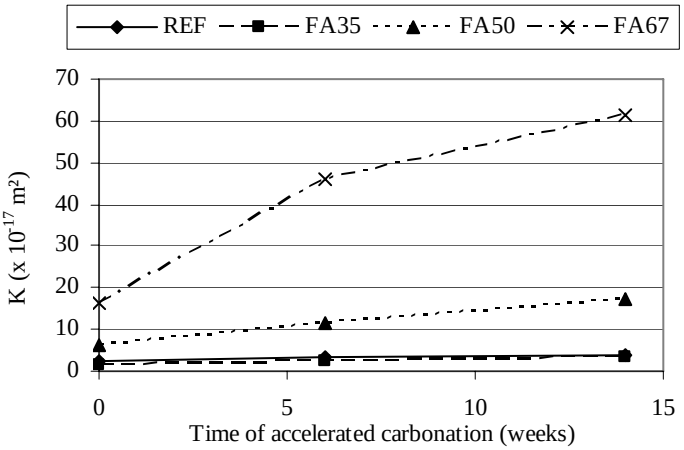

Figure 4. Coefficient of gas permeability K (3 bar) after 0, 6 and 14 weeks of exposure to 10% CO_2

5 CONCLUSIONS

The porosity, gas permeability, carbonation and their interaction were studied in concrete mixtures with different levels of fly ash replacement (up to 67%) and a constant W/CM ratio. The capillary and total permeable porosity increased with increasing fly ash replacement level. A considerable decrease in porosity was noticed for the fly ash mixtures between 1 and 3 months of age as a result of the pozzolanic reaction and the transformation of capillary pores into gel pores. Following the results of capillary porosity, the gas permeability at the age of 3 months increased with increasing fly ash content, but also other factors influenced gas permeability. Since the gas permeability increased and the amount of carbonatable material decreased with increasing fly ash content, the carbonation rate at all ages was much higher in HVFA concrete than in OPC concrete. Thermogravimetric analysis showed that the amount of $Ca(OH)_2$ decreased with increasing fly ash level, and that it was rapidly depleted by accelerated carbonation in FA50 and FA67. Carbonation did not have a negative effect on porosity, while the gas permeability increased significantly for the fly ash mixtures as a result of exposure to CO_2.

Concerning gas permeability and carbonation HVFA concrete (FA50, but certainly FA67), with a W/CM = 0.4 en CM = 400 kg/m³, performed worse compared to OPC concrete with the same W/CM and CM. Therefore the use of reinforced HVFA concrete with these mixture proportions does not seem advisable in practice. Further research on HVFA concrete with lower W/CM ratios, and therefore lower porosities, is needed to improve the durability performance of HVFA concrete.

ACKNOWLEDGEMENTS

This research was made possible through the financial support of the Research Foundation – Flanders (FWO-Vlaanderen), project G.0135.05.

REFERENCES

Abbas, A., Carcasses, M. & Ollivie,r J.-P. 1999, 'Gas permeability of concrete in relation to its degree of saturation', *Materials and Structures*, 32[215], 3-8.

Audenaert, K., De Schutter, G. 2007, 'Relation between vacuum water absorption and porosity of self-compacting concrete'. Proc. 5th Int. RILEM Symp. SCC, Ghent, 3-5 September 2007, 701-706.

Berry, E., Hemmings, R., Zhang, M., Cornelius, B. & Golden, D. 1994, 'Hydration in high-volume fly ash concrete binders'. *ACI Materials Journal*, **91**[4], 382-389.

Bilodeau, A., Sivasundaram, V., Painter, K. & Malhotra, V. 1994, 'Durability of concrete incorporating high volumes of fly ash from sources in the U.S.' *ACI Materials Journal*, **91**[1], 3-12.

Jiang, L., Lin B. & Cai, Y. 2000, 'A model for predicting carbonation of high-volume fly ash concrete', *Cement and Concrete Research*, **30**[5], 699-702.

Khan, M. 2003, 'Permeation of high performance concrete', *Journal of Materials in Civil Engineering*, **15**[1], 84-92.

Kosmatka, S., Kerkhoff, B., Panarese, W. 2002, *Design and control of concrete mixtures*. PCA, Naples.

Malhotra, V.M. & Mehta, P.K. 2005, *High-performance, high-volume fly ash concrete (2nd edition)*. Supplementary Cementing Materials for Sustainable Development Inc., Ottawa.

McCarthy, M. & Dhir, R. 2005, 'Development of high volume fly ash cements for use in concrete construction', *Fuel*, **84**[11], 1423-1432.

Ngala, V. & Page, C. 1997, 'Effects of carbonation on pore structure and diffusional properties of hydrated cement pastes', *Cement and Concrete Research*, **27**[7], 995-1007.

Papadakis, V., Fardis, M. & Vayenas, C. 1992, 'Hydration and carbonation of pozzolanic cements', *ACI Materials Journal*, **89**[2], 119-130.

RILEM TC 116-PCD. 1999, 'Permeability of concrete as a criterion of its durability', *Materials and Structures*, **32**[217], 174-179.

Tange Jepsen, M., Mathiesen, D., Munch-Petersen C. & Bager D. 'Durability of resource saving "green" types of concrete'. *Proc. FIB-symposium "concrete and environment"*, Berlin, 2001.

11DBMC International Conference on Durability of Building Materials and Components
ISTANBUL, Turkey 11-14 May 2008

Analysis of Rebar Cross Sectional Area Loss by Reinforced Concrete Corrosion

Angela Gaio Graeff [1]
Luiz Carlos P. da Silva Filho [2]

T 11

ABSTRACT

One of the most important pathological manifestations which occur in reinforced concrete structures is the rebar corrosion. This deteriorative process is known by its high frequency of incidence and, mainly, by the destructive effect that it causes to structures. Several researches focused on the corrosion initiation phase can be found in the literature. However, restricted knowledge is available on the propagation phase, which is the broad aim of this work: to focus on the analysis of the consequences, in terms of structural properties, due to corrosion incidence on rebar. Among these properties, it is emphasized the loss of cross sectional area, loss of bond between concrete and reinforcement, and cracking due to rust accumulation on the bar length – which can lead to concrete spalling in advanced stages. The loss of cross sectional area can be highly responsible for several consequences on reinforced concrete structures. This property is the one of the key outputs of building design methods and, therefore, variations on its properties during the structure's life-cycle, along with other pathological manifestations that may occur, or yet with the misuse of the building, can put the structure under an unusable status or even cause its failure. This work focuses on the study of rebar cross sectional area loss of reinforced concrete specimens subject to accelerated corrosion process stimulation, at specific levels of deterioration (0, 2, 5 and 10% of weight loss), under chloride action. The specimens were induced to corrosion through the use of constant current and immersion in an isotonic solution of sodium chloride. The losses of cross section were measured by using a 3D image reconstruction with laser. The results show that the loss of bars section under corrosion effect is significant, and these values should be taken in consideration when an assessment of these structures is carried out.

KEYWORDS

Corrosion, Reinforced concrete, Propagation phase, Cross sectional area loss

[1] The University of Sheffield, Department of Civil and Structural Engineering, Sheffield, England, Phone +44 (0) 7794281131, a.graeff@sheffield.ac.uk
[2] Federal University of Rio Grande do Sul, Civil Engineering Post-Graduate Program, Porto Alegre, Brazil, Phone +55 51 33083333, Fax +55 51 33083333, lcarlos@cpgec,ufrgs.br

1 INTRODUCTION

Among the pathological manifestations that accelerate the performance loss of reinforced concrete structures, rebars' corrosion is one of the most important, due to its occurrence and damage potential. According to Helene [1993], reinforcement corrosion is known as a destructive interaction with the environment, which leads to damage reaction of chemical or electro-chemical nature, associated or not to deterioration processes (both physical or mechanical).

The reinforcement corrosion modifies some of the basics parameters used in the structural design and its incidence leads to some considerable consequences, for instance: the loss of rebar cross sectional area; the increase of radial tensile forces in the concrete – with subsequent cracking of the cover concrete due to rust along the rebars surface and along the surrounding pore structure of the concrete – eventually leading to spalling of concrete on advanced stages; and the loss of bond between concrete and reinforcement.

All of these effects are relevant, not only from the durability impact perspective, but also from the structural performance point of view. On account of these issues, reinforcement corrosion has received special attention by the scientific community over recent years. However, it has been observed in the literature a great amount of researches about the initiation phase of corrosion, i.e. period on which the structural effects have not yet evidenced [Breit 2001; Vu and Stewart 2000; Li 2003a; Glass *et al.* 2000; Val and Trapper 2006; Morris *et al.* 2002 and 2004; Engelund and Sorensen 1998]. The approaches used in some of these works rely on the simulation of chloride penetration and the advance of carbonation front in concrete elements. In general, these researches aim to determine the moment on which steel depassivates. Both experimental and numerical analysis have been investigated in this area. Nevertheless, only a reduced number of researches are dedicated to study the propagation phase of corrosion [Wang and Liu 2006; Coronelli 2002; Li 2003b and Vu *et al.* 2005].

The initiation phase is the period of time comprised between the time the corrosion first appears on the structure's construction and ends when the steel is depassivated. During this period, the structural damage may not occur, or it can be considered null, on the assumption that the corrosion intensity is very low in this phase: it does not represent a risk to the life-cycle.

The propagation phase attends the period after the steel depassivation is triggered, when corrosion current is established in the rebar, which is considered damaging to the life-cycle. By the time this phase starts, some changes in the steel alloy occur and an amount of expansive iron oxide is formed. This process should be interrupted in order to avoid the structure loss of performance or, in some critical situations, in order to avoid the failure of the building.

This study focused on delivering guidelines to assess the deterioration level of reinforced concrete structures by creating an equivalency between the corrosion level and the loss of cross sectional area of the reinforcement bars through the use of experimental laboratory test. This study also aims to determine the effect of the formation of pitting regions in the bars by using an accurate method to measure the cross sectional areas at 5.0mm spacing along the bar element.

2 LOSS OF REBAR CROSS SECTIONAL AREA

The reinforcement used in the majority of structural elements is a result of accurate and complex designing processes. The key output of a structural design, following the necessary data input, e.g. applied loads, element geometry and the materials properties, is the rebar cross sectional area. Hence, changes on its value may lead to significant impact in the construction stability/serviceability.

The chloride attack is considered one of the most critical pathological manifestations which occur in reinforced concrete structures. When the corrosion is due to this chloride attack, it is expected the

formation of some pitting regions. In these specific pitting points it is possible to evaluate a considerable loss of cross sectional area or even the total failure of certain fragments of the bars.

Some researches found in the literature suggest a linear correlation between the loss of cross sectional area and the corrosion level [Apostolopoulos et al. 2006; Graeff 2007].

3 EXPERIMENTAL PROGRAMME

In order to evaluate the loss of rebar cross sectional area, an experimental analysis was carried out. The method consisted basically in accelerating the corrosion process in reinforced concrete specimens by means of a chloride attack. The experimental program was divided into three stages: the first of them being in regard to the research variables and the materials' characterization; the second, concerning the corrosion acceleration method employed and the third referring to the measurement of cross sectional area loss resulting from the corrosion stimulation.

3.1 Research Variables and Materials

The research variables were established considering the rebar corrosion level, for instance, 0, 2, 5 and 10% of weight loss. The concrete and materials' quality were kept constant, as well as the rebar diameter used (12.5mm). The concrete was produced in laboratory by using a vertical mixer; the quantities showed in the Table 1 were used in order to produce a concrete with a 25MPa of compressive strength.

Table 1. Concrete mixture to produce a 25MPa concrete.

Material	*kg per m^3 of concrete*
Cement	289.95
Sand	840.85
Coarse Aggregate	1043.82
Water	191.37

The cement used to cast the specimens was the High Initial Strength Portland cement. Its composition is formed of 95-100% clinquer and 0-5% limestone and fly ash. The sand is from Jacuí River (Southern Brazil) and its gradation is considered as medium. The origin of the coarse aggregate is basaltic. The gradation curves of both the sand and the coarse aggregate are shown in Fig. 1.

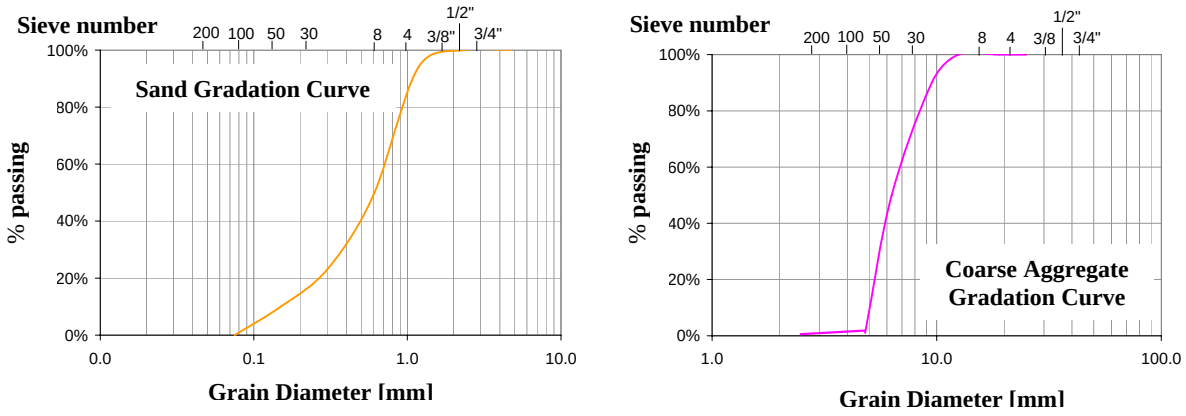

Figure 1. Gradation curves of gravel and coarse aggregate.

Samples sizing 100x100x200mm were cast with one rebar of 12.5mm of diameter and 145mm long placed in the midst of it. The samples were left into the moulds for a period of 24 hours after casting.

After this first 24 hours, the specimens were demoulded and placed in a humid and temperature controlled chamber for a period of 20 days for curing.

3.2 Corrosion acceleration in the samples

An accelerated test modifies the natural environment conditions and, therefore, makes more difficult the establishment of correlations between the test and the environment to which the material would be legitimately exposed to. Hence, it becomes impracticable to estimate the life-cycle of the material in analysis considering the test's periods of time. Nonetheless, accelerated tests can be useful tools to establish comparative analysis. It helps identifying how variations in the materials may affect their behaviour and express long term effects in shorter scales, allowing, for instance, the evaluation of long-term degradation effects caused by corrosion in this research.

The majority of the tests found in the literature are based in electrochemical process to accelerate corrosion in reinforced concrete specimens. A great number of corrosion stimulation and chloride penetration tests are based on the application of constant voltage. In order to decrease the test's duration some test methods use higher values of voltage to accelerate corrosion [e.g. ASTM 1202C 1999]. However, the use of high voltages cause strong heating of the samples due to the elevated passing electric current associated with the resistance decrease of the concrete. Thus, it has been observed in the newest studies a strong preference for using constant electric current to study the propagation phase in lieu of constant voltage.

The method used to accelerate the corrosion is based on exposing concrete samples in a chloride solution (3.5g/l) and applying an electric current in order to stimulate chlorides to migrate from the solution to the rebar, as shown in Fig. 2.

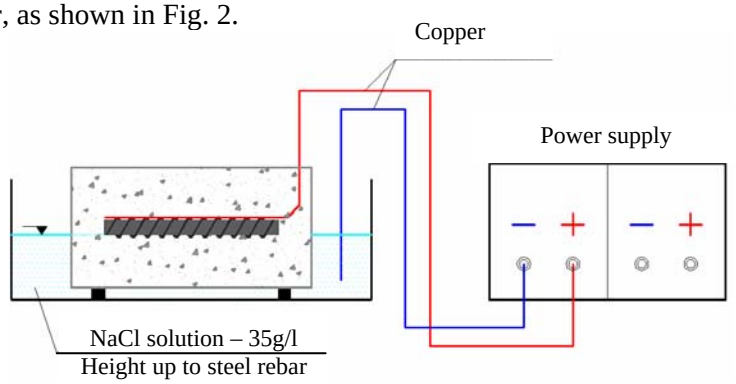

Figure 2. Test layout to accelerate corrosion.

Samples are partially immersed in an isotonic solution of sodium chloride, which was used in a similar concentration to the salt found in the Atlantic Ocean. The solution depth in the chamber was equivalent to the concrete cover thickness: this condition is important to allow the entrance of both the humidity and the oxygen. A copper wire was placed over the rebar, with no electric contact with the steel, prior to the casting of the samples. During the test, the wire was connected in the positive pole of the power supply, while the other copper wire, showed in the previous figure, was connected to the negative pole. The current density applied was 500 A/cm^2.

Faraday's Law was used to predict the period of time required to reach the specific corrosion levels of 2, 5 and 10%. This theory is widely used in the literature, for instance, the work of Fang et al. [2004] and El Maaddawy and Soudki [2003]. One previous calibration was done in order to verify the accuracy of the Faraday's Law. Information about this calibration study can be found elsewhere [Graeff, 2007].

3.3 Measurement of the Loss of Cross Sectional Area

After achieving the desired corrosion level by the acceleration procedures employed, the samples were broken in order to retrieve the rebar placed on its core. The excess of concrete around the rebars was manually removed and the bars were immersed in a solution of 3,5g hexamethylene tetramine diluted in 500ml of hydrochloric acid and 500 ml reagent water according to the procedures of ASTM G1-03 (2003) for a period of 40min time. After this period, the bars were removed from the solution and washed with clean water. Finally, the rebars were placed in the oven for 30min, with an average temperature of 25ºC, in order to completely dry the steel fragments. After the careful cleaning process, the bars were weighted to measure the mass loss and placed inside a three-dimensional scanner which is able to acquire the co-ordinates of the bar surface by applying a laser beam. The bar is rotated at least three times in order to allow the scanner to read the entire surface of the bar. When the scanner is done with the readings, a graphical software is used to render the surface of the bars. After the images have been graphically reconstituted, the measurements of the cross sectional areas in all sections of rebars tested were carried out using the software. In this research, the areas were measured at 5.0mm spacing apart from each other. Two non-corroded bars were placed in the scanner prior to the corrosion induction, in order to get the areas at 0% corrosion level, preventing errors caused by differences in the samples used. Only the samples that yielded corrosion levels of 2 and 5% were measured using this technique. Samples with 10% of corrosion level were not tested before the corrosion acceleration because it was noticed a strong similarity between the results of the two previous scanned bars; hence, it was decided to reduce costs and time on scanning the specimen, with no damage to the analyses.

4 RESULTS

A comparison was carried out between the actual weight losses and the foreseen values determined using the calibration study based on the Faraday's Law previously cited [Graeff, 2007]. This comparison is important in order to prove that the targeted corrosion levels were in fact achieved. The values from this comparison are show in the Table 2.

Table 2. Comparison between the target corrosion level and the calibration study based on the Faraday's Law.

Corrosion level targeted	*Calibration study based on the Faraday Law – actual weight loss*
2%	2.29%
5%	5.03%
10%	10.33%

The following pictures (Fig. 3 and Fig. 4) are the models obtained from the 3D rendering, before and after the corrosion acceleration test. Figure 5 shows the results, in terms of area loss for each analysed section, for the corrosion levels of 2, 5 and 10%, respectively.Table 3 shows the mean of the areas of the total amount of bar sections analysed, with the standard deviation and general percentage of area loss. It can be observed in the graphics on Fig. 5 and on the above table that the cross sectional areas corresponding to the corrosion levels of 2 and 5% did not decrease considerably, and they were also similar in value (around 2.5%). In regard to the corrosion level of 10%, however, a considerable decrease of the cross sectional area has occurred, equivalent to approximately 7.5% (almost more than three times the area loss observed in the 5% of corrosion level).

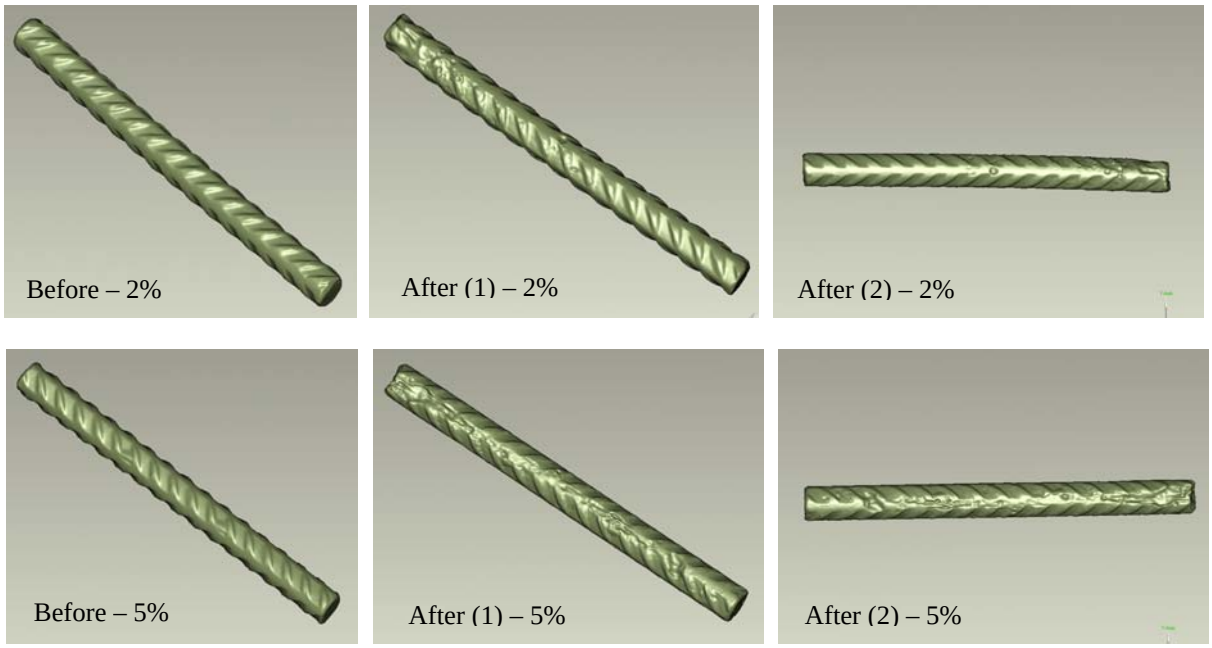

Figure 3. Digital images before and after corrosion acceleration (corrosion levels of 2 and 5%).

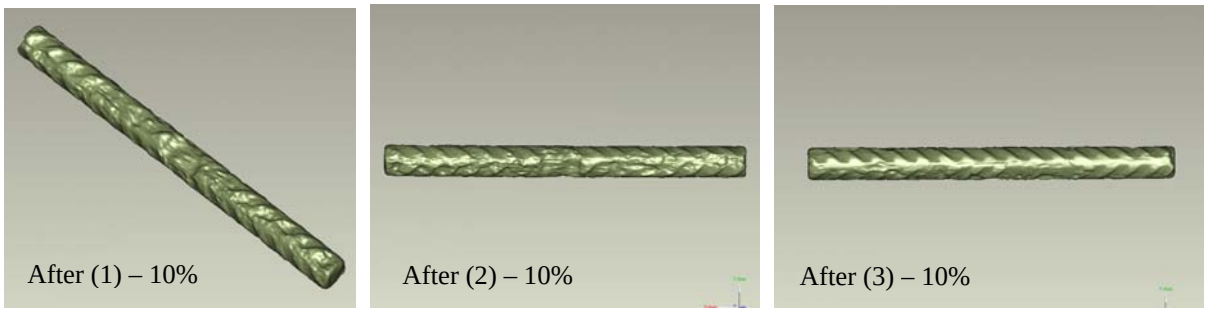

Figure 4. Digital images after corrosion acceleration (corrosion level of 10%).

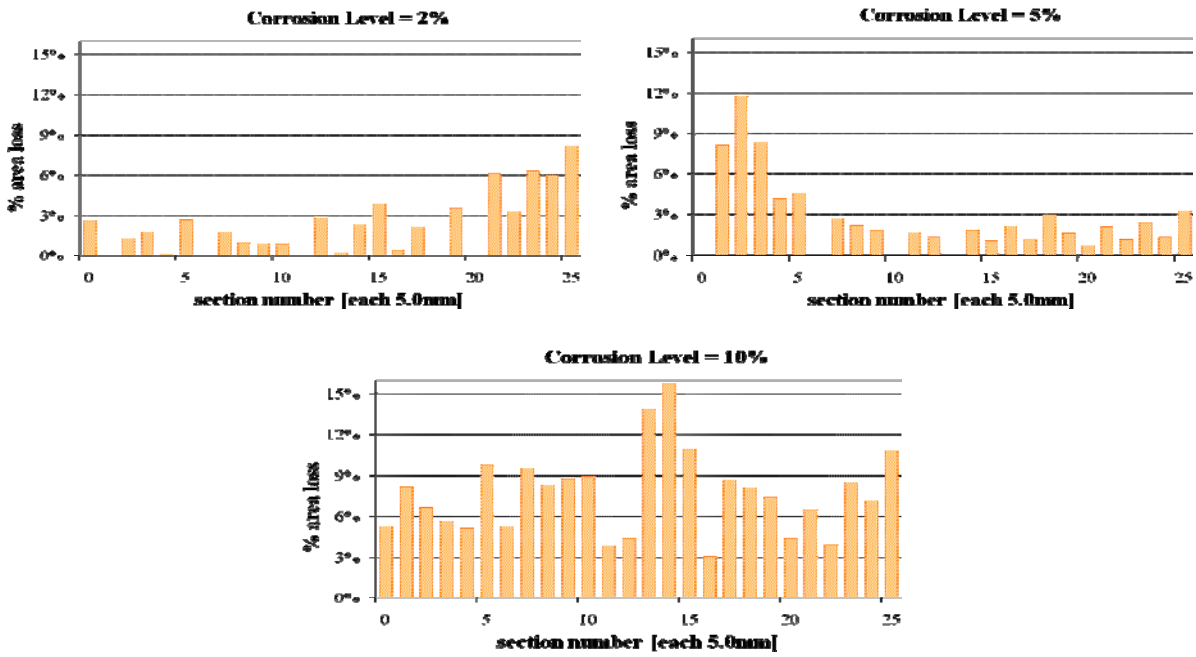

Figure 5. Graphics of the area loss considering each section analysed.

Table 3. General calculus of the cross sectional areas.

Corrosion Level		*Areas mean (mm²)*	*Standard Deviation (mm²)*	*% area loss*
2%	Before	120,64	1,14	2,20
	After	117,98	2,98	
5%	Before	118,75	1,54	2,75
	After	115,49	4,16	
10%	Before	119,66	0,55	7,64
	After	110,52	3,49	

Figure 5 shows that the bars with 2 and 5% of corrosion level presented a larger decrease of area nearer the bar end. In these points, 8% and 12% of area loss were obtained for the corrosion levels of 2 and 5%, respectively. For the corrosion level of 10%, the major values of area loss were concentrated in the middle of the bar length, with a peak of 16% of area loss. These points where the area loss was more intense than the other sections are, probably, a result of the pitting effect, due to chloride attack.

5 CONCLUSIONS

- Although corrosion acceleration test methods are not entirely effective to simulate the real corrosion phenomenon which occur in the environment, the method used in this research seems to be reliable. It appears to adequately simulate the corrosion process, allowing the rust to re-locate in the concrete pores due to its slower speed.
- The measurement of the cross sectional area loss confirmed that corrosion due to chloride attack does not occur uniformly. In some points it is observed values of area loss higher than three times the mean of the area loss of the entire bar. These points are considerably critical and can cause the structure's failure.
- The technique used to measure the rebars' cross sectional area by using the 3D scanner proved to be a very accurate method. It can be considered as a great instrument to measure the effects of the corrosion propagation phase in concrete samples. The results can be used as an important tool to predict the degradation in structures, and in some models of life-cycle.
- An increment of the cross sectional area loss was noticed when the corrosion level is higher.

ACKNOWLEDGMENTS

The autors would like to acknolodge the support of research assistants and technicians of the Laboratory of Structural Tests and Materials (LEME) of the Federal University of Rio Grande do Sul. For the finance support, the autors are grateful for the assistance of CNPq.

REFERENCES

American Society for Testing and Materials. Annual book of ASTM Standards. 2003, *Standard practice for preparing, cleaning, and evaluating corrosion test specimens*, ASTM G1-03. Philadelphia.

American Society for Testing and Materials. Annual book of ASTM Standards. 1999, *Standard test method for electrical indication of concrete's ability to resist chloride ion penetration*, ASTM 1202 C. Philadelphia.

Apostolopoulos, C. A., Papadopoulos, M. P. & Pantelakis, S. G. 2006, 'Tensile behavior of corroded reinforcing steel bars BSt 500s', *Construction and Building Materials,* 20, 782-789.

Breit, W. 2001, 'Critical corrosion inducing chloride content – state of the art and new investigations results', *Betontechnische Berichte, Concrete Technology Reports 1998/2000*. Düsseldorf: VBT - Verlag Bau und Technik, 168p.

Coronelli, D. 2002, 'Corrosion cracking and bond strength modeling for corroded bars in reinforced concrete', *ACI Structural Journal,* 99[3], 267-276.

El Maaddawy, T. A., Soudki, K. A. 2003, 'Effectiveness of impressed current technique to simulate corrosion of steel reinforcement in concrete', *Journal of Materials in Civil Engineering.*

Engelund, S., Sorensen, J. D. 1998, 'A probabilistic model for chloride-ingress and initiation of corrosion in reinforced concrete structures', *Structural Safety***,** 20, 69-89.

Fang, C., Lundgren, K., Chen, L. & Zhu, C. 2004, 'Corrosion influence on bond in reinforced concrete', *Cement and Concrete Research,* 34[11], 2159-2167.

Glass, G. K., Reddy, B., Buenfeld, N. R. 2000, 'The participation of bound chloride in passive film breakdown on steel in concrete', *Corrosion Science.* 42, 2013-2021.

Graeff, A. G. 2007, *Avaliação Experimental e Modelagem dos Efeitos Estruturais da Propagação da Corrosão em Elementos de Concreto Armado.* Dissertation (Master in Engineering) – Civil Engineering Post-Graduate Program, Federal University of Rio Grande do Sul, Porto Alegre.

Helene, P. R. L. 1993, *Contribuição ao estudo da corrosão em estruturas de concreto armado.* Tese de Livre Docência – Departamento de Engenharia de Construção Civil, Escola Politécnica da Universidade de São Paulo, São Paulo.

Li, C. Q. 2003a, 'Life-cycle modeling of corrosion-affected concrete structures: initiation', *Journal of Structural Engineering.*

Li, C. Q. 2003b, 'Life-cycle modeling of corrosion-affected concrete structures: propagation', *Journal of Structural Engineering*

Morris, W., Vico, A., Vasquez, M., Sanchez, S. R. 2004, 'Chloride induced corrosion of reinforcing steel evaluated by concrete resistivity measurements', *Electrochimica Acta,* 49, 4447-4453.

Morris, W., Vico, A., Vasquez, M., Sanchez, S. R. 2002, 'Corrosion of reinforcing steel evaluated by means of concrete resistivity measurements', *Corrosion Science.* 44, 81-99.

Val, D. V., Trapper, P. A. 2006, 'Probabilistic evaluation of initiation time of chloride-induced corrosion', *Reability Engineering & System Safety.*
Vu, K., Stewart, M. G. & Mullard, J. 2005, 'Corrosion-induced cracking: experimental data and predictive models', *ACI Structural Journal,* 102[5], 719-726.

Vu, K. A. T., Stewart, M. G. 2000, 'Structural reliability of concrete bridges including improved chloride-induced corrosion models*', Structural Safety,* 22, 313-333.

Wang, X., Liu, X. 2006, 'Bond strength modeling for corroded reinforcements', *Construction and Building Materials***,** 20, 177-186.

11DBMC International Conference on Durability of Building Materials and Components
ISTANBUL, Turkey 11-14 May 2008

Durability Of Metakaolin Based Cement Mortar To Chloride Attack Under Wet – Dry And Freeze – Thaw Exposure

Shweta Goyal [1]
Maneek Kumar [2]
B. Bhattachargee [3]

ABSTRACT

This study investigates the effect of metakaolin as replacement of cement on durability of mix to chloride attack when subjected to freezing / thawing and wetting / drying exposure conditions. Two metakaolin replacement levels were considered in the study: 5% and 10% by weight of cement. The effect was investigated at water-to-binder ratios of 0.5. The mortar specimens were cast for each mix and after 7 days of initial water curing period, specimens were immersed in various chloride salts (3% concentration), with or without corrosion inhibitor, for a total period of 42 days. The progressive deterioration was evaluated through visual inspection, relative change in mass and relative strength determinations.

The investigations indicated that metakaolin as replacement of cement increased the chloride resistance of mortar. The various chloride salts have different penetration rates into the given mix, resulting in different degree of damages. Calcium chloride was found to be most destructive under the applied exposure conditions. Also, the compatibility of corrosion inhibitor was found to depend on the type of salt solution to which the specimens were exposed. Among the exposure conditions, freezing – thawing cycles were found to be more detrimental as compared to wetting – drying cycles.

KEYWORDS
Metakaolin, Wetting – drying, Freezing – thawing, Chloride solutions

[1] Thapar University, Civil Engineering faculty, Patiala, India, Phone +91 175 2393016, shweta@tiet.ac.in
[2] Thapar University, Civil Engineering faculty, Patiala, India, Phone +91 175 2393354, maneek@tiet.ac.in
[3] IIT Delhi, Civil Engineering Faculty, New Delhi, India, Phone +91 11 26861763, bishwa@civil.iitd.ernet.in

1 INTRODUCTION

Mineral admixture concrete is one of the most significant new material available worldwide for utilization in new construction and in rehabilitation of buildings, highways and bridges. Economics (lower cement requirement) and environmental considerations have a role in the growth of mineral admixture usage. Studies have shown [Bouzoubaa et al 2002; Mazloom et al 2004; Tan & Pu 1998; Ozyildirum & Halstead 1994] that mineral admixtures such as blast furnace slag, fly ash and silica fume enhance the strength and durability of concrete. Recently, there is a growing interest in the use of metakaolin (MK) as a mineral admixture in the concrete industry. It is well known that metakaolin is produced by calcining purified kaoline clay in the temperature range of 700 to 800˚C to derive off the chemically bound water and to destroy the crystalline structure [Ding and Li 2002; Khatib & Wild 1996; Al-Akhras 2007; Lee et al 2005]. The end product of this reaction is nearly 100% reactive pozzolana which actively combines with calcium hydroxide to form C-S-H gel.

Extensive research has been reported in the literature regarding the effect of MK on different properties of concrete [Gruber et al 2001; Boddy et al 2001; Ding & Li 2002; Sabir et al 2001; Wild et al 1996; Khatib & Wild 1998]. However, limited research has been carried out on the effect of MK when the concrete is exposed to deicing chemicals (sodium chloride and calcium chloride) under freeze-thaw and wet-dry exposure conditions. The deicing chemicals increase the concrete damage originating from freeze-thaw due to many reasons. Firstly, deicing chemicals increase the degree of concrete saturation and therefore, keep pores at maximum fluid saturation that leads to the increase in risk of frost damage [Litvin 1976]. It also decreases the freezing point of concrete pore solution, leading to hydraulic pressure. Along with this, the pressure is also generated in between the layers because salt concentration varies with the distance from the concrete surface [Wang et al 2006]. Apart from the above stated physical interactions, the concrete materials also interact chemically with the deicing salts that lead to decomposition of cement hydration products [Heukamp et al 2001]. These chemical reactions become more vulnerable after the formation of cracks formed due to the physical interaction between the deicers and the concrete materials [Mehta & Gerwick 1982]. Looking at the wide range of effects of deicer chemicals of the concrete mix, it becomes imperative to study the effect on MK mixes as well. The purpose of the present investigation is to examine the effect of various deicing solutions and exposure conditions on mortars containing MK. The study is further extended to cover corrosion inhibitors with the deicer salts.

2 EXPERIMENTAL DETAILS

2.1 Materials

ASTM Type I Portland cement was used throughout the investigation. The physical properties and the chemical composition is given in Table 1. The MK used is Metacem of 85-C grade with properties given in Table 1. Locally available river bed sand confirming to Zone III of IS: 383-1970 was used as fine aggregates to make mortar specimens. The specific gravity, absorption and fineness modulus of the aggregates were 2.68, 1.02% and 2.507 respectively.

2.2. Aggressive Chemicals

Four chemical, sodium chloride (NaCl), calcium chloride ($CaCl_2$), sodium chloride with the corrosion inhibitor (NaCl + inhib), calcium chloride with corrosion inhibitor ($CaCl_2$ + inhib) were considered in the present study. The percentage of the salt solution used was 3% and the percentage of corrosion inhibitor was kept at 1%. Triethanolamine was used as corrosion inhibitor.

Table 1. Chemical properties of cement and MK.

Chemical (%)	CaO	SiO_2	Al_2O_3	Fe_2O_3	SO_3 (%)	MgO	K_2O	Na_2O
Cement	61.7	22.4	5.93	4.91	2.28	1.5	0.65	0.122
MK	2.8	55.3	37.1	2.4	-	0.3	0.6	0.25

2.3 Mixtures details

Three different mortar mixes were prepared for water-to-binder ratios of 0.5. For this water-to-binder ratio, cement was partially replaced by 5% and 10% of MK. The binder to sand was kept as 1:3 for all mixes. For each mix, 70.5 mm cubes were cast to study the variation of compressive strength. The specimens were demoulded after 24 hours and then cured in tap water for initial 7 days. After the initial water curing period, the samples were subjected to different chemical, as stated earlier, in plastic containers. For wet-dry (W-D) exposure, samples were immersed in the solution at room temperature for 16 hours followed by 8 hours of air drying. Similarly, for freeze-thaw (F-T) cycles, the specimens were stored in a freezer at -15 ± 1˚C for 16 hours, followed by 8 hours of thawing in large tubs having the same solution at room temperature. Thus, one W-D and one F-T cycle was of 24 hours duration. The tests were conducted at the end of 14, 28 and 42 cycles.

Prior to compressive strength tests, the specimens were visually investigated for any signs of cracking, spalling, delamination etc. Weight change was also monitored throughout the test and compared with the initial weight of the specimen before it was immersed in the salt solution.

3. RESULTS AND DISCUSSIONS

3.1. Strength Results

Figs. 1 to 3 present the compressive strength development of mortar specimens under F-T and W-D exposure conditions, made at water-binder ratios of 0.5 and different percentages of metakaolin. In these graphs, data represented in columns indicate the effect of F-T exposure while line representation is made for W-D exposure. It can be observed that for all mixes, the strength development of the mixes under both W-D and F-T exposure follows similar pattern, however, it is more for W-D exposure than that under F-T exposure condition. Such a small increase in strength can be due to slowing of cement hydration at low temperature. Analyzing F-T exposure condition thoroughly, it can be seen from the Fig. 1 that for control mix, the addition of sodium chloride did not cause great damage in mortar specimens although the increase of strength is lower than the mix exposed to F-T under distilled water. Addition of corrosion inhibitor further reduced the damage caused by the aggressive chloride salt. Attack by calcium chloride is worst. Addition of corrosion inhibitor to calcium chloride could not produce the effect it caused in sodium chloride salt. In this case, addition of corrosion inhibitor delayed the damage but could not diminish it.

Similar to the control mix, the effect of sodium chloride salt is less aggressive than the calcium chloride salt. However, the presence of corrosion inhibitor has a different effect on the specimens containing MK. In this case, the strength educed regardless of the type of salt present.

The strength loss is very high when the corrosion inhibitor is present along with calcium chloride salt. It means that the corrosion inhibitor used in this study is not compatible with MK. It emphasizes the need of a pre-study to check the compatibility of the ingredients with corrosion inhibitors.

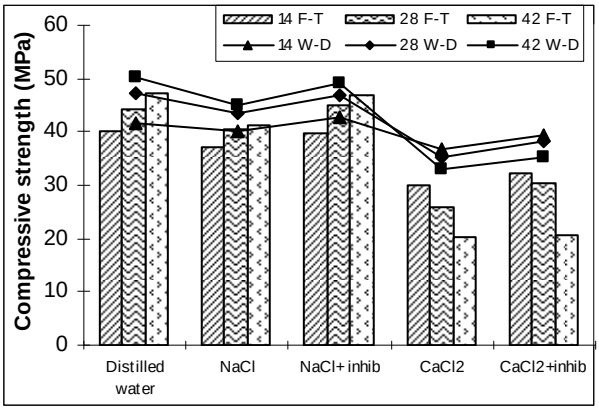

Fig. 1. Compressive strength of the control mix under F-T and W-D cycles.

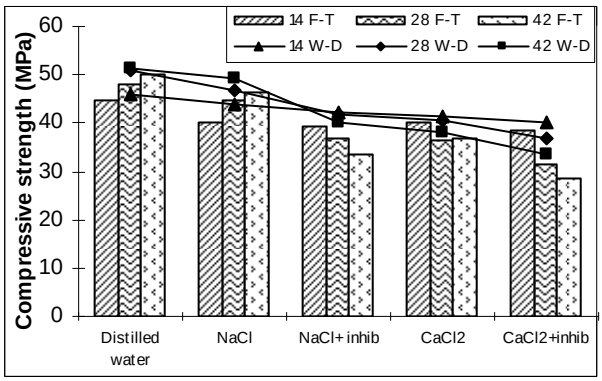

Fig. 2. Compressive strength of mix with 5% metakaolin under F-T and W-D cycles.

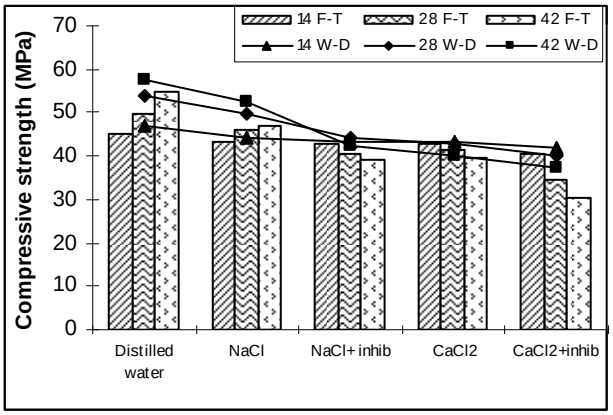

Fig. 3. Compressive strength of mix with 10% metakaolin under F-T and W-D cycles.

3.2 Mass Loss and Scaling

Fig. 4 and 6 shows the mass change of the mortar specimens with percentage replacement of metakaolin varying from 0% to 10%. The mass change data is presented for F-T cycles only, because, it is established in the compressive strength studies that F-T exposure is more aggressive than W-D exposure. Secondly, it

was observed weight change was negligible for W-D exposure. The mass change of the specimens was calculated as follows:

$$\text{Percentage mass change} = \frac{M_2 - M_1}{M_1} \times 100$$

Where M_1 (gm) is the mass of the specimen at 7 days of initial water curing, i.e., before immersion in salt solution and M_2 (gm) is the mass of cleaned specimens after immersion in salt solution. Negative value of percentage mass change will indicate decrease in mass with the number of F-T cycles.

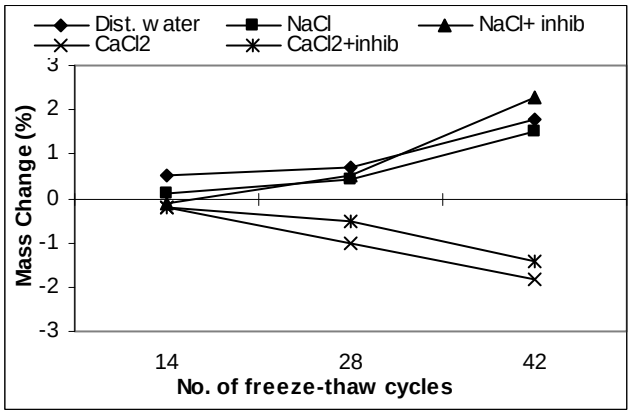

Fig. 4. Mass change of control mix under F-T cycles at 0.5 water-to-binder ratio.

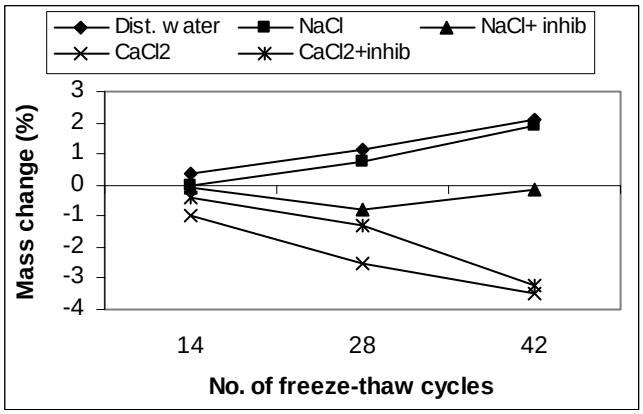

Fig. 5. Mass change of mix with 5% metakaolin under F-T cycles.

It is found that the specimens containing only OPC as binder and exposed to distilled water and NaCl displayed a small amount of mass gain. Mass loss of the specimens with metakaolin and exposed to NaCl started a bit late, i.e. after 28 cycles of freeze-thaw. The specimens exposed to $CaCl_2$, with or without corrosion inhibitor, showed a higher mass loss indicating that $CaCl_2$ salt is more aggressive than NaCl and its aggressivity does not depend on presence or absence of mineral admixture. Also, the initial mass loss of the specimens containing corrosion inhibitor was lesser than when $CaCl_2$ alone is present, however, the final losses are almost the same. This result once again implies that the presence of corrosion inhibitor postpones the damage but does not eradicate it completely.

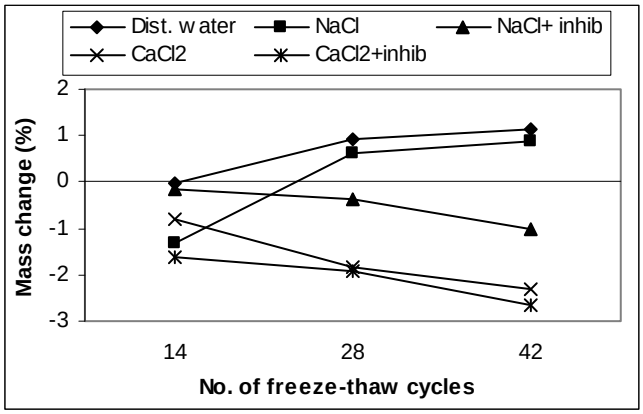

Fig. 6. Mass change of mix with 10% metakaolin under F-T cycles.

Visual investigation indicated that the intensity of damage of the specimens submerged in distilled water and NaCl solution is less and they showed very small scaling damage throughout the test, indicating that these solutions are less aggressive. Samples containing mineral admixture and immersed in NaCl solution containing corrosion inhibitor showed the presence of micro-pores (Fig. 5) at the surface of the specimen that increased with the increase in number of exposure days indicating the loss of material due to stresses developed in alternate freeze-thaw. However, the samples immersed in $CaCl_2$ with or without corrosion inhibitor, demonstrated increased scaling with the increase in freeze-thaw cycles. In this case, the damage is more at the edges and it is traveling to the surfaces indicating the rate of loss will increase with exposure (Fig. 6).

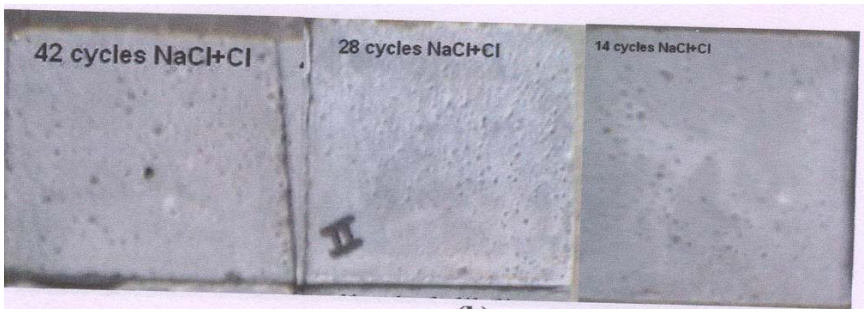

Fig. 5. Cubes containing 10% MK and exposed to NaCl + inhib. under F-T exposure.

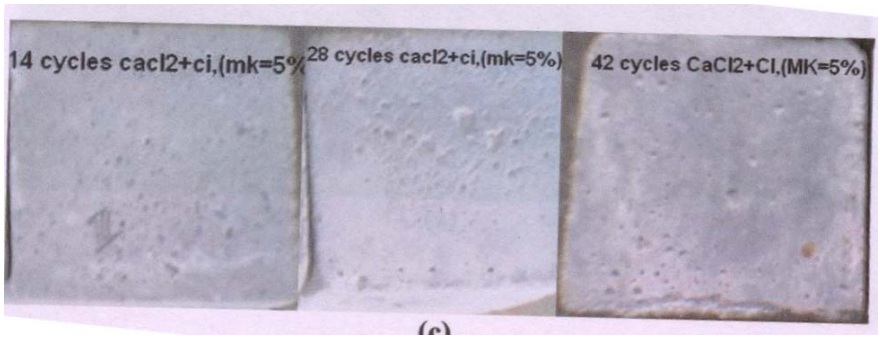

Fig. 6. Cubes containing 5% MK and exposed to $CaCl_2$ + inhib. under F-T exposure.

4 CONCLUSIONS

The following conclusions can be drawn from the present investigation:

1. F-T exposure condition is more aggressive than the W-D exposure condition. The damage of specimens was aggravated under F-T cycles.
2. Among the chemicals studied, $CaCl_2$ solutions, with or without corrosion inhibitor, displayed more severe damage on the specimens in terms of compressive strength loss and weight loss.
3. Metakaolin replacement of cement was found to be effective in improving the resistance against aggressive chemicals under W-D and F-T exposure conditions. However, the performance was dependent on the percentage replacement level.
4. While using corrosion inhibitor with MK, it is essential to check the compatibility of both by conducting small experiment on the strength development pattern.

REFERENCES

Bouzoubaa, N., Fournier, B., Malhotra, V.M. & Golden, D. 2002, 'Mechanical properties and durability of concrete made with high volume fly ash blended cement produced in cement plant', *ACI Materials Journal*, 99[6], 560 – 567.

Mazloom, M., Ramezanianpour, A.A. & Brooks, J.J. 2004, 'Effect of silica fume on mechanical properties of high strength concrete'. *Cement and Concrete Composites*, 26, 347 – 357.

Tan, K. & Pu, X. 1998, 'Strengthening effects of finely ground fly ash, granulated blast furnace slag, and their combination', *Cement and Concrete Research*, 28[12], 1819 – 1825.

Ozyildirum, C. & Halstead, W.J. 1994, 'Improved concrete quality with combination of silica fume and fly ash', *ACI materials Journal*, 91[6], 587 – 594.

Ding, J. & Li, Z. 2002, 'Effect of metakaolin and silica fume on properties of concrete', *ACI Materials Journal*, 99[4], 393-398.

Khatib, J.M. & Wild, S. 1996, 'Pore size distribution of metakaolin paste', *Cement and Concrete Research*, 26[10], 1545-1553.

Al-Akhras, N.M. 2007, 'Durability of metakaolin concrete to sulfate attack', *Cement and Concrete Research*, 36, 1727-34.

Lee S.T., Moon H.Y., Hooton R.D. & Kim J.P. 2005, 'Effect of solution concentration and replacement levels of metakaolin on the resistance of mortars exposed to magnesium sulfate solutions, *Cement and Concrete Research*, 35, 1314-1323.

Gruber K.A., Ramlochan T., Boddy A., Hooton R.D. & Thomas M.D.A. 2001, 'Increasing concrete durability with high-reactive metakaolin', *Cement and Concrete Composites*, 23[6], 479-484.

Boddy A., Hooton R.D. & Gruber K.A. 2001, Long-term testing of the chloride penetration resistance of concrete containing high-reactive metakaolin', *Cement and Concrete Research*, 31[5], 759-765.

Sabir B.B., Wild S. & Bai J. 2001, 'Effect of metakaolin and calcined clays as pozzolans for concrete: a review', *Cement and Concrete Composites*, 23[6], 441-454.

Wild S., Khatib J.M. & Jones A. 1996, 'Relative strength, pozzolanic activity and cement hydration in superplasticized metakaolin concrete', *Cement and Concrete Research*, 26[10], 1537-1544.

Khatib J.M & Wild S. 1998, 'Sulfate resistance of metakaolin concrete', *Cement and Concrete Research*, 28[1], 83-92.

Litvan G.G. 1976, 'Frost action in cement in the presence of deicers', *Cement and Concrete Research*, 6[3], 351-356.

Wang K., Nelsen D.E. & Nixon W.A. 2006, 'Damagimg effects of deicing chemicals on concrete materials', *Cement and Concrete Composites*, 28[2], 173-188.

Heukamp F.H., Ulm F.J. & Germaine 2001, 'Mechanical properties of calcium leached cement pastes: triaxial stress states and the influence of the pore pressure', *Cement and Concrete Research*, 31[5], 767-774.

Mehta P.K. & Gerwick B.C. 1982, 'Cracking-corrosion interaction in concrete exposed to marine environment', *Concrete International*, 4[10], 45-51.

Alternative Reinforcement for Durable Reinforced Concrete Structures

Marijana Serdar [1]
Irina Stipanović Oslaković [2]
Dubravka Bjegović [3]

T 11

ABSTRACT

The enormous costs and safety issues associated with corrosion of steel in concrete have resulted in the development of a wide range of new technologies and materials to increase the durability of reinforced concrete structures and their repairs. One of these methods is the use of certain types of stainless steel, which are resistant to corrosion in concrete environment even when the concrete is highly contaminated with chlorides, as substitution of part or all reinforcement in concrete. The use of stainless steel as a replacement for carbon steel reinforcement has been limited to vital structures exposed to aggressive environments by concerns over the increase in initial construction costs.

Recent results indicate that some alloy steels under certain conditions behave significantly better than ordinarily used black steel reinforcement. Since the price of alloy steel reinforcement is comparable to the price of normal black steel reinforcement, the idea of using alloy steel as reinforcement is economically justified.

In this paper the experimental program that will be used to evaluate corrosion behaviour of different types of alloy steel when used as reinforcement in concrete is presented. Results of so far performed corrosion testing of different types of alloy steel in alkaline media are presented as well. The aim of the research is to evaluate the influence of chloride ions and carbonation on passivity of alloy steel in alkaline media such as concrete. Corrosion performance and material cost of alloy steel will be compared to black and stainless steel.

KEYWORDS

Alloy steel, Stainless steel, Reinforced concrete, Electrochemical corrosion testing

[1] University of Zagreb, Faculty of Civil Engineering, Department for Materials, Zagreb, Croatia, Phone +385 1 4639 118, Fax +385 1 4828 051, marijana.serdar@grad.hr
[2] Civil Engineering Institute of Croatia, Concrete and Masonry Structures Department, Zagreb, Croatia, Phone +385 1 6125 125, Fax + 385 1 6125 103, irina.stipanovic@igh.hr
[3] University of Zagreb, Faculty of Civil Engineering, Department for Materials; Civil Engineering and Institute of Croatia, Zagreb, Croatia, Phone +385 1 4639 212, Fax +385 1 4828 051, dubravka.bjegovic@grad.hr

1 INTRODUCTION

Nowadays the main responsibility of construction engineers is not only to design and construct structures that are functional, safe and aesthetic but that these structures remain such during their whole service life. Inspections of reinforced concrete structures exposed to aggressive (marine or continental) environment have shown that almost all of them have degraded due to chloride induced corrosion of reinforcement and that corrosion is the main reason for their reduced service life (Bertolini *et al.*, 2004). Maintenance and repair costs constitute a major part of the current spending in infrastructure worldwide and often overhead the costs of structures themselves. The enormous costs and safety issues associated with corrosion of steel in concrete have resulted in the development of a wide range of new technologies and materials to increase the durability of reinforced concrete structures and their repairs. One of these methods is the use of certain types of stainless steel, which are resistant to corrosion in concrete environment even when the concrete is highly contaminated with chlorides, as substitution of part or all reinforcement in concrete (Nürnberger, 1996). The use of stainless steel as a replacement for carbon steel reinforcement has been limited to vital structures exposed to aggressive environments by concerns over the increase in initial construction costs. Recent results indicate that some low alloy steels under certain conditions behave significantly better than ordinarily used black steel reinforcement. Since the price of low alloy steel reinforcement is comparable to the price of normal black steel reinforcement, the idea of using low alloy steel as reinforcement is economically justified. All this is the main scope of working package 3.1 “Validation and application of low-alloyed steel” of the specific targeted research project ARCHES “Assessment and Rehabilitation of Central European Highway Structures” (031272), funded by the European Community under the Sixth Framework Programme, Priority 1.6.2 Sustainable Surface Transport. The aim of this part of the ARCHES project is to validate the application of low alloyed steel in the concrete and finally to produce Guidelines for the use of low-alloyed steel. In this paper detailed experimental program that will be used in this part of the project ARCHES is presented. Experimental program is designed with the aim of evaluating corrosion behaviour of alloy steel in high alkaline media, such as fresh concrete and media with lower alkalinity, such as carbonated concrete with different concentrations of chlorides, simulating aggressive marine environment.

2 STATE OF THE ART

At the beginning of this research the task of the researchers was to evaluate all corrosion resistant types of steel available on the market and to classify them concerning the content of alloying elements. The aim was to find those types of steel that contain lower content of alloying elements, which makes them cheaper than stainless steel, but still have satisfying corrosion behaviour (better resistance than black steel).

Research has shown that corrosion behaviour of different steel types depends on type and quantity of alloying elements and on the nature of the corrosive environment. By the comparison of corrosion behaviour of ordinary (black) steel and low alloy steel it was calculated that low alloy steels corrode almost two times slower than black steel in the first two years of service life and four times slower from sixth till fifteen year of service life. (Shreir *et al.*, 1994). Steel commercially called TOP12 produced by Swiss Steel, is a ferritic stainless steel (X2Cr12, basis 1.4003). TOP12 is manufactured by a new production process, where the material properties are achieved by only two production steps: hot rolling of the billets in several steps to the final product and controlled cooling (Schiegg *et al.*, 2004). This type of steel has a lower content of Nickel and a somewhat higher content of Silicon than austenitic stainless steels and around 12 % of Chromium, which sets it into the category of corrosion resistant steel. Recent research of steel TOP12 shows that its corrosion resistance is significantly better than corrosion resistance of black steel (Hasler *et al.*, 2000). Since the behaviour of TOP12 has not been fully researched in alkaline media such as concrete and its application as reinforcement in concrete has not been validated this type of steel was chosen for testing in present research. Research of the low-Ni type 204Cu stainless steels showed that, in chloride contaminated pore solution, they

have corrosion behaviour very similar to that of traditional austenitic stainless steels. Since Nickel very much contributes to the price of stainless steel, the price of this steel is 35-40% lower than the price of stainless steel (Bautista *et al.*, 2006). Newer research of duplex steel, type 1.4362, show that this type of steel has good corrosion resistance in concrete contaminated with chlorides (Chauveau *et al*., 2007). The price of this steel type is lower than the price of stainless steel grade 316 because of the lower content of nickel and molybdenum. During the project corrosion resistance and price of chosen types of steel will be compared to normal black steel, whose corrosion resistance is very weak (Berke *et al.*, 1990; Bentur *et al.*, 1997) and with stainless steel, whose corrosion resistance is proven in laboratory research (Bertolini *et al.*, 2000; Veleva *et. al*, 2005; Blanco *et al.*, 2006) and on site application (Castro-Borges *et al*., 2007).

3 EXPERIMENTAL PROGRAM

In the first stage of the research accelerated corrosion testing will be performed on electrodes made of chosen types of steel in highly alkaline media (pH 12,5), such as fresh concrete, and middle alkaline media (pH 10), such as carbonated concrete, all with different concentrations of chloride ions. In the second stage of the research electrochemical testing will be performed on concrete "lollipops" with the embedded steel specimens. In the third stage of the research concrete specimens with steel reinforcement will be prepared and placed into salt spray chamber to simulate aggressive marine environment. In the last part of the research a testing field near Croatian seacoast will be established. At this testing field concrete beams reinforced with chosen steel types will be exposed to natural aggressive marine environment and their corrosion behaviour will be evaluated.

3.1 Materials

During this research, corrosion behaviour of six different steel types will be researched: two types of steel with lower content of alloying elements (TOP12 and 204Cu), two grades of duplex steel (1.4362 and 1.4462), two grades of stainless steel (1.4301 (AISI 304) and 1.4306 (AISI 304L)) and black steel B500B. Till now three types of steel have been delivered and tested: TOP12, stainless steel grade 1.4301 (AISI 304) and black steel. Their chemical composition is given in Table 1 and mechanical properties in Table 2.

Table 1. Chemical composition of the researched steel types.

Quality	TOP12	AISI 304	Black steel B500B
C	0,03	0,058	0,190
Mn	1,50	1,460	0,620
S	≤0,015	<0,001	0,022
Cr	10,50/12,50	18,240	0,070
Mo		0,036	<0,020
Ni	0,0,30/1,00	7,930	0,020
N	0,030	0,051	0,005
Fe		71,450	98,910

Table 2. Mechanical properties of researched steel types.

Type	TOP12	AISI 304	Black steel B500B
Yield strength, $R_{p0,2}$ [MPa]	566	882	500
Tensile strength, R_m [MPa]	748	992	540
Stress ratio, $R_m/R_{p0,2}$	1,32	1,12	1,08
Elongation, A_{gt} [%]	8,2	10,3	5,0

3.2 Corrosion Testing of Steel in Pore Solution

Investigation of corrosion behaviour of different steel types will be performed in pore solution with pH value 12,4 (non carbonated concrete), pH 9,5 (carbonated concrete) and pH 10,1 with different concentration of NaCl using anodic linear polarization (LP). Potentiodynamic polarization is performed after one hour submersion in the potential range between -0.2 V and 0,8 V with scan rate 10 mV/s. The aim is to evaluate which concentration of chloride ions will surely cause corrosion initiation of steel, in other words which concentration of chloride ions is for given system the critical one. Measurements will be performed using PAR VMP2 potentiostat / galvanostat with three-electrode arrangement. For electrochemical testing working electrodes were prepared manually (Bjegovic *et al.*, 2007). Small specimens of steel were connected to copper wire that was inside a glass tube. All sides of steel specimen were protected with 5 mm thick epoxy coating, except one unprotected side with area of 0,196 cm^2. After the epoxy coating had firmed, electrodes were mechanically abraded on 400 and 600 grade emery paper, rinsed in distilled water, degreased with ethanol and dried. Counter electrode was carbon rod and reference electrode saturated calomel electrode (SCE). All potentials reported, refer to SCE. Working electrode is shown in Figure 1 a) and three-electrode experiment setup in Figure 1 b).

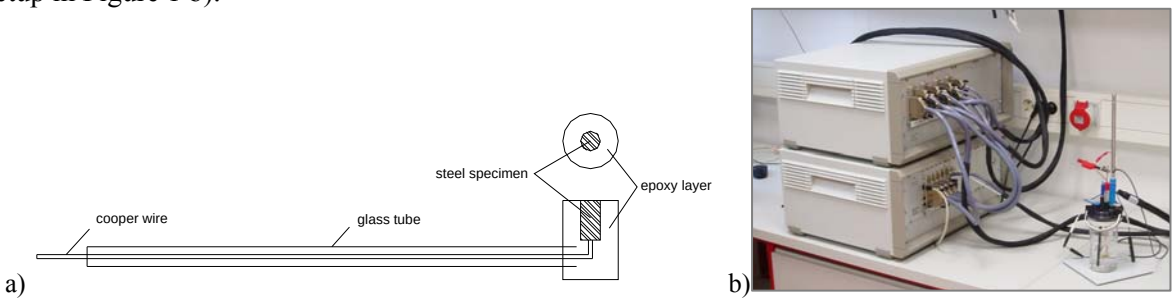

Figure 1. a) Steel specimens for corrosion testing; b) Experiment setup for steel specimens

3.2 Accelerated Corrosion Testing of Steel in Concrete

Investigation of corrosion behaviour of different steel types embedded into smaller concrete specimens ("lollipops") will be performed in 3,5% of NaCl contaminated water using potentiostatic anodic polarization. Anodic potential of 10 V will be applied and change of current in time will be measured. Rapid increase of current is considered to be a sign of corrosion initiation (Stipanovic et al., 2007). Measurements will be performed using PAR VMP2 potentiostat / galvanostat with three-electrode arrangement. Working electrodes were prepared manually. Concrete specimens with embedded steel were prepared in this way: isolated copper wire is connected to 10 cm long steel bars and the connection is protected with layer of water resistant material. These steel specimens are then embedded in 12 cm high and 4 cm thick moulds in which fresh concrete will be poured, Figure 2 a). Concrete specimens prepared this way will be cured for 28 days and then used in accelerated corrosion testing. Counter electrode is carbon rod and reference electrode is saturated calomel electrode (SCE). All potentials reported, refer to SCE. Experiment setup is shown in Figure 2 b).

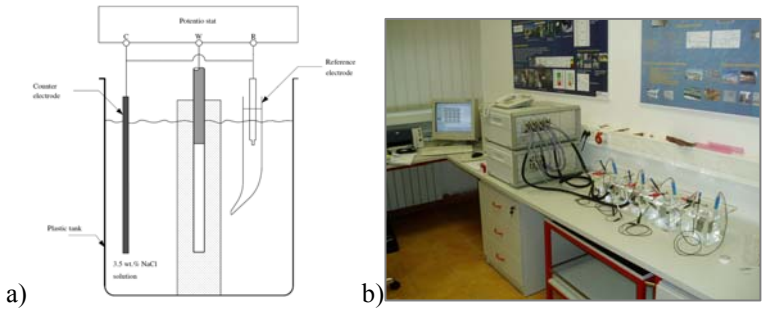

Figure 2. a) Three electrode system for corrosion testing; b) Experiment setup for concrete specimens

3.3. Corrosion Testing of Steel in Concrete Exposed to Artificial Atmosphere

During this part of the project task concrete specimens reinforced with different types of steel rebar will be exposed to artificial marine environment with the use of salt spray chamber, Figure 3. Concrete specimens will be exposed to conditions simulating splashing zone in marine environment: 60 - 100% moisture, temperatures between 35 °C and 50 °C and continuous spraying of 3,5% sodium chloride solution. During the exposure in salt spray chamber half cell potential, corrosion current and concrete resistance measurements will be performed.

a)  b) 

Figure 3. a) Concrete specimens; b) Salt spray chamber

3.4 Corrosion Monitoring of Steel in Concrete Exposed to Marine Atmosphere – Testing Field

In the last part of the task an exposure site will be established in the real marine environment. Testing site is situated near Rijeka in Croatia at the Adriatic coast in very aggressive chloride environment, as it can been seen in Figures 4 a and b. Larger concrete beams reinforced with different types of steel with embedded probes for corrosion monitoring will be exposed to aggressive marine environment. Corrosion behaviour will be monitored with electrical resistant probes embedded in concrete specimens and periodically with the use of galvanostatic pulse instrument (half cell potential, corrosion current and concrete resistance measurements).

a)  b) 

Figure 4. Testing site in very aggressive environment at the Adriatic coast.

4 RESULTS

Till now corrosion testing of three types of steel (TOP12, stainless steel grades 1.4301 (AISI 304) and black steel) have been performed. Testing have been performed on steel electrodes (Figure 1 a) in pore solution with pH 12,4 and with the following chloride concentration: 0%, 0.1%, 0.3%, 0.5% and 1%. Pore solution was prepared with addition of $Ca(OH)_2$ and KOH to distilled water. The change of corrosion potential in time and relation potential versus current of black steel, TOP12 and AISI 304 are given in Figures 5, 6 and 7 respectively.

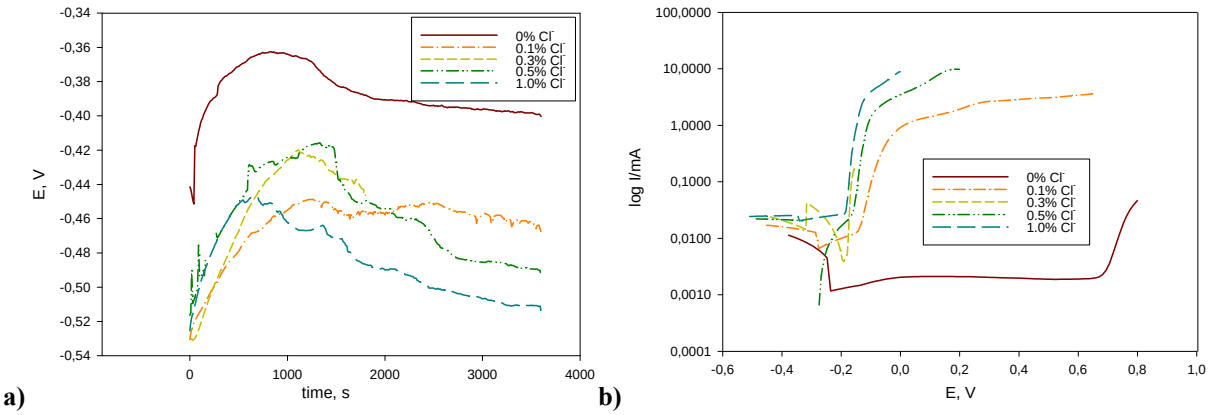

a) **b)**

Figure 5. Black steel: a) corrosion potential vs. time; b) potentiodynamic anodic polarization.

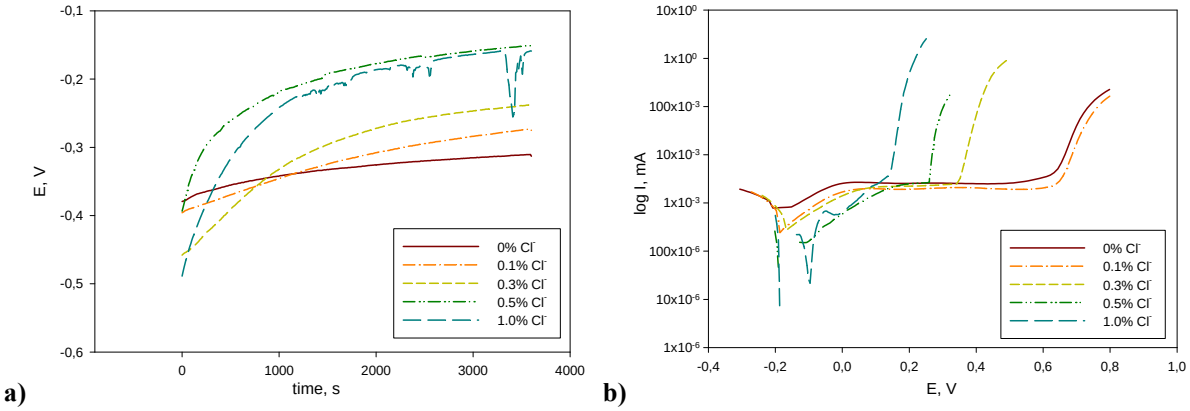

a) **b)**

Figure 6. TOP12: a) corrosion potential vs. time; b) potentiodynamic anodic polarization.

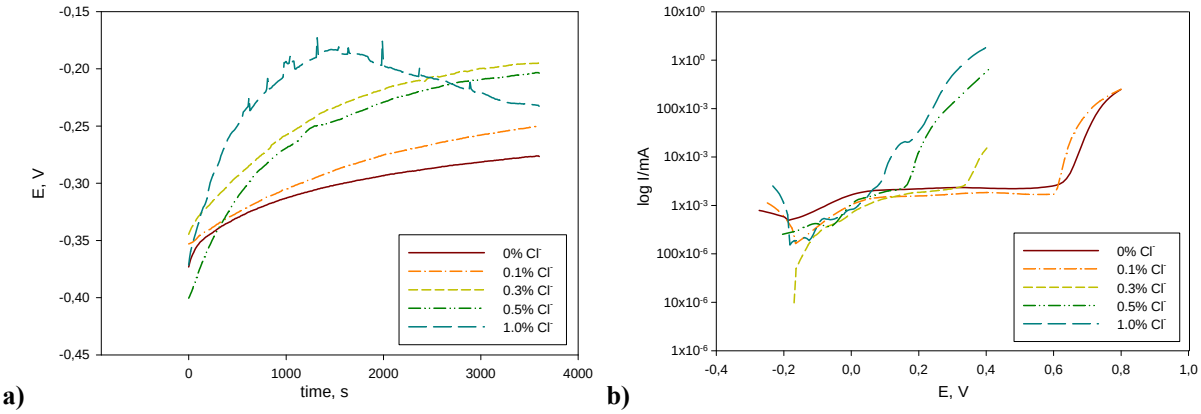

a) **b)**

Figure 7. AISI 304: a) corrosion potential vs. time; b) potentiodynamic anodic polarization.

From the results shown in Figure 5 a) it can be seen that even a small concentration of chloride ions (0.1%) causes a decrease of corrosion potential in time which is an indication that passive layer of black steel that is formed in alkaline media is not stable. This conclusion is confirmed during polarization, because even a concentration of 0.1% of Cl^- caused immediate increase of current and formation of corrosion pit on surface of black steel specimen. On the other side, only chloride concentration of 1.0% managed to unstable the corrosion potential of steels TOP12 (Figure 6 a) and AISI 304 (Figure 7 a). From the results shown in Figure 6 b and Figure 7 b it can be seen that steel TOP12 and AISI 304 have the same behaviour after addition of 0.1%, 0.3% and 0.5% of Cl^-. Only after addition of 1.0% of Cl^- their behaviour changes; pitting potential of steel TOP12 is -120 mV, while pitting corrosion occurs almost immediately after polarization on steel type AISI 304.

5 CONCLUSION

In this paper detailed experimental program that will be used to evaluate corrosion behaviour of different types of alloy steels in concrete is presented. The idea of the research is to evaluate corrosion behaviour of different steels in chemically simplified systems (pore solution) to more complex systems (concrete). Since this research has just begun, till now testing of three types of steel has been performed in pore solution with pH 12,4 and with different concentrations of Cl^-, from 0.1% to 1.0%. From the results of performed testing, which are presented in this paper, it can be concluded that steel TOP12 has satisfying corrosion behaviour when used in high alkaline media such as new concrete. While comparing corrosion behaviour of steel TOP12 to corrosion behaviour of black steel and AISI 304, TOP12 showed longer passivity range in non carbonated pore solution with high concentration of Cl^-.

In order to fully research behaviour of steel TOP12 and other chosen steel types further research will be carried out during the project.

ACKNOWLEDGMENTS

This research was performed within scientific project "The Development of New Materials and Concrete Structure Protection Systems" (082-0822161-2159), funded by Croatian Ministry of education, science and sport and scientific project "ARCHES – Assessment and Rehabilitation of Central European Highway Structures" (031272), funded by the European Community under the Sixth Framework Programme. Authors would like to thank companies Roldan S.A. (ACERINOX group), Spain and Swiss Steel AG, Switzerland for providing steel samples used in this research.

REFERENCES

Bautista, A., Blanco, G. & Velasco, F. 2006, 'Corrosion behaviour of low-nickel austenitic stainless steels reinforcements: A comparative study in simulated pore solutions', *Cement and Concrete Research* 36, Issue 10, p. 1922-1930.

Bentur, A., Diamond, S. & Berke N.S. 1997, *Steel Corrosion in Concrete*, E & FN Spon, UK.

Berke, N. S., Chaker, V. & Whiting, D. 1990, *Corrosion Rates of Steel in Concrete*, ASTM STP 1065, Baltimore.

Bertolini, L., Gastaldi, M., Pedeferri, M. P. & Pedeferri, P. 2000, *Stainless Steel in Concrete*, European Community, COST 521 Workshop, Utrecht.

Bertolini, L., Elsener, B., Pedeferri, P. & Polder, R. B. 2004, *Corrosion of Steel in Concrete Prevention, Diagnosis, Repair*, Wiley – VCH, Weinheim.

Bjegovic, D., Stipanovic, I., Serdar, M. 2007, 'Corrosion of Prestressing Steel in High Performance Grouts', 12th International Congress on the Chemistry of Cement, Montreal, Canada.

Blanco, G., Bautista, A. & Takenouti, H. 2006, 'EIS study of passivation of austenitic and duplex stainless steels reinforcements in simulated pore solutions', *Cement and Concrete Composites*, Volume 28, Issue 3, p. 212-219.

Castro-Borges, P., Cardenas, A., Torres-Acosta, A., Martinez-Madrid, M., Moreno, E. & Troconis de Rincon, O. 2007, 'Chloride profiles in a 63-year old concrete pier reinforced with 304 stainless steel in

Mexico', Proceedings of the 5th International Conference on Concrete under Severe Conditions of Environment and Loading, Tours, France, p. 143-150.

Chauveau, E. & Demelin, B. 2007, 'New lean duplex stainless steel rebar: pitting corrosion resistance and galvanic coupling behaviour', Proceedings of the 5th International Conference on Concrete under Severe Conditions of Environment and Loading, Tours, France, p. 1859-1866.

Hasler, S., Heinmann, W. A., Nussbaum, G., Urlau, U., Schiegg, Y., Voute, C. H., Böhni, H., Lima, M., Kurz, W., Kohler, H. R. & Bischoff, C. 2000, 'TOP12—The innovative reinforcing steel', Materials Week, Munich, Paper No. 665.

Nürberger, U. 1996, *Stainless Steel in Concrete, State of the Art Report*, Publication No. 18, Institute of Materials, London; UK.

Schiegg, Y., Voûte, C.-H., Peter, H., Hasler, S. & Urlau U. 2004, 'Initiation and Corrosion Propagation of Stainless Steel Reinforcements in Concrete Structures', Proceedings Eurocorr'04, Nice, France.

Shreir, L. L., Jarman, R.A. & Burstein, G. T. 1994, *Corrosion. Vol. 1, Metal/Environment Reactions and Alloys*, Butterworth-Heinemann, 3rd Edition, Oxford, UK.

Stipanovic, I., Serdar, M. & Bjegovic, D. 2007, 'Using Inhibitors to Protect Steel Prestressing in High Performance Grouts', *Materials Performance* 46, 3, p. 40-44.

Veleva L., Alpuche-Aviles M. A., Graves-Brook, M. K. & Wipf, D.O. 2005, 'Voltammetry and surface analysis of AISI 316 stainless steel in chloride-containing simulated concrete pore environment', *Journal of Electroanalytical Chemistry*, Volume 578, Issue 1, p. 45-53.

11DBMC International Conference on Durability of Building Materials and Components
ISTANBUL, Turkey 11-14 May 2008

Modeling of Time Depended Changes of Chloride Diffusion Coefficient

Irina Stipanović Oslaković [1]
Marijana Serdar [2]
Dubravka Bjegović [3]
Dunja Mikulić [4]

T11

ABSTRACT

Today engineers have to consider durability of structures in the design process which is realized through the choice of materials and material's performance. Chloride diffusion coefficient is main parameter of durability properties of concrete, like compressive strength is of mechanical properties. In this paper chloride diffusion coefficient was determined for the structure of Krk bridge, which is located in aggressive marine environment, exposed to direct influence of chlorides for the period of more than 25 years. Chloride diffusion coefficient was calculated from chloride profiles measured on specimens taken from different testing places on bridge within inspection and maintenance works on the bridge. In this research results from 1989, 1994, 2000 and 2003 are taken into account and analysed. In order to evaluate change of chloride diffusion in time, results of on site testing were compared with chloride penetration testing in laboratory. Specimens for these testing were prepared from the same concrete mixture that was used during construction of this bridge. All results obtained during the research were compared with calculated chloride coefficient from existing durability models (*DuraCrete, Life-365* and *Chlodif*) for given mixture and exposure time.

KEYWORDS

Chloride diffusion, marine environment, service life modelling, time dependency.

[1] Civil Engineering Institute of Croatia, J.Rakuse 1, Zagreb, Croatia, Phone +385 1 6125 103, Fax +385 1 6125 100, irina.stipanovic@igh.hr
[2] University of Zagreb, Faculty of Civil Engineering, Department for Materials, Zagreb, Croatia, Phone +385 1 4639 118, Fax +385 1 4828 051, marijana.serdar@grad.hr
[3] University of Zagreb, Faculty of Civil Engineering, Department for Materials, Zagreb, Croatia, Phone +385 1 4639 212, Fax +385 1 4828 051, dubravka.bjegovic@grad.hr
[4] University of Zagreb, Faculty of Civil Engineering, Department for Materials, Zagreb, Croatia, Phone +385 1 4639 119, Fax +385 1 4828 051, dunja.mikulic@grad.hr

1 INTRODUCTION

For years, reinforcement corrosion has been recognised as the major problem with respect to the durability of reinforced concrete structures. For structures in marine environment chlorides are the most critical environmental load, which are causing serious corrosion damages. Reliable prediction of chloride ingress in concrete is, therefore, one of the key elements for determining the service life of the structure; which can be theoretically determined by mathematical modelling of a chloride transport mechanism. Existing service life models are mainly based on chloride diffusion process in the concrete, described by Fick's 2nd law, resulting in a prediction model based on an error function complement solution.

In this paper chloride diffusion coefficient was measured on Krk bridge located in aggressive marine environment, exposed to direct influence of chlorides for the period of more than 25 years. Chloride diffusion coefficient was calculated from chloride profiles measured on specimens taken from different testing places on bridge. In order to evaluate change of chloride diffusion in time, results of on site testing were compared with chloride penetration testing in laboratory. Specimens for these testing were prepared from the same concrete mixture that was used during construction of the Krk bridge. All results obtained during the research were compared with calculated chloride coefficient from existing durability models (*DuraCrete, Life-365* and *Chlodif*) for given mixture and exposure time.

2 CHLORIDE PENETRATION TESTING

2.1 Description of the Structure and Location

Chloride analyses were performed on structural elements of Krk bridge, situated at very aggressive marine environment at the Adriatic coast. Krk bridge is a 1430 m long reinforced concrete arch bridge connecting the Croatian island of Krk to the mainland and carrying over a million vehicles per year. It consists of two arch bridges, one with a span of 244 m (the small arch), and the second, between the islet St. Marko and the mainland, with a span of 390 m (the big arch), which is the second longest concrete arch in the world. The bridge was built from 1976 and completed in 1980 [Sram 1981].
Main winds in this area are gale and sirocco, which are producing high waves (few meters) and swirls in the sea, which disperses the sea drops very high, up to 60 meters. The gale wind (from north) as a storm wind is occurring more often in this area, then the wind from south. The average salinity of the sea-water in Adriatic sea is relatively high, around 3.8 %, and by the coast due to the spring of sweet water is decreased to 3.5 %.

2.2 General on the Concrete Quality

For concrete production during the construction of Krk bridge following concrete mix design and materials were used:

- ca 450 kg of Portland Cement class 45 with 20% slag per m^3 of built-in concrete,
- alluvial mined carbonate gravel, with the maximum grain size of 16 mm, divided in fractions 0-4, 4-8 and 8-16 mm,
- 0.15% of air entrainer and 0.2% superplastizicer
- w/c ratio 0.37 by D_{max} = 16 mm.

The same materials and concrete mix design was used in the laboratory chloride penetration testing during 2007. Average compressive strengths of control samples were between 48.8 N/mm^2 and 55.6 N/mm^2. All together 4400 control samples were tested, with the standard deviation from 3.9 to 5.4 N/mm^2. Laboratory testing of capillary suction gave the result of 0.65%, bending tensile strength 9.3 N/mm^2 and static modulus of elasticity 41 300 N/mm^2.

Design values of concrete cover for structural elements of the Krk bridge were 25 and 30 mm, which is one of the main reason why the structure is today locally damaged by sever corrosion [Sram 1981, Beslac 2003].

2.3 Chloride Testing

Chloride profiles had been determined on different parts of bridge several times during its service, performed within the inspection and maintenance works. In this paper results from 1989, 1994, 1997, 2000 and 2003 are taken into account and analysed [Beslac 1997, 2003, IGH 1994, 2003, Durekovic & Calogovic 1991]. From chloride profiles apparent chloride diffusion coefficients were calculated with the application of Fick's 2nd law. In order to evaluate change of chloride diffusion coefficient in time, results of on site testing were compared with chloride penetration testing in laboratory, which simulated concrete diffusion properties at the beginning of structural service life. Specimens for these laboratory testing were prepared from the same concrete mixture (with the same type of cement – CEM II/A-S 42,5), aggregate and same admixtures) that was used during construction of this bridge and tested according NT BUILD 492 in order to get non-steady state migration coefficient [Nordtest, 1999]. It was not possible to compare systematically the change of chloride concentrations in time on the same structural elements and at the same micro environment conditions, since there was no systematic approach in the execution of chloride testing during the service and maintenance of Krk bridge. Typical chloride profiles have been chosen for the analysis, on which basis the calculation procedure for the determination of chloride diffusion coefficient was performed. In Figure 1 is shown longitudinal view of the Krk bridge with marked places of chloride testing during inspections in the period from 1989 to 2003.

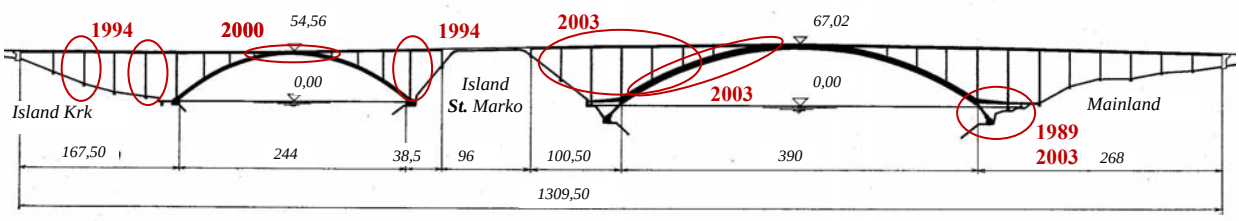

Figure 1. Scheme of Krk bridge with marked places of chloride testing

In Figures 2, 3 and 4 chloride profiles are presented for arch foundation (1989), main beams (2000), arch and columns (2003), depending on the position of testing and height above or under the sea level.

In the *Mathematica* program, the diffusion coefficient for the representative chloride profiles was calculated by curve fitting along with the defined solution of Fick's second law by means of inverse error function. Results of D_{Cl} calculation are presented in Table 1, as well as chloride migration coefficient calculated from NT BUILD 492 measurements.

Results of calculated apparent diffusion coefficients are within the limits from 0.24 to 0.84× 10^{-12} m^2/s for the age of structure from 13 to 23 years, which is in a very good correlation with the values from the literature [Bentz et al. 1996, DuraCrete 1999].

3 APPLICATION OF MATHEMATICAL MODELS

In this research three mathematical service life models were used for the comparison with experimental results, and those are *Life-365*, *CHLODIF* and *DuraCrete*. [Stipanovic 2005]All three models are based on the assumption that the diffusion is the predominant process of chlorides penetrating into the concrete, which can be described mathematically by Fick's second law of diffusion. The time to initiation of corrosion (t_i) may be calculated as the time necessary for the concentration of chloride ions to reach the critical value C_{cr} at the level of reinforcement, which is a

function of the transport properties of concrete (usually the apparent diffusion coefficient), the surface chloride concentration defined by the environment, the thickness of the concrete cover and the chloride threshold value. Within the models *Life-365* and *CHLODIF* deterministic approach is used for the calculation of initiation period t_i and chloride profiles after certain time of exposure, while *DuraCrete* model calculates the probability of corrosion initiation in relation to the time of exposure. By defining the acceptance criteria it is possible to predict structural performance for a pre-determined design service life with a selected level of reliability [Krstic 1994, Bjegovic *et al.* 1995, Bentz, Thomas 2001, DuraCrete 1999]. Each model has different definitions of time-dependency of the chloride diffusion coefficient, which are described in following paragraphs.

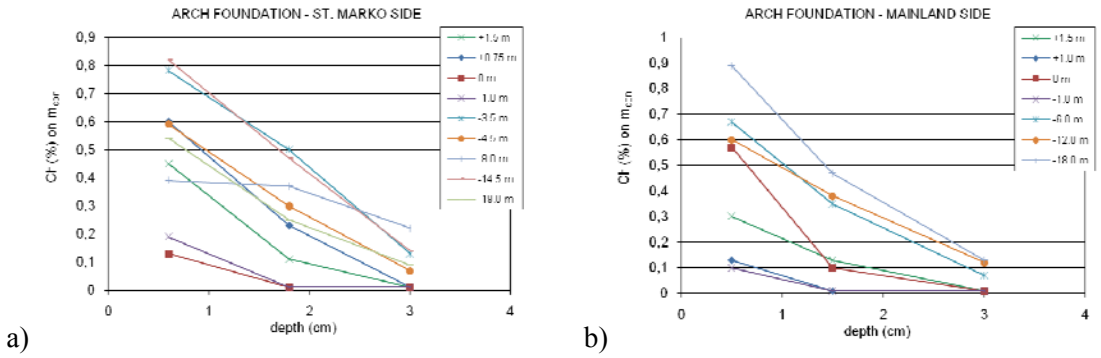

a) b)

Figure 2. Chloride profiles for the arch foundation: a) St. Marko, b) Mainland side measured in 1989.

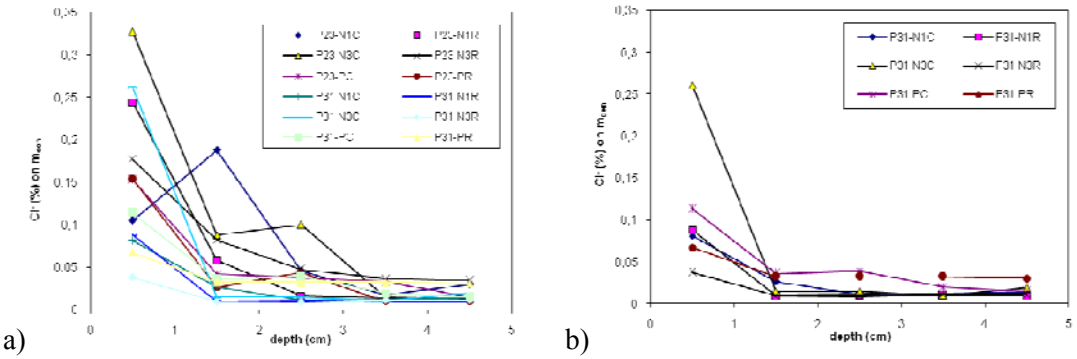

a) b)

Figure 3. Chloride profiles for main beams in: a) field 23; b) field 31, measured in 2000.

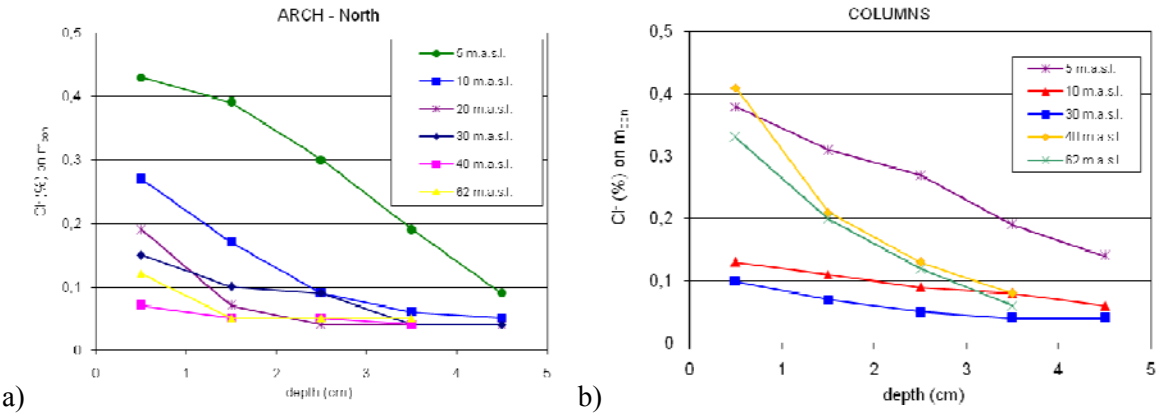

a) b)

Figure 4. Chloride profiles for: a) arch; b) columns, measured in 2003.

Table 1. Overview of calculated apparent chloride diffusion coefficients for Krk bridge.

Age of structural element (years)	Year	Method of D_{Cl} determination	Structural element	Number of chloride profiles analyzed	Value of D_{Cl} [$\times 10^{-12}$ m^2/s]	Standard deviation σ [$\times 10^{-12}$ m^2/s]
0	2007	NT BUILD 492 non-steady state migration test	laboratory concrete	3	6,05	0,39
13	1989	natural diffusion, non-steady state, saturated concrete	submerged	8	0,82	0,43
13	1989	natural diffusion, non-steady state, non-saturated concrete	foundation arch support (above sea level)	8	0,24	0,04
14	1994	natural diffusion, non-steady state, non-saturated concrete	columns C21, C28, C30	14	0,44	0,23
20	2000	natural diffusion, non-steady state, non-saturated concrete	main beams (small arch)	12	0,47	0,18
21	2000	natural diffusion, non-steady state, non-saturated concrete	small arch	20	0,39	0,20
24	2003	natural diffusion, natural diffusion, non-steady state, non-saturated concrete	columns C15, C16, C17, C19	24	0,84	0,34
24	2003	natural diffusion, non-steady state, non-saturated concrete	big arch	10	0,74	0,28
27	2003	natural diffusion, non-steady state, non-saturated concrete	foundation arch support (above sea level)	2	0,46	-

3.1 Service Life Model *Life-365*

Life-365 is based on a 1-D and 2-D finite difference implementation of Fick's Second Law, the general advection-dispersion equation [Bentz, Thomas 2001]. The theoretical value of the apparent chloride diffusion coefficient at 28 days maturity, D_{28}, can be calculated by the model with the following relationship:

$$D_{28} = 1 \times 10^{(-12.06 + 2.40\ w/c)}\ \text{m}^2/\text{s} \qquad (1)$$

where; *w/c* is water-cementitious material ratio of the concrete.

The chloride diffusion coefficient is furthermore a function of time and temperature:

$$D(t,T) = D_{ref} \cdot \left(\frac{t_{ref}}{t}\right)^m \cdot \exp\left[\frac{U}{R} \cdot \left(\frac{1}{T_{ref}} - \frac{1}{T}\right)\right] \qquad (2)$$

where: $D(t,T)$ = diffusion coefficient at time t and temperature T

D_{ref} = diffusion coefficient at some reference time t_{ref} (= 28 days in *Life-365*)
m = constant (depending on mix proportions)
m = 0.2 + 0.4 (*%FA*/50 + *%GGBS*/70) ,
FA = Fly ash; *GGBS* = ground granulated blast furnace slag
U = activation energy of the diffusion process (35000 J/mol)
R = gas constant
T = absolute temperature

In this study only time-dependency of chloride diffusion coefficient is analysed. Concrete mixture used in Krk bridge was produced with *w/c* ratio 0,37 and with 20% of slag in the cement, which gives the *m* value of 0.31, and $D_{ref} = 6.73\times10^{-12}$ m^2/s at 28 days and $D_{t1} = 3.04\times10^{-12}$ m^2/s after 1 year. Time dependency of chloride diffusion coefficient calculated by *Life-365* is shown in Figure 5.

3.2 Service life model *Chlodif*

Numerical model *Chlodif* was developed at the University of Zagreb, Faculty of Civil Engineering in the early nineties. The process of a continuous diffusion process of chloride ions into a reinforced concrete structure is also based on a time-varying diffusion coefficient and varying chloride surface concentration [Krstić 1994,Takewaka & Matsumoto 1988]. The empirical formula for the chloride diffusion coefficient depending on *w/c* ratio, based on the conducted research work in Japan [Takewaka & Matsumoto 1988], was accepted in *Chlodif*:

$$log_{10} D_{w/c} = -6.274 - 0.076 \times w/c + 0.00113 (w/c)^2 \quad (3)$$

where: $D_{w/c}$ = "basic" diffusion coefficient (cm^2/s),
w/c = water-cement ratio (%).

The research work was performed on concrete specimens with the age between 1 and 20 years, which were exposed to different marine environment (tidal, splashing, submerged and atmospheric zone). The conclusion of these testing was that diffusion coefficient is not depending on the environment conditions, but it is strongly depending on type of cement and especially on the age of concrete: the older concrete, the lower diffusion coefficient. Accordingly the following relationship was suggested for describing the change of diffusion coefficient with the age of concrete [Takewaka & Matsumoto 1988]:

$$D_{Cl^-} = D_{w/c} \times D_0 \times t^{-0.1} \quad (4)$$

where: D_0 = coefficient which takes into account type of cement,
t =the age of structure (years).

For the cement with the slag addition D_0 is 0.30, which gives the theoretical value of chloride diffusion coefficient for this case study $D_{w/c} = 5.68\times10^{-11}$ m^2/s and $D_{Cl^-} = 4.68\times10^{-12}$ m^2/s after 1 year. Time dependency of chloride diffusion coefficient calculated by *Chlodif* is shown in Figure 5.

3.3 Service Life Model *DuraCrete*

In *DuraCrete* model corrosion initiation is defined as serviceability limit state (SLS) which gives the design service life. The design equation for this SLS is described over Fick's 2nd law of diffusion, where each variable is defined over its design and characteristic value. The design value of the time dependent concrete resistance is derived from:

$$R_{cl}^{d}(t) = \frac{R_{cl,0}^{c}}{k_{e,cl}^{c} \cdot k_{c,cl}^{c} \cdot \left(\frac{t_0}{t}\right)^{n_{Cl}^{c}} \cdot \gamma_{R_{cl}}} \quad (5)$$

where $R_{cl,0} = \left(\frac{1}{D_{\mathrm{RCM},0}} \right)$

where $D_{RCM,0}$:is chloride migration coefficient in [m^2/s] , measured according to NT BUILD 492 test,

$k_{c,cl}$ = curing factor,
$k_{e,cl}$ = environment factor,
t_0 = the age of the concrete when the compliance test is performed,
n_{cl} = age factor,
γ_{Rcl} = partial factor for the resistance with respect to chloride ingress (1.50; 2.35; 3.25 depending on the risk relative to the cost of repair)

For the concrete which was 28 days cured $k_{c,cl}$ is 0.79, while environment and age factors are given in Table 2 [DuraCrete 1999]. For this case study $D_{RCM,0}$ was 6.05×10^{-12} m^2/s after 28 days, which gives $R_{cl,0}$ 1.65×10^{11} s/m^2. Time dependency of chloride diffusion coefficient calculated by *DuraCrete* is shown in Figure 5.

Table 2. Characteristic values of the environment and age factor for GGBS concrete.

Variable	GGBS, Submerged	GGBS, Tidal Zone	GGBS, Splash zone	GGBS, Atmospheric
$k_{e,cl}$	3.88	2.70	0.78	1.98
n_{cl}	0.71	0.60	0.60	0.85

4 ANALYSIS OF RESULTS AND CONCLUSION

In these three chloride ingress models the diffusion coefficient is treated as time-dependent, based on the power law, as given in eq. (2), with some specifics in each of them as previously described. Time dependencies of chloride diffusion coefficient calculated by *DuraCrete*, *Life-365* and *Chlodif* are shown in Figure 5, for this specific type of concrete and exposure conditions, and compared with the experimental results for the Krk bridge.

A number of researches have shown that a chloride diffusion coefficient decreases with time, due to the continuous hydration and binder reactions which densify the concrete with time. The time-dependency is varying very much for different types of concrete, especially for different binders. [Stipanovic et al. 2007].

In this study a comparison of results of initial chloride ingress testing on new concrete and condition survey testing performed in 1989, 1994, 2000 and 2003 showed that chloride diffusion coefficient significantly decreased, about one order of the magnitude. For the age of structure from 13 to 23 years results of calculated apparent diffusion coefficients are within the limits from 0.24 to 0.84×10^{-12} m^2/s. Measurements of chloride migration coefficient D_{Cl} (according NT BUILD 492) at the age of 28 days performed on the copy of concrete mixture built into the Krk bridge, gave the average result of 6,05 $\times$ 10^{-12} m^2/s. Based on these experimental results regression analysis concerning the time dependent decrease of D_{Cl} were performed. Curve fitting of the power law relationship to the experimental results gave the m value 0.47 for this type of concrete (w/c = 0.37, 20 % slag). These results are in a very good correlation with the values from the literature and with the prediction of D_{Cl} decrease in mathematical model *Life-365* and partially with *DuraCrete* model [Bentz et al. 1996, Thomas & Bentz 2001, DuraCrete 1999, Tang & Gulikers 2007].

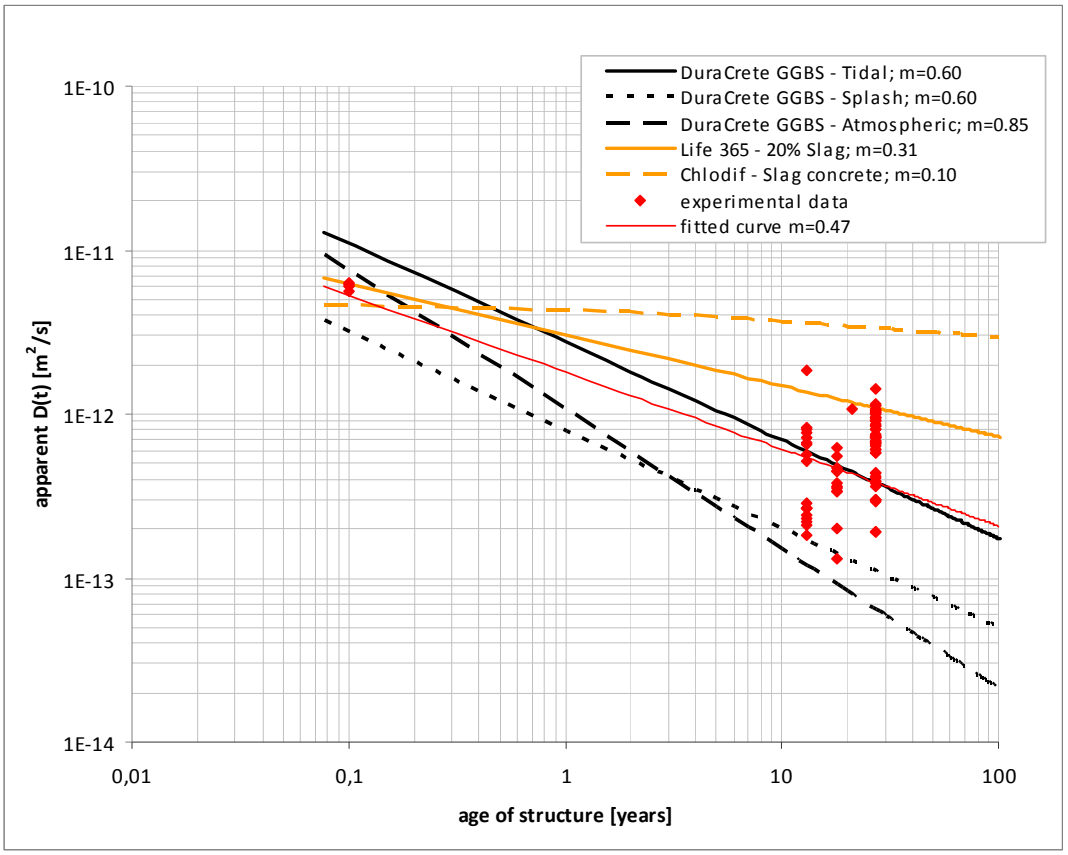

Figure 5. Time-dependency of chloride diffusion coefficient described by 3 mathematical models, depending on binder and environment conditions.

ACKNOWLEDGMENTS

This research was performed within two scientific projects "The Development of New Materials and Concrete Structure Protection Systems", 082-0822161-2159, and "From Nano- to Macro-structure of Concrete", 082-0822161-2990, funded by Croatian Ministry of education, science and sport.

REFERENCES

Bentz, D.P., Clifton, J.R., & Snyder, K.A. 1996, A Prototype Computer-Integrated Knowledge System: Predicting the Service Life of Chloride-Exposed Concrete, *Concrete International*, **18** (12), 42-47, Dec. 1996.

Beslac, J. & Bogovic, M. 1997, *'Enhanced maintenance of the Krk bridge'*, GRAĐEVINAR **49** 8, pp. 427-434. (in Croatian)

Beslac, J. 2003, '*Maintenance of the Krk bridge'*, IGH. (in Croatian)

Bjegovic D., Krstic V., Mikulic D. & Ukrainczyk V. 1995, 'C-D-c-t Diagrams for Practical Design of Concrete Durability Parameters', *Cement and Concrete Research*, Vol. **25**, No. 1, pp. 187-196.
Durekovic, A. & Calogovic, V. 1991, 'Investigation on Bridge Support after 11 Years of Exposure to Seawater', Second International Conference Durability of Concrete, ACI SP-126, Montreal, Canada, pp. 627-641.

EU – Brite EuRam III: *DuraCrete Final Technical Report*, Probabilistic Performance Based Durability Design of Concrete Structures, Document BE95-1347/R17 May 2000.

IGH, Department for masonry and concrete structures: REPORT, research work and evaluation on materials in reonforced concrete structure of Big arch of the Krk bridge, Book 3, Zagreb, March 2003. (in Croatian)

IGH, Repair work project and protection of column on Small arch of krk bridge, 1994. (in Croatian)
Krstic, V.: Numerical model for durability design of reinforced concrete structures, Master Thesis, Faculty of Civil Engineering, University of Zagreb, 1994. (in Croatian)

Luping, T., Gulikers, J. 2007, 'On the mathematics of time-dependent apparent chloride diffusion coefficient in concrete', Cement and Concrete Research 37 589 – 595.

Nordtest method NT BUILD 492 Concrete, Mortar And Cement-Based Repair Materials: Chloride Migration Coefficient From Non-Steady-State Migration Experiments, 1999.

Sram, S. 1981, *Execution of the Krk bridge,* Građevinar **33**, 2, 77-106. (in Croatian).

Stipanovic, I.: Service life modeling of reinforced concrete structures exposed to chlorides, Master Thesis, Faculty of Civil Engineering, University of Zagreb, 2005 (in Croatian).

Stipanovic, I., Bjegovic, D. & Serdar, M. 2007, 'Durability properties of ecologically friendly concrete', Proceedings of FIB Symposium May 2007, Cavtat, Croatia, 20-23, 337-346.

Takewaka, K. & Mastumoto, S. 1988, 'Quality and Cover Thickness of Concrete Based on the Estimation of Chloride Penetration in Marine Environments', ACI-SP 109-117, Concrete in Marine Environment, pp. 381-400, Detroit (USA).

Thomas, M.D.A. & Bentz, E.C. 2001, *Life-365*, Service Life Prediction Model, Computer Program for Predicting the Service Life and Life-Cycle Costs of Reinforced Concrete Exposed to Chlorides, University of Toronto, December 2001.

Prediction of Elastic Properties of Concrete Using the Virtual Cement and Concrete Testing Laboratory

Sinan T. Erdoğan [1]
Edward J. Garboczi [2]
Jeffrey W. Bullard [3]

T 11

ABSTRACT

The Virtual Cement and Concrete Testing Laboratory (VCCTL) project was initiated at the National Institute of Standards and Technology (NIST) in 2001. The VCCTL is being developed by NIST and a consortium consisting of universities, materials manufacturers and trade associations.

VCCTL has the goal of modeling the materials used in concrete during mixing, and curing so that both fresh and hardened concrete properties can be predicted. Its impact on modeling concrete mixtures could potentially be similar to the effect finite element modeling of structures has had on structural analysis and design. It will permit optimum designs of concrete mixtures to be determined, eliminating a large amount of laboratory mixing and testing now required, and resulting in time and monetary savings. Rheology, curing time, strength, and durability are now or are planned to be within the scope of its predictions.

The elastic properties of concrete, the quintessential building material, have an important effect on the strength and durability of structures. An overview of the capabilities of VCCTL v5.0 is given with emphasis on mechanical property prediction. VCCTL models are able to accurately predict the results of some standard laboratory tests such as ASTM C109 and ASTM C215, when given well-characterized mixture material data as input.

KEYWORDS

Concrete, Mortar, Computer modeling, Virtual testing, Elastic properties

[1] Middle East Technical University, Dept. of Civil Engr., Ankara, Turkey 06531, Phone +90 312 210 2428, Fax +90 312 210 5401, sinante@metu.edu.tr
[2] National Institute of Standards and Technology, Inorganic Materials Group, Gaithersburg, MD 20878 USA, Phone +1 301 975 6708, Fax +1 301 990 6891, edward.garboczi@nist.gov
[3] National Institute of Standards and Technology, Inorganic Materials Group, Gaithersburg, MD 20878 USA, Phone +1 301 975 5725, Fax +1 301 990 6891, jeffrey.bullard@nist.gov

1 INTRODUCTION

The design of concrete mixtures and the evaluation of the properties of fresh and hardened concrete have been done mostly empirically until the present day. Conventional laboratory testing methods are costly and time-consuming, requiring the purchase and disposal of materials, allocation of human resources and money, and sometimes long wait periods before obtaining results.

The Building and Fire Research, and Information Technology Laboratories within the National Institute of Standards and Technology (NIST) formed, in 2001, a NIST/industry consortium to develop a Virtual Cement and Concrete Testing Laboratory (VCCTL) with the goal of developing a world wide web-based virtual laboratory for evaluating and optimizing cement-based materials. Virtual, computer testing of cement and concrete properties permits substantial savings in time, materials, human resources, and money by reducing the number of physical concrete tests performed by private industry [Web reference 1]. Table 1 summarizes the need for the development of a virtual testing laboratory by comparing current (physical) testing with virtual testing.

Table 1. Comparison of current testing methods and virtual testing.

Current Testing	**Virtual Testing**
physical based	computer based
manpower intensive	computationally intensive
materials intensive	small material needs
weeks/months	hours/days
high disposal costs	low disposal costs

A computer model for the hydration and development of cement-based materials, based on over 10 years of research at NIST, is at the core of the VCCTL. Details of this research are available in [Web reference 1]. Other models, including those that predict rheological, mechanical, and transport properties and simulate degradation mechanisms, will eventually allow for durability modeling and service life prediction. In addition to the models, databases of fully characterized cements and aggregates exist which can be used as sources of input data for the models. Figure 1 shows the input needed for the microstructure-based models of VCCTL and the kinds of problems VCCTL can address.

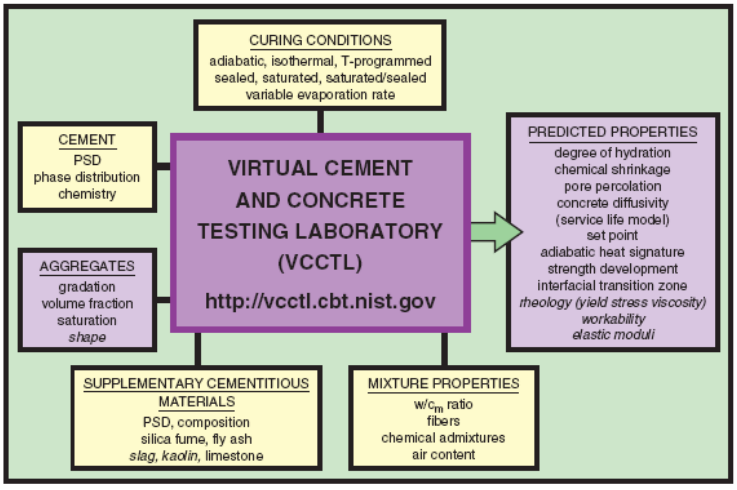

Figure 1. The input required for and the properties predicted by VCCTL [Bullard *et al.* 2005].

Enhancements and additions to the base models and web interface, based on the specific interests of the consortium members, are performed continuously and a new version of the software is made

available to the members annually. An educational version of VCCTL, with limited capabilities compared to the full consortium version, is scheduled to be released in 2008 and will be available at [Web reference 1].

The elastic properties of concrete greatly influence the strength and durability of structures and are particularly important for tall structures. VCCTL can perform standard tests 'virtually' by simulating hydration reactions for well-characterized mixture material data and performing calculations on the hydrated microstructure. Some standard laboratory tests performed regularly in many countries, such as ASTM C109, Standard Test Method for Compressive Strength of Hydraulic Cement Mortars (commonly referred to as the mortar cube strength test) and ASTM C215, Standard Test Method for Fundamental Transverse, Longitudinal, and Torsional Frequencies of Concrete Specimens, can currently be performed virtually, with appreciable accuracy.

2 WHAT VCCTL CAN OR WILL BE ABLE TO DO

As it is, the hydration model satisfactorily predicts the influences of particle size distribution, volume and surface area fractions of cement phases on hydration, and several phenomena involved with the addition of pozzolans. The rheology model uses a multi-phase approach to predict concrete plastic viscosity using a combination of simulation and measurements. In this approach, the paste viscosity can be measured using a paste rheometer and the effect of aggregate size, shape and grading can be added through computer simulations to obtain a concrete viscosity prediction. Work is being done on the interaction between particles in the model to account for the influence of chemical admixtures on the flow of cement paste. The flow of concrete in various geometries is also being investigated.

In the future, VCCTL software will allow users to generate and test virtual concrete mixtures, by selecting cements and fine and coarse aggregates from a database. The user will be able to choose from the fully characterized input materials in the database materials which are similar to the material actually being used or input new values obtained from the users laboratory characterization of the actual materials. The end-product will be a powerful tool for: predicting important values such as degree of consumption of starting ordinary portland cement (OPC) compounds, capillary porosity, non-evaporable water, hydroxyl ion concentration in the pore solution etc.; for conducting virtual rheology tests to check for flow properties thus minimizing the number of physical trial mixtures needed for selecting a mixture with desired properties; and for conducting virtual cylinder or cube tests for strength determination, reducing the number of physical validation tests drastically. The accurate predictions of the hydration model will make it possible to predict durability problems before they occur, potentially preventing great financial losses.

The mechanical properties model can, for a wide-range of water-to-cement ratio (W/C) values and curing ages, predict elastic moduli of cement paste, mortar and concrete accurately. The model can also make compressive strength predictions based on elastic moduli. Future research will investigate the accuracy of elastic modulus predictions of blended cement pastes and concretes. Viscoelastic properties, to be able to make accurate predictions of mechanical properties at early ages, and the effect of aggregate shape on strength are also being investigated. The virtual determination of the compressive strengths of mortars is explained in the following section and the results compared with physical tests on the mortars made using well-characterized cements and prepared under carefully controlled mixing and curing conditions.

3 PREDICTION OF MECHANICAL PROPERTIES OF MORTARS USING VCCTL

Three cements with contrasting chemical composition were selected to evaluate the accuracy of VCCTL predictions: Cement A, an ASTM Type I cement; Cement B, an ASTM Type V cement; and Cement C, an ASTM Type I white cement. Since virtual tests to determine mortar strength require

cement characteristics, and mixing and curing conditions to be input, polished specimens containing cements dispersed in epoxy were analyzed using a combination of scanning electron microscopy/back scattered electron images and x-ray images. This allowed the identification of different phases within cement grains in two-dimensions, and this area fraction was used to calculate the volume fraction of each phase in three-dimensions. This process has been described in detail in [Bentz and Stutzman 1994, Bentz *et al.* 1999, Bentz *et al.* 2003]. The particle size distributions for the cements were measured using wet (with isopropanol used to disperse the cements) low-angle light spectroscopy (laser diffraction - LD). Table 2 gives some characteristics of the three cements used.

Table 2. Chemical (based on SEM/EDS images) and physical characteristics of the cements. The fineness values are based on wet laser diffraction measurements. All units are volume fractions.

	Cement A	**Cement B**	**Cement C**
C_3S (%)	58.85	65.02	65.39
C_2S (%)	17.64	16.43	24.92
C_3A (%)	4.42	3.14	7.13
C_4AF (%)	11.68	8.35	0
Gypsum (%)	5.55	5.58	2.37
K_2SO_4 (%)	0.44	0.44	0.11
Mg/Ca (%)	0.13	1.04	0.08
Free lime (%)	0.67	0	0
Silica (%)	0.36	0	0
Kaolin (%)	0.16	0	0
Slag (%)	0.1	0	0
Fineness (m^2/kg)	483	545	614

The cement composition and some mixture properties were input into the hydration model to create a starting microstructure in 3-D, in which cement particles were randomly placed in a 3-D system of chosen dimensions so that the particle size distribution (PSD) matched experiment. By choosing a system, it is meant that a collection of voxels (3-D pixels), each containing a single starting phase such as C3S, C4AF, or water, is simulated. A water to cement mass ratio (W/C) of 0.485 was chosen for each simulation in accordance with ASTM C109. The system sizes were chosen to be (90 x 200 x 200) µm for cements A and C and (88 x 200 x 200) µm for cement B. Each system had a 10 µm thick aggregate slab dividing the shortest dimension in half to allow the simulation of an interfacial transition zone (ITZ) (see Fig. 2).

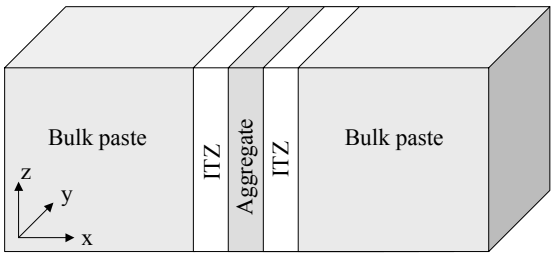

Figure 2. Shape and construction of the system chosen to simulate geometry and elastic properties of ITZ and bulk cement paste.

The system sizes were calculated [Sun *et al* . 2007] to attain the chosen W/C in the bulk of the starting microstructure, outside of the ITZ. The thickness of the ITZ was assumed to be equal to the median of the cement PSD [Bentz *et al.* 1993], and the required system size was determined considering the knowledge of the amount and physically measured PSD of Ottawa sand used in ASTM C109 (and assuming spherical sand particles), and calculating the total amount of paste in the system and the ratio

of the volume of the paste in the ITZ to the bulk paste (outside of the ITZ). Thus, the size of the system in the direction perpendicular to the aggregate surface was restricted so as to maintain the ITZ-to-bulk paste volume ratio. So, for example, the different sections/phases along the shortest dimension (88 μm) of the system for Cement B (for which ITZ thickness was 15 μm) were: bulk paste-24 μm; ITZ paste-15 μm; aggregate slab-10 μm; ITZ paste-15 μm; bulk paste-24 μm. The ITZ was taken as 15 μm for cements A and B, and 12 μm for the finer cement C. The size of the system in the directions parallel to the aggregate surface was made large enough in order to fit in the largest cement grains allowed by the cement PSD used.

Mixing and curing information such as aggregate fraction (to be used in tracking paste temperature), curing temperature and saturation conditions were input, as well as some other hydration parameters like a time conversion factor used to relate simulation time to actual time. The aggregate fraction was 0.53 to 0.54 for the three cements, varying because of their different measured densities). The starting microstructure was then hydrated virtually to age 28 d (6 h to 7 hours in actual computer time) and the resulting paste microstructure with a distribution of various hydration products was obtained. The elastic/mechanical property predictions were based on this hydrated microstructure in each of the three mortar cases. Predictions for different ages were made using the hydrated microstructures after the corresponding amount of time in the simulations, with the degree of hydration increasing with increasing computer time.

The time conversion factor used to relate simulation time to actual time was determined by matching the predicted degree of hydration (doh) to the experimental doh, measured at various ages (more frequently at early ages), using loss of bound water mass on ignition [Bentz, 1997]. The elastic moduli for the hydrated paste was determined using the elastic moduli of individual hydrated phases (from literature, available in Haecker *et al.* [2005]) and a program which, assuming cement paste is linearly elastic, treats each cubic voxel (containing only one hydrated phase) as a tri-linear finite element upon which the elastic equations are discretized and solved using a relaxation algorithm. The average stress for a given strain is used to determine the composite moduli, which are averaged over direction to minimize the effects of having a small, periodic model of a large microstructure. Details of this program and the assumptions involved are available in [Garboczi 1998, Garboczi and Day 1995]. The elastic moduli for the ITZ paste was calculated separately from the bulk paste by averaging the elastic properties of the voxels near the aggregate slab surface at a distance less than the assumed ITZ thickness, which is important because elastic moduli of the ITZ paste are lower than those of the bulk paste, due to its lower density. At the W/C used, this ratio was observed to be about 0.83 to 0.87, at an age of 28 d, for the cement pastes simulated with the ratio increasing with increasing age for a given cement paste. The elastic moduli for the mortars were predicted using the calculated/predicted cement paste moduli, the measured Ottawa sand PSD, elastic moduli for the sand determined averaging published elastic constants for alpha quartz, and a model air content, which was based on physical measurements. The air content for the mortars A, B, and C were determined to be 6.1 %, 5.3 % and 4.8 % by volume, respectively. The calculated mortar moduli were compared with resonant frequency experimental measurements (ASTM C215), on 51 mm x 51 mm x 203 mm (2 in x 2 in x 8 in) mortar prisms that were cured indentically to the ASTM C109 mortar cubes.

Compressive strength predictions were made semi-empirically, using equations relating measured dynamic Young's modulus, E_d, to measured static Young's modulus, E_c [Lydon and Balendran 1986], and relating measured static Young's modulus to measured compressive strength, fc [ACI 318]:

$$E_c = 0.83E_d \quad (1)$$

$$E_c = 4.73\sqrt{f_c} \quad (2)$$

The predicted dynamic Young's modulus was related to compressive strength by combining Eqns 1 and 2:

$$f_c = (E_d / 5.7)^2 \quad (3)$$

The compressive strength predicted for the three mortars and measured (using 2 in cubes as per ASTM C109) for different testing ages are given in Table 3. One standard deviation is reported for the C109 and C215 strength results. The uncertainty for VCCTL predicted strength is uncalculable because the error in Eqns 1 and 2 are meaningful only for the cements used in their development. This research serves in a way to estimate the uncertainty of predicted strength. The only uncertainty involved in the prediction of dynamic Young's modulus comes from the randomization of the placement of cement particles in the microstructure and is negligible. For each age in Table 3, the VCCTL predicted result and the ASTM C215 result are both based on using the dynamic Young's modulus, predicted or measured, in Eqn. 3 to give the predicted compressive strength.

Table 3. Comparison of predicted and measured (using 2 in cubes for ASTM C109 and 2 in x 2 in x 8 in prisms for ASTM C215) strength values for the three mortars. The VCCTL predicted and ASTM C215 based strength values were calculated by using Eqn. 3. All values are in MPa.

Age	Method	Cement A	Cement B	Cement C
3-day	VCCTL predicted	29.24	31.65	37.80
	ASTM C215 based	25.35 ± 0.17	26.00 ± 0.14	36.92 ± 0.23
	ASTM C109	26.58 ± 1.13	29.63 ± 0.31	41.07 ± 1.91
7-day	VCCTL predicted	32.55	34.86	40.79
	ASTM C215 based	30.41 ± 0.16	31.85 ± 0.16	41.15 ± 0.25
	ASTM C109	31.40 ± 0.99	32.59 ± 0.85	49.01 ± 0.95
28-day	VCCTL predicted	36.03	38.19	43.97
	ASTM C215 based	35.58 ± 0.16	39.23 ± 0.16	44.37 ± 0.26
	ASTM C109	38.21 ± 1.47	41.51 ± 1.30	54.39 ± 2.47

4 ANALYSIS OF THE RESULTS AND OBSERVATIONS

Since the VCCTL predicts the dynamic Young's modulus (E_d) for mortars and then uses Eqn. 3 to relate E_d to the compressive strength, f_c, comparison of VCCTL predicted f_c results with f_c results based on the ASTM C215 resonant frequency test, which are also calculated using Eqn. 3, actually gives an indication of how accurately VCCTL predicts E_d. The VCCTL predicted and the C215 predicted compressive strength values are within 18 % at 3 d, within 9 % at 7 d, and within 3 % of each other at 28 d. The percent difference between the predicted and measured E_d values is approximately doubled by using Eqn.3 to predict strength, so that the predictions of VCCTL for E_d are within 9 % of the C215 measurements at 3 d, 5 % at 7 d, and within about 1 % at 28 d. The accuracy of the predictions increases with increasing mortar age because, as mentioned, the VCCTL models assume linear elastic behavior and the effect of viscoelasticity is greater at early ages than at later ages.

It is also useful to compare VCCTL predictions with a direct measurement of strength, the ASTM C109 mortar cube uniaxial compression test, frequently performed to compare the strength of mortars made using different cements. It is seen in Table 3 that VCCTL predicted strengths were consistently lower than the C109 measured strengths, at 28 days. The difference at 28 days was within 8 % for cements A and B, but nearly 20 % for cement C. While this difference is obviously quite large, the C109 28 d strength result is also nearly 20 % higher than the C215 based result for cement C. This suggests that what is predicted by VCCTL, namely $E_{dynamic}$, may be quite accurate, but the equations used to relate $E_{dynamic}$ to f_c do not apply to cement C. This is supported by the observation that the difference between VCCTL predicted and C215 strength results are close for all three cements used. In

fact, the VCCTL and C215 strengths are within 2.5 %, whereas the C109 strength is more than 8 % greater than the VCCTL predictions for cement C at all three ages. Equations 1 and 2 were developed empirically, using a limited data set containing mostly common cement types, therefore it should not be surprising that they work well for some cements and less well for others. In addition, these relations were developed using results for concrete specimens at 28 days. Examining the composition of cement C in Table 2, it is seen that it is very finely ground and contains greater then 25 % of C_2S, notably higher than in typical cements, which may help explain the low accuracy of the strength predictions for the mortars made with this cement, using Eqn. 3.

A reported ASTM C109 strength is the average of three test results and the maximum difference between any result and the average must be less than 8 %. This shows that there is a certain amount of uncertainty in these results and that a compressive strength prediction within 5 % to 10 % of measured values is reasonably accurate. Some other factors that affect strength predicted in this way are air content, sand PSD and Young's modulus, state of saturation, and ITZ thickness. Air content is particularly influential on predicted strength and it was determined that a one percent change in air content used resulted in a ≈ 4 % change in strength. It was observed that the use of two different PSD results on Ottawa sand from the same container at two different times resulted in a ≈3 % change in the strength results. This is probably due to the assumption of a uniform ITZ thickness. It is assumed that the aggregate size is significantly larger than the cement particles and so the aggregate surface can locally be taken as a flat surface. Then, the ITZ thickness can be assumed to be due to the packing of cement particles on the surface. It was observed that varying the ITZ by 3 μm from the median cement size resulted in a 5 % to 6 % change in predicted strength. Considering all these factors, which are difficult to accurately control or determine, it can be said that VCCTL can predict the strength of mortars made using cements A and B quite well, and less accurately for cement C.

5 CONCLUSIONS

VCCTL is a powerful tool which allows the simulation of hydration reactions for cements and to a certain extent, supplementary cementitious materials. This enables or simplifies the prediction of many properties of cement pastes, mortars, and concrete which relate to durability and can eventually significantly reduce the amount of physical testing required for projects. It is well known that the mechanical properties of cementititous materials, such as strength, are closely tied to their performance in different environmental conditions. It was shown that VCCTL can, for well characterized starting materials, accurately predict the Young's modulus of cement mortars, which can then be related to strength. The accuracy of the strength prediction is limited only by the correctness of the equations relating Young's modulus and strength, for the cement used. Development of a better relation will increase the effectiveness of VCCTL as a tool to evaluate the durability of mortars and concrete.

ACKNOWLEDGMENTS

The authors wish to thank Mr. Rémy Leroy for performing some of the experimental tests.

REFERENCES

Web reference 1: http://ciks.cbt.nist.gov/monograph

Bullard, J.W., Ferraris, C.F., Garboczi, E., Martys, N. & Stutzman, P. 2004, 'Virtual Cement' Reprinted from *Innovations in Portland Cement Manufacturing*, Chapter 10.3, eds J.I. Bhatty, F.M. Miller & S.H. Kosmatka, Portland Cement Association, 5420 Old Orchard Road, Skokie, IL 60077, pp. 1311-1331.

Bentz, D.P. & Stutzman, P.E. 1994, 'SEM Analysis and Computer Modelling of Hydration of Portland Cement Particles', in *Petrography of Cementitious Materials*, eds S.M. DeHayes & D. Stark, ASTM, Philadelphia, PA, p. 60.

Bentz, D.P., Stutzman, P.E., Haecker, C.J. & Remond, S. 1999, 'SEM/X-ray Imaging of Cement-Based Materials', Proc. 7th Euroseminar on Microscopy Applied to Building Materials, eds H.S. Pietersen, J.A. Larbi & H.H.A. Janssen, Delft University of Technology, pp. 457-466.

Bentz, D.P., Haecker, C.J., Feng, X.P. & Stutzman, P.E. 2003, 'Process Technology of Cement Manufacturing', Proc. 5th International VDZ Congress, September 23-27, 2002, Düsseldorf, Germany, pp 53-63.

Sun, Z.; Garboczi, E. J.; Shah, S. P. 2007, 'Modeling the Elastic Properties of Concrete Composites: Experiment, Differential Effective Medium Theory and Numerical Simulation', *Cement and Concrete Composites*, **29** [1], 22-38.

Bentz, D.P., Garboczi, E.J. & Stutzman, P.E. 1993, 'Computer modeling of the interfacial transition zone in concrete', in *Interfaces in cementitious composites*, ed J.C. Maso, E and FN Spon, London, pp. 259–268.

Bentz, D.P. 1997, 'Three-Dimensional Computer Simulation of Portland Cement Hydration and Microstructure Development,' *J. Amer. Ceram. Soc.*, **80**, 3-21.

Haecker, C.J, Garboczi, E.J., Bullard, J.W., Bohn, R.B., Sun, Z., Shah, S.P. & Voigt, T. 2005, 'Modeling the linear elastic properties of Portland cement paste', *Cement and Concrete Research* **35** [10], 1948-1960.

Garboczi, E.J., 1998, *Finite element and finite difference programs for computing the linear electric and elastic properties of digital images of random materials*, NIST Internal Report 6269.

Garboczi, E.J. & Day, A.R. 1995, '*An algorithm for computing the effective linear elastic properties of heterogeneous materials: 3-D results for composites with equal phase Poisson ratios'*, J. Mech. Phys. Solids **43**, 1349-1362.

Lydon, F.D. & Balendran, R.B. 1986, 'Some Observations on Elastic Properties of Plain Concrete', *Cement and Concrete Research* **16**, 312-24.

ACI 318, 1989, Building Code Requirements for Structural Concrete and Commentary.

11DBMC International Conference on Durability of Building Materials and Components
ISTANBUL, Turkey 11-14 May 2008

Chloride Ion Measurement for Cement-Based Materials

Ceki Halmen [1]
David Trejo [2]

T 11

ABSTRACT

Measurement of the chloride concentration of cement-based materials is an important issue because chloride ions are known to cause corrosion of metals embedded in cement-based materials. ASTM C 1152 is the widely used standard to determine the chloride concentration of cement-based materials. The method uses potentiometric titration to determine the chloride ion concentration of cement-based materials. A faster and less expensive method to determine the chloride ion concentration of cement-based materials was developed under the Strategic Highway Research Program (SHRP). Samples of grout, flowable low-strength concrete, and normal-strength concrete with different amounts of chloride ions added during mixing were tested using the ASTM C1152 method and the rapid SHRP method. The rapid method was used with 1.5 and 3.0 gram samples. Results indicate that for grout and normal-strength concrete samples both methods are very well correlated for both 1.5 and 3.0 g samples. The slope values of calculated linear regression models were close to unity. Results also indicate that for mixtures that contain unconventional aggregates and supplementary cementitious materials such as the flowable low-strength concrete samples the slope value of the linear regression model is significantly different from unity. Samples of high volume fly ash containing mortar with different amounts of chloride ions added during mixing were tested using the ASTM C1152 and the rapid SHRP method using an internal calibration procedure. Results indicate that the use of internal calibration procedure did not improve the correlation of results of the two methods for mixtures containing high volumes of supplementary cementitious materials, however changed the slope of the linear regression model to unity. These results will allow for the use of the faster testing procedure that can save significant time and money.

KEYWORDS

Durability, Rapid chloride content measurement, Concrete, Corrosion

[1] Texas Transportation Institute, Texas A&M University, Post Doctoral Research Associate, College Station, TX, 77843, Phone 979 8625660, Fax 979 8456554, ceki-halmen@tamu.edu
[2] Texas A&M University, Zachry Department of Civil Engrg. Faculty, College Station, TX, 77843, Phone 979 8452416, Fax 979 8625660, trejo@civil.tamu.edu

1 INTRODUCTION

One of the most important deterioration mechanisms for reinforced concrete structures is the corrosion of metallic reinforcement embedded in concrete. Aggressive ions such as chlorides can diffuse through concrete to the steel interface. They can initiate corrosion by attacking the passive layer of the steel when they reach a threshold concentration level. Therefore accurate determination of chloride concentration in concrete and other cement-based materials is very important to evaluate the current conditions of reinforced concrete structures and to estimate their remaining service lives. To be statistically valid these chloride concentration measurements should be done with a large number of samples collected from different parts of the structures.

The most commonly used method to determine the chloride concentration of cement-based materials is potentiometric titration following the ASTM C 1152. Ground concrete powder is digested in nitric acid, heated, and filtered. The chloride concentration of the filtrate is determined through potentiometric titration using an ion specific electrode and a standard silver nitrate solution. This is a time consuming, labor intense, and costly procedure.

A rapid method to determine the chloride concentration of cement-based materials was developed under the Strategic Highway Research Program (SHRP) [Herald et al. 1993]]. This method requires ground concrete powder to be digested in a mixture of acetic acid and isopropyl alcohol. After the addition of a dilute sodium chloride solution, potential readings are collected from the solution using a chloride specific electrode and a high resistance voltmeter. Potential readings are then converted to chloride concentrations using a linear calibration curve. To obtain the linear calibration curve, potentials of a series of calibration solutions with known chloride concentrations are measured and logarithms of known chloride concentrations are plotted against their corresponding potential readings.

In a separate study related to this rapid method Clemeña and Apusen [2002] stated that using the described calibration procedure may lead to erroneous results due to unaccounted effects of ions in solution coming from different sources. To solve this problem they suggested an internal calibration procedure. In this procedure, small volumes of a solution with known chloride concentration are added to the digested sample solution and successive potential readings are recorded. Then the initial chloride concentration of the digested sample solution is calculated using the change in potential readings for each successive addition. The changes in the volume of the digested sample solution due to the additions are neglected.

If the results of the rapid method are well correlated with the potentiometric titration method results of the ASTM C 1152 standard, it can allow for more frequent and statistically accurate examination of reinforced concrete structures for chloride concentrations. This would lead to substantial cost and time savings

2 EXPERIMENTAL PROGRAM

The study presented in this paper compares the chloride concentrations of cement-based materials measured using the rapid method and the potentiometric titration method following the ASTM C 1152, and evaluates their correlation. The rapid method was used with 1.5 and 3.0 g samples and also an internal calibration method was evaluated. Four different cement-based materials were used in the study; normal strength concrete, low strength flowable concrete (LSFC), grout, and mortar mixtures containing fly ash (fly ash up to 60% by weight of cement replacement).

Grout mixtures were prepared using a proprietary repair grout for post-tensioned bridges that compensates for shrinkage in plastic and hardened states and that contains no chlorides or fine-aggregates. Two grout mixtures with 3 and 6 percent sodium chloride by weight of total mixture were prepared. Both mixtures had a water cement ratio (w/c) of 0.24. They were prepared by mixing 11.34

kg of grout with 2.72 kg of laboratory tap water that had 0.42 and 0.84 kg dissolved sodium chloride for 3 and 6 percent sodium chloride mixtures, respectively. A total of 12 cylindrical samples, 75x150 mm in size, were prepared for each mixture to use in chloride concentration determination.

Four different normal strength concrete mixtures with two different w/c's (0.4 and 0.6) and two different chloride concentrations (3 and 6 percent by weight of total mixture) were prepared. The normal strength concrete mixture with a w/c of 0.4 consisted of 872 kg/m^3 cement, 349 kg/m^3 water, 1359 kg/m^3 crushed limestone, and 1390 kg/m^3 sand. Sodium chloride in the amount of 119 and 238 kg/m^3 was added to obtain 3 and 6 percent sodium chloride by total mixture weight. The normal strength concrete mixture with a w/c of 0.6 consisted of 582 kg/m^3 cement, 349 kg/m^3 water, 1359 kg/m^3 crushed limestone, and 1621 kg/m^3 sand. Sodium chloride in the amount of 117 and 235 kg/m^3 was added to obtain 3 and 6 percent sodium chloride by total mixture weight. A total of 6 cylindrical samples, 100x200 mm in size, were prepared for each w/c and percent chloride combination.

Mortar mixtures had a water cementitious material ratio (w/cm) of 0.33. Mortar mixtures were prepared at four different fly ash contents by replacing 0, 35, 50, and 60 percent by weight of cement with fly ash. Class F fly ash was used. For each fly ash content three mixtures with 0, 1, and 3 percent chloride by weight of total cementitious material (cement and fly ash) were prepared. Table 1 shows the mixture designs of mortars with different fly ash and chloride contents. For each fly ash and chloride content combination 3 mortar cubes, 50 mm in size, were prepared.

Table 1. Mixture designs for mortars with different fly ash and chloride contents.

Fly ash [%][1]	NaCl [%][2]	Cement [kg/m^3]	Fly Ash [kg/m^3]	Water [kg/m^3]	Sand [kg/m^3]	NaCl [kg/m^3]
60	0	225	338	186	1394	0
60	1	225	338	186	1388	4.6
60	3	225	338	186	1377	13.9
50	0	282	282	186	1409	0
50	1	282	282	186	1403	4.6
50	3	282	282	186	1392	13.9
35	0	366	197	186	1433	0
35	1	366	197	186	1427	4.6
35	3	366	197	186	1416	13.9
0	0	563	0	186	1487	0
0	1	563	0	186	1481	4.6
0	3	563	0	186	1470	13.9

[1]percent by weight of cement
[2]percent by weight of total cementitious material (cement and fly ash)

Unlike normal strength concrete, grout, and mortar samples, 15 LSFC cylinders, 75x150 mm in size, were prepared without adding any chlorides into the batch water. These 15 cylinders were selected randomly from a large number of samples that were exposed to a 3 percent sodium chloride solution for 26 months. Compressive strength of LSFC cylinders varied from a minimum of 0.12 MPa to a maximum of 1.09 MPa. Table 2 shows the mixture designs of randomly selected samples and the numbers of samples from each mixture.

All cement based materials contained ASTM C 150 type I cement. Normal strength concrete, grout, and mortar samples were cured for 28 days following ASTM C192/C 192M-02, before they were ground using a profile grinder. All ground samples were passed through a No. 20 sieve and tested for chloride content following the ASTM C 1152 and the rapid method. Because LSFC samples were too weak for grinding, they were cut and a sample collected from their center was ground using a ceramic

mortar and pestle. Rapid method was performed using 1.5 and 3.0 g powder samples of normal strength concrete and grout. For mortar and LSFC the rapid method was performed using only 3 g powder samples. Potentiometric titration was performed using 10 g powder samples as required by the ASTM C 1152 standard. A chloride ion specific electrode and a high resistance multi-meter combination with accuracy of 0.001 mV was used to perform the rapid method.

Table 2. Low strength flowable concrete mixtures and the number of samples tested.

No of samples	Cement [kg/m^3]	Fine Aggregate [kg/m^3]	Fine Aggregate type	Fly Ash [kg/m^3]	Fly Ash Type	Water [kg/m^3]
2	63	0	.	1200	F	432
1	63	0	.	1200	F	515
1	30	1500	sand	0	.	98
1	30	1500	sand	0	.	111.7
2	15	1500	sand	180	F	190
1	15	1500	sand	180	C	168
1	30	1500	sand	180	C	186
2	30	1500	sand	180	C	144
1	30	1500	sand	180	C	184
1	30	1500	sand	180	HC[1]	472
1	30	1500	foundry sand	180	HC[1]	494
1	15	1500	bottom ash	180	HC[1]	324

[1]High carbon fly ash

3 STATISTICAL ANALYSIS AND RESULTS

Two multiple linear regression analyses were performed with the chloride concentrations measured using the titration method as the response variable. Chloride concentrations were measured from 1.5 and 3.0 g normal strength concrete and grout samples. Chloride concentrations measured using the rapid method and mixture type were used as explanatory variables. Mixture type was a classification variable with three values; grout, normal strength concrete with w/c of 0.4, and normal strength concrete with w/c of 0.6. Both models were significant with an R^2 of 0.98. However, analysis of variance indicated that the mixture type was not a statistically significant variable. Therefore two simple linear regression analyses were performed for 1.5 and 3.0 g samples using the chloride concentrations measured using the titration method as the response variable and the chloride concentrations measured using the rapid method as the explanatory variable. Both models were again statistically significant with an R^2 of 0.98. However, analysis of residuals indicated that the spread of residuals was increasing with increasing chloride concentration for both models. This indicates that the assumption of constant variance of residuals for regression analysis was not satisfied.
If the spread of residuals is dependent on the value of measured chloride concentration then using the model shown in equation 1 to define the relationship between the measured chloride concentrations would be more appropriate.

$$\frac{\left[Cl^-\right]_{ASTM\,C1152}}{\left[Cl^-\right]_{rapid}} = c + k\frac{1}{\left[Cl^-\right]_{rapid}} \qquad (1)$$

Where
$\left[Cl^-\right]_{ASTM\,C1152}$ is the chloride concentration measured using the titration method

$\left[Cl^-\right]_{rapid}$ is the chloride concentration measured using the rapid method

If the assumption of dependence is correct then the simple linear regression model between the chloride concentrations measured using the titration and the rapid method can be obtained by switching the coefficients of equation 1 as shown in equation 2. This model should satisfy the regression assumption of constant spread of residuals.

$$\left[Cl^-\right]_{ASTM\,C1152} = c\left[Cl^-\right]_{rapid} + k \qquad (2)$$

Simple linear regression analysis was performed for the chloride concentration values measured from 1.5 and 3.0 g samples using the form shown in equation 1. Analysis of residuals indicated that all assumptions of linear regression were satisfied. Later the coefficients were switched to get the simple linear regression models in the form shown in equation 2. Figures 1 and 2 show simple linear regression models and their 95% confidence intervals about the mean and their 95% confidence interval for prediction for 1.5 and 3.0 g samples, respectively.

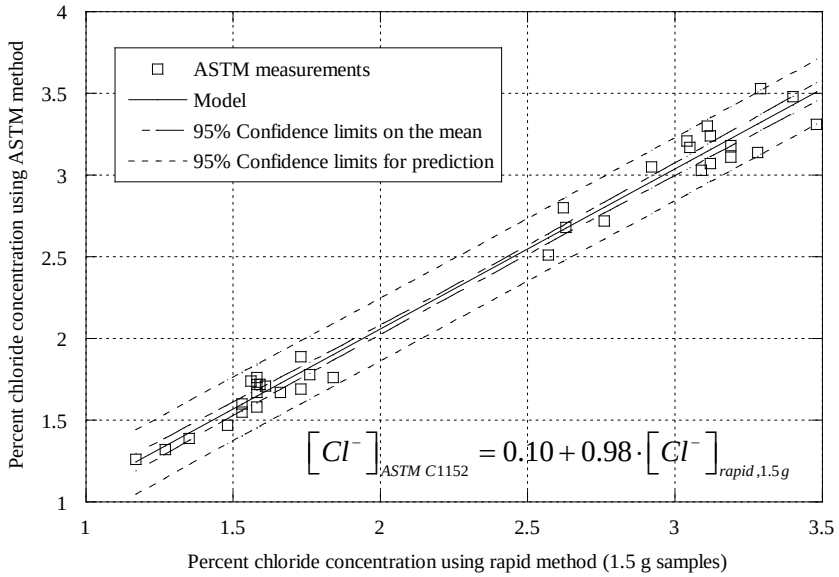

Figure 1. Chloride concentration measured using rapid vs. titration method for 1.5 g samples.

The 95% confidence interval about the mean defines the range of values where the mean of predicted chloride concentration values using the titration method will be with 95% probability. The prediction interval defines the range of values where each individual measured chloride concentration will be with a 95% probability. Since the spread of the means of predicted values is expected to be lower than the individual predicted values the confidence interval about the mean is narrower than the confidence interval for prediction.

Analysis shows that the slope values for both models are statistically significant and they are very close to unity, i.e. a change in the value of chloride concentration measured using the titration method corresponds to an equal change in the value of chloride concentration measured using the rapid method. For the 3.0 g samples the intercept is not statistically significantly different from zero and for the 1.5 g samples there is significant intercept value of 0.1. Both models have an R^2 of 0.98. This means that 98% of variability of the chloride concentration data measured using the titration method could be explained by the model.

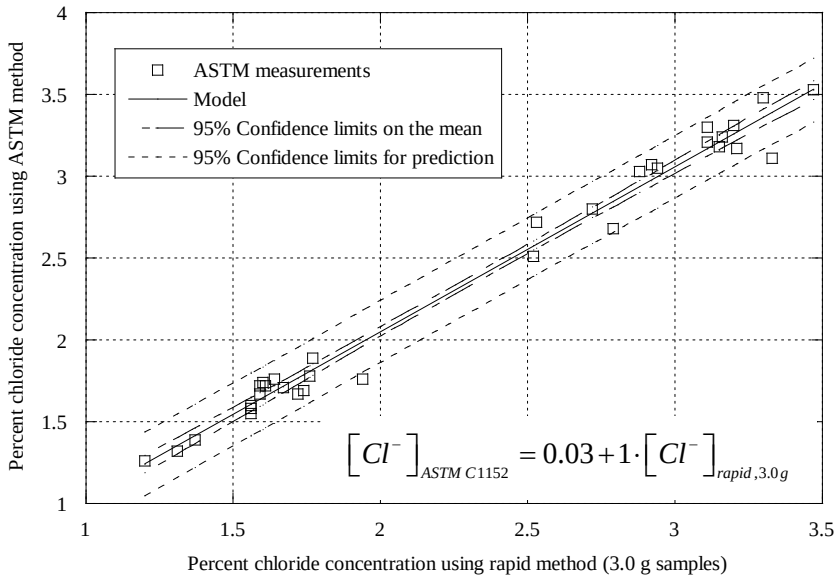

Figure 2. Chloride concentration measured using rapid vs. titration method for 3.0 g samples.

A simple linear regression analysis was also performed between the chloride concentration values measured using the titration method and the rapid method for the LSFC samples. Analysis indicated that using a model in the form shown in equation 1 was not necessary. It should be pointed out that because chlorides were not mixed into these samples, the measured chloride concentrations were much lower compared to the normal strength and grout samples. Figure 3 shows the regression model and its 95% confidence intervals about the mean and for prediction.

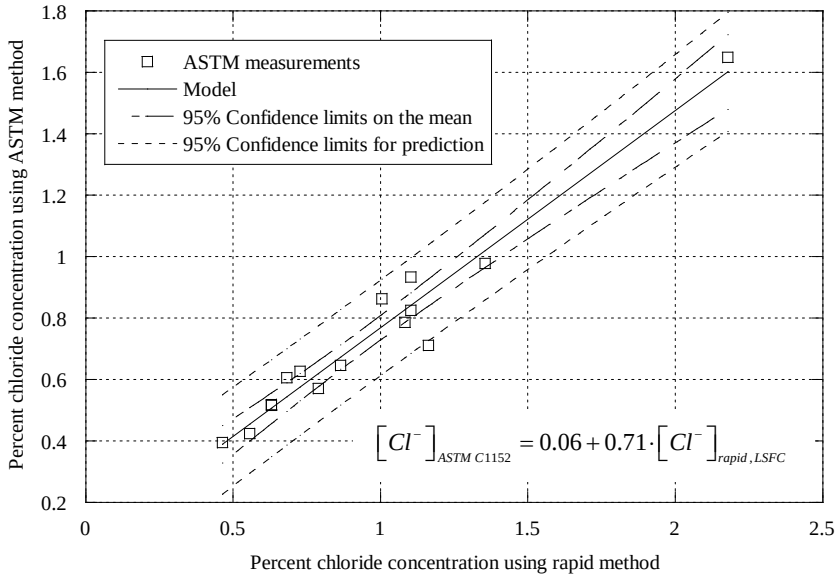

Figure 3. Chloride concentration measured using rapid vs. titration method for LSFC samples.

Analysis indicates that the intersection value was not statistically significantly different from zero similar to the results obtained from 3.0 g normal strength concrete and grout samples. The slope was statistically significant and less than unity (0.71). The model had an R^2 value of 0.95. The LSFC samples are inherently different from normal strength concrete and grout samples due to their low cement content, high w/c ratio, and high amounts of supplementary cementitious materials.
To examine if the difference in results obtained from the LSFC samples and the normal strength concrete and grout samples were due to the calibration procedure used for the rapid method as suggested by Clemeña and Apusen [2002] mortar mixtures containing fly ash were tested. Mortar

mixtures containing fly ash up to 60% by weight of cement were prepared and evaluated using the titration method and the rapid method. The potential readings obtained from the rapid method were converted to chloride concentration values using the internal calibration method described by Clemeña and Apusen [2002].

Analysis indicated that performing simple linear regression using the form of model shown in equation 1 was necessary. Figure 4 shows the regression model and its 95% confidence intervals about the mean and for prediction. The chloride concentration values shown on the x-axis were measured using the rapid method with the internal calibration procedure.

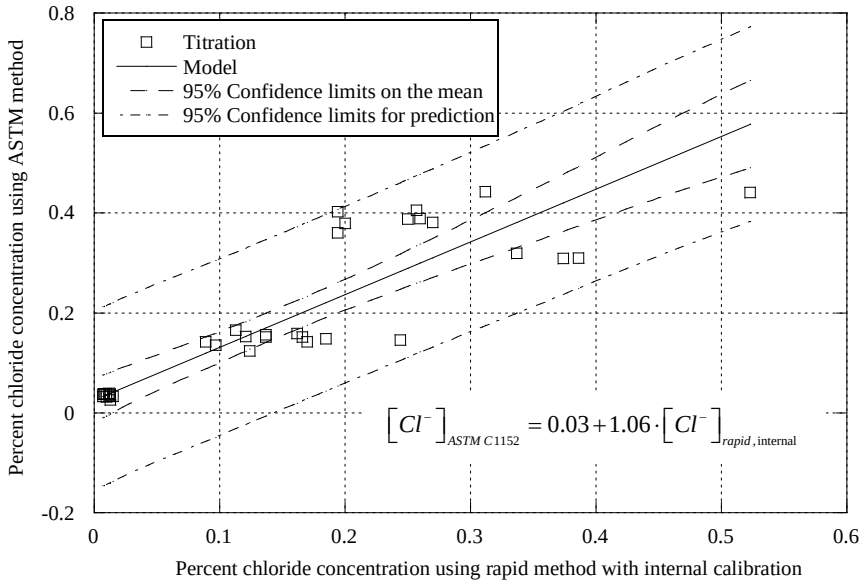

Figure 4. Chloride concentration using rapid method with internal calibration vs. ASTM method.

Analysis indicated that the slope of the simple regression model was statistically significant and close to unity similar to the normal strength concrete and grout samples. However, the R^2 value of the model was 0.89. This indicates that although the slope value was similar to normal strength concrete and grout samples, a smaller portion of the chloride concentration variation measured by the titration method could be explained by the developed model, i.e. predictions made using this model will be less accurate compared to the models developed for normal strength concrete and grout samples. This is also indicated by the wide 95% confidence interval for prediction shown in Fig. 4.

4 SUMMARY AND CONCLUSIONS

The rapid chloride concentration measurement method developed under the SHRP was compared to the commonly used potentiometric titration method for determining chloride concentration of cement-based materials. Normal strength concrete, low strength flowable concrete, grout, and mortar mixtures were used. In general, analysis indicates that the results of both methods are well correlated for a wide variety of cement-based materials.

For normal strength concrete samples and grout samples used in this study, testing performed with 3.0 g samples indicated a very well correlation between the results (R^2 of 0.98). A statistically not significant intercept value and a significant slope value close to unity showed that the results obtained from both methods were almost the same. Neither the type of mixture, concrete or grout, nor the w/c of the mixtures did have an effect on the relation of the results. For 1.5 g samples addition of a constant to the results obtained from the rapid method was necessary to convert them to the results measured using the titration method. The slope was close to unity and the R^2 was 0.98.

For LSFC samples the results of both methods were again very well correlated but the slope and intercept of the model were statistically significant and they were different from zero and unity, respectively. This indicated that chloride results obtained from both methods were not similar for these samples and the simple linear regression model was necessary to convert the results. However, the R^2 of the model was 0.95 showing that a high amount of variation could be explained by the model.

To check the hypothesis that the chloride concentrations measured using the rapid method with the internal calibration will be more accurate for cement-based materials containing supplementary cementitious materials, mortar mixtures containing fly ash were tested. Analysis indicated that the results were highly correlated and the slope of the model was close to unity. However, the R^2 of the model was 0.89 which indicated that a lower amount of variation of the results could be explained by this model. Based on these results authors recommend to test a group of samples with both methods (titration method and the rapid method) to establish a conversion model when the rapid method is going to be used to measure the chloride concentrations of mixtures with supplementary cementitious materials.

REFERENCES

Herald, S.E., Henry, M., Al Qadi, I.L., Weyers, R.E., Feeney, M.A., Howlum, S.F., & Cady, P.D. 1993, *Condition Evaluation of Concrete Bridges Relative to Reinforcement Corrosion, Volume 6: Method for Field Determination of Total Chloride Content*, SHRP-S-328, Strategic Highway Research Program (SHRP), National Research Council, Washington, DC.

Clemeña, G.G., & Apusen C.M. 2002, *An Alternative Potentiometric Method for Determining Chloride Content in Concrete Samples from Reinforced Concrete Bridges*, Report VTRC 02-R18, Virginia Transportation Research Council, Charlotsville, VA.

11th International Conference on Durability of Building Materials and Components
Istanbul Turkey May 11-14, 2008

Fungal Colonization on Fiber Cement Exposed to the Elements in a Tropical Climate

Márcia Aiko Shirakawa [1]
Edson Yoshio Aihara [2]
Cleber Marcos Ribeiro Dias [3]
Christine Claire Gaylarde [4]
Vanderley Moacyr John [5]

T 11

ABSTRACT

This study describes a preliminary assessment of non-asbestos fiber cement samples exposed to the elements for forty months in a tropical climate. Fungal colonization was determined by culture, optical and scanning electron microscopy. Preliminary assessment of its correlation with quantitative colour change was carried out. A positive Pearson's coefficient (r = 0.9) was observed only between total fungal structures and color change on the reverse surface, but not on the surface exposed to the north**;** on the latter particulate material from the burning of fossil fuels contributed to the dark colour. *Cladosporium*, *Pestalotia/Pestalopsis* and *Trichoderma* were three main fungal genera detected on fiber cement exposed for 40 months in the tropical climate of São Paulo. Mycelia sterilia also had high frequency.

KEYWORDS

Fiber cement, Cellulose fibers, Fungal colonization, Natural weathering

[1] São Paulo University, Escola Politécnica, Dept. Construction Eng., São Paulo, Brazil, Phone +0055 11 3091 5248, Fax 11 3091 5544, shirakaw@usp.br
[2] Colégio Universitário Taboão da Serra, Taboão da Serra, Brazil, Phone + 0055 11 4788 7978, osaihara@terra.com.br
[3] São Paulo University, Escola Politécnica, Dept. Construction Eng., São Paulo, Brazil, Phone +0055 11 3091 5248, Fax 11 3091 5544, cleber.dias@poli.usp.br
[4] University of Portsmouth, Microbiology Research Laboratory, Portsmouth , United Kingdon, Phone + 44 07981 066615, Fax 0239384 2147, cgaylarde@yahoo.com
[5] São Paulo University, Escola Politécnica, Dept. Construction Eng., São Paulo, Brazil, Phone +0055 11 3091 5248, Fax 11 3091 5544, vanderley.john@poli.usp.br

1 INTRODUCTION

Fiber cement is a composite building material that can be used in a wide range of applications. Since asbestos is considered carcinogenic [Chiappino, 2006] there is a tendency to increase the use of asbestos free fiber cement composed of natural and synthetic fibers. These fibers increase strength and toughness of the composite hence they are extremely important to the mechanical performance of fiber cement products [Dias, 2005].

Cellulose fiber deterioration in the alkaline cement matrix has been considered the main problem of durability of fiber cements [Gram 1983, Sarja 1988, Bentur & Akers 1989]. Synthetic fibers like poly (vinyl (alcohol)) (PVA), on the other hand, have been considered durable in the cement matrix [Kalbskopf et al. 2002]. The main effects of fibers deterioration are embrittlement and decrease of mechanical strength.

Biodeterioration is not a frequent worry in fiber cement technology. Some researchers declare that the alkalinity of the matrix inhibits the deterioration of fiber cement products by this mechanism. De Souza et al. [1997] have studied composites of cement-bonded wood particleboard, which presents a high organic/inorganic ratio compared with conventional fiber cement formulations. These authors concluded that fungi and termites did not cause significant deterioration (weight loss) even after accelerated carbonation of composite. In this research the fungi studied were basidiomycetes (Phylum Basidiomycota).

In the current work the term fungi is designated to moulds (Fungi Imperfecti, also sometimes known as Deuteromycota); they are composed of filamentous structures called hyphae, which can differentiate and produce rounded forms called spores or conidia.

Fungi can grow on the surface of materials and cause dark discoloration. On roofs this can compromise the thermal comfort inside the buildings. However colour changes roof surfaces affect the thermal performance of the entire building, users comfort or energy consumptions, they also can affect urban microclimate due to spectral reflectance and infrared emmitance [Synnefa et al, 2006].

Cellulose is easily transformed by cellulolytic microorganisms including bacteria and fungi. Due to high alkalinity of fresh cement materials usually microorganism can not grow before carbonation occurs. There have been some patents registered for the incorporation of biocides into cellulose to prevent microbial attack on fiber cement. Nevertheless there is little literature describing the colonization of fiber cement in natural weathering conditions and which microorganisms are more frequent.

This study describes mould colonization of non-asbestos fiber cement composed of PVA and cellulose fibers exposed to the elements for forty months in a tropical climate, in São Paulo, Brazil.

2 MATERIAL AND METHODS

2.1 Materials

Table 1 presents the materials and the formulation (labeled PVA 14) that were used for the preparation of specimens. Six-millimeter length poly (vinyl (alcohol) (PVA) fibers, unbleached long cellulose fibers and newspaper waste were employed as reinforcement. Densified silica fume, ordinary Portland cement and limestone filler from the Brazilian market were also employed.

2.2 Natural Aging

Fiber cement specimens were exposed in São Paulo, a large industrial metropolis with a mean annual temperature of 19.5 °C, an annual rainfall of ~1500 mm, a mean relative humidity of 78% and

presence of urban and industrial pollution. These specimens were exposed in metallic racks facing to the true north with a slope of approximately 45° (Fig. 1). After 40 months of exposure they were submitted to fungal analysis.

Table l. Materials and fiber cement formulations [Dias 2005].

Materials	**Dry weight fraction (%)**
Portland cement	75.20
Limestone filler	12.72
Silica fume	6.68
PVA fibers	1.40
Unbleached cellulose fibers	1.20
Newspaper waste	2.80
	Volume fraction (%)
PVA fibers	3.00
Cellulose fibers	8.60

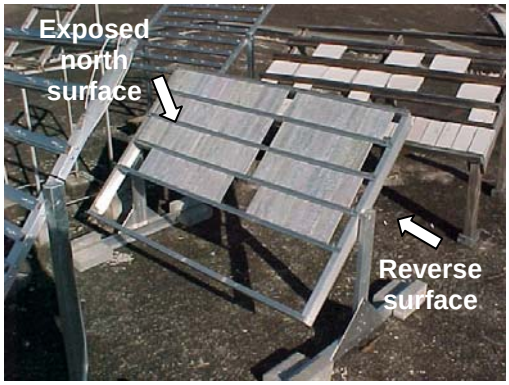

Figure 1. Rack with fiber cement specimens.

2.3 Fungal Sampling Method

Brush sampling was carried out by mean of a toothbrush previously packaged in aluminuim foil and sterilized for 15 minutes at 120° C at 1 atmosphere of pressure and dried for 2 days at 80° C. The toothbrush was moistened in saline sterile solution and brush sampling was performed five times in a clockwise direction. Afterwards toothbrushes were kept in closed tubes containing 10 mL of sterile saline solution (0.85%). Fungi were recovered from the brush in an ultra-sonic bath Thornton C/7, T7 for 10 minutes and diluted 1:10 in sterile saline solution. This suspension was used to evaluate culture and total fungal structures.

2.4 Quantitative Culture

Culture was carried out with 100 µL of the fungal suspension as described in 2.3 and inoculated by spread plate method in two Petri dishes containing Sabouraud Dextrose Agar. The plates were incubated at 25° C for 48-72 hours and colony forming units (CFU) were recorded.

2.5 Quantification of Total Fungal Structures by Neubauer Chamber[1]

Fungal suspensions as produced in Section 2.3 were analyzed in Neubauer chamber[1] in optical microscope in order to quantify total fungal structures (hyphae and spores).

[1] Chamber used in to count biologic structures

2.6 Color Analysis by Spectrophotometry

BYK Gardner Color-Guide 45/ 0.6805 equipment was used. According to CIE Lab, L* : Luminosity (black L*=0 to white L*=100); a*: red to green (positive and negative values respectively) and b*: yellow to blue (positive and negative values respectively) were analysed.

The total difference of colour was defined as $\Delta E = \sqrt{(\Delta L^*)^2 + (\Delta a^*)^2 + (\Delta b^*)^2}$, in this case the average values of L*, a* and b* of unexposed samples were used as initial reference color.

2.7 Scanning Electron Microscopy

The samples were submitted to SEM. A LEO Leika S440 microscope with an acceleration voltage of 20 kV and current of 150 mA was used to examine the fractured section and the surface of specimens. All samples received carbon coating in a Spputering Baltec SCD 050 equipment before SEM examination.

2.8 Statistical Analysis

Statistical analysis of fungal quantification was carried out according to the non parametric Mann-Whitney test (α=0.05%). Pearson's correlation was used to analyze differences between colour and fungal quantification. BioEstat program was used for both analyses.

3 RESULTS

Results of fungal growth measurements are presented in Table 2 for both viable fungi and total fungal structures. According Mann-Whitney test viable fungi is significantly lower than total fungal structures in both exposed and reverse surfaces of fiber cement.

Viable fungal colonization assessment by culture method, according Mann-Whitney test, was higher in reverse surface than exposed surface. However, for total fungal structures evaluation there is no significant difference between exposed and reverse surface.

Table 3 presents L*, a* and b* of unexposed samples which average is used as initial reference. Besides of this L*, a* and b* of exposed to north and reverse ones. This Table also presents total difference of colour (ΔE**)** between each measure and the average of unexposed samples as describes in 2.6.

Fungal relative frequency is presented in Table 4. *M. sterilia*, a group of fungi that does not produce spores, was found in high frequency (54% and 67% on exposed and reverse surfaces, respectively).

Table 2. Fiber cement quantification per 5.4 cm^2 of sampled area of viable fungi in CFU and total fungal structures.

Viable fungi CFU		*Total fungal structures*	
Exposed surface	*Reverse surface*	*Exposed surface*	*Reverse surface*
470	1990	1.7×10^6	1.3×10^6
350	1230	1.9×10^6	1.6×10^6
335	513	2.4×10^6	2.2×10^6
285	650	3.4×10^6	3.7×10^5
216	570	1.3×10^6	1.1×10^6
265	1680	8.5×10^5	1.0×10^6

Table 3. L*,a*,b* of unexposed samples, exposed to north, reverse surface and ΔE, after 40 months aging.

Unexposed			*Exposed to north*				*Reverse surface*			
*L**	*a**	*b**	*L**	*a**	*b**	*ΔE*	*L**	*a**	*b**	*ΔE*
63.15	-0.67	1.84	53.36	-0.27	4.56	7.30	54.15	0.10	3.24	6.28
59.64	-0.33	1.25	51.48	-0.05	5.58	9.42	53.18	0.04	3.30	7.24
54.80	-0.23	2.52	53.94	-0.10	4.56	6.76	53.73	-0.30	3.62	6.72
59.57	-0.76	2.11	54.15	-0.11	5.24	6.81	57.07	0.21	2.74	3.30
61.49	-0.62	3.09	53.29	0.24	5.45	7.71	53.64	0.10	2.96	6.75
63.40	-0.63	3.73	52.95	0.21	4.10	7.61	55.94	0.18	3.18	4.48
60.34	-0.54	2.42	53.19	-0.01	4.91	7.60	54.61	0.05	3.17	5.79

The last line in the Table 3 is the average of above values of the column.

Pearson's correlation was significant (r= 0.9) only between total fungal structures and total color difference on the reverse surface (Figure 2) after 40 months aging. There was no correlation between viable fungi (CFU) and colour diference on both surfaces.

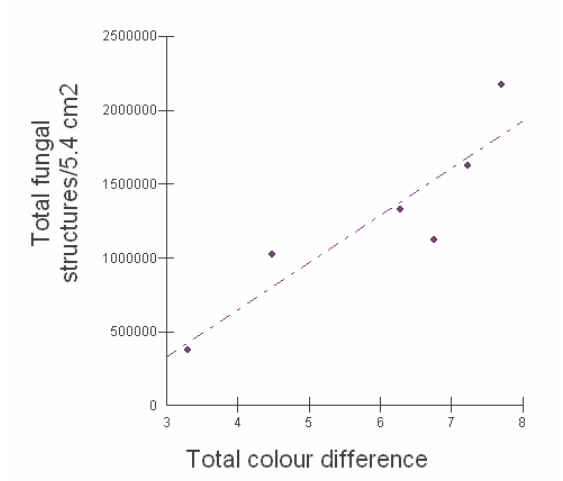

Figure 2. Diagram showing strong correlation between total fungal structures and color difference on the reverse surface (Pearson's correlation r=0.9).

Table 4. Relative frequency of viable fungi detected by culture.

	Exposed surface (%)	Reverse surface (%)
Cladosporium	31	67
Pestalotia/Pestalopsis	54	40
Trichoderma	31	27
Aspergillus	8	20
Nigrospora	23	0
Chaetophoma	23	7
Aureobasidium	8	20
Phoma	8	13
Alternaria	0	7
Monilia	8	0
Helminthosporium	8	0
Curvularia.	8	0
Fonsecaea	0	7

Scanning electron microscopy images obtained after 40 months aging are presented in Figures 3 and 4. Figure 3 (a) shows a fractured region of fiber cement**;** cellulose fibers are bigger and more irregular than PVA fibers. Figure 3 (b) shows fungal hyphae growing on cellulose fiber.

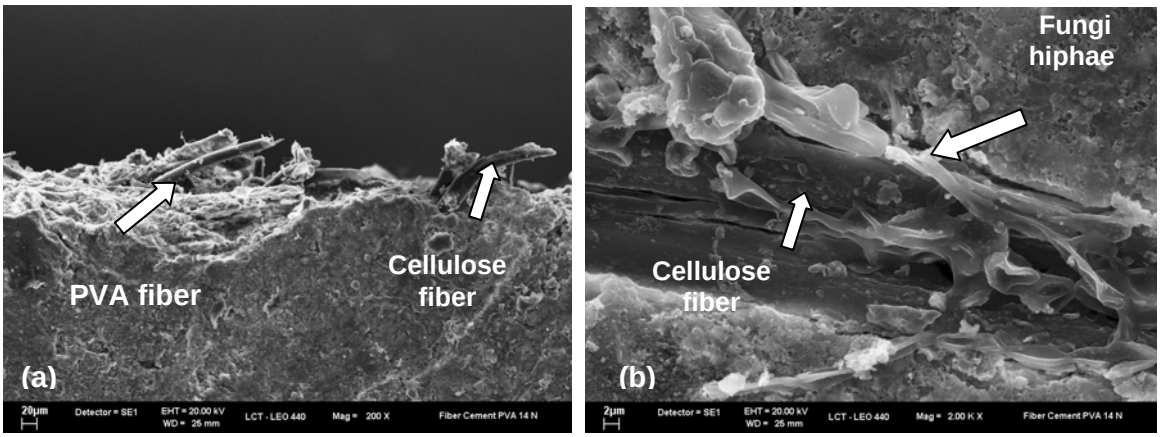

Figure 3. (a) Fractured sample after 40 months exposure, (b) Fungi colonization on cellulose fiber.

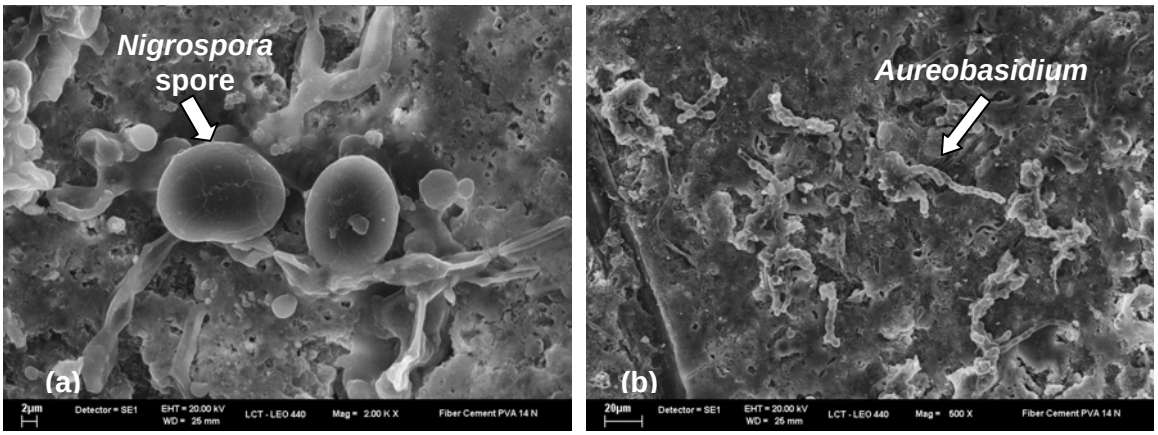

Figure 4. Fungal colonization on fiber cement matrix after 40 months exposure. Round structure is similar to *Nigrospora* spore (a). Structures are similar to *Aureobasidium* genus (b).

4 DISCUSSION

There is no correlation between total fungal structures quantified by Neubauer chamber in the optical microscope and viable fungi quantified by culture. Some portions of these fungal structures could be non viable and hence resistant to culture in the media due to environmental conditions like UV irradiation, temperature and desiccation**.** Another reason could be that the media used were not suitable for xerophilic fungal growth. In addition, some fungal structures detected by Neubauer chamber can be already dead.

As shown by scanning electron microscopy, in this preliminary assesment PVA fibers did not present fungal colonization. The cellulose fibers were colonized by fungi as well as the cement matrix.

In the surface exposed to the north irregular particles about 20% larger than fungal structures were found more often than on the reverse surface. The presence of particulate material from burning of fossil fuels is to be expected, since the natural aging station is located in São Paulo, the biggest city of Brasil with high pollution records.

Regarding L* (black L*=0 to white L*=100) measurement both north-exposed and reverse samples showed significant lower values in relation to unexposed reference ones, confirming the darker surface in relation to unexposed samples after aging.

Fungi can contribute to the darkening of fiber cement as well as particulate material from the burning of fossil fuels. Some species of *Trichoderma* are quoted in the literature as cellulolytic fungi [Persson, 1991] and they are found in a relative frequency of about 30%. Others relevant fungal genera detected in this work, such as *Cladosporium* and *Pestalotia/Pestalopsis*, are also being isolated in different building materials in Brazil. *Cladosporium* has also been described as a cellulolytic fungus [Abrha, 1992]. *Mycelia sterilia*, a non sporulating group, was found in high frequency.

As described above the focus of this study was not to investigate the degradation of fiber cement by fungi, but the influence of fungal colonization on the surface darkening of this material. Future studies will focus on cellulose colonization inside the specimens submitted to natural aging.

5 CONCLUSION

Fungi detected in the current work contribute to darkening of fiber cement since most of them are usually melanin producing and their structures like hiphae or spores are brown to black. Particulate materials from burning of fossil fuels, typical from urban areas, contribute to dark discoloration, mainly on the specimens' surface exposed to the north.

ACKNOWLEDGMENTS

The authors thank Conselho Nacional de Desenvolvimento Científico e Tecnológico (CNPq) and Fundação de Amparo à Pesquisa do Estado de São Paulo (FAPESP) for sponsoring this research and for the grants to M.A. Shirakawa and C.M.R. Dias.

REFERENCES

Abrha, B. & Gashe, B.A. 1992, "Cellulase production and activity in a species of *Cladosporium*", *World Journal of Microbiology and Biotechnology*, 8: 164-166.

Bentur, A. & Akers, A.S. 1989, "The microstructure and ageing of cellulose fibre reinforced cement composites cured in a normal environment", in: The *International Journal of Cement Composites and Lightweight Concrete*, 11(2):99-109

Chiappino, G. 2006, "Asbestos fibre dimensions and mesothelimoa", *Epidemiol Prev*.,30(4-5): 289-94.

De souza, M.R.; Geimer, R.L.& Moslemi, A. 1997, "Degradation of conventional and CO_2 injected cement-bonded particleboard by exposure to fungi and termites", *Journal of Tropical Products*, 3(1): 63-69.

Dias, C. M. R. 2005, "Aging effects on the microstructure and mechanical performance of fiber cements", *Thesis of University of São Paulo*, São Paulo, [In Portuguese].

Gram, H-E., 1983, *Durability of natural fibres in concrete*. Stockholm.

Kalbskopf, R.; De Lhoneux, B.; Van Der Heyden, L.; Aladerweireldt, L. 2002, "Durability of fiber-cement roofing products", in: *Inorganic-Bonded Wood and Fiber Composite Materials,* V8. Sun Valley.

Sarja, A. 1988, "Wood fibre reinforced concrete" in: *Natural Fibre Reinforced Cement and Concrete*, Blackie, London, pp.63-88.

Persson, I., Tejerneld, F. & Hahn-Hägerdal, B. 1991**, "**Fungal cellulolytic enzyme production: A review", *Process Biochemistry***,** 26: 65-74.

Synnefa, A., Santamouris, M. & Apostolakis, K. 2007, "On the development, optical properties and thermal performance of cool colored coatings for the urban environment", *Solar Energy*, 81(4):488-497.

Durability of the HPC Cured in Sulphate Environment

Rabah Chaid [1]
Raoul Jauberthie [2]
Mohamed Tahar Abadlia [3]
Abderrahim Bali [4]

T 11

ABSTRACT

The use of integral high performance concrete of the cementitious additions as the fly ash, the silica fume or the cementitious hydraulic slag increased considerably during two last decades. The works in HPC last longer and involve maintenance costs less low than those out of ordinary concrete. Moreover, the HPC uses less cement, which decreases the CO_2 emissions. A vaster use of the integral high performance concrete of the cementitious additions could thus involve benefit as well environmental as financial and build more durable works.

In the current state, research on the concretes with high performances in Algeria is especially centered on their formulations in order to produce concretes of better resistances and durable.

However, an optimal composition depends on several parameters, in particular on the choice of the ingredients. The effect of the cementitious additions and their smoothness remains little undertaken. This is why we propose in this work, to formulate of high performances concretes with and without cementitious addition. And, to treat the influence of the slag of the iron and steel plant of El-hadjar (Algeria), finely crushed and substituted for part of cement, on the physicomechanical characteristics of the elaborate concretes. The mode of conservation is the gypsum water (corrosive condition).

KEYWORDS

HPC, Slag, Durability, Sulphate.

[1] Laboratory of Mineral & Composite Materials, University of Boumerdes, Algeria 35000, Phone 213 78731284, Fax 213 24818915, chaidr@yahoo.fr
[2] Laboratory of Civil Engineering and Mechanical Engineering, INSA-Rennes, France 35043, Phone 33 23238314, Fax 33 23238314 raoul.jauberthie@insa-rennes.fr
[3] Laboratory of Mineral & Composite Materials, University of Boumerdes, Algeria 35000, Phone 213 24816408, Fax 213 24816408, abadlia_tahar@yahoo.fr
[4] Laboratory of Construction & Environment, ENP, Alger, Algeria 16200, Phone 213 21525303, Fax 213 21522973, balianl@yahoo.fr

1 INTRODUCTION

The concrete of high resistances to fact the object of many research, since strong a long time, from the very start of the century, the concretes of resistance higher than 50 MPa were obtained on building site, result very meritorious if one compares the quality of materials available at the time to that of cements and aggregates of today. However, for a few years, a renewed interest has appeared, in the whole world, for the concrete with high performances, obtained thanks to the use of thinners and silica smoke. The reason of this new reversal must be sought, makes some not only in the possibility of reducing the structures by an increase in the pressures in services, but rather in the improvement of the durability of material in service in chemically aggressive mediums [Mekki 2002].

The action of sulphated underground water offers the simplest case of an aggression giving rise to expansive new compounds starting from the components of cement. The calcium sulphatic combines with aluminates of cement to form a salt (the ettringite) or salt of Candlot $C_3A.3CaSO_4.32H_2O$, whose crystallization accompanied by expansion causes the cracking of the concrete. It facilitates the penetration of the aggressive agents to the reinforcements which are, in their turn attacked.

It is possible to modify the microstructure of the concrete by incorporating mineral products. These cementitious additions modify the microstructure of the concrete in term of physical and chemical characteristics. The pozzolanic mechanism of reaction of the cementitious additions can be briefly described like the reaction of silica with the lime released by the hydration of cement, in the presence of water. It results from it from the C-S-H with poor Ca/Si report/ratio. Although this reaction is prompt and early, it is limited by the quantity of water in the HPC.

The slag of blast furnace is a by-product of the manufacture of the cast iron in blast furnaces starting from flux and coke, iron ore (the oxides FeO, Fe_2O_3, Fe_3O_4 in variable proportions) possibly. One collects it liquid towards 1550°C above the cast iron. The vitrified slag, granulated is a product hydraulic, i.e. likely to give by basic activation, of the stable products of hydration. It is obtained by brutal cooling by water under pressure; it is a sand of granulometry 0/5 mm.

In the slag cements, the clinker is the principal activator of the slag; however the first produced hydrates will be those of the clinker; C-S-H and $Ca(OH)_2$ which uniformly cover the grains with the slag and the clinker ; thereafter the lime excess activates the hydration of the slag with a texture C-S-H similar to that of cements; it then results from it from calcium silicate hydrates and hydrated aluminates tetracalcic [Baron and Olivier [1997]; Jiang and Grandet [1989]].

What allows the solubilization of a new quantity of products until a concentration involving a new precipitation of hydrated compounds. It is this repetition of the cycle dissolution - concentration - precipitation (several years), which constitutes the catch and the hardening of the slag vitrified [Alexandre and Sebileau [1988].

Resulting precipitations are normally intended to seal the large pores; however, precipitations of the slag cements are fixed and impermeable whereas those of Portland cements are not it. Consequently the ordinary concrete is more porous than the concrete with the slag [ACI [1974]; Venuat [1971]].

[Sarkar *et al.* 1970] had shown that with a ground slag with a smoothness of 800 m^2/kg, one obtains a significant reduction of the heat of hydration of cement, a high-strength concrete and with more compact structure. [Péra *et al.*1988] showed that more the granulometry of the slag is high, better are its performances.

2 EXPERIMENTAL

2.1 Materials

2.1.1 The Cement

The *Portland cement* used is a CPA CEM I 52,5 of the factory Saint Pierre Lacour, whose chemical composition is deferred on table 1.

Table 1. Chemical composition of cement CEM I 52,5

Elements	*CaO*	*SiO_2*	*Al_2O_3*	*Fe_2O_3*	*MgO*	*SO_3*	*K_2O*	*Na_2O*	*IR*	*PF*	*CaO_l*
%	64,50	21,01	4,90	2,80	0,90	3,00	0,90	0,20	0,20	1,10	0,45

The mineralogical composition of this cement calculated by Bogue's method is as follows :
- C_3S ..... 65,94 %
- C_2S ..... 10,47 %
- C_3A ..... 8,24 %
- C_4AF ..... 8,52 %

2.1.2 The Slag

The slag used is a by-product of the manufacture of the cast iron, factory of El-hadjar ' Annaba'. It is a sand of granulometry 0/3 mm, granulated slag cooled with the jet of water, vitrified i.e. amorphous. Table 2 gives its chemical composition. It is tiny room powders some until obtaining a large surface specific compared to cement.

The slag of El-hadjar has the advantage of being rather acid (the CaO/SiO_2 report/ratio varies within the limits of 0,95 - 1,04); it is relatively stable. The result of the micro-analysis (figure 1) comes to confirm this assumption.

Table 2. Chemical composition of slag.

Elements	*CaO*	*SiO_2*	*Al_2O_3*	*Fe_2O_3*	*MgO*	*SO_3*	*K_2O*	*Na_2O*	*IR*	*PF*
%	39,77	41,69	7,05	1,41	5,49	0,15	0,44	0,10	0,12	0,11

Other physical properties: Specific surface = 8 500 cm^2/g.

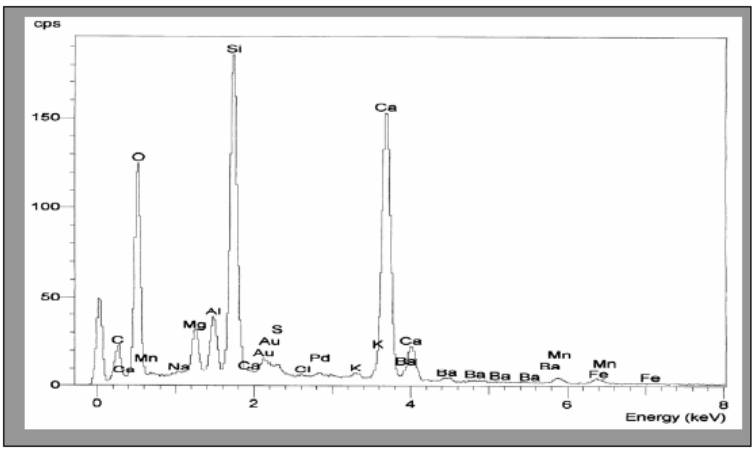

Figure 1. Micro-analysis (x2000) of slag.

In addition to its pozzolanic capacity, the slag with such a granularity (specific surface doubles cement), will ensure the thickening of the matrix : these particles can fit between the cement grains [Behim *et al.* 2002].

2.1.3 Aggregates

Obtaining the characteristics necessary for the concrete passes imperatively by the settling of optimal compositions of the various aggregates.

These aggregates for a great part are rolled: quaternary deposit of Unpleasant (Ille and Vilaine, France), primarily siliceous in the form of quartz and, for a weak part, crushed : corneal and metaquarzite.

For this work, after preliminary tests relating to as well the rheology of the mixtures of concrete as its crushing as a hardened material, the choice was concerned the aggregates of class 3/8 and 8/15.

As for sand used, it is a coarse river sand, whose fineness modulus is worth 2,47.

2.1.4 The Additive

The additive used is a plasticizing water reducer for concretes with high performances in conformity with standard *NF EN 934-2* provided by company SIKA.

The SIKAMENT FF 86 allows the concrete clothes industry very weak report/ratio W/C having mechanical resistances very high in all term and in particular to the youths.

2.2 Formulation

The final composition of High Performances Concrete (HPC) without addition and that of High Performances Concrete with addition of slag (HPCS), after optimization [Chaïd *et al.* 2004] are reported on table 3.

Table 3. Compositions of concretes with and without slag.

Components	*Cement*	*Sand*	*Gravel 3/8*	*Gravel 8/15*	*Water*	*Additive*	*Slag*
(HPC)	500 kg/m^3	573 kg/m^3	130 kg/m^3	915 kg/m^3	150 l/m^3	8 l/m^3	-
(HPCS)	425 kg/m^3	573 kg/m^3	130 kg/m^3	915 kg/m^3	150 l/m^3	8 l/m^3	75 kg/m^3

The procedure of malaxation to make the concrete specimens is the following :

1 - The aggregates and the binder (cement + slag) are mixed dry during for one minute.

2 - The mixing water is added with a third of the volume of superplastifiant and malaxation continues for 2,5 mn.

3 - The remaining superplastifiant is added with a final malaxation of one minute.

The concrete specimens are preserved in their mould in wet place (20°C, 95% HR) during 24 hours. They then undergo immersed in gypsum water at 20° C until the fixed terms.

The physical, mechanical and microstructural characteristics of the concretes with and without addition of slag are compared.

3 FINDINGS AND ANALYSIS

3.1 Densities and mechanical resistance

Figure 2 shows the evolution of the density of the various concretes preserved in gypsum water. One note a thickening of the concrete with slag addition. Indeed, the high grinding of the slag, combined with its interaction with Portlandite to form no soluble calcium hydrosilicates, favors the increase of the compactness of the hardened concrete. This explains the increase of its density compared to the control concrete.

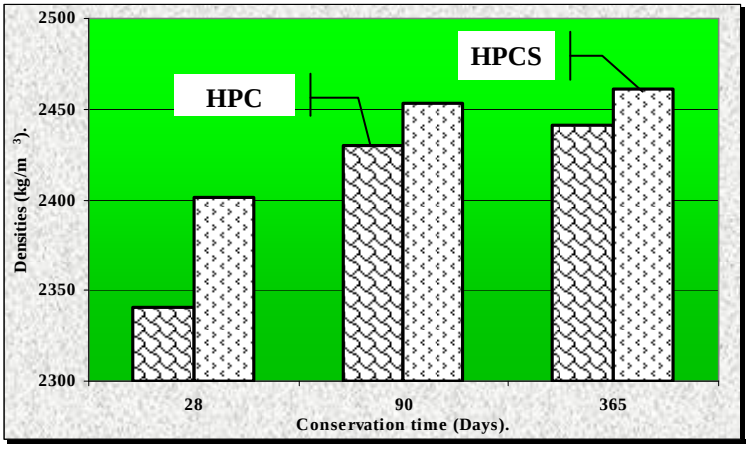

Figure 2. Evolution of the densities of the concretes according to the cured time.

Figure 3 shows the increase in resistance, with respect to the period of conservation in gypsum water. It is definitely higher for the concrete with the addition of slag (HPCS). After 365 days of conservation, the constraint reached is about 100 MPa, whereas for the concrete without addition (HPC) it is only 69 MPa.

The thorough grinding of the slag supported the increase in the compactness of the HPCS, which explains the increase in its density compared to the HPC. On the physicomechanical level, the slag reacts by its fineness and its pozzolanic activity, thus generating a more coherent skeleton and consequently a more resistant and more durable concrete in gypsum water.

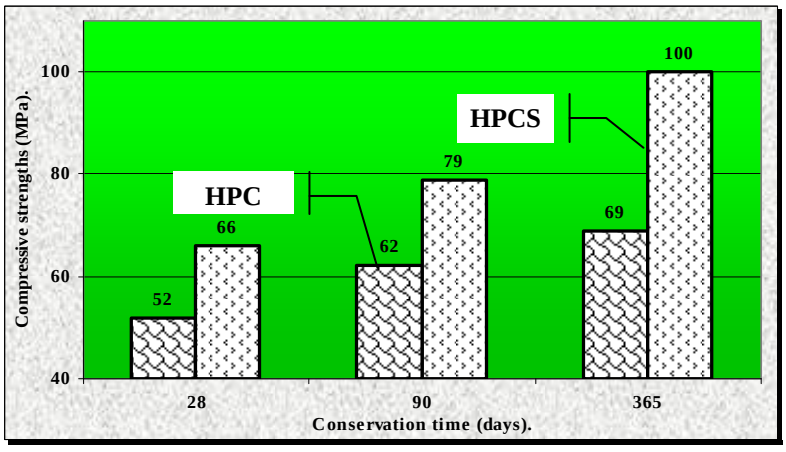

Figure 3. Evolution of the compressive strengths according to the cured time.

3.2 Internal Structure

The reactions known as pozzolanic are faster because of the very low dimension of the reactive particles. On the one hand the newly formed products are more easily dispersed or better set out in materials; on the other hand their composition is more favorable to the incorporation of alkaline in their crystalline structure.

The reactions known as pozzolanic are faster because of the very low dimension of the reactive particles. On the one hand the newly formed products are more easily dispersed or better set out in materials; on the other hand their composition is more favorable to the incorporation of alkaline in their crystalline structure.

The microstructure of cement with addition of slag is characterized by a dense matrix with a growth of the C-H-S on the surface of the particles of the slag. Compared with cement, products of hydrations of the cement mixture - slag also have a weak Ca/Si ratio but rich in magnesia and alumina [Sarkar and XU [1996].

The observation under the scanning electron microscope (Figure 4) enabled us to examine the microstructure of the hydrates formed within the concretes after 365 days of hardening. A microstructure relatively improved in the concretes with addition of slag was noticed with interfaces relatively more densified and rich in C-S-H, characteristic of the high quality concretes.

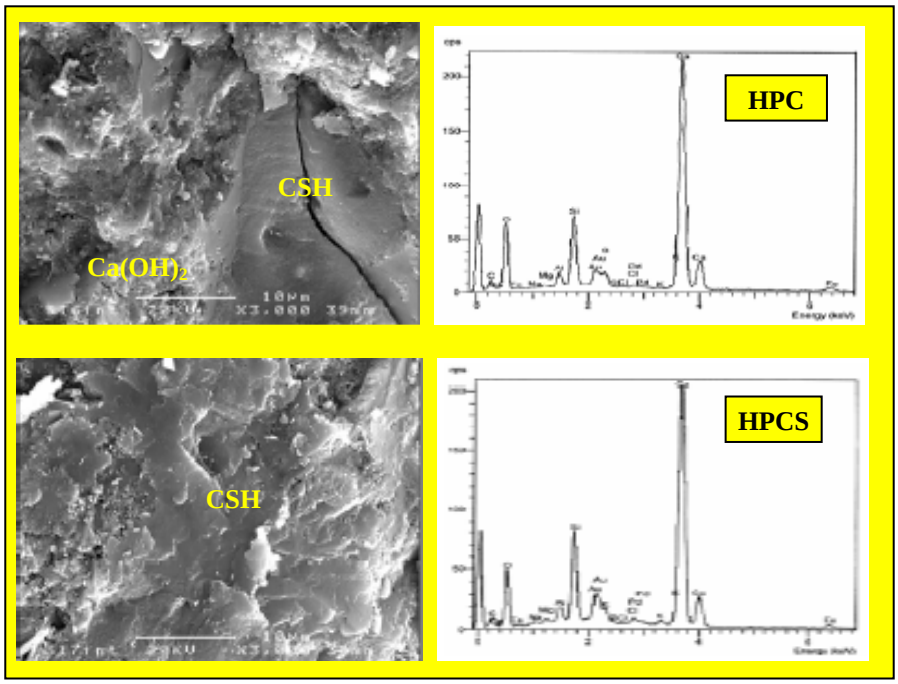

Figure 4. SEM Observation of the internal structural of concrete specimens after 365 days of curing.

However, one can notice some plates of the lime and the presence of needles of ettringite in the cavities of the HPC. For the HPCS, the matrix having become very dense, it does not support the blooming of certain products, which thus find a free field only in the bubbles of air and the interfaces stamps aggregates.

The analysis by x-ray diffraction (Figure 5) illustrates the various crystalline phases. Which are identical for the concretes with and without slag. However, the hydration of the anhydrous compounds of the slag concrete is considerably slowed down, contrary to that of the concrete without addition.
This is the consequence of the thickening of the matrix. By supporting the formation of a more compact skeleton (structure) and consequently of much higher chemical resistances.

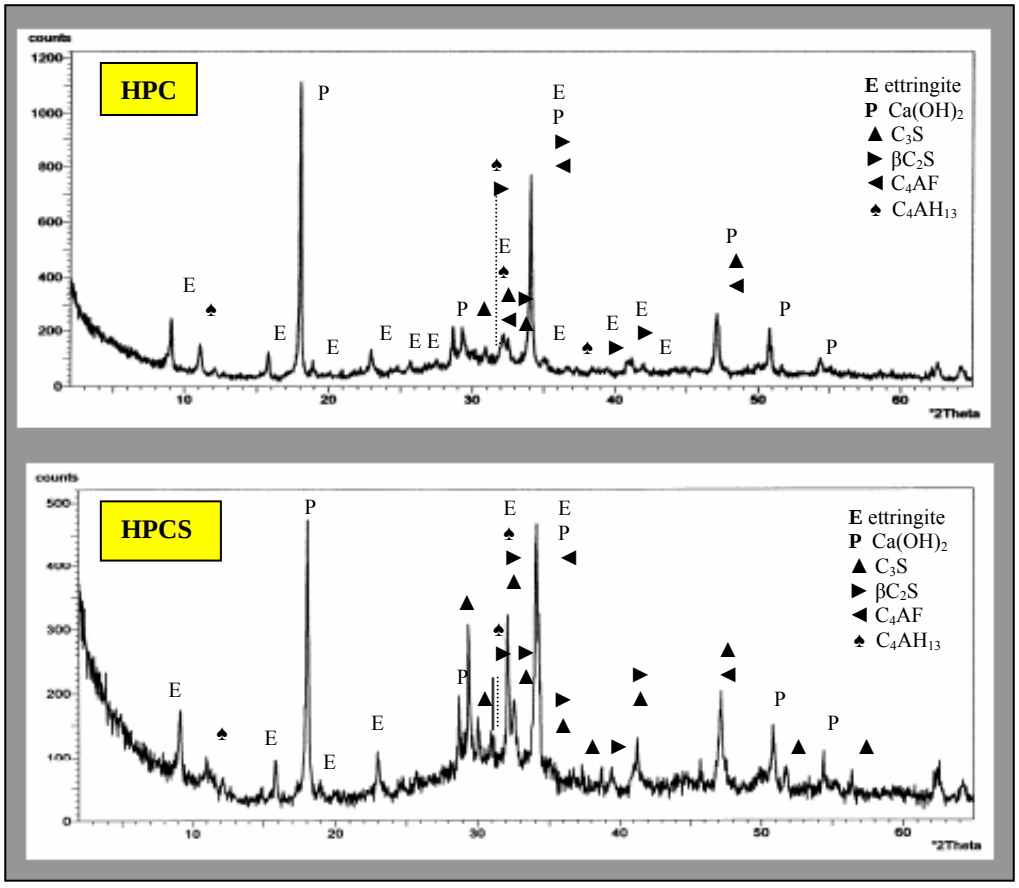

Figure 5. Radiogram of different concretes cured in gypsum water.

In addition, the incorporation of the finely crushed slag also generates a granular effect related to the induced modifications on compactness of the granular skeleton. This effect acts during the hardening of the concretes and influences the extent of the modifications made on the porosity of the cementitious matrix. This explains the high propagation velocities of wave measured on the slag concrete specimens compared to the concrete without addition (Figure 6), on various terms with an increasing rise and this in spite of the character prejudicial of the medium of conservation (gypsum water).

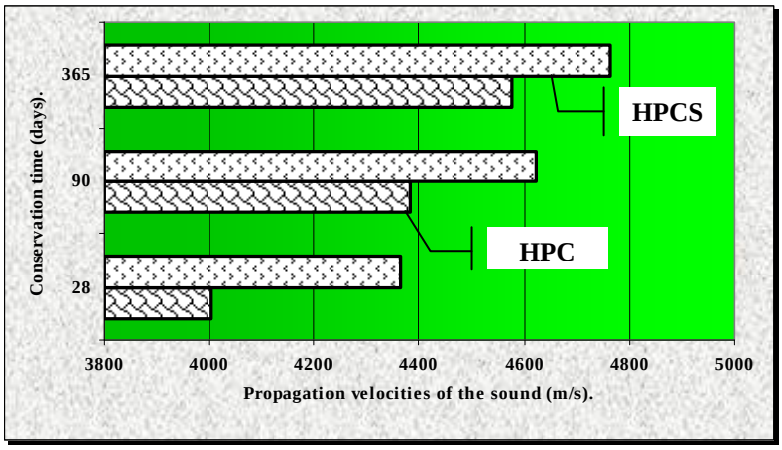

Figure 6. Evolution of propagation of sound velocities through the concretes according to the cured time.

3.3 Concrete Skin

On the surface of the specimens preserved in gypsum water one observe an important deposit of gypsum needles (Figure 7), covering almost all the surface of the concrete of control unlike that of the slag concrete where the presence of the calcite crystals on the surface of the concrete is relatively more noticed compared to the concrete of control.

In addition, one note that the slag which presents the strongest contribution to the mechanical resistance also contributes in reducing the degradation of the external surface of the concrete specimens preserved in gypsum water and consecutively contributes to increase their chemical resistance.

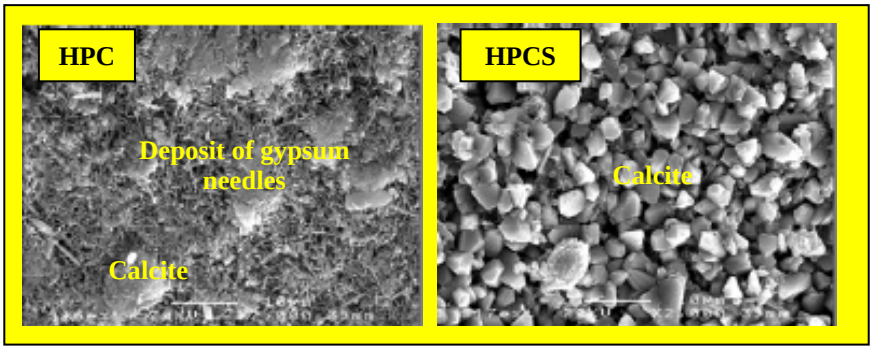

Figure 7. SEM observation of the surface of concrete specimens cured in gypsum water.

In other words, the addition of slag contributes to the reinforcement of the connections in the cementitious matrix and also contributes to its chemical resistance by the formation of an impermeable layer made up of calcite crystallites.

A considerable deposit of the gypsum needles observed on figure 7 for the concrete of control puts in danger the permeability of the skin of concrete without addition of slag, this yield weaker chemical resistance.

CONCLUSION

The study undertaken in this communication deals with the study of degradation of the concretes with and without addition of slag by the sulphates ions.

The thorough grinding of the slag has favoured the increase in the compactness of the concretes. This explains the increase in their resistance compared to the resistance of the concrete without addition.

The observation by the scanning electron microscope enabled us to examine the microstructure of the hydrates formed within the concretes after of 365 days of hardening. A microstructure relatively improved in the concretes with addition of slag has been noticed with interfaces relatively more densified and rich in C-S-H.

The incorporation of the finely crushed slag also generates a granular effect related to the modifications induced on compactness of the granular skeleton. On the physicochemical aspect, the slag entails the formation of a concrete skin relatively more impermeable and, consequently a more durable concrete.

In conclusion, it is important to emphasis on the fact that the influence of the fineness of the slag becomes more and more significant, when one seeks to manufacture more powerful concretes.

REFERENCES

A.C.I, *Fall convention REVEW journal American concrete institute*, 1974.

Alexandre, J. & Sebileau, J-L. 1988, 'Le laitier de haut fourneau', *Centre Technique et de Promotion des Laitiers (C.T.P.L)*, Paris, p. 340.

Baron, J. & Olivier, J-P. 1997, 'Les bétons – bases et données pour leur formulation', *Association technique de l'industrie des liants hydrauliques*, Éditions Éyrolles, Paris.

Behim, M., Redjel, B., Jauberthie R. 2002, 'Réactivité des laitiers de haut fourneau d'Annaba en substitution partielle du ciment' , *Journal de Physique IV*, Pr6 - vol. 12, Sept., 223-228.

Chaïd, R., Jauberthie, R., Bali, A. & Abadlia, M-T. 2004, 'Formulation des bétons de hautes performances avec des ajouts cimentaires locaux', *Revue : Algérie Equipement*, n°38, ISSN 111-5211, janvier 2004, p. 3-7.

Chaïd, R., Jauberthie, R. & Rendell, F. 2004, 'Influence of a natural pozzolana on the properties of high performance mortar', *Indian Concrete Journal*, volume 78, number 8, August 2004, p 22-26, ISSN : 0019-4565.

Mekki, B. 2002, 'Étude de l'endurance du matériau composite, polymère béton armé avec des fibres', *Algérie Équipement*, n° 36, décembre 2002, p. 15-18.

Jiang, S-P. & Grandet, J. 1989, 'Évolution comparée des porosités des mortiers de ciments au laitier et mortiers des ciments portland', *Cement and concrete research*, vol. 19, p. 487-496.

Lea, F-M. 1970, 'Pozzolans and pozzolanic cements', *In :The chemistry of cement and concrete*, par F-M. Lea, Great Britain : Edward Arnold, p.414-453.

Pera, J. & Rols, S., Chabannet and Ambroise J. 1998, 'Influence of cement the type on the resistance on concrete to an agricultural environment', *In : Sidney Diamond Symposium on Materials science concrete*, Edited by Menashi Cohen, Sidney Mindess and Jan Skalny, p. 419-431.

Sarkar, S-L. & XU, A. 1996, 'Why use mineral admixture in high performance concrete', *In : L'Industria Italiana del cemento*, October 1996, p. 715-726.

Venuat, M. 1971, 'Adjuvant et traitement des mortiers et bétons' *1ere éd. Venuat*, Paris, p. 40-45.

Effects of Ternary Blended Binders on Chloride Diffusivity of Concrete

Özkan Şengül [1]
Mehmet Ali Tasdemir [2]

T 11

ABSTRACT

There are several studies on the microstructure, production, durability and mechanical properties of high strength concrete using superplasticizers and mineral particles such as fly ash, ground granulated blast-furnace slag and silica fume. In recent years, for ultrafine particles it was shown that the filler effect is more important than its pozzolanic effect. Thus, the fineness of the pozzolan is very important for the modification of aggregate-cement interface zone in high strength concretes. The main objective of this study is to investigate the combined effects of finely ground blast furnace slag and fly ash on the resistance of concrete against chloride penetration. In the experimental study 16 concrete mixtures were prepared in which ordinary portland cement was replaced by the ground fly ash and ground slag up to 60 % with the increments of 10%. The average particle size of both the fly ash and slag used were relatively low with Blaine fineness of 600m^2/kg. Water/binder ratio was kept constant in all concrete mixtures. Chloride diffusivity of the concretes were obtained using a non-steady state migration testing. Electrical resistivities of the concretes were also recorded. The results indicate that concretes containing the pozzolanic materials show a significantly better resistance against chloride penetration compared to that of the pure portland cement concrete. Electrical resistivities obtained with the two electrode method were significantly higher for the pozzolan blended binders.

KEYWORDS

Ternary blended binder, Pozzolan, Durability, Chloride diffusivity, Electrical resistivity

[1] Istanbul Technical University, Faculty of Civil Engineering, Istanbul, Turkey 34469, Phone +90 212 2853756, Fax 212 2856587, osengul@ins.itu.edu.tr
[2] Istanbul Technical University, Faculty of Civil Engineering, Istanbul, Turkey 34469, Phone +90 212 2853855, Fax 212 2853336, tasdemirme@itu.edu.tr

1 INTRODUCTION

Poor durability; and as a result uncontrolled and short service life, is a major concern for structures and can lead to great economical losses. One of the effective ways of minimizing the chloride diffusivity of concrete is to substitute a part of Portland cement by pozzolanic materials which are fine particles and can react with calcium hydroxide at ordinary temperatures to form calcium silicate hydrates. The most widely used pozzolanic materials are fly ash and granulated blast furnace slag which are industrial by-products.

Fly ash is a by-product of the combustion of coal in thermal power plants for electricity production. It is also known as pulverized fuel ash. It is removed by the dust collection system as a fine particulate residue from the combustion gases before discharging into atmosphere. Fly ash is the most common artificial pozzolan worldwide. It is estimated that about 450 million tons of fly ash is produced worldwide annually, but only about 6 percent of the total available fly ash is used as a pozzolan in blended cements or in concrete mixtures [Mehta, 2000]. There are twelve active coal-burning power plants in Turkey [Bayat, 1998] and the annual fly ash production capacity in the country is about 15 million tons [Tokyay, 1998]. Fly ash includes meta-stable alumino-silicates that react with calcium ions, in the presence of moisture and lime to form silicate hydrates. The reaction of fly ash depends on the breakdown and dissolution of the glass phase which occurs when the pH value of pore solution is higher than 13 [Fraay, 1989]. The increase in the alkalinity of the pore water is because of the hydration of portland cement. The amount of CH formed during the first days is not enough for the dissolution of the glass phase of fly ash and because of this, the fly ash is usually considered inert during the early days of hydration. Fly ash can be utilized as a blending component in blended cement or can be added separately during the concrete production.

Ground granulated blast-furnace slag is a by-product of iron production. During the iron production process about 300 kg of slag is obtained for each ton of pig iron [Neville, 2004]. In production plants with older technology, however, the amount of slag obtained is usually higher. About 100 million tons of slag is produced annually worldwide but only a very small fraction is utilized. Today slag is widely used in Europe as a component in blended cements but the degree of usage varies significantly between different countries. Netherlands, for example, utilizes about 90 % of its slag production [Regourd, 2004] and slag cement has a market share of about 60 % in the country [Bijen, 1996]. The pozzolanic reaction of the blast furnace slag is more rapid when compared to that of the fly ash [Bijen, 1996]. For the dissolution of the glass phase of blast furnace slag, pore water pH of about 12 is enough and this alkalinity level occurs in a short period after mixing the slag – portland cement blend with water. This more rapid reaction is one of the factors causing a higher early strength of slag concretes.

By using pozzolans in concrete with higher amounts, it is possible to obtain better properties than normal concrete. Replacing high amounts of portland cement by pozzolans, however, may have some drawbacks such as low early strength or high early permeability. In order to overcome the disadvantages of using pozzolans in high amounts, pozzolanic reactions can be increased using very fine paricles and different pozzolans in combination.

The main objective of this study was to investigate the combined effects of finely ground blast furnace slag and fly ash on the resistance of concrete against chloride penetration. In the experimental study, 16 concrete mixtures were prepared in which ordinary portland cement (OPC) was replaced by the ground fly ash and ground slag up to 60 % with the steps of 10%.

2 EXPERIMENTAL

2.1 Materials

The same ordinary Portland cement (PC 42.5), finely ground fly ash and finely ground blast furnace slag were used in the concretes. The 7- and 28-day compressive strengths of the standard RILEM-Cembureau cement mortars were 45.8 MPa and 57.3 MPa, respectively. The fly ash used in this study was brought from Catalagzi power plant, which is located in the northwest coast region of Black Sea in Turkey. The Blast furnace slag was obtained from Karabük iron production plant. The fly ash and blast furnace slag were ground in a laboratory ball mill. The original Blaine fineness of the fly ash was 222 m^2/kg and was increased to 604 m^2/kg by grinding. The ground blast furnace slag used in this study also had a Blaine fineness of 600 m^2/kg.

2.2 Mixture Proportioning

In the study, 16 concrete mixtures were prepared in which ordinary portland cement was partially replaced by the ground fly ash and slag up to 60 % with the steps of 10%. Water/binder ratio was 0.35 and kept constant in all the mixtures. In all concretes, partial replacement of cement by fly ash and slag was made on one to one weight basis. Portland cement concrete without any pozzolan was also produced for comparison. Basalt type coarse aggregate was used in all concretes in order to obtain better concrete strengths [Sengul et al. 2002]. The aggregates were washed and used in saturated air-dry state. The grading curve of concrete aggregate was chosen between ISO A32-B32 and closer to B32. The aggregate grading, water-binder ratio, and the maximum particle size were kept constant in all concrete mixtures. A superplasticizer was used to maintain approximately the same slump. The mixture proportions are shown in Table 1.

Table 1. Compositions of the concretes containing ground fly ash and slag.

Mixtures	*Cement, kg/m³*	*Slag, kg/m³*	*Ground Fly Ash, kg/m³*	*Water, kg/m³*	*S.plasticizer, kg/m³*	*Aggregates, kg/m³*	*Unit weight, kg/m³*	*Slump, cm*
100 PC	472	0	0	165	5.2	1816	2459	19
20S	379	95	0	166	5.3	1816	2462	23
10S10F	377	47	47	165	4.8	1792	2442	21
20F	377	0	94	165	5.2	1793	2435	19
40S	286	190	0	166	5.2	1820	2467	20
30S10F	282	141	47	164	4.8	1792	2431	21
20S20F	282	94	94	164	5.2	1785	2424	20
10S30F	283	47	142	165	5.2	1781	2423	22
40F	283	0	189	165	5.4	1773	2415	21
60S	190	285	0	166	5.1	1808	2456	21
50S10F	189	236	47	165	5.0	1790	2432	19
40S20F	190	190	95	166	5.0	1798	2446	22
30S30F	188	141	141	164	4.9	1765	2402	21
20S40F	188	94	188	164	4.3	1761	2401	20
10S50F	187	47	234	163	5.2	1746	2383	21
60F	188	0	282	165	5.4	1750	2391	22

Concretes were coded as follows; PC shows the concrete with ordinary portland cement, xySwzF defines the concretes with pozzolan replacements where; S shows slag and F: the fly ash. xy and wz represent the replacement amounts for slag and fly ash, respectively. For example 40S20F represents the concrete with 40% slag and 20% fly ash. All mixtures were prepared in a laboratory mixer with vertical rotation axis by forced mixing. All the specimens were demolded after 24 hours, stored in a water tank saturated with lime at 20°C until the testing day.

2.3 Testing Procedures

Chloride diffusivity of the concretes were measured according to NT 492 which is a non-steady state migration testing. Concrete disc specimens of 100 mm in diameter and 50 mm thickness were used for the test. Electrical resistivity of the concretes were also recorded. Some mechanical properties of the specimens were also obtained. Mechanical properties of the concretes were obtained at the ages of 7, 28 and 180 days. Due to limited amount of specimens, chloride diffusivity and electrical resistivity tests were carried out on only one year old specimens. Pozzolanic reaction continues for a long period and diffusivity testing carried out at later ages indicates the potential diffusivity that can be achieved. For the same materials and similar mixture proportions, resistance to chloride ion penetration at 28 and 90 days were given in another study [Şengül et al., 2003].

3 RESULTS AND DISCUSSION

3.1 Chloride Diffusivity

Chloride diffusivity of the concretes produced with ternary blend of ordinary portland cement, ground fly ash and slag are given in Figures 1 and 2. For a clearer and easier evaluation of the chloride diffusivity of the concretes, the results obtained for different replacement ratios are presented together with that of the portland cement concrete without pozzolan.

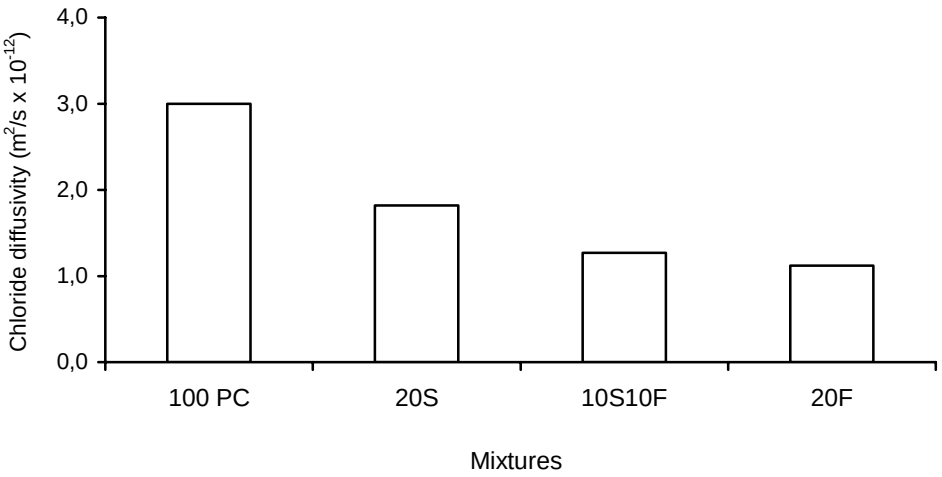

Figure 1. Chloride diffusivity of the mixtures containing 20% pozzolans.

As seen in the figures, partially replacemenet of portland cement by fly ash or blast furnace slag improves the chloride diffusivity of the concrete substantially. The chloride diffusivity of the portland cement concrete is $3.0x10^{-12}$ m^2/s, but it drops to $1.8\ x10^{-12}$ m^2/s for the concrete produced with 20% slag (20S) and $1.1x10^{-12}$ m^2/s for the mixture with 20% fly ash (20F) replacement, respectively. As the replacement amount increases lower diffusivity values are obtained. For example, the diffusivities of the mixtures containing 40% and 60% slag (40S and 60S) are $1.4x10^{-12}$ m^2/s and $1.1x10^{-12}$ m^2/s, respectively.

The test results indicate that, for a given replacement ratio, the fly ash used in the study is more effective than the slag in reducing the diffusivity and this reduction is more significant for the replacement ratio of 20%. For each replacement ratio, the mixtures containing the highest amount of the fly ash have the lowest chloride diffusivity. Although the concretes containing less amounts of fly ash have slightly higher diffusivities, the values for the various mixtures were close to each other. As seen in the Figures 1 and 2, mixtures containing ternary blends of cement, slag and fly ash performed similar to the binary blended mixtures.The chloride diffusivity test was carried out on one year old

specimens which were cured in water and extensive pozzolanic reaction took place during this period which reduced the diffusivity further. As a result of the long pozzolanic reaction, the difference in the diffusivity of the fly ash and slag concretes become smaller.

The lower chloride permeability of the concretes with high volume pozzolans is a result of a denser microstructure. The pozzolanic reaction may cause lower amount of capillary pores and clogging of the pores, which reduce the chloride ion transport in concrete [Li and Roy 1986]. Improvement of the aggregate – cement paste interface by the pozzolanic reaction may also play a role in decreasing the chloride ion permeability. Better chloride ion resistance of high volume fly ash concretes was also shown in other studies [Sengul et al. 2005; Zhang et al. 1999]. The ground fly ash and slag used in this study has a high fineness which may have contributed to obtaining lower chloride ion permeability [Dhir and Jones 1999].

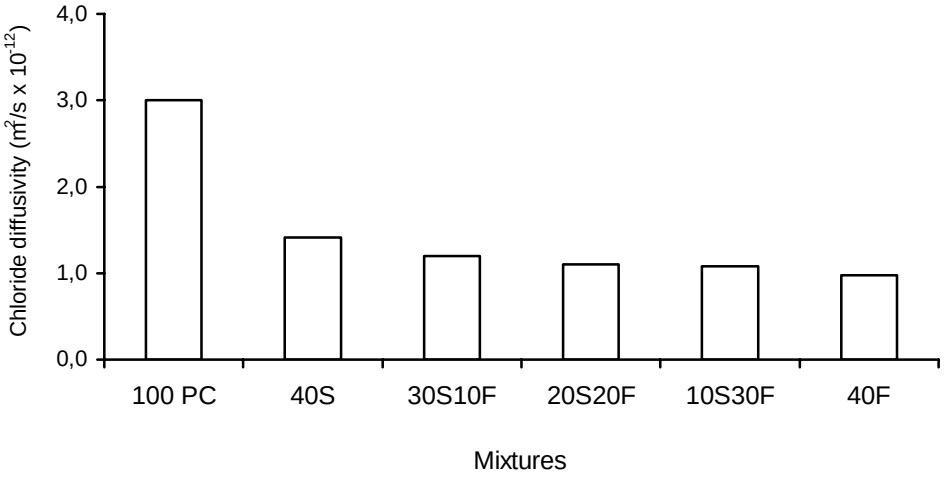

Figure 2. Chloride diffusivity of the mixtures containing 40% pozzolans.

3.2 Electrical Resistivity

Electrical resistivity of the concretes obtained by the two-electrode method are presented in Figures 3 and 4. As expected, the resistivity of the concretes containing slag or fly ash are substantially higher compared to that of the pure Portland cement concrete. For example, the increases in resistivity are about 65% and 250% for the mixtures containing 20% slag (20S) and 20% fly ash (20F), respectively (Figure 3). With the increase in the replacement ratio, higher electrical resistivities were obtained. For example, the electrical resitivity of the mixture containing 20%, 40% and 60% slag are 65%, 140% and 270% higher than that of the control mixture. Most significant increase in the resistivity was obtained for the mixture containing 60% fly ash which is about 8 times higher than that of the portland cement concrete (Figure 4). Test results indicate that for a given replacement ratio, fly ash is more effective in obtaining higher resistivity. As illustated in the figures, for the ternary blended mixtures resistivity increased slightly with the fly ash amount.

Electrical resistivity is a material property and can be defined as the resistance of concrete to an electrical current. Electrical current is carried by the dissolved ions in the pore solution and the factors affecting the pore structure of concrete also affect the resistivity of the concrete. As illustrated in the Figures 1 to 4, there is a good aggrement between the diffusivity and resistivity values obtained. For example, the portland cement concrete which has the highest chloride diffusivity but the lowest electrical resistivity. However, the mixtures containing pozzolans have lower diffusivity but higher resistivity. Based on these test results, it may be concluded that electrical resistivity can be used as an indication of the diffusivity of concrete.

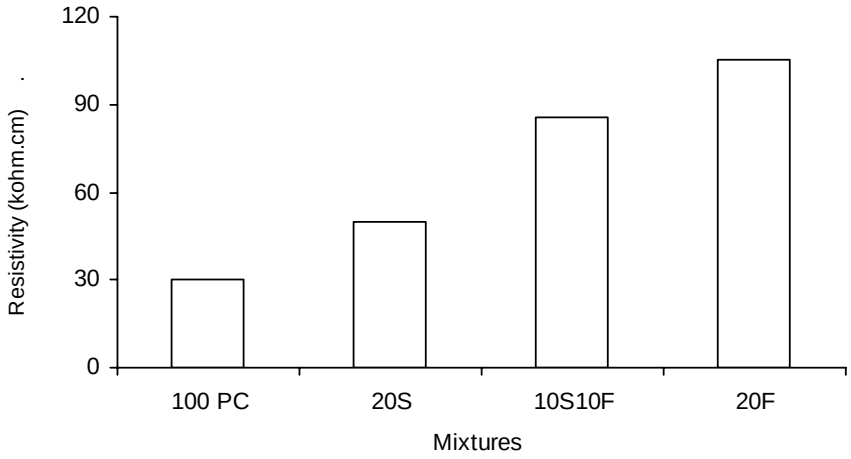

Figure 3. Electrical resistivity of the mixtures containing 20% pozzolans.

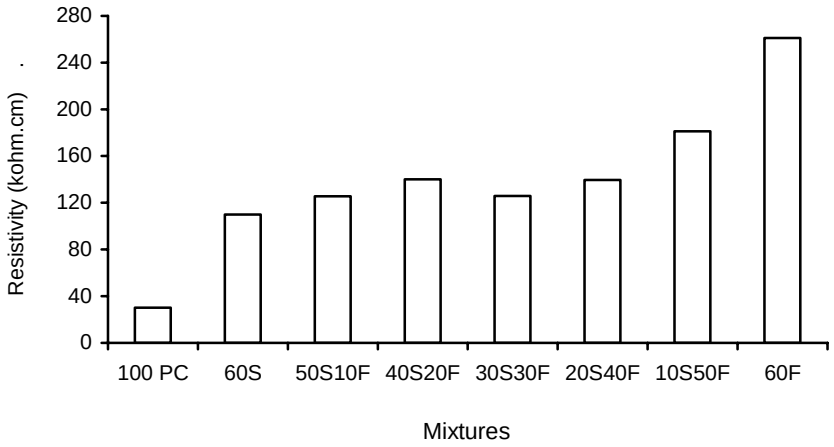

Figure 4. Electrical resistivity of the mixtures containing 60% pozzolans.

3.3 Mechanical Properties

Mechanical properties of the concretes are shown in Table 2. Compressive strength tests were carried out on the specimens at the ages of 7, 28 and 180 days. At the 20% replacement level and age of 7 and 28 days, there are slight decreases in the strengths of the concretes containing slag or fly ash. At the age of 180 days, however, the concretes produced with 20% pozzolans perform better. Similar results were also recorded for the mixtures containing 40% pozzolans. For the concretes containing 60% pozzolanic materials, at the age of 7 days, concrete strength decreased with the increase in fly ash content. Compared to portland cement concrete, concrete cast with 60% fly ash have about 55% lower strength at the age of 7 days. Although this strength reduction is substantial, the strength is 29.4 MPa. Strength decreases with the increase in fly ash content was observed also for the 28 and 180 days. The test results obtained indicate that for obtaining higher compressive strength, the slag used in this study is more effective than the fly ash used.

Modulus of elasticity and brittleness index of the specimens were obtained at the age of 28 days. Test results indicate that modulus of elasticity of the concrete is not affected significantly at the 20% and 40% replacement levels. For the 60% replacement level, however, the modulus elasticity decreased slightly with increasing fly ash content. The lowest value was obtained for the 60% fly ash concrete which is about 16% lower than that of the portland cement concrete. Test results indicate that the brittleness index increases with compressive strength. Brittleness index is an indication of the strength of aggregate – cement interface and a higher brittleness index value represents a stronger interface.

This result may be attributed to the modified interface in these concretes. As the inteface becomes more dense and homogeneous, mechanical properties and also permeability of this region is improved. The permeability of concrete depends on the permeability of the cement paste phase and also that of the interface. As the interface becomes less permeable, the permeability of the concrete decreases. Thus, the brittleness index can indirectly indicate the permeability of the concrete. For the concretes containing pozzolans, the brittleness index decreases with the increase in fly ash content. Compared to the slag, the slower pozzolanic reaction of the fly ash can be responsible for the slightly lower brittleness index. For all the replacement levels, however, the brittleness index of the concretes containing slag and fly ash are higher than that of the portland cement concrete.

Table 2. Mechanical properties the concretes.

Mixture	Compressive strength (MPa)			Splitting strength at 28 days (MPa)	Modulus of elasticity at 28 days (MPa)	Brittleness index at 28 days
	7 days	28 days	180 days			
100 PC	65.3	74.5	80.0	8.9	40700	2.86
20S	62.5	74.8	83.3	8.6	42300	4.94
10S10F	58.8	73.8	83.8	9.7	40700	3.94
20F	61.3	71.7	84.8	9.5	41100	3.92
40S	54.5	71.6	87.9	8.8	39100	5.83
30S10F	53.8	70.3	83.1	8.8	40000	4.40
20S20F	50.2	73.6	81.2	9.1	38100	4.83
10S30F	50.8	71.8	74.6	8.9	37000	5.15
40F	48.9	64.5	71.7	9.4	38600	3.80
60S	53.2	66.1	83.1	9.2	37700	4.65
50S10F	50.3	65.7	80.8	8.5	36200	4.12
40S20F	48.5	68.1	80.2	8.3	35900	4.67
30S30F	46.3	61.4	79.4	8.2	35500	3.68
20S40F	45.2	59.9	75.1	8.0	35100	4.02
10S50F	37.8	56.2	69.8	7.5	35100	2.94
60F	29.4	53.9	70.3	7.4	34100	2.77

4 CONCLUSIONS

Following conclusions could be drawn from the results obtained in this study:

1. Chloride diffusivity of the concrete is substantially reduced with the partial replacement of portland cement by the slag or fly ash. The test results indicate that for the reduction of chloride diffusivity, the fly ash used in this study is more effetive than the slag used.

2. Electrical resistivity of the concretes containing slag or fly ash are substantially higher compared to that of the pure portland cement.

3. High compressive strengths were obtained with the use of finely ground fly ash or slag. Compared to the fly ash used, better mechanical properties were obtained using the slag.

ACKNOWLEDGMENTS

The authors wish to acknowledge the financial support of TUBITAK (The Scientific and Technical Research Council of Turkey) Project: MAG 104M390.

REFERENCES

Bayat, O. 1998, 'Characterization of Turkish Fly Ashes', *Fuel*, 77, 1059 – 1066.

Bijen, J. 1996, *Blast Furnace Slag Cement*, Association of Netherlands Cement Industry, The Netherlands.

Dhir, R.K., Jones, M.R.. 1999, 'Development of chloride-resisting concrete using fly ash', *Fuel*, 78 [2], 137-142.

Fraay, A.L.A., Bijen, J.M. and Haan, Y.M.D. 1989, 'The Reaction of Fly Ash in Concrete; A Critical Examination', *Cement and Concrete Research*, 19, 235 – 246.

Mehta, P.K., 2000, 'Reflections on Recent Advancements in Concrete Technology', Second International Symposium on Cement and Concrete Technology in the 2000s, Istanbul, 6-10 September, Vol.1, 43-57.

Li, S., and Roy, D.M. 1986, 'Investigation of relations between porosity, pore structure and chloride diffusion of fly ash and blended cements', *Cement and Concrete Research,* 16[5], 49-759.

Neville, A.M. 2004, *Properties of Concrete*, Pearson Prentice Hall, Essex.

Regourd, M.M. 2004, 'Cements Made from Blast-furnace Slag', in *Lea's Chemistry of Cement and Concrete*, Ed. Hewlett, P.C., Elsevier Ltd, Oxford, pp. 637-678.

Şengül, Ö., Tasdemir, C. and Tasdemir, M.A. 2002, 'Influence of Aggregate Type on the Mechanical Behavior of Normal and High Strength Concretes', *ACI Materials Journal*, 99 [6], 528-533.

Şengül, Ö., Tasdemir, C., and Tasdemir, M.A. 2005, 'Mechanical Properties and Rapid Chloride Permeabilites of Concretes with Ground Fly Ash', *ACI Materials Journal*, 102 [6], 414-421.

Şengül, Ö., Taşdemir, M.A., Yüceer, Z. and Erenoğlu, T. 2003, 'Effects of Fly Ash and Ground Granulated Blast Furnace Slag on the Compressive Strength and Chloride Permeability of Concrete', *5th National Congress on Concrete*, The Chamber of Turkish Civil Engineers Istanbul Branch, Istanbul, 1-3 October, pp. 483-492.

Tokyay, M., 1998. *Characterization of Turkish Fly Ashes*, Turkish Cement Manufacturers Association, Ankara, 70 pp.

Zhang, M.H., Bilodeau, A., Malholtra, V.M., Kim, K.S., Kim, J.C. 1999, 'Concrete incorporating supplementary cementing materials: Effects on compressive strength and resistance to chloride ion penetration', *ACI Mater. J.*, 96 [2], 181-189.

11DBMC International Conference on Durability of Building Materials and Components
ISTANBUL, Turkey 11-14 May 2008

Critical Evaluation of the Definition of "Sulfate-Resistance" A Focus on the Flexural Strength Performance of SR Cements

Pınar Akpınar [1]*
Ignasi Casanova [2]

T 11

ABSTRACT

Sulfate attack in concrete has different consequences such as expansion, cracking, reduction in overall strength and cohesion depending on the type of the attack products that may be formed. Secondary ettringite, secondary gypsum and thaumasite, are the attack products that can be formed individually or sometimes even simultaneously, causing severe deteriorations in concrete

Current standards define sulfate-resistant cement by limiting only the amount of aluminates in the clinker phases. Limiting the aluminates is known to be effective in reducing the occurrence of ettringite-related expansions in the concrete. On the other hand, the formation of other attack products like secondary gypsum does not depend on the aluminates in the clinker. Therefore, reduction in the overall strength of concrete can still be possible as the result of a sulfate attack in a concrete made with a "sulfate-resistant" cement.

This study focuses on the strength performance of the "sulfate-resistant" cements. A sulfate resistant (low C_3A content) and a non-sulfate resistant (high C_3A content) cement were used throughout the experiments. The length change behavior and the flexure strength development of these two cements that were exposed to sulfate solutions of different concentrations were observed systematically for more than a year. Results show that even though their expansion behavior can be quite different, the strength performance of these two cements can be very similar.

This paper involves the results obtained from the experiments and the detailed interpretation of these results.

KEYWORDS

Sulfate attack in concrete, Sulfate-resistant cement, Flexure strength testing

[1] Near East University, Department of Civil Engineering, Lefkosa, TRNC, Phone +90 392 223 64 64/236, Fax +90 392 223 64 61, apinar@neu.edu.tr
[2] Universitat Politècnica de Catalunya, Centre for Research in Nanoengineering(CRnE), Barcelona, Spain, Phone +34 934 017 350, Fax +34 934 017 262, ignasi.casanova@upc.edu
* Previously involved in: Universitat Politècnica de Catalunya, School of Civil Engineering.

1 INTRODUCTION

Majority of cement standards define "sulfate-resisting" cement by limiting the aluminates in its clinker composition. The limit defined varies from country to country, depending on the exposure conditions and other specific requirements that each geographical zone might have.

Besides these national standards, one of the most world-widely recognized and commonly used standards is for sure the ASTM. ASTM C150, Standard Specification for Portland cement [2000], defines clinker composition of high sulfate resistant cement by limiting C_3A and (C4AF+2(C3A)) to maximum values of 5% and 25%, respectively. These limiting values were estimated according to results of the experimental studies carried out by using another ASTM test method, C452 [1995]. ASTM C452 basically involves the submersion of Portland cement mortars prepared with the addition of gypsum in the mixing stage, into distilled water for 14 days. The expansion recorded in the samples, at the end of the test period is compared by some expansion limits that are previously defined by ASTM, in order to be able to classify the tested cement as severe, moderate or non-sulfate resistant.

However, it is well known that expansion is not the only type of damage that the concretes under sulfate attack may experience. Different sulfate attack products may be formed in the concrete micro structure due to the reactions between the attacking sulfates and the hydration products of cement, leading a variety of durability problems, such as loss of overall strength and cohesiveness, disintegration and spalling, besides the expansion and cracking. Secondary ettringite, result of the reactions between the sulfates and the C_3A or C_3A-based hydration products, is known to be the main responsible of the expansion. On the other hand, secondary gypsum and thaumasite are the sulfate attack products causing strength-related problems. It is generally accepted that thaumasite is a special type of sulfate attack product that forms only under some specific conditions. Secondary ettringite and gypsum are the most commonly seen attack products, causing damage to the concretes exposed to sulfates.

Secondary gypsum is formed from the reactions between the sulfates and CH and/or C-S-H, which are the hydration products of cements that do not depend on the initial C_3A content of the cement's clinker composition. Therefore, the "sulfate-resistant" cements that are defined according to their C_3A contents might not be necessarily providing a better resistance against secondary gypsum-related durability problems. This study investigates the strength resistance of low-C_3A sulfate resistant cements. Cements of high and low C_3A content are exposed to sulfate solutions having both high (commonly used in standard accelerated tests) and moderate (field-like) sulfate concentrations. Besides the length change behavior (usual measurement approach in standard tests), the flexural strength development of the mortar samples was also measured systematically up to an age of maximum 72 weeks. The results obtained, as well as the details about the experimental campaign are discussed in the following sections.

2 MATERIALS AND METHODS

Two commercial Portland cements were used throughout the experimental campaigns. They were chosen on the basis of their relative C_3A contents, and labeled as HA and LA (for high- and low-aluminates contents, respectively), as shown in Table 1. Standard method ASTM C1012 [1995] was used as a reference for the preparation and storage of mortar samples in two different solutions of sodium sulfate (50000 ppm as originally described in the method, and also additionally 6000 ppm).

Six mortar bars were produced from two different batches of each cement to be tested for expansion and stored in the prepared sodium sulfate solutions. Although this standard method suggests just a 6-month testing period, we extended the observations for 88 weeks (1.7 years) in order to have a more complete data set of the long-term behavior. In each test, length changes were recorded twice with two Sylvac S229 digital extensometers that had been independently calibrated to ±3µm before each

measurement. The bars were placed in the extensometer with the same orientation (same face is kept in front with the same edge being kept at the top each time). As a result of this procedure, twelve length changes (6 samples by 2 extensometers) are obtained each time.

Table 1. Oxide and calculated Bogue's compositions of high-aluminate (HA) and low aluminate (LA) cements.

	Cements	
Oxide	**HA**	**LA**
SiO_2	19.86	19.73
Fe_2O_3	3.40	4.24
Al_2O_3	5.61	4.43
CaO	62.38	63.34
MgO	2.14	1.68
K_2O	0.97	0.59
Na_2O	0.15	0.14
SO_3	3.36	3.03
LOI	2.14	2.3
Phase		
C_3S	50.86	63.48
C_2S	18.57	8.68
C_3A	9.13	4.56
C_4AF	10.34	12.89

Twelve additional mortar bars (6 from each batch) of each type of cement were fabricated for tensile strength measurements carried out for a total period of up to 72 weeks, with a Multitester-Normatest type Universal Press. Span length and loading velocity of the equipment are 100 mm and 5.08 mm/min, respectively.

3 RESULTS

3.1. Length-Change Data

I. HA and LA cements are observed to experience similar expansion values for the *initial* ages (i.e. t<24weeks), under both concentrations (please note the y-scale differences in figs 1 & 2).

II. HA cement mortars are observed to experience higher *final* expansions compared to LA samples both at high and moderate sulfate concentrations.

III. Both cements yield in higher expansion values under high concentrations than what they yield in under moderate concentrations.

IV. The rate of the expansion at the later ages is observed to be increased, for both cements under both concentrations. This increase in the expansion rate is observed to be higher for HA cement.

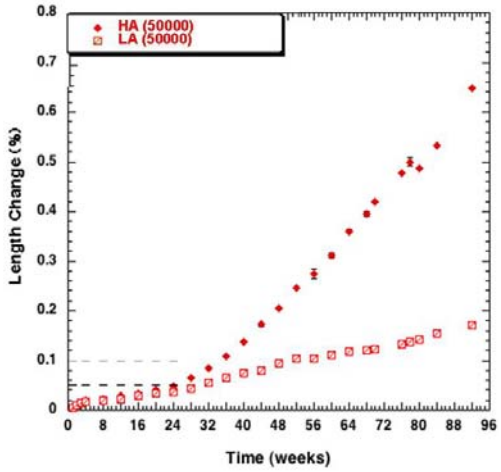

Figure 1: (Left) Expansion behavior of HA and LA cements exposed to a 50000ppm sodium sulfate solution.

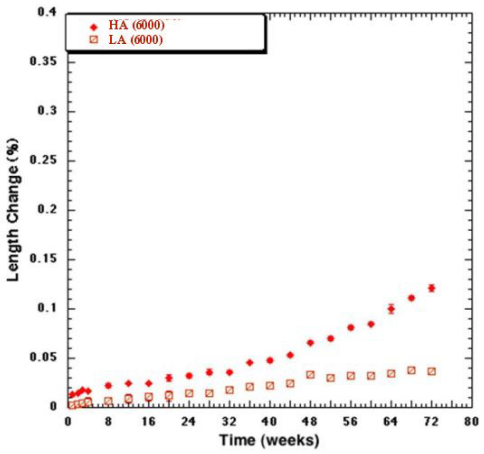

Figure 2: (Right) Expansion behavior of HA and LA cements exposed to a 6000ppm sodium sulfate solution.

3.2. Flexural Strength Data

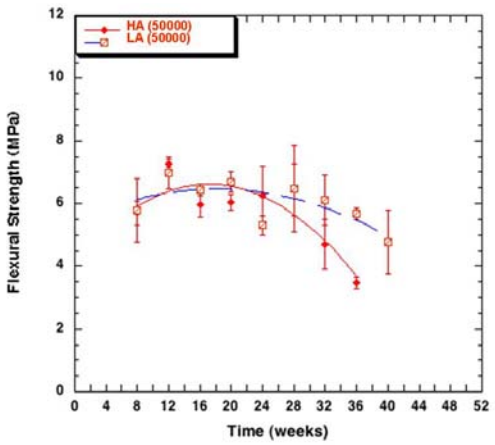

Figure 3: (Left) Flexural strength evolution of HA and LA cements exposed to a 50000ppm sodium sulfate solution.

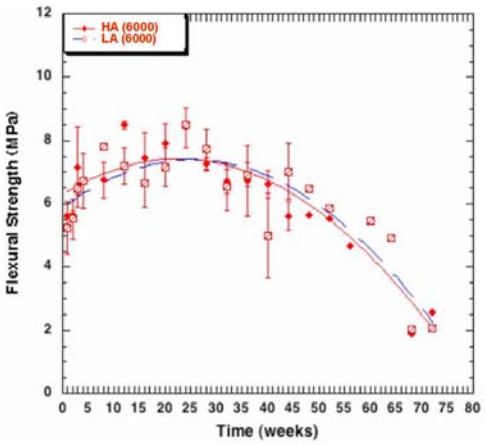

Figure 4: (Right) Flexural strength evolution of HA and LA cements exposed to a 6000ppm sodium sulfate solution.

I. The evolution of flexural strength show an increase during the early ages (first 24-25 weeks), reaching a peak strength and then an evident decrease in a manner that can be fitted with a second degree polynomial, in the cases of both cements under all sulfate concentrations.

II. Before reaching the peak flexural strength at a given concentration, HA and LA perform similarly (i.e. similar strength values). After the time for peak strength, especially at high sulfate concentration, HA looses strength more rapidly; LA has higher strength till the end of testing period. (See Fig. 3).

III. For lower sulfate concentrations, like 6000 ppm, the compositional differences of HA and LA cements do not seem to have a critical effect on the flexural strength behavior of the mortars (seeFig. 4). It seems that at 50000 ppm the difference in the behavior of the two cements can be defined as more notable (Fig. 3).

4 DISCUSSIONS

4.1. Discussions on Length-Change Data

It is observed that at higher concentrations (e.g. 50000ppm) both HA and LA cements experience higher length changes. In their paper dealing with sulfate attack mechanisms, Santhanam et al. [2001] report that Na_2SO_4 yields firstly in secondary gypsum formation when the sulfate concentration is high (e.g. >8000 ppm). Later, it is known that by the consumption of secondary gypsum formed, secondary ettringite is produced [Taylor 1990; Irassar et al. 2000]. In accordance with this suggestions, samples submerged into the 50000ppm solution in this study expand more than the samples in 6000ppm (see figures 1 & 2), since there are more sulfate ions present in the system capable of producing more secondary gypsum, which later is used to produce more secondary ettringite.

More total expansion is also observed in HA cement's samples when compared to LA samples that are stored in the sulfate solutions of same concentrations. This can be considered as a commonly expected result, since LA cement is defined by standards to have less susceptibility sulfates.

The sudden increase in the rate of expansion noted at the last stage is expected to be due to the initiation of micro cracks in the samples under sulfate attack, strongly suggesting that the samples in the 50000 ppm solution get into the micro cracking stage earlier than those in the 6000 ppm solution (see figs 1 & 2). Another coherent observation can be made when the behavior of HA and LA samples compared: HA samples is observed to experience a sudden increase in their lengths with a higher expansion rate; indicating that the expected micro cracking that the HA samples have experienced is much more significant than that of samples made with sulfate-resisting LA cement.

It is observed that the difference in the sulfate reactivity of HA and LA samples cannot be clearly detected before the micro cracking stage (i.e. before the start of the sudden increase in length change) of the samples. The difference in the performance of different cements becomes more evident in later ages, as Cao et al.[1997] had reported as well. Although the HA cement has much more C_3A than the LA cement, the majority of the observed difference in the expansion behavior of these cements could only be recorded after an age of an at least 24 weeks, under the exposure conditions suggested for accelerated tests (see fig 1). Therefore, especially in the case of testing PC blends with previously unknown characteristics, the decision on the level of their sulfate resistance should not be taken by considering their length-change behavior only at initial ages, which does not succeed in reflecting the reality completely.

In any case, although the length change measurements might be carried out for a longer period, authors emphasize the importance of using additional measurement approaches, like flexure strength testing, in order to be able to evaluate the resistance of cements against *all* aspects of sulfate attack. Secondary ettringite is usually accepted to be the cause of the most of expansion recorded [Collepardi 2001]. In our tests, the difference in the etrringite-based expansion behavior of both high- and low-aluminate cements is observed to be well detected by length change measurements, at the end of the whole testing period. However, gypsum is not considered to be expansive, when compared to ettringite [Kurtis et al. 2001; Irassar et al. 2000]; but, it may have a "filling effect" like ettringite as they both may accumulate in the porosity, and may result in an increase of strength of the tested sample. It is presumed that gypsum is not likely to be present in the system in high amounts, since it is continuously used for secondary ettringite formation [Irassar 1990]. Apart from its effects as an attack product, the formation process of gypsum is also very important: CH is consumed during the process and the pH level in the system eventually drops, causing decalcification of C-S-H. As in the case of leaching in which low alkalinity of the system causes dissolution of CH for balancing the pH, leading the decomposition of hydrated silicate and aluminates, gypsum formation also yields severe strength loss and disintegration. [Kurtis et al. 2001] However, these possible influences of secondary gypsum on the overall strength of the samples could not have been observed, if the length change was the only measurement approach used during this study.

4.2. Discussions on Flexure Strength Data

One of the most significant results obtained from the flexural strength testing is the convenience to use a second degree polynomial fit for the observed strength development behavior of the samples. This result is in accordance with the findings of Irassar (1990). Using second degree polynomial curve-fits could be a promising approach to be used in future modeling studies aiming to simulate the mechanical consequences of sulfate attack in concrete. This mathematically definable behavior observed in the samples has the potential to enable us to detect and interpret the different stages of sulfate attack that progresses in the samples.

The initial increase in the flexural strength is expected to be the strength development due to hydration process of cement. In addition to this, Irassar (1990) suggests that the increase in the flexural strength can be also attributed to pores being filled by secondary ettringite and gypsum. Samples in the 50000ppm solution show a faster strength drop, when compared to the samples in 6000ppm solution, after reaching to their peak strengths (figure 3). As discussed before, higher amounts of secondary gypsum is formed during the early ages under such high sulfate concentrations. Accordingly, this higher amount of gypsum formed, later yields in the formation of more secondary ettringite, especially in the high-aluminate cement samples, causing more expansion and consequent crack formation faster than it can be observed in the low-aluminate samples in the same solution, justifying the faster strength loss observed in the HA samples. The effect of CH consumption during the formation of secondary gypsum (more under 50000ppm) should be also taken in to account as an important cause of the detected faster strength loss. However, it should be emphasized that 50000ppm is a value mainly used in laboratory tests to accelerate the reactions. Most of the standards define the sulfate concentration level for severe sulfate attack always around or less than 10000ppm [Neville 2004; and references therein].

The samples stored in 6000ppm solution also experience the second degree polynomial strength evolution that is observed in the samples in 50000ppm solution: After an increase during the first ages, both HA and LA samples reaches to their peak flexural strength and then experience the expected strength loss (fig 4). However, the differences observed in the time to reach to peak strength and the evolution of the flexure strength loss of both cements are in fact too small to be taken into account to classify HA and LA cements to be "non-sulfate-resistant" and "sulfate-resistant" cements, respectively. Both cements experience practically the same strength development; even though their length-change behaviors were significantly different (see figures 2 and 4).

These findings show that low-C_3A cements are only good at minimizing expansion-related problems; in spite of being generally classified as “sulfate-resisting” cements, they do not necessarily provide a better strength, or better resistance against all aspects of sulfate attack. Similar findings were also reported by Mehta [1993]. Therefore, limiting only the C_3A content of the cements as suggested by many standards may help to improve the performance only in some aspects, but seems to fail to be an adequate solution to the entire problem of sulfate attack. Properties like strength performance, which is crucial for civil engineering, should also be covered with a more extended definition of “sulfate resistance”.

These findings also imply the importance of using adequate testing approaches during the evaluation of cements’ sulfate attack performance. Using only one type of measurement approach might not be sufficient to detect all consequences of sulfate attack going on in the samples. On the other hand, using length change and strength development approaches at the same time, like it was done in this study, provides us a more complete overview of the resistance of the tested cements against consequences of all sulfate attack products being formed.

5 CONCLUSIVE REMARKS

This study involves a data-based evaluation of the strength performance of "sulfate-resistant" cements. Meso-scale laboratory experiments focusing on the systematical measurements of the length change and the flexural strength development of two Portland cements, having a high and a low C_3A content, were carried out. A high (accelerated laboratory tests) and moderate (more realistic) sulfate concentrations were used in the exposure solutions, in order to be able to compare the performance results obtained under standard conditions with the ones that may occur in the real cases.

Results show that the cement having high C_3A content, which is defined to be not "sulfate-resistant" by the standards, experiences more expansion, in both sulfate concentrations, when compared to low C_3A content cement. However, when their strength development is compared, both cements show a very similar performance, especially under the more realistic moderate sulfate concentration. This finding implies that the so-called "sulfate-resisting" cements do not always provide a high resistance against all known consequences of sulfate attack, and also that the definition of sulfate resistance should perhaps be extended to include strength-related requirements, as well.

Another remarkable observation is the necessity of using different measurement approaches at the same time, in order to be able to determine the resistance of cements against all aspects of sulfate attack. Using only length change measurement approach, as suggested in many test methods, is observed to be not adequate to detect the influence of the strength reducing attack products, such as secondary gypsum.

ACKNOWLEDGEMENTS

This work was partially supported by grants MAT2002-00077 and BIA2006-12717 from the Spanish Ministry of Education and Science, through the National Plans of Materials and Construction, respectively. Financial support to P.A. from the International Graduate School of Catalonia is also gratefully acknowledged. We also wish to thank Paulo J.M. Monteiro (UC Berkeley) and Silvia Vieira (Holcim) for insightful comments, Eufronio Beyret (Laboratory of Construction Materials, UPC) for technical assistance, and Joan Puig (Ciments Molins) for providing the cement and continuous encouragement and support to this study.

REFERENCES

'ASTM C150-Standard Specification for Portland Cement', 2000, in *Annual Book of ASTM Standards*, Vol 04.02. American Society of Testing and Materials, Philadelphia, PA, USA.

'ASTM C452- Standard test Method for Potential Expansion of Portlan Cement Mortars Exposed to Sulfate', 1995, in *Annual Book of ASTM Standards,* American Society of Testing and Materials, Philadelphia, PA, USA.

'ASTM C1012-Standard Test Method for Length Change of Hydraulic-Cement Mortars Exposed to a Sulfate Solution', 1995, *Annual Book of ASTM Standards*, Vol 04.01. American Society of Testing and Materials, Philadelphia, PA, USA.

Cao H.T., Bucea L., Ray A. & Yozghatlian S. 1997, 'The effect of cement composition and pH of environment on sulfate resistance of Portland cements and blended cements', *Cement and Concrete Composites*, 19[2], 161-171.

Collepardi, M. 2001, 'Ettringite Formation and Sulfate Attack in Concrete', ACI International Symposium on Concrete Technology, Singapore, 21-38.

Irassar, E.F. 1990, 'Sulfate resistance of blended cement: Prediction and relation with flexural strength', *Cement and Concrete Research* 20, 209-218.

Irassar, E. F., Gonzalez, M. & Rahhal, V. 2000, 'Sulphate resistance of type V cements with limestone filler and natural pozzolana', *Cement Concrete and Composites*, 22, 361-368.

Kurtis, K. E., Shomlin, K. & Monteiro, P. J. M. 2001, 'Accelerated Test for Measuring Sulfate Resistance of Calcium Sulfoaluminate, Calcium Aluminate and Portland Cements', *Journal of Materials in Civil Engineering*, May/June, 216-221.

Mehta, P.K. 1993, 'Sulfate Attack on Concrete – A Critical Review', Materials Science of Concrete, The American Ceramic Society, Vol.3, 105-130.

Neville, A. 2004, 'The confused world of sulfate attack on concrete', *Cement and Concrete Research*, 34, 1275-1296.

Santhanam, M., Cohen, M. D. & Olek, J. 2001, 'Sulfate attack research—whither now?', 2001, *Cement and Concrete Research*, 31, 889– 897.

Taylor, H. F. W. 1990, *Cement Chemistry*, Thomas Telford Publishing, London.

Durability and Mechanical Properties of Fiber Reinforced Cement Composites Exposed to High Temperatures

Eva Vejmelková [1]
Jan Toman [2]
Pavel Padevět [3]
Petr Konvalinka [4]
Robert Černý [5]

T 11

ABSTRACT

Fiber reinforced cement composites are often employed in severe conditions. These might be exposed for instance to high temperatures and/or high mechanical loads. However, their durability and mechanical properties are mostly measured in laboratory conditions only, so that designers cannot take into account changes in their material parameters after loading. In this paper, basic durability and mechanical properties of hybrid (glass and polypropylene) fiber reinforced cement composite material are determined as functions of thermal load, the loading temperatures being 600 °C, 800 °C and 1000 °C. Water vapor diffusion coefficient, water absorption coefficient, moisture diffusivity, adsorption isotherms, thermal conductivity, specific heat capacity, tensile strength and bending strength are the investigated parameters. The experimental results show that the decomposition of calcium hydroxide is the principal factor affecting the behavior of thermally loaded specimens. The most important changes in moisture diffusivity, water vapor diffusion resistance factor, adsorption isotherm and thermal conductivity occur between the unloaded state and the loading temperature of 600 °C which is safely above the calcium hydroxide decomposition temperature.

KEYWORDS

Fiber reinforced cement composites, High temperatures, Durability properties

[1] Czech Technical University in Prague, Faculty of Civil Engineering, Department of Materials Engineering and Chemistry, Thákurova 7, 166 29 Prague 6, Czech Republic, Phone +420224354694, Fax: +420224354446, eva.mnahoncakova@fsv.cvut.cz

[2] Czech Technical University in Prague, Faculty of Civil Engineering, Department of Materials Engineering and Chemistry, Thákurova 7, 166 29 Prague 6, Czech Republic, Phone +420224354694, Fax: +420224354446, toman@fsv.cvut.cz

[3] Czech Technical University in Prague, Faculty of Civil Engineering, Department of Mechanics, Thákurova 7, 166 29 Prague 6, Czech Republic, Phone +420224354484, Fax: +420224310775, pavel.padevet@fsv.cvut.cz

[4] Czech Technical University, Faculty of Civil Engineering, Experimental Center, Thákurova 7, 166 29 Prague 6, Czech Republic, Phone +420224354306, Fax: +420224354306, conwa@fsv.cvut.cz

[5] Czech Technical University in Prague, Faculty of Civil Engineering, Department of Materials Engineering and Chemistry, Thákurova 7, 166 29 Prague 6, Czech Republic, Phone +420224354429, Fax: +420224354446, cernyr@fsv.cvut.cz

1 INTRODUCTION

Cement-based materials are characterized by very good properties in compression but their brittle manner of failure under tensile or impact load was a limiting factor for their applicability range from the very beginnings. Fiber reinforcement is a traditional and effective method how to improve the toughness and durability of cement-based products. The steel rod reinforcement became very popular during the whole last century and remains the most frequently used type of concrete reinforcement until now. However, in the second half of the 20th century, an application of uniformly dispersed short fibers strengthening the brittle cementitious matrices appeared with an increasing frequency. In the current practice, steel, glass, carbon and various polymeric fibers such as polyethylene, polypropylene, nylon, polyester, polyurethane, cellulose, etc., are commonly used in cement-based materials.

Glass-fiber reinforced cement composites (GFC) are produced by incorporating a small amount of alkali-resistant glass fiber in cement mortar to overcome the traditional weakness of inorganic cements, namely poor tensile strength and brittleness [Majumdar 1991], [Young 1978], [True 1986]. The length and content of the glass fiber reinforcement can be chosen to meet the strength and toughness requirements of the product. Also, the type of aggregates can be varied in order to control thermal properties. GFC are often employed in severe conditions. These might be exposed for instance to high temperatures and/or high mechanical loads.

The properties of glass fiber reinforced cement composites were studied in an insufficient way until now. However, the most frequently analyzed were the mechanical properties. The durability properties such as hygric and thermal properties were measured only rarely. In addition, the specimens were tested mostly in the reference state, i.e., in room temperature conditions. The properties of this type of materials in high-temperature conditions or after high-temperature loading were studied only exceptionally.

A basic survey of mechanical properties of various Portland cement GFC, namely bending, tensile and impact strength and Young's modulus can be found in Majumdar [1991] where the work until 1990 is compiled. Basic values of thermal and hygric properties, such as thermal conductivity, thermal expansion coefficients, air and water vapor permeability are also included. Within the last ten years, the number of references describing measurements of GFC properties decreased significantly compared to 1970s and 1980s, and the few remaining were concentrated on mechanical properties. For instance, Zhang et al. [1997] measured flexural strength of GFC with high content of fly ash, Huang et al. [1997] analyzed the interfacial mechanical properties of carbon-coated GFC, Marikunte et al. [1997] determined the flexural and tensile strength of GFC after hot-water durability tests, Park et al. [1999] measured compressive strength, compressive modulus of elasticity, tensile strength, flexural strength of low-density/low cost GFC, Mu et al. [2000] determined tensile strength and impact resistance of short fiber GFC with high slag content, Mu et al. [2002] analyzed the possibilities of improving the interface bond between fiber mesh and cementitious matrix of GFC and used fracture toughness to evaluate the flexural behavior of GFC.

It seems to be quite logical that mechanical properties of GFC under common environmental conditions are in the center of interest of most researchers working on those materials, particularly taking into account why GFC were developed, i.e., to improve the tensile and flexural strength of cement based composites. However, there are numerous applications where determination of mechanical properties is not sufficient. There are also situations when testing in normal conditions does not provide enough information on the behavior of GFC in a structure. For instance, lightweight GFC can be used as thermal insulation materials. Here certainly thermal properties are very important. GFC can also be used as fire protection materials. In this case, it is useful to know not only the properties in usual conditions but also the material's response to high temperatures. For GFC used in any wall systems hygrothermal performance should be assessed so that both hygric and thermal properties are to be known.

In this paper, basic mechanical, thermal and hygric properties of hybrid glass and polypropylene fibers reinforced cement composite were measured in reference state and after heating up to 1000 °C.

2 MATERIAL AND SAMPLES

The measurements were done on glass and polypropylene fibers reinforced cement composite produced in the laboratories of VUSTAH Brno. The composition of the material is shown in Table 1. Water in the amount corresponding to the w/c ratio of 0.33 was added to the mixture. The samples were produced by vacuum technology using the OMNI MIXER 10 EV mixing device.

Table 1. The mixture composition.

Composition [% of dry substances]	
Cement CEM I 52.5 Mokrá	54
Quartz sand aggregates 0-1 mm Bzenec	40
Microsilica	3
Glass fibers - 12 mm length	2.7
Polypropylene fibers	0.3

In the experimental measurements the following specimens were tested:

- reference specimens not exposed to any load (denoted as SC in what follows)
- specimens exposed to a gradual temperature increase up to 600, 800 and 1000 °C during two hours, then left for another 2 hours at the final temperature and slowly cooled (denoted as SC-600, SC-800 and SC-1000 according to the loading temperature).

3 EXPERIMENTAL METHODS

3.1 Basic Physical Properties

As fundamental physical material characteristics, bulk density ρ [kgm^{-3}], vacuum saturation moisture content w_{sat} [kgm^{-3}], porosity Ψ_0 [Vol.-%] and matrix density ρ_m [kg m^{-3}] were determined. They were obtained using the vacuum saturation method [Roels et al. 2004].

3.2 Mechanical Properties

The measurement of tensile strength was done using the electromechanical testing device MTS Alliance RT 30 with the maximum tension force of 30 kN. The rate of loading was 0.025 mm/min. The bending strength was measured in the same device provided with the three-point bending track 642.01A which allows the maximum load of 27.80 kN. The rate of loading was 0.04 mm/min. The values of tensile strength and bending strength were calculated from the measured force values using the common formulas.

3.3 Water Vapor Transport Properties

The wet- and dry cup methods were employed in the measurements of water vapor transport parameters [Roels et al. 2004]. The water vapor diffusion coefficient D [m^{2}s^{-1}] and water vapor diffusion resistance factor μ [-] were determined.

3.4 Adsorption Isotherms

In the measurements of adsorption isotherms the samples were placed into the desiccators with different solutions to simulate different values of relative humidity [Roels et al. 2004]. The initial state for all the measurements was dry material. The experiment was performed parallel in all desiccators in

a common way. The mass of samples was measured in specified periods of time until steady state value of mass was achieved. Then, the moisture content by mass was calculated.

3.5 Water Vapor Transport Properties

The water sorptivity A [kg m^{-2} s $^{-1/2}$] and apparent moisture diffusivity κ [m^2 s^{-1}] were measured using a water suction experiment [Černý et al. 2002].

3.6 Thermal Properties

Thermal conductivity λ [W m^{-1} K^{-1}] and specific heat capacity c [J kg^{-1} K^{-1}] were measured using the commercial device ISOMET 2104 (Applied Precision, Ltd.). ISOMET 2104 is a multifunctional instrument. The measurement is based on analysis of the temperature response of the analyzed material to heat flow impulses. The heat flow is induced by electrical heating using a resistor heater having a direct thermal contact with the surface of the sample.

4 EXPERIMENTAL RESULTS AND DISCUSSION

4.1 Basic Physical Properties

Table 2 shows basic parameters of the studied material depending on the loading temperature. The most important change in porosity occurred between the unloaded state and the loading temperature of 600 °C where the increase of porosity was as high as 35 %. Later porosity changes were lower than 10 %. This is in accordance with the behavior of most Portland cement based composite materials where the most important chemical reaction in the high temperature range is decomposition of calcium hydroxide at about 460-480 °C [Černý and Rovnaníková 2002].

Table 2. Basic physical properties.

Material	Ψ_0 [%]	ρ [kg m^{-3}]	ρ_m [kg m^{-3}]
SC	24	2021	2660
SC-600	32	1947	2899
SC-800	35	1909	2954
SC-1000	33	1871	2799

4.2 Mechanical Properties

Tables 3 and 4 show deformation, tensile strength and bending strength. The most important changes in tensile strength were observed between the loading temperatures of 600 °C and 800 °C. After heating to 800 °C the tensile strength decreased to about 9 % of its reference value. The most remarkable changes of bending strength were observed between the reference state and the specimens heated to 600 °C, where the bending strength decreased to about one fifth of its original value. The results are in a reasonable qualitative agreement with the basic parameters in Section 4.1.

Table 3. Deformation and tensile strength

Material	*Deformation* [mm]	*Tensile strength* [MPa]
SC	0.51	4.18
SC-600	0.49	3.73
SC-800	0.30	0.32

SC-1000	0.16	0.14

Table 4. Deformation and bending strength

Material	*Deformation* [mm]	*Bending strength* [MPa]
SC	0.32	15.08
SC-600	0.17	3.78
SC-800	0.17	2.43
SC-1000	0.16	1.93

4.3 Water Vapor Transport Properties

Table 5 shows water vapor transport properties of the studied SC material. We can see that the values of water vapor diffusion resistance factor decreased very rapidly with the increasing load temperature for both configurations of the cup experiment. The most important was the change between the unloaded state and the loading temperature of 600 °C. This is in basic agreement with both the porosity and mechanical parameters data. The water vapor diffusion resistance factor for wet-cup arrangement was significantly lower than in dry-cup measurement. This concurs with the measurements obtained for many other building materials and reflects the partial inclusion of liquid water transport into the water vapor transport coefficient in the wet-cup experiment [Černý and Rovnaníková 2002].

Table 5. Water vapor transport properties

Material	*Dry cup*		*Wet cup*	
	D [m^2s^{-1}]	μ [-]	D [m^2s^{-1}]	μ [-]
SC	2.9E-07	77	6.0E-07	38
SC-600	9.6E-07	24	1.5E-06	15
SC-800	1.2E-06	19	2.7E-06	8.4
SC-1000	1.2E-06	19	5.1E-06	4.5

4.4 Adsorption Isotherms

Figure 1 shows that water vapor adsorption capacity of the studied material increased with increasing loading temperature. This behavior can be explained by the changes of the porous structure after high temperature exposure. The observed increase in porosity (see Table 2) due to the thermal decomposition reactions was apparently caused by the increase of the amount of larger pores but the amount of smaller pores probably did not decrease on that account in a significant way as it is usual in similar cases. This seems to be a positive effect of polypropylene fibres which decomposed at lower temperatures. In this way, they could provide channels for vapor escape and thus help to reduce the further thermal damage in some extent.

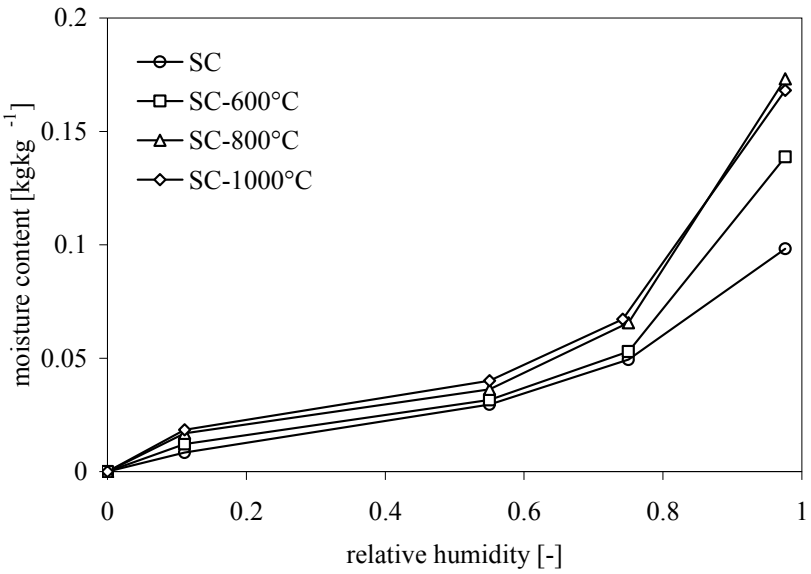

Figure 1. Adsorption isotherms.

4.5 Water Transport Properties

Table 6 presents liquid water transport properties. Once again, the thermal decomposition processes at high temperatures were the dominant factor for the differences in water transport parameters measured for thermally loaded samples. The increase of both water absorption coefficient and moisture diffusivity of thermally loaded specimens was in a comparison with reference specimens very high, up to two orders of magnitude, which indicated very remarkable damage of the structure of the analyzed material. The most important increase in water transport parameters was observed between the reference state and the samples exposed to 600 °C, similarly as for all other studied parameters in this paper.

Table 6. Water transport properties.

Material	*A* [$kgm^{-2}s^{-1/2}$]	κ [m^2s^{-1}]
SC	0.0096	1.65E-09
SC-600	0.0465	2.13E-08
SC-800	0.0718	4.20E-08
SC-1000	0.275	6.91E-07

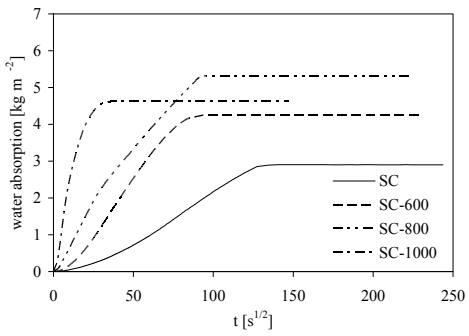

Figure 2. Water absorption.

4.5 Thermal Properties

The results of measurements of thermal parameters in Table 7 showed that thermal conductivity in dry state significantly decreased after high temperature loading. This is in qualitative agreement with the increase of porosity due to decomposition reactions in high temperature range leading to an increase of significance of the low thermal conductivity of air in the cement matrix-air system. The principal loading temperature was again 600 °C where the thermal conductivity decreased by about 10 % compared to unloaded specimens. The specific heat capacity was affected in a similar qualitative way. The changes were only up to 5 % in this case, which may reflect the mass loss due to the thermal decomposition reactions. The thermal diffusivity basically followed the changes of thermal conductivity which were more remarkable than changes of specific heat capacity.

Table 7. Thermal properties in dry state.

Material	λ [$Wm^{-1}K^{-1}$]	c [$Jkg^{-1}K^{-1}$]	a [$10^{-6}\,m^2s^{-1}$]
SC	1.02	810	0.65
SC-600	0.90	790	0.54
SC-800	0.84	780	0.55
SC-1000	0.63	760	0.44

5 CONCLUSIONS

The cement-based composite material with hybrid glass-polypropylene fiber reinforcement studied in this paper was found to resist to high temperatures only slightly better than similar composites with common fiber reinforcement. The decomposition of calcium hydroxide at about 460-480 °C remained clearly the most important factor for the damage of the porous matrix after high-temperature exposure. The use of polypropylene fibers in addition to glass fibers led to certain improvement of water vapor adsorption capacity but the majority of other mechanical and durability properties was not affected in a very significant way.

ACKNOWLEDGMENTS

This research has been supported by the Ministry of Education, Youth and Sports of Czech Republic, under grant No MSM: 6840770031.

REFERENCES

Černý R., Poděbradská J., Drchalová J. 2002, Water and Water Vapor Penetration Through Coatings, *Journal of Thermal Envelope and Building Science,* 26, 165-177.

Černý, R., Rovnaníková, P. 2002, *Transport Processes in Concrete.* Spon Press, London.

Huang, C. M., Zhu, D., Cong, X.D., Kriven, W. M., Loh, R. R., Huang, J. 1997, Carbon-coated-glass-fiber-reinforced cement composites I: fiber pushout and interfacial properties, *Journal of American Ceramic Society*, 80, 2326-2332.

Majumdar, A.J., Laws, V. 1991, *Glass Fibre Reinforced Cement*, BSP, Oxford.

Marikunte, S., Aldea, C., Shah,S. P. 1997, Durability of glass fiber reinforced cement composites, *Advanced Cement Based Materials*, 5, 100-108.

Mu, B., Meyer, C., Shimanovich, S. 2002, Improving the interface bond between fiber mesh and cementitious matrix, *Cement and Concrete Research*, 32, 783-787.

Mu, B., Li, Z., Peng, J. 2000, Short fiber-reinforced cementitious extruded plates with high percentage of slag and different fibers, *Cement and Concrete Research*, 30, 1277-1282.

Park, S. B., Yoon, E. S., Lee, B. I. 1999, Effects of processing and materials variations on mechanical properties of lightweight cement composites, *Cement and Concrete Research*, 29, 193-200.

Roels, S., Carmeliet, J., Hens, H., Adan, O., Brocken, H., Černý, R., Pavlík, Z., Hall, C., Kumaran,K., Pel, L., Plagge, R. 2004, Interlaboratory Comparison of Hygric Properties of Porous Building Materials, *Journal of Thermal Envelope and Building Science*, 27, 307-325.

True, G. 1986, *GRC Production and Uses*, Palladian Publications Ltd., London.

Young, J. 1978, *Designing with GRC*, Architectural Press, London.

Zhang, Y., Sun, W., Shang, L., Pan, G. 1977, The effect of high content of fly ash on the properties of glass fiber reinforced cementitious composites, *Cement and Concrete Research,* 27, 1885-1891.

Implementation of Durability in the Design of Glass Fibre Reinforced Concrete Structures

Heidi Cuypers [1]
Petra Van Itterbeeck [2]
Tine Tysmans [3]
Jan Wastiels [4]

T 11

ABSTRACT

When concrete is reinforced with technical textiles, a cheap load bearing concrete composite can be produced. Since – in contrast to classical reinforced concrete – no concrete cover is necessary, very thin plates and shells of any desired shape can be produced without necessarely increasing the need for skilled labourers and consequently increasing the cost price. When glass fibres are used to form technical textiles, a relatively high strength and stiffness can be combined with the formation of a finer crack pattern and relatively low cost price.

One of the main reasons why glass fibre reinforced concrete (grc) has seldomly been used as structural reinforcement in concrete structures is the durability. Common glass fibres are attacked by the alkalinity of the concrete matrix and rapidly lose strength. In the past a proper lifetime of a grc structure could not be guaranteed, but recent developments led to more durable material combinations.

In this paper the potential of TRC with glass fibres is illustrated by means of a dimensioning example. A roof structure, made of a shell with a hypar surface shape will be dimensioned and the effect of durability will be evaluated. The minimal thickness to provide a certain lifetime will be calculated for several material combinations with different ageing behaviour.

KEYWORDS

Durability, Textile reinforced concrete, FEM, Glass fibres

[1] Vrije Universiteit Brussel, Department of Mechanics of Materials and Constructions, 1050 Brussel, Belgium, Phone +32 2 6292955, Fax +32 2 6292928, heidi.cuypers@vub.ac.be
[2] Vrije Universiteit Brussel, Department of Mechanics of Materials and Constructions, 1050 Brussel, Belgium, Phone +32 2 6292989, Fax +32 2 6292928, petra.van.itterbeeck@vub.ac.be
[3] Vrije Universiteit Brussel, Department of Mechanics of Materials and Constructions, 1050 Brussel, Belgium, Phone +32 2 6292921, Fax +32 2 6292928, tine.tysmans@vub.ac.be
[4] Vrije Universiteit Brussel, Department of Mechanics of Materials and Constructions, 1050 Brussel, Belgium, Phone +32 2 6292924, Fax +32 2 6292928, jan.wastiels@vub.ac.be

1 INTRODUCTION

Textile reinforced concrete (TRC), which is the material that will be discussed in this paper, is a special type of fibre reinforced concrete (FRC). Classical fibre reinforced concrete can be used to enhance the thoughness and to obtain a better crack control of cementitious mixtures, but seldomly leads to an enhanced load-bearing capacity. The production techniques (mixing and casting/pressure forming or use as shotcrete) allows the implementation of a limited amount of fibres (approximately 1-2 vol%). Moreover, the spatial homogenity and orientation of the fibres are not easily controlled.
When fibres are introduced in the form of textiles, orientation and spatial homogenity carefully controlled. When other production techniques – which are more conforming to composite technology than to concrete technology (hand lay-up, calendering, pulltrusion) – are used, a higher fibre volume fraction (approximately 15%) can also be obtained. As a consequence, textile reinforced concrete can be used as a load bearing material and steel rebars could be ommited. Therefore, no concrete cover is needed and very thin plates (1mm minimal thickness) and thin shells with a high curvature (thanks to the high flexibility of the textile) can be produced. The aim of this paper is therefore to study the potential and the limits of TRC for shells. This evaluation will be limited to structural analyses (design-examples) of shells of different spans and this with several materials combinations. Within the subsequent discussions, only the effects of the possible use of a smaller thickness (material saving effect) will be discussed in detail. Other advantages concerning e.g. the fact that less skilled labourers are needed (for bending and forming of the reinforcement) and the consequent lower cost price are not discussed in detail.

Fig. 1 shows the type of structure that will be analysed for illustrative purposes in this paper. A hypar shell was chosen for several reasons: (1) it is a typical shape which can be produced easily with TRC, but is less obvious with a classical steel reinforced concrete, (2) the use of technical textiles as flexible and reusable moulds for TRC is currently under study. The presented shape can be constructed, using a textile mould under pre-tension (3) due to the curvature, the external load will be transferred partially through 'compression-arc' and 'tensile-chain' paths within the shell, but the shell can also withstand bending. Although relatively complex stress patterns could already occur, interpretation of the global behaviour is still not too awkward.

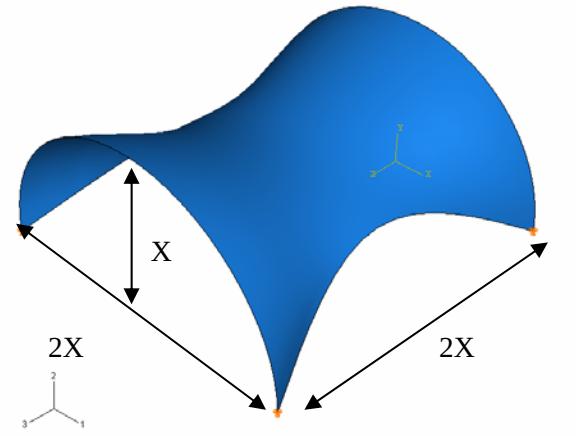

Figure 1. Global shape of the studied hypar surface. X is the maximal height of the surface and is variable. The projection of the hypar surface fits into a plane with dimensions 2X*2X.
(X = 1, 5 or 7.5m)

Three values were chosen for the height in the FEM analyses: 1, 5 and 7.5m. The length of the sides of the horizontal square in which the hypar shell can be projected is twice the height for the three studied cases. This means that the mathematical description (and thus also the curvature) of the three studied surfaces is the same and only the global dimensions are varied.

Since the material behaviour of TRC is rather complex, it will be briefly explained, before it is implemented into the finite element models. Focus is put on the stress-strain behaviour and the durability.

2 MATERIAL BEHAVIOUR

There are two points of attention that should be considered when a structure, comprising TRC, is to be dimensioned. (1) Although the behaviour of TRC is linear elastic in compression up to failure, the stress-strain behaviour in tension is nonlinear – as is shown in figure 2. In serviceability limit state, the variation of the stiffness with increasing load will have its consequences on the total deflection of the structure. (2) Since for some material combinations a considerable loss of strength can be expected within the lifetime of the studied structure, this is also included in the dimensioning examples. Two types of TRC materials (with different fibres and matrix) will be discussed in more detail and will be included into the FEM analyses. The behaviour of these two exemplary TRC materials is discussed in this section. The influence on the dimensioning is discussed in the next section. The first material combination under study in this paper is a mortar matrix with ordinary Portland cement (OPC), reinforced with AR-glass fibres. The second material under study consists of a combination of E-glass fibres with an Inorganic Phospate Cement (IPC). The similarities and differences between these materials will be discussed in more detail in following sections.

2.1 Tensile Loading

The global behaviour of TRC in tension and the underlying mechanisms are briefly explained in this section. Fig. 2 shows the three stages of a typical stress-strain curve. These three stages are globally defined as follows:

1. in the linear elastic stage or pre-cracking stage, the matrix and fibres both carry part of the applied load and generally exhibit the same deformation.
2. within the multiple cracking stage, matrix cracks are formed and stabilised by the fibres, which bridge these cracks. A fine crack pattern is built with increasing stress and existing adhesive bonds between matrix and fibres are releaved in the vicinity of the crack faces and replaced by a purely frictional stress transfer.
3. in the post-cracking stage, no new cracks develop any more in the matrix. Only the fibres contribute to the load bearing capacity with the increasing load and thus define the composite stiffness. The TRC composite fails when the fibres eventually fail or when they are pulled out of the matrix.

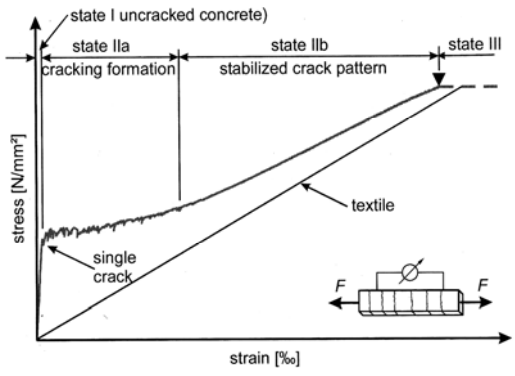

Figure 2. Typical stress-strain behaviour TRC composites

Several models, based on the global description explained above, have been developed, verified and described in detail over the years [e.g. Aveston *et al.*[1971]; Cuypers and Wastiels [2006]]. In the scope of this paper, it is sufficient to know that the stress-strain behaviour is nonlinear. The specific

curves that were implemented into the FEM calculation are shown in Fig. 3. This figure shows that the OPC mixture has a higher stiffness in the pre-cracked state (mainly due to the higher stiffness of the matrix), which can be advantageous in serviceability limit state, but the IPC combination shows higher strength (mainly due to the higher fibre volume fraction).

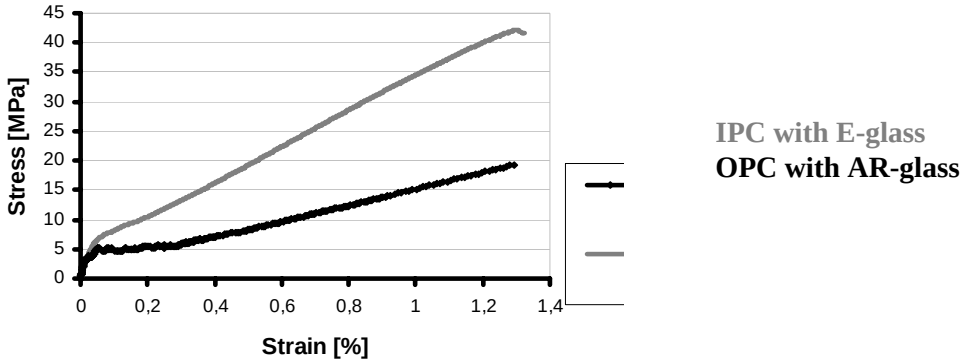

Figure 3. Stress-strain behaviour of the two studied types of TRC composites

2.2 Durability

In the early days of glass fibre reinforced concrete (grc), it was soon recognised that the fibres were aged under chemical attack by the matrix material itself (see e.g. Budd [1961]; Majumdar and Tallentire [1968]). This degradation of glass fibres in a concrete matrix occurs slowly but surely during the service life of the structure. Ageing of materials due to chemical attack under service conditions can globally be determined in two ways: (1) from specimens which were subjected to real environmental conditions and (2) from results obtained on similar specimens stored in a well-controlled environment in the laboratory. Unfortunately, when the studied processes are slow the first method is not a viable option to study "new" material combinations. Basic knowledge of the degradation mechanisms can however be used to study the materials of interest under "accelerated" ageing, meaning that the nature of the attack is not modified and processes are only accelerated within a laboratory environment. For grcs this method is commonly used (e.g. Litherland *et al.*[1981]). Rather than focussing on the description of detailed chemical reactions for several material combinations, this section aims to present a global methodology for the modelling of ageing due to chemical attack from an engineering point of view. Nowadays the majority of the authors agree on some important conclusions that can be used to model the loss of strength of glass fibres due to chemical attack in simulated pore solutions as function of temperature, humidity and time:

1. The remaining strength of the glass (and thus also of glass fibres) is determined by fracture mechanics: the loss of strength of the fibres is thus not due to global loss of fibre diameter, but due to the growth of the flaws (small defects) inherently present in the fibre. The order of magnitude of these flaws is about 10-100nm (e.g. Gao *et al.* [2003]; Orlowsky *et al.* [2005]). The rate of loss of strength is directly linked to the flaw growth rate.
2. The temperature dependency of the rate of chemical attack is expressed according to an Arrhenius relationship (Litherland *et al.* [1981]; Purnell et al. [2001]). Usually it is assumed that only one (e.g. Litherland *et al.* [1981]; Purnell et al. [2001]) or two (according to Orlowsky *et al.* [2005]) mechanisms occur as a function of the studied time-temperature frame. This Arrhenius relationship is thus usually used to express the dependency of maximal two rate constants as function of temperature.

3. The rate of chemical attack of glass is function of the humidity. For example Wiederhorn [1967] and Freiman [1980] noted that the rate of chemical attack of glass increases with increasing partial pressure of water within the surrounding environment. Orlowsky [2005] describes an increasing rate of ageing of full composite TRC specimens with increasing relative humidity.

The OPC material combination discussed in this paper has been tested under several temperatures and relative humidities at several ageing times. Based on these callibration tests, that were conducted in a well-controlled laboratory environment, a theoretical prediction of the loss of strength with time under real outdoor weathering was performed. Details are described by Cuypers and Orlowky [2007] and Fig. 4 shows the theoretically predicted loss of strength within four years of weathering in Aachen together with the experimental values.

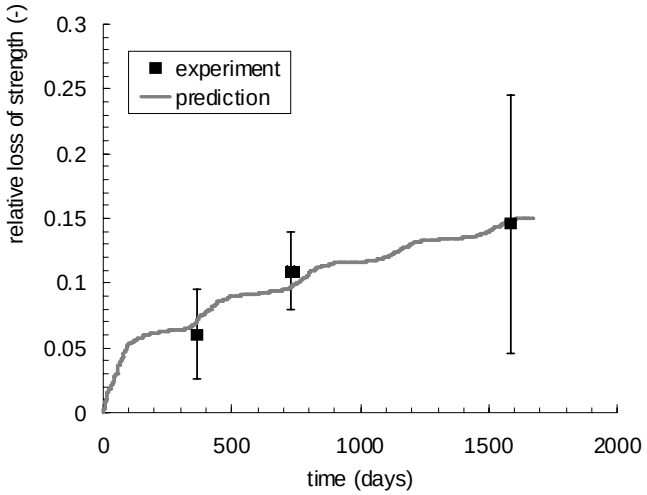

Figure 4. Evolution of the experimental and theoretical loss of strength of the OPC composite under natural ageing in Aachen after 4.5 years

Based on Fig. 4 it is clear that the required lifetime of the structure will have an influence on the necessary thickness: the remaining strength at the end of the lifetime of the structure will be lower when the ageing time increases. With the above mentioned methodology the remaining strength of the studied OPC composite is calculated for a lifetime of 10 years and for a lifetime of 50 years. It was found that for the OPC material combination under study, that the calculated loss of strength was 30% after 10 years of outdoor weathering and 40% after 50 years of outdoor weathering.

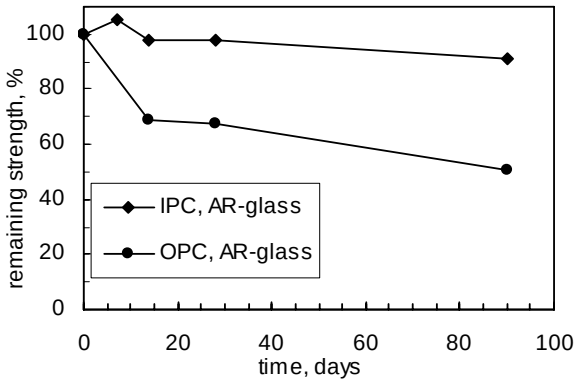

Figure 5. Evolution of the experimental loss of strength of OPC with AR-glass and IPC with E-glass under water at 50°C

Fig. 5 shows the evolution of the loss of strength of the OPC composite, as discussed before, and of the IPC composites within the same environment: after storage under water at at 50°C. This figure clearly shows that, although the OPC composites show distinct loss of strength, this is not the case for the IPC composite. It can therefore reasonably be assumed that the loss of strength of the IPC composites can be neglected.

3 FEM ANALYSIS

3.1 Implementation of Loads and Materials

Dimensioning was done following the Eurocodes as much as possible. This means that in ultimate limit state (ULS) it was checked whether the shells do not fail under all possible load combinations (including snow, wind, own weight) that can be defined under ULS. In serviceability limit state, no load combination that should be considered, is allowed to lead to too large deflections. In this case the maximum deflection was limited to span/250. In serviceability limit state (SLS), the engineering constants of the materials that are used, are average values. The non-linear stress-strain curves, as shown in Fig.1, represent the average behaviour of the two studied TRC materials and can thus be inserted into the FEM model as such. In ULS however, design values should be determined for the strength. The characteristic values of the strength (< 5% probability of failure, assuming a Weibull probability distribution function for the strength) were determined from series of experiments. After a material safety factor was applied to these characteristic values, the dimensioning values - which were then used in the FEM analysis and dimensioning – that were found were approximately 10MPa for the OPC composite and 20MPa for the IPC composite. These values represent the initial strength of the used materials and do not include possible effects of ageing yet.

In order to obtain representative values for the external loads, according to the Eurocodes, it was assumed that the building resides in Belgium on a flat topography terrain in an urban area, in which at least 15% of the surface is covered with buildings and their average height exceeds 15m. The design loads in ULS and SLS are determined according to this assumption.

The shell is pin supported at its four corners; the edges are free. This design leads to stress concentrations in the four corners. Therefore, the contact surface will be enlarged when constructing the doubly-curved shell. The global minimal thickness of the doubly-curved shells will be determined without considering these stress concentrations.

3.2 Overview of results and discussion

The minimal values of the necessary thickness of the hypar shells are listed in Table 1. For all dimensioning examples, the ultimate limit state was the decisive design state. As can be seen from Table 1, the necessary thickness is relatively low for all calculated cases. Since it was assumed, based on experimental results, that the E-glass reinforced IPC does not show considerable loss of strength with time, the calculated necessary thickness was not considered to be a function of time.

The calculation example with AR-glass fibre reinforced OPC shows that the necessary minimum thickness should be increased when the required lifetime of the studied structures is increased. Globally, for the studied type of hypar surface, the combination of IPC with E-glass seems to be the most advantageous from point of view of minimal thickness.

Table 1. Calculated necesarry mimimum thickness of hypar surfaces: influence of span, material combination and lifetime used.

material	*2m span*	*10m span*	*15m span*
IPC + E-glass	0.8	4.0	6.0
OPC + AR-glass, initial	1.1	5.5	8.5
OPC + AR-glass, 10 years	1.3	6.5	9.5
OPC + AR-glass, 50 years	1.4	7.0	10.5

Note: the calculated values for minimal thickness are depicted in cm

4 CONCLUSION

In this paper, the potential of TRC (textile reinforced concrete) in structural applications was studied by means of some illustrative design examples. The type of structure that was chosen here was a doubly-curved shell with varying span. The influence of the material choice was also discussed briefly. Generally, the design examples showed that shells with relatively limited thickness could be theoretically designed with TRC. If a newly developed durable material combination is used, only 6cm thickness should be sufficient to span a doubly curved shell with 15mx15m ground surface. If a less durable (but slightly cheaper) material combination is used, the necessary thickness increases up to about 10cm for a required lifetime of 50 years. The next step that is foreseen in the near future is an experimental verification on the studied shells with 2mx2m ground surface.

ACKNOWLEDGMENTS

Funding by the Flemish Fund for Scientific Research (FWO) of the post-doctoral research of the first author is acknowledged. Funding for the scientific Research (FWO) under the contract FWOAL320 is gratefully acknowledged.

REFERENCES

Aveston, J., Cooper, G.A., Kelly, A. 1971, 'Single and multiple fracture, The Properties of Fibre Composites', National Physical Laboratories Conference Proceedings, IPC Science & Technology Press Ltd. London, 15-24.

Budd, S.M. 1961, 'The mechanisms of chemical reaction between silicate glass and attacking agents', *Phys. Chem. Glasses*, **2**, 111-114.

Cuypers, H. and Wastiels J. 2006, 'Stochastic matrix-cracking model for textile reinforced cementitious composites under tensile loading', *Materials and Structures*, **39**, 777–786.
Cuypers, H., Orlowsky, J., 2007, 'Chemical Ageing mechanisms of glass fibre reinforced concrete', in A*geing of composites*, ed. Rod Martin, Woodhead Publishing, in press

Freiman, S.W. 1980, 'Fracture Mechanics of Glass', *Glass: Science and technology*, **5**, 21-78.

Gao, S.L., Mäder, E., Abdkader, A., Offermann, P. 2003, 'Environmental resistance and mechanical performance of alkali-resistant glass fibers with surface sizings', *J. Non-Crystalline Solids*, **325**, 230-241.

Litherland, K.L., Oakly, D.R., Proctor, B.A. 1981, 'The use of accelerated ageing procedures to predict the long term strength of grc composites', *Cement and Concrete Research*, **11**[3], 455-466.

Majumdar, A.J., Tallentire, A.G. 1973, 'Glass fibre reinforced cement', Intern. Symposium on Applications of Fibre reinforced concrete, Ottawa, Canada, 11 October 1973, American Concrete Insitute

Orlowsky, J., Raupach, M., Cuypers, H., Wastiels, J. 2004, 'Durability modelling of glass fibre reinforcement in cementitious environment', *Materials and Structures*, **38**, 155-162.

Orlowsky, J. 2005, Zur Dauerhaftigkeit von AR-glasbewehrung in Textilbeton, Deutscher Ausschuss für Stahlbeton, Heft 558. (in German)

Purnell, P., Short, N.R., Page, C.L. 2001, 'A static fatigue model for the durability of glass fibre reinforced cement', *Journal of Material Science*, **36**, 5385-5390.

Wiederhorn, S. 1967, 'Influence of Water Vapor on Crack Propagation in Soda-Lime Glass', *Journal of the American Ceramic Society*, **50**, 407-141.

11th International Conference on Durability of Building Materials and Components
Istanbul Turkey May 11-14, 2008

Permeability and Porosity as an Essential Factors in the Long-term Durability of Steel Fibres Reinforced Concrete

Beddar Miloud [1]

T11

ABSTRACT

Steel fibres have gained popularity in recent decades for use in concrete at relatively low volume fractions, mainly to ameliorate toughness, strength and shrinkage cracking. However, little information is available about the effects of fibers on the permeability and the porosity, which play an important role in long –term durability of concrete.

This paper presents the results of an experimental study that was carried out to examine the influences of steel fiber addition on the permeability and porosity of a concrete prepared mainly from local materials. The results tests are discussed in this paper and many interpretations of the results are reported as well as many reliable conclusions regarding effects of steel fibers on water and gas permeability of concrete.

KEYWORDS

Porosity, Permeability, Voids, Steel fiber concrete.

[1] M'sila University, Laboratory of Geomaterials, Civil Engineering Department, Faculty of Science and Engineering, 28000, Algeria, Phone 00213 72455813, Beddarm@yahoo.fr

1 INTRODUCTION

Permeability of concrete generally refers to the rate at which water or other aggressive substance (sulphates, chlorides ions, etc.) can pass through the concrete. It plays an important role in the long-term durability of concrete material [Jackson, 1978]. Low permeability is an important requirement for hydraulic structures and in some cases water tightness of concrete may be considered to be more significant than strength although, other conditions being equal, concrete of low permeability will also be strong and durable. A concrete, which readily absorbs water, is susceptible to deterioration. This deterioration is determined largely by the ability of the cover zone concrete to resist the ingress of deleterious agents from the environment.

Concrete is inherently a porous material. This arises from the use of water in excess of that required for the purpose of hydration in order to make the mix sufficiently workable and the difficulty of removing all the air from the concrete during compaction. If the voids are interconnected concrete becomes pervious although with normal care concrete is sufficiently impermeable for most purposes.

Steel fibres have gained popularity in recent years and are used in concrete mainly to improve flexural and toughness strength, to reduce shrinkage cracking [Antoine, 1985; ACI Committee, 1984]. The arrest cracks shrinkage in young concrete by fibres could lead to reduce permeability of SFRC when compared with plain concrete [Tsukamoto and Worner, 1991]. But, little information is available about the effect of fibre addition on both porosity and permeability of concrete.

The main aim of this experimental study is to examine the influence of fibre length and fibre content on the porosity and permeability as essential factors in the long-term durability of a concrete prepared mainly from local materials. The work reported herein is based on laboratory experiments and carried out according to the ASTM standards [Astm, 1982] concerning the porosity property while gas and water Permeability were measured using the test rigs illustrated in Figures 1and 2.

2 MATERIALS AND METHODS

2.1 Basic Ingredients. The basic ingredients of steel fibre reinforced concrete were:

2.1.1 Portland cement

Type CPJ45, comes from AIN TOUTA factory and is conform to NF.P. 15.301. Chemical composition and physical properties are given in tables 1 and 2.

Table 1 Physical and mechanical test results

Blaine fineness m^2/ kg	Autoclave expansion, percent	Setting time(Vicat) Initial	Final	Compressive strength, MPa	Shrinkage µm/ml
324	0.01	105	220	45 (28days)	800

Table 2 Chemical composition (%, by weight) of CPJ cement

Constituent, %	SiO_2	Al_2O_3	Fe_2O_3	Ca O	Mg O	Ca O free	SO_3	P.F	Insoluble
CPJ45	19.48	5.06	3.72	61.95	0.85	1.63	1.1	3.44	1.26

2.1.2 Coarse aggregate

this is local aggregate obtained by crushing of the limestone rock from the COSIDER carry. It has two fractions 3/8 and 8/15. Its physical properties are given in tables 3 and 4.

Table 3 Some characteristics of the sand and gravel used in the tests

Materials	Density	Porous/dense	Compactness	Porosity	Sand equivalent
Sand	2.56	1.64/1.83	36.42/70.76	36.58/29.24	75.4/77.2
Gravel 3/8	2.68	1.28	47.46	52.24	……
Gravel 8/15	2.68	1.32	49.25	50.75	……

Table 4 Some physical and mechanical and morphological properties of the gravel used

Gravel Grading	Superficial tidiness (P)	$CaCO_3$ (%)	Flattening Coef	Los Angles (LA) MDE
3/8	1.5	8.5	18	20	16
8/15	1.28	8.3	13	23	17

2.1.3 Dune sand

this is a clean, siliceous and fine sand of fraction 0/5 taken from BOUSAADA region. Its characteristics are regrouped in tables 3 and 5.

Table 5 Chemical composition (%, by weight) of the dune sand used.

Constituent, %	SiO_2	Al_2O_3	Fe_2O_3	Ca O	Mg O	Ca O free	SO_3	P.F	Insoluble
Sand of dune	86.04	1.35	0.86	6.63	0.08	…..	…….	5.00	…….

2.1.4 Steel fibers: all fibers used in this study were steel fibers having 1.2 mm diameter, 10÷30 mm length, the average fiber density was 7.89. The fiber content was varying from 0.5 to 2% by volume. Its characteristics are regrouped in table 6.

Table 6 Some physical and mechanical properties

Density	Tensile strength MPa	Elasticity modulus MPa	Dilatation Coef (µ/m)	Fire resistance °
7.8	1000 to 3000	2×10^5	11	1500

2.2 Mix Proportioning

Concrete mixes were designed to provide a slump of (60±10mm) for ease of handling, placing and finishing. The air content of all mixes is 3 ± 0.5 %. The concrete mix proportion used (class 350 dan/m^3) has been determined by absolute volume method [Komar, 1982] and were follows: Cement 350 kg/m^3, Sand 758 kg/m^3, Gravel 1073 kg/m^3 and total water 215 l/m (This quantity takes into account the degree of aggregates absorption)

3 SPECIMEN PREPARATIONS AND CONDITIONNING

3.1 Mixing, Casting and Curing

A total of nine plains (three for porosity tests, three for gas permeability tests and three for water permeability tests) and forty five fibre reinforced mixes were prepared. Materials were mixed in a linear-cum-flow mixer type 'O' which had a capacity of 0.043 cubic metres and a power driven rotating pan and paddle. This mixer was sturdy enough for fibrous mixes, and a good uniformity of fibre distribution could be achieved. The mixer was first loaded with the coarse aggregate and a portion of the mixing water; after starting the mixer; sand, cement and the rest of water were added and mixed for 5 min. The fibres, in the case of fibrous mixes, were added following the addition of all mix ingredients.

Three 16×32 mm cylinders were cast from each mix. They were cast in cylindrical steel moulds and compacted on a vibrating table. Specimens were placed under plastic sheet membrane for 24 hours in an ambient temperature. Following removal from the moulds, they were individually sealed in plastic bags and stored at room maintained at 24°C and 65% relative humidity until testing at an age of 7, 14 and 28 days for porosity tests and only at age of 28 days for permeability tests. But, before testing, the cylinders were removed from the plastic bags, and cut (in the case of porosity and gas permeability tests) using specimen cutting machine into 50 mm- thick slices having removed a 10mm thick slice from the top and the bottom.

4 POROSITY AND PERMEABILITY TESTS

4. 1 Porosity Test in Hardened Concrete

The porosity of steel fibre reinforced concrete, as well as plain concrete, is an important characteristic, which determines to a large extent their mechanical properties. High porosity is strongly detrimental to the strength and permeability of a concrete, particularly if the pores are of large diameter.
To evaluate the porosity of hardened concrete and following ASTM C642 testing procedures, apparent, bulk saturated surface dry, and bulk dry specific gravities of hardened concrete (in both cases: plain concrete and steel fibre reinforced concrete) were evaluated by using the following formula:

$$T.V = (1 - y_1 / y) \times 100 \ldots\ldots..(1)$$

Where T.V = Volume of permeable pore space in concrete, percent
y_1 = Concrete bulk dry specific gravity
y = Concrete apparent specific gravity

4.2 Water Permeability Test in Hardened Concrete

Water permeability was measured using the apparatus illustrated in Figure 1. It consists of a metal stand with three permeability cells, unit pressure regulator range from 0 to 30 bars, and a graduated gauge glass. Each cell comprises a top and bottom steel plate which bolt together by three steel shafts fixed on the stand (Fig. 2). The base plate is mild steel with a 20mm diameter hole drilled to form the water inlet. The top is also steel but with a circular window, through which the top face of the test specimen can be observed. After putting the test specimen in the cell and making the water pressure on, Flow test is normally measured by observing the rate of flow of water through the calibrated glass

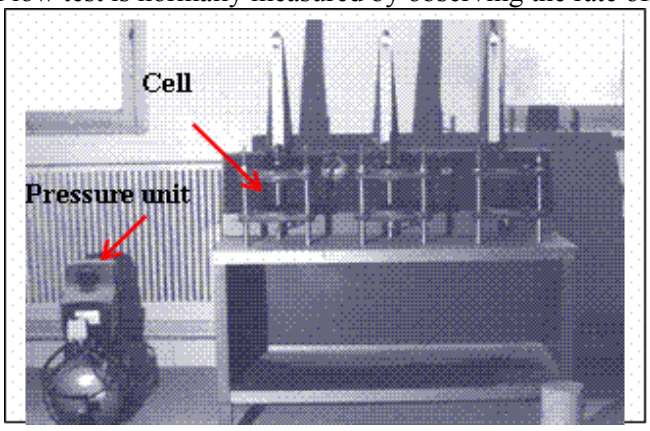

Fig .1 Water Permeability Test Rig

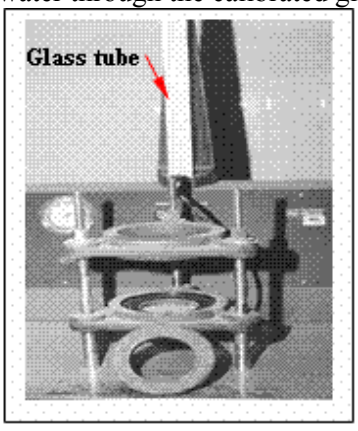

Fig .2 General View of the Cell

Generally, for concrete complete penetration of the specimen may take several days or more. In our case, the specimens are removed from the test after one week, and the permeability coefficient calculated from the depth of water penetration.

4.3 Water Permeability Coefficient

The test, in this case, consists in making an amount of water, under a determined pressure, flows through a cylindrical specimen of concrete and then measure the flow.

♦ To measure the coefficient of water permeability by flow, the DARCY'S Law [Darcy, 1856] can be applied as the flow is continuous:

$$K_{1D} = Q.X \ / A.\ h \qquad (2)$$

Where Q is the volume flow rate given in (m^3/s), A is the cross-sectional area of the test specimen in (m^2), h is the head of water given in (m), X is the specimen thickness in the direction of thickness (m), K is the permeability coefficient.

♦ To measure the water coefficient by penetration, VALENTA'S Law |Valenta,1970] can be applied if the material is less permeable:

$$K_{1V} = \chi^2_{P}.\ V / 2.h.t \qquad (3)$$

Where K_{1V} : Water permeability coefficient (m/s)
χ^2_P : depth of penetration (m) V : Volume of voids filled by water in the penetrated zone.
t : Time to penetrate to depth χ_P (s) , h : Applied press ion (eg: 1 bar = 10m)

The two coefficients calculated from equation 2 and 3 are derived for a specific fluid flowing through a specific porous medium. To compare the permeability of concretes obtained from tests using different liquids it is necessary to define the "intrinsic permeability" K_i, which should depend only on the pore structure of the concrete:

$$K_{1c} = Q\ \chi\ \eta\ /\ A(\ P_1 - P_2) \qquad (4)$$

Where K_{1c} = intrinsic permeability of concrete (m^2) η = viscosity of liquid
P_1 = upstream pressure (N/m^2) P_2 = downstream pressure (N/m^2)
$P_1 - P_2$ = pressure differential = h ρ g, P = density (kg / m^3) and g = 9.81 m/s

Substituting for $P_1 - P_2$ in equation 4.

$$K_{1c} = Q\ \chi\ \eta\ /\ A\ h\ \rho\ g \qquad (5)$$

Then $K_{1c} = K_{1D}\ \eta\ /\ \rho\ g$; for water $\rho = 1000 kg/m^3$, hence $K_{1c} = K_{1D}.\ 10^{-3}/1000.\ 9.61 = 1.02.\ 10^{-7}\ .\ K_{1D}$
For water, therefore, the intrinsic permeability coefficient in units of m^2 is approximately 10^{-7} times the Darcy coefficient in units of m/s.

4.4 Gas Permeability Test

The test rig used to measure gas permeability is illustrated in Figure.3. It is an apparatus with measurement of bubble flow, it is made up mainly:

- A pressure unit automatically-controlled leading to cell entry
- Glass tubes of different volumes (1.5-5-15-150ml)

The test cell is made up of 5 parts: an aluminium receiver, two milled plates being used for recuperating oxygen crossing the concrete disc, a polyurethane membrane surrounding the disc of concrete and a lid (Fig 4).

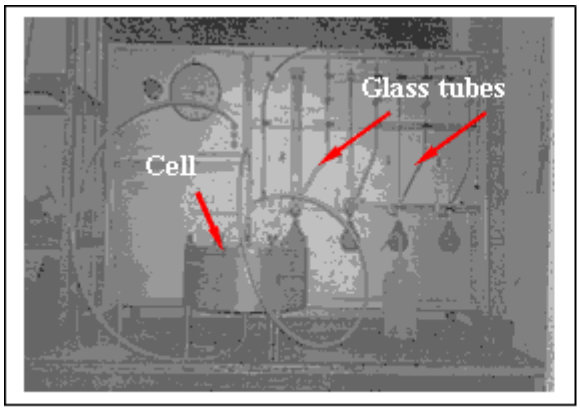

Fig 3. Gas permeability test rig

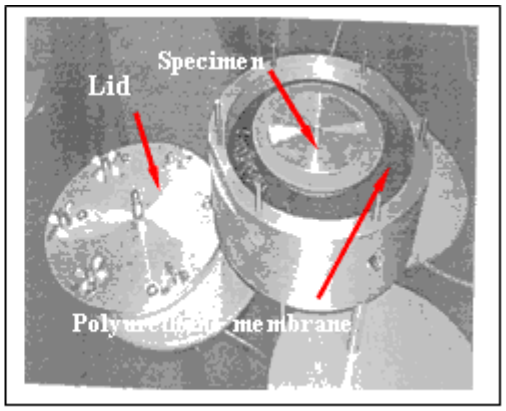

Fig 4. General view of the cell

4.5 Gas Permeability Coefficient

The principle is the same one as for water, a gas overpressure is applied to one of the test disc and a flow is measured at the exit. Thus, The permeability coefficient obtained using a gas normally defined by the Hagen-Poiseuille 's formula:

$$Kg = 2.\ Q.x.P_0.\ \mu.\ /\ A\ (\ P^2 - P_a^{\ 2}\ ) \qquad (5)$$

Where K_g is the intrinsic permeability coefficient of gas in units of m^2,μ is the dynamic viscosity of liquid, P is the downstream pressure , P_0 is the pressure at which the flow is measured (generally =Pa), Pa is upstream pressure , Q , A, x are as defined previously. Here, it very important to mention that the flow rate is measured at downstream face. If the flow rate is measured through the upstream face, then P replaces $P_a$in the numerator.

5 TEST RESULTS

5.1 Porosity Test Results and Discussion

Porosity in hardened concrete (nine unreinforced concrete specimens and twenty seven steel fibres reinforced concrete specimens) was determined according To ASTM C642 standard method. The results given in this paper are the average values obtained from three specimens per mix. A relationship between porosity and curing age, fibre content, fibre length and slice position was established using data calculated by equation 1.
In this investigation, pores distribution throughout the plain and reinforced concrete specimens were evaluated after slicing each cylindrical specimen into six cylindrical slices (from top to the bottom).

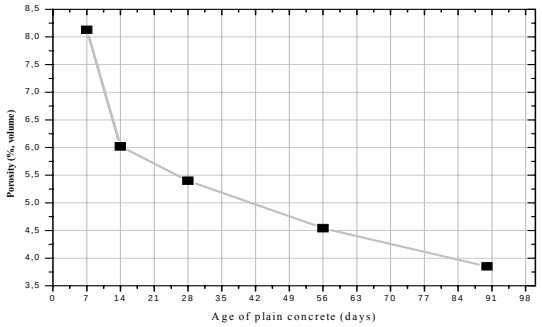

Fig 5. Relationship between pores percent and cure age (Average values of the whole specimen)

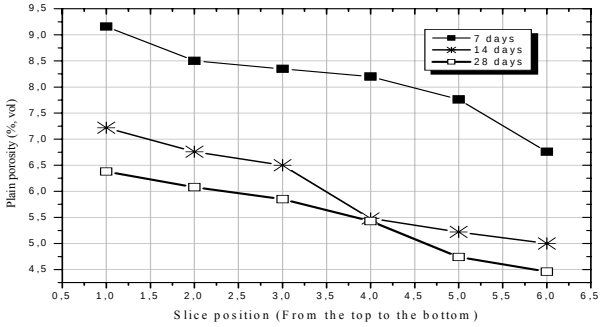

Fig 6 Relationship between pores and cure age at different positions

The porosity percentage decrease from 6.38 % in the top slice to 4.46 % in the bottom slice, which is the most compacted part of the specimen. This indicates that pores content are not uniformly distributed throughout the specimen .The 28 days porosity values for plain concrete specimens cured in the laboratory were shown in figure 5. These values were in the range of 4.46 percent (in the bottom slice) to 6.38 percent (in the top slice). It can be also seem from figure 5 that porosity content decrease with increasing cure age. The 7 days porosity content value was 8.13 percent. But this percent was only on the average of 5.49 at the age of 28 days. This can be explained by the hydration process in which the capillary pores and air voids are partially or completely filled with the hydration products and the possibility of water flow is gradually reduced. This fact is also confirmed by other researchers [Brandt, 1995; Husseyin, 1995] who reported that the duration and quality of cure of the fresh mix determine the process of hydration and the volume of hydration products, which may eventually fill the capillary pores and reduce their permeability.

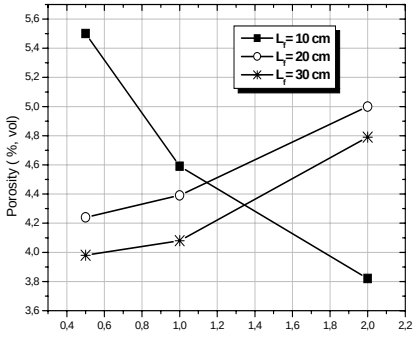

Fig 7 Relationship between porosity and

Generally, it can be seen from figure 6 that the value of porosity is lower after 28 days at ambient temperature, because the pores accrete. On the contrary, concrete with steel fibers exhibits lower porosity values compared with plain concrete at the same slice and in the same direction. With fiber amount varied in the range of 0.5 to 2 % by volume (L_f= 10mm), the porosity varied from 5.5 to 3.82 %, as it can be seen from figure 7, whereas with fiber length of 20mm the porosity increased with increasing fiber content. The addition of fibers, with length of 30mm, did not affected the porosity in the amount values ranged from 0.5 to 1 % but, beyond the 1 % there was a slight increase in the porosity. The slight decrease reported in the porosity of specimens reinforced with steel fibers compared to the plain concrete can be explained by the fact that reinforced concrete specimens needed a long duration of vibration which surely affected the pores rate and their sizes and their distribution. It is important to mention that many studies [Brandt, 1995; Husseyin, 1995; Bencheick &Baali, 2003; Bhattacharjee et al., 2004] have reported that fibers addition did not significantly increase the amount of pores above those calculated for plain concrete.

6.2. Water permeability results and discussion

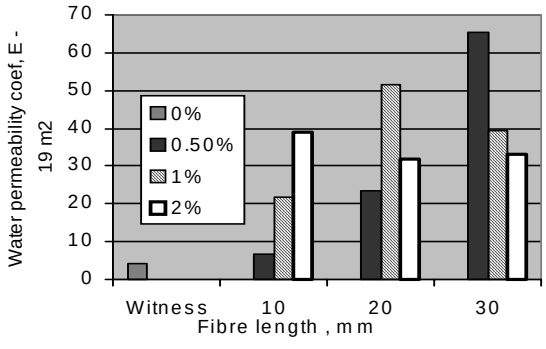

Fig 8. Relationship between Kw and Fibre length

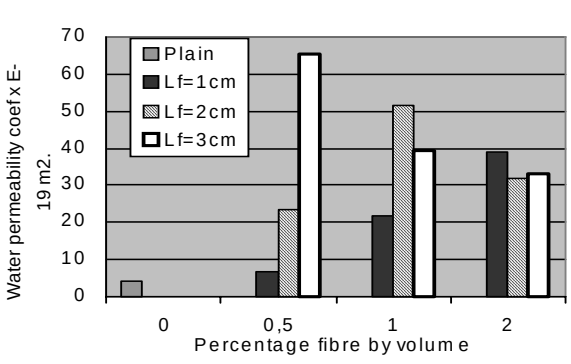

Fig 9. Relationship between Kw and fibre content

Generally in the cases of a concrete as a composite a great porosity does not mean high permeability. Indeed only the interconnected of these pores is significant for permeability. The results given in this paper are average values obtained from three specimens per mix and were derived from penetration measurements using the Valenta equation 3. All results are reported in figure 8 and 9. Steel fibre addition to concrete clearly increases water permeability coefficient whatever fibre amounts or fibre lengths as it can be seen from figure 9 and 10. Water permeability coefficient of a plain concrete was around 4.02×10^{-19} m^2, while it can be said that all the three fibre lengths, with an amount of 0.5% by volume, caused water permeability coefficient to range from 6.71×10^{-19} m^2 for L_f =10 mm to 23.36×10^{-19} m^2 for L_f =20mm and 65.49×10^{-19} m^2 for L_f = 30mm. At 1 % fibre content, water permeability coefficients were 21.87×10^{-19} m^2, 51.39×10^{-19} m^2 and 39.21×10^{-19} m^2 for 10mm, 20mm and 30mm fibres respectively. But, at 2% fibre content this coefficient varied from 38.83×10^{-19} m^2 L_f = 10mm to 33.18×10^{-19} m^2 for L_f = 30mm.

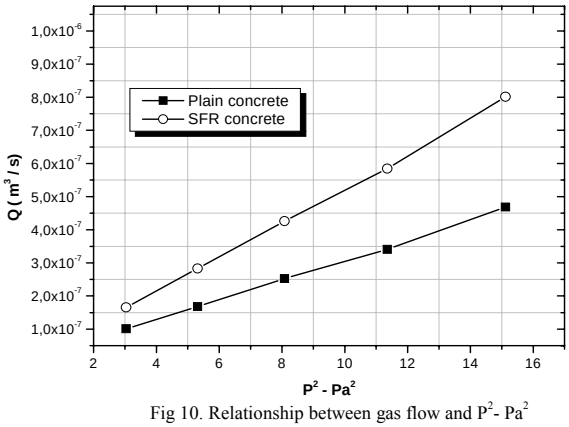

Fig 10. Relationship between gas flow and P^2- Pa^2

Generally water permeability tests are very complicated to be realized and results given in this paper can be explained by the fact that the presence of fibres, whatever their lengths or their contents facilitated the interconnection between pores which were reduced according to the porosity results. The fibre acted as a bridge between pores so that the flow rate had been increased and water permeability coefficient was subsequently increased.

6.3.Gas Permeability Results and Discussion.

The permeability was determined by using equation 3 of Hagen-Poiseuille. Tests were carried out on a ordinary concrete disc with thickness of 65 mm, having undergoes a 28 cure days as mentioned before. A pressure of 5 bars is selected on the pressure gauge of the permeameter and fluid movement is observed in the tubes during 5 minutes. This enables us to check that oxygen does not pass by the disc edges when the tire is inflated. Typical results of a plain concrete specimen as an example are given in table7, while some results, which represent steel fibres reinforced concrete specimens, are given in table 8. The average value of permeability coefficient K_g for plain concrete is 3.6950×10^{-17}, while that of concrete reinforced with 1 % by volume of steel fibres is 4.0916×10^{-17} . This means that steel fibres increased gas permeability coefficient. To explain such increase in the gas permeability coefficient of steel fibre reinforced concrete, it may be assumed that even permeability is determined more by matrix properties [Brandt, 1995; Husseyin, 1995, Bamforth, 1987] than the fibres ones.
Particularly, the matrix-fibre interface has the largest content of pores and micro cracks that effect overall permeability. Also, it is very important to mention here that fibres act as ties between pores so that great interconnections can be created which allow gas flow to penetrate easily inside the concrete structure.
All results were obtained at the time of a rise in pressure followed by a descent. The final result being an average of each pressure of the calculated permeability.In the large majority of the cases, the average value obtained in the downward phase in the pressure is the same as that measuring of the rising phase.

All results of the gas flow (Q_g) can be plotted against pressure variation. Figure 10 is a typical example that can confirm the influence of fibre addition on gas permeability concrete. It can be seen from figure 10 and from all other obtained that all curves are very close to be approximately straight lines which ensure the correct operation of the equipment, of the assembly carried out and the aptitude of oxygen to cross material.

Table 8: Typical results of steel fibre concrete

P (bars	0.5	1	1.5	2	2.5	3
T1	33	39	29	39	44	32
T2	34	40	30	40	44	32
T3	34	39	30	39	44	32
T4	35	40	30	40	44	32
T5	34	40	30	40	44	32
T moy (s)	34	39.6	29.8	39.6	44	32
V (ml)	1.5	4	5	10	15	15
Pa (bars)	1.02	1.02	1.02	1.02	1.02	1.02
P^2- Pa^2	1.27	3.04	5.31	8.08	11.35	15.12
Q(m^3/s). E-07	0.4411	1.01	1.6779	2.5253	3.409	4.6875
Ki (m^2). E-17	4.081	3.9035	3.7121	3.6716	3.5286	3.6421
K (m^2)	3.7565					

6 SUMMARY AND CONCLUSIONS

At 0.5, 1 and 2 percent volume fraction, effects of steel fibres, with three different lengths, on water and gas permeability of concrete were investigated experimentally. Results of this investigation indicate that high porosity does not mean high permeability. The only factor which governs the permeability process is the pores interconnections. The porosity results presented in the paper indicates that steel fibres can reduce porosity. This reduction may be referred to the vibration duration that was longer with steel fibres reinforced concrete specimens compared to plain concrete specimens. More tests will be required to allow the determination of the exact influence of the fibres in this respect. Steel fibre addition to concrete clearly increases water permeability coefficient whatever fibre amounts or fibre lengths. This increase is also observed with gas permeability coefficients. The fibers acted as bridges between pores so that the flow rate had been increased and both water and gas permeability coefficients were subsequently increased. As a conclusion, it is important to mention that with 1 % fibre content, water permeability coefficient was 21.87×10^{-19} m^2, while the average value of gas permeability coefficient K_g for a concrete reinforced with 1 % by volume of steel fibres was 4.0916×10^{-17}. So, concrete permeability coefficients obtained using water and gas was considerably different, due to the phenomenon of gas slippage.

REFERENCES

ACI COMMITTEE 554, “State Of The Art Report On FRC”, J. Am. Concrete. Inst., 1984, Pp 140-146

ANTOINE, E.N. “Fibre-Reinforcement Concrete” Conc. Intern, March1985, Pp 21-25

ASTM C 6426-82 “ Standard Test Method.” American Standard Of Testing Materials, 1982, Pp 395-97

BAMFORTH, P.B “The Relationship Between Permeability Coefficient For Concrete Obtained Using Liquid And Gas ” Magazine Of Concrete Research: Vol. 39, N°. 138: March ,1987, Pp 3-10.

Bhattachrjee, B Et Al " Permeabile Porosity Of CM" J M In C Eng, 2004,16(4), 322-330.

Bencheick, M., Et Al, " Permeability And Porosity Of Concrete " Conf, , M'sila University, 2003, 263-274.

BRANDT, A.M « Cement-Based Composites: Materials." E & FNSPON, London, 1995.

DARCY, H.P "Les Fontaines Publiques De La Ville De Dijon". Paris, 1856, Pp. 19-20.

HUSSEYIN, S Et Al " Permeability And Durability Of Plain And Blended Cement Concretes Cured In Field And Laboratory Conditions." ACI Materials Journal, V: 92 N°12, March-April , 1995, Pp 111-116.

JACKSON, N. Civil Engineering Materials,3rd Edition, Mack Press Ltd,1978, London.

KOMAR, A. "Matériaux Et Eléments De Construction ". Edition Mir, Moscow, 1982.

TSUKAMOTO, M. WORNER, J.D « Permeability Of Cracked Fibre Reinforced Concrete." Darmstadt Concrete: Annual Journal On Concrete & Concrete Structures, 6 (1991),Pp 123-135.

VALENTA, D " The Permeability And Durability Of Concrete In Aggressive Conditions", Proceedings Of The 10th International Congress On Large Dams, Montreal, 1970.Pp. 103-117.

11DBMC International Conference on Durability of Building Materials and Components
ISTANBUL, Turkey 11-14 May 2008

Accelerated Weathering Effects on the Mechanical and Surface Properties of CFRP Composites

Saud Aldajah [1]
Ashraf Biddah [2]
Abd Alsattar Noureldin [3]
Ammar Al-Omari [4]

T 11

ABSTRACT

This study provides data regarding the characteristics of three carbon fiber reinforced polymer (FRP) laminates with three types of resins exposed to accelerated natural weathering conditions according to ASTM G-154-00a for 1000hrs. The FRP laminate consists of three layered CFRP sheets bonded together with an adhesive. Three-point bend testing according to ASTM D790 showed that ultra violet (UV) light exposure decreased the flexural modulus of the three- layered FRP samples by 10%, 36% and 2% for samples A, B and C respectively. While the reduction for the resin samples was 11.8%, 8.3% and 14.3% for samples A, B and C respectively. SEM analysis showed cracking and deterioration in the resin and FRP systems as a result of the exposure to natural weathering.

KEYWORDS

FRP, Weathering, Durability

[1] Mechanical Engineering Department, UAE University P. O. Box 17555. , Phone +971-50 733 4817, Fax +971 3762 3158, s.aldajah@uaeu.ac.ae
[2] Civil Engineering Department, UAE University P. O. Box 17555. , Phone +971-50 763 6202, Fax +971 3762 3158, abiddah@uaeu.ac.ae
[3] Mechanical Engineering Department, UAE University, P. O. Box 17555. , Phone +971-3 713 3054, Fax +971 3762 3158, A.Noureldin@uaeu.ac.ae
[4] Mechanical Engineering Department, UAE University P. O. Box 17555. , Phone +971-50 713 3584, Fax +971 3762 3158, a.alomari@uaeu.ac.ae

1 INTRODUCTION

FRP composite materials have been widely used in strengthening concrete structures in the past few decades. One of the most important issues with using FRP materials to strengthen concrete structure is the durability and long term performance, especially in hot and humid environments. FRP composite materials can provide longer lifetimes and lower maintenance than equivalent structures fabricated from conventional materials if it is designed and applied appropriately. The feasibility of strengthening concrete structures through the external bonding of FRP composites has been extensively demonstrated through laboratory tests and field applications [1-11], there are still significant unanswered questions related to durability and extent of service life that can be expected. For any application it is critical that a designer know not just the short-term behavior of the materials under consideration, such as strength and modulus, but also the rates of deterioration of these properties as a function of exposure condition and time. In the case of strengthened structures, the assessment of service life is complicated and difficult to define precisely since it depends on the intrinsic durability of not only the FRP system used to strengthen the structure, but also on the integrity of the adhesive bond between the FRP and the concrete substrate. There are many factors affect the performance of an FRP and adhesive materials. Among these factors is the ultraviolet (UV) exposure [12]. UV exposure is usually confined to the top few microns of the surface [13]. This causes surface degradation which can affect the mechanical properties disproportionately, as flaws that results from degradation can serve as stress concentrators and initiate fracture at stress levels much lower than those for unexposed specimens.

The purpose of this research was to evaluate the three different types of FRP laminates and resins and assess the UV impact on their mechanical behavior. These systems are to be used in stregthening the concrete structure in Abu Dhabi Company for Onshore Oil Operations (ADCO), hence the most durable system was recommended.

2 EXPERIMENTAL PROGRAM

2.1 Materials and Sample Preparations

A group of carbon fiber reinforced polymer sheets and resins were considered for this experimental program. These materials were provided by three different manufacturers and are labled as A, B and C. A total of six samples per group of FRP materials were made by gluing three layers together using the corresponding adhesive. The size of these samples was 25 mm width and 150 mm length. The above mentioned adhesives were applied to the FRP sheets using a brushing process followed by a rolling process to evacuate the entrapped air between the different layers. Similarly six resin samples were made with the same size and a thickness of 4 mm. In the case of the resin samples, the resins were prepared and poured into a mould of the required dimensions.

2.2 Exposure Environment

WETHEROMETER BS3900 UV accelerated testing machine was used to expose a total of 18 samples for a total of 1000h. The exposure cycle consisted of 8 hr UV exposure at 60˚C and 4h condensation at 50˚C.

3 RESULTS AND DISCUSSION

3.1 Mechanical Behavior Testing

The three point bending flexural test provides values for the modulus of elasticity in bending EB, flexural stress σf, flexural strain εf and the flexural stress-strain response of the material. The three-point bending machine, shown in figure 1, was used to evaluate the flexure behavior of controlled and

weatherd samples. The Modulus of elasticity of resin samples are shown in figure 2. All weathered resin samples have experienced reduction in the modulus of elasticity due to the UV exposure. The percentage in modulus of elasticity reduction are 11.8%, 8.3% and 14.3% for A, B and C samples, respectively. It should be noted that the highest modulus of elasticity is for sample C with values of 5.6 GPa and 4.8 GPa for the control and weathered samples respectively.

Figure 3 shows the elastic modulus comparison for the three-layered FRP system. The three-layered FRP samples have shown the same trend, UV exposure has reduced the elastic modulus elasticity by 10%, 36% and 2% A, B and C samples, respectively.

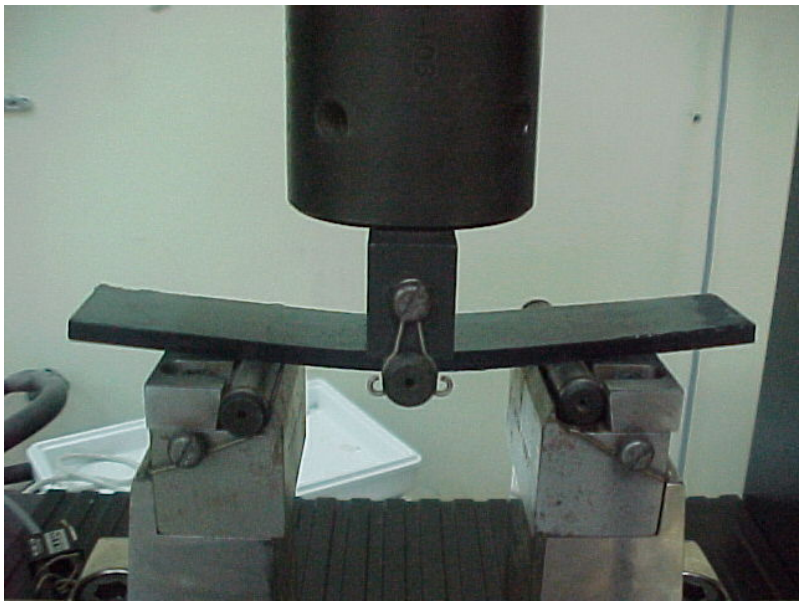

Figure 1. Three-point testing machine.

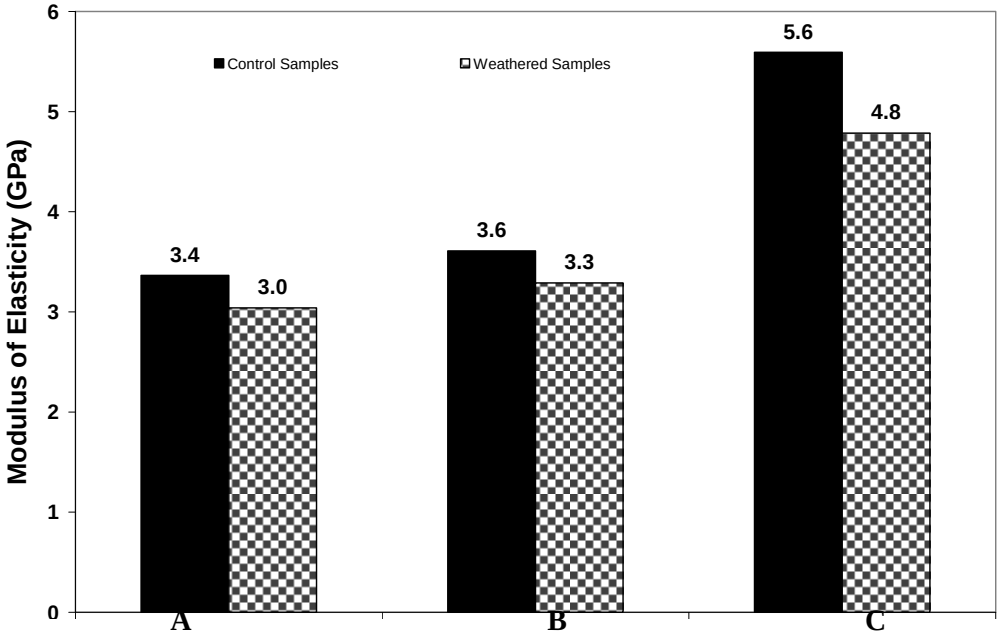

Figure 2. Modulus of elasticity for weathered and control resin samples.

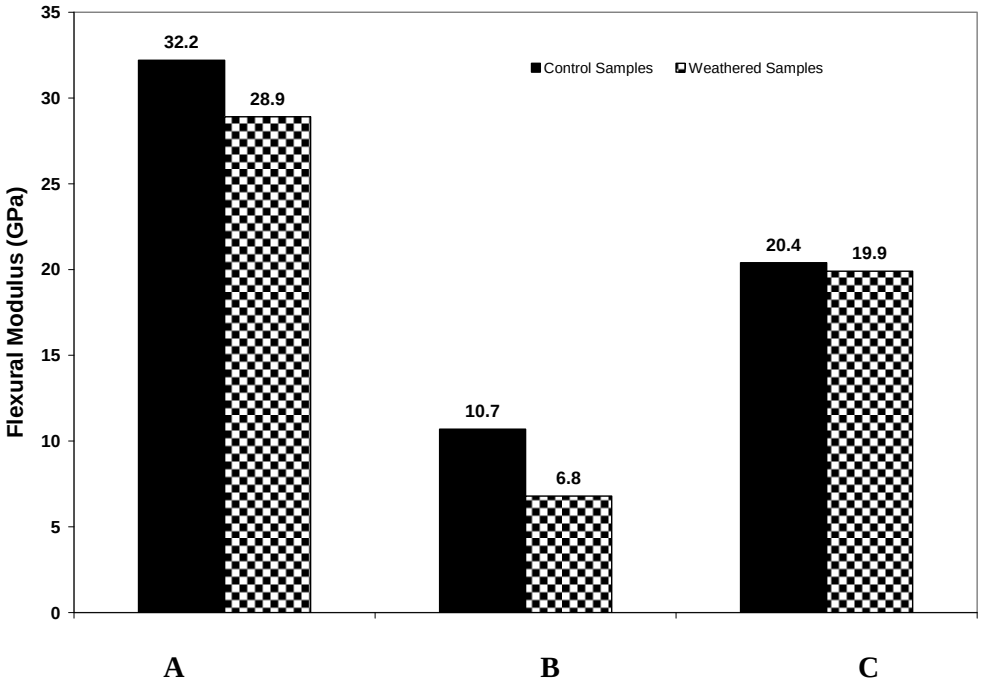

Figure 3. Modulus of elasticity for weathered and control three-layered FRP samples.

3.2 SEM Analysis

Specimens that were subject to accelerated weathering were tested under a three point flexural bending test and the fractured surfaces were analyzed using the scanning electron microscope. Fractured surfaces of virgin samples were also analyzed for benchmarking. For the virgin specimens, failure occurred mostly through matrix delamination as shown in figure 4-6. It can be seen from this figure that fibers and matrix exhibited a strong bond for the control samples. For the specimens subjected to environmental testing, the failure resulted from a matrix cracking and matrix fiber debonding.

Similary it was obvious to see the resin deterioration under the scanning microscope. All resin samples exhibited deterioration with microcracking as a result to the UV exposure. Figures 8-10 show SEM pictures of control and weathered samples.

(a) **(b)**

Figure 4. Enhanced magnification showing fractured **A** samples with (a)good adhesion between the fibers and the matrix for virgin samples, and (b) matrix cracking.

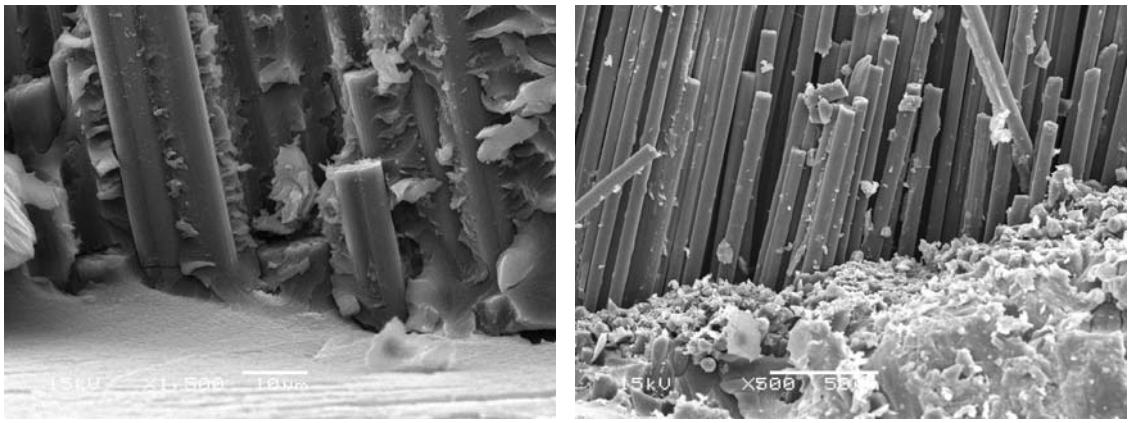

(a) **(b)**

Figure 5. Enhanced magnification showing fractured **B** samples with (a)good adhesion between the fibers and the matrix for virgin samples, and (b) matrix cracking.

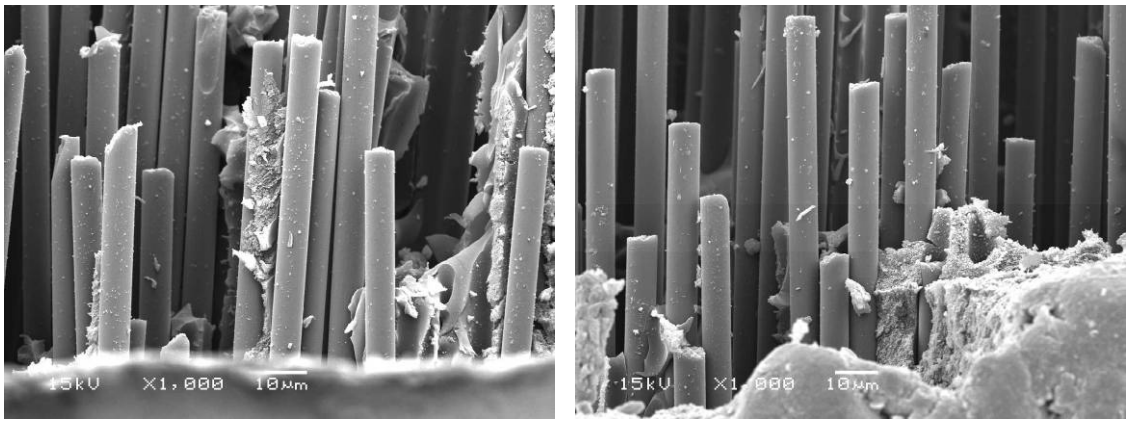

(a) **(b)**

Figure 6. Enhanced magnification showing fractured **C** samples with (a)good adhesion between the fibers and the matrix for virgin samples, and (b) matrix cracking.

4 CONCLUSIONS

The extended exposure of UV light to the composite materials would decrease the mechanical strength and flexure modulus. Examinations of composite and resin fractured samples under SEM revealed that the failure of the weathered three-layered samples was due to debonding between the matrix and fibers, while for the control samples failure occurred due to delamination. This is attributed to the reactions between the UV ray and the matrix. T

Based on the results of this research it was reccommended to use sample A FRP composites wraps for sregthening ADCO concrete structures due to the fact that the modulus of elasticity value was higher than B and C samples.

ACKNOWLEDGMENTS

This project was supported by ADCO.

REFERENCES

Saadatmanesh, H. & Ehsani, M.R. 1991, 'Reinforced concrete beams strengthened with GFRP plates-I. Experimental study', *ASCE Journal of Structural Engineering*;117(11):3417-33.

Ritchie, P.A., David, A.T. Le-Wu, L. & Guy, M.C. 1991, 'External reinforcement of concrete beams using fiber reinforced plastics', *ACI Structural Journal*, 88(4):490-500.

Meier, U. & Kaiser, H.P. 1991, 'Strengthening of structures with CFRP laminates' Proceedings on Advanced Composite Materials in Civil Engineering Structures, MT. Div./ASCE/Las Yegas,. p. 224-32.

Meier, U., Deuring, M., Meier, H. & Schwegler, G. 1992, 'Strengthening of structures with CFRP laminates: research and applications in Switzerland'. In: Neale KW. Labossiere P, editors. *Advanced Composite Materials in Bridges and Structures*. Canadian Society for Civil Engineering.

Shahawy, M.A., Arockiasamy, M., Beitelman, T. & Sowrirajan, R. 1996, 'Reinforced concrete rectangular beams strengthened with CFRP laminates', Composites Part B;27B(3/4):225-33.

Shahawy, M.A., Beitelman, T., Arockiasamy, M. & Sowrirajan, R. 1996, 'Experimental investigation on structural repair and strengthening of damaged prestressed concrete slabs utilizing externally bonded carbon laminates', Composites Part B;27B(3/4):217-24.

Takada, K., Mitsui, Y. & Murakami, K. 1996, 'Flexural strength of reinforced concrete beams strengthened with carbon fibre sheets', Composites Part A;27A(10):981-7.

Faza, S.S. & Ganga Rao H.Y.S. 1994, 'Fiber composite wrap for rehabilitation of concrete structures', Proceedings of the Materials Engineering Conference 804. ASCE. 1135-9.

Ross, A.C., Jerome, O.M., Tedesco, T.W. & Hughes, M.L. 1999, 'Strengthening of reinforced beams with externally bonded composite laminates', *ACI Structural Journal*;96(2):212-20.

Spadea, G., Bencardino, F. & Swamy, R.N. 1998, 'Structural behavior of composite RC beams with externally bonded CFRP', *ASCE Journal of Composites for Construction*; 2(3):132-7.

Buyukozturk, O. & Hearing, B. 1998, 'Failure behavior of precracked concrete beams retrofitted with FRP', *ASCE Journal of Composites for Construction*; 2(3): 138-44.

Delre, L.C. & Miller, R.W. 1988, 'Characterization and Weather Aging and Radiation Susceptibility', *Engineered Materials Handbook: Vol.2-Engineering Plastics*, Metals Park, OH: ASM International, p.576-580

Yamaguchi, T. 1998, '*Study on deterioration of FRP Rods for Concrete Reinforcement on Ultra-Violet Rays and Creep Rupture'*, Doctoral Thesis, University of Tokyo.

11DBMC International Conference on Durability of Building Materials and Components
ISTANBUL, Turkey 11-14 May 2008

Monitoring Moisture Content in Autoclaved Aerated Concrete as a Mean to Achieve Higher Durability

Zbyšek Pavlík [1]
Lukáš Fiala [2]
Zbigniew Suchorab [3]
Robert Černý [4]

T 11

ABSTRACT

Autoclaved aerated concrete (AAC) is a structural material which is commonly used around Europe, particularly as it combines ease of construction with excellent combination of its mechanical and thermal properties. However, the empirical principles employed in construction design until now have led in many countries to a series of failures which are beginning to have serious consequences for the practical applications of the material. High moisture content in AAC blocks in the construction phase belongs to most serious flaws because it can lead to hygric shrinkage related problems in the structure. In this paper, the time domain reflectometry (TDR) method is presented as a universal method for monitoring moisture content in AAC both during the production phase and in situ. TDR can be generally classified as a dielectric method, based on an analysis of the behavior of dielectrics in a time-varying electric field, and consists in the measurement of permittivity of moist porous media. In contrast to most methods used for determination of moisture content, TDR method does not require calibration for every material. Another advantage of the TDR method is that it is well applicable for the materials with higher salinity, where an application of methods such as the resistance method or the capacitance method is impaired by a significant loss of accuracy. TDR also enables continuous long-term non-destructive monitoring of moisture content in constructions.

KEYWORDS

Autoclaved aerated concrete, Moisture content, Time-domain reflectometry method

[1] Czech Technical University, Faculty of Civil Engineering, Department of Materials Engineering and Chemistry, Thákurova 7, 166 29 Prague 6, Czech Republic, Phone: +420224354371, Fax: +420224354446, pavlikz@fsv.cvut.cz
[2] Czech Technical University, Faculty of Civil Engineering, Department of Materials Engineering and Chemistry, Thákurova 7, 166 29 Prague 6, Czech Republic, Phone: +420224354371, Fax: +420224354446, fialal@fsv.cvut.cz
[3] Lublin University of Technology, Faculty of Civil and Sanitary Engineering, Department of Environmental Protection Engineering, Nadbystrzycka 40b, 20-618 Lublin, Poland, Phone: +48815384322, zibi@fenix.pol.lublin.pl
[4] Czech Technical University, Faculty of Civil Engineering, Department of Materials Engineering and Chemistry, Thákurova 7, 166 29 Prague 6, Czech Republic, Phone: +420224354429, Fax: +420224354446, cernyr@fsv.cvut.cz

1 INTRODUCTION

In spite of the autoclaved aerated concrete (AAC) is a structural material commonly used around Europe, high frequency of AAC structures defects has become well known among the potential investors what leads in consequence to the weakening of the position of AAC on the European building materials market which is unfortunate because the material can be considered as environmentally friendly and has considerable potential for future applications. The new precise walling technologies (thin joint systems) lead to much better thermal properties of the envelopes because the thermal bridges characteristic for classical brick-like walling with AAC are practically excluded, and this results in significant savings of both heat energy and the amount of material necessary for construction.

The main problem with the current applications of AAC is that the major European AAC producers (with their whole corporate chain in different European countries including Czech Republic) restrict themselves just to the advertisement of their products and neglect further research work. They often prescribe unrealistic conditions of walling for instance concerning the initial moisture content in AAC blocks. Unsuccessful applications of "user-unfriendly" technologies offered by the AAC producers logically lead to a negative response of both designers and investors, and if the producers would insist on these improper technologies, the development could aim to a dead end.

In the current building practice one can find different walling technologies of AAC structures based on classical walling principles or on precise-walling technology (thin joint system). The differences are as follows. In the classical way of walling the AAC blocks are built using standard mortar joint of 10 mm nominal size. The AAC walls are built on site in standard masonry construction and productivity can often be low. Problems such as the use of overstrong mortar or missing movement joints can lead to cracking of AAC walls. However, problems are generally not found with classical AAC masonry providing that good practice is followed.

Precise walling requires the use of mortar joints that are not greater than 3 mm thick, typically 1 - 2 mm. The blocks are often larger than those used in classical walling. The potential benefits of precise walling are improved productivity and better thermal performance of the completed building. The system can be constructed faster than classical systems and it does not rely so heavily on traditional masonry methods. The precise walling also generates less waste from both blocks and the mortar on site and the amount of mortar used is much less than in classical walling. These precise-walling systems are often referred to as thin joint AAC blockwork.

The precise-walling technologies are being employed over Europe with an increasing frequency but they are still considered as innovative. Compared to the classical walling technologies (large joints), precise walling technologies lead to much better thermal properties of the envelopes because the thermal bridges characteristic for classical brick-like walling with AAC are practically excluded. Therefore, the use of precise-walling technologies should be encouraged and a growth in the use of the technology should be expected. However, good design parameters are required for precise-walling AAC with render systems.

There are clearly benefits to be gained from precise-walling AAC but problems have become evident and this could diminish the growth and use of the technology. When problems do occur they are often due to the differences between AAC and the traditional renders that are used. In particular, the moisture conditions and transfer between the materials often determines the suitability of the AAC system with a particular render finish.

The design of AAC building envelopes has mostly been done by empirical rules for construction until now. As a result, approaches to design have differed case by case and failures have resulted as a result of incorrect specifications and errors in construction. Typical failure examples are cracking of both

external and internal finishes, detachment of renders from the AAC block (sometimes with the AAC itself), cracks around windows and doors, frost failure of external render.

Experience has shown that reasons of defects were due to the use of methods for brick structures being employed by the designers for AAC blockwork. However, the brick-based technologies which were proven by their successful applications over centuries cannot be applied to anything other than brick structures. The properties of AAC differ from those of bricks to such a degree that any analogy between systems based on AAC and on bricks has always to be doubtful.

The current standards cannot help to the designers in preventing failure. Moisture analysis in both Czech and European codes is restricted to water vapor transport in steady-state conditions. This presents a risk for a designer as water suction, water vapor convection, and the cross effects between heat and moisture transport are not considered and this can often lead to the underestimation of the amount of liquid water in the envelope or the condensation zone can appear in another place than predicted by the standard calculation. Hygric and thermal movements are also not considered in standards and the designer is not required to evaluate the thermo- and hygro-mechanical response of the envelope.

On this account, there is very difficult to perform durability and service live assessment of AAC-based envelope systems because complex view on AAC material performance is missing and a precise and serious analysis of hygro-thermo-mechanical performance of the new AAC technologies based on sound scientific knowledge is a very actual problem.

From the above given information results the necessity to determine moisture transport and storage parameters of AAC that will enable to estimate its hygric performance. Since the experimental assessment of hygric material parameters requires measurement of liquid moisture content, the suitable moisture measurement method for application for AAC has to be chosen and calibrated.

Because water possesses many anomalous properties that also affect the properties of materials, various methods of determination of moisture content were devised and various moisture meters constructed which can take advantage of it. Basically, the measuring methods can be divided into two main groups; absolute and relative methods. The absolute methods (or direct methods), which are based on the removal of water from the specimen (by drying, extraction, etc.) are usually used as reference methods for calibration of relative methods. The disadvantage of these methods consists in fact that they are time consuming and they are not applicable for instantaneous determination of moisture profiles. Therefore, relative methods which determine the amount of water in material on the basis of measuring another physical quantity (permittivity, electrical conductivity, absorption of radiation energy etc.) are widely used in technical practice. However, the application of particular methods is limited for prescribed types of materials and specific conditions of measurement. For instance, frequently used resistance moisture meters are practically inapplicable for materials with a higher amount of salts, because the measuring errors rapidly increase with the increasing moisture content. The same problem can be found for capacitance moisture meters working on lower frequencies.

On the basis of the theoretical analysis of the currently used moisture measurement method we have chosen for the moisture measurement in AAC the time domain reflectometry (TDR) method that has proved to be very reliable for various applications and materials. Already in 1930s it became a recognized technique in cable testing. Other applications were focused on investigation of electrical properties of liquids. A fast development of the TDR technology was initiated in 1980s in soil science where the method found an increasing use in soil moisture measurement (see e.g. [Topp *et al.*, 1980], [Dalton & van Genuchten, 1986]). Nowadays is the TDR technique frequently used in many fields for instance for moisture measurement in building materials and structures [Kupfer & Trinks, 2005], [Kupfer *et al.*, 2007], [Aghaei *et al.*, 2005], for monitoring of quality of food products [Schimmer *et al.*, 2007], etc.

Since the possibilities of using TDR method for measurement of moisture content were proven for wide range of materials, in this paper we present the TDR method as a universal method for monitoring moisture content in AAC both during the production phase and in situ.

2 TIME-DOMAIN REFLECTOMETRY METHOD

TDR method can be generally classified as a dielectric method, based on an analysis of the behavior of dielectrics in a time-varying electric field, and consists in the measurement of permittivity of moist porous media. The determination of moisture content using the permittivity measurements is based on the fact that the static relative permittivity of pure water is equal to approximately 80 at 20 °C, while for most dry building materials it ranges from 2 to 6 [Katze, 1989], [Owen *et al.*, 1961].

The permittivity of materials is strongly affected by the orientation of molecules in the electric field. This characteristic is high for water in gaseous and liquid phase, but is significantly lower for water bound to a material by various sorption forces, which makes the orientation of water molecules more difficult. This feature makes it possible to distinguish between the particular types of bond of water to the material using the permittivity but on the other hand, it results in the dependence of the sensitivity of moisture measurements to the amount of water in the material. The relative permittivity of water bonded in a monomolecular layer is approximately 3.1, but for further layers it increases relatively fast. Therefore, the dependence of relative permittivity on moisture content is generally characterized by a more or less gradual change at the transition from a monomolecular to a polymolecular layer. Consequently, the methods of moisture measurements based on the determination of changes of relative permittivity have lower sensitivity in the range of low moistures where their application is rather limited.

The principle of TDR device consists in launching of electromagnetic waves and the amplitude measurement of the reflections of waves together with the time intervals between launching the waves and detecting the reflections. The fundamental element in any TDR equipment used for the determination of moisture content in porous materials is a device to observe the electromagnetic pulse echo in time domain. The method application originates from the application of electric cable tester. The measuring device usually consists of four main components: a step or needle pulse generator, a coaxial cable wave guide, a sampler and an oscilloscope to register or visualize the trace of echo.

The pulse generator produces the electromagnetic wave that propagates through the measured medium. The Fourier transform of an electrical pulse consists of sine waves covering a large frequency range but dependent on the shape of pulse. The highest frequency present in the pulse depends on its slew rate. This means that step pulse and needle pulse can be used equivalently if their rise time is comparable.

A very important part of TDR equipment is the probes. Rods of the probes are the signal conductors. There are a lot of probe constructions available for TDR measurements. They generally differ in shape, material and number of rods but general idea is that TDR probe is an extension of the coaxial cable with specified geometry. The TDR probe itself is conductively connected to the coaxial cable in such a way that the cable is open ended and the probe forms this open end. In principle, the coaxial cable and the probe differ not only in the shape but also in a type of dielectric material. While the cable has usually polyethylene as a dielectric, the measured material serves as a dielectric of the probe. Thus, the cable dielectric is nearly ideal but the measured moist material usually contains dissolved salts and therefore conducting current appears. This is, however, not disturbing the measurement because of the high frequency of the pulse.
The sampler detects the electromagnetic waves launched by the pulse generator and transmitted through the coaxial cable and TDR probe system. TDR meter consists of two main components, a high precision timing device and a high precision voltmeter. When the electromagnetic waves launched by

the generator are detected by the sampler, the sampler measures the voltage between the shield and the conductor at a certain time interval. The set of data obtained consists of voltage as a function of time when the transmitted pulse echo comes back to the device. The coaxial cable connects the step-pulse generator and the sampler. The shield of the coaxial cable is connected to earth and its electric potential is 0 V. The electromagnetic waves produced by the step- or needle-pulse generator are launched into the coaxial cable with a voltage drop of several tenths of a volt between the conductor and the shield.

The evaluation of data obtained by a tester is based on the following basic principles. Any change of impedance in the cable-probe system causes a partial or total reflection of the pulse. Therefore, one reflection will be on the cable/probe interface, where the dielectric is suddenly changed, and therefore the impedance must also be changed, while the second reflection is on the open end of the probe, where the impedance tends towards free space impedance and the wave is reflected in phase.

Reflected pulses can be either in phase with the incident pulse, which happens in the case when the electromagnetic waves pass an increase in impedance, or in counter phase, when a decrease of impedance is met.

Time/velocity of pulse propagation depends on the apparent relative permittivity of the porous material, which can be expressed using the formula

$$\varepsilon_r = \left(\frac{ct_p}{2L} \right)^2 , \tag{1}$$

where ε is the complex relative permittivity of the porous medium, c the velocity of light ($3 \cdot 10^8$ m/s), t_p the time of pulse propagation along the probe rods measured by TDR meter and L the length of the sensor's rod inserted into a measured porous medium.

Complex relative permittivity of porous medium consists of the real part ε_r' and imaginary part ε_r'',

$$\varepsilon_r = \varepsilon_r' + \varepsilon_r'' . \tag{2}$$

Both parts of the complex relative permittivity depend on applied measuring frequency. From Figure 1 it is evident that imaginary part of the complex relative permittivity can be in case of TDR measurement neglected and the real part is more or less constant.

Knowing the relative permittivity of the studied material we can estimate water content in a medium in a few of possible ways for example using empirical calibration, homogenization techniques and empirical conversion functions.

Complex relative permittivity exhibits also temperature dependence which can be described according to [CRC, 2002] by equation

$$\varepsilon = 249.21 - 0.79069 \cdot T + 0.00027997 \cdot T^2 \quad (273 < \mathrm{T\ (K)} < 373). \tag{3}$$

Therefore, in practical application of TDR technique for moisture measurement especially in situ temperature compensation has to be done.

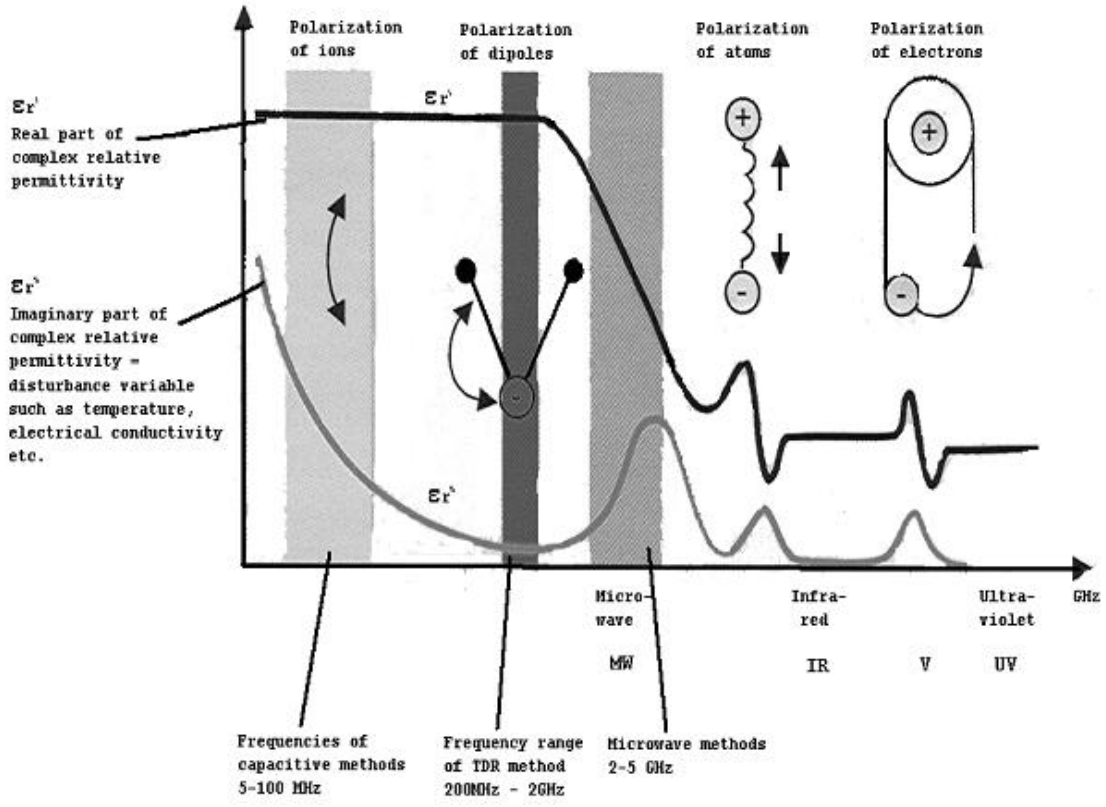

Figure 1. Illustration of complex relative permittivity dependence on frequency.

3 MEASURING TECHNOLOGY, MATERIALS AND SAMPLES

For the TDR measurements in this paper, the cable tester LOM/RS/6/mps produced by Easy Test which is based on the TDR technology with $\sin^2$-like needle pulse having rise-time of about 200 ps, was employed. It is computer aided instrument [Malicki & Skierucha, 1989] originally designed for measurements of soil moisture. The built-in computer serves for controlling TDR needle-pulse circuitry action, recording TDR voltage versus time traces, and calculating the pulse propagation time along particular TDR probe rods and the relative permittivity of measured material.

A two-rod miniprobe LP/ms (Easy Test) was used for the determination of moisture content that was designed by Malicki et al. [Malicki *et al.*, 1992]. The sensor is made of two 53 mm long parallel stainless steel rods, having 0.8 mm in diameter and separated by 5 mm. The sphere of sensor's influence was determined with the help of a simple experiment. The probe was fixed in the beaker and during the measurement, there was added water step by step. From the measured data (relative permittivity in dependence on water level) there was found out that the sphere of influence creates the cylinder having diameter about 7 mm and height about 60 mm, circumference around the rods of sensor. The accuracy of moisture content reading given by producer is ± 2% of displayed water content.

The measuring technology can be divided into three basic steps; probe calibration, sample arrangement and probes placing, data evaluation and determination of moisture content. The probe calibration was done for every probe using the known dielectric constants of water and benzene (see Pavlík *et al.*, 2006, for details).

The moisture measurements were done on the AAC samples provided by Polish producer PPH FAELBED Inc.. Three different types of AAC based materials were studied. Nominally, AAC 500,

AAC 600 and AAC 700 having different densities and porosities were tested. The experiment was done on samples having dimensions of 40 x 40 x 100 mm. At first, two parallel holes having the same dimensions as the sensor rods were bored into each sample. Then, the sensors were placed into the samples and sealed by silicon gel. The samples were partially saturated by water and insulated to prevent water evaporation. The relative permittivity of wet samples was then continuously monitored until the measured values reached the constant value. Then, the experiment was interrupted, sensors removed from the samples and moisture content in the samples was determined using gravimetric method. In this way, the empirical calibration curve of particular measured materials was accessed that in future work can be used for evaluation of measured relative permittivity data.

4 EXPERIMENTAL RESULTS

The obtained results (see Figure 2) clearly document the dependence of relative permittivity of the studied materials on moisture content. The empirical calibration curves have more or less exponential shape for all studied materials. We can observe relatively similar results in the range of lower moisture contents whereas for higher moisture contents (typically from 30%) the effect of different densities plays an important role. However, for rough estimate of moisture content of AAC the results can be considered similar and no extra calibration for every AAC material is supposed to be done.

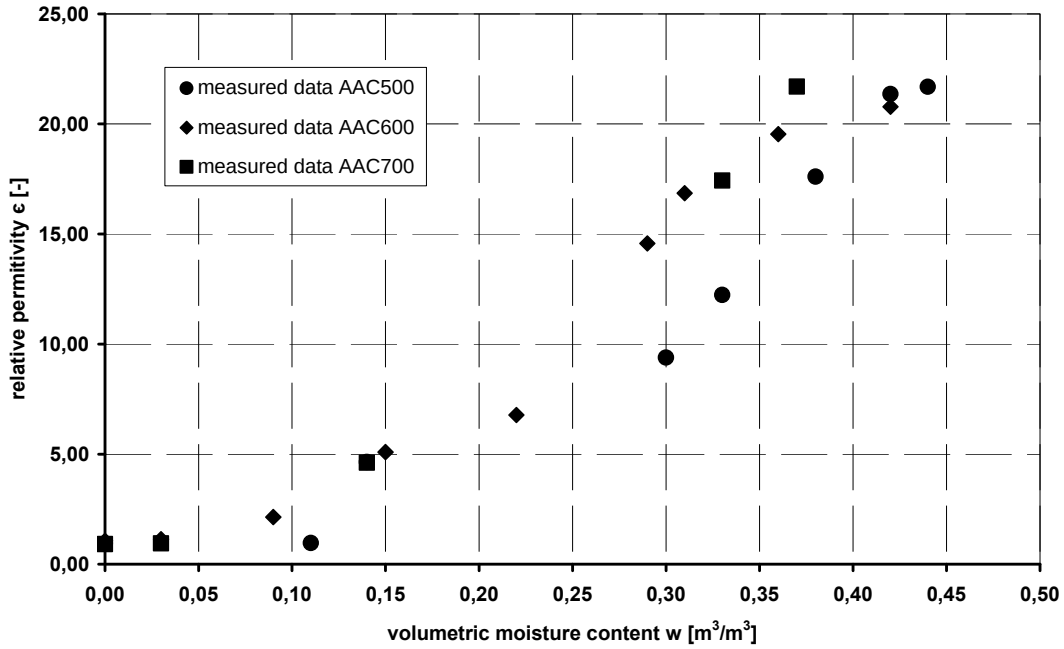

Figure 2. Empirical calibration curves of the measured AAC materials.

5 CONCLUSIONS

From the point of view of the applicability of TDR methodology for moisture measurement of building materials on AAC basis, the experiment presented in this paper has clearly shown a good perspective of the TDR method for such type of measurements. The obtained results can find use for example in long term monitoring of moisture content in AAC structures which can contribute to the accurate assessment of hygric function of building structures and in consequence to the higher durability and service life of AAC structures. The results can also be used for the determination of hygric parameters of tested materials, particularly moisture diffusivity and water absorption coefficient. It should also be noted that the TDR method has a high potential not only in laboratory

measurements, but it also makes possible long term monitoring of moisture content in situ, directly on building site.

ACKNOWLEDGMENTS

This research has been supported by Czech Ministry of Education, Youth and Sports of Czech Republic, under project No MSM: 6840770031.

REFERENCES

Topp G. C., Davis J. L. & Annan A.P. 1980, 'Electromagnetic determination of soil water content: measurements in coaxial transmission lines', *Water Resources Research*, vol. **3**, pp. 574-582.

Dalton F. N. & van Genuchten M. T. 1986, 'The time domain reflectometry for measuring soil water content and salinity', *Geoderma*, vol. **38**, pp. 237-250.

Kupfer K. & Trinks E. 2005, 'Simulations and Experiments for Detection of Moisture Profiles with TDR in a Saline Environment', *Electromagnetic Aquametry*, Springer Verlag Heidelberg Berlin, pp. 349-365.

Kupfer K., Trinks E., Wagner N. & Hübner Ch. 2007, 'TDR Measurements and Simulations in High Losy Bentonite Materials', *Measurement Science ad Technology*, London.

Aghaei A., van Der Zanden A. J. & Hendriks N. A. 2005, 'TDR technique for measuring moisture content in brick', *Proceedings of the Sixth Conference on Electromagnetic Wave Interaction with Water and Moist Substances*, Weimar, Germany.

Schimmer O., Oberheitmann B., Baumann F. & Knöchel R. 2007, 'Instantaneous Distinction Between Double and Single Frozen Fish Using a New Handheld Time Domain Reflectometer', *Proceedings of the 7th International Conference on Electromagnetic Wave Interaction with Water and Moist Substances*, Hamamatsu, Japan, pp. 167-174.

Katze U. 1989, 'Complex permittivity of water as a function of frequency and temperature', *J. Chem. Eng. Data*, **34**, pp. 371-374.

Owen B. B., Miller R. C., Milner C. F. & Cojan H. L. 1961, 'The dielectric constant of water as a function of temperature and pressure, *J. Phys. Chem*., **65**, pp. 2065-2071.

CRC Handbook of Chemistry and Physics, 83rd Edition, D. R. Lide, CRC, 2002.

Malicki M. A. & Skierucha W. M. 1989, 'A manually controlled TDR soil moisture meter operating with 300 ps rise-time needle pulse', *Irrigation Science*, vol. **10**, pp. 153-163.

Malicki M. A., Plagge R., Renger M. & Walczak R. T. 1992, 'Application of time-domain reflectometry (TDR) soil moisture miniprobe for the determination of unsaturated soil water characteristics from undisturbed soil cores', *Irrigation Science*, vol. **13**, pp. 65-72.

Pavlík Z., Jiřičková M., Černý R., Sobczuk H. & Suchorab Z. 2006, Determination of Moisture Diffusivity Using the Time Domain Reflectometry (TDR) Method, *Journal of Building Physics*, vol. **30**, no. **1**, pp. 59-70.

11DBMC International Conference on Durability of Building Materials and Components
ISTANBUL, Turkey 11-14 May 2008

Durability Properties of High Performance Concrete Containing Alternative Silicate Binders

Eva Mňahončáková [1]
Pavla Rovnaníková [2]
Robert Černý [3]

T 11

ABSTRACT

Alternative silicate binders such as fly ash, ground granulated blast furnace slag, silica fume and metakaolin/calcined clay have a high potential to replace a part of Portland cement in concrete due to the generally recognized necessity to decrease the amount of carbon dioxide in atmosphere. Fly ash, ground granulated blast furnace slag and silica fume are waste materials. Metakaolin is produced by thermal decomposition of kaolin without production of CO_2. Main durability properties, namely moisture and heat transport and storage parameters, of high performance concrete belong to the most critical parameters in designing and using complex reliability based models for service life prediction of concrete structures. In this paper, durability properties of high performance concrete containing two selected alternative silicate binders, namely metakaolin and ground granulated blast furnace slag, are studied. Moisture diffusivity is determined by a method utilizing the results of water sorptivity measurement, water vapor diffusion permeability is measured by the cup method. Thermal conductivity and specific heat capacity are measured by an impulse technique. The experimental results indicate that the chosen composition of the two studied concrete mixtures can ensure both sufficiently high compressive strength and reasonable resistance against water transport which makes good prerequisites for the achievement of high durability.

KEYWORDS

Concrete, Alternative silicate binders, Durability properties.

[1] Czech Technical University in Prague, Faculty of Civil Engineering, Department of Materials Engineering and Chemistry, Thákurova 7, 166 29 Prague 6, Czech Republic, Phone +420224355405, Fax: +420224354446, eva.mnahoncakova@fsv.cvut.cz

[2] Brno University of Technology, Faculty of Civil Engineering, Institute of Chemistry, Žižkova 17, 602 00 Brno, Czech Republic, Phone +420541147631, Fax: +420541147667, rovnanikova.p@fce.vutbr.cz

[3] Czech Technical University in Prague, Faculty of Civil Engineering, Department of Materials Engineering and Chemistry, Thákurova 7, 166 29 Prague 6, Czech Republic, Phone +420224354429, Fax: +420224354446, cernyr@fsv.cvut.cz

1 INTRODUCTION

The progressive building materials development improves their quality and utility value. In order to achieve better material properties, besides the new technologies also specific admixtures are employed. The accurate admixture dosage and technological conditions observation can improve the material parameters like strength and durability. Most frequently, such admixtures as silica fume, ground granulated blast furnace slag, metakaolin, fly ash or flue cinder are used in concrete production.

Traditional concrete was characterized essentially by its compressive strength. Therefore, when first high performance concretes (HPC) appeared they were supposed to be considered as just high strength concretes (HSC). However, within the last several decades this basic view was changed substantially. In the new HPCs some other properties such as water and salt transport and storage parameters, freeze-thaw resistance or abrasion resistance began to gain higher importance and in some cases they even became decisive for the solutions made in the design process. As these parameters depend more or less on the porosity of a material, the reduced porosity became the main characteristic of HPC. Despite the gradual shift in the HPC design and application philosophy towards a generally recognized necessity to measure a wider scale of HPC parameters the mechanical properties still remain the far most frequent parameters investigated in the research work being done on HPC.

We will give only a few examples of the investigations done during the last couple of years. Donza et al. [2002] measured the compressive strength and the elasticity modulus of HPC depending on the aggregate fineness and realized that granite crushed sand appeared as the most advantageous. Gao et al. [2001] found that the compressive strength of HPC was improved after using superfine mineral powder of phosphoric slag. Beshr et al. [2003] reported the positive effect of the coarse aggregate quality on the compressive strength, split tensile strength and modulus of elasticity of HPC. The effect of silica fume on the mechanical properties was reviewed in an extensive way by Chung [2002].

Water and water vapor transport and storage properties of HPC were not yet in the center of interest of most researchers until now although they possess a very high predicative potential concerning the HPC quality. So, only couple of references was found in common sources within the last years. Jooss and Reinhardt [2002] measured water permeability and water vapor diffusion coefficient of five HPC mixtures with the compressive strength of 86-93 MPa and found both the transport coefficients to decrease several times compared to the reference B35 concrete. Nilsson [2002] determined desorption isotherms and hygroscopic moisture diffusion coefficients of twenty HPC mixtures and realized that moisture diffusion coefficient was not only several times lower but also much less moisture dependent for HPC than for normal concrete. Sun et al. [2001] measured the relative water permeation coefficient of several HPC with expansive agents and hybrid fibers and found that the impermeability resulted from the combined use of both admixtures. Khan [2003] determined the sorptivity of several HPC incorporating fly ash and microsilica prepared with different water/binder ratios and found the incorporation of 8-12 % of microsilica as cement replacement as the optimum value.

In this paper, measurements of basic moisture and heat transport and storage parameters of two different HPCs, the first with groundgranulated blast furnace slag admixture and the second with metakaolin admixture, are presented.

2 MATERIALS

Two different types of concrete, namely the high performance concrete containing ground granulated blast furnace slag and the same material with metakaolin, were studied. Table 1 presents the composition of the studied concrete mixtures.

Table 1. The composition of concrete mixtures [kgm^{-3}].

Component	Type of concrete mixture	
	BM	BS
CEM I 42.5 Mokrá	440	440
aggregates 0-4 mm	812	812
aggregates 4-8 mm	910	910
plasticizer Mapei Dynamon SX	5.3	5.3
metakaolin MEFISTO	44	-
ground granulated blast furnace slag Štramberk	-	44
water	188	188

3 EXPERIMENTAL METHODS

3.1 Basic Physical Properties

Among the basic properties, the bulk density, matrix density and open porosity were measured. Each sample was dried in a drier to remove majority of the physically bound water. After that the samples were placed into the desiccator with deaired water. During three hours air was evacuated with vacuum pump from the desiccator. The specimen was then kept under water not less than 24 hours.

From the mass of the dry sample m_d, the mass of water saturated sample m_w, and the mass of the immersed water saturated sample m_a, the volume V of the sample was determined from the equation

$$V = \frac{m_w - m_a}{\rho_l}, \tag{1}$$

where ρ_l is the density of water.

The open porosity ψ_0 [m^{3}m^{-3}], the bulk density ρ [kgm^{-3}] and the matrix density ρ_m [kgm^{-3}] were calculated according to the equations

$$\psi_0 = \frac{m_w - m_d}{V\rho_l} \tag{2}$$

$$\rho = \frac{m_d}{V} \tag{3}$$

$$\rho_{mat} = \frac{m_d}{V(1-\Psi_0)} \tag{4}$$

The samples for determination of basic properties had the size of 50 x 50 x 20 mm.

3.2 Compressive Strength

The compressive strength was determined using the standard 500 kN testing device. It was calculated as the ratio of the measured ultimate force and the load area.

3.3 Water Vapor Transport Properties

The common cup method was used in the measurements of water vapor transport parameters [Roels et al. 2004]. The specimens were water and vapor proof insulated by epoxy resin on all lateral sides, put into the cup and sealed by technical plasticine. The impermeability of the plasticine sealing was achieved by heating it first for better workability and subsequent cooling that resulted in its hardening. Two different experiments were done. In the first one (the dry cup method), the sealed cup containing silica gel (the equilibrium relative humidity above the desiccant was 5 %) was placed in a controlled climatic chamber with 30% relative humidity and weighed periodically. In the second one (the wet cup method), the cup containing saturated K_2SO_4 solution (the equilibrium relative humidity above the solution was 97.8 %) was placed in a controlled climatic chamber with 30 % relative humidity. The measurements were done at 25±1°C for a period of two weeks. Steady state values of mass gain or loss were determined by linear regression for the last five readings.

The water vapor diffusion permeability δ was calculated from the measured data according to the equation

$$\delta = \frac{\Delta m \cdot d}{S \cdot \tau \cdot \Delta p_p}, \tag{5}$$

where δ is the water vapor diffusion permeability [s], Δm the amount of water vapor diffused through the sample [kg], d the sample thickness [m], S the specimen surface [m^2], τ the period of time corresponding to the transport of mass of water vapor Δm [s], Δp_p the difference between partial water vapor pressure in the air under and above specific specimen surface [Pa].

In an analogous way, the water vapor diffusion coefficient D was calculated as

$$D = \frac{\Delta m \cdot d \cdot R \cdot T}{S \cdot \tau \cdot M \cdot \Delta p_p}, \tag{6}$$

where D is the water vapor diffusion coefficient [m^2s^{-1}], R the universal gas constant, M the molar mass of water, T the absolute temperature [K].

On the basis of the diffusion coefficient D, the water vapor diffusion resistance factor μ was determined,

$$\mu = \frac{D_a}{D}, \tag{7}$$

where D_a is the diffusion coefficient of water vapor in the air.

The samples for determination of water vapor transport properties were cylindrical, with the diameter of 110 mm and height of 20 mm.

3.4 Water Transport Properties

The water sorptivity A and apparent moisture diffusivity D_w were measured using a water suction experiment [Kumaran, 1994]. For the determination of water sorptivity a common experimental setup was chosen. The specimen was water and vapor-proof insulated on four lateral sides and the face side was immersed 2 mm in the water. Constant water level in the tank was achieved by a Mariotte bottle with two capillary tubes. One of them, inside diameter 2 mm, was ducked under the water level, second one, inside diameter 5 mm, was above water level. The automatic scale allowed recording the increase of mass. The known water flux into the specimen during the suction process was then

employed to the determination of water sorptivity. The samples were tested in constant temperature conditions.

The water absorption coefficient A [kgm^{-2}s$^{-1/2}$] was then calculated using the formula

$$i = A \cdot \sqrt{t}\,, \tag{8}$$

where i is the cumulative water absorption [kg/m^2], t is the time from the beginning of the suction experiment.

For the calculation of apparent moisture diffusivity, the following approximate relation was employed

$$D_w \approx \left(\frac{A}{w_c} \right)^2 \tag{9}$$

where w_c is the saturated moisture content [kgm^{-3}].

The samples for determination of water transport properties had the dimensions of 50 x 50 x 20 mm.

3.5 Thermal Properties

The thermal conductivity as the main parameter of heat transport and the specific heat capacity as the main parameter of heat storage were determined using the commercial device ISOMET 2104 (Applied Precision, Ltd.). ISOMET 2104 is a multifunctional instrument for measuring thermal conductivity, thermal diffusivity, and volumetric heat capacity. It is equipped with various types of optional probes, needle probes are for porous, fibrous or soft materials, and surface probes are suitable for hard materials. The measurement is based on the analysis of the temperature response of the analyzed material to heat flow impulses. The heat flow is induced by electrical heating using a resistor heater having a direct thermal contact with the surface of the sample. The measurements in this paper were done in dependence on moisture content. The samples for determination of thermal properties had a size of 70 x 70 x 70 mm.

4 EXPERIMENTAL RESULTS AND DISCUSSION

4.1 Basic Physical Properties

The basic properties of studied HPCs are shown in Table 2. BM containing metakaolin achieved higher porosity and thus lower bulk density compared to BS containing ground granulated blast furnace slag. So, the voids in the cement matrix in BS were filled more successfully than in BM.

Table 2. Basic physical properties of studied HPCs.

HPC	ρ [kg m^{-3}]	ρ_m [kg m^{-3}]	Ψ_0 [%]
BM	2370	2706	12.4
BS	2398	2674	10.3

4.2 Compressive Strength

Table 3 shows the compressive strength of the studied HPCs after 28 days. The results were very similar for both materials. The differences were within the error range of the experimental method.

Table 3. Mechanical properties of studied HPCs.

HPC	Compressive strength [MPa]
BM	84.0
BS	83.3

4.3 Water Vapor Transport Properties

The water vapor transport parameters of the studied HPCs are shown in Table 4. The measured data revealed basic information that the values of water vapor diffusion coefficient corresponding to the lower values of relative humidity (5/30 %) were always lower than those for higher relative humidity values (97/30 %). This is in accordance with the previous measurements on many other materials including concrete [Kumaran 1996]. The main reason for this finding is coupling of water vapor transport with liquid water transport in a material with higher relative humidity where the capillary condensation takes place in a much higher extent than in the range of lower relative humidity [Černý and Rovnaníková 2002]

Comparing the data measured for the two studied HPCs, we can see that the values of water vapor diffusion coefficient of BM was in the both ranges of higher and lower relative humidity higher than for BS. This is in a general agreement with the open porosity data in Table 2 as it is quite obvious that a material with higher porosity should transport water vapor faster than a material with lower porosity.

Table 4. Water vapor transport properties of studied HPCs.

HPC	*5/30%*			*97/30%*		
	δ [s]	D [m^2s^{-1}]	μ [-]	δ [s]	D [m^2s^{-1}]	μ [-]
BM	1.11E-11	1.53E-06	16.87	2.27E-11	3.12E-06	7.47
BS	9.82E-12	1.35E-06	17.27	1.67E-11	2.30E-06	10.08

Table 5. Water transport properties of studied HPCs.

HPC	A [kg $m^{-2}s^{-1/2}$]	D_w [m^2 s^{-1}]
BM	0.0080	4.03E-09
BS	0.0076	5.64E-09

The results of measurements of water transport parameters are presented in Table 5. The comparison of water absorption coefficients showed that the material BM with higher porosity transported liquid water slightly faster than the material BS. Differences in the intensity of water transport in both materials are illustrated in more detail in Fig.1 where an example of the course of water absorption is presented. The lower value of apparent moisture diffusivity of BM in Table 5 is clearly due to the higher open porosity of the material and thus its higher saturated moisture content. This indicates the possible shortages in estimating the moisture diffusivity using Eq. [9]. The more laborous and for concrete much more time consuming way of determination of moisture diffusivity using inverse analysis of moisture profiles [Černý and Rovnaníková 2002] should apparently be given precedence in such cases.

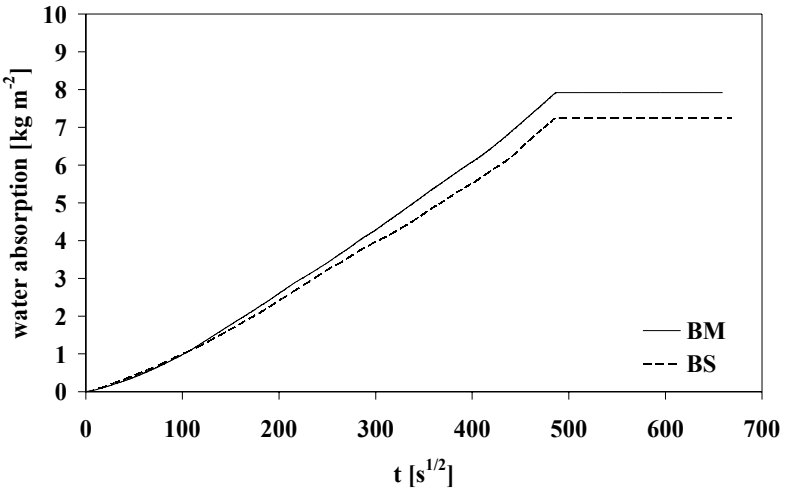

Figure 1. Water absorption of studied HPCs.

4.4 Thermal Properties

The thermal parameters data in Table 6 show that the material BS had systematically higher values of thermal conductivity than BM in the whole range of moisture content analyzed but the differences were relatively low, up to 10%. This is in a qualitative agreement with the open porosity data in Table 2. The specific heat capacity of BM was slightly higher than of BS in the whole range of moisture content. Some small discrepancies were observed for BS where the specific heat capacity in some cases decreased with increasing moisture content. However, this was apparently an experimental uncertainty which was within the error range of the measuring method of ±10%. The thermal diffusivity of BM was very similar to that of BS in whole the moisture range except for the dry state where for BM it was about 10% lower. This reflects the changes in thermal conductivity and specific heat capacity data.

Table 6. Thermal properties of studied HPCs.

HPC	*w* [kgkg^{-1}]	λ [Wm^{-1}K^{-1}]	*c* [Jkg^{-1}K^{-1}]	*a* [m^{2}s^{-1}]
BM	0.000	1.57	727	0.90
BM	0.037	1.84	734	1.06
BM	0.040	1.98	742	1.13
BM	0.047	2.08	761	1.15
BS	0.000	1.71	683	1.04
BS	0.034	1.94	743	1.09
BS	0.038	2.00	727	1.10
BS	0.042	2.13	719	1.13

5 CONCLUSIONS

The results of the experimental work presented in the paper indicated that both metakaolin and ground granulated blast furnace slag were materials having good perspectives as partial cement replacement in future use. The compressive strength of HPCs with either metakaolin or ground granulated blast furnace slag in the amount of only 10% of the mass of cement in the mixture was after 28 days higher than 80 MPa which with the CEM I 42.5 type of cement was a very good result. The water and heat

transport properties of both studied concretes were found to meet reasonably the basic requirements necessary to achieve such a durability which is expected for HPC.

ACKNOWLEDGMENTS

This research has been supported by the Czech Science Foundation, under grant No 103/07/0034.

REFERENCES

Beshr, H., Almusallam, A.A., Maslehuddin, M. 2003. Effect of coarse aggregate quality on the mechanical properties of high strength concrete. *Construction and Building Materials*, 17, 97-103.

Černý R, Rovnaníková P. 2002. *Transport Processes in Concrete.* Spon Press, London.

Donza, H., Cabrera, O., Irassar, E.F. 2002. High-strength concrete with different fine aggregate. *Cement and Concrete Research*, 32, 1755-1761.

Gao, P., Deng, M., Feng, N. 2001.The influence of superplasticizer and superfine mineral powder on the flexibility, strength and durability of HPC. *Cement and Concrete Research*, 31, 703-706.

Chung, D.D.L. 2002. Review. Improving cement-based materials by using silica fume. *Journal of Materials Science*, 37, 673-682.

Jooss, M., Reinhardt, H.W. 2002. Permeability and diffusivity of concrete as function of temperature. *Cement and Concrete Research*, 32, 1497-1504.

Khan, M.I. 2003. Permeation of High Performance Concrete. *Journal of Materials in Civil Engineering,* 15, 84-92.

Kumaran M.K. 1996. IEA Annex 24 Final Report, Vol. 3, Task 3: Material Properties. KU Leuven, Leuven.

Nilsson, L.O. 2002. Long-term moisture transport in high performance concrete. *Materials and Structures,* 35, 641-649.

Pliskyn, L. 1992. High Performance Concretes – Engineering Properties and Code Aspects. In: *High Performance Concrete: From Material to Structure*. Edited by Y. Malier. E & FN Spon, London, 186-195.

Sun, W., Chen, H., Qian, H. 2001. The effect of hybrid fibers and expansive agent on the shrinkage and permeability of high performance concrete. *Cement and Concrete Research*, 31, 595-601.

11DBMC International Conference on Durability of Building Materials and Components
ISTANBUL, Turkey 11-14 May 2008

Multidisciplinary Collaborations for a Qualitative Systemization towards a Durable Structure

Shohre Shahnoori [1]
Liek Voorbij [2]

T 11

ABSTRACT

Optimization in order to ensure efficiency plays a major role in the construction industry. However, efficiency has a very broad definition, even in the defined area of the pragmatic construction. The context of this study is an efficient building system in a seismic desert area in which declining the vulnerability of the structure to increase the safety of the inhabitants, in earthquakes is the main goal. Sustainability, however, is the key issue to elaborate the system.

With such complex constraints, materialization of the structure is very sensitive. It has to deal with the earthquake resonance effects as well as the desert climatic conditions. Compared with some other industries technology transfer had slow adoption in construction industry. Nevertheless, it can revolutionize the ways to find solutions for the long lasting construction problems. In this study with a collaborative knowledge from different discipline, modern technology will be implemented in the materialization of a qualitative structure. For this, the data collection and laboratory tests were consequences of the design conceptions.

KEYWORDS

Durable material, Concrete structure, Sustainable construction, Seismic resistance, Fiber reinforcement

[1] Delft University of Technology, Department of Building Technology, BerlageWeg 1, 2628 CR Delft, the Netherlands, Phone +31152783972, Fax 152784178, s.shahnoori@tudelft.nl
[2] Delft University of Technology, Department of Building Technology, BerlageWeg 1, 2628 CR Delft, the Netherlands, Phone +31152783626, Fax 152784178, A.I.M.voorbij@tudelft.nl

1 INTRODUCTION

Material selection and optimization in design and construction is a major issue (Ashby, 2005). However, extra consideration is required when this selection and construction is going to happen for a context with additional constrains such as seismicity and desert climatic conditions (Shahnoori et al. 2007). Engineers from various fields work on this particular subject concentrating on different aspects. Conventionally, safety and economy are always the most important principle aspects. However environmental considerations also became of high concerns (Brundtland, 1987) to designers (e.g. engineers), scientists and authorities (Troyer, 1990). Durability of buildings including the building materials, as an essential part of construction, can be defined as a common issue between these three essential aspects (i.e. safety, economy, and sustainability). Because durability of building materials will, first, improve the life safety for inhabitants. Secondly, it enhances the economical aspects with more efficiency (relatively) over time, requiring less repair and replacement (Newman et al., 2003). Besides, using durable materials in the building, relatively saves more natural resources of being distracted for raw materials (Yu, et al. 2006). Moreover, eco- costs relate to both the environment and the economy, that decline by using durable materials (Hendriks, et a. , 2002). Implementing durable materials, in fact, assists the material minimization on a long term (Groot, 2005) to ensure an eco-efficient system for a sustainable construction. For this, Vogtlander et al. (2004) takes also the Virtual Pollution prevention costs into the account. These are the required costs to reduce the emissions of the production process to a sustainable level.

The main context of the research is reconstruction after a destructive earthquake. Therefore for a sustainable reconstruction, this study, focuses on materialization of houses seeking for more durability. Durably materializing houses is very effective. Because, earthquakes happen in large numbers and in various places on the planet. Table number 1.1 shows the high rate of earthquakes occurrence in the world since 1900. This table indirectly emphasizes/ensures the efficiency of application of strong durable materials. However, the statistics are only about earthquakes with a magnitude of 5 and more, which are called strong earthquakes (CERCESJ, 2006).

Table 1. Magnitude- average annually (The data was collected from the USGS and wikipedia)

Date / Magnitude	1900-20	1920-40	1940-60	1960-80	1980-2000	2000-2007	Total
Magnit.5	-	-	-	75	79	70	224
6≥	21	34	37	71	164	43	370
7≥	45	48	69	69	30	22	283
8≥	5	6	9	8	8	2	38
9≥	-	-	2	1	-	1	4
Total	71	88	117	224	281	138	919

For building collapse as the main consequence of large earthquakes, causing huge economic and social impacts, lacking systemization and material qualification were identified as two important items (Shahnoori, 2005). A very important part of systemization for such a purpose in a seismic area is also materialization (Booth et al., 2006). The former research proved that a concrete composite as the main base for materializing structures in many seismic cities is a good alternative (Shahnoori et al., 2007). Concrete, being a very flexible material, has the potential to be combined with a large variety of materials for upgrading its mechanical properties (Li, 2003). This material has a good compression strength while it is weak in tension. Thus, normally the efforts in the structural design aim at enhancing the tension (Macdonald, 2003). For which using reinforcement materials that are good at tension such as stainless steel, in this composite, are conventions. Besides, concrete is a brittle material, which causes it to include cracks. But in the normal situation these cracks are not counted as serious problem (Markovic, 2006). However, for a seismic design they can cause consequent problems. The main problem resulting in a huge scale death toll and sever injuries in earthquakes is de-fragmentation of construction materials. Therefore, a strong material that can not easily be segmented (that is the case in the bricks and other similar materials especially with weak mortars) is a

good alternative. A qualified concrete composite with an appropriate performance is conditionally a good solution. There are two conditions to be met: first, being affordable. Secondly, declining the chance of propagation of cracks to a bigger or larger size, resulting in serious structural problems (Marcovich, 2006). This study concentrates on investigating the possible options to meet these requirements by using fiber reinforced concrete.

2. APPROACH AND METHODOLOGY

This study is part of a wider research on reconstructing the houses in seismic desert cities. The focus of this study lies in materialization of the structure, which is related to the work presented in this piece. The aim of the total study is improvement of the durability of an appropriate concrete composite for such a situation and at the same time declining the vulnerability of the inhabitants. For that developing a durable concrete aiming at improving the ductility of the composition is required. For that two models were materialized with a time difference of about 2 years, using the earth-casting technique for molding the composite (i.e. figure. 2.1.and 2.2.).

Figure 2.1

Figure 2.2

Models are based on Portland cement and aggregates as a conventional concrete in the scale of 1:25, thus the thickness of the shell structures were 8 mm for each. Different reinforcement materials in various typology and geometry were used to make a shell structure of reinforced concrete. The characteristics of these fibers are shown in table 2. Fibers were mainly divided in two groups of woven and individuals; the individuals were mixed in the composite. However the woven fibers were positioned in the middle of the walls.

Table 2. typology, geometry, and time of use of reinforcement materials in the concrete composite

Typology / Fibers	Short fibers	Long & straight	Woven fibers
E-glass	4.5 mm First period	50 mm Second period	50 mm wide, First and second
Carbon	-	-	60 mm wide, Second period
Aramid	-	-	50 mm wide, Second
Poly Propylene	-	-	First and second
Natural fibers	-	30-120 First &second	-

The models were built in the indoor climate and curing for the concrete was done also in such an environment. W/C ratio was about 1/3, fibers in the woven type were locally positioned. Two main task were necessary before the observation, including first the sample preparation, and second, making the thinsections. These processes were done as the specimens were made by cuting the samples, stabilzation through vacuum impregnation, and then cutting them into sections (25-30 µm) by DBT Diamond Roller and preparation by Grinder/86. By Gluing the HELP glass to flatten, resin impregnation, then gluing the object glass to pulish and hardening them under the UV-light, the specimens of about 0.5 mm were cut, grind and pulished. Observation, investigate, and analyzing the

composite on micro scale to investigate the interactions were assisted by the Polarized ligh and the UV-fluorescence.

3. RESULTS

The basic composite matrix (liquid phase) with E-glass, carbon fibers, aramid, and poly propylene were similar therefore the differences were related to the various effects of different fibers. Table 3 shows a comparison of density for the different reinforcing materials used in the composite in addition to some other mechanical properties involved in the durability.

Table 3. comparison of some mechanical properties of reinforcement materials used in the composite

Property reinforcement	Density (g/cm^2)	Strength (MPa)	Young modulus (GPa)	Elongation (%)
Stainless steel fibers	7.8	480-2240	189-210	05-3.5
E-glass	2.5	2500-3500	70-75	2.5
Carbon	1.4	2500-5500	220-700	1.4-1.8
Aramid	1.4	3000-4000	85-135	3.3-3.7
Poly Propylene	0.9	27.6-41.4	7	20
Natural fibers	1.5	80-840	9-22	2.0-2.5

Main results from the tests related to this study are as:
- There was an adhesion problem between the cement matrix and the natural fibers (Figure 3.1. &2)
- The cement is more porous around the bio-fibers
- In the end of the bio-fibers the cement particle does not go through (too big to go, i.e. Figure 3.1.)

Figure 3.1. a, and **b** the bio fibers, and **c**, glass fibers for comparison

- Distribution of the glass fibers is not homogenous in all the specimens (i.e. Figure 3.2).
- In the samples from the second model a good adhesion was observed between the carbon and Aramid fibers and the matrix
- Long glass fibers show a better bond with the matrix
- Around the glass fibers in the older version, alkaline problem is observable while in the samples from the model number 2 this was not seen
- The polypropylene fibers have a better bonding with the cement matrix even in the older version they do not show particular problems
- The matrix in the second model is more homogenous (from the mix), however the interface structure between the matrix with the expanded clay, fibers and the bulk still shows problems including the pullout, and unbundling.

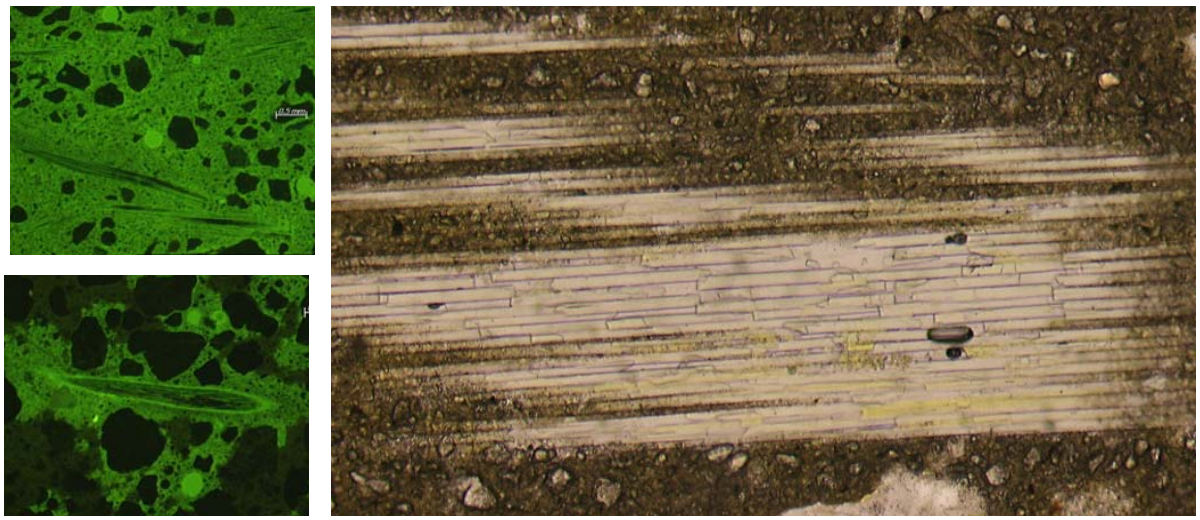

Figure 3.2. a, **b**, and **c** the glass fibers and the concrete matrix

4. DISCUSSION

Reinforcing materials that are weaker in tension than in compression with fibers to achieve better properties is not new. For example in Aqur Quf (i.e. near Baghdad) straw was used to strengthening the sun-baked bricks in about 3500 (Bentur et al. 2007). However, from 1900 with the invention of Hadscheck process asbestos cement was the first widely used manufactured composite (Bentur et al. 2007). This is called the first version of modern fiber reinforced composites. Since 1960 polymers have been used as reinforcement for concrete which was accompanied by further application of the reinforced concrete system (Dolan et al., 1999). Although since then the application of these fibers had an ordinary progression, recently it has been developed revolutionary.

An example of the latest version of these advanced technology is Engineered Cementitious Composite (ECC). This concrete is a very progressed version of a ductile concrete while it is 40% lighter in weight (Li, 2005). The economical efficiency of this composite lies in its long life, so, with a better bonding achieved by micro scale fibers acting like ligament as it is much more durable than the conventional concrete (SNR & ECSS, 2005). Nevertheless the application of such an material in a seismic desert city requires more research.

Predicting the durability of concrete is difficult because so many items (e.g. compressive strength and permeation properties) are involved (Jones et al. 2002). The observation for durability in this study is not based only on the reactions insides one time modeling but it includes also model with about 1.5 year time difference. Some effects such as alkali pollutions are more obvious in the samples from the older model, but most of the problems were generally similar.

As a biodegradable and renewable source, bio-fibers, recently attracted many scientists. One might expect that these fibers are the most sustainable solution for fiber reinforced concrete. For example these kind of fibers (that are industrially produced and implemented) have been used as filters for air and water or bio-fiber geo-textiles in the form of a mat. Annually about 4 billion tons bio fibers is being produced world wide. 60% comes from agriculture and 40% from forests. (Svennerstedt, 2002). Many building products that are made of these fibers are highly applicable and desired (e.g. door panels). The basic structure of bio fibers consists of cellulose, hemi-cellulose, and lignin. The cellulose molecules consist of glucose units linked together in long chain while hemi-cellulose are polysaccharides bonded together in branching chain. Lignin, a three dimensional polymer with an amorphous structure (Olesen, 2001), is the compound that gives rigidity to the plant. For which pectin is the glue to hold them together (Svennerstedt, 2002). The relative high strength and low density and the heat, sound, and electrical insulation ability are of other main advantages of these fibers. However,

they are prone to water absorption and many of them are hygroscopic, thus the water absorption is high (due to the cohesion of hydrogen by hydrogen molecules to groups of hydroxyl in cellulose in cell-wall polymers). Problem is that reactive organic chemicals are tied to the cell-wall hydroxyl groups of cellulose, hemi-cellulose and lignin (Svennerstedt, 2002). Although this problem can be decreased and controlled by some methods (e.g. acetylation and heat treatments), it needs extra improvements and costs. These extra costs lower the applicability in building.

Additionally, the nature of such fibers causes them to have a big range of variety in diameter, length, and shape/geometry, which makes it much more difficult to create a reliable concrete with them compared to the industrially produced fibers such as glass fibers. This size problem needs extra attention and costs during the production process, but the quality is affected in either situation. Another problem that comes from the nature of such fibers is the low fire resistance. With temperatures above 200 ºC most of natural fibers ignite, thus for the exposed structural application this should be taken into the account. Moreover, bio-fibers can not be basically counted as durable (i.e. in the concrete composites for building products), because of destructive effect of alkaline pore solution on them. Especially in a long time as Swamy (1990) reported the lignin content may influence the hydration of the cement composite matrix. The decomposition of the fibers takes place more rapidly at high temperature (Gram et al. 1984). Thus, making a durable strong concrete structure by using bio-fibers, for improving some mechanical properties such as tensile strength, needs much more research and extra considerations. Although John et al. (1990) proved that producing load bearing bio fiber concrete is possible, and although Brazilian (RILEM & CIB, 1990) proved that by changing the concrete matrix prolongation of the durability of bio-fiber concrete is possible, the mentioned consequences prevent generalization of this use of bio-fibers for a durable concrete composite at least for a load bearing shell structure.

For the application of bio fibers in a seismic desert area it needs to be mentioned that even though the water absorption might not cause to much problems the availability of these fibers in these areas is low. Furthermore because of the long term and other construction problems with the use of these fibers they are not suitable for application in seismic areas.

From the results of the test samples the longer glass fibers showed a better bonding and better matrix-fiber interface structure than the shorter fibers, specially in the samples taken from the younger model. This might be caused by the higher need to water for the shorter fibers. Although Benmokrane et all (1999) proved that the fiber glass applied in the Juffre bridge worked well, the durability of structures is a time dependant item. Particularly for this bridge the fiber optic sensors were installed for the long and short term control to investigate future problems. These first applications had a great effect on the implementation of the glass fibers for reinforcing the concrete for such structures. However, for structural application, in seismic desert areas it would be the aim to replace steel bars wit glass fiber reinforcements. Alsayed et al. (1999) tested this application for a column, which showed that such a replacement in columns reduces their capacity by about 13% when subjected to monotonic-concentric loading (Alsayed et al., 1999). The axial capacity of the columns containing Glass fibers ties was 10% lower than those containing an equal volume of steel ties. However, for ductility and crack prevention, which is a very important goal of this study, Sato et al. (1999) proved that the prevention of propagation of cracks improved, based on the finding that the crack spacing decreased as the reinforcement ratio increased. In the test results of this study, no crack was reported in the samples of high ratio glass fiber reinforced composite. Nevertheless, it is not certain that glass fiber reinforcement will be suitable for the seismic desert application. This will require further study.

The ductility of the concrete reinforced with fibers such as glass fiber, carbon, and aramid increase was similar to the test done by Sato et al. (1999). Sato et al. (1999) showed that the effect to improve strength is the biggest in carbon fibers while aramid improves the ductility. For the shear strength carbon fibers are more effective than the aramid (Sato et al., 1999).

Intensive fiber pull-out indicates a fairly weak matrix/fiber interface bonding of the composite. Suzuki et al (1992) states that this prominent behavior of fiber pull-out is very significant for attaining high fracture energy (γρο). As it occurred in the work of Suzuki et al (1992), the few fragments of broken matrices imply the absence of chemical bonding at the interface between the matrix and the fibers in the older samples. The individually pull-out of the fibers and no observation of fiber bundles is different from the dominant mixed mode pullout of individual fibers and fiber bundles in the carbon fiber. Similar to carbon fiber the bonding is stronger in polypropylene fibers than the glass fibers. The alkali problem, which was observed in the matrix in the edges of the glass fibers is less than the problem caused by the high porosity of the matrix around the bio-fibers. This problem is not generally observable for the polypropylene fibers. Thus, for some mechanical properties such as strength, glass fibers have priority to the polypropylene fibers, but the propylene fibers similar to the carbon fibers showed a better bundling in these tests. Although carbon and aramid fibers can be mentioned as creating durable composite, the affordability is a subject for the general application of such materials.

5. SUMMARY AND CONCLUSION

Bio fibers are naturally lacking durability, and thus to implement them in a liquid like concrete which may even be exposed to the water after the hardening, needs extra costs and attentions. With interaction of extra risk possibility, and regarding the current applied techniques, this is not a good alternative to be used in a concrete composite for load bearing structures in seismic areas yet. However, desert climate creates two contradictories. First, because of dry-ness of a dry desert, it is a good option, (as water creates the most crucial problems for such fibers) but, secondly, for the same reason growing such fibers in a large scale does no seem feasible in the desert.

In the concrete as a composite with brittle ceramic matrix, the problems associated with the process of fiber pullout are much more complex than that in a monolithic material. However, as fibers generally prevented cracks and crack propagation and increased the ductility, appropriately using a fiber reinforced concrete composite is a good solution to decrease the vulnerability of the inhabitants of houses in seismic areas. With all of these, polymers showed better comprehensive characteristics, however further research for the most suitable polymer to be mixed in the composite is required.

ACKNOWLEDGMENT

Many thanks to Dr. Timo Nijland from Micro-Lab TNO Delft for his generously supports, guides, and helps. Thanks to Dr. Joe Larbi Micro-Lab TNO Delft, and to the Hormozgan University for sponsoring the research program.

REFERENCES

Ashby, M., 2005. Materials selection in mechanical design, third edition, Amsterdam: Elsevier. ISBN: 0-7506-6168-2

Alsayed, S. H., Al-Salloum, Y. A., Almusallam, T. H., Amjad, M. A., 1999. *Concrete Column a Reinforced by Glass Fiber Reinforced Polymer Rods.* Proc. fourth int. symp. Fiber Reinforced Polymer Reinforcement for Reinforced Concrete Structures, ACI, USA, card number: 99-066598.

Benmokrane et al., 1999. Benmokrane, B, Masmoudi, R, Chekired, M. , Rahman, H. , Debbache, Z. , and Tadros, G.. *Desiign Construction and Monitoring of Fiber Reinforced Polymer Reinforced Concrete Bridge Deck.* Proceeding 'Fourth International Symposium, fiber Reinforced polymer Reinforcement for Reinforced Concrete Structures', ISBN: , pp87-102

Booth, E., Key, D., 2006. *Earthquake design practice for buildings*. Second edition, London, Thomas Telford, ISBN: 0-7277-2947-0

Brundtland, 1987. *Our Common Future*, Report of UN World commission on Environment and Development, Geneva, Switzerland, April 1987

CERCESJ, 2006.*Committee of Earthquake Resistance of Civil engineering Structure in Japan* **.** Japan Society of Civil Engineering, Special Task Committee of Earthquake Resistant of Structures

Dolan et al. , 1999. Dolan, W. C. ; Rizkalla, H. S. ; and Nanni, A. *Fourth International Symposium, fiber Reinforced polymer Reinforcement for Reinforced Concrete Structures*. ACI

Gram, H-E, Persson, H., Skarendahl, A., 1984). *Natural Fiber Concrete-Report from a SAREC- financed research and development project. Sarec ReportsR2: 1984, Stokholm*

Hendriks, C. F., 2002. *Durable and sustainable construction materials and the building cycle*, Best, Aeneas ISBN 90-75365-49-7

Kahl, 2005. Steve Kahl Super Visor experimental studies group with the Michigan Department of Transportation's (MDOT), The University RECORD for Faculty and Staff, 17 May 2005

Lauritzen, E. K., 1998. 'The Global Challenge of Recycled Concrete', in Sustainable Construction: 1-Use of Recycled Concrete Aggregates, Thomas Telfort, London, pp. 505- 519.

Li, 2005. Professor Victor Li, Environment and Civil Engineering University of Michigan. In 'The University RECORD for faculty and staff of the University of Michigan, 17 May 2005

Lura, P. van Breugel, K., 2002. *Volume Changes of LWAC at early ages.* Proc. Int. conf. '9DBMC, 17th-20th March 2007 Brisbane, Australia

Marcovich, I., 2006. *High-performance hybrid-fibre concrete: development and utilization*. Delft, Delft University Press, ISBN: 90-407-2621-3

Newman, J. Choo, B. S., 2003. *Advanced Concrete* Technology: constituent materials, Amsterdam, Elsevier ISBN 0-7506-5103-2

Olesen, P. O., Plackett, D. V., 1999. 'Perspectives on the performance of Natural' plant fibers proceedings of the International conference Natural Fibers Performance Foroum, May 27-28, 1999. Copenhagen, Denmark.

Pietersen et al. 2002. Ietersen, H. S. , Fraaij, A. L. A., Veries, H. J. De. *Durability of concrete with recycled aggregates- Results of Dutch laboratory and Pilot tests.* Proceeding 9dbmc, ISBN: 0643068279

Proverbio, E. , Bonaccorsi L. M., 2002. *Failure of Prestressing Steel Induced by Cervise Corrosion In Prestressed Concrete Structure.* Prce. 9th Int. Conf. Durability of Building Materials and Componenets, Brisbane, Australia, 17th -20th March 2002

Sato, Y., Fijii, S. Seto, Y., Fujii, T., 1999. *Structural behavior of Composite Reinforced Concret Members Encased by Continuous Fiber-Mesh reinforced Mortar Permanent forms*. Proc. fourth int. symp. Fiber Reinforced Polymer Reinforcement for Reinforced Concrete Structures, ACI, USA, card number: 99-066598.

Shahnoori, S., 2005. Reconstruction in Bam inrespect to seismic aspects. Proceedings of International Conference of Earthrn Cities, Cerpic05, 5-7 July 2005, Istanbul, Turkey, ISBN: 975-561-269-6 pp. 316-324.

Shahnoori, S. Voorbij, A. I. M., 2007. *A Multidesciplinary challenge for technological adaptation* , proceedings of the conference 'Building Stock activation 2007', November 4-7, Tokyo, Japan. CIB pp. 237-244

Shahnoori, S., Voorgij, A. I. M., 2007. *Glocal Structural System in a seismic desert c*ity, proceedings of 'Sustainable Construction, Materials and practices' 12-14 September 2007, Lisbon ISBN: 978-1-58603-785-7; pp. 959-967

SNR and ECSS, 2005. The School of Natural Resources and Environment Center for Sustainable Systems. PHYSORG; Science: Physics: Tech: Nano: News, May 04 2005

Suzuki, T., Sato, M., Sakai, M. 1992. *Fiber pullout and Mechanisms of a carbon fiber silicon nitride ceramic composite*. Journal of Material research, Volume 7, number 10, October 1999.

Svennerstedt, B., 2002.*Durability and life cycle aspects on bio-fiber composite materials*, proceedings of International Conference of 9DBMC, 14th-17th March 2007, Brasbane, Australia.

Swammy, R. N., 1990. Vegetable Fiber Reinforced Cement Composites- A false dream or a Potential Reality? Proceedings of the second international symposium, RILEM & CIB. September 17-21. 1990, Salvador, Brazil.

Symonds, 1999. report to DGXI, European Commission. Construction and demolition waste management practices, and their economic impact. Final report February 1999.

Troyer, W., 1990. Preserving Our World, A consumer guide to the Brundtland Report; Warglen International Communication INC, second printing, ISBN: 0-9694538-1-7.

Vogtlander, J. G. Hendriks, C. F., 2004. *The Eco-costs/Value Ratio (EVR): materials and ecological engineering*, Boxtel, Aeneas. ISBN: 90-75365-50-0.

Yu, C. W. Bull, J. W., 2006. *Durability of materials and structures in building and civil engineering,* Boca Raton, CRC Press, ISBN: 1-870325-58-3.

11th International Conference on Durability of Building Materials and Components
Istanbul Turkey May 11-14, 2008

Concrete Crack Width under Combined Reinforcement Corrosion and Applied Loads

Chun-Qing Li [1]
Shangtong Yang [2]
T K Ho [3]

T 11

ABSTRACT

Concrete crack width is a parameter of the most practical significance for the design and assessment of reinforced concrete structures. Practical experience and observations suggest that corrosion affected reinforced concrete structures are more prone to cracking than other forms of structural deterioration. The situation is exacerbated when the applied loads add additional radial pressure to that induced by corrosion expansion. It is well known that concrete cracking incurs considerable costs of repairs and inconvenience to the public due to interruptions. This gives rise to the need for thorough examination of concrete cracking under both reinforcement corrosion and applied loads so as to achieve cost-effectiveness in maintaining the serviceability of concrete structures.

This paper attempts to derive a model for concrete crack width under the combined pressure of corrosion expansion and applied loads. A recently developed corrosion model will be used to determine the corrosion volume. The concrete fracture mechanics will be employed in the derivation whereby cracks are modelled as smeared cracks and concrete be quasi-brittle. With the values of the basic variables of the model taken form literature review, a worked example is presented for illustration. A merit of the derived model is that it is directly related to design variables used by practical engineers. The paper concludes that the model presented herein can be used to estimate concrete crack width under the combined effects of reinforcement corrosion and applied loads with reasonable accuracy.

KEYWORDS

Corrosion expansion, Applied load, Crack width, Concrete structures, Fracture mechanics

[1] Department of Civil Engineering, the University of Greenwich, England, ME4 4TB, Phone +44 1634 883518, Fax, 1634 883153, c.q.li@greenwich.ac.uk
[2] Department of Civil Engineering, the University of Greenwich, England, ME4 4TB, Phone +44 1634 883031, Fax, 1634 883153, s.yang@greenwich.ac.uk
[3] Department of Civil Engineering, the University of Greenwich, England, ME4 4TB, Phone +44 1634 883709, Fax, 1634 883153, t.k.ho@greenwich.ac.uk

1. INTRODUCTION

Corrosion of reinforcement in concrete has been identified as one of the most predominant factors for the deterioration of reinforced concrete structures [Bhargava et al. 2006]. The corrosion products occupy much greater volume than the original steel. When steel corrosion develops, the corrosion products first accumulate at the steel surface and try to fill the closest voids. After that the corrosion products exert expansive pressure to the surrounding concrete as the corrosion continues. This expansive pressure could induce tensile stresses in the concrete whose tensile strength is usually very low which leads to longitudinal cracking of concrete. This situation will be exacerbated when applied loads introduce additional radial forces to the surrounding concrete due to the bond action between the concrete and reinforcement. The bond depends primarily upon mechanical action which through ribs of deformed bars imposes radial stress components to the concrete. As a result, there are more cracks on the surface of concrete, incurring considerable costs of repairs and inconvenience to the public due to interruptions [Li et al. 2006].

Considerable studies have been carried out on corrosion-induced concrete cracking [Dagher and Kulendran 1992; Liu and Weyers 1998] and on loading-induced concrete cracking [Colotti and Spadea 2004; Goto 1971; Tepfers 1979]. Liu and Weyers [1998] examine the time from corrosion initiation to cracking of the cover concrete both theoretically and experimentally and developed a model to calculate the critical amount of rust products. Li et al. [2006] establish an analytical model for corrosion-induced crack width which gives quantitative relationships between the critical factors affecting cracking and crack width. Ueda et al. [1998] use finite element methods to examine the factors that affect corrosion-induced cracking in concrete and find that the tensile strength and creep of the concrete are important factors. Tepfers [1979] conduct a research on the cracking resistance of the cover concrete without considering the corrosion effect and obtain the stresses in concrete for an elastic stage, a plastic stage and an elastic stage with internal ring cracks. Goto [1971] presents the results of experiments on the characteristics of internal cracks, secondary cracks and longitudinal cracks around tensile reinforcing bars, and points out the longitudinal cracks are more probable when primary crack spacing is near the maximum. The review of research literature (see references) shows that there is little research focusing on both corrosion and loading effects on concrete cracking.

This paper attempts to investigate the combined effects of both loading and corrosion on concrete cracking and to develop an analytical model for crack width. In this study, both effects are examined on three different stages – no cracking, partly cracked, and completely cracked based on which three different mechanisms are taken into account for both effects together. Fracture mechanics is employed for the analysis of stress and strain in the cracked concrete where isotropic property is no longer applicable. The developed model can be used as a tool to assess the serviceability of corrosion affected concrete infrastructure.

2. FORMULATION OF THE PROBLEM

Although considerable research has been undertaken on corrosion-induced, or loading-induced concrete cracking, little work has been conducted directly on corrosion-induced crack width over time [Li et al. 2006], and almost no research is carried out on both corrosion and loading induced crack width as a function of time.

Concrete with embedded reinforcing bar can be modelled as a thick-wall cylinder [Bažant 1979; Pantazopoulou and Papoulia 2001; Tepfers 1979] where elastic mechanics [Timoshenko and Goodier 1970] and fracture mechanics [Bažant and Jirasek 2002; Noll 1972] are employed to analyse the stress distribution. This is shown in Fig. 1 (a), where D is the diameter of reinforcement bar, d_0 is the thickness of the annular layer of concrete pores at the interface between the bar and concrete and C is the concrete cover. $P(t)$ is the expansive pressure at the interface between the rust band and concrete, and it consists of two parts: $P_1(t)$ induced by corrosion and P_2 induced by loading.

$$P(t) = P_1(t) + P_2 \tag{1}$$

Under the expansive pressure, the concrete cylinder undergoes three phases in terms of cracking: 1) no cracking; 2) partially cracked; 3) completely cracked.

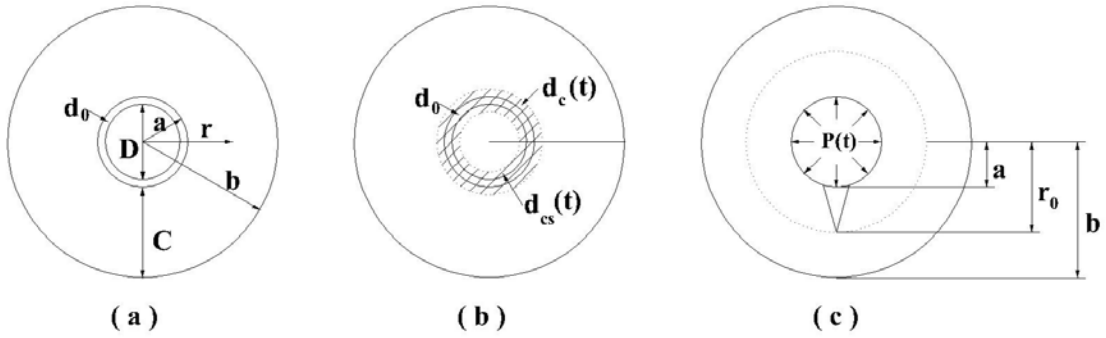

Figure 1. Schematic of corrosion-induced concrete cracking process

2.1 Effect of Corrosion Products

As shown in Fig. 1 (b), $d_c(t)$ is the thickness of the band of rust which is formed after the corrosion products fill in the full layer of concrete pores, $d_{cs}(t)$ is the thickness of corroded steel. Usually d_0 is constant once concrete has hardened. The inner and outer radii of the thick-wall cylinder are $a = D/2 + d_0$ and $b = C + D/2 + d_0$. As steel corrodes, the corrosion products first fill in the pore band of d_0, which does not cause stresses in the concrete cylinder. After that, as the corrosion propagates in the concrete cylinder, a ring of corrosion products forms, the thickness of which as mentioned above, is $d_c(t)$. According to Liu and Weyers [1998], $d_s(t)$ is the sum of d_0 and $d_c(t)$, and can be determined as

$$d_s(t) = \frac{W_{rust}(t)}{\pi D}\left(\frac{1}{\rho_{rust}} - \frac{\alpha_{rust}}{\rho_{st}}\right) \tag{2}$$

where α_{rust} is a coefficient related to the type of corrosion products, ρ_{rust} is the density of corrosion products, ρ_{st} is the density of steel, and $W_{rust}(t)$ is the mass of corrosion products. Then $d_c(t)$ can be obtained from

$$d_c(t) = d_s(t) - d_0 \tag{3}$$

It is assumed in this paper that $d_c(t)$ is the displacement of the concrete cylinder caused by corrosion only.

In Figure 1, $d_{cs}(t)$ can be expressed in terms of $W_{rust}(t)$ as

$$d_{cs}(t) = \frac{\alpha_{rust} W_{rust}(t)}{\rho_{st}} \tag{4}$$

According to Li et al. [2006] and Liu and Weyers [1998], $W_{rust}(t)$ can be expressed as

$$W_{rust}(t) = \sqrt{2\int_0^t 0.105(1/\alpha_{rust})\pi D i_{corr}(t)dt} \tag{5}$$

2.2 Effect of Applied Loads

This paper only concerns load-induced longitudinal cracks which are due to radial component of the bond forces between deformed rebar and surrounding concrete as schematically shown in Fig. 2.

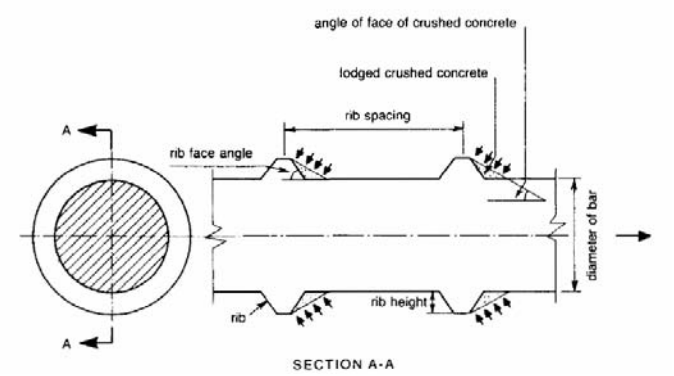

Figure 2. The mechanical interaction [Tepfers 1979]

The radial pressure to concrete can be calculated from Tepfers [1979]

$$P_2 = \frac{D}{4}\frac{d\sigma_s}{dx}\tan\theta \tag{6}$$

where σ_s is the steel stress under loads, x indicates different position over the length of the rebar, and θ is the angle between the bond force and the axis.

For a simply supported reinforced concrete beam subject to distributed load with magnitude ω, from theory of concrete structure, σ_s can be determined as follows

$$\sigma_s = \frac{M(x)}{A_s(h_0 - \frac{f_y A_s}{2\alpha_1 f_c b})} = \frac{\frac{\omega L}{2}x - \frac{\omega x^2}{2}}{A_s(h_0 - \frac{f_y A_s}{2\alpha_1 f_c b})} \tag{7}$$

where L is the length of the beam, f_y is the tensile strength of the reinforcement, f_c is the compressive strength of the concrete, A_s is the area of the reinforcement in the concrete, h_0 is the effective height and b is the width of the concrete beam.

It follows that P_2 can be expressed as

$$P_2 = \frac{D}{4}\frac{\frac{\omega L}{2} - \omega x}{A_s(h_0 - \frac{f_y A_s}{2\alpha_1 f_c b})}\tan\theta \tag{8}$$

3. DERIVATION OF CRACK WIDTH

At no-cracking stage, the concrete cylinder can be considered to be elastically isotropic so that the theory of elasticity can be employed to determine the radial stress $\sigma_r(r)$ and tangential stress $\sigma_\theta(r)$ at any point (r) in the cylinder. According to [Timoshenko and Goodier 1970], the radial and tangential stresses can be expressed as

$$\sigma_r(r)=\frac{E_{ef}}{1-\upsilon_c^2}\left[(1+\upsilon_c)c_1-\frac{(1-\upsilon_c)c_2}{r^2}\right] \tag{9}$$

$$\sigma_\theta(r)=\frac{E_{ef}}{1-\upsilon_c^2}\left[(1+\upsilon_c)c_1+\frac{(1-\upsilon_c)c_2}{r^2}\right] \tag{10}$$

At the partially cracked stage, the concrete cylinder is divided into two coaxial cylinders: inner cracked and outer uncracked ones. For the outer uncracked concrete cylinder, the theory of elasticity still applies. For the inner cracked one, however, fracture mechanics is employed to determine the stress distribution by assuming that the cracks are smeared and uniformly distributed on the circumference of the cracked cylinder [Pantazopoulou and Papoulia 2001]. To account for this, a tangential stiffness reduction factor α (<1) is introduced.

For the outer uncracked concrete, the stress components are

$$\sigma_r(r)=\frac{E_{ef}}{1-\upsilon_c^2}\left[(1+\upsilon_c)c_3-\frac{(1-\upsilon_c)c_4}{r^2}\right] \tag{11}$$

$$\sigma_\theta(r)=\frac{E_{ef}}{1-\upsilon_c^2}\left[(1+\upsilon_c)c_3+\frac{(1-\upsilon_c)c_4}{r^2}\right] \tag{12}$$

For the inner cracked concrete the radial and tangential stresses are

$$\sigma_r(r)=\frac{\sqrt{\alpha}E_{ef}}{1-\upsilon_c^2}\left[c_5(1+\upsilon_c)r^{(\sqrt{\alpha}-1)}-c_6(1-\upsilon_c)r^{(-\sqrt{\alpha}-1)}\right] \tag{13}$$

$$\sigma_\theta(r)=\frac{\alpha E_{ef}}{1-\upsilon_c^2}\left[c_5(1+\upsilon_c)r^{(\sqrt{\alpha}-1)}+c_6(1-\upsilon_c)r^{(-\sqrt{\alpha}-1)}\right] \tag{14}$$

At the completely cracked stage, the governing equation for the concrete cylinder is the same as that of inner cracked part for the partially cracked stage with different boundary conditions. Thus, the stress components are as follows

$$\sigma_r(r)=\frac{\sqrt{\alpha}E_{ef}}{1-\upsilon_c^2}\left[c_7(1+\upsilon_c)r^{(\sqrt{\alpha}-1)}-c_8(1-\upsilon_c)r^{(-\sqrt{\alpha}-1)}\right] \tag{15}$$

$$\sigma_\theta(r)=\frac{\alpha E_{ef}}{1-\upsilon_c^2}\left[c_7(1+\upsilon_c)r^{(\sqrt{\alpha}-1)}+c_8(1-\upsilon_c)r^{(-\sqrt{\alpha}-1)}\right] \tag{16}$$

In the above equations, C_1 - C_8 are coefficients of differential equations to be determined based on initial and boundary conditions which cannot be described in details here due to page limit.

Before corrosion initiates, there is only applied load induced pressure P_2, under which the concrete cylinder could be either not cracked or partially cracked. Completely cracked case can be designed out. This needs to be checked before corrosion induced pressure is considered.

Assuming under P_2 at t=0 the concrete cylinder has no cracking, apply $\sigma_r(a) = -P_2$ and $\sigma_r(b) = 0$ (see Fig 1) as the boundary conditions, the stresses components could be obtained

$$\sigma_r(r) = \frac{a^2 P_2}{b^2 - a^2}(1 - \frac{b^2}{r^2}) \tag{17}$$

$$\sigma_\theta(r) = \frac{a^2 P_2}{b^2 - a^2}(1 + \frac{b^2}{r^2}) \tag{18}$$

If $\sigma_\theta(a) < f_t$, it means no cracking for concrete cylinder at t=0,
If $\sigma_\theta(a) \geq f_t$ and $\sigma_\theta(b) < f_t$, it means partially cracked for concrete cylinder at t=0.

When there is no cracking, applying $u(a) = d_c(t)$ and $\sigma_r(b) = 0$ as the boundary conditions, the corrosion-induced radial stress at $r = a$ could be found as

$$\frac{E_{ef} d_c(t)}{a(\frac{a^2 + b^2}{a^2 - b^2} - \upsilon_c)}.$$

Then applying

$$\sigma_r(a) = \frac{E_{ef} d_c(t)}{a(\frac{a^2 + b^2}{a^2 - b^2} - \upsilon_c)} - P_2$$

and

$$\sigma_r(b) = 0$$

as new boundary conditions, the radial and tangential stresses at any point (r) under the combined effect can be obtained. The same methodology applied to the second phase and third phase is employed to determine all the coefficients. Finally, the solution to crack width is

$$w_c = 2\pi b\left[c_7 b^{(\sqrt{\alpha}-1)} + c_8 b^{(-\sqrt{\alpha}-1)} - \frac{f_t}{E_{ef}}\right]$$

$$= \frac{4\pi d_s(t)}{(1-\upsilon_c)(a/b)^{\sqrt{\alpha}} + (1+\upsilon_c)(b/a)^{\sqrt{\alpha}}} + \frac{4\pi a P_2}{E_{ef}\sqrt{\alpha}((b/a)^{\sqrt{\alpha}} - (a/b)^{\sqrt{\alpha}})} - \frac{2\pi b f_t}{E_{ef}} \tag{19}$$

When the concrete is partially cracked before corrosion starts, the initial cracking time $t_1 = 0$. The concrete cylinder undergoes from the phase of partially cracking and the stresses expressions of (11) to (14) are applicable. Under these two scenarios the coefficients of differential equations are the same. It needs to be checked, however, at the very beginning, which scenario occurs and analyse for the correct phase.

4. WORKED EXAMPLE

To demonstrate the application of the derived model, a numerical example is carried out using the values of basic variables in Table 1. In this case, a reinforced concrete beam with the dimension 100 x

200 x 3000 (length) mm is used. The beam is subjected to a uniformly distributed load of 2e4 N/m and is (assumed) located in a marine environment which inevitably causes reinforcement corrosion in the beam and eventually concrete cracking. Under this situation, equation (19) can be used to estimate the crack width. Firstly, computer program written in MATLAB is developed for all the computation for different phases as described above. The program is run 1001 times for a 10 years service life with a time increment of 0.01 year. The value of crack width is obtained once the stiffness reduction factor α is determined in each run. The results for the crack width, the expansive pressure and the tangential stiff reduction factor are presented as function of time in Fig.3.

Table 1. Values of some basic variables

Symbol	Values
α_1	0.85
h_0	163mm
f_y	400MPa
A_s	226 mm^2
b	120mm
C	31mm
D	12mm
d_0	12.5μm
f_t	5.725 MPa
α_{rust}	0.57
ρ_{rust}	3600 kg/m^3

As can be seen in Fig 3, the crack width increases with time as well as the displacement of concrete cylinder at r=a. At time t=0, the expansive pressure is caused by applied loads only; therefore the pressure keeps constant until corrosion induces the additional pressure. At about 2 years, the concrete surface cracks leading to an abrupt increase in crack width, accompanied with sudden decreases in the tangential stiffness reduction factor α and expansive pressure P. The sudden decreases in the expansive pressure and α indicate that the consistency in deriving the crack width based on both isotropic, elastic concrete and anisotropic, quasi-brittle concrete. At nearly 3 years, the tangential stiffness reduction factor α approaches zero which means almost no tangential stress in concrete from then.

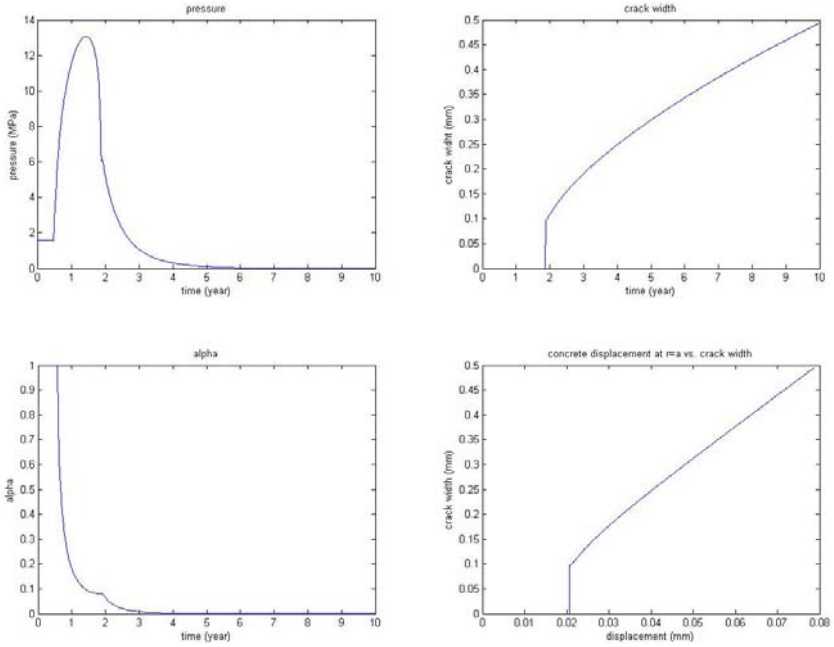

Figure 3. Relationships between some important factors and time

5. CONCLUSIONS

An analytical model for concrete crack width under both reinforcement corrosion and applied loads has been derived based on a combination of elastic mechanics and fracture mechanics. The model is directly related to the causal factors of corrosion rate and applied load, as well as the concrete geometry and properties. Due to page limit, details of the derivation of the solution to the differential equations cannot be presented. A worked example is given and the numerical results seem to be quite reasonable to reflect the engineering reality. It can be concluded that the model derived in the paper can serve as a useful tool for engineers, operators and asset managers in decision-making with regard to the serviceability of corroded concrete structures.

ACKNOWLEDGMENTS

Financial support from the Engineering and Physical Sciences Research Council with Grant No. EP/E00444X/01 and the Royal Academy of Engineering with Award No. 10177/93 is gratefully acknowledged.

REFERENCES

Bažant, Z.P. 1979, 'Physical model for steel corrosion in concrete sea structures – theory', Journal of Structural Division, ASCE, 105, (ST6), 1137 – 1153.

Bažant, Z.P. & Jirasek, M. 2002, 'Nonlocal integral formulations of plasticity and damage: survey and progress', Journal of Engineering Mechanics, ASCE, 128, (11), 1119 − 1149.

Bhargava, K., Ghosh, A.K., Mori, Y. & Ramanujam, S. 2006, 'Model for cover cracking due to rebar corrosion in RC structures', Engineering Structures, 28, 1093-1109.

Dagher, H.J. & Kulendran, S. 1992, 'Finite element modeling of corrosion damage in concrete structures', ACI Structural Journal, 89, (6), 699 – 708.

Li, C. Q., Melchers, R. E. & Zheng, J. J. 2006, 'Analytical model for corrosion-induced crack width in reinforced concrete structures', ACI Structural Journal, V. 103, No. 4.

Liu, Y. & Weyers, R. E. 1998, 'Modeling the time-to-corrosion cracking in chloride contaminated reinforced concrete structures', ACI Materials Journal, 95, (6), 675 – 681.

Noll, W. 1972, 'A new mathematical theory of simple materials', Archive for Rational Mechanics and Analysis, 48, 1 – 50.

Goto,Y. 1971, 'Cracks formed in concrete around deformed tension bars', ACI Journal, April.

Pantazopoulou, S.J. & Papoulia, K.D. 2001, 'Modeling cover-cracking due to reinforcement corrosion in RC structures', Journal of Engineering Mechanics, ASCE, 127, (4), 342 – 351.

Tepfers, R. 1979, 'Cracking of concrete cover along anchored deformed reinforcing bars', Magazine of Concrete Research, 31, (106), 3 – 12.

Timoshenko, S.P. & Goodier, J.N. 1970, *Theory of Elasticity,* McGraw-Hill Book Company, New York, 400.

Ueda, T., Sato, Y., Kakuta, Y. & Kameya, H. 1998, 'Analytical study on concrete cover cracking due to reinforcement corrosion', *in Concrete Under Severe Condition 2,* Proceedings of an Int. Conf., Tromso, Norway, 678 – 687.

11DBMC International Conference on Durability of Building Materials and Components
ISTANBUL, Turkey 11-14 May 2008

Deterioration of Cement Hydrates Containing Mineral Admixtures Due to Sulfuric Acid Attack

Kenji Kawai [1]
Akihiro Sako [2]
Tomoya Ikuta [3]
Takeo Ishida [4]

T 11

ABSTRACT

Concrete in sewage and wastewater treatment plants are deteriorated by sulfuric acid. To prevent this deterioration, some coutermeasures are taken. The use of mineral admixtures such as blast furnace slag, fly ash and silica fume is one of the countermeasures. In this study, the effect of mineral admixturs on resistance of cement hydrates to sulfuric acid attack was investigated.

Cement paste and mortar specimens were prepared with different water cement ratios. A part of cement was replaced with blast furnace slag, fly ash and silica fume. After curing, the specimens were immersed in sulfuric acid solutions of pH=1.0 and 2.0. To simulate a circumstance of sewage, some specimens were immersed in flowing sulfuric acid solution. The erosion depths and mass losses of the specimens were measured. For some specimens, the calcium hydroxide contents were determined before and after immersion.

As a result, specimens containing silica fume showed much better resistance to sulfuric acid attack than those containing blast furnace slag and fly ash. Specimens containing three mineral admixtures of blast furnace slag, fly ash and silica fume also showed good resistance. The flow of the solution accelerated the erosion of specimens immersed in sulfuric acid solution of pH=2.0.

KEYWORDS

Acid attack, Sulfuric acid, Mineral admixture, pH

[1] Hiroshima University, Department of Social and Environmental Engineering, Higashi-Hiroshima, Japan 739-8527, Phone +81 82 424 7788, Fax 82 424 7788, kkawai@hiroshima-u.ac.jp
[2] Tokyo Metropolitan Government Bureau of Sewerage, Tokyo, Japan 132-0021, Phone +81 3 5662 7215, Fax 3 3652 6299, Akihiro_Sako@member.metro.tokyo.jp
[3] Hiroshima University, Graduate School of Engineering, Higashi-Hiroshima, Japan 739-8527, Phone +81 82 424 7786, Fax 82 424 7786, tomoya-ikuta@hiroshima-u.ac.jp
[4] Hiroshima University, Department of Social and Environmental Engineering, Higashi-Hiroshima, Japan 739-8527, Phone +81 82 424 7786, Fax 82 424 7786, ishidax@hiroshima-u.ac.jp

1 INTRODUCTION

Concrete structures in sewage and wastewater treatment plants are severely damaged by sulfuric acid attack. Generally some kind of resin material is coated on the concrete surface when severe acid attack is expected against the concrete. But this coating is effective only if there is no defect such as a pinhole. Otherwise concrete deterioration will be developed from the surrounding of a pinhole. To prevent such deterioration, it is demanded that concrete itself has the resistance to sulfuric acid solution in some extent. The use of mineral admixtures such as blast furnace slag, fly ash and silica fume will be one of the countermeasures against the concrete deterioration due to acid attack because calcium hydroxide which reacts with sulfuric acid to produce gypsum is consumed by hydration of blast furnace slag and pozzolanic reaction of fly ash and silica fume.

Recently the design method of a concrete structure has been shifting to the performance-based design method. If a concrete is placed under a circumstance where its deterioration is supposed, the deteroiration prediction will be demanded in the design stage. In this study, the effect of mineral admixtures on resistance of cement hydrates to sulfuric acid attack was investigated to establish an estimation method for predicting deterioration of cement hydrates containing mineral admixtures due to sulfuric acid attack.

2 EXPERIMENTAL PROCEDURES

2.1 Materials

Ordinary portland cement, blast furnace slag, fly ash and silica fume were used as binding material. The physical and chemical properties of these materials are shown in Table 1. Silicious sand was used as fine aggregate. In Japan, a new type of acid resistant cement has been developed [Kawai *et al.* 2007]. This cement is composed of 20% of ordinary portland cement, 30% of blast furnace slag, 30% of fly ash and 20% of silica fume. In this study, this cement was also used as binding material.

Table 1. Physical and chemical properties of binding materials used in this study

Binding material	*Chemical component* [%]							
	SiO_2	Al_2O_3	Fe_2O_3	CaO	MgO	SO_3	Na_2O	K_2O
Ordinary portland cement	20.41	5.18	3.17	64.25	2.06	2.16	0.4	0.39
Blast furnace slag	33.86	14.92	0.29	42.24	6.09	0.23	0.36	0.65
Fly ash	57.8	29.1	3.9	3.2	1.1	0.3	0.49	0.46
Silica fume	96.3	---	---	0.3	0.6	0.2	---	---

Binding material	*Chemical component* [%]			*Density* [g/cm^3]	*Blaine specific surface area* [cm^2/g]
	TiO_2	P_2O_5	MnO		
Ordinary portland cement	0.24	0.69	0.06	3.15	3 460
Blast furnace slag	0.65	0.01	0.34	3.05	3 950
Fly ash	1.67	0.04	0.01	2.28	3 900
Silica fume	---	---	---	2.22	---

2.2 Specimens

Cement paste specimens with a water binding material ratio of 0.35 and mortar specimens with a water binding material ratio of 0.40 were prepared. Both cement paste and mortar specimens are prisms of 40 mm x 40 mm x 160 mm in size. Specimens were demolded 24 hours after casting and cured in water at 20 ^{o}C for given periods. The mix proportions of cement paste and mortar specimens are shown in Tables 2 and 3, respectively.

Table 2. Mix proportions of ccement paste specimens

Mark	*W/B*	*Mass ratio of binding materials*			
		Ordinary portland cement	*Blast furnace slag*	*Fly ash*	*Silica fume*
OPC	0.35	100	--	--	--
BFS30		70	30	--	--
FA30		70	--	30	--
SF20		80	--	--	20
ARC		20	30	30	20

Table 3. Mix proportions of mortar specimens

Mark	*W/B*	*S/B*	*Mass ratio of binding materials*			
			Ordinary portland cement	*Blast furnace slag*	*Fly ash*	*Silica fume*
OPC	0.40	3.0	100	--	--	--
BFS40			60	40	--	--
ARC			20	30	30	20

2.3 Immersion Test

After cured in water for 8 weeks, cement paste specimens were cut into 40 mm x 40 mm x 40 mm in size and immersed in sulfuric acid solution with a pH value of 1.0. Mortar specimens were cut into 40 mm x 40 mm x 80 mm in size and four sides of mortar specimens were sealed with an acid-resistant resin so that sulfuric acid solution penetrated into the specimens one-dimensionally only from both ends of the specimens. After that the mortar specimens were immersed in sulfuric acid solution with pH values of 1.0 and 2.0. Before immersion, all surfaces of these specimens were ground with a grinder since calcium leaching during the water curing was suspected in the vicinity of the surfaces.

For mortar specimens, some were immersed in flowing sulfuric acid solution to simulate a circumstance of an actual sewage [Kawai *et al.* 2005] and the deterioration of them was compared with that of specimens statically immersed in sulfuric acid solution. The flow was generated by circulating the solution with a pump.

The mass losses of cement paste specimens and the erosion depths of mortar specimens were measured at given periods. The value of pH of the solution was continously measured with a pH meter to hold it constant by adding sulfuric acid.

3 RESULTS AND DISCUSSIONS

3.1 Immersion Test of Cement Paste Specimens

Calcium hydroxide contents of cement paste specimens at the age of 28 days are shown in Fig. 1. The calcium hydroxide contents of the specimens containing blast furnace slag (BFS30) and silica fume (SF20) decrease more than the replacement percentage of the mineral admixture, compared with the calcium hydroxide content of the specimen using ordinary portland cement (OPC). Hydration of blast furnace slag and pozzolanic reaction of silica fume consume calcium hydroxide while pozzolanic reaction of fly ash does not proceed. It is found that the specimen using acid resistant cement (ARC) remains very few calcium hydroxide contents.

Figure 2 shows the calcium hydroxide amount consumed by each mineral admixture which was calculated from the calcium hydroxide contents of cement paste specimens at the age of 56 days. A very large amount of calcium hydroxide is consumed by silica fume compared with blast furnace slag

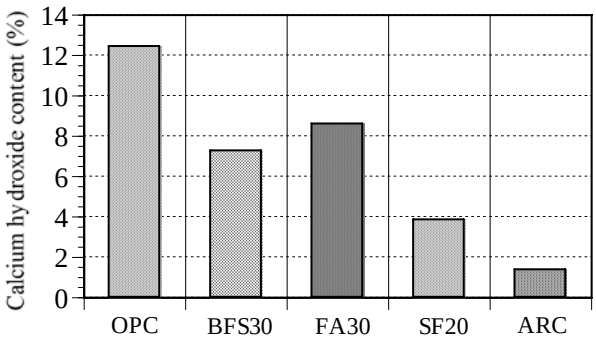

Figure 1. Calcium hydroxide content of each cement paste specimen at the age of 28 days

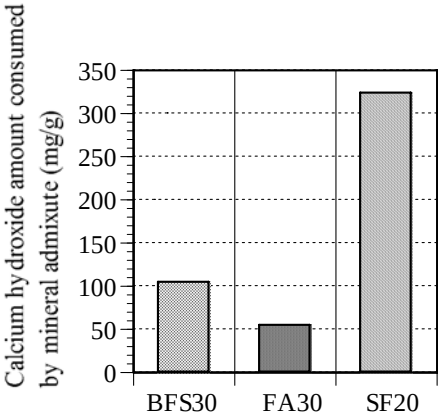

Figure 2. Calcium hydroxide amount consumed by each mineral admixture for 56 day curing

and fly ash. From this result, it is suitable to replace ordinary portland cement with silica fume in order to consume calcium hydroxide in the cement paste and improve the resistance of cement hydrates to sulfuric acid. The addition of silica fume, however, may reduce the consistency of cement paste. Therefore the addition of an appropriate amount of blast furnace slag or fly ash in addition to silica fume could be needed to keep the consistency of cement paste and improve the resistance of cement paste to sulfuric acid.

Changes in the mass loss of each specimen immersed in sulfuric acid solution of pH=1.0 are shown in Fig. 3. For BFS30, FA30, SF20 and ARC, the larger the calcium hydroxide content, the larger the mass gain of the specimen. The change in the mass of the specimen depends upon the remaining calcium hydroxide content. Therefore the addition of blast furnace slag instead of fly ash in addition to silica fume will be better from the result of the mass change.

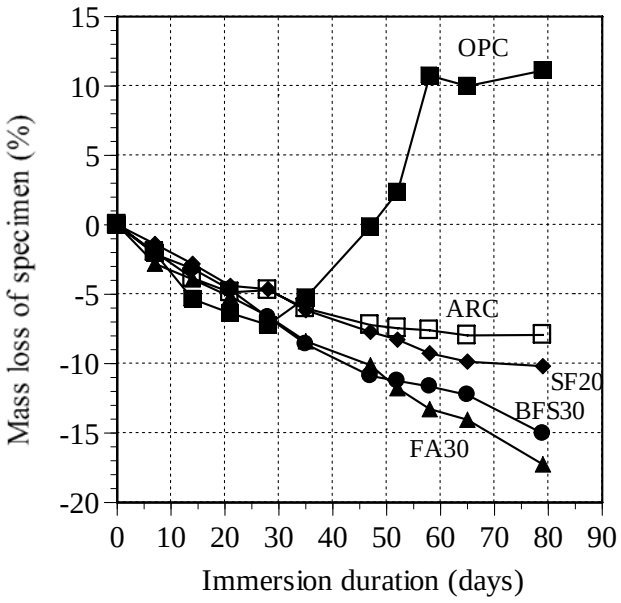

Figure 3. Mass loss of each cement paste specimen immersed in H_2SO_4 solution of pH=1.0

Photograghs of cement paste specimens immersed for 79 and 116 days in sulfuric acid solution of pH=1.0 are shown in Figs 4 and 5, respectively.

For the specimens using ordinary portland cement (OPC), gypsum was precipitated on the surfaces and removed. As a result, the size of the specimen reduced (Fig.5 (a)). On the other hand, for the

(a) OPC

(b) BFS30

(c) FA30

(d) SF20

(e) ARC

Figure 4. Photographs of specimens immersed for 79 days in H_2SO_4 solution of pH=1.0

(a) OPC

(b) BFS30

(c) FA30

(d) SF20

(e) ARC

Figure 5. Photographs of specimens immersed for 116 days in H_2SO_4 solution of pH=1.0

specimens using blast furnace slag and fly ash (BFS30, FA30), gypsum was precipitated on the surfaces but remained there. Gypsum layers were formed on the surfaces of the specimens and cracks which will be caused by swelling of gypsum production can be seen around the corners of the

specimens (Fig. 5 (b), (c)). It is thought that the gypsum layer for FA30 is gray because it contains fly ash particles together with gypsum. Comparing with gypsum produced in OPC, gypsum produced in BFS30 and FA30 should have higher cohesiveness which leads to control of acid penetration into a specimen. Little deterioration can be seen apparently for the specimens using silica fume and acid resistant cement (SF20, ARC) although some alternation is observed around the surfaces (Fig. 5 (d), (e)). This alternation, however, was so strong that there was no separation.

3.2 Immersion Test of Mortar Specimens

Erosion depths of mortar specimens immersed in flowing and static sulfuric acid solution with pH values of 1.0 and 2.0 are shown in Figs 6 and 7, respectively.

For specimens immersed in sulfuric acid solution of pH=1.0, the erosion depths of the specimens using ordinary portland cement, blast furnace slag and acid resistant cement differed largely, while the difference of the specimens immersed in flowing and static sulfuric acid solution was small. The specimens using acid resistant cement show good resistance to sulfuric acid solution and the addition of blast furnace slag also improves the resistance to sulfuric acid solution.

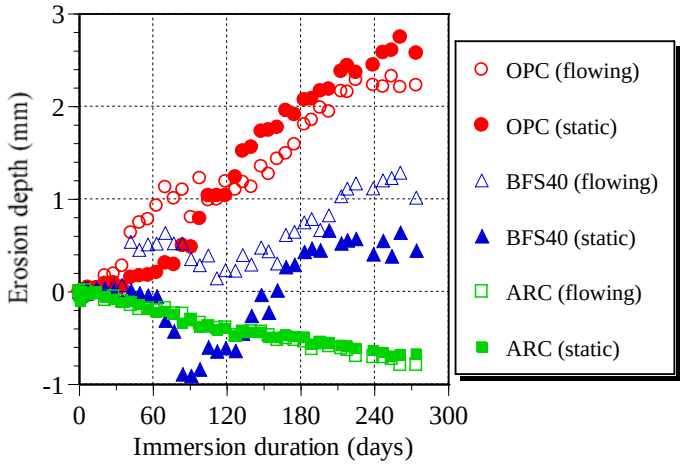

Figure 6. Changes in erosion depth of each mortar specimen immersed in H_2SO_4 solution of pH=1.0

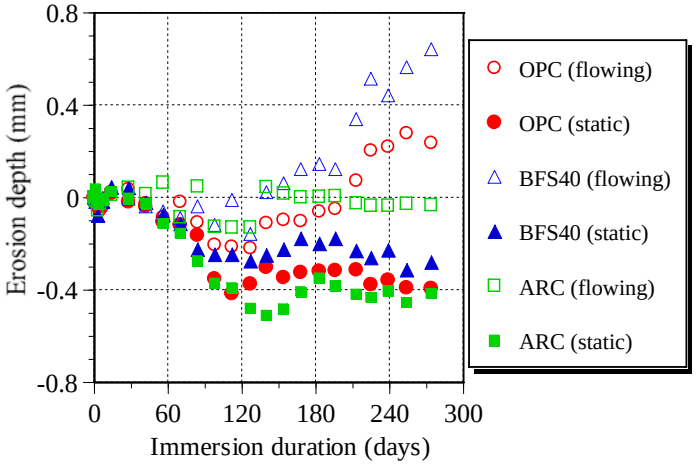

Figure 7. Changes in erosion depth of each mortar specimen immersed in H_2SO_4 solution of pH=2.0

For specimens immersed in sulfuric acid solution of pH=2.0, the erosion depths of the specimens immersed in flowing and static sulfuric acid solution differed significantly in every binding material. Since the acid attack at pH=2.0 is weaker than at pH=1.0, the production of gypsum by calcium

hydroxide and sulfuric acid is slow enough to remove the product by the shearing force of the flow in flowing sulfuric acid solution. It can be said that the shearing force of the flow accelerates the erosion of the specimen.

Mass losses of mortar specimens immersed in flowing and static sulfuric acid solution with pH values of 1.0 and 2.0 are shown in Figs 8 and 9, respectively.

The results do not wholly correspond to the results for the erosion depths. For instance, the erosion depths of the specimens for OPC and BFS40 immersed in flowing sulfuric acid solution are largely different in Fig. 6 but the mass losses of both specimens are almost same in Fig. 8. This will be because the specimen for BFS40 was not eroded very much but the microstructure near the surfaces became porous. Such microstructural change could be reflected to the mass losses.

Comparing the results between pH=1.0 and pH=2.0, the specimens for OPC immersed statically in sulfuric acid solution show very different tendency, which can be seen also in the results for the erosion depth. This will explain that the reaction rate of calcium hydroxide and sulfuric acid is quite different at pH=1.0 and pH=2.0.

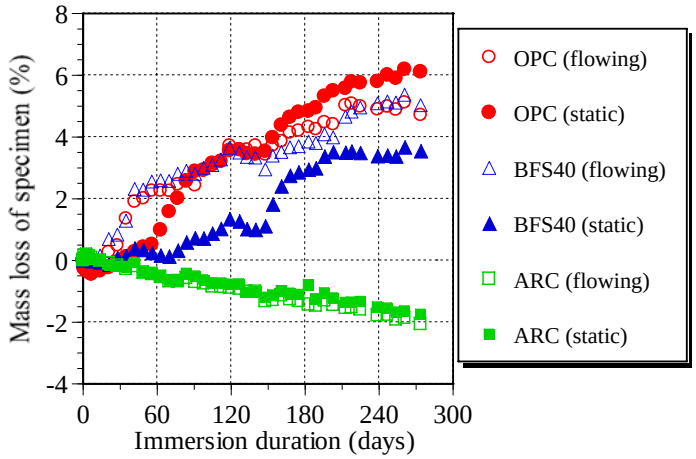

Figure 8. Changes in mass loss of each mortar specimen immersed in H_2SO_4 solution of pH=1.0

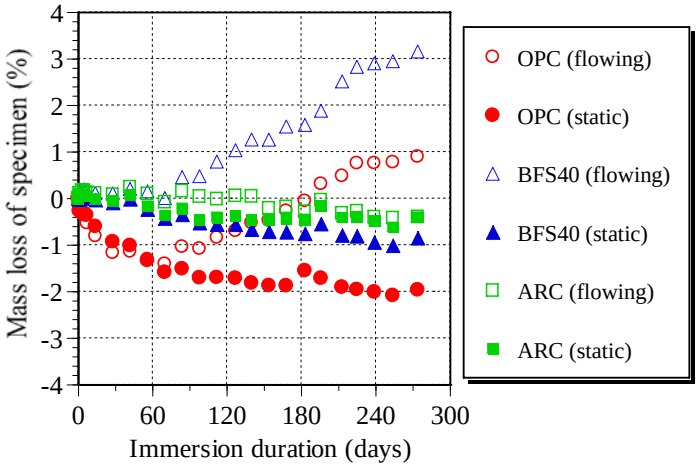

Figure 9. Changes in mass loss of each mortar specimen immersed in H_2SO_4 solution of pH=2.0

4 CONCLUSIONS

In this study, the effect of mineral admixtures on resistance of cement hydrates to sulfuric acid attack was investigated. As a result, the following conclusions can be drawn.

1. Coment paste specimens containing silica fume showed good resistance to sulfuric acid attack compared with specimens containing blast furnace slag and fly ash. Cement paste specimens containing three mineral admixtures of blast furnace slag, fly ash and silica fume also showed good resistance to sulfuric acid attack.

2. When mortar specimens were immersed in sulfuric acid solution of pH=1.0 and pH=2.0, changes in erosion depths and mass losses were different in the value of pH for specimens containing no mineral admixture and blast furnace slag. Specimens containing three mineral admixtures of blast furnace slag, fly ash and silica fume showed very little changes in both erosion depths and mass losses.

3. When mortar specimens were immersed in flowing sulfuric acid solution at pH=2.0, the erosion of the specimens was accelerated compared with specimens immersed statically in sulfuric acid solution.

ACKNOWLEDGMENTS

A part of this study was supported by Grant-in-Aid for Scientific Research (B), Japan Society of the Promotion Science.

REFERENCES

Kawai, K., Yamaji, S., & Shinmi, T. 2005, ‘Concrete Deterioration Caused by Sulfuric Acid Attack’, Proc. 10th Int. Conf. on Durability of Building Materials and Components, 17-20 Lyon, April 2005, 7p. (in CD-ROM).

Kawai, K., Ishida, T., Sako, A., Higuchi, S. & Nito, N. 2007, ‘Resistance to sulfuric acid of mortar using acid resistant cement’, Proc. 5th Int. Conf. on Concrete Under Severe Conditions - Environment and Loading, Tours, France, 4-6 June 2007, vol. 1, pp. 579-588.

11th International Conference on Durability of Building Materials and Components
Istanbul Turkey May 11-14, 2008

Corrosion Resistance of GGBS Concrete

M. Hulusi Ozkul [1]
Unal Anil Dogan [2]
Ali Raif Saglam [3]
Nazmiye Parlak [4]

T11

ABSTRACT

Owing to the fact that corrosion of steel is the key concern of service life of reinforced concrete structures, researchers have been dealing with this subject for many years. Pozzolanic materials, most of which are by products of industries, are widely used in concrete production, especially to increase the durability properties. Fly ash, ground granulated blast furnace slag (GGBS) and silica fume are the most common pozzolans together with natural pozzolans used in concrete technology.

In this experimental research, resistance to chloride induced corrosion of reinforcing steel bars embedded in GGBS concrete has been studied. Two classes of concrete have been prepared; such as C25 and C35 at two different binder ratios. Cement in the concrete was replaced with GGBS at the ratios of 30%, 50% and 70%. Lollipop specimens with steel bars located in the center were prepared and stored in 1M NaCl solution for corrosion testing. Two levels of continuous potential difference, i.e. 6V and 12V, were applied to accelerate the corrosion and corrosion rate, corrosion potential and resistivity of concrete were monitored by using the linear polarization method. Efficiency factor of GGBS on corrosion initiation and threshold chloride concentration are calculated. Test results showed that higher the GGBS content in concrete lower the chloride diffusion and longer the corrosion initiation time.

KEYWORDS

Slag, Reinforcement corrosion, Chloride

[1] Istanbul Technical University, Civil Engrg. Faculty, Istanbul, Turkey 34469, Phone +90 212 2853762, Fax 212 2856587, hozkul@ins.itu.edu.tr
[2] Istanbul Technical University, Civil Engrg. Faculty, Istanbul, Turkey 34469, Phone +90 212 2853769, Fax 212 2856587, adogan@ins.itu.edu.tr
[3] Sika Construction Chemicals, Istanbul, Turkey 34899, Phone +90 216 5810600, Fax 216 5810699, saglam.ali@tr.sika.com
[4] Sika Construction Chemicals, Istanbul, Turkey 34899, Phone +90 216 5810600, Fax 216 5810699, parlak.nazmiye@tr.sika.com

1 INTRODUCTION

It is well known that the most common cause of deterioration of reinforced concrete structures is corrosion of reinforcing bars. Under normal conditions, high alkalinity of concrete keeps the embedded steel passive; however corrosion may initiate due to either carbonation of cover, or chloride attack or both. Permeation of such aggressive substances through concrete cover controls the time to corrosion onset.

Sustainability of construction industry can only be achieved by using supreme amount of pozzolanic material replacements in concrete [Mehta 1997]. Pozzolanic materials improve the impermeability by both filling and pozzolanic effects, the latter occurs between pozzolans and $Ca(OH)_2$, generated during the hydration of C_3S and C_2S components of cement, to form calcium silicate hydrate (C-S-H). Hence, utilization of mineral admixtures in concrete mitigates the heat of hydration, improves the durability, recycles the waste products and reduces the cost.

Fly ash and GGBS are widely employed in concrete production. In the production of GGBS, grinding is needed, however, the energy requirement for grinding is only 25% of that of clinker production [Song & Saraswathy 2006]. Neville [1993] denoted that the content of GGBS must be at least 50% by mass of the total cementitious material, and preferably 60-70% to be effective. In order to maintain a significant influence in reducing reinforcement corrosion, more than 40% of cement in concrete should be replaced by GGBS [Mangat & Molloy 1991]. Aldea *et al.* [2000] reported an increase on compressive strength up to 25% slag replacement and a decrease above this level, and concretes with 50% slag replacement had compressive strength similar to control mixture. However, increasing slag replacement continuously improved microstructural properties and decreased chloride penetrability. In another study [Thomas & Bamforth 1999], it is estimated that diffusion coefficients for slag or fly ash concretes decrease to one or two order of magnitude than similar grade Portland cement concrete during 100-year service life. Robins *et al.* [1992] obtained lower permeability values for slag concretes just in case of water curing under hot climate conditions. In a more recent study, significant improvements in corrosion rate, corrosion potential and carbonation depths of slag added concretes were reported compared to those of plain concrete having similar compressive strength [Pal *et al.* 2002]. Leng *et al.* [2000] found 50% reduction in the coefficient of chloride permeability, provided 30% of cement is replaced with GGBS.

2 EXPERIMENTAL

2.1 Materials

Concretes were cast by using CEM I 42.5 cement. The aggregates were composed of crushed stone II, crushed stone I, crushed stone sand and natural sand, with the specific weights of 2.70, 2.70, 2.66, 2.59 kg/dm^3 and in the percentages of 0.25;0.25;0.25;0.25, respectively. Physical and chemical properties of cement and GGBS are presented in Table 1.

In order to observe the effect of concrete quality on the corrosion behavior of embedded steel bars, two water/cement ratios of 0.65 and 0.49 were tested. A lignin based water reducer was employed in the dosages of 0.7% and 1.2% (as wt. percentage of cement) for high and low water/cement ratios, respectively. Mixture propotions of concretes are given in Table 2. Cubes of 150x150x150 mm specimens were cast for compression tests and lollipop cylinders of ϕ100x200 mm specimens containing a ϕ10 steel bar located in the center for corrosion tests were cast. Prior to casting concrete, steel bars were cleaned by a metal brush and partially coated with an epoxy based coating as shown in Figure 1. Thus, the exposed area of each steel was equal to 31.4 cm^2. Two sets of lollipop specimens were prepared for each batch. Following demoulding the specimens, uncoated parts of the steel bars of the lollipop specimens were

coated with vaseline to avoid corrosion and specimens were partially immersed in a water tank for 28 days for curing.

Table 1. Physical and chemical compositions of cement and GGBS

			Cement	*GGBS*
Physical properties	Specific gravity		3.17	2.92
	Fineness	Passing 32μ(%)	87.2	-
		Blaine cm^2/g	3071	4520
	Compressive Strength, MPa	2-day	25.7	-
		28-day	56.8	-
	Setting time (h:min)	Initial	2:49	-
		Final	3:49	-
	Strength activity (N/mm^2)		-	13.3
Chemical analysis	Silicon dioxide (SiO_2)		20.73	38,02
	Aluminum oxide (Al_2O_3)		4.14	10,12
	Ferric oxide (Fe_2O_3)		3.65	2,75
	Calcium oxide (CaO)		65.10	34,06
	Magnesium oxide (MgO)		0.99	10,16
	Sulfur trioxide (SO_3)		2.60	3,13
	Sodium oxide (Na_2O)		0.50	0,52
	Potassium oxide (K_2O)			1,10
	Free lime		1.11	-
	Loss on ignition (%)		1.35	0.00
	Bogue potential compound composition	C_3S	62.51	-
		C_2S	12.28	-
		C_3A	4.80	-
		C_4AF	11.11	-

Table 2. Mix design of concretes

Mix code	**Cement [kg/m³]**	**GGBS [kg/m³]**	**W/B**	**Water reducer**
C25	280	-	0.65	0.7
C25-30%	196	84	0.65	0.7
C25-50%	140	140	0.65	0.7
C25-70%	84	196	0.65	0.7
C35	340	-	0.49	1.2
C35-30%	238	102	0.49	1.2
C35-50%	170	170	0.49	1.2
C35-70%	102	238	0.49	1.2

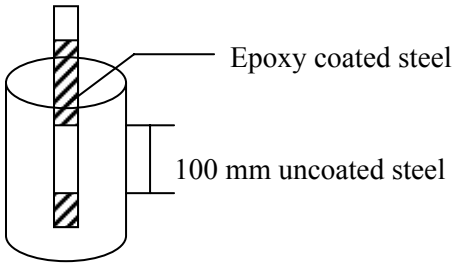

Figure 1. Lollipop specimens

2.2 Methods

The corrosion in rebars was electrically accelerated by using a 6-volt direct current to find out the time to corrosion initiation and 12-volt direct current to observe crack propogation. Each exposing cycle consist of keeping the lollipop specimens in 1M NaCl solution for 24 hours, followed by 48 hours of drying in air (Fig. 2a). All the specimens were monitored by the Gecor 8 corrosion ratemeter (Fig. 2b) which can perform in accordance with linear polarization method and can also measure half-cell potential and resistivity, at the end of each cycle. Chloride profiles of specimens for corrosion initiaton were measured at the end of acceleration.

Figure 2. a) Accelerated corrosion test setup, **b)** Gecor 8 corrosion ratemeter

3 TEST RESULTS AND DISCUSSION

Compressive cube strengths of concretes with and without GGBS are demonstrated in Figure 3. For both type of concrete classes, increasing amount of GGBS exhibited reduced 7-day to 28-day compressive strength ratios. This ratio decreased from 0.80 to 0.28 for C25 and from 0.82 to 0.21 for C35 grade concretes, which can be attributed to the lower hydration reaction rate of GGBS at early ages.

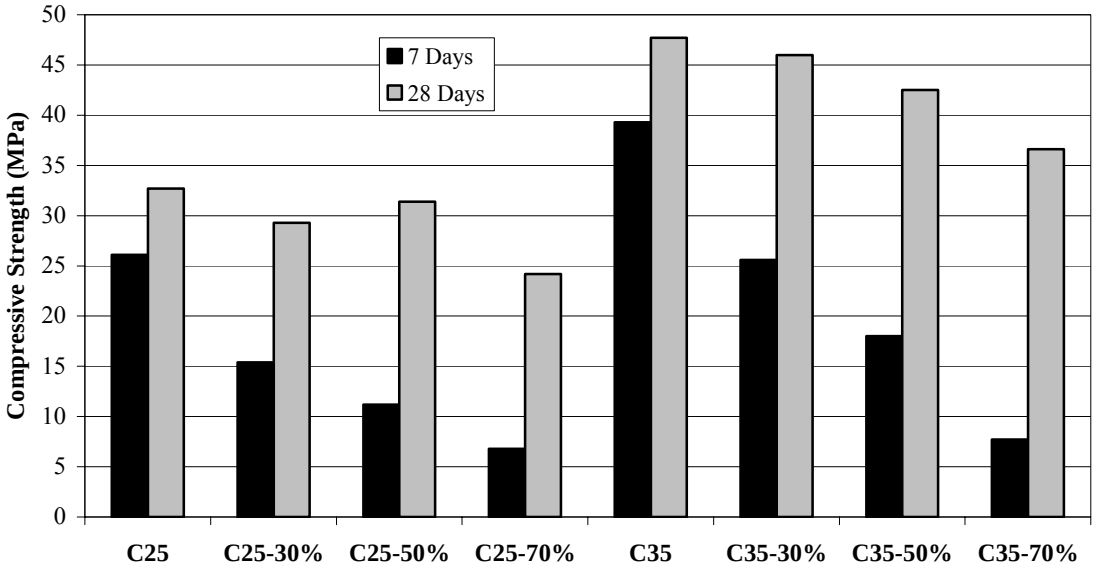

Figure 3. Compressive cube strengths of concretes

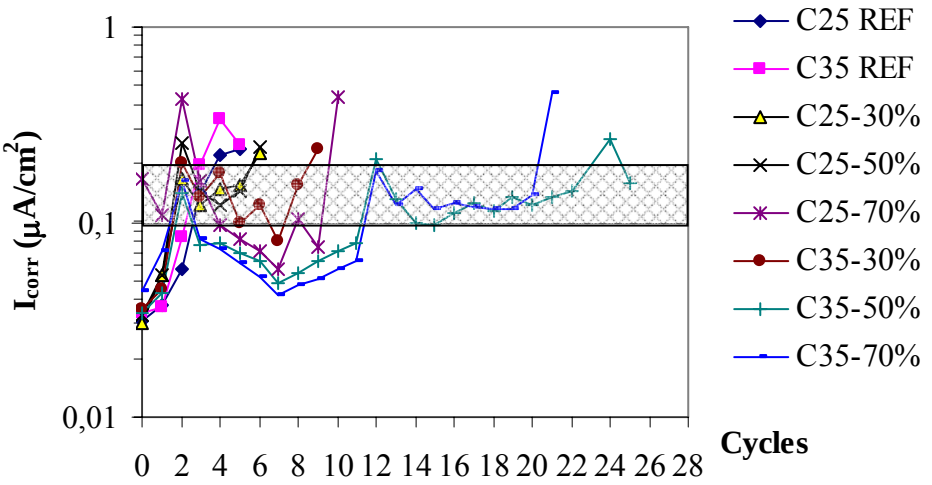

Figure 4. Corrosion rate measurements of lollipop specimens subjected to 6V potential difference.

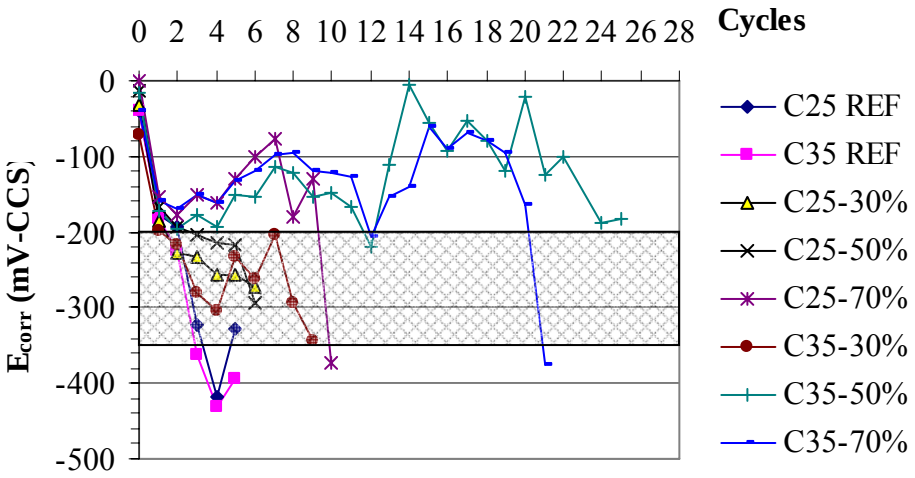

Figure 5. Corrosion potential measurements of lollipop specimens subjected to 6V potential difference.

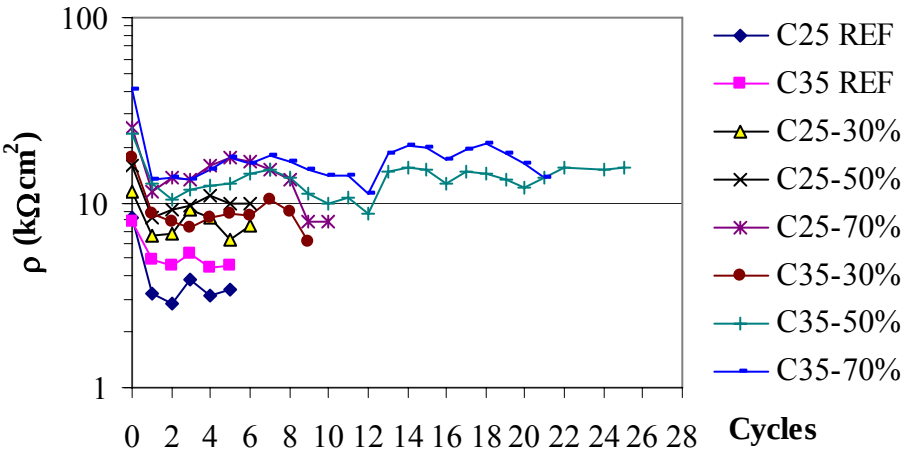

Figure 6. Resistivity measurements of lollipop specimens subjected to 6V potential difference.

In order to determine the corrosion initiation time of the lollipop specimens, corrosion rate (I_{corr}), corrosion potential (E_{corr}) and resistivity (ρ) tests were carried out under a potential difference of 6V

and the results are shown in Figures 4-6, respectively. Critical zones for I_{corr} and E_{corr} values are shaded in these figures and tests were finalized when the I_{corr} values exceeded the critical zones. Test results exhibited that for the 70% GGBS replaced specimens of C25 grade concretes, the longest corrosion initiation times were obtained and those of 30% and 50% replaced specimens followed them. No difference was seen between the performances of 30% and 50% replacement levels for C25. On the other hand, for C35 concretes, the best performance belongs to the specimens of 50% GGBS replacement instead of 70% replaced ones, showing a kind of optimum GGBS replacement ratio. The tests of E_{corr} supported the results of I_{corr}, as can be seen in Figures 4 and 5.

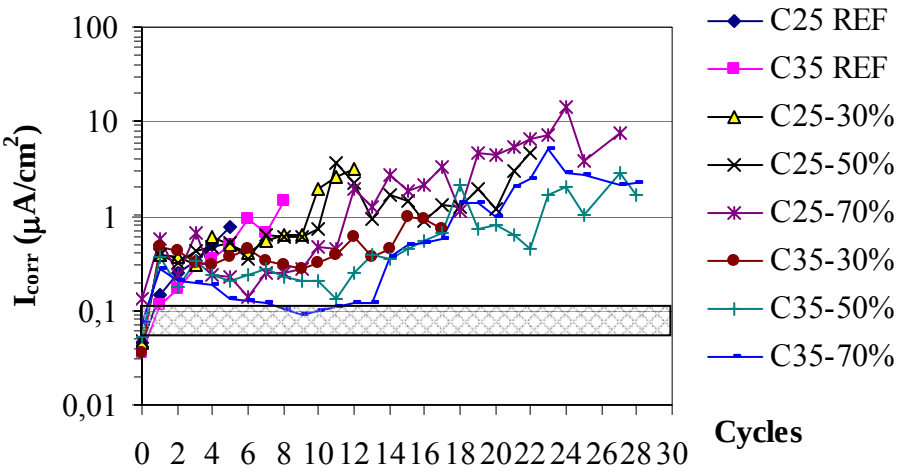

Figure 7. Corrosion rate measurements of lollipop specimens subjected to 12V potential difference.

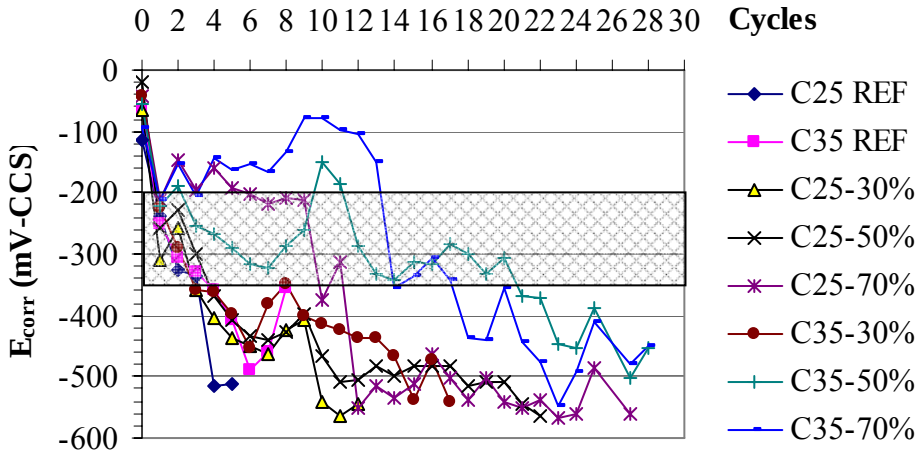

Figure 8. Corrosion potential measurements of lollipop specimens subjected to 12V potential difference.

In the corrosion data obtained from the specimens subjected to 12V potential difference (Figures 7-9) no cracks were seen below the corrosion rate of 1µA/cm^2 and above the corrosion potential of -500 mV (vs. CCS). Besides, resistivity values were seen as the main indicator on failure of concrete cover, particularly after corrosion onset. Concretes with higher resistivities, as a function of binder composition, cracked at elevating corrosion rates. Increasing slag content prevented crack formation even at very high corrosion rates and at very low corrosion potentials for longer periods. In other words, for 45 mm concrete cover (for lollipop specimens), C25 grade specimens with GGBS contents of 0, 30%, 50% and 70% cracked at corrosion rates of 0.78 µA/cm^2, 3.19 µA/cm^2, 4.54 µA/cm^2 and 7.58 µA/cm^2, respectively. At the end of 28 cycles, no cracks have been observed yet on the C35-50% and C35-70% specimens.

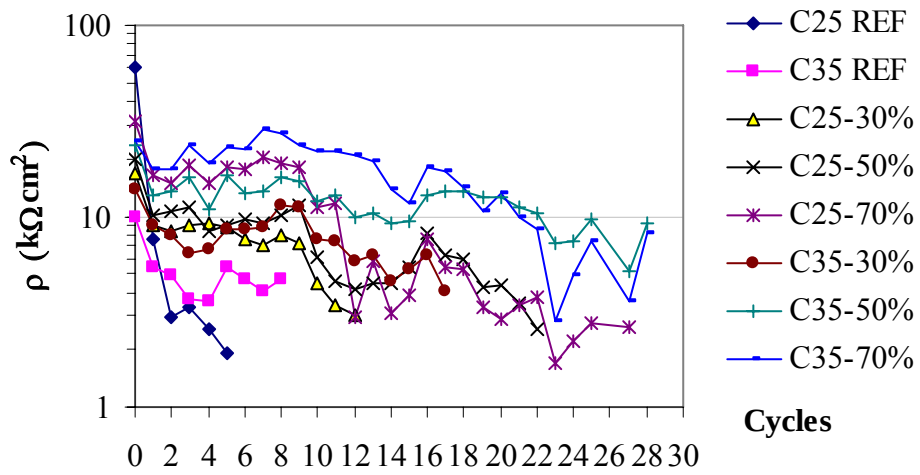

Figure 9. Resistivity measurements of lollipop specimens subjected to 12V potential difference.

Figure 10 demonstrates the number of cycles needed for corrosion initiation (CI) and crack formation (CF) of all concretes. Apart from C35-50%, it can be concluded that higher the GGBS content longer the time to corrosion initiation and the time to crack formation.

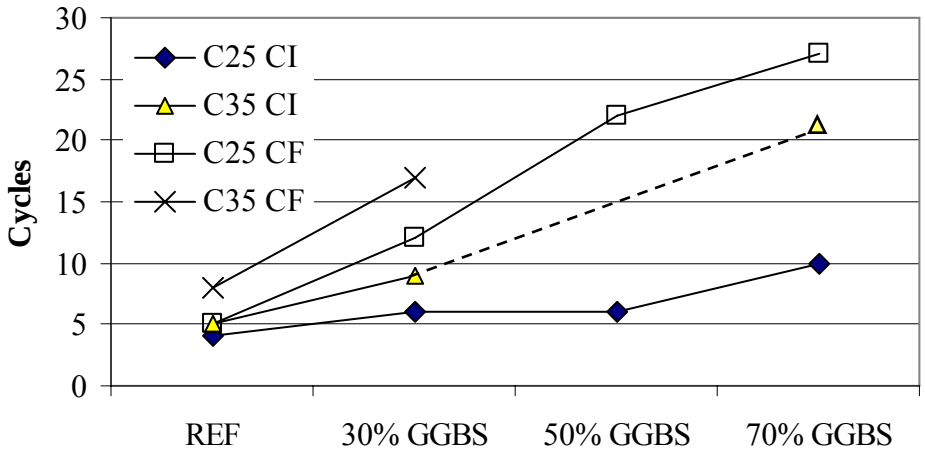

Figure 10. Number of cycles needed for corrosion initiation (CI) and crack formation (CF) of concretes

Chloride profiles of C25 coded concretes with the number of cycles for corrosion initiation are illustrated in Figure 11. Similar profiles of C35 were not shown, because corrosion has not initiated yet for high content slag added concretes at this grade. Figure 11 shows that, regardless of the number of cycles for corrosion onset, the higher the chloride content at peak values, the greater the binding capacity. Therefore, it can be deduced that ascending chloride binding capacity extends corrosion initiation period. Critical chloride concentration of reference concrete is higher than those of GGBS concretes, probably due to the consumption of hydroxide ions in pozzolanic reaction of slag.

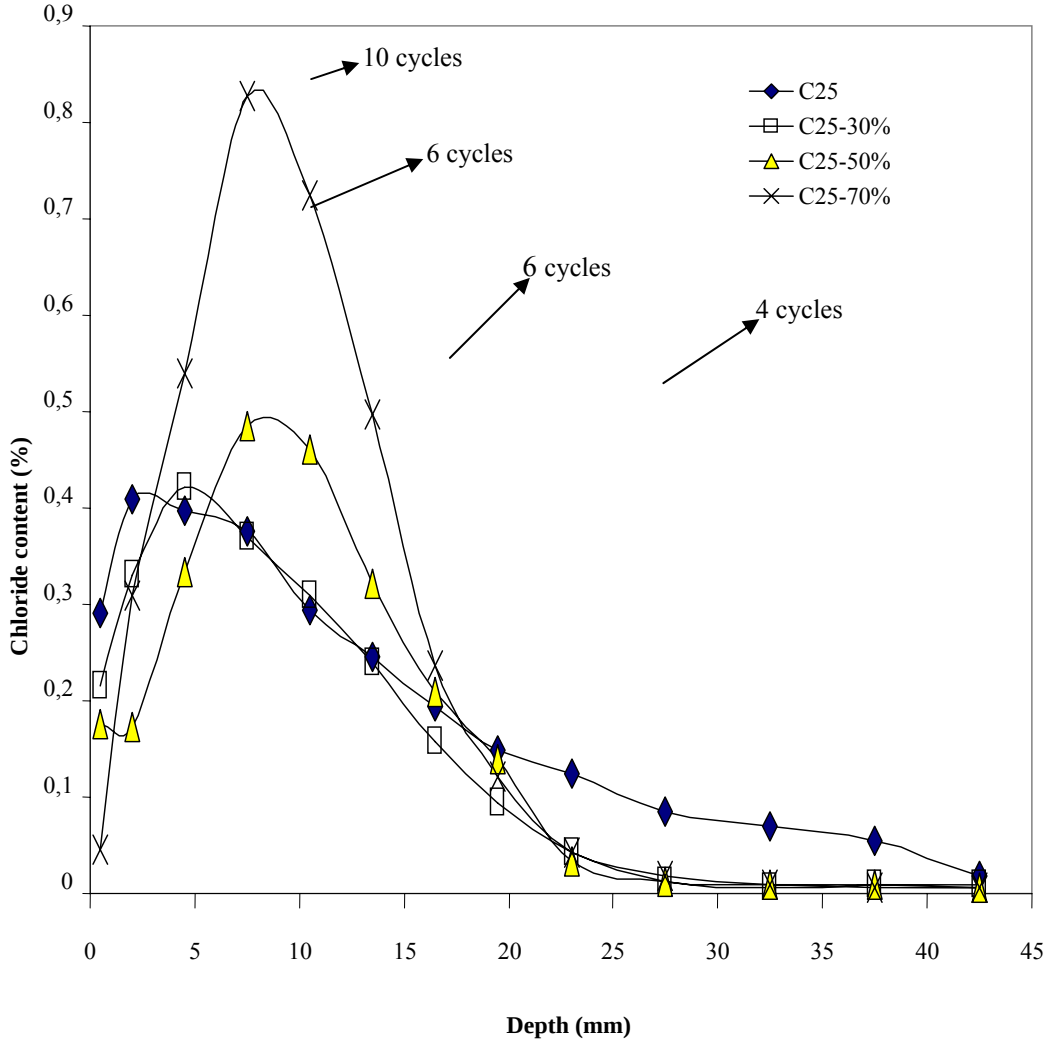

Figure 11. Chloride profiles of C25 coded concretes subjected to 6V potential difference.

4 CONCLUSION

In this paper, resistance of GGBS concrete against chloride-induced corrosion phenomenon with respect to migration test is studied. Significant reductions in compressive strength were obtained for high amount of slag replacement compared to OPC concretes. Besides, time to corrosion onset of C25 concretes containing %30, %50 and %70 GGBS, took 1.5, 1.5 and 2.5 times longer than that of plain concrete, respectively, while extention was 1.6, 4.2 and 5 times for C35 ones, in the same order.

More importantly, crack formation period, indicating the end of service life, for C25-30%, C25-50% and C25-70% concretes, extended 2.4, 4.4 and 5.4 times longer than that of OPC concrete, respectively.

Improvement in corrosion resistance of slag added concretes can be due to the chloride binding capacity of slag and affecting the resistivity by changing the pore solution chemistry. It can be concluded that usage of slag as cement replacement in concrete seems to be a good solution against chloride-induced corrosion, such as in marine environment.

REFERENCES

Aldea, C.M., Young, F. Wang K. and Shah S.P. 2000, 'Effects of curing conditions on properties of concrete using slag replacement', *Cement and Concrete Research*, **30**[3], 465-472.

Leng, F.G., Feng N.Q. and Lu X.Y. 2000, 'An experimental study on the properties of resistance to diffusion of chloride ions of fly ash and blast furnace slag concrete', *Cement and Concrete Research*, **30**[6], 989-992.

Mangat, P.S. and Molloy B.T. 1991, 'Influence of PFA, slag and micro silica on chloride induced corrosion of reinforcement in concrete', *Cement and Concrete Research*, **21**[5], 819-834.

Mehta, P. K., 1997, 'Durability – Critical Issues for the Future', *Concrete International*, **20**[7], 27-33.

Neville, A.M. 1993, *Properties of Concrete,* Longman Scientific & Technical, Harlow, Essex.
Pal, S.C., Mukherjee A. and Pathak S.R. 2002, 'Corrosion behavior of reinforcement in slag concrete', *ACI Materials Journal*, **99**[6], 521-527.

Robins, P.J., Austin S.A. and Issaad A. 1992, 'Suitability of GGBFS as a cement replacement for concrete in hot arid climates', *Materials and Structures*, **25**[154], 598-612.

Song, H.W. and Saraswathy V. 2006, 'Studies on the corrosion resistance of reinforced steel in concrete with ground granulated blast-furnace slag – An overview', *Journal of Hazardous Materials*, **138**[2], 226-233.

Thomas, M.D.A. and Bamforth P.B. 1999, 'Modelling chloride diffusion in concrete: Effect of fly ash and slag', *Cement and Concrete Research*, **29**[4], 487-495.

11DBMC International Conference on Durability of Building Materials and Components
ISTANBUL, Turkey 11-14 May 2008

Durability of Autoclaved Aerated Concrete

Berit Straube [1]
Peter Langer [2]
Andreas Stumm [3]

T 11

ABSTRACT

A main requirement of the "Construction Products Directive (CPD)" for buildings and building materials is their mechanical resistance and stability. A relevant part of the safety of components and buildings is their durability. The requirements for durability are affected by the economically useful life and the ambient conditions, such as physical- and chemical-environmental influences. The durability of cementious building materials is based on Calcium-Silicate-Hydrate phases (C-S-H), and is crucially defined by the formation of their mineral phases. The crystalline C-S-H phase, tobermorite, directly affects the mechanical properties of autoclaved aerated concrete (AAC). The formation of tobermorite is influenced by raw materials and process parameters. Well crystallised C-S-H phases in AAC must not be compared to the poorly crystallised C-S-H phases in normal concrete. C-S-H phases in normal concrete have a low ordered structure, with highly variable amounts of calcium, silicon and water, which lead to structural changes with increasing lifetime. In this study, the durability of AAC was investigated in order to assess the quality of AAC after long term application. Correlations between phase formation, mechanical properties and durability were proved with examples. AAC with well crystallised tobermorite is not substantially influenced by CO_2 under normal atmospheric conditions. Due to these results, it was conducted that AAC is durable and does not loose its function of stability during long term application.

KEYWORDS

AAC, C-S-H phases, Tobermorite, Calcium sulphate, Durability

[1] Xella Technologie- und Forschungsgesellschaft mbH, Hohes Steinfeld 1, 14797 Kloster Lehnin, Germany, Phone +49 33844752111, Fax 33844752110, berit.straube@xella.com
[2] Xella Technologie- und Forschungsgesellschaft mbH, Hohes Steinfeld 1, 14797 Kloster Lehnin, Germany, Phone +49 33827060189, Fax 33827060120, peter.langer@xella.com
[3] Xella Technologie- und Forschungsgesellschaft mbH, Hohes Steinfeld 1, 14797 Kloster Lehnin, Germany, Phone +49 33844752120, Fax 33844752110, andreas.stumm@xella.com

1 INTRODUCTION

Autoclaved aerated concrete (AAC) is produced of natural inorganic raw materials such as sand, lime, cement, water and the rising agent aluminium.
AAC has an unique structure, formed by millions of small air pores, which leads to an optimum correlation between compressive strength and low materials weight. Moreover, air has a low thermal conductivity which makes AAC one of the best insulating building materials.
A requirement of the "Construction Products Directive (CPD)" for buildings and building materials is their mechanical resistance and stability. A relevant part of the safety of components and buildings is their durability. The requirements for durability are affected by the economically useful life and the ambient conditions such as physical- and chemical-environmental influences. Well crystallised C-S-H phases, like tobermorite in AAC, are resistant to carbonation and cannot be compared to the poorly crystallised C-S-H gels in ordinary concrete.

Poorly crystallised AAC contains so called C-S-H(I), which is from the structural point of view, between C-S-H gel and tobermorite (CaO/SiO_2 = 0.83). C-S-H(I) has highly variable amounts of calcium, silicon ($0.75 < CaO/SiO_2 < 1.5$) [Taylor 1964] and water, which easily leads to structural changes with increasing lifetime.

C-S-H(I) encourages the carbonation process in autoclaved aerated concrete like in ordinary concrete. Internal investigations assume, that the amount of C-S-H(I) directly influences the shrinkage.
In the production of AAC the formation C-S-H(I) has to be avoided. The addition of calcium sulphate, such as anhydrite and gypsum, improves the material, i.e. higher compressive strength and a intensified formation of better crystallised tobermorite. The tobermorite formation is intensified with lower shrinkage, and probably better resistance upon carbonation.

Additional calcium sulphate has been used in AAC production since 1967 [Clementi 1967]. The mechanisms are not completely understood.

In this study, the durability of AAC was investigated to assess the material properties of AAC during long term application using X-ray powder diffraction, carbon/sulphur-analysis and compressive strength testing. Correlations between phase formation, mechanical properties and durability were proved with model substances, drilling cores taken from buildings and stored AAC units.

2 EXPERIMENTAL

2.1 Sample Preparation

2.1.1 Model samples synthesis

Four model samples of AAC with the raw density of 440 kg/m^3 were produced (6 h at 190 °C) in lab sized moulds (10 litres) by using the usual method for the production of AAC [RILEM 1993]. The recipes are shown in Table 1. The content of calcium sulphate ($CaSO_4$ = anhydrite) was subsequently increased by substituting the non-reactive filler calcite ($CaCO_3$).

Eight AAC units (AU) with a bulk density 400 kg/m^3 from the identical production mixture were stored under a roof protected from rain. These materials were produced in 1980. Calcium sulphate was added to the mixture. The surface of the material was not protected by either mortar or paint.
These AAC units have been subsequently sampled and analysed for compressive strength after various time periods from the time of production (0 year) up to 26 years [Table 2].

Table 1. Recipes of the model mixes

sample	*quartz-sand* [% mass]	*CEM I 52.5 N* [% mass]	*lime* [% mass]	*anhydrite* [% mass]	*calcite-filler* [% mass]	*aluminium-powder* [% mass]	*water/solid ratio*
M0	58	15	15	0	12	0.05	0.65
M1	58	15	15	1	11	0.05	0.65
M3	58	15	15	3	9	0.05	0.65
M4	58	15	15	4	8	0.05	0.65

2.1.2 Drilling cores and stored AAC units

Four drilling cores (DC) were taken from four different buildings distributed over Germany [Table 2].

Table 2. Location and ages of taken cores.

sample	*age* [years]	*geographic region*
DC1	42	south-western Germany
DC2	37	central Germany
DC3	34	south-eastern Germany
DC4	28	eastern Germany
AU	0,1,2,3,5,8,13,26	southern Germany

2.2 Sample Characterisation

2.2.1 Sulphur analysis and qualitative phase analysis

The material was characterised in the centre of the drilling core [Fig. 1]. A Philips PW 1800 diffractometer with autosampler employing CuKα radiation and graphite secondary monochromator was used. Measurements were performed over a 4-60° 2Θ range, with a 0.02 2Θ step size and a exposure time of 1s/step. Automatic divergent slits were used to maintain an illuminated sample length of 10 mm. Qualitative analysis was performed by using Panalytical's High Score.

The samples were treated before measurement with isopropanol in a McCrone micronising mill. The milled material was prepared into a back loaded sample holder. Carbon/sulphur analysis was performed by the use of an Eltra CS 800 device. The results are given as SO_3 total from sulphate in the final product.

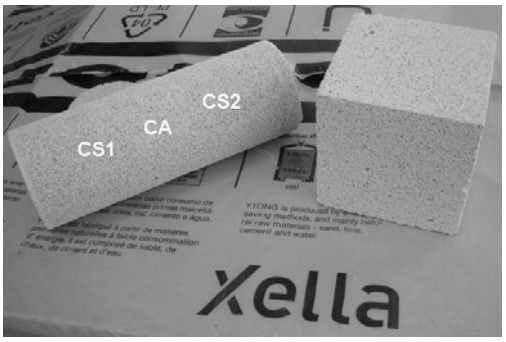

Figure 1. Photograph of a taken core sample (on the left) with the analysed areas CS1 = compressive strength 1, CS2 = compressive strength 2, CA = chemical sulphur analysis and qualitative phase analysis; (on the right) compressive strength testing cubes

2.2.2 Compressive strength testing

An universal hydraulic compressive strength testing device from Toni Technik was used. The compressive strength of the drilling cores was determined from two cylinders with a length and diameter of 75 mm [Fig. 1].

The compressive strength of both the model substances and the stored AAC units was measured on three cubes of the size 100 mm x 100 mm x 100 mm. The cubes were cut out from the base, mid and top of the AAC unit. In the lab samples they were taken from the base.

In this paper, the samples are compared with their compressive strength as well as with their so called A-value. The A-value represents a relative level of the strength of AAC.

The bigger the A-value the better the level of stability. The A-value depends on the raw density and the compressive strength and can be described as followed: A-value = CS / RD^2 x 0.016; with: CS = compressive strength [N/mm^2], RD = raw density [kg/dm^3], 0,016 = const. [Zürn 1997].

2.2.3 Determination of the shrinkage behaviour

According to RILEM [1993] water saturated specimens (40 mm x 40 mm x 160 mm) were dried at a temperature of 20 °C and a relative humidity of 43 % to the equilibrium moisture content, where the shortening of the specimens was recorded. The value of shrinkage in this paper is the complete change of the length from water saturated to equal moisture for this climate.
All tests were performed in a climate chamber (Feutron KPK 400.V).

3 RESULTS AND DISCUSSION

3.1 Model substances

The X-ray powder diffraction patterns of the model substances are shown in Fig. 2. The mineral phases are tobermorite, quartz, calcite and anhydrite. The peaks of tobermorite and anhydrite increase with increasing sulphate content [Fig. 2]. Calcite peaks gain intensity with decreasing calcite filler content. The AAC samples also show increasing compressive strength with increasing sulphate content. Finally, the measurement of the shortening shows decreasing shrinkage values with increasing amount of calcium sulphate.

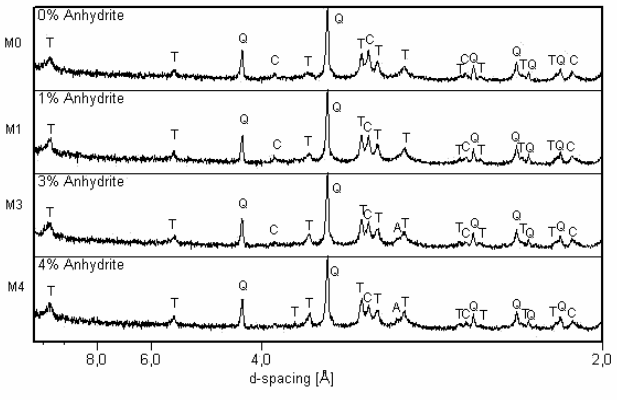

Figure 2. X-ray diffraction patterns of AAC with various amounts of sulphate. T = tobermorite, Q = quartz, C = calcite, A = anhydrite.

Table 3. Material properties of the model substances

Sample	*Anhydrite* [% mass*]	*SO_3* [% mass**]	*Raw density* [kg/m^3]	*Compressive strength* [N/mm^2]	*A-value* [a.u.]	*Shrinkage value* [mm/m]
M0	0	0.63	454	3.02	917	0.40
M1	1	0.91	440	3.45	1113	0.38
M3	3	1.99	441	3.80	1224	0.36
M4	4	2.29	433	3.90	1299	0.34

* of dry mix; ** of final product

3.2 Drilling Cores

The chemical analysis reveals, that sample DC1 has the highest amount of SO_3 (3.41 % mass), followed by DC2 (2.17 % mass), DC3 (1.98 % mass) and DC4 (0.89 % mass) [Table 4].

The compressive strength testing shows that sample C1 has the highest A-value (1104) followed by DC2 (1245), DC3 (972) and DC4 (686). The amount of sulphate determines the durability of the material, since the A-value increases with increasing amount SO_3 from sulphate. The compressive strength is less dependent from time than from the optimum mixture with its sulphate content. The samples (D1-D4) still fulfil the essential compressive strength values for building materials and buildings.

The X-ray diffraction analysis reveals in all samples tobermorite, quartz, anhydrite and calcite [Fig. 3]. Quartz is an residual product whereas anhydrite is a new formation. The amount of anhydrite increases parallel to the amount of SO_3. The intensity of calcite increases from sample DC1 to DC4. Low calcium sulphate content leads to an increasing formation of calcite, due to the higher CO_2 uptake [Fig. 3].

Table 4. Material's properties of the taken cores.

Sample	*Age* [years]	*Raw-density* [kg/m^3]	*Compressive strength* [N/mm^2]	*A-value* [a.u.]	*SO_3* [% mass*]
DC1	42	442	3,45	1104	3,41
DC2	37	496	4,90	1245	2,17
DC3	34	593	5,47	972	1,98
DC4	28	656	4,72	686	0,89

* of final product

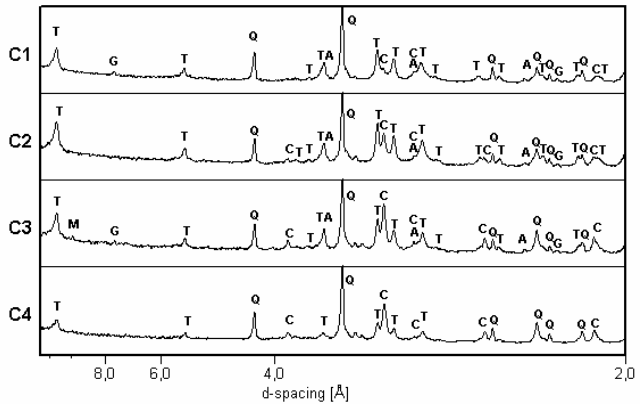

Figure 3. X-ray diffraction patterns of the 4 AAC drilling cores. T = tobermorite, Q = quartz, C = calcite, A = anhydrite, G = gypsum, M = muscovite.

3.2 Stored AAC units

Due to subsequent compressive strength testing, there is no detectable loss of compressive strength during the last 26 years of storage [Fig. 4]. The material did not loose its function of stability. AAC is durable, because it obviously has not changed its properties within 26 years.

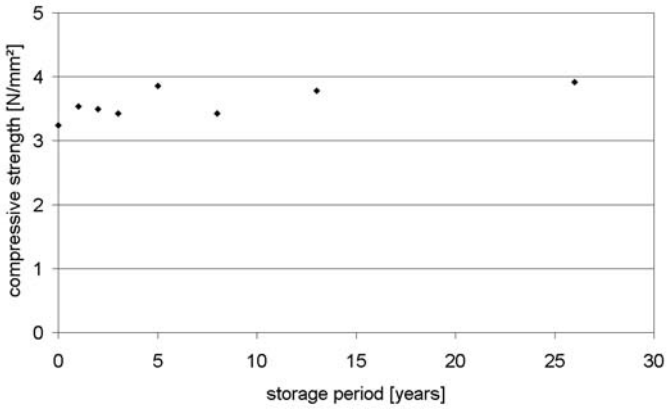

Figure 4. Compressive strength of sample AU after various storage periods.

4 CONCLUSIONS

Correlations between phase formation, mechanical properties and durability were proved with examples. The compressive strength testing reveals, that there is no loss of compressive strength over life time if calcium sulphate is used in the production of AAC. The addition of calcium sulphate leads to an intensified formation of the better crystallised C-S-H phase tobermorite.
AAC with well crystallised tobermorite is not substantially influenced by CO_2 under normal atmospheric conditions.
Due to these results, it was conducted that AAC is durable and does not loose its function of stability during long term application.

REFERENCES

Taylor, H.F.W. 1964, 'The Calcium Silicate Hydrates', in *The Chemistry of Cements,* Academic Press, London, pp. 167-232

Clementi, F. 1967, 'Verfahren zur Herstellung von dampfgehärtetem Gasbeton', *German patent, Aktenzeichen DE 16 46 580.8-45 (H 62442)*, Bundesrepublik Deutschland, Deutsches Patentamt

Zürn, S.G. 1997, 'Einfluss der Sandminerale auf die Bildung von Caclciumsilikathydraten (CSH-Phasen), das Gefüge und die mechanischen Eigenschaften von Porenbetonprodukten', Logos Verlag Berlin

RILEM 1993, *Autoclaved Aerated Concrete – Properties, Testing and Design*, eds. S. Aroni, G.J. de Groot, M.J. Robinson, G. Svanholm & F.H. Wittman, E & FN SPON, London

11DBMC International Conference on Durability of Building Materials and Components
ISTANBUL, Turkey 11-14 May 2008

Prediction of Residual Stress Due to Early Age Behaviour of Massive Concrete Structures: On Site Experiments and Macroscopic Modelling

Jihad Zreiki [1]
Vincent Lamour [2]
Mohend Chaouche [3]
Micheline Moranville [4]

T 11

ABSTRACT

Early age behaviour of concrete is based on complex multi-physical and multiscale phenomena. The predication of both cracking risk and residual stresses in hardened concrete structures is still a challenging task. We propose in this paper a practical method to characterize in the construction site the material parameters and to identify a macroscopic model from simple tests. We propose for instance to use a restrained shrinkage ring test to identify a basic early age creep model based on a simple ageing visco-elastic Kelvin model. The strain data obtained from this test can be treated through an early age finite element incremental procedure such that the fitting parameters of the creep law can be quickly identified. The others properties of concrete have been measured at different ages (elastic properties, hydration kinetics, and coefficient of thermal expansion). From the identified early age model, we computed the temperature rise and the stress development in a non reinforced concrete stress for nuclear waste. The good agreement between in-situ measurement and predicted behaviour allowed us to validate our approach.

KEYWORDS

Basic creep, Kelvin model, Residual stresses, Early age concrete.

[1] LMT-Cachan Laboratory of Mechanic and Technology, Sector Civil Engrg, Cachan, France 94230, Phone +33 (0)1 47 40 22 38, Fax +33 (0)1 47 40 22 40, zreiki@lmt.ens-cachan.fr
[2] LMT-Cachan Laboratory of Mechanic and Technology, Sector Civil Engrg, Cachan, France 94230, Phone +33 (0)1 47 40 22 38, Fax +33 (0)1 47 40 22 40, lamour@lmt.ens-cachan.fr
[3] LMT-Cachan Laboratory of Mechanic and Technology, Sector Civil Engrg, Cachan, France 94230, Phone +33 (0)1 47 40 22 38, Fax +33 (0)1 47 40 22 40, chaouche@lmt.ens-cachan.fr
[4] LMT-Cachan Laboratory of Mechanic and Technology, Sector Civil Engrg, Cachan, France 94230, Phone +33 (0)1 47 40 22 38, Fax +33 (0)1 47 40 22 40, moranville@lmt.ens-cachan.fr

1 INTRODUCTION

Early age behaviour of concrete is based on complex multi-physical and multiscale phenomena. The predication of the cracking risk and the residual stresses in the hardened concrete structures is still a challenging task. The use of the restrained shrinkage ring test to identify a basic early age creep model is based on a simple ageing visco-elastic Kelvin model.
We propose in this article to identify a simple macroscopic model with a reduced number of parameters. First we model the total behaviour of the structure in various configurations, and then specimens of building site are used to accomplish the identification.
The behaviour of the concrete at early age is generally described as visco-elastic. The rheological models based on Kelvin chains are used to model this behaviour [De Schutter 1996] and [Bǎzant *et al.* 1997], or they are based on Maxwell chains to take into account the humidity or temperature effects [Bǎzant & Chern 1985] and [Bǎzant and *al.*2004]. However, others models have used the Burger model [Hauggaard et *al.* 1999] and [Bǎzant et *al.*2004]. In section 2 we begin with the model used to describe elastic modulus of concrete at early age, and then we proposed a model based on the hydration degree. Section 3 focuses on the basic creep's and the function of creep, and then we describe the hydration kinetic. After having exposed the behavioural model of concrete at early age and having identified its parameters, a comparison is done between real measurements and outputs of the numerical model are detailed in section 4 before concluding.
The stake of such tool is to limit the early age cracking risk in order to increase the durability of the prefabricated products of concrete and to determine of the residual stresses of fabrication.

2 EVOLUTION OF THE MODULE OF ELASTICITY

There are several models describing the evolution of the Young modulus. Some of them require more tests to reproduce the material behaviour. Researches have shown that models using the Apparent Setting time will be more robust against effects of insufficiency in amount of experimental data [Larson & Jonasson 2003]. Larson proposed a Linear Logarithmic Model (LLM) for the creep of concrete, in which the Young modulus is given by equation 1:

$$E(t_0) = E_{ref}.\beta_E(t_0) \tag{1}$$

Where: E_{ref} is a reference value, which here is chosen as the Young modulus at 28 days age, and $\beta_E(t_0)$ is a parameter expressed as:

$$\beta_E(t_0)\begin{cases} 0 & t_0 < t_s \\ b_1.\log(t_0/t_s) & t_s \le t_0 < t_s \\ b_1.\log(t_B/t_s)+b_2.\log(t_0/t_B) & t_B \le t_0 < 28j \\ 1 & t_0 \ge 28j \end{cases} \tag{2}$$

The traditional equations which describe the non-aging Young modulus, based on the compressive strength at age of 28 days, as in [Table 1], [Takács 2002].

Table 1. Formula for the Young modulus at age of 28 days.

Code	**Formula de E_c (MPa)**
CEP-FIP model code 1990	$E_c = 9980(f_{cm})^{1/3}$
Euro code 2	$E_c = 9500(f_{cm})^{1/3}$
ACI 318	$E_c = 4733(f_{cm})^{0.5}$

We find in ACI-209R-82 a recommendation for the prediction of creep and shrinkage, and they gave a relation for calculates the aging Young modulus [Rajeev *et al.* 2007] Equation 3.

$$E_c(t) = 0{,}04326\sqrt{\rho^3 . \mathrm{f}_{\mathrm{cm}}\left(\frac{t}{a+b.t}\right)} \tag{3}$$

Where: a, b: constants depend on cement type and treatment conditions; $E_c(t)$: The Young modulus of concrete at age t; ρ: The density of the concrete (kg/m^3).
The Young modulus given in CEB-FIP for a concrete of strength (12-80 MPa) at 28 days by the following form equation:

$$E_c(t_0) = E_c . \sqrt{\exp\left\{s\left(1-\sqrt{\frac{18}{t_0}}\right)\right\}} \tag{4}$$

Where: $E_c(t_0)$ The Young modulus of concrete at age t_0; c: Constant dependent on the type of cement.
In reality the Young modulus (E) of concrete evolves with time according to a chemical reaction of cement hydration [Ignacio & Bǎzant 1993] and [De Schutter 1999].
The Young modulus is given by De Schutter according to the degree of hydration for a concrete (CEM III/B 32.5) [De Schutter 1999].

$$E_0(\chi) = 37000.\left(\frac{\chi - 0.25}{1-0.25}\right)^{0.62} MPa \tag{5}$$

χ : The degree of hydration.
You can see a relation which depends on time, in which the Young modulus evolves in a potential way [Hauggaard *et al.* 1999].

$$E(t) = a.e^{-\left(\frac{b}{t}\right)^c} \tag{6}$$

Where a, b, c are parameters depend on material, and t is the equivalent time defined at temperature 20±C.
Byfor used to define the Young modulus as function of degree of hydration [Eduardo *et al.* 2004] like:

$$E(\xi) = E_\infty . \frac{1+1{,}37(f_{c,\infty})^{2{,}204}}{1+(f_c(\xi))^{2{,}204}}\left(\frac{f_c(\xi)}{f_{c,\infty}}\right) \tag{7}$$

$E_\infty = E(\xi = 1)$: The Young modulus at the end of hydration.

3 MACROSCOPIC MODEL OF CONCRETE AT EARLY AGE:

3.1 The creep's function:

The simplest and the oldest models of creep for concrete is the effective modulus method (EMM) [Bǎzant & Wittmann 1980], which consists only of a single linear elastic solution, as $E_{effective} = 1/J(t,t_0) = E(t_0)/(1+\phi(t,t_0))$, where J is the creep compliance function, t_0 is the age at loading, $E(t_0)$ is the initial Young modulus, and ϕ is the creep coefficient. The linear treatment of visco-elastic of ageing materials as the concrete can be characterised by the compliance function $J(t,t')$ or the relaxation function $R(t,t')$. $J(t,t')$ Presents the strain at time t caused by a constant

stress applied at the time t' [Ignacio & Bǎzant 1993]. For a stress different of 1, the strains are calculated by the following equation:

$$\varepsilon(t) = \Delta\sigma.J(t,t') \tag{8}$$

For $t = t_0$, we have $J(t_0,t_0) = 1/E(t_0)$. By applying the principle of superposition, we find the equation of Volterra which constitute the law of linear visco-elastic behaviour of aging material:

$$\gamma(t) = \int_{t'=0}^{t} J(t,t')d\sigma(t') \tag{9}$$

The use of Dirichlet series to expresser the function of creep $J(t,t')$, and the integral of the equation give more effective differential equations for the numerical solutions:

$$J(t,t') = \frac{1}{E_0(t')} + \sum_{\mu=1}^{n} \frac{1}{E_\mu(t)}\left(1 - e^{\frac{-E_\mu}{\eta_\mu}(t-t')}\right) \tag{10}$$

$J(t,t') = q_1 + C(t,t')$ Where q_1 is the instantaneous elastic strain. The equation of creep can be written like a sum of exponentials (i.e., Dirichlet series). It is possible to convert the equation (9) to linear differential equations. These equations can be simulated well by rheological models like Kelvin or Maxwell chains with an aging spring $E_\mu(t)$ and aging dashpot $\eta_\mu(t)$ [Ignacio & Bǎzant 1993]. There are several possibilities of arranging the spring and the dashpot, but it is shown that the behaviour of creep generally can be described by Maxwell or Kelvin chains [Bǎzant & Santosh 1989].
If we consider only one element of the chains of Kelvin (μ=1) 'Fig 1', we can write the differential equation:

$$E_1(\chi)\gamma + \eta_1(\chi)\dot{\gamma} = \sigma \tag{11}$$

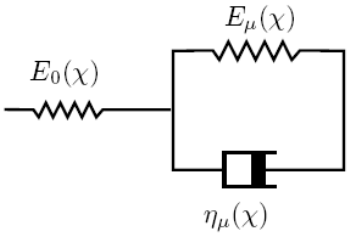

Figure1. The Rheological model of Kelvin

3.2 Thermal model:

We can write the equation of heat describing the thermal transfers in concrete at early age:

$$C(\chi)\frac{\partial T}{\partial t} = div(k(w,\chi).grad(T) + Q_{hy}(\chi) - Q_{ev}(\chi) \tag{12}$$

Where C and K are the thermal capacity and conductivity, Q_{hy} the heat provided by the hydration, Q_{ev} the waste heat by evaporation in skin in the event of fast unmoulding in conditions of extreme drying.

3.3 Hydration kinetic:

With simplicity the kinetics of hydration of cement can be modelled by an equivalent chemical affinity according to Arrhenius's law:

$$A(\chi) = \dot{\chi} = \widetilde{A}(\chi).\exp\left(\frac{-E_a}{RT}\right) \tag{13}$$

With: $\widetilde{A}(\chi)$ the chimical affinity equivalent standardized given for an isothermal reation of hydration.

The evolution and the heat of hydration of concrete can be followed by a quasi-adiabatic test on insulated cylindrical. We can determine the equivalent endogenous affinity and the evolution of the reaction advancement degree for various thermal paths.

We consider that the advancement of hydration reaction is stabilized at 28 days ($\chi = Q/Q_{28d} \approx 1$) 'Fig.2'.

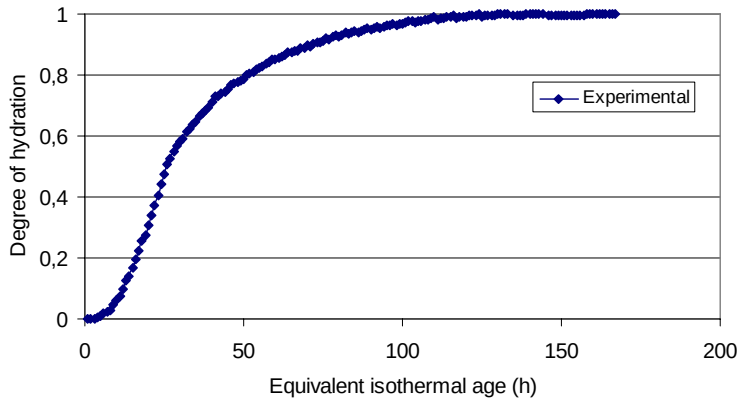

Figure 2. Evolution of degree of advance of reaction (activation energy = 46 KJ/mol)

3.4 Mechanic model:

We used a mechanical model based on the deformation partition principle:

$$\dot{\varepsilon} = \dot{\varepsilon}_e + \dot{\varepsilon}_c + \dot{\varepsilon}_T + \dot{\varepsilon}_{Sh} \tag{15}$$

With: $\dot{\varepsilon}_T = \alpha.\dot{T}$ the thermal deformation, α the thermal dilation coefficient; $\dot{\varepsilon}_{Sh}$ the shrinkage's deformation, $\dot{\varepsilon}_e$ elastic deformation, $\dot{\varepsilon}_c$ creep's deformation equation (11).

4 IDENTIFICATION OF MODELE

4.1 Used Concrete

We used to identify the model a self compression fibred concrete with a low heat of hydration, the composition of this concrete is presented in the Table 2

4.1 Mechanical proprieties

To identify the creep model, we propose a shrinkage ring test. In fact the ring test is a simple test by which we measure the visco-elastic deformation in a ring of concrete. The geometry of the ring is presented in the 'Fig.3'.

Table 2. Formulation of concrete (W/C = 0.35).

Materials	*Concrete fractions* [Kg/m^3]
Cement CEM V / A (S-V) 42.5 N CE PM ES CP1	454
Silica fume	45
Calcareous sand 0/4mm	984
Calcareous aggregate	672
Affective water	173
Superplasticizer	5.2
Fibre (L30mm, Ø0,6mm)	85

The section of the brass ring: 2*7cm, the section of concrete: 7*7cm, the outside diameter of concrete: 64 cm, and the inside diameter: 50cm, the inside diameter of ring: 46 cm. We measure orthoradial deformation by four gauges presented in 'Fig.5'. The rheological diagram of the ring test is represented on 'Fig 4' [Lamour & *al* 2007]. The result of the ring test allows us to determine the parameters of the creep model by an explicit diagram of integration. 'Fig 5'

Figure 3. The ring test

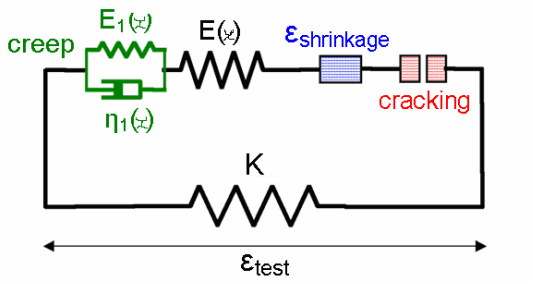

Figure 4. Simplified 1D parallel model for the ring test.

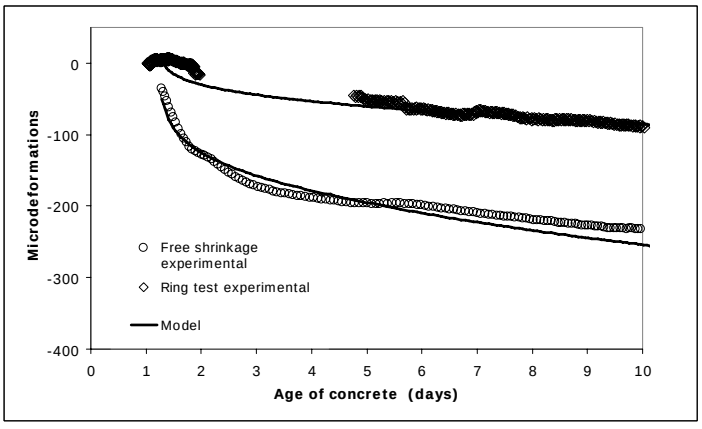

Figure 5. Simplified 1D parallel model for the ring test

The evolution of the elastic modulus was measured on specimen (7*7*28 cm) by using the Ultrasound velocity measurement, where transversal wave velocities were measured, the elastic modulus (E) was determined by using wave propagation theory in homogeneous bodies.
We propose for fitting elastic modulus a model (see eq.5)based on χ (hydration degre) like the model proposed by [De Schutter G. 1999].

$$\left\{ E(\chi) = E_{\max}\left(\frac{\chi - \chi_0}{\chi_{\max} - \chi_0} \right)^b \right\} \tag{16}$$

Where : χ the hdration degre; $\chi_{\max} \approx 1$ the hydration degree at end of test; $\chi_0 = 0.25$ the hydration degree at unmoulding, $E_{\max} = 35GPa$ the elastic modulus at fin of essais, b = 0.5 coefficient . The experimental resalting and modele proposed showen in 'Fig 6 '

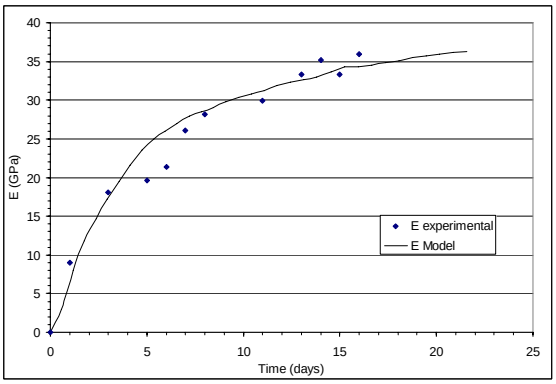

Figure 6. Elastic modulus

5 CALCULUS OF THE RESIDUAL CONSTRAINT ON REAL STRUCTURE

The studies structure corresponds to a piece of fibres massive concrete none armed including four reservations 'fig 7'. The measurement of the deformation and temperature is automated via an autonomous power station of acquisition.

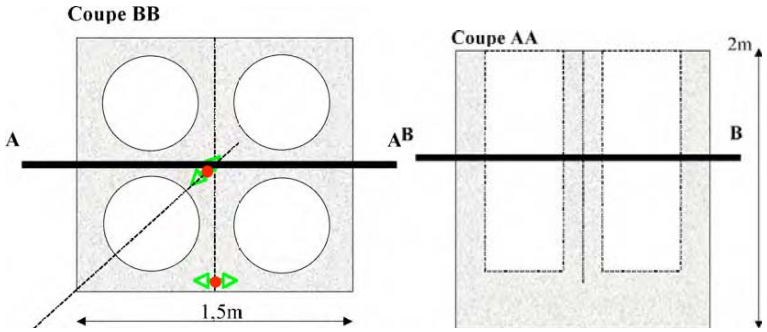

Figure 7. The piece of concrete with two vibrating cord sensor installation (red and green)

The model is implanted in code of element finis (CAST3M) developed by [CEA-France], the resolution of problem is done in an iterative way: for each step of time corresponding to an increment of the advance of the reaction of hydration in each element [Lamour & *al* 2007]. The deformations are calculated from an identified model on specimen, moreover the modelling of structure makes it possible to evaluate the mechanical constraints generated in the structure 'Fig 8'. We verify in particular that the generated constraints are lower than resistances in traction of the concrete.

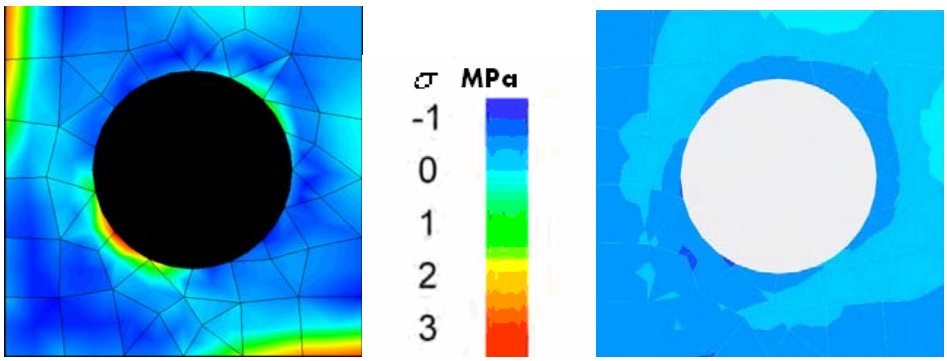

a) At peak of heat (40 h) b) Residual stresses après cooling

Figure 8. Simulated cartography of the principal stress in a quarter of the piece
(The blue zones are a compression zones, the orange zones represent the zones at the risk with respect to cracking at early age).

6 CONCLUSIONS

We proposed in this paper a practical method to characterize the material parameters in the construction site and to identify a macroscopic model from simple tests. We proposed for instance to use the restrained shrinkage ring test to identify a basic early age creep model based on a simple ageing visco-elastic Kelvin model.

Model identification of elastic modulus based on hydration degree has given good resultants. The identification of creep's deformation was done by a rheological model in using the ring test.
This model makes it possible to quantify the risk of cracking and to evaluate the residual stresses of manufacture by taking into account the clean creep identified by the ring test.

REFERENCES

De Schutter, G. 1999, 'Degree of hydration based Kelvin model for the basic creep of early age concrete'. *Materials and Structures*, May, vol. 32, pp. 260-265.

Bǎzant, Z. P., Hauggaard, A. B., Baweja S. & Ulm F.J. 1997, 'Microprestress-solidifcation theory for concrete creep. I:Aging and draying effects'. *Journal of Engineering Mechanics*, vol. 123, No. 11.

Bǎzant, Z.P. & Chern J.C. 1985, 'Concrete creep at variable humidity: constitutive law and mechanism'. *Materials and Structures*, January, vol. 18, No. 1.

Bǎzant, Z.P., Cusatis G. & Cedolin L. 2004, 'Temperature effect on concrete creep modeled by microprestress-solidification theory'. *Journal of Engineering Mechanics*, June, vol. 130, No. 6.

Hauggaard, A. B., Damkilde, L. & Hansen, P. F. 1999, 'Transitional thermal creep Of early age concrete'. *Journal of Engineering Mechanics*, April 1999, vol. 125, No. 4.

Larson M., Jonasson J. E. 2003, 'Linear Logarithmic Model for Concrete Creep, I. Formulation and Evaluation'. *Journal of Advanced Concrete Technology*, July, vol. 1, No. 2, 172-187.

Takács, P. F. 2002, 'Deformations in Concrete Cantilever Bridges: Observations and Theoretical Modelling'. Doctoral Thesis, Norwegian University of Science and Technology. 205p.
Rajeev G., Kumar R., Paul D. K. 2007, 'Comparative Study of Various Creep and Shrinkage Prediction Models for Concrete. *Journal of Materials in Civil Engineering*, March, vol. 19, No. 3.

De Schutter G. 1999, 'Degree of hydration based Kelvin model for the basic creep of early age concrete'. *Materials and Structures*, May, vol. 32, pp 260-265.

Eduardo F., Silvoso M. M., Filho R. D. T. , Alves J. L. D., Ebecken N. F. F. 2004, 'Optimization of mass concrete construction using genetic algorithms'. *Computers and Structures*, 82:281-299.

De Schutter G. & Taerwe L. 2000, 'Fictitious degree of hydration method for the basic creep of early age concrete'. *Materials and Structures*, July 2000, vol. 33, pp 370-380.

Sathikumar S., Karihaloo B. L. & Reid S. G. 1998, 'A model for ageing viscoelastic tension softening materials'. *Mechanics of Cohesive-Frictional Materials*, 1998, vol. 3, 27-39.

De Borst R., Van Den Boogaard A.H. 1994, 'Finite-element modeling of deformation and cracking in early age concrete'. *Journal of Engineering Mechanics*, December 1994, vol. 120, No. 12.

Băzant Z. P., Boe Hauggaard A., Baweja S., Ulm F.J. 1997a, 'Microprestress-solidifcation theory for concrete creep. I: Aging and draying effects'. *Journal of Engineering Mechanics*, August 1997, vol. 123, No. 11.

Commissariat à l'Energie Atomique CEA - DEN/DM2S/SEMT, Cast3m finite element code, available at http://www-cast3m.cea.fr/.

Lamour V., Zreiki J., Moranville M. et Chaouche M. 2007, ' *Détermination des contraintes mécaniques dans les pièces massives en béton au jeune age : instrumentation in situ et modélisation*'. Huitième édition des Journées scientifiques du Regroupement francophone pour la recherche et la formation sur le béton (RF)2B.

Repair & Rehabilitation of Initially cracked RCC Beams by CFRP

Liaqat. A. Qureshi [1]
Imran A. Bukhari [2]
Kamran A. Qureshi [3]

T 11

ABSTRACT

This paper presents the comparison of different repairing techniques commonly used for cracked RCC beams. Six RCC beams (each 3 meter x 225 mm x 300 mm) designed as under-reinforced beams were cast, cured and tested by two-point loading. One beam was loaded up to failure and treated as "Control Beam". Its failure load was noted and deflections were continuously measured by deflection gauges installed at middle and quarter points. Other beams were loaded up to ¾ th of the failure load of control beam. The five cracked beams were repaired by using different ratios of "Carbon Fiber Reinforced Polymers (CFRP) strips". When repair process was over, all five beams were tested again and loaded up to their ultimate load. Again deflections were noted and overall performance of beams was analyzed.

It was noted that the ratio of "Carbon Fiber Reinforced Polymers (CFRP) strips" used will affect the load carrying capacity of the beam and will lead to decreased deflection and increased brittleness of the beams. All patterns used were found to be able to restore or enhance the structural capacity of cracked sections.

KEYWORDS

Cracked, Carbon Fiber, Polymers, Deflection

[1] University of Engg. & Technology, Department of Civil Engineering, Taxila, Pakistan, Phone: 00923215519776, Fax: 0092519047420, lqtqureshi@yahoo.com
[2] University of Engg. & Technology, Department of Civil Engineering, Taxila, Pakistan, Phone: 00923005202890, Fax: 0092519047420, iabukhari@yahoo.com
[3] Baha-u-din Zakria University , Department of Civil Engineering, Multan, Pakistan, Phone: 00923008731120

1 INTRODUCTION

A devastating earthquake, measuring 7.6 on the Richter scale, hit the northern part of Pakistan on the morning of 8th October, 2005. With the death toll of about 90 thousands and injuries in the same range, it is a catastrophe on a scale never before seen in this region. The earthquake also resulted in destruction of all types of buildings and other infrastructure. The buildings which survived are also suffering from severe major cracks. The rehabilitation and repair of cracks in order to make the structure safe for human use is a major problem. To restore their structural capacity, retrofitting and/or strengthening are badly needed. There are different techniques available for retrofitting and strengthening of initially cracked reinforced concrete beams reported in literature. In this research, laboratory investigation regarding use of carbon fiber reinforced polymers to strengthen a given structure or part of it to restore its serviceability and strength is discussed.

Studies have shown that fiber reinforced plates (FRP) increase the strength of flexural members significantly. CFRP has a high strength to weight ratio, favorable fatigue behavior and excellent resistance to electrochemical corrosion to make it practically suited for structural application [Clarke and Waldron 1996]. A study conducted by Alfarabi et al.[1994] showed that, although the FRP increase the failure loads, most of the beams strengthened by FRP started the failure at the curtailment zones of the plates. The epoxy used to laminate the plate at the soffit of flexural members only failed at loads much higher than the required level [El-Mihimly & Tedesco 2000]. Similar study also found that the failure modes for repaired structures may change from ductile to brittle [Arduni et al. 1997]. The probability of this change depends largely on the percentage of FRP being used, the location of FRP and the presence of shear reinforcement in the existing structures. Toong and Li [2000] investigated the effect of using carbon fibre reinforced polymer (CFRP) plates to strengthen one-way spanning slab to increase the flexural capacity with particular emphasis on the cracking behavior at working load. All the CFRP strengthened specimens exhibited large increase in load carrying capacity ranging from 60% to 140% [Wauud & Jaafar 2005].

In this research work CFRP plates were applied at the soffits of initially cracked RCC beams in different proportions in order to observe their strengthening effect as compared to control beam which was loaded up to its failure load. Furthermore this study focuses on the serviceability, strength and ductility performance for each of the CFRP ratio used to ascertain their potential application in initially cracked reinforced beams.

2 EXPERIMENTAL PROGRAM

In order to investigate the effect of repair by using various patterns of CFRP, on the structural response of initially cracked RCC beams, a total of six full-scale RCC beams were cast, cured and tested. All beams were designed by ultimate strength method as under-reinforced and having dimensions 3 meter x 225 mm x 300 mm and singly reinforced by 3 # 4 bars, without using shear reinforcement. All specimens were tested under two pint loading. One beam, designated by C1, was loaded up to failure and named as “Control Beam”. Its failure load was noted and during loading, deflections were measured by deflection gauges installed at middle and quarter points. Other beams were loaded up to ¾ th of the failure load of control beam. Subsequently, the load was removed and specimens removed from the testing frame, so that repairs may be carried out.

Five beams were retrofitted by using different amounts of CFRP and when repair process was over, these were again tested by the same loading arrangement till failure and deflections noted. The response of each of the five retrofitted specimens in terms of deflection, stiffness, cracking load, ultimate load, and failure pattern was analyzed

2.1 Materials Used in the Beams

2.1.1 Cement
Ordinary Portland Cement (TYPE 1) was used.

2.1.2 Fine Aggregate
Sand from Lawrencepur (Pakistan), free from deleterious substances was used. Gradation of sand was carried out in accordance with ASTM Standards. Fineness Modulus was found as 2.62.

2.1.3 Coarse Aggregate
Coarse Aggregate consisted of clear, hard, strong, sound and uncoated crushed stones quarried from Margala Hills, best source of aggregate in Pakistan near Islamabad. These were free from deleterious amount of soft, friable, thin elongated or laminated pieces. Gradation of coarse aggregates was carried out in accordance with ASTM Standards.

2.1.4 Water
Water fit for drinking, as proved by water quality tests, was used in concrete work.

2.1.5 Formwork
Steel formwork (moulds) was used for casting beams.

2.1.6 Size of Beams
All beams were identical in X-section, length and materials:

Cross-section of beams = 225mm x 300 mm
Length of beams = 3 meter

2.1.7 Reinforcement
Deformed steel of grade 40 for 3 # 4 bars was used as main reinforcement. # 4 stirrups were used @100 mm c/c up to 0.7 meter from each end.

2.1.8 Concrete Mix. Design
Concrete Mix. Proportion 1:2:4 (by weight) was used. Water cement ratio was kept as 0.50 and slump was measured as 38 mm (average). Average cube crushing strength at 28 days was achieved as 4258 psi.

2.2 Materials for Retrofitting

2.2.1 Sika Carbudur Laminates
Type used was **S812**, 80 mm wide and 1.2 mm in thickness with cross sectional area of 96 mm^2, Black color, having base of carbon fiber reinforced with an epoxy matrix. Fiber volumetric content is greater than 68%. Main properties for this type as provided by manufacturer are as under:

Shelf life	Unlimited (no exposure to direct sunshine)
E-Modulus	> 165,000 N/mm^2
Tensile strength	> 28,000 N/mm^2
Mean value of Tensile strength at break	> 3, 050 N/mm^2
Elongation at break	> 1.7 %
Density	1.5 g/cm^3

2.2.2 Sikadur-30 Adhesive
For bonding Sika Carbudur laminates on the prepared substrate of beams, Sikadur-30 adhesive was used. It has following properties as per manufacturer technical data:

Appearance	Component A:	White paste
	Component B:	Black paste
	Component A + B:	Light grey after mixing
Mix. Ratio	A : B = 3 : 1	(Parts by weight)
Density	1.5 Kg/lit	(A + B)
Pot life	40 minutes	(at 35°C)
Open time	30 minutes	(at 35°C)
Shrinkage	0.04 %	

Static E-Modulus	12,800 N/mm^2	
Adhesive Strength	Concrete failure	(4 N/mm^2)
Shear Strength	Concrete failure	(15 N/mm^2)
Coefficient of expansion	9 x 10^{-4} per ^{o}C	(-10^{o}C to + 40^{o}C)

2.2.3 Colma Cleaner
The behavior of concrete elements strengthened or retrofitted with Sika Cabudur Laminates is highly dependent on a sound concrete substrate and proper preparation and profiling of the concrete surface. Surfaces of the beams were grinded and smoothened with the help of hand grinder and cleaned with Colma Cleaner before applying adhesive over the surface of Sika Cabudur laminates.

2.3 Strengthening of Beams

Five beams were retrofitted at their soffits as under:

- **Two Beams** - One S812 laminate was bonded in the center along the length of beams as shown in Fig. 1.
- **Two Beams** - One 1.5 meter piece of S812 laminate was bonded in the centre over mid span, shown in Fig. 2.
- **One Beam** - Two S812 laminates were bonded in the center along the length of beams. The schematic diagram is shown in Fig. 3).

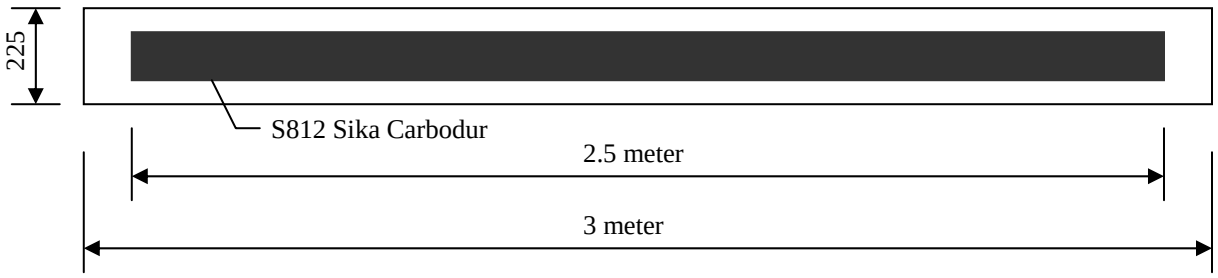

Figure 1. Strengthening by one strip of full beam length

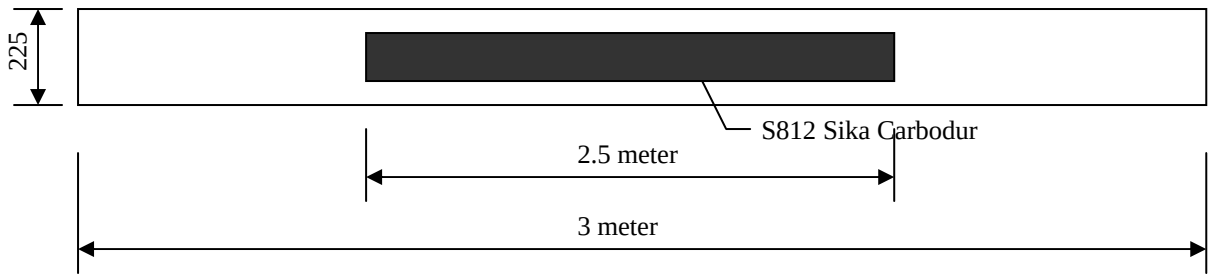

Figure 2. Strengthening by one strip of 1.5 m length.

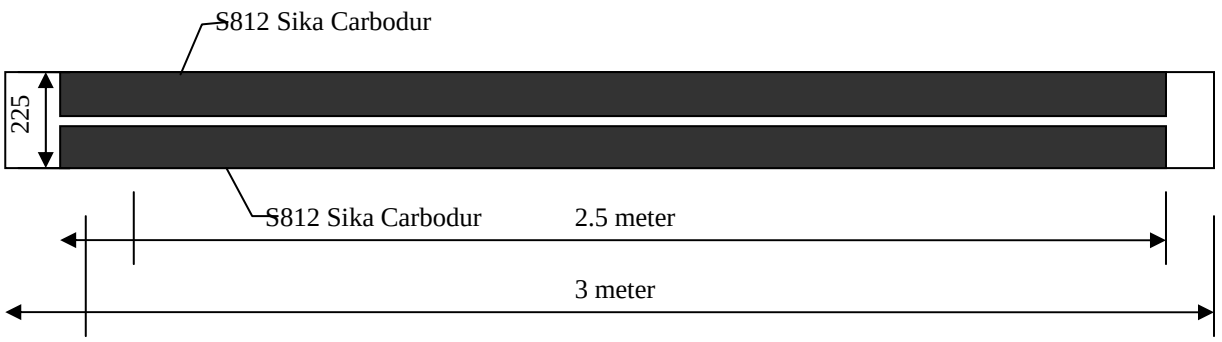

Figure 3. Strengthening by two strips of full beam length

2.4 Testing of Beams

First of all, beams were tested for flexural strength in a staining frame before strengthening. One dial gauge was installed at mid span to record the mid span deflection and two gauges were installed at quarter points to record deflection at those points. Two point loads were applied at the centre of beam and deflections recorded for each increment of load. One beam was tested up to failure and designated as control beam. Other beams were tested up to $3/4^{th}$ of failure load of control beam. These beams were then removed from the testing frame and strengthened with the help of CFRP strips as shown in figs 1 to 3. The strengthened beams were tested again up to ultimate load and deflections noted. The results of two beams, strengthened with one CFRP strip, are averaged as B1. Similarly average results of two beams strengthened with one 1.5 meter length of strip are designated as B2 and the results of beam strengthened by two CFRP strip are designated by B3.

3 RESULTS AND DISCUSSION

Figures 4 - 6 show load-deflections curves of B1, B2 and B3 before and after repair. The deflections recorded at mid-span are used in these curves. All results reflect less deflection after repair, which is an indication of non-ductile behavior of the beams. Also load-deflection curve of control beam shown in fig. 7 indicates high deflection at failure load. The decrease in deflection is more prominent at advanced stages of loading. Beams strengthened with two CFRP plates show least deflection at the highest ultimate load i.e., 275 KN, which reveals that these beams are more brittle as compared to control as well as other repaired beams. A comparison of ultimate loads, taken by control and repaired beams, is shown in figure 8.

In case of control beam, failure load was 200 KN. First crack appeared at 134 i.e., 67 % of the ultimate load. Crack pattern showed that failure mode was tension failure.

In case of B1, failure load of repaired beams was 210 KN, a little bit greater than that of control beam. First crack appeared at an average load of 114 KN i.e., 54 % of failure load. After strengthening, ultimate load bearing capacity increased by 5 %. Failure mode was CFRP plates end interfacial de-bonding.

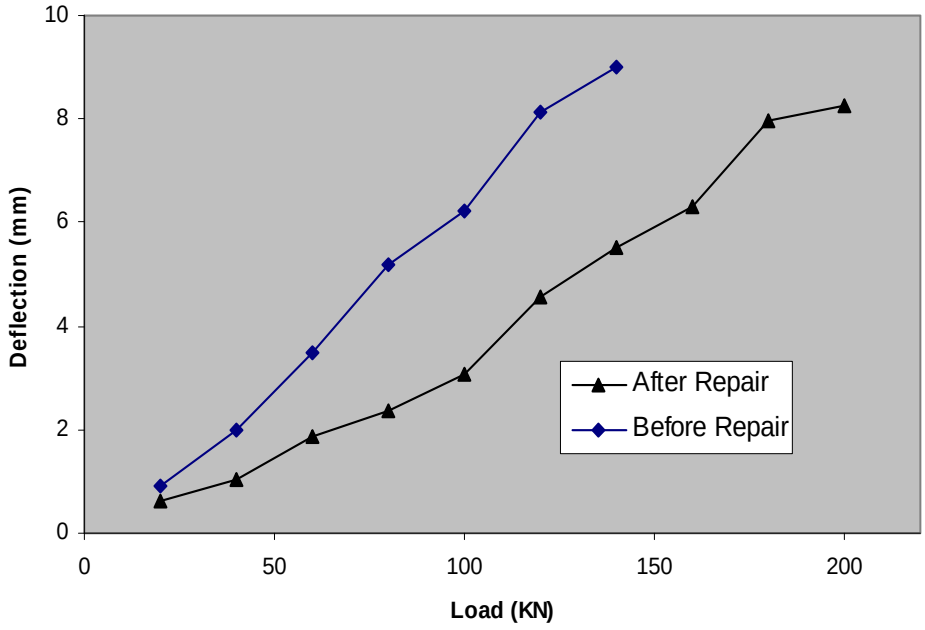

Figure 4. Load versus Deflection graph for B1.

In case of B2, beams failed at an average failure load of 180 KN. Ultimate load bearing capacity of repaired beams decreased by 10 % as compared to the control beam. Failure was flexural tension failure

near ends of CFRP laminates. Both tested beams failed in the same manner with CFRP plates intact with bottom.

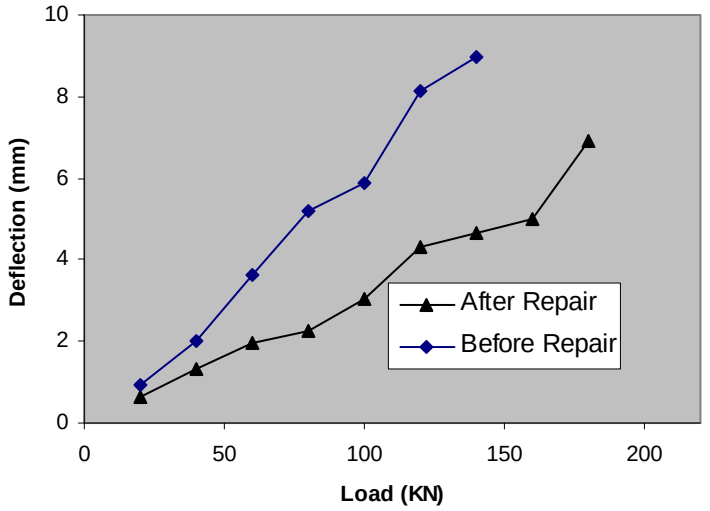

Figure 5. Load versus Deflection graph for B2.

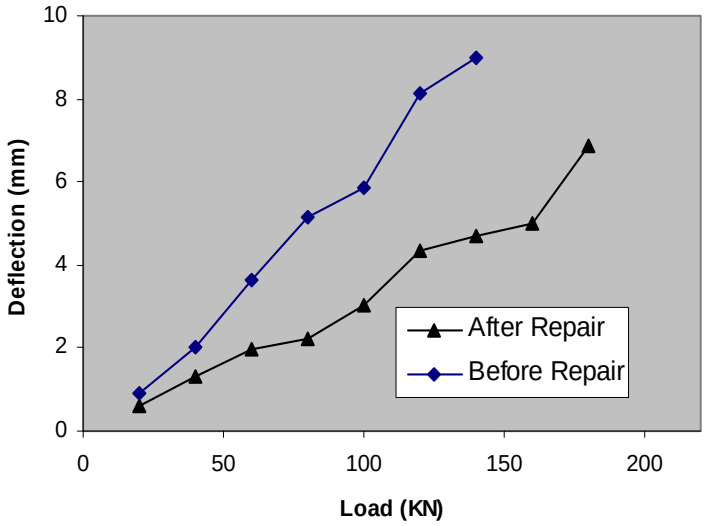

Figure 6. Load versus Deflection graph for B3

When two CFRP laminates of full beam's length were used for repair of cracked beams, more favorable results were found. Both beams failed at 275 KN load. Ultimate load bearing capacity increased by 138 % over the control beam. This ultimate bearing capacity is 31 % more than B1 and 53 % more than B2. Cracks started at load of 220 KN, which is 80 % of the ultimate failure load. Mode of failure involved the concrete cover separation (peeling off) along with laminate from one end.

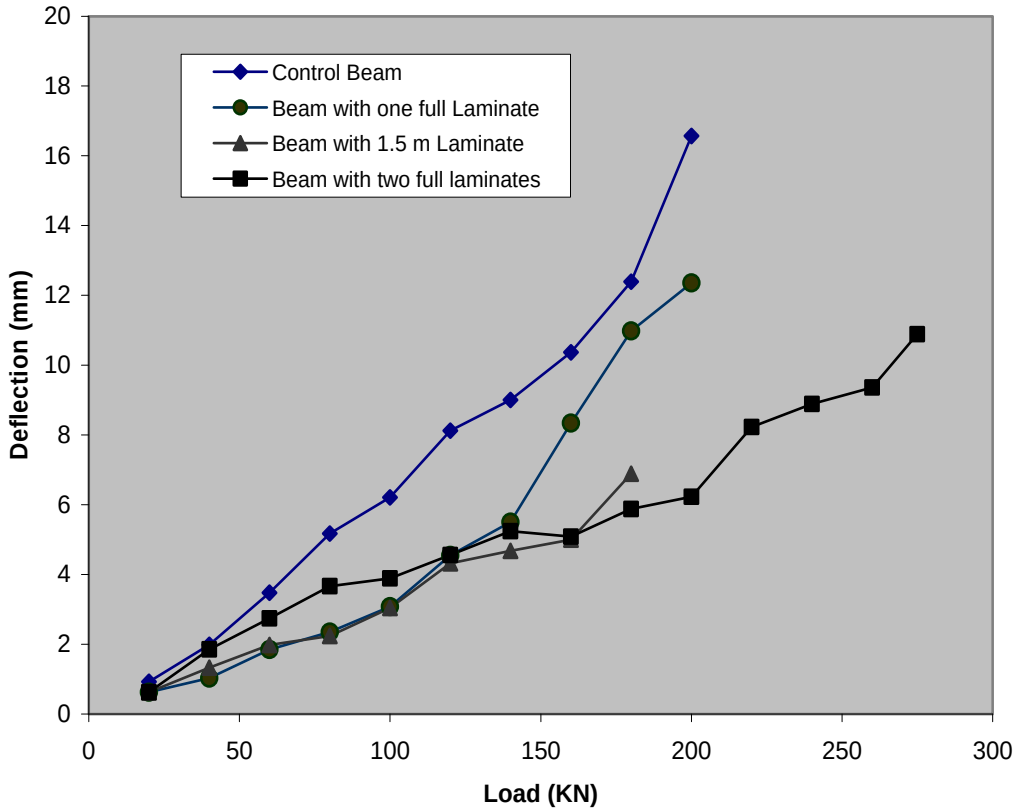

Figure 7. Comparison of Load versus Deflection graphs for strengthened beams and control beam.

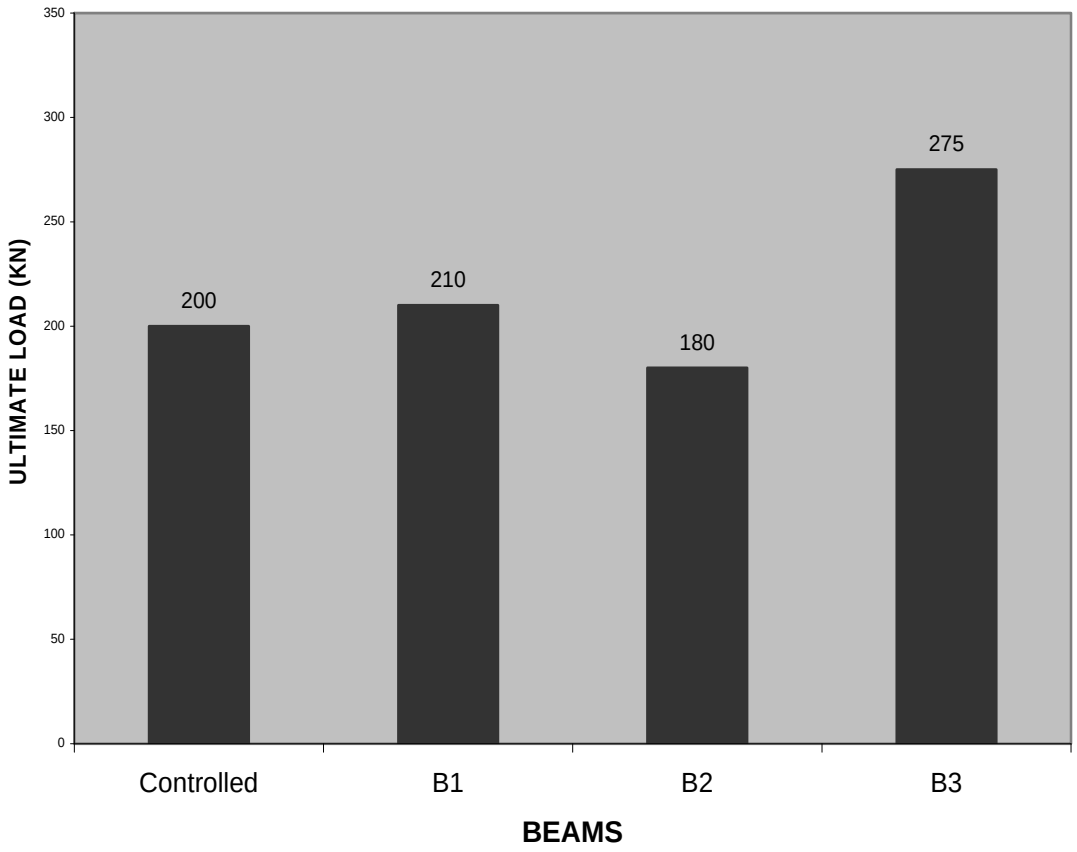

Figure 8. Comparison of ultimate loads taken by all beams

4 CONCLUSIONS

Based on this study, the following conclusions can be made:

- Strengthening of initially cracked RCC beams with externally bonded CFRP plates is effective and leads to increased load carrying capacity.
- The repaired beams had similar or higher cracking loads compared to the control beam.
- The deflection values of all the CFRP-strengthened tested beams are reduced.
- The retrofitted beams possess less ductility compared to the original beams before cracking. This is the result of the brittleness nature of the encountered failure modes of the retrofitted beams (concrete cover separation along with CFRP plates and de-bonding of CFRP plates from ends).
- In order to achieve full capacity of the laminate and to avoid brittle failure by de-bonding, special attention should be paid to provide adequate anchorage length for the fibers either longitudinally or transversely.
- Best results regarding ultimate failure load were achieved in case of two CFRP strips having lengths equal to full beam's length. On the other hand, the same is associated with high cost of CFRP strips used. This factor should be kept in mind while finally selecting this mode of repair.

5 REFERENCES

Clarke, J.K. & Waldron, P. 1996, 'The reinforcement of concrete structures with advanced composites', *Struct Eng* 74 (17/3), p. 1996.

Alfarabi, S., Alsulaimani, G.J., Basunbul, I.A., Bamch, M.H. & Ghaeb, B.N. 1994, 'Strengthening of initially loaded reinforced concrete beams with using FRP plates' *ACI Struct Journal*, March, pp. 160-168.

El-Mihimly, M.T. & Tedesco, J.W. 2000, 'Analysis of reinforced beams strengthened with FRP laminates', *J Struct Eng*, June, pp. 684-691.

Arduni, M., Tomasso, A.D. & Nanni, A. 1997, 'Brittle failure in FRP plate and sheet bonded beams', *ACI Struct J* 94, pp. 363-370.

Toong, K. Chan, & Li Xiaoan, 2000, 'Improving crack behavior of one-way slabs with carbon fiber plates', In: *Proc of the 4th Asia-pacific structural engineering and construction conference*, September 13-15, Kualalampur, Vol. 2, pp. 351-358.

Razali, M., Kadir, A. & Noorzaci J. 2005, 'Repair and structural performance of initially cracked reinforced concrete slabs', *Construction and Building Material J*, Vol. 19, Issue 8, October, pp. 595-603.

Chloride Transport in Concrete Structures Exposed to Marine Environments Considering Time Dependent Characteristics

Ha-Won Song [1]
Seung-Woo Pack [2]
Ki Yong Ann [3]

T 11

ABSTRACT

The present study surveyed published data on chloride transport in concrete structures exposed to a marine environment for the duration ranging from 1 to 49 years. In particular, time-dependent characteristics of the diffusion coefficient (D) and surface chloride concentration (C_S) were extensively investigated for the prediction of the ingress of chlorides. As a result, it was found that both D and C_S are time dependent; D decreases and C_S increases with time. A build-up of the C_S was considered to solve the Fick's 2nd law and the time dependency of the D was applied to the solution for the chloride ingress, and then chloride profiles were comparably predicted, using both time dependent and time independent models. From the comparison, the chloride profiles calculated by the time dependent model are always higher than those by the time independent model. Consequently, the time dependent model predicts shorter service life which is the shorter time to corrosion initiation of rebar. It was found that decreased D with time is more influencing on the rate of chloride ingress than the increased C_S. It was also found that the conventional model, utilizing constant values of D and C_S may underestimate the rate of chloride transport and thus predict less risk of chloride-induced corrosion.

KEYWORDS

Concrete structures, Marine environments, Corrosion, Diffusion coefficient, Surface chloride concentration

[1] Yonsei University, School of Civil and Environmental Engineering, Professor, Seoul 120-749, Korea, Phone +82 2 2123 2806, Fax +82 2 364 5300, song@yonsei.ac.kr
[2] Yonsei University, School of Civil and Env. Engineering, PhD candidate, ditto, yannism@cmme.yonsei.ac.kr
[3] Yonsei University, School of Civil and Env. Engineering, Research Professor, ditto, k.ann@cmme.yonsei.ac.kr

1 INTRODUCTION

The assessment of chloride-induced corrosion of steel embedment in concretes exposed to marine environments has received increasing attention, because of its widespread occurrence and high cost of repair. Corrosion of steel in concrete reduces the service life of concrete structures, and thus the service life should be predicted by comparison between the amount of chloride concentration at cover depth by chloride transport and chloride threshold value [Song et al. 2006a]. In the majority of previous studies on the service life prediction, a conservative chloride threshold value for corrosion initiation such as 0.2 or 0.4% by weight of cement has been used to predict the service life [Ann & Song 2007]. For chloride transport, the Fick's 2nd law is often used to predict chloride penetration in terms of diffusion [Collepardi et al. 1972], due to its convenient and easy calculation with constant values of the apparent diffusion coefficient (D) and surface chloride concentration (C_S), which are in fact dependent on concrete mix proportion and exposure condition to a salt environment (eg. submerged, tidal, splash and aerated zones in marine environments) [Song et al. 2007a]. The diffusivity decreasing with time due to development of the pore structure with time has been currently considered in assessing the rate of chloride transport [Thomas & Bentz 2000, Bamforth 1999]. Due to the hypothesis that chloride ions and surface concrete make a chemical equilibrium in the form of di-electric layer, the time dependency of the C_S has been intuitively ignored in conventional chloride transport model, so that a constant value of the C_S has been widely used in modeling chloride transport. Only when concrete structures are exposed to a marine atmospheric condition, a build-up of the C_S has been taken into account [Kassir & Ghosn 2002]. It was, however, observed in a survey on in-situ that a build-up of the C_S occurs, even when concretes are exposed to direct contact to seawater such as in tidal/splash zones [Uji et al. 1990].
The present study examined 6 concrete bridges located in the West Sea side of Korea exposed to tidal zone, where data on the D and C_S were obtained. These data were fitted as a function of time, and used in modelling to predict chloride profiles and the corrosion risk of concrete structures exposed to marine environments. The characteristic of a C_S build-up was considered in solving the Fick's 2nd law and the time dependency of the diffusivity was subsequently applied for the solution of the chloride ingress in concrete.

2 TIME DEPENDENCY OF CHLORIDE TRANSPORT

In this study, 6 concrete bridges exposed to marine environments were examined to assess the rate of chloride transport, depending on exposure duration. The bridges at ages ranging from 0.65 to 48.65 years were built in ordinary Portland cement (OPC) concrete as a binder. Concrete samples ground from surface concretes were obtained from a pier of the bridges in tidal zone at the time of tide down by drilling and grinding with 2 mm increments up to 50 mm. The chloride content of each sample was determined by acid soluble extraction in a nitric acid solution followed by potentiometric titration against silver nitrite. The chloride profiles at the time of sampling were also obtained. Then, the D, non-steady state diffusion in a semi-infinite medium, was determined for each specimen by fitting the error function solution to the Fick's second law, for.
Fig. 1 describes the D and C_S for target structures exposed to tidal zone. The best fit curves for the D are expressed as a power function of time, and for the C_S as a logarithm function of time. It is seen that the D decreased with exposure duration, despite their high deviation at exposure conditions, including different degrees of wave, weathering and presumably segregation of concrete in mixing. The D initially at 0.65 years ranged from 5.53×10^{-12} to 7.89×10^{-12} m^2/s and at 48.65 years from 4.47×10^{-12} to 5.55×10^{-12} m^2/s respectively. The C_S were also much affected by the exposure duration. The C_S ranged from 1.85 to 2.21% by weight of cement at 0.65 years and from 2.71 to 3.11% at 48.65 years respectively. These results were used to model chloride penetration considering its time dependency in terms of only diffusion in the present study.

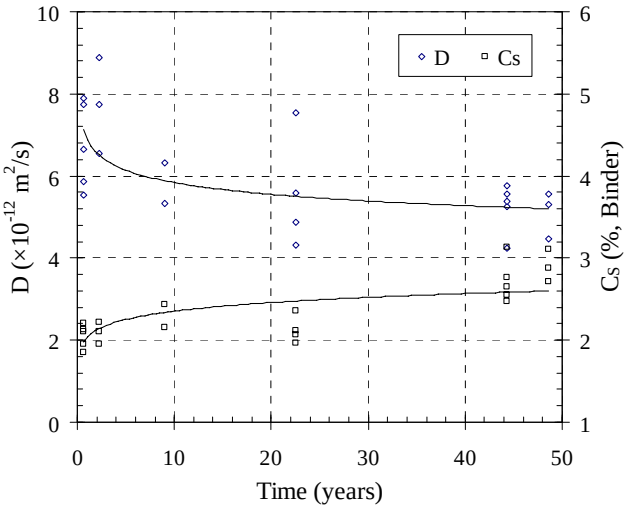

Figure 1. Time dependent change in the apparent diffusion coefficient and surface chloride

3 MODELLING OF CHLORIDE TRANSPORT

3.1 Time independent transport

The Fick's 2nd law is commonly used to describe chloride ion diffusion in concrete as given in Eq. 1, which is used for the time independent model. Theoretically, the D can be calculated by measuring the concentration of the C_S and the concentration of chloride ions $C(x, t)$ at the depth x and the exposure duration t.

$$C(x,t) = C_S(1 - erf\frac{x}{2\sqrt{Dt}}) \quad (1)$$

where, *erf* is an error function.

3.2 Time dependent diffusion coefficient

The diffusivity often decreases with time, as cement hydration proceeds to refine the concrete pore structure, thereby letting connectivity of the pores significantly decrease [Thomas & Bentz 2000]. A package program [Thomas & Bentz 2000] for service life prediction uses a model in determining the D in predicting a chloride profile as follows.

$$D(t) = D_R\left(\frac{t_R}{t}\right)^m \quad (2)$$

where, $D(t)$ is the diffusion coefficient at time t, D_R is the diffusion coefficient at reference time t_R (i.e. usually 28 days), and m is an age factor. This model is known to fit well for marine environments, as a change in the pore structure imposes a development of cement hydration [Bamforth 1999]. However, a direct application of this model for predicting the rate of chloride transport has a defect, that the historic change of the D for a given exposure duration is not considered, which may lead to an erroneous judgment on chloride ingresses and thus the risk of chloride-induced corrosion.
In this study, in order to remedy the defect by consedering hysteresis of the D, the mean value of the D for exposure duration to marine environments was used to predict a chloride profile. Thus, the mean D was calculated by integrating the definite D for a given exposure duration, and then by dividing the exposure duration, as given in Eq. 3.

$$D_m(t) = \frac{1}{t}\int_0^t D(\tau)\cdot d\tau \tag{3}$$

where $D_m(t)$ is the mean diffusion coefficient for the exposure duration, t. In this study, the time dependency of the D was expressed in the same power function as seen in Eq. 2. Thus the mean D can be obtained by substituting Eq. 2 into Eq. 3:

$$D_m(t) = \frac{D_R}{1-m}\left(\frac{t_R}{t}\right)^m \tag{4}$$

This equation is more useful to solve the Fick's 2nd law for a chloride profile, rather than a constant D, since both the time dependency and the hysteresis of the diffusivity are encompassed [Song et al. 2006b].

3.3 Time dependent surface chloride

A build-up of the C_S for concrete structures exposed to seawater was obviously observed in previous survey [Uji et al. 1990]. In this study, the time dependency of the C_S as well as the D is considered in solving the Fick's 2nd law, based on the in-situ data (Fig. 1). The time dependency of the C_S was observed as shown in Fig. 1. Hence, a build-up of the C_S was taken into account in calculating a chloride profile using the best fit of a change in the C_S with time [Song et al. 2006b] from the field data as Eq. 5.

$$C_S(t) = \alpha[\ln(\beta t + 1)] + k \tag{5}$$

Here, t is the time of exposure in years and α, β and k are constants obtained from in-situ environments as given in Fig. 1.
The chloride content, $C(x, t)$, at a given time t and a depth x, can be expressed with the time dependent C_S, by utilizing a heat conduction solution in solids [Carslaw & Jaeger 1959].

$$C(x,t) = \frac{2}{\sqrt{\pi}}\int_{\frac{x}{2\sqrt{Dt}}}^{\infty} C_S\left(t - \frac{x^2}{4D\omega^2}\right)\cdot e^{-\omega^2} d\omega \tag{6}$$

Eq. 6 was derived from the Fick's law by considering C_S variation with time while D remains constant. Although consideration of the time dependent D to solve the Fick's 2nd law could provide a more accurate prediction on the ingresses of chlorides, the calculation for the solution could be subject to an extreme complexity. Hence, the term D in the solution Eq. 6 was substituted by the time-varying D as Eq. 4, even it produce a marginal error. Thus, a final expression for the chloride transport can be written by the following equation.

$$C(x,t) = \frac{2}{\sqrt{\pi}}\int_{\frac{x}{2\sqrt{D_m(t)t}}}^{\infty} C_S\left(t - \frac{x^2}{4D_m(t)\omega^2}\right)\cdot e^{-\omega^2} d\omega \tag{7}$$

4 Results

4.1 Chloride penetration

The chloride penetration by both the time-dependent model and time-independent model at 25, 50, and 100 mm of concrete covers is calculated in Fig. 2. The chloride content was calculated with 2.5 years of the time interval. It is seen that the penetrated chloride ions calculated from the time dependent model is always higher than the time independent model. At an early age within 5-10 years, the penetration of chloride ions seems not to be affected by time dependency of chloride transport; there is no particular difference between the time-dependent model and the time- independent model.

However, for chloride content penetrated through the depths of cover concrete, the time dependent model predicts higher chloride content than that by the time independent model. It can be seen that the influence of the increased C_S is very dominant for chloride penetration due to higher concentration gradient of chloride ions on the concrete surface. However, as the cover depth increases, the difference of penetration of chlorides between two models decreases, since the increased C_S is less influencing and only D governs the rate of chloride ingress.

The influence of the time dependency of C_S to chloride profiles is given in Fig. 3. The chloride profiles show up to the depth 100 mm of the concrete cover at 5, 20, and 100 years. The chloride ingresses by the time dependent model were always higher than those by the time independent model, and the chloride ingress increases much higher with time, presumably due to the higher C_S by time-dependent build-up of C_S. The concentration gradient of chloride ions on the surface concrete significantly increases with time and thus the higher level of chloride ingress at all depths occurs.

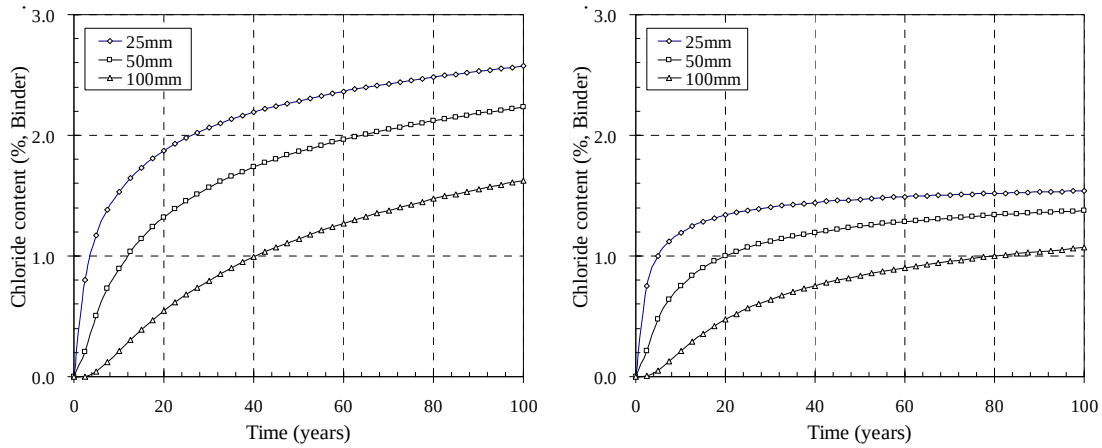

(a) Time dependent model (b) Time independent model

Figure 2. Penetration of chloride ions at different concrete cover depths

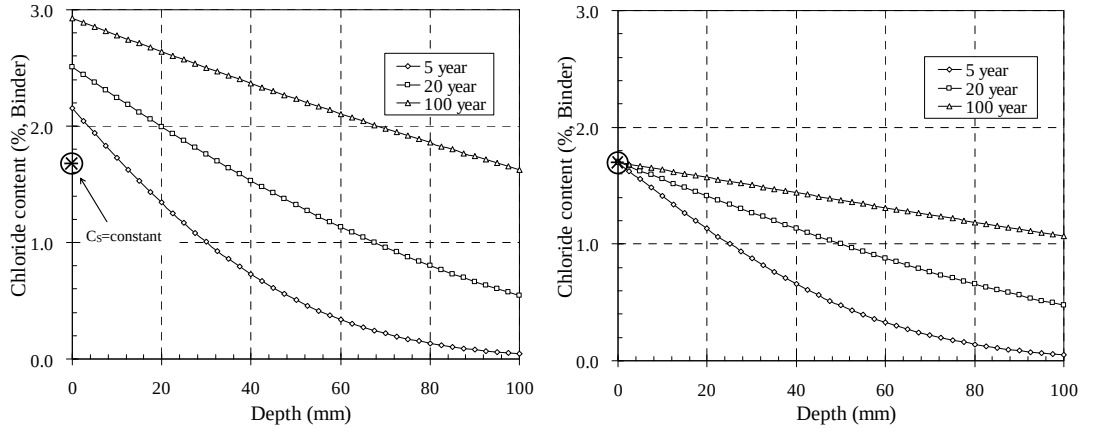

(a) Time dependent model (b) Time independent model

Figure 3. Chloride profiles with time

4.2 Time to corrosion

The time to corrosion, i.e. corrosion initiation, is calculated as in Fig. 4 with different chloride threshold level, C_{lim}, of 0.4%, 0.6%, and 0.8% by weight of binder, respectively. The concrete cover depth of up to 100 mm in a tidal zone is considered. It was found that the time dependent model predicts earlier corrosion initiation due to greater build-up of the C_S with time and relatively lower

decrease in the D. With 0.4% of C_{lim}, the difference in prediction of corrosion initiation by two models is negligible, whereas corrosion initiation predicted by time independent model is greater up to by about 50% than that by time dependent model for 0.8% of C_{lim}. It was also found that the defference by two models becomes large with a increase of C_{lim}.

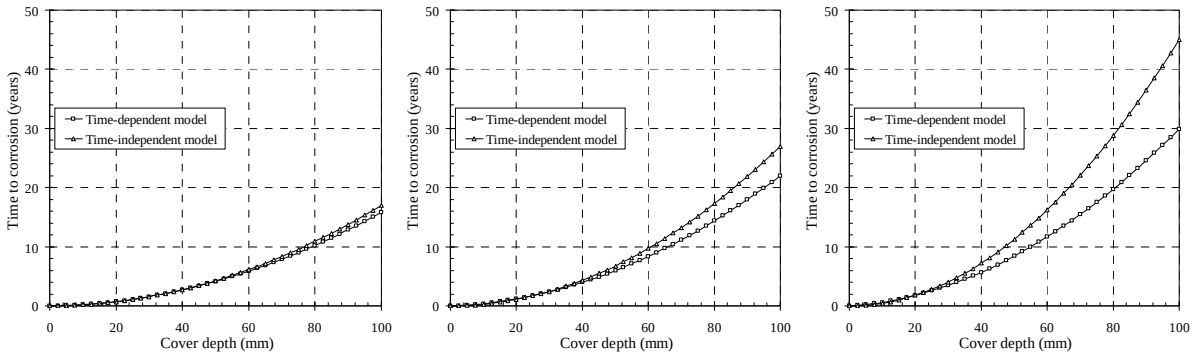

(a) C_{lim} = 0.4 (%,binder) (b) C_{lim} = 0.6 (%,binder) (c) C_{lim} = 0.8 (%,binder)

Figure 4. Time to corrosion for a concrete structure exposed to marine environments (tidal zone)

5 DISCUSSION

5.1 Chloride transport

The chloride transport via capillary pores is dependent on volume fraction and connectivity of the pores inside concrete, and it can be depending on the W/C ratio, cement content, cement type, and use of secondary cementitious materials. For example, low W/C, good curing and use of pozzolanic materials result in the capillary pores being blocked with gel and reduced permeability to water containing aggressive ions such as chlorides. The reduction of the rate of chloride transport is also ascribed to the development of cement hydration. Cement matrix usually completes 85-90% of the hydration within 28-56 days after casting. The rest of hydration takes place in a very long term, ranging from a couple of years to decades. When cement hydration proceeds, the hydration products expand twice of the volume and thus may occupy the capillary pore or block the interconnected network. Thus, the rate of chloride transport could significantly decrease with time. This effect was once modelled using a computational technique [Garboczi & Bentz 1992], but the results was less conclusive, since only the change of geometry in the capillary pore network (i.e. volume fraction) with time was taken into account. In fact, the rate of chloride transport is much affected by other factors including chemistry between chloride ions and cement matrix [Ann et al. 2007], and physical condition of the interfacial zone between cement paste and aggregate, which are also attributed to the chloride ions' mobility. Hence, it seems to be necessary to further investigate the time dependency of the rate of chloride transport, considering the complexity of physical and chemical change in cement matrix.

A proportion of chloride ions present in concrete is chemically bound, primarily by tricalcium aluminate (C_3A) to form Friedel's salt. Recent studies have modelled the influence of binding on the penetration of chloride [Glass & Buenfeld 2000]. Glass & Buenfeld [2000] found that with increased chloride binding capacity, total chloride contents increase nearer the surface of the concrete, but decrease deeper in the concrete. An increase in the C_S is induced by the binding effect which allows the progressive build-up of higher total chloride content at increasing distances from the concrete surface. Chloride binding also reduces the content of free chloride within concrete and the concentration gradient at depth, because chloride binding removes chloride from the transport process [Song et al. 2007b]. It is notable that the content of bound chloride depends on the binding behaviour of cement matrix and the concentration of chloride source.

5.2 Corrosion of steel

A reduction of ionic diffusivity through concrete with time is beneficial in delaying the onset of chloride-induced corrosion and thus enhancing the corrosion free life of structures. However, a build-up of the C_S may mitigate the benefit of decreased diffusivity. It can be seen from the analytical results between two models that the increased C_S with time plays a more important role than the decreased D does in penetration of chloride ion. Pulverised fly ash (PFA), ground granular blast furnace slag (GGBS) or silica fume (SF) in concrete is effective in enhancing the resistance to chloride diffusion as compared with concrete with plain Portland cement as binder. The decrease in D for PFA, GGBS or SF concretes generally arises from (1) refinement of pore structure, and (2) increased binding capacity of GGBS [Luo et al. 2003]. These influences of concrete containing PFA and GGBS on the chloride diffusivity seem to continue for a long period of time. The D reduces more dramatically in concrete mixtures containing pozzolans showing their long-term hydration properties rather than in the OPC concrete [Bamforth 1999]. Even the structures investigated in the present study were built in OPC as binder, and then a reduction of diffusivity in concrete with time did not affect significantly to the diffusion resistivity, it is possible to delay the corrosion initiation of the structures by using the pozzolanic admixtures, such as PFA and GGBS, when considering time dependent characteristics.
The presence of moisture and oxygen are necessary for corrosion to proceed at a significant rate after initiation, so corrosion propagation is dependent on cathodic reaction in terms of oxygen and moisture, the estimates of corrosion rates may be given on the bases of oxygen pemeability [Andrade et al. 1989]. Concrete permeability depends largely on diameter, shape, and connectivity of pores. Pore volume in PFA concrete and SF concrete is rapidly reduced with time, permeability of 50% PFA concrete is approximately 50% less than that of OPC concrete [Day et al. 1985]. Therefore, pozzolanic materials give low permeability of oxygen and moisture inside concrete, and it results in delaying time to repair and/or mitigate corrosion development.

6 CONCLUSION

The conclusion of this study is as follows.

(1) Diffusion coefficient (D) of chloride ions in concrete obtained from in-situ marine environments decreased with time, whereas surface chloride concentration (C_S) increased. The D decreased dramatically for the first 20 years after exposure in marine environments and then still decreased but at a lower rate up to about 75% of the initial D, while the C_S highly increased up to by about 70% compared to the initial C_S.
(2) The chloride profiles were calculated by both the time dependent and independent models. The time dependent model predicted higher chloride ingress than the time independent model did and the chloride ingress increased with time at a much higher rate, since the decreased D with time is more influencing on the rate of chloride ingress than the increased C_S.
(3) Using the time dependent model, the time to corrosion initiation was predicted shorter than that by the time independent model, mainly due to a higher build-up of the C_S and relatively a lower fall of the D. It was found that the time independent model for chloride transport, which has been used for the prediction of service life, may underestimate the risk of chloride-induced corrosion in concrete structures.

ACKNOWLEDGMENTS

The authors would like to acknowledge financial supports from a project on standardization of performance based construction specifications and design, Korea and a Center for Concrete Corea, Korea.

REFERENCES

Andrade, C., Alonso, C., Rz-Maribona, I. & Garcia, M. 1989, 'Suitability of the measurement technique of oxygen permeability in order to predict corrosion rates of concrete rebars', *Paul Klieger Conference*, ACI, San Diego.

Ann, K.Y., Buenfeld, N.R. & Head, M.K. 2007, 'The effect of electrochemical treatment in inhibiting the corrosion of steel in concrete, *Materials and Structures*, in press.

Ann, K.Y. & Song, H.-W. 2007, 'Chloride threshold level for corrosion of steel in concrete', *Corrosion Science,* in press.

Bamforth, P.B. 1999, 'The derivation of input data for modelling chloride ingress from eight-years UK coastal exposure trials', *Magazine of Concrete Research*, Vol. 51, 87-96.

Carslaw, H.S. & Jaeger, J.C. 1959, *Conduction of Heat in Solids*, The Clarendon Press (2). Oxford.

Collepardi, M., Marcialis, A. & Turriziani, R. 1972, 'Penetration of chloride ions into cement pastes and concrete', *Journal of American Ceramic Society*, Vol. 55, 534-535.

Day, R.L., Joshi, R.C., Langan, B.W. & Ward, M.A. 1985, 'Measurement of the permeability of concretes containing fly ash, in *Proc. 7th Int. Ash Util. Symp. and Exp.*, Orlando, Vol. 2, 811-821.

Garboczi, E.J. & Bentz, D.P. 1992, 'Computer simulation of the diffusivity of cement-based materials', *Journal of Materials Science*, Vol. 27, 208-392.

Glass, G.K. & Buenfeld, N.R. 2000, 'The influence of chloride binding on the chloride induced corrosion risk in reinforced concrete', *Corrosion Science*, Vol. 42, 329-344.

Kassir, M.K. & Ghosn, M. 2002, 'Chloride-induced corrosion of reinforced concrete bridge decks', *Cement and Concrete Research*, Vol. 32, 139-143.

Luo, R., Cai, Y., Wang, C. & Huang, X. 2003, 'Study of chloride binding and diffusion in GGBS concrete', *Cement and Concrete Research*, Vol. 33, 1-7.

Song, H.-W., Pack, S.-W., Lee, C.-H. & Kwon, S.-J. 2006a, 'Service life prediction of concrete structures under marine environment considering coupled deterioration', *Restoration of Buildings and Monuments*, Vol. 12, 265-283.

Song, H.-W., Pack, S.-W. & Moon, J.S. 2006b, 'Durability evaluation of concrete structures exposed to marine environment focusing on a chloride build-up on concrete surface', *Proc. of the Int. Workshop on Life Cycle Management of Coastal Concrete Structures*, Nagaoka Japan, 1-9.

Song, H.-W., Lee, C.-H. & Ann. K.Y. 2007a, 'Factors influencing chloride trasnport in concrete structures exposed to marine environments', *Cement and Concrete Composites*, in press.

Song, H.-W., Lee, C.-H. & Ann, K.Y. 2007b, 'Prediction of chloride profile considering binding of chlorides in cement matrix', *International Corrosion Engineering Conference*, Seoul Korea.

Uji, K., Matsuoka, Y. & Maruya, T. 1990, 'Formulation of an equation for surface chloride content of concrete due to permeation of chloride', *Cor. of Rein. Concrete*, Elsevier Applied Science, 258-267.

Thomas, M.D.A. & Bentz, E.C. 2000, *Life-365 Manual*, released with program by Master Builders.

11DBMC International Conference on Durability of Building Materials and Components
ISTANBUL, Turkey 11-14 May 2008

Improvement of durability of RC column by transverse prestressing

Yasuji Shinohara[1]

T 11

ABSTRACT

Experiments and 3-D FEM analyses were performed on reinforced concrete columns laterally prestressed by high strength shear reinforcement to study the influence of the active confinement on shear crack behaviors and shear strength. Flexure-shear tests were performed on RC columns that were laterally prestressed (LPRC) and not prestressed (RC), respectively. The lateral prestress was introduced into concrete as follows: (1) the high strength transverse hoops were pretensioned to approximately 40-60% of the yield strength using the rigid steel molds and special jigs, (2) concrete was placed vertically into the steel molds and cured until the strength of the concrete increased sufficiently, and (3) the core concrete was laterally prestressed by removing the steel molds. All columns were designed to undergo shear failure before the longitudinal reinforcements yield. Six strain gauges were attached to each shear reinforcement (hoop), and the width of each shear crack near the shear reinforcement was measured by a digital microscope with a resolution of 0.01 mm three times during loading and two times during unloading. The results of the flexure-shear tests indicate that the shear capacity at first diagonal cracking is increased and the width values of shear cracks, especially their residual opening, are remarkably reduced by transverse prestressing. This reduction of the shear crack opening improves not only durability but also earthquake resistance.

FEM analysis can be used to evaluate the shear capacity at first cracking and the ultimate shear strength with a fair degree of precision. The FEM analysis using the smeared crack model cannot be used to evaluate a localized crack accurately, but can provide valuable information about the total damage in the overall depth of a specimen and about the effect of the active confinement on shear cracking by evaluating the intensity of confinement in the triaxial state of stress.

KEYWORDS

Transverse prestressing, Active confinement, Shear crack, Residual opening, FEM analysis

[1] Tokyo Institute of Technology, Structural Engineering Research Center, Yokohama, Japan 226-8503, Phone +81 45 924 5326, Fax +81 45 924 5526, shinohara.y.ab@m.titech.ac.jp

1 INTRODUCTION

Prestressing in concrete structures is generally performed to control flexural cracks by the arrangement of tendons in the axial direction of a given member. On the other hand, in an attempt to delay the onset of shear cracking and reduce the crack width, experimental studies have been conducted on reinforced concrete (RC) columns that have been laterally prestressed by high strength shear reinforcement [Watanabe *et al*. 2004]. The results of flexure-shear tests have indicated that transverse prestressing increases the shear capacity at first diagonal cracking (shear crack strength) and decreases remarkably the width of shear cracks, especially their residual opening. This reduction of the crack opening improves not only durability but also earthquake resistance.

The main purposes of the present study are (1) to investigate how transverse prestressing in RC columns affects the shear behavior with respect to the propagation of cracks and the triaxial state of stress, (2) to clarify the relationship between the width of a shear crack and the strain of a shear reinforcement, and (3) to determine the extent to which FEM analysis with a smeared crack model can evaluate the actual shear crack behavior.

2 OVERVIEW OF TEST AND ANALYSIS

2.1 Test Specimens and Analytical Models

The details of the test specimen and the finite element model are shown in Fig. 1. The specifications of the specimens are summarized in Table 1. Flexure-shear tests were performed on RC columns that were laterally prestressed (LPRC) and not prestressed (RC), respectively. The test specimens have a square cross section of 340 mm x 340 mm and a height of 900 mm. The specimens were designed to reach shear failure before the longitudinal reinforcements yield, in accordance with design guidelines of the Architectural Institute of Japan [1999]. For this reason, high strength steel bars (D22 in Fig. 1,

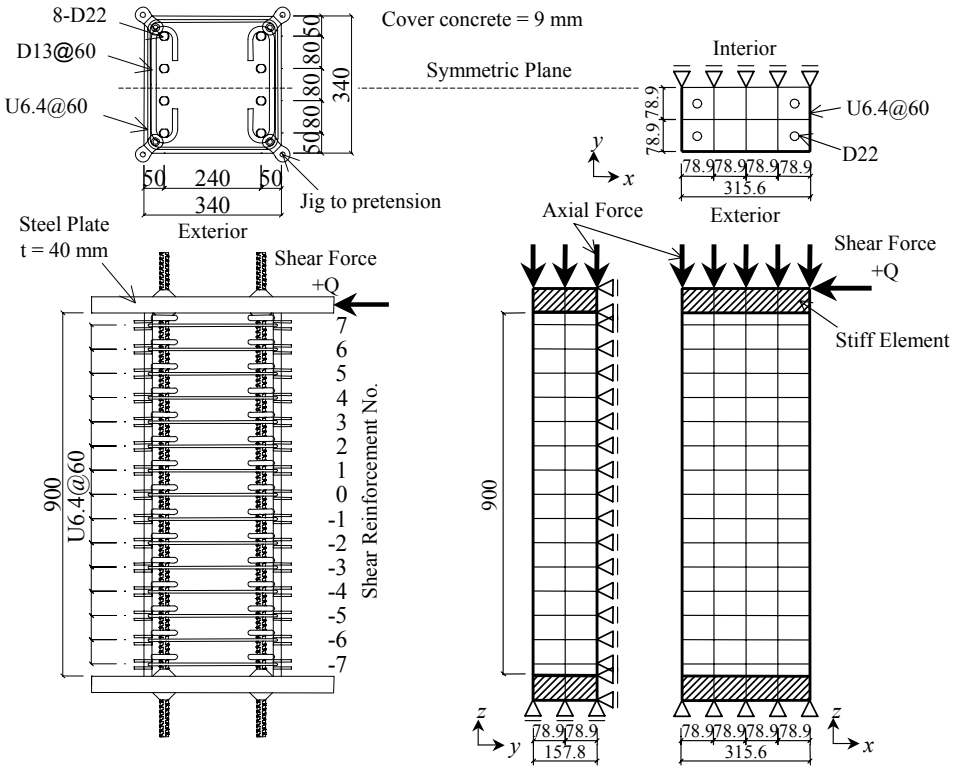

Figure 1. Details of test specimen and finite element model

σ_y=1196 N/mm^2) was used for the longitudinal reinforcements. Moreover, an additional reinforcement (D13 in Fig. 1) was arranged to prevent columns from splitting by bond failure. The lateral prestress was introduced into concrete as follows: (1) the high strength transverse hoops (U6.4 in Fig. 1) were pretensioned to approximately 40% of the yield stress using the rigid steel molds and special jigs shown in Fig. 1, (2) concrete was placed vertically into the molds and cured until the strength of the concrete increased sufficiently, (3) the core concrete was laterally prestressed by removing the steel molds. The product of the ratio (p_w) and the stress (σ_{wp}) of the pretensioned transverse reinforcements is defined as the average lateral prestress σ_L (=$p_w\sigma_{wp}$) to indicate the intensity of lateral prestress. The mix proportion of concrete used in the test specimens is given in Table 2. The coarse aggregate used in the mix is natural round sea gravel with a maximum aggregate size of 25 mm. The mechanical properties of the concrete and reinforcements are shown in Figs 2 and 3, together with their idealizations in FEM analysis.

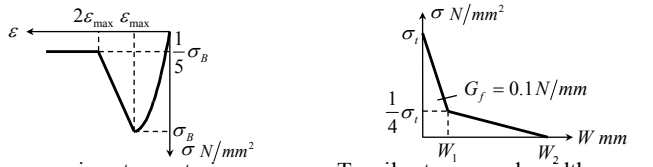

Compressive stress-strain curve Tensile stress-crack width curve

Test series	σ_B N/mm^2	ε_{max}	E_c N/mm^2	σ_t N/mm^2	W_1 mm	W_2 mm	ν
RC	50.8	-0.002	3.51E+4	2.9	0.031	0.15	0.2
LPRC	46.5	-0.002	3.45E+4	2.9	0.031	0.15	0.2

E_c: secant modulus at 1/3σ_B, ν: Poisson's ratio

Figure 2. Mechanical properties and analytical models for

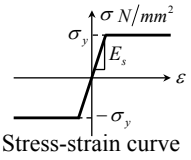

Stress-strain curve

Type	σ_y N/mm^2	σ_{max} N/mm^2	E_s N/mm^2
D22	1196	1281	1.92E+5
U6.4	1459	1499	2.04E+5
D13	344	488	1.92E+5

Figure 3. Mechanical properties and analytical model for

Table 1. List of test specimens

Test Series	b=D mm	M/QD	p_w %	σ_0/σ_B	σ_{wp} N/mm^2	σ_L N/mm^2
RC	340	1.3	0.29	0.30	0	0.0
LPRC					536	1.6

b and D: width and depth of column, M/QD: shear span-depth ratio, p_w: ratio of transverse hoop, σ_0: axial stress of column, σ_B: compressive strength of concrete, σ_{wp}: prestress introduced in transverse hoop

Table 2. Mix Proportion

Proportion, by weight			
Cement	Sand	Coarse Aggregate	Water
1	2.04	2.53	0.50

Maximum aggregate size: 25 mm
Admixture: Super plasticizer

2.2 Loading and Measuring Methods in Tests

The loading apparatus is shown in Fig. 4. The vertical force on the test specimen was supplied by a 2 MN hydraulic jack, and the ratio of axial load to axial strength was maintained constant at 0.3 during

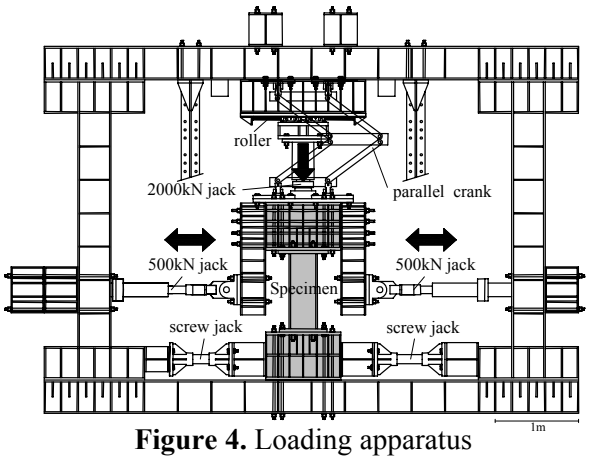

Figure 4. Loading apparatus

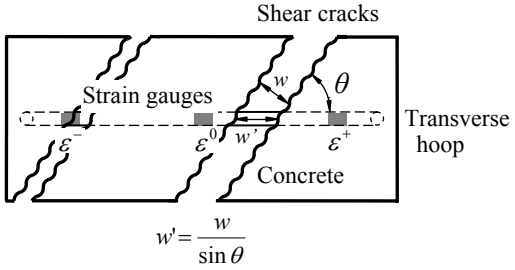

Figure 5. Definition of crack width and designations of strain gauges

the test. The horizontal force was supplied by two hydraulic jacks having a capacity of 500 kN and was controlled in displacement. The cyclic horizontal load was applied so as to produce an antisymmetric moment in a column. The horizontal load was reduced when the rotation angle of a column, R, reached ±1/400, ±1/200, ±1/100, ±1/67, and ±1/50, until reaching the peak load. The width of each shear crack near the shear reinforcement was measured using two digital microscopes with a resolution of 0.01 mm three times for each loading cycle and twice for each unloading cycle. The crack width used in the present study is defined as the distance normal to the direction of the crack, as illustrated in Fig. 5. Three strain gauges, the locations and designations of which are also shown in Fig. 5, were attached to each leg of all transverse hoops.

3 RESULTS AND DISCUSSIONS

3.1 Shear Load-Rotation Angle Curves and Shear Strength

The shear load Q-rotation angle R curves obtained from the tests are shown in Fig. 6, compared with the results of FEM analysis. For the typical crack behavior observed during tests, flexural cracks first appeared and then extended to flexural shear cracks near both ends of the specimen. Finally, shear cracks occurred with increasing shear load. The maximum shear loads for RC and LPRC columns are 617 kN when R = 1/100 and 762 kN when R = 1/67, respectively. The shear loads for both RC and LPRC were gradually reduced without any reinforcement yielding due to concrete being crushed in the compressive zone at the top and bottom ends. The shear crack strength and ultimate shear strength obtained from experiments and FEM analyses are presented in Table 3 together with the calculation results reported by Watanabe [2004] that take into account the lateral prestress. The shear crack strength of analysis is defined as the shear load, which causes the strain in the shear reinforcements to increase rapidly. As shown in Table 3, both FEM analysis and the calculation can predict with a fair degree of precision the difference between the shear strengths of the RC and LPRC columns.

The relationships between shear crack stress ${}_{exp}\tau_{sc}(={}_{exp}Q_{sc}/bD)$ and lateral prestress, and between ultimate shear stress ${}_{exp}\tau_{su}(={}_{exp}Q_{su}/bD)$ and lateral prestress are plotted in Fig. 7 together with

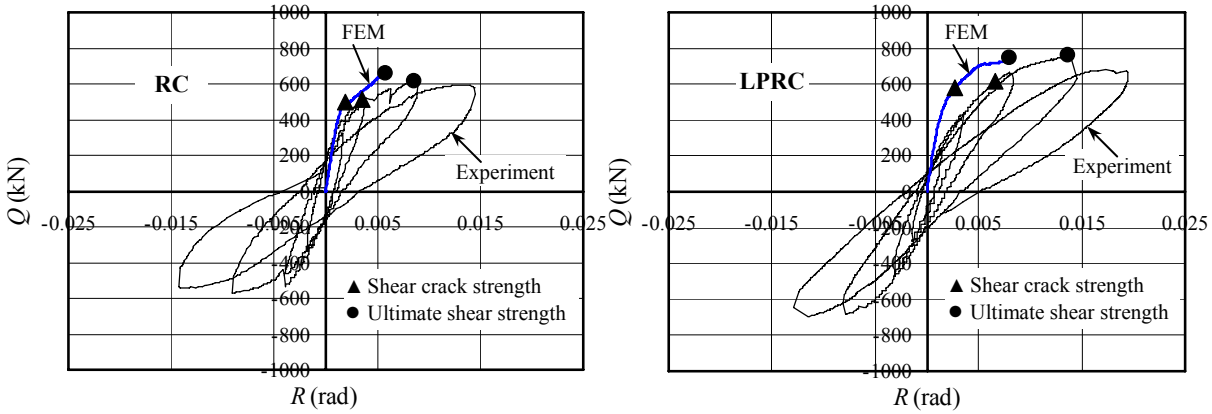

Figure 6. Comparisons between analytical and experimental Q-R curves for RC (left) and LPRC (right)

Table 3. Shear crack strength and ultimate shear strength

Test Designation	${}_{exp}Q_{sc}$ (kN)	${}_{exp}Q_{su}$ (kN)	${}_{FEM}Q_{sc}$ (kN)	${}_{FEM}Q_{su}$ (kN)	${}_{cal}Q_{sc}$ (kN)	${}_{cal}Q_{su}$ (kN)
RC	515	617	495	655	496	648
LPRC	611	762	577	747	606	725

${}_{exp}Q_{sc}$ =shear crack strength by experiment, ${}_{exp}Q_{su}$ =ultimate shear strength by experiment
${}_{FEM}Q_{sc}$ =shear crack strength by FEM, ${}_{FEM}Q_{su}$ =ultimate shear strength by FEM

Watanabe's data [2004] marked in solid white (σ_B = 35 N/mm^2). The difference in strength of concrete was adjusted by dividing them by the characteristic strength to determine their failure modes. Figure 7 shows that the shear crack strength and ultimate shear strength have increased in proportion to the increasing lateral prestress. Furthermore, Fig. 8 shows a comparison of the shear strengths obtained experimentally and analytically. The predictions of FEM analysis are consistent with all existing experimental data for the shear crack strength and the ultimate shear strength.

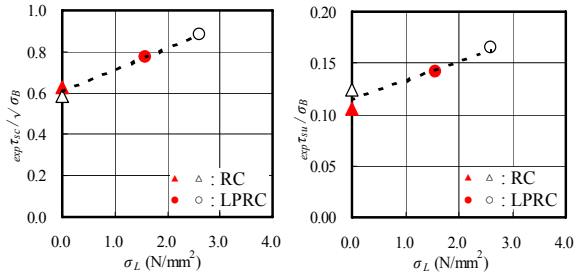

(1) Shear crack strength (2) Ultimate shear strength

Figure 7. Increase in strength with increasing lateral prestress σ_L

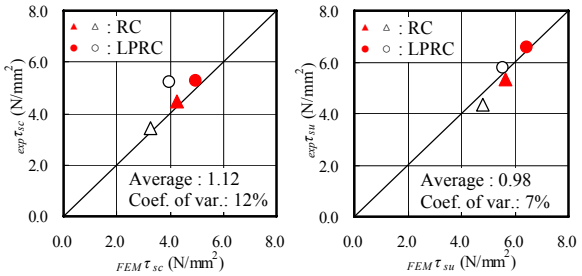

(1) Shear crack strength (2) Ultimate shear strength

Figure 8. Comparison of strength from experiment and FEM analysis

3.2 Comparison of Shear Crack Patterns, Strains in Shear Reinforcement, and FEM analysis

Figure 9 shows a comparison of the propagations of shear cracks in the front of RC and LPRC specimens when the rotation angle is 1/200, 1/100, and 1/67. The crack patterns in the front and back of specimens were essentially similar. The contours of the crack strain obtained by analyses and the diagrams of shear cracks observed experimentally are shown in Fig. 10. The lateral confinement in the LPRC specimen greatly restrained the shear cracks from propagating at a shear load similar to the peak load of the RC specimen, and the final crack pattern of the LPRC differed drastically from that of the RC. Shear cracks developed scatteringly in the upper and lower sides of the LPRC specimen, whereas they developed intensively in the center of the RC specimen. The spacing and width of the scattered cracks in the LPRC specimen are smaller than those of the localized cracks in the RC specimen. Since the ability to transmit shear force across a rough crack is exponentially reduced with increasing crack width [Shinohara *et al*. 1999], a scattered crack with a smaller width can reduce to some extent the decrease in shear stiffness of a column. This small crack spacing that developed in the LPRC specimen is probably due to an increase in bond strength [Braam 1990] and to the tensile stress generated by introducing lateral prestress. FEM analysis using the smeared crack model cannot evaluate an individual crack but can assess the difference in crack patterns between the RC and LPRC specimens. Figure 11 shows the distribution of strains in the shear reinforcement at the maximum shear loads obtained from experiments and analyses to discuss the relationship between the shear crack patterns and the strains in transverse hoops. As shown by Figs 10 and 11, the strain increment in

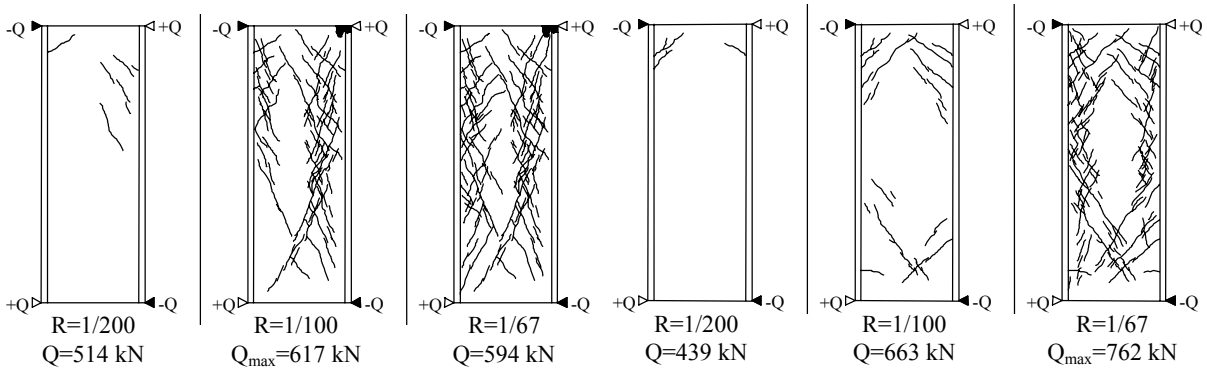

(1) RC specimen (2) LPRC specimen

Figure 9. Comparison of shear crack propagations in front of RC and LPRC specimens

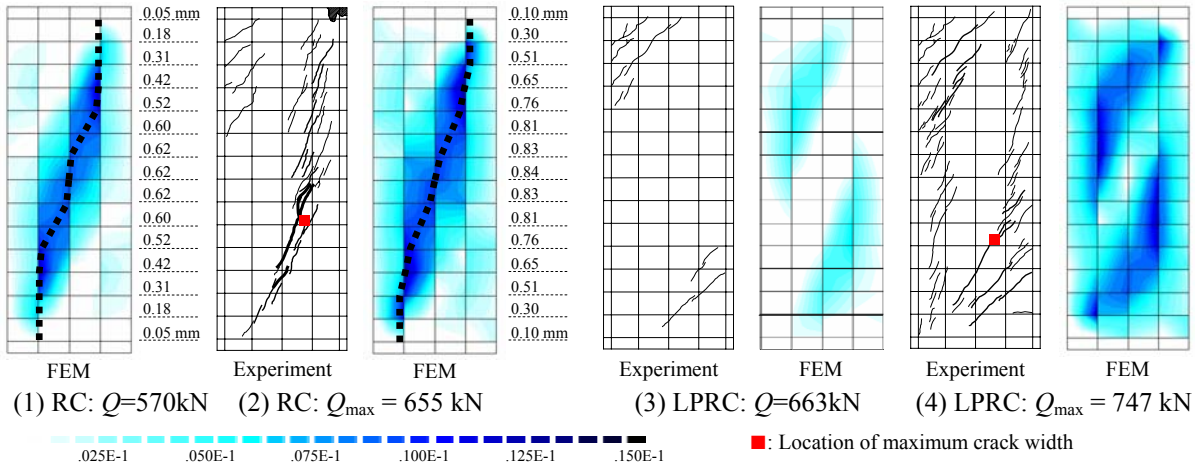

Figure 10. Comparisons between crack pattern from experiment and crack strain from FEM analysis

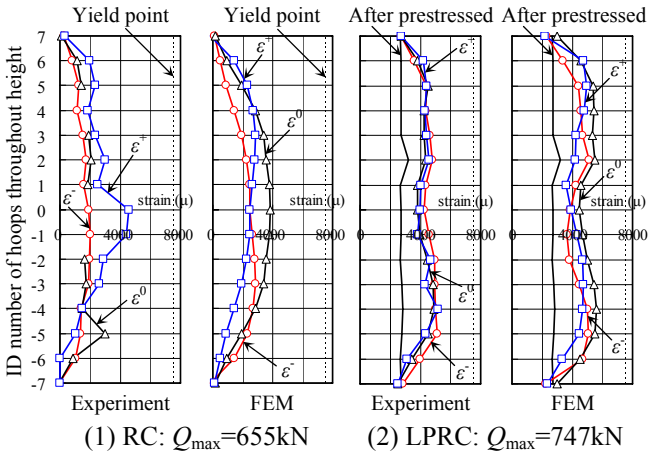

Figure 11. Comparisons between strain distribution of shear reinforcement by experiment and analysis

the shear reinforcement is roughly consistent with the width of shear cracks. In the case of the RC experiment, since the shear cracks localized and deviated to the right around mid-height, the corresponding strain ε^+ was highest, and the three strains of gauges attached at each reinforcement differed from ε^- by a maximum of 2,700 μ. In the case of the LPRC experiment, on the other hand, since the shear cracks did not localize and were scattered over the depth of the column, the differences among three strains on each reinforcement were within 800 μ. The strain distributions obtained by analysis for the RC specimen are anti-symmetric with respect to half height and do not fully correspond with those obtained experimentally because of localized shear cracks, whereas the analytical result for the LPRC shows good agreement with the experimental result, including the shape of the vertical distribution showing higher strains in the upper and lower sides due to the existence of numerous distributed shear cracks.

The relationship between the width of shear cracks and the elongation of shear reinforcements is shown in Fig. 12, where the total crack widths over a reinforcement observed by microscope, $\Sigma_{exp}w$' (see Fig. 5), are plotted as the abscissa and the elongations of the corresponding reinforcement calculated using the strains, $\Sigma_{cal}w$, are plotted as the ordinate. The elongation, $\Sigma_{cal}w$ in Fig. 12(1) is calculated using only one strain at the center, and $\Sigma_{cal}w$ in Fig. 12(2) is calculated using all three strains. If shear cracks are scattered over shear reinforcements, as in the LPRC specimen, the total crack widths, $\Sigma_{exp}w$', can be estimated fairly accurately by one strain of the reinforcement. In the case of localized shear cracks, as in the RC specimen, a better estimate of $\Sigma_{exp}w$' can be obtained by integrating the strain distribution of the three gauges. In addition, the estimated crack width, $\Sigma_{cal}w$, is

over 20% larger than the observed crack width, $\Sigma_{exp}w$', because the tensile strain of concrete between cracks was neglected and micro cracks might have been overlooked.

In order to investigate how accurately the FEM analysis with a smeared crack model can evaluate the extent of actual shear crack damage, the total crack width by FEM analysis, $\Sigma_{FEM}w$, which is estimated from the nodal displacements at both ends of a shear reinforcement by neglecting the strains of concrete, is shown in Fig. 13 together with $\Sigma_{exp}w$' observed by microscope and $\Sigma_{cal}w$ obtained by the strains in hoops. Although $\Sigma_{exp}w$' is observed on the surface of concrete, while $\Sigma_{cal}w$ and $\Sigma_{FEM}w$ are estimated by a reinforcement, these three crack widths exhibit broadly similar behavior due to the small concrete covering of 9 mm (see Fig. 1). The difference between the crack width behaviors of the RC and LPRC specimen is basically consistent with that of shear crack behaviors shown in Fig. 10 and strain behaviors of shear reinforcement shown in Fig. 11 because the total crack width faithfully reflects their behaviors. In particular, the experimental and analytical crack widths, $\Sigma_{cal}w$ and $\Sigma_{FEM}w$, behave in a similar manner. Comparison among the three crack widths indicates that most of the apparent Poisson's ratio is due to the shear cracks. Moreover, FEM analyses using the smeared crack model cannot accurately evaluate a localized crack but can provide valuable information about the total damage in the overall depth of a specimen.

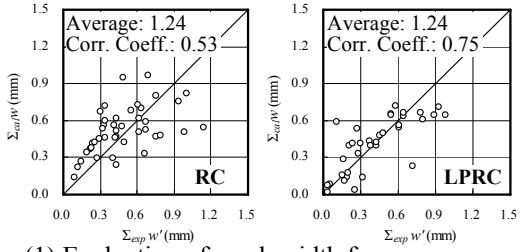

(1) Evaluation of crack width from one gauge

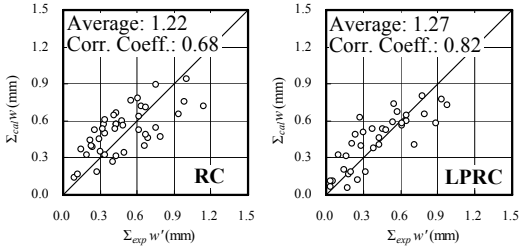

(2) Evaluation of crack width from three gauges

Figure 12. Relations between shear crack width and strain of shear reinforcement

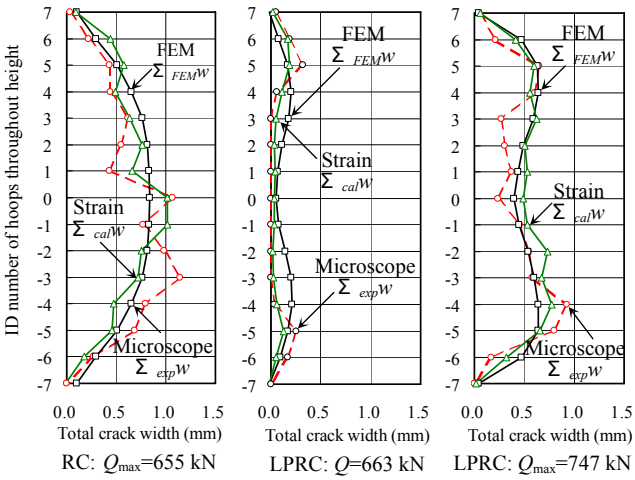

Figure 13. Total crack width obtained by microscope, strain of hoop, and FEM analysis

3.3 Shear Crack Width at Peak Load and Unloading, and Hysteresis

Figure 14 shows the relationship between the width of a shear crack at peak load ($_{exp}w_p$) and that at unloading ($_{exp}w_r$) in front of and behind specimens when the rotation angle is 1/100 cycle for the RC specimen, and 1/100 cycle and 1/67 cycle for the LPRC specimen. The individual crack width of the LPRC specimen is less than that of the RC specimen because numerous scattering cracks developed over the depth of the column, as shown in Figs 9 and 10. In addition, the average ratio of $_{exp}w_r$ to $_{exp}w_p$ in the LPRC specimen is smaller than that in the RC specimen. Specifically, the residual width of a shear crack in the LPRC specimen is reduced considerably compared to that in the RC specimen. The relationship between the shear load and the maximum crack width marked by ■ in Fig. 10 is plotted in Fig. 15 for both surfaces. As for the RC specimen, the crack width increases rapidly immediately after cracking and exceeds 1 mm at the maximum load. The increase in shear load is only 100 kN after cracking. As for the LPRC specimen, the shear load increases by 150 kN after cracking, and the crack width is less than 0.5 mm at peak load and 0.2 mm when unloaded. The transverse prestressing reduces the width values of shear cracks, especially their residual opening, and increases shear

stiffness after shear cracking. Consequently, this prestressing improves durability as well as earthquake resistance for RC structures.

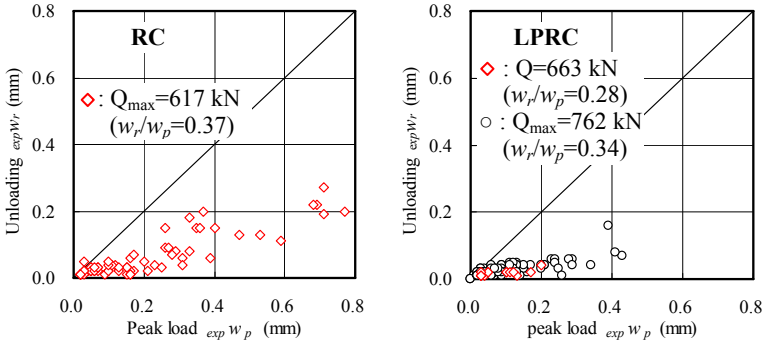

Figure 14. Relationships between crack width at peak load and crack width at unloading

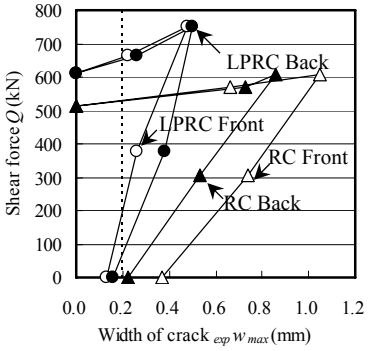

Figure 15. Relationships between shear force and naximum crack

3.4 Compression Strut based on Minor Principal Stress Distribution

Figure 16 shows the distributions of the minor principal stress in the center of the RC and LPRC specimens obtained by FEM analysis [Shinohara *et al*. 2005]. For the RC specimen, the compressive strut formed by a large compressive stress is clearly revealed at a shear load of 550 kN. The width of the strut then reduces slightly and localizes in a diagonal direction at the maximum load. For the LPRC specimen, on the other hand, the compressive strut appears at a shear load similar to the maximum load of the RC, and the width of the strut increases gradually up to the maximum load. As a result, the ultimate shear strength becomes higher. This difference is probably due to the crack patterns of the RC and LPRC specimens described previously.

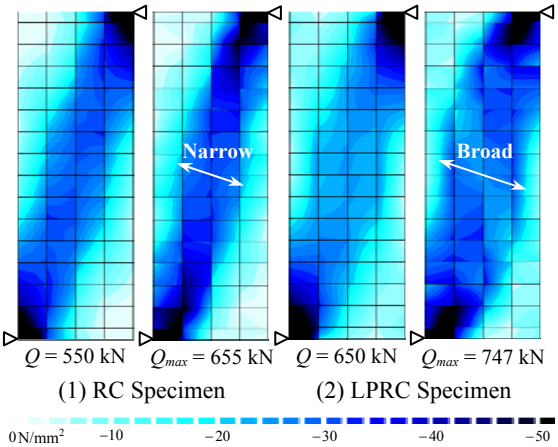

Figure 16. Compression strut based on minor principal stress distribution

4 CONCLUSIONS

The following conclusions are obtained from experiments and 3-D FEM analyses performed on reinforced concrete columns prestressed laterally to investigate the effect of the active confinement on the shear strength and crack behaviors.

1) The shear crack strength and ultimate shear strength have increased proportionally with increasing lateral pressure.
2) The shear crack patterns have changed appreciably, and the spacing and width of cracks have decreased drastically by introducing lateral prestress into a RC column.

3) The close relationship between the width of shear cracks and the distributed strain in reinforcements has been proven both experimentally and by FEM analyses.
4) The transverse prestressing reduces the width values of shear cracks, especially their residual opening after shear cracking, improving durability as well as earthquake resistance.

REFERENCES

Watanabe, H. *et al*. 2004, 'Shear crack control by lateral prestress on reinforced concrete column andevaluation of shear strength', *J. Struct. Const. Eng.*, AIJ, [577], pp.109-116. (in Japanese)

Architectural Institute of Japan 1999, Design Guidelines for Earthquake Resistant Reinforced Concrete Buildings Based on Inelastic Displacement Concept, AIJ. (in Japanese)

Shinohara, Y. and Kaneko, M. 1999, 'Compressive shear behavior in fracture process zone of concrete', *Journal of Structural and Construction Engineering*, AIJ, [525], pp.1-6. (in Japanese)

Braam, C. R. 1990, 'Control of Crack Width in Deep Reinforced Concrete Beams', *HERON*, **35**[4], pp.3-105.

Shinohara, Y. *et al*. 2005, 'Active confining effect and shear crack behavior for R/C columns prestressed laterally', *J. Struct. Const. Eng.*, AIJ, [587], pp.147-153. (in Japanese)

Durability Properties of Geopolymer Mortars

David W Law [1]
Andi A Adam [2]
Tom K Molyneaux [3]
Indubhushan Patnaikuni [4]

T 11

ABSTRACT

Environmental concerns related to the production of cement in terms of energy consumption and emission of CO_2 are driving the search for more sustainable alternatives. One possible alternative is to use industrial by-products as the binder. At present both fly ash and slag are frequently used as cement replacement materials. Both of these materials provide a more sustainable alternative to concrete and have been shown to increase durability in aggressive environments. Recent research has shown that it is possible to use fly ash or slag as a sole binder by activating them with an alkali component. The development of these materials is still at the early stages, with little knowledge about the long term performance of the materials.

This paper reports the early age durability characteristics of three geoplymer mortars. It reports the compressive strength, resistivity and ultrasonic pulse velocity data at 28, 90 and 150 days, together with the results of sulphate exposure test.

KEYWORDS

Geopolymer, Ultrasonic pulse velocity, Resistivity, Sulphate

[1] RMIT University, School of Civil and Chemical Eng, Melbourne, Australia, Phone +61 3 99253824, Fax +61 3 96390138, david.law@rmit.edu.au
[2] RMIT University, School of Civil and Chemical Eng, Melbourne, Australia, Phone +61 3 99255287, Fax +61 3 96390138, andi.adam@student.rmit.edu.au
[3] RMIT University, School of Civil and Chemical Eng, Melbourne, Australia, Phone +61 3 99253232, Fax +61 3 96390138, tom.molyneaux@rmit.edu.au
[4] RMIT University, School of Civil and Chemical Eng, Melbourne, Australia, Phone +61 3 99252197, Fax +61 3 96390138, patnaikuni@rmit.edu.au

1 INTRODUCTION

Environmental concerns related to the production of cement in terms of energy consumption and emission of CO_2 has led to the search for more environmentally viable alternatives. One of these alternative materials is the use of alkali-activated binder using industrial by-products containing silicate materials. The most common industrial by-products used as binder materials are fly ash (FA) and blast furnace slag. Slag has been used as cement replacement material due to the latent hydraulic properties, while fly ash has been used as pozzolanic material to enhance physical, chemical and mechanical properties of cements and concretes. However, research has indicated that a limit of 70% for slag and 40% for fly ash can be used to replace Portland cement while maintaining acceptable strength and durability (Neville 1996). The utilisation of large proportion of by-products would contribute to the elimination of an environmental problem and to the development of potentially new high-performance material (Puertas 2000).

Recent research has shown that it is possible to use fly ash or slag as a sole binder in mortar by activating them with an alkali component (Adam et al. 2007a; Adam et al. 2007b). There are two models of alkali activation of fly ash/slag, Activation by low to mild alkali of a material containing essentially silicate and calcium will produce calcium silicate hydrate (C-S-H) with low C/S ratio (Bakharev and Patnaikuni 1997). On the other hand, the activation of material containing mostly silicate and aluminates by a highly alkaline solution will form an inorganic binder through a polymerization process (Palomo et al. 1999). In 1979 Davidovits defined this second model as geopolymer (Davidovits 1991).

2 FLY ASH BASED GEOPOLYMER

The reaction mechanism of geopolymer can be described in two steps (Buchwald and Schulz 2005):

1. *Activation*. The alkaline pore solution disintegrates the solid network to produce reactive silicate and aluminate species with low molecular weights. The activation of the solid is achieved with alkaline solutions containing alkali hydroxides, alkali silicates and/or alkali carbonates.
2. *The setting reaction*. Pure alumino-silicate materials, e.g., metakaolin and some types of fly ash, set by a condensation reaction which leads to the formation of alumino-silicate polymers.

The later reaction differentiates geopolymer from other types of alkali activated materials (such as: alkali activated slag) since the product is a polymer rather than C-S-H.

The best known material for producing geopolymer is metakaolin, however due to the limitation on the quantity available it is not suitable as a concrete binder, this has resulted in the substitution of metakaolin with other aluminosilicate materials such as, fly ash and rice husk ash.

To study the strength and durability of fly ash based geopolymer mortars, three different mixes were prepared with fly ash activated by a different weight ratio of sodium oxide in activator to fly ash (Na_2O to FA ratio). The compressive strength, ultrasonic pulse velocity, and resistivity were examined together with the sulphate resistance of the specimens

3 MATERIALS

3.1 Cementitious material

Fly ash, from Gladstone quarry, was provided by Cement Australia Ltd. Chemical analysis of the material is given in Table 1.

Table 1. Oxide composition of the fly ash (mass %)

Oxide	SiO_2	Al_2O_3	Fe_2O_3	CaO	MgO	K_2O	Na_2O	TiO_2	P_2O_5	Mn_2O_3	SO_3	S^{2-}	Cl
Mass %	49.45	29.61	10.72	3.47	1.3	0.54	0.31	1.76	0.53	0.17	0.27	0.21	0.001

3.2. Activator

The activator used in this study was a sodium silicate based solution which means that the activator contained sodium silicate and sodium hydroxide. Grade D sodium silicate solution (Na_2O = 14.7% and SiO_2 = 29.4%) was supplied by PQ Australia. Sodium hydroxide solution (NaOH) was prepared by dissolving sodium hydroxide pellets with deionised water at least 1 day prior to mixing.

4 MIX PROPORTIONS AND TESTING SPECIMENS

Three different mass ratio of Na_2O in activator to fly ash (Na_2O to FA ratio) were used (i.e. 7.5%, 10%, and 15%). Alkali modulus in activator, which is defined as AM = $[(SiO_2)/(Na_2O)]$ was fixed to 1.25.

Water to solid ratio of 0.37 was used to prepare all the fly ash based geopolymer mortars. The amount of water in the mix was the sum of the water contained in the sodium silicate, sodium hydroxide and the added water, while the amount of solid was the sum of the weight of fly ash, and the solid contained in the activator solution. The sand-cementitious binder ratio was 2.75:1. Table 2 summarizes the composition of the mortar specimens.

Table 2. Details of the mixes (1 liter)

Mortar		*Fly ash (gram)*	*Activator*		*Sand (gram)*	*Added water (gram)*
ID	*Na_2O to FA ratio*		*NaOH 15M (gram)*	*Na_2SiO_3 (gram)*		
Mix1	7.5%	523	46	167	1438	108
Mix2	10%	514	60	218	1412	78
Mix3	15%	496	87	316	136	20

The mixing was performed using a 5-liter Hobart mixer, the mix was then poured into the moulds and vibrated for 1 minute. The structural integrity of the geopolymer specimens left at room temperature was not sufficient to allow the specimens to be demoulded until three days had elapsed, therefore a heat curing regime was applied. After leaving for 24 hours at room temperature, the specimens were wrapped with cling-film and left in the oven for 24 hours at 80ºC. The specimens were then allowed to cool in the mould at room temperature before they were demoulded. Following demoulding, the specimens were left at room temperature until testing.

Compressive strength measurements of 50 mm cube mortars were performed on an MTS machine under a load control regime with a loading rate of 20 MPa/min. Three to five cubes were tested for each data point.

The ultrasonic measurement is conducted on 170x50x50 mm specimens using a portable ultrasonic non-destructive digital indicating tester (Pundit Plus) with a 54 kHz transducer. The resistivity was measured using Wenner probe by the four-point method at 50 mm spacing. All tests were conducted at 28, 90, and 150 days after casting. While the sulphate exposure was conducted by immersing Φ50mm x100 mm cylinders in 4.4% Na_2SO_4 solution, the mass change was measured every 2 weeks up to 12 weeks.

5 RESULTS AND DISCUSSIONS

5.1 Effect of Na_2O to FA ratio on strength

Figure 1 indicates that an increase in the Na_2O to FA ratio resulted in a significant increase in the compressive strength. Increasing the Na_2O to FA ratio means an increase in both alkali content and soluble silicates and consequently an increase in the reaction rate (a higher concentration of reactants induces a higher reaction rate). In geopolymer mortar, alkali hydroxide is needed to dissolve silicate and aluminate monomer from the fly ash grain. A small increase in strength, with age, was observed at the lowest Na_2O to FA ratio (7.5%). At higher concentrations, the strength remained constant with time.

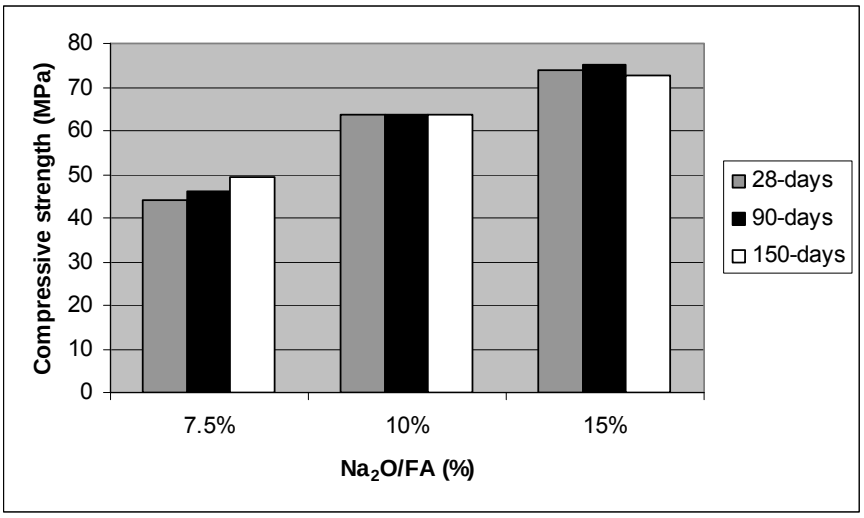

Figure 1. Strength of geopolymer mortars with different Na_2O to FA ratio

5.2. Effect of Na_2O to FA ratio on ultrasonic pulse velocity

The effect of the Na_2O to FA ratio on the ultrasonic pulse velocities is shown in Fig. 2. It was found that mixtures with a higher percentage of Na_2O in the activator had higher values of the UPV. Since the ultrasonic pulse will propagate more easily through the solid phase than that of empty space, the higher UPV would indicate a higher solid volume fraction/density and a lower porosity of the specimens.

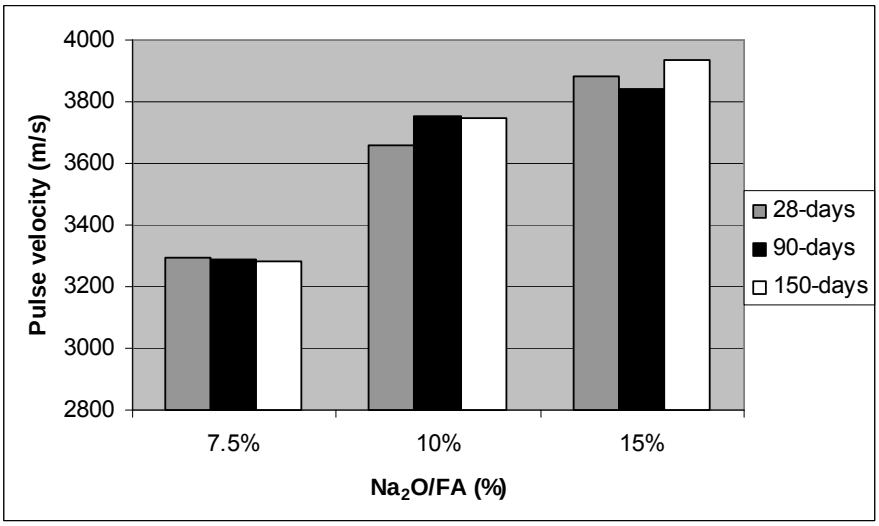

Figure 2. UPV of fly ash based geopolymer mortars with different Na_2O to FA ratio

There was a strong relationship between strength and UPV of geopolymer mortars, as can be seen from Fig. 3. By regression analysis using Microsoft excel the relationship may be described as :

$$\mathbf{f_c} = 3.9556e^{0.0007V} \quad (1)$$

Where f_c = compressive strength of the mortar (MPa)
V = pulse velocity (m/s)

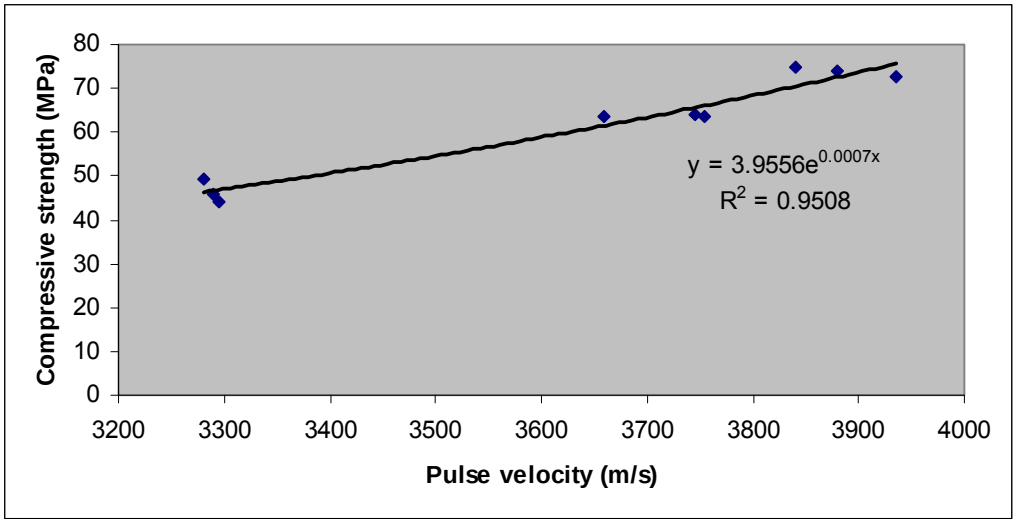

Figure 3. Relationship between UPV and Strength of geopolymer mortars

5.3. Effect of Na_2O to FA ratio on sulphate resistance

The deterioration of concrete from sulphate attack is due to the formation of ettringite and gypsum, caused by the sulphate reacting with the C_3A and lime in the cement (Neville, 1996). Both the gypsum and ettringite form expansive products which are less structurally stable than the cement matrix. Both the fly ash and slag have reduced C_3A content compared to OP cement and as such would be expected to be more resistant to sulphate attack. The density of the material will also influence the sulphate resistance, with the higher density giving a greater resistance.

The change in mass for the geopolymer specimens are given in Fig. 4. The data shows that the 7.5% and 10% Na_2O follow a similar trend, with an initial fall in mass followed by a slight rise. The 15% Na_2O shows an initial rise, followed by a fall and then a further rise. All variations are within 1.5% of the initial mass and may be a function of the handling a weighing procedure.

None of the specimens displayed any visual sign of deterioration, Fig. 5, although a slight discolouration due to crystallisation on the surface of the mortars was observed. There was no cracking of the specimens or an indication of ettringite or gypsum products.

Overall there is no indication, to date, of any variations in the performance of the specimens. All are displaying a good level of resistance to sulphate attack.

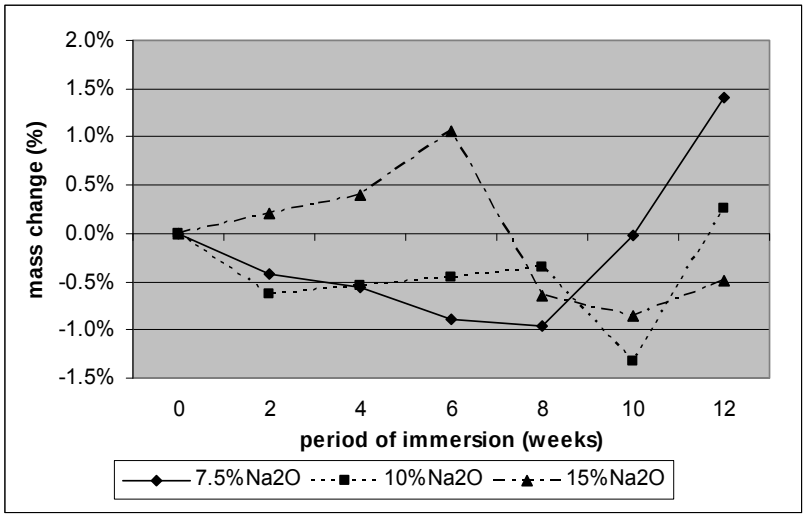

Figure 4. Mass change of fly ash based geopolymer mortars with different Na_2O to FA ratio after several periods of immersion

Figure 5. Geopolymer mortars with different Na_2O to FA ratio after 12 weeks of immersion

5.4 Effect of Na_2O to FA ratio on resistivity

The resistivity of concrete is one of the parameters used to assess the likelihood of corrosion of steel in concrete, Table 3, although the value can only be used if half-cell potential measurement shows that corrosion is probable (Bungey et al. 2006).

As can be seen from Table 4, the resistivity of geopolymer mortar exposed to laboratory environment was very high (more than 100 kΩ cm) at 90 & 150-days for all mixes. However, the value was very low when the specimens were saturated. This condition is attributed to the high amount of hydroxyl ion in the pore solution of geopolymer mortar, which in the presence of moisture leads to a high conductivity, and hence a low resistivity. When the specimens are dry, the hydroxyl ions are not able to move in the pore solution and hence a low conductivity and high resistivity is observed.

This finding is similar to that of Portland cement mortar, Fig. 5, since the average relative humidity in the lab was 40%. Contrary to the resistivity measurements of saturated specimens at 180-days, the 28-

day tests showed that the resistivity decreased as the ratio of Na_2O to FA increased. The higher ratio of Na_2O to FA increased the density of geopolymer mortar, thus slowed the rate of drying.

Table 3. Interpretation of resistivity measurement (Bungey et al. 2006)

Resistivity (kΩ.cm)	*Likelihood of significant corrosion when steel activated (for non-saturated concrete)*
< 5	Very high
5 – 10	High
10 – 20	Low/moderate
> 20	Low

Table 4. Resistivity of geopolymer mortars with different Na_2O to FA ratio and ages

Mix	*Resistivity (kΩ cm)*			
	Laboratory environment (air dry)			*180-days saturated*
	28-days	*90-days*	*150-days*	
7.5%Na_2O	>100*	>100*	>100*	8
10%Na_2O	71	>100*	>100*	8.9
15%Na_2O	43	>100*	>100*	15

*the equipment can only measure up to 99 kΩ cm

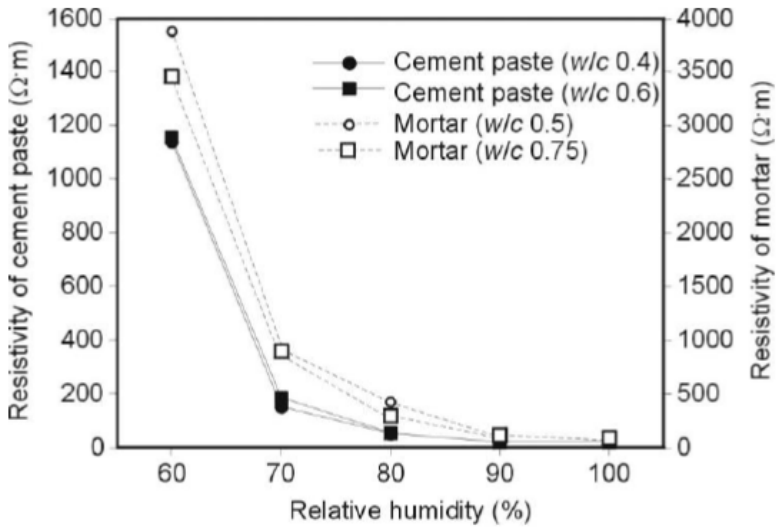

Figure 5. Dependence of resistivity of cement paste and mortar on water/cement ratio and relative humidity of the environment (Bertolini et al. 2004)

CONCLUSIONS

- The Na_2O to FA ratio has significant influence on the strength of fly ash based geopolymer mortars.
- Strength development with age was only observed on lower concentration of activator, while at higher concentration, no further strength development was observed after 28 days

- The ultrasonic pulse velocity was influenced by Na_2O to FA ratio, the mixtures with a higher Na_2O to FA ratio had higher values of the UPV which is related to the density of the mortar
- There is a strong relationships between strength and UPV for geopolymer mortar
- The Na_2O to FA ratio exhibits no observable effect on the sulphate resistance to date, with all specimens showing good resistance to sulphate attack.
- The resistivity of geopolymer mortar depends on the density and the pore-water composition which is related to the Na_2O to FA ratio
- The moisture content of mortar and the humidity of the environment also affected the resistivity of the geoplymer mortar

ACKNOWLEDGEMENT

The authors wish to acknowledge Independent Cement & Lime Ltd., Cement Australia Ltd., and PQ Australia Ltd. for providing the raw materials for the research. The authors also wish to acknowledge the work of three undergraduate project students, Kerry Walton, Laurence Harrison and Clinton Hare.

REFERENCES

Adam, A. A., Molyneaux, T. C. K., Patnaikuni, I., and Law, D. 2007, 'Strength of Mortar Containing Activated Slag' Proc. 4th International Structural Engineering and Construction (ISEC-4) Conf., RMIT University, Melbourne, Australia, 26 – 28 September, vol. 1, pp. 505 - 508.

Adam, A. A., Patnaikuni, I., Law, D. W., and Molyneaux, T. C. K. 2007, 'Strength of Mortar Containing Activated Slag and Fly Ash' Proc. Concrete 07 Conf., the Concrete Institute of Australia, Adelaide, Australia, 18 – 20 October 2007, pp. 353 – 359

Bakharev, T., and Patnaikuni, I. 'Microstructure and durability of alkali activated cementitious pastes' Proc. 5th International Conference on Structural Failure, Durability and Retrofitting, the Singapore Concrete Institute, Singapore, 27 – 28 November 1997, pp.200 – 209

Bertolini, L., Elsener, B., Pedeferri, P., and Polder, R. 2004. *Corrosion of Steel in Concrete: Prevention, Diagnosis, Repair*, Wiley-VCH Verlag GmbH & Co. KGaA,, Weinheim.

Buchwald, A., and Schulz, M. 2005. 'Alkali-activated binders by use of industrial by-products' *Cement and Concrete Research*, **35**(5), 968-973.

Bungey, J. H., Millard, S. G., and Grantham, M. G. 2006. *Testing of Concrete in Structures*, Taylor & Francis, Oxon

Davidovits, J. 1991. 'Geopolymers: Inorganic Polymeric Materials' *Journal of Thermal Analysis*, **37**, 1633-1656.

Neville, A. M. 1996. *Properties of concrete*, Wiley and Sons, Inc., New York.

Palomo, A., Grutzeck, M. W., and Blanco, M. T. 1999. 'Alkali-activated fly ashes: A cement for the future, *Cement and Concrete Research*, **29**(8), 1323-1329.

Puertas, F., Martinez-Ramirez, S., Alonso, S., and Vazquez, T. 2000. 'Alkali-activated fly ash/slag cements: Strength behaviour and hydration products' *Cement and Concrete Research*, **30**(10), 1625-1632.

Concrete Mix Proportions with Ultra-High Electrical Resistivity

Mohammad Shekarchizadeh [1]
Mohammad Tahersima [1]
Amir Hajibabaee [1]
Hamed Layssi [1]

T 11

ABSTRACT

Durability is the ability of concrete to withstand any deterioration process during its service life. Different concretes require different degrees of durability depending on the exposure environment and properties desired. The long-time behavior of concrete structures has shown that their main cause of distress is reinforcement corrosion. This type of damage is responsible for the huge financial cost spent each year on the repair of deteriorated structures.

The electrical resistivity of concrete is one of the main parameters controlling the initiation and propagation of reinforcement corrosion specially in railway ties or in structures in which concrete is used for protection from stray currents. Electrical resistivity is well correlated with durability parameters such as diffusion coefficient, capillary absorption and porosity.

The main aim of this study is achiving to ultra high electrical resistivity in concrete; in this paper, bulk electrical resistivity of concrete is measured using a new instrument in which bulk electrical resistivity is calculated in different frquency ranges. The effect of silica fume and metakaolin as pozzolanic admixtures has been investigated. Also the effect of aggregate content types is studied in this research.

KEYWORDS

Electrical Resistivity, Metakaolin, Silica fume

[1] University of Tehran, School of Civil Engineering, Tehran, Iran 34469, Phone +98 21 88973631, Fax +98 21 88959740, amirtech.doc@gmail.com

1 INTRODUCTION

Corrosion of steel reinforcment is responsible for premature deterioration of concrete structures worldwide, particularly in marine environment of hot regions such as Persian Gulf. It is well known that the durability of materials and structures depends both on the environmental conditions at the exposed surfaces of the structures and on the material resistance to the action of aggressive substances [Antonio Costa and Julio Appelton 2002].

Electrical resistivity is an important durability characteristic of concrete to resist the passage of electrical current and it may directly affect the rate of steel corrosion. This would be of more importance in electrically powered rapid transit lines, where high resistivities are required.

Electrical resistivity is fundamentally related to the permeability of fluids and diffusivity of ions through porous materials such as concrete. Therefore, electrical resistivity also can be used as an indirect measure of the ability of concrete to prevent penetration of chloride salt solutions that may cause corrosion of the reinforcing steel [David A. Whiting and Mohamad A. Nagi 2003].

In other words, electrical resistivity may be considered as a function of concrete quality and pore structure. Consequently parameters such as water to cement ratio, cement content, cement type, pozzolanic materials, compaction, curing period, age of concrete may affect electrical resistivty.

In the case of metals embedded in concrete, the electrolyte for the corrosion cell is the concrete itself. A resistivity of less than 5 K.Ohm.cm can support very rapid corrosion of steel [Brown, 1980]. If the electrolyte has high resistance to the passage of current, or if the electrolyte is dry and unable to support ionic flow, then corrosion will occur only at a very low rate, if at all. Various researchers [Tremper, 1958; Vassie, 1980; Alonso et al., 1988] have determined that corrosion can be limited by increasing resistivity. A table of suggested values [Langford and Broomfield, 1987] is shown in Table 1.

When resistivities exceed a value of 20 K.Ohm.cm the risk of corrosion is low. Where steel is actively corroding, however, Broomfield et al. [1993] state that resistivity must exceed 50 K.Ohm.cm to reduce corrosion to an acceptable rate, and that resistivity must exceed 100 K.Ohm.cm to stop corrosion entirely.

Table 1. Relationship between resistivity and corrosion rate of steel in concrete

Electrical resistivity (KΩ.cm)	Corrosion rate
<5	Very High
5-10	High
10-20	Moderate
>20	Low

Purpose of this study is to increase the bulk electrical resistivity of concrete in laboratory condition. The effect of cementitous materials, aggregate content, and different pozzolans on electrical resistivity are investigated using a new commercial electrical resistivity-meter.

2 EXPERIMENTAL INVESTIGATION

2.1 Materials

The cementitious materials used in this study were Portland cement (PC) equivalent to ASTM Type II, silica fume (SF) obtained from Azna ferro-silicon alloy manufacture. Metakolin used in this research

was provided from ASAN SERAM Company, Iran. The chemical composition of the Cement, Silica fume and Metakaolin are given in Table 2.

Table 2. Chemical composition of Metakaolin, cement and silica fume.

Components	SiO_2	Al_2O_3	Fe_2O_3	CaO	Na_2O	K_2O	MgO	TiO_2	P_2O_5	L.O.I
Metakaolin	51.85	43.87	0.99	0.20	0.01	0.12	0.18	1.74	0.03	-
Cement	22.42	4.68	3.68	63.2	0.25	0.75	3.63	-	-	0.45
Silica Fume	93.16	1.13	0.72	-	-	-	1.6	-	-	1.58

Silica aggregates were provided from Techno-Silica plant, Iran. Polycarboxylate ether polymer superplasticizer and lignosulphonate plasticizer were used for the mixes in order to improve the workability of fresh concrete.

Aggregates with maximum size between 12-19 mm must be used for preparing ordinary concrete. Therefore, S-curve graph has been served for optimized grading, also the cost of raw aggregates and the quality of aggregate packing is to be optimized [Genadij Shakhmenko and Juris Birsh 1998] (shows in 'Fig. 1').

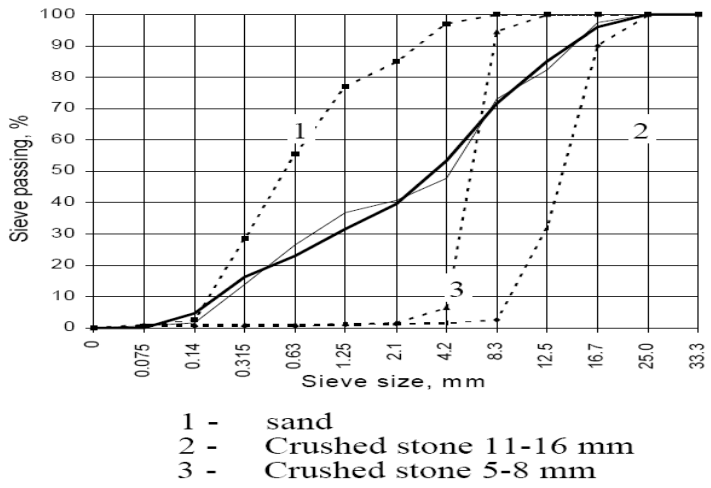

Figure 1. S-Curve for grading aggregates.

2.2 Mix proportions

Concrete of 6 different mix designs were selected among many mix designs studied during the research program. The mixes are presented in Table 3. Fine and coarse aggregates were used in 30% and 70% proportions, respectively.

2.3. Sample Preperation, Casting and Curing

Three specimens were made for each mix proportion. Concrete of each mix was casted into 10 cm cubic molds. In order to reduce void space, compaction was done using a steel tamper in 4 layers, each layer compacted by 30 impacts. The molds were covered with the burlap kept wet for 24 hours after casting. The specimens were removed from the molds and were allowed to cure in water saturated with calcium hydroxide at 80 °C for 28 days. Specimens were tested for the electrical resistivity at the ages of 7, 14, 21 and 28 days.

Table 3. Details of concrete mixtures

Materials	Mix					
	1	2	3	4	5	6
Cement (kg/m^3)	600	550	550	400	650	650
Water (kg/m^3)	300	250	250	200	350	350
W/C ratio	0.5	0.45	0.45	0.5	0.5	0.5
Silica-fume (kg/m^3)	400	320	350	320	-	350
Metakaolin (kg/m^3)	250	230	180	135	350	-
Cementitous Materials (kg/m^3)	1250	1100	1080	855	1000	1000
Aggregates (kg/m^3)	900	1100	1100	1350	1100	1100
SP (% by weight of cement)	1	1	1	1	1	1

It has been found that hot water curing will accelerate electrical resistivity growth [David A. Whiting and Mohamad A. Nagi 2003]. It seems specimens with smaller amount of cementitiuos materials have higher growth in resistivity at the end of the curing period.

2.4 Test Procedure and Measurement

Sudden temperature variations may lead to microcracks in concrete. To prevent initiation of microcracks, temperature of specimens should be slightly declined a few hours before testing. Specimens were tested at saturated surface dry condition.

It's important to dry the surface before testing as the moist surfaces may cause resistivity declining and inaccurate measurement. After drying the surfaces, electrical resistivity of concrete has been determined by two cuprous plates. Sufficient fresh cement paste has been injected between cuprous plate and specimen surfaces for complete connection (as shown in 'Fig. 2').

The new instrument innovated in Construction Materials Institute has been applied. It should be noted that the alternative current has been used in testing procedure and the resistivity hase been determined by measuring the respective voltage. The device which is shown in the follwing picture Measures the bulk electrical resistivity of concrete by providing measurement in different frequency ranges.

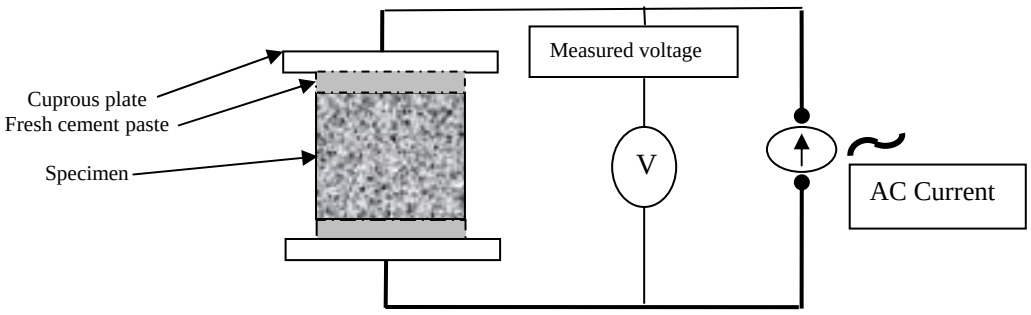

Figure 2. schematic diagram of testing procedure

3 RESULTS AND DISCUSSIONS

3.1 Results

The Results of the electrical resistivity of are illustraed in Table 4. Values are avarage of the three specimens of each mix design.

Table 4. Electrical Resistivity of specimens at the ages of 7,14,21 and 28 days

Age (days)	Electrical Resistivity (K.Ohm.cm)						
	Mix	1	2	3	4	5	6
7		1930	1970	5880	8340	17	600
14		3040	4940	8160	16590	46	1350
21		6460	8510	10130	18090	163	3340
28		7000	11090	17610	18500	217	3730

The above results in Table 4 compared with Table 1, show that concrete with ultra-high electrical resistivity has been gained.

3.2 Disscussions

3.2.1 Effect of Aggregates Content

According to the Figure 3, increasing the aggregate contents can accelerate the electrical resistivity. The electrical resistivity of aggregate is much higher than that of cement paste. While there is no specific study on the effect of aggregate type on electrical resistivity of concrete, one would expect that resistivity of concrete made with limestone aggregate would be less than that of concrete made with silica aggregate [David A. Whiting and Mohamad A. Nagi 2003].

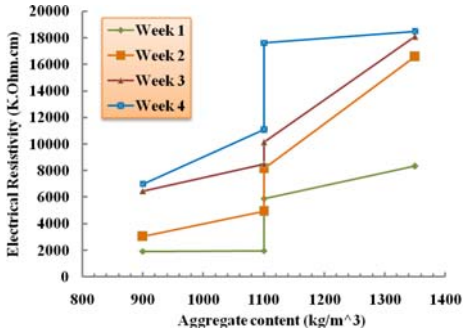

Figure 3. Relation between aggregate content and electrical resistivity

3.2.2 Effect of Cementitious Materials

Supplementary cementing materials such as silica fume and metakaolin have been used in concrete production of this research in relatively large amounts to improve durability charactersitics of concrete. Because of their pozzolanic effect and their physical properties, these materials improve microstructure of the cement matrix, and reduce concentrations and mobilities of the ions in the pore solution. Therefore they exert an influence on the electrical resistivity of concrete. In most cases, these materials create a finer pore size distribution and lower ionic concentration, which leads to higher electrical resistivity than in normal Portland cement concrete [Whiting et al., 1993].

The relation between cementitious materials and electrical resistivity has been shown in 'Fig. 4' obtained from samples NO. 1,2,3 and 4.

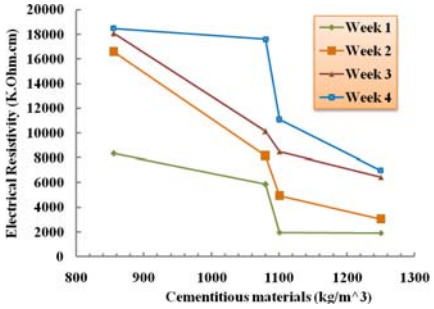

Figure 4. Relation between cementitious materials and electrical resistivity

Concerning the increase of cement content, it seems that decreasing the aggregate content decreases the electrical resistivity in concrete.

3.2.3 Effect of Different types of Pozzolanic Materials

According to relatively high w/c=0.5 in this study, there are some cappilary pores in cement paste. Because of a low cement content, even by a complete hydration process, there would not be sufficient CH for applying the whole pozzolns, considering the high content of pozzolanic materials. Therefore a considerable amount of pozzolanic materials remains non-reactive in the paste and it must be expected a physical effect not chemical; the pores have been filled by non-reactive pozzolans, so grading of non-reactive pozzolans becomes more important.

Comparison between resistivity of silica-fume, metakaolin and combination of them has been shown in 'Fig. 5' obtained from samples NO. 1 (Silica Fume+Metakaolin), 5 (Metakaolin), and 6 (Silica Fume).

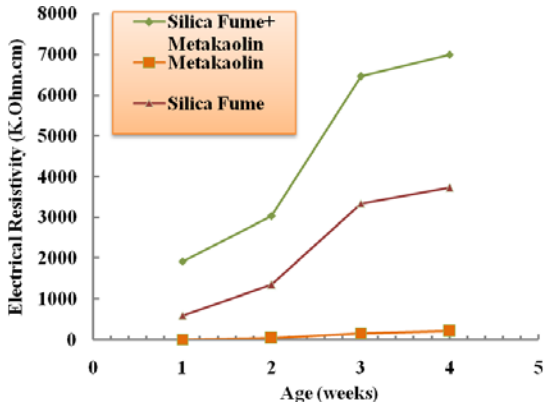

Figure 5. Comparison between resistivity of silica-fume, metakaolin and combination of them

In this research, optimum amounts of pozzolanic materials were found in each sample (about 37% and 16% by weight of cementitous materials for silica-fume and metakaolin respectively). Silica-fume and metakaolin separately has lower enhancement in electrical resistivity rather than their combination, however silica-fume is more efficient than metakaolin. This is shown in Fig 5.
Silica fume has a better effect on improving electrical resistivity than metakaolin for its finer particles and when using a combination from both pozzolans, there would be another grading beside the aggregate grading merely, so blank spaces like capillary pores will be filled more because of better physical role of non-reactive pozzolans.

4 CONCLUSION

In this study, the fundamentals of electrical resistivity have been reviewed and a concrete mix proportion with ultra-high electrical resistivity has been found. The electrical resistivity of concrete is a measure of its ability to resist passage of electric current and ionic migritaion within the concrete.

In general, following factors seem to be effective for increasing the electrical resistivity of concrete:

- Since cement paste has higher conductivity, limiting the amount of cementitous materials would be effective
- Optimum combination of silica-fume and metakaolin has been deduced from presented review instead of applying them seperately.
- Hot water curing may be useful to achieve higher values of electrical resistivities.
- For achiving higher electrical resistivity, effect of physical parameters are significant like the chemical parameters, too.

ACKNOWLEDGMENTS

Continued regards of Construction Materials Institute at the University of Tehran is highly appreciated. The authors also appreciate Alireza Javadian and Amir Ghods during this experimental study.

REFERENCES

Ant onio Costa, ulio Appelton J. 2002, *Case studies of concrete deterioration in a marine environment in Portugal*, Cement and Concrete Composites, pp. 169-179.

Broomfield, J.P., Rodriguez, J., Ortega, L.M., and Garcia, A.M. 1993, "Corrosion Rate Measurement and Life Prediction for Reinforced Concrete Structures," *Proceedings of Structural Faults and Repair – 93*, Engineering Technical Press, University of Edinburgh, U.K., Vol. 2, pp. 155-164.

Brown, R.D. 1980, "Mechanisms of Corrosion of Steel in Concrete in Relation to Design, Inspection, and Repair of Offshore and Coastal Structures," ACI SP-65, *Performance of Concrete in Marine Environments*, American Concrete Institute, Farmington Hills, MI, pp. 169-204.

Genadij Shakhmenko and Juris Birsh 1998, *Concrete mix design and optimization*, Riga Technical University, Department of Building Materials, 2nd Int. PhD Symposium in Civil Engineering Budapest.

Langford, P. and Broomfield, J. May 1987, 'Monitoring the Corrosion of Reinforcing Steel' *Construction, Repair*, Vol. 1, No. 2, pp. 32-36.

Tremper, B., Benton, J.L., and Stratfull, R.F. 1958, 'Fundamental Factors Causing Corrosion', HRB Bulletin 182 *Corrosion of Reinforcing Steel and Repair of Concrete in a Marine Environment*, Highway Research Board, Washington, D.C., pp. 18-41.

Whiting, David A., and Nagi, Mohamad A. 2003, *Electrical Resistivity of Concrete—A Literature Review*, Portland cement Association, Skokie, Illinois, USA, R&D Serial No. 2457, 57 pages.

Non destructive Test Methods for evaluation of concrete: the case study of Punta Perotti (Italy)

Luprano Vincenza [1]
Caretto Flavio [1]
Labia Nicola [2]
Ciniglio Gabriele [3]
Tatì Angelo [2]
Tundo Antonella [1]
Pfister Valerio [1]

T 11

ABSTRACT

There is often a need to evaluate the in place strength of concrete in existing structure for an accurate assessment of structural capacity. In place test methods can be used for a quantitative assessment of the strength, for this goal it is necessary to establish a strength relationship for the concrete in the structure. The relationship can be developed only by performing in –place tests at selected locations and taking companion cores for strength testing. The use of in place testing do not eliminate the need for coring, but it can reduce the amount of coring required.

A statistical study was carried out on a building (Punta Perotti) in Bari before its demolition. Punta Perotti, a building exposed for more than 10 years to particular aggressive environmental conditions (near the sea and in a windy area), of which are well known the technical schedules of original materials, was selected in order to study the life cycle of the materials and structures, until the demolition process. About 180 cores (10 cm diameter) and 290 microcores (2 cm diameter) were taken from the pillars of the structure made in concrete at different planes (-1, 0,1,2,3,6) after the non destructive testing (ultrasonic tests and rebound hammer tests) made on the same pillars. The Italian (OPCM 3274), European (PrEN 13791) and USA (ACI 228) guide lines were followed both in the in situ measurements and in the data analysis. The statistical data analysis was carried out by means of one – way ANOVA method. Some of the possible correlations between non destructive testing and mechanical testing, and between compressive strength of cores and microcores will be analyzed in this work.

KEYWORDS

Non destructive testing, Concrete statistical analysis, Core compressive strength

[1] ENEA, Brindisi Research Center, 72100 Brindisi, Italy, Phone +39 0831 201452, Fax +39 0831 201581, vincenza.luprano@brindisi.enea.it
[2] ENEA Casaccia Research Center, Roma, Italy
[3] ENEA Portici Research Center, Portici (Naples), Italy

1 INTRODUCTION

In Italy, for the seismic reliability, the Decree 3274 of 2003 and its successive modification (OPCM 3431/2005), predicts a founded quantitative process on following phases: structural knowledge, definition of the required performances, evaluation of the existing structure in accord to actualised performing level, plan of adaptation and at last, evaluation of the adequate structure.

The interventions of seismic reliability imply the necessity to elaborate in opportune way the data concerned the material properties.

In the verification of structural reliability , methods of analyses compatible with the acquaintance of the building must be chosen. It is necessary to redefine a complete and reliable model of the structure. It must be reduced the total outlay for the intervention of the structural reliability.

About the structure to analyse, it must be necessary to know the technical norms utilized in phase of planning. It is necessary to know the constructive practice at the age of the building and the original function. The characteristic strength of the concrete in the existing buildings is obtained from the results of tests in situ divided the "Factor of confidence". This last one depends on the level of the knowledge of the all structure. To obtain the appropriate type of analyses and the relative levels of "confidence", three different types of knowledge must be defined:

- LC1: Limited knowledge
- LC2: Adequate knowledge;
- LC3: Accurate knowledge.

The aspects that define the levels of knowledge are: geometry (the geometric characteristics of the structural elements), structural details (the numbers and disposition of the armours, the consistency of the not structural elements), materials (the mechanical properties of the materials). The acquired level of knowledge determines the method of analysis, and the values of the factors of confidence to apply to the property of the materials.

For the knowledge of the characteristic compression strength of the concrete, the mentioned Norm makes possible to substitute (not more than 50%), with a large number of non destructive tests (at least the triple one).

The same Norm indicates in the surface of plan of 300 m^2 the minimal cores number to extract, variable from three to nine in accord to the plan of investigation (limited, extensive or exhaustive). Apart from these general indications for the evaluation of the strength of the concrete in situ, do not exist consolidates procedures of combined investigations (destructive tests and non-destructive tests).

As shown in literature [OPCM 3274 2003] the relationship between concrete compression strength measured by means of mechanical testing and the measurements obtained by means of in situ non destructing testing results to be disperse and does not easily correlated.

The main object of this work is to try to validate the use of non destructive testing (ultrasonic measurements, rebound number and so on) through the identification of reliable correlation curves reducing the cores number to extract from the studied structure.

It is necessary to identify a good practice to select the eligible test stations of the same structural element on which to do the cores to minimize the errors in the technical evaluation.

To reach this goal a consistent number of experimental data (mainly ultrasonic measurements, rebound number and mechanical compressive test) was raised in order to lead statistical studies. ENEA has identified the Punta Perotti structure in Bari (Fig. 1) as a good case of study. Punta Perotti

was a building (14 levels high, about 1560 m^2 for level) exposed for more than 10 years to particular aggressive environmental conditions (near the sea and in a windy area), of which are well known the technical schedules of original materials and was selected in order to study the life cycle of the materials and structures, until the demolition process.

2 EXPERIMENTAL

On the complex of Punta Perotti it has been carried out a wide campaign of destructive and non destructive tests (Fig. 2-3-4). In particular the tests used for the data analysis reported in the present article are:

- ultrasound and rebound Hammer tests were carried out in situ on 90 pillars at three different heights (test stations) on six different floors of the building (-1, 0, 1, 2, 3, 6) and were extracted cores and microcores from the same places of the test stations.
- ultrasound velocity measurements obtained in laboratory on 180 cores and 290 microcores and on which have been executed relative strength measurements.

The used instrumentations for the tests in situ are:

- Schmidt Concrete Test Hammer for normal concrete structures. Impact energy 2,207 N/m.
- Digital CM42 CoverMaster Concrete Pachometers (microprocessor COVERMASTER CM9) equipped with an standard probe from 7 to 90 mm
- Low frequency Ultrasonic Instrument RP5000 SIRIO equipped with a microcomputer and two probes of 50Hz frequency and crystal of 1’’
- Professional hydraulic core drill for manual use with endowed column of sliding of diamond crowns of diameter 3,5 cm and 10 cm, for perforation to water on all the superficial ones of armed concrete

The used instrumentations for the laboratory tests are:

- Low Frequency RP5000 SIRIO Ultrasound instrument endowed of microcomputer and two probes of 50 KHz frequency, crystal from 1"½
- Low Frequency KrautKramer 23 LF Ultrasound instrument, computer laptop inside acquisition board A/D converter and two probes of 50 KHz frequency, crystal from 1"
- Low Frequency Boviar Ultrasound instrument endowed of palm computer and two probes of 50 KHz frequency, crystal from 1"½
- Low Frequency Numeric Ultrasound instrument and two probes of 50 KHz frequency, crystal from 1"
- 250 KN CONTROLS Press for automatic compression tests equipped with computer for data acquisition

Figure 1. Punta Perotti building

Figure 2. In situ ultrasonic test

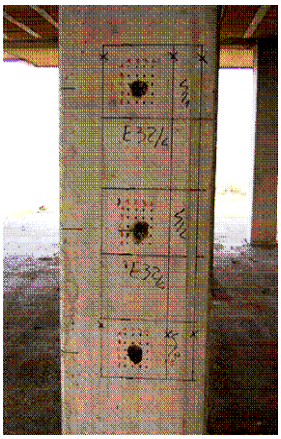

Figure 3. Pillar test stations

Figure 4. Microcores

Studied pillars	*Pachometric tests*		87
	Rebound hammer		68
	Ultrasonic tests		64
	Thermographic analysis		3
Non destructive testing	*Pachometric tests*		365
	Rebound hammer		298
	Ultrasonic tests		152
	Thermographic analysis		3
	Carbonation tests		180
Destructive testing	*Cores*	*micro*	293
		standard	180

Table 1. Number of the analysis done in situ on the Punta Perotti building.

3 DATA ANALYSIS

All the acquired data were used to try to establish a quantitative assessment of the strength for the concrete in the existing structures of Punta Perotti. In order to develop the strength relationship, it is generally necessary to correlate the in place tests parameter with the compressive strength of cores obtained from the structure. Furthermore by combining results from more than one in place test (for example ultrasonic test and rebound hammer), a multivariable correlation can be established to estimate strength. Combined methods are reported to increase the reliability of estimated strength. For example an increase in moisture content increases pulse velocity but decrease the rebound number, so their combined use results in a cancelling effect that improves the accuracy of the estimated strength [ACI 228 1R -03].

For this reason it was decided to evaluate the in situ experimental results both with the strength versus the alone ultrasonic velocity variable ($R\_ac = a \times V^{c}$) and versus the ultrasonic velocity and rebound variables ($R\_abc = a \times IR^{b} \times V^{c}$).

The result of the comparison between the multivariable and single variable correlation, Fig. 5, shows that the calculated values are quite similar. For this reason it was decided to work on the curve correlation obtained only versus the ultrasonic velocity.

A further interpretation of the data is carried out in order to try to define the homogenous groups of data with the aim to define a wide statistical sample to obtain the best correlation curves.

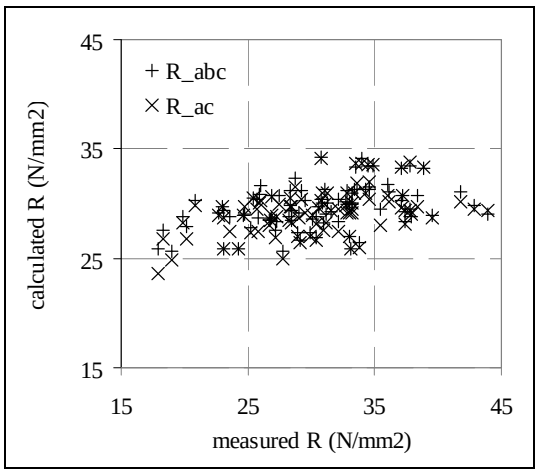

Figure 5. Comparison between multivariable (R_abc) and single (R_ac) correlation.

For this purpose it was used the software Analyse-it in order to use methodology ANOVA (ANalysis Of VAriance). ANOVA is one instrument of statistics, developed in order to verify the significance of the differences between the arithmetic means of two or more similar statistics populations.

ANOVA allows to decompose and to measure the incidence of the various variation sources on the values observed of two or more groups of data [Analyse-it for Microsoft Excel].
The concrete for its nature it is a material that has strongly variable physical characteristics if measured in punctual way.

ANOVA is, in your opinion, a good statistical instrument to deal the data obtained from this type of experimental campaigns. ANOVA is more suitable of the t of Student, commonly used for this type of analysis.

The base hypotheses of this methodology are that the data must be between independent each other, normally distributed and that the variances of several the groups must be homogenous. These hypotheses turn out satisfied on the measures that we carried out on the structure of Punta Perotti.
The totality of the data has been decomposed in various groups in which a single parameter varied (i.e.: the floor, the test stand, the instrument of measure etc.).

Through the elaboration of the data, they were defined the groups of different specimens for physical causes, and those with similar behaviour have joined, to the aim to carry out one statistical study on the maximum number of data between homogenous samples.

The obtained results can be therefore synthesized:

- ANOVA has confirmed that there is a variation of the compression strength and of the ultrasound velocity in the concrete of Punta Perotti versus the analyzed floors (Figure 6).
- From the statistical analysis carried out on the same pillar of the same floor at different height, it turns out that there are not meaningful differences between the values of velocity (Figure 7) and strength (Figure 8); therefore in the subsequent analyses we have considered indifferently all the measurements obtained from the pillars of the same floor.
- Always with ANOVA it was verified that there is not a meaningful difference between the measurements of ultrasound velocity carried out in situ on the pillars and the ultrasound measurements carried out in laboratory on the cores with same ultrasound instrument (Figure 9). Therefore for the statistical analysis the ultrasonic velocity values measured on the cores were used in order to have approximately the double quantity of the data.

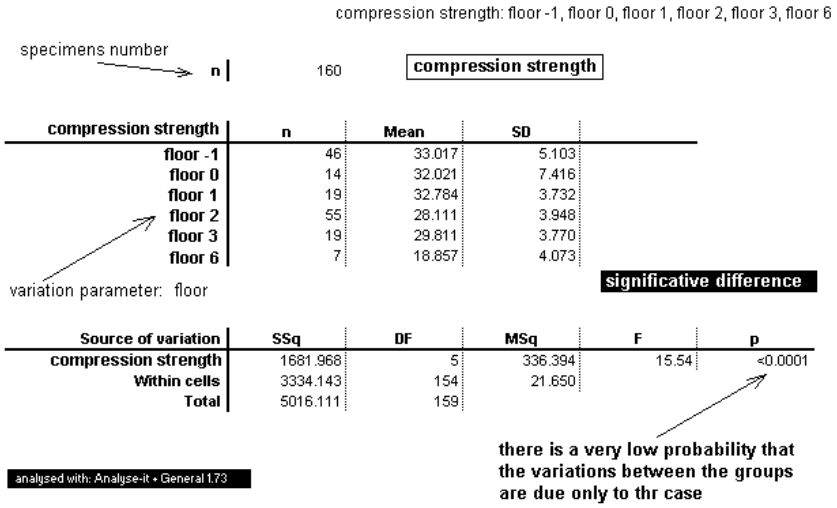

Figure 6. ANOVA results: comparison between compression strength obtained on different floors

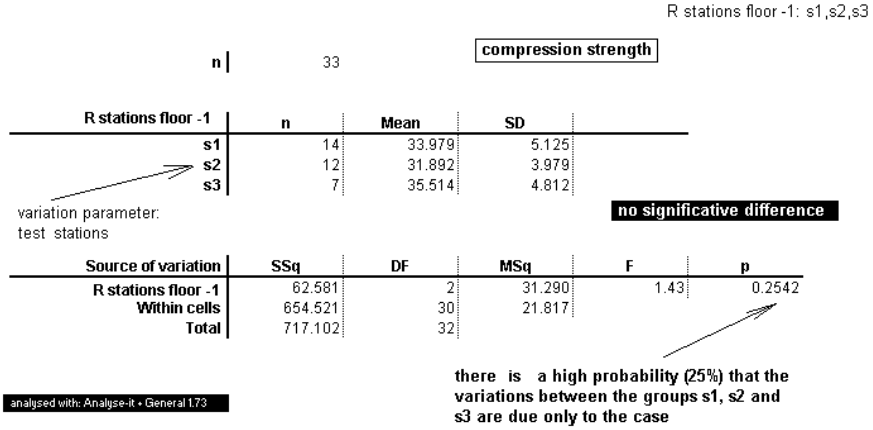

Figure 7. ANOVA results: compression strength on floor -1 versus the 3 different heights of the same pillar

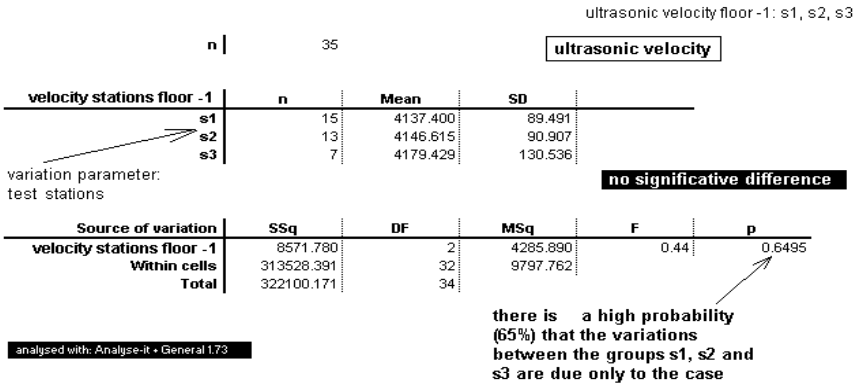

Figure 8. ANOVA results: ultrasound velocity on floor -1 versus the 3 different heights of the same pillar.

ultrasonic velocity pillars and ultrasonic velocity cores

n	275

ultrasonic velocity

pillars/cores velocity	n	Mean	SD
cores velocity	180	4132.428	142.582
pillars velocity	95	4097.081	443.658

varation parameters:
pillars and cores

no significative difference

Source of variation	SSq	DF	MSq	F	p
pillars/cores velocity	77687.552	1	77687.552	0.96	0.3286
Within cells	22141281.138	273	81103.594		
Total	22218968.690	274			

there is a high probability (33%) that the variations between the groups pilaters and carrots are due only to the case

analysed with: Analyse-it • General 1.73

Figure 9. ANOVA results: comparisons between ultrasonic velocity measurements obtained on pillars in situ and on cores in laboratory.

4 CORRELATION CURVES ANALYSIS

The main goal of this study is to try to minimise the number of cores on the structure and obtain a representative correlation curve. To reach this goal, first of all ad hoc correlation curves between ultrasonic velocity and strength measurements for every floor using all cores available were calculated. The second step was to calculate the correlation curve using only 10 ultrasonic and strength measurements, that is the number of the cores indicated by the Italian Guide Lines [OPCM 3431 2005] for a structure as Punta Perotti. At the beginning it was calculated the correlation curve with 10 measurements choosing the ultrasonic velocity measurements in the range of the minimum, medium and maximum values.
To evaluate the goodness of the correlation curve obtained with 10 measurements with respect that one obtained with the measurements available on the same floor, it was considered as parameter the ***S***um of ***S***quared ***E***rrors (*SSE*) that is minimised with the regression calculation. It was then defined the $SSE_{population}/SSE_{10selected}$ ratio. If this ratio is near 1 then the two regressions result to be quite similar. In this way it was possible to establish that there is a very good correspondence between the correlation curve obtained in all floors with both the 10 medium and maximum values of the ultrasonic velocity, with except the floor 2 (Figures 10-11).

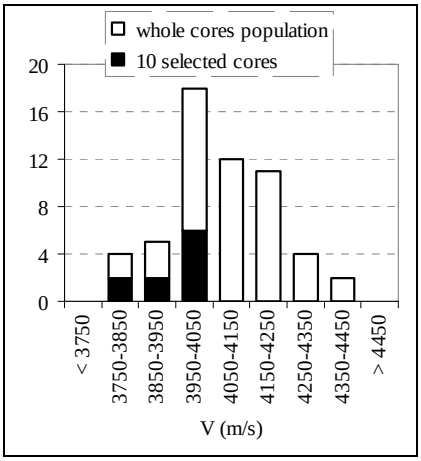

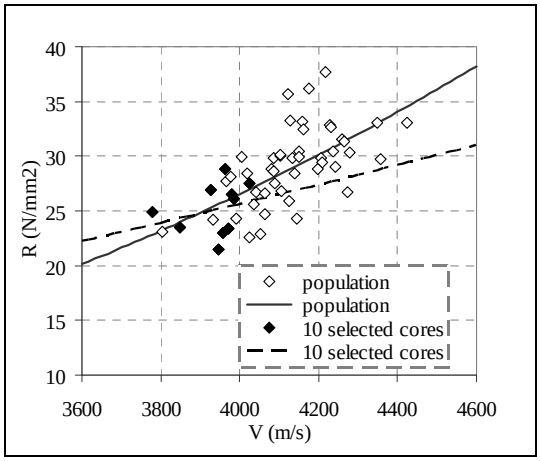

Figures 10-11. Distribution of the ultrasonic velocity measurements and regression curves of the 10 selected data considering the minimum values of ultrasonic velocity.

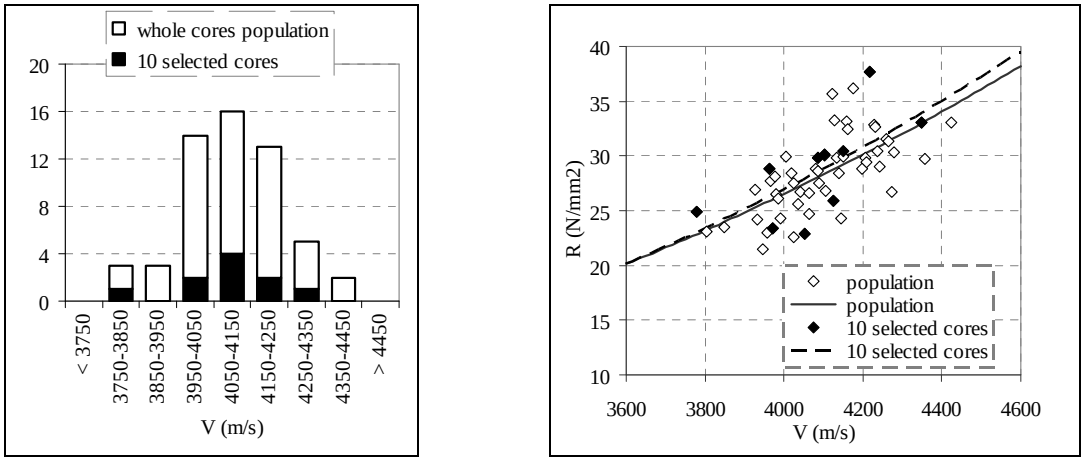

Figures 12-13. Distribution of the ultrasonic velocity measurements and regression curves of the 10 selected data considering similar mean value and standard deviation.

Due to this singularity, it was decided to identify another methodology and it was chosen 10 measurements with mean value and standard deviation of the ultrasonic velocity similar to the values obtained from all the measurements of the same floor.

This kind of analysis was applied to the 2nd floor obtaining a good correlation between the two curves (Figures 12-13).

It can be concluded that in the selection of the core locations, it is appropriate to include the widest range of concrete strength in the structure as it is possible.

In order to verify the hypotheses of pre-selected zones on which carrying out the cores, an exhaustive analysis of all the possible decuples of cores is in progress. For giving to an order of magnitude of the problem, the exhaustive analysis of the possible decuple for floor -1 in the structure of Punta Perotti is estimated in about 400.000.000 possible cases, while for floor 2 is estimated in more than 3.300.000.000 possible cases.

5 CONCLUSIONS

A wide campaign of non destructive and destructive tests on the same structure (Punta Perotti) was carried out in order to study a methodology to built up the best correlation curve to define the mechanical strength of the concrete.

The main goal of this research work is to support the designer to assess the reliability of an existing structure, without having a complete knowledge of its present condition, in the choise of the best position in which to do the cores. To reach this goal it was used an statistical approach. Preliminary results seems to demonstrate that a previous campaign of non destructive testing and an accurate statistical analysis of the results can help to identify the most appropriate zone in which doing the cores. Further studies are underway to improve this method.

ACKNOWLEDGMENTS

The Authors acknowledge Dr. Massimo Puccini (Head of MATQUAL Department of ENEA) for scientific and economic support to this tests campaign.

REFERENCES

OPCM 3274, 2003, 'Primi elementi in materia di criteri generali per la classificazione sismica del territorio nazionale e di normative tecniche per le costruzioni in zona sismica', *Gazzetta Ufficiale* 8/5/2003.

OPCM 3431, 2005, 'Norme tecniche per il progetto, la valutazione e l'adeguamento sismico degli edifici esistenti'.

CEN (2004). European standard EN1998-3:2004: Eurocode 8: Design provisions for earthquake resistance of structures. Part 3: Assessment and retrofitting of buildings. European Committee for Standardisation.

A. Masi, 2007, 'L'adeguamento sismico del patrimonio edilizio pubblico: il ruolo delle indagini per la riduzione dei costi di intervento', Proc. Controllo e monitoraggio di edifici in c.a. Il caso studio di Punta Perotti, Bari, Italy, 20th June 2007.

ACI 228 1R -03, 'In place methods to estimate concrete strength'

prEN 13791 (2005) 'Assessment of in-situ compressive strength in structures and precast concrete components'

Analyse-it for Microsoft Excel, http://www.analyse-it.com/ .

Influence of Fibers Weight Fraction and Nature of Fibers on Thermal and Mechanical Properties of Vegetable Fibers / Cement Composites

Cristel Onésippe [1]
Fernando Toro [2]
Ketty Bilba [3]
Silvio Delvasto [4]
Marie-Ange Arsène [5]

T 11

ABSTRACT

Nowadays, in the purpose of energy saving and eco-friendly technologies and materials, increasing interest is accorded to natural vegetable fibers. Many studies have shown that vegetable fibers are an alternative to asbestos in fiber reinforced cement products manufacturated by the Hatscheck process. Few works have demonstrated the low thermal conductivity of such composite materials resulting from effect of the mixture fiber/matrix.

The aim of this study is to produce low–cost building materials in the purpose of saving energy using heat-treated and chemically treated sugar cane bagasse and fique fibers as reinforcement in cement (OPC) based materials. Consequently, the influence of the type and weight of additives on the insulating thermal properties (conductivity) and on the mechanical properties (flexural strength) are prospected.

This study evidences that composites composed with pyrolyzed bagasse fibers have better thermal properties than others composites. The higher mechanical properties are noted for composites manufactured with alkali treated fibers.

KEYWORDS

Vegetable fibers/cement composites, Thermal properties, Flexural strength, Alkali treatment, Heat treatment

[1] Laboratoire COVACHIMM, Université des Antilles et de la Guyane UFR SEN BP 250, 97157 Pointe-à-Pitre Cedex, Guadeloupe (France), Phone +590590483057, Fax +590590483072, cristel.onesippe@univ-ag.fr
[2] Grupo de Materiales Compuestos, Escuela de Ingenieria de Materiales, Universidad del Valle, Cali, Colombia
[3] Laboratoire COVACHIMM, Université des Antilles et de la Guyane UFR SEN BP 250, 97157 Pointe-à-Pitre Cedex, Guadeloupe (France), Phone +590590483057, Fax +590590483072, ketty.bilba@univ-ag.fr
[4] Grupo de Materiales Compuestos, Escuela de Ingenieria de Materiales, Universidad del Valle, Cali, Colombia, delvasto@visionsatelite.com.co
[5] Laboratoire COVACHIMM, Université des Antilles et de la Guyane UFR SEN BP 250, 97157 Pointe-à-Pitre Cedex, Guadeloupe (France), Phone +590590483057, Fax +590590483072, maarsene@univ-ag.fr

1 INTRODUCTION

Composite materials incorporating vegetable natural fibers have known an increasingly interest during the past few decades [Toledo Filho et al. 2003, Savastano et al. 2000, Savastano et al. 2003, Bilba et al. 2003, Arsène et al. 2007, Coutts 1988]. These environmentally friendly materials are low-cost [Coutts 1988] and offer advantages such as reduction of electrical consumption by air conditioning. Moreover, the use of vegetable fibers in replacement of synthetic fibers is interesting in developing countries where the availability of tropical plants and agricultural wastes is important. Due to health reasons, since 1973, various regulations are applied to restrict and ban the use of asbestos in France [Bilba et al. 2004] and other countries. Many studies have shown that, regarding the mechanical behaviour, vegetable fibers are an interesting alternative to asbestos in fiber reinforced cement products manufactured by the Hatscheck process [Savastano et al. 2000, Savastano et al. 2003, Savastano et al. 2001] although few works have demonstrated the low thermal conductivity of such vegetable fiber-Portland cement based composite materials [Toledo Filho et al. 2003, Savastano et al. 2001] resulting from effect of the mixture fiber/matrix.

The aim of this study is to produce low–cost insulating materials for building construction in order to obtain habitability and to save energy. Although thermal properties are really involved in applications of such materials, it is essential to evaluate if their mechanical properties are in good agreement with the civil engineering codes [Blankenhorn et al. 2001]. Consequently, the influence of the type of treatment and amount of fibers on the mechanical and thermal properties are prospected.

2 MATERIALS AND METHODS

Samples were elaborated at Universidad del Valle (Cali, Colombia) using a process followed by Delvasto [2006] and de Gutiérrez and al. [2005] while the thermal and mechanical studies were developed at Université des Antilles et de la Guyane (Guadeloupe, France).
Two types of vegetable fibers were used: bagasse, solid residue of sugar cane after juice extraction (provided by Sugar Cane Factory in Guadeloupe) and Colombian plant fique (provided by a Colombian Fique sacks factory). They will be noted respectively “BAG” and “FIQ”.

Two types of treatments were applied:

- Heat–treatment : pyrolysis under controlled atmosphere (N_2 flow, 2L/h) during 2 hours and at 200°C which is the optimal temperature to obtain retified fiber without formation of char [Bilba & Ouensanga 1996]. The pyrolyzed fibers will be named “BAGP”.
- Chemical treatment: attack by a 5% by mass alkaline solution of $Ca(OH)_2$ for bagasse and fique fibers. The alkali treated fibers will be named “BAGB” and “FIQB”.

A Portland cement marketed as ASTM type I usually used in Colombia, a graded natural river sand, a limestone filler and water were used as the matrix. 93.5 % by weight of the limestone filler is Calcium carbonate ($CaCO_3$). The size distribution, determined by using a Malvern laser diffraction analyzer, of Portland cement gives an average granulometry of 15µm and the limestone filler has an average particle size about 1 µm.

According to these results, the Portland cement has a factory addition what is a calcareous material. The sand is appropriated for use in cement based mortars, its apparent density is about 2605 kg/m^3 and its average particle size is approximately 0.6 mm.

2.1 Composites Preparation

The content of sand and calcium carbonate were kept constant at 50% and 30% by weight of cement respectively. The composites studied were elaborated with a matrix based on Portland cement. The

proportions of the matrix compounds were in weight percent with respect to Portland cement (wrtc): sand 50 %, limestone powder 30 %, bentonite 1.5 and 3 %, cellulose pulp 4 %, silica fume 5 %, an aqueous copolymer dispersion of butyl acrylate and styrene from BASF (Acronal® 296 D) 7.5 %. The amount of fibers was changed from 0 % to 3 % wrtc. Slurry of each mix contains a water/cement ratio of 0.9 (weight by weight) being prepared before its pouring on a casting bed that was subjected to vacuum to obtain a flat sheet. After the slurry dewatering process, pads (160 x 50 x 8 mm^3) cut from the fresh laminate were cured for 21 days at 100% of relative humidity and left to air dry in the laboratory for 7 days at room temperature.

About 19 mixes were elaborated: 3 samples for the 3 types of fibers for 2 fiber contents and 1 as control (without any fiber). The detail of the mixes is shown in [Table 1]. The mixes reinforced with fique alkali treated (FIQB) correspond to codes: M86, M90; The mixes reinforced with bagasse alkali treated (BAGB) correspond to codes: M71, M74. The mixes reinforced with pyrolyzed bagasse (BAGP) correspond to codes: M80, M83. The composites will be noted “CBAGP”, “CBAGB” and “CFIQB”.

Table 1: Proportions of the mixes elaborated.

Composites	**Fibres and treatment**	**Bentonite (% wrtc)**	**Fibres (% wrtc)**	**Acrylic Polymer (% wrtc)**	**Silica Fume (% wrtc)**	**Pulp (% wrtc)**
Control (M 75)		3	0	7,5	5	4
CFIQB (M90)	FIQB	3	1,5	7,5	5	4
CBAGB (M74)	BAGB	3	1,5	7,5	5	4
CBAGP (M83)	BAGP	3	1,5	7,5	5	4
CFIQB (M86)	FIQB	3	3	7,5	5	4
CBAGB (M71)	BAGB	3	3	7,5	5	4
CBAGP (M80)	BAGP	3	3	7,5	5	4

2.2 Thermal conductivity testing

Thermal tests were conducted under controlled laboratory conditions (temperature ~ 20°C and relative humidity of 70–80%) on 112 days old specimen. The apparatus used was a thermal conductivimeter “CT–mètre” with a thermal probe commercialized by Controlab (Saint–Ouen, France). Six measurements were conducted for each composite with one hour interval between each measurement in order to evaluate the standard deviation of the results.

2.3 Flexural strength testing

Composites flexural strength was measured under three-point bend loading with a span of 50mm. The tests were conducted 112 days after specimen fabrication. The specimens were loaded continuously to failure at a speed rate of 0.5 mm/minute. The tests were carried out in an Instron (model 3367 - Guyancourt, France) testing machine equipped with a 500N load cell.

3 RESULTS AND DISCUSSION

In this paper, results of the tests on 112 days old specimen are presented. At this age, the principal hydration processes of cement have almost completely been done and the formulations of the composites are very stable [Bilba et al. 2004, Taylor 1997]. The evolution of thermal conductivity according to the amount of fibers is reported in [Figure 1]. Dash lines correspond to control specimen. The thermal conductivity values are of same order of magnitude whatever the type of fibers. Evolution of mechanical properties determined by three-point bending test is presented in [Figure 2].

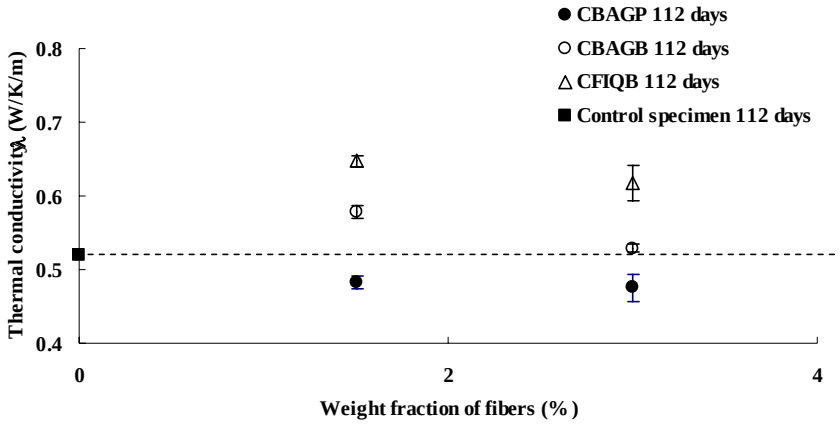

Figure 1. Evolution of thermal conductivity of 112 days old vegetable fibers/cement composites according to weight fraction of fibers.

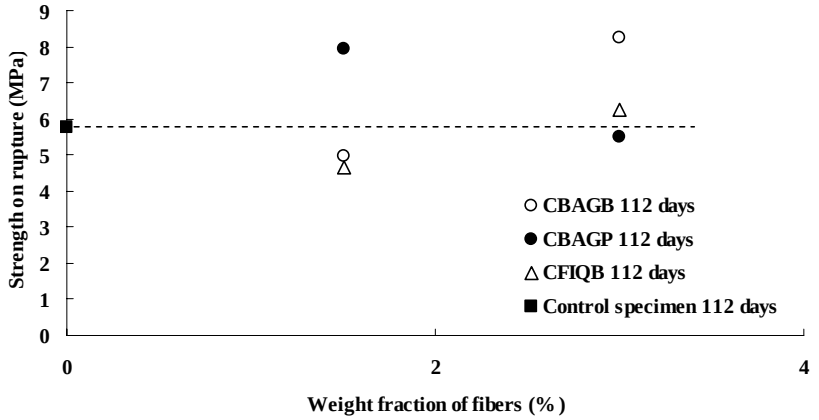

Figure 2. Evolution of flexural strengths of 112 days old vegetable fibers/cement composites according to weight fraction of fibers.

3.1 Influence of weight fraction of fibers

By increasing the weight fraction of fibers, there is a progressive decrease of the thermal conductivity. This result is in good agreement with Asasutjarit et al. [2007] results: when cement/fiber is higher, the thermal conductivity of a cement board increases. The weaker heat conductor materials are CBAGP because the more pronounced addition of fibers effect is for those composites; indeed all the thermal conductivity values of CBAGP are lower than the control specimen one.
The effect of fiber content has been correlated with the treatment. At low fiber content (1.5% wrtc), strengthening effect is observed only for composites with pyrolyzed bagasse fibers. On the contrary, at 3% (wrtc) of fibers, the better mechanical properties are measured for composites elaborated with bagasse and fique fibers using alkaline treatment.
In case of thermally treated fibers, the flexural strength decreases with increasing fiber content. A strengthening effect of mechanical properties, with increasing fiber content, is noted for composites containing chemically treated fibers. However, at low content of chemically treated fiber (1.5 %), the composites flexural strength is lower than for the control specimen. This behaviour with 1.5% weight fraction of fibers points out the importance of fiber adhesion and porosity.
Between 1.5% and 3% (wrtc) of fiber content, mechanical properties are supposed to follow a linear variation. By extrapolation, a fiber content of 2% is found. In these conditions, flexural strengths are closer for the two composites made of bagasse fibers and remain higher than the control specimen one.

These results are confirmed by former results **[5]** that evidence an optimal pyrolyzed bagasse fiber content of 2% (wrtc) for improved mechanical properties and an increase of mechanical strength thanks to the addition of pyrolyzed bagasse fibers or alkali treated fique fibers.

3.2 Effects of fiber treatment

As shown in [Figure 3], pyrolysis at 200°C significantly improves thermal properties of these composites because thermal conductivity values of CBAGP are lower than the control specimen one. The value of thermal conductivity is more than 20 % lesser for the CBAGP than for the commercial cellulose boards which report 0.68 W/K/m [Asasutjarit et al. 2007].
The most important decrease of thermal conductivity values is noted for alkali treated fibers/cement composites. Nevertheless, up to 3% of alkali treated fibers, the values keep higher than for the control specimen. This means that the inclusion of pyrolyzed fibers limits the heat transfer.
With 3% of pyrolyzed bagasse fibers, the composites do not offer greater mechanical properties because the strength of CBAGP is lower than the control specimen, whereas strengths of alkali treated fibers/cement composites are higher than the control specimen one. At 3% weight fraction of fibers, CBAGB and CFIQB behave better and seem to be well designed for improved mechanical properties of building materials.

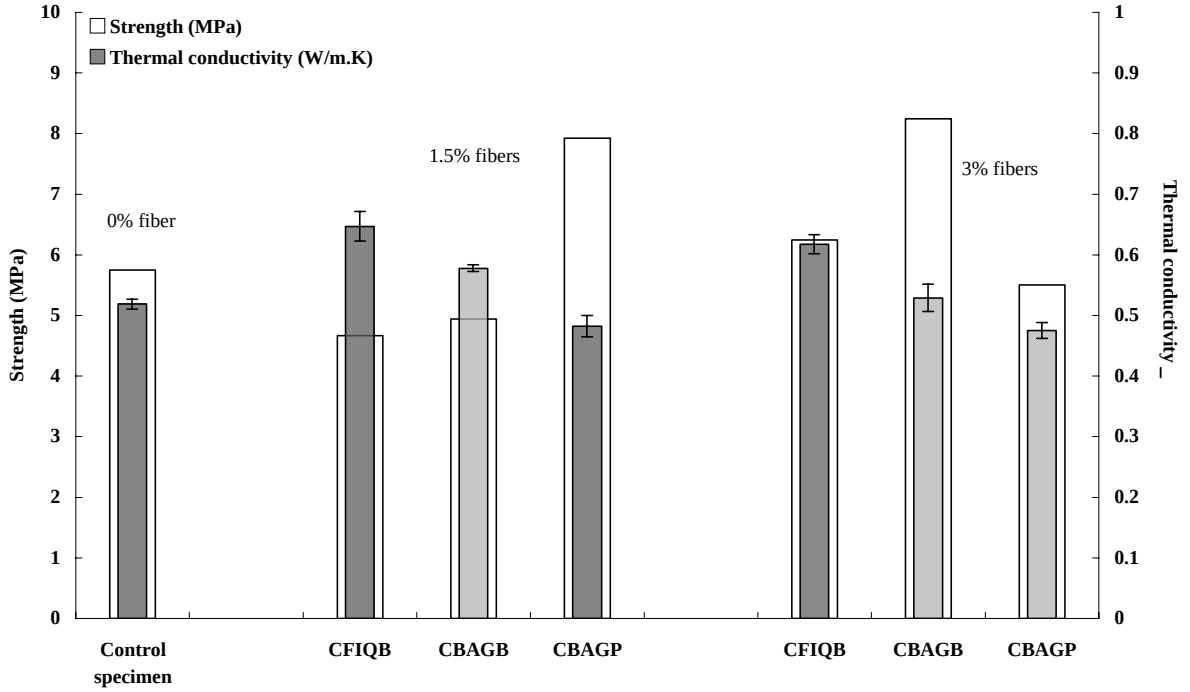

Figure 3. Comparison of thermal conductivity and flexural strengths of 112 days old vegetable fibers/cement composites according to weight fraction of fibers.

3.3 Influence of nature of fibers

A comparison of mechanical and thermal properties of CFIQB and CBAGB allows an assessment of effect of botanical origin of fibers.
According to Fig. 3, the less insulating materials are elaborated with alkali treated fique fibers as all thermal conductivity values for CFIQB are higher than the others.
Regarding the strength values (Fig. 2 and 3), its trend according to the weight fraction of fibers is similar for CBAGB and CFIQB but we note that CBAGB present higher flexural strength than CFIQB.

Alkali treatment dissolves the hemicellulose matrix of vegetable fibers and thus, increases surface roughness. However, it improves little or degrades slightly the vegetable fibers properties. While heat treatment (pyrolysis), which increases significantly fibers mechanical strength, increases in a less way the vegetable fibers roughness in comparison with alkali treatment [Arsène et al. 2007]. Thus, these two factors allow the interpretation of the flexural strength according to fiber weight fraction and nature of fibers.

4 CONCLUSIONS

Thermal conductivity of vegetable fibers/cement composites is an important parameter in the use of such materials in construction for saving energy. In this study, particular attention is given to the influence of weight fraction of fibers, fibers treatment and nature of fibers on thermal properties. Composites elaborated with bagasse fibers are weaker heat conductor materials than those elaborated with fique fibers. Although for thermal insulating applications, one should prefer the weaker heat conductor that is to say CBAGP. But if requirements on mechanical strength are more severe, composites with alkali treated fibers have to be preferred.
Treatment effectiveness can be limited by roughness or fiber/matrix adhesion problems.
In order to evaluate the interest of a treatment or the nature of reinforcement, we have to compare the composites characteristics to control specimen (without any fiber) characteristics. In this study, the reference specimen contains aggregates and plasticizers and fiber content is limited to 3% (wt). In such conditions, improving effect of alkali treatment is not noted, at the contrary of results reported by Arsène et al. [2007] in the case of an ordinary Portland cement paste.
This study allows the determination of an “optimal” weight fraction of fibers. Indeed, if one wants to find a good deal between great thermal and mechanical properties, a formulation within 2.25% of bagasse fibers appears to be optimal.
Composites with fique fibers present weaker mechanical properties than composites with bagasse fibers.
This study has to be supplemented by additional experiments on specimen containing higher fiber content. Indeed, it will be useful in order to determine the potentialities of use of these composites as insulating materials.

ACKNOWLEDGMENTS

This work was supported by the ECOS-Nord Project “Vegetable fibers-cement composites” (Ref: C05P03). ECOS-Nord is also supported by MEN/ICETEX/COLCIENCIAS from the Colombian Government and by the French Government.

REFERENCES

Arsène, M.-A., Okwo, A., Bilba, K., Soboyejo, A.B.O. & Soboyejo, W.O. 2007, ‘Chemically and thermally treated vegetable fibers for reinforcement of cement-based composites’, *Materials and Manufacturing Processes*, **22**, 214-227.

Asasutjarit, C., Hirunlabh, J., Khedari, J., Charoenvai, S., Zeghmati, B. & Cheul Shin, U. 2007, ‘Development of coconut coir-based lightweight cement board’, *Construction and Building Materials*, **21**, 277-288.

Bilba, K., Arsène, M.-A. & Ouensanga, A. 2003, ‘Sugar cane bagasse fibre reinforced cement composites. Part I. Influence of the botanical components of bagasseon the setting of bagasse/cement composites’, *Cement & Concrete Composites*, **25**, 91-96.

Bilba, K., Arsène, M.-A. & Ouensanga, A. 2004, 'Influence of chemical treatment of vegetable fibers on insulating behavior of vegetable fibers/cement composites', Proc. Conferencia Brasileira de materiais e tecnologias de nao-convencionais, Pirassununga, Brasil, 29 October 3 November 2004, pp 51-59.

Blankenhorn, P.R., Blankenhorn B.D., Silsbee, M.R. & DiCola M. 2001, 'Effects of fiber surface treatments on mechanical properties of wood fiber-cement composites', *Cement and Concrete Research*, **31**, 1049-1055.

Coutts, R.S.P. 1988, Wood Fibre Reinforced Cement and Concrete.

De Guttierez, R.M., Diaz, L.N. & Delvasto, S. 2005, 'Effects of pozzolans on the performance of fiber-reinforced mortars', *Cement and Concrete Composites*, **27**, 593-598.

Delvasto, S. 2006, IIBCC 10th Int. Inorganic-Bonded Fiber Composites Conference, pp 218-228.

Savastano, H.J., Warden, P.G. & Coutts, R.S.P. 2000, 'Brazilian waste fibres as reinforcement for cement-based composites', *Cement & Concrete Composites*, **22**, 379-384.

Savastano, H.J., Warden, P.G. & Coutts, R.S.P. 2001, 'Performance of low-cost vegetable fibre-cement composites under weathering', CIB Worl Building Congress, Wellington, New-Zealand, April 2001, pp 1-11.

Savastano, H.J., Warden, P.G. & Coutts, R.S.P. 2003, 'Mechanically pulped sisal as reinforcement in cementitious matrices', *Cement & Concrete Composites*, **25**, 311-319.

Savastano, H.J., Warden, P.G. & Coutts, R.S.P. 2003, 'Potential of alternative fibre cements as building materials for developing areas', *Cement & Concrete Composites*, **25**, 585-592.

Toledo Filho, R.D., Ghavami, K., England, G.L. & Scrivener K. 2003, 'Development of vegetable fibre-mortar composites of improved durability', *Cement & Concrete Composites*, **25**, 185-196.

A Study on the Addition of Extra Water Which Affects the Durability Degradation of Concrete

Young Je, Woo [1]
Hwa Sung, Ryu [2]
Sang Hwa, Jung [3]
Sung Tae, Chae [4]

T11

ABSTRACT

Various problem such as durability degradation may happen when extra water is added to concrete. Because of these reasons, the change of water content is managed by using rapid evaluation method of unit water content such as electric capacity method, heat drying method making use of micro wave, unit capacity mass method among various methods. Especially, in Japan, guidance for the change of water content(±10, 15, 20kg/m^3 etc.) were regulated and used. However, it is the real situation that the guidance which was regulated in Japan evaluate suitability only considering production and measurement error under the circumstances which are not considering the degree of durability degradation.

Therefore, this study tries to investigate the influence of addition of extra water in the concrete on the durability degradation of concrete when it was added by artificial manipulation or by management error. From the test results, a guideline of the contents of extra water for the quality control is suggested with the consideration of the degree of durability degradation and the probable error resulted from the addition of extra water.

The contents of extra water for tests are set as 0, 15, 25, 35kg/m^3. To examine the durability degradation of concrete, freezing and thawing, carbonation, chloride penetration and compressive strength are tested.

KEYWORDS

Extra water, Durability, Degradation, Concrete

[1] Korea Institute of Construction Materials, Standardization Research Group, Construction Material Research Center, Structural Material Team, Senior Researcher, South Korea, Phone +82 2 3415 8811, Fax 3415 8790, imgod@kicm.re.kr
[2] Korea Institute of Construction Materials, Standardization Research Group, Construction Material Research Center, Structural Material Team, Researcher, South Korea, Phone +82 2 3415 8818, Fax 3415 8790, rhsung@kicm.re.kr
[3] Korea Institute of Construction Materials, Standardization Research Group, Construction Material Research Center, Structural Material Team, Team Leader, South Korea, Phone +82 2 3415 8808, Fax 3415 8790, jsh2593@kicm.re.kr
[4] Korea Institute of Construction Materials, Standardization Research Group, Construction Material Research Center, Structural Material Team, Head, South Korea, Phone +82 2 3415 8781, Fax 3415 8790, concre@kicm.re.kr

1 INTRODUCTION

Water is indispensable in order to cause hydration reaction and secure a certain level of liquidity when fabricating concrete. Generally, as shown in Figure 1, when the unit water content within concrete increases, such materials as coarse aggregate or mortar are segregated, and the increase in bleeding or the shrinkage crack due to an increase in drying shrinkage might also generate porosity on the lower part of aggregate or reinforcing bar, which deteriorates adhesiveness between reinforcing bar and the concrete. Besides, other deterioration might be lead such as settlement cracking, a surface deterioration through water transfer or the drop in penetrating resistance for salt, water and gas with internal porosity increases. Accordingly, such methods as electric capacity method, heat drying method are being suggested to improve the durability of concrete structure and the credibility of quality control and to quantitatively manage the quality of concrete at the construction site.

Especially in Japan, guidance for the change of water content (±10, 15, 20kg/m^3 etc.) were regulated by relevant institutions such as Ministry of land, infrastructure and transport, as shown in Figure 2. However, it is the real situation that the guidance which were regulated in Japan evaluate suitability only considering production and measurement error under the circumstances which are not considering the degree of durability degradation, which means that the Ministry of land, infrastructure and transport of Korea set $\sqrt{10^2+10^2} \fallingdotseq \pm 15\,\mathrm{kg/m^3}$ as a standard for an evaluating, considering such probable errors as fabrication error of ±10kg/m^3 and measurement error of 10kg/m^3.

Therefore, this study tries to investigate the influence of addition of extra water in the concrete on the durability degradation of concrete when it was added by artificial manipulation or by management error. From the test results, a guideline of the contents of extra water for the quality control is suggested with the consideration of the degree of durability degradation and the probable error resulted from the addition of extra water.

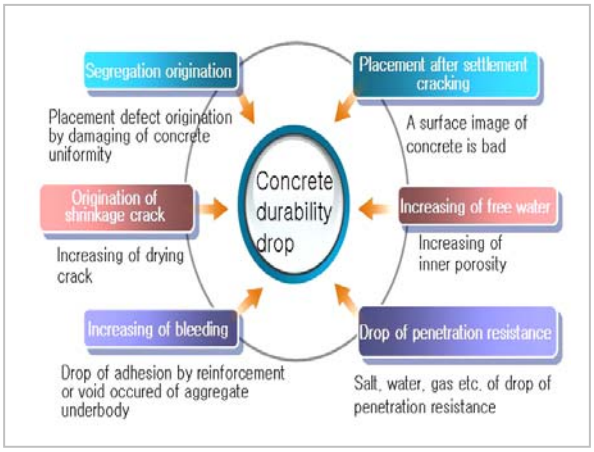

Figure 1. Drop in durability according to unit water content

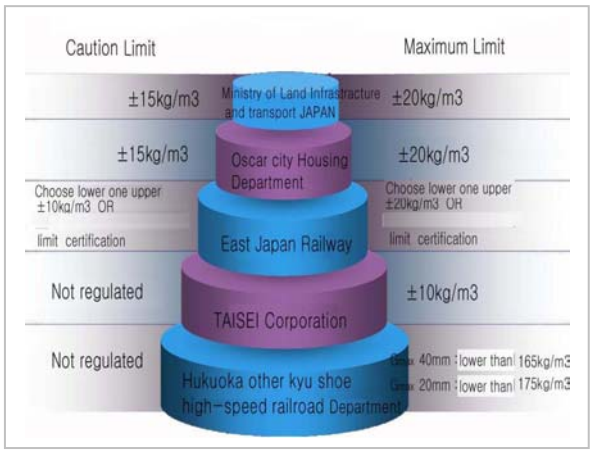

Figure 2. Japanese guideline on unit water content

2 TEST PLAN AND PROCEDURE

2.1 Test Plan

As shown in Table 1, we set five-step test variables of 155, 165, 175, 185 and 195kg/m^3 as standard test variables, based on the unit water content, considering most frequently used concrete mixture among three major ready-mixed concrete companies. In order to examine the possible problems by the change in unit water content at the plant for ready-mixed concrete, we also established four-step increase in water content (0, +15, +25, +35kg/m^3) at each unit water content as test factors. As for the accelerated concrete, the evaluation on compressive strength for each age, freeze-thaw resistance, penetration resistance of chlorine ion and carbonation had been implemented in accordance with the test methods specified in the Korean Standards (KS).

Table 1. Test Plan and A Mix of Concrete

Water-Cement Ratio (%)	Fine Aggregate Ratio (%)	Unit Weight (kg/m^3)				
		Water		Cement	Fine Aggregate	Coarse Aggregate
48	45.7	155	0 +15 +25 +35	320	885	1050
52		165	0 +15 +25 +35	320	872	1036
55		175	0 +15 +25 +35	320	860	1021
58		185	0 +15 +25 +35	320	848	1007
61		195	0 +15 +25 +35	320	836	993

2.2 Materials

Physical properties of materials used in this concrete experiment are shown in Table 2.

Table 2. Physical properties of materials used

Cement	Type : Normal Portland Cement (Type I), Density : 3.15g/cm^3, Fineness : 3,200cm^2/g	
Aggregate	Fine Aggregate	Type : Sea Sand, Density : 2.61g/cm^3, FM : 2.57
	Coarse Aggregate	Type : Ground gravel, Maximum size : 25mm, Density : 2.64g/cm^3, FM : 6.96

2.3 Test Items and Evaluation

The evaluation on the test items and the durability of concrete had been implemented in accordance with the KS, as shown in Table 3.

Table 3. Items of Measurement

Items of Measurement	Instantaneous compliance
Compressive Strength	3, 7, 28day
Freezing-Thawing Resistance	0,50,100,150Cycle
Penetration Resistance of Chlorine Ion	28day
Accelerated Carbonation	7, 14, 21, 28day

The test for the penetration resistance of chlorine ion was implemented in accordance with RCPT (Rapid Chloride penetration test) and ASTM.

Freeze-thaw resistance test was conducted by 10 × 10 × 40cm of specimen, a test of KS F 2456's (resistance test of rapid freeze-thaw of concrete) B type was freezing in air and thawing in water. It makes 1 cycle of -18℃ ~ +4℃ feeze-thaw for 4 hours. The test for rapid carbonation resistance conditions on temperature(20±2)℃, relative humidity(60±5)% by KS F 2584(rapid carbonation test of concrete). The measurement for carbonation depth was sprayed a reagent by KS M 8238, it measured depths of discoloration to madder from concrete surface. The measurement ages are 7, 14, 21, 28 days

3 TEST RESULTS AND CONSIDERATION

3.1 Test result of Compressive Strength

Test result of compressive strength by the change in water content within concrete in Figure 3 shows that compressive strength increases as it ages 3, 7, to 28 days and it increases as Water-Cement Ratio and Unit water content are low. In other words, when the water content within concrete increases, compressive strength decreases overall.

At each water-cement ratio vs. unit water content, when we say that W0's compressive strength rate in the 28th day without summand is 100, and if a summand of + 15 occurs as shown in Figure 4 (a figure describing a relative compressive strength rate according to summand in percentage, a relative compressive strength rate is 84~87%. If a summand of +25 occurs, a relative compressive strength rate is 67~76% and +35 summand results in relative compressive strength rate of 61~62%.

This result is calculated adding safety rate to design standard strength. But, it is evaluated to take into consideration of possible compressive strength result below the design standard strength if +25 of summand occurs. In case of B Class with 59%-185, 61%-195, material segregation occurs from +15 summand. Therefore, it was intended to exclude from the test analysis.

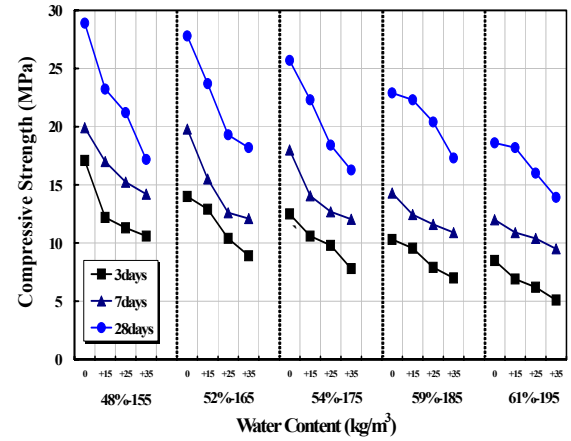

Figure 3. Compressive strength of concrete according to unit water content

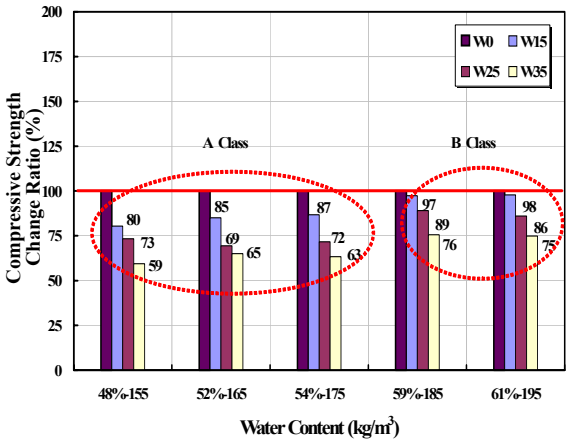

Figure 4. Decrement of compressive strength according to unit water content

3.2 Resistance to Freezing and Thawing

Figure 5 illustrates that the relative dynamic modulus of elasticity for 48%-155 decreases to 73~75% and the relative dynamic modulus of elasticity for 52%-165 decreases to 61~71% at the cycle 150 with an increase in water content. However, at 54%-175 and 59%-185, there is no such difference caused by adding water, showing great similarity in the results either adding water or not. When adding +25, +35 kg/m^3 of water to the specimen, it might cause the problem of fracturing during the freezing and thawing test, making it impossible to measure. Especially at 61%-195, all specimens were fractured at the cycle 150. From the results above, it might be inferred that freezing-thawing resistance caused by an increase of the unit water content shows relatively slight degradation when the water-cement ratio have higher compressive strength.

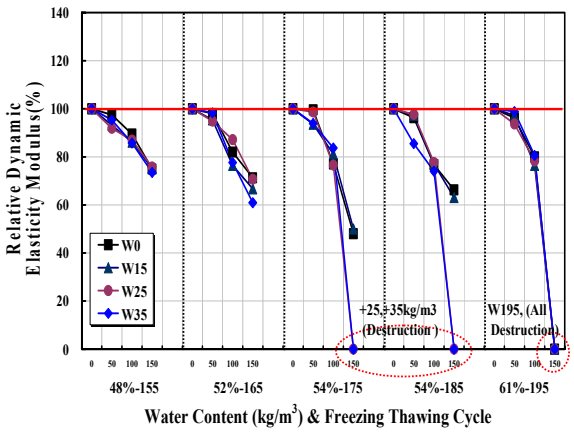

Figure 5. Relative Dynamic Elasticity coefficient

3.3 Penetration Resistance of Chlorine ion

As shown in Table 4 and Figure 6, which indicates a test result of penetration resistance of chlorine ion by adding extra water, Class B with relatively lower strength undergoes greater influence by the

change of unit water content and has thicker chloride ion penetration, compared to Class A. When adding +15 or +25kg/m^3 of water , in all cases compared to W0, the result shows a thicker penetration of chlorine ion with approximate thickness of 0.08~0.61mm for Class A and 1.29~2.55mm for Class B. However, when adding +35kg/m^3 of water, chloride ion penetration grows greater with approximate thickness of 3.23~7.97mm. Therefore, it is suggested that the addition of water would not exceed +25kg/m^3 considering penetration resistance of chlorine ion at normal strength even when the water content within concrete increases due to the artificial addition and the addition caused by management or fabrication error.

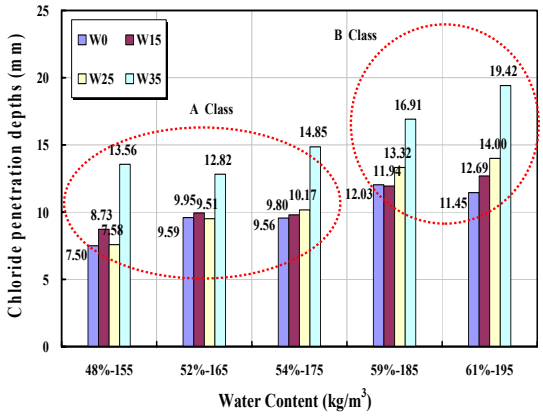

Figure 6. Depth of penetration of chlorine ion according to unit water content

Table 4. Depth of penetration of chlorine ion according to unit water content

Unit water content	W0(mm)	W15(mm)	W25(mm)	W35(mm)
155	7.50	8.73	7.58	13.56
165	9.59	9.95	9.51	12.82
175	9.56	9.80	10.17	14.85
185	12.03	11.94	13.32	16.91
195	11.45	12.69	14.00	19.42

Table 5. Photograph of penetration of chlorine ion according to unit water content

Unit water content	W0	+15	+25	+35
155				
165				
175				
185				
195				

3.4 Resistance to Carbonation

1) Thickness of Carbonated Penetration

While the increase rate of carbonated thickness ranges from 4 to 17% when adding +15 kg/m^3 of water, the addition of +25 or +35kg/m^3 of water lead an increase 24~77% and 35~130%, respectively, suggesting a consideration for the resistance to carbonation. (See Table 6.)

Table 6. Depth of penetration of Carbonation according to unit water content

Unit water content		W0(mm)	W15(mm)	W25(mm)	W35(mm)
155	28days	7.50	8.73	7.58	13.56
165	28 days	9.59	9.95	9.51	12.82
175	28 days	9.56	9.80	10.17	14.85
185	28 days	12.03	11.94	13.32	16.91
195	28 days	11.45	12.69	14.00	19.42

2) Durability Estimation by using Coefficient of Carbonation Speed

As shown in Figure 7 and Table 7, a coefficient at the same condition of CO_2 concentration of 5±0.2% could be calculated in accordance with the formula (1). The coefficient, ranged from 2.0 to 4.0mm/day$^{0.5}$, increases as the water content within concrete increases.

$$C = A \cdot \sqrt{t} \quad (1)$$

Where, C is carbonated thickness, t is the time passed, A is a Coefficient of Carbonation Speed

As given in Figure 8 through Figure 12 and Table 8, the estimation of durability using the coefficient of carbonation speed showed that it would take approximately 100 years to reach 30mm in its cover at the ratio of 48% - 155% while it would take 55 to 60 years with a higher ratio ranged from 52%-165 to 61%-195. When adding +15kg/m^3 of water, it showed comparatively gentle decline its durability with an average decreasing rate of 14% while its decreasing was considerably rapid with the average of 36% and 52%, respectively, when adding +25, +35kg/m^3 of water The water gain from the manufacturing or management error had a great influence on the process of long-term carbonation of concrete, which led an increase in internal porosity and a decrease in the resistance to carbonation which had been resulted from the penetration of carbon dioxide or water. Therefore, the water-cement ratio should not exceed 48% and the unit water content should be less than 155kg/m^3 to secure the durability of 100 years for the carbonation of concrete. Especially, in order to secure the durability on the carbonation of concrete structure even when the unit water content within concrete increases due to its manufacturing error caused by adding water, the water added to the concrete might not +25kg/m^3.

Table 7. Velocity Coef. of carbonation according to unit Water content

Unit water content	W0(mm/day $^{0.5}$)	W15(mm/day $^{0.5}$)	W25(mm/day $^{0.5}$)	W35(mm/day $^{0.5}$)
155	1.37	1.61	2.42	3.15
165	2.24	2.57	2.81	3.50
175	2.48	2.64	3.07	3.44
185	2.87	2.99	3.55	3.89
195	2.76	2.97	3.81	5.18

Table 8. A taking time of carbonation progress from concrete surface into 30mm depth in concrete

Unit water content	W0(year)	W15(year)	W25(year)	W35(year)
155	100	90	60	40
165	60	45	33	25
175	58	50	43	35
185	46	45	32	28
195	55	45	33	20

Table 9. Photograph of penetration of carbonation according to unit water content

Unit water content/days	195	185	175	165	155
	W0 +15 +25 +35	W0 +15 +25 +35	W0 +15 +25 +35	W0 +15 +25 +35	W0 +15 +25 +35
7					
14					
21					
28	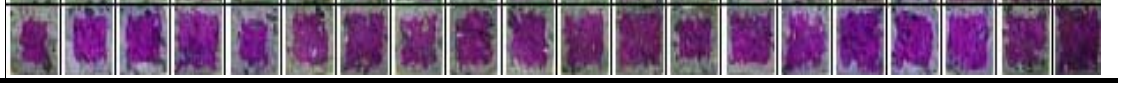				

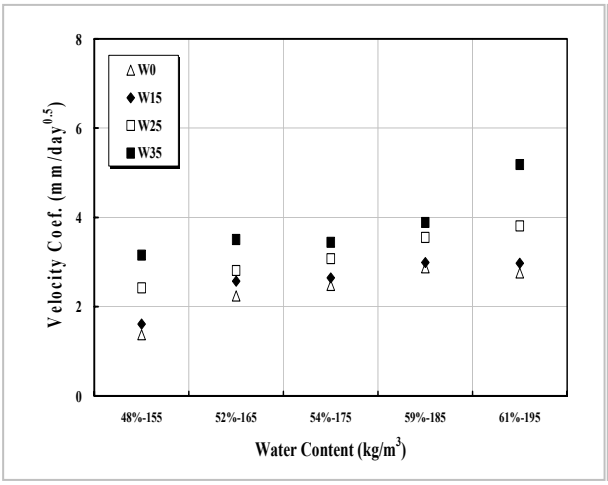

Figure 7. Velocity Coef. of carbonation according to unit Water content

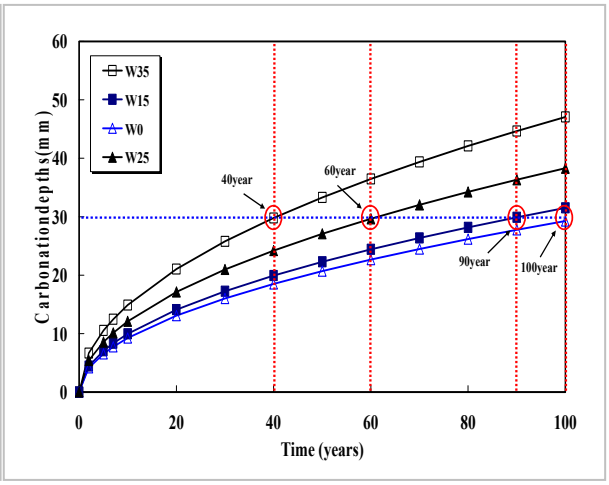

Figure 8. Carbonation depth of concrete with time(48%-155)

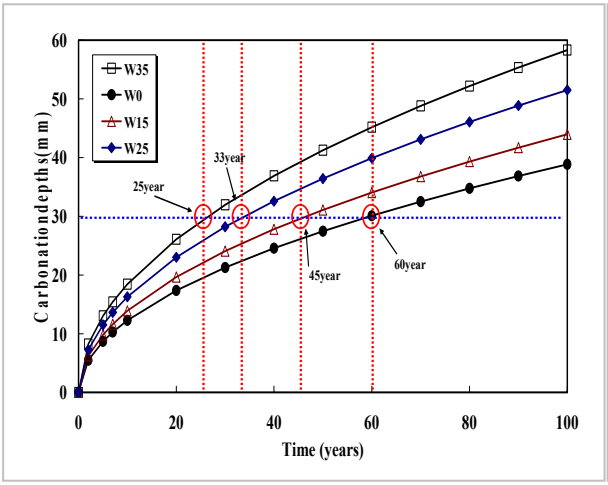

Figure 9. Carbonation depth of concrete with time(52%-165)

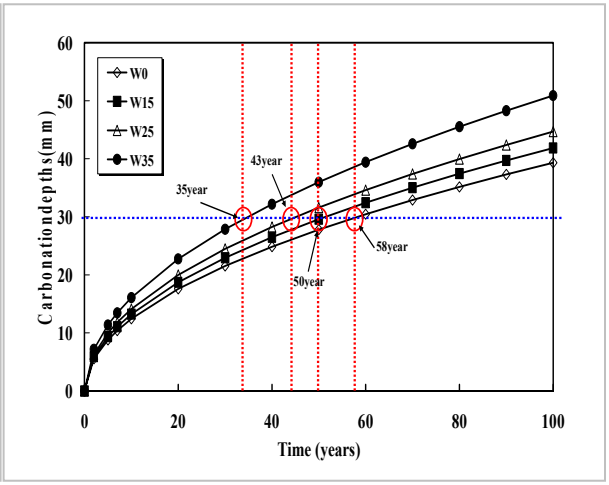

Figure 10. Carbonation depth of concrete with time(54%-175)

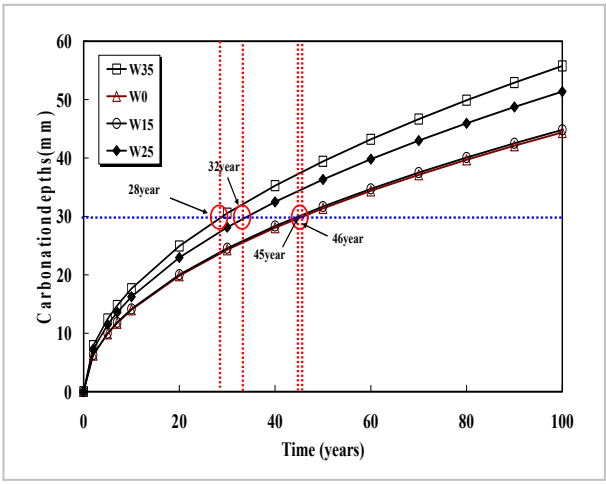

Figure 11. Carbonation depth of concrete with time(59%-185)

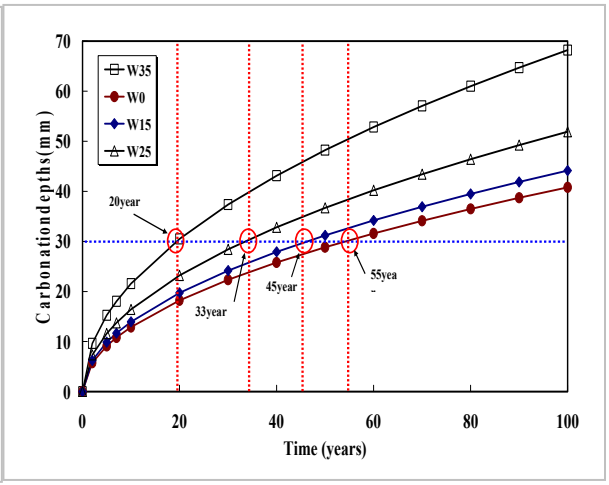

Figure 12. Carbonation depth of concrete with time(61%-195)

4 CONCLUSION

Based on the test results above, we might draw a conclusion that when the unit water content within concrete increases due to the errors caused during the quality control or the manufacturing, compressive strength decreases, not to mention of durability of concrete such as Freezing-Thawing Resistance, Penetration Resistance of Chlorine ion, Carbonation Resistance. The results of this research might be summarized as follows:

1) From the result of compressive strength test, it could be inferred that when adding +15, +25 and +35 kg/m^3 of water, relative compressive strength would decrease to the level of 84 ~ 87%, 67 ~ 76% and 61 ~ 62%, respectively. Therefore, it is recommended to take into consideration for not adding more than +25kg/m^3 of water in order to maintain a certain level of designed compressive strength.

2) From the result of the test for freeze-thaw resistance, it could be inferred that an increase in compressive strength would lead a decrease in freeze-thaw resistance with the change in the unit water content, especially with lower than 52%-165.

3) From the result of the test for penetration resistance of chloride ion, it could be inferred that when adding +15 or +25kg/m^3 of water , in all cases compared to W0, the result shows a thicker penetration of chlorine ion with approximate thickness of 0.08~0.61mm for Class A and 1.29~2.55mm for Class B. However, when adding +35kg/m^3 of water, chloride ion penetration grows greater with approximate thickness of 3.23~7.97mm. Therefore, it is suggested that the addition of water would not exceed +25kg/m^3 considering penetration resistance of chlorine ion at normal strength even when the water content within concrete increases due to the artificial addition and the addition caused by management or fabrication error.

4) From the result of carbonation test, it could be inferred that the water gain from the manufacturing or management error had a great influence on the process of long-term carbonation of concrete, which led an increase in internal porosity and a decrease in the resistance to carbonation which had been resulted from the penetration of carbon dioxide or water. Therefore, the water-cement ratio should not exceed 48% and the unit water content should be less than 155kg/m^3 to secure the durability of 100 years for the carbonation of concrete. Especially, in order to secure the durability on the carbonation of concrete structure even when the unit water content within concrete increases due to its manufacturing error caused by adding water, the water added to the concrete might not +25kg/m^3.

5) From the test results above, it could be inferred that the quality control on the mix designed unit water content should be noted in order to maintain a certain level of durability performance when there is an increase more than +25kg/m^3, which might lead considerable deterioration of concrete.

ACKNOWLEDGMENTS

This research was supported by a grant(06-CIT-A02: Standardization Research for Construction Materials) from Construction Infrastructure Technology Program funded by Ministry of Construction & Transportation of Korean government.

REFERENCES

Young Je, Woo Hwa Sung, Ryu, "A study of endurance quality change by increasing of water content in concrete", Korean society of hazard mitigation of a collected papers, vol7, no2, 2007.06, pp 1~6

Ministry of Land, Infrastructure and Transport Japan, Ready-mixed Concrete, Water content Measurement outline(proposal), 2004. 3

L.Tang and L.O.Nilsson, Rapid Determination of the Chloride Diffusivity in Concrete by Applying an Electrical Field, ACI MATERIALS Journal, Jan.-Feb., 1992, p.p.49-53

ASTM C 1079-87 : Standard Test Methods for Determining the Water Content of Freshly Mixed Concrete

Behaviour of Four Repair Materials Under Accelerated Testing of Carbonation and Chloride Penetration

Carmen Andrade [1]
Unal Anil Dogan [2]
Nuria Rebolledo [1]
Isabel Martinez [1]

T11

ABSTRACT

The main objective of repair mortars, usually applied in patching is to restore the geometry and integrity of the material and the repassivate the reinforcing steel. Repair materials can be of two different natures: cement based or polymer based. In the case of cementitious repair materials, a polymer may be added that will dissolve or disperse during mixing. With any of these alternatives the steel should exhibit after repair a very low corrosion rate which is described as "be repassivated". An additional property appreciated in repair mortars is their resistance to the penetration of the aggressive substances: carbonation and chloride ions.

In present paper, four different repair materials are tested in an accelerated manner in order to rank them for application in a particular structure. The tests performed have been water absorption, mercury porosimetry, corrosion potential and corrosion rate after carbonation and after chloride penetration. The accelerated carbonation was made in a chamber at 100% CO_2 and the accelerated chloride ingress by applying an electrical field. The results indicate very different performance regarding corrosion of the steel: While one of the mortars exhibited immediate corrosion depassivation when tested, there is another not depassivated after one year in the same conditions. These different behaviours claim for the need to test these materials. In the paper attempts are made to justify the very different performance from the results obtained on the microstructure.

KEYWORDS

Repair materials, Ccarbonation, Chloride, Corrosion

1 Institute of Construction Sciencie, "Eduardo Torroja", CSIC, Serrano Galvache s/n, Apdo 19002, E-28003, Madrid, Spain, andrade@ietcc.csic.es
2 Istanbul Technical University, Civil Engrg. Faculty, Istanbul, Turkey 34469, Phone +90 212 2853769, Fax 212 2856587, adogan@ins.itu.edu.tr

1 INTRODUCTION

Steel embedded in concrete is protected against corrosion due to its alkaline nature as a result of $Ca(OH)_2$ evolution during hydration of cement. However, concrete structures are subjected to aggressive environments which may cause degradation depending on their performance, throughout their service life. In alkaline concrete with a pH value greater than 12, a passive layer of ferro-oxides is formed over the reinforcing steel. This passivity may break down mainly in two ways; ingress of chloride ions and carbonation of concrete cover which lead into reinforcement corrosion.

Many repair operations involve only patches where the repair material to be used is in the form of (polymeric/cementitious) mortar. Cementitious mortars are recently preferred because of the repassivation effect of cement hydration but polymer latex utilization is also common in order to improve permeability and bonding properties.

Although cementitious repair mortars reproduce passive layer over the steel, primers applied on rebar surfaces are also used to overcome the risks resulting from poor compaction of these rapid hardening repair mortars. On the other hand, they are used in order to achieve a complete bond between mortar and steel.

In this study, four different commercially available rapid hardening cementitious repair mortars and steel primers are tested against carbonation and chloride induced corrosion by Polarization Resistance electrochemical technique. To characterize the repair materials regarding the corrosion resistance and able to make a comparison, accelerated chloride migration tests, accelerated carbonation tests, capillarity and mercury intrusion porosimetry (MIP) tests are applied.

2 EXPERIMENTAL

The four commercial pre-mixed repair mortars used are of cementitious nature and the contents are unknown . Water-to-cement ratios of mortar were adjusted according to the specifications of set of fats. For the accelerated chloride migration tests 7x7x7 cm cubic specimens and for accelerated carbonation tests, 2x5.5x8 cm prisms containing two identical steel bars were cast. In both of the tests, half of the steel bars embedded in mortars were coated with the primer of each brand. Before embedding the steel bars into the mortars, they were cleaned in an HCl solution, washed with water, immersed in acetone and dried with hot air. Prisms, having the same dimensions, without steel bars were also produced to perform capillarity test. After being demoulded, carbonation and chloride migration specimens were put in a chamber having a 95% RH and 20±2^{o}C for 7 and 28 days, respectively.

2.1 Carbonation experiments

Specimens for accelerated carbonation were stored in laboratory conditions for drying during 28 days and then are subjected to accelerated carbonation under 100% CO_2, 50% RH and 20±2^{o}C. Prior to location of the samples in the carbonation chamber and in the following days, weights and corrosion rates were measured every day. On account of CO_2 binding of hydration product (calcium hydroxide) of cementitious mortars, weight propagations were observed. When the rate of increase became negligible, it is assumed that carbonation process had finished and specimens were immersed in water. Daily corrosion measurements were continuously taken after immersion.

2.2 Migration experiments

A container, filled with a 1 M of NaCl solution, was sealed on a face parallel to the rebar axis [Castellote *et. al.* 2002]. Migration of the chloride ions is accelerated by 12V potential difference between the solution container and opposite side of the specimen as shown in Figure 1. Some days

after initiation of the test, catholyte solution was neutralized with 0.05 M of HCl solution, in order to maintain a pH value of around 6 – 8.

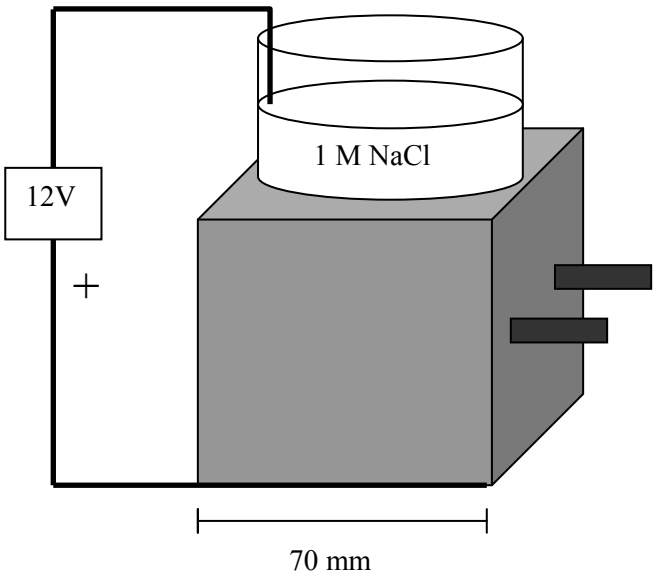

Figure 1. Accelerated chloride migration test setup

Prismatic specimens without rebar and for capillary water absorption tests were cured in a chamber having a 95% RH and 20±2°C for 28 days. Afterwards, they were left for drying in laboratory conditions for 60 days. The capillary water absorption by means of increase of weight per unit area is illustrated in Figure 3. The test and the calculation of coefficients m and k, resistance to water penetration and coefficient of capillary absorption, respectively, are performed according to Fagerlund [1982].

3. TEST RESULTS

Figure 2 illustrates the increase in weights of specimens during carbonation. In the figure, first letter denotes the coded mortar brand and the second one shows the situation of the embedded steel. Here, C is the abbreviation of 'coated'with primer and B is 'bare'.

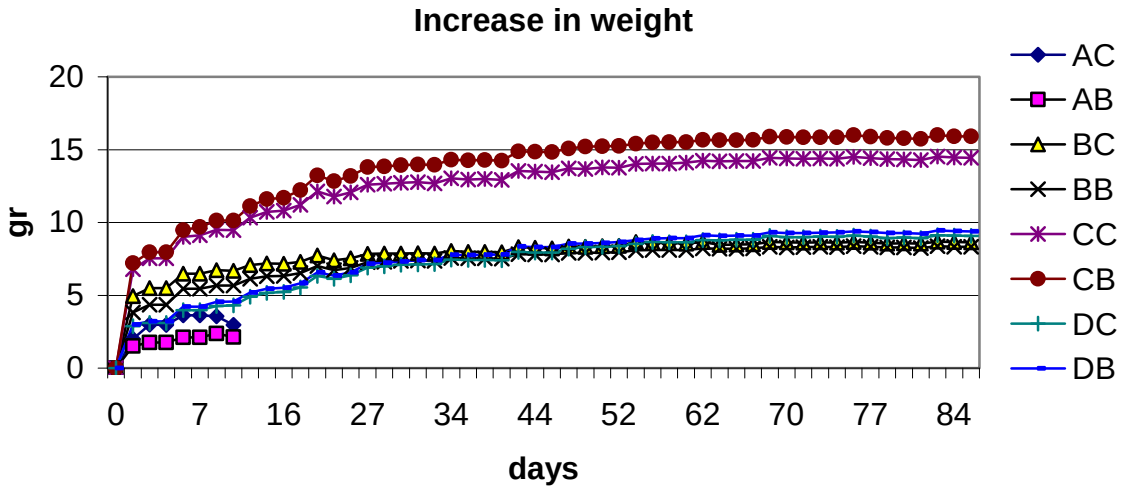

Figure 2. Weight rise of specimens subjected to accelerated corrosion tests

In order to investigate the pore structure of the hardened mortars, mercury intrusion porosimetry test was also applied.

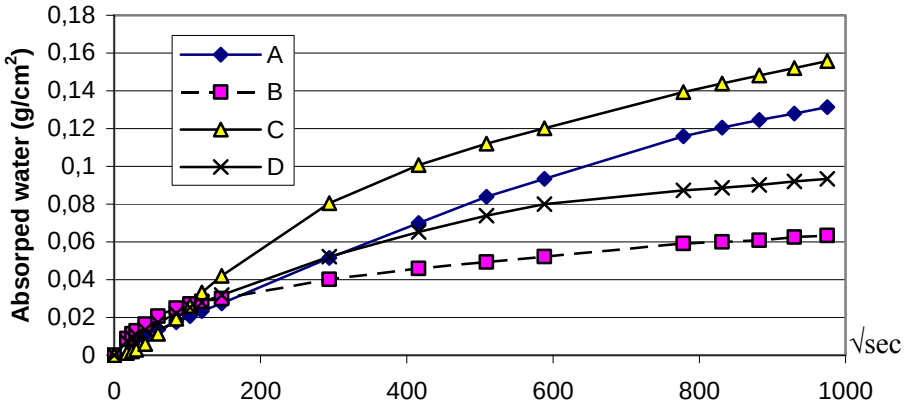

Figure 3. Capillary water absorption of the four repair mortars

Figure 2 and 3 show the increase in weight due to capillary suction and during carbonation, respectively. Except mortar A, rate of carbonation and water absorption by capillarity of mortars are in the same order.

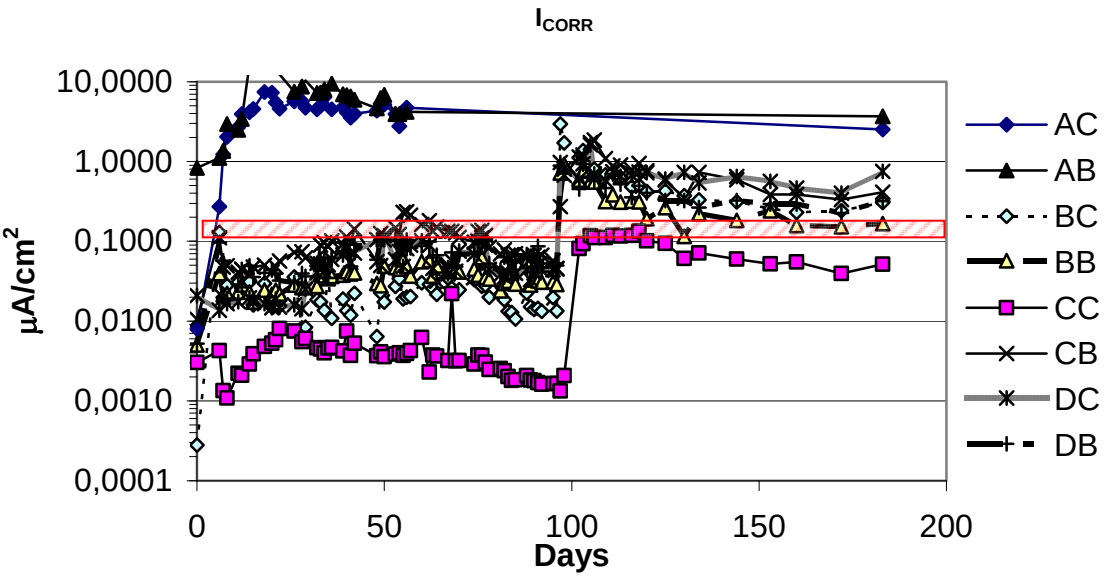

Figure 4. Corrosion rate evolution of accelerated carbonation specimens

Corrosion rate and corrosion potential evolution of the rebars embedded in repair mortars, during the accelerated carbonation tests is demonstrated in Figures 4,5 and 6. Other than the rebars in mortar A, none of the embedded steels seemed to corrode during the carbonation period until they contact to water. At the time all mortars are completely carbonated, they were immersed in water so corrosion rates were drastically increased and corrosion potentials decreased. These results prove again that steel does not depassivate in a dry concrete even if in low pH value-environments. Following the immersion in water, primer of mortar C showed the best performance followed by mortar B.

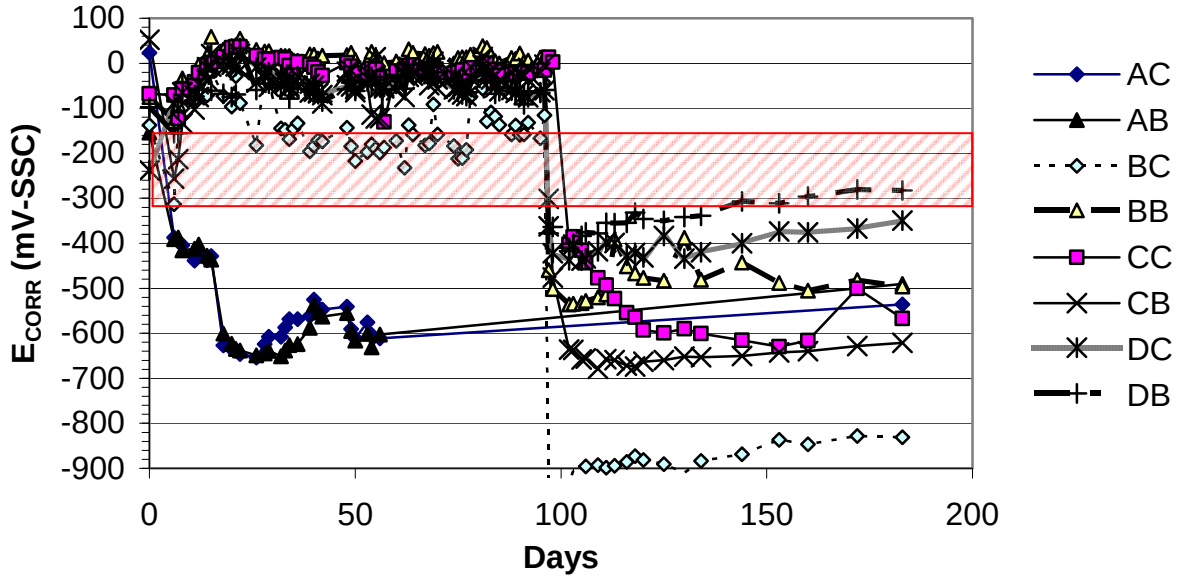

Figure 5. Corrosion potential evolution of accelerated carbonation specimens

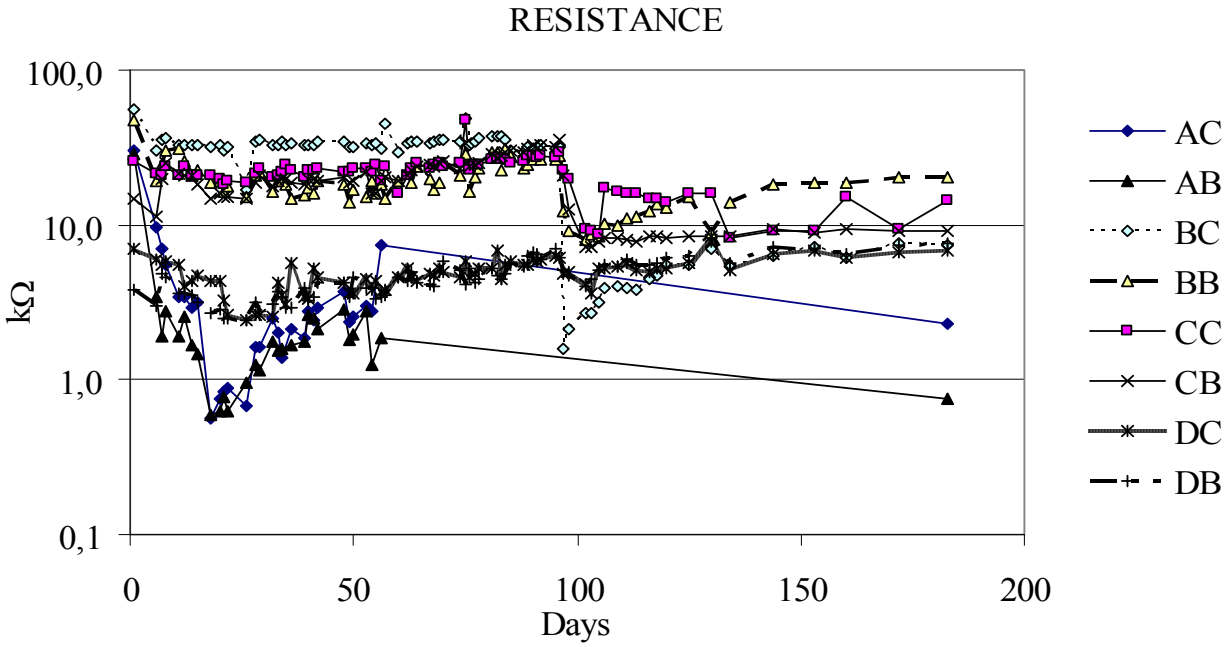

Figure 6. Electrical resistance evolution of accelerated carbonation specimens.

Results of the accelerated chloride migration test on the same mortars can be seen in Figures 7-9. Corrosion initiation of the steels in mortars by means of corrosion rate (Fig. 7) and corrosion potential (Fig. 8) was in correspondence. Also, for all mortars, bare steels started to corrode earlier than coated ones as expected. Surprisingly, onset of corrosion in mortar A was immediate as the carbonation specimens and mortar B remained passive after almost one year of 'accelerated' migration test while the latest initiation of all mortars was at about two months (mortar C). Time to corrosion initiation was similar for mortars C and D.

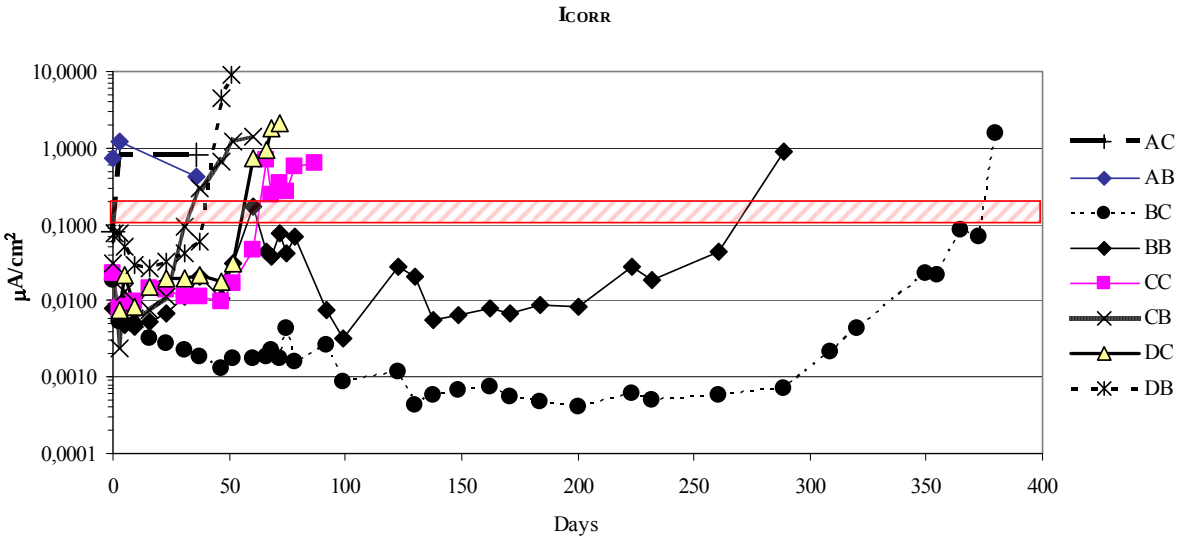

Figure 7. Corrosion rate evolution of accelerated chloride migration specimens

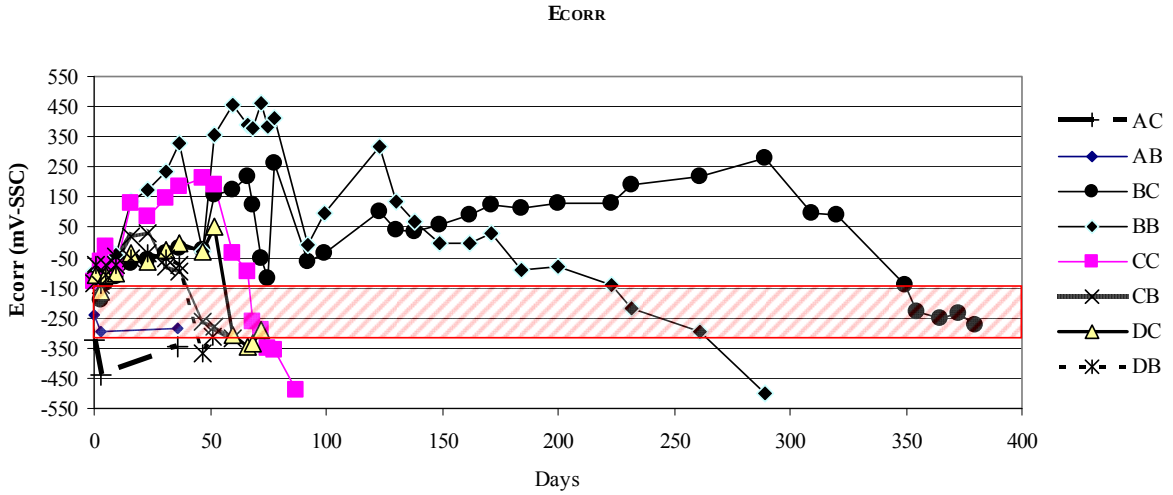

Figure 8. Corrosion potential evolution of accelerated chloride migration specimens

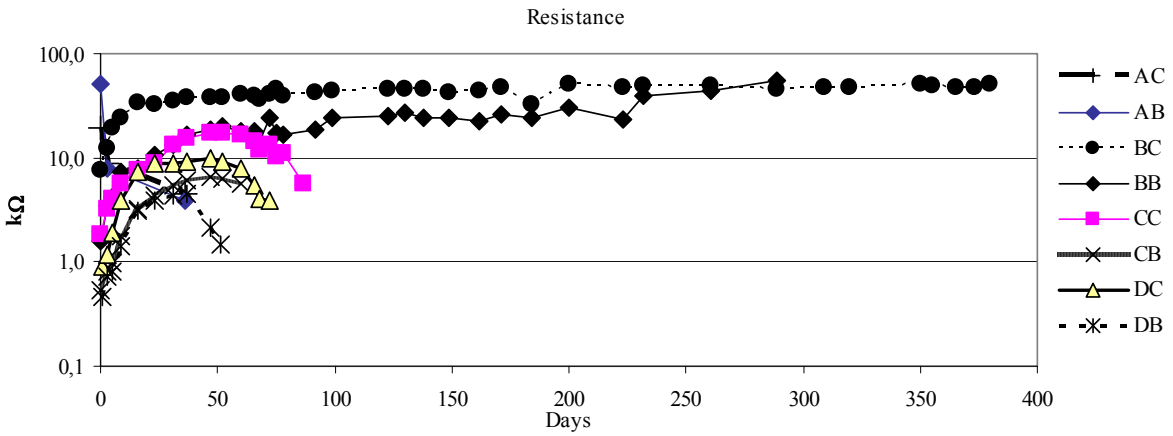

Figure 9. Electrical resistance evolution of accelerated chloride migration specimens

The pore size distribution and pore volume characterization of repair mortars is defined in Figures 10 and 11. Cumulative and incremental relative volumes by means of pore size are plotted versus pore

diameter. In Figure 11, it can easily seen that the peaks, called threshold diameter and defined as 'The highest amount of porosity per change in equivalent diameter in MIP method' [Cook & Hover 1999] are located between 1 nm and 0.01 nm. Provided these results are compared with the chloride-induced corrosion test results, it can be deducted that the smaller threshold diameters, the later corrosion initiation on account of chloride attack.

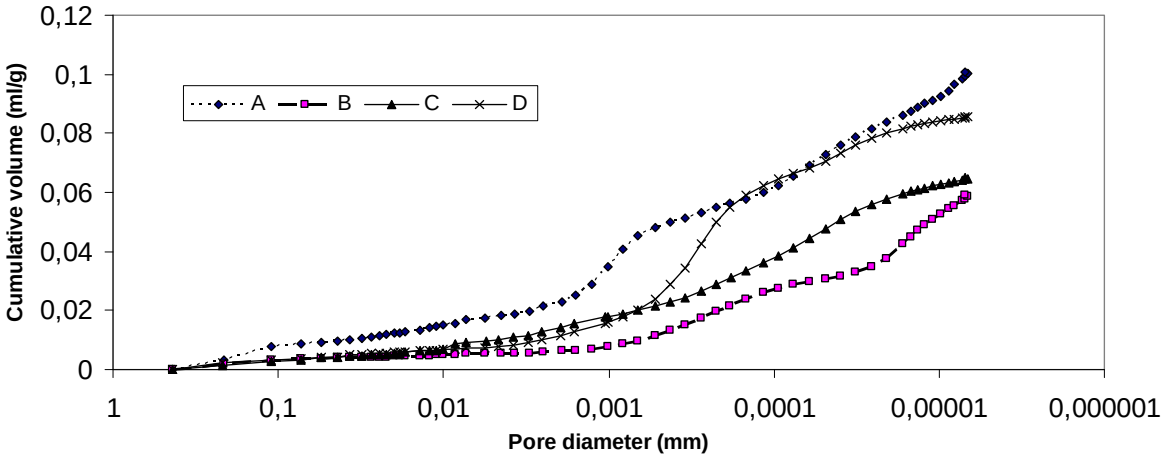

Figure 10. Cumulative pore size distribution of hardened repair mortars

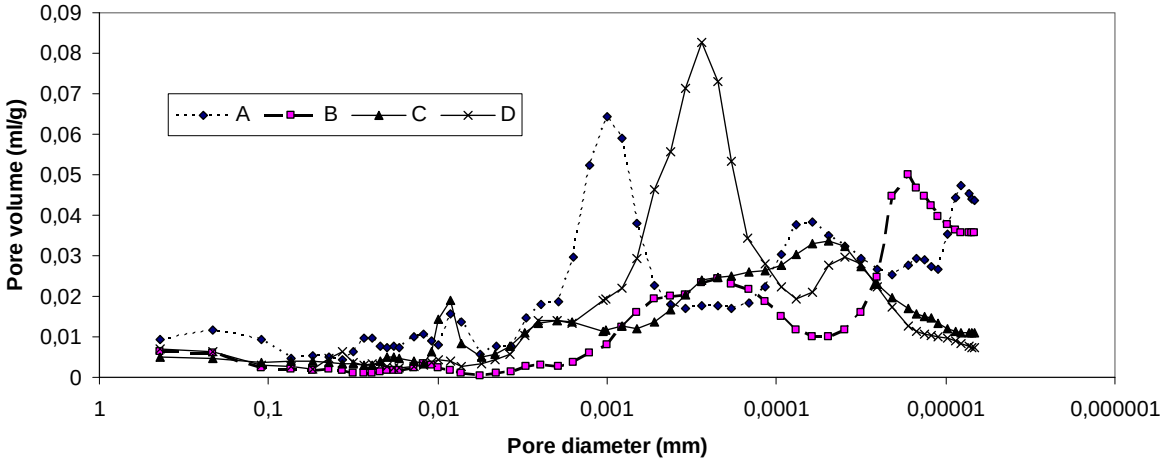

Figure 11. Incremental pore volume distribution of hardened repair mortars

4 DISCUSSION

The four different repair mortars perform very differently regarding protection against corrosion in spite the four are for the same use and purpose. In all cases the presence of a primer has been beneficial.

Regarding carbonation, primer of mortar C seemed somewhat more protective than the rest of the primers. Although mortar C had the highest amount of continuous capillary pores, coated rebars in this mortar didn't corrode after total carbonation. When an electrical field of 12V is applied to the mortars to accelerate chloride diffusion into concrete, mortar B showed an excellent performance through one year. Time to corrosion initiation was earlier but similar for mortars C and D.

Regarding the techniques to monitor the corrosionperformance, the most illustrative is the measurement of the polarization resistance because the electrical resistance or corrosion potential alone may be misleading as can be deduced from Figure 12.

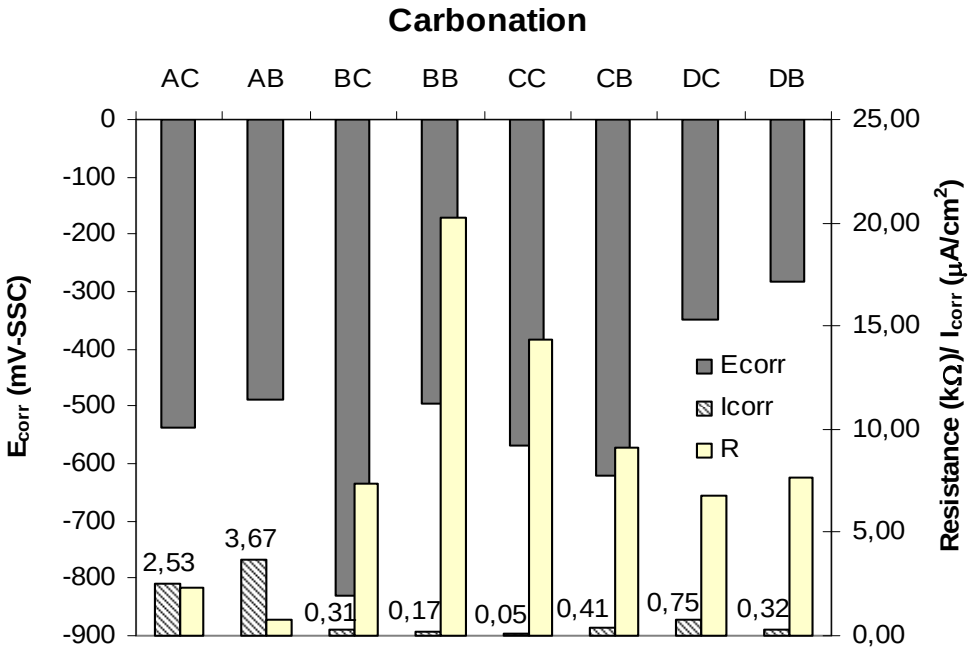

Figure 12. Ultimate values of carbonation specimens regarding with I_{corr}, E_{corr} and R_{ohm}.

CONCLUSION

Although more work is necessary to link composition of the repair mortars with corrosion performance, in present results evidences have been shown on the relation between low porosity or averaged pore radius and resistance to carbonation and chloride penetration.

The other main deduction made is that the presence of a primer has always delayed the corrosion onset and has contributed to lower further corrosion rates.

ACKNOWLEDGMENTS

The financial support of The Scientific and Research Council of Turkey to the second author is gratefully appreciated. The authors would like also to thank SIKA for the fruitful collaboration in these kinds of studies.

REFERENCES

Castellote, M., Andrade, C. and Alonso, C., 2002 'Accelerated simultaneous determination of the chloride depassivation threshold and of the non-stationary diffusion coefficient values', *Corrosion Science*, Vol. 44, 2409-2424.

Cook, R. A. and K. C. Hover 1999 'Mercury porosimetry of hardened cement pastes', *Cement and Concrete Research*, Vol. 29, 591-601.

Fagerlund, G.; "On the capillarity of concrete". Cement AB, Head technical development. Nordic Concrete Research, Oslo - 1982.

Coarse aggregate mineralogy, size and water content influence on concrete permeability

C. Gonilho Pereira [1]
J.P. Castro-Gomes [2]
A. Pereira de Oliveira [3]

T 11

ABSTRACT

The main objective of the experimetal work carried out was the evaluation of the influence of coarse aggregates geological source, dimension and water content in the concrete permeability. Four different aggretates, obtained from different geological environments, were selected, like granite, basalt, calcareous and marble coarse aggregates. After their mechanical and physical characterization, three concrete mixtures were produced with constant volume proportions, workability, mixing and curing conditions using different sizes of each aggregate type. Concrete durability parameters, such as capillary water absorption and oxygen permeability, measured at 28 days, were found to be affected by coarse aggregate size and its water content rather than aggregate mineralogy, as presented and discussed.

KEYWORDS

Coarse aggregate, Permeability, Water absorption, Concrete permeability, Durability

[1] Setubal Polytechnic, Barreiro College of Technology, 2830 Barreiro, Portugal, Phone +351 21 2064660, Fax 21 2075002, cristiana.pereira@estbarreiro.ips.pt
[2] University of Beira Interior, Department of Civil Engineering, 6200 Covilhã, Portugal, Phone +351 275 329990, Fax 275 329969, castro.gomes@ubi.pt
[3] University of Beira Interior, Department of Civil Engineering, 6200 Covilhã, Portugal, Phone +351 275 329738, Fax 275 329969, luiz.oliveira@ubi.pt

1 INTRODUCTION

The most common natural coarse aggregates used for concrete production are crushed rock extracted from pits and quarries of different geological sources. In what concerns the european aggregates industry, more than 28000 extraction sites across Europe produce around 3 billion tons of aggregates per year [UPEG 2006] and a quarter of this value is used in new residential building. Regarding the production of aggregates per EU citizen per year, the average annual production represents 7 tons per citizen [BGS 2006]. Nevertheless, the economic relevance of aggregates differs significantly among the member states. While some countries are interested in recycling others have a significant internal market, being Portugal one of the countries where the aggregates industry reveals economic relevance. More than 82 millions tons of aggregates were produced in Portugal, during the year of 2004, representing about 8.4 tons per citizen [Bleishwitz & Banhn-Walkowiak 2006].

Igneous, sedimentary and metamorphic rocks represent 30, 20 and 40% of national land, respectively [IGM 2000]. Igneous rocks are mainly granites and basalts and are predominant at North and Centre of Portugal, respectively. Sedimentary rocks are of calcareous nature and metamorphic are schist, quartzite and marble, and can be extracted at Centre and South of Portugal.. "Lisboa" and "Vale do Tejo" regions are responsable for 80% of total sand produced in Portugal [Gonilho Pereira 2005].

Large urban centres, like Lisboa and Setúbal (Centre of Portugal), Braga and Porto (North of Portugal), represents the higher production and consumption of aggregates. Therefore, calcareous and granite aggregates represent more than 70% of total of aggregates produced and consumed in Portugal.Thus, in the portuguese scenario, the selection of the coarse aggregate type for concrete production is determined by its demand and production in a specific region. However the choice of aggregate type should be decided based on concrete requirements [Ribeiro *et al* 2002]. Mechanical and physical characteristics of concrete, such as density, compressive strength or abrasion, are mainly determined by the mechanical and physical properties of aggregates [Aitcin & Perraton 2001]. This experimental work presents and discusses the relevance of coarse aggregate type, dimension and water content in concrete permeability and durability.

2 EXPERIMENTAL PROGRAMME

2.1 Aggregates selection and properties evaluation

The most common and relevant aggregates from Portuguese quarrying industry, were selected for this experimental work: granite (G), basalt (B), calcareous (C) and marble (M).

Aggregates mechanical and physical properties were evaluated according to European and Portuguese standards and laboratory tests were carried out in core specimens extracted from rock as well as in coarse aggregates obtained from quarries. Compressive strength and properties related to durability were determined in rock core specimens and coarse aggregates. Core specimens were evaluated in what concerns their compressive strength [ISRM 1981], capillary water absorption [LNEC-E392 1993], absorption and capillary coefficient [NF B 10-502] [DIN-52617], and oxygen and water permeability [Pacheco Torgal *et* al 2006]. Sieve analysis, particle volume index [LNEC-E223 1968], crushing values [BS-812 1990], bulk and particle density, particle water absorption and Los Angeles abrasion were evaluated in coarse aggregates [LNEC-E227 1970]. Experimental details of equipment used and procedures for each of these tests are described elsewhere [Pacheco Torgal *et* al 2006].

2.2 Concrete mixing conditions

A total of 12 different concrete mixes were produced with the four aggregate types. For each aggregate type, three different concrete compositions were produced, and designated as mix (A1A2), mix (A1), and mix (A1SAT) [Table 1]. Coarse aggregates of different particles size, were mixed in concrete in

both dry (mix A1A2 and mix A1) and water saturated states (mix A1SAT). Faury composition method was used for each mix formulation. Parameters like cement content, aggregate size distribution, water/cement ratio and voids volume were kept constant. To maintain the aggregate particle size distribution, standard sieve analysis curves were produced in laboratory for each type of aggregates, thus obtaining a constant modulus of fineness (aggregate size A1=6,4 and aggregate size A2=7,0).

Concretes were produced with constant workability, mixing and curing conditions and were cured for 28 days, at 90% of relative humidity and approximately 20ºC constant temperature.

Table 1. Concrete mix proportions

	Aggregate type			
	Basalt	*Granite*	*Calcareous*	*Marble*
Cement CEM II/B-L 35.2 (kg/m^3)	450.0			
Water (l/m^3)	198.0			
Mix (A1A2) Sand (kg/m^3)	697.5	697.5	697.5	697.5
Aggregate A1 (kg/m^3)	511.9	475.7	459.4	502.8
Aggregate A2 (kg/m^3)	471.4	345.2	418.7	448.4
Added water during mixing (%)*	-	1.5	35	1.5
Final slump (cm)	13	11	11	13
Mix (A1) Sand (kg/m^3)	813.8	813.8	813.8	813.8
Aggregate A1 (kg/m^3)	839.9	780.5	753.8	825.1
Additional water during mixing (%)*	4	13	16	5
Final slump (cm)	10	11	10	11
Mix (A1SAT) Sand (kg/m^3)	813.8	813.8	813.8	813.8
Aggregate A1 (kg/m^3)	839.9	780.5	753.8	825.1
Water adjustment (%)**	-	-	-	20
Final slump (cm)	10	10	10	10

* Added water includes water aggregates absorption and water adjustment to obtain approximately constant workability measured by slump test (12 ±2cm).
** Water adjustment to obtain constant slump.

Mixes (A1A2) and (A1) were produced using coarse aggregates in a relatively dry state. Therefore additional water was used to compensate aggregates initial absorption, considering that aggregates can absorb 70% of total water corresponding to its saturation [Ribeiro *et al* 2002]. A second water adjustment was preformed, during mixing, to obtain maintain concrete workability. Mix (A1SAT) was produced with water saturated with dry surface coarse aggregates particles that were saturated by water immersion during 24 hours and dry surface was obtained by leaving water to evaporate, in laboratory environment.

3 RESULTS AND DISCUSSION

3.1 Aggregates properties

Mechanical and physical properties of aggregates, obtained in core rock specimens and in fine and coarse aggregates, are presented in table 2.

Basalt presents the highest compressive strength, of about 140MPa followed by granite with 100MPa. Compressive strength mean results of calcareous and marble rocks are between 60 to 70MPa. The

compressive strength results of calcareous and marble are within the minimum value (60MPa) recommended for aggregates to be used in concrete production [Coutinho 1997].

Table 2. Mechanical and physical properties of fine and coarse aggregates.

	Aggregate type				
	Sand	*Basalt*	*Granite*	*Calcareous*	*Marble*
Maximum particle sizes (mm) *	2,4	12,7 / 19,1	12,7 / 19,1	2,7 / 19,1	12,7 / 19,1
Faury Modulus of Fineness *	3,3	6,4 / 7,0	6,4 / 7,0	6,4 / 7,0	6,4 / 7,0
Particle volume index *	-	0,25 / 0,25	0,12 / 0,19	0,20 / 0,26	0,17 / 0,22
Bulk density (kg/m^3)	1690	1630	1420	1360	1490
Particle density (kg/m^3)	2620	2850	2640	2540	2750
Particle water absorption (%)	0,5	1,5	0,3	2,8	0,05
Los Angeles abrasion (%)	-	15	26	37	41
Crushing value (%)	-	16	24	32	29
Compressive strength (MPa) **	-	138	100	61	71
Absorption coef. ($kg/m^2/h^{0,5}$) **	-	0,03	0,03	1,30	0,015
Capillarity coef.($g/cm^2/min^{0,5}$) **	-	0,04	0,04	1,68	0,02
Oxygen permeability (m^2) x 10^{-16} **	-	0	0,01	0,32	0
Water permeability (m^2) x 10^{-16} **	-	0	0,006	6,97	0

* obtained for particles size coarse aggregates A1 / A2
** obtained in core rock specimens

Aggregates are considered regular, suitable for the production of ordinary concrete, whenever their bulk density is between 1200 and 1700 kg/m^3, and particle densities are between 2300 and 3000 kg/m3 [Coutinho 1997]. All coarse aggregates presented Los Angeles abrasion lower than 50%, maximum mass loss recommended for aggregate to be used for concrete production. Aggregates are considered acceptable for concrete production when present aggregate crushing value, equal or lower than 45% [Coutinho 1997], which was verified for the four different aggregates.

Calcareous presented the highest oxygen permeability while basalt and marble did not allow the oxygen penetration, in the performed test conditions. In what concerns water penetration, basalt and marble are impermeable, granite has a very low permeability and calcareous presents the highest water penetration. However, both oxygen and water permeability results were very low in all cases. Calcareous presented the highest water absorption, in opposition to the marble that presented almost none absorption.

Granite, basalt and marble are almost impermeable, presenting very low capillarity, and that calcareous is water inhibitor, presenting weak capillarity [Tables 3-4].

Table 3. Aggregates class according to its absorption coefficient [NF B 10-502].

DIN 52617 absorption class	Absorption coefficient ($kg/m^2/h^{0,5}$)	Category of the aggregate
Rapid suction	> 2	
Water inhibitor	$0,5 < A \leq 2$	Calcareous
Almost impermeable	$0,001 < A \leq 2$	Granite, basalt and marble
Impermeable	$\leq 0,001$	

Mechanical and physical properties of the four types of aggregates [Table 2, Table 3], are characteristic of regular aggregates of good quality.

Table 4. Aggregates class according to its capillarity coefficient [DIN-52617].

NF B 10502 capillarity class	Capillarity coefficient ($kg/m^2/h^{0,5}$)	Category of the aggregate
Strong capillarity	> 4	
Weak capillarity	$1,5 \leq C \leq 4$	Calcareous
Very low capillarity	C < 1,5	Granite, basalt and marble

3.2 Concretes produced

Compressive strength, determination of absorption and capillary coefficients, vacuum water absorption and oxygen permeability were carried out to characterize concrete and mortars produced, at 28 days of age.

Compressive strength test was performed in 15cm high and 7,5cm diameter size cylinders.The absorption and capillary coefficients were obtained as performed in rock cores. Permeability to oxygen and water was also carried out in cylindrical specimens of 5cm high and 4cm diameter extracted from concrete cubes. Experimental details of equipment used and procedures for each of these tests are described elsewhere [Pacheco Torgal *et* al 2006], [Pacheco Torgal & Castro-Gomes 2006].

The influence of coarse aggregate type, size, as well dry or water saturated conditions, on the concrete durability parameters were determined. The average results of the tests carried out in the different types concrete mixtures, (A1A2), (A1) and (A1SAT), are presented in tables 5, 6 and 7, respectively.

Table 5. Average test results obtained in concrete mixtures A1A2.

	Aggregate type			
	Basalt	*Granite*	*Calcareous*	*Marble*
Compressive strength (MPa)	33	35	33	33
Absorption coefficient ($kg/m^2/h^{0,5}$)	2,09	1,78	2,32	2,01
Capillarity coefficient ($g/cm^2/min^{0,5}$)	2,72	2,30	3,00	2,58
Vacuum water absorption (%)	15	15	18	15
Oxygen permeability (m^2) x 10^{-16}	2,2	2,0	2,5	2,2

Table 6. Average test results obtained in concrete mixtures A1 type.

	Aggregate type			
	Basalt	*Granite*	*Calcareous*	*Marble*
Compressive strength (MPa)	33	27	29	31
Absorption coefficient ($kg/m^2/h^{0,5}$)	1,75	2,11	2,18	1,70
Capillarity coefficient ($g/cm^2/min^{0,5}$)	2,25	2,72	2,81	2,20
Vacuum water absorption (%)	15	15	17	14
Oxygen permeability (m^2) x 10^{-16}	2,0	1,5	2,4	1,9

Table 7. Average test results obtained in concrete mixtures A1SAT type.

	Aggregate type			
	Basalt	*Granite*	*Calcareous*	*Marble*
Compressive strength (MPa)	33	31	32	30
Absorption coefficient ($kg/m^2/h^{0,5}$)	1,65	1,89	2,06	1,69
Capillarity coefficient ($g/cm^2/min^{0,5}$)	2,15	2,44	2,67	2,20
Vacuum water absorption (%)	13	13	14	13
Oxygen permeability (m^2) x 10^{-16}	1,7	1,7	1,6	1,5

All concrete mixes have quite similar compressive strength values, of the same level of magnitude. In concrete mix (A1A2) the compressive strength obtained is slightly higher than in other mixes, which is caused by the use of aggregates of larger particle size A2. Regarding capillary coefficients, all concrete mixes have showed weak capillarity. Some mixtures can be classified as having fast suction behaviour and others can be classified as water inhibitors in what concerns absorption coefficient results.

The highest values of vacuum water absorption results are presented by mixtures produced using calcareous aggregates. Regardless the aggregate type, (A1A2) mixtures presented higher vacuum water absorption, followed by (A1) mixtures and (A1SAT) mixtures, which have presented the lowest of all results. Following this trend,oxygen permeability is higher for (A1A2) mixtures than those obtained for (A1) mixtures, which in turn is higher than the results obtained for mixtures (A1SAT).

Considering all concrete results of absorption and capillarity coefficients, vacuum water absorption and oxygen permeability, a decreasing tendency is observed from mixes (A1A2) to mixes (A1) and (A1SAT). Thus, the production of concrete using smaller size aggregates reduces capillary and vacuum absorption, as well as permeability. This phenomenon can be explained once the existence of larger coarse aggregates contributes to the increase of path length of capillary pores and its interconnectivity and the increase of porous cement-aggregate interface zone, where absorption of water by capillary phenomenon occurs [Metha 1986]. The trend found of decreasing absorption, capillary coefficient or even oxygen permeability, is clear in all cases except in concrete produced with granite aggregates. Nevertheless, tendency of diminishing results of these tests is quite evident, particularly vacuum water absorption, which decreases in all cases of different aggregates when aggregate size is reduced and water saturated. It is possible that vacuum water absorption, that measures total open porosity, is less affected by sample drying than pores interconnectivity which may strongly affect capillary absorption or oxygen permeability.

When comparing the performance of concrete mixes (A1) and (A1SAT), it is evident that mixes with saturated aggregates present lower results than with dried ones. Since aggregate sizes did not change from mixes (A1) to (A1SAT), there is not any modification of capillary pores pathways, but rather a change of cement aggregate interface porosity might have occurred [Aitcin & Perraton 2001]. It is believed that since the aggregate is water saturated before mixing it does not absorbs water from the cement mortar fraction, during hydration. Consequently the cement aggregate interface will have lower porosity when aggregate is water saturated.

Finally the results of different properties presented in tables 5, 6 and 7, obtained in concretes produced with different aggregates are of same level of magnitude, thus indicating that aggregates mineralogy and geological source appears to not influence it significantly.

4 CONCLUSIONS

Concretes using coarse aggregates of different geological sources, granite, basalt, calcareous and marble, were produced in specific mix proportions and laboratory controlled conditions. The influence of coarse aggregate type, particle size, as well as dry or water saturated conditions, on the concrete mechanical and durability parameters were determined. It was found that aggregates type, particle size or water content during mixing does not influence significantly concrete mechanical behaviour. Regardless of aggregate geological type, concrete durability properties are significantly influenced by aggregates particles size and water content. Concrete mixtures produced using larger size aggregates presented higher vacuum water absorption and oxygen permeability, than mixtures using smaller size aggregates. Concrete mixtures using saturated aggregates presented lower vacuum water absorption and oxygen permeability than mixtures were aggregates were introduced in a relatively dry state.

ACKNOWLEDGMENTS

Authors are grateful to Portuguese Foundation for Science and Technology for project grant - POCTI36027/99 "Influence of Physical Properties and Morphological Parameters of Granites and Calcareous Aggregates on the Permeability of Concrete".

REFERENCES

Aitcin P, Perraton D. Perméabilité du béton de peau, Le choix du granulat peut-il s'avérer un élément plus déterminant que le rapport E/C Bulletin des Laboratoires des ponts et chaussées 2001:59–72.

BGS (British Geological Survey). Office of Deputy Prime Minister, European Mineral Statistics 2000-04, Keyworth Nottingham, 2006.

Bleishwitz, R. and Bahn-Walkowiak, B. Sustainable Development in the European aggregates industry: a case for sectoral strategies, Wuppertal Institute for Climate, Environment and Energy, October, 2006.

British standard BS812, part 110. Methodos for determination of aggregate crushing value, 1990.

DIN 52617: Determination of the water absorption coefficient of construction materials.

Gonilho Pereira, C.N. Study of aggregates influence on structural concrete: Durability and interface zone, Master Thesis, University of Beira Interior, Covilhã, Portugal, July, 2005. (only available in Portuguese)

IGM (Portuguese Mining and Geology Institute). Portugal – Rock Extraction Portuguese Industry Report, 2000. (only available in Portuguese)

ISRM. Suggested method for determining the uniaxial compressive strength and deformability of rock materials: In: Brown Et, editor, International Society of Rock Mechanics, ISRM suggested methods. NJ: Pergamon Press; 1981.

LNEC Portuguese Standard E223. Aggregates: determination of volumetric index, Lisboa, 1968.

LNEC Portuguese Standard E226. Concrete: compressive strength test, Lisboa, 1968.

LNEC Portuguese Standard E227. Aggregates: Los angeles abrasion test, Lisboa, 1970.

LNEC Portuguese Standard E392. Concrete: oxygen permeability determination, Lisboa, 1993.

LNEC Portuguese Standard E393. Concrete: determination of capillary water absorption, Lisboa; 1993.

Metha, P.K. Concrete: structure, properties and materials. Englewood: Prentice-Hall; 1986.

NF B 10-502: Produits de carrières. Pierres calcaires. Mésure de lábsortion de l'eau par capillarité.

Pacheco Torgal, F. and Castro-Gomes, J.P. Influence of physical and geometrical properties of granite and limestone aggregates on the durability of a C20/25 strength class concrete, Construction and Building Materials 20, 2006.

Ribeiro, A.B., Gonçalves, A., Salta, M.M. Influence of aggregates on concrete durability. Portuguese Congress of Structural Concrete, LNEC, Lisbon, 2002. (only available in Portuguese)
Sousa Coutinho, A. Production and properties of concrete. LNEC, 3ªEd., Vol I., Lisbon, 1997. (only available in Portuguese)

UPEG (European Aggregates Association). Providing essential materials for Europe, Annual Report, Brussels, 2006.

Mechanical and Durability Properties of Concrete with Ground Waste Glass Sand

L. A. Pereira de Oliveira [1]
J.P. Castro-Gomes [2]
P. Santos [3]

T 11

ABSTRACT

This paper examines the possibility of using finely ground waste glass as partial natural sand replacement in concrete. The reduction of waste glass particle size was accomplished in the laboratory by crushing and grinding the waste glass in a jar mill. The compressive strength at 7, 28 and 90 days, was determined for different ground waste glass sand percentage replacement in concrete.

Absorption and permeability tests were also carried out. A test method was followed to verify the potential concrete expansion caused by the alkali silica reaction.

The results showed a very significant compressive strength improvement with the increasing of percentage replacement of natural sand by ground waste glass. A higher compressive strength was obtained with a lower expansion verified by the bar tests. The same trend for durability properties were also observed in this study.

The results obtained attested the high possibility of recycling and using of the ground waste glass collected in central region of Portugal as natural sand replacement in concrete mixtures.

KEYWORDS

Fine aggregate, Ground waste glass, Concrete expansion, Durability

[1] University of Beira Interior, Dept. of Civil Engineering and Architecture, Covilhã, Portugal, Phone +351 275 329738, Fax 275329969, luiz.oliveira@ubi.pt
[2] University of Beira Interior, Dept. of Civil Engineering and Architecture, Covilhã, Portugal, Phone +351 275 329990, Fax 275329969, castro.gomes@ubi.pt
[3] University of Beira Interior, Dept. of Civil Engineering and Architecture, Covilhã, Portugal, Phone +351 275 329968, Fax 275329969, luiz.oliveira@ubi.pt

1 INTRODUCTION

Nonrecyclabe waste glass constitutes a problem for solid waste disposal in many municipalities in Portugal. Traditionally, most nonrecyclabe mixed-colour broken glass results of the bottling industry. The current practice is still to landfill most of the nonrecyclabe glass. Since the glass is not biodegradable, landfills do not provide an environment-friendly solution. Nowadays, the civil construction industry search the alternatives for satisfy the increasing needs for the concrete production. The attractive use of the waste glass in the construction materials is caused by the fact that not all waste glass can be recycled into new glass. For the glass industry, the impurities, transports costs and mixed colour waste streams difficult the useful raw glass stocks. United Nations estimates the volume of yearly disposed solid waste to be 200 million tons, 7% of which is made up of glass the world over [Topçu & Canbaz 2004]. In Portugal, 7.5% of 4 712 458 tons of solid waste produced during 1999 and 2005 was glass. In fact, only 30% of the total used bottles are actually reuse and recycled, it means 70% is disposed as landfill. The efforts to reduce the landfilling of waste glass, because they are not biodegradable, has been done over past few decades by several others researches by studies using the waste glass as an aggregate, including Schmidt & Saia [1963], Johnston [1974], Figg [1981], Polley at al [1998] and Shayan & Xu [2004]. Our earlier results [Oliveira at al 2007] also showed that glass particles 75µm-150µm size range did not cause expansion in the accelerated mortar bar test, which agree with the observations of Shayan & Xu [2006], but according to Bazant at al [1998] the glass particle around 1.5 mm caused excessive expansions.
Using waste glass, as coarse aggregate in concrete, did not have a marked effect on the workability of concrete, but the compressive strength decrease in proportion to an increase in waste glass [Topçu & Canbaz 2004]. According to Park at al [2004], the increase in the content of waste glass fine aggregate on concrete showed a slump decrease tendency influenced by the grain shape and the fineness modulus of the waste glass aggregates. These authors observed a decreasing compressive strength along with an increase in the mixing ratio of the waste glass aggregate. They found the highest compressive strength in concrete containing 30% of waste glass aggregates.
Thus, taking in account the influence of the waste glass as fine aggregate on the concrete workability an additive was used to maintain the same slump for all mixtures tested in this work. A basic experimental study on the mechanical and durability properties of concrete containing waste glass collected in the central region of Portugal was carried out.

2 METHODS

2.1 Materials

A commercial Portland cement type CEM I 42.5R conforming to European Standards EN–197-1 with Blaine fineness of 384.8 m^2/kg and with a particle density of 3140 kg/m^3 was used for all mixes. A fly ash with Blaine fineness of 400.9 m^2/kg and with a particle density of 2380 kg/m^3 was used for all mixes As the aggregate for producing concretes, natural sand was used with maximum particle size 4.76 mm, a particle density of 2520 kg/m^3 and Modulus of Fineness of 3.47. The coarse aggregate was a 12.7 mm crushed granitic stone with a particle density of 2698 kg/m^3 .The amber waste glass was ground in a jaw crusher to produce a fine glass sand with maximum particle size 4.76 mm, a particle density of 2509 kg/m^3 and Modulus of Fineness of 2.40. Fig. 1 show the grading distribution of fines aggregates determined in according of the ASTM C136.

2.2 Concrete mixtures

A reference mix 1:0.29:1.87:3.14 (cement : fly ash : fine aggregate : coarse aggregate) with a water/cement ratio of 0.60 was used. Other mix proportions were formulated based on this mix to include the fine glass sand mentioned above. The purpose of the trial was to determine the effect of glass sand as natural sand replacement, at 25, 50 and 100% dosage rates. Table 1 gives details of the 4 mixes used in field trial.

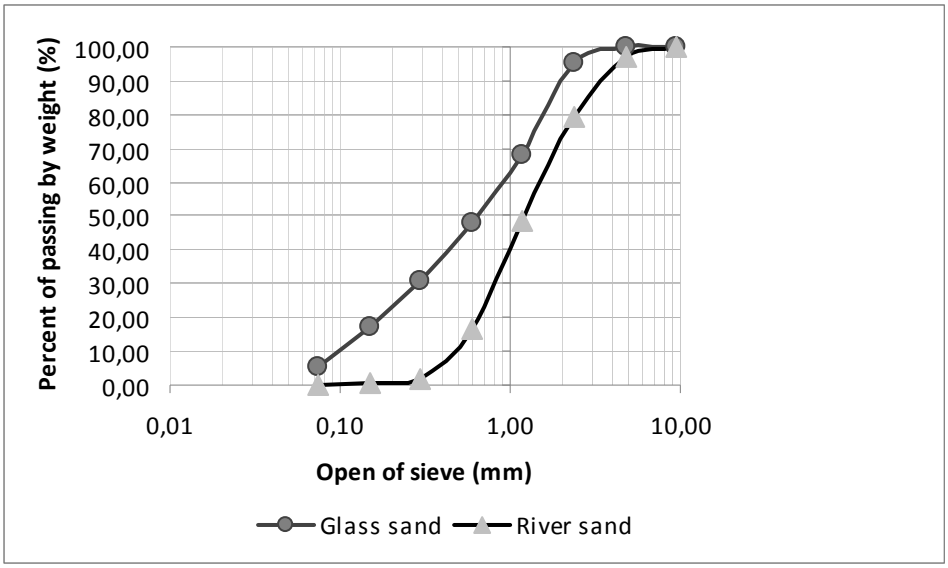

Figure 1. Grading curves of aggregates

Table 1. Mix proportions (kg/m^3).

Description	*Cement*	*FA*	*Coarse aggregate*	*Fine sand*	*Crushed glass*	*Water*
Control mix	350	101.5	1099	654.5	0	210
25%CGS[a]	350	101.5	1099	490.8	163.6	210
50% CGS	350	101.5	1099	327.25	327.25	210
100% CGS	350	101.5	1099	0	654.5	210

[a] GCS = crushed glass sand

2.3 Workability

The tests conducted on the fresh concrete included the slump test and flow table test, in according to EN 12350-2 and EN 12350-5, respectively. The workability was evaluated by conducting slump test in accordance with EN 12350-2. The slump for control mix was was 100 mm ± 10 mm. As the sand content increases, the slump decreases due to the reduction of equivalent fineness modulus. For concretes with sand glass content, high-range water reducer admixture was used to obtain the same workability as indicated for control mix. The dosage of admixture is about 0.2% by weigth of cement for 25% sand glass content and 0.3% for 50% and 100% of sand glass content.

2.4 Compressive strength test

The compressive strength tests were conducted, in according with EN 12390-3, at 7 and 28 days for 150 mm concrete cubes maintained in fog room (21 ± 2ºC, 100% RH).

2.5 Expansion test

The alkali silica reaction (ASR) test was was applied to check the influence of sand glass percentage replacement in concrete expansion. Three concrete bar specimens, with the dimensions 40 x 40 x 160 mm, were made for each mixing containing glass sand. Normal procedure was to cure them for 24 h, immerse them in water for 24 h, and then store them in 1 N NaOH solution at 80ºC in a closed container. Changes in the length of the concrete bars were checked for the following 14 days after their surface was dried by using a comparator, a length comparison measuring device with an accuracy less than 0.002 mm.

2.6 Capillary sorptivity test

The sorptivity tests were carried out on samples, with 7.5 x 7.5 x 15cm, after drying in oven, at a temperature of 60ºC ± 5ºC. The samples were stored until the weight loss was negligible. The preparation of samples also included water impermeability of their lateral faces, reducing the effect of water evaporation. The test started with the registration of samples weight and, afterwards, they were placed in a recipient in contact with a level of water capable to submerge them about 5 mm. After a predefined period of time, the samples were removed from the recipient to proceed to weight registration. Before weighing, the samples superficial water was removed with a wet cloth. Immediately after the weight, the samples were replaced in the recipient till reach the following measuring time. The procedure was repeated, consecutively, at various times such as 10, 20, 30, 40, 50, 60, 70, 90, 130 and 150 min (min = minutes) until the last reading. Because of small initial surface tension and buoyancy effects, the relationship between cumulative water absorption (kg/m2) and square root of exposure time ($t^{0.5}$) shows deviation from linearity during first few minutes [3]. Thus, for the calculation of sorptivity coefficient, only the section of the curves for exposure period from 10 min to 90 min, where the curves were consistently linear, was used. The sorptivity coefficient (k), was obtained by using the following expression:

$$\frac{W}{A} = k\sqrt{t} \tag{1}$$

where W= the amount of water adsorbed in (kg); A= the cross section of specimen that was in contact with water (m^2); t = time (min); k = the sorptivity coefficient of the specimen ($kg/m^2/min^{0,5}$).

2.7 Water and oxygen permeability test

For determination of concrete oxygen and water permeability it is used a permeability cell and the tests were conducted by the procedures described by Gomes at al [2002]. For these tests, cylindrical test specimens are prepared with 5cm of diameter and about 4 cm of height. This permeability cell allows submitting samples, with the referred dimensions, to a certain pressure, guaranteeing that the flow of oxygen through the sample is uniaxial. So much plus, that in the adopted methodology, specimens are first dried in oven at 60ºC, for 48 hours. The water permeability test can take place after the oxygen permeability test, in a similar way and with in the same specimen.

3 RESULTS AND DISCUSSION

3.1 Compressive strength

The compressive test results for concretes containing amber waste glass fine aggregates are shown in the Fig. 2. It was observed that with increase of amber waste glass content, the strength of concrete increase. For each mixing rate of the amber waste glass (25%, 50% and 100%), the compressive strength increased by 26%, 26% and 34%, respectively, at 7 days. For 28 days the increase was 24%, 25% and 29%. It was observed a strength development coefficient from 7 to 28 days of 1.30 for the reference mix, 1.27 for the mix with 25% of waste glass, 1.29 for 50% mixing rate and 1.25 for 100% mixing rate. These results are in opposition of the results obtained by Park at al [2004] and by Topçu & Canbaz [2004]. In general, the strength of concrete containing glass is lower than that with natural aggregate. Strengths are particularly low when high alkali cement is used. This apparent disagreement was probably caused by replacement of cement with around 30% fly-ash that demonstrated effective in controlling the large retrogression of strength. By the other hand, the use of a more fine aggregate as natural sand replacement can improve the aggregates particle packing by the filler effect. When the specific surface of aggregate is increased for a constant mix proportion, the amount of cement relative to the surface of the aggregate decreases. Lallard & Belloc [1997] state that as the maximum paste

thickness between aggregate particles decreases the compressive strength increases. In dry packing of particles, it has been observed that the highest stresses exist at the contact points of aggregate particles. Thus, when paste is introduced into the packing and it is placed between two close aggregates, the paste will be highly stressed, yielding a greater matrix strength.

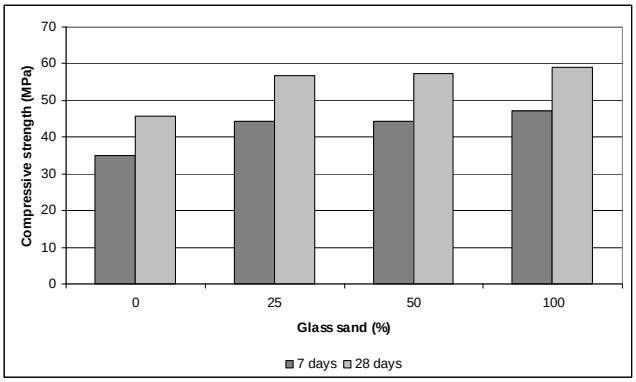

Figure 2. Compressive strength vs sand glass content for 7 and 28 days.

3.2 Influence of glass sand content on the concrete expansion

All the concretes prisms stored at the conditions described in 2.5 showed insignificant expansion (<0.1%) at the age of 14 days (Fig. 3), indicating that no deleterious alkali silica reaction expansion took place by that age. In Fig. 3, curves for mixes with natural sand replaced by 100% and 50% of waste glass sand presents an expansion development with the age inferior or similar to the control mix. Despite the expansion increasing at 14 days, about 60% more than control mix, for the mix with 25% of waste glass sand, it is observed that the fly ash content in the mixes lead for a more stable behaviour. This effect provide ample evidence that both fly ash and waste glass sand can be used together to produce concretes with relative high strength without any adverse reaction.

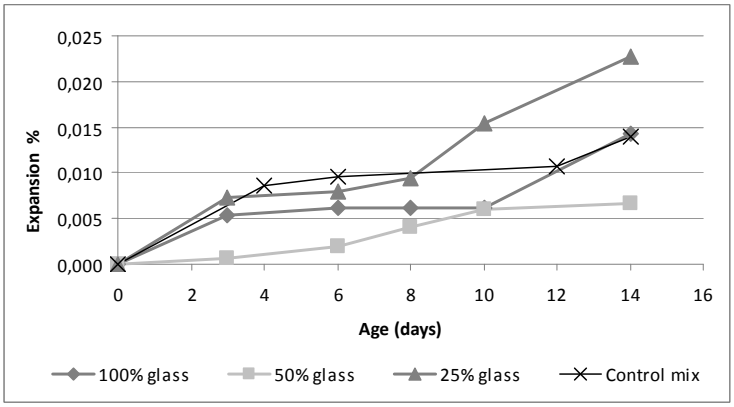

Figure 3. Expansion of concrete bars with various sand glass content imersed in NaOH solution.

3.3 Mix proportions and durability evaluation.

It was observed that the sand replacement by the waste glass sand reduced the concrete sorptivity coefficient. Fig. 4 shows that the reduction attaint a maximum of 39% for 28 days with 100% of natural sand replacement and 29% of reduction at 63 days for the same waste glass rate. This reduction can be influenced by the favorable effect of waste glass sand gradings that improve the particles packing almost certainly reducing the quantity of capillary pores.

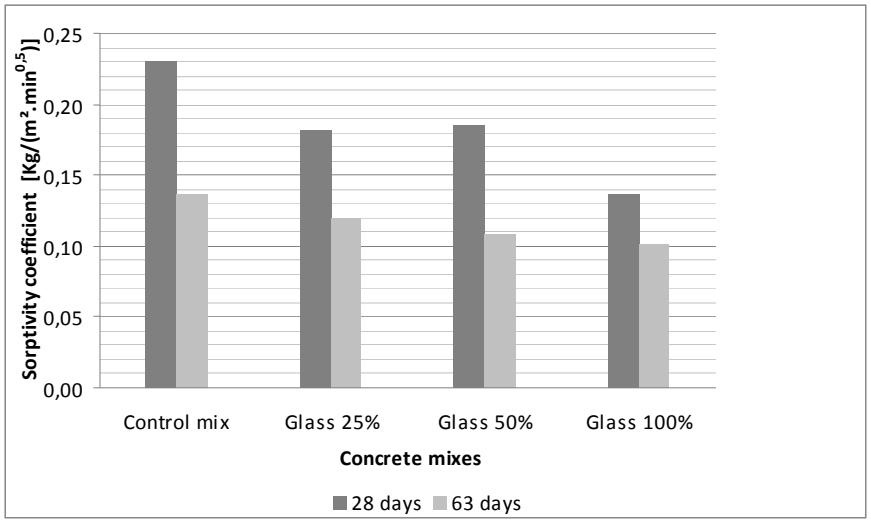

Figure 4. Sorptivity coefficient of different concrete mixes at 28 and 63 days

Figs. 5 and 6 presents the results obtained on concretes produced with different waste glass sand replacement rate. All results presented in both figures are medium values obtained from testing of 4 specimens. Fig.5 shows the influence of natural sand replacement by waste glass sand on the oxygen permeability cofficient at the concrete age 28 and 63 days. At 28 days it was observed an increase, between 20 and 30%, in the oxygen permeability for mixes with 25% and 50% of waste glass sand, but a significantly decreasing when the total natural sand was substituted by waste glass sand. In general, the oxygen permeability is reduced by an half with the concrete age evolution. At the end of 63 days the oxygen permeability of the concrete with waste glass sand is the same order of the concrete with natural sand.

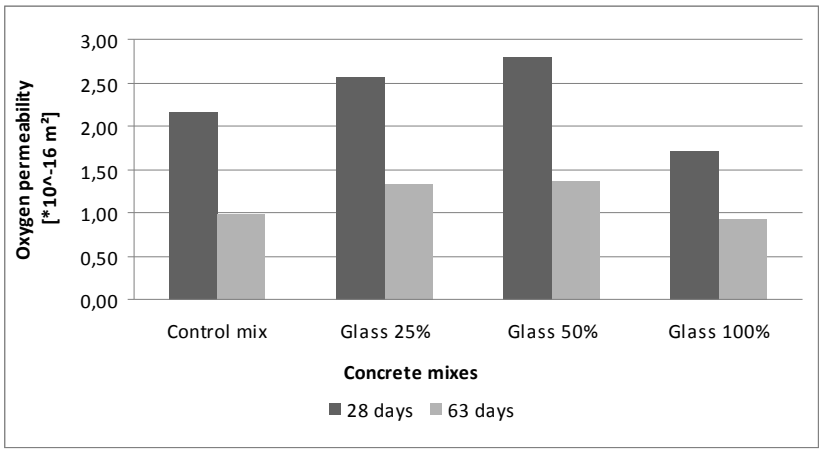

Figure 5. Oxygen permeability coefficient of different concrete mixes at 28 and 63 days.

Fig. 5 shows a similar behaviour for the concrete water permeability, which means a reducing with the time, an increase with combination of natural sand and waste glass sand and the same order values for concrete produced with waste glass sand and for natural sand.

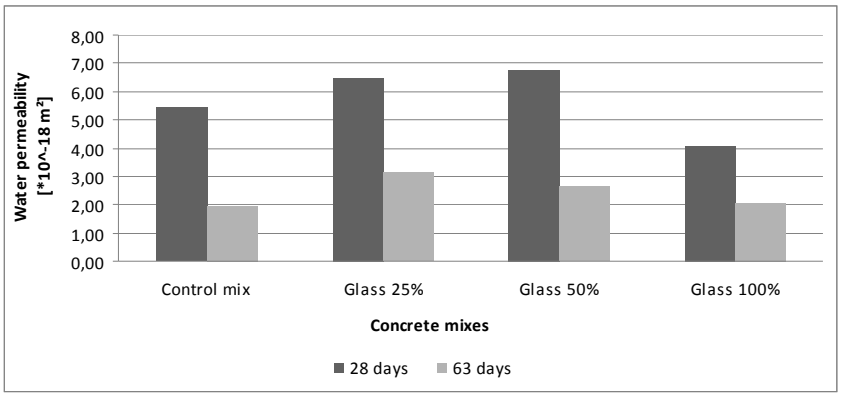

Figure 6. Water permeability coefficient of different concrete mixes at 28 and 63 days.

4 CONCLUSION

The effect of using waste glass sand in concrete mixes has been investigated. Four different mixes having a specified characteristic compressive strength of 40 MPa were prepared. It was necessary to use a high range water reducer with waste glass sand to maintain adequate workability at required constant w/c ratio. The compressive strength was increasead with the waste glass sand rate in concrete, where the alkali silica reaction was largely mitigated by addition of a suitable fly ash. The increase of waste glass sand is also beneficial to reduce the concrete sorptivity coefficient, but give a control mix similar permeability behaviour only for 100% waste sand rate. Finally, the results of this study indicate waste glass sand to be a satisfactory substitute for natural fine aggregate providing considerable economic and environmental benefits to the community.

ACKNOWLEDGMENTS

The authors gratefully acknowledge “Fundação para Ciência e Tecnologia” by the support throughout the project POCI/ECM/55588/2004.

REFERENCES

Bazant Z. P., Jin W. & Meier C. 1998, “Fracture mechanics of concrete structures”, Proc. FRA MCOS, 3, 1687-1693.

Figg, J. W. 1981, “Reaction between cement and artificial glass in concrete”, Proc. Conf. on Alkali-Aggregate Reaction in Concrete, Cape Town, South Africa.

Gomes, J. P.C, Oliveira, L.A.P., Gonilho, C.N.P. & Torgal, F.M.A.S.P. 2002, “Discussion of Aggregate and Concrete Water Absorption and Permeability Testing Methodology**”**, XXX IAHS World Congress on Housing, Coimbra, Portugal, Oktay U, Abrantes V, Tadeu a (Eds.), Vol. III, pp 1761- 1768.

Johnston, C. D. 1974, “Waste glass as coarse aggregate for concrete”, J. Testing and Evaluation, **2**(5), 344-350.

Lallard, F. & Belloc A. 1997, “The influence of aggregate on the compressive strength of normal and high-strength concrete”, ACI Materials Journal, Vol. 94, No. 5, pp. 417-426.

Oliveira L. A. P., Gomes J. P. C. & Santos P. 2007, "Optimization on pozolanic reaction of ground waste glass incorporated in cement mortars", Portugal SB07 Sustainable Construction, Materials and Practices, L. Bragança et al (Eds.) IOS Press, 2007, Part 2, pp. 928-934.

Park, S.B., Lee B. C. & Kim J. H. 2004, "Studies on mechanical properties of concrete containing waste glass aggregate", Cement Concrete Research, 34, 2181-2189.

Polley, C., Cramer, S. M. & Cruz R.V. 1998, Potential for using waste glass in portland cement concrete" Journal of Materials in Civil Engineering, **10** (4), 210-219.

Schmidt, A. & Saia, W. H. F. 1963, "Alkali-aggegate reaction tests on glass used for exposed aggregate wall panel work", ACI Mat. J., 60, 1235 – 1236.

Shayan A. & Xu A. 2006, "Performance of glass powder as a pozzolanic material in concrete: a field trial on concrete slabs", Cement Concrete Research, 36, 457-468.

Shayan A. & Xu A. 2004, "Value-added utilisation of waste glass in concrete", Cement and Concrete Research, 34, 81-89.

Topçu, I. B. & Canbaz M. 2004, "Properties of concrete containing waste glass" Cement and Concrete Research 34, 267-274.

11DBMC International Conference on Durability of Building Materials and Components
ISTANBUL, Turkey 11-14 May 2008

Durability Modelling of Behaviour of Different Concrete Types as Tunnel Lining Elements

Marijan Skazlic [1]
Nenad Gucunski [2]
Dubravka Bjegovic [3]

T 11

ABSTRACT

Development of novel building materials based on a cement binder, and improvement of the properties of existing materials made considerable progress at the end of last century and at the beginning of this century. One of innovative types of concrete that occurred in this period is a high-performance fibre-reinforced concrete (HPFRC). To the present day a small number of structures made of this kind of concrete were constructed. Tunnelling is one of rare fields of civil engineering in which application of HPFRC has not been closely investigated so far.

In this paper is shown an experimental research work carried out on different concrete types: Conventional concrete and high-performance fibre-reinforced concrete. Experimentally obtained values of mechanical properties of the said concrete types were used in modelling the behaviour of secondary tunnel lining. In numerical analyses, the parameters that were varied were the following: the type and cross-section of concrete in secondary tunnel lining and the type of durability loading. The analyses carried out showed that HPFRC used for fabrication of secondary tunnel lining has higher durability and safety than other concrete types.

KEYWORDS

Durability behaviour, High-performance fibre-reinforced concrete, Tunnel lining

[1] University of Zagreb, Faculty of Civil Engineering, Kaciceva 26, 10 000 Zagreb, Croatia, Phone +385 1 4639 361, Fax +385 1 4828 051, skazle@grad.hr
[2] Rutgers-The State University of New Yersey, 623 Bowser Road, Piscataway, New Yersey, USA, Phone 732-445-4413, Fax 732-445-0577, gucunski@rci.rutgers.edu
[3] University of Zagreb, Faculty of Civil Engineering, Kaciceva 26, 10 000 Zagreb, Croatia, Phone +385 1 4639 212, Fax +385 1 4828 051, dubravka@grad.hr

1 INTRODUCTION

The New Austrian Tunnelling Method (NATM) is a method for excavation of large cross-section underground structures without using temporary supports. This method has been developed as a result of relevant experience, a number of measurements both on structures and models, and theoretical analyses. According to NATM, a tunnel consists of primary and secondary supports. Primary support is used to permanently support the tunnel cross-section and, in interaction with rock mass, to carry the total load. Secondary support, i.e. tunnel lining is installed after settlement and deformation of the primary support system has been completed. [Kovacevic et al. 2004]

All theories to date suggested that secondary lining has not been considered as a static portion of the system, but rather as structural and protective element and thus it is designed as such. Measurements of deformations in the secondary lining of constructed tunnels showed significant growth in stress and deformations during use. [Kovacevic 2003, University of Zagreb 2004] It was found that durability of the primary support elements is being reduced over time and the mechanical properties are being lost. Loss of mechanical properties of the primary support system results in additional load on secondary lining, causes changes in the state of stress and deformations, and consequently affects durability of the secondary tunnel lining. Such loss is caused, in most cases, by (1) creep, swelling or weathering of the rock mass, (2) corrosion of steel anchors and/or loss of shotcrete durability, and (3) creep of shotcrete. The factors influencing durability of primary and secondary support systems can be analyzed through numerical simulations. [Skazlic 2005]

In this paper a description is given of the test results obtained experimentally for main mechanical properties of conventional concrete (C25/30) and of two types of high-performance fibre-reinforced concrete (HPFRC 1 and HPFRC 2). HPFRC 1 and HPFRC 2 differed according to the values obtained for compressive and flexural strengths, and modulus of elasticity. The said materials were selected because conventional concrete is the material that is most used for installing secondary tunnel lining, and HPFRC is a new type of concrete that has not been widely used for this purpose. Compared with other concrete types used for installing secondary tunnel lining, HPFRC has much higher strengths, stiffness, toughness and durability. Such higher tensile strength and toughness of HPFRC, relative to conventional and fibre-reinforced concretes, provide the mobilization of the rock mass and thus preservation of its strength, which is one of the main principles of NATM and modern tunnelling in general. By the use of materials having higher tensile strength and toughness, higher stability and durability of structures are ensured. [Skazlic 2005, Skazlic & Bjegovic 2005]

The values of mechanical properties obtained in experimental investigation for the above three concrete types were used in modelling the behaviour of secondary tunnel lining. In numerical analyses, the parameters varied were: (1) the type and cross-section of the concrete in secondary tunnel lining; and (2) the kind of load. In addition, the durability of the secondary tunnel lining was analysed with respect to the parameters varied. The analyses carried out illustrated that loss of mechanical properties of some elements of the primary tunnel support can have significant effects on durability of secondary tunnel lining. Thus, it was established that secondary tunnel lining has higher bearing capacity and safety when HPFRC is used instead of conventional concrete.

2 EXPERIMENTAL WORK

In experimental work, the values of mechanical properties required to numerically model the state of stress and deformations in secondary tunnel lining were determined. The mechanical properties tested were the following: (1) compressive strength (according to HRN.EN12390-3 and HRN.EN196-1 standards); (2) flexural strength (according to HRN.EN12390-5 and HRN.EN196-1 standards); and (3) static modulus of elasticity (according to HRN.U.M1.025 standard). All the values of the above mechanical properties were used in the case when specimens were cured in water until the date of testing. The results are shown in Table 1. The illustration of mechanical properties tests is given in Figure 1.

Table 1. Mechanical properties of various concrete types necessary for numerical modelling.

Property	Concrete type		
	Conventional concrete (C25/30)	HPFRC 1	HPFRC 2
Compressive strength (MPa)	38.9	141.7	211.3
Flexural strength (MPa)	5.5	13.3	40.1
Static modulus of elasticity (GPa)	29.2	40.8	48.7

Figure 1. Concrete mechanical properties tests required to numerically model compressive strength (left), flexural strength (middle), and modulus of elasticity (right).

3 NUMERICAL MODELLING OF THE BEHAVIOUR OF SECONDARY TUNNEL LINING

The numerical simulation of the behaviour of the secondary tunnel lining was carried out using the final difference method by means of the Fast Lagrangian Analysis of Continua program package (FLAC).

The tunnel was modelled on the basis of the parameters of the Konjsko Tunnel constructed on the Zagreb-Split Motorway. Mechanical properties of rock mass employed in calculations were the following: ρ = 2.3 Mg/m^3, c = 100 kPa, φ = 20°, E = 200 MPa and ν = 0.3. The height of tunnel overburden was 30 metres. Primary support system was installed using shotcrete C25/30 of 25 cm-average thickness and steel IBO anchors of ϕ = 25 mm, L = 8 m, and steel RA 400/500. Non linear models of material behaviour were used in numerical modelling.

The numerical simulation of excavation stabilization with primary support system was run in the following steps (Figure 2):

1. Determination of primary state of stress,
2. Excavation phase 1.and application of shotcrete and ground anchors, and
3. Excavation phase 2 and application of shotcrete and ground anchors.

In the numerical analyses of the state of stress and deformations of the secondary tunnel lining the parameters varied were the following: (1) the type of concrete with which the tunnel lining elements were constructed (C25/30, HPFRC 1, and HPFRC 2); (2) the thickness of secondary lining (10, 20, 30 and 40 cm); and the main load on secondary tunnel lining causing the loss of its durability (failure of ground anchors; failure of shotcrete; loss of rock strength by 50 %; failure of the primary tunnel support; and loss of rock strength by 25 %). For the chosen concrete types and cross-section of the

secondary tunnel lining, and for given combination of permanent load, the maximum stresses in the tunnel cross-section obtained by parameter analysis are shown in Figures 3 and 4.

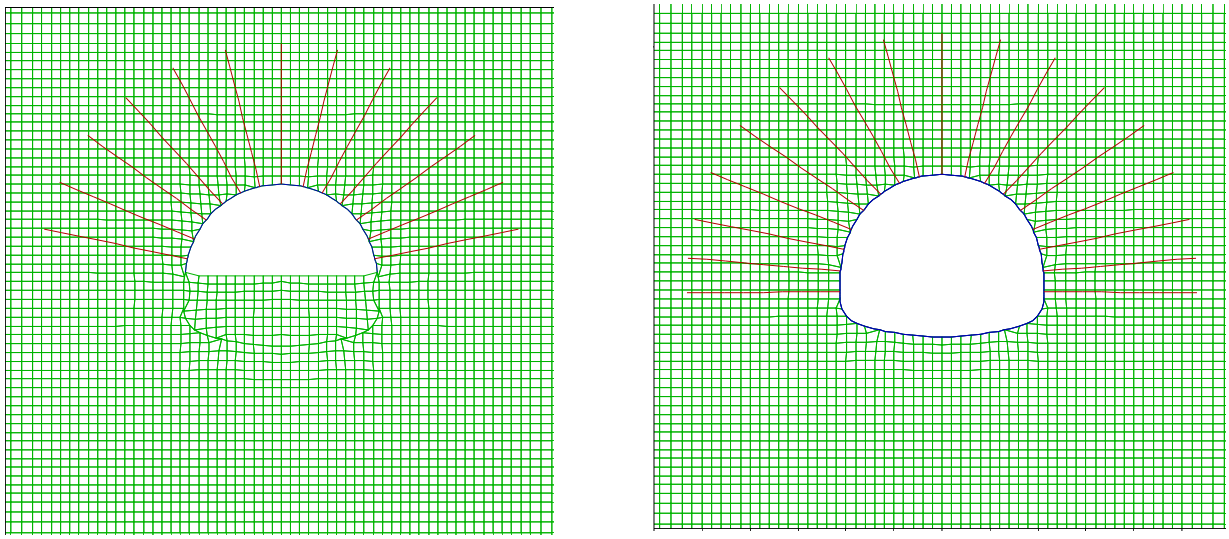

Figure 2. Numerical simulation of excavation phase 1 (left) and excavation phase 2 (right).

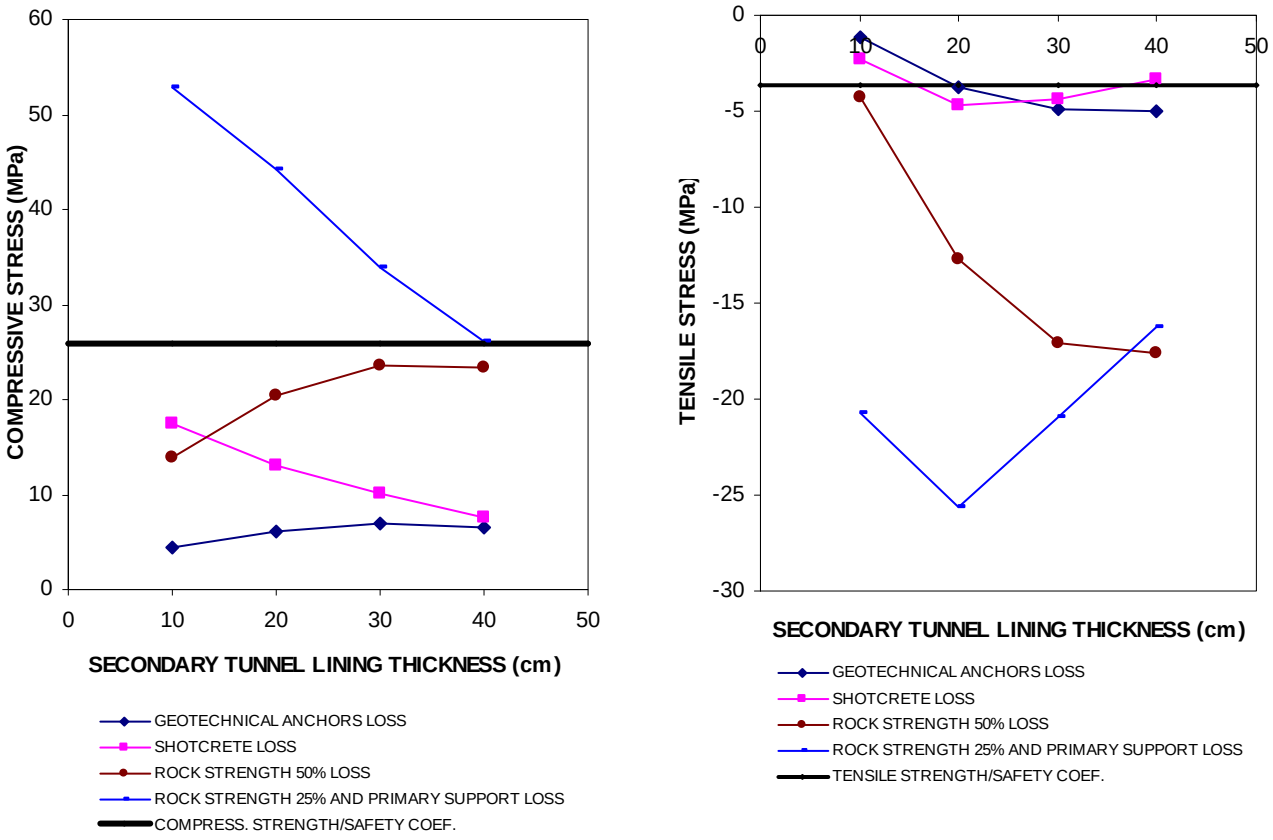

Figure 3. Results of numerical modelling of the behaviour of the secondary tunnel lining installed with concrete C25/30.

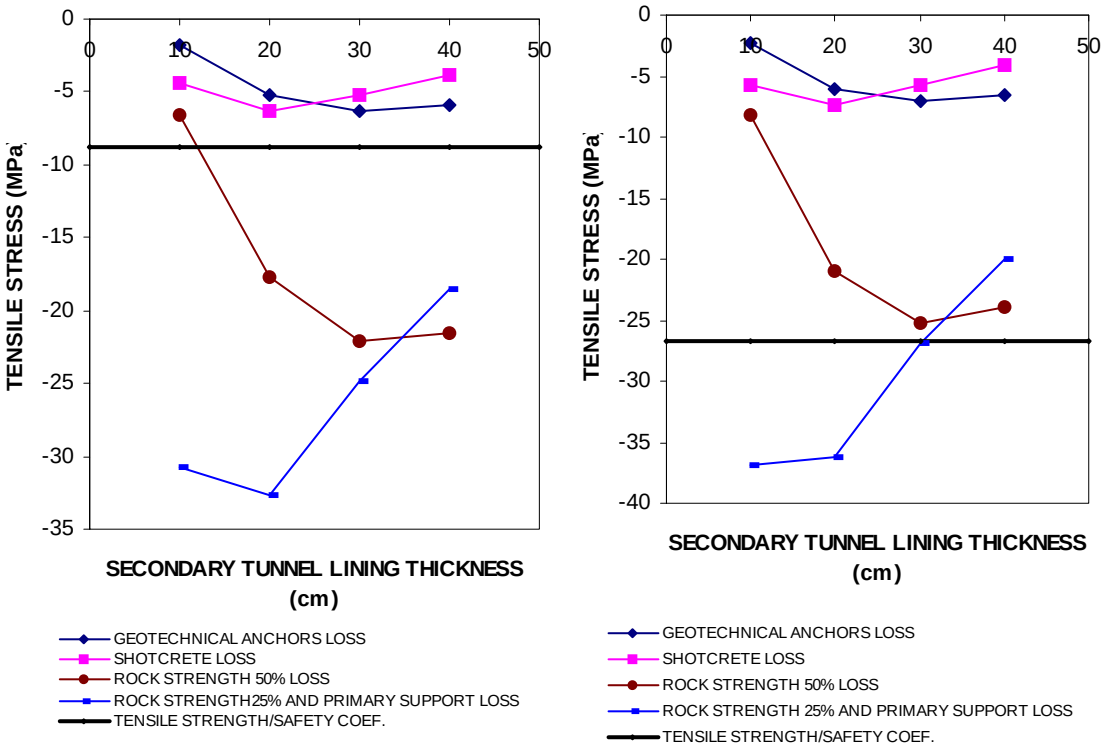

Figure 4. Results of numerical modelling of the behaviour of secondary tunnel lining with HPFRC 1 (left) and HPFRC 2 (right).

4 ANALYSIS OF RESULTS

The analysis of the results obtained for the behaviour of the secondary tunnel lining was made taking into consideration the criterion of allowed stresses (See Figures 5, 6 and 7). Resistance, i.e. computational strength of secondary tunnel lining was obtained by dividing the values of strength shown in Table 1 by factor of safety. The factor of safety used was 1.5, based on French recommendations for HPFRC. [AFGC/SETRA Working Group, 2002]

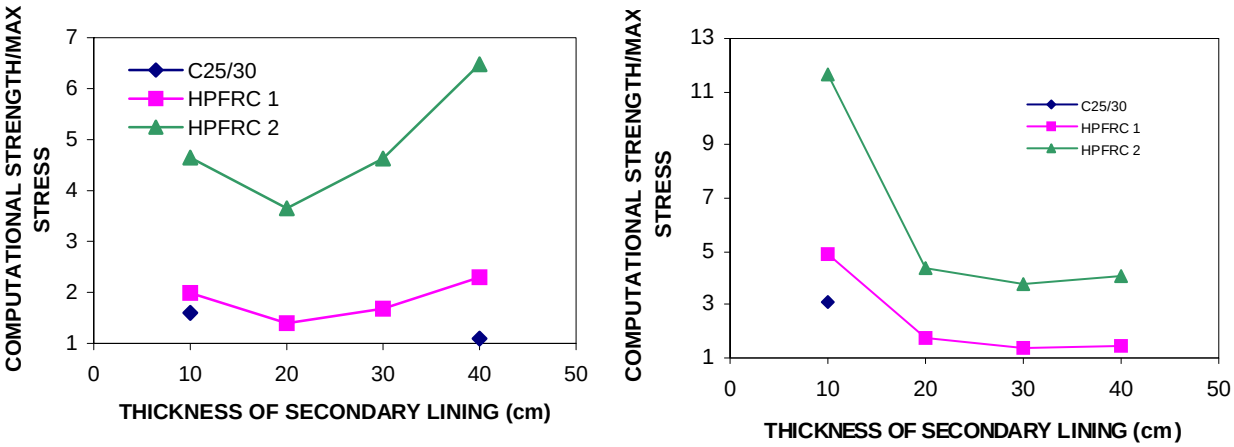

Figure 5. Safety factors in tension obtained for different types of concrete in secondary tunnel lining in the case of shotcrete failure (left) and anchors failure (right).

In Figures 5, 6 and 7, safety factors in compressive and flexural failure of the secondary tunnel lining are shown versus the thickness of secondary lining and load. The safety factor is defined as a ratio between computational strength and maximum compressive strength and/or tensile stress. Only the cases are illustrated for which the safety factor is higher than or equal to 1, i.e. in which secondary tunnel lining has permanent bearing capacity for the load analyzed.

The Table 2 presents the analysis of the results of numerical modelling of the behaviour of the secondary tunnel lining. For particular concrete types and the cross-section of the secondary lining, the cases are illustrated when bearing capacity in compression or in tension under main permanent loads is not allowed.

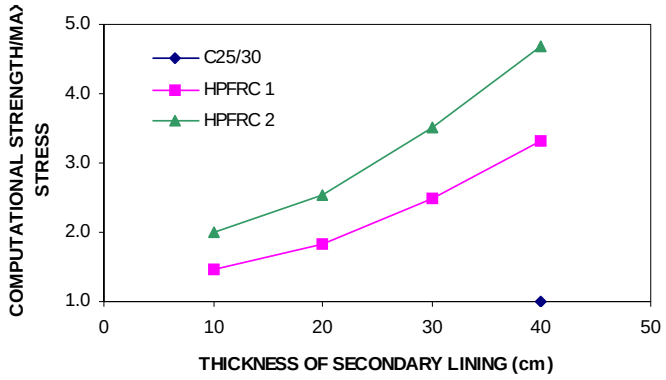

Figure 6. Safety factors in compression obtained for different types of concrete in secondary tunnel lining in the case of rock strength loss of 25 % and primary support failure.

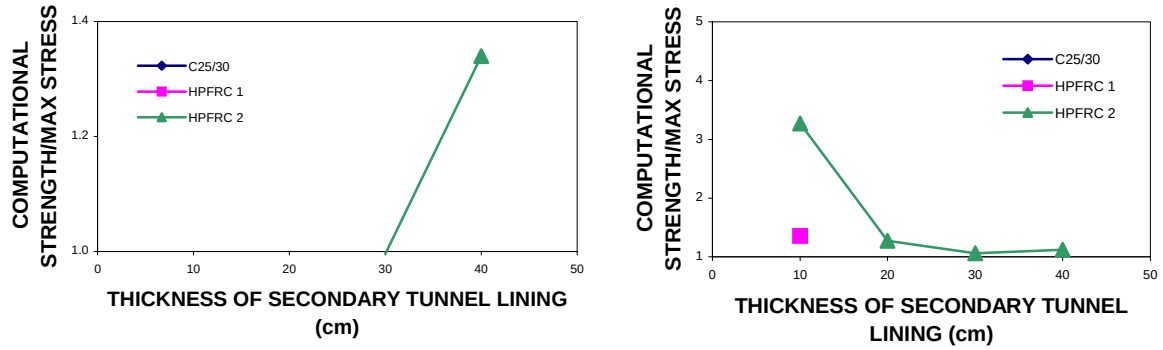

Figure 7. Safety factors in tension obtained for different types of concrete in secondary tunnel lining in the case of loss of rock strength by 25 % and primary support failure (left) and loss of rock strength by 50 % (right).

The analyses described above showed that the mixtures of new concrete types, i.e. HPFRC 1 and HPFRC 2, exhibit significantly higher bearing capacity and safety than the concrete type used so far for installation of secondary tunnel lining. As for durability aspect, it can be said that secondary tunnel lining may, in time, be exposed to high load due to loss of mechanical properties in some primary tunnel lining elements. The calculations described did not take into account extraordinary actions on these structural elements such as possible explosion from terrorist attacks. When this kind of load is considered together with permanent loads, it is safe to conclude that HPFRC is the optimum concrete composition for secondary tunnel lining because it has significantly higher safety and bearing capacity than concrete types used for this purpose up to date. As in this paper two different types of HPFRC were analyzed, when deciding between these two HPFRC types, the site conditions and total costs should be taken into account.

Table 2. Results of numerical modelling in the cases when bearing capacity of the secondary tunnel lining, due to its reduced durability, cannot to carry main loads.

Concrete type	Type of failure	Main load	Thickness of secondary lining (cm)
C25/30	tension	- primary support failure and loss of rock strength by 25 %	10, 20, 30, 40
C25/30	tension	- primary support failure and loss of rock strength by 25 % - loss of rock strength by 50 % - shotcrete failure -anchors failure	10, 20, 30, 40 10, 20, 30, 40 20, 30, 40 20, 30, 40
HPFRC1	tension	- primary support failure and loss of rock strength by 25 % - loss of rock strength by 50 %	10, 20, 30, 40 20, 30, 40
HPFRC2	tension	- primary support failure and loss of rock strength by 25 %	10, 20, 30

5 CONCLUSIONS

In this paper analyses were made of the durability of secondary tunnel lining installed with three different materials (two different types of HPFRC and conventional concrete). The material that has been most commonly used for this purpose so far is conventional concrete, and HPFRC is a new concrete type exhibiting higher tensile strength and toughness the use of which for tunnel lining is yet to be more widely applied. In numerical modelling of the behaviour of the secondary tunnel lining the experimentally obtained values of mechanical properties of these concrete types were used. In numerical analyses the parameters varied were: (1) the type and cross-section of the concrete in secondary tunnel lining, and (2) the type of load (failure of ground anchors; failure of shotcrete; loss of rock strength by 50 %; failure of primary tunnel support; and loss of rock strength by 25 %). In addition, the durability of the secondary tunnel lining with regard to the above parameters was analyzed. The analyses performed illustrate that loss of mechanical properties of some elements of the primary tunnel lining may have significant effect on durability of the secondary tunnel lining. It was also found that secondary tunnel lining has higher bearing capacity and safety when HPFRC is used for its construction instead of conventional concrete.

ACKNOWLEDGMENTS

The authors express their acknowledgements to Ministry of Science, Education and Sports of the Republic of Croatia for their support. The experimental research described in this paper has been carried out as part of two research projects (Modern methods of engineering materials testing, 082-0822161-2996, Project Leader Marijan Skazlic, PhD, Assistant Professor, Development of new materials and systems of concrete structures protection, 082-0822161-2159, Project Leader Dubravka Bjegovic, PhD, Professor) supported by the above Ministry.

REFERENCES

Kovacevic, M.S., Skazlic, Z., Skazlic, M. 2004 ′Durability of Tunnel Primary Support′, Proceedings of the International Symposium «Durability and Maintenance of Concrete Structures», Dubrovnik, Croatia, 21-33 October, 2004, pp. 257-264

Kovacevic, M.S. 2003 ′The Observational Method and the use of geotechnical measurements′ , Proceedings Geotechnical problems with man-made and man influenced grounds, XIII European conference on soil mechanics and geotechnical engineering, Prague, Czech Republic, 25-28 August, 2003, pp. 575-582

University of Zagreb, Faculty of Civil Engineering, Geotechnical Department 2004, *Stabilization Measurements on Konjsko Tunnel, south and north tunnel tubes, the Zagreb-Split-Dubrovnik Motorway* (in Croatian)

Skazlic, M. 2005, *High performance fiber reinforced precast segments for secondary tunnel lining*, dissertation, University of Zagreb, Faculty of Civil Engineering

Skazlic, M., Bjegovic, D. 2005 ′High performance fibre reinforced concrete-composition, structure and technology′ , in *Research and development of new materials*, ed. Filetin, Croatian society of materilas and tribology, Zagreb, Croatia, pp. 189-225 (in Croatian)

AFGC/SETRA working group 2002, *Ultra-High Performance Fibre-Reinforced Concrete, Interim Recommendations*

11DBMC International Conference on Durability of Building Materials and Components
ISTANBUL, Turkey 11-14 May 2008

Chloride Threshold Determination in Prestressing Steel Beams

C. Alonso [1]
F.J. Recio
M. Sanchez
C. Andrade

T 11

ABSTRACT

In last years a lot of effort has been devoted to the determination of chloride threshold values for service life prediction of concrete structures. Both data and determination methods are being collected using many different experimental conditions, either in laboratory or in real structures. Most of the information dealing with critical chlorides relates to conventional reinforcement, but there is a lack of information on chloride threshold for prestressing steel, and even practically inexistent in prestressed concrete elements.

Present paper gives preliminary results of a more ambitious experimental study being carried out in prestressed beams of 1.5m length. Four methods for chloride penetration are being considered, those are: 1) Natural-1: ponding method, using a pool on one surface of the beam, which contains the Chloride dissolution, 2) Natural-2: using wetting/drying cycles, 3) Migration test, using a field of 12V and 4) Potentiostatic test, controlling the surface potential of the wire by polarising at different potentials. The source of chloride used was a 0.5M NaCl dissolution. Besides, several methods to determine the critical time for rebar depassivation are also being used, through the measurement of E_{corr}, i_{corr}, and Potential and Current variations in the wires of the beam.

After depassivation, the profile of chloride penetration along the wires of the beams is determined through the measurement of different parameters: % of free and % of total chloride. Finally the apparent diffusion coefficient, D_{app} has being calculated. In present paper results are given from the beam tested under migration induced method, the only one between the tested methods that, till now, has shown depassivation of the wires. The D_{app} values found for the prestressed concrete beam are in the order of 10^{-10} cm^2/s.

KEYWORDS

Chloride Threshold, Prestressing Steel, Corrosion Onset Methods, Free and Total Chlorides

[1] Inst. of Construction Science Eduardo Torroja, c/Serrano Galvache 4, 28033, Madrid, Spain. mcalonso@ietcc.csic.es

1 INTRODUCTION

Penetration of chloride ions from de-icing salts or marine environments are common causes for degradation of concrete structures and responsible for most of the damages and investment in repair works. By these reasons efforts are being devoted in standards and construction codes in order to give rules and guidelines for designing durable structures. Also efforts are being derived to the developing of models, deterministic or probabilistic, [Andrade *et al*. 2000, Duracrete 2000, Tanner & Andrade 2000], to more accurately approach to the calculation of the service life of concrete structures; however most of them are based on Tuutti´s Model [Tuutti 1982].

Service life models consider that reinforced concrete exposed to chloride polluted environment initiate corrosion when a certain amount of chlorides arrives to the rebar surface [Lambert *et al* 1967, Hope 1987, Glass & Buenfeld 1997, Alonso *et al* 2002]. The so-called chloride threshold level is considered an essential parameter for assessing the probability of reinforcement corrosion, and becomes one of the key parameters needed for service life prediction, being of interest to have tests methods and expressions to introduce in the models.

In spite of the numerous studies performed to establish the critical chloride level for the onset of corrosion, a wide range of chloride threshold values have been suggested even using apparently similar testing conditions and materials, which makes not feasible to define a single value. Thus, a reliable quantification of the critical chloride content is considered a prerequisite for service life calculation. The reason has been attributed to the number of variables that affect the chloride threshold, among them are: the type and content of cement, the exposure conditions, the distance from the sea in marine environments, the time of exposure, the environmental temperature, the oxygen availability at the rebar surface, the type of steel, the electrical potential of the rebar surface, etc.[Rasheduzafar *et a*, 1990, Hansson & Sorensen 1990, Hussain *et al* 1995, Arya & Xu 1995, Sandberg 1995, Mammoliti *et al* 1996, Thomas 1996, Pettersson 1996, Glass & Buenfeld 1997, Alonso *et al* 2002]. Besides, few of these studies include statistical approach to the problem [Breit & Schiesl 1995, Izquierdo *et al* 2004]. Other reasons exist for a non unique chloride threshold value derived from the methodology employed to detect depassivation and the parameter to express the threshold [Hausman, 1967, Lamdberg *et al* 1991, Kayyali & Hake 1995, Arup 1996, Alonso *et al* 2002, Castellote *et al* 2002]. From this analysis it can be concluded that, at present, a significant lack of critical analyses on the chloride threshold is observed resulting in a large uncertainty in the values used for reinforcement. It is therefore a great practical importance to reduce this uncertainty based on a common approach supported by appropriate experimental investigations.

When dealing with prestressing structures the knowledge concerning chloride threshold is practically inexistent; however construction codes include different levels for prestressing steel. In fact present codes specify a lower value for prestressing steel (0.2%) than for reinforcing steel (0.4-0.6%). The reasons for this difference are unclear and should be clarified on the basis of understanding of the corrosion process and experimental determination of chloride levels. Present paper gives an initial attempt to determine chloride threshold values in prestressed concrete beams.

Relatively small samples can be acceptable for reinforcement chloride threshold determination to be used in the laboratory. But for prestressing concrete, not only the steel composition changes, but also the wire works under load (70-80% max. load), what makes unsuitable the use of similar samples than for conventional concrete. Beams are being used in this work having a 1.5 m length of exposed steel wire, which makes feasible to perform several determinations of chloride threshold at the wire level and to perform statistical analyses of chloride threshold levels. Four penetration methods are being used: two Natural methods, ponding and wetting/drying Cycles, one Potentiostatic method, controlling the surface potential of the wire and one Migration method, using an electrical field.

2 EXPERIMENTAL PROCEDURES

2.1 Prestressed Beams Preparation

Prestressed concrete T beams of 1.5m length are being used for the experimental study. The beams were fabricated in an industrial line and cut from a 140m initial prestressed concrete element. Three prestressed ribbed wires of 5mm in diameter were embedded, two at 1.5 cm and separated 5cm and the third wire centred at 8 cm, as shown in figure 1. The beams were fabricated using 380k/m^3 of 42.5 OPC, the slump of the concrete was 1-2 cm (dry) and 40 MPa of compressive strength. After fabrication the elements were left for hardening during 3 days covered with a plastic to avoid drying, then were cut into beams of 1.5m.

Three faces of the T beams were painted with epoxy resin in order to prevent the interaction with the atmosphere. A pool was fixed on the biggest face "Fig 1" in order to introduce the 0.5M NaCl solution for chloride penetration tests. Electrical cables were welded to the wires that appear at the lateral faces of the beams.

Initially water was included in the pool for 20 days and the passive state of the steel wires was confirmed through the measurement of corrosion potential, E_{corr} and corrosion rate, i_{corr}. Mean values of E_{corr} in the order of -175 mV vs. SCE and $i_{corr} < 0.1$ μA/cm^2, (mean $i_{corr} = 0.06$μA/cm^2) indicate the passive state.

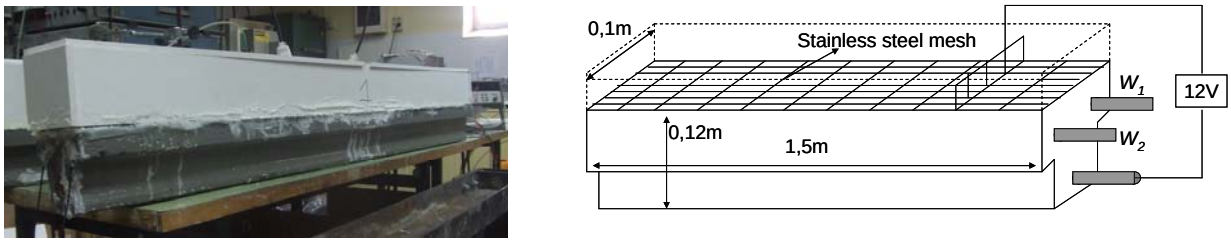

Figure 1. Prestressed T beam dimensions, with a pool fixed at the surface containing 0.5M NaCl (left) and connections for accelerated Cl penetration test (right).

2.2. Chloride Penetration Tests for Chloride Threshold Determination

Four different types of tests are being carried out: 2 considered as natural (ponding and wetting/drying), 1 potentiostatic method and 1 accelerated, the migration induced method.

In the natural-1 method, the pool containing the chloride is maintained continuously and periodically the E_{corr} and i_{corr} of the wires are measured in order to identify the initiation of corrosion. In the natural-2 method, wetting and drying cycles are employed; the pool is maintained with the chloride solution for two weeks and then emptied and leaved for drying during one week. E_{corr} and i_{corr} of the wires are also measured during the wetting period. The criteria for corrosion initiation were: stable measurements of $E_{corr} < -350$ mV SCE or $i_{corr} > 0.2$ μA/cm^2

Potentiostatic method, the wires are continuously polarised at a constant potential, in this case the potential selected was -350mV SCE through a potentiostat and a silver/silver chloride electrode. A stainless steel mesh was used as external counter electrode introduced inside the solution. Periodic monitoring of the current evolving from the system is recorded, for the individual wires and for the whole system. When the system is suffering a sharp and continuous increase of the current above 0.2 μA/cm^2 is considered as criteria for depassivation and pitting corrosion initiation, as demonstrated in a previous paper [Alonso *et al* 2002].

Finally a more accelerated test was employed, the migration induced method, as described in [Castellote *et al* 2002]. In this case an electrical field of 12 V is applied between two counter electrodes. The field has been imposed from an external counter electrode (stainless steel mesh) connected to the negative pole of the power supplier and the rebar embedded at 8 cm was connected to the positive pole, so that chlorides penetration is accelerated from the pool to inside the concrete. The two wires embedded at 1.5cm are affected by the action of the electrical field and suffer an inductive polarisation. During the test a continuous record of the potential of the wires, using Mn/MnO_2 electrode and a multi-channel data logger, was made. The electrical field was switch off when a sharp evolution of the potential of the wire to more positive values is detected, considered as indicative of pitting corrosion; although the electrical field was maintained longer to guarantee that the pits activity is permanent. Also periodically the electrical field is switched off and maintained for 1 hour to reach stable values of E_{corr} and i_{corr} of the wires to contribute to more accurate determination of depassivation time, evolution to more negative potentials in the E_{corr} or to high i_{corr} values are considered indicative of activation of corrosion.

2.3. Chloride Content Measurements

Two methods are being employed to identify chloride penetration:

a) % of free Chlorides at the rebar level, determined through titration of soluble chlorides in water, and expressed by weight of cement.
b) % of total Chlorides, determined by XRF and expressed by weight of cement, used to profile penetration and content distribution at the rebar level

The chloride content was determined in small concrete samples taken 5 mm as maximum from the rebar level and at several points along the beam. Also concrete cores of 5 cm in diameter were taken between the two parallel wires, in order to determine the profile of chloride content and for further calculation of the chloride diffusion coefficient of prestressed concrete.

3 RESULTS AND DISCUSSION.

3.1 Influence of the Method on the Determination of the Onset of Corrosion

The two natural tests used have showed no signs of corrosion initiation after five months of exposure of prestressed beams to chloride penetration in the E_{corr} measurements and neither in the i_{corr}. Values above -350mV, SCE and $i_{corr} < 0.1\ \mu A/cm^2$ respectively were recorded, as shown in 'Fig. 2 left' for wetting and drying test.

With regard potentiostatic test, the initial values of the current measured were around $0.2\mu A/cm^2$ that diminishes within three months up to $0.08\ \mu A/cm^2$. Around four months the current again increases up to $0.3\ \mu A/cm^2$ and maintain till 1 year, as showed in 'Fig. 2 right', however a continuous increase of the current was not detected. Finally after 15 months the potentiostatic polarisation was switch off and the E_{corr} and i_{corr} of the wires was measured in order to better identify the corrosion state. Values of $E_{corr} \approx$ -125 mV, SCE and $i_{corr} \approx 0.05\mu A/cm^2$ were measured which confirm the passive state.

In previous work [Alonso *et al* 2002] was detected that the critical chloride threshold linearly increases for surface potential of the rebar below -200mV/ SCE, (from 0.5-0.7% at -200 mV to 1-1.5% at -350mV/SCE). The reason was attributed to differences in composition and homogeneity of the passive layer as the polarisation potential becomes more negative. Chloride threshold values determined at more positive potentials, > -200mV/SCE, do not affect Cl^- threshold and significantly reduce the test duration for the onset of corrosion. This region of potentials is more representative for passive state of concrete structures at the atmosphere. Further experiments at potential values within the region that do not affect the chloride threshold will be also carried out.

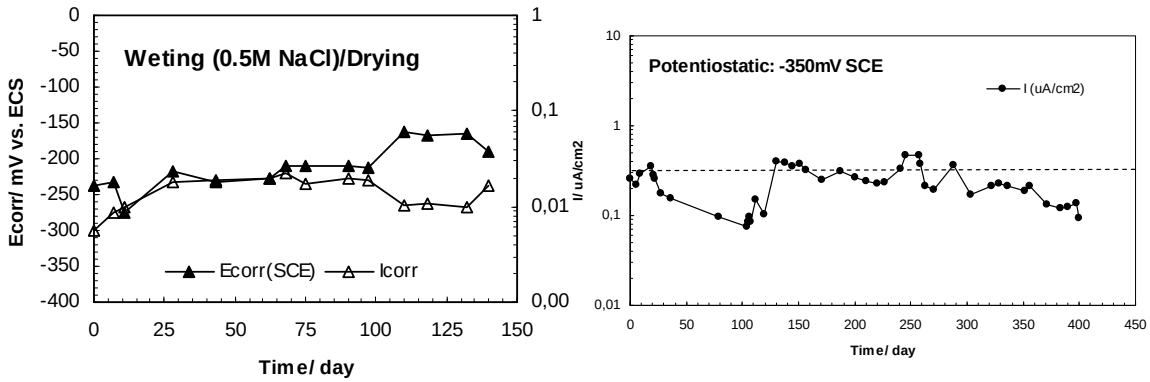

Figure 2. E_{corr} and i_{corr} evolution of prestressed wires exposed to wetting/drying cycles in 0.5M NaCl (left). Current evolution of the prestressed wires of the beam polarised at -350mV/SCE (right).

The migration test has been more accelerated and after 60 days of testing, rebar showed signs associated to pitting corrosion initiation. The inductive potential polarisation (V) measured in the wire evolves from -1V/SCE to +0.5V/SCE, as can be observed in 'Fig. 3' identified as 1st pitting. Simultaneously a decay to more negative values of the E_{corr} of the wire (< -500mV SCE), square points of 'Fig. 3 left', and high $i_{corr} \approx 1$ μA/cm^2, square points of 'Fig. 3 right', were also measured. However if the electrical field is maintained, a new decay of the inductive potential of the wires to more negative values is newly observed, which has being interpreted as a repassivation of the initial pits, also followed by increase of E_{corr} and decrease of i_{corr}. At longer testing times, 140 days, a new evolution of the polarised potential of the wires to more positive values is detected and interpreted as 2nd pitting, which also corresponds with decay of E_{corr} and increase of i_{corr}. These last positive polarisations of the wires are maintained with time and indicate that pitting is permanent.

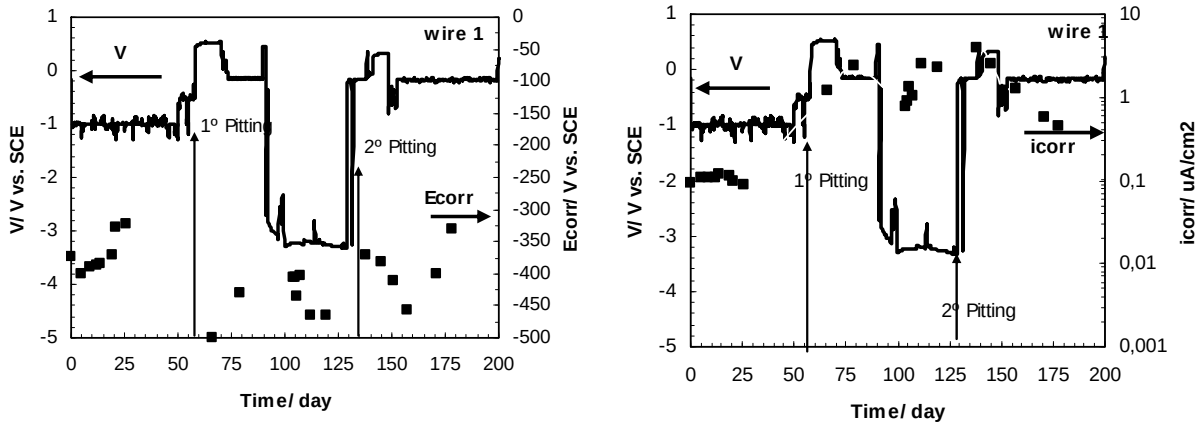

Figure 3. Inductive polarisation potential of beam prestressed wires exposed to chloride threshold migration test. Evolution of E_{corr}, (squares-left) and i_{corr} (square right) at depolarisation.

3.2 Chloride Penetration. Profile and Diffusion Coefficient Determination

The chloride profile was determined in concrete cores taken at 30, 60, 90 and 120 cm length of the beam. The profiles, given in 'Fig. 5 left', show a decrease in chloride content with the concrete depth, at 0.5 cm, 1.2-1.6% total Cl^- by weight of cement, and decreasing to 0.2-0.5 % at 3 cm. The total chloride content expected at the rebar level varies from 1 to 1.4%.

The profiles of the total chlorides represented in 'Fig. 3 left' have being used to determine the non-stationary diffusion coefficient of the concrete of the prestressed beam. The migration diffusion coefficient, D_{mig}, has been determined, from the use of a modified Fick's second law [Andrade *et al*

1994] and following the suggestion of a previous paper [Castellote *et al* 2002] the D_{app} of the prestressed concrete of the beam has been obtained.

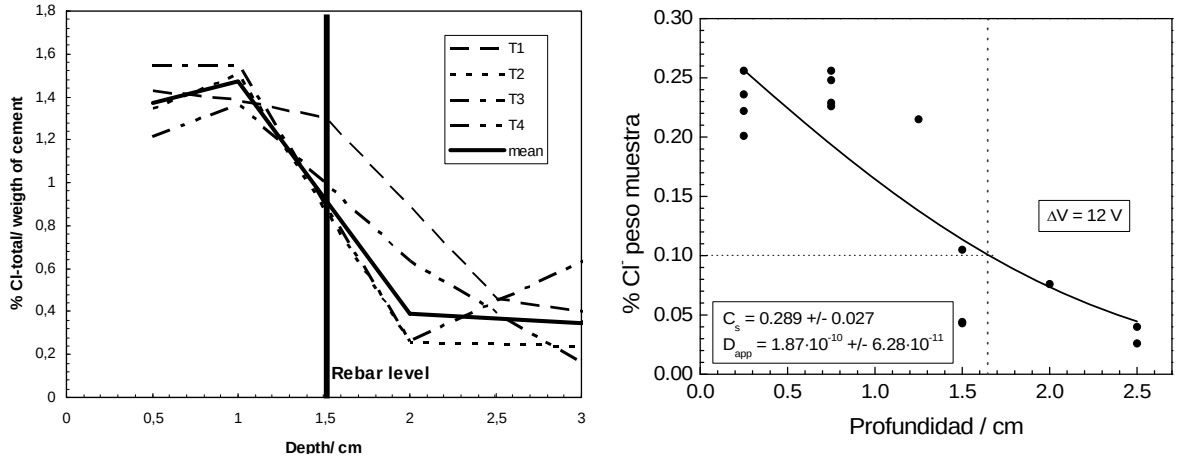

Figure 4. Chloride profiles in the concrete cores, in % total Chloride by weight of cement (left). Chloride profile for apparent diffusion coefficient determination (right)

A mean value for a D_{app} of $2.65 \cdot 10^{-10} \pm 7.32 \cdot 10^{-11}$ has been found. Table 1 shows the D_{app} coefficients for each core and the average. These values are more than one order of magnitude lower to those published in literature for conventional concrete, non prestressed. However further tests are needed from non accelerated chloride penetration methods to confirm previous values.

Table 1. D_{app} of concrete prestressed beam calculated from migration coefficient test

T1 (cm^2/s)	*T2 (cm^2/s)*	*T3 (cm^2/s)*	*T4 (cm^2/s)*	*Media (cm^2/s)*
$4.31 \cdot 10^{-10}$ $\pm 1.68 \cdot 10^{-10}$	$1.91 \cdot 10^{-10}$ $\pm 1.38 \cdot 10^{-10}$	$1.54 \cdot 10^{-10}$ $\pm 1.45 \cdot 10^{-10}$	$2.95 \cdot 10^{-10}$ $\pm 1.67 \cdot 10^{-10}$	$2.65 \cdot 10^{-10}$ $\pm 7.32 \cdot 10^{-11}$

At the end of the migration experiment, the chloride content distribution near the rebar surface was determined at different points along the beam, in order to know the variability of the chloride threshold. The % of total amount of chlorides and the free chlorides were analyzed. “Figure 5 left” shows the results. The average % for free chlorides is 1.37±0.34 and for total chlorides 1.73±0.48% by weight of cement. After broken and observations, the wire surface shows pits with different sizes. These pits are more developed in areas with higher free chloride content.

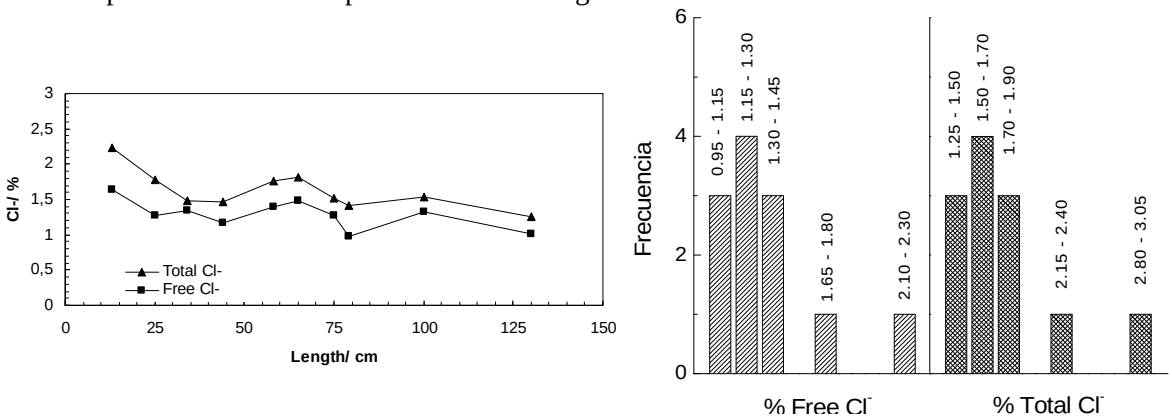

Figure 5. % of total and free chlorides content, in weight of cement at the rebar level (left)**.** Chloride distribution probability at the wire level (right).

The statistical distribution of the chlorides values shows that the higher probability of chloride threshold at the rebar level is around 1.15 to 1.30 for free chlorides and 1.5 to 1.7 for total Cl^-, as shown in "Fig. 5 right". Besides, more than 70% probability of free Cl^- content is among 1 to 1.5, and for total chloride the 80 % is between 1.2 to 2%. However these chloride thresholds can be considered representative if corrosion pits are completely developed and certain penetration of attack is accepted. However lower values should be found if the time for first pitting is considered, as shown in "Fig. 3"

4 CONCLUSIONS

From the preliminary results presented in the paper several conclusions have been derived:

- It has been possible to develop an experimental procedure for determining chloride threshold using real prestressed concrete samples.
- Several methods have been considered based on natural or accelerated determination, which varies significantly the time to onset of corrosion.
- The accelerated method based on migration has been confirmed to be a method able to give information on chloride threshold in reasonable testing time. The method has allowed the simultaneous determination of the time to depassivation at different levels of corrosion.
- The higher dimension of the samples needed for prestressed concrete, which includes large length of wire exposed, allows on the same sample several determinations of chloride threshold at the wire surface and to perform statistical analyses.
- The simultaneous determination of D_{app} is possible from the same test sample.

ACKNOWLEDGES

The authors wish to acknowledge to the Minister of Science and education of Spain for the financial of the research (Proj. BIA 2004-02239). Also are gratefully to SOMAPRE-HISPANIA for the supply of the prestressed beams.

REFERENCES

Alonso, C., Andrade, C., Castellote, M *&* Castro, P. 2000, "Chloride threshold values to depassivate reinforcing bars embedded on standardised OPC mortars", *Cem. & Conc. Res*., 30, pp 1047-1055.

Alonso, C., Castellote, M *&* Andrade, C. 2002, "Chloride threshold dependence of pitting potential of reinforcement", *Electrochemica Acta*, 47, pp 3469-3481.

Andrade, C., San Juan M.A., Recuero, A. *&* Rio, O. 1994, "Calculation of chloride diffusivity in concrete from migration experiments in non-steady state conditions", *Cem. & Con. Res.*, Vol. 24, No. 7, pp 1214-1228.

Andrade *et all*, 2000, "A validated users manual for assessing the residual service life of concrete structures, CONTECVET", *IETcc electronic publication, www.ietcc.csic.es*, Pp 1-152.

Arya C. *&* Xu, Y. 1995, "Effect of cement type on chloride binding and corrosion of steel in concrete. *Cem & Conc. Rs*., 25,4, pp 893.

Arup, H. 1996, "A new method for determining chloride thresholds as a function of potential in field exposures tests". *Durability of concrete in saline environment*. Edt. Cementa, pp 107.
Breit W. *&* Schiesl P. 1995, "Investigations on the threshold value of the critical chloride content". *Int. RILEM Workshop on Chloride penetration into concrete*. Edt. L.O. Nilsson and J.P. Olivier. France,pp 441.

Castellote, M., Andrade, C. & Alonso, C. 2002, "Accelerated simultaneous determination of chloride depassivation threshold and of non – stationary diffusion coefficient values", *Corros. Sc.*, 44, pp 2409-2424.

Duracrete Project, 2000. *Probabilistic performance based design of concrete structures*, EC BE95-1347.

Izquierdo D., Alonso C., Andrade, C. *&* Castellote M., 2004, "Potentiostatic determination of chloride threshold values for rebar depassivation. Experimental and statistical study". *Electrochemica Acta*, 40 pp 2731-2739.

Glass, G.K. *&* Buenfeld, R.N., 1997. "The presentation of the chloride threshold level for corrosion of steel in concrete". *Corros. Sc*. 39, 5, pp 1001.

Hansson, C. *&* Sorensen, B. 1990, "The threshold concentration of chloride in concrete for the initiation of the reinforcement corrosion". *Corrosion rates of steel in concrete*. ASTM STP 1065, Edt. S. Berke, V. Chaker and D. Whiting. 3.

Hausman, D.A. 1967, "Steel corrosion in concrete. How does it occurs?". *Mater. Prot*., pp 19.

Hope, B.B. *&* Alan K.C. 1987. "Chloride corrosion threshold in concrete". *ACI Mat. J*. pp 306.

Hussain, S.E., Rasheeduzzafar, Al-Musallan, A. *&* Al-Gahtani A.S.. 1995. "Factors affecting threshold chloride for reinforcement corrosion in concrete". *Cem. & Con. Rs*., 25, 7, pp 1543.

Lambert, P. Page, C.L. *&* Vassie, P.R.W.1991, "Investigations of reinforcement corrosion. 2. Electrochemical monitoring of steel in chloride-contaminated concrete". *Mat. & Struc.* 24, pp 351.

Kayyali, O.A. *&* Haque, M.N. 1995. "The Cl-/OH- in chloride contaminated concrete. A most important criterion". *Magz. of Con. Rs*., 47, 172, pp235.

Mammoliti, L.T., Brown L.C., Hansson C. *&* Hope, B.B. 1996. "The influence of surface finish of reinforcing steel and pH of test solution on the chloride threshold concentration for corrosion initiation in synthetic pore solutions". *Cem. & Con. Rs.* 26,4, pp 545.

Pettersson, K. 1996. "Factors influencing chloride induced corrosion of reinforcement in concrete". *Int. Conf. of Durability of Building Materials and Components*. Edt. C. Sjostrom. Chapman *&* Hall, London, pp 1001.

Sandberg, P., 1995, "*Critical evaluation of factors affecting chloride initiated reinforcement corrosion in concrete*". Unv. of Lund, Report TVBM-7088, pp 4-113.

Rasheduzafar, M., Al-saadoun S.S., Al-Gahtani A.S. *&* Dakil F.H. 1990. "Effect of tricalcium aluminate content of cement on corrosion of reinforcing steel in concrete". *Cem. &Con. Rs.* 20, pp723.

Tanner, P. *&* Andrade, C. 2000, Corrosion models for structural design, proceedings of the RILEM/CBI/ISO Int Symp. On Integrated life cycle design of materials and structures, RILEM Publ., Helsinki.

Thomas M. 1996. "Chloride thresholds in marine concrete". *Cem. & Con. Rs*., 26, 4, 513

Tuutti, K. 1982, "*Corrosion of steel in concrete*". CBI Publ. Stockholm (1982) pp 291.

11DBMC International Conference on Durability of Building Materials and Components
ISTANBUL, Turkey 11-14 May 2008

Analysis of Reinforced Concrete Flexural Members Strengthened with Near-Surface Mounted CFRP

N. Chikh [1]
G. Foret [2]
B. Bousalem [3]
S. Firas [4]

T 11

ABSTRACT

Carbon fiber reinforced polymer (CFRP) materials are currently produced in different configurations and are widely used for the strengthening and retrofitting of concrete structures and bridges. Recently, considerable research has been directed to investigate the use of CFRP strips as near surface mounted (NSM) reinforcement, primarily for strengthening applications. The technique is based on fixing, by epoxy adhesive, CFRP strips into pre-cut grooves made on the concrete cover of the elements to be strengthened. In several cases the NSM technique has shown substantial advantages when compared with externally bonded laminates.

This paper investigates the flexural behaviour of reinforced concrete beams strengthened with NSM CFRP laminate. A simple and direct analytical procedure for evaluating the ultimate flexural capacity of NSM CFRP strengthened reinforced concrete beams is presented. The procedure is derived from equilibrium equations and compatibility of strains and is applicable to both singly and doubly reinforced concrete rectangular sections. Upper and lower limits of NSM CFRP strips that may be bonded into slits made on the concrete cover of a reinforced concrete cross section to ensure ductile behaviour are established. Design charts to facilitate the implementation of the procedure were also developed. The procedure is validated by comparisons with results of some experimental data available in the literature.

KEYWORDS

RC beam, Flexural strengthening, Near surface mounted, Carbon fiber reinforced polymer, Design

[1] University of Mentouri, Materials and Durability of Constructions Laboratory, Constantine 25000, Algeria, Phone +213 31 90 92 41, chikh_ne@yahoo.fr
[2] Ecole Nationale des Ponts et Chaussées, Material Analysis and Identification Laboratory, Marne la Vallée, France F77455, Phone +33 164153713, Fax +33 164153711, foret@lami.enpc.fr
[3] University of Mentouri, Materials and Durability of Constructions Laboratory, Constantine 25000, Algeria, Phone +213 31 90 92 52, bbousalem_dz@yahoo.fr
[4] Ecole Nationale des Ponts et Chaussées, Material Analysis and Identification Laboratory, Marne la Vallée, France F77455, Phone +33 164153704, Fax +33 164153711, sayed_firas@yahoo.fr

1 INTRODUCTION

Fiber-Reinforced Polymers (FRP) materials have been used extensively, in different configurations and techniques, in the last decade for strengthening bridges and buildings. Externally bonded (EB) FRP sheets and strips are currently the most commonly used technique for flexural and shear strengthening of concrete beams and slabs. This method of strengthening has been the subject of extensive experimental investigations, and codes and design guidelines have been published that address many aspects of this technology. Several researchers reported that the failure of concrete members strengthened with EB FRP sheets or strips could be brittle due to debonding and/or peeling of the FRP reinforcements especially in the zones of high flexural and shear stresses [Spadea *et al.* 1998]. To improve the efficiency of this technique, some anchorage systems have been proposed [Khalifa e*t al.* 1999]. However, the reinforcing performance of these composites can be negatively affected by the effect of freeze/thaw cycles, significantly decreased when submitted to high and low temperatures and are also susceptible to vandalism acts.

To minimize these problems, to improve utilization of the FRP materials, and to ensure long service life for the selected system, near-surface mounted (NSM) reinforcement was recently introduced as a promising strengthening technique and a valid alternative to the EB FRP technique for increasing flexural strength of reinforced concrete members [De Lorenzis e*t al.* 2000, Taljesten e*t al.* 2003, El-Hacha e*t al.* 2004]. In the NSM FRP method, grooves are first cut into the concrete cover of an RC beam/slab and FRP bars/strips are then inserted and bonded therein with an appropriate binding agent typically epoxy paste or cement grout. Configuration of the FRP reinforcements used for the NSM technique is controlled by the depth of the concrete cover.

Compared to externally bonded FRP reinforcement, the NSM system has a number of advantages [De Lorenzis & Teng 2007]: (a) the amount of site installation work may be reduced, as surface preparation other than grooving is no longer required (e.g., plaster removal is not necessary; irregularities of the concrete surface can be more easily accommodated; removal of the weak laitance layer on the concrete surface is no longer needed); (b) NSM reinforcement is less prone to debonding from the concrete substrate; (c) NSM bars can be more easily anchored into adjacent members to prevent debonding failures; this feature is particularly attractive in the flexural strengthening of beams and columns in rigidly-jointed. Thus, this method is relatively simple and considerably enhances the bond of the FRP reinforcements, thereby using the material more effectively.

Published literature on the use of NSM FRP rebars and strips for structural strengthening is still very limited when compared with that of EB FRP sheets and strips. This paper presents a design procedure for flexural RC beams with NSM CFRP reinforcement. The procedure is derived from equilibrium equations and compatibility of strains and is applicable to both singly and doubly reinforced concrete rectangular sections. Upper and lower limits of NSM CFRP ratios to ensure ductile behaviour are established. Design charts to facilitate the implementation of the procedure are also presented. Some experimental results currently available on this topic are used as basis and support to the proposed equations.

2 SECTION ANALYSIS

2.1 Failure Modes

The possible failure modes of beams flexurally-strengthened with NSM CFRP reinforcement are of two types: those of conventional RC beams, including concrete crushing or NSM CFRP rupture generally after the yielding of internal steel bars, for which the composite action between the original beam and the NSM CFRP is practically maintained up to failure, and ‘‘premature’’ debonding failure modes which involve the loss of this composite action. Although debonding failures are less likely a problem with NSM CFRP compared with externally bonded FRP, they may still significantly limit the

efficiency of this technology [De Lorenzis & Teng 2007]. In the present analysis, it is assumed that the beam is properly detailed so as to preclude debonding failure modes.

2.2 Assumptions of Present Analysis

The design equations presented herein are based on the following assumptions:

- Linear strain distribution across the section depth.
- Compressive force in concrete, at crushing, is determined by Whitney's equivalent rectangular stress block. The ultimate compressive strain in concrete is assumed to be 0.0035.
- Tensile stresses in concrete, at ultimate strength, are ignored.
- Reinforcing steel is assumed to have elastic-perfectly plastic response.
- CFRP behaves linearly up to brittle failure since its fibres are aligned with the beam axis.
- Perfect NSM CFRP strip bond is considered for strain compatibility equations.
- The governing failure mode is concrete crushing, preceded by steel yielding, prior to CFRP rupture. A minimum NSM CFRP ratio is formulated to ensure this failure mode.

3 DESIGN OF SINGLY REINFORCED RECTANGULAR SECTIONS

The approach developed by Hayder [Hayder & Shariq 2003] is followed here, as closed form equations are formulated to establish a direct procedure for flexural strength design of FRP-strengthened beams. They differ from the current state of the art iterative procedure which may lead to tedious calculations [Chaallal e*t al.* 1998, EI-Mihilmy e*t al.* 2000]. Referring to figure 1, the force equilibrium equation is used to define the CFRP strip ratio as follows:

$$f_c\, a\, b = A_s\, f_y + A_f\, f_f \tag{1}$$

$$A_f = \frac{f_c\, a\, b - A_s\, f_y}{f_f} \quad \text{with} \quad f_c = 0.85\, f_c' \quad \text{and} \quad a = 0.8\, x \tag{2a}$$

$$\rho_f = \frac{f_c}{f_f} 0.8\alpha - \rho_s \frac{f_s}{f_f} \tag{2b}$$

where $\rho_f = \dfrac{A_f}{b\,d}$, $\rho_s = \dfrac{A_s}{b\,d}$ and $\alpha = \dfrac{x}{d}$.

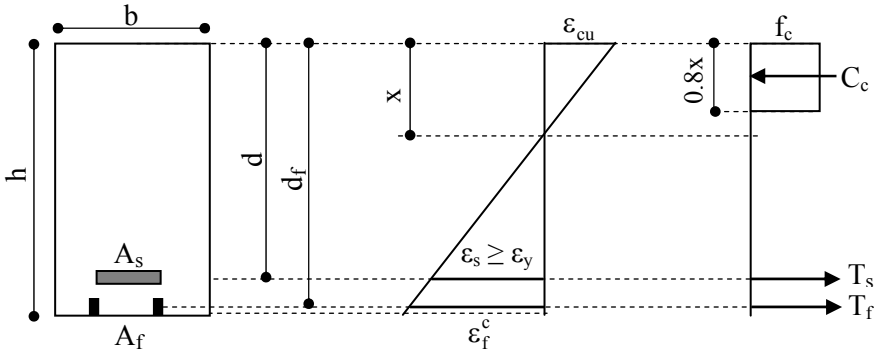

Figure 1. Singly reinforced cross-section with strain distribution and force profile.

Using strain compatibility, the strain in the NSM CFRP strip ε_f^c is given by

$$\varepsilon_f^c = \frac{d_f - x}{x} \varepsilon_{cu} \tag{3}$$

Considering that $\alpha_d = \frac{d_f}{d}$, the above equation is rewritten as follows

$$\varepsilon_f^c = \left(\frac{\alpha_f}{\alpha} - 1\right)\varepsilon_{cu} \tag{4}$$

where ε_f^c is the CFRP strain at failure, considering zero initial concrete strain during strengthening. The actual CFRP strain ε_f^c is found by subtracting the initial concrete strain ε_0:

$$\varepsilon_f = \varepsilon_f^c - \varepsilon_0 \tag{5}$$

Thus, the tensile stress in NSM CFRP strip is

$$f_f = \varepsilon_f E_f = \left(\frac{\alpha_f}{\alpha} - 1\right)\varepsilon_{cu} E_f \tag{6}$$

The expression of the ultimate moment of resistance may be obtained by summing the moment of the forces acting on cross section about the centroid of the concrete stress block

$$M_r = A_s f_y (d - 0.4x) + A_f f_f (d_f - 0.4x) \tag{7}$$

Equation (7) can be expressed in a non-dimensional form

$$\mu_r = \rho_s \frac{f_y}{f_c}(1 - 0.4\alpha) + \rho_f \frac{f_f}{f_c}(\alpha_f - 0.4\alpha) \tag{8}$$

where $\mu_r = \frac{M_r}{bd^2 f_c}$.

Replacing Eq. (1) into Eq. (2) gives

$$\alpha^2 - 2.5\alpha_d \alpha - 3.125\left[\rho_s \frac{f_y}{f_c}(1 - \alpha_d) - \mu_r\right] = 0 \tag{9}$$

Equation (9) directly yields α, which is used to solve ρ_f by substituting into Eqs. (4) and (6).

3.1 Maximum NSM CFRP Reinforcement Ratio

To ensure ductile failure, steel yielding needs to take place prior concrete compression failure. This can only happen if the area of NSM CFRP strip is kept lower than that causing balanced failure (i.e. simultaneous yielding of steel and crushing of concrete). Thus, the maximum NSM CFRP ratio may be expressed in terms of the difference between the balanced and actual steel ratios of the original unstrengthened section, as follows:

$$\frac{\varepsilon_{cu}}{x_{bal}} = \frac{\varepsilon_{cu} + \varepsilon_y}{d} \quad \Rightarrow \quad x_{bal} = \frac{0.0035}{0.0035 + \frac{f_e}{E_s}} d = \frac{700}{700 + f_e} d \tag{10}$$

$$\frac{\varepsilon_{cu}}{x_{bal}} = \frac{\varepsilon_{cu} + \varepsilon_f^{cbal}}{d} \quad \Rightarrow \quad \varepsilon_f^{bal} = \left(\frac{d_f}{x_{bal}} - 1\right)\varepsilon_{cu} - \varepsilon_0 = 0.0035\left(\frac{700 + f_e}{700}\frac{d_f}{d} - 1\right) - \varepsilon_0 \tag{11}$$

$$0.8 f_c\, b\, x_{bal} = A_s f_y + A_f^{bal} E_f \varepsilon_f^{bal} \tag{12}$$

Substituting Eqs. (9) and (10) into Eq. (11) and rearranging:

$$\frac{E_f \varepsilon_f^{bal}}{f_y}\rho_f^{bal} = 0.8\frac{f_c}{f_y}\frac{700}{700 + f_e} - \rho_s \quad \Rightarrow \quad \rho_f^{bal} = \frac{f_y}{f_f^{bal}}\left(\rho_s^{bal} - \rho_s\right) \tag{13}$$

where $\rho_f^{bal} = \frac{A_f^{bal}}{bd}$, ε_f^{bal} is computed by Eq. (10).

It is clear from Eq. (13) that cross-sections originally reinforced with the balanced steel ratio cannot exhibit a pseudo-ductile failure when strengthened with NSM CFRP strips. Fortunately, in current code

practice the steel ratio ρ_s is limited to 75% of the balanced steel ratio [ACI 2002]. This same percentage may be used here to limit the maximum NSM CFRP ratio so that the same type of pseudo-ductile failure is ensured:

$$\rho_s^{max} = 0.75\,\rho_s^{bal}, \quad \rho_f \le \rho_f^{max} = 0.75\,\rho_f^{bal} \tag{14}$$

3.2 Minimum NSM FRP Reinforcement Ratio

As stated earlier, the desired mode of failure is yielding of steel reinforcement followed by concrete crushing prior to NSM CFRP rupture. The latter cannot be guaranteed unless the NSM CFRP stress, at concrete crushing, is lower than its design ultimate strength f_{fu}. This may be conveniently prescribed by keeping the NSM CFRP ratio greater than that minimum needed to attain NSM CFRP design ultimate strength (f_{fu}) upon concrete crushing. Accordingly, the strain compatibility and force equilibrium equations are used to define such a ratio. If Eq. (7b) above yields a lower NSM CFRP ratio, the minimum should be obviously used to avoid any possible NSM CFRP failure.

$$\frac{\varepsilon_{cu}}{x_{min}} = \frac{\varepsilon_{cu} + \varepsilon_{fu}^{c}}{d_f} \quad \Rightarrow \quad x_{min} = \frac{0.0035}{0.0035 + \varepsilon_{fu} + \varepsilon_0} d_f \tag{15}$$

$$0.8\,f_c\,b\,x_{min} = A_s\,f_y + A_f^{min}\,f_{fu} \quad \Rightarrow \quad \rho_f^{min} = 0.8\frac{f_c}{f_{fu}}\frac{x_{min}}{d} - \rho_s\frac{f_y}{f_{fu}} \tag{16}$$

Except for lightly reinforced sections, the second term of Eq. (15) is typically larger than the first term, yielding negative values of ρ_f^{min} which indicate that reaching NSM CFRP design ultimate strength (f_{fu}) prior to concrete crushing is not possible.

4 DESIGN OF DOUBLY REINFORCED RECTANGULAR SECTIONS

The equations governing the NSM CFRP strengthening design for doubly reinforced sections are similar to those of Eqs. (1)–(9) with the contribution of the compression steel included. The strain compatibility is used to define the compressive steel strain, Fig. 2:

$$\frac{\varepsilon_{cu}}{x} = \frac{\varepsilon_{cu} - \varepsilon_s'}{d'} \quad \Rightarrow \quad \varepsilon_s' = 0.0035\left(1 - \frac{d'}{x}\right) = 0.0035\left(1 - \frac{\delta'}{\alpha}\right) \quad \text{with} \quad \delta' = \frac{d'}{d} \tag{17}$$

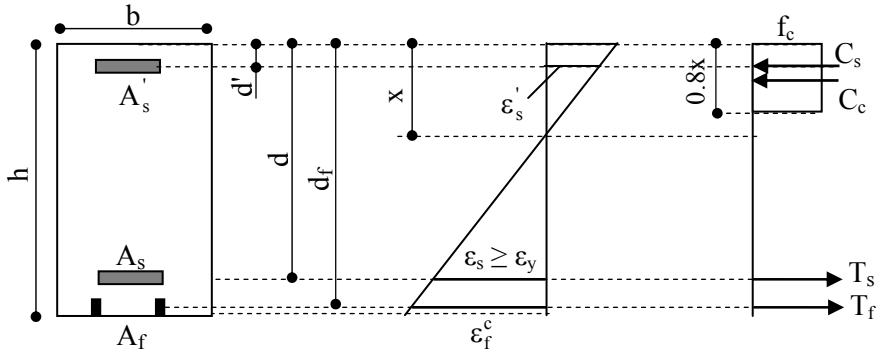

Figure 2. Doubly reinforced cross-section with strain distribution and force profile.

Using the force equilibrium and the sum of moments about the centroid of the concrete compressive force, we obtain the following expressions:

$$\rho_f = \frac{f_c}{f_f} 0.8\alpha + \rho_s' \frac{f_s'}{f_f} - \rho_s \frac{f_s}{f_f} = \rho_{f\,singly} + \rho_s' \frac{f_s'}{f_f} \tag{18}$$

$$\alpha^2 - 2.5\alpha_d\,\alpha - 3.125\left[\rho_s \frac{f_y}{f_c}(1-\alpha_d) + \rho_s' \frac{f_s'}{f_c}\left(1 - \frac{\delta'}{\alpha}\right) - \mu_r\right] = 0 \tag{19}$$

Equation (19) may be directly solved for α if the compression steel has yielded. f_s' is substituted by f_y assuming that $\varepsilon_s' > \varepsilon_y$. The value of α obtained is then substituted into Eq. (17) to verify this yielding. If yielding actually takes place, the solution is complete. Otherwise, Eq. (17) is substituted into Eq. (19) resulting in a cubic expression, which may also be directly solved for α using a scientific calculator.

$$\alpha^2 - 2.5\alpha_d\,\alpha - 3.125\left[\rho_s \frac{f_y}{f_c}(1-\alpha_d) + \rho_s' \frac{f_s'}{f_c}\left(1 - \frac{\delta'}{\alpha}\right) - \mu_r\right] = 0 \tag{20}$$

Once α is found as the lowest positive root of Eq. (20), A_f is determined using Eq. (18).

4.1 Maximum and Minimum NSM CFRP Reinforcement Ratio

The derivation of the maximum and minimum NSM CFRP ratios follows analogous steps to those of Eqs. (10)–(16) yielding the following expressions

- Maximum NSM CFRP ratios: $$\rho_f^{max} = \frac{1}{f_f^{bal}}\left(0.6\rho^{bal} + \rho_s' f_s' - \rho_s f_y\right) \tag{21}$$

- Minimum NSM CFRP ratios: $$\rho_f^{min} = 0.8\frac{f_c}{f_{fu}}\frac{x_{min}}{d} + \rho_s' \frac{f_s'}{f_{fu}} - \rho_s \frac{f_y}{f_{fu}} \tag{22}$$

with $$x_{min} = \frac{0.0035}{0.0035 + \varepsilon_{fu} + \varepsilon_0} d_f \quad \text{and} \quad f_s' = 700\frac{d_f - x_{min}}{x_{min}}$$

5 DESIGN CHARTS

To facilitate the analysis and design of reinforced concrete beams strengthened with NSM CFRP strips, several design charts were developed employing the results of the section analysis previously discussed. The following assumptions were made in the development of these charts:

- Linear strain distribution at failure
- Failure is controlled by the tension failure mechanism
- NSM CFRP strips are bonded to unloaded reinforced concrete beams ($\varepsilon_0 = 0$).

Due to lack of space, the development of the design expressions is presented only for the case of singly reinforced rectangular sections. Referring to Figure 1 and using the same parameters defined in section 3, Eq. (2b) yields to

$$\alpha = \frac{\rho_s f_y + \rho_f f_f}{0.8 f_c} \tag{23}$$

f_f is given by Eq. (6). Substituting this latter into Eq. (23) and taking ε_{cu}=0.0035 and f_c=0.85 f_{c28} leads to

$$\alpha = \frac{\rho_s f_y + \rho_f \left(\frac{\alpha_f}{\alpha} - 1\right) 0.0035 E_f}{0.8 f_c} \tag{24}$$

Rearranging Eq. (24) into a quadratic form and defining ω and ω_f respectively as the mechanical ratio of the reinforcing steel and the CFRP strip:

$$\alpha^2 - \frac{1}{0.68}(\omega - 0.0035\omega_f)\alpha - \frac{0.0035\,\omega_f\,\alpha_d}{0.68} = 0 \qquad (25)$$

where $\omega = \rho_s \dfrac{f_y}{f_{c28}}$ and $\omega_f = \rho_f \dfrac{E_f}{f_{c28}}$

Equation (25) may be used to determine directly the value of α. Substituting Eq. (6) into Eq. (8) and using the parameters ω and ω_f leads to

$$\mu_r = \omega(1 - 0.4\alpha) + 0.0035\,\omega_f \frac{f_f}{f_c}\left(\frac{\alpha_d}{\alpha} - 1\right)(\alpha_d - 0.4\,\alpha) \qquad (26)$$

Considering the section equilibrium, μ_r must be greater or equal to μ_s $(= M_a / bd^2 f_c)$ where M_a represents the design moment. An iterative procedure was employed to determine ω_f for each assumed values of ω and μ_s. The following flow chart resumes the different steps to be carried out to perform the various calculations.

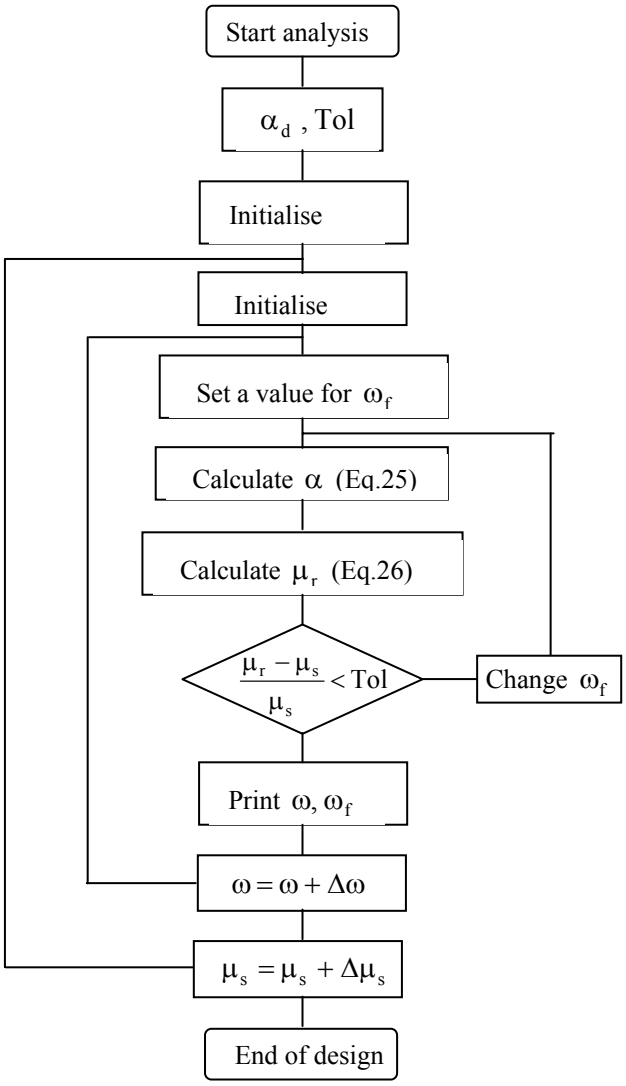

Figure 3. Flow chart of the design procedure for the analysis of NSM CFRP strengthened singly reinforced rectangular section.

The calculations were performed using a computer program developed for this study, and the results are presented in the form of design graphs such as the one presented in Fig. 4. Each family of curves is a function of the ratio d_f/d only. It is interesting to note that these charts are valid for any specific CFRP modulus of elasticity and tensile strength as long as beam failure is controlled by the tension mechanism. Thus, the required NSM CFRP cross-sectional area should be checked against $A_f^{max} (=\rho_s^{max}\, b\, d)$ and $A_f^{min} (=\rho_s^{min}\, b\, d)$ as previously discussed. Therefore, for a reinforced concrete beam requiring an increased moment capacity M_u, the required NSM CFRP cross-sectional area A_f is determined from the following expression:

$$A_f = \rho_s\, b\, d = \omega_f \frac{f_c}{E_f} b\, d \qquad A_f^{min} \le A_f \le A_f^{max} \tag{27}$$

where ω_f is determined from Fig. 4. The exam of this latter reveals that:

- NSM CFRP strips can significantly increase the ultimate flexural capacity of reinforced concrete beams.
- This effect is more pronounced for beams having relatively small steel reinforcement ratios, ρ.
- For any particular reinforced concrete beam, the rate of increase in ultimate flexural capacity decreases as the NSM CFRP strip cross-sectional area is increased.

For the purpose of illustration, design graphs for the case of a doubly reinforced concrete rectangular section are shown in Fig. 5 with $\rho_s^{'} = 0.5\%$, $f_s^{'} = 400\text{MPa}$ and $f_{c28} = 25$ MPa ($\omega^{'} = \frac{\rho_s^{'} f_s^{'}}{f_{c28}}$).

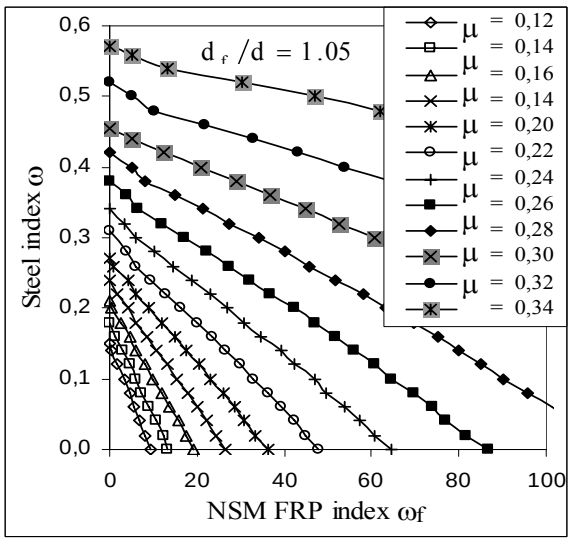

Figure 4. Design charts for singly reinforced concrete rectangular section

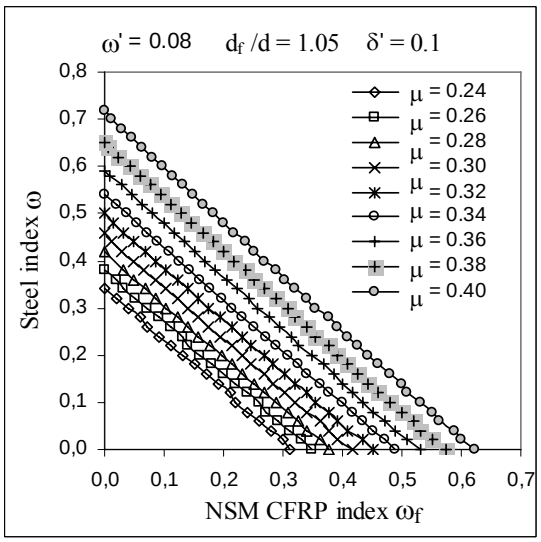

Figure 5. Design charts for doubly reinforced concrete rectangular section

6 SECTION ANALYSIS VERIFICATION

Most of the experimental data available on this topic do not provide all parameters values so as to perform calculations for comparison purposes. The results published by Barros [Barros & Fortes 2005] indicate fortunately all the details regarding tested specimens and materials used. In this respect, a comparison is made and the results are summarized in Table 1. All beams were tested in

Table 1. Comparison of results

Beam Designation	b (mm)	d (mm)	As (mm^2)	A's (mm^2)	f_y (MPa)	f'_y (MPa)	f_{c28} (MPa)	A_f (mm^2)	E_f (GPa)	Exp. ult. load (KN)	Calc. ult. load (KN)
V2R2	100	152	339	402	730	530	48	28.5	160	78.5	75.9
V3R2	100	150	427	402	730	530	43	28.5	160	81.9	83.6
V4R3	100	155	603	402	730	530	46	42.75	160	94.9	108.2

four-point bending over a simple span length. The ultimate load represents the sum of the two equal concentrated loads applied to the beams at failure. The results from this limited comparison clearly indicate that the proposed procedure is quite satisfactory in predicting the ultimate flexural capacity of reinforced concrete beams strengthened with NSM CFRP strips. The absolute average percent difference between the experimental ultimate loads and the ultimate loads predicted by the section analysis procedure was 6.7%, which is very acceptable. In fact, this difference is quite small when one considers the expected variation associated with the behaviour of reinforced concrete structures.

CONCLUSIONS

Strengthening of structures with NSM FRP reinforcement is a technique that represents a feasible and economic alternative to the technique of strengthening structures with EB FRP reinforcement. Research in this field started only a few years ago but has by now attracted worldwide attention. A significant amount of research has been conducted on this emerging technique. This paper presents a design procedure for flexural RC beams with NSM CFRP reinforcement. A simple and a direct approach was developed on the basis of equilibrium and strain compatibility. Design graphs to facilitate implementation of the procedure were also developed. Upper and lower limits for NSM FRP strip cross-sectional area to ensure ductile behaviour of the strengthened beams were introduced. To verify the accuracy of the proposed procedure, comparison of results obtained by the section analysis with some reported experimental results was performed. Good correlation of the predicted results with experimental results was noted.

REFERENCES

ACI 318-02, Building code requirements for structural concrete. 2002. American Concrete Institute, Detroit, Michigan, 443p.

Barros J.A.O. & Fortes, A.S. 2005, 'Flexural strengthening of concrete beams with CFRP laminates bonded into slits', *Cement Concr Compos*, **27** [4], 471–480.

Chaallal O., Nollet M.J. & Perraton D. 1998, 'Strengthening of reinforced concrete beams with externally bonded fiber-reinforced-plastic-plate: design guidelines for shear and flexure', *Can J Civil Eng*, **25** [4], 692–704.

De Lorenzis L., Nanni A. & La Tegola A. 'Flexural and shear strengthening of reinforced concrete structures with near surface mounted FRP rods', Proc. Int. Conf. on Advanced Composite Materials in Bridge and Structures (ACMBS-III), Ottawa, Canada, 15-18 August 2000, pp. 521–528.

De Lorenzis L. & Teng J.G. 2007, 'Near-surface mounted FRP reinforcement: An emerging technique for strengthening structures', *Compos Part B: Eng*, **38** [2], 119-143.

El-Hacha R. & Rizkalla S.H. 2004, 'Near-surface-mounted fiber-reinforced polymer reinforcements for flexural strengthening of concrete structures', *ACI Struct J*, **101**[5], 717–726.

Hayder A. R. & Shariq P. 2003, 'Closed form equations for FRP flexural strengthening design of RC beams', *Compos Part B: Eng*, **34** [6], 539-550.

Khalifa A., Alkhrdaji T., Nanni A. & Lansburg S. 1999, 'Anchorage of surface mounted FRP reinforcement', *Concrete Int.: Design Constr*, **21** [10], 49–54.

EI-Mihilmy M.T. & Tedesco J.W. 2000, 'Analysis of Reinforced Concrete Beams Strengthened with FRP Laminates', *J of Struct Eng ASCE*, **126** [6], 684-691.

Spadea G., Bencardino F. & Swamy R.N. 1998, 'Structural behaviour of composite RC beams with externally bonded CFRP', *J Compos Constr*, **2** [3], 132–137.

Taljsten B, Carolin A, Nordin H. 2003, 'Concrete structures strengthened with near surface mounted reinforcement of CFRP', *Adv Struct Eng*, **6** [3], 201–213.

11DBMC International Conference on Durability of Building Materials and Components
ISTANBUL, Turkey 11-14 May 2008

Effect of Cement Type on the Resistance of Concrete against Rapid Chloride Permeability

Tolga Ilıca [1]
Hasan Yıldırım [2]
Özkan Şengül [3]

T11

ABSTRACT

In chloride containing environment, chloride permeability of concrete is a very important quality parameter affecting the service life of concrete structures. The primary objective of this experimental study was to investigate the effect of different types of cement on the resistance of concrete against chloride penetration. These cements included two different types of granulated blast furnace slag cement (CEM III/A 32.5N and CEM III/A 42.5N), a sulfate resisting cement (SRC 32.5), and a portland cement blended with fly ash, all compared to an ordinary type of portland cement (CEM I 42.5R). For each cement type, four concretes at different strength classes were produced and as a result 20 mixtures were obtained. Workability of the concretes was kept constant. Maximum size of the aggregate and aggregate grading was kept constant in all mixtures. Rapid chloride ion penetration tests according to ASTM C 1202 were conducted. Capillary water absorption tests were also carried out. In order to characterize the concrete quality, compressive strength of the specimens were obtained. The test results clearly demonstrated that the blast furnace slag cements gave the highest resistance against chloride penetration, while the pure portland cements gave the lowest resistance. Sulfate resisting cement also had a low resistance against chloride penetration. Concrete produced using the sulfate resisting cement had substantially higher capillary sorption compared to other mixtures.

KEYWORDS

Cement type, Rapid chloride permeability, Compressive strength, Capillarity.

[1] Civil Engineer MSc, ilica@itu.edu.tr
[2] Istanbul Technical University, Faculty of Civil Engineering, Istanbul, Turkey 34469, Phone +90 212 2853761, Fax 212 2856587, yildirimhasan63@hotmail.com
[3] Istanbul Technical University, Faculty of Civil Engineering, Istanbul, Turkey 34469, Phone +90 212 2853756, Fax 212 2856587, osengul@ins.itu.edu.tr

1 INTRODUCTION

Chloride induced corrosion of embedded reinforcement is the most severe durability problem of concrete structures in marine environment. Concrete composition is one of the main factors affecting the transport of chlorides into concrete. One of the effective ways of minimizing the chloride diffusion of concrete is to substitute portland cement by mineral admixtures [Neville 2004]. These materials are finely divided and can react with calcium hydroxide at ordinary temperatures to form calcium silicate hydrates (ASTM C618, 2000). The most widely used pozzolanic materials are fly ash and granulated blast furnace slag which are industrial by-products. Fresh and hardened concrete properties can be improved by using pozzolanic materials. Utilization of such materials in cement and concrete technology also has important environmental benefits. Since these by-product materials are obtained in very high amounts, storage can also be a major issue. By reducing the clinker amount used, more economical mixtures can be obtained (Aïtcin, 2000).

Pure portland cements are the dominating type of cement in many countries. However, it is expected that the production of blended cements are bound to increase in the years to come (Mehta and Monteirio 1996). Blended cements are produced by replacing parts of the portland cement by various types of pozzolanic materials. For many years, special cements such as granulated blast-furnace slag cements have proved to give a very high resistance of concrete against chloride penetration compared to that of pure portland cements (Bijen, 1998). In recent years, however, more optimized, high-performance cements and combinations of cements with pozzolanic materials have been used for improved durability of concrete structures in severe chloride containing environments.

The main objective of the present project is to study the effect of various types of cements on the resistance of concrete against chloride penetration. In the experimental program four different cements were used to produce concretes. A series of mixtures in which portland cement partially replaced by 25% fly ash, were also produced.

2 EXPERIMENTAL STUDY

2.1 Materials

In the study, four different types of cement were used (Table 1), including two blast furnace slag cements (CEM III/A 32.5N and CEM III/A 42.5N) with 35-40% and 52-58% slag, respectively, a sulfate resisting cement (SRC 32.5) and an ordinary portland cement (CEM I 42.5R) used as reference. For structures in a marine environment, sulfate resisting cement is recommended in many specifications in the country. However, the performance of this cement against chloride effect is not taken into account.

In addition to these cements, the ordinary portland cement blended with fly ash was included in the study. The fly ash used in this study was brought from Catalagzi power plant which satisfies the Class F requirements according to ASTM C 618 [Sengül et al. 2005]. It is known that the pozzolanic reaction of the fly ash is slow and its effect on improving the concrete properties can be limited. In order to obtain the performance of the concrete containing the fly ash equivalent to that of the pure portland cement concrete, 10% of the portland cement was replaced by 25% fly ash by weight.

The grading curve of concrete aggregate was chosen between ISO A16-B16 and closer to B16. In all the mixtures the aggregate grading and the maximum particle size of aggregate were kept constant. The basis of moisture content of the aggregates used in the concrete mixtures was saturated surface dry.

For each cement type, four concretes at different strength classes were produced and as a result 20 mixtures were obtained. The compositions of these concrete mixtures are shown in Table 2. Mixture proportioning was based on previous experience with the cements and trial mixtures to obtain the same compressive strengths. The concrete classes were C25/30, C30/37, C35/45 and C40/50 which are

the most widely used concrete grades in Turkey. These classes were based on the compressive strengths at the age of 28 days. For all the concrete mixtures, a superplasticizer was used to maintain approximately the same slump of 150±10 mm.

Table 1. Compositions of the cements.

Composition (%)	Portland cement CEM I 42.5R	Blast furnace slag cement CEM III/A 32.5N	Blast furnace slag cement CEM III/A 42.5N	Sulfate resisting cement
SiO_2	19.83	26.94	25.38	20.57
Fe_2O_3	2.71	2.35	2.72	3.96
Al_2O_3	4.95	8.63	7.65	4.18
CaO	64.28	50.36	55.29	64.29
MgO	1.56	3.92	2.99	0.95
SO_3	2.65	1.51	1.70	2.53
$Na_2O+0.658\ K_2O$	0.65	0.81	0.79	0.58
Cl^-	0,01	0,01	0.01	0,006
Loss on ignition	2.68	2.34	2.55	1.84
Slag content (%)	–	56.00	37.50	–
Blaine fineness, cm^2/g	3350	3593	3593	3226

2.2 Testing Procedures

The concrete mixtures were prepared in a laboratory mixer with vertical rotation axis, from which a number of 150 mm cubes and Ø100 x 200 mm concrete cylinders were produced. After demolding the next day, all specimens were kept in water saturated with lime at 20°C±2°C until time of testing.

The resistance of concrete against chloride penetration was obtained by the rapid chloride ion permeability test according to ASTM C1202-05 standard was applied. This test is based on the electrical conductivity of concrete. The concrete sample was subjected to a potential difference of 60 V and the total charge passing through at the end of 6 hours was measured and expressed in terms of Coulombs.

Capillary water suction and water absorption tests were carried out according to TS 4045 [1984]. The test is based on the water absorption of specimen by capillarity. The test is performed on specimens dried at 50ºC until constant weight. The specimens are covered with paraffin on four of their six faces to ensure that water is absorbed only from the given surface. Specimens are then placed in a container filled with few mm of water and the change in water is recorded at different intervals.

3 RESULTS and DISCUSSION

3.1 Rapid Chloride Permeability

Figure 1 shows the effect of cement type on the rapid chloride permeability of the concretes. The ASTM C1202-05 test is based on the electrical conductivity of concrete. A decrease in the charge value obtained at the end of the test indicates better resistance to chloride ion penetration and thus, lower permeability. As presented in Figure 1, the rapid chloride permeability of the concretes produced with the blast furnace slag cements are substantially lower than those of the other cements. For example, for the concrete grade of C25, the rapid chloride permeability of the pure portland cement concrete is about 6 times higher than the slag cement concretes. Similar results are obtained also for the C30 and C35 concrete classes. As seen in the Figure 1, for the pure portland cement concrete substantial reduction in the chloride permeability was obtained between the C35 and C40

grades. However, at the concrete class of C40, the chloride permeability of the portland cement concrete is still about 3 times higher than those of the slag cement concretes.

Table 2. Concrete mixture proportions (kg/m^3).

Mixture Code	Cement	Water	Fly Ash	w/b	Plasticizer	Natural Sand	Crushed Sand	Crushed Aggregate	Unit Weight
CEM I 42.5 R – C25	260	195	-	0,75	2.1	449	303	1142	2350
CEM I 42.5 R – C30	300	195	-	0,65	2.4	441	297	1124	2360
CEM I 42.5 R – C35	342	205	-	0,60	2.7	428	290	1092	2360
CEM I 42.5 R – C40	379	170	-	0,45	6.1	436	294	1110	2395
CEM I+FA-C25	239	214	66	0,70	2.4	415	293	1140	2370
CEM I+FA-C30	270	207	75	0,60	2.8	398	280	1088	2320
CEM I+FA-C35	313	228	87	0,57	3.2	387	272	1060	2350
CEM I+FA-C40	345	198	96	0,45	4.4	386	271	1058	2360
SRC – C25	247	210	-	0,85	2.0	445	300	1136	2340
SRC – C30	294	206	-	0,70	2.4	440	296	1121	2360
SRC – C35	337	186	-	0,55	2.7	432	292	1101	2350
SRC – C40	377	170	-	0,45	3.8	434	292	1104	2380
CEM III/A 32.5N-C25	369	203	-	0,55	2.9	423	286	1077	2360
CEM III/A 32.5N-C30	451	216	-	0,48	3.6	398	268	1013	2350
CEM III/A 32.5N-C35	490	225	-	0,46	3.9	384	258	978	2340
CEM III/A 32.5N-C40	585	263	-	0,45	4.7	355	239	903	2350
CEM III/A 42.5N-C25	289	196	-	0,68	2.3	441	298	1124	2350
CEM III/A 42.5N-C30	353	198	-	0,56	2.8	428	288	1091	2360
CEM III/A 42.5N-C35	404	194	-	0,48	3.2	419	282	1068	2370
CEM III/A 42.5N-C40	451	203	-	0,45	4.4	408	275	1038	2380

As seen in the Figure 1, partially replacing portland cement by the fly ash had an important effect on the rapid chloride permeability. Compared to the permeability of the pure portland cement concrete, the reduction in the chloride permeability due to fly ash is not significant at the concrete class of C25, but for the other concrete grades, this reduction is more than 50%. At the concrete class of C40, the chloride permeability obtained for the fly ash concrete was close to those of the slag cement concretes.

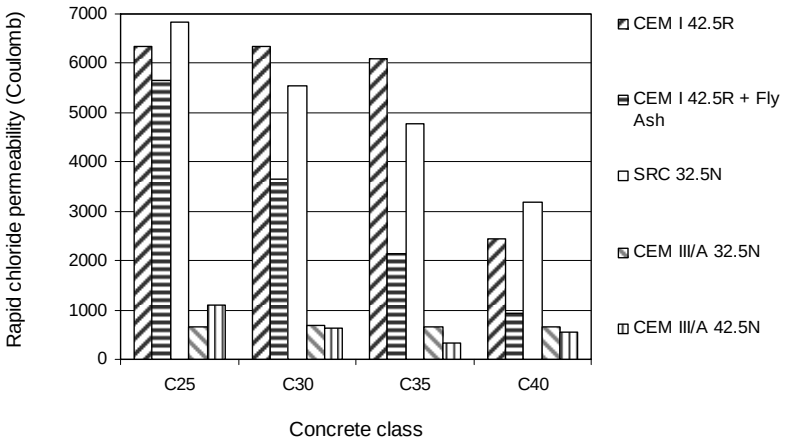

Figure 1. Effect of cement type on rapid chloride permeability of the concretes.

Concretes produced with the sulfate resisting cement were slightly lower than those of the pure portland cement concrete. The rapid chloride permeability of the concretes containing the sulfate resisting cement were about 6 times higher than the slag cement concretes at the C25, C30 and C35 grades and about 3 times higher for the C40 concrete grade. In many construction projects in Turkey, sulfate resisting cements are specified for structures exposed to marine environments. The chloride effect, however, is usually disregarded. These test results clearly indicate that sulfate resisting cements performance is close to portland cement in a chloride containing environment.

As expected, the rapid chloride permeability of the concretes decreased with the increase in concrete strength class. As seen in Figure 1, the chloride permeability of the portland cement concrete was almost the same for the concrete classes of C25, C30 and C35. At the C40 class, however, a substantial reduction was recorded for this type of concrete. The concretes containing the slag cements had very low chloride permeability at all classes, but the changes of rapid chloride permeability of these concretes due to the increase in concrete class were not significant.

The ASTM C 1202-05 suggests values for evaluating the rapid chloride permeability test results. The comparison is based on total charge passing at the end of 6 hours. The chloride ion penetrability is considered high for the test results more than 4000 coulombs. When the test results are between 100 and 1000 coulombs, the concrete can be classified as very low chloride permeability concrete. As presented in Figure 1, the concretes in this study produced with the slag cements can be considered as concretes of very low chloride permeability for all the concrete classes. The lower chloride permeability of the concretes with slag is a result of a denser microstructure. The pozzolanic reaction may cause lower amount of capillary pores and clogging of the pores, which reduces chloride ion transport in concrete [Li and Roy 1986].

As seen in the Figure 2, the concretes produced with the slag cements had very low chloride permeability according to the ASTM C 1202-05 even if they have high water-binder ratios such as 0.68. Except the water-binder ratio of 0.45, the chloride ion permeability of the specimens produced with portland cement and sulfate resisting cement are over 4000 coulombs and these concretes can be classified as concretes with low resistance to chloride penetration. As presented in the figures, the use of fly ash increases the resistance to chloride ion penetration.

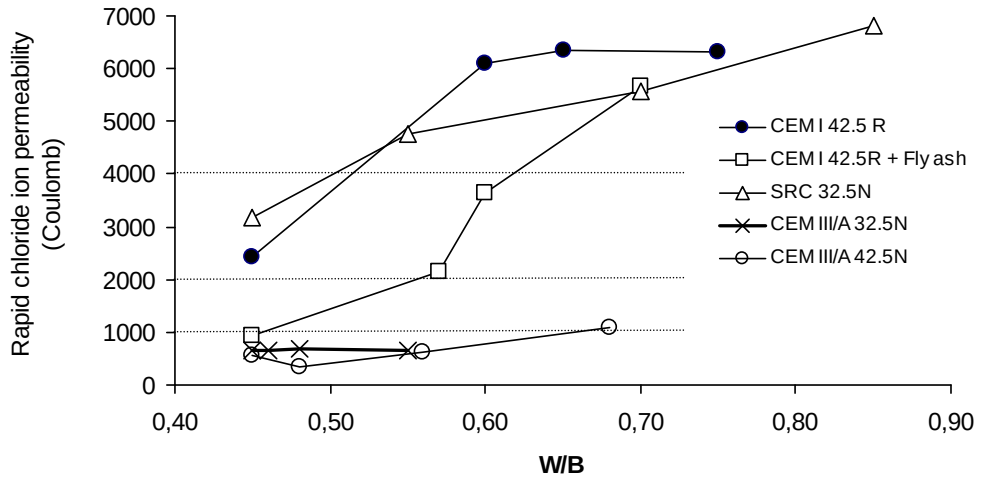

Figure 2. Effect of water-binder ratio on rapid chloride permeability of the concretes.

3.2 Capillary Water Absorption

Capillary water absorption test was carried out to physically characterize the mixtures. This test indicates possible macroscopic pore structure changes as a measurement of the changes in mass for partially submerged specimens. Capillary absorption is the mass of water per unit area that can be

absorbed in the material capillary when the specimen is in contact with water. It represents effective porosity or porosity that is accessible to water and, therefore, to aggressive environmental agents.

The capillary water absorption test is based on the water absorption of the concrete only from a given surface. The changes in weight due to water absorption are recorded at different intervals. The capillary absorption coefficient (k) is obtained from the "weight change per unit area vs. time" graphic. Figure 3 shows the effect of cement type on capillary water absorption of the concretes. An increase in the capillary water absorption coefficient is an indication of the increased water absorption.

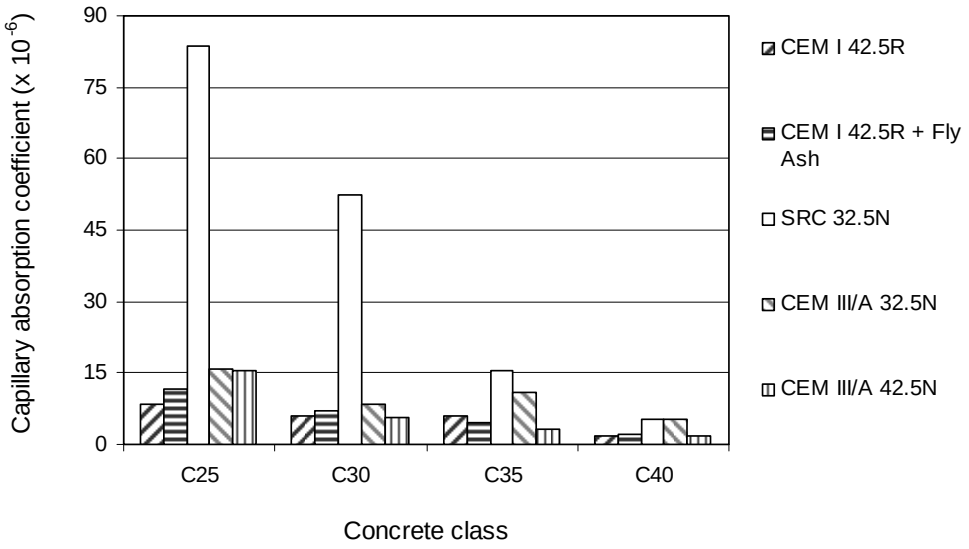

Figure 3. Effect of cement type on capillary water absorption of the concretes.

As seen in Figure 3, the capillary water absorption decreases with the increase in concrete strength class, as expected. This reduction, however, is more significant for the concrete with sulfate resisting cement. The capillary water absorption of the concretes produced with the sulfate resisting cement is substantially higher than those of the other cements, especially for the lower concrete grade. For the concrete class of C25, the capillarity is about 10 times higher than that of the portland cement concrete. At the concrete grade of C40, however, the capillary of the sulfate resisting cement and slag cement 32.5 are almost the same.

Although the concretes produced using the slag cements have substantially lower chloride permeabilities (Figure 1), the capillary water absorption of these concretes are not the lowest. The test results indicate that the capillarity of the concretes with slag cements is similar to those of the portland cement concrete (Figure 3).

3.3 Water Absorption

The specimens used for the capillary water absorption test are also used for obtaining the total water absorption. After the capillarity test, the specimens are immersed into water for 3 days to ensure complete saturation. Based on the dry weight, the water absorption of the concretes was calculated. Pores open to surface affect the water absorption, thus, the water absorption value may be accepted as an indirect indication of the porosity of the specimen. Figure 4 shows the effect of cement type on water absorption of the concretes.

The water absorption test results indicate the high water absorption of the concretes produced using the sulfate resisting cement. Except for the concrete class of C40, this concrete had the highest water absorption which supports the capillarity test results. As seen in Figure 4, the water absorption of the concretes decreases slightly with the increase in concrete class. For a given concrete class, it seems that the effect of cement type is not significant and similar results were obtained. When the rapid

chloride permeability test results (Figure 1) are compared to the capillary suction results (Figure 3) and the water absorption test results (Figure 4), it can be concluded that the better performance of the concretes produced with slag cement is not reflected in the water absorption and capillarity tests.

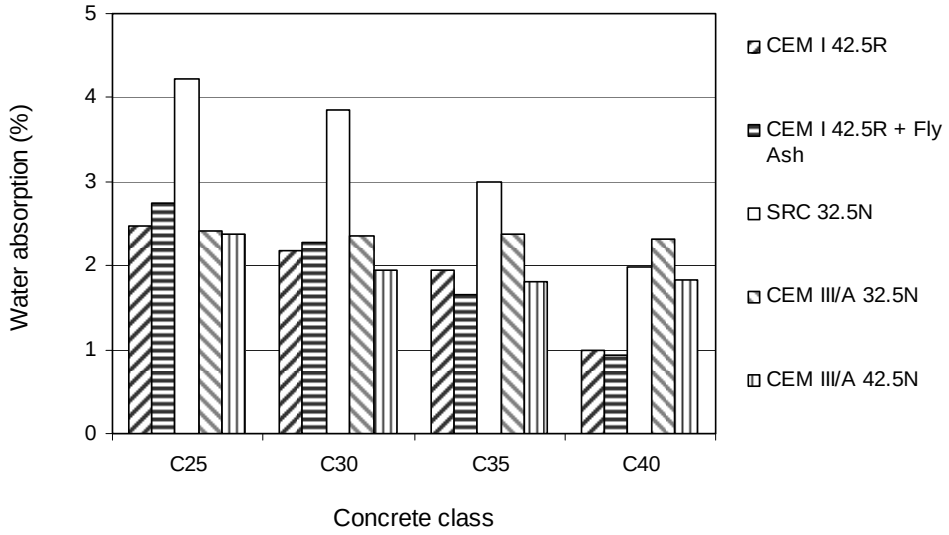

Figure 4. Effect of cement type on water absorption of the concretes.

4 CONCLUSIONS

The experimental investigation was based on a limited number of variables, and the testing was carried out according to accelerated methods. However, based on the test results obtained, the following conclusions appear to be warranted:

1. Concretes produced using the slag cements have substantially lower rapid chloride permeability compared to those of other cements. The concretes produced using the ordinary portland cement had the highest chloride permeability for all the concrete classes. The test results indicate that concretes with the sulfate resisting cement had low chloride permeability performance for all the classes investigated.

2. Concretes produced using the sulfate resisting cement had the highest capillary suction. For the concrete class of C25, the capillary coefficient of this type of concrete was about 10 times higher that of the portland cement concrete. Total water absorption of the concretes with sulfate resisting cement were also the highest among the concretes investigated.

3. The concretes produced using the slag cements have substantially lower chloride permeabilities compared to other mixtures. However, this performance is not reflected in the capillary water absorption test or total water absorption test.

REFERENCES

Aïtcin, P.C., 2000. Cement and Concrete Development from an Environmental Perspective, in *Concrete Technology for a Sustainable Development in the 21st Century*, pp. 206-217, Eds. Gjørv, O.E. and Sakai, K., E&FN Spon, London.

ASTM C 618, 2000, Standard Specifications for Coal Fly Ash and Raw or Calcined Natural Pozzolan for Use as Mineral Admixture in Portland Cement Concrete, *The American Society for Testing and Materials*, Pennsylvania.

ASTM C 1202 – 05, 2005, 'Standard Test Method for Electrical Indication of Concrete's Ability to Resist Chloride Ion Penetration', 6 pp.

Bijen, J. 1998, "Blast Furnace Slag Cement for Durable Marine Structures", *VNC/BetonPrisma*, The Netherlands, 62 p.

Li, S., & Roy, D.M. 1986, 'Investigation of relations between porosity, pore structure and chloride diffusion of fly ash and blended cements', *Cem. Concr, Res.*, 16[5], 49-759.

Mehta, P.K. & Monterio, P.J.M. 1996, Concrete, Prentice Hall, New Jersey.

Neville, A.M. 2004. Properties of Concrete, Pearson Prentice Hall, Essex.

Şengül, Ö., Taşdemir, C., & Taşdemir, M.A. 2005, 'Mechanical Properties and Rapid Chloride Permeabilites of Concretes with Ground Fly Ash', *ACI Materials Journal*, 102[6], 414-421.

TS 4045, 1984, 'Determination of the Capillary Water Absorption of Building Materials', Turkish Institute of Standards, Ankara.

Effects of Cement with Mineral Additive and without Mineral Additive on the Concrete Durability

Hasan Yıldırım [1]
Özlem Yörük [2]
Aslı Özbora [3]

T 11

ABSTRACT

The fly ash effect on the concrete durability was investigated in this study. For this purpose, 12 types of concrete were produced. 4 of them were prepared with only Portland cement, 6 of them were produced by adding fly ash in Portland cement and 2 of them were produced using Portland pozzolana cement. Maximum aggregate size was 16 mm; 7x7x7 cm cubic specimens and 7x7x28 cm prismatic specimens were prepared. On cubic specimens, compressive strength and capillary absorption tests and on prismatic specimens, ultrasonic velocity measurement and flexural tests were carried out. Some of the specimens were put into a solution that includes 10 % sodium sulphate, some of them were placed into lime-saturated water and some of them were kept under a wet burlap. Sodium sulphate solution was renewed at every 21 days.

At the end of 120 days of exposure, the compressive and flexural strengths as well as the weight and ultrasonic velocity of specimens were measured. These values were compared to those of normally cured specimens. According to the results, the resistance loss of the concrete specimens which were produced by fly ash was smaller than those which did not contain any fly ash; high strength concrete specimens were less effected by sodium sulphate solution. The specimens without any fly ash had higher water permeability and they were easily broken and lost weight when kept in the sodium sulphate solution. Parallel to the increasing water/cement ratio, capillary absorption was increased, thus the durability was negatively effected. The results showed that fly ash addition decreased water permeability by filling the pores in the concrete; and the cement paste-aggregate interfacial zone which is the weakest link in concrete could be improved by the pozzolanic and filler effect of fly ash.

KEYWORDS

Fly ash, Water permeability, Sulphate resistance, Durability

[1] Istanbul Technical University, Civil Engrg. Faculty, Istanbul, Turkey 34469, Phone +90 212 2853761, +90 542 2342125, Fax 212 2856587, yildirimhasan63@hotmail.com
[2] Msc Civil Engineer.
[3] Msc Civil Engineer, EPO Construction Chemical

1 INTRODUCTION

One of the most important properties of tbe concrete is its durability. Durable concrete should continue to perform its intended functions, maintain its required strength and serviceability , during the specified or traditionally expected service life [1]. Concrete durability has been defined by the American Concrete Institute as its resistance to weathering action, chemical attack, abrasion and other degradation processes such as freeze-thaw damage (physical effects, weathering), alkali-aggregate reactions (chemical effects), sulfate attack (chemical effects), microbiological induced attack (chemical effects), corrosion of reinforcing steel embedded in concrete (chemical effects), abrasion (physical effects), mechanical loads (physical effects), etc.

In the last years, many efforts has been focused on the development of concrete mix design with enhanced durability performances. In the present study, the effect of fly ash on the concrete durability was compared to the effect of Portland and pozzolanic cement.

2 EXPERIMENTAL STUDY

2.1 Materials

It has been used CEM I 42,5 and CEM II 32,5 conforming to TS EN 197-1. Fly ash, procured from Çatalağzı thermal power plant, was used as additive. Its specific surface was 2280 cm^2/g.
The maximum aggregate size was 16 mm; for all the trials, aggregates of the same type and of the same granulometry were used.
A lignosulfonate based plasticizer was utilised as admixture at the rate of 0,4 % of the binder weight.

2.2 Concrete Mixes

12 concrete mixes were prepared, the composition of these concrete mixes are shown in Table 1.

Table 1. Mix Designs

Mixture Code	w/b	Fresh Concrete Unit Weight (kg/m^3)	Cement (kg)	Fly Ash (kg)	Air Content (%)	Admixture (kg)	Sand (kg)	Crushed Sand (kg)	Crushed Aggregate (kg)
P250+00	0,83	2310	249	0	2,4	0,82	538	279	1036
P300+00	0,70	2310	297	0	2,6	1,20	522	274	1008
P350+00	0,60	2320	346	0	2,6	1,40	513	266	986
P400+00	0,53	2350	400	0	1,6	1,60	505	265	970
P250+10	0,75	2290	246	26	3,0	1,20	523	273	1013
P300+10	0,63	2270	293	29	1,8	1,28	506	261	972
P350+10	0,54	2310	346	34	1,8	1,52	499	260	959
P250+20	0,70	2320	252	50	1,6	1,20	521	275	1011
P300+20	0,58	2290	297	59	3,2	1,40	500	262	964
P350+20	0,50	2290	348	72	3,0	1,37	480	254	927
T330	0,65	2330	334	—	2,0	1,33	516	266	994
T380	0,56	2290	377	—	2,0	1,51	491	257	948

3 RESULTS AND DISCUSSION

3.1 Flexural Strength

According to the Table 1 and Figure 1, concrete with low cement content is much more effected by sodium sulphate solution than those with high cement content and compressive strength is decreased parallely. If fly ash is added, the negative effect on flexural strength of sodium sulphate solution is less important.

Concrete with cement content of 300 kg/m^3 and fly ash content of 20% is the more economical and have better strength values.

Table 2. Flexural Strength.

	Flexural Strength (N/mm^2) (120 days)	
Mixture Code	wet burlap	sodium sulphate solution
P250+00	6,6	1,2
P300+00	6,6	4,9
P350+00	7,8	8,8
P400+00	8,8	8,8
P250+10	7,6	3,9
P300+10	8,6	5,7
P350+10	9,0	9,4
P250+20	7,2	5,5
P300+20	8,7	8,7
P350+20	8,8	8,9
T330	4,9	2,8
T380	8,6	6,6

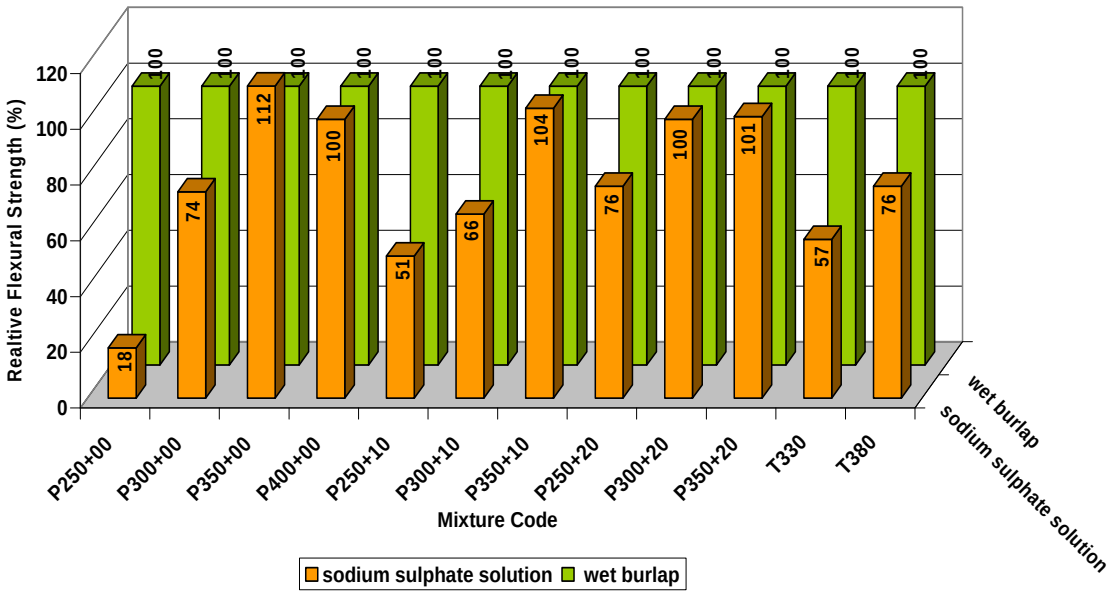

Figure 1. Concrrete Relative Flexural Strengths.

2.3 Compressive Strength

According to the Table 3 and Figure 2, the negative effect of the sodium sulphate solution on the compessive strengths is obvious, this effect is more emphasized for concrete with low cement content.

Against sulphate attack on concrete, the use of concrete with cement content of 300 kg/m^3 and fly ash content of 20% is advised. It is preferable to use concrete with cement content of at least 350 kg/m^3 if no fly ash is added. It is advised not to use Portland pozzolana cement with a cement dosage below 380 kg/m^3.

Table 3. Compressive Strength

		Compressive Strength (N/mm^2) (120 days)		
Mixture Code	w/b	lime- saturated water	sodium sulphate solution	wet burlap
P250+00	0,83	32,8	3,6	33,2
P300+00	0,70	38,7	25,8	38,8
P350+00	0,60	52,7	43,9	52,1
P400+00	0,53	62,2	52,6	59,8
P250+10	0,75	38,2	26,5	37,9
P300+10	0,63	43,0	28,0	42,2
P350+10	0,54	54,9	40,7	62,7
P250+20	0,70	40,3	25,1	38,6
P300+20	0,58	47,1	39,5	49,2
P350+20	0,50	56,4	48,3	52,7
T330	0,65	17,0	15,9	21,9
T380	0,56	40,9	34,5	39,9

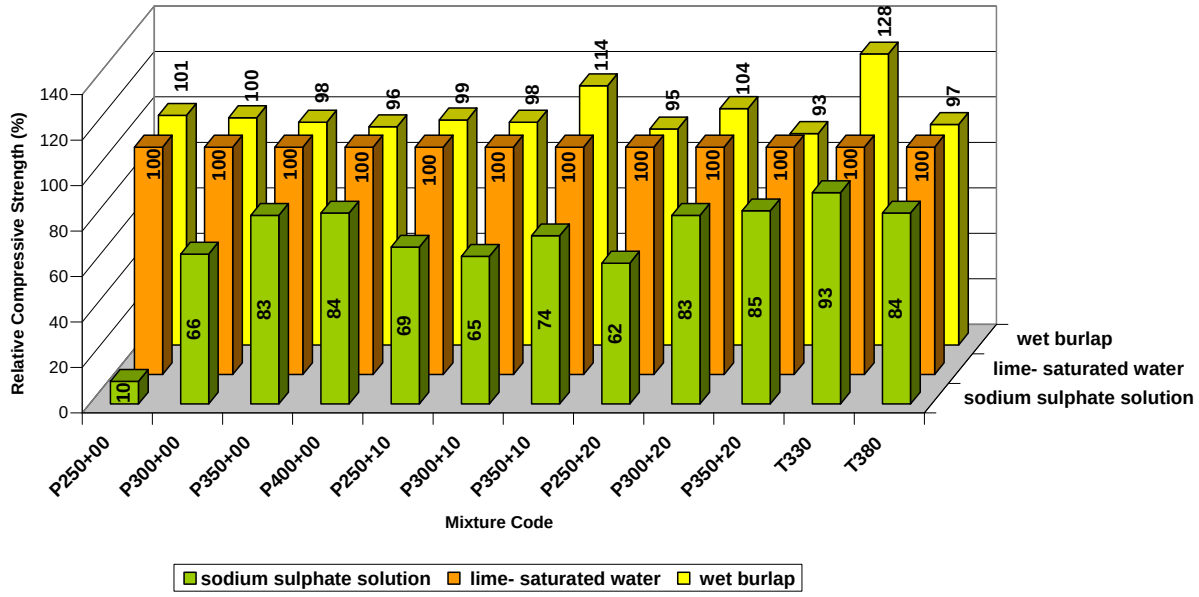

Figure 2. Concrete Relative Compressive Strengths

3.3 Ultrasonic Velocity Measurement

By the ultrasonic velocity measurement which is a non-destructive test method, the velocity of the sound through the concrete is obtained. The velocity data indicates that a condition of craking and deterioration exists in the concrete. If the concrete is porous, the time taken for the sound to pass between the transducers is prolonged , thus the velocity is decreased.

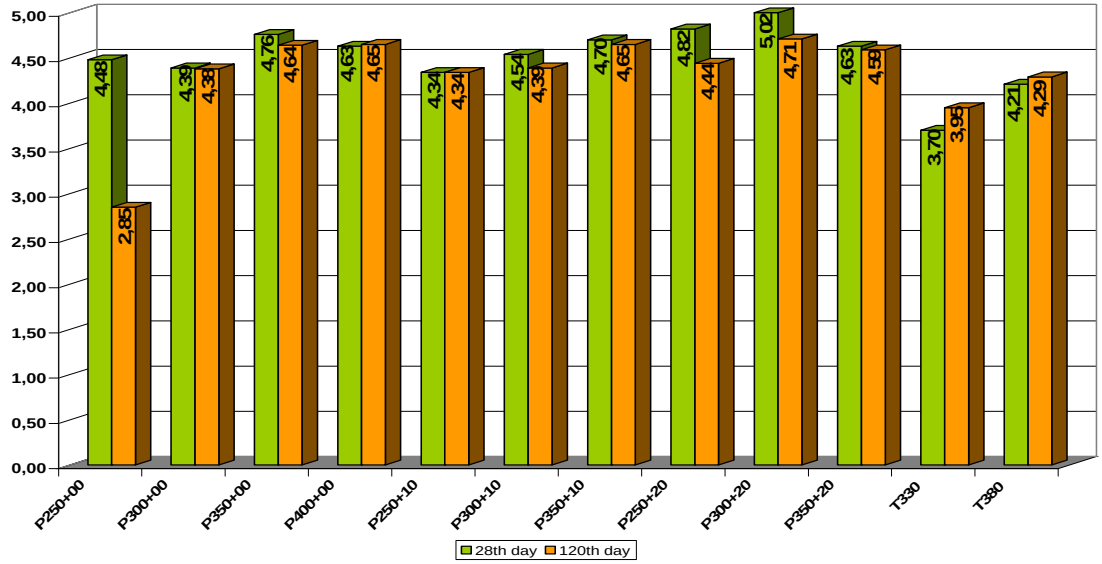

Figure 3. Ultrasonic Velocity Values

From Figure 3 arises that the negative effect of the sodium sulphate solution on the concrete structure is more evident for the sample with cement content of 250 kg/m^3. As the velocity values of other samples are not as much decreased as P250+00, we can conclude that the sodium sulphate has not such a defective effect on the internal structure of concrete with higher cement content.

2.3 Capillary Absorption

The cubic specimens of 7x7x7 cm were cured under a wet burlap during 120 days. Then, they are dried in an oven at 50^{o}C for 24 hours. After reaching the ambient temperature, the lateral surfaces of the specimens were coated with paraphine. The specimens are then placed on a grating in a water vessel, and the weight gains are recorded at 0., 1., 4., 9., 16., 25., 36., 49. seconds.

$$q^2 = (Q/A)^2 \quad (3.1.)$$
$$q^2 = k.t \quad (3.2.)$$

Permeability coefficient of each sample is calculated according to the 3.1. and 3.2. formulas.

As seen in the Figure 4, the permeability coefficient increases with the decreasing cement content. This permeability coefficient increase is more emphasised for the concrete samples with cement content of 250 kg/m^3 and for those containing Portland pozzolana cement. According to the Figure 5, the fly ash has a filler effect on the concrete samples filling the capillary voids, especially for those having low cement content, thus permeability coefficients are less important.

Figure 6 shows that capillary coefficients increase with increasing w/b ratio. This increase is especially emphasized for samples which do not contain any fly ash. It is important to notice that increasing capillary coefficient values have negative effects on the durability.

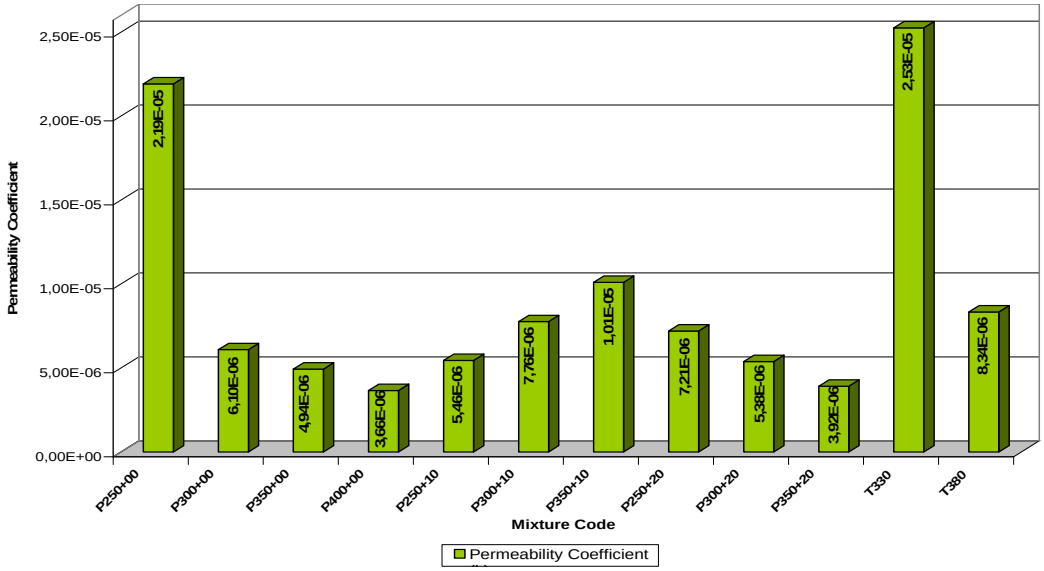

Figure 4. Permeability Coefficients

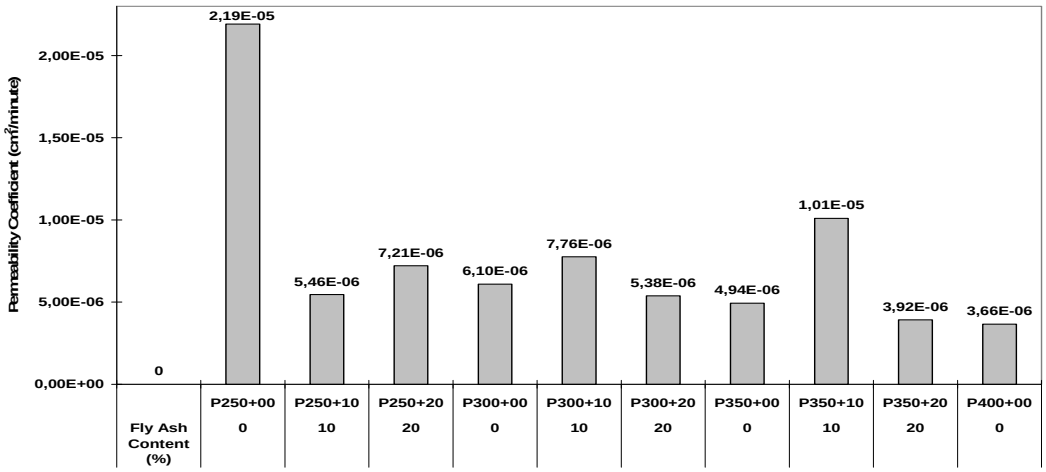

Figure 5. Fly Ash Content and Permeability Coefficient Relation

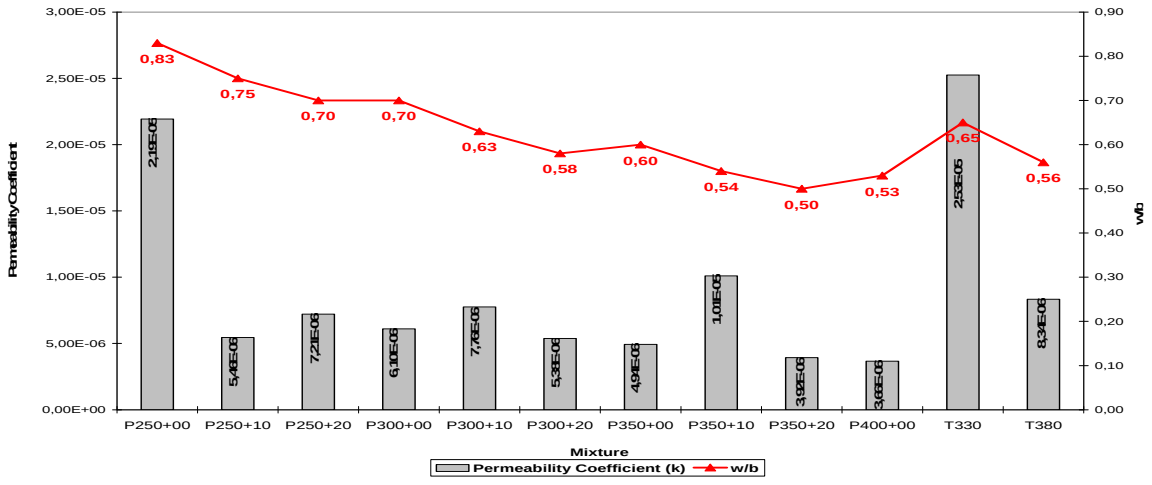

Figure 6. w/b Ratio and Permeability Coefficient Relation.

3 CONCLUSIONS

According to the results, fly ash addition decreases the flexural and compressive resistance loss of the concrete specimens. Concrete with high cement content is less effected by sulphate attack.

The specimens without any fly ash have higher water permeability and they are easily broken and lose weight when kept in the sodium sulphate solution.

Parallel to the increasing water/cement ratio, capillary absorption increases, thus the durability is negatively effected.

These results showes that fly ash addition decreases water permeability by filling the pores in the concrete; and the cement paste-aggregate interfacial zone which is the weakest link in concrete could be improved by the pozzolanic and filler effect of fly ash.

REFERENCES

Aitcin, P. C., et al 1986, 'Comparative study of the cementitious properties of diffrenet fly ashes', 2nd International Conference CANMET / ACI on Silica Fume, Fly Ash, Slag and Natural Puzzolans in Concrete, Madrid, vol. 1, pp. 91-114.

Akman, M. S., Öztekin, E., & Erdinç, M., 1994, 'Düşük çimento dozajlı ve uçucu kül katkılı hazır betonlarda dayanım ve dayanıklılık', III. Ulusal Beton Kongresi, Istanbul.

Chengzhi, Z., Aiqin, W., & Mingshu, T., 1996, 'The filling role of pozzolanic material, Cement and Concrete Research, vol. 26, no. 6, pp. 943-947.

Freeman, R.B., & Carrasquillo, R.L., 1992, 'Effects on the sulphate resistance of fly ash concrete', Concrete Fourth CANMET / ACI International Conference on Fly Ash, Silica Fume, Slag and Natural Puzzolans in Concrete, vol. 1, pp.281-297, Istanbul.

Goldman, A., & Bentur, A., 1994, 'Properties of cementitious systems containing silica fume or nonreactive microfillers, Advanced Cement Based Materials, pp.209-215.

Khatri, R.P., & Sirvivatnanon V., 1997, 'Role of permeability in sulphate attack', Cement and Concrete Research, vol. 27, no. 8, pp. 1179-1189.

Lamond, J. F., 1991, 'Low water-cement ratio concrete improves many aspects of concrete durability', 2. CANMET/ ACI International Conference, pp. 195-203.

Mehta, P. K. 1992, In Material Science of Concrete II, Jan Skalny Ed., American Ceramic Society, pp. 102-130.

Schiessl, P., & Hardtl, R. 1194, 'Relationship between durability and pore structure properties of concrete containing fly ash', P. K. Semp. On Durability of Concrete, Nice, pp. 99-118.

Tian, B., & Cohen, M.D., 2000, 'Does gypsum formation during sulphate attack on concrete lead to expansion?', Cement and Concrete Research 30, 117-123.

Yong, J.F., 1998, 'A review of the pore structure of cement paste and concrete and it's influence on permeability', ACI, pp. 108.

11DBMC International Conference on Durability of Building Materials and Components
ISTANBUL, Turkey 11-14 May 2008

Effect of Fire on Microstructure and Mechanical Properties of Blended Cement Pastes Containing Metakaolin and Silica Fume

M. S. Morsy [1]
S. S. Shebl [2]
A. M. Rashad [3]

T 11

ABSTRACT

The influence of high temperature on microstructure and mechanical properties of cement paste is vital to characterize fire resistance. Some experimental investigations on the microstructure and compressive strength of pre-heated metakaolin-silica fume blended cement pastes are presented in this paper. The aim of this investigation is to study the effect of substitution of metakaolin (MK) by silica fume (SF) on thermal stability of Portland cement-MK blended pastes. The kaolinite was thermally activated at 850 ^{o}C for 2 hours. The cement pastes were prepared using standard water of consistency. The pastes were kept in moulds at 20 ^{o}C and 100% relative humidity for 24 hours and then hydrated for 28 days under water. The hydrated pastes were exposed for 2 hours to temperature 200, 400, 600 and 800 ^{o}C. The pre-heated specimens were tested for compressive strength, thermal stability, microstructure and phase composition. The thermal shock resistances were performed on cement pastes after hydration. The results of investigation showed that the compressive strength of pre-heated blended cement increases with temperature up to 400 ^{o}C and then, it decreases as the pre-heated temperatures increase up to 800 ^{o}C. The replacement of Portland cement, PC, by 15% MK and 15% SF in cement pastes increases the thermal shock resistance by about 20 times than control

KEYWORDS

Blended cement, Microstructure, Thermal Shock Resistance, Compressive Strength, DSC

[1] Housing & Building National Research Center, Building Physics Department, Cairo, Egypt, Phone +20237617062, Fax +20233351564, msmorsy@yahoo.com
[2] Housing & Building National Research Center, Building Physics Department, Cairo, Egypt, Phone +20237617062, Fax +20233351564, ssshebl@yahoo.com
[3] Housing & Building National Research Center, Strength of Building Materials and Quality Control Department, Cairo, Egypt, Phone +20237617062, Fax +20233351564, alaarashad@yahoo.com

1 INTRODUCTION

When reinforced concrete is subjected to high temperature as in fire, there is deterioration in its properties. Of particular importance are losses in compressive strength, cracking and spalling of concrete, destruction of the bond between the cement paste and the aggregates and the gradual deterioration of the hardened cement paste. Assessment of fire-damaged concrete usually starts with visual observation of color change, cracking and spalling of the surface. The replacement of ordinary Portland cement by pozzolanic material improves mechanical properties and fire resistance Morsy & Shebl [2007], Rojas & Cabrera [2002].

The most common cementitious materials that are used as concrete constituents, in addition to Portland cement, are fly ash, FA, granulated blast furnace slag (BFS) and silica fume. They save energy, conserve resources and have many technical benefits He *et al.* [1994]. Metakaolin, produced by controlled thermal treatment of kaolin, can also be used as a concrete constituent, since it has pozzolanic properties Dunster *et al*. [1993], Sha & Pereira [2001]. According to the literature, the research work on metakaolin is focused on two main areas. The first one refers to the kaolin structure, the kaolinite to metakaolinite conversion and the use of analytical techniques for the thorough examination of kaolin thermal treatment Kakal [2001]. The second one concerns the pozzolanic behavior of metakaolin and its effect on cement and concrete properties Shvarzman *et al.* [2002]. Although there is a disagreement on specific issues, the knowledge level is satisfactory and is being continuously extended.

When fine pozzolana particles are dispersed in the paste, they generate a large number of nucleation sites for the precipitation of the hydration products. Therefore, this mechanism makes the paste more homogeneous and dense as for the distribution of the fine pores. This is due to the reaction between the amorphous silica of the pozzolanic and the calcium hydroxide produced by the cement hydration reactions Rojas & Cabrera [2002]. In addition, the physical effect of the fine grains allows denser packing within the cement and reduces the wall effect in the transition zone between the paste and aggregate. This weaker zone is strengthened due to the higher bond developed between these two phases, improving the concrete microstructure and properties. In general, the pozzolanic effect depends not only on the pozzolanic reaction, but also on the physical or filler effect of the smaller particles in the mixture.

The study aims to investegate the effect of high temperature treatment on the microstructure, mechanical and physical properties as well as the thermal shock resistance of cement-metakoline-silica fume blended pastes.

2 EXPERIMENTAL

The materials used in this investigation were Portland cement with a Blaine surface area of 3000 cm^2/g, metakaolin of Blaine surface area of 3600 cm^2/g and silica fume of very high Blaine surface area 220000 cm^2/g. The chemical composition of starting materials is shown in Table 1. The cement pastes were prepared using Portland cement that was partially substituted by metakaolin and silica fume as illustrated in Table 2. The kaolin was fired at 850 ^oC for 2 hours to give active amorphous metakaolin Dunster *et al.* [1993]. The starting materials were initially mixed with ethanol to attain ascertain homogenity. The pastes were prepared using the standard water of consistency. Table 3 illustrates the used water of consistency for different blended cement pastes.

The pastes were molded into 1 inch cubes for compressive strength determination. The moulds were vibrated for one minute to remove any air bubbles. The samples were kept in moulds at 100% relative humidity for 24 hours, then it was cured under water for 28 days.

Table 1. The chemical composition of starting material.

Oxide composition	*Portland cement (%)*	*Metakaolin (%)*	*Silica fume (%)*
CaO	62.56	1.24	0.21
SiO_2	20.85	58.52	96.10
Al_2O_3	4.70	35.54	0.5
Fe_2O_3	3.86	1.15	0.70
MgO	1.23	0.19	0.48
SO_3	2.79	0.06	0.10
Na_2O	0.49	0.25	0.31
K_2O	0.12	0.05	0.49
Cl^-	---	0.05	---
Ignition loss	2.82	2.74	1.14

Table 2. The dry mixes composition of blended cement, (mass %).

Mixes	*Portland cement*	*Metakaolin*	*Silica Fume*
M0	100	0	0
M1	70	30	0
M2	70	25	5
M3	70	20	10
M4	70	15	15

Table 3. The standard water of consistence for blended cement.

Mixes	M0	M1	M2	M3	M4
Water/ Bender	0.25	0.2569	0.2692	0.2885	0.2886

The hardened cement pastes were dried at a temperature of 105 ^oC for 24 hours in an oven. Then, they were kept for 2 hours at temperatures 200, 400, 600, and 800 ^oC. Each tested temperature was maintained for 2 hours to achieve the thermal steady state. The specimens were allowed to be cool gradually inside the furnace to room temperature.

The compressive strength was performed on dried and pre-heated specimens. The crushed samples (dried and fired) result from compressive strength tests were ground for thermal analyses and X-ray diffraction.

Differential scanning calorimetry run were conducted using a Shimadzu DSC-50 thermal analyzer at a heating rate of 20 ^oC/min. The sample chamber was purged with nitrogen at a flow of 30 ml/min. The thermal shock resistance were determined by heating the molded cement pastes after 28 days of curing under water (1" cubes) for 40 minutes at 800 ^oC followed by quenching in water for 5 minutes. Such cycles are repeated until the samples are broken, damaged or deteriorated.

The crystalline phases present in the hydrated product were identified using the X-ray diffraction technique. Nickel-filtered Cu-Kα radiation at 40 KV and 20 mA were used throughout in a Philips PW 1390 diffractometer with scanning speed of 2^o/min. The scanning electron microscope, Philips–XL 30, was used for identification of the changes occurring in the microstructure of the formed and/or decomposed phases.

3 RESULTS AND DISSCUSION

Figure 1 illustrates the development of compressive strength for control and blended cement pastes thermally treated at 200, 400, 600 and 800 ^{o}C for 2 hours. It is evident that, the compressive strengths of control, M0, M1 and M2 cement pastes increase with temperature up to 200 ^{o}C then decrease up to 800 ^{o}C. It also, shows that, the compressive strengths of blended cement pastes, M3 and M4 increase as the treatment temperature increases up to 400 ^{o}C then decrease as the treatment temperature increases up to 800 ^{o}C. Evidently, the increase of compressive strength up to 200 ^{o}C may be due to the additional hydration of unhydrated cement grains as a result of steam effect under the condition of the so-called internal autoclaving effect. The increase of compressive strength of blended cement pastes may be due to the pozzolanic reaction of metakaolin and silica fume with free lime to produce more CSH and CAH phases that deposit in the pore system. The compressive strengths of control, M0, M1 and M2 cement pastes start to decline at 200 ^{o}C whereas those of other blended; M3 and M4 cement pastes even at 400 ^{o}C. This phenomenon is contributed to higher volumes of CSH and CAH phases formed in the blended cement pastes on the one hand and reduction in $Ca(OH)_2$ contents on the other hand relative to those developed in control, M1 and M2 cement pastes. Cement matrix with higher volumes of gel-like hydration products, and lower crystallic $Ca(OH)_2$ contents has improved fire resistance. The decrease in compressive strength with temperature may be due to the dehydration of the calcium hydroxide at about 500 ^{o}C producing CaO and H_2O. Over 600 ^{o}C strength losses are mainly caused by calcium carbonate dissociation and subsequent CO_2 escape from $CaCO_3$. Strength losses of M3 and M4 blended cement pastes are less significant than that of control M0, M1 and M2 cement paste.

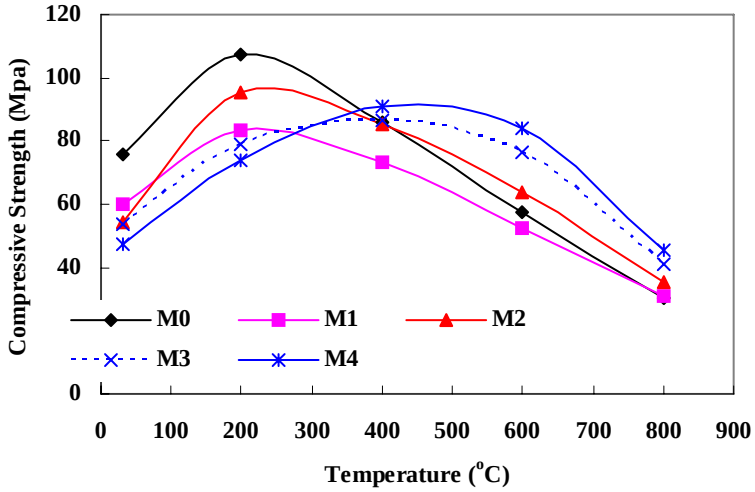

Figure 1. Variation of compressive strength of cement pastes with temperature for different admixtures blended cements.

The formation of CSH as a results of pozzolanic reaction is deposited in porous as well as the filler effect of fine MK and SF. Evidently, this leads to bridge the porous as well as reducing the internal thermal stress. Therefore, the increase of compressive strength can be partially due to the strengthened hydrated cement pastes during the evaporation of free water, which leads to greater Van der Waal's forces as a result of the cement gel layers moving closer to each other Hossain [2006]. Because transportation of moisture in concrete is rather gradual, residual moisture in concrete allowed accelerated hydration at the early stage of heating concretes to high temperatures. Further hydration of cementitious materials is another important cause of the hardening of hydrated cement pastes. The compressive strength of blended cement pastes M3 and M4 has higher values than other control and blended cement pastes up to 800 ^{o}C. This may be due to the principal reaction between the metakaolin ($Al_2O_3.2SiO_2$) and the calcium hydroxide derived from cement additional, cementitious aluminium containing CSH gel, together with crystalline products, which include calcium aluminate hydrates and

alumino-silicate hydrates (i.e., C_2ASH_8, C_4AH_{13} and C_3AH_6). The decrease in compressive strength after 400 °C, may be due to the propagation of microcracks. The crystalline products formed depend principally on the metakaoline/calcium hydroxide ratio and reaction temperature. The formation of CAH and CASH phases, increase the compressive strength.

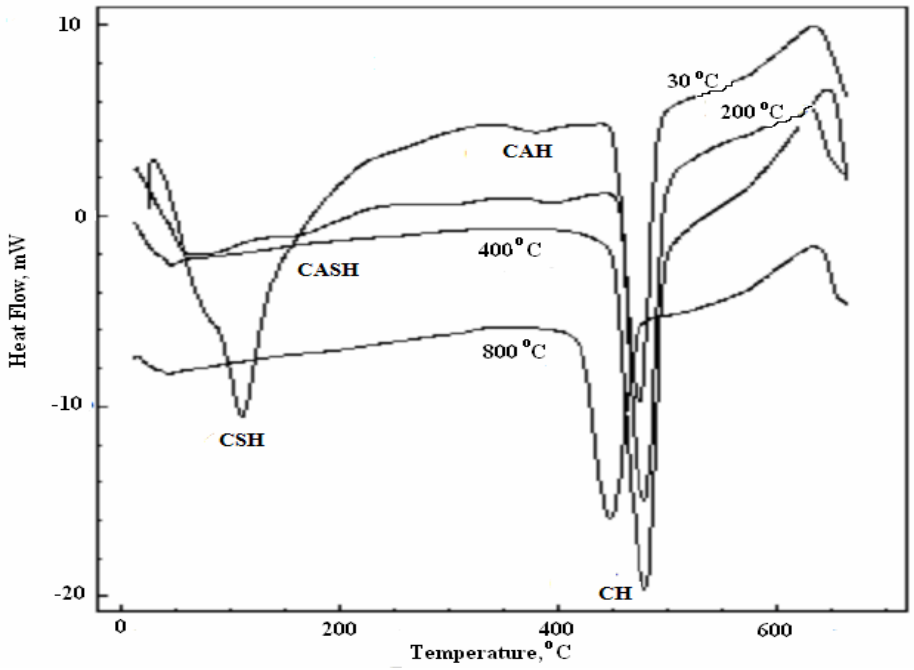

Figure 2. DSC thermograms of the Portland cement paste thermally treated at different temperatures.

The variations of the DSC thermograms of control, M0, and blended cement pastes, M4 at ambient temperature, pre-heated at200, 400 and 800 °C are shown in Figs 2 and 3. Evidently, there are almost four endothermic peaks. The first peak located at about 110-120 °C, is mainly due to the decomposition of calcium silicate hydrates; CSH. The second endothermic peak observed at about 160 °C represents the decomposition of the calcium sulpho-aluminate. The third endothermic peak at about 350 °C is due to the dissociation of C_2SH. The forth endothermic peak was observed at around at 470 °C represents the decomposition of Ca $(OH)_2$. As the pre-heated temperature increases the peak area of calsuim hydroxide increases up to 600 oC and shefted to word lower temperature at 800 °C pre-heated control cement paste, M0, as shown in Fig. 2. This is due to the formation of ill-crystals of $Ca(OH)_2$. Also it is clear that the thermograms of the blended cement paste M4 that pre-heated at 200, 400 and 800 °C show very weak endothermic peaks Fig. 3. It is clear that the calcium hydroxide peak area decreases as pre-heated temperature increases. Evidently, this is due to further reaction between metakaolin, silica fume and CaO at high temperature up to 800 °C. It is obvious that the enthalpy of calcium hydroxide phases in control cement paste, M0, Fig. 2 decreases from 60.22 J/g to 48.58 J/g as the treatment temperature increases up to 800 °C. On the other hand, the enthalpy of calcium hydroxide phase in the blended cement paste, M4, Fig. 3 decreases from 13.06 J/g to 1.9 J/g as the pre-heated temperature increases up to 800 °C. This is due to the formation of ill-crystals (this is indicated by the decrease in enthalpy) of free lime as a result of further reaction of pozzolana at elevated temperatures.

The effects of admixtures on thermal shock resistance of hydrated blended cement pastes are shown in Fig.4. Evidently, the thermal shock resistance increases as the silica fume ratio increases in blended cement pastes. Therefore, the higher replacement of metakaolin by silica fume in investigation blended cement pastes leads to higher thermal shock resistance. This may be due to consumption of free lime released during hydration. During heating, the outer layers of the test specimen tend to expand more than inner layers. Subsequent sudden cooling will unbalance the internal equilibrium, with significant

internal stresses developed as the outer layers attempt to contract relative to the inner Morsy & Shebl [2007]. The differential deformation between the different layers leads to further crack activities. Evidently, the hardened Portland cement paste, M0, can resist only 3 cycle's thermal shock. This is due to the free lime released during hydration of Portland cement. The $Ca(OH)_2$ crystals transform into CaO crystals during heating. Since CaO is often rehydrates in the humid environment and forms $Ca(OH)_2$ again with increase in volume leading to complete failure of the hardened cement paste Morsy & Shebl [2007] [1].

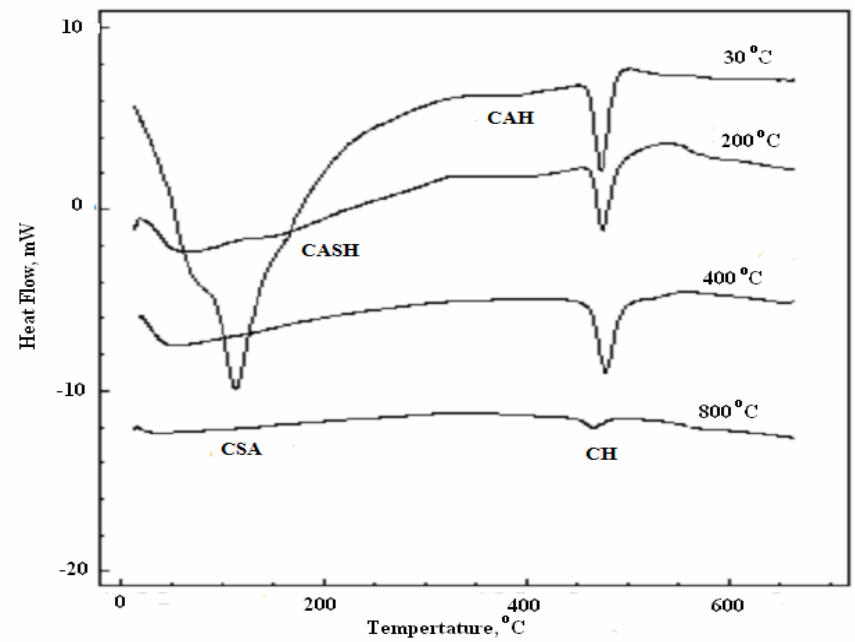

Figure 3. DSC thermograms of the blended cement pastesM4 (70% Portland cement, 15% MK, and 15% SF) thermally treated at different temperatures

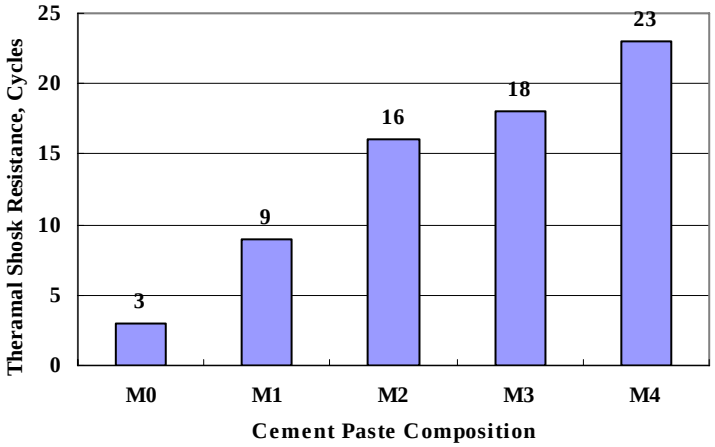

Figure 4. Thermal shock resistance of control and blended cement pastes

The replacement of Portland cement by 30% metakaolin in blended cement paste, M1, leads to increase the thermal shock resistance up to 9 cycle's. This is due to the pozzolanic activity of metakaolin during hydration and at 800 °C, the SiO_2 and Al_2O_3 of metakaolin react with CaO. It also clear that, the replacement of metakaolin by 5% in the blended system, M2; leads to thermal shock resistance of 16 cycle's. The results show that the 30 % wt. replacement of Portland cement by pozzolanic admixture consisting of 15 % wt. of metakaolin and 15 % wt. of silica fume creates the most durable hydrate phase to thermal shocks. Evidently, the thermal shock resistance of blended cement pastes is considerably higher when highly effective microfiller-microsilica is added. Figures 5

and 6 illustrate the XRD patterns of pre-heated control and blended cement pastes. It is clear that, the XRD patterns of the OPC cement pastes pre-heated at ambient temperature, 200, 400 and 800 ^{o}C are presented in Fig. 5. Evidently, the crystalline phase of CH (portlandite) was decreases as the pre-heated temperature increases up to 800 ^{o}C. This is due to thermal decomposition of calcium hydroxide phase at 570 ^{o}C. The replacement of OPC by metakaolin and silica fume is shown in Fig. 6. Basically, the calcium hydroxide phase decreases as the ratio of MK and SF increase, while the weak peaks of CAH and CASH in pastes replaced by SF and MK, slightly increase. The XRD patterns of the hydrate products are plotted in Fig. 6, the MK were replaced by 15% SF. It can be observed that the crystalline peak of CH decreases as the replacement rate increases while the weak peak of CSH and gehlenite hydrate (C_2ASH_8) increases. In Fig.6, the decrease of the CH peak is related with the consumption by pozzolanic reaction of MK and SF Sha & Pereira [2001].

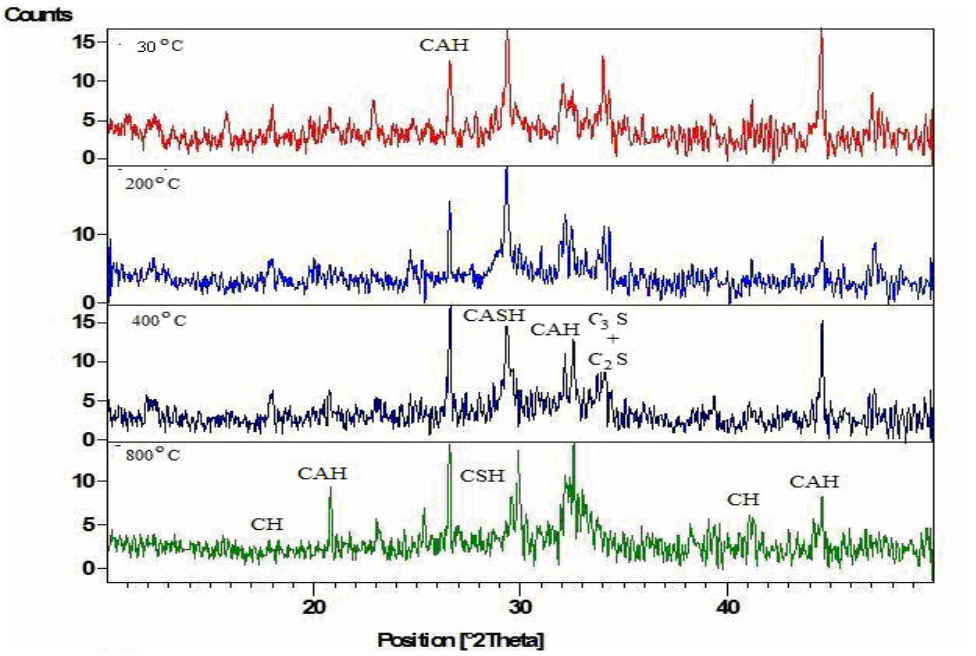

Figure 5. X-ray pattern of pre-heating hydrated cement pastes (M0).

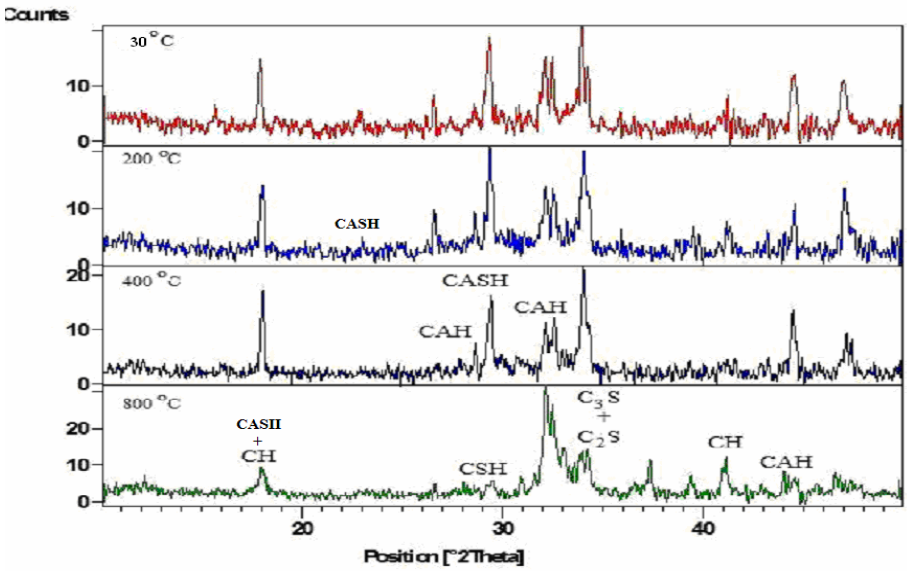

Figure 6. X-ray pattern of pre-heating hydrated blended cement pastes (M4).

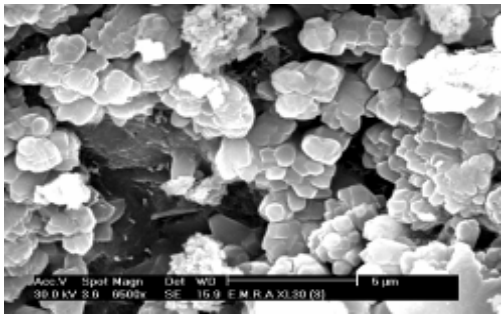

a) SEM micrograph of OPC cement paste at 30°C

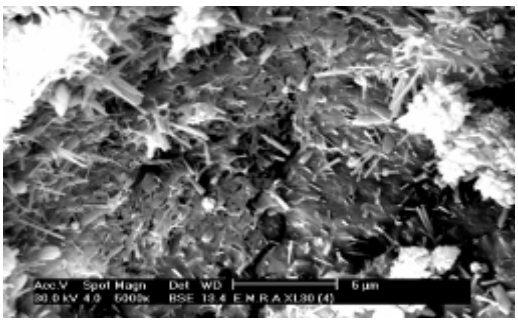

b) SEM micrograph of blended cement paste at 30°C

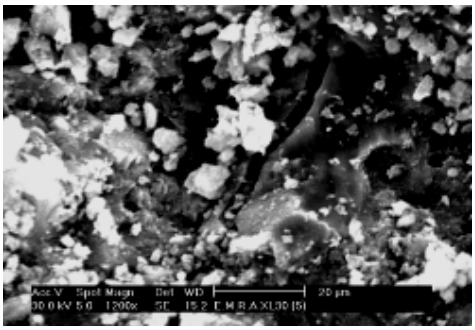

c) SEM micrograph of OPC cement paste at 200°C

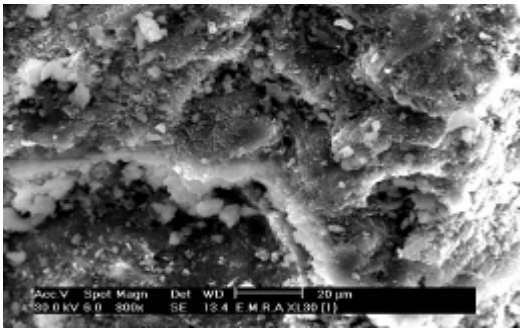

d) SEM micrograph of blended cement paste at 200°C

e) SEM micrograph of OPC cement paste at 400°C

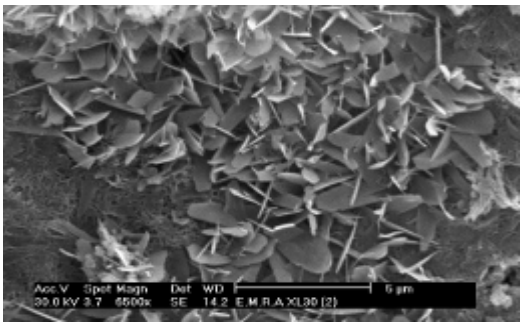

f) SEM micrograph of blended cement paste at 400°C

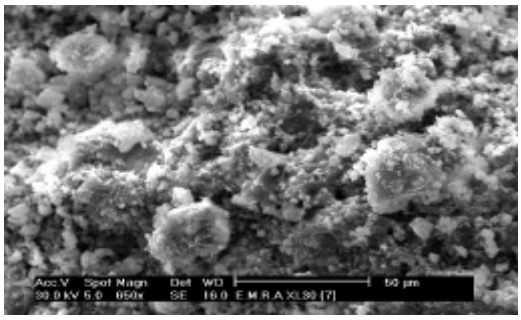

g) SEM micrograph of OPC cement paste at 800°C

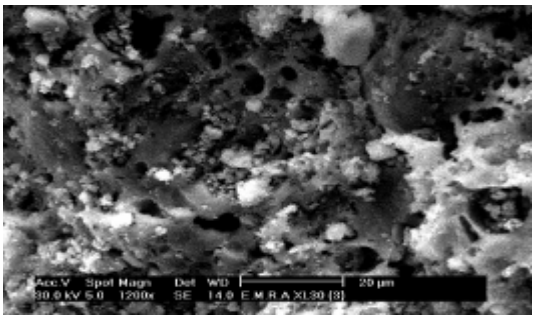

h) SEM micrograph of blended cement paste at 800°C

Figure 7. SEM micrograph of OPC (M0) and blended cement pastes (M4) pre-heated at different temperature.

Figure 7 illustrates the SEM micrograph of pre-heated control and blended cement pastes. Figs (7-a, c, e and g) shows the SEM micrograph of OPC pastes hydrated at ambient temperature and pre-heated at 200, 400 and 800 °C for 2 hours respectively. It is clear that the hydration products formed up to 200 °C having a massive structure of well crystalline C-S-H and sheets of $Ca(OH)_2$ representing the microstructure; Figs (7-a and c). Evidently, the micrograph of sample pre-heated at 400 °C safer partial

decomposition in formed phases. The micrograph of the pre-heated OPC pastes at 800 °C Fig. 7- g; shows a week structure with appearance of micro cracks and pores. However, these leading to a destruction of binding forces as represented by the low compressive strength. On the other hand, the 800 ^{o}C pre-heating was already identified as a critical temperature for the water saturation moisture content of the material and thus for the open porosity as well as the significant increase in porosity due to the $CaCO_3$ decomposition was accompanied by the micro-structural damage of the Portland cement matrix that was also documented in the SEM analysis. Figures (7-b, d, f and h) illustrates the SEM micrographs of blended cement pastes M4, 15% metakaolin and 15 % silica fume, after pre-heated at 200, 400 and 800 ^{o}C. Clearly, the microstructure was relatively compact; the cement binder exhibited a low porosity. Evidently, the microstructure of blended cement paste pre heated at 800 ^{o}C Fig. 7-h; displayed the formation of dense masses of hydration products having micro- and narrow pores. However, these to relatively high compressive strength values as compared with those of OPC paste at 800 ^{o}C.

4 CONCLUSIONS

The main conclusion derived from this study may be summarized as follows

1. The residual compressive strength of the above cement blend paste heated to 800 ^{o}C is higher than the residual compressive strength of the Portland cement. In addition, the microstructure of blended cement pastes, M4, pre-heated at 800 ^{o}C is dense than OPC pastes at the same condition.
2. The replacement of OPC by 15% wt. of metakaolin and 15% wt. of silica fume increase the thermal shock resistance by 20 times than control.
3. The blended M4 can be applied as a fire resistance bonding materials.

REFERENCES

Dunster, A. M., Parsonage, J. R., & Thomas M. J. K., 1993, "Pozzolanic reaction of metakaolinite and its effects on Portland cement hydration", *J Mater Sci*., 28, 1345–1351.

He, C. Makavicky, E., & Osback, B., 1994, "Thermal stability and pozzolanic activity of calcined kaolin", *Appl Clay Sc.i*, 9, 165-187.

K. M. Anwar Hossain., 2006, “High strength blended cement concrete incorporating volcanic ash: Performance at high temperatures”, *Cement & Concrete Composites*, 28, 535–545.

Kakali, G., Perraki, T., Tsivilis, S., & Badogiannis, E. 2001, "Thermal treatment of kaolin: the effect of mineralogy on the pozzolanic activity", *Appl Clay Sci*, 20, 73–80.

Morsy, M. S., & Shebl, S. S., 2007, "Effect of silica fume and metakaolin pozzolana on the performance of blended cement pastes against fire", *Ceramics Silikaty*, 51 [1], 40-44.

Rojas, M. F., & Cabrera, J., 2003, “The effect of temperature on the hydration phase of metakaolin-lime-water system”, *Cem. Concr. Res.*, 32, 133-138.

Sha, W., & Pereira., B. 2001, "Differential scanning calorimetry study of ordinary Portland cement paste containing metakaolin and theoretical approach of metakaolin activity", *Cement Concrete Compos*, 23, 455–61.Shvarzman, A., Kovler, K., Schamban, I., Grader, G. S. & Shter, G. E. 2002, "Influence of chemical and phase composition of mineral admixtures on their pozzolanic activity", *Adv Cement Res*., 14[1], 35–41.

11DBMC International Conference on Durability of Building Materials and Components
ISTANBUL, Turkey 11-14 May 2008

Easy Evaluation Method of Self-Compactability of Self-Compacting Concrete

Masanori Maruoka [1]
Hiromi Fujiwara [2]
Erika Ogura [3]
Nobu Watanabe [4]

T 11

ABSTRACT

The use of self-compacting concrete (SCC) in construction is designed to improve the durability of the structure, by creating as far as possible a comletely filled, voidless and faultless concrete state. However, even with SCC, achieving complete self-compaction is extremely difficult. Therefore, before construction starts, the self-compactability of SCC is examined using, for example, a real-size model formwork in order to determine whether the self-compactability in the construction is adequate. However, the cost of such examinations is high, and so a cheaper and easy examination method is desirable. In this study, we investigated an evaluation method for evaluating the self-compactability of SCC easily by varying several parameters of concrete, mortar and construction properties, such as the rheological properties of mortar, unit volume of coarse aggregate of concrete, and state of obstacle distribution in the formwork. Our cost-effective and simple method enabled pressure force loss of flowing SCC around the ostacles to be evaluated in a formwork. We believe that this method will contribute to the improvement of durability of constructions using self-compacting concrete.

KEYWORDS

Self-compacting concrete, Self-compactability, Rheology, Force loss of flowing concrete

[1] Utsunomiya University, Faculty of Architecture and Civil Engineering, Utsunomiya, Japan, Phone +81 28 689 6211, Fax 28 689 6211, mmaruoka@cc.utsunomiya-u.ac.jp
[2] Utsunomiya University, Faculty of Architecture and Civil Engineering, Utsunomiya, Japan, Phone +81 28 689 6209, Fax 28 689 6209, fhiromi@cc.utsunomiya-u.ac.jp
[3] Utsunomiya University, Faculty of Architecture and Civil Engineering, Utsunomiya, Japan, Phone +81 28 689 6211, Fax 28 689 6211, t042807@cc.utsunomiya-u.ac.jp
[4] Utsunomiya University, Faculty of Architecture and Civil Engineering, Utsunomiya, Japan, Phone +81 28 689 6211, Fax 28 689 6211, mt063433@cc.utsunomiya-u.ac.jp

1 INTRODUCTION

If concrete can be poured completely and is voidless and faultless, the durability of a concrete structure will not deteriorate through the influence of, for example, carbonation and freezing and thawing action. However, producing such a state of concrete is difficult and thus deterioration of the durability remains an important consideration. The use of self-compacting concrete (SCC) in construction is designed to improve the durability by creating, as far as possible, a completely filled, voidless and faultless concrete state.

There are currently two estimation methods of the self-compactability of SCC. One involves the SCC filling test using the real-size model formwork modeled from a real structure and determining whether or not the formwork is filled completely or not. The other is a simulation method of numerical analysis. To date, few investigations of the former method have been conducted, and the latter method requires model parameters of the structure as well as parameters of the fresh SCC properties and mix content design of SCC which are very difficult to obtain. Moreover, numerical analysis does not always provide sufficient information.

In this study, we aimed to develop an easy method for evaluating the degree of self-compactability of SCC using a model experiment involving a visualization method of concrete. In this experiment, we use a model of self-compacting concrete that maintains the same fluidity, such as slump flow. The important parameters for this evaluation are unit content of coarse aggregate, rheological properties of mortar, and interspace size of obstacles in the formwork. We alter these parameters and evaluate self-compactability via the “pressure loss” parameter in the model experiment. The results of investigations of this new method are presented and discussed.

2 WHAT IS PRESSURE LOSS ?

We define pressure loss for use in the evaluation of self-compactability of SCC as follows. In the case of SCC flowing in the channel form with steel bars as obstacles (see Figure 1), the stream line of SCC is changed around the obstacle.

If unit coarse aggregate content is small, for example, the unit absolute volume of coarse aggregate is less than about 0.28 m^3/m^3, SCC flow is continued and flows around the obstacle slowly, and there is little height difference between the upstream and downstream surfaces of SCC that is bounded by the obstacle (Case (a) of Figure 1).

If unit coarse aggregate content of SCC is very large, for example, the unit volume of coarse aggregate is more than about 0.33 m^3/m^3, and if segregation occurs, SCC flow stops due to coarse aggregate blockage around the obstacle, such that SCC in the section containing coarse aggregate is changed by the effect of the obstacle (Case (b) of Figure 1). In this case, a difference in surface height is observed.

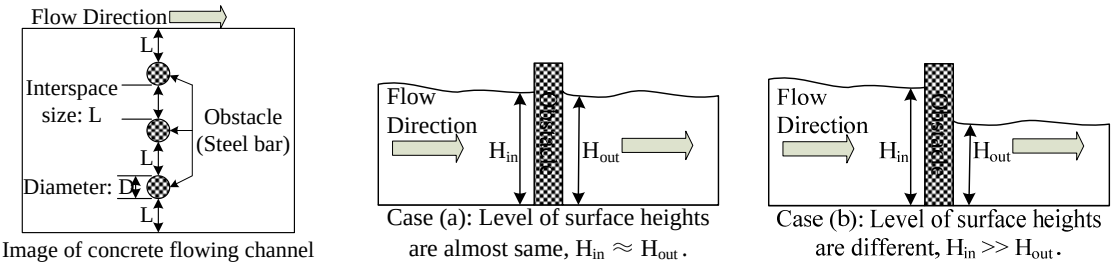

Figure 1. Differences in surface height between upper and lower sections divided by an obstacle.

Pressure loss is calculated by Eq. (1) using the difference in surface height. Then, we considered that the pressure loss value can be used as an index of the evaluation of self-compactability.

$$\Delta P = \rho g \Delta h \quad (1)$$

3 OUTLINE OF EXAMINATIONS

3.1 Examination Method

3.1.1 Measuring Method of Pressure Loss

In this examination, we use a model form made of clear acrylic sheet with obstacles made of pipe, as shown in Figure 2. The method, also shown in Figure 2, is as follows. [1] The gate of the form closes and Tank A is filled with model concrete (see section 3.3 for details). [2] The gate opens and concrete flows out from Tank A to Tank B through the obstacle interspaces. [3] The flow velocity becomes slow and eventually stops. [4] We then measure the height of the concrete surface in Tanks A and B, and calculate the height difference between them Δh, and calculate the pressure loss value ΔP using Eq. (1).

The main parameters for this examination are interspace size of obstacle: *L* (by changing diameter of obstacles; 4 types, 21, 24, 26 and 30 mm diameter) and coarse aggregate volume of model concrete: *Xv* (3 types, 0.26, 0.30 and 0.34).

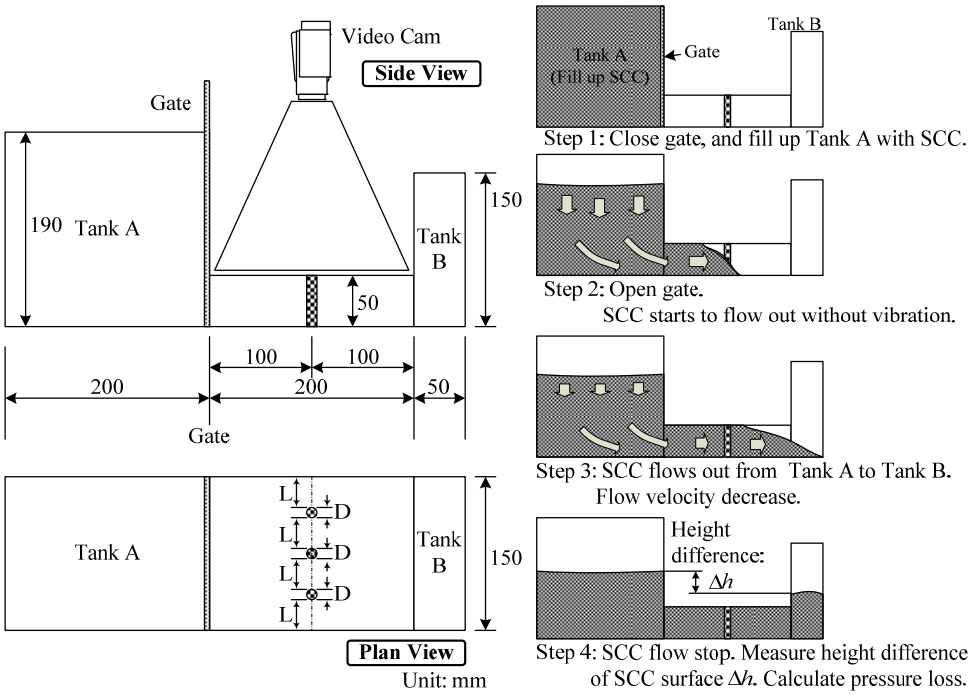

Figure 2. Details of model form and measuring method of height difference Δh between surface of SCC in Tanks A and B.

3.1.2 Visualization Test to Investigate Flow State

Next, we try to estimate the changing coarse aggregate volume divided into two sections by the obstacle. The method is shown in Figure 3. The increase in the volume of coarse aggregate *Xv*' was then measured and calculated. A still image was taken, and Area 1 and Area 2 were defined as shown in Figure 3. Image processing showed the coarse aggregate in white in the image, and the ratios of the white area (contained in Area 1) to Area 1 and the white area (contained in Area 2) to Area 2 were defined as S_1 and S_2, respectively. Then, the difference in the volume ratio of coarse aggregate

between upstream of and downstream of the obstacle ΔXv and the increased coarse aggregate ratio Xv' is given by Eq. (2),

$$\Delta Xv = \frac{S_1 - S_2}{S_1 + S_2} Xv, \quad Xv' = Xv + \Delta Xv = \frac{2S_1}{S_1 + S_2} Xv \tag{2}$$

where ΔXv is the increase in the volume ratio of coarse aggregate, Xv is the initial unit volume ratio of coarse aggregate, S_1 is the area ratio of coarse aggregate in Area 1, S_2 is area ratio of coarse aggregate in Area 2, and Xv' is the volume ratio of coarse aggregate increased in Area 1.

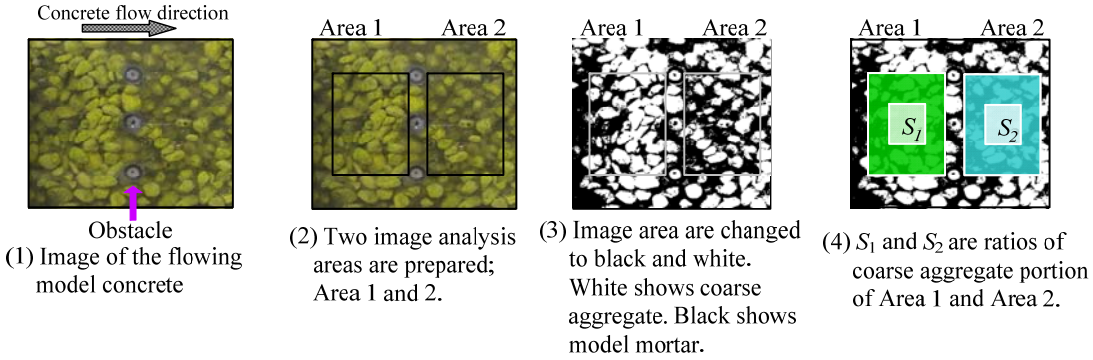

Figure 3. Method of measuring coarse aggregate area using image analysis.

3.2 Materials Used

In these examinations, we must be able to view the coarse aggregate particles, which cannot be done using real SCC. Therefore we use model concrete containing water and a viscosity agent typically used for concrete material as model mortar, and processed lightweight aggregate (density: 1.35 g/cm^3, maximum size: 15 mm) as model coarse aggregate.

The model mortar is therefore almost clear, allowing the distribution of the model coarse aggregate to be observed in the model formwork. In order to capture the coarse aggregate movement data easily, we paint the coarse aggregate yellow.

3.3 Mix Content of Concrete

Mass ratios of the viscosity agent content of the model mortar were 12.5, 15 and 17.5 %. In these conditions, mortar flow with no vibration is almost around 250 mm. The unit volume content of the coarse aggregate was 0.26, 0.30 and 0.34.

3.4 Examination Results

3.4.1 Measuring Pressure Loss

Figure 4 shows the relationship between pressure loss ΔP and interspace size L. These results show that in the case of small L, ΔP increases more than in the case of large L, and this relationship is similar to that obtained for model mortar with a different Xv and viscosity. This means that under the condition of small L and large Xv, it is difficult for the model SCC to flow around the obstacle, and it is considered that the resistance force of the steel bars disturbs and decreases the flow of model SCC, resulting in an increase in ΔP. In the case in which high viscosity mortar is used, ΔP decreases; the occurrence of contact and friction between the coarse aggregate particles decreases, and this has a large effect of the stress transfer mechanism.

3.4.2 Flow State of Coarse Aggregate

In every case we observed that the measured coarse aggregate volume of the upstream section divided by the obstacle was greater than the downstream section. The reasons are thought to be that the stream line of SCC flow around the obstacle changes from being linear to curved and coarse aggregate particles cannot move easily because of the obstacle disturbance and thereby restrict particle movement in the interspaces and the upstream section, making the SCC flow more difficult. In the downstream section, however, where there is no obstacle, the coarse aggregate volume is smaller.
We consider the phenomenon of SCC passing around the obstacle to be an important mechanism when describing increasing pressure loss.

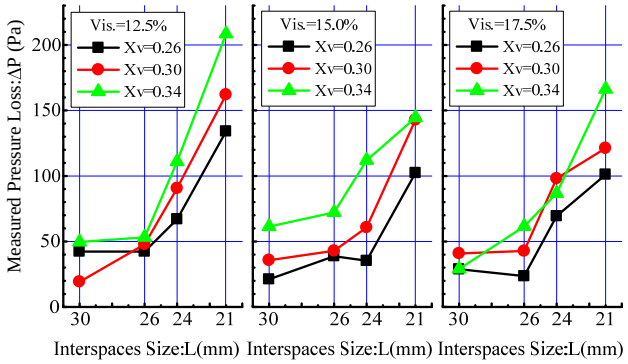

Figure 4 Relationship between interspaces size of obstacle L and measured pressure loss ΔP

4 BUILDING UP THE THEORETICAL AND EXPERIMENTAL FUNCTIONS TO DESCRIBE INCREASING PRESSURE LOSS

4.1 Modeling the Mechanism of Generating and Increasing Pressure Loss

To investigate the mechanism model of generating and increasing pressure loss, we consider the phenomenon of increasing pressure loss when SCC flows through the obstacle interspaces as follows.

[1] Coarse aggregate in flowing SCC is delayed in front of obstacles
When SCC flows through the formwork with steel bars, the flow line of SCC changes from being linear to curved as a result of having to flow around the steel bars, and movement of coarse aggregate contained in the SCC around the steel bars is obstructed and the flow velocity of coarse aggregate is decreased.

We considered one of the reasons causing this phenomenon is coarse aggregate volume change in the SCC. We considered the change to be caused by original coarse aggregate volume *Xv*, increased volume of coarse aggregate *Xv*', interspace size *L*, mortar viscosity, and yield stress. Considering these parameters, we show the relationship between *Xv* and *Xv*'/*Xv* in Figure 5 left side and the equation to explain the phenomenon in Eq. (3) [Kanematsu *et. al.* 1999].

$$\frac{Xv'}{Xv} = \Gamma Xv + 1 \qquad (3)$$

In the case of small *L*, the slant Γ of the relationship is larger than for large *L*. We introduce the idea of relative interspace size *Lr* that is defined in Figure 6 right side and Eqs. (4) and (5). We will verify these relationships later.

$$\Gamma = a \cdot Lr^{-b} \quad (4), \qquad Lr = \frac{L}{L+D} \qquad (5)$$

where a and b are parameters including the rheological properties of mortar, L is the interspace size (mm), and D is the diameter of the obstacle (mm).

[2] Volume of coarse aggregate in front of the obstacle increases
Coarse aggregate particles accumulate in front of the obstacles due to the phenomenon described in [1].

[3] Change in the stress transfer mechanism inside SCC
We consider that, inside the SCC, the sheer stress σ and shearing stress τ act on the surfaces of the coarse aggregate particles, as shown in Figure 6 left side. In the case of SCC having low volume of coarse aggregate particles and high volume of mortar, shearing stress has no influence on sheer stress. However, as the volume ratio of coarse aggregate particles to mortar increases, coarse aggregate particles can come into contact with each other easily. As a result, we consider that the mechanism of the stress transfer model changes and the relationship between σ and τ becomes linear, as shown in Figure 6 center.

[4] Increases in yield stress of SCC and sheer stress at the surface of coarse aggregate particles
The shearing stress increases with increasing sheer stress. Thus, the deformation resistance force of SCC also increases, and the yield stress of SCC increases.

[5] Increasing pressure loss
When SCC flows through the interspaces between the steel bars, it seems a balance of dynamics is arrived at around the steel bars, as shown in Figure 6 right side and Eq. (6). Furthermore, it seems that the force acting on the steel bars from the SCC is related to the decrease in pressure around the steel bars, as described by Eq. (6) for estimating pressure loss. This formula shows that pressure loss increases as the yield stress increases.

Thus, we have derived a model explaining the increasing pressure loss mechanism by means of the above steps [1]-[5].

$$\Delta P = \frac{2D}{D+L}\tau_c \qquad (6)$$

where τ_c is the yield stress of SCC, ΔP is the pressure difference present in the interspaces between the steel bars, D is the diameter of the steel bars, and L is the distance between adjacent steel bars.
In the next section, we will explain about the increase coarse aggregate volume mechanism described in [1], and investigate it through examination.

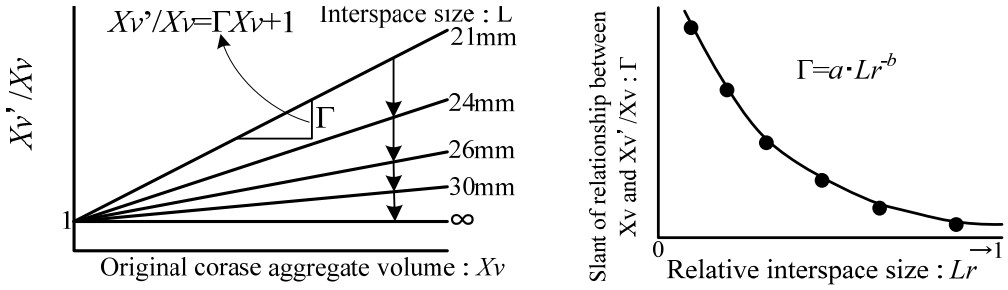

Figure 5. Concepts of relationship between original coarse aggregate volume Xv and relative Xv'/Xv (left side), and relationship between relative interspace size Lr and Γ which is the slant of the relationship between Xv'/Xv and Xv (right side).

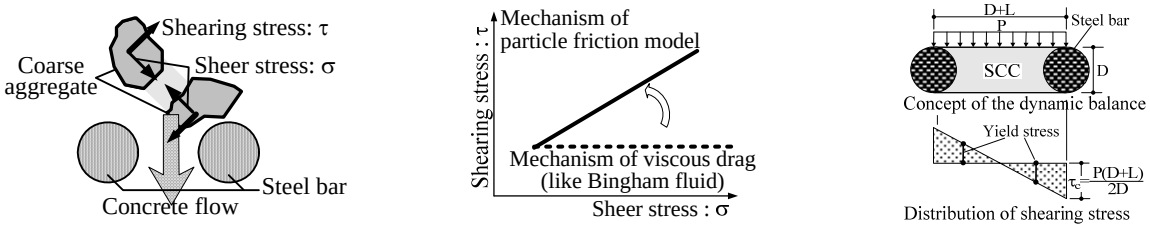

Figure 6. Concepts of sheer and shearing stress (left side), change in stress transfer mechanism (center), and dynamics model of the steel bar interspaces (right side).

4.2 Investiagation of the Model

4.2.1 Relationship between Xv'/Xv and Viscosity of Mortar

The left side of Figure 7 shows the relationship between *Xv*'/*Xv* and *Xv*, as calculated by image analysis. *Xv*' increases with narrowing *L*, and increasing *Xv*'/*Xv* is smaller when high viscosity mortar is used.

The right side of Figure 7 shows the relationship between Γ and *Lr*. Curves indicate the approximate curves of plots in these relationships for each mortar viscosity case applied. In the case of small *Lr*, Γ decreases with increasing mortar viscosity. This suggests that the increase in coarse aggregate volume is controlled partly by increase in mortar viscosity.

Equations in this figure show the approximate curves of the relationship between Γ and *Lr*, and are shown in Eq. (7).

$$\Gamma = \left\{ \begin{array}{l} 0.0189Lr^{-4.34} \left(\eta_m = 0.507\text{Pa}\cdot\text{s}\right) \\ 0.0177Lr^{-4.30} \left(\eta_m = 0.545\text{Pa}\cdot\text{s}\right) \\ 0.0158Lr^{-4.21} \left(\eta_m = 0.748\text{Pa}\cdot\text{s}\right) \end{array} \right\} \tag{7}$$

The left side of Figure 8 shows the relationship between mortar viscosity and coefficient *a*, *b*.
In this test, there are only three types of mortar viscosity, but they have linear relationships. These are shown in Eq. (8).

$$a = -0.01167\eta_m + 0.02447\,, \quad b = -0.5064\eta_m + 4.587 \tag{8}$$

This allows us to explain the increase coarse aggregate is partly due to the influence of mortar viscosity.

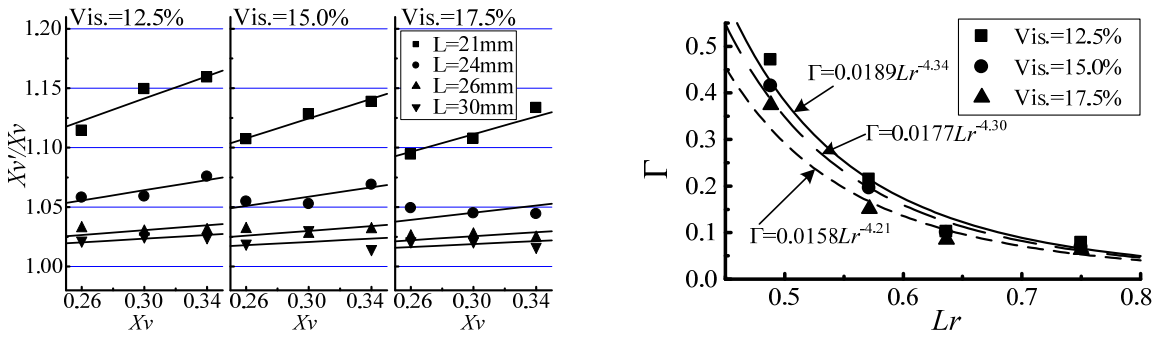

Figure 7. Relationship between relative increase in coarse aggregate volume *Xv*'/*Xv* and *Xv* (left side) and relationship between Γ that is the slant of the relationship between *Xv*'/*Xv* and *Xv*, and relative interspace size *Lr* (right side).

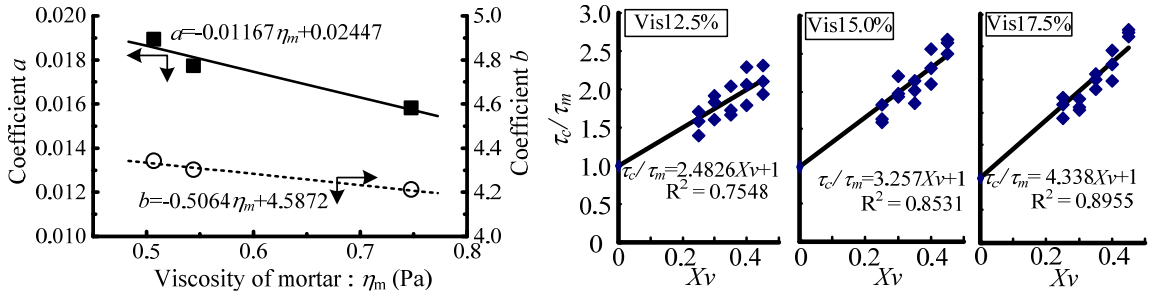

Figure 8. Relationship between coefficients of *a*, *b* and mortar viscosity (left side) and relationship ratio of yield stress of concrete and mortar τ_c/τ_m and original coarse aggregate volume of SCC *Xv* (right side).

4.2.2 Relationship between Yield Stress of Concrete and Mortar and Coarse Aggregate Volume

In this examination, we used a concrete viscometer, and investigated the relationship between relative yield stress of concrete and mortar τ_c/τ_m and coarse aggregate volume *Xv*.

The results are shown in Figure 8. Each relationship has essentially a straight relation, like Eq. (9), and the slants of the lines increase with increasing mortar viscosity.

Thus, there is a relationship between coefficient *c* and mortar viscosity as shown in Eq. (10).

$$\frac{\tau_c}{\tau_m} = cXv + 1 \quad (9), \qquad c = 6.816\eta_m - 0.509 \tag{10}$$

4.2.3 Calculating and Estimating Pressure Loss

We consider that pressure loss can be estimated easily from the aforementioned relationships between the rheological parameters of mortar, coarse aggregate volume, interspace size and diameter of the obstacle.

Equation (11), which has been published previously [Maruoka, et al. 2005], is as follows,

$$\tau_m = -0.553(2R_0) + 203.7\,,\quad \eta_m = 0.0251t_{14} + 0.387\,,\quad \tau_c/\tau_m = (6.816\eta_m - 0.509)Xv + 1\,,$$
$$\Delta P = \frac{2D}{D+L}(cXv+1)\tau_m\,,\quad c = 6.816\eta_m - 0.509 \tag{11}$$

where, τ_m is the yield stress of mortar (Pa), η_m is the viscosity of mortar (Pa*s), R_0 is the radius of mortar flow with no vibration (mm), and t_{14} is the mortar flow through time of the J_{14} type funnel (s).

5. COMPARISON OF MEASURED AND ESTIMATED PRESSURE LOSS

Figure 9 shows the comparative results of measured pressure loss and estimated pressure loss. For low pressure loss (under 200 Pa), the results are similar. However, in certain cases they are dissimilar, i.e., when mortar viscosity is low and interspace size is narrow.

The reason that the model generates pressure loss is in the condition of using low viscosity mortar, where there is large friction between the coarse aggregate particles and modeling this is difficult. Hereafter, we will attempt to improve the precision of the modeling.

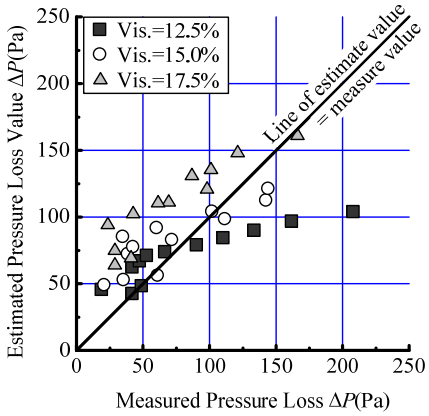

Figure 9. Comparison of measured and estimated pressure loss.

6 CONCLUSIONS

We attempted to estimate the self-compactability of SCC by considering the pressure loss phenomenon. We proposed an easy method for estimating pressure loss, using the rheological parameters of mortar and concrete, coarse aggregate volume and diameter of the obstacle. Using a visualization method to make clear the state of concrete flowing through a channel with obstacles, we detected changes in coarse aggregate volume and observed differences between upstream and downstream SCC flow.

On the basis of the rheological proprties and some derived equations, we estimated the pressure loss, finding that the measured value of pressure loss and estimated value was generally similar, enabling us to estimate pressure loss and self-compactability easily.

REFERENCES

Kanematsu, M., Nagai, H., Oh Sang-Gyun, Noguchi, T. & Tomosawa F., 1999, 'Evaluation of Passing Ability of Self-Compacting Concrete Part1.Evaluation Method', Summaries of technical papers of Annual Meeting Architectural Institute of Japan. A-1, Materials and construction, 361-362.

Maruoka, M., Fujiwara, H., Watanabe, Y., Iwasaki, A., & Fujie, Y., 2005, 'Experimental investigation of estimating method of pressure loss of self-compacting concrete pass through the gaps between re-bars', Journal of material, japan society of civil engineers, concrete structures and pavement, No.795/V-68, 111-126.

On Durability of Fiber Reinforced Concrete

M.A. Aiello [1]
E. Vasanelli [2]
G.A. Plizzari [3]

T 11

ABSTRACT

Costs for maintenance and repair of conventional reinforced concrete (RC) buildings and structures have become a serious economical, ecological and social problem. A large percentage of worldwide infrastructure needs nowadays repair measures.

This situation motivates great care when developing new construction materials, such as Fiber-Reinforced Concrete (FRC), whose enhanced toughness contributes to more durable structures. In fact, fibers could be introduced in RC structures to reduce the cracking phenomena thus helping the structural durability.

In the present paper, fracture behavior and water permeability of fiber reinforced concrete are studied. The effect of different crack openings is analyzed in order to study its influence on the mechanism of ingress of water.

KEYWORDS

Fiber Reinforced Concrete, Crack width, Water permeability, Steel fibers, Fracture tests

[1] University of Salento, Department of Innovation Engineering, Lecce, Italy Phone +39 0832 297248, Fax 0832 359872, antonietta.aiello@unile.it.
[2] University of Salento, Department of Innovation Engineering, Lecce, Italy Phone +39 0832 297266, Fax 0832 312013, emilia.vasanelli@unile.it.
[3] University of Brescia ,Dept. of Civil Engineering, Architecture, Land and Environment, Brescia , Italy Phone +39 030 3711 213, Fax , +39 030 3711 312, plizzari@ing.unibs.it.

1 INTRODUCTION

Costs for maintenance and repair of conventional reinforced concrete (RC) buildings and structures have become a serious economical, ecological and social problem. A large percentage of worldwide infrastructure needs repair measures.

The durability of concrete is intimately related to its permeability and the presence of cracks significantly increases the ability of aggressive agents to penetrate into the matrix, accelerating the deterioration processes. This is because concrete is susceptible to degradation through corrosion, alkali-silica reaction, sulphate attack, freeze-thaw damage and other mechanisms that result from the ingress of water [Neville 1981]. Although the permeability of dense concrete with a water-to-cement ratio approximately lower than 0.45, is nearly negligible in an uncracked condition, it becomes significant by the introduction of cracks and increases with the crack width [Ludirdja *et al.* 1989, Wang *et al.* 1997]. In addition, the increased permeability due to cracking, can accelerate other deterioration processes such as freezing and thawing damage.

This situation motivates great care when developing new construction materials, such as Fiber-Reinforced Concrete (FRC), whose enhanced toughness contributes to reduce cracking phenomena [Di Prisco *et al.* 2004, Carpinteri *et al.* 2007]. In a cracked matrix, the presence of fibers improves concrete durability since fibers influence the crack development by causing more distributed cracks with a smaller width. During the last 30 years many different fiber types made from many different materials have been successfully used to reinforce concrete and to enhance its durability [Tsukamoto & Wörner 1991, Aldea *et al*. 2000, Lawler *et al*. 2002].

After decades of research efforts on FRC properties, some structural applications came up and, during the last few years, design guidelines for FRC structures were proposed [Rilem 162 TDF 2002, CNR 2006]. However, the lack of results on durability of FRC does not allow to provide satisfactory information.

In the present paper, early results from an extensive research program (in progress) on fracture properties and water permeability of Fiber Reinforced Concrete are presented. The effect of the level of crack opening is analysed in order to study its influence on the mechanism of ingress of water.

2 EXPERIMENTAL METHODS

2.1 Materials

The concrete mix proportion used for the tests is given in Table 1. The steel fibers used had hooked ends and the characteristics reported in Table 2. The main properties of concrete at fresh and hardened state are reported in Table 3.

Table 1. Mixture proportions.

Materials	
Cement CEM 42,5R II-A/LL	400 Kg/m^3
Water/Cement ratio	0.55
Sand (0-4 mm)	936 Kg/m^3
Gravel (4-10 mm)	643.7 Kg/m^3
Superplasticizer	2.136 Kg/m^3
Fibers	47 Kg/m^3

Table 2. Fiber charachteristics.

Type	*Shape*	*Diameter*	*Length*	*Tensile Strength*
Steel	Hooked	500 μm	30 mm	1200 MPa

Table 3. Physical properties of concrete .

Entrained air (%)	4.9
Slump at fresh state (mm)	265
Compressive strength after 28 days (MPa)	28.93
Tensile strength after 28 days (MPa)	7.35
Dynamic elastic modulus (MPa)	30.96

Workability of fresh concrete was measured by performing a slump test (UNI 12350-2), entrained air was measured according to UNI 12350-7, the compressive strength was measured on cubes (150 mm side, according to UNI 12390-3), the tensile strength was determined by 3 Point Bending Tests (UNI 12390-5) while the dynamic elastic modulus was measured according to UNI 9524 FA-1.

2.2 Fracture Tests

Concrete Toughness was measured according to the Italian Standard (UNI 11039). Four point bending tests were performed on notched beams having a size of 150x150x600 mm and a notch depth of 45 mm 'Fig. 1a'. The Crack Mouth Opening Displacement (CMOD), measured by a Clip Gauge, was adopted as feedback signal. The Crack Tip Opening Displacement (CTOD) was also measured on both faces of the beam during the test 'Fig. 1b'.

Six beam specimens were cast in order to determine the fracture properties of each type of FRC. The latter were determined by using a 250 kN hydraulic testing machine (CONTROLS ADVANT TEST 9) with a closed loop control that permits to compensate the finite stiffness of the load system.

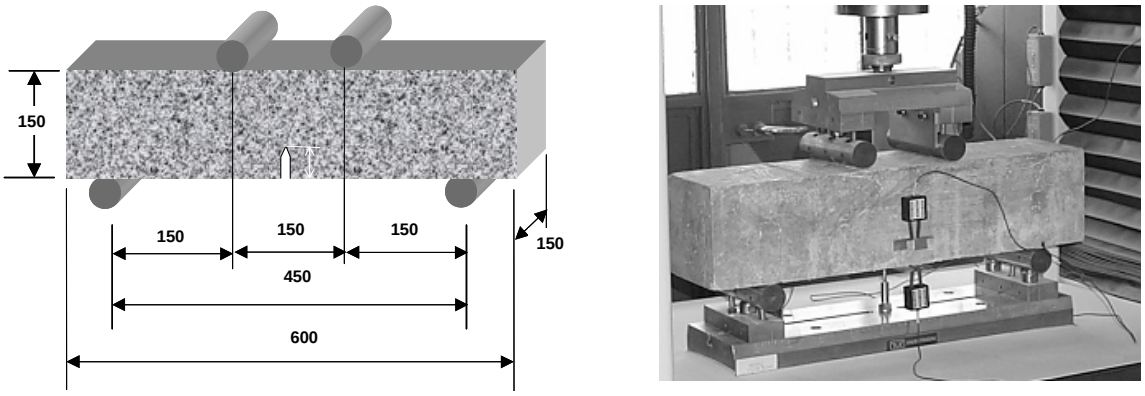

(a) (b)

Figure 1. Geometry (a) and instrumentation (b) of the notched specimen for the bending tests, according to UNI 11039 (2003).

'Figure 2' exhibits typical experimental results from beams tested. Diagrams report the applied load vs. the Crack Tip Opening Displacement (CTOD); it can be noticed that the remarkable residual post-cracking strength of steel fiber reinforced concrete.

'Table 3' summarize the main results from all fracture tests on beam specimens, including the tensile stress at crack onset (f_{If}), the equivalent strength for a crack tip opening displacement (CTOD) in the range 0-0,6 mm ($f_{eq(0-0,6)}$), typical for service loads, and in the range of 0,6-3 mm ($f_{eq(0,6-3,0)}$), typical for ultimate loads.

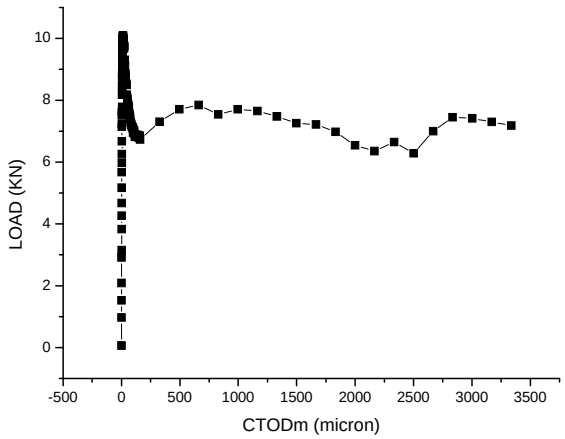

Figure 2. Typical experimental results of fracture tests (Load vs. CTOD).

Table 3. Fracture test results.

	f_{If}	$f_{eq(0-0,6)}$	$f_{eq(0,6-3,0)}$
Mean value (MPa)	2.76	2.05	2.0
Coefficient of variation %	16	29	39

2.3 Water Permeability Test

The concrete specimens for water permeability tests were slices (25 mm thick) cut from cylinders 200mm high with a diameter of 100mm.

The water permeability test was conduced on both cracked and uncracked specimens. Seven cracked specimens were tested. Specimens were pre-cracked by performing splitting tests ('Fig. 3'). Six measurements of the crack width were taken on both sides of the specimens by using an optical microscope ('Fig. 4'); the mean value was assumed as reference crack opening. The mean values of the crack width obtained at the end of the splitting tests are reported in [Table 4].

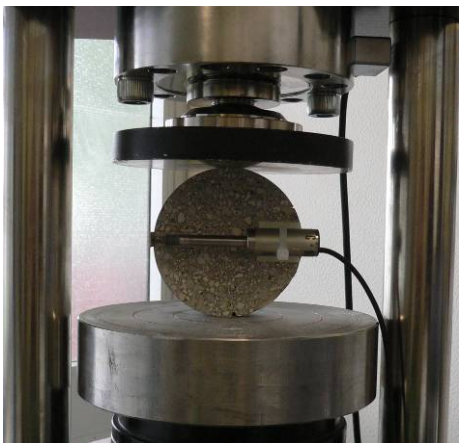

Figure 3. Splitting test performed to pre-crack the specimen**.**

Table 4. Crack width measurements.

Specimen	*Mean value of the crack width*	*Coefficient of Variation %*
A	113.17	24.5
B	26.75	29.2
C	39.05	32.2
D	117.73	45.2
E	160.31	53.4
F	106.21	27.5
G	236.23	13.7

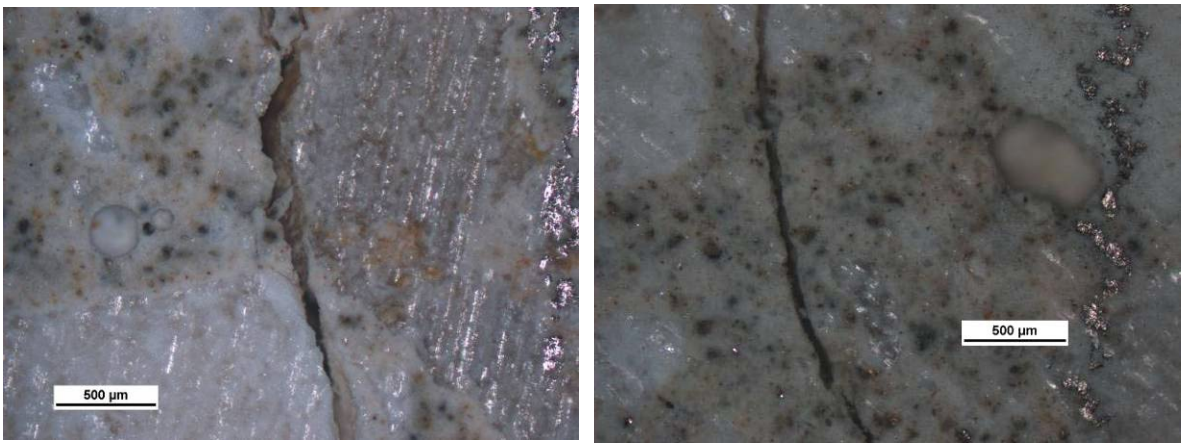

(a) (b)

Figure 4. Optical microscope images: (a) crack width of 100 microns; (b) crack width of 50 microns.

All specimens (cracked and uncracked) were conditioned before the water permeability test. The specimen preparation followed the procedure of chloride permeability tests (ASTM C1202-97 "Electrical indication of concrete's ability to resist chloride ion penetration"). Samples were firstly coated with a silicone building sealant on their side surface in order to prevent leakage during the water permeability test; afterwards, they were placed for three hours under vacuum. With the vacuum pump still running, the distilled water stopcock was opened in order to fill the specimen container: this step takes another hour. After the vacuum saturation, specimens were soaked until the water permeability test. After conditioning, the specimens were mounted and clamped in the water permeability test apparatus, as shown in 'Fig. 5'.

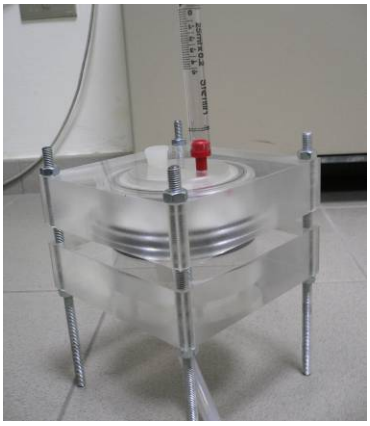

Figure 5. Water permeability cell.

The water permeability cell used in this work ('Fig. 6a') resembles that fully described by Wang et al [1997] ('Fig. 6b'). The cell A and B are slightly different: in the cell A there are two Plexiglas chambers instead of the Plexiglas plates and tubes used in the cell B. In this way it is possible to avoid problems in centering the sample between the Plexiglas tubes of the cell B.

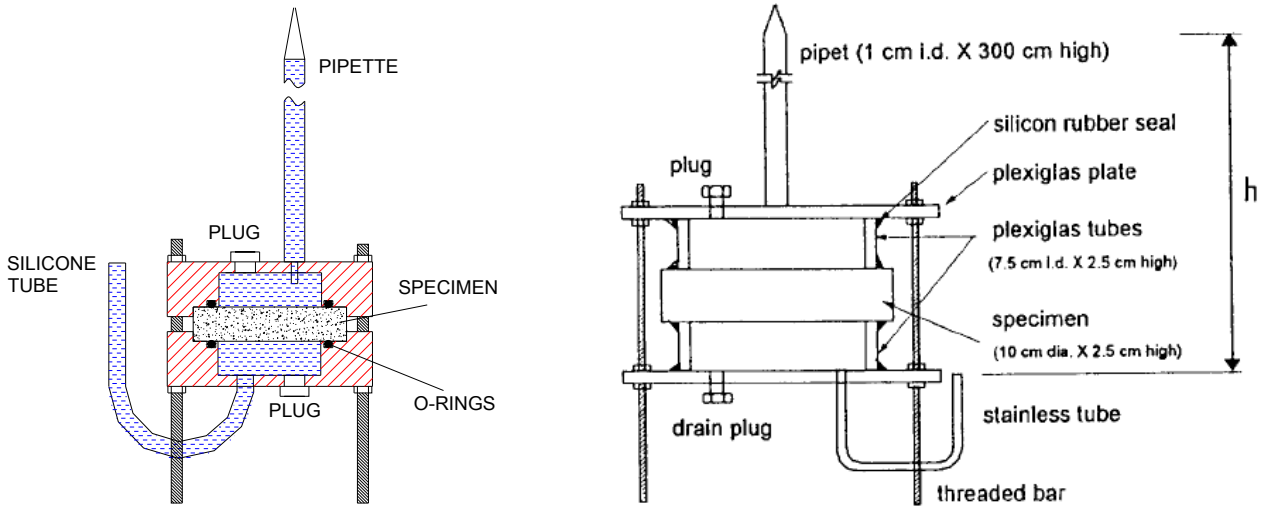

(a) (b)

Figure 6. Comparison between: the water permeability cell used in this work (a) and the water permeability cell used by Wang et al. (1997) (b).

The water permeability test started by filling the pipette with water. The water pass through the specimen under the pressure head given by the difference between the height of water in the pipette and the height of water in the silicone drain tube.

The water flow rate and the procedure of measuring the coefficient of water permeability were different if the specimen was cracked or uncracked.

For uncracked specimens, the water drop was measured once a day in the first week of testing and every two or seven days during the rest of the testing period, in order to minimize the reading errors. After each measurement the water in the pipette was restored to the original level. The test results were plotted with a curve of the cumulative water flow versus time. When the curve becomes linear, a steady state flow is reached and the Darcy's law can be applied to the permeability analysis [Wang *et al.* 1997]. The coefficient of water permeability can be calculated according to the following equation:

$$\frac{dQ}{dt} = \frac{khA}{L}$$

where:

Q is the water flow (cm^3);
k is the coefficient of permeability (cm/sec);
h is the water head (cm);
A is the cross-sectional area of the specimen (cm^2);
L is the specimen thickness (cm).

'Figure 7' shows the curves obtained for two uncracked specimens.

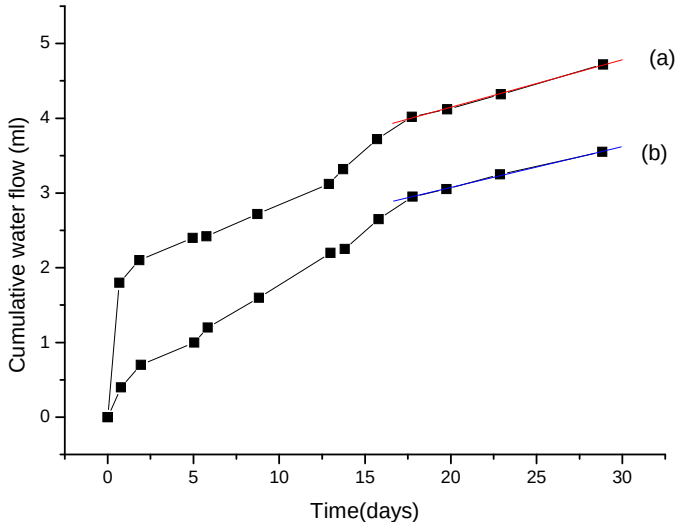

Figure 7: Cumulative water flow vs. time for two uncracked specimens (a, b).

For cracked specimen with a small crack width (specimens B and C), the procedure of measuring the water permeability coefficient was quite different from that used for uncracked specimen. The water flow rate was quite high so the readings of water drop were taken twice a day. Therefore, unlike uncracked specimens, in this case the water head could not be considered as a constant during the test, because the water drop was quite high in the reading time interval. The coefficient of permeability was calculated by integrating the Darcy's law from initial water head h_0 to measured water head h_1, as follows:

$$dQ = -A'dh$$

where A' is the cross-sectional area of the pipette;

$$\frac{\mathrm{dQ}}{\mathrm{dt}} = -A'\frac{dh}{dt} = \frac{khA}{L} \Rightarrow -\frac{dh}{h} = k\frac{A}{A'L}dt$$

$$-\int_{h_0}^{h_1}\frac{1}{h}dh = \int_0^t k\frac{A}{A'L}dt \Rightarrow k = \frac{A'L}{At}\ln\frac{h_0}{h_1}$$

For cracked specimens with a crack width larger than 100 μm, it took less than three minutes for the water to drop from the top to the bottom of the pipette. In this case, the time of the water drop was recorded with a stopwatch and the average of five flow rate, which were all very close, was used for permeability coefficient calculation [Wang *et al*. 1997].

The values of coefficient of water permeability 'k' obtained by using the procedure described above are reported in 'Table 5'.

'Figure 8' shows the relationship between water permeability and crack widths (in 'Fig. 8b' the water permeability coefficient is reported in a log scale). It can be notice that crack openings smaller than 50 microns have a little effect on concrete permeability: the value of k is about 10^{-6} cm/min compared with 10^{-8} for uncracked specimen. The increase in water permeability become significant for specimen with crack openings larger than 100 μm. In this case the order of magnitude of 'k' is about 10^{2} cm/min and become higher for cracks larger than 200 microns (about 10^{-1}). With such high permeability, considerable leaking may occur in the concrete structure during a limited service period.

Table 5. Values of the coefficient of water permeability.

Specimen	*Crack width*	*k (cm/min)*
Uncracked a	-	5.40E-08
Uncracked b	-	6.17E-08
Cracked A	113.17	0.018
Cracked B	26.75	5.70-06
Cracked C	39.05	5.31E-06
Cracked D	117.73	0.022
Cracked E	160.31	0.040
Cracked F	106.21	0.025
Cracked G	236.23	0.25

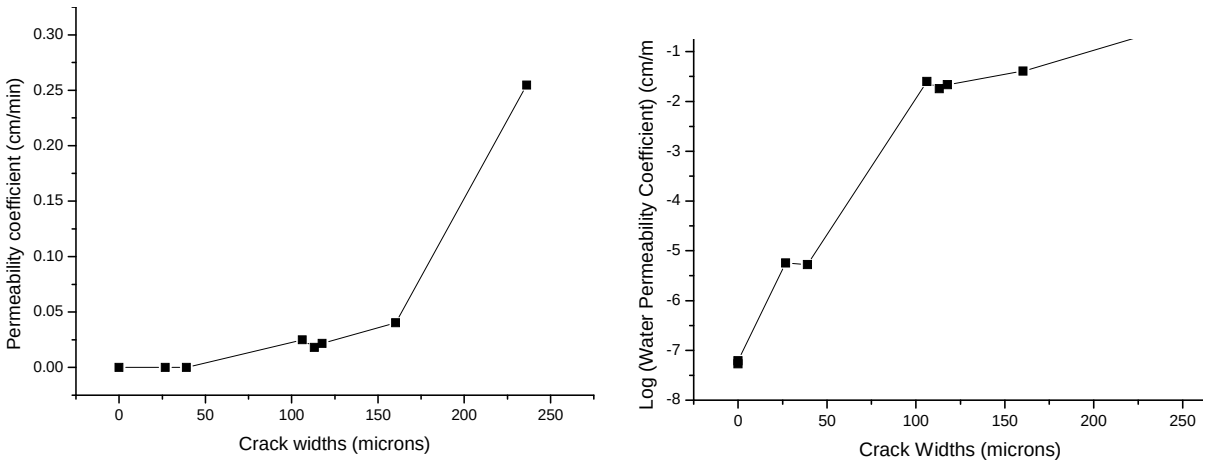

Figure 8. Permeability coefficient vs. crack width.

The results obtained from the present permeability tests on FRC specimens are in accordance with the ones reported in the literature for plain concrete [Wang *et al*. 1997] having similar crack opening: the permeability of cracked concrete with crack widths below 100 μm is nearly identical to that of uncracked concrete. Referring to RC structures, the Italian building code limits the design crack widths in the range 200÷300μm for aggressive and moderately aggressive environmental conditions, depending also on the sensibility of reinforcing steel to corrosion. As the design crack width is affected by a coefficient equal to 1.7, the allowable crack width is below 200 μm. This value is empirical, based on experience, and is in accordance with results obtained herein for FRC.

3 CONCLUDING REMARKS

Fracture behavior and water permeability of Fiber Reinforced Concrete with different crack widths was experimentally studied. Specimens were made of concrete with water cement ratio of 0.55 and a volume fraction of hooked steel fibers equal to 0.6%.

From fracture tests, it was observed that the volume fraction of fibers adopted, significantly improved the material toughness.

Results from water permeability tests indicates that crack openings smaller than 50 μm have a little effect on concrete permeability. The increase in permeability becomes significant for specimens with

crack openings larger than 100 μm where the order of magnitude of the coefficient of permeability (k) is about 10^{-2} cm/min and becomes higher for cracks larger than 200 μm (about 10^{-1}). With such high permeability, considerable leaking may occur in the concrete structure during a limited service period. The results obtained in this work for Fiber Reinforced Concrete are in accordance with those reported in the literature for plain concrete. Although it seems that the presence of fibers doesn't affect the influence of crack width on matrix permeability, smaller crack openings are expected in FRC. However, further research is needed to investigate the influence of the fiber content on the permeability of both cracked and uncracked matrices.

ACKNOWLEDGEMENTS

The Authors wish to express their gratitude and sincere appreciation to the Ministry of University and Research (MIUR) for financing this research work within the National Project (PRIN 2006) "Optimisation of the Structural, Technological and Functional Performance of Construction Methodologies and Materials in Tunnel Linings".

A special acknowledgement goes to Eng. Massimo Borsa of CTG Italcementi Group of Brindisi (Italy) for his valuable help in performing the experiments. The Authors are also grateful to Mr Giuseppe de Rossi (La Matassina Technology s.r.l.) for providing all the fibers.

REFERENCES

Aldea, C.-M., Peled, A., & Shah, S.P. 2000. 'Permeability of Cracked High Performance Fiber Reinforced Cement Based Composites', *BEFIB 2000*, RILEM, Lyon, France.

Carpinteri, A., Gambarova, P., Ferro, G. & Plizzari, G.A. Eds. 2007. 'Proceedings of the 6th International Conference on Fracture Mechanics of Concrete and Concrete Structures', FraMCoS 6, Catania, 18-21 June, Balkema, Volume 3: *HPC, brick masonry and environmental aspects*, 1886 pp.

CNR-DT 204 2006. 'Guidelines for the design and construction of fibre reinforced concrete structures', National Research Council of Italy.

di Prisco, M., Felicetti, R. & Plizzari G.A. Eds. 2004. 'Proceedings of the 6th RILEM Symposium on Fibre Reinforced Concretes (FRC)', *BEFIB 2004*, RILEM PRO 39, 1514 pp.

Lawler, J.S., Zampini, D. & Shah, S.P. 2002. 'Permeability of cracked hybrid fiber-reinforced mortar under load', *ACI Materials Journal,* 99[4], 379-385.

Lepech M. & Li V.C. 2005. 'Water permeability of cracked Cementitious composites', *ICF 11*, Torino, Italy, March 20-25 (on CD ROM).

Ludirdja, D., Berger, R.L. & Young, J.F. 1989. "Simple Method for Measuring Water Permeability of Concrete," ACI Materials Journal, Vol. 86[5], 433-439.

Neville, A.M. 1981. 'Properties of concrete' (Third Ed.), Longman Scientific and Technical, 779 pp.

Rapaport, J., Aldea, C.M., Shah, S.P. & Ankenman, B. 2001. 'Permeability of cracked steel fiber-reinforced concrete', *Technical Report* Number 115, National Institute of Statistical Sciences.

Tsukamoto, M. and Wörner, J.-D. 1991. 'Permeability of Cracked Fibre-Reinforced Concrete', *Darmstadt Concrete*, Vol. 6, 123-35.

RILEM TC 162 TDF 2002. "Test and design methods for steel fibre reinforced concrete : Design of steel fibre reinforced concrete using the σ-w method: principles and applications", Materials and Structures, Vol.35, 262-278.

Wang, K., Jansen, D.C., Shah, S.P. & Karr, A.F. 1997. 'Permeability study of cracked concrete', *Cement and Concrete Research*, 27[3], 381-393.

11DBMC International Conference on Durability of Building Materials and Components
ISTANBUL, Turkey 11-14 May 2008

Effect of High Temperature on Mechanical and Microstructural Properties of Cement Mortar

Özge Andiç-Çakır [1]
Oğuzhan Çopuroğlu [2]
Kambiz Ramyar [3]

T 11

ABSTRACT

This study investigates the effect of high temperature on some mechanical and microstructural properties of 6 different cement types (CEM I, CEM II/A-P, CEM II/B-P, CEM IV/A-W, CEM IV/B-W, CEM III/A). Blended cements are prepared by adding appropriate amounts of supplementary cementing materials to CEM I. Mortar mixtures prepared in accordance with TS EN 196-1 are cured in water for 28 days and in air for the following 28 days. In addition to control mixture, the specimens are exposed to 150°C, 300°C, 450°C, 600°C and 900°C for 4 hours and are allowed to cool to room temperature. Strength testing is applied to these specimens 24 hours after exposure. Flexural tensile and compressive strength of the mortars are determined in accordance with TS EN 196-1. Blended cements exhibit a higher compressive strength compared to CEM I at high temperatures. Mechanical test results are discussed by considering the microstructural changes in the mortar specimens.

KEYWORDS

Heat resistance, Cement type, Compressive strength, Flexural strength, Microstructure

[1] Ege University, Engineering Faculty, Department of Civil Eng., Bornova, Izmir, Turkey 35100, Phone +90 232 3886026, Fax 232 3425629, ozge.andic@ege.edu.tr
[2] Delft University of Technology, Faculty of Civil Engineering and Geosciences, Microlab, P.O.Box 5048, 2600GA Delft, The Netherlands, o.copuroglu@tudelft.nl
[3] Ege University, Engineering Faculty, Department of Civil Eng., Bornova, Izmir, Turkey 35100, Phone +90 232 3886026, Fax 232 3425629, kambiz.ramyar@ege.edu.tr

1 INTRODUCTION

The resistance of portland cement concrete to high temperature depends mostly on the type of the materials used in concrete design. Considering the deteriorations in concrete after exposing to high temperatures, cement paste is the least stable constituent. Chemical and physical deteriorations such as loosing the interlayer and chemically combined water from C-S-H and further decomposition of CH and C-S-H phases takes place in cement paste after exposure to high temperatures. The porosity and mineralogy of the aggregate are other important factors which affect the severity of deteriorations at different temperatures.

Temperature rise has different effects on cement paste [Baradan *et al.* 2002];

- capillary and gel water evaporates at ~100-150^{o}C,
- shrinkage and cracking takes place at ~150-250^{o}C accompanying reduction in tensile strength,
- evaporation of chemically combined water from aluminous and ferrous constituents takes place at ~250-300^{o}C, compressive strength of concrete starts to decrease,
- CH transforms into CaO at ~400^{o}C with accompanying 33% volume reduction,
- C-S-H starts to decompose at ~400-600^{o}C, strength reduction becomes considerable,

Xu *et al* [2001], studied the mechanical and durability properties of concretes incorporating fly ash at 0%, 25% and 55%; w/b ratios of 0.3 and 0.5 after exposure to temperatures of 250^{o}C to 800^{o}C. After exposure to 250^{o}C, plain concretes gained 8-9% compressive strength and fly ash incorporated one gained 10-15% compressive strength compared to the specimens tested before heating. This behavior is attributed to the strengthening of cement paste upon the evaporation of free water, which leads to greater Van der Waals of attraction forces as a result of the cement gel layers moving closer to each other. After exposure to 450^{o}C, the strength loss of fly ash incorporated mixtures was less than plain ones. The beneficial effect of 55% fly ash incorporation was still significant for concretes exposed to 650^{o}C, while the beneficial effect of fly ash diminished after 800^{o}C. It was evident that, C-S-H was decomposed after the exposure temperature of 650°C. The authors also concluded that reduction of CH constituent in fly-ash incorporating concrete increased the heat resistance of concrete by two ways given below:

- the reduction in cracking around CH crystals at ~300^{o}C,
- upon availability of extra water, rehydration of CaO give rise to 44% volume increase, cracking and strength loss at ~400-600^{o}C. The reduction of $Ca(OH)_2$ in cement paste prevents deterioration.

Sarshar and Khoury [1993], investigated the effect of high temperature on compressive strength of pastes and concretes prepared by using ordinary portland cement and cements incorporating 10% silica fume, 30% fly ash and 65% slag. The specimens were cured at 100% relative humidity for 1 year. High temperatures were applied to unloaded specimens after the curing period and compressive strength testing was performed. The authors concluded that plain cement incorporating mixtures started to lose compressive strength after 200^{o}C, the decrease in strength was obvious at 300^{o}C. Concrete and mortar specimens containing fly ash and slag expressed a better performance than plain mixtures and silica fume-bearing mixtures at high temperatures. This behavior was attributed to the fact that mineral admixture-bearing samples had less $Ca(OH)_2$ than plain mixtures.

Savva *et al* [2005] investigated the effect of elevated temperatures on the mechanical properties of blended cement concretes prepared with a siliceous aggregate and a limestone aggregate. Water to binder ratio of the mixes was constant (0.60), blended cements were prepared by using different amounts of two different fly ashes and a natural pozzolan. The authors concluded that concretes with pozzolanic materials showed better resistance at elevated temperatures until 300^{o}C, while they were more sensitive to elevated temperatures above 300^{o}C. Between 100-300^{o}C, the residual strength of almost all the mixtures increased. The effect was more significant for siliceous aggregate-containing concretes. A continuous decrease in the compressive strength of the specimens was observed irrespective of the type of the aggregate at 600^{o}C and 900^{o}C.

The aim of this study is to investigate the effect of elevated temperatures on flexural and compressive strength of 6 different cement types (CEM I, CEM II/A-P, CEM II/B-P, CEM IV/A-W, CEM IV/B-W, CEM III/A). Mortar mixtures were cured in water for 28 days and in air for the following 28 days in laboratory conditions. After curing period, the specimens were exposed to 150°C, 300°C, 450°C, 600°C and 900°C for 4 hours and were allowed to cool to room temperature. The specimens were tested in flexure and in compression 24 hours after exposure. It was concluded that blended cements exhibit a higher compressive strength compared to CEM I when exposed to high temperatures. Microstructure of control and exposed specimens containing CEM I and CEM III-A were observed under ESEM (environmental scanning electron microscope).

2. MATERIALS AND TEST METHODS

2.1 Composition of Binders

The chemical composition of ordinary portland cement (CEM I 42.5R) and mineral admixtures (fly ash, natural pozzolan and slag) are provided from İzmir Çimentaş Cement Factory (Table 1).

Table 1 Chemical composition of CEMI 42.5R, fly ash, natural pozzolan and slag.

Oxide Composition (%)	CEM I 42.5 R	Fly Ash	Natural Pozzolan	Slag
MgO	1.54	1.54	1.27	5.47
Al_2O_3	5.17	23.55	12.22	10.43
SiO_2	18.71	45.98	51.82	41.33
SO_3	2.88	1.47	0.07	0.07
K_2O	0.84	1.8	2.56	1.21
CaO	63.74	18.67	12.32	32.60
Fe_2O_3	2.38	4.91	4.47	1.18
Na_2O	0.30	0.24	1.01	---
Loss on Ignition	3.88	2.31	10.32	---

2.2 Cement Types

The cement types used in this study were prepared by mixing the reference cement (CEM I 42.5 R) with different amounts of mineral admixtures. The contents of different cements are given in Table 2.

2.3 Aggregate (Standard Sand)

The mortars used in this study were cast by using siliceous standard sand in order to compensate the effect of aggregate mineralogy in different mixtures. Standard sand complies with the requirements given in TS EN 196-1.

Table 2 Cement types and their contents

	CEM I 42.5 (reference cement)	Fly Ash	Natural Pozzolan	Slag
CEM I 42.5	100%	0%	0%	0%
CEM IIA-P	85%	0%	15%	0%
CEM IIB-P	70%	0%	30%	0%
CEM IVA-W	70%	15%	15%	0%
CEMIVB-W	55%	15%	30%	0%
CEM III-A	55%	0%	0%	45%

2.4 Mixture Proportions and Test Method

Mortars were cast in accordance with TS EN 196-1 method by using 450 g cement, 1350 g standard sand and 225 g tap water. Six mortar specimens were cast into 40x40x160 mm prismatic molds for each mixture. The demolded specimens were cured in water for 28 days and in air for the following 28 days. The control mixture was tested in 20°C, other specimens were exposed to temperatures of 150, 300, 450, 600 and 900°C for 4 hours and cooled to room temperature for 24 hours. Exposed specimens were weighed before and after exposure to high temperatures.

Strength tests were performed in accordance with TS EN 196-1 by using a test machine of 10 ton capacity which can measure the loads and deflections automatically. Three-point loading was applied in order to evaluate the flexural tensile strength of the specimens. The broken portions were tested in compression as 40x40x40 mm modified cubes.

2.5 Microstructural Investigation

Epoxy-impregnated plane sections were prepared for the microstructural analysis. To obtain the desired smooth surface finish, impregnated specimens were subsequently lapped with 1200 and 4000 mesh bonded Carborundum and polished with 6µm, 3µm, 1µm and 0.25µm diamond paste on a lapping table. Polished specimens were finally rinsed in an ultrasonic bath to remove polishing paste and debris. Surface quality was checked under an optical microscope.

Polished specimens were investigated using a Philips XL30 environmental scanning electron microscope (ESEM). The instrument was operated at 15kV accelerating voltage, beam current 20mA, 0.3Torr pressure and at 10 mm working distance, with these settings applied for imaging.

3 RESULTS AND DISCUSSION

Flexural test results are the average of 6 specimens and compressive strength test results are the average of 12 specimens. Relative compressive strength, relative flexural strength and relative weight loss values were calculated with respect to the control specimen (the specimens tested at 20°C) of each cement type.

Relative compressive strength – temperature relationship is given in Figure 1. The compressive strength of CEM IV/A-W and CEM IV/B-W mortars were slightly increased at 300°C. The relative compressive strength of all mixtures was decreased by increasing temperature and blended mixtures showed higher relative compressive strength values beyond 300°C. The relative compressive strength of all of the mixtures was reduced to approximately 10% at 900°C.

Relative flexural strength-temperature relationship of the mixtures is given in Figure 2. There is a considerable increase in the relative flexural strength value of CEM I mixture at 150°C. Relative flexural strength of all mixtures was reduced at temperatures beyond 300°C. The relative flexural strength of all of the mixtures was reduced to approximately 15% at 600°C, while these values were reduced to about 10% at 900°C. Blended cements are more resistant to high temperatures when compared to CEM I at 450°C. Beyond 450°C, the effect of type of cement on flexural strength of mortars becomes negligible. Figure 3 shows the relative weight loss – temperature relationship. The weight loss of the samples are close to each other for each temperature level, weight loss of all of the mixtures are around 10-12% at 900°C.

Considering the compressive strength-temperature relationships, CEM IV (Pozzolanic) cements containing both fly ash and natural pozzolan and CEM III-A cement containing slag seems to be more resistant to high temperatures when compared to CEM I (plain) cement and CEM II (Portland-pozzolan) cements containing different amounts of natural pozzolan. Similar findings were observed for flexural tensile strength test results which are remarkable at 450°C.

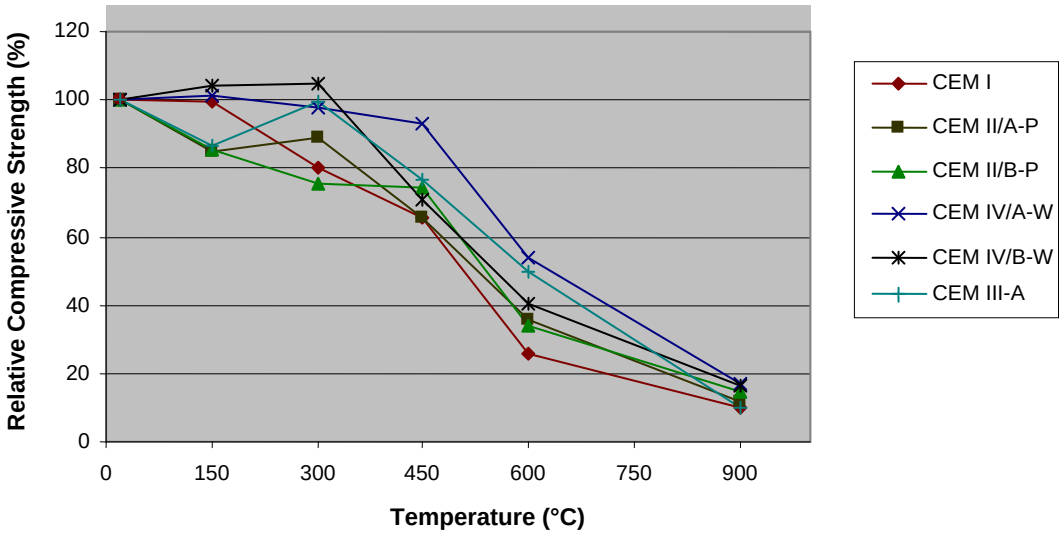

Figure 1 Relative compressive strength – temperature relationship of mortars

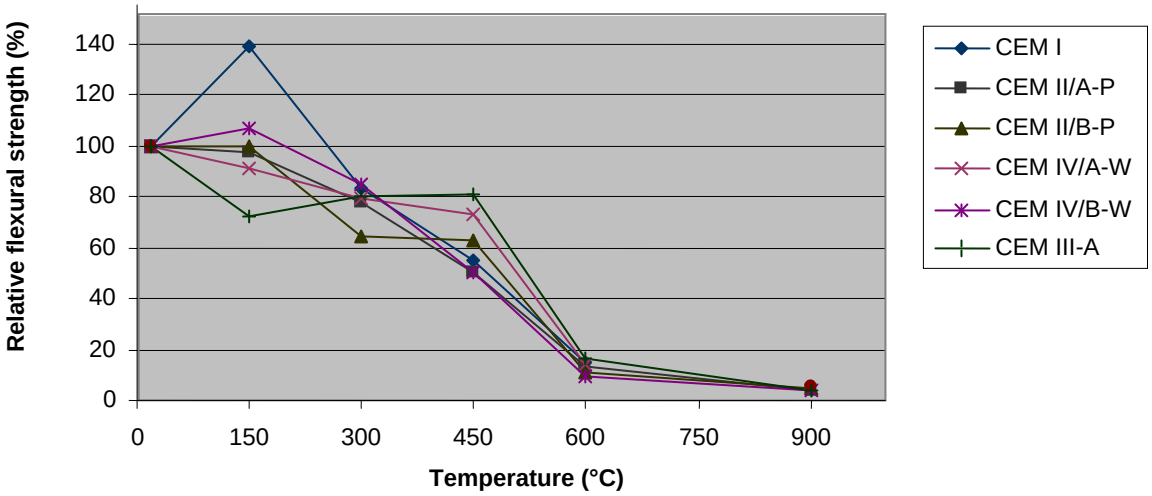

Figure 2 Relative flexural strength-temperature relationships of mortars

Microscopy findings concerning the effect of elevated temperature on the CEM I and CEM III-A mortars is presented in Figure 4. Up to 300°C, no significant structural damage was observed. Bonding between aggregate particles and cement paste was visually in rather good quality. However, significant crack development was observed at the microstructures of mortars exposed to 600°C. Micro cracks were observed throughout the microstructure but the most critical ones were traveling (connecting) individual coarse aggregate particles. De-bonding of the unreacted cement particles was also seen. This effect was probably because of significant volume alteration of hydration reaction products (CH, CSH).

The mineral admixture particles (in this case slag) showed no extensive debonding and appeared to be unaffected by the temperature attack. The microstructural investigation showed that crack size in CEM I paste microstructure was larger in comparison to the CEM III-A paste cracks. Information obtained from microstructural observations seems to support the findings obtained from mechanical tests.

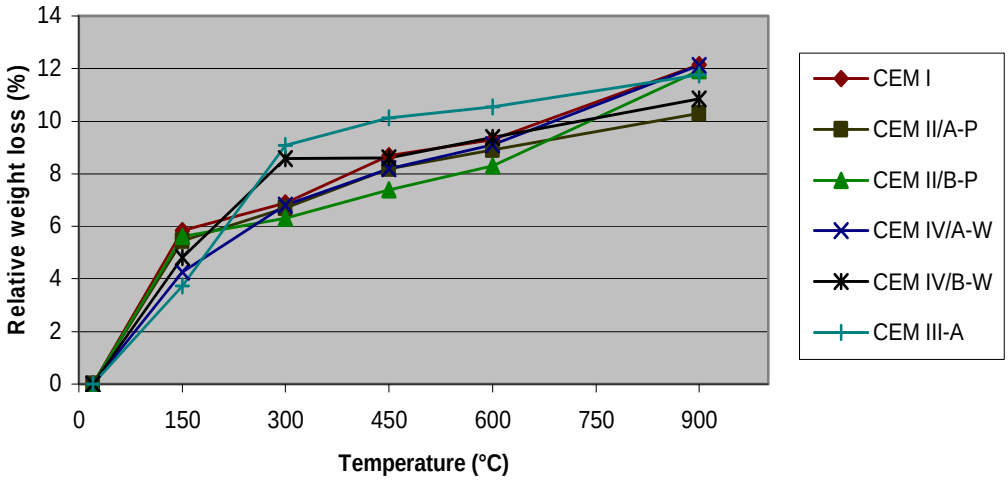

Figure 3. Relative weight loss-temperature relationship.

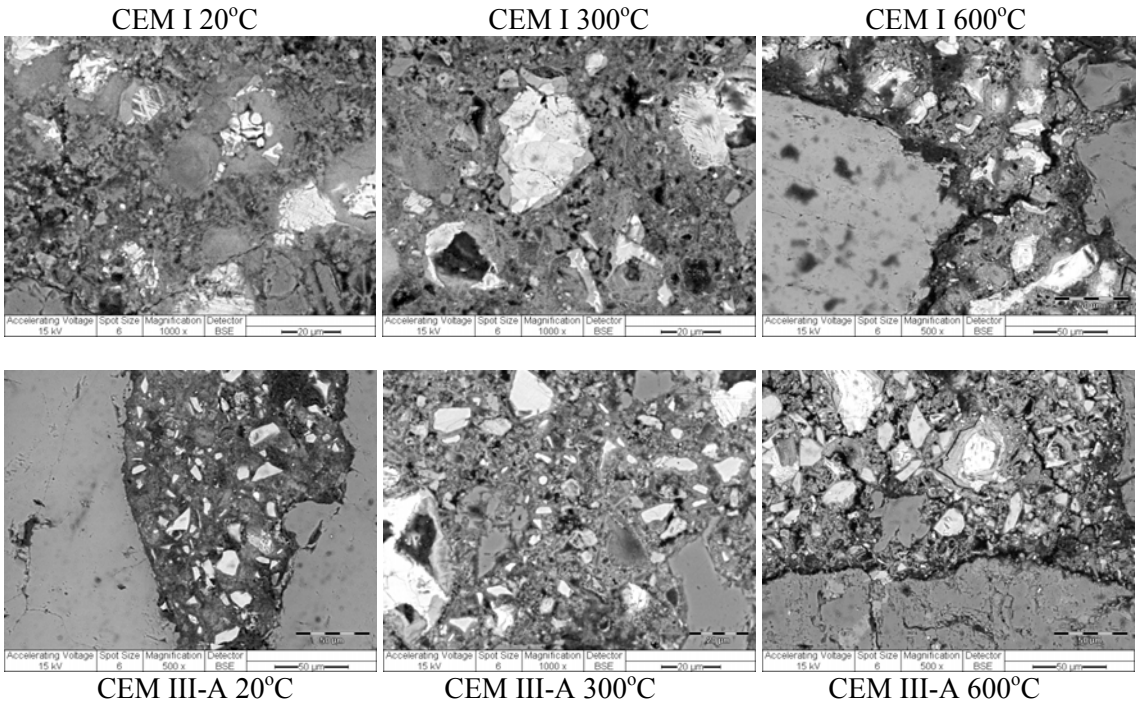

Figure 4. Effect of temperature elevation on the mortar microstructure, CEM I vs. CEM III-A.

4. CONCLUSIONS

- ✓ Relative compressive and flexural tensile strength of all mixtures was decreased by increasing temperature and blended mixtures showed higher relative strength values beyond 300°C.
- ✓ Considering flexural and compressive strength values, CEM IV and CEM III-A type cements are more resistant to high temperatures when compared to CEM I and CEM II type cements.
- ✓ The microstructural investigation showed that crack size in CEM I paste was larger in comparison to the CEM III-A paste cracks.

- ✓ Information obtained from microstructural observations seems to support the findings obtained from mechanical tests.

ACKNOWLEDGMENTS

The authors would like to acknowledge The Scientific and Technological Research Council of Turkey for their financial support during this study.

REFERENCES

Baradan, B., Yazıcı, H., Ün, H., 2002, *Betonarme Yapılarda Kalıcılık (Durabilite)*, DEU Mühendislik Fakültesi Yayınları, No: 298, İzmir.

Sarshar, R., & Khoury, G.A., 1993, Material and environmental factors influencing the compressive strength of unsealed cement paste and concrete at high temperatures, *Magazine of Concrete Research,* **45 [**162], 51-61.

Savva,A., Manita,P., & Sideris,K.K., 2005, Influence of Elevated Temperatures on the Mechanical Properties of Blended Cement Concretes Prepared with Limestone and Siliceous Aggregates, *Cement & Concrete Composites*, **27,** 239-248.

Xu, Y., Wong, Y.L., Poon, C.S., & Anson, M., 2001, Impact of high temperature on PFA concrete, *Cement and Concrete Research*, **31**, 1065-1073.

Durability of Cement Mortars with Carbon Material Admixtures

Pedro Garcés [1]
Juan Alcaide [2]
Eva G. Alcocel [3]
Emilio Zornoza [4]
Luis G. Andión [5]

T 11

ABSTRACT

Using a constant water/cement ratio of 0.42 and different amounts of carbonaceous materials and different curing periods the evolution of the corrosion process in the embedded reinforced bars has been determined. The addition of small quantities of carbonaceous materials to the mixture produces a reduction of the concrete permeability. The higher is the cement paste conductivity, the higher is the instant corrosion rate in embedded steel.

KEYWORDS

Carbon materials, Durability, Reinforced concrete, Corrosion

[1] University of Alicante, Dept. Ingeniería de la Construcción, Alicante, Spain 03690, Phone +34 965903400 (Ext. 3324), Fax +34 965903678, pedro.garces@ua.es
[2] University of Alicante, Dept. Construcciones Arquitectónicas, Alicante, Spain 03690, Phone +34 965903400 (Ext. 2572), Fax +34 965903678, juan.alcaide@ua.es
[3] University of Alicante, Dept. Construcciones Arquitectónicas, Alicante, Spain 03690, Phone +34 965903400 (Ext. 2950), Fax +34 965903678, eva.garcia@ua.es
[4] University of Alicante, Dept. Ingeniería de la Construcción, Alicante, Spain 03690, Phone +34 965903400 (Ext. 3707), Fax +34 965903678, emilio.zornoza@ua.es
[5] University of Alicante, Dept. Ingeniería de la Construcción, Alicante, Spain 03690, Phone +34 965903400 (Ext. 9499), Fax +34 965903678, luis.garcia@ua.es

1 INTRODUCTION

There is a wide range of potential applications of general purpose carbon fibers (GPCF). One of the most important is in the construction industry as addition to concrete mixes in order to develop or enhance special properties.

Although the use of carbon fiber materials in the construction industry means a significant cost increase, the highly promising benefits of their use, not only because of the improvement of mechanical properties but also in obtaining more efficient, smaller concrete element sections, make it interesting.

Durability of both the concrete matrix and reinforcements governs the service life of structures. In spite of the above mentioned advantages of carbon fibers, there are very few works published in the technical literature regarding the effect that the addition of different carbon materials produce in the concrete strength properties and the corrosion of embedded steel reinforcement [Hou & Chung 2000, Garcés *et al.* 2005, Garcés *et al.* 2007]. The purpose of the present work is to characterize the durability properties of steel embedded in mortars specimens in which different types of carbon materials have been used.

2 EXPERIMENTAL

2.1 Materials and methods of mortar specimens fabrication

Portland cement type CEM I 52.5 R (CP) and silica sand normalised under UNE-EN 196-1 standard were used for all mortar specimens.

Figure 1 shows the SEM images of the carbon materials used. Note the irregular particle shape. Sofacel graphite powder (PGS) is a commercial brand of Le Carbone Lorraine Company with particle size lower than 0.63 mm. Figure 2 shows PGS in detail. The marked lamellar structure and the rough surface can be observed.

No. 9 Graphite Powder (PG9) is a commercial brand supplied by Superior Graphite Company, particle size lower than 75 µm, also shown in Fig. 2. The morphological differences between PGS and PG9 are notorious.

The graphite electrode maker Grafitos Barco has supplied two types of by-products of the fabrication of furnace conductor electrodes for the steel industry. Both have identical composition and the difference is based on the particle size distribution. PGA type contains a minimum 90% of particles under 50 µm size, whereas PGC type contains a 90% of particles with average size in the range 0.5-1 mm. Table 1 shows the element composition of each type of graphite powder. The high content of carbon in all of them (more than 98%) is to be noted.

Table 1. Chemical analysis of carbon admixtures.

Sample	*Elemental Analysis (% wt.)*			
	C	*H*	*N*	$(S+O)_{dif}$
PGS	99.35	-	-	0.65
PG9	99.00	-	-	1.00
PGA and PGC	98.48	-	0.05	1.47

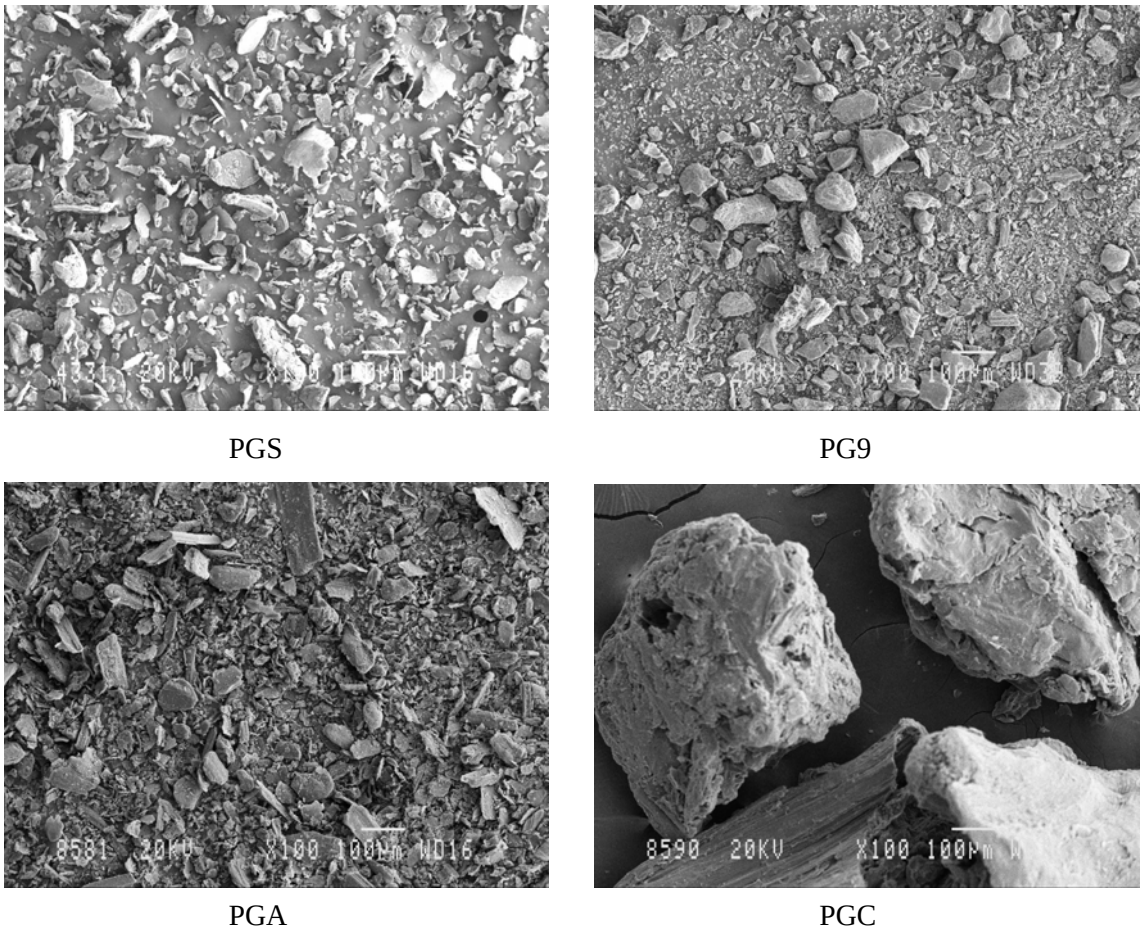

Figure 1. SEM images of carbonaceous materials.

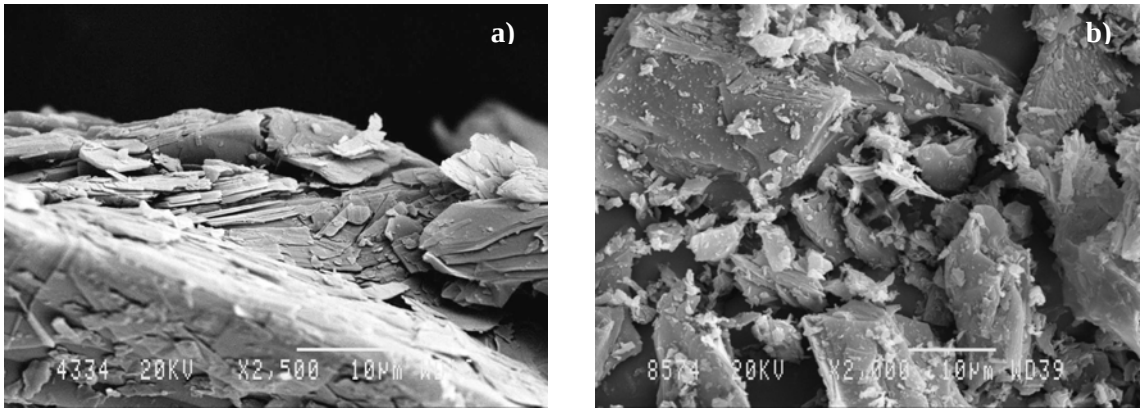

Figure 2. Details of (a) PGS and (b) PG9.

Figure 3 shows the particle grading curves obtained by laser light diffraction of the materials used in mortar fabrication. Only the fraction of sand passing through 0.16 mm sieve was used. The mean size value D50, that is the size value in µm under which 50% of the particles lay, is as follows: 15.9 µm for cement, 28.1 µm for PG9, 28.8 µm for PGA, 41.2 µm for PGS, 79.7 µm for sand and 355.7 µm for PGC. With the exception of PGC all graphite powder types have grading curves laying in between the cement and the sand grading curves. A filler effect can then be expected for those materials.

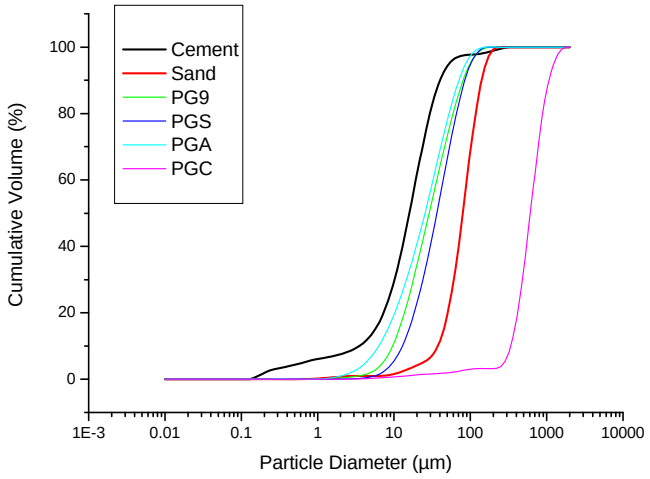

Figure 3. Particle size distributions of the GP types, cement and sand in the experiments.

2.2 Corrosion tests

For corrosion testing the GP ratio used was 1% as addition. Corrosion tests were carried out using mortar prismatic specimens of 80x55x20 mm size. Each specimen contained two cylindrical carbon steel electrodes, 8 mm diameter, and a graphite counter-electrode in the middle. The resulting cover thickness is 6 mm. The steel exposed area is 6.3 cm^2 (two electrodes). The instant corrosion rate Icorr for each electrode was assessed and the average of the two electrodes of each specimens was taken as the result value. Measuring was carried out until stable values of Icorr were obtained.

Corrosion test specimens were cured in a 100% RH chamber, and later, some of them, subjected to haste carbonation (CO_2 saturated atmosphere, 70% RH).The others were partially immersed in a 0.5 M NaCl dissolution simulating seawater.

Half of the specimens were hastily carbonated inside a glass recipient internally filled with a CO_2 saturated atmosphere. In the internal bottom of the recipient a glycerine dissolution kept the inside relative humidity at about 70%. A perforated tray was used to separate and store the specimens above the glycerine dissolution. The progress of the carbonation front was monitored using the phenolphthalein method on separate 80x20x20 mm prismatic specimens. After cutting 1 cm thick slices of the control prisms the carbonated areas were detected by dropping some phenolphthalein on the cut face.

The other half of specimens were hastily carbonated, dedicated to chloride attack study, were placed inside recipients with a 0.5 M dissolution of NaCl simulating seawater. Specimens remained partially immersed in the dissolution leaving only 2 cm of their height above the liquid surface in order to avoid contact of the electrodes with the dissolution. The liquid level was checked periodically and maintained constant. The portions of the electrodes extending outside the mortar were covered with Vaseline to avoid corrosion on this parts.
The electrochemical technique used to asses the instant corrosion rate Icorr of steel was the Polarization Resistance, Rp. After measuring the Rp value the Icorr vas calculated using the Stern and Geary formula [Stern & Geary 1957]: Icorr = B/Rp . Constant B was set to 26 mV for corroding steel and to 52 mV for steel in passive state [Andrade & González 1978].

The value of Rp was measured periodically through the experimental time, along with the corrosion potential Ecorr. At the end of experiments, the total electrochemical mass loss was calculated for each electrode and checked against the gravimetric loss (obtained by weighing). All values of potentials

refer to a calomel saturated electrode. A Princetone 362 EG&G galvanostat was use in the measurements. The result values of Icorr are the average of the measurements of four electrodes (two specimens, two electrodes each). The electrochemical mass loss was calculated by integration of the Icorr vs. time curves and the Faraday Law. The calculated values matched quite well with the gravimetric values, confirming the adequacy of the value used for B.

3 RESULTS

The results of the corrosion behavior of steel embedded in these conductive mortars are shown in Fig. 4 as the evolution of corrosion rate in mortar specimens with additions of PGA, PGC and PG9 types. Initially, the specimens were stored in a 100% RH ambience. Icorr values were monitored periodically since the instant of specimen demoulding until steady values.

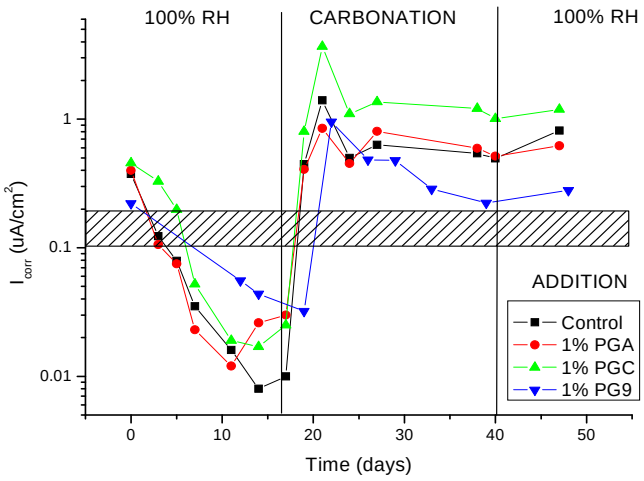

Figure 4. Evolution of corrosion rate in mortars with 1% addition of different GP types and subjected to different ambient conditions: 100% RH, carbonation and again 100% RH.

Under the first 100% RH period, the Icorr values were decreased continuously with the highest values of 0.04 µA/cm^2 for PG9 addition. All values lay under the 0.10 µA/cm^2 threshold, that is in passive state and usually continue so until a change in the conditions occur.

Specimens were then stored in the carbonation chamber and a sudden increase of the corrosion rate was detected in all cases. For example, the PGC addition mortar reached Icorr values of about 4 µA/cm^2. Later on, steady values were recorded but with important difference between some of them. The highest steady value obtained was 1.3 µA/cm^2 for PGC addition specimens. These steady values were almost the same when the specimens were again stored in a 100% RH ambience.

The Icorr values of GP added specimens were similar or higher than the ones of the reference specimens (no GP), except for PG) additions. One possible explanation of it could be the high fineness of this addition and the smaller porosity of the specimens that would compensate the effect of a higher conductivity due to the presence of the carbon material. The lower porosity would mean a limitation of the oxygen diffusion current and consequently of the cathodic reaction.

Figure 5 shows the evolution of Icorr in mortar specimens fabricated with 1% additions of PGA; PGC and PG9 types, cured in a 100% RH chamber and then partially immersed in seawater. Right after demoulding, the first Icorr values were obtained. The recorded values were in the range 0.3-07 µA/cm^2.

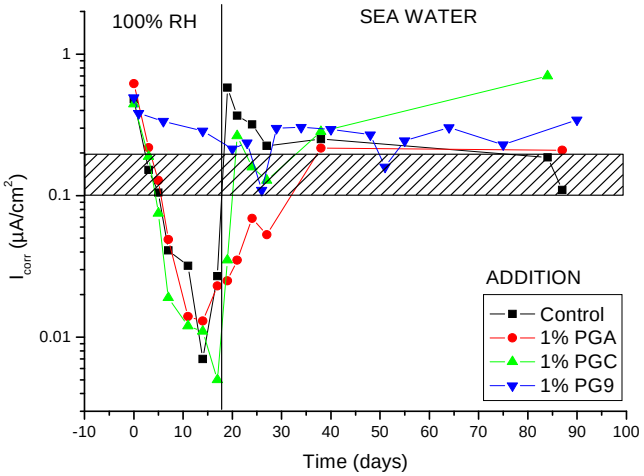

Figure 5. Evolution of corrosion rate in mortars with 1% addition of different types of GP, cured in 100% RH chamber, and later partially immersed in seawater.

In the period of 100% RH ambience the Icorr values were decreasing to values well under 0.1 µA/cm^2, except for PG9 added specimens that provided values in the higher limit of the passivity marking band [Andrade & Alonso 1996, Andion *et al*. 2001].

The immersion in seawater implied in all cases a sudden increase in corrosion rates which after some time reached stationary values.. The PGC type added mortars provided the highest Icorr values of about 0.6 µA/cm^2. The result differences between PGA, PG9 and PGC added specimens can be explained by their different particle size grading curves.

The reference specimens provided smaller Icorr values than any GP added specimen. To explain this, the role of the galvanic couple between steel and the carbon materials is to be considered. The contact of conductive materials of different nobility levels implies that the less noble material will develop a corrosion level higher than the one it would have being alone in the same environment. This would be compensated by a decrease in the corrosion level of the more noble material. The electrons from the oxidation of the less noble material will act as some kind of cathodic protection on the more noble material surface. In our case the more noble material is graphite and the less noble is steel. Consequently the presence of graphite in the mortars contributes to an increase in the Icorr levels registered in steel.

The presence of GP implies an increase in steel corrosion rates due both to the higher conductivity of the mortar and to the galvanic effect that the carbon materials produce on the embedded steel.

4 CONCLUSIONS

1. The higher the carbon material addition content ratio, the higher is the porosity.

2. Tests demonstrate that a increase of the corrosion level occurs when the content ratio of carbon material addition is increased.

REFERENCES

Andión, L.G., Garcés, P. & Cases, F. 2001, 'Metallic corrosion of steel embedded in calcium aluminate cement mortars', *Cement and Concrete Research* **31**, 1263-1269.

Andrade, C. & González, J.A. 1978, 'Quantitavie measurements of corrosion rate of reinforcing steels embedded in concrete using polarization resistance measurements', *Werkst. Korros.* **29**, 515-521.

Andrade, C. & Alonso, C. 1996, 'Corrosion rate monitoring in the laboratory and on-site', *Construction and Building Materials* **10**, 315-328.

Garcés, P., Fraile, J., Vilaplana-Ortego, E., Cazorla-Amorós, D., Alcocel, E.Gª & Andión, L.Gª. 2005, 'Effect of carbon fibres on the mechanical properties and corrosion levels of reinforced portland cement mortars', *Cement and Concrete Research* **35**, 324-331.

Garcés, P., Andión, L.Gª, De la Varga, I., Catalá, G. & Zornoza, E. 2007, 'Corrosion of steel reinforcement in structural concrete with carbon material addition', *Corrosion Science* **49,** 2557-2566.

Hou, J.Y. & Chung, D.D.L. 2000, 'Effect of Addition in concrete on the Corrosion Resistance of Steel Reinforced Concrete', *Corrosion Science* **42**, 1489-1507.

Stern, M. & Geary, A.L. 1957, 'A theoretical analysis of the shape of polarization curves', *Journal of Electrochemical Society*, **104**, 56-63.

Durability Properties of Polypropylene Fiber Reinforced Concrete

Hamed Layssi [1]
Mehrdad Mahoutian [1]
Mohammad Shekarchi [1]

T 11

ABSTRACT

Concrete is an inherently brittle material with a relativity low tensile strength compared to its compressive strength. Reinforcing with randomly disturbed short fibers presents an effective approach to the stabilization of the crack system, improving the ductility and tensile strength of concrete. Polypropylene (P.P) fiber reinforcement is considered to be an effective method for improving the shrinkage cracking characteristics, toughness and impact resistant of concrete material. Even though fibers are widely used to improve mechanical properties of concrete, they may affect the workability and the flow characteristics of plain concrete.

Durability characteristics of plain concrete may be improved using polypropylene fibers. Several researchers have been carried out on the mechanical properties of polypropylene fiber reinforced concrete; yet there are a few investigations on the durability properties of concrete containing polypropylene fibers.

In this paper, the effect of adding various percentages of P.P fibers to concrete on the durability of concrete is investigated. Water penetration, gas permeability, electrical resistivity and shrinkage were studied. Results show that adding P.P fibers to the concrete will decrease the shrinkage of concrete significantly. Although using these fibers does not improve the permeability of concrete notably.

KEYWORDS

Polypropylene fiber, Durability, Shrinkage

[1] University of Tehran, School of Civil Engineering, Tehran, Iran 34469, Phone +98 21 88973631, Fax+98 21 88959740, cmi@ut.ac.ir

1 INTRODUCTION

Rapid development in concrete technology in line with advances in concrete additives has lead in the application of ultra high performance concrete in the field of construction materials. High strength concrete offers more options for the design of tall buildings and makes it possible to be used for long span beam and slab design. Although increasing mechanical properties of concrete such as compressive strength are useful and beneficial, but it reduces the ductility of such concrete which in turn reduces the safety of concrete structures against seismic loads [Tayyib1990].

Adding fibers into the concrete is an efficient method in increasing the ductility of concrete. The most famous of fibers used in the concrete are steel and polypropylene fibers. Thus application of fibers in UHPC is indispensable.

Numerous investigations have been carried out on the application and behavior of the fiber reinforced concrete. Research has been performed on the behavior of fiber reinforced concrete subjected to various load conditions, including flexural and tensile loadings [Khaloo 2005].

1.1 Steel Fibers

The addition of steel fibers significantly improves many of the engineering properties of mortar and concrete, notably impact strength and toughness. Tensile strength, flexural, failure strength and ability to spalling are also enhanced.

Moreover addition of fibers makes the concrete more homogeneous and isotropic material. When concrete cracks, the randomly oriented fiber arrested a micro cracking mechanism and limit crack propagation, thus improving strength and ductility [duzgun et al 2005].

Despite the mentioned advantage of steel fiber, steel fiber could not to be used in the concrete elements which placing in the sever conditions. Durability problems should be concerned when using steel fibers in concrete structures exposed to severe conditions. Constant maintenance and repairing is needed to enhance the life cycle of these structures [Sargaphuti et al 1993].

1.2 Propylene Fibers

Many investigations have performed on the mechanical properties of propylene fiber reinforced concrete.

The results showed that, the use of polypropylene fibers has successfully increased the toughness of concrete. Although polypropylene fibers are characterized by low elastic modules and poor physiochemical bonding with cement paste, it is quite apparent that the load carrying ability of a structure under flexural loading is considerably increased. On the hand, it may be used instead of steel fibers in severe exposure conditions.

Propylene fibers may improve thermal behavior of UHPC although it does not significantly modify the residual mechanical properties of UHPC.

Beside these investigations carried out on the mechanical properties of concrete, There are a few investigations on the durability properties of concrete containing polypropylene fibers. The ability of concrete to withstand the penetration of liquid and oxygen can be described as the durability of concrete [Mahoutian et al 2007].

In this paper, the effect of different percentages of P.P. fiber on durability properties of fiber reinforced concrete is investigated. The effect of fiber on the Water penetration, gas permeability, electrical resistivity and shrinkage of concrete is investigated in this study.

Results obtained from this study indicate that adding fibers into concrete does not significantly improve the durability parameters such as water penetration depth and oxygen permeability, while it reduces shrinkage of concrete.

2 EXPERIMENTAL PROGRAM

In order to investigate the effect of propylene fiber on the properties of fresh and hardened concrete, several mixes of different fiber contents and lengths were designed and tested.

Aggregates used in this experiment are derived from Metosak Company, Iran and are graded in accordance with ASTM C 33. Propylene fiber was provided from Bonyad Alyaf Propylene, Iran.

2.1 *Mix Proportions*

Mix proportions for concrete specimens are shown in Table 1. The water to cement ratio of 0.4 is kept constant for all mixes. Fibers of two different lengths are used in order to investigate the effect of fiber length on workability of fresh concrete. Superplasticizer is used in order to improve the workability.

Table 1. Mix proportions.

	Unit	P_0	P_1	P_2	P_3
Cement	Kg/m^3	350	350	350	350
Coarse Agg.		950	950	950	950
Fine Agg		1000	1000	1000	1000
Water		184	184	184	184
w/c		0.4	0.4	0.4	0.4
SP	Kg/m^3	4.72	4.72	4.72	4.72
Propylene fiber		0	0.9	0.9	3.6
Fiber length	mm	-	12	19	12
Fiber content	%		0.1	0.1	0.4

2.2 Laboratory Tests

To investigate different properties of fresh and hardened concrete containing propylene fibers, laboratory tests according to most well-known standards and recommendations were carried out.

3 FRESH CONCRETE TESTS

3.1 Slump Test

Slump test of fresh concrete is determined regarding ASTM C 143. Although this test is not recommended for Fiber reinforced concrete structures, but it can be used as investigate the effect of adding fibers on the workability of fresh concrete. For mixes containing fibers, the value of slump is determined before and after adding the fibers.

3.2 The Time of Flow Through Inverted Slump Cone

Workability and consistency of fiber-reinforced concrete is best measured by determining the time of flow of fiber-reinforced concrete through inverted slump cone according to ASTM C 995.

The inverted slump-cone time is a better indicator than slump of the appropriate level of workability for fiber reinforced concrete placed by vibration because such concrete can exhibit very low slump due to the presence of the fibers and still be easily consolidated.

Results of these two tests are shown in Tables 2.

3.3 Air Content of Fresh Concrete

Air content of freshly mixed concrete was determined using pressure method in accordance with ASTM C 231. Results are shown in Table 2.

Table 2. Air content, slump and time of flow.

	Units	P_0	P_1	P_2	P_3
Air Content	%	3.9	3.8	3.3	2.8
Slump before adding fibers	mm	90	90	100	105
Slump afteradding fibers	mm	-	25	18	3
Time of flow	sec	-	71	84	188

4 HARDENED CONCRETE TESTS

4.1 Compressive and Flexural Strengths

Compressive strength and flexural strength of concrete specimens of 28 days age according to ASTM C 39 and ASTM C 293 respectively. Results are shown in Table 3.

Table 3. Compressive strength and flexural strength.

	Unit	P_0	P_1	P_2	P_3
Compressive strength at 7 days		39.4	42.3	41.7	38.4
Compressive strength at 28 days	MPa	49	51.8	51.6	49.3
Flexural strength at 28 days		8.7	9.2	8.9	9.7

4.2 Flexural Toughness

Toughness is generally defined as energy absorption capacity of a cracked concrete specimen. Test method in this experiment is in accordance with ASTM C1018. The schematic illustration of the method and calculation is shown in Fig. 1. Toughness indices I5, I10 and I20 correspond to the area under load-deflection curve in steps of 3, 5.5 and 10.5 times of the first crack deflection. Regarding this standard, the indices are calculated as shown below:

$$I_5 = \frac{areaO' ACD}{areaO' AB} \quad , \quad I_{10} = \frac{areaO' ACEF}{areaO' AB} \quad , \quad I_{20} = \frac{areaO' ACEGH}{areaO' AB}$$

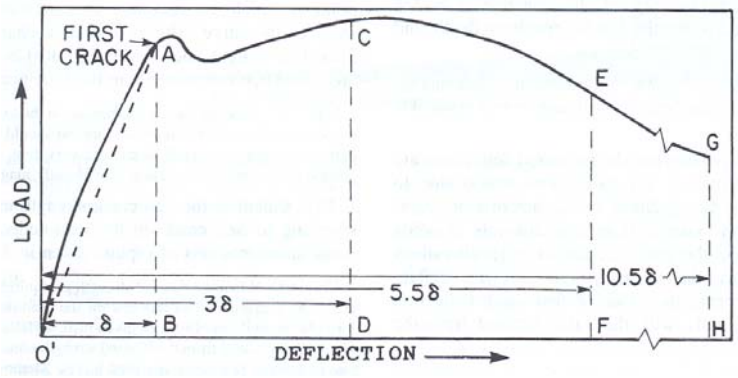

Figure 1. Load deflection curve for concrete specimens under flexural test.

Results obtained from the test are shown in Table 4.

Table 4. Flexural toughness of concrete.

	P_0	P_1	P_2	P_3
Flexural toughness`	0.73	1.22	2.31	2.53
Toughness index I5	-	1.29	1.28	1.25
Toughness index I10	-	-	1.52	1.47
Toughness index I20	-	-	-	1.68

5 DURABILITY TESTS OF HARDENED CONCRETE

5.1 Water Penetration Depth

Water permeability test and determining the depth of water penetrated into concrete is done according to DIN-1048 Part1. The test is carried out on cylindrical specimens of 30 cm height and 15 cm diameter at the age of 28 days. Specimens are kept at water pressure of 1, 3 and 7 atmosphere for duration of 48, 24 and 24 hours sequentially. Results are shown in Table 5.

5.2 Oxygen Gas Permeability Test

Permeability is a microstructure property of concrete which indicates the ability of concrete to bypass a fluid with specific viscosity under a pressure gradient [Bamforth 1987].

The permeability of porous environments is still governed by Darcy's law. Although it has its own limitations and is just valid if:

1- Considering the flow regime laminar.
2- The penetrating fluid should be neutral. There should be no physical or chemical reaction (absorption, capillarity) between the porous milieu and the fluid.
3- The fluid should be incompressible.

Permeability of concrete specimens against oxygen gas is determined in accordance with RILEM-TC116 recommendations. Cylindrical concrete specimens of 30 cm height and 15 cm diameter were tested at the age of 28 days. Results are shown in Table 4.

Table 5. Water permeability test and gas permeability of concrete specimens.

	Unit	P_0	P_1	P_2	P_3
Water penetration depth	mm	13.4	13.5	14.0	14.2
Gas Permeability coefficient * 10^{-17}	m^2	6.485	6.098	7.042	7.872

6 DRYING SHRINKAGE

Determining the shrinkage of specimens was done according to UNI-6555 recommendation. Specimens of 10*10*50 cm were casted in order to measure the shrinkage of concrete within 28 days after casting. Specimens are kept in laboratory condition of Temperature 20 ±1 C0 and the relative humidity of 50 ± 3%. Results are shown in Table 6.

Table 6. Drying shrinkage at the ages of1, 2, 3, 7, 14, 28 days.

	Length change – mm			
Age (days)	P_0	P_1	P_2	P_3
1	-2.92	-0.84	-0.84	-0.76
2	-3.52	-1.54	-1.86	-1.22
3	-3.94	-1.72	-2.48	-2.34
7	-4.66	-2.80	-3.74	-3.54
14	-7.54	-5.48	-5.72	-4.14
28	-8.78	-5.66	-5.88	-5.38

7 CONCLUSION

Results obtained from this study indicate that adding propylene fibers to concrete improves flexural toughness of concrete significantly; while it does not improve other mechanical properties such as compressive and flexural strength.

Adding propylene fibers into concrete has significantly reduced the drying shrinkage of concrete. Although it does not improve durability parameters such as water permeability or oxygen gas penetration into concrete.

ACKNOWLEDGMENTS

Authors should thank Bonyad Propylene Co. for providing fibers required for test preperation.

REFERENCES

Tayyib A., & ZahraNni M., “Corrosion of Steel Reinforcement in Polypropylene Fiber Reinforced Concrete Structures”; *ACI materials journa*l, 1990, P.P. 108-113.

Khaloo, A., & Afshari, M., 2005, ‘Flexural behaviour of small steel fiber reinforced concrete slabs’, cement and concrete composit, pp 141-149.

Duzgun, O, Gul, R., & Aydin, A., 2005, ‘Effect of steel fiber on the mechanical properties of natural lightweight aggregate concrete’, material letter, pp 3357-3363.

Sargaphuti, M., Shah, S. & Vinson, K., ‘ Shrinkage cracking and durability characteristics of cellous fiber reinforced concrete’, 1993, ACI Material Journal, vol 90.

Mahoutian, M., Libre, N., Shekarchi, M. & Moradi, F., 2007, 'durability properties of fiber reinforced lightweight aggregate concrete', IABSE, weimar, Germany.

Bamforth P.B., "The Relationship between Permeability Coefficients for Concrete Obtained Using Liquid and Gas"; *Magazine of Concrete Research*, 1987, vol. 39, P.P. 3-11.

The Use of Maturity Method in Estimating Early Concrete Strength

Amr E. Salama [1]
Gouda M. Ghanem [2]
Sayed Mohamed Abd El-bakey [3]
Esraa Emam Ali [4]

ABSTRACT

Prediction of the early age strength of concrete is essential for modernized concrete for construction as well as for manufacturing of structural parts. Safe and economic scheduling of such critical operations as form removal and reshoring, application of post-tensioning or other mechanical treatment, and in process transportation and rapid delivery of products all should be based upon a good grasp of the strength development of the concrete in use. This research work investigates the use of "*Maturity method*" in estimating the concrete strength and presents a brief review on the previous experimental and theoretical studies carried out on estimating maturity method. An experimental program is designed to estimate the concrete strength by using the maturity method .Where fourty eight concrete mixes are designed. Using available local materials, Ordinary Portland Cement was used with different contents (300, 350,400 and 450 kg/m^3) at curing temperatures (10,25 and 40ºC) and constant water to cement ratio= 0.45, the different mixes are examined woth respect to(compressive strength, indirect tensile strength, flexural strength and elastic modulus).

KEYWORDS

Maturity, Concrete strength, Concrete temperature, Curing temperatures.

[1] Prof. of Strength & properties of Materials, Chairman of Housing & Building National Research Center,Egypt, Cairo, Phone +202-3356722, Fax +202-3356853
[2] Prof. of Strength & properties of Materials Civil Engineering Department, Faculty of Engineering Helwan University,Egypt, Cairo, Phone +202-2416298, Fax +202-2416298
[3] Prof. of Strength & properties of Materials, Building Materials and Quailty Control Institute, Housing & Building National Research Center,Egypt, Cairo, Phone +202-3356722, Fax +202-3356853
[4] Assistant Lecturer , Building Materials and Quailty Control Institute, Housing & Building National Research Center,Egypt, Cairo, Phone +202-3356722, Fax +202-3356853

1 INTRODUCTION

For years, 28-days cube tests have been employed during construction in order to estimate the compressive strength of concrete, since it makes no allowance for the effects of placing, compaction, or curing. Nondestructive in-place test methods have been developed for estimating the compressive strength of concrete in structures. These tests are essential for realistic depiction of the in-place strength in concrete elements. One of the techniques for estimating the strength gain of in-place concrete is the maturity method. This technique is based upon the measured temperature history of concrete during the curing period. The combined effects of time and temperature lead to a single parameter termed "maturity". McIntosh [1], was probably the first to develop a parameter in 1949, which called "basic age", to combine the influence of temperature and time. The basic age was calculated as the multiple of time and temperature above minus 1.1ºC. Numerous maturity functions since the early 1950. Saul [2], proposed the following relation to compute the maturity of concrete.

$$M(t,T) = \sum (T - T_O)\Delta t \tag{1}$$

Where;

M (t, T) = Maturity of concrete as a function of time (t) and temperature (T)
T = Temperature of concrete
To = Datum temperature, and
Δ t = time interval

A model based on the Arrhenius function for thermal activation is widely used in some European countries and also in North America [3].

$$M(t,T) = \int_0^t K.EXP\left(\frac{-E}{RT_k}\right)dt \tag{2}$$

Where;

K = Constant
T_K = Temperature of concrete in degrees Kelvin
E = Activation energy in kilo joules per mol, and
R = Universal gas constant.

Rastrup .[4] presented a time-temperature function of the form:

$$t_1 = 2^{\frac{(T + T_r)}{10}} t_2 \tag{3}$$

Where;

t_1 = Curing time at the temperature Tr
t_2 = The curing time at the temperature T, and
Tr= The reference temperature

The function proposed by Rastrup is based on a well-known physicochemical rule, which states the speed of reaction is doubled when the temperature is increased by 10 ºC.

Nurse [5], used the multiple of the time and temperature above 0 ºC as a parameter to combine the effects of curing history. In this investigation, prism specimens were subjected to steam curing at atmospheric pressure and were tested for strength properties including compressive strength using various types of aggregates and cement.

In 1956, Plowman [6], attempted to develop a relationship between concrete strength and maturity. He used cube specimens that were initially subjected to normal curing for 24 hours prior to being cured at various curing temperatures.

In this study, concrete mixes are designed. Using Ordinary Portland Cement with different contents at curing temperatures (10,25 and 40 ^{o}C) and constant water to cement ratio= 0.45, the different mixes are tested (compressive strength, indirect tensile strength, flexural strength and elastic modulus) with the maturity index [7].

2 EXPERIMENTAL PROGRAMME

The experimental programme includes selection of materials, preparation of mixtures, and testing of specimens.

2.1 Selection of Material

The used cement was CEM I 42.5N according to Egyptian Standard Specification 4756/2005, crushed limestone coarse aggregate according to Egyptian Standard Specification 1109/2001 with maximum nominal size of 14 mm, and sand fine aggregate according to Egyptian Standard Specification 1109/2001, silica fume and fly ash from Mcc. company are also used.

2.2 Perpartation of Mixes

The following Table (1) shows the different concrete mixes used in the experimental programme.

Table 1. Concrete mixes proportions.

Mix no.	Cement content (Kg/m^3)	Coarse agg. (Kg/m^3)	Fine agg. (Kg/m^3)	W/C ratio	Silica Fume (Kg)	Fly Ash (Kg)
1	300	1280	640	0.45	-	-
2	350	1220	610	0.45	-	-
3	400	1154	577	0.45	-	-
4	450	1090	545	0.45	-	-
5	350	1306	653	0.35	35	35

Mixing was done in a standard drum-type mixer. Coarse and fine aggregates were first mixed in dry state until the mixture became homogenous.

For each mix twelve cubes were prepared (15*15*15 cm) for testing compressive strength at (1,3,7 and 28 days) for each degree of temperature (10, 25 and 40°C), also three cylinders (15*30 cm) for splitting tension test, three cylinders (15*30 cm) for determining the modules of elasticity and three beams (10*10*70 cm) for determining the flexural strength of concrete for cement content (350 Kg/m3) at temperature 25°C. During each age of testing the concrete temperature was measured by using a device to monitor and record the concrete temperature at each curing temperature (10, 25 and 40°C) where thermocouples sensors installed at critical location in the specimens.

Figure 1. A device to Monitor and Record Concrete Temperatures.

Figure 2. Thermocouples Sensors Installed in Specimens.

2.3 Determination of Datum Temperature

The testing required to experimentally determine the datum temperature can be performed using mortar specimens, the basic approach is to establish the compressive strength versus age relationships for mortar specimens cured in water baths maintained at three different temperatures.

Two baths should be at the maximum and minimum concrete temperatures expected for the in place concrete during the period when the strengths are to be estimated. The third water bath temperature should be midway between the extremes. (10, 25 and 40 °C).

After knowing the final setting times at the three temperatures, prepare a graph with the reciprocal of strength as the y-axis and reciprocal of age as the x-axis then determine the slope and the intercept of the best-fitting straight line through the data for each curing temperature.

For each straight line divide the value of the intercept by the value of the slope resulting in the k-values which are used to calculate the datum temperature.

Fourty eight mixes were carried out to achieve the strength-maturity relationship at three different curing temperatures (10, 25 and 40 °C).

3 RESULTS AND DISCUSSIONS

Table 2. The Compressive Strength Test Results for Cement Content 350 kg/m^3.

Ages (Days)	Ambient Temp.˚C	Measured Temp.˚C	K-Values 1/Day	Datum Temp.˚C	Strength kg/cm^2	Maturity Index (˚C.Day)
1	10	11.8	0.77	2.7	136.5	9.1
	25	24.7	1.18		183.3	22
	40	42	2.98		189.6	39.3
3	10	10.2	0.77	2.7	188.6	22.5
	25	24.5	1.18		211.1	65.4
	40	40.8	2.98		302.1	114.3
7	10	10.5	0.77	2.7	244.4	54.6
	25	24.2	1.18		250.4	150.5
	40	40.2	2.98		410.2	262.5
28	10	10.4	0.77	2.7	308.2	215.6
	25	24	1.18		325.6	596.4
	40	40.3	2.98		389.2	1052.8

Table 3. The Compressive Strength Test Results for Cement Content 450 kg/m^3.

Ages (Days)	Ambient Temp.˚C	Measured Temp.˚C	K-Values 1/Day	Datum Temp.˚C	Strength kg/cm^2	Maturity Index (˚C.Day)
1	10	12.5	0.33	3.2	199.4	9.3
	25	25.8	1.03		198.6	22.6
	40	43.2	1.77		212.2	40
3	10	12.5	0.33	3.2	236.5	27.4
	25	24.6	1.03		214.2	64.2
	40	41.8	1.77		325.1	115.8
7	10	11	0.33	3.2	314.6	54.6
	25	25.1	1.03		345.2	153.3
	40	40.9	1.77		436.5	263.9
28	10	10.2	0.33	3.2	412.5	196
	25	25.1	1.03		448.2	613.2
	40	40.1	1.77		388.5	1033.2

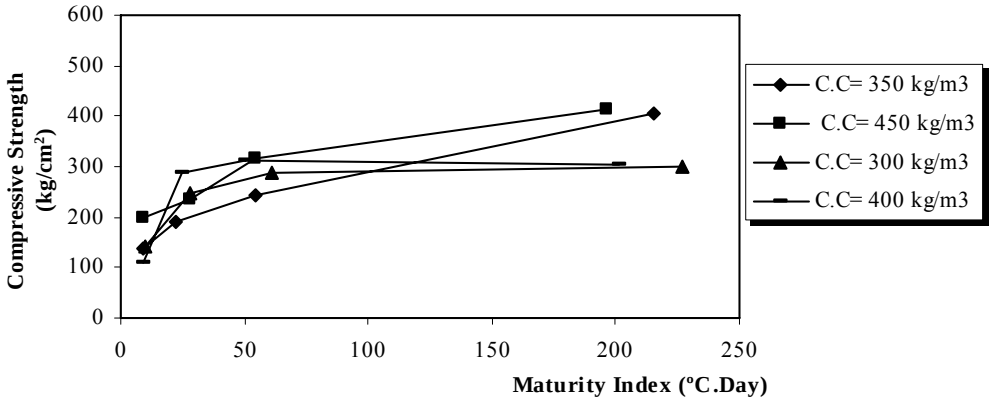

Fig(3-a) Strength- Maturity Relationship at 10°C

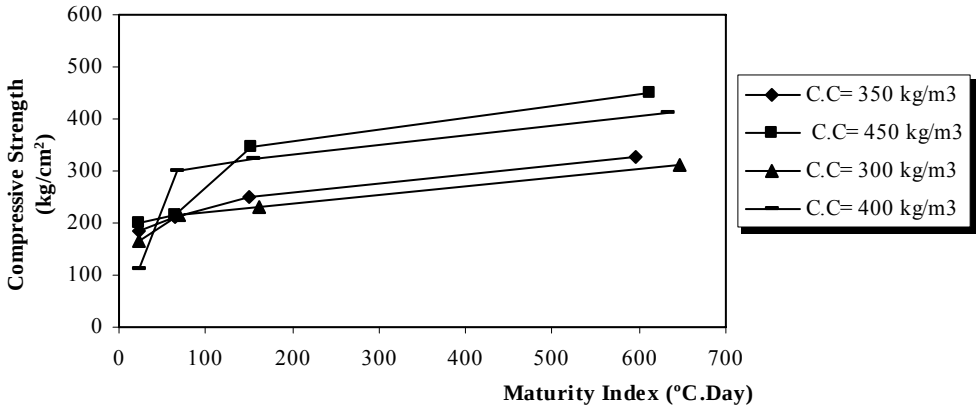

Fig(3-b) Strength-Maturity Relationship at 25°C

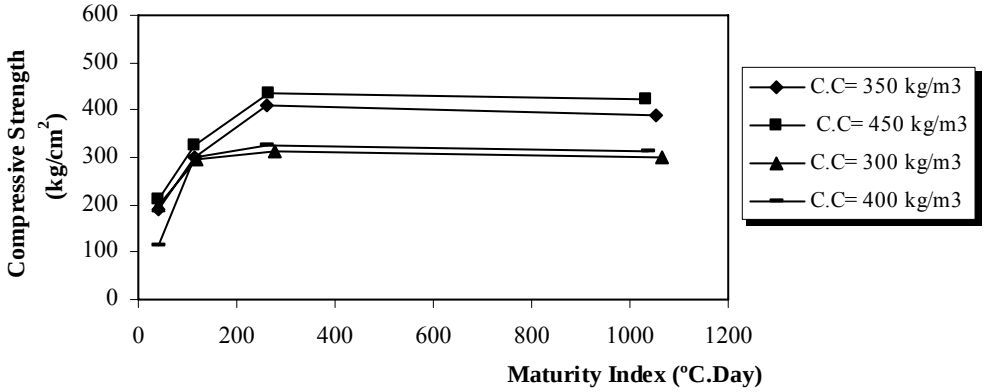

Fig(3-c) Strength-Maturity Relationship at 40°C

4EFFECT OF DIFFERENT CEMENT CONTENTS ON STRENGTH-MATURITY RELATIONSHIP.

The strength-maturity relationship for cement contents (350,450,300,400 kg/m^3) and constant w/c=0.45 are as shown in Fig 3 (a ,b and c) and Tables (2 and 3) respectively.

The rate of strength gained is increases at the first 7 days while the rate slow at later ages up 28 days. At mixes which have 0% silica fume and 0% admixtures, at 10°C, the rate of strength gain is smaller compared to the other two degrees of temperatures (25 and 40°C), where for the same mix the 28 days concrete strength at 10°C is more or less equals to the 7 days concrete strength at 40°C, while the slope equals 1.2,1.05,0.48 and 0.53 , (the ratio between the strength and maturity index) for cement contents (350,450,300 and 400 kg/m^3) respectively, it can be seen that cement content 350 kg/m^3 shows the higher slope, while at 25°C and 40°C were (0.22,0.40,0.2 and 0.34) and (0.13,0.14,0.052and 0.10) for cement contents (350,450,300 and 400 kg/m^3) respectively, it can be seen that cement content 450 kg/m^3 shows an increase than the other cement contents.

At 25°C, the strength shows a higher value compared with two degree of temperatures (10 and 40°C) by (8%,8.6%,15% and 10%) and (8%,15.5%,15% and 13.2%), for cement contents (350,450,300 and 400 kg/m^3) respectively.

At 40°C, the rate of strength gain is increased at the first 7 days then decreased at later ages. This is due to the increase of rate of hydration of cement at early ages at higher temperatures which creates a porous concrete matrix hence leading to decrease the compressive strength at later ages.

For maturity index, it increases with an average (1.5 to 5.5 times) as temperature increases from 10 to 40°C for all cement contents.

Table 4. The Splitting tensile Strength Test Results for Cement Content 350 kg/m^3.

Mix Code	Ambient Temp.˚C	Measured Temp.˚C	Datum Temp.˚C	Strength kg/cm^2	Maturity Index (˚C.Day)
0% SP,0%SF,0%FA	25	26.9	2.7	15.4	24.2
	25	26.3		20.3	70.8
	25	25.9		27.2	162.4
	25	24.3		31.8	604.8
10%SF,10%FA	25	27.9	-12	15.8	39.9
	25	27.4		18.6	118.2
	25	26.9		30.2	272.3
	25	25.5		43.5	1050

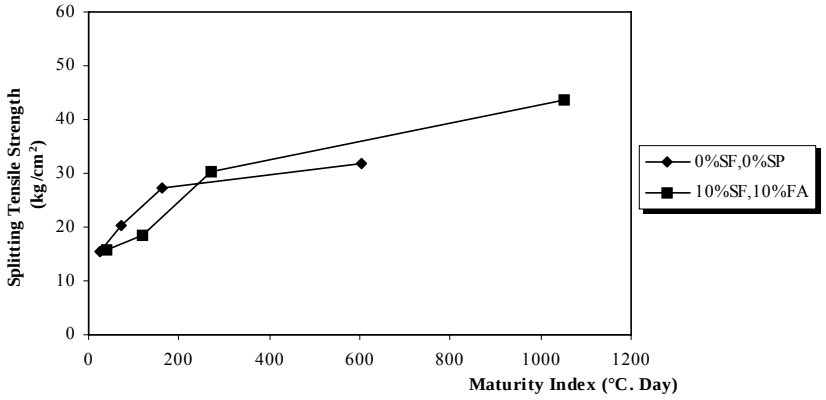

(c) Splitting Tensile Strength-Maturity Relationship for C.C=350 kg/m^3 at 25 °C for W/C=0.45

Table 5. The Flexural tensile Strength Test Results for Cement Content 350 kg/m^3.

Mix Code	Ambient Temp.˚C	Measured Temp.˚C	Datum Temp.˚C	Strength kg/cm^2	Maturity Index (˚C.Day)
0% SP,0%SF,0%FA	25	26.4	2.7	37.8	23.7
	25	25.9		99.75	69.6
	25	25.7		112.35	161
	25	25.3		136.5	632.8
10%SF,10%FA	25	27.4	-12	57.75	39.4
	25	26.9		140.7	116.7
	25	26.5		155.4	269.5
	25	25.8		162.75	1058.4

The splitting strength-maturity relationship Table (4), for cement content 350 kg/m^{3}at temperature 25°C at w/c=0.45 the mix which have 10% silica fume and 10% fly ash shows an increase in strength 37%, while the maturity index increase by 74% from the mix which have no silica fume and fly ash.

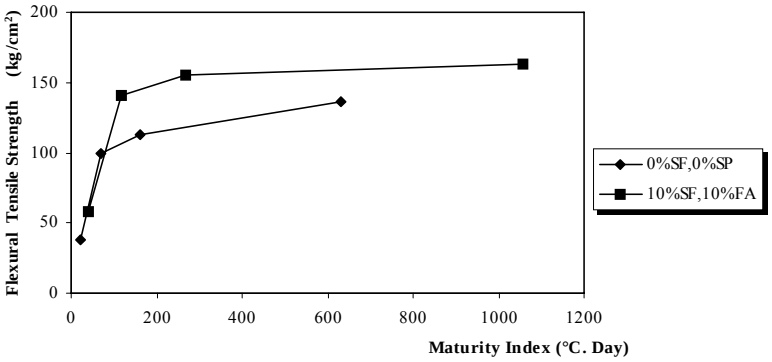

(c) Flexural Tensile Strength-Maturity Relationship for C.C=350 kg/m^3 at 25 °C for W/C=0.45

Table 6. The Static Modulus of Elasticity Test Results for Cement Content 350 kg/m^3

Mix Code	Ambient Temp. ˚C	Measured Temp. ˚C	Datum Temp. ˚C	Youngs Modulus (kg/cm^2)	Maturity Index (˚C.Day)
0% SP,0%SF,0%FA	25	25.2	2.7	152	630
10%SF,10%FA	25	25.8	-12	284.7	1058.4

The flexural strength-maturity relationship Table (5), for cement content 350 kg/m^{3}at temperature 25°C at w/c=0.45 the mix which have 10% silica fume and 10% fly ash shows an increase in strength 19%, while the maturity index increase by 67% from the mix which have no silica fume and fly ash.

At w/c=0.45, mix which have 10% SF and 10% FA Table (6), shows an increase in Young's modulus and maturity index (87%, 68%) compared with mixes which have no silica fume or fly-ash respectively.

5 CONCLUSTION

1-The maturity concept can be used to predict strength of concrete at early ages, provided that the actual concrete temperature which used in estimating maturities during the early part of hydration of cement.

2- Compressive, splitting, and flexural strength development of concrete are related to mixture proportioning and curing temperature history.

3- The maturity index increases (1.5- 6 times) as temperature increase from 10 to 40°C depending on the mix proportions.

4- Curing temperature 25°C shows an increase in strength and maturity index for all cement contents (300, 350, 400 and 450 kg/m^3) respectively, while at 40°C at the first 7 days shows a higher increase in strength as the rate of hydration of cement increases hence the strength decrease at later ages.

5- W/C=0.45 shows an increase in strength and maturity index for all cement contents (300,350,400 and 450 kg/m^3) respectively.
6- Critical construction operations should not be initiated on the basis maturity index values and the strength-maturity relationship without further verification that the in place concrete has the expected strength potential.

ACKNOWLEDGMENT

The experimental work was carried out at Housing and Building National Research Centre Laboratories. The great help of the laboratory technical staff is highly appreciated.

REFERENCES

McIntosh, J.D., 1949, " Electric Curing of Concrete " Magazine of concrete research, Vol. 1, No. 1, January, pp. 21-28.

Saul,A.G.A., 1951, "Principles Underlying of The Steam Curing of Concrete at Atmospheric pressure", Magazine of concrete research, Vol. 2, No. 6, March, pp. 127-140.

Naik, T.R., 1983, "Maturity Functions For Concrete Cured During Winter Conditions", ASTM STP 858, Philadelphia, pp. 107-117.

Rastrup, E., 1954, "Heat of Hydration of Concrete", Magazine of concrete research, Vol. 6, No. 17, January, pp. 79-92.

Nurse, R.W., "Steam Curing of Concrete", Magazine of concrete research, Vol. 1, No. 2, January 1949, pp. 79-88.

Plowman, J.M., 1956, "Maturity and The Strength of Concrete", Magazine of concrete research, Vol. 8, No. 22, March, pp. 13-22.

Esraa, E. A., 2005, "The Use of Maturity in Estimating Concrete Strength" M.Sc. Thesis, Faculty of Engineering, Helwan University, Egypt.

11DBMC International Conference on Durability of Building Materials and Components
ISTANBUL, Turkey 11-14 May 2008

Concrete for Durability at Marmaray Project

Serap Erdoğdu [1]
Steen Lykke [2]

T 11

ABSTRACT

The aim of this paper is to present information about the study performed during the construction work of Marmaray Project to obtain the target of 100 years service life of RC concrete structures.

The Marmaray Project in İstanbul includes part of the upgrading of the 76 km commuter rail from Halkalı, in the European end, to Gebze, in the Asian end. This line includes 1.4 km of immersed tunnel, 10.1 km of bored tunnels, 1.3 km of cut and cover tunnel and four underground stations.

Serviceability is influenced from various effects such as cracking, deformation, vibration, durability, water tightness and fatigue. Durability is one of the parameters of serviceability of the structure and therefore during the design stage all parameters were evaluated together in order to check compliance with the service life time requirement which was targeted for the overall project.

In the Project, concrete classes were determined according to the design requirements of typical structures. The composition of the mixture was optimized by pre-testings and trials to resist the relevant exposure conditions that impact concrete's durability. This means appropriate cementitious materials for sulfate ressistance, air void system for freezing and thawing and scaling resistance, adequate protection to prevent corrosion either from carbonation, chloride ingress or depth of cover a low paste content to minimize the drying shrinkage and thermal cracking, and the appropriate combination of aggregates and cementitious materials to minimize the potential for expansive cracking related to alkali silica reactivity.

Methods to be applied during construction for ensuring durability requirements is another step of the studies which are; proper quality control system for constituent materials, hardening and hardened concrete besides curing of concrete and finally adequate repair method.

[1] Chamber of Geology Engineers, Avrasyaconsult, Istanbul, Turkey, 34716, Phone +90 216 3495997, Fax 216 3495009.
[2] Institution of Engineers, Denmark (M.C.I.F), Danish society for Structural Engineering, Danish Academy of Technical Sciences Association of Consulting Engineers, Denmark Danish Concrete Association, Chairman of the Board.

1 INTRODUCTION

The durability of concrete is one of its most important properties because it is essential that concrete should be capable of withstanding the conditions for which it has been designed throughout the life of a structure. Lack of durability can be caused by external agents arising from the environment or by internal agents within the concrete. Causes can be categorized as physical, mechanical and chemical. Physical causes arise from the action of frost and from differences between the thermal properties of aggregate and of the cement paste, while mechanical causes are associated mainly with abrasion and physical load conditions. Chemical causes are attacks by sulphates, acids, sea water and also by chlorides which include electrochemical corrosion of steel reinforcement.

Durability studies for Bored Tunnels (TBM) and Immerse Tube Tunnel (IMT) which are the major structures of the project will be presented here.

For the bored tunnel, durability was analyzed for the carbonation of concrete and the attack of chloride ion in consideration of the design life of 100 years. As a result, it was confirmed that the carbonation is no problem if the cover is 25 mm or above. However, for the attack of chloride ion it was decided to ensure a cover of 70 mm in all structures potentially exposed to salin water (the Bosphorus Strait). The concrete cover of 70 mm is decided according to the actual measurement value of chloride ion. The result show that chloride ion content in water is extremely small, thus the influence on the tunnel lining is considered to be small. Therefore a concrete cover of 70 mm is used from the strait part to the above mentioned boringhole location. The typical cross section of the Bored and Immerse Tunnel is shown in Figure 1.

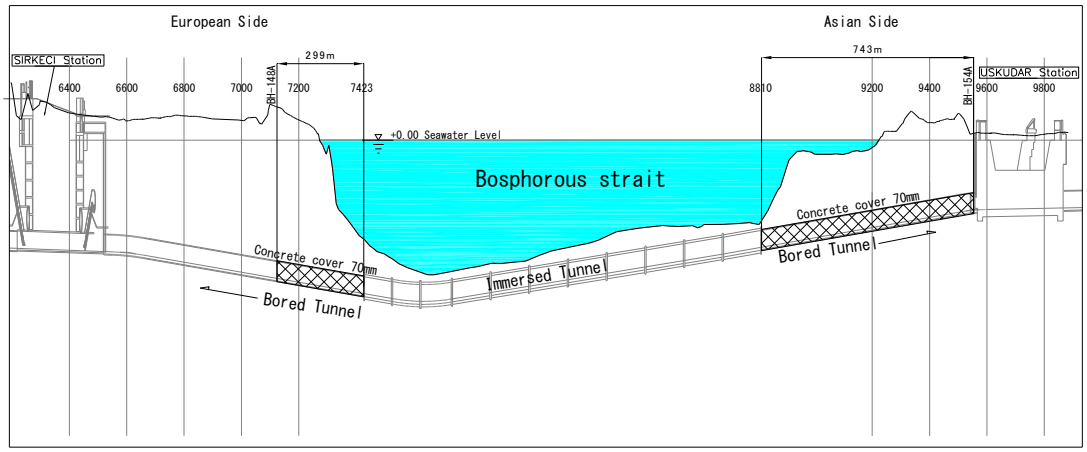

Figure 1. The range in which the concrete cover is 70 mm.

For the Immersed Tunnel (IMM), reinforced structure is enclosed in a steel membrane and waterproofing sheet and isolated from the aggresive environment.

According to British Standard BS 6349 for Maritime Structures, the condition of exposure for the immersed tunnel can be classified as frequently wetted condition, designated as XC2, with the structure totally submerged in seawater at all time. For this exposure condition, the nominal cover required by standard is 50 mm. Although there is an isolation of concrete with a layer of steel membrane and waterproofing sheet, 70 mm minimum cover is appropriate for severe environmental exposure conditions in case the external face of the member should have the waterproofing membrane fail and exposes the concrete structure to seawater seepage. Additionally, steel membrane is protected against corrosion by cathodic protection. Figure 2 shows that the thypical section of Immerse Element.

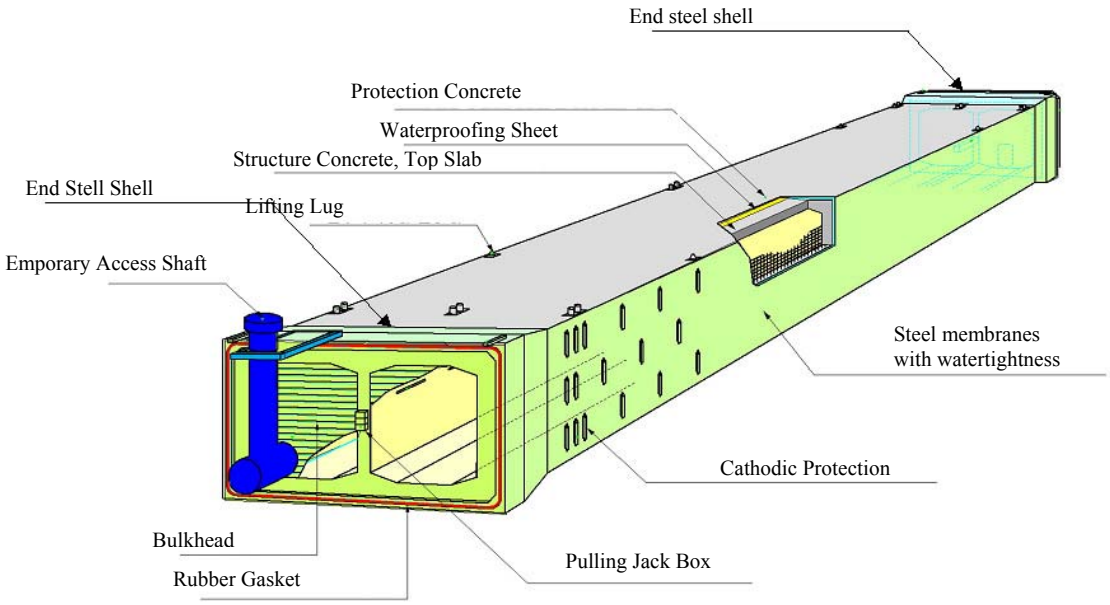

Figure 2. Typical Section View of Immersed Element.

2 DESIGN OF CONCRETE

2.1 Concrete Mix Design

For ensuring durability of concrete, mix design has been optimized according to the following limits;

- Maximum free water/cement ratio : 0.4
- Minimum cement content : 375 kg/m^3
- Minimum strength class : C40
- Minimum nominal cover : 70 mm (external faces), 32 mm (internal faces)
- Maximum crack widths : 0.2 mm (except early-age cracking)

The main characteristics of the mix determined by considering the limitation mentioned above used in the project are;

- High characteristic cylinder compressive strength (fck : 40-50 MPa)
- Low water/cement ratio (Between 0,30 to 0,40)
- Well graded aggregate
- Admixture for water reducer
- Air-entraining admixture
- Supplementary cementitious materials (Fly ash and Micro Silica)

2.2 Pre-testing of Concrete

A comprehensive pre-test programme was developed and executed. A part of the pre-testing was full scale trial casting (FSTC) executed under realistic circumstances. FSTC was not allowed to start until the pre-testing of the concrete mix was completed and should be done using the proposed construction methods and equipment performed by operators and staff whould be involved in the execution of the concreting works.

Following tests were conducted during pre-testings and also production;

2.2.1 Constituent Materials

All tests of constituent materails (Cement , Aggregates (Fine & Coarse), Sand, Fly-Ash, Micro -Silica, Admixtures and Water) according to related standards were realized and certified as Inspection Section.

2.2.2. Fresh Concrete Tests

Workability, Density, Temperature, Air-content

2.2.3 Hardening Concrete Tests

Activation Energy, Compressive Strength Tets, Tensile Strength Test, Modulus of Elasticity, Adiabatic Heat, Early-age Shrinkage, Strains due to Creep, Thermal Expansion, Maximum Temperature.

2.2.4. Hardened Concrete Tests

Compressive Strength, Density, Air Content, Chloride Diffusion, Petrographic Testing (Thin & Plane Section)

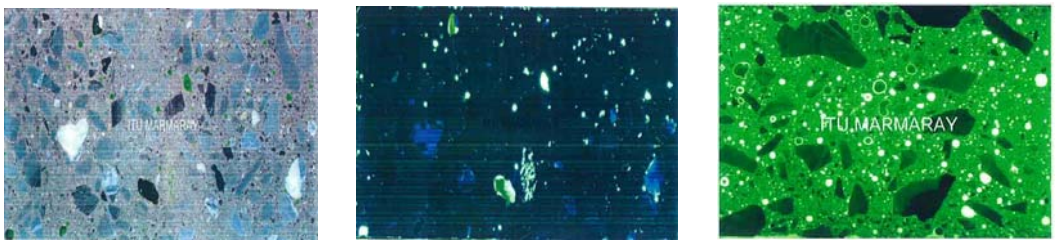

Figure 3. Polished impragneted plane section and thin section analysis.

Concrete Petrography Laboratory which is a part of İTÜ Marmarmaray Laboratory is the first in Turkey. At this laboratory concrete characteristichs are investigated closely during the production. Figure 3 is showing the image of polished impragnated plane and thin section.

3 CRACK CONTROL

Crack control studies of concrete comprises evaporation protection, early age crack control and frost resistance.

3.1 Evaporation Protection

All surfaces of the newly cast concrete is protected against evaporation. The protection is established after completion of compaction and surface treatment is applied to prevent cracking due to plastic shrinkage. The protection against evaporation is maintained until a minimum degree of hydration of 90% has been reached at the concrete surface, except for internal formed surfaces in tunnel items where the requirement for 90% degree of hydration may be replaced by a requirement to reach 96 maturity hours.The degree of hydration in the concrete surface is determined from measurements of the temperature at a depth of a maximum 10 mm, except for construction joints where a maximum depth of 20 mm is allowed. For concrete surfaces cast against formwork, an accaptable evaporation protection to leave the formwork in place.

3.2 Early-Age Crack Control

For hardening concrete structures, early-age cracks may be caused by reastraint to deformations due to combinations of thermal movements, early shrinkage, creep and settlements. Theoratical crack risk must not exceed 0.7. In the project early age cracking is generally not allowed.

For each type of structural element and all water-retaining structures planned risk of early-age cracking are determined through temperature and stress analysis (Figure 4). If cracking occurs, craks are injected in case they exceed the design crack widths.

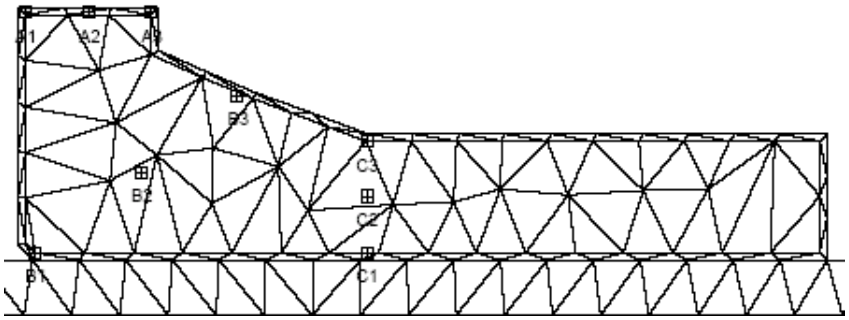

Figure 4. Temperature and Stress Simulation Model.

1) Temperature simulation is based on all relevant input data such as;
- the model (geometry, element mesh and boundary conditions),
- the maturity function for the concrete,
- the documented values for the adiabatic heat development, the content of powder in the concrete,
- the thermal conductivity of the concrete,
- the specific heat of the concrete,
- the concrete density, the fresh concrete temperature,
- the ambient temperature and wind velocity, the temperature, thermal conductivity, specific heat and density of surrounding materials,
- the documented values for the thickness and thermal conductivity of formwork and insulating materials,
- the design and control of arrangements for temperature control,
- the control of curing activities,
- casting sequence.

2) The output from the temperature simulation comprise information such as;
- temperature graphs showing the development of the mean temperatures of the structural elements (figure 5),
- graphs showing the development of the mean temperature of the newly cast items and the mean temperature of previously cast items (Dext),
- graphs showing the temperature difference between the mean temperature of newly cast items and the surface temperature of the newly cast items (Dint),
- graphs showing the maximum temperature in the concrete.

3) Stress simulation is performed using a well-documented computer program based on the Finite Element Method. Stress simulation shall be based on documented values for the thermal expansion coefficient, the E-modulus, the early-age shrinkage and the creep for the actual concrete. Stress simulation is based on all relevant input data such as;
- the model (geometry, element mesh and boundary conditions/restraint)
- the simulated temperatures,
- the documented value for the thermal expansion coefficient,
- the documented value for the thermal expansion coefficient,
- Poission's ratio
- The documented development of the early-age shrinkage,
- The documented development of the parameters that describe the development of strains due to creep.

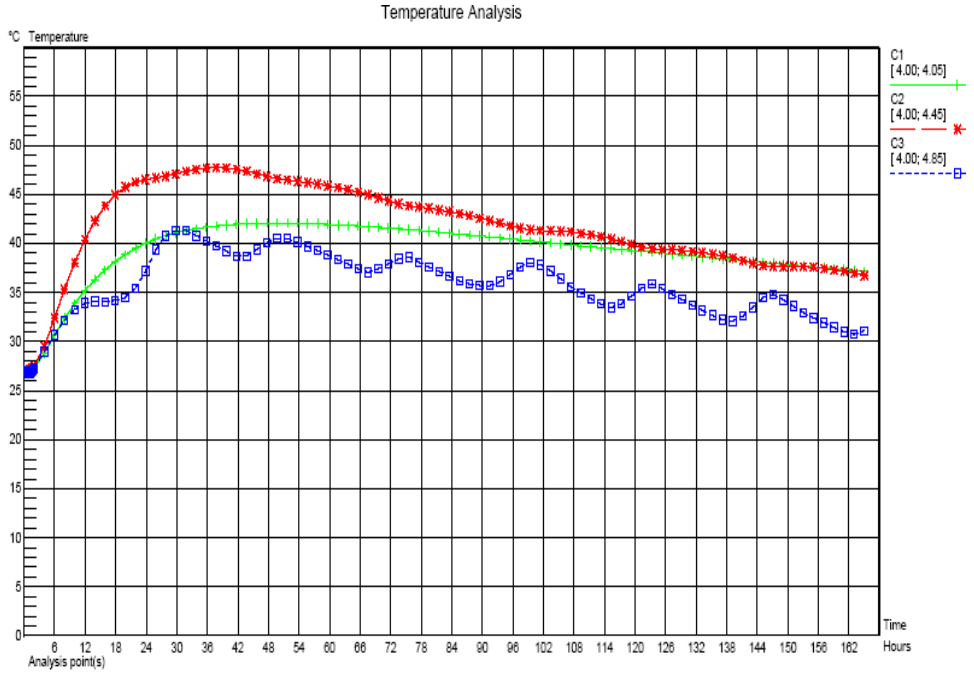

Figure 5. Temperature simulation model.

4) The output from stress simulation shall comprise information such as,
   - a general presentation of the stress level in the structure (iso-curves)
   - the development of the principal tensile stresses in selected points
   - the development of the risk of cracking (P) shall at any time be defined as:

5) The risk of cracking (P) is at any time be defined as:
   P= maximum principal tensile stress / the axial tensile strength
   The maximum crack risk simulation is shown in figure 6.

6) The axial tensile strength of the concrete ($f_{ct,ax}$) is determined from the splitting tensile strength ($f_{ct,sp}$) according to:

$$f_{ct,ax} = 0.9 \times f_{ct,sp}$$

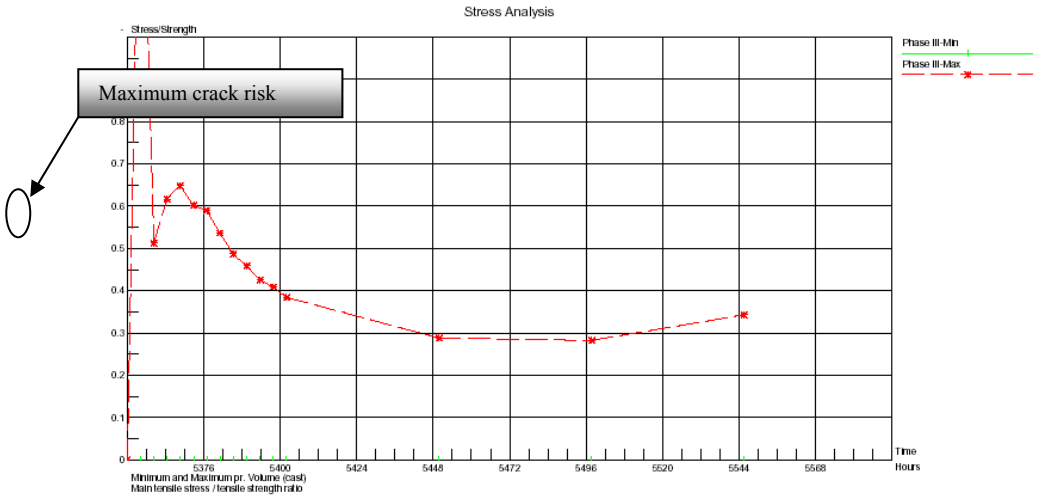

Figure 6. Crack risk simulation.

7) The risk of cracking must comply with the requirements given in Table 1.

Table 1. Overview of Parameters Reletad to Early-Age Cracking.

Location/Structure	Max. W (mm)	Max P	Max D_{ext} (^oC)	Max ΔT_{inc} (^oC)
Tunnels				
- water-retaining parts	0,2	0,70	15	8
- other parts		1,00	20	12
Ramps and C&C				
- water- retaining parts	0.2	0.70	15	8
- other parts		1.00	20	12
Stations				
- water- retaining parts	0.2	0.70	15	8
- other parts		1.00	20	12

8) Based on stress analysis, limiting temperature differences for each structural element are established corresponding to the following two limits;

(a) For structural items that are restrained by neighbouring elements, a maximum temperature difference between the mean temperature of the newly cast element and the mean temperature of previously cast items (D_{ext}) should be defined. The maximum allowable temperature difference during hardening should comply with the requirements given in table 1, regardless of the result of the stress simulation.

(b) For all structural elements, a maximum temperature difference between the mean temperature of the element and the temperature of the element (D_{int}) should be defined. The maximum allowable temperature difference during hardening shall be less than 15 ^oC regardless of the stress simulation.

9) The maximum temperature of the concrete is 50 ^oC in the central part of bottom slabs. If higher than 50 ^oC special consideration of Deleyaed Ettringite Formation (DEF) must be given.

10) A graphical comparison to the requirements is possible. Graphs showing the temperature developments is available on site for execution of the temperature control and other actions related to the temperature and maturity development, e.g. stripping of formwork.

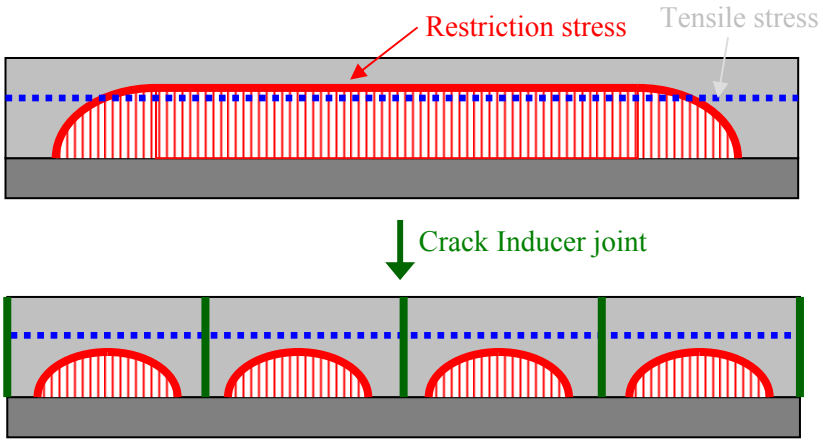

Figure 7. Effect of crack inducer joint.

In the project, temperature and Stress Simulation program is being effectively used in order to determine the casting method. As shown in figure 7, location of crack inducer joints are determined according to the outputs getting from T&S Analysis.

3. 3 Frost Resistance

The concrete is protected against freezing until frost resistance is obtained. Frost resistance is considered obtained when the concrete has reached a compresive strength of 10 Mpa.

In order to provide resistance to the damaging mechanism resulting from freezing is achieved through the use of air-entraining admixtures that stabilize and help distrubute air bubbles within the concrete.

4 CONCLUSION

In conclusion, sub-aqueous tunnels are subject to extraordinary conditions with regard to outside pressure and chemical aggresivity. Therefore, special measures with regard to avoiding or delaying the development of concrete deteriotion and reinforcement corrosion needs to be considered. In this paper, studies regarding the concrete durability have been presented to obtain the target of 100 years of service life of the structures in Marmaray Project.

REFERENCES

ACI COMMITTEE 201.2R-92 Guide to durable concrete, Part 1: Materials and General Properties of Concrete, *ACI Manual of Concrete Practice,1994*.

ACI COMMİTTEE 318-89 Building Code requirements for reinforced concrete, Part3: Use of Concrete in Buildings-Design, Specification and Related Topics, *ACI Manual of Concrete Pracyice,1994.*

ACI COMMITTEE Guide to durable concrete, Part1, *ACI Manual of Concrete Practice, 1994.*

BS 6349 Maritime Structures part 1: Code of practice for general criteria.

A.M. NEVILLE, Corrosion of Reinforcement, Concrete, pp 48-50 (London, June 1983).

A.M. NEVILLE Concrete Technology, (1999)

ERQ (Employer's Requirement) for the Marmaray Project.

11DBMC International Conference on Durability of Building Materials and Components
ISTANBUL, Turkey 11-14 May 2008

Rebound and Composition of in-Situ Polypropylene Fibre-Reinforced Shotcrete

Atef Badr [1]
Jeff Brooks [2]

T 11

ABSTRACT

This paper presents the results of an experimental investigation into the rebound of polypropylene fibre reinforced shotcrete (PPFRSC). The effects of polypropylene fibre (PPF), fly ash (FA) and silica fume (SF) on the total rebound material and the composition of the in-situ shotcrete were investigated.

Six mixes were sprayed of which four mixes were initially optimised and investigated by laboratory tests. The remaining two mixes were commercially pre-packed shotcrete mixes. The total material rebound was measured and the factors affecting it were analysed. Samples were taken from the rebound and the freshly placed shotcrete for composition analysis.

About 80 % of the initial PPF dosage did not reach the mould and dropped in the area between the nozzle and the target surface. In general, the total rebound material was combined aggregate, of which the coarse aggregate represented about 60 to 75 %. Consequently, the presence of PPF had no effect on the total rebound material, whereas the coarse aggregate content, experience of nozzleman and binder type had noticeable influences. Mixes without coarse aggregate showed the least rebound. Fly ash was effective in reducing the total material rebound, particularly in the presence of silica fume. A reduction of 35 % and 55 % was observed for mixtures containing FA in the absence or presence of SF, respectively.

The composition of the in-situ shotcrete was significantly different from the proportions of the batched constituents. The in-situ shotcrete had much higher binder content and lower coarse aggregate content. The internal layer of the in-situ shotcrete was affected by the rebound more than the external layer.

KEYWORDS

Shotcrete, Rebound, Fly ash, Silica Fume, Polypropylene fibre

[1] University of Bolton, School of BE & Engineering, BL3 5AB, UK, Phone +44 1204 903840, a.badr@bolton.ac.uk
[2] University of Leeds, School of Civil Engineering, Leeds, LS2 9JT, UK, jj.brooks@ntlworld.com

1 INTRODUCTION

Fibres offer many advantages over traditional mesh reinforcement in shotcrete as they provide considerable benefits to all end-users including designers, contractors and owners. The most common fibres that are added to shotcrete are mainly steel fibres [Adams 1993; Cengiz and Turanli 2004]. However, using steel fibres has some disadvantages such as, hose wear and high cost. Polypropylene fibres (PPF), in contrast, do not have these adverse effects. Polypropylene fibre reinforced concrete (PPFRC) has an impact resistance and flexural toughness that compare favourably with those observed in concrete made with many other commercial fibres utilised at higher dosage rates [Malhotra *et al.* 1994]. The properties of PPFRC have been extensively researched [Badr *et al.* 2001; Bayasi and Zeng 1993; Zellers and Ramakrishnan 1994; Song *et al.* 2005; Badr *et al.* 2006; Sivakumar and Santhanam 2007]. However, there is very little information about using PPF in shotcrete. In particular, there is almost no information about the rebound of PPF and its effect on the total material rebound and, consequently, the composition of the in-situ shotcrete.

The process of applying shotcrete generally ensures that most of the aggregates and cementitious materials combine to form a mixture, which adheres well to the substrate. Unfortunately, considerable amounts miss the target or do not adhere to the substrate [Wood *et al.* 1993]. Rebound, which is the material that strikes the surface but does not adhere to it, is the most important and significant proportion of the total production losses. The rebound greatly influences the economic efficiency and also has an inconvenient environmental impact [Pfeuffer and Kusterle 2001]. The main questions that always arise with shotcrete applications are related to the amount of rebound [Jolin *et al.* 1999]. In addition to the economical and environmental factors, the amount of rebound and its composition has a direct effect on the composition of the in-situ shotcrete. Therefore, studying the amount of rebound and the factors affecting it are of great interest to the shotcrete industry.

2 MATERIALS, MIXES AND SPRAYING

2.1 Materials

Portland Cement (CEM1), conforming to BS EN 197-1 [2000], was used as main binder in this study. Fly ash and silica fume were used as cement replacement materials. The coarse aggregate used was quartzite natural gravel of 10-mm nominal maximum size. It had a specific gravity of 2.64, bulk density of 1585 kg/m3 and water absorption of 0.60 percent. Quartzite sand which complies with zone M of BS EN 12620 [2002] was used as a fine aggregate, with specific gravity and water absorption of 2.68 and 0.10 percent, respectively. Fibrillated PPF (Figure 1) were used in this study. The fibre has a length of 18mm and an average diameter of 55μm.

Figure 1. Polypropylene fibres used in this investigation.

2.2 Mixes

Six mixes were sprayed in this study. Four of these mixes were initially optimised from laboratory tests. The pre-sprayed composition of these four mixes is given in Table 1. The water content was decided during spraying by the nozelman according to the ease of 'shotability' of each mix.

The remaining two mixes were pre-packed mixes, which are commercially available for shotcrete applications. Both mixes (RDY1 and RDY2) were plain mixes (without fibres). A dosage of 2 kg/m^3 PPF was added to RDY1 in order to compare it to the other fibre-reinforced mixes. However, the producer of mix RDY2 recommended not to add fibres to the mix and, therefore, mix RDY2 was sprayed without fibres. Due to commercial reasons, the compositions of RDY1 and RDY2 are unknown except that both mixes did not contain coarse aggregate.

Table 1. Pre-sprayed mix proportions (kg *per m*^{3}).

Mixes	*CEM1*	*FA*	*SF*	*Gravel*	*Sand*	*Fibre*
CEM0	400	-	-	948	948	-
CEMF	400	-	-	948	948	2.0
FA30	280	120	-	948	948	2.0
FASF	248	120	32	948	948	2.0

2.3 Spraying

Shotcrete panels were produced by the dry process, which was more appropriate for this study due to economical and practical reasons. A dry-process pneumatic spraying machine was used with two rotary feed wheels for mixtures with and without coarse aggregates. For the former mixes, a 38-mm nozzle and material hose were used while a 25-mm nozzle and hose were used for the latter mixes.

Wooden square moulds of 1200-mm side and 100-mm depth were manufactured specially for this investigation. Before spraying, the moulds were positioned as vertically as possible (within 5 to 10°). Polyethylene sheets were placed underneath and around the moulds to collect the rebound.

For the laboratory developed mixes (CEM0, CEMF, FA30 and FASF), all ingredients except water were first mixed in the dry state in a conventional concrete mixer. Where applicable, PPF fibre was added after two minutes of dry mixing, which then continued for another two minutes. The dry mix was then fed through the hopper of the spraying machine, which conveyed the mix pneumatically through the material hose to the nozzle where water was added through the water ring. For all the shotcrete mixes, variations in the spraying process were minimised by keeping the shooting distance between the nozzle and the target-surface around one meter. Also, the spraying angle was as close to 90° as possible, as shown in Figure 2.

Figure 2. Spraying distance and angle were kept around one meter and 90°, respectively.

2.4 Measuring the Rebound and Composition Analysis

On completion of each shotcrete panel, the rebound was collected before starting the finishing process. After weighing the total material rebound, two representative samples were taken from each mix. The shotcrete surface profile was levelled to the edges of the mould using metal trowel. Immediately after finishing, samples of the in-situ shotcrete were taken from different locations.

The fresh samples taken from the rebound material and in-situ shotcrete were used for analysing the composition. A small part from each sample was immediately weighed and dried using a microwave oven to determine its water content, as recommended by BS 1881-128 [1997]. The remaining concrete was washed with an excessive amount of water and drained to separate the aggregate, which was then weighed to determine the total aggregate content in the sample. Using sieve analysis, the combined aggregate was then analysed to estimate the fractions of fine and coarse aggregates.

3 RESULTS AND DISCUSSION

3.1 Total Material Rebound

The total material rebound is shown in Figure 3. The values are given as a percentage of the finished in-situ shotcrete and also as a percentage of the total sprayed materials. The rebound values obtained for the different mixes are in good agreement with values reported by other investigators for dry-process shotcrete [Wood *et al.* 1993; Austin *et al.* 1996].

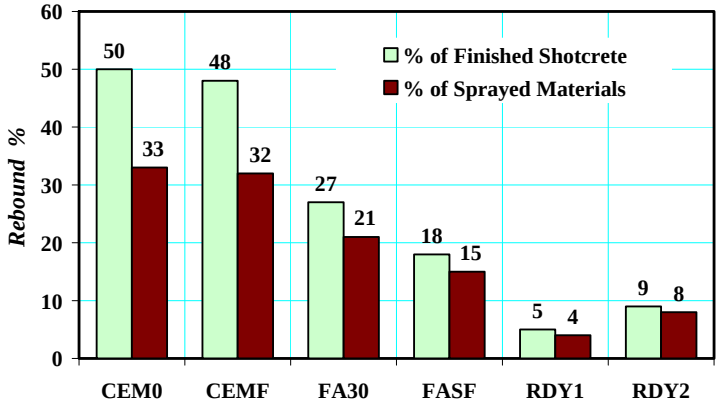

Figure 3. Total rebound as percentages of the finished shotcrete and of the sprayed materials.

It can be seen that the two ready-mixes RDY1 and RDY2 showed the least rebound due to the absence of coarse aggregate. In addition, since the nozzleman was familiar to spraying those mixes regularly his experience may have been a factor in reducing their rebound. The effect of the experience of nozzleman was previously reported [Adams 1993; Lars 1996]. The rebound of mixes containing fly ash (FA30 & FASF) was the best among the laboratory developed mixes.

The presence of PPF had no effect on material rebound, as the difference between the rebound of the control mix CEM0 and its counterpart fibre reinforced mix (CEMF) was negligible, as shown in Figure 3. Fly ash and silica fume effectively reduced the total material rebound. The use of fly ash reduced the rebound of the sprayed materials by about 35 % compared to the CEMF mix. Fly ash was even more effective in the presence of silica fume as the combination between them resulted in a reduction of about 55 % so that the rebound was only 15 % of the total sprayed material.

3.2 PPF Rebound

Most of the polypropylene fibres did not reach the target surface. On exiting from the nozzle, PPF separated from the concrete mixture due to the insufficient wet mixing. Consequently, and as a result of a different density, PPF gained a lower velocity compared to other constituents. Therefore, a considerable amount of PPF dropped down between the nozzle and the target surface, as shown in Figure 4. It was estimated that only 20 % of the fibres reached the mould. It can also be seen from the same figure that other constituents rebounded adjacent to the mould, unlike the fibres. The authors suggest that producing PPFRSC using the wet-process could probably eliminate this problem. It is expected that PPF would not be separated from a well-mixed matrix. However, the dry-process should still be able to produce this type of concrete if the initial fibre dosage was much higher the original fibre content. A factor of 5 could be used as a rough guide. Although this might appear a high factor, the low cost of PPF would not cause a noticeable increase on the total cost of the shotcrete.

It should be mentioned that the problem of embedding fibres in fresh-shotcrete is common regardless of the fibre type. For example, high number of steel fibres in the rebound and the insufficient adhesion of steel fibres to the shotcrete are always observed and have been subject to theoretical studies in attempts to understand and minimise this problem [Burge 1986; Cengiz and Turanli 2004].

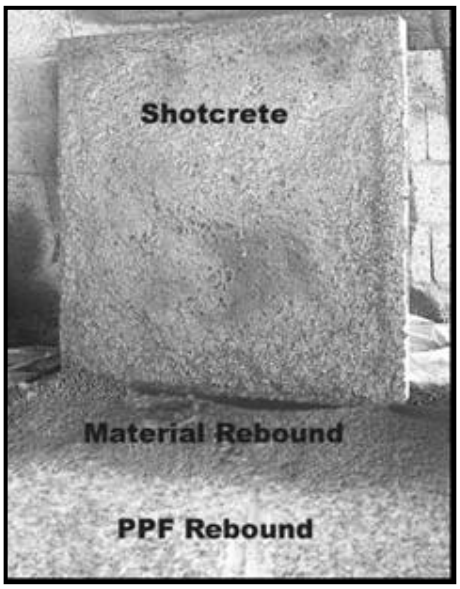

Figure 4. Material and fibre rebound.

3.3 Composition of the Rebound

Individual constituents rebound by different amounts due to their different sizes and densities. Samples from the rebound material were analysed in order to estimate the amount of each constituent. The estimated quantities were used to calculate important ratios such as coarse aggregate-to-rebound (g/R) and fine aggregate-to-rebound (s/R), as shown in Table 2.

The composition of the rebound was mainly combined aggregate with a high percentage of gravel. On average the combined aggregate in the rebound was about 80% of the total rebound material. About two-thirds of the combined aggregate in the rebound consists of coarse aggregate, which represented more than 50 % of the total rebound material compared to 27% fine aggregate in the rebound. Therefore, the gravel-to-sand ratio in the rebound was 2:1, whereas it was 1:1 in the pre-sprayed mixture. This can be attributed to the fact that heavier particles rebound more than the lighter sand grains and cementitious materials. This finding explains the low rebound values for the ready-mixes RDY1 and RDY2 as they did not contain coarse aggregate. However, it can be seen that neither PPF nor the binder type has clear effect on the total aggregate content in the rebound.

Table 2. Constituents of the rebound materials.

	Composition (kg *per* m^3)				*Ratios*			
	Binder *(b)*	Gravel *(g)*	Sand *(s)*	Water (w)	*(g+s)/R*	*g/(g+s)*	*g/R*	*s/R*
CEM0	433	1361	757	63	0.81	0.64	0.52	0.29
CEMF	564	1277	646	95	0.74	0.66	0.49	0.25
FA30	520	1178	796	90	0.77	0.60	0.46	0.31
FASF	383	1602	544	69	0.83	0.75	0.62	0.21
Average	475	1355	686	79	0.79	0.66	0.52	0.27

3.4 Composition of the in-Situ Shotcrete

Samples of fresh in-situ shotcrete were analysed and the proportions are shown in Table 3. Comparing Table 3 to Table 1, it can be seen that the in-situ concrete proportions were different from those of the batched concrete. The shotcrete had much higher binder content and lower coarse aggregate content. The average binder content was about 700 kg/m^3, which is 75 % more than the intended 400 kg/m^3. This very high binder content could provide potential for alkali-silica reaction and early cracking through high heat of hydration [Cabrera and Woolley 1996]. It can also be noticed that the increase of the binder content was at the expense of coarse aggregate, which on average decreased to 592 kg/m^3, whereas the average fine aggregate content actually increased slightly from 948 to 994 kg/m^3.

Table 3. Composition of the in-situ shotcrete.

	Composition (kg *per* m^3)				*Ratios*	
	Binder *(b)*	Gravel *(g)*	Sand *(s)*	Water (w)	w/*b*	*(g+s)/b*
CEM0	727	487	1079	179	0.25	2.15
CEMF	730	585	916	202	0.28	2.06
FA30	749	674	924	159	0.21	2.13
FASF	605	623	1057	174	0.29	2.78
Average	703	592	994	179	0.26	2.28

The w/*b* ratios of in-situ shotcrete varied from 0.21 to 0.29, with an average of 0.26, which can be considered as low values. This, in fact, is the main advantage of the dry-process because a high workability is not a requirement as the case for the wet-process.

There was no significant difference in the w/*b* and *(g+s)/b* ratios for mixes CEM0 and CEMF, indicating that PPF had no effect on the composition of in-situ shotcrete. As with conventional concrete, fly ash reduced the water demand for the shotcrete. However, adding silica fume to the fly ash mix resulted in a w/b ratio equal to that of the CEMF mix.

It was interesting to notice that the internal layer of the in-situ shotcrete was affected more by the rebound than the external layer. Most aggregate rebound from the first layer, as the particles hit the hard substrate with high velocity and rebound. The first layer forms a relatively soft substrate for the next layer and, therefore, the rebound from the external layer was less, as can be seen from Figure 5 (the yellow line indicates the demarcation between the first and subsequent layers). It can be seen that the internal layer (mould side) had very little aggregate compared to the external layer (spraying side).

Figure 5. Composition of external and internal layers of the FASF in-situ shotcrete.

4 CONCLUSIONS

For the shotcrete mixes and PPF used in this investigation, the following conclusions can be made:

- About 80 % of the initial PPF dosage did not reach the mould and dropped in the area between the nozzle and the main rebound material, which was next to the target surface. Consequently, the addition of PPF had no effect on the total rebound material, whereas the binder type had an obvious influence.

- Fly ash was effective in reducing the total rebound, particularly in the presence of silica fume. FA reduced the rebound by 35 % and 55 % in the absence or presence of SF, respectively.

- The sprayed materials rebound by different amounts due to different sizes and densities. The composition of the rebound was mainly aggregate with high percentage of coarse aggregate. On average, the combined aggregate was about 80 % of the total rebound material, of which the coarse aggregate represented about two-thirds. Neither PPF nor the binder type had a clear effect on the total aggregate content in the rebound.

- The composition of the in-situ shotcrete was significantly different from the proportions of the batched constituents. The in-situ shotcrete had much higher binder content and lower coarse aggregate content. The internal layer had less aggregate compared to the external layer.

- PPF had no effect on the composition of in-situ concrete, whereas the binder type has noticeable effect on the water-to-binder and aggregate-to-binder ratios.

REFERENCES

Adams, F.R., 1993, 'Steel Fibre Reinforced Shotcrete: An End-User Prospective', Proc. 6th Engineering Foundation Conf., Shotcrete for Underground Support VI, Niagara-on-the-Lake, Canada 1993, pp. 33-40.

Austin, S., Robins, P., Seymour J. & Turner, N.J., 1996, 'Wet Process Shotcrete Technology for Repair', Proc. ACI/ SCA International Conf. on Sprayed Concrete/Shotcrete, Shotcrete Technology, Edinburgh University, UK, vol. 1, pp. 157-165.

Badr, A., Richardson, I.G., Hassan, K.E., & Brooks, J.J., 2001, 'Performance of Monofilament and Fibrillated Polypropylene Fibre-Reinforced Concretes', Proc. 2nd International Conf. on Engineering Materials, San Jose, CA, USA 2001. pp. 735-744.

Badr, A., Ashour, A.F. & Platten, A.K., 2006, 'Statistical Variations in Impact Resistance of Polypropylene Fibre-Reinforced Concrete', *International Journal of Impact Engineering*, **32**[11], 1907-1920.

Bayasi, Z., & Zeng, J., 1993, 'Properties of Polypropylene Fibre Reinforced Concrete', *ACI Materials Journal*, **90**[6], 605-610.

British Standards Institute 1997, Methods for Analysis of Fresh Concrete, BS 1881-128, UK.

Burge, T.A., 1986, 'Fibre Reinforced High-Strength Shotcrete with Condensed Silica Fume', *ACI Special Publications*, **91**(57), 1153-1170.

Cabrera, J.G., & Woolley, G.R., 1996, 'Properties of Dry Shotcrete Containing Ordinary Portland Cement or Fly Ash-Portland Cement,' Proc. ACI/ SCA International Conf. on Sprayed Concrete/Shotcrete, Shotcrete Technology, Edinburgh University, UK, vol. 1, pp. 8-25.

Cengiz, O., & Turanli, L., 2004, 'Comparative Evaluation of Steel Mesh, Steel Fibre and High-Performance Polypropylene Fibre Reinforced Shotcrete in Panel Test', *Cement and Concrete Research*, **34**[8], 1357-1364.

Jolin, M., Beaupré, D. & Mindess, S., 1999, 'Tests to Characterise Properties of Fresh Dry-Mix Shotcrete', *Cement and Concrete Research*, **29**[5], 753 –760.

Lars, B.J., 1996, 'Why Certify Shotcrete Nozzlemen?', *Concrete International*, **18**[2], 68-69.

Malhotra, V.M., Carette, G.G. & Bilodeau, A., 1994, 'Mechanical Properties and Durability of Polypropylene Fibre reinforced High-Volume Fly Ash Concrete for Shotcrete Applications', *ACI Materials Journal*, **91**[5], 478–486.

Pfeuffer, M., & Kusterle, W., 2001, 'Rheology and Rebound Behaviour of Dry-Mix Shotcrete', *Cement and Concrete Research*, **31**[11], 1619 -1625.

Sivakumar, A., & Santhanam, M., 2007, 'Mechanical Properties of High Strength Concrete Reinforced with Metallic and Non-Metallic Fibres', *Cement and Concrete Composites*, **29**[8], 603-608.

Song, P.S., Hwang, S. and Sheu, B.C. 2005, 'Strength Properties of Nylon and Polypropylene Fiber-Reinforced Concretes', *Cement and Concrete Research*, **35**[8], 1546-1550.

Wood, D.F., Banthia, N., & Trottier, J.F., 1993, 'Comparative Study of Different Steel Fibres in Shotcrete', Proc. 6th Engineering Foundation Conf., Shotcrete for Underground Support VI, Niagara-on-the-Lake, Canada 1993, pp. 57-66.

Zellers, R.C., & Ramakrishnan V., 1994, 'Fbrillated Polypropylene Fiber-Reinforced Concretes', *Transportation Research Record*, **1458**, 27-66.

11DBMC International Conference on Durability of Building Materials and Components
ISTANBUL, Turkey 11-14 May 2008

Mechanical Behaviour of GFRP-Confined Concrete after Exposure to Severe Conditions

Francesco Micelli [1]
Maria Antonietta Aiello [2]
Alfonso Maffezzoli [3]
Rossella Modarelli [4]

T 11

ABSTRACT

In the last decade fibre-reinforced polymer (FRP) composites have been successfully used for confinement of reinforced concrete (RC) and masonry columns. Their high mechanical properties, light weight and low installation costs have contributed to making the wet lay-up wrapping one of the most affordable techniques for column confinement. Although previous studies have demonstrated the high performance of FRP strengthening systems, several concerns are related to the long-term behaviour of wrapped columns, which has limited implementation. Environmental effects, such as freeze-thaw cycles, wet-dry cycles, ultra violet (UV) radiations exposure, high temperatures and de-icing salts, may affect the material properties and the structural response of the wrapped elements. In this paper an experimental work is presented in order to study the long-term behaviour of Glass FRP-confined columns. A commercial GFRP system was used to wrap thirty-two small-scale concrete cylinders that were subjected to extreme conditions such as freeze-thaw cycles, immersion in water and saline solution, immersion in alkaline or HCl solutions. Epoxy adhesives, cured at four different temperatures, used for FRP bonding, were also studied after immersion in water, diffusion properties were measured after different times of exposure, also changes in glass transition temperature were monitored by using a differential scanning calorimeter. Changes in mechanical and physical properties of FRP-confined cylinders and adhesives are discussed herein.

KEYWORDS

Fibre Reinforced Polymer, Confinement, FRP-confined concrete, Structural Strengthening

[1] University of Salento - Innovation Engineering Dept. - Via per Monteroni, 73100 Lecce – ITALY, Phone +39 0832 297380, francesco.micelli@unile.it
[2] University of Salento - Innovation Engineering Dept. - Via per Monteroni, 73100 Lecce – ITALY, Phone +39 0832 297248, antonietta.aiello@unile.it
[3] University of Salento - Innovation Engineering Dept. - Via per Monteroni, 73100 Lecce – ITALY, Phone +39 0832 297254, alfonso.maffezzoli@unile.it
[4] Department of Materials and Structures Engineering, CETMA, Cittadella della ricerca, s.s. 7 Appia km 706 – 72100 Brindisi – ITALY, Phone +39 0831 449111, rossella.modarelli@cetma.it

1 INTRODUCTION

When structural deficiencies are present in the columns of a reinforced concrete (RC) building, collapse of the entire structure happens without system redundancy. These dangerous occurrences may be due to insufficiencies caused by incorrect design assumptions, deterioration in section capacity due to steel corrosion, vehicular impact damage, construction defects or damage caused by seismic forces.

Although several experimental studies demonstrated the effectiveness of FRP-confinement in repairing damaged or inadequate compressed concrete elements, important questions related to long-term behaviour and durability were not adequately highlighted. Knock-down factors to address environmental conditioning are an important design consideration for long-term performance, thus research efforts are needed in this field.

Environmental agents, over time, may reduce the durability in infrastructure applications including bridges and marine structures. The most important effects that need to be investigated are those related to low temperatures in cold regions, aggressive environments such as marine or industrial areas, de-icing salts that are used to avoid frost in infrastructures, fluid penetration and absorption such as rain waters, thermal cycles, typical of seasonal changes.

Earlier studies revealed that external agents can significantly reduce the effects of confinement, due to material degradation, embrittlement of the resin and fibres and chemical attack that reduces the effectiveness of reinforcement [Toutanji and Balaguru 1999]. In particular it was observed that different resin systems and wet-dry cycling affect the ductility of Glass FRP (GFRP) confinement, reducing the ultimate capacity by 18% [Toutanji 1999]. Freeze-thaw cycles combined with moisture showed reduction of more than 30% in the ductility of GFRP-confined concrete [Karbhari and Eckel 1994]. The effect of freeze-thaw cycling was found to be very low in a dry environment; only the radial strain is affected, resulting in more brittle failure modes [Karbhari et al. 2000]. Combined effects, including moisture and freeze-thaw cycling, different pH environments, were investigated and reduction in mechanical properties was found to be more than 20% of the compressive strength and axial strain, while a reduction of 50% was found in radial strain [Kshirsagar et al. 2000]. According to the results obtained by Corvaglia et al. [2006] it was highlighted that durability of FRP-confined concrete is related to three main issues: type of aggressive environment; constituent materials of FRP systems; wrapping technique used for confinement.

In this study a set of forty-eight concrete cylinders were tested in compression. The experimental variables were different geometry and different exposure programs. The effects of aggressive fluids and low temperature were studied for FRP-confined concrete and for the epoxy adhesive. Thus the scope of this research is defined by the possible effects of external aggressive agents on retaining of carrying capacity and structural ductility of FRP-confined concrete columns. Experimental results furnished in this research may be taken into account for future calibration of existing guidelines, including environmental factors that can be addressed to particular service conditions.

2 EXPERIMENTAL PROGRAM AND TEST SET-UP

The experimental program consisted of specimen preparation, a period of accelerated aging, mechanical and physical tests. A laboratory-protocol was used to investigate the durability effects on conditioned cylinders and FRP specimens under different conditions. Compression testing was used to measure the possible changes in mechanical properties of FRP-confined concrete, while differential scanning calorimetry (DSC) was used to measure possible changes in resin properties, such as glass transition temperature, that may assist in understanding the degradation processes that occurred in the FRP layer. Tensile tests according to ASTM D3039 were used for characterization of FRP systems. Mechanical properties of FRPs in the following will be related to the thickness of dry sheets. The variables investigated were geometry of concrete cylinders (full-core and hollow-core), accelerated

aging, including immersion in water, also followed by freeze-thaw cycles, immersion in aggressive solutions (acidic, alkaline, saline). In all cases the conditioning regime of cylinders did not take place in presence of axial stress (i.e. sustained loading). However, it may also be noted that in real RC columns the stress in FRP jacket is negligible under service conditions. Unconditioned specimens and unconfined concrete cylinders were also tested as control specimens. Four compressive tests were made for each type of control and conditioned cylinder.

Concrete cylinders were poured with the same mix at the same time, a low quality concrete was chosen in order to simulate more real conditions (20 MPa of compressive strength). Forty cylinders were cast with a diameter of 150 mm and height of 300 mm; eight cylinders were cast with the same geometry but with hollow core, having a wall thickness of 50 mm.

E-glass fibre sheets were used for external strengthening; mechanical properties of GFRP were measured by tensile tests that were conducted according to ASTM D-3039. Testing was performed in displacement-control mode on a 150-kN universal testing machine, with a crosshead displacement rate of 2 mm/min. An electrical extensometer was used to measure the strain of CFRP under tensile force. Average experimental results (with standard deviation) were: tensile strength 1957 MPa (173 MPa), Young modulus 86 GPa (6 GPa), ultimate strain 2.29 % (0.003 %). Tensile tests of epoxy adhesive were also conducted according to ASTM D-638. Average experimental results (with standard deviation) were: tensile strength 22 MPa (5 MPa) and tangent modulus 2 GPa (6 GPa). Flexural tests, according to ASTM D-790, were performed to measure the flexural properties of the resin, the average strength was 56 MPa (2.7 MPa), the modulus was 1.84 GPa (0.16 GPa).

The strengthening process was done using the manual wet lay-up technique, in a laboratory environment with a controlled temperature of 21 °C and 45% of relative humidity. The same experienced worker applied the composite jackets in order to reproduce the same conditions for all specimens, since the comparative aspect of the results was the main issue. Properties of the epoxy adhesive were studied also in terms of absorption capacity; twenty-five circular plates of resin (diameter was 80 mm and thickness was 5 mm) were cured at different temperatures: 20°C, 30°C, 40°C, 55°C. All specimens were immersed into distilled water for 1440 hours at 40°C; weight measurements were made every 72 hours, except for the first ten days, in which the possible weight increase was measured every 12 hours. A supplementary group of five resin specimens that was cured at 20°C, after immersion in water was also subjected to 166 freeze-thaw cycles, with a range of temperature from -15°C to 25°C. Weight increase law that was recorded was about the same for all specimens, as it is illustrated in Figure 1. According to these results a diffusion coefficient was computed, and an average value of $D=3.36 \times 10^{-3}$ mm^2/hrs was found. Assuming a saturation point of 90% and a thickness of 2 mm for the FRP cured sheet, from the Fickian diffusion law, it was found that a period of 1010 hours is necessary for the saturation of the epoxy adhesive at 40°C.

Differential scanning calorimetry (DSC) was used to measure the glass transition temperature (T_g) range of the resin cured at room temperature (21°C), and activation of T_g resulted at 56°C. Therefore, a conditioning temperature of 40°C was chosen, since it resulted far from possible thermal degradation of the resin or thermal activation of post-cure polymerization.

GFRP confined cylinders were subjected to different exposure programs, each group was made by four samples. Two groups were immersed into distilled water at 40°C for a period of 2600 hours, one of them was also subjected to 80 freeze-thaw cycles from – 8 °C to +8 °C, the duration of a single cycle was of 24 hours.

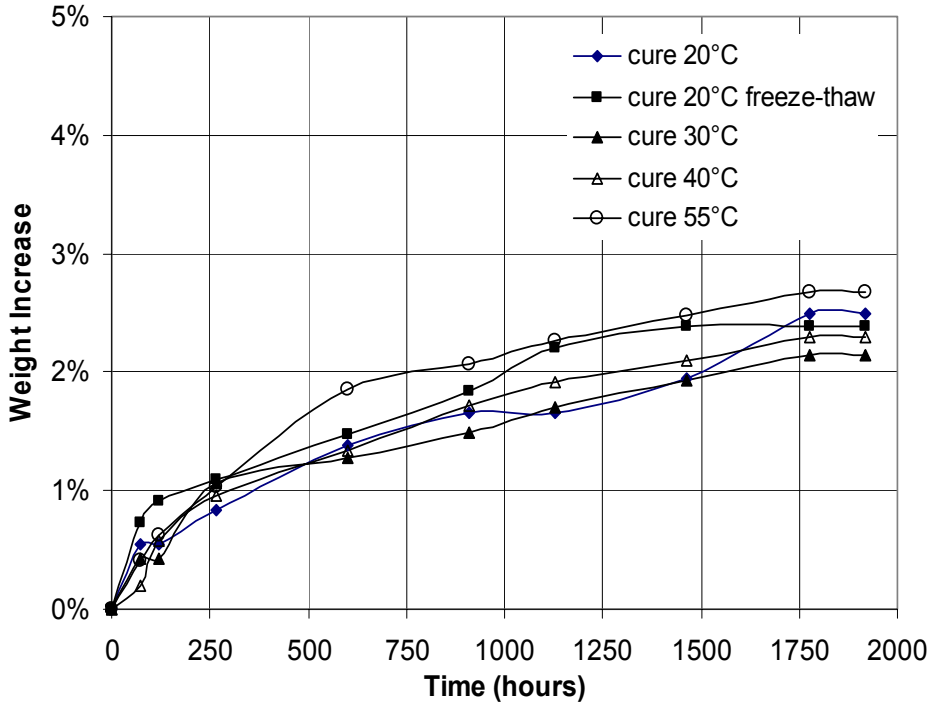

Figure 1. Water absorption in epoxy resins cured at different temperatures.

A third group of cylinders was immersed in a HCl aqueous solution (pH=3.0) at 40°C for 2600 hours. Four groups of cylinders (two with full core and two with hollow-core) were immersed in a NaCl aqueous solution (5% weight) at 40°C for 2600 hours; one group for each type was also subjected to 80 freeze-thaw cycles from – 8 °C to +8 °C, the duration of a single cycle was of 24 hours. The last group of cylinders was immersed in alkaline solution (0.16% $Ca(OH)_2$+1%Na(OH)+1.4% K(OH) in weight) at 40 °C for 2600 hours. Table 1 shows the details of the experimental program.

Table 1. Experimental program for GFRP-confined cylinders.

Specimen	# of samples	Geometry	Strengthening	Exposure
C	4	full-core	unconfined	laboratory - control
H	4	hollow-core	unconfined	laboratory - control
C-F	4	full-core	1 layer GFRP	laboratory - control
C-H	4	full-core	1 layer GFRP	laboratory - control
W	4	full-core	1 layer GFRP	distilled water 40°C 2600 hrs
W-FT	4	full-core	1 layer GFRP	distilled water + freeze-thaw cycles
HCl	4	full-core	1 layer GFRP	HCl solution 40°C 2600 hrs
NaCl	4	full-core	1 layer GFRP	NaCl solution 40°C 2600 hrs
NaCl-FT	4	full-core	1 layer GFRP	NaCl solution + freeze-thaw cycles
HC-NaCl	4	hollow-core	1 layer GFRP	NaCl solution 40°C 2600 hrs
HC-NaCl-FT	4	hollow-core	1 layer GFRP	NaCl solution + freeze-thaw cycles
A	4	full-core	1 layer GFRP	alkaline solution 40°C 2600 hrs

Plain and wrapped concrete cylinders were tested under axial compression using a 3000-kN compression machine in load-control mode. Two LVDTs were used to monitor the relative displacement between the extreme faces of the cylinder. Four strain gauges, two in the longitudinal

and two in the hoop direction, were applied on each cylinder at mid-height to measure load vs strain values.

In all specimens the FRP wrap did not cover the full height of the cylinder. This avoided that the axial load be applied directly on the FRP resulting in local buckling of the composite close to the loaded surfaces. Thus a narrow gap was left between the end concrete surfaces and the extreme composite fibres.

3 RESULTS AND DISCUSSION

Differential calorimetry tests revealed that after immersion in water, and after freeze-thaw cycles the glass transition temperature showed a difference respect to the control samples within a range of 4°C. Thus it is assumed that the wet conditioning did not produce any significant change in the properties of adhesive, respect to a premature glassy/rubbery transition.

It was observed after different cure temperatures in a range from 20 °C to 55 °C, so the tested epoxy adhesive may be applied at room temperature, higher temperatures of cure did not showed to activate an higher rate of polymerization.

Compressive tests on plain concrete cylinders showed a strength of 26.5 and 26.1 N/mm^2 respectively for full and hollow-core samples. Confinement with one layer of GFRP produced a dramatic increase in mechanical properties, it was expected due to the low quality of plain concrete: an average increase of about 70% was observed in both cases. Axial strain at ultimate crushing state was more than 4 times that of unconfined cylinders. Those results are very encouraging since both ultimate capacity and ductility are enormously modified with a single layer. Long-term behaviour showed that this advantage may be lower since a damage of the FRP-confined system may occur.

Immersion in water produced a reduction of about 20% in ultimate load, while the presence of freeze-thaw cycles after wet exposure showed a positive effect as shown in Figure 2 and in Table 2. Reduced capacity is due to a degradation of the confinement effect that is practiced by the FRP jacket, in this case the presence of an aqueous solution may have produced a damage at fibre/matrix interface that modifies the stress distribution inside the composite cylindrical layer.

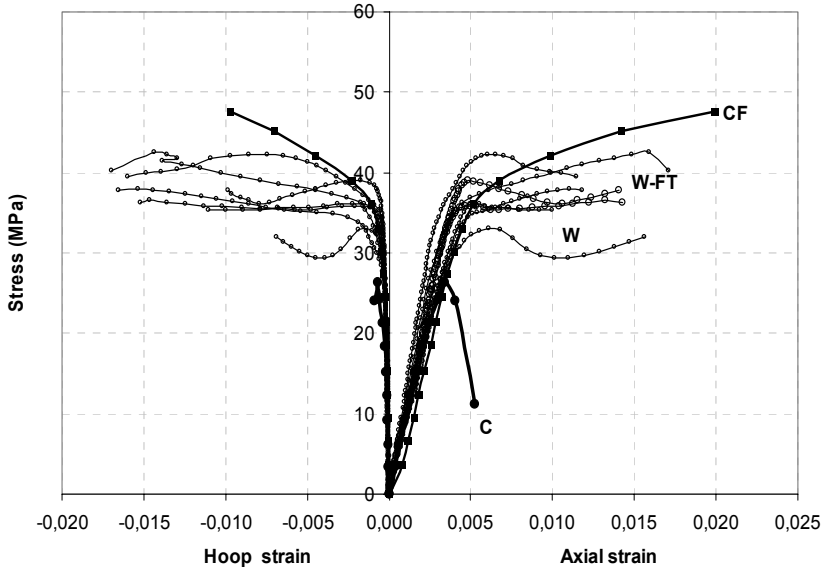

Figure 2. σ-ε curves for specimens immersed in water (W and W-FT).

Cylinders subjected to immersion in acidic solution showed a reduction in their capacity. The difference between control and aged specimens in terms of ultimate load was almost the same observed for specimens immersed in water, while a significant reduction (more than 40 %) was recorded for axial displacement. This indicates decay in terms of enhanced ductility due to the presence of the GFRP. Curves in Figure 3 and average results of Table 2 illustrate the experimental results for this group of specimens.

GFRP-confined concrete subjected to marine environment (NaCl solution), that is typically very aggressive for steel rebars, when concrete has an undesired porosity, showed a moderate reduction in terms of ultimate compressive strength (about 20% for both full and hollow-core cylinders). Additional freeze-thaw cycles that were applied after immersion in NaCl of hollow-core cylinders did not produce any effect, as seen in Figure 4 and Table 2.

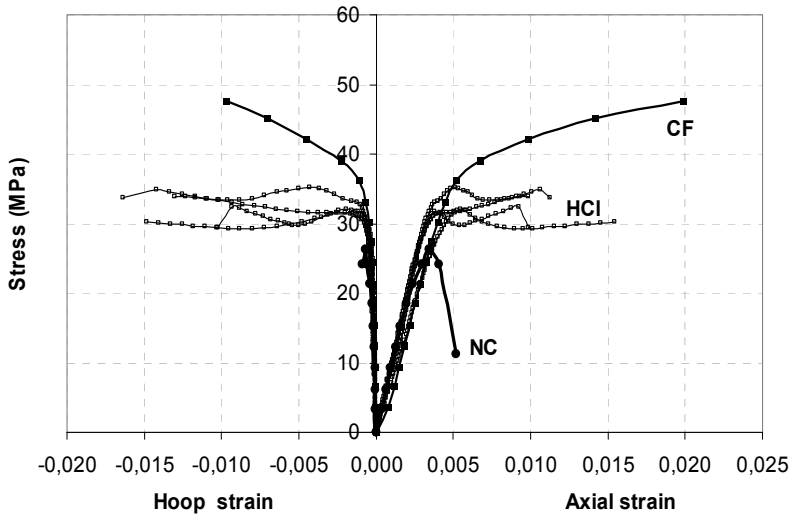

Figure 3. σ-ε curves for specimens immersed in HCl solution (HCl).

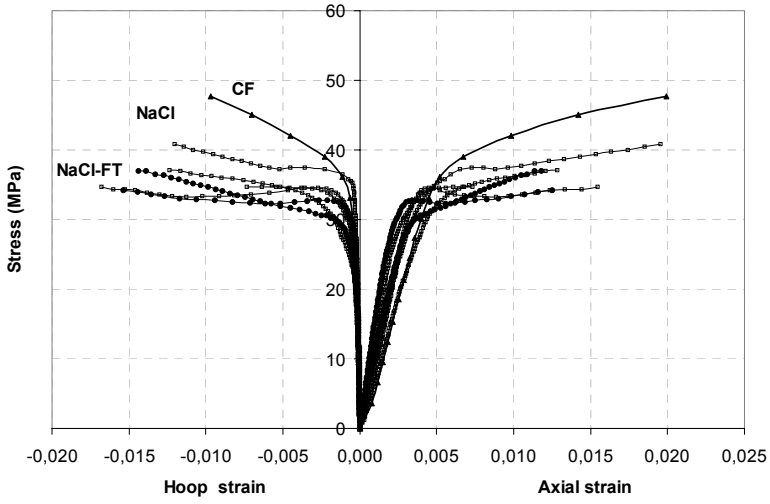

Figure 4. σ-ε curves for specimens immersed in NaCl solution (NaCl and NaCl-FT).

The alkaline attack to E-glass fibres resulted the most dangerous for GFRP-confined concrete since the average compressive strength was 29.8 MPa that is very close to that of unconfined concrete. The alkaline environment produced a chemical attack, so it can be assumed that the presence of alkaline ions produced an embrittlement of the glass fibres and damage at the fibre resin interface level produced by the growth of hydration products. These effects lead to a dramatic loss in tensile strength and interlaminar transverse properties of the GFRP jacket.

Also the ductility, measured as deformation capacity until failure, was very close to that of plain concrete, therefore the effects of confinement were negligible after alkaline conditioning. It is clear from the observation of Figure 5 and Table 2, where experimental results are reported in form of average values.

From the mechanical tests it was observed that wet environment may produce a saturation of the resin that influences the ultimate properties, this may be due to a change in interface properties. When different types of ions are present, the chemical attack is extended to the fibres, which are prone to premature failure. It was seen in fact that immersion in water, saline and acidic fluids reduces the mechanical performance of GFRP-confined concrete, while the presence of an alkaline solution erases the advantages of external confinement.

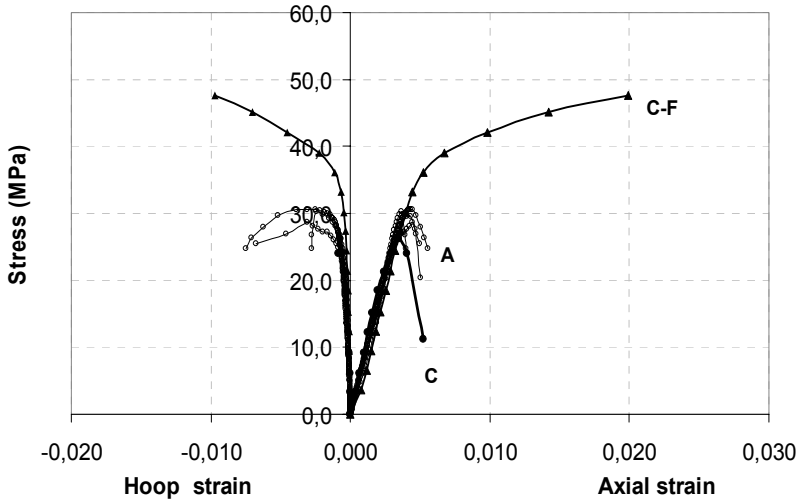

Figure 5. σ-ε curves for specimens immersed in alkaline solution (A).

Table 2. Experimental results for GFRP-confined cylinders.

Specimen	f'_{cc} (N/mm^2)	ε_{axial} %	ε_{radial} %	$f'_{cc\text{-}AGED}/f'_{cc}$	$\varepsilon_{acc\text{-}AGED}/\varepsilon_{acc}$	$\varepsilon_{rcc\text{-}AGED}/\varepsilon_{rcc}$
C	26.5	0.35	0.10	-	-	-
H	26.1	0.35	0.02	-	-	-
C-F	44.5	1.97	0.93	-	-	-
C-H	42.3	1.43	1.12	-	-	-
W	35.9	1.34	1.07	0,81	0,68	1,14
W-FT	40.9	1.30	1.62	0,92	0,66	1,73
HCl	33.3	1.16	1.34	0,75	0,59	1,43
NaCl	36.9	1.37	1.21	0,83	0,70	1,29
NaCl-FT	35.4	1.22	1.54	0,80	0,62	1,65
HC-NaCl	35.0	1.22	1.21	0,83	0,85	1,08
HC-NaCl-FT	34.2	1.04	1.36	0,81	0,72	1,21
A	29.8	0.49	0.57	0,67	0,25	0,61

where:
f'_{cc} is the average value of the compressive strength of the specimens
ε_{axial} is the average value of the ultimate axial strain of the specimens
ε_{radial} is the average value of the ultimate hoop strain of the specimens
$f'_{cc\text{-}AGED}/f'_{cc}$ is the ratio between the strength of aged specimens and strength of control specimens
$\varepsilon_{acc\text{-}AGED}/e_{acc}$ is the ratio between the axial strain of aged specimens and that of control specimens
$\varepsilon_{rcc\text{-}AGED}/e_{rcc}$ is the ratio between the hoop strain of aged specimens and that of control specimens

4 CONCLUSIONS

An experimental study has been presented in order to investigate important issues related to the long-term behaviour of GFRP-confined concrete. A preliminary study was made to understand the properties of the epoxy adhesive since this is the matrix that should be able to protect the glass fibers from external agents.

Glass transition temperature was measured for different temperatures of polymerization and after different conditioning programs. Significant changes were not observed in terms of glass transition.
Results of gravimetric tests after immersion in water at 40 °C were calibrated in order to obtain the diffusion properties of the resin and its capacity respect to reach a saturation point.

Based on these preliminary results different exposure programs were applied to GFRP-confined concrete cylinders that were aged in aqueous solutions at 40 °C for 2600 hour, including saline ions, acidic ions and alkaline ions. Freeze-thaw cycles were also applied after conditioning in wet environment.

A moderate reduction (about 20%) was observed in terms of ultimate strength and ultimate axial strain, in all cases, except for alkaline solution, which produced a dramatic drop of mechanical properties. In this last case the properties of aged GFRP-confined concrete resulted close to that of plain concrete. Freeze-thaw cycles did not affect the mechanical properties.
Authors know that accelerated extreme conditions reproduced in laboratory are more dangerous than those that affect structural systems in real applications, but the results of this study help to individuated which conditions are more critical in presence of E-glass fibres. Results may be considered very helpful in calibrating durability safety coefficients that are present in current design guidelines.

ACKNOWLEDGMENTS

This research was funded by the project MITRAS “Materials, Technologies and Methods for Innovative Design of Structural Strengthening in Road Infrastructures”.

REFERENCES

Corvaglia, P., Feo, A., Micelli, F., Nenna, S. & Pugliese, L. 2006, ‘Durability of FRP-confined concrete subjected to severe conditions’, Proc. of the 2nd International FIB Congress, Naples - June 5-8 2006 (CD-ROM).

Karbhari, V. M., & Eckel, D. A., 1994, ‘Effect of cold regions climate on composite jacketed concrete columns’, *ASCE - J. Cold Regions Eng*., **8** [3], pp. 73-86.

Karbhari, V. M., Rivera, J., & Dutta, P. K., 2000, ‘Effect of short-term freeze-thaw cycling on composite confined concrete’, *ASCE - J. Comp. Constr*., **4**[4], pp. 191-197.

Kshirsagar, S., Lopez, R. A. & Gupta, R. K., 2000, ‘Environmental ageing of fiber-reinforced polymer wrapped concrete cylinders’, ACI Materials Journal, **97**[6], pp. 703-712.

Toutanji, H., & Balaguru, P., 1999, ‘Effects of Freeze-Thaw Exposure on the Performance of Concrete Columns Strengthened with Advanced Composites’ ACI Materials Journal, **96**[5], pp. 605-611.

Toutanji, H. A., 1999, ‘Durability characteristics of concrete columns confined with advanced composite materials’, Comp. Struct., **44**, pp. 155-161.

11DBMC International Conference on Durability of Building Materials and Components
ISTANBUL, Turkey 11-14 May 2008

The Characteristics of Boron Modified Active Belite (BAB) Cement and its Utilization in Mass and Conventional Concrete

Aydın Sağlık [1]
Oya Sümer [2]
Ergin Tunç [3]
M.Fatih Kocabeyler [4]
Rahmi Sencer Çelik [5]

T 11

ABSTRACT

Energy, natural resources and environmental protection are the most important factors for the sustainability of technology. The production of Portland cement constitutes about 8% of the total CO_2 emission in the world today. The production of boron modified active belite (BAB) cement reduces the emission of CO_2 by up to 25% and saves a significant amount of energy due to low clinkering temperatures around 1325°C. These two factors are the main propulsive forces for the trial production of this cement. The production process of BAB cement is still in the test scale, however, first findings of the technical characteristics of the BAB cement are very noticeable. In this paper, by using boron modified active belite (BAB) and normal Portland cement, produced in Goltas Cement Factory, some chemical, physical and mechanical tests were carried out to investigate characteristics of the cement and concrete phases and evaluate the results in this first part of the research. In the second part of the research, besides some other tests, the microstructure of concrete made with BAB cement will be investigated mostly. BAB cement was standardized by Turkish Standard Institution as a type of Portland cement called "boron modified active belite cement" It has been found out that BAB cement has very low heat of hydration and less than 52,5 Cal/g at 7 days. Moreover, its early strength at first 7 days is less than that of normal Portland cement, however, beyond 7 days it gives same levels of strength values up to 28 days and later ages displays higher strength values than the normal Portland cement. In the durability part of tests like water permeability and chloride penetration resistance tests, concrete specimens made with BAB cement indicated more resistance as comparing to the specimens made with normal Portland cement even at lower cement contents.

KEYWORDS
Boron oxide, Active belite cement, Heat of hydration, Strength, Durability

[1] DSİ Genel Müdürlüğü, TAKK Dairesi Başkanlığı, Ankara, Turkey, 06100, Phone +90 312 3992796, Fax 312 3992795, aydinsaglik@dsi.gov.tr
[2] DSİ Genel Müdürlüğü, TAKK Dairesi Başkanlığı, Ankara, Turkey, 06100, Phone +90 312 3992796, Fax 312 3992795, oyasumer@dsi.gov.tr
[3] DSİ Genel Müdürlüğü, TAKK Dairesi Başkanlığı, Ankara, Turkey, 06100, Phone +90 312 3992796, Fax 312 3992795, ergint@dsi.gov.tr
[4] DSİ Genel Müdürlüğü, TAKK Dairesi Başkanlığı, Ankara, Turkey, 06100, Phone +90 312 3992793, Fax 312 3992795, mehmetf@dsi.gov.tr
[5] DSİ Genel Müdürlüğü, TAKK Dairesi Başkanlığı, Ankara, Turkey, 06100, Phone +90 312 3992792, Fax 312 3992795, sencerc@dsi.gov.tr

1 INTRODUCTION

Boron modified active belite (BAB) cement, a hydraulic binder, is finely ground and an inorganic material and forms cement paste hardening with hydration reactions when mixed with water. This cement paste maintains its strength and stability by the means of stable hydrate phases formed after hydration. This definition is completely compatible with Portland cement definition in TS EN 197-1 standard. Main component of BAB cement clinker is di-calcium silicate (α and/or α'-C_2S modifications), which is in active belite phase. Other mineralogical components are tri-calcium aluminates (C_3A) and tetra-calcium alumina ferrite (C_4AF) phases. Difference of BAB cement clinker from Portland cement clinker is that the main component is hydraulically high active belite phase instead of the alite phase. Hydraulically hardening of BAB cement rely on hydration of active belite phase, but other cement phases can also play some roles in the hardening process.

According to the results of tests carried out on boron modified belite (BAB) cement produced by adding one of the boron ores, Colemanite, to other cement raw materials (e.g. farine), it has been determined that C_3S phase, formed at high ratios in normal Portland cement, did not form at all or formed in very small amounts. At the same time, when producing BAB cement, the production temperature in the rotary kiln does not exceed 1325°C and as such, a decrease of about 25% in CO_2 emission is observed. In BAB cement, instead of C_3S (alite), one of the polymorphs of C_2S, having α or α'-C_2S crystal structure forms; this belite phase is quite active and stable phase. It is for this reason that this cement has been named as boron modified active belite cement (BAB).

In this research, the chemical, physical and mechanical properties of boron modified active belite (BAB) cement were examined. The composition of BAB cement contains about 3.0% (wt.) of B_2O_3 (boric oxide). The chemical composition of boron modified active belite cement has no C_3S, there is active and stable structured α and/or α'- C_2S crystal phase in extremely high amounts and the rate of hydration is significantly higher than cement containing the β-C_2S phase; consequently this results in the formation of a more compact and more dense concrete microstructure. In normal conditions the hydration of the β-C_2S phase of cement is very slow as compared to that of C_3S and gaining strength values is lately. However, the final strength is the same or greater than that for C_3S. Reaction of the β-C_2S (or the α- or α'-C_2S phases) and the reaction of the C_3S phase with water can be summarized as follows:

$2C_3S + 6H_2O \rightarrow C\text{-}S\text{-}H\ (C_3S_2H_8) + 3Ca(OH)_2$ (Fast Reaction)
$2C_2S + 4H_2O \rightarrow C\text{-}S\text{-}H\ (C_3S_2H_8) + Ca(OH)_2$ (Slow Reaction)

The hydration reaction of C_3S with water forms 2 times more $Ca(OH)_2$ than that of C_2S. Calcium hydroxide constitutes about 20% or 25% by volume of Portland cement paste. This component is the weakest component in the concrete and it mostly tends to gather on the interfacial and transition zone between the aggregate and cement paste. Failure in concrete generally begins on the surface between aggregate and cement paste and continues. Another negative aspect with normal Portland cement (including C_3S) is that high calcium hydroxide formation leads to increase of porosity ratio of concrete. However, in concretes made with BAB cement with high α and/or α'- C_2S, the ratio of calcium hydroxide will be rather low and this will lead to less porosity ratios (capillary pores) and therefore strength and durability of concrete will be higher with a more dense structure.

The fineness of BAB cement is a critical parameter because the strength development depends on the degree of fineness. In this research, the degree of fineness of BAB cement and normal Portland cement were chosen to be almost the same. The degree of fineness of both cements was around 3300 cm^2/g. For mass concrete structures the fineness of BAB cement is considered acceptable at around 3500 cm^2/g. However, when high early strength values are needed in structures such as concrete bridges, concrete roads and residence buildings and the like, it is possible to attain early strength development when using BAB cement as compared to normal Portland cement by increasing the fineness value of the BAB cement to 4000 ± 50 g/cm^2. Moreover, without increasing the fineness of the cement, high early strength values can easily be accomplished by using concrete chemical admixtures.

2 MATERIALS

Cement: All chemical, physical and mechanical tests of cements and all concrete tests were conducted on BAB and CEM I 42,5R Portland cement conforming to TS EN 197-1 and manufactured at the Goltas Cement Factory, Isparta, Turkey. The results of chemical analysis of the BAB cement is given in Table 1 and the results of the physical and mechanical tests of four different Blaine values of BAB cement are given in Tables 2 and 3. Moreover, some mechanical test results of normal Portland cement (CEM I 42,5R) conforming to TS EN 197-1 and very finely grounded Denizli BAB cement were given on Table 3.

Table 1 . Results of Chemical Analysis of Goltas BAB Cement.

Results of Chemical Analysis of BAB Cement, %	
Silicon Dioxide (SiO_2)	19.1
Aluminum Dioxide (Al_2O_3)	4.68
Ferric Oxide (Fe_2O_3)	3.42
Calcium Oxide (CaO)	57.1
Magnesium Oxide (MgO)	1.32
Chloride (Cl^-) (%)	0.001
Sulphur trioxide (SO_3)	2.68
Loss on Ignition	3.82
Insoluble Residue	0.70
Equivalent Alkalies (Na_2O+0,658.K_2O) (Na_2O=0,34 K_2O=0,78)	0.86
Boric Oxide (B_2O_3)	3.00
Clinker	86.1
Gypsum	4.85

Table 2. Results of physical test of Goltas BAB cement with different Blaine values.

Test and Standard	Blaine-1	Blaine-2	Blaine-3	Blaine-4
Density, TS EN 196-6, g/cm^3	3,09	3,09	3,15	3,14
Specific Surface (Blaine), TS EN 196-6, cm^2/g	3562	3778	4056	4273
Setting Times, TS EN 196-3, (Initial and Final), Min.	145 - 180	130 - 180	100 - 145	90 - 125
Soundness, TS EN 196-3, mm (<10,0 mm)	1,0	1,0	0,5	1,0
Standard Consistency Water, TS EN 196-3 (Normal Portland CEM I 42,5R Water = 28 g)	22,0	23,0	24,2	25,2

Table 3. Compressive strength development of Goltas BAB cements with different Blaine values, very fine Denizli BAB cement and normal Portland cement CEM I 42,5R.

Days	Compressive Strength Development of Goltas BAB Cement With Different Blaine Values, MPa				Denizli BAB Blaine : 4309 cm^2/g	Normal Portland CEM I 42,5R
	Blaine-1 3562 cm^2/g	Blaine-2 3778 cm^2/g	Blaine-3 4056 cm^2/g	Blaine-4 4273 cm^2/g		
2	13,4	13,6	15,5	16,9	17,4	26,8
4	23,1	29,0	31,6	34,0	30,5	34,0
7	28,4	38,0	40,6	43,5	41,5	40,6
14	35,5	44,5	49,0	55,0	55,0	46,0
28	41,5	50,0	54,0	61,0	65,0	50,0
90	50,2	58,5	61,5	67,0	70,0	55,0
180	51,6	62,5	66,0	69,5	72,0	57,0
365	58,5	67,0	70,0	72,0	74,0	58,0

Aggregate: In concrete tests, three classes of crushed aggregate (two classes of coarse and one class of fine aggregate) were used. Some physical tests results about the aggregates are given on Table 4.

Table 4 – Some physical test results of aggregates used in concrete specimens.

Classes of Aggregates	Specific Gravity	Water Absorption (%)	Aggregate Ratios Used in Concrete Mixes (%)	Fineness Modulus of Fine Aggregate
Coarse Agg. 1 (15-30 mm)	2,71	0,2	25,0	In Concrete F.M.= 2,63
Coarse Agg. 2 (7-15 mm)	2,70	0,3	25,0	
Fine agg. (0-7 mm)	2,70	1,2	50,0	2,57

3 EXPERIMENTAL STUDY

Cement Tests: the chemical, physical and mechanical tests conducted on both BAB and normal Portland cement produced at the Goltas Cement factory gave quite significant findings. All the results obtained with both cements are given in Tables 1 to 3. The most important characteristic of the BAB cement is that it has a very low heat of hydration even less than very low heat cement. The heat of hydration measurements were carried out with an isothermal conduction calorimeter for the BAB cement, normal Portland cement and Portland cement plus fly ash and the results are given on Figs 1 and 2.

Concrete Tests: with the lights of cement test results, concrete tests were started. In concrete tests, by using both BAB and normal Portland cement produced at Goltas Cement factory, same kinds of tests were conducted and the results were compared with each other. In concrete tests, especially durability aspect and strength development of samples were investigated. All concrete mixtures prepared in the laboratory are given on Table 5 in detail.

Table 5. Cement, mixing water contents and w/c ratios of concrete designs prepared in the laboratory. No chemical admixture was used in the mixtures.

Concrete Code	BAB or CEM I 42,5R Portland Cement Content, kg/m^3	Water Content kg/m^3	Water/Cement Ratio
BAB Cement Concrete with Slump 15 cm (Water Bleeding Exist)			
BD-1	250	200	0,80
BD-2	275	200	0,73
BD-3	300	200	0,67
BD-4	325	200	0,62
BD-5	350	200	0,57
BD-6	375	200	0,53
BD-7	400	200	0,50
BD-8	450	200	0,44
Normal Portland Cement Concrete with Slump 15 cm (Slump Loss Exist)			
ND-1	250	200	0,80
ND-2	300	200	0,67
ND-3	350	200	0,57
ND-4	400	200	0,50
ND-5	450	200	0,44
BAB Cement Concrete with Slump 10 cm (Slump Protection Exist)			
BD-9	250	190	0,76
BD-10	300	190	0,63
BD-11	350	190	0,54
BD-12	400	190	0,48
BD-13	450	190	0,42

Note: BD and ND abbreviations define different concrete mixtures as BD: BAB cement concrete mixtures and ND: normal CEM I 42,5R Portland cement concrete mixtures.

Concrete tests were carried out at the same amount of cement contents and same slump values with both cement types and all concrete mixes were made without using any chemical admixtures. The results of concrete mixes with different chemical admixtures will be given in the second part of research. At the beginning, the slump values of concrete mixes were chosen to be between 13 and 15 cm for pumpable concrete. However, it was observed that concrete mixes with BAB cement with a slump value of 15 cm showed some bleeding after moulding due to the slow hydration of BAB cement. Because the rate of hydration of C_2S containing BAB cement is slow and for this reason concrete mixes were not being subjected to any slump loss for a period of time and there was a long enough time to work with the concrete to be placed in a structure. For this reason it was decided that new concrete mixes should be made to obtain a slump value of 10 cm without showing any bleeding. With this method, 5% less mixing water was used in the concrete mixtures made with BAB cement resulting in a reduced w/c ratio. Whereas the concrete mixes with slump values of 15 cm were made with a mixing water dosage of 200 kg/m^3, the concrete mixes made with BAB cement and a slump value of 10 cm were made with a mixing water dosage of 190 kg/m^3. In the meantime, concrete mixes made with normal Portland cement with a slump value of 15 cm showed a significant level of slump loss, however, concrete mixes made with BAB cement with a slump value of both 10 cm and 15 cm did not show any significant slump loss for about 30 min.

4 TEST RESULTS

Tests results obtained from both types of cement and concrete phases are given in this section. A comparison among measurements for the development of heat of hydration over time for the BAB cement, normal Portland cement and Portland cement plus fly ash using an isothermal conduction calorimeter at constant temperature of 20 C are given in Figures 1 and 2. In technical specifications for mass concrete, values for the heat of hydration are limited to 60 Cal/g and 70 Cal/g for 7 and 28 days respectively. In any case, the rate of heat of hydration of BAB cement at early age is very low and the cement significantly reduces the adiabatic temperature rise of concrete. Given this property, BAB cement has many advantages in terms of economical, technical and logistical points of view as compared to other types of cement and binders. In Figures 1 and 2, the rate of heat of hydration and total heat of hydration results of BAB cement, normal Portland cement and normal 65% Portland cement plus 35% fly ash are given comparatively.

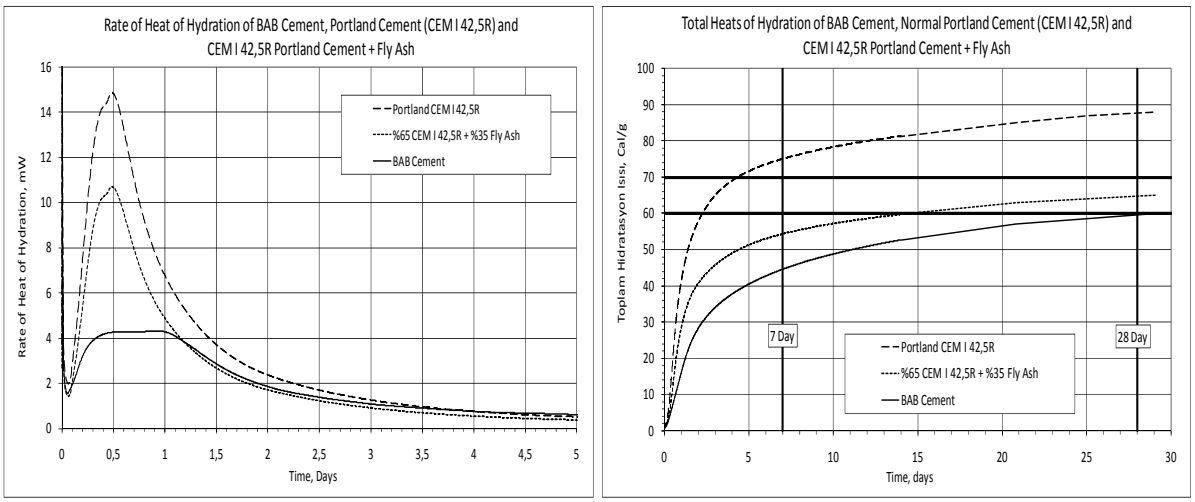

Figures 1 and 2 . The results of the rate of heat of hydration and total heat of hydration of BAB cement, CEM I 42,5R Portland cement and 65% CEM I 42,5R+35% Fly ash with I.C. Calorimeter.

The heat of hydration of BAB cement is very low in comparison with other types of cement and binders. For this reason, BAB cement can be utilized in all mass concrete structures without taking any extra precautions such as the installation of pre-cooling and post-cooling systems.. On the other hand, the

strength development of BAB cement is also in good levels except for at early ages. In later ages, the strength of BAB cement exceeds that of normal Portland cement as can be clearly seen in Figure 3.

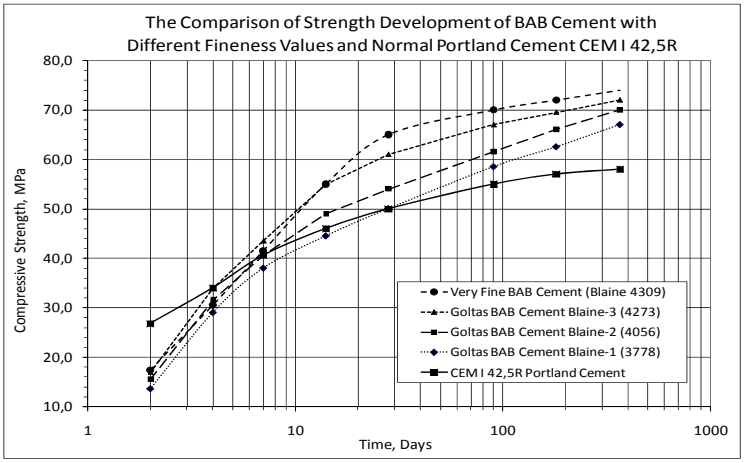

Figure 3. The strength developments of BAB cement with different Blaine fineness values and normal Portland cement.

Some experiments have been carried out with BAB cement in its concrete phase especially intended for measuring its durability and performance properties and considerable results have been attained. Studies were carried out with both cement types for quite a wide range of cement dosages (between 250 kg/m^3 and 450 kg/m^3) and tests were made for measurement of strength development, water permeability and resistance against chloride penetration. In Figures 4 and 5, the 7 and 28 day compressive strength values of concrete with different cement contents and with a slump value of 15 cm made with BAB cement and normal Portland CEM I 42,5R cement are given. The compressive strength changes with cement contents as is evident from the Figures. In Figures 6 and 7, values for concrete strength development for concrete having a 10 cm slump and made with BAB cement as compared to with a 15 cm slump made from normal Portland CEM I 42,5R cement. For these two cement types, a gap has been observed between the 7-day strengths of concrete specimens with 15 cm slump values. For the 28-day strengths, this gap disappears and the values were noted as almost the same. Moreover, concrete strength values of 10 cm slump concretes made with BAB cement are higher than concrete strength values of 15 cm slump concrete specimens made with normal Portland CEM I 42,5R cement at both the 7 day and 28 day cure.

Water permeability tests were carried out on concrete samples made with different cement contents of BAB cement and normal Portland cement according to EN 12390-8 Standard. From this work, a relation was obtained (shown in Fig. 8) that relates depth of water penetration to cement content. It has been determined that the degree of water permeability of concretes made with BAB cements is less than that of concretes made with normal CEM I 42,5R Portland cement. While concrete with 250 kg/m^3 cement content and with 10 cm slump value made with BAB cement was determined as almost impermeable against water and harmful chemicals, concrete made with BAB cement and 15 cm slump was determined almost impermeable to water. However, when concrete made with normal CEM I 42,5R Portland cement was examined, it has been determined that only concrete with 300 kg/m^3 Normal Portland cement content and higher cement contents are almost impermeable against water.

In Table 6, tests results for resistance to chloride penetration conducted according to ASTM C1202-05 are given. Results for concretes made with BAB cement with slump values of both 15 cm and 10 cm and concretes made with normal Portland cement with a slump value of 15 cm are provided. As can be clearly seen in Table 8, concretes made with the BAB cement are more resistive to chloride penetration than those made with normal CEM I 42,5R Portland cement. The resistance to chloride ion penetration of concrete made with normal Portland cement at 400 kg/m^3 cement content resulted in a high permeability class, whereas in comparison,, concrete made with BAB cement, even a lower

cement contents of 250 kg/m^3,resulted in a moderate permeability class. As a result, concrete made with BAB cement appears more durable than that made with normal Portland cement. The reasons for this were explained in detail in the introductory section. The theory and the test results gave quite parallel findings.

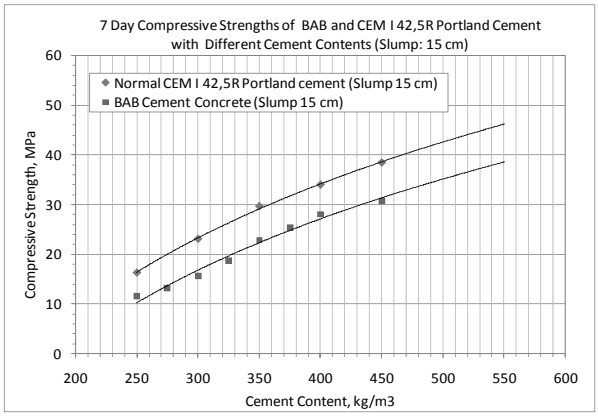

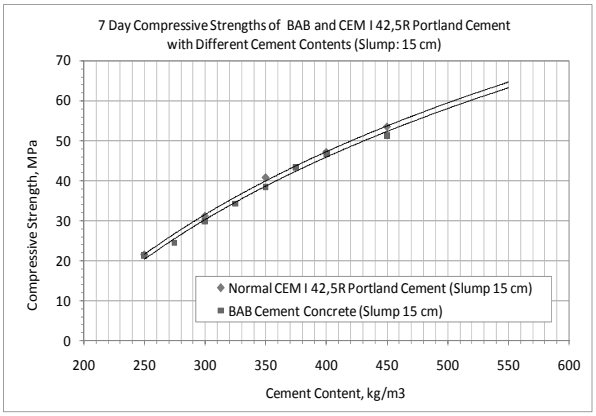

Figures 4 and 5 – The comparison of 7 and 28 days strengths test results of BAB cement concrete and normal Portland cement concrete with different cement contents and slump value of 15 cm.

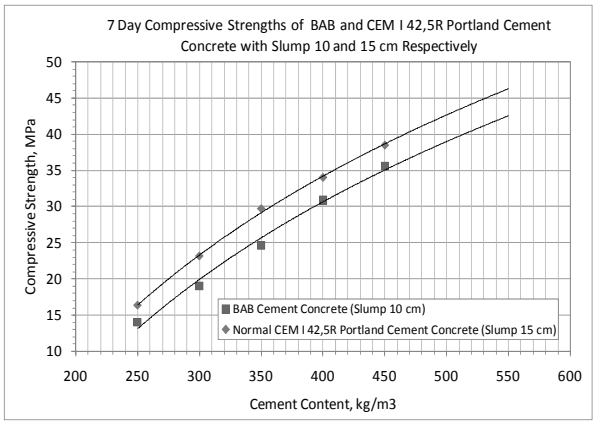

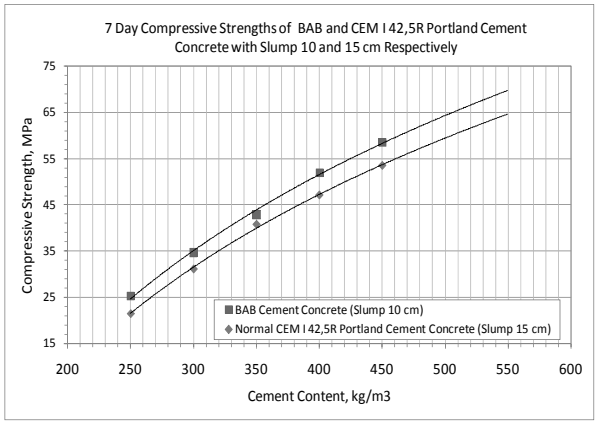

Figures 6 and 7 – The comparison of 7 and 28 days strengths test results of BAB cement concrete and normal Portland cement concrete with different cement contents and slump value of 10 cm.

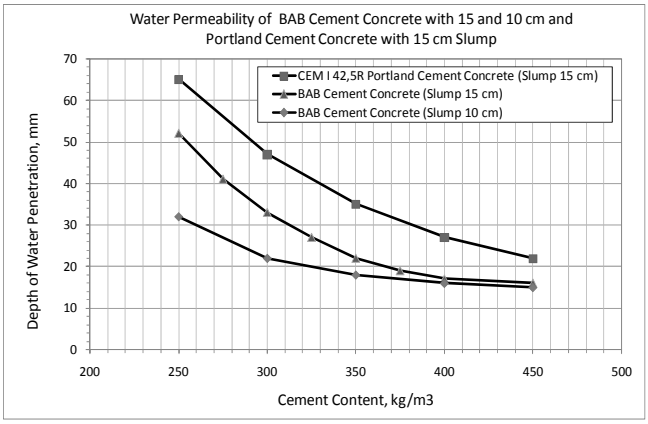

Figure 8 – The comparison of water permeability of concrete samples.

Table 6. The test results of chloride penetration resistance of concrete samples.

Concrete Code	BAB or CEM I 42,5R Portland Cement Content, kg/m^3	w/c ratios	Coulomb Value (Electrical Potential)	Permeability Class of Concrete
BAB Cement and Normal CEM I 42,5 Portland Cement Concrete (Slump = 15 cm)				
BD-3	300	0,67	4461	Moder.
BD-5	350	0,57	3622	Moder.
BD-7	400	0,50	3588	Moder.
ND-2	300	0,67	6830	High
ND-3	350	0,57	4849	High
ND-4	400	0,50	4833	High
BAB Cement Concrete (Slump = 10 cm)				
BD-9	250	0,76	4400	Moder.
BD-10	300	0,63	3512	Moder.
BD-11	350	0,54	3460	Moder.
BD-12	400	0,48	3289	Moder.

5 RESULTS AND DISCUSSION

The partial test results of both cement and concrete with BAB and normal Portland cement showed that this new BAB cement could be used in all massive concrete and in some conventional concrete structures where durability is of main concern. Despite the fact that early strength development seemed to be disadvantageous as comparing to normal Portland cement, however if necessary, by taking some precautions, this obstacle can be overcome most likely. During the pre-tests, a few chemical admixtures such as set-accelerator and high range water reducer were tried in concrete castings in order to investigate the early strength development of BAB cement concrete at 1, 3, 7 and 28 days. With a set-accelerator chemical admixture 5,0 MPa, 18,0 MPa and 29,0 MPa compressive strength values were obtained at 1, 3 and 7 days respectively. Also with a high range water reducer chemical admixture 8,8 MPa, 31,2 MPa and 54,2 MPa compressive strength values were obtained at 1, 3 and 7 days respectively. If needed Blaine value of BAB cement can be increased by up to 4300 cm^2/g in order to obtain higher early strengths of concrete. Moreover, dynamic modulus of elasticity, velocity of longitudinal pulses and transit times were measured on both concrete specimens made with either BAB or normal Portland cement. The first results showed that there is no significant difference between the concrete specimens made with both cement.

In the second part of the research, a more detailed research will be conducted; in particular, focus will be placed on characterising the microstructure of concrete and the effects of mineral and chemical admixtures on the properties of concrete. As well, tests on concrete specimens made with different Blaine values of BAB cement will be carried out to investigate the durability against different environmental effects.

ACKNOWLEDGEMENTS

The authors would like to deeply thank those individuals who provided the DSİ Genel Müdürlüğü with useful and helpful assistance and in particular the National Boron Institute (BOREN) and the Turkish Cement Manufacturers Association (TCMA).

REFERENCES

Türk, S., Gürbüz, G., Ertün, T. , Yeginobali, A., 2006,'Heat of hydration and shrinkage properties of Boron containing active belite cements', ConcreteLife'06 - International RILEM-JCI Seminar on

Concrete Durability and Service Life Planning: Curing, Crack Control, Performance in Harsh Environments, RILEM Publications SARL, pp.397 – 404.

Hewlet, P. C., 1998, '*Lea's Chemistry of Cement and Concrete'*, 4th Edition, London, UK.

'*Mass Concrete*' reported by ACI Committee 207.1R-05, *ACI Materials Journal*; November 1996.

Jinyu, L., Peng Xiaoping, Cao Jianguo, Chen Gaixin, Tian Juntao, Wang Xiujun, Lin Li, Wang Aiqin, Sui Tongbo, Wen Zhaijun, Zhang Chaoran and Shi Zhenhuan, 'Development and research of high belite cement dam concrete with low heat and high crack resistance', China Institute of Water Resource and Hydropower Research, Beijing, 100038, PRC, China Institute of Building Materials Research, Beijing, 100024, PRC, China Three Gorges Construction Corporation General, Yichang County, Hubei, Province, 443100, PRC.

Tongbo, S., Lei, F., Zhaijun, W., Jing, W., Zhonglun, Z., 2004, "Study on the Properties of High Strength Concrete Using High Belite Cement", *Journal of Advanced Concrete Technology*, Vol. 2, No.2, pp. 201-206, Japan Concrete Institute.

The Efficiency Comparison of Polyester, Acid Catalyzed Lacquers and Nitrocellulose Lacquers on *Fagus Orientalis* Wood and Plywood

Saeed Keshani Langroodi [1]
Mehrdad Sedghi [2]
Davood Parsapajouh [3]
Azad Henareh Khalyani [4]

T 12

ABSTRACT

Variety of consumption in wood products, new situations, variety of chemicals which are used for wood finishing, finishing process and necessity of wood preservation illustrate the necessity for choosing the best materials for wood and wood product finishing.

In this research, in order to study the effects of wood finishing materials on wood and plywood durability, nitrocellulose lacquers, acid catalyst lacquers and polyesters are applied on wood and plywood; next, the specimens are imposed to accelerate aging situation according to D3459 ASTM standard. Then, their physical and mechanical properties are measured.

The results have indicated that in bending strength and modulus of elasticity, polyesters are the best material; however, their efficiency are perceived only on plywood's specimens. On the other hand, there aren't many differences between paints in the case of massive wood. In glue-line shear strength, results have indicated that polyesters are the best materials after aging situation. In water absorption tests, acid catalyst lacquers are suitable finishes for water absorption; although, the rate of water absorption in polyesters are slower at first but this finishes couldn't endure aging and after accelerate aging the rate absorbed water increased. In Swelling Thickness, like water absorption, acid catalyst lacquers are the best water resistant paints; while, in long run, it could be useful after aging; but generally in short term preservation polyesters are the best of all.

KEYWORDS

Finishing, Aging, Plywood

[1] University of Tehran, Faculty of Natural Resources, Karaj, Iran, Phone 0098 911 245 4015 , saeedkeshani@libero.it
[2] Gonbad High Education Center, Gorgan University Of Agricultural Science & Natural Resources, Gonbad, Iran, Phone 0098 911 371 6385, mehrsedghi@yahoo.com
[3] University of Tehran, Faculty of Natural Resources, Karaj, Iran, Phone 0098 261 2223045, Fax 0098 261 2227565, parsa@nfr.ut.ac.ir
[4] University of Tehran, Faculty of Natural Resources, Karaj, Iran, Phone 0098 912 809 4409 henareh@nrf.ut.ac.ir

1 INTRUDUCTION

In Regard to limited resources of wood, the necessity of wood products' preservation is clear. Wood surface treatment is a method that is applied for preservation of wood and wood substrates. In addition, woods and wood products' durability against decay, temperature, moisture, chemicals and etc, makes their appearance more attractive and improve their efficiency to some extent. 'T. Eldwson *et al* [2003] find that the method of painting had the most effects on water movement in wood'. 'W.C.Feist and R. C. Williams [2004] studied on strength of plywood and paints efficiency that imposed in outdoor places. The results showed that the efficiency of oil based and latex against decay was excellent. In addition, paints had better durability in comparison to film forming paints. But their resistance against decay was more than film forming paints after 16 years of aging in the same situations'.

Application of surface treatments in comparison to other methods is simpler and make it possible to use it in structures that have built before; furthermore, it can be used easier with less limitation in wood substrates for example plywood.

Temperature, moisture, their interactions and periodical changes are critical factors on mechanical properties of wood and wood substrates; besides, these can change the solid wood properties and influence on glues in wood substrates. Therefore, these agents not only affect wood, but also they influence on internal glues and defects occur because of glue failures. 'B.H. River [1994] studied on outdoor effects on wood and wood substrates. They compare their efficiency to specimens that subjected to aging in laboratory tests. Results covey that solid wood have the best properties in comparison to wood substrates; that is because of the effects on glues, certainly density, the amount of chemicals and wood spices are influential on the results'. 'C.G.Carll and W.C. Feist [1989] prepare wafer board panels with different finishing and imposed them to weathering. Results showed that weathering and subsidence of application properties are touch on their finishing'.

There are many researches on practical properties of wood and wood substrates in outdoor situations but there are a few studies on properties and aging on wood and wood substrates on indoor spaces. As far as a perfect finishing may increase the efficiency of wooden structures, so the prospect of this research is the efficiency comparison of polyester, acid catalyzed lacquers and nitrocellulose lacquers, three chemicals that used for wood finishing and aging on wood and plywood on indoors spaces. These comparisons are based on mechanical and physical properties of specimens.

2 MATERIALS AND METHODES

At the first stage, the specimens which are *Fagus Orientalis* wood and plywood cut into standard tests dimensions according to ASTM D1037 with the exception of specimens that are used for water absorption and thickness swelling. In these specimens because of the limitation in the size of the logs the ISO standard are applied. After preparation of specimens all of them except those are used as untreated specimens paint with sealers; after that each group of them separately are painted with polyester, acid catalyzed lacquers and nitrocellulose lacquers.

Before the main aging stage, all specimens put in laboratory situations 23±2°C and 65±3% relative humidity (RH). Then, accelerate aging are used for this research according to ASTM D3459 standard. Half of the specimens are put in accelerate aging situation and others are put aside as untreated specimens. In accelerate aging, at first, the specimens are placed in oven 50±2°C while the air circulated around them to prevent overheating. After 48 hours the specimens are put in 50 ±2°C and 97±2% RH; germinator are used for this purpose. After 48 hours in germinator the specimens are put in 23±2°C and 65±3% relative humidity (RH). We repeat these periods five times and after that physical and mechanical properties of all specimens are measured, according to ASTM D1037. INSTRUN® machine are applied for measurement of these properties. The data analyzed by statistical

methods. In addition, the data are compared separately reaching the rate of changes in mechanical and physical properties of specimens.

3 RESULTS AND DISCUSSION

Statistical analyses and comparison of data showed these results which are mentioned here:

3.1 Bending Strength and Modulus of Elasticity in Grains Direction

In plywood specimens the effect of aging and finishing on modulus of elasticity (MOE) and bending strength (BS) in grains direction showed significant different of 1% in statistical analyses. Interaction of two factors on MOE is not significant and bending strength was significant in 1%. In solid wood the effect of aging, finishing and their interaction effect on MOE and bending strength are not significant in exception of aging on MOE that are significant in 5%. The rates of changes are showed in [Table1 and Table2] . The numbers in [Table 1] convey the differences between physical and mechanical properties of the specimens before and after accelerate aging. We can see that all the specimens lose their efficiency to some extent when they encounter to the aging situation. But these rates show a dramatic change in plywood, especially in the physical properties, (water absorption, and thickness swelling).

Table 1. The rate of decrease in physical and mechanical properties after accelerate aging in plywood and wood in all specimens.

tests	*plywood [%]*	*wood [%]*
MOE Parallel to grains direction	-6.9	-3.7
MOE vertical to grains direction	-7.5	-2.8
BS Parallel to grains direction	-9.9	-8.2
BS Vertical to grains direction	-7.4	-2.8
Glue-line shear	-24.7	-
Water absorption 2hours	-37.3	-25
Water absorption 24hours	-15.5	-21.5
Swelling in thickness 2hours	-33.9	-2.5
Swelling in thickness 24hours	-25.2	-11.7

We could find from these results that aging in bending strength were effective on plywood rather solid wood and it approximately hasn't effect on MOE and bending strength. For example, [Table1] show 6.9 percent decrease in MOE parallel to grains in comparison to 3.7 percent decrease in wood. We can find their reasons in the structure of these materials. In plywood urea formaldehydes as glue are sensitive in periodical changes of temperature and moisture. Temperature and moisture cause fail in performance of glue that it eventually decrease the mechanical properties in plywood but in solid wood temperature and moisture periodical changes can't influence on wood properties because of its solid and massive structure; however, it may cause some cracks that it happen in plywood too, but, it's less than we observed in solid wood.

In the case of paints polyesters show the best resistance in accelerate aging situation [Table2]. Furthermore, it increases MOE and bending strength of specimens. That is because of the solid structure of polyesters that enhanced the mechanical properties; in addition, it preserved wood materials from periodical changes of temperature and moisture. Also, it's found in comparison of nitrocellulose lacquers and acid catalyst lacquers (A.C. lacquers) to untreated specimens that these paints have positive effects on preservation of specimens in accelerate aging situation, but they don't strengthen the mechanical properties of specimens because of the more flexible structure of these film layers that they have.

In the case of solid wood polyesters are the best materials for surface preservation against aging and then nitrocellulose lacquers and at last A.C. lacquer; but this difference generally is not significant in statistical analyses in wood specimens. 'According to River [1994] decrease in MOE and bending strength in solid wood specimens was less than the same properties in plywood specimens'. Therefore, in this case the best material for aging preservation is polyester; however, its efficiency on plywood and in the case of solid wood doesn't show many differences between paints in statistical analyses.

Table 2. Comparison of polyesters [A], A. C. Lacquers [B] and nitrocellulose lacquers [C] to untreated specimens in plywood and wood in all specimens before and after aging.

tests	*plywood*			*wood*		
	A	*B*	*C*	*A*	*B*	*C*
		[%]			*[%]*	
MOE Parallel to grains direction	+8.9	+2.4	+5.7	+2.3	+2.8	+1.6
MOE vertical to grains direction	+6.68	+7.26	+4.68	+1.8	+6.8	+4
BS Parallel to grains direction	+11.5	+3.01	+8.41	+0.5	+0.6	+0.2
BS Vertical to grains direction	+7.5	+1.9	+2.1	+1	+0.01	+0.3
Glue-line shear	+34.7	16.1	+12.1	-	-	-
Water absorption 2hours	+81.4	+77.7	+74.9	+57.8	+78.6	+77.7
Water absorption 24hours	+62.9	+44.9	+43.3	+57.2	+53.3	+54.1
Swelling in thickness 2hours	+61.3	+68.6	+43	+13.1	+49.5	+42.6
Swelling in thickness 24hours	+52.2	+27.7	+25.5	+27	+44.9	+33.2

3.2 Glue Line Shear Strength

Statistical analyses results show a significant difference 5% after aging in this property and it isn't significant about finishing and finishing - aging interaction. However, [Table1 and Table2] show the efficiency of paints in accelerate aging situation; but, they can't improve the mechanical properties in specimens that aren't imposed in accelerate aging situation. Aging affect the glue line and decrease this property. This test is measurable only in plywood.

3.3 Water Absorption

It can be inferred from results that aging is an initial factor in water absorption and it affect on finishing performance. In accordance with statistical analyses and the amount of water absorption that are showed in [Table 1 and Table 2] a large amount of water absorption are observed in solid wood. We can come to conclusion that the amount of water absorption in specimens are because of the water that absorbed by wood material itself; of course, the amount of absorbed water in plywood is more than solid wood and it might be because of the remained water between wood layers and broader surface that face to water. A. C. lacquers specimens can be the best finishing in water absorption. In spite of that the amount of water absorption in polyester specimens is rather than other paints at first. But these paints can't tolerate accelerate aging situation that lead to absorption of more water that is because of the fine cracks occur on the surface of the paint's layer. So, water can penetrate easily under paint but the efficiency of these paints is like nitrocellulose lacquers after aging. In the case of A.C. lacquers thanks to their flexible structure, the paint's layer can protect the wood and plywood better; therefore, it's an ideal paint against water absorption in long run.

3.4 Thickness Swelling

In this case results indicate that the most important factor in thickness swelling in plywood is the separation of wood layers in plywood. Statistical analyses show that there aren't significant differences between paints and specimens that are imposed to accelerate aging situation and those that aren't. In regard to [Table 1 and Table 2], thickness swelling in polyesters are not so high because of theirs solid molecule structure. Solid structure hold wood layers tightly in theirs solid structure; but

fine crakes appear after aging. When these fine cracks develop the solid structure may break up and layers separate because of more water absorption and it causes more thickness swelling. But in nitrocellulose lacquers their flexible layer are more stable in periodical change of moisture and temperature; therefore, in long term preservation can be the best materials; however, polyesters are the best one in short term periods of preservation. Nitrocellulose lacquers in comparisons to others are in the lower level. More water absorption and thickness swelling of these specimens are because of their chemical properties. A complete polymerization that there are in polyesters and A.C. lacquers don't happen in these paints; therefore, water can penetrate easier under the paints layers.

4 CONCLUSIONS

The results have showed that in bending strength and modulus of elasticity, polyesters are the best materials, but, these paints are effective only on plywood and there aren't many differences between wood finishing materials in the case of massive wood .it is because of that aging effect on glues more than wood itself. Therefore, when plywood imposed to aging situation, the paints can show their efficiency better.

In glue-line shear strength, results have indicated that polyesters are the best materials after aging situation. In water absorption tests, acid catalyst lacquers are suitable finishes for water absorption; however polyesters absorb less water at first but this finishes can't endure aging and after accelerate aging situation the amount of absorbed water increase. We can find its reason in different chemical properties that paints have.

In Swelling Thickness, like water absorption, acid catalyst lacquers are the best water resistant paints; then in long term, it can be useful after aging; however, in short term preservation polyesters are the best of all.

REFERENCES

Carll, C.G., & Feist, W.C., 1989, 'Long-term weathering of finished *Aspen* waferboard', *Forest Product Journal.* **39**, 25- 30.

Eldwson, T., Bergstrom M., & Hamalainen M., 2003, 'Moisture dynamics in *Norway spruce* and *Scots pin* during outdoor exposure in relation to different surface treatments and handling condition'. *Holzforschung*. **57**, 219- 227.

River, B.H., 1994, 'Outdoor aging of wood- based panels and correlating with laboratory aging'. *Forest Product Journal.* **44**, 55-65.

Williams, R.S., & Feist, W.C., 2004, 'Durability of *yellow-poplar* and *sweetgum* and service life of finishes after long- term exposure'. *Forest Product Journal*. **54**, 96-101.

11DBMC International Conference on Durability of Building Materials and Components
ISTANBUL, Turkey 11-14 May 2008

Modification of Wood with Si and B Compounds

S. Nami Kartal [1]
Tsuyoshi Yoshimura [2]
Yuji Imamura [3]

T 12

ABSTRACT

In the study, tetraethoxysilane and methyltriethoxysilane were tested as modifying Si-compounds to limit boron leachability from modified wood and to increase biological durability of the wood against fungi and termites. Both silane compounds were used in silane state in where acidified ethanol was added and stirred at ambient temperature for 30 min. There were two different processes for preservative treatments: double and single treatments. In double treatments, specimens from sugi wood were first treated with boric acid at 1% concentration and the specimens were then treated with the silanes. In single treatments, boric acid was mixed with the silane compounds in silane state yielding 1% boric acid concentration. After treatments, the wood specimens were subjected to laboratory leaching tests and leachates were analyzed for boron content by using Induced Coupled Plasma Spectrometry (ICP). ICP analyses showed that silane treatments in the study were able to limit boron leaching from treated wood by about 40% in all cases for each silane compound. The specimens were subjected to laboratory termite and decay resistance tests using the subterrenean termites, *Coptotermes formosanus*, and the wood decaying fungi, *Fomitopsis palustris* and *Trametes versicolor*. Termite and fungal decay resistance tests revealed that resistance of modified wood with the silane compounds and boron increased when compared to untreated and boron-only treated wood specimens. More detailed studies are in progress to obtain a better understanding of the mechanisms of interaction between the silicon compounds, boron element and wood components.

KEYWORDS

Wood modification, Boron, Silicone, Silane, Biological resistance

[1] Istanbul University, Forestry Faculty, Istanbul, Turkey 34473, Phone: +90 212 226 11 00, Fax: +90 212 226 11 13, snkartal@istanbul.edu.tr
[2] Research Institute for Sustainable Humanosphere (RISH), Kyoto University, Kyoto, Japan 611-0011, Phone: +81 774 38 3664, Fax: +81 774 38 3664, tsuyoshi@rish.kyoto-u.ac.jp
[3] Research Institute for Sustainable Humanosphere (RISH), Kyoto University, Kyoto, Japan 611-0011, Phone: +81 774 38 3662, Fax: +81 774 38 3664, imamura@rish.kyoto-u.ac.jp

1 INTRODUCTION

Various chemical compounds have been used for the modification of wood to improve its several characteristics [Donath *et al*. 2004; Rowell 1983; Militz *et al*. 1997; Norimoto 2001]. Many types of silicon compounds have been applied for this purpose. Silanes are long known as modification agents in a number of applications and they are used for hydrophobication of ceramics, scratch resistant surfaces, soil proofing and anti-graffiti coatings or as adhesion promoters between organic and inorganic materials [Donath *et al*. 2004; Hill *et al*. 2004; Mai *et al*. 2003]. The silanol groups of silanes can react with hydroxyl groups of cell wall polymers forming a covalent bond between the silicon compound and cell wall polymers; however, Si–O–C-bonds are weak and susceptible to hydrolysis. Alkylalkoxysilanes bear at least one alkyl group which remains after the sol–gel process because, in contrast to Si–O-bonds, the Si–C-bonds are stable against hydrolysis [Brinker and Scherer 1990; Sebe and Brook 2001; Donath *et al*. 2004].

Besides improved wood properties, modification may have potential for limiting preservative release from treated wood and increasing biological resistance against wood degrading fungi and insects. Kartal *et al*. [2004] found that acryl-silicon type resin emulsion and boron-treated wood specimens resulted in about 54% boron release after a 10-day leaching process; however, nearly all boron was leached out from boron-only treated specimens. Similar results were obtained when wood specimens were treated with both boron containing quaternary ammonia compound (DBF) and the same emulsion in surface treatments Kartal *et al*. [2004]. A study by Lin and Chen [2005] has showed that a series of cleavable water-soluble silicon surfactants prepared by the reaction of a hydroxyl-terminated polyester and an organopolysiloxane bear siloxane as the functional group of water repellency effect.

Since several silicon compounds may have ability to increase water repellency and reaction with cell wall components, such compounds can be used for limiting boron release from boron-treated wood. In this study, tetraethoxysilane and methyltriethoxysilane compounds as modifying Si-compounds were tested to limit boron leachability from chemically modified wood and to increase biological durability of the wood against wood degrading fungi and termites.

2 MATERIALS AND METHODS

Wood specimens, 20 (radial) by 20 (tangential) by 10 (longitudinal) mm, were cut from sapwood portions of sugi wood (*Cryptomeria japonica* D. Don). Before treatment, all wood specimens were conditioned at 20°C and 65% relative humidity (RH) for 2 weeks. The specimens were free of knots and a visible concentration of resins, and showed no visible evidence of infection by mold, stain, or wood-degrading fungi.

As modifying agents, tetraethoxysilane (Si-I) and methyltriethoxysilane (Si-II) were used in silane state where acidified ethanol (1 mol) was added to the silanes and stirred at ambient temperature for 30 min as described by Donath *et al*. [2004]. As catalyst, 2.1 and 0.9 mg/l HCl (37%) was added to tetraethoxysilane and methyltriethoxysilane compounds, respectively [Donath *et al*. 2004].

There were two different processes for preservative treatments: double treatments and single treatments. In double treatments, wood specimens were first treated with boric acid (BA) at 1% concentration. The specimens were then reconditioned at 20°C and 65% RH for one day and treated with the silane compounds in silane state. In single treatments, BA was mixed with the silane compounds in silane state yielding 1% boric acid concentration.

In both treatments, treatment cycle consisted of a 40-minute vacuum (-88 kPa absolute pressure) in a treatment desiccator. After all treatments, the specimens were blotted dry and reweighed to determine

the uptake chemical retention. All treated specimens were then reconditioned at 20°C and 65% RH for one day and then dried at 105°C for one day before leaching process.

The leaching process was conducted according to Japanese Industrial Standard (JIS) K 1571 [2004] The process involved immersing wood specimens in distilled water, stirring with a magnetic stirrer (400-450 rpm) at 27°C for 8h followed by drying at 60°C for 16 h. This cycle was repeated 10 times. After each leaching cycle, the water was renewed with fresh distilled water to a ratio of 10 volumes of water to 1 volume of wood. The sample preparation for boron analyses was similar to the American Wood Preservers' Association (AWPA) A2-98 standard method [AWPA 1999]. The specimens were ground to pass through a 40-mesh screen in the Wiley Mill, oven-dried, and 1.5 g of ground wood was weighed to the nearest 0.001 g into a 250 ml flask. For each treatment group, two specimens were ground and analyzed. One hundred ml of deionized water was added to the flask containing the ground wood. The flask was placed in a water bath at 90-95°C for 60 min with agitation every 15 minutes. After cooling, the contents in the flask were filtered through Whatman #4 filter paper, rinsed 3 times with 20 ml of hot deionized water, and diluted to 200 ml in a volumetric flask. Leachates sampled from the leaching cycles for 10 days and extracts from the treated wood were analyzed with an ICP Sequential Plasma Spectrometry (ICP-S 1000III Shimadzu Co Ltd, Japan). The percentage reduction of boron in the specimens was calculated based on the initial amount of boron in the specimens.

Untreated and treated specimens were exposed to the subterranean termites, *Coptotermes formosanus* Shiraki, according to the JIS K 1571 standard method [(2004]. An acrylic cylinder (80 mm in diameter, 60 mm in height) whose lower end was sealed with a 5 mm thick hard plaster (GC New Plastone, Dental Stone, G-C Dental Industrial Corp., Tokyo, Japan) was used as a container. A test specimen was placed at the centre of the plaster bottom of the test container. A total of 150 worker termites collected from a laboratory colony of RISH, Kyoto University were introduced into each test container together with 15 termite soldiers. Five wood specimens per treatment were assayed against the termites. The assembled containers were set on damp cotton pads to supply water to the specimens and kept at 28°C and >85% RH in darkness for three weeks. The mass losses of the specimens due to termite attack were calculated based on the differences in the initial and final oven-dry (60°C, 3 days) weights of the specimens after cleaning off the debris from the termite attack.

Decay resistance test was conducted according to Japanese Industrial Standards [JIS K 1571 2004] using the brown-rot fungus, *Fomitopsis palustris* (Berkeley et Curtis) Murrill (FFPRI 0507) and the white-rot fungus, *Trametes versicolor* (L. ex Fr.) Quel. (FFPRI 1030). After the oven-dried weights were determined, the specimens were sterilized with gaseous ethylene oxide. Three wood specimens per treatment were placed in a glass jar on the surface of 250 g quartz sand wetted with 80 ml nutrient solution and inoculated with liquid fungal cultures. Liquid fungal cultures were prepared inoculating 1000 ml liquid medium which contained 40 g glucose, 3 g peptone, 15 g malt extract and 1000 ml distilled water. The medium was shaken at 26°C for 10 days at 100 rpm. The nutrient solution used for wetting the quartz sand contained 40 g glucose, 3 g peptone, 15 g malt extract and 1000 ml distilled water for the white-rot fungus and 20 g glucose, 1.5 g peptone, 7.5 g malt extract, and 1000 ml distilled water for the brown-rot fungus. The test jars were then incubated at 27°C for 12 weeks. Nine replicates were tested for each decay fungus. The extent of the fungal attack was expressed as the percentage of mass loss.

3 RESULTS AND DISCUSSION

Figure 1 shows a scheme for the sol-gel deposition of alkoxysilane on the wood surface, causing covalent bonds with the wood surface and resulting in hydrophobication. Sebe *et al*. [2004] has stated that silicon-based monomers undergo selective bond cleavage and recombination to form macromolecular layers based on Si-O-Si and Si-O-C linkages. Covalent grafting of silicon polymers is considered as another potential reaction of wood hydrophobization. Saka *et al*. [2001] have suggested that silane compounds react with the cell wall via the sol-gel process to achieve a deposition of the

silicon in the wood. They also observed that the silicon compounds in the lumina of the wood did not make any contribution to decreased water absorption [Saka *et al*. 1992]. Sol-gel polycondensation networks of alkoxysilanes deposited within the wood cell wall enhance the water resistance properties of wood [Tshabalala *et al*. 2003].

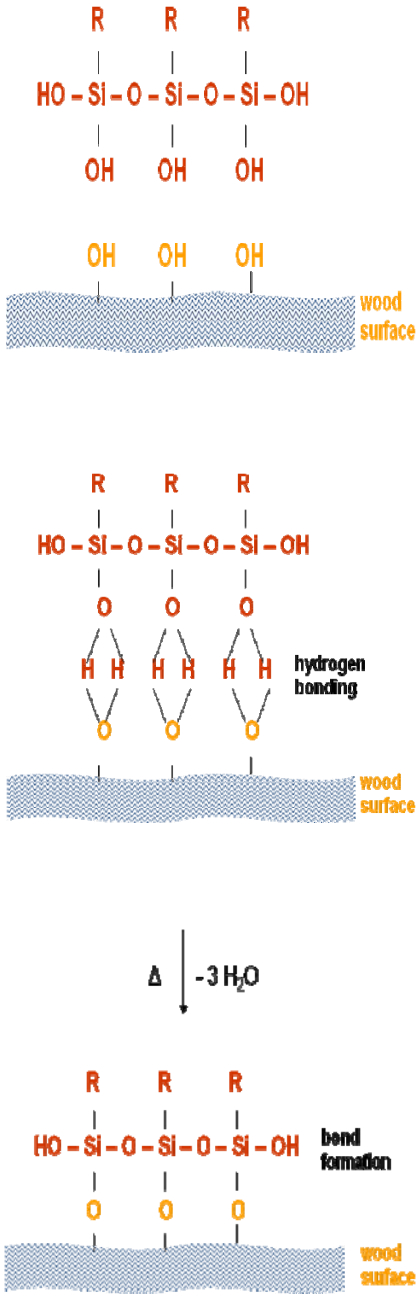

Figure 1. Scheme for deposition of alkoxysilane on wood and hydrophobication - covalent bond formation in silanol groups of alkoxysilane, and hydrophobication on wood surface.

Figure 2 shows the amount of boron released from the specimens during the 10-day leaching course as ppm. In BA-only treated specimens, totally 212 ppm boron release was determined and only 189 ppm boron was released on the first day of leaching. Si-I and Si-II treated specimens showed less boron release during the course.

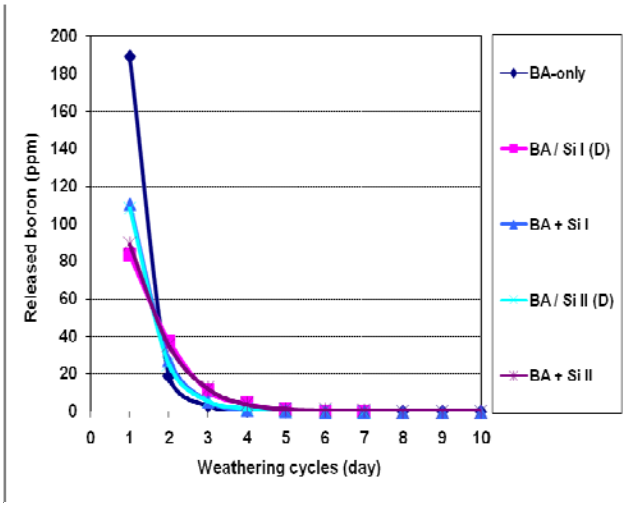

Figure 2. Released boron from treated specimens.

Figure 3 shows the percentage boron release from the specimens at the end of the leaching course. Nearly all boron was leached out from BA-only treated wood specimens; however, about 40% of total boron remained in the specimens treated with either Si-I or Si-II compounds. It should be noted that original BA retention was in the specimens nearly 7 kg/m^3 before leaching. Less boron leachability in Si-I nd Si-II treated specimens likely resulted from a reduction in the pore size and spaces within the cell wall, which are a pathway for the adsorption of water. Similar results were obtained by Donath *et al*. [2004]. They treated wood specimens with various types of alkoxlysilanes and has suggested that the chemical modification of wood requires the reaction of chemicals with cell wall components to achieve mechanical fixation of the compounds in the wood. In our study, most of the boron located in the wood lumina was leached out from the treated specimens, since there was no reaction between either boron or silicon precipitated in the lumina. It is assumed that some parts of boron located in the cell wall together with the silicon emulsion remained in the wood after the leaching process.

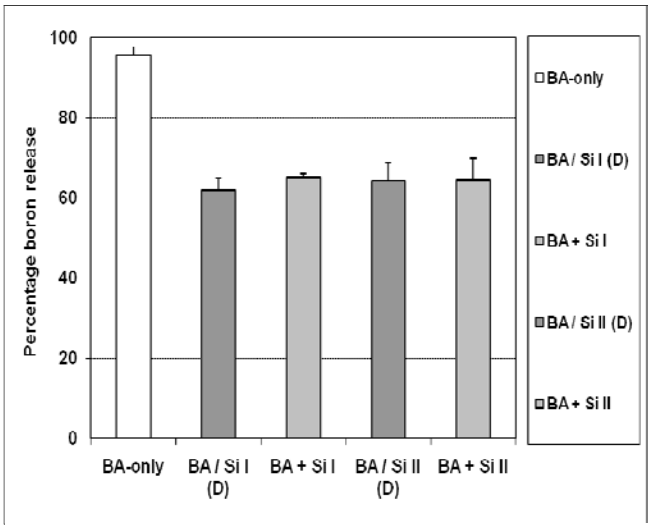

Figure 3. Percentage boron released from treated specimens.

Figure 4 shows mass losses in the specimens occurred after a 3-week exposure to the subterranean termites, *C. formosanus*. All unleached specimens showed perfect protection against the termites; however, mass losses in control specimens and BA only treated and leached specimens were nearly 30%. The more interesting results were obtained in Si-I and Si-II treated specimens. In those specimens, mass losses were considerably lower than BA-only and untreated control specimens. As

mentioned before, about 40% of total boron remained in those specimens suggesting that remaining parts of boron along with the silicon compound increased the resistance. In our study, it was found that nearly 2.5 kg/m^3 BA-retention in the specimens was achieved after leaching. Commercial retentions to provide protection against termites are usually in excess of about 4.5 kg/m^3 boric acid equivalent (BAE). However in the UK, treatments require 1.8 kg/m^3 BAE minimal cross-sectional retention because termite risks are considerably lower. Lumber receiving commercial treatment with borates in the United States is treated with DOT (disodium octoborate tethrahydrate) and receives a borate retention of 2.7 kg/m^3 BAE to control decay, beetles, and native termites or 4.5 kg/m^3 BAE to protect against Formosan subterranean termites [Lloyd 1997].

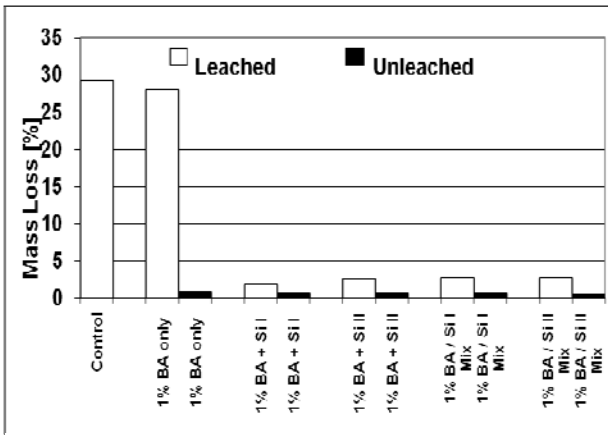

Figure 4. Mass losses in the specimens exposed to termite resistance tests.

Mass losses in the specimens exposed to 12-week fungal resistance tests followed by a 10-day leaching process are given in Fig. 5. Mass losses in untreated control specimens for both fungi, *F. palustris* and *T. versicolor* exceeded 30%. BA-only treated specimens also showed similar mass losses due to high boron release from the specimens during the leaching process. However, unleached specimens of this treatment group showed no mass losses. Mass losses in Si-I and Si-II treatments were lower than 5% suggesting that remaining boron in the specimens after leaching was able to protect wood against the fungi tested.

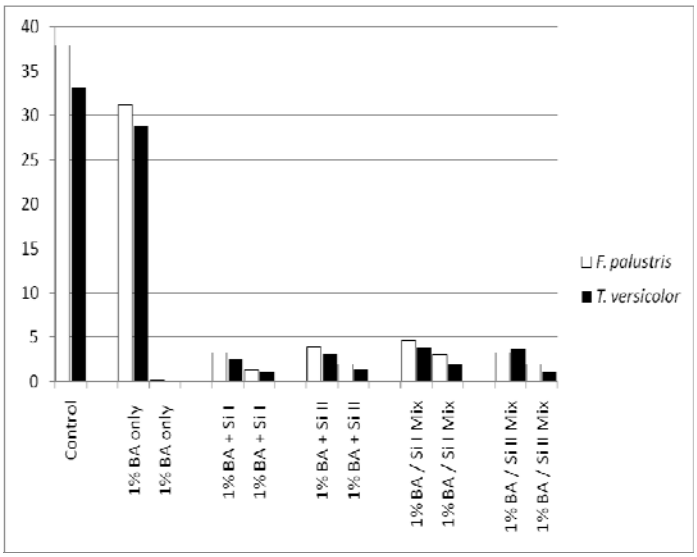

Figure 5. Mass losses in the specimens exposed to decay resistance tests.

European standards usually require 0.76, 0.59, 0.32, and 0.30 kg/m^3 DOT retention levels for protection against *Trametes versicolor*, *Gloeophyllum trabeum*, *Coniophora puteana*, and *Poria placenta*, respectively [Lloyd 1997]. Na-borate retention levels of 0.8-1.1 kg/m^3 were needed to protect wood against *Neolentinus lepideus*, *C. puteana* and *P. placenta*, but more Na-borate retention levels were needed against *T. versicolor* and *G. trabeum*, respectively [Abbot *et al*. 2000]. Tsunoda [2001] found that the toxic threshold values for sugi sapwood specimens treated with BA were 0.8 kg/m^3, 0.9-1.8 kg/m^3, and 0.9-1.8 kg/m^3 BAE against *T. versicolor*, *F. palustris*, and the subterranean termites, *C. formosanus*, respectively. A study by Akbulut *et al*. [2004] showed that 0.1% BAE borax treatment in the MDF specimens decreased mass losses to below 3% against *F. palustris* and *T. versicolor*.

4 CONCLUSIONS

The effects of two silane compounds, tetraethoxysilane and methyltriethoxysilane on both boron leaching and decay and termite resistance of wood specimens under laboratory conditions were evaluated. The silane treatments helped wood retain about 2.5 kg/m^3 boric acid retention in the specimens after the leaching process. Several previous studies showed that termite resistance usually requires retention levels of BAE of more than 1 kg/m^3 in the wood; however, less than 1 kg/m^3 retention is needed to protect wood against wood decaying fungi. In our study, the specimens treated with BA and the silane compounds showed resistance against the fungi and the subterranean termites, *C. formosanus* after the leaching process.

ACKNOWLEDGMENTS

The first author acknowledges The Turkish Academy of Sciences (TUBA) for the grant given under the Program to Reward Successful Young Scientists (TUBA-GEBIP), and RISH and National University Corporation, Kyoto University, Japan.

REFERENCES

American Wood Preservers' Association (AWPA). 1999, 'Standard methods for analysis of waterborne preservatives and fire-retardant formulations', AWPA A2-98. AWPA, Birmingham, AL.

Abbot, W., Woodward, B., & West, M., 2000, 'Efficacy of copper borax preservative against wood decay', Proceedings of 97th Annual Meeting of the American Wood-Preservers' Association (AWPA). Minneapolis Marriott City Center Minneapolis, Minnesota, May 20-23, 2000. Volume 97. American Wood-Preservers' Association Granbury, Texas.

Akbulut, T., Kartal, S.N., & Green, F., 2004, 'Properties of medium density fiberboard (MDF) treated with N'-N-(1, 8-Naphthalyl) hydroxylamine (NHA-Na), borax and boric acid', *Forest Products Journal* **54[**10], 59-64.

Brinker, C.F., & Scherer, G.W., 1990, *Sol-Gel-Science*. Academic, San Diego.

Donnath, S. Militz, H. & Mai, C. 2004, 'Wood modification with alkoxysilanes', *Wood Science and Technology* **38**, 555-566.

Hill, C.A.S., Farahani, M.R.M., & Hale, M.D.C., 2004, 'The use of alkoxysilane coupling agents for wood preservation', *Holzforschung* **58**, 316-325.

JIS K 1571. 2004, 'Test methods for determining the effectiveness of wood preservatives and their performance requirements (in Japanese)'. Japanese Standard Association.

Kartal, S.N., Yoshimura, T. & Imamura, Y., 2004, 'Improvement of boron leachability from disodium octoborate tetrahydrate (DOT)-treated wood by *in situ* copolymerization of allyl glycidyl ether (AGE) with methyl methacrylate (MMA)', *International Biodeterioration and Biodegradation* **53**[2], 111-117.

Lin, L.H., & Chen, K.M., 2006, 'Surface activity and water repellency properties of cleavable-modified silicone surfactants', *Colloids and Surfaces A: Physicochem. Engineering Aspects* **275**, 99-106.

Lloyd, J.D., 1997, 'International status of borate preservative systems', Proceedings of the Second International Conference on Wood Protection with Diffusible Preservatives and Pesticides. Proceedings No. 7284, Forest Prod. Soc., Madison, WI. pp. 45-54.

Mai, C., Donath, S. & Militz, H., 2003, 'Modification of wood with silicon compounds', Proceedings of the First European Conference on Wood Modification. Gent, Belgium. pp. 239–251.

Militz, H., Beckers, E.P.J., & Homan, W.J., 1997, 'Modification of solid wood: research and practical potential', IRG International Research Group on Wood Preservation, Stockholm. Document No. IRG/WP 40098.

Norimoto, M., 2001, 'Chemical modification of wood', In: Hon DNS, Shiraishi N (eds) *Wood and Cellulosic Chemistry*, 2nd Edition, Dekker, New York, pp 573–598.

Rowell, R.M., 1983, 'Chemical modification of wood', *Forest Products Abstracts* **6**, 363–382.

Saka, S., Sasaki, M., & Tanahashi, M., 1992, 'Wood–inorganic composites prepared by sol-gel processing. 1. Wood–inorganic composites with porous structure', *Mokuzai Gakkaishi* **38**, 1043–1049.

Saka, S., Miyafuji, H., & Tanno, F., 2001, 'Wood-inorganic composites prepared by the sol-gel process', *Journal of Sol-Gel Science Technology* **20**, 213–217.

Sebe, G., & Brook, M.A., 2001, 'Hydrophobization of wood surfaces: Covalent grafting of silicone polymers', *Wood Science and Technology* **35**[3], 269–282.

Tshabalala, M.A., Kingshott, P., VanLandingham, M.R., & Plackett, D., 2003, 'Surface chemistry and moisture sorption properties of wood coated with multifunctional alkoxysilanes by sol-gel process', *Journal of Applied Polymer Science* **88**, 2828-2841.

Tsunoda, K., 2001, 'Preservative properties of vapor-boron-treated wood and wood-based composites', Journal of Wood Science **47**, 149–153.

The Old, Wooden Window
a Balance between Romantism and Performance

Ana-Maria Dabija [1]

T 12

ABSTRACT

As the knowledge and technology increases, it is interesting to observe how the expression of the building components becomes… poorer. The most important measure that is being used to compare buildings as a whole or parts of buildings is in terms of performance, either thermal, energy, acoustic, durability and so on Mies van der Rohe's *"Less is more"* became a universal statement as in recent years the preoccupation for the decoration of the building components almost vanished (and unfortunately, where it did not, the result is rather catastrophic). While discussing the glazed part of the envelope we observe how more and more new, performant windows take the place of old, "worn out" wooden ones, in existing buildings. Traditional windows, old bow-windows, shutters and blinds are replaced with modern windows with special glazing, with performant hardware, with ever-lasting self-maintaining finishing. In less than one century a time-verified window system left the market and will eventually vanish even from the facades of the old buildings. The paper aims to present these types of windows – in principles and performances – as well as some exquisite sculptures that were carried out on the wooden components of the old window.

KEYWORDS

Window, Wood, Opening system, Decoration

[1] Ion Mincu University of Architecture and Urbanism, Bucharest, Romania, Phone: +40 (0)752 230 646, Fax: +40 21 312 39 54, am.dabija@iaim.ro

1 INTRODUCTION

During the last twenty years we have assisted – helplessly – at the declining of the traditional windows: everywhere the wooden windows are replaced with new, contemporary, PVC or metallic windows, that use performant insulated glass units. The theory goes that these high quality windows ensure better energetic performances, better economic performances .

The wooden window, on hinges, is the most commonly used type of windows and has carried us through the last centuries, mainly in the housing programme but also in other types of buildings: schools, offices, theatres etc.

In a country like Romania, with a very rough climate*, the windows had to be double. Even old, peasants' houses [see Figure 1] have two lines of sashes mounted on the same frame, in order to protect better against weathering.

Figure 1. XVIII Century house, Peasants' Museum, Bucharest.

2 CHARACTERISTICS OF WOODEN WINDOWS

The wood is a "warm" material and has the natural quality of "breathing". Therefore the thermal performances of the wooden elements have only recently been achieved by PVC profiles with at least 4 chambers.

Wood also has a capacity of absorbing a certain amount of vapours from the atmosphere, thus contributing to a natural balance of the humidity in the interior environment.

However, beyond that critical amount, humidity deforms and deteriorates wood. The deformations are different according to the type of wood.

Common wood species that are used in Romania are fir and oak. For the windows of the more expensive buildings, oak profiles were used.

The mechanical resistance of the window is different, according to the mechnical resistance of the type of wood. Deformations at the joining of the wooden parts, especially of the sashes, are caused also by the shrinking of the elements.

* excessive continental temperate climate, with very high summer temperatures (as high as +45 C^0 in Bucharest in 2007) and winters with very low temperatures (going down to -20 C^0 in 2004)

The sealing between the frame and the sash is made by the overlapping of the grooves, thus resulting a reduction of the air and water tightness.

This is not altogether bad, in the case of wooden windows that are in a good state, as the imperfect overlapping of the elements allows a (hopefully) feeble air movement between the two environments: the interior and the exterior of the building. If the gap between the elements increases, however, steps should be taken in order to keep it in controlled parameters [Dabija, 2002]. Wood is flammable and combustible.

3 COMMON TYPES OF WOODEN WINDOWS

In the less heated spaces (cellars, staircases that lead to appartments etc.) – or unheated altogether – of the "civilian" buildings (dwellings, etc), simple windows were used (with a single sash).

In some situations of double windows the second sash was taken off the frame, considering that the space needs not to be comfortably warm. In the heated spaces of the buildings double windows are used (two sashes that accomplish a window).

Currently, in the interior warm environment we deal with two main types of wooden windows, that practically cover the market; both of them on hinges applied on the vertical elements of the window: customary opening windows and interior opening windows.

In Romania, the double window in which one sash opens towards the interior and one towards the exterior is called "customary opening window" (see Figure 1and Figure 2).

It was the usual system of opening windows; therefore the name of the type of opening is "customary".

Figure 2. "Customary" opening window – University of Bucharest, arch. Al. Orascu, 1857-1869.

The interior opening system is accomplished by two sashes on a common frame or on two independent frames that open towards the interior (Figure 3).

While the *declared* thermal performances of these types of windows are similar (as there is a mathematical formula by which the performance is established), the effective protection against dust, cold air and rain penetration is different [Dabija, 2004] from one system to another.

Figure 3: "Interior" opening window – Bucharest, early XX-th Century.

There are several levels of discussion about windows:

1. the characteristics of the two main types (advantages, disadvantages)
2. the supplementary devices that can be adapted for these types of windows
3. the decorative approach, according to the geometric features of the types of windows

3.1 The Characteristics of the Two Main Types (Advantages, Dissadvantages) of Windows

One common feature is the depth of the profile of the massive wooden sash: 42mm. Laminated wood profiles of today, mainly built according to norms [DIN 68121], are over 20mm deeper (currently 68mm). It is true that these profiles bear the load of insulated glass (I.G.) units. Also in terms of widthness, the old massive wooden sashes were slimmer than the ones used today (mainly due to the same reason, the load of the insulated glass unit).

3.1.1 Features of the "customary" opening windows

Without considering the material that the windows are made from (metal, plastic, wood), the main advantage of the "customary" opening windows is that it acts like a storm window: when the wind blows on a facade, the exterior sash is being pressed against the frame, thus increasing the air and water tightness of the window assembly. Rain water, pushed by the wind on the window, will not penetrate between the sash and the frame. This is the reason for which the "customary" opening windows are not provided with larmiers on the inferior traverse. However, in the case of fanlights the principle does not apply: water can penetrate on the traverse of the window and from there inside, at the top of the lower window. In this case a larmier is attached, either on the inferior traverse of the fanlight sash or on the intermediary traverse of the window (see Figure 4).

Among the defficiencies of the customary opening windows are the problems of maintenance (the exterior opening sash is difficult to clean; if left open for longer periods, the hardware can be more easily rot as it is more exposed to weathering).

Also, the position of these windows should be well thought of, as there is a danger for the pedestrians to be hit by an opening window, if the window is placed on the ground floor of a building at the street front.

More than the advantages, the dissadvantages (in maintenance, mainly) led to the abandon of these types of windows. However, in countries with rough, windy climates (near the sea for instance or in the Northern countries) the traditional way of building includes the "customary" opening windows.

Figure 4. Customary opening window, with fanlight and larmier
School of Architecture, Bucharest arch. Grigore Cerchez, 1912 – 1927.

3.1.2 Features of the "interior" Opening Windows
In the case of the "interior" opening windows, the wind pressure (applied on a façade) pushes the sash away from the frame. The measures to avoid water penetration between the sash and the frame are the provision of larmiers on the horizontal elements of the window and the geometry of the sash (with grooves that allow the water to flow on "channels" to the base of the element and lead it out through special perforations).

No special maintenance measures have to be taken for the "interior" opening windows.One of the geometrical characteristics of these double windows is that, due to the necessity of opening both sashes at an angle of 90^0, the exterior frame is broader than the interior one (Figure 5) and also broader than the one of the "customary" opening windows (where both frames – interior and exterior – were identical). In order to give the appearance of a slimmer window, the masonry can partly cover and hide the broad frame.

Figure 5. Interior opening window – School of Architecture arch.
Grigore Cerchez, 1912 – 1927.

3.2 The Supplementary Devices that can be Adapted for these Types of Windows

Most wooden windows are provided with blinds and shutters. In some situations they may fulfill a triple role [Dabija, 2005]: sun protection, aditional thermal insulation and protecton against the intruders.In the case of "customary" opening window, textile rolling blinds or venetians are provided between the sashes (the distance between the sashes is about 9 cm, so there is plenty of space).
These systems are not as efficient as if they were provided on the exterior, but it is the only way to achieve some protection and open the window as well. At the end of the ninteenth and the beginning of the twentieth Century both types of wooden windows were set on buildings with two or three

storeys: on the ground floor the double windows with interior opening that would protect pedestrians from being slammed by a window pane – and which, in the case of dwellings, were provided with shutters for safety reasons as well as for summer sun protection and winter thermal protection – on the higher levels, "customary" opening windows, excelent for protection against weathering (see Figure 6).

Figure 6. Interior opening and customary opening windows
School of Architecture, Bucharest, arch. Grigore Cerchez, 1912 – 1927.

In the case of the interior opening windows, the supplementary devices can be either rolling blinds or shutters, as the protection is operating on the exterior of the window and allows the window to open independently for ventilation. In most of the situations they are provided on the exterior of the window, as this position ensures the most efficient sun protection as well as the protection agains intruders. In order to keep them in the open position, metalic (decorated, in many situations) elements are fixed onto the façade wall. In old houses the groundfloor windows are protected with traditional shutters on sashes. They are sometimes lively painted (Figure 7).

Figure 7. Exterior shutters, discontinuous or continuous; Peasants' Museum, Bucharest.

3.3 The Decorative Approach, according to the Geometric Features of the Types of Windows

Another characteristic that has not been mentioned, as it is obvious, is that wood can be easily carved. It is an important feature, as it allows a vaste variety of shapes and decorations to be worked out, thus ensuring specificity and personality for each window.

In the Art Nouveau period, all over Europe curves were emphasized. Gaudis' windows in Barcelona for instance are world famous (Figure 8). Curved windows have been used throughout the Art Nouveau period in all the countries touched by this architectural style.

Figure 8. Door and windows at Gaudi's Casa Bathllo, Barcelona.

Not only the geometry of the window frame is more easily shaped in wood, but – and this is specific to the wooden windows of the end of the nineteenth century – the perfect subdivision of the vertical or horizontal wooden components was done by means of decoration, if the dimension of the profile requested it.

In the case of windows with fanlight, for instance, the intermediary traverse is very broad. The field is usually subdivided, like in the example given in figure 9, with decorations taken from the means of expression of the classic architecture.

Figure 9. "Customary" opening windows, with decorations on the intermediary traverse.

In the case of windows with more than one leaf, the performance request is to ensure the sealing between the frame and the sash by overlapping of the elements. Therefore, the mullion becomes broader, so that both sashes can be pressed onto it. The vertical field is not let flat, but decorations are applied, in the form of columns with capitels and consoles or cable mouldings. The image is being corrected and the window seems slimmer (Figure 10).


Figure 10. "Customary" opening windows, with decorations on the intermediary mullions.

In (very) rare cases of buildings the decorations on the frames and the sashes are also painted, thus integrating the window more organically into the façade, as presented in Figure 11.


Figure 11. Windows at the Central School in Bucharest, arch. Ion Mincu 1890.

CONCLUSIONS

The contemporary era is associated with an intense building activity. New needs appear and higher requests are formulated for the building components. Higher technical performances lead to changes in the concepts of buildings altogether. *Speed of execution* is a key word. *Technological performance* is another one. The time in which a building is finished decreases as the performances of the components increases. Industrializaton also means simplicity: profiles are more or less the same and windows have a more or less anonymus aspect. Due to the difficulties of maintenance, the "customary" opening windows are also almost lost, even if their performances are better than the ones of any other type.

While the principles for opening are kept and, of course, respected, the refined concepts in how to individualize buildings by their elements, how to divide a surface in order to obtain the maximum aestetical effect, is lost.

Contemporary demands of energy savings of the tennants or owners of buildings have led to the replacement of the old, almost centenary windows, sometimes altering the holistic image of the building (see figure 12.a). The simple approach is the replacement of an old, wooden window with new ones, provided with gaskets and carrying IG units. The fair approach would be to analyze the quality of the buildings, of the windows and instead of replacing, to **add** a performant window, **inside** the building. This way the improvements are made and the cultural, historical and professional heritage are also kept (Figure 12.b).

a. aggressive intervention (replacement)

b. discrete intervention (adding an interior window)

Figure 12. Interventions on existing wooden windows.

The romantic old wooden windows, witnesses of another epoch, are sadly and quietly dissapearing, their place being taken by more modern – but not always necessary better performing – ones.

REFERENCES

Dabija, A-M, Stan A., 2002, Technical Guide for thermal refurbishing of joineries in existing buildings, Minstry of Transportation, Constructions and Tourism, pp 21.

Dabija, A-M, 2004, Notions for designing joineries in civil buildings, Editura Universitara “Ion Mincu”, pp 17-18.

DIN 68121 - Holzprofile für Fenster und Fenstertüren.

Dabija, A-M, 2005, A bridge between old and new. Thermal window refurbishment of the dwellings in Romania, Proc. 10DBMC International Conference On Durability of Building Materials and Components, Lyon, France, 17-20 April 2005.

11DBMC International Conference on Durability of Building Materials and Components
ISTANBUL, Turkey 11-14 May 2008

Hurricane Katrina: An Overview of Damage to Timber Structures

Anthony J. Lamanna [1]
Brian Metrovich [2]
Jeremy Martin [3]

T 12

ABSTRACT

On August 29, 2005, hurricane Katrina made its second landfall as a Category 3 storm in South-Eastern Louisiana. Levees separating Lake Pontchartrain and several canals from New Orleans were breached a few days after the storm had passed, subsequently flooding 80% of the city and many areas of neighboring parishes for weeks. The storm is estimated to have caused over $81.2 billion (in 2005 U.S. dollars) in damage. Whether damage to a structure was caused by wind or flood waters has been a subject of great importance to homeowners with insurance for only wind or water.

Structures away from the immediate vicinity of levee breaches contained structural damage caused by floodwaters that was primarily due to the lack of connection between the timber structure and the foundation. In many instances the combination of rising and moving floodwaters swept structures off of their piers. The standing floodwaters from canals containing harmful chemicals and brackish water from Lake Pontchartrain caused corrosion problems in nails, screws, and other connectors.

Wind induced structural damage was observed primarily in the removal or loosening of roof decking from the underlying framing. Building claddings also suffered significant damage, especially where the stiffness of the cladding was significantly different than that of the underlying structure, such as brick cladding on a timber house.

KEYWORDS

Wind damage, Flood damage, Wood structure

[1] Lamanna Engineering Consultants, LLC, New Orleans, LA 70118, Phone +504 861 9076, Fax +504 861 9076, DrTony@LamannaEngineering.com
[2] Department of Civil, Architectural and Environmental Engineering, University of Miami, Coral Gables, FL 33146, Phone +305 284 3465, Fax +305 284 3492, bmetrovich@miami.edu
[3] Modjeski and Masters Consulting Engineers, New Orleans, LA 70130, Phone +504-524-4344, Fax +504-561-1229, jmartin@modjeski.com

1 INTRODUCTION

On August 29, 2005, Hurricane Katrina made its second landfall as a Category 3 storm in South-Eastern Louisiana. Levees and floodwalls along Lake Pontchartrain and the outfall and navigational canals breeched, causing the city to flood. Due to a variety of factors, including the approach of Hurricane Rita a few weeks later, parts of the city were not drained of water until a month later.

This paper is intended to provide an overview of the damage caused by Hurricane Katrina, and present some design advice and practices that can be learned. It is not intended to serve as a complete catalog of damage nor a complete design guideline for construction in hurricane prone regions, nor does it address the social and economical implications of the damage caused.

2 FLOOD DAMAGE

Flowing floodwaters in the vicinity of breeches caused a good deal of damage similar to that caused by the storm surge which preceeds a hurricane as it makes landfall. Building materials were also affected by long term sumbersion in the brackish water from Lake Pontchartrain.

2.1 Rapidly Moving Waters

The most readily apparent damage was in the immediate vicinity of the levee breeches. Timber frame structures which were inadequately tied to their foundations were often lifted off their foundations by water passing under the raised floors and/or pushed horizontally. A one story timber framed structure is shown in Fig. 1. There was no evidence of a mechanical connection between this structure and the foundation piers which used to support the floor framing, shown in Fig. 2. This particular structure showed a poor foundation layout, where the concrete masonry unit (CMU) piers were set on a very small concrete “spread footing.” In other instances, sill plates were firmly attached to the concrete foundation with anchor bolts; however, the wall studs framing into the bottom sill plates were only attached with toe nails, as seen in Fig. 3. These toe nails were unable to resist the horizontal forces imposed by the flowing waters.

Figure 1. One story timber frame structure pushed away from the concrete porch.

Figure 2. Foundation pier without evidence of mechanical connection.

Figure 3. Sill plate attached to knee wall with anchor bolt.

When a structure was adequately attached to the foundation, the rapidly flowing floodwaters often induced failure elsewhere in the structure. Entire sections of wall were destroyed by flowing water. These walls were standard load bearing portions of the timber frame structure. Walls which had brick cladding appeared to be more protected from lower velocity flowing water; however, in the immediate vicinity of a breech brick clad walls exhibited similar damage to walls clad with timber weatherboards or vinyl siding. Often, failures were clearly initiated in the vicinity of large door or windows,

indicating that unsecured or unprotected openings provided a weak point in the structure which allowed propagation of more significant damage. Some examples are shown in Figs 4 & 5.

Figure 4. Brick clad wall damaged in vicinity of a levee breech.

Figure 5. Wall clad with vinyl siding damaged in vicinity of a levee breech.

As a result of the damage caused by the floodwaters and the potential for portions of the city to flood, structures in New Orleans that were substantially damaged, substantially improved, or new construction must meet new elevation requirements. These structures must be elevated to either the Base Flood Elevation (BFE) or at least 3 feet above the higest exsiting adjacent grade elevation at the existing site. The Base Flood Elevation (BFE) represents the average floodwater elevation for a 100 year flood event. These new requirements adopted in the region assumes the U.S. Army Corps of Engineers is actively repairing and improving the flood control systems.

ASCE 24-05 Flood Resistant Design and Construction requires enclosures below the BFE to either have breakaway walls or have openings designed to allow equalization of hydrostatic pressure between the interior and exterior of the enclosure. The asthetics of raising structures is of concern to many residents. An example of a recently elevated house is shown in Fig. 6.

Figure 6. Structure recently elevated to above the BFE.

2.2 Long Term Submersion

There was a wide range of observed damage attributed to the long term submersion in the brackish waters of Lake Pontchartrain. Some homes remained partially under water for up to four weeks. While we focus on structural materials in this paper, it is worthy to note the severe mold issues that arose on drywall.

The paper layer remained wet for an extended period of time after the flood waters receeded, and grew mold in most instances. This mold was not seen on walls that were covered with plaster or cement board. This mold may be a significant health hazard.

The most easily observed type of damage was the rusting of metal fasteners, which can be seen above in Fig. 3. Other metal hardware, such as lintels in brick cladding over windows, exhibited some signs of rusting, which could lead to further water ingress if not repaired along with the rest of the structure.

The timber members became saturated in many cases. Timber structural members which were restrained or under load while saturated suffered damage to their grain structures. Many timbers became twisted or warped while in this saturated condition; many remained so upon eventual drying. Tounge and groove hardwood floors were the most visible example of this type of damage.

Some red brick walls which were submerged in the brackish waters showed a degradation in the mortar, which was apparent when the mortar was scraped with a knife blade. Calcium leaching has been shown to degrade the material properties of cementitious materials [Heukamp et al. 2005]. The high porosity of the red bricks and insulation board along the inside of red brick exterior walls likely trapped moisture, which extended the amount of time past flood subsidence that leaching could occur.

It is important to note that damage caused by long term exposure to brackish water, such as the corrosion, warping, and leeching described above, may not be readily apparent. Post disaster inspections of structures exposed to these elements should keep a special look out for these effects as they may otherwise go undetected until they fail in some future, perhaps less extreme condition.

3 WIND DAMAGE

On August 29th, 2005 Hurricane Katrina passed over New Orleans with maximum sustained winds estimated to be around 105 mph (170 km/h) [Knabb et al. 2005]. It is important to keep in mind while observing and analyzing damage from high winds that several factors affect the wind speeds near structures such as height above the ground, type of terrain surrounding the structure, dependence of measured wind speed on averaging time, and turbulence features such as flow separation and vortex shedding around a structure.

3.1 Lack of Uplift Load Path Continuity

The most spectacular form of this failure was the removal of entire sections of roof. Figure 7 shows the removal of a church roof from the supporting walls. Large uplift pressures on the overhangs helped contribute to the failure in this case; however, there was no evidence of tie downs between the roof rafters and the supporting walls.

Cases were also oberved where porches and carports, which were open to the wind, lifted up off of the support columns. If structurally attached to the primary structure, the porch or carport would cause damage to the primary structure when it collapsed. An example of a collapsed porch is shown in Fig. 8.

Figure 7. Removal of a church roof from the supporting walls.

Figure 8. Porch collapsed from uplift forces and lack of tie downs.

3.2 Poor Construction Practices

It is sometimes difficult to separate poor construction practices from poor design practices. The decision to construct a building with a gabled roof instead of a hipped roof in a high wind area would be an example of a poor design practice. The lack of adequate fasteners attaching the sheathing to the structure or fasteners driven through the sheathing and missing the underlying framing would be an example of poor construction practices. Often builders use pneumatic nailguns, which do not provide feedback to the user whether or not the nail entered a structural member. Figure 9 shows decking nails that missed the supporting rafter. Figure 10 shows poorly fastened sheathing that was blown off of a gabled end wall. It is important to realize that while some construction practices are poor, they may be typical and accepted for a particular region.

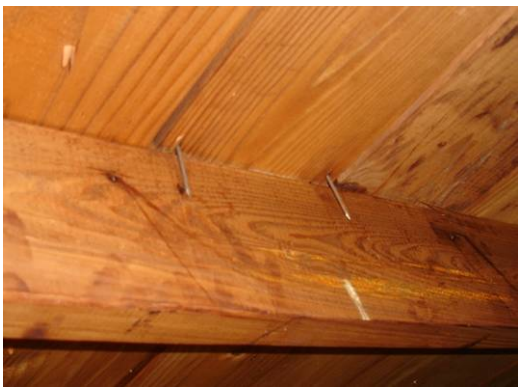

Figure 9. Decking nails that missed the supporting rafter.

Figure 10. Poorly fastened sheathing that was blown off of a gabled end wall.

Another poor construction practice that was observed throughout property inspections was the reduced number of fasteners in hurricane ties. The majority of ties are engineered to have a nail in each hole; a reduced number of fasteners means a reduced load capacity for the anchor. Many contractors do not install the full compliment of fasteners because they must be installed by hand and not with a pneumatic nailgun (it is very difficult to line up the nail with the hole in the connector).

Lack of oversight on small timber framed buildings during the construction process can lead to poor quality and many of the errors previously explained. Some local goverments have instituted inspection processes which can reduce the amount of errors and increase overall quality; for example, Jefferson

Parish in Southern Louisiana requires the design engineer to inspect and approve the construction before the interior gypsum board and other wall and floor coverings are installed.

4 UPLIFT AND LATERAL LOAD PATH DESIGN

Wind design has evolved significantly recent years. The design of timber structures for high winds can be easily completed utilizing manufactured connections and tie downs. Story offsets and geometric irregularities (such as large dormers or porch awnings, which are common in New Orleans) make wind analysis and design more difficult than a simple rectangular building with a gabled or hipped roof. An overview of typical uplift and lateral load paths is shown in Fig. 11.

Structural sheathing and structural sub-flooring plays an important role in resisting lateral wind forces through diaphragm action. The sheathing thickness, size and amount of fasteners must be designed so that the diaphragm can adequately resist the imposed loads. Openings in floor diaphrams need to be engineered so as not to interfere with the lateral resistance of these diaphragms.
The State of Louisiana will soon move to the 2006 versions of the International Building Code and International Residential Code. All new construction will be required to be designed to the high wind levels required in these codes which should help to mitigate some of the damage discussed in this paper. Although local permitting processes differ, most additions, repairs, and major remodelling will also be required to meet these new high wind requirements.

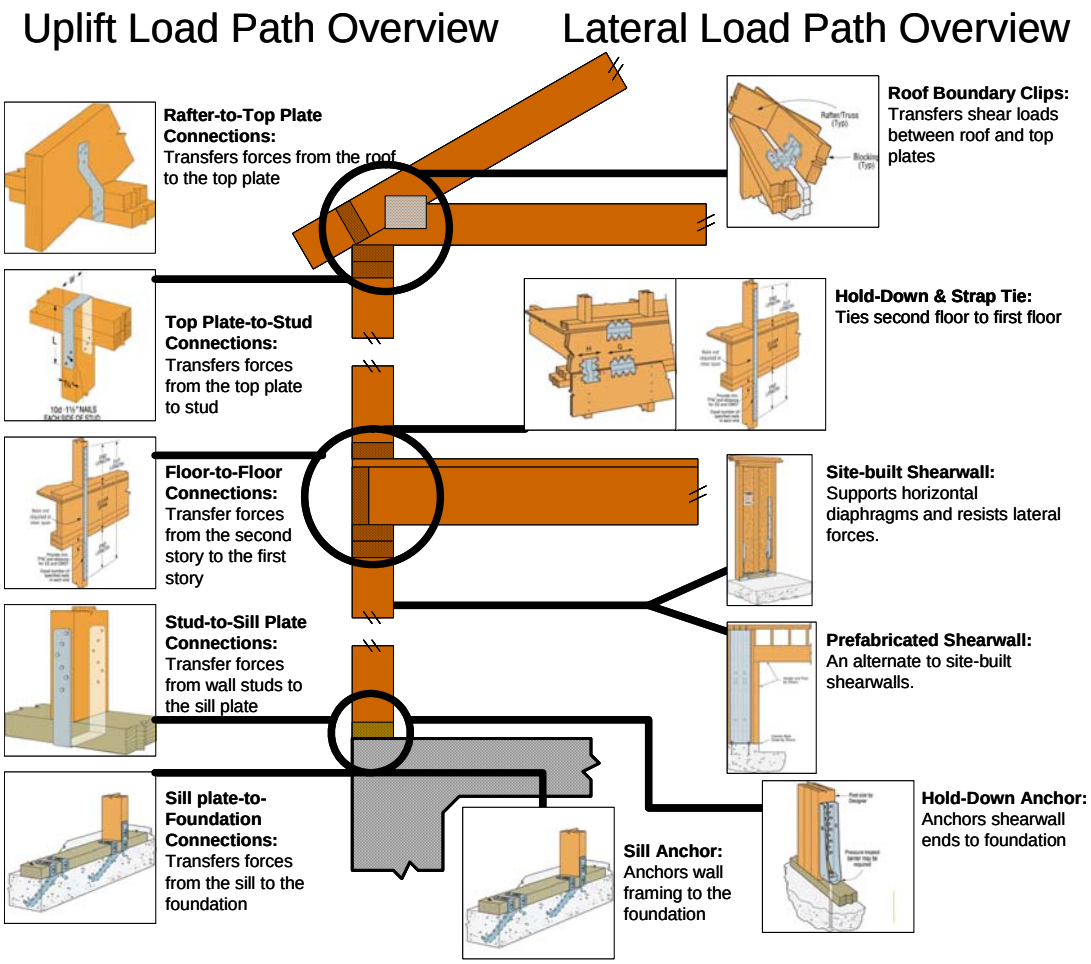

Figure 11. Overview of uplift and lateral load paths [Adapted from Simpson 2006].
With the recent passage of House Bill No. 558, owners in Louisiana can also expect to see discounts in their insurance premiums if they retrofit their buildings to resist high winds. While the details are

still being developed, there is a possibility of partial premium discounts for partial retrofit. This legislation is intended encourage owners to retrofit older buildings, which are typically exempt from the more current building codes which include design for high wind resistance. These measures should prove to be a significant incentive to improve existing structures as insurance premiums have more than tripled for some residents of New Orleans, while coverage has declined.

5 CONCLUSIONS

Large scale disasters like hurricane Katrina subject timber structures to a combination of destructive forces from both flood water and wind. Damage from these forces varies significantly and can be mitigated with different improvements to the structures, which can be addressed in local building codes. Building codes and construction requirements change over time. As we learn more about the forces imposed upon structures by natural and manmade disasters with magnitudes such as Hurricane Katrina, it is imperative to take these lessons and apply them to future designs and building practices. Accordingly, the State of Louisiana and its parishes have been adpoting and updating building codes and practices as a direct result of Hurricane Katrina, and have been taking steps to encourage owners to upgrade existing buildings which are exempt from the new codes.

ACKNOWLEDGMENTS

The author would like to thank Dr. William Micah Hale, of the University of Arkansas, for his assistance in editing this paper.

REFERENCES

ASCE 24-05. 2006, *Flood Resistant Design and Construction*, American Society of Civil Engineers, Reston, Virginia.

Heukamp, F. H., Ulm, F. J., & Germaine, J. T., 2005, 'Does Calcium Leaching Increase Ductility of Cementious Materials? Evidence from Direct Tensile Tests,'Journal of Materials in Civil Engineerng, **17**[3], 307-312.

ICC. 2006, *2006 International Building Code (IBC)*, International Code Council, Falls Church, Virginia.

ICC. 2006, *2006 International Residential Code (IRC)*, International Code Council, Falls Church, Virginia.

Knabb, R. D., Rhome, J. R., & Brown, D. P., 2005, *Tropical Cyclone Report Hurricane Katrina*, National Hurricane Center, Miami.

Simpson Strong Tie 2006, *High Wind Framing Connection Guide*, Simpson Strong Tie Company, Inc., Pleasanton, CA.

Wood as a Structural Material

N.Papatya Seçkin [1]

T 12

ABSTRACT

Wood has high strength, is easily worked, is relatively abundant, and its grain structure is naturally attractive. By the way, wood is probably the single most widely used structural material, and some of the most beautiful structures have been constructed with wood.

There are as many different types of wood as there are species of trees. Each species has its own unique qualities. Some have very beautiful grain patterns. Some of extremely strong and stable, and others have natural resistance to rot and decay. Before selecting a species for a project application, designers must know the characteristics of the species of wood. They are contemplating using. Often the qualities of a particular species will vary from tree to tree and can even vary within an individual tree. How the wood is processed can complicate the selection of a type of wood even further. Damage incurred during felling, the saving method used to convert the timber into boards, the method used for seasoning, the introduction of preservatives, and laminating or gluing separate pieces together can all have a dramatic impact on the quality and characteristics of the final product.

In some societies, wood is revered and endowed by the people with mystical properties. Craftsmen in these societies consciously seek to express these qualities in the structures that they design and build.

The majority of structural wood used in the world comes from softwoods. Softwoods are typically preferred over hardwoods for structural purposes because they are generally lighter, more easily worked, less prone to structural defects, and available in greater quantity and in larger size ranges than hardwoods.

KEYWORDS

Wood, Wood composites, Structural material.

[1] Mimar Sinan Fine Arts University, Faculty of Architecture, Division of Construction Physics and Materials, Istanbul, Turkey 34427, Phone +90 212 2521600, npseckin@msgsu.edu.tr

1 INTRODUCTION

Forests and the wood they produce, have played an important role in human activity since before recorded history. Indeed, one of the first major innovations of humankind was utilizing fire, fueled by wood, for cooking and heating. Since this ancient beginning, the uses of wood, and the value of the forest, have expanded dramatically, as the population of humans and their economies grew.

Wood has remained as an important substance throughtout history because of its recyclable, renewable and biodegradable unique and useful properties. Today, wood is used in tools, paper, buildings, bridges, guardrails, railroad ties, posts, poles, decks, fences, gazebos, play structures, mulches, furniture, packaging, and thousands of other products.

As known, wood as a structural material has high strength, is easily worked, is relatively abundant, and its grain structure is naturally attractive. It has probably been the single most widely used construction material in the world.

Architects and Landscape Architects often design projects that use wood as a structural material. The designer who wishes to utilize wood in a Project needs to understand its capabilities and limitations in order to maximize its potential.

Some of the most beautiful structures in the world have been constructed with wood and have been designed to last indefinitely. Conversely, some of the most homely and pitiful structures have also been constructed of wood.

The versatility of wood can be seen in the houses in Figs 1 and 2. The classic revival houses emphasizes the flexible nature of wood and the ease with which it can be worked into a multitude of shapes and forms. The modern house relies more on the inherent beauty of the grain and color of the wood and its utilitarian as a building material.

Figure 1. Classic revival home, Adalar-Istanbul.

Figure 2. Modern house, House Into –Finland [Seçkin, 2006].

2 UTILISATION OF WOOD

Wood is used in both solid wood (timber) and manufactured wood products (wood composites).Our subject in this paper is only to concentrate on the types of wood composites and applications. In following, first is described laminated timbers (such as glulam) and structural composite lumber. These materials are primarily used in load-bearing building applications in the form of beams; then wood composition boards such as plywood, flakeboard, particleboard and fiberboard. The wood composition boards can be classified according to density, raw material form and process type (Fig 3).

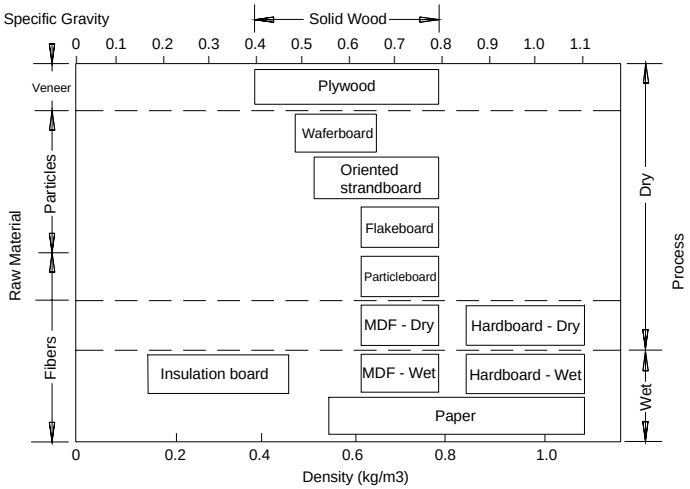

Figure 3. Classification of wood composite board materials by particle size, density and processing principle [Rowell, 2005].

2.1 Laminated Timbers

Structural glued laminated beams (Glulam) is a structural product that consists of two or more layers of lumber glued together with the grain all going parellel to the length. Typically the laminates are 25 to 50 mm in thickness.

The biggest advantage of using glulam is that large beams can be made using small trees. In addition, lower quality wood can be used, thinner lumber can be dried faster than large, thick beams, and a variety of curved shapes can be produced.

Common wood species used to make glulam are softwoods such as Douglas-fir, Southern pine, Hemlock-fir and spruce.

For example, The roof system of Disney ICE rink in Anaheim is a combination of southern yellow pine glulam girders and solid sawn Douglas-fir purlins spaced at 48" on center (Fig. 4). Curved supporting columns are steel encased in concrete. The arched glulam girders are 8-3/4" x 50-7/8" in section. The curved girders are spaced at 22 feet on center and span 116 feet.

Figure 4. Glulam and plywood roof system of Disney Ice, in California, create a modern sculptural quality and recall traditional [APA, 2002].

The roof sheathing is 1-1/8" tongue-and-groove AFA trademarked plywood. Bending the thick 1-1/8" plywood over the glulam beams by hand was very challenging because the arches were curved to a 75-foot radius and to span 48 inches between purlins (Fig. 5).

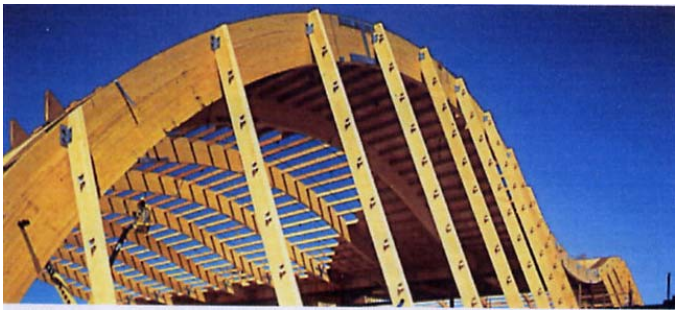

Figure 5. Glulam arches were curved to a 75-foot radius to form the ice center's roof system [APA, 2002].

Glulam can be used in almost any type of structure for architectural and structural purposes including domestic construction, recreational buildings, industrial structures requiring large column free spaces, and high quality architectural/structural uses in churches, shopping centres etc. Glulam is also used in joinery, benchtops, stairtreads, stringers, handrails, etc where both the structural properties and aesthetic appeal of the timber are required.

2.2 Plywood

Thin veneers can be glued together for plywood. Different thickness of plywood can be produced using multi-layers of veneers. The alternation of grain direction in adjacent plies provides plywood panels with dimensional stability across their width.

This material is used as a structural underlayment in floors and roofs and in furniture manufacturing. There are two basic types of plywood: construction and decorative. Construction-grade plywood has traditionally been produced using softwoods such as Douglas-fir, Southern pines, White fir, Larch and Western hemlock. Decorative plywood is usually produced using softwoods for the back and inner layers, with a hardwood layer on the outer surface.

The Sydney Opera House is an example for the use of plywood and laminated hardwood in a public building (Fig. 6).

Figure 6. The use of plywood and laminated hardwood at the Sydney Opera House [Toogood, 2006].

2.3 Structural Composite Lumber

Structural composite lumber (SCL) is manufactured by laminating strips of veneers or strands of wood glued parallel to the length. There are many types of SCL products: oriented strand lumber (OSL), parallel strand lumber (PSL) (Fig. 7), laminated veneer lumber (LVL) (Fig. 8), laminated strand lumber (LSL), and oriented strand board (OSB) (Fig. 9). Usually Douglas-fir, Southern pines, Western hemlock and Yellow-poplar are used, but other species are also used. The major adhesives used to produce SCL products are phenol-formaldehyde or isocyanates. All of these SCL products are used as replacements for solid wood.

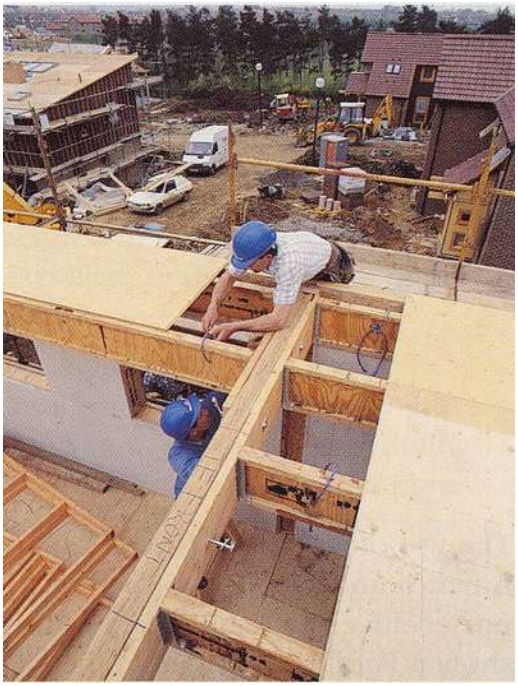

Figure 7. The use of PSL on wall, floor and roof panels of a building [Seçkin, 2006].

The store building in Australia is a 32m span fixed portal frame structure with 9 bays at 8.5m centres and one at 5m. The portal is 12m clear at the eaves and rises to 15m at the ridge (Fig. 8). Columns and rafters are fabricated from 63mm thick LVL forming a box section 900 x 426mm. The roof purlins and wall girts are 300 x 45mm LVL spaced at 1200 centres. The walls were trussed with 50 x 2mm steel straps and 90 x 45mm pine noggings.

Figure 8. The use of LVL at the store building in Australia [Ferguson, 2006].

Figure 9. Use of OSB in wall sheathing, roof sheathing, and floor sheathing [LP Building Products 2005].

2.4 Composite Beams

Composite structural beams can be produced by combining several elements such as sawn, or structural composite lumber flanges and plywood, hardboard, flakeboard and oriented strandboard, bonded together with exterior type adhesives. Especially, prefabricated I-beams are used by builders because they are lightweight, uniform, and easy to use (Fig. 10).

Figure 10. I-joist compatible glulam beams are supplied in depths of 9-1/2", 11-7/8", 14", and 16" [APA 2003].

2.5 Flakeboard

Large, thin wafers or smaller flakes can be produced by several methods and used to produce a composite board. Wafers are thicker than flakes. Wafers are almost as wide as they are long while flakes are much longer than they are wide. Wafer and flakeboard are made with a waterproof adhesive, such as phenol formaldehyde or an isocyanate.

2.6 Fiberboard

Fiberboards can be formed using a wet-forming or a dry-forming process. There are three types of fiberboard: low-density fiberboard (LDF), medium-density fiberboard (MDF) and high-density fiberboard (HDF, insulation board).

2.6.1 Low-Density Fiberboard (LDF)

Low-density fiberboards are usually produced by a dry process that uses a ground wood fiber. They are used for insulation and for light-weight cores for furniture.

2.6.2. Medium-Density Fiberboard (MDF)

Medium-density fiberboard is mainly used as a vore for furniture (Figure 11).

Figure 11. The use of MDF walls panels [Stahl and Benschneider 2007].

2.6.3. High-Density Fiberboard (HDF)

High-density fiberboard is produced both with and without wax and sizing agents. The wax is added to give the board water resistance. HDF is used as an overlay on workbenches and floors, and for siding. There are the different types of high-density fiberboards.

3 CONCLUSIONS

Wood is probably the most widely used structural material in the world. It is universally available, also a renewable resource. In addition, wood is easily worked and shaped with simple hand tools. A skilled carpenter can build marvelous structures with nothing more complicated than hammer, saw, square, and a few other common tools. Moreover, if properly protected from moisture and insects, wood can be considered a permanent material. There are numerous examples of structures around the world that are hundreds of years old and are still in perfect condition.

As mentioned before, there are two primary classifications of woods: Hardwoods and softwoods. Hardwoods are used most often for furniture, flooring, veneers, and other applications for which appearance of grain and durability are paramount. Softwoods are typically preferred over hardwoods for structural purposes because they are generally lighter, more easily worked, less prone to structural detects, and available in greater quantity and in larger size ranges than hardwoods.

Wood composites constitute a wide variety of materials, such as glulam and laminated veener timber used in beams, as well as board materials such as particleboard, fiberboard and oriented strand board. Waste-wood and smaller trees can be used in wood composites, strength is increased since defects are removed, and structural shape can be designed. The scale of the wood element, its orientation, and material density are important factors controlling performance.

Optimization of structural shape, in combination with variations in material and material compositions, has great potential for components in building systems. I-beams with different materials in the flange and in the web are simple examples already in existance, although the concept may be brought much further.

REFERENCES

APA 2002, '*Disney Ice'*, The Engineered Wood Association, Form No: W120A.

APA 2003, '*Glulam Product Guide'*, The Engineered Wood Association, Form No: EWS X440B.

Desch, H.E., & Dinwoode J.M., 1996, '*Timber- Structure, Properties, Conversion and Use'*, Macmillan Press, London, 1996.

Ferguson, S., 2006, '*Store Building'*, Forest and Wood Products Research and Development Corporation, Australia.

Gibbs, H.L., 1976, 'Wood & Wood Structures', *Handbook of Landscape Architecture Construction, Volume Four: Materials for Landscape Construction*, ed. S.S. Weinberg & G.A. Coyle, The Landscape Architecture Foundation, Washington, D.C., pp. 231-288.

LP Building Products 2005, '*A structurally sound idea from the world leader in OSB'*, LP OSD Sheating Broshure.

Rowell, R.M., 2005, *Handbook of Wood Chemistry and Wood Composites*, Taylor & Francis Group, Boca Raton.

Seçkin, N.P. 2006, '*Ekolojik Değerlere Göre Ahşap Kompozit Malzemenin Seçim Kriterleri'*, MSGSÜ Fen Bilimleri Enstitüsü, Yüksek Lisans Tezi.

Toogood, B., 2006, *'Sydney Opera House'*, Forest and Wood Products Research and Development Corporation, Australia.

Stahl, D,. & Benschneider, B., 2007, 'Shaped Smart', Pacific NW 4 Agust 2007, Seattle Times Newspaper

Youngquist, J.A., 1999, 'Wood-based Composites and Panel Products', *Wood Handbook-Wood as an Engineering Material*, Forest Products Laboratory, U.S. Department of Agriculture, Forest Service, Madison, pp.10/6.

Preparation Method and Service Condition Effects on the Performance and Durability of Epoxy Adhesives Used in Structural Timber Repairs

João Custódio [1]
Helena Cruz [2]
James Broughton [3]

T 12

ABSTRACT

Rehabilitation/restoration systems involving structural adhesives represent an efficient method for the repair and/or reinforcement of both new and existing timber members. Epoxy adhesives have been used for many years in the repair and strengthening of timber structures, and are currently the most appropriate adhesive type for in-situ operations. Nevertheless, there is still a lack of knowledge about their durability and long-term performance derived from the absence of standards on this issue. This paper describes an experimental campaign developed to address these concerns, which included the development of a test procedure to assess long-term behaviour of bonded-in rod connections. The effect that the type of mixing, curing, and post-curing had on the epoxy adhesive's mechanical properties was also assessed.

From the results, it was seen that the mixing procedure influences the mechanical properties of the cured adhesive, and its effects varied with the different adhesives tested. Post-curing the adhesives was beneficial, but with different magnitudes for each adhesive. The data obtained using the new test procedure are, so far, encouraging, providing very different behaviours depending on the system employed.

KEYWORDS

Epoxy adhesives, Service conditions, Performance, Durability assessment.

[1] Laboratório Nacional de Engenharia Civil (LNEC), Structures Department, Timber Structures Division, Av. Brasil 101, 1700-066 Lisboa, Portugal, Phone +351 218443933, Fax +351 218443025, jcustodio@lnec.pt
[2] Laboratório Nacional de Engenharia Civil (LNEC), Structures Department, Timber Structures Division, Av. Brasil 101, 1700-066 Lisboa, Portugal, Phone +351 218443295, Fax +351 218443025, helenacruz@lnec.pt
[3] Joining Technology Research Centre (JTRC), School of Technology, Oxford Brookes University, Wheatley Campus, OX33 1HX, United Kingdom, Phone +44 1865483556, Fax 1865484179, jgbroughton@brookes.ac.uk

1 INTRODUCTION

Adhesives have been used for many years in the aerospace and automotive industry. A great deal of research has been carried out on the behaviour of adhesively bonded joints of the types used by those industries. However, there is a lack of appropriate guidance for their use in the construction industry. As far as the various construction materials are concerned, the largest use of adhesives for structural applications is with timber, either in the form of pre-fabricated products, or for connections between members. Some applications for structural adhesives are well established (*e.g.* anchors and fixings, including dowels in concrete and timber; ground anchors; timber composites; timber-timber connections; steel plate bonding; pre-cast concrete segmental construction; fibre composites; etc), with the appropriate guidance readily available, while other applications are still being developed (*e.g.* like the repair and strengthening of timber structures).

Rehabilitation of buildings has an increasing economical and social importance in most countries, due to the historical value of the built heritage and to the need to maintain and improve the built environment of cities. Rehabilitation/restoration systems involving structural adhesives represent an efficient method for the repair and/or reinforcement of both new and existing timber members. Epoxy adhesives have been used for many years in the repair and strengthening of timber structures, and are currently the most appropriate adhesive type for in-situ operations. They can be used on their one or in conjunction with steel plates, rods or fibre reinforced polymer (FRP) composite materials for the consolidation or reinforcement of wood structures. Structural epoxy adhesives are generally used in service conditions equivalent to service classes 1 and 2 (EN 1995-1:2004). However, because they exhibit excellent initial joint strength when tested in standard climate conditions, there has not been a major concern about its service durability. The lack of knowledge about the way in which high service temperature affects their performance lead the authors to develop research studies to address those concerns. The results from those studies clearly showed that the performance of an adhesive is severely influenced by service temperature, and its immediate effects may be critical for structural safety [Cruz et al. 2005; Cruz & Custódio 2006; Custódio et al. 2007]. In addition, reliable and realistic accelerated ageing tests do not yet exist, and the application of the existing European or national test and performance standards to epoxy bonded products are much too penalising, since they merely impose severe conditions that are not verified in service because they were developed originally for other adhesives, namely for phenolic and aminoplastic adhesives. The lack of standards in this field impedes the objective evaluation of the reliability of a glued connection, causing engineers to avoid this type of solution and sometimes to commit errors with potential disastrous results [U. S. National Transportation Safety Board 2007; Hansson & Larsen 2005].

The European Committee for Standardization (CEN) has already identified the need for development of standards for the evaluation of bond durability and long-term performance of epoxy adhesives, but so far, no standards have been produced. To address these concerns a test programme was developed to assess the effect that the preparation method, application environment and service conditions, have on the performance and durability of epoxy adhesives. In addition, using the findings from the above, a test procedure to assess and to predict the long-term behaviour of bonded-in rod connections was developed.

2 EXPERIMENTAL PROGRAM

The study undertaken at LNEC and JTRC is divided in two main experimental campaigns. The first deals with the influence of the preparation method on the short-term properties of the epoxy adhesives. The second part focus on the long-term effects of service environment on the timber bonded joints durability. Since this study involves long-term tests, the experimental campaign is still ongoing so that this paper presents the results obtained until this moment, more results will be available at the time of the conference presentation.

2.1 Preparation Method Effect on the Performance of Epoxy Adhesives

The viscoelastic properties of the adhesives were determined through dynamic mechanical analysis (DMA) in the 3 point bending deformation mode. The DMA multi-frequency stress/strain mode was used, because it allows the assessment of the temperature dependence of the stiffness, loss modulus, and tan δ, while the oscillation amplitude (15 μm) is held constant, using a frequency of 1 Hz, a temperature ramp rate of 2°C/min, and a temperature range of 10-140ºC. Three replicates were used for each test. The test specimens had a rectangular prism shape measuring 60 mm in length, 10 mm in width and 4 mm in thickness. The width and thickness varied along the specimen length by less than 2 % of the mean value. The tests involve 4 different two-component structural epoxy adhesives, 2 mixing procedures, and several different conditioning and ageing (artificial accelerated weathering, AAW, and natural weathering, NW) processes. Figure 1 summarizes the test campaign.

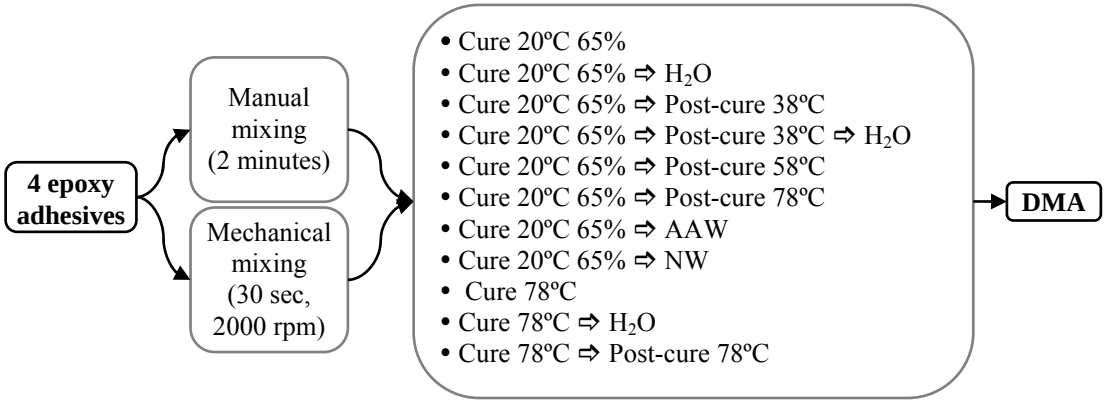

Figure 1. Description of the DMA test campaign.

2.2 Service Conditions Effect on the Durability of Epoxy Adhesives

The method developed to assess and predict the long-term durability of a bonded timber joint, consists of submitting test specimens to natural and artificial accelerated weathering, and to evaluate periodically any creep deformation and residual bond strength. These tests were performed in loading rigs specifically developed and designed for this purpose (Figure 2). The loading rigs were created with the objective of testing several replicates at the same time, with the minimum possible amount of materials (adherents and adhesives), the space occupied by the set up was to be as small as possible, and it was necessary to be able to take measurements during the ageing of the specimens with minimum disruption. The bonded joints are being aged in laboratory-controlled environments and out-door conditions (both in the United Kingdom and Portugal). The latter will simulate the real conditions that this type or repair system is exposed to in service, and will allow the comparison of the results obtained in this way to the ones obtained from laboratory test procedures. The load applied to the specimens is equivalent to approximately three times what they experience in service, which corresponds to about 20% of its ultimate failure load.

Daily weather information (temperature and relative humidity) registered in Lisbon and London in the last seven years, and the weather data registered in two roof covers (one in Lisbon and one in Oxford) since October 2005 was collected, compiled and analyzed. This allowed the determination of the expected service conditions to which a joint in this type of repair technique is likely to be exposed in both countries, as well as to the definition of the artificial weathering conditions to which joints will be exposed (Table 1).

Table 2 illustrates briefly the planning of the on-going long-term durability tests in both countries. Several different combinations of adherend/adhesive/weathering/load/rods were tested in order to verify their influence on the durability of the bonded joints.

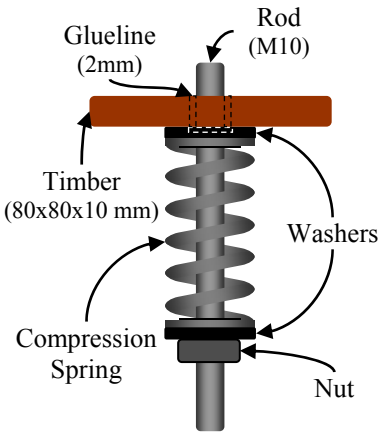

Figure 2. Loading rig sketch.

Table 1. Artificial accelerated weathering cycle.

Duration [Hours]	*Temperature* [ºC]	*Relative Humidity* [%]
48	17	80
24	50	40
48	17	80
24	50	40
20	20	65
48	17	80
24	10	90
48	17	80
24	10	90
20	20	65

Table 2. Description of the durability tests with pine, oak and steel specimens.

Adherend	*Type of*	*Load on*	*Type of Rod*	*Number of*	*Location*	*Age when*
Pine & Oak	None (20ºC & 65% R. H.)	Unloaded	Zinc plated threaded steel	2	UK & PT	0 months 60 months
			No rod	No adhesive	UK	0 months 60 months
		Loaded	Zinc plated threaded steel	2	UK	12 months 60 months
	Natural Weathering	Unloaded	Zinc plated threaded steel	2	UK & PT	12 months 60 months
			No rod	No adhesive	UK & PT	12 months 60 months
		Loaded	Zinc plated threaded steel	2	UK & PT	6 months 12 months 24 months 36 months 60 months
Pine	Artificial Accelerated Weathering	Loaded	Zinc plated threaded steel	2	UK	3 months 6 months 9 months 12 months
Steel	None (20ºC & 65% R. H.)	Unloaded	Zinc plated threaded steel	2	UK	0 months 60 months
			Steel rod	2		0 months 60 months
	Natural Weathering	Loaded	Zinc plated threaded steel	2	UK	12 months 60 months
			Steel rod	2		12 months 60 months

3 RESULTS AND DISCUSSION

3.1 Preparation Method Effect on the Performance of Epoxy Adhesives

Considering the effect of type of mixing in the glass transition temperature, Tg, of the adhesives (Table 3), we observe that for two of the adhesives (A, C) there is not a substantial difference between the Tg of the hand- and machine-mixed specimens (average Tg increase of 0.3ºC for A and 0.1ºC for C). Nevertheless, for adhesive B it seems that the machine mixed specimens had a slightly lower Tg (average Tg decrease of 2.3ºC).

Regarding the post-curing effects on the Tg, it can be concluded that there is always an increase in its value, and that the magnitude of the Tg increment is different for each adhesive. The post-curing was more effective for adhesive C (average increase of 7, 21, and 29ºC) and A (average increase of 5, 11, and 8ºC), and the least influenced was adhesive B (average increase of 2, 1, and 3ºC).

Table 3. Glass transition temperatures obtained for hand- (HM) and machine-mixed (MM) specimens.

Glass transition temperature (ºC)		*No post-cure*		*Post-cure 38ºC*		*Post-cure 58ºC*		*Post-cure 78ºC*	
		Avg.	*S. D.*	*Avg.*	*S. D.*	*Avg.*	*S. D.*	*Avg.*	*S. D.*
Adhesive A	HM	56.7	0.27	61.6	0.04	67.5	0.46	64.6	0.30
	MM	57.2	0.40	61.8	0.34	67.5	0.60	65.3	0.41
Adhesive B	HM	46.6	0.72	47.9	0.29	48.8	0.54	49.7	0.38
	MM	44.7	0.13	46.7	0.87	45.2	1.69	47.0	0.44
Adhesive C	HM	58.9	0.25	66.0	0.20	79.6	0.41	87.2	0.37
	MM	58.2	0.23	65.4	0.41	80.2	0.05	88.3	0.23

NOTES: Avg. = average of three replicates; S. D. = standard deviation associated.

Due to the large amount of experimental data concerning the DMA tests, the authors opted by not presenting the actual stiffness values obtained, but instead showing the variations obtained in the stiffness for each adhesive. Thus, Table 4 presents the stiffness variation with temperature obtained with the different curing conditions. The 100% value corresponds always to the stiffness of the hand-mixed adhesive at 20ºC. All the other percentages were calculated in respect to that stiffness value.

Table 4. Stiffness variation obtained for hand- (HM) and machine-mixed (MM) specimens.

Stiffness variation (%)		*No post-cure*		*Post-cure 38ºC*		*Post-cure 58ºC*		*Post-cure 78ºC*	
		HM	*MM*	*HM*	*MM*	*HM*	*MM*	*HM*	*MM*
Adhesive A	20ºC	**100**	99	94	99	89	97	92	105
	30ºC	93	94	88	92	83	90	85	98
	40ºC	81	83	77	82	73	78	69	83
	50ºC	25	29	44	49	46	49	36	44
	60ºC	3	3	7	8	20	21	13	16
Adhesive B	20ºC	**100**	107	107	96	109	106	107	110
	30ºC	85	82	91	63	95	87	94	92
	40ºC	28	16	36	17	44	22	48	27
	50ºC	2	1	2	2	3	2	4	2
	60ºC	1	1	1	1	1	1	1	1
Adhesive C	20ºC	**100**	88	99	87	100	90	103	77
	30ºC	95	84	95	84	97	87	100	75
	40ºC	88	79	90	79	92	82	96	72
	50ºC	61	49	82	71	83	75	88	67
	60ºC	6	4	34	27	74	67	77	60

The effect of type of mixing is quite different for each adhesive. Only adhesive A seems to benefit with the machine mixing procedure, but this does not mean that the other adhesives could not also benefit from it, this only means that the mixing conditions used (30 seconds at 2000 r. p. m.) are more favourable for adhesive A. For adhesives A and C the stiffness difference magnitude for the two mixing processes seems to stay constant up to a temperature of 40ºC and then decreases gradually until 60ºC. Adhesive B, which has the lowest Tg, showed the opposite behaviour.

Post-curing had also resulted in very different influence in the mechanical properties of each adhesive, as was the case for the glass transition temperature. For adhesive A the post-curing resulted in a stiffness increase only above 40ºC, the best result was obtained with a post-curing temperature of 58ºC. Adhesives B and C benefit from it, from ambient temperature, the best result was obtained with a post-curing temperature of 78ºC (except for MM adhesive C that was 58ºC). It can be concluded that post-curing is beneficial and, for some adhesives, even advisable.

3.2 Service Conditions Effect on the Durability of Epoxy Adhesives

The results presented here refer to the bonded timber specimens subjected to natural and artificial accelerated weathering having 6 and 3 months of ageing, respectively. Table 5 exhibits the temperature and relative humidity to which the test specimens were subjected to during the weathering. It can be seen that the conditions experienced in Portugal were, as expected, far more severe than the ones registered in the UK. Also, the artificial accelerated cycle had temperatures closer to those of Portugal and the relative humidity somewhere in between, at least for this period. Table 6 presents the results obtained for the durability tests undertaken in Portugal (PT) and in the United Kingdom (UK).

Table 5. Temperature and Relative Humidity registered during the weathering.

	Temperature (ºC)			*Relative Humidity (%)*		
	Maximum	*Minimum*	*Average*	*Maximum*	*Minimum*	*Average*
PT Shed	46	8	**22**	87	15	**58**
UK Shed	31	5	**16**	89	26	**70**
A.A.W	50	9	**22**	94	11	**64**

Table 6. Creep results for the specimens using zinc plated threaded steel rod and loaded.

Weathering	*Adhesive*	*Country*	*Timber*	*Creep (mm)*			
				No load	*0 months*	*3 months*	*6 months*
None	A	UK	Pine	0.00	0.02	0.00	0.03
			Oak	0.00	0.03	0.04	0.04
	B	UK	Pine	0.00	0.07	0.16	0.19
			Oak	0.00	0.09	0.30	0.33
Natural	A	UK	Pine	0.00	0.03	0.20	0.05
			Oak	0.00	0.04	0.16	0.06
		PT	Pine	0.00	0.16	0.44	0.44
			Oak	0.00	0.19	0.44	0.45
	B	UK	Pine	0.00	0.06	0.39	0.46
			Oak	0.00	0.10	0.42	0.57
		PT	Pine	0.00	0.22	1.81	2.34
			Oak	0.00	0.33	1.56	2.02
Artificial Accelerated	A	UK	Pine	0.00	0.02	0.45	–
	B	UK	Pine	0.00	0.04	Failed*	–

NOTES: Creep 3 months * = specimens failed after 1 week of AAW.

Comparing the creep behaviour of specimens kept in a controlled environment with that of the naturally and artificially aged specimens, we observe that the former was always lower. As expected adhesive B always showed more creep than adhesive A. Globally, the specimens aged in PT had a more pronounced increase in the creep value, which is consistent with the more severe weathering conditions in Lisbon. In addition, for adhesive A the creep seems to be slowing down, while for adhesive B it continues to rise. Considering the creep values for adhesive A specimens aged in PT and the ones from the specimens aged artificially, we observe that 3 months in AAW correspond to 6 months of NW. However, the creep values in the UK after 6 months are still below the ones verified in AAW. Adhesive B specimens subjected to AAW failed immediately after the first half of the weathering cycle, and several NW specimens failed during the first 3 months in PT. Considering the pronounced creep of the adhesive B specimens aged in PT, it seems likely that all of them will fail before or during the next summer. In the UK, no adhesive B specimens have failed so far.

On Table 7 we can observe the pull-off strengths obtained and the number of specimens that failed during ageing. Comparing the pull-off strengths of the specimens aged naturally with those of the artificially aged specimens, we observe that with adhesive A the loss of strength was of 9% for pine and 11% for oak aged naturally in the UK during 6 months, and 11% for pine aged artificially during 3 months. Interestingly, for adhesive A aged naturally in Portugal during 6 months, the pull-off strength actually increased, possibly as result of an additional post-curing of the adhesive. Regarding the failure type, there seems to be a decrease in cohesive wood failure and an increase in cohesive adhesive failure with the weathering.

The results for adhesive B are quite different. The loss of strength was of 24% for pine and 10% for oak aged naturally in the UK during 6 months. For the specimens that did not suffer premature failure in PT, the pull-off strength was maintained for oak and seemed to increase for pine, but these may be influenced by the fact that only the strongest specimens in the group survived long enough to be tested. Regarding the failure type, there seems to be a decrease in cohesive woof failure and an increase in cohesive adhesive failure with the weathering.

Table 7. Pull-off tests results.

Weathering	*Adhesive*	*Country*	*Timber*	*Pull-off strength (MPa)*		
				0 months	*3 months*	*6 months*
Natural Weathering	A	UK	Pine	19.2 (4.0)	None failed	17.5 (2.9)
			Oak	18.7 (2.3)	None failed	16.7 (1.5)
		PT	Pine	16.9 (3.4)	None failed	18.2 (3.2)
			Oak	17.1 (1.3)	None failed	17.4 (1.4)
	B	UK	Pine	22.8 (3.8)	None failed	17.4 (2.6)
			Oak	21.1 (2.6)	None failed	18.9 (1.5)
		PT	Pine	17.6 (3.5)	Failed 32/50	19.6 (3.0)
			Oak	18.3 (0.9)	Failed 8/50	18.4 (2.7)
Artificial Accelerated	A	UK	Pine	19.2 (4.0)	17.1 (2.6)	–
	B	UK	Pine	22.8 (3.8)	Failed 40/40*	–

NOTES: Pull-off strength with standard deviation in parentheses; *specimens failed after 1 week of AAW.

4 CONCLUSIONS

One behaviour common to all three adhesives tested was the pronounced decrease in their strength with the increase in temperature. If one considers the service temperatures that this adhesives will have to withstand in service (usually up to 50ºC), the results indicate that a very careful selection of the adhesive is necessary. A great number of commercial product data sheets do not give this kind of detailed information about their mechanical properties changes with temperature. If this is the case then it is necessary to obtain that information from the manufacturer or to determine them experimentally. With the data obtained so far, it seems that the main factor influencing the durability

of an epoxy-bonded repair was the temperature induced creep behaviour. With that said, it could be tempting to state that the DMA technique could be used alone to predict the durability of these repair systems. However, the data analysed so far refers only to 3 months of artificial accelerated and 6 months of natural weathering. Furthermore, we must always consider the bonded system as a whole, and the intherphase between the adherend and adhesive plays also an important role in the system durability. We saw that the failure behaviour at the wood-adhesive interphase was different for each adhesive and timber tested, which means that when considering different combinations of adhesives and timbers the results could also be different.

The type of mixing, curing, and post-curing affected the mechanical properties of all the epoxy adhesives investigated, and consequently their durability. The mixing procedure influences the mechanical properties of the cured adhesive, and its effects varied with the different adhesives tested. Since they can be either beneficial or detrimental, the optimum mixing procedure needs to be determined for each adhesive. Post-curing the adhesives was always beneficial, but to different extents for each adhesive, again an optimum post-curing regime should be determined separately. The data obtained using the new test procedure is, so far, encouraging, providing very different results depending on the system employed.

ACKNOWLEDGMENTS

This work was carried out within the scope of a PhD research project (SFRH/BD/17210/2004/DGW8) and a POCI project (POCI/ECM/60089/2004) both financed by "Fundação para a Ciência e a Tecnologia, Portugal". The authors wish to acknowledge this financial support.

REFERENCES

EN 1995-1-1:2004 Eurocode 5: Design of timber structures – Part 1-1: - General - Common rules and rules for buildings. 36 rue de Stassart, B - 1050 Brussels, Belgium, European Committee for Standardization (CEN).

Cruz H., Custódio J. E. P., & Machado J. S., 2005, "A temperatura de serviço elevada e o recobrimento no desempenho de colas epoxídicas usadas em reforço estrutural" (High service temperature and the timber embedment effects on the performance of epoxy structural adhesives), *International Journal Construlink*, 3[10], 1-8.

Cruz H., & Custódio J. E. P., 2006. "Thermal performance of epoxy adhesives in timber structural repair", Proc. 9th World Conference on Timber Engineering - WCTE 2006, Portland, OR, USA.

Custódio J. E. P., Cruz H., & Broughton J. G., 2007, "Performance and Durability of Composite Repair and Reinforcement Systems for Timber", Proc. 9th annual Conference for Young Researchers, London, UK.

U. S. National Transportation Safety Board. 2007. *Ceiling Collapse in the Interstate 90 Connector Tunnel, Boston, Massachusetts, July 10, 2006*. Highway Accident Report NTSB/HAR-07/02. Washington, DC.

Hansson M. & Larsen H. J. 2005. "Recent failures in glulam structures and their causes", *Engineering Failure Analysis*, 12[5], 808-818.

11DBMC International Conference on Durability of Building Materials and Components
ISTANBUL, Turkey 11-14 May 2008

Reduction of Water Absorption and Swelling of Fiberboard

Javad Torkaman [1]

T 12

ABSTRACT

In order to reduce water absorption and swelling of fiberboard, waterproof paraffin and beet molasses with ratio 5,10,15,20 and 25 percentage of solution as sizing agent were used. The fiberboards were made with both materials and were compared with control boards. The results showed 42 and 49 % reduction in water absorption and swelling by using15% waterproof paraffin respectively. The values that obtained for 20 % beet molasses were 3 and 15.5% reduction in water absorption and swelling respectively. At 15 % waterproof paraffin and 20% beet molasses thickness swelling were reduced 49.78 and 15.53% respectively. Also the fiberboards were tested at 30 ,66 ,80, 98% RH and 100%(liquid water) after 30 days. In all relative humidities tests, except 100% the maximum water absorption was 2.4 % without increase in swelling.

KEYWORDS

Water proof paraffin, Beet molasses, Water absorption, Swelling, Fiberboard

[1] University of Guilan,Faculty of Natural Resources, P.O. Box 1144, Sowmehsara, Rasht, Iran, Phone +98 182 3223023 ,Fax 182 3222102, j_torkaman@yahoo.com

1 INTRODUCTION

Sizing is a processing which by adding Suitable chemical materials to pulp can control water absoption and swelling thickness in fiberboard or paper. The aim of sizing is cover the fiber surface by materials which reduction surface energy of fiber caused them hydrophobic [Suchsland 1986].

The hydrophilic characteristic of fiber can be explained by sorption behavior of the chemical wood components such as cellulose ,lignin and their proportions in the chemical composition of the wood as well as their different thermal constancy[Kollman and Schnider 1963].

The usual size in fiberboard is paraffin size which is solid and doesn't solve in water and chemically is neutral. Therefore must be emulsion and we need to use positive alum[$AL_2(SO_4)_3$] to settle over the negetive fibers.Whereas our waterproof paraffin is Ionic compounds and dosenot need alum.The cost of Ionic paraffin is a little more than solid paraffin but the beet molasses is low-priced and available.The other materials which were tested for dimentional stability of fiberboards except paraffin are polyethylene glycol, formaldehyde, acetic anhydride.The treatment of fiberboard with formaldehyde at low temperature was increased dimentional stability of cell walls[Minato 1995].

Aspen fiber was reacted with either ketene gas or liquid acetic anhydride to product acetylated fiber. Board made from ketene-reacted fiber were not as dimentionally stable as boards made from acetic-anhydride-reacted fiber[Rowell 1989,1991].

The possibilities of intraction between wood *pinus sylvestris* (60%RH) and Polyethylene glycol (PEG 1500) have been investigated.The Dynamical Mechanical Techniques (DMTA) measurements shows interaction on the molecular level between wood and PEG 1500 [Wallstrom 1995].

The purpose of this research are dimensional stability and thickness swelling decrease of fiberboard according to cost and capable to use in industry scale.

2 EXPERIMENTAL

Sampling was done before add any additives to fibers.The fibers were spryed only with five levels of solution of waterproof paraffin and beet molasses 5,10,15,20 and 25 percentage. The fibers which were used for control boards didn't used this additives.The fiber was hand-formed into 100by 22 mm randomly oriented mats.then they were pressed to a maximum thickness of 3 mm at time and temperature press of factory condition.The swelling percentage and reduction of water absorption were calculated according to primary and seccondry weight and thickness of samples after 24 hours immersion at 20 ºC.The Anti-Swelling Efficiency and Water Repellency Efectiveness values of the treatment and control samples are determind on basis of oven dried measurement. Anti-Swelling Efficiency (ASE) and Water absorption (WRE) were calculated as:

$$S(\%)=\left(\frac{V_2}{V_1}-1\right)\times 100$$

S=Volumetric Swelling

V_2= the volume of the swollen samples

V_1= the volume of the oven dried samples

$$ASE(\%)=\left(1-\frac{S_2}{S_1}\right)\times 100$$

S_1=Average Swelling of untreated samples(control)

S_2=Average Swelling of treated samples

$T(\%)=({}^{Ww}/_{Wo} -1) \times 100$

T= Rate of the water absorption Specimen
W_W = Weight of wet samples
W_O=Weight of oven drying samples

$WRE\ (\%)=(1-{}^{T2}/_{T1})\times 100$

T_1= Rate of the water absorption of control specimen
T_2=Rate of the water absorption of test specimen

Same of other wood products fiberboard is absorbent and repellent air humidity.Therefore fiberboard specimens(50by50 mm) were placed in a humidity dessicator at 30,66,80, 98% RH and 100% (liquid water) and 20 ºC separately water absorption and thickness swelling were determined after 30 days.

3 RESULTS AND DISCUSSION

The water absorption and thickness swelling of treatment boards were campared with control boards obtained 77.2 and 46.5 % respectively. The results of treatment specimens were showed in Table1 and 2.

Table 1. Results of measuring of water absorption and swelling percentage of fiberboards which were treated with water proof paraffin.

Measurement factor	*Water proof paraffin* [%]				
	5	10	15	20	25
Water absorption [%]	71.6	54	44.6	70.6	79.4
Swelling percentage [%]	26.3	25.5	23.4	36.2	41

As can be seen from table1.Decrease and increase in waterproof paraffin from point of 15% increasing water absorption and swelling percentage of fiberboards while in comparison with control boards. Water absorption and swelling percentage were showed 42 and 49 % decrease respectively.

Table 2. Water absorption and Swelling percentage of fiberboards made at various amounts of beet molasses.

Measurement factor	*Beet molasses* [%]				
	5	10	15	20	25
Water absorption [%]	91.4	82.4	84.7	76.94	79.5
Swelling percentage [%]	41.02	40.12	43.12	39.28	41.97

According to table 2.The use of 20 % beet molasses decreased maximum 3 and 15.5% in water absorption and swelling percentage respectively. These are lower than values were obtained in use of 15% water proof paraffin. Both materials improve water absorption and swelling in low values but these materials can also play a major role in adhesion and in high values damage fiber bonds. Consequent the water absorption and swelling increase in fiberboard.

Table 3. The Anti-swelling and Anti-water absorption efficiency of fiberboards were treated with paraffin and beet molasses.

Size type	*Amount* [%]	*Anti-swelling efficency (ASE)* [%]	*Anti-water absorption(WSE)* [%]
Paraffin (Water proof)	5	43.44	7.25
	10	45.16	30
	15	49.78	42.2
	20	22.15	8.55
	25	11.83	-2.85
Beet molasses	5	11.78	-18.39
	10	13.72	-6.73
	15	7.26	-9.71
	20	15.53	0.34
	25	9.74	-2.98

Attention to Table3. Maximum Anti-Swelling and Anti-Water absorption efficiency were obtained at 15 percentage of waterproof paraffin and 20 percentage of beet molasses.The data show that the effect of waterproof paraffin in Anti-Swelling and Anti-Water absorption is more than beet molasses.By using 15% waterproof paraffin the amount of decrease in thickness swelling and water absorption of fiberboards are 49.75 and 42.2 percentage respectively.

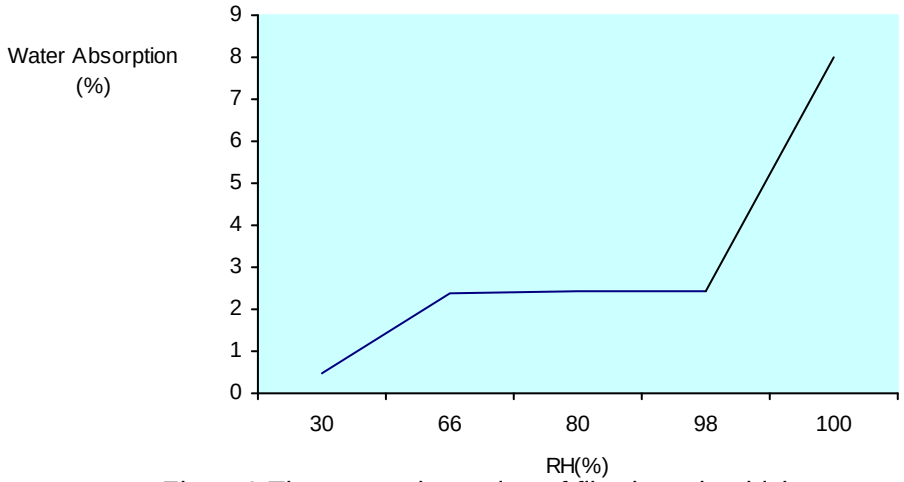

Figure1.The water absorption of fiberboards which were treated with paraffin in various relative humidity(RH)

In range of 30-100% relative humidity(RH) water absorption of fiberboards have been showed in figure1.The fiberboards which were treated with waterproof paraffin have lowest absorption (2%) in expose to below 100% relative humidity that doesn't show sensible swelling in this amount. Anti-swelling efficiency and Anti-water absorption were obtained 49.78% and 42.2% respectively.This material was tested in Iranian fiberboard factory processing and suitable results were obtained.

Generally the research showed that between two materials waterproof paraffin and beet molasses as size for decreasing of water absorption and swelling we can repleace 15 % waterproof paraffin solution instead of total additives materials in manufacturing fiberboards was given the better results. And also this material is economical and available.

ACKNOWLEDGMENTS

The author wish to thank to Prof, Dr.GH, Ebrahimi (University of Tehran; Iran)for his collaboration and assistance to this work and Mr.Bahremand and Mrs Naseri staff of Iranian fiberboard company for their invaluable advice and their supplying of materials.

REFERENCES

Kollmann,F.,& Schneider,A., 1963.On the sorption behavior of heat stabilized wood,Holz als Roh- und Werkstoff,21[3],77-85.

Minato.K.,& Seto.Y., 1995.Formaldehyde treatment of Medium Density Fiberboard in the Low Temperature Range I. Reaction Kinetic aspects.Mokuzai Gakkaishi .Vol.41, No.3, p.318-323.

Minato.K.,& Seto.Y.1995.Formaldehyde treatment of Medium Density Fiberboard in the Low Temperature Range II. Physical and mechanical properties.Mokuzai Gakkaishi .Vol.41, No.3, p.324-329.

Rowell,R.M & Youngquist,J.A., 1991.Dimensional Stability of Aspen Fiberboard made from Acetylated fiber.Wood and Fiber Science.23[4],pp.558-566.

Rowell,R.M&Imamura,Y., 1989.Dimensional Stability,Decay Resistance and Mechanical Properties of Veneer-Faced Low- Density Particleboards made From Acetylated Wood.Wood and Fiber Science, 21[1],pp.67-79.

Suchsland,O & Woodson,GE., 1986.Fiberboards manufacturing practies in the united states.(Agriculture handbook No.640) USDA Forest Service,Madison.263pp.

Wallstrom,L., & Lindberg,K.A.H.,1995.Wood Surface Stabilization with Polyethylene Glycol(PEG).Wood Science and Technology.29:109-119.

Attenuated Total Reflectance (ATR) Fourier Transform Infrared (FTIR) Radiation Studies of Wood Rot Decay andMould Fungi Growth on Building Materials

Bjørn Petter Jelle [1]
Idar Myklebost [2]
Jonas Holme [3]
Per Jostein Hovde [4]
Tom-Nils Nilsen [5]

T 12

ABSTRACT

The attenuated total reflectance (ATR) fourier transform infrared (FTIR) radiation experimental technique represents a powerful measurement tool on various materials. The ATR technique may be applied on both solid state materials, liquids and gases with none or only minor sample preparations, also including materials which are non-transparent to IR radiation. This facilitation is made possible by pressing the sample directly onto various crystals, e.g. diamond, with high refractive indices, in a special reflectance setup. Thus ATR saves time and enables the study of materials in a pristine condition, i.e. the comprehensive sample preparation by pressing thin KBr pellets in traditional FTIR transmittance spectroscopy is avoided.

Ageing processes in building materials, both ageing by natural and accelerated climate exposure, decomposition and formation of chemical bonds and products, may be studied in an ATR-FTIR analysis. In this work the ATR-FTIR technique is attempted utilized to detect wood rot decay and mould fungi growth on building material substrates. An experimental challenge and aim is to be able to detect the wood rot decay and mould fungi growth at early stages when it is barely visible to the naked eye. Another goal is to be able to distinguish between various species of fungi and wood rot.

KEYWORDS

ATR, FTIR, Wood Rot Decay, Mould Fungi, Building

[1] SINTEF and NTNU BAT, Phone +47 73 593377, Fax +47 73 593380, bjorn.petter.jelle@sintef.no
[2] NTNU BAT, Phone +47 73 595040, Fax +47 73 595045, idarm@stud.ntnu.no
[3] SINTEF and NTNU BAT, Phone +47 73 593387, Fax +47 73 593380, jonas.holme@sintef.no
[4] NTNU BAT, Phone +47 73 594547, Fax +47 73 595045, per.hovde@ntnu.no
[5] NTNU CHEM, Phone +47 73 594112, Fax +47 73 594080, tom-nils.nilsen@nt.ntnu.no

SINTEF: Department of Building Materials and Structures, SINTEF Building and Infrastructure, NO-7465 Trondheim, Norway.
NTNU BAT: Department of Civil and Transport Engineering, Norwegian University of Science and Technology, NO-7491 Trondheim, Norway.
NTNU CHEM: Department of Chemical Engineering, Norwegian University of Science and Technology, NO-7491 Trondheim, Norway.

1 INTRODUCTION

Wood rot decay and mould fungi growth on materials represent a problem. In addition to the building damages, e.g. wood rot decay, often due to unwanted water ingress, one of the large risks is related to mould fungi growth.

Trapped water or moisture, e.g. between water tight barriers, which has no possible way to dry or drain out, may lead to mould fungi growth under certain conditions. Unfortunately, these conditions are often fulfilled. The mould fungi initiation and growth are dependent upon the following factors:

- Availability of fungal spores, which are almost always present, except under sterile conditions.
- Nourishment, e.g. wood.
- Moisture.
- Temperature.
- Oxygen.
- Time.

There exists many different species of mould fungi, each of them with various requirements to the above initiation and growth factors. For example, a specific fungi specie may be latent with no growth below a certain temperature and might be exterminated above a certain temperature, where the temperature range will vary for each specie.

The exact relationship between mould fungi growth, with release of airborne fungi, and health problems is not yet fully understood. Nevertheless, that there is a health risk is not questioned, and many people have got ill due to moisture entrapment and the subsequent fungi growth. Occasionally, it has been necessary to evacuate buildings infected with mould fungi.

In this work we are trying to utilize the attenuated total reflectance (ATR) fourier transform infrared (FTIR) radiation experimental technique in order to detect wood rot decay and mould fungi growth on building material substrates. The ATR-FTIR technique makes it possible to study materials which are non-transparent to IR radiation in a pristine condition. That is, the extensive, time-consuming and often cumbersome sample preparation by pressing thin KBr pellets as in traditional FTIR transmittance spectroscopy, which might even change the sample material in question, is avoided. The ATR technique is based on a special reflectance setup where the sample is pressed directly onto various crystals with high refractive indices, e.g. diamond.

Of special interest, and an experimental challenge, is to be able to detect the wood rot decay and fungi growth at early stages when it is barely visible to the naked eye. Ultimately, one might think of future hand-held instruments scanning over a larger area and being able to detect wood rot decay or mould fungi growth before it is visible. Experimentally, the task is challenging, both to differentiate the biological growth and decay impact on the attacked material from the substrate material itself, as well as to being able to distinguish between various species of fungi and wood rot. Populistic, one may say that you are becoming what you are eating, i.e. with respect to FTIR spectra differentiation between the wood rot and mould fungi products versus the substrate material.

Several works are carried out applying infrared spectroscopy in various studies of microorganisms, e.g. by Fischer et al. [2006], Irudayaraj et al. [2002], Kos et al. [2002], Mohebby [2005], Naumann et al. [2005], Ngo-Thi et al. [2003], Orsini et al. [2000], Pandey and Pitman [2003, 2004] and Wenning et al. [2002]. Kos et al. [2002], Mohebby [2005] and Orsini et al. [2000] performed their works by employing the ATR-FTIR spectroscopical technique, which they describe as promising and with many advantages in these types of investigations.

2 EXPERIMENTAL

2.1 Sample Materials

The small sample materials for the FTIR measurements have been collected from the larger field samples depicted in Figure 1, with the following sample categories (no further details are given here):

- **Mould fungi on GU plaster board (GU = exterior grade gypsum board)**
  - Unexposed GU plaster board
  - Exposed GU plaster board with mould fungi scraped off, i.e. measured on plaster board
  - Mould fungi on GU plaster board
  - Mould fungi scraped off from GU plaster board, i.e. measured on a small mould fungi powder pellet
- **Mould fungi on wood**
  - Unexposed wood (30 mm below surface), the wood piece is in reality an exposed sample, but the measured sample is taken 30 mm below the outer surface of the wood piece, where there are no signs of mould fungi
  - Exposed wood (2 mm below surface), some mould fungi may be present 2 mm below the outer surface
  - Mould fungi on wood
  - Mould fungi scraped off from wood, i.e. measured on a small mould fungi powder pellet
- **Wood with wood rot decay**
  - Unexposed wood (30 mm below surface), the wood piece is in reality an exposed sample, but the measured sample is taken 30 mm below the outer surface of the wood piece, where there are no signs of wood rot decay
  - Exposed wood (2 mm below surface), some wood rot decay may be present 2 mm below the outer surface
  - Wood surface damaged by wood rot, measured sample close to wood rot on wood, i.e. adjacent to (but not onto) wood surface heavily infected with wood rot
  - Wood rot on wood, area on wood piece heavily infected with wood rot
  - Wood rot scraped off from wood, i.e. measured on a small wood rot powder pellet
- **Reference materials (for check/comparison of FTIR absorbance peaks)**
  - Water, distilled
  - Gypsum, non-dried
  - Gypsum, dried

Figure 1. Photos of the large field samples from where smaller samples have been collected for the FTIR measurements. Mould fungi on GU plaster board (left photo) and mould fungi on wood and wood rot (right photo). GU = exterior grade gypsum board (”outdoor use”).

2.2 FTIR Measurements

The FTIR material characterization was carried out with a Thermo Nicolet 8700 FTIR spectrometer with a Smart Orbit accessory, i.e. a horizontal attenuated total reflectance (HATR) accessory (single reflection) with a diamond crystal, in the wavelength range 4000 cm^{-1} (2.5 μm) to 400 cm^{-1} (25 μm) in an atmosphere with minimalized CO_2 and H_2O content through purging by a Parker Balston 74-5041 FTIR Purge Gas Generator. Each FTIR spectrum presented is based on a recording of 32 scans at a resolution of 4 cm^{-1}. In order to ensure satisfactory contact between the HATR diamond crystal and the sample, a minimum of three or more FTIR spectra were recorded at various locations on the sample.

The FTIR spectra given in this work have not been ATR corrected, neither with respect to penetration depths nor absorbance band shifts, which both are dependent on the refractive indices of the sample and the ATR crystal (diamond in this case) and the angle of incident radiation. The penetration depth is in addition also dependent on the radiation wavelength.

The FTIR measurements were performed on several samples within each sample category as described above (ch.2.1), of which only one single representative spectrum for each sample category is shown in the following (ch.3).

3 RESULTS AND DISCUSSION

FTIR absorbance spectra versus wave number for the various mould fungi and wood rot samples are presented in Figs.2-6. Mould fungi samples at various exposure degrees on GU plaster board are shown in Figure 2. Mould fungi samples at different exposure levels on wood are given in Figure 3. Wood rot samples at various decay levels are shown in Figure 4.

As the absorption of electromagnetic radiation, e.g. IR radiation, follows the Beer-Lambert law, i.e. the radiation is decreasing exponentially with the penetration depth in the actual material, it is often helpful to plot the spectra on a logarithmic absorbance scale vs. wavelength. Hence, a representative spectrum is chosen from each of the samples and plotted on a logarithmic absorbance scale for quantitative studies. Mathematically and physically it follows that a doubling of the logarithmic absorbance, also called optical density, is interpreted as a doubling of material thickness or a doubling of concentration of absorption active agents.

The mould fungi growth and wood rot decay makes the sample material undergo chemical changes and may then as a result of the chemical reactions change the actual thickness of the sample. In this work the experiments are conducted by applying the ATR equipment with the FTIR spectrometer. Hence, the IR radiation is only penetrating into a thin surface layer of the actual sample. With respect to the experiments carried out in this work, the material thickness will then be regarded as approximately constant, i.e. the change in the IR absorbance is explained by an increase or decrease of absorption active species within the sample material undergoing the chemical transformation.

Figure 5 gives the FTIR absorbance versus wave number between 4000-400 cm^{-1} for mould fungi on GU plaster board, mould fungi on a wood sample and wood rot at selected exposure levels (from Figs.2-4). In addition, the water spectrum is also plotted as a comparison.

Figure 6 shows the FTIR absorbance versus wave number between 1800-1400 cm^{-1} for mould fungi on GU plaster board, mould fungi on a wood sample and wood rot at selected exposure levels (from Figs.2-5). In addition, the water, non-dried gypsum and dried gypsum spectra are also plotted as a comparison.

In Figure 6 the narrow, large ellipse encircles FTIR absorbance peaks which may be related to mould fungi and/or wood rot, but this is more uncertain due to the water peak at this location. Note that any microbiological growth may increase the water content. Furthermore, in order to quantify any potential pollution (error) from any astray gypsum powder, the gypsum peaks are also depicted, as these falls in the same wave number range.

Also note that different adjacent neighbour atoms in a compound, e.g. in a polymer chain, will shift the wave number somewhat for the absorbance peak corresponding to the chemical bond in question.

The thick, small ellipse in Figure 6 encircles FTIR absorbance peaks which are found to be characteristic for the mould fungi and wood rot. These peaks, also including the other samples depicted in Figs.2 - 4, lies between 1558 cm^{-1} and 1535 cm^{-1}.

That is, the chemical bonds which is the source for the absorbance peaks at these wave numbers, are found to be present and characteristic for the various mould fungi and wood rot products studied in this work.

Hence, in this preliminary study it has been demonstrated that the ATR-FTIR spectroscopical technique may be applied in order to detect wood rot decay and mould fungi growth on building materials. Further studies and experimental investigations are needed in order to elaborate the suitability, the reliability, the limitations and the future potential possibilities of this method.

In future applications of this experimental method as a detection tool capable of differentiating between various wood rot and mould fungi species, there is a need to build up large reference databases containing FTIR spectra of the different species.

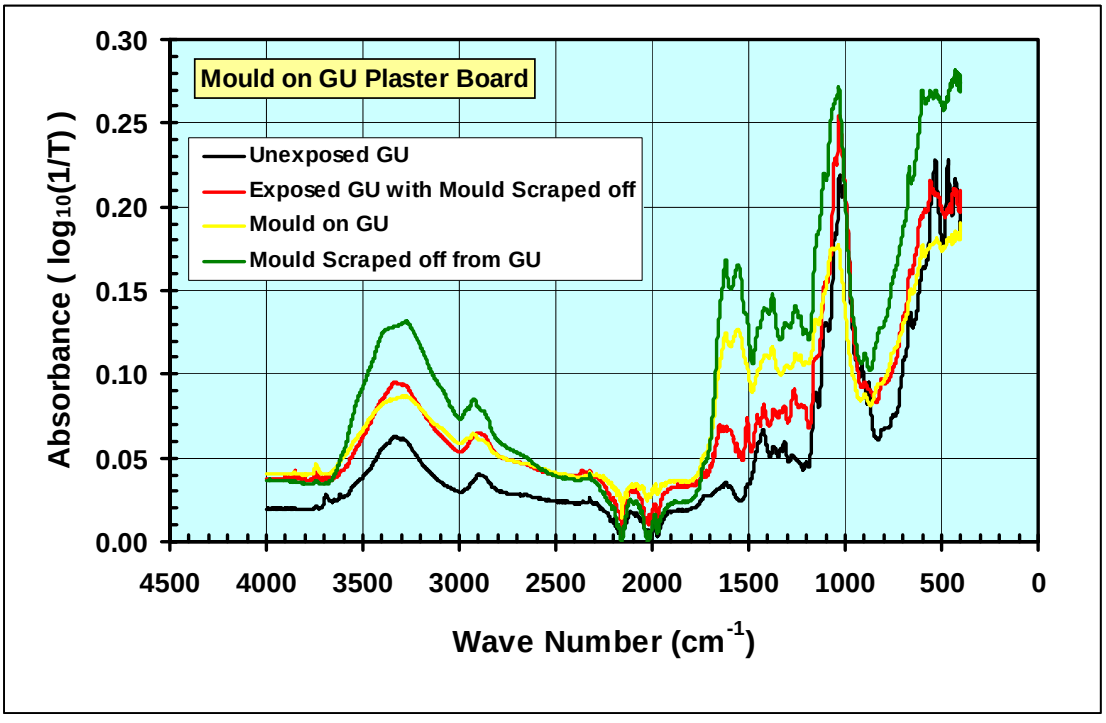

Figure 2. Absorbance (logarithmic) versus wave number between 4000-400 cm-1 for mould fungi at various exposure levels on GU plaster board. (T = Transmittance).

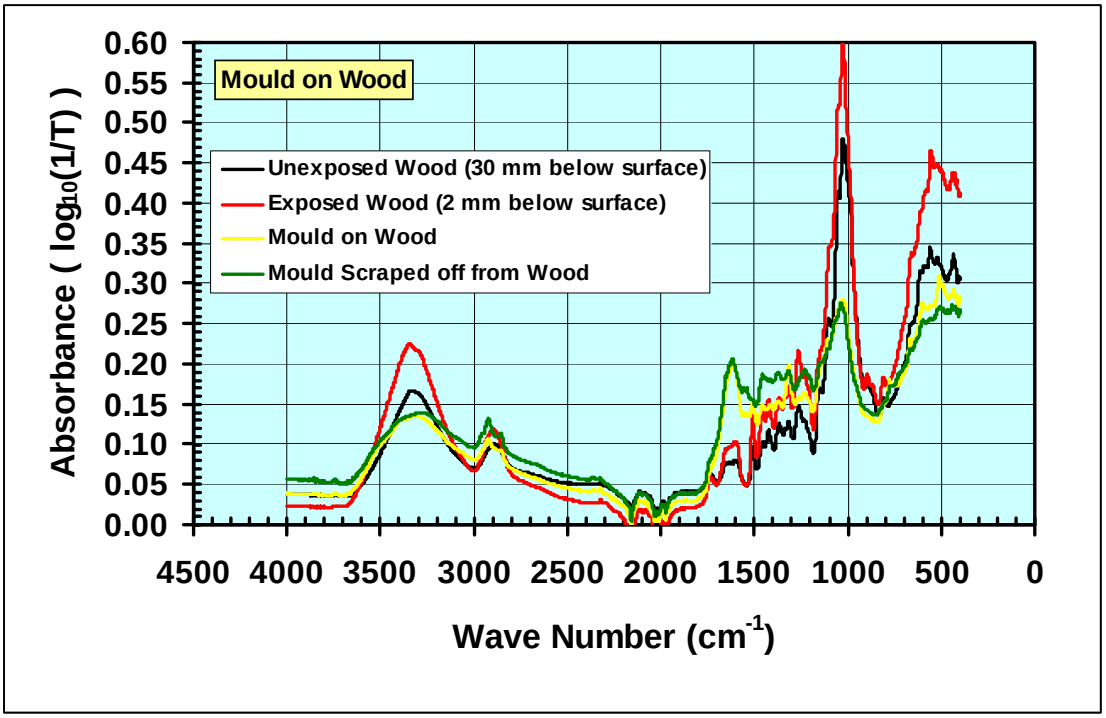

Figure 3. Absorbance (logarithmic) versus wave number between 4000-400 cm^{-1} for mould fungi at various exposure levels on a wood sample.

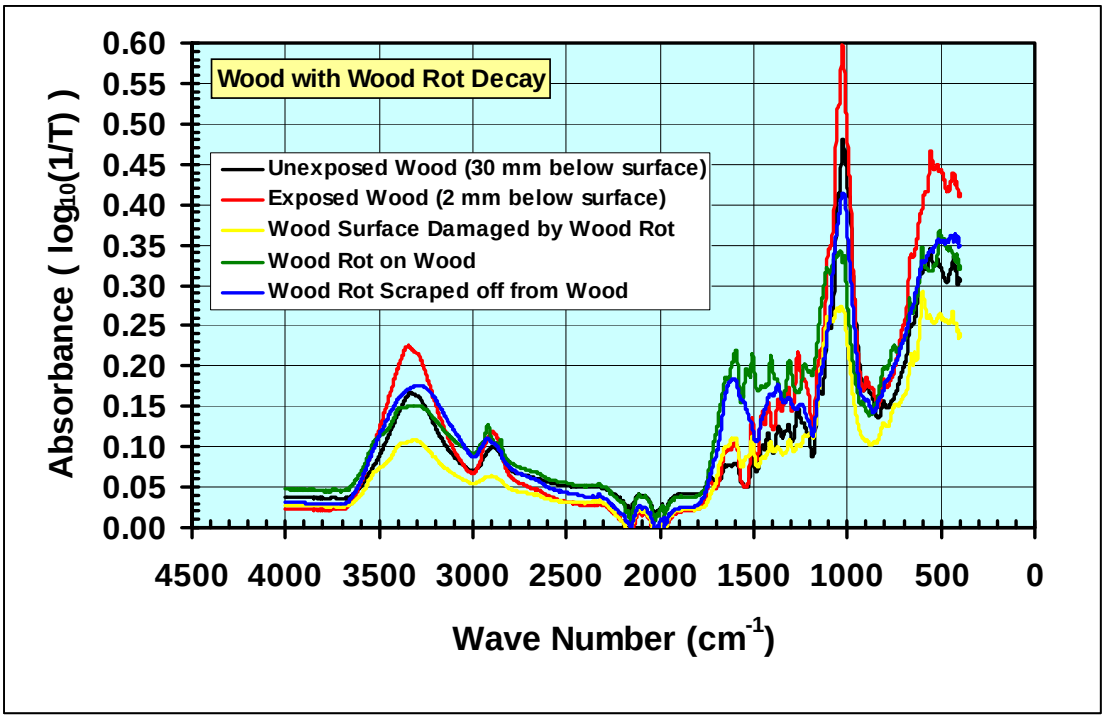

Figure 4. Absorbance (logarithmic) versus wave number between 4000-400 cm^{-1} for wood rot at various exposure levels of wood rot decay.

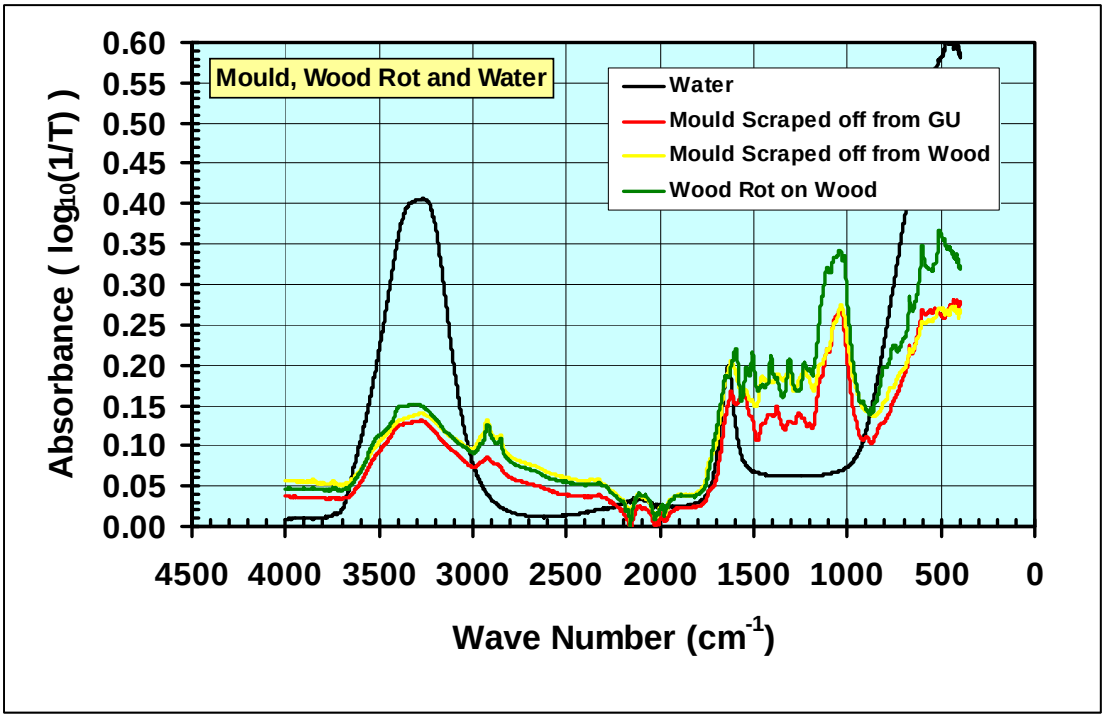

Figure 5. Absorbance (logarithmic) versus wave number between 4000-400 cm^{-1} for mould fungi on GU plaster board, mould fungi on a wood sample and wood rot at selected exposure levels. In addition, the water spectrum is also plotted as a comparison. From Figs.2-4 (except water spectrum).

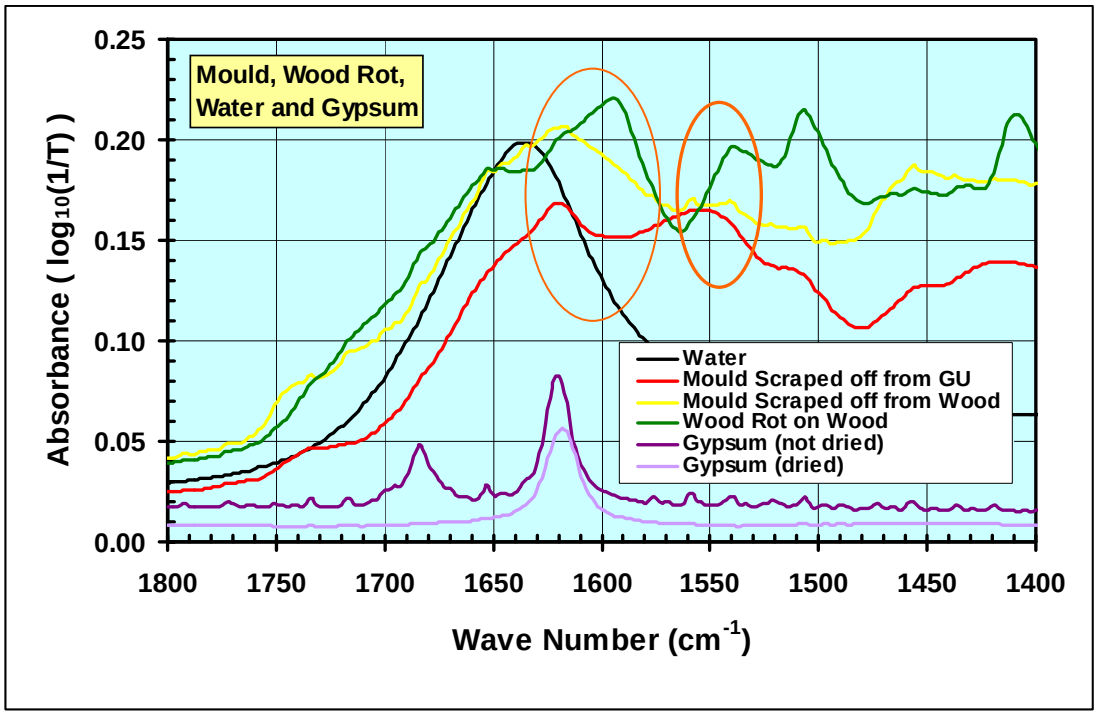

Figure 6. Absorbance (logarithmic) versus wave number between 1800-1400 cm^{-1} for mould fungi on GU plaster board, mould fungi on a wood sample and wood rot at selected exposure levels. In addition, the water, non-dried gypsum and dried gypsum spectra are also plotted as a comparison. From Figure 5 (except gypsum spectra). See discussion in text about the FTIR absorbance peaks within the narrow, large (left) and thick, small (right) ellipse encircling the absorbance peaks.

4 CONCLUSIONS

This preliminary study has demonstrated that the attenuated total reflectance (ATR) fourier transform infrared (FTIR) spectroscopical technique may be applied in order to detect wood rot decay and mould fungi growth on building materials. However, further studies and experimental investigations are needed in order to elaborate the suitability, the reliability, the limitations and the future potential possibilities of this method.

REFERENCES

Fischer, G., Braun, S., Thissen, R. & Dott, W., 2006, 'FT-IR spectroscopy as a tool for rapid identification and intra-species characterization of airborne filamentous fungi', *Journal of Microbiological Methods*, **64**, 63-77.

Irudayaraj, J., Yang, H. & Sakhamuri, S., 2002, 'Differentiation and detection of microorganisms using Fourier transform infrared photoacoustic spectroscopy', *Journal of Molecular Structure*, **606**, 181-188.

Kos, G., Lohninger, H. & Krska, R., 2002, 'Fourier transform mid-infrared spectroscopy with attenuated total reflection (FT-IR/ATR) as a tool for the detection of Fusarium fungi on maize', *Vibrational Spectroscopy*, **29**, 115-119.

Mohebby, B., 2005, 'Attenuated total reflection infrared spectroscopy of white-rot decayed beech wood', *International Biodeterioration & Biodegradation*, **55**, 247-251.

Naumann, A., Navorro-González, M., Peddireddi, S., Kües, U. & Polle, A. 2005, 'Fourier transform infrared microscopy and imaging: Detection of fungi in wood', *Fungal Genetics and Biology*, **42**, 829-835.

Ngo-Thi, N.A., Kirschner, C. & Naumann, D., 2003, 'Characterization and identification of microorganisms by FT-IR microspectrometry', *Journal of Molecular Structure*, **661-662**, 371-380.

Orsini, F., Ami, D., Villa, A.M., Sala, G., Bellotti, M.G., & Doglia, S.M., 2000, 'FT-IR microspectroscopy for microbiological studies', *Journal of Microbiological Methods*, **42**, 17-27.

Pandey, K.K. & Pitman, A.J. 2003, 'FTIR studies of the changes in wood chemistry following decay by brown-rot and white-rot fungi', *International Biodeterioration & Biodegradation*, **52**, 151-160.

Pandey, K.K., & Pitman, A. J., 2004, 'Examination of the lignin content in a softwood and a hardwood decayed by a brown-rot fungi with the acetyl bromide method and fourier transform infrared spectroscopy', *Journal of Polymer Science: Part A: Polymer Chemistry*, **42**, 2340-2346.

Wenning, M., Seiler, H., & Scherer, S., 2002, 'Fourier-transform Infrared Microspectroscopy, a novel and rapid tool for identification of yeasts', *Applied and Environmental Microbiology*, October 2002, 4717-4721.

11DBMC International Conference on Durability of Building Materials and Components
ISTANBUL, Turkey 11-14 May 2008

Attenuated Total Reflectance (ATR) Fourier Transform Infrared (FTIR) Radiation Investigations of Natural and Accelerated Climate Aged Wood Substrates

Bjørn Petter Jelle [1]
Petra Rüther [2]
Per Jostein Hovde [3]
Tom-Nils Nilsen [4]

T 12

ABSTRACT

The attenuated total reflectance (ATR) fourier transform infrared radiation (FTIR) experimental technique represents a powerful measurement tool on various materials. The ATR technique may be applied on both solid state materials, liquids and gases with none or only minor sample preparations, also including materials which are non-transparent to IR radiation. This facilitation is made possible by pressing the sample directly onto various crystals, e.g. diamond, with high refractive indices, in a special reflectance setup. Thus ATR saves time and enables the study of materials in a pristine condition, i.e. the comprehensive sample preparation by pressing thin KBr pellets in traditional FTIR transmittance spectroscopy is avoided. Ageing processes in building materials, both ageing by natural and accelerated climate exposure, decomposition and formation of chemical bonds and products, may be studied in an ATR-FTIR analysis. In this work the ATR-FTIR technique is attempted utilized to detect changes in selected wood building material substrates subjected to natural weather exposure and various accelerated climate exposure conditions. One aim is by ATR-FTIR analysis to be able to quantitatively determine the length of the wood ageing time before priming/treatment. Climate parameters like temperature (including freezing/thawing), relative air humidity, wind-driven rain amount, solar and/or ultraviolet radiation and exposure duration are controlled in different climate ageing apparatuses. Both impregnated and raw wood samples have been employed in the experimental investigations.

KEYWORDS

ATR, FTIR, Climate Ageing, Wood, Building.

[1] SINTEF and NTNU BAT, Phone +47 73 593377, Fax +47 73 593380, bjorn.petter.jelle@sintef.no
[2] NTNU BAT, Phone +47 73 594579, Fax +47 73 595045, petra.ruether@sintef.no
[3] NTNU BAT, Phone +47 73 594547, Fax +47 73 595045, per.hovde@ntnu.no
[4] NTNU CHEM, Phone +47 73 594112, Fax +47 73 594080, tom-nils.nilsen@nt.ntnu.no
SINTEF: Department of Building Materials and Structures, SINTEF Building and Infrastructure, NO-7465 Trondheim, Norway.
NTNU BAT: Department of Civil and Transport Engineering, Norwegian University of Science and Technology, NO-7491 Trondheim, Norway.
NTNU CHEM: Department of Chemical Engineering, Norwegian University of Science and Technology, NO-7491 Trondheim, Norway.

1 INTRODUCTION

Wood deterioration of building materials due to natural climate ageing processes represents a problem. In natural climate ageing the wood materials, e.g. wood claddings, are exposed to several climate factors like for example:

- Solar radiation including ultraviolet (UV), visible (VIS) and near infrared (NIR) radiation.
- Ambient infrared (IR) heat radiation (the resulting elevated temperature increases the rate of chemical degradation reactions, and also the rate of growth of rot and fungus up to limiting temperatures).
- Temperature changes/cycles (relative temperature movements between different materials, number of freezing point passes during freezing/thawing).
- Water, e.g. moisture, relative air humidity, rain (precipitation), wind-driven rain.
- Wind.
- Erosion (also from above factors).
- Pollutions (e.g. gases and particles in air).
- Time (for all the factors above to work).

Note that wood rot and mould fungus are not listed as climate factors, i.e. the wood rot and mould fungus are in this context viewed as (unwanted) results of the specific climate factors moisture and temperature for a certain exposure time with a sufficient supply of nourishment (e.g. wood). Although commonly not regarded as so, the availability of fungal spores may be seen as a special climate exposure factor. Fungal spores are almost always present, except under sterile conditions. See Jelle et al. [2007] for FTIR investigations of wood rot decay and mould fungi growth on building materials.

In this work we are trying to utilize the attenuated total reflectance (ATR) fourier transform infrared (FTIR) radiation technique in order to study wood decomposition in (accelerated) climate aged building material substrates. The ATR-FTIR technique makes it possible to study materials which are non-transparent to IR radiation in a pristine condition. That is, the extensive, time-consuming and often cumbersome sample preparation by pressing thin KBr pellets as in traditional FTIR transmittance spectroscopy is avoided. This traditional technique might even change the sample material in question. The ATR technique is based on a special reflectance setup where the sample is pressed directly onto various crystals with high refractive indices, e.g. diamond. One goal is to be able to quantitatively determine the wood decomposition by performing an ATR-FTIR analysis, including to determine the length of the wood ageing time before priming/treatment of the wood has to be done.

Experimentally the task is challenging. Firstly, it may be difficult to differentiate the wood deterioration products on the attacked wood sample from the wood substrate material itself. Secondly, it may be complicated to be able to distinguish between various wood decomposition products. Thirdly, the wood material is not homogenous, which may complicate the measurements. Finally, with the ATR technique it is important to achieve and ensure a good contact with no air pockets between the sample and the ATR crystal in order to obtain correct quantitative results. With wood samples having relatively hard and rough surfaces such a good contact might be difficult to achieve and especially to ensure that the actual contact is the best one attainable. Several works are carried out applying infrared spectroscopy in studies of wood weathering and wood photodegradation, e.g. by Anderson et al. [1991], Colom et al. [2003], Humar et al. [2006], Mohebby [2005], Pandey and Pitman [2003], Pandey [2005], Sudiyani et al. [2003] and Yamauchi et al. [2004]. Anderson et al. studied the effects of artificial weathering of softwoods and hardwoods with water alone, sunlight (xenon lamp) alone and both water and sunlight applied in conjunction. ATR analyses were performed by Humar et al. [2006] and Mohebby et al. [2005]. The common practice and most widely applied experimental method is the traditional KBr pellet sample technique in infrared transmittance modus. Although there exists many experimental challenges using the ATR-FTIR method on wood, this method is nevertheless very promising and with many advantages and is therefore the subject of our investigations in this work.

2 EXPERIMENTAL

2.1 Sample Materials

Altogether, nine different wood sample materials, five raw, non-impregnated and four impregnated wood samples, have been tested in various accelerated climate ageing apparatuses, in addition to natural outdoor weather ageing. Due to length limitations for this publication, only two samples are discussed in the work presented here. The two wood samples are:

Sample A Norway Spruce, *Picea Abies L. Karst.* (Ruptimal® Surface, mechanically treated surface), measured dry mass density of 0.41 kg/dm^3. Raw, non-impregnated sample.

Sample H Pressure Treated Pine Class NP5 (chemical treated according to EN 351-1:2007), *Pinus Sylvestris L.*, measured dry mass density of 0.50 kg/dm^3. Impregnated sample.

The small wood pieces needed for the FTIR measurements have been collected from the larger samples depicted in Figure 1.

Figure 1. Photos of wood sample A (left) and wood sample H (right) after 115 days of accelerated ageing in the Atlas Solar Simulator climate chamber. Direct solar radiation exposed side shown upwards. Small wood pieces are cut from the samples for use in the FTIR investigations.

2.2 Short Description of the Overall Study

The results presented here is part of a larger on-going study where several different wood samples are being subjected to both natural weather ageing and various accelerated climate ageing apparatuses, including comparisons between the natural and the artificial weathering methods. The various ageing apparatuses include an Atlas SC600 MHG Solar Simulator (see next section for details), a QUV apparatus weathering tester horizontal option with ponding and water spray (The Q-Panel Company, Cleveland, Ohio, USA) and a vertical accelerated climate simulator subjecting the sample area in turns to four different climate zones (1 hour in each climate zone), that is, one UV (UVA and UVB intensities are averaged to 14 W/m^2 and 1.4 W/m^2, respectively) and IR irradiation zone (black panel temperature of 63ºC), one water spray zone (15 dm^3/(m^{2}h)), one freezing zone (-20ºC) and one indoor laboratory climate zone according to Nordtest Method NT Build 495 (”Building materials and components in the vertical position: Exposure to accelerated climatic strains”). However, due to length limitations for this publication, only some of the results from the accelerated ageing in the Atlas Solar Simulator are presented here.

2.3 Accelerated Ageing in Atlas Solar Simulator

The accelerated ageing was carried out in an Atlas SC600 MHG Solar Simulator climate chamber with a 2500 W MHG lamp. The wood samples were tilted a bit from the horizontal (8 ± 2º) in order to let the water run off the surface. The samples were placed in the climate chamber with a distance of approximately 55 cm from the climate chamber glass ceiling to the samples, where the solar radiation intensity is reported to be 1200 W/m^2 at 100 % lamp power intensity. During the ageing period the

UVA and UVB radiation intensity was measured at various times to be lying within the interval 60-80 W/m^2 and 3-6 W/m^2, respectively. The UV measurements were performed with a radiometer/photometer Model IL 1400A (International Light) with an UVA sensor and an UVB sensor. Note that a 6 % UVA fraction (like in sunlight) of the total solar intensity (1200 W/m^2) yields 72 W/m^2 UVA radiation. The exposure duration consisted of 115 whole cycles of 24 hours, each cycle divided into 20 hours with a solar radiation intensity of 1200 W/m^2 and 4 hours with water spray application and no solar radiation exposure. The two water spray nozzles gave each 0.5 dm^3/min, i.e. 1 dm^3/min in total, which gives approximately 1.7 dm^3/(m^{2}min) assuming an even horizontal water distribution at the sample location in the whole climate chamber. Integrated up, the solar radiation (MHG lamp) energy is 24 kWh/m^2 per day and 2760 kWh/m^2 during 115 days. Likewise, assuming 70 W/m^2 as an average, the UVA radiation energy is 1.4 kWh/m^2 per day and 161 kWh/m^2 during 115 days. The temperature and relative air humidity were held constant at 63ºC and 50 % RH during the solar radiation exposure and at 10ºC and close to 100 % RH during the water spray application.

2.4 FTIR Measurements

The FTIR material characterization was carried out with a Thermo Nicolet 8700 FTIR spectrometer with a Smart Orbit accessory, i.e. a horizontal attenuated total reflectance (HATR) accessory (single reflection) with a diamond crystal, in the wavelength range 4000 cm^{-1} (2.5 μm) to 400 cm^{-1} (25 μm) in an atmosphere with minimalized CO_2 and H_2O content through purging by a Parker Balston 74-5041 FTIR Purge Gas Generator. Each FTIR spectrum presented is based on a recording of 32 scans at a resolution of 4 cm^{-1}. In order to ensure satisfactory contact between the ATR diamond crystal and the sample, a minimum of three or more FTIR spectra were recorded at various locations on the sample. Figure 2 shows a wood piece from sample A pressed onto the diamond crystal in the HATR accessory connected to the FTIR spectrometer.

Figure 2. Photos of a wood piece from sample A pressed onto the diamond crystal in the HATR accessory connected to the FTIR spectrometer. In the close-up photo to the right, the lower steel pin is only a reflection of the above steel pin in the polished mirror-like sample plate.

The FTIR spectra given in this work have not been ATR corrected, neither with respect to penetration depths nor absorbance band shifts, which both are dependent on the refractive indices of the sample and the ATR crystal (diamond in this case) and the angle of incident radiation. The penetration depth is in addition also dependent on the radiation wavelength. Note that it should always be stated if an ATR-FTIR spectrum has been ATR corrected or not, e.g. important during computerized database spectra comparison searches.

3 RESULTS AND DISCUSSION

FTIR transmittance spectra versus wave number between 4000-400 cm^{-1} for the sample A and sample H at various accelerated ageing levels are presented in Figure 3 and Figure 4. Further close-ups of these spectra are shown as FTIR absorbance versus wave number between 1900-700 cm^{-1} in Figure 5 and Figure 6. Finally, as a reference to avoid any misinterpretations, the distilled water FTIR transmittance spectrum is plotted together with the fresh and aged 115 days sample A spectra in Figure 7. Note that the irregularities in the FTIR spectra between 2200-1900 cm^{-1} (Figure 3 and Figure 4) are due to the very large absorption in the ATR diamond crystal between these wave numbers, which represents the weak point in an otherwise excellent material choice for ATR applications.

As the absorption of electromagnetic radiation, e.g. IR radiation, follows the Beer-Lambert law, i.e. the radiation is decreasing exponentially with the penetration depth in the actual material, it is often helpful to plot the spectra on a logarithmic absorbance scale vs. wavelength. Hence, a representative spectrum is chosen from each of the samples and plotted on a logarithmic absorbance scale for quantitative studies. Mathematically and physically it follows that a doubling of the logarithmic absorbance, also called optical density, is interpreted as a doubling of material thickness or a doubling of concentration of absorption active agents.

The wood sample material undergoes chemical changes and may then as a result of the chemical reactions change the actual thickness of the sample. In this work the experiments are conducted by applying the ATR equipment with the FTIR spectrometer. Hence, the IR radiation is only penetrating into a thin surface layer of the actual sample. With respect to the experiments carried out in this work, the material thickness will then be regarded as approximately constant, i.e. the change in the IR absorbance is explained by an increase or decrease of absorption active species within the sample material undergoing the chemical transformation.

By inspecting the FTIR spectra (Figs.3-6) more closely it is found that several absorbance peaks in the fresh, non-aged wood samples (both A and H) are diminished and finally vanished during the accelerated ageing in the Atlas Solar Simulator. These absorbance peaks are located around 1730-1710 cm^{-1} (varying with different wood specimens), 1510 cm^{-1}, 1260 cm^{-1} and 810 cm^{-1}. The peak around 1730-1710 cm^{-1} are attributed to carbonyl (C=O) stretching in hemicellulose, whereas the peak around 1510 cm^{-1} arises from the C=C stretching of the aromatic ring in lignin. These two peaks located around 1730-1710 cm^{-1} and 1510 cm^{-1} represent good candidates for studying wood decomposition by climate ageing through FTIR analysis.

In addition, for wood sample H (impregnated sample), the two sharp and distinct characteristic absorbance peaks between 3000-2800 cm^{-1} (CH stretch, which may be attributed to the impregnation agent) disappear after some ageing time. The fresh, non-aged wood sample A does not have these two distinct absorbance peaks, only a broad peak in the same wavelength range (similar to the aged peak for sample H).

There are some other changes (i.e. increase and/or decrease) in the absorbance peaks during the ageing period also, but generally no completely disappearance of peaks and neither appearance of new peaks. Note that the water absorbance peaks are located at 3265 cm^{-1} (broader peak, -OH) and 1637 cm^{-1} (narrower peak, -O-), and changes in the FTIR spectra around these wave numbers might also be due to various moisture levels in the samples. Also note that different adjacent neighbour atoms in a compound, e.g. in a polymer chain, will shift the wave number somewhat for the absorbance peak corresponding to the chemical bond in question.

Hence, in this preliminary study it has been demonstrated that the ATR-FTIR spectroscopical technique may be applied in order to detect different levels of climate induced wood decomposition or ageing. Further studies and experimental investigations are needed in order to elaborate the suitability,

the reliability, the limitations and the future potential possibilities of this method. In future applications of this experimental method as a detection tool capable of differentiating between various wood decomposition or ageing levels, there is a need to build up large reference databases containing FTIR spectra of the different species.

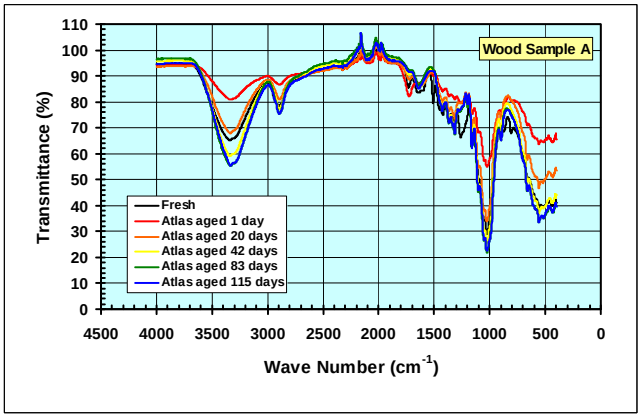

Figure 3. Transmittance versus wave number between 4000-400 cm^{-1} for wood sample A during accelerated ageing in an Atlas Solar Simulator.

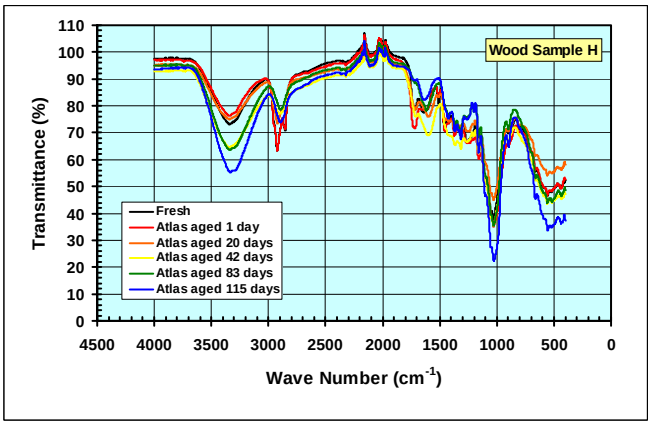

Figure 4. Transmittance versus wave number between 4000-400 cm^{-1} for wood sample H during accelerated ageing in an Atlas Solar Simulator.

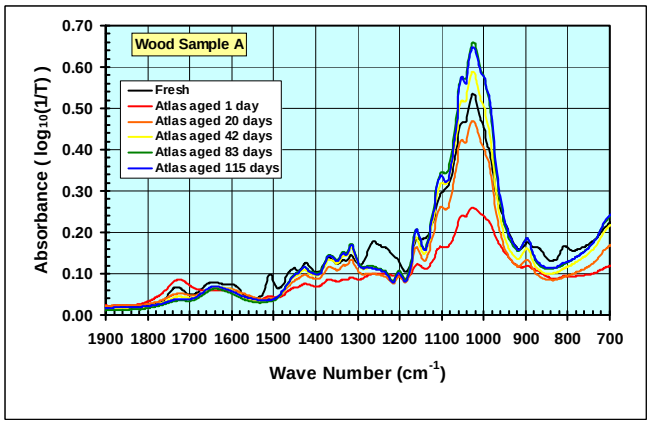

Figure 5. Absorbance (logarithmic) versus wave number between 1900-700 cm^{-1} for wood sample A during accelerated ageing in an Atlas Solar Simulator.

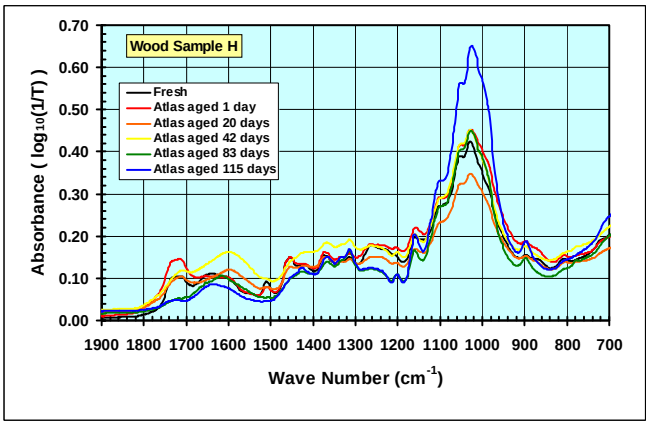

Figure 6. Absorbance (logarithmic) versus wave number between 1900-700 cm^{-1} for wood sample H during accelerated ageing in an Atlas Solar Simulator.

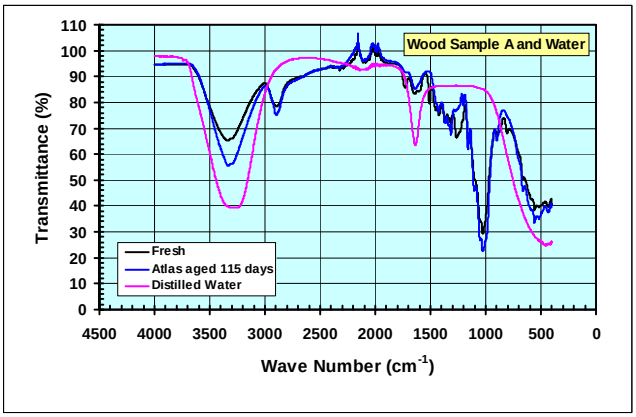

Figure 7. Transmittance versus wave number between 4000-400 cm^{-1} for wood sample A during accelerated ageing (fresh and 115 days, see Figure 3 for more) in an Atlas Solar Simulator including a comparison with the distilled water spectrum.

4 CONCLUSIONS

This preliminary study has demonstrated that the attenuated total reflectance (ATR) fourier transform infrared (FTIR) spectroscopical technique may be applied in order to detect different levels of climate induced wood decomposition or ageing. However, further studies and experimental investigations are needed in order to elaborate the suitability, the reliability, the limitations and the future potential possibilities of this method.

REFERENCES

E. L. Anderson, Z. Pawlak, N. L. Owen & W. C. Feist, ”Infrared studies of wood weathering. Part I: Softwoods”, *Applied Spectroscopy*, **45**, 641-647 (1991).

E. L. Anderson, Z. Pawlak, N. L. Owen & W. C. Feist, ”Infrared studies of wood weathering. Part II: Hardwoods”, *Applied Spectroscopy*, **45**, 648-652 (1991).

X. Colom, F. Carrillo, F. Nogués & P. Garriga, ”Structural analysis of photodegraded wood by means of FTIR spectroscopy”, *Polymer Degradation and Stability*, **80**, 543-549 (2003).

M. Humar, B. Bučar & F. Pohleven, ”Brown-rot decay of copper-impregnated wood”, *International Biodeterioration & Biodegradation*, **58**, 9-14 (2006).

B. P. Jelle, I. Myklebost, J. Holme, P. J. Hovde & T.-N. Nilsen, ”Attenuated Total Reflectance (ATR) Fourier Transform Infrared (FTIR) Radiation Studies of Wood Rot Decay and Fungus Growth on Building Materials”, *Proceedings of the 11th International Conference on Durability of Building Materials and Components*, Istanbul, Turkey, 11-14 May, 2008.

B. Mohebby, ”Attenuated total reflection infrared spectroscopy of white-rot decayed beech wood”, *International Biodeterioration & Biodegradation*, **55**, 247-251 (2005).

K. K. Pandey & A. J. Pitman, ”FTIR studies of the changes in wood chemistry following decay by brown-rot and white-rot fungi”, *International Biodeterioration & Biodegradation*, **52**, 151-160 (2003).

K. K. Pandey, ”Study of the effect of photo-irradiation on the surface chemistry of wood”, *Polymer Degradation and Stability*, **90**, 9-20 (2005).

Y. Sudiyani, Y. Imamura, S. Doi & S. Yamauchi, ”Infrared spectroscopic investigations of weathering effects on the surface of tropical wood”, *Journal of Wood Science*, **49**, 86-92 (2003).

S. Yamauchi, Y. Sudiyani, Y. Imamura & S. Doi, ”Depth profiling of weathered tropical wood using Fourier transform infrared photoacoustic spectroscopy”, *Journal of Wood Science*, **50**, 433-438 (2004).

EN 351-1, ”Durability of wood & wood-based products - Preservative-treated solid wood - Part 1: Classification of preservative penetration and retention”, 2007.

Performance-based Specification of Wooden Components

Christian Brischke [1]
Andreas O. Rapp [2]

T 12

ABSTRACT

The need for a unified and harmonised system for performance classification and specification of wood and wood-based products in Europe emanates from requirements of users and the European Construction Products Directive (CPD). A road to a feasible specification system is outlined. Exposure-related performance prediction was worked out as a key task on the way to product specification. Therefore suitable tools, field test methods as well as short-term/laboratory test methods, are sought to allow the determination of reference service lives for different exposure categories. On the one hand, performance factors, which derive from service lives in field tests, allow the specification of wood products. On the other hand, the calculation of inter-site factors may allow the modelling of service lives and the drawing of hazard mappings.

KEYWORDS

Wood, Commodity, Field tests, Service life prediction, Performance factors

[1] Leibniz Universität Hannover, Institute of Vocational Sciences in the Building Trade (ibw), Hannover, D-30419 Germany, Phone +49 762-5829, Fax +49 762-3196, brischke@ibw.uni-hannover.de

[2] Leibniz Universität Hannover, Institute of Vocational Sciences in the Building Trade (ibw), Hannover, D-30419 Germany, Phone +49 762-4595, Fax +49 762-3196, rapp@ibw.uni-hannover.de

1 INTRODUCTION

A unified and harmonised system for performance classification and specification of wood and wood-based products in Europe is still lacking. At the same time the need for such a system becomes more and more obvious. Users and consumers have a strong interest in reliable information on the expected performance of wooden products. They are the decision makers in the market place and will particularly decide, if wood-based products or substitute building materials will be used.

For the user, the only valuable product information needs to be based on a performance characterisation. For example when attempting to chose among different products, is not very helpful to the user to determine the relative protective effectiveness of a wood preservative as is done according to different European standards, e.g. EN 113 (1996), ENV 807 (2001). For potential customers it is essential to have useful information in a form that helps assess whether the product will meet its performance requirements (*i.e.* the desired service life). Ideally what is needed for this purpose is a reliable service life estimate, but at the very least, a product specification having performance classes would be useful information for a consumer to make an informed choice. Furthermore, such a system should not be limited for a particular group of wood products only, but universally applicable for all wood-based products including, for example:

i. Wood treated with classical wood preservatives
ii. Wood treated with new organic preservatives
iii. Natural durable wood
iv. Modified wood
v. Wood-based composites.

Secondly, the need for performance classification emanates from the European Construction Products Directive, CPD (1988) on the approximation of laws, regulations and administrative provisions of the member states relating to construction products. The CPD requires in particular "products fit for an intended use", which may be translated as meaning, “a sufficient level of performance” over a particular time period – the time period of the intended use.

Thus, for the wood industry, as well as for wood scientists, three important needs may be derived from the CPD:

1. Provide data that are applicable for performance estimations of wood-based products
2. Deliver suitable test methods to assess the performance over time of wood-based products
3. Establish a European-wide harmonised classification and specification system.

The objectives of this work were to identify the necessary steps towards a feasible performance classification system and to provide a roadmap for the specification of wood-based products. The approach presented in the following should be seen as a proposal and a base for the discussion about different aspects related to wood product specifications. Valuable comments and subjects of the discussion, which took place in the frame of COST Action E37 “Sustainability through new technologies for enhanced wood durability”, were considered in this paper.

2 ROADMAP FOR THE SPECIFICATION OF WOOD AND WOOD-BASED PRODUCTS

2.1 General Aspects

A roadmap for the specification of wood and wood-based products to be drawn in this paper can be defined by its start and ending point. The starting point of this road is the expectancy regarding a specification system by the user of wood-based products and the CPD (1988) as described in Section 1. As is shown in Figure 1, a feasible product specification is the final destination at the end of the road intended to meet user requirements. From the beginning it is clear that the end of this road can only be reached by performance prediction, which somehow need to be realized . In the following

sections, the different stopovers on the roadmap to developing a useful product specification will be described and discussed that focus on the steps necessary to achieve performance prediction .

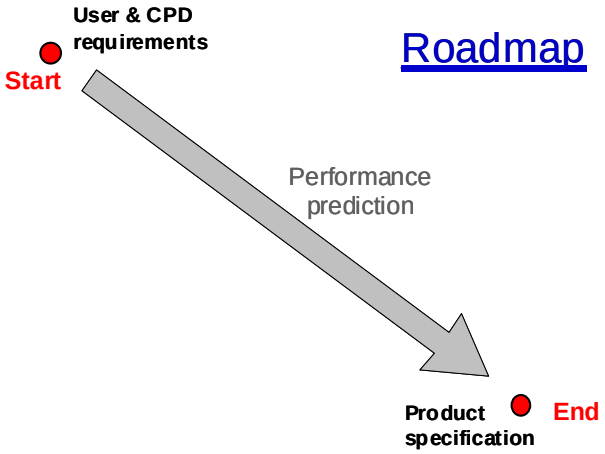

Figure 1. Start and ending point of a road towards the specification of wood and wood-based products.

2.2 Necessary Number of Reference Service Lives

To predict the performance of a wood-based product means nothing else than to predict its service life. The service life of a product ends, when the performance level becomes lower than the performance requirements, whether they are functional, static, or aesthetic. Therefore performance prediction can be equated with service life prediction, and the principles of service life planning as given by the ISO standard 15686 should be considered. According to ISO 15686-1 (2000) a service life can be estimated by considering a reference service life and different modifying factors as follows:

Estimated service life (ESL) = Reference service life (RSL) • modifying factors,

whereby the modifying factors include all conditions that deviate from defined reference conditions, e.g. climate, design measures, or maintenance intervals.

From the laws of error propagation it can be seen that the more unknown variables considered in an equation, the higher the total statistical error to be expected. Therefore, it is obvious, that working with only a single RSL is no solution. Thus, the question arises as to how many different RSLs need to be considered to obtain a reliable service life estimate, and how can these RSLs be determined (i.e. what are suitable test methods?). Different wooden commodities, even if they are made from the same material, can perform very differently. Depending on the exposure situation different service lives will be obtained. Consider, for example, wooden poles in ground contact or the same material used as beams in a roof construction. Table 1 shows information on the relation between commodities, exposure situations, and the expected performance for related use classes described in EN 335-1.

Different commodities can be merged into commodity groups having similar expected performance. At the same time, different exposure categories can be defined and related to the different commodity groups. However, a simple equalisation of exposure and commodity is not possible, as for window joinery, which is usually coated, the same exposure situation is given compared to a cladding, but a completely different performance of these two commodities can be expected. In this case one needs to distinguish between coated and uncoated commodities within the same exposure category "above ground". A second example for the need of a more discerning classification of commodity/exposure groups is the hazard of termite attack. This regionally occurring special hazard concerns nearly all commodities and requires therefore a separate category.

Table 1. Different exposure categories with related use classes according to EN 335-1 (2006), commodities and potentially suitable test methods.

ID	Related to use class	Exposure category	Commodity group	Close to reality Test method
A	1	Interior	Roof beams, rafters	Not known, Not available
B	2	Above ground covered	External walls, ground floor joist	Not known, Not available
C	3.1	Above ground coated	Window joinery	L-joint EN330
D	3.2a	Above ground slight	Cladding, fence rails	Not known, Not available
E	3.2b	Above ground severe	Decks	Double layer / multiple layer
F	4	Ground contact	Poles, posts, sleepers	EN 252
G	5	Sea water contact	Ships, wharfs	EN 275
H		Termite hazard		Not known, Not available

Some exposure categories are identical with the use classes described in EN 335-1 (2006) and may be taken over. However, the range of use class 3 seems to be unacceptably broad and needs therefore to be subdivided. In Table 1 coated and uncoated commodities are first distinguished, and thereafter, slight and severe hazards are distinguished for uncoated materials. The need for further differentiations should be discussed.

To summarize, the essential finding is that the agreement on a certain classification of exposure categories, which represent different commodities close to reality, gives the necessary number of RSLs to be considered for service life prediction. The rule should hence be to distinguish between as

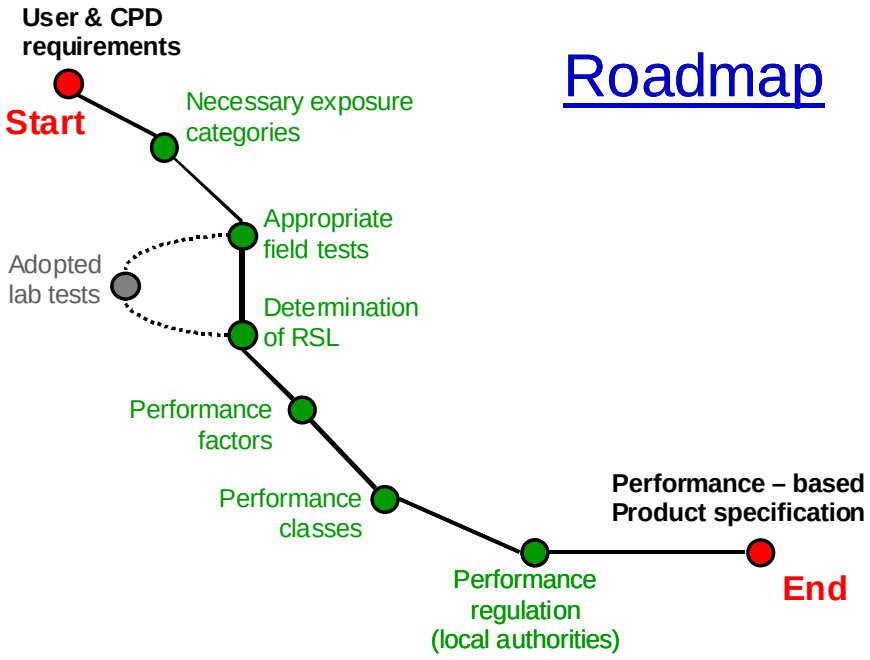

Figure 2. Roadmap for the specification of wood and wood-based products.

many categories as necessary, but as few as possible. Thus, the first stopover "Necessary exposure categories" is reached, as given in Figure 2.

2.3 Determination of Reference Service Lives with Appropriate Field Test Methods

Once a certain number of exposure categories are agreed on, the next task is to determine RSLs for all of them. Therefore, suitable test methods, which represent the different exposure categories, and commodity groups respectively, need to be determined. Table 1 gives some examples for field test methods, which may be helpful to determine RSLs for the particular categories. For example, the EN 252 (1989) test for in-ground exposure and the L-joint-test (EN 330, 1993) for coated window joinery are well-established methods, and a lot experience with these tools exists.

For other exposure categories suitable tools are still missing and the adoption of existing methods or the development of new methods should be the next stopover on the map ("Appropriate field tests", Fig. 2).

2.4 Determination of Reference Service Lives with Adopted Laboratory Tests

Appropriate test methods for the determination of RSLs are not necessarily only field test methods. The wood industry in particular, but also scientists and testing laboratories, are seeking short-term methods that take less time to conduct, not at least to allow a sufficiently rapid approval of a product for specific applications. However, as a starting point in the development of such methods, is that these should replicate in-use conditions as close to reality as possible. These are typically conducted, in general and apart from in-service performance, as field trials.

Some guidance on how to incorporate short-term tests into performance classification is given by the ISO standard 15686-2 (2001). An extract of the systematic methodology for service life prediction of building components, adopted and closely related to wood products is given in the scheme provided in Fig. 3.

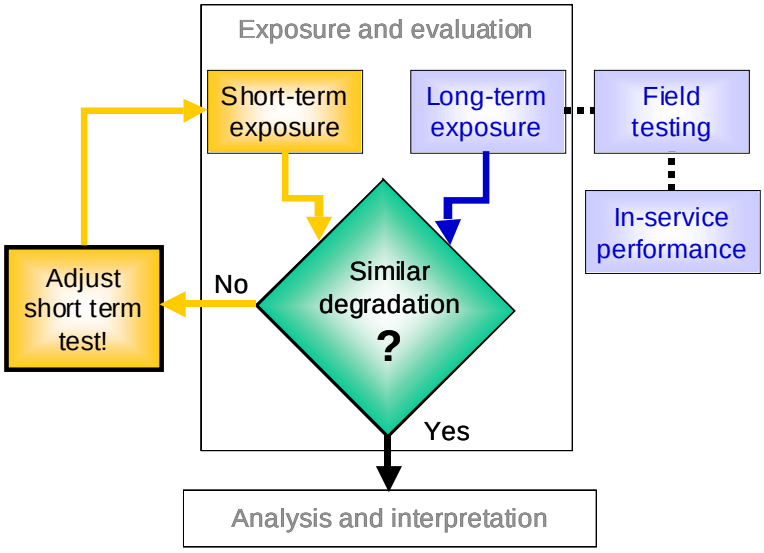

Figure 3. Systematic methodology for service life prediction of building components (according to: ISO 15686 -2 (2001)).

Whenever one wants to make use of the results derived from short-term tests, it is indispensable to compare the degradation patterns between long-term and short-term tests. As long as no similar degradation pattern can be observed, the short-term test should be adopted. However, if similar degradation is provided, nothing argues against the inclusion of laboratory short-term tests. Quite the contrary, there are also some exposure categories conceivable, where short-term tests appear as the only suitable solution: For commodities exposed above ground and protected, e.g. external walls, the occurrence of decay will probably take years or even decades. In this case, moisture measurements over a limited period of time may be an alternative to long-term field trials.

However different the test methods, for the roadmap it is essential that for every exposure category, a method having test conditions closely related to in-use conditions should be established to obtain a RSL for each exposure category, as given in Table 1. From this, “Determination of RSL” is the next stopover on the product specification roadmap provided in "Fig. 2. The adoption of short-term test methods may be seen as a side route on the map.

2.5 Performance Factors

The results of the different tests, representing the different exposure categories, can be used to predict and classify the performance of wood-based products. Actually, the primary result of every field trial is the service life in years of, on the one hand, a material X to be tested, and on the other hand, a reference material. The reference material can be Scots pine sapwood (*Pinus sylvestris* L.), as it is used in many existing European standards, but may be also different for a particular test method. At this stage it is particularly important to note that the service life of a reference material or reference product ($SL_{reference}$) is different from the reference service life (RSL) of a certain material X determined at a particular test site. Thus, two main results arise from each field test:

$SL_{material\ X}$ = service life of a material X to be tested
$SL_{reference}$ = service life of the reference

To become independent from the influence of the different test sites it seems appropriate to express the performance of the test material as a factor, the performance factor (PF), given as:

$$PF = SL_{material\ X} / SL_{reference} \quad [y/y]$$

In accordance to the classification of exposure situations (Table 1) the performance factors must be related to the different exposure categories. For each exposure category a performance factor needs to be determined as the following example shows:

Exposure category F: ground contact Test method: EN 252 (1989)

$SL_{material\ X}$ = 6.9 years
$SL_{reference}$ = 3.0 years

$$PF_F = SL_{material\ X} / SL_{reference} = 6.9/3.0 = 2.3$$

PF_F = 2.3 → 2.3 longer service life than the reference in ground contact (exposure category F)

With the help of performance factors for each exposure category considered, a very detailed and precise characterization for a material to be tested is possible. From the stopover "Performance factor" the final destination is already reachable on the roadmap. In principal, every material can be specified with a certain number of performance factors.

2.6 Performance Classes and Performance Regulation

The use of numerous different performance factors may cause confusion during its implementation in practice. Therefore it could be an option to combine performance factor intervals in performance classes, e.g. according to the classification of durability (EN 350, 1994), as schematically shown in Fig. 4. Again the creation of performance classes needs to be done separately for the different exposure categories.

To define, which product may be used for a certain application, is a task for the local authorities. They need to devise requirements related to the different performance classes (example given in Fig. 4). On the roadmap the final destination is reached. The task "performance regulation" appears as a stopover on the road to a "performance-based product specification".

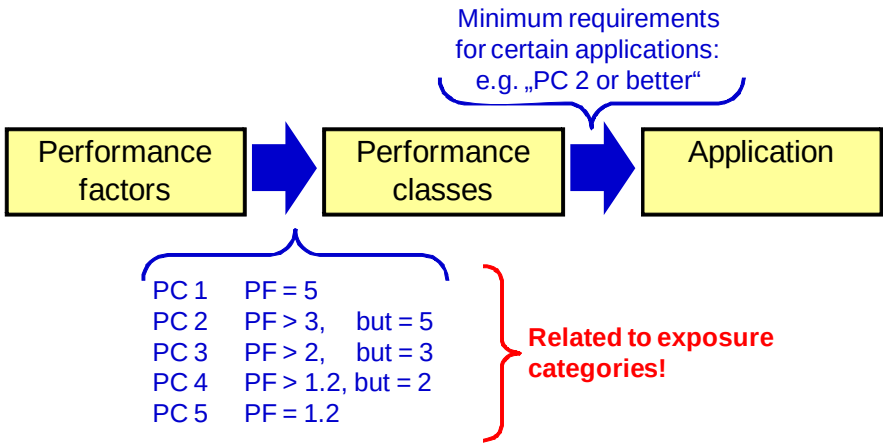

Figure 4. Relationship between performance factors, performance classes, and performance regulation.

2.7 Test-site Relationships

In section 2.5 relating to performance factors, the influence of the test site was not considered. In fact, performance factors were created in order to eliminate the influence of the test site. However, the test site nonetheless has a strong influence on the test results. Testing the same material at different field test sites will inevitably lead to different service lives. Table 2 gives a fictitious example of test results from L-joint tests (EN 330, 1993), carried out at three different test sites, *e*.g. London, Hamburg, and Bordeaux.

Table 2. Fictitious example for the calculation of performance factors from service lives of a material X to be tested and a reference material determined at different test sites.

Test site	$SL_{material\ X}$ [y]	$SL_{reference}$ [y]	*PF3.2a (L-Joint)*
London	18	9	2.0
Hamburg	24	12	2.0
Bordeaux	30	15	2.0

The material X to be tested revealed different service lives at the three sites as well as the reference material. Ideally, the calculation of performance factors leads to the same performance classification (here: $PF_{3.2.a}$ = 2.0) for all test sites. Certain variations of the performance factors determined at different sites should be expected, but may be in an acceptable range.

The relation between two test sites can be calculated from the service lives of the reference material in terms of an inter-site factor, e.g. between London and Bordeaux:

Inter-site factor $_{BDX/LON} = ISF_{BDX/LON} = SL_{reference\ /\ BDX} / SL_{reference\ /\ LON}$ = 15 years / 9 years = 1.67

Another example shows a possible practical use of knowledge related to inter-site relationships. Consider the following:

1. Material X shall be used in Bordeaux
2. Material X is so far tested only in London

A question might be posed as to what the estimated service life (ESL) of material X in Bordeaux would be? With the help of knowing the inter-site factor between London and Bordeaux, the ESL of material X in Bordeaux can be calculated as:

$ESL_{material\ X\ /\ BDX} = SL_{material\ X\ /\ LON} \bullet ISF_{BDX/LON} = 18\ years \bullet 1.67 = 30\ years$

To summarize, two important measures can be obtained as a result of different field tests at different test sites: 1.) The performance factor, which is the service life of a certain material relative to a reference, can be used to specify a product. 2.) As a by-product, inter-site factors, which describe the relation between different test-sites by means of their decay hazard, can be used for service life prediction models and hazard mappings.

For the roadmap a second sideway with the stopover "Inter-site factors" resulted from reflecting on the inter-site relationships (Fig. 2). Together with the tasks "product specification" and "performance regulation" it represents the basis for performance based building, which can be seen as a super ordinate aim, when working on performance prediction and product specification.

3 CONCLUSIONS

A strong need for performance classification derives from the user of wood and wood-based products on one hand, and is required by the CPD on the other hand. On the way to fulfilling these requirements service life prediction can be seen as the link between "user needs" and a feasible "product specification". The results from service life prediction are always numbers in years and consequently satisfy the perceived needs of the user, whereas performance factors, determined for a sufficient number of different exposure categories, can represent the connection between use and hazard classes and durability classes.

The roadmap outlined in this paper shows that all necessary tools for an exposure-related performance specification are, in principal, already available. Different field and laboratory tests need to be adopted to in-service related test situations, but do already exist, as well as the use classes and durability classes, which are adaptable to performance classes. The challenge for the wood industry practitioners and wood scientists is to bring all these single elements together – a proposal is made in this paper. Finally, the cornerstones for a performance-based building can be established on the way to developing a feasible product specification.

4 REFERENCES

CPD, 1988, Council directive of 21 December 1988 on the approximation of laws, regulations and administrative provisions of the member states relating to construction products. 89/106/EEC, Brussels, Belgium.

EN 252, 1990, `Wood preservatives. Field test methods for determining the relative protective effectiveness in ground contact´.

EN 335-1, 2006, `Durability of wood and wood-based products – Definition of use classes – Part 1: General´.

EN 335-2, 2006, ` Durability of wood and wood-based products – Definition of use classes – Part 2: Application to solid wood´.

EN 350-1, 1994, `Durability of wood and wood-based products. Part 1: Guide to the principles of testing and classification of the natural durability of wood´.

EN 350-2, 1994, `Durability of wood and wood-based products. Part 2: Guide to natural durability and treatability of selected wood species of importance in Europe´.

EN 113, 1997, `Wood preservatives. Test method for determining the protective effectiveness against wood-destroying basidiomycetes. Determination of toxic values´.

ENV 807, 2001, `Wood preservatives - Determination of the effectiveness against soft rotting micro-fungi and other soil inhabiting micro-organisms´.

ISO 15686-1, 2000, `Building and constructed assets – Service life planning – Part 1: General principles´.

ISO 15686-2, 2001, `Building and constructed assets – Service life planning – Part 2: Service life prediction procedures´.

11DBMC International Conference on Durability of Building Materials and Components
ISTANBUL, Turkey 11-14 May 2008

Fire Resistance Performance Study on the Compartment Walls in Wood Platform Construction

Chun-Ta Tzeng [1]
Hung-Chi Su [2]
Pang-An Hsiao [3]

T12

ABSTRACT

This study refers to the North America construction methods and adopts the foreign and native materials in Taiwan to fabricate the specimens for experiments. Several full-scale experiments were carried out to explore the effects of factors regarding fire resistance performance according to the fire resistance test for structural parts of building stated in the CNS 12514 which is similar to ISO834-1.The experiments had shown that the covering board materials and the dimensions of studs directly affect the properties of thermal resistively. With covering board material selected, the nail length does affect the fire resistance performance. It was found that by decreasing the nail spacing, the fire resistance performance exhibits improvement. The research results revealed that the wood-framed compartment wall specimens specified as above-mentioned sustain at least one hour fire rating performance according to the current Building Technique Regulations.

KEYWORDS

Platform construction, Wood framing, Compartment walls, Fire resistance performance

[1] Dep. of Architecture, National Cheng-Kung University, Taiwan
[2] Dep. of Architecture, National Cheng-Kung University, Taiwan
[3] Dep. of Asset Management Science, Hsing Kuo University of Management, Taiwan

1 INTRODUCTION

The wood structure buildings provide with the advantages of low contamination, low energy consumption, swift construction, earthquake-resistace and is beneficial to our health. It also conforms to the sustainable development as well as the green building policy in Taiwan.

According to the mechanical behavior, the system of platform wood-framing wall can be classified into bearing wall and non-bearing wall. The fire prevention division wall is the main structure on prevention of horizontal fire spread, and it plays a extremely important role on fire control and safety evacuation. This research refers to the fire preventing regulations in America, Japan and Canada.

This study carried out several full-scale experiments according to the CNS 12524 standard "method of fire resistance rest for structural parts of building" in Taiwan to investigate the fire resistance of platform wood framing non-bearing wall.

The intent of this research is to provide practical applications and thus make the Taiwan fire resistance performance and standard of wood framing building harmonize with the international.

2 EXPERIMENT LAYOUT

The structure of wood framing compartment wall mainly consists of structural material of wall body, stud cross section and spacing, cover board, insulation material, fastener etc. The study adopts the rock fiber as insulation material in our experiments. The wood material of stud, size of stud section and cover material type are taken as the primary factors in this research. Each factor contained two sets of settings which listed below :

1. Structure material for wall body : the stud had chosen the local material china fir and foreign material SPF which was the compose wood of Spruce (Picea Spp)、Pine (Pinus Spp) and Fir (Abies spp.).
2. Size of stud section(studs pacing) : the section dimension of stud for this experiment used 2 inch × 4 inch and 2 inch × 6 inch.
3. Covering material type and Fastener: the experiment used the level 1 fire resistance gypsum board with thickness of 15mm, which was most commonly used in foreign wood framing cover board, and also the rating 1 fire resistance silicate board with thickness of 12mm, which was used in local production on covering board material for light interval wall. The nails and glues were adopted to fasten the gypsum board and the screw is used for the silicate board. The previous factors with each two setting are shown below on Table1.

Table 1. Setting of experimental factors.

Factor		Material of Stud		Section of Stud		Covering Board	
Setting Of Experimental Factors		SPF	china fir	2×4	2×6	Gypsum Board	Silicate Board
Detail	**Performance**	1.CNS14631 2.CNS14632 3.CNS14633	1.CNS14631 2.CNS14632 3.CNS14633	1.CNS14631 2.CNS14632 3.CNS14633	1.CNS14631 2.CNS14632 3.CNS14633	1.CNS6532 rating1	1.CNS6532 rating1
	Scale	-	-	1.section : 2in×4in (38mm×89mm) 2.interval : 16in (406mm)	1.section : 2in×6in (38mm×140mm) 2.interval : 24in (610mm)	1.thickness : 15mm	1. thickness : 12mm

3 TEST CONDITIONS AND PROCEDURE

The heating equipment used for the experiment was the furnace from Architecture and Building Research Institute, Ministry of Interior as shown in Figure 1.The heating control for the experiment was through the 16 thermocouples within the furnace. The relevant standard for heating time and temperature curving were shown below in Figure 2.

The determination conditions for the experimenting fire resistance performance had shown below in Table 2. The specimen wood frame was consisting according to previous conditions. The stud sections for 2 inch × 4 inch and 2 inch × 6 inch are shown in Figures 3 and 4.The positions of thermocouples on the elevation of a wall are shown in Figure 5 and Figure 6. Specimen number and construction material list are shown in Table 3.

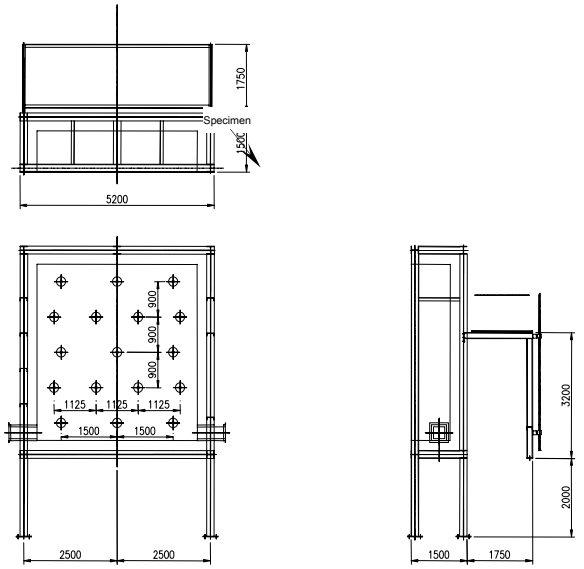

Figure 1. Elevation view of furnace(unit; cm).

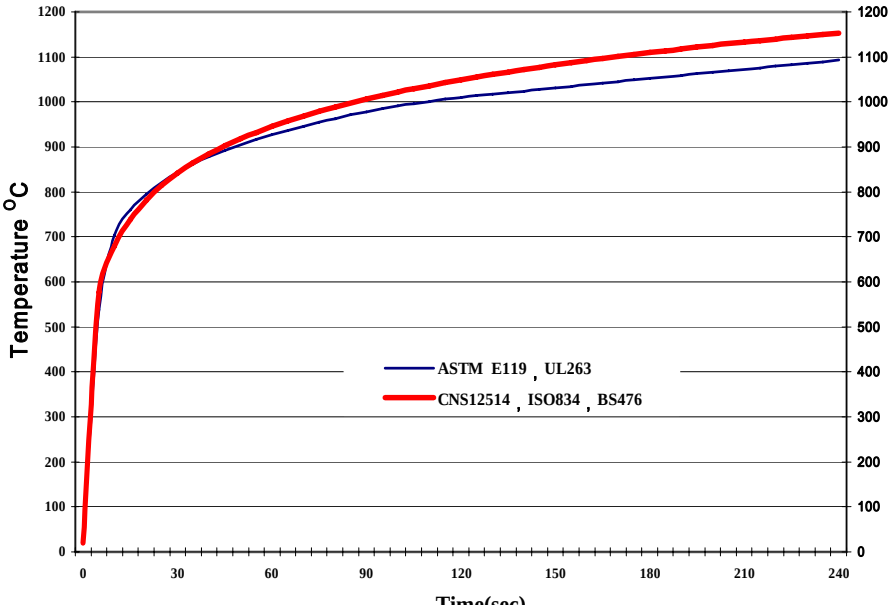

Figure 2 Time-temperature curve for CNS12514.

Table 2 CNS12514 determination for fire resistance performance.

Item	Source	Explanation	Determination detail	Determination taken
Fire Insulation	CNS12514 9.2	During the heating procedure ,the non-heating side temperature should not exceed the regulation number under certain.	(1) average temperature exceed 170□ during experiment.	○
			(2) temperature under any position exceed 210□ (include the measure form mobile thermocouple)	○
Fire Inegrity	CNS12514 9.3	During the heating procedure ,the building construction should prevent fire penetration under certain amount of time .	(1) wool on fire	×
			(2) continuous fire on non-heating side over 10 seconds.	○
			(3) fire penetrate form heating side to non-side for over 10 seconds.	○
Fire Stablity	CNS12514 9.1	The building structure and construction should prevent collapse when taking loads under certain amount of time.	(1) maximum axial compression volume (mm) : C=h/100	×
			(2) maximum axial compression velocity (mm/min) : dC/dt=3h/1000	×

○ : indicate using by the experiment , × : indicate will not be use by the experiment

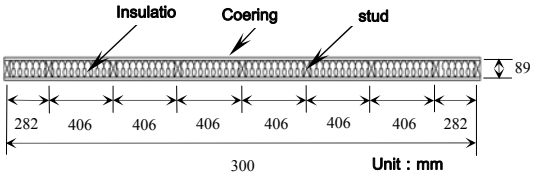

Figure 3. 2×4 specimen section view.

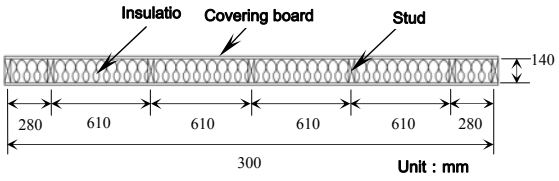

Figure 4. 2×6 specimen section view.

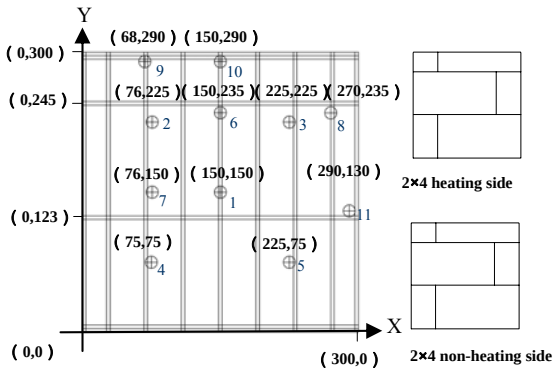

Figure 5. Position of thermocouples in elevation of 2×4 wall (unit; cm).

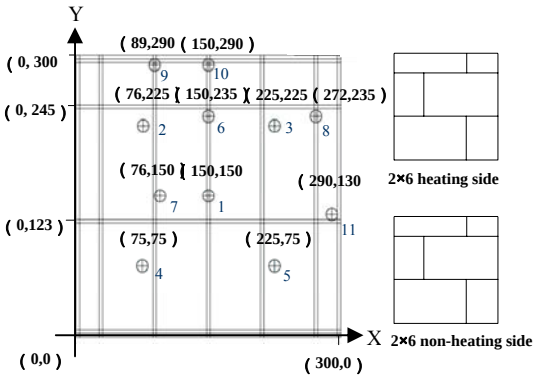

Figure 6. Position of thermocouples in elevation of 2×6 wall (unit; cm).

Table 3. Specimen number and construction material list.

Specimen number	Type	A Covering Board		B Section Of Stud		C Wood Material of Stud		Insulation	Fastener			
		Gypsum Board	Silicate Board	2×4	2×6	SPF	china fir	rock fiber 60k	screw		nail + glue	
		(G)	(C)	(4)	(6)	(S)	(T)		length 31.8mm spacing 300mm amount 130	length 63.5mm spacing 180mm amount 216	length 50.0mm spacing 150mm amount 260	length 60.0mm spacing 150mm amount 260
W1	G-4-S	○		○		○		○	○			
W2	G-4-T	○		○			○	○	○			
W3	G-6-S	○			○	○		○		○		
W4	G-6-T	○			○		○	○		○		
W5	C-4-S		○	○		○		○			○	
W6	C-4-T		○	○			○	○			○	
W7	C-6-S		○		○	○		○				○
W8	C-6-T		○		○		○	○				○

4 RESULTS AND DISCUSSION

4.1. Performance Discussion of Fire Resistance for CNS12514

Although the experimental results shown that the heating time for each specimen is different , it does not show any sign of continuous fire last over 10 seconds on non-heating side or any fire penetration from heating side to non-heating side for more than 10 seconds within 60 minutes, this had proved the specimen did have at least 1 hour of fire integrity performance. The construction technical regulation term 70 had listed for fire resistance compartment wall should be at least one hour fire rating , and all the specimen had reach this requirement. Which the related statistic results of fire insulation and fire integrity had shown in Table 4.

Table 4. Experiment results.

Specimen Number	Type	Fire Insulation		Fire Integrity	
		Time for temperature under any position exceed 210□ on non–heating side	Time for average temperature exceed 170□ on non–heating side	continuous fire on non-heating side over 10 seconds.	fire penetrate form heating side to non-side for over 10 seconds
W1	**G-4-S**	65：50 (3950 sec)	69：40 (4180sec)	×	×
W2	**G-4-T**	64：50 (3890 sec)	71：40 (4300sec)	×	×
W3	**G-6-S**	80：10 (4810 sec)	86：00 (5160sec)	×	×
W4	**G-6-T**	77：40 (4660 sec)	81：50 (4910sec)	×	×
W5	**C-4-S**	77：00 (4620 sec)	88：40 (5320sec)	×	×
W6	**C-4-T**	72：50 (4370 sec)	75：00 (4500sec)	×	×
W7	**C-6-S**	82：40 (4960 sec)	98：50 (5930sec)	At 125 min 20 sec the flame occured and continue for 2 min 40 seconds.	At 125 min 20 sec the flame occured and continue for 2 min 40 seconds.
W8	**C-6-T**	83：20 (5000 sec)	108：50 (6530sec)	×	×
× indicates event did not occur , heating stop at 86 min					

4.2. Temperature Discussion on Non-Heating Side of Specimen

For all specimens, most of the temperature points on non-heating side of specimens did not show large variations through the first 60 minutes of the experiment. Take specimen W6 for example illustrated in Figure7. However, when the heating time exceeded 60 minutes, some temperature points exhibited

sudden increase due to the collapse of the cover board on the heating side and drop of the rock fiber when the supporter was gone. The inner furnace was then directly heated the cover board of non-heating side and caused all the non-heating side temperature points climbed abruptly.

By camparing with the same specimen, the time taken for single point on the non-heating side to reach 210 were shorter then average temperature reached 170. Due to the temperature of single point on the non-heating side reached 210 faster, the time determination of fire insulation should mainly focus on the temperature point reached 210. Thus the analysis for fire insulstion quality is mainly on time taken for single point on non-heating side to reach 210.The range for the fire insulation performance for all specimens were about 64 minutes to 83 minutes, which proved all the specimen possess the performance of fire insulation for at least 60 minutes.

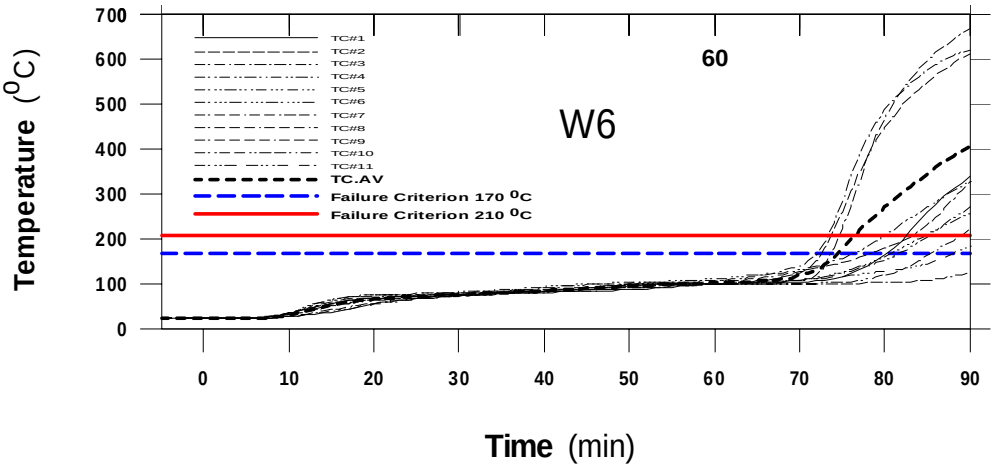

Figure 7. W6 non-heating side temperature recording.

4.3 Inner Furnace Temperature Discussion

The inner furnace temperature curve had fitted the CNS12514 requirement as shown in Figure 8, as for the inner temperature climbed abruptly 40 minutes after the experiment started for specimen W1、W2 and W4 . Through the observation window on the side of furnace, the cause of sudden increase on the inner furnace temperature could be the reason of widely collapse in cover board material, and the wood framing structure burned down on the heating side of the specimen. About 75 minutes after the experiment started, the cover board on the non-heating side for specimen W6 had been half destroyed and collapsed, the temperature of the inner furnace had then leaked from the collapse area and thus caused the inner temperature to drop.

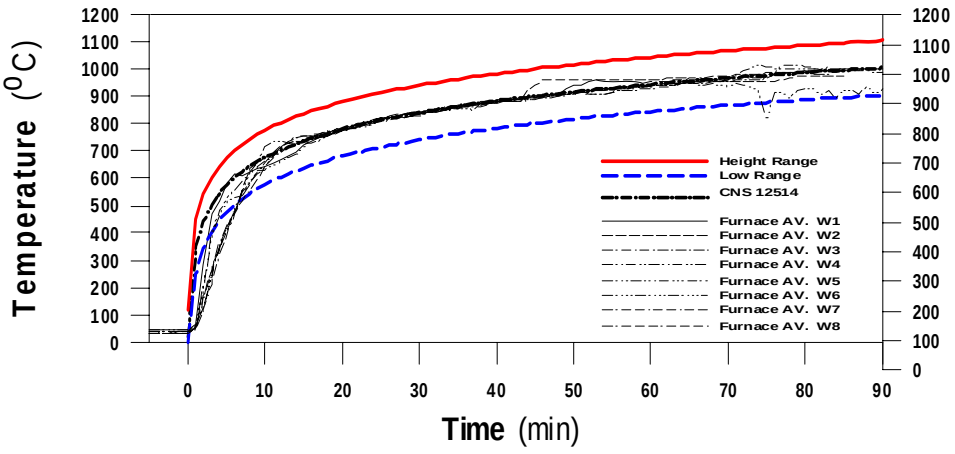

Figure 8. Furnace temperature versus time.

4.4 Experimental Factors

By comparing and analysis the effect of the fire resistance performance for the wood framing compartment wall as shown in Table 5. When the wood material had been changed from SPF to china fir, the fire resistance performance would had a slight reduction about 0.025%. As the size of stud changed from 2×4 to 2×6, the fire resistance performance would had an average increase of 18.88%. As for the cover board material, the observation had shown that by switching gypsum board to calcium silicate board, the fire resistance performance would have an average increase of 15.17%.

Table 5. Comparison of experimental factor.

Comparison of structure material					
Group	1	2	3	4	**Average**
【S】：SPF	W1（3590sec）	W3（4810sec）	W5（4620sec）	W7（4960sec）	
【T】：China Fir	W2（3890sec）	W4（4660sec）	W6（4370sec）	W8（5000sec）	
【T】-【S】	300sec	-150sec	-250sec	40sec	-60 sec
（【T】-【S】）/【S】×100%	8.35%	-3.11%	-5.41%	0.08%	**-0.025%**
Comparison size of stud					
【4】：Size Of Stud 2×4	W1（3590sec）	W2（3890sec）	W5（4620sec）	W6（4370sec）	
【6】：Size Of Stud 2×6	W3（4810sec）	W4（4660sec）	W7（4960sec）	W8（5000sec）	
【6】-【4】	1220sec	770sec	340sec	630sec	740 sec
（【6】-【4】）/【4】×100%	33.98%	19.79%	7.35%	14.41%	**18.88%**
Comparison of covering board					
【G】：gypsum board	W1（3590sec）	W2（3890sec）	W3（4810sec）	W4（4660sec）	-
【C】：silicate board	W5（4620sec）	W6（4370sec）	W7（4960sec）	W8（5000sec）	-
【C】-【G】	1030sec	840sec	150sec	340sec	590 sec
（【C】-【G】）/【G】×100%	28.69%	21.59%	3.11%	7.29%	**15.17%**

Under the condition of using 2×4 stud wood frame, the change of cover board material had conspicuous increased on fire resistance performance. The fastener could be the factor that caused the difference since both type of the cover board had conform the term of level one fire resistance, thus the construction method altered from increasing the length of nail from 31.8mm to 50.0mm and spacing distance between each nail from 300mm down to 150mm should applied on the same 2×4 stud. In this case, when the wood frame was under the same carbonize rate. The calcium silicate board would had longer and more fixed nail which extended the time taken till the cover board collapsed from the wood frame, thus increased the fire resistance performance.

5 CONCLUSIONS

This research focused on the subject of wood framing compartment wall, Referenced from foreign standard, and combined foreign and localize wood material to run a full scale experiment on verify the fire resistance performance of wood framing compartment wall . The experimental results had pointed out the type of cover board material and size of stud had greater effect on the performance of fire insulation then material of stud. This study had found that the fire resistance performance for wood framing compartment wall rely mainly on the cover board material and insulation. The change size of stud factor would also alter the element of fastener. By extended the time for the cover board to stayed fixed on the wood frame would also increased the fire resistance performance. During the heating progress, the wood frame material would gradually carbonize. At the same the wood frame would lost the bond strength of fastener, and thus the shear stresses of fastener would gradually disappeared; the nail spacing distance reduced meaning the number of nail amount increased, relatively the shear

stresses every nail had to bear would decreased, thus the longer the nail length is and shorter the spacing distance is between each nail would enhance the fire resistance performance conspicuously.

As for the use of the cover board material, the fire insulation for calcium silicate board was slightly better than gypsum board. Except considering the nature of the material itself, the difference in fastener for both of the materials could cause variety factors for fire insulation. The gypsum board only used screw, where the calcium silicate board had higher density and heavier in weight, thus screw stabilized would be un-appropriate. The metal frame when stabilized normally used screw, but the kind of screw were not suitable for wooden materials, thus by using the glue to bind and stabilized by adding nail during the construction, were considered to be the practical method for calcium silicate board. Our results had also indicated that the fire resistance performance by adopting foreign and localize wood material, and the fabricated wall refer to foreign construction standards can satisfy the technical building regulation of one hour fire resistance performance.

REFERENCES

CNS 12514, 2007, '*Method Of Fire Resistance Test For Structural Parts Of Building'*, Chinese National Standards, Taiwan.

ISO834-1, 1999, '*Fire Resistance Tests-Elements Of Building Construction Part 1'*, International Organization for Standardization, Geneva.

CNS 14631, 2002, '*Structural Sawn Lumber Used In Platform Construction'*, Chinese National Standards, Taiwan.

CNS 14632, 2002, '*Finger Joined Lumber Used In Platform Construction'*, Chinese National Standards, Taiwan.

CNS 14633, 2002, '*Grading Rules Softwood Lumber Used In Platform Construction By Machine Stress Rating'* , Chinese National Standards, Taiwan.

Editor Committee of Construction and Planning Agency, Ministry of The Interior, 2003, '*Technical Code for Design and Construction of Wood-Framed Building'*, Construction Magazine Corporation, Taipei.

Canada Mortgage and Housing Corporation, 1997a, '*Glossary of Housing Terms'*, P.109, Canada.

Canada Mortgage and Housing Corporation, 1997b,'*Canadian Wood-Frame House Construction'*, Canada, p.56-p.85.

Lin, C.Y., Cheng, S.T., & Wang, K.C., 1992, 'A study of the relationship between the constitution and fire resistive performance of sprayed fire resistive materials applied to steel structures', The 13th Sino-Japanese Modern Engineering And Technology Symposium ,p.82-p.106.

Chen, C.J., 2003, 'Fire Resistance And Earthquake Resistance of RC Beams and Columns-Comparison of International Standards of Timber Structure', Architecture And Building Research Institute, Ministry of the Interior, Taipei.

Tzeng, C.T., 2004, 'Framed Wall Construction Fireproof Function Verification', ROC-Canada Cooperative Conference on Wooden Structure Architecture—Fire Resistance, Sustainability and Market, Conference Proceedings, pp.81-90, The Representative Office of British Columbia, Canada.

Yeh, S.W., Tzeng, C.T., & Chen, C.R., 2004, 'Wooden Structure Fireproof Function Design and Verification', A Topic Research Paper, 2004 Joint Research Project Conference, Architecture and Building Research Institute, Ministry of the Interior, Taipei.

Kodur, V.K.R., Sultan, M.A., Latour, J.C., Leroux, P., & Monette, R.C., 2002, '*Fire Resistance Tests on Cellulose and Glass Fiber Insulated Wood Shear Walls'*, National Research Council Canada.

Sultan, M.A., & Lougheed, G.D., 2002, '*Result of Fire Tests on Full-Scale Gypsum Board Wall Assemblies'*, National Research Council Canada.

DURABILITY OF EXTERNAL WOOD-FRAME DOOR SYSTEM, A CASE STUDY

Fatih Yazıcıoğlu [1]
Kevser Coşkun [2]

T12

ABSTRACT

The aim of this paper is to determine the causes of the damages occurred in the external wood frame door systems. Environmental agents affect external wall systems of buildings. Hence, external wall systems are one of the most risky components of the buildings. On the other hand wood is the most used material in buildings in the history. Wood is commonly used in the structure systems, claddings, floorings, doors, and windows of the buildings. Wooden components used in the doors and windows are the most damageable parts.
Some external wood-frame door systems in the Taşkışla Building were studied in this study. In order to determine the durability of these wood-frame doors, firstly a process-oriented study in which damages are observed has been done. In this study the design, construction and usage processes of the doors are examined. Afterwards an object oriented study has been made and in this study survey conducted. In this survey, exact damages were analyzed and the reasons of these damages were classified. Lastly, environmental agents that affected these doors are analyzed. In conclusion, the classification of these damages will be used to evaluate the design of external wood-frame doors.

KEYWORDS

Wood frame, Door systems, Durability

[1] Istanbul Technical University, Faculty of Architecture, Istanbul, Turkey 34437, Phone +90 212 2931300-2206, Fax 212 2514895, fyazicioglu@gmail.com
[2] Istanbul Technical University, Faculty of Architecture, Istanbul, Turkey 34437, Phone +90 212 2931300-2390, Fax 212 2514895, kevsercoskun@yahoo.com

1 INTRODUCTION

The deterioration and demise of one building element critically affects the function of the entire building. External walls, which are parts of the envelope systems, are mainly designed to be a barrier between the natural outdoor and the artificial indoor, and they may perform a structural role. On the other hand, external walls are far more inclined to be pierced with holes, better known as windows and doors (2). In this study, damaged exterior doors are examined and causes of deterioration and principles of diagnosis and cure are explained.

The durability of building elements and materials is a massive subject. The failures of a building component is usually due to one of the following four factors: The first factor is poor design, the second factor are failures which are related to construction, the third factor is environmental agents and the last one is usage, user behavior and the lack of maintenance and its frequency. Principles of diagnosis process are respectively; information gathering, site investigation and last step is diagnosis and evaluation of collected data (1).

The doors of the courtyard of the southwest tower of Taşkışla Building are bad in condition and a diagnosis and cure process is needed to be applied to them. In order to determine the most suitable process, damage of the doors are examined and photographed, a survey has been conducted and the possible reasons of the damages are determined. At the end of the study proposals are given to increase the overall condition of the doors.

2 DAMAGE TYPES OF THE WOOD FRAME WINDOWS & DOORS

The nature of deterioration mechanisms is that not only are they progressive, but the resulting damage is cumulative and irreversible (2). From the time the construction process finishes, a building starts, albeit usually very slowly, to decay. Estimating the expected life of a building component is often a complex and difficult task (1).

The door system, which is the subject of this study, is made of wood. And the most serious effect is loss of structural integrity which occurs with the decay of the wood, which usually occurs both externally and internally (1). There are two common environmental factors with related to wooden made external door systems: *a)* agents is related to water: water, moisture, condensation and rain, *b)* agents is related to sun: solar radiation, sunlight and temperature.

Generally the moisture content is the predominant factor when considering the durability of a building element. The chemical agent that is most prevalent is water. It is probably also the agent with greatest influence on the properties of materials, particularly when it is combined with extremes of temperature. In many instances the presence of moisture is necessary to enable physical, chemical or biological reactions to take place. The agency of decay is fungal attack is the other important factor.

The orientation of the joinery and whether it is exposed to full sunlight is one of the other important factors that effects wooden doors. The ultraviolet radiation causes degradation of the surface, particularly of softwood species, which will affect the adhesion of paint and other finishes. Many organic dyes, bituminous materials and some synthetic polymers such as those used in sealant are degraded by ultraviolet light. Changes of temperature are also relevant when assessing the consequences of thermal expansion and contraction-such as stresses within materials when changes of size are restrained and strains imposed on jointing materials when components are free to change size. Thermal radiation can also act from within a component. When timber is used externally it must be remembered that most species are susceptible to damage from prolonged exposure to sunlight. The ultraviolet radiation causes degradation of the surface, particularly of softwood species, which will affect the adhesion of paint and other finishes (1). Blistering, cracking, peeling and flaking of the paint coating, deterioration of stains or varnishes, resin exudation and the rot of the timber are the causes of the deterioration of the external wood doors.

3 A CASE STUDY: 1940 DATED WOODEN DOORS

Taşkışla building is approximately 140mx100m sized, and it has a 70mx40m sized main courtyard. There are also four other 9mx7m sized courtyards in the four 26mx20m sized towers of the building. Taşkışla Building has many obsolete parts and the sixteen external wood-frame doors of the south-west tower courtyard are some of them. These wood-frame doors are dated to 1944 and they are the doors which was studied. The damages that is determined about the external doors of the courtyard of Taşkışla can be categorized in three groups:

3.1 Damage of the Dye of the Doors

The dye of some different parts of the doors are cracked, expanded and spilled. The deterioration of the doors increases in the parts which are nearer to ground level (Figure 1a). The dye of the horizantal components are totally spilled (Figure 1b).

Figure 1. (a) The damage of the paints of the doors increases near to ground level
(b) All of the horizontal elements of the doors are damaged

3.2 Damages Of The Wooden Components Of The Studs

Damage of the wooden structural components can be categorized in two main groups: Decay of wood, especially in parts near to ground level (Figure 2). Surface and pattern deteriorations of wood which can be seen as dye is spilled (Figure 3a).

Figure 2. Decay in the components near to ground level.

Figure 3. (a) Damage on the surface of wooden components of doors.
(b) Deformation of door handle.

3.3 Damages Of The Accessories Of The Stud

Secondary structural components of the doors like hinges and door handles are deteriorated because of getting old. The connection of door handle to door has become loosen and deteriorated from its axe. The locking mechanism of some of the doors do not work and some of the doors can not be closed properly. Most of these doors are screwed to eachother. Some hinges are rusted and make sound while opening or closing (Figure 3b).

4 ANALYSIS OF CAUSE OF DAMAGES OF 1940 DATED EXISTING DOORS

At the end of this study, which is about the doors of the administrative tower of Taşkışla building, realistic results have been determined. The method of the study is; making an analysis which is based upon experience and comparing this analysis with other similar analysis about doors which are found from literature.

4.1 Damages Related With The Design Of The Doors

Water related agents, which are determined as the major damaging factors of doors, effect doors negatively because of the failures and deficiency about the design of them. The first failure about design of doors is about the shape of door sills which cover the intersection point of horizontal wooden components and glasses (Figure 4). Water related agents can not escape from these points easily and force intersection points and as time went by pass over these points and reach to the core of the wooden components which are not protected with paints.

The second failure about the design of doors is; the most near to ground level parts of doors, which lean on the doorsteps, was not designed water proof. Water related agents that pass the sills and that is pushed with the wind can not pass the intersection point of door and doorstep and accumulated in these points. The accumulated water demolished wooden components in time (Figure 5a).

The third failure about the design of doors is; the deterioration of the plumb line of doors (Figure 5b). One of the reasons of this situation is the wrong decision about the connection type of horizontal and vertical components. Another reason of this situation is about the sizes of horizontal wooden components. These elements are smaller than needed for the moment effect effecting the doors. Also the type of the wood of doors, which is determined as pine, may be a reason for this failure.

Figure 4. Failure about the design of the connection point of glass and wooden components of door

Figure 5. (a) Failure about the design of the connection point of doors and ground
(b) Failure about the plumb line of the door

4.2 Damages Related With the Production and Assembly

In this study, one sample door from each direction was disassembled in order to determine possible failures related with the assembly. With this experiment it was understood that doors are good examples of traditional wooden door craftsmanship. Every connection was made with tongue & grooves, wooden connectors & nails, and glue. No extra metal material is used and all the connections stayed tight. Further more, the cores of wooden studs are also stayed well. The middle horizontal wooden components and the surfaces are problematic parts but as doors are dated to 1950 and haven't had any maintenance, it can be said that they stayed well. The assembly of the doors with the walls were also examined but no failure could be observed (Figure 6, Figure 7).

Figure 6. Detail of wooden nail for connection of the stud

Figure 7. Detail of wooden connector for connection of the stud

4.3 Damages Related With the Environmental Effects

The effects of the environmental effects change according to the direction of the facades of the Taşkışla building's administrative courtyard, which is located in Istanbul, Sisli. Environmental effects can be categorized in two main groups; water related and sun related environmental effects. Water related environmental effects effect doors negatively because of the design failures which were discussed in section 4.1. but in addition to the information given in that section, it can be said that the negative effect of water related environmental agents increase on the south and north facing façade and decrease in the north and east facing façades as the dominant wind and rain directions in Istanbul is form north and south.

Another problem with the south facing façade is the direct sun light in the entire sunny days. Direct sun light effects firstly paint and then combining with water related agents decay the wooden components. The east and west façades also get direct sunlight but not for entire day and so they are not effected as bad as the south facing. The north facing façade is not effected negatively with the sun, as it does not get any direct sunlight (Figure 8).

4.4 Damages Related With the Usage

In order to analyze failures related with usage, the characteristics of the surrounding spaces of courtyard should be examined. Courtyard is surrounded by administrative rooms from north and west, a private restroom for lecturers from east and a hall to sit and rest, which is mostly used by lecturers, from north. Students usually use these places as a transition space, they rarely use to sit and rest, and they mostly use if they have something to do with administrators. So, the primary users of courtyard and surrounding places are lecturers and administrators. The interaction of them with these places can be categorized in two seasonal periods, winter and summer. In winter courtyard is usually not used and its doors are kept closed, whereas in summer courtyard is both used for sitting and resting and passing. On the other hand both in winter and summer, same doors of same facades are used which are; the doors in the middle of the south, east and west facing facades and the far eastern door of the north facing façade. In conclusion, the user profile of courtyard and surrounding places is mostly formed with lecturers which expose that a failure related with usage is hard to say.

Figure 8. Examples of doors looking different directions. From left to right; north facade, east facade, south facade and west facade. All the examples are the doors which is positioned in the middler of the facades. Doors belonging to north and east are the worst in condition, door of south facade have some painting related problems and door from the west facade is the best.

5 PROPOSALS FOR CURE

The proposals for cure, which are made considering their costs and application duration, are listed below:

The paint of all doors should be stripped or burnt off and the timber should be protected until it has dried out. But as it is not possible to leave the openings without a door until they are dried a micro porous paint can be applied to doors which would allow doors to dry while stop surface water entering the timber.

Condensation which occurs on the inner face of the glasses of doors should be prevented to enter the core of the studs. A bead seal of clear silicone sealant to BS 5889 type B can be used to avoid the condensation water enter the core. But the best solution for this problem is to stop condensation occur, for this the glasses of the doors may be changed with double glazed glasses.

Two common causes of blistering of paint finish are resin exudation from knots and resin pockets in the timber, and water vapors expansion from moisture in the timber. For the resin exudation, which will show as brown sticky resin or, when dried, as a whitish powder, then the cure is to strip affected areas and apply shellac knotting. An aluminum primer should be used before repainting, with a light color. If it is vital to avoid recurrence, the timber component should be replaced by one in a different species of timber, that contains less resin.

The treatment of timber with chemical preservatives, preferably through pressure impregnation, will protect it from both insect and fungal attack (1). The rotten parts of the wooden components of the doors must be cut out and replaced with preservative-treated timber, the new timber being spliced into the old or being fitted to replace complete sections. Adjacent timber can be injected with solvent based preservative or drilled and fitted with borax rods. When repairs are being undertaken, rebates and exposed and grain should be sealed with a primer coat.

6 CONCLUSION

Environmental agents, design, production and user behavior oriented damages, and absence of maintenance & repair program are the main reasons of failures in buildings. The failures should be correctly determined and effective precautions which will end the reasons of the failures should be

taken. It should always be kept in mind that diagnosis & cure of an existing product is a better approach, but costs and application duration of a diagnosis & cure process should be carefully examined and the product should be renewed as a last way.

Water and sun related agents are found out to be the reasons of the damages of the doors. Failures about the decisions that was made in the design process of the doors combined with the absence of a maintenance and cure program made the doors have damages. These failures made the paints of the doors demolish, wooden components of the doors decay, and accessories of the studs fray. Cure proposals were made according to the types of the failures.

In conclusion, in order to use building elements successfully, diagnosis and cure of them should be made periodically. The diagnosis and cure of building elements can be summarized as fallows: To avoid decay, these applications are used; using timbers of suitable durability or employ preservative treatment, any dowels used should be of a durable timber or pretreated with a water-repellent preservative, designing to avoid water traps and horizontal surfaces, avoiding jointed sills and bottom rails, sealing effectively all joints between components and the edges of plywood, using durable glues, not doing fit mortise locks in the region of a dowelled joint. If condensation has been the chief cause of decay then, apart from repairing the door frame, a drainage channel should be incorporated that will allow the condensation to drain to the outside. In situations where there is heavy moisture production, more ventilation and/or heat may be necessary in addition. For provision of a drainage channel in a timber door sill to reduce the risk of wood decay. If decay is localized, cut away the affected parts and renew them with preserved timber. Allow the timber to dry and then repaint. If decay is extensive, renew the door completely. It is important that any migration from the masonry to the timber frame is prevented.

REFERENCES

Carillion, 2001. Defects in Buildings: Symptoms, investigation, diagnosis and cure, London:TSO.

Harris, S.Y., 2001. Building Pathology-Deterioration, Diagnostics, and Intervention, John Wiley&Sons, Inc.

Addleson, L., 1992. Building Failures: a guide to diagnosis, remedy, and prevention, Oxford : Butterworth Architecture.

Wakita, O.A., Linde, R.M., 1999. The Professional Practice of Architectural Detailing, John Wiley&Sons, Inc.

Allen, E., 1993. Architectural Detailing, John Wiley&Sons, Inc.

Eriç, M., 2002. Yapı Fiziği ve Malzemesi, Literatür Yayınları

11DBMC International Conference on Durability of Building Materials and Components
ISTANBUL, Turkey 11-14 May 2008

Production of Dimensionally Stable and Decay Resistant Wood Components Based on Acetylation

Roger M. Rowell [1]
Bert Kattenbroek [2]
Peter Ratering [3]
Ferry Bongers [4]
Francesco Leicher [5]
Hal Stebbins [6]

T 12

ABSTRACT

Wood is a renewable, biodegradable and sustainable composite of cellulose, hemicelluloses, lignin, extractives and inorganics in a three-dimensional matrix. Nature is programmed to recycle it, in a timely way, back into its basic building blocks of carbon dioxide and water through biological, thermal, aqueous, photochemical, chemical, and mechanical degradations. The properties of wood are the result of the chemistry of its cell wall components and the matrix they are in. If the chemistry is changed at the molecular level, the properties change and performance changes. Based on performance requirements of wood, chemical modifications can be carried out to change properties and performance. Dimensional stability, resistance to decay fungi and destructive insects, as well as other positive performance improvements can be greatly increased by reacting wood with acetic anhydride (acetylation) resulting in a new generation of value added wood-based products that perform very well in adverse environments.

KEYWORDS

Chemical modification, Acetylation, Dimensional stability, Decay resistance, Mechanical properties

[1] University of Wisconsin (Professor Emeritus), Madison, WI phone 608-231-1821, rmrowell@wisc.edu and Titan Wood Ltd., Westervoortsedijk 73, 6827 AV, Arnhem, Netherlands, roger.rowell@titanwood.com
[2] Titan Wood Ltd., Westervoortsedijk 73, 6827 AV, Arnhem, Netherlands, Phone 06-51-70-28-32, bert.kattenbroek@titanwood.com
[3] Titan Wood Ltd., Westervoortsedijk 73, 6827 AV, Arnhem, Netherlands, Phone 06-38-78-85-93, peter.ratering@titanwood.com
[4] Titan Wood Ltd., Westervoortsedijk 73, 6827 AV, Arnhem, Netherlands, Phone 06-23-43-35-95, ferry.bongers@titanwood.com
[5] Titan Wood Ltd., Westervoortsedijk 73, 6827 AV, Arnhem, Netherlands, Phone 06-29-25-23-67, Francesco.leicher@titanwood.com
[6] Titan Wood Ltd, 5000 Quorum Dr. #310, Dallas, Texas 75254 USA, Phone 972 233 6565 x203, hal.stebbins@titanwood.com

1 INTRODUCTION

Wood changes dimension with changing moisture content because the cell wall polymers contain hydroxyl and other oxygen-containing groups that attract moisture through hydrogen bonding. The hemicelluloses are mainly responsible for moisture sorption, but the accessible cellulose, noncrystalline cellulose, lignin, and surface of crystalline cellulose also play roles. Moisture swells the cell wall which expands until it is saturated with water (fiber saturation point, FSP). Beyond this saturation point, moisture exists as free water in the void structure and does not contribute to further swelling. This process is reversible, and the fiber shrinks as it loses moisture below the FSP. Wood exposed to moisture frequently is not at equilibrium, having wetter areas and drier areas within the same board. This exacerbates the moisture problem resulting in differential swelling followed by cracking and/or compression set. Over the long term, wood undergoes cyclic swelling and shrinking as moisture levels change resulting in more severe moisture effects than those encountered under steady moisture conditions.

Wood is degraded biologically based on an organisms' ability to recognize a potential food source mainly in the carbohydrate polymers [primarily the hemicelluloses] in the cell wall and having both non-specific chemical and highly specific enzyme systems capable of hydrolyzing these polymers into digestible units. Biodegradation of both the matrix and the high molecular weight cellulose weakens the fiber cell wall. Strength is lost as the matrix and cellulose polymer undergoes degradation through oxidation, hydrolysis, and dehydration reactions. As degradation continues, removal of cell wall content results in weight loss. All of these biological reactions take place in a high humidity condition.

Wood exposed outdoors undergoes photochemical degradation caused by ultraviolet radiation. This degradation takes place primarily in the lignin component, which is responsible for the characteristic color changes. The surface becomes richer in carbohydrate polymer content as the lignin degrades. In comparison to lignin, carbohydrate polymers are much less susceptible to ultraviolet degradation. After the lignin has been degraded, the poorly bonded carbohydrate-rich fiber surface easily erodes which exposes new lignin to undergo further degradative reactions. In time, this "weathering" process causes the surface of the composite to become rough and can account for a significant loss in surface fibers.

2 CHEMICAL MODIFICATION

Chemical modification of wood has been used to improve performance properties of wood. Many chemical reaction systems have been published for the modification of wood, however, the reaction of wood with acetic anhydride has been the most studied. The reaction with acetic anhydride with wood results in esterification of the accessible hydroxyl groups in the cell wall with the formation of byproduct acetic acid [Hill, 2006, Rowell 1983, 1984, 2005, 2006]. The byproduct acid must be removed from the product as the human nose is quite sensitive to the smell of acetic acid. While this is easily done in the case of wood particles and fiber, it is somewhat difficult to do in solid wood.

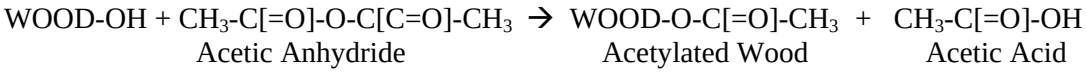

Acetylation is a single-site reaction that means that one acetyl group is on one hydroxyl group with no polymerization. This means that all of the weight gain in acetyl can be directly converted into units of hydroxyl groups blocked.

All woods naturally contain acetyl groups. In general, softwood has an acetyl content between 0.5 to 1.5% and more durable hardwoods between 2 to 4.5%.

3 HISTORY OF WOOD ACETYLATION

The acetylation of wood was first done in Germany in 1928 by Fuchs using acetic anhydride and sulfuric acid as a catalyst. He found an acetyl weight gain of over 40% which meant that he decrystalized the cellulose in the process. He used the reaction to isolate lignin from pine wood. In the same year, Horn [1928] and Suida and Titsh [1928] acetylated beech wood to remove hemicelluloses in a similar lignin isolation procedure. In 1929, Suda and Titsch acetylated powdered beech and pine using pyridine or dimethylaniline as a catalyst and got an acetyl weight gain of 30 to 35% after 15 to 35 days at 100 ºC. In 1945, Tarkow first demonstrated that acetylated balsa was resistant to decay [Tarkow 1945]. In 1946, Tarkow, Stamm and Erickson first described the use of wood acetylation to stabilize wood from swelling in water. Since the 1940's, many laboratories around the world have looked at acetylation of many different types of woods and agricultural resources.

In spite of the vast amount of research on chemical modification of wood, and, more specifically, on the acetylation of wood, commercialization has not come easily, The first patent on the acetylation of wood was filed by Suida in Austria in 1930. Later, in 1947, Stamm and Tarkow filed a patent on the acetylation of wood and boards using pyridine as a catalyst. In 1961, the Koppers Company published a technical bulletin on the acetylation of wood using no catalysis but with an organic cosolvent [Goldstein et al. 1961, Dreher et al. 1964]. In 1977, in Russia, Otlesnov and Nikitina came close to commercialization but the process was discontinued presumably because it was not cost-effective. In the late 1980's, Daiken, in Japan, started a small commercial production of acetylated wood for flooring called alpha-wood that is still in production today.

There is one large commercial-scale production facility of acetylated wood today. It is produced by TitanWood in The Netherlands [www.titanwood.com] at an expanding 30,000 m^3 pa plant capable of acetylating lumber up to 100mm thick Their technology is being used to build additional facilities with capacities in excess of 100,000 m^3pa each.

5 PRODUCTION OF ACETYLATED WOOD

In large scale production of acetylated wood, lumber is stickered and placed in a high pressure vessel using advanced handling equipment for efficiency. Acetic anhydride is introduced into the vessel and the temperature raised to the reaction temperature. Pressure is applied as needed. After the reaction is complete, the excess anhydride is recycled and the by-product acetic acid is processed back into anhydride. The acetylated wood is then dried, removed from the vessel and stored until shipment. The entire process has minimal by-products which have ready end-uses and is environmentally benign. When combined with the use of sustainable grown wood from certified sources as input, acetylated woods provide and improved building material that address a range of environmental factors.

6 PROPERTIES OF ACETYLATED WOOD

The properties presented in this paper are mainly a combination of results on southern yellow pine, aspen, radiata pine, poplar, beach and birch, demonstrating that wood acetylation properties apply to a range of species.

6.1 Volume Changes

Table 1 shows the increase in volume of pine after reaction with acetic anhydride and the calculated volume of chemical added to the cell wall after re-drying the wood. Since the volume increase due to reactions with acetic anhydride is equal to the calculated volume of chemical added, this shows that the reaction has taken place in the cell wall and not in the void spaces of the wood.

Table 1. Changes in pine volume and volume of chemical added as a result of chemical reactions.

WPG[1]	Increase in wood volume[2]	Calculated volume of added chemical[3]
17.5	3.0	2.9
22.8	3.9	4.0

[1] Weight Percent Gain [2] Difference in oven-dry volume between reacted and non-reacted wood.
[3] Density used in volume calculations: acetic anhydride 1.049

There is a change in color due to acetylation. Light colored woods tend to darken slightly while dark colored woods become slightly lighter.

6.2 Acetyl Stability

Table 2 shows the stability of acetyl groups in southern yellow pine and aspen to cyclic exposure to 90% and 30% relative humidity [RH] [Rowell et al. 1992]. Each cycle represents exposure for three months at 30% RH and then three months at 90% RH. Within experimental error, there is no loss of acetyl over 41 cycles of humidity changes.

Table 2. Stability of acetyl groups in southern yellow pine and aspen flakes after cyclic exposure between 90% relative humidity [RH] and 30% RH.

Wood	Acetyl content [%] after cycle [number]				
	0	13	21	33	41
Pine	18.6	18.2	16.2	18.0	16.5
Aspen	17.9	18.1	17.1	17.8	17.1

This data was collected starting in 1992 and this experiment has continued to this day. After more than 20 years of cycling these samples from 30 to 90% RH, analysis shows that there is still no loss of acetyl resulting from humidity cycling and thus other benefits reviewed below are likely to, or have been proven in separate field tests, to be ongoing as well.

6.3 Moisture Properties and Dimensional Stability

By replacing some of the hydroxyl groups on the cell wall polymers with bonded acetyl groups, the hygroscopicity of the wood material is reduced. Table 3 shows the fiber saturation point for acetylated southern yellow pine and aspen. As the level of acetylation increases the fiber saturation point decreases in both the soft and hard wood.

Table 3. Fiber saturation point for acetylated southern yellow pine and aspen.

WPG	Pine [%]	Aspen [%]
0	45	46
6	24	--
8.7	--	29
10.4	16	--
13.0	--	20
17.6	--	15
18.4	14	--
21.1	10	--

Figure 1 shows the sorption isotherm of control Pine and acetylated Pine. The lower curves are for the acetylated pine shows much lower moisture content at a given relative humidity as compared to non-acetylated pine.

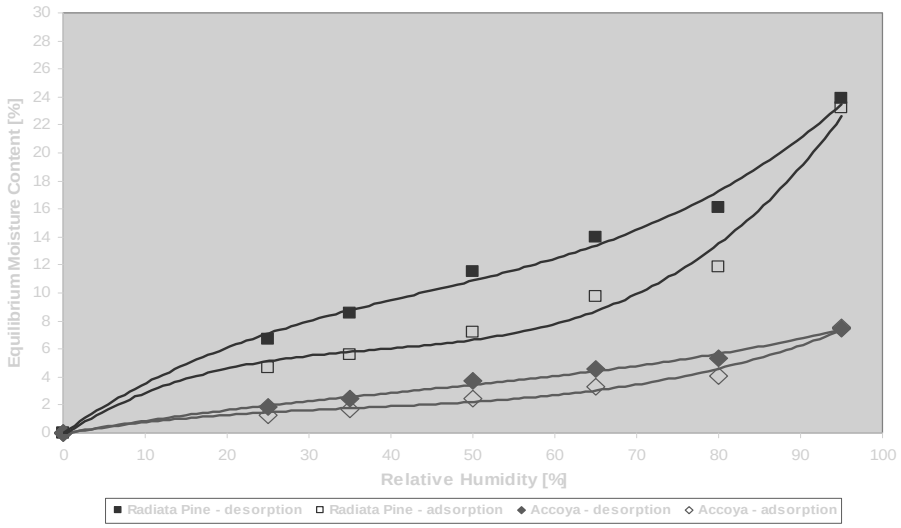

Figure 1. Sorption isotherm of control and acetylated pine.

Table 4 shows the equilibrium moisture content [EMC] of control and acetylated pine and aspen at several levels of acetylation and three levels of relative humidities. In all cases, as the level of chemical weight gain increases, the EMC of the resulting wood goes down.

Table 4. Equilibrium moisture content of acetylated southern yellow pine, aspen and radiata pine.

Specimen	WPG	Equilibrium Moisture Content at 27 ºC		
		30%RH	65%RH	90%RH
Southern Yellow Pine	0	5.8	12.0	21.7
	6.0	4.1	9.2	17.5
	10.4	3.3	7.5	14.4
	14.8	2.8	6.0	11.6
	18.4	2.3	5.0	9.2
	20.4	2.4	4.3	8.4
Aspen	0	4.9	11.1	21.5
	7.3	3.2	7.8	15.0
	11.5	2.7	6.9	12.9
	14.2	2.3	5.9	11.4
	17.9	1.6	4.8	9.4
Radiata Pine	0	5.1	11.9	22.2
	15	2.3	5.4	10.6
	20	2.2	4.1	8.7

Dimensional stability is recorded as antishrink efficiency [ASE] [Stamm 1964]. It is calculated as:

$$S = \frac{V2 - V1}{V1} \times 100$$ [S = Swelling coefficient; V1 = Volume dry; V2 = Volume wet]

$$ASE = \frac{S1 - S2}{S1} \times 100$$ [S2 = Acetylated; S1 = Control]

Figure 2 shows the reduction in swelling in control and acetylated pine. The un-acetylated pine shows much greater shrinkage especially in the tangential direction as compared to acetylated pine. Less shrinkage is observed in the radial direction.

Table 5. Dimensional stability of acetylated southern pine.

WPG	ASE
10	35
15	55
17	63
20	72

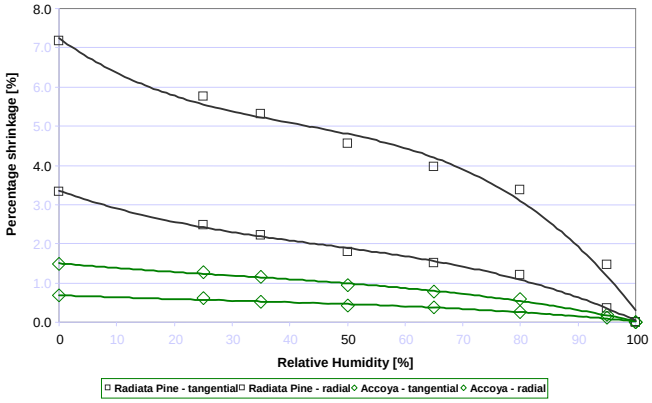

Figure 2. Reduction in shrinkage in radiata pine.

6.4 Resistance to Biological Attack

6.4.1 Fungi

Various types of solid wood, particleboards and flakeboards made from acetylated wood have been tested for resistance to several different types of organisms [Imamura et al. 1987, Rowell et al. 1987, 1989, 1997, Beckers et al. 1994, Militz 1991, Wang et al. 2002].

Acetylated radiata has been tested against several types of decay fungi in an European Union standard [EN 113] decay test using the brown rot fungus *Gloeophyllum trabeum* and white rot fungus *Coriolus versicolor*. Table 6 shows the resistance at several levels of acetylation to attack by brown- and white rot fungi. As the level of acetylation goes up, the resistance to attack goes up.

Table 6. Resistance of southern yellow pine against fungi.

WPG	Weight Loss After EN 113 test	
	Brown-rot Fungus	White-rot Fungus
[%]	[%]	[%]
0	58.8	7.3
6	32.7	4.1
10	6.3	2.2
15	2.7	<2
20	<2	<2

Another test for fugal and bacterial resistance that has been done on acetylated composites is with brown-, white-, and soft-rot fungi and tunneling bacteria in a fungal cellar. Control blocks were destroyed in less than 6 months while samples made from acetylated wood above 16 WPG showed no attack after 1 year. [Nilsson et al. 1988, Rowell et al. 1988]. This data shows that no attack occurs until swelling of the wood occurs [Rowell et al. 1988]. This fungal cellar test was continued for an additional 5 years with no attack at 17.9 WPG. This is more evidence that the moisture content of the cell wall is critical before attack can take place [Ibach and Rowell 2000, Ibach et al. 2000].

In-ground tests have also been done on acetylated solid wood and flakeboards [Rowell et al.1997, Larsson Brelid et al. 2000]. Specimens have been tested in the United States, Sweden, and New Zealand . The specimens in test in Mississippi are showing little or no attack after 10 years.

Acetylated fiberboards in three in-ground locations in Gulf Port, Mississippi show no attack after 14 years. Recent results show that acetylated pine at a WPG of 21.2 is outperforming CCA [copper-chromium-arsenic] at 10.3 kg/m^3 after 8 years in test in Sweden [Larsson Brelid et al. 2000].

Table 7. Fungal rating data on control and acetylated stakes in Gulf Port, Mississippi test plot.

WPG	Rating at [years]									
	1	2	3	4	5	6	8	10	12	14
0	3	4	--							
20	0	0	0	0	0	0	0	0	0	0
Rating system: 4=Destroyed, 3=Badly attacked, 2=Some attack, 1=Evidence of attack, 0=No attack										

6.5 Other Properties

6.5.1 Strength

Table 8 shows the bending stiffness [MOE] and bending strength of [MOR] of acetylated radiate pine. The table shows strength properties are retained even after of acetylation.

Table 8. Bending stiffness [MOE] and bending strength of [MOR] of control and acetylated radiata pine.

Specimen	Density [Kg/m^3]	Moisture [%]	MOE [N/mm^2]	MOR [N/mm^2]
Radiata Pine	417	12.2	9664	43
Acetylated Radiata Pine	492	5.2	8788	39

6.5.2 Hardness

Table 9 shows the Janka hardness of acetylated and control radiata pine. Acetylated radiata is much harder in all directions as compared to unacetylated pine but this is partly due to the lower moisture content of compared to unacetylated radiata pine.

Table 9. Janka hardness of samples according to ASTM D143.

Specimen	Density	Moisture Content	Janka hardness ASTM D143		
			Radial	Tangential	End Grain
	[Kg/m^3]	[%]	[N]	[N]	[N]
Radaita Pine	479	12.1	2750	2748	3637
Acetylated Radiat	521	4.2	4046	4187	6595

6.5.3 Machinability

In general, acetylated wood has the same machining properties [sawing, planing, drilling, routing] as unacetylated wood. Gluing and coating properties are also similar to unacetylated wood using the present industrial gluing and coating systems. Due to the dimensional stability of wood acetylated to its core, coatings typical have a life of 2-3 times that of control samples.

The surface of acetylated wood after planing is smoother than unacetylated wood resulting in less sanding before coating application.

7. PRODUCTS IN TEST AND APPLICATION

Acetylated wood has been in commercial use for several years. As an early test acetylated poplar was placed in test in the walls of one of the canals in The Netherlands [Figure 4 (left)]. After 13 years it was removed and determined to have minimal damage due to UV or biological degradation Figure 4 (right).

Figure 4. Acetylated poplar in test in a canal [left]
and the sample after 13 years [right].

Leading applications of acetylated wood include use in windows doors, siding, decking, and exterior load-bearing glulam beams for buildings, bridges and other structures. Acetylated pine is now being used by many manufacturers for windows and doors [Figure 5] in the European market.

Figure 5. Examples of acetylated wood applications.

Acetylated wood has also been successfully tested for use in load-bearing glulam structural beams for multiple purposes. As an example, two 40 meter long heavy road traffic bridges are currently under construction in Sneek, Netherlands due for completion in 2009.

All beams have been produced for the projects. This following extensive testing for the application by leading independent institutes. Laminated beams up to 1080 x 1400 mm were produced. Superior strength-to-weight, durability, dimensional stability and low maintenance costs were cited as reasons for selection.

8 CONCLUSIONS

Acetylation of both softwoods and hardwoods gives a product which has a very high degree of dimensional stability and durability. Strength properties and hardness are not reduced. This technology provides an environmentally safe method of protecting sustainable common woods to give a new generation of value-added products with increased stability and durability without the use of toxic chemicals. This method can take stress off of endangered tropical hard wood species that have been the traditional means of meeting durability requirements.

REFERENCES

All referenced used in this paper can be found in the following books.

Hill, C.A.S., 2006, Wood modification: chemical, thermal and other Processes. John Wiley & Sons, Chichester, England, 239 pp.

Rowell, R.M., 2005, Handbook of Wood Chemistry and Wood Composites, Taylor and Francis, Boca Raton, FL, 487 pp.

11DBMC International Conference on Durability of Building Materials and Components
ISTANBUL, Turkey 11-14 May 2008

Development of an Automated Artificial Ageing Test Apparatus for Sealants and Comparison with Outdoor Exposure Testing

Hiroyuki Miyauchi [1]
Yoshiaki Takemoto [2]
Michael A. Lacasse [3]
Kyoji Tanaka [4]

T 14

ABSTRACT

The long-term performance and degree of deterioration of sealants due to ageing effects is currently evaluated using artificial accelerated test methods such as those described in JIS A 1415. However, there are many issues related to correlating the deterioration of sealants subjected to outdoor tests that are not yet resolved. In this study, a computer-controlled, automated artificial ageing test apparatus was developed that subjected sealants to a deterioration process similar to exposure outdoors. Three kinds of sealant product were selected: a 1-component modified silicone, a 2-component modified silicone, and a 1-component polyurethane, all manufactured in Japan. Outdoor environmental data was collected over one year that included, joint movement of the dynamic outdoor exposure test apparatus and specific weathering factors such as temperature of the sealant, and quantity of solar radiation and rainfall at the exposure site. The data acquired from the outdoor test was simultaneously transferred to the artificial ageing test apparatus. As a result, the movement, temperature, total radiation and wetting conditions of the artificial ageing test were nominally the same as those extracted from the outdoor test with the exception of the wavelength distribution for solar radiation. Comparing results of the deterioration of the sealant, the artificial ageing test apparatus offered a high degree of correlation to results obtained in outdoor tests for both of the modified silicone products but not for the polysulphide product. The results suggest that the development of the proposed indoor test using the automated artificial accelerated test method appears promising given the degree to which results can reproduce those obtained from ageing sealant products outdoors.

KEYWORDS

Sealant, Artificial ageing, Joint movement, Test method, Test apparatus

1. Tokyo Institute of Technology, Structural Engineering Research Center, Kanagawa, Japan 2268503, Phone +81-45-924-5329, Fax +81-45-924-5339, miyauchi@serc.titech.ac.jp
2. Shimizu Institute of Technology, Tokyo, Japan 1358530, Phone +81-3-3820-8487, Fax +81-3-3820-5959, y.takemoto@shimz.co.jp
3. National Research Council Canada, Institute for Research in Construction, Ottawa, Canada K1A0R6, Phone +1 613 993 9715, Fax +1 613 954 5984, Michael.Lacasse@nrc-cnrc.gc.ca
4. Tokyo Institute of Technology, Structural Engineering Research Center, Kanagawa, Japan 2268503, Phone +81-45-924-5329, Fax +81-45-924-5339, tanaka@serc.titech.ac.jp

1 INTRODUCTION

Factors causing the deterioration of construction sealants may be classed as, e.g., weathering, i.e. due to ultraviolet radiation, temperature and rainfall, and due to movement, that occurs by the behaviour of external walls to solar radiation [Wolf 1990; Wolf 1996]. Evidently these are the most significant factors that influence the performance of sealants over time [Wolf 1999]. Typically it is necessary to evaluate the durability of sealant products by testing before the sealant is used in building construction. At present, a dynamic outdoor exposure testing apparatus has been used at an outdoor exposure test site in Japan that provides information on the simultaneous deterioration due to weathering and movement [Enomoto et al. 2006a; Enomoto and Tanaka 2007]. However, outdoor exposure tests take considerable time to perform since the deterioration of sealants in such tests occurs in real time and from natural environmental conditions.

On the other hand, it is of evident practical importance to evaluate the durability and deterioration of sealants using test that can be completed in a short period of time and in this context, various artificial weathering tests have previously been developed and carried out in Japan [Ito et al. 2004; Miyauchi et al. 2004]. However, being able to provide verification that results derived from outdoor exposure tests reasonably correlate to those from accelerated weathering test remains a significant research issue and a challenging task and despite the fact that a number of studies have been carried out on resolving issues regarding correlation of outdoor and accelerated weathering test results [Beasley 1996; Wolf et al. 1999; Enomoto et al. 2006b].

Various studies have been carried out to investigate the durability of sealed joints against joint movement of external walls in Japan and from these fatigue tests for sealants have been developed [Matsumoto et al. 1981; Koike et al. 1983; Miyauchi and Tanaka 2004]; this highlights the importance of joint movement in the durability of sealed joints. Hence, when considering an accelerated weathering test for sealants, it is necessary to include movement in the weathering test and to match the movement conditions with those that may be derived from the outdoors. However, it is very difficult to evaluate the deterioration of sealants using an accelerated weathering test method without outdoor test data that can be used as a basis of correlation. Therefore, in was considered that for the first stage of this study, the deterioration effects used in the artificial weathering test and their rate of application would be the same as that of the outdoor test such that the deterioration of sealants subject to both tests could be compared and the results correlated. Thereafter it is supposed that the accelerated weathering test method can be used to evaluate the deterioration of sealants given the relationships derived from correlation between test methods.

Hence, for this study, a dynamic outdoor exposure apparatus incorporating an integral joint movement system was used in outdoor exposure test [JSIA 2004] and a prototype, computer-controlled, automated artificial test apparatus was developed that permitted subjecting sealant products to a deterioration process that was similar to that obtained from outdoor exposure. Using both apparatus, the condition of sealants exposed to outdoor and artificial (indoor) testing was compared by visual observation, and by observation with a light microscope.

2 OUTLINE OF TEST METHOD FOR THE DETERIORATION OF SEALANTS

2.1 Deterioration Factors and Method of Evaluation of Sealants

There are several factors that cause deterioration in sealants however, of these factors, those selected as the basic test parameters for weathering included: solar radiation, temperature, moisture and the expansion–contraction brought about by joint movement. Figure 1 shows the basic notions from which was developed a method for the performance evaluation of sealants based on artificial deterioration of products combined with outdoor environmental conditioning. First of all, environmental factors causing deterioration are divided into two components: (i) weathering effects, i.e. effects such as total

solar radiation, material temperature, and moisture, and (ii) movement. Both these set of factors are measured by the dynamic outdoor exposure testing apparatus as shown in Figure 2. Next, the data obtained from the outdoor exposure testing apparatus in respect to the test parameters are input to instruments on the artificial test apparatus (fabricated by TiTech*) and are automatically synchronized to the outdoor conditions. The sealant surface conditions showing deterioration as characterised by both visual observation and observation by light microscope, permitted correlating results derived from either test method. Tests were carried over a 1-year period under two conditions: weathering alone and combined weathering and movement.

2.2 Test Specimen

Three kinds of sealant products were selected as shown in Table 1. The tensile testing was carried out in accordance with conditions specified in JIS K 6251 [2004] and the test specimens were prepared with a

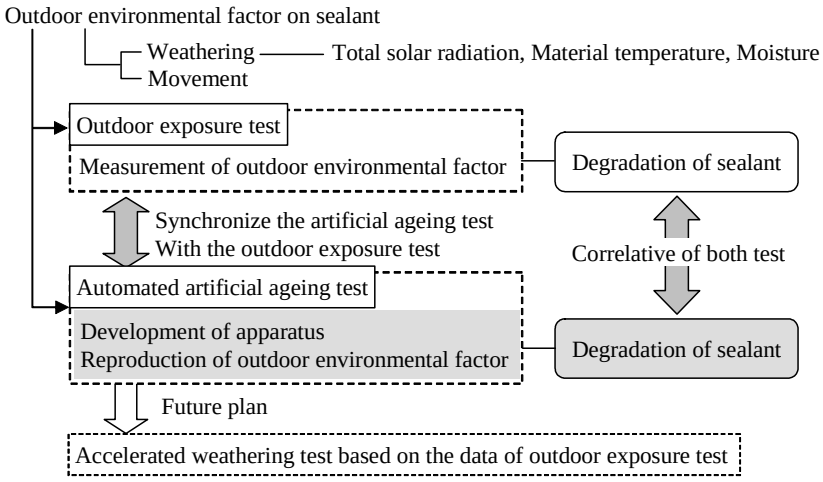

Figure 1. Artificial ageing test philosophy synchronized outdoor environmental condition

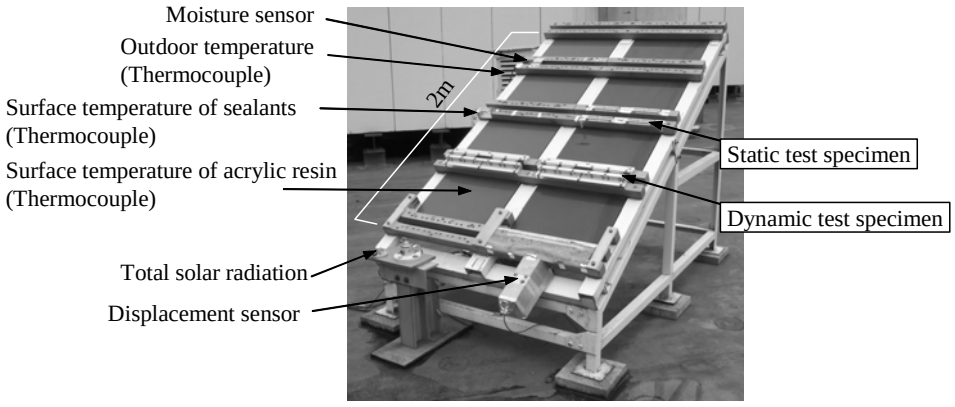

Figure 2. Dynamic outdoor exposure testing apparatus

Table 1. the physical properties of sealants

Sealants	*50% Modulus* (N/mm²)	*Maximum tensile stress* (N/mm²)	*Elongation* (%)
1-component modified silicione(MS-1)	0.16	0.57	520
2-component modified silicone (MS-2)	0.15	0.49	650
1-component polyurethane (PU-1)*	0.17	1.32	800

*PU-1 is not coating on the surface of sealant

* TiTech – Tokyo Institute of Technology, Yokohama, Japan

joint width and depth of 12 mm, conforming with conditions specified in ISO 13640 [1999]. The sealant
was cured in accordance with conditions specified in JIS A 5758 [2004]. The surface of PU-1 was not painted to evaluate the deterioration condition of the sealant in the short term.

2.3 Dynamic Outdoor Exposure Test

2.4.1 Dynamic Outdoor Exposure Testing Apparatus

The dynamic outdoor exposure testing apparatus, shown in Figure 2, is able to evaluate the influence of weathering and joint movement on sealants. It is composed of a steel frame of white colour and a black coloured acrylic board. The joint movement occurs by virtue of the difference between the coefficients of linear thermal expansion of the steel frame as compared to the acrylic board.

2.4.3 Method of Measuring Outdoor Environmental Data

Total horizontal solar radiation was measured by installing a pyranometer (wavelength: 305-2800 nm) in front of the test apparatus. The surface temperature of the sealant was measured with a thermocouple embedded in the sealant 1-mm from the surface. Joint movement of test specimen was measured and calculated as follows: (i) The joint movement between the fixed and the movable structural member of the test apparatus was measured with a displacement sensor; (ii) The movement of the test specimen was calculated considering the measured value of displacement and the length of an acrylic board. The displacement sensor is protected with a metal cover to avoid the effects of solar radiation and rainfall. The presence of rainfall was measured with the rainfall sensor that made the principle of the difference of the electrical resistance between metallic needles. The amount of ultraviolet radiation was measured with a portable type UV dosimeter (UV-A type sensor).

3 OVERVIEW OF AUTOMATED ARTIFICIAL AGEING TEST APPARATUS

3.1 Method to Deteriorate Sealants

The automated artificial ageing test apparatus is shown in Figure 3 and in Figure 4, the method for installing test specimens and the measurement-control method for the test apparatus is provided. This test apparatus operates by a purposely designed control program, that is synchronized to the dynamic outdoor exposure testing apparatus.

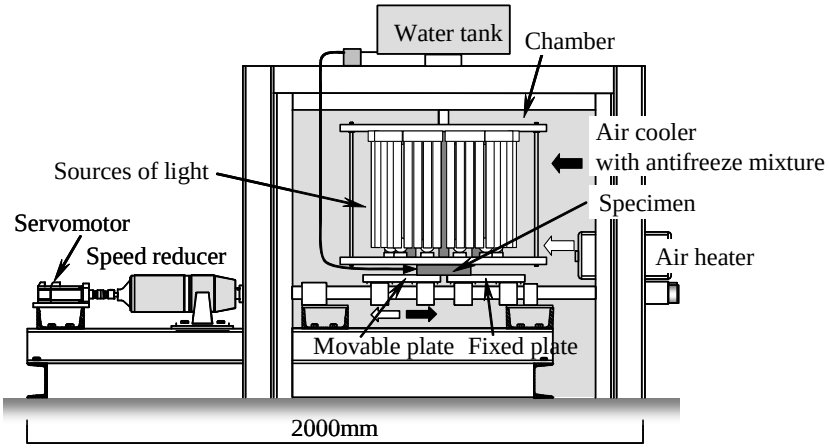

Figure 3. Artificial wweathering and movement apparatus (Side view)

Solar radiation in the apparatus was recreated using three sources of radiation each providing for different wavelength spectrums; the ultraviolet region was re-created using a black light, the visible region with a fluorescent lamp, and the infrared region re-created with a high-intensity filament lamp. The spectral irradiance of sunlight was used as reference. Given that the spectral irradiance differs is

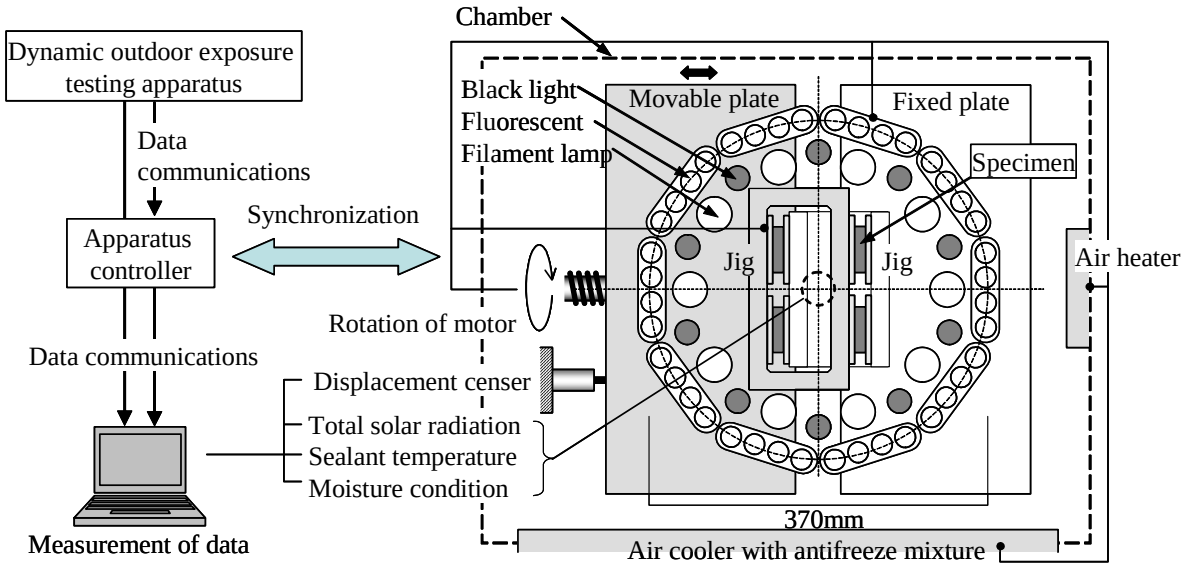

Figure 4. Specimen arrangement details and method of controlling deterioration factors
（Only the specimen given movement is shown in the figure.）

according to specific weather conditions, the amount of irradiation from the artificial light sources was controlled by measuring the total solar radiation obtained from the pyranometer attached to the dynamic outdoor exposure testing apparatus. The quantity of total solar radiation for each weather condition was re-created by changing the number of operable sources of artificial light. The temperature condition within the apparatus was based on the surface temperature of the sealant in the outdoor test apparatus. A heating-cooling system was used to maintain the specified temperature in the test chamber. Distilled water contained atop the apparatus in a water tank was the source of moisture used to wet the sealant surface; water was admitted via a solenoid valve through a silicon tube to the surface of the sealant as required to provide the wet conditions. A servomotor and the movable plate connected to the motor controlled joint movement. Joint movement was measured with a displacement sensor installed on the moveable plate; monitoring the movement permitted synchronization of joint movement to that of the dynamic outdoor exposure testing apparatus.

3.2 Testing Period and Condition

The testing period was one year (May 18, 2005 - May 17, 2006) and the deterioration in the surface condition of the sealant was investigated after 3, 6 and 12 months exposure. Test specimens were exposed to two (2) types of deterioration effects: weathering and the combined effects of weathering and movement. The temperature condition when initiating the test influences the behaviour of the expansion-contraction joint movement after the test. In this research, the temperature at the reference position (0 mm) was 20 °C, and the test started when the temperature was 20 °C on May 18th at 17:00 hrs. The data from both the outdoor and artificial deterioration tests were recorded every ten minutes.

3.3 Measurement Result of Outdoor Exposure Test

Figure 5 shows the results of measurement of relevant climate data and joint movement for a one year period using the dynamic outdoor exposure testing apparatus. The quantity of total solar radiation is relatively high from spring to summer, reaching a maximum of 0.97kW/m^2 on the 25th and 27th July, 2005. The highest sealant surface temperature was 61.4 °C on 27 July, 2005 and the lowest surface temperature was -6.6 °C obtained on 24 January, 2006. The maximum difference in sealant surface temperature over one year was 68.0 °C. In regard to the moisture condition on the sealant surface, considerable amounts of rain fell over the rainy and the typhoon season. The maximum value of joint movement in compression was -4.35 mm on 27 July, 2005 and the minimum value in expansion was 2.12 mm, occurring on 24 January, 2006. These results indicated that there was direct correlation

between the temperature and joint movement; the higher the temperature, the smaller the joint opening. Given that the joint movement for the "zero-point" was calibrated at a temperature of 20 °C, the degree of movement in compression was larger than that in extension.

4 REPRODUCIBILITY OF DETERIORATION EFFECTS OF TEST APPARATUS

Figure 6 provides a comparison between results of test conditions obtained from the automated artificial ageing test apparatus (indoor) and the dynamic outdoor exposure testing apparatus. Comparative information over the test period (11 to 17 August, 2005) is provided in regard to total solar radiation ($kW \cdot m^{-2}$), ultraviolet radiation ($W \cdot m^{-2}$), sealant surface temperature (°C), surface moisture condition (rain or dry), and joint movement (mm). It can be observed that the amount of ultraviolet radiation from the artificial ageing test apparatus is smaller than that derived from the outdoor exposure test and consequently, the UV-radiation spectrum from the artificial test does not completely recreate that of the outdoors.

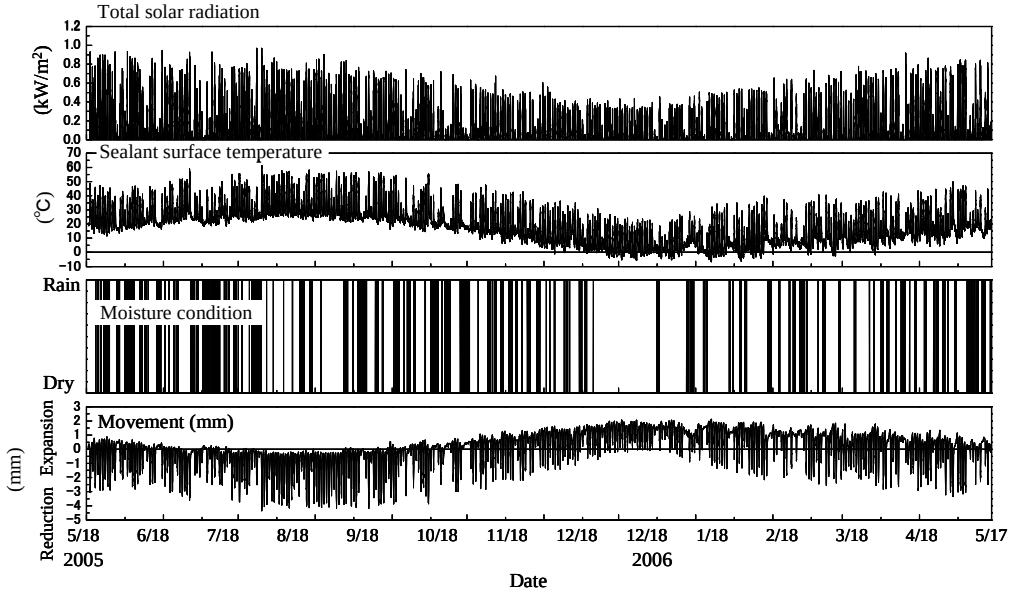

Figure. 5 the Results of meteorological observation and movement occurred in joint for 1 year (2005.5.18 – 2006.5.17)

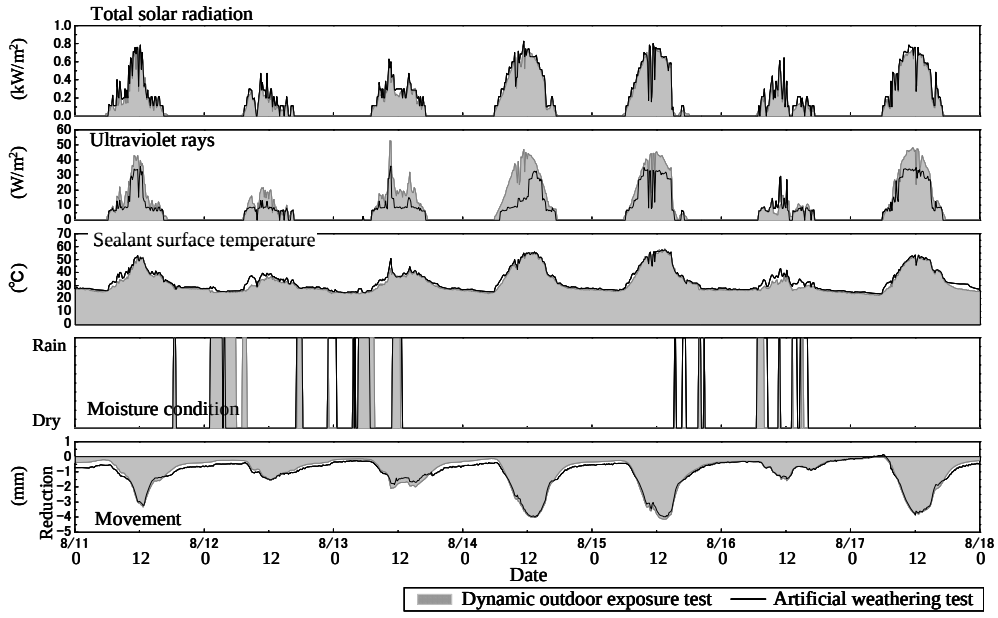

Figure.6 comparison of artificial weathering test and dynamic outdoor exposure test (2005.8/11～8/17)

5 COMPARISON OF SEALANT DETERIORATION FROM BOTH TESTS

5.1 Method of Observation for Surface Cracks on Sealants

The presence of surface cracks on sealants was investigated by two methods: that observed by using a digital camera (visual) and that with the use of an optical microscope having an attached digital scanning instrument. The detection of the presence or absence of cracks on the surface of the sealant with the optical microscope was determined by visual observation with the same magnification. The differentiation between areas having or not having cracks was determined using a light-contrasting binarization technique in which areas containing cracks appeared black and those not having cracks white in colour.

5.2 Result of Observations of Surface Cracks of Sealants

Table 2. The crack condition of sealants

Sealant	*Term (month)*	*Weathering*		*Weathering + Movement*	
		Outdoor	*Indoor*	*Outdoor*	*Indoor*
MS-1	12	12mm No crack	No crack		
MS-2	3	No crack	No crack		
	6				
0.1 0.5mm	12				
PU-1	3		No crack		No crack
	6		No crack		No crack
0.1 0.5mm	12				

Table 2 shows the sealant crack condition for the three (3) sealants investigated (i.e. MS-1; MS-2; PU-1), the upper most set of digital photographs for MS-1, and those of sealants MS-2 and PU-1, characterised by binary imaging, provided in the lower two sets of images. The images in all three sets are those taken of the surface of the respective sealant products following exposure to outdoor testing and the corresponding artificial ageing test (indoor) for three (3), six (6) or twelve (12) months. The test results are arranged such that images can be compared between products having been subjected to only “weathering” or with “weathering and joint movement” combined.
In regard to product MS-1, large cracks occurred to same degree in the sealant specimens exposed to the “weathering and movement” conditions of both test apparatus; that is, the crack depth on the

surface of sealants exposed in the outdoor test was 6.5 mm and for the artificial (indoor) ageing test, 5 mm. For product MS-2, the small cracks on the surface of sealants subjected to "weathering" conditions alone occurred with both test apparatus after 6 months exposure and only after 3 months when subjected to combined "weathering and joint movement". However, larger crack sizes were evident for the same sealant exposed to the dynamic outdoor exposure testing procedure as compared that of exposure to the artificial (indoor) ageing test. For product PU-1, the surface cracks occurred after 3 months of dynamic outdoor exposure testing, whereas this occurred after 1 year for the same sealant subjected to the artificial ageing test.

5.3 Correlation of Dynamic Outdoor Exposure Testing and Artificial Ageing Test

The degree of surface crack formation of sealants subjected to the combined action of "weathering and movement" occurs earlier than those subjected to "weathering" alone. Hence the results of tests on MS-1 suggest that the joint movement has a significant influence on the occurrence of surface cracks of this product. Additionally, and most significantly, it was observed that the surface crack pattern of sealants changed from a generalised random cracking (crazing) to a series of parallel cracks by the influence of joint movement.

From a comparison of results of the sealant crack condition derived from the two test methods, it appears that the degree of factors casing deterioration in the artificial ageing test is slightly less important than that achieved with the dynamic outdoor exposure testing apparatus. It was surmised that the reason for the differences between test methods were most likely due to the influence of ultraviolet rays, specifically, the difference in UV-spectrum between outdoor and artificial ageing methods. However, other factors might also be considered to influence ageing results; e.g., the harmful effects of gas and that of acid rain. In the future it will be useful to further examine the influence of different factors causing deterioration in sealants by combining the lesser effects with the effect of UV radiation.

Additionally it would be useful to test different types of products not as susceptible to deterioration from joint movement given that for product MS-1, the influence of joint movement on the formation of cracks was clearly evident. However, it was not easy to discern differences in the degree of deterioration achieved using either test method on the basis of results of tests on this product.

Nonetheless, the results suggest that the test method that incorporates both "weathering and joint movement" best recreates outdoor exposure and hence most closely replicates natural exposure conditions.

6 CONCLUSIONS

The following conclusions were obtained.

(1) The sun light spectrum of the artificial ageing test differs from the dynamic outdoor exposure test, the difference, in particular, being the ultraviolet radiation spectrum of the artificial ageing test. However, the total solar radiation, sealant surface temperature and moisture condition from the outdoor environmental conditions were readily replicated in the artificial ageing test apparatus..
(2) The surface crack condition for the PU-1 sealant product when subjected to the artificial ageing test was different than that of the same product exposed to the dynamic outdoor exposure test, however, the surface crack condition of sealant products MS-1and MS-2 resulted in nominally the same conditions from the artificial ageing as compared to that of the outdoor exposure test.
(3) The degree of crack propagation in similar sealant products occurs earlier in those sealants subjected to the combined action of weathering and joint movement as compared to those subjected to weathering alone.

ACKNOWLEDGEMENTS

The authors would like to express their sincere gratitude to committee members of the JAPAN SEALANT INDUSTRY ASSOCIATION and to Mr. Duong Minh Nhut and Mr. Wataru Hirasawa.

REFERENCES

Beasley, J. L., 1996, "The Correlation of Modulus Changes in Building Sealants after Artificial Ageing with those that Occur after Natural Weathering", in: Durability of Building sealants, Proceedings of the International RILEM Symposium (11-12 October, 1994, Garston, UK), J. C. Beech and A. T. Wolf editors, E & F N Spon, London, UK, pp. 17-26.

Enomoto, N., Ito, A., Takemoto, Y. and Tanaka, K., 2006a, "New test specimen and method for evaluation of weatherability of sealants", Journal of Structural and Construction Engineering, Architectural Institute of Japan, No.602, pp. 67-71, 2006.

Enomoto, N., Ito, A., Shimizu, I., Matsumura, T., Takane, Y., Okamoto, Y., Yoshiaki, T. and Tanaka, K., 2006b, "Weatherability test of membrane roofing and sealants - Part 19 Study on weatherability test of construction sealants", Summaries of technical papers of Annual Meeting Architectural Institute of Japan, pp. 887-888, 2006.

Enomoto, N., and Tanaka, K., 2007, "A study on the quantification of the effect of dynamic transformation for the weatherability of construction sealants", Journal of Structural and Construction Engineering, Architectural Institute of Japan, No.619, pp. 27-32, 2007.

ISO 13640 1999: Building construction - Jointing products - Specifications for test substrates.

Ito, A., Enomoto, N., Shimizu, I., Matsumura, T., Takane, Y. and Tanaka, K.,2004, "Weatherability test of membrane roofing and sealants - Part 5 Study on accelerated exposure test of construction sealants", Summaries of technical papers of Annual Meeting Architectural Institute of Japan, pp. 885-886, 2004.

JIS K 6251 2004: Tensile testing methods for vulcanized rubber.

JIS A 5758 2004: Building Construction Sealants.

JSIA, 2004, Handbook of Construction Sealants, Japan Sealant Industry Association, 2004.

Koike, M., Tanaka, K., Tomiita, T. and Oda, S., 1983, "Observation on behavior of sealed joints in moving joint apparatus", Transactions of the Architectural Institute of Japan, Architectural Institute of Japan, No.329, pp. 150-159, 1983.

Matsumoto, Y., Ono, T. and Maruichi, T., 1981, "Dynamic outdoor exposure test for building construction sealants - Performance of sealants during construction in construction in winter", Proceedings of the Architectural Research Meetings, Kanto Chapter, Architectural Institute of Japan, pp. 361-364, 1981.

Miyauchi, H. and Tanaka, K., 2004, "Estimation of the Fatigue resistance of Sealants to Movement at Intersections of Sealed Joints and Improvement in the Joint Design Method", ASTM Symposium on Durability of Construction Sealants and Adhesives (29 January, 2003; Ft. Lauderdale, FL), ASTM STP 1453,A. T. Wolf Editor, ASTM International, West Conshohocken, PA, pp. 156-170.

Miyauchi, H., Enomoto, N., Sugiyama, S. and Tanaka, K., 2004, "Artificial Weathering and Cyclic Movement Test Results Based on the RILEM TC139-DBS Durability Test Method for Construction

Sealants", ASTM Symposium on Durability of Construction Sealants and Adhesives (29 January, 2003; Ft. Lauderdale, FL), ASTM STP 1453,A. T. Wolf Editor, ASTM International, West Conshohocken, PA, pp. 206-212.

Wolf A T., 1990, "Studies on the Ageing Behaviour of Gun-Grade Building Joint Sealants – The State of the Art" Materials and Structures 23 (134), pp. 142-157.

Wolf, A. T., 1996, "Ageing Resistance of Building and Construction Sealants, Part I", in: Durability of Building sealants, Proceedings of the International RILEM Symposium (11-12 October, 2004, Garston, UK), J. C. Beech and A. T. Wolf editors, E & F N Spon, London, UK, pp. 63-89.

Wolf, A T., 1999, "Environmental Degradation Factors, Their Characterisation and Effects on Sealed Building Joints", in: Durability of Building Sealants, State-of-the-Art Report of RILEM Technical committee 139-DBS, Durability of Sealants, Report 21, A.T. Wolf editor, RILEM, Cachan, France, pp. 41-72.

Wolf, A T., Bolte, H. and Boettger, T., 1999, "Attempts at Correlating Accelerated Laboratory and natural Outdoor Ageing Results", in: Durability of Building Sealants, State-of-the-Art Report of RILEM Technical committee 139-DBS, Durability of Sealants, Report 21, A.T. Wolf, Ed., RILEM, Cachan, FR, pp. 181-202.

Quantification of Effect of Dynamic Movement for Weatherability of Construction Sealants

Noriyoshi Enomoto [1]
Kyoji Tanaka [2]

T 14

ABSTRACT

Construction sealants are materials that ensure the waterproofing function of external joints of building, and the weatherabilty of sealant is a very important performance to sustain the functional performance of the joint. Sealant deterioration is a complex phenomenon influenced by factors such as joint movement and environmental agents whose intensity depends on the regional climate. Though many studies related to the weatherability of sealants have previously been completed, the evaluation of the surface degradation of sealants requires quantitative performance criteria. Prior to this study, a new type of test specimen was developed to assess the weatherabilty of sealants. The configuration of the test specimen is such that extension and of the joint can be applied continuously on a single specimen. For the quantitative evaluation of the surface degradation of sealants an equation based on the ISO 4628 assessment criterion was used. The approach adopted in this study for the quantitative evaluation of sealant degradations due to weathering thus included the new test specimen configuration and the ISO assessment method. The weatherability of sealants was considered to be composed of three factors: degree of degradation in the static conditions: increased rate of degradation due to joint movement, and: effects of environmental agents derived from the regional climate to which the sealant is exposed. In this study, eight sealants, commercially available in Japan, were subjected to a 4-year weathering test program carried out in the Yamanashi Prefecture, Japan. The exposure of sealants in this location was intended to exclude the effects of regional environmental factors on the degradation of the sealants. A functional equation is proposed that gives a surface degradation index of sealants subjected to static and dynamic conditions after a given exposure time. The following results were obtained in regard to the deterioration of sealants subjected to this weathering test program: silicone sealants did not deteriorate, though modified silicone sealants deteriorated slightly in static conditions. The degradation was greatly accelerated by adding joint movement. The degradation of polyurethane sealants was less influenced by joint movements as compared to the degradation of other types of sealant evaluated in this study.

KEYWORDS

Construction sealant, Out-door exposure, Weatherability, Dynamic transformation

[1] Product Development Dept., Sunstar Engineering Inc., Yamanashi, Japan, Phone +81 552845661, Fax +81 552827105,noriyoshi.enomoto@sunstar.com
[2] Structural Engineering Research Center, Tokyo Institute of Technology, Yokohama, Japan, Phone +81 459245329,Fax+81 459245339tanaka@serc.titech.ac.jp

1 INTRODUCTION

Construction sealant is the material used to maintain the waterproof and airtight functions over the long term, and the weatherability is an important performance criterion for maintaining these functions. Though the degradation of sealants in the outdoors proceed by UV irradiation, heat, water and many factors in general, the dynamic movement to which the sealant is exposed in actual joints accelerates the degradation. Many reports concerning outdoor exposure test employing testing device providing dynamic movements have been published, but there were usually large devices and only a limited number specimens could to be attached to them. [Matsumoto & Ono 1981][Koike & Tanaka 1983] This report presents information on the weatherability of construction sealants based on a newly developed test specimen [Enomoto & Tanaka 2006] that allows simultaneous exposure of the sealant to forced movement and outdoor environment.

2 TEST PROCEDURES

2.1 Sealants and Test Specimen

Eight commercially available sealants (see Table 1), typically used in Japan , conforming to JIS A 5758 [2004] and tested in accordance with JIS A 1439 [2004], were used to carry out the exposure test.
The configuration of the test specimen that enabled exposure of the sealant to continuous degrees of extension and compression in a single specimen is shown in Figure 1.

Table 1. Sealants tested.

Sealant	Mark	Physical Properties*		
		50%M (N/mm2)	Tensile Strenght (N/mm2)	Elongation (%)
2 part Silicone	SR-2	0.14	0.81	1170
2 part Polyisobutylene	IB-2	0.11	0.38	490
2 Part Modified silicone (General Purpose type)	MS-2(GP)	0.13	0.49	550
2 part Modified silicone (Stress Relaxation type)	MS-2(SR)	0.17	0.52	550
1 part Modified silicone	MS-1	0.12	0.51	800
2 part Polysulfide	PS-2	0.19	0.56	350
2 part Polyurethane	PU-2	0.11	1.15	790
1 part Polyurethane	PU-1	0.18	0.97	800

*Physical Properties : based on JIS A 1439

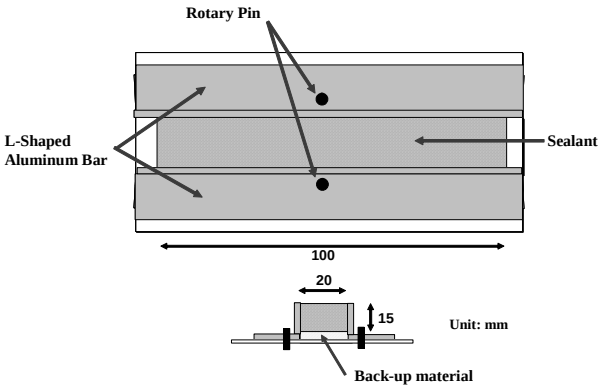

Figure 1. Test specimen.

2.2 Outdoor Exposure Conditions

The exposure test was carried out at one single site of Yamanashi Prefecture, located in central Japan. The choice of this exposure location permitted excluding variations in regional exposure factors. The exposure conditions and a summary of the weather at the exposure site are given in Table 2 and 3 respectively. The test specimen was exposed to both static and dynamic conditions, i.e. the static condition was without movement and the dynamic condition exposed the specimen to extension and compression cycle that were periodically reversed twice every week. The evaluation of surface degradation on the specimen was determined at four locations: i.e. for the static specimen, at ±0% movement amplitude, and: for the dynamic specimen, at ±1.5%, ±15% and ±25% movement amplitude as shown in Figure 2. The centre of the dynamic specimen was exposed to a movement of ±1.5% due to the gap between the rotary pin and the edge of the specimen.

Table 2. Exposure conditions

Location of exposure	Term of exposure	Direction/Angle	Interval of extension/compression exchange	Position of evaluation
Yamanashi Pref., Japan	2003.01.16 – 2007.01.15	South/30°	* Non (Static) * Twice/week (Dynamic)	* ± 0% * ± 1.5% * ± 15% * ± 25%

Table 3. Weather summary.

Temperature (℃)	Max.	40.4
	Min.	-7.8
	Ave.	15.2
Accumulated total solar radiation (0 °MJ/m2)		21,004
Accumulated precipitation (mm)		4,277

*Term: 2003.01.16 – 2007.01.15

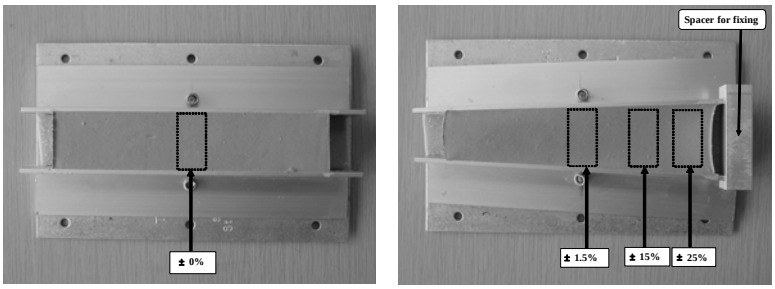

[Extension/Compression: Non] [Extension/Compression : Twice/week]

Figure 2. Evaluation position of test specimen.

3 EVALUATION

3.1 Determination of Degradation

The determination of the degradation was based on the rating scheme provided ISO 4628-4 [2003] with additional rating criteria introduced to determine the influence of minute cracks on the surface of the sealant. (see Table 4 – indicated by Italic letters, and Figure 3)

Table 4. Crack Rating index.

Rating	Quantity of cracks (Q)	Rating	Size of cracks (S)
0	None	0	*Not visible × 100 magnification*
0.5	*Trace*	*0.3*	*Only visible under magnification up to× 50*
1	Very few	*0.5*	*Only visible under magnification up to× 30*
2	Few	1	Only visible under magnification up to× 10
3	Moderate	2	Just visible with normal corrected vision
4	Considerable	3	Clearly visible with normal corrected vision
5	DEnse	4	Large cracks generally up to 1mm wide
		5	Very large cracks generally more than 1mm wide

*Italic letter : new added rating to decide minute cracks

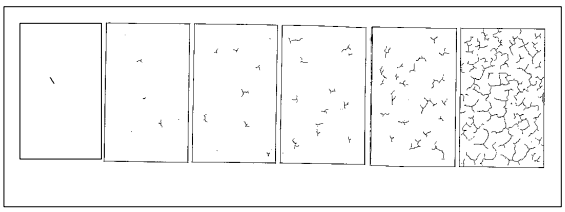

0.5 1 2 3 4 5

Figure 3. Crack patterns for quantity.

3.2 Evaluation of Degree of Degradation

The degree of degradation (QS-value) was based on the product of the rating of quantity (Q) and Size (S) of cracks as provided Equation 1. The approximate relationship between the QS-value and the surface condition is indicated in Figure 4. The digital photo of the crack surface given in Figure 4 illustrates the effectiveness of the QS-value to assess the state of degradation of the sealant.

$$QS(t)=Q(t)\times S(t) \quad (1)$$

where QS(t): QS-value after t months, Q(t): rating of Q after t months, S(t): rating of S after t months.

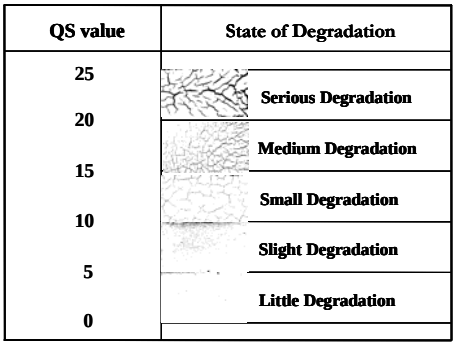

Figure 4. Surface degradation condition rating.

4 TEST RESULT

The changes in QS-value for the different sealants are provided in Figure 5. A summary of the test results is given below.

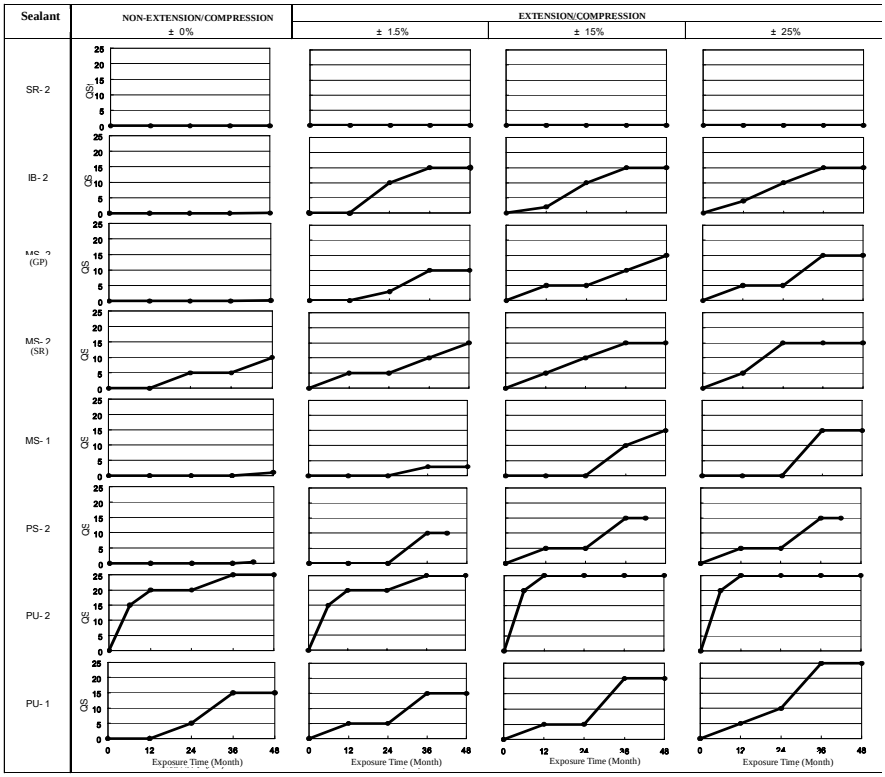

Figure 5. Changes of QS-value of sealants.

1) 2-part silicone sealants did not show degradation for any of the test conditions.
2) Though 2-part polyisobutylene, 2-part modified silicone (general purpose type), 1-part modified silicone and 2-part polysulfide showed a reduced rate of degradation in the static condition, the enforced movement in the dynamic condition accelerated the degree of degradation.
3) The degradation of 2-part modified silicone (stress relaxation type), 2-part polyurethane and 1-part polyurethane showed a gradual degradation with an increase in degree of movement.

5 DISCUSSIONS

5.1 Quantification of Degradation

A three dimension model (response surface) of the QS-value as a function of exposure time and extension-compression ratio was generated from the test results as shown in Figure 6.

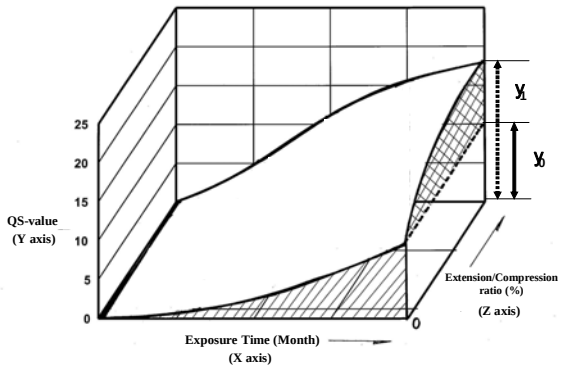

Figure 6. Response surface model of change in QS-value.

5.1.1 Degradation in Static Conditions

The change in QS-value with weathering in the static conditions is given in Equation 2.

$$QS_0(t)=a \cdot t^{b} \quad (2)$$

where, $QS_0(t)$: QS-value obtained from weathering in static conditions after t months; t: exposure months; a and b: constants.

5.1.2 Effect on Degradation due to Dynamic Joint Movement

When sealants as subjected to dynamic joint movement conditions, the equation for the acceleration of degradation due to movement is described in Equation 3. The relationship is derived from the response surface model given in Figure 6.

$$B=y_1/y_0 \quad (3)$$

where, B: coefficient of acceleration, y_0: QS-value on the static condition after t months, y_1: QS-value on the dynamic condition at the ε % of extension-compression ratio after t months.

From the model provided in Figure 7, the relation between the increased QS-value to that of y_0 induced by movement can be described by equation 4.

$$(y_1-y_0)/y_0=c \cdot \varepsilon^{d} \quad (4)$$

where, ε : extension-compression ratio, c and d: constant.

Substituting Equation 4 into Equation 3 yields Equation 5.

$$B=y_1/y_0$$
$$=(y_0+y_0\times c\cdot \varepsilon^{d})/y_0$$
$$=(1+c\cdot \varepsilon^{d}) \quad (5)$$

The change of value of $c\cdot \varepsilon^{d}$ for each year is shown in Figure 8. The parameters c and d are constants that were obtained from an average of each year.

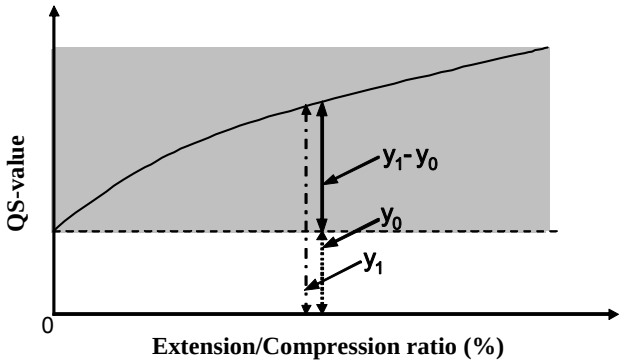

Figure 7. Model of QS-value change for movement.

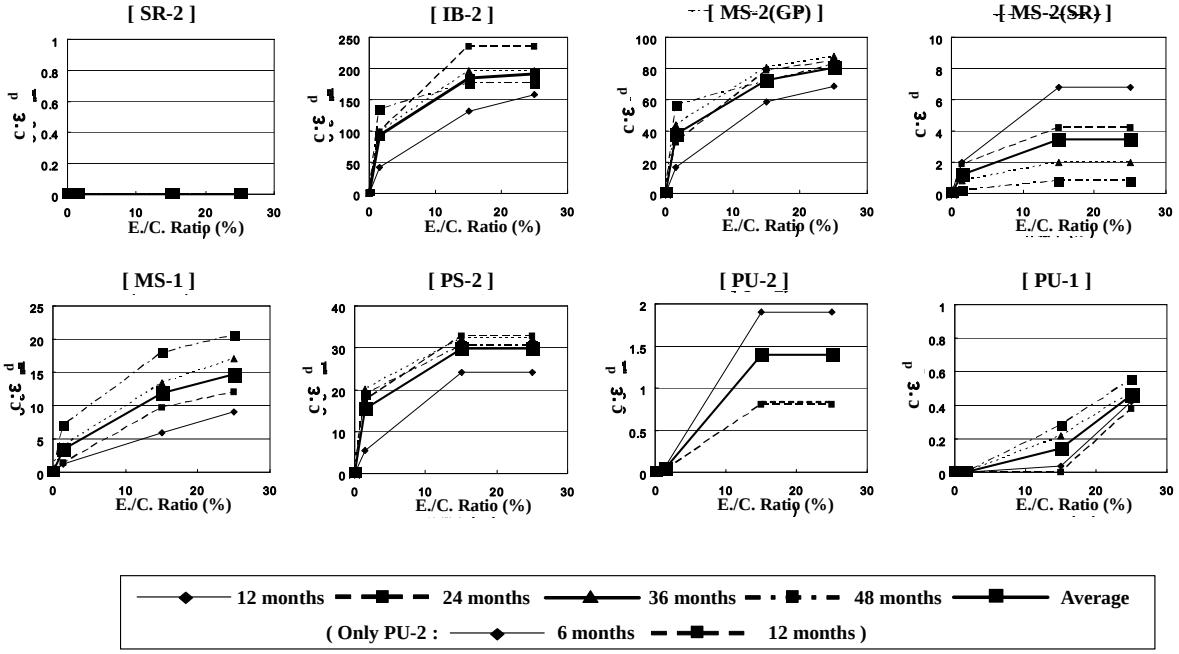

Figure 8. Change of $c\cdot \varepsilon^{d}$ value.

5.2 Proposal for The Equation of Degradation

Based on Equation 2 to 5, the equation for the QS-value was expressed as shown in equation 6.

$$QS(\varepsilon \cdot t)=QS_0(t)\times B$$
$$=(a\cdot t^{b})\times(1+c\cdot \varepsilon^{d}) \quad (6)$$

where, QS(ε ・ t): QS-value at ε % after t months, $QS_0(t)$: QS-value on the static condition after t months, t: exposure months, ε : extension-compression ratio, a,b,c and d: constant. The equation derived for each sealant is given in Table 5.

5.3 Comparison between Calculated and Observed Results

The relationship between QS-value and those calculated are shown in Figure 9.

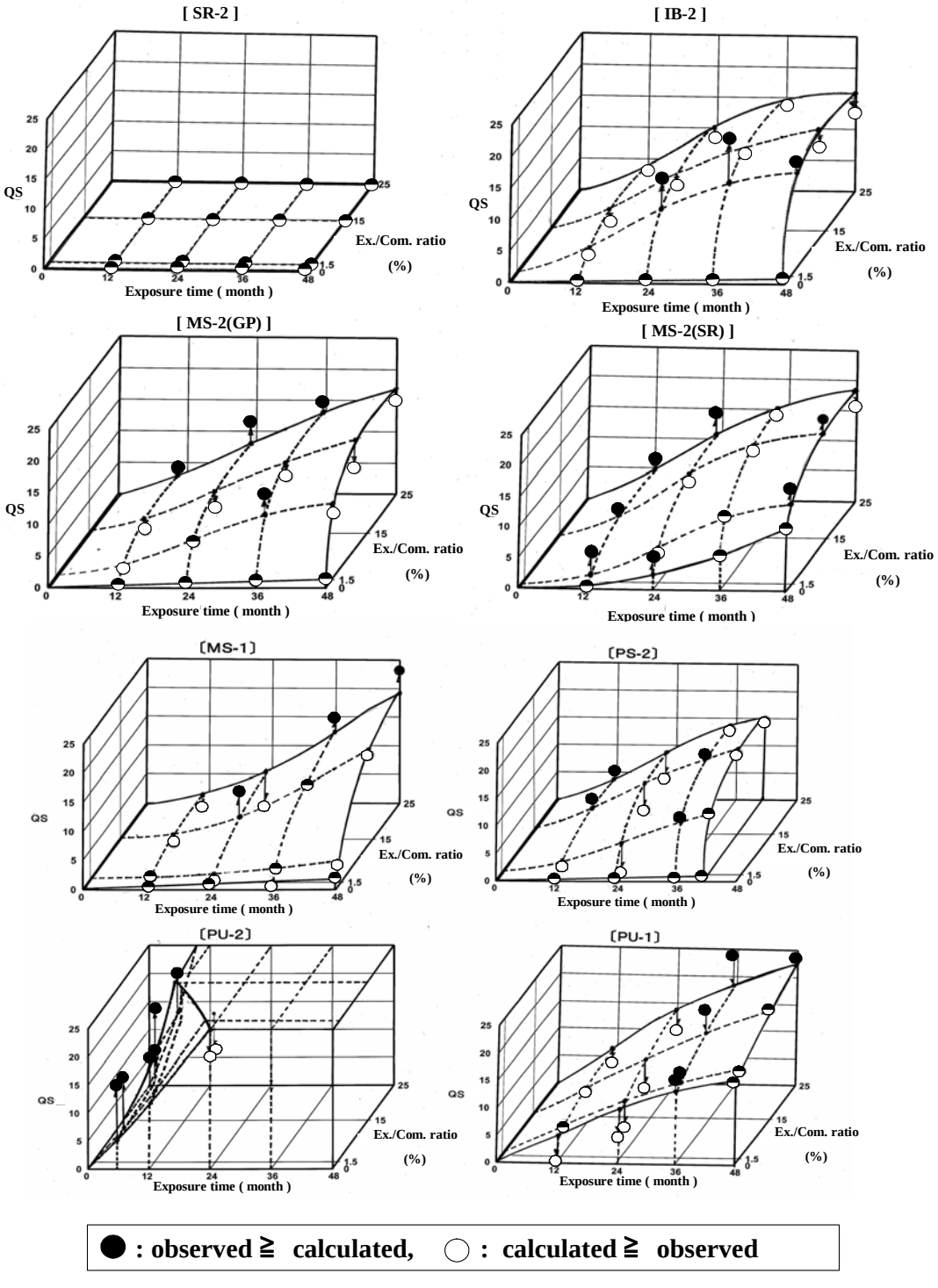

Figure 9. Relationship of QS-value between observation and calculation.

Table 5. Equations of degradation for each sealant.

Sealant	Equation for $QS(\varepsilon \cdot t)$
SR-2	$QS(\varepsilon \cdot t) = (0 \times t^{1.0}) \times (1 + 0 \times \varepsilon^{1.0})$
IB-2	$QS(\varepsilon \cdot t) = (0.002 \times t^{1.0}) \times (1 + 104 \times \varepsilon^{0.2})$
MS-2(GP)	$QS(\varepsilon \cdot t) = (0.005 \times t^{1.0}) \times (1 + 40 \times \varepsilon^{0.2})$
MS-2(SR)	$QS(\varepsilon \cdot t) = (0.005 \times t^{1.9}) \times (1 + 1.6 \times \varepsilon^{0.3})$
MS-1	$QS(\varepsilon \cdot t) = (0.02 \times t^{1.0}) \times (1 + 4 \times \varepsilon^{0.4})$
PS-2	$QS(\varepsilon \cdot t) = (0.01 \times t^{1.0}) \times (1 + 18 \times \varepsilon^{0.2})$
PU-2	$QS(\varepsilon \cdot t) = (3.8 \times t^{0.6}) \times (1 + 0.4 \times \varepsilon^{0.4})$
PU-1	$QS(\varepsilon \cdot t) = (0.7 \times t^{0.8}) \times (1 + 0.003 \times \varepsilon^{0.9})$

6 CONCLUSIONS

1) The new rating criteria for determining minute cracks on the surface of sealants were an effective means to evaluate the degree of degradation of sealants.
2) The equation for the QS-value of the sealant products provides a reasonable relationship between experimental observations and the calculated index of degradation of sealants over the exposure period of this test program.

REFERENCES

Enomoto, N., & Tanaka, K. 2006, 'New test specimen and method for evaluation of weatherability of sealant", *Architectural Institute of Japan*, Vol. 604, pp.17-22.

ISO 2003, 4628-4: "Paints and varnishes - Evaluation of degradation of coatings - Degradation of quality and size defects and intensity of uniform change in appearance – Part 4.

JIS A 5758, 2004, "Sealants for sealing and glazing in buildings"

JIS A 1439, 2004, "Testing methods of sealants for sealing and glazing in buildings"

Koike, M., and Tanaka, K. 1983, 'Observation for stress of sealants by joint movement using dynamic testing device', Architectural Institute of Japan, Vol. 329, pp.150-159.

Matsumoto, Y., and Ono, T.,1981, "Outdoor exposure test of sealant - Performance during curing stage on winter construction", Kanto Branch, *Architectural Institute of Japan*, pp.361-364.

11DBMC International Conference on Durability of Building Materials and Components
ISTANBUL, Turkey 11-14 May 2008

Acrylic Foam Structural Glazing Tapes

Steve Austin [1]
Uwe Manert [2]

T 14

ABSTRACT

The use of Acrylic Foam Structural Glazing Tapes to replace conventional structural silicone sealant and conventional structural glazing tape for 4-sided structural glazing applications has grown rapidly over the last few years. While the use of Acrylic Foam Structural Glazing Tapes is new in many parts of the world they have been used successfully since 1990 across the globe. Thousands of buildings have been successfully glazed around the world in countries such as USA, Germany, Brazil, Israel, India and Thailand with Acrylic Foam Structural Glazing Tapes.

Conventional structural glazing methods of bonding glass lites to a metal frame use either one-part or two-part structural silicone sealants. Acrylic Foam Structural Glazing Tape provides an alternative bonding method with the performance needed for the application yet with some significant benefits over conventionally glazed systems. The successful application history of Acrylic Foam Structural Glazing Tapes and the testing of glass lites bonded with Acrylic Foam Structural Glazing Tape at third party test institutes demonstrate this alternative bonding material has the capability to meet established requirements for the application. Test results according to application specific ASTM standards show that select Acrylic Foam Tapes have acceptable performance when compared to more traditional structural silicone sealants. Additional testing of Acrylic Foam Structural Glazing Tape according to EOTA ETAG 002 was conducted by the CSTB in France. UV accelerated weathering studies have also been conducted demonstrating the strength and durability of Acrylic Foam Structural Glazing Tapes compared to structural silicone sealants.

KEYWORDS

Acrylic Foam Structural Glazing Tape, Curtain wall, Structural glazing, Durability

[1] 3M Industrial Adhesives & Tapes Division, Technical Service Specialist, St. Paul, MN USA 55144, 651-736-1259 sraustin19@mmm.com
[2] 3M Deutschland GmbH, European Technical Service Specialist, Neuss, Germany D-41453, +49 (0) 2131 14 2669 umanert@mmm.com

1 INTRODUCTION

The use of an adhesive to attach glass lites to glazing profiles independent of mechanical fastening began in the mid 1960s as described by Schmidt et al [1988] in a paper titled Performance Properties of Silicone Structural Adhesives published in ASTM STP 1054 Science and Technology of Glazing Systems. This method of attaching glass lites gained popularity over the next few decades as architects and building owners desired the clean look of an adhesively bonded curtain wall system. This method of glazing is now commonly called structural glazing. Structural silicone sealant was the first adhesive to be used in a structurally glazed curtain wall system. The structural glazing industry has done an excellent job of developing test methods, standards and quality control procedures that has lead to a wide acceptance of this type of glazing method. More recently beginning in 1990 according to 3M™ VHB™ Structural Glazing Tapes Technical Guide [2007], acrylic foam structural glazing tapes have been successfully used in thousands of buildings globally as the adhesive bonding glass lites to glazing profiles in curtain wall and commercial glazing window systems.

The use, composition and performance of an acrylic foam structural glazing tape is significantly different than that of a conventional structural glazing tape also known as a spacer tape. Conventional structural glazing tapes are employed in a structural glazing system to create a space between the glass and a typical metal glazing profile. The thickness of the structural silicone sealant is determined by the thickness of the conventional structural glazing tape. This tape keeps the space or face clearance constant during the curing of the liquid applied structural silicone sealant. It does not provide a structural bond of the glass to the glazing profile. The structural bond is provided by the structural silicone sealant once it is fully cured. Conventional structural glazing tapes are characterized by a foam core with a thin adhesive skin on two opposing sides. The only adhesive portion is the thin skin which contacts the glass and glazing profile. The internal foam strength of a conventional structural glazing tape is generally low as high strength is not required from this tape in this application.

Conversely, an acrylic foam structural glazing tape used in this application must assume the same bonding role of a structural silicone sealant as it replaces both the sealant and the conventional structural glazing tape. That role is to adhesively bond the glass lite and transfer incidental windloads to the building facade structure. Acrylic foam structural glazing tapes are adhesive throughout their entire construction including the foam core. It is this unique construction that give acrylic foam structural glazing tape the strength and performance properties suitable to be used as the primary structural bond in a structural glazing system.

As with the use of a structural silicone sealant, the use of an acrylic foam tape for structural glazing applications requires careful consideration. The performance and durability of any adhesive used for this application should be well demonstrated before ever being considered for a structural glazing project. The objective of this paper is to demonstrate the performance and durability of a class of acrylic foam tapes known as 3M™ VHB™ Structural Glazing Tapes. The primary criteria used to demonstrate this performance is based on the test methods and design standards developed specifically for this application by the structural silicone and commercial glazing industry.

1.1 History of Acrylic Based Pressure Sensitive Adhesives

Early use of pressure sensitive adhesives began in the 1800s and was focused on attachment solutions for the medical industry according to Satas in the Handbook of Pressure Sensitive Adhesive Technology [1989]. The early examples were based on simple resins and beeswax. Rubber was later introduced in this century as a key component in pressure sensitive adhesives. Satas also states that more recent advancements were made in the automotive area when designers were looking for a method to hold paper sheets or masks during the painting process. The area of masking tapes was invented by 3M Corporation to address this need in the 1920's and is now widely accepted for this and many other uses. This tape generation was based on natural

and later synthetic rubber often characterized by a short shelf life and durability. In the early 1960s 3M also developed a special long lasting cellophane office tape which could remain on paper without turning yellow. The basis for this new tape was acrylic adhesive chemistry. This new acrylic based adhesive technology was also used to make thick double coated tapes for mirror bonding applications. The first thick double coated tapes consisted of a polyurethane or polyethylene foam core. In this construction the only adhesive component is the thin outer skin of the tape. The 1980s saw further advancement of the acrylic adhesive technology. For example, thick double coated acrylic foam tapes which were based solely on acrylic adhesive technology were developed by 3M as described in 3M™ VHB™ Durability Technical Bulletin [2001]. This construction was different than the previous thick double coated tapes as the acrylic foam tapes were adhesive throughout the entire construction. This characteristic is what leads to its unique viscoelastic high strength properties. These products were named 3M™ VHB™ Tapes as they exhibited higher dynamic and static load strength than conventional double coated foam tapes.

1 ETAG 002 TEST STUDY

The European Organization for Technical Approval (EOTA) developed the ETAG 002 Guideline for European Technical Approval for Structural Sealant Glazing Kits (SSGK). A part of this European guideline contains the manner and methodology to which structural silicone sealants are tested and characterized for a structural glazing application (kit). This methodology has acted well to characterize structural silicone sealants and is also a good initial method of evaluating an alternative bonding agent such as acrylic foam structural glazing tapes. However, structural silicone is a cold liquid applied, chemically curing sealant while acrylic foam structural glazing tapes are a fully cured, ready to apply tape. Thus, not all listed test procedures are directly applicable for an evaluation of an acrylic foam structural glazing tape. It must also be noted that 3M™ VHB™ Structural Glazing Tapes have a lower dynamic tension design strength of 85 kPa which is lower than that of a structural silicone sealant which is most commonly listed as 140 kPa.

The CSTB institute in France was consulted to conduct an independent evaluation of VHB™ Structural Glazing Tape according to ETAG 002. This study focused on an evaluation according to the appropriate test methods that would help to determine the performance and suitability of this acrylic foam tape for a structural glazing application. The mechanical properties evaluated in this test regime were tensile strength, shear strength, cyclic fatigue, UV accelerated aging resistance and water immersion strength retention characteristics.

2.1 CSTB Test Reports According to ETAG 002 on ER4 – Safety in Use

The following tables summarize the data from the standard test regime conducted at the CSTB. All test samples consisted of aluminum bonded to glass. While 3M™VHB™ Structural Glazing Tape is more temperature and rate/time sensitive due to its viscoelastic characteristics than structural silicone sealants this data demonstrates its ability to meet the performance demands of this application. The final version of the EOTA approval will take more time to complete but only to make a precise specification for acrylic foam structural glazing tapes which have different properties than those of liquid applied, chemically curing structural silicone sealant.

Table 1. Dynamic tensile and shear strength at -20°C, +23°C & +80°C (ETAG 5.1.4.1.1&2). Additional testing was conducted at 100°C.

Aluminum/Glass	**-20°C (-4°F)**	**+23°C (73°F)**	**+80°C (176°F)**	**+100°C (212°F)**
Shear Strength	706 kPa	562 kPa	409 kPa	-
Tensile Strength	3130 kPa	412 kPa	185 kPa	221 kPa

Table 2. Dynamic tensile strength after UV exposure - 4000 hr (ETAG 5.1.4.1.1).

Aluminum/Glass	**0 hr**	**1000 hr**	**2000 hr**	**3000 hr**	**4000 hr**
Tensile Strength	412 kPa	387 kPa	394 kPa	422	453

Table 3. Dynamic tensile strength after high temperature (45°C) water immersion & UV exposure (ETAG 5.1.4.2.1).

Aluminum/Glass	**0 hr**	**504 hr**	**1008 hr**
Tensile Strength	412 kPa	400 kPa	325 kPa

Table 4. Dynamic tensile strength after NaCL immersion (ETAG 5.1.4.2.2).

Aluminum/Glass	**0 hr**	**480 hr**
Tensile Strength	412 kPa	416 kPa

Table 5. Dynamic tensile strength - cyclic load/fatigue (ETAG 5.1.4.6.5).

Aluminum/Glass	**0 cycles**	**5350 cycles**
Tensile Strength	412 kPa	406 kPa

3 VISCOELASTIC NATURE OF 3M™ VHB™ SRUCTURAL GLAZING TAPE

The main purpose of the test study according to ETAG 002 was to gain a further understanding of the mechanical properties of 3M™ VHB™ Structural Glazing Tape. The challenge now with the data is to take the viscoelastic properties of this unique adhesive into consideration. Adhesives typically are elastic in nature. This means in general it is easy to determine maximum stress and modulus. This changes significantly if testing is done with a viscoelastic adhesive like 3M™ VHB™ Structural Glazing Tape. In Fig. 1 is an example of a stress/strain curve of a typical elastic adhesive compared to 3M™ VHB™ Tape when they are extended to a certain point of strain. This graph also demonstrates the capability of 3M™ VHB™ Structural Glazing Tape to stress relax when a constant strain is applied to a glazing joint for example from a differential thermal expansion and contraction type stress. This unique property of a viscoelastic adhesive will act to protect the bond line interface. This property is not typical of elastic adhesives and the associated stress relaxation effect would not be expected as observed with a viscoelastic adhesive.

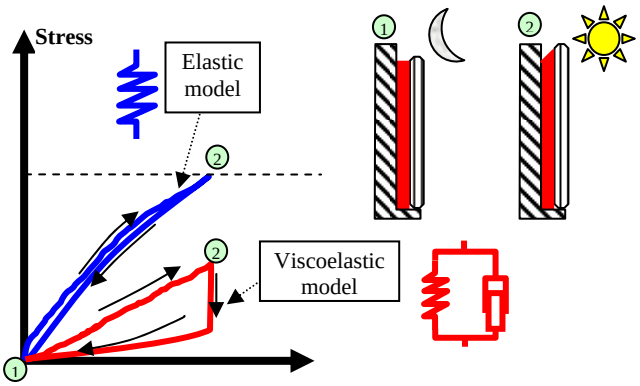

Figure 1. Typical stress vs. strain curves of elastic adhesive compared to viscoelastic adhesive for concept representation.

As stated earlier the main challenge is to find a significant characterization model for these types of adhesives and to accurately describe viscoelastic behavior. The following characteristic of viscoelastic 3M™ VHB™ Tape is used to help explain this. 3M™ VHB™ Tape will exhibit

different modulus and ultimate strength based on the rate (speed) of the applied load. This means that 3M™ VHB™ Structural Glazing Tape tested at 500 mm/min shows much higher values than when tested at a slower rate of 5 mm/min (an elastic adhesive would be relatively constant). It also must be noted that a faster strain rate is associated with a high wind event as described in a section titled "Pull Rate" by the Schmidt et al [1988] paper referenced earlier in Section 1 of this paper. Tests conducted with 3M™ VHB™ Structural Glazing Tape at various strain rates yield a logarithmic curve as described below in Fig. 2.

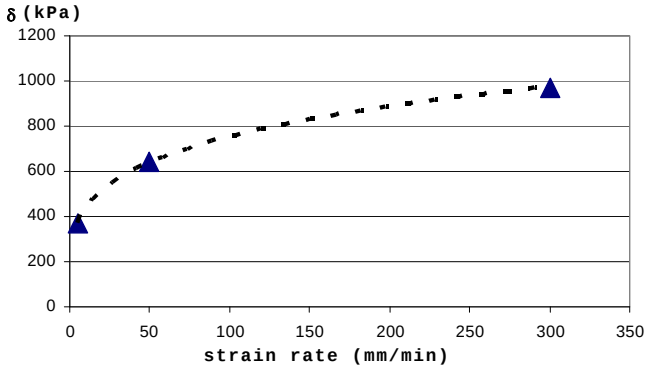

Figure 2. Ultimate stress vs. strain rate of 3M™ VHB™ Structural Glazing Tape.

Figure 2 is an accurate depiction of the viscoelastic adhesive. By using the maximum elongation (strain) for each strain rate one can then calculate the load duration. This graph is then transferred into an exponential formula. This formula is used to calculate the dynamic and the static design strength of 3M™ VHB™ Structural Glazing Tape. This characterization data confirms the currently used 3M design guideline strength values of 85 kPa for dynamic loads such as windload and 1.7 kPa for static loads such as panel bonding for curtain walls.

4 ASTM STRUCTURAL PERFORMANCE MOCK-UP TEST STUDY

The test study conducted by the CSTB demonstrates several of the material property characteristics of 3M™ VHB™ Structural Glazing Tape and the methodologies used for determining appropriate and safe design guidelines. A test study was also conducted at an accredited independent 3rd party test facility (Winwall Technology Pte Ltd - Singapore) to demonstrate the validity of these design guidelines in a real life based on ASTM mock-up tests under stresses and environmental conditions that glass panels would typically experience in a glazed curtain wall system.

This test study consisted of bonding double glazed unit glass panels (insulated glass) as well as monolithic glass panels to a typical structural glazing metal profile. A side by side comparison was conducted comparing glass panels bonded with 3M™ VHB™ Structural Glazing Tape to samples bonded with a one-part structural silicone sealant - Dow Corning® 795. The glazed panels were constructed following the respective design guidelines for both 3M™ VHB™ Structural Glazing Tape and the structural silicone sealant for a windload design pressure of 2.9 kPa. The first test sequence consisted of a polyvinyl butyral (PVB) laminated glass panel bonded with 3M™ VHB™ Structural Glazing Tape, a double glazed unit (DGU) bonded with 3M™ VHB™ Structural Glazing Tape and a DGU bonded with the structural silicone sealant.

The test protocol began with air infiltration testing according to ASTM E 283 *Standard Test Method for Determining Rate of Air Leakage Through Exterior Windows, Curtain Walls, and Doors Under Specified Pressure Differences Across the Specimen* and water penetration according to ASTM E 331 *Standard Test Method for Water Penetration of Exterior Windows, Skylights, Doors, and Curtain Walls by Uniform Static Air Pressure Difference*. Thermal cycling was also conducted for 20 cycles from -25°C to 70°C followed again by the air infiltration and water penetration test methods. After these initial tests there were no water or air leakages identified in any of the three window units. Testing then progressed with the same glazed panels

tested according to ASTM E 330 *Standard Test Method for Structural Performance of Exterior Windows, Doors, Skylights and Curtain Walls by Uniform Static Air Pressure Difference.* No failure was observed with either the 3M™ VHB™ Structural Glazing Tape glazed panels or the structural silicone sealant glazed panel in this wind load structural test at ambient as well as cold and hot temperatures (32ºC, -25ºC, and 70ºC) up to the design pressure of 2.9 kPa, corresponding to a wind speed of 250 kph (155 mph). After this, positive and negative pressures were gradually increased in 1 kPa increments up to 8.4 kPa at ambient temperature conditions. At this negative pressure point the laminated glass failed and blew out of the chamber. However, glass was still attached and bonded to the 3M™ VHB™ Structural Glazing Tape around the perimeter of the glazing frame. Testing was then stopped at this point.

A second test sequence patterned after the first test sequence was run consisting of two monolithic tempered glass lites bonded with either 3M™ VHB™ Structural Glazing Tape or the structural silicone sealant. The DGU panel bonded with 3M™ VHB™ Structural Glazing Tape was also subjected to this second test sequence after surviving the first test sequence. No failure was observed with either the 3M™ VHB™ Structural Glazing Tape glazed panels or the structural silicone sealant glazed panel in any of the tests including wind load structural tests up to a positive and negative pressure of 10 kPa which corresponds to a sustained wind speed of 467 kph (290 mph). The ability of the panels to survive pressure loads well beyond the original design pressure demonstrates the use of safety factors for both structural silicone sealant and 3M™ VHB™ Structural Glazing Tape. This testing protocol also demonstrated that no air or water leakage can be obtained with proper assembly methods. The glazed panels constructed with the acrylic foam structural glazing tape provided excellent performance overall compared to control panels glazed with a well accepted one-part structural silicone sealant. Table 6 below is a summary of this 3rd party test study.

Table 6. Summary of application specific performance tests.

Test Sequence	Test Method	Laminated Glass - 3M VHB SGT	Insulated Glass (DGU) - One Part SS	Insulated Glass (DGU) - 3M VHB SGT	8mm Tempered Glass - One Part SS	8mm Tempered Glass - 3M VHB SGT
Air Infiltration	ASTM E283 (at +0.3kPa)	No air leakage from panel	No air leakage from panel	No air leakage from panel	No air leakage from panel	No air leakage from panel
Water Penetration	ASTM E331 (at +0.72kPa)	No water leakage	No water leakage	No water leakage	No water leakage	No water leakage
Temperature Cycling	20 cycles (-25^{0}C to 70^{0}C)	For each cycle, temperature is maintained at -25^{0}C for 15 minutes and 70^{0}C for 15 minutes		Subjected to 40 cycles	For each cycle, temperature is maintained at -25^{0}C for 15 minutes and 70^{0}C for 15 minutes	
Air Infiltration	ASTM E283 (at +0.3kPa)	No air leakage from panel	No air leakage from panel	No air leakage from panel	No air leakage from panel	No air leakage from panel
Water Penetration	ASTM E331 (at +0.72kPa)	No water leakage	No water leakage	No water leakage	No water leakage	No water leakage
Windload Structural	ASTM E330 (-25^{0}C, 32^{0}C, 70^{0}C, hold for 1 minute)	+/-2.9kPa (60psf, 250kph)		+/-2.9kPa (60psf, 250kph)	+/-2.9kPa (60psf, 250kph)	
Air Infiltration	ASTM E283 (at +0.3kPa)	No air leakage from panel	No air leakage from panel	No air leakage from panel	No air leakage from panel	No air leakage from panel
Windload Structural Max.	ASTM E330 (32^{0}C, hold 10 sec)	+/- 6kPa (125psf, 360kph)	+/- 6kPa (125psf, 360kph)	+/- 8kPa (167psf, 416kph)	+/- 8kPa (167psf, 416kph)	+/- 8kPa (167psf, 416ph)
Windload Structural Destructive	Maximum Pressure (+/-)	Glass burst at -8.4kPa (175psf, 426kph)	> -8.4kPa (175psf, 426kph)	>10kPa (209psf, 465kph)	>10kPa (209psf, 465kph)	>10kPa (209psf, 465kph)

Subjected to 2x test cycles

5 DURABILITY OF 3M™ VHB™ STRUCTURAL GLAZING TAPES

The best measure of the durability of a structural silicone sealant or acrylic foam structural glazing tape is how it performs in real life applications. Structural silicone sealants have demonstrated durable performance over the last four decades when used properly in structural glazing applications. Acrylic foam structural glazing tapes such as 3M™ VHB™ Structural Glazing Tape has demonstrated durable performance since 1990 for this same application. Thus, it was appropriate to conduct an accelerated weathering study to evaluate the durability of 3M™ VHB™ Structural Glazing Tape compared to that of a two-part structural silicone sealant -Dow Corning® 983.

This test study was conducted at the 3M Weathering Resource Facility in St. Paul, Minnesota. Test samples consisted of 6 mm clear float glass bonded to black anodized aluminum with either the two-part structural silicone sealant or 3M™ VHB™ Structural Glazing Tape. These samples were then placed in a high intensity UV light chamber (Xenon Arc lamp) with cycling heat and humidity (water spray). Samples were then taken out of the chamber at various time intervals and tested for tensile strength. The maximum exposure time in this cycling chamber was 10,000 hours. Figure 3 below depicts the tensile strength retention of both the two-part structural silicone sealant and 3M™ VHB™ Structural Glazing Tape in this test study.

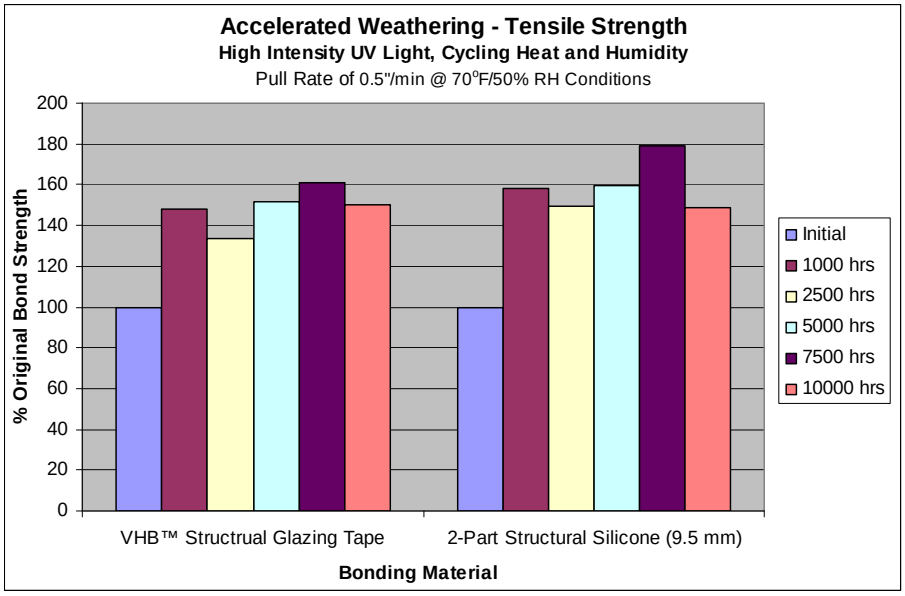

Figure 3. Tensile bond strength after accelerated weathering.

Both the two-part structural silicone sealant and the 3M™ VHB™ Structural Glazing Tape exhibit good tensile strength retention even after 10,000 hours in this harsh accelerated weathering chamber. This 10,000 hour test is a more severe UV cycling test with a higher total dose of radiation than that of the accelerated weathering tests described in both ETAG 002 and ASTM C 1184 *Standard Specification for Structural Silicone Sealants*.

6 SUMMARY

Select grades of Acrylic Foam Tapes have proven their performance and durability for structural glazing applications since 1990 as described earlier in Section 1 Introduction of this paper. While these tapes may be new to the world in some locations they have earned acceptance in the marketplace in other parts of the world and their growth continues.

The data presented in this paper demonstrates the properties, performance and durability of an Acrylic Foam Structural Glazing Tape. The contract glazer, fabricator or curtain wall designer must be sure to use only an appropriate Acrylic Foam Structural Glazing Tape if they intend to use a tape for glass bonding in structural glazing applications. It is also critical to follow the design guidelines and quality control procedures as outlined by the Acrylic Foam Structural Glazing Tape manufacturer.

The material properties of a viscoelastic Acrylic Foam Structural Glazing Tape are different than those of a structural silicone sealant. Both have demonstrated their performance in structural glazing applications for many years. The standards, codes and specifications currently written for structural glazing are focused on the properties of cold liquid applied, chemically curing elastomeric structural silicone sealants. While these documents are useful as a starting point to help characterize an Acrylic Foam Structural Glazing Tape, there exists a great need to develop appropriate standards, codes and specifications for Acrylic Foam Structural Glazing Tapes to ensure only suitable products are used for this critical application.

ACKNOWLEDGEMENTS

The authors wish to acknowledge Christophe Magniez for his work with the CSTB (France), Ken Goh for his work with the Winwall Technology Pte Ltd (Singapore) and Dick Fischer of the 3M Weathering Resource Center.

REFERENCES

EOTA 2005, ETAG 002 Guideline for European Technical Approval For Structural Sealant Glazing Kits (SSGK), Kunstlaan 40 Avenue des Arts, B, 1040 Brussels.

Schmidt, C.M., Schoenherr, W.J, Carbary, L.D., & Takish, M.S., 1989, 'Performance Properties of Silicone Structural Adhesives', ASTM STP 1054 Science and Technology of Glazing Systems, pp. 22-45, ASTM International, West Conshohocken, PA, USA.

3M Corporation, 2007, *3M™ VHB™ Structural Glazing Tapes Technical Guide*, pp. 5.

Satas, D. 1989, *Handbook of Pressure Sensitive Adhesive Technology*, Van Nostrand Reinhold, New York, pp. 2-3.

3M Corporation, 2001, *3M VHB Durability Technical Bulletin*, pp. 1.

ASTM E283-04 2004, 'Standard Test Method for Determining Rate of Air Leakage Through Exterior Windows, Curtain Walls, and Doors Under Specified Pressure Differences Across the Specimen', ASTM International, West Conshohocken, PA, USA.

ASTM E331-00 2000, 'Standard Test Method for Water Penetration of Exterior Windows, Skylights, Doors, and Curtain Walls by Uniform Static Air Pressure Difference', ASTM International, West Conshohocken, PA, USA.

ASTM E330-02 2002, 'Standard Test Method for Structural Performance of Exterior Windows, Doors, Skylights and Curtain Walls by Uniform Static Air Pressure Difference', ASTM International, West Conshohocken, PA, USA.

ASTM C1184-05 2005, 'Standard Specification for Structural Silicone Sealants', ASTM International, West Conshohocken, PA, USA.

11DBMC International Conference on Durability of Building Materials and Components
ISTANBUL, Turkey 11-14 May 2008

Non-Destructive Testing of Elastomeric Joint Sealants in Construction

Huff, Daniel N. [1]

T 14

ABSTRACT

Durability of buildings depends on adequate testing and quality assurance programs during construction. Lack of good testing during construction can result in construction defects. In the United States, construction lawsuits have become so costly that construction insurance in now one of the largest costs of doing business for contractors.

This is particularly true in the field of leaking buildings and toxic mold related lawsuits. For that reason, the author has spent the past 7 years in research and development of a comprehensive 100% capable non-destructive method and device for evaluating weather seal sealants. Recently, the author has developed a similar test system that can be used on SSG (Silicone Structurally Glazed) sealants as well.

This paper is focused on the use of non-destructive Quality Assurance systems for sealants in construction that can perform at the rate of 100% if necessary. The current industry standards call for testing of these sealants at the rate of one destructive "pull test" per 1000 lineal feet [305 m]. It is the belief of the author that this standard is woefully short of the needs of the industry. On one project alone, where the author was able to conduct 100% testing, it was discovered that a 0.2% failure rate of the weather seal resulted in over 400 potential leaks on the 227,000 square foot [69,190 m] building, in 35,000 lineal feet [10,668 m] of wall sealant. Statistics related to perfect versus real life application of sealants are also discussed in this paper. ASTM C1521 is cited as a new approach to seal and sealant testing.

KEYWORDS

Sealants, Non-destructive testing, ASTM C1521.

[1] Daniel Huff, 4915 Swegle Road NE #18, Salem, Oregon USA 97301, +1 503 910 0968.

1 INTRODUCTION

Imagine that you belong to a family that suffers from a genetic flaw that can cause serious health problems. However, your doctor has good news; a test exists to find out if you have any of the health problems associated with the gene. After the test, you will be issued a report of the test results. The problem is that the test is only accurate from between one chance in 4,000, and one chance in 192,000, depending on how you figure the odds.

Now imagine that you are a sealant installer on a construction project that relies on sealants for weatherproofing or safety. A manufacturer's sealant warranty can be obtained if certain project specific tests for substrate compatibility, primer requirements, and field adhesion are performed. An official report follows each test, proving your due diligence. Unfortunately, the odds of finding a seal continuity problem using the industry standard field test is between one in 4,000, and one in 192,000, depending on how you figure the odds. Later, when the building leaks or glass is dislodged, you find yourself in the position of trying to defend your installation with test reports, but you are told that the problems are caused by installation error.

This paper focuses on adhesion field-testing of construction sealants. This is because durable and functional building facades using construction sealants in critical areas require continuous adhesion of the sealant in all joints at all locations.

2 INCONVENIENT STATISTICS

Dr. Joseph Lstiburek,a principle of Building Science Consulting stated: *"It may be possible to install sealant in one joint perfectly –but how about installing sealant perfectly in 10 joints? Now how about 100 joints? Recall, that the joints must be perfectly prepared and installed. How about 1,000 perfect joints? Or 10,000 perfect joints? To put this into perspective, there are more than 1,000 sealant joints per building in most commercial buildings. Many of the joints leak from day one. More joints leak as the building ages."* [Lstiburek 2007].

An associate of the author, a principle of Morrison Hershfield, Ltd., Canada, & Morrison Hershfield Inc., USA, made the following comment when presented with some of the data included in this paper: *"Even with above average workmanship, there will always be a failure rate. Even if sealant joints on any given project are as good as 99.5% successful (an extraordinary achievement in any human endeavour), the remaining 0.5% can cause significant damage. Submarines have bilge pumps to catch the leaks from the 0.5%. There needs to be a second line of defence. Nothing we do is perfect enough to rely on a sealant joint 100% of the time, and in my opinion, this is a foolhardy approach to building design"* [Gallant 2005].

The average commercial building in the United States contains about 35,000 lineal feet [10,668 m] of sealant, or 6.62 miles [10.7 km]. With volumes of face-sealed joints this high, a very small failure rate can result in significant trouble for the building.

In 2002, the American Society for Testing and Materials (ASTM) Committee C24 ("Building Seals and Sealants") adopted a new Field Practice C1521 ("Standard Practice for Evaluating Adhesion of Installed Weatherproofing Sealant Joints") that codified several testing procedures that were already considered industry standards [ASTM 2002]. These procedures include the destructive tail and flap "pull tests", a water immersion procedure, and a non-destructive joint probe procedure that uses a blunt instrument to induce strain to the bond line of the sealant.

The frequency of the destructive pull testing recommended by ASTM is one test per 100 lineal feet [30.48 m] for the first 1000 feet [304.8 m], and one test for every 1000 lineal feet thereafter. This is the recommended test procedure by all of the major sealant manufacturers worldwide. Most

manufacturers recommend cutting a 3-inch tab into the sealant bead, and then pulling the tab either to an elongation percentage keyed to the movement capabilities of the particular sealant, or to cohesive failure [Dow Corning 2007].

Assuming that the full 3 inches qualify as the test parameters, the odds of finding continuity problems in the sealant installation is 4,000 to 1. In actuality, the true test is taking place at the interface of the tab to the sealant at the bottom of the tab in perhaps 1.6 mm [1/16"]. This means that the true statistical odds of finding a continuity problem in the sealant joint with this test is closer to approximately 192,000 to 1. Even at the once every 100 feet frequency (impractical, material waste, costly), the odds of finding a problem is 19,200 to 1.

The destructive testing procedure is concerned with, A) the quality of the sealant, and B) whether or not it is able to adhere to the substrate. It is a sealant material Quality Assurance process, not a seal continuity Quality Assurance process.

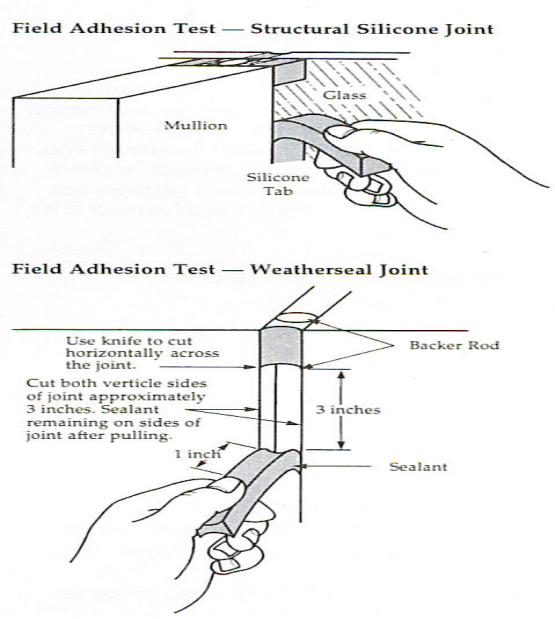

Figure 1. These are depictions of the hand pull test recommended by sealant manufacturers as a standard Quality Assurance program for sealant adhesion for weather seals and SSG. Frequency of the test as recommended by manufacturers varies, but the ASTM recommendation in C1521 is one test per 100 lineal feet [30.5 m] for the first 1000 lineal feet [304.8 m] tested, and one test per 1000 feet thereafter.

3 CONTINUOUS TESTING USING A ROLLING DEVICE – TRUE CONTINUITY QUALITY ASSURANCE

In the ASTM document C1521, a non-destructive procedure is outlined that offers an alternative to the pull test. It suggests that the evaluator subject the sealant bead to pressure with a blunt probe. The objective is to strain the sealant bead inducing stress on the sealant bond line in order to reveal failed or poor adhesion. Put simply, one pokes the sealant with a blunt instrument, with a goal of depressing the bead 50% of its movement capability.

For the reasons discussed above, some Building Enclosure Professionals have been using simple rolling devices such as a window screen roller or a "backer rod placement device" to affect the non-destructive procedure mentioned above. Notably, David Nicastro, principle with Engineering Diagnostics, Inc. and the former chair of ASTM Committee C24, and Patrick Gorman of Gorman

Moisture Control and former Vice Chair of C24 have been using the screen roller approach for a number of years. Currently, C24 has taken under consideration adding rolling devices as a test option. This will be in addition to the "blunt instrument" in the current C1521 Non-Destructive test protocol. The advantage of being able to determine the relative condition of a sealant joint using this approach is obvious – a 100% evaluation of the sealant is now possible.

The problem with any of the un-controlled rolling devices is that they generate non-reproducible subjective test data. For that reason, the author embarked several years ago on a quest for a scientific, objective approach to this idea by creating an adjustable, controlled, and calibratable device.

4 DESCRIPTION OF CONTROLLED CALIBRATED CONSTANT PRESSURE DEVICE

The device is a hand held instrument able to exert pressure in a controlled manner to the sealant joint. Extending from the housing at the front of the device is an armature with a roller at the tip. Behind the armature is a piston charged with compressed gas delivered from a pressurized tank. The amount of pressure behind the piston translates directly into the amount of force that is applied to a surface to which the roller probe is engaged. The amount of gas pressure delivered from the pressurized tank is adjusted with a regulator. Pressure within the device and behind the piston is monitored from a gauge visible on the control box. Within the pressure control box the gas is manipulated in such a way that the pressure is constant within the entire stroke of the piston in the hand held portion of the device. Pressure in the apparatus as derived from the gas source resulting in strain at the probe contact point is maintained if the armature is somewhere within the stroke of the piston. The operator pushing in or pulling away from the joint with the device during operation cannot alter the pressure at the probe contact point. This means that the pressure that the test probe exerts on the sealant remains constant. To maintain constant pressure, the piston must simply be kept within its' 3-inch [7.6cm] stroke range.

Using this device, accurately applied pressure to the joint is not dependant on adjacent surfaces (as in the case of a backer rod placement style device) or the judgment of the user (as in the case of a screen roller or similar device) when testing. The result is a reproducible and objective evaluation system. The user simply dials up the predetermined pressure for the device to operate on and then lets the device do the rest. A predetermined pressure is set for the specific sealant through calibration of the device.

Figure 2. The picture is a depiction of the pressure-controlled as discussed in this paper.

Calibration of the device is aimed at a 50% elongation of the sealant based on the sealant movement capability, following the guideline for the non-destructive procedure found in ASTM C1521. The calibration numbers used in the field are an average based on the particular sealant and the average joint width on the building. If the test practitioner wishes to, adjustments for joint width changes can

be made as often as is necessary, but as a practical matter, using an average pressure is more efficient. When testing organic sealants, it is important to consider temperature changes. Reporting all of the pressures used is important for the archive in order for future reproducibility.

To obtain calibration data, sealant calibration specimens are constructed in three rectangular joint configurations held within a rigid metal grid. Joint configurations are constructed as follows:

- [12.70 mm by 6.35 mm] 500 mil by 250 mils
- [19.05 mm by 9.52 mm] 750 mil by 375 mils
- [25.4 mm by 12.70 mm] 1000 mil by 500 mils

Each specimen is approximately 508 mm (20 inches). Various colors are used in order to factor batching and pigmentation (during the initial 6-month calibration study, pigmentation was discovered to have a slight but detectable effect on sealant movement capability). Movement dial indicators are spaced evenly along the underside of the specimen in order to record the deflection created during a pass of the roller through the sealant on the topside. Differing pressures are used to strain each specimen. A significant number of passes with the roller probe are completed and the deflections recorded. The information is reduced and translated into "target deflections". These target deflections are a percentage of elongation as defined by the specific sealants' movement capability. For example, a target of 50% elongation in a 50% movement capability sealant in a 1 inch (25.4 mm] wide joint would be ¼ inch (6.35 mm) deflection. The result of this process is sealant specific calibrations chart such as is depicted in the example below (Table 1). The table describes the calibration of sealant #1, average Shore "A" Durometer Hardness 28, movement capability ± 50%. Numbers following targets are calibration numbers for the device as a percentage of available force in the control box.

Table 1. Calibration of Sealant #1.

Joint:	Target Deflection:	50%	75%	100%
500 by 250mil (12.70 by 6.35 mm):		40	55	73
750 by 375mil (19.05 by 9.52 mm):		32	51	68
1000 by 500 mil (25.4 by 12.7 mm):		26	43	62

5 STATISTICS FROM FIELD USE

Experience using this device in the field has demonstrated that if at least 5% to 10% of a building is sampled, and the sampling is conducted in a thoughtful scientific manner, the results are usually representative of the entire sealant installation.

For example, on an 11-story building, with 24 grid locations for suspended scaffolding, two grids were sampled. This represented an 8.3% sampling rate. Found were 14 adhesion failures on 1 grid section, and 20 on the other, for an average of 17 failures per grid section. From this sample, it was predicted that 408 failures would be found on the entire building. 427 adhesive failures were uncovered during the ultimate 100% evaluation process. This means that sampling has a solid basis for obtaining a realistic view of the sealant installation on a building.

Figure 3. This is an example of the type of "invisible" seal failure uncovered by using the non-destructive method and device described elsewhere in the paper. Prior to finding this seal breach, the entire sealant bead depicted looked exactly like the area above and below the breach.

What did we learn from sealant testing at the rate of 100%? In the case cited above, the failure rate was a mere 0.2%. Yet it resulted in 427 breaches in the building seal. This demonstrates that a very low failure rate can pose a significant potential problem for a building simply because the volume of sealant used is typically a large number. A 99.8% successful installation is not a bad job, and as Mr. Gallant suggested, a 99.5% rate of success is all one could ever hope for in a "human endeavour".

On one project, a twin 18 story condominium in Long Beach, California, we found a 5.6% failure rate in the Exterior Insulation and Finish System. We started with a 1% sample, and then sampled 5%, then 10%. What was significant is that the failure rate remained constant despite the sample size. This has been a consistent finding on all of the projects where this system has been used. As a result, we recommend that sampling be conducted at a minimum rate of 5% to a maximum of 10% prior to 100% testing as a way of determining the severity of the problem and determining the reasons for the failures. This can also provide the practitioner information for establishing a protocol for using the test system as a repair program. The failed samples should be removed for analysis. This will reveal the reasons for the failure, most often from contaminated substrates, but in some cases, laboratory analysis is appropriate. We have also found that when full scale testing is undertaken, it is often cost effective to coordinate the testing with a contractor able to implement repairs. After the repairs are made, a 10% re-sample is useful in confirming the success of the test and repair program.

The information in Table 1 provides basic statistics obtained during a 100% sealant evaluation of the newly constructed building (specimen A) using the pressure controlled and calibrated device and used in accordance with the principles of the non-destructive test protocol outlined in ASTM C1521 [ASTM 2002a].

Table 2. Statistics Generated from Sealant Testing (Specimen A).

Number of Lineal Feet of Sealant:	35,000 feet [10,668m]
Number of Adhesive Failures:	427
Average Length of Failure:	two inches [50.8mm]
Failure Rate in Lineal feet:	one in 82 feet [25m]
Total Lineal feet of Sealant Failure:	71 feet [21.6m]
Percentage Rate of Sealant Failure:	**.2% Failure**
Percentage Rate of Sealant Success:	**99.8% Success**

The author is currently involved in an adaptation of the non-destructive testing technology described in this paper for use in evaluating Silicone Structural Glazing (SSG). This new test system is designed for non-compressible sealant joints and gaskets.

6 CONCLUSIONS

The future of field-testing of sealants should therefore necessarily include non-destructive procedures that have the ability to test 100% of sealant joints. Continuous testing using rolling devices have been demonstrated to be a good choice. The program should have a goal of finding the seal breaches and simultaneously repairing them immediately. This approach to building seal verification has the potential to save many dollars in building maintenance, litigation, health care costs, insurance, and owner borne construction costs, to name a few. In the case of SSG applications, life safety issues are involved. Improved testing technology can provide all concerned with a new level of confidence that durable building seals and structural silicone glazing adhesives can be realized. The question now is not whether we have methods and technology to accomplish durability of construction, the question is whether we have the will to use it.

REFERENCES

ASTM C1521-02, 2002a, 'Field Practice for Evaluating Adhesion of Installed Weatherproofing Sealant Joints'.

Dow Corning Corporation, 2007, 'Contractors Guide'.

Huff, D. 2003, 'Non-Destructive Testing of Installed Weatherproofing Sealant Joints' ASTM STP 1453, pp. 335 – 345, certain sections reprinted, with permission, copyright ASTM International, 100 Barr Harbor Drive, West Conshohocken, PA 19428."

Huff, D. 2005, 'Non-destructive Testing of Installed Weatherproofing Sealant Joints – Questions and Answers', ASTM STP 1488, certain sections reprinted, with permission, copyright ASTM International, 100 Barr Harbor Drive, West Conshohocken, PA 19428."

Lstiburek, J. 2007, 'EIFS – Problems and Solutions', Building Digest 146.

11DBMC International Conference on Durability of Building Materials and Components
ISTANBUL, Turkey 11-14 May 2008

The Sandstone Conundrum

Edward Gerns [1]
Rachel Will [2]

T 15

ABSTRACT

In the Midwestern United States, the use of Lake Superior sandstone was very popular at the end of the 19th Century. The rich red color and ease of workability resulted in many architects, owners and builders choosing Lake Superior sandstone as a cladding material. While the stone was quite attractive, the physical characteristics of the stone, as well as quarring methods, have resulted in numerous and dramatic failures. Severe erosion and delamination of the bedding planes became a widespread problem beginning in many instances as early as the beginning of the 20th Century.

This paper will be divided into two parts. The first will discuss the physical characteristics of sandstone in general and specifically Lake Superior sandstone. This will include a discussion of deterioration mechanisms and repair techniques which have been implemented or proposed in an attempt to maintain the original material as well as the desired aesthetics. These include chemical treatments, patching, pinning, selective replacement, substitute materials and alternate stone materials.

The second part of the paper will present a case study of a residence in Chicago and the approaches considered and finally implemented to address severe deterioration of the stone. The residence provides a dramatic example of previous unsuccessful repairs and the process of developing a new facade system which was sensitive to the original design intent while employing more durable materials. The process of the facade reconstruction will be discussed from investigation of the existing conditions, alternative approaches considered, design development and installation of the new cladding system.

KEYWORDS

Sandstone, Facade, Recladding

[1] Consultant, Wiss, Janney, Elstner Associates, Inc., Chicago, Illinois, Phone 312-372-0555, Fax 312-372-0873, egerns@wje.com
[2] Associate II, Wiss, Janney, Elstner Associates, Inc., Chicago, Illinois, Phone 312-372-0555, Fax 312-372-0873, rwill@wje.com

1 INTRODUCTION

Like many cities, Chicago experienced dramatic changes in the later part of the 19th Century. Following the Great Fire of 1871, Chicago experienced significant population growth becoming the second largest city in the United States by 1900. The fire had virutally cleared the slate for the introduction of new building technologies and styles. Residential construction, in what is now known as the Gold Coast area of Chicago, began shortly after the fire as the city center continued to expand. In response to the fire, numerous changes in construction practices and building codes were introduced to reduce the risk of fire. Residential construction never fully embranced the notion of fireproof construction largly because of economics, as well as, the scale of the structures. In Chicago, lots sizes ranged between 8 and 10 m wide and between 40 m and 60 m deep. As a result, row houses were a popular residential form borrowed from European archetypes. The row houses in Chicago typically had a highly adorned main facade facing the street and, where exposed, the remaining utilitarian load bearing facades were monolithic multi-wythe common brick walls. In the midwestern United States, decorative residential cladding materials of the time included stone, brick and terra cotta. Of these materials, stone was the most desirable and therefore many of the most prestigious residences of the late 19th century incorporated facades of richly carved limestone, granite and sandstone ornament. The main facades were typically monolithic walls with the decorative outer wythe of masonry and a multi-wythe clay brick backup wall. Floor and roof systems were typically wood joists spanning parellel to the main facade.

2 LAKE SUPERIOR SANDSTONE

Sandstone is a sedimentary stone consisting of deposits of sediment materials in prehistoric river and lake beds. The sediment is the result of the decomposition and erosion of other rocks, minerals and organic matter which are bonded together through compaction and naturally created cementitious products. The cementing material can consist of silica, calcarious materials, iron oxide or clay and generally determine the color of the stone [Merrill 1889]. Distinct bedding planes between individual layers of material and grain size characterize sedimentary stone. Lake Superior sandstones, generally classified as a ferruginous sandstones [Ashurst 1990], compositionally vary depending on the specific formation of the region, but generally are composed of quartz cemented with iron oxide, calcite, authigenic quartz or silica [Ekert 2000].

The durability of sandstone is generally dependant on exposure, water shedding details, orientation of the bedding planes as well as the cementing agents which hold the quartz grains together. Natural weathering will erode the surface of the stone through continued cycles of rain and freeze thaw deterioration will breakdown the cement bond over time. The rate of deterioration changed as a result environmental changes of the 19th and 20th centuries with increasing concentrations of carbon dioxide, sulfates and nitrates in the air. If the particles of the stone are held together by calcareous materials, the bond is easily broken by the polutants present in acid rain [Warland 2006].

3 LAKE SUPERIOR SANDSTONE IN CHICAGO

Lake Superior sandstone was first used as a building material in Chicago just prior to the Great Fire of 1871. At the time, Lake Superior sandstone was touted to resist the detrimental effects of fire when compared with other contemporary stones. As a result, it gained great popularity throughout the city as a durable, fireproof, decorative and coveted building material. In the wake of the Chicago fire, builders and architects sought durability above all else in materials, as evidenced by the Tribune Building constructed in 1872 by Burling and Adler as the first Tribune Company Building, constructed of Niagara limestone and cast iron had been destroyed by the 1871 fire [Eckert 2000].

Lake Superior sandstone, while not indigenous to the region of Chicago, was made more readily available through the canal system and more so with the introduction of the Chicago, St. Paul Minneapolis, and Omaha Railroad in 1883 [Chicago Tribune 1873].

The Boyce Block (now demolished), located at the corner of Madison and State streets was partially finished at the time of the fire which led to the many conclusions about the durability of the stone in relation to fire. It was touted as one of the best examples displaying the texture and building capacities of Lake Superior sandstone [Chicago Tribune 1871]. The Masonic Temple on Forrest Avenue between 32nd and 33rd Streets also illustrates the splendor of this material, thus indicating this material was not primarily limited to commercial, residential or religious structures.

Prestige and regard for Lake Superior sandstone were also gained through the opinions of architects in Detroit, Chicago and Cleveland on the value of Lake Superior sandstone. Cudell and Blumenthal of Chicago, architects of the Cyrus McCormick House, spoke highly of the stone, as described below:

> Having used [Marquette brownstone/Lake Superior sandstone] to a considerable extent, we consider it an excellent building stone, especially adapted to elegant residences and structures where its beautiful color appears to an advantage. This latter feature must ever secure it favor with the true artist, being rich and warm, and suggestive of vitality. As a working material, it is all the artist can desire, being soft and tenacious, thus enabling the stonecutter to cut and carve the most elaborate and intricate designs of the architect…[Eckert 2000]

The beauty, warmth, sculptural qualities and perceived durability of Lake Superior sandstone caught the attention of many architects, builders and wealthy residential commissioners. Among the costly residences constructed of Lake Superior sandstone are the Hough House on Prairie Avenue, the W.M. Crilley House on Michigan Avenue, the Cyrus McCormick House [Eckert 2000], the Crane House on Wabash Avenue, the Boughton House on Indiana Avenue, the Boyington House on Indiana Avenue, the Henry Furst House (one of the early distributors of Lake Superior sandstone) and the Potter Palmer House [Chicago Tribune 1871]. Unfortunately many of these structures have not survived, for various reasons, one being the extensive deterioration of Lake Superior sandstone.

4 REPAIR APPROACHES

Several options exist to address deterioration of sandstone. These range from topical application of chemicals to complete replacement. When considering replacement materials given the poor performance characteristics of Lake Superior sandstone, a cursory review of the various preservation philosophies is worth considering. The Secretary of Interior's Standards for Rehabilitation stresses matching and blending replacement materials with the adjacent original material:

> *Deteriorated architectural features shall be repaired rather than replaced, wherever possible. In the event replacement is necessary, the new material should match the materials being replaced in composition, design, color, texture and other visible qualities.* [NPS 1992]

This contrasts to Venice Charter which states:

> *Replacements of missing parts must integrate harmoniously with the whole, but at the same time must be distinguishable from the original so that restoration does not falsify the artistic or historic evidence.* [US/ICOMOS 1992]

In many instances, the state of extreme deterioration of the stone results in having to reconsider traditional preservation approaches. "Preservation is defined as the act or process of applying measures necessary to sustain the existing form, integrity, and materials of an historic property." [NPS 1992]. Preservation respects the historic material and enables the structure to continue to age. "Rehabilitation is defined as the act or process of making possible a compatible use for a property

through repair, alterations, and additions while preserving those portions or features which convey its historical, cultural, or architectural values." [NPS 1992]. Both of these approaches were can be unrealistic given the extreme state of deterioration that many Lake Superior sandstone facades experience. "Reconstruction is defined as the act or process of depicting, by means of new construction, the form, features, and detailing of a non-surviving site, landscape, building, structure, or object for the purpose of replicating its appearance at a specific period of time and in its historic location." [NPS 1992]. Reconstruction effectively eliminates the original time line and introduces a completely new element which is a gesture to a past element [Murtagh 1997]. This is generally considered the approach of last resort due to loss of original fabric as well as economics.

4.1 Chemical Treatments

Chemical treatments are divided into four main groups, according to their composition. These groups are inorganic materials, alkoxysilanes, synthetic polymers, and resins. These products are generally inexpensive to apply, but require extensive testing and evaluation to determine if they are appropriate and effective treatments. Even if effective, chemical treatments do not reverse the loss of detail of the ornamant due to erosion and freeze thaw damage.

Inorganic stone consolidants were extensively used during the 19th century and are still being used. Most inorganic consolidants produce an insoluble phase within the voids and pores of a stone, either by precipitation of a salt or by chemical reactions with the stone. It has been rationalized that the development of a new matrix similar in composition to the matrix of a stone will bind together the particles of deteriorated stone. Little success has been achieved in consolidating stone with inorganic materials, and in some cases their use has greatly accelerated stone decay. Among the problems are formation of a shallow and hard crust, the formation of soluble salts as reaction by-products, the growth of precipitated crystals, and the inability of some of them to bind stone particles together.

Alkoxysilanes are being highly regarded because of their ability to penetrate deeply into porous stone and polymerization can be delayed until deep penetration has been achieved. In addition, the polymerize produces materials similar to the binder in siliceous sandstone [Clifton, 2007].

Two general types of polymer systems are used to treat stone. In the first, monomeric molecules are first polymerized, dissolved in appropriate solvents, and then applied to stone. They are deposited within the voids and pores of the stone as the solvent evaporates. The second type is monomeric molecules, either pure or dissolved in a solvent, which are polymerized within the voids and pores of a stone [Clifton, 2007].

Resins have been applied to stone for over 2,000 years. Resins are effective in increasing the water repellency of stone. Many other water repellents of various more complex compositions have been developed and employed in attempt to reduce water absorption and subsequent deterioration.

4.2 Patching

Various proprietary patching materials are commercially available. These products combine various polymers in a cement-based blend of select graded aggregates, additives fillers and pigments.

Patches are installed by first removing all deteriorated areas of stone to solid stone substrate which will receive the patch material. Depending on the depth of the patch, anchors may be installed to provide a mechanical connection of the patch to the substrate. Another approach is to install screws that project to within about 1 cm of the finished surface and installing a net of corrosion resistant wire to provide mechanical bond for the patch.

4.3 Selective Replacement

Performance characteristics of the original sandstone may make retaining replacement material very difficult. The appropriateness of installing a less durable material is philosophically not appropriate in

most instances. If only limited units required replacement, salvaging, harvesting and recycled material could be considered.

Appropriate substitute materials, depending on the extent of replacement required, could include terra cotta, limestone and alternative sources of sandstone. Each option offers advantages and disadvantages both economically and philosophically as will be discussed in the case study presented.

5 CASE STUDY

The project presented in this case study is representative of the issue currently being addressed by owners of sandstone buildings. The three story residence was constructed in the 1880s. The west facade fronts the street and is clad almost entirely with Lake Superior sandstone except for areas of ornament at the roof level which is composed of terra cotta units. The east, north and south facades are mostly concealed by adjacent buildings with the exposed areas clad with Chicago common brick.

Figure 1. Representative example of previous repair which has subsequently failed and face bed unit.

The sandstone units were installed with a multi-wythe common brick backup wall varying between two and four wythes. Galvanized metal ties were installed into the backup wall and engage the bed joints of the sandstone. The sandstone units varied in thickness between 10 cm and 40 cm.

Deterioration of the sandstone has been an ongoing issue with many buildings in the area. Ongoing deterioration was the result of prolonged exposure to rain and erosion of the binders between the sand particles. Several of the units also appear to have been face bedded. Deterioration was further exacerbated by the physical characteristics of Lake Superior sandstone which contains shale and clay within some of the bedding planes as well as susceptibility of face bedded units to rapid failure.

In the 1990s, a repair campaign was undertaken which included the removal of deteriorated and delaminated areas of sandstone. A proprietary cementitious patching material was used to reform the areas which had been severely eroded. The depth of deterioration in many instances exceeded 4 cm with significant loss of carved detail. The patch material was installed over a stainless steel wire mesh that was fastened to self drilling-self tapping fasteners driven into sound substrate as shown in Figure 1. Massive failure of the repairs by 2005 prompted the owner to seek alternative repair approaches. Deficiencies in the patch material included fading of the color and bond failure at the interface of the material and the substrate.

A survey of the facade revealed that more than 75 percent of the units had been previously patched. In many instances the entire exposed surface was composed patch material. The majority of units which had not been previously patched were ashlar units or units which were protected by water tables or drip courses.

The owner had retained a masonry restoration contractor that recommended another campaign of patching be considered. The authors were retained by the owner to provide a second opinion regarding possible repair approaches. The owner expressed the desire to comprehensively restore the facade and achieve a very durable restoration. Several alternatives were presented for consideration which while being more expensive would provide the 75 year restoration that the owner had requested. It was the author's opinion that a restoration which included patching and limited repair could potentially achieve the owner's goals, but the patches would likely not last more than 10 to 15 years regardless of the quality of the installation. Further, availability of replacement Lake Superior sandstone is very limited since most of the quarries have been long closed. Given the poor performance history of the material, the wide spread installation of a poor quality material was not an appropriate approach for the restoration. Alternative cladding materials were considered included terra cotta, limestone and other sandstones.

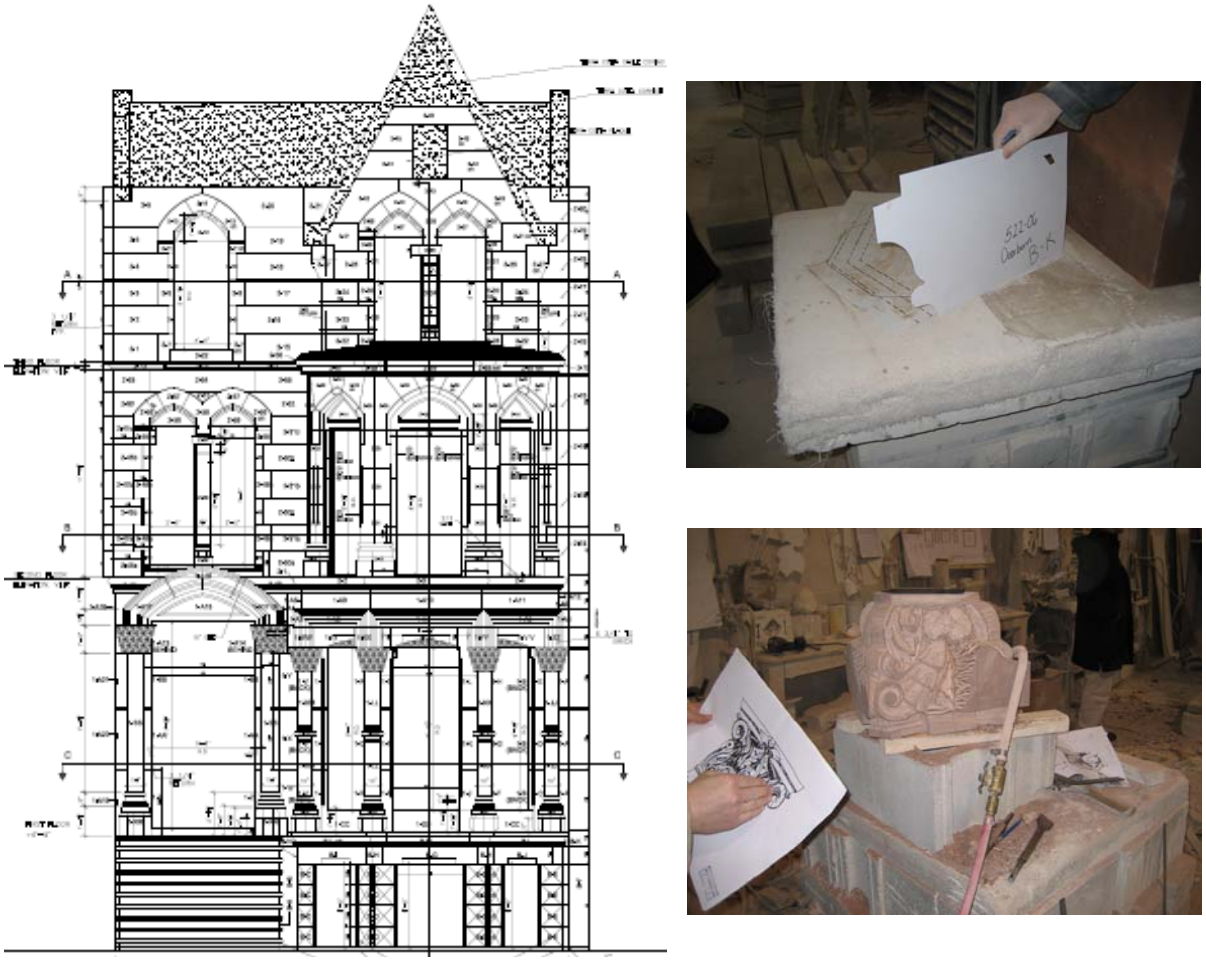

Figure 2. Shop drawing and stone fabrication process

Terra cotta was deemed an appropriate substitute material if the replacement units could be grouped to maintain a cohesive appearance. Regardless of the skill of the glaze formulation, the ability to match the sandstone was recognized to be limited. Had the severely deteriorated units been limited to the column capitals, water tables and window surrounds, terra cotta may have been appropriate. The extent of deterioration however would result in limited areas of sandstone and large areas of terra cotta.

A very common and economical replacement cladding material in the Midwest United States is Indiana limestone which has a long history of successful applications. The obvious drawback of Indiana limestone is the uniform gray color. Staining the limestone, to match the sandstone, was considered, but matching the color and the long term stability of the stain was difficult to accurately predict to achieve the desired 75 year service life.

Another option considered was using red sandstone which was more durable than Lake Superior sandstone. Like Indiana limestone, the sandstone would be closer in color, but would not match the texture and hue of the original material.

Ultimately, the owner opted to entirely reclad the main facade of the building using an alternative red sandstone; St. Bees Red sandstone, which is quarried in England. The new sandstone had excellent physical characteristics and the color and texture were similar to Lake Superior sandstone. Due to the quantity of feldspar, St. Bees is described as sub-arkose, a well consolidated medium grained sandstone primarily consisting of quartz (80 percent), alkali feldspar (10 percent), chert (3 percent), muscovite (1 percent) and a matrix of approximately 5 percent clay.

A detailed survey of each unit on the building was performed by the stone fabricator, masonry contractor and owner. Material was shipped from England to Toronto Canada where it was cut, caved and sculpted to match the original units as shown in Figure 2.

Figure 3. Representative example of new sandstone installation.

A systematic cataloging approach for removing the original units, taking necessary and appropriate dimensions and stockpiling the units was employed by the masonry contractor. The original galvanized ties were cut flush with the brick backup wall and open joints in the backup wall were repointed.

During the fabrication process, a temporary enclosure was installed to allow the residence to remain in use during the recladding. Pipe scaffolding had been in place and remained in place as further protection for the interior.

During the installation of the new sandstone, limited areas of the backup had to be modified to accommodate the new sandstone units. In general, a minimum of two wythes of the backup wall existed, but in many areas as many as four wythes existed. To accommodate some of the larger units, some of the backup wythes were removed. New sandstone units were installed using stainless steel lateral anchors which were fastened using stainless steel straps into the repaired backup wall as shown in Figure 3.

Installation of the stone offered several challenges for the fabricator and contractor. Though durable, the new sandstone was very soft and easily damaged during handling. To minimize damage during shipping, units were carefully packaged together or in some instances individually packaged and shipped. Units ranged in size and weight. Smaller units were set by hand. Several of the lintel units over the windows weighed in excess of 500 kg and had to be set using a combination of Lewis pins, chain falls and extreme care.

6 CONCLUSION

While good preservation philosophy stresses repairing, restoring and conserving orignal building fabric whenever possible, in some instances these approaches may be impractical. While Lake Superior sandstone is a beautiful building material, it does not offer good long term performance. Depending on the condition of the material and when treatment programs are initiated, complete replacement can be avoided.

REFERENCES

Ashurst, John& Francis Dimes, 1990, *Conservation of Building and Decorative Stone*, Hartnolls Ltd, Cornwall, pp 61-62.

Chicago Tribune 1873, *The Upper Peninsula*; March 20, 1873, ProQuest Historical Newspapers.

Chicago Tribune 1871, *Building Materials*; Dec. 2, 1871, ProQuest Historical Newspapers.

Bishop Eckert, Kathryn 2000, *The Sandstone Architecture of the Lake Superior Region*. Wayne State University Press, p. 22 and p. 58-59.

National Park Service 1992: Secretary of Interiors Standards for the Treatment of Historic Properties; Introduction: Choose an Appropriate Treatment for the Historic Building.
http://www.cr.nps.gov/hps/tps/standguide/overview/choose_treat.htm [Accessed 22 February 2005]

Merrill, George 1889, *The Collection of Building and Ornamental Stones in the U.S. National Museum: A Handbook and Catalogue*, Smithsonian Institute, p. 443.

Murtagh, William 1997, *Keeping Time: The History and Theory of Preservation in America*, John Wiley & Sons, New York, pp. 184-188.

Search Conservation Online: Clifton, James R., *Stone Consolidating Materials: A Status Report*
http://palimpsest.stanford.edu/search.html

US/ICOMOS Scientific Journal, Volume 1, Number 1, 1999, ICOMOS Charters and Other International Doctrinal Documents, pp. 7-8 (Charter of Venice).
Warland, Edmund 2006, *Modern Practical Masonry*, Donhead Publishing Ltd, London, p. 127.

11DBMC International Conference on Durability of Building Materials and Components
ISTANBUL, Turkey 11-14 May 2008

The Perception of Small Scale Damage and Repairs of Natural Stone

Wido Quist [1]
Rob van Hees [2]
Silvia Naldin [3]
Timo Nijland [4]

T 15

ABSTRACT

By means of a questionnaire a study was carried out to investigate the perception of small scale damage and repairs of natural stone used in buildings. Participants were asked to evaluate damage to natural stone shown on pictures. They were also asked to give their opinion on interventions needed to preserve or restore the material. Significant differences can be found between specialists and non-specialists in conservation.

Respondents consider some cases as "damage" situations, even though no intervention is deemed as necessary, as if damage was a sort of natural weathering, thus to be expected and accepted. In other cases, also defined as "'damage" situations, interventions are considered necessary. This seems to imply the use of a different criterion to define "damage", maybe including the expected risks related to its development. This study contributes to the definition of damage, and to a better understanding of the criteria used by different people to decide on the need of interventions.

KEYWORDS

Perception, Conservation, Damage, Natural Stone, Intervention.

[1] Delft University of Technology, Faculty of Architecture, Department of Building Conservation. P.O. Box 5043, 2600 GA Delft, The Netherlands, Phone +31 15 2788496, Fax +31 (0)15 2781028, w.j.quist@tudelft.nl
[2] Delft University of Technology, Faculty of Architecture, Department of Building Conservation. P.O. Box 5043, 2600 GA Delft, The Netherlands, Phone +31 15 2784153, Fax +31 (0)15 2781028, r.p.j.vanhees@tudelft.nl
[3] Delft University of Technology, Faculty of Architecture, Department of Building Conservation. P.O. Box 5043, 2600 GA Delft, The Netherlands, Phone +31 15 2784133, Fax +31 (0)15 2781028, s.naldini@planet.nl
[4] TNO Built Environment and Geosciences, Department of Structures and Safety, P.O. Box 49, 2600 AA Delft, The Netherlands, Phone +31 15 2763219, Fax +31 15 2763018, timo.nijland@tno.nl

1 INTRODUCTION

Decisions about the conservation of monuments often depend on different technical considerations, such as the acute need of preservation, material properties or arguments regarding the artistic value of the object. It includes sometimes a reconstruction, and in practice, non-technical arguments relating to public appreciation, tourist concerns, or even political purposes [e.g., Von der Dunk 2006]. Assuming that these considerations are often made by persons with different interpretative frameworks, depending on their education and professional experience, a clear definition of damage is absolutely necessary as a starting point for any decision on interventions. The definition of damage should be objective and commonly accepted. Several glossaries combined with damage atlases have been developed over the years, involving a wide range of specialists in conservation [e.g., Van Hees & Naldini 1995, Franke et al. 1998, Van Balen et al. 1999, Fitzner & Heinrichs 2002, Naldini et al. 2006; see also the *ICOMOS International Scientific Committee for Stone*, http://www.lrmh.culture.fr/-icomos/icomos/consult/index.htm]. Still the definition of damage is not unambiguous, but rather subjective, which partly explains the different approaches shown in monument conservation.

Situations (i.e., damaged buildings) that are technically identical are often handled in different ways, depending on the building concerned and the people involved in the conservation process. Apparently, the technical arguments are not decisive. Probably, decisions are also based on non-technical arguments like intuition, aesthetics and perception. Further, it is not clear whether, from the same perspective of intuition, aesthetics and perception, the results of the intervention (repairs, cleaning) are considered to be an improvement, especially by non-specialists. Though they play a major role in everyday decision making on conservation, non-technical arguments such as perception in relation to replacement or preservation have not been widely researched. This study is aimed at assessing which factors are involved in deciding whether deteriorated building parts should be preserved, restored, reconstructed or replaced.

In this study, pictures of small scale damage (i.e., damage to individual stones or small sections of a wall) have been submitted to the participants for evaluation, because it is expected that in these cases non-technical arguments would determine their decisions far more than in the case of large scale damage (i.e., entire façades). When facing large scale damage, technical surveys are commonly carried out and decisions based on perception are supposedly minimized.

2 METHODOLOGY

2.1 Questionnaire

The methodology of this study was inspired by research of Andrew [2002] on the perception of weathered stone façades, and earlier studies on perception by Van Wegen [1970] De Jonge [1971] and Steffen [1983].

A questionnaire was composed of 20 images of natural stone; both weathered/damaged and repaired (Fig. 1). Each of the images was accompanied with 11 statements to be answered on a 7-point scale ranging from “totally agree” to “totally disagree”. The research was related to the Dutch conservation world, therefore, the questionnaire was in Dutch. The questionnaires were sent to people known to be interested in and/or working in the field of conservation of natural stone, architects, geologists and students attending courses on building conservation. To have the layman’s opinion, the questionnaire was also sent to family and friends who do not have a professional relation to conservation of natural stone. The questionnaires were distributed in colour-printed form. All the images had a printed size of 80 mm height. The returned questionnaires have been processed using standard spreadsheet software, where the 7-point scale is entered as 1-2-3-4-5-6-7 (1 being totally agree and 7 being totally disagree).

Figure 1. A-T. The twenty images that have been used in the questionaire.

2.2 Statements

Several historic examples show the diversity of arguments used to underline a conservation approach [e.g., Quist & Van Hees 2006]. Based on an overview of the most recurrent arguments, 11 statements have been used to capture the perception of small scale damage and repair of natural stone:

1. The stone shows damage.
2. The stone is attractive.
3. The stone needs maintenance.
4. The stone shows natural weathering.
5. The stone is well looked after.
6. The stone needs to be repaired.
7. The stone is in good condition.
8. The stone is ugly.
9. The stone needs to be cleaned.
10. The stone looks neglected.
11. The stone needs to be replaced.

2.3 Response

Out of 230 questionnaires, 102 usable questionnaires have been returned, a response of 44%. Respondents had to choose a profession out of a list; it was allowed to choose more than one profession. It is remarkable that almost all architects working in the field of conservation chose both the profession of "specialist" and "architect". The distribution is as follows: Student: 12 (10%); Specialist in the field of conservation: 49 (39%); Architect: 26 (21%); Geologist: 13 (10%); Other: 25 (20%). Due to a low response in most of the predefined populations, only the "specialists" and "the others, not being specialist" can be used as a different population within the analyses. The architects-population seems usable, but 17 out of 26 respondents are also part of the specialists-population. The remaining 9 respondents can not be used as a separate population.

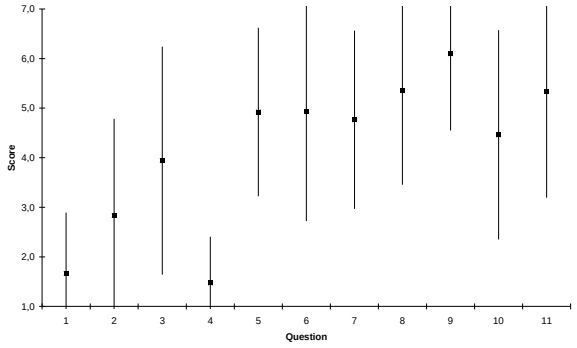

Figure 2. $\bar{x}$ and σ of all the statements regarding image 9 (Fig. 1-I).

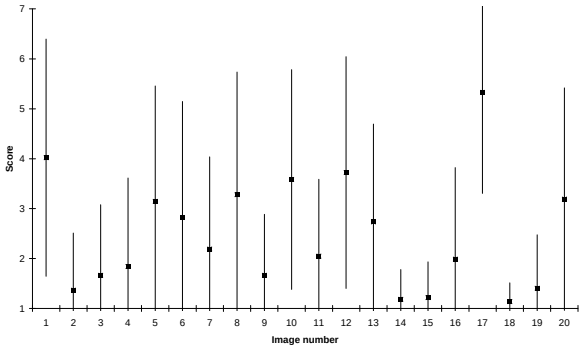

Figure 3. $\bar{x}$ and σ of all the first statements (damage) regarding all images (Fig. 1 A-T).

3. INTERPRETATION

3.1 Mean Average and Standard Deviation

For every question on the questionnaire, the mean average ($\bar{x}$) and the standard deviation (σ) were calculated. Figure 2 shows a graphical representation of $\bar{x}$ and σ of all statements regarding the ninth image. Figure 3 shows a graphical representation of $\bar{x}$ and σ of the first statement (damage) regarding all images (see Fig.1 A-T). In both cases all the respondents were taken into account. Figure

2 and 3 serve as an example to illustrate the high statistical dispersion. All the other $\bar{x}$ and σ show the same tendency. In general, the dispersion is lowest for image 18, and highest for image 5; images 2, 7, 8, 16 and 20 also show a very high statistical dispersion.

There are 2 possible explanations for this high statistical dispersion:
1. The total population is not homogeneous. The perception of the specialist population significantly differs from the non-specialist population.
2. The statements used in the questionnaire do not distinguish enough.

3.1.1 The Total Population Is Not Homogenous

To check whether there is a significant difference in perception for the specialist-population and the non-specialist-population, the student's homoscedastic t-test, with a two tailed distribution was carried out. With this test, 220 data ranges (20 images with 11 statements each) were processed (see table 1). For 85 out of the 220 data ranges can be concluded that $\bar{x}$ differs significantly (p=5%). This proves that, in relation to a lot of statements and images, there is a different perception of small scale damage and repair of natural stone for both populations.

Six out of twenty images show significantly different mean averages for both populations. These images are 3, 5, 11, 12, 16 and 20, of which four images concern repaired natural stone. Looking at the statements, four (statement 2, 8, 9 and 10) appear to differ significantly for over 10 images. The specialists tend to judge the images more positively in relation to the statements "attractive", "ugly" and "neglected". The opinion of the specialists in relation to "cleaning" differs for 18 out of 20 images significantly.

Table 1. p-values to check whether differs significantly for both populations.

	Question										
Image	**1 (%)**	**2 (%)**	**3 (%)**	**4 (%)**	**5 (%)**	**6 (%)**	**7 (%)**	**8 (%)**	**9 (%)**	**10 (%)**	**11 (%)**
1	51	0	4	24	30	48	40	7	0	0	22
2	5	27	69	100	48	40	17	84	0	42	41
3	93	5	5	1	5	4	37	1	0	2	3
4	75	1	72	86	5	94	11	1	0	89	0
5	7	0	0	14	0	0	0	1	0	0	0
6	41	51	83	11	25	29	60	48	0	28	6
7	41	51	83	11	25	29	60	48	0	28	6
8	34	37	12	67	9	33	8	31	0	16	8
9	79	93	20	35	94	24	2	44	34	3	70
10	10	0	82	62	30	70	9	1	48	2	1
11	50	0	5	1	0	14	2	0	0	0	0
12	6	4	0	48	0	0	3	24	0	0	71
13	29	76	38	4	12	91	67	88	0	15	78
14	80	93	35	7	87	18	9	61	0	49	11
15	25	0	82	47	1	37	0	0	1	94	22
16	70	4	24	2	7	18	3	3	0	0	5
17	33	13	33	14	1	61	53	0	0	0	8
18	79	1	10	3	30	6	62	0	0	10	18
19	39	23	13	100	71	6	18	21	0	5	25
20	1	0	0	66	0	0	0	0	0	0	1

3.1.2 Explaining High Standard Deviations

Further analyses of the frequency distributions of scores on statements with high standard deviations show that there are two types leading to the same high σ, namely:
1. The scores are almost evenly distributed to all seven items on the 7-point scale. The histogram shows an almost horizontal linear trend. This concerns statements 2, 5, 7, 8 and 10.
2. There is a high concentration of scores on either the "agree-side" and the "disagree-side". The histogram shows a parabolic trend. This concerns statements 1, 3, 6, 9 and 11.

This division can be assigned to types of statements. The evenly distributed scores all concern the more "soft", personal statements and the polarized scores all concern the more "expert, technical, objective" statements. These phenomena can be found in all three populations (total, specialists, and non-specialists). Two opposite opinions exist with regard to damage, maintenance, repair, cleaning and replacement.

3.2 Correlation

Both the specialist-population and the non-specialist-population show four pairs of statements indicating linear regression: $-0.6 < r\ (PMCC) > 0.6$, see table 2. In addition, two more correlations can be found in the non-specialist-population.

Table 2. Statements that show linear regression.

Population specialists	Population non-specialists
The stone is attractive and the stone is ugly (r = -0.82)	The stone is attractive and the stone is ugly (r = -0.77)
The stone needs maintenance and the stone needs to be repaired (r = 0.68)	The stone needs maintenance and the stone needs to be repaired (r = 0.72)
The stone is well looked after and the stone is in good condition (r = 0.64)	The stone is well looked after and the stone is in good condition (r = 0.67)
The stone is well looked after and the stone looks neglected (r = -0.65)	The stone is well looked after and the stone looks neglected (r = -0.67)
	The stone is in good condition and the stone looks neglected (r = -0.63)
	The stone is in good condition and the stone needs to be replaced (r = -0.63)

The strong negative regression between "attractive" and "ugly" indicate that these statements are considered to mean the opposite. The same counts for "well looked after" and "neglected". The linear regression between "maintenance needed" and "to be repaired" shows that in most of the cases when talking about maintenance, people want to intervene by repairing the natural stone.

After a first analysis of the results, some images have been grouped to investigate whether linear regressing according to comparable cases of damage can be demonstrated:

1. Sandy limestone on several scales (images 1, 9 & 13)
2. Repair (images 5, 7, 8, 11 & 20)
3. Larger scale, "wide-angle" (images 1, 10, 13 & 17)
4. Obvious loss of material (images 2, 3, 15 & 19)
5. Scaling (images 3, 9, 16, 18)
6. Sandstone degradation (images 2, 16)

Despite the assumed similarity between these groups of images, no correlation can be found.

4 DISCUSSION AND CONCLUSIONS

If all respondents are evaluated as one group, some interesting observations can be made on a number of situations regarding the question whether a situation is considered to be damage (statement 1) and if so, whether or not intervention (statements 6, 9 and 11) is necessary (Fig. 4). In some cases, the situation shown by the images is considered as damage, but accepted, without any intervention deemed to be necessary. This holds for images 6 (pronounced layering due to weathering), 9 (exfoliation), 13 (wide angle view of blocks with exfoliation) and 19 (spalling). Perhaps, these cases are considered as a kind of natural weathering. In contrast, regarding images 2 (sanding), 14 (joint), 15 (strong exfoliation) and 18 (strong powdering and exfoliation), the situation is also associated with

"damage" (statement 1), but most respondents consider intervention to be necessary. An explanation for the different inclination (whether to intervene or not) between both series of images may be the observed impact or expected future development of the damage. Another interesting situation is provided by image 10, an example of biological growth on tuff stone masonry. About 50% of the respondents consider this situation as damage. Also, about 60% states that an intervention is necessary. Obviously, those who consider biological growth to be damage, always deem that repair is necessary.

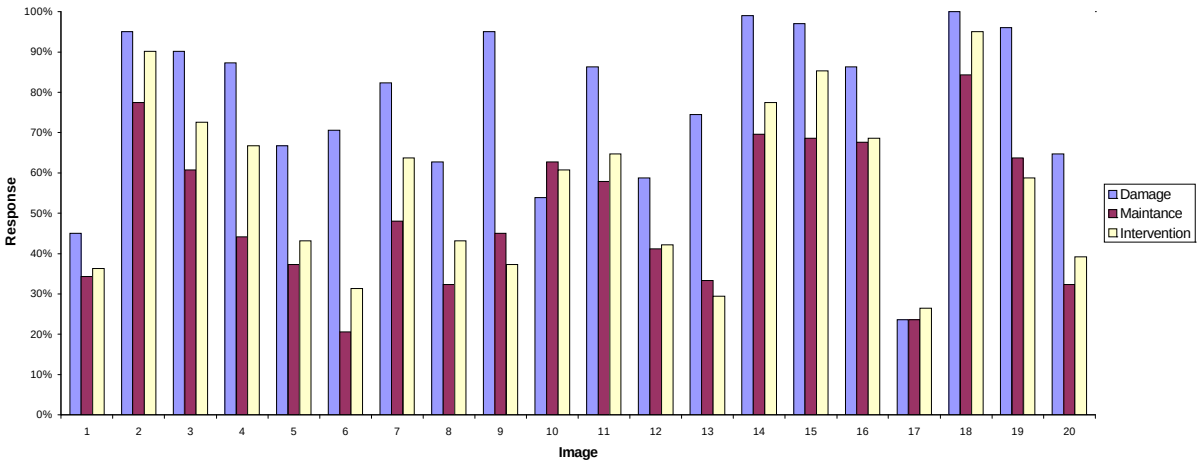

Figure 4. Comparison of the response on the issues of damage (statement 1), maintenance (statement 3) and intervention (statements 6, 9 and 11) of all respondents together.

It is impossible to point out the exact differences between predefined groups of people due to a low response within most of the groups and the high σ. Despite this, it is possible to observe some tendencies, especially in relation to statement 1 (damage). In general (Fig. 5): Students tend to give low scores (i.e., tend to agree); Geologists tend to give high scores (i.e., tend to disagree) especially image 6, 8 and 10; Response of the conservation specialists and architects on the images 5, 12 and 20 tend to diverge from the others.

The response by the students may possibly be explained by a lack of knowledge and experience, which makes them consider all kinds of degradation as "damage". The response from geologists clearly shows that (small scale) damage to natural stone is not an objective term. It is defined depending on the background and interpretative framework of different specialists. This is illustrated by the fact that geologists do not consider material degradation due to natural processes (i.e., weathering) as damage, and, consequently as reason for intervention. Apparently, the fact that internal characteristics of the stone, such as layering or presence of fossils, become more pronounced and better visible due to weathering processes (as in image 3), may even be appreciated. The stone is considered to express itself to a larger extent, and to gain charm by ageing. To some extent, this concept is comparable with the noble patina of age and (referring to paintings) *time as a painter* [Gombrich, 1988] sometimes invoked in art theory. On the contrary, conservation specialists and architects tend to associate the same result with damage, probably because it changes the original conception of a façade, and tends to erase the working of the stone by stone masons and artists. The definition of damage depends on the education and professional experience of the person involved, rather than on objective criteria, which influences how decisions about intervention are made.

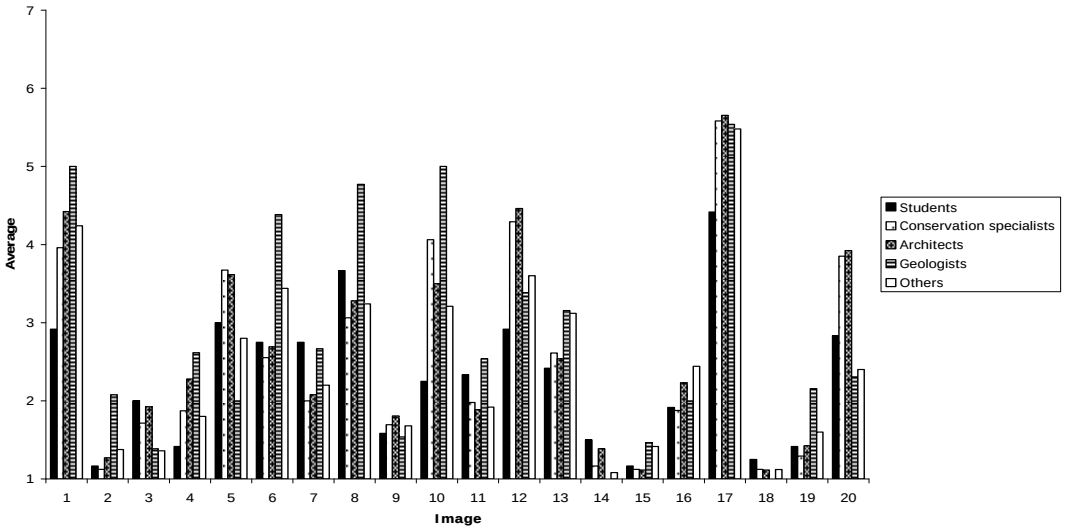

Figure 5. Average score on statement 1 (damage), regarding images 1-20.

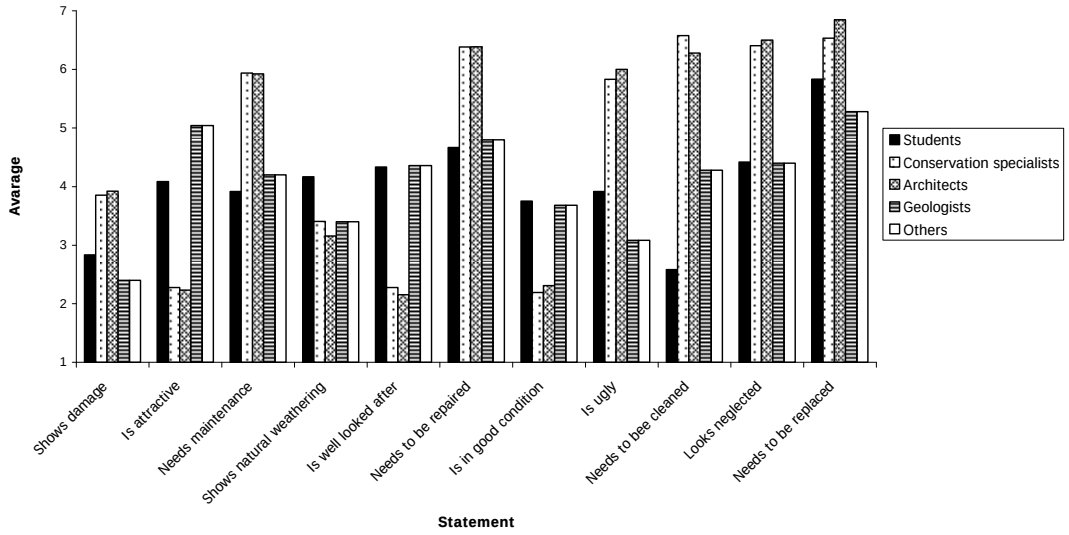

Figure 6. Average score on the statements, regarding image 20.

Decisions about interventions are not only based on the direct need of conservation in order to preserve material and building, but are also made to enhance a building, street or neighbourhood in a way 'the general public', 'visitors' or 'tourists', supposedly appreciate. A clean façade or neat blocks of stone are often regarded as ways to get this appreciation. The results allow some interesting reflections on this point.

Images 11 and 20 show situations in which a repair is visible. However, if all respondents are grouped together (Fig. 5), most of them (c. 85 %) consider the repair shown in image 11 to be damage. Many of those 85 % even consider intervention to be necessary. The situation shown in image 20 - a close-up of a recently executed sandstone repair - is clearly seen as the more successful one (Fig. 4). However, conservation specialists and architects apparently feel different about what is a successful repair from the general public. Architects and monument specialists highly appreciate the repair, in contrast with the other respondents (Fig. 6).

In general, conservation specialists and architects seem to have a greater appreciation of repairs than the general public. The latter still tend to consider a repaired stone "damaged". The specialists recognize the situation from their professional experience, and assume that this was the only option to

preserve the block of stone. Contrary, the non-specialists do not judge the actual repair, but "the disturbed, not naturally looking, not original situation". Opinions of "creators", judging the repairs positively, and "observers", judging the repairs negatively, consequently diverge. This implies that, when appreciation by the general public is one of the motives for intervention, initiators of this intervention (such as owners of a building, authorities, etc) may not obtain the desired result.

With regard to cleaning, the situation is the opposite. Whereas non-specialist in general do not appreciate the repairs, they tend to opt for cleaning as an intervention. In contrast, specialists are (very) negative to cleaning, whilst they appreciate the repairs. Specialists are probably aware of the technical implications of cleaning, and the damage that may result from it. In this case, new methods enabling damage-free cleaning might combine public appreciation with professional care.

REFERENCES

Andrew, C., 2002. Perception and aesthetics of weathered stone façades. In: Přikryl, R. & Viles, H.A., eds., *Understanding and managing stone decay*. Karolinum Press, Prague, 331-339.

Balen, K. van, Mateus, J., Binda, L., Baronia, Hees, R.P.J. van, Naldini, S., Klugt, L. van der & Franke, L., 1999. *Expert system for the evaluation of the deterioration of ancient brick structres*. EU Environment Program, EV5V-CT92-0108, Research report 8.

Conti, A., ed. *Sul Restauro*, Einaudi, Torino, 1988.

Dunk, T.H. von der, 2006. De moeizame vormgeving van het verleden. *Bulletin van de KNOB* 105(4):108-122.

Fitzner, B. & Heinricks, K., 2002. Damage diagnosis on stone monuments – weathering froms, damage categories and damage indices. In: Přikryl, R. & Viles, H.A., eds., *Understanding and managing stone decay*. Karolinum Press, Prague, 11-56. See also: http://www.stone.rwth-aachen.de

Franke, L., Schumann, I., et al., 1998. *Damage atlas*. Fraunhofer IRB, Stuttgart.

Hees, R.P.J. van & Naldini, S., 1995. Masonry Damage Diagnostic System. *International Journal for Restoration of Buildings and Monuments* 1:461-473.

Jonge, D. de, 1971. *Over de belevingswaarde van enige bouwmaterialen*. Centrum voor Architectuuronderzoek. TH Delft, Delft.

Naldini, S., Hees, R.P.J. van & Nijland, T.G., 2006. Definitie van schade aan metselwerk. In: *Praktijboek Instandhouding Monumenten* 28. SDU uitgeverij, 's-Gravenhage.

Quist, W.J. & Hees, R.P.J. van, 2006. De reiniging van de Grote Kerk in Breda – tien jaar later. In: *Praktijkboek Instandhouding Monumenten* 27. SDU uitgeverij, 's-Gravenhage.

Steffen, C., 1983. *De beleving van gevelvervuiling*. TH Delft, Delft.

Wegen, H.B.R. van, 1970. *Onderzoek naar de belevingswaarde van vier bouwmaterialen met behulp van de semantische differentiaal – techniek*. TH Delft, Delft.

Biofilm Effect and Microbiological Deterioration on the Material Surface

Sedat Kurugöl [1]
Dilek Dilhan Hatipoğlu [2]

T 15

ABSTRACT

Under natural circumstances, microorganisms preferably tend to continually show progress on a surface. Generally, other building materials like wood and plastics as well as most metals, except the ones that are toxic, natural stones, concrete cannot resist this progress of bacterial colonies in convenient environments and circumstances. Formation of this microbial organization on the material surface and the intensity of the colonization do not depend on random circumstances, but become obvious as the result of various factors gathering together. Microbiological activities can be also considered as an indicator and a reflection on the material of the variety and the transformation of ecological circumstances. On the other hand, they are critically important also with regard of durability, because of the deterioration mechanisms due to the physicochemical effects they generate in time on the material surface underneath the biofilm they have formed. In this study, by explicating the formation and progress stages of biofilms, the effects of these activities on various building materials like metal, stone and concrete are discussed.

KEYWORDS

Surface, Biofilm, Microbiological deterioration, Concrete, Metal, Stone.

[1] Mimar Sinan Fine Arts University, Istanbul, Turkey 34427, Phone +90 212 2435343, Fax 212 2435343, sedkur@msu.edu.tr
[2] Mimar Sinan Fine Arts University, Istanbul, Turkey 34427, Phone +90 212 252 16 00 / 250, dilhan@msu.edu.tr

1 INTRODUCTION

Biofilms are naturally growing bacterial activities and bacterial coatings by clinging and adhering of various microorganisms to generally stable and humid surfaces. They constitute several negative physicochemical effects on the surface of the material in terms of durability by chemical mechanisms they develop with the influence of the ambient. Biofilim is an activity on the surface of the material. All technological and physicochemical effects like adhesion, abrasion, friction, corrosion may grow up depending on surface qualities of materials. Therefore, in this sense surfaces are always reactive and behave in accordance with all effects they suffer. One of the interactions on material surface is the surface film formed in consequence of microbiological activities, which is called 'biofilm'. Microbiological activities within an ecosystem show themselves as biofilm formations on the surface of material. These activities, ultimately, cause surficial deteriorations and decompositions on the material due to surface properties and environmental circumstances.

In natural environments, microorganisms cling to various organic or inorganic surfaces and provide the required vital energy by utilizing the surrounding environment to pursue their lives and generations. Generally, biofilm is described as "a sum of microorganisms formed by gathering and getting organized in a matrix of organic molecules which cling to a surface" [Chevrou&Rodiere 2004]. The existence of biofilms seems to be the source of also industrial and economic problems besides serious and important issues in every field. Biofilms, as well as being emphasized in various scientific fields like industry, medicine, biology, chemistry, microbiology, geology, etc., are confronted as a remarkable phenomenon in terms of physicochemical effects they generate on the surface of building materials and the damage they give seem to be high beyond the suppositions.

Biofilm grows up on the surface of the material as a result of its relationship with the environment and almost all materials are covered with a biofilm layer in their non-sterile natural environments. Biofilm bacteria can be colonized in all humid surfaces whether organic or inorganic [Bergeli 2005]. Depending upon the environments they develop, 1 mm^3 of a biofilm may contain a huge amount of microorganisms and there may be various bacteria, fungi and algae within a biofilm [Haras 2005]. In aquerous, humid and stuffy environments, these microorganisms use compounds of oxygen, carbon, nitrogen and sulfur in the soil for growing up and providing energy by benefitting from them. Biofilm microorganisms also give rise to growing up of biofilm layers by generating various organic molecules (EPS: Extracellular Polymeric Substances) as a result of nutrition. The EPS matrix is composed of organic molecules like polysaccharide and protein and they can take up 75-95 % of a matured biofilm capacity [Haras 2005, Suci *et al*. 1994]. 80-95 % of a biofilm and 85-98 % of an EPS matrix consist of organic items. Additionally, in biofilm, there can be various inorganic items (humic substances, debris, clay, silica, gypsum, etc.) [Flemming 1998]. Biofilm shows itself when four components come together. These factors are : 1- Generally a bit aggressive environment and its characteristics. 2- A material affected by the environment and its surface characteristics. 3- Various types of microorganisms whose existence had been ignored or not considered [Chevrou & Rodiere 2004, Bergeli 2005, Suci *et al*. 1994, Flemming 1998, Féron 2005]. 4- Time (Figure 1).

In this structure, there may be different types of bacteria, fungi, microalgae and moulds together and they may cause a biofilm to grow up. These bacteria, which have various types depending on their ways of nutrition, are organisms that have very tiny constructed elementary morphology that can be merely seen under a microscope, they can stay alive in every environment like air, liquid, soil, and can grow up up to the various circumstances of the environment like oxygen, temperature, pH, hydrostatic pressure and salinity [Magot 1998]. And the primal terms of biofilms to grow up are: 1-A nutrition source 2-An energy source 3-Water and damp 4-An adequate temperature 5-An adequate pH 6-An adequate amount of oxygen and [Chevrou&Rodiere 2004] 7-Surface characteristics of the material. For a biofilm to form and grow up, primarily physicochemically, microorganisms have to hang on to the surface and be accepted by the surface. Formation of a biofilm formation with bacterium on a solid surface in adequate and aggresive environment seems like a complex case where are lots of parameters. A biofilm formation ready to increase in numbers occurs in four steps that follows one another [Féron 2005].

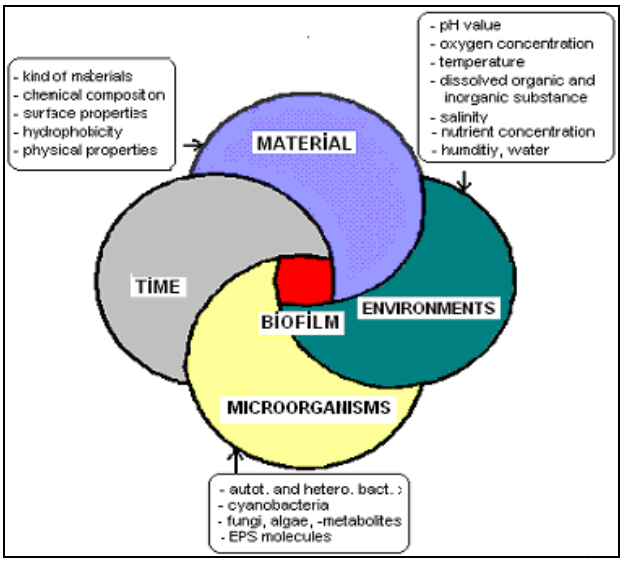

Figure 1. The factors that determine the formation of a biofilm.

1. Transport : It is a matter of microorgansims being moved to a surface with many different ways.
2. Absorption: It is an instant matter, it causes the surface to have physico-chemical transformation.
3. Adhesion: The theories about the adhesion mechanism besides being interpreted in various ways according to different scientific disciplines, generally occurs depending on a two-stepped activity. At the first step, a reversible phase that holds the bacteria on surface and can be easily washed away and gone is formed, and at the second step which follows this, stiff and solid matrix (like scratching&brushing) that causes the irreversible adhesion of the bacterium and requires a huge energy to take these back is formed.
4. Colonization: This activity may take a few months or a few hours depending on the terms the microorganism is in and this colonization ends up with a formation of a biofilm. In a formation of a biofilm, not only the effect of bacterium and damp but also at the same time the organic items that has been created by the organisms on the surface (EPS) play a role (Figure 2,3). Colonization may take place in different times depending upon the type of material and the environment. For instance, it is formed in a few hours in sea water on stainless steel (inoxydable AISI 304), few days on AISI 316 steel [Lemaitre *et al.*1990], seven days in a fluid water on a mild steel [Donlan *et al*. 1990], few months in fresh water [Feugeas *et al.* 1997]. On the surface of the material, there might not be a coordinated and uniformed spread of the biofilm. Microorganisms that created biofilms can show themselves in various types in this structure. This colonization can occur on the whole surface or in one part of the surface based on the relationship between the surface characteristics of the material & bacteria structures [Haras 2005].

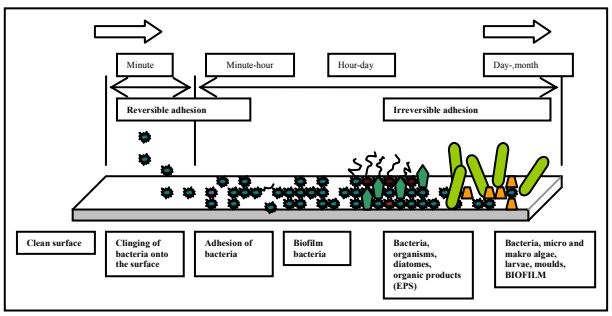

Figure 2. Presentation of a biofilm formation image on a surface as schematic.

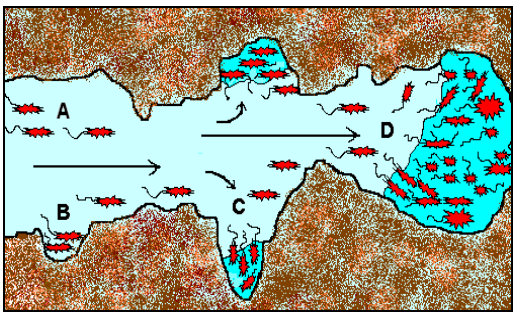

Figure 3. Presentation of steps of the biofilm formation in a covern as schematic.A-Actions of water and the bacteria(absorbation), B-Bacteria's holding to the surface(adhesion), C-Creation of the EPS molecules, D-Colonization. Bacteria fill in the

Substantial environments created by organic items is counted as the reason of the variety of microorganisms that can be seen in biofilms. Accordingly, corruption of the environment and various organic items they have are effective like a formative factor in the formation of a biofilm and correspondingly the microcolonization and biofilm formations on the surface raises.

2 EFFECT OF BIOFILM ON THE MATERIAL

Biofilms seem to have a capability of growing up in suitable cases on every kind of structure material like metal, concrete, stone, wood and plastic. Biofilm activities which are on various materials are discussed in the subtitles.

2.1 Microbiological Effect on Concrete

Concrete which is a structure material and widely used worldwide can be deteriorated because of the biofilm on the surface created by various autotroph and hetotroph bacteria, cyanobacteria, alga and fungus [Saad & Gaylarde 2004]. Main problems of the abrassion of concrete below the biofilm layer with the effect of bacterium show itself in drain water and canalization systems generally made by this material because of the reason that there is hydrogen sulfur (H_2S) in the environment.

Underground waters that contain sulphate and chloride ions, sea water, waters that contain free CO_2 or H^+ ions which mix up with industrial contaminations and dirty waters may therefore cause harmful reactions [Yeğinboğalı 1999]. This situation, although observed in many countries, was first analyzed in ABD and Germany. The effect of sulfuric acid on concrete had been known time out of mind. In addition to this, the mechanism of the transformation of H_2S to H_2SO_4 was not a well known thing. Afterwards, the investigations made have revealed that this thing originates from bacterium. To determine the existence and types of microorganisms, with the investigations made on concrete, mortar and limestones [Graef *et al.* 2004, Muynck *et al.* 2005], the existence of the *T.bacillus* bacterium on concrete elements have been proved, lichen formations have been seen, and it has been appointed that gypsum stone cristals are formed with the effect of sulfuric acid released by the *T.bacillus* bacterium and (Fig.4) therefore the ettringit cristals have grown up on concrete.

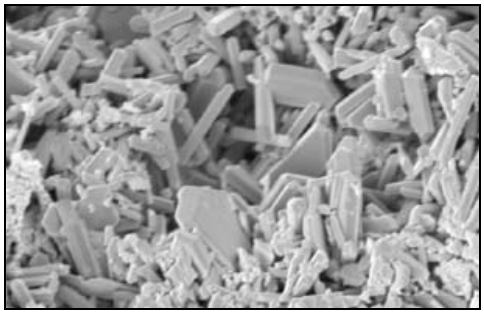

Figure 4. Gypsum cristals in concrete due to H_2SO_4 created by Thiobacillus [Welton *et al.* 1998].

In these environments, offensive odor, toxicity, corrosion of metals and the deteriorations seen on the concrete in the course of time are the prominent indicators. Generally, it has the characteristic feature of dampish concrete that damaged by the effects with microbiologic source and has a whitish appearance. It is covered by a sticky and thin layer of film. The pH value on the surface is approximately 1. This case mostly shows itself in not much aerated environments that contain acid and bacteria. Sulfur oxidizing microorganisms that become effective in these kinds of environments are gathered under three categories [Tache 1998]: 1- Colorless Chimiolithotrophes (*Thiobacillus, T.spira, T.bacterium, T.microspira, T.vulum, Macromonas, Sulfolobus* etc). These bacteria grow up as autotroph. They use the CO_2 in the environment for their synthesis. 2- Colorful Photosynthetic bacteria (reddish color). These are anaerobic bacteria which can make oxidation in an oxygen-free environment with light and reduce sulphate. And their basic type is known as *Desulfovibrio, D.fomonas,*

D.fococcus, D.fobacter and *D.fobalbus.* 3- Heterotroph microorganisms which are capable of oxidizing sulfur compounds without taking energy. In another example [Belie *et al*. 1997] dept of deterioration and microcracks have been detected. Here it has been found that the acids created by bacteria affects the material much, and especially in the exterior surface of the concrete, the connection phase between cement and aggregate has been deteriorated enormously. In another study, [Silva 1994, Silva 1997] it has been shown that the microbiological activities on the concrete grow up in not only water systems but also every environment. Studies have been made by using six different investigation technique to analyze these activities on the concrete samples taken from the three buildings that are in different climates, (among the buildings of 7 or 30 years old and exposed to the temparature between -5, + 35C^{o}). As a result, the deterioration of the concrete by organisms occurs even in different climates which can be regarded as normal, and in concrete surfaces, in addition to the same type microorganisms characterized morphologically, we may happen to meet non-characterized various types (*Diatom algea, Actinomycete, Cladosporium, Protozoa* etc). On the other hand, on the surface of concrete and cement, other than sea water and drain water,even in natural fresh water, it has been seen that various microorganisms, by growing up, can create biofilms that may cause cement to deteriorate [Roux *et al*. 2005]. Biodeterioration is caused mainly by 1-bacteria; 2- fungi; 3- algae and lichens and; and 4- organisms that erode an drill the concrete [Gaylarde *et al.* 2003]. Among those that cause concrete biodeterioration some of the most important are: 1- cyanobacteria; 2- nitrobacteria; 3- sulfur-reducing bacteria; and 4- sulfur-oxidizing bacteria. Their main characteristics and influence on concrete are presented in Table 1 [Bastidas-Artega *et al.*2008].

Table 1. Effect of bacteria on reinforced concrete.

Bacteria type	*Lifestyle*	*Temperature*	*pH*	*Consequence on concrete*
Cyanobacteria	Autotrophic, aerobe or anaerobe	-60 to 85 ^{o}C	wide range pH	Generate tensile stress leading to an increment in the size of cracks.
Nitrobacteria	Heterotrophic and anaerobe	18 – 25 ^{o}C	< 7,5	Nitrifying bacteria (*nitrosomona and nitrobacter*) produce calcium nitrate by solubilising some of cement components.
Sulfur-reducing bacteria	Heterotrophic and anaerobe	25 – 44 ^{o}C	5.5< 9	Produce H_2S that is used for the *sulfur-oxidizing bacteria* to produce sulfuric acid. This prosess is commonly called *concrete corrosion*.
Sulfur-oxidizing bacteria	Heterotrophic and anaerobe	25 – 44 ^{o}C	2< 9	Produce sulfuric acid, acetic acid, sulfates, sulfur, sulfites and polythionates that affect the concrete chemically.

According to the similar studies on this issue, various microorganisms use both concrete and stones as substrats and shows that they cause activities to deteriorate the concrete by creating acids.According to the investigations [Tache 1998] with the effect of this activitiy,there is a loss of material which has 2-3 mm thickness on the concrete surface. H_2S created in an anaerobic environment by *Desulfovibrio* type of bacteria, H_2SO_4 created in an aerobic environment by *Thiobacillus* type of bacteria shows themselves on the concrete as a source of microbiological deterioration. On the concrete, the simplified mechanism of sulfuric acid effect is like this: Cement paste, attacked by this acid created, causes calcium hydroxide [$Ca(OH)_2$] to dissolve. Sulphate, by reacting with calcium ionics, forms gypsum (hydrate calcium sulfate) and as a result they create silica gel.

$$Ca(OH)_2 + H_2SO_4 \rightarrow CaSO_4.2H_2O \text{ (gypsum)} \quad (1)$$

$CaSO_4.2H_2O$, later on, can react with the tricalcium alluminate (C_3A) in cement and gives way to the formation of ettringite ($3CaO.Al_2O_3.3Ca_2O_4.32H_2O$) causing concrete to swell and burst, and then may cause an increase in permeability [Aviam *et al.* 2004]. These activities go on like this by following each other and as time goes by, give way to durability problems like reinforcement corrosion besides decompositions in concrete.

2.2 Microbiological Effect on Metal

Biofilm effect on metal confronts us as microbiological corrosion (*MIC*). Biological corruption of metal materials, biochemical corrosion, biocorrosion, microbial corrosion, bacterial corrosion, corrosions created by microorganisms, or MIC/CIM, all these terms expresses the same reality and expresses the active and crucial role of various microorganisms, bacteria, fungi in corrosion [Féron 2005]. Biocorrosion is the dissolution of a metal or a blend electrochemically. These reactions occur in many different steps with the mutual interaction of metal and biological structure on the surface. [White *et al.* 1990]. First step of biocorrosion begins with the biofilm formations which grow up by necessity on the surface of the metal [Magot 1998]. In addition to this, it must be stated that a biofilm layer is not always a reason for corrosion. And there may not be always a relationship between biolayer and biocorrosion. [Bach *et al.* 1990]. Bacteria that cause corrosion have different metabolic features. They have an ability to oxidize irony ionics and sulfur and reduce oxygen, sulphate, tiosulphat and iron. Environment and the physicochemical features of the environment have also indicative roles in growing of biocorrosion activities. The physico-chemical compositions like temperature, pH value, oxygen contents, organic production they have, moisture content affect the growings of the microbiological formations. In formation of a biofilm, surface roughness of the metal is not seen as a formative factor, and in waxed and polished surfaces (like polishing), compared with raw and rough surfaces, sensitivity towards the formation of MIC reduces [White *et al.* 1990]. But however engraving of the surface of metal raises this sensitivity (e.g. as if brushing).

Bacteria that seem very aggressive steel and its blends encounter are sulphurogen type bacteria. These (Flemming 1998, Bach *et al.* 2005]; make up two important groups under the name of 'sulfur reducer'(BSR) and 'thiosulfide reducer'(BTR). BSRs generally use sulfur as electron receiver, so many substrats on the surface or from carbon sources as electron transmitter, acids (lactic, fumarate, acetate) hydrogen, from ethanols (methanol, ethanol, propanol), saturated hydrocarbon big molecular oil acids, simple aromatic compounds (phenol, benzene) and sucrose (fructose) [Chevrou *et al*. 2004, Haras 2005]. H_2S that appears during the reduction of sulfur transforms the iron in the environment to the FeS. Deterioration of the metal is generally the vallecula (or redd) type of corrosion. In case the metal which faces corrosion is an iron, sulfur reduction occurs in following reactions [Doruk 1982].

Anodic occurrence	$4Fe \rightarrow 4Fe^{2+} + 8^{e-}$	(2)
Kadotic occurrence	$8H_2O \rightarrow 8H^+ + 8OH^-$	(3)
	$8H^+ + CaSO_4 \rightarrow 4H_2O + CaS^+ - 8^{e-}$	(4)
	$CaS + 2H_2CO_3 \rightarrow Ca(HCO_3)_2 + H_2S$	(5)
Total amount occurrence	$4Fe+2H_2O+CaSO_4+2H_2CO_3+2H_2CO_3 \rightarrow 3Fe(OH)_2+FeS+Ca(HCO_3)_2$	(6)

Biofilm colony formations formed on the surface of the metal by microorganisms and diffused to several parts create different aerated part figures on the surface. So the place between these parts and the colonies are oxided differently and for this reason the center of the colonies is suddenly oxided as a result of contact to metal. This different oxidizing at the two parts of the metal causes potential electric discrepancy and ultimately a corrosion drift [Haras 2005, Féron 1998]. This formation is in the image of corrosion that is created by different airing. (Figure 3, 4). The MIC formation can grow up on several types of steel.

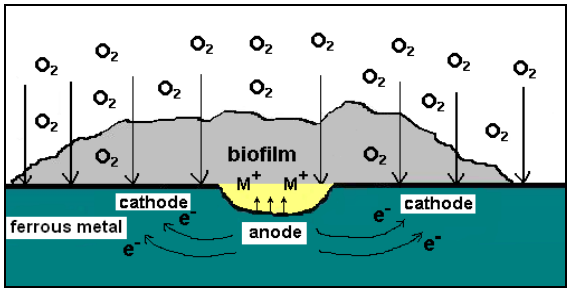

Figure 3. Little or much oxygenic biofilm part.

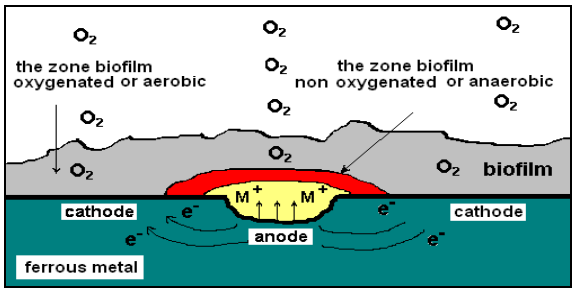

Figure 4. Biofilm in anaerobic parts.

2.3 Microbiological Effect on Stone Material

As stone has the quality of a traditional material in the way of its usage in historical process, it is the mostly analyzed material because of biological deterioration as much as various disintegration mechanisms. Out of the parts of the stone that is exposed to the effect of water, especially in the parts on which earth humid is effective, and which is very near to the soil, it is known that bacteria and fungi colonizations become activated. There is a relationship between disintegration mechanisms biofilm caused and stone types and climatic conditions. In addition to this, in all types of climatic conditions, on various stones bacterial activities can be mentioned. For example, Kumar and Kumar [1999] have analyzed microbiological formations on different stone types in various tropical environments of the world, their types, characteristics and accordingly their types of deterioration. In the environments where temperature decrease to -25 ^{o}C (Erzurum), it is seen that on surfaces of several monuments, microorganisms, which make stones deteriorate, grow up under the biofilm layer due to air pollution. [Nuhoğlu *et a*l. 2005].

Researchers have shown that bacteria on stone surfaces produce corrosive organic acids when exposed to pollutants, resulting in significant stone degradation. The scientific understanding of these processes remains limited because of the major variables involved. It is difficult to assess the relative importance of microbial processes in microbial-induced stone degradation. Chemoautotrophic sulfur oxidizing bacteria attack stones under aerobic conditions by producing inorganic sulfuric acid. Sulfuric acid reacts with the constituents of the stone to form sulphate crusts, precipitated within the pores of the stone, which upon recrystallization exert tremendous stress on the pore walls due to increase in volume, thereby causing damage to the stone [Khobragadeı *et al*. 2006]. The effect and composition of various biofilms growing up in carbonate stone monuments have some features in common and it is possible to see lichens on the stone surfaces of all the historical monuments. Cynobacteria, fungi, algae and heterotrophic bacteria are the typically seen microorganisms in these biofilms. It is observed that the acid effect of the grainy and laminal decays and cracks on the stones appear in the parts where these microorganisms are colonized.

Cyanobacteria create variously coloured microbial films on stone surfaces and facilitate adherence of airborne particles of dust, pollen, oil and coal ash, giving rise to hard crust of patinas18. Respiration and photosynthetic reactions of cyanobacteria also produce acids as by-products causing etching of mineral components and dissolution of binding minerals [Khobragadeı, *et al*., 2006]. These activities effect the stones aesthetically, chemically and physically [Rois *et al.* 2005], cause especially in calcareous Cynobacteria stones, decays by creating patinas with their biochemical activities. [Crispim & Gaylarde 2005, Albertona 2004]. Besides algas, protozoas, fungus, bacteria (cyanobacteria), limestones, they can be colonized on other types of rocks. [Ortega-Morales 2006]. Algae cause deterioration primarily by staining the stone surfaces resulting from different coloured pigments of the algae. Algae also produce organic acids which increase solubility of the stone in water, and alter the physico-chemical properties of stone [Griffin, *et al*. 1991].

The colonization of *Tihobasills* and nitrifying bacteria grows up to the existence of sulfur and nitrogen compounds. These are sulfur and nitrogen oxidizing and heterotrophic bacteria and show themselves

with the color change. The activities of nitrogen bacteria carbonate rocks is explained with the following balance and accordingly we draw a conclusion that external decay is predicated on nitrification. As a result of these activities, decays ending up with the dissolving of minerals and their transportation from the surface.

$$2CaCO_3 + (NH_4)_2 + 4O_2 \rightarrow Ca(NO_3)_2 + CaSO_4 + 2CO_2 + 4H_2O \quad (7)$$

3 CONCLUSION

Biofilm forms, in various processes, in one sense a type of corrosion, a type of biological deterioration for most materials. In this study, several researches related with the subject performed on materials like concrete, metal and stones are summarized. Besides the corrosion and decomposition mechanisms in these materials, biofilms also constitute various physico-chemical effects like splitting of molecular bonds in some polymers, decay in wood, surface erosion, spots and loss in the optical characteristics in glass and may cause significant problems in durability of the material. Measures which might be taken against biofilms may include physical, chemical and biological studies. In this respect, material type together with the composition of the biofilm form the characteristic criteria in common prevention and preservation studies. Hence, the methods to be chosen and protective materials should be assessed in this context. In general, studies of preventing and struggling against the biofilm formation on the surface of the material consist of two-phase practices which are a) to prevent the colonization on the surface (in the reversible step of the biofilm) and b) to remove them from the place they settled (in the irreversible step). The methods to be chosen have to be decided on only after the required analysis.

REFERENCES

Chevrou,M., Rodiere, A., 2004, 'Les Biofilms". Ecole Nationale Supérieure de Chimie de Rennes. Option méthodologies d'analses Projét binome, France.

Bergeli, A. 2005, 'Création du Pnir-Biofilms". *Laboratoire de Génie Chimique- CNRS* . La Revue trimestrielle du réseau Ecrin – no: 60, France.

Haras.D., 2005, 'Bioflims et Altération des Matériaux: de L'Analyse du Phenomene aux Stratégies de Prevention'. *Materiaux et Techniques 93*.

Suci, P.A., Mittelman, M.W., Yu, F.P., Geesey, G.G., 1994, 'Antimicrob.Agents Chemother' 38, 2125-2133.

Flemming, H.C., 1998, "Biofilms" Biodétérioration des Matériaux. EDP Sciences, , pp 74, France.

Féron, D., 2005, 'Comportement des aciers en environnement naturel : cas des aciers inoxydables en eau de Mer' EDP Science, *Matériaux and Téchniques* 93, 43-58

MAGOT, M., 1998, 'Introduction à la Microbiologie des Bactéries' *Biodétérioration des Matériaux.* EDP Sciences, ISBN: 2-86883-329-2, pp 31,33, France.

Lemaitre, C., Hernandez, G., Beranger, G., Guezennec, J., 1990, 'Matérials et Téchniques', 25-33.

Donlan, R., Munia, R., Gibbon, D. 1990, 'Sulphate Reducing Bacterial Colonization of Mild steel in Recirculating coolin Water, Microbially Infulenced Corrosion on Biodeterioration.' NJ Dowling, M.W.Mittel. and J.C. Danko, Eds., 2 ,Duke Power Inco Alloys Inter.Inc., Tennnesse Eastman, 69-74.

Feugeas.F., Mangin, J.P., Cornet, A., Rameau, J.J., 1997, 'Corrosion Influence par les Micro-organisme: Influence du Biofilm sur Corrosion des Aciers, Téchniques et Resultats Recents'. *Journal Physique III* France.

Saad, S.D., Gaylarde, C., 2004, 'Biodeterioration of Concrete-A Brief". Second International RILEM Workshop on Microbial Impact on Buildings Materials. RILEM Publications SARL, 37-46.

Yeğinboğalı, A., 1999, 'Betonun Dayanıklılığı-II'. Türkiye Çimento Müstahsilleri Birliği Çimento ve Beton Araştırma-Geliştirme Enstitüsü, Ankara, 1-17.

Graef, D.B., Windt, D., Belie, D.N., Verstraete, W., 2004, 'Cleaning of Concrete Fouled by Algea with the aid of Thiobacilli'. *Proc.of the second Intern. RILEM Workshop on Microbial Impact on Building Materials*. RILEM, TC 183-MIB, Vitoria-ES, Brazil.

Muynck, D., Dick, J., Graef, B., Windt, D.W. Verstraete, W., Belie, D.N., 2005, 'Microbial Ureolytic Calcium Carbonate Precipitation for Remediation of Concrete Surfaces'. *Inter. Conf. on Concrete Repair, Rehabilitation and Retrofittin*, Cape Town, South Africa, 21-23.

Welton, R.G., Silva, R.M., Gaylarde, Ch., Herrera, L.K., Anleo, X., Belie, D.N., Mondry, S., '2005, Techniquest Applied on the Study of Microbial Impact on Building Materials'. *RILEM TC 183-MIB, Materials ant Structures* 38,

Tache, G., 1998, "Corrosion bacterienne des Betons". *Biodéterioration des Matériaux*. EDP Sciences, 115-126.

Belie, D.N., Verschoore, R., Gemert, V.D., 1997, 'Microscopic study on concrete attacked by organic acids', Proceedings of the Sixth Euroseminar on Microscopy Applied to Building Materials, Reykjavik, Iceland, 25-27 June 1997, 250-258.

Silva, R.M., 1994, 'La diversification climatique et la dégradation du béton', in 'Dealing with Defects in Building', *Proceedings of an International Symposium, Varenna, Sept. 1994* (Sartori, Internat. Council for Building Research Studies and Documentation, Varenna, 1994) v.1. 471-480.

Silva, R.M., 1997, "The role of the scanning electron microscopy on the study of concrete biodeterioration', in 'Sixth Euroseminar on 64 Microscopy Applied to Building Materials', *Proc. of an International Sem., Reykjavik, June 1997* (Iceland Building Research Institute, Reykjavik,) 325-334.

Roux, S., Feugeas, F., Cornet, A., 2005, 'Biedégradation des bétons: analyse des bétons et mortiers en contact avec une eau douce naturelle' *Materiaux & Techniques 93*, pp.123-135 EDP Sciences.

Bastidas-Arteaga, E., Sanchez-Silva, M., Chateauneuf, A., Ribas Silva, M., 2008, 'Coupled Reliabilitiy Model of Biodeterior, Chloride Ingress and Cracking for Reinforced Concrete Structures' Elsevier, Structural Safety, Vol.30, 110-129.

Gaylarde, C., Ribas Silva, M., Warscheid, Th., 2003, 'Microbial impact on Building Materials: An Overview', Mater. Structural, 36, 342-352.

Aviam, O., Nes.G.B., Zeiri, Y.,Sivan, A. 2004 "Accelerated Biodegradation of Cement by Sulfur-Oxidizing Bacteria as a Bioassay for Evaluating Immobilization of Low-Level Radioactive Waste". *American Society for Microbiology. Applied and Environmental Microbiology*, Oct. 2004, p. 6031–6036 Vol. 70, No. 10 .

White. D., Jack, R., Dowling, N., 1990, 'The Microbiology of MIC, Microbially Influenced Corrosion and Biodeterioration', Duke Power Inco Alloys Internat., Inc, Tennesse Eastman, 1, 10.

Bach. M., Feugeas. F., Farcas. F., Dupont. I., Victoire-M.E., Cornet. A., 2005, 'Influence Bactérienne et l'efficacite d'un inhibiteur de Corrosion Organo-Mineral pour des elements Metaliques en Fer Pur'. *Matériaux, Technhiques 93*, France.

Doruk. M., 1982, '*Korozyon ve Önlenmesi*', ODTÜ.

Féron, D., Thierry, D., 1998, 'Corrosion Bactérienne Des Métaux'. *Biodétérioration des Matériaux*. EDP Scien., 89-101.

Nuhoğlu, Y., Oğuz, E., Uslu, A., İpekoğlu, B., Ocak, İ, Hasenekoğlu, İ., 2006, 'The Accelerating effect of the Microorganisms on Biodeterioration of Stone Monuments under air Pollution and Continental-cold Climatic Conditions in Erzurum, Turkey'. *Science of The Total Environment, Volume 364, Issues 1-3,* 1 July 2006, pp 272-283.

Kumar, R., Kumar, V.R., 1999, 'Bioteterioratin of Stone in Tropical Environments'. *The Getty Conservation Institute*.

Rois, A., Garcia, C., Wierzchos, J., Ascaso, A., 2005, 'Microbial Biofilms in Carbonate rocks from Spanish Monuments' *Geophysical Research* Vol.7, 08371, Eurepean Geosciences Union.

Crispim, C.A., Gaylarde, C.C., 2005, 'Cyanobacteria and Biodeterioration of Cultural Heritage: A Review'. *Springer Science-Business Media,* Inc. Volume 49, 1–9 .

Ortega-Moralles, B.M., 2006, 'Cyanobacterial diversty and Ecology on Historic Monuments in Latin America'. *Rev. Latinoamericana de Microbio., Presen. en simposios.*, Vol 48 No:2, 188-195.

Albertona, P., 2004, 'CATS-Cyanobacteria attact rocks: developments after a three years project on control and preventive strategies to avoid damage caused by cyanobacteria and associated microorganisms in Roman hypogean monuments' *6 th European Commision Conference on Sustaining Cultural Heritage*. UK, 1-3 sept.2004 London.

Griffin, P.S., Koestler, R.J., 1991, Int. Biodeterior., 28, 187-207.

Khobragadeı, C.N., Srinivasa, Rao, R., PRITA S. Borkar Prita, S., RAHUL S. Yangade Rahul, S., 2006, 'Microbially induced impact on physico-chemical properties of porous lime stones: A case study from Kandhar fort' Current Science, Vol.91, no.10.

11DBMC International Conference on Durability of Building Materials and Components
ISTANBUL, Turkey 11-14 May 2008

Determination of Water and Nitrate Transport Properties of Sandstone Used in Historical Buildings

Zbyšek Pavlík [1]
Lukáš Fiala [2]
Milena Pavlíková [3]
Robert Černý [4]

T 15

ABSTRACT

Coupled water and nitrate transport in sandstone frequently used in historical buildings on the Czech territory is investigated in the conditions of one-sided water and KNO_3 solution uptake. In the experimental work, rod-shaped samples are used for the determination of moisture and nitrate concentration profiles in simulated 1-D water and nitrate solution transport. The moisture content is determined by gravimetric method, the nitrate concentration is measured using the pH/ION 340i device with utilization of ion selective electrode. Experimentally determined KNO_3 concentration profiles and moisture profiles are used for identification of nitrate diffusion coefficient and moisture diffusivity on the basis of inverse analysis using the diffusion-advection model. The moisture diffusivity in dependence on moisture content is calculated in three different ways. First, the moisture diffusivity is calculated from moisture profiles measured for the penetration of distilled water into a specimen. Then, the moisture diffusivity vs. moisture content function is calculated from moisture profiles measured for the penetration of KNO_3 solution. Finally, the third moisture diffusivity vs. moisture function is obtained by the inverse analysis of nitrate concentration profiles under assumption that no nitrate diffusion takes place in the liquid phase. The results of inverse analysis show that the possible neglect of nitrate diffusion in the liquid phase is apparently wrong because the moisture diffusivity calculated from nitrate concentration profiles under this assumption is two to three orders of magnitude higher than moisture diffusivity calculated from moisture profiles.

KEYWORDS

Sandstone, Historical buildings, Water and nitrate transport.

[1] Czech Technical University, Faculty of Civil Engineering, Department of Material Engineering and Chemistry, Thákurova 7, 166 29 Prague 6, Czech Republic, Phone +420224354371, Fax: +420224354446, pavlikz@fsv.cvut.cz
[2] Czech Technical University, Faculty of Civil Engineering, Department of Material Engineering and Chemistry, Thákurova 7, 166 29 Prague 6, Czech Republic, Phone +420224354371, Fax: +420224354446, fialal@fsv.cvut.cz
[3] Czech Technical University, Faculty of Civil Engineering, Department of Material Engineering and Chemistry, Thákurova 7, 166 29 Prague 6, Czech Republic, Phone +420224354688, Fax: +420224354446, jiricko@fsv.cvut.cz
[4] Czech Technical University, Faculty of Civil Engineering, Department of Material Engineering and Chemistry, Thákurova 7, 166 29 Prague 6, Czech Republic, Phone +420224354429, Fax: +420224354446, cernyr@fsv.cvut.cz

1 INTRODUCTION

A part of building damages assigned to the negative moisture effects would not arise if only pure water would be present. Water represents very often only transport medium for other harmful pollutants that take part in the process of surface degradation of building materials. Water transport in porous materials makes possible salt transport or accumulation as well. Salt accumulation in specific places of building structures can lead in consequence to their failure or destruction.

Salts are from the chemical point of view binary or multi-component compounds consisting of simple or complex cations and anions. Only specific group of salts represents real danger in building practice or restoration. In light of danger for facades, paints, mortars, stones, bricks and other building materials, the salt solubility is the most important criterion. In corrosive processes only those salts take part, which are well soluble in water, whereas the influence of insoluble salts is more or less negligible.

The most frequent salts that cause damages of building materials and structures are sulphates, chlorides and nitrates and in some particular cases also water-soluble carbonates. The most important harmful salts that occur in building materials including their solubility are given in Table 1.

Table 1. The most frequent harmful salts that occur in building materials.

Salt	*Solubility* [g/L of solution]
Sulphates	
$CaSO_4 . 2H_2O$	2.4
$MgSO_4 . 7H_2O$	1172
$Na_2SO_4 . 10H_2O$	583
Na_2SO_4	481*
K_2SO_4	111
Chlorides	
$CaCl_2 . 6H_2O$	5359
$CaCl_2 . 2H_2O$	1281
$MgCl_2 . 6H_2O$	3051
NaCl	360
KCl	340
Nitrates	
$Mg(NO_3)_2 . 6H_2O$	2805
$Ca(NO_3)_2 . 4H_2O$	4305
$NaNO_3$	880
KNO_3	316
NH_4NO_3	1920
Carbonates	
$Na_2CO_3 . 10H_2O$	217
$Na_2CO_3 . 7H_2O$	489*
$Na_2CO_3 . H_2O$	261
$K_2CO_3 . 2H_2O$	110
the solubility is given at 20°C, * the solubility is given at 40°C	

The salts sources can be divided into four main groups; salts primarily contained in building materials, salts transported into the structures by means of moisture rising from subsurface or moisture transport from different part of structure, salts originated in chemical corrosion of building materials induced by polluted atmosphere and salts originated from biological sources.

The destructive effect of water-soluble salts is the consequence of two main processes – crystallization and salt hydration in porous materials. In case of salts solution penetration into the porous structure of building materials, at the water evaporation the salts concentration in the solution is rising. The critical moment for salt crystallization is so called salt crystallization threshold that represents state, when the salt concentration in the solution exceeds the solubility of specific salt in water. Salt crystals can gradually fulfill the porous space and the crystallization pressures are exerted on the porous space. In dependence on temperature, supersaturation rate and pores dimensions, the destruction of materials can occur.

The second degradation process evoked by water-soluble salts is related to the salts that enable to bind defined amount of water molecules in their crystal lattice. The formation of hydration products is characteristic by changes of salt volume that are accompanied by hydration pressures. Also in this case, the harmful effect on the durability of building materials can be observed.

The extent of possible salt damage gives sound arguments for its thorough investigations; thus damage assessment of building materials and structures due to the effect of salts is very actual topic for researchers and building practice. In literature, two basic possibilities how to evaluate the danger of salts contained in building materials can be found. The first possibility is to take specimens from damaged structures and analyze them in laboratory. This provides information on water content and on the type and amount of ions in material which is very useful for assessment of the current state and for discovering the possible reasons for the presence of the particular ions. However, it is very difficult to make reliable predictions of further damage on the basis of these data. This requires years or even decades of on site measurements, aside from the fact that the extent of such analyses is logically restricted by the amount of material which can be taken from a historical building.

Another method of prediction of water and salt movement and salt crystallization in building structures represents mathematical and computational modeling. In this way, the time development of water and salt concentration fields can be obtained which is crucial for a proper assessment of possible future damage. However, the accuracy of simulated water and salt concentration fields critically depends on the availability of all input parameters.

There are two types of these parameters which have to be known in advance. The first are initial and boundary conditions. Initial conditions can be determined using on site analysis of water and salt concentration fields in the walls. Boundary conditions are of two types. The first of them are meteorological data for temperatures, relative humidities, rainfall and solar radiation, possibly also concentration of acid-forming gases in the atmosphere. The second type of boundary conditions involves water content and salt concentration in the underground soil close to the studied building. These data can be obtained again by on site analysis.

The second type of input parameters are water and salt transport and storage parameters of the materials of the wall which appear in water and salt mass balance equations. For the studied problem of coupled water and salt transport, these parameters include moisture diffusivity and water vapor diffusion resistance factor as water transport parameters, sorption isotherm and water retention curve as water storage parameters, ion binding isotherm as salt storage parameter and salt dispersion coefficient as salt transport parameter. These parameters can be determined by common laboratory methods.

In this paper, determination of moisture diffusivity and nitrate diffusion coefficient of sandstone in dependence on moisture and salt concentration is done on the basis of inverse analysis of experimentally determined moisture and salt concentration profiles.

2 MECHANISMS OF MOISTURE AND SALT TRANSPORT AND DETERMINATION OF TRANSPORT PARAMETERS

Determination of material parameters describing the mechanism of coupled salt and moisture transport is based on the assumed mode of this transport. In this work, the moisture dependent moisture diffusivity is calculated in three different ways on the basis of inverse analysis of experimentally obtained moisture and salt concentration profiles. First, the moisture diffusivity is calculated from moisture profiles measured for penetration of distilled water into the dry specimen. Then, the moisture diffusivity vs. moisture content function is calculated from moisture profiles measured for the penetration of KNO_3 solution. Finally, the third moisture diffusivity vs. moisture function is obtained by the inverse analysis of nitrate concentration profiles under assumption that no nitrate diffusion takes place in the liquid phase.

The diffusion mechanism of moisture transport where the dependence of moisture diffusivity κ [m^2s^{-1}] on moisture concentration w [m^3/m^3] was taken into account was assumed in the first two cases. For the inverse analysis of experimentally determined moisture profiles $w(x, t)$ Matano method [Matano, 1933] was employed. Its application leads to the following solution for moisture diffusivity.

$$\kappa(w_0) = \frac{1}{2t_0\left(\frac{dw}{dz}\right)_{z=z_0}} \int_{z_0}^{\infty} z \frac{dw}{dz} dz \ . \tag{1}$$

where t_0 =*const.* is a given time where the moisture field $w(z,t_0)$ is known and z is the space variable (for details see Drchalová *et al.* [2002]).

For description of coupled salt and moisture transport, diffusion-advection model proposed by Bear and Bachmat [Bear & Bachmat, 1990], [Pel *et al.*, 2000] was used. This model employs the system of parabolic equations describing salt and moisture transport. System of equations can be subjected to an inverse analysis in a similar way as for one parabolic equation, provided the initial and boundary conditions are simple enough, and the material parameters D and κ can be identified as functions of water content and salt concentration. The simplest possibility of such an inverse analysis is again an extension of the Boltzmann-Matano treatment under the same assumptions of constant initial conditions and Dirichlet boundary conditions on both ends of the specimen for both moisture content and salt concentration where one of the Dirichlet boundary conditions is equal to the initial condition. After applying Boltzmann transformation and performing some straightforward algebraic operations, we arrive at the following formula for the determination of salt diffusion coefficient.

$$D(z_0) = -\frac{C_f(z_0)\kappa(z_0)\left(\frac{dw}{dz}\right)_{z_0}}{w(z_0)\left(\frac{dC_f}{dz}\right)_{z_0}} + \frac{\int_{z_0}^{\infty} z\left(\frac{d(wC_f)}{dz} + \frac{dC_b}{dC_f}\frac{dC_f}{dz}\right)dz}{2t_0 \cdot w(z_0)\cdot\left(\frac{dC_f}{dz}\right)_{z_0}}, \tag{2}$$

where z is the space variable, t_0 the time corresponding to the chosen moisture and concentration profiles $w = w(z,t_0)$, $C_f = C_f(z,t_0)$, the chosen values of moisture and concentration are $w_0 = w(z_0, t_0)$, $C_{f0} = C_f(z_0, t_0)$, the corresponding moisture diffusivity and salt diffusion coefficient $\kappa(z_0) = \kappa(w_0, C_{f0})$, $D(z_0) = D(w_0, C_{f0})$ and $C_b = f(C_f)$ is the ion binding isotherm.

Using diffusion-advection model, the third moisture diffusivity function was also calculated neglecting the nitrate diffusion in the liquid phase ($D = 0$). The relation for moisture diffusivity calculation using this procedure is given as

$$\kappa(z_0) = \frac{\int_{z_0}^{\infty} z\left(\frac{d(wC_f)}{dz} + \frac{dC_b}{dC_f}\frac{dC_f}{dz}\right)dz}{2t_0 \cdot C_f(z_0) \cdot \left(\frac{dw}{dz}\right)_{z_0}}. \quad (3)$$

3 EXPERIMENTAL

Many historical buildings in the Czech Republic were built using sandstone. The sandstone studied in this paper originated from Mšené-lázně quarry and was originally used for ornamental parts of architecture. It is psamitic equigranular rock, about 95% of which is made up of suboval quartz clasts. Other mineral grains are present only as accessories (tourmaline, epidote, muscovite and zircone). Quartz grains reach up to 0.1 mm in diameter, but those of muscovite are larger, up to 0.3 mm. The matrix is formed by clay minerals (mainly kaolinite). In Table 2, the basic parameters of the studied material are given, ρ_b is the bulk density, ρ_{mat} matrix density and ψ total open porosity.

Table 2. Basic material properties of the studied sandstone.

ρ_b [kg m^{-3}]	ρ_{mat} [kg m^{-3}]	ψ [m^3 m^{-3}]
1807	2627	0.31

The rod shaped samples with the dimensions of 20 x 40 x 160 mm were used for the determination of moisture and nitrate concentration profiles in simulated 1-D water and nitrate solution transport. The dry, on lateral sides vapour-proof insulated samples were exposed by their 40 x 20 mm face to the penetrating KNO_3 solution (concentration 101.1 kg/m^3 of solution). Duration of the experiment was 30, 60 and 90 minutes for three different groups of samples. After this time, the samples were cut into 8 pieces and in each piece water content and nitrate concentration were measured. Moisture content was determined by the gravimetric method using weighing the moist and dried specimens. In the determination of nitrate concentration, the particular samples were after drying first ground by a vibration mill so that grains smaller than 0.063 mm were obtained. Then the ground samples were overflowed by 80 °C warm distilled water and leached. The nitrate contents in particular leaches were determined using an ion selective electrode.

For the determination of ion binding isotherm, Tang and Nilsson modified absorption method was chosen. This modification consisted in using the specimens of more realistic dimensions (40 x 40 x 10 mm) instead of crushed specimens [Jiřičková & Černý, 2006]. On the basis of the measured ion binding isotherm of KNO_3, $C_b = f(C_f)$, the profiles of bound and free nitrates were determined.

4 RESULTS AND DISCCUSION

The experimentally determined moisture and nitrate concentration profiles are presented in Figs. 1-3. For the computational inverse analysis it was necessary to smooth the measured data to obtain continuous functions. The linear filtration method was used for that purpose (see Figs. 1-3).

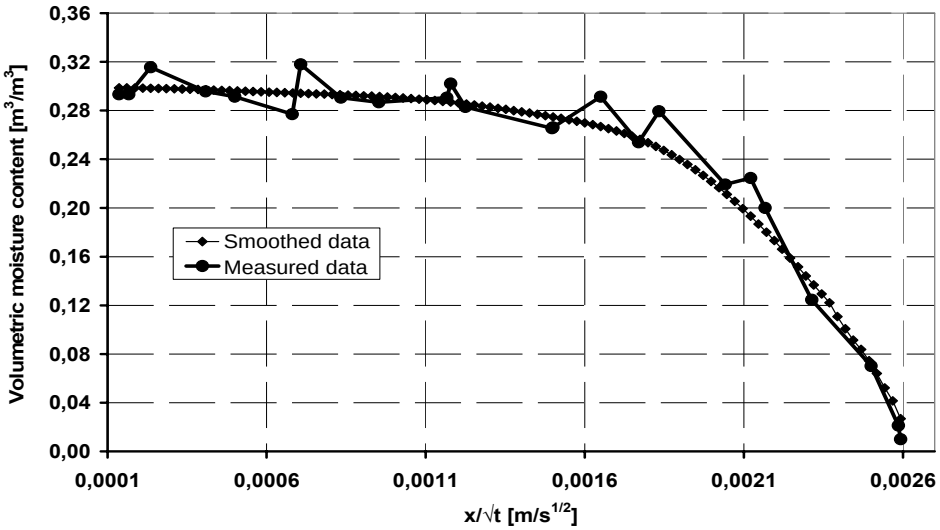

Figure 1. Volumetric moisture content for penetration of distilled water.

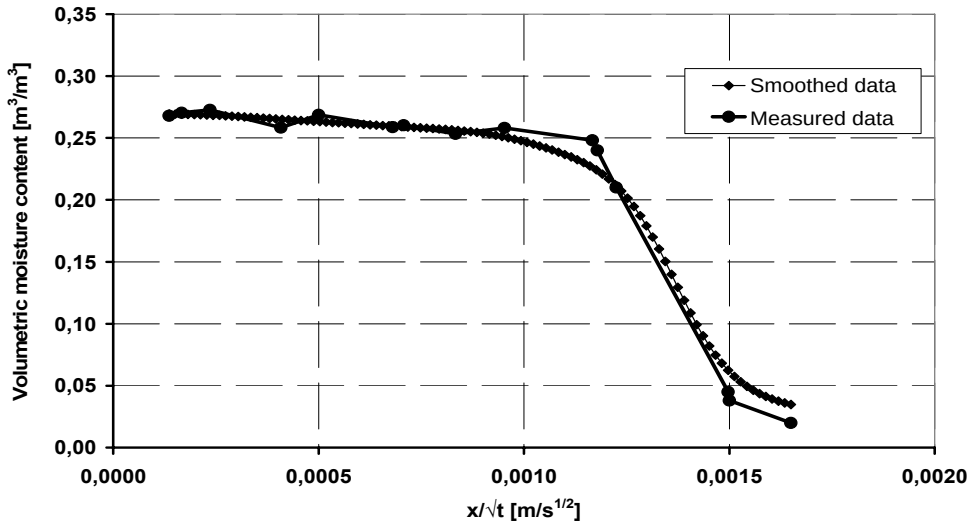

Figure 2. Volumetric moisture content for penetration of KNO_3 solution.

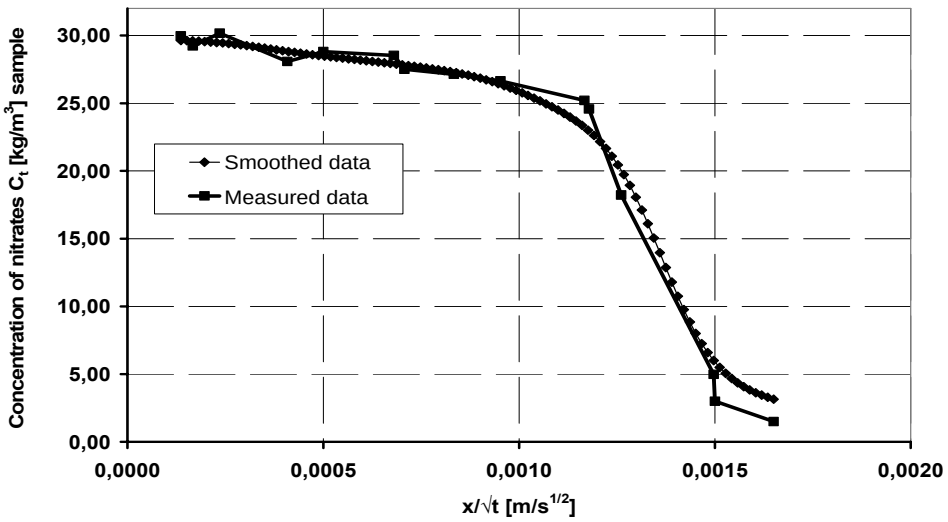

Figure 3. Total nitrates concentration.

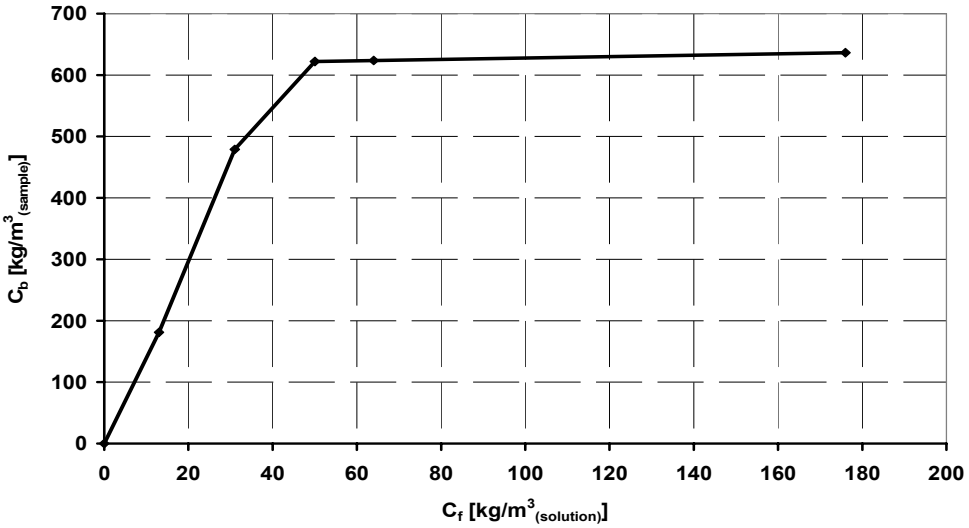

Figure 4. Binding isotherm of KNO_3 for the studied sandstone.

The nitrate binding isotherm measured by modified Tang and Nilsson adsorption method is shown in Fig. 4. The obtained binding isotherm gives evidence about the very high nitrate binding capacity of the studied material. The results of moisture diffusivity calculations are presented in Fig. 5. The moisture diffusivity calculated for penetration of distilled water is systematically higher than the moisture diffusivity obtained for KNO_3 water-solution. This is probably the consequence of the higher viscosity of KNO_3 solution compared to viscosity of distilled water. The results of inverse analysis also show that the possible neglect of nitrate diffusion in the liquid phase is apparently wrong, because the moisture diffusivity calculated from nitrate concentration profiles under this assumption is two to three orders of magnitude higher than moisture diffusivity calculated from moisture profiles. The dependence of nitrate diffusion coefficient on concentration is shown in Fig. 6. From the quantitative point of view, the calculated nitrate diffusion coefficient is quite high, about three orders of magnitude higher than the diffusion coefficients of most ions in free water. Therefore, the common diffusion mechanism is probably not the only driving force for nitrate transport within the liquid phase and some other driving forces are taking place here. This acceleration of nitrate transport can be attributed most probably to surface diffusion on pore walls and/or to osmotic effects.

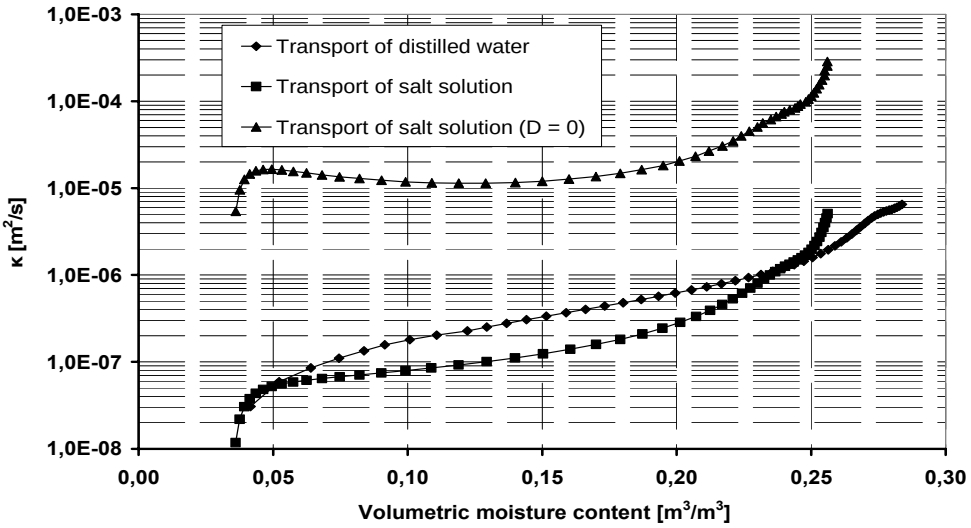

Figure 5. Moisture diffusivity of sandstone determined in three different ways.

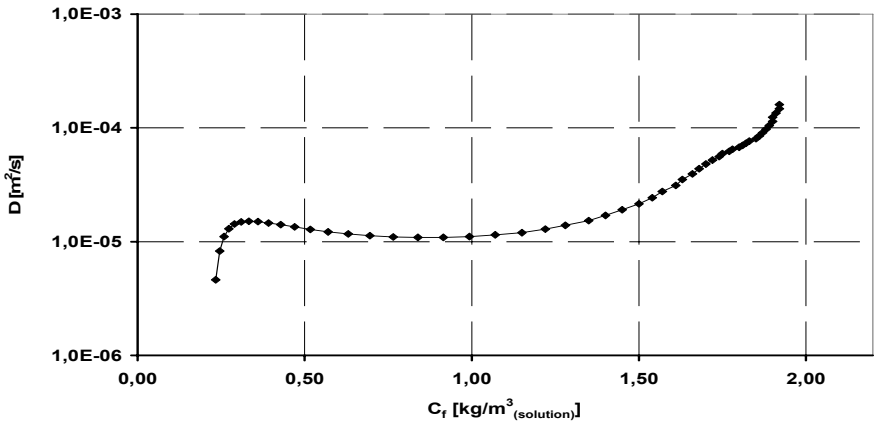

Figure 6. Nitrate diffusion coefficient of sandstone.

5. CONCLUSIONS

The main contribution of the work presented in this paper consists in the determination of two basic parameters describing the moisture and nitrate transport capability of the studied sandstone which make possible to perform damage assessments. The obtained results revealed very fast salt transport within the liquid phase affecting the total nitrate concentration in the material in a very significant way. From the point of view of exact explanation of mechanisms of coupled water and nitrate transport in porous materials, the presented experiments and calculations revealed the necessity to implement some other effects (e.g., surface diffusion and osmosis) into the diffusion-advection model.

ACKNOWLEDGMENTS

This research has been supported by Czech Ministry of Education, Youth and Sports of Czech Republic, under project No MSM: 6840770031.

REFERENCES

Bear J., & Bachmat Y., 1990, *Introduction to Modelling of Transport Phenomena in Porous Media*, Vol. 4, Kluwer, Dordrecht.

Drchalová J., Pavlík Z., & Černý R., 2002, 'A Comparison of Various Techniques for Determination of Moisture Diffusivity from Moisture Profiles', Proceedings of the 6th Symposium on Building Physics in the Nordic Countries, Trondheim, Norwegian University of Science and Technology, vol. 1, pp. 135-142.

Jiřičková M., & Černý R., 2006, 'Chloride Binding in Building Materials', *Journal of Building Physics* vol. 29, pp. 189-200.

Matano, C., 1933, 'On the relation between the diffusion coefficient and concentration of solid metals', *Jap. J. Phys.*, **8**, pp. 109-115.

Pel, L., Kopinga, K., & Kaasschieter, E. F., 2000, 'Saline absorption in calcium-silicate brick observed by NMR scanning', *J. Phys. D: Appl. Phys*, **33**, pp. 1380–1385.

The Correlation of Electric Emissions with Stress and Strain on Stressed Rock Samples

Ilias Stavrakas [1]
Antonis Kyriazopoulos [2]
Panayiotis Kyriazis [3]
Konstantinos Ninos [4]
Cimon Anastasiadis [5]
Dimos Triantis [6]

T 15

ABSTRACT

Laboratory experiments on rock samples have shown electric signal emissions when the samples are subjected to temporal stress variation. These electric signals are attributed to the generation and propagation of microcracks that guide the sample to mechanical failure.

In this work such electric emissions will be demonstrated for marble samples subjected to stress at a rate 0.3MPa/s approximately. The emissions become intense when the relative compressional stress becomes approximately 70% of the ultimate stress while it reaches its maximum value for relative stress value 0.95. Consequently the emission diminishes. Based on the sample stress-strain diagrams the electric emissions are directly related to the deviation of the linearity in the stress- strain diagram. The emitted electric current is correlated to the deformation of the sample through the measured strain. These emissions are attributed to the movement of dislocations and cracks that cause electric polarization and consequently charge flow. The damage in the bulk of the sample increases with stress while there is a stress level beyond which damage increases rapidly as new cracks form and connect to the growing existing cracks until a failure plane is formed and the sample collapses.

KEYWORDS

Pressure Stimulated Currents, Electric current emissions, Crack opening, Marble fracture, Mechanical stress.

[1.] Technological Educational Institution of Athens, Department of Electronics, Laboratory of Electric Properties of Materials, Athens, Greece, 12210, Phone +30 210 5316525, Fax +30 210 5316525, ilias@ee.teiath.gr
[2.] Technological Educational Institution of Athens, Department of Civil Engineering, Athens, Greece, 12210, Phone +30 210 5316525, Fax +30 210 5316525, akyriazo@teiath.gr
[3.] Technological Educational Institution of Athens, Department of Electronics, Laboratory of Electric Properties of Materials, Athens, Greece, 12210, Phone +30 210 5316525, Fax +30 210 5316525, pankyriazis@gmail.com
[4.] Technological Educational Institution of Athens, Department of Electronics, Greece, 12210, Phone +30 210 5316525, Fax +30 210 5316525, kninos@ee.teiath.gr
[5.] Technological Educational Institution of Athens, Department of Electronics, Laboratory of Electric Properties of Materials, Athens, Greece, 12210, Phone +30 210 5316525, Fax +30 210 5316525, cimon@ee.teiath.gr
[6.] Technological Educational Institution of Athens, Department of Electronics, Laboratory of Electric Properties of Materials, Athens, Greece, 12210, Phone +30 210 5316525, Fax +30 210 5316525, triantis@ee.teiath.gr

1 INTRODUCTION

Laboratory investigations that show the existence of electric signal emissions during a full cycle of rock deformation have received considerable attention in recent years. These electric emissions have been attributed in the past at several potential sources like the quartz existence [Nitsan, 1977; Ogawa *et al.,* 1985; Eccles *et al.,* 2005], fluid movement causing electrokinetic effect [Eccles *et al.,* 2005; Ishido & Mizutani, 1981; Yoshida *et al.,* 1998], point defects [Varotsos & Alexopoulos, 1986] and electron emissions [Brady & Rowell, 1986; Enomoto & Hashimoto, 1990].

At the same time acoustic emissions (AE) have been studied when applying stress to rocks and it was shown that they are highly indicative of rock deformation and failure processes [Lavrov, 2005; Lockner *et al.,* 1991; Sammonds *et al.,* 1992].

When dealing with quartz free rocks with extremely low internal moisture and low porosity the piezoelectric and the electrokinetic effects are not considered as strong underlying physical mechanisms to support the existence of electric signal emissions. A model that is applicable for this case was proposed by Slifkin [Slifkin, 1993] and was further developed by [Vallianatos & Tzanis, 1999; Tzanis & Vallianatos, 2002] and explains electric signal emissions due to the dislocation and other defect movements that cause local polarization. This model is known as Moving Charged Dislocations (MCD) model.

Papers of experimental laboratory recordings and analyses of electric signals emitted under temporally varying uniaxial compressional stress upon rock samples like marble and amphibolite have been conducted [Anastasiadis *et al.,* 2004; Stavrakas *et al.,* 2004; Triantis *et al.,* 2007; Anastasiadis *et al.,* 2007a,b]. The electric current emitted during such temporal stress variation leading to a catastrophic process and to sample fracture has been rendered under the term “Pressure Stimulated Current” (PSC).

The technique applied in order to show up and record the above described signals is rendered under the term «PSC technique».

The Pressure Stimulated Currents are characterized by very low peak values (1pA up to 100pA) and they reveal from the background noise level when the applied stress on the sample leads to the non-linear deformation region (out of the limits of Hooke’s law) and specifically when the sample is led to the Crack Propagation Zone (CPZ). Intense PSC emissions are observed slightly before the fracture of the sample.

According to the MCD model the observed transient electric variation is related to the non-stationary accumulation of deformation. The expected emission of Pressure Stimulated Current (PSC), is proportional to the strain rate [Vallianatos *et al.,* 2004]. When a PSC emission psc(t) is recorded during a process of a continuously increasing axial compressional stress it should obey the following law:

$$\mathrm{psc}(t) \propto \frac{d\varepsilon(t)}{dt} \tag{1}$$

where ε(t) is the temporal variation of the strain during the axial compressional stress variation σ(t). According to the Eq. 1 the total charge Q, released during that process is given as:

$$Q(t) = \int_0^t \mathrm{psc}(t)\,dt \propto \varepsilon(t) \tag{2}$$

During this work marble samples were subjected to constantly increasing compressional stress from early stress levels up to fracture. The stress rate was 0.3MPa/s. The PSC emissions were recorded

during all the experimental procedure. The emitted PSC is discussed with respect to the deformation and the applied compressional stress.

2 SAMPLES AND EXPERIMENTAL TECHNIQUE

In this section marble, which is the material under examination, is described. Rock materials and especially marble have been used in the past in constructions and therefore results concerning their strength may serve in many restoration works that are in progress as for example on the Parthenon temple of the Acropolis of Athens as well as on other civil engineering applications.

Marble is a geomaterial of known physical and chemical properties. The marble samples under examination were collected from Mt. Penteli (Dionysos) and are mainly composed of calcite (98%) and other minerals i.e. 0.5% of muscovite, 0.3% of sericite, 0.1% of chlorite, it also contains 0.2% of quartz (Kourkoulis et al. 1999). Its specific density is 2730 kg/m^3, its apparent density is 2717 kg/m^3 and its porosity is very low, varying from 0.3% for pristine marble to 0.7% for marble that has suffered natural weathering and has been exposed to corrosive agents [Kleftakis *et al.*, 2000].

The used samples were prismatic and the stress was applied in parallel axis to the long edge. The dimensions of the used specimens were 35mm x 35mm x 60mm and their fracture limit was 47MPa approximatelly.

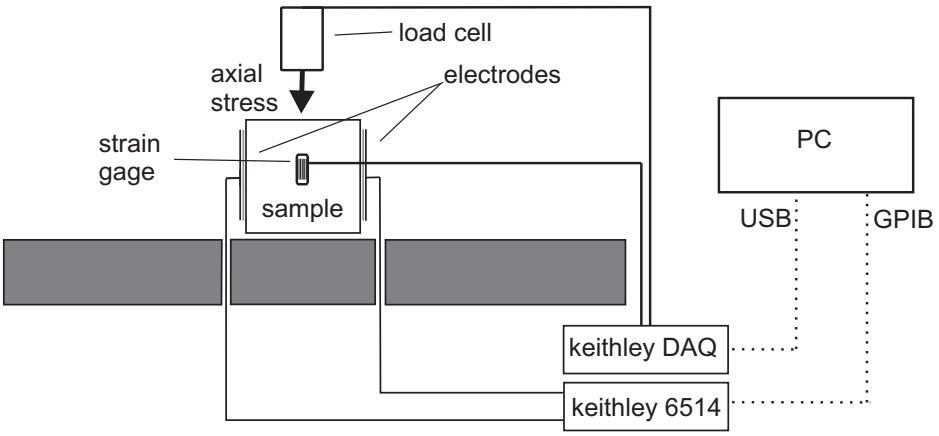

Figure 1. A schematic representation of the experimental set-up to conduct PSC experiments.

Figure 1 shows the schematic representation of the experimental PSC-techniques. The experiment was conducted in a Faraday shield to prevent from electric noise from affecting the measurements. The shield protects the mechanical parts that transfer the stress on the sample (i.e hydraulic stressing cylinder Enerpac-RC106, plates, sample underlay holder), the stress and strain sensors and the electrodes that measure the PSC.

The sample was placed on a steel anvil and thin Teflon plates were placed between the anvil and the stressing plates to provide electric insulation. The electrodes were attached to the marble sample, using conductive paste. Two gold plated electrodes were attached on the sample where the conductive paste was applied in a direction perpendicular to the axis of the applied axial compressive stress.

The stress sensor (load cell) is placed on the axis of stress and the strain sensor is placed in the free edges of the sample in a direction perpendicular to the stress (see Fig. 1).
Properly shielded Keithley cables that minimize electric noise lead through interfaces the PSC to the programmable electrometer placed outside the shield. PSC measurements were conducted using the programmable electrometer Keithley 6514. The communication of the Keithley electrometer and the PC that stored the measurements was achieved through a GPIB interface.

The stress was measured through a stress sensor ADW 15 that converts the applied stress to voltage. The strain was measured using Kyowa strain gauges attached on the Microlink-770, 120Ω resistance bridge. The stress and the strain were directly recorded on the PC through a 8 differential channel, high sampling rate, and 500x maximum amplification, Keithley A/D converter. All the data were stored in a computer hard disk through the described interfaces at a sampling rate 3samples/s.

3 EXPERIMENTAL RESULTS – DISCUSSION

The applied compressional uniaxial stress was constantly increasing on the sample at a rate of 0.3MPa/s from very low stress levels up to fracture. Figure 2 (curve a) presents the temporal development of the emitted PSC. It becomes obvious that the PSC starts to show an excitation only after time t=220s. It is significant to notice at the curve b of the same figure that time t-220s corresponds to a strain value slightly higher than 0.004. This strain value corresponds to the stress-strain curve (Fig3. curve a) at the point were stress and strain are no more linearly related. It is known [Lavrov, 2005] that this value corresponds to the crack formation and propagation region, regarding the sample's mechanical behaviour. Since PSC emissions are mainly attributed to crack formation and propagation it is expected that when these mechanisms are activated they dominate the sample bulk and PSC excitation is expected to be observed.

Another significant observation is that despite the fact that the stress increases linearly the PSC values after time t=270s approximately seem to grow fast following a corresponding change of the deformation. This is the point that the yielded strain changes much faster than the applied stress. In terms of cracking and damage mechanisms in general it can be stressed that this is the region where dynamic processes take place, macrocracks are created, the fracture plane is formed and the irreversible failure process initiates.

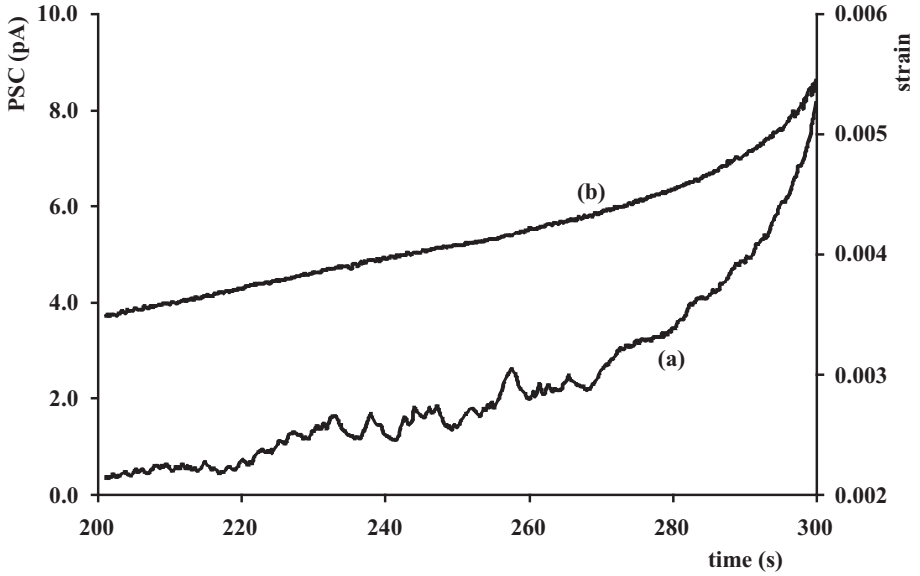

Figure 2. The temporal development of the emitted PSC (curve a) and the temporal development of the deformation while applying constantly increasing stress (curve b).

Studying the totaly released charge with respect to deformation some significant results can be drawn. Figure 3, curve a, clearly shows that the stress and the strain are linearly related up to a stress value of the order of 40MPa approximatelly. Beyond that point the stress and the strain are no more linearly related to each other and the strain starts to grow faster than the applied stress. At a value of stress 47MPa approximately the failure of the sample occurs. Regarding the total released charge with

respect to the stress-strain curve of the marble samples it can be stressed that no significant charge is released when the stress and the strain are linearly related. For a strain value of the order of 0.004 it can be seen on the curve that the total released charge Q is of the order of 20pC. When the stress increases further and stress and strain are no more linearly related the released charge increases linearly with the yielded strain. This process goes up to the vicinity of fracture for stress levels of the order of 46MPa approximately which corresponds to the 98% of the ultimate compressional strength.

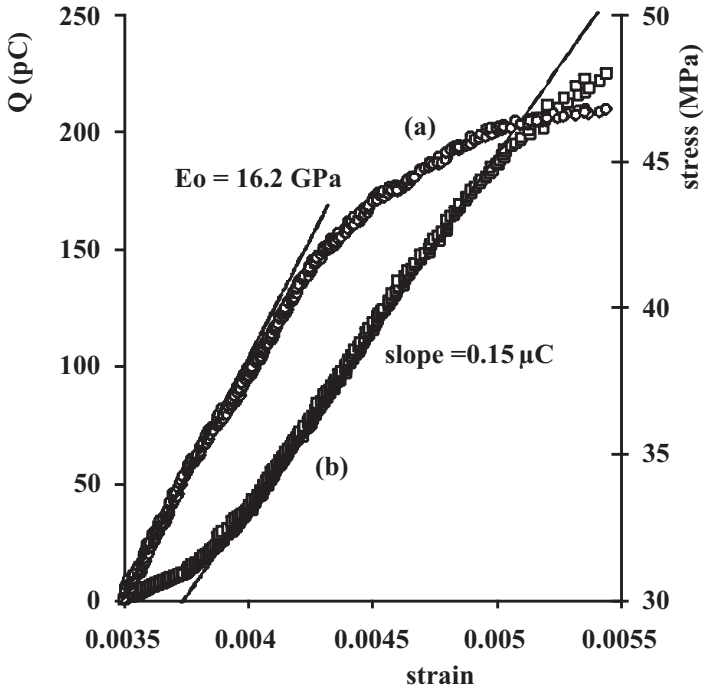

Figure 3. A representative stress strain curve of the used marble samples (curve a) in the same diagram with the totaly released charge with respect to the strain (curve b).

4 CONCLUDING REMARKS

This work demonstrates that during a stressing process of marble samples the total released charge is linearly related to the deformation change in a good approximation. This linearity is valid from the point that both stress and strain are no more linearly related (see the stress-strain curve at about 60% of the ultimate compressional stress strength) up to the near fracture range (98% of the ultimate compressional stress strength of the sample).

When the released charge and the strain are no more linearly related this indicates the upcoming event of fracture.

After all these the PSC technique and specifically by the study of the totally released charge was proved to be a valuable tool in laboratory conditions that can detect the mechanical status of marble samples. The underlying mechanisms of the generation of the PSC are based on the Moving Charged Dislocation Model.

REFERENCES

Anastasiadis, C., Triantis, D., Stavrakas, I. & Vallianatos, F., 2004, 'Pressure stimulated currents (PSC) in marble samples after the application of various stress modes before fracture', *Annals of Geophysics*, 47, 21-28.

Anastasiadis, C., Triantis, D., & Hogarth, C.A., 2007a, 'Comments on the phenomena underlying pressure stimulated currents (PSC) in dielectric rock materials', *Journal of Materials Science*, 42, 2538-2542.

Anastasiadis, C., Stavrakas, I., Triantis D., & Vallianatos F., 2007b, 'Correlation of Pressure Stimulated Currents in rocks with the damage parameter', *Annals of Geophysics*, 50, 1-6.

Brady, B.T. & Rowell, G.A., 1986, 'Laboratory investigation of the electrodynamics of rock fracture', *Nature*, 321, 448-492.

Eccles, D., Sammonds, P.R., & Clint, O.C., 2005, 'Laboratory studies of electrical potential during rock failure', *International Journal of Rock Mechanics and Mining sciences*, 42, 933-949.

Enomoto, J., & Hashimoto, H., 1990, 'Emission of charged particles from indentation fracture of rocks', *Nature*, 346, 641-643.

Ishido, T., & Mizutani, H., 1981, 'Experimental and theoretical basis of electrokinetic phenomena in rock-water systems and its applications to geophysics', *J. Geophys. Res.*, 86, 1763-1775.

Kleftakis, S., Agioutantis, Z., & Stiakakis C., 2000, 'Numerical Simulation of the uniaxial compression test including the specimen-platen interaction', *Computational methods for shell and spatial structures*, IASS-IACM.

Lavrov, A., 2005, 'Fracture-induced Physical Phenomena and memory Effects in Rocks: A Review', *Strain*, 41, 135-149.

Lockner, D.A., Byerlee, J.D., Kuksenko, V., Ponomarev, A., & Sidorin, A., 1991, 'Quasi-static fault growth and shear fracture energy in granite', *Nature*, 350 [7], 39-42.

Nitsan, U., 1977, 'Electromagnetic emission accompanying fracture of quartz-hearing rocks', *Geophysical Research Letters*, 4, 333-337.

Ogawa, T., Oike, K., & Mirura, T., 1985, 'Electromagnetic radiations from rocks', *J. Geophys. Res.*, 90, 6245-6249.

Sammonds, P. R., Meredith, P.G., & Main I.G., 1992, 'Role of pore fluids in the generation of seismic precursors to shear fracture', *Nature*, 359, 228-230.

Slifkin, L., 1993, 'Seismic electric signals from displacement of charged dislocations', *Tectonophysics*, 224, 149-152.

Stavrakas, I., Triantis, D., Agioutantis, Z., Maurigiannakis, S., Saltas, V., Vallianatos, F., & Clarke, M., 2004, 'Pressure stimulated currents in rocks and their correlation with mechanical properties', *Natural Hazards and Earth System Sciences*, 4, 563–567.

Triantis, D., Anastasiadis, C., Vallianatos, F., Kyriazis, P., & Nover, G., 2007, 'Electric signal emissions during repeated abrupt uniaxial compressional stress steps in amphibolite from KTB drilling', *Natural Hazards and Earth System Sciences*, 7, 149-154.

Tzanis, A., & Vallianatos, F., 2002, 'A physical model of electrical earthquake precursors due to crack propagation and the motion of charged edge dislocations', in M. Hayakawa and O.A. Molchanov (eds), *Seismo Electromagnetics: Lithosphere-Atmosphere-Ionosphere Coupling*, TERRAPUB, Tokyo, 117-130.

Vallianatos, F., & Tzanis, A., 1998, 'Electric current generation associated with the deformation rate of a solid: Preseismic and coseismic signals', *Physics and Chemistry of the Earth*, 23, 933-938.

Vallianatos, F., Triantis, D., Tzanis, A., Anastasiadis, C. & Stavrakas, I. 2004, 'Electric Earthquake Precursors: From Laboratory Results to Field Observations', *Physics and Chemistry of the Earth*, 29, 339-351.

Varotsos, P., & Alexopoulos, K., 1986, 'Thermodynamics of point defects and their relation with bulk properties' North-Holland, Amsterdam.

Yoshida, S., Clint., O.C. & Sammonds, P.R., 1998, 'Electric potential changes prior to shear fracture in dry and saturated rocks', *Geophys. Res. Lettters*, 25, 1577-1580.

Freeze Thaw Susceptibility of Natural Stone – Characterization of the Mechanical Strength and Microstructure During Frost Cycling

T. Yates [1]
A. Mauko [2]

T 15

ABSTRACT

Frost resistance of natural stones is complex phenomena. Different intrinsic properties (e.g. porosity and mineral composition) as well as extrinsic properties (e.g. presence of salts, temperature variation, humidity) influence frost resistance of stone. In some countries frost is consider as being one of the most potent causes of decay, although attribution of deterioration features of in-built stone only to one factor is ambiguous.

The test method for determination of susceptibility of natural stone to frost deterioration is standardised with CEN standard EN 12371. Additional requirements for testing are given in appropriate harmonised standards for natural stone products, e.g. EN 1469 for cladding slabs. Although standard EN 12371 has been used for some years now, it has been established that a robust correlation of test results to actual condition is difficult to make.

The main objective of the research presented in this paper was to give insight into frost deterioration of two selected marbles and two limestones during 104 cycles of standardised test. Relationships between intrinsic properties of stone (porosity and mineral composition) and frost resistance, which was determined by mechanical characterization of stone (flexural strength and USV measurement) after 12, 24, 56 and 104 frost cycles, are given. The results of research can be used as input information for modelling the life span and risk assessment of natural stone façade when subjected to frequent freezing.

KEYWORDS

Frost resistance, Natural stone, Porosity, USV, Strength

[1] BRE, Watford, United Kingdom, Phone +44 (0)1923 664341, Fax +44 (0)1923 664991, yatest@bre.co.uk
[2] Slovenian National Building and Civil Engineering Institute (ZAG Ljubljana), Ljubljana, Slovenia, Phone +386 1 280 4 251, Fax +386 1 436 7 449, alenka.mauko@zag.si

1 INTRODUCTION

During its life span natural stone product is exposed to various degradation processes. Their damage effects can be additive, antagonistic or synergetic [Wessman 1997]. Among many acting mechanism the actual cause for stone deterioration ['Fig. 1'] is sometimes difficult to define. Nevertheless, freeze-thaw cycles are generally considered as one of the main decay factor of natural stone, especially in northern and central European countries.

Although generally assessed as important parameter, detailed mechanisms of stone frost deterioration are still not fully understood. Freeze-thaw durability depends greatly upon stone's intrinsic and extrinsic parameters. Porosity, the moisture content and presence of dissolved salts highly influence performance of stone while exposed to frost action [Lindqvist *et al.* 2007].

Current practice of assessing the effect of freeze-thaw cycles on natural stone product's characteristics (flexural strength, dowel hole strength, compressive strength) is based on CEN standard EN 12371. After certain number of cycles of freezing in air and thawing in water [e.g. 48 cycles for stone pavements – EN 1341 and 1342, or 12 cycles for stone cladding – EN 1469], the frost resistance is determined as the change of mean strength or as the number of cycles necessary to initiate cracks or rupture. However, such concept is difficult to apply to in-built performance of stone products, since some products show cracks and spalling after a while, although they have passed the frost test, while others not passing the test exhibit good performance during their life span in building [Ingham 2005].

In this study, susceptibility to freeze and thawing was determined for four selected natural stones, two marbles and two limestones. With flexural strength and USV measurements after 12, 24, 56 and 104 cycles, different performance for four selected stone was determined. Additionally, materials were characterised by measurements of open porosity and apparent volume.

In this study, hypothesis about deterioration rate differences between studied samples is examined. Following this hypothesis, prediction of life span of natural stone products exposed to natural cycling of freezing and thawing must be based on detailed studies, since different behaviour can be established even among same rock types.

Figure 1. Here, deterioration of calcitic marble in the form of intense cracking is visible. The actual cause for deterioration is difficult to define; probably it is due to simultaneous action of freezing and thawing and thermal degradation, or even mechanical loading.

2 MATERIALS AND METHODS

Four samples have been chosen for determination of frost resistance; two marbles (one dolomitic, one calcitic) and two limestones. In [Table 1] a list of samples is presented. Samples were tested according to CEN standards or other methods, e.g. EN 12371 – Determination of frost resistance, EN 12372 – Determination of flexural strength, EN 14579 – Determination of sound speed propagation, EN 1936 – Open porosity and apparent volume, OM – Optical microscopy, SEM – Scanning electron microscopy, Hg – Mercury porosimetry, EN 13755 – Water absorption at atmospheric pressure, EN 13364 – Determination of dowel hole strength. Only part of results (mechanical strength, apparent volume and porosity) is presented in this paper.

Table 1. List of samples tested in the frame of frost resistance study.

Sample no.	*Petrographic name*	*Number of specimens*	*Dimension of specimens [mm]*	*Method according to standard*
1	Dolomitic marble	63	30x50x180	EN 12371, EN 12372, EN 14579*
		57	30x30x30	EN 1936, OM, SEM, Hg
		12	30x30x30	EN 13755*
		10**	200x200x30	EN 13364
2	Calcitic marble	63	30x50x180	EN 12371, EN 12372, EN 14579*
		57	30x30x30	EN 1936, OM, SEM, Hg
		12	30x30x30	EN 13755*
		10**	200x200x30	EN 13364
3	Limestone	63	30x50x180	EN 12371, EN 12372, EN 14579*
		57	30x30x30	EN 1936, OM, SEM, Hg
		12	30x30x30	EN 13755*
		10**	200x200x30	EN 13364
4	Limestone	63	30x50x180	EN 12371, EN 12372, EN 14579*
		57	30x30x30	EN 1936, OM, SEM, Hg
		12	30x30x30	EN 13755*
		10**	200x200x30	EN 13364

* Deviations from standard's requirements regarding size of specimens

Freeze-thaw cycling was carried out according to test procedure described in EN 12371:2001. Five batches of specimens with denotations *A – E* were sawed from cladding panels of 20 and 30 mm thickness. On specimens from batch *A*, initial properties of fresh samples [flexural strength, speed of sound propagation and open porosity] were determined according to corresponding standards [EN 12372, EN 14579, EN 1936]. Specimens from batches *B*, *C*, *D* and *E* were then exposed to freeze-thaw cycling. After every 12th cycle apparent volume and visual examination were carried out. After 12, 24, 56 and 104 cycles, specimens of corresponding batches were taken out from frost chamber, dried at 70 ^{o}C in ventilated oven to constant mass, after which USV, flexural strength and open porosity, were again determined.

3 RESULTS AND DISCUSSION

3.1 Visual Examination

Four samples exhibit different characteristics during frost exposure. The most decaying material is white calcitic marble (sample no. 2), in the case of which signs of deterioration had been observed even before exposure. Poor cohesion between mineral grains in sample no. 2 is marked by degranulation or "sugaring".

During frost exposure this material becomes progressively deteriorated. After no more than 12 cycles changes in colour can be observed and thin hair-like cracks start to form, although none of the specimen had completely disintegrated during 104 cycles. During exposure other samples didn't change significantly, with exception of slight rounding of edges. Cohesion between stylolites in sample no. 3 is good even after the end of exposure.

3.2 Mechanical Strength

Results of initial flexural strength measurements and measurements of flexural strength after 12, 24 and 56 cycles, are given in [Table 2] and 'Fig. 2 and 3'.

The lowest flexural strength can be observed in the case of sample no. 2, while the highest flexural strength has micritic limestone with stylolits, sample no. 3 ['Fig. 2'].

On 'Fig. 3' different characters of flexural strength decrease, or in the case of #3 slight increase, can be observed.

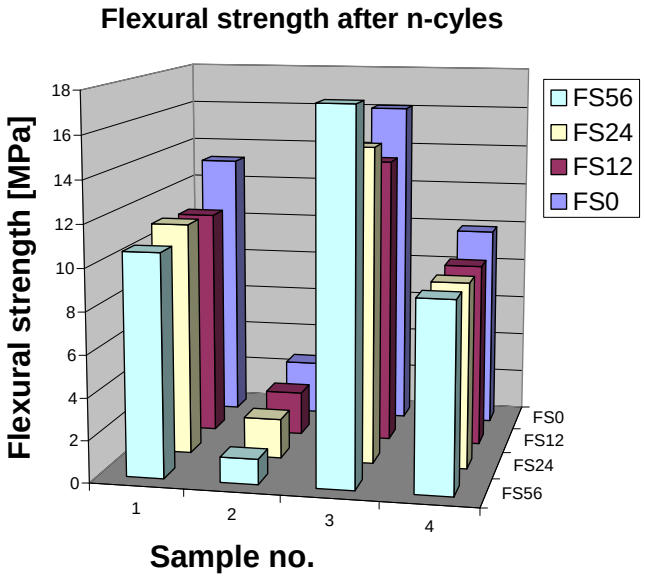

Figure 2. Flexural strength of samples before exposure (*FS0*) and after 12 (*FS12*), 24 (*FS24*) and 56 (*FS56*) *c*ycles.

Table 2. Decrease/increase of flexural strength before exposure [Rtf_0] and during 12, 24 and 56 cycles [Rtf_{12}, Rtf_{24}, Rtf_{56}, respectively].

Sample		*Rtf_{nave}*	*$Stdev_0$*	*Δ [%]*
1	Rtf_0	13,2	1,8	0
	Rtf_{12}	11	0,5	-16,7
	Rtf_{24}	11,2	0,9	-15,2
	Rtf_{56}	10,6	0,8	-19,7
2	Rtf_0	2,6	0,6	0,0
	Rtf_{12}	2,1	0,5	-19,2
	Rtf_{24}	1,9	0,4	-26,9
	Rtf_{56}	1,2	0,3	-53,8
3	Rtf_0	16,1	2,6	0,0
	Rtf_{12}	13,9	1,5	-13,7
	Rtf_{24}	15,1	2,3	-6,2
	Rtf_{56}	17,5	2,5	8,7
4	Rtf_0	9,9	0,9	0,0
	Rtf_{12}	8,9	3,2	-10,1
	Rtf_{24}	8,9	1,2	-10,1
	Rtf_{56}	9,0	0,8	-9,1

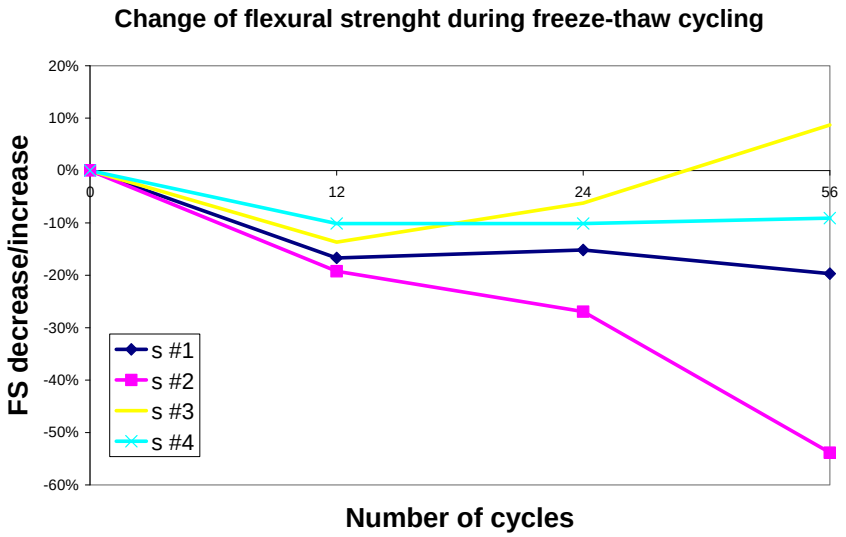

Figure 3. Change of average flexural strength (in percentage) during 56 cycles.

3.3. Ultrasonic Velocity

Average speeds of sound propagation and rates of decrease [increase] during exposure are listed in [Table 3]. In general, USV degradation curve ['Fig. 4'] follows the flexural strength degradation curve ['Fig. 3]. Again, velocity of sound propagation decrease with the highest rate in the case of sample 2, while sample 3 shows constant increase in speed propagation.

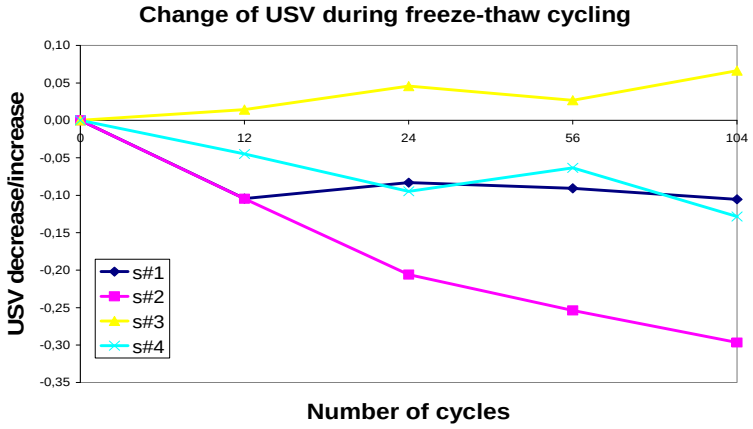

Figure 4. Change of USV during 104 cycles.

Table 3. Change of USV after 12, 24, 56 and 104 cycles.

Sample		USV_{0ave} [km/s]	$Stdev_0$ [km/s]	USV_{nave} [km/s]	$Stdev_n$ [km/s]	Δ [%]
1	v_{12}	5,94	0,18	5,32	0,36	-10,4
	v_{24}	6,02	0,29	5,52	0,19	-8,3
	v_{56}	5,95	0,29	5,41	0,25	-9,1
	v_{104}	6,07	0,21	5,43	0,18	-10,5
2	v_{12}	2,87	0,51	2,57	0,43	-10,5
	v_{24}	3,06	0,55	2,43	0,37	-20,6
	v_{56}	2,60	0,23	1,94	0,19	-25,4
	v_{104}	3,17	0,34	2,23	0,18	-29,7
3	v_{12}	6,97	0,65	7,07	0,69	1,4
	v_{24}	7,00	0,4	7,32	0,45	4,6
	v_{56}	7,07	0,36	7,26	0,46	2,7
	v_{104}	7,08	0,6	7,55	0,57	6,6
4	v_{12}	5,63	0,41	5,61	0,37	-0,4
	v_{24}	6,02	0,41	5,75	0,24	-4,5
	v_{56}	5,91	0,51	5,35	0,48	-9,5
	v_{104}	5,99	0,45	5,61	0,45	-6,3

3.4 Apparent Volume

No significant change in apparent volume can be seen during freezing and thawing, although with other methods deterioration trend could be observed. Following this, despite of different broad range regarding frost resistance of studied materials [material with high rate of deterioration, material with no deterioration], method of measurement apparent volume after every 12 cycles is too robust to determine susceptibility of stone to frost action.

On 'Fig. 5' apparent volume of sample no. 2 after 12, 42 and 104 cycles is presented.

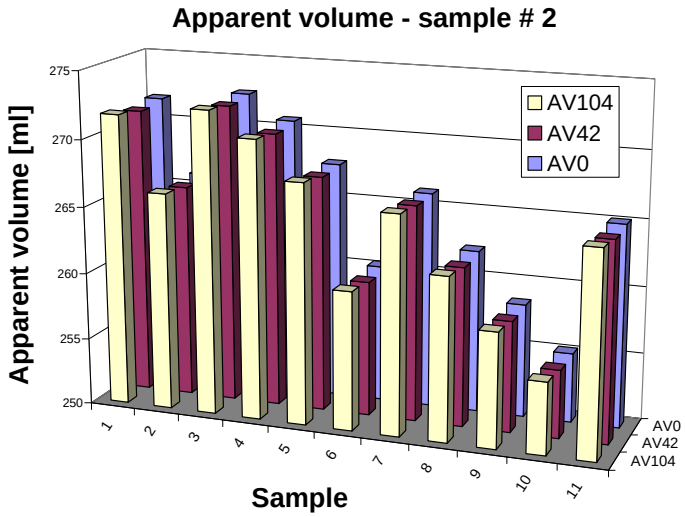

Figure 5. Apparent volume of sample no. 2 after 0, 42 and 104 cycles.

3.5 Open Porosity

In the state of art only open porosity for marbles has been determined [Table 4]. No change in porosity is observed in the case of dolomitic marble, which also shows good performance after exposure and a relatively moderate decrease of USV and flexural strength. A slight increase of open porosity was measured in the case of calcitic marble.

Table 4. Open porosity of sample no. 1 and 2 before exposure and after 104 cycles.

Sample	*Average open porosity before exposure*	*Average open porosity after 104 cycles*
Sample 1	0.5	0.5
Sample 2	0.6	0.7

5. CONCLUSIONS

Frost susceptibility of four samples of two different marbles and limestones has been studied. It has been established that there is significant difference in deterioration rate due to freeze thaw cycling even among samples of the same rock group. While three of the studied samples show general decrease in flexural strength and USV, compact micritic limestone shows distinctive increase of mechanical properties.

While in the case of flexural strength this could be explained on the first glance by heterogeneity of natural stone, steady increase of USV shows this is not so. The detailed mechanism of improvement of

mechanical properties of some samples during frost exposure can not be explained in this stage. Further explanation of the mechanism could be given after detailed study of nature of porous and rock microstructure.

ACKNOWLEDGMENTS

The authors would like to thank to Geoff Ashall for carrying out the flexural strength tests. One of the authors, Alenka Mauko, would also like to thank to Scientific and Educational Foundation of the Republic of Slovenia - *Ad Futura* for granted financinal support for researchers exchange.

REFERNCES

BS EN 1341:2001, 'Slabs of natural stone for external paving – Requirements and test methods', BSI, London, UK, 44 pp.

BS EN 1342:2001, 'Setts of natural stone for external paving – Requirements and test methods', BSI, London, UK, 40 pp.

BS EN 1936:2006, 'Natural stone test methods – Determination of real density and apparent density, and of total and open porosity', BSI, London, UK, 14 pp.

BS EN 12371:2001, 'Natural stone test methods – Determination of frost resistance', BSI, London, UK, 18 pp.

BS EN 12372:2006, 'Natural stone test methods – Determination of flexural strength under concentrated load', BSI, London, UK, 18 pp.

BS EN 14579:2004, 'Natural stone test methods – Determination of sound speed propagation', BSI, London, UK, 16 pp.

Ingham, J.P., 2005, 'Predicting the frost resistance of building stone', *The Quarterly Journal of Engineering Geology and Hydrogeology*, 38[4], 387-399.

Lindqvist, J.E., Malaga, K., Middendorf, B., Savukoski, M., & Pétursson, P., 2007, 'Frost resistance of natural stone, the importance of micro- and nano- porosity', www.sgu.se/dokument/fou_extern/Lindqvist-et-al_2007.pdf, last visited on 29th of October, 2007.

Wessman, L., 1997, 'Studies on the frost resistance of natural stone', Report TVBM-3077, Lund Institute of Technology, Division of Building Materials, Lund, Sweden, 199 pp.

11DBMC International Conference on Durability of Building Materials and Components
ISTANBUL, Turkey 11-14 May 2008

Visual Effects of Building Stone Texture

Jun Tsuchiya [1]
Shoji Sunaga [2]

T 15

ABSTRACT

Durability of buildings is an important issue of social demand. For this demand it is necessary to maintain not only structural durability but also visual performance, which pertains to the pleasant appearance of building materials. However, currently there is no common evaluation method for the visual performance of building materials, so it is still difficult to find a general standard for selecting finishing materials. Due to its durability and appearance, many stones has used as finishing materials. On the other hand, little research has been done on the visual performance of building stone finishing.

In this research, the effect of surface properties on the visual evaluation of building stone finishing was investigated.

One of the important characteristic appearances of stones is a feeling of depth,which gives high quality impression by a deep color. Factors affecting the visual depth of natural stone surface were analyzed by performing a sensory test using natural stone specimens which varied in stone type, surface finishing method and surface pattern. And appearance of glossy and glitter surface especially analyzed by performing a sensory test using 7 level polished black stone specimens.

Physical values of luminance, and surface color were measured and the relationship between them and the results of the sensory tests were considered. It was shown that the visual evaluation of stone specimens is affected by various factors, visual gloss and the feeling of depth are related to the physical value of the surface luminance and dark color. There was no definite relationships between luminance and other evaluation items such as flavor , comfort and calmness.

KEYWORDS

Stone, Texture, Visual effect, Feeling of depth, Sensory test

[1] User Science Institute, Kyushu University, 4-9-1, Shiobaru, Minami-ku, Fukuoka, 815-8540, Japan, Phone +81 92 553 4654, Fax +81 92 553 4654, tsuchiya@usi.kyushu-u.ac.jp
[2] Department of Visual Communication Design, Faculty of Design, Kyushu University, 4-9-1, Shiobaru, Minami-ku, Fukuoka, 815-8540, Japan, Phone +81 92 553 4508, Fax +81 92 553 4508, sunaga@design.kyushu-u.ac.jp

1 INTRODUCTION

Durability of buildings is an important issue of social demand. For this demand it is necessary to maintain not only structural durability but also visual performance, which pertains to the pleasant appearance of building materials. This is a performance relates to the aging effect for the visual materials deeply.However, currently there is no common evaluation method for the visual performance of building materials, so it is still difficult to find a general standard for selecting finishing materials. Due to its durability, the use of stone has increased as finishing material in recent years. On the other hand, little research has been done on the visual performance of building stone finishing. It is thought that the stone has the aging characteristic.

Kitamura and Isoda (1998) evaluated the appearance of building materials by visual sensation and tactile sensation. Nakayama (1998) examined the deterioration and discoloration of natural stones used for building. However, there does not seem to be a full examination of stone finishing only. In addition to the many kinds of stone types, building stone has some traditional surface finishing, and the visual impression changes with the finish. Moreover, there are other factors which affect the impression of stone, such as colors, patterns and surface forms. These factors influence each other. The purpose of this study is to extract the features and determine the factors affecting the visual evaluation like the feeling of depth of various stones.

2 SENSORY TEST ON THE IMPRESSION OF STONE

2.1 Outline

In order to grasp the factors which influence the impression of a stone, a sensory test was performed on specimens of natural stone of various types and surface finishing. For comparison, surface properties such as surface colors were measured. The relationship between these surface properties and the evaluated sensory values were analyzed.

2.2 Procedure of Sensory Test

2.2.1 Preliminary Sensory Test (Test 1)

Stone specimens of size 90×150×10 mm were cut out of actual stone. Thirteen kinds of stone types generally used as stone finishes for the interior or exterior of buildings in Japan were selected. The surface finishing of these stones was changed (Table 1). The sensory test was performed on 13 stone specimens by 33 subjects, all of whom were students and teachers with normal eyesight (19men & 14women who were about 20 ~ 50years old). The laboratory was arranged such that the stone specimens were illuminated with 700 lx fluorescent light (5000 K). The test was conducted under the controlled lighting condition. The subjects were asked to evaluate the feeling of depth and similar words to depth. The results were quantified.

2.2.2 Sensory Test of Granite (Test 2)

Stone specimens of size 90×90×10 mm were cut out of actual stone. The surface finishing of these stones was changed (Table 2). The sensory test was performed on 7 stone specimens by 22 subjects, all of whom were students and graduate students with normal eyesight (11men & 11women who were about 20 ~ 30years old). The laboratory was arranged as well as test1. The test was conducted under the controlled lighting condition. The subjects were asked to evaluate 10 items (Table 3) which extracted from test1, and results were quantified.

Table 1. Stone images and measurement results (Test 1).

Name	A	B	C	D	E
Stone	granite	granite	granite	granite	granite
Source	South Africa	South Africa	USA	USA	Norway
Finish	polished	burned	polished	burned	polished
Luminance	85.38cd/㎡	51.01 cd/㎡	99.83 cd/㎡	80.17 cd/㎡	76.21 cd/㎡
L*	94.05	76.69	99.93	91.76	89.96
a*	12.86	11.06	17.49	20.62	12.69
b*	31.34	30.03	35.73	37.34	29.68
Image					
Name	F	G	H	I	J
Stone	granite	granite	granite	granite	granite
Source	Norway	India	India	Angola	Angola
Finish	burned	polished	burned	polished	burned
Luminance	44.0 cd/㎡	87.96 cd/㎡	66.03 cd/㎡	84.37 cd/㎡	59.9 cd/㎡
L*	72.24	95.14	85.01	93.61	81.78
a*	12.21	18.58	24.15	13.20	11.76
b*	31.05	34.22	35.67	30.89	29.71
Image					
Name	K	L	M		
Stone	marble	marble	granite		
Source	Norway	Turkey	India		
Finish	polished	polished	polished		
Luminance	163.4 cd/㎡	57.06 cd/㎡	81.86 cd/㎡		
L*	120.63	80.21	92.51		
a*	24.38	16.91	13.28		
b*	47.35	29.76	30.72		
Image		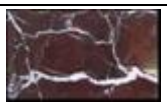			

Table 2. Granite images and measurement results (Test 2).

Name	GB1	GB2	GB3	GB4	GB5	GB6	GB7
Grind	#80	#200	#400	#800	#1500	#3000	Buff
Luminance	44.52	42.39	40.77	33.88	57.95	68.58	99.07
L*	72.58	71.138	70.01	64.86	80.71	86.29	99.63
a*	9.95	9.39	9.02	8.92	12.15	12.44	13.79
b*	25.16	23.83	22.65	21.08	27.81	29.31	32.21
Image							

Table 3. Evaluation items.

Massiveness	thin - massive
Depth	shallow - deep
Flavor	flavorless - flavorful
Expensiveness	cheap - expensive
Comfort	uncomfortable - comfortable
Oldness	new - old
Calmness	restless - calm
Brightness	dark - bright
Third dimension	planar - stereoscopic
Glossiness	matte - glossy

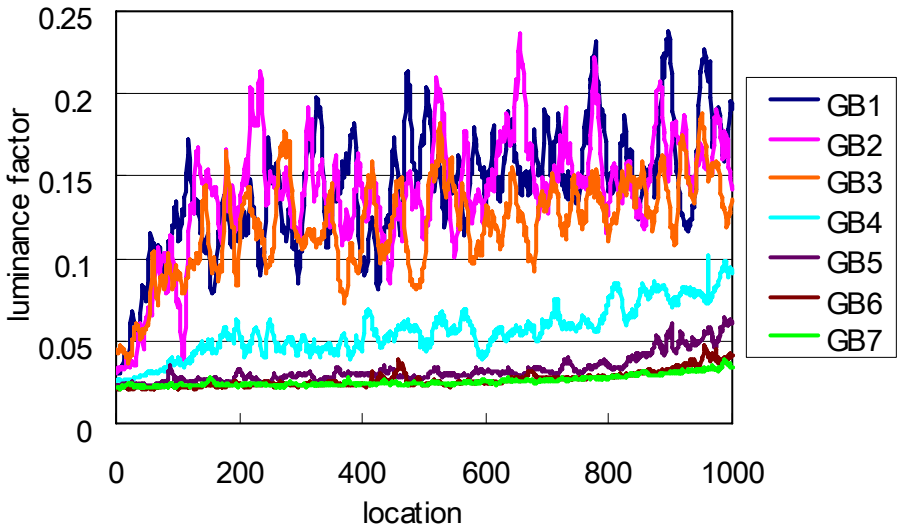

Figure 1. Luminance factor of granite specimens.

2.3 Measurement Surface Properties

Surface color was measured by spectoral photometer (MINOLTA CS-1000A) in test1 and luminance factor was measureed by multi spectoral imaging method. Figure 1 shows the result of the luminance factor of the granite specimens in Test 2.

3 RESULTS AND CONSIDERRATIONS

3.1 The Evaluation of The Feeling of Depth of Various Kind of Stone

Figure 2 shows the result of the evaluation of the stone specimens.This is the avereage of the evaluation of the feeling of depth (Test 1). The polished finish A, E, I were estimated to be deep. For granite E, whose surface has glitter minerals, there was a high feeling of depth. The feeling of depth of specimens D, E were the lowest of all specimens. The value of a* was high in these specimens. Figure 3 shows the results of the multi dimensional scaling of specimens (MDS). MDS is a set of related statistical techniques often used in data visualization for exploring similarities or dissimilarities in data. It is a special case of ordination. An MDS algorithm starts with a matrix of object-object similarities, and then a location for each object is assigned in a low-dimensional space that is suitable for graphing.

The tendency of the feeling of depth depend on surface finishes, surface color. The polished finish granite specimens were high feeling of depth, however the different tendency in colored and colorless specimens. Especially uneven surface color specimens were high feeling of depth.

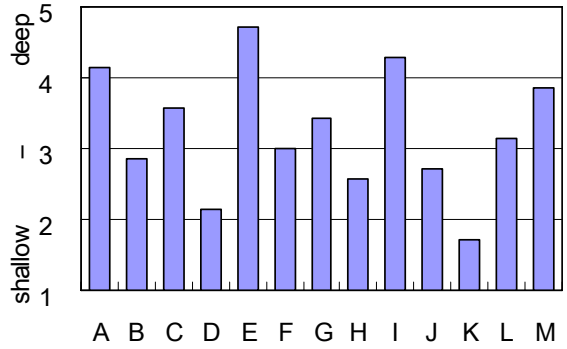

Figure 2. Evaluation of the stones (Test1).

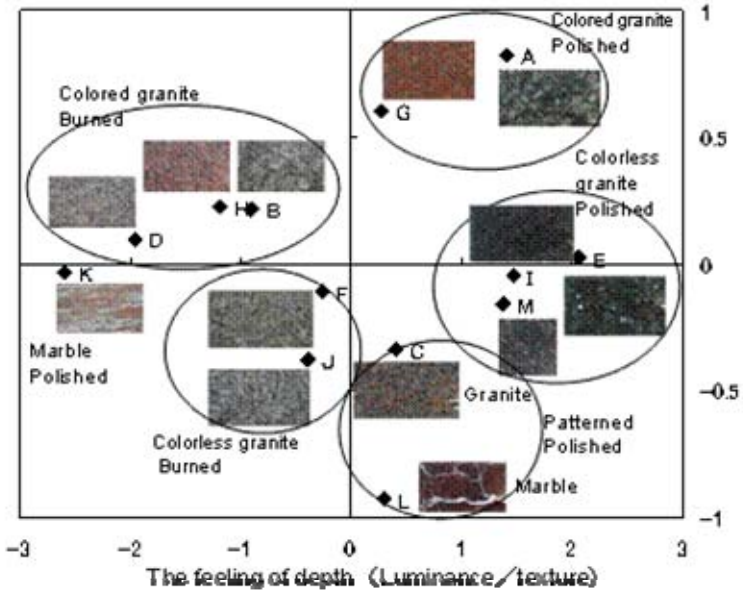

Figure 3. The Result of Multi Dimensional Scaling.

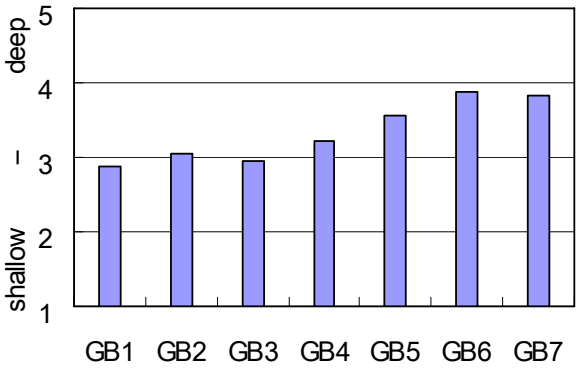

Figure 4. Evaluation of the stones（Test 2).

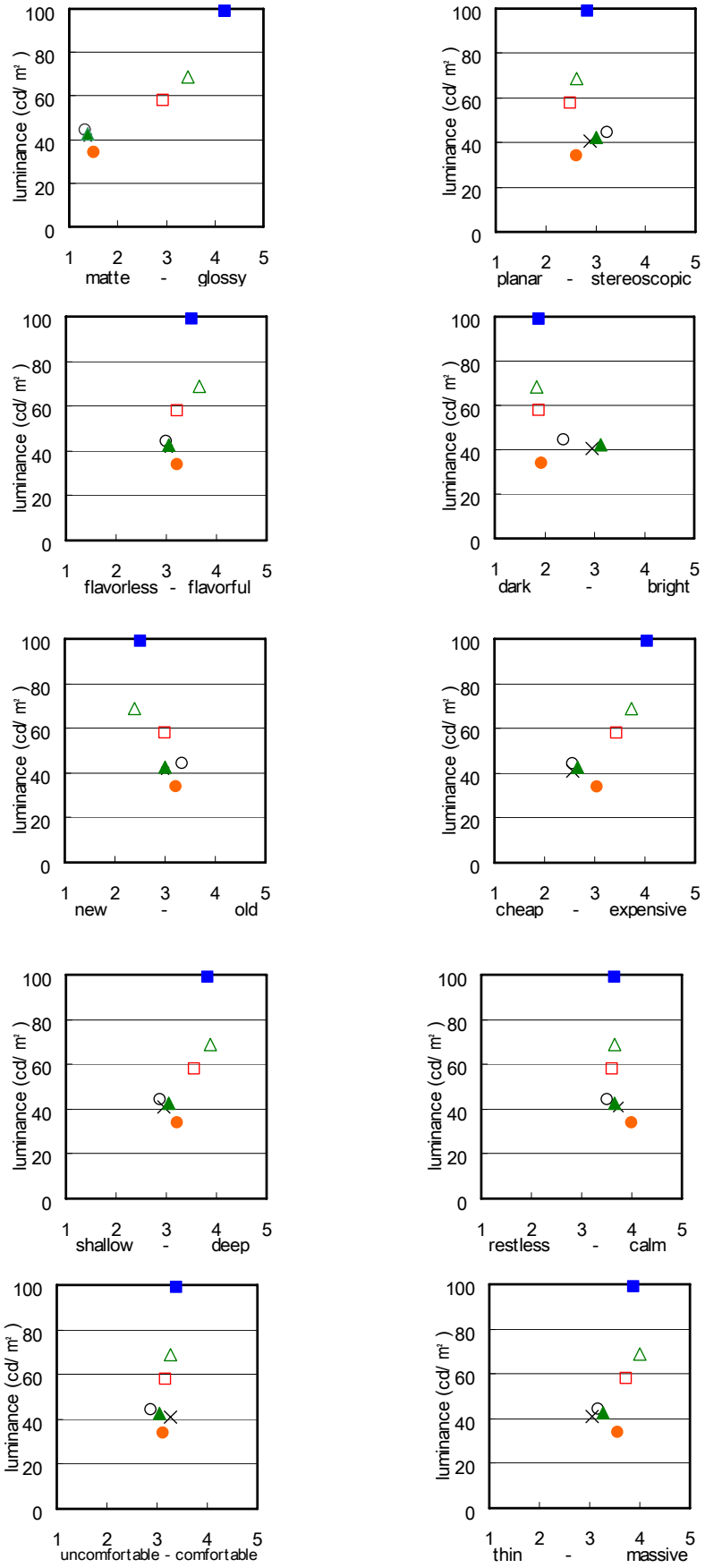

Figure 5. Relationship between luminance and the each evaluation items.

3.2 The Evaluation of 7 Surface Finishing Granite

Figure 4 shows the average of the evaluations of feeling of depth (Test 2).These 7specimens changes surface gloss by grindstone gradually. The rough surface finish changed stone whitish, then it was affecting the evaluation as well as surface gloss.

Although the order from least to most rough was G1B, G2B, G3B specimens, there was little difference of the feeling of depth because the effect of whitish and high L* surface in those three specimens.

For GB6, the evaluation was the highest of all specimens. The value of luminance and L*a*b* of this specimen were lower than GB7. It indicated that the optimum conditions of surface finishes in the feeling of depth.

Figure 5 shows the relationship between luminance and the each evaluation items. The evaluations of gloss and feeling of depth showed a correlation with luminance. There were no definite relationships between luminance and other evaluation items.

4 CONCLUSIONS

The conclusions of this study are as follows.
(1) The polished finish granite was high feeling of depth.
(2) Uneven surface color affected the evaluation of feeling of depth.
(3) The evaluations items of gloss and feeling of depth showed a correlation with luminance.
(4) There was no definite relationships between luminance and other evaluation items.

ACKNOWLEDGMENTS

This result was supported partly by User Science Institute in Kyushu University (Special Coordination Funds for Promoting Science and Technology).

REFERENCES

Okuda, S., & Honda, S., 1968, ‘A study on gloss of building finishing materials,’ Summaries of Technical Papers of Annual Meeting AIJ, Japan, October.1968, pp.185-186.

Kitamura, K., Isoda, N., & Yanase, T., 1998, ‘Interpretation of the evaluation scales for appearance, and a quantitative analysis of appearance using simple texture-Evaluation of the appearance of building materials by visual sensation and tactile sensation (Rept.1),’ J.Archi.Plann.Environ.Eng., AIJ,Japan,September.1998, No.511, pp69-74.

Nakayama, M., 1998, ‘Investigation of deterioration associated with natural inherent in stones - Consideration of deterioration which occurs stone surface by onsite surveys’ J.Struct.Constr. Eng., AIJ, August.1998, No.510, pp7-14.

Tsuchiya, J., Kitsutaka, Y., Tamura, M., 2005, ‘Visual Evaluation of Building Stone Finishing on the View Point of Aging Effect’, 10DBMC International Conference On Durability of Building Materials and Components, LYON ,France, 2005.4, TT-95.

Outdoor Wall Painting Semi-Natural Test

Alberto Giacardi [1]
Luigi Morra [2]

T 16

ABSTRACT

This research is the result of experimentation of two Authors. It proposes a study on durability of two kinds of wall painting. The target of the study is to value degradation of wall painting superficial film for exteriors. Hence, it is crucial to:

- collect adequate information on geographic area;
- establish sample shape (hollow flat block already selected at laboratory);
- decide the means necessary to hold up samples;
- determine the superficial treatment to be used [two kinds of painting have been chosen: Metilsilossanico (CVP 60) and Vinilversatico (CVP 45)];
- define the superficial film application steps;
- explain the method applied as well as the results achieved.

On these premises, the Authors have deepened aspects of the problem (according to the instruction contained in ISO 2810:2004, UNI EN ISO 7783-1:2001 and EN 1062-3:1998 standards), leading to the following outcomes:

- measurement of permeability to water vapour and liquid water transmission of samples prepared and exposed outside (vs. the witness specimens preserved in laboratory);
- definition of different behaviours of wall painting film during two years of exterior exposition.

The final goal is to demonstrate which kind of lesions are more frequent on wall painting film, which sort of water and vapour transmission may be observed during the coming years and which type of superficial treatment is better to adopt (naturally, between the two issues here above mentioned).

KEYWORDS

Degradation, Wall painting, Laboratory testing.

[1] Turin Institute of Technology, Department of Building Engineering and Territorial Systems, Turin, Italy 10129, Phone +39 011 5645329, Fax 011 5645399, alberto.giacardi@polito.it
[2] Turin Institute of Technology, Department of Building Engineering and Territorial Systems, Turin, Italy 10129, Phone +39 011 5645309, Fax 011 5645399, luigi.morra@polito.it

1 INTRODUCTION

Research activity on degradation of superficial film of wall painting for exteriors follows the guidelines proposed by fundamental ISO 15686-2:2001 standard and related UNI 11156:2006.

Eight samples have been tested. Six of them have been exposed to climate agents and air pollution in Vercelli (2nd Faculty of Engineering) and stressed from May 2005. The others have been stored and preserved in Turin at Department of Building Science and Technology.

2 MODALITY OF TEST

2.1 Framework

Every single framework, on which wall painting was applied, has been personally constructed by the Authors in all its details (design, realisation, selection of components used for plasterwork, maturation, ground support, ...).

For the selection of components used to prepare plasterwork layer for wall painting (see Table 1), the results of a research brought out by Polytechnic of Milan and Professional University School of Italian Switzerland [Maggi 2001] have been greatly significant.
Plasterwork necessary to apply painting (thickness about 15mm), has been reinforced with a netting of anti-crack fiberglass.

Table 1. Granule distribution of sand for finish plasterwork, for a total quantity of 6 kg.

Filler <*0.075* mm	*from 0.075 to 0.15* mm	*from 0.15 to 0.3* mm	*from 0.3 to 0.6* mm	*from 0.6 to 1.18* mm	*from 1.18 to 2.36* mm	*from 2.36 to 4.75* mm	*Total*
3%	12%	13%	13%	19%	27%	13%	100%
180g	720g	780g	780g	1,140g	1,620g	780g	6,000g

2.2 Sample Dimension

The choice of sample format depends on measures of hollow flat block available (dimension: 40x24x2.5cm) and on possibility of making element movement easier. Final format of samples (mortar included) is 47.5x28x4.5cm with a band (28x10cm) having a thickness increased to 5.5cm (Fig. 1).

Figure 1. Sample in its final configuration.

2.3 Support For Exterior Exposition of Samples

Two fir frameworks of appropriate dimensions have been designed and produced in order to support samples in exteriors. They have been equipped with bracings and protected by impregnation for open-air conditions (Fig. 2). Top edge has been covered with an aluminium facing and inclination of sample surfaces has been carried out in compliance with the guidelines proposed by the ISO standard 2810:2004 («Paints and varnishes - Natural weathering of coatings - Exposure and assessment»). Inclination value is about 45° on horizontal plan. Framework has been oriented to south.

The research has pointed out that, in comparison with traditional solution (vertical painting on massive wall), worsening of surface integrity is linked not only to inclination but also to the low mass of support. Superficial temperatures are, from time to time, either particularly high or extremely low. In the last case, it's possible to realize the presence of a periodic ring of condensation during the morning. This reaction proves the presence of a heat exchange due to a nocturnal re–radiation without that "inertia" or "thermic capability" shown by heavy and massive structures.

Figure 2. Frameworks placed outside in Vercelli.

2.4 Monitoring of Meteorology Condition of Exposition

In order to collect data on nature of real prodding, for the whole trial period, the monitoring of meteorology conditions has been kept. Thanks to ARPA station located in Ruggerina (2.4 km westward from Vercelli exposition site), it has been possible to keep information up to date.

Table 2. Historical data (1994-2002) regarding city of Vercelli.

Months	*Daily Average Temp. Max* (°C)	*Daily Average Temp. Min* (°C)	*Average Humidity* (%)		*Average Rainfall* (mm)
			Max	*Min*	
January	6.9	-1.9	99.9	28.1	58.4
February	10.9	-1	99.1	17.6	42.6
March	16.5	2.4	99.8	14.7	40.2
April	18.9	7.3	100	15	71.8
May	23.8	13	99.6	25.6	106.5
June	27.7	15.5	99.8	23	64.1
July	29.9	17	99.8	27.3	55
August	29.2	16.5	99.4	30.9	67.5
September	23.8	11.1	98.9	25.4	84.7
October	18.8	7.9	98.9	27	71.7
November	11.6	2.9	99	27.9	103.1
December	7.2	-0.1	99.8	37.6	45.5

2.5 Choice of Painting Cycle to Apply

Two kinds of painting have been chosen: Metilsilossanico (CVP 60)* and Vinilversatico (CVP 45). Both of them have been acquired by companies Caparol and Melzi. The cycle of Metilsilossanico is a recent compound having - according to manufacturer - a great resistance to environmental pollution, while the Vinilversatico has already been tested before and the result of that research shows that it is not so resistant to severe environmental pollution.

2.6 Application of MetilsIlossanico Cycle

Drafting process of product on samples implies (before exposition):

1) wetting of screen test with sponge;
2) overcoat of AMPHISILAN TIEFGRUND LF followed by natural dry out for 55';
3) first paintbrush drafting (no dilution) of AMPHISILAN VOLTON UND ABTÖNFARBE - "oxidrot" color, with 1 h and 40' room temperature drying;
4) second paintbrush of AMPHISILAN VOLTON UND ABTÖNFARBE - "oxidrot" color;
5) 27 days of concrete maturation.

On the basis of consumption of painting, it has been possible to notice that thickness of coating has been certified on an average measure of 220 µm (more or less constant for four sample realized). This result is comparable to the one visible with optical microscope (Fig. 3). In this case the value of reference sample is about 230 µm.

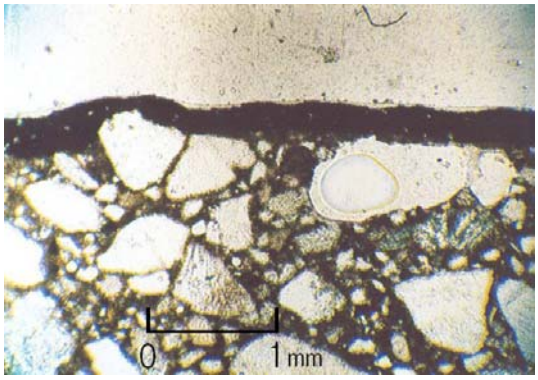

Figure 3. Thin film section of Metilsilossanico cycle.

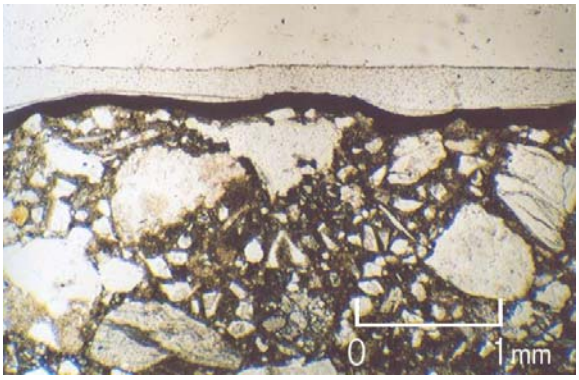

Figure 4. Thin film section of Vinilversatico cycle.

2.7 Application of Vinilversatico Cycle

Procedure has involved:

1) paintbrush undercoat of oxide red color (14 % dilution compared with subsequent painting coats) and natural drying period of 16 h;
2) first paintbrush coat with a drying time of 8 h (room temperature);
3) second and last resin paintbrush.

Depending on consumption of painting, thickness of coating has been rated on an average measure of 100 µm (variable for four sample realized). This result is in step with the thin film section: 120 µm (while the reference value for control group is about 110 µm - see Fig. 4).

**Notation "CVP" means value of volumetric powder concentration measured in %.*

2.8 Look of Protected Surfaces

The following images (Figs. 5 and 6) refer to the surface aspect of sample kept intact in our laboratory.

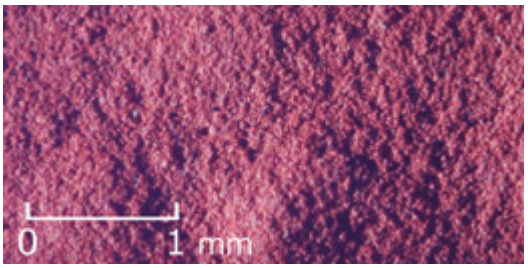

Figure 5. Close-up photo of Metilsilossanico cycle.

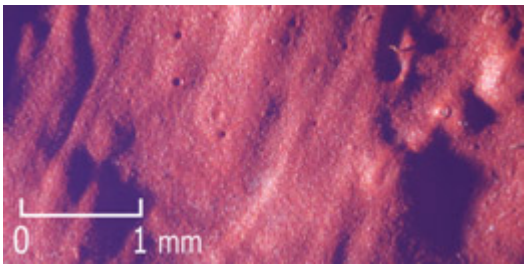

Figure 6. Close-up photo of Vinilversatico cycle.

3 MEASUREMENTS

3.1 Measurement of Permeability to Water Vapour

Test has been carried out following procedure proposed by UNI EN ISO 7783-1:2001 standard [«Paints and varnishes - Coating materials and coating systems for exterior masonry and concrete - Determination and classification of water-vapour transmission rate (permeability)»]. Preparation of laboratory specimens has implied:

1) cut of rectangular portions (4.5 x 10 cm);
2) subsequent dehydration of these sections;
3) arrangement of aluminium boxes to be used as capsules (as mentioned by UNI EN ISO standard to point 7.1);
4) introduction, before complete sealing of sample inside capsule, of saturated solution made with ammonium dihydrogen phosphate (as scheduled at point 7.2 of the standard);
5) measurement of mass loss through weighing during well-known time steps.

UNI EN ISO standard mentioned above, foresees that test ends when change of mass for atmosphere exposition time unit becomes a constant.

Achieved results (Fig. 7) show that original Metilsilossanico cycle has a transmission level of water vapour equal to 13.25 g/m^2·d. Numeric value determination comes from formula reported in Fig. 9.

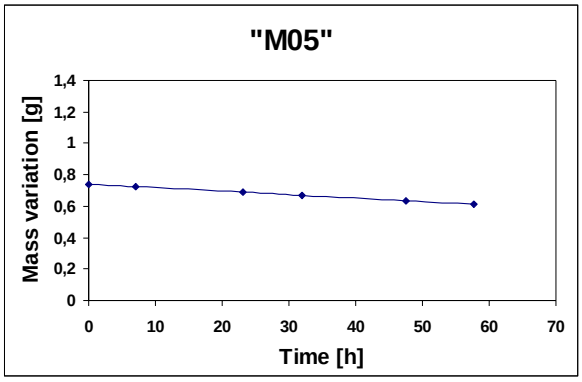

Figure 7. Transmission of water vapour for Metilsilossanico cycle.

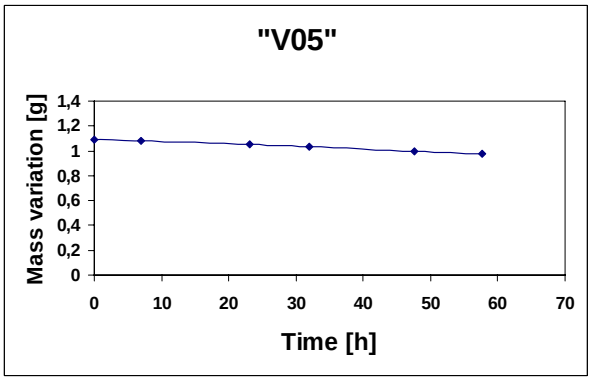

Figure 8. Transmission of water vapour for Vinilversatico cycle.

On the other hand (see Fig. 8), Vinilversatico cycle (concerning screen tests stored in laboratory) has a transmission level of water vapour equal to 10.52 g/m^2·d (numeric value determination comes from formula reported in Fig. 9).

$$WVT \left[\frac{g}{m^2 \cdot d}\right] = \frac{240 \cdot Dm}{A}$$

read as follows:

$$Dm \left[\frac{mg}{h}\right] = \frac{(m_1 - m_2)}{(t_2 - t_1)}$$

m_{1-2} : mass at selected points (on straight line)
t_{1-2} : time at selected points (on straight line)
A : sample surface area

Figure 9. Calculation formula of water vapour transmission (WVT).

$$LWT \left[\frac{kg}{m^2 \cdot h^{0.5}}\right] = \frac{Dm}{A \cdot Dt^{0.5}}$$

read as follows:

$$Dm \left[g\right] = (m_2 - m_1)$$

m_{1-2} : mass at selected points (on straight line)
A : sample surface area

$$Dt^{0.5} \left[h^{0.5}\right] = (t_2^{0.5} - t_1^{0.5})$$

t_{1-2} : time at selected points (on straight line)

Figure 10. Calculation formula of liquid water transmission (LWT).

3.2 Measurement of Liquid Water Transmission

Test has taken place following procedure proposed by EN 1062-3:1998 [«Paints and varnishes - Coating materials and coating systems for exterior masonry and concrete - Determination and classification of liquid-water transmission rate (permeability)»].

After a brief settlement period (not highlighted in diagrams), the results (Figs. 11 and 12) show that Metilsilossanico cycle (in its original version) has a transmission level of liquid water equal to 0.04 kg/m^2·h$^{0.5}$, while original Vinilversatico is certifiable to 0.16 kg/m^2·h$^{0.5}$. Numeric value determination comes from formula reported in Fig. 10.

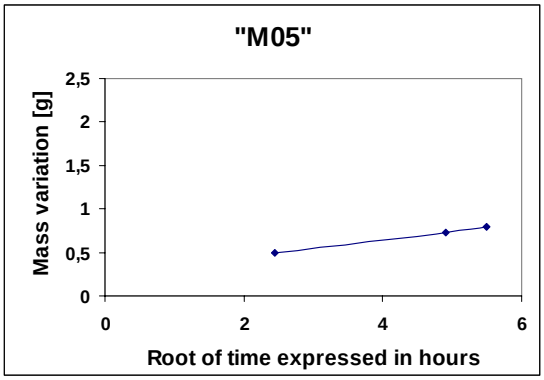

Figure 11. Liquid water transmission of Metilsilossanico cycle.

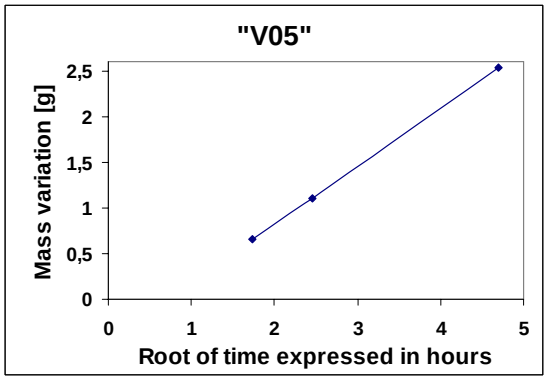

Figure 12. Liquid water transmission of Vinilversatico cycle.

4 RESULTS

4.1 Phenomena of Semi-Natural Obsolescence Pointed out in The Course of Time

It is evident, in Figs. 13 and 14 that the Metilsilossanico cycle has a bigger degradation than the other one. Vinilversatico treatment shows only the presence of some close-fitting particles on its surface and

no interruption of film continuity, whereas Metilsilossanico sample has displayed, in isolated portions, some film damages.

The real evaluation of superficial transformations is based on data collected on permeability features of film surface (water vapour and liquid water).

Change of water vapour permeability: as shown in Fig. 15, the level of Metilsilossanico cycle - after two years of exposition - has slightly decreased down to 11.15 g/m^2·d. Numeric value determination comes from formula reported in Fig. 9.

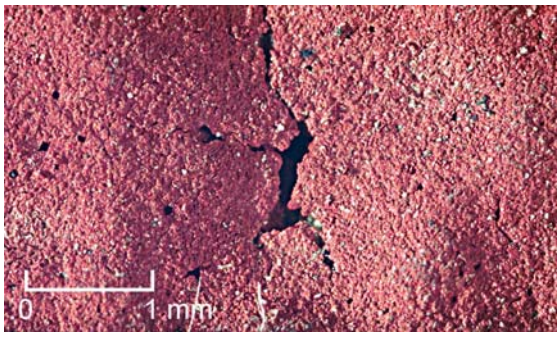

Figure 13. Close-up of Metilsilossanico cycle.

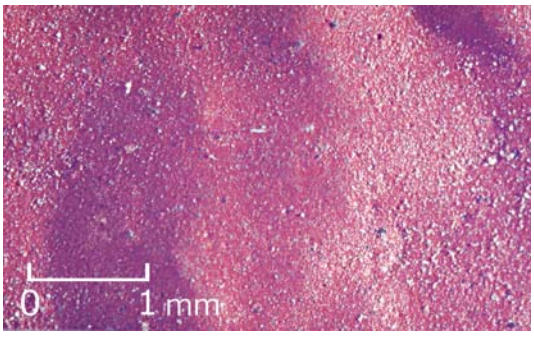

Figure 14. Close-up of Vinilversatico cycle.

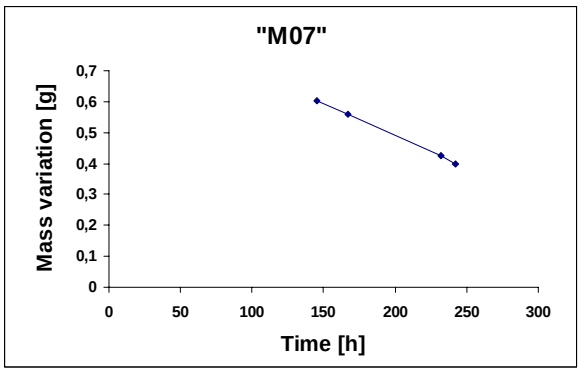

Figure 15. Water vapour transmission of Metilsilossanico cycle.

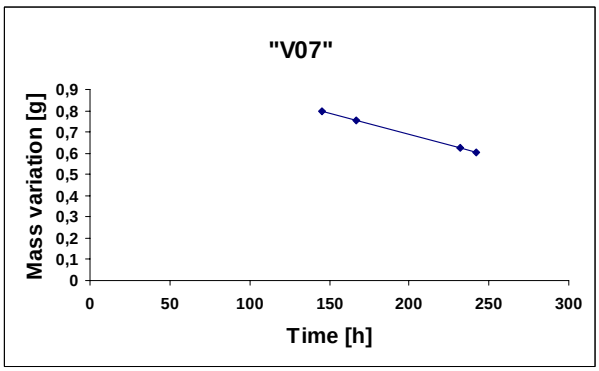

Figure 16. Water vapour transmission of Vinilversatico cycle.

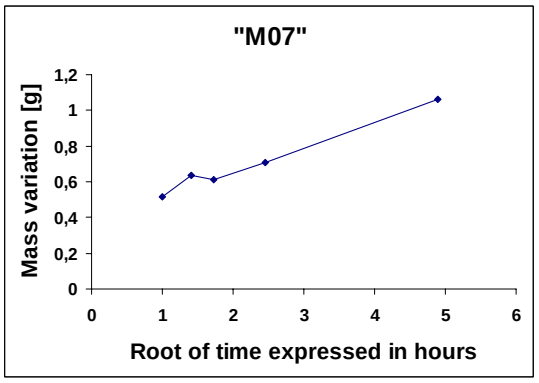

Figure 17. Liquid water transmission of Metilsilossanico cycle.

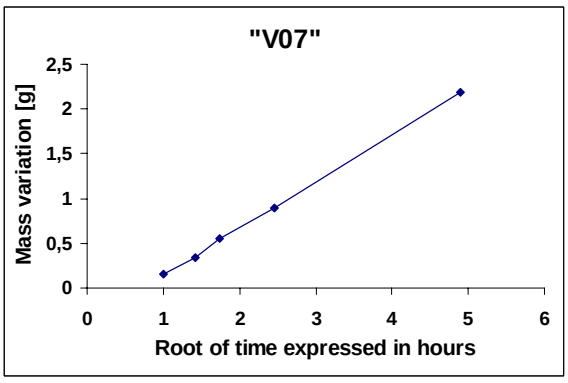

Figure 18. Liquid water transmission of Vinilversatico cycle.

Change of vapour permeability: as shown in Fig. 16, the level of Viniversatico cycle - after two years of exposition - has slightly reduced, achieving the value of 9.07 $g/m^2 \cdot d$. Surface tested has not shown visible phenomena of film break. Numeric value determination comes from Fig. 9 formula.

Regarding the transmission level of liquid water, Metilsilossanico aged cycle (two years) (Fig. 17) has a value of 0.023 $kg/m^2 \cdot h^{0.5}$, while Vinilversatico (Fig. 18) - after two years of outdoor exposition - shows a permeability value of 0.079 $kg/m^2 \cdot h^{0.5}$. For these two determinations has been applied formula reported in Fig. 10.

5 CONCLUSION

First laboratory results show that structure of resins permits to mantain a good water vapour permeability (with a 16 % value reduction), whereas greater impermeability to liquid water may lead to hardening of exposed surfaces. As visible in the diagrams, both solutions have shown a minor liquid water transmission level: about sixty percent for Metilsilossanico and fifty percent for Vinilversatico.

Moreover, it is also possible to point out a strong adherence of hydrocarbonous pollutants, made worse by 45° inclination of the specimen. Such inclination may determine significant casual lack of cleanness.
Obviously samples tested have excluded points of evident crack.

Outdoor exposition has been influent in the same way on Metilsilossanico and Vinilversatico samples, even if the Metilsilossanico film has a double average thickness compared with the Vinilversatico. To justify this reaction, it must be underlined that resin used to constitute the thickest film has a volumetric powder concentration equal to 60 %, while the value for Vinilversatico is limited to 45 %.

ACKNOWLEDGMENTS

Special thanks to ing. Tedeschi of Caparol GmbH and Co. (Vermezzo - MI) and dott. Melzi of Melzi s.n.c (Albignasego - PD).

REFERENCES

Maggi, P.N., (edited by) 2001, *La valutazione della durabilità*, DISET Milan Institute of Technology, Epitesto Publishing, Milan.

UNI 11156:2006, [«*Durability evaluation of building components*»].

ISO 2810:2004 [«*Paints and varnishes - Natural weathering of coatings - Exposure and assessment*»].

ISO 15686-2:2001, [«*Service life planning - Service life prediction procedures*»].

UNI EN ISO 7783-1:2001, [«*Paints and varnishes - Coating materials and coating systems for exterior masonry and concrete - Determination and classification of water-vapour transmission rate (permeability)*»].

EN 1062-3:1998, [«*Paints and varnishes - Coating materials and coating systems for exterior masonry and concrete - Determination and classification of liquid-water transmission rate (permeability)*»].

11DBMC International Conference on Durability of Building Materials and Components
ISTANBUL, Turkey 11-14 May 2008

Durability Evaluation of Newly Developed Water-Based Paint Systems for Buildings

Kenji Motohashi [1]

T 16

ABSTRACT

According to the report, about 30% of total amount of organic carbons emitted into the atmosphere due to human activities have been considered to come from paint works. Different from coating work in manufacturing factories, it is difficult to collect organic solvents evaporated in the air because paint works in construction are carried out on construction site. The only method for decreasing organic solvent emission is to use coating materials including little organic volatile. In this context, various water-based emulsion paint products have been developed in Japan and applied to coating works for buildings.

This paper outlines the results of durability evaluation test for these new water-based paint systems. An accelerated ageing test and an outdoor exposure test for 10 years have been conducted for both newly developed water-based paint more than 10 years ago and existing organic solvent type paint.

High durability performance of some water-based paint systems has been demonstrated through the evaluation tests. It was confirmed that some of the newly developed water-based paint systems show competitive durability against existing organic solvent type of paint systems.

KEYWORDS

Accelerated aging test, Air pollution, Organic solvent type paint, Outdoor exposure test, Water-based paint

[1] Building Research Institute, Dept. of Building Materials & Components, Tsukuba-City, 305-0802 Japan, Phone +81 298646622, Fax +81 298646772, ken-moto@kenken.go.jp

1 INTRODUCTION

According to Sakamaki [1986], about 30% of the total amount of volatile organic carbons (VOC) which were emitted into the atmosphere due to human activities has been considered to come from painting works. Ministry of Environment in Japan also reported VOC emission percentages from the fixed facility sources as shown in Fig. 1. Paint coating is the most important source of VOC emission to the environment. Moreover, in case of coating works on construction sites, it is difficult to control VOC evaporation into the atomosphere because they are carried out in outdoor conditions.

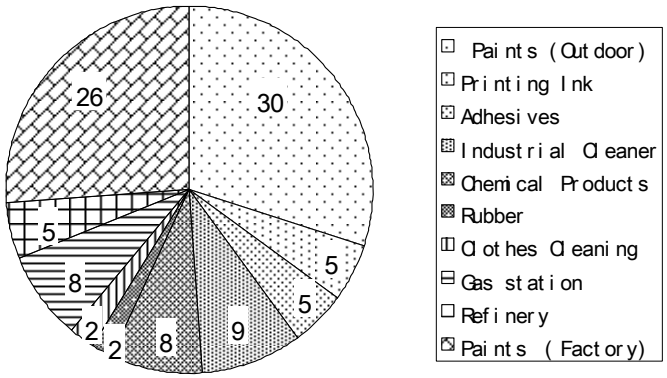

Figure 1. The percentages of VOC emission from the fixed facility sources in Japan.

For this reason, use of water-based paint has been recommended from the viewpoint of environment protection. This demand has become very strong recently. Paint manufacturers are intensively developing safer and more durable paint. Figure 2 shows fundamental methodologies for developing safer paint to the environment.

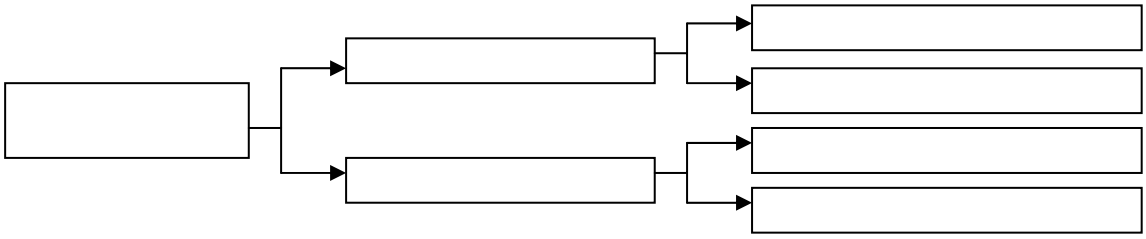

Figure 2. Basic methodology for developing environmentally safer paint.

Among the various types of paint shown in Fig. 2, poor solvent (mineral sprits, solvent with higher boiling point) type of paint, water-based paint and high solid type of paint have been on the market aiming at substituting for existing solvent type of paint used in construction works. Especially, water-based paint is considered to be most suitable from the viewpoint of environment protection. However, water-based paint is generally less durable than organic solvent type of paint. Therefore, it is not so easy to replace water-based emulsion paint for existing solvent type of paint especially where high durability is required.

Because of insufficient data on the durability of newly developed water-based paint, few types of durable water-based paints have been standardised in Japanese Industrial Standards (JIS) and other public material standards. In addition, few coating work specifications with durable water-based paint have been standardised in public construction works. The accumulation of durability data is a crucial point to promotion of water-based paint in construction works.

On this background, Building Research Institute has been conducting both outdoor exposure tests and accelerated ageing tests to obtain durability data for such durable water-based coating products which

are rather new on the market. The results of the 10 years outdoor exposure test and the acceleration test are reported in the paper.

2 EXPERIMENT

2.1 Outdoor Exposure Test

The coating products listed in Table 1 were evaluated in the outdoor exposure test. Water-based fluoropolymer emulsion paint [Motohashi et al. 1998] , acrylic silicon emulsion paint, and polyurethane emulsion paint were evaluated. A solvent type of fluoropolymer paint, acrylic silicon paint, and acrylic paint which had been already standardised in the material standards were also tested for comparison.

Table 1. Types and numbers of objected coating products in the outdoor exposure test.

Type of top coating paint	*Material standard*	*Number of tested brands*
Water-based fluoropolymer emulsion paint	Not standardised	17
Water-based acrylic silicon emulsion paint	Not standardised	17
Water-based polyurethane emulsion paint	Not standardised	10
Solvent type fluoropolymer paint	JIS K 5658:2002*	1
Solvent type acrylic silicone paint	JASS 18 M-404**	1
Solvent type polyurethane paint	JIS K 5656:2003*	1

* Japanese industrial standard, **Japanese architectural institute material standard

Each paint product listed in Table 1 was applied on the 70 mm x 150 mm x 6 mm (thickness) fibre reinforced cement sheet after application of a water-based emulsion primer. Paint (white opaque paint) listed in Table 1 was applied twice. Total coating amount of each paint product was about 150g/m^2.

The outdoor exposure test was carried out in the outdoor exposure site of Building Research Institute, Japan which is located some 50 km north of Tokyo and in rural district area. The painted specimens were mounted to the exposure rack facing the south at an angle of 30 degrees for 10 years.

2.2 Accelerated Ageing Test

The open-flame carbon-arc type of irradiation test was also conducted for most of the coating products which were evaluated in the outdoor exposure test in accordance with ISO 4892-4:1994 [ISO 1994]. The objected coating products are listed in Table 2.

Table 2. Types and numbers of objected coating products in the accelerated aging test.

Type of top coating paint	*Material standard*	*Number of tested brands*
Water-based fluoropolymer emulsion paint	Not standardised	9
Water-based acrylic silicon emulsion paint	Not standardised	13
Water-based polyurethane emulsion paint	Not standardised	8
Solvent type fluoropolymer paint	JIS K 5658:2002*	1
Solvent type acrylic silicone paint	JASS 18 M-404**	1
Solvent type polyurethane paint	JIS K 5656:2003*	1

* Japanese Industrial Standard, **Japanese Architectural Institute Material Standard

The acceleration test was carried out up to 5,000 hours. Water spraying was applied for 18 minutes in every 120 minutes. The painted test specimens were prepared by the same preparation method in the outdoor exposure test.

2.2 Optical Measurement

Gloss retention percentages were monitored periodically in both the outdoor exposure test and the acceleration test. Gloss reflection percentages were measured at angle of 60 degrees. In case of the outdoor exposure test, the gloss reflection values of the specimens were measured after washing with water and drying in order to eliminate dirt from the specimens.

3 RESULTS AND DISCUSSION

The changes in gloss retention of the fluoropolymer paint, acrylic silicon paint, and polyurethane paint in the outdoor exposure test are shown in Fig. 3, 4, and 5, respectively. Those in the acceleration test are also shown in Fig. 6, 7, and 8.

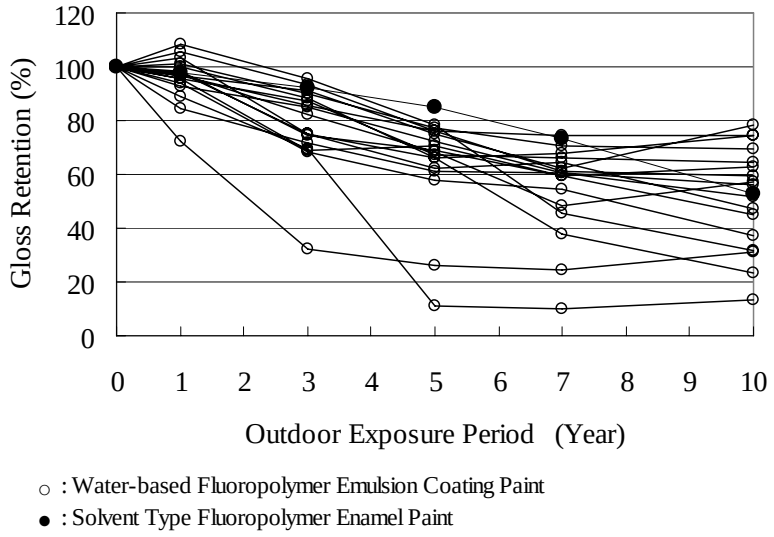

Figure 3. Gloss retention percentages of the fluoropolymer paint in the outdoor exposure test.

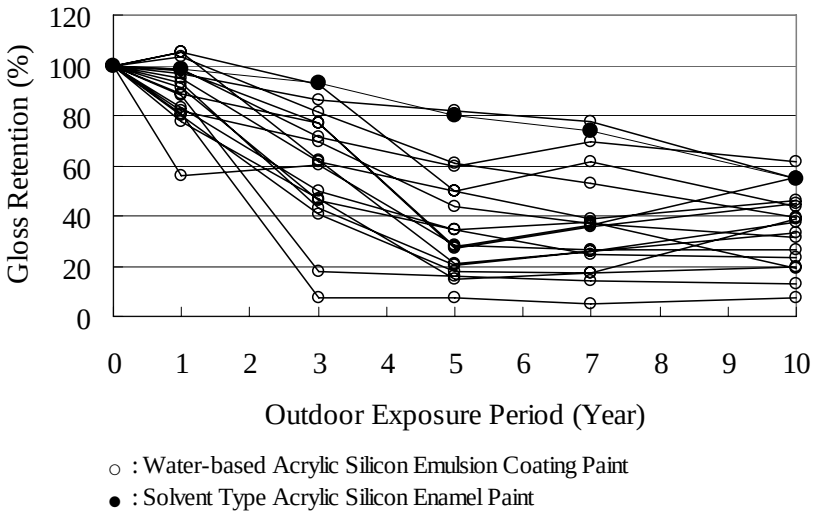

Figure 4. Gloss retention percentages of the acrylic silicon paint in the outdoor exposure test.

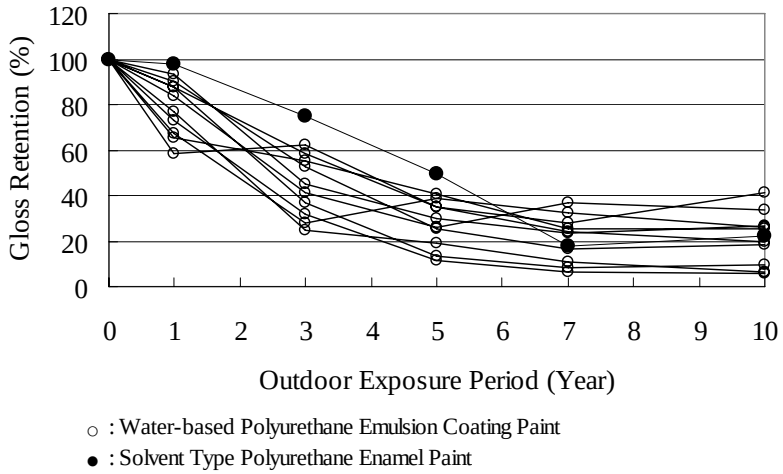

Figure 5. Gloss retention percentages of the polyurethane paint in the outdoor exposure test.

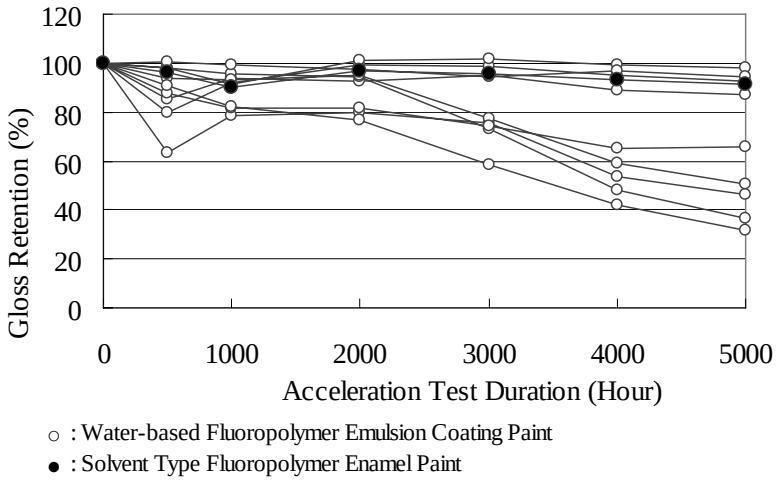

Figure 6. Gloss retention percentages of the fluoropolymer paint in the acceleration test.

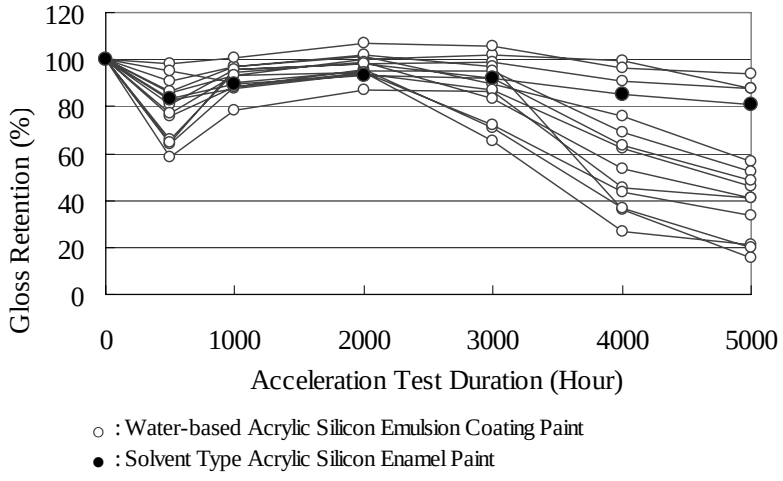

Figure 7. Gloss retention percentages of the acrylic silicon paint in the acceleration test.

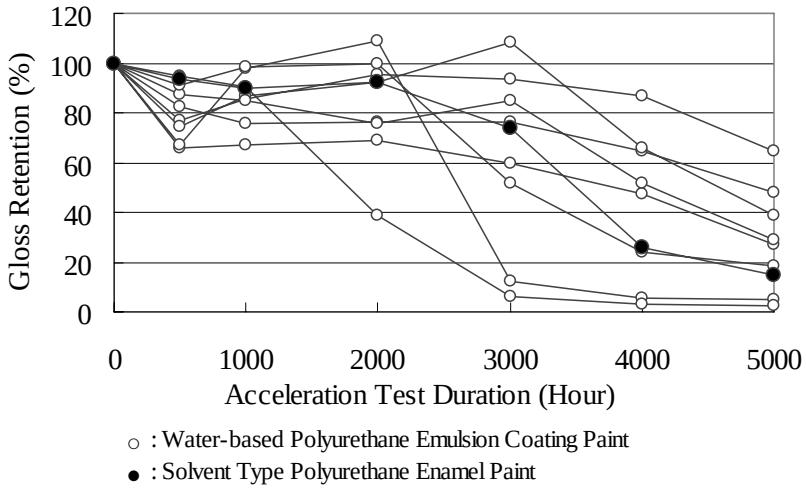

Figure 8. Gloss retention percentages of the polyurethane paint in the acceleration test.

First, when the three different types of polymers (fluoropolymer, acrylic silicon polymer, and polyurethane polymer) are compared one another by referring to the data obtained in the outdoor exposure test and the acceleration test, it can be said that fluoropolymer coating paint products are generally most durable among the three types of polymers and that the acrylic silicon coating paint products are generally more durable than the polyurethane coating paint products.

Second, in each type of polymer coating, it can be said that the standardised solvent type of paint is generally more durable than most of the water-based emulsion paint products made of the same type of polymer. However, on the other hand, it is possible to find a few water-based emulsion paint products whose durability is similar to that of the solvent type paint product among the evaluated water-based coating products. This fact could be confirmed in both the outdoor exposure test and the acceleration test.

Through Fig. 3 to 8, it is recognized that there was large variation in durability performance of the water-based emulsion products on the market. It means that the performance level of material standards for the durable water-based emulsion paint is very important. If we would like to select water-based emulsion paint which is as durable as solvent type of paint, the level of material standards for water-based emulsion paint products should be silmilar to that of the existing material standards of the organic solvent types of durable coating products. Through this experimental study, the durability data of the existing water-based paint products could be obtained and such data are very helpful for establishing rational material standards for durable water-based emulsion paint.

4 CONCLUSION

The 10 years outdoor exposure test and the accelerated ageing test were conducted for the durable water-based emulsion paint products on the market in order to investigate durability levels and their variation of fluoropolymer emulsion paint, acrylic silicon paint, and polyurethane emulsion paint which have been intensively developed in Japan. The organic solvent types of durable paint products were also evaluated in the same tests.

The results obtained can be summarised as follows:

1) When fluoropolymer emulsion paint products, acrylic silicon emulsion paint products, and polyurethane emulsion paint product are compared one another, the durability in the outdoor exposure

test and the acceleration test is generally superior in the order of fluoropolymer, acrylic silicon, and polyurethane.

2) Solvent type of paint is generally more durable than water-based emulsion paint which was synthesized by use of a similar type of base polymer. However, it is possible to find a few water-based emulsion products whose durability is comparable to that of solvent type of paint.

3) There is large variation in durability performance of the durable water-based emulsion paint products on the market. It is important to establish rational material standards for selection of proper products. Through this experimental study, the useful data could be obtained for establishing rational material standards of durable water-based paint products.

REFERENCES

ISO 4892-4:1994, Plastics - Methods of exposure to laboratory light sources - Part4: Open-flame carbon-arc lamps.

Motohashi, K., Hirano T., Miyazaki N., & Yamauchi M., 1998, 'Durability evaluation of newly developed fluoropolymer emulsion paint', Proc. 14th CIB World Building Congress, Gavle, Sweden, 7-12 June 1998, vol. 1, pp. 357-364.

Sakamaki, F., 1986, 'Hydrocarbons in the Global Troposphere', in *Res. Rep. Natl. Inst. Environ. Stud., Jpn.*, No. 102, 31-42.

11DBMC International Conference on Durability of Building Materials and Components
ISTANBUL, Turkey 11-14 May 2008

Effect of Anti-Graffiti Coatings on the Drying Behaviour of Building Materials

Barbara Lubelli [1]
Rob P.J. van Hees [1,2]
Teun van de Weert [3]

T 16

ABSTRACT

Anti-graffiti coatings are used to protect façades against unwanted graffiti. Despite the fact that anti-graffiti are widely used, not much is known about their effect on the drying behaviour of treated materials. Existing recommendations generally only take into account the water vapour transport values, not considering that the drying behaviour of a material is largely affected by the liquid moisture transport.
This paper reports the results of a research on 6 types of anti-graffiti coatings (permanent and sacrificial, water repellent and not) applied on two substrate materials (fired-clay brick and calcium silicate brick). The effect of the treatment on the drying behaviour is evaluated by means of drying tests performed at different RH. The obtained results are explained in the light of the product composition and the properties of the substrate materials (porosity and pore size distribution). The possible consequences of the application of the tested anti-graffiti coatings on common damage processes, as e.g. frost, salt crystallization, are discussed.

KEYWORDS

Anti-graffiti coating, Drying behaviour, Brick

[1] Delft University of Technology, Faculty of Architecture, Delft, The Netherlands, Phone +31 15 2781004, Fax +31 15 2781028, b.lubelli@tudelft.nl
[2] TNO Built Environment and Geosciences, Delft, The Netherlands, Phone +31 15 2763164, Fax +31 15 2763016, rob.vanhees@tno.nl
[3] Rebeon Advice, Scherpenzeel, The Netherlands, tgvandeweert@planet.nl

1 INTRODUCTION

Anti-graffiti coatings are used to protect façades against unwanted graffiti. They have the aim of limiting or avoiding the penetration of the graffiti into the substrate, thus making graffiti removal easier.
Anti-graffiti coatings can be grouped into three distinct categories [Bunnink et al 2004]:

a) *Permanent coatings:* these coatings are generally based on epoxy or polyurethane. Graffiti can be removed (with solvents) without the loss of properties, performance or appearance of the coating itself. These coatings have a service life of about 10 years and can be re-applied only after an adequate pre-treatment consisting in sand blasting or laser cleaning of the wall to eliminate the residue of the old anti-graffiti coating.
b) *Sacrificial coatings:* are mostly based on acrylates, polymer waxes, biopolymers (polysaccharides) or combinations of these. After soiling with graffiti, the anti-graffiti layer and the graffiti are removed together. After the removal, the coating has to be re-applied. Most of these products can be easily removed with (warm) water. Their solubility in water limits their durability: the service life of a sacrificial coating is about 3 years, but in façades or objects exposed to rain the service life can be shorter. They have good transparency and do not alter the aesthetical aspect of the treated material.
c) *Semi-permanent coatings:* These systems can be of two types: (i) a combination of a permanent base layer and a sacrificial top-layer or (ii) a semi-permanent one layer coating. In the first case the properties of the two layers are the same described in a) and b). During removal of the graffiti (by a solvent) the oleophobic part is removed, while the hydrophobic part is maintained. After the removal of graffiti a new layer of coating should be applied. These systems do not usually alter the aesthetical aspect of the treated substrate and have a long service life (about 10 years).

Within each of the categories, a distinction can be made between anti-graffiti with water repellent properties (e.g. silane) and without water repellent properties (e.g. polysaccharides) and between film forming (e.g. polyurethane based products) and not film forming (e.g. polysaccharide based products) coatings.

Depending on its chemical composition, an anti-graffiti coating will have a minor or a relevant influence on the drying behaviour of the material on which it is applied.

In spite of the fact that drying is a combination of both liquid and vapour transport, recommendation related to anti-graffiti coatings generally consider only water vapour transport [WTA 2005]. It can be expected that anti-graffiti coatings having water repellent properties or forming a water-tight film on the surface may strongly reduce the moisture transport by hindering the liquid water transport. Drying will therefore take longer, even if the product does not have any effect on the water vapour transport. This may enhance some processes as e.g. salt decay, frost damage and biological growth; moisture and salt related damage processes are in particular important for ancient buildings and monuments.

In this research the relevance of the effect of anti-graffiti coatings on the drying behaviour of treated material has been investigated. A drying test has been performed on two common building materials (a fired-clay brick and a calcium silicate brick) treated with a selection of 6 types of anti-graffiti coatings. At the end of the drying test the specimens have been cut and their surface and cross section observed by means of optical microscopy.

2 MATERIALS AND METHODS

2.1 Anti-graffiti Products

Six anti-graffiti coatings have been selected, including sacrificial, semi-permanent and permanent systems. The most relevant properties of the products are summarized in Table 1.

Table 1. Properties of the selected anti-graffiti coatings.

Composition	*Type*	*No of layers*	*Solvent*	*Film forming*	*μd** [m]
Wax based	Sacrificial	2	no	no	0.050
Polysaccharides	Sacrificial	2	no	no	0.024
Acrylic	Sacrificial	2	no	yes	0.200
Acrylic (mixed with siloxane emulsion)	Semi-permanent	2	no	yes	0.200
Polyurethane (water based)	Permanent	3	water	yes	0.950
Acrylic + polyurethane	Permanent	2	no	yes	0.575

** relative water vapour diffusion resistance : it depends on the thickness of the anti-graffiti layer and expresses the thickness of the air layer having a water vapour diffusion equal to the one of the applied layer of anti-graffiti (determined on the anti-graffiti layer according to DIN 52615 – Bestimmung der Wasserdampfdurchlässigkeit von Bau- und Dämmstoffen, November 2007).*

The natural wax used in this experiment is a commonly used, sacrificial anti-graffiti treatment. It does not alter the aesthetical properties of the treated object and it is not harmful for the building or for the user. It confers to the substrate some water repellency. It has a limited service life.
The polysaccharide product is a commonly used, sacrificial anti-graffiti treatment. It swells if in contact with liquid water, thus it can be washed away by longer periods of rain. As a result its service life is limited.

Two acrylic products have been selected: one semi-permanent (mixed with a siloxane micro-emulsion), the other sacrificial. Both acrylics form a water-tight film on the surface of the treated material.

The one component polyurethane anti-graffiti used in this test is a water based coating, which forms a water-tight film on the surface of the treated material. It is a moisture curing product, thus a RH of at least 50% is necessary for the polymerization reaction to occur.

The acrylic and polyurethane combination constitutes a film-forming, permanent system.

2.2 Materials

Two building materials commonly used in the Netherlands have been selected: a fired-clay brick and a calcium silicate brick. These substrates have been chosen also because largely different in colour and smoothness of the surface (this is important for the aesthetical influence of the anti-graffiti coating) and in pore size distribution (this is the most relevant parameter determining the moisture transport behaviour). The total porosity and the pore size distribution have been measured by means of mercury Intrusion Porosimeter (Autopore IV/9500 by Micromeritics).

The fired-clay brick has a red colour, 5 sanded surfaces and a porosity of 29.25 % by volume with pore sizes mainly in the range between 2 and 10μm (Fig. 1). The calcium silicate brick is greyish, has smooth surfaces and a total porosity of 27.24 % by volume, distributed in very wide range of pore sizes (Fig 2).

During testing it has been found that the outer surface of this calcium silicate brick was treated at the production with a water repellent. The penetration depth of the water repellent has been measured by wetting a broken cross section of the calcium silicate brick and was found to be limited to the outer 2mm.

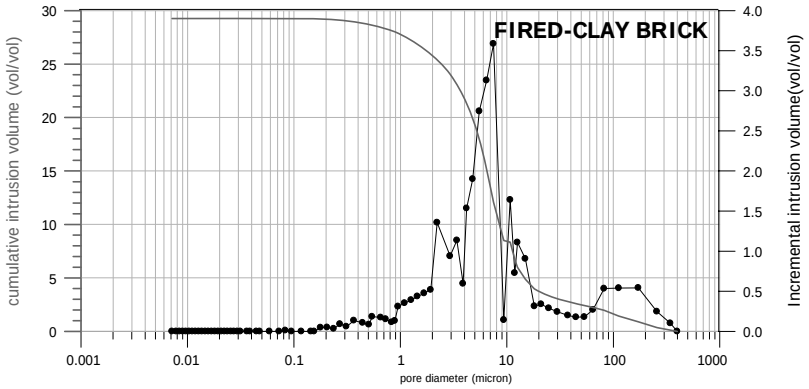

Figure 1. Pore size distribution of fired-clay brick.

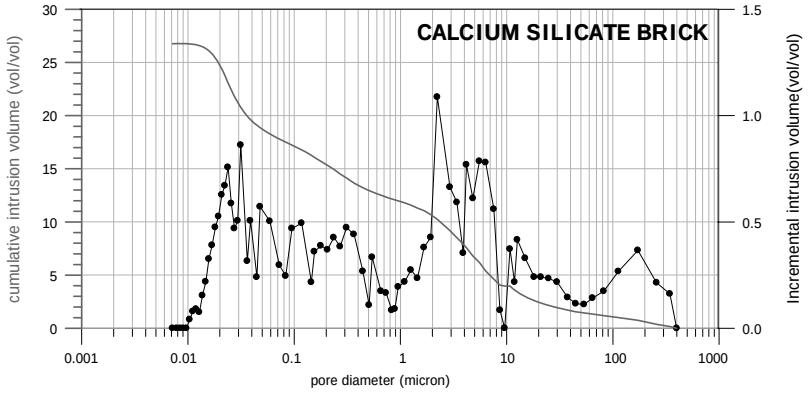

Figure 2. Pore size distribution of calcium silicate brick.

2.3 Procedure

The specimen consists in a half brick having the size of approximately 110 x 50 x 100 mm (b x l x h) in the case of the fired-clay brick and of 120 x 70 x 100 mm in the case of the calcium silicate brick.

Before the application of the anti-graffiti, the specimens were coated with epoxy resin on the 4 lateral sides, dried in the oven until they reached the constant mass and then conditioned at room temperature for one day.

The anti-graffiti coatings have been applied by roll, in 2 or three layers, on the upper surface of the specimen by an experienced person according to the prescriptions of the producer.

The treated substrates have been cured for 1 week at 20 °C 50% RH and then partially immersed in water until they reached the constant mass (mass change less then 0.1% per day). It was paid attention not to wet the upper surface of the specimens to avoid swelling and further dissolution of the polysaccharide. Then the bottom of the specimens was sealed with tape, so that drying could occur only through the treated surface. The specimens were stored in climatic rooms.

In the case of the fired-clay brick two drying conditions were used: 20°C 50% RH and 80% RH. In this way the effect of the anti-graffiti coating on the drying was studied not only at typical lab conditions (20 °C 50% RH) but also at more realistic environmental conditions (in the Netherlands the average RH is 82%). In the case of calcium-silicate brick only 20°C 50% RH conditions have been used, because of the very slow drying of this material. For each material/anti-graffiti/climatic condition combination 3 specimens have been used. Not treated specimens were used as reference.

At the end of the drying test the water repellency and the water tightness of the fired-clay brick treated with anti-graffiti have been tested by a drop test, i.e. by observing the shape of a water drop which was put on the surface and on a cross section of the material.

The cross sections were dried at 30°C before performing the test. This temperature was chosen to avoid re-emulgation of the wax and any possible shrinkage crack to the polysaccharide film. Both surface and cross section of the specimens have been observed by means of optical microscopy to study the thickness and adherence of the anti-graffiti layer.

3 RESULTS

3.1 Drying Behaviour

The drying behaviour at 50% RH of fired-clay and calcium-silicate bricks is reported in Fig. 3 and 4 respectively. The drying behaviour of the fired-clay brick at 80% RH is illustrated in Fig. 5.

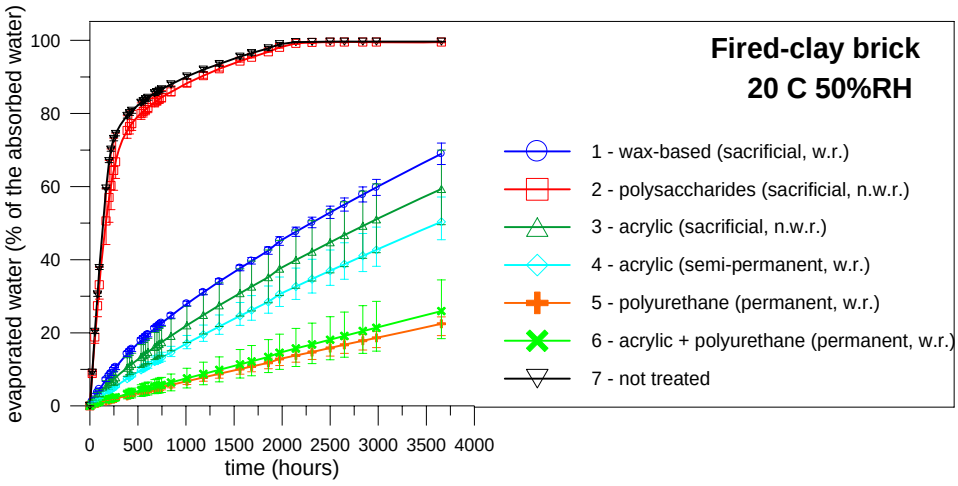

Figure 3. Drying behaviour at 20°C 50% RH of fired-clay brick treated with anti-graffiti coatings.

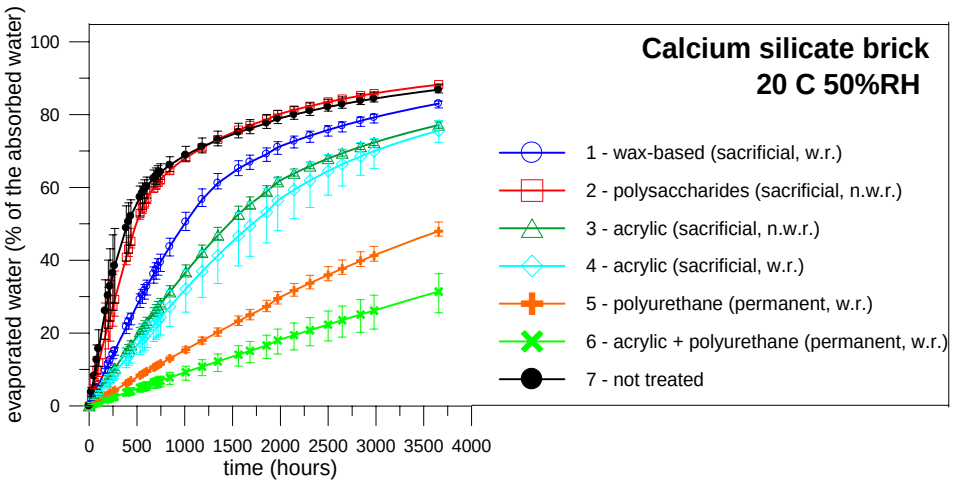

Figure 4. Drying behaviour at 20°C 50% RH of calcium silicate brick treated with anti-graffiti coatings.

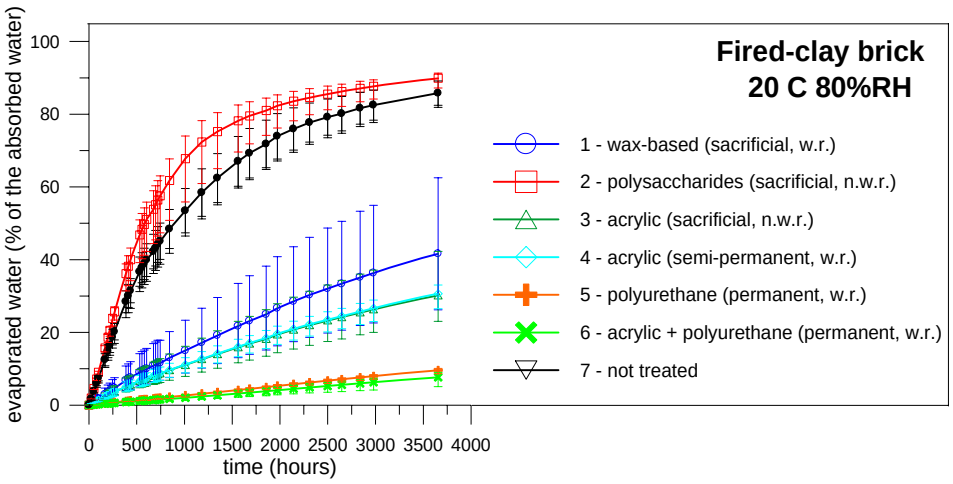

Figure 5. Drying behaviour at 20°C 80% RH of fired-clay brick treated with anti-graffiti coatings.

3.1.1 Reference Materials

The fired-clay brick dries faster than the calcium silicate brick. This is due to the presence of a water repellent layer on the calcium silicate brick and to the fact that the calcium silicate brick has finer pores than the fired-clay brick.

The drying behaviour of the reference fired-clay brick shows, as expected, two distinct drying phases: a first phase in which drying by liquid water transport prevails followed by a second phase during which drying occurs mainly through water vapour transport.

A porous material treated with a water repellent will not allow any liquid moisture transport and will therefore show no change in the slope of the drying curve, but a constant evaporation rate. This was expected for the calcium silicate brick the surface of which was treated during the production process with a water repellent. Figure 4 shows that this is not true in this case: two phases of drying are still distinguishable. This means that the water repellent layer is not completely effective and some liquid moisture transport remains possible.

3.1.2 Materials Treated with Anti-graffiti Coatings

The effect of the anti-graffiti coatings on drying of the fired-clay brick is clearly visible, both at 50% and at 80% RH. On the basis of the effect on the drying behaviour three “classes” of anti-graffiti can be distinguished:

- Anti-graffiti which do not significantly reduce the drying rate of the substrate: the polysaccharide belongs to this group. The drying behaviour of both fired-clay brick and calcium silicate brick treated with polysaccharide is about the same as the one of the reference materials.
- Anti-graffiti which reduce the drying rate: wax and acrylic products (sacrificial and permanent) belong to this category. These products significantly reduce but not completely stop liquid water transport: in fact a change in the slope is still visible in the drying curves.
- Anti-graffiti which strongly reduce the drying rate: polyurethanes coatings, alone or in combination with an acrylic primer, belong to this category. Due to the presence of a water-tight film on the surface of the treated material, liquid water transport is completely stopped and drying can occur only through water vapour diffusion, as shown by the constant drying rate. In the case of the calcium silicate brick the drying reduction due to the 3 layer polyurethane is less than for the combination acrylic primer and polyurethane. In the case of the fired-clay brick no relevant differences between the two anti-graffiti coatings are observed.

A correspondence exists in general between the water vapour diffusion data (see Table 1) and the drying behaviour measured on treated fired-clay brick and calcium silicate bricks: low water vapour diffusion resistance values correspond to a minor hindering effect on the drying. Nevertheless, the drying test gives more information about the simple water vapour diffusion resistance value, since it takes into account both phases of the drying and the effect of the material properties. In fact it has been observed that the properties of the material on which the anti-graffiti is applied play an important role. The hindering effect of anti-graffiti coatings on the drying is more pronounced for the fired-clay brick than for the calcium silicate brick. This can be explained by the fact that these products limit the liquid moisture transport, therefore they have a large impact on the first phase of the drying. As can be seen by the drying of the reference specimens, the first phase of the drying is more important for the fired-clay brick than for the calcium silicate brick (the fired-clay brick looses 60% of the initial moisture content in the first phase, while the calcium silicate brick only looses 30%), therefore the effect of these products on the drying will be more relevant for materials with a faster drying rate than for slow drying materials.

3.2 Water Drop Test

The water repellency and the water tightness of the fired-clay brick treated with anti-graffiti have been tested by performing the drop test (see section 2.3). As expected, the specimens treated with polysaccharide showed no water repellency: the water drop was immediately absorbed by the brick. On the surface of the specimens treated with acrylic products the drop remained spherical, while it was immediately absorbed on the cross section, indicating this anti-graffiti forms a water-tight film on the surface, and it has no penetration depth. The 3 layers polyurethane and the acrylic-polyurethane combination showed a reasonable (inferior to the acrylic) water tightness at the surface. The wax anti-graffiti show a good water repellency on the surface and some penetration depth (about 0.5mm).

3.3 Microscopy Observations

The microscopy observations of the surface and cross section of the specimens (Fig. 6) show that:

- The presence of the anti-graffiti is clearly distinguishable on the surface of the brick. Only in the case of the polysaccharide the amount of anti-graffiti left seems to be very limited.
- The surface is still opaque in the case of the brick treated by wax, the polysaccharide and acrylic anti-graffiti coatings, while it has assumed a glossy appearance in the case of the polyurethane and, in minor extent, of the acrylic and polyurethane combination.
- Wax and polysaccharide do not form a film on the surface of the brick. The other products form a more or less thick film. The thickness of this layer, observed in cross section, is not homogeneous.

4 DISCUSSION

The drying rate of a building material may influence its durability. Materials which retain water for a long time are generally more susceptible to decay.

The drying rate depends both on liquid and vapour transport; being the first much more effective than the second mechanism, hindering liquid water transport has a larger effect on the drying rate than reducing the water vapour transport. For this reason we believe that the effect of a surface treatment should be evaluated by measuring the drying behaviour of treated materials, instead of referring to water vapour transport values only, as usually done by the existing guidelines [WTA 2005].

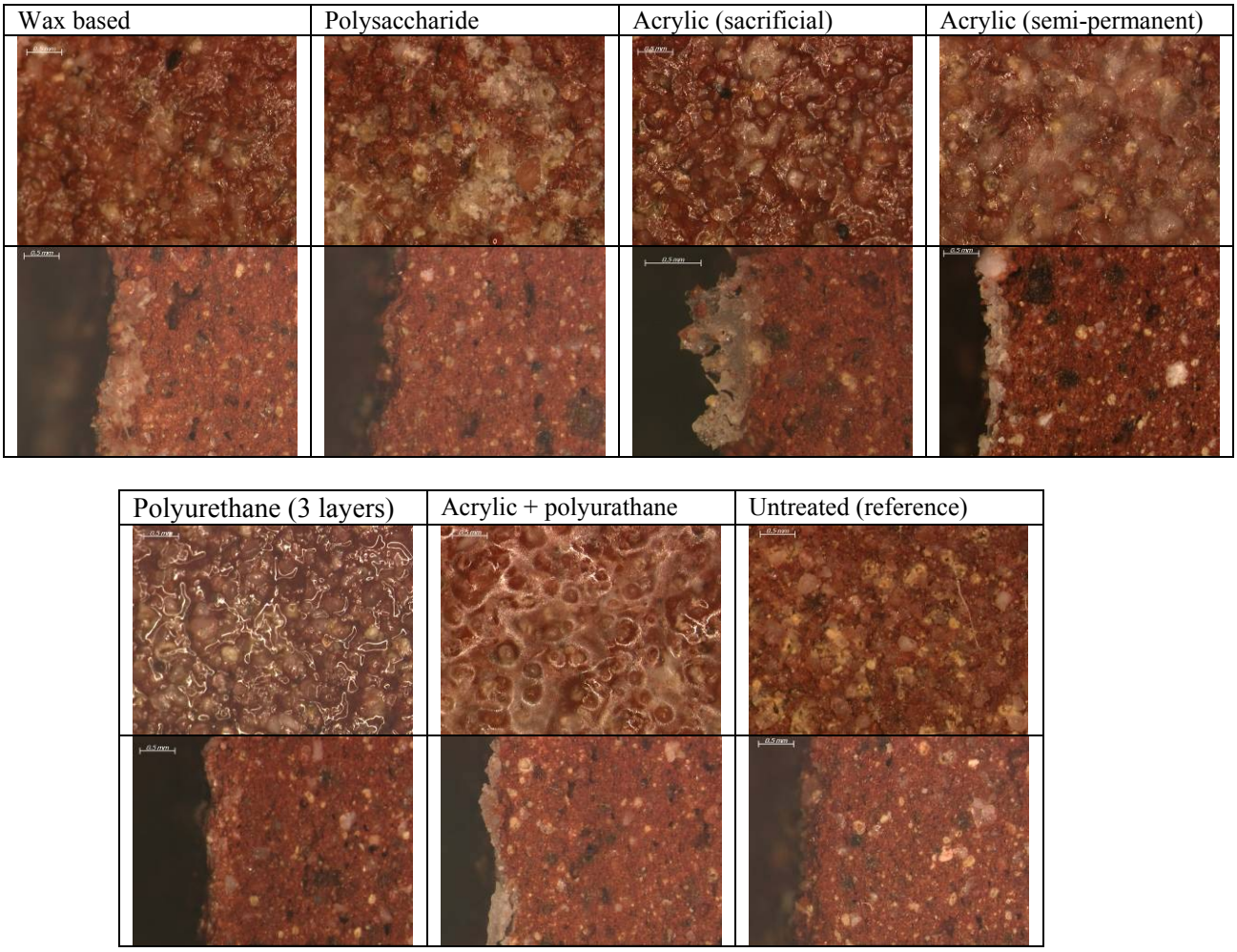

Figure 6. Pictures of the surface (above) and the cross section of fired-clay bricks treated with anti-graffiti.

This research has shown that some anti-graffiti coatings can strongly reduce the drying rate of a material. This may have negative effects not only on decay processes affecting high moisture loaded materials (like frost and biological growth) but also on salt crystallization damage. Similarly to what is observed in substrates impregnated with water repellents [van Hees & Brocken 2001], the salts, which can be transported only in liquid water and not in vapour, accumulate beneath the treated layer and may cause its detachment.

It is interesting to notice that the delaying effect of the anti-graffiti on the drying process is more evident in materials having larger pores and thus faster drying rate: the amount of water evaporated after one week from the fired-clay brick treated with a polyurethane is only 2.3% of the water evaporated from the untreated substrate, while in the case of the calcium silicate brick it is about 10%. The physical properties and in particular the pore size distribution of a material should therefore be taken into account when selecting the appropriate type of anti-graffiti coating.

5 CONCLUSIONS

This research has shown that some anti-graffiti coatings can strongly reduce the drying rate of a material. Polysaccharide has no or a very limited effect on the drying. Differently, wax, acrylic and, in larger extent, polyurethane based products partially or totally hinder liquid moisture transport, thereby

significantly reducing the drying rate of a treated material. This hindering effect may have negative consequences on the damage development in the case salts and/or moisture are present in the masonry.

REFERENCES

Bunnik T., an Hees R., van Hunen M., van de Weert T., 2004, *Graffiti – het verwijderen van en beschermen tegen graffiti*, Rijksdienst voor de Monumentenzorg en WTA Nederland –Vlaanderen,

R.P.J. van Hees, H., Brocken 2001, Interaction of the solvent based water repellent treatment with Na_2SO_4, NaCl and $NaNO_3$, in *Salt compatibility of surface treatments*, EC research report, (E. de Witte Ed.), pp. 109-119, unpublished

WTA, Merkblatt 2-8-04/D 2005, Bewertung der Wirksamkeit von Anti-Graffiti-Systemen (AGS).

11DBMC International Conférence on Durability of Building Materials and Components
ISTANBUL, Turkey 11-14 May 2008

Durability of Surface Protection Systems in Harsh Marine Climates

Claus K. Larsen [1]
Jan-Magnus Østvik [2]

T 16

ABSTRACT

The Norwegian Public Roads Administration owns and manages about 17.000 bridges, with several hundred concrete bridges in harsh marine environment along the long Norwegian coast-line. During the last 15-20 years a lot of work has been done on the effect of various surface protection systems for concrete in harsh marine environments. This paper summarises the work and the main conclusions drawn from some of the various field and laboratory investigations.

The objective for the various investigations has been at least two-folded: a) To investigate the effect of different types of surface protection systems in the field, both on the short and on the long term; b) to identify critical parameters with respect to technical performance of hydrophobic treatments and flexible cement-based coatings. Four large field investigations are reviewed; two large marine concrete bridges, one inland highway concrete bridge and one marine concrete quay.

Some of the results from the long-term investigations (up to 12 years) reveal systematically that impregnation of concrete with hydrophobic agents is very sensitive to the initial concrete moisture content. The penetration depth seems to be a critical parameter with respect to long-term chloride barrier effects. Coatings that are not flexible, or cracked after application, will fail due to cracking and subsequent loss of bond due to water accumulation and freeze/thaw actions. Surface protection systems might be very efficient over time when right products are chosen and applied properly.

KEYWORDS

Concrete, Surface protection, Durability, Maintenance, Bridges

[1] Norwegian Public Roads Administration, Technology dep., Materials Technology Section, Oslo, Norway, Phone +47 2207 3223, claus.larsen@vegvesen.no
[2] Norwegian Public Roads Administration, Technology dep., Materials Technology Section, Trondheim, Norway, Phone +47 480 36 750, jan-magnus.ostvik@vegvesen.no

1 INTRODUCTION

Concrete coastal bridges, ferry quays and wharf docks, especially those situated in harsh climatic conditions, suffer from various deteriorating mechanisms. The most severe is considered to be steel reinforcement corrosion due to chloride ingress from sea-water. Concrete bridges situated inland also suffer from steel reinforcement corrosion due to chloride ingress, but in this case from de-icing salt used on roads. The winter season requiring use of de-icing salt is normally 4-5 months in Norway, in some parts even longer. Especially for horizontal parts of a bridge, e.g. edge beams and concrete pavements, the chloride load can be rather high. Freeze/thaw actions in combination with salty water can lead to frost damages on the edge beams.

Maintenance of reinforced concrete structures is necessary to fulfil the designed or assumed service life [*fib* 2006]. The proper way of maintaining the concrete structure, i.e. the choice of repair/maintenance method, materials, application techniques and time of action is not always obvious. Wrong decisions can lead to increased problems, for instance if a coating starts to crack and fall off shortly after application. The chloride ingress is not necessarily affected by this, but the costs of repairing the surface protection system might be high. In many cases there is a need for repair of damaged areas (corroded steel and delaminated concrete) prior to surface treatment. Such repair is complex since the concrete has to be removed to a depth where the chloride content is lower than a certain critical level, a level that in many cases is difficult to identify as an unique value. Another uncertainty during maintenance and repair work is, of course, the weather conditions on site. Doing maintenance and repair work in a harsh and rough climate (strong winds, low temperatures and rough sea) is very challenging and demanding.

2 BACKGROUND AND EXPERIMENTAL

2.1 "OFU Gimsøystraumen Bridge Repair Project"

This EUR 4 million project ended in 1997, and was concluded in the international conference *Repair of Concrete Structures. From Theory to Practice*, held in Svolvær, Norway, May 1997. Main results up to 2005 from the on-going follow-up project that started in 1997, are summarised and discussed in [Larsen & Østvik 2005]. In addition to full-scale maintenance and repair work on the bridge, a research program was undertaken on the effect of various surface treatments on small-scale concrete slabs with two different initial moisture contents and two different surface preparations. Results from up to 10 years exposure will be reported and discussed in this paper.

Gimsøystraumen Bridge is a cantilever bridge finished in 1981 and situated in Northern Norway with a harsh marine environment. The bridge is 840 meters long with 5 long spans (126-148 m) and 4 short spans (25-65 m). The post tensioned box girder has a height that varies from 2.2 to 7.4 m. The highest and lowest point of the bridge deck is 36.5 m and 6.3 m above the sea level, respectively.

Small concrete slabs, 500mm by 500mm with thickness 50 mm, were cast with an OPC concrete with w/b-ratio 0.40 and 5% silica fume (by cement mass). A total of 87 slabs were cast, and they were all wrapped in plastic after de-moulding, and cured for 10 weeks in sealed conditions (no moisture exchange), i.e. the concrete was self-desiccated after curing. The degree of capillary saturation was measured to 79%. After 10 weeks, half the number of slabs was taken directly from the sealed condition, i.e. the concrete was still self-desiccated at the time of application, while the other half was immersed in water for five days to bring the concrete close to water saturation prior to application of the various surface protection systems. Immediately before application, half the number of slabs in each of the two moisture conditions was sand-blasted, i.e. there were four different concrete surface conditions available for application:

A.	Semi-dry; sand-blasted surface	B.	Wet; sand-blasted surface
C.	Semi-dry; virgin surface	D.	Wet; virgin surface

For each surface condition, nine different surface protection systems were applied on two parallel slabs and two parallel slabs served as untreated reference slabs – a total of 80 slabs. The slabs were placed on the North and West side, respectively, of one of the pillars of the bridge in August 1995. Many of the applied products were part of a development plan and are not commercially available today; therefore only four products will be reported. The products are (numbers refer to the original research plan and are therefore not in sequence):

1. Hydrophobic impregnation; a mixture of silane and siloxane in White Spirit (20% active substance).
4. Hydrophobic impregnation; pure silane (100% active substance).
6. Hydrophobic impregnation (same as #4) with a silane-acrylic based top-coat.
7. Flexible cement-latex-based coating
10. Untreated reference

The idea behind the topcoat for system #6 is to prevent degradation of the silane impregnation by UV-radiation. It is accepted that UV-radiation is the major reason for braking down a silane hydrophobic treatment [Basheer *et al*. 1992].

In 1998, five extra slabs that were cast, but not treated in 1995, were subjected to a new research plan. The slabs had been stored wrapped in plastic inside the box-girder of the bridge for three years. The slabs were treated with three different hydrophobic impregnations without any moisture conditioning or sand-blasting, i.e. the surfaces were comparable with condition C (but even drier). Two slabs served as untreated references. One of the products was in the development stage at the time of application, and is therefore not included in the results.

I. Reference N
II. Reference S
III. Pure silane (same as product #4)
IV. Silane gel (pure silane made slightly thixotropic with clay minerals)

2.2 “Skarnsundet Bridge”

Skarnsundet Bridge, once the longest cable stayed bridge in the world and still the world’s longest cable stayed bridge with a super structure in concrete, was finished in 1991 and is situated in marine environment close to Trondheim in the middle part of Norway. In 1993 it was decided to investigate various surface protection systems and their long term effect as chloride barriers on this bridge. The lowest part of the two pillars that form one of the towers of the bridge was divided in 28 sections, each 1m wide and 5m high, such that ten different surface protection systems could be applied on two opposite sides of the pillars, in addition to eight untreated reference areas (one section on each side of the two pillars). The different products are divided in two hydrophobic impregnations (silane diluted in White Spirit with 13% and 40% active substances, respectively), two impregnations (thin-film paints) and six cement based coatings (two flexible and four non-flexible). Results from up to 12 years exposure will be reported in this paper.

The concrete substrate is a typical Norwegian concrete used for bridges, with w/b-ratio 0.40, 5% silica fume and high strength OPC. Prior to application, the chloride content in the reference areas was determined by profile grinding, and each section was carefully investigated with respect to cracking and other surface failures that could influence the effect of the surface treatments. One idea behind the project was to let the suppliers find their best chloride barrier, suggest the proper pre-treatment of the concrete surface and apply the products themselves. This would lead to the very best application any

supplier could get for such a research project. Each application was carefully monitored with measurement of the amount of agents applied.

2.3 "Lundevann Bridge"

Lundevann Bridge is a 12-span beam bridge on the E18 highway in the southern part of Norway. It is situated in inland-climate and suffers from intensive use of de-icing salts 4 to 5 months per year. During repair work on the edge beams in 1998, due to heavy reinforcement corrosion after nearly 30 years in service, a field investigation on the effect of surface protection systems was started. The new parts of the edge beams and test specimens (small concrete slabs, 300 mm x 500 mm x 50 mm placed on top of the edge beams), were cast with a OPC concrete with w/b-ratio 0.40 and 5 % silica fume (by cement mass). Both the edge beams and the slabs were treated with four different products, two hydrophobic impregnations and two flexible cement based coatings. Results from up to 9 years exposure will be reported and discussed in this paper.

2.4 "Sjursøya Quay"

The Sjursøya Quay is part of the Oslo Harbour, and serves as an important quay for the oil industry in the Oslo region. The quay was repaired in 1999, due to heavy chloride induced corrosion of the steel reinforcement and subsequent loss of load bearing capacity. The quay is a traditional concrete beam-slab structure, about 300 meters long divided in 48 beam-slab sections. The chloride contaminated concrete in the bottom part of the slabs and the beams was removed by water-jetting, and replaced by shotcrete for the slabs and ordinary concrete for the beams, both OPC concretes with w/b-ratios 0.40 and 5% silica fume. A few weeks after concreting eight of the sections (a section includes one beam and the corresponding slab underside) were treated with different surface protection systems; five hydrophobic impregnations and three cement-based coatings. Some results from up to five years exposure will be reported and discussed in this paper.

2.5 Chloride Ingress

The chloride ingress was measured on specimens either cut from the various slabs or on cores taken from the various structures. Concrete powder was carefully grinded in thin layers parallel to the exposure face of the specimens, and the acid-soluble chloride content measured with potentiometric titration.

2.6 Penetration Depth of Hydrophobic Impregnation

The penetration depth of the hydrophobic impregnations was measured on freshly split concrete surfaces that immediately after splitting were submerged for a few seconds in water. The concrete that is hydrophobic will not turn dark grey due to wetting, and the depth of impregnation is therefore easily measured. The reported impregnation depths are the average value of ten single measurements along the split surface (typically about 100mm long).

3 RESULTS AND DISCUSSION

3.1 Chloride Ingress

Figure 1 shows the chloride ingress for the 1995 Gimsøystraumen slabs after 10 years exposure.

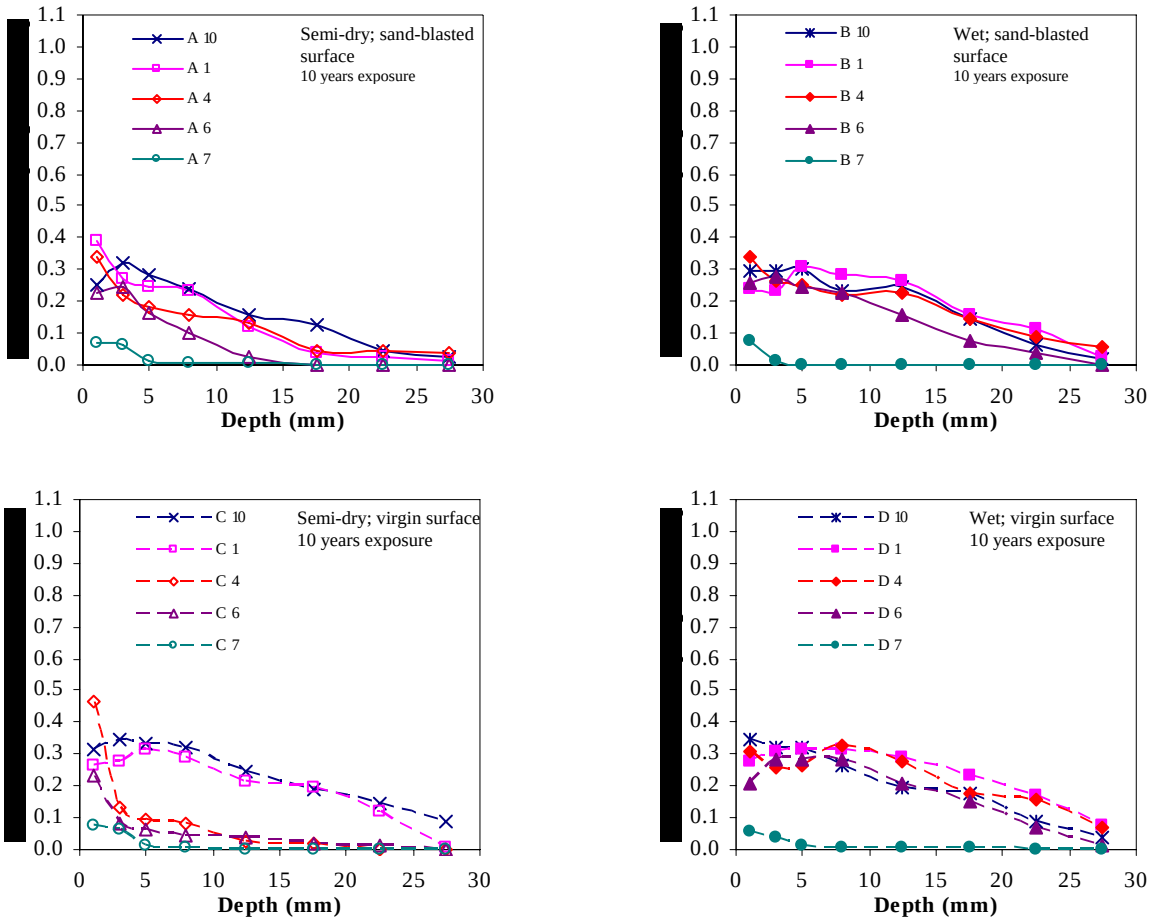

Figure 1. Chloride ingress after 10 years exposure, 1995 Gimsøystraumen slabs.

It can clearly be seen that the long-term effect of the surface protection systems to decrease chloride ingress is affected by the pre-treatment of the concrete substrate. The concrete moisture content plays an important role as all the hydrophobic treatments (#1, #4 and #6) on initially wet concrete have very little effect after 10 years in service, whereas the same products applied on semi-dry virgin concrete, except product #1 (20% silane/siloxane), still are fairly good chloride barriers. This can be visualized by plotting the chloride barrier effect (the filtration degree, i.e. the ratio of the total amount of penetrated chlorides in a treated sample versus the untreated reference), as seen in Fig. 2.

From the right part of Fig. 2 it is obvious that the effect of the hydrophobic treatments have been reduced gradually over the years, as one would expect for a UV-exposed silane-treated surface. A UV-filter on top of a hydrophobic treatment seems to prevent some of the degradation process, as product #6 has a better long term barrier effect than product #4.

The most important factor for preventing degradation of the impregnated surface is perhaps the penetration depth of the hydrophobic treatment. If the silane agents can penetrate deep into the concrete surface, the idea is that no UV-radiation can reach and destroy the impregnation. It was reported after application that penetration depths were hardly measurable and always less than 0.5mm for the wet concrete slabs, whereas the penetration depths for the semi-dry slabs were measured to 2-4mm.

This difference in penetration depth might explain the difference between the wet and the semi-dry substrate as seen in Fig.2.

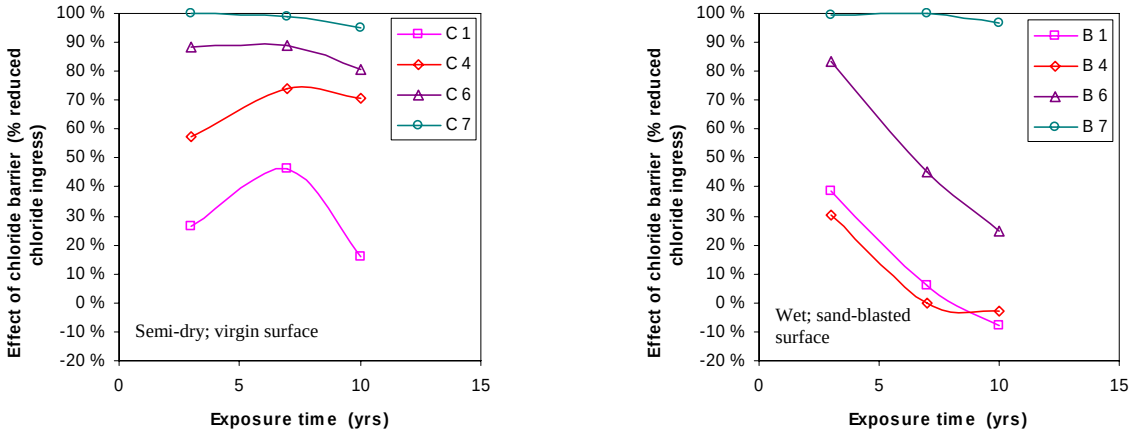

Figure 2. Chloride barrier effect for Gimsøystraumen slabs (1995).

Another marked effect from Figs 1 and 2, is the very good chloride barrier effect over time for the flexible cement-latex based coating (#7). This system has a chloride barrier effect above 98% even after 10 years in harsh marine environment and it still is flexible and adheres very well to the concrete as visually observed on-site during condition assessment.

To follow up the promising long-term effect of a large penetration depth, some of the 1998 Gimsøystraumen slabs were treated with a silane-gel that in the laboratory had proven to penetrate this type of concrete to very large depths (product #IV). The average penetration depths for the silane-gel and the pure (liquid) silane are 22 mm and 2 mm, respectively. The same trend was found on the Lundevann-slabs, where the same two products (silane-gel and liquid silane) were applied on self-desiccated concrete. In that project the ratio between silane-gel and liquid silane was on average 7.1. The penetration depth for the silane-gel is therefore on average about one order of magnitude larger than for the liquid silane.

The chloride ingress over time for the 1998-Gimsøystraumen slabs is shown in Fig. 3.

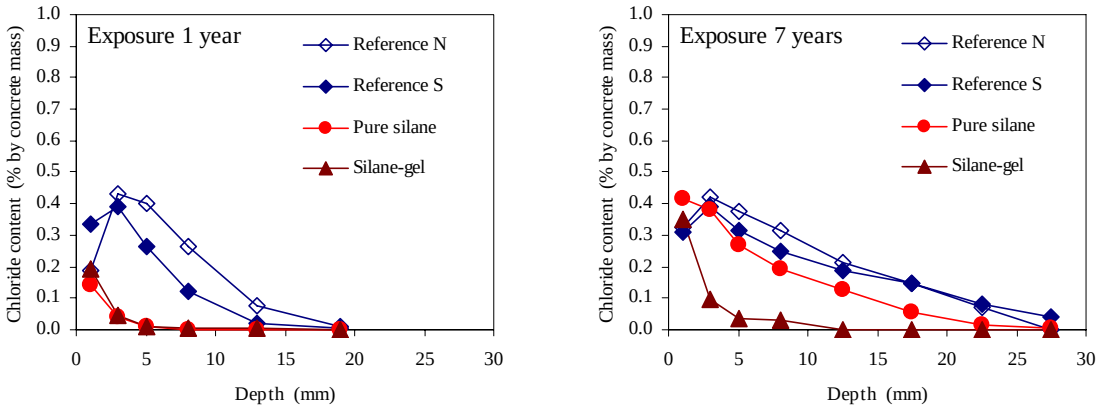

Figure 3. Chloride ingress for the 1998-Gimsøystraumen slabs.

It is clear that the pure silane (liquid) has lost most of its chloride barrier effect (decreased from 87% to 28%) from one to seven years exposure, whereas the silane-gel has more or less kept its barrier effect (decreased slightly from 83% to 80%) in the same period of time.

Figure 4 shows the chloride ingress in the sprayed concrete slab (underside) of the Sjursøya Quay after 5 years exposure. It is clear that all the surface protection systems, even the hydrophobic treatments, have a very good chloride barrier effect.

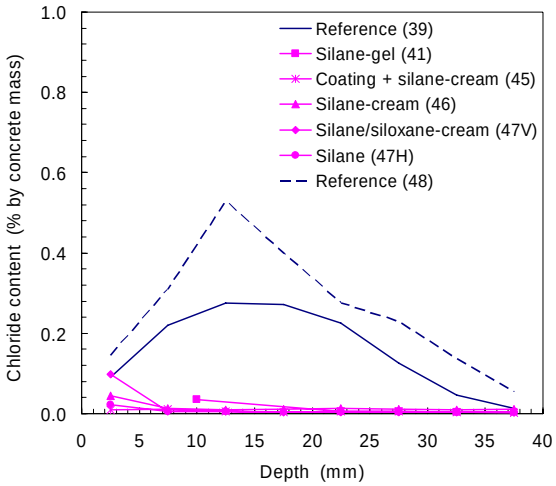

Figure 4. Chloride ingress in the sprayed concrete slab (underside) of the Sjursøya Quay, 5 years exposure.

On the Sjursøya Quay the measured penetration depths for the various hydrophobic impregnations were: silane-gel (41), 17.5 mm; silane-cream (46), 15 mm; silane/siloxane-cream (47V), 7 mm; and silane (liquid) (47H), 4.5 mm. The large penetration depths probably explain the high chloride barrier effect over time for all the impregnations. The reason for the high penetration depths might be the rather high porosity of the shotcrete used for repair of the slab underside. Measurements indicate a capillary porosity of about 22 % for the shotcrete, which is very high compared to the ordinary concrete used for the beam-repair, at about 13 %. A higher porosity will of course lead to an improved penetration of the impregnation agents, and not to forget increased chloride ingress into the untreated concrete. Both these factors would lead to a bigger difference between treated and untreated concrete. Another reason for the good long-term effect might be the fact that the underside of the quay-slab is protected against direct sun-shine, as the slab extends several meters towards open sea from where the samples have been extracted. However, there are signs of a degradation of the impregnations, as a thin outer layer of the surface no longer is hydrophobic after five years exposure. This can be seen in Fig. 5.

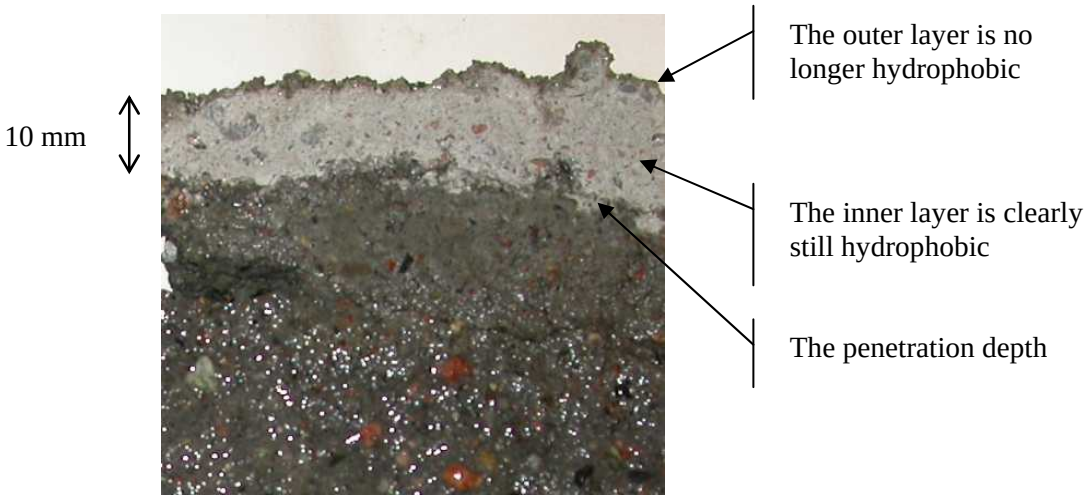

Figure 5. Degradation of a hydrophobic treatment, the Sjursøya Quay, 5 years exposure.

Figure 6 shows the chloride ingress on the surface facing south of the north and south pillar on Skarnsundet Bridge after 12 years exposure.

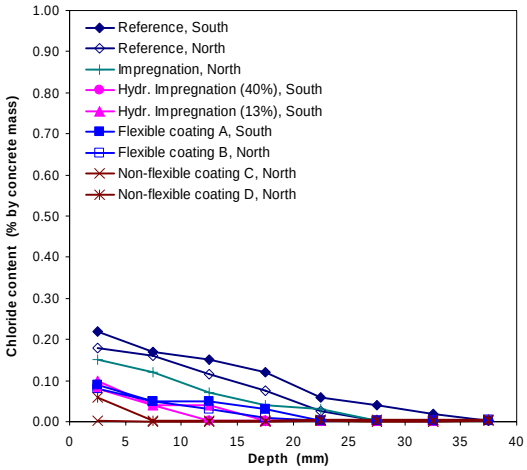

Figure 6. Chloride ingress on the south face of the north and south pillar on Skarnsundet Bridge, 12 years exposure.

In the Skarnsundet project it is clear that most of the surface protection systems have a rather good chloride barrier effect after 12 years in service. The hydrophobic impregnations, both being diluted solutions, have more or less the same chloride barrier effect as coatings, which is very unusual especially when considering the fact that it was not possible to measure any penetration depth (zero penetration, i.e. no measurable hydrophobic layer) for these two products. The product with the poorest chloride barrier effect is the impregnation, or more precisely a thin-film coating on the northern pillar. This product showed already after one year in service signs of degradation, as the thin-film coating cracked and started to change colour. After four years in service the product was no longer visible on the surface, it was simply worn off due to the harsh marine climate (rough winds combined with heavy rain).

3.2 Cracking of Coatings

The chloride barrier effect for flexible cement-based coatings is excellent, as have been shown in this paper. However, there is one major concern for these coatings – the risk of cracking. The Lundevann Bridge project demonstrated clearly the destructive effect of cracks when the structure is exposed to harsh climates, with heavy use of de-icing salts and long winters with a lot of freeze-thaw action. Half the height of the edge beams of the bridge was removed by water-jetting, the corroded reinforcement was replaced with new rebars and concrete was thereafter cast to fully repair the edge beams.

The surface protection systems (two flexible cement-latex based coatings and two hydrophobic impregnations) were applied about two weeks after demoulding, in such a way that the edge beams were fully covered.

The problem occurred after a few weeks when the concrete started to crack, probably due to shrinkage. The cracks penetrated the coatings, even though both were flexible. However, this is not strange if one considers that when cracking occurres after application of the coating, the coating suffers from an infinite strain at the cracking point. Only the most extreme products will withstand this.

Figure 7 shows three pictures from three different stages of the crack-failure. The first stage (Fig.7 a) is the cracking of the coating it selves with subsequent water penetration/accumulation and a microscopic freeze-thaw damage in the crack. After a few years the freeze-thaw damage expands from the crack and outwards (Fig.7 b) until the entire coated area is affected (Fig.7 c).

(a) (b) (c)

Figure 7. Crack-failure for the flexible coatings on Lundevann Bridge; (a) initial stage with cracked coating; (b) advanced stage with loss of bond adjacent to the crack; (c) final stage with a massive loss of bond originating from the crack.

After the first winter it was obvious that there was only a matter of time before the coatings would fail and fall off. For one of the coatings this was the case after two years in service, whereas the other coating lasted for another three to four years before large areas started to loose bond and fall off. There was little doubt that freeze-thaw damage was the main cause of loss of bond, as there was a thin layer of concrete still adhering to the scaled off coating indicating a surface freeze-thaw action. This suggests that application of coatings must be done after any initial cracking of the concrete.

4 SUMMARY AND CONCLUSIONS

Concrete surface protection systems can, if properly applied and the right product is used, be very efficient chloride barriers on the long-term even in harsh exposure climates. The most important results reported in this paper, indicates that:

- the long term effect of hydrophobic impregnation is influenced by the penetration depth, possibly due to the improved UV-protection at larger penetration depths
- the wetter the concrete substrate is before application, the smaller is the penetration depth
- silane-gel and silane-cream show a much larger penetration depth than pure liquid silane
- flexible cement-based coatings perform excellent as chloride barriers if the coating remains un-cracked
- cracks in coatings can have a devastating effect on the service-life of a treatment in harsh climates with freeze-thaw actions

REFERENCES

Basheer, P.A.M., Long, A.E., & Montgomery, F.R., 1992, *Durability of surface treated concrete.* Report No. SMRG-03-1992. Belfast. The Queen's Univ. of Belfast

fib 2006, *Model code for service life design*, Bulletin 34, ISBN: 978-2-88394-074-1, 116 p

Larsen, C K., & Østvik, J-M., 2005, '10 years experience with repair of a costal concrete bridge', Proc. ICCRRR, Cape Town, South Africa, 21-23 November 2005, pp 777-783

Proceedings of the International Conference Repair of Concrete Structures. From Theory to Practice in a Marine Environment; Svolvær, Norway, May 1997, Norwegian Public Roads Administration.

Long-term Performance of Extruded Polystyrene Thermal Insulation Products

Holger Merkel [1]

T 17

ABSTRACT

One of the essential requirements of the European Construction Products Directive (CPD) is the durability of products. This is closely linked to the sustainability of buildings and their energy consumption. Hence thermal insulation products have to provide evidence that they are durable over their service life.

The paper presents ways how to adress this complex issue using the example of factory made extruded polystyrene foam XPS according to the harmonized European standard EN 13164.
XPS insulation is applied in numerous constructions which are subjected to different combined loadings, such as combined mechanical, moisture and heat impact.

In particular the hygrothermal and mechanical durability of XPS products were investigated. Both laboratory results and practical results will be presented in order to show the correlation between short-time durability tests and practical performance of products.

The application of insulation products under sustained load is another topic which will be adressed in the paper. The durability of insulation products against mechanical degradation when subjected to long-term loading is characterized by its creep performance (EN 13164 Annex ZA). The method according EN 1606 and the results of creep performance measurements for XPS products will be presented and discussed.

KEYWORDS
Thermal insulation, Extruded polystyrene foam, Creep, Moisture

[1] Dow Deutschland Anlagenges.mbH, 65824 Schwalbach, Deutschland, Phone +49 6196 566 158, Fax +49 6196 566 426, hmerkel@dow.com

1 INTRODUCTION

One of the essential requirements of the European Construction Products Directive (CPD) is the durability of products. Durability is defined as *the ability of a product to maintain its required performance over a given or long time, under the influence of foreseeable actions, subject to normal maintenance* [EC 2004].

To attest its conformity with the CPD, a product put on the market must carry CE marking. CE marking attests that the product complies with the applicable technical specification (hENs, ETAs). In addition, it is compulsory for the manufacturer to declare the performance of the product for the mandated characteristics which are required by the technical specifications[CEPMC 2005].

The concept of durability related to CE marking means the permanence of the mandated characteristics of a product**,** linked to one or more of the 6 essential requirements. This permanence is dependent on the evolution in time, or ageing, of one or several performances of the characteristics and implies resistance to deterioration during exposure to normally foreseeable external or specific agents[EC 2004].

Table 1. Illustrative assumed working life (design working life) of works and construction products [EOTA 1999].

Assumed working life of works (years)		Working life of construction products to be assumed in ETAG's, ETAs, hENs (years)		
Category	Years	Category		
		Repairable or easily replaceable	Repairable or replaceable with some more efforts	Lifelong [2)]
Short	10	10 [1)]	10	10
Medium	25	10 [1)]	25	25
Normal	50	10 [1)]	25	50
long	100	10 [1)]	25	100

[1)] in exceptional and justified cases ; e.g. for certain repair products a working life of 3 to 6 years may be envisaged (when agreed by EOTA TB or CEN respectively)
[2)] When not repairable or replaceable "easily" or "with some more efforts"

Thermal insulating products are repairable or replaceable "with some more efforts" in many cases. There are exceptional applications, e.g. foundation insulation where the product must be assumed at least in category "Normal" which means 50 years of working life according to Table 1.

2 ASSESSMENT OF DURABILITY OF INSULATING PRODUCTS

The assessment of durability of thermal insulating products is possible by:

- Laboratory short-term test methods
- Laboratory ageing test methods
- Testing products in application under natural climatic conditions.

2.1 Laboratory Test Methods

In the following two mandated characteristics which are specified in the European product standards will be addressed:

- durability of thermal resistance against wheatering, degredation and freeze-thaw

- durability of compressive strength against ageing and degradation.

2.1.1 Durability of Thermal Resistance against Wheathering, Degradation and Freeze-Thaw

One of the most important tests for extruded polystyrene is the freeze-thaw test. It comprises two separate tests. The test for water absorption by diffusion [EN 12088] and the test for water absorption after freezing and thawing cycles [EN12091].

The test is mandatory for applications like Inverted Roofs and any insulation below ground level; e.g. perimeter insulation and insulation of road- and railways [EN 14934].

The Figures 1 and 2 show schematically the test build-up and the boundary conditions of the diffusion and freeze-thaw test.

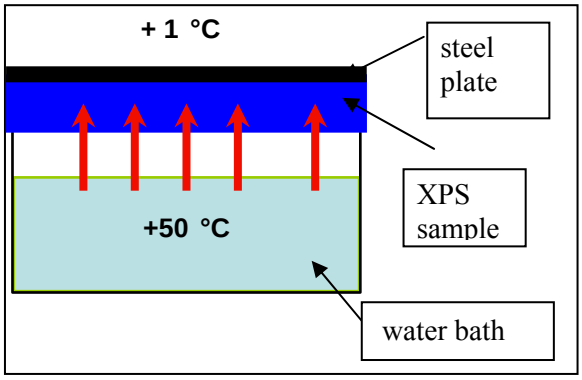

Figure 1. Diffusion test (schematically), 28 days.

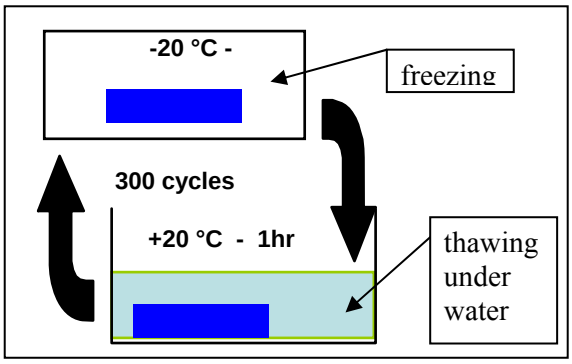

Figure 2. Freeze-thaw test (schematically), 28 days.

After a 28 days diffusion test the samples are used for the freeze-thaw test. The boundary conditions are more severe than climatic conditions in most of the European countries. But the results are in good agreement with practical long-term results. Thus the test conditions are simulating short-term the performance of the product under climatic conditions.

The requirements for both water absorption by diffusion and after freeze-thaw cycling are listed in Tables 2 and 3.

Table 2. Levels of water absorption by diffusion in relation to nominal thickness d_N according to EN 13164 [EN13164] for extruded polystyrene.

level	Requirement [m³/m³ (Vol-%)]		
	d_N = 50mm	d_N = 100mm	d_N = 200mm
WD(V)5	≤ 5	≤ 3	≤ 1,5
WD(V)3	≤ 3	≤ 1,5	≤ 0,5

The actual values from test results of various notified bodies in Europe are shown in Figure 3.

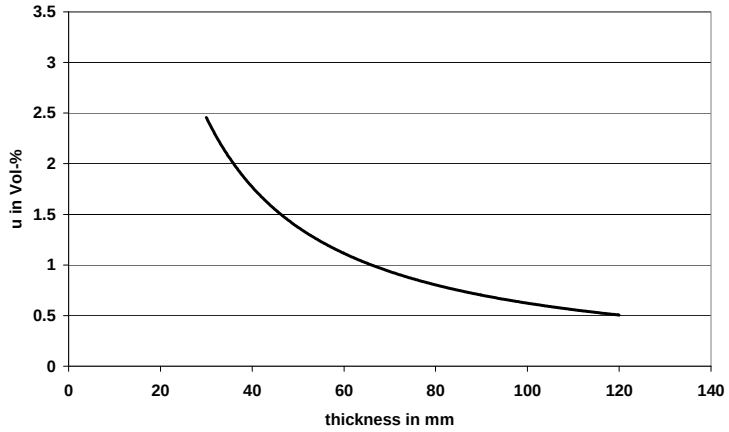

Figure 3. Water absorption by diffusion, typical values for XPS products (Roofmate).

The values in Figure 3 lead to a declaration WD(V)3 according to EN 13164. It can be assumed that such a product is durable against water impact.

Table 3. Levels of resistance against freez-thaw cycling, water absorption after freeze-thaw cycling for extruded polystyrene according to EN 13164.

level	Requirement [m³/m³ (Vol-%)]
FT 1	≤ 2
FT 2	≤ 1

After freeze-thaw cycling the reduction of compressive strength shall not exceed 10% of the initial value before the freeze-thaw test. This requirement ensures that the material structure of the foam has not been deteriorated during the freezing and thawing processes.

Actual values from tests performed by European notified bodies, show nearly no reduction of compressive strength for XPS products such as Styrofoam.

2.1.2 Durability of Compressive Strength

There are applications where it is not possible or not affordable to repair or replace insulating products. In particular when products are applied under foundations or within other structural parts of a building. In such a case the products must comply with the category “NORMAL” specified in Table 1. Normal means a lifetime of at least 50 years.

Extruded Polystyrene Foam has been successfully used for many years under road-and railway constructions as well as under load-bearing concrete slabs, such as foundations or industrial floors. It is necessary to know the stress-strain behavior (compressive creep) of XPS under sustained load. The assessment of thermal insulating products shall follow the European test standard EN 1606 [EN1606].

The standard comprises the measurement method and a calculation method to predict the long-term creep according to the FINDLEY approach [Merkel 2004].

This method describes the viscoelastic behavior of cellular plastic foam.

$$X_t = X_0 + m \cdot t^b \quad (1)$$

where:
X_0 : initial deformation 60s after the load has been applied
m,b : material parameters (FINDLEY parameters)

The equation (1) is known as Findley equation. The second term describes the visco-elastic part of the deformation. The material parameter m and b are stress dependent.
Equation (1) can also be expressed in a linear form by introducing logarithmic terms:

$$\log (Xt - X0) = \log m + b \cdot \log t \quad (2)$$

The parameters m and n can be obtained from a linear regression curve, which is calculated using the measured values starting 168 hours after initial measurement. From equation (2) it follows the parameter b as the slope of the curve and log m the intercept of the ordinate.

Figure 4 shows a typical linear regression curve for XPS from which m and b can be determined. The details of this procedure are described in EN 1606. An extrapolation 30 times the testing time is permitted when $R^2 \geq 0.9$.

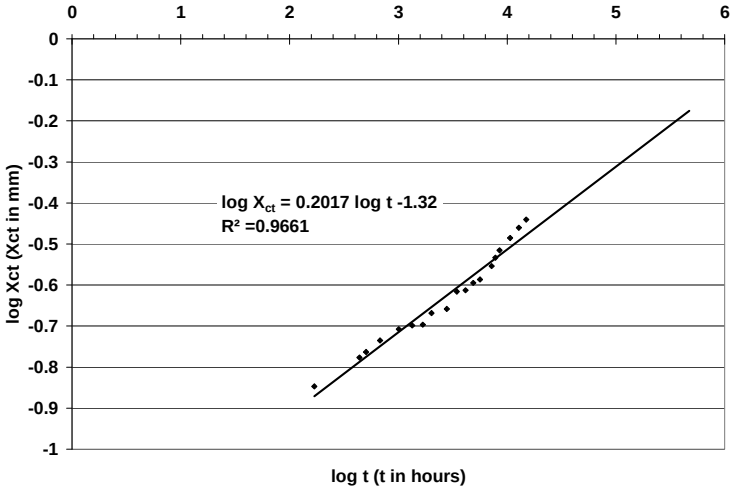

Figure 4. Typical regression curve for XPS to determine the FINDLEY parameter m and b (Dow Building Solutions).

Taking the given example, the FINDLEY parameters are determined to be: b = 0.2017 and m = 0.048. For building applications such as thermal insulation of foundations a total reduction of ≤ 2% of the initial thickness and an extrapolation time of 50 years are generally required.

Conclusively, thermal insulating products have to be tested for 608 days at a stress level which will finally result in deformations less than 2%.

Figure 5 shows a creep curve for an XPS product according EN 1606.

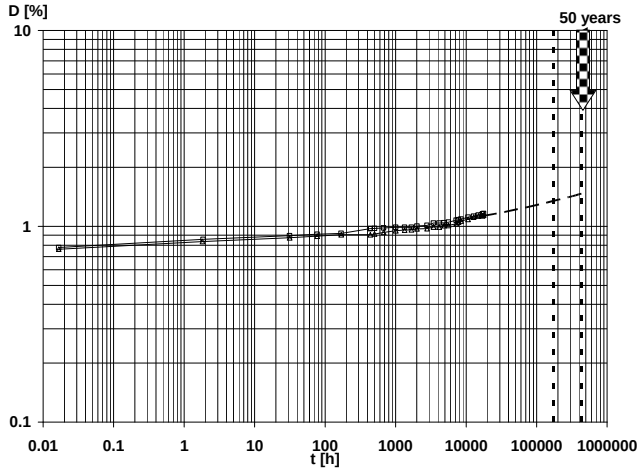

Figure 5. Creep deformation of an XPS product under constant load of 270 kPa (Graph: Dow Building Solutions).

It is obvious that after a short period of initial response to the load applied the remaining creep part of the deformation is pretty small. The dashed perpendicular lines on the right side of the figure are at 20 years and 50 years. Between 20 years and 50 years of service the creep deformation is practically negligible.

The foam remains structural stable during the entire test-period. This means extruded polystyrene foam is highly durable against sustained mechanical loads.

2.2 Long-term Performance Under end-use Conditions - Examples

2.2.1 Civil Engineering Application

The performance of XPS frost insulation layers in roadway application in Siberia were studied over a time period of 20 years [Polukhina et. al. 2003].

The insulation layer was located about 50cm to 65cm below ground level. The climatic conditions were characterized by typical continental climatic conditions with temperature variations of about 90K between summer and winter. The results which characterize the durability of XPS products applied in this project are listed in Table 4.

Table 4. Results of long-term performance of XPS in roadway application [Polukhina et. al. 2003].

property	1983	1995	2003
Compressive strength [N/mm²]	0,40	0,48	0,52
Thermal conductivity at 20°C, dry sample [W/(mK)]	0,028	0,0286	0,0295
Thermal conductivity at 20°C, wet sample [W/(mK)]	-	0,0301	0,0309

The XPS product investigated showed no deterioration under very severe climatic and complex soil and hydrological conditions over 20 years of service. The increase in thermal conductivity due to moisture impact is less than 5%. The time dependent change in thermal conductivity due to cell gas exchange is about 5 %. This is well below the increase predicted at 10% according to previous German standards.

2.2.2 Building Application

The application of XPS outside of the water-proofing layer requires high mechanical and moisture resistance. In such applications the insulation product is exposed to a combined impact of heat, moisture and mechanical loads. Hence, the long-term performance of XPS is of topical interest.

XPS products have been tested after 5 to 22 years of service in different roofing applications and in perimeter insulation below groundwater level.

Figure 6. Sampling of XPS boards from a green roof (Photo: Dow Building Solutions).

The results are summarized in Table 5.

Table 5. Results of long-term performance of XPS in Inverted Roof (IR) and Perimeter application (Dow Building Solutions).

construction	**service-life [years]**	**thickness [mm]**	**compr.strength [kPa]**	**$\lambda_{10\ measured}$ [W/(mK)] 1)**	**λ_{design} [W/(mK)] 2)**
gravel ballasted IR	8	140	not measured	0,036	0,038
gravel ballasted IR	22	80	359	0,029	0,033
Roof garden IR	22	60	459	0,029	0,033
Perimeter below ground-water level	5	60	357	0,031	0,035

1) unconditioned sample as taken from the building
2) design values according National regulations in Austria, Germany and Switzerland

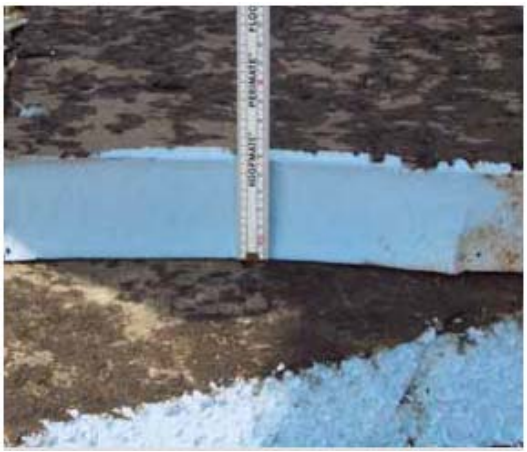

Figure7. Cross section of XPS insulation board after more than 20 years of service in an Inverted Roof outside of the water-proofing layer (Photo: Dow Building Solutions).

The sample shown in Figure 7 was taken from the roof and cut in half to investigate whether the foam structure has been deteriorated over the life-time. No change in cell structure could be detected. This explains why the properties of the foam are practically unchanged.

3 REFERENCES

EC2004. 'Durability and the Construction Products Directive', European Commission, DG Enterprise and Industry, Brussels, Dec. 2004

CEPMC 2005, 'Durability of the performance of construction products',CEPMC, Brusssels Sept. 2005

EOTA1999, 'Assumption of working life of construction products in ETAG, ETA and harmonized standards', Guidance Document 002, Brussels Dec. 1999

EN12088. EN 12088 'Thermal insulating products for building applications – Determination of long term water absorption by diffusion'

EN12091. EN 12091' Thermal insulating products for building applications- Determination of freeze-thaw resistance'

EN14934. EN14934:2007 'Thermal insulation and light weight fill products for civil engineering applications – Factory made products of extruded polystyrene (XPS) – specification

EN13164. EN 13164 'Thermal insulation products for buildings- Factory made extruded polystyrene foam products (XPS)'

EN1606. EN 1606 'Thermal insulating products for building applications – Determination of compressive creep'

Merkel, H., 2004, 'Determination of Long-Term mechanical Properties for Thermal Insulation under Foundations. BUILDINGS IX, Proc. International Conference Clearwater, Florida 2004, ASHRAE 2004.

Polukhina, L.A., Nikitin, V.P, Shestakov, V.N., 2003, 'Study of the operating condition of the Omsk-Novosibirsk motorway section (km 1304, PK 101+40 – PK 106+00) with STYROFOAM foamed plastic heat insulating layers' (in Russian) , Siberian state road transport academy,Research Division, Omsk 2003.

11DBMC International Conference on Durability of Building Materials and Components
ISTANBUL, Turkey 11-14 May 2008

Durability of Roof Underlays Exposed to Natural Climate

Birgitte Dela Stang [1]
Erik Brandt [2]
Morten Hjorslev Hansen [3]

T 17

ABSTRACT

Durability of roof underlays is of large importance as they serve as the ultimate barrier against water ingress in roof constructions. This is especially true in Denmark because of the frequent use of clay tiles on buildings with low pitched roofs where wind-driven rain has fairly easy access to the roof underlay. Also, some tiles allow a high amount of solar radiation to pass through the corner joints.

A large part of roof underlays used in Denmark are based on flexible polymer sheets that are not supported by a rigid underlay. A popular trend in contemporary Danish architecture is low pitch roofs with ceilings parallel to the roof surface leaving no or very poor accessibility for inspection of the roof underlay.

The paper presents results from testing of watertightness and tensile strength on 5 different types of flexible sheet roof underlays, a woodfibre board, and a bituminous roof underlay supported by plywood. The 7 roof underlays were exposed to natural climate on a south-facing roof with a pitch of 20° and without roof covering. Tests were carried out at various exposure times between 3 months and 32 months. Also, supplementary samples of the 7 roof underlays were exposed to accelerated ageing according to EN 13859-1. Reference data were obtained from unexposed material.

KEYWORDS

Roof underlays, Deterioration, Natural exposure, Tensile stength, Watertightness

[1] Danish Building Research Institute, Aalborg University, 2970 Hoersholm, Denmark, Phone +45 4586 5533, Fax +45 4586 7535, bds@sbi.dk
[2] Danish Building Research Institute, Aalborg University, 2970 Hoersholm, Denmark, Phone +45 4574 2370, Fax +45 4586 7535, ebr@sbi.dk
[3] Danish Building Research Institute, Aalborg University, 2970 Hoersholm, Denmark, Phone +45 4586 5533, Fax +45 4586 7535, mhh@sbi.dk

1 INTRODUCTION

For quite some years Danish common practice has been use of roof underlays (also designated sarking felt or underlayments) for sloping roofs with roof coverings of tiles or slates. Roof underlays are also used for metal roof coverings to catch drips from condensation on the backside of the roof covering.

The main purpose of the roof underlay is to act as a barrier against water penetrating the roof covering itself. In Denmark some types of roof coverings – especially clay pantiles with small overlapping joints and fibre cement slates – are fairly open to water, especially in the form of wind-driven rain. When it comes to drifting snow, all tile or slate roof coverings will allow snow to pass unless special solutions e.g. mechanically tightened joints are used.

In addition, the roof underlay must not jeopardize the natural moisture transportation by diffusion through the roof construction. Traditionally this has been achieved by using roof constructions with a vented cavity between the insulation and the roof underlay. In such cases vapour tight materials perform very well as long as the cavity has sufficiently large openings to the surroundings. During recent years a new type of materials has been introduced to the market. These materials which are very open to water vapour diffusion are used in a different way than previously as they are placed directly on the insulation i.e. such roofs do not have the possibility of removing moisture by ventilation. Moisture penetrating from the interior of the building must consequently be removed by diffusion instead of ventilation. These materials must be water vapour permeable to such extend that moisture is not accumulated inside the construction.

Further, some clay pantiles allow a relatively high amount of solar radiation to pass through the corner joints. Hence, the roof underlay must be resistant to UV-radiation.

A relatively large part of roof underlays used in Denmark are based on flexible polymer sheets that are not supported by a rigid underlay. A popular trend in contemporary Danish architecture is low pitched roofs with ceilings parallel to the roof surface leaving no or very poor accessibility for inspection of the roof underlay.

In a previous study [Brandt & Hansen, 1998] the most important properties for roof underlays were found to be:

Tightness against precipitation - this property is especially required during the construction period until the primary roof has been laid.

Tightness against water - this property covers standing water as well as water running on the surface. When well constructed no ponding should occur on the roof underlay.

No tent effect - tent effect refers to the well-known fact that touching of the inside of a tent during rain may cause penetratiom of water. For underlayments laid directly on wood and insulation, no tent effect should occur, as it would impair the watertightness.

Water vapour permeability - for unventilated constructions it is evident that moisture from the interior of the building can only escape through the underlayment by diffusion. Consequently the material shall be very permeable to diffusion of water vapour.

Moisture accumulating properties - are a supplementary asset if all other requirements to the roof are fulfilled. It allows the take-up and accumulation of moisture during periods with high exposure. The moisture is allowed to be removed during other periods.

Dimensional stability against changes in RH - is an important property but is not a problem with current materials.

2 THEORY AND TEST SET-UP

Degradation of polymer based materials is mainly caused by UV-light, heat and moisture. Most roof underlays are used as interim roof in the construction period – which often lasts several weeks – where it is exposed to UV-light (together with ambient temperature, precipitation and wind). Further, it has been shown that for some clay pantiles with small overlapping joints as much as 5 % of the UV-light in the environment may reach the roof underlay [Holck & Rosenfeld, 2005]. In an earlier study, [Brandt & Hansen, 1998], it was found that the temperature of the roof underlay is normally below 45° C in the finished roof. It is anticipated that temperatures in the construction period is at the same level.

When used as a provisional roof the roof underlay is exposed to precipitation and consequently is moist a fair part of the time dependent on the weather conditions. In the finished roof the roof underlay will only be exposed to water occasionally but it will more regularly be exposed to high relative humidity from the environment due to diurnal and seasonal changes in temperature etc.

Based on the conditions described above and problems seen in practice it is assessed that the main degradation factor for roof underlays is UV-light [Brandt *et al.*, 2007].

One purpose of the study was to compare results from natural ageing with results from accelerated ageing according to EN 13859-1. In Denmark it is common to test roof tile underlays for so called tent effect after accelerated ageing to a somewhat harsher UV-exposure than used in EN 13859-1, cf. [Nordtest Method 488]. Testing of the same specimens used for this study is currently being performed.

2.1 Test set-up

The paper presents results from testing of watertightness and tensile strength for roof underlays after exposure to natural climate and after accelerated ageing testing according to EN 13859-1.

The study encompasses 5 different types of flexible sheet, 1 wood fibre board, and 1 bituminous roof underlay supported by plywood. The test specimens of the 7 roof underlays were exposed to natural climate on a south-facing roof with a pitch of 20° and without roof covering.

Figure 1. Test set-up for exposure to natural climate. The 7 roof underlays where placed on a south-facing roof with a pitch of 20°.

2.1.1 Test Material

Table 1. Materials used for the testing were 5 different types of flexible sheets, 1wood fibre board, and 1 bituminous membrane.

Material name	*Type of roof underlay*	*Material type*	*Area mass [kg/m^2]*
A	Permeable	Laminate of HD-PE & PP	125
B	Permeable	Laminate of polypropylene	135
C	Non-Permeable	Laminate of polyester mesh and bitumen	450
D	Non-permeable	PE-foil with reinforcement mesh (12x12 mm)	530
E	Non-permeable	Bitumen impregnated polyester mesh	1500
F	Permeable	Wood fibre board*	3000
G	Non-permeable	Bitumen impregnated polyester mesh**	2200

*: Not a flexible sheet
**: Supported by plywood

3 TEST RESULTS

Natural ageing was carried out at various exposure times between 3 months and 32 months (2,75 years). Accelerated ageing was performed according to EN 13859-1. After exposure, tensile strength, deformation at maximum load and watertightness were tested. Reference data were obtained from testing of unexposed material.

3.1 Results of Tensile Testing

Tensile testing was performed using rectangular specimens with a length of 300 mm. Materials A-E had a width of 100 mm. The sides (25 mm) were folded to the centre resulting in a 50 mm 2-folded specimen. Test results for materials A-E were divided by 2 representing the strength of a 50 mm wide specimen. Materials F and G were tested according to EN 12311-1. Specimens had a width of 50 mm. The crosshead speed was the same in all tests: 100 mm/min. Simultaneous measurements of load and crosshead movements were logged.

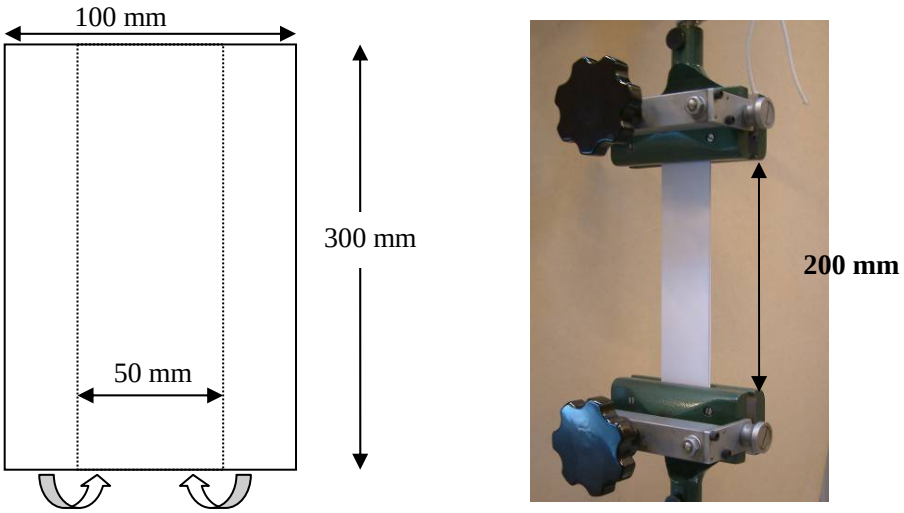

Figure 2. Test set-up tensile tests. Tests of materials A-E were performed according to EN 13859-1. Specimens were folded according to the sketch.
Tests of materials F and G were performed according to EN 12311-1.

Table 2. Maximum load, P, average of 5 tests. Results are representing specimens of 50 mm width.

Test material	*Unexposed*	*EN 13859-1*	*Exposed to natural climate*		
			3 months	5 months	32 months
	P_U [N]	P_S [N]	P_3 [N]	P_5 [N]	P_{32} [N]
A	441	428	393	289	170
B	255	230	240	201	146
C	386	338	374	344	301
D	371	349	264	268	289
E	884	876	820	830	819
F	3231	3438	3821	3553	2468
G	1014	982	936	944	1036

Table 3. Deformation, d, at maximum load presented as average of 5 tests. Deformation is referring to crosshead movements relative to initial position.

Test material	*Unexposed*	*EN 13859-1*	*Exposed to natural climate*		
			3 months	5 months	32 months
	d_U [%]	d_S [%]	d_3 [%]	d_5 [%]	d_{32} [%]
A	17	14	12	7,9	3,3
B	44	31	37	31	17
C	32	29	27	29	27
D	16	14	14	14	13
E	40	37	37	36	37
F	0,52	1,10	1,19	1,2	1,11
G	36	28	35	38	32

Table 4. Maximum load, P, and deformation at maximum load, d, normalized to maximum load, P_u, and deformation, d_u, at maximum load of unexposed test materials. Average of 5 tests.

Test material	*EN 13859-1*		*Exposed to natural climate*					
			3 months		5 months		32 months	
	$\frac{P_S}{P_u}$ [-]	$\frac{d_S}{d_u}$ [-]	$\frac{P_3}{P_u}$ [-]	$\frac{d_3}{d_u}$ [-]	$\frac{P_5}{P_u}$ [-]	$\frac{d_5}{d_u}$ [-]	$\frac{P_{32}}{P_u}$ [-]	$\frac{d_{32}}{d_u}$ [-]
A	0,97	0,86	0,89	0,72	0,66	0,47	0,39	0,20
B	0,90	0,72	0,94	0,83	0,79	0,71	0,57	0,39
C	0,88	0,89	0,97	0,84	0,89	0,91	0,78	0,83
D	0,94	0,93	0,71	0,88	0,72	0,93	0,78	0,81
E	0,99	0,93	0,93	0,92	0,94	0,92	0,93	0,93
F	1,06	2,13	1,18	2,30	1,10	2,22	0,76	2,13
G	0,97	0,77	0,92	0,97	0,93	1,05	1,02	0,88

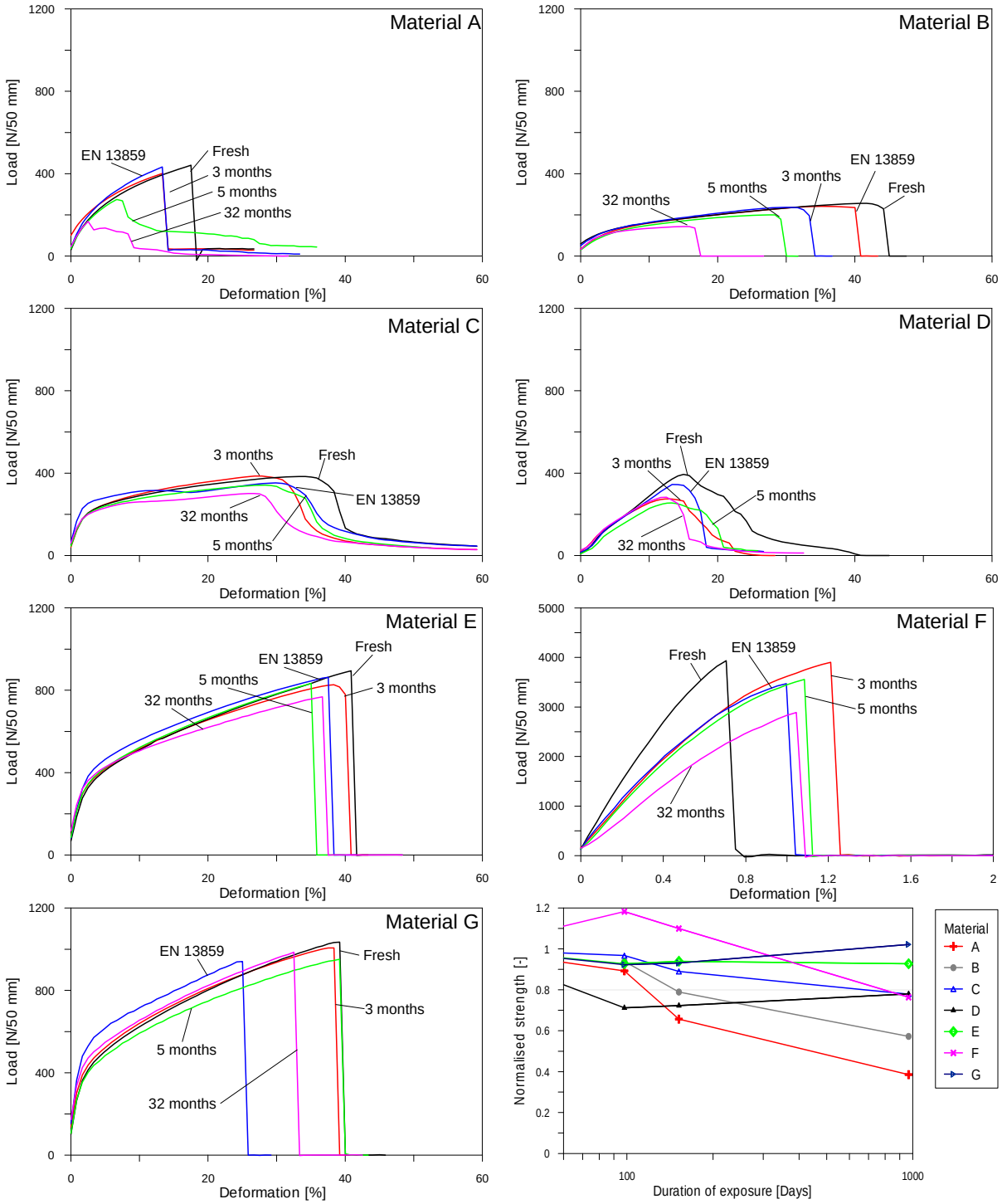

Figure 3. Subfigures 1-7: Examples of load-deformation curves for the 7 tested materials at different levels of exposure. Note that material F is presented with different axis values.
Subfigure 8 (bottom right): Strength for the 7 tested materials at different duration of exposure normalized to the unexposed testing materials.

3.2 Results of Watertightness Testing

Tests of watertightness were performed in a plexiglass cylinder with a 200 mm head of water. A filter paper was placed under the testing materials to simulate tent-effect. Watertightness between test material and container is obtained by silicone grease. The container is bolted to the lower plate in the 4 corners. Water is poured along the cylinder until a water level of 200 mm above the test material. The

weight of the filter paper was determined before and after 60 minutes of testing (materials D-F were tested for at least 15 hours). The tests were considered failed if the water uptake exceeded 0.5 g.

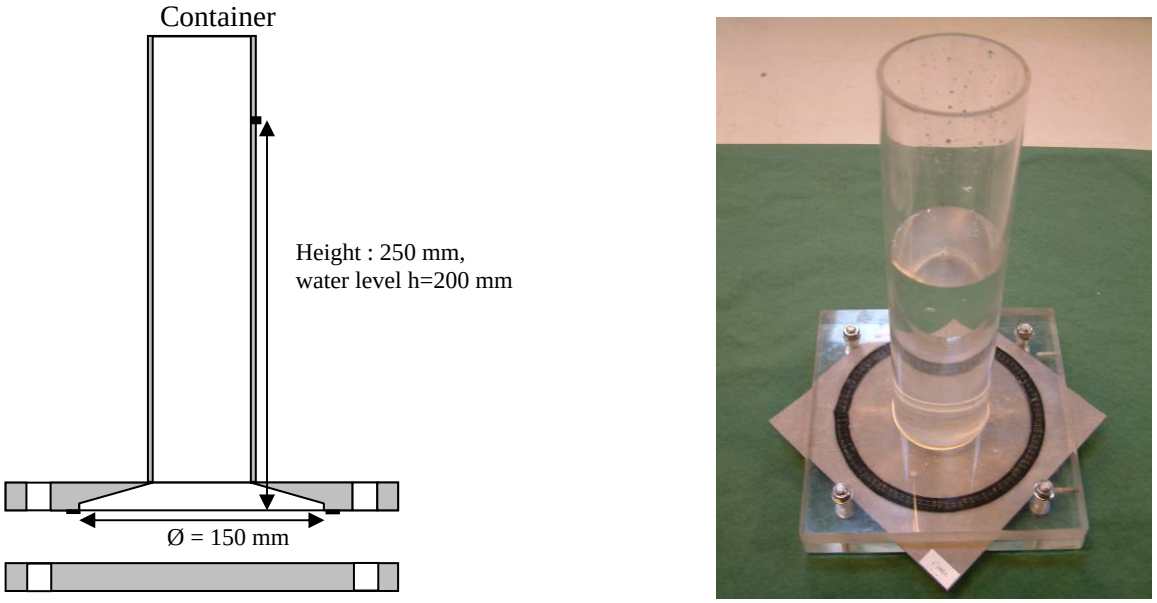

Figure 5. Test set-up for watertighness. A filter paper and the test material are placed on the lower plexiglass plate. The container is bolted to the lower plate in the 4 corners. Water is poured along the cylinder until a water level of 200 mm above the test material.

Table 5. Watertightness. Ratio between number of failed and tested specimens at different levels of exposure.

Test material	*EN 13859-1*	*Exposed to natural climate*		
		3 months	5 months	32 months
	Fail/test	Fail/test	Fail/test	Fail/test
A	1/3	0/3	0/3	3/3
B	0/3	0/3	0/3	3/3
C	0/3	0/3	1/3	3/3
D	-	-	-	0/3
E	-	-	-	0/3
F	-	-	-	0/2
G	-	-	-	0/1

4 DISCUSSION AND CONCLUSION

4.1 Tensile Testing

As generally expected, it can be seen from figure 3 that results from naturally aged materials are ranked according to the exposure period, i.e. the longer exposure the bigger changes are seen.

In contrast to this, results from natural ageing differ from results for materials aged according to EN 13859-1. For example it appears that for material B ageing according to EN 13859-1 corresponds to

less than 3 months natural ageing whereas for material G it corresponds to more than 32 months of natural ageing.

From figure 2, subfigure 8, it can be seen that the change in tensile strength not only differs considerably from material to material but also that it is extremely difficult to predict long term changes from short term testing.

There is no obvious correlation between results from short term natural ageing and long term natural ageing. Therefore, long term natural ageing appears to be necessary. Neither, any correlation can be observed between natural ageing and accelerated ageing according to EN 13859-1. The reason for this is believed to be too weak UV-radiation in the test (UV radiation ought to be at least partly UV-B radiation). EN 13859-1 appears to be unsuitable for accelerated ageing of roof underlays as it is not able to rank materials in accordance with natural ageing.

Materials A, B, C and F continue to loose strength after 5-32 months whereas materials D, E and G only show minor changes throughout the period of natural exposure.

4.2 Testing of Watertightness

Tests of watertightness show that after 32 months of natural exposure the lightweight materials A, B and C failed the watertightness test. The tests showed that the filter paper under the test materials was soaked after only 5 minutes of water exposure. However, only one test failed after 5 months of natural exposure. Unfortunately, no test results are available for materials exposed between 5 months and 32 months making it difficult to estimate a time of failure. The heavier materials D-G proved to be watertight after 32 months of exposure. These materials were tested for a longer period of water exposure (15 hours).

REFERENCES

Brandt, E., & Hansen, M.H., 1998, *Undersøgelser af uventilerede undertage (Investigations on unventilated roof underlayments)*, SBI-report 292. (in Danish).

Brandt, E., Hansen, M.H., & Bunch-Nielsen, T., 2007, *'Unventilated roof tile underlayments'*, Interface. The Journal of RCI. **25**[9], 21-30.

EN 13859-1. 2005, *Flexible sheets for waterproofing - Definitions and characteristics of underlays for discontinuous roofing.* CEN European committee for standardization.

EN 12311-1. 1999, *Flexible sheets for waterproofing. Bitumen sheets for roof waterproofing - Determination of tensile properties.* CEN European committee for standardization.

DS/EN 12311-2. 2000. *Flexible sheets for waterproofing. Determination of tensile properties - Plastic and rubber sheets for roof waterproofing.* CEN European committee for standardization.

Holck, O., & Rosenfeld, J.L.J., 2005, *'Estimation of exposure to sunlight of the liner under a tiled roof'*. Solar Energy, **78**[2], 199-209.

NT BUILD METHOD 488. 1998. *Roof tile underlays: Watertightness – tent effect.* Nordic Innovation Centre.

Polymer-based Building Materials: Effects of Quality on Durability

Esin Kasapoğlu [1]

T 17

ABSTRACT

Polymer is the main substance of plastic. Monomers are the 'building blocks', polymer is the completed plastic and the reaction is called polymerization. During production processes, as well as oil-based chemicals, chlorine, hydrochloric acid, fluorine, nitrogen, oxygen and sulphur are the substances used. Nearly all plastics include additives like plasticizers, pigments, stabilizers against solar radiation, preservatives and perfumes. Plastic is a substance that contains natural or synthetic high molecular organic material which can be liquefied and thereby cast in specific moulds.

Quality can be defined as the appropriateness level of a product to the desires of the consumer. The quality of a product or a complete building or other construction is the totality of its attributes. Quality enables to perform a stated task or to fulfil a given need satisfactorily for an acceptance period of time. If the material has low level of quality, durability of the material will be shortened. Plastic building materials are used in floors, roofs and walls. It is difficult and expensive to repair or replace them. Plastics should have a functional life-span at least 50 years equivalent to other materials in the building. It is unlikely that any of today's plastics can satisfy such conditions.

In this paper, the meaning of quality will be defined again through the view of polymer based (plastics) building materials. Quality properties which will enable the durability of polymer based materials with a more functional life span will be discussed. The last developments in plastics industry and their effects on durability will also be reported.

KEYWORDS

Polymer, Plastic, Building material, Quality, Durability

[1] Istanbul Kultur University, Faculty of Engineering Architecture, Bakırkoy, Istanbul, Turkey 34156, Phone +90 212 4984286, Fax 212 6618563, ekasapoglu@iku.edu.tr

1 INTRODUCTION

Throughout the 1990s, polymer based building materials, especially plastics, have been used widely in construction industry. Superior strength in weight performance, corrosion resistance, environmental stability, insulation properties, lower cost are the main properties of polymer based building materials.

Although, polymer based building materials have some important superior properties compared to traditional materials, they have some disadvantages, like their flammability and smoke toxity. However employing additives or combining with other materials, helps plastics gaining superior properties. Quality level of polymer based building materials can be evaluated through the new results. Durability of the material will be affected also by the quality level of the material.

2 POLYMER BASED BUILDING MATERIALS

Polymers are organic compounds which are the main substance of plastic. Monomers are the 'building blocks', polymer is the completed plastic and the reaction is called polymerization. During production processes, as well as oil-based chemicals, chlorine, hydrochloric acid, fluorine, nitrogen, oxygen and sulphur are the other substances used. Nearly all plastics include additives like plasticizers, pigments, stabilizers against solar radiation, preservatives and perfumes. Plastic is a substance that contains natural or synthetic high molecular organic material which can be liquefied and thereby cast in specific moulds [Berge 2001].

Plastics were first used as ornament, superficial finish, or as secondary parts for enclousure systems, in building and construction. Although, plastics are in construction industry as a wider scope of uses such as interior finishes, glazing, plumbing fixtures and even structural components today, only recently they began to gain respect and appreciation as a viable primary material. Having a lower fire-rating and limited usage in applications of requiring fire resistance are the weakness of plastics compared to other construction materials. However, there are some advantages plastics can offer like they are lightweight, lower in cost, resistant to corrosion and moisture, can be relatively strong and are readily shaped. One of the other disadvanges of plastics was their being short-lived fad that is brittle and prone to discolor, but has recently been revised due to enormous advances in the plastics industry, which has manufactured unprecendented variety of new products with improved physical properties. Since the material is intrinsically man-made, there is no limit for the charasteristics and expanding will continue [Bell 2006].

Plastics can be divided into two basic categories: thermo plastics and thermosetting plastics. Thermosetting plastics and thermoplastics are both used in building. Thermosetting plastics are generally harder and stronger than thermoplastics. Adhesives, laminates, rigid foam insulation, waterproofing membrances and window frames are typical applications of thermosetting plastics. Polyvinyl chloride (PVC), polycarbonate and acrylic are the three types of thermoplastics which are most often used in building construction. PVC is the most commonly used plastic in building construction. Resistance to water, and some chemicals, low cost and resistance to tearing are the main charasteristics of PVC. [Bell 2006] When produced as a foam, many plastics have high thermal insulation properties and good water- and vapour-proofing properties. Paint, sheeting, paper, sealing strips and mastics are the guises plastic can take as a sealant. Polyisobutyl, polyehylene and PVC are the three plastics used for sheeting. Sheetings can be used as damp-proofing for foundations, vapour barrier or moisture-proofing. A mastic has to fulfill the conditions of constant elasticity and durability. Polysulphide, silicone, polyurethane and various acrylic substances are used as mastic. The composition is usually based on at least five chemical substances with at least eight different additives. Sealing strips are the materials used mainly between the sheets of glass in window and door reveals. Polyurethane, polyamide, PVC, ethylene-propylene rubber, chloroprene rubber and silicone rubber are the important plastics used in sealing strips. The products include different additives also. Polystyrene, polyurethane and urea formaldehyde are the plastics used to produce different insulation materials [Berge 2001].

Plastics is rarely used as a structural material in building. In the western world, a large amount of unspecified plastic waste exists now which can be possible raw material for simple structural elements. If supporting substances are added in proportions of 10-15 percent, polystrene waste can be cast into solid beams and columns. The components are suitable for sawing and nailing and the structural properties are approximately the same as timber. [Berge 2001] For structural applications, pultruded glass-fiber-reinforced polymer (GFRP) profiles have a great potential; the higher strength to weight ratio, the lower weight, the electromagnetic transparency, the ease of installation, the lower maintenance requirements, and the improved durability in aggressive environments are the advantages over traditional materials. Although (GFRP) profiles have been used mainly in nonstructural or secondary structural elements up to now, such as ladders, handrails and pavement grids, according to the results of researches, they offer a very good mechanical performance and lightness, as well as good durability charasteristics, compared with those of traditional structural materials [Correia *et al*. 2006].

Crack repair systems have been used for many years and polymer based building materials are one of the most common crack repair materials. Epoxy resins generally have very good bonding and durability characters that commonly used repair materials. According to Calder and Thompson the overall structural performance of reinforced concrete slabs repaired using epoxy resin injection performed best compared to other materials such as polyester and methl methacrylate resins. The use of carbon fiber reinforced polymers (CFRP) is a new development in the repair and the rehabilitation of reinforced concrete. In recent years, the applications of these materials to structural repair and retrofit have grown significantly. Carbon fiber reinforced polymers fabrics offer supperior performance such as resistance to corrosion, and a high stiffness-to-weight ratio. [Ekenel & Myers 2007] As the results of researches with advanced composites had shown that plastic composites were more durable than steel and conrete and also they are lightweighted, energy-absorbent, less corrosive and low cost new methods to strenthen bridges, buildings and other forms of civil infrastructure with plastic composites are being developed. According the results plastic ‘wraps’, which are only a few millimetres thick and consist of a fibreglass-graphitecomposite, around concrete structures can increase their strength [Jones 2007].

3 QUALITY OF POLYMER BASED BUILDING MATERIALS

Construction quality is a measure of the level of meeting a particular work the requirements demanded by the building project. [Mora 2007] The quality of a product or a complete building or other construction is the totality of its attributes. Quality enables to perform a stated task or to fulfil a given need satisfactorily for an accepted period of time. If the material has low level of quality, durability of the material will be affected negatively. During the construction process by ensuring to use materials of the same durability, the use of raw materials is reduced, by producing more durable products. Therefore it is possible not sacrificing better quality components in a building when there is decay elsewhere. When there are any materials with less quality, it is important to be easily replaced while the more durable materials can be dismantled for re-use or recycling in the case of demolition. There is a clear advantage in using robust materials and allowing buildings lasting as long as possible. [Berge 2001] Energy required to produce the material, CO2 emissions resulting from the manufacture of the material, toxity of the material are some of the factors determined by the quality of the materials. Like quarry pit, wood taken from forest, oil spills from an oil well, the impact on the local environment resulting from the extraction of the material is the other factor of quality of the materials. Degree of pollution resulting from the material at the end of itsuseful life, lifetime of the material and its potential for reuse if the building is demolished are the other factors that can be taken into consideration while determining quality of a material. [Roaf *et al.* 2003].

Plastic composite building materials obtain much of their versatility because they can be engineered to provide specific performance charasteristics including durability, light weight, corrosion resistance, high strength, and low maintenance requirements. In cooler climates, fiber-reinforced polymers (FRP)

could increase the use of concrete in architectural cast fences. As the thread of freeze-thaw and corrosion require substantial concrete coverage forrebar protection, concrete is not a suitable material for thin wall structures. FRP composites could present a solution, when a structural element, such as a wall or beam can benefit from additional support. A combination of wood fibers and plastics is wood-plastic composites (WPCs). Their durability and weather-resistance can be appropriate for outdoor environments. Wood-plastic composites (WPCs) are commonly used, where durability is an important performance attribute. In order to improve processing and performance, small amounts of other materials can be added to wood-plastic composites (WPCs) as with inorganic-fiber composites. WPC lumber rarely rots, cracks, warps, or splinters, when properly manufactured and installed. WPC are typicaly stain resistant, waterproof, ultraviolet (UV) light-resistance and impervious to insects and can be made strong enough for applications such as load-bearing deck boards. A good dimensional stability and a lower coefficient of expansion than solid plastics are the other properties WPCs tend to have [Krebs 2006].

Plastics will burn, like all organic materials. As such, increasing the temparature necessary before ignition and/or lower the rate of burning, plastics used in construction contain fire-retarding. The various building codes typically have regulations require specific fire performance characteristics that deal with plastics. These characteristics are for fire/flame retardation and safety. Today's plastic construction materials, when used in the proper application and correctly installed, can meet or exceed the fire performance charasteristics required by most codes and standarts, can help provide a nice living environment by performing their intended function. Different performance requirements are specified, when foam plastic materials are installed on the exterior of buildings. As the foam plastic insulation material contribute to upward flame spread over the surface or within the exterior wall, additional specialized tests are also specified to prevent. [Parker & Beitel 2006]

Including acrylic, some interesting products have left their mark in recent years. Acrylic plastic products are known with the virtue of material lying in its clarity and ultraviolet (UV)- resistant attributes. When the material is extruded, thin UV-resistant coatings can be applied to polycarbonate, offering enhanced protection for performance and aesthetics. Besides, light-diffusing charasteristic of the celular structure can leave any strach or dirt almost undetectable. A simple hosing or pressure-washing usually suffices, when cleaning is desired. [Bonenfant 2006] Vinyl can be easily kept clean and disinfected, since it can be washed or scrubbed. This is an important consideration for healthcare projects the spreading of germs and bacteria must be minimised. Vinyl can be versatile and durable. Strong and scratch-resistant vinyl products are continually becoming easier to apply, partly due to bette pastes. Especially for high-traffic areas, vinyl coverings are ideally suited. Vinyl becomes a wide variety of price and design options. [Jacop 2006] In window applications, although other plastics are also employed, PVC is often used as the thermoplastic matric. 80- to 200- mesh wood fiber which is a wood-filled PVC product is usually employed in windows and doors, offers thermal stability, moisture resistance, and stiffness. Wood flour have been combined with both vinyl and polyolefin to form exterior trim in new exterior applications that resists rot and weathering. A wide range of design can be shaped by the resulting material that typically do not require painting or the use of special cleaning agents [Krebs 2006].

Polycarbonate, among the first window glazing materials certified, can resist the impact of a 2.4m. (8-ft) long 2x4 fired from an air cannon at 55 km/h (34 mph). A polycarbonate barrel-vault skylight was impact load and high-pressure winds. Polycarbonate can offer opportunuties for day lighting, in addition to impact resistance. Daylighting is not only a matter of bringing in the sun's light but also efficient systems must insulate well [Bonenfant 2006].

4 DURABILTY OF POLYMER BASED BUILDING MATERIALS

Durability is an ability of a building or a material to maintain its performance over time and use. It can be measured in terms of the time until some loss of function occurs that renders the service provided

unacceptible. It depends on the degrading effects of the service and the environment to which it is exposed, it is not a fundamental property of a material. Refering to service, life, is more appropriate, as this properly implies the effects of the particular conditions of service. Being long lasting, can reduce maintenance and repair costs, and often cost-effective from a life-cycle perspective are advantages of durable materials and building systems. Minimized disruption of building operations and environmental benefits resulting from the reduced disposal and replacement of materials.

Durability is not only a quantifiable technical property, but has also an aesthetic and fashionable aspect. Designing a product that can outlast the swings of fashion is also quite a challenge. Rather than a maximum durability, it is also important to consider an optimal durability, especially with technical equipment. The lifespan of a material depends on mainly four factors which are the material itself, its physical structure and chemical composition; construction and its execution, where and how the material is fitted into the building; the local environment, the climatic and other chemical or physical conditions; maintenance and management. [Berge 2001] Durable materials will not need to be replaced or repaired as frequently, so the raw materials, energy, and environmental impacts invested in them can be spread out over more time. Durable materials provides a long period of time to amortize the environmental and economic costs that were incurred in building it. Durability is an issue of water management to a significant extent. The ratio of durability problems in buildings are fully 80 percent about moisture. By causing materials to expand and contract, thermal stress can reduce durability. This can affect, for example, long-term window performance. Making windows leaking over time, including vinyl and aluminum certain frame materials expand and contract at a higher rate than glass. Roofing materials are also affected by high roof temparatures. Ultraviolet light (UV) degrades most plastics. Along with heat, degradition of roofing materials is a major problem. Including vinyl siding, although in some cases UV stabilizers themselves carry environmental burdens, plastics that are used outdoors are typically treated with these stabilizers. Ozone and acid rain, various atmospheric pollutants, can damage building materials. Ozone and other air pollutants damage materials, including rubber, nylon, dyes polyster, and certain paints, many synthetic materials.[Wilson 2007] Heat, cold, wind, snow, hail, ice, mechanical stress, acids, animals, plants, water and other liquids and micro-organisms are some of the external factors which can break down plastics. The type and the position of the plastic and the local climate determines the life-span of a plastic [Berge 2001].

It is difficult to anticipate the lifespan of most new materials like plastics. Although it is possible to create accelarated deterioration in laboratories, these are not the results of actual situation which is more complex. [Berge 2001] Causing embrittlement and a change in surface appearance short-wave solar radiation affects plastics negatively. In coastal and rural areas the risk is greatest. Using some additives incorparated into the plastic the effects can be reduced or increased. Adding fire retardants reduces resistance to degradition. Although, moisture in general has little effect but can reduce bond strength between glass fibre and polyester resin. Depending on the control exercised in manufacture greatly, the extend of any weakening of bond strength can be controled also. In general, contact with other building materials do not harm plastics, though the use of oil base jointing compounds cause cracking of polyethylene cold-water cisterns [Ransom, 1987].

PVC and polycarbonates have high thermal expansion and varieties of polyethylene have even greater thermal movement. Down pipes can cause joint failure and leakage, when the movement of PVC gutters, unless properly allowed for. Under continued, loads plastics creep when stresses are high, as in filled cold-water cisterns, special precautions are needed. [Ransom, 1987] It is also difficult to make a picture, as the plastics are often full of additives. Although PVC is known as a plastic with a very good durability, it has been known to undergo very rapid breakdown. Sometimes addiditives can be harmful, just the opposite of the expectations. One of the examples is crumbling of 10-year-old plastic skirtings made of PVC, because of an added acrylonitrile butane styrene (ABS)-plastic which should have increased the strength and durability. All plastics oxidize easily. Another plastic polyethylene sheeting, had an effective lifespan of ten years and used as a moisture barrier until 1975. As the sheeting is usually in accessible within the fabric of a building and often supposed to prevent

condensation within the walls, this is extremely low. Some additives included polyethylene to make it more stable [Berge 2001].

When the material has to be replaced or the use that material had is brought to an end, durability ends. A durable material is useful for longer. Durability is an indicator which informs if a material maintains its original requirements over time. The material durability will increase, when the time and resources required to maintain it decrease. [Mora 2007] Sometimes 1 year is enough losing functionality. Ethylene proppylene rubber (EPDM) is used as sealing strips between the elements in prefabricated building of timber and concrete. According to researches certain makes have lost elasticity after only one year and causing the joints open and the material does not function. As many of the plastic products currently on the market have been around for less than 15 years, there is very little feedback on their life span. Altough some of the products have been on the market, for a longer period, todays' components are very different from those that were used in products of 20 years ago, as it is well known by the polymer technicians. It is difficult to find examples giving a picture of the lifespan of the plastics products made today, as the design of products has changed so much recently [Berge 2001].

5 CONCLUSION

In construction industry, polymer based building materials have a rapid development and have been used widely throughout 1990s. Especially having different kinds and offering different types of design enabled them gaining popularity among architects. Polymer based building materials, especially plastics, are man-made, therefore there is no limit for the charasteristics and development will continue. New products with improved properties can be manufactured. This continuous development is the main difference between polymer based building materials and traditional materials. Additives help improving charasteristics against resistance to fire, UV ray and other disadvantages. Especially as an element of composite material specific performance charasteristics can be improved. The combination of distinctly different components of composites can make new high-strength, lightweight materials with corrosion resistance, long-term durability, low maintenance requirements, design flexibility, good vibrational damping and resistance to both fatigue and temperature extremes. The performance capabilities of the composites can be developed and high-performance composites can be manufactured. This means, quality of polymer based building materials can be developed also. Every material have some specific characters but a general definition of quality for polymer based building materials can be written as:
"A polymer based building material should be resistant to fire, UV ray, water and some chemicals, corrosion, moisture, thermal and mechanical stress, ozone and other air pollutants; should have good water and vapour proofing, high thermal insulation properties, and high strength and should be load bearing, lightweighted, appropriate for outdoor environment and lower in cost."

The characteristic of a building material being durable affects the level of quality or on the other hand improving the level of quality of a building material can affect the material being more durable. As quality enables to perform a stated task or to fulfill a given need satisfactorily for an accepted period of time, quality is improving the characteristics of a building material. Improving characteristics can also affect the material being more durable. Being a wall covering more durable it is needed to have an average compressive strength, a negligible level of moisture content, resistant to thermal stress, ultraviolet light and high wind pressure and it is also preferred to be sustainable. Improving a material having more compressive strength or decreasing the level of moisture, affects its quality level positively also. As the level of quality is increasing, the material can be more durable also. Polyvinyl chloride (PVC) or vinyl is perhaps the most versatile of all plastics. In construction vinyl is used as flooring, siding, piping and single-ply membrane roofing. Vinyl is generally self-extinguishing and resists weathering, oils, greases, acids, fungus and moisture and and abrasion-resistant depending on the type. One of the vinyl types used in building commonly is siding. There is little that challenges vinyl's versatility, durability and possible textures, colors and shapes. Vinyl siding requires little

maintenance, remaining attractive for years. These are the characteristics of vinyl siding and they can be listed as the quality criteria, also. Being recycling can be added as a quality criterion that nearly all waste of vinyl is recycled. [Knowles 2003] As a durable material lasts a long time and provides a long period of time to amortize the environmental and economic costs that were incurred in building it, durable materials and materials will not need to be replaced or repaired as frequently. So, the raw materials, energy and environmental impacts invested in them can be spread out over time. The longer-lasting building's higher economic and environmental costs can usually be justified by its durability.

Another building material is spray polyurethane foam (SPF) which is one of the fastest growing polymers in construction and can be used for specific purposes including roofing insulation, wall insulation, air barrier systems, and below-grade foundation insulation and below slap-on-grade. According to performance studies and research suggest SPF roofing systems can last 30 or more years. They require low maintenance, resist high wind blow-off, add structural strength and minimize moisture damage within the building envelope which are among the quality criteria. [Knowles 2003] Characteristics of the material can be developed also by using closed-cell formulations or open-cell formulations which is also enables developing the charasteristics of the material. Developing charasteristics of a material affects quality level positively, also, which will affect durability positively. Closed-cell formulations typically range in density from 27 kg/m3 to 51 kg/m3, while compressive strength ranges from 103 kPa to 345 kPa. The density and composition of closed-cell foams help the building gaining more structural integrity. When closed-cell MD-SPF is sprayed in place, makes the applied place seamless and 100-percent fully adhered. This means, SPF roofing limits moisture intrusion because of its 90-percent closed-cell properties. Damage to the system typically does not cause leaks into the building and moisture intrusion is isolated to the areas of damaged foam cells. SPF roofing system has exceptional wind uplift resistance. According to the researches SPF roofs applied over a built-up roof and metal increased the wind uplift resistance of roof coverings. The tests showed similar results for concrete, metal and wood. It requires no fasteners or adhesives, and may not shrink or sag over time, making it ideal for use in vertical wall and below-grade exterior applications. [Harris 2004] [Knowles 2003] Having needed characteristics of a building envelope also refers to the building material having needed quality level which means also affecting durability positively. According to the researches existing performance attributes of SPF has an average compressive strength and core density, offers a very high wind uplift resistance rating and average moisture content was negligible. SPF air barriers offer long-term durability greater than or equal to the building's life span which means the developed charasteristic of the material that affected quality positively, also.

As the type and the place where the material is used changes, needed quality criteria differs. The quality of a building material is the totality of its attributes. When there are any materials with less quality, it is important to be easily replaced with the more durable materials. A different quality definition is needed for every product which can be defined again through the view of durability. For instance the definition of quality for PVC can be written as: "A PVC building material should be resistant to water, some chemicals, tearing, thermal stability and moisture, should have high strength and low cost." When produced as a foam, PVC should have high thermal insulation properties and good water, moisture and vapour proofing properties. The more efficient use of building materials mainly tendencies like the improvement of the quality of the materials, affects improvement of durability, also. Having needed characteristics of a building envelope also refers to the building material having needed quality criteria. It means; if there is a stable interaction between heat, air and moisture transports, the building material will have needed characteristics which also show the level of quality. It affects also the durability. The durability of a material in a building envelope not only depends on the quality level of the building material but also the outdoor and indoor climate, type of construction and conditions of service, also.

REFERENCES

Bell, V. B., 2006, *'Materials for architectural design'*, Laurance King Publishing, London, UK.

Berge, B., 2001, *'The ecology of building materials',* Architectural Press Elsevier Science Ltd., Oxford, UK.

Bonenfant, N., 2006, 'Cellular polycarbonate glazing', *Modern Materials,* 4[1], 15-18 .

Correia, J. R., Cabral-Fonseca S., Branco, F. A., Ferreira, J. G., Eusebio, M. I., Rodrigues, M. P., 2006, 'Durability of pultreded glass-fiber-reinforced polyerster profiles for structural applications', *Mechanics of Composite Materials*, 42 [4], 325-338.

Ekenel, M., Myers, J. J., 2007, 'Durability performance of RC beams strengthened with epoxy injection and CFRP fabrics', *Construction of Building Materials,* 21, 1182-1190.

Harris, T., 2004, 'High Performance Buildings Drive', *Modern Materials*, 2[1], 19-23.

Jacop, J., 2006., 'Design & durability with vinyl wall coverings', *Modern Materials,* 4[1], 26-28.

Jones, R., 2007, 'A future set in plastic', www.monash.edu.au/pubs/eureka/Eureka_95/plastic.html

Knowles, M., 2003, 'Sustainability charasteristics of SPF roofing and insulation systems', *Modern Materials*, 1[1], 16-21.

Krebs R., 2006, 'Composites as high-performance solutions', *Modern Materials,* 4[1], 21-25.

Mora, E. P., 2007, 'Life cycle, sustainability and the transcendent quality of building materials', *Building and Environment,* 42, 1329-1334.

Parker, A. J., Beitel J. J., 2006, 'Flammability requirements for plastic materials', *Modern Materials,* 4[1], 10-12.

Ransom, W. H., 1987, '*Building Failures'* E & FN Spon, London, UK.

Roaf, S., Fuentes, M., Thomas S., 2003, *'Ecohuse2'*, Architectural Press Elsevier Science Ltd., Oxford, UK.

Wilson A., 2007, 'Durability: A key component of green building', www.greenerbuildings.com/news_detail.cfm?NewsID=29240

11DBMC International Conference on Durability of Building Materials and Components
ISTANBUL, Turkey 11-14 May 2008

Service Life of Light Weight Bathrooms

Erik Brandt [1]

T 17

ABSTRACT

Traditionally bathrooms in Denmark have been made from heavy inorganic materials like masonry and concrete clad with ceramic tiles. To make it simpler, easier and cheaper to make bathrooms – including installation of bathrooms in old houses where no bath was available earlier – there has been a wish to make light weight bathrooms i.e. mainly made from wood based products or building boards, e.g. gypsum boards.

In Denmark the use of light weight bathrooms has been allowed since the 1970'es. The use has not been without problems as a lot of the early constructions proved not to be watertight – at least not over time. The experience was such that some organisations tried to make it illegal to use light weight bathrooms due to the large number of errors and the very large sums used for repair work.

The paper describes the problems experienced over the years including identification of the most important properties for light weight bathrooms and the prerequisites for the use. In addition the changes in requirements over time are discussed. The changes are generally more rigorous requirements first of all to secure the watertightness of the construction. In order to use light weight bathroom constructions documentation must be available for example from testing and subsequent approval. The test procedures used is currently - in a slightly modified form - being treated by EOTA in connection with a Technical Guideline for "Watertight covering kits for wet room floors and walls". The test methods which to a certain extent takes durability into consideration is shortly described.

It is discussed how long a service life might be anticipated for a light weight bathroom in comparison with a traditional solution. Finally the importance of regular survey and maintenance is discussed.

KEYWORDS

Bathrooms, Watertightness, Service life.

[1] Danish Building Research Institute, Aalborg University, DK-2970 Hoersholm, Denmark, Phone +45 4574 2370, ebr@sbi.dk

1 INTRODUCTION

In Denmark bathrooms have traditionally been made from heavy inorganic materials e.g. floors of concrete with iron beams and walls made from masonry or concrete. These constructions were considered to be watertight provided that they had a water repellent surface, e.g. ceramic tiles.

Different solutions have been invented to install bathrooms in older houses which originally did not have bathrooms. Typically old houses have floor constructions with wooden beams and walls containing wood in some form. The old wooden beams have e.g. been used to support a concrete slab used as floor in the new bathroom. Also lighter construction materials have been used, e.g. wooden studs, plywood or gypsum boards.

The advantage is that they are cheap, easy to install and without excess water. The drawback is damages resulting in reduced service life and excessive repair costs.

The use of lightweight constructions was introduced in Denmark some 35 years ago. The use has always been restricted to constructions and/or materials either with a national approval for a specific material or construction or approved via directions issued by the Danish Building Research Institute.

Experience gathered in the 1990'es, e.g. by the so called “building defects funds”, showed quite a few problems with light weight bathrooms due to insufficient watertightness of the solutions in practice. The problems were almost entirely connected to bad workmanship or use of unsuited materials e.g. watertight membrane was missing or there were failures around details especially floor gullies.

As a consequence of the findings a series of changes were made to the requirements for obtaining an approval as well as to the constructions described in the directions from the Building Research Institute with the purpose to improve the service life of the light weight constructions.

2 PERFORMANCE ANALYSIS AND PROPERTIES

Before light weight bathroom constructions were allowed in Denmark an analysis was made in order to identify all the functions of bathroom walls and floors and all the agents acting on them. Based on the performance analysis it was possible to set up a list of performance properties for bathroom walls and floors. The five most important properties related to service life are found to be:

2.1 Watertightness

Watertightness which is especially required in areas exposed to water. In Denmark the use of bathtubs or shower units is not common and consequently the floor and the walls are directly exposed to water.

2.2 Water Vapour Permeability

In bathrooms a high relative humidity can be expected. This causes a high vapour pressure in the bathroom and consequently diffusion of moisture through floor, ceiling and walls. Especially for constructions that are part of the building envelope it is necessary to take precautions to avoid condensation of moisture inside the structure – this is normally done by the use of a vapour barrier.

2.3 Resistance against Mechanical Loads

The floor and wall constructions in bathrooms shall be able to resist ordinary loads from persons and furniture. This is also the case for vulnerable details like floor gullies and pipe penetrations.

2.4 Dimensional Stability against Changes in RH or Temperature

The constructions must not be damaged by dimensional changes in the materials e.g. due to unavoidable changes in RH due to seasonal variations. For materials where dimensional variations are unavoidable, e.g. wood, precautions must be taken to accommodate the dimensional changes envisaged.

2.5 Compatibility

The materials used shall be compatible including materials used for cleaning and maintenance. Besides the above mentioned the bathroom shall ensure that the functions foreseen can take place, for example must the floor be safe to walk on and the surfaces shall be easy to clean.

3 MATERIALS AND CONSTRUCTIONS USED

To ensure a satisfying service life the requirements to materials and constructions for bathrooms are generally higher than for ordinary rooms due to the exposure to water: Besides the consequences of failures are most often very severe. For constructions the requirements are expressed as stricter rules regarding strength and stability in order to ensure they are strong and stiff enough to prevent damages to the watertight membrane. Further the materials in the construction should either have small dimensional changes when exposed to variations in relative humidity (unavoidable due to seasonal changes) or measures should be taken to accommodate them. In Denmark it was in the first years required that wood based materials were pressure impregnated in order to make them resistant to water. This requirement was given up after a few years due to a philosophy stating that water shall not be present in the interior of the construction. Surfaces in wet rooms are required to be water repellent or even watertight in order to ensure that water runs of and to avoid ingress of water to any vulnerable materials in the construction. The following is a brief description of materials and constructions used in floor, wall and surface constructions respectively.

3.1 Floor Constructions

Light weight floors in bathrooms are normally made from board materials supported by wooden beams. The board material may either act directly as sub-floor or as underlay for a levelling compound.

To increase the stiffness of the floor compared to ordinary rooms a reduced distance is used between beams/joists. The distance is dependent on the material used and the intended surface material. Boards for floors are most often plywood or chipboard. The latter is nowadays only allowed for resilient floor coverings due to insufficient dimensional stability. Other materials used are polystyrene (PS) boards with a facing or wood based boards with a coating to make them inherently watertight. For inherently watertight boards it is in addition to the watertightness of the board itself required that the joints are watertight. PS boards and gypsum boards are only allowed with a national approval and they both have special requirements to the underlay to ensure a sufficient strength and stability.

Service life for light weight floors is good as regards resistance against mechanical loads and dimensional stability. There are only few examples on insufficient stiffness and this has especially been in connection with a change from PVC floor covering to ceramic tiles where the requirements are higher. Problems with floors are usually connected with watertightness.

3.2 Wall Constructions

For walls there have earlier been problems with insufficient stability. This has resulted in increased requirements to stiffness which may be fulfilled by a combination of 1) reduced distance between studs, 2) greater dimensions of studs (the standard is now a 70 mm stud - i.e. a 70 mm cavity in the

wall), 3) thicker boards or 4) two layers of boards. Studs may either be wood or steel. Boards come in several materials of which gypsum board are most popular probably due to the price and the fact that they are dimensionally very stable. Due to earlier problems gypsum boards in Denmark now comes as special "wet room boards" with a higher density than normally and with silicone impregnated gypsum. The carton is not impregnated as this would jeopardize later application of watertight membranes etc. Gypsum boards are also available as fibre reinforced boards without carton. Other materials include calcium silicate boards (water resistant) with or without a watertight facing, plywood, chip board and plastic laminate. Finally are used - as for floors - polystyrene (PS) boards with a facing and wood based boards with a coating to make them inherently watertight.

The experience with performance and service life for the current constructions are good as regards resistance against mechanical loads and dimensional stability. There have only been a few cases of insufficient stability, e.g. where studs have been cut to make room for pipe penetrations or where walls are not provided with 2 layers of boards. Problems with water tightness are mainly due to lack of watertight membrane or bad detailing. A special problem is seen for walls supplied both with a vapour barrier behind the boards AND a watertight membrane on the face of the board, see below.

3.3 Watertight Layer

For lightweight constructions it is of utmost importance that vulnerable materials are protected from water and moisture. To ensure watertightness not only the materials but the entire construction including joints, penetrations etc. must be watertight if a long service life shall be achieved.

For stud walls protection against moisture is normally achived with a vapour barrier. In bathrooms the watertight layer shall replace the ordinary vapour barrier which consequently shall be left out. If not, water may under unfortunate conditions – e.g. due to an even minor leak – penetrate into the board where it is trapped between the two impermeable layers without possibility to escape. This might lead to accumulation of moisture and severe damages.

To day watertightness of a light weight construction is achieved in one of the following ways:

- application of a watertight membrane (in fluid form) on the underlay. The membrane is normally protected by a wearing surface most often tiles. In Denmark it is to day a requirement that the membrane shall be at least 1 mm thick.
- application of a pre-fabricated membrane. Prefabricated membranes include PVC floor and wall coverings (with welded joints to achieve watertightness). For membranes placed inside the construction all materials over the membrane shall be able to withstand exposure to water.
- application of a watertight paint system with a glass fibre cloth as reinforcement. The watertightness is normally achieved by the use of a special adhesive for application of the glass fibre cloth.
- inherently watertight boards with watertight joints.

Earlier other watertight layers have been used. For example systems based on polyurethane or acrylic materials were used as a combined watertight layer and wearing surface. These systems were used in accordance with national approvals but were given up may be due to problems with crack propagating from the substrate, i.e. insufficient crack bridging ability of the material. Glass fibre reinforced polyester was used to a limited extent but was given up due to safety problems for the workers. For many years all suppliers in Denmark had systems where the watertightness was based on a combination of a primer and a tile adhesive. In principle it is still possible to use such systems provided that watertightness can be documented. However, they are not on the market anymore. Some 12 years ago the building defects funds preferred pre-fabricated membranes because they had seen a lot of problems with fluid applied membranes. This led to a requirement of a minimum 1 mm thickness of the fluid applied membranes. This requirement has resulted in a change so to day the fluid applied membranes are the preferred. Both systems have their advantages and drawbacks. A prefabricated membrane has a well defined thickness but may cause problems with the joints

especially in the corners. A fluid applied membrane has no problems with joints but may cause problems if the thickness is to low.

4 COMMON FAILURES IN BATHROOMS

Failures in bathrooms are generally related to ingress of water or condensation of moisture in the construction. Failures will normally lead to reduced service life and quite often renovation is comprehensive and associated with excessive costs. Failures are seen in all bathrooms including the traditional ones made from concrete, masonry etc. However, the traditional constructions are often more "tolerant" against small failures i.e. the consequences are less severe and renovation not as comprehensive as for light weight constructions.

For light weight constructions the most common problems are:

- watertight layer/membrane missing or not thick enough resulting in ingress of water in the construction, see figure 1.
- lack of detailing for floor gully, pipe penetrations and joints resulting in ingress of water around details, see figure 2.
- insufficient stiffness resulting in cracks in tiles – and in some cases damages to the membrane, see figure 3.
- insufficient welding of joints in PVC floor and wall coverings resulting in ingress of water through the joints, see figure 4.
- illegal changes to floor gully – normally made in connection with renovation of floor where the existing floor gully is extended to a new floor surface. Many problems are seen due to ingress of water through the extensions, see figure 5 and 6.
- the bathroom is not designed to resist moisture transport, e.g. vapour barrier is used in connection with watertight membrane or less permeable layers are used inside the construction resulting in accumulation of moisture and deterioration of materials.

Besides other problems are seen, e.g. insufficient slope and inaccessible floor gully, which do not have direct influence on the service life.

Figure 1. Example of a bathroom wall made from wood based material without a watertight membrane. The lack of watertightness resulted in a total renovation of the bathroom due to fungus and dry-rot in the constructions.

Figure 2. Example of pipe penetrations in a floor construction. The tubes (for the pipe in tube system) are finished just over the floor allowing water to run into the construction.

Figure 3. Example of cracks in a floor with underlay of plywood but with insufficient stiffness.

Figure 4. Example of insuffiient welding – worst example ever seen – with repair of the joint with tape. Probably a do-it-yourself work.

Figure 5. Example of new floor covering on top of the old. The floor gully has been extended with a plastic frame but unfortunately it is not watertight, see figure 6.

Figure 6. The result of lacking watertightness of the extended floor gully is seen as a drop on the water lock (inside the marking) in the flat underneath after floding the floor above under 10 mm water for about 10 minutes.

5 APPROVAL AND TESTING

In Denmark the use of new light weight constructions for bathrooms is only allowed with an approval. So far approvals have been national and issued by ETA-Denmark (national approvals are in Denmark designated MK-approval i.e. approval of materials (M) and constructions (K)). Shortly it will also be possible to get European approvals (ETA's).

All approvals are for systems, e.g. a bathroom partition with specified studs, specified boards and specified screws assembled in a specified way. Approvals are issued on basis of a testing. Approval can be obtained for constructions, i.e. floor constructions, or for watertightening systems.

Testing of constructions is done in order to ensure that the strength and stiffness is sufficient for use in a bathroom. For example walls are tested according to ETAG 003 (European Technical Guideline for testing of partitions in general and partitions in bathrooms in particular), [EOTA, 2003], with hard and soft body impacts.

Testing of watertightening systems has until recently mainly been performed according to Nordtest methods, [Nordtest, 1994], [Nordtest, 1991], [Nordtest, 1987]. These methods were developed as a sort of accelerated test methods with exposure to mechanical loads, humidity changes and cycles of hot and cold water. The exposure was chosen to simulate exposure under use conditions but with

tougher extremes. The test specimens include all types of details to be expected in bathrooms, e.g. in- and outgoing corners, floor gullies and pipe penetrations. The details are included to ensure that not only can they be made in the intended way but they shall also be able to resist in-use conditions under a long period of use. Actually problems most often occur at the details. It can not be said how much the testing accelerates the real life exposure as this very much depend on the actual use.

New products appear regularly and even though standard procedures exist for some products these can not always be followed. New products may have properties different from what have been seen earlier and consequently may call for a different test. In such cases it might be necessary to develop new or modified test procedures with the aim of ensuring a sufficient performance and service life.

During the past five years an EOTA (European Organisation for Technical Approval) working group has been working on a European Technical Guideline (ETAG 022) for waterproofing of wet rooms. The first part dealing with watertight membranes applied in fluid form is now finished and the remaining two parts (dealing with watertight systems applied as pre-fabricated sheets and inherently watertight boards respectively) are currently under finalisation [EOTA, 2007].

The properties dealt with in the ETAG guideline 022 comprise performance properties as well as properties used for characterisation and production control. The performance properties include, e.g. watertightness, tensile strength (initial and after different exposure conditions), crack bridging ability and water vapour permeability. A number of the test methods in the EOTA work are full scale tests very similar to the NORDTEST methods used in Denmark, Norway and partly in Sweden and Finland until now, i.e. with testing of all relevant details like floor gully and corners.

Some of the above mentioned properties are compulsory, whereas others are dependent on national requirements and consequently only need to be documented in the relevant country. For example there are requirements in the Nordic countries (dependent on country) as regards water vapour permeabilty and thickness of membrane.

6 FACTORS AFFECTING THE SERVICE LIFE

The service life of light weight bathrooms is dependent on several factors. Besides the factors already mentioned the following should be taken into account:

The workmanship is crucial for a good result. Even a good product/system is worth nothing if not installed properly. In Denmark the most common problem is probably that too little watertight membrane is applied. The reasons are believed to be that the membrane is expensive and the application time consuming. This calls for a quality control of the work best performed by the contractor himself and followed up by an independent body. In Denmark a voluntary control scheme has so far only been used for works with PVC floor and wall coverings used as watertight membrane. For PVC works the contractor – actually the individual craftsman – controls his own work and this is followed up by independent surveys of randomly chosen bathrooms. The control scheme has led to a significant improvement of the quality of the work.

Maintenance is important and is best performed on basis of regular inspections. Any sign of leakage or potential risk of leakage should be reported and repaired as soon as possible in order to avoid damages. In Denmark light weight bathroom shall be designed so any leakage shows immediately, e.g. by water from a leak dripping out a conspicuous place. Thereby it is possible to make necessary repair works before a damage spread out and gives serious and expensive problems in the entire construction.

7 DISCUSSION

Light weight bathrooms have now been used in Denmark for more than 30 years. A number of light weight bathrooms have been in use since the use was allowed in the beginning of the 1970'es and still perform well.

The increased requirements introduced over the past 12 years have proved to have a good effect as the number of problems has been reduced significantly. Contributing to the reduced number of problems is also that a huge effort to teach consultants and contractors about the importance of good design and workmanship has been fruitful. Today most architects, engineers and craftsmen are very much aware that bathrooms constructions are complicated and require special attention.

It is believed that good performing bathrooms with long service lives can be achieved if the earlier mentioned factors affecting the performance and service life are taken into account when designing and executing a light weight bathroom, i.e.:

- the bathroom shall be designed taking into account not only the constructions but also the installations and any complications that may arise due to the severe exposure to water and high relative humidity,
- floor and wall constructions shall be stable enough to avoid deflections that may damage the watertight layer and the surface covering,
- vulnerable materials shall be efficiently protected by a watertight layer, e.g. a membrane. The watertight layer shall be approved for the intended use or sufficient documentation for performance and service life shall be provided by the supplier,
- vulnerable materials shall be protected from condensation of humidity, e.g. by a membrane (normally the watertight membrane),
- all details shall be well described and tested for watertightness,
- design as well as execution shall be under quality control,
- the contractor shall be made aware of the importance of good workmanship,
- the bathroom shall be maintained regularly preferably on basis of regular inspections.

Based on the experience gained after the implementation of the stricter requirements it is assessed that light weight bathrooms are able to function properly. On condition that the above mentioned requirements are met it is assessed that light weight bathroom have service lives of 30 years or more.

REFERENCES

EOTA, ETAG 003, 2003, *"Guideline for European Technical Approval: Internal partition kits for use as non-loadbearing walls"*,].

EOTA, ETAG 022, 2007, *"Guideline for European Technical Approval: Watertight covering kits for wetroom flors and/or walls", Part 1 "Liquid applied membranes"*.

Nordtest Method 230, 1994, *"Bathroom floors - watertightness"*.

Nordtest Method 058, 1987, *"Bathroom Walls: Watertightness and Resistance to Water and Moisture"*.

Nordtest Method 389, 1991, *"Wall coverings: Waterproofing on small test pieces"*.

Properties of Concrete with Shredded Waste Tyres

Özer Dogan [1]
Gülser Çelebi [2]
Soofia Tahira Elias-Ozkan [3]

T 18

ABSTRACT

The ever-increasing volume of discarded tyres poses a serious problem from the point of view of solid-waste disposal as well as its derogatory environmental impact. Research is being carried out to solve this problem by reusing or recycling material from such tyres. One such study was undertaken to determine the effects of incorporating shredded rubber tyres into Portland cement concrete mixes. Tests were carried out on experimental blocks prepared with concrete mixes in which predetermined portions of coarse aggregates were replaced by two lengths of rubber fibres from shredded tyres, separately, to the order of 10, 15, 30 and 45%. A total of 9 mixes, including the control mix, were prepared and 17 samples of each were tested for their unit weight, slump, flow, air content, density, water absorption, porosity, water permeability, durability after freeze-thaw cycles, compressive and flexural strengths. This paper presents the findings of experiments related to the physical and mechanical properties of concrete with varying ratios of the rubber fibres from waste tyres.

KEYWORDS

Rubberized concrete, Waste tyres, Shredded tyres.

[1] Gazi University, Arch. & Eng. Faculty, Ankara, Turkey 06570, Phone +90 312 440 94 77, mimrozer@hotmail.com
[2] Gazi University, Arch. & Eng. Faculty, Ankara,, Turkey 06570, Phone +90 212 2317400/ 2659, Fax 212 2310183, gulser@gazi.edu.tr
[3] Middle East Technical University, Faculty of Architecture, Ankara, Turkey 06531, Phone +90 312 2102221, Fax 312 2107966, soofia@metu.edu.tr

1 INTRODUCTION

The production of tyres has increased proportionally to the production of automobiles, in Turkey. In the year 2000, total sales of tyres was around 126,000 tons of which 86,000 tons were sold directly to vehicle owners; hence, the assumption that approximately 90,000 tons of rubber tyres are replaced annually. In addition to locally manufactured tyres, imported tyres are also sold in the domestic market. Thus, based on these figures, it is estimated that the total volume of waste tyres needing disposal is approximately 120,000 tons annually [DPT Report 2000a].

Most of the discarded tyres in Turkey are recycled in some ways; for instance, 11% of the waste tyres are used in the production of rubber soles for shoes [DPT Report 2000b]. Hence, the number of discarded tyres to be disposed of as solid waste is small compared to Western countries. On the other hand, the ever increasing production of vehicles may lead to a higher rate of tyres being discarded than can be recycled. Consequently, even Turkey can face a dilemma similar to that of the EU, Japan or USA where the number of tyres discarded per annum is in the region of 240, 100 and 285 millions, respectively.

Up until the eighties, the only way to dispose off waste tyres was to burn them; but the oil and soot thus produced caused tremendous environmental pollution, which was not only a health hazard but also in contradiction to the environmental policies and legislation in place. In order to use up this waste in an environmentally acceptable manner, the first attempt to recycle rubber from discarded tyres was in the form of rubber crumbs, which was used as light aggregate in hot asphalt for paving roads [Lougheed and Papagiannakis 1996].

Recycling or reusing any kind of discarded material is always a better option than dumping it as waste, from the point of view of environmental impacts as well as the country's economy. Of the many ways being investigated to accomplish this objective, using rubber from waste tyres as coarse aggregate in concrete mixes is an option that is being tested in many parts of the world. Rubber is chopped up into granules of predetermined sizes; however, for this research project, rubber was shredded into fibres of lengths 1cm and 4 cm with diameters of 0.1cm and 0.4cm, respectively [Dogan 2005]. A literature survey regarding experiments with recycled rubber concrete has shown that with the addition of rubber granules into the concrete mix the properties of concrete change. Compressive and flexural strength of such concrete are lower than conventional concrete, while this decrease is directly proportional to the amount of crumb rubber present in the mix, and its size. On the other hand, presence of some rubber helps improve crack resistance and the ability to absorb shocks from impacts; hence, it is more tough and durable. The decreased brittleness prevents concrete from disintegrating under compressive or flexural loads. Since the unit weight is reduced and the surface is not as hard, Recycled Rubber Fiber Concrete (RRFC) provides better acoustics control and heat insulation [Rad 1967, Fang *et al*. 1992, Sukontasukkul & Chaikaew 2006].

2 EXPERIMENTAL PROCEDURE

Predefined ratios of coarse aggregate in the concrete mix were replaced separately with two sizes of fibres from shredded rubber tyres, while ratios of other material were kept constant. Samples were then prepared with these mixes and tested for various physical and mechanical properties, keeping in mind the following three objectives:

- To test the performance of concrete when coarse aggregate (crushed stone) is partially replaced with rubber fibre and to compare it with the control mix.
- To investigate the effect of the size of the rubber fibres replacing crushed stone aggregate, on the properties of concrete.
- To investigate the effects of increasing the ratio of rubber fibre in the concrete mix.

2.1 Materials

The following materials were used to prepare the various concrete mixes:

- Portland cement: complying with EN 197-1 and having a 28-day strength of 42.5N/mm².
- Sand: complying with EN 12620 and having granule size of less than 4 mm, unit weight of 1740 kg/m^3, specific gravity of 2640 kg/m^3, water absorption ratio of 0.99%, and fineness module of 2.44.
- Crushed stone: aggregate complying with with EN 12620 and having sizes of 1-12 mm and 1-24 mm with unit weights of 1520 kg/m^3 and 1490 kg/m^3, specific gravities of 2720 kg/m^3 and 2720 kg/m^3,water absorption ratio of 0.50% and 0.25%, and fineness modules of 5.31 and 6.58.
- Water: complying with EN 206-1 standards, suitable for use in concrete mixes.
- Recycled rubber fibres (RRF): produced by shredding discarded tyres into two sizes of fibres, which had a specific gravity of 650 kg/m^3, modulus of elasticity E= 5-15 N/mm^2, and heat conductivity of 21 Kcal/m^{2}h^{0}C. The shorter fibbers (RRF1), of length 1cm and a diameter of 0.1cm, had a unit weight of 405 kg/m^3 and a modulus of fineness of 2.2; while the longer fibres (RRF4) of length 4cm and diameter 0.4cm had a unit weight of 370 kg/m^3 and a modulus of fineness of 4.9 (Figure 1). Since the rubber was shredded into fibres instead of granules, sieve sizes used were 4-31.5 mm and 1-16 mm for the long and short fibres, respectively. The granulometric charts are shown in Figs 2 a and b below.

Figure 1. Short and long rubber fibres (RRF1 and RRF4) obtained by shredding discarded tyres.

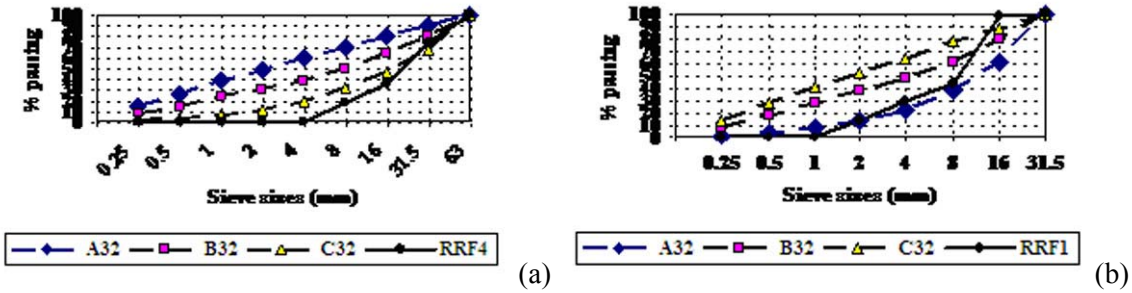

Figure 2. Granulometric chart for: (a)long rubber fibres (RRF4) and (b) short rubber fibres (RRF1)

2.2 Mix Design

Apart from the control mix, 8 varieties of recycled rubber fibre concrete (RRFC) mixes were prepared by replacing 10%, 15%, 30%, and 45% of the coarse aggregate (crushed stone) with the short and long rubber fibres. Of these, 4 mixes were prepared with the short and the other 4 with long recycled rubber fibres (RRF1 and RRF4) separately. Thus, a total of 153 specimen were cast for testing, of which 17 were prepared with the control mix (without any rubber fibre) and 17 each with 10%, 15%, 30%, and 45% of coarse aggregate replaced with RRF1 and then with RRF4.

Table 1 below lists the proportions of Portland cement, water, sand, fine aggregate and coarse aggregate in the mixes for the control specimen, along with the four mixes prepared by replacing 10%, 15%, 30%, and 45% of the coarse aggregate with the long recycled rubber fibre RRF4 (denoted by 4RRFC10, 4RRFC15, 4RRFC30, 4RRFC45) and the four mixes prepared by replacing 10%, 15%,

30%, and 45% of the coarse aggregate with the shorter recycled rubber fibre RRF1 (denoted by 1RRFC10, 1RRFC15, 1RRFC30, 1RRFC45).

Table 1. Materials used to prepare the nine varieties of concrete mixes, by weight and by volume.

Concrete mix		*Portland Cement*	*Water*	*Sand*	*Fine crushed stone*	*Coarse crushed stone*	*Recycled rubber fibre*	*Air content*
Control Mix	kg	313.86	191.16	736.03	379.17	758.34	0.00	0.00
	dm^3	101.57	191.16	278.80	139.40	278.80	0.00	0.10
1RRFC10	kg	313.86	191.16	736.03	342.07	682.08	27.19	0.00
	dm^3	101.57	191.16	278.80	125.76	250.77	41.84	0.10
1RRFC15	kg	313.86	191.16	736.03	321.59	645.24	40.79	0.00
	dm^3	101.57	191.16	278.80	118.23	237.22	62.75	0.10
1RRFC30	kg	313.86	191.16	736.03	266.05	530.51	81.58	0.00
	dm^3	101.57	191.16	278.80	97.81	195.04	125.51	0.10
1RRFC45	kg	313.86	191.16	736.03	207.73	417.71	122.37	0.00
	dm^3	101.57	191.16	278.80	76.37	153.57	188.26	0.10
4RRFC10	kg	313.86	191.16	736.03	342.07	682.08	27.19	0.00
	dm^3	101.57	191.16	278.80	125.76	250.77	41.84	0.10
4RRFC15	kg	313.86	191.16	736.03	321.59	645.24	40.79	0.00
	dm^3	101.57	191.16	278.80	118.23	237.22	62.75	0.10
4RRFC30	kg	313.86	191.16	736.03	266.05	530.51	81.58	0.00
	dm^3	101.57	191.16	278.80	97.81	195.04	125.51	0.10
4RRFC45	kg	313.86	191.16	736.03	207.73	417.71	122.37	0.00
	dm^3	101.57	191.16	278.80	76.37	153.57	188.26	0.10

2.3 Preparation of Test Samples

All the dry ingredients were first mixed for two minutes in the Pan Mixer, with a capacity of 20 dm^3, before adding the water and mixing again for another two minutes, after which the concrete was poured into the moulds. Two types of plastic moulds were used to prepare the samples; cubic ones of dimensions 15cmx15cmx15cm and cylindrical ones with 15cm diameter and a height of 30cm. The mixes were filled and compacted in the cubic and cylindrical lubricated moulds placed on the vibration table, in accordance with the EN12390-1 and 2 procedures. After leaving them in the laboratory for 24 hours at room temperature, the moulds were removed and the samples were left in the curing room at a uniform temperature of 20 °C.

Some samples were taken out after 7 days and others after 28 days of curing and were then left to dry at room temperature for another 24 hours, before performing the tests.

Figure 3. Mixing the concrete in the pan-mixer and Preparing test-samples by compacting concrete mix into moulds placed on the vibration table.

2.4 Experimental Tests

Various tests were carried out to determine the physical and mechanical properties of the 9 mixes. These tests were carried out according to Turkish standards complying with European norms; the relevant standard notations are given next to the tests applied as listed below:

1. Unit weight of fresh concrete (TS EN 12350–6)
2. Unit weight of hardened concrete (TS EN 12390–7), which was determined for 7 and 28 day old samples
3. Slump test (TS EN 12350–2)
4. Flow table test (TS EN 12350–5)
5. Air content – pressurized testing (TS EN 12350–7)
6. Density, water absorption, and porosity tests (TS 3624)
7. Water permeability test (TS 4045): 27 cubic specimens were tested. (3 each for the 9 mixes)
8. Compressive strength (TS EN 12390–3): a constant loading speed of 0.2 MPa/sec to 1.0 MPa /sec was applied to the samples until they failed.
9. Flexural strength (TS EN 12390–5): a constant loading speed of 0.04 MPa/sec to 0.06 MPa /sec was applied to the samples until they failed.
10. Durability; after freeze-thaw cycles (ASTMC290,C291,C292, and C310): the 28-day samples were frozen for 12 hours at a temperature of -25 ^{o}C and the left to thaw for another 12 hours at 25 ^{o}C. This freeze-thaw cycle was repeated for 25 days and then the samples were tested for their unit weights and compressive strengths.

Figure 4. Slump test.

Figure 5. Water permeability test.

Figure 6. Determining the air content in the concrete mix with pressurized vessel testing.

(a)


(b)

Figure 7. Behaviour of control mix (a) and RRFC (b) samples when tested for compressive strength.

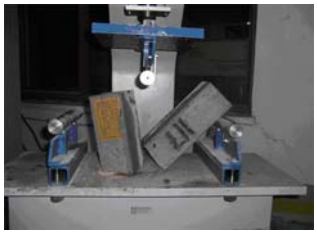
(a)

(b)

Figure 8. Behaviour of control mix (a) and RRFC (b) samples when tested for flexural strength: control-mix sample breaks while RRFC only cracks.

3 EXPERIMENTAL RESULTS

Data collected as a result of the various tests applied to samples of the 9 mixes has been condensed and presented in Tables 2 and 3 below.

Table 2. Physical properties of control mix and recycled rubber-fibre concrete mixes.

Physical Properties	*Control Mix*	*1RRFC10*	*1RRFC15*	*1RRFC30*	*1RRFC45*	*4RRFC10*	*4RRFC15*	*4RRFC30*	*4RRFC45*
Unit weight of fresh concrete (kg/cm³)	2.384	2.301	2.264	2.123	2.008	2.376	2.328	2.185	2.155
Unit weight of 7-day concrete (kg/cm³)	2.359	2.281	2.219	2.102	1.927	2.331	2.319	2.174	2.145
Unit weight of 28-day concrete (kg/cm³)	2.373	2.303	2.243	2.143	1.960	2.335	2.313	2.196	2.153
Slump (cm)	5.10	4.37	3.77	2.83	1.63	4.30	3.63	2.83	1.90
Flow table test (cm)	32.17	35.33	38.67	43.00	47.33	36.67	41.00	44.50	51.50
Air content (%)	0.48	0.81	1.05	2.62	3.11	0.58	0.71	1.18	1.31
Water absorption (%)	1.76	1.83	2.60	4.83	5.91	1.79	2.70	3.32	3.51
Porosity (%)	4.14	4.16	5.87	10.12	12.23	4.15	6.13	7.19	7.38
Water permeability (gm)	28.17	27.18	28.54	25.10	27.35	27.76	34.64	25.93	29.85
Capillarity (cm²/s)	2.35×10^{-6}	2.19×10^{-6}	2.40×10^{-6}	1.87×10^{-6}	2.02×10^{-6}	2.28×10^{-6}	3.70×10^{-6}	1.99×10^{-6}	2.71×10^{-6}

Table 3. Mechanical properties of control mix and recycled rubber-fibre concrete mixes.

Mechanical Properties	*Control mix*	*1RRFC10*	*1RRFC15*	*1RRFC30*	*1RRFC45*	*4RRFC10*	*4RRFC15*	*4RRFC30*	*4RRFC45*
Compressive strength of 7 day cubic sample (MPa)	32.53	25.00	23.07	15.57	13.67	26.47	24.23	17.80	14.70
Compressive strength of 28 day cubic sample	38.57	29.57	26.73	18.50	16.20	31.50	29.67	21.07	15.33
Compressive strength of 7 day cylindrical sample (MPa)	27.26	20.00	18.74	13.04	11.44	22.76	21.15	15.47	12.92
Compressive strength of 28 day cylindrical sample (MPa)	32.31	24.75	22.90	16.15	14.08	25.20	24.10	17.65	13.32
Flexural strength of 28 day cubic sample (MPa)	6.89	5.44		3.85		5.34		4.01	
Compressive strength of conc. after freeze-thaw cycles (MPa)	38.90		25.97		15.13		27.43		13.97
Density of conc. after freeze-thaw cycles (g/cm^3)	2.359		2.284		2.106		2.329		2.183

4 DISCUSSION OF RESULTS

As a result of the experiments carried out on RRFC samples prepared with 8 types of concrete mixes by incorporating different ratios of two lengths of rubber fibres from shredded recycled tires, the following physical and mechanical properties were determined:

- The unit weight of fresh concrete is reduced from 2.384g/cm³ to 2.008g/cm³ by replacing 45% of the coarse aggregate with RRF1, and to 2.155g/cm³ by replacing the same amount with RRF4; i.e. an increase in the percentage of rubber fibre decreases the unit weight of concrete. This decrease is less for RRF1 than for RR4 replacements.
- The unit weight of 28 days old concrete samples is reduced from 2.337g/cm³ to 1.960g/cm³ by replacing 45% of the coarse aggregate with RRF1, and to 2.153g/cm³ by replacing the same amount with RRF4; i.e. an increase in the percentage of rubber fibre decreases the unit weight of concrete. This decrease is less for RRF1 than for RR4 replacements.
- As the percentage of rubber fibres increased, segregation and settlement of aggregates decreased. In other words, the high frictional resistance of the rubber aggregate decreases the workability of the cement.
- As the amount of rubber fibres increased, fluidity of the concrete also increased. It was observed that when shaken repetitively, the rubber fibres in the cement lost their frictional force and the fluidity increased.
- As the amount of rubber fibres increased, air content in the concrete also increased. When fresh concrete with RRF is subjected to pressure, the rubber fibres contract in size and when the pressure is released they spring back, causing an increase in porosity within the concrete.
- The water absorption capacity of RRFC is more for RRF4 than for the shorter fibre, RRF1. Due to the porosity of the rubber fibres themselves, the higher the percentage of RRF in the concrete, the higher is its water absorption capacity and volume of air pockets within.

- As the amount of rubber fibres increases, capillary action in the concrete also increases.

Tests related to compressive strength, flexural strength, and durability, applied on the recycled rubber fibre concrete samples gave the following results:

- Compressive strengths of cubic RRFC samples (15x15x15cm³), which had been cured for 28 days dropped from 38.57 MPa to 16.2 MPa for 45% RRF1 replacements and to 15.33 MPa for 45% RRF4 replacements. Replacing coarse aggregate in concrete mixes with 10%, 15%, 30%, and 45% RRF1 caused a decrease in the compressive strength by 23, 31 , 52 , and 58 percent respectively; while replacements with RRF4s caused a decrease of 18, 23, 45, 60 percent, respectively.
- Compressive strengths of cylindrical RRFC samples (15x30 cm³), which had been cured for 28 days, dropped from 32.31 MPa to 14.08 MPa for 45% RRF1 replacements and to 13.32 MPa for 45% RRF4 replacements. Replacing coarse aggregate in concrete mixes by 10%, 15%, 30%, and 45% RRF1s caused a decrease in the compressive strength by 23, 29, 50, and 56 percent respectively; while replacements by RRF4s caused a decrease of 22, 25, 45, and 59 percent, respectively..
- Flexural strengths of cubic RRFC samples, which had been cured for 28 days dropped from 6.89 MPa to 3.85 MPa for 30% RRF1 replacements and to 4.01 MPa for 30% RRF4 replacements. It was observed that an increase in the amount of RRFs caused a reciprocal decrease in the flexural (tensile) strength of the concrete. Samples made with the control mix or with 10% RRFs exhibited brittleness and broke under tensile strain; however, when the amount of RRFs was increased to 30% the concrete samples cracked but did not break under the same loads.
- The Unit weights of RRFC samples that had undergone 25 freeze-thaw cycles increased slightly after this treatment; this behaviour is in contrast to normal concrete where unit weights drop after the freeze-thaw cycles. The unit weights of the control mix, 1RRFC15, 1RRFC45, 4RRFC15 and 4RRFC45 increased from 2.37, 2.24, 1.96, 2.31, and 2.15 g/cm^3 to 2.36, 2.28, 2.11, 2.33 and 2.18 g/cm^3, respectively.
- The compressive strengths of RRFC samples that had undergone 25 freeze-thaw cycles decreased slightly after this treatment; this behaviour is in contrast to normal concrete where compressive strengths increase after the freeze-thaw cycles. The decrease is more for the longer fibres as compared to the shorter ones. The compressive strengths of the control mix, 1RRFC15, 1RRFC45, 4RRFC15 and 4RRFC45 dropped from 38.57, 26.73, 16.20, 29.67, and 15.33 MPa by 0%, 3%, 7%, 7.5%, and 8.8%, respectively, to 38.90, 25.97, 15.13, 27.43, and 13.96 MPa.

5 CONCLUSION

The experiments conducted by incorporating two lengths of rubber fibres into the concrete mixes have demonstrated that the compressive and flexural strengths of RRFC decrease with the addition of rubber fibre from shredded waste tyre. The reduction in mechanical properties is directly proportional to the amount of fibre and also the size of the fibre that replaces the coarse aggregate in the concrete mix. However, with the increase in compressive or flexural loads, the RRFC did not disintegrate like conventional concrete, but held together in spite of surface cracks. Furthermore, when the applied load was removed, the samples were seen to have undergone plastic deformations. On the other hand, the presence of RRFs led to a reduction in the unit weight of concrete, which was proportional to the amount of fibre present in the mix; therefore, it is lighter than conventional concrete. Despite the reduction in compressive and flexural strengths, RRFC was observed to be more durable as it is more impact resistant and has higher plasticity. Also, RRFC is able to absorb more energy; hence, it has better sound absorption and heat retention properties.

ACKNOWLEDGMENTS

This study was supported by the Turkish Cement Manufacturers' Association.

REFERENCES

Dogan O., 2005, *'Investigation of rubberized concrete characteristics with experiments'*, Unpublished M.Sc. Thesis, Gazi University, Institute of Science and Technology, Ankara.

Fang, H.Y., Topçu, I.B., Hitchens, D., & Hontz, D., 1992, *'Use of scrap rubber tires for construction materials'*, Proc. 24th Mid-Atlantic Industrial Waste Conf., West Virginia University, Morgantown, USA. pp.563-72.

Lougheed, T.J., & Papagiannakis, A., 1996, 'Viscosity characteristics of rubber-modified asphalts', *Journal of Materials in Civil Engineering,* ASCE, **8** [3], pp. 153-156.

Rad, R. 1967, 'Rubberized concrete', *New Horizons in Construction Materials*, Vol. l, pp. 287-292.

Sukontasukkul P., Chaikaew C., 2006, 'Properties of concrete pedestrian block mixed with crumb rubber', *Construction and Building Materials*, **20** [7], pp. 450-457.

T.C. Başbakanlık Devlet Planlama Teşkilatı Müsteşarlığı. 2000a, *"Araç Lastiği Özel İhtisas Komisyonu"*, DPT Report, Yayın No:2235-ÖİK:365, l-3 7, Ankara.

T.C. Başbakanlık Devlet Planlama Teşkilatı Müsteşarlığı. 2000b, *"Lastik ve Plastik Eşya Özel İhtisas Komisyonu"*, DPT Report, Yayın No: 2218-ÖİK:362, 1-36, Ankara.

11DBMC International Conference on Durability of Building Materials and Components
ISTANBUL, Turkey 11-14 May 2008

Oriented Straw Cable Composites for Housing Applications

Seda Yeşilmen [1]
Anthony J. Lamanna [2]
Gerhard Piringer [3]

T 18

ABSTRACT

A low strength cementitious matrix composite that is reinforced with oriented wheat straw cables was investigated in the study. The composite can offer an inexpensive, locally available, renewable and environmentally friendly construction material that can be used in regions where these criteria are critical for housing needs. They can offer a solution for the housing problems throughout the world as their assembly will also be quick and effortless considering their light weight. The composites can be used for housing applications in low income areas of developed and developing countries or in emergency situations where housing needs emerge due to force majeure events or places such as refugee camps.

A series of experiments were performed on the composites to obtain their mechanical properties. The load carrying capacity average for small scale composite columns tested in compression was 12,663 N (2,847 lbf). A life cycle assessment (LCA) study was also performed to identify the environmental burdens associated with the composite as a building material. The critical processes in the life cycle of a wall system of the composite were identified using Simapro.

KEYWORDS

Biocomposites, Mechanical properties, LCA

[1] Assistant Professor, Department of Civil Engineering, Atılım University, Ankara, Türkiye
[2] President & Consulting Engineer, Lamanna Engineering Consultants, LLC, New Orleans, LA 70118, USA
[3] Professor of Practice, Department of Earth and Environmental Sciences, Tulane University, New Orleans, LA 70118, USA

1 INTRODUCTION

Natural fibers are grown throughout the world and are mostly byproducts of agriculture. The use of natural fibers in building components is an important research area since a large portion of natural fibers are being burned or disposed of with serious environmental consequences. Composites based on natural fibers offer a wide variety of advantages in the building sector. They can be expected to be renewable, at least partially biodegradable, and not highly energy-intensive. Potential uses for such composites can be either as non-load bearing elements such as wall and insulation panels, or they can be used as load bearing elements for simple building frames.

Natural fibers are great alternatives for housing applications where very high strengths are not required [Satyanarayana et al. 1984]. Natural fiber reinforcement have been used both in cement and in polymer composites [Burgueno et al. 2004]. The main advantages in cement composites of natural fibers were listed as increased flexural capacity, post crack load bearing capacity, increased impact toughness and improved compressive strength [Sera et al. 1990]. The performance of discontinuous and randomly distributed natural fiber was investigated in cement board applications, wall panels, and suggested as a substitute for asbestos cement [Ghavami et al. 1999]. Natural fibers such as bamboo and date palm fronds were used as continuous reinforcement because such fibers are quite strong even as individual fibers.

Wheat straws as an abundantly available agricultural fiber have only been investigated as discrete fibers in a composite. A wheat-straw based particleboard was found to meet industrial standards [Boquillon et al. 2004]. In addition to the environmental and economical advantages, natural fibers are good insulators; low density straw panels have been suggested in thermal insulation applications [Strivasta and Grupta 1990].

This paper presents information on basic mechanical properties and the environmental impacts of a novel composite building material - oriented straw cable composite (OSCC). Wheat straws were oriented in parallel and assembled into cables which were then embedded in a low strength cementitious matrix. No literature on this particular subject has been found by the authors.

Reinforcing matrix materials with organic fibers can be expected to increase the compressive and flexural strength compared to non-reinforced matrix material. The tensile strength of the fibers constitutes an ideal flexural reinforcement. Wheat straw, like most agricultural residue, does not behave elastically under loads. The behavior has been defined as viscoelastic or even as a combination of plastic, viscous and elastic behavior [Moustafa et al. 1968]. As a first approximation however, the calculations in this preliminary study are based on a linear analysis.

The environmental impact of the OSCC material was another aspect of this study. Natural fiber composites are claimed to offer various environmental advantages over conventional composites such as reduced dependence on non-renewable energy sources, lower pollutant and green house gas emissions, and end-of-life biodegrability [Joshi et al. 2004]. Environmental burdens of the OSCC manufacturing processes were quantified to identify critical processes. The Life Cycle Assessment (LCA) methodology was used for the environmental burden analysis. There is no specific LCA study for wheat reinforced composites; therefore, in this study the scope and boundaries were set according to similar studies found in the literature [Corbiere-Nicollier et al. 2001].

2. MATERIALS AND PRODUCTION

Specimens to be tested were manufactured by Ashland Prototypes (Ashland, Oregon, USA). An extrusion machine was used in production of the OSCC, mounted on a combine chassis and used to harvest a portion of the remaining wheat plant after harvest. Wheat straw, clay, clay bearing subsoil,

recycled newspaper, cement, polyethylene string, were the materials used for the production of the OSCC. The length of the straw was dependent on the type or setting of the combine.
The OSCC prototypes studied here were small scale columns and beams. The OSCC columns consisted of four 50.8 mm (2.28 in.) diameter straw cables and the matrix covering the cables, the nominal cross section being a 101.6 × 101.6 mm (4 in. × 4 in.) square 'Fig 1'. Seven different column specimens with average length of 457 mm (18 in.) were tested. Two OSCC beams were also tested, with an average length of 1626 mm (64 in.) and rectangular cross sections of approximately 102 × 203 mm (4 × 8 in.). A total of eight continuous straw cables were running through the whole beam length. The specimens were stored and tested in normal room conditions (22 ± 2 °C).

Figure 1. A small scale OSCC (oriented straw cable composite) column.

3. MECHANICAL TESTING

3.1 Experimental Method

The overall objective of this part of the study was to investigate the loading behavior of OSCC. The composite specimens were tested in compression and bending. Testing was carried out in the Materials Testing Laboratory of the Civil and Environmental Engineering Department at Tulane University (New Orleans, Louisiana, USA). Compression tests were conducted at a rate of 0.025 mm/sec (0.00098 in./sec), and for the bending tests the rate was 0.017 mm/sec (0.00066 in./sec).

Wheat straw is an anisotropic and heterogeneous material with a loading response of combined elastic, inelastic, and viscous behaviors. It is highly complicated to evaluate its response to any type of loading [Liu et al. 2004]. Considering the limited scope of this research, a number of assumptions were made to simplify the evaluation of the wheat straw behavior. The strain calculations were based on the engineering strain definition. Stress calculations were based on the bulk area of the specimens. The modulus of elasticity calculations were based on the linear portions of the stress-strain graphs.

Testing for small scale OSCC columns was conducted on an MTS 311.31 load frame, with a 244.51 hydraulic actuator (the motor that converts hydraulic energy to mechanical work) and a Flex Test III CTM controller. The MTS Basic TestWare software was used to carry out the experiments and to acquire data. The bending tests on small scale OSCC beams were performed in a MTS fixture with the 355.86 kN (80 kips) hydraulic MTS actuator. The beams did not show sudden deflections or failure, but they underwent large deflections with small increments of applied load. Deflections were measured to analyze the behavior of the beams. Extensometers and string pots were used at multiple positions of the test set-up to monitor displacements. The test fixture for the bending tests was shown in 'Figure 2'.

Figure 2. The bending test set up for a small scale OSCC beam.

3.2 Mechanical Testing Results

The average load carrying capacity value for OSCC columns was 12,663 N (2,847 lbs). A typical load displacement graph for the OSCC columns is shown in 'Figure 3'. The average stiffness value for the wheat straw reinforced composite group was 257.98 MPa (35,407 psi). The composite beams had ultimate flexural stresses of 331 and 462 kPa (48 and 67 psi) for the elastic portion of their load behavior. The load versus mid-span deflection graph was shown in 'Figure 4' for one of the beams.

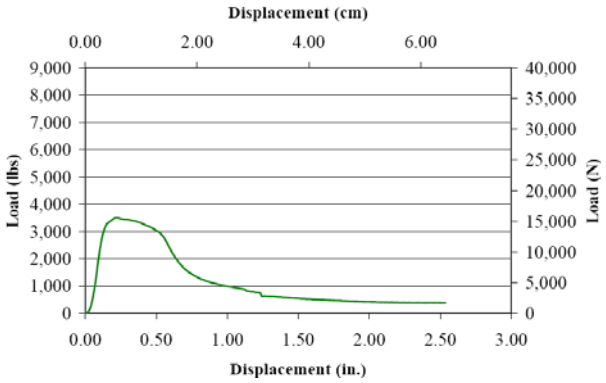

Figure 3. Load-displacement graph for an OSCC tested in compression.

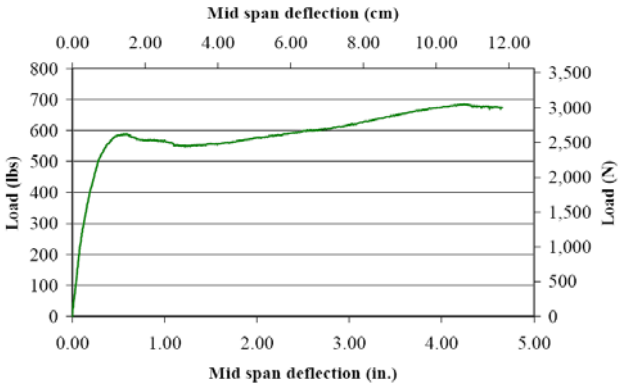

Figure 4. Load-mid span displacement graph for 4-point bending test on an OSCC beam.

4 ENVIRONMENTAL IMPACTS OF OSCC PRODUCTION

The life cycle assessment (LCA) method was used to quantify the environmental impacts associated with the production of an OSCC beam. The use of renewable sources such as OSCC can also increase material efficiency corresponding to the goals of sustainable development. The life cycle assessment is expected to extend the knowledge base on the environmental impact of bio-based building materials. The target audiences are sustainable materials researchers and LCI practitioners.

The function of the beams as building materials was defined as the structural support, thermal and sound insulation, and protection against water and air intrusion. The functional unit for the comparison study was selected as an OSCC beam with a 20.3 × 20.3 cm (8 × 8 in.) square cross section and a length of 3.05 m (10 ft).

4.1 Method, Data Quality and Sources

The composition of the OSCC was obtained from the strawjet manufacturer (Smith, 2004). Life cycle inventory and life cycle impact assessment results were obtained using the Simapro v.7 software (Pre-Consultants bv. Amersforth, NL). As a first step, an LCI was compiled for the materials used in the beams and burdens associated with these materials. Life cycle inventory contributions to different environmental impact categories were assessed using the impact assessment method TRACI (Tool for the Reduction and Assessment of Chemical and other environmental Impacts) (Bare 2002) which was part of the Simapro software.

Since the material is new and unique, the primary data - the data about the OSCC production process itself - are prospective data estimated by the designer of the composite production process. The geographic scope was the US region, time coverage was from 1995 to 2005, and the technology is the only technology currently available for OSCC production. The secondary data – the data on pre-production and disposal processes – were obtained from various databases as listed below. The geographical coverage for all secondary data was the US and Canada, except the Ecoinvent database which is mainly based on European data. The time coverage, technological coverage, representativeness, precision, completeness, consistency, and reproducibility of the secondary LCI data varies with the source database used.

Databases used for the study include the Franklin US LCI Database, the Ecoinvent database, and the US Input/Output database. These databases were included with the commercial LCA software used in the study. The inventory for the wall systems also includes data from other sources, the US LCI Database, the ATHENA Environmental Impact Estimator software database ,and the 2002 commodity flow survey (CFS) [Franklin 2003 & NREL 2001]. The data were reviewed for consistency with the system boundaries set for the project. The environmental impact categories included in the impact assessment method were: global warming, acidification, human health (HH) cancer, HH non-cancer, HH criteria air pollutants -point source, HH criteria air pollutants -mobile source, eutrophication, ozone depletion, ecotoxicity, smog.

4.2 System Boundaries and Description

The system includes “cradle-to-gate” processes; that is, the use phase and disposal of the beams were not considered. All the processes related to raw materials extraction, and production were taken into account in the study. Capital goods such as the infrastructural facilities needed for the manufacture of products were not included in beam system definition with the exception of the strawjet machine and the processes taken from two databases that routinely consider capital goods contributions - the Ecoinvent database and the US input/output library. These two databases were only used when data from other sources were not available. Ancillary materials such as engine oil for the OSCC production machinery, as well as human labor were not considered.

The allocation considerations in this study simply followed those by the databases used for the processes. Transportation distances were considered in two parts for each beam component purchased off-farm. The products were transported from the manufacturing plant to a retailer, then from the retailer to the on-farm construction site. The distances for the first part of the transportation varied by material and US average distances were obtained from the US Bureau of Transportation Statistics 2002 Commodity Flow Survey (CFS). The second part of the transportation - from a retailer to the OSCC production site - was represented for all materials purchased off-site by the same ad-hoc estimate. A wide triangular probability distribution was assumed to reflect the large uncertainty, with an average distance of 30 km (18.64 mi.), a minimum of 3 km (1.86 mi.), and a maximum of 75 km (46.60 mi.).

The OSCC has two main components; the matrix and the straw bundle. The materials used in the composite are listed in [Table 1] showing the amount of each material needed per functional unit. In the production stage, oriented straw cable composite was assumed to be extruded at the site of the wheat straw harvest. When the straw is used for the composite, its normal processing – tilling into the soil - is prevented, so the environmental burdens from tilling were counted as negative burdens, or credits, to the life cycle inventory.

Table 1. Inputs per 3.05 m (10 ft) composite beam used for the LCA

Inputs per Functional Unit	**Amount kg (lb)**
Cementitious Matrix :	
Clay-bearing subsoil	23.7 (52.2)
Recycled newspapers	2.3 (5)
Portland cement	1.1 (2.5)
Mortar Clay	2.5 (5.4)
Straw Cable	
Straw	16.8 (37.1)
Polyester Yarn	0.04 (0.1)

4.3 Environmental Burden Results

The environmental burdens of the components of the OSCC beams were compared. The contribution of the matrix was higher than that of the straw bundle in all impact categories except eutrophication and ecotoxicity. The high contributions of the straw bundle in these categories were due to fertilizers required to replace the nutrient content of wheat straw that was not tilled into the soil, because it was used in OSCC. As a benefit of this avoided tillage of straw, the straw bundle showed negative contributions to the categories of global warming, HH criteria air pollutants, and smog. Extrusion of the beam had its highest contribution in HH criteria air pollutant category, mainly due to air emissions resulting from cutting the extruded OSCC composite.

The components of the matrix materials were more thoroughly investigated for their contributions to the environmental burden of the composite beam [Table 2]. Clayey subsoil was the critical component of the cementitious matrix for global warming, acidification, HH criteria, and smog categories. Portland cement was the critical component for the HH cancer and non-cancer categories and mortar clay caused the highest impact in the ozone depletion category. For the composite beam, the cementitious matrix was the critical component according to the impact scores for most impact categories. The composition of the matrix can be modified using products carrying lower environmental burdens.

Table 2. Percent contribution of each matrix component to the impact score for the categories considered in the LCA study.

Impact category	Portland Cement	Clayey subsoil	Old Newspaper	Mortar Clay	Matrix Mixing
	Percentage %				
Global Warming	3.05	49.10	3.21	43.40	1.24
Acidification	15.60	55.00	21.10	7.18	1.10
HH Cancer	99.60	0.03	0.04	0.320	5.18E-4
HH Non-cancer	99.10	0.29	0.30	0.35	2.25E-3
HH Criteria Air-Point Source	2.79	72.90	5.05	18.20	1.05
HH Criteria Air-Mobile	2.88	71.80	5.61	18.70	1.04
Eutrophication	16.10	57.40	19.40	5.95	1.17
Ozone Depletion	6.15	0.12	0.14	93.60	2.14E-3
Ecotoxicity	69.50	2.32	2.69	25.40	0.04
Smog	5.77	67.50	20.10	5.27	1.38

5 DURABILITY ASPECT

The durability of OSCC is an important property for both mechanical behavior and environmental impact aspects. The exterior coating-the matrix- of the OSCC specimens that were exposed to weathering were observed to disintegrate with time. The application of exterior coatings used in the buildings like paint, stucco or plaster will help enhance the durability performance of the material for outside conditions. The durability characteristics of some organic materials in cement matrix such as wheat straws are found to be in desirable limits (Soroushian, 2004).

6 CONCLUSIONS AND FUTURE WORK

The oriented straw cable composites can be used as low cost structural components manufactured with locally available materials. The experimental and environmental investigations into the oriented wheat straw cable composites have provided a basic understanding for the overall properties of the material. Introducing the oriented straw cable composite as a building material would be a challenge because it is a new material and there is no design method developed; however, this work shows that natural fibers are feasible candidates as a reinforcement to cement matrix for affordable housing. Straw fiber reinforcement increased the compressive strength of low strength cementitious matrix material. They are also degradable and energy efficient, especially compared to some materials currently used in construction. These characteristics are highly advantageous for a building material as environmental considerations are a growing concern in most countries.

More detailed experimental investigations are needed to define the material behavior parameters and thus allow modelling the behavior of OSCC. A larger number of replicate tests are necessary to account for the high deviations in the material behavior and to allow statistical analyses that should be performed to increase the reliability of testing data. The proper design code should be developed for

the materials. The material's performance related to the dynamic loading and time dependent structural behavior, thermal and sound insulation characteristics and durability should also be studied.

Comparisons of other biodegradable materials with conventional materials should be performed. The methodology should be applied to compare the composite with load bearing and non load bearing elements used in the construction market. Optimization of the OSCC composite design will be an interdisciplinary process where structural and environmental efficiency has to be balanced to approach a better composite in both areas. Sensitivity analyses should be performed for various assumptions made in the LCA model, such as impact assessment method, impact categories used. Uncertainty analyses should be performed to investigate the effect of data uncertainties on the model.

Improvements in the cement matrix composition can easily enhance the durability characteristics of the material. The aging characteristics of the OSCC are not investigated in this paper but it is definitely necessary to examine the variation of mechanical properties with age in future studies.

ACKNOWLEDGEMENTS

The authors wish to thank David Ward, Norton Smith and Martin Lee from Ashland Prototypes. We also would like to acknowledge the support provided by Dr. S.H. Aung and graduate students of the former Tulane University Civil and Environmental Engineering Department.

REFERENCES

Satyanarayana, K.G., Sukumaran, K., Ravikumar K.K., Bramhakumar, M., Pillai S.G.K., Pavithran, C., Mukherjee, P.S., Pai, 1984, B.C. 'Possibility of Using Natural fiber Composites as Building Materials', International Conference on Low Cost Housing for Developing Countries, April 1984, pp. 177-181.

Burgueno, R., Quagliata, M.J., Mohanty, A.K., Mehta, G., Drzal, L.T., Misra, M., 2004, 'Load-Bearing Natural Fiber Composite Cellular Beams and Panels', *Composites Part A: Applied Science and Manufacturing*, **35** [6], 645-656.

Sera, E.E., Robles-Austriaco, L., Pama, R.P., 1990, 'Natural Fibers as Reinforcement', *Cement and Concrete Composites*, vol. **20** [2], , 109-124.

Ghavami, K., Toledo Filho, R.D., Barbosac, N.P. 1999, 'Behaviour of Composite Soil Reinforced with Natural Fibers', *Cement and Concrete Composites*, **21** [1], 39-48.

Boquillon, N., Elbez, G., Schonfeld, U., 2004, 'Properties of wheat straw particleboards bonded with different types of resin', *Journal of Wood Science*, **50** [3], 230-235.

Strivasta, A.C., Grupta, R., 1990, 'Feasibility of using thrash and straw as a thermal insulator', *Biological Waste*, **33** [1], 63-65.

Moustafa, S.M.A., Stout, B.A., Bradley, W.A., 'Elastic and Inelastic Stability of Biological Structure', *Journal of Agricultural Engineering Research*, **13**[1], 1968, 64-82

Joshi, S.V., Drzal, L.T., Mohanty, A.K., Arora, S., 2004, 'Are natural fiber composites environmentally superior to glass fiber reinforced composites?', *Composites Part A: Applied Science and Manufacturing*, **35** [3], 371-376.

Corbiere- Nicollier, T., Laban, B.G., Lundquist, L., Letterie, Y., Manson, J.A.E., Jolliet, O., 2001, "Life Cycle Assessment o f Biofibers Replacing Glass Fibers as Reinforcement in Plastics," *Resource Conversation Recycling*, **33**[4], 267-287.

Liu, Z-M., Wang, F-U., Wang, X-M., 2004, 'Surface Structure and Dynamic Adhesive Wettability of Wheat Straw', Wood and Fiber Science, **36** [2], 239-249.

Smith, N. Personal communication.

Bare, J.B., 2002, 'Developing a Consistent Decision-Making Framework by Using the U.S. EPA's TRACI,' Annual AICHE conference.

Franklin Associates LTD, 2003, Life Cycle Services, ATHENA Sustainable Materials Institute Documentation.

2001, NREL (National Renewable Energy Laboratory) U.S. Life-Cycle Inventory Database.

Soroushian, P., Aouadi, F., Chowdhury, H., Nossoni, A., Sarwar, G., 2004, 'Cement-bonded Straw Board Subjected to Accelerated Processing' Cement&Concrete Composites, **26**, 797-802.

11DBMC International Conference on Durability of Building Materials and Components
ISTANBUL, Turkey 11-14 May 2008

Experimental Study of Geopolymer Concrete Resistance to Sulphuric Acid Attack

Robert Munn [1]
Xiujiang Song [2]
Marton Marosszeky [3]

T 18

ABSTRACT

Geopolymer concrete is well known for its high chemical resistance. Class F fly ash was firstly activated in a highly alkaline sodium silicate environment to obtain Geopolymer, which was further mixed with silica sand and aggregates to make Geopolymer concrete. The resultant Geopolymer concrete developed a compressive strength of 70MPa at age of 28 days, after being initially cured at 70ºC for 12 hours. The Geopolymer concrete samples at age of 28 days were exposed in either a 10% sulphuric acid for 8 weeks or a 1% sulphuric acid for up to 18 months. The visual appearance, mass loss, residual compressive strength and acid neutralisation depth were measured regularly. The mass loss was about 5% while the compressive strength reduction was about 30%. It was also found that the sulphuric acid attack on Geopolymer concrete samples in a 10% acid for 8 weeks resulted in an equivalent degree of loss (in terms of compressive strength reduction and acid neutralisation depth) as the Geopolymer concrete samples exposed to a 1% acid for about 14 months. Finally the SEM-EDS analysis indicated that acid affected Geopolymer concrete mainly consisted of silica gel, differing from the aluminosilicate structure present in the original Geopolymer before acid exposure test. Moreover, the silica gel in the acid affected Geopolymer concrete was still able to fulfil a cementitious function, which agrees with the observation that the Geopolymer concrete samples remained structurally intact after sulphuric acid exposure.

KEYWORDS

Geopolymer, Alkaline activated material, Acid resistance, Fly ash

[1] Building and Construction, Research and Consultancy, Brookvale, NSW, Australia 2100, Phone +61 2 9939 7533, Fax +61 2 9939 7544, r.munn@bcrc.com.au
[2] Building and Construction, Research and Consultancy, Brookvale, NSW, Australia 2100, Phone +61 2 9939 7533, Fax +61 2 9939 7544, t.song@bcrc.com.au
[3] Building and Construction, Research and Consultancy, Brookvale, NSW, Australia 2100, Phone +61 2 9939 7533, Fax +61 2 9939 7544, m.morosszeky@bcrc.com.au

1 INTRODUCTION

An accelerated test is normally used in a laboratory for acid resistance test of concrete. The Los Angles County [Redner et al 1998] examined the sulphuric acid resistance of concrete by exposing concrete samples to a 10% sulphuric acid for 8 weeks. When tested by a similar method, fly ash based Geopolymer concretes have been noted for its high acid resistance [Song et al 2005]. The low mass loss of about 5% agrees with the acid exposure testing undertaken by Bakharev (2005). Both tests indicated the high resistance to degradation of Geopolymer concretes in acidic environments and suggested it be a promising binder against acid attack in sewer pipes as corroded sewer pipes have been reported to have the sulphuric acid concentration of about 1% [Thistlethwayte et al 1972]. In order to reduce assessment time, it is important to compare the acid resistance of Geopolymer concretes in a 1% sulphuric acid for a relative long term with the results in an accelerated test (i.e. in a 10% sulphuric acid) for a short term. The comparison is made by examining four properties; visual inspection, mass loss, compressive strength reduction and acid neutralisation depth after acid exposure of Geopolymer concrete samples.

2 MATERIALS AND METHODS

2.1 Materials and Geopolymer Concretes

The Geopolymer binder used in this investigation was synthesised from two Class F fly ashes and a mixed alkaline activator of sodium hydroxide and sodium silicate. The median particle size was 20.4 micrometers for the fly ash No.1 and 3.14 micrometers for the fly ash No.2. The sodium hydroxide solution had a concentration of 14M (moles per litre). The sodium silicate solution was composed of 30.6% of SiO_2, 9.5% of Na_2O and 59.9% of H_2O by mass. Table 1 shows the mix design of the Geopolymer concrete used in this experiment. All raw materials were locally sourced and met the requirement of respective Australian standards.

Table 1. Mix proportions of the Geopolymer concrete.

Material types	*Fly ash No.1*	*Fly ash No.2*	*Aqueous NaOH*	*Aqueous Na_2SiO_3*	*Silica sand*	*10mm Basalt*
Mass ratio (%)	13.5	4.9	3.4	4.1	26.2	47.9

Geopolymer concrete samples were cast in 50mm steel cubic moulds and wrapped with plastic sheets. The samples were initially cured at 70˚C for 12 hours in an oven followed by air curing in the laboratory at approximate 23˚C. The resultant Geopolymer concrete had its 28-day compressive strength of 70MPa. Samples of a Portland cement based concrete with the similar strength grade served as the reference concrete.

2.2 Acid Exposure Tests

A modified ASTM C267 test method was used for the sulphuric acid exposure tests.

Sulphuric acid solution, 10% or 1% by mass, was directly diluted from 98% concentrated sulphuric acid with tap water. The ratio of the sulphuric acid volume to specimen exposure area was fixed at 8 ml/cm^2 [Chang et al 2005]. The acid concentration was monitored via titration and adjusted weekly.

Masses and compressive strengths of concrete cubes were monitored regularly over the acid exposure period. At age of 28 days, twelve Geopolymer concrete cubes were immersed in a 10% sulphuric acid solution. Three cubes were weighed for mass change and the rest were crushed to test for residual

compressive strength after being immersed in sulphuric acid for 1, 4 and 8 weeks. Meanwhile, eighteen cubes were immersed in 1% sulphuric acid solution, three of them for monitoring mass change and the rest for crushing to determine compressive strength after acid exposure of 2, 6, 9, 12 and 18 months.

The acid neutralisation depth was determined using the following method. At age of 21 days, twelve concrete cubes were coated with an acid resistant epoxy and only one surface of each sample was left uncoated for exposure to acid. The samples were immersed in a 10% or a 1% sulphuric acid when the concrete was 28 days old. At the end of each period of acid exposure (in the 10% acid after 1, 4, 8 and 12 weeks and in the 1% acid after 2 and 14 months) two concrete cubes were removed and rinsed slightly with tap water.

The epoxy coat was ground off and the exposed concrete surfaces were then sprayed with the Universal pH Indicator to detect the degree of alkalinity by colouration. Three distinct layers, in the colour of pink, yellow and light blue, were normally observed on the sample sections with the pH value of approximate 3, 7 and 11 respectively. The depth of the pink and yellow layers was measured from the acid exposed surface. The average of six readings taken from two samples was recorded as the "acid neutralisation depth" after each period.

2.3 Microscopic Examination and Analysis by SEM-EDS

Acid affected Geopolymer samples were prepared and a Hitachi 4500II Scanning Electronic Microscopy (SEM) coupled with an Oxford Energy-dispersive Spectrometer (EDS) was used to examine microscopic images and to undertake the semi-quantitative analysis of the chemical composition of the resultant Geopolymer.

3 RESULTS

3.1 Visual Inspection

In distinct contrast to the damage of the control concrte observed in Figure 1, samples of Geopolymer concretes remained intact after acid exposure, though some fine cracks has developed. This comparison demonstrated that the Geopolymer matrix is far superior to Portland cement paste in resisting sulphuric acid attack.

Figure 1. Visual comparison of concrete samples after acid exposure (left) Control concrete in a 10% sulphuric acid for 4 weeks, (middle) Geopolymer concrete in a 10% sulphuric acid for 8 weeks, (right) Geopolymer concrete in a 1% sulphuric acid for 18 months.

3.2 Mass Change

Further to the visual inspection, the mass change (average of three concrete cubes) was compared with that of the control concrete in Figure 2. The negative values indicate mass loss. The mass change in Figure 2 is shown as proportion of the dry mass, which is intended to eliminate the influence of adsorbed water in the open pores in the acid affected layer.

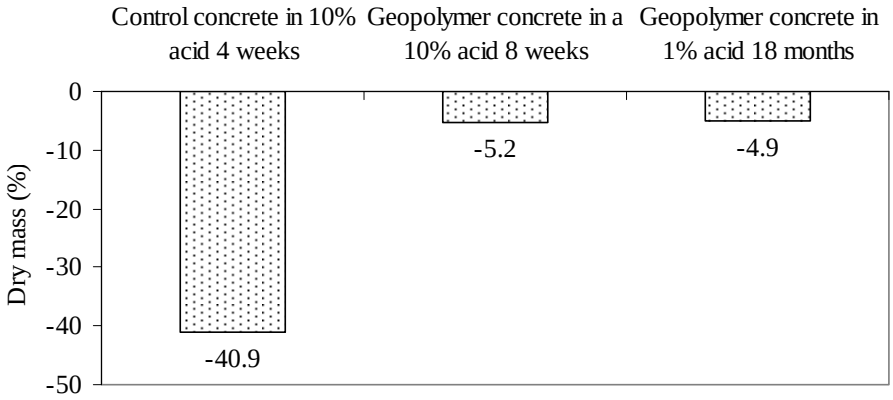

Figure 2. Dry mass comparison of concrete samples after sulphuric acid exposure for different times (negative values indicate mass loss).

In addition to the dry mass change as shown in Figure 2, the change of saturated surface dry (SSD) mass was also measured. It is intended to observe the relationship between the SSD mass loss and the exposed time. The SSD mass loss was the average of three concrete cubes tested in accordance to ASTM C267.

As seen in Figure 3, Geopolymer concretes lost mass at higher rates at the beginning of the acid exposure test, whilst the mass loss became almost constant after a longer period of acid exposure (i.e. in the 1% sulphuric acid after 224 days).

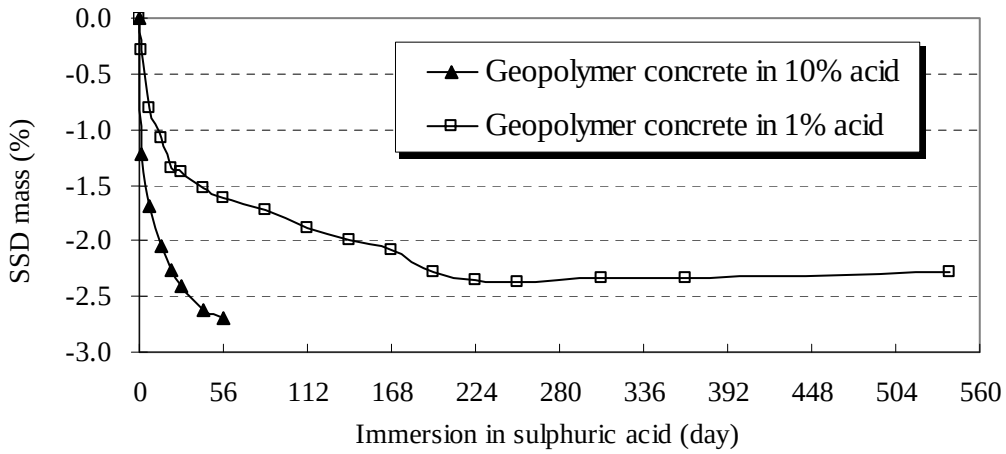

Figure 3. SSD mass comparison of Geopolymer concretes in a 10% sulphuric acid for 8 weeks vs in a 1% sulphuric acid for 18 months (negative values indicate mass loss).

Unlike the dry mass, the SSD mass contains the absorbed free water in the open pores. As a result, the total SSD mass loss in Figure 3 is smaller than the dry mass loss in Figure 2. However the advantage of using SSD mass change is to monitor the mass change with exposure time without risking any undesired side effects on the samples during the immersing-drying process.

3.3 Compressive Strength Reduction

Following immersion in sulphuric acid, the Geopolymer concrete cubes were tested to detect the change in structural characteristics as indicated by changes in the compressive strength. The residual strengths, expressed as a percentage to the initial strength (before acid exposure) and after exposure in 1% or 10% sulphuric acid are compared in Figure 4. It was observed that Geopolymer concretes recorded strength reductions of about 33% after 8 weeks exposure in a 10% acid. It took about 14 months to achieve the same percentage of strength reduction in a 1% sulphuric acid.

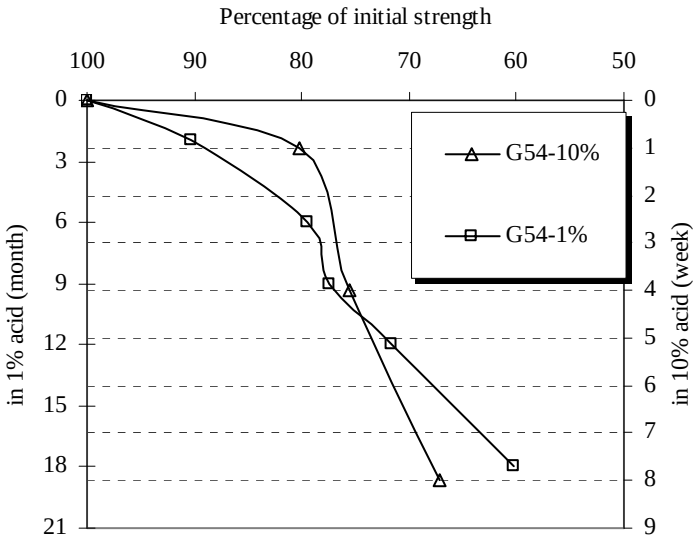

Figure 4. Residual compressive strength comparison of Geopolymer concretes in a 10% sulphuric acid for 8 weeks vs in a 1% sulphuric acid for 18 months.

3.4 Acid Neutralisation Depth

The hardened Geopolymer concretes were found to be alkaline with pH values of about 11. However, this alkaline environment was gradually neutralised when the material came into contact with acid solutions. The Universal pH indicator was employed to identify the changes in alkalinity in Geopolymer concrete matrices after exposure to acid.

As shown in Figure 5, after exposure in sulphuric acid, the alkalinity of the outer concrete layer (bottom
part) was neutralised as demonstrated by the pink colouration. The concrete in this layer was considered to be “severely affected” because its pH value dropped to 3 (the lowest range of the Universal indicator) or lower. By contrast, concrete at the far inner layer (top part) had a pH value of about 11, close to its original alkalinity. The concrete in this layer is thus called “unaffected”. The transition layer was a very thin yellowish layer with a pH value in the range of 6 ~ 7. The thickness of the “severely affected” and “transition” layers are described as the “neutralisation depth” because the pH values in these two layers have been reduced to a value less than 7 after acid exposure.

It was noticed that the neutralisation depth in Figure 5 was about 10 mm after the Geopolymer samples were exposed in a 10% sulphuric acid for 8 weeks. A similar depth of about 11 mm was measured after exposure in a 1% sulphuric acid for 14 months.

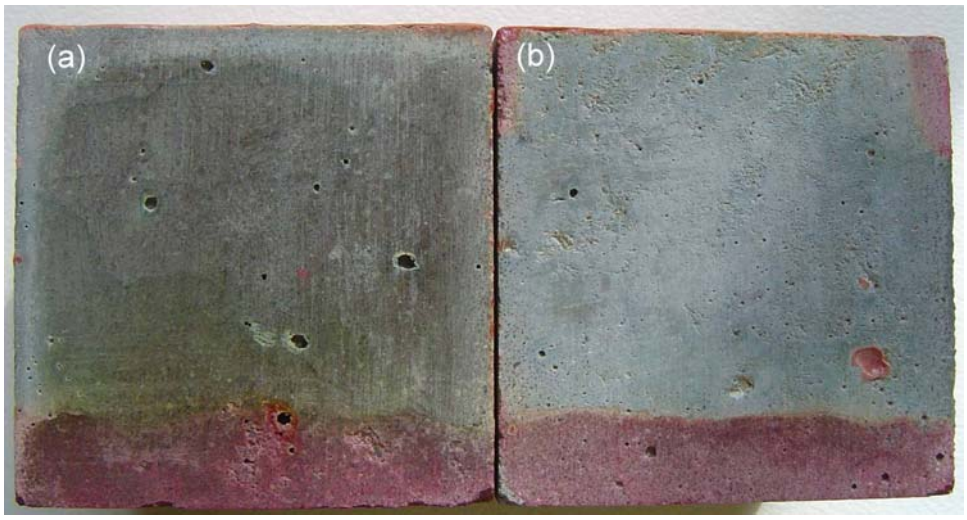

Figure 5. Acid neutralisation depth comparison of Geopolymer concretes (a) in a 1% sulphuric acid for 14 months vs (b) in a 10% sulphuric acid for 8 weeks.

4 DISCUSSION

As seen in Figure 1, Geopolymer concretes have high sulphuric acid resistance. The mass losses reported in Figures 2 and 3 agree well with observations by visual inspection. The reason for the significant mass loss observed in the control concrete is simply due to the dissolution of the paste by the acid. The mass decrease of Geopolymer concrete is considered to be mainly due to the dissolution of minor components from Geopolymer concrete. In general, it was found that the mass loss of the Geopolymer concrete after sulphuric acid attack was quite small. The dry mass loss was about 5% (Figure 2) while the SSD mass loss was about 3% (Figure 3).

This lower mass loss in current research on Geopolymer concretes agrees with the published data in the technical literature, such as about 1.13% [Wastiels et al 1993], about 3% [Silverstrim et al 1997], and about 2% [Bakharev 2005] over similar periods of exposure.

Despite the small mass losses of the Geopolymer concretes (about 5%), the compressive strength reductions were much more significant. This appears to suggest that the microstructure of Geopolymer in the outer layer of the concrete samples must have been damaged to some extent due to sulphuric acid attack, although the visual appearance of the Geopolymer cubes in Figure 1 still remained unaltered.

As can be seen in Figure 4 the Geopolymer concretes show similar trends in strength reduction as compared by the respective lines for 1% and 10% acid. It was observed that Geopolymer concrete in a 10% acid for 8 weeks had a similar strength reduction to those samples of the same concrete soaked in a 1% acid for about 14 months. Moreover, the neutralisation depth of Geopolymer concrete in a 10% sulphuric acid for 8 weeks is similar to that in a 1% acid for 14 months as shown in Figure 5. The similar behaviours of the strength reduction shown in Figure 4 and the acid neutralisation depth shown in Figure 5 indicate that exposing concrete to a 10% sulphuric acid for 8 weeks is indeed a valid accelerated test method and may replace the traditional acid exposure method, based on exposure in 1% acid for 14 months to determine the acid resistance of concrete.

The microstructural images and elements of Geopolymer gel, before and after acid exposure, are compared in Figures 6 and 7. As seen in Figure 6, the original Geopolymer looks sound and has three primary elements typically silicon, aluminium and sodium. These features were changed substantially as a result of acid attack. The images in Figure 7 show that after acid attack the material looks soft and

has very low sodium content but contained more silicon and sulphur compounds. The appearance of sulphur indicates the ingress of sulphuric acid into Geopolymer matrix. The important finding from Figure 7 is the silica gel that has the appearance of a "sponge-like substance". However it still maintains a cementitious function binding the aggregate and undissolved fly ash particles. This explains the visual observation that the outer layer of Geopolymer concretes in Figure 1 still had a stable shape after being neutralised by sulphuric acid.

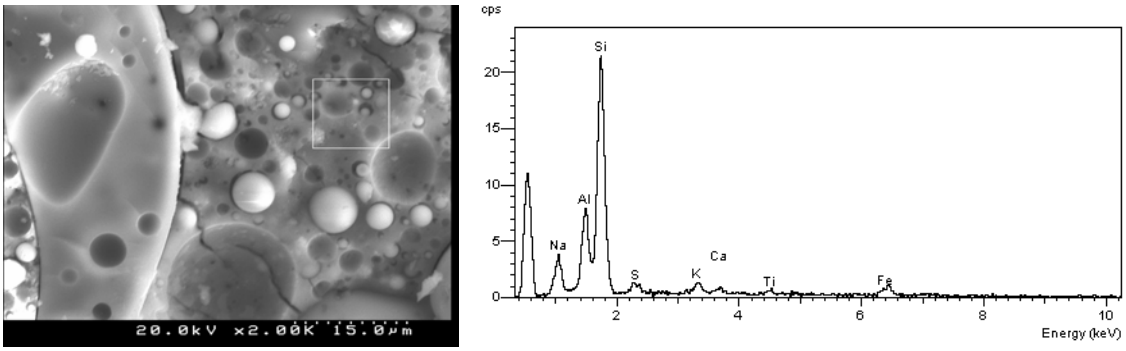

Figure 6. SEM-EDS of Geopolymer gel before acid exposure.

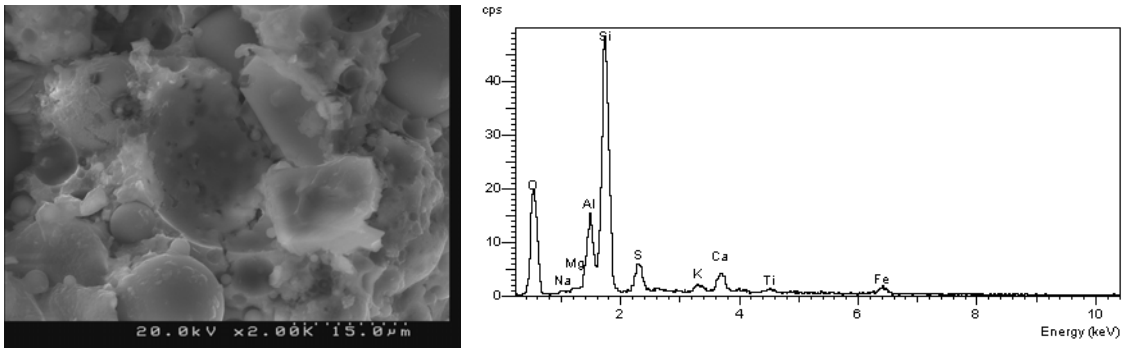

Figure 7. SEM-EDS of acid affected Geopolymer gel.

4 CONCLUSIONS

This test confirmed that Geopolymer concrete has high sulphuric acid resistance following immersion in a 10% acid for 8 weeks or in a 1% acid for 18 months. Sulphuric acid has penetrated into Geopolymer matrix about 10mm. However, Geopolymer test samples remained structurally intact. The mass loss was about 5% but the compressive strength was typically reduced about 30%.

Exposing concrete to a 10% sulphuric acid is proposed as a valid accelerated test method to examine the acid resistance of concrete. It was found that immersion in a 10% acid for 8 weeks achieved similar results, in terms of compressive strength reduction and acid penetration depth, to immersion in a 1% sulphuric acid solution for about 14 months.

The SEM-EDS analyses showed that due to acid attack, the aluminosilicate Geopolymer has converted into a soft sponge-like substance with much less sodium but more silicon and sulphur compounds present. This residual silica gel is still able to maintain the function of a cementitious binder in the acid affected Geopolymer concrete.

REFERENCES

Bakharev, B., 2005, 'Resistance of Geopolymer materials to acid attack,' *Cement and Concrete Research,* **35**(4), 658-670.

Chang, Z-T,. Song, X-J, Munn, R., & Marosszeky, M., 'Usng limesone aggregates and diferent cement for enhnacing resistance of concrete to sulphuric acid attack', *Cement and concrete research*, **35**[8], 1486-1494.

Redner, J. A., His, R. P., Esfandi E., T., & Sydney, R., 1998, *Evaluation of Protective Coatings for Concrete,* County Sanitation Districts of Los Angeles County, Calfonia, August.

Silverstrim, T., Rostami, H., Clark, B. & Martin, J., 'Microstructure and properties of chemically activated fly ash concrete', The 19th International Cement Microscopy Association, Cincinnati, OH, USA, 1997, pp.355-373.

Song, X. J., Marosszeky, M., Brungs, M., & Munn, R., 'Durability of fly ash based Geopolymer concrete against sulphuric acid attack', International Conference 10th on Durability of Building Material and Components, Lyon, France, 17-20 April 2005, TT3-48.

Thistlethwayte, D. K. B., Davy, W. J. & Technological Standing Committee on Hydrogen Sulphide Corrosion in Sewerage Works (Australia). 1972, *The control of sulphides in sewerage systems*, Sydney, Butterworths.

Wastiels, J., Wu, X., Faignet, S., & Patfoort, G., 'Mineral polymer based on fly ash', Proceedings of the 9th International Conference on Solid Waste Management, Philadelphia, PA, USA, 14-17 November, 1993.

Physical and Mechanical Properties of Rubberized Concretes

Albéria C. Albuquerque [1]
Luiz Carlos P. Silva Filho [2]
João Luiz Calmon [3]
Moacir A. S. Andrade [4]

T 18

ABSTRACT

The incorporation of tire rubber granules into concrete has been studied for several researchers as an alternative disposal of this material. In this study, a control mix (without rubber addition) was set against mixes with rubber aggregates, obtained from shredded non-reusable tires, in five treated and untreated contents (2%, 4%, 6% 8% and 10% rubber contents). An acrylic polymeric admixture was used in order to improve the bonding between rubber and cement paste. The samples were investigated about the mechanical and physical properties, including permeability. It was verified that both rubber content and surface treatment did not influence significantly the properties. Such findings have demonstrated that the contents of non-reusable tire rubber can have viable applications, because there was no damage to the physical and the mechanical properties of the concrete.

KEYWORDS

Tire Rubber, Concrete, Permeability, Mechanical Properties

[1] Federal Center of Technological Education of Mato Grosso, Civil Buildings Department, Mato Grosso, Brazil, Phone +55 65 33143566, Fax 65 36611643, albuquerque@ccivil.cefetmt.br
[2] Federal University of Rio Grande do Sul, Civil Engineering Department, Rio Grande do Sul, Brazil, Phone +55 51 33083333, Fax 51 33083333, lcarlos@cpgec.ufrgs.br
[3] Federal University of Espírito Santo, Civil Engineering Department, Espírito Santo, Brazil, Phone +55 27 33352174, Fax 27 33352650, calmont@npd.ufes.br
[4] FURNAS Centrais Elétricas S/A, Civil Engineering Center, Goiás, Brazil, Phone +55 62 32396300 Fax 62 32396500, concreto@furnas.com.br

1 INTRODUCTION

The environmental and social gains are important features for using non-usable tire rubber in concrete mixes. Some of them are the reduction of natural resources consuming and the diminution in ecological and public health problems, due to increasing amounts in waste tires at the dumps.

The incorporation of tire rubber into cement-based composite has been studied for several researchers all around the world in order to get different applications. Benefits such as increase of the tenacity and the capacity of deformation have been observed. However, the studies have shown that the main problem in the combination of these materials is the bond weakness between the cement matrix and tire rubber particles, which is revealed through the reduction of the material strength [Topçu [1995]; Toutanji [1996]; Khatib & Bayomy [1999]; Hernández-Olivares *et al.* [2007]].

Rubber tire is a non-hydrophilic material and, consequently, when incorporated to fresh concrete it creates a barrier against the cement paste which obstructs the hydration reaction in the interfacial transition zone (Segre, 1999). Tests were conducted in order to modify the rubber surface and to improve the cement paste / rubber interface. Some successful tests were observed; meantime, these surface treatments imply higher material and processing cost [Rostami *et al*. [1993]; Li *et al*. [1998]; Segre & Joekes [2000]; Marques et al. [2005]].

A certain amount of caution is advisable at this point since making comparisons between the studies is a hard task because several authors carried out diverse types, dimensions and methods to incorporate tire rubber into cement based materials. At the same time, there are some points in which there is some agreement:

- tire rubber fiber (from retreading) or granules (from non-reusable tire grinding);
- maximum 4.8 mm - size tire rubber particles use;
- tire rubber use in replacement of aggregate volume fractions;
- steady the cement consumption value and the water/cement ratio;
- workability control through plasticizer admixtures.

The present work is part of a wide-ranging project, developed in the Technological Center of Civil Engineering of Furnas Centrais Elétricas S/A, in the context of the Civil Engineering Post-Graduation Program at the Federal University of Rio Grande do Sul (UFRGS), being financially supported by the Electrical Power National Agency (ANEEL) and by the National Council of Scientific and Technological Development (CNPq –Brazil).

2 EXPERIMENTAL PROCEDURE

Pilot tests were performed in order to assess the most suitable way of incorporating the tire rubber into the concrete in a way that could minimize the decrease in compressive strength and maximize the reduction in elasticity modulus. The results have indicated that the use of tire rubber particles in place of sand volume fractions contributes more to attenuate the reduction of mechanical properties than a total aggregate replacement [Albuquerque et al. 2004]. This behavior was also observed by Akasaki et al. [2001].

Subsequent experiments on tire rubber particles replacing 5% to 25% of the sand volume have indicated a higher increasing resistance about 0% and 10%. It was also observed that tire rubber granules promote better workability than tire rubber fibers and that among surface treatments, the acrylic polymer was the most efficient for attenuating the diminution of strength [Albuquerque et al. 2005].

In this work, one of the the goals was to identify the ideal tire rubber content (until 10%) that replaces the sand volume. Therefore, the following independent variables were selected:

- tire rubber content in place of sand volume: 0%, 2%, 4%, 6%, 8% e 10%;
- maximum 1.5mm - size tire rubber granules;
- treated and untreated with acrylic polymer tire rubber granules;
- age of test.

The material description, examined properties and mixtures are presented in the Tables 1 and 2, respectively. Variance analyses (ANOVA) were performed in order to calculate significant differences on the obtained results. According to ANOVA, the averages will be statistically different if *p-value* < 0.05, and the more this difference will be the more the *F value* with reference to *critical F* will be.

Table 1. Materials.

Materials	*Investigated Properties*
Portland cement - Ordinary Portland Cement	Compressive strength
Coarse aggregate – 19 mm and 38 mm MSA - Crushed granite	Modulus of deformation
Fine aggregate- Natural sand	Splitting tensile strength
Crumbed tire rubber - Granules : ∅ 1.5 mm	Axial tensile strength
Chemical admixtures - Super plasticizer and Air entrainer admixtures	Specific gravity
Admixture based acrylic polymer for surface treatment of tire rubber	Permeability

Table 2. Properties of Fresh Concrete.

Mix		*Tire Rubber Contents (% of aggregate volume)*										
		0%	*2%*		*4%*		*6%*		*8%*		*10%*	
		C	*U*	*T*	*U*	*T*	*U*	*T*	*U*	*T*	*U*	*T*
Composition data (kg/m³)	*Portland cement*	306	310	306	305	307	309	304	307	305	308	304
	Water	151	153	151	150	151	152	150	151	150	151	150
	Natural sand	624	620	612	597	601	593	593	576	572	565	558
	Crumbed tire rubber	-	5.8	5.7	11.5	11.6	17.4	17.2	23.2	23.0	29.0	28.6
	19 mm crushed aggregate	533	540	533	531	535	538	529	535	531	536	530
	38 mm crushed aggregate	678	687	678	676	681	685	974	681	676	683	674
	Super plasticizer admixture	-	-	-	-	0.03	0.07	0.03	0.10	0.06	0.12	0.09
	Air entrainer admixture	0.09	0.08	0.07	0.06	0.06	0.04	0.04	0.03	0.03	0.02	0.02
	Acrylic polymer	-	-	1.219	-	2.454	-	3.642	-	4.876	-	6.072
Properties of Fresh Concrete	*W/C ratio*	0.49	0.49	0.49	0.49	0.49	0.49	0.49	0.49	0.49	0.49	0.49
	% mortar w/ entrained air	52.92	52.98	52.13	52.70	52.63	52.37	52.79	52.03	52.10	53.13	52.20
	Fineness module	5.81	5.82	5.82	5.83	5.83	5.84	5.84	5.85	5.85	5.86	5.86
	% sand in mass	34.0	34.0	34.0	34.0	34.0	34.0	34.0	34.0	34.0	34.0	34.0
	Slump (mm)	60	50	50	60	60	50	50	55	60	31	60
	Entrained air (%)	4.0	3.4	3.2	4.0	3.6	3.0	3.8	3.0	3.4	4.0	3.6
	Specific gravity (kg/m³)	2282	2308	2273	2262	2274	2292	2248	2267	2248	2261	2229

C – Control ; U – Untreated rubber granules ; T – Treated rubber granules.

3 EXPERIMENTAL RESULTS AND DISCUSSION

Mechanical Properties

All mix proportions behaved as usual cement-based materials. It was observed the influence of the age on the increase of mechanical properties on all specimen. This understanding seems to corroborate results obtained by analysis of variance (ANOVA) whose *p-value* < 0.05 and great *F value* as seen on Figs 1 to 4.

Mixes with treated and untread tire rubber have shown similar performance. There were few differences, but ANOVA test demonstrated that *surface treatment* have no or little effect on the

studied properties. This indicates *p-value* > 0.05 (Figs 1 and 2) or *p-value* < 0.05 but with low *F values* (Figs 3 and 4).

According to the tests, when there is an increase of *rubber content* the mechanical properties of concrete tends to reduce. However, this fact is not significant enough as it was confirmed by ANOVA results: p-value < 0.05 but low F values (Figs 1 to 4). In this investigation was possible to obtain until 10% of reduction on elasticity modulus having little effect on tensile and compressive strength.

Entrained air ratings strongly affects concrete mechanical properties. Some researchers have detected that bigger tire rubber content makes entrained air content gets higher levels. (Albuquerque et al. 2004b, Macedo 2005). In this work, all mixes were inoculated with entrainer air admixture in order to obtain 3% to 4% of air entrained content. This procedure was taken to minimize the action of this variable on the results. Table 2 shows that the entrainer air admixture amount is inversely proportional to the tire rubber content.

Other authors have shown that compressive strength of rubberized concretes usually drops in a drastic way when rubber content is raised (Eldin e Senouci 1993, Topçu 1997, Turantzine at al. 2003). Keeping strength levels is important because it can avoid the increase in cement consumption and, consequently, put final product costs up. On the other hand, elasticity modulus reduction can be suitable for structures in which toughness and strainability are required. In this present work was possible to combine elasticity modulus reduction and resistance levels maintenance.

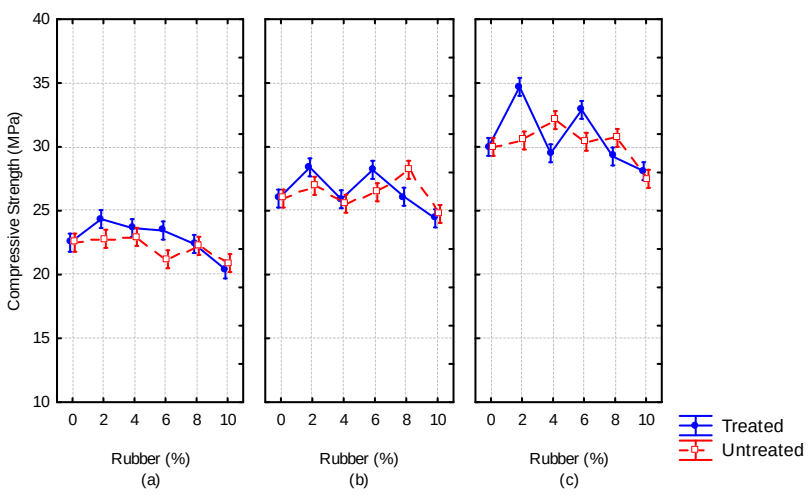

Variable	*Square sum*	*Degree of Freedom*	*Mean square*	*Critical F*	*F relation*	*P-value*
Rubber content	86.80	5	17.36	2.36	15.03	0.000000
Age	772.86	2	386.43	3.14	334.60	0.000000
Treatment	4.01	1	4.01	3.99	3.48	0.066944
Error	72.76	63	1.15			

Figure 1. Compressive strength x Rubber content x Surface treatment – Results at (a) 7 days, (b) 28 days and (c) 91 days.

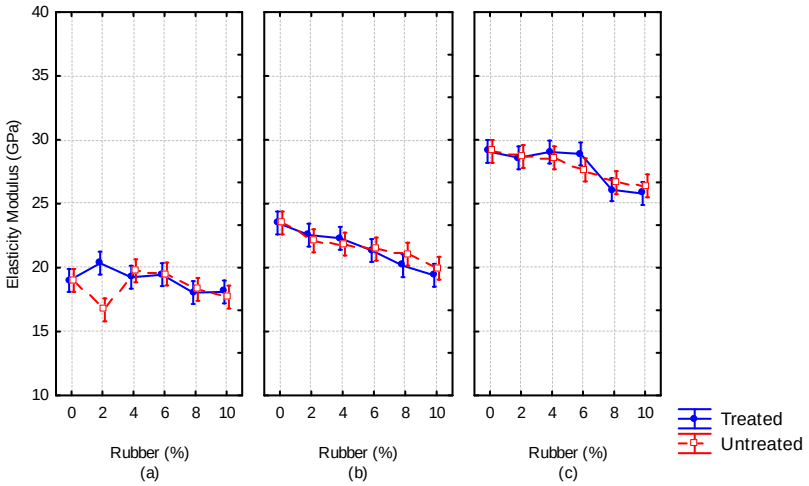

Variable	*Square sum*	*Degree of Freedom*	*Mean square*	*Critical F*	*F relation*	*P-value*
Rubber content	65.01	5	13.00	2.36	17.81	0.000000
Age	1047.03	2	523.51	3.14	717.23	0.000000
Treatment	0.52	1	0.52	3.99	0.71	0.403279
Error	45.98	63	0.73			

Figure 2. Elasticity modulus x Rubber content x Surface treatment – Results at (a) 7 days, (b) 28 days and (c) 91 days.

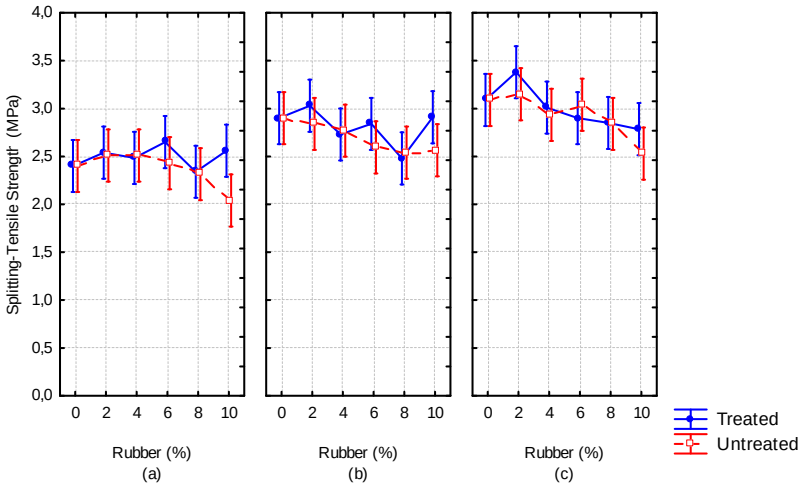

Variable	*Square sum*	*Degree of Freedom*	*Mean square*	*Critical F*	*F relation*	*P-value*
Rubber content	1.0993	5	0.2199	2.36	6.24	0.000092
Age	3.4907	2	1.7454	3.14	49.54	0.000000
Treatment	0.1964	1	0.1964	3.99	5.57	0.021344
Error	2.2196	63	0.0352			

Figure 3. Splitting-tensile strength x Rubber content x Surface treatment – Results at (a) 7 days, (b) 28 days and (c) 91 days.

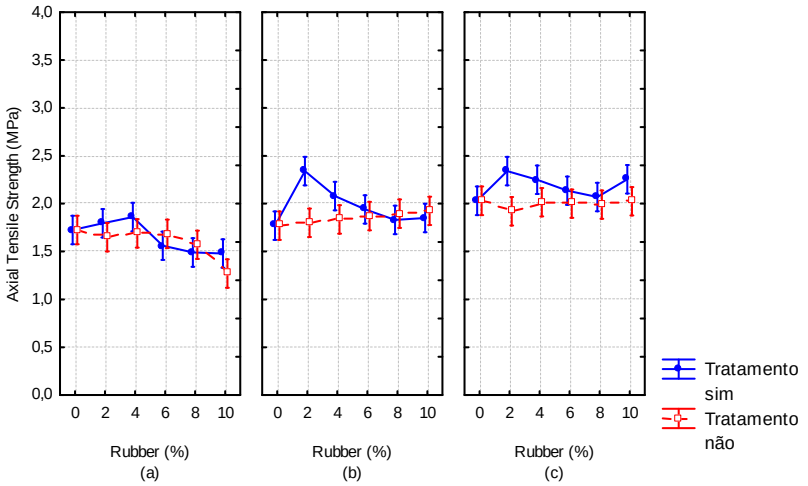

Variable	*Square sum*	*Degree of Freedom*	*Mean square*	*Critical F*	*F relation*	*P-value*
Rubber content	0.3300	5	0.0660	2.36	3.19	0.012552
Age	2.6195	2	1.3098	3.14	63.25	0.000000
Treatment	0.2532	1	0.2532	3.99	12.23	0.000868
Error	1.3046	63	0.0207			

Figure 4. Axial tensile strength x Rubber content x Surface treatment – Results at (a) 7 days, (b) 28 days and (c) 91 days.

Physical Properties

Age and surface treatment have had no significant influence on specific gravity or permeability of the studied concretes. ANOVA test reports p-value > 0.05 or small F value (Figs 5 and 6).

Rubber content have had significant influence on specific gravity or permeability. ANOVA test reports p-value < 0.05 (Figs 5 and 6).

Some specific gravity reduction was expected as a result of the increase of the rubber tire content. This behavior is common because of two factors: 1) tire rubber specific gravity is smaller than sand specific gravity and 2) when rubber tire content increases, it makes the entrained air content get higher levels. In this investigation, as the entrained air content in the concrete mixes was controlled, any variance observed can be attributed exclusively to the difference found between rubber tire and sand relative density. In this case, only the 10% rubber tire content mixes have demonstrated specific gravity significantly lower than the one in the control mix.

All mixes presented pressurized water permeability at level of 10-13 m/s to 10-12 m/s, that can be considered good numbers and were also observed by other researchers for conventional concretes (FURNAS, 1997). According to Choinska et al. (2007), the fluid flow occurs in a porous network, that includes, not necessarily connected, the initial porosity of the material and the micro and macro cracking induced by mechanical loads, environment and time effects.

In this investigation, the mixes with tire rubber exhibited smaller pressurized water permeability than the control (Figure 6). This behavior indicates that rubberized concretes may have greater resistance to the penetration of aggressive agents and hence greater durability than conventional concrete. However, tests of durability over time are needed to confirm their performance.

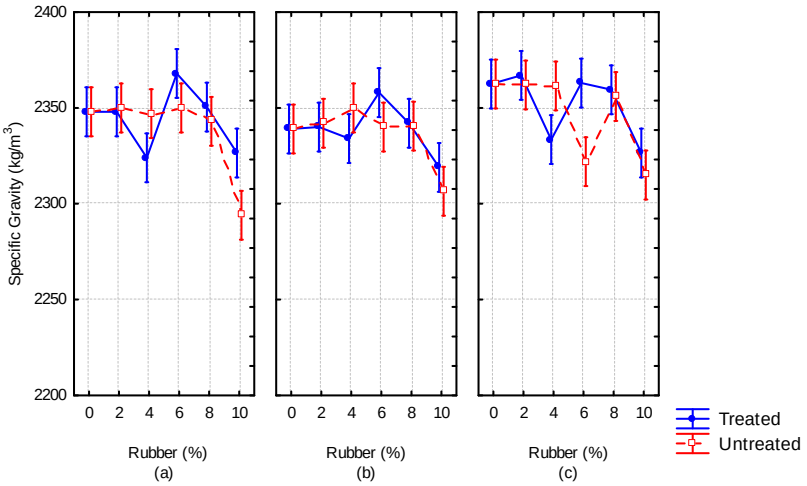

Variable	*Square sum*	*Degree of Freedom*	*Mean square*	*Critical F*	*F relation*	*P-value*
Rubber content	12124	5	2425	2.36	15	0.000000
Age	1718	2	859	3.14	5	0.006862
Treatment	356	1	356	3.99	2	0.140002
Error	10027	63	159			

Figure 5. Specific gravity x Rubber content x Surface treatment – Results at (a) 7 days, (b) 28 days and (c) 91 days.

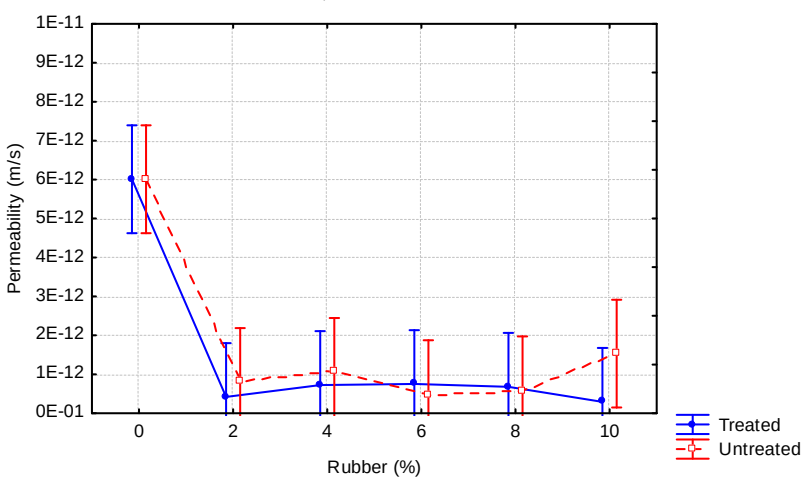

Variable	*Square sum*	*Degree of Freedom*	*Mean square*	*Critical F*	*F relation*	*P-value*
Rubber content	0.0000	5	0.0000	2.81	28.4539	0.000000
Treatment	0.0000	1	0.0000	4.45	0.66350	0.426591
Error	0.0000	17	0.0000			

Figure 6. Permeability x Rubber content x Surface treatment – Results at 91 days.

4 CONCLUSIONS

In this paper, rubberized concrete mixes as well as concrete control were examined, under different contents and treated and untreated surface treatment. After analising all results, the following conclusions are feasible :

- *rubber content and surface treatment* have had no significant influence on mechanical and physical properties of the concrete;
- the use of tire rubber granules in substitution of until 10% of sand volume was viable and do not imply any harm to physical and mechanical properties;
- mixes with treated and untreated tire rubber have similar performance;
- was not possible to evaluate the effect of the surface treatement with acrylic polymer;
- the use of tire rubber particles tends to reduce the pressurized water permeability.

ACKNOWLEDGMENTS

The authors thank very much to the FURNAS Centrais Elétricas S/A, in special the Laboratory of Concrete team. The authors are also grateful to the Electric Energy National Agency (ANEEL) and to National Council of Scientific and Technological Development (CNPq-Brazil), being that latter well-known in Brazil as organizations that supports research projects, and that has contributed to the development of this study by providing financial support.

REFERENCES

Akasaki JL., Nirschl GC., Fioriti CF., 2001. *Análise experimental da resistência à compressão do concreto com adição de fibras de borracha vulcanizada*, Anais do 43º Congresso Brasileiro do Concreto, Foz do Iguaçú.

Albuquerque AC., Andrade MAS., 2004. *Use of Tire Rubber as Concrete Aggregate*. 7th ICCTDC, Malásia.

Albuquerque AC., Hasparyk NP., Andrade MAS., 2004(b). *Investigation of Different Treatments in Tire Rubber with a View to Concrete Application.* RILEM, Barcelona.

Albuquerque AC., Hasparyk NP., Andrade MAS., Andrade WP., 2005. *Polymeric Admixtures as Bonding Agent between Tire Rubber and Concrete Matrix.* ACI - Special Publication 229, Michigan/USA, p. 479-496.

Choinska M., Khelidj A., Chatzigeorgiou G., Pijaudier-Cabot G., 2007. *Effects and interactions of temperature and stress-level related damage on permeability of concrete*, Cem Concrete Res, 37;79-88.

Hernández-Olivares F., Barluenga G., Parga-Landa B., Bollati M., Witoszek B., 2007. *Fatigue behaviour of recycled tyre rubber-filled concrete and its implications in the design of rigid pavements*. Const Build Mat, 21.

Eldin N., Senouci AB., *Rubber-Tire Particles as Concrete Aggregate*, J Mater Civil Eng, 1993;5(4).

FURNAS – 1997. *Concretos: Massa, Estrutural, Projetado e Compactado com Rolo* – Ed. Pini, São Paulo-SP.

Khatib ZK., Bayomy FM., 1999. *Rubberized Portland Cement Concrete*, J Mater Civil Eng, 1, 11(3)206-213.

Li Z, Li F, Li JSL, 1998. *Properties of concrete incorporating rubber tyre particles*, Mag Concrete Res, 50(4).

Macedo DCB, 2005. *Estudo da viabilidade técnica de placas pré-moldadas utilizando borracha de pneu em matrizes cimentícias*. Dissertação de Mestrado. Universidade Federal de Goiás. Brazil.

Marques ML., Marques AC., Trigo APM., Akasaki JL., 2005. *Avaliação do comportamento da argamassa adicionada de diferentes granulometrias de borracha após o tratamento com NaOH*, 47º IBRACON, Brazil.

Rostami H., Lepore J., Silverstrim T., Zandi I., *Use of Recycled Rubber Tyres in Concrete,* Concrete 2000: Economic and Durable Construction Through Excellence - Scotland, UK, 1993;2;391-399.

Segre N., 1999. *Reutilização de borrachas de pneus usados como adição em pasta de cimento*, PhD Thesis.

Segre N., Joekes I., 2000. *Use of tire rubber particles as addition to cement paste*.Cem Concrete Res, 30.

Topçu IB, *The properties of rubberized concretes*, 1995. Cement and Concrete Research, 25(2); 304-310.

Toutanji HA., 1996. *The Use of Rubber Tire Particles in Concrete to Replace Mineral Aggregates*, Cem Concrete Comp, 18(2);135-139.

Turatsinze A., Bonnet S., Granju JL., 2003. Cement-based materials incorporating rubber aggregates: shrinkage length changes, Proceedings of International Symposius Brittle Matrix Composites 7. Warsaw, pp.359-368.

Durability of Mortars Prepared with Innovative Eco-compatible Binders

Raffaele Cioffi [1]
Francesco Colangelo [1]
Luciano Santoro [2]

T 18

ABSTRACT

The possibilities of using waste materials from different manufacturing activities in the preparation of innovative mortar and concrete is the aim of this paper. Two kinds of waste were identified: marble sludge, from marble processing, and cement kiln dust. The use of these wastes was proposed in different percentages both as an addition to and as substitution of cement, for the preparation of Self Levelling Mortars. As comparison, two mixtures containing natural aggregates were also prepared, one using limestone powder as a mineral addition and the other with no addition. A total of sixteen different mixtures were prepared containing 10, 20 and 30% of wastes compared to the total quantity of aggregates and 10, 15 and 20% compared to the amount of cement. The two residues were characterised from a chemical, physical and morphological point of view. The prepared mixtures were then studied in terms of their properties both in fresh and in hardened state. In particular, compressive strength, water absorption and capillary absorption tests were conducted on the mortars cured for 28 -day water curing and after 500-day immersion in a sodium and magnesium sulphate solution.

KEYWORDS

Cement kiln dust, Sulphate solution, Marble sludge, Mechanical properties, Self-levelling mortars

[1] University of Naples Parthenope, Department of Technology, Naples 80143, Phone +39 081 5476732, Fax 081 5476777, raffaele.cioffi@uniparthenope.it, colangelo@uniparthenope.it
[2] University of Naples Federico II, Department of Chemistry, Naples 80125, Phone + 39 081 674028, Fax 081 674033, santoro@unina.it

1 INTRODUCTION

Nowadays, the ecological trend aims at limiting the use of natural resources in the field of building materials. Thus, there is an increased interest in the use of alternative materials , mainly wastes coming from industrial activities, which presents significant advantages in economic, energetic and environmental points of view.

Only in Italy, the concrete industry uses about 100 million tons of aggregates with an extremely high environmental impact [CRESME Research Centre, Italy, 2003].

Moreover, the Italian legislation decree 22/97 was passed with the aim of incentivating the recycling of industrial solid waste as alternative to landfill disposal. Subsequently, the Italian ministerial decree DM 5/2/98 supplied the technical indications needed to implement the recycling procedures and indicated the preliminary treatments to be carried out for different types of wastes. In particular, one of the main form of recycling suggested is their reuse in road foundations.

Two important aspects need consideration : although the possibilities of using waste in the preparation of road foundations is great, it is unimaginable that all types of waste could be used in such applications. Some particular categories of wastes, with specific physico-chemical and mechanical characteristics, would be under utilized were they to be used in such applications.

For instance, residues such as marble sludge from stony material manufacturing and cement kiln dust are characterised by an average diameter in the order of a few microns at the end of the industrial processes from which they come from [Colangelo, F *et al.* 2004.1]. This important physical characteristic makes them potential candidates for use in the production of self-levelling mortars (SLMs) and self-compacting concretes (SCCs). These building materials can be compacted under their self-weight, with no external action, providing considerable time and energy saving [Collepardi, M., 2002, Ouchi, M. & Okamura, H., 1999, Colangelo, F. *et al.* 2004.2].

These products require much higher quantities of fine components than traditional concretes, making them potentially capable of incorporating large quantities of fine wastes [Colangelo, F. *et al.* 2003]. Very often the production of SCC envisages an expensive material such as powdered limestone as a filler. Therefore, recycling fine wastes in SLMs and SCCs has both environmental and economical advantages, provides incentives for their development currently hampered by a higher cost in respect to ordinary concretes.

The feasibility of the waste material recycling process is particularly influenced by the fulfilment of the economic, technical and normative aspects for each field of use. In fact, once the economic convenience has been assessed, the experimentation must verify that the physico-chemical characteristics attained after treatment are suitable to the specific proposal for which they are intended.

This work proposes the use of industrial wastes, such as marble sludge from stony material manufacturing activities and cement kiln dust, in an innovative Self Levelling Mortar preparation. A limestone filler has also been used to provide a reference benchmark.

The aim of the work is to investigate the influence of the above wastes on the rheology of fresh mortars and on the physical-mechanical properties of hardened self-levelling mortar before and after immersion in a sodium and magnesium sulphate solution.

2 MATERIALS AND METHODS

The cement employed was CEM II/A-LL 42,5 R, according to European Standards EN 197/1, made by the Cementi della Lucania factory (Potenza, Italy), and its chemichal composition is shown in table 1.
The aggregate used was a 4 mm maximum size siliceous sand. Powder limestone employed had about a 99% $CaCO_3$ content .

The superplasticizer (SP) used was an acrylic one with 40% solid content and a specific gravity of 1.2 kg/dm^3. It was used in all SLM mixtures and its amount was proportioned to ensure a constant workability. The water content of the superplasticizer was considered during the mix-design phase.

To enhance stability, an inorganic Viscosity Modifying Agent (VMA) was also used in all SLM mixtures

Table 1. Chemical composition of cement.

SiO_2	Fe_2O_3	Al_2O_3	CaO	MgO	SO_3	L.O.I.
20.55%	3.20%	4.90%	60.95%	1.64%	2.76%	5.73%

The extraction and processing of stony material inevitably results in the production of a huge mass of wastes of different natures and characteristics [Colangelo, F. *et al.* 2003., Miletic, S. *et al.* 2003]. In fact, stone extraction produces a yield in blocks which usually does not exceed 60% of the extracted material, so waste accumulation is a major problem, causing damage to environment and landscape. Their possible recycling would thus offer sensible and multiple advantages, as reported by Colangelo et al. 2004.1.

In this work, the sludges from twenty Southern Italian marble processing factories was characterized and proposed for use as a filler in SLM.

The results of chemical and physical characterization performed on different samples show the presence of $CaCO_3$ in weight percentages ranging between 96% and 98%, as well as more modest percentages of SiO_2 (0.8-1.2%), Al_2O_3 (0.1-0.3%), Fe_2O_3 (0.06-0.09%), MgO (0.6-0.8%), etc. The sludge employed is characterized by a diameter at 90% equal to 10.1 μm.

The main constraints in recycling industrial waste are linked to the qualitative constancy of the following parameters: chemical composition, very small size and absence of heavy metal.

Marble sludge morphological analysis was performed by a scanning electron microscope, (SEM) ands as shown in figure , SEM images reveal an irregular shape of all particle, some of them are also sharp-edged.

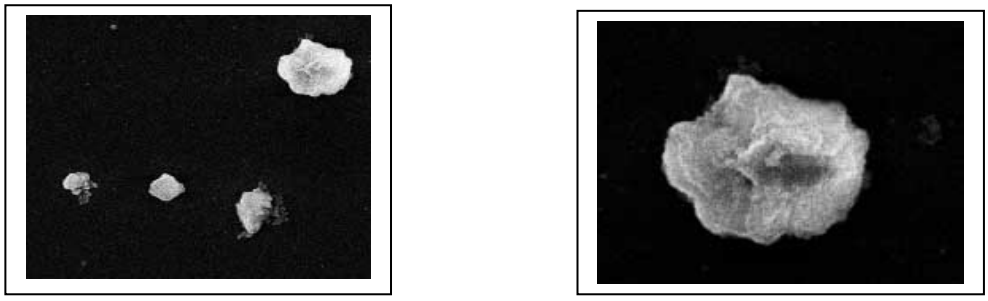

Figure 1. SEM pictures of marble sludge (left), SEM particular of marble sludge (right).

Cement kiln dust (CKD) is a waste generated by the cement industry. It is a powder mainly composed of micron-sized particles collected from electrostatic precipitators during the manufacture of cement clinker. The CKD chemical composition and particle size depend on the raw materials used to produce clinker, fuels and kiln types. The USA Environmental Protection Agency (EPA) estimated that the amount of CKD could range from 0 to 25% of the clinker produced, depending on the above-mentioned factors.

A huge quantity of CKD is produced every year throughout the world; for example, USA alone produces 4 to 12 million tons [Duchesnea, J. & Reardonb, E.J. 1998]. In this work CKD supplied by Cementi della Lucania, Potenza, Italy, was used. The CKD chemical composition is shown in Table 2.

Table 2. Chemical composition of CKD.

SiO_2	Fe_2O_3	Al_2O_3	CaO	MgO	SO_3	Na_2O	K_2O	L.O.I.
14.65 %	2.13 %	4.75 %	41.72 %	1.12 %	0.72 %	0.9 %	0.6 %	32.30 %

The fineness of CKD power is quite high with a Blaine specific surface area greater than 5000 cm^2/g . CKD grading curve and density population are shown in Figure 3.

The morphologic analysis was performed by a scanning electron microscope, as shown in figure 2. Both images show that CKD particles seems quite regular and rounded.

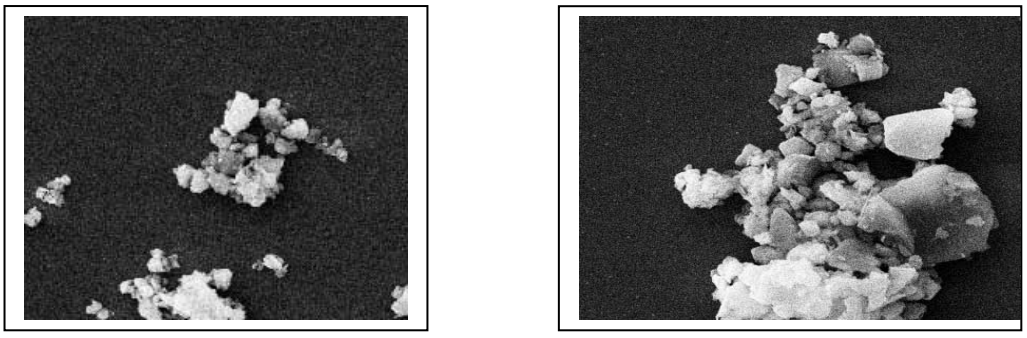

Figure 2. SEM picture of CKD (left) and SEM particular of CKD (right).

Twelve mixtures were prepared employing, alternatively CKD and marble sludge both in addition to cement, in substitution of the natural siliceous aggregate, and in replacement of cement. A reference mixture (B), without industrial waste, was also prepared.

Moreover, mixtures containing marble sludge, in partial substitution of the sand (in addition to cement), were compared with similar powdered limestone based ones.

Table 3 shows mixture proportions for all the mortar specimens. In this table the first part of the mixture code gives information on the waste and the addition contained in the mortar (S for marble sludge, L for limestone, C for cement kiln dust), the second letter (A or S) indicates the usage of the CKD, sludge and limestone (addition to cement or its substitution).

Table 3. Mortar mixture proportion.

	Composition, g						
Mix code	Sand	CEM II	CKD	S	L	SP	VMA
B	1350	500				23.2	0.6
CS10	1350	450	50			23.2	0.6
CS15	1350	425	75			24.5	0.6
CS20	1350	400	100			26.0	0.6
CA10	1215	500	135			26.4	0.6
CA20	1080	500	270			26.4	0.5
CA30	945	500	405			33.2	0.6
LA10	1215	500			135	27.5	0.6
LA20	1080	500			270	27.5	0.6
LA30	945	500			405	27.5	0.6
SS10	1350	450		50		22.7	0.6
SS15	1350	425		75		22.9	0.6
SS20	1350	400		100		23.6	0.6
SA10	1215	500		135		26.0	0.5
SA20	1080	500		270		26.4	0.5
SA30	945	500		405		27.3	0.5

In order to prepare all the mortar mixtures, a 5 dm^3 mixer was used. After mixing, fresh mortar was employed for the determination of slump flow. The slump flow test measures the mean diameter of concrete spread after the removal of the slump cone. A spread of at least 250 mm is required for self-levelling mortar [Bignozzi, M.C. *et al.* 2003]. All the mixtures prepared were characterized by slump values according to this limit and did not show any segregation phenomena. By varying the amount of superplasticizer the same value of 260 mm was reached for all mixtures.

To evaluate the strength development, compressive tests were carried out after 28 days of water curing. The specimens were kept during the first 24 hours in a curing chamber at 20 ±1 °C and R.H. ≥ 98 %; after this period, they were removed from the mold and cured in water, maintained at 20±2 °C, until the test age. The specimens were dried in air for half an hour before testing. Four specimens were tested for each data point. A 150 kN capacity compressive testing machine was used according to Standard EN UNI 196/1.

Water and capillary absorption were also measured, according to the procedure Italian Normal -11/85 Water absorption and capillary absorption of the mortars.

The above two kinds of tests were carried out after 500-day immersion in a sulphate solution and at fixed times during sulphate immersion period, respectively. Furthermore, the compressive stregth was also determine after 500-day immersion in a sulphate solution. Hardened specimens for each mix were immersed in a combined sulfate solution (mixed solution of 10% sodium sulfate and 10% magnesium sulfate). The cylinders were fully immersed in solutions in stainless steel baths. The cylinder was kept apart at a distance of 5 cm. The stainless steel baths were covered in order to minimize the evaporation. The solutions were replaced once a month with fresh ones and the pH was maintained at 7 during 500-day test.

3 RESULTS AND DISCUSSION

Table 3 reports the amounts of superplasticizer (SP) added to the mixtures in order to obtain the same workability without changing the water to cement ratio. It can be seen that in the case of the mixtures containing CKD in partial substitution of cement, CS10 required the same amount of SP as reference mixture B. Furthermore, in the case of CS15 and CS20 mixtures the amounts of SP are slightly higher than that employed in mixture B.

When the same waste was used in addition to cement (in partial substitution of the aggregates) the fresh behaviour of the mixtures was different. The increase in the amount of SP was equal to about 14%, 14% and 43% for the mixtures CA10, CA20 and CA30, respectively. In particular, the CA30 mixture was very cohesive and no addition of viscosity modifying agent was required.

The amount of SP added to the mixtures SS, prepared with marble sludge in partial substitution of cement, was similar to that required for the reference one. While in the case of the SA mixtures, prepared with marble sludge in addition to cement (in partial substitution of aggregates), the increase in the amount of SP was equal to 12%, 13.7% and 17.2% for mixtures SA10, SA20 and SA30, respectively. The SA mixtures required smaller amounts of SP than the CA ones. This is probably due to the smaller mean diameter of CKD particles. These are 3.62 and 4.45 μm for the CKD and marble sludge, respectively.

Particle morphology did not significantly affect workability, probably due to the very small dimensions of waste particles. In fact, it is well known that the workability of mixtures significantly depends on the shape of the larger particles.

Figures 3 and 4 report the compressive strength results after 28-day water and 500-day immersion in sulphate solution of all the kinds of mortars. After 28-day water curing (Figure 3) a significant increase in mechanical strength is observed with respect to the reference mortars in the case of waste being employed in addition to cement (in partial substitution of aggregates).

It is important to point out that, after 500-day immersion in sulphate solution, the increases in compressive strength for the mixtures CS10 and SS10 compared to the reference mixture was equal to 8% and 5%, respectively. After 28 day of curing in water all the CS and SS mixtures showed values of compressive strength lower than that of the B mixture, as reported by other authors for the concrete containing CKD [Shoaiba, M.M. *and al.* 2000, Ravindrarajah, R., 1992].

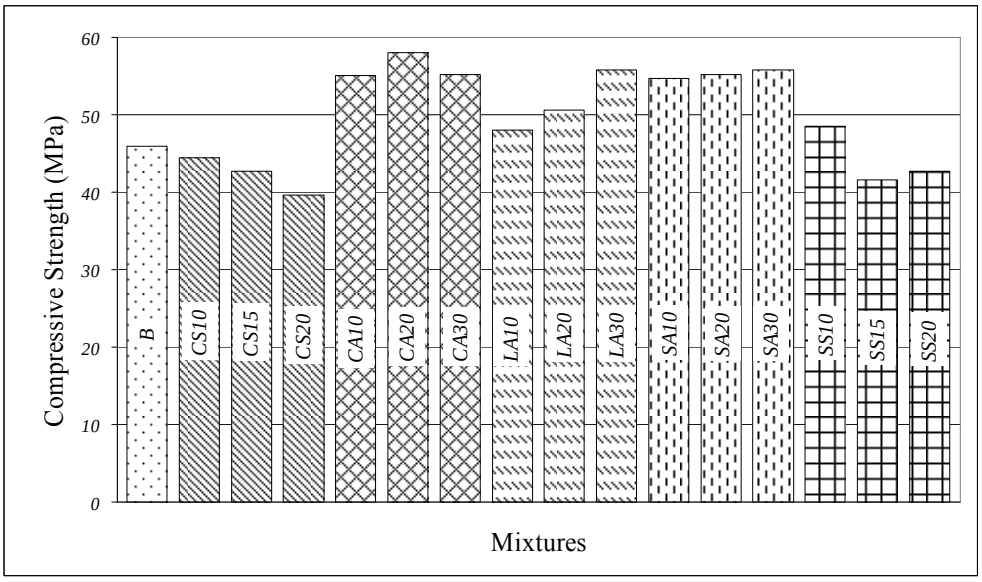

Figure 3. Compressive Strength after 28-day water curing.

In comparison to L mixtures, prepared with limestone filler, the SA mixtures showed higher values of compressive strength for all the amounts of wastes added both after 500-day immersion in sulphate solution (Figure 4) and 28-day water curing (Figure 3).

Figure 5 reports the values of the capillary absorption development with age during sulphate solution immersion. These data are very useful to predict the behaviour of mortars and concrete in the presence of capillary phenomena which can be responsible for decay caused by aggressive solutions.

Lower water capillary absorption coefficient values were observed for the mixtures containing the higher amount of wastes employed in addition to cement and in partial substitution of aggregates (CA20, CA30, SA20, SA30) compared to reference mixture B. Whereas when the wastes were used in partial substitution of cement the same coefficients were similar or slightly higher than those of the mixture B.

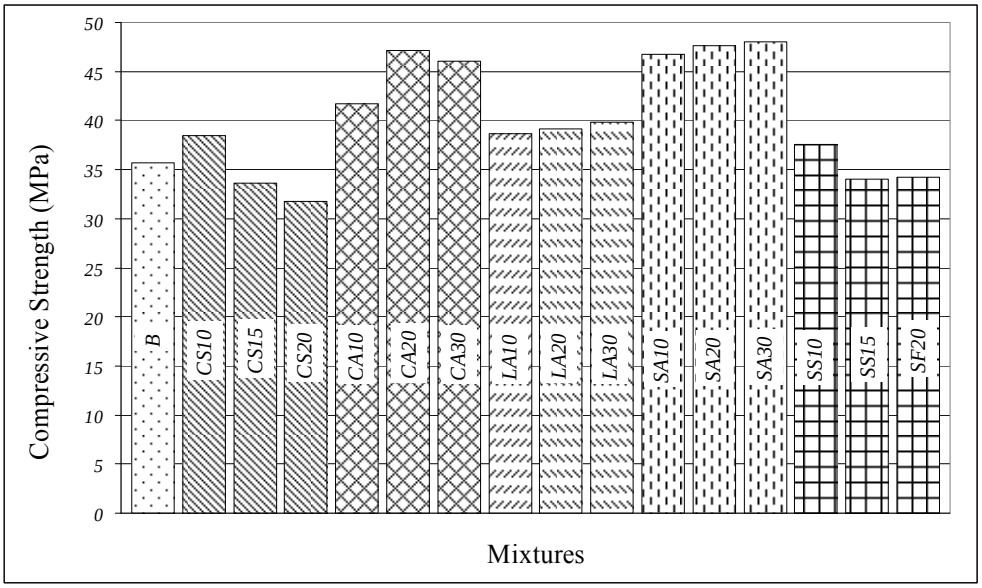

Figure 4. Compressive Strength after 500-day immersion in sulphate solution.

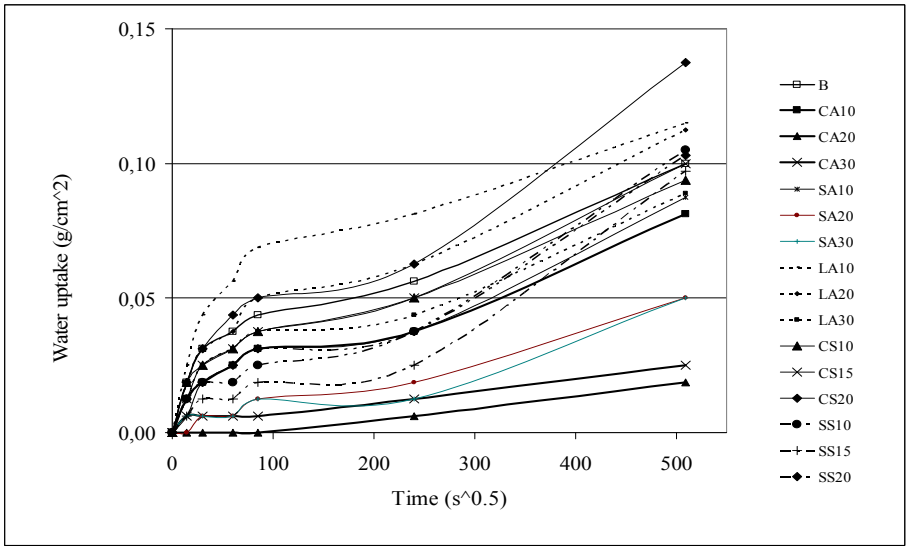

Figure 5 Capillary absorption development during the immersion in sulphate solution.

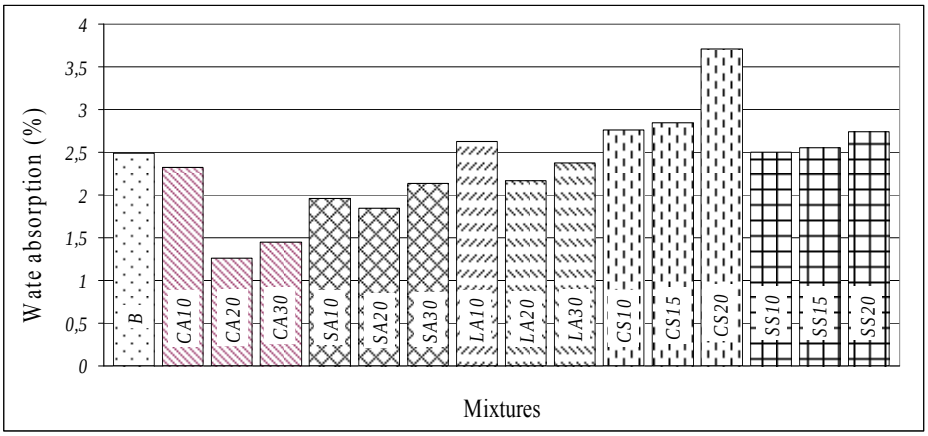

Figure 6. Water absorption after 500-day of immersion in sodium sulphate solution.

The values of water absorption coefficient after immersion in sulphate solution are shown in Figure 6. Also in these cases the presence of wastes in addition to cement improve the properties of hardened mortars in terms of lower permeability when immersed in water. In fact, it is well known that the values of water accessible porosity is an important factor in assessing the durability of mortars and concrete. In particular, slightly and much lower values were observed for SA and CA mixtures respectively. In the case of the CA20 mixture a 50% decrease was observed.

3 CONCLUSIONS

All the experimental data show that it is possible to use both selected wastes in the manufacturing of self-levelling mortars. Furthermore, in many cases, the addition of the wastes improves the physical and mechanical properties. These results are of great importance because this kind of innovative mortar requires large amounts of fine particles.

When the wastes are employed in addition to cement and in partial substitution of aggregates, amounts up to 30% can be used to provide mortars of higher physical and mechanical properties than the reference ones. Furthermore, attention to water demand must be taken into account, especially in the case of addition of CKD.

The use of the wastes in partial substitution of cement is possible for lower amounts than the cases described above. The maximum substitutions are 10% in the case of marble sludge, while the presence of CKD results in a decrease of properties for all quantities used.

Furthermore, experiments conducted on these specimens immersed in sulphate solution show that the presence of CKD and marble sludge in the manufacture of self-compacting concrete make mortars with high chemical resistant to aggressive solutions.

ACKNOWLEDGMENTS

The authors wish to thank the National Research Programme PRIN 2006 for financial support of this work.

REFERENCES

Bignozzi M.C., Franzoni E., Sandolini F. 2003. 'Waste Materials employed in the manufacture of self-compacting mortars' Proc. of the 4th International Congress Added Value and Recycling of Industrial Waste, L'Aquila – Italy, pp. 24-27.

Colangelo, F. Pandolfo, R., Cioffi, R., Masi, S., 2004. 'Recycling of industrial wastes in geo-environmental applications', *Recycling*, **8** (4) 109-113.

Colangelo F., Marroccoli M., Cioffi R., Molfetta M. 2004. 'Influence of mineral additions on the properties of Self-Compacting Concrete', Proc. of the International Congress IMTCR, Lecce – Italy, pp. 153-161.

Colangelo, F., Marroccoli, M., Cioffi, R., 2003. 'Reuse marble sludges as artificial aggregates in sel-compacting concrete', Proc. Seminar: Researches and technologies in treatment and recycling of wastes, ECOMONDO, Rimini, , 126-131.

Collepardi, M., 2003. 'New concrete', Enco s.r.l., Spresiano, Italy.

Duchesnea, J., Reardonb, E.J., 1998 'Determining controls on element concentrations in cement kiln dust leachate', *Waste Management*, **18** 339-350.

Martini, A., et al. 2003. 'Precast concrete, industry and marketing', CRESME.

Miletic, S., Ilic, M., Milosevic, M., Mihajlov, A., 2003. 'Building Materials based on waste stone sludge', Proceedings Intern. Conf. WASCON 2003, Inasmet, 323-328.

Ouchi, M., & Okamura H. 1999. 'Self-compacting concrete development, Present and future' Proc. 1st Int. Symposium on Self-compacting Concrete, RILEM, Sweden, pp. 212-220.

Ravindrarajah, R., 1992. 'Usage of cement kiln dust in concrete', *International Journal of Cement Composites and Lightweight Concrete*, **4** (2) 95-101.

Polarization Behavior of Carbon Fiber as an Anodic Material in Cathodic Protection

Mahdi Chini [1]
Roy Antonsen [2]
Øystein Vennesland [3]
Jon Håvard Mork [4]
Bård Arntsen [5]

T 18

ABSTRACT

In impressed current CP systems, an insoluble anode is used on the surface or within the concrete structure, and in some parts an electrical connection between the anode and rebars are established. The most frequently and widely used anode material is titanium covered with noble metal oxides. Meanwhile much work is carried out to replace the anode material or improve the application technique such as using conductive coatings and paintings. In this regard, carbon fiber meshes have been introduced as an alternative for the last decade.

By studying the Pourbaix diagram of carbon, one could conclude that it is a not a stable material in alkaline solution at its own corrosion potential. Unfortunately, scientific work and publications concerning electrochemical properties of carbon embedded in concrete are scarce. Hence, a series of experiments have been designed and carried out in order to improve knowledge of its behavior as anode.

As a first step, polarization behavior of carbon was investigated and the results are presented in this paper. The polarization curves, from 20 mV up to 5000 mV polarization, indicate that carbon has a passive-active-passive behavior in alkaline solution. It is in passive condition up to 500 mV polarization and then enters to active area up to 2500 mV. From that point, it starts the second passive condition. The effect of addition of 1% and 3% chloride ions has also been investigated. The addition of chloride ions into the solution would increase the corrosion rate of the carbon but it seems that it is due to the characteristic of chloride. In other words, the amount of chloride has a very slight effect on the corrosion.

KEYWORDS

Carbon fiber, Corrosion, Cathodic protection, Alkaline solution, Polarization

[1] Norut Teknologi, Narvik 8514, Norway, mahdi.chini@tek.norut.no
[2] Norut Teknologi, Narvik 8514, Norway, roy.antonsen@tek.norut.no
[3] Department of Structural Engineering, NTNU, Trondheim 7491, Norway, oystein.vennesland@ntnu.no
[4] Maxit Group AB, Oslo, Norway, jon-havard.mork@maxit-group.com
[5] Norut Teknologi, Narvik 8514, Norway, baard.arntsen@tek.norut.no

1 INTRODUCTION

During the last decades, widespread problems of deterioration of civil engineering structures have been experienced in many countries. The major portion of these structures consists of reinforced concrete and the corrosion of reinforcing steel is the principal cause of deterioration. Therefore the registered need for rehabilitation and repair and the associated costs is a matter of great concern for those responsible for assessment and maintenance of affected structures. Due to this matter, several protection and prevention methods and technique have been developed.

Cathodic protection and prevention are one of the effective techniques in this regard. Cathodic protection (CP) of steel reinforcement in concrete structures, as schematically illustrated in Fig.1, is obtained by applying a direct current through the concrete from an anode system which is usually applied on the concrete surface. Anode material is connected with the positive terminal of a low voltage direct voltage source towards reinforcement; in this case rebars are acting as cathode and connected with the negative terminal [Pedeferri 1996]. The anode material is perhaps the most critical component of a CP system, because it serves to distribute the protective current across the structure and provides the locations for anodic reactions to take place in lieu of the reinforcing steel. Therefore, while the system is in service, the anode, instead of the reinforcing steel, will degrade. There are some materials which are used as anode. Although the most frequently used anode material is titanium mesh covered by activated metal oxides, as a more recent anode material the carbon fiber meshes have been used for some years in some countries.

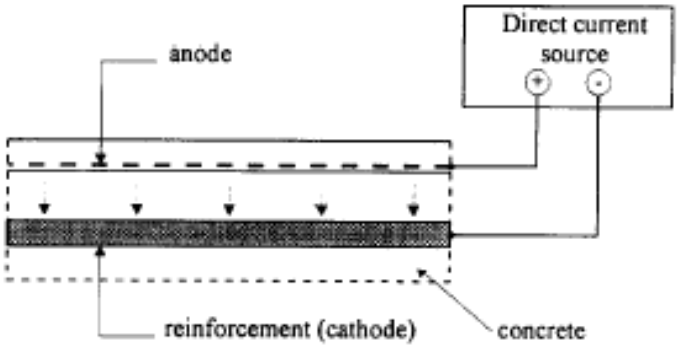

Figure 1. Schematic illustration of CP system [Pedeferri 1996].

By studying the Pourbaix diagram of carbon (graphite), which is illustrated in Fig.2, one could conclude that it is a not a stable material in alkaline solution at its own corrosion potential [Pourbaix 1974]. Unfortunately the published papers about this anode material are scarce [Chini 2007]. Hence, a series of experiments have been designed and applied in order to improve knowledge of its behavior as anode. In this paper the first results are presented. Potentiostatic behavior of carbon in simulated concrete pore solution and also in present of different amount of chloride would be illustrated.

2 TEST DESIGN

The first property of carbon interested was corrosion current density in different polarization potentials (E-I plot). In order to reach that, the corrosion current density of carbon was measured in different anodic polarization potential from open circuit corrosion potential as 20, 40, 60, 100, 150, 300, 500, 750, 1000, 1500, 2000, 2500, 3500, 5000 mV. These measurements were operated by Electrochemical Interface 1287 from Solartron Company. By using Solartron 1287 the potentials were continuously applied and the data was stored. A titanium mesh was used as counter electrode and the reference electrode was SCE (Hg/Hg_2Cl_2 in saturated KCl).

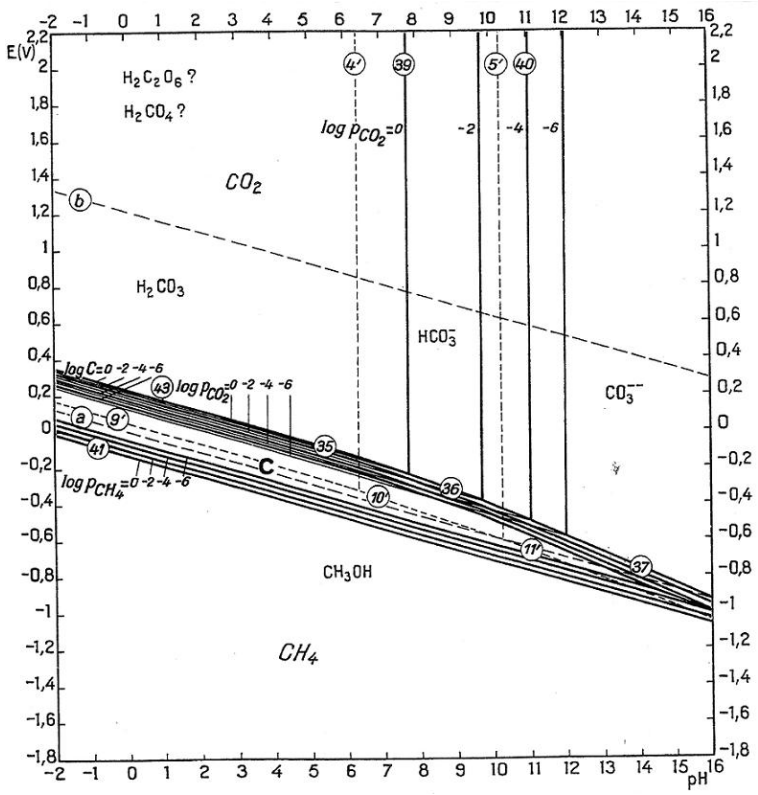

Figure 2. Pourbaix diagram of Carbon.

Since existence of chloride ion plays an important role in corrosion process, effect of different amount of chloride were also investigated. Therefore measurements were also made in chloride contents of 0, 1 and 3 percent of solution volume.

3 SPECIMENS AND SOLUTION PREPARATION

In CP system the carbon is used as mesh. The applied anode material is a continuous, highly flexible mesh woven of carbon fibers. This makes the anode easy to install. The threads may consist of thousands of filaments with a thickness of 7 µm of each filament. In a common industrial product, a thread consists of 6000 or 24000 filaments which make a very narrow thread [Vennesland et al. 2005]. Since it was impossible to find a carbon rod from industry, it is very difficult to measure the corrosion current density among longitude of fibers, due to the fact that it is impossible to measure the exact surface area of exposed fibers. Although some techniques have been introduced [Mork et al. 2006], there are still uncertainties on measurement of surface area. Hence, in order to have more accurate active surface area after various experiments, the cross section corrosion monitoring was designed.

In this method 10 bundles of 24000-filament thread were cast in a non-conductive epoxy. Transparent pipe was used as mold in order to monitor the accuracy of the procedure. After molding, the specimen was cut and ground to have a smooth and clear cross section. This method gives a surface area of around 10 mm^2. A chamber was also designed for this method. It is a rectangular prism with dimensions of 15cm length, 12.5 cm width and 12 cm depth which is filled by 1.75 liter solution. Figure 3 shows the final version of sample. New samples were made by cutting 4 to 5 millimeters from the head of the used specimen. Therefore 20 cm length specimen could be used for several experiments.

To reach a stable status in polarization the following procedure was applied. First, system was run in open circuit condition for 2 hours to stabilize the carbon in this alkaline solution. After that anode was

polarized between 30 minutes and 150 minutes, depends on polarization value. All procedure was monitored and saved by Solartron 1287.

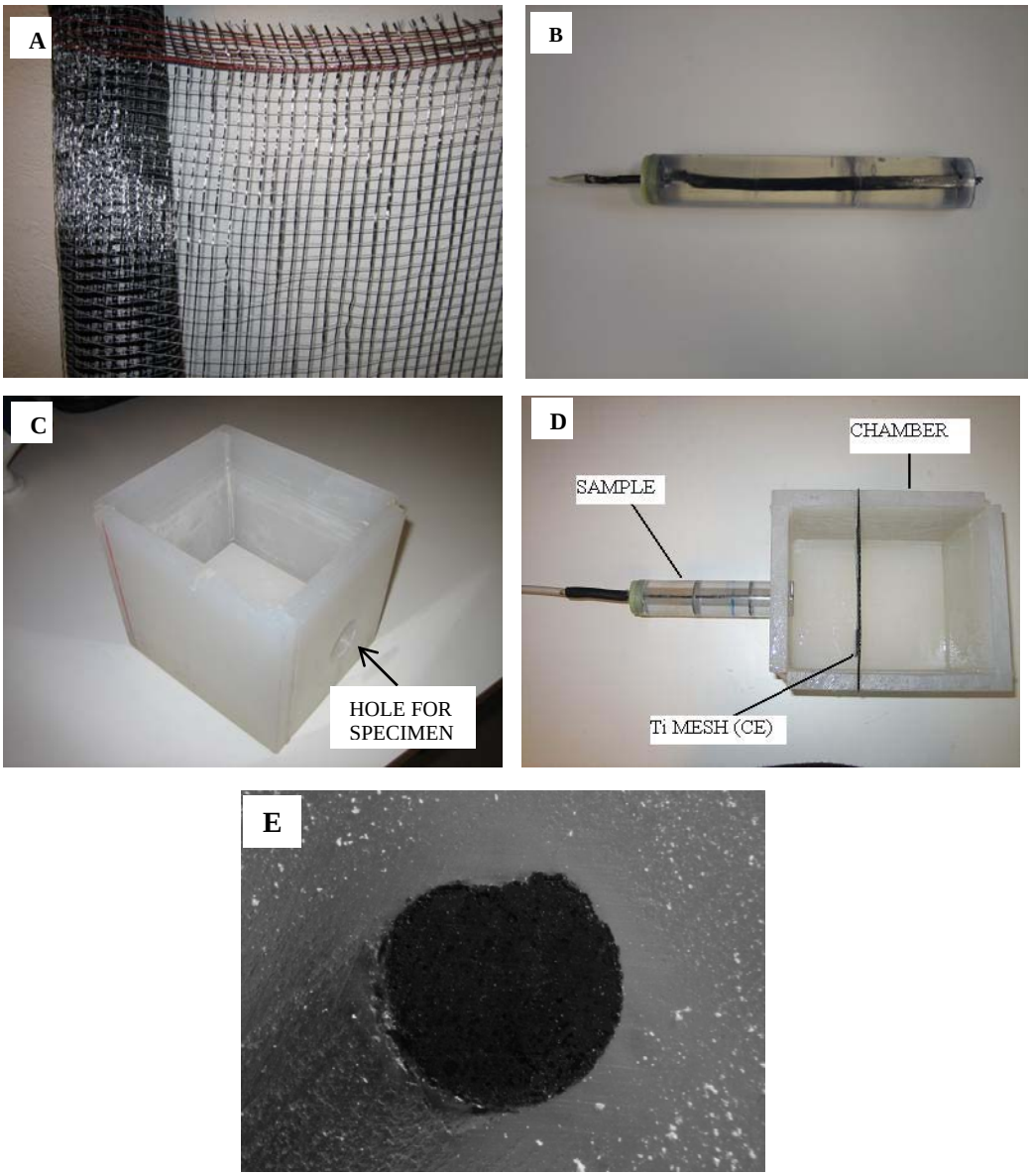

Figure 3. Photos of specimen and chamber.
A) Carbon mesh. B) Carbon specimen. C) Chamber. D) Test setup E) Cross section.

To simulate the concrete pore solution, a mixture of sodium, potassium and calcium hydroxide was used. pH of the solution was 13.2 and the measurements made in room temperature between 22 and 25 centigrade. Chloride ions were added as NaCl to make 1% and 3% chloride solutions.

4 RESULTS

The potentiostatic results were measured for different chloride contents. Figures 4 and 5 show examples of open circuit curve and 750 mV-polarization curve in 3% chloride solution. The E-I plot (potentiodynamic curve) for all 3 different chloride contents is illustrated in Fig. 6. Unfortunately the last read in 3% chloride content was out of range due to destabilization of the system. The result for

applied potential less than 500 mV are showed in separate plot. As it is observed in Fig. 4, before exposing the carbon to the alkaline solution, it is in immune area. After exposing by passing time, it eventually reaches to its open circuit corrosion potential. The open circuit value for testing carbon material is around -410±10 mV vs. SCE. Moreover during polarization, it took time to stabilize the current and that depended on polarization amount (Fig. 5).

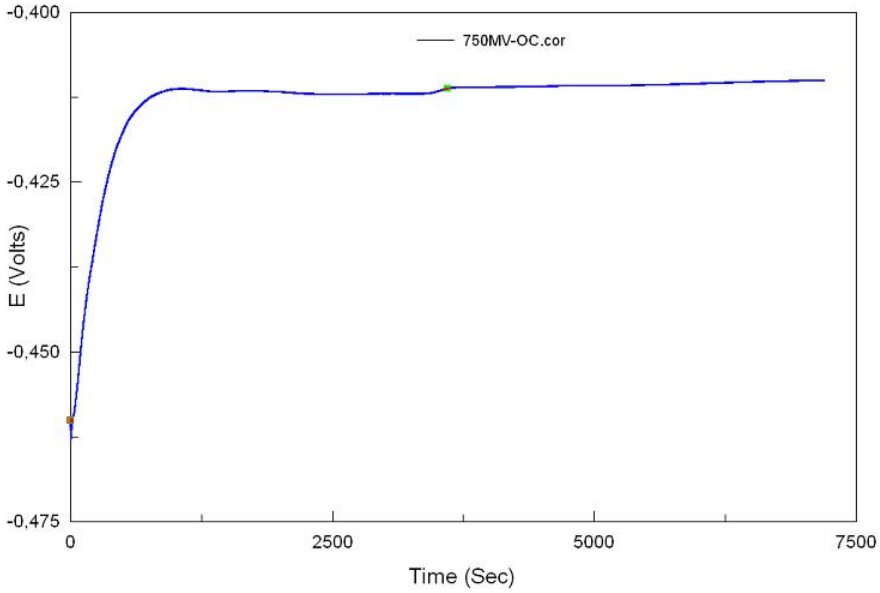

Figure 4. Open circuit measurement in 3% chloride content.

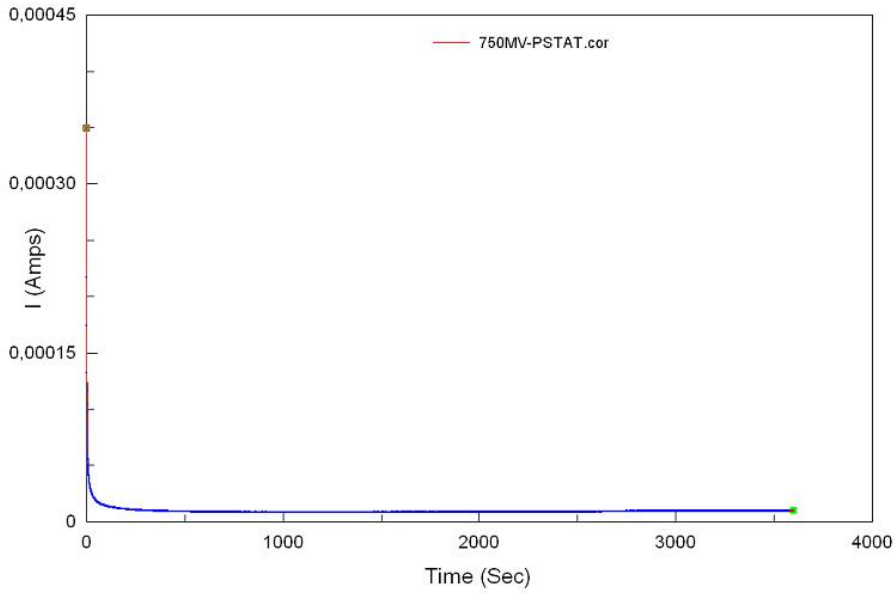

Figure 5. Potentiostatic measurement in 750 mV polarization and 3% chloride content.

As it is showed in Fig. 6, behavior of carbon in different chloride contents was mostly the same. There is a very small shift in curves to right by increasing the chloride content. In all three conditions there is a small area of passivation up to 300 mV polarization. In this area the corrosion current density is low, between 2E-8 ~ 7E-8 A/mm^2. It is more obvious in non chloride contaminated condition. After that carbon has an active behavior with a very rapid slope up to 2500 mV polarization. In this point, corrosion current density reaches to values of 1E-3 A/mm^2. After this point there is another passive

area in non-chloride content solution. But is both 1% and 3% chloride content this passive area is started after a jump from 1E-3 to 1E-2 A/mm2 in 2500 to 3500 mV polarization respectively.

It should be also mentioned that the oxygen reduction theorically should happen in 220 mV vs. SCE. This potential is equal to 630 mV polarization for the test material. During tests formation of bubbles on the surface of the carbon was observed after 750 mV polarization. Unfortunately monitoring the changes in pH value of the solution due to oxygen reduction could not be possible because of small surface area of working electrode compared with solution volume.

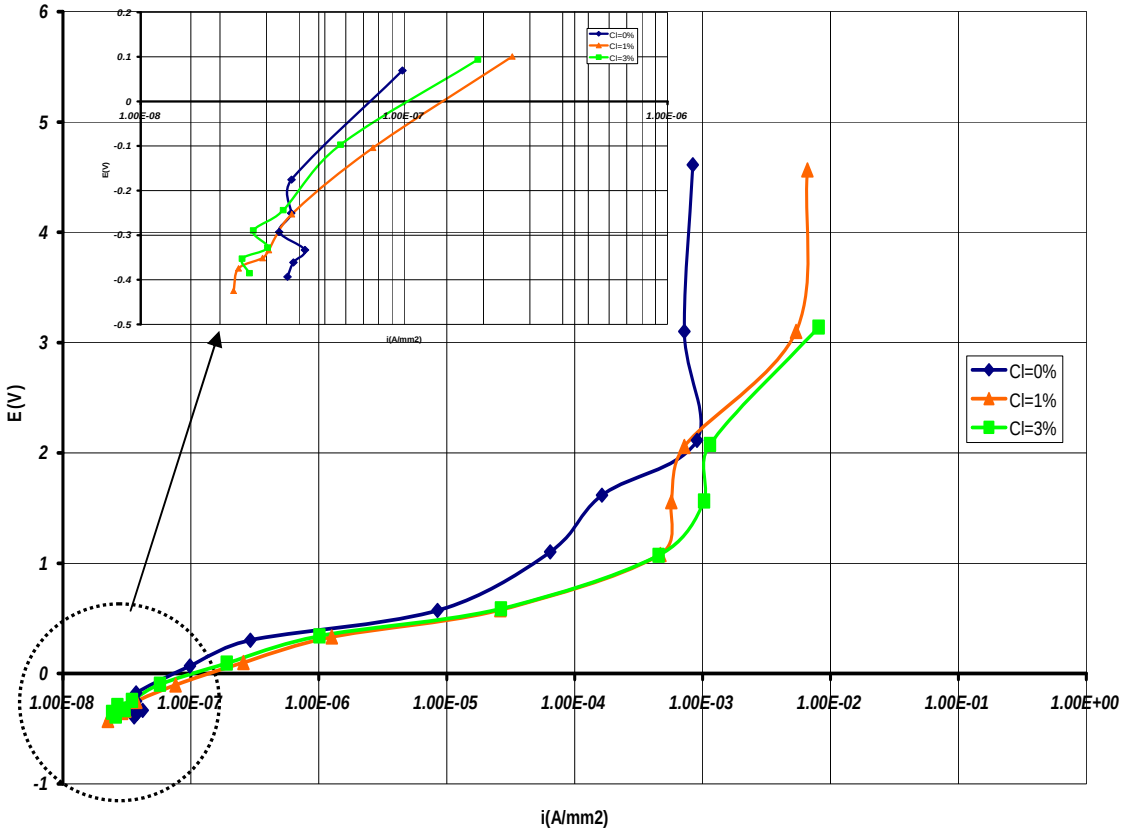

Figure 6. E-i plot for different chloride contents.

However the formation of corrosion products was observed on the surface of the samples after 1500 mV polarization, but these products were solid and didn't released to the solution in non-chloride solution case. But in 1% and 3% chloride contents conditions, changing color to brown around the working electrode surface was observed from 3500 mV and 2500 mV polarization respectively by researcher.

5 CONCLUSIONS

The results have been presented of carbon fibre material which could be used as an anode material in CP systems. To improve the knowledge about behavior of this material in alkaline media, the polarization tests were fulfilled.

The performed investigations have shown that carbon has a passive-active-passive behavior in alkaline solution. It is in passive condition up to 500 mV polarization and then enters to active area up to 2500 mV. From that point, it starts the second passive condition.

Corrosion current density is 2E-8 A/mm^2 in low potentials up to 1E-3 A/mm^2 in high polarization potentials. This value would be increased up to 1E-2 A/mm^2 by adding chloride ions in the solution. Addition of chloride into the solution increases the corrosion current densities in high polarization values. But it seems that this effect is slight in low polarization values and amount of chloride ions do not play a great role in that.

Oxygen reduction has been observed from 750 mV polarization. It could make some mechanical damage to the surface of the carbon. But the change in solution color to brown was monitored just only in very high polarization potentials.

ACKNOWLEDGEMENT

A part of this work is financed by the Norwegian Research Council through the strategic research program RECON at Norut Teknologi in Narvik, Norway. Additionally the support from maxit Group AS is highly appreciated both by sharing their scientific and practical experience and financing part of this work.

REFERENCES

Pedeferri, P., 1996, 'Cathodic protection and cathodic prevention', *Construction and Building Materials*, 10[5], 391-402.

Pourbaix, M., 1974, *Atlas of electrochemical equilibria in aqueous solutions*, National association of corrosion engineering, Houston, Texas.

Chini, M., Antonsen, R., Vennesland, Ø., Arntsen, B. & Mork, J. H., 2007, 'A review of utilization of carbon fibers as an anodic material in cathodic protection', International RILEM Workshop on Integral Service Life Modeling of Concrete Structures, Guimarães, Portugal, 5 6 November 2007.

Vennesland, Ø., Haug, R. & Mork, J. H., 2005, 'Cathodic protection of reinforced concrete – a system with woven carbon mesh', International Conference on Concrete Repair, Rehabilitation and Retrofitting (ICCRRR), Cape Town, South Africa, November 2005.

Mork, J. H., Mayer, S., Rosenbom, K., Tuveson-Carlstrom, L., Sederholm, B. & Sandberg, B., 2006, 'Cathodic protection of concrete structures with a carbon fibre mesh anode', EUROCORR2006, MAASTRICHT, Netherlands, September 2006.

Vegetable Materials in Architecture

Dora Francese [1]
Ida Orefice [2]
Cristian Filagrossi Ambrosino [3]

T 18

ABSTRACT

Nowadays design procedures in the sphere of architectural culture are generally focused on environmental issues, and more and more often it is finally accepted at least the need of looking for alternative systems aimed at saving energy from fossil fuels, and studying and testing various options in the production of components and materials for construction able to create a better environment, an higher vivibility and a less polluted planet. The paper we present reports some results from a research aimed at testing a number of these systems, which could create a valid alternative to those conventional components and materials that happen to be increasingly toxic for the users' health, damaging for the biotic and a-biotic parts of the earth ecosystem, and requiring great amount of fossil fuels for running. In particular the research has been focused on a peculiar field of systems, which can employ vegetable materials as a base for the production of building components, because these materials, having a very high level of naturality, being very durable, and capable of re-entering the circularity of the earth processes, will save energy, will reduce the environmental load, will create an healthy environment and thus a better way of living for humans. The research shows that the use of such materials as wood, cork, bamboo, cellulose or rammed earth, will require a different way of thinking, of designing, of constructing the architecture, depending mainly on the fact that a number of components made out of these materials have different characters from the usual conventional systems in concrete, steel and plastic. Great sensibility of the designer is then required any time the selection of vegetable material is considered an option in order to integrate the building in the circle of nature. The study here presented, beginning from the analyses of such characters of these natural materials, will define in the end a number of guidelines as basis for helping the designer to do the right choice according to different using purpose. The results of such studies could help to promote the production and the use of these vegetable components and to outline the procedures for employing new methodologies of application in architectural intervention.

KEYWORDS

Vegetable materials, Bioclimatic architecture, Sustainable architecture, Health

[1] Università degli Studi di Napoli Federico II, Architecture Faculty, Dipartimento di Configurazione ed Attuazione dell'Architettura, Napoli, Italy 80135 Phone +39 081 2538403 Fax +39 081 2538406, francesedora@virgilio.it
[2] Università degli Studi di Napoli Federico II, Architecture Faculty, Dipartimento di Configurazione ed Attuazione dell'Architettura, Napoli, Italy 80135 Phone +39 081 2538403 Fax +39 081 2538406, ida.orefice@libero.it
[3] Università degli Studi di Napoli Federico II, Architecture Faculty, Dipartimento di Configurazione ed Attuazione dell'Architettura, Napoli, Italy 80135 Phone +39 081 2538403 Fax +39 081 2538406, cristian.filagrossi@gmail.com

1 INTRODUCTION

The building market proposes a large range of industrial products with higher and higher performances; although one of the aspects that seems to be more attractive for the professional figures involved in the design process (enterprises, designers and users) is the ecological character of the element, i.e. its capacity to minimize negative impacts on ecosystems and users and its ability to cut energy consumption by fossil fuels. According to the latest European and Italian law this latest aspect seems to prevail so much that often the real performance levels are defined only as far as energy consumption is concerned, ignoring the other environmental loads that, during all the life cycle, from the pre-production till the recycling, the component provides. Nonetheless we think that the duty of researchers and designers will be to grasp the real eco-sustainability and bio-compatibility characters of such components, not only during production, transport, etc., but also and mainly during the employment, which represents the longer and the more polluting phase, both for the users and the ecosystems, and the only one in which the building role, combined with the various produtcs, can actually answer in an olistic way to the comfort needs.

2 VEGETABLE MATERIALS AS ALTERNATIVE CONSTRUCTION SYSTEMS

The environmental questions had achieved, in the latest years, a vital importance, not only in the specific bulding field, but also in the political, economical and cultural sphere. Nowadays speaking about sustainable design seems almost pointless, since the sustainability should be included in any type of intervention. The problem of cutting energy consumption in buildings is today widely discussed and studied, nonetheless the same approach does not often occur in the eco-sustainibility and bio-compatibility of building materials.

In a changing world, flexible, re-generative, intelligent and sustainable materials and solutions are required for architecture. Vegetable materials seem to be a good answer for such a goal.

The need of employing these alternative materials, rather than more conventional ones, such as steel, concrete and others, is due to a great number of reasons, mainly belonging to the sphere of socio-economical and technical fields.

Figure 1. Cork.

Table 1. Energy in MJ for the production of 1 mc per unit strength [MPa].

Material	MJ/m^{9}MPa
Steel	1500
Concrete	240
Wood	80
Bamboo	30

The first one includes production of low cost construction materials; very low amount of energy needed for the production [Table 1]; substitution of the whole or part of polluting materials with environmentally friendly ones; new design possibilities using non-conventional materials and techniques; use of local materials; protection of non-renewable energy resources; very high potentiality of recycling.

Technical reasons can be focused on the chance of having simple processing materials and higher mechanical properties and performances (i.e. the bamboo) similar to those of conventional building materials.

Nevertheless, there are also some limits for the employment of vegetable materials. It is possible to distinguish three different kind of limits: biological, technical and temporal. The first ones are due to the growth of the upper plants; the technical limits are various but the most frequent are related to the problem of root compenetration; finally the time limits are linked to the need of working within or without the growth time [Figure 2].

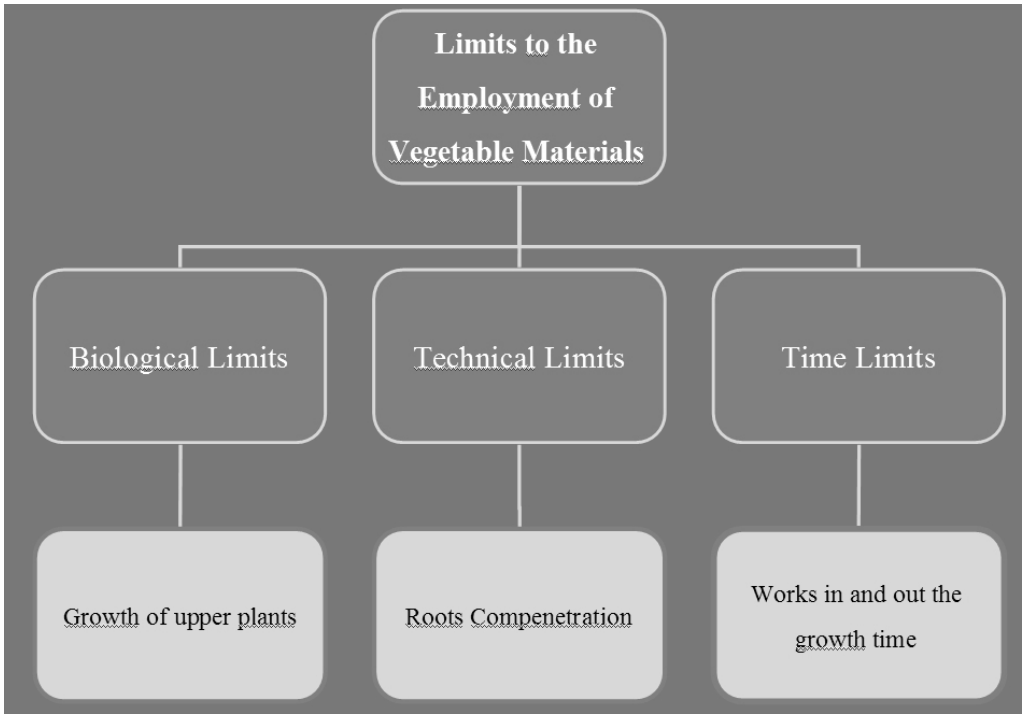

Figure 1. Limits to the employment of vegetable materials.

3 BAMBOO

One of the vegetable materials, lately come unto fashion again among designers, the bamboo, has been investigating as far as its potentialities are concerned. The term "bamboo" describes a range of woody perennal evergreen plants (Family Poaceae, Sub-family Bambusoideae), mainly diffused in the tropical zones, but also in the temperate and sub-tropical zones. It includes 1250 species, most of which have a very fast growth, reaching their maturity in less than five years. Upon time different types of bamboo were used all over the world for variuos purposes depending on cultures, traditions and climatic characters [Janssen, 2003].

In Europe the use of such material began more than 300 years ago, but it remained neglected till few years ago when the designers had started again to look at bamboo as a building material. Nowadays many European researchers (for example the Eindhoven University, Holland) are performing tests for checking the structural potential of this material (Table 2). These bamboo researches are aimed to establish its physical and mechanical behaviour so as to make possible its employment as a substitute of the structural steel.

Table 2. Comparative properties between bamboo and others conventional building materials.

Material	Strength N/mm2	Mass/ Volume	Ratio	Emodulus MN/m2	Mass/Volume	Ratio
Concrete	8	2.400	0.003	25.000	2.400	10
Steel	160	7.800	0.020	210.000	7.800	27
Wood	7.5	600	0.013	11.000	600	18
Bamboo	10	600	0.017	20.000	600	33

Among vegetable materials, bamboo is the one on which the scientific community - linked to construction sector - has better hopes for an efficient structural use.

Thank to the arising consciousness about the serious environmental crisis in which we currently live, the research for new building materials is still developing. So far the bamboo seems to be very interesting for its physical and technical properties: in fact, like all vegetable building materials with circular section (wood, straw, sugar cane, etc.) it offers a very high tensile and torsion strengths, as well as elastic properties independent form shape and load distribution [Hidalgo, 1981].

Frei Otto, within the programme of activities carried out for the Institut für Leichte Flächentragwerke, had extensively shown how the bamboo is more resistant and lighter than other "conventional" building materials. For these reasons is now impossible to ignore a material that offers a twice bigger strength compared with the glass fiber and six times an higher lighthness than the steel, and it can also be reminded that it is not a chance bamboo is called "the vegetable steel". Moreover, its ecological features are very interesting. It is the plant with the higher growth rate (some bamboo species can grow up to 1 meter in a day). Thus, the employment of bamboo guarantees a large availability, also in brief times, and at the same time insures a regular control over the oxygen/ carbon dioxide balance in the atmosphere. In particular, the Guada Angustifolia specie is one of the essences that offers an higher percentage of carbon dioxide particle absorption, giving an helpful hand to the fight against global warming [Cusak, 2000].

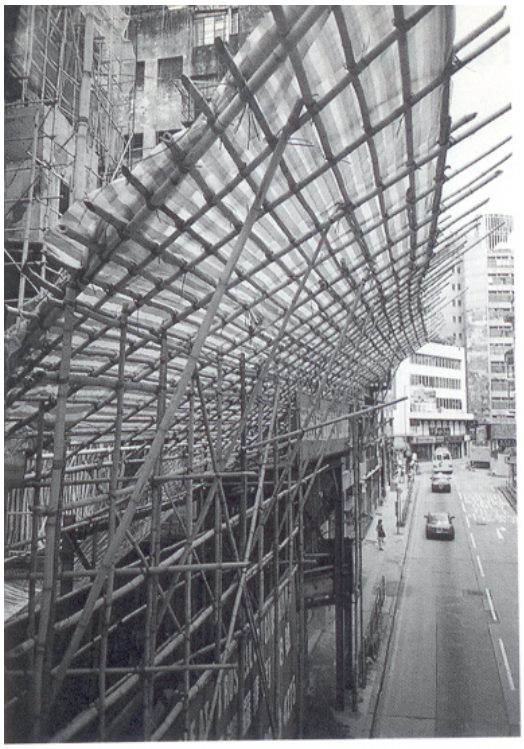

Figure 3. Bamboo used as scaffolding.

The use of bamboo in building sector can play an important role also in relation to the well-known deforestation problem and can provide, in brief times, enough material for building houses for millions of people that live in the developing areas of the world. Building with the bamboo, also in Europe, becomes nowadays a task with a benefit for environment, next generations and poor commuities that fund their economy on its production. The chance that had allowed the meeting between Occident and the bamboo culture was the Hannover Expo (2000), where the architect Simon Velez realised the Padiglione Zeri, the bigger bamboo structure ever built, measuring 40 meters by 9. In the 2002 the Vergiate Municipality (near Milan) commisioned the EmissioneZero society (the same who built the Padiglione Zeri) by doing a huge structure in bamboo, inside the Ticino Park, that was the first permanent bamboo building in Europe.

4 CLASSIFICATION AND EVALUATION

The first stage of our research was meant to classify those vegetable materials, that are usually employed in architecture and urban planning, in two big categories: living vegetable materials and organic dead materials. The first one includes seeds, scions, grass, plants with roots and, generally, all the vegetable materials that are used in landscape architecture. The second one, instead, includes building materials such as wood, coconut and juta fiber, cork, etc. [Figure 4].

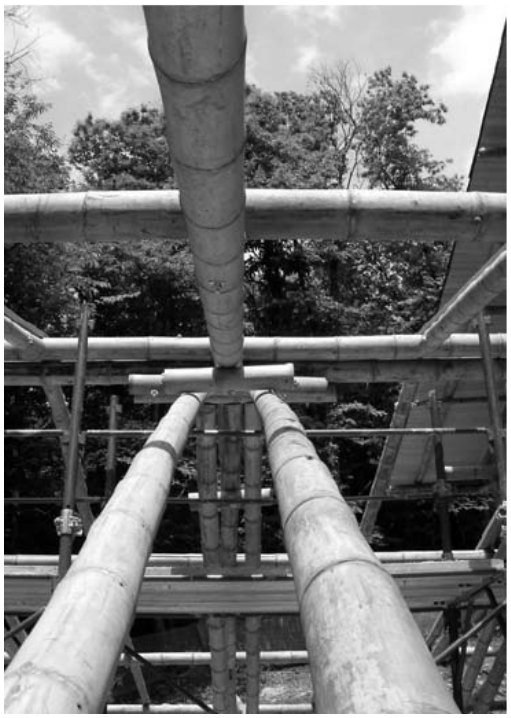

Figure 2. The bamboo structure of the public space built in Vergiate (near Milan)

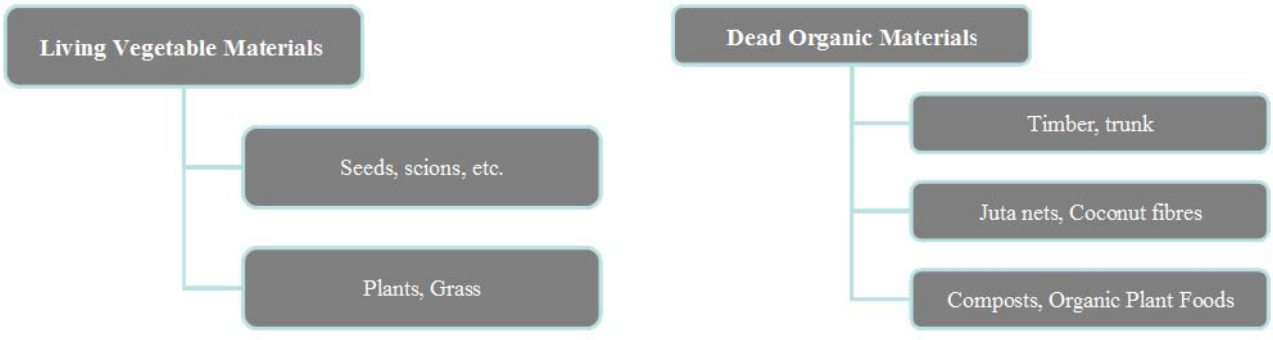

Figure 3. Classification of vegetable materials.

The following table [Table 3] shows some important characters (linked to their ecological aspect) of the principal vegetable materials. For each of them, thermal conductivity, energy consumption values, chance for the product to be recycled or to be made by recycled elements and finally some notes about the physical performances, are listed.

Table 3. Characters of the principal vegetable materials.

Material	Thermal Conductivity (λ)	Energy Consumption in Production	Recycling	Characters
TIMBER FIBER CARDBOARD	$\lambda \sim 0.0050$	Very low	Yes as fuel	Transpiring, antistatic, toxic emissions free
CORK	$0.030 \leq \lambda \leq 0.100$	KWh/m= 30-60 (+ 30 for cardboard depth)	Yes	Good insulation, Impermeable to the water, transpiring, good fire resistance, toxic emissions free, no need of adhesives.
MINERALIZED TIMBER CARDBOARD	$0.050 \leq \lambda \leq 0.100$ $\lambda \geq 0.100$	KWh/m= 30-50	Yes as inert for concrete	Transpiring, antistatic, toxic emissions free
COCONUT FIBER	$\lambda = 0.045$	KWh/m=30		Resistant, transpiring, antistatic. Good resistance to insects, mold and humidity. Inflammable, high costs.
JUTA FIBER	$\lambda = 0.055$	Very low		Transpiring, antistatic. Inflammabale. Low costs.
NATURAL WOOL	$\lambda = 0.033$	Very low	Yes, often is already produced by recycled wool	Good insulation (thermal and phono), transpiring. Fears attacks from parasites and mites. High costs.
CELLULOSA FIBER FLAKES	$\lambda = 0.032$	KWh/m=6		Good insulation (thermal and phono), transpiring. Excelent resistance to parasites, insects and rodents. Toxic emissions free. Fire resistant, Fears water.

The output of this research is the creation of an evaluation method for the sustanibility of the vegetable materials, which can be applied to other materials. Such method consists into a format divided in two classes: ecosustinability and biocompatibility [Francese, 2007]. The first is related to the impacts that the material/product provides on the environment (in terms of material and energy consumption and of polluting emissions), the second instead to the impacts provided on the users' health (in terms of emissions, radioactivity, smells, etc.).

Any class can be identified by a number of parameters, which define performances and requirements of the employed material. Each parameter is, on its turn, specified by qualitative and quantitative indicators, to which a value will be given. The points for each indicator are given considering a defined range of values, every range corresponds to a determinated point, from 1 (worse performance) to 5 (best performance).
In the next table, a sample of thus type of classification is shown for some indicators.

Table 4. Examples of ranges and values.

Indicator	Values
Permeability/Impermeability	1 - perm. > 2 μg/N s 2 – 1 μg/N s < perm. < 2 μg/N s 3 – 0,5 μg/N s < perm. < 1 μg/N s 4 – 0,067 μg/N s < perm. < 1 μg/N s 5 – perm. < 0,067 μg/N s
Thermal Conductivity	1 – C > 1,3 2 – 0,75 < C < 1,3 3 – 0,1 < C < 0,75 4 – 0,05 < C < 0,1 5 – 0,02 < C < 0,05

The satisfaction level of performance for each indicator provided by each material is thus represented by the specific value (from 1 to 5) appointed to the indicator. Moreover different weights are provided for each class and for groups of parameters, according to their importance (as known in the AHP method). So the ecosustainability class has a weight corresponding to the 45% of the total, and the biocompatibility weights for the remaining 55 %. The weights for the parameters are shown in the Table 5.

The final result will be provided as a comparison value within the multicriteria method, for the ecosustainability and biocompatibility of two different materials.

5 THE CASE STUDY: BAMBOO HOUSE (ARCH. KENGO KUMA)

We have tested our evaluation method analazying one of the most famous bamboo buildings: the Bamboo House by Kengo Kuma.

The building was part of an initiative to develop a series of houses, all by Asian architects along the Great Wall of China. His composition is based on a central zone called bamboo lounge: it is a common space with gardens and water; around it all the rooms are articulated. Two small paths link the bambo lounge with the daily and the nightly zones. Kuma varied the spacing and thickness of the bamboo canes creating the walls of the house, each defining a different level of fluidity from one space to the next. Dappled light penetrates between the thin stalks. Kuma is in a sense a traditionalist, aiming to restore the historical Japanese buildings.

Figure 6. The Lounge Bamboo (Bamboo House).

However his approach is a modern one, in which he focuses on “light and natural materials to get a new kind of transparency.” [Pavarini 1999].

The evaluation method tested on the Bamboo house had shown the evidence that bamboo can be considered, at a first sight, an ecological and healthy material, due to the high values for both the requirement classes, the ecosustainability and the biocompatibility.

Both from the point of view of secutiry and friendly features, it has a good chance to become the material of the future. Durability and environmental resistance contribute to provide it with high quality and appeal.

Table 5. The case study: evaluation of the use of bamboo in the Bamboo House by Kengo Kuma.

Bamboo					
Classes		*Parameters*	*Indicators*	*Values*	*Total*
Ecosustainibility 45%	Resources Saving (45%)	Material Consumption	Availability	5	3,77
			Water consumption	4	
			Durability	3	
			Maintenance	3	
			Reparability	5	
			Re-use	5	
			Biodegradability	5	
			Wastes Produced	4	
			Rigeneration	5	
		Energy Consumption	Preproduction	5	4,4
			Production	5	
			Distribution	4	
			Use	3	
			Dismantle/Recycling	5	
	Ecosystem Protection (55 %)	Polluting Emissions: CO_2	Preproduction	3	3,6
			Production	3	
			Distribution	4	
			Use	4	
			Dismantle/Recycling	4	
		Polluting Emissions: CFC	Preproduction	4	4
			Production	4	
			Distribution	4	
			Use	4	
			Dismantle/Recycling	4	
		Polluting Emissions: COx, NOx, SOx	Preproduction	3	3
			Production	3	
			Distribution	3	
			Use	3	
			Dismantle/Recycling	3	
Biocompatibility 55 %	Health (55 %)	Toxic Emissions: VOC	Effects to target	4	2,66
			Intensity of emission	3	
			Time of emission	1	
		Toxic Emissions: Radon	Effects to target	4	4
			Intensity of emission	3	
			Time of emission	5	
		Toxic Emissions: Formaldeyde	Effects to target	5	5
			Intensity of emission	5	
			Time of emission	5	
		Toxic Emissions: Microrganisms	Effects to target	4	4,33
			Intensity of emission	4	
			Time of emission	5	
	Comfort (45 %)	Acoustic Comfort	Phonoabsorption	3	3
			Phonoinsulation	3	
			Thickness	3	
			Superficial Resistance	3	
			Localization	3	
		Hygrometric Comfort	Specific Heat	3	3
			Thermal Conductivity	3	
			Thermal Resistance	3	
			Heat Storage	2	
			Emissivity	3	
			Permeability/Impermeability	3	
			Transpirability	4	

Table 6. Summary scheme of the evaluation output.

Ecosustainability					
45 %	Resources Savings		III level points	II level points	I level points
	45 %	Material Consumption	3,77	4,08	3,77
		Energy Consumption	4,4		
	Ecosystems Protection				
	55 %	Polluting emissions: CO2	3,6	3,53	
		Polluting emissions: CFC	4		
		Polluting emissions: COx, NOx, SOx	3		
Biocompatibility					
55 %	Health				
	55 %	Toxic emissions: VOC	2,66		3,57
		Toxic emissions: Radon	4	4	
		Toxic emissions: Formaldeyde	5		
		Toxic emissions: Microrganisms	4,33		
	Comfort				
	45 %	Acoustic Comfort	3	3	
		Hygrometric Comfort	3		

5 CONCLUSIONS

Sustainable construction will be more and more challenging in the next years, first of all because it appears as the only possible way of reducing the big impact on the planet health in terms of both energy and material consumption, and then because the European as well as other continent regulations are increasing the mandatory requirements for environmental tasks.

The field of research should, in the future, be aimed at investigating new technological solutions and new materials for achieving the result of a low environmental load during the whole life cycle of building process. The first aspects on which such a reasearch focused regard environmental and social performances of those innovative technical solutions: this is in fact one of the aim of the reasearch we are presenting, which is mainly oriented at demonstrating that vegetable materials, being recyclable, durable, clean, ecological and healthy, could represent an actual alternative to oil derived solutions. At the same time any innovation in the field of vegetable material should be tested and investigated so as to find out their real ecosustainable and biocompatible performance. The example of the bamboo, whose performance we had started to evaluate with our verification method, provide a good sample of such a direction in the research, because it is demonstrated that the impact on earth and human health is minimum, and at the same time its technical properties could really be compared with other more conventional but more polluting materials. Moreover the high levels of social as well as sustainable characters of vegetable materials will push the building market into the direction of assuming and employing these innovative technical solutions as good challenge for future architectural design.

The research will go on, with the aid of our laboratory (LICA) in which deeper and various investigating procedures are planned and arrange for verifying bamboo performances, such as monitoring its thermal properties, its structural characters and its environmental care degree.

The last stage of our research will be outlining a number of guidelines useful for designers who wants to employ such materials, as the vegetable ones and in particular the bamboo in which the connection with the evaluation tool will help to take the decision in the direction of environmental care.

We believe in fact that not only the formal, strategic, bioclimatic approach to architecture is expected to be employed for future improvement of the building sector, but also the selection of the appropriate solutions and materials can provide the planet with an holistic view for achieving sustainable development.

REFERENCES

Benyus J.M., 1997, *Biomimicry,* HarperCollins Publishers, London.

CRATerre (Centre de Recherche et d'Application - Terre) 1995, *Construire en terre*, Editions L'Harmattan, Paris.

Cusak V., 2000, *Bamboo World*, Simon e Schuster, New York.

Dunkelberg K., 1989, *Bambus Bamboo (bamboo as a building material)*, Institut for Lighweight, Stuttgart.

Francese D., 2007, *Architettura e Vivibilità*, Franco Angeli, Milano.

Giagnoni, J.M., 2003, "71 Kengo Kuma Great (Bamboo) wall" in *Materia n° 42, Settembre-Dicembre 2003* p. 50-59.

Hidalgo O., 1981, *Manual de construccion con bamboo*, Estudios tecnicos Colombianos Ltda Editores, Bogotà.

Janssen J., 2000, *Building with bamboo - a handbook*, Intermediate Technology Publications, London.

Pavarini, Stefano., 1999, "Una nuova architettura", in *L'arca: la rivista internazionale di architettura, design e comunicazione visiva,* n° 142, Gennaio 1999, p. 66.

11DBMC International Conference on Durability of Building Materials and Components
ISTANBUL, Turkey 11-14 May 2008

Ultra-High Strength Concrete Using Limestone Powder

Kazuo Yamada [1]
Kazuhisa Tsukada [2]
Hikotsugu Hyodo [3]

T 18

ABSTRACT

Lowering water to cement ratio (W/C) is a popular way to enhance durability. Ultra-high strength concrete having compressing strength over 100 MPa is usually made by using nano-size silica fume and expected very durable. Excepting pozzolanic effect of silica fume, the foundamental role is to fill the fine spaces where cement particles are not able to filfull because of its limited particle size distribution in nano order. From foundamental point of view, other powder that has similar particle size with silica fume is expected to work similarly to silica fume. One candidate is nano-size limestone powder (LSP).

In this study, nano-size LSP is made from commercial LSP having an average particle size of 8 μm by using ball mill. Various powders having average sizes from 0.3 to 2.3 mm and BET specific surface area from 19.9 to 3.2 m^2/g, respectively were produced.

These LSPs were added as mineral admixture by replacing 10 mass% of cement. The addition of LSP improve the fluidity at very low W/C around 13–16 %. The most suitable size of LSP was around 1 μm. The performance of fluidity and compressive strength that was around 140 MPa at 28 days and comparable with silica fume. This limestome powder is also effective after drying. Another characteristic point of LSP was the significant shortening effect of setting time.

KEYWORDS

Limestone powder, Ultra-high strength, Silica fume, Particle size, Setting time

[1] Taiheiyo Cement Corp., R&D Center, Chiba, Japan 285-8655, Phone +81 43 498 3907, Fax +81 43 498 3849, kazuo_yamada@taiheiyo-cement.co.jp
[2] Taiheiyo Cement Corp., R&D Center, Chiba, Japan 285-8655, Phone +81 43 498 3909, Fax +81 43 498 3849, kazuhisa_tsukada@taiheiyo-cement.co.jp
[3] Taiheiyo Cement Corp., R&D Center, Chiba, Japan 285-8655, Phone +81 43 498 3909, Fax +81 43 498 3849, hikotsugu_hyoudou@taiheiyo-cement.co.jp

1 INTRODUCTION

In order to realize high durability, increasing strength by lowering water to cement ratio (W/C) is a popular method. Simultaneously, workability should be maintained constant. Limestone powder (LSP) is sometimes used as a kind of mineral additives [JCI Committee 1995]; [Ramachandran & Zhang 1986]; [Pera *et al.* 1999]; [Sato & Beaudoin 2007] for high strength concrete in order to improve the workability. Silica fume (SF) has pozzolanic reactivity and this contributes better durability. Besides this effect, SF is also important to make ultra-high strength concrete of very low W/C less than 20 % from the aspect of workability. Although ultra-high strength concrete is expected as very durable, without the addition of SF, the mixture of cement and water is too stiff even if plenty amount of superplasticizer is added. By the additio of small amout of SF around 10 mass% of cement, the cement paste starts to show fluidity. This effect has been considered as filling effect of missing particle grade of cement in the finer part.

Usually, cement has an average grain size of 10 several μm and the ratio of particles less than 1 μm is very limited. Some amounts of water trapped among the spaces made of these relatively larger particles can be released by packing finer particles in these spaces and the trapped water is changed to media for particles to move.

If this mechanism is correct, the kind of particle is not the essential factor but only the size is expected to be important. The particle shape may have a secondary effect. In order to verify this assumption, LSP is selected as the material for study.

There are two reasons to select LSP. One is the grindability. Calcite, main component of limestone, is easy to grind compared to other materials such as blast furnace slag, fly ash, and silicate rocks. Usually it is not easy to grind inorganic materials less than 1 μm because of the surface charge that makes particles flocculated. Calcite is not so hard compared to other silica or silicate minerals and is expected easy to grind to fines and to control the average size easily to check the most suitable size to maximize the fluidity of cement paste. Another interesting characteristics of calcite is the supression of decreasing hydration speed of C_3S after second peak of hydration. After the initiation of second peak of cement hydration, crystals of C-S-H deposit on C_3S and C-S-H forms a kind of layer to prevent its dissolution. For hydration progress, water or dissolved ions must diffuse through this layer to dissolve from C_3S and to precipitate C-S-H in the surrounding space of C-S-H covering C_3S. Therefore, with the progress of hydration, the thickness of C-S-H becomes more and the required time to diffuse this layer becomes longer and the hydration speed of C_3S decreases. In this hydration process, calcite takes one interesting role. C-S-H can be precipitate on calcite but not or limited on SF or maybe not on fly ash. Blast furnace slag may act like calcite in some degree. Because C-S-H precipitates on calcite, the thickness of the C-S-H layer on C_3S becomes less and the increase of required time to diffuse C-S-H layer is expected less. Then, the hydration of C_3S in the second peak and in early ages is increased.

In order to make ultra-high strength concrete, plenty amount of superplasticizer is added. For this purpose, special superplasticizers whose retarding effect of cement hydration is minimized are used. However, the dosage is so much and significant retardation is typical phenomena. Then, the addition of LSP is expected to shorten the retardation and the effect is estimated to correlate the surface area.

Based on these background and technical estimation, in this study, limestone was ground by a wet process and nano-size limestone was used as a candidate of fine powder. The optimum particle size was investigated and the effects of fluidity, setting time and strength were examined.

2 EXPERIMENTS

2.1 Materials

For mortar and paste tests, cement used was low heat portland cement (LPC) for fluidity evaluation and normal portland cement (NPC) for the evaluation of heat generation. Both were commercial products and specified by JIS. The original LSP was commercial one (LSP1) having 1.5 m^2/g of Blain specific surface area and was made by dry ball milling from limestone. For comparison, chemically synthesized calcite LSP2 and SF were used. Two kinds of SF used were commercial available products and their BET specific surface area was 10.8 and 22.4 m^2/g. The characteristics of cement, LSP, and SF are shown in Table 1. The superplasticizer used was a commercial product specialized for ultra-high strength concrete. The main component is polycarboxylate polyether polymer.

2.2 Grinding Procedure of Limestone Slurry

Limestone slurry, SL was prepared by a following procedure. In a ceramic pot mil, limestone, water, superplasticizer, and alumina balls having a diameter of 5 mm were added and the pot was rotated on a rotating mill for certain time and several SL having different particle size were obtained. One SL was dryed in a dryer at 105 ℃, ground and sieved to pass 0.077 μm. The information of particle size is summarized in Table 2.

2.3 Evaluations

Hydration heat was evaluated by a conduction micro calorimeter. 5 to 10 mass% of NPC was replaced by 0.3μmSL and 8μmLSP. Cement paste having 0.30 of W/P was mixed with a superplasticizer with the amount of 2 mass% of powder and the heat generation was measure for 56 hours. Particle size was evaluated by three methods, *i.e.,*BET specific surface area using one point N_2 adsorption, scanning electron microscope, SEM, and Lazer diffraction scattering particle size distribution method.

Fluidity was evaluated by mortar. In a Hobart mixer, 900 g of LPC, 1350 g of JIS standard siliceous sand, 2.5 mass% of superplasticizer against powder, and mixing water containing 1 mass% of defoamer against powder were added and mixed for 10 min at the low speed. The dosage is usually plenty enough to have saturated dispersing effect. The flow by using a cone having 10 cm of bottom diameter and 5 cm of height was measured to evaluate the workability. For the evaluation of the adding effects of LSP and SF, 10 mass% of LPC was replaced by them.

Table 1. Characterics of materials used (mass%, except Blaine* specific surface area in cm^2/g).

Type	Blaine*	ig.loss	Chemical composition												Mineral composition			
			SiO_2	Al_2O_3	Fe_2O_3	CaO	MgO	SO_3	Na_2O	K_2O	TiO_2	P_2O_5	MnO	Cl	C_3S	C_2S	C_3A	C_4AF
LPC	3504	0.85	26.3	2.6	3.0	62.7	0.6	2.5	0.1	0.3	0.1	0.05	0.10	0.004	26.2	55.8	1.8	9.2
NPC	3347	0.68	21.9	4.6	3.1	64.6	1.6	2.0	0.2	0.3	0.2	0.22	0.06	0.005	55.1	21.2	7.2	9.3

Type	Blaine	Purity	Chemical composition							
		[$CaCO_3$%]	SiO_2	Al_2O_3	Fe_2O_3	CaO	MgO	SO_3	Na_2O	K_2O
LSP1	5000	97.7	0.06	0.05	0.04	55.25	0.49	0.0	0.0	0.0
LSP2	32000	99	0.03	0.05	0.03	55.49	0.27	0.0	0.0	0.0

Type	BET [m^2/g]	SiO_2	MgO	SO_3	Cl^-
SF1	10.8	96.7	-	0.03	-
SF2	22.4	> 97.5	< 0.5	< 0.4	< 0.1

Table 2. Characteristics of LSPs.

Type	Ave. size [μm]	BET surface area [m^2/g]	Production method
1.5μmSL	1.5	4.2	Wet milling (solid content = 70%)
0.3μmSL	0.3	20	Wet milling (solid content = 40%)
1.5μmSL-dry	1.5	4.2	Drying after milling
0.15μmLSP2-syn	0.15	8.0	Chemically synthesized
8μmLSP	8	1.5	Dry milling

3 RESULTS AND DISCUSSIONS

3.1 Particle Size of LSP

In Figure 1, SEM photos of ground LSP1 and SF1 are shown. As is shown, the original 8 μmLSP (LSP1) was ground to smaller particles. The particles size of the finest 0.3μmSL is comparable with SF.

In Figure 2, the particle size distributions of LSP are shown. The particle size distribution of 8μmLSP is relatively wide and by milling the distribution became narrower.

In Figure 3, the particle size distributions of LPC and LPC mixed with LSP are shown. The particles less than 1 μm in LPC is limited.

By the addition of 1.5mmSL or 0.3mmSL, the lack of fine particles are compensated.

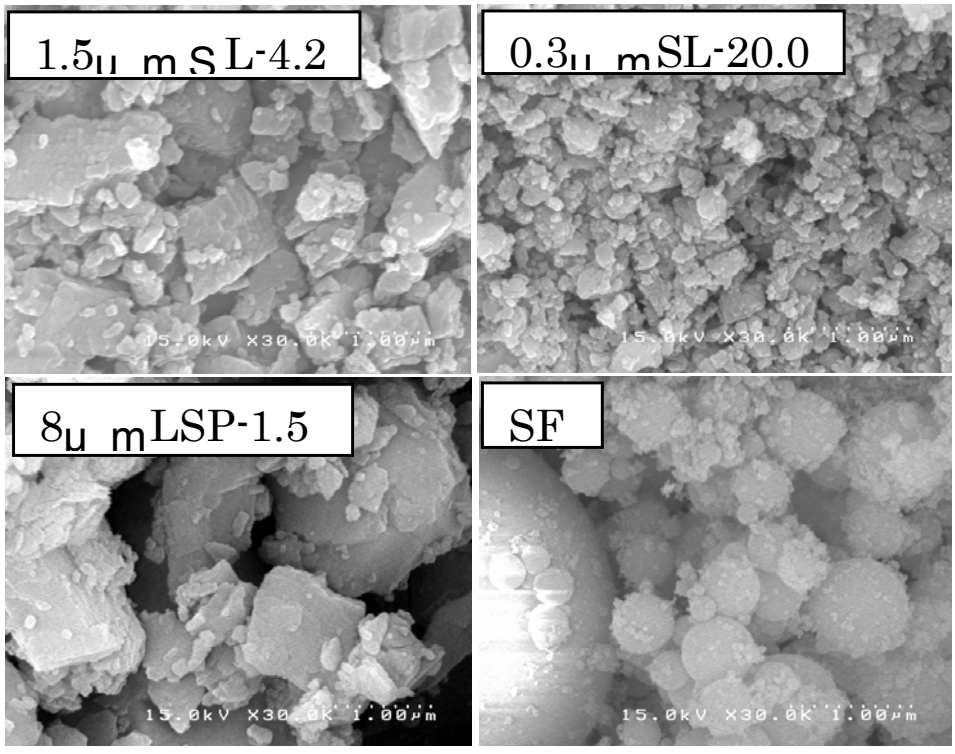

Figure 1. SEM photos of ground LSP and SF1.

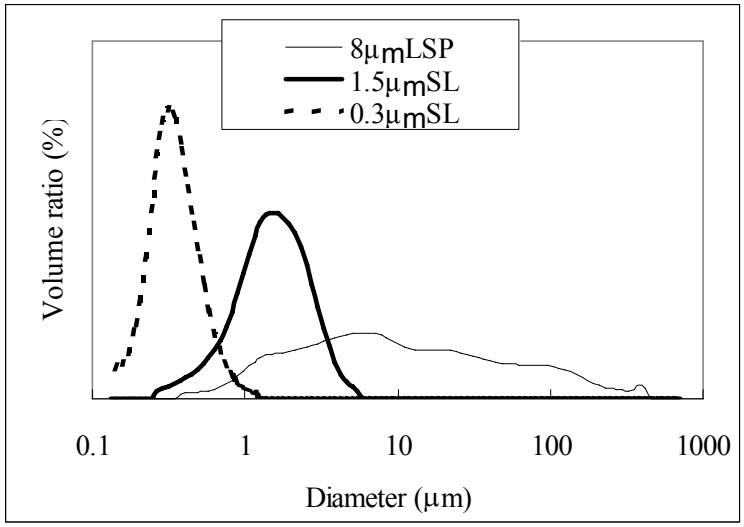

Figure 2. Particles size distribution of LSPs.

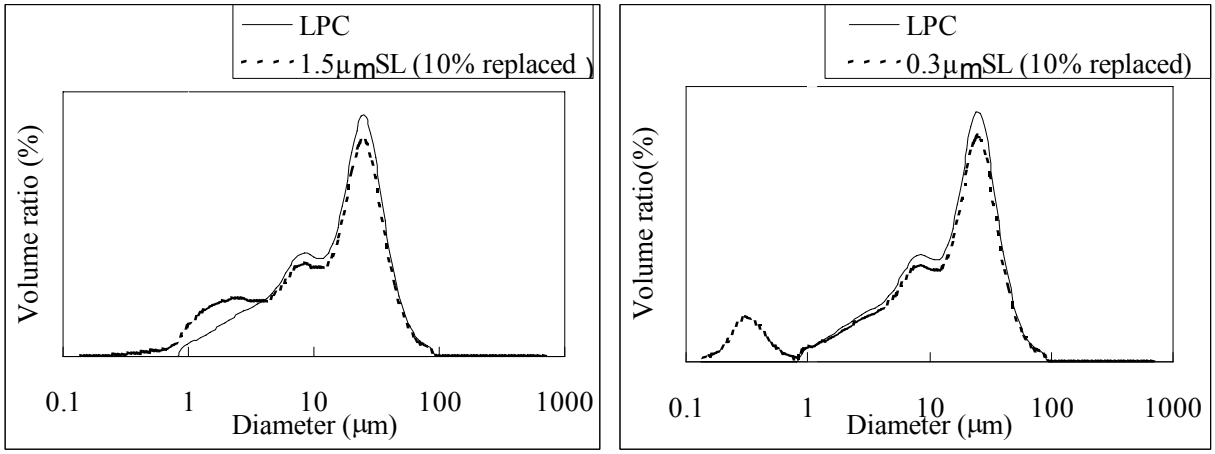

Figure 3. Particle size distribution of LPC and mixed cement with 10 mass% of 1.5μmSL-4.2.

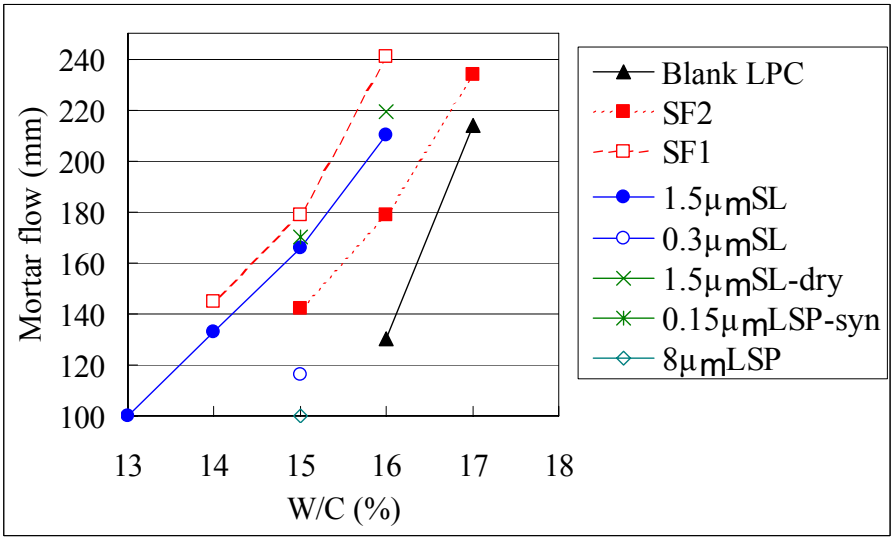

Figure 4. W/C and Mortar flow.

3.2 Effects of LSP Addition on Fluidity at Very Low W/C

Figure 4 shows the correlation between W/C and mortar flow. Without LSP or SF, blank LPC did not show fluidity at W/C lower than 15 %. At 15 % of W/C, the addition of 8μmSL showed almost no fluidity increase. By the addition of 1.5μmSL, the fluidity was improved and in the range of W/C larger than 13 %, some level of fluidity was obtained. The adding effects were almost the same for 1.5μmSL-dry and 0.15μmSL-syn but less for 0.3μmSL. Regarding SF, the finer SF2 showed less fluidity than the coarser SF1. There are suitable particle size to show high fluidity. By wet-grinding process, around 1.0 μm is the best particle size in this experiments. However, when producing method is different, the optimum particle size may be different because 0.15μmSL-syn showed relatively high fluidity even it has finer particle size. For SF, 10 m^2/g of BET specific surface area is preferable than the finer 22 m^2/g.

The results obtained indicates that there is an optimum particle size corresponding to the kind and the procuding process of powders. At least, SF and LSP with appropriate particle size showed the similar fluidity. The effect of shape on the fluidity is expected limited. SF is round in shape and LSP is relatively rectrangulr. Therefore, when the particle size distribution is optimized, this shape effect becomes visible. However, the optimization of grading is thought to be the more important factor. The fluidity improving effect of SF is not the intrinsic character of SF but just the matter of appropriate particle size because LSP having average particle size around 1 μm showed the similar fluidity with SF. Furthermore, some preliminarly fine tuning of particle size distribution by the combination of 0.3 and 1.5 μm SL was carried out but no better fluidity was obtained at this moment. It is effective to fulfill the missing submicron particles of portland cement by some other particle. However, there seems to be a limitation of this method in the range of 10–100 nm order. One interesting point worthy to mention is the required time to show fluidity. When mortar is mixed, at first they are only wet powders. After several 10s seconds or several minutes, the mixture becomes to one stiff lump. After more several minutes, the mixture starts to show fluidity. Interesting point is the required time to show this behavior. Even the final mortar flow is same, the required time for mixign is considerably different sometimes. SF1 and 1.5μmSL showed relatively shorter time. This is one of the crucial factors for actual production.

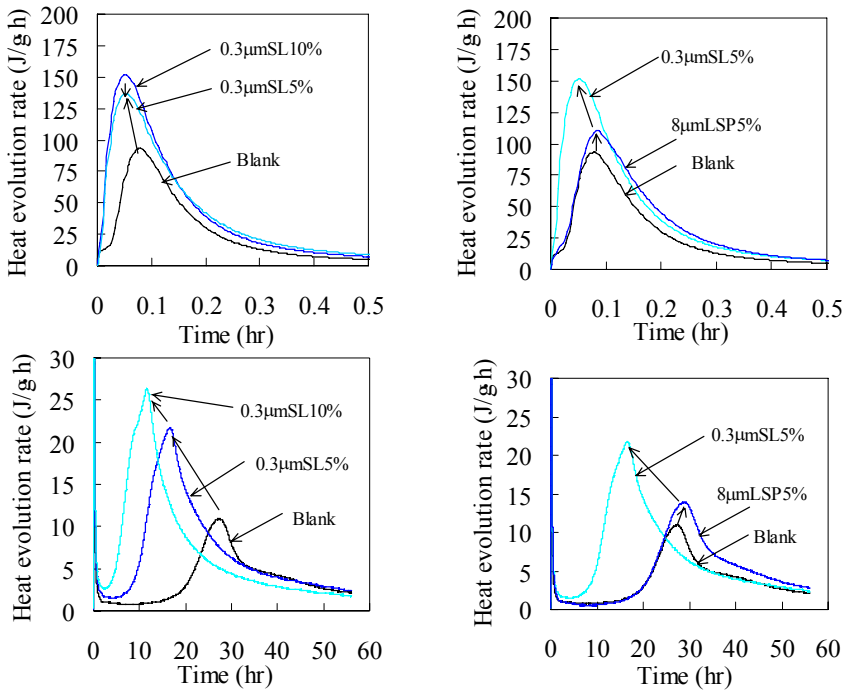

Figure 5. Heat generation behaviors of LSP replaced by 0.3μmSL and LSP1. Upper: 1st peak, lower: 2nd peak.

3.3 Heat Generation Behaviors

In Figure 5, the heat generation behaviors of LPC partially replaced by SL and LSP1 are shown. By the more addition of finer limestone powder, the first and second peaks appears the earlier and higher. These effects are estimated as the hydration acceleration of C_3A and C_3S by fine calcite.

3.4 Behavior in Concrete

The adding effect of SL should be confirmed by concrete tests because the mixing efficiency and the grading of the total particles are completely different. By the preliminary tests of concrete, flowable concrete having 650 mm of slump flow was obtained at 13 % of W/C for the mixiture of 10 mass% replacement by 1.5μmSL and SF1. The setting time of 1.5μmSL was 5 hours faster than 13.5 hrs of SF1. The compressive strength were almost the same level of 145 MPa at 28days. From the view point of durability, the behaviors of autogeneous shrinkage are significantly different each other. During first several days, 1.5μmSL-concrete showed more shrinkage but the shrinkage tends to saturated. Later, SF1-concrete continuously shrunk and after 10s days it showed more shrinkage than 1.5μmSL-concrete. Further evaluations are now under examinations.

4 CONCLUSIONS

(1) 1.5μmSL showed fluidity enhancing effect at very low W/C around 13–16 %. The performance was comparable or betther than SF. This effect is considered as the filler effect fulfilling the finer parts around and less than 1 μm range of the particle distribution of portland cement. There is an optimum particle size to improve the fluidity. For the combination of LPC and LSP, the LSP have an average particle size around 1μm is preferable.

(2) Hydration behaviors indicated by the first and second peaks of heat generation are enhanced by finer and more amount of LSP. This effect was much more characteristic for LSP than SF as confirmed by preliminary concrete test of setting time.

(3) Low W/C concrete having 650 mm of slump flow is possible as low as around 13 % by using SF1 and 1.5μmSL. Compressive strength at 28 days concrete including 10 mass% of LSP or SF are almost same around 145 MPa.

REFERENCES

JCI Committee on Limestone Powder. 1998, *Committee report on the properties of limestone powder and its application for concrete*, Japan Concrete Institute (in Japanese).

Ramachandran, V.S., & Zhang, C., 1986, 'Influence of $CaCO_3$ on hydration and mictostructural characteristics of tricalcium silicate', *Il Cemento*, **3**, 129-152.

Pera, J., Husson, S., & Guihot., B. 1999, 'Ingluence of finely ground limestone on cement hydration', *Cement and Concrete Composite*, **21**[2], 99-105.

Sato, T., & Beaudoin, J.J., 2007, 'The effect of nano-sized $CaCO_3$ addition on the hydration of cement paste containing high volumes of fly ash', Proceedings on 12th International congress on the Chemistry of Cement, 18.

11DBMC International Conference on Durability of Building Materials and Components
ISTANBUL, Turkey 11-14 May 2008

Heat Transfer in the Thermo-Efficient BIPSE Bricks

Yuri Z. Totoev [1]

T 18

ABSTRACT

According to Australian Greenhouse Office, energy consumption in Australia will increase by 60% from 1990 to 2010. Almost 40% of energy used in households is for space heating and cooling. It is believed that these numbers are even higher in other developed countries with climate not as mild as Australian. There is a great potential to achieve significant savings in energy consumptions, costs, greenhouse effect etc. by increasing passive solar efficiency of structures including brick walls.

Passive solar efficiency works in several ways. Solar radiation is absorbed and stored by materials with high thermal mass (usually masonry and concrete) in a house. It is re-released at night when it is needed to offset heat losses to lower outdoor temperatures. Passive shading allows maximum winter solar gain and prevents summer overheating. This is simply achieved with orientation to the sun of appropriate areas and well designed eaves or other external devices. It is possible to achieve the same or even better effect on masonry walls not by using external devices but by building the principles of passive solar efficiency into brick design.

A new design for brick with built in passive solar efficiency was developed at the University of Newcastle, Australia. This brick absorbs more heat in winter because the external area of the brick exposed to solar radiation is significantly increased in comparison to a conventional brick and also because of reflection. It also absorbs less heat in summer because the area exposed to direct sun is significantly reduced. The new brick design also has some potentially unique architectural properties.
Thermal properties of new bricks were studied experimentally. This paper will present details of the thermo efficient brick and also first results of experimental comparison to conventional bricks.

KEYWORDS

Heat transfer, bricks, passive solar efficiency

[1] The University of Newcastle, Faculty of Engineering, University Drive, Callaghan, NSW 2308, Australia, Phone +612 49215290, Fax 49216991, ceyuri@civeng.newcastle.edu.au

1 INTRODUCTION

Household energy demand is increasing following the increase in the number of electrical appliances used and also due to larger building floor areas. Passive energy efficient design philosophy appears to rise and fall in popularity with increasing and decreasing energy prices. It is also generally recognised that the passive energy efficient design philosophy is not only beneficial financially but environmentally beneficial too.

The following quote from Underwood and Yik [2004] is a good introduction to a new design for bricks with built-in passive solar efficiency. “Buildings consume between 40 and 60% of all energy used in most developed economies and an increasing proportion in many developing and emerging economies… …what is not in doubt is that our current dependency on carbon based fossil fuels for providing comfort and amenity in buildings cannot be sustained and that alternative strategies require to be explored, designed, implemented, tested and demonstrated in the immediate years ahead. At the heart of this is the need to both extend and improve our knowledge of the processes of energy exchange in buildings whether they be ‘high tech’ commercial buildings in the centres of our cities or the simpler and often naturally ventilated buildings and residential habitats that surround them”.

1.1 Building Energy Use

Average household energy demand in Australia is rising. A study in by the Australian Greenhouse Office [AGO, 1999] indicated that by 2010 household energy demand could be 160% of 1990 value. Approximately 40% of household energy use is for space heating and cooling. Residential energy use accounts for approximately 10% of total energy use. This means that residential space heating and cooling accounts for approximately 4% of total energy use in the country.

1.2 New Energy Regulations

The Building Code of Australia [BCA, 2005] sets out minimum requirements for energy efficiency of new buildings. At the moment, different Australian states require different star ratings (out of five stars) for new buildings to be met. A blanket five star rating will probably be included in any new release of the BCA.

Software programs are used to calculate the energy ratings of buildings; the two most common in Australia are NatHERS and FirstRate. Both computer programs are versions of software developed by CSIRO. A nation-wide trial of a new improved program, AccuRate, is currently being implemented to replace both NatHERS and FirstRate.

All these developments show that the government is determined to reduce energy consumption. This can only be done through legislation that will enforce the use of “cleaner” energy sources

1.3 Basics of Passive Energy Efficient Design

Passive technology in building design involves the use of natural energy flows to maintain a comfortable living environment in the building. A passive system is concerned with controlling the capture of incidental solar radiation and controlling captured energy through the thermal mass and insulating properties of different building materials and through air movement.

Much research has been done in the area of passive design. The focus of this research has been on:

- Building orientation;
- Building plan;
- Window arrangement;
- Insulation techniques;

- Airflow patterns;
- Energy capture and release from the building materials.

All these aspects have been considered with respect to the dynamic nature of the building environment over time in the particular space and with respect to each other in a systems design approach. However, design of a brick with built-in passive solar efficiency presented in this paper is primarily concerned with the first and the last aspect from the list above.

Building orientation is important for gaining maximum benefits from the control of incoming solar radiation. Positioning a building so that the side with the largest surface area faces the sun will allow the building to capture more solar radiation during the colder period of the year. A trade-off however is that potentially it will also capture more unwanted solar radiation during the hot period of the year. To cut unwanted solar radiation designers use shading devices. For example, the design of the eaves of the building with respect to the windows is important in providing maximum solar penetration to thermal masses in winter when there is a low sun angle and minimum solar penetration in summer when there is a high sun angle as shown in Figure 1.

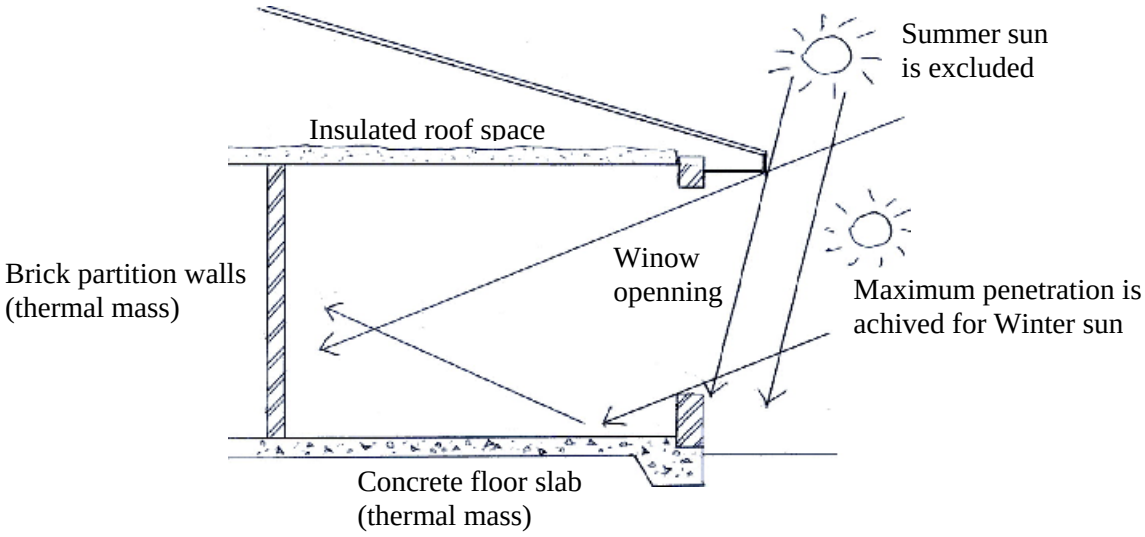

Figure 1. Key principles of passive solar design

Also important for passive design is the thermal mass of the building material. In mild climates where it is mostly the day-night cycle of warm days and cooler nights that requires the use of space heating or cooling, thermal mass is quite effective at averaging out the day-night temperature fluctuations. Brick is one of the most suitable materials to act as thermal mass and maintain comfortable temperature within the building. When the external temperature is hotter than is comfortable, external brick walls can absorb large amounts of energy with a small increase in temperature keeping the internal environment cool. When the external temperature is colder than is comfortable they will release energy keeping the internal environment warm. Windows can be used during colder periods of the year to allow internal walls to absorb solar energy in the day time and then release it at night as the temperature decreases. During hot periods of the year windows can be screened to prevent energy absorption by internal walls. The house is opened up at night and building materials release their energy to the cooler night air. During the heat of the day their thermal mass allows them to stay cool for longer.

2 BRICK WITH BUILT-IN PASSIVE SOLAR EFFICIENCY (BIPSE BRICK)

The major idea for development of a new brick was to achieve on the northern (mostly exposed to the sun in Australia) masonry walls better solar energy absorption in winter and better shading in summer

not by using large windows and external shading devices but by building the principles of passive solar efficiency into brick design. The design (Australian Patent No. 2005902375 Building Cladding Element with Built-in Passive Solar Efficiency) proposed by the author in 2004 is shown in Figure 2.

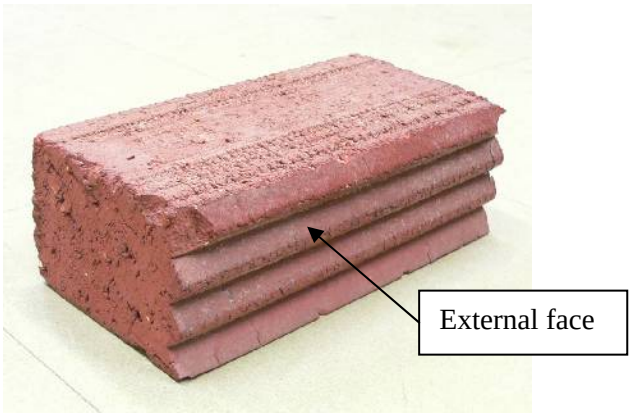

Figure 2. Extruded clay brick with built-in passive solar efficiency

The external face of the brick is not flat as in a traditional brick, but has horizontal ribs designed to increase the brick surface exposed to solar radiation in winter and reduce exposure in summer. It is also designed to capture in winter time some of the solar radiation reflected by the ribs back onto the brick surface as shown in Figure 3.

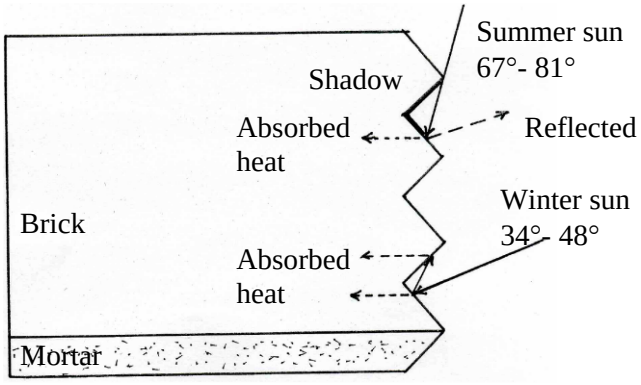

Figure 3. Principles of built-in passive solar efficiency (for Sydney latitude)

The angles of the ribs are designed to work best at certain latitude. Figure 4 on the next page show how a brick wall built out of new solar efficient bricks would look at midday in summer and winter. This new brick design will have some implications in brick manufacturing, brick storage and brick laying. It will also have some architectural benefits apart from improved energy efficiency.

2.1 Implications for Brick Manufacturing Industry

- Clay bricks will be extruded as usually. There will be one additional operation – ribs on the external surface of fresh bricks will be formed by rolling them with a specially designed gear;
- Dry pressed bricks or moulded blocks must be formed with the external ribs at the bottom of a mould form;
- There will be approximately a 5% saving in the material for bricks with the overall width of 110mm.

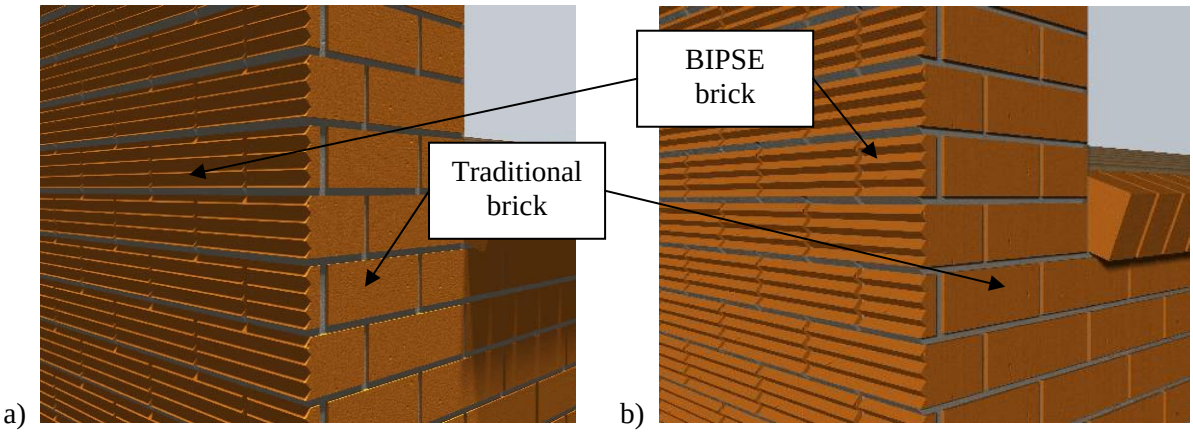

Figure 4. Computer simulation of passive shading on the northern wall at midday for Sydney: a). in summer; b). in winter.

2.2 Implications for the Brick Laying

- Struck bed joints are preferred because mortar joint forms the lower surface of every forth rib;
- At the external corners of walls conventional quoin bricks, or both new and conventional, or bricks cut at 45^{o} can be used;
- A bricklayer's trowel needs to be modified – corners near the handle need to be approximately 90^{o}.

2.3 Additional Architectural Benefits of BIPSE Bricks

This new design of brick completely changes the appearance of such a traditional material as brickwork giving to an "old" material a new face. A wall made of BIPSE bricks will have horizontal articulations in the form of ribs. This contemporary articulated look will be amplified in summer by horizontal shadows on the wall. If glazing is used on the upper surface of ribs, a brick wall will appear to have a different colour depending on the view angle. The colour of the wall will also appear to change when the observer moves to or from the wall. These architectural features of BIPSE bricks, although by-products of original solar efficient design, may prove popular among house designers and consumers.

3. COMPARISON OF THERMAL PERFORMANCE OF CONVENTIONAL AND BIPSE BRICKS

Laboratory tests were performed at the University of Newcastle (Australia) to compare the thermal performance of BIPSE bricks and conventional bricks. Tests on the heat absorption were performed by Mr. Mathew Turner [2004] as a part of his final year civil engineering project. These results were summarised and analysed in [Totoev, 2006]. Tests on the heat conduction were performed by Mr. Ryan Tranter [2007] as a part of his final year civil engineering project. Both sets of results are presented in these paper for completeness. The objective of tests was to assess the heat absorption and heat conduction capacity of new bricks in comparison to conventional bricks by measuring heat flux through the brick.

3.1 Principles of Heat Transfer Theory for Bricks

It is commonly accepted that heat transfer though the brick occurs by conduction due to the temperature differential on external and internal surfaces of the brick. The convection of hot air though pores of the brick, although theoretically possible, is assumed negligible in comparison to the

heat conduction. Most of the heat energy is delivered during the day time to the external surface of a northern wall by solar radiation. Part of it is absorbed into the brick and the remainder is reflected away from the wall. Absorbed and reflected parts are believed to be comparable in magnitude. Part of the absorbed energy heats the brick and the rest of the energy passes through the internal surface of the brick. At night this process is usually reversed because external temperature is lower than internal. Brick walls at night radiate energy back to the external environment.

3.2 Test Specimens

Test specimens were single bricks. Bricks were extruded solid clay units. Four types of bricks were tested for heat absorption:

- Conventional brick with flat external face;
- BIPSE brick with 50º inclination of the upper face of ribs;
- BIPSE brick with 60º inclination of the upper face of ribs;
- BIPSE brick with 70º inclination of the upper face of ribs.

First two types were also tested for heat conduction.

The thickness of the conventional brick was reduced to achieve the same volume as BIPSE bricks. This was done to ensure that exactly the same amount of energy is used to heat all the bricks. Therefore the amount of energy passing through the internal surface of a brick was proportional to the amount of energy absorbed into the external surface of a brick.

In the Sydney/Newcastle area an angle of 50º for the inclination of upper face of ribs on the northern wall was expected to be the most efficient at midday. However, before and after midday the sun is lower in the sky. Two other angles of inclination designed to work better with a reduced incident angle of the sun were tested.

3.3 Testing Rig

A purpose-built testing rig was developed for the laboratory heat conduction tests. Similar arrangement was used previously for heat absorption tests. The testing arrangement is shown in Figure 5.

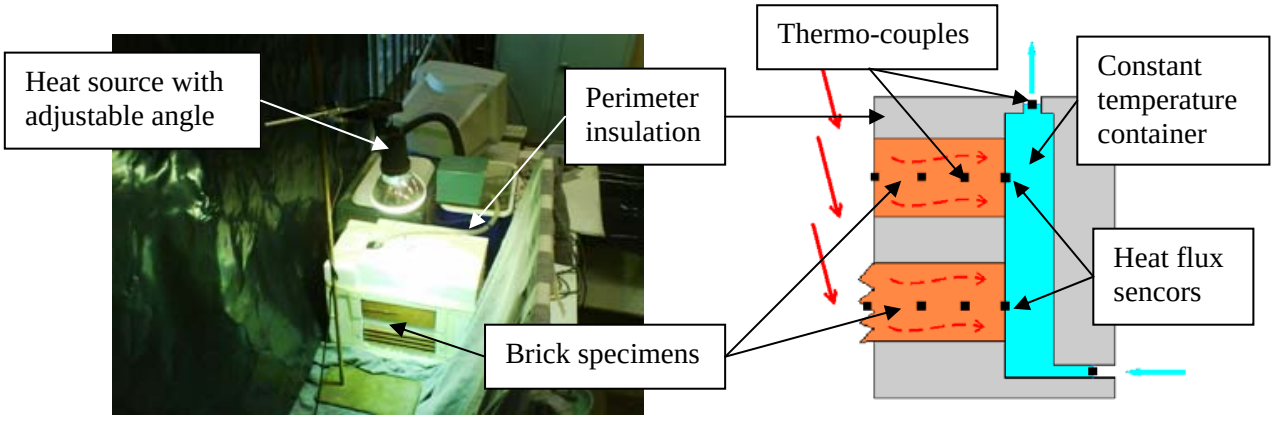

Figure 5. Rig configuration for heat absorption and heat conduction tests

Alternative test methods based on in situ atmospheric measurements have been considered. Laboratory testing was preferred at the first stage because it has less expensive set up and because it is easy to repeat this test with exactly the same heat input into specimen.

Bricks were placed on the aluminium water container. The water in the container was kept at a constant temperature of 22ºC for heat conduction tests and 25ºC for heat absorption tests. These

temperatures are from a comfortable temperature range in a house. The heat flux sensor was attached to the back of the test brick. The heat transfer compound was used to dismiss of any air gaps between the specimen, the flux sensor and the water container. A foam box was installed around the perimeter of the specimen for insulation leaving only the external face of the brick exposed to heat. The insulation box was glued to the water container and a gap filling compound was used between it and the specimen to minimise the heat losses though the sides of the specimen.

A 275W light globe was used in these tests as a heat source. In preliminary tests it was found that this heat lamp if positioned 620mm from the centre of the brick is capable of heating the specimen's external surface to a temperatures between 30 and 50ºC depending on the inclination angle of the lamp. This temperature range was comparable to temperatures recorded on northern walls of masonry buildings in spring. The inclination angle of the lamp was adjustable to represent the incident angle of the sun.

The set up was instrumented with a heat flux sensor and thermo-sensors. The heat flux sensor measured the heat transfer through the internal surface of the specimen. Thermo-sensors were positioned to measure temperature temperature through the depth of the brick. The laboratory air temperature and the water temperature in the container were also constantly measured. All sensors were connected to the data taker and continuously uploaded to the computer.

3.4 Testing Procedures

3.4.1 Heat Absorption Tests

Each specimen was tested at six different angles of lamp inclination: 30º, 40º, 50º, 60º, 70º, and 80º. For reference, the highest summer sun angle in Sydney is approximately 81º and the midday winter sun can be as low as 34º. It should be noted that before and after midday in winter and for walls not directly facing true North this angle is lower than 34º.

Each test was 24 hours long. Heat flux measurements recorded at night were more consistent than daily measurements because at night all energy input into the specimen was from the heat lamp radiation without any interference from the sun radiation and also because it was easy to maintain constant room air and water temperatures. After an initial transient period of approximately 2 hours, daily fluctuations of the heat flux were up to 25%. Nightly fluctuations were less than 5%. Therefore nightly records were used for comparison.

3.4.2 Heat Conduction Tests

Specimen was tested over six consecutive days in complete darkness; no radiant heet was absorbed into the external surface of the bricks. For the first three days the room temperature was bellow the water temperature in the tank. It was done to generate conduction of heat from internal to external surface of the brick as it happens during the colder time of the year and at night. For the next three days the room temperature was above the water temperature in the tank. This conditions generated conduction of heat from external to internal surface of the brick as it happens during the hot time of the year and during the day time.

3.5 Test results

3.5.1 Heat Absorption Tests

Test results for the heat absorption tests are summarised in Figure 6. In this Figure the heat flux through the internal surface of bricks is plotted against the angle of the heat radiation source.

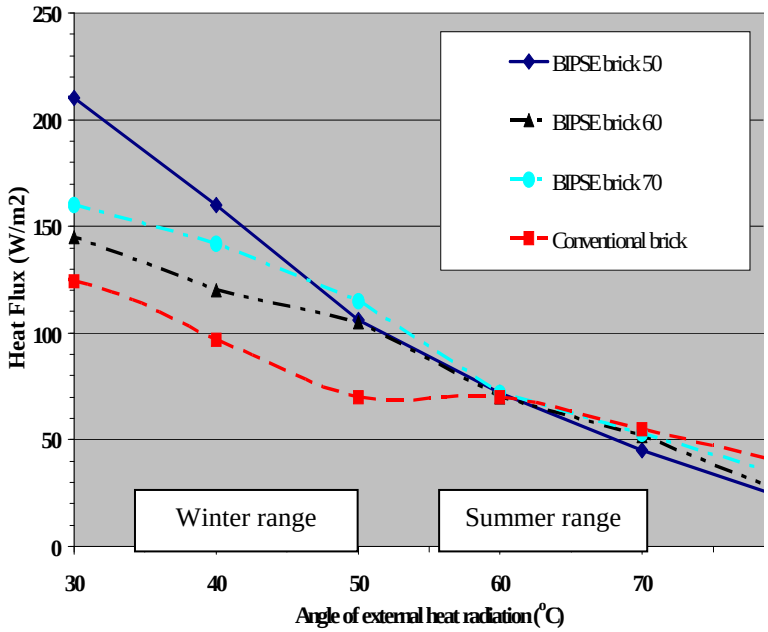

Figure 6. Summary of the heat absorption test result

In these tests all BIPSE bricks outperformed the conventional bricks at both ends of the heat source angle range. They absorbed more heat at low angles of the heat source and less heat at high angles of the heat source.

As was expected, the highest efficiency overall have BIPSE bricks with a 50º inclination of the upper rib face. The maximum heat flux of 210 W/m2 was recorded through BIPSE50 bricks. The maximum heat flux was achieved at a 30º angle of the heat source. At this angle of heat source the heat flux through the conventional brick was 124 W/m2, which is 41% lower than for BIPSE50 bricks. The minimum heat flux of 23 W/m2 was also recorded in BIPSE50 bricks at an 80º angle of the heat source. Corresponding heat flux in the conventional brick was 39 W/m2, which is 59% higher. In the middle of the heat source angle range (approximately 50º-60º) the heat flux though BIPSE70 bricks was higher than though other bricks.

3.5.2 Heat Conduction Tests

Test results for the heat conduction tests are summarised in Figure 7. In this Figure the heat flux through the internal surface of bricks is plotted over six days. Also in this Figure included plots for the room air temperature and for water temperature in the tank.

In these tests BIPSE brick was conducted more heat in both directions. It was expected because of its larger external surface. During the simulated “hot” days, the net effect of heat conduction was almost zero. BIPSE brick conducted more heat then the conventional brick from the external environment during the day. But it also conducted more heat into external environment at night. During the simulated “colder” days, heat conduction was unidirectional from internal to external surface of both bricks. BIPSE brick conducted approximately 70% more heat both during the day and at night.

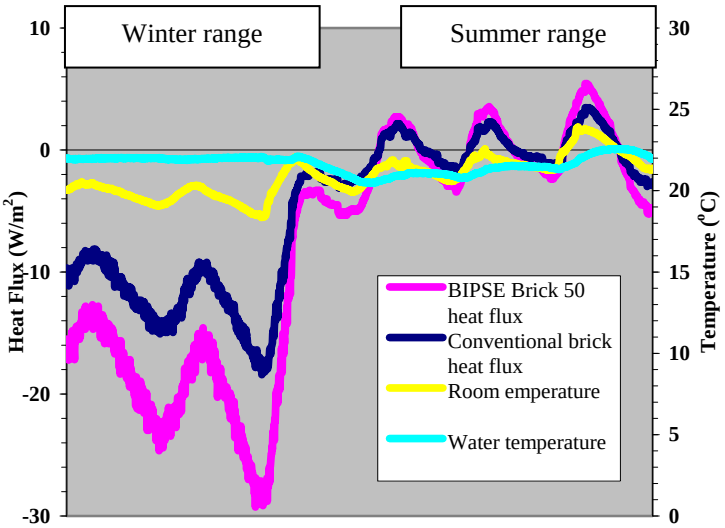

Figure 7. Summary of the heat conduction test result

Comparison of the heat absorption results in Figure 6 and the heat conduction test results in figure 7 reveals that the net effect in colder environment could be much smaller than observed in heat absorption tests.

4. CONCLUSION

A new brick with built-in passive solar efficiency (BIPSE brick) was designed at the University of Newcastle, Australia. The external face of this brick is not flat as in traditional brick but has horizontal ribs designed to increase the brick surface exposed to solar radiation in winter and reduce summer exposure.

BIPSE bricks can be made with minimal implications for the manufacturing industry and do not require any special bricklaying techniques. Apart from the improved solar efficiency BIPSE bricks have some additional architectural benefits: shades, texture, colour effects, contemporary appearance etc.

The experimental set up was developed to perform the heat conduction and the heat absorption tests and to compare thermal performance of traditional and BIPSE bricks. In this test the heat flux though the internal face of brick is was measured at different incident angles of the heat radiation on the external side of prisms or at different temperatures of external and internal surface of brick.

A series of heat absorption tests were performed on conventional and BIPSE bricks with different angles of inclination of the upper face of ribs. In these tests BIPSE bricks demonstrated better heat absorption properties to the conventional brick at both ends of the heat radiation angle range. They absorbed more heat at low incident angles of the heat radiation and less heat at high angles of the heat radiation. From these results it is possible to conclude that BIPSE bricks can potentially absorb up to 40% more solar energy in winter and up to 60% less solar energy in summer in comparison to traditional bricks.

A series of heat conduction tests were also performed on conventional and BIPSE bricks with 50^{o} angle of inclination of the upper face of ribs. In these tests the net heat flow through the brick was almost zero in warm environment. In colder environment BIPSE brick conducted approximately 70% more heat from the internal to the external surface both during the day and at night.

It is concluded that more testing is required and that the long term atmospheric in situ tests could be a better indicator of thermal efficiency of BIPSE bricks.

BIPSE bricks would be better suited to temperate or subtropical climate regions with mild winters and hot summers. The angle of rib inclination needs to be designed depending on a region's latitude. Body text is to be 11 points Times New Roman. All paragraphs should be right justified and single spaced, and there should be one blank line between paragraphs. References should be set in hanging indent, as shown later.

ACKNOWLEDGEMENTS

The help of Mr. Roger Reece of the civil engineering laboratory at the University of Newcastle in building and instrumenting the test set up is gratefully acknowledged. I also would like to thank my daughter Miss Anastacia Totoeva for proof reading this text and editing my English.

REFERENCES

Australian Building Codes Board, *BCA 2005: building code of Australia*, CanPrint Communications on behalf of the ABCB, Fyshwick, ACT.

Australian Greenhouse Office, AGO 1999, *Final report: Australian residential building sector greenhouse gas emissions 1990-2010*, Parkes, ACT.

Totoev, Y.Z. 2006, " Thermal properties of bricks with built-in passive solar efficiency", in *Proceedings of the 7th International Masonry Conference*, London.

Tranter, R., 2007, *Heat Conduction by BIPSE Bricks*, Final year project for Bachelor of Engineering (Civil), The University of Newcastle, NSW, Australia.

Turner, M. 2004, *Thermal properties of "comfy-brick"*, Final year project for Bachelor of Engineering (Civil), The University of Newcastle, NSW, Australia.

Underwood, C.P. and Yik, F.W.H. 2004, *Modelling methods for energy in buildings*, Blackwell Publishing Ltd., Melbourne.

11DBMC International Conference on Durability of Building Materials and Components
ISTANBUL, Turkey 11-14 May 2008

Strength of Cement Mortars with Carbon Material Admixtures

Luis G. Andión [1]
Juan Alcaide [2]
Eva G. Alcocel [3]
Emilio Zornoza [4]
Pedro Garcés [5]

T 18

ABSTRACT

The use of electrical conductors such as graphite powder (GP) as mortar admixtures in order to obtain conductive cement-based materials suggests the idea of designing multifunctional materials for specific purposes. The main goal of the present work is to evaluate the effect of GP admixtures in the mechanical properties of cement mortars fabricated with different types of graphite powder. Four different types of GP were used as admixtures to Portland cement mortar samples: two of them are commercially available products and the other two are by-products of the fabrication of graphite electrodes. The carbon ingredients have been added both as an addition to the mix and as a substitutive of a portion of cement weight.

For all studied graphite powder types the mechanical properties decrease as the addition rate increases. For addition rate of 3%, the loss of compressive strength is between 0 and 10%. Therefore it is possible to obtain conductive mortars without important loss of mechanical properties.

KEYWORDS

Carbon materials, Mechanical properties, Mortars

[1] University of Alicante, Dept. Ingeniería de la Construcción, Alicante, Spain 03690, Phone +34 965903400 (Ext. 9499), Fax +34 965903678, luis.garcia@ua.es
[2] University of Alicante, Dept. Construcciones Arquitectónicas, Alicante, Spain 03690, Phone +34 965903400 (Ext. 2572), Fax +34 965903678, juan.alcaide@ua.es
[3] University of Alicante, Dept. Construcciones Arquitectónicas, Alicante, Spain 03690, Phone +34 965903400 (Ext. 2950), Fax +34 965903678, eva.garcia@ua.es
[4] University of Alicante, Dept. Ingeniería de la Construcción, Alicante, Spain 03690, Phone +34 965903400 (Ext. 3707), Fax +34 965903678, emilio.zornoza@ua.es
[5] University of Alicante, Dept. Ingeniería de la Construcción, Alicante, Spain 03690, Phone +34 965903400 (Ext. 3324), Fax +34 965903678, pedro.garces@ua.es

1 INTRODUCTION

Concrete is a very versatile material because its properties can be changed by incorporating to the mix ingredients such as chemical products, mineral materials, fibers, etc. The mixes so obtained make it possible multiple applications of the new material using its new properties. Traditionally the research on cement-based materials for building and civil construction have been oriented to the material strength because of their main structural function. However in recent years new research lines have been conducted in order to obtain complementary functions of such materials, that is to convert them into "multifunctional materials" [Chung 2004]. Different categories of cement-based multifunctional materials can be distinguished. One of them is the electrically conductive cement-based materials. As regular concrete is a poor conductor (dielectric), different electrical properties can be obtained by the addition of conductive materials, for example graphite powder (GP) or carbon fibers. This way the resulting composite materials have special physical and chemical properties that make them suitable for new technologically advanced products [Chung 2000].

Even though the use of these materials means an important cost increase, the highly promising benefits that can be obtained, apart of the mechanical properties improvement, make them interesting. Among the functions that a conductive cement-based material can realise are the self sensing of internal strain, electromagnetic signal arrestor (EMI shielding) and deicing action on frozen pavements [Chung 2003].

The electrical resistance of concrete have been under study for many years [Hammond & Robson 1955]. Its efficiency as electrical isolator was demonstrated by the use of concrete sleepers for railways. It has been reported that concrete behaves as a dielectric when perfectly dry and shows resistivity values in the range of semiconductors when is humid or water-saturated.. In the latter conditions it has been demonstrated that that the internal pore system was the responsible of the conductive path [Monfore 1968]. Under the influence of an electrical field the migration of ions in the pore dissolution occurs and the material becomes an electrical conductor. Further studies have demonstrated that the concrete resistivity is closely related to the cement hardening and hydration progress [Roberts 1980] and that resistivity is a key control parameter in the reinforcing steel corrosion [Alonso *et al*. 1988], because it is dependent on the degree of water saturation of the pore system.

The residual service life of a concrete structure depends on the state of both the conglomerate and the reinforcing steel. In spite of the potential advantages that the addition of carbon material provide, there are very few references in the specialised literature on the effect that different types of carbon additions in concrete mixes produce on the mechanical properties and particularly in the corrosion rates of the reinforcing steel [Hou & Cheng 2000, Garcés *et al*. 2005].

Consequently, the objective of the present study is to provide an insight knowledge of the strength properties of mortars fabricated with different types of carbon materials. Four types of graphite powder (GP) were used in this research: two commercial types and two by-products of the graphite electrode industry.

2 EXPERIMENTAL

2.1 Materials and Methods of Mortar Specimens Fabrication

Portland cement type CEM I 52.5 R (CP) and silica sand normalised under UNE-EN 196-1 standard were used for all mortar specimens. Figure 1 shows the SEM images of the carbon materials used. Note the irregular particle shape. Sofacel graphite powder (PGS) is a commercial

brand of Le Carbone Lorraine Company with particle size lower than 0.63 mm. Figure 2 shows PGS in detail. The marked lamellar structure and the rough surface can be observed.

No. 9 Graphite Powder (PG9) is a commercial brand supplied by Superior Graphite Company, particle size lower than 75 µm, also shown in Fig. 2. The morphological differences between PGS and PG9 are notorious.

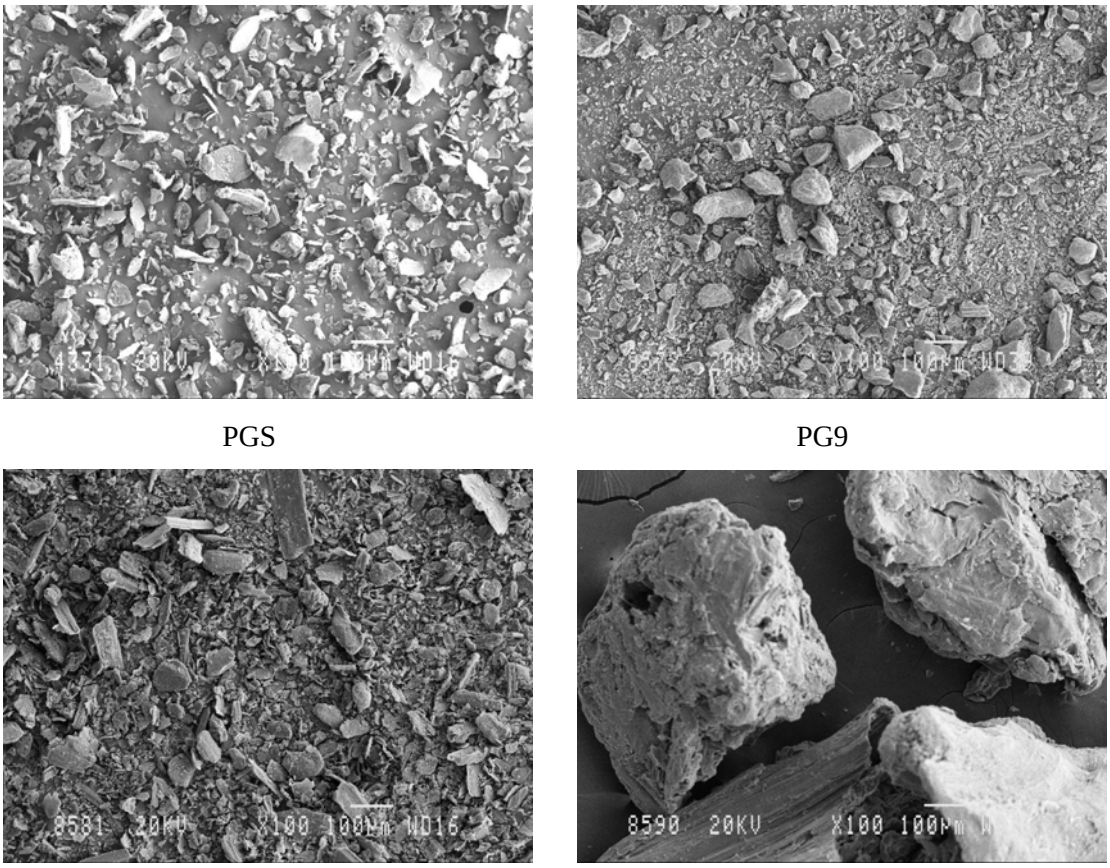

Figure 1. SEM images of carbonaceous materials.

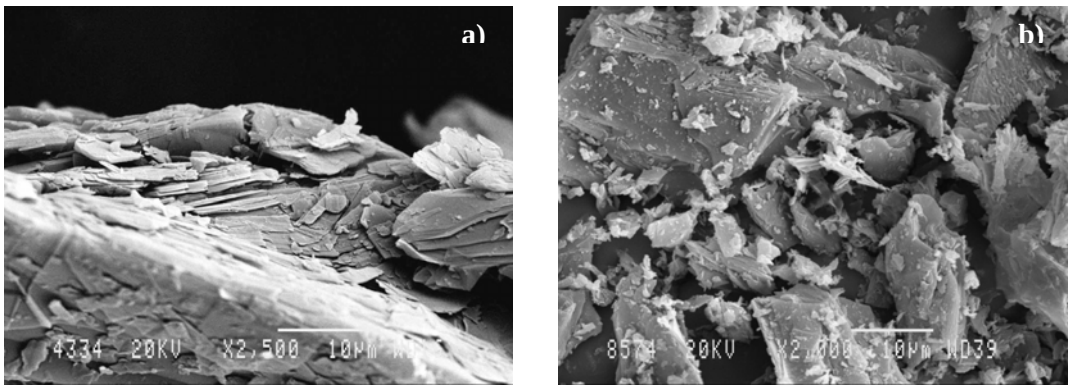

Figure 2. Details of (a) PGS and (b) PG9.

The graphite electrode maker Grafitos Barco has supplied two types of by-products of the fabrication of furnace conductor electrodes for the steel industry. Both have identical composition and the difference is based on the particle size distribution. PGA type contains a minimum 90% of particles under 50 µm size, whereas PGC type contains a 90% of particles with average size in

the range 0.5-1 mm. Table 1 shows the element composition of each type of graphite powder. The high content of carbon in all of them (more than 98%) is to be noted.

Table 1. Chemical analysis of carbon admixtures.

Sample	*Elemental Analysis (% wt.)*			
	C	*H*	*N*	$(S+O)_{dif}$
PGS	99.35	-	-	0.65
PG9	99.00	-	-	1.00
PGA and PGC	98.48	-	0.05	1.47

Figure 3 shows the particle grading curves obtained by laser light diffraction of the materials used in mortar fabrication. Only the fraction of sand passing through 0.16 mm sieve was used. The mean size value D50, that is the size value in µm under which 50% of the particles lay, is as follows: 15.9 µm for cement, 28.1 µm for PG9, 28.8 µm for PGA, 41.2 µm for PGS, 79.7 µm for sand and 355.7 µm for PGC. With the exception of PGC all graphite powder types have grading curves laying in between the cement and the sand grading curves. A filler effect can then be expected for those materials.

All paste and mortar specimens were fabricated and cured at 20ºC. The GP was included in the mix either as an additional component of the binder or as a substitute of part of the cement mass. In the first case the binder is only the cement mass, whereas in the latter case (substitution) it has been considered that the binder is the cement mass plus the content of GP. With these premises the weight ratios used in the mix formulation were 0.5 for water/binder and 3.0 for sand/binder. For strength testing the GP weight ratios in mortar specimens were 0% (reference), 0.5%, 1% and 3% both as addition and as cement substitution.

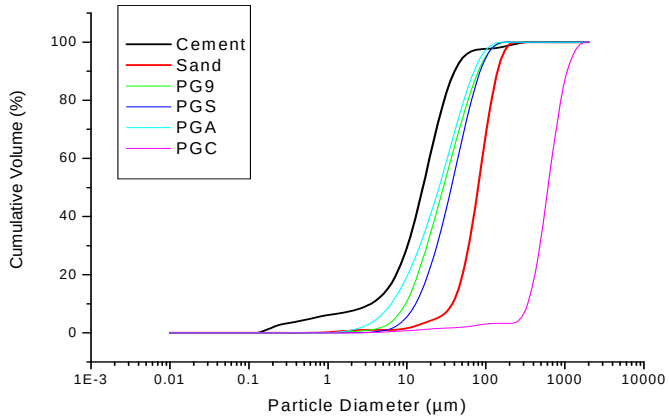

Figure 3. Particle size distributions of the GP types, cement and sand in the experiments.

2.2 Mechanical Tests

The mortar consistency was determined according to standard UNE 1015-3. The mechanical tests were performed in laboratory ambient conditions according to standard EN 196-1. Prismatic mortar specimens of 4x4x16 cm size were fabricate in two layers with mechanical compaction. Specimens were cured submerged in water and the tests were carried out at ages of 2, 28 and 120 days. Flexural and compressive strengths as well as accessible porosity were determined in the mechanical test specimens.

3 RESULTS

Chart of Fig. 4 shows the 120 day flexural strength results of mortar specimens fabricated with 0.5%, 1% and 3% of GP (relative to cement weight), for each of the GP types under study. Chart values are the ratio Rf_i/Rf_0, where Rf_i is the strength result of the specimen and Rf_0 is the strength of the reference sample. The chart reveals that with only 0.5% addition of any type of GP some improvement of flexural strength was obtained, being clearly GPC the type with the highest strength gain.

When the addition rate is increased to 1%, the flexural strength still improves, except for PGS type. The lamellar structure of this type of GP could be responsible for this result. However for 3% addition rate, none of the studied GP types reach the flexural strength of the reference specimens, with strength drops of 7%, 6%, 2% and 1% for types PGA, PGS, PG9 and PGC, respectively. The lack of continuity of the cement paste is not beneficial for the flexural strength when the GP addition rate exceeds some threshold value between 1% and 3%.

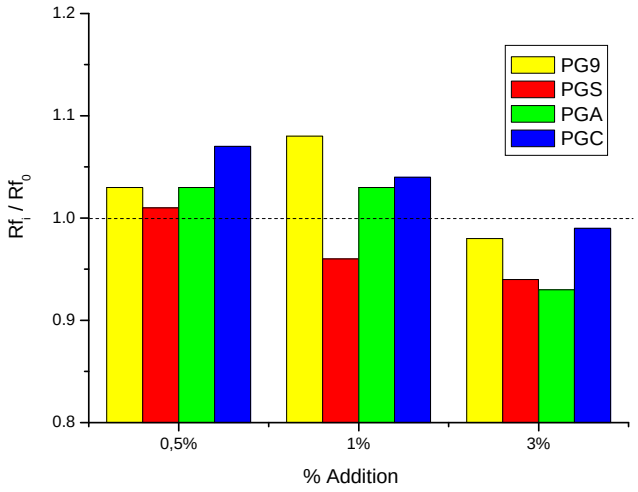

Figure 4. 120-day flexural strength of mortars with different GP types used as admixtures in various ratios. Y-axis values are Rf_i/ Rf_0, that is the ratio of specimen strength (Rf_i) to the reference mortar (no GP) strength (Rf_0).

Figure 5 shows the compressive strength values (Rci) at 120 days of mortars fabricated with different types of PG with addition rates of 0.5%, 1% and 3% of the cement weight. Y-axis values are Rci/ Rc0 where Rc0 is the compressive strength of the reference mortar (no PG). PG9 and PGS significantly improve the reference mortar strength for addition rates up to 1%. By-products PGA and PGC are only beneficial for addition rate of 0.5%. For higher addition rates of 3%, only the PG9 type reach the strength of the reference mortar. PGS, PGC and PGA types added at 3% rate produce strength losses of 8%, 9% and 10%, respectively.

Therefore, with the exception of PG9 type, the addition of GP in rates exceeding 1% produce a significant reduction of strength.

Table 2 shows the average diameter of consistency tests (mm) and the porosity values at 120 days of mortars fabricated with 3% additions of the four types of GP. The specimens with lower diameter show high porosity. These results are consistent with the ones of the compression tests because, with the exception of PGS, the drier is the mortar mix (lower diameter) the lower is the compressive strength.

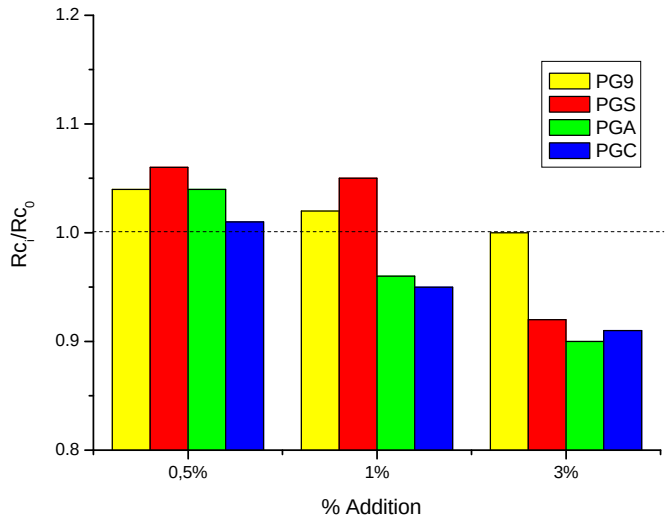

Figure 5. 120-day compressive strength of mortars with different GP types used as admixtures in various ratios. Y-axis values are Rc_i/ Rc_0, that is the ratio of specimen strength (Rc_i) to the reference mortar (no GP) strength (Rc_0).

Table 2. Average consistency test diameter values (mm) and porosity (%) of mortar fabricated with 3% of different types of graphite powder.

Parameter	*Control*	*3% PG9*	*3% PGS*	*3% PGA*	*3% PGC*
Slump (mm)	184	178	162	170	173
Porosity (%)	16.8	16.5	18.4	18.3	16.5

In general, it can be observed that the mortar strength decreases when the addition rate increases. According to Fig. 1 and Fig. 2, the shape of particles, rather similar for all types, does not seem to be responsible for the different behavior. The GP particle size does not explain it either, because the strength values trend is not consistent to the mean GP particle size trend and the grading curves are closed to each other and in between the curves of sand and cement. The differences in strength are then attributed to the different graphitation level of GP types (higher in the commercial types).

Figure 6 shows the 120-day compressive strength values, Rc_i of mortars fabricated with substitution of of 0.5%, 1% and 3% of cement weight by the four different types of GP. Y-axis values are expressed as the ratio Rc_i/Rc_0 with respect to the reference mortar (no GP) values, Rc_0. For 0.5% substitution rate, all types reach the reference mortar strength, except type PGA that shows a strength loss of 10%. For substitution rate of 1%, the loss of strength is 3% for all types, except for PGS that equals the reference mortar value. For substitution values of 3% all types show strength losses in the range 5%-10%.

Consequently, with strength loss smaller than 5%, it can be concludes that the substitution of cement by GP in rates up to 1%, it is possible to fabricate mortars in accordance to the mechanical prescriptions of standard UNE en 197-1.

This way it is possible to put in market value some graphite by-products (PGA and PGC) for the fabrication of mortars with cement content savings.

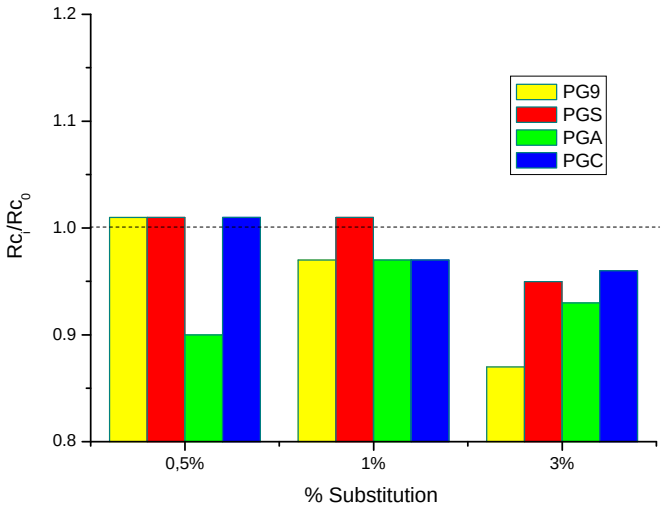

Figure 6. 120 day compressive strength of mortars with different GP types used as cement substitution admixtures in various ratios. Y-axis values are Rc_i/ Rc_0, that is the ratio of specimen strength (Rc_i) to the reference mortar (no GP) strength (Rc_0).

Nevertheless, the purpose of the fabrication of these mixes, specially with commercial types, is not to obtain gains in the mechanical behavior , but changes in the electrical conductivity of the resulting materials. The inclusion of a conductive material, such as GP transforms the non conductive mortar into a conductive mortar or concrete, making it possible the use for other functions and becoming a multifunctional material.

4 CONCLUSIONS

The overall review of the results allows the following conclusions.

1) For all studied graphite powder types the mechanical properties decrease as the addition rate increases. For addition rate of 3%, the loss of compressive strength is between 0 and 10%. Therefore it is possible to obtain conductive mortars without important loss of mechanical properties.

2) For the by product GP types (PG9 and PGC) the results show that their use for conductive mortars with some cement savings is feasible. This can be a contribution on sustainability and can be a way of making some GP products more valuable.

REFERENCES

Alonso, C., Andrade, C., & González, J.A., 1988, 'Relation between resistivity and corrosion rate of reinforcements in carbonated mortar made with several cements types', *Cement and Concrete Research* **18**, 687-698.

Chung, D.D.L., 2000, 'Cement reinforced with short carbon fibers: A multifunctional material', *Composites Part B: Engineering* **31**, 511-526.

Chung D.D.L., 2003, 'Multifunctional cement-based materials', Ed. Michael Meyer editor. Marcel Deeker, Inc., New York.

Chung, D.D.L., 2004, 'Electrically conductive cement-based materials en Multifunctional cement-based materials', Ed. Marcel Dekker, Inc., The State University of New York, Buffalo, New York.

Hammond, E., & Robson, T.D., 1955, 'Comparison of electrical properties of various cements and concretes', *The Engineer* **199**[5165], 78-80 and [5186], 114-115.

Hou, J., & Cheng, D.D.L., 2000, 'Effect of admixture in concrete on the corrosion resistance of steel reinforced concrete', *Corrosion Science* **42**, 1489-1507.

Garcés, P., Fraile, J., Vilaplana-Ortego, E., Cazorla-Amorós, D., Alcocel, E.Gª & Andión, L.Gª., 2005, 'Effect of carbon fibres on the mechanical properties and corrosion levels of reinforced portland cement mortars', *Cement and Concrete Research* **35**, 324-331.

Monfore, G.E., 1968, 'The electrical resistivity of concrete', *Journal of PCA Research and Development Laboratories* **10**, 35-48.

Roberts, J.J., 1980, Cement and Concrete Association, Technical report nº 532.

Seismic Rehabilitation of an Ancient Masonry Infill Steel Frame Building

Nouredine Bourahla [1]
Salim Tafraout [2]
Tahar Boukhamacha [2]

T 21

ABSTRACT

Ancient buildings constructed in urban areas, particularly in Algiers, are typically 4 to 6 storey high and are made of stone masonry walls or infill light steel framing. These types of buildings are reputed to be vulnerable to seismic effects.

This paper presents a study on the renovation and required seismic upgrading of a 100 year old masonry infill steel frame building located in the centre of Algiers. The building is to be renovated for use as a modern art museum. The structure primarily consists of a light steel structure made of riveted steel trusses and columns having thick stone and brick masonry walls along its perimeter. The basement floor is made of shallow arches supported by steel beams (jack arch system) and the upper floors are wood-framed diaphragms. The building endured several moderate earthquakes that occurred in proximity to Algiers and as well sustained no significant damage from the Boumerdes earthquake (M 6.8) that occurred in 2003. The structure was numerically simulated using 3D finite elements models. The data, obtained from an extensive program of non-destructive and destructive tests on the constituent materials, were introduced into the numerical models and a series of ambient vibration tests together with modal analyses were performed to validate the mathematical models. A linear elastic analysis was carried out on the calibrated numerical model of the structure using the most recent elastic spectrum of the Algerian seismic code (RPA99 rev.2003).

Results of load combinations helped identify critical regions and seismic deficiencies. On the basis of these findings upgrade strategies and a solution for strengthening the structure are proposed.

KEYWORDS

Masonry strengthening, Ambient vibration, Structural assessment, Seismic vulnerability

[1] Saad Dahlab, Blida University, Civil Eng. Dept, Blida, Algeria 09000, Phone +213 25433939, Fax +213 254339393, nbourahla@mail.univ-blida.dz
[2] SCTE, Division Etudes, Algiers, Algeria, Phone +213 21 552895, Fax +213 21404920, scte_algiers@yahoo.fr

1 INTRODUCTION

In seismic prone areas, structural masonry is seldom used for new buildings since most collapses and deaths in recent earthquakes are due to inadequate performance of unreinforced masonry buildings. However, most of ancient buildings constructed in those regions are made of stone or brick masonry walls or infill light steel framing in which masonry panels play dominant role in resisting lateral forces. Research on the seismic behaviour of masonry structures is nowadays almost entirely dedicated to existing buildings and to the issues related to assessment and reduction of their seismic vulnerability [Magines G. 2007]. Because of different degrading agents, old masonry buildings become even more fragile and need to be strengthened. The determination of the material characteristics in terms of stiffness, strength and energy dissipation capacity (cyclic behaviour) is required to assess the actual resistance capacity and to design an efficient retrofit scheme [Bourahla & al. 2002]. In this context fiber reinforced polymer (FRP) materials offer viable solutions to solve or lessen the effects of overloading. Extensive research work investigated the seismic behaviour of rettrofitted masonry structures both analytically and experimentally [Triantafillou T. C. 1998, Tumialan G. Et al. 2001, Elgawady M. 2006, Shrive N. 2006]. This paper focuses on the structural diagnostic of an old masonry infill steel frame to identify the structural degradations and assess the overall dynamic and damping characteristics using ambient vibration testing. On the basis of the dynamic analysis, critical zones were identified and a strengthening technique based on fibre-reinforced polymers was adopted.

2 DESCRIPTION OF THE BUILDING

The edifice is an ancient building constructed in 1909 and intended to be used as a modern art museum. The construction is an L shaped four storey building located in the centre of Algiers. It comprises two patios in the middle with a roof incorporating five domes made of steel frames with glass infill. A 16 m height minaret is located at one corner of the building (Fig. 1).

Figure 1. Interior and exterior views of the building.

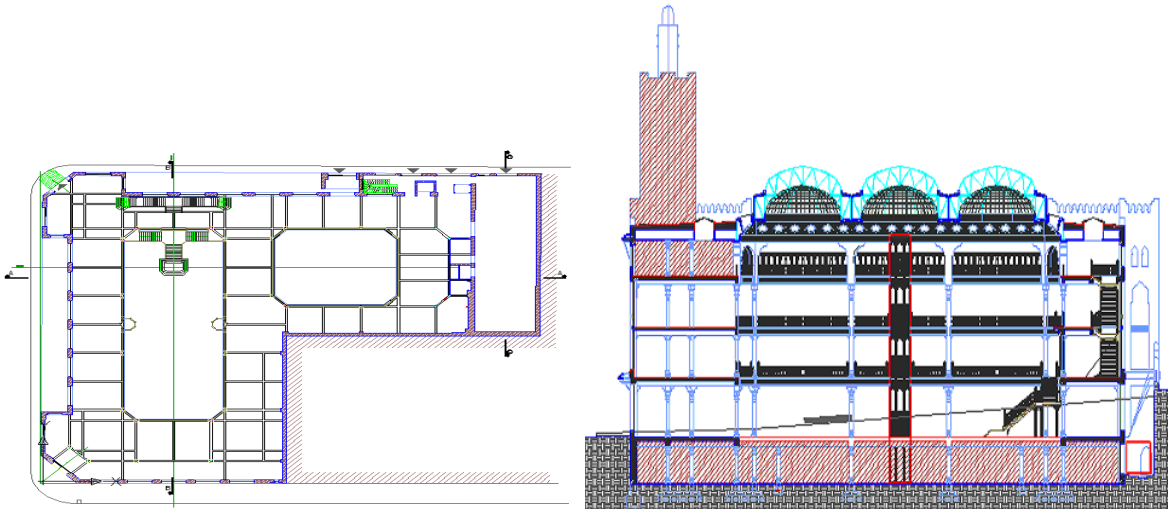

Figure 2. a- Plan view of the building b- Elevation view of the building

The edifice is supported by riveted light steel framing with peripheral stone/brick masonry walls of 90 cm thick used as a structural element to resist horizontal forces and part of the vertical loads. These walls are perforated by numerous window and door openings.
The slender steel columns are embedded in circular micro concrete sections to enhance their stability performance.

The building withstand several moderate earthquakes that occurred in the vicinity of Algiers and recently a major far field earthquake that occurred in Boumerdes 2003 about 40km away. An investigation of the building was carried out by a multidisciplinary engineering team. Beside the classical tests for material characteristics identification, a special attention was particularly made to investigate the building physically in search of any imprint the earthquakes might have left. The structural damage consists almost exclusively of widespread corrosion observed on certain steel elements because of humidity in areas subjected to water leak and exposed to sea environment. (Fig. 3).

Figure 3 a- Typical steel element corrosion b- column cross section

Damage inflicted by earthquakes is insignificant. It is thus somewhat extraordinary for such type of old building ---especially one with very tall stories, no substantial cross walls, a spacious multi-story interior sanctuary space and an irregular domed and gabled roof --- to resist the seismic activity for more than a century with almost no damage. On the basis of our studies, we conclude that certain specific dynamic characteristics of the structure and the exceptionally high material quality are largely responsible for this performance.

3 AMBIENT VIBRATION TESTING

The assessment of the structural resistance of existing constructions uses often mathematical models whose parameters can hardly be precisely estimated by analytical procedure only. Therefore, the elastic, mass and damping characteristics of the structure to be assessed must be known to a sufficient degree of accuracy in order to evaluate the actual structural capacity of the construction. The elastic dynamic properties, particularly the natural frequencies and the corresponding mode shapes are a combined measure of the structural characteristics of the construction. These model characteristics can be successfully estimated, especially in elastic range, using the well known ambient vibration testing. In this paper we present briefly the main issues pertaining to this particular modal testing; FRF measurement techniques, testing procedure, and modal parameter estimation method.

For this particular case preliminary modal analyses were first carried out and the fundamental modes were predetermined. On the base of these results optimum sensor locations were chosen nevertheless additional measurement points were also included to take account of any other modes that were not predicted by the analytical model. Measurement near the nodal point of any of the modes will omit that particular mode and aliasing effect is to be prevented by avoiding intersection regions of the fundamental modes to be identified.

The tests were performed using three degrees of freedom seismometer type Lennartz electronic (Le3Dlite) and a data acquisition system type City Shark II. The measured signals were processed using the GEOPSY program [Wathelet 2005] capable to perform most of the signal processing operations for the analysis of ambient vibration data. The sensors were located and oriented according to the previously defined test programme. The recording time for each sequence was set to 10 mn and found to be largely sufficient to obtain smooth transfer function curves. In total 24 measurement points were performed. Figure 4 shows the locations and the orientations of the sensors on the top floor.

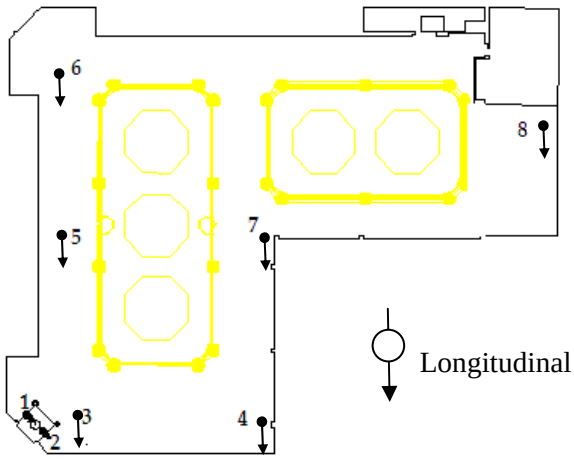

Figure 4. Locations and orientations of the sensors on the roof and the minaret

The natural frequencies of the structure were simply identified using a “peak cursor” on the Frequency Response Functions (FRF). Due to the complex shape of the structure, the individual vibration modes do not exhibit purely translational motions, but generally a coupled transversal, longitudinal and rotational motion. Thus individual Frequency Response Functions (FRF) have peaks corresponding to several modes. In one hand this enables to cross-check the measured frequencies but in the other hand closely spaced frequencies are difficult to identify.
The first few lower frequencies were identified (Table 1) and representative FRF curves are shown in Figs. 5 and 6. The continuous lines represent the average curves and the dashed lines are the limits of standard deviations.

Table 1. Natural frequencies and corresponding damping ratios.

Mode	*Frequency* [Hz]	*Direction*	*Damping* [%]
1	2.45	Longitudinal	1.05
2	2.70	Torsional	1.34
3	2.90	Transversal	1.05
4	3.35	Transversal	1.42
5	3.50	Longitudinal	1.88
6	4.25	Longitudinal	1.97
7	5.30	Longitudinal	2.21

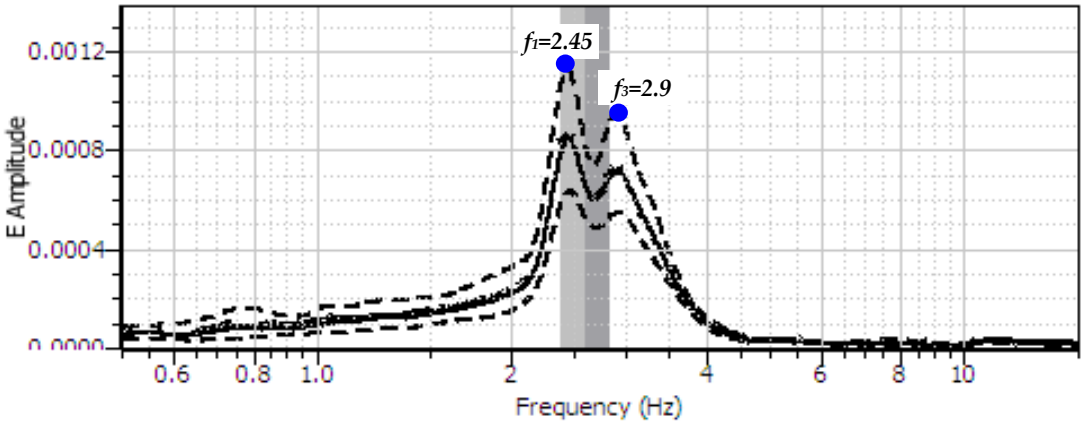

Figure 5. FRF curve recorded on point 2.

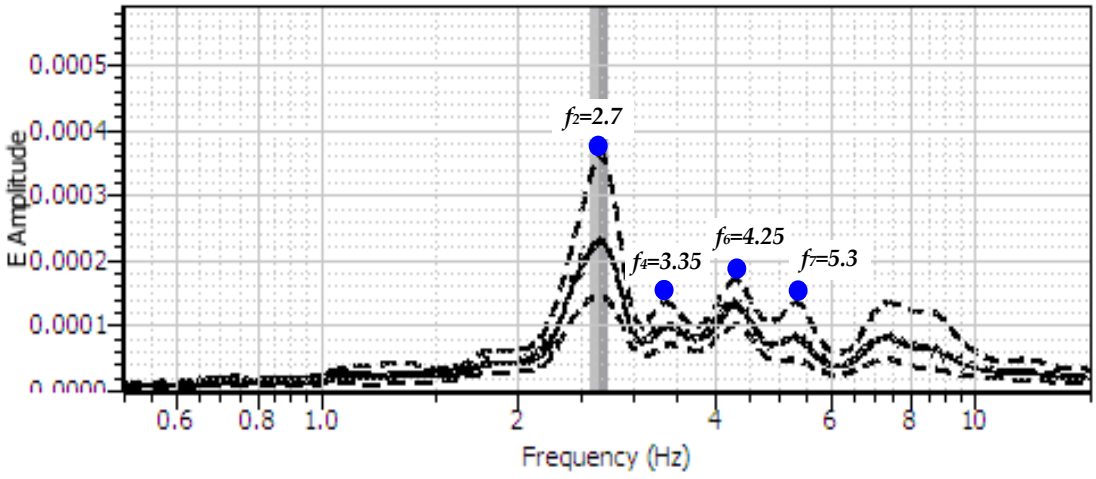

Figure 6. FRF curve recorded on point 5.

4 MODAL AND SEISMIC ANALYSES

In order to portrayed the elastic seismic behaviour of the building a three-dimensional analytical model was developed using SAP2000 [CSI 2004]. The model included the entire peripheral masonry wall system, the floor and roof diaphragms, and the steel framing (Fig. 7). A modal analysis was first carried out to validate the model. A minor adjustment of the elastic modulus of the masonry achieved reasonable correlation with the experimental results.

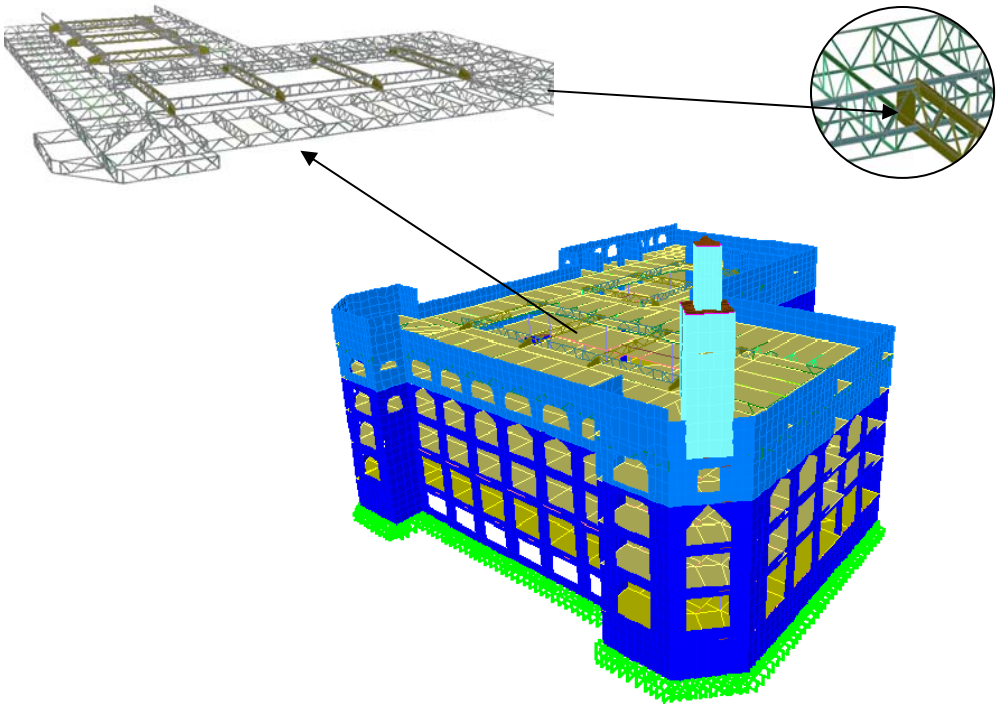

Figure 7. Three-dimensional analytical model.

A spectrum response analysis was performed by applying an acceleration spectra derived from the RPA99v2003 (Algerian seismic code). The seismic response of the building was studied in details to understand the vulnerability of each structural element particularly the masonry walls.
Figure 8 shows the stress distribution in the masonry walls where we can notice that the masonry around openings is subjected to substantially greater stress demand. On the basis of these results, several critical zones were identified for strengthening.

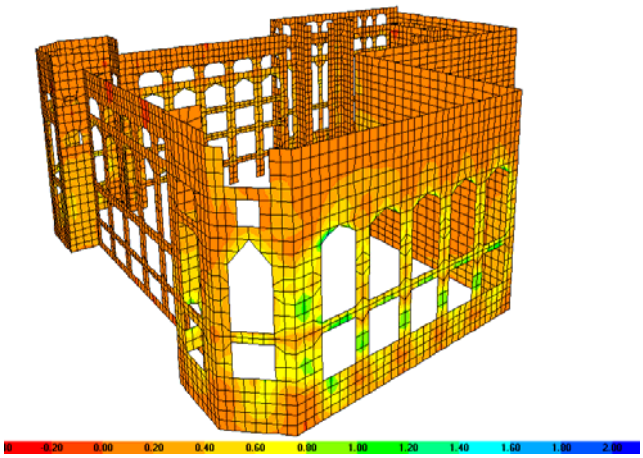

Figure 8. Stress distribution in the perimeter masonry walls.

5 STRUCTURAL STRENGTHENING

As outlined earlier, critical components are localised in the vicinity of the lower openings of the masonry walls. Considering the different strengthening schemes of masonry walls to enhance their in plane strength capacity, it was decided to use the technique based on the fibre-reinforced polymers

which is most suitable in this case because of the high demand to capacity ratio. Fibre reinforced polymers (FRPs) can be adhered to the surface of a masonry wall with epoxy to provide strength across potentially weak planes. Because of the high tensile strength of FRP materials, a fairly thin sheet can provide substantial strength and confinement to the masonry. Though lateral strength of masonry wall can be enhanced several fold using FRP sheets, inelastic deformation capacity may be limited as a result of debonding of the sheets which occurs suddenly with little ductility. Thus, FRP materials should be placed strategically on those piers that are likely to attract damage first so that alternate, and more ductile, mechanisms can occur. The locations and directions of the FRP sheets are indicated on Figure 9 according to the results obtained from the dynamic analysis. In order to relieve the high stresses around the lower openings on the wall, a reinforced concrete rings are provided as shown on Figure 10.

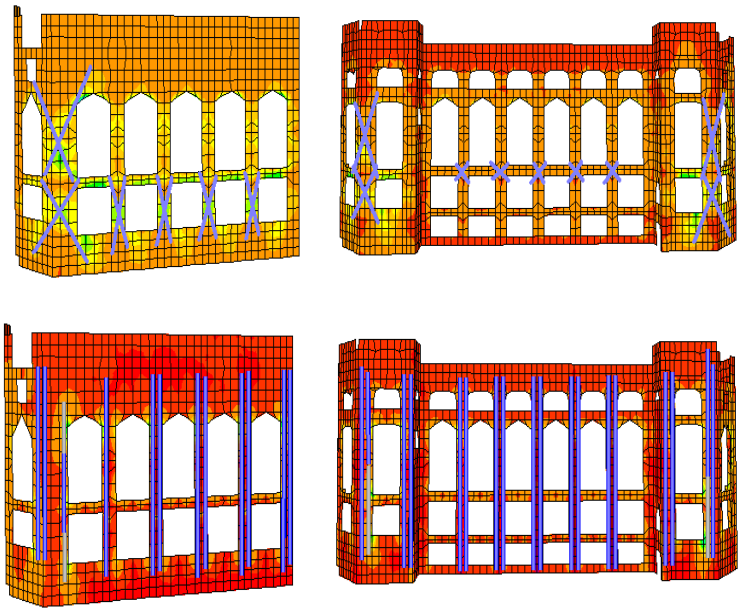

Figure 9. Fibre reinforced polymer locations.

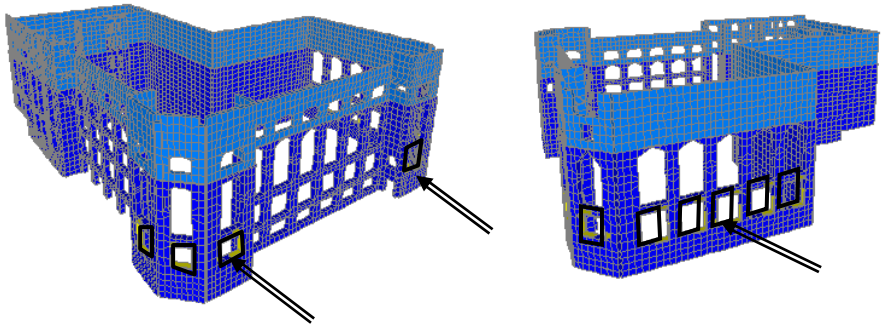

Figure 10. Reinforced concrete windows frames.

6 CONCLUSION

Ancient masonry bearing walls are reputed to be vulnerable to seismic loading. The old masonry becomes even weaker because of the effect of degrading agents which alter the strength and energy dissipation capacity that are distinctive characteristics to resist earthquakes. To rehabilitate such buildings, it is of paramount importance to evaluate their actual resistance capacity. In addition to

conventional material testing, the use of ambient vibration testing is efficient to determine the overall dynamic characteristics of the building. Based on simple dynamic analysis it is possible to determine the critical or deficient zones. Strengthening techniques based on fibre reinforced polymers is appropriately used for the particular cases of high demand to capacity ratio that had been detected in many locations of the perimeter walls. In addition, the high stress concentration around the big openings was relieved by using reinforced concrete rings. The combined upgrading technique offers an acceptable stability and strength increase and preserves the architectural aspect of the building.

REFERENCES

Bourahla N., Bouriche F., Benredouane M. and Ould-Amara M. 2002, 'Structural Assessment by Modal Analysis, case study of the new Algiers Airport', Proceedings of the Sixth International Conference on Computational Structures Technology, B. H. V. Topping and Z. Kumar (editors), Civil-Comp Press, Sterling, U.K, paper 53.

Triantafillou T. C. 1998, 'Strengthening of Masonry Structures Using Epoxy-Bonded FRP Laminates' Journal of Composites for Construction, Vol. 2, No. 2, May 1998, pp. 96-104

Tumialan j. G., Micelli F., and Nanni A. 2001, 'Strengthening of Masonry Structures with FRP Composites', Proceedings of the 2001 Structural Congress and Exposition. section 52, chapter 5, ASCE, Washington D.C.

ElGawady M. A., Lestuzzi P. and Badoux M. 2006, 'Analytical model for the in-plane shear behavior of URM walls retrofitted with FRP, Composites Science and Technology, Volume 66, Issues 3-4, Pages 459-474

Shrive N. G., 2006, The use of fibre reinforced polymers to improve seismic resistance of masonry Construction and Building Materials, Volume 20, Issue 4, Pages 269-277

CSI 2004, Computer and Structures Inc., SAP2000 User's Manual.

Magines G. 2007, 'Masonry building design in seismic area: recent experiences and prospects from a European standpoint', Proceedings of the First European Conference on Earthquake Engineering and Seismology, Geneva 3-8 September 2006, paper K9.

Wathelet M. 2005, *GEOPSY geophysical Signal Database for Noise Array Processing*, Software, LGIT, Grenoble, France.

11DBMC International Conference on Durability of Building Materials and Components
ISTANBUL, Turkey 11-14 May 2008

Evaluation of Ceramic Tiles Frost Resistance Using Frequency Inspection Method

Marta Korenska [1]
Zdenek Chobola [2]
Iveta Plskova [3]
Jan Martinek [4]
Radomir Sokolar [5]

T 21

ABSTRACT

The frequency inspection method is based on the physics of elastic stress wave propagation in bodies. An exciting impulse, being realized, for example, by a mechanical impact on the specimen surface, gives rise to low-frequency stress waves to propagate within the structure and reflect on cracks and the specimen surface. The specimen response to the exciting impulse is picked up on the surface by means of a sensor and transmitted to a computer for frequency analysis. The predominant frequencies may be associated with multiple reflections within the structure, carrying information on the structure integrity and defect localization.

The present paper deals with an experimental study of the frequency inspection method applicability to assess the long frost resistance of ceramic tiles. In order to verify the frequency inspection results and examine their application to the ceramic tile frost resistance assessment, we have also analysed some of the tiles' other properties, such as, porosity, the modulus of elasticity and deformability.

KEYWORDS

Frequency inspection, Frost resistance, Structure integrity, Defect

[1] Brno University of Technology, Faculty of Civil Engineering, Czech Republic 602 00, Phone +420 541 147 657, Fax 541 147 666, korenska.m@fce.vutbr.cz
[2] Brno University of Technology, Faculty of Civil Engineering, Czech Republic 602 00, Phone +420 541 147 650, Fax 541 147 666, chobola.z@fce.vutbr.cz
[3] Brno University of Technology, Faculty of Civil Engineering, Czech Republic 602 00, Phone +420 541 147 664, Fax 541 147 666, plskova.i@fce.vutbr.cz
[4] Brno University of Technology, Faculty of Civil Engineering, Czech Republic 602 00, Phone +420 541 147 623, Fax 541 147 666, martinek.j@fce.vutbr.cz
[5] Brno University of Technology, Faculty of Civil Engineering, Czech Republic 602 00, Phone +420 541 147 510, Fax 541 147 502, sokolar.r@fce.vutbr.cz

1 PASSIVE ACOUSTIC EMISSION

1.1 Introduction

The analysis was applied sets of ceramic tiles, which had been fabricated in HOB in year 2002. To assess the long frost resistance, the ceramic tiles were subject to 300 freezing - thawing tests to EN ISO 10545-12 [EN ISO 10545-12,1998].

1.2 Test Method

Prior to the tests, the ceramic tiles were immersed into a vessel containing water whose temperature was t_1 = 5°C. After having been pulled out from water, the specimen was wiped with a wet rag. Immediately after the removal from water, the ceramic tiles were placed in a refrigerating chamber. The tiles being frozen, the refrigerating chamber temperature was maintained at t_2 = -5°C for 15 minutes.

The freezing cycle being completed, the tiles were immersed into water for 1 to 2 hours in order to thaw out. The ceramic tiles were left lying in water till the test continuation.

A check measurement was carried out prior to stress cycle start and, subsequently, after the completion
of 50, 100, 150, 200 and 300 cycles.

A metal hammer of a mass of 169 g, which was hinged in a fixture ensuring a constant release level, h=2 cm [Plšková 2004], was used to hit the tile. The tile response to the exciting impulse was picked up by means of a piezoelectric sensor of Sedlák S7 type, whose operating frequencies range from 100 Hz to 50 kHz. The sensor was fitted to the tile surface at a point of coordinates x = 18 cm, y = 16,5 cm, i.e., in the maximum amplitude region [Martinek 2003, Plšková 2003].

The response voltage was fed into the input of a Yokogawa DL1540CL digital oscilloscope and further processed by means of a special signal-analysis software package. Fig. 1 shows the measuring apparatus.

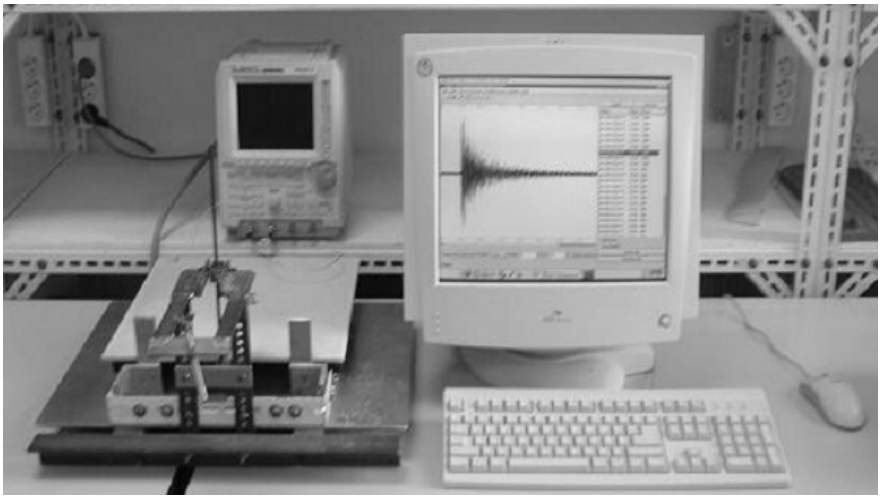

Figure 1. Measuring apparatus.

1.3 Experiment Results and Discussion

Fig. 2 shows the power spectral density (in relative units) versus frequency plot for specimen No.203. A dominant frequency f_0 = 5760 Hz may be observed.

Fig. 3 shows the power spectral density (in relative units) versus frequency plot for specimen No.203 after the 150 freezing and thawing cycles. A dominant frequency f_0 = 5785 Hz may be observed.

Fig. 4 shows the power spectral density (in relative units) versus frequency plot for specimen No.203 after the completion of 300 freezing and thawing cycles. A dominant frequency f_0 = 5936 Hz may be observed.

Fig. 5 shows average incremental values of a dominant frequency versus numbers of freezing and thawing cycles for a ceramic tiles.

Mean values of average values of a dominant frequency and the respective variance coefficients are shown in Fig. 6 - after the 150 and the completion of 300 freezing and thawing cycles.

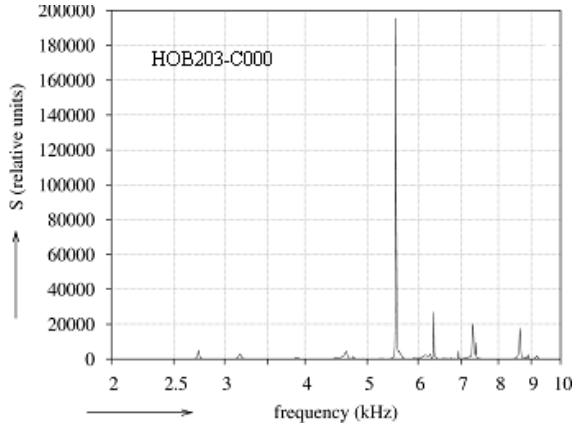

Figure 2. The power spectral density versus frequency plot for a ceramic tile No.203 before degradation.

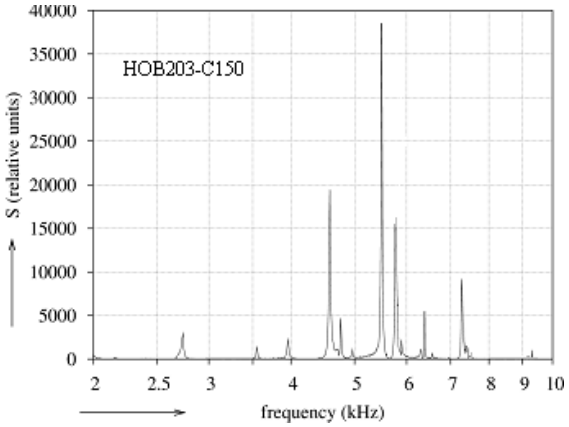

Figure 3. The power spectral density versus frequency plot for a ceramic tile No.203 after the 150 freezing and thawing cycles.

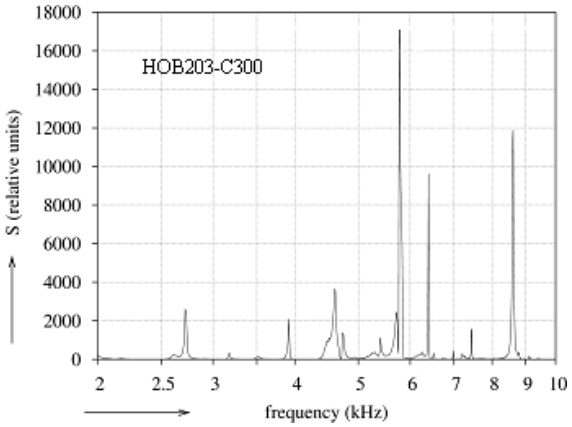

Figure 4. The power spectral density versus frequency plot for a ceramic tile No.203 after the completion of 300 freezing and thawing cycles.

The changes that were observed in the tile may be taken as an indication of certain structure impairment. The structure impairment appeared to be reflected in a change of the resonance frequency distribution.

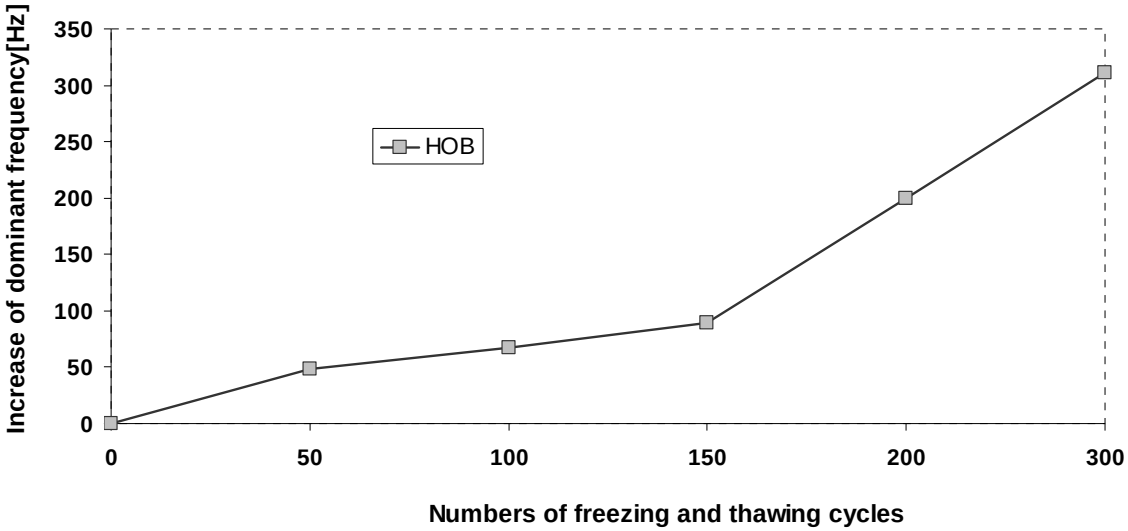

Figure 5. Average incremental values of a dominant frequency versus numbers of freezing and thawing cycles for a ceramic tiles.

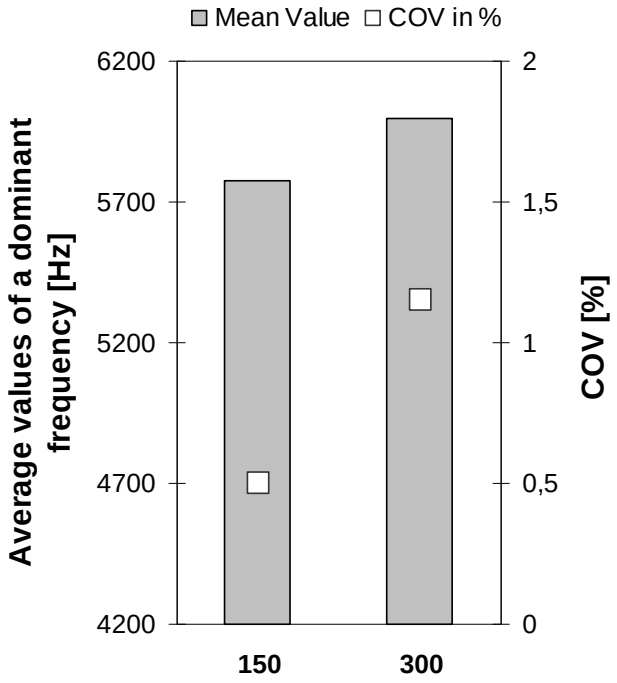

Figure 6. Average values of a dominant frequency after the 150 and the completion of 300 freezing and thawing cycles: Mean values and variance coefficients.

2 MODULUS OF ELASTICITY AND DEFORMABILITY

2.1 Introduction

We have studied the variations in the modulus of elasticity and deformability using the bending test, and, furthermore, the flexural tensile strength values for ceramic tiles. Ceramic tiles had been fabricated in HOB in year 2002.

For the measurements to be practicable on a measuring apparatus complying with ČSN 736174 [ČSN 736174 1994], the ceramic tiles were cut longitudinally by means of a diamond saw, thus producing flat strips of a thickness of 100 mm. In this way, two test specimens arose from each ceramic tile. The first specimen was subject to the flexural tensile strength measurement, the second, to the determination of the modulus of elasticity and deformability from the bending test. Once the bending strength is known, the various loading steps can be specified. Table 1. presents the ceramic tiles.

Table 1. Description of ceramic tiles.

Type of ceramic tyles (Year of production)	*Specification of ceramic tyles*	*Number of freeze - thaw cycles to [EN ISO 10545-12,1998]*	*Dimension of ceramic tyles [mm]*	*Average value of water absorption [%]*	*Surfacing of ceramic tyles*
HOB (2002)	1, 2, 3	0	330 x 330 x 8	0,4	glaze
	4, 5, 6	150			
	7, 8, 9	300			

2.2 Test Method

The test specimen is loaded stepwise by forces F_1 through F_n, generating mechanical tension, which are growing up in steps of 10% of the flexural tensile strength, R_1. The load application and release is performed continuously at a rate of 250 Ns^{-1}. Let the transverse deflection corresponding to F_1 be $S_{tot,1}$. Then the load is increased to $F_2 = 2F_1$ and the total transverse deflection is $S_{tot,2}$. Subsequently, the load is reduced to F_1 and an elastic transverse deflection, $S_{t,2}$, is determined.

The total transverse deflection at the specimen span centre corresponding to F_n is calculated from the following equation:

$$f_{tot,n} = \frac{1}{2}(S_{tot,n} - 2S_{tot,1} + S_{tot,2}), \tag{1}$$

The elastic transverse deflection at the beam span centre corresponding to F_n is calculated from:

$$f_{e,n} = \frac{1}{2}(S_{tot,n} - S_{t,n} + S_{tot,2} - S_{t,2}) \tag{2}$$

Finally, the modulus of elasticity, E, and the modulus of deformability, E_n, are calculated from following equations:

$$E = \frac{F \,.\, l}{f_e \, b \,.\, h}\left[0{,}213\,\frac{l^2}{h^2} + 0{,}46\right] \tag{3}$$

$$E_o = \frac{F \,.\, l}{f_{tot} \,.\, b \,.\, h}\left[0{,}213\,\frac{l^2}{h^2} + 0{,}46\right] \tag{4}$$

where F denotes the specimen load in N, f_e is the elastic transverse deflection in mm, f_{tot} is the total transverse deflection in mm, b is the specimen width in mm, h and l are the respective specimen height and length in mm.

The flexural tensile strength, $R_{f,max}$, can be calculated from the following equation:

$$R_{f,\max} = \frac{M}{w}, \tag{5}$$

where M is the maximum flexural modulus in v N.mm and w is the section modulus in mm^3 with respect to the bottom filaments at the failure point.

The load was applied to the specimen via hard rubber bands. Two identical weights were applied at the 1st and 2nd thirds of the specimen span l. The maximum bending moment is calculated from the formula

$$M = \frac{F.l}{6}, \tag{6}$$

where F is the fracture load in N and l is the support distance in mm.

2.3 Experiment Results and Discussion

A HACKERT/FP2 100/1 pressing machine was employed for the measurements. To measure the transverse deflection, a dial gauge to 0,001 mm was used. The specimen dimensions were as follows: length L = 330 mm, width b = 100 mm, and height h = 8 mm. Fig. 7 presents a diagram showing the test specimen loading with a force F.

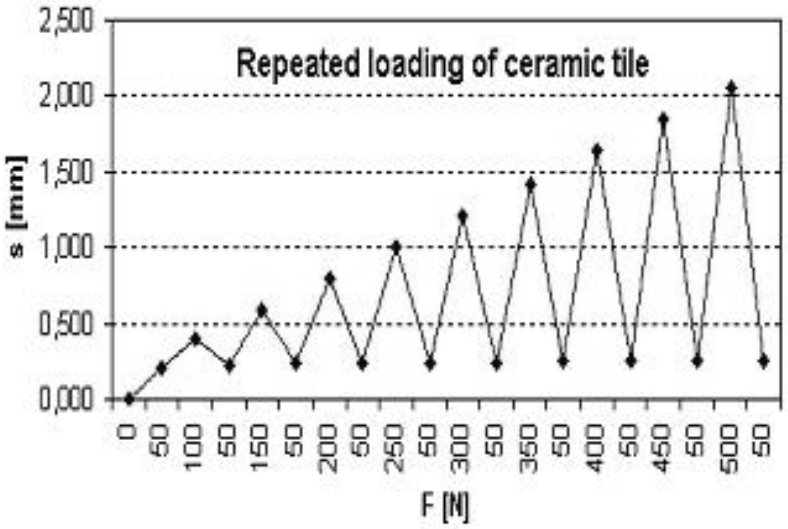

Figure 7. Repeated loading of ceramic tile.

The ceramic tiles, which have not been subject to the freeze-thaw cycles, exhibit an average flexural tensile strength of about 28 MPa. After the ceramic tile had been subject to 150 freeze-thaw cycles the above-mentioned quantity dropped to 27 MPa, i.e., 95.5 % of the initial value; and after 300 cycles, to 25 MPa, which is about 89 % of the initial value. Fig. 8 presents a value of modulus of elasticity and deformability of ceramic tiles. Fig. 9 shows a value of tensile strength of ceramic tiles.

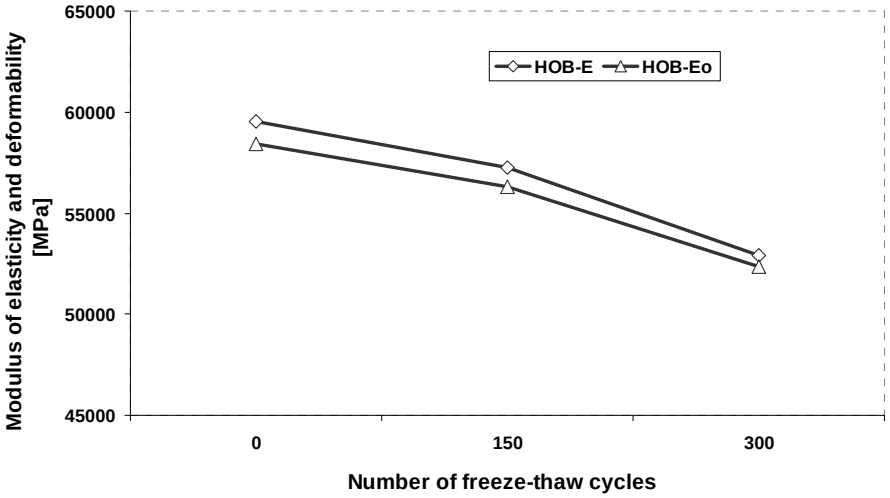

Figure 8. Modulus of elasticity and deformability of ceramic tiles.

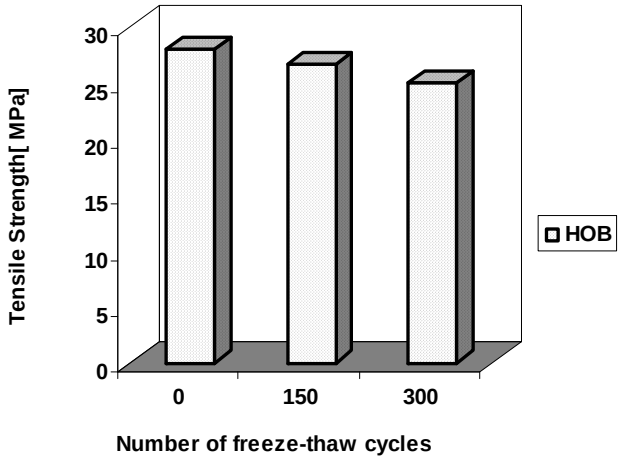

Figure 9. Tensile Strength of ceramic tiles.

3. CONCLUSIONS

The analysis was applied a sets of ceramic tiles, of a plain tile type, which had been fabricated in HOB in 2002. To assess the long frost resistance, the ceramic tiles were subject to 300 freezing - thawing tests.

With the exception of a single ceramic tile, only insignificant resonance frequency changes. Average values of changes of resonance frequency were 313 Hz by type HOB in the course of the freezing and thawing cycles. This gives evidence of a very good quality as well as frost resistance of this ceramic tiles types, from which a long service life may therefore be predicted.

From the results we can also see that the frequency inspection method is a useful non-destructive testing method being applicable to the evaluation of the ceramic tile structure condition and allowing predicting of the frost resistance and service life of these products.

An experimental study designed to determine the modulus of elasticity and deformability for ceramic tiles loaded by freeze-thaw cycles has been carried out. It is apparent that the ceramic tiles under test exhibited a very high flexural tensile strength and a surprisingly high modulus of elasticity.

With an increasing number of the freeze-thaw cycles applied, the flexural tensile strength goes down gradually. Fortunately, this decrease is rather moderate. After the ceramic tiles HOB undergo 150 freeze-thaw cycles, the strength decrease amounts to some 4.5% and after 300 freeze-thaw cycles the strength decrease to 11%. Thus giving evidence of a very good frost resistance of these products.

ACKNOWLEDGMENTS

This research has been supported by project of MSMT 1M6840770001 and GA CZ project 103/06/1711.

REFERENCES

ČSN EN ISO 10545-12 Ceramic tiles- Part 12:Determination of frost resistance.ČNI,1998

Plšková, I.; Trebuláková, P.; Martinek, J.; Chobola, Z., 2004 *Passive Acoustic Emission Method as a Tool to Analyze the Homogeneity of Ceramic Tiles*. In Workshop NDT 2004. Brno. p. 178 - 180. ISBN 80-7204-371-4.

Martinek, J.; Chobola, Z., 2003, *Computation of Decay Coefficient of Acoustic Signal*. In: Proceedings of International Workshop on Physical and Material Engineering 2003, Richňava, Slovakia: Bratislava, Slovak University of Technology, p. 149-152. ISBN 80-227-1924.

Plšková, I.; Martinek, J.; Chobola, Z., 2003, *A Study of the Response Signal Amplitude Versus the Sensor Position on the Ceramic Tile Surface.* In Proceeding of the Workshop NDT CMC 2003 Non-Destructive Testing of Civil Engineering Structures and Constructions. Brno, Technikal University of Brno. p. 123 - 126. ISBN 80-7204-318-8.

ČSN 736174, 1994.Stanovení modulu pružnosti a přetvárnosti betonu ze zkoušky v tahu ohybem. Praha:Český normalizační institut

Influence of the Mix Proportion of Mortars and Paint Formulation on the Behaviour of the Mortar/coating system in Water Transport Phenomena

Kai L. Uemoto [1]
Neide M. N. Sato [2]
Vanderley John [3]

T21

ABSTRACT

The development of biological microorganisms on external walls of buildings painted with acrylic latex or PVA latex paints (emulsion paints) is frequent, generating unexpected building maintenance expenses. Inspections in painted façades identified stained areas due to biological growth of organisms such as fungus, while structural parts of the wall, in concrete, exhibit the original colour, indicating that the characteristics of the substrate are fundamental factors in the growth of these organisms.

The aim of this paper is to show the influence of the mix proportion of mortars and the paint formulation on the behaviour of the mortar/coating system in relation to water absorption and evaporation. The study was conducted with different painting systems: two acrylic latex, matt-finish and mid sheen-finish (semi-gloss), and one PVA latex, matt finish, were applied on mortars, with two different mix proportions, 1:0:3 and 1:2:9 in volume. Water absorption and evaporation were measured during one week and the water vapour transmission of paint films was also measured.

The experimental data showed that all coating systems, when applied on a porous substrate, are permeable to water to different extents. These substrates, when exposed to water, present high water absorption and the absorbed water is eliminated slowly.

KEYWORDS

Biological microorganisms, Paints, Mortars, Latex paint, Water transport phenomena

[1] São Paulo University, Escola Politécnica, Dept. of Construction Eng., São Paulo, Brazil, Phone +55 11 3091 5789, Fax 11 3091 5544, kai.loh@poli.usp.br
[2] Nove de Julho University Center, Civil Engineering Faculty, São Paulo, Brazil, Phone +55 11 3665 9000, Fax 11 3743 6917, neide.sato@uninove.br
[3] São Paulo University, Escola Politécnica, Dept. of Construction Eng., São Paulo, Brazil, Phone +55 11 3091 5794, Fax 11 3091 5544, vanderley.john@poli.usp.br

1 INTRODUCTION

Absorbed water is the main deterioration factor of external wall surfaces [Uemoto et al 2001]. In order to prevent water penetration, the walls are protected by paints that provide a barrier on the surfaces and thus reduce the volume of absorbed water. The rate at which water moves in a material is determined by its permeability, which is strongly affected by the nature of the pores, both in terms of their size and the extent to which they are interconnected [Chew & Ping 2003] [Uemoto et al 2001].
Microbial growth in external painted façades is considered to be one of the most important maintenance problems throughout the world, especially in sub-tropical and tropical regions [Sato et al 1995]; [Chew & Ping 2003]. This problem is quite common in typical façades of Brazilian buildings (Figs. 1 and 2), as well as in other areas of the world [Sedlbauer 2001, 2002]; [Becker & Putterman 2002].

Figure 1. Dark stains caused by biological growth

Figure 2. Areas with dark stains caused by rainwater, on the façade of the building

The presence of biological microorganisms is the most significant factor in the performance of paints when the aesthetic function is desired. These organisms do not usually cause significant damage to the paint film or mortar, but they do produce disfiguring stains on wall surfaces. Different mortars and paints present different characteristics such as permeability, vapour diffusion and water absorption, resulting basically from the differences in the mix proportion of the mortars and the paint formulation.
If a painted façade presents high water absorption and has difficulty in diffusing the absorbed water due to the characteristics of the wall, like the presence of hollow blocks, the rainwater accumulated inside the wall can facilitate the development of biological microorganisms.
Paints are complex materials, formulated by combining a binder (resin), pigments, fillers, stabilizers, surfactants, solvents and thickeners. The proportion of raw materials defines the paint film performance. For example, the pigment-binder ratio (P/B), usually calculated on a weight basis, controls paint film gloss – a consequence of surface gloss and permeability to water and vapour. Gloss decreases and permeability increases as the pigment-binder ratio increases. However there is no linear relationship between these two factors, since changes are normally most rapid in the range from 0.9:1 to 1.1:1 [Tyssal 1964]. The relation between pigment and resin is internationally known as Pigment Volume Content (PVC), which is the volume of pigment (and filler) in the dry film divided by the volume of the whole dry film, and it is expressed as a percentage. This expression is often used by the paint industry and sometimes it is also referred to as Pigment Weight Content (PWC).

$$PVC = 100\left(\frac{V_p}{(V_p + V_v)}\right) \quad (1)$$

Where: Vp is the pigment (and filler) volume and Vv is the binder (resin) volume
PVC is a factor that directly influences the porosity of the paint, thus resulting in differences in permeability, adhesion, gloss, degree of protection to the substrate, mechanical properties like tensile

strength and elongation, etc. Table 1 shows the typical gloss and permeability obtained for different PVC values.

Table 1. Paint formulations associated with gloss levels.

PVC (%)	*Gloss*	*Permeability*
10 to 15	High gloss	Low
15 to 30	Semi-gloss	Medium
30 to 35	Sheen or "silk"	-
35 to 45	Low sheen or "matt"	High

Most of the published data measures the influence of paint formulation on vapour permeability by using a paint film. However, the paint substrate also affects the paint film performance in terms of mass transfer. This can be caused by variation in paint film characteristics and also due to the suction of liquid paint by substrate porosity. In practical terms, the paint and the substrate work as a system: both parameters control the surface mass transport phenomena. This fact is not well documented in the literature.

German standards establish limits of water vapour permeability and water absorption (DIN 18550-1; DIN 4108-3), based on Künzel's studies [1977 apud Wagner, 2000], to limit the effects of driving rain and condensation on building constructions in such a way that damage (e.g. fungus growth, corrosion) is avoided. However, these limits are climate dependent and have not been adapted to the Brazilian climate. Therefore further studies need to be developed in order to establish performance criteria for building constructions, including painting systems.

This paper examines the water absorption and loss of water by evaporation of mortars, with two mix proportions, painted with different water-based systems (latex sealer and latex paints). All products are commercially available.

2 EXPERIMENTAL PROGRAM

To evaluate the performance of different painting systems in inhibiting the infiltration of water in the substrate as well as to understand the water transport mechanism through latex paints, three latex paints with different resin compositions and pigment/binder ratios were collected from the consumer market, and two mortar substrates with different mix proportions were prepared. The evaluation method is based on the comparison of the water absorption and evaporation over a period of time in painted and unpainted mortar substrates.

2.1 Materials

2.1.1 Basic composition of the paint samples

In the study, one acrylic sealer, one PVAc latex (matt finish) and two acrylic latex (matt and semi-gloss finishes) were collected from the consumer market in the city of São Paulo. The products were characterized according to ASTM D3723-05 Standard Test Method for Pigment Content of Water-Emulsion Paints by Low-Temperature Ashing. The non-volatile content was determined by drying the sample at 105oC, and the pigment content, by drying at 450oC. The resin content was estimated through the difference between non-volatile content and pigment content. Table 2 shows the main characteristics of the products and the pigment/binder ratio (g/g).

2.1.2 Mortar specimen (substrate)

For a better simulation of in-service conditions, mortar specimens, measuring approximately 20cm x 10cm x 3 cm, were prepared and cured during 28 days. They were prepared with Portland cement, lime and sand, with the mix proportions most commonly used in Brazil: 1:0:3 and 1:2:9 (cement: lime: sand, by volume). After casting, the mortar specimens were kept for seven days in a wet

chamber with 95% relative humidity (RH) and then stored for over 30 days in a laboratory environment at (25 ± 2) oC and (50 ± 5) % RH.

Table 2. Basic composition of the paints.

Tests	*Acrylic Semi-gloss*	*Acrylic Matt*	*PVAc Matt*	*Acrylic sealer*
Volatile content (%)	53.1	47.9	51.7	34.0
Pigment content (%)	22.7	33.2	32.9	54.1
Binder (resin) content (%)	24.2	18.9	15.4	11.9
Pigment/binder ratio (g/g)	0.94	1.76	2.14	4.55

2.1.3 Specimen preparation

After the curing period of the mortar, one coat of sealer and two coats of latex paint were applied on the mortar specimens, with a nylon brush, according to the manufacturers' instructions. A set of unpainted specimens was used as control. All specimens (painted and unpainted) were sealed with a silicone sealant in the 10 x 3cm faces.

2.1.4 Film preparation

Liquid paint was applied to a PVC substrate (plate) with a drawdown bar (film applicator), with a nominal wet thickness of 150μm. The liquid paint films were dried at ambient temperature for seven days and, after this period, were separated from the plate. The "free" film was used to determine water vapour permeability through the paint films.

3 TEST METHODS

The effect of the latex paint samples on the relative change of water content in mortar substrates was determined by measuring water absorption and evaporation of the specimens and permeability of paint films according to the following methods.

3.1 Water Absorption

The test was based on BS 6477-92 Specification for water repellents for masonry surfaces. One of the 20cm x 10cm faces of both sets, painted and unpainted specimens, was immersed in deionised water, with the painted face down, to measure uni-directional water absorption. Water depth was maintained at 1/3 of the height of the specimens during the test. Water gain was determined by weighing the specimens at predetermined time intervals. The measurements were performed until the set of unpainted specimens, used as control, reached complete saturation. The tests were carried out in an environment at 25oC and 50-60% RH. The relative water absorption of unpainted and painted specimens is shown in Fig. 3. The results were expressed in terms of mass change as a function of time. The mean values of the results obtained from five determinations were expressed in kg/m2.

3.2 Loss of Water

The same specimens previously used in the water absorption test were displayed face up for drying in a controlled environment. In this test the faces that had not been exposed to water in the water absorption test were sealed with aluminium foil, and the face previously exposed to water was kept unsealed so that the loss of water occurred only through this surface. The loss of water was measured by weighing the test specimen at predetermined time intervals, until a constant weight was reached. The mean values of the results obtained from five determinations were expressed in kg/m2.

3.3 Permeability of Water Vapour through Paint Films

The rate of water vapour transmission through the paint film was determined without the influence of the mortar. Film permeability was measured according to ASTM D1653-03 Standard Test Methods for Water Vapour Transmission of Organic Coating Films, Dry Cup Method. The "free" films are fixed on top of a glass recipient containing an amount of anhydrous calcium chloride (desiccant). The whole set (recipient with the film) is weighed and placed in a climatic chamber, in a controlled environment, with temperature of 25oC and relative humidity of 50%. The sets are weighed at predetermined time intervals. The increase in weight is due to vapour passing through the paint film. The difference in weight was a measure of the permeability of the latex films. The medium results obtained from three determinations were expressed in ng/(Pa.s.m).

4 RESULTS

Table 3 presents the water absorption by capillarity (mean values of five specimens and standard deviation, Sd), after 24 hours of exposure, of unpainted mortar specimens with mix proportions of 1:0:3 and 1:2:9. Table 4 shows the results of water vapour transmission (mean values of three specimens and standard deviation, Sd) through the sealer paint films.

Table 3. Water absorption by capillarity (24h) of unpainted mortar specimens.

Mix proportion (volume)	*Water absorption (kg/m^2)*	*Sd*
1:2:9	4.63	0.21
1:0:3	3.04	0.10

Table 4. Water vapour transmission.

Samples	*Permeability (ng/(Pa.s.m)*	*Sd*
Acrylic sealer	0.330	0.0100
PVAc paint	0.067	0.0188
Acrylic paint (matt)	0.012	0.0004
Acrylic paint (semi-gloss)	0.011	0.0004

Figures 3 and 4 show the results of water absorption of the mortar specimens, unpainted and painted with PVAc latex (matt finish) and acrylic latex (semi-gloss and matt finish). Figures 5 and 6 show the results of loss of water of the mortar specimens, unpainted and painted with PVAc latex and acrylic latex.

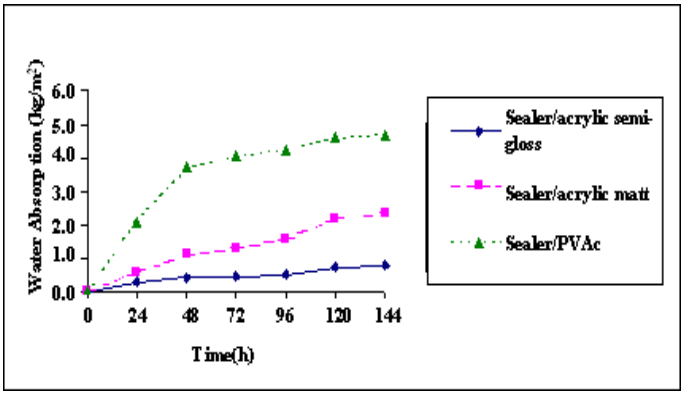

Figure 3. Water absorption of 1: 2: 9 mortar specimens, unpainted and painted.

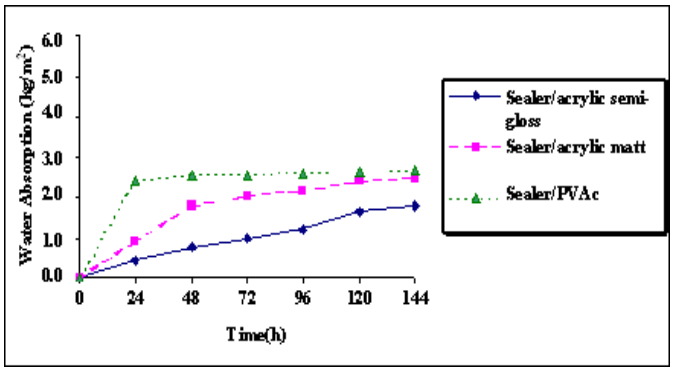

Figure 4. Water absorption of 1: 0: 3 mortar specimens, unpainted and painted.

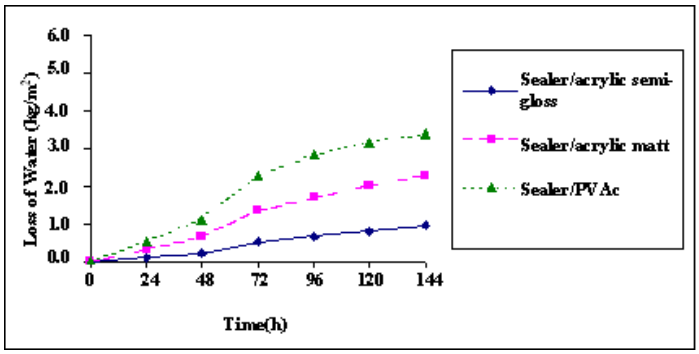

Figure 5. Loss of water of 1: 2: 9 mortar specimens, unpainted and painted.

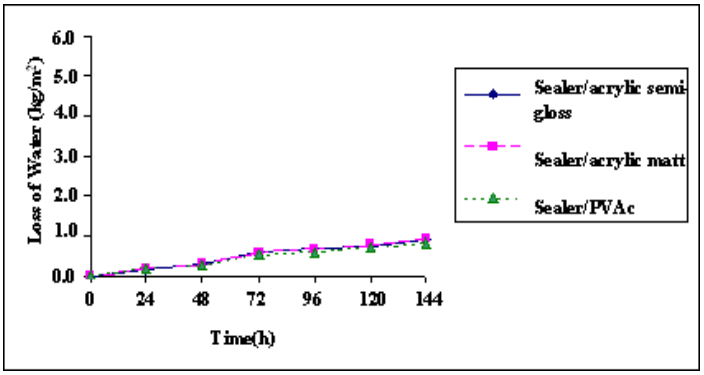

Figure 6. Loss of water of 1: 0: 3 mortar specimens, unpainted and painted.

5 DISCUSSION

5.1 Permeability of Water Vapour through Paint Films

According to Table 1, PVAc (matt) and acrylic (matt and semi-gloss) paints have different resin contents. According to the first author's studies [Uemoto 1998], the higher the resin content, the lower the water permeability. In this study the two acrylic paints did not show a significant difference in water vapour permeability: 0.012 (ng/(Pa.s.m) for matt finish and 0.011 (ng/(Pa.s.m) for semi-gloss finish. In the case of PVAc latex a more significant difference (0.067 ng/(Pa.s.m)) was observed, resulting from the higher difference in P/B and also from the difference in resin composition.

5.2 Water Absorption

According to Table 2, mortars with different mix proportions (1:2:9 and 1:0:3) present differences in water absorption capacities. Figs. 3 and 4 show that the paint formulation also affects the performance

of the mortar; the level of protection against water penetration varies according to the PVC and resin composition of the paint. The influence of the paint is more significant on more porous mortars, with a mix proportion of 1:2:9 (Fig. 3).

According to Figs. 3 and 4, the acrylic latex paint, semi-gloss finish, has the highest level of protection against water absorption, and the PVAc latex has the lowest level of protection. The water absorption rate shows a sudden decrease after 48 hours; longer exposure periods do not affect the moisture content of the specimens very significantly. Both unpainted mortars (1:2:9 and 1:0:3) reached saturation in 24 hours.

5.3 Loss of Water

Figure 5 shows that the evaporation (loss of water) process in porous mortar, mix proportion 1:2:9 (cement : lime : aggregate), is affected by the paint formulation. Paints such as acrylic latex, semi-gloss finish, greatly reduce the water evaporation rate, while more permeable paints such as acrylic latex or PVAc latex, both with matt finishes, allow faster loss of water. Also, the difference between the two acrylic paints is significant, despite the fact that their films present almost the same water vapour permeability, which suggests an interaction between the paint and the substrate.

Figure 6 shows that the evaporation (loss of water) process in less porous mortar, mix proportion of 1:0:3 (cement:aggregate; without lime), is independent of the paint composition. In such formulation, the paint had no influence on the loss of water, which is governed by the porosity of the mortar.

The rate of loss of water is always much lower than that of water absorption. In more porous mortar, mix proportion of 1:2:9 (cement: lime: aggregate), the paint's water vapour permeability is important to control the drying process. On denser substrates, like 1:0:3 mortar and concrete, the paint formulation does not seem to affect the drying process significantly.

5.4 Final Discussion

All the systems studied (mortar/sealer/paint) are permeable to water to different extents and the time necessary to eliminate the absorbed water is much longer than the absorption time. The water vapour permeability results (Table 3) of "free" films did not have any correlation with the evaporation results of painted mortar (Figs. 5 and 6). The permeability of the system is not only determined by the paint film, but also affected by the mortar characteristics; in the water evaporation process the phenomenon is very clear.

In more permeable mortar (1:2:9) it could be seen that the acrylic semi-gloss paint (low PVC) provides greater protection against water and probably other potentially harmful substances present in the environment. The acrylic matt paint (high PVC), with P/B of 1.76, as determined in the characterization test, does not protect the mortar against water penetration as well as paints with low PVC, with P/B of 0.94. In this case, the paint has only decorative but not protective purposes. In less porous mortar (1:0:3), the effect of acrylic paints with different P/B is observed mainly in the first 24 hours of water exposure. After this period the effect of different PVC is not as visible.

The application of paint is an efficient protection practice only in more porous mortar. For low porosity mortar the protection provided by the paint is of minor importance, once the substrate itself already presents low permeability. A less permeable paint such as acrylic semi-gloss reduces water absorption of the mortars; however, the loss of the absorbed water is also impeded by this paint. The water accumulated inside the wall can facilitate the development of microorganisms. Ideal "paintwork" needs to have low water absorption, such as acrylic latex, semi-gloss finish, and simultaneously allow the evaporation of the absorbed water, such as PVAc latex.

6 CONCLUSIONS

This study allows the conclusion that both paint formulation and mortar substrate mix proportion influence water absorption kinetics. In general, paints can reduce the water absorption rate in both substrates tested. The lower the pigment ratio, the higher the absorption reduction. On the other hand, paint formulation did affect water evaporation on the more porous 1:2:9 mortar. On the denser 1:0:3 mortar the porosity was the single factor which controlled evaporation.

ACKNOWLEDGEMENTS

The authors gratefully acknowledge the support of FAPESP (Research Support Foundation of the State of São Paulo) for this research project.

REFERENCES

Becker, R.; Putterman, M. 2002, 'Patterned mold growth on rendered facades in Israel – A consequence of substrate thermal insulation'. in: The 6th Symposium on Building Physics in Nordic Countries. Trondheim. Proceedings... Norway, June 2002, pp.17-19.

Chew, M.Y. L.; Ping, T. P. 2003, 'Staining of facades'. Singapore.

Loh, Wah S. 2006, Product development for Green productivity – A case study of the development of algae resistant surface coating for building facades in the human tropics. Available at: <http:www.apo-tokyo.org/gp/manila_conf02/resource_papers/narrative/dr_loh-wah.sing.pdf. Accessed 26 September 2006.

Parnham, Phil. 1997, Premature staining of new buildings-causes and remedies. *Structural Survey*. vol.15.n. 4.pp.166-171.

Sato, N. M. N.; Vittorino, F., Agopyan, V, Uemoto, K. L. 1995, Penetração de umidade e crescimento de fungos em fachada. in: *Entac - Encontro Nacional De Tecnologia Do Ambiente Construído*. Rio de Janeiro. 1995

Sedlbauer, K. 2001. Prediction of mould fungus formation on the surface of and inside building components. Stuttgart, 2001. 247 pp PhD-thesis – University Stuttgart.

Sedlbauer, K.; Krus, K.; Zillig, W. 2002, Prediction of mould growth by hygrothermal calculation. in: The 6th Symposium on Building Physics in Nordic Countries 2002. Trondheim. Proceedings... Norway, June 2002, pp.17-19.

Tyssal, L. A. 1964, Industrial paints: Basic principles. Pergamon Press Ltd, London.

Uemoto, K. L. 1998, Influência da formulação das tintas de base acrílica como barreira contra a penetração de agentes agressivos nos concretos. São Paulo, 1998. 178p. Thesis (PhD) Escola Politécnica, Universidade de São Paulo.

Uemoto, K. L., Agopyan, V., Vitorino, F. 2001, Concrete protection using acrylic latex paints: Effect of the pigment volume content on water permeality. *Materials and Structures*. EUA, p.172 - 177.

Wagner, M. C. 2000, La teoria de la protection de fachadas segun Künzel como base para una futura normalización. Revista Bit, Marzo 2000. Chile.

11DBMC International Conference on Durability of Building Materials and Components
ISTANBUL, Turkey 11-14 May 2008

The Maintenance of Colour on Finishing Coats

Pietro Zennaro [1]
Katia Gasparini [2]

T21

ABSTRACT

The maintenance of finishing coats is usually thought of as an activity relating to how the outermost surfaces of buildings affects the quality of the environment, today considered a matter of strategic importance. Appearance has gained in importance in its relation to substance, and this new way of reading the streetscape has meant that colour planning is an increasingly important activity. In many new constructions, particularly in non-residential buildings once banished to chromatic empiricism, more and more attention is being paid to choosing the colour of the external surfaces. However, if we are witnessing a new renaissance in the colour of buildings, the same cannot be said about the maintenance of these colours. The finishing coat is considered to be either strictly dependent on the behaviour of the underlying layers or completely independent of them. In the first case the skin is considered independently of the colour, in the second the inverse: the hue of the finishing layer is the most important aspect, independent of the behaviour of the support. It should be remembered that there is a long-standing tradition in which the finishing layer is considered a 'sacrifice layer' that does not require maintenance. The common idea of maintaining coloured layers involves the removal of the old layer and/or the application of a new one. If this method of maintaining the skins of buildings was acceptable in the past, the introduction of new products for the creation of thicker outer layers or products made from particular materials means that a new approach must be developed for the maintenance of entire blocks of layers. It would seem that durability, or persistency, is no longer considered to be an essential factor. Hue, lightness and saturation are no longer aspects that need to be conserved. The maintenance of colour finishing coats is considered of fundamental importance only in the restoration of historical buildings. On a hypothetical scale of priorities, where should colour maintenance lie today?

KEYWORDS

Colour, Maintenance, Coatings

[1] Venice Iuav University, Architecture Faculty, Venice, Italy, Phone +39 41 2571957, Fax 041 5246296, pietro.zennaro@iuav.it
[2] Venice Iuav University, Architecture Faculty, Venice, Italy, Phone +39 41 2571957, Fax 045 7152291, katiag@iuav.it

1 INTRODUCTION

The perception of material reality occurs through the detection of the outer layer of entities, apart from when they are transparent. Of course, no architectural product can avoid this rule. Both on the outside and the inside of configured spaces only the periphery of architectures is perceived: the last material threshold that is visible (or tangible, or that can be tasted, smelt or heard). This skin-like layer is that which, to a greater extent than other material aspects, is able to determine the quality of spaces, a quality strictly related to appearance. If this outer layer is visible it is bound to be coloured.

In fact a number of characteristics of materials contribute to the quality of the environment, the most important being the chromatic aspect of physical bodies and places. Visual perception occurs thanks to the variable presence of light that determines the chromatic sensation for each object. Colour is a psycho-physical sensation generated by the perception of a number of luminous frequencies emitted directly – or reflected – by physical bodies. The absence of light or the inability of the ocular-cerebral system to perceive certain frequencies produces a colour interpreted by the brain as black, black being the result of the inability of an object to reflect light in the range of visible frequencies (an object might reflect infrared or ultraviolet rays, but these cannot be perceived by the human eye).

The frequencies of the visible spectrum range from 4×10^{14} to 7.5×10^{14} Hz approximately; the simultaneous confluence of all the visible frequencies is perceived as white. A vast number of colours can be perceived between these two frequencies which, for convenience, are divided into six bands of tones (as defined by the CIE, Commission Internationale de l'Eclairage): violet, blue, green, yellow, orange and red.

The entire, complex set of materials and techniques used in the field of architecture relies on the thin layer of visible surfaces to stimulate our emotions. And if spatial configuration appears to be one of the fundamental concerns of architecture, it should be remembered that this is perceived – at least in visual terms – as chromatic variations which are dependent on a multiplicity of conditions (intensity and variation of the incident and/or reflected light, changes in the environmental conditions due to climate, season, humidity, changes in the colours of the surroundings, differences between the viewers, subjective and cultural interpretations, psychosomatic conditioning, defects in eyesight, etc.).

The outer layer of architecture, especially (but not exclusively) when covering the external surfaces of buildings, has always performed the function of representation to the public. In fact all buildings are seen more frequently from the outside by an indefinite number of people, many more than those who normally occupy its spaces. The external walls are also those that hardly ever display the same, constant colour due to variations in daylight caused by the rising and the setting of the sun, the changing seasons, the reflections of traffic, and many other external factors. These walls are also those that suffer most from decay as they are constantly exposed to the elements and to aggressive pollutants.

Apart from a few exceptions, the surfaces of the internal walls of buildings undergo a much less incisive chromatic variation than the external surfaces (thanks to artificial lighting, control of lighting obtained via curtains, blinds, windows with solar filters and other systems), and fewer variations caused by the reflections of the activity or movement of people and objects.

When external surfaces survive the filter of time then the whole building, or some of its parts, become historical because it constitutes a cultural inheritance left by past epochs, an aspect considered fundamental in the material evolution of mankind. Even if many of the architectures of past epochs are today completely stripped of their original colours and given different colours to those they had in the past, in turn becoming more or less illicitly part of history (for example the stones, marble and bricks stripped of their original plaster or of their intense colour or repainted with more recent materials), they can convey new images, the result of a fascination derived from a glorious, hypothetical, dreamlike past. This need to hypothesise a dreamlike past is the fruit of an idea conceived after the

events. All hypotheses, whether they concern the past or the future, seem to be forcedly adapted to the present.

The present era, in particular, refuses to accept the decaying of organic bodies or of man-made works. "Decaying and putrefied bodies" are repudiated in history as a method of contrasting the obscene… "Death is tolerated only when the bones are white: if architects are unable in their studies of 'healthy and robust, active and useful, ethical and happy peoples and homes' (Le Corbusier in *Vers une architecture*), they can at least find themselves at ease in front of the white ruins of the Parthenon. A young life and a decorous death, this was the motto of architecture" [Tschumi 1996] until almost the end of the XX century. Today life must be perennially young and any sign of yielding duly smothered using any method able to gloss over the signs of ageing, both in people and in buildings.

What we know in the field of the culture of materials is a story of external surfaces, a story subject to interpretation which can misrepresent the original as it is based on the reality of the present where plaster is perfectly smoothed, covered in flashy colours whose intensity is influenced by cinema or television where advertising promotes the increase in the level of tones and their chromatic saturation. Because nuances are no longer appreciated, an unprecedented violence is transferred to the walls of buildings, even in historic centres and even where so-called 'colour regulation plans' have been adopted.

In reality, the methods used to plaster and paint walls in the past led to the creation of rugged surfaces, covered with protrusions, planar irregularities, colours spread unevenly in several coats to the extent that they would break off in flakes or would be scraped away so that they could be seasonally 'refreshed', a new coat of paint being applied over the existing one. This is what maintenance consisted of. Today, from the point of view of the maintenance of finishing coats, especially where the choice of materials such as paint and lime has been imposed (materials which are inherently susceptible to decay), one must deal with a specific set of maintenance proposals.

2 MAINTENANCE

If, on one hand, the greater respect for places and an awareness of local cultures has led to the necessity to regulate the chromatic aspect of architecture of longstanding historical importance, on the other hand for new buildings – and for the renovation of relatively recent constructions or emblematic buildings – colour continues to be a 'surplus': a feature that is not considered necessary, applied following vague parameters. The final decision on the choice of colour is usually left to the amateur skills of the client and the contractors who are more used to addressing economic problems than those of environmental quality.

Furthermore, the considerable advance obtained with the introduction of materials and techniques by manufacturers means that there are very few limitations in the choice of possible colours. In the past the application of the colour blue (for example) on surfaces directly exposed to the sun's radiation was not considered suitable because it faded rapidly, today this problem has been sufficiently overcome by means of the production of materials that, exposed to ultraviolet rays, are altered to a much lesser extent than their predecessors. The choice of colours, no longer limited by the duration of the materials and the specificity of their application, is blatantly influenced by advertising. Tones and saturations reach levels never seen before in the field of construction.

Added to these developments in materials is the availability of a vast range of colours. Accustomed to hearing of printers or video screens that can produce millions of colours, it is easy to think that such a broad choice could be made available for the finishing coats of buildings. However, a standard observer is unable to distinguish between more than 100,000 colours. So what is the point of offering a range of hundreds of millions of colours? Of course this is a marketing technique that results in the disorientation and confusion of the users: chromatic background noise with no real utility whatsoever.

Also the materials used are no longer dedicated to a particular use. There is no material for the colouring, painting, tinting of surfaces and decoration in general that does not contain a percentage of polymers. Even the basic colours of lime, imposed by a number of town councils for the facades of historic centres, contain a significant quantity of polymeric substances introduced in the materials to reduce the effects of being washed out by rain. Adopting these non-traditional products allows the colour to remain constant for a much greater length of time than when traditional lime-based tints with no additives are used.

Many products used for finishing can be applied to any kind of supporting layer as long as the support is pre-treated. To be more precise: as well as the adequate treatment of the support, the basic colouring product is the same and the variation occurs only by means of additives, a small percentage compared to the final quantity of product applied. This procedure is considered an innovation in which more know-how and less material is incorporated. In effect, this is the result of the optimization in production and storage of the materials.

To the external membrane, then, are attributed functions (thermal protection, salubrity, interactivity, etc.) that often cannot be supported by the layer of paint except for brief periods of time as they have to be, in the first case, useful for the protection of the underlying layers and, at the same time, representative. This tendency, of using any kind of supporting layer, seems to cry out to those who attempt to penetrate into the world of products for the construction industry the logic of specialization of the functional layers: one external membrane dedicated and specialized according to the context in which it is applied. Surely the approach to the maintenance of these layers, made with the materials referred to above, presents problems that are not easy to resolve, as this involves trying to identify the 'ingredients' of the materials, details of which are hardly ever revealed by the companies that produce them.

It is possible to obtain, as well as extemporaneous tones and saturations, materials with equally extemporaneous finishes, introducing a new representation of the external spaces. An emblematic case, in some situations in Italy, is the spread of the plaster or polished finishes in the external walls of buildings, as well as an unprecedented increase in the use of the same finishes for internal walls. The polished plaster finish, typical of certain interiors built in past epochs, when used externally will certainly present problems of lack of durability and accelerated decay, even if the materials have been specially produced for exteriors. Early crazing, microcracking or cracks that are more or less visible are the order of the day in these circumstances. The lack of elasticity and the low level of porosity lead to a condition of accelerated decrease in reliability of the surface finish. What form of maintenance should be adopted in these cases? Once the finish has started to deteriorate and depending on the result that needs to be obtained, one can:

1. substitute the previous layer with another of the same or different type, after having removed the old layer;
2. apply a protective layer of another type;
3. patch up the finish by re-plastering only the areas that have been damaged.

This is the procedure that is usually followed every time that an external surface needs to be repaired. Perhaps it should be remembered that "The purpose of colouring of walls is as much for the conservation of buildings as for the improvement of their appearance" [Donghi 1920]. The colouring or painting of buildings, and other structures, is the technique that – by means of the deposit of a very thin layer of material, carried out in various ways – is able to improve the appearance and increase the durability of the building. Usually this means mechanically depositing substances onto the surface of the bodies using tools such as brushes, rollers, pads, spatulas, etc. or with spray guns. A similar effect is produced chemically or electrochemically. In this case one can no longer refer to it as mechanical application, but rather as coating or surface treatment. The most suitable techniques are chosen

according to the materials that make up the support on which the protective or expressive layer (colour) is deposited.

In constructions the supporting layer, usually treated so as to best receive these deposits, is extremely varied: from plaster to walls consisting of various materials (bricks, concrete, plasterboard, etc.), metallic surfaces, woods, glass, plastic, and new composite materials. Thus the building sector offers a range of possibilities of chromatic coating that is so vast that it seems to be difficult to find a single way of approaching the problem of maintenance. Carrying out maintenance work on buildings treated with a plaster finish or with an anodized finish is clearly not the same thing. Specific methods are required to return the finishing coat to the desired degree of quality. Once the colouring product has been applied to a support, it provides performance levels derived from its composition, from the method used for its application, from the behaviour of the supporting layer and from the external actions that it undergoes, being subjected to chemical, physical, mechanical and biological actions and actions related to the building's use. The intensity and duration of these actions contribute to determining its durability 'in the field'. Any kind of maintenance work has the task of prolonging the useful life of the building and guaranteeing levels of performance congruent with the potential that a painting product applied to a building can provide.

Carrying out maintenance is useful only if it never stops. But what is the point of discussing maintenance of finishing coats when these no longer exist? This is the case, for example, with finishes that are thick or with the insertion of pigment materials within plaster, the latter solution becoming operative in order to eliminate a phase of work: painting. Pigments are added to the mixture of the last layer of plaster so as to form a coloured finishing mortar. But while this requires a certain amount of technical know-how and suitable equipment for its application, in the application of plaster the workmanship is expressed by the plasterers. The figure of the painter is eliminated both for the exterior and the interior of buildings, with the use of white mortar and plaster finishing. Another professional figure is thus disappearing from the building site, caused by the desire to economise, the constant loss of professionalism and fact that technical and practical know-how is no longer passed on.

A practice that is becoming more and more accepted in the creation of surface finishes relies heavily on the need for continual mutation and the elimination of the need to carry out maintenance work (for example, the self-cleaning or pollutant-resistant glass or paints already widely used in infrastructures such as tunnels, road constructions, etc.). In a society used to instant change, the restoration of facades is of little interest because they should be frequently and easily modified. The buildings that make the skin a qualifying element of variation are significant, and the glossy architectural magazines are full of them. Maintenance seems to be considered a 'poor' activity, going against the idea of staying eternally young, beautiful and efficient. A comparison with cosmetic surgery, however, can remind us that to be in line with what is required by the rules of beauty one needs botox crèmes, injections of silicone and anything else that can modify one's image. The idea is not so much to maintain the efficiency of the skin but to obtain an appearance that can satisfy current fashions, even if the end result can appear monstrous. Thus in architecture it seems unnecessary for skins to perform their given function, as long as they appear congruent and can adapt to new styles. In this way even the action of maintenance becomes an action that modifies the pre-existing state with the aim of conforming to fashions, and the resulting 'new image' can be more or less different in relation to the preceding one, whether or not this change is useful or functional. The important thing is to *appear* adequate, despite not being adequate at all.

3 CONCLUSIONS

The change in the ways we perceive man-made environments, in particular man-made structures, has given rise to a number of changes that – in certain respects – can be considered epoch making, at least in the sector of coloured finishes. The application of colour on the walls of buildings is currently considered an operation of little interest from the point of view of the behaviour of the materials. It is

considered a cosmetic option having a lower priority than other processes; it follows the fashion of the moment and a subculture of the building sector.

Despite being considered strategic in terms of the image projected by a building (in a society in which image is decisive for the market), the outermost surface is normally thought of as unnecessary either for the improvement of the efficiency of the building system or for the layers to which it is applied. The decline in interest in this aspect is the result of a number of questions that have decreed its obsolescence. The first of these is the cost of labour.

A process such as applying colour to the walls of buildings has always required qualified and sensitive – and therefore expensive – skilled labour. To succeed in eliminating the need for this, or to reduce the time and number of methods needed for the application of colour, has required the availability of special materials that can be used on any kind of support. Thus the sector of painting products, or rather pigmenting products, has worked to create products that can have an almost infinite chromatic range and degrees of saturation that were previously unimaginable in the building sector. The drive to raise the level of saturation comes from the world of the media and of the need to make buildings emerge from their surroundings, the opposite of the historical assumption that buildings should be integrated with the landscape.

This has brought about an epoch-making change in the use of materials; these are no longer developed within the building sector but in that of polymers and chemicals in general, as well as the in the field of nanotechnologies. Methods and techniques have been studied to obviate the need for the stratum of colour to protect the underlying layer. The materials employed today are indifferent to the substrate, being able to adhere to nearly all types of building material. This has given rise to a radical change in the way maintenance is carried out. If in the past it was necessary to protect the last coloured layer, but above all the underlying layers, now – when the choice of materials and their behaviours is no longer restricted – the coloured layer serves a purely aesthetic function. The approach to maintenance has become specific, or rather specialized. Also the inclusion in the colouring material of substances that repel dirt and pollution has given the coup de grace even to operations of normal cleaning. In short, we have arrived at the threshold at which products can be used that repair themselves, clean themselves and regenerate themselves. Probably everything that approaches the level of nanotechnology is showing a potential similar to that of human skin whenever it suffers minor damage. And the layer of colour, exactly for this connotation of thin coating film, is heading in this direction, where maintenance can only be carried out following sophisticated, specialized and dedicated technologies, a long way from the historical repainting or 'patching up'. The other layers are left to their destiny, denied the precious protection that has always completed most works of architecture.

REFERENCES

Le Corbusier 1923, *Vers une architecture*, Paris (eng. tr. 2007, *Towards an Architecture*, Getty Research Institute, Los Angeles).

Tschumi, B. 1996, *Architecture and Disjunction*, The Mit Press, Cambridge (MA) (ita. tr. 2005, *Architettura e disgiunzione*, Pendragon, Bologna, p. 60).

Donghi, D. 1920, *Manuale dell'architetto. Lavori da decoratore e da tappezziere*, vol. I, Parte II, cap. VI, Torino.

Zennaro, P. ed. 2007, *Il colore nella produzione di architettura (The colour on production of architecture)*, Ipertesto Edizioni, Verona.

Investigation of Physical and Mechanical Properties of Clay Bounded Plasters Applied on Kerpic Buildings from Diyarbakir

Şefika Ergin Oruç [1]
Bilge Işık [2]

T 21

ABSTRACT

Earthen material is preferred all over the world due to its easily workability, economical and ecological concern. Both on rural and urban areas some of the earthen structures can be considered as architectural heritage of the country. For that reason investigation must be carried for maintenance, restoration as well as for new buildings.

Earthen material is mostly used in wall (Kerpic), floor and plaster applications. The wall surfaces can be plastered or not. In case of wall plastering, the physical and mechanical properties of earthen wall should be taken into consideration. Clay bounded plaster is widely used on earthen wall surfaces. Clay affects the durability of plaster in terms of resistance against external impact. Therefore, plaster properties should be investigated in detail for determining their durability. The study can run on new test sample program or test can be carried out on existing walls or plasters.

This is a study on clay bounded plaster on existing earthen wall in rural areas of Diyarbakir. In the study, physical properties of the plasters have been examined on the samples that were taken from Yuvacik village, Diyarbakir/Turkey. Experimental results have showed that the material does not deteriorate due to water absorption and vapor permeability properties are determined as suitable.

KEYWORDS

Earthen material, Earthen architecture, Properties of plasters, Clay as binder, Water absorption

[1] Dicle University, Civil Engrg.-Architecture Faculty, Diyarbakir, Turkey, 21280, Phone +90.412.248 8403, Fax +90.412.2242374, sefika@dicle.edu.tr
[2] Istanbul Technical University, Faculty of Architecture, Istanbul, Turkey 34437, Phone +90.212 288 7879, Fax +90.212 266 0279, bilge.isik@kerpic.org

1 INTRODUCTION

Earthen material (Kerpic) is mostly used in wall, floor and plaster applications. The wall surfaces can be plastered or not. In case of wall plastering, the physical and mechanical properties of earthen wall should be taken into consideration. Clay bounded plaster is widely used on earthen wall surfaces. Clay affects the durability of plaster in terms of resistance against external impact. Therefore, plaster properties should be investigated in detail for determining their durability. The study can run on new test sample program [1] or test can be carried out on existing walls or plasters.

This is a study on clay bounded plaster on existing earthen wall in rural areas of Diyarbakir. In the study, physical properties of the plasters have been examined on the samples that were taken from Yuvacik village, Diyarbakir/Turkey. Experimental results have showed that the material does not deteriorate due to water absorption and vapor permeability properties are determined as suitable.

2 ADOBE WALL SURFACES

Structural walls can be constructed with various earthen materials. Earthen walls and their surface **perform** according to the properties of the main material and the additives. The wall surfaces are exposed to different environmental conditions. To reduce damages from environmental conditions, plaster can be applied to the surfaces of the walls. If so, the plaster should possess some properties considering the required durability.

Environmental **impact** leads to damages at external wall surfaces throughout the time. These effects could be physical, chemical and mechanical damages on the wall or plaster.

3 CLAY BOUNDED PLASTERS

Clay bounded plasters are vulnerable to water. Erosion can occur due to water exposure. Such cases new plaster can be applied for renovation. The study will contribute to the new plaster decision.

The properties of plasters that can be used on to earthen wall vary in respect to origin and amount of binders, aggregates and additives. The most used binders are clay-cement, clay-gypsum, clay-lime, hybrid and straw fiber [2]. Straw added into clay based plaster prevent cracks due to shrinkage after applied to the wall [3]. Whitewashing on plasters contributes to durability of the envelope while decreasing the water permeability. Lime plastering could be also applied to external plasters.

Clay-cement bounded plasters have high strength and low elasticity. These plasters are sensitive against mechanical and thermal movements and can easily crack. Such plaster types should not be used as indoor plaster or external plaster over light-wall-materials (wall materials having unit weight less than 1000 kg/m^3) [4] which have low strength and part of building that any structural movement were expected [5] [6]. Therefore, their application is limited to buildings. They can be used externally on basement walls (stone or concrete) and reinforced concrete ceiling of buildings which are exposed to external conditions. Clay-cement bounded plasters are used in structure where continuous high humidity ratios and high abrasion exist. Usually shrinkage cracks occurred if the plaster is smoothed with trowel. Drying duration of the plaster is very closely related with atmospheric conditions. Flowering on the surface of the plaster can occur if soluble salts are in the soil.

Clay-gypsum mixed plaster type has low strength and elastic behavior. Gypsum in the clay undergoes reaction with clay minerals during hydration and the plaster gains durability. Plaster deterioration is low when compared with unstabilized clay bounded plaster. Clay particle in unstabilized plaster extends when exposed to water. Clay-gypsum shows a balancing behavior to heat and humidity [7]. They have smooth surface and dust production does not develop.

Clay-lime bounded plasters have low strength. They have good binding property and are less affected by water and humidity. These plasters can be easily applied to indoor and outdoor surface of the building. Clay-lime bounded plaster types should be preferred in applications on low strength and light structural materials and also active parts of a building. Its abrasion strength is low. Clay-lime plaster should be applied in two layers. In the first layer middle size sand and in the second layer fine sand should be used. Lime-composite has long duration for hardening process so, the second layer should not be applied immediately.

Hybrid plaster is composed of more than one binder; like lime and gypsum or lime and cement. Gypsum and lime bounded plasters should be applied to elastic surfaces with low strength. Cement and lime bounded plasters can be applied on heavy duty surfaces, both indoors and outdoors [8].

Cracking of earthen material or clay material is frequently encountered; therefore this deficiency should be resolved. The best solution for this problem is adding fibers like straw, linen, cotton stem and similar organic fibers into it. Straw is generally added to plasters for increasing its tensile properties [8].

4 EXPERIMENTAL STUDY

In this study, physical and mechanical properties of external plasters bounded with clay from existing wall were examined.

A structure built in 1967 at Yuvacik village of Bismil county, Diyarbakir province was chosen in order to conduct experimental study (Figure.1). Straw added earthen (Kerpiç) blocks were used in the structure and for plastering.

The samples for experimental study were taken from external plaster of the building and categorized as east (D1), north (K1) and south (G1).

Figure 1. The structure where samples were taken from.

4.1 Sieving Analysis

Sieving analysis of the samples was performed to determine particle size distribution and physical properties of the material according to TS 130 standard [9].

The results of sieving analysis are given in Table 1.

Table 1. Results of Sieving Analysis.

Sieve size (mm)	Over sieve weight (gr)	Sample percentage (%)
2	6,55	2,183
1	23,2	7,733
0,5	24,75	8,25
0,25	47,38	15,793
0,125	94,54	31,513
0,63	62,56	20,853
Under Sieve	41,02	13,673

4.2 Unit Weight, Composite-Porosity, Specific Weight

The experimental studies were conducted according to the Code TS EN 1936 in order to determine Unit Weight, Composite-Porosity, and Specific Weight of the material [10]. The results are given in Table.2.

Table 2. Results of the experiments.

Sample	Size (cm)	Weight (gr)	Unit Weight gr/cm^3	Composite %	Porosity %	Specific Weight gr/ cm^3
D1	1,53×2,23×2,91	9,98	1,01	41.06	58.94	2,46
G1	1,63×2,50×3,68	16,48	1,10	42.95	57.05	2,56
K1	1,28×1,28×3,32	6,24	1,15	44.75	55.25	2,57

4.3 Water Absorption Capacity due to Capillary Effect

The experiment for determination of water absorption capacity was carried out in compliance with TS EN 1925 standard [11]. Three samples were prepared as regular geometrical shapes and named as G1, K1, and D1 (Figure 2).

Figure 2. G1, K1, and D1 Samples Preparation.

The samples G1, K1, and D1 were completely wet in 25, 81 and 154 minutes respectively and the first one dissolved in 169 minutes, the second one dissolved in 121 minutes and the third one did not dissolve.

D1 sample was illustrated in Figure 3.

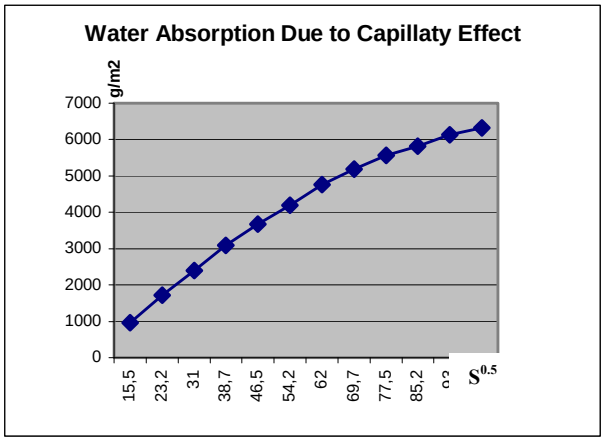

Figure.3 Water Absorption of the Samples D1 Due to Capillary Effect.

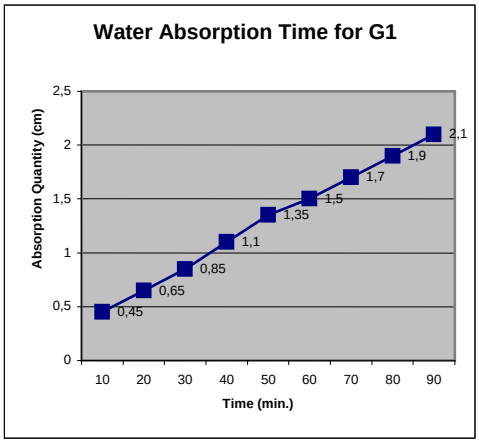

Figure.4 Water Absorption Time for G1.

4.4. Water Absorption Time

Water Absorption Time experiments for G1, K1, D1 samples were conducted according to TS EN 1936 standard [10]. Figure 4-6 represents water absorption times of the samples. The sample procedure is illustrated in Figure 7.

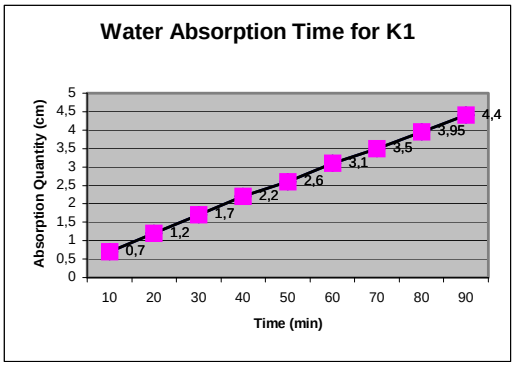

Figure.5 Water Absorption Time for N1.

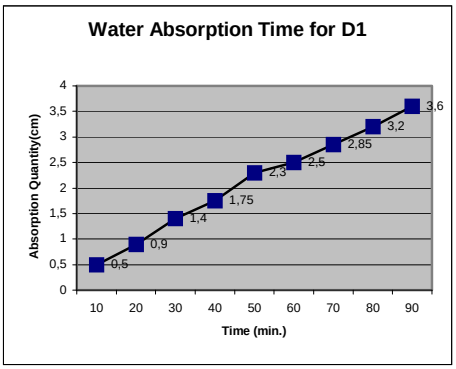

Figure.6 Water Absorption Time for E1.

Figure.7 Water Absorption Test.

Figure.8 Vapor Permeability Test.

4.5 Vapor Permeability

Vapor permeability experiments were performed according to TS 7847 standard [12] (Figure 8). The experiments were carried out for each sample and the results are given in Table 3.

Table 3. Results of Compressive Strength Experiments.

Sample	Dimensions (cm)	P_{max} Fracture Load (kg)	A Load Application Area of Samples (cm^2)	σ_k Compressive Strength (N/mm^2)
E1-1	2.58*2.89*5.15	450	7.46	6.03
E1-2	2.23*3.62*5.76	260	8.07	3,22
E1-Average				4,6

4.6 Compressive Strength

Compressive strength of the samples was determined according to TS 2514 standard [13] (Figure 9). The samples were cut as rectangular prism and the experimental results of two samples pertaining to E1 are given in Table 4.

Figure 9. Compressive Strength Experiments.

5 RESULTS

Properties of the materials used for structures are crucial for long duration and healthy buildings. Durability of envelope can be achieved through paints, plasters etc. The aim of the study is to determine performance of the clay binder plaster on earthen walls.

The samples for experimental studies were taken from external plaster of a house built in 1967 at Yuvacik Village of Bismil County, in Diyarbakir. Straw was added into plaster for better bounding in local technique. Damage at the external plaster was very low. Mechanical and physical properties of the samples were examined and the results are as follows:

Water absorption due to capillary effects of a sample according to TS 2514 standard states that a sample should not be dissolved before 45 minutes. In this study the G1 sample dissolved at 169th minute, K1 sample dissolved at 121st minute and D1 sample did not dissolve during the experimental period, which was 169 minutes. The results of this experiment show that the samples are resistant enough against deterioration.

Water absorption from 14mm tube measured is 3.6, 2.1 and 4.4 cm for E1, S3 and N3, respectively.

Water vapor permeability according to TS 7847 standard should be at least (1/μ.d) 0,5 m^{-1}. In this study these values are 5,13 m^{-1} 4,89 m^{-1}, and 5,33 m^{-1} for E1-, S1- and N1-, respectively. These results show the validity of the sample for vapor permeability period

TS 2514 standard for compressive strength on earthen block is minimum 0.8 N/mm^2 and the average of all samples should not be less than 1 N/mm^2. In the study these values were 6.03 N/mm^2 for E1-1, 3.22 N/mm^2 for E1-2 and the average was 4.63 N/mm^2. The results show that the samples are appropriate according to the TS 2514 standard.

REFERENCES

[1] Taylor M, 1986, Fort Selden Test Wall Status Report, New Mexico State Monuments, Museum of New Mexico.

[2] Kömürcüoğlu, E.A.,1962, Earth as construction material, and earthen construction systems, (Yapı Malzemesi Olarak Kerpiç ve Kerpiç İnşaat Sistemleri), Istanbul Technical University, Faculty of Architecture.

[3] Houben, H., Guillaud, H.,1994, "Earth Construction, A Comprehensive Guide", Intermediate Technology Publication.

[4] TS 1262, 1988, Sıva Yapım Kuralları- Bina İç yüzeylerinde Kullanılan, TSE, Ankara.

[5] Anon., 1993, VKF Vereinigung Kant. Feuerversicherungen, Brandschutzregister, Ausgabe.

[6] Klingsohr, K., 1994, "Vorbeugender Baulicher brandschutz".

[7] IŞIK, B.: 1993 "Outdoor-Plaster Applications on Gypsum&Adobe Wall" Post, CIB Congress, Vanquver, Canada, 20/26 June.

[8 Ersoy, H.Y., 2001, "Kompozit Malzeme", Literatür Yayıncılık, İstanbul.

[9] TS 130, 1978, Agrega karışımlarının elek analizi deneyi için metot, TSE, Ankara.

[10] TS EN 1936, 2001, Doğal Taşlar- Deney Metotları- Gerçek Yoğunluk, Görünür Yoğunluk, Toplam ve Açık Gözeneklilik Tayini, TSE, Ankara.

[11] TS EN 1925, 2000, Doğal Taşlar- Deney Metotları- Kılcal Etkiye Bağlı Su Emme Katsayısının Tayini, TSE, Ankara.

[12] TS 7847, 1990, Hazır Sıva – Dış Cepheler İçin, Sentetik Emülsiyon Esaslı, TSE, Ankara.

[13] TS 2514, 1977, Kerpiç Bloklar ve Yapım Kuralları, TSE, Ankara.

Table 3. The Results of Water Permeability Experiment.

	Thickness d (m)	Diameter m	Area m^2	Date	Time between two successive measurements (h)	Sample Weight (kg)	The Weight Difference Δm	Vapor Quantity (G) (kg/h)	Vapor Diffusion Resistance Factor (μ)	1 / μ*d
S1	d= 0.01137	0.06960	$3,80.10^{-3}$	27.04.2004	0	0,10611535	0	0	18	4,89
				28.04.2004	24	0,10669053	$5,75.10^{-4}$	$23,96.10^{-6}$		
				29.04.2004	24	0,10711226	$4,22.10^{-4}$	$17,58.10^{-6}$		
				30.04.2004	24	0,10741133	$2,99.10^{-4}$	$12,46.10^{-6}$		
				02.05.2004	48	0,10808952	$6,78.10^{-4}$	$14,13.10^{-6}$		
				03.05.2004	24	0,10847322	$3,84.10^{-4}$	$16,00.10^{-6}$		
				04.05.2004	24	0,10886101	$3,88.10^{-4}$	$16,17.10^{-6}$		
				05.05.2004	24	0,10920959	$3,49.10^{-4}$	$14,54.10^{-6}$		
				06.05.2004	24	0,10962318	$4,14.10^{-4}$	$17,25.10^{-6}$		
				07.05.2004	24	0,10999859	$3,75.10^{-4}$	$15,63.10^{-6}$		
				10.05.2004	72	0,10999921	$10,00.10^{-4}$	$13,89.10^{-6}$		
E1	d= 0.01218	0.07060	$3,91.10^{-3}$	27.04.2004	0	0,10641432	0	0	16	5,13
				28.04.2004	24	0,10692752	$5,13.10^{-4}$	$21,38.10^{-6}$		
				29.04.2004	24	0,10738312	$4,56.10^{-4}$	$19,00.10^{-6}$		
				30.04.2004	24	0,10771101	$3,28.10^{-4}$	$13,67.10^{-6}$		
				02.05.2004	48	0,10846637	$7,55.10^{-4}$	$15,73.10^{-6}$		
				03.05.2004	24	0,10889201	$4,26.10^{-4}$	$17,75.10^{-6}$		
				04.05.2004	24	0,10931364	$4,22.10^{-4}$	$17,58.10^{-6}$		
				05.05.2004	24	0,10969011	$3,76.10^{-4}$	$15,67.10^{-6}$		
				06.05.2004	24	0,11013146	$4,41.10^{-4}$	$18,38.10^{-6}$		
				07.05.2004	24	0,11053827	$4,07.10^{-4}$	$16,96.10^{-6}$		
				10.05.2004	72	0,11162201	$10,84.10^{-4}$	$15,06.10^{-6}$		
N1	d= 0.01043	0.07171	$4,04.10^{-3}$	27.04.2004	0	0,10287144	0	0	18	5,33
				28.04.2004	24	0,10340338	$5,32.10^{-4}$	$22,17.10^{-6}$		
				29.04.2004	24	0,10388227	$4,79.10^{-4}$	$19,96.10^{-6}$		
				30.04.2004	24	0,10422566	$3,43.10^{-4}$	$14,29.10^{-6}$		
				02.05.2004	48	0,10502938	$8,04.10^{-4}$	$16,75.10^{-6}$		
				03.05.2004	24	0,10547517	$4,46.10^{-4}$	$18,58.10^{-6}$		
				04.05.2004	24	0,10592834	$4,53.10^{-4}$	$18,88.10^{-6}$		
				05.05.2004	24	0,10633344	$4,05.10^{-4}$	$16,88.10^{-6}$		
				06.05.2004	24	0,10680141	$4,68.10^{-4}$	$19,50.10^{-6}$		
				07.05.2004	24	0,10723465	$4,33.10^{-4}$	$18,04.10^{-6}$		
				10.05.2004	72	0,10838351	$11,49.10^{-4}$	$15,96.10^{-6}$		

11DBMC International Conference on Durability of Building Materials and Components
ISTANBUL, Turkey 11-14 May 2008

Mechanical Behaviour of Non-bearing Brick Masonry Facades

Ignacio Oteiza [1]
José P. Gutiérrez [1]
Juan Monjo [1]
Juan R. Rey [1]

T21

ABSTRACT

The non-bearing, fair-face brick masonry wall is one of the most commonly used enclosure systems in Spanish building, applied in over 80% of new construction. This system is a descendant of the bearing wall facades used ever since the Middle Ages. The solution initially adopted with the routine implementation of two-way concrete structures in the mid-twentieth century, consisting in a one-foot outer wythe, soon gave way (in the nineteen sixties) to a ½-foot outer wythe of fair-faced brick, a non-ventilated (insulated or otherwise) chamber and an inner stretcher bond wythe made of four-cm face brick laid on edge. This system poses mechanical, damp, thermal and on site construction issues that may lead to a series of pathologies, including facade collapse in some extreme cases.

The study presented forms a part of a research project (PROFIT) funded by the Ministry of Industry and Trade in conjunction with a number of contractors, the Spanish association of brick and tile manufacturers (Hispalyt), quality control organizations, the Polytechnic University of Madrid and the Eduardo Torroja Institute (IETcc). The paper discusses the results of structural trials conducted at the IETcc in connection with the mechanical behaviour of walls and their constituent materials. The results of these trials are compared to the mathematical models under evaluation at the Polytechnic University of Madrid to determine the form, recommendable dimensions and the use or otherwise of ancillary elements in non-bearing brick masonry facades.

KEYWORDS

Facades, Fired clay brick, Mechanical tests

[1] Madrid, Spain. Instituto Eduardo Torroja- CSIC. C/Serrano Galvache, 4. Phone +34 913020440 Ext. 275, Fax +34 9130204 40, ioteiza@ietcc.csic.es , jpgutierrez@ietcc.csic.es, director.ietcc@csic.es, jrrey@ietcc.csic.es

1 INTRODUCTION

Brick masonry, one of the elements most profusely used throughout the history of western construction, continues to be the most common housing enclosure typology to be found in Spain. And yet design and construction records often contain very little information on this unit of work, a circumstance that is particularly significant against the backdrop of the recent entry into effect of Spain's new Technical Building Code. In the early twentieth century, masonry walls which since the Middle Ages had been designed to bear structural weight adopted a new function, with the attendant thinning of their dimensions from the prior 1 ½' to the present ½ foot. This reduction has posed mechanical, damp, thermal and on site construction issues that need to be explored and analyzed to prevent their degeneration into a series of pathologies associated with masonry exposure to the elements and on site construction conditions, which may in some cases lead to collapse of the building enclosure.

Recent studies on damage detected in masonry in-fill show that mechanical erosion is still routinely found in the form of scaling, cracks and fissures. This justifies an experimental study to substantiate present solutions, improve their implementation and attempt to eliminate the most common causes underlying such pathology.

2 DAMAGE IN WALLS

Generally speaking, damage may be classified into three main groups: physical, mechanical and chemical. Moreover, damage can rarely be attributed to a single cause. Mechanical damage may be **caused directly** by loading, overloads, thrust, impact or friction and **indirectly** as a result of faulty design, workmanship, materials or maintenance. Damage to masonry in-fill may be classified as mechanical, one of the most prominent causes being the disparities between portal frame and brick masonry stiffness values, which generate different degrees of tolerance to deformations; these, in turn, tend to appear at joints connecting the two elements.

2.1 Statistical Data and Trends

A number of surveys were conducted on the different types of damage detected in brick masonry in-fill and possible causes, from which the following trends were identified:

- Mechanical damage was found in at least 42% and in some cases nearly 50% of all the brick masonry in-fill surveyed.
- Mechanical stress was the direct cause of such damage in at least 18% of the cases.
- Inappropriate design was the source of at least 40% of the damage, presently accounting for 47%.
- Although in blank walls the percentage of damage per construction unit has declined slightly, it continues to be found in at least 25% of the total.

3 EXPERIMENTAL PROCEDURE

3.1 Characterization of Materials

In the first stage, research focused on characterizing the materials comprising brick masonry, via an experimental study performed at the Eduardo Torroja Institute for Construction Science (IETcc - CSIC, a Spanish National Research Council body). Six types of standard brick were analyzed. A photograph of perforated fair-face brick, the object of the research described below, is reproduced in Fig. 1. Its dimensions are: 240 mm x 115 mm x 49 mm. The mortars studied were all made from 42.5R CEMII/B-V type cement.

The characterizing of the components of walls built with conventional (designated type C) perforated fair face brick was conducted to the specifications laid down in Spanish and European standard UNE-EN 772-1 "Methods of tests for masonry units. Part 1: Determination of compressive strength"

Figure 1. Brick type C , Brick capping and Brick after testing

The results of the compression tests run on perforated brick (Figure 1) showed that the mean compressive strength of these units was 35.04 N/mm^2.

3.2 Standard-compliant Mechanical Testing on Small Walls

The primary aim of this part of the study was to analyze compressive and bending strength in brick masonry walls.

3.2.1. Compression tests on low perforation brick masonry walls, to Spanish and European standard UNE-EN 1052-1

Specimens measuring approximately 50 x 50 cm were prepared, each consisting of eight rows of perforated brick with one exposed face, received in a 16.6-MPa sand and cement mortar. One of the specimens is shown in Figure 2, both before testing, fitted with strain gauges on both sides, as well as during and after failure.

Figure 2. Test specimen before and after compression failure.

The specimens tested to a mean compressive strength of 12.55 N/mm^2. A second series of tests was conducted on three 50 x 50-cm specimens, made with 13.9 N/mm^2 mortar. In this case, the mean compressive strength recorded was 10.04 N/mm^2 and the modulus of elasticity was found to be 13092.63 N/mm^2, although the values of the latter parameter showed a wide scatter. The instantaneous stress-strain ratio, E, specified in the SpanishTechnical Building Code for masonry, is 1000·f_k. Applied to the mean strength obtained in the tests, this would call for a value of between 10000 and 12500 N/mm^2, i.e., generally lower than the mean values found with the standard tests.

3.2.1 Bending tests on low perforation brick masonry walls, to Spanish and European standard UNE-EN 1052-2, Part 2 (2000)

The object of this standard is the determination of the bending strength of clay-based brick and cement mortar walls. The standard envisages two different situations: where the failure plane is parallel and

where it is perpendicular to the bed or horizontal joints. Figure 3 shows walls tested for bending strength along a plane parallel to the horizontal joints. The specimens tested to a mean bending strength of 0.80 N/mm^2.

Figure 3. Failure parallel to bed joints.

Figure 4. Failure perpendicular to bed joints.

The mean bending strength found for walls tested along a plane perpendicular to the horizontal joints (Fig. 4) was f_{x2} = 2.19 N/mm^2.

3.3 Bending Tests in Full Size Walls

Two 5-m wide specimens, 2.5 and 3 m high, respectively, were tested. This test was run on walls ½ foot thick, supported at the top and bottom but not on the sides. The intention was to simulate the conditions prevailing in actual brick facades. A testing frame was built with rolled steel shapes, to be able to apply both vertical loads and horizontal loads perpendicular to the plane of the wall.

The first specimen measured 5 x 3 m. Figure 5 shows the wall after it was built, on the compression side, A (left) and side B (right), prepared for testing. The failure sequence is depicted in Fig. 6.

Figure 5. View of 5 x 3-m wall, side A (left) and side B (right).

A 6-kN/m (30 kN total) linear vertical pre-load was first applied to the top of the wall. This was followed by a five-minute stabilization period before the horizontal load was applied to the steel shapes used to distribute the load. The shapes were positioned one quarter and three quarters up the wall, generating two uniform horizontal load lines. A displacement gauge was positioned at the centre of the

wall to measure its horizontal movement. Deformation was measured with strain gauges placed on both sides of the wall. Three gauges were positioned along the centreline (1.50 m from the top) on both sides, one in the centre and the other two at 1.50 m from each edge of the wall. Data were recorded on a Solartron IMP datalogger connected to a PC.

Figure 6. Bending failure sequence for a 3 x 5-m wall.

The graph in Fig. 7 depicts the load – horizontal displacement curve at the centre of the wall, from the time the horizontal load was applied. A slight change was observed in the slope of the curve at between 12 and 13 kN due to the appearance of cracks in the masonry. At a load of about 18 kN, which prompted a 2-mm displacement, the slope changed abruptly due to cracking in the failure section, located around the upper horizontal load line in the wall. Failure occurred at a load of 24.42 kN and displacement of 6.90 mm.

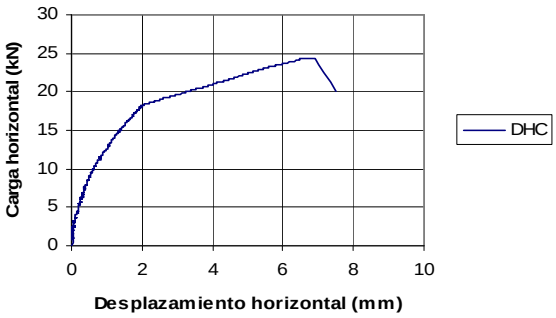

Figure 7. Load – horizontal displacement at centre of wall

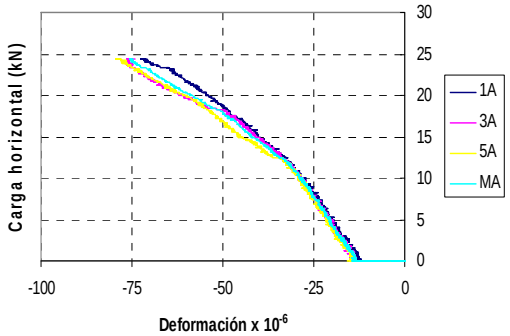

Figure 8.
Load – deformation on side A of the wall.

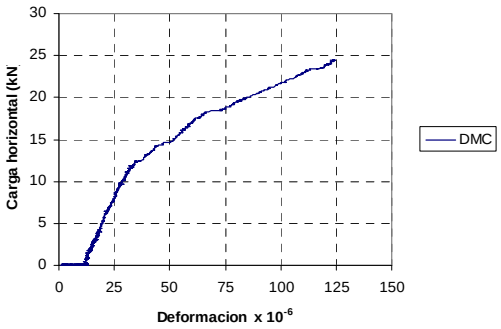

Figure 9.
Load – deformation on side B of the wall.

The graph in Fig. 8 shows the deformation at the centreline of side A of the wall, the side subjected to compression stress, recorded by gauges 1A, 3A and 5A when the horizontal load was applied. The curve labelled MA represents the mean of the measurements recorded by the three gauges. The initial deformation shown on the graph was due to the vertical pre-loading that preceded horizontal loading. This pre-loading generated bending stress due to load eccentricities (the eccentricities generated when

the load was applied to the shape positioned on the wall for this purpose cannot be determined exactly) and flawed construction, namely lack of plumb with the concomitant deviations in wall verticality or flatness.

The graph in Fig. 9 shows the mean deformation generated along the centreline on side B of the wall. Wall behaviour was approximately elastic and linear up to a horizontal load of between 12 and 13 kN. Up to this loading, the measurements recorded by the tensile side gauges were similar to the data logged by the gauges on the compression side. At higher loads, the wall began to crack, stiffness declined and buckling became more intense.

The failure load obtained was found to be 24.42 kN, or 12.21 kN per load line, while the surface load was 1.628 kN/m^2. The peak ultimate horizontal moment, disregarding both additional vertical pre-loading and second order eccentricities, as well as initial construction errors, was 0.75 x 12.21 = 9.157 kNm across the entire 5-m wide section (9.157/5 = 1.831 kNm/m).

For the central section of the wall, the vertical pre-loading-induced second order moment at failure due to horizontal deformation was 2.2% of the first order moment, i.e., practically negligible. Based on the initial deformation values obtained, the initial moment generated by vertical pre-load eccentricity plus eccentricity due to flawed construction may be estimated to be around 20% of the moment generated by the horizontal load. While hardly negligible, in engineering standards this load is taken into account as part of the additional eccentricities generated by construction errors, slenderness and lack of precision in the point where the vertical load is applied.

The second test was conducted on a wall measuring 5 x 2.5 m. The three snapshots in Figs 10 to 12 depict the failure sequence and the failure line generated.

Figures 10 to 12. Failure sequence, 5 x 2.5-m wall.

The wall was first subjected to a 30-kN/m (150 kN in all) linear vertical pre-load from the top down. This was followed by a stabilization period, after which the horizontal load was applied

The graph in Fig. 13 depicts the load – horizontal displacement curve at the centre of the wall, from the time the horizontal load was applied. The initial deformation or displacement recorded was due to the eccentricity induced by the vertical pre-load as well as other additional eccentricities occasioned by construction errors, namely lack of plumb and the resulting imperfect verticality.

At a load of approximately 15.54 kN, the wall cracked longitudinally at the lower horizontal load line, where the displacement recorded was 3.11 mm. The ensuing deformation to 10.63 mm was so abrupt that the testing machine was unable to maintain the thrust, resulting in a decline in both pressure and load. After this first failure stabilized, the horizontal load process continued until the peak test load was reached. Failure occurred at a load of 31.68 kN, when displacement was 13.02 mm.

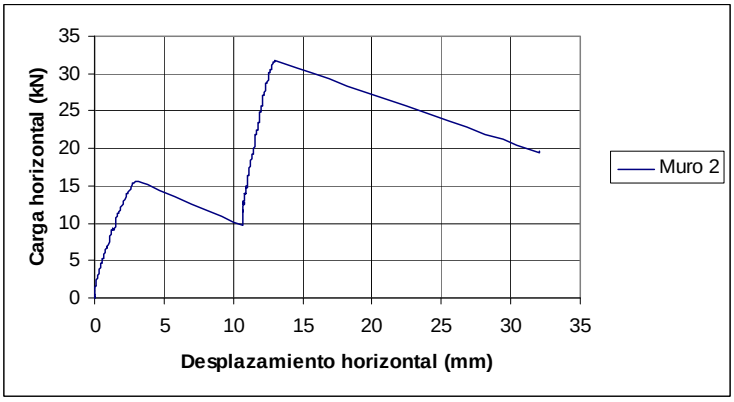

Figure 13. Load – horizontal displacement at centre of wall

The graph in Fig. 14 shows the deformation at the centreline on side A of the wall, the side subjected to compression stress, recorded by central gauge 3A when the horizontal load was applied. The initial deformation observed on the graph was due to the vertical pre-loading that preceded horizontal loading.

The graph in Fig. 15 shows the mean deformation generated along the centreline on side B of the wall, as recorded by gauges 3B and 5B. The graph shows the abrupt rise logged at a load of 15.54 kN.

The ultimate load found was 31.68 kN, or 15.84 kN per load line applied, for a surface load of 2.53 kN/m^2.

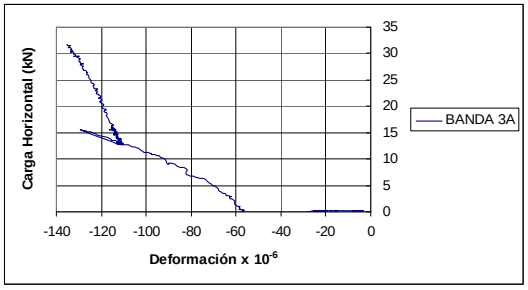

Figure 14. Load – deformation on side A.

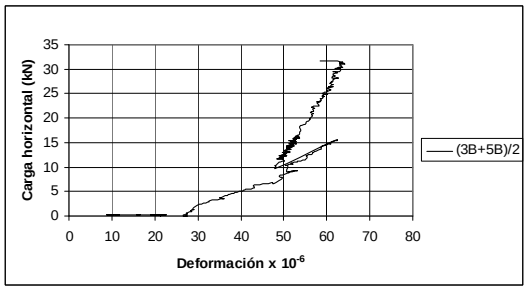

Figure 15. Load – deformation on side B.

4 CONCLUSIONS

Some of the results of a research project relating to the mechanical behaviour of walls and their component materials are discussed in the present paper. Compressive strength and modulus of elasticity were found for low perforation brick masonry walls with brick and mortar combinations used in standard construction. The values found for compressive strength ranged from 10 to 12.5 N/mm^2, while the modulus of elasticity varied widely, from 13000 to 24000 N/mm^2. Bending strength was also determined along the planes parallel and perpendicular to the bed joints, with the former showing mean strengths of from 0.8 to 1 N/mm^2 and the latter mean values on the order of 2.2 N/mm^2.

In addition, two full size walls one half-foot (11.5-cm) thick were tested to failure under horizontal loads. For the first wall, vertically pre-loaded at 6 kN/m (30 kN in all), the uniform surface failure load was 1.628 kN/m^2, with a deformation of 6.90 mm at the centre of the wall. For the second, vertically pre-loaded at 30 kN/m (150 kN in all), the uniform surface failure load was 2.53 kN/m^2. These values may serve as a reference for wind action calculations in wall enclosure design.

ACKNOWLEDGEMENTS

This paper presents some of the results of the 2006 PROFIT research project titled **"Cooperative project to analyze the problems and most suitable solutions affecting non-bearing clay brick walls".** The authors wish to thank the IETcc-CSIC mechanical testing team for their assistance.

REFERENCES

UNE-EN 772-1:2000 -Methods of test for masonry units Part 1: Determination of compressive strength.

UNE-EN 1052-1 Methods of test for masonry Part 1: Determination of compressive strength.

Project Profit 2006.Ministerio of Industry Tourism and Trade Cooperative Project
Analysis of the problems and the most appropriate solutions for the construction of walls does not Bearing ceramic brick.

11DBMC International Conference on Durability of Building Materials and Components
ISTANBUL, Turkey 11-14 May 2008

Durability of Highly-Insulated Timber-Frame Flat Roofs

Christoph Buxbaum [1]
Oskar Pankratz [2]

T 22

ABSTRACT

European roof structures in industrial and commercial construction (warehouses, etc.) are usually carried out in prefabricated reinforced concrete or with metal sandwich-panels. Due to the increasing requirements for the thermal protection of the building envelope, highly-insulated timber-frame flat roof constructions have become an alternative energy efficient method of construction.

The aim of the present study is the analysis and comparision of the hygrothermal performance and furthermore durability of non-ventilated light-weight flat roofs. The main focus is the assessment of potential risks of mold and especially wood decay funghi growth due to moisture accumulation inside constructions, if they are smooth-surfaced (i.e., without aggregate surfacing), or covered with gravel aggregate. Within the investigations, several numerical simulations were done. In particular, the effect of the selected modeled constructions (i.e., the interaction of different types of vapor retarders and membrane systems) on moisture behavior was estimated.

KEYWORDS

Condensation, Moisture accumulation, Mold and wood decay funghi growth

[1] Carinthia University of Applied Sciences, Department for Architecture, Spittal an der Drau, Austria, Phone +43 4762 90500 1132, Fax +43 4762 90500 9910, c.buxbaum@fh-kaernten.at
[2] Architect and Consulent for Heat and Moisture Simulations, Haidershofen, Austria, Phone +43 7434 42353, Fax +43 7434 42353, pankratz@kt-net.at

1 INTRODUCTION

This paper presents initial results of a study concerning the durability performance of non-ventilated, highly-insulated timber-frame low-slope roofs in the climate of Central Europe. The primary aim was to investigate the possible interaction of varying roof membranes and vapor retarders on the hygrothermal conditions of the chosen constructions. The calculations were performed for partially-attached systems with smooth-surfaced roof membranes and alternatively for gravel-surfaced membranes, which are often required due to fire regulations, protection from ultra violet (UV) radiation, against wind uplift forces, or simply demanded due to architectural aspects. The basic approach was to analyze the drying potential of unvented low-sloped roofs when different roof membranes and varying code-approved or modern vapor retarders are alternately used. It is important to note, that usally in Austria, according to code OENORM B8110-2, the protection against condensation is evaluated by using the dew-point- method (Glaser scheme). However this method only considers steady-state and very simplified boundary conditions. Neither realistic influences like solar radiation, wetting processes, etc., nor hygroscopic sorption or liquid transport are taken into account. The scope of this study is therefore to predict the long-term and therefore especially durability performance as realistically as possible by using transient hygrothermal calculations.

2 DESCRIPTION OF CASES

In frame of the research, prefabricated low-sloped roof timber constructions, which are uusally used in Austria, were analyzed with regard to their drying potential. These roof structures are typically constructed of a simple static structure consisting of timber beams 300mm (12´´), which are faced with bracing oriented strand boards on both sides. The space between the beams is assumed to be filled with mineral wool insulation. Based on this standard case, 10 different systems with varying roof membranes (having varying permeance and color) and vapor retarders were analyzed.

Table 1. Description of the investigated roof assemblies cases 1 to 10.

<table>
<tr><th colspan="10">Investigated Cases (Layers from out- to inside)</th></tr>
<tr><td>Case 1</td><td>Case 2</td><td>Case 3</td><td>Case 4</td><td>Case 5</td><td>Case 6</td><td>Case 7</td><td>Case 8</td><td>Case 9</td><td>Case 10</td></tr>
<tr><td colspan="4">Without Gravel</td><td colspan="6">Gravel Covering 50mm (2´´)</td></tr>
<tr><td colspan="2">Roof Membrane
Type: Plastic (Polyolefin)
Permeance = 0.2187perm
(s_d- Value = 15m)</td><td colspan="2">Roof Membrane
Type: Rubber (EPDM)
Permeance = 0.029perm
(s_d- Value = 110m)</td><td colspan="2">Roof Membrane
Type: Plastic (Polyolefin)
Permeance = 0.2187perm
(s_d- Value = 15m)</td><td colspan="2">Roof Membrane
Type: Rubber (EPDM)
Permeance = 0.029perm
(s_d- Value = 110m)</td><td colspan="2">Roof Membrane
Type: Plastic (Polyolefin)
Permeance = 0.0104perm
(s_d- Value = 315m)</td></tr>
<tr><td colspan="10">Oriented Strand Board (OSB) 15mm (5/8´´)</td></tr>
<tr><td colspan="10">Mineral Wool 300mm (12´´)</td></tr>
<tr><td>R 1</td><td>R 2</td><td>R 1</td><td>R 2</td><td>R 1</td><td>R 2</td><td>R 1</td><td>R 2</td><td>R 1</td><td>R 2</td></tr>
<tr><td colspan="10">Oriented Strand Board (OSB) 15mm (5/8´´)</td></tr>
<tr><td colspan="10">Gypsum Board 15mm (5/8´´)</td></tr>
</table>

R 1	Vapor Retarder, Permeance = 0.0252perm (s_d- Value = 130m)
R 2	Humidity-Adaptive Vapor Retarder; Permeance = 13.12/0.328perm (s_d- Value = 0.25/10m)

As stated, the primary aim of this paper is to demonstrate the impact of different roof membranes with and without gravel surfacing and varying vapor retarders on the hygrothermal and durability performance of highly-insulated timber-frame low-sloped roof constructions. Thus, two types of vapor retarders were included; specifically those meeting Austrian standards and code-approved, as well as modern, humidity-adaptive products. Regarding surfacing, the chosen simulations were calculated without gravel and with gravel surfacings to investigate whether reduced surface temperatures might decrease the inward drying.

It is noted that the analyses were conducted under the assumption that the roof structures had good air tightness and insulation installation, and thus without convective vapor flow affecting moisture build-up.

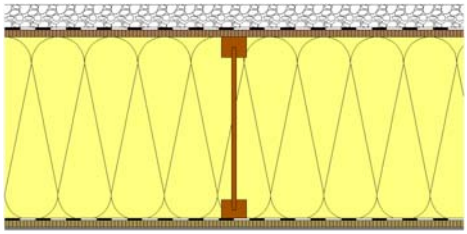

Figure 1. Schematic draft of standard case.

3 DESCRIPTION OF CALCULATION

The simulations were carried out by using the software WUFI®. (Wärme und Feuchte instationär – Transient Heat and Moisture), which was developed at the Fraunhofer Institute for Building Physics (Kuenzel 1994) in Holzkirchen / Germany and validated using data from outdoor and laboratory tests.

3.1 Default Program Settings

The heat transfer coefficient at the exterior surface was 19 W/(m²K), while that at the interior was 8 W/(m²K). For cases without gravel surfacing, short-wave solar radiation absorptivities of 0,5 and 0,9 were chosen for the grey-colored plastic membrane and for the black-colored rubber membrane, respectively. The slope of the roof was 2° northwards. Hourly weather data measured in 1995 in Holzkirchen / Germany represented the outdoor climatic conditions. The room climate varied as a sine curve between 20 °C and 30 % relative humidity in winter and 22 °C and 60 % relative humidity in summer. The initial conditions of the materials were chosen with a temperature of 20 °C and a higher initial RH. of 80 % (Karagiozis 1998). It`s noted that such a higher moisture content (i.e., 80 %) may be possible due to rain wetting during transport, erection work of large roofs structures or even flank diffusion over adjacent masonry (Kuenzel 1996). The material parameters required for each material were taken from the WUFI® material data base. The hygrothermal behaviour was simulated over a period of seven years.

4 SIMULATION RESULTS

This paper focuses on the “generally” hygric behaviour of the chosen roof assemblies. As is commonly recognized, the control of moisture is a critical part in the design of building envelopes. Hence the total water content and results concerning moisture accumulation in the “assumedly critical” exterior oriented strand boards were taken as the indicators of drying potential and risk of mold or even wood decay fungi growth.

A high intitial humidity of 80 % which is equivalent to ~ 16 % by mass in case of the oriented strand boards. These higher moisture conditions were chosen due to the fact that a non-regular dampening (i.e., wetting) of construction materials can always be possible due to rain penetration. Moreover for the evaluation undertaken in this paper, higher initial moisture conditions are quite useful in estimating the "real" drying potential of the materials (WTA, 2002).

4.1 Roof Systems without Gravel Surfacing:

Total Water Content (TWC)

First, simulations using roof systems (i.e. cases) 1 to 4 without gravel surfacings were carried out. Figure 2 shows the trend of the total water content (TWC) of these cases during the seven year period. It is clearly seen that all cases are showing a constant drying performance over the course of the seven years. It is also determinable that the humidity-adaptive vapor retarders, applied in cases 2 and 4, are having an significant effect on the moisture accumulation within these constructions. In these cases, the drying inwards is relatively fast; hence, it is not limited due to a vapor-tighter vapor retarder. The humidity-adaptive retarders have reduced vapor restistance at higher relative humidity levels and the vapor flow inwards is therefore not reduced. The total water content (TWC) of case 2 is leveling off at a seasonal maximum of ~ 2.25 kg/m² after about 4 years. In addition to that, the black coloring of the rubber in case 4 affords a higher drying rate. Higher temperatures at the exterior due to a higher radiation absorptivity of the membrane generates increased vapor pressure inwards and optimizes therefore the drying rate. So it is is clear to see that the capacity of inward drying should be considered as an important design factor (Powell and Robinson, 1971, Straube, 2001, Desjarlais, 1995).

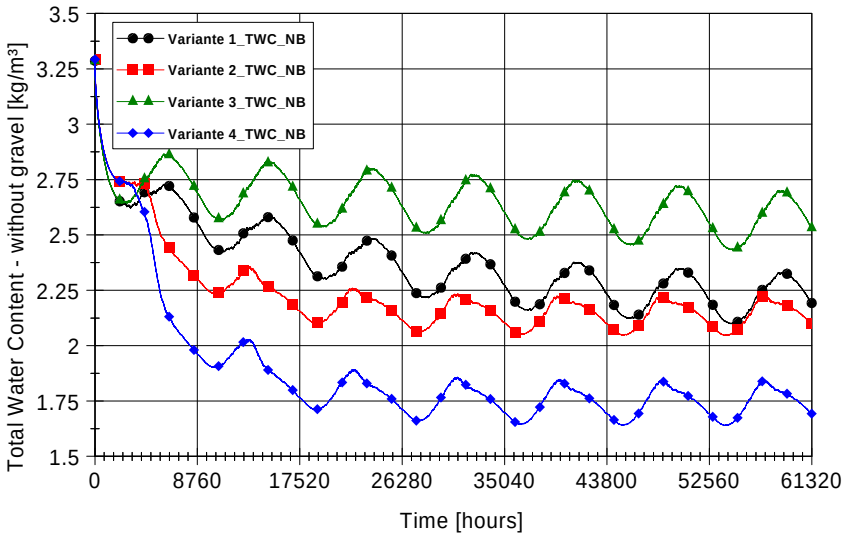

Figure 2. Total Water Content (TWC) of Cases 1 to 4, without gravel surfacing.

Water Content (WC) Exterior OSB Decking

The next step in this parametric study was to predict the moisture response of the wooden components and especially the exterior OSB decking. One can observe in Figure 3 that the moisture content of the OSB for cases 1 through 4 is decreasing over the years. In cases 1 and 2 it levels off at about ~ 13 % by mass, and in case 4 at ~ 9.5 % by mass. Only the moisture content of the exterior OSB in case 3 remains at a high humidity level for the whole period, decreasing from 18 % by mass to only ~ 16.8 % by mass. This effect is quite crucial for practical application, since the unscheduled moisture within the construction will be trapped between the vapor-tight exterior rubber and the interior vapor-tight conventional retarder for a longer time. This potential higher humidity level during long periods would endanger the risk of mold or even decay funghi growth and hence a potentially premature constuction failure.

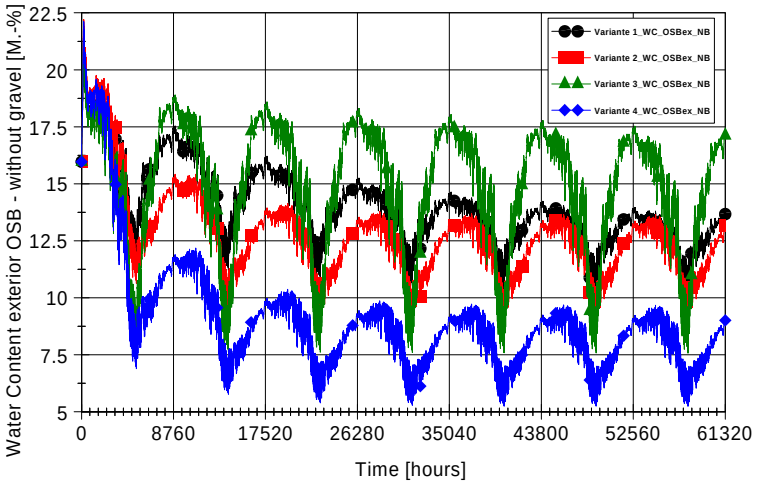

Figure 3. Moisture content (by mass) of the exterior oriented strand boards for cases 1 to 4, without gravel surfacing.

4.2 Roof Systems with Gravel Surfacing:

Total Water Content (TWC)

Next the previously discussed roof assemblies were again subjected to simulated modeling with a 5cm gravel surfacing above the membrane layers. Figure 4 depicts the TWC for cases 5 to 10. Starting again with initial moisture conditions of 80 %, it is now observeable that cases 5 and 7, which contain vapor-tight, code-approved vapor retarders, are showing a constant moisture accumulation. Especially the TWC of case 5 with the less vapor tight exterior plastic membrane increases rapidly. That would suggest that the lower vapor resistance of the exterior membrane is influencing the moisture uptake in a very special way. This affect is due to the high relative humidity level within the gravel layer during most time from spring to fall. Higher vapor pressures above the membrane are generating vapor flows from the outside, through the membrane, to the exterior OSB. That means that a vapor-tight membrane in cases with gravel surfacing would reduce the risk of an extraordinary moisture impact due to vapor flow from the exterior. Combined with vapor-adaptive retarders at the interior, the constructions are able to dry out.

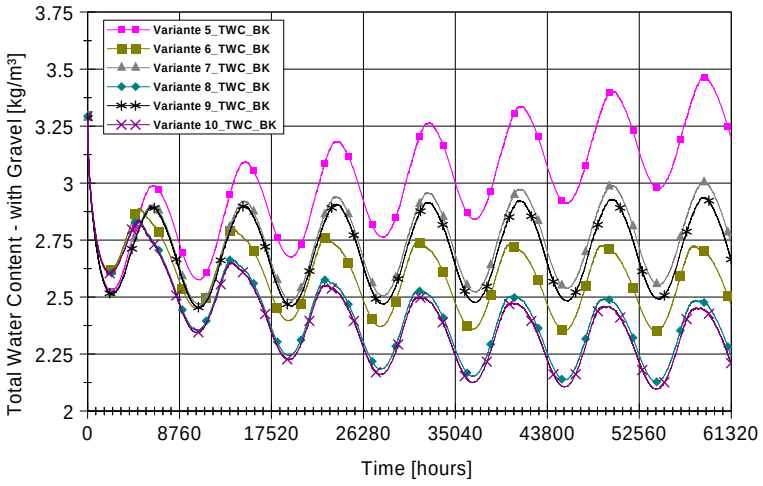

Figure 4. Total Water Content (TWC) of Cases 5 to 10, with gravel surfacing.

These effects are observable for roof assemblies 6 and 8, which include humidity-adaptive vapor retarders and therefore dry out over the course of the years. Tis is especially true for case 8 with the vapor-tight rubber membrane, which is showing an optimized moisture performance. It is also clearly evident that roof assemblies 9 and 10, which contain similar vapor-tight plastic membranes show comparable behavior to those cases with the exterior rubber membrane.

Water Content (WC) Exterior OSB Decking

The increased total water content ratios accentuate the need for a detailed investigation concerning the moisture contents in the exterior OSB. Note that according to the literature (Weiß et. al., 2000), wood decay funghi growth is normally possible at higher moisture contents, i.e., > 20 % by mass. The temperature tolerance varies between +3 °C and +40 °C with an optimum depending on fungi species lying at about +18 °C to +20 °C, but usually in building constructions a critical limit of about > 5 °C should be considered. The calculated results diplayed in Figure 5 indicate that the moisture content of the exterior OSB in roof assembly 5 after the 3rd year remains over 20 % and rises up to ~ 26 % during the simulation period. This wetting process, combined with favorable temperatures, dramatically assists the possibility of mold and wood funghi growth within a few years.

In addition to that, even the OSB in case 7, which includes a rubber membrane, tends to a slightly increasing moisture gradient over the course of the years. The moisture content per mass goes up from 18 % at the start to ~ 20 % in the 7th year. Hence moisture related problems like mold growth, but sooner or later even wood rot is likely to occure.

In contrast, the OSB WC of Case 9 is showing a steady state performance throughout the calculation period, apart from seasonal fluctuations, and remains under 20 % by mass. Anyway it is clearly observed that the drying potential is also limited, which means that unforeseen wetting processes will keep higher moisture levels over a longer period – a certain amount of risk can therefore also not be excluded.

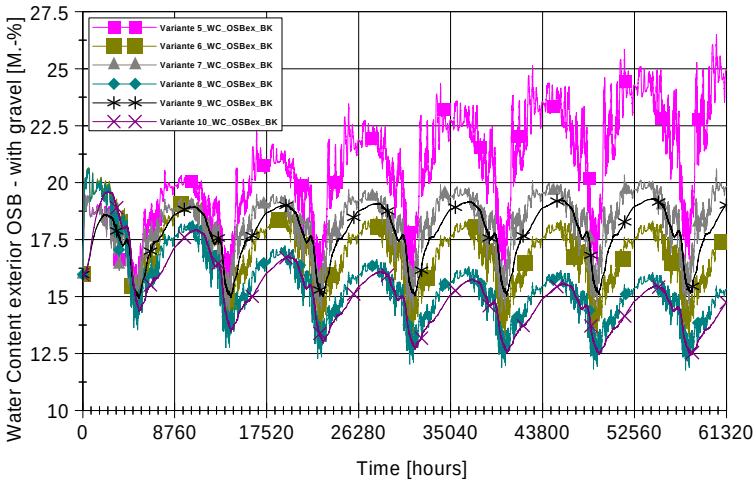

Figure 5. Moisture Content per mass of the exterior oriented strand boards in Cases 5 to 10, with gravel surfacing.

Only in cases 6, 8 and 10, where humidity-adaptive vapor retarders were applied, can it be observed that the assemblies are showing a drying performance and hence the risk of moisture related problems is limited.

6 CONCLUSIONS

This paper presents initial theoretical results concerning the hygrothermal behavior of non-ventilated, highly-insulated timber-frame flat roofs in the climate of Central Europe. The investigations indicated that the interaction of membrane systems and vapor retarders are strongly influencing the moisture migration and accumulation and therefore durability performance of low-sloped roofs in such timber constructions. Darker membranes are increasing the temperatures in the exterior part of the roof assemblies and therefore optimizing the solar-driven diffusion to the interior. Combined with humidity-adaptive vapor retarders at the inside, the drying process can rapidly be improved.

Timber-based roof structures covered with gravel surfacing are, as a matter of principles, more vulnerable. A sufficient drying rate is only found to be realizable if humidity-adaptive vapor retarders are incoporated in the system. For avoiding moisture build-up due to diffusion from the exterior, rather vapor-tight membrane systems should be used.

REFERENCES

Desjarlais, A., 1995, Self-drying roofs: What?! No dripping!, Conference Proceedings Thermal Performance of the Exterior Envelopes of Buildings VI, Clearwater Beach, Florida, page 763.

Karagiozis, A., 1998, Applied moisture engineering, Conference Proceedings Thermal Performance of the Exterior Envelopes of Buildings VII, Clearwater Beach, Florida, page 241.

Kuenzel, H.M., 1994, ‘Verfahren zur ein- und zweidimensionalen Berechnung des gekoppelten Waerme- und Feuchtetransportes in Bauteilen mit einfachen Kennwerten’, Dissertation Universitaet Stuttgart.

Kuenzel, H.M., 1996, Tauwasserschaeden im Dach aufgrund von Diffusion durch angrenzendes Mauerwerk, wksb 41/1996, Heft 37, Seite 34-36.

OENORM B7220, 2002, ‘Daecher mit Abdichtungen – Verfahrensnorm’, Austrian Standards Institute.

Powell, F.J, and Robinson, H.E., 1971, The effect of moisture on the heat transfer performance of insulated flat-roof constructions, Building Sciences Series 37, Gaithersburg, National Bureau of Standards.

Straube, J.F., 2001, ‘The Influence of Low-Permeance Vapor Barriers on Roof and Wall Performance’, Proceedings of ASRHAE Thermal Performance of the Exterior Envelopes of Buildings VIII.

Weiß, B., Wagenführ, A., Kruse, K., 2000. Beschreibung und Bestimmung von Bauholzpilzen.

WTA – Wissenschaftlich Technische Arbeitsgemeinschaft für Bauwerkserhaltung und Denkmalpflege, 2002, Merkblatt 6-2-01/D ‘Simulation waerme- und feuchtetechnischer Prozesse’.

Refurbishing the Roof: Possibilities, Consequences and Policies in Building Rehabilitation

Ana-Maria Dabija [1]

T 22

ABSTRACT

There are some well-known axioms in regards to roofs:

- the roof is an important part of the building envelope and therefore it should fulfill the performance needs of the envelope, and in particular those associated with specific functions related to it's position in the building.
- the roof is the fifth façade of a building (many architects know this, from their own experience).
- the roof is one of the very important subsystems of the building that costs about 6 – 10% of the building and yet investors think it costs too much. (This is usually a statement of the roof builders.)

The roof is a component of the building that fulfills more than one major function – protection against incoming rain, snow, and wind. In different architectural cultures, the space below it accomplishes the task of storage, of drying room, smoke house, or of regular rooms, with the same hygrothermal performances as the rest of the house. According to the geographic location, the roof may be traditionally low-sloped or pitched. During the Art Nouveau and the Modernist Architecture period – and up to the present day – low-sloped roofs were designed in parts of the world where traditionally pitched roofs were used.

This paper presents some possible interventions for renovating roofs and problems the designer may have to deal with when refurbishing a building, and changing the geometry or the function of a roof.

KEYWORDS

Roof, Building refurbishment, Mansard-roof, Garden-roof, Renovation

1 INTRODUCTION

As everybody knows, the envelope of the building is a system that separates two different environments: the exterior one from the interior one. Therefore its contribution to achieving and maintaining a constant, comfortable (appropriate for the specific use) microclimate is very important.

Equipment (i.e., HVAC systems) is of course very important as well but the first barrier that receives the input from the exterior or interior environment is composed by three elements that "close" the building: walls, roof and the slab on the ground or over the cellar (or other type of cold basement). Both walls and roofs have the main task of protecting the building against weathering.

The main functions that an envelope should fulfill for the spaces it encloses are the following [Dabija, 2000]:

- protection against water (liquid and solid) intrusion
- hygrothermal protection
- acoustic protection
- fire and wind protection
- natural lighting and visual contact between these spaces and the environment exterior of the envelope
- natural ventilation

The roof, as a part of the envelope, has a role in fulfilling all these functions, but of course the performance needs of protection against rain, snow, wind are the ones that define traditionally this subassembly.

2 TYPES OF ROOFS

Historically, climatic conditions have generally dictated the type of the roof: low-sloped or pitched. Low-sloped roofs are often associated with warm European countries that experience little rain or snow; pitched roofs are common in countries where the quantities of rain and snow are significant. Of course, there are the modern high-rise buildings with low-sloped roof systems that have nothing to do with the traditional way of building. They represent another issue.

In Romania (and probably in other South-Eastern European countries as well), the attic was traditionally an auxiliary space (Figure 1) for preserving goods (sausages, for instance, were smoked there). In such instances due to the use of space, the roof was supposed to be cold and more ventilated. Thus, it was very much like a buffer space.

Figure 1. A traditional Romanian village house with smoke stains resulting from the "domestic" activity of preparing supplies for winter; smoke passes through the joints of the roof elements.

In many European countries (Central and Western Europe) the space under the roof was traditionally used for living. In these cases, the structural system of the roof as well as the corresponding walls were designed based on this hypothesis.

Today, contemporary houses in Romania normally consider the attic as a possibility for increasing the living area of the dwelling, so most of them have mansards (warm attics) under the roofs (Figure 2).

Figure 2. A newly built pension in Sinaia, Romania (courtesy, arch. Cristina Sandulescu).

Nowadays, when undertaking renovation, modernization or general repair projects, owners increase the living area of their houses by transforming the attic into comfortable dwellings.

The low-sloped roof is, in Romania as well as in other northern European countries, a consequence of the intensive, vertical development of the built environment. It is highly improbable that a high rise building (more than 5-6 levels) would have a pitched roof. The higher is the building, the more severe are the measures taken for ensuring it against wind and not only water and snow.

Taking advantage of general repair, the owners – or the designers – aim to improve the functionality or the performances of their buildings. Usually in such situations or in general repair, the existing waterproofing membrane is replaced - maybe (i.e., hopefully) - by another waterproofing system that would provide improved durability performance.

A frequent proposal for the renovation of the roof, that alters the functionality and adds to the modernisation of the entire building, is to add practically a condominium with a pitched roof that shelters a mansard. There are situations when such an approach is appropriate, but normally this step is presented in a too optimistic light, without mentioning the implications of such an action (see 3.2.3).

3 TYPES OF INTERVENTIONS

The paper focuses on appropriate and non-appropriate systems of renovations applied to existing buildings, and in particular the roof system. We will not address the most common types of repairs or current interventions.

3.1 Transforming an Existing Attic into a Mansard.

According to Romanian regulations [Athanasescu *et al* 2005], the attic is the space sheltered by the roof. It is not a warm space; thus, in other words, it is not a part of the envelope. The floor between the attic and the level below has to ensure the necessary thermal protection of the envelope. The roof

represents the protection against weathering but the space beneath it is a ventilated space that provides sun and wind protection and a possibility for the air vapours to migrate to the exterior.

The mansard is a part of the envelope; it is an attic with the same hygrothermal conditions as the rest of the building. Another feature of the mansard is that at least a part of the ceiling has to be sloped, in other words the roof geometry has to be – more or less - emphasized. To transform the attic of a 1 – 2 storey building into a mansard is technically and theoretically not too difficult. Some steps have to be taken by each of the different specialists:

3.1.1 Architectural Considerations

- The entire space beneath the roof cannot be used. The steeper the slope, the more the space can be functional [Athanasescu *et al* 2005]. The living area can be defined only from the point where people can stand (the minimum free height of at least 1.90m), as presented in Figures 3 and 4.
- Evaluations should be made to ensure adequate functional circulation in these rooms (heights, distances etc) as well as appropriate placement of the furniture and equipment (see Figure 3).

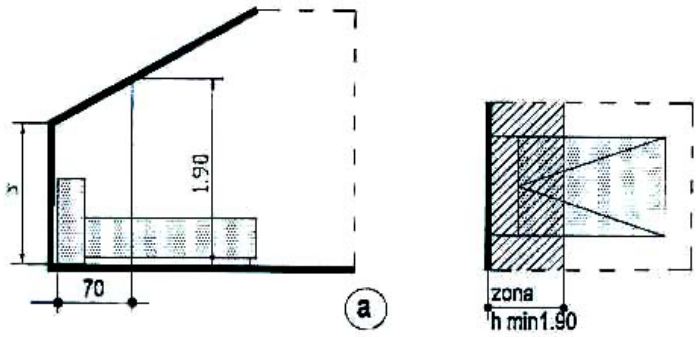

Figure 3. Recommended placement of the bed in a bedroom; the height of the room at 0.70m from the mansard wall should allow an adult to stand comfortably.

- special care should be taken for co-ordinating the architecture design with the other sections of the building and its given spaces (in particular with sanitation; for example, the placement of the sanitary objects determines the particular line for the pipes). The placement of such objects has to allow their use in normal conditions.

Observation: Not only the plans are important in this situation, but also needed is very careful evaluation of the height where the different objects are to be placed and – more than that – the relation between the user and the position of these objects so that the user may actually be able to reach to them (Figure 4).

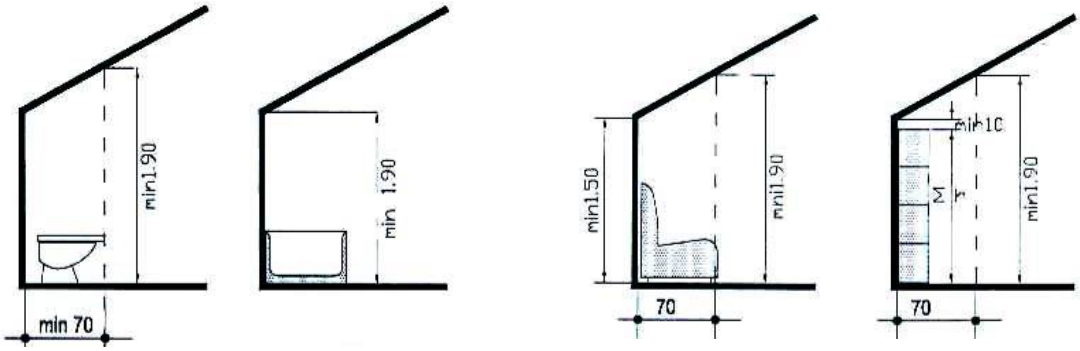

Figure 4: Recommended placement of sanitary facilities or living room furniture;
the height of the room at 0.70m from the mansard wall should allow an adult to stand comfortably.

- The building of an appropriate access to the attic is required in many situations but not in all cases because the space under the roof was already readily accessible. In many cases the access was provided through a trap door so stairs have to link these spaces with the rest of the house.

3.1.2. Structural Considerations

- an evaluation has to be made to ensure that the building can stand the extra load.
- the design of a new set of stairs may induce consequences on the structural system of the building that have to be taken into consideration.
- an evaluation has to be made to check if the existing roof structure can bear the extra load of roof tiles, which are in most situations considered necessary for ensuring improved waterproofing performance of the roof system.

3.1.3 Hygrothermal, Acoustic and Light Control Considerations

Installation of thermal wall insulation must be undertaken. (This step is necessary if improving the thermal performance of the walls is not taking place anyway. Many private houses are being insulated with mineral wool or expanded polystyrene to increase thermal behaviour of the envelope.) Accordingly, measures to protect the thermal insulation against vapour must occur.

- Thick thermal insulation of the roof must be provided with necessary action taken that protects against vapours (barriers, ventilated space above the thermal insulation, and the like). In many situations, due to the fact that the attic was only an auxiliary space, the thickness of the exterior walls of the attic is smaller and therefore, in order to achieve the same thermal performance, the thermal insulation thickness should be increased.
- Any thermal insulation between the attic and the floor beneath it should be removed, because this space becomes part of the warm interior environment.
- Satisfactory measures must be taken to prevent the roof from leaking, either due to poor protection against water intrusion, or from too tightly sealing this upper floor (circulation of air between the roof structure and the roof cladding elements (different types of shingles, metal sheets, etc).
- Acoustic protection should be provided (especially in the case of metal roofing) against the sound of rain or hail.
- Roof windows (i.e., skylights), used for a minimal ventilation of the original space, should be replaced with appropriate windows that ensure necessary daylighting and that also fulfill the performance needs for thermal, acoustic and sun protection comfort.

3.1.4 Installation Consideration

- Electric, heating, sanitary and ventilation components have to be ”lifted” to this new floor, sometimes with high costs.

3.2 Interventions for Low-Sloped Roofs of Existing Buildings

The difference of temperature extremes on low-sloped roof surfaces in Romania is around 100^0C. We can compare ourselves with some parts of the USA where substantial temperature differences can occur within 24 hours. In 2007 the air temperature went as high as 45^0C in Bucharest, while in the winter the temperature went sometimes as low as -20^0C in the same city). In foreign documentations [Parker&Barkaszi, 1994], [Bass&Baskaran 2003], we found references to temperature differences of 60^0C.

Normally, in Romania, the durability of a well protected, bituminous waterproof membrane can reach 25 years. If we have a traditional (bituminous) waterproof membrane, what is happening is that it absorbs thermal radiation during the day, heating the whole assembly including the space beneath the roof. During the night the heat is transmitted both to the inside and outside environment.

These temperature fluctuations can create strong thermal shocks and decrease the life-cycle of the membrane (not to mention the discomfort of the users of the space beneath it). A primary measure is to protect the membrane with a reflective coating.

Figure 5. Example of unprotected bituminous waterproof membrane (courtesy Prof. Alexandru Stan).

There are three possibilities for interventions on the low-sloped roofs of multi-storey buildings:

3.2.1 Replacement of the Roof Membrane System
Replacement of the roof membrane system with a similar one. This is performed without consequence to the functionality of the building. The implications on the environment are the same as before the intervention.

3.2.2 Replacement and Improvement of the Roof Membrane System
Replacement and improvement of the roof membrane system while increasing the energy savings of the building and preserving the natural environment;

As shown above, in Romania, the first measure of protection of the roof membrane, with repercussions also on the energy consumption is to provide a protective reflective coating. From a strictly thermal performance and energy-savings point of view such a measure reduces the use of air conditioning systems by about 10%.

Figure 6. Images of roof-gardens in Paris on the Montparnasse Railway station.

Another possibility for saving energy (and reducing heating costs) is the use of green (terrace) roofs. By using these systems, the state of the exterior environment is at least preserved, if not improved.

Creating spaces for parks, gardens and trees in the center of the cities is rather unlikely in these days. Some western countries (such as Germany, Austria, Switzerland, France, some parts of Canada and USA) have developed a strategy of creating "green space" on the top of new or existent buildings. [Bass & Baskaran]. Polluted areas might even be thus rehabilitated (as we note the case of Linz in Austria where the politics of the "green roof" helped to "de-pollute" this industrial city). Briefly, among the advantageous aspects of green (terrace) roof performance, we can mention [Dabija 2006]:

- retention of an important quantity of the rain water (vegetation acts like an absorbent sponge), thus reducing the pressure imposed on water collectors placed on the terrace.
- reduction of the noise level felt by users who live on the top floor. This is due to the additional mass represented by the soil and the plants. In general, persons living near noisy environments such as airports, discotheques, parking structures, and industrial areas are better protected against noise with a rather non-expensive means.
- protection against electromagnetic radiations [Parker&Barkaszi, 1994];
- achievement of a constant interior temperature with no heating peaks in the apartments situated on the top floor under the roof. This is due both to the additional thermal protection represented by the soil and plants as well as to the increased percentage of humidity produced by the breathing of the plants, that cool the air in the vicinity of the roof.
- preservation of the natural environment, as represented by these systems. As mentioned, in polluted industrial areas, the environment might be "healed" after the installation of green roof terraces (see the Linz case [Municipality of Linz, 2006]).

Unfortunately, in Romania, such approaches are rare, because these systems are still considered to be very expensive.

3.2.3 Building Condominiums on the Terraces of Existing Buildings

Currently in Romania the building activity f is extremely intense. Not only are new buildings from residential houses to high-rise offices appearing, but the need for renovating the old stock has become more acute, as the costs of utilities (heating, in particular) increase. On the other hand, like everywhere else in the world, the prices of houses in the centers of the cities are very high. In order to build in this expensive area, either one expects some buildings to be demolished (unlikely, unless catastrophes occur) or ways to be found to build condominiums (on top of the roofs of existing buildings).

The owners are presented the bright side of the problem: building a condominium, with a pitched roof, is an advantage, as it ensures
- better protection against water and snow (given strictly by the geometry of the traditional roof)
- a fairly rapid pay-off of the investment, once you rent the mansard that results.

The true colours are, however, not as radiant. Supposing the structure of the building allows the extra storey, there are legal problems as well as technical, design, structural, construction, economical other implications that are extremely complicated:

1. Legal, sociological, financial and juridical aspects: In multi-storey dwellings, where each apartment is owned by a different person, it is not a simple task to have everyone accept building a condominium. The nuisance (debris, dust, noise, shocks) of demolishing the roof system (waterproof membrane, thermal insulation, slope, concrete) to reach to the reinforced concrete floor is differently felt by persons on the different floors. Those under the roof are most exposed while those on the ground floor have almost no problems about it. Once the condominium is built, new problems appear: how and who gets the money, how is it spent, and so forth.

2. Structural and installation aspects: The new structure is different from the rest of the building. It has to be a light structure with light walls. This type of construction leads to a completely different regime of use of the installations, thus creating problems with the other occupants. It is easier (in terms of inter-human relations) to design and build an entirely new, autonomous utility system (heating, sanitation, electricity) exclusively for the mansard; it is however very expensive.

3. Functional, structural, equipment (and economical) aspects: The staircase has to be taken to the condominium, unless the condominium is a two-storey apartment. (Then other discussions appear: for example, why should everybody pay in terms of discomfort for somebody's wish of having extra space?) In the case of three storey buildings (that are not provided with elevators), the addition of the condominium necessitates providing an elevator for the transformed building, because the number of levels increases from 3 to 4, where an elevator is compulsory. The costs are very high and the possibilities to place such equipment inside the building are very reduced (if ever possible). To fulfill the requirements of the regulations, exterior, panoramic elevators should be provided. In the case of buildings that have elevators, the problem of taking the elevators to the top (newly built) floor also implies changing the existing elevator, if possible.

4. Construction aspects (technology): While working on the condominium, extra costs have to be taken into account for protecting the building. Once the roofing membrane has been ripped off, it be immediately replaced. There have been cases of buildings (at least one every year), when the rain destroyed from top to bottom all apartments and produced short-circuits, because the roof was not protected any more.

All these problems have sociological and economical implications, and to be sure are difficult to solve.

CONCLUSIONS

Interventions on the roof are not ever simple. However, there are some major directions for renovating roofs that have appeared in the last years. These interventions correlated with the needs to preserve and improve the environment. In the case of existing sloped (i.e., pitched) roofs, the possibility to renovate and refunctionalize the space of the attic is valid. In the case of low-sloped roofs of multi-owned, multi-storied dwellings, the apparent advantage of an extra level with pitched roof and mansard should, in our opinion, be reconsidered. The green terraces seem to be the answer to many requirements and the "legend" of the high costs that such systems incur should fade due to the important gains.

REFERENCES

Dabija, A-M., 2000, *Implications of the use of new technologies in the buildings in Romania*, PhD Thesis, 'Ion Mincu' University of Architecture and Urbanism, pp 25-26.

Athanasescu I, Stan A., Dabija A-M., 2005, *Technical Norm for Designing Mansards*, Indicative NP 064-02, Ministry of Public Works, Bucharest, pp 14-15.

Parker, D., Barkaszi, S., May/June 1994, *Saving Energy With Reflective Roof Coatings*, Home Energy Magazine Online, in www.homeenergy.org/archive/hem.dis.anl.gov/eehem/94/940509.html

Bass, B., Baskaran, B., 2003, *Evaluating Rooftop and Vertical Gardens as an Adaptation Strategy for Urban Areas, pp 1 – 16,* in http://irc.nrc-cnrc.gc.ca/pubs/fulltext/nrcc46737/nrcc46737.pdf (NRCC-46737, CCAF Impacts And Adaptation Progress Report April 1, 1999 – March 31, 2001, Project Number A020).

Dabija, A-M., 2006,*Pleading For The Roof*, Proc. Nat. Conf. The Behaviour 'in situ' of constructions, Raul Mare, Romania.

Municipality of Linz, Planning Department, 2006, Editor: Edmund Maurer, in http://www.shef.ac.uk/landscape/greenroof/pdf/edmundmaurer.pdf

Durability of Clay Roofing Tiles: Assessing the Reliability of Prediction Models

Mariarosa Raimondo [1]
Michele Dondi [2]
Claudia Ceroni [3]
Guia Guarini [4]

T 22

ABSTRACT

The indirect prediction of frost resistance of construction materials has been widely investigated in recent years giving rise to several models based on pore size, open porosity, water absorption and/or capillary rise. This study is aimed at appraising these models on 13 industrially-manufactured roofing tiles with a different frost resistance determined by severe freeze/thaw testing (EN 539-2). Samples were characterised by measuring pore size distribution (MIP), pore specific surface (BET), open porosity and water absorption (ASTM C67 and C373), capillary rise (UNI 10859) and phase composition (Rietveld-XRPD). No model is able to foresee reliably the product frost resistance since all models exhibit a strong dependence on the data population and probably succeed only with a homogeneous sample in terms of both composition and manufacturing technology. Among them, the Arnott's model seems to be the most reliable to discriminate among scarcely (<100 freeze/thaw cycles) and highly frost resistant products (>250 cycles); however, a complete understanding of the excellent performance (>400 cycles) provided by some roofing tiles is still lacking. Looking at their phase composition, tiles with the best performance contain also abundant calcium-magnesium silicate phases formed during firing while products with a frost resistance lower than expected are characterised by large amounts of amorphous phase or residual mica-illite and quartz. This circumstance indicates new ways to achieve highly frost resistant products that is alternative to the conventional design imposing microstructural rearrangements (low porosity and coarse pore size) through drastic batch changes and/or firing at higher temperature.

KEYWORDS

Roofing tiles, Frost resistance, Microstructure, Phase composition, Clay.

[1] Institute of Science and Technology for Ceramics, ISTEC-CNR, Faenza, Italy 48018, Phone +39 0546 699718, Fax 0546 46381, mrosa@istec.cnr.it
[2] Institute of Science and Technology for Ceramics, ISTEC-CNR, Faenza, Italy 48018, Phone +39 0546 699728, Fax 0546 46381, dondi@istec.cnr.it
[3] Department of Applied Chemistry and Material Science, Faculty of Engineering, University of Bologna, Bologna, Italy 40100, Phone +39 051 2093205, Fax +39 051 2093213
[4] Institute of Science and Technology for Ceramics, ISTEC-CNR, Faenza, Italy 48018, Phone +39 0546 699718, Fax 0546 46381, guiagrn@istec.cnr.it

1 INTRODUCTION

Nowadays clay roofing tiles are widely used as exterior masonry components and their durability, defined as the ability to withstand adverse climatic conditions, is one of the most important requirements to be considered in the structural design of modern buildings.

The deterioration of construction materials can be due to several factors; among them, design and construction techniques, material properties and environmental conditions, which may be, in most cases, considered more predominant than others. Particularly, in cold regions the service lifetime of masonry components is heavily affected by the frost action and salt crystallization.

Frost action is produced when the external temperature falls below 0°C and the water included in the porous structure starts freezing; the density change of the liquid-solid water transition involves the development of an internal pressure, leading to the formation of micro-cracks whose extent can overcome the strength resistance of the material and promote inescapable damage. The extent of these damages will be strictly dependent on the exposed surface area, the saturation degree of the material, as well as on the number and size of pores. Specifically, for pore dimensions greater than a critical value and/or for a low saturation degree, the developed pressure, and hence damage, will be negligible since the free space in the pores accommodates the expansion of the freezing water; in contrast, severe structural damage can occur. Owing to these circumstances, the material characteristics, which in turn depend on the raw material formulations, the forming process, and the firing cycle, become key factors in the evaluation of the deterioration risk.

Many papers in the field of civil engineering analyse the factors affecting the durability of construction materials going also through the elaboration of prediction models. In the last years, for example, Maage [Maage [1990], Arnott [Arnott [1990], Franke and Bentrup [Franke and Bentrup è1993], Koroth [Koroth *et al.* [1998], Robinson [Robinson *et al.* [1995] and Vincenzini [Vincenzini [1974] elaborated different models which basically relate to technological (i.e., water absorption in different experimental conditions, capillary coefficient) or microstructural (i.e., porosity amount, size, and internal specific surface of pores) properties, deriving then equations able to define the product durability on the basis of the calculated indices.

This study is aimed at appraising these models on industrially-manufactured roofing tiles with varying frost resistance, experimentally determined by severe freeze/thaw testing, assessing both their reliability and restrictions. The role played by phase composition on products durability has been also analysed.

2 MATERIALS AND METHODS

Thirteen (13) industrially-manufactured roofing tiles, obtained from different working plants, were selected. On the basis of different shape and colour, they have been classified as *Marseilles* (samples A, C, F, H and L), *Portuguese* (samples B, D, E, G, I, J and M) and *Coppo* (sample K) tiles. All were produced by extrusion and fired at a maximum temperature between 850 and 1150°C with a thermal cycle of 24-48 hours from cold -to -cold.

Products were characterized by the determination of phase composition, open, closed and total porosity, bulk density, pore size distribution and pore specific surface. Phase composition (Table 1) was determined by X-ray powder diffraction (Rigaku DIII, experimental conditions: monochromated $CuK_{1,2\ \alpha}$ radiation in the 5-80°2θ range, scan rate 0.02 °2θ, 2 sec per step) and quantitative analyses were performed by Rietveld method using the GSAS software; the relative error is ± 5%

Open porosity (OP) and bulk density (BD) were quantified according to ASTM C373; specific weight (SW) was measured by He pycnometry (Micromeritics MVP 1305) according to ASTM C329 and total porosity (TP) was calculated by the equation: TP = (1-BD/SW) ·100. In addition, the following

porosity-related properties were also measured: 24-hours (WA_{24h}) and 4-hours (WA_{4h}) cold water absorption, 5-hours boiling water absorption (WA_{5h}) according to UNI 8942/3; the ratio WA_{24h}/WA_{5h} being defined as the saturation coefficient C_s (Table 2).

Table 1. Phase composition of roofing tiles.

Sample	*Quartz* (%)	*K-Feldspar* (%)	*Plagioclase* (%)	*Pyroxene* (%)	*Hematite* (%)	*Illite* (%)	*Ghelenite* (%)	*Amorphous* (%)
A	38	8	22	14	4	-	-	14
B	24	3	11	1	5	13	-	42
C	26	7	33	12	2	5	6	8
D	20	5	22	32	5	-	1	17
E	33	7	30	3	2	-	1	23
F	24	7	26	3	3	-	-	37
G	42	13	5	6	7	-	-	27
H	23	6	41	2	2	-	2	24
I	31	6	19	1	6	9	-	27
J	20	6	36	1	1	8	-	27
K	6	1	24	9	2	-	-	58
L	24	4	44	2	2	-	1	23
M	39	7	-	-	4	10	-	40

Table 2. Open (OP), total (TP) and closed (CP) porosity, bulk density (BD), water absorption (WA), 24-hours (WA_{24h}) cold water absorption, 5-hours boiling water absorption (WA_{5h}) of roofing tiles.

Sample	*OP* (%)	*TP* (%)	*CP* (%)	*BD* (g/cm^3)	*WA* (%)	WA_{24h} (%)	WA_{5h} (%)
A	20.3	30.4	10.1	1.877	10.8	10.7	15.4
B	18.0	25.1	7.1	2.020	8.9	8.8	11.1
C	27.8	32.6	4.8	1.817	15.3	14.9	16.1
D	21.0	29.6	8.6	1.899	11.1	10.6	11.4
E	13.0	29.2	16.2	1.910	6.8	8.0	13.6
F	22.3	29.1	6.8	1.912	11.7	11.1	13.0
G	19.3	25.9	6.7	1.997	9.6	10.1	12.3
H	23.2	29.6	6.3	1.899	12.2	12.2	14.3
I	21.1	27.2	6.1	1.962	10.8	11.1	13.1
J	25.2	31.0	5.8	1.861	13.5	13.1	14.7
K	24.3	29.7	5.4	1.895	12.8	11.6	14.5
L	22.4	28.6	6.2	1.924	11.7	11.6	13.5
M	19.4	23.2	3.9	2.070	9.3	9.9	11.1

The pore size distribution (in the 0.01 – 100 μm range) was determined by MIP (ThermoFinningan Pascal 140) with an experimental uncertainty of about 1% relative; the experimentally measured mercury - brick contact angle of 166.4° was inserted into the Washburn equation [34] and the porosimetric results corrected by a factor of 1.24. Data were expressed as medium pore diameter (MD), PV (cumulative volume of pores, cm^3/g), P3 (relative amount of pores having a diameter larger than 3 μm), Φ_{50} (median pore size, μm) and Φ_{90} (ninetieth percentile, μm); the pore specific surface analysis was performed by nitrogen absorption (Micromeritics FlowSorb II 2300) following the B.E.T. single point method (ASTM C1069) (Table 3).

Table 3. Medium pore diameter (MD), cumulative volume of pores (PV), relative amount of pores having a diameter larger than 3 μm (P3), Φ_{50} (median pore size), Φ_{90}, pore specific surface (BET) and capillary coefficient (K_s) of roofing tiles.

Sample	*MD* (μm)	*PV* (cm^3/g)	*P3* (%)	Φ_{50} (μm)	Φ_{90} (μm)	*BET* (m^2/g)	*Ks* ($g/cm^2\ s^{1/2}$)
A	1.88	0.146	56.0	1.8	4.5	0.728	5.8
B	0.52	0.134	3.3	0.5	1.2	1.712	2.2
C	0.41	0.189	0.7	0.4	0.8	1.808	5.2
D	0.34	0.161	1.6	0.4	0.7	1.613	2.6
E	0.70	0.151	14.2	0.5	3.0	1.110	0.1
F	0.36	0.157	2.42	0.4	0.8	1.530	4.5
G	0.74	0.132	12.9	0.7	3.5	1.565	0.8
H	0.50	0.168	1.9	0.5	1.3	1.179	4.0
I	0.40	0.146	2.4	0.4	1.2	1.841	4.8
J	0.38	0.182	3.1	0.4	0.8	1.630	4.4
K	0.41	0.179	1.4	0.4	0.7	1.312	3.0
L	0.37	0.161	2.4	0.4	0.9	1.837	3.6
M	0.34	0.117	8.6	0.3	1.4	2.190	3.3

The capillary absorption was determined according to UNI 10859 on small pieces of about 5 cm^3 obtained from each roofing tile. Plotting the specimen mass recorded after 10, 20, 30 and 60 minutes versus the square root of the elapsed time, a graph was obtained presenting an initial straight line, whose slope is the experimental capillary coefficient K_s (Table 3). Frost resistance was assessed by severe freeze/thaw testing (EN 539-2) on 10 samples for each industrially-manufactured product. Tests were carried out in a climatic cell at temperatures ranging from -15°C to +15°C performing 400 different freeze/thaw cycles; this number of cycles - much higher than those (150) scheduled by the reference standard - was chosen in order to simulate very extreme conditions.

Table 4. Frost resistance of roofing tiles determined according to EN 539-2.

Sample	*Number of freeze/thaw cycles*	*Overcame freeze/thaw cycles*	*Defects found after freeze/thaw testing*
A	400	400	Several chips on the back of the sample
B	400	375	Loss of interlocking ribs, hairline cracks
C	50	25	Large exfoliations on both sample sides
D	400	400	none
E	300	275	Several exfoliations on both sample faces
F	125	100	Loss of interlocking ribs, delaminations, flaking, hairline
G	125	100	Breaking of test sample into three pieces
H	400	400	Detachment of a sample projection
I	100	75	Exfoliations, hairline cracks
J	125	100	Delaminations, exfoliations, hairline cracks, loss of interlocking ribs
K	125	100	Surface cracks, delaminations, exfoliations, structural cracks, pits
L	300	275	Exfoliations, loss of interlocking ribs, hairline cracks
M	150	50	Loss of interlocking ribs, chips, hairline cracks, delaminations

The product durability was evaluated from the analysis of both the mass loss and the structural changes standing out during and after the test; the freeze/thaw resistance was expressed as the fraction of samples which are able to withstand test conditions (Table 4).

Both microstructural and porosity-related parameters were utilized to calculate durability indices according to the models proposed by Maage, Robinson, Vincenzini, Arnott, Franke and Bentrup and Koroth; the variables considered by the authors to elaborate their models and the resulting indices are summarized in Table 5 and 6, respectively.

Table 5. Prediction models and classification of frost behaviour as proposed by the authors**.**

Durability Factor (DF)	*Models*	*Frost resistant products*	*Non-frost resistant products*
Maage	3.2/PV + 2.4P3	DF > 70	DF < 70
Robinson	$[K_s/10(1-C_s)] + (WA_{24h} - 10)$	Low values of DF	-
Arnott	$9.2\ P3 - 0.5\ K_s + 423\ (WA_{5h}/WA) - 100\ K_s\ C_s - 84.5$	High values of DF	-
Vincenzini	Φ_{90}	$\Phi_{90} \geq 1.80$ µm	$\Phi_{90} \leq 1.80$ µm
Franke & Bentrup	Φ_{50}	$\Phi_{50} \geq 1.65$ µm	$\Phi_{50} \leq 0.60$ µm
Koroth	$450(2.94 + WA_{5h}) + 330\ (1-WA_{4h}/WA_{5h})$	DF > 85	DF < 70

Table 6. Calculated durability factors of roofing tiles.

Sample	*Durability factors*					
	Maage	*Robinson*	*Arnott*	*Vincenzini Φ90 (µm)*	*Franke-Bentrup Φ50 (µm)*	*Koroth*
A	156.3	0.9	962	4.5	1.8	220
B	31.8	-1.2	394	1.2	0.5	288
C	18.7	4.9	273	0.8	0.4	238
D	23.9	0.6	272	0.7	0.4	277
E	55.2	-2.0	835	3.0	0.5	355
F	26.1	1.1	321	0.8	0.4	233
G	55.0	0.1	495	3.5	0.7	328
H	23.6	2.	343	1.3	0.5	254
I	27.7	1.2	365	1.2	0.4	227
J	25.0	1.7	314	0.8	0.4	246
K	21.2	3.1	327	0.7	0.4	279
L	25.6	1.7	339	0.9	0.4	259
M	47.9	-0.1	410	1.4	0.3	255

A statistical elaboration of data was performed by simple (linear binary correlation) and multivariate analysis techniques (factor and multiple regression analyses) using the StatSoft Statistica 6.0 software. Factor analysis was carried out on the main physical, compositional and microstructural variables extracting principal components (3 factors according to the scree test for eigenvalues). Multiple linear

regression was executed by the forward stepwise method, including intercept in the model and setting F = 1.00 to enter and F = 0.00 to remove.

3 RESULTS AND DISCUSSION

3.1 Reliability of Models

The durability factors of table 6 account for a quite different behaviour of samples in terms of their ability to overcome frost action. In order to verify the reliability and the validity range of the models, a comparison between the experimental results – in terms of number of freeze/thaw cycles – and the calculated indices haves been undertaken (Figure 1).

As shown in Fig. 1, the following considerations can be drawn out:

- Maage durability factor (Figure1A), although presents a positive relationship with the number of freeze/thaw cycles, is not able to discriminate among frost (DF >70) and non-frost resistant (DF<70) products, with sample A being the only one that can be considered as frost resistant; in addition, the model provides no reasons for the excellent performance (>400 cycles) of samples B, D and H. Looking in detail at the microstructure of sample A, it is clear that the Maage factor mainly accounts for its quite high percentage of pores having a diameter greater than 3 μm (P3 = 56%).
- Any statistical significant correlation was detected plotting the durability factor, calculated according to Robinson's model, and the experimental behaviour of samples (Figure 1B); however, the index seems to decrease when the behaviour of products becomes better.
- The model proposed by Arnott (Fig. 1C) seems to present a good agreement with the experimental performance of scarcely resistant (<100 cycles) and highly resistant (>250 cycles) products; the main exceptions are always represented by samples L, B, H and D having excellent durability. The insertion into the multiple regression analysis of different physical and technological parameters provides a model (Table 5) where the role of each variable is quantified by a statistical different weight: the amount of greater pores (P3) seems to be the most influent so that, accordingly, index values increases as the percentage of P3 increases.
- The limit value of Φ_{90} = 1.8 μm proposed by Vincenzini to discriminate among non-frost (Φ_{90} <1.8 μm) and frost (Φ_{90} >1.8 μm) resistant products revealed in this case not to be reliable. Specifically, examining Fig 1D, the correspondence between the experimental performance and the index can be validated only for samples A and E, while sample G, although presenting a Φ_{90} value as high as 3.5 μm, does not show an acceptable durability.
- The evaluation of the median pore size values Φ_{50}, as proposed by Franke and Bentrup (Figure 1E), presents more or less the same limitations of Maage factor. In fact, A and G are the only samples which could be considered as frost resistant, though the experimental results indicate that good (samples E and L) or excellent (samples B, D, H) performance belong to products having a reduced value of pore size (Φ_{50} <0.5-0.6 μm).
- Finally, according to Koroth's model (Figure 1F), all samples should be considered frost resistant since the durability factor calculated for each of them is much higher than the limit value of 85; however, any significant relationship between the calculated index and the experimental results occurs.

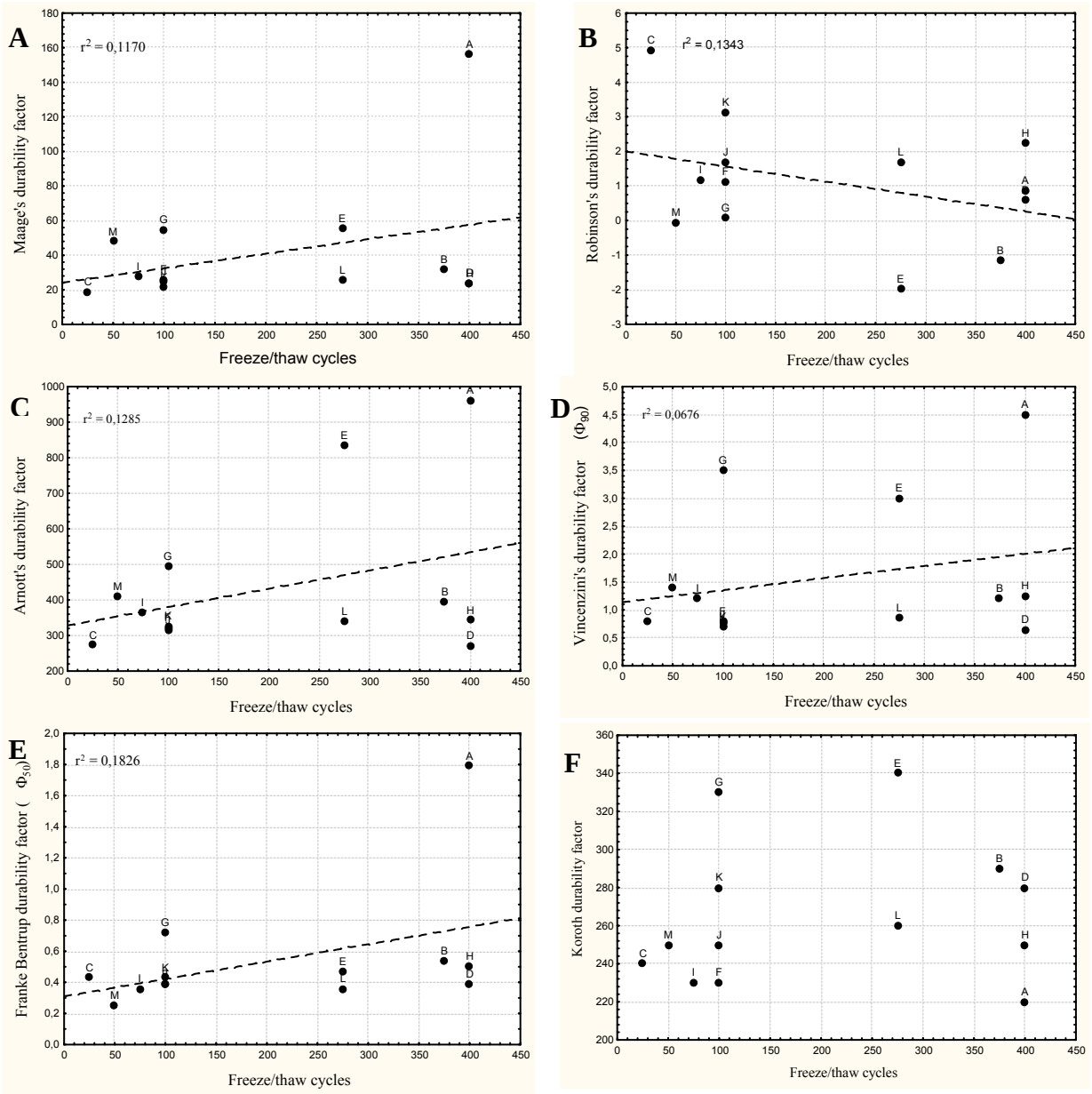

Figure 1. Experimental behaviour of roofing tiles (number of freeze/thaw cycles) vs durability factors of A) Maage; B) Robinson; C) Arnott; D) Vincenzini; E) Franke and Bentrup; F) Koroth.

3.2 Statistical Elaboration

Since simple binary correlations between the calculated indices and the experimental behaviour of roofing tiles were not satisfactory, a statistical elaboration of data (factor analysis and "stepwise" multiple regression analysis) was undertaken considering, besides the number of freeze/thaw cycles, physical (TP, BD, P3, BET, Φ_{50} and Φ_{90}) and compositional (amount of quartz, amorphous phase and Ca-silicates) properties of products as well.

- The extraction of the principal components (Table 7) highlights that, as expected, the frost resistance of products is correlated in a quite complex way with all the other variables so that the hypothesis that more than one parameter could simultaneously influence the materials real performance is in some way confirmed.

Table 7. Extraction of the principal components.

Variable	*Factorial weights*		
	Factor 1	Factor 2	Factor 3
Freeze/thaw cycles	0.535	-0.001	0.457
TP	0.545	-0.794	-0.123
P3	0.813	0.495	0.056
BET	-0.837	0.04	-0.438
BD	-0.542	0.794	0.127
Φ_{50}	0.864	0.381	0.115
Quartz	0.250	0.793	-0.528
Ca-silicates	0.457	-0.841	-0.008
Amorphous	-0.610	0.178	0.691
Φ_{90}	0.707	0.649	-0.042
Variance	4.132	3.446	1.214

Anyway, looking at the mutual relationships of figure 2, the following conclusions can be drawn out:

- a positive correlation exists between frost resistance and the amount of pores greater than 3 μm (P3), the median pore size (Φ_{50}) and Φ_{90} values;
- frost resistance is inversely related to the pore specific surface (BET) but also to the amount of amorphous phase, so that the highest its content, the lowest is the product performance;
- concerning the amount of quartz and Ca-silicates, their role on the frost resistance seems to be the opposite: a higher amount of new formed phases (such as Ca-silicates) increases the ability of products to withstand frost action, which in turn is decreased by the presence of high quartz amounts.

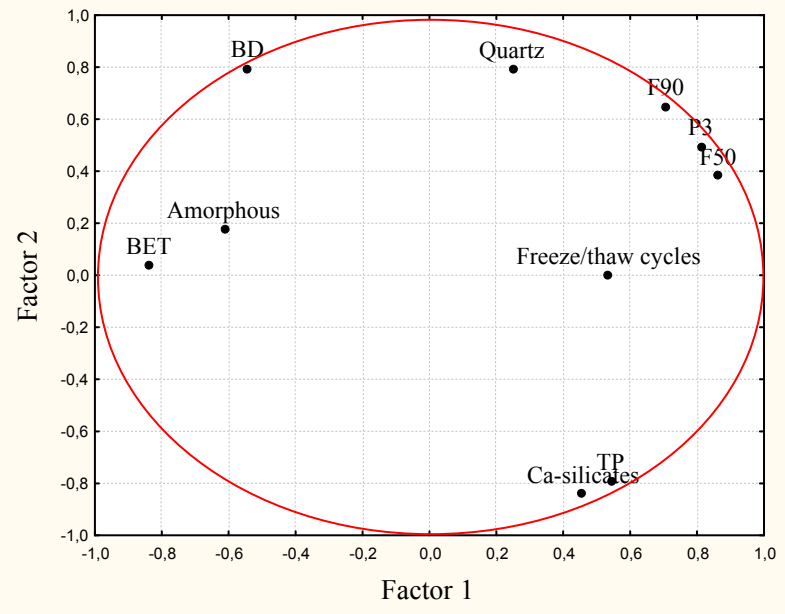

Figure 2. Extraction of the principal components: factor 1 vs factor 2.

The results of the multiple regression analysis (R^2= 0.94138, p<0.00184), taking into account the product frost resistance as dependent variable and the physical and compositional parameters as independent ones, made possible to confirm some of these indications (Table 8):

- according with the values of β factors, the statistical procedure selected the following as the most influent parameters: BD, quartz amount, BET, Ca-silicates amount, amorphous amount and Φ_{50};
- it is worth noting that the statistical weight (as expressed by β factors) of the mineralogical phases are quantitatively equivalent to that of BET and prevailing on the pore size represented by Φ_{50};
- concerning the positive or negative role played by each selected variable, it is confirmed that the amount of Ca-silicates, on one side, and that of quartz and amorphous, on the other side, work in the opposite way; a higher amount of new formed phases increases the frost resistance of products, while the presence of both quartz and amorphous potentially involves the risk of frost damage;
- the evaluation of the p-level corresponding to each selected parameters allows to assess the reliability of the results of the statistical procedure which can be considered satisfactory.

Table 8. Results of the multiple regression analysis.

Stepwise multiple regression analysis R = 0.970; R2 = 0.941; p-level < 0.002

N = 13	β	Std. Error	B	Std. Error	p-level
Intercept			-7063.22	1052.63	0.0005
BET	-0.821	0.201	-338.80	83.12	0.0065
Amorphous	-0.775	0.381	-9.20	4.53	0.0885
BD	1.857	0.231	4227.63	527.29	0.0002
Quartz	-0.882	0.368	-14.33	5.98	0.0054
Ca-silicates	0.779	0.223	7.34	3.99	0.0110
Φ_{50}	0.252	0.182	101.05	73.41	0.2180

Following these results, it can be pointed out that the production of roofing tiles with excellent frost resistance – which are able to overcome a number of freeze/thaw cycles much higher that those required by the current standard – involves the evaluation of both product and processing variables. As far as the composition of raw mixtures, their CaO content should be improved paying in the meantime great attention to the development of a highly porous microstructure and controlling the pore dimensions (to get lower BET values). Analogously, the amount of new formed Ca-silicates should be improved (≥ 40%), while the amount of amorphous phase reduced under about 20%. These requirements, together with the need to obtain a microstructure having a higher quantity of pores greater than 3 μm, can be satisfied through the modification of the firing process, i.e., increasing the maximum firing temperature.

4 CONCLUSIONS

This study has taken into account the frost behaviour of 13 industrially-manufactured roofing tiles which were assessed through a double approach: performing severe freeze/thaw testing (EN 539-2) and calculating the durability indices, according to some of the models present in the literature. The products microstructure, in terms of physical, technological and compositional parameters, was fully investigated and the results correlated with the frost resistance of roofing tiles.

Looking at the correlation between the experimental frost behaviour and the calculated durability factors, we can conclude that no model is able to foresee reliably the product performance since the models exhibit a strong dependence on the data population and probably succeed only with a homogeneous sample in terms of both composition and manufacturing technology.

Inserting into a statistical procedure all the microstructural and compositional variables, together with the experimental number of freeze/thaw cycles, new indications came out concerning the design and production of roofing tiles able to withstand adverse climatic conditions. Following these results, it can be pointed out that the production of roofing tiles with excellent frost resistance involves the evaluation of both product (i.e., raw materials composition, microstructure and phase composition of tiles) and processing (i.e., firing temperature) variables.

REFERENCES

Maage M., 1990, 'Frost resistance and pore size distribution in bricks', part 1, *Ziegelindustrie Int.* **9**, 472-481.

Maage M., 1990, 'Frost resistance and pore size distribution in bricks', part 2, *Ziegelindustrie Int.* **10**: 582-588.

Robinson, G. C., 1995 'Relation between physical properties and durability of commercial marketed bricks'. *Amer. Ceram. Soc. Bull*., **56** [12], 1071-1075.

Arnott, M., 1990 'Investigation of freeze-thaw durability', NRC-IRC Report N. CR 5680.1 Nat. Res. Council of Canada, Ottawa, Canada

Vincenzini, P., 1974 'Le prove di laboratorio nella previsione del comportamento al gelo dei materiali ceramici per l'edilizia' *Ceramurgia,* **3**, 176-188.

Franke, L., & Bentrup H., 1993 'Evaluation of the frost resistance of bricks in regard to long service life', part 1, *Ziegelindustrie Int.* **7-8**, 483-492.

Franke, L., & Bentrup H., 1993 'Evaluation of the frost resistance of bricks in regard to long service life', part 2, *Ziegelindustrie Int.*, **9**, 528-536.

Koroth, R., Fazio P., Fedman D., 1998 'Development of new durability index for clay bricks'. *Journal of Architectural Enginnering*, **9**, 87-93.

The Assessment of Durability of Discontinuous Roofing: An Experiment on Sandwich Panels

Giuseppe Alaimo [1]
Francesco Accurso [2]

T 22

ABSTRACT

The sustainable development of the construction trade requires a more rational use of the resources used. In light of this, the knowledge of building components and systems durability becomes fundamental in planning the service life of those components and to forestall unexpected deterioration and pathologies. Within the framework of more general research on the durability of building components, which involves various Italian universities, Palermo university has been concerned with discontinuous roofing. After the theoretical study on the reliability of a range of twenty-four technical solutions within the discontinuous roofing class, the sandwich panel, made up of two sides of metallic sheet with expanded polyurethane, was investigated. The research, carried out, in accordance with ISO 15686, concerns the behaviour in time of the sandwich panel, established through the monitoring of its performance characteristics (aspect, weight, colour, thermophysical and mechanical characteristics) when it is subjected to natural and artificial aging using an accelerated aging cycle in a climatic chamber. This was done for typical conditions of the Mediterranean climate. The tests on samples of different sizes, concerned the analysis of colour (light and dark), the measurement of conductivity, thermal resistance and resistance to tensile stress and bending moments. These were carried out on new samples, samples exposed externally and samples subjected to accelerated aging. The results allow the development of correlations between the variations of thermophysical and mechanical parameters and the deteriorations after the first two years of outdoor aging and the first sixty cycles of accelerated aging (rescaling). In such a study, particular attention should be given to the polyurethane interface sheet, in terms of criticality of thermophysical behaviour of the panel and the colour, appearance which compete to imply the quality of the whole building envelope.

KEYWORDS

Sustainability, Maintenance, Durability, Reliability, Sandwich panels.

[1] Università degli Studi di Palermo, Dipartimento di Progetto e Costruzione Edilizia, Palermo, Italy 90128, Phone +39 091 234151, Fax 091 488562, alaimo@unipa.it
[2] Università degli Studi di Palermo, Dipartimento di Progetto e Costruzione Edilizia, Palermo, Italy 90128, Phone +39 091 234151, Fax 091 488562, ing.accurso@alice.it

1 INTRODUCTION

Durability deals with the maintenance of performances associated with a component at the beginning of its working life and the ways in which performance decays in time. Important aspects required to achieve building quality are maintenance planning and control of resources which will be used in all phases of the building process.

This paper presents the results of a research study on "Methodologies of planning and experimental evaluation of the durability of discontinuous roofing", within a national research program (P.R.I.N.) which involves the University of Palermo, the Polytechnics of Milano and Torino, the Universities of Brescia, Napoli and Catania. They constitute a network of research centres, where, in the last years they have developed experimental methodologies to evaluate the durability on different building components, for a range of environments. The results reached, until now, have been presented at Palermo's Conference on 15 September 2006, they furnish contribution to the international research of the CIB W80 RILEM 175 "Service Life Prediction Methodologies", e ISO TC 59/SC14 "Building Construction".

The roof has always been a fundamental component of the building envelope, and a determinant of the environmental quality of the indoors, because it contributes to controlling energy flows between the interior and exterior of the building. The roofs contribute to maintain the planned environmental conditions, with the control of technological functions of the technical elements of the class. That's why there's a need to make reference to the class of technical elements (classification UNI 8290) and to each technological performance level. Within the National Program, the Research Unit of Palermo is carrying out a study on pitched roofs, through a first phase of functional and technical analysis of a catalogue of technical solutions of the class by performing an assessment of natural reliability. We have chosen sandwich panels, used either as roof or wall elements, as the building components for our research, and of which Italy is a leading manufacturer in the world.

2 THE METHODOLOGY

Based on the latest national and international standards (UNI 11156-2006; ISO 15686), the methodology we have followed consists of evaluation using two distinct and complementary procedures for the two parameters of durability: reliability and service life [Maggi et al. 2000, 2001]. Reliability is estimated through a method that permits a qualitative evaluation following a comparative procedure involving the elements of a catalogue of technical solutions of the class, which is considered out of system and with no intended use [Rejna 1995]. Service life is estimated through experimental tests on samples of technical elements exposed to natural agents and accelerated aging test in the laboratory. The results must be compared to determine the time re-scaling of the performance decay of the component.

This methodology for the evaluation of service life results is in accordance with the approach designed by ISO 15686 "Building service life planning". The assessment of reliability proceeds through the evaluation of the four components of reliability:

Functional reliability which, through the functional analysis, individualizes the distribution of the functions inside the solution, on which the degree of fatigue of the element depends on its operation;

Executive reliability which, through the technical analysis, verifies the degree of executive correspondence in comparison to the design;

Inherent reliability which concerns possible dimensional changes of the component during the phases of the exercise due to the different thermal and humidity stress of the functional elements;

Critical reliability which considers physical-chemical compatibility between adjacent materials of a different nature, and which constitute the technical solution.

The global reliability expresses in qualitative and comparative terms the degree of probability that the technical solutions have to last in time, whereas its complementary to 1 expresses the risk of failure during the service life. The estimate qualitative of reliability, both in global terms and of its components, offers useful information on the choice of maintenance procedure. Allowing by means of comparison, assessment of technical solutions other than those studied, both to estimate the reliability of a solution data and to plan new solutions of data reliability. The method permit to express reliability on the basis of its components: functional, inherent and critical reliability refer to planning choices and their complement of 1 expresses the risk failure for errors in the planning phase; executive reliability concerning activity in the construction phase and its complement of one expresses the risk failure for errors committed in that phase.

3 THE RANGE OF TECHNICAL SOLUTIONS

A range of 24 technical solutions were evaluated, which also included representative solutions by local builders. As well, “innovative” solutions were studied and compared to "traditional" constructions. The technical solutions of the repertoire (some are illustrated in Figure 1), have been characterized by: type of seal element; nature of load bearing structure; presence of insulation and ventilation layers.

The type of seal element (in small or large elements) can be made of brick (plain roofing or channel tiles), cement, fibrous concrete, metal or sandwich panel. The load bearing seals can be mixed with brick and reinforced concrete, of prestressed concrete or with timber and metal. The innovative solutions are those which use sandwich or composite panels, insulated and ventilated. These are also used in residential building.

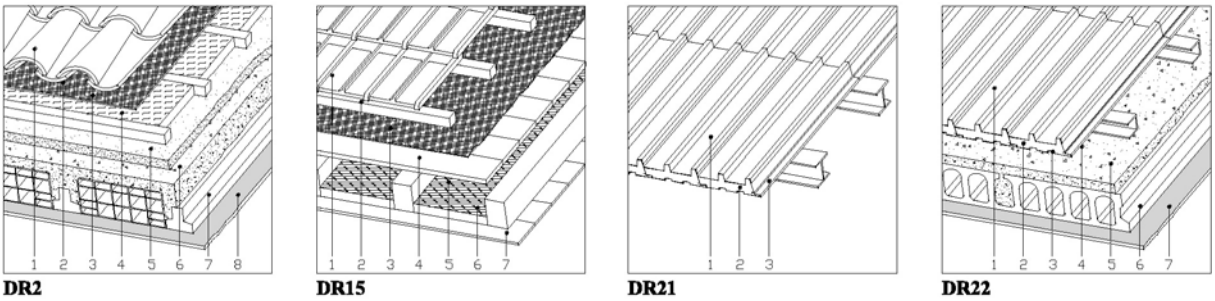

Figure 1. Some technical solutions of the repertoire.

4 THE EXPERIMENTS, SAMPLES AND PARAMETERS

The following parameters and properties were recorded for each sample: aspect; weight; colour; thermo-physical properties; mechanical properties. Such characteristics were determined for samples aged outdoors and in the laboratory using destructive and not-destructive tests, in the following manner:

1) not-destructive tests: aspect (using visual and measurement methods); weight; difference of colour; measurement of thermal conductivity and thermal resistance on the whole sample.
2) destructive tests: mechanical characteristics (traction, shearing and bending); thermo-physical properties (thermal conductivity and thermal resistance on PUR sections).

The original panel was made of two pre-painted galvanized steel skin, with a thickness of 0.45 mm, and an insulated core of expanded polyurethane, with a thickness of 40 mm. The specimens cut from the panel were of sizes 100 x 100 mm, 100 x 250 mm and 100 x 1000 mm are differentiated by colour in bright (White-grey) and dark (Siena red).

5 NATURAL AGING

The samples were exposed outdoors, directed toward South and with slope of 30° (Figure 2a). Before the exposure, the edges of the specimens were protected with a special polyurethane paint. On some samples, we applied some programmable data-loggers (Figure 2b), in order to record the surface temperatures reached (exposed and shade side) during the exposure. The collected data, between March 2004 and March 2006, have been used to determine trends of the maximum, minimum and averages temperatures reached on the surface of the samples in Palermo with the different seasons of the year.


a

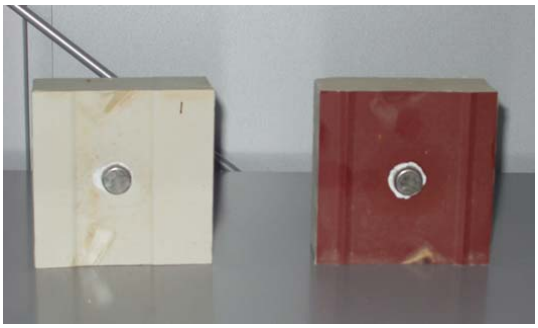
b

Figure 2. a: The samples exposed in outdoor; **b**: Temperature data-logger.

6 ACCELERATED AGING

The aging of samples was done inside a climatic chamber (Figure 3) that reproduces the principal climatic agents: rain, sunlight, high and low temperatures, variations of relative humidity. A necessary methodological preamble to the experimental phase included the definition of the range of weathering agents - actions - effects [Daniotti 2000] and corresponding deteriorations that can arise in the specimens. The artificial cycle (Figure 4a) has been developed on the basis of the specific climatic context of Palermo, and with the results of values measured outdoors, after initial calibration (Figure 4b).

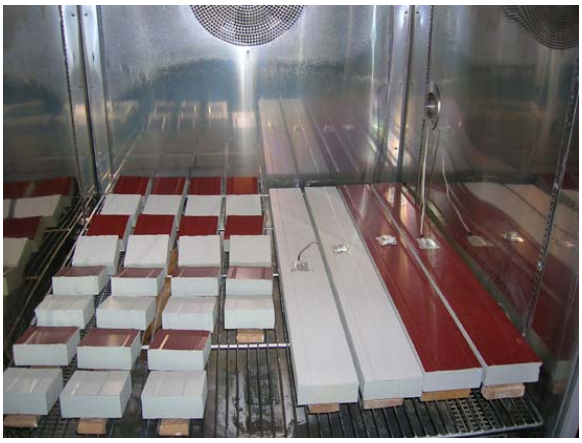

Figure 3. Samples inside of the Climatic chamber with temperature data-loggers.

The weathering accelerated cycle had a duration of 12 hours and consisted of the following phases:

Phase 1 - The samples were sprinkled with water at a temperature of about 20°C for 3 hours. In this phase the relative humidity inside the chamber was 95%;
Phase 2 - Temperature of the chamber was brought to 2°C for 1.5 hours;
Phase 3 - The samples were submitted to the action of warm dampness (T = 35°C, RH = 87%) for around 3.5 hours. This phase was preceded by a transition sub-phase of about 1.5 hours;
Phase 4 - In this phase the samples were exposed to the light produced by the UV lamp that together with the elevated temperature served to simulate the action of dry heat. The temperature was brought to around 80°C and the RH to 56% and maintained for about 2.5 hours.

The artificial aging has been conducted over 120 cycles corresponding to about 1500 hours of accelerated aging.

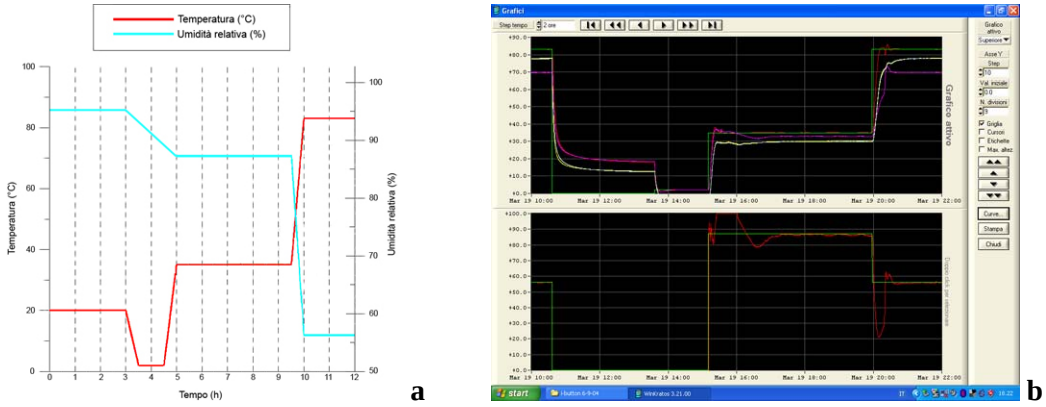

Figure 4. a: Theoretical accelerated aging cycle;
b: Experimental accelerated aging cycle (by Winkratos software).

The tests, destructive (thermal and mechanical properties) and non-destructive (aspect, colour, weight), were performed on the initial samples at time zero; the external aged samples after each year and after every 30 cycles for samples aged in laboratory.

7 RESULTS AND CONCLUSIONS

Surface Effects
Both with natural aging and accelerated aging, a slow evolution of degradation was observed. Initially, the phenomena of chromatic and yellowing alterations of the metallic surface were observed. Then the appearance of local oxidation marks, and with the increase of cycles, the formation of blisters and cavities in the foam, thus variations of shape at the interface foam-metal skin. After 120 cycles cracks on the interface appeared, which is certainly a critical point, both for thermo-physical and mechanical behaviour.

Tensile tests
The test has the purpose of evaluating the tensile strength of the polyurethane foam (Figure 5a,b) and its adhesion to the metallic support (ETAG 016-1, UNI EN 1607, EN 14509).

The specimen showed an improvement of the traction resistance up to 60 cycles, subsequently such tendency is reversed with the increase of cycles (Figure 6a).

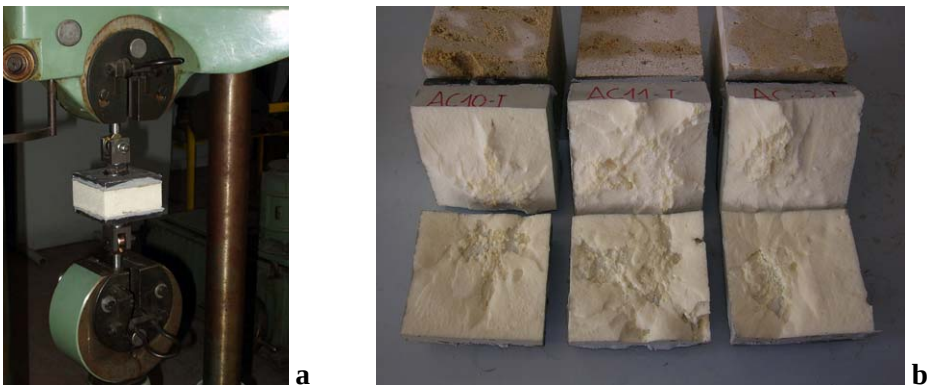

Figure 5. a: Tensile test; **b**: Type of failure (PUR).

It is important to underline the relationship found between the tensile strength, the percentage of uncovered metal skin (Figure 6b) and the length of the aging. The aging causes in fact an increase of the percentage uncovered after the failure. This effect was more accented in the dark samples. From comparison of the effects of the two types of aging in this type of tests, a correspondence can be noticed between the effects of 60 cycles and those of 2 years of natural exposure.

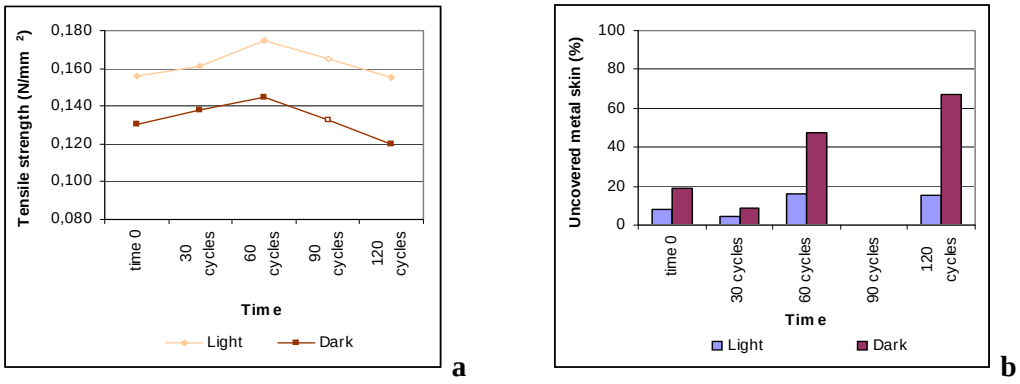

Figure 6. **a**: Tensile test; **b**: Metal skin after the failure (accelerated aging).

An analogue behaviour was observed, from a qualitative point of view, between the resistance to traction and thermal conductivity and thus a decrement of the characteristic up to 60 cycles and a successive reversal of the trend with an increasing number of cycles.

Thermal conductivity
Measurements have been conducted both on whole samples and on the polyurethane sections (extracted from the core of every samples two sections with a thickness of 10 mm) (Figure 7a), with the purpose to evaluate the influences of the external metallic elements and the interfaces with polyurethane.

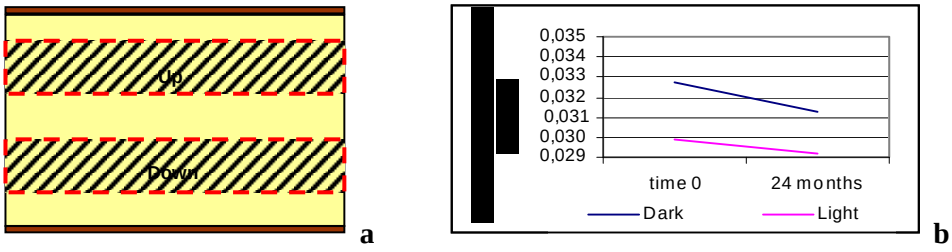

Figure 7. a: Sections of PUR; **b**: Change of conductivity (natural aging).

For up to 24 months of external exposure the conductivity of the samples remains substantially constant, both in the whole samples and in the sections of PUR (Figure 7b). In general the changes in thermal conductivity of the whole samples are greater than the changes in the PUR sections, because of the lower contact resistance due to the cover sheets glued to the PUR.

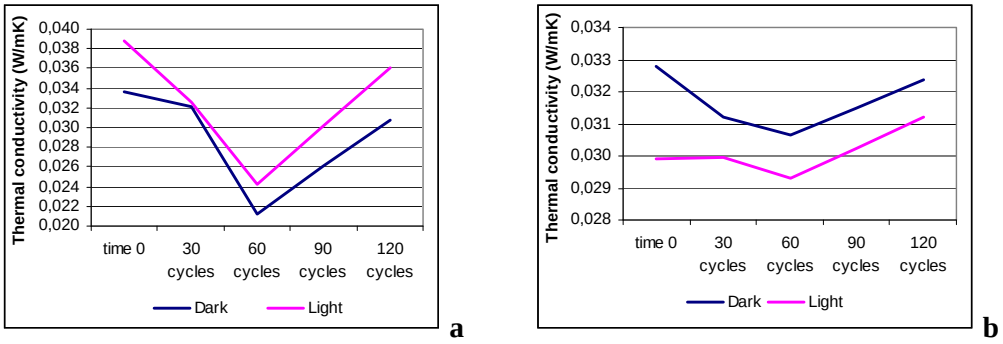

Figure 8. Change of conductivity – **a**: whole samples;
b: sections of PUR (light and dark samples -accelerated aging).

There is a substantial consistency among the measurements on the samples marked "Up" with those of the samples marked "Down". The results of the tests in the climatic chamber show an analogous behaviour from the qualitative point of view among the whole samples (Figure 8a) and the sections of PUR (Figure 8b) both for the samples White Grey and for those Siena Red.

Also in this type of tests after 60 cycles, an inverse relationship is observed with substantial consistency, involving the thermal conductivity both in the first year of natural aging, and in the first 30 cycles of accelerated aging. Definitively, the results show a significant qualitative relationship between variations of thermo-physical and mechanical parameters and a corresponding trend between the observed degradations after the first two years of external aging and the first 60 cycles of accelerated aging (re-scaling).

Colour
The results of the measurement of colour, in the CIEL*, a*, b* space, show:
• after about two years of natural aging, the light samples have been shown a significant variation of colour (ΔE) and a tendency to yellowing;
• in the samples that were artificially aged, we can see a difference of colour in two ways.

The light samples show a tendency to yellowing and a progressive variation of colour, the dark ones have a more significant variation after 30 cycles and a decrease in this difference with the increase of cycles. Results, for the light samples, are shown in Figure 9.

Between the different aspects investigated, the study of colour assumes particular value, both from an aesthetic and architectonic point of view, on the visible impression, on the individual psychological effects as the “Sick Building Syndrome”. Thus, the colour is able to reflect not only the quality of the building product, but also that of the existing environment.

Another important social aspect is the maintenance, in particular that carried out on the aesthetic appearance of buildings in the outskirts of the city, where social decadence is almost always accompanied by the lack of urban and building quality. Therefore, this is an aspect which requires adequate attention also from a normative point of view.

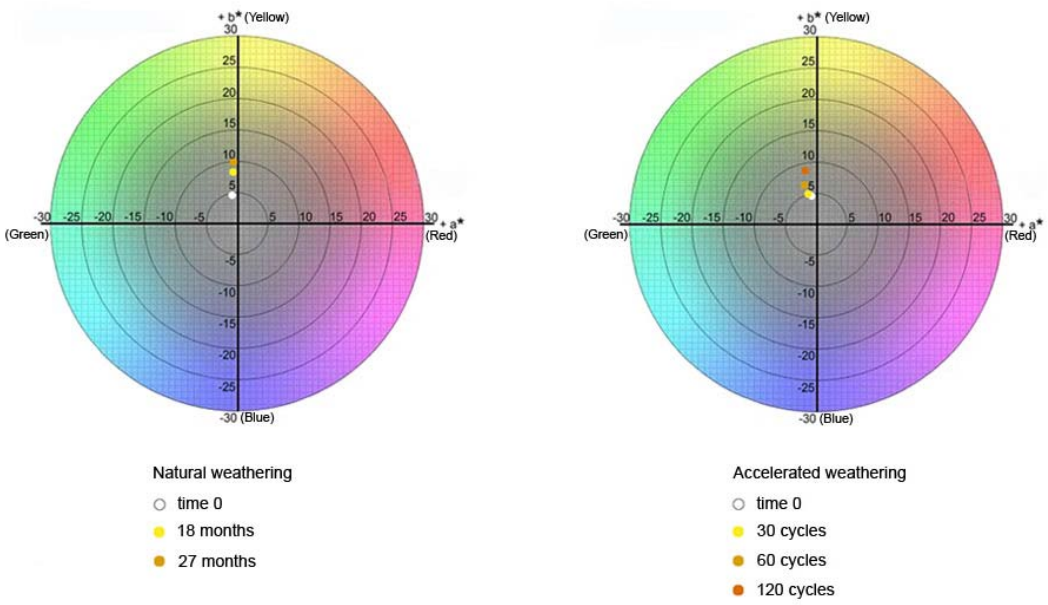

Figure 9. Chromatics diagrams a*, b* for the light samples.

It will be useful continue to check the course of the thermal conductivity of the samples exposed outdoors to shed new light on the role of the skin-core interface and on the variability of the insulating property. The study could establish properties of the aged polymer and the gas contained inside the cells to provide an explanation to the improvement of the characteristics (tensile strength, thermal conductivity) measured in the initial phase of the panel's aging.

REFERENCES

Alaimo G. et al., 2006, Valutazione sperimentale della durabilità di coperture discontinue. Un'applicazione al pannello sandwich, EdiTecnica, Palermo.

Alaimo G., 2004, L'affidabilità funzionale delle coperture discontinue, EdiTecnica, Palermo.

Alaimo G., Accurso F., 2006, La stima dell'affidabilità delle coperture discontinue, EdiTecnica, Palermo.

Maggi P.N. et al., 2000, La qualità tecnologica dei componenti edilizi - La durabilità, Epitesto, Bologna.

Maggi P.N. et al., 2001, La qualità tecnologica dei componenti edilizi - La valutazione della durabilità, Epitesto, Bologna.

Rejna M., 1995, Valutazione della qualità tecnologica utile dei prodotti complessi per l'edilizia, Quaderno DISET vol. 4, Esculapio, Bologna.

ISO 15686-1 (2000) Buildings and constructed assets - Service life planning - General principles.

ISO 15686-2 (2001) Buildings and constructed assets - Service life planning - Service life prediction procedures.

UNI 11156-1-2-3 (2006) La valutazione della durabilità dei componenti edilizi.

11DBMC International Conference on Durability of Building Materials and Components
ISTANBUL, Turkey 11-14 May 2008

Roof Management Program for Multiple Roof Systems

Steven P. Bentz [1]
Walter J. Rossiter, Jr. [2]

T 22

ABSTRACT

Roof management programs are intended to extend the service life of roofing systems, while maximizing the efficient use of available funding whenever repairs or replacements are performed. The requirements of an acceptable roof management program include: good roof design and installation using quality materials in applications where the materials are appropriate, satisfactory maintenance of the roof to acceptable standards, preventive maintenance before costly deficiencies occur or timely repairs immediately after deficiencies are found, and documentation of information regarding roof performance for utilization on future projects. This paper presents an overview of a roof management program developed to provide a methodology for performing these actions while understanding the limitations of time, manpower, and funding with which to do so.

Within this program, evaluations of roof systems are based on ten factors which are quantified (i.e., scored) and thus provide the basis for a prioritization schema. A key consideration is enabling the scoring by minimally trained personnel with little roofing experience. The ten factors to be scored for the roofing prioritization schema, in no particular order, are durability, age, roof criticality, susceptibility to damage, membrane condition, flashing condition, attachment, slope and drainage, constructability, and leak history. Each factor is ranked on a comparative scale from 1 to 10, with 1 being a low or poor score, and 10 being a good or high score. The individual scores for the ten factors are then added together to develop an overall score for the roof, which is then used to objectively develop a prioritization for the repairs or replacements. Representative evaluations at several large U.S. campus-type facilities have demonstrated the utility of this approach, and will be described in the paper as examples of using this program to extend roof service life.

KEYWORDS

Durability, Management program, Prioritization, Roof.

[1] Facility Engineering Associates, P.C., Project Manager, Fairfax, Virginia 22030, USA, Phone 703 5914855, Fax 703 5914857, bentz@feapc.com
[2] W.J. Rossiter & Associates, Clarksburg, Maryland 20871, USA, Phone 301 2533534, wjrossiter@verizon.net

1 INTRODUCTION

Roofing practitioners have long acknowledged that successful low-sloped roofing performance relies on a combination of four key elements namely; sound design, suitable materials, good workmanship, and proper and timely maintenance [1]. Historically, in spite of such acknowledgement, far too often little attention was paid to putting this tenet into practice, particularly with regards to maintenance. For example, almost 20 years ago, Firman chastised that in general the industry is geared towards new and re-roof construction, with very little emphasis given to maintenance needs [2]. He further stated that owners were mainly responsible for this because they were not demanding an emphasis on maintenance. The result, in his opinion, was that owners contributed to most roof leaks due to lack of maintenance. Reasons for this attitude have not been explored, but the present authors believe that it was associated with a short-sighted, outright unwillingness to allocate the funds necessary to perform the needed maintenance. Fortunately, as time elapsed, many practitioners awoke to realize that the roof represents a sizeable investment that needs to be protected, and began to promote roof maintenance management programs as a formal mechanism for doing so. Bradford evidenced this shift in attitude clearly and succinctly in 1996 when he called the need for roof maintenance indisputable [3]. To be sure, we can readily say in 2007 that widespread use of roof maintenance programs has been realized in the United States. Here we quote Bradford's 2004 writings that during the past several years, roofing contractors and roof consultants have seen substantial increases in requests for roof preventive maintenance services [4]. He opined also that everyone in the roofing business-from manufacturers to consultants to contractors of every size—has seemingly developed a program, system, or department to address owners' roof system maintenance needs. Today, any building owner in the United States can search the World Wide Web for 'roof maintenance management' and find web sites for hundreds or more firms that offer such services ranging from limited inspections and repairs to full management.

The objective of a roof maintenance program is to extend the Expected Useful Life (EUL) of a roof system [5]. The elements comprising such a program are periodic inspections, routine maintenance and repair, and correct application of quality roofing products [5]. Historically, one of the first major organizations in the United States to adopt a formal roof maintenance management program was the U. S. Air Force (USAF) [6]. Although controversial because of some of its requirements, a generally accepted feature of the USAF program was the assignment of a quantitative rating of the condition of a roof as determined through its inspection. In turn, the individual ratings for a number of roofs at a facility were used for ranking their relative conditions to establish priorities for completing necessary repairs [1]. Such prioritization is particularly important in the case of multi-building complexes. Today many maintenance programs incorporate roof-condition ranking systems for determining the allocation of maintenance funds. In the United States, perhaps the most widely known maintenance management program is the ROOFER Program of the U.S. Army Corps of Engineers (USACOE) [7]. This program, which incorporates relative ratings of roof condition among its many features, is not only used at Army facilities but has also been adopted and adapted in the private sector. Such programs can be costly due to the amount of information needed to populate the database. Today's computer technology has aided in the development of maintenance programs but, at the same time, has increased the amount of information that is input. The cost to obtain the data is sometimes the governing factor, exceeding the cost of the software itself.

This paper presents an overview of a newly developed roof maintenance management program for use on multi-building complexes such as campus, military bases, and office parks. Examples of its features are given from limited practical experiences in the field. The goals of this program are to prioritize roofs, train on-site personnel, and simplify the process. One key feature of this program, consistent with those developed for example by the USAF and the USACOE, is the inclusion of a quantitative ranking of a roofs' conditions. Another key feature is the training of on-site personnel and the use of those trained personnel in conducting the inspections. Regarding this latter feature, we note with interest that Sinderman, in his web article discussing roof maintenance management, quoted a U.S. roofing consultant as saying that a lot of roof maintenance "is just having someone walk your roof who is competent, trained, and knows what to look for and how to evaluate repairs" [8].

2 ROOF PRIOTIZATION SCHEMA FACTORS

The foundation of the program presented here is the delineation of ten factors used in ranking the relative conditions of the roofs (entire buildings or roof sections at one building) inspected. These ten factors, referred to as the "Roof Prioritization Schema," are, in no particular order:

- **Age** (EUL of the existing roof system)
- **Importance Factor** (use of the building
- under the roof area)
- **Susceptibility to Damage** (roof traffic
- indicator)
- **Membrane Condition** (existing
- membrane)
- **Flashing Condition** (existing flashings)

Attachment (type of attachment)
Slope and Drainage (slope to drains and general roof slope, size/amount of drains, gutters, scuppers, etc. and functionality)
Constructability (difficulty of repairs/replacements)
Leak History (observed or reported leaks)
Durability (existing membrane toughness)

These factors are scored on a relative scale of 1 to 10, based on a ranking system developed for this program. In general a score of 1 for a factor is a poor rating and a score of 10 is a good rating, except as noted in the descriptions that follow.

The methodology behind the Prioritization Schema is to aid in development of recommendations and prioritization of maintenance needs and roof replacement scheduling. The documentation provided in AFI 32-1051 [5] can serve as a primer for evaluations performed with these factors in mind. The technical basis for each of the factors in the ranking system is as follows:

2.1 The Age Factor

While the age of a roof system may seem like a fair metric by which to measure a roof's performance, not all roof systems age the same. Therefore, having a multi-building complex with various different EPDM, single-ply, gravel-surfaced built-up roof (GSBUR), metal, and other types of roof systems of varying age presents the question of how old is too old? For the purpose of scoring roofs on the basis of age, roofs are rated on the expected useful life of the existing membrane as compared to the current age. For example, the expected useful life of an EPDM membrane roof system is approximately 12-15 years (Cash or Schneider Reference), therefore, an age of 6 years results in a score of 5, while an age of 1 year would result in a score of 9. A built-up roof has an expected life of about 25-30 years; therefore an age of 12 years would result in a score of 5, while an age of 24 years would result in a score of 1.

Based on the Author's experience a minimal percentage of roofs fail extremely prematurely, within 1 to 2 years. Conversely, we have seen a similar minimal percentage of roofs to fail after an extremely long service life of maybe 30 years. The largest majority of failures seen in practice tend to occur within one standard deviation of the average failure age. Using EPDM as an example, and taking the average failure age to be 12-years with a three year standard deviation, approximately 60% of EPDM roofs might be expected to fail within 9 to 15 years. Similar predictions based upon our experiences have been established for the other types of roofs.

However, with the longer service lives for many roof types, the range of the statistical failure point (standard deviations) increases, resulting in larger ranges for the expected failures.

Table 1 summarizes the expected useful life of some typical roof systems based on the Author's field experiences and complimented with data from roofing literature.

2.2 The Importance Factor

This ranking prioritizes roofs based upon the function of the building use or occupancy. That is, the level of importance is rated by how important the roof integrity is to the operation of the space below and how the occupants would be impacted by roofing damage or failure.

For example, a building housing sensitive electronic gear would score a 1 (i.e. failure is worse here) while a building housing spare machine parts would score a 10 (i.e. failure results in little damage).

Table 1. Expected useful life scoring.

Roofing System	Surface Type	EUL*	Score for 10-year old Roof
Built-up (3 or 4-ply)	Gravel	25-30 years	7=((30-10)/30) x 10
Modified Bitumen (2-ply)	Granules	20-25 years	6=((25-10)/25) x 10
Single-ply (TPO, PVC – heat-welded)	Un-surfaced/Exposed Membrane	15-20 years	5=((20-10)/20) x 10
Single-ply (EPDM – adhered)	Un-surfaced/Exposed Membrane	10-15 years	3=((15-10)/15) x 10
Metal (standing-seam)	Fluoropolymer Paint	40 years	8=((40-10)/40) x 10

*Note: The EUL shown assumes a minimal roof slope of ¼" per foot.
Formula Explanation: Ranking Factor = ((Upper End of EUL-Age)/Upper End of EUL)*10

2.3 Susceptibility to Damage

This factor addresses the probability of damage due to concerns such as foot traffic and surrounding conditions (overhanging trees, runways, taxiways, adjacent buildings, etc.). Are there multiple mechanical units on the roof that require access? Are there pavers or walkpads to protect the roof ?

Are traffic paths clearly identified? Each of these different types of traffic can cause undue stress on the roof system. Table 2 is a general rating system of the resistance of a roof surface relative to roof traffic and a general guide to scoring roofs with respect to this factor. Note that the metal roof system is scored based on the possibility of paint scraping, denting of panels, the possibility of seams being bent, etc.

Table 2. Resistance to roof traffic.

			Relative score					
			FT		SC		Access	
Roof System	**Surfacing**	**Traffic Resistance**	**Low**	**High**	**Low**	**High**	**Low**	**High**
Built-up (3 or 4-ply)	Gravel	High	10	8	10	8	10	8
	Smooth Surfaced	Moderate to High	9	6	9	6	9	6
Modified Bitumen (2-ply)	Gravel	High	10	8	10	8	10	8
	Granular Surface	Moderate to High	9	7	9	7	9	7
	Smooth Surfaced	Moderate to High	9	6	9	6	9	6
Single-ply	Exposed Membrane	Low to Moderate	7	5	7	5	7	5
	Ballasted	Low to Moderate	7	4	7	6	7	4
Metal	Fluoropolymer Paint	Low to Moderate	8	6	8	6	8	5
PMA	Ballasted	High	10	9	10	9	10	9

FT = Foot Traffic; SC = Surrounding Conditions; Access = Ability and/or need to access the roof.

2.4 Membrane Condition

This is a subjective view of the membrane based on the inspection of each roof for defects. The number, type, and extent of defects are included in the rating.

Table 3 summarizes some typical defects for roof systems.

Table 3. Typical roof membrane defects.

Roof System	Typical Defects
Built-up (3 or 4-ply)	Exposed felts, wind scour, blisters, asphalt migration (down slope), ply slippage (down slope), exposed embedded metal, inadequately filled pitch pockets, splits, or tears
Modified Bitumen (2-ply)	Open seams, inadequate bleed-out, exposed bleed-out, blisters, fish mouths, wrinkles, exposed reinforcing scrim, loss of granules, inadequately filled pitch pockets, punctures, tears, or splits.
Single-ply (heat-welded polymer)	Open lap seams, short lap seams, fish mouths, wrinkles, inadequately filled pitch pockets, punctures, tears, or splits.
Single-ply (adhered rubber)	Open lap seams, short lap seams, fish mouths, wrinkles, inadequately filled pitch pockets, punctures, tears, or splits.
Metal (standing-seam)	Open seams at standing-seams, missing or backed-out fasteners, buckling of pans, scratches, dents, or corrosion.

A membrane in good condition could be a 10, even if the membrane is 30 years old. A membrane in poor condition would be a 1, even if it is relatively new. The key in this factor is not to take extensive time to document each deficiency, but rather to use the general visual inspection to provide a relative magnitude of the defects. In our experience, with training most facilities personnel can subjectively rate a membrane condition to a reasonable degree to consistency.

2.5 Flashing Condition

In general, the assessment of flashings is similar to the assessment of the membrane in so far as the number, type, and extent of defects are included in the rating. Two important concerns not associated with membranes but included in flashings are the vertical attachment method and the counterflashing. Vertical flashings should be attached with continuous terminations. Counterflashings should be provided. The lack of either of these may necessitate the issuance of a lower value in this category. Flashings that do not appear to be performing well are to be rated lower than those that appear to be water tight and performing well.

2.6 Attachment

Attachment provides resistance to wind loads, and most design codes have very specific requirements for wind uplift resistance. Attachment methods are at times compromised by force-fitting a particular attachment method to a roofing deck that does not readily lend itself to the method. Figure 1 shows the three most commonly used roof attachment methods. The fourth method shown, the Protected Membrane Assembly, is a hybrid of the basic attachments in that the roof membrane may or may not be fully adhered, but the insulation clearly requires the ballast to keep it in place.

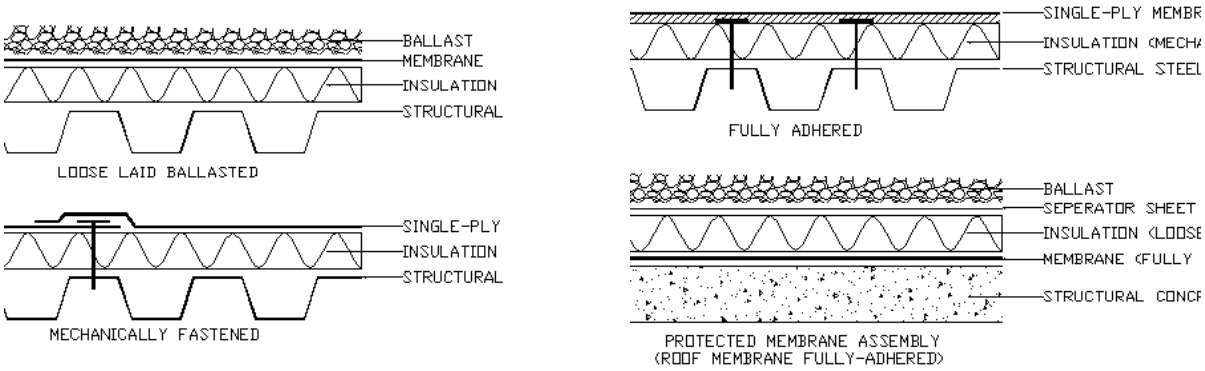

Figure 1. Attachment methods.

Deficiencies in attachment are a cause of roofing failures. Membrane blow-off causes failure of the weatherproofing system at the very least, and can be accompanied by structural failure of the roof

under certain circumstances. Another example is failure of the attachments causing failure of the waterproofing membrane. Examples include fasteners backing out through the membrane, or fasteners penetrating the roof deck and causing condensation and water issues in the spaces below. Either deficiency can have significant adverse effects on the long term use of the existing roofing installation. Evaluating the appropriateness of the attachment method for the specific type of roof deck and evaluating the condition of the attachment devices is critical to the long term performance of the deck. Attachment is evaluated by comparing an appropriately attached roof system with no apparent failures (score a 10) with an inadequately fastened, but functioning well roof system (score of 5) with fastener back out puncturing the membrane (score of 1). Typically fastener defects are difficult to detect in a surface visual review of the roof system. For this reason, it becomes important that the personnel performing the rankings also perform review of the construction documents, looking for fastening requirements and also access the interior of the building to attempt to verify fastening type and pattern from the underside of the roof deck. IN our experience, this factor is likely to be evaluated as either a 10, a 5, or a 1 by most assessors.

2.7 Slope and Drainage

Slope is an important factor in the proper function of a roof system. Adequate slope can compensate for inferior materials and construction quality; therefore, a roof with positive slope to drain (greater than ¼ inch per foot) should receive higher score than one with less slope. The waterproofing ability of the membrane is less likely to be compromised by draining water quickly away from the roof surface. Roof drainage and slope are two distinctly different parameters. An adequately sloped roof can have inadequate drainage, and a flat roof deck can have adequate drainage. Inadequate drainage on a well-sloped roof can lead to slower water runoff, taxing the roofs' flashing systems and potentially leading to leaks. A relatively flat roof system can have adequate drainage, which becomes a requirement when designing protected membrane assemblies. Well sloped roofs with minimal or no indications of ponding should score a 10, while no slope roofs with extensive ponding score a 1. Drainage is an important factor in the proper functioning of a roof system. Drainage refers to the ability of the roof system to carry water away from the roof and the building. The building code usually dictates the minimum level of drainage required for a roof system. Conventional roof design calls for at least four drains for larger roofs, a minimum of two drains for roofs under 10,000 square feet, and a maximum spacing of drains in any direction of 75 feet. Roofs that meet these criteria should receive a higher score; those not meeting the requirement should be scored lower. In addition, drainage also covers the adequacy and function of the existing roof drains. Roof drains that are clogged, that inadequately carry water away from the roof and building, or that overflow during severe events, should be scored appropriately lower when evaluating drainage. Roofs with good drainage, adequate for the flow of water, well placed to divert water from the roof and building score a 10, while roofs with minimal drainage that retain water score a 1. Scoring within the slope and drainage category should be an average of the 1 to 10 recorded for Slope and the 1 to 10 recorded for Drainage.

2.8 Constructability

This factor is associated with the human element of postponing needed repair or renovation of failed roof systems only because they are difficult to access. In our experience with multi-building complexes, the more difficult it is to reach a roof, the longer the replacement is avoided. To overcome this tendency toward procrastination, we rank relatively inaccessible roofs with lower values than those that are readily accessible. Constructability refers to the construction factors involved in maintaining or replacing a particular roof, taking into account building location, height, type, roof location and number, use, and occupancy. Roofs on taller buildings are more difficult to access than those on lower buildings. A building located in cramped conditions with inaccessible roof edges will be more difficult to replace. Roofs that can be easily and readily replaced or repaired due to their location, height, use, etc. should be scored a 10. Roofs that will be difficult to replace due to inaccessible locations or extensive restrictions should be scored a 1.

2.9 Leak History

Leak history can be quickly determined based upon interviews with building occupants or visual inspection of the interiors. A roof that leaks extensively each time it rains scores a 1. A roof that never leaks would be scored a 10. Scores between 1 and 10 are based on a count of the number of leaks and a comparison of the total number of leaks at each building across the complex. It should be noted that the leaks need to be considered purely on number, not on what is damaged. Additionally, the determination of leak history scoring could be augmented with knowledge gained from Non-Destructive Evaluation (NDE) such as infrared or nuclear moisture scanning, if performed; however, NDE is not necessarily a requirement for completion of the ranking system.

2.10 Durability

Material durability refers to the roof system's ability to resist weathering and natural or man-made impact without breaking down. Membrane type, thickness and surface treatment have a significant effect on roof system durability. The roof membrane and surfacing must have the capability to expand and contract to prevent splits and tears from extreme temperature changes. This capability must be present when a roof is constructed, and remain at adequate levels throughout the EUL of the roof. Thus, in order for a roof system to perform adequately, it must have adequate material durability when it's constructed and not have a tendency to lose those characteristics as it ages. For the most part, roof membrane materials today possess the material durability to resist weathering and building-related movement. However, some roofing materials may not be suitable for the climatic conditions of the site. A relatively thin, single-ply membrane that is suitable for a sunny, mostly dry climate with no foot traffic in the southwestern United States is likely inadequate for a mid-Atlantic U.S. environment where large seasonal swings in temperature are experienced. A particular membrane assembly that is used in environments where insulation is not needed or used may not be appropriate in a heavily insulated assembly. Many manufacturers have multiple membrane products for numerous surfacing configurations. Table 4 provides a summary of the author's durability scoring methodology used in this prioritization schema. These scores are based on the author's experience and relate similarly to the age scoring EUL as shown above. It should be noted that scoring the age factor is purely based on the numerical age of the roof compared to its EUL, while scoring the durability factor is more related to the relative durability of one material to another.

Table 4. Durability scoring.

Roofing System	Surface Type	Relative Durability	Score
Built-up (3 or 4-ply)	Gravel	High	10
Modified Bitumen (2-ply)	Granules	Moderate to High	9
Single-ply (TPO, PVC – heat-welded)	Un-surfaced/Exposed Membrane	Low to Moderate	8
Single-ply (EPDM – adhered)	Un-surfaced/Exposed Membrane	Low to Moderate	7
Metal (standing-seam)	Fluoropolymer Paint	High	10

3 USING THE FACTORS

Based upon the evaluations performed at a multi-building complex in the Northeastern Atlantic Region each roof was given a ranking score in the 10 categories as defined above. The scores were determined by minimally trained field personnel and compared to the opinions of two Registered Roof Professionals who had also accessed each roof. Table 5 summarizes the scores for selected buildings at the complex to provide an idea of how the system works. Table 6 summarizes the resultant score for the selected roofs and ranks them in order of priority. It should be noted that the complex surveyed consisted of approximately 130 buildings, with a total gross building area of approximately 1.4 million square feet. In this phase of the work, 30 buildings were surveyed totaling approximately 512,000 square feet in area, or an approximate 33% sampling. Typically, scores below 60 would be considered a priority for replacement, while scores above 80 would indicate roofs that

were recently installed, or were in good condition. As can be seen from this ranking, the complex has many roofing systems that rank between 50 and 70, indicating a great need at the facility both for roofing maintenance activities to keep the roofs from deteriorating further and for funding to begin to replace those roofs with scores below 50 indicating a roofing system that is on the verge of failure.

Table 5. Sample Individual Roof Ranking Scores.

Bldg. Letter	Age	Crit.	Mem.	Flash.	Attach.	Slope/ Drainage	Const.	Leaks	Suscep.	Dura.
A	1	3	1	3	8	10	8	6	10	10
B	5	3	8	8	9	8	8	4	10	7
C	1	4	5	5	6	10	10	9	10	10
D	1	4	5	4	6	10	9	7	10	10

Note: Generic buildings considered, to show how rankings would be tallied, does not match those in Table 6.

Table 6. Roof Prioritization.

Bldg. Num.	Roof Size	Roof Age	Roof Type	Ranking Score
1	107300	1988	EPDM	42
2	5640	1991	EPDM	44
3	5640	1991	EPDM	44
4	5640	1991	EPDM	45
5	5640	1991	EPDM	45
6	5640	1991	EPDM	48
7	5640	1991	EPDM	49
8	5640	1991	EPDM	49
9	5640	1991	EPDM	50
10	51400	1994	Hypalon	52
11	2350	1940	Metal	52
12	5640	1991	EPDM	53
13	2350	1940	Metal	53
14	2350	1940	Metal	53
15	2350	1940	Metal	53
16	2350	1940	Metal	53
17	5640	1991	EPDM	54
18	2350	1940	Metal	54
19	2350	1940	Metal	54
20	2350	1940	Metal	54
21	51400	1994	Hypalon	55
22	51400	1994	Hypalon	55
23	25185	1987	EPDM	56
24	2350	1940	Metal	56
25	2350	1940	Metal	56
26	51400	1994	Hypalon	58
27	14760	1994	EPDM	59
28	6550	1978	Built-up	60
29	51400	1994	Hypalon	63
30	8515	1979	Built-up	66
31	10270	1956	Built-up	70
32	2680	2002	EPDM	70

Need Replacement

Watch List

Fair Condition

4 SUMMARY

In summary, these 10 items can be subjectively rated by minimally trained individuals to obtain a roof rating. This roof rating can then be tracked in a database to obtain information on the relative degradation of the roof, and from this information, projected deterioration rates and replacement time frames determined. In addition, the rating can be used to rank multiple roofs across one or more multi-building complex in order to more efficiently spend the limited budgets.

REFERENCES

Rossiter, W.J., Cullen, W.C., and Mathey, R.G., "Roof Management Programs," NBS Report 85-3239, U.S. National Bureau of Standards (now NIST), Gaithersburg, MD (Nov. 1985).

Firman, D.M., "Maintenance Needs: An Owner's Perspective," 9th Conference on Roofing Technology, U.S. National Roofing Contractors Association Rosemont, IL (May 1989), pp.15-19.

Bradford, D., "An Industry Perspective on Roof Maintenance," Sustainable Workshop on Low-Slope Roofing, Conf-9610200, Oak Ridge National Laboratory, Oak Ridge, TN (Oct. 1996), pp.77-81.

Bradford, D., "Roof Maintenance: What Building Owners Need to Know," Professional Roofing (April 2004), pp. 24-27.

"Roof Systems Management," Air Force Instruction (AFI) 32-1051, U.S. Air Force, AFCESA/ENC (March 1989), 19 pages.

Built-Up Roof Management Program, Air Force Manual AFM 91-36, U.S. Department of the Air Force (3 Sept. 1980).

Bailey, D.M., Brotherson, D.E., and Tobiasson, W., "ROOFER: A Management Tool for Maintaining Built-Up Roofs," 9th Conference on Roofing Technology, U.S. National Roofing Contractors Association Rosemont, IL (May 1989), pp. 6-10.

Sinderman, M., "Staying on Top of the Roofing Business," Retail Traffic (Aug. 2000), http://retailtrafficmag.com/mag/retail_staying_top_roofing/.

Cash, Carl G., "The Relative Durability of Low-Slope Roofing," Proceedings of the Fourth International Symposium on Roofing Technology, U.S. National Roofing Contractors, Association, Rosemont, IL (Sep 1997).

Schneider, K.G., Jr. and Keenan, A.S., "A Documented Historical Performance of Roofing, Assemblies in the United States 1975-1996," Proceedings of the Fourth International Symposium on Roofing Technology, U.S. National Roofing Contractors Association, Rosemont, IL (Sep 1997), pp. 132-137.

Development of Test Method for Evaluating Root Resistance of Waterproofing Membrane

Kyoji Tanaka [1]
Saori Ishihara [2]
Soonju Pyo [3]
Hiroyuki Miyauchi [4]

T 22

ABSTRACT

The area of rooftop gardens has increased in Japan. As for waterproofing membranes used for rooftop gardens, the resistance to penetration by root systems such as roots or rhizomes of plants is needed in addition to the fundamental performance of waterproofing. Evaluation of root resistance of a membrane in advance is therefore required for actual roof application. The test method where trees or grass are planted in a container inside of which a test membrane was applied, and is then inspected for root penetration, has been widely adopted. However, the method takes a long time to obtain a result, and the development of a simple test method is needed for both users and manufacturers. It is well known from our experiences that rhizomes of bamboo grass are very hazardous for waterproof membranes. We therefore measured actual penetration force of the tip of a bamboo rhizome and observed the penetrating force of 9.8N. A new test method such as a needle penetrating method was developed on the basis of the results. The three penetrating needles of 0.1 mm, 0.3 mm and 0.5 mm in tip diameter were first prepared on the basis of the shapes of bamboo grass and lawn grass tips. Penetrating loads by the needles were then measured for various waterproofing membranes: five PVC sheets, five polyurethane membranes and five EPDM sheets. As for root resistance tests using actual plants, bamboo grass and lawn grass were also planted in containers, inside of which the same kinds of waterproofing membranes were applied. After the 1 year, the membranes were inspected, and the two results from the needle penetrating test and the container test were compared. It was found that the maximum strength in the needle penetrating tests and the strength at 1 mm penetration correponded well with the results of the container test. The proposed needle penetrating test and the two values as indices were considered to be useful for estimating the resistance of waterproofing membranes to root penetration.

KEYWORDS
Waterproofing membrane, Roof membrane, Green roof, Rooftop gardens, Root penetration, Test method, Root, Rhizome, Needle penetrating test, Bamboo grass, Lawn grass.

[1] Structural Engineering Research Center, Tokyo Institute of Technology, Yokohama, Japan, Phone +81 45 924 5329, Fax +81 45 924 5339, tanaka@serc.titech.ac.jp
[2] Structural Engineering Research Center, Tokyo Institute of Technology, Yokohama, Japan, Phone +81 45 924 5329, Fax +81 45 924 5339, saori@serc.titech.ac.jp
[3] Korea National Housing Corporation, Seongnam, Korea, Phone +82 31 786 0561, pyoju-@hanmail.net
[4] Structural Engineering Research Center, Tokyo Institute of Technology, Yokohama, Japan, Phone +81 45 924 5329, Fax +81 45 924 5339, miyauchi@serc.titech.ac.jp

1 INTRODUCTION

Rooftop gardens have been rapidly spreading in recent years. Unlike conventional systems having a heavy layer of concrete to protect the waterproofing membrane, soil for planting is directly placed on the waterproofing membrane without a concrete protective layer. In such a case, the tips of roots and rhizomes can come into direct contact with the membrane or even penetrate it if it is not strong enough. Such penetration by roots and rhizomes can lead to critical damage to the system directly leading to water leakage.

For this reason, waterproofing membranes for rooftop gardens are required to be root-resistant. However, root resistance has not been regarded as an evaluation item for conventional waterproofing membranes. At the present time, penetration resistance of waterproofing membranes has had to be judged solely by actually planting, waiting for the plant to grow, and observing if its roots or rhizomes have penetrated the membrane after a certain period. Though this method is realistic in that it uses actual plants, it requires a period of over a year to obtain the results, and above all, the results depend on the growth characteristics of the plants. If the plants are poorly growing, the forces of their roots are not strong enough to penetrate the waterproofing membranes, possibly leading to misjudgment of the root resistance of membranes. A mechanical test method for root resistance independent of the plant characteristics similar to other performance items for waterproofing membranes is desirable in order to evaluate root resistance of a membrane in an objective manner. With this as a background, the authors investigated a mechanical method of evaluating the root resistance of waterproofing membranes that is reproducible and simple.

In regard to past studies on this subject, methods have been standardized such as DIN 4062[1)] and the test method by FLL (the Landscaping and Landscape Development Research Society e.v.)[2)], in which actual plants are planted in containers applied inside by test membranes and the state of the membranes is investigated after intermittent observation over a period of several years. However, there have been few studies were found that evaluate the root resistance of waterproofing membranes using a mechanical apparatus instead of actual plants.

2 APPARATUS AND METHOD OF MEASURING PENETRATING LOAD

2.1 Shapes of Rhizome Tips

Whereas both roots and rhizomes can penetrate waterproofing membranes, severe damage to membranes is mostly caused by rhizomes. Therefore, in this study, the development of an apparatus for testing root resistance was intended for rhizomes. Since the shapes of rhizome tips were considered to produce a significant effect on the root resistance evaluation, the tips of bamboo grass and lawn grass were microscopically observed as representative rhizome tips.

Bamboo grass and lawn grass, both of which reportedly cause damage to membranes, are commonly used for Japanese style gardens and turf, respectively.

Typical shapes of their rhizome tips are shown in Figure 1. As these rather sharp shapes vary from one rhizome to another depending on the growth conditions, the tip shapes were approximated to hemispheres to examine their diameters.

The results, superimposed on the photo, are approximately in the range of 0.1 to 0.5 mm in diameter, though with differences depending on growth and time.

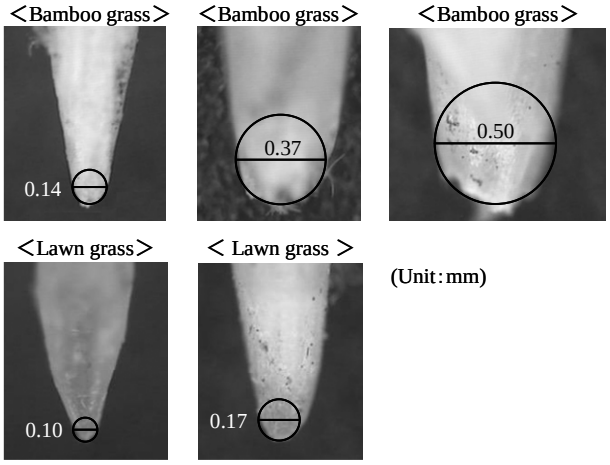

Figure 1. Tip of Rhizomes.

2.2 Simulated Needles

Needle-like tips simulating these rhizomes were fabricated based on the results of observation. The diameters of hemispherical tips were 0.1, 0.3, and 0.5 mm, with the axis diameter being 3 mm. Steel was selected as the material, as robust tips were required to test the root resistance of waterproofing membranes having a wide range of hardness.

2.3 Specimens

Specimens were prepared by sandwiching a membrane between two 8 mm-thick disks with a through hole in the center as shown in Figure 2. Since the diameter of the hole could affect the test results, tests were conducted using disks with the diameter of a hole of 2, 3, 5, and 10 mm to examine its effect. Figure 3 shows typical results. Whereas the stroke of the needle tip at puncture tended to increase as the diameter of the hole increased, the load at puncture remained nearly the same independent of the diameter of the hole. A hole diameter of 3 mm was therefore adopted for ease of measurement.

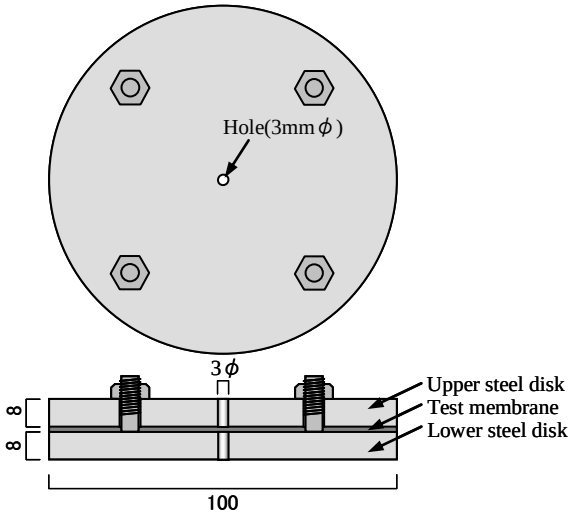

Figure 2. Membrane fixing disk (Unit:mm).

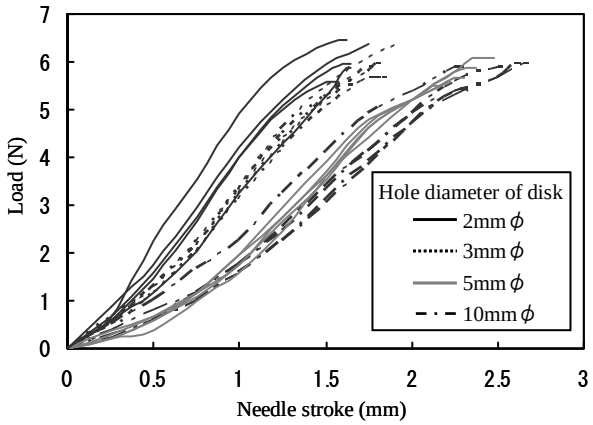

Figure 3. Relation between load and needle stroke at various diameter of disk in needle penetration test（PVC membrane: 0.5mm thick, Needle tip diameter: 0.3mm., Stroke rate: 1.0mm/min）

2.4 Test Procedure

As shown in Figure 4, the needle tip was pressed onto a waterproofing membrane, while measuring the load and the needle stroke. The penetrating speed of the needle was 1.0 mm/min for ease of testing. Also, as most waterproofing membranes are polymeric materials and are affected by temperature, tests were conducted partially at three levels, 10, 20, and 30 ℃, while the test temperature assuming the soil temperature was basically set at 20℃. Five specimens were tested for each type of waterproofing membrane.

3 MEASUREMENT OF PENETRATING LOAD

3.1 Tested Waterproofing Membranes

For the purpose of developing a test method, it is necessary to obtain data using, to the extent possible, a wide variety of waterproofing membranes having different mechanical properties. Tested membranes included the following: five mixes of elastic polyurethane rubber/urea resin fluid-applied membranes, five thicknesses of PVC sheet-applied membranes, and five types of EPDM sheet-applied membranes with and without reinforcement of different compositions. The types and mechanical properties of these membranes are listed in Table 1. Not all of these materials are available on the market. Some were specially manufactured as trial products for this study.

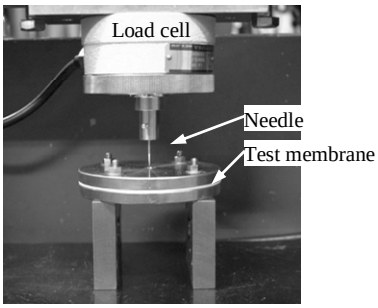

Figure 4. Test apparatus for measuring needle penetrating load.

Table 1. Test membrane.

Membrane	Sample Name	Thickness (mm)	Strength at peak*	Strength at break* (N/mm^2)	Elongation at break* (%)
Polyurethane fluid-applied membrane	PU-1	3.2	-	4.3	520
	PU-2	3.1	-	11.8	595
	PU-3	3.2	-	14.1	370
	PU-4	3.5	-	19.9	136
	PU-5	4.2	-	22.5	29
PVC sheet-applied membrane	PVC-1	0.1	-	22.0	232
	PVC-2	0.2	-	24.7	272
	PVC-3	0.5	-	12.0	223
	PVC-4	1.5	-	13.3	247
	PVC-5 (reinforced by glass fiber mesh)	1.5	101.8(N/mm)	82.9(N/mm)	232
EPDM sheet-applied membrane	EPDM-1	1.0	-	10.5	523
	EPDM-2	1.4	-	10.1	502
	EPDM-3 (reinforced by glass fiber mesh)	1.5	66.3(N/mm)	65.8(N/mm)	405
	EPDM-4 (reinforced by polyester fiber mesh)	1.4	122.0(N/mm)	51.0(N/mm)	453
	EPDM-5 (reinforced by polyester nonworen cloth)	1.5	-	55.7(N/mm)	374

* Date are shown as the averaged value of five specimens obtained from tensile test at 100mm/min.

3.2 Measurement Results

Figure 5 shows the measured penetrating load of simulated needles with a tip diameter of 0.1, 0.3, and 0.5 mm. Figure 6 shows the results at different test temperatures. Note that measurement was terminated when the needle tip punctured the membrane or when the load exceeded 50 N.

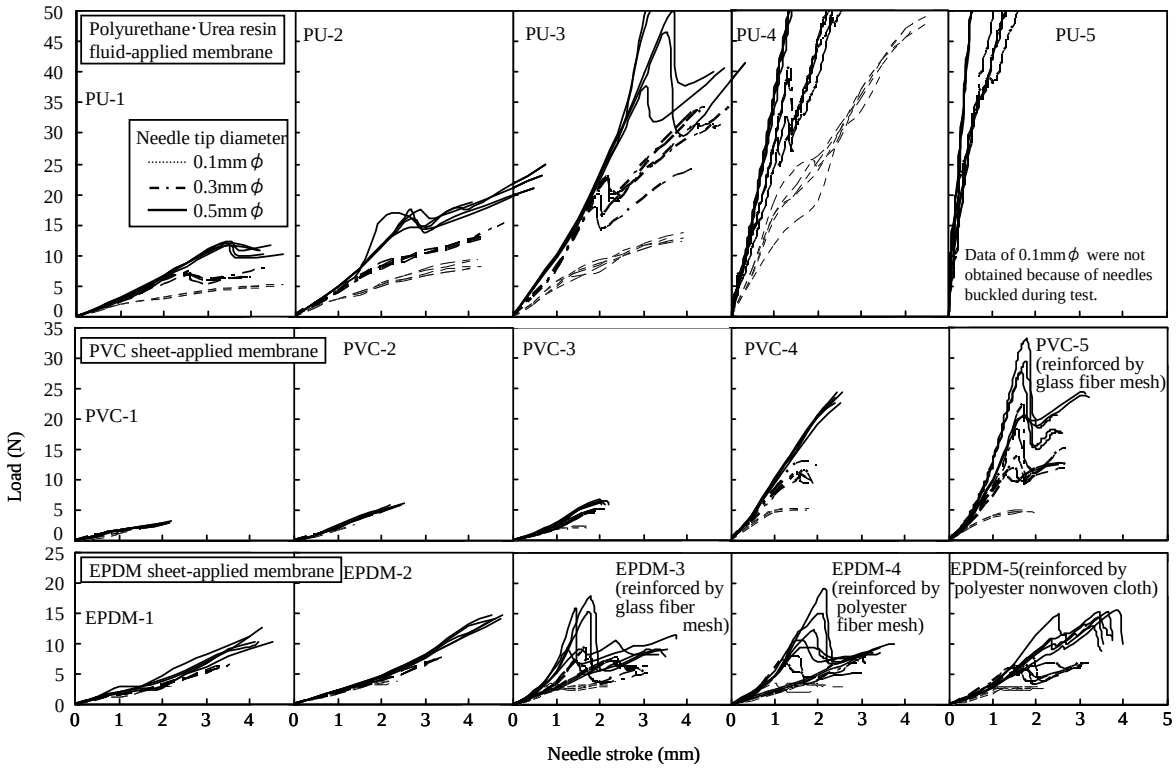

Figure 5.Load-needle stroke behavior at various needle tip diameters in needle penetration test.

3.2.1 Load-Stroke Relationship

The load increased as the needle penetrated into the waterproofing membrane. For most membranes, the load peaked when the needle tip pierced through the membrane and immediately decreased thereafter. The load behaviour tended to be complicated when the needle tip penetrated into thick membranes, such as urethane rubber/urea resin liquid-applied membranes, presumably because of the side surface of the needle coming into contact with the membrane. Also, for PVC and EPDM reinforced membranes, the load did not drop immediately after the peak but slowly decreased.

3.2.2 Effect of Needle Tip Diameter

In regard to the size of needle tips, which were worked into hemispheres, the peak load tended to increase as the needle tip diameter increased. However, the load behaviour of needle tips penetrating into reinforced membranes tended to be complicated presumably due to friction and interruption by reinforcement in membranes during penetration.

3.2.3 Effect of Temperature

Within the temperature range of this study, the load slightly tended to increase as the temperature decreased. However, no marked difference in the load was observed in the region of small strokes in which the penetration of actual roots and rhizomes causes problems.

This may be because the temperature range of 10 to 30℃ could not cause significant changes in the mechanical properties of membranes.

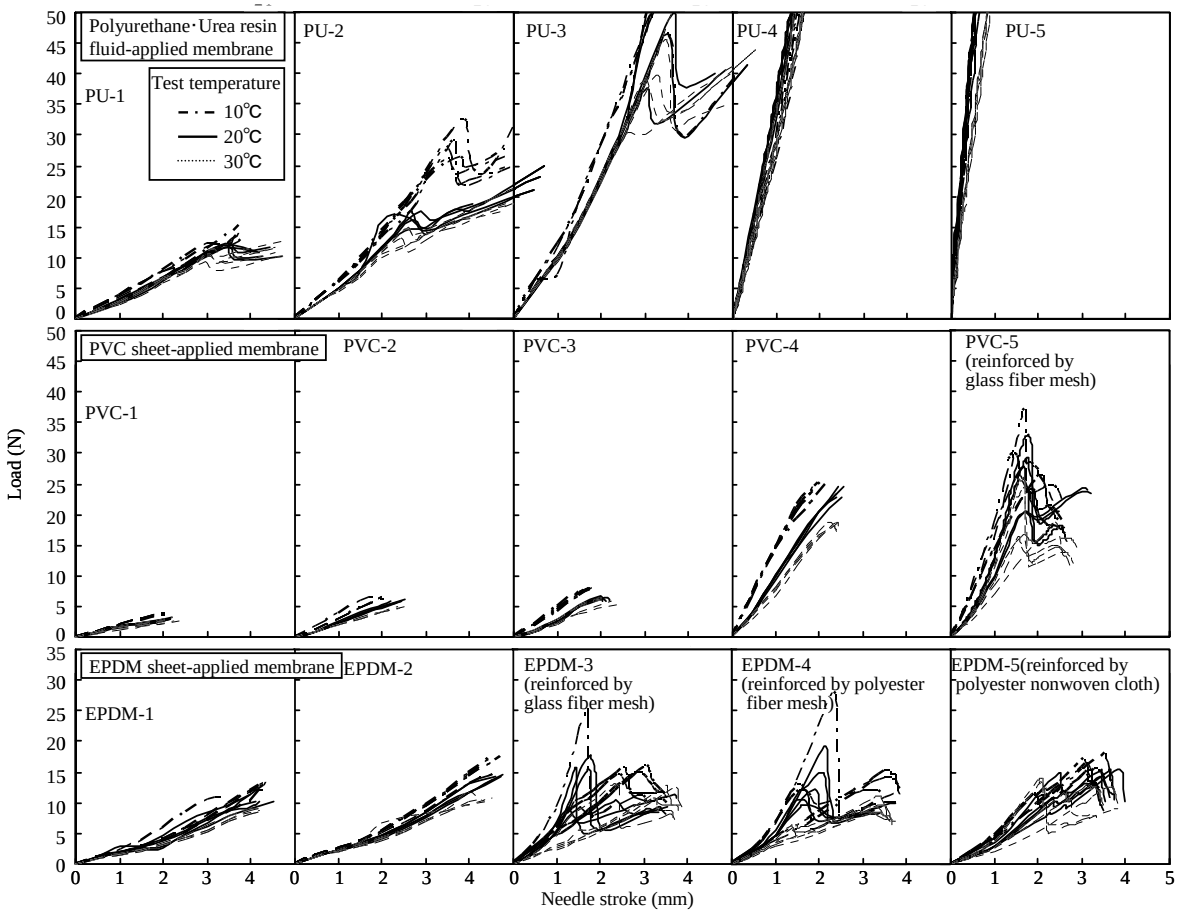

Figure 6. Load-needle stroke behavior at various temperature in needle penetration test.

4 ROOT RESISTANCE TESTS USING ACTUAL PLANTS

4.1 Test Plants

Bamboo grass and lawn grass were used again.

4.2 Specimens

A specimen consisted of an inner container, which was made of punched metal with many holes 20 mm in diameter, a test waterproofing membrane, and an outer container as shown in Figute 7. Soil was placed on the membrane to plant the grass, as well as between the inner and outer containers to let the roots and rhizomes that would penetrate through the membrane and holes grow out without being interrupted.

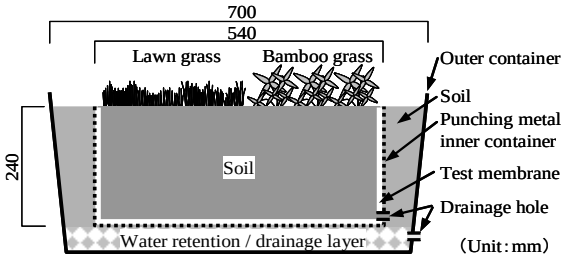

Figure 7. Test apparatus of investigateresistance.

4.3 Test Procedure

4.3.1 Specimen Preparation

A waterproofing membrane was laid on the inside of each inner container made of punched metal. As for the liquid-applied material, a box-shaped membrane was produced beforehand in a laboratory so as to fit into the inner container. Soil was then placed in the container, in which bamboo grass and lawn grass was planted. The inner container with the plants was then embedded in an outer container containing soil.

4.3.2 Growth Control of Plants

As shown in Figure 8, the specimens were placed in a greenhouse, which was not air-conditioned but was under rough temperature control by shading from the sunlight and ventilation, and watered according to the plant condition so as to let them grow well.

Figure 8. Specimens in greenhouse.

4.3.3 Observation of Specimens

During the test period, each inner container was periodically removed from the outer container to observe the state of root/rhizome penetration through the sides and bottom of the membrane. After observation, the container was fitted back into place to continue testing. Observation was carried out for a year from July 27, 2004 to July 27, 2005.

4.4 Test Results

Figures 9 and 10 show the test results. In the root systems of bamboo grass and lawn grass, which comprise rhizome portions and root portions, only the rhizome portions punctured some of the waterproofing membranes. Generally speaking, puncture by bamboo grass was observed at earlier times than by lawn grass. The rhizomes of plants more often penetrated through softer or thinner membranes.

When examined in more detail, however, the order of time to penetration does not necessarily agree with the order of the thickness of membranes. For instance, a PVC sheet-applied membrane 0.5 mm in thickness was punctured by bamboo grass earlier than the same membrane 0.2 mm in thickness, and an EPDM sheet-applied membrane 1.5 mm in thickness was punctured but the same membrane 1.0 mm in thickness was not punctured. Detailed observation by dismantling the specimens after a year revealed that, in specimens with non-punctured membranes, rhizomes were bent at the membrane surfaces and grew along the membranes thereafter. Whether rhizomes penetrate the membranes or bend at the membrane surfaces appears to depend on the relative strengths of rhizomes and membranes. These vary due to the fact that the penetrating forces vary form one rhizome to another in actual plants. Generally speaking, however, soft membranes tended to be punctured more than hard membranes.

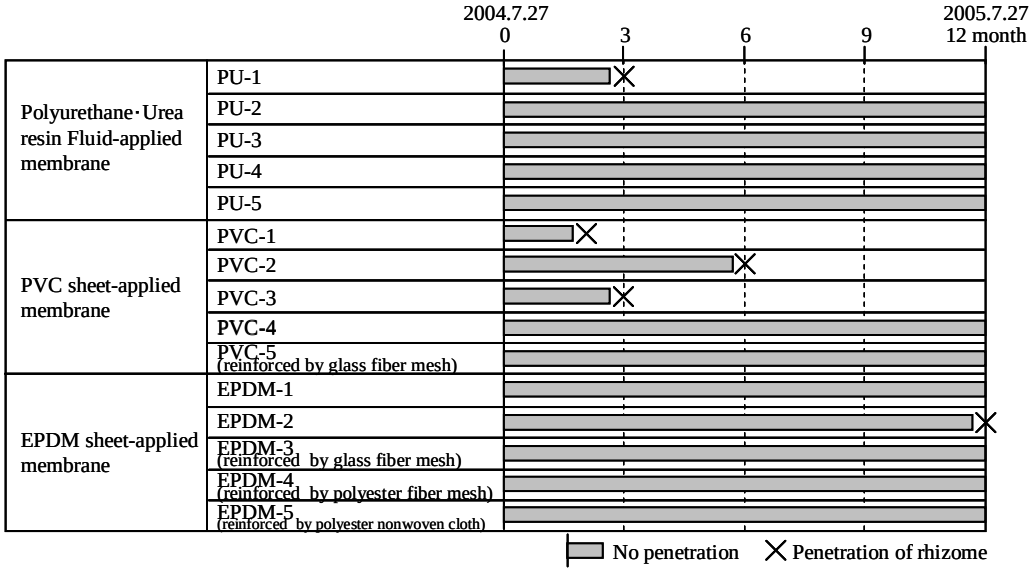

Figure.9 Results of resistance test to root/rhizome penetration(Bamboo grass).

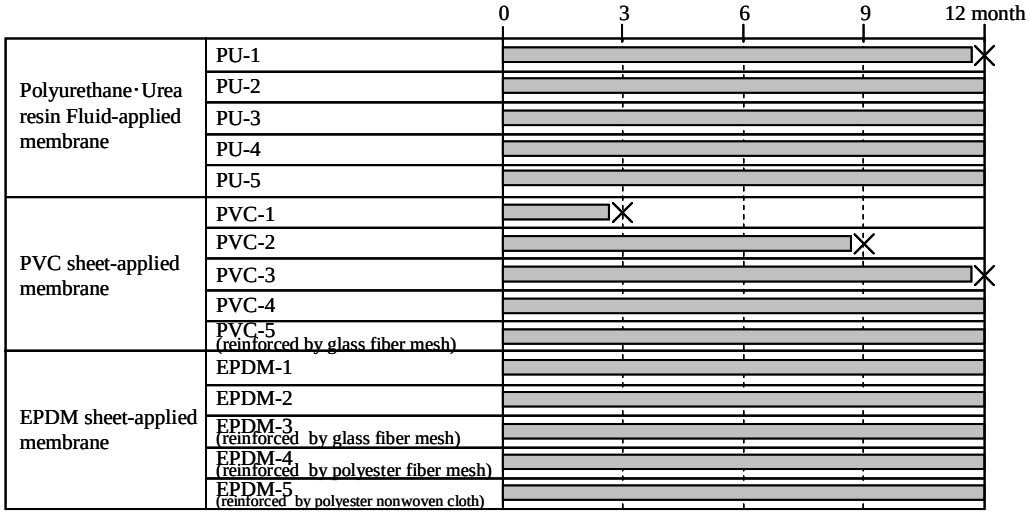

Figure.10 Results of resistance test to root/rhizome penetration(Lawn grass).

5 DISCUSSION

Various physical values in the penetration tests of waterproofing membranes using simulated needles were compared with root resistance test results by using actual plants. The load-stroke curves up to 50 N were organized in the four values such as the maximum load, load at 1.0 mm of needle stroke, maximum needle stroke at penetration, and deformation energy to penetration (i.e., area under the load-stroke curve to penetration) as shown in Figure 11. The results of membranes punctured by actual plants are shown in black in the figure.

5.1 Relationship between Maximum Load and Root Resistance Test Results

When the needle tip diameter was 0.1 mm, five membranes with a maximum load of 4.9 N or less were penetrated by testing using actual plants. However, four membranes with a maximum load lower than this remained intact. When the needle tip diameter was 0.3 mm and 0.5 mm, membranes with a maximum load of 7.2 N and 14.3 N, respectively, were penetrated. Membranes with maximum loads lower than these were all penetrated excepting two types in both cases. These maximum penetrating

loads of simulated needles 0.3 mm and 0.5 mm in diameter can therefore be utilized as an index of root resistance evaluation.

5.2 Relationship between Load at 1 mm of Needle Stroke and Root Resistance Test Results

With a needle tip diameter of 0.1, 0.3, and 0.5 mm, membranes with a load at 1 mm of needle stroke of 2.1, 2.7, and 2.9 N or less, respectively, were penetrated by rhizomes in testing using actual plants, excepting only one type of the EPDM sheet-applied un-reinforced membrane. The load at 1 mm of needle stroke appears to strongly correlate with the root resistance and also be usable as a measure of root resistance evaluation for waterproofing membranes.

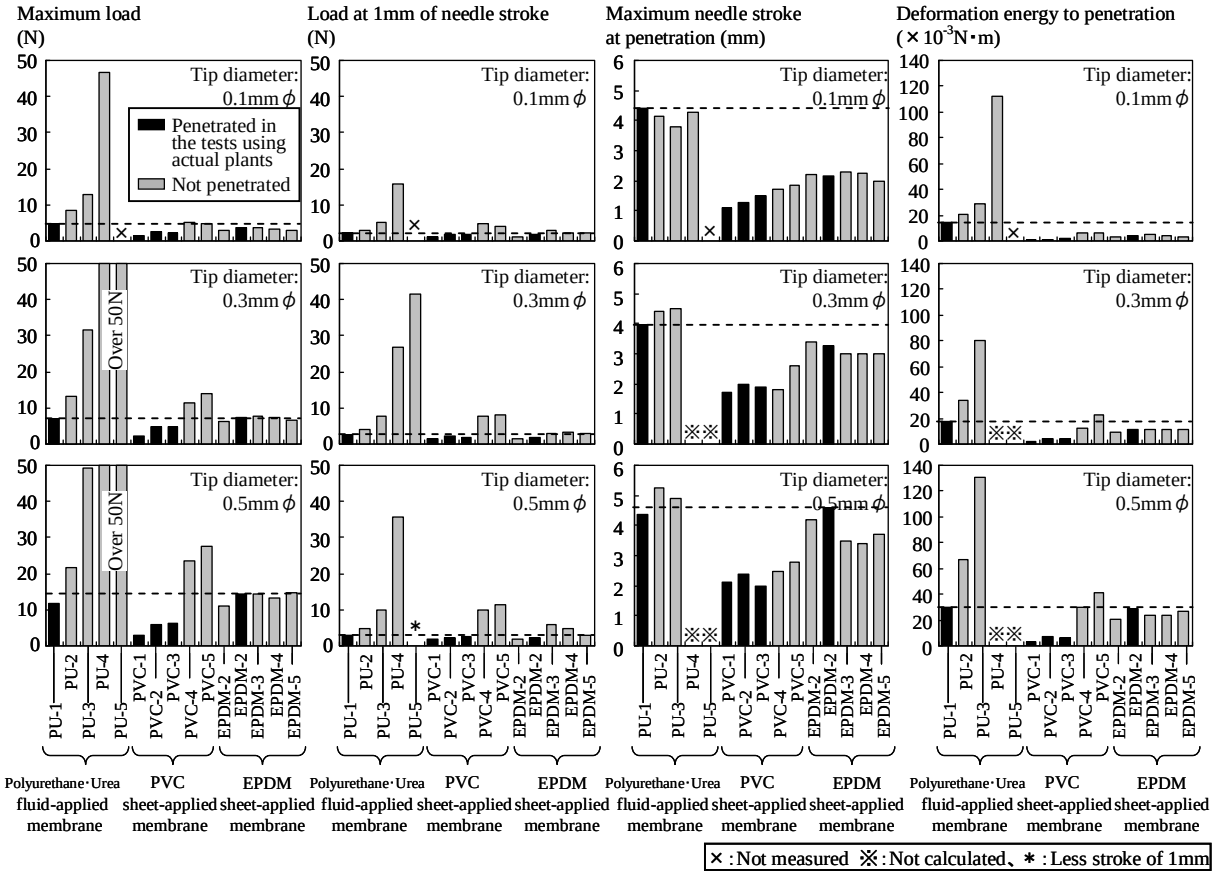

Figure 11. Various physical values obtained from needle penetration test and 1year result of root enetration test for bamboo grass.

5.3 Relationship between Needle Stroke at Penetration and Root Resistance Test Results

It is difficult to draw a line by a specific value of the needle stroke at penetration, and no correlation with the test results is observed.

5.4 Relationship between Deformation Energy to Penetration and Root Resistance Test Results

Membranes with a deformation energy to penetration of 14×10^{-3} N·m, 18×10^{-3} N·m, and 30×10^{-3} N·m were penetrated by rhizomes when the needle tip diameter was 0.1, 0.3, and 0.5 mm, respectively. However, 6, 5, and 4 membranes with a deformation energy to penetration lower than these remained intact with the needle tip diameter of 0.1, 0.3, and 0.5 mm, respectively. This parameter is therefore not likely to be usable as an index of root resistance evaluation.

Judging from all these results, the load at 1 mm of needle stroke and the maximum load may be used as rough indices of root resistance evaluation. Simulated needles with a tip diameter of 0.3 and 0.5 mm are particularly correlated with the root resistance test results. Nevertheless, it is also necessary to consider the effect of factors other than mechanical breakage in regard to penetration of the tips of root systems, such as chemical effects of acid secreted from root systems. Therefore, it is desirable to use this test method for the purpose of screening for root resistance evaluation.

6 CONCLUSIONS

The conclusions of this study are as follows:

(1) A simple test method for root resistance evaluation was proposed using needles simulating the rhizome tips of bamboo grass and lawn grass.
(2) The load required to penetrate various waterproofing membranes were measured by this test method to elucidate their load-stroke relationships.
(3) Root resistance tests were conducted using actual bamboo grass and lawn grass. Rhizomes penetrated thin or soft membranes.
(4) The results of penetration tests using simulated needles and root resistance tests using actual plants were compared. The maximum load and load at 1 mm stroke with needle tip diameters of 0.3 and 0.5 mm were found usable as simple indices of root resistance evaluation for waterproofing membranes, such as for screening of these materials.

REFERENCES

DIN 4062: *Testing the Weed Resistance of Everlast-Roofskin.*

P.Fischer., R.Bohlen., R.Klein., J.Lieseche., G.Losken., P.Siegert., W.Tebart & R.Walter., 2002. *Procedure for investigation resistance to root penetration at green-roof sites*; The Landscaping and Landscape Development Research Society e.v.(FLL), January.

11DBMC International Conference on Durability of Building Materials and Components
ISTANBUL, Turkey 11-14 May 2008

Condensation Problems in Cool Roofs

Christian Bludau [1]
Daniel Zirkelbach [2]
Hartwig M. Künzel [3]

T 22

ABSTRACT

In some regions of the United States so called cool roofs have become mandatory in order to save cooling energy in summer and it is expected that these roofs will also become more widespread in other parts of the world. A cool roof uses a bright surface to reflect incident solar radiation which significantly lowers the day-time surface temperature compared to conventional roofs with bituminous felt. However, since most energy savings measures involve some sort of moisture related issue, the question is whether the widespread application of these roofs may lead to durability problems. There are already rumors that the so-called self-drying roofs that do not have a vapor barrier might face moisture accumulation when equipped with a reflective surface, because the solar vapor drive helping to dry out the roofs during summer time is diminished.

In order to clarify this important durability issue experimentally verified hygrothermal simulations have been carried out on light-weight flat roofs with and without reflective surface layer. Because the long-wave radiation to the sky is an important factor for the night-time roof temperature and thus also for the risk of interstitial condensation, the sky radiation has been measured as part of the meteorological data collection at the field test site in Holzkirchen. Together with continuous surface temperature recordings of different roofs these meteorological data have been used to validate the new radiation exchange model of a hygrothermal simulation tool. Afterwards a typical light-weight cool roof has been selected and its moisture behavior simulated under different outdoor conditions. The results show that severe moisture accumulation will only occur in colder regions of Europe and North-America. However, among these regions there are also some where cool roofs could be beneficial for cooling energy savings.

KEYWORDS

Cool roof, Interstitial condensation, Nightime radiative cooling

[1] Fraunhofer Institute for Building Physics, Department of Hygrothermics, Fraunhoferstr. 10, 83626 Valley, Germany Phone +49 8024 643 290, +49 8024 643 366, christian.bludau@ibp.fraunhofer.de
[2] Fraunhofer Institute for Building Physics, Department of Hygrothermics, Fraunhoferstr. 10, 83626 Valley, Germany Phone +49 8024 643 229, +49 8024 643 366, daniel.zirkelbach@ibp.fraunhofer.de
[3] Fraunhofer Institute for Building Physics, Department of Hygrothermics, Fraunhoferstr. 10, 83626 Valley, Germany Phone +49 8024 643 345, +49 8024 643 366, hartwig.kuenzel@ibp.fraunhofer.de

1 INTRODUCTION

In order to build energy efficient buildings nowadays it is very important to optimize the building envelope. The roof provides a large part of the envelope so it is obvious to try saving energy at this area. There are already some approaches and solutions to save energy by building a so called 'cool roof'. A cool roof uses a bright surface to reflect incident solar radiation which significantly lowers the day-time surface temperature compared to conventional roofs with bituminous felt. Cool roofs bring along the risk of moisture accumulation in colder regions of Europe and North America due to the reduced surface temperature during the day. Furthermore the long wave radiation can lead to overcooling of the surface beneath the ambient temperature. Such low temperatures during the night can cause the temperature to drop beneath the dew point followed by condensation of moisture in the construction. New simulation models are able to consider this effect.

2 FUNDAMENTALS

2.1 Cool Roofs

The temperature occurring on a roof depends on several factors. When the solar radiation hits the roof's surface, a part is reflected, another is absorbed. A part of the received energy is emitted back to the sky as infrared radiation. Another part of the heat is exchanged with the environment by convection. The remaining heat flows through the roof and interacts with the room. This heat flow depends on the temperature gradient between the roof surface and the interior temperature, the thermal conductivity and the thickness of the construction materials (e.g. insulation) of the roof. Unlike conventional roofs, cool roofs keep a moderate temperature even during hot summer days by having a higher solar reflectance and higher thermal emittance than conventional roofs. Many publications, especially from the United States, talk about cooling energy savings of up to 25%.

2.2 Self Drying Roofs

Self-drying roofs are designed to eliminate accumulation of moisture in the construction. The occurring moisture can dry out to the interior of the building (downward drying). The construction is usually sealed to the outside by a roofing membrane acting as water and vapor barrier. In the interior the construction consists of an insulation core made from materials which do not rapidly degrade mechanically in the presence of moisture. To the inside no vapor retarder is used to guaranty the possibility to dry out. The interior finish can be formed for example by a gypsum board in habitations or profiled sheeting in industrial buildings. A widespread research about self-drying roofs was performed by Dejarlais [Desjarlais *et al.* 1995 and 1998].

3 CALCULATIONS

3.1 Climatic Data

For the studies performed at the Fraunhofer Institute for Building Physics in Holzkirchen measured climatic data are used. The climate at Holzkirchen is representative for a critical climate situation in Germany. At the institute's weather station many kinds of metrological data are collected. To carry out these investigations the following data have a significant influence. The surface temperature on black and white surfaces (measured since 1998), the global, diffuse and west radiation (measured since 1987) and the atmospheric counter radiation (measured since 2002). A further experimental setup was built up in 2007, to research the influence of the night time long wave radiation in detail.

3.2 Hygrothermic Simulations

A validated method for simultaneous calculation of heat and moisture transport in building components WUFI® [Künzel 1994] was used for the simulations in this paper. As boundary conditions the climatic reference data (hourly values) from the investigated location was used. This file contains hourly values for temperature, humidity, rain, wind, solar-, atmospheric radiation etc.. For the interior climate the specifications from EN 15026 [2007] for 'normal moisture load' was used. The interior conditions are shown exemplary for Holzkirchen in Fig. 1. In this standard the indoor conditions are derived from the outdoor climate. Depending on the outdoor air temperature the indoor conditions vary between 20 and 25°C, respectively 30 and 60% RH. The material properties needed to perform the calculations are taken from the WUFI material database.

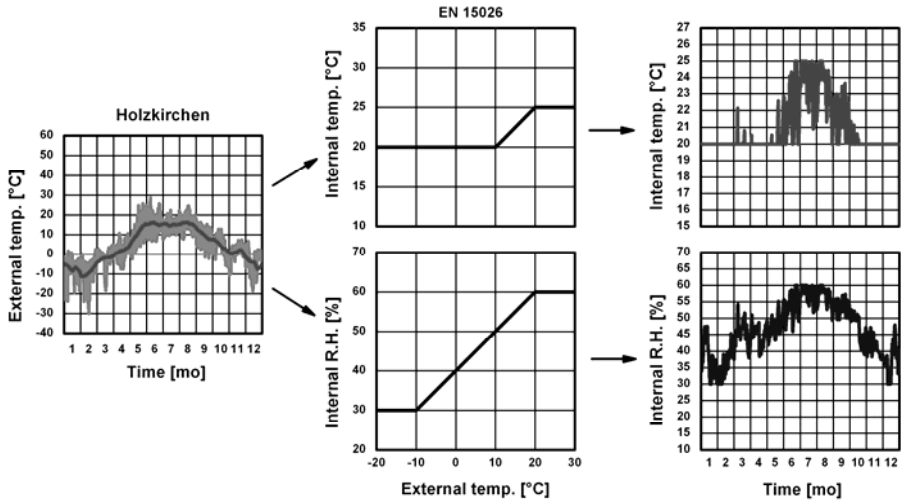

Figure 1. Example of the used interior conditions for the calculation in Holzkirchen derived from the outdoor temperature according to EN 15026 [2007].

3.3 Comparision of Measurement and Calculation Using An Explicit Long-Wave Radiation Model

For validating of an explicit long-wave radiation model in WUFI® [Kehrer and Schmidt 2006] many calculations where performed. This model considers an explicit exchange of the long wave radiation while in earlier applications the radiation effects were only lumped together with the convective heat transfer coefficient. In this section only one example is shown comparing measurement with calculation. In this case a flat roof is considered, built up with mineral wool insulation and sealed with an elastomeric bitumen roofing sheet covered with dark red colored mineral granules.

In Fig. 2 the measured surface temperature of the flat roof is displayed in blue. The red line is the temperature calculated by WUFI® using the measured ambient air temperature (green graph) as boundary conditions and the radiation values collected by the weather station. The surface temperature values are in a range of -10°C to 50°C while the air temperature only show values between -3°C and 20°C. Surface temperatures below ambient air temperature are due to long-wave radiation to the clear sky at night. The calculation shows a good accordance to the measured values; the lower temperatures during night time as well as the higher temperatures during day are captured. The days between the second and fifth November during which the calculation shows a much higher temperature than the measurement, the roof was covered with snow. The model does currently not take into account the effect of snow.

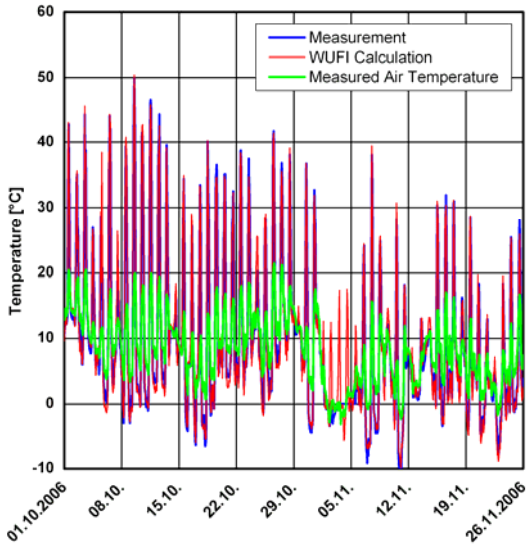

Figure 2. Comparision between measuremnet and calculation.

3.4 Self-Drying Flat Roofs in North America

The considered self-drying roof is built up as shown in Fig. 3. To the outside it is sealed by a roofing membrane, to the inside the construction is completed with profiled sheeting. The interior is filled with foam insulation (Polyisocyanurate).

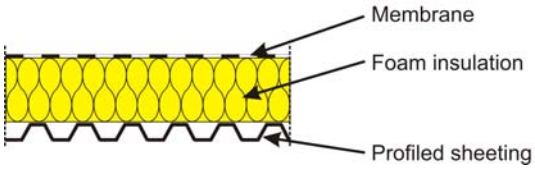

Figure 3. Composition of the self-drying roof.

The simulations were carried out for different locations in North America to find out, if there is a problem using a reflective layer on a self-drying roof. Phoenix (Arizona) was selected as warm location, Chicago (Illinois) as temperate location and Anchorage (Alaska) as cold location. The following parameters were used for the calculation: Vapor permeability of the profiled sheeting was set to s_d=3.3m (1US perm – equivalent diffusion resistance considering perforations and joints) according to Desjarlais [1995] and for the roofing membrane to s_d=1000m. The short-wave absorption factor for a white surface is 0.2 and for a black surface is 0.88. For the long-wave emission ε=0.9 is used. The calculation starts at the first of October and is continued for five years to see if a moisture accumulation will occur. The simulations results are compared by examining the total water content in the construction. If a water content of more than 0.5kg/m^2 occurs there is a risk of water dripping out of the construction. Furthermore the annual average of the moisture content should not increase over time.

The temperatures at the examined locations are shown in Fig. 4. The curves displayed in gray are hourly values of the temperature; the black curve is the floating monthly average. Comparing the average curves, in Phoenix the temperature ranges between 10 and 35°C with minimum temperatures of 0°C and maximum values of about 45°C. In Chicago the average temperature fluctuates between -9 and 23°C with minimum values of about -22°C and maximum values of about 34°C. The average temperature in Anchorage lies between -12 and 15°C with minimum values of -29°C and maximum values of 24°C.

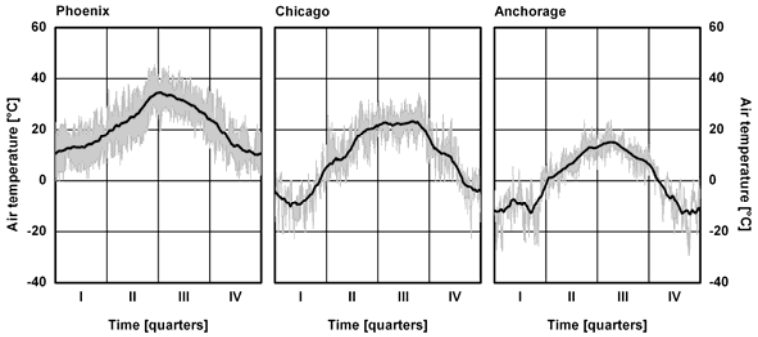

Figure 4. Air temperature in Phoenix, Chicago and Anchorage. The gray line are hourly values, the black line shows the floating monthly average.

The temporal variations of the total moisture content in the construction are displayed in Fig. 5. For the warm location Phoenix the total water content reaches up to 0.05 kg/m^2 in case of the white surface. The roof with the black surface stays dry almost all year. Concerning the roof in Chicago, a difference between the black and the white surface is recognizable. The bright roof reaches a total water content of about 0.3 kg/m^2, the dark roof about 0.1 kg/m^2. At the cold location Anchorage the roof with the dark surface shows maximum total water content of 0.35 kg/m^2 while the roof with the white surface is not able to dry out during the summer time. An accumulation of water over the years is clearly visible.

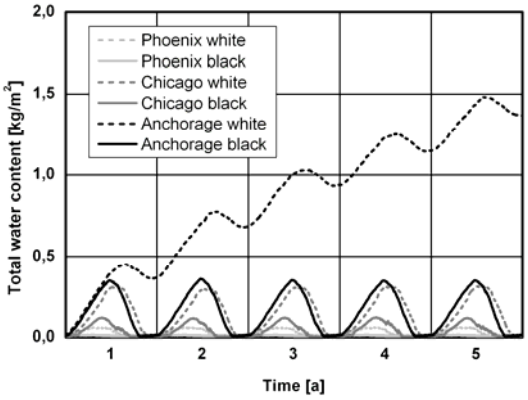

Figure 5. Total water content flat roof at different locations with white and black surface.

The self-drying roof works in most locations independent of the applied surface color under the conditions that the only source of moisture is vapor diffusion from the interior. Only in locations with low average temperatures moisture accumulation due to a bright surface color cannot be ruled out.

3.5 Bright and Dark Flat Roof in Holzkirchen

For the following comparison of the influence of the different surface colors on the moisture behavior a flat roof which is typical for European constructions is considered.

The composition is shown in Fig. 6. The roof is constructed with mineral insulation between wooden rafters, sheeted by an OSB panel and is sealed with an elastomeric bitumen roofing sheet. This roofing sheet is calculated with a radiation reflecting white surface (absorption factor 0.2) and a typical used black surface (absorption factor 0.88). The long-wave emission factor ε=0.9. To the inside the construction is closed using a vapor retarder (s_d=2m) and a gypsum board. In this example the insulation layer has a thickness of 200mm.

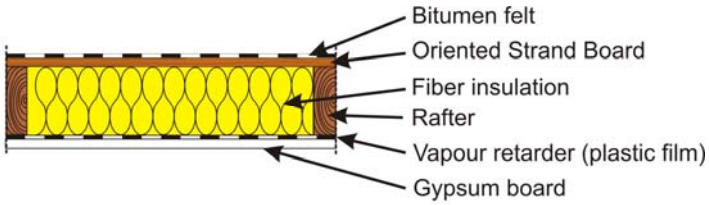

Figure 6. Composition of the flat roof.

For the calculations the Holzkirchen climate data are used. For the interior conditions 'normal occupacy' is assumed according to EN 15026 [2007] (see also paragraph 3.2). The calculation starts at the first of October and is performed for five years to see if a moisture accumulation will occur.

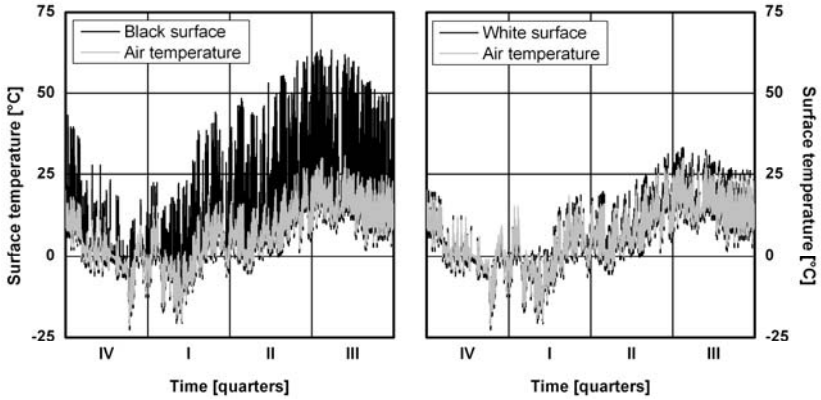

Figure 7. Comparision of black and white roof surface temperature and air temperature in Holzkirchen.

The calculated surface temperatures are shown in Fig. 7. On the black surface maximum temperatures of about 60°C develop. The fluctuation of the white roof temperature is similar to that of the ambient air temperature, with maximum values of about 30°C. On both roofs there is some overcooling below the outdoor temperature.

The cold time during night and winter is the crucial factor for vapor diffusion into the roof. If there is no sufficient drying during daytime or summer moisture accumulation can occur.

Fig. 8 shows the development of moisture in the OSB layer beneath the roofing membrane. Using a bright roof membrane the construction cannot dry out due to the reduced temperatures during the day. During night time moisture is permeating into the construction and leads to an increasing accumulation of water in the OSB layer. The moisture penetrating during winter cannot dry out during the summer time due to the reduced solar heat gain.

After five years a water content higher than 26M.-% will occur and it is still increasing. The moisture content in the wood over 20M.-% is considered to be critical because it may lead to degradation of the material. The roof with the dark sheeting shows a much better behaviour, the moisture content of the OSB layer varies between 11 and 16M.-%.

These calculations show the problems of using bright, energy saving roof sheeting in areas with cold winters. Before using such bright membranes for this kind of construction the moisture behaviour should be checked by hygrothermal simulations using the regional climate conditions.

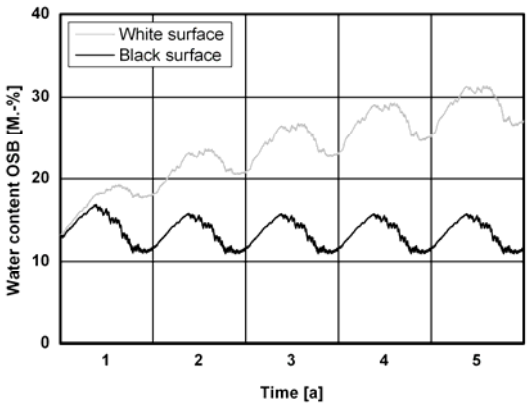

Figure 8. Comparision of the development of moisture in the OSB layer under a black and white roof sheeting in Holzkirchen.

3.6 Bright and Dark Flat Roof at North American Locations

The same construction shown in chapter 3.5 was investigated using North American climate conditions. As locations Phoenix, Chicago and Anchorage are selected again (annual temperature variations see Fig. 4). The calculations were performed for white surfaces and only if the moisture content in the OSB layer exceeded the limit of 20M.-% the simulations were repeated for black surfaces.

Figure 8 shows the water content developing in the OSB layer depending on the surface color. The white surface in Phoenix shows moisture contents between 11 and 16M.-%. In this warm region the flat roof works with every surface color.

The flat roof in Chicago reaches values between 17 and 23M.-% in the OSB sheet. For this reason the roof with the black surface is simulated as well. The black surface in Chicago leads to a water content of 10 to 15M.-%. In Chicago such a construction should be built up with a dark surface to avoid damage by accumulating moisture.

In Anchorage the white roof shows a fast increase of the average moisture content in the OSB layer signifying that such a roof will fail. If a black roofing membrane is used the moisture in the OSB layer ranges between 14 and 20M.-% which is just below the critical limit. A brighter color can not be recommended for this location.

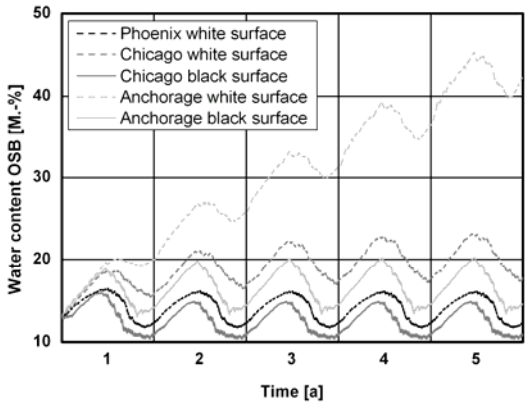

Figure 9. Comparision of the development of moisture in the OSB layer roof sheeting in North America.

3 CONCLUSIONS

Self drying roofs with foam insulation can be applied with all kind of surface colors in most parts of Northern America. Only in regions with very cold ambient temperatures there is a risk of moisture accumulation especially in case of using a bright surface. Bright roof sheeting is saving cooling energy during hot summer days. Using this sheeting at temperate climatic locations an accumulation of moisture can occur in constructions where a vapor retarder is applied at the interior side.

If a cool roof is designed for a temperate or cold climate its moisture behavior should be analyzed by hygrothermal simulations in order to avoid critical water content in the construction. If necessary a darker color of the roof surface should be considered.

REFERENCES

Desjarlais, A., 1995, *Self-Drying Roofs:What ?! No Dripping!*, Conference Proceedings of the Thermal Performance of the Exterior Envelopes of Buildings VI, 1995, Cleawater, FL, pp. 763-773.

Desjarlais, A. O., Petrie, T. W., Childs, P. W. and Atchley, J. A., 1998, *"Moisture studies of a self-drying roof: tests in the large-scale climate simulator and results from thermal and hygric models"*, Thermal Performance of the Exterior Envelopes of Buildings VII, Clearwater Beach, Florida, pp. 41-54.

EN 15026, 2007, *Hygrothermal performance of building components and building elements – Assessment of moisture transfer by numerical simulation*; European Committee for standardization, Brussels.

Kehrer, M., Schmidt, T., 2006: *Temperaturverhältnisse an Aussenoberflächen unter Strahlungseinflüssen*, Proceedings BauSIM2006, 9.-11. Okt., TU München, Germany.

Künzel, H.M. 1994, *Simultaneous Heat and Moisture Transport in Building Components. One- and two dimensional calculation using simple parameters.* Dissertation Universität Stuttgart 1994.

WTA-Guideline 6-2-01/ E 2004, *Simulation of heat and moisture transfer*. Fraunhofer IRB Verlag, ISBN 978-3-8167-6827-2.

11DBMC International Conference on Durability of Building Materials and Components
ISTANBUL, Turkey 11-14 May 2008

Design of Mineral Fibre Durability Test Based on Hygrothermal Loads in Flat Roofs.

Daniel Zirkelbach [1]
Hartwig M. Künzel [2]
Christian Bludau [3]

T 22

ABSTRACT

The durability of mineral fiber insulations depends to a large extent on coinciding temperature und humidity conditions within these materials. Existing test procedures use combinations of rather extreme temperature and humidity conditions above 60 or 70 °C and 95 to 100 % RH. However, these test conditions lead to a significant reduction of the mechanical strength of glass fiber insulation materials which cannot be observed in real life. Subject of this work is to evaluate these loads in light-weight flat roofs with mineral fiber insulation and dark roofing membranes. Therefore a test roof was built up at the field test site of the Fraunhofer IBP in Holzkirchen (alpine region of Germany, 680 m a.s.l.). The solar radiation and the night sky radiation at this altitude lead to rather extreme temperature conditions in the test roof. In order to achieve the most unfavorable humidity conditions within the insulation two liters of water per m² were inserted to the roof before closing the construction. The measured conditions in the roof serve also to validate hygrothermal simulation results which allow in a second step to “transfer” the test roof to other locations in northern and southern Europe. Thus, the most extreme temperature and moisture conditions likely to occur in the glass fiber insulation layer of light-weight flat roofs can be determined. A material test procedure for durability assessments should accelerate the normal degradation process but not make fail a solution which performs well in reality. Therefore, new test conditions are proposed which are closer to the conditions occurring in real life while still allowing the normal aging process to be accelerated. The result will be a more realistic decrease of the material strength compared to the present procedures.

KEYWORDS

Mineral fiber insulation, Mechanical strength, Roof, Durability test procedure

[1] Fraunhofer-Institut of Building Physics, Department Hygrothermics, 83601 Holzkirchen, Germany, Phone +49 8024 643229, Fax +49 8024 643366, zirkelbach@hoki.ibp.fraunhofer.de
[2] Fraunhofer-Institut of Building Physics, Department Hygrothermics, 83601 Holzkirchen, Germany, Phone +49 8024 643245, Fax +49 8024 643366, kuenzel@hoki.ibp.fraunhofer.de
[3] Fraunhofer-Institut of Building Physics, Department Hygrothermics, 83601 Holzkirchen, Germany, Phone +49 8024 643290, Fax +49 8024 643366, cbludau@hoki.ibp.fraunhofer.de

1 INTRODUCTION

To assess the durability of mineral fibre insulation there are currently several different laboratory tests available, e.g. Nordtest, DUR2 (prEN 14509), Florida test. All these tests have in common that the hygrothermal conditions are rather extreme which often cause durability problems for glass fibre insulation products. While it makes sense to perform tests which allow an acceleration of the natural degradation process, it is also important to ensure that tests do not make products fail that perform well in reality. Therefore the hygrothermal conditions prevailing during these tests should not exceed the temperature and humidity conditions in real life by far. An acceleration of product aging can still be achieved by prolonging the duration of peak loads derived from field tests.

The aim of this study is therefore to determine test conditions that allow an acceleration of the natural aging process without damaging the insulation product in a way that will never occur in reality. The testing conditions have to be backed up by results from field tests and validated hygrothermal simulations to develop the basis for new test methods with more realistic temperature and humidity conditions.

2 INVESTIGATIONS

2.1 Field Test

Subject of this study are the measured and simulated hygrothermal conditions in an insulated flat roof with the following composition from inside to outside:

- Load bearing wooden sheathing
- Vapour barrier (aluminium foil, s_d > 1500 m)
- Insulation layer: 90 mm respectively 175 mm glass fibre boards
- Impermeable roofing membrane (elastomer bitumen)

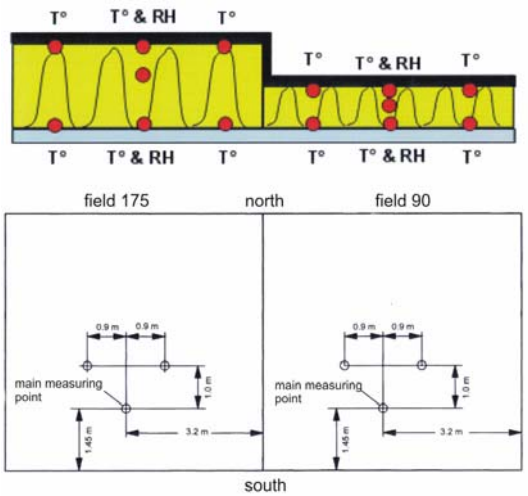

Figure 1. Sensor positions in the test roof (side and top view). The data recorded at the centre positions are used for validating the hygrothermal simulations.

A schematic drawing of the flat roof construction with the measurement positions is displayed in Fig. 1. The placement of the sensors at the positions where peak loads are expected has been selected according to preliminary calculations. The temperature measurements are performed by using PT100 temperature sensors. The relative humidity is determined by capacitive sensors. Prior to the installation, all sensors are calibrated in the laboratory. The roof was set up at the field test site of the Fraunhofer Institute for Building Physics (IBP) in Holzkirchen (South Germany) in August 2006.

In order to get an extreme scenario with a high initial moisture content about 2 kg/m² of water are added to the glass fibre insulation. It is expected that this moisture will be trapped in the construction between the vapour barrier and the vapour-tight roofing membrane. With the temperature variations during changing seasons or during a night and day cycle the moisture is expected to migrate between bottom and top of the insulation.

2.1 Hygrothermal Simulations

The hygrothermal simulations are performed by applying WUFI® [Künzel 1995], which allows the transient calculation of the coupled heat and moisture transport in building components under real climate conditions. The model was developed at the Fraunhofer Institute for Building Physics and has been experimentally validated by comparison with numerous field tests. For the mineral wool a moisture retention curve based on the paper by Peuhkuri *et al.* [2005] and adapted to fit the measured results was used. The other material parameters are taken from the WUFI® database. As outdoor conditions the measured climate from August 2006 to January 2007 in Holzkirchen including solar radiation and long wave sky radiation from the atmosphere is used. As indoor climate serve the recorded temperature and humidity conditions in the attic space beneath the flat roof. The time period for which experimental and calculation results are compared lasts from August 2006 to January 2007.

If a good agreement between measurement and calculation in Holzkirchen can be achieved, the investigation may be broadened by repeating the simulations with climate conditions at other locations. The selected locations are Copenhagen in Denmark representing a Northern European climate and Naples in Southern Italy representing the warm regions of Europe. The meteorological data sets for Copenhagen and Naples are taken from the ASHRAE [2001] climate data which were compiled for building energy calculations. While the climate of Copenhagen appears to be mild compared to Holzkirchen, Naples shows higher air temperatures but not much difference in peak radiation. The indoor climate is assumed to be the same at all locations. According to the WTA-Guideline 6-2 [2004] sinusoidal curves between 20 °C / 40% RH in winter and 22 °C / 60 % RH in summer represent the indoor conditions in residential buildings with normal moisture load. However, since the roof is water and vapour tight the humidity conditions are rather irrelevant.

3 RESULTS

3.1 Field Test

The field test described above is still ongoing - for the current paper a time period of six months from August 2006 to January 2007 is analyzed. The temperatures during the winter 2006 / 07 were quite moderate with only little snow. There were only a few days with temperatures below -5 °C while in a normal cold winter the temperatures can drop to -20 °C at times. The measured temperature and relative humidity within the construction are shown and discussed in comparison with the calculated results in the Figs 3 to 5. In the result diagrams the three sensor positions located at the centre of the roof sections are labelled from outside to inside with “exterior”, “middle” and “interior”.

3.2 Comparision of Calculation and Experiment

Figure 2 shows the measured (blue curve, sensor beneath the roofing membrane) and calculated (red curve) surface temperature of the roof with 90 mm insulation layer. The agreement between the two curves is very good - only sometimes the peak values show a small difference of two or three degree Celsius. The comparison with the outdoor air temperature (black curve) shows the strong influence of solar radiation (energy source during day-time) and sky radiation (energy sink during night-time) which is accurately captured by the new model for radiation and surface heat exchange in WUFI® version 4.1.

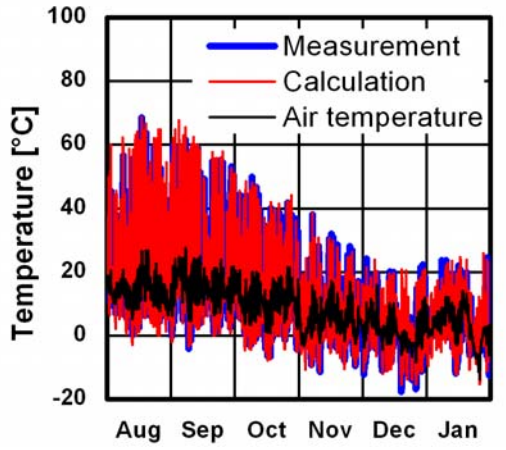

Figure 2. Comparison of measured and calculated exterior surface temperature variations of the roof with 90 mm insulation and the outdoor air temperature at Holzkirchen.

Figure 3 shows the relative humidity at the three positions within the insulation layer. The overall agreement between measured and calculated curves is quite acceptable. At the exterior position of the insulation the calculated and the measured curves coincide rather well. This is important, since the most extreme temperature and humidity conditions in the insulation layer are observed at the exterior sensor. In summer the RH at this position varies between 20 % at noon (when the sun shines and heats up the exterior surface) and 100 % during night. With lower temperatures and shorter days in autumn and winter the RH at noon increases and remains from midmonth of November permanently at 100 %. At the middle and the interior positions of the insulation layer the mean progression of the curves is very similar, but the spread of the measured values is slightly larger to both directions compared to the calculation. This difference may be due to a remaining uncertainty concerning the material properties (sorption isotherm, vapour diffusion resistance) of the glass fibre boards or the assumption of the initial water content in the roof.

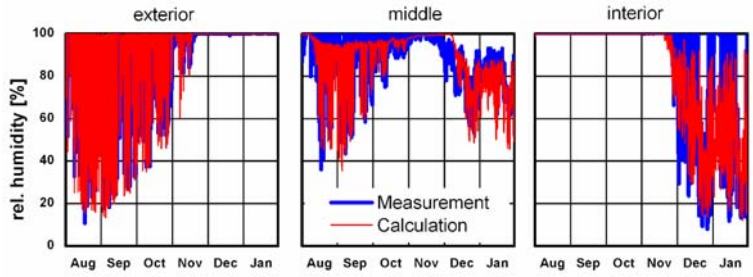

Figure 3. Comparison of measured and calculated relative humidity variations at the three sensor position in the roof with 90 mm insulation under the indoor and outdoor climate conditions recorded during the test in Holzkirchen.

A more detailed plot of the hygrothermal conditions for two single weeks in summer and winter (Fig. 4) at the exterior sensor position confirms the generally good agreement between simulation and experiment. The deviation in surface temperature on Dec. 20 is due to a thin snow cover of the roofing membrane which is disregarded in the simulation. An important observation concerning the durability assessment of the glass fibre insulation is the opposed variation of temperature and RH beneath the surface of the roofing membrane in Fig. 4. Every time, the temperature rises the relative humidity measured res. calculated for the same position drops in an inverse manner. That means high temperature and high RH never coincide at this point.

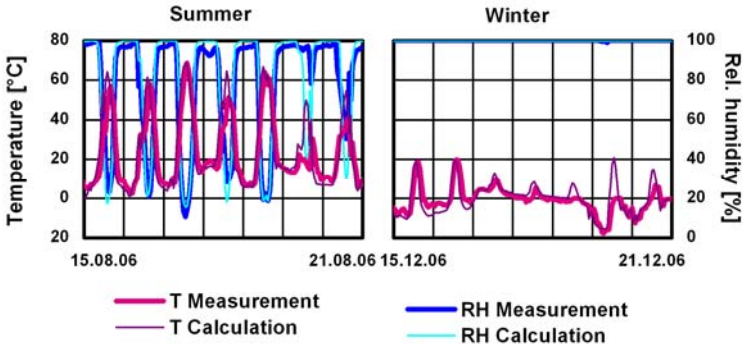

Figure 4. Comparison of measured and calculated temperature and humidity variations at the exterior sensor position in the roof with 90 mm insulation for two selected weeks in August and December.

The results of the roof with 175 mm insulation layer show less severe hygrothermal conditions with similar good agreement between measurement and calculation. Therefore these results are not plotted and discussed in this paper.

3.3 Evaluation of Peak Conditions

Laboratory test have shown that the coincidence of high temperature and high humidity has a significant degradation effect on glass fibre insulation. Under dry conditions, a high temperature doesn't do any harm and a high relative humidity is not a great problem as long as the temperature remains low. Therefore, the measured and calculated hygrothermal conditions in the roof are displayed in a special graph where temperature and humidity are plotted against each other for time intervals of one hour. Such a graph is shown in Fig. 5 for the three sensor positions in the roof with 90 mm thick insulation. The highest temperatures with more than 60 °C (maximum 70 °C) occur at the exterior position beneath the roofing membrane. However, the coinciding RH values remain very low, between 10 % and 30 %. The maximum RH of 100 % is frequently reached at all sensor positions. While the coinciding temperatures stay around 20 °C at the bottom of the roof (interior position) they can reach a maximum of nearly 40 °C in the middle and upper parts of the roof. The limit curve that will not be exceeded at any position in the insulation layer of the investigated roof can be drawn as a straight green line from 40 °C / 100 % RH to 80 °C / 0 % RH.

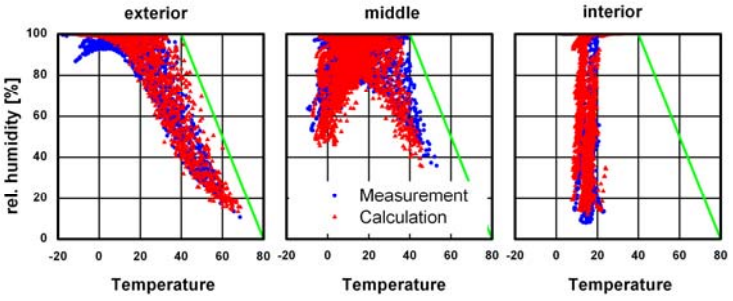

Figure 5. Coinciding temperature and humidity conditions on an hourly basis measured and calculated at three sensor positions in the roof with 90 mm insulation. The green line represents the limiting curve for the hygrothermal conditions determined for the climate conditions in Holzkirchen.

The selected locations for the further hygrothermal simulations are Copenhagen and Naples. The plot of the calculated hourly RH plotted over temperature at Copenhagen is displayed in Fig.6. The results are very similar to the data of the flat roof in Holzkirchen (Fig. 5). However, the Copenhagen results for the exterior position come a bit closer to the limit curve (green line) and go even slightly over the limit a couple of times.

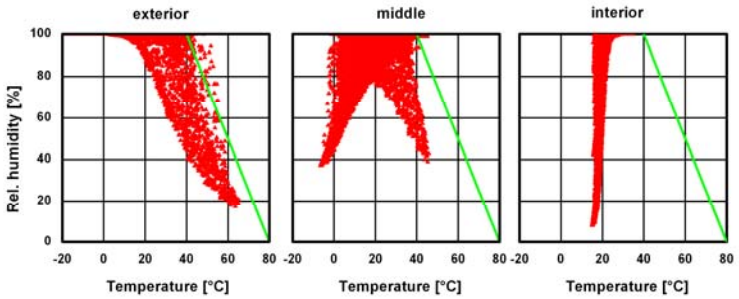

Figure 6. Coinciding temperature and humidity conditions on an hourly basis calculated at three monitor positions within the roof with 90 mm insulation located in Copenhagen. The green line represents the limiting curve defined in Fig. 5.

In order to obtain more detailed information the coincident temperatures and relative humidities are classified in steps of 10 % RH starting with 50 % and steps of 10 K between -10 and +80 °C to analyse the different peak levels. The accumulated results are listed in Table 1. About 7700 hours a year a RH between 90 % and 100 % prevails, more than 3200 hours thereof at a temperature range between 0 and 10 °C and 1600 between -10 and 0 °C. In the higher temperature ranges the hours where RH exceeds 90 % become increasingly scarce. At Copenhagen the temperature within the construction never exceeds 70 °C. A temperature above 40 °C and a coincident relative humidity of above 80 % occurs during about 90 hours a year - this represents only 1.0 % of the service life of a roof.

Table 1. Hourly classification of the simultaneous RH and temperature at the exterior position of the flat roof with 90 mm of glass fibre insulation for Copenhagen.

Temperature °C	*Relative Humidity* [%]					
	0 - 50	50 - 60	60 - 70	70 - 80	80 - 90	90 - 100
< -10						189
-10 - 0						1634
0 - 10						3262
10 - 20					1	1618
20 - 30			8	47	86	640
30 - 40	16	48	86	61	74	305
40 - 50	143	67	52	52	35	49
50 - 60	197	14	7	6	3	2
60 - 70	56					
70 - 80						
>80						

The same hygrothermal analysis is repeated with the climate data for Naples. The relative humidity over temperature plot is displayed in Fig. 7. Compared to Copenhagen the values show a similar distribution - only the maximum temperature level in summer is 15 K higher but with a lower humidity of just about 10 % RH.

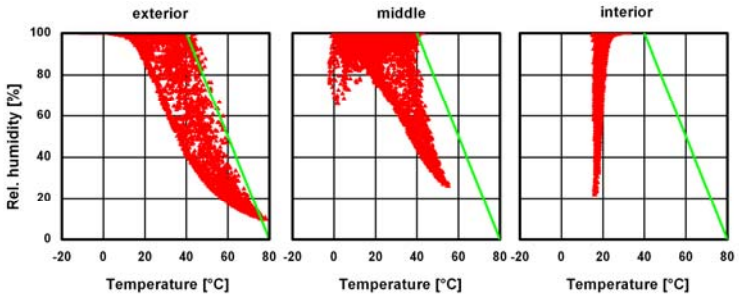

Figure 7. Coinciding temperature and humidity conditions on an hourly basis calculated at three monitor positions within the roof with 90 mm insulation located in Naples. The green line represents the limiting curve defined in Fig. 5.

The hourly classification of temperature and humidity in Table 2 shows with about 6600 fewer hours between 90 and 100 % RH than the locations further north. Due to the higher surface temperature in summer the RH decreases faster during day. Most frequent in Naples are with about 2700 hours conditions from 90 to 100 % RH combined with a temperature between 10 and 20 °C followed by 2200 hours with the same RH at temperatures between 0 and 10 °C. Values above 80 % RH and 40 °C occur during less than 100 hours - so apart from the higher temperatures of 80 °C the number of hours in a higher range of RH and temperature differs hardly from the situation in Copenhagen.

Table 2. Hourly classification of the simultaneous RH and temperature at the exterior position of the flat roof with 90 mm of glass fibre insulation for Naples.

Temperature °C	*Relative Humidity* [%]					
	0 - 50	50 - 60	60 - 70	70 - 80	80 - 90	90 - 100
< -10						11
-10 - 0						599
0 - 10						2177
10 - 20					26	2659
20 - 30			37	56	166	778
30 - 40	41	108	53	67	110	348
40 - 50	240	80	83	41	49	48
50 - 60	384	26	10	4		
60 - 70	409					
70 - 80	148					
>80						

4 CONCLUSION

The measured conditions in the flat roof in Holzkirchen as well as the simulation results for locations in northern and southern Europe show, that a RH above 95 % in combination with a temperature of more then 60 °C will never occur in a vapour permeable insulation material like mineral fibre - even if there is a high initial water content in the roof of about 2 kg/m². The simultaneous occurrence of humidity conditions above 80 % RH and maximum temperatures between 40 and 50 °C at the most critical position within the insulation layer of a flat roof (beneath the roofing membrane) does generally not exceed 100 hours a year under European climate conditions. It should be noted that these conditions do not prevail continuously for several subsequent hours and they do not affect the entire insulation layer. They represent only short peaks that happen under particular weather situations at the most exposed part of the insulation layer, the zone directly below the roofing membrane. Other parts of the glass fibre boards experience less severe conditions.

It is therefore proposed to define new durability test conditions based on the study presented here. Both the experimental results and the simulations have shown that coinciding peaks of temperature und relative humidity ranging from 40 °C to maximum 50 °C res. from 80 % to 100 % (average 90 % RH) add up to less than 100 hours per year. Consequently, there is good reason to set the durability test conditions to 50 °C and 90 % RH. However, the question concerning the duration of such test remains. Field tests periodically checking the durability of mineral fibre insulation in external wall insulation systems have shown that the greatest loss in pull-off strength happens in the first few month of service life. After that period the mechanical properties remain stable [Zirkelbach *et al.* 2005]. Continuous exposure of mineral wool to constant test conditions in the laboratory may show a slightly different picture (e.g. [Franke & Deckelmann 1999]), but they do not reflect the permanently altering hygrothermal conditions in the real world. The field tests indicate that there are periods (probably those with dominantly dry conditions) where the insulation material seem to recover its strength. This cannot happen during prolonged laboratory tests with constant peak conditions lasting 1000 hours or more. Thus, a test period in excess of the summed-up intervals of peak conditions occurring during a year in a real flat roof do not make much sense. It is therefore proposed to limit the test period to one week which is still on the safe side compared to the 100 hours of peak conditions actually occurring.

For this conclusion, the long-term performance of glass fibre boards in flat roof constructions is assumed to be comparable to that of mineral fibre boards in external thermal insulation composite systems (ETICS), where the temporal development of the pull-off strength has been determined by field tests. In order to confirm this assumption field tests monitoring the compressive strength of glass fibre insulation in flat roofs should be carried out in future.

REFERENCES

Künzel, H.M.,1995. Simultaneous Heat and Moisture Transport in Building Components. One- and two-dimensional calculation using simple parameters. IRB-Verlag Stuttgart.

Peuhkuri, R., Rode, C., & Hansen, K.K., 2005. Effect of method, step size and drying temperature on sorption isotherms. 7th Nordic Symposium on Building Physics, Reykjavík, pp. 31-38.

ASHRAE: International Weather for Energy Calculations (IWEC) CD-ROM, Atlanta 2001.

WTA-Guideline, 2004. 6-2-01/ E: Simulation of heat and moisture transfer. Fraunhofer IRB Verlag, ISBN 978-3-8167-6827-2.

Zirkelbach, D., Holm, A. & Künzel, H.M., 2005. Influence of temperature and relative humidity on the durability of mineral wool in ETICS. Proceedings 10DBMC, Lyon April, TT2-87.

Franke,L. & Deckelmann, G., 1999. Vergleich der Auswirkungen hygrothermischer Beanspruchungen von Mineralfaserdämmstoffen im baupraktischen Einsatz und unter Laborbedingungen. Proceedings 10th International Symposium for Building Physics, Dresden, pp 587-596.

A Model for Determining Accelerated Ageing Cycles in Durability Research: A Case Study on Continuous Roofing

Maurizio Nicolella [1]
Alba De Pascale [2]

T 22

ABSTRACT

This paper introduces research about a model for determining the experimental ageing cycle in laboratory tests for evaluating durability. The model has been implemented with computer software that uses an algorithm in which the input is comprised of a series of climatic data that was obtained from various national climatic database sources. The model was implemented specifically for evaluating a continuous roofing sub-system, as part of a broader Italian national research project, related to the durability of building components. The Italian national research project has one that encompassed a network of research organisations from the Universities of Brescia, Catania, Milan, Naples, Palermo and Turin. Research on the durability of continuous roofing has typically been based on a comparison between the results from artificial ageing tests (conducted in a laboratory) with those obtained from natural weathering tests on the same sample. The approach taken in this research project was to attempt to simulate - in the laboratory - the environmental actions that roofing sub-systems are typically exposed to, in relation to the various climatic conditions in which they are expected to perform. The computer output derived from an application of the model provides for the duration of laboratory ageing sub cycles - each one representing, and essentially reproducing a climatic season - with respect to temperature, humidity, sunlight radiation, and rainfall to which the sample is subjected. In this way a "virtual year" is obtained comprising four climatic seasons, each having different values for temperature, humidity, sunlight radiation and rainfall. The values to consider in laboratory tests are those, for the region and the time of year, which represent the season in question. The necessary values for implementing the model proposed are fixed and given in the research for three particular contexts (Milan, Naples and Palermo). Actually, a method to compose the cycles test in any climatic context for various kinds of experimentation in laboratory about the simulation of environmental effects on each part of building has been already implemented.

KEYWORDS

Accelerating ageing test, Environmental effect, Re-scaling, Artificial ageing test

[1] University of Naples Federico II, D.IN.E., Naples, Italy, Phone +39 081 7682141, Fax +39 081 7682141, maurizio.nicolella@unina.it
[2] University of Naples Federico II, D.IN.E., Naples, Italy, Phone +39 081 7682141, Fax +39 081 7682141, adepasca@unina.it

1 INTRODUCTION

This paper introduces the first part of a study project (part of a national research on the durability of building components) that was conducted and coordinated by Prof. M. Nicolella,. The Naples part of this research concerned the behaviour of roofing subsystems in specific climatic contexts, estimated by comparing laboratory ageing tests with natural weathering tests on similar samples of roof systems. To obtain successful and suitable laboratory tests, and, therefore, a more reliable re-scaling of data, the research group has defined some specific ageing cycles that simulate the appropriate environmental test conditions. Building from that model, the research group has generalized a system defining the method to determine the ageing cycles to apply in the laboratory for the simulation of every specific environmental context. In this paper, we intend to introduce this model and, in so doing, provide a general method to determine the accelerated ageing cycles in durability research. This effort comes from the lack of standardized approaches in defining accelerated ageing tests.

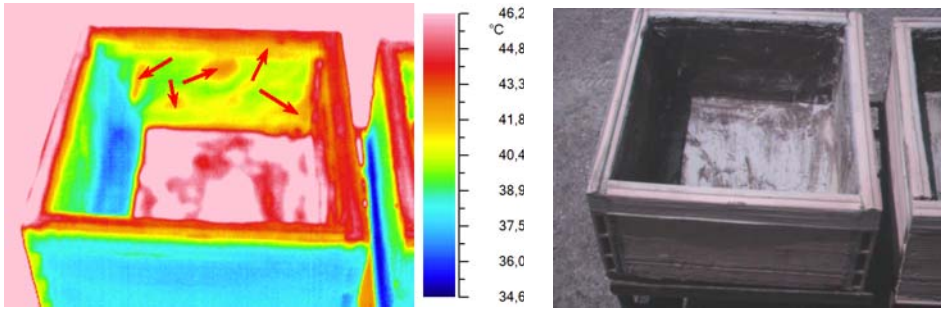

Figure 1. Infrared videothermography inspection on a sample of one of the roofing systems analyzed.

2 IMPORTANCE OF THE STANDARDIZATION OF ACCELERATED AGEING TEST METHODS

Durability standards for building materials and components provide different approaches for estimating service life, but, nevertheless, only generic procedures are given. A general approach is also adopted when determining the service life of components in comparison to results from laboratory ageing with natural weathering tests. For example, the ASTM E 632-82 - "*Standard Practice for Developing Accelerated Test to Aid Prediction of the Service Life of Building Components and Materials*" –one of the most important references on the matter - does not provide a detailed description of the way in which accelerated, or in-service performance testing, should be carried out.

The accelerated ageing tests advocated in this standard have been carried out by imposing higher than normal stress levels on components in order to increase the rate of degradation such that the component will fail within a relatively short period of time in relation to its expected service life. The performance and failure-time data derived from these tests have been analyzed by fitting a degradation model to the data to estimate the relationship between performance, time to failure (age), and stress level.

Although the theoretical procedure introduced in the standard ASTM is very clear, some important and typical shortcomings about the use of accelerated tests to estimate the service life, include:

- Difficulty simulating the degradation mechanisms of the various materials and their interaction;
- Difficulty reproducing the stochastic nature of the degradation factors affecting the building components;
- Difficulty correlating accelerated laboratory test results with the actual in-service results;
- Difficulty defining suitable accelerated ageing tests to reproduce the effects of specific environmental conditions.

Generally, in National and International standards dealing with ageing test methods, as is the case with this ASTM standard, only a limited series of criteria for determining the environmental conditioning cycle is provided. This, in turn, leaves a certain degree of attitude for defining experimental ageing conditions in the laboratory.

On the contrary, we believe, that the obligation to proceed to a re-scaling should influence the conditioning cycle, which must necessarily be differentiated according to the diverse contexts in which the re-scaling occurs. Otherwise, only comparative tests and studies would be possible, through which we could only determine analogous patterns of behaviour between the different ways in which the same element is used. In other words, we do not believe to be reliable a re-scaling performed in significantly different climatic contexts, where a sample is subject to the same artificial action.

On this basis, an attempt was made to design an ageing conditioning cycle which provides an accelerated reproduction of what really occurs to different extents, and in different environmental conditions, to which components may be subjected to over their service life.

3 COMPOSITION OF THE AGEING CYCLE FOR A SPECIFIC TEST CONDITION

The starting point in an attempt to standardize a procedure for the definition of accelerated ageing tests on building components was the need to outline a correct cycle within the national study on roofing sub-systems. We tried to simulate a specific context in the laboratory,, the typical environmental conditions of the city of Naples, and later, we tried to extend and generalize the results by designing a cycle which provides an accelerated reproduction of what occurs in different environmental contexts. This model uses an algorithm in which the input data comprises a series of climatic data which can be obtained from various sources (principally, air force). The output provides the duration of the sub cycles (each one of which represents, and reproduces a climatic season) with the temperatures, humidity, sunlight radiation, and rainfall to which the sample has been subjected. In this way, we obtain a kind of “virtual year”, comprising the four seasons in succession, with different values for temperature, humidity, sunlight radiation, and rainfall, with the values inserted for the region and time of year that represents the season in question (as shown in Table 1 below):

Table 1.

Sub cycle	*Action*	*Value inserted*
Freezing	Temperature Humidity Sunlight radiation Rainfall	Absolute minimum Mean - -
Hot / Dry	Temperature Humidity Sunlight radiation Rainfall	Highest among means Mean Xenon lamp lights -
Hot / Humid	Temperature Humidity Sunlight radiation Rainfall	Absolute maximum 95% Xenon lamp lights -
Rainy	Temperature Humidity Sunlight radiation Rainfall	Lowest among means Mean - Splash or puddling

Climatic data was collected in advance from various official sources, covering a period no longer than the last 5 years, on account of the extreme variability in recent times. The values necessary for implementing the proposed model together with related definitions are given in Table 2 below:

Table 2.

Action	*Value inserted*	*Definition*
Rainfall	Number of rainy days in one year	Value obtained from mean annual value
	Intensity of rainfall	Value obtained from mean annual value
Temperature	Absolute minimum	Value obtained from mean absolute minimum value
	Mean minimum	Value obtained from mean monthly value, calculated as daily mean minimum value, taking lowest value into account
	Absolute maximum	Value obtained from mean absolute maximum value
	Mean maximum	Value obtained from monthly mean value, calculated as daily mean maximum value, taking highest value into account
Humidity	Relative humidity	Value obtained from monthly mean for work for each year
Sunlight radiation	Number of sunny days in one year	Value obtained from annual mean value
	Sunlight radiation hourly trend	Value obtained from annual mean values

It is interesting to note that across the different climate zones in Italy there is little difference between the absolute values for many of the environmental actions.

Two examples suffice to illustrate this point:

- Where absolute maximum temperature is concerned, there is no significant difference between Milan and Palermo. What distinguishes the two contexts is the *number* of days per year in which they reach high temperatures;
- The intensity of rainfall recorded in Naples in the last five years exceeds, to a considerable extent, that of Milan in some winter months.

It so happens that for contexts and climates which differ significantly, the seasonal sub cycles determined have (for example) similar temperatures. It is the length of the segment, or the combined effect of the other environmental actions, which characterizes each context.

The final output generated by special simulation software providing the values for Naples are shown in Table 3 below:

Table 3.

Sub cycle Naples	*Dur.*	*Temp.*	*Hum.*	*Sun rad.*	*Rainfall*
Freezing	6 hrs	4 C°	70%	No	No
Hot / Dry	9 hrs	25 C°	60%	Yes	No
Hot / Humid	9 hrs	40 C°	95%	Yes	No
Rainy	6 hrs	10 C°	75%	No	Yes

The values in the Table are provided in Figure 2 below.

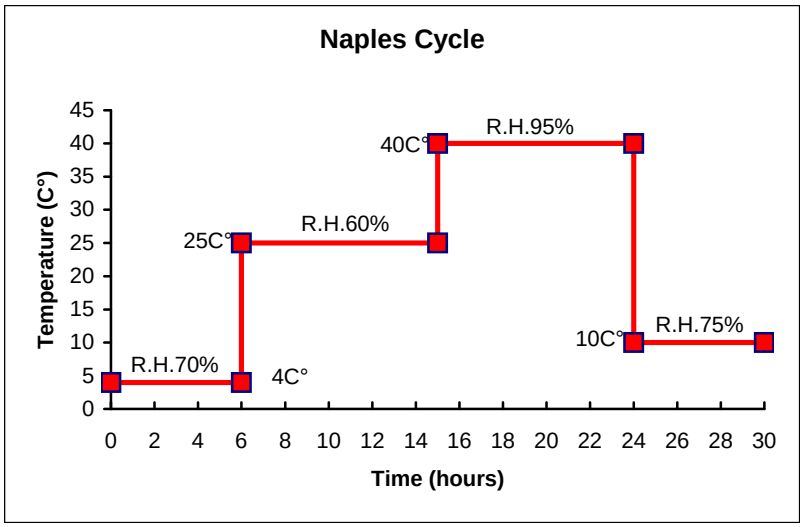

Figure 2. Proposed accelerated ageing conditioning cycle for ageing components in Naples.

4 COMPOSITION OF AGEING CYCLE FOR ANY CLIMATIC CONTEXT

By adopting the criteria previously described, one can develop – as was done for Naples – a simulated cycle for any environment. A schematization has been provided with the options to be exercised by the operator with regard, not only to specifically climatic data (temperature and humidity) but, also, the lamp activation mode in the two heat segments, and, above all, the duration of the various segments in which the sub cycles are contained. Therefore, the process should first be conducted for the individual sub cycles, and then, used as a direct indicator for the selection of climatic data and durations by the user wishing to compile and customize the cycle for the local climatic context. Note that the length of the segments is not only established in relation to climatic data in terms of temperature and humidity, but is also evaluated, as mentioned above, in terms of the longevity of the season in relation to the annual climate. For example, maximum temperatures recorded in the hottest months in Milan are as much as those in Palermo, regardless of the fact that these two locations belong to climatically diverse contexts. What is important is the duration of elevated temperatures, indeed, and the effect on the climatic trend for the entire year. Such periods of oppressive heat in which temperature peaks occur, can vary significantly from location to location. To assist in the schematization of this process, the Italian National Zoning Plan (Italian directive 412/93) has been used, based on the number of degree-days* recorded for the different districts. This directive provides information on the delineation of Italy into 6 subdivisions**. For the present purposes, given the similarities of performance between pairs of subdivisions, they were examined two by two; hence the observed subdivisions include zones A and B, C and D, and E and F , for. By crossing the climatic data (absolute or mean values) with the impact percentage of the reference climatic season for the trend of the climatic year (here illustrated by zones A to F, as determined by the legislation), we will be able to correctly estimate the duration for which the season in question must be schematized in the reference sub cycle.

* The "degree-days" of a designated district are the sum, for all the days in a conventional annual warm period, with the daily positive differences between ambient temperature, conventionally set at 20 degrees centigrade, and the daily mean outdoor temperature; the unit of measurement used is the degree-day (DD).

** The Italian territory is divided into six climate zones according to their degree-days, regardless of their geographic location:

Zone A: districts with degree-days less than 600; Zone B: districts with degree-days between 600 and 900; Zone C: districts with degree-days between 900 and 1,400; Zone D: districts with degree-days between 1,400 and 2,100; Zone E: districts with degree-days between 2,100 and 3,000; Zone F: districts with degree-days greater than 3.000.

In light of the above considerations, the following schematizations are proposed:

Sub cycle A – FREEZE: Definition of climate conditions		
Parameter	*Instruction*	*Value*
Temperature	Enter absolute zone minimum value recorded in period of year represented by season in question	X C°
Humidity	Enter zone mean value for season in question	Y %
Sunlight radiation	Keep lamp switched off from now on	---
Rain	Switch off water	---
Climate zone	Establish zone	Zones A/B/C/D/E/F

Sub cycle A – FREEZE: Definition of length of segments	
Climate zone	*Value*
Zones A/B	4 hrs
Zones C/D	6 hrs
Zones E/F	9 hrs

Sub cycle B – HOT / DRY: Definition of climate conditions		
Parameter	*Instruction*	*Value*
Temperature	Enter the absolute zone mean maximum value recorded in the period of the year represented by the season in question	25 C°
Humidity	Enter the zone mean value for the season in question	Y %
Sunlight radiation	Light lamp for zones A/B/C	Maximum value
Rain	Switch off water	---
Climate zone	Establish zone	Zones A/B/C/D/E/F

Sub cycle B – HOT / DRY: Definition of length of segments	
Climate zone	*Value*
Zones A/B/C	9 hrs
Zone D	6 hrs
Zones E/F	4 hrs

Sub cycle C – HOT / HUMID: Definition of climate conditions		
Parameter	*Instruction*	*Value*
Temperature	Enter the absolute zone maximum value recorded in the period of the year represented by the season in question	X C°
Humidity	Enter a fixed value	95 %
Sunlight radiation	Keep lamp switched on always	Maximum value
Rain	Switch off water	---
Climate zone	Establish zone	Zones A/B/C/D/E/F

Sub cycle C – HOT / HUMID: Definition of length of segments	
Climate zone	*Value*
Zones A/B/C	9 hrs
Zone D	6 hrs
Zones E/F	4 hrs

Sub cycle D - RAIN: Definition of climate conditions		
Parameter	*Instruction*	*Value*

Temperature	Enter the mean zone minimum value recorded in the period of the year represented by the season in question	X C°
Humidity	Enter the zone mean value for the season in question	Y %
Sunlight radiation	Keep lamp switched off from now on	---
Rain	Water	30 mm of water
Climate zone	Establish zone	Zones A/B/C/D/E/F

Sub cycle D - RAIN: Definition of length of segments	
Rainfall band	*Value*
Band 1: less than 50 days/year	4 hrs
Band 2: 50 – 90 days/year	6 hrs
Band 3: over 90 days/year	9 hrs

From these results, we have also developed specific software to automatically compose the seasonal sub-cycles using the criteria introduced above. An image of this software is provided in Figure 3.

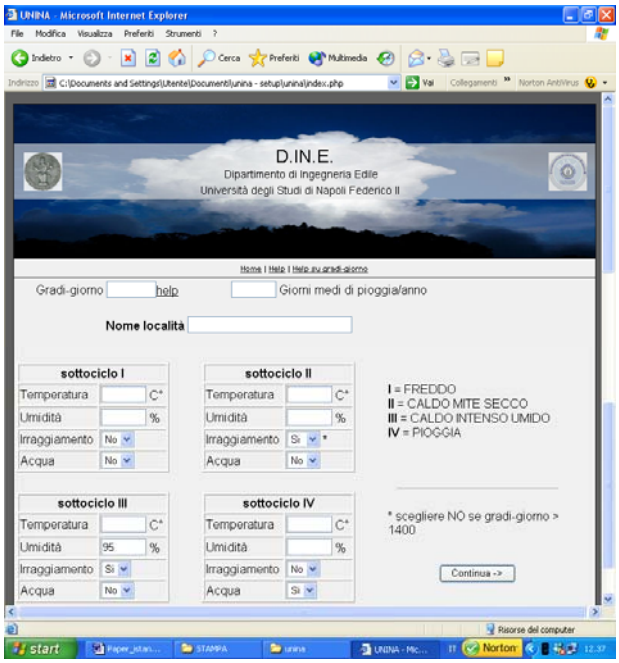

Figure 3. A screen from the software for the automatic composition of accelerated ageing sub-cycles in any climatic context.

5 REFERENCES

ASTM E 632-82, *Standard Practice for Developing Accelerated Test to Aid Prediction of the Service Life of Building Components and Materials.*

BS 7543, *Guide to durability of buildings and building elements, products and components*, BSI, London.

ISO 6241, *Performance standards in building – Principles for their preparation and factors to be considered*, ISO, Geneva.

ISO 15686, *Buildings and constructed assets — Service life planning - Part 1/ Part 2.*

UNI 11156, *Valutazione della durabilità dei componenti edilizi – Part. 1,2,3*, UNI, Milano.

Maggi, P.N., 2003, *Qualità tecnologica dei componenti edilizi*, Epitesto, Milano.

De Pascale, A. Nicolella., M. 2005, *Service life of building components. Analysis and proposals of definition of the modifying factors,* in Atti del 10th International Conference on *Durability of Building Materials and Components,* Lyon (France).

De Pascale, A., 2002, *Modifying factors of a method for estimating service life* in Atti del 9th International Conference on *Durability of Building Materials and Components,* Brisbane Convention & Exhibition Centre, Queensland (Australia).

Jernberg, Sjöström, Lacasse, Brandt, Siemes, 2004, *Guide and Bibliography to Service Life and Durability Research for Buildings and Components*, Joint CIB W080 / RILEM TC 140, CIB Publication, Rotterdam.

Lounis, Z., Lacasse, M.A., Vanier, D.J., and Kyle, B.R., *Towards Standardization of Service Life Prediction of Roofing Membranes*, Roofing Research and Standards Development: 4th. Volume, ASTM STP 1349, T. J. Wallace and W.J. Rossiter, Jr., Eds., American Society for Testing and Materials, 1998.

Nicolella, M., 2006, *La durabilità delle coperture continue*, Ediltecnica srl, Palermo.

Nicolella, M., 2004, *Programmazione degli interventi in edilizia*, UNI, Milano.

Nicolella, M., 2003, *A methodological hypothesis for estimating service life*, in Atti del Convegno Internazionale *Management of durability in the Building process*, Milano 25-26 Giugno.

Nicolella, M., 2002, *Components service life: from field test to methodological hypothesis*, in Atti del 9th International Conference on *Durability of Building Materials and Components,* Brisbane Convention & Exhibition Centre, Queensland (Australia).

Nicolella, M., 2000, *Affidabilità e durabilità degli elementi costruttivi in edilizia*, CUEN, Napoli.

Durability of Clay Roofing Tiles under Salt Mist Atmosphere

Cláudio Cruz [1]
M. Rosário Veiga [2]
Victor M. Ferreira [3]

T 22

ABSTRACT

Clay tiles are largely used in traditional construction in Portugal. In coastal zones some cases of accelerated decay have been affecting the roofing tiles durability, apparently due to the exposition to a salt mist atmosphere. To evaluate the performance of the clay roofing tiles subjected to a sea environment, an experimental study is being carried out based on artificial accelerated weathering tests. The study includes the roofing tiles characterization, the development of accelerated weathering tests, the evaluation of the weathering effect through observation and physical and chemical tests and also the comparison with roofing tiles that suffered natural weathering in coastal zones of Portugal. The study aims at reproducing the pathology mechanisms observed in real conditions, and identifying the parameters - of both composition and manufacture - having a higher contribution to the decay of roofing tiles to provide industry with relevant data to improve the manufacturing process.

This paper presents tests performed on several kinds of tiles and the results obtained regarding soluble salt effects in the specimens' microstructure. Mercury Intrusion Porosimetry (MIP) was used to assess differences in the porous structure. Soluble salt content profiles after weathering were also performed, aiming to determine the depth of salt crystallization.

Accelerated weathering tests can cause different levels of alteration and degradation to ceramic roofing tiles. Hydrophobic tiles may resist longer to salty mist but they can suffer high damage if there is some penetration of salty solution. Tiles present rather diverse porosimetric structures. The concentration of salt crystallization on the outer layers may induce the destruction of thin superficial layers.

KEYWORDS

Durability, Clay roofing tiles, Accelerated weathering tests, Salt mist.

[1] LNEC, Laboratório Nacional de Engenharia Civil, Materials Department, Av. Brasil 101, 1700-066 Lisboa, Portugal, Phone +351 21 844 32 41, Fax +351 21 844 30 23, ccruz@lnec.pt
[2] LNEC, Building Department, Av. Brasil 101, 1700-066 Lisboa, Portugal, rveiga@lnec.pt
[3] UA, Universidade de Aveiro, Civil Eng. Department / CICECO, Campus de Santiago, 3810-193 Aveiro, Portugal, Phone +351 234 370 258, Fax +351 234 370 094, victorf@ua.pt

1 INTRODUCTION

The crystallization of soluble salts is considered one of the main causes for the degradation of porous construction materials [Rodrigues J. D. and Gonçalves T. D. 2006]. To simulate, in the laboratory, the weathering defects due to salty mist, specimens from different types of tiles have been subjected, in a climatic chamber, to artificially accelerated weathering test sets of 10, 20 and 30 cycles of wetting with a salty mist and subsequent drying. The effects of weathering cycles were studied through visual assessment, weight variations and water absorption tests performed before and after weathering. The changes in microstructure were assessed through determination, before and after weathering, of the pore size distribution by Mercury Intrusion Porosimetry (MIP). After weathering, soluble salt content profiles were performed, to determine the depth of salt crystallization.

2 MATERIALS AND METHODS

2.1 Test Specimens

5 specimens from each tile were prepared through transversal cuts. In these tests the specimens cut from the mid transversal area of the roofing tiles were preferentially used, having the width of the tile and circa 9 cm length (Fig. 1). The cut faces of the specimens were sealed with epoxy resin. Roofing tiles from two manufacturers (F1 and F2) were used:

F1 NH - manufacturer 1, model 1, non-hydrophobic red tiles
F1 B - manufacturer 1, model 1, non-hydrophobic white tiles
F1 H - manufacturer 1, model 1, hydrophobic red tiles
F2 NH - manufacturer 2, model 1, non-hydrophobic red tiles
F2 B - manufacturer 2, model 1, non-hydrophobic white tiles
F2 H - manufacturer 2, model 1, hydrophobic red tiles
F2 T2 NH - manufacturer 2, model 2, non-hydrophobic red tiles
F2 T3 NH - manufacturer 2, model 3, non-hydrophobic red tiles

2.2 Artificial Accelerated Weathering Tests

Tests were designed based on the European Norm EN 14147:2003 and adapted to what was thought to be realistic conditions for this product [Cruz et al, 2007]. These tests were carried out in a climatic chamber where the specimens are subjected to sets of cycles of wetting under salt mist atmosphere and subsequent drying, the temperature in the chamber maintained at 35ºC. Salt mist is produced by spraying a salt solution into the chamber with a concentration of 110g of sodium chloride per litre of de-ionised water. The results of two preliminary tests with cycles of 48 h (10 h of salt fog + 38 h of drying) and 24 h (8 h + 16 h) allowed the selection of the 24 h cycles for the final tests. For each type of tiles, one or two specimens were subjected to 10 cycles, another one or two to 20 cycles and three or four to 30 cycles.

Figure 1. Specimens before and during tests.

2.3 Characterization Tests

Before the cycles, the specimens were dried at a temperature of 60ºC to constant mass, as a basis for the weight variations tests. They were also subjected to a water immersion test based on Annex B of EN 539-2:2006, which measures the specimen's weight increase after 48 h of water immersion. For some types of tiles, 'new condition' specimens taken from the same tile as those used for weathering tests, where subjected to Mercury Intrusion Porosimetry (MIP) tests, based on ASTM D 4404 [ASTM 2004], to determine their microstructure.

After weathering and desalinization, specimens of all but one type were subjected to water immersion under vacuum, for characterization purposes. This test, based on EN 1936:1999, measures the weight increase after 72 h of immersion (24 h under vacuum followed by 24 h under water + vacuum and more 24 h under water at atmospheric pressure). Finally, the specimens are weighed twice: once submerged, and after being wiped. This test permits the determination of apparent density, open porosity, and water absorption under vacuum.

2.4 Weathering Effect Evaluation Tests

During the weathering tests, the specimens were visually inspected. After desalinization, they were submitted to water absorption, and samples of some specimens were subjected to Mercury Intrusion Porosimetry. These tests were carried out for comparison of results and evaluation of their sensitivity to the degradation suffered by the specimens. To determine the depth of salt crystallization, salt content profiles were obtained on weathered and non-desalinised samples of two different kinds of specimens, using the hygroscopic moisture content (HMC) method [Gonçalves T. D. and Rodrigues J. D. 2006]. After being submitted to 30 cycles of salt mist wet/drying, one specimen of F2T3NH and another of F2B4 were dry cut and, in this way, two C1 samples were obtained (Fig. 2). In each of the C1 samples 5 layers were marked and from them 5 samples were obtained using sandpaper (from the upper face to the under face: C1 A, C1 B, C1 C, C1 D and C1 E), control samples with sodium chloride by itself and with new tile powder were also used (Fig.3). All the samples were dried at 60ºC and then inserted in a climatic chamber at 20ºC 85%HR, their weights were measured to constant mass and HMC values were calculated.

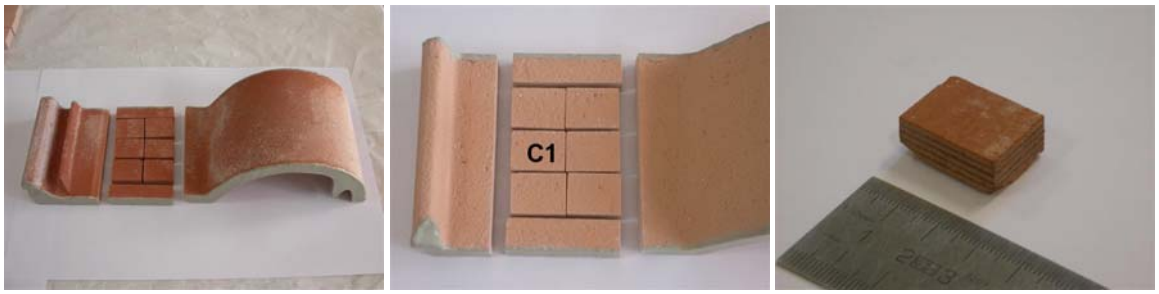

Figure 2. C1 samples.

Figure 3. Grounded layers and control samples.

3 RESULTS

3.1 Visual Assessment, Weight Variations and Water Absorption

Visual inspection results (Table 1) demonstrate different types and levels of degradation caused on the specimens by the weathering tests.

Table 1. Alteration and degradation forms with some examples.

Specimens	*Degradation*	*Examples*
F1 NH	Pitting Granular disaggregation	
F1 B	Pitting Granular disaggregation Peeling	
F1 H	None Bowing Plaques	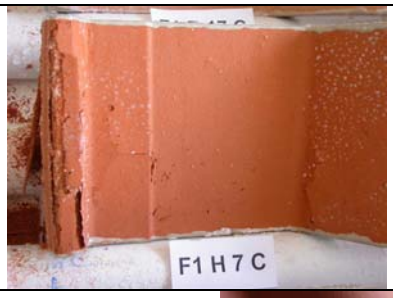 
F2 NH	Pitting Granular disaggregation	
F2 B	Pitting Granular disaggregation Peeling	
F2 H	None	---
F2 T2 NH and F2 T3 NH	Pitting Granular disaggregation Peeling	 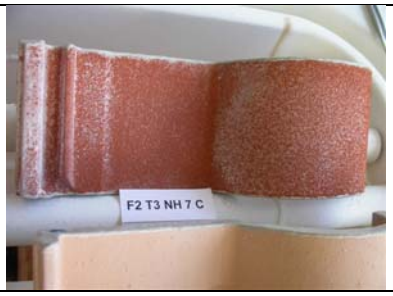

Hydrophobic specimens didn't show immediate defects but some of them suffered huge degradation following the access of the salty solution to the material under the protected surface. Hydrophobic tiles from manufacturer 2 seem to be more resistant to weathering than those from manufacturer 1. Non-hydrophobic tiles, both red and white, showed low to medium degradation levels characterized mainly by pitting, some disaggregation and peeling, with a slightly higher level in the white ones.

In general, weight determinations before and after weathering didn't show significant differences, thus they do not quantify the visual degradation at the present level. However, for white tiles of both manufacturers and some hydrophobic red tiles of manufacturer 1, where degradation is higher, weight loss is more significant.

The results of water absorption under vacuum obtained (Table 2) show that the white tiles present higher porosity and higher water absorption than the red tiles, for both manufacturers. Concerning the red tiles, the water absorption and porosity are higher for those from manufacturer 1. The lowest values concern the hydrophobic tiles from F2 and the model T3 also from F2. There is a significant increase of water absorption after weathering (Table 3) in the hydrophobic red tiles of manufacturer 1 (F1H). For the other specimens, so far the water absorption does not quantify the visual degradation.

Table 2. Water immersion under vacuum test results (characterization tests).

Manufacturers 1 and 2				*Manufacturer 2*			
Specimens	*Apparent density* [Kg/m3]	*Open porosity* [% V]	*Water absorption under vacuum* [% W]	*Specimens*	*Apparent density* [Kg/m3]	*Open porosity* [%]	*Water absorption under vacuum* [% W]
F1NH	2070	23.0	11.1	F2NH	2200	18.4	8.4
F1B	2020	24.3	12.0	F2B	2060	21.8	10.6
F1H	---	---	---	F2H	2200	17.9	8.1
F2T2NH	2130	21.3	10.0	F2T3NH	2210	17.9	8.1

Table 3. Water absorption.

Number of cycles	*Manufacturers 1 and 2*			*Manufacturer 2*		
	Specimens	*Before weathering* [%]	*After weathering* [%]	*Specimens*	*Before weathering* [%]	*After weathering* [%]
10	F1NH	9.34	9.21	F2NH	5.83	5.83
20		9.37	9.26		5.81	5.86
30 (3 spec)		9.22; 9.22; 10.15	9.20; 9.08; 10.03		5.89; 5.90; 6.46	5.86; 5.90; 6.49
10 (1 or 2)	F1B	9.89	9.78	F2B	7.26; 7.26	7.26; 7.25
20 (1 or 2)		9.04	9.00		7.30; 6.80	7.31; 6.83
30 (3 spec)		9.12; 9.59; 9.20	9.07; 9.57; 9.06		7.24; 6.83; 6.79	7.25; 6.84; 6.76
10	F1H	3.89	3.03	F2H	0.58	0.24
20		8.75	10.68		0.57	0.37
30 (3 spec)		4.24; 6.16; 4.31	9.15; 10.00; 8.92		0.61; 1.19; 0.42	0.53; 0.56 ; 0.28
10 (1 or 2)	F2T2NH	8.24	8.17	F2T3NH	5.97; 5.95	5.80; 5.74
20 (1 or 2)		8.31	8.31		6.08; 5.85	5.88; 5.66
30 (3 spec)		8.30; 8.23; 8.20	8.30; 8.22; 8.15		5.68; 5.71; 6.13	5.55; 5.56; 6.00

3.2 Mercury Intrusion Porosimetry

The pore size distributions obtained (Fig. 4) show some differences among the various tiles: the red non-hydrophobic model 1 tiles of both manufacturers F1 and F2 have the largest pores within a very thin range of values (around 0,2-0,5 μm); the white tiles from manufacturer F1 show a large range of pore dimensions, including the finest pores around 0,05-0,09 μm and some larger pores of the range 0,2-0,4 μm; the non-hydrophobic tiles of the model T2 from manufacturer F2 have finer pores than the other non-hydrophobic red tiles (mainly in the range 0,1-0,3 μm).

The curves also show that the deterioration didn't provoke significant changes on the pores dimensions. Possibly, the type of degradation obtained is still rather superficial and only longer tests will produce the rupture of pores due to salt crystallisation.

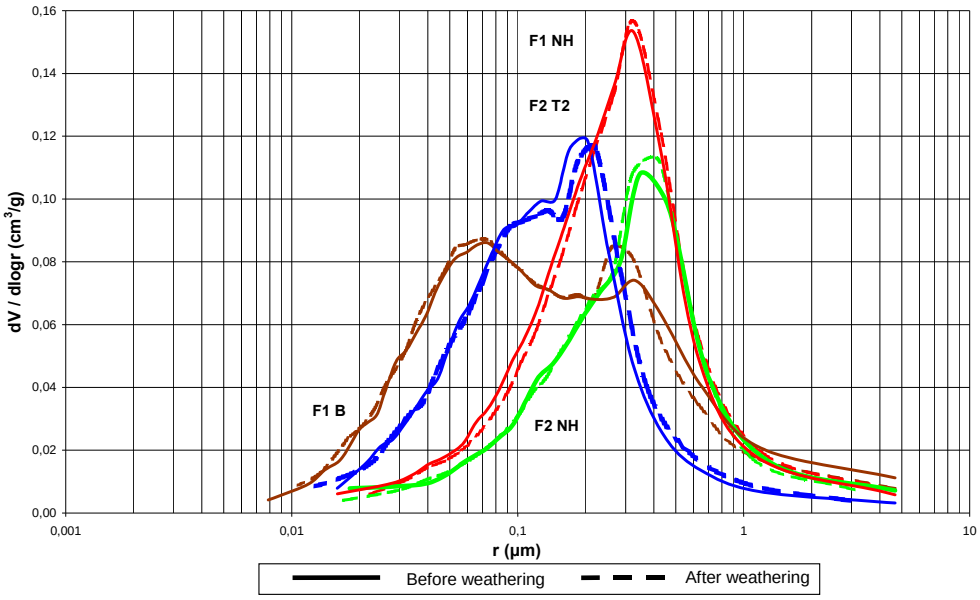

Figure 4. Pore size distribution.

3.3 Salt Content Profiles

Figure 5 shows the Hygroscopic Moisture Content over time of the five grounded layers (Fig. 3) of each of two C1 samples (Fig. 2) obtained from weathered non-desalinised specimens F2T3NH7C and F2B4C.

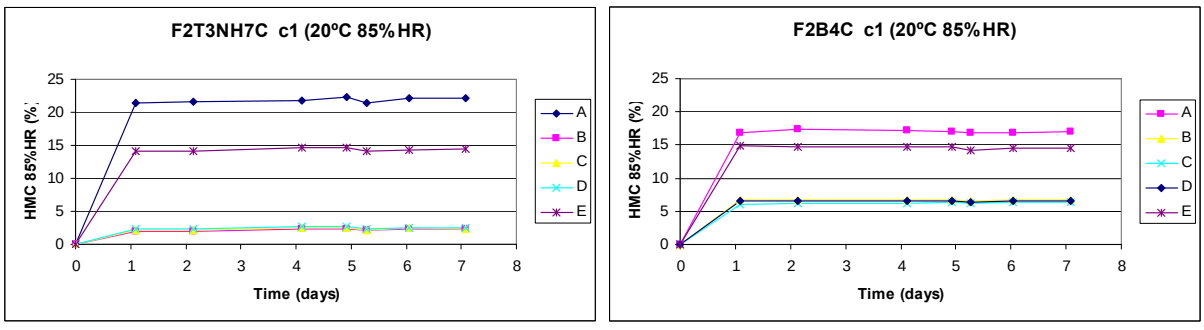

Figure 5. HMC graphics of grounded layers A, B, C, D and E.

Figure 6 shows the same HMC over time of the grounded layers, but now together with the HMC of sodium chloride control samples (Fig. 3). The last chart shows the HMC over time of control samples with powder from new tiles (Fig. 3).

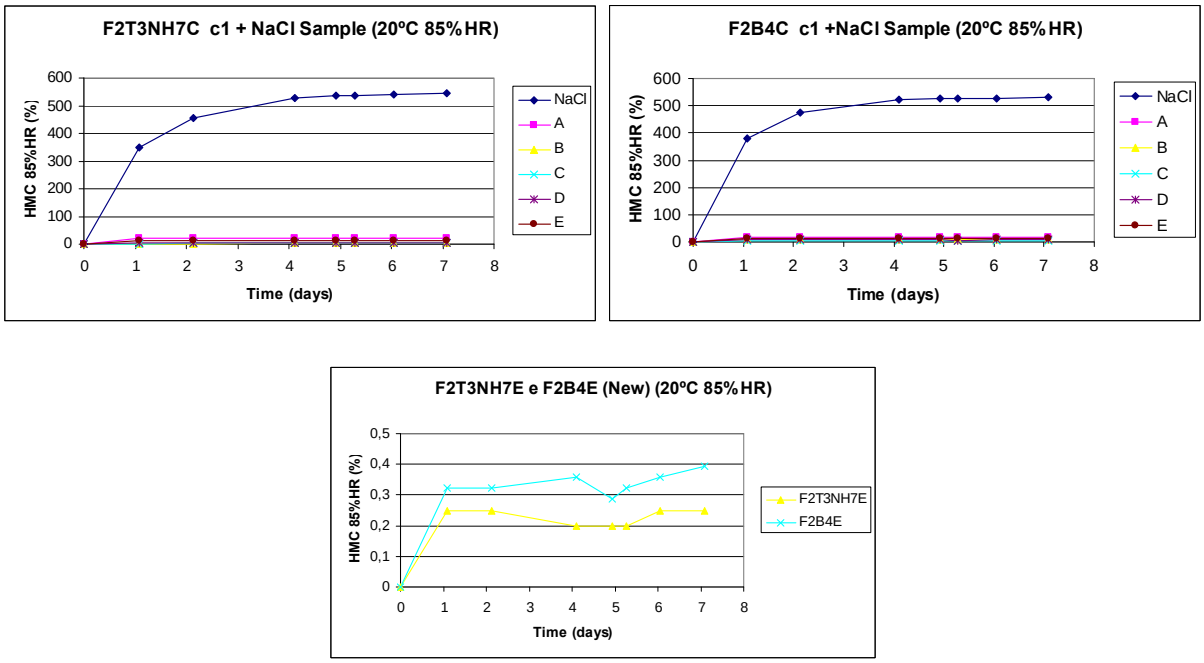

Figure 6. HMC graphics of grounded layers and of control samples.

From HMC values on day 7 the NaCl content of each layer was obtained (Table 3). In both types of samples, NaCl content is much higher in the outer layers. In the inner layers of the white sample the content of NaCl is higher than in the inner layers of the model 3 red tiles.

Table 3. NaCl contents

Layers	NaCl content (%)	
	F2T3NH	F2B
C1 A	4.0	3.1
C1 B	0.4	1.2
C1 C	0.4	1.1
C1 D	0.4	1.1
C1 E	2.6	2.7

4 DISCUSSION OF RESULTS

Visual inspection results demonstrate different types and levels of degradation caused by the weathering tests on the specimens. Hydrophobic specimens don't show immediate defects but they can suffer huge degradation if the solution can pass through the protected surface. Hydrophobic tiles from manufacturer 2 seem to be more resistant to weathering than those from manufacturer 1. Non-hydrophobic tiles, both red and white, show low to medium degradation levels, with a slightly increased level in the white ones. Characterization tests demonstrate different physical characteristics of the various types of tiles. Naturally, hydrophobic tiles show much lower water absorption than non-hydrophobic tiles, especially in manufacturer 2 tiles. This difference is less evident in vacuum conditions. For both absorption conditions, non-hydrophobic tiles from manufacturer 1 have higher absorption than model 1 tiles from manufacturer 2, whose model T2 is nevertheless the most

absorbent. White tiles show slightly higher water absorption and higher porosity than non-hydrophobic model 1 red tiles. These characteristics can explain the difference also detected in visual degradation. In general, weight variations and water absorption tests do not quantify the visual degradation at the present level. The MIP results show some differences in the porous structure of the four models tested. Tiles F1 B and F2 T2 present larger ranges of pore sizes and they are also those where higher degradation was observed. The finest and more homogeneous range of pores is of non-hydrophobic model 1 red tiles from both manufacturers, which showed intermediate levels of degradation. The salt content profiles demonstrate higher concentration of sodium chloride in the outer layers, in the upper and lower faces, especially in the case of the red tile tested. These crystals may be harmless if they are upon the surface but they may also provoke peeling if they concentrate under a very thin layer of material, which can be easily detached. The concentration in outer layers may thus indicate a potential for quick deterioration.

5 CONCLUSION

Cycles of wetting with a salty mist and subsequent drying can be used to cause different levels of artificial weathering alteration and degradation to ceramic roofing tiles. Hydrophobic tiles may resist longer to salty mist but they can suffer high damage if there is some penetration of salty solution. White tiles showed higher levels of degradation than the non-hydrophobic red ones. The tiles present rather diverse porous structures, which could be the cause of different behaviour under the testing cycles. The white and the non-hydrophobic model T2 red tiles, which show higher degradation, have larger ranges of pore sizes. The concentration of salt crystallization on the outer layers may induce the destruction of thin superficial layers.

To simulate real adverse conditions it is necessary to get higher degradation levels. The intention is to pursue the study and achieve these results by increasing the number of cycles or changing some of the parameters of the weathering tests.

ACKNOWLEDGMENTS

The authors thank the manufacturers of the roofing tiles and CTCV (Centro Tecnológico da Cerâmica e do Vidro) for the specimens and information delivered and acknowledge the collaboration of the Materials Department of LNEC and its personnel, where the tests have been done.

REFERENCES

ASTM International 2004, *Standard Test Method for Determination of Pore Volume and Pore Volume Distribution of Soil and Rock by Mercury Intrusion Porosimetry*. ASTM International, West Conshohocken, PA, USA, ASTM D 4404 – 84 (Reapproved 2004).

Cruz, C., Veiga, M. R., & Ferreira, V. M., 2007, ‘Evaluation of Durability of Clay Roofing Tiles’, Materiais 2007, IV Int. Materials Symposium, Porto, Portugal, 1-4 April 2007.

Gonçalves T. D., & Rodrigues J. D., 2006, ‘Evaluating the salt content of salt-contaminated samples on the basis of their hygroscopic behaviour. Part I: Fundamentals, scope and accuracy of the method’, *Journal of Cultural Heritage*, 7 (2006), 79-84.

Rodrigues J. D., & Gonçalves T.D., 2006, ‘Sais solúveis nas construções históricas’ (Soluble salts in historic constructions. Introduction and summary), CS 32, LNEC, Lisboa, 2006, pp. 1-13.

11DBMC International Conference on Durability of Building Materials and Components
ISTANBUL, Turkey 11-14 May 2008

Designing Replacement Roof Systems to Achieve Long Term Service Life: A Sustainable Solution

Thomas W. Hutchinson [1]

T 22

ABSTRACT

As an architect who has chosen to specialize in roof system design I have come to realize that roof system design is a skill set unto itself and equal in importance with structural, mechanical, plumbing and electrical design. Replacement roofing and the unknown conditions dealt the designer require knowledgeable and skilled designers. This paper will endeavor to review the process by which roof system designers should approach replacement roofs in order to achieve sustainable low slope roof systems with service lives in excess of 30 years and how the replacement roof system design should take into consideration all the building elements that impinge upon the roof.

KEYWORDS

Replacement roofing, Long Term Service Life. Sustainability, Thermal performance, 30 year roof systems

[1] Hutchinson Design Group, Ltd., Principal, Barrington, Illinois 60010, USA, Phone 1-847-756-4450, Fax 1-847-756-4451, hutch@hutchinsondesigngroup.com

1 INTRODUCTION

Every roof system ultimately reaches a stage where serviceability cannot be maintained by repairs; an investment in a new roofing system is necessary to preserve the usefulness of the building. Sixty percent (60%) of all roofing work in the United States of America is roofing replacement. Of the sixty percent (60%), two thirds (2/3) is considered recovery and one-third (1/3) involves the complete tear-off of the existing roofing system down to the existing roof deck. A large inventory of aging buildings in the United States assures a continued growth of reroofing opportunities*.

Roofing replacement, defined as removal of the existing roof systems and the installation of a new roof system, allows for the opportunity to improve upon the existing roof system, bringing it into line with current codes and standards, while also providing an opportunity to design a new sustainable, robust roof system increasing thermal efficiency thus enhancing the buildings energy conservation, reducing the buildings carbon foot print and striving to achieve long term service life (defined as having a service life of at least 30 years)**, the essence of sustainable construction.

The difficulties facing today's architects and roof consultants are almost overwhelming. Roofing replacement design is exceedingly more difficult, time consuming, and complex than new roofing system design. Today's multiple varieties of roof systems and components, code requirements and the interjection of 'cool roofing' concepts that are typically not very well thought out, require that the architect/roof consultant or roofing contractor have a full knowledge and understanding of the existing building structure and reroofing options. The investigation and analysis of existing building components, selection of the appropriate solution, and acumen to properly detail a project requires a great deal of knowledge and experience that few possess. Therein lays a major concern contributing to poor roofing replacement design. All too often the designer possesses one, or possibly two, rarely all three qualities required to succeed. While many architects may be knowledgeable about building components, they are lacking in knowledge about appropriate roof design, let alone roofing replacement design. They are a product of our educational system, which places roofing design at the lowest of priorities. Contractors often lack empirical knowledge of building systems, and roof consultants often lie somewhere in the middle.

Further complicating the roofing replacement design is the need to maintain the building's use during the reroofing construction. Ultimately, reroofing is an exercise in roof analysis, the subtle balancing of advantages and liabilities requiring knowledgeable and clean judgment in weighing design factors***.The roof system designer must not only possess a great deal of knowledge and empirical experience, but he must also possess an enthusiasm for his work, as the challenge before him is formidable, a challenge that can only be satisfied by the complete dedication of a competent designer.

The options in roofing replacement are great as there are numerous differing types of low slope and steep slope roof systems, each with differing requirements. In order for a roofing replacement system design to be successful, two conditions must exist: An excellent working relationship between architect/roof consultant, owner and contractor must be established, and work must be predicated on a set of construction documents that reflect a roof system design consideration of all building components. It further requires the education of building owners. Owners seldom comprehend the technical complexities and substantial risks entailed in roofing replacement. The owner almost always concludes that if the building leaks it is because of a faulty roof system. Not only may this not be a faulty assumption, but may lead to the errant spending of money, which will not correct a supposed problem. It is also inherent on the roof system designer to inform the owner about the cost involved in correcting original design errors.

* RSI, "Tear-off or recover: That is the question." Oct. 1989, pg. 82-85.
** Roofing Canada, "Keys to Sustainable Roofing", Spring/Summer 2007, pg. 16-30.
*** Roof Design, "A conservative approach to reroofing." Sept/Oct 1985, pg. 24.35, 51.

In order to accurately determine the condition of the existing roof system, an accurate investigation and analysis of the existing roof system, building components that impinge upon the roof and the activities both within the building and atop the roof system is required. Inappropriate selection of corrective action will lead to less than desirable results. The installation of a new roofing system without giving consideration to the results of the investigational analysis, code review and the owner's goals may lead to a new roofing system selection that does not provide a long term, sustainable design solution.

2 INVESTIGATION / ANALYSIS

Prior to giving consideration to the selection of a roofing system, a complete and thorough investigation and analysis of all existing building components impinging upon the roof system must be undertaken. Failure to do so may not only result in the failure of the new roof system, but also reflect a complete misunderstanding of the roofing replacement design process, as well as be a disservice to the client. Neglecting to respond to the investigation and analysis of existing building components may not only result in the repeat of previous errors such as continued ponding of water, but may also assist in the deterioration of the existing building components; a condition which will compound existing problems.

Roofing replacement design needs to take into account the "whole picture". A successful solution will address all concerns. The smallest of details must be examined. Most roof leaks are caused by inappropriate attention to the design and detailing of building components that impinge upon the roof. All too often, building owners conclude a building leak is the result of a faulty roof system, but unfortunately, this is not always true. Most leaks are a result of faulty building components, faulty roof system component installation, or faulty building interfaces.

2.1 Investigation

Prior to the design of a new roofing system, a complete investigation of the existing roof system as well as related building components which impinge upon the existing roofing system must be undertaken. The intent is to understand the existing conditions and the causes of concern. Designers must know the existing conditions and problems before they can propose a solution for them. The existing roof system must be examined. The current causation of problems and condition of the existing roof should be determined by analysis, observation, and possibly testing, including moisture surveys and destructive analysis such as 'test cuts'. This analysis will provide the designer with a set of parameters on which to design the new roof system. Results of test cuts performed on the existing roof system will provide data on the existing roof systems to be removed as well their thickness.

A thorough investigation should endeavor to review: 1) Historical records, including a leak history of the existing roof system; 2) existing "as-built" drawings; and 3) any warranties that may exist on the roof system, and through discussions with the owner, determine the existing building use, its occupancy and future plans. The existing roof system should be observed, noting concerns such as the areas and depth of ponding water, wind damage and evidence of repeated foot traffic. It is very important that drainage deficiencies are noted, as they are a major contributor to roof problems.

The existing roof perimeter, as well as the exact location of existing roof drains, penetrations, HVAC curbs, penthouses, chimneys, and all building components impinging upon the roof should be observed, their condition investigated and their exact location noted. The exact location of these components is imperative, especially as they affect the design of a tapered insulation system.

All details of the existing conditions should be sketched. A complete photo record of the entire roof system, its building components and all conditions that may require detailing should be taken and labeled accordingly. This photographic record will prove invaluable in aiding the designer in the

design and detailing of the new roof system. Test cuts should be performed to determine not only the material components of the existing roof system, but also the depth of the roof system; information which is required when designing tapered insulation systems and their results on roof edge design considerations. The existing roof system should also be tested for asbestos containing materials (ACM).

The condition of building components such as the following; should be observed, photographed, sketched, and their existing condition fully evaluated:

a) Roof drains: Their size, location, and condition.
b) Parapets and adjacent masonry walls: Examine the masonry and mortar for deterioration, structural cracks; is tuckpointing and sealing required, are the coping stones and joints in need of restoration, do weep holes and through wall flashing exist, if so, what are their locations in relation to the existing roof system and base flashings?
c) Previous roof patching: Quality of patch, check roof deck condition below.
d) Gutters: What is their general condition? Are they rusted? Is repainting required? Are they properly sized? Are they well supported? Are expansion joints properly located? Are the gutter downspouts properly sized? Are downspouts missing? Do they properly displace the water at grade?
e) Roof deck: Age must be considered for the potential mechanical fastener attachments. Are there any visible areas of deterioration? Were there any "soft" areas experienced during the walk through?
f) HVAC equipment, curbs, associated piping, and the existing condition of these penetrations as they penetrate the roof system. Are there multiple pipes penetrating through a single pitch pan? Is the unit itself leaking? Are weep holes plugged? Are there penetrations from the unit through the top of the curb cap that may be taking on water?
g) Expansion joints: Are the cover joints watertight? Are the expansion joints properly located? Is the height proper?
h) Penthouse walls, base flashings considerations: Metal siding on penthouses is often notoriously low to the roof membrane. Identification of the siding support system is required as the new roof system may rise higher than the bottom of the siding.
i) Cooling towers: How are they supported? Does any associated piping penetrate the roof membrane? Is the piping grouped together?
j) Drain pipes: Is the roof drain/downspout connection watertight?
k) Abandoned curbs, pipes, etc. that may be removed should be noted. These items should be reviewed with the owner's maintenance personnel who may be of great assistance in identifying roof top penetrations that could be removed.
l) Structure: It must be analyzed. Is it a viable structural system to carry any additional weight that you may be adding? Columns and beams should be checked for structural integrity as well as the roof deck. Are there any new adjacent tall buildings which may have changed the design and roof load considerations involving snow loads? Are there any new tall additions that would also change the loading factor?
m) What is the current access, not only to the existing roof system via scuttles or ladders to the high roofs, but also to the site for construction equipment ?
n) Location of any IT cabling, tower conduit and refrigerant piping that currently transverses the roof.
o) Current roof top maintenance traffic patterns.
p) Interior Conditions: Evaluate and determine the interior occupancy, climate conditions and space use, and whether they have contributed to the existing roofs deterioration or will affect the performance of the new roof system.

The roof designer, while investigating, analyzing and documenting the existing roof system, must ask himself/herself questions such as the following:

a) Are there sufficient roof drains to adequately and quickly remove water from the roof? Can additional drains be installed and/or the existing moved to facilitate efficient tapered insulation layouts.
b) Are existing HVAC units currently in working order? Does the owner wish to upgrade existing units or incorporate additional units? Can any abandoned units and their curbs be removed.
c) Are there masonry parapets or walls that require restoration or maintenance that can be performed prior to the installation of the new roof system?
d) Are there any roof penetrations that are not currently in use and may be removed?
e) Are skylights currently cracked, requiring replacement and/or removal? Are additional required?
f) What are the conditions of the existing roof drain-downspout connections? Are the roof drain bowls secured to the roof deck?
g) What kind of access is available for the construction equipment such as dumpsters and cranes?
h) On adjacent masonry walls, are weep holes and through wall flashing present? Is their location above the existing roof system? What is the distance to the existing roof drains and will the incorporation of tapered insulation rise above the through wall flashing?
i) Has the base flashing and/or counterflashing covered existing through wall flashing and weep holes?
j) Are there TV antennas, IT equipment of antennas or weather stations that need to be removed and reinstalled? How will they be anchored, and will they penetrate through the roof? How will this be detailed?
k) Are there gas pipes, electrical conduit or other types of piping transversing the roof, and can they be relocated along a parapet, wall or below the roof deck?
l) Are parapet coping stones loose? Do they require restoration, replacement or installation of a throughwall flashing below? Should they be removed or abandoned and covered with sheet metal? What are the joint conditions, do they need to be restored?
m) Are the parapet walls structurally sound? Will they require rebuilding, tuckpointing and sealing, or should they be covered with metal siding?
n) Are there any masonry components, such as interior parapet walls that can be removed?
o) What is the integrity of the large masonry chimneys? Do they require tuckpointing and sealing, rebuilding, new chimney caps? Can their heights be reduced as a result of new boiler systems? Have they been abandoned?
p) What type of access is there to the roof from the interior? Is it through a roof scuttle? Is a new scuttle required? A new ladder? Are exterior ladders required to high roof areas?
q) What type of roof traffic is anticipated on the new roof system? How often? Foot or mechanical traffic? Where?
r) Are air intakes located such that fumes from the new roof system installation could enter the building's air circulation systems?
s) What is the intended use of the roof system beyond that of water repelling? Will it be required to perform as a working surface?
t) What is the height of the specific roof areas and what is the climate and type of geographical location the building in? Urban? Rural?
u) What types of wind can be expected?
v) What is the existing height of all roof curbs? How much will they be required to be raised to accommodate the new roof surface height?
w) What type of effluents from below will come in contact with the new roofing system? From adjacent or neighboring buildings? From planes?
x) Grouped piping penetrating the roof through pitch pans: What will be involved in separating them?
y) Are new expansion joint covers required? Can roof penetrating expansion joints be eliminated and designed into the roof substrate below the roof membrane?
z) How would increased roof top energy efficiency affect the interior HVAC air balancing?

aa) How will roof top construction disturb interior finishes and worker production?

bb) How are the roof areas laid out? Will any specific roof areas require special consideration or roofing replacement priority over other areas, e.g., high roofs over low roofs?

2.2 Analysis

With the results of the field investigation and assessment, an analysis of the existing building conditions can be undertaken, roof cover type selected and the scope of work determined. This decision, as well as all others, must be based on sound engineering principles so that enhanced and/or long term roof system service life can be attained. A sustainable roof system cannot be achieved if decisions are made that 'short circuit' the optimization of the roofs service life and the attainment of the long term performance.

Tear-off and removal of the existing roof system down to the existing roof deck, prior to the installation of a new roof system allows for the inspection of, and if required, replacement of deteriorated roof deck. Unknown conditions that may affect obtaining long term service life are often eliminated in total or at least observed corrected when the old roofing is removed. It also allows for the clean installation of thermal insulation, especially tapered insulation, thus enhancing drainage and thermal performance (energy conservation and a reduction of carbon footprint).

Once the analysis phase has been completed and a scope of work delineated, a budgetary construction estimate can be arrived at and reviewed with the building owners for approval. Following approval of this budget, the roof replacement design process may begin.

3 DESIGN

Items that must be given design consideration, researched and answered include:

a) Potential roofing systems.
b) The appropriate insulation, type and method of attachment must be investigated. What are the owner's energy efficiency requirements?
c) Calculation of the dew point and the decision whether to use a vapor retarder.
d) The fifth façade: The roof is part of the building envelope, and as such should be considered the fifth façade after the walls. The interface of the wall and roof systems needs to be understood and considered. Is there an air barrier in the wall construction that the new roof air or vapor barrier should be incorporated into? Planning for potential façade replacement and the implementation of a wall air barrier may also be prudent.
e) Future maintenance concerns: All roofs require maintenance, whether they are new or existing. In designing a roof replacement an opportunity exists for minimizing the required maintenance. That means the installation of maintenance-free components such as prefinished sheet metal.
f) Give consideration in designing the new roof system to easily provide for future recover or partial removal and replacement.
g) Plan for future reroofing with conditions such as copings, gravel stops, and counter flashings that can be screw fastened and facilitate future removal and reinstallation.
h) Appropriateness of materials.
i) Availability of materials. Are the materials available during the time of the year when the reroofing will be undertaken?
j) The roof system design should have a respect for and reflect the intent of the existing building design.
k) What is the availability of local knowledgeable installers? When working on a project in southern Japan, it was found that although SPM installers existed in Japan, they were almost exclusively located in the north. Qualified installers of metal roof systems existed in southern Japan, and lead to the design of a structural standing seam roof system, which was installed with excellent workmanship.

l) Are there experienced roofing contractors who are able to correctly install the selected roof system?
m) What is the existing building's expansion and contraction requirement across the roof? Are expansion joints required? Can they be eliminated?
n) Plumbing: Do the existing roof drain locations facilitate the layout of new tapered insulation? If not, you may wish to relocate some drains. Will the new roofing system require the installation of new roof drains and downspouts? Can the current drainage systems handle the anticipated water volume? Do existing roof drain conditions require the replacement of existing with new? The renovation of existing? The abandonment of existing? Consideration should also be given to the type of appurtances required by the drains, including sump pans, extension rings, and under deck clamps. Plumbing concerns also involve the raising of existing vent stacks.
o) Drainage: On steep slope roofing, gutters and downspouts should be sized for the appropriate design parameters. The dispersement of the water at grade should be given consideration as to the effect on the surrounding area during the various seasons. Do not install downspouts to sidewalks or driveway locations in areas in which the winter seasons will cause icing. The appropriate method of downspout support should be determined, as well as appropriate downspout materials to protect against anticipated vandalism.
p) With the multitude of insulations on the market today, the roofing designer must be cognizant of the differing types and the densities that are available. Chlorofluorocarbon (CFC) free insulation should be used? Consideration at this time should be given to the use of utilizing tapered insulation in order to remove water from the roof as expeditiously as possible. Rapid removal of roof top water is paramount to a successful long term roof system design. How do HVAC roof curbs, masonry walls, and roof edge considerations impinge upon this tapered insulation, especially at valleys? Consideration should also be given to the required R-value. Double layers of insulation with offset joints to create thermal breaks from the roof deck to the roof cover is mandatory for optimizing energy performance, and in many climates for preventing the formation of condensation below the roof cover.
q) Asbestos removal should also be reviewed. In the United States, regulations exist that govern the removal of asbestos containing materials, including those imbedded in asphalt as well as pipe installation around drains and asbestos siding. Penalties for ignoring the appropriate removal and disposal of asbestos containing materials can be severe. Personal opinions must be set aside in adherence to the law.
r) Many older buildings have beautiful, albeit deteriorating masonry and lime stone detailing that impinge upon the roof and will require restoration and waterproofing at the time of roof replacement. This is work that should be performed prior to the installation of any new roofing system; so that foot traffic is minimized and chemicals utilized by various trades do not come in contact with the new roofing system.
s) Building height, geographic location, climate and wind considerations and requirements should be considered.
t) The aesthetic appearance of the roof system should be given consideration, especially in steep slope roofing work and when observable from building areas above.
u) Consideration should be given to sheet metal materials for uses and detail appropriateness. Remember the long term performance goal and maintenance free aspect; under no circumstances utilize galvanized metal.
v) Recognize that unknown conditions will exist, and in your specifications, incorporate unit prices for materials in which potentially unknown conditions or replacement of existing building components will be necessary. Such items include roof deck, HVAC curbs, roof drains, wood blocking, skylights, and labor.
w) Evaluate the existing roof edge construction as it pertains to the installation of the new roof edge wood blocking to increased thermal (tapered) insulation systems and in regards to wind uplift considerations. Raising the roof edge is often required to accommodate the increased thermal insulation installed.
x) Whenever raising a roof edge, it is imperative that the new roof edge wood blocking be adequately secured to the existing building and structure. If the existing wood blocking or

perimeter conditions are not adequately fastened, they themselves should be fastened. Detailing such as requiring scarfed joints will reduce the deformation of roof edge sheet metal due to the warping of treated lumber.

y) Are there any building components, abandoned or otherwise not required that could be removed from the roof?

z) How will the removal of the existing roof system affect structural components with camber; for example, with the weight removed camber will manifest itself and may cause interior damage such as cracked plaster and/or masonry unit light lens displacement.

aa) Will heavy equipment, utilized during roofing replacement construction work vibrate the deck and cause damage or disruption of the work place?

bb) Will the building's security system or fire alarm be disturbed?

cc) Will the use of ballast or reflective membrane be beneficial over the life of the roof?

dd) If a garden roof is a consideration, structural integrity, soaked weight, growing medium depth and type of plantings need to be considered.

Review and consideration of the "Tenants of Sustainable Low Slope Roofing" arrived at by the CIB/RILEM Joint Committee on Roofing Issues should be undertaken.

Once the appropriate decisions to the above referenced design considerations are made, the architect or roof consultant may proceed to the design of the new roofing replacement system. Beginning with the preliminary design and roof plan, the designer should lay out the new roof system and insulation systems. It should be noted here that if a roof system did not incorporate a sloped structure, under no circumstances should a flat roof be incorporated into the design. If the roof deck is not structurally sloped then tapered insulation should be incorporated into the new roof system design. This may require the intensive design and detailing of roof edge conditions, especially of existing gravel stop conditions. Following the completion of a preliminary plan, all building components must be given consideration and thought for detailing.

Once this overall roof plan layout has been conceived, thought given to other building components and reviewed, the designer now enters the most critical phase of the roof replacement design; that is producing a final set of construction documents taking into account all of the information gathered. Attempts to perform roof replacement without quality contract documents (and quality is the key word), often result in roof systems with premature failure. The goal of the construction documents is to clearly communicate to the roofing contractor your design intent. In association with bringing the roof plan up through final stages in the construction document phase, roof details such as roof edges, are to be sketched simultaneously. Following completion of the roof plan, roof edge details are finalized. All details should be drawn to the largest scale possible so as to indicate as much detail as possible. Each detail should be thoroughly noted so as to leave no question as to what is required. These are the details that specifically relate to the building components. Following the completion of general details, attention should be given to specific details; the details that will make or break your roofing replacement system design.

They should include: 1) Elevation drawings of terminations such as when a roof edge terminates into a masonry wall; 2) counter flashing; 3) intersection of gravel stops, copings and masonry as they abut adjacent structures; 4) end wall gutter details; 5) built-in gutter details; 6) ridge vents; 7) tie-in details between two differing roof systems, etc. The general thought in this phase of detailing is to do whatever is necessary to properly communicate to the roofing contractor as to what is required. Sometimes this may require three or four isometrics in a series that build on each other as they progress to indicate exactly how the concern is to be handled. The details should indicate existing components to be removed, existing components to remain, as well as indicating new roof systems and their attachment.

Following a final review of the construction drawings, the specifications should be prepared specifically for the project in question. These specifications should include technical sections on all building components involved in the new roofing replacement system construction, i.e., new roof drains, wood blocking, masonry and limestone restoration, as well as components of the building system that may be damaged during construction or will require repair such as existing grass and landscaping areas, and bituminous and concrete paving.

4 BIDDING

Following a review of the contract documents and specifications, and the coordination of same, the project is ready for bidding. In order to arrive at a set of construction documents for bidding purposes, the architect/roof consultant designer has gone through a painstaking and comprehensive investigation of not only existing building components, but of roof system options, materials, causes and effects, as well as having been involved in a multitude of decisions, and an evaluation of value between costs and results. This author firmly believes that the architect/roof consultant must continue to be involved during the bidding process, to be available to answer questions, issue addenda, hold pre-bid conferences, inform the roofing contractors of the specific requirements of the project, and to answer all questions concerning the project design.

5 CONSTRUCTION PHASE

Once bids have been received, references should be contacted, verified and confirmed prior to making a recommendation to the building owner. Preconstruction meetings must be held; verification of submittals, as well as continued observation of the installation of same must be upheld. Site visits allow for the verification of compliance with the contract documents, allow for the answering of questions as well as to review unknown conditions and to advise the roofing contractor on how to proceed. Continued communication between the roof system designer and the contractor during all phases of construction is invaluable to the success of the roofing replacement system and the achievement of a sustainable long term roof systems.

6 CONCLUSION

The successful completion of a roofing replacement system design with a goal of sustainability and long term service life is not easy. It involves a tremendous amount of work by the roof system designer; involving investigation, analysis, design, decision making, continued communication and problem solving, and the observation of the construction. A well thought out systematic procedure will lead to successes. Owners will be happy with results, the built environment enhanced and the roofing replacement designer will obtain the self satisfaction of knowing that they have been involved in one of the most important comprehensive construction processes that a building owner can undertake.

REFERENCES

Building Design & Construction, 1988, “Repair, re-cover or replace?” Sept. pg. 82-85.

Exteriors, 1988, “Sorting out complexity of options in reroofing.” Autumn, pg. 24-29.

Hutchinson, T.W. 2007 ‘Keys to Sustainable Roofing’, Proc. of RoofTech 2007, Calgary, Canada, 4-6 June.

Hutchinson, T.W. 2004 'Sustainable Low-Slope Roof Systems Designed for the Long-Term – Getting it Right the First Time', Proc. of the 2004 CIB World Building Congress, Toronto, Canada, 1-7 May.

Professional Roofing, 1988, "Reroofing: An opportunity for improvement.", Sept. pg. 15-17.

Roof Design, 1985, "A conservative approach to reroofing,", Sept/Oct. pg. 24-33, 51.

Roofing Spec, 1986, "Identifying markets key to success in reroofing.", Aug. 1986, pg. 21-24.

Roofing Spec, 1986, "1001 reasons not to roof over wet insulation.", Aug. pg. 27-30.

RSI, 1989, "Recover boards join old systems with new.", Oct. pg. 36-38.

RSI, 1989, "Tear-off or recover: That is the question.", Oct. pg. 36-38.

11DBMC International Conference on Durability of Building Materials and Components
ISTANBUL, Turkey 11-14 May 2008

The Specification and Selection of CE Marked Reinforced Bitumen Membranes for Low Sloped Roofs to Ensure Their Durability in the UK

Gerry Saunders [1]

T 22

ABSTRACT

In order to ensure the specifier can select the right quality of reinforced bitumen membrane for a given roof type a new British Standard , BS8747, has been developed. This paper presents the development process and the methodology used to establish BS8747. It shows how the key parts of BS8747 lead to the successful specification and selection of reinforced bitumen membranes so that a durable roof is achieved.

Bitumen membranes have been used in the United Kingdom for waterproofing low sloped roofs for many years. They have been covered by a British Standard (BS747) where the membrane is identified by the materials it contains. The standard can be called a recipe standard which had 5 separate types of base reinforcement. The best membrane type in terms of performance and durability is type 5 which uses a polyester based carrier. If a high performance membrane is required the specifier could easily require those to BS747:type 5 to be used.

Recently a new European standard (EN13707) has been produced by CEN TC254 which refers to flexible sheets for roof waterproofing. This presents data according to a number of test methods which have been based upon the regulatory requirements of the various member states. It is a requirement that EN13707 refers to all products that are legally placed on the market. This means the CE mark covers low quality as well as high quality products. The product information given with CE marking is in the form of results from a series of tests. This means that an in-depth knowlede of material properties would be needed to assess quality and durability.

KEYWORDS

Bitumen, Membranes, Durability

[1] Building Research Establishment, Watford, WD25 9XX United Kingdom , Phone +44 1923 664382, Fax +44 1923 664991, saundersg@bre.co.uk. Chairman CEN TC254 Flexible sheets for waterproofing.

1 THE HISTORICAL USE OF BS747

BS 747:2000 – Reinforced bitumen sheets for roofing - Specification [British Standards Institution] was first published in 1937. Other editions have been published in 1952, 1961, 1968, 1970, 1977, 1994 and the last in 2000. The products that have been covered by this standard have been traditionally known as 'bitumen felt' but to better reflect the latest European standards they are now referred to as ' reinforced bitumen sheets for roofing'.

The various types of materials covered by this standard have a matted fibre base which is coated with bitumen. There are a number of types which have been identified according the material used for the base. These are shown in table 1 together with their reference within the standard.

Table 1. The types of pre-formed base materials covered by BS747.

Types of pre-formed base roofing sheets	*Type 1 Fibre base*	*Type 2 Asbestos base*	*Type 3 Glass fibre base*	*Type 5 Polyester base*
Fine mineral surfaced sheet, e.g. fine sand, talcum etc.	-	-	3B	5B and 5U
Granule surfaced sheet, e.g. slate, granite or ceramic	-	-	3E	5E
Reinforced sheet	1F	-	-	-
Venting base layer	-	-	3G	-

There are marked differences in the performance and durability of the various materials. Those of type 1 with a base of organic fibres, often referred to as 'ragfelt', performed so poorly in the application of waterproofing for flat roofs that they were removed from BS747 in the 1994 amendment. The only reference for type 1 products (type 1F) is for use as underlays for the use beneath slates or tiles in pitched roof construction.

Type 2 products were manufactured using an asbestos base but these were formally withdrawn probably in the 1977 version.

Type 3 products are manufactured using a glass fibre base are for general use in what are now considered to be relatively low performance situations. The building may be temporary or the substrate maybe be stable so the membrane is at low risk of failure due to building movements. The life of this type of membrane, usually comprising at least two layers is generally accepted as being about 10 years.

The type 3G is specifically manufactured to provide a venting base layer. This was developed to lay over new concrete decks and avoids blisters due to entrapped moisture during construction. More recently it has been used as a first layer over certain types of insulation board.

Type 4 is a specialist product for a specific application beneath mastic asphaltic and is not included in table 1 and are not considered further here.

Type 5 products are made from polyester. The base is provided in a variety of weights (mass per unit area) and has been manufactured by one of two methods. The lighter and medium weight sheets are non-woven materials while the heaviest can be needle punched. The combination of a light weight underlay (125 g/m^2) and a heavyweight capsheet (350 g/m^2) has been responsible for a service life of at least 30 years.

The last version of BS747 developed in 2000 also recognised that different weights of membranes based on polyester were in use so the additional types were added. These included the refined types 5B/180, 5B/250 and 5B/350. Type 5E with a mineral surface were also denoted in this way.

In the manufacturing process the base material maybe impregnated first with straight run bitumen and then coated with oxidised bitumen. BS747 does not cover products developed more recently that use polymer modified bitumen. Reinforced bitumen membranes manufactured using polymer–modified bitumen have generally been covered by third party certification.

2 THE INTRODUCTION OF EN13707:2006 – BITUMEN SHEETS FOR ROOF WATERPROOFING [CEN]

The reason for the development of a series of Europen Norms (ENs) was the agreement of the Construction Products Directive in 1989 between the member states of the European Union (EU). The intention was to establish free trading of construction products throughout the EU. After an initial period of development the European Committee for Standardization Technical Committee 254 (CEN TC254) was established to produce test methods and product standards for a particular group of products callled 'flexible sheets for waterproofing'.

The requirements for product standards was established by the requirements in member states based on their (building) regulations. These requirements were collated by the Standing Committee for Construction and issued as a mandate. This mandate was sent to CEN or European Office for Technical Approval (EOTA) who responded with a reply which contained relevant product standards and test methods.

Within the structure of CEN TC254 bitumen sheets for roof waterproofing were dealt with by Sub-committee 1 (SC1) and the same for plastics and rubbers in SC2. It was recognised that there would be some common test methods and separate working groups (WGs) were established by CEN TC254 to produce test methods.

EN13707 is the product standard developed by CEN TC254/SC1 for bitumen sheets for roof waterproofing. It refers to a series of test methods and contains information which leads a manufacturer to be able to CE mark a product. The CE mark on a product or a label, can contain information based on results of test methods. This information may only refer to a few tests results (such as external fire performance) necessary for satisfying the regulation of any member state where the product may be sold. A wider range of information about the product can be found on the manufacturers data sheet including tensile properties, tear resistance and shear and peel of joints.

The value assigned for a particular material property may not give the same value as stated by a manufacturer. This is because EN13707 requires information to be stated as a manufacturers declared value or a manufacturers limiting value and there are rules which relate to both of these.

EN13707 contains reference to product characteristics for which a series of test methods have been developed. They are for initial characterisation of the product or for factory production control. The characteristics as listed in Table 2.

Table 2. Product characterisitcs in EN13707.

Initial type tests	*Tests for Factory Production Control*
Watertightness	Visible defects
External Fire performance	Length & width
Reaction to fire	Straightness
Watertightness after stretching at low temperature	Mass per unit area and thickness
Joint strength (peel and shear resistance)	Tensile properties
Water vapour properties	Resistance to tearing (nail shank)
Resistance to impact	Dimensional stability
Resistance to static loading	Flexibility at low temperature
Resistance to root penetration	Flow resistance at elevated temperature
Form stability under cyclic temperature change	Adhesion of granules
Artificial ageing behaviour	

3 THE DEVELOPMENT OF BS8747:2007 [BRITISH STANDARD INSTITUTION]

BS8747:2007 was developed by a British Standards Institution (BSI) committee reference B 546/1. The committee has been Chaired by the author of this paper for over 10 years.

The initial decisions made were firstly to refer to bituminous products as ‘reinforced bitumen membranes’ (RBMs). Previously the word ‘felt’ had been used and tended to convey a meaning of poor performance and failure. Secondly, it was found to be possible to retain the numbers ‘747’ in the new British Standard thereby ensuring a continuance with the industry in the use of these numbers in reference to bituminous products.

The task faced by the committee was to determine how to link the old standard BS747 and the new European standard EN13707 so that the end user and would be able to select and specify bituminous products based on performance and durability.

The committee identified a need to concentrate on a number of items of work;

- To identify the product characteristics from the list in EN13707 which could best be used to determine a change in levels of performance and durability
- To match the chosen product characteristics with the end use conditions ensuring compliance with existing Codes of Practice
- To produce a simple coding system which would allow specifiers to select bituminous products according to performance
- To compile a list of test results for the product characteristics for a range of the most widely used reinforced bitumen membranes.

All of these were needed to develop the final document so two working groups were established, a users group and a manufacturers group.

The committee were mindful that a system had been developed in France called the 'FIT' system (Chaize 1991). This was based on fatigue, impact and temperature. Impact and temperature are referred to in the product characteristics in EN13707 i.e. resistance to impact and flexibility at low temperature.

A problem that was recognised was that as far as end users were concerned they only needed 3 levels of performance – low, medium and high. This was also strongly linked to short, medium and long term requirements for service life (and hence durability). On the other hand the typical manufacturer has about 40 different bituminous products and wants to sell all of them. A standard with just 3 levels of performance would not be acceptable to the industry.

This can be considered against the old standard which had effectively 3 levels of performance through type1, 3 and 5 products. However, this only referred to products manufactured using oxidised bitumen. BS8747 needed to encompass those manufactured with polymer-modified bitumen also.

3.1 The Coding System Developed

A classification for RBMs for roofing was developed. The system is based on two parameters, tensile strength and indentation and is used to define the following:

a) the performance achieved by any particular membrane
b) the performance required by any particular roof construction.

The characteristics chosen from EN 13707 were tensile strength (S) and resistance to puncture or indentation (P). Hence the SP classification. Each letter is assigned a numerical suffix that increases with performance level. The lowest perfoming membrane is hence S1P1. A total of 5 levels were chosen so the highest performing is S5P5.

The tensile strength is determined according to EN12311-1:2000 [CEN]. The S class is determined by a number levels e.g. 150 to 350 N/50mm for S1 and 350 to 450 N/50mm for S2. The values stated are minimum values as quoted by the manufacturer and are required in both the longitudinal and transverse direction. The class for the P parameter is determined from 2 sub-classes based on the resistance to impact (EN 12691:2006 [CEN]) for Dx and resistance to static loading (EN12730:2001[CEN]) for Lx. Table 3 below shows how these are combined to determine the P class.

Table 3. Combinations of D subclass and L subclass to give P class.

Subclass D	*Subclass L*	*Combination*	*P class*
D1	L1	D1L1	P1
D2	L2	D2L2	P2
D2	L3	D2L3	P3
D2	L4	D2L4	P4
D3	L4	D3L4	P5

The values from the impact test are a drop height e.g. up to 700mm for subclass D1. The values for static loading are expressed as a load e.g. 5 kg for subclass L1.

3.2 How to Use The Snpn Classification System.

Two approaches have been taken in BS8747 to use the SnPn system.

The French FIT system was used as a basis to deveop a table which gave membrane classification by performance requirement. A small part of the performance table is shown in Table 4 as an example.

Table 4. A small part of the performance table.

Substrate below the membrane	*Slope/Falls*	*Roof use and type of protection*	
		No access apart from maintenance	
		Self-protected	*Ballast (coarse gravel)*
Concrete	1 to 5	S3P2	S2P3
	>5	S3P2	-
Plywood, OSB or timber boarding	1 to 5	S3P2	S2P3
	>5	S3P2	S2P3

In the performance approach the specifier is free to modify the performance if other factors are involved. An example may be to increase the puncture resistance (Pn +1) if a softer substrate is used i.e. thermal insulation.

A flow chart was also developed which gave a system selection for warm deck roofs and for inverted roofs. Table 5 is based on a small section of the flow chart.

Table 5. System selector for a typical warm deck roof.

Step 1	Choose a deck/substrate Preparation	Close boarded timber Correct any uneven planks and punch in nail heads
Step 2	Select a vapour control layer	RH low: nailed RBM to minimum of S2P2 with sealed laps RH medium: nailed RBM as above, and fully bond a second S2P2 layer RH high: nailed RBM S2P2 and fully bond a metal-cored second layer
Step 3	Select thermal insulation After bonding/fixing insulation boards, for pour and roll or torch-on systems the following preparations are needed before the application of the first working layer	e.g Polyurethane (PUR) Apply a type 3G layer (specialised product originally developed in BS747 for use over wet concrete. Experience has shown blisters can develop when membranes are fully bonded to PUR boards)
Step 4	Select working waterproofing layer	First working layer: could be S2P2 but specifier is free to choose Final Layer: depends on application (see performance table) typical choice could be S3P2

3.3 Other Information in BS8747

Before considering the specification of the RBM waterproofing layer it has been assumed that the roof has been designed by a competent person and that the roof design has been considered for wind loading, condensation risk, designed for drainage and complies with the UK building regulations. For consideration as an RBM in BS 8747 the RBM must pass the following tests in EN13707:

- watertightness , for all applications
- root resistance for green or garden roofs.

BS 8747 also considers other product information and gives a typical range of values for tensile strength, elongation, nail shank tearing, static load resistance, impact resistance, flexibility at low temperature, flow resistance at elevated temperature, durability, external fire performance and reaction to fire.

Information is also given as to what performance level would be acceptable. For example a minimum value for nail shank tearing of greater than 175 N would be acceptable in all instances. Durability is

assessed by exposure to heat aging in an oven for 12 weeks (EN1296 [CEN]) and then assessing flexibility at low temperature. The UK expectation is that no change will take place for durable products. Such is the performance of polymer-modified polyester reinforced bitumen membranes that a service life in excess of 50 years is anticipated.

3.4 Worked Examples

The BSI committee did realise that the new approach taken to help the specification and selection of RBMs might, in the first instance, not be readily understood so a series of worked examples have been given in an annex. The worked examples chosen are:

- Single-storey rural school classroom
- Three-storey block of flats/offices
- Swimming pool
- Hospital refurbishment
- Garage block(domestic).

All of the worked examples follow the same format and blank forms are included for copying to aid the development of a specification.. The reasons for the choices made in the worked examples are given in each case.

4 CLOSING COMMENTS

The BSI committee reaslised the need to develop guidance for the specification and selection of reinforced bitumen membranes. This has in part been due to the active UK participation in the relevant meetings of CEN TC254 in developing EN13707. It has been the case that British Standards tend to lag behind the current practices of the day and only incorporate these practices into a Standard as they become the accepted and successful method of construction. In this context BS8747 is ground breaking in that it leads the industry into the use of EN13707 products rather than waiting to see what the industry would do. It would be difficult to produce effective specifications without the guidance in BS8747. The rag based felts were withdrawn from the old BS747 sometime ago because of their poor perfromance in construction methods incorporating thermal insulation on flat roofs. Such products will be legally marketed within Europe with a CE mark. It is therefore essential that a system is developed so that the lower performing products are used only in those applications for which they are suited. The use of low perfoming products could result in unexpected costs due to early replacement. It is anticipated that the use of BS 8747 will avoid such expense and result in the correct selelction and specification of reinforced bitumen membranes.

5 REFERENCES

Chaize, Alain., 1991, Classification FIT des systemes d'etancheite de toitures, Third Internation Symposium on Roofing Technology, National Roofing Contractors Association, USA.

BSI – British Standards Institution. Customer Services +44 (0)20 8996 9001.http://www.bsi-global.com.

CEN – European Committee for Standardization. Management Centre: rue de Stassart, 36 B-1050 Brussels.

11DBMC International Conference on Durability of Building Materials and Components
ISTANBUL, Turkey 11-14 May 2008

Wind Tunnel Tests of Various Mechanically Anchored Waterproofing Membranes

Hirokazu Ichikawa [1]
Nobuo Kato [2]
Hiroyuki Miyauchi [3]
Kyoji Tanaka [4]

T 22

ABSTRACT

The wind resistance of mechanically anchored waterproofing systems depends on the reliability of the fasteners. For designing safer mechanically anchored various waterproofing membrane systems, it is necessary to make clear the behaviour of them under strong wind. In this study, the wind tunnel test with various mechanically anchored waterproofing membranes was carried out to gain an understanding of the behaviour of waterproofing membranes and its relation to wind parameters against high wind speed. Two types full-scale size waterproofing membranes were exposed to high wind speed in wind tunnel. They are polymer-modified asphalt roofing sheet layered and poly-vinyl-chloride (PVC). The size of test specimen is 2.4-m wide by 5.5-m length and 0.5-m height without parapet. The space of fasteners used for the mechanically attached membrane was 600-mm. Wind tunnel test was carried out in condition of uniform flow and wind speed from 18m/s to 35m/s. The behaviour of membrane to high wind speed was observed, and the strain of waterproofing membrane and the axial force occurring at a fastener was measured. Both membranes were lifted up by negative pressure of wind and tensile force induced in a fastener. Each modulus in waterproofing membrane is different, and modulus in same type is different depending on the direction. The billowing condition of waterproofing membranes depended on their modulus and the strain was greater at the bias direction of fastener. The modulus of waterproofing membrane exerted an influence upon the frequency and fluttering patterns. It is necessary to consider the mechanical property of waterproofing membranes when the waterproofing membrane system was designed against high wind speed.

KEYWORDS

Mechanically anchored waterproofing system, Wind resistance, Waterproofing membrane, Wind tunnel

[1] Building Engineering Dept., Engineering Div., Tokyu Construction Co., Ltd., Tokyo, Japan, 1508340, Phone +81-3-5466-5293, Fax 3-5466-6259, ichikawa.hirokazu@tokyu-cnst.co.jp
[2] Institute of Technology, Tokyu Construction Co., Ltd., Kanagawa, Japan, 2291124, Phone +81-42-763-9511, Fax +81-42-763-9502, katou.nobuo@tokyu-cnst.co.jp
[3] Tokyo Institute of Technology, Structural Engineering Research Center, Kanagawa, Japan 2268503, Phone +81-45-924-5329, Fax +81-45-924-5339, miyauchi@serc.titech.ac.jp
[4] Tokyo Institute of Technology, Structural Engineering Research Center, Kanagawa, Japan 2268503, Phone +81-45-924-5329, Fax +81-45-924-5339, tanaka@serc.titech.ac.jp

1 INTRODUCTION

Typhoons 18 and 22 caused great damages to waterproofing membranes in Japan in autumn, 2004. In particular, as for the mechanically anchored waterproofing system for which waterproofing membrane are fixed only by fasteners on a ground, it was found that some of such membranes could not endure strong winds. In recent years, use of this method increases rapidly mainly on repair works since it is hard to be influenced by grounds however immaturity of such system was exposed in the technical aspects by occurrence of these damages. In particular, it seems the cause of such damages is the point that wind-resistant designs of the waterproofing membranes were performed with static wind loads as references and behaviours of a mechanically anchored waterproofing membrane system under strong winds were not clarified for the said designs. A number of studies on wind resistance of waterproofing membranes have been conducted by tests with simple and easy suction box systems. However, behaviours under a windy condition have not been actually reproduced. Winds, as an external force, were clarified by wind tunnel tests Baskaran & Savage [2003] conducted however behaviours of an entire waterproofing system have not been clarified yet.

The authors have undertaken a study on behaviours of mechanically anchored waterproofing membrane systems in a wind tunnel to grasp such behaviours. There are various types of waterproofing membranes and it is assumed that their dynamic behaviours are greatly affected by mechanical properties of waterproofing materials. From the above viewpoint, for this study, the authors selected waterproofing materials with different mechanical properties and discussed differences on behaviours of waterproofing membranes under a strong wind by wind tunnel tests of a mechanically anchored waterproofing membrane system using the materials.

2 WIND TUNNEL TESTS BY ACTUAL-SIZED SPECIMENS

2.1 Type of Waterproofing Membrane and Basic Physical Property

The authors selected two types of waterproofing membranes with different mechanical properties as specimens for the study, an asphalt waterproofing membrane in which two polymer-modified asphalt roofing sheets (reinforced type) are layered (denoted as "layered asphalt membrane") and a poly-vinyl-chloride (PVC) membrane (general composite type) as roofing sheets of synthetic polymer. Test pieces of 200 mm in length and 50 mm in width were cut off from the same materials as those used for the tests (three pieces from each of lengthwise, crosswise and diagonal 45 degrees directions). Woodcuts of 50 mm square was affixed to both ends of a specimen to prevent fractures of chucks during a tensile test and an effective test piece length was 100 mm. These test pieces were strained at 100 mm/min in a temperature condition of 20 degrees Celsius, and tensile strengths and extension rates were measured. Fig. 1 shows results obtained from the tests. Waterproofing sheet layers or reinforcing materials were inserted to the specimens. And so tensile strengths of the

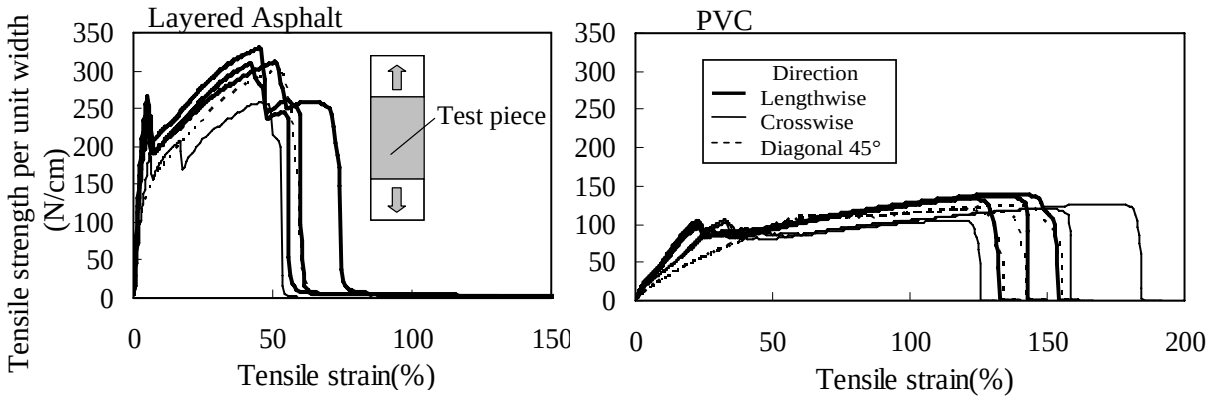

Fig.1 Results of tensile test concerning waterproofing membranes.

membranes were not uniform. The results were presented in "tensile strength per unit width". In the process of their behaviours, a reinforcing material breaks at first, then a waterproofing material strains and finally reaches a fracture. However, in the test piece cut off in a diagonal 45 degrees direction, remarkable tensile peaks were not found at an initial stage of straining.
According to Ichikawa *et al.*[2005], mechanical properties with an expansion lower than 1% in an initial region of a tensile test engage with a waterproofing membrane's behaviours under a strong wind. 1% modulus (tensile strength at 1% deformation) was higher in a layered asphalt membrane for all directions and the lower 1% moduluses were obtained from a PVC sheet respectively.

2.2 Measurement Item and Measurement Condition

2.2.1 Wind Tunnel and Specimen
Specimens without parapets of 2.4m in width, 5.5m in length and 0.5m in height shown in Fig. 2. They were set in a circuit boundary layer wind tunnel with a section area of 2.3m in height and 2.4m in width. According to Bienkiewicz & Sun [1997], various wind tunnel tests were carried out by their great efforts. Using models of roof pavers made of plexiglass and graphic tape as spacers were excellent. However, their objects are solid and thick. It is impossible to reduce the waterproofing membrane to be thin, transformable and not uniform. Though problem in the effect of the scale had been understood, to make clear the behavior of mechanically anchored waterproofing membrane against strong wind, it was necessary that the specimen used real material was exposed high wind speed of a wind tunnel. The tests were conducted under a condition without obstructions on the windward. A blockage rate of this wind tunnel test was 21.7%(= aspect area of specimen/wind tunnel cross section * 100). An ALC panel with a thickness of 100mm was used as a bed for membranes. The membranes were fixed in the bed with M12 bolts and nuts in 0.6m intervals(0.5m intervals for the upwind edge) through a circular metal plate of 75mm in diameter and 1.7mm in thickness.

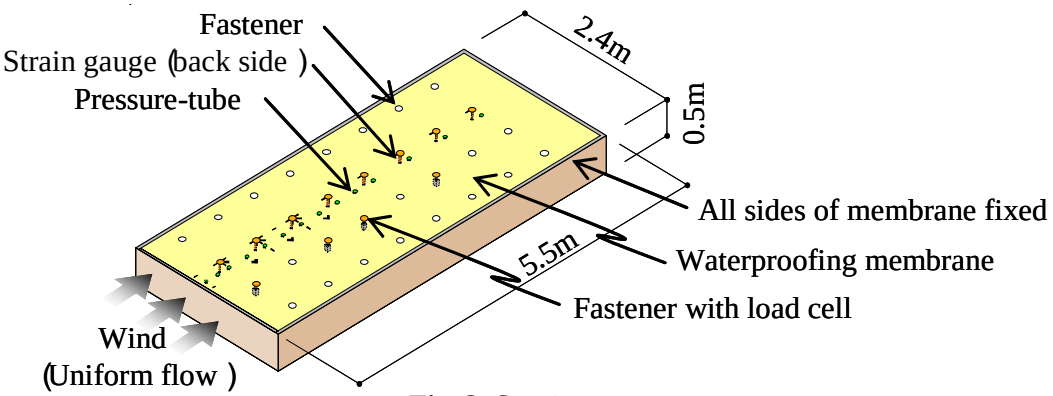

Fig. 2. Specimen.

2.2.2 Measurement Method
Figure 3 shows the measurement method. 14 wind pressure measuring taps were placed in the wind direction in a straight line. For wind pressures act on waterproofing membranes, pressures on the external and underneath (a gap between the membrane and the bed) of a membrane were led to a pressure anemometers from vinyl tube installed on the waterproof membrane with the aluminum pipe and differential pressure of external and internal on sheet were measured. The scale was put on the window of the wind tunnel, and the top of the swelling of the membrane was measured. Wind speed in the wind tunnel were measured in a pitot static tube installed at the position of 0.9m above the specimen's center. Deformations of membranes were measured by strain gauges (strain limit: 5%) attached on the membranes' back side. The temperature in the wind tunnel was around 15 degrees Celsius. Axial forces of the fastener fixing the membranes were measured by load cells (rated capacity: ±9.8kN, non-linearity : within 5%) set in the vicinity of the center, which was not affected by the wall effect. 8192 values were obtained from a tubing compensation for the data measured at 200Hz for 60 seconds in each measuring point.

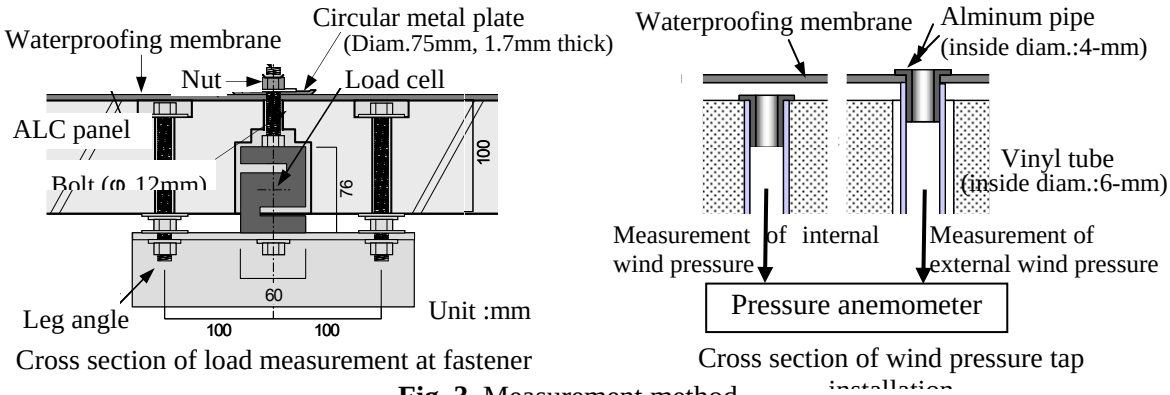

Fig. 3. Measurement method.

3 TEST RESULTS AND DISCUSSIONS

3.1 Observation Results of Waterproofing Membranes' Behaviours Caused by Wind

Figure 4 shows blister shapes in a fastener line of the specimen's center part at a wind speed of around 30m/s, for which the shapes are five times strained in the height direction as in the length direction.

Waterproofing membranes are sucked up by a wind and their shape become a swollen shape however the swells are divided since the membranes are fixed in the bed at certain intervals. Swellings on a PVC membrane were identified visually from wind speeds of around 10m/s and those on a layered asphalt membrane were identified visually from a wind speed of around 20m/s.

The wind speed at which a waterproofing membrane begin to swell is related to its mass. Large swellings are seen in the windward on each membrane. Swellings are higher in the PVC, followed by the asphalt and the membranes tend to be easy to swell as modulus is lowered. Fluttering motions were quick in the windward direction and slow in the leeward direction for all the membranes.

3.2 Wind Pressures Acting on Waterproofing Membranes

Distributions of wind forces coefficient acting on each waterproofing membrane are shown with a plane surface without waterproofing membranes in Fig. 5. One of the relation between the and the wind speed simulated beforehand shown in the right of Fig.5. A layered asphalt membrane has small swells and its wind pressure distribution is similar to the plane surface. On the other hand, for a PVC membrane, negative pressures, which are larger than those on the plane surface, are generated at the windward end and they decrease drastically on the leeward since their shapes change irregularly by behaviours of the waterproofing membranes.

The difference of wind force coefficient is thought to be an influence by the swelling of the membrane. A layered asphalt membrane has small swells and its wind pressure distribution is similar to the plane surface. On the other hand, for a PVC membrane, negative pressures, which are larger than those on the plane surface, are generated at the windward end and they decrease drastically on the leeward since their shapes change irregularly by behaviours of the waterproofing membranes.

The difference of wind force coefficient is thought to be an influence by the swelling of the waterproofing membrane.

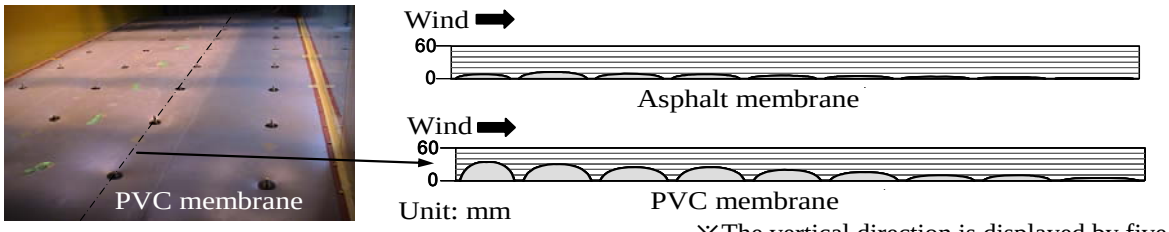

Fig.4. Swelling of waterproofing membrane by wind (wind speed: 30m/s).

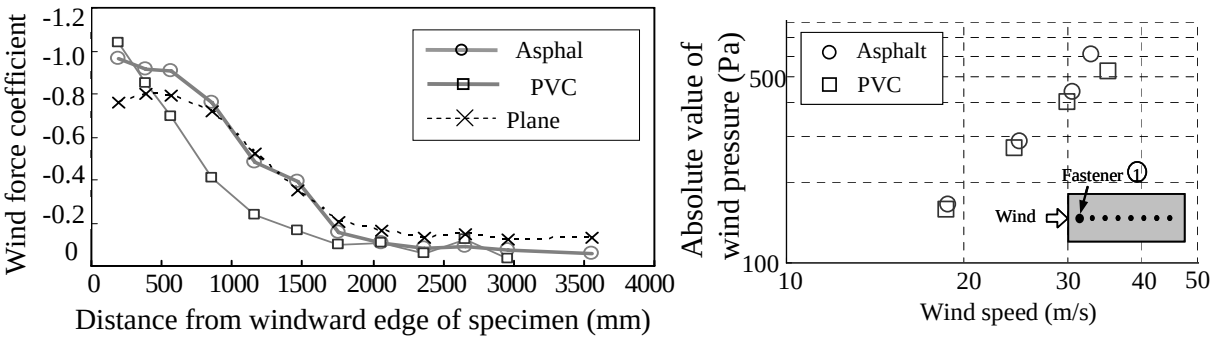

Fig.5. Distributions of wind force coefficient on each waterproofing membrane

3.3 Deformations and Behaviours of Waterproofing Membranes

Figure 6 shows strain changes of layered asphalt and a PVC membrane in one second in the upwind direction at the wind speed of 33m/s.

Tensile strains of the membranes are large on the windward, and small on the leeward same as the average wind pressure distributions.

This is similar to swells on membranes visually observed. Frequencies of the waterproofing membranes' fluttering motions were 10-16Hz on the windward and around 10Hz on the leeward therefore the cycle of fluttering motions on the leeward are longer than those on the windward. Moreover, a layered asphalt membrane with high modulus billows small and slowly, and a PVC membrane with low modulus do quickly and greatly.

Strains, variations and frequencies of the waterproofing membranes are influenced by mechanical properties of themselves.

Figure 7 shows tensile strain and tensile force of the membranes in one second in each direction from the fastener. For waterproofing membranes studied this time, strains around the fasteners were large. The average maximum strain for the PVC membrane was 0.27% and that for the layered asphalt membrane was 0.12% at the wind speed of 33m/s. Each maximum strain was measured at the first point on the windward or the second point on the leeward approximately 1m away from the windward, at which negative pressures are large, and in crossward direction or diagonal 45 degrees direction, in which moduluses are low.

The maximum momentary strain for the PVC membrane was 0.39%.

The tensile strain of the PVC membrane with lower modulus is larger, and the membrane in the directions in which modulus is lower deform easily as shown in the left of Fig. 7. However, the tensile force of the asphalt membrane with higher modulus is larger as shown in the right of Fig. 7.

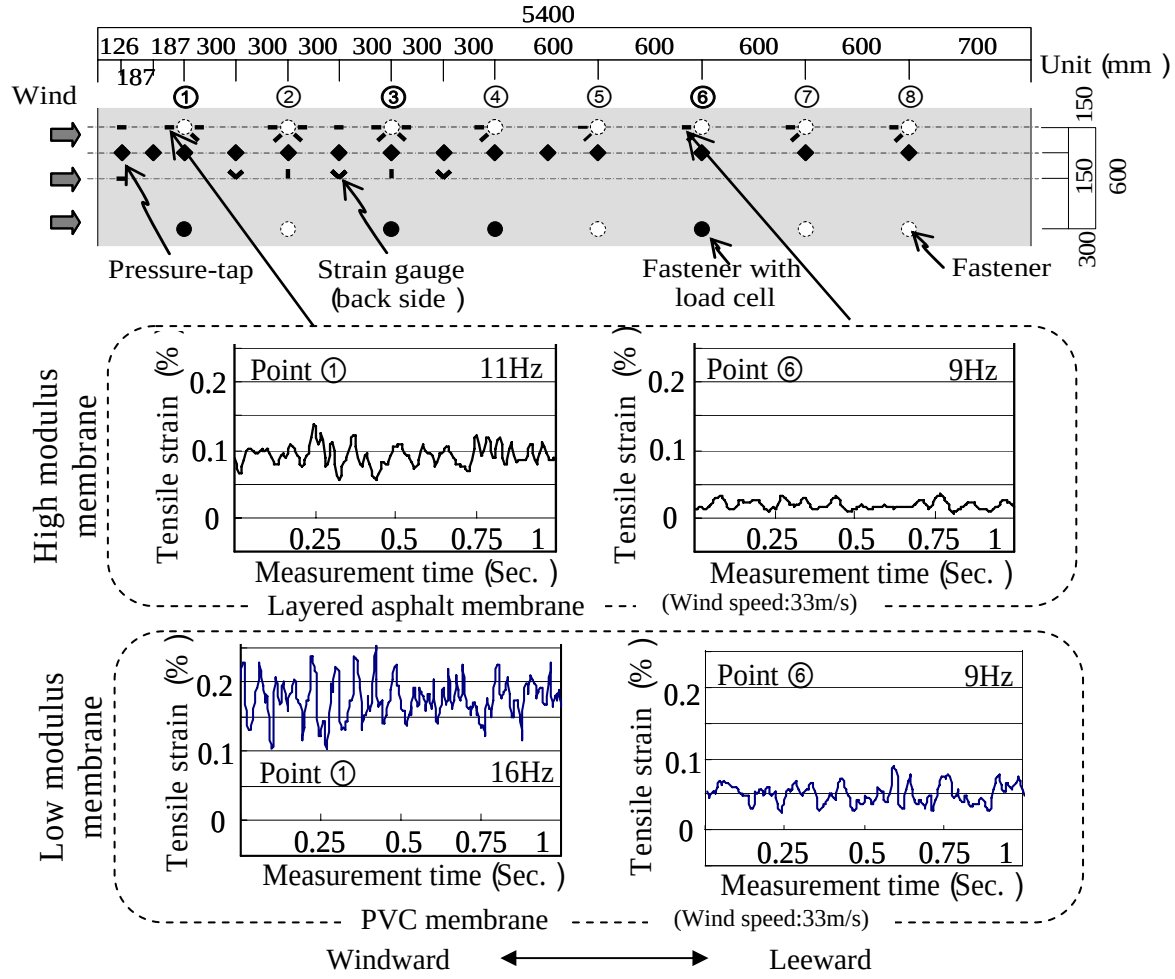

Fig.6. Tensile strain of membranes in one second on the windward direction of each position.

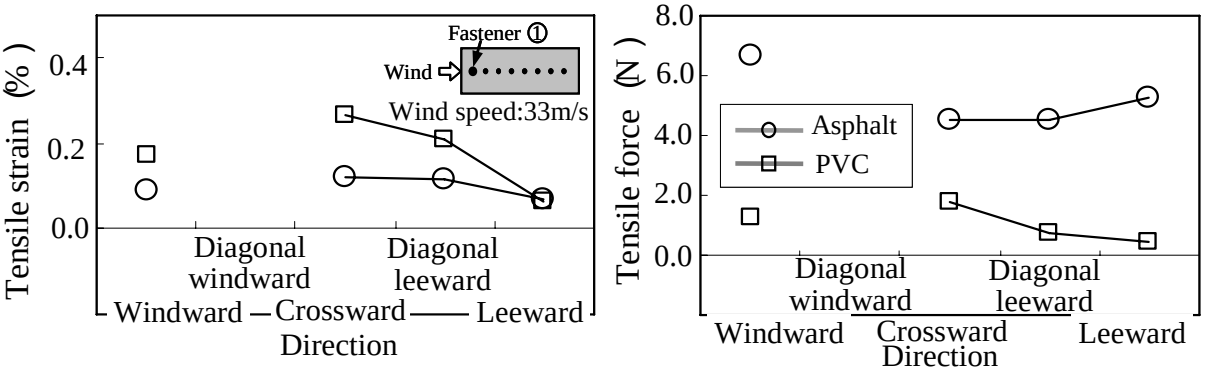

Fig.7. Tensile strain and tensile force of the membranes in each direction from the fasteners.

3.4 Relations of Wind Load and Waterproofing Membrane Tensile Forces

Figure 8 shows wind effect on mechanically anchored waterproofing membrane system. A typical mechanically anchored waterproofing membrane swells by the suction of the wind on them, as shown in the left of Fig. 8. Thus, tensile forces are generated in the waterproofing membrane as well as tensile and shear loads induced in the fasteners. The tensile force of the membrane balances wind force with perpendicular element. Therefore, the total of the perpendicular element force caused by the tensile force of the membrane on the edge of a fixing plate becomes equal to wind load on membranes that one fastener bears as shown in the right of Fig. 8. The axial force is generated in the fastener resisting the force pulling out fastener. Similarly, it is thought that the difference of the horizontal

component of the tension on the membrane around a fixed plate generates the shearing force in the fastener.

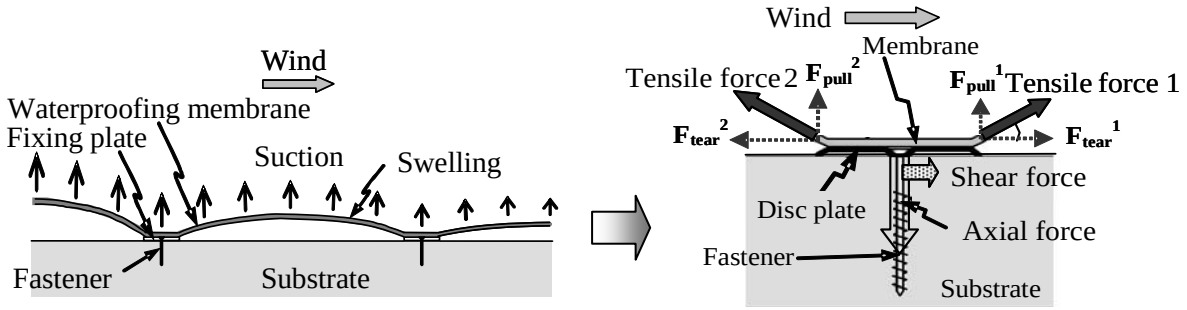

Fig.8. Wind effect on mechanically anchored waterproofing membrane system.

Figure 9 shows relations between tensile forces of the membranes and wind loads acting on them. The area of wind loads acting on membranes that the first fastener on the windward bears is 0.33m^2. In the case of the same wind speeds, larger tensile forces are generated in almost horizontally on a layered asphalt membrane with high moduluses than them in a upward direction on PVC membrane with low moduluses.

As previously mentioned, this means the tensile forces of the membranes balance wind force with their perpendicular element. Furthermore, in a same waterproofing membrane, a tensile force turns up as a wind load increases.

This is because the membrane expands by the wind load as shown at the right of Fig. 9. Therefore, the tensile force of membranes does not double even if the wind loads doubles. This tendency is strong because asphalt with high moduluses is horizontally near as shown in Fig. 9. On the other hand, the tensile force of PVC membrane with low moduluses does not change so much.

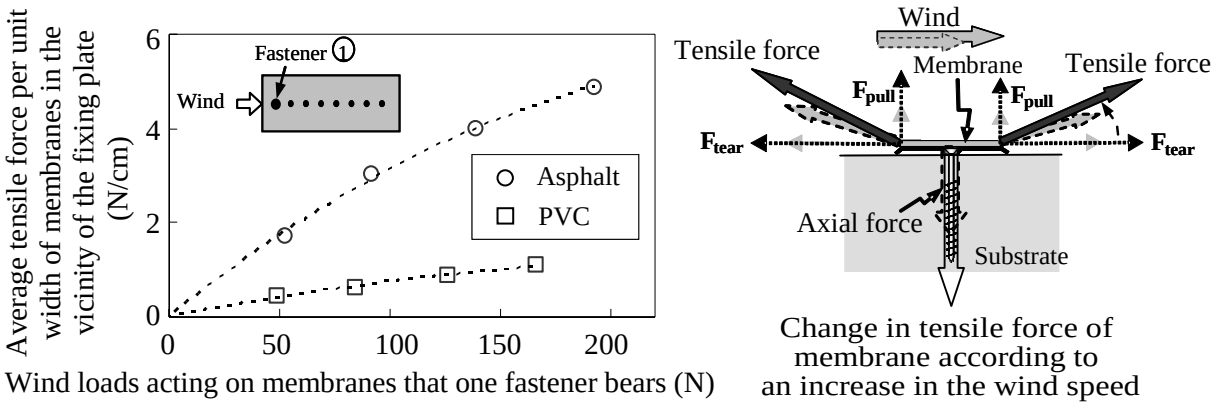

Fig.9. Relations between tensile forces of the membranes and wind loads acting on membranes.

3.5 Relations between Wind Speeds and Fastener Axial Forces

Relations between wind speeds and fastener axial forces in each membrane are shown in Fig. 10.

It has the fastener axial force and the wind speed in a linear relation. An axial force at a wind speed of around 30m/s (wind force = 551Pa) was an almost constant value of around 130N in a PVC and layered asphalt membrane, considering the mass of the membrane. Therefore, the mechanism that each membrane transmits the wind force to the fastener was confirmed.

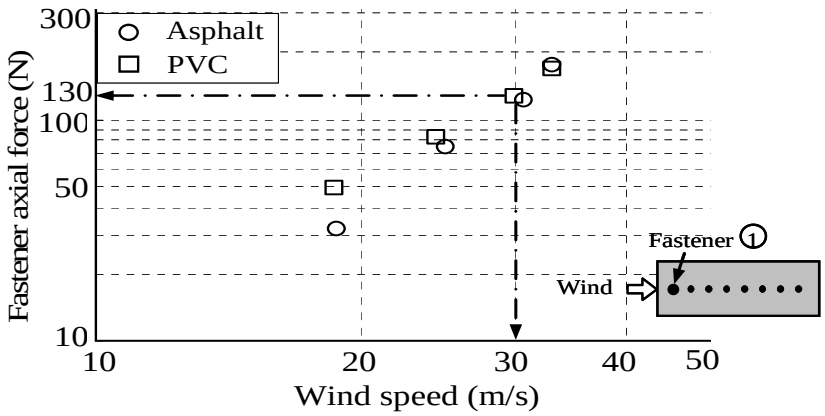

Fig.10. Fastener axial force and wind speed.

4 CONCLUSIONS

For two types of waterproofing membranes with various mechanical properties, behaviours of them in strong wind were studied by wind tunnel tests. Results are summarized as follows.

(1) A height of a waterproofing membrane's swell is related to a modulus of a waterproofing material and a waterproofing membrane with low modulus is easy to swell. In addition, a waterproofing membrane does not swell uniformly since it strains in a direction where a modulus is low.
(2) Behaviours of a waterproofing membrane are quickly in a windward and slowly in a leeward. Behaviours are different in each waterproofing material. A layered asphalt membranes with high modulus billows small and slowly and a PVC membrane with low modulus do quickly and greatly.
(3) A waterproofing membrane strains greatly around of a fastener and tensile forces are generated accompanied with such a motion. In the same wind speed, larger tensile forces are generated in a waterproofing membrane with high modulus around a fastener, and tensile forces of a waterproofing membrane with low modulus are small.

Wind tunnel tests of a mechanically anchored waterproofing membrane system were performed by waterproofing materials with various mechanical properties. From the tests, we have clarified some qualitative properties of strains of waterproofing membranes with various waterproofing materials and those of forces generated in a fastener. The study will be continued so as to propose safer wind-resistant designs for mechanically anchored waterproofing membrane systems.

REFERENCES

Ichikawa, H., Bartoko M., Kato, N., Miyauchi, H., Sasaki, T. & Tanaka, K. 2005, 'Behavior of mechanically anchored waterproofing membrane exposed to high wind speed of wind tunnel' *J. Struct. Cnstr. Eng., AIJ,* No.593, pp.17-24. *in japanese.*

Miyauchi, H., Kato, N., Ichikawa, H. & Tanaka, K. 2006, 'Behavior of mechanically anchored waterproofing membrane exposed in high wind speed of actual wind' *J. Struct. Cnstr. Eng., AIJ,* No.610, pp. 29-34. *in japanese.*

Ichikawa, H., Kato, N., Miyauchi, T. & Tanaka, K. 2007, 'Wind tunnel tests of various mechanically anchored waterproofing membranes' *J. Struct. Cnstr. Eng.*, AIJ, No.615, pp. 47-52. *in japanese.*

Baskaran, B.A. & Savage, M.G. 2003, 'Wind pressure measurement on fullscale flat roofs', in *Journal of the Roof Consultants Institute*, 21, (4), pp. 17-21.

Baskaran, B.A. 2004, 'News update - standard test method for the dynamic wind uplift resistance of mechanically attached membrane roofing systems', in *Journal of the Roof Consultants Institute*, RCI Interface, 22, (2), pp. 1.

Baskaran, B. A. & Ko. S.K.P. 2005, 'A Guide for the Wind Design of Mechanically Attached Flexible Membrane Roofs', in *Construction Innovation, Volume 10, Number 4*, NRC-IRC.

Baskaran, B. A. 2005, 'Newsbrief - SIGDERS project, Phase IV,' Construction Innovation, 10, (4), December, pp. 5.

B. Bienkiewicz & Y. Sun, 1997, 'Wind loading and resistance of loose-laid roof paver systems', in *Journal of Wind Engineering and Industrial Aerodynamics, Volume 72,* pp. 401-410.

B. Bienkiewicz & Y. Sun. 1992, 'Wind-tunnel study of wind loading on loose-laid roofing systems' in *Journal of Wind Engineering and Industrial Aerodynamics, Volume 43, Issues 1-3*, pp.1877,

11DBMC International Conference on Durability of Building Materials and Components
ISTANBUL, Turkey 11-14 May 2008

Service Life (Model) for Bituminous Roofing

Erik Brandt [1]
Tommy Bunch-Nielsen [2]

T 22

ABSTRACT

Leaking low-sloped roofs, i.e., roofs with roofing felt or roofing membranes, have been responsible for extensive major damage to buildings all over the world. The causes have been several, e.g., bad materials – or rather materials and materials combination used in a way they were not suited for - bad design with difficult details hard to make at a building site and bad workmanship. In Denmark the problems have been dealt with in different ways including requirements for minimum slope, for the substrate and for the roofing felt/membrane. To avoid problems a model for service life prediction of low-sloped roofs was developed some years ago. The model was based on experience. The paper explains the background for the model and discusses how the model fits also with later gained experience. In addition, the paper describes an investigation on service life of SBS modified bituminous roofing carried out in cooperation between the Danish Bituminous Roofing Manufacturers, The Danish Roofing Advisory Board and the Danish Building Research Institute. The findings confirm the predictions of the model as regards SBS modified roofing felt.

KEYWORDS

Roofing material, Roofing felt, Low-sloped roofs, Service life, Modelling.

[1] Danish Building Research Institute, Aalborg University, DK-2970 Hoersholm, Denmark, Phone +45 4574 2370, ebr@sbi.dk
[2] Danish Roofing Advisory Board, DK-2970, Hoersholm, Denmark, Phone +45 4566 2922, tbn@bmd.dk

1 INTRODUCTION

Leaking low-sloped roofs, i.e., roofs with roofing felt or roofing membranes, have been responsible for extensive major damage not only to the roof covering itself, but also to the underlying parts including underlay, trusses and occasionally to furniture and fixtures In Denmark the causes for the problems have been several.

Earlier the use of horizontal roofs was quite common, as it gave an architectural impression which was popular at the time and besides alterations or expansion of the buildings was relatively simple. However the horizontal roofs led usually to ponding of water followed by destruction of the roofing felt/membrane due to formation of ice and prolonged exposure to humidity. Also the materials used earlier were less durable than materials used today, e.g., the glass fibre reinforcement in earlier generations of roofing felt led to brittle products and for PVC-roof membranes big problems were caused by shrinkage due to evaporation of plasticisers. Finally problems occurred due to the use of materials or combinations of materials used in a way they were not suited for, bad design with difficult details hard to make at a building site and bad workmanship.

In Denmark the problems have been dealt with in different ways. The horizontal roofs were abandoned when requirements for minimum slope were introduced in the building codes in 1981. New generations of materials have come to the market e.g., new reinforcement and plastic modified bitumen for the roofing felt and more suited plasticisers for PVC membranes. Also the underlay for the roofing is of importance for the service life of the entire constructions and here requirements have been set by the involved key partners, e.g., Danish Roofing Advisory Board.

2 SERVICE LIFE MODEL FOR ROOFS

It is not possible to state a precise service life for roofing materials because it is dependent on a number of different factors. Some years ago a model for service life prediction of low-sloped roofs was developed based on experience taking into account the factors considered most important for the deterioration of roof membranes in the past [Bunch-Nielsen, T., 1997]. The factors in the model are:

- The type of roof membrane (p - product)
- The number of plies (n)
- The slope of the roof (s)
- The substrate (u – underlay)
- The fastening to the substrate (f)
- The design, especially the details (d – design)
- The traffic on the roof (t – traffic)
- The maintenance (m)

Based on the factors the service life can be expressed as:

$$L = T \bullet p \bullet n \bullet s \bullet u \bullet f \bullet d \bullet t \bullet m$$

T is the anticipated service life for a reference roofing material. The remaining factors all have values between 0 and 1, i.e., T is the maximum service life on condition that all other factors are at their maximum.

2.1 Roof Membrane – The Product

In Denmark an important property for a roofing membrane is its ability to function in a cold climate with many freeze-thaw cycles. From assessments, we find that this is, on the average, best achieved with a SBS-modified bitumen. Consequently a roofing felt made from SBS-modified bitumen and reinforced with polyester carrier - which is the most commonly used roof membrane in Denmark – is

used as the reference in the model and the service life for a roof of this type is estimated to be 50 years, i.e., the factor T in the formula is 50 years. For other types of roof coverings a reduction factor is used according to the following:

Roof covering	SBS-modified bitumen	APP-modified bitumen	Oxidized bitumen	PVC reinforced	EPDM
Factor p	1.0	0.7-0.9	0.8	0.8	1.0

2.2 Number of Plies

The number of plies in a roof covering has bearing on the service life. In Denmark roof coverings are traditionally made with 2 plies (earlier in built-up roofs even more plies were used). The factors used are the following:

Number of plies	2	1
Factor n	1.0	0.8

2.3 Slope of The Roof

The slope of the roof is of importance for the time of wetness and for the risk of water ponds. Ponds on the roof may lead to a risk of a build-up of ice which can remove the protective granules or even tear the roofing material apart due to temperature movements under freeze-thaw cycles. The influence of the slope is expressed according to the following:

Slope	≥ 1:5	≥ 1:20	≥ 1:40	< 1:40
Factor s	1.0	0.9	0.8	0.6

2.4 The substrate – Roof Underlay

In Denmark a number of different substrates have been used and quite a few have been abandoned due to problems, e.g., lack of dimensional stability under in use conditions. Nowadays are used products with a record of satisfying performance under in use conditions, mainly boards such as plywood, oriented strand board (OSB), and insulation materials. In case "soft" insulation materials (compressive strength less than 40 kN/m²) are used it is necessary to apply a hard load distributing layer on top of the insulation. In addition, it is normal to renovate old roofs with roofing felt by applying a new layer on top of the old. The influence from the substrate is expressed as the following:

Substrate/underlay	"Soft" insulation	"Hard" insulation	Boards, Plywood, OSB	Old roofing On hard substrate	Other substrates without documentation
Factor u	0.7-0.9	0.9-1.0	1.0	1.0	0.6- 0.4

2.5 The Fastening to The Substrate

Fastening of a roof membrane to the substrate can be achieved in different ways. Traditionally roofing felt is bonded or torched to the substrate, but mechanical fastening has been the dominant method for the last 15 years. Membrane securement might also be achieved by ballasting the membrane. The influence from the fastening is expressed as the following:

Fastening	Bonded or welded roofing felt	Mechanically fastened 2 ply roofing felt	Mechanically fastened 1 ply roofing felt	Membrane fastened with ballast	Mechanically fastened synthetic membrane
Factor f	1.0	1.0	0.9	0.9	0.8

2.6 The Project – Design of Details

The design has a major influence on the service life and especially the design of the details. It is important to include here a requirement that the details shall be buildable, i.e., it shall be possible to construct the details on a building site. The risk for failures increases with the number of details on a roof and consequently the factors mentioned below should be reduced, e.g., by a factor 0.8 for roofs with many details. The factors used are the following:

Details	Details in accordance with TOR[1] directions	Details not in accordance with TOR
Factor d	1.0	0.8

[1)] TOR is the Danish Roofing Roofing Advisory Board

2.7 Traffic on the Roof

The roofing material and the details can been damaged due to compression of the underlay from traffic on the roof. The influence of the traffic is expressed according to the following.

Traffic	Pedestrian traffic for maintenance of roof only	Pedestrian traffic for maintenance of mechanical installations, rooflights etc.	
		Hard substrate e.g., plywood	Soft substrate e.g., mineral wool
Factor t	1.0	0.8	0.6

2.8 Maintenance

The roof membrane itself is not anticipated to require maintenance, but details, e.g., flashings and joints and the drainage system need maintenance as part of preventive maintenance. The influence of the maintenance is expressed according to the following:

Maintenance	Maintenance according to TOR requirements	Maintenance not in accordance with TOR req.	No maintenance
Factor s	1.0	0.8	0.6 – 0.4

Because the assessments naturally are performed with a considerable uncertainty, the service life should only be given as the closest 5 year interval found as result of the calculation, e.g., 25-30 years.

3 SURVEY OF ROOFS WITH ROOFING FELT

To verify some of the assumptions in the service life model, 12 roofs have been surveyed. The roofs were all with bituminous roofing produced by Danish manufacturers. The inspected roofs are taken from a database of more than 15000 roofs under a warranty system for roofs in Denmark.

The warranty system was established in 1989 and was in full service in 1991 with approximately 1 x 10^9 m^2 of roofs added each year. The warranty period is 10 years and in that period less 0.5 percent of the roofs experience problems.

Please note that service life and warranty period are two different things and the expected (and experienced) service life time is fortunately much longer than the 10 year warranty period.

UV- radiation and heat from the sun is normally considered to be the main mechanism regarding ageing of bituminous roofing. To protect the surface of the membrane against UV-radiation it is normally protected by slate granules. It is of utmost importance that the uppermost protective layer is not damaged e.g., during the laying of the roof, from ice build-up or during maintenance in the service life of the roof.

The survey included a visual inspection of the roofing felt as such, the condition of the details and a subjective assessment on the remaining service life of the roof covering.

Besides specimens of the membrane were taken out form the surveyed roofs and the membranes were tested on the labs of the producers to detect any changes in properties during the use.

3.1 Visual Inspection of Roofs

The surveys were done according to an inspection list made for the purpose. The list included relevant information about the building owner, geographical position, etc. The technical evaluation was assessed as shown in the following example:

Roof covering:	2 ply SBS-modified bitumen Slope about 30°
When applied:	1991
Description:	The roof is made as a saddle roof with felting on angle fillets. The roof is build together with a lower low-sloped roof. This roof is assessed separately.

Visual inspection:

Overall impression:	Some deformations in the substrate (roof elements) are clearly visible. The roof covering itself looks acceptable.
Granule covering:	Generally good. ”Surface cracks” on the west side of the building
Tightness of welding seams:	Ok
Fastening:	Ok
Cracks in the roofing felt:	Starting to appear on angle fillets
Blisters:	None
Folds in the covering:	None
Cracks at flashings etc.:	None
Damage around roof lights:	No rooflights
Algae etc.:	Some algae on north facing surfaces of angle fillets
Valleys:	No valleys
Drain:	The roof is drained over the edge of the roof
Further remarks:	None

Estimated remaining service life based on the visual inspection: at least 15 Years

Using the service life model for this roof gives the following result:
L = 50 • 1 • 1 • 1 • 1 • 1 • 0.9 • 1 • 1 = 45 years.

Similar, the other roofs give in average results corresponding to the subjective assessment of the roof.

3.2 Laboratory Analysis on Test Samples

Laboratory tests on samples taken from the inspected roofs were performed by the 2 Danish producers in their own laboratories. The properties tested were those considered most crucial for a long service life. The roof membrane must remain watertight, weather-resistant and be able to resist influence from the underlying substrate.

All roofs are exposed to high temperatures in summer time and it is for that reason important that the bitumen is high quality and not sensitive to heat ageing. Temperatures of 70 to 80 ^{o}C can easily be reached on a hot summer day even in Scandinavia.

Table 1. Relevant properties for bituminous roofing.

Softening point/flow resistance	The flashings must be fastened so that they remain intact.
Cold bending:	The membrane must remain flexible in cold weather to resist traffic on the roof and the protective bitumen must not crack
Adhesion of the protective layer:	The membranes granule coating must remain intact to protect the bitumen from UV-radiation.
Tensile strength and elongation:	The membrane must remain flexible and be able to resist small movements in the substrate.
Shear and peel strength of joint:	The shear and peel strength of the joint must remain high to render the membrane watertight.

It is not possible to test the shear and peel strength of the joint on samples taken out from the roof as all roofs inspected are 2 layer systems. The results of the laboratory investigations were:

Table 2. Test results for the test samples taken from the surveyed roofs.
L = longitudinal, T = transversal.

Roof #	Tensile strength, L[1]	Tensile strength, T	Elong-ation, L	Elong-ation, T	Cold bending[2)]	Softening Point	Adhesion of granules	Flow resistance	Year of Installa-tion
1	1356	1030	45	53	-20	103,6	95	90	1992
2	1056	826	32	33	-8	99,4	95	80	1992
3	1196	836	49	48	-20	107,6	93	80	1993
4	1218	968	51	53	-20	105,7	94	90	1992
5	460	931	42	48	-6	122	97	100	1991
6	754	1025	41	36	4	91	97	70	1991
7	709	1082	45	46	-6	112	94	100	1991
8	734	970	43	38	-6	99	94	80	1991
9	714	957	41	35	-2	100	91	90	1991
10	641	679	39	40	4	89	92	70	1991
11	1167	1006	39	47	-2	115	94	100	1991
12	-	-	-	-	-4	109	-	100	1991
Sum	10005	10310	467	477	-86	1253.3	1036	1050	
Mean	909.5	937.3	42.5	43.4	-7.2	104.4	94,2	87.5	[3)]

[1)] It is difficult to see on samples what is parallel to production direction
[2)] Cold bending is on the top side of the product
[3)] Samples are taken in 2003

Table 3. Test results for the test samples taken from the surveyed roofs compared with the requirements.

Properties	*Test method*	*Unit*	*Requirement*	*Results from samples mean value*
Tensile strength, longitudinal	EN 12311-1	N/50 mm	500	909,5
Tensile strength, transversal	EN 12311-1	N/50 mm	500	937,3
Elongation, longitudinal	EN 12311-1	%	35	42,5
Elongation, transversal	EN 12311-1	%	35	43,4
Cold bending	EN 1109	ºC	-20	
Cold bending after ageing	EN 1109/1296	ºC	0	-7,2
Flow resistance	EN 1110	ºC	100	87,5
Adhesion of granules[1)]	EN 12039	g/m²	770-910	834,3
Softening point		ºC	125 [2)]	104,4

[1)] Amount of granules varies from 1100 to 1300 g/m
[2)] No requirement, typical value

4 DISCUSSION AND CONCLUSION

Based on the findings from the visual inspections it is believed that well performing membrane roofs can be achieved provided that the above mentioned factors are taken into account when designing and executing the roof, i.e.:

- to obtain a good roof a high class roof covering is necessary,
- two plies will generally provide better protection than one layer,
- a roof with a well defined slope will eliminate/reduce the risk of ponding and decrease the time of wetness and the risk of ice building,
- the construction including the underlying substrate shall be stable enough to avoid deflections that may damage the roof covering,
- the roof shall be designed taking into account not only the constructions but also the installations and any complications that may arise due to the severe exposure to water and high relative humidity,
- the structure that supports the roof shall be stable enough to avoid deflections that may damage the watertight layer and the surface covering,
- the fastening shall secure the roof covering and must not cause unintended, increased load on the membrane itself,
- all details shall be well described/illustrated, easy to construct at the building site and preferably with a good use record (or tested for watertightness),
- pedestrian traffic should be avoided as far as possible or measures should be taken to protect the membrane from direct contact,
- the roof shall be maintained regularly--preferably on the basis of regular inspections and especially regarding details etc.

Undoubtedly the factors mentioned are crucial for the service life . The findings from the visual inspections and the laboratory tests seems to confirm that the service life model - at least for bituminous roof membranes - gives a good estimate of the service life.

It should be emphazised that the model is rough and with considerably uncertainties as some of the factors are based on individual evaluation.

The experience from the few problems in the warranty shows that it is often the details of the roof that fail – which is in accordance with the findings in the survey.

Therefore the service life time model should emphazise the use of correct details in the roof design more in order to secure against water infiltration etc. It is proposed that the model is improved by using a more detailed factor for design as shown below.

Details	No critical details[1)]	≤2 critical details per 100 m² roof	≤10 critical details per 100 m² roof	≤20 critical details per 100 m² roof	>20details per 100 m² roof
Factor d	1.0	0.8	0.6	0.4	0.3

[1)] Critical details are details not in accordance with the design rules as stated in the Danish design guide for roofs or wrongly executed details, e.g., too close together to ensure watertightness. An example of a critical detail is a flashing with a height lower than the minimum height 150 mm as stated in the Danish design guide. In the table 1 m flashing is considered equivalent to 1 penetration.

Figure 1. Example on two roofs with different slope but same roofing felt. Both were assessed during the survey.

Figure 2. Example of a dead low-sloped roof with ponding water. Ponding water leads to a risk of reduced service life due to increased exposure of the roof membrane to moisture and freeze-thaw cycles.

Figure 3. Example on different penetrating details normally seen on a roof.

Figure 4. Superficial "cracking" in the bitumen on steep surfaces leads to reduced protection by the granules.

Figure 5. Example of ponding water in a valley. In this case the water remained in the valley almost permanently and, as a consequence, the protective granules were gone.

Figure 6. Sampling of specimen for laboratory testing.

REFERENCES

Bunch-Nielsen, T., 1997. Designing roofs with roofing felt and roof membranes (in Danish), Danish Roofing Advisory Board.

EN 13707. Flexible sheets for waterproofing. Reinforced bitumen sheets for roofs.

ETAG 006. "Guideline for European Technical Approval: Mechanically fastened waterproofing". EOTA 2007.

Flexible Polyolefin Roofing Membranes: 15 Years Of Field Experience

Hans-Rudolf Beer [1]
Anthony Mayr [2]

T 22

ABSTRACT

Flexible polyolefin (FPO/TPO) roofing membranes were introduced in 1991 and have since gained wide acceptance in the European as well as in North American market place. The first TPO test roofs were installed in 1988. Hence in 2008 there are data available looking back on twenty years of field experience. At the occasion of 15 years of experience with installed TPO roofs a European TPO manufacturer has undertaken a field study on the long term behaviour of such products.

The paper presents the results of the constant monitoring of 42 installed roofs aged up to 15 years old. These data are compared with two specific sampling and testing projects carried out on six roofs by a third party testing institute after 10 and 15 years of field exposure, respectively.

Mechanically-attached and gravel-ballasted roofs have been considered. On site roof inspections showed all investigated roofs in good and fully functional conditions. Samples were taken for subsequent laboratory testing. All sample cutting spots could be securely patched by overwelding with new membrane pieces. Laboratory testing included properties such as tensile strength and elongation at break, low temperature flexibility, peel and shear strengths of the welded seams, accompanied by surface examinations using optical and electronic microscopy. No or marginal deterioration of the material properties were found.

The conclusions are that the investigated types of flexible polyolefin roofing membranes will fulfil their waterproofing and protection function for at least several decades.

KEYWORDS

Roofing, FPO, TPO, Longevity, Roofing membrane

[1] Sika Technology AG, CH-6060 Sarnen, Switzerland, Phone +41 41 6669966, Fax +41 41 666 97 90, beer.hans-rudolf@ch.sika.com
[2] maxon motor ag, CH-6072 Sachseln, Switzerland, Phone +41 41 6661500, Fax 41 41 6661650, anthony.mayr@maxonmotor.com

1 INTRODUCTION

Durability of building materials is – besides aesthetics – the most often discussed topic among building owners and architects. Upon introducing new materials, the subject of service life is of crucial importance. Lacking track records, the extrapolation of accelerated ageing tests data is the only means for meaningful predications on the durability of the new products.

Flexible polyolefins for roof waterproofing have been introduced to the market in 1991. Since then they have gained wide acceptance in the European as well as in the North American market place [Baxter, 1998; Beer, 1995; Beer, 1997; de Palo, 1995, Foley]. The common designation for flexible polyolefins is FPO in Europe, whereas they are named TPO (for thermoplastic polyolefins) in North America. Taking into account the trial phase prior to market introduction more than 15 years of field experience in roofing applications have now been gained with these materials.

When TPO roofing membranes were first introduced in Europe for flat roofs the service life of the product was predicted at several decades. This prediction was supported by manufacturer experience, testing programmes, and a series of field tests which had begun in 1989. Definitive statements on the durability of roofing membranes are only possible on the basis of long-term field investigations. Several such studies on the durability of the first TPO membranes have been conducted.

The most comprehensive study was carried out by Rieche and Wehrle [1999] on behalf of the membrane manufacturer at the occasion of ten years of field experience. The results were presented to the waterproofing community by Beer and Keiser [10]. The overall assessment of these studies was very positive regarding the durability of the manufacturer's TPO roofing membrane.

The fact that the observed deterioration of the material properties was only marginal, supports the previous assumption of a service of several decades.

Having reached 15 years of field experience with TPO membranes the study carried out after 10 years has been repeated. The results of this 15 year update are presented in this paper.

2 METHODOLOGY

The investigation described here is based on a field study of roofing membranes on 42 roofs covered with TPO membranes with fibre glass mat reinforcement (G type) or combined reinforcement of fibre glass mat and polyester scrim (S type). On behalf of the manufacturer the German Institute for Building Protection, Building Materials and Construction Physics [11] examined and evaluated four roofs of various age, taking into consideration the overall evaluation roofs monitored by the manufacturer. Thus a total of 162 samples (Fig. 1) of TPO roofing membranes with ages up to 15 years were collected and examined.

The roof assessment and testing of samples of the four roofs was done by the Institute independently of the manufacturer's surveys, according to the following criteria:

Roof assessments: General condition of roofing, roof assembly, flashings, welded seams, construction technology aspects.

Material samples: Thickness, tensile strength, elongation at break, low-temperature flexibility, peel strength and shearing tensile strength of site-welded seams, and microscopic investigation of the membrane surface.

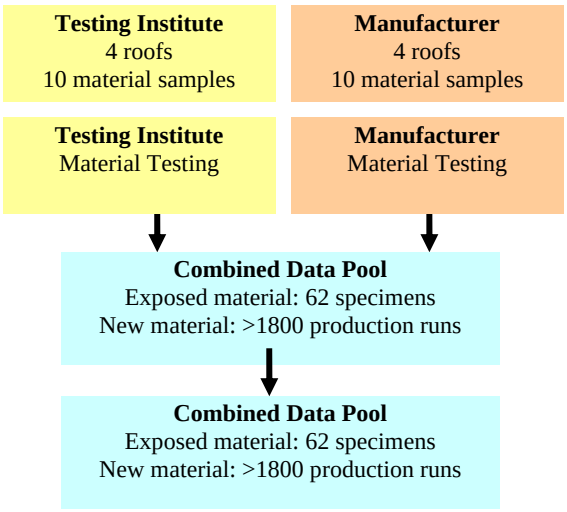

Figure 1. Data structure.

These properties are essential for predicting the durability of polymeric waterproofing membranes. By merging the data of the Institute and the manufacturer the long-term stability and durability of TPO roofing membranes of types G and S can be predicted, supported by a broad base of data and using methods of accelerated artificial weathering. The longer the observation period and the larger the number of investigated roofs, the more reliable the data obtained through field investigation is for predicting service life. A more detailed discussion on providing a forecast in the product and system development phase and subsequent reviews of the forecast in the utilisation phase has been presented by Beer and Keiser (2000).

3 RESULTS

3.1 Roof Assessments

All four examined roofs were found to be in good general condition (Fig. 2). The edge securement (Fig. 2) and the flashings at penetrations such as curbs (Fig. 3) were intact. All seams probed with a screwdriver were tight. All sampling locations (Fig. 4) could be patched without problem by welding using the standard methods described in the installation guidelines.

Figure 2. Two roofs investigated by Rieche [2004]. Left: Gravel ballasted industrial roof at Flawil, Switzerland (a typical application of G-type membranes). Right: Mechanically attached industrial roof at Ehingen, Germany (a typical application of S-type membranes).

Figure 3. Curb flashing detail, industrial building at Ehingen, Germany.

Figure 4. Sampling location on industrial building at Fellbach, Germany.

Comparing with the study conducted in 1999 [9], no changes to the technical or visual condition of the roofs were detected.

3.2 Mechanical Properties

To summarize the characteristics of various polymeric waterproofing membranes in uniform terms, one can express the change of properties over time in relation to the properties of new material. This method was used in this study. Mechanical properties of new material show a range of values, due to certain technical aspects of production and measuring. This distribution of values can be quantified using standard deviation methods. For the graphic display, a confidence interval of 99% was chosen. Of 100 measured values of new material, 99 are within the range of distribution.

If values measured on a sample from an exposed roof are within this confidence interval, the material properties have not changed significantly in comparison with the new condition.

3.2.1 S-type Membranes

Material investigations of S-type membranes showed that the mechanical values for elongation at break and tensile strength even after up to 15 years of exposure lie within the described distribution range for new material. Hence, there is no significant change of properties.

Figure 5 contains representative examples displaying the tensile strength of the S-type membrane specimens.

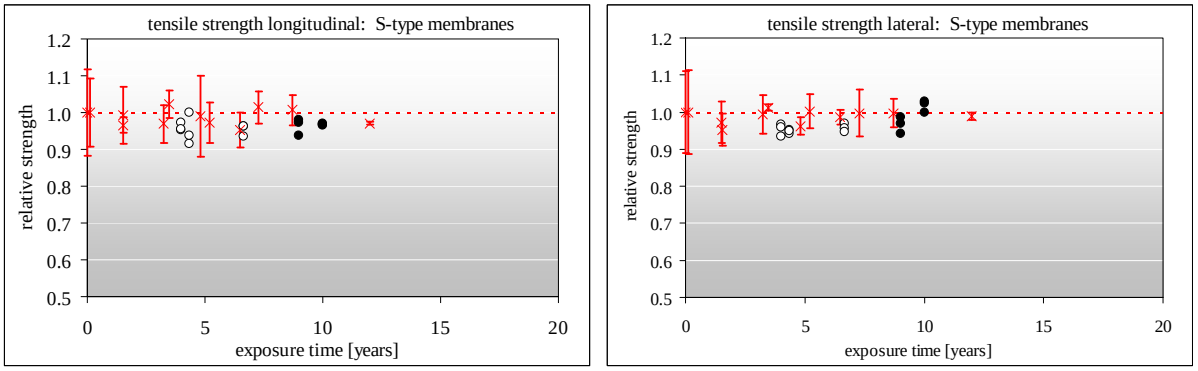

Figure 5. Relative tensile strength of S-type membranes after field exposure.
● data Rieche, 2004, ○ data Rieche, 1999, x manufacturer's continuous roof monitoring data.

3.2.2 G-type Membranes

Measured values of elongation at break for G-type membranes were similar to the results of S-type membranes; there was no significant change over time (Fig. 3: Elongation at break).

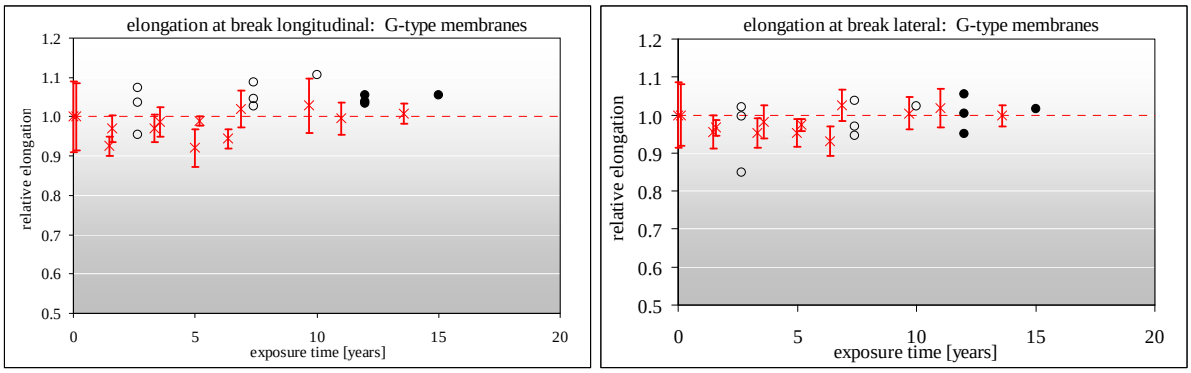

Figure 6. Relative elongation at break of G-type membranes after field exposure.
● data Rieche, 2004, ○ data Rieche, 1999, x manufacturer's
continuous roof monitoring data.

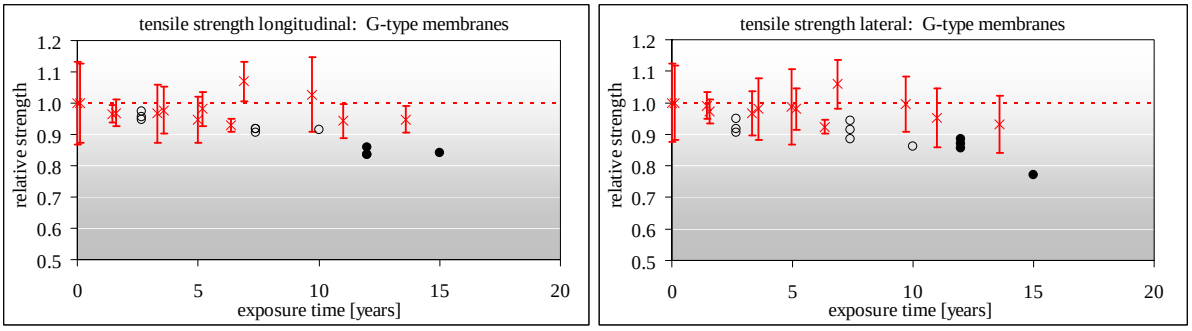

Figure 7. Relative tensile strength of G-type membranes after field exposure.
● data Rieche, 2004, ○ data Rieche, 1999, x manufacturer's
continuous roof monitoring data.

In the study conducted by Rieche [2004] the tensile strength of a G-type membrane showed a drop of 15% in machine direction (longitudinal) and 22% in cross direction (lateral) after 15 years of field exposure (see Fig. 7).

The manufacturer's continuous monitoring of field roofs reveals a decrease in tensile strength of G-type membranes as well, however, to a lower degree than Rieche's [2004] findings.

3.3 Other Properties

The thickness of aged membranes samples was measured according to standard methods (DIN 18531). Only the overall thickness was determined, but not the thickness of different membrane layers. For both G- and S-type membranes no change in material thickness due to exposure on the roof was found (Figure 7).

The low-temperature flexibility test produced no cracks in spite of using a testing temperature more stringent than that prescribed by standards (-35 °C instead of -20 °C) [DIN 18531, 2005], [SIA 280, 1996].

Optical microscope inspection at 30x enlargement showed no surface cracks. Seam strength of field samples was tested in shear mode and peel mode. All welded seams tested tore outside the seam area, as required by standards [DIN 18531, 2005], [SIA 280, 1996].

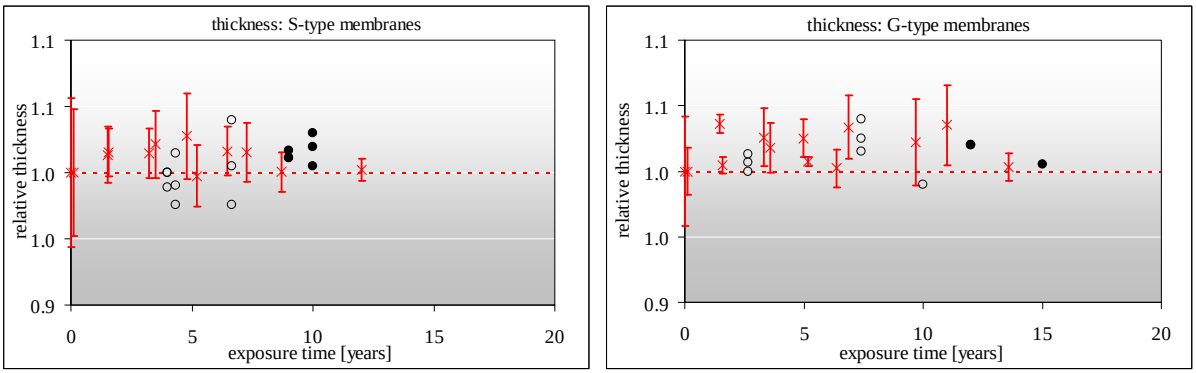

Figure 8. Relative thickness of G-type membranes after field exposure.
● data Rieche, 2004, ○ data Rieche, 1999, x manufacturer's continuous roof monitoring data.

4 DISCUSSION AND ASSESSMENT OF DURABILITY

4.1 S-type Membranes

S-type membranes are designed for application in mechanically attached roof waterproofing. The prime requirement of these types of membranes is a high tensile strength in order to cope with the mechanical stresses induced by wind uplift forces. The polyester reinforcement scrim provides for the necessary mechanical strength.

Rieche's [2004] investigations of S-type membranes show that the results for specimens from roofs 9 to 10 years old lie within the distribution ranges of results obtained by the manufacturer's internal monitoring, or in other words, within the normal ranges encountered in production. To the extent that a comparison with specimens from that year's production (2004) was possible, the studies also show that after 9 years and 10 years no significant change in mechanical properties had occurred. Thus Rieche's [2004] investigation results confirm the data collected by the manufacturer for roofs up to 12 years old. The 1999 assessment [Rieche and Wehrle 1999] of the durability of S-type membranes (10 years old) is confirmed by the results of the update investigation [Rieche 2004] 5 years later (15 years old).

4.2 G-type Membranes

The roofs investigated with G-type membranes in Rieche's [2004] update study have been exposed for periods of 12 and 15 years. The properties tested, for example elongation at break, showed results similar to those of S-type membranes, i.e. no significant change over time could be detected.

A somewhat different behaviour was found for the G-type membranes' tensile strength: It dropped by 15% (longitudinal) and by 22% (lateral) after 12 years outdoor weathering. Considering the results from 1999, [Rieche and Wehrle] this shows a further reduction of tensile strength in comparison to the reduction during the first 7 and/or 10 years. However, the manufacturer's monitoring data with hundreds of data points indicate only a minor decrease of the G-membranes tensile strength. Most samples between exposure times between 2 and 14 years have tensile strength values whose scatter bands are still within the original values. An explanation for some lower strength data could lie in changes of the crystallinity degree of the polymers. However, a strength reduction by such an effect is not regarded as a damage to

the material since the relevant mechnical property of G-type materials is their elongation, which is virutally unaltered (cf. Fig. 6)

Nevertheless, the Rieche's observation of decreased tensile strength of G-membranes give rise to a deeper examination of the material durability. There are two ways to predict the service life of G-type membranes. The German standard DIN 18531 requires for new materials a value of at least 5 N/mm^2. Model calculations produce a period of time of 24 to 44 years before tensile strength drops to 5 N/mm^2. The requirement for tensile strength of at least 5 N/mm^2 applies to new material. For calculating the service life of G-type membranes the authors consider a requirement of 3 N/mm^2 for tensile strength reasonable and sufficient. Using the same considerations, this requirement of 3 N/mm^2 produces a time period of 40 to 64 years. Therefore all the data would indicate a service life of 40 to over 60 years for G-type membranes. Rieche's 1999 assessment of the durability of G-type membranes (10 years old) is confirmed by the results of this investigation 5 years later (15 years old).

The main application field of G-type membranes is in ballasted conditions, such as gravel or paver ballasted roofs or green roofs. The tensile strength is of far minor importance in these applications. Since all the other measured properties showed no deterioration during up to 15 years exposure duration the slight decrease of the g-type membranes' tensile strength is weighted low.

5 CONCLUSIONS

The studies the Institute for Building Materials [Rieche and Wehrle, 1999 and Rieche, 2004] as well as the manufacturer's continuous monitoring of 106 roofs (Figs. 3-6) support the previous assumption of a service life of the manufacturer's TPO membranes of several decades. The data give evidence that at least 20 years of service life are secured. An extension by one or two decades seems reachable, provided that proper maintenance of the roofs and the membranes are carried out.

REFERENCES

Baxter D., 1998, 'Observations from the field during 1997', *Professional Roofing*, ', **2**, 22-30.

Beer, H.R., 1995, 'Flexible Polyolefin Roofing Membranes - Properties and Ecological Assessment', Proc. IXth International Waterproofing Association Congress,, April 26-28, Amsterdam, Netherlands, pp 81-89.

Beer, H.R., 1997, 'Longevity and Ecology of Polyolefin Roof Membranes', Proc. IVth. Intl. Symp. on Roofing Technology, Sept. 17-19, Gaithersburg, USA.

Beer, H.R and Keiser, S., 2000, 'Flexible Polyolefin Roofing Membranes: Ten Years of Field Experience', Proc. XIth International Waterproofing Association Congress, Florence, Italy, October 4-6, 154-172.

de Palo, R., 1995, 'Flexible Polypropylene Alloys', Proc. IXth International Waterproofing Association Congress,, April 26-28, Amsterdam, Netherlands, pp. 309-320.

DIN 18531, 2005, German Standard, 'Dachabdichtungen', Berlin, Germany.

Foley, R.K. and Rubel, W., 1997, 'Polyolefines – The New Roofing Technology', *Interface*, October, 30-32.

Graham, M., 2006, 'Putting TPOs to the test', *Professional Roofing*, **6**, 42-50.

Graham, M., 2003, 'TPO membrane standard', *Professional Roofing*, **10**, 64.

Paroli, R.M., Liu K.Y., Simmons, T.R., 1999, 'Thermoplastic Polyolefin Roofing Membranes', Construction Technology Update, National Research Council Canada, 30 (Dec.).
Rieche, G. and Wehrle, S., 1999, 'Expert report 3460 on the durability of flexible polyolefin roofing membranes of type Sarnafil TS and Sarnafil TG for roofs', Institute for Building Protection, Building Materials and Constructional Physics, D-70736 Fellbach. Germany.

Rieche, G. , 2004, 'Expert report 4708 on Durability of Sarnafil T polymeric roofing membrane', Institute for Building Protection, Building Materials and Constructional Physics, D-70736 Fellbach. Germany.

SIA 280, 1996, Swiss Standard, SN 564 280: 'Polymer Membranes, Materials Testing and Requirements', Zürich, Switzerland.

Tatum R., 1997, 'Newest Kid on the Roof', *Building Operating Management*, **9**, 114.

Performance of Silicone Water Repellent for FRC Corrugated Roof Tiles

Flávio L. Maranhão [1]
David Selley [2]
Cleber Dias [3]
Kai Loh [4]
Vanderley M. John [5]

T 22

ABSTRACT

Cellulose fibre has been used to substitute asbestos on Fibre Reinforced Cement (FRC) roof tiles, despite the fibre's deterioration caused by alkaline atack and intensified by wet-dry cycles resulting in embrittlement of composite. Mould growth is another problem in FRC because of its impact on the aesthetical and thermal performance of components. Mould Growth is largely influenced by the water absorption rates.

This paper investigates the effect of water-repellents on the accelerated aging of asbestos-free fibrecement sheets reinforced with PVA and cellulose fibres, under accelerated wet-dry aging cycles. Laboratory-scale produced fibrecement sheets were treated by foam roller brushing with different concentrations of a water-based silane/siloxane emulsion. After 28 days of curing both treated and untreated samples were submitted to up to 150 wet-dry cycles.

Composite deterioration was measured by water absorption kinetics, mechanical properties (MOR and specific energy) and thermogravimetric analysis (DSC).

The results show that: (i) the aging program causes important reduction in untreated fracture toughness and water intake results, (ii) for the treated samples, the higher the water repellent concentration, the lower the water absorption; (iii) the accelerated aging test did not cause any significant influence on the water repellency performance (iv) the silane/siloxane products prevented toughness degradation by aging and cellulose fibre degradation, (v) there is a correlation between cellulose degradation and fracture toughness.

KEYWORDS

Fibrecement, Durability, Water repellents, Performance

[1] University of Sao Paulo and São Judas Tadeu University, Brazil, Phone + Tel: +55-11-3091.5459 flavio.maranhao@poli.usp.br
[2] Dow Corning Corporation, Midland, EUA, david.selley@dowcorning.com
[3] University of Sao Paulo, Phone + Tel: +55-11-3091.5382 cleber.dias@poli.usp.br
[4] University of Sao Paulo, Brazil, Phone + Tel: +55-11-3091.5234, kai.loh@poli.usp.br
[5] University of Sao Paulo, Brazil, Phone + Tel: +55-11-3091.5234, vanderley.john@poli.usp.br

1 INTRODUCTION

Cellulose fibre has been used to substitute asbestos on Fibre Reinforced Cement (FRC) roof tiles, despite the fibre's mineralization caused by wet-dry cycles resulting in embrittlement of the composite [Gran, 1983]. Mould growth is another problem caused by water absorption and it influences the FRC aesthetical and thermal performance.

Many alternatives has been used to prevent those degradation: a) low alkalinity cement [Savastano Jr 2001; Warden & Coutts 2001); b) pozzolanic addictions; c) increase the matrix carbonation rates [Tolêdo *et al.* 2003]; d) fibres treatment [Lin *et. al.* 1997] and ; e) water repellent products.

The last one, althouth the little information already published, has a potential advantage compared to the others because it could increase the FRC overall performance by reducing the soiling rate, mainly influenced by mould growth.

The water repellents most widely used for FRC are the silicone-based materials (mainly silane and siloxane). These products have good hydrophobic properties (by the apolar radical) and a potential long-term performance due to the Si-O and Si-C bond stability.

There are different ways to introduce the water repellent products in FRC plants. The first one is to treat the cellulose fibres (Abdelmowlett et. al, 2004), with the advantages of protecting only the fibres that show degradation and optimizing water repellent consumption.

The second is to add the water repellent during the mixing of raw materials, which may potentially reduce water absorption rates but may also influence the MOR and the sheet layer adhesion (Selley *et. al.*, 2006).

The third way is to protect the sheet surface as post-treatment application (Selley et. al,. 2006), which is the most used method in other building materials. The main factors that influence this method performance are: (i) application method (spray, paint or dipping), (ii) product concentration, and (iii) application moment (before or after curing).

Comparing the different methods is not easy, mainly because no complete published research has been identified in the literature. For industrial plants, the application as post-treatment is the easiest to put in action but its performance under service conditions is largely influenced by cracks (Lunk; Wittmann, 1998). The other application methods influence the FRC mechanical properties, and modify the flocculation process in the Hatcheck machine, thus requiring further researche before any industrial application.

This paper investigate the performance of one silicone water-repellent product applied as post-treatment in fibre cement sheets before and after accelerated aging.

2 EXPERIMENTAL DESIGN

The research was developed in laboratory. The water repellent performance were evaluated by means of the water absorption rates, modulus of rupture (MOR) and specific energy. In addiction changes in the chemical and mineralogical composition were evaluated using thermogravimetric analysis.

2.1 Materials and Specimens Preparation

Table 1 presents the main raw materials properties as well as the formulation of the composite used in the experiment. The formulation is similar to the commonly used for fibercement production and includes an ordinary Portland cement, densified silica fume, limestone filler, short bleached cellulose fibre and 6.0millimiters leght PVA fibres.

The following steps were used to produce the specimens: 1-mixing the raw materials and water to produce the pulp (Table 1) using a solid/water ratio of 0.20; 2-applying vacuum (300mmHg for two minutes); 3-compression using 3.2MPa dead load for one minute; 4-curing in a ventilated oven at 65^0C and 90%RH for 18 hours; 5-applying the water repellent as post-treatment; 6- curing in a plastic bag for 28 days; 7-cutting the specimens in the dimension 16 cm x 3.7 cm x 0.5 cm; 8- sealing the borders using liquid rubber; 9 - drying in an oven at 65^0C and 50% RH for two days.

The water repellent product used in the experiment was a silane/siloxane emulsion (table 2). It was used three different dilution rates: 3%, 5% and 10%. All of them based on the water weight. The first and the last concentration are the lowest and the highest recommended by the manufacturer. The untreated specimens were used as reference.

The hydrophobic agent was applied after curing using a foam roller in two coatings. After the application the specimens were cured in a plastic bag for 28 days.

Table 1. Properties of raw materials and formulation used in the research.

Materials	Density (g/cm^3)	BET Surface area (m^2/g)	Fraction (w/w%)
Portland cement	2.97	1.43	70.2
Limestone filler	2.69	1.50	20.0
Silica fume	2.18	18.18	5.0
Cellulose fibres	1.56	---	3.0
PVA fibres	1.35	---	1.8

Table 2. Properties of water repellent used in the experiments.

Active content	40 %
Color	Milky white
Density	1.01 g/cc
pH	6 to 8
Shelf life	720 days
Volatile organic content	< 200 g/L

2.2 Test Methods

Accelerated aging was performed in a laboratory at USP (University of São Paulo), in an automatic machine. Specimens were submitted to 150 wet-dry cycles, each of then lasting six hours: 2 hours and 50 minutes wetting, 2 hours and 50 minutes drying at 70^0C with a 10minute interval between these steps. During the cycles only one side of the specimens was wetted.

Water absorption was measured by immersion test in five different moments: after 30 seconds, 60 seconds, 3 minutes, 1 hour and 24 hours.

The modulus of rupture (MOR) and specific fracture energy were measured in an Instron Universal Machine 5569, with a load cell unit of 1kN. It consists in a four-point bending test, with 13.5cm bending spans, a load distance point of 5.0cm. Displacement ratio was controlled (5 mm/min) and deflection measured with a LVDT positioned under the specimens in the middle of the span. For each concentration of water repellent and reference a minimum of 5 specimens were evaluated.

Thermogravimetric analysis (TG) was conducted with a NETZSCH STA409PG on a 1.0 g sample mass in a nitrogen atmosphere (flow ratio = 60 ml/min), with a heating rate of 10°C/min from 10°C to 1000°C. Prior to the test, the specimens were first deep frozen in liquid nitrogen and then lyophilized for 16 hours to sublimate the absorbed water.

3 RESULTS AND DISCUSSION

3.1 Water Absorption

Figure 1 shows the water absorption results before and after aging. Continuous lines represent unaged specimens, while the dashed lines represent aged specimens. The higher the water repelant concentration the lower is the water absorption, for both aged and unaged samples.

Ageing caused a 23% of water absorption reduction (after 24h of immersion) for the untreated samples. This probably is a combined effect of increase of both, degree of hydration and carbonation [Dias 2005; Tonoli et al. 2006].

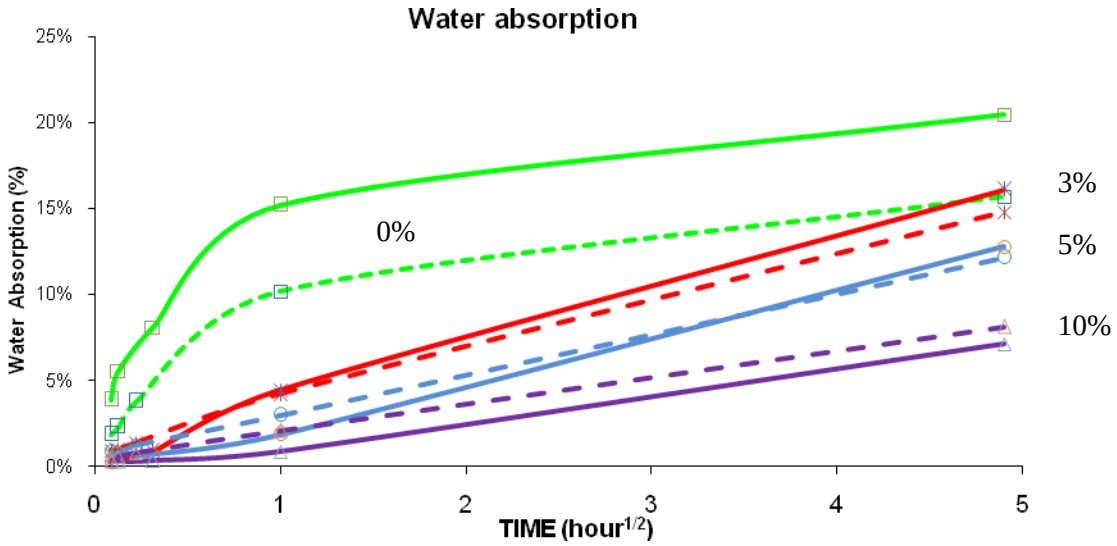

Figure 1. Water absorption kinetics before and after accelerated aging. Continuous line = unaged, dashed line = aged.

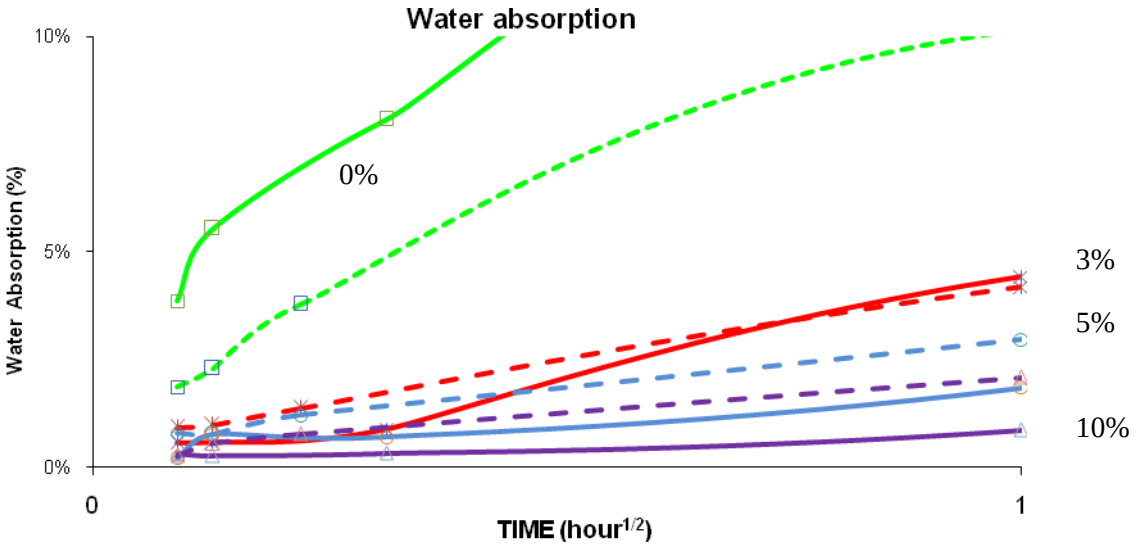

Figure 2. Water absorption kinetics along the first hour before and after accelerated aging. Continuous line= unaged, dashed line = aged.

For the treated samples, for all concentrations tested, artificial ageing showed only a slight influence on water absortion at 24 h. However, for shorter periods of immersion the aged treated specimens showed higher water absorption (Figure 2) than unaged ones. For instance, on the concentration of

10%, ageing caused water absorption to increase around 150% over unaged ones. This is problaly caused be an superficial degradation of the water repellent or composite cracking that enable water penetration.

3.2 Mechanical Properties

Figure 3 and Figure 4 show the MOR results. Figure 5 presents the typical curves for the highest water repellent concentration and for the reference (0%). The MOR of untreated samples was not influenced by accelerated aging (figure 4), while fracture toughness was reduced by around 70% (Figure 5). This conclusion and the absolut values are in accordance with other authors when a similar PVA fibre content was used [Dias, 2005; Caldas e Silva, 2002] and caused by cellulose sibre degradation by artificial ageing. This degradation cause the fibers to break during bending, therefore reducing fracture toughness. Another problem is the fibre mineralization (John et. al. 2005).

For the treated samples, on the other hand, aging caused reduction of MOR. The explanation of this unexpected result is not clear. One possibility is the reduction in water intake limited the increase the degree of hydration. In consequence, for samples with water repellant the increase of hydration wasn't enougth to counteract the other degradation mechanisms. By the other side, water repellant treatment was efficient to prevent fracture toughness reduction during ageing (Figure 5) because it protected fibers from degradation.

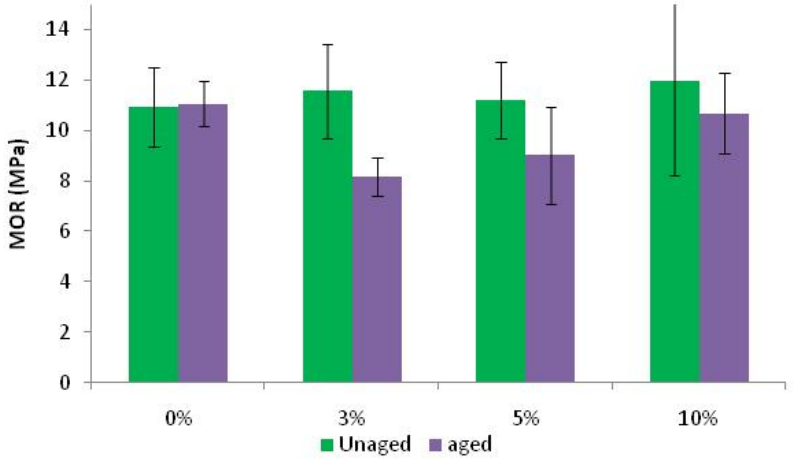

Figure 3. MOR results.

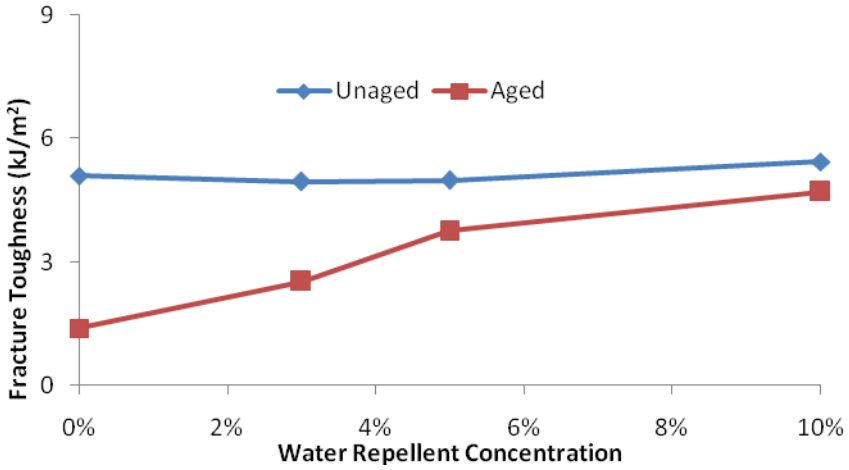

Figure 4. Fracture Toughness results.

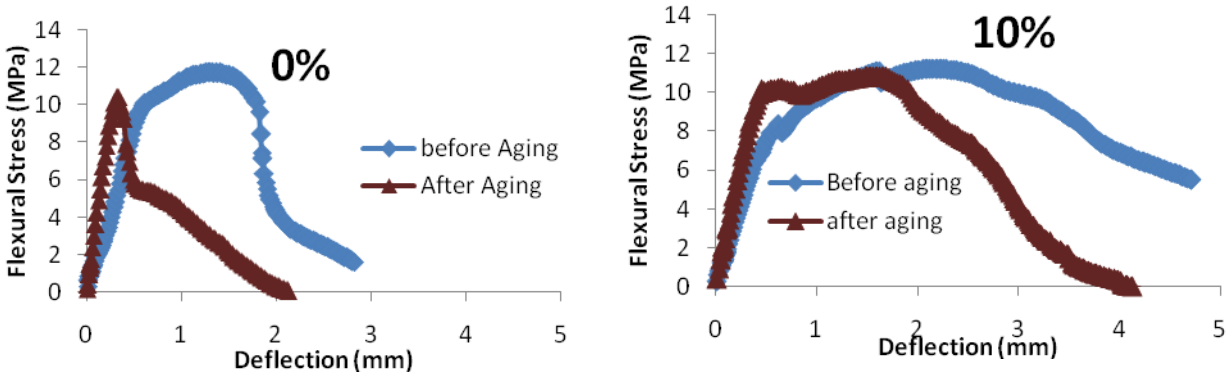

Figure 5. Typical curves of flexural stress versus deflection.

3.2 Thermogravimetric Analysis

In Figures 6 and 7 the thermal analysis results are presented. For the untreated samples (0%) ageing increased the CSH content and decreased the cellulose fibre peak. For the treated samples (10%) ageing increased the first carbonate peak and decreased Ca(OH)2. Comparing the thermal analysis results, it is clear that the water repellent treatment reduced cellulose fibre degradation and the matrix hydration. Figure 8 plots fracture toughness after aging and the cellulose fibre peak intensity ratio before and after aging as identified by the thermal analysis. The higher is this ratio (based in the composite non-volatil content) the higher is the cellulose mass loss intensity after aging compared to the unaged ones. The results shows an important correlation. However other researchers such as Dias (2005) did not identify differences in the cellulose peak by accelerated and natural aging, this must be confirmed by futher investigation.

CONCLUSIONS

The results show that: (i) the aging program causes an important reduction in the untreated samples' fracture toughness and water intake results; (ii) for the treated samples, the higher the water repellent concentration, the lower the water absorption; (iii) the accelerated aging test did not cause any significant influence on the water repellency performance; (iv) the silane/siloxane product prevents cellulose fibre degradation and toughness degradation by aging; (v) there is a correlation between cellulose degradation and fracture toughness.

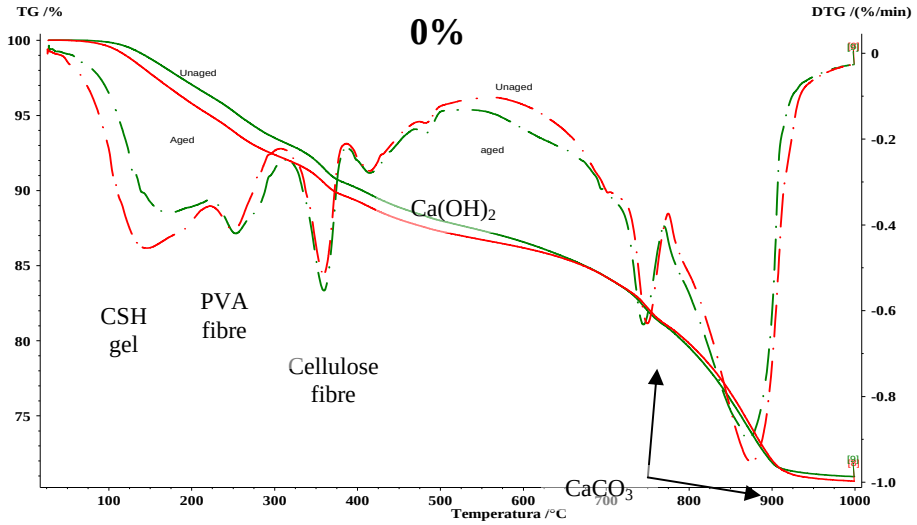

Figure 6. TG and DTG curves for the untreated specimens.

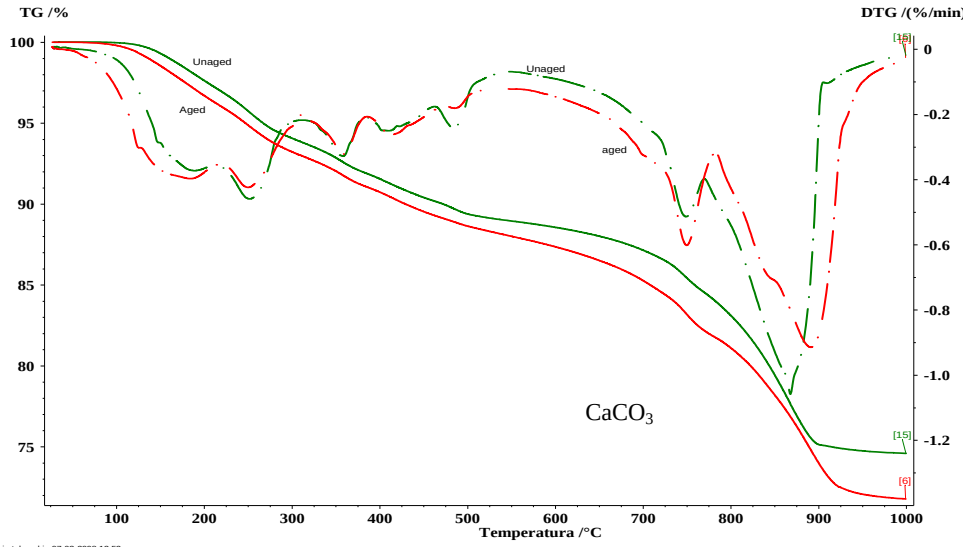

Figure 6. TG and DTG curves for the highest concentration (10%) specimens.

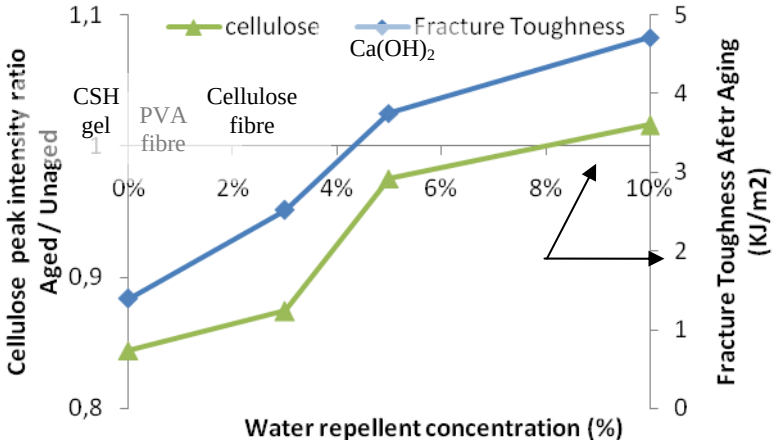

Figure 7. Correlation between cellulose degradation and fracture toughness after aging.

ACKNOWLEDGMENTS

The authors would like to thank the Dow Corning Corporation Team, specially: Jennifer Kempf, Gislene Attilo, Marco Souza, Jorge Venardos and Emerson Oliveira.

REFERENCES

Bentur, A., Akers, A.S., 1989, *The microestruture and ageing of cellulose fibre reinforced cement composites cured in a normal environment*. The International Journal of Cement Composites and Lightweight Concrete V11 N2.

Caldas e Silva A., 2002, Durability of Composite Reinforced with Celulose Fibre**.** *Master Dissertation, University of São Paulo. (in Portuguese).*

Dias, C., 2005, Aging Effects in the Porous Structure and the Mechanical Properties of Fiber Reinforced Composite. Master Dissertation, University of São Paulo. (in Portuguese**)**.
GRAM, H-E., 1983, *Durability of natural fibres in concrete.* Stockholm.

Lin, X., Silsbee, M. R., Roy, D. M., 1997, *Improvements in the durability of cellulose reinforced cementitious composites*. In: Mechanisms of Chemical Degradation of Cement-based Systems. London.

John, V.M,, Cincotto,M.A., 2005, Sjöström, C., Agopyan[a], V., Oliveir, C.T.A. Durability of slag mortar reinforced with coconut fibre. *Cement and Concrete Composites*, V. 27, Issue 5, Pages 565-574.

Lunk, P., Wittmann, F. H., 2998, The *Behaviour of Cracks in Water Repelent Concrete Structures with Respects to Capillary Water Transport*. Proceedings of Hydrophobe II, Aedificatio Publishers pp.63-76.

Sarja, A., 1988, *Wood fibre reinforced concrete*. In: Natural Fibre Reinforced Cement and Concrete. London: Blackie, p.63-88.

Savastano Jr, H., Warden, P. G., Couts, R. S. P., 2001, Ground iron blast furnace as a matrix for cellulose-cement materials. *Cement and Concrete Composites* 23. Elsevier Science Ltd. p389-397.

Selley, D.; Maranhão, F. L.; Loh, K., John, V., 2006, Silicone water repellents for (FRC) Fibre-Cement Boards. In: 10th International Inorganic-Bonded Fiber Composites Conference, 2006, São Paulo. Proceedings of the IIBCC 2006. São Paulo, v. 1. p. 14-24.

Tolêdo Filho, R.D., Scrivener, K., England, G.L., Ghavami, K., 2000, *Durability of alkali-sensitive sisal and* coconut fibres in cement mortar composites. *Cement and Concrete Composites* 22,. p127-143.

Tonoli, G. H. D. *.et. al.*, 2006, Accelerated carbonation on vegetable fibre reinforced Cementitious roofing tiles. In: 10th International Inorganic-Bonded Fiber Composites Conference, 2006, São Paulo. Proceedings of the IIBCC 2006. São Paulo, v. 1. p. 14-24.

11DBMC International Conference on Durability of Building Materials and Components
ISTANBUL, Turkey 11-14 May 2008

Effects of Wet and Dry Cycles on the Performance and Microstructure of Asbestos-free Fiber Cement

C. M. R. Dias [1]
H. Savastano Jr. [2]
Vahan Agopyan [3]
Vanderley M. John [4]

T 22

ABSTRACT

In this work we study the effects of wet and dry cycles on the performance of asbestos-free fiber cement. Two accelerated ageing methods are analyzed, including the heat-rain ISO standard test and up to 500 scaled-down wet and dry cycles. Four-point bending tests were performed to evaluate the modulus of rupture (MOR), limit of proportionality (LOP), modulus of elasticity (MOE) and specific fracture energy of specimens. SEM with EDS analysis and mercury intrusion porosimetry (MIP) were used to evaluate the ageing effects on the microstructure. The results show that the effect of the heat-rain test and scaled-down wet and dry cycles on the mechanical performance of fiber cement results from a balance of positive and negative effects. Embrittlement of the composite was the main effect in both ageing tests as a result of cellulose fiber deterioration and enhancement of the bond between PVA fibers and the cementitious matrix.

KEYWORDS

Asbestos-free fiber cement, Accelerated ageing, Wet and dry cycles, Mechanical performance, Microstructure.

[1] University of São Paulo, Polytechnic School, Department of Construction Engineering, São Paulo, SP, Brazil, Phone +55 11 3091-5794, Fax +55 11 3091-5544, cleber.dias@poli.usp.br
[2] University of São Paulo, Faculty of Animal Science and Food Engineering, Pirassununga, SP, Brazil, Phone +55 19 35654153, FAX +55 19 35654004, holmersj@usp.br
[3] University of São Paulo, Polytechnic School, Department of Construction Engineering, São Paulo, SP, Brazil, Phone +55 11 30915794, Fax +55 11 30915544, vahan.agopyan@poli.usp.br
[4] University of São Paulo, Polytechnic School, Department of Construction Engineering, São Paulo, SP, Brazil, Phone +55 11 30915794, Fax +55 11 30915544, vanderley.john@poli.usp.br

1 INTRODUCTION

The introduction of asbestos-free fiber cement technology is relatively recent in developing countries, including Brazil, where fiber cement industries have used poly (vinyl alcohol) (PVA) or polypropylene fibers combined with cellulose fibers in the manufacture of building components.

Durability is an important parameter when developing and producing fiber cement components, because the expected service life of such products is usually high. Therefore a set of accelerated ageing tests has been developed to help to forecast long-term performance. Most of these tests are variations of wet and dry cycling or of carbonation combined with wet and dry cycling. ISO 9933 [ISO 1995], adopted in many countries, recommends 25 cycles of heat and rain test (or wet and dry test) on full-scale 10 m² samples. Many other small-scale wet and dry cycles have been used in several studies [Mohr et al. 2005; Mohr et al. 2006; Gram 1988; Agopyan 1991; Soroushian & Marikunte 1992] in which most researchers adopt modulus of rupture (MOR) and fracture toughness as deterioration indicators. Despite the fact that ISO 9933 controls only watertightness and the occurrence of visible cracking, variations in mechanical strength and fracture toughness are also relevant for such products. No work has been published so far comparing different accelerated ageing methods. Moreover, the number of wet-and-dry cycles deserves investigation.

In this paper we present two case studies. In the first case, full-scale industrially produced corrugated sheets available in the Brazilian market were submitted to heat-rain ISO 9933 test [ISO 1995]. These roof sheets were evaluated before and after 25 wet and dry cycles. In the second case, laboratory-produced fiber cement specimens were submitted to up to 500 scaled-down accelerated wet and dry cycles. In both case studies, the effects on microstructure and mechanical performance were evaluated.

2 EXPERIMENT

Results of a full-scale 10 m² roof submitted to ISO 9933 ageing heat-and-rain test were compared with those obtained with a scaled-down wet and dry test (up to 500 cycles). The corrugated sheets used in the ISO 9933 test were produced via Hatscheck method and presented a similar composition, except for the limestone content, to that of the laboratory-produced samples used in the wet and dry test (Table 1). Variation in LOP, MOE, MOR, fracture toughness and microstructure, due to accelerated ageing tests, were measured in selected samples.

2.1 Heat-Rain ISO Test on Asbestos-Free Industrial-Scale Produced Corrugated Sheets

The heat-rain ISO 9933 consists in submitting a 10 m² assembled 15° ± 5° sloped roof to twenty-five (25) wet and dry cycles. Rain is simulated by a water outflow of (2.5 ± 0.5) L/(min.m²) for 2 h and 50 min. Drying is performed by infra-red (IR) lamps capable of maintaining a surface temperature (black body) of (70 ± 5)°C for 2 h and 50 min. Between each heat and rain step there is an interval of ten (10) minutes, totalizing 6 h/cycle.

The roof used in the test was constituted of nine entire corrugated sheets with 6 mm nominal thickness, 1.10 m width and 1.20 m length, approximately 60 days after production. The standards require the examination of the roof for cracking, delamination, and other visible effects.

In addition to the ISO 9933 requirements, microstructure and mechanical performance were also characterized. For the mechanical tests, low-dimension specimens with approximately 35 mm width and 160 mm length were extracted from the straight regions of the corrugated sheets using a water-cooled rotary saw.

2.2 Wet and Dry Cycles on Asbestos-Free Laboratory-Produced Fiber Cement

This study was performed to evaluate the effects of up to 500 accelerated wet and dry cycles on the microstructure and mechanical performance of laboratory-produced asbestos-free specimens. The employed materials, formulations, and the methodology for the characterization of microstructure and mechanical performance are described below.

2.2.1 Materials, Formulation, and Preparation of Specimens

Table 1 presents the materials and the formulation that were used to prepare the specimens. Densified silica fume, ordinary Portland cement and limestone filler from the Brazilian market were also employed. Six-millimeter length PVA fibers and long unbleached cellulose fibers (average length of 1.24 mm) were employed as reinforcement. In this formulation, the cellulose volume fraction is 8.5% and the PVA volume fraction is 4.2%. The group of laboratory-produced specimens was labeled PVA_2.0%.

Fiber cement pads (~5 x 200 x 200 mm³) were laboratory-produced by using slurry vacuum dewatering method [Savastano Jr. et al. 2005]. Immediately after preparation, each green pad was pressed at 3.2 MPa for 5 min. Next, these sheets were maintained in plastic bags for one day, soaked in water for 5 days, and air-cured for up to 28 days. Low-dimension specimens with 40 mm width and 160 mm length were extracted from the pads using a water-cooled rotary saw. These specimens were submitted to the mechanical tests before and after the ageing tests.

Table 1. Materials and formulation of PVA_2.0%.

Materials	Portland cement	Limestone filler	Silica fume	PVA fibers	Cellulose fibers
Dry mass fraction (%)	75.20	12.72	6.08	2.0	4.0

2.2.2 Scaled-down Wet and Dry Cycles

Up to 500 scaled-down accelerated wet and dry cycles were performed with low-dimension specimens in automatic equipment. Fig. 1 shows a schematic drawing of the equipment. Wetting and drying times were similar to those previously described for the heat-rain test.

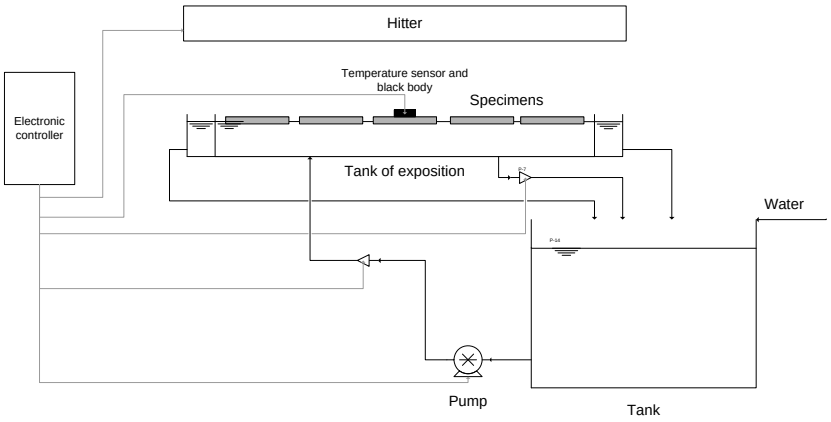

Figure 1. Schematic drawing of wet and dry cycle equipment.

2.3 Evaluation of Ageing Effects

The ageing effects were evaluated by microstructural analysis and mechanical tests. A high-vacuum LEO Leika S440 microscope with an acceleration voltage of 20 kV and current of 150 mA was used to examine a fractured section and a polished cross-section of the specimens. Samples for evaluation by secondary electron image (SEI) and backscattering electron image analysis (BSEI) were vacuum

(200 mbar) impregnated with epoxy resin and air cured for 24 h before grinding with silicon carbide and polishing with diamond paste (3, 1 and 1/4 mm grain size respectively). All samples received carbon coating before examination.

MIP tests were carried out using a Micromeritics Auto Pore III. For each treatment, three randomly selected 1 g specimens were cut with a precision rotary disk saw, subsequently dried at 70 + 5 °C with -60 kPa vacuum pressure and finally submitted to evaluation. The Washburn equation with a contact angle of 130° and mercury superficial tension of 0.485 N/m was employed to assess the pore size distribution.

Four-point bending tests were conducted with an INSTRON 5569 using bending span of 135 mm. Displacement ratio was controlled (1.5 mm/min) and deflection was measured with an LVDT positioned under the specimens in the middle of the span. Modulus of rupture (MOR), limit of proportionality (LOP), modulus of elasticity (MOE) and specific fracture energy of specimens were evaluated. All specimens, 15 specimens/group, were soaked in water for 24 h before the bending tests.

3 RESULTS AND DISCUSSIONS

3.1 Microstructural Changes

Accelerated ageing reduced the porosity of all samples. Significant reduction in porosity, from 30.7 to 27.5%, was observed in the corrugated sheet specimens that were submitted to heat-rain cycles. A similar effect was observed in laboratory-produced specimens (Fig. 2a), which presented lower porosity than corrugated sheets.

Fig. 2b shows that the reduction in porosity of corrugated sheets was expressive in the diameter range lower than 100 nm and higher than 10,000 nm. The large pores (>10,000 nm) are manufacturing defects and their volume is significantly higher than that observed in the laboratory-produced samples. Porosity reduction is a characteristic effect of hydration and matrix carbonation [Bier et al. 1987; Matsusato et al. 1992]. Both hydration and carbonation are positive effects that help to improve the mechanical strength of the composite matrix. However, they also cause densification of interface zones between fibers and matrix, thus resulting in embrittlement of the composite [Bentur and Mindess 1990].

The peak between 100 nm and 10,000 nm, present in all samples, is typical of fiber cement formulations that have cellulose fibers in their composition and it is probably associated with cellulose fiber lumens and with the fibers-matrix interface. This peak varied slightly with heat-rain cycles, as shown in Fig. 2.Wet and dry cycles also changed significantly the pore size distribution of laboratory-produced composites in a similar way to what was observed in corrugated sheets, except for the increase in the volume of pores with diameter lower than 10 nm (pore refinement) (Fig. 2c). Pore refinement is related with C-S-H formation by matrix hydration and by pozzolanic reaction.

In both cases a reduction in porosity was expected within the diameter range corresponding to the cellulose pores, as a result of the filling of cellulose lumens with cement products [Bentur & Akers 1989]. However, in both samples, the pore size distribution presented minor changes within this range after accelerated ageing.

Therefore, it is reasonable to suppose that wetting and drying times influence the filling rate of cellulose lumens.

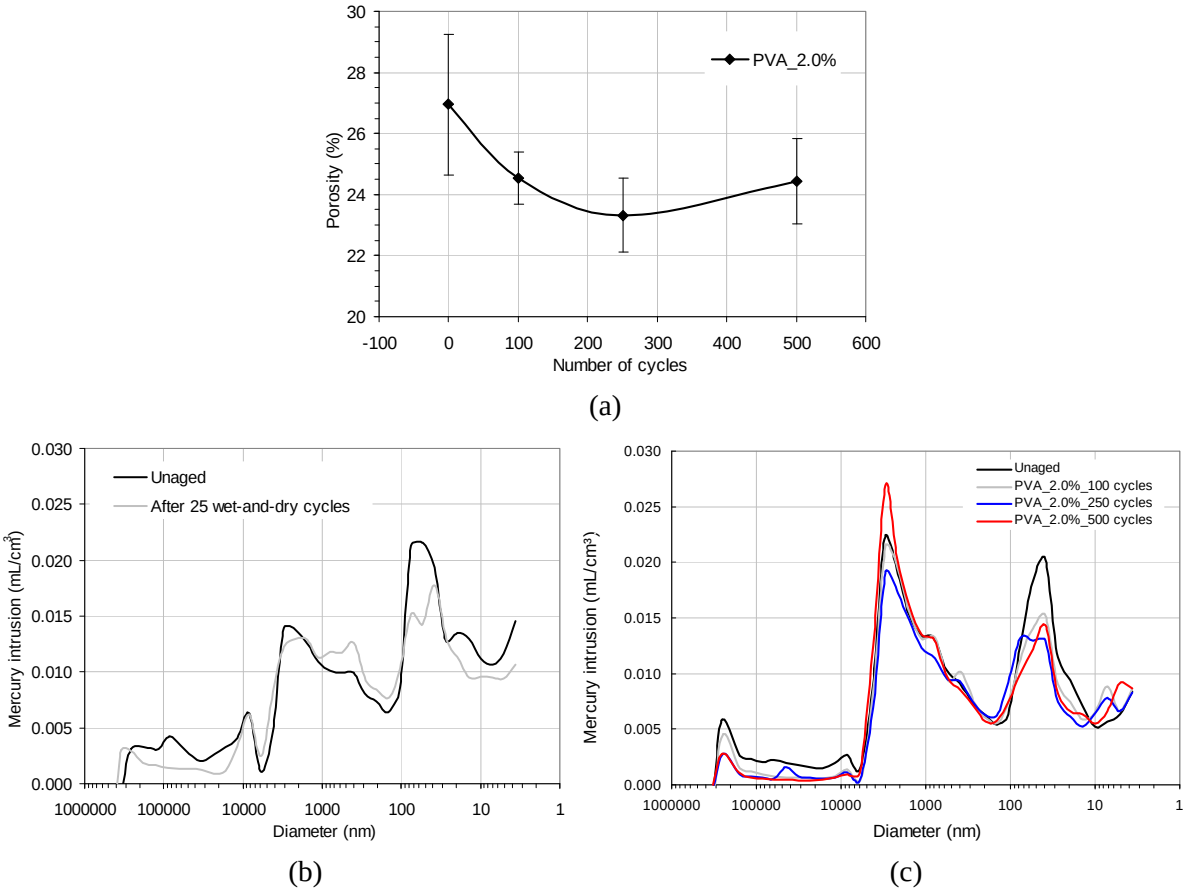

Figure 2. Porosity and pore size distribution of asbestos-free fiber cement corrugated sheets: a) porosity of specimens PVA_2.0%; b) small samples extracted from corrugated sheets and c) laboratory scale-produced specimens.

Images obtained by SEM of fracture and polished sections of laboratory-produced specimens show that, in the unaged PVA_2.0% samples (Fig. 3a), the fibers are predominantly pulled out of the matrix during the fracture process. However, accelerated aged samples presented predominantly broken cellulose fibers during fracture (Fig. 3b), which is a result of cellulose fiber degradation and interface densification. As a result, the composite suffered significant embrittllement. In addition, accelerated ageing did not fill the lumens of cellulose fibers.

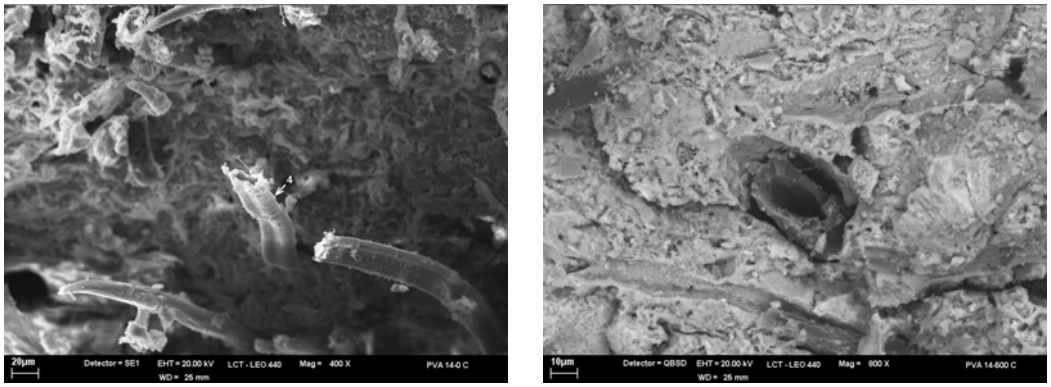

Figure 3. Images obtained by SEM of fracture and polished sections of laboratory-produced specimens: a) unaged and b) after 500 wet and dry cycles.

PVA fibers did not appear to undergo significant deterioration in the composites after wet and dry cycles and interface densification probably did not increase the pull-out force above the mechanical strength of the fibers, so they were predominantly pulled out both in aged and unaged specimens.

3.2 Effect of Ageing on Mechanical Properties

Fig. 4 shows the flexural stress versus deflection curves of both aged and unaged specimens and Table 2 summarizes their properties. Statistical analysis of data showed that, for the small specimens of corrugated sheets, embrittlement was the single significant effect (significance level of 0.05) of heat-rain cycles on the mechanical performance of the composite. Embrittlement means loss of toughness, which is proportional to the area under the flexural stress versus deflection curves. Both fiber deterioration and densification of the interface zone between fibers and matrix lead to the increase in the occurrence of fiber rupture instead of pull-out during the process of composite fracture, resulting in a decrease in the energy necessary to fracture the material [Bentur and Akers 1989].

The slope of the flexural stress versus deflection curve after the first crack on small specimens of corrugated sheets increased with heat-rain cycles, indicating the densification of the interface zone (Fig. 4a). Limited densification of the interface zone between PVA fibers and the matrix is a positive effect for MOR (maximum flexural stress). Cellulose fiber deterioration, on the other hand, contributes negatively to the mechanical strength. The balance of positive and negative effects can explain the maintenance of the modulus of rupture of small samples extracted from corrugated sheets.

Fig. 4b shows the flexural stress versus deflection curves of laboratory-produced specimens. The results show that MOR and specific energy are significantly changed after the first cycles, probably due to cellulose deterioration and deterioration of the interface zone. After 250 cycles the balance between the positive PVA fiber interface densification and the negative effect of cellulose degradation results in an increase in MOR. Thermogravimetric analysis showed that hydration, instead of matrix carbonation, predominated on the laboratory-produced specimens. In contrast, carbonation predominated on corrugated sheet specimens.

Results show that degradation is dependent on the number of cycles, and the exposure to a number of cycles above the ISO 9933 determination yields additional information. The large difference of toughness between laboratory and industrial products is at least partially due to fiber orientation on the Hatschek machines.

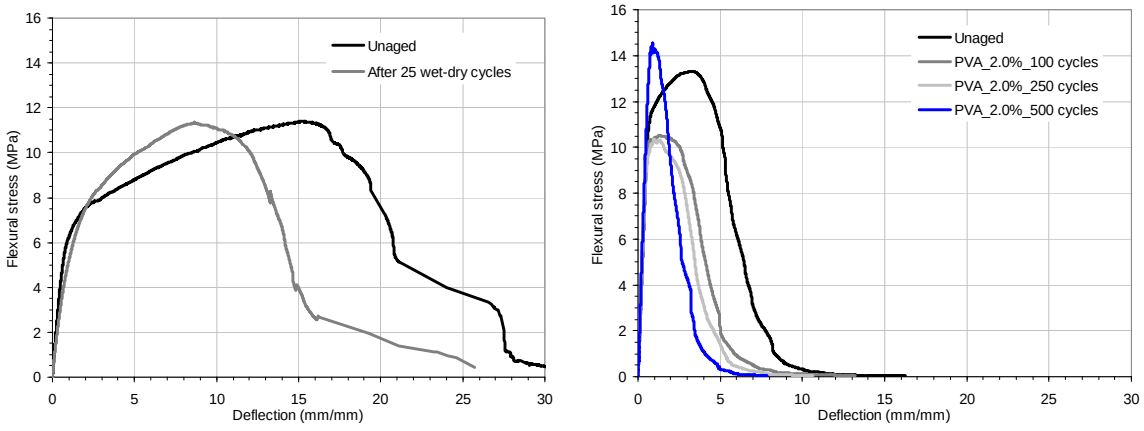

(a) (b)

Figure 4. Typical flexural stress – deflection curves of aged and unaged asbestos-free fiber cement: a) specimens extracted from corrugated roof sheets before and after ISO 9933 test (left) and b) laboratory-produced samples before and after up to 500 wet and dry cycles.

Table 2. Mechanical properties of industrially produced asbestos-free fiber cement small samples.

Properties	Unaged	25 heat-rain cycles
LOP (MPa)	5.6 ± 0.8*	6.6 ± 1.5
MOR (MPa)	11.7 ± 0.9	12.1 ± 1.1
MOE (GPa)	9.1 ± 2.1	6.8 ± 3.3
Specific fracture energy (kJ/m²)	6.8 ± 1.1	4.5 ± 1.1

* Average ± standard deviation.

Table 3. Mechanical properties of laboratory-produced asbestos-free fiber cement small samples.

Properties	Unaged	100 cycles	250 cycles	500 cycles
LOP (MPa)	9.29 ± 1.5*	9.4 ± 1.2	9.10 ± 1.47	13.8 ± 2.91
MOR (MPa)	13.8 ± 1.4	11.1 ± 0.9	10.6 ± 0.9	15.6 ± 2.4
MOE (GPa)	13.6 ± 1.5	14.6 ± 1.8	15.7 ± 1.3	15.8 ± 1.5
Specific fracture energy (kJ/m²)	2.8 ± 0.5	1.64 ± 0.6	1.4 ± 0.4	1.22 ± 0.2

* Average ± standard deviation.

3.3 Visual Inspetion

The samples did not present any visible damage in the performed tests. This was confirmed by many other full-scale heat and rain tests conducted by the team.

4 CONCLUSIONS

Changes in porosity and pore size distribution were evidenced after wet and dry cycles. Fiber cement porosity decreased after wet and dry cycles and this is mainly related with hydration and matrix carbonation. The effect of heat-rain and scaled-down wet and dry cycles on the mechanical performance of fiber cement is a result of a balance of positive and negative effects. Accelerated wet and dry cycles promoted significant changes in the mechanical properties of asbestos-free fiber cement and the main effect was embritlement of the composite. The number of wet and dry cycles influences degradation and there is an interest to increase this number above the minimum requirement specified by ISO 9933.

ACKNOWLEDGMENTS

The authors would like to thank Fundação de Amparo à Pesquisa do Estado de São Paulo (FAPESP), CNPq, Financiadora de Estudos e Projetos (FINEP, HABITARE Program), INFIBRA and IMBRALIT for their financial support.

REFERENCES

INTERNATIONAL ORGANIZATION FOR STANDARDIZATION (ISO). ISO 9933: *Products in fibre-reinforced cement - Long corrugated or asymmetrical section sheets and fittings for roofing and cladding*. 1995.

Mohr B.J., Nanko, H., Kurtis, K.E., 2005, *Durability of kraft pulp fiber–cement composites to wet/dry cycling*. Cement & Concrete Composites 27. 435–448.

Mohr, B.J., Biernacki, J.J., Kurtis, K.E. 2006, *Microstructural and chemical effects of wet/dry cycling on pulp fiber–cement composites*. Cement and Concrete Research 36. 1240–1251.

H-E Gram., 1988, *Natural fibre concrete roofing*, Concrete Technology and Design 5: natural fibre reinforced cement and concrete, Glasgow and London.

Agopyan, V., 1991, *Fibrous materials for building construction in development countries: the use of vegetal fibers* [Thesis of Polytechnic school of University of São Paulo]. São Paulo, In Portuguese.

Soroushian, P., Marikunte, S., 1992, *Long-term durability and moisture sensitivity of cellulose fiber reinforced cement composites.* In: Fibre Reinforced cement and concrete [Edited by R. N. Swamy]. RILEM. London.

Savastano Jr., H., Warden, P G, Coutts, R S P., 2005, *Microstructure and mechanical properties of waste fibre–cement composites*. Cement and Concrete Composites; 27(5), pp 583-592.

Bier, TH.A., Kropp, J., Hilsdorf, H.K., 1987, *Carbonation and realkalinization of concrete and hydrated cement paste*, Durability of Construction Materials 3, Proceedings of the 1st Congress from Materials Science to Construction Materials Engineering, RILEM.

Matsusato, H., Ogawa, K., Funato, M., Sato, T., 1992, *Studies on the carbonation of hydrated cement and its effect on microstructure and strength*. In: 9th International Congress on the Chemistry of Cement, vol5, New Delhi, pp 363-369.

A. Bentur, S. Mindess, 1990, *Fibre Reinforced Cementitious Composites*, Elsevier Applied Science, London and New York,

Bentur, A., Akers, A.S., 1989, *The microstructure and ageing of cellulose fibre reinforced cement composites cured in a normal environment*. In: The International Journal of Cement Composites and Lightweight Concrete vol 11, N2.

11DBMC International Conference on Durability of Building Materials and Components
ISTANBUL, Turkey 11-14 May 2008

Polyolefin Roof Membranes on Site Durability Evaluation

Sergio Croce [1]
Matteo Fiori [2]

T 22

ABSTRACT

Thermoplastic polyolefins are a new generation of single-ply roofing. Polyolefin roof membranes were introduced to the international markets already from 1991 with the North American designation as TPO (Thermoplastic Polyolefins) or with the European as FPO (Flexible Polyolefins). Flexibility of such membranes depends on internal chemical structure: unlike other thermoplastic membranes, they do not contain plasticizers. This fact provides the membranes with the property of a pronounced longevity.

A special type of polyolefin is represented by TPO-FPA (Flexible Polypropylene Alloy), obtained from polypropylene semi-crystalline matrix (PP), in which is incorporated an high percentage of ethylene-propylene rubber (EPR), through a patented catalloy process. The aim of this paper is to present the results of a research commissioned by a company manufacturer, oriented to estimate the durability and the residual properties of TPO-FPA non-reinforced membranes, exposed in different latitudes directly to the solar radiation after 5/10 exposition year.

KEYWORDS

Flat roof, Membranes, Polyolefin, TPO, FPA, FPO, Durability

[1] Politecnico di Milano, Building Engineering-architecture Faculty, Milan, Italy, Phone +39 0223996032, Fax +39 02 23996020, sergio.croce@polimi.it
[2] Politecnico di Milano, Building Engineering-architecture Faculty, Milano, Italy, Phone +39 023996014, Fax +39 02 23996020, matteo.fiori@polimi.it

1 INTRODUCTION

Polyolefin membranes were introduced in Europe around 15 years ago. This time is sufficient to study their behaviour over time and therefore their reliability. The objective of the study was to check whether the main functional features of a mechanically-attached, polyolefin non-reinforced synthetic membrane are maintained.

The study was conducted by inspecting three flat roofs located in sites with different sun exposure and temperatures, by means of laboratory tests on samples taken in field. In the cases of Bourges (France) and Cordoba (Spain), the membrane had been laid more than 10 years before the inspection, in the case of Wattrelos (France) the membrane had been laid around 5 years before the inspection.

For the purposes of the study, the behaviour of membranes directly exposed to sunrays (UV) was compared with that regarding membranes in non-exposed areas (Fig.2). The data were then compared with those mentioned in the product technical specifications issued at the time of membrane production.

2 POLYOLEFINS

Polyolefins represent a large family of thermoplastic polymers. They can be formed by olefin monomers of the same type, such as, for example ethylene or propylene (homopolymer polyolefins) or result from a chain of monomers having different nature (copolymer polyolefins). In the case of polypropylene-based polyolefins (TPO-PP), like whose on which the experiment was carried out, materials have now become established which are generated by means of innovative polymerization processes: these are essentially ethylene-propylene copolymers that, upturning the conventional distinction between different homopolymers and their relevant packages of proprieties and performances, go beyond the behaviour profiles of the original polypropylene or polyethylene, somehow combining their features in one single polymer alloy whose architecture is directly obtained in the reactor. Precisely because of their structure, polypropylene-based membranes feature better hot mechanical properties in hot exposition: this is particularly important when membranes are applied on exposed roofs, without protection and with mechanical fasteners. Besides this, unlike polyethylene-based membranes, polypropylene based membranes can also be used without reinforcement.

3 INSPECTIONS

The inspections were performed on roofs located in Cordoba (Spain), Bourges (France) and Wattrelos (France). Eight samples were taken from each of the roofs, two with a size of 80x80 cm and six, with a size of 8x20 cm, on the overlaps. The areas where the samples were taken were repaired by means of new material, working on the inner side of the membrane without any welding problems. Inspections were performed in 2004 and 2005.

Table 1. Summary table of the main features of the analyzed roofs.

Description	*Bourges (France)*	*Cordoba (Spain)*	*Wattrelos (France)*
Type of building	industrial	industrial	industrial
Roof area	8800 m2	25000 m2	10000 m2
Year when the sealing membrane was laid	1994	1994	2000
Face thickness sealing membrane	1.2	1.14	1.2
Type of climate	Continental	Mediterranean	Continental
Latitude	47.50 N	37.53 N	50.42 N

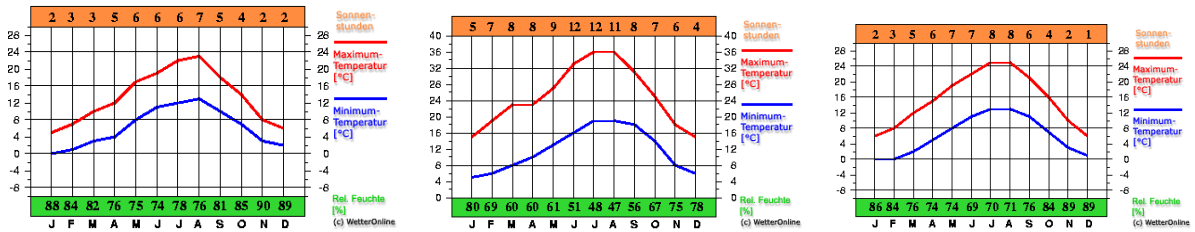

Figure 1. Average minimum and maximum temperatures in Bourges, Cordoba, Wattrelos.(Source WetterOnline).

4 IN SITU INSPECTIONS

Inspections were carried out on three flat roofs located in three different sites.

4.1 In situ Inspection of The Roof in Bourges (France)

The size of the roof is approx. 8800 m2 and it is characterized by six pitches, with little slope. The roof was re-built in 1994, with the presence of reliefs and skylights. Before it was rebuilt in 1994, the roof had been waterproofed by means of a bitumen membrane self-protected by aluminium foil. The waterproof membrane is of the polyolefin type with a polypropylene base, nominal thickness 1.2 mm, ply width of 1 m, homogeneous, fixed on the support by means of mechanical fasteners on the overlaps (Fig. 4); the distance between the fasteners is variable (16-20 cm). The membrane is laid crosswise with respect to the slope. No particular signs of decay were detected after a careful inspection of the waterproof membrane. The joints on the overlaps appeared efficient. No corrugations were detected on flat areas or on reliefs.

Fig. 1. General view

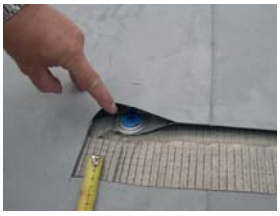

Fig.2. Non- exposed area

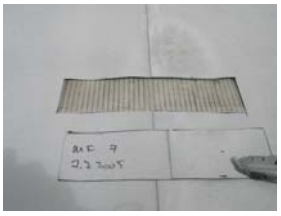

Fig.3. Sample extraction

Fig.4. Repair area

4.2 In situ Inspection of The Roof in Cordoba (Spain)

The size of the roof is approx. 25000 m2 and it was built in 1994. There are skylights and construction joints. The sealing membrane is of the polyolefin type, two-colours, nominal thickness 1.2 mm (required 1.14 mm on US standard), homogeneous, and is fixed to the support by means of mechanical fasteners in line on the overlaps; the distance between the fasteners is variable (16-20cm).

Fig.5. General wiev

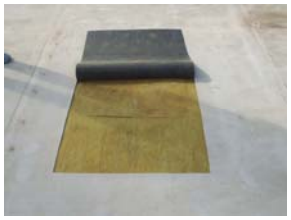

Fig.6. Sample extraction

Fig.7. Sample extractio in overlapping area

Fig.8. Non-exposed areas

No particular signs of decay were detected after a careful inspection of the waterproof membrane. The joints on the overlaps appeared efficient. No significant corrugations were detected on the flat areas or on overlaps and reliefs.

4.3 In situ Inspection of The Roof in Wattrelos (France)

The size of the roof is approx. 10000 m″. The roof is characterized by various pitches, each with a slope of around 25%. There are many skylights and system terminals. Water is collected on the roof flashings. The water is discharged through spouts at the ends of the flashings. The sealing membrane is fixed on the support along the overlaps at a distance of approx. 30 cm. The width of the plies is 210 cm. The nominal thickness of the membrane is 1.2 mm. The roof was rebuilt in 2000.

Fig.9. Skylight

Fig.10. General view

Fig.11. Old membrane before the renovation

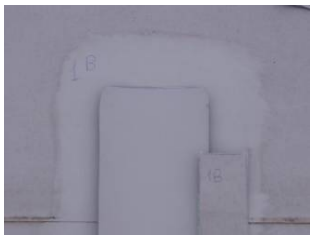

Fig. 12. Repair area

No particular signs of decay were detected after a careful inspection of the waterproof membrane. The joints on the overlaps appeared efficient. No corrugations were detected on flat areas or on reliefs.

5 ANALYSIS OF THE RESULTS OF LABORATORY TESTS

The samples were subject to experimental tests shown in Table 2. The table summarizes the results.

Table 2. Summary table of the features analysed.

Standard of reference	Results of the experimental tests
Thickness (UNI EN 1849-2)	The samples analyzed show a very similar behaviour. In all cases, there is an extremely low change in thickness, equal to maximum 5% between the area exposed and the area not exposed to sun radiation. This value is however comparable to membrane production tolerance, equal to 5%.
Crosswise and longitudinal tensile strength (UNI EN 12311-2, B Method: handlebar test strip)	Values obtained from the experimental test were similar to nominal values, without significant differences between exposed and unexposed samples.
Elongation (UNI EN 12311-2, B Method: handlebar test strip)	Values obtained from the experimental test were similar to, and sometimes higher than, the nominal value, without significant differences between exposed and unexposed samples.
Foldability at low temperature (UNI EN 495-5)	All tests performed, at a temperature of –30°C, had a positive outcome, without indications of damage or cracks.
Peel resistence of joints (UNI EN 12316-2)	Values obtained from the experimental tests were similar to or higher than nominal values.
Resistence to tearing (UNI EN 12310-1 and UNI EN 12310-2)	Values obtained from the experimental tests were similar to or higher than nominal values.
Dimensional stability (UNI EN 1107-2)	Tests performed, with an accuracy of 0.1 mm, proved that dimentional stability did not change over time.

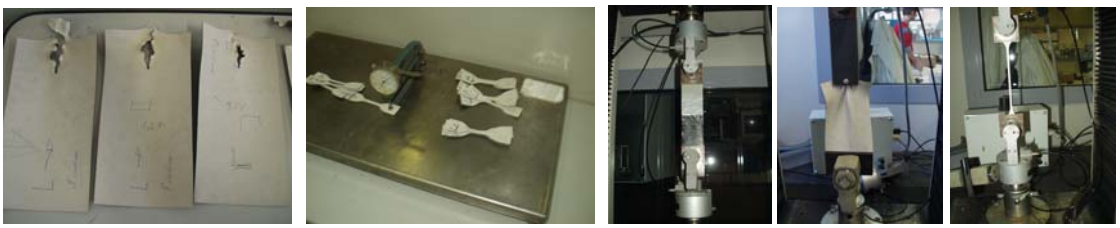

Figure 13. Pictures of laboratory tests.

Specifically, below are the diagrams of the results of the main experimental tests broken down by site. The values of the technical specifications at the moment of production are compared with the current values for the exposed and protected samples – and therefore not directly exposed to sun radiation.

Bourges (Fr)

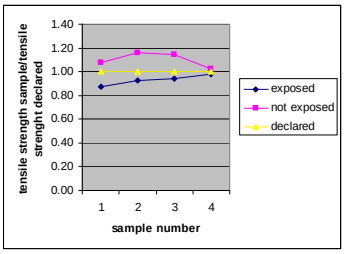

Graphic 1. Crosswise tensile strength

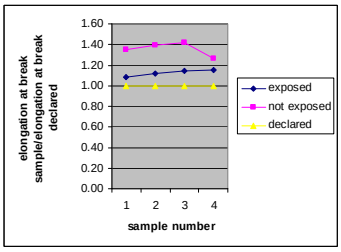

Graphic 2. Crosswise elongation at break

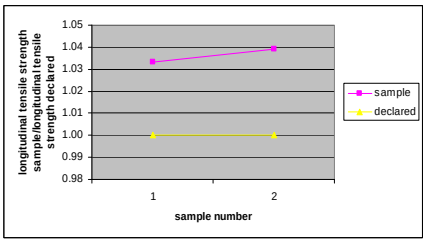

Graphic 3. Longitudinal tensile strength

Cordoba (Sp)

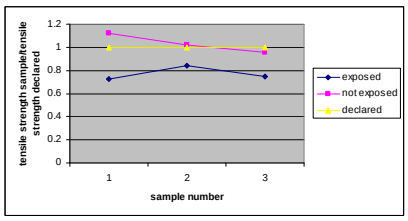

Graphic 4. Crosswise tensile strength

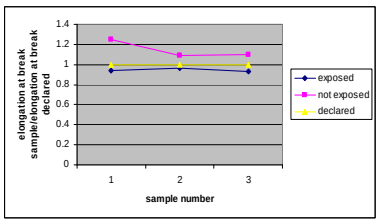

Graphic 5. Crosswise elongation at break

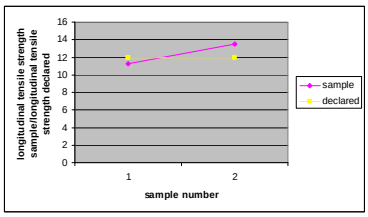

Graphic 6. Longitudinal tensile strength

Wattrelos (Fr)

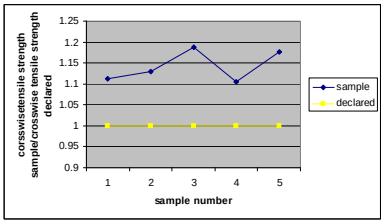

Graphic 7. Crosswise tensile strength

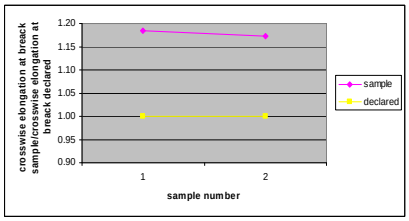

Graphic 8. Crosswise elongation at break

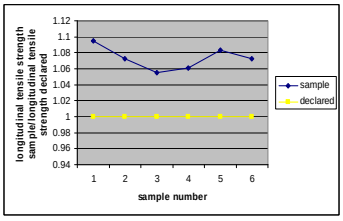

Graphic 9. Longitudinal tensile strength

6 SUMMARY RESULTS OF EXPERIMENTAL TESTS

Below are some figures that summarize the outcome of laboratory tests

Crosswise and longitudinal tensile strength (UNI EN 12311-2) B method (handlebar test strip):
The longitudinal tensile strength stated for the membranes were different: 12 N/mm2 for Bourges and Cordoba, 18 N/mm2 for Wattrelos. The values obtained from the experimental tests were similar to the ones stated. An additional indication is the comparison between the tests on exposed and non-exposed samples, performed for the Bourges and Cordoba test strips.

In this case, the difference between the two values was approximately 15%, while values were significantly different only in two cases (sample 3S1 and 3S6), of around 25%.

Elongation (UNI EN 12311-2) B (handlebar test strip):
The stated value of longitudinal tensile strength was different for the utilized membranes: 500% for Bourges and Cordoba, 700% for Wattrelos. The values obtained from the experimental tests were similar to the ones stated. An additional indication is the comparison between the tests on exposed and non-exposed samples, performed for the Bourges and Cordoba test strips. In this case, the difference between the two values was approximately 15%.

Peel resistance of joints (UNI EN 12316-2)
The values obtained from the experimental tests were similar to or higher than the ones stated.

Shear resistance of joints (UNI EN 12317-2)
The values obtained from the experimental tests were similar to or higher than the ones stated.

Longitudinal and crosswise resistance to tearing (UNI EN 12310-1 and UNI EN 12310-2)
The values obtained from the experimental tests were similar to or higher than the ones stated.

7 CONCLUSIONS

The objective of the research study was to analyse the behaviour over time of polyolefin membranes in TPO-FPA without reinforcement. Three flat roofs were examined, waterproofed with membranes having a nominal thickness of 1.2 mm, laid by means of mechanical fasteners, located in different climates, with operating times of 5, 10, and 12 years.

In all inspections the covers showed, on the flat areas section and in detail, an absence of visible signs of decay. The favourable overall assessment of the cover in place was confirmed by laboratory tests performed on the samples taken: measurements made showed similar behaviours in the three geographical sites.

Membranes had very different exposures to sun radiation, both in terms of intensity and duration: in Bourges (France) and Cordoba (Spain), the membrane had been laid more than 10 years before the inspection, in Wattrelos (France) the membrane had been laid 5 years before the inspection.

Sampling actions on the roofs showed the perfect weldability and therefore the full possibility to repair membranes, even after years of operating exposure, by working on the inner side of the existing membrane.

It should be noted that the assessments made refer exclusively to the specific experimented polyolefin material and therefore to membranes with a polypropylene base (TPO-PP), resulting from a particular polymerization processes.

REFERENCES

Beer, H.R., Keiser, S., 2000,"Flexible polyolefin roofing membranes: ten years of field experience", Proceedings of Waterproofing technology and the environment, IXth International Waterproofing Association Congress, Amsterdam, pp. 154-172.

Beer, H.R. 1997, 'Longevity and ecology of polyolefin roof membranes', Proceeding of the fourth international symposium on roofing technology, Gaithersburg, MD, pp. 14-21.

Beer, H.R., 1995, 'Flexible polyolefin roofing membranes properties and ecological assessment', Proceedings of waterproofing technology and the environment, IXth International Waterproofing Association Congress, Amsterdam, Holland, pp. 81-89.

de Palo, R., 1995 'Flexible polypropylene alloys: a new generation of materials for waterproofing application', Proceedings of Waterproofing technology and the environment, IXth International Waterproofing Association Congress, Amsterdam, Holland, pp. 309-320.

Paroli, R.M., Simmons, T.R., Smith, T.L., Baskaran, B.A., Liu, K.K.Y., Delgado, A.H., 2000, 'Thermoplastic polyolefin (TPO) roofing membrane: the north American experience', Proceedings of Waterproofing technology and the environment, IXth International Waterproofing Association Congress, Amsterdam, Holland, pp. 173-200.

Rotolo, A., 2000, 'The most recent frontiers of performance in APP modified bitumen waterproofing membranes with the use of new generation polyolefins' proceedings XIth International Waterproofing and Roofing Congress, Florence, Italy, pp. 65-79.

Simmons, T.R., Runyan, D., Liu, K.K.Y., Paroli, R.M., Delgado, A.H., Irwin, J.D., 1999, 'Evaluation of in-service thermoplastic olefin (TPO) roofing membranes', Roofing research and standards development: Fourth volume, ASTM STP 1349, pp. 19-42.

Simmons, T.R., Runyan, D., Liu, K.K.Y., Paroli, R.M., Delgado, A.H., Irwin, J.D., 1999, 'Effects of welding parameters on seam strength of thermoplastic polyolefin (TPO) roofing membranes', Proceedings of the north American conference on roofing technology, Toronto, ON, Canada, pp. 56-65.

Materials Used in Transparent Facades: an Approach Towards Building Maintenance

Geísa Gaiger de Oliveira [1]
Oliveira, Roberto de Oliveira [2]
Cláudio Renato de Camargo Mello [3]

T 24

ABSTRACT

Transparent facades have been widely used in construction as a way to promote user interaction with the external environment combined with an attractive and a modern appearance. Designing transparent facades, however, requires the understanding of intrinsic variables that, otherwise neglected, may result to user dissatisfaction. This work aims at identifying the main types of materials that are utilized in transparent facades in the city of Porto Alegre, Rio Grande do Sul State, as well as presenting a checklist for the evaluation of the maintenance process. The research method adopted for this work is composed of three main stages: a bibliographic search followed by the development of a checklist for evaluation purposes. The third stage was accomplished based on a checklist applied to a non-random sample of buildings located in Porto Alegre, Brazil. From the study of the sample, it was possible to observe a series of problems such as dirty stains, colour mismatch due to material replacement, and a series of complaints regarding the buildings' conditioning. It was also noticed that the solar orientation of some facades requires the use of internal shades, which, in turn, prevent integration with the external environment. In many cases, the lack of building details to facilitate maintenance was another noticeable problem. The most utilized materials in facades were reflective laminated glass and common tempered glass. Based on this study, it was possible to conclude that designers can count on a variety of materials available in the market. However, extra care should be taken when specifying a given material in order to avoid any mistakes that might later compromise the life cycle of the building.

KEYWORDS

Transparent facades, Maintenance, Materials

[1] PPGEC – UFSC, SC. Universidade de Cruz Alta, RS. Cruz Alta RS, Brazil Phone 5551 3779-8680, ggaiger@gmail.com
[2] Universidade Federal de Santa Catarina SC, Florianópolis SC, Brazil, ecv1rdo@ecv.ufsc.br
[3] Architecture and Urbanism Course at Universidade de Cruz Alta RS, Cruz Alta RS, Brazil. mello@unicruz.edu.br

1 INTRODUCTION

In the past few years, the use of natural light has become a trend in modern architecture as a design element for energy efficiency purposes and visual comfort. Optimization of natural light in buildings can significantly contribute to reduce energy consumption and to improve visual comfort and welfare of users. Natural daylight provides more pleasant and preferred atmospheres than artificial lighting (ABNT 02:135.02-001, 1998).

Appearance is the first thing to attract the attention of the client. But the task of designing a building requires the understanding of several variables that, if disregarded, may result in user dissatisfaction especially in terms of comfort. It is important to mention that comfort in this case means satisfaction and safety in a building.

Within this context, this work aims at identifying the main types of materials utilized in transparent facades, as well as proposing a checklist to evaluate facades with a view on maintenance process. The growing interest on this topic is due to the fact that a number of materials once employed as mere detail have become part of the facade itself.

2 TRANSPARENT FACADES

Major heat exchanges in a building usually occur through glazing devices such as windows, skylights, glass facades or any other transparent material employed in the architecture. Convection, conduction, and radiation are the three types of heat exchange. The radiation is the main aspect to be considered, since it is the amount of heat directly transmitted to the inside of the building and it depends on glass transmissivity (τ). When considering transparent glazing, the designer has many options of materials available such as glass and polycarbonates. However, employing these materials without a previous evaluation of their characteristics may cause a series of pathologic manifestations from aesthetic issues to more serious matters related to thermal comfort.

According to Alucci (1999), choosing a type of facade should take into account the activities for which the building was designed, as well as the weather conditions of the region.

The solar radiation transmitted to a building is either absorbed or reflected by the facade. A temperature increase implies higher infrared emission, which, in turn, is reflected back to the environment, resulting in air overheating and, consequently, the greenhouse effect. In architectural projects for facades, the main variables that may affect the heat input through glazing facades are: orientation and size, type of glass or transparent material, and use of internal and external solar protection. According to Silva (2001), for optimization of natural light, the glazing devices should be designed to allow a balance between the losses and gains that result from heat radiation transmission inward and outward the building and the light that comes inside the building.

The natural light available inside of a building depends on the amount of natural daylight available outside. The levels of natural light depend on cloudy sky conditions, on the period of the day and year, on the geometric characteristics of the building and compartments, on the dimensions and the spectrophotometric characteristics of glazed areas, on the level of external obstruction and, also, on the reflectometric characteristics of interior surface materials (SANTOS, 2000).

In the case of surface materials, the designer must evaluate the viability of the material that is being proposed – a material wrongly specified or a forgotten detail may compromise the whole performance of the building. In general, external sunshades with *brise soleil* or architectural details tend to be more efficient than internal protections.

3. MOST PREFERABLE MATERIALS FOR TRANSPARENT FACADES

Due to its transparency, the glass allows solar radiation to pass through, where it is converted to heat. Depending on the building location and position, the transparent facades should count on a shading device. It is important to mention that external shading devices are more effective than internal ones, since they reduce the amount of heat entering into the building and the consequent greenhouse effect.

The dark glass, whether laminated, normal or with some type of film, is designed to reduce solar radiation, but it also reduces the amount of natural light inside of a building. In this case, extra opening areas are often required. The use of reflective glass represents a good option to minimize the radiation. However, it is important to consider mobile elements to allow solar radiation and optimization of natural light.

Lamberts (1997) classifies glass for building purposes into simple, green glass, film and absorbing glass, film and reflective glass, and plastic. Although plastic (polymers) are not glass, they are entering the market as polycarbonates and acrylics for transparent shading elements.

Santos (2003) studied the main types of glass and materials used in transparent facades. They are presented below:

1)Coloured float glass or Absorbing glass - the main purpose of this glass is to reduce solar transmittance by absorbing a great amount of incident energy, reducing direct heat gain and glare inside of the building.
2) Laminated glass – is a type of safety glass composed of two or more layers of glass bonding together by up to four interlayers, usually made of polyvinyl butyral (PVB).
3) Reflective glass – based on colored or colorless float glass, the reflective glass receives a metallic coating (semi-conducted metal oxides) that is directly applied to one of its surfaces during production.
4) Polyester film with solar control layer – used for enhancing solar control. A solar control film is applied on the glass.
5) Polycarbonate – a material with outstanding impact resistance and transparency. Lighter than glass, it can be cold-moulded and it also provides UV protection.
6) Acrylic – a linear thermoplastic polymer obtained from addition polymerization of Methyl Methacrylate.

4 MAINTENANCE CONSTRAINTS

Performance losses of a building or of one of its elements often require recovery maintenance, which, inevitably, results in costs for users. Although this is a known fact, maintenance planning for buildings does not seem to be of great concern to many designers. The problem becomes more serious when the damage is not repaired. According to Perez (1988, p.611), it is taken for granted that maintenance begins when construction ends, but the process actually starts on the drawing board. For Vasconcelos (1998), a change in mentality towards the builder/client relationship at the moment the product is delivered is crucial. Based on that, Vasconcelos (1998) provides some guidance on how to prepare a program for periodical building maintenance and on how to turn maintenance into a facilitator component in the building/client relationship.

A building process with integrated stages (planning, project, execution) results in better quality product (building). In this case, the decision making process will not be based on a single stage, but on all stages. This type of procedure may minimize problems and costs of future maintenance. It is possible to perceive that for building matters, maintenance is seen as a cost when, in reality, it should be considered as an investment on the property. This investment not only increases users satisfaction, but it also adds value to the property.

The principle that maintenance adds value to a property is not often exercised by users, since they are usually unaware of how to perform maintenance and the advantages of doing so.
Many users mistakenly believe that once a building is finished it will remain in favourable conditions for a long period of time.

The interest in maintenance is based on the fact that, every year, condominiums are forced to spend great sums of money on this activity. Many problems that require maintenance could be avoided if only the materials and the architectural details received more attention during the project phase.

Performance requirements, however, are not officially in place yet. This fact makes Calmon and Grilo (2000) to affirm that the absence of crucial requirements throughout the decision making process in construction – associated with the lack of indicators to evaluate conformity of product and processes to the quality required during the production phase – favours pathologic manifestations and contributes to consolidate inadequate and counterproductive building techniques. This type of procedure procedure leads to the need of more frequent maintenance and, consequently, higher cots to users.

5 RESEARCH METHOD

The research method adopted in this work comprises four main stages. Figure 1 presents the research design. According to figure 1, the stages were divided into bibliographic search, checklist development, checklist application, and data analysis.

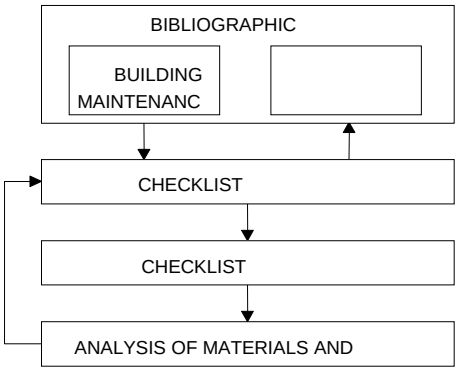

Figure 1. Research design.

During the bibliographic search an attempt was made to collect the theoretical framework related to building maintenance and transparent facades. The aim of this stage was to identify types of facades, materials as well as considerations and procedures for building maintenance. Once the theoretical review was concluded, a proposal of a checklist (Table 1) was developed and applied in a sample of buildings located in the city of Porto Alegre/RS – Brazil. The checklist was based on the topics approached in the theoretical framework and it was developed in order to facilitate the data collection process. The checklist was applied to a **non-random** sample of buildings. The authors decided to contemplate those neighbourhoods that are known for aggregating buildings with transparent facades. For this study, the authors decided not to classify the age or the cost of maintenance processes of the buildings in the sample, since the study aimed at developing a data collection instrument (the checklist) that may be used for a broader classification to be conducted in the future. A study of materials and typologies of facades was thus conducted. The data was analyzed with the aim at identifying – in the sample – the types of facades and the materials of which they were composed. During this stage, the authors attempted to raise considerations regarding ease of maintenance execution. After the analysis, some changes in the original checklist – to be used in further researches – were suggested.

Table 1. The checklist used in this work.

FEDERAL UNIVERSITY OF SANTA CATARINA		
Date of Inspection	Commercial ( ) Residential ( )	
Building Address		
Responsible for the Inspection		
Checklist Number		
Number of Photographs:		
	YES	**NO**
Type of transparent facade:		
Glass skin		
Windows with frames		
Curtain wall		
Articulated glass skin		
Other:		
Position of the facade– vertical		
Position of the facade – horizontal		
Position of the facade – inclined		
Solar Position of the facade		
East		
West		
North		
South		
Types of materials used in the facade		
Colourless float glass:		
Coloured float glass:		
Laminated glass:		
Reflexive glass:		
Glass with polyester film:		
Tempered glass:		
Polycarbonate:		
Acrylic:		
Other:		
Solar protection		
External solar protection? Specify:		
Internal solar protection?		
Types of internal protection		
Brise soleil		
Awnings		
Roof edges		
Mobile Venetian blinds		
Blinds		
Other? Specify		
General		
Is the building surrounded by intense traffic?		
Is there any mismatched component on the facade, non-conform with the whole appearance?		
Was the facade under maintenance during the inspection?		
Does the facade require any specific cleaning product?		
Does the facade offer easy access for cleaning?		
Was there any visible safety device for maintenance during the inspection?		
Is it possible to identify if there are designed elements in the facade in order to facilitate the use of external maintenances equipments?		
Does the type of frame facilitate maintenance?		
Are there any details to facilitate the maintenance process?		
Recommendations/Observations:		

6. ANALYSIS AND DISCUSSION

Based on the non-random sample, composed of 15 buildings located in the city of Porto Alegre, Brazil, it was possible to observe that in commercial buildings there is a predominance of reflective glass skin facades combined or not with architectural details in masonry and concrete or, in some cases, with aluminum sheets (Figure 2). In residential buildings, it was observed a predominance of laminated glass in the composition of the facades. In this case, the laminated glass was employed as frames, as shown in Figure 3

Figure 2. Transparent facade with aluminum sheets.

Figure 3. Laminated with frames.

Table 2 presents the most used types of glass observed during the study.

Table 2. Most preferable types of glass.

	Reflective Glass	Laminated glass	Tempered Glass
Commercial building	8	1	1
Residential Building	0	4	1

Polycarbonates and Acrylics were only observed in architectural details, such as skylights. But even in those cases the maintenance process should be performed with care in order to avoid major problems, as shown in Figure 4. From Figure 4, it is possible to observe a build up of dirt on the left lower portion of the window frame. It reveals a lack of maintenance or faulty assembly without adequate devices to prevent this kind of problem.

Figure 4. Glazing with alveolar polycarbonate with build up of dust.

The typology of the facade does not significantly interfere with maintenance. However, the majority of the inspected buildings lacked the necessary devices – scaffolds, safety belt d-rings, platforms, among others – to perform or facilitate this task:

None of the buildings presented specific construction details for maintenance or, at least, elements to facilitate the procedure. It is possible to perceive that, in the buildings with skin glass, the maintenance process, the replacement of a component or even a simple cleaning procedure often require external scaffolds. In one of the buildings, the facade was away from the structure (Figure 5). In this case, an internal scaffold was necessary. Glass with architectural detail or frame pyramidal shape of the upper floor would not allow any kind of device or scaffold for external cleaning.

Figura 5. Transparent facade displaced from the structure.

The dirt that builds up on the illuminating surfaces, that is, on the transparent facades reduces transmittance e reflectance. This dust that accumulates on the facade will interfere with the illuminance calculation, which depend on the measures of the room and on the natural light that can be lateral or zenithal. Transparent facades should be free from any kind of dirt; they require extra care since its differential lies exactly on their transparency. Cleaning products should be suitable for each material, otherwise they may cause damage to the facade.

Facades that are made of transparent or translucid material require more frequent maintenance; for that reason, the project for those facades should include devices to facilitate maintenance procedures. Those devices vary from structures to adapt scaffolds or similar devices to internal devices for fixing safety belts.

A great number of commercial buildings are located on streets or avenues of intense traffic of buses and cars a fact that considerably increases the amount of dirt. It is important to mention that, in some of the buildings, it was not possible to conduct an internal inspection. For these cases, it is not possible to affirm if the buildings with reflective glass facade had some kind of internal shading, except in a few buildings where it was possible to identify the use of curtains. With respect to solar orientation of the facades, it was not observed any significant predominance that could or could not justify the choice for transparent facades, taking into account thermal comfort, as shown in Table 3. This fact may lead to the conclusion that, in some cases, the solar orientation is directly related to the choice of facade. This issue, however, should be the topic for a further study.

Table 3. Orientation of the transparent facades.

Solar Orientation	Buildings
North	5
South	2
East	5
West	3

7 FINAL CONSIDERATIONS AND RECOMMENDATIONS

As final consideration, the authors are able to affirm that: i) the project for buildings with transparent facades did not include any specific device to facilitate maintenance procedures; ii) the projects should specify materials and procedures as well as construction details that could facilitate maintenance procedures; iii) nowadays, with a variety of materials available, architectural designers are able to fully express their creativity; but it is important to be cautious when specifying a given material in order to avoid mistakes that may compromise the project.

The technology employed in new materials or in the improvement of existing ones offers a number of options available in the market, which, in turn, helps the architect or the engineer to design and specify materials. This availability, however, demands a much deeper understanding of a great number of different materials. Knowing the types and specifications of the desired materials will avoid future problems, such as pathologic manifestations and unplanned maintenance procedures.

The understanding of these facts and a sense of responsibility result in human comfort and promotes a harmonic relationship among people, their home and the environment, with less effort, lower energy costs, and fewer equipment.

The checklist not only aids the identification of tendencies in the use of certain materials, but it also helps in the classification of the state-of-art of the maintenance process performed in the city of Porto Alegre, Rio Grande do Sul State

As recommendation for further works, it is possible to highlight:

- Analysis – with professionals of the field – of the level of maintenance easiness of some facades;
- Interview with designers to identify tendencies of project;
- Analysis of the use of materials for transparent facades

REFERENCES

ALUCCI, M. P. ‘Fachadas transparentes: do conforto ao consumo de energia’. *Revista Thécne*, mai/jun , 1999 n.40, p.53-55.

ASSOCIAÇÃO BRASILEIRA DE NORMAS TÉCNICAS, ABNT. Iluminação natural – Parte: Conceitos básicos e definições. Junho 1998, 7 páginas.

BILLMEYER Jr, F. W. *Ciencia de los Polímeros*. Espanha, Editorial Reverté S. A., 1978.

CALMON, J,L., GRILO. ‘Falhas externas em edificações multifamiliares segundo a percepção dos usuários’. In: Encontro Nacional de Tecnologia do Ambiente Construído. Salvador, Bahia. 2000.

LAMBERTS, R. DUTRA, L. PEREIRA, F. o. R. *Ciência Energética na Arquitetura*. ed. PW Editores, São Paulo, 1997.

OLIVEIRA, G.G. Vidro na Construção. Notas de aula. Universidade de Cruz Alta, Disciplina de tecnologia das edificações, 2005.

PEREZ, A .R. 'Manutenção dos edifícios'. In: *Tecnologia das Edificações*. São Paulo: Ed. Pini - IPT 1988. p. 611-614

Policarbonato disponível em www.metálica.com.br acessado em 20/07/2005.

SILVA, Geziel da. 'Uso de superfícies transparentes em edificações'. Disciplina de Térmica Aplicada. Universidade Federal de Santa Maria – Programa de Pós-graduação em Engenharia Civil, 2001.

SANTOS, A. J. 'Metodologia de caracterização das condições ambientais de iluminação natural nos edifícios'. Proc. NUTAU 2000 – Tecnologia do desenvolvimento, p. 995-1002. São Paulo, 2000. *Anais:* São Paulo, FAU-USP.

SANTOS, J. C. P. Desempenho Térmico e Visual de Elementos Transparentes á Radiação Solar, Tese (Doutorado em Ciências e Engenharia de Materiais), São Carlos, São Paulo SP, 2003 Universidade de São Paulo.

VASCONCELLOS, L.A .C. Planejamento da manutenção predial visando à pós entrega. Disponível em http://www.infohab.org.br. Acessado em 07/09/2003

Use of a Peltier Element to Increase Time of Wetness of Unglazed Solar Collector Specimens in a Natural Field Exposure Test

Bojan Stojanović [1]
Jan Akander [2]

T 24

ABSTRACT

In accelerated testing, material specimens are exposed to completely artificial environments, where exposure to individual degradation agents is enhanced. In contrast, field-testing exposes specimens to multiple degradation agents. When performing a semi-natural test, the influence of a selected degradation agent may be increased while the specimen is still situated in its natural environment. Moisture is such an agent. In an experimental set-up for evaluating long-term optical performance of an building integrated Unglazed Solar Collector, a sub-task was to increase Time of Wetness (TOW) for several collector specimens for two reasons: to "simulate" an active cooling of the component as is the case for solar collectors; and to assess the role of TOW on optical degradation of the solar collector. Specimen cooling and increase in TOW was achieved by utilisation of a Direct-Air Peltier Element. TOW was estimated through measurements with WETCORR sensors (monitoring surface temperatures and moisture) and climate parameters (temperature and relative humidity) at site. At this particular test site in Gävle, Sweden, TOW was more than doubled in comparison to non-cooled surfaces. The Peltier Element proved to be inexpensive and flexible for this purpose.

KEYWORDS

Peltier Element, Time of wetness, Semi-natural environment, Optical durability

[1] University of Gävle, Building Materials Technology, Centre for Built Environment, Gävle, Sweden, Phone +46 26 648137, Fax +46 26 648181, bojan.stojanovic@hig.se
[2] University of Gävle, Building Materials Technology, Centre for Built Environment, Gävle, Sweden, Phone +46 26 648118, Fax +46 26 648181, jan.akander@hig.se

1 INTRODUCTION

The durability issues of solar collectors are in general related to a number of problems: erroneous manufacturing, installation or freezing [Wennerholm 2003]. Other durability issues are the exposure to various strains (solar radiation, wind, rain/humidity, snow and airborne pollutants) as a result of outdoor placing and in-service use. These contribute to a degradation process and contamination of the collector material (surface) that affects its energy performance due to change in optical properties (e.g. see Carlsson et al. [1994]). These changes will in turn be transposed throughout the system, lowering its degree of efficiency, which directly relates to the economical and environmental aspects of the system. As a result of these types of changes, a performance-over-time assessment is needed, so that the progression and effects of the performance lowering degradation processes can be assessed. This paper presents a study on optical surfaces degradation of a building (roof) integrated Unglazed Solar Collector (USC), by exposing USC specimens to a field test consisting of a natural and semi-natural test set-up. When performing a semi-natural test, the influence of a selected degradation agent is increased while the specimen is still situated in its natural environment; moisture is such an agent. The paper specifically presents the semi-natural test set-up procedure and its proficiency evaluation, in order to increase Time of Wetness (TOW) and highlights USC humidity exposure and its accompanying effects. The exposed USC was developed and used in the EU project Endohousing (Endothermic Technology for Energy Efficient Housing in the EU, Project No: NNE5-2001-00565). The project used solar-assisted heat pumps (e.g. see Ozgener & Hepbasli [2007] and Kjellsson [2004]) to provide the thermal energy to meet space heating, cooling and hot water requirements for domestic houses in different regions of the EU throughout the year. Five demonstration sites (Endosites) were established, equipped and evaluated across the EU; one of which was located in the central parts of Sweden (Sandviken), Fig. 1. The USC is made of extruded aluminium 6060, where the ends and in/outlet pipes are welded to the extruded profile. The USC surface is zinc chromate yellow etched prior to coating application, in which a polyester powder coating is used, in this case with colour RAL 7022; see Fig. 1.

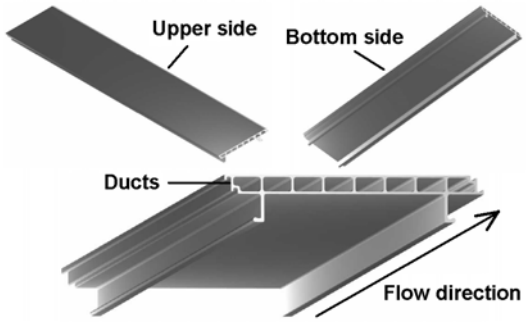

Figure 1. The Swedish demonstration site (Endosite) in Sandviken, showing the roof integrated USC. A drawing showing a top and bottom isometric view of the roof integrated USC used in the Swedish demonstration site (Sandviken).

A major degradation agent acting on all outdoor exposed building materials and components is humidity, whether it is in the form of rain, moist air or condensation. A roof-integrated USC is not merely a component in an energy system, it also has accompanying building technology functions and criteria, e.g. rain protection etc, which makes it highly exposed to the outdoor weather due to its function and placing.

An USC does not solely work as a solar collector since it also works as a convective heat-transfer surface, by absorbing heat from the ambient air. During this operating mode, there will be occasions when air is cooled at the USC surface to the extent that condensation occurs. Roofs also have the tendency for condensation due to night sky radiation (emitting long wave radiation), as these have a large view factor towards the sky. All of these scenarios demonstrate the USC humidity exposure and necessity of endurance. The evaluation and assessment of USC surface response to outdoor humidity exposure, is an important part in the field exposure testing (semi-natural test). In order to highlight humidity exposure and its accompanying effects, a number of USC samples were cut into rectangular shape and mounted onto a Direct-Air Peltier-Element (PE), which cools the samples to increase TOW. One of the main questions is, as the roof-integrated USC being an active energy system component (experiencing different temperatures and surface wetness), if it will have a different durability and Service Life (SL) in comparison to regular architectural surfaces. As the metallic USC is a regular outdoor surface (not as the absorber coating of a glazed solar collector), the coating applied on to the USC component will most likely be of the same type as for regular architectural surfaces (e.g. tin roofs), and have the same durability requirements. These requirements usually do not express optical durability related to the radiation energy transfer parameters: solar absorptance (α) and IR emittance (ε), which are vital for solar collector performance [Duffie & Beckman 2006], or regard the possibly harsher degradation environment as a result of the USC being an active component. This raises the question if current coating requirements and durability tests are adequate for this type of application.

2 FIELD EXPOSURE TESTING

In order to test the optical durability of the USC due to outdoor strain and in-service use at a pre-testing stage [ISO 15686-2], a natural and semi-natural field exposure test was set-up; see Fig. 2 and 3. The main idea behind the division into these two test procedures is to have a field test set-up that assesses in-service use and highlights the extremes of outdoor strain, without having a full USC test component in operation (in-use exposure [ISO 15686-2]). One extreme being a surface (component) absorbing as much as possible solar radiation, hence experiencing high surface temperatures and UV radiation (this is related to the natural test set-up), the other being rain and humidity – humidity due to that an USC in operation can/will convectively absorb heat from the ambient air to the extent that condensation occurs and condensation due to long wave radiation towards a clear night sky. In order to facilitate the collection of test sample specimens from the exposed USCs, pieces were beforehand cut out from the collector and exposed to the outdoor environment. This was achieved by first separating the upper side of the USC and thereafter cutting this aluminium sheet to smaller pieces. The necessity of doing so is due to the USC material thickness of $2 * 10^{-3}$ m, which makes it difficult to cut the test samples on site without damaging or contaminating the test and USC surface. The prepared specimens were then assembled into larger homogenous surfaces (see Fig. 2 and 3) in attempt to reduce the size effect of having smaller material test specimens [Marteinsson 2004]. Size effect implies that small specimens will statistically have fewer faults than is common for a larger surface. Small specimens are also more likely to behave as points in space rather than continuous component surfaces, e.g. experiencing different wind patterns, surface temperatures and moistures due to area and mass. The natural test set-up consists of USC specimens mounted onto a Plexiglas panel (see Fig. 2). The attachment is realised as holes were drilled through the Plexiglas panel. The USC specimens were placed over these holes, which thereafter were filled with silicone from the backside, thereby attaching the specimens with silicone fillings. This approach enables an easy detachment of test specimens and replacement with an aluminium dummy, in order to preserve the homogenous panel surface. The main purpose of this procedure is the ability to expose entire test panels as opposed to single small specimens (see discussion above). A total of five test panels were mounted onto a rack facing south which is inclined 45° (see Fig. 2). Each test panel holds 16 pre-cut specimens, 0.05 * 0.05 m².

In order to assess and characterize the exposure environment and its degradation agents, local and microenvironment monitoring was conducted during the exposure testing. The monitored local meteorological parameters used in the study (at a pretesting stage [ISO 15686-2]) were: air

temperature (°C), relative humidity (%), global- and diffuse solar-, and UV- (0.295-0.385 µm) irradiance at a horizontal surface ($W \cdot m^{-2}$). The microclimate (temperature and TOW) was monitored on the surface of the exposed test specimens with a WETCORR measuring equipment (see Fig. 2, 3 and 4). A WETCORR sensor consists of a ceramic plate with a grid of gold [Norberg 1998] that is connected to an adapter which provides a 100 mV DC excitation voltage, with a polarity reversal every 30 seconds. The resulting current flow, which is proportional to moisture on the grid, is sampled continuously and the average over one minute is logged and (in this study) set to be stored as a 30-minute average value. In addition to moisture, the sensor is also sensitive to pollutants, which may accumulate and thereby modify the electric conductivity of the moisture film on the gold grid [Norberg 1998]. An embedded PT-1000 element samples the surface temperature simultaneously. For further description of the WETCORR equipment, see Norberg [1993] and Norberg [1998]. WETCORR sensors were placed on two separate panels in the natural field exposure test and one on the semi-natural field exposure test. The mean of the two measured values in the natural field exposure testing is considered to be representative for the microclimate for these test surfaces. As for the semi-natural test, only one sensor is used as a representative measure. The USC test samples in this study were placed outdoors at the natural and semi-natural field exposure-testing site on the first of November in 2005. Measurements started simultaneously in order to monitor the exposure environment. The test site is located on the roof of the Centre for Built Environment at the University of Gävle, Gävle, Sweden.

Figure 2. The natural field exposure set-up of the USC optical durability test. 5 test panels mounted onto a rack facing south and having an incline of 45°.

2.1 Semi-Natural Field Exposure Testing

When performing a semi-natural test, the influence of a selected degradation agent may be increased while the specimen is still situated in its natural environment [Jernberg et al. 2004]; moisture is such an agent. Moisture is often a major degradation agent that acts on all outdoor exposed building materials and components, whether it is in the form of rain, moist air or condensation. The evaluation and assessment of USC surface response to outdoor humidity exposure, is an important part in the field exposure testing. In order to highlight humidity exposure and its accompanying effects, a number of USC samples were cut into rectangular shape and mounted onto a PE, which cools the samples to increase TOW, see Fig. 3 and 4. The PE unit used in the study for accomplishing this task is a Direct-Air system, which absorbs heat through a cold plate and "*pumps*" it through the PE, emitting the heat to the air (cooling fins) by an air heat sink at the backside. The used PE (DA-160-24-02) [Supercool 2007] is a product from the company Supercool. It has an active cold plate of 0.18 * 0.13 m² and a maximum cooling power of 160 W at $\Delta T = 0$ (cold plate – ambient temperature). The PE is assembled into a box (see Fig. 3), which incorporates the PE cold plate with the box front.
The exposed plate has a larger aluminium surface onto which USC specimens are mounted, thereby isothermally cooling hence increasing USC TOW while being situated in a natural environment.

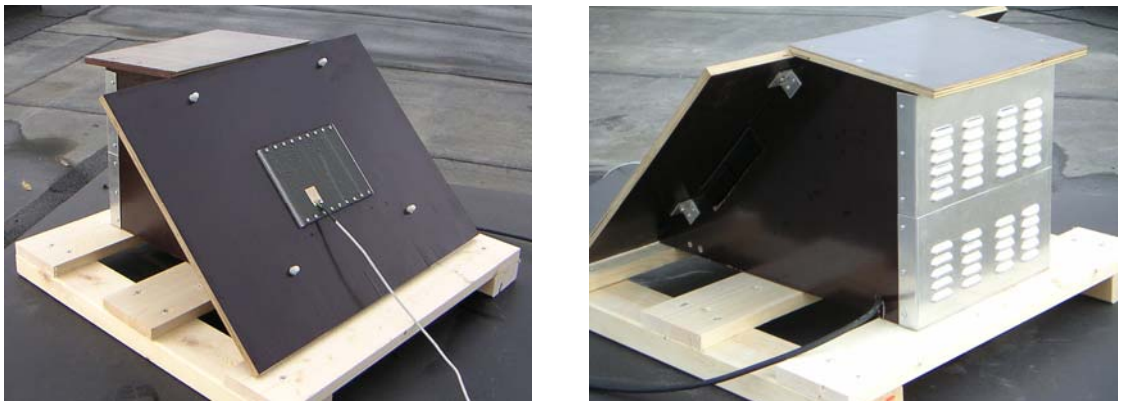

Figure 3. The Peltier Element test set-up in the semi-natural field exposure testing. *To the right*: box front side with exposed specimens. *To the left*: box back side with slots for removal of absorbed heat.

The specimens in the so-called semi-natural field exposure testing have the size of 0.14 * 0.02 m² and are screwed onto a lager cooled aluminium surface of 0.14 * 0.19 m², which is attached onto the PE cold plate. The 9 specimens make up a larger test panel (see Fig. 3). The test set-up has an inclination of 45° facing north. The sides of the PE set-up are also shaded to assure that no direct solar radiation reaches the PE cooled surfaces. This set-up is chosen in order to avoid surface heating and drying up, thereby increasing humidity exposure. The control strategy of the PE was to set a fixed temperature difference between the surface and ambient air, such as to obtain continuous visible surface condensation. As the PE is a Direct-Air type, the directly cooled aluminium surface (USC specimens) temperature will follow the outdoor temperature variations with a fixed cooling temperature difference. The set point temperature is chosen by guidance of monthly outdoor mean air temperature and humidity of a reference year of the test site. This rough and simple control strategy can in combination with time-to-time visual checkups and adjustments render a significant overall TOW increase. The convenience of using a PE is the simplicity of only being dependent on electricity. Other set-ups for cooling, usual require some circulating brine or other cooling fluid, in combination with a refrigerator unit. The semi-natural test set-up proved to cool the exposed USC test specimens in en proficient way, by actively maintaining a homogenous surface temperature lower than the ambient (see Fig. 4); making the assumption that all semi-natural USC test specimens are exposed to equivalent conditions, fair.

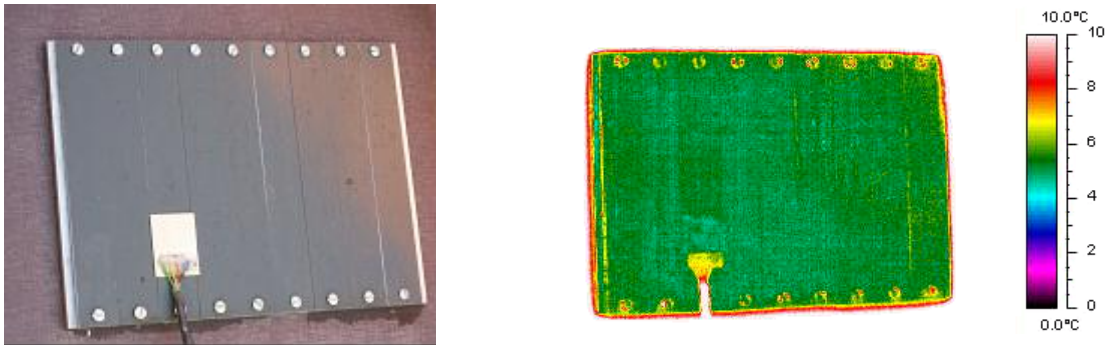

Figure 4. A Close-up picture of the cooled test surfaces in the semi-natural field exposure testing and a thermograph picture of the Peltier Element cooled USC specimens exposed in the field test, showing that the cooled specimens are isothermal.

3 MICRO AND LOCAL CLIMATE MEASUREMENTS

Compiling the monitored exposure environment attained a lucid view of the USC test surface conditions. The quantified surface exposure parameters presented within the scope of this paper is surface temperature and TOW; as the objective of the paper is to present the TOW increase proficiency of the semi-natural field exposure test set-up.

The processed data presented below range for approximately 21 months, from November 2005 to September 2007. Measured surface temperatures (sampled by the WETCORR PT-1000 sensor) are presented in cumulative graphs in Fig. 5, for the total exposure time. In these figures N and SN denote natural and semi-natural.

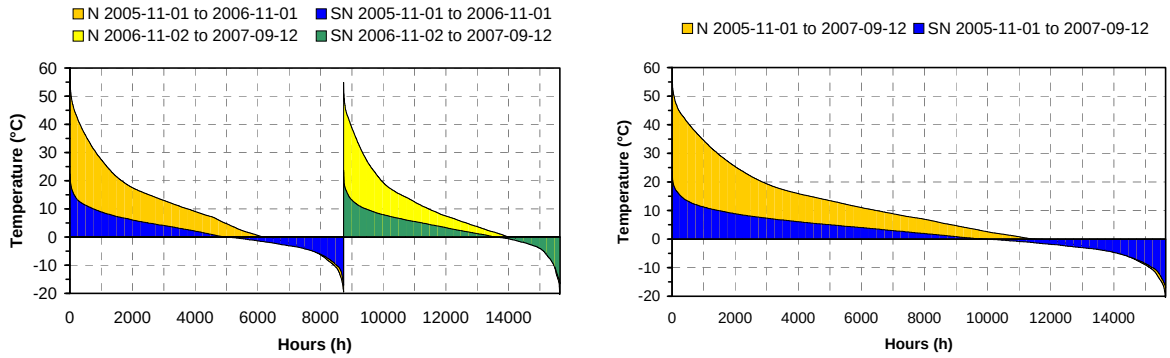

Figure 5. Cumulative graphs of the measured test surface temperature of the natural (N) and semi-natural (SN) exposure for the test period.

In order to estimate TOW of the USC surface, a WETCORR sensor signal limit was identified to indicate the wetness status of the surface (wet/not wet). The limit of 10 nA was found adequate, as can be observed in Fig. 6, which represents a period in July 2006 that was used as limit guidance. The limit of 10 nA, was also found adequate and used by Norberg [1993] in an earlier study, performed at the same test site.

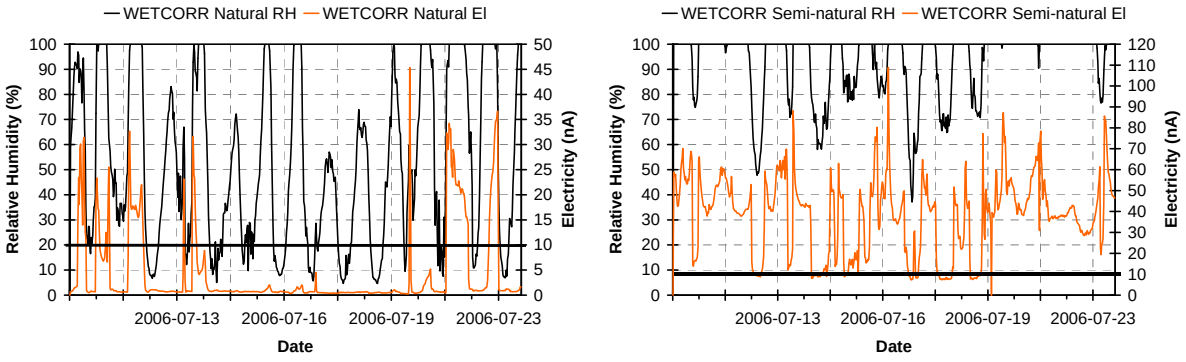

Figure 6. *To the left:* Calculated relative humidity at the natural exposed test sample surface (*surface temperature vs. ambient humidity*), and electrical signal from the WETCORR sensor. *To the right:* Calculated relative humidity at the semi-natural exposed test sample surface, and electrical signal from the WETCORR sensor. Note that the 10 nA limit is marked.

The estimated TOW is presented in Fig. 7 for the USC specimen exposure time. Fig. 7 shows duration time of the electric signals from the WETCORR sensors, with the electrical current criteria of >10 nA

when the surface temperature is >0 °C. The surface in question is considered wet when the electric current and temperature criteria is fulfilled.

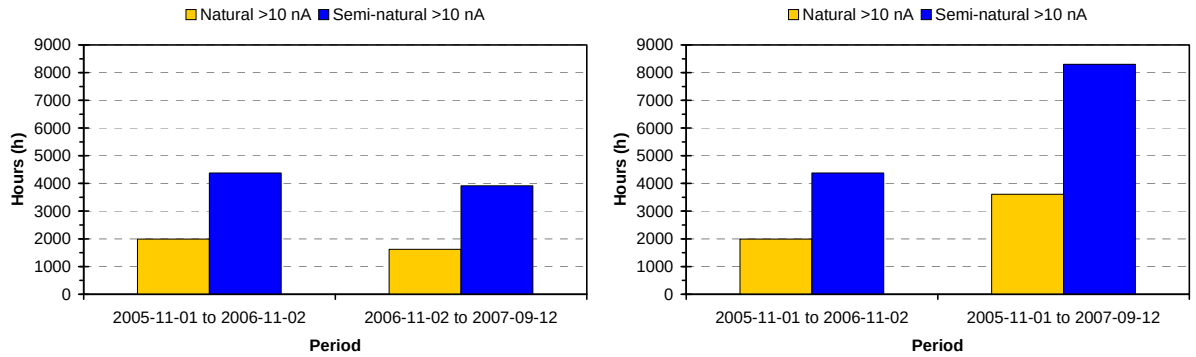

Figure 7. Cumulated measured (estimated) TOW for the natural and semi-natural exposure with the electrical current criteria of >10 nA (from the WETCORR sensor) when the surface temperature is >0 °C, for the presented periods. These periods represent the exposure time.

4 DISCUSSION AND CONCLUSIONS

The semi-natural test set-up showed a considerable increase in USC test surface TOW in comparison to the natural test set-up (~2.3 times longer TOW), due to lower surface temperatures; see Fig. 5 and 7. This shows that it is possible to achieve a significantly increased moisture exposure, through a relatively simple cooling device (PE) and rough control strategy. The test set-up also proved to be cost effective, as well as convenient for attaining a prolonged surface TOW and highlight humidity exposure, as the PE is only dependent on electricity. Other set-ups for cooling usual require some circulating brine or other cooling fluid in combination with a refrigerator unit. The down side of PE units is the difficulty of homogeneously cooling larger specimens or a number of specimens, as commercially available PE units usually have a limited cooling surfaces size. An optical (solar absorptance (α) and IR emittance (ε) [Duffie & Beckman 2006]) USC surface coating durability evaluation [Stojanović et al. 2007] performed after about 11 months of exposure, showed (at time) no significant optical degradation induced by the natural or semi-natural field exposure testing, at this particular test site. However, measurements revealed a significant impact on the specular reflectance due to surface pollution (predominantly quarts in this case). The natural and semi-natural test procedures present an approach for field testing and assessing the optical durability of solar thermal active building envelope components, acting in an energy system. Future work will be conducted and contain a continued USC test specimen exposure and monitoring, as well as additional optical and material durability evaluations.

REFERENCES

Carlsson, B., Frei, U., Köhl, M., Möller, K. 1994, *Accelerated life testing of solar energy materials – Case study of some selective solar absorber coating materials for DHW systems.* A technical Report of Task X of the International energy Agency programme on Solar Heating and Cooling, February 1994, SP-Report 1994:13, ISBN 91-7848-472-3.

Duffie, J.A. & Beckman, W.A. 2006, *Solar Engineering of Thermal Processes 3ed*. Wiley, New York, ISBN-13 978-0-471-69867-8.

ISO 15686-2 *Building and Constructed Assets - Service Life Planning Part 2: Service life prediction procedures.* ISO 15686-2:2001.

Jernberg, P., Lacasse, M. A., Haagenrud, S. E., Sjöström. 2004, *Guide and Bibliography to Service Life and Durability Research for Building Materials and Components.* CIB W80/RILEM 175-SLIM, Publication 295, ISBN 90-63 63-041-7.

Kjellsson, E. 2004, *Solvärme i bostäder med analys av kombinationen solfångare och bergvärmepump, (in Swedish).* Licentiate Thesis, Division of Building Physics, Lund Institute of Technology, Lund, Sweden.

Marteinsson, B. 2005, *Service Life Estimation in the Design of Buildings - A Development of the Factor Method*. Doctoral Thesis, The Royal Institute of Technology, KTH Research School, Centre for Built Environment, Department of Technology and Built Environment, University of Gävle, Gävle, Sweden.

Norberg, P. 1993, Evaluation of a new surface moisture monitoring system. 6th International Conference on Durability of Building Materials and Components (6DBMC), Omiya, Japan, October 26-29 1993, vol. 1, pp. 637–646.

Norberg, P. 1998, *Microclimate measurements in the built environment - Development and applicability of the WETCORR method for measurements of surface moisture and time of wetness.* Doctoral Thesis, The Royal Institute of Technology, Centre for Built Environment, Gävle, Sweden.

Ozgener, O. & Hepbasli, A. 2007, A review on the energy and exergy analysis of solar-assisted heat pump systems. *Renewable & Sustainable Energy Reviews 11: 482-496.*

Stojanović, B., Akander. J., Eriksson. B. 2007, Natural and Semi-Natural Field Exposure Testing and Analysis, on Optical Degradation of a Building Integrated Unglazed Solar Collector Surface. *Materials and Structures, Online first, DOI: 10.1617/s11527-007-9306-1.*

Supercool. 2007, *Peltier Element manufacturing company*, http://www.supercool.se, accessed 2007-09-14.

Wennerholm, H. 2003, *Värmebärare i solvärmesystem - Etablerade medier och nya system, (in Swedish).* Vattenfall Utveckling AB, Sweden, FUD-program solvärme 2001-2003, Reprt no U 03:51.

11DBMC International Conference on Durability of Building Materials and Components
ISTANBUL, Turkey 11-14 May 2008

Minimum Required Performance Level for Rendered Facades

Pedro Lima Gaspar [1]
Jorge de Brito [2]

T 24

ABSTRACT

Service life ends when buildings and components fail to meet a predefined minimum required performance level. However, performance levels are relative concepts that vary according to time, place, available budget, building regulations, existing and expected comfort standards or even the pressure to keep up with the neighbours.

This paper focuses on minimum required performance levels for cement-rendered facades, based on an on-going field research. First, field data on the condition of in-service residential buildings is used to identify a degradation pattern for rendered facades. Different condition levels for rendered facades are then discussed, according to varying building ownership status (public owned, private owned or rented), previously identified as paramount for the durability of rendered facades.

The final aim of the paper is to identify a set of criteria that can be adapted to different building and social contexts and used in service life prediction methodologies, most notably those relying on degradation curves. In practice, for each situation, a combination of criteria should be identified and the minimum required performance level accordingly adjusted in order to obtain the predicted service life. The emphasis is placed on the decision maker, for experience shows that most refurbishing decisions are made due to subjective criteria – before the actual physical degradation threshold of buildings and components is reached.

KEYWORDS

Minimum required performance level, Performance criteria, Rendered facades, Facades

[1] Technical University of Lisbon, Faculty of Architecture, Lisbon, Portugal, Phone +351 918 203 804, Fax 213 645 818, pmgaspar@fa.utl.pt
[2] Technical University of Lisbon, Instituto Superior Técnico, Portugal, Phone +351 218 419 709, Fax +351 218 497 650, jb@decivil.ist.utl.pt

1 INTRODUCTION

All building and building parts go through a deterioration process from the moment they are finished, during which they increasingly lose their ability to fulfil their users' needs and expectations. Loss of performance manifests itself through construction defects – or failures – that occur due to design problems, lack of construction quality or wrong choice of materials, under the specific maintenance, in-use and environmental conditions, for any given construction [Burati *et al.*, 1992].

Degradation of a building part can be plotted in scatter diagrams, expressing *Condition* (that is, the deterioration level of the part considered) as the dependent variable versus *Time* (as the independent variable). Degradation paths are hence obtained through simple linear regression techniques, best suited to express continual degradation mechanisms, such as environmental actions that affect a facade [Shohet *et al.* 2002]. Once the minimum required performance level for the sample studied is known, it is possible to establish the estimated service of the building part considered.

Building facades are particularly sensitive to the effects of environmental agents for they present a large exposed surface (under the direct influence of rain, wind, sunlight and atmospheric pollutants) but a relatively thin thickness. Visual degradation and disfigurement of the facade are therefore often pointed out as a widespread problem, which has a strong impact on the aesthetic performance of a building envelope and on the quality of the urban environment. [Parnham 1997, Flores & de Brito 2003]. It also generally implies high maintenance costs associated with cleaning and repair actions [Watt 1999, Chew & Ping 2003].

In this paper, fieldwork data relative to the condition of cement-rendered facades of residential buildings are used to identify the deterioration path of the sample studied. Different condition levels for rendered facades are discussed, according to varying ownership status, in order to identify different thresholds of the required performance of rendered facades that can be adapted to different building and social contexts.

2 MINIMUM REQUIRED PERFORMANCE LEVEL OF A BUILDING PART

The minimum required performance (MRPL) of any building or building part is a changing, relative (and often a subjective) concept. In fact, one has just to remember past comfort standards (such as available room area per person, protection against heat, humidity or noise) to realize the changing nature of minimum required performance levels. Evidence of evolving performance standards can also be gathered through the increased performance demands on building legislation and codes, in such distinct areas as structural and fire safety, cost and maintainability, environmental protection, energy consumption, waste control and recycling, access to disabled users or durability.

Finally, even when performance levels can be clearly and objectively defined, previous research demonstrates that changes in buildings occur mostly due to subjective reasons [Aikivuori 1999, Sarja 2005] according to time, place, budget available, building regulations, existing and expected quality standards or the pressure to "keep up with the neighbours". As far as exterior building surfaces are concerned, Balaras *et al.* [2005] have shown that "owners tend to decide on exterior renovation actions on the basis of the general appearance of the building", that is, on its aesthetic appearance.

2.1 Defining Varying Minimum Required Performance Levels for Render Facades

In this research, different performance levels for rendered facades are identified based on a fieldwork survey of 50 residential buildings in real-life service conditions, located in Lisbon, Portugal. First, data collected are measured and computed into one single degradation indicator: overall degradation level (ODL). The latter is then plotted against time in order to identify a degradation path that can model the typical deterioration process of rendered facades. Finally, different deterioration stages are

described and related to the respective case studies (and most notably to their ownership status) so that different 'profiles' associated with distinct minimum reference levels can be identified.

3 FIELDWORK DATA

3.1 Fieldwork Data Collection

A sample of buildings was randomly chosen and filtered in order to select case studies matching the following criteria: a) buildings with cement-rendered facade, b) no known records of deterioration as a result of accidental actions, and c) with known records of past maintenance actions or the date of construction. The last condition was regarded as indispensable so that the pattern of variation in time of the ODL could be identified.

Fieldwork surveys were performed between July 2006 and July 2007. Each facade was visually assessed and photographed. Defects were registered and classified based on a discrete level classification system – from "0" (no degradation) to "4" (immediate action required) [Balaras *et al.* 2005]. Finally, each photograph was converted into drawn elevations in which deteriorated areas were measured, according to their condition level, for each of the three main defect categories: "staining", "cracking" and "detachment" of render. After completing the fieldwork, it was possible to quantify ODL of each facade, improving on earlier research [Gaspar & de Brito 2005].

3.2 Overall Degradation Level

The overall degradation level of a facade (ODL) represents the severity of degradation (area and depth of defects) relative to a reference degradation area that corresponds to the total exposed rendered area of the facade, affected by the most unfavourable condition for all possible defects, see equation (1).

$$ODL = \sum (A_n \,.\, k_n \,.\, k_{a,\,n}) \,/\, (A_r \,.\, k \,.\, k_{a,\,n}) \qquad (1)$$

where,

ODL	overall degradation level, in percentage;
A_n	area of a facade affected by defect n, in square meters;
k_n	condition level for defect n, where $k_n \in K$;
k	constant, equivalent to the value of the worst condition level within K;
$k_{a,\,n}$	relative importance of the defects detected, where $k_{a,\,n} \in]\,0, +\infty\,[$;
A_r	exposed rendered area of a facade, in square meters;
$K = \{0, 1, 2, 3, 4\}$	space with all condition levels.

To obtain the value of ODL for the cases studied, defects are weighted according to their hazard level. Such distinction is based on empirical evidence that suggests that, for normal ageing processes, light degradation (associated to staining, soot and dust deposition) occurs before heavy degradation (cracking and detachment of render) [Parnham 1997]. Furthermore, as deterioration progresses situations of simultaneous action of different degradation agents tend to occur more frequently. The combined effects of different degradation types (such as cracking and water penetration) also lead to increasingly hazardous defects (such as salt attack or freeze-thaw cycles that penetrate deeper in the render thickness) [Henriques 1992].

Different scenarios for $k_{a,\,n}$ (see equation 1) were therefore studied and the best-fitting combination of values was selected: staining, cracking and detachment defects are affected by $k_{a,\,n}$ indexes of 0.67, 1.00 and 1.50 respectively.

3.3 Modelling Loss of Performance Over Time

The ODL indicators obtained for the cases surveyed can be plotted in scatter diagrams, expressing Condition (as the dependent variable) versus Time (as the independent variable), as shown in A degradation path for the sample studied - obtained through linear regression - is also plotted in Fig. 1.

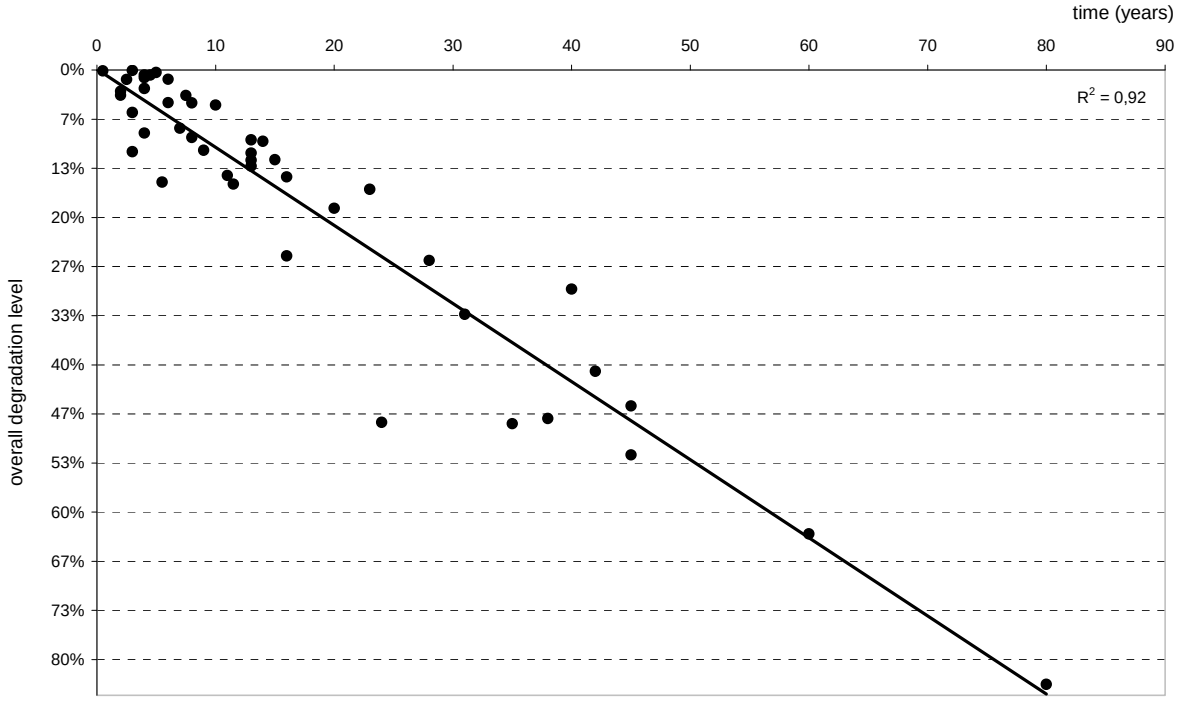

Figure 1. Overall degradation path for 50 cement-rendered facades, expressing loss of performance over time.

Analysis of figure 1 shows that degradation of cement-rendered facades tends to increase over time, according to a linear pattern. ODL seems also to provide a good correspondence between results and a linear regression pattern (Pearson R^2 of 0.92) for the 50 facades surveyed.

3.4 Analysis of Fieldwork Results

Analysis of fieldwork results suggest that the cases surveyed can be classified according to five groups corresponding to different ODL levels:

a) Renders with ODL ≤ 5%, corresponding to cases with no signs of degradation or to cases with very small areas of very light staining (condition levels of "1" or "2") and no cracking nor detachment of render; with no exceptions, all of these renders are less than five years of age;

b) Renders with ODL between 6 and 10%, corresponding to situations of staining (levels "1" to "3") and cracking (levels "1" and "2"); most staining corresponds to light soot and dirt deposition; all of these renders are less than 10 years of age;

c) Renders with ODL between 11 and 20%, corresponding to extensive areas of staining (levels "1" to "4"), including early manifestations of algae and moss, and broader areas affected by cracking (of all condition levels); all cases with ODL higher than 14% show signs of small detached areas as well; within this group, age of render tends to group around 10 to 15 years, although two cases studied correspond to renders with less than five years of age (suggesting a defective intervention) and two cases correspond to renders of about 20 years of age (that is, cases with above standard quality levels);

d) Renders with ODL between 21 and 30%, corresponding to just three situations of heavily stained facades with significant parts of render cracked and some detachment (especially in corners and below balconies); age of render in this group is also scattered (from 16 to 40 years);

e) Finally, renders with ODL above 30%, corresponding to extensive degradation of all three type of defects: heavy staining (all condition levels), significant areas of render cracked (levels "3" and "4") and sometimes large portions of detached render; these situations correspond to the older renders of the sample – although it is quite difficult to confirm the age of renders with more than 40 years.

Data collected show that there is some correlation between the ODL of cement-renders and the age of the latter (older renders tend to present higher deterioration levels, as expected) that makes it possible to identify groups of renders with similar degradation patterns.

Furthermore, the results obtained seem to confirm the empirical view that deterioration of renders progresses from light staining defects (soot and dirt deposition), to more significant forms of disfigurement (runoff marks on the facade due to defective or non-existent drips in ledges and window sills). Over time, more hazardous types of defects tend to occur, such as cracking and detachment. For the most deteriorated situations (high values of ODL), all types of defects occur simultaneously leading to increasingly higher degradation levels (for instance, cracked areas allow runoff water to penetrate into the render and deposit salts that destroy the matrix of the render and originate efflorescence, more extensive cracking and even the detachment of the render).

4 IDENTIFYING MINIMUM PERFORMANCE REFERENCE LEVELS

As a facade progresses in its deterioration path (and reveals increasing levels of disfigurement as well as diminishing performance levels) owners and users are also increasingly confronted with the need to correct such process. At an early stage, deterioration may remain unnoticed for some time. When defects are consciously considered, the decision to repair may be affected by considerations of cost, opportunity and difficulty of intervention. MPRL therefore correspond to different acceptance levels from end users and owners – and to accordingly different demands for repair work to be scheduled.

Previous research [Balaras *et al.* 2005] has shown that more affluent owners (private companies that strongly rely on their perceived image – such as hotels or banks – or private owned condos) will maintain and repair the facade even at earlier stages of deterioration, whilst in rented or state-owned residential houses the decision to repair may tend to be postponed until unacceptable or dangerous levels of degradation occur. Finally, if no intervention is performed, the building may enter a stage of neglect and decay [Wyatt 1999].

To test these assumptions, data on the ownership status of the building surveyed were collected and crossed with the degradation level of the latter and the time of intervention.

4.1 Minimum Performance Reference Levels for Private Owned Buildings

Analysis of fieldwork data reveals that all cases with ODL less than 5% (condition level "0") are privately owned buildings that have had recent interventions on the facade, despite the age of the building. In such situations, interventions at facade level may result from a desire to improve recently acquired buildings – perhaps due to a keep-up-with-the-neighbour attitude – or from the will to sell for a better price, for indeed many buildings correspond to constructions with more than 50 years of age that are experiencing a renovation of dwellers. Two company-owned buildings were actually subjected to repair work despite the fact that their ODL was no higher than 10%.

Privately owned buildings are still dominant in groups of condition level "1" and "2", although there are some situations of rented buildings (town-owned) with somewhat recent interventions. Noteworthy is the fact that repair work was actually initiated in private owned buildings with ODL of less than 15% and age of render of 13 years.

With two exceptions, rented buildings correspond to the majority of cases with ODL more than 20%. Within these cases, no major distinction can be identified between buildings that belong to a private landlord or town-owned dwellings. However, renovation work does eventually occur in the latter group – especially under specific programs that finance such interventions in low rent dwellings – whilst the former may undergo a process of neglect and decay, as described.

4.2 Degradation Patterns Associated With Ownership Status

To better visualize the correspondence between ownership status and ODL, all cases studied were grouped according to four ownership categories (company owned, private owned, town-owned, and rented buildings). Although the available data prevents the sample from being statistically significant, cases studied and their regression lines are plotted in figure 2.

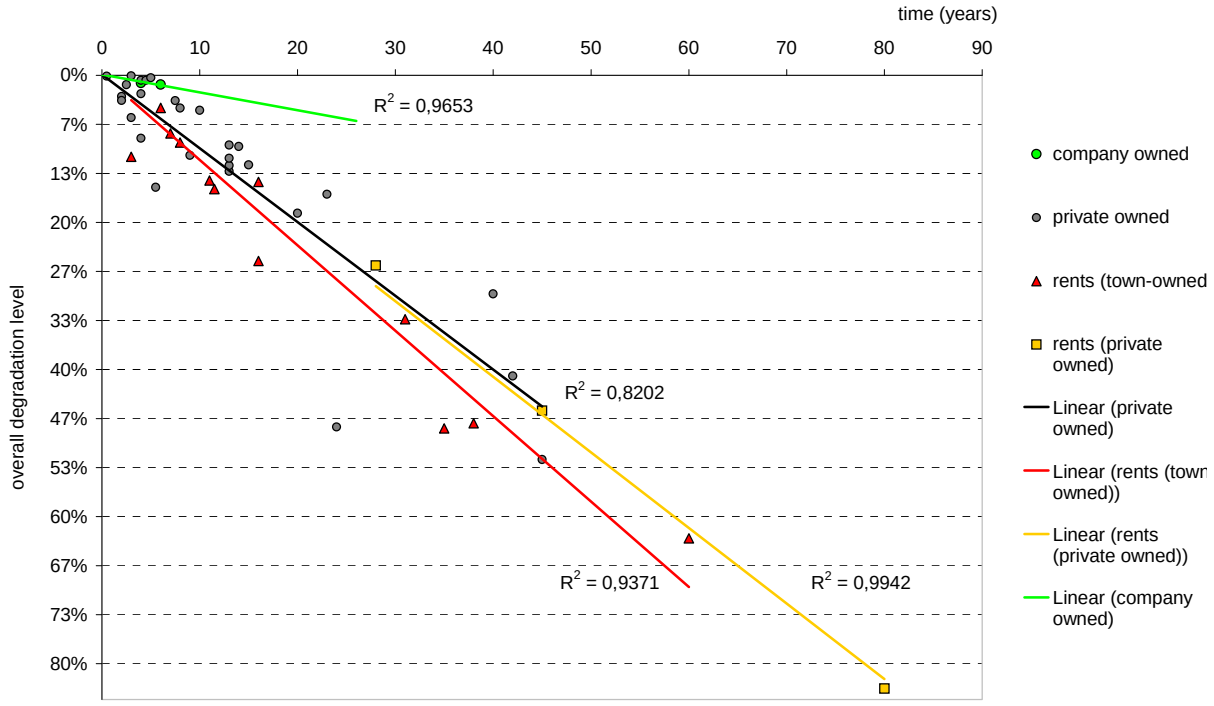

Figure 2. Overall degradation path for 50 cement-rendered facades, grouped by ownership status.

Not surprisingly, analysis of Fig. 2 reveals that the majority of the situations accessed corresponds to privately owned buildings, which can be explained by the specificity of the Portuguese real estate context: scarce rental market (due to the compulsory maintenance of the values of existing rents, which led to very low age-old rents and only a small percentage of market-value rents) and widespread purchase of private dwellings (especially fostered by low interest rates).

Further analysis of figure 2 also shows a clear distinction of the degradation pattern for town owned, privately owned and company owned dwellings. Each of these groups seems to have increasingly demanding performance reference levels inasmuch as they show slower degradation patterns. Distinction of the degradation pattern between 'privately owned' and 'rented (to a private landlord) dwellings' is not so clear, except that the latter show higher deterioration levels and older renders

whilst the former tend to display more recent renders. This may be an indication that facades of privately owned buildings tend to be repaired sooner, as indicated during the fieldwork phase.

5 DISCUSSION OF RESULTS

Despite the scarce sample of renders assessed that prevent the results obtained from being statistically significant, some conclusions can be drawn:

a) Fieldwork data seems to confirm a deterioration pattern for cement-render facades, from light staining due to dirt and soot deposition to increasingly hazardous defects (water runoff stains, cracking and detachment of render) and simultaneous effects of the latter;
b) Renders can be classified according to their degradation level into five broad categories that illustrate the deterioration pattern of this type of cladding;
c) In accordance to the work of other authors [Balaras *et al.* 2005], age and ownership status seem to influence the condition level of the renders;
d) Older renders tend to show higher levels of degradation over time, according to a linear pattern with a rather good correspondence of results, especially as data have been gathered in buildings in real-life service conditions;
e) Ownership status influences the perceived degradation level: privately owned cases of the sample reveal better performances than town-owned (rented) buildings;
f) Rented buildings have been found to have lower performances than private owned condos: not only do the latter undergo repair work sooner, but also the former tend to remain unattended for longer periods and eventually experience a process of neglect and decay [Wyatt 1999] (ODL higher than 60%); this situation can be explained by the very low rents associated with much of these dwellings due to the Portuguese real-estate context;
g) Town-owned buildings tend to deteriorate considerably before repair work is scheduled, perhaps due to financial constraints, but also on account of the low lobbying power of their tenants; when finally repair work is performed these buildings seldom return to very high performance levels, especially when compared to privately owned condos that have been recently repaired as well;
h) Finally, different minimum performance levels can be proposed, based on the degradation level of the cases studied before repair work on the facade is scheduled: thus a pattern was identified in which company owned buildings were repaired before they reached 10% of ODL; as a rule, privately owned and town owned were repaired before they reached 15 and 20% of ODL respectively.

6 CONCLUSIONS

In this paper a methodology is proposed to identify minimum performance reference levels according to the ownership status of buildings, based on a sample of 50 rendered facade buildings located in Lisbon, Portugal. The results obtained confirm the strong correlation between ownership status and degradation and suggest that buildings can be grouped according to their degradation level, following a linear pattern of degradation.

The degradation level of the sample is then used as an indicator of performance or, indeed, of loss of performance. Through analysis of fieldwork data it is possible to identify different degradation patterns associated with ownership status and thus deduce the minimum performance level for each group. Although minimum accepted performance is a relative (and changing) concept and the decision to repair highly subjective, the methodology presented is able to propose distinct minimum performance levels in relation to the ownership type, for the Portuguese context. It also provides benchmark information concerning the expected service life time of cement-renders for life-cycle analysis and service life estimation methodologies.

ACKNOWLEDGMENTS

The authors thankfully acknowledge the support of the ICIST Research Institute from IST, Technical University of Lisbon and of FCT (Foundation for Science and Technology).

REFERENCES

Aikivuori, A. 1999, 'Critical loss of performance - what fails before durability', Proc. 8th Int. Conf. on Durability of Building Materials & Components, Vancouver, Canada, 30 May 3 June 1999, pp. 1369-1376.

Balaras, C., Droutsa, K., Dascalaki, E., Kontoyiannidis, S. 2005, 'Deterioration of European apartment buildings', *Energy and Buildings*, **37**[5], 515-527.

Burati, J., Farrington, J. & Ledbetter, W. 1992, 'Causes of quality deviations in design and construction', *Construction Engineering and Management*, **118**[1], 34–49.

Chew M. & Ping T. 2003, *Staining of facades*, World Scientific Publishing, Singapore.

Flores-Colen I. & de Brito J. 2003, 'Premature stains in facades of recent buildings', Proc. CIB/W87 2nd International Symposium. Lisbon, Portugal, 6 8 November 2003, pp. 311-320.

Gaspar, P. & de Brito, J. 2005, 'Assessment of the overall degradation level of an element, based on field data', Proc. 10th Int. Conf. on Durability of Building Materials & Components, Lyon, France, 17-20 April 2005, pp. 1043-1050.

Henriques, F. 1992, *Humidity on walls*, PhD thesis (in Portuguese), Technical University of Lisbon, Lisbon.

Parnham P. 1997, *Prevention of premature staining of new buildings*, E & FN Spon, London.

Sarja, A. 2005, 'Generic limit state design of structures', Proc. 10th Int. Conf. on Durability of Building Materials & Components, Lyon, France, 17 20 April 2005, pp. 420-467.

Shohet, I., Putterman, M., Gilboa, E. 2002, 'Deterioration patterns of building cladding components for maintenance management', *Construction Management and Economics,* **20**[4], 305-314.

Watt D. 1999, *Building pathology: principles and practice*, Blackwell Science, Oxford.

Wyatt, D. 1999, 'A natural progression: neglect to decay', Proc. 8th Int. Conf. on Durability of Building Materials & Components, Vancouver, Canada, 30 May 3 June 1999, pp. 2126-2135.

Durability of Sandwich Panels

Çiğdem Çelik Tekin [1]
Ülger Bulut [2]

T 24

ABSTRACT

Durability of a material is its ability to resist changes of its properties. In design process of a building or system or component cannot be considered rationally except in the context of that material in service and the environment in which it must function since it is the interaction of elements of environment with a material that determines its durability.

In this context, durability and performance characteristics might require modification or innovation in process of choosing material and compound design. Necessity of more durable and high performance building materials causes to development of composite materials. In this study composite sandwich panels which are used for industrial buildings, prefabricated buildings, sport buildings, hypermarkets, except housing, are researched

Distributed load bearing capacity, wind load, indoor comfort criteria, heat and sound insulations, fire load effect, expansion, durability of environmental conditions affect sandwich panel compounds. All above mentioned factors determine service life of sandwich panels.
In this study, it is explained how the different selection of paint, metal and layer of heat insulation affects servis life and durability of panels and indoor comfort level. Additionally to this, the faults in transportation, storage and the application of sandwich panels are examined.

KEYWORDS

Sandwich panel, Insulated panel, Durability, Roof cladding, Wall cladding

[1] Mimar Sinan Fine Arts University, Architectural Faculty, Istanbul, Turkey 34427, Phone +90 212 2521600, cigdemad@hotmail.com
[2] Istanbul Technical University, Architectural Faculty, Istanbul, Turkey 34437, Phone +90 212 2931300, ulgerbulut@hotmail.com

1 INTRODUCTION

All buildings are aimed to be durable and comfortable during their service life. Durability which also effects the comfort conditions-criteria, is the ability of resistance and tolerance of the features of materials and systems against negative factors in the buildings. Besides the production, storage, transportation, application and use features, durability is also closely related to avoiding from the radiation, temperature, water, freeze and chemicals that affect-ruin-damage the materials when exposed and the environmental conditions.

Sandwich panels also have a wide range of possibility of use with compatiblity-applicablity for many kinds of buildings such as industrial buildings, prefabricated buildings, gym centers, supermarket buildings and shopping malls, but excluding residences. Same as the buildings, sandwich panels also have service lives. In general they might be considered having long service lives like 30-40 years. However, the durability term of the panels might decrease owing to the choice of types of panels, production, transportation, storage or adjustment-mountage, and a discomfort of inner space conditions and service quality might be observed.

Most of the mistakes on choosing the component combinations forming the sandwich panels, made by the consumers, mainly depend on economical worries. On the other hand, most of the mistakes on the production, transportation, storage, mountage and application of the sandwich panels are caused by inexperience and lack of knowledge.

2. SANDWICH PANELS

Sandwich panels are multi-layered/laminated composite materials used for roofing and wall systems that are formed of metal panels on both sides and certain thickness of isolation material in between. The metal panels are usually aluminum, galvanized plate, pvc membrane or craft paper, and the coating paints are polyester, plastisol or PVdf, and the isolation fill material might be polyurethane, rockwool, glasswool or expanded polystren. The optimum result solutions choosing the sandwich panels, are determined according to the function, the physical features of the panel components, the environmental conditions and the fulfilling of certain needs.

One of the main parts of the panels; galvanized plate, should be galvanized with “hot-immersion” method, be in TS EN 10142 standarts and 100-275gr/ m^2 zinc plated. As the proportion of the galvanize determines the durability of the plate, this proportion should be determined according to the environmental conditions where the sandwich panels will be used. Aluminum is used straight or after crimping. Although, aluminum, is a corosion-resistant, conductive material, its coefficient of expansion is much higher compared to galvanized plate. (for carbon steel-galvanized plate = 10,8x10-6 /C; for aluminum = 23 X 10-6 /C)

Depending on these features, it is preffered for asidic conditions and / or heavy industry conditions. Galvanized and aluminum plates are painted with coil coating technique. Within this coil coating technique, a painted metal with homogenious paint thickness for continuous production line and metal surfaces is obtained. In this technique, galvanize or aluminum roll is opened on the continuous painting line and surface cleaning is first applied. The surface to be painted, is purified from grease and unwanted substances which is followed by the chromate coating process for a convenient surface before painting. Then, first both sides of the metal is primed and kiln-dried. As the last process, the chosen color and type from the RAL catalogue is applied then kiln-dried again and covered with folio.

2.1 The Effect of Panel Combination on Durability

The low costs while constructing a building does not mean that it is an economical building. The criteria of an economical building are; the ability of energy saving during the presumed service life,

low costs of maintenance and the qualification to reduce the environmental effects to the least both inside and outside the building.

Sandwich panels are composed of multi-layers with different mechanical features. Depending on the paint, metal and isolation features, many different panel combinations can be obtained and closely related with the comfort, cost of maintenance and long service life of the building. Each component has different and limited rigidity and one alone cannot resist the load as they can compositely. As a whole, the bending momentum is met by the metal panels, and the shear momentum is met by the filling layer. The choice of insufficient thickness of panels and fillings caused by economical worries may result as stated below.

a. Type, thickness, dimension of trapeze form of metal plate for sandviç panel, determined results of statical analyses. According to the carcasse system, purlin span and the distributed load, suitable galvanized or aluminum plate should be used. Under constant load, the filling material of roof panels are deformed more slowly. For this reason, under constant load, the panel deformation would increase gradationally. But, there is not constant load on wall panels. Thus, especially for roof panels, the calculations should be made according to the type of load and the type of filling to be used. The calculations should be made considering the effects of climatical conditions, snow, wind, temperature, dead and live loads, and the components like construction and the purlin spans of the building should be calculated each alone then together considering the worst scenario the convenient filling and metal plate thicknesses should be chosen. The thickness of the metal panels is different; the carrier upper plate is thicker. Galvanized carrier plates should be at least 0, 50 mm; and for aluminum plain and trapeze plates 0, 70 mm. The load capacity of the panel can be increased with a better metal and filling adherency. The adhered surface between metal plates and filling reinforces the endurance of the sandvich panel. The "in situ application" systems where the metal panels are not adhered to the fillings are less endurant to torsion than the sandwich panels. As there should be a good adherency between the metals and the filling, the filling itself should also be able to meet the flexibility. Metal panels meet the bending momentum and the filling the shear momentum. Especially, the mineral fillings should be adhered carefully. Sandwich panels should definetely be tested for resistance and long-term effects. Before choosing the panels, the applicator and the consumer should demand TSEK and production proficiency certificates from the producer. The adherent surface of filling should be tested against aging and loss of strength. With these tests, the effects of water steam and temperature on stress strength should be determined.

b. Places where the day-night, summer-winter temperature flactuations are observed, the final coating material should be chosen carefully. Besides the atmospheric temperature effects, radiation also affects the buildings. Direct and spread radiation, causes a higher temperature than the atmospheric temperature on surfaces relevant with the color and texture of the wall. In winter, especially during nighttime, again relevant with the radiation effects and depending on the features of the wall, a temperature lower than the atmospheric temperature appears. As a result of these thermal changes, the expansion causes contractions or extensions on the building. If the thermal expansion coefficiencts of the panels and fillings are different, this effect causes damage and disintegration. Choosing different metals for the upper and lower panels of a sandwich might be unpreferrable since the expansion coefficient of metals may vary. Even the reaction of the same metal may vary for the thermal expansion inside and outside are different. So, the choice of metals for the panels should be made considering the inner and outer weather conditions and changes. In summer, the temperature of the outer panel depends on the coating color and the reflectivity of the panel surface. For this reason, the determination of the color of coating should be made considering the temperature changes, like in hot climates, use of dark colors should be avoided. High temperatures usually accelerate the deformation-decomposition of materials. For example, in the Mediterranean Region, while the surface heat of light color panels are 55°C, the dark color panels might increase until 80°C. Using light colors or reflective elements on the roofs, the expansion activities caused by the thermal changes might be reduced.

c.The thickness and density of the fillings of sandwich panels should be determined according to the climatical data of the location of the building. The thickness of the filling is calculated according to the thermal conductivity coefficient of the substance used. Mainly, polyurethane, glasswool, rockwool or EPS are used as fillings. The thermal conductivity coefficients and densities of the substances are important for the rigidity and load-bearing features of the panels. The necessary features for the isolated sandwich panel fillings are shown below on Table 1. As shown on Table 1, the thermal conductivity coefficient of polyurethane between 10-20°C is around <0,025 W/mK. But, for lower temperatures, the thermal conductivity coefficient value also decreases and a better heat isolation is provided. Because of this feature, polyurethane is convenient for cold storage spaces. For hygiene-must spaces, the panels should be produced with folios on both sides.

Table 1. The technical features of the filling materials

	Polyurethane	Rockwool	Glasswool	EPS
Thermal conductivity coefficient (W/Mk)	≤ 0,025	≤ 0,040	≤ 0,040	≤ 0,040
Density (kg/m3)	40 kg/m3	100-110kg/m3		20kg/m3
Thermal endurance of filling material °C	-50/+110 °C	-50/+700-750°C	-50/+250°C	-50/+75°C
Fire classification	B1-B2	A1	A1	B1-B2
Location & use in the building	Roof-wall systems, cold storage buildings	Roof-wall systems	Roof-wall systems	Roof-wall systems
The contribution of the material to isolation	Only thermal isolation	Thermal-sound and fire isolation	Thermal-sound and fire isolation	Only thermal isolation

d. The metal and the filling material of the sandwich panels used as roof or wall systems effect the extension of the fire and the damage that might be caused on panels. When the filling materials of the sandwich panels, which generally are used on industrial buildings, are being determined, the features should be evaluated considering the function of the building, the materials used and the risk of fire. Polyurethane and polysiyanurat, which are thermosets, become liquidified during fire and move in between the panels dropping. EPS in the thermoplastic category is 1,5 times flammable than polyurethane. EPS when exposed to high temperatures, before flaming it softens and shrivels (Eren, 2005). The shrinkage, softening or the melting of the filling materials cause the continuous and non-cavity structure sandwich panel to loose its strength. Plastic originated filling materials have the disadvantages such as causing high heat and toxic gases during fires and hinder the intervention, cause gas-affected deaths and accelerate the extension of the fire. The behaviors of metal panels during fire are also important. Steel materials are 2 or 3 times stronger than aluminum and affected by temperature at 585°C. Aluminum is affected from about 100-225 °C. While a 10 mm. steel beam at 500°C expands 600 mm., under same circumstances, an aluminum beam expands double and melts at 660°C (url. 1). Polyisocyanurat are resembled to polyurethane but different indeed. Polyisocyanurat, when exposed to a source of heat, does not soften but gets parched in limits. When parched, might melt and flammation might occur if the steam comes out. But, if a certain amount of parching occurs and then the heat source is stopped, the material loses isolation features. Normally, in low flame heat source might not cause flaring and shows a fire-resistant behavior; but in big scale fires, might combust and cause the fire to extend quickly. Polyurethane exhales a dense smoke, toxic gases, hydrogen cyanid and carbon monoxide (url. 2). For fire safety priority buildings, A class, non-flammable, mineral wool filled panels should be preferred. These panels do not increase the fire load, exhale toxic gases, drop, soften or shrink in case of fire. The melting point of rockwol and glasswool is 1000°C. According to the building fire instructions, use of A class filling materials are necessary relevant with the type of building.

e. The metal plates of the sandwich panel should be protected against corosion, ultraviolet rays and sufiric acids. For this reason, the galvanized plates or aluminum plates are painted on the continuous production line with coil coating technique. With the last layer, the preferred color is given and a homogenious paint thickness is obtained on each and every point of the plate. According to the climatical and environmental conditions where the sandwich panel would be located, metal plates are coated with epoxy prime followed by polyester and PVdf or plastisol paint. These paints with different feature have the common point to be wet paints. Paint helpsthe metal to longlast. Metals coated with coil coating technique can easily be processed. Painted surfaces are not affected by trapeze shaping processes. And another important feature of painted metal is the prime layer applied to the isolated side of the metal (Karasu 2006). With this layer, isolation filling is adhered to the metal and isolated panel gains a composite structure. The last coating layer of the metal panels should be determined not considering the type of the metal, but the location and environmental data. Standart polyester paint is applied 20 microns on 5-7 microns of prime on the metal surface. Sandwich panels possible to be exposed to chemical materials, plastisol paint should be preferred. But, in 2007, according to ISO14001 Environmental Management Systems instructions, production of plastisol paint is forbidden. Paints widely used and features are given on Table 2. According to this, the best UV resistant paint is PVdF and the worst is plastisol.

Table 2. Technical features of paints.

UV resistance	*thermal resistance*	*corrosion resistance*	*Hardness*	*flexibility*
PVdF	*PVdF*	*Plastisol*	*Polyester*	*Plastisol*
Polyester	*Polyester*	*PVdF*	*PVdF*	*PVdF*
Plastisol	*Plastisol*	*Polyester*	*Plastisol*	*Polyester*

f. There are alternative roof and wall systems to the prefabricated sandwich panels composed of two panels and filling in between. These systems do not cause any changes on the inner space physical comfort features, but only production, application and constructional needs are different; such as “cast-in-situ”, “waffle system” and “clamp system”. The preferred roof and wall systems should be decided in design state, not after the building is constructed. Before the construction starts, the necessary details should be designated; the thickness for thermal isolation, filling for water and sound isolations and loadbearing system should be decided.

g. The main purpose and function of roof and wall systems are to protect the inner space comfort from the outer conditions. This function can be provided by waterproof materials. The risk of a roof to leak, especially from horizontal connections, is higher than the walls. The risk of leak for roofs changes according to the roof plans. The risk increases for low pitches. Materials and connection elements used for plain or low pitch roofs should be 100 % waterproof. To prevent deformations caused by humidity, the formation of humidity on the surfaces of elements and the inner building should be prevented. If humidity and dampening are inevitable, the dampening time should be tried to be kept minimum. Moreover, the quantity of galvanize to be used on the plates of the sandwich panels should be increased and the type of paint should be decided upon the corosion-resistance listed on Table 2. Water caused by the intensification of damp, especially causes the mineral wool fillings to get wet and its thermal conductivity increases and as a result, a loss of energy occurs. Mineral wool (glasswool, rockwool) filling panels should be kept away from water and damp during storage and transportation.

2.2. The Effects of Production Defects on Durability

The metal plates to be used as panels, painted or unpainted, are brought to the factory in rolls. The rolls are opened by the quality control department to be checked for **TS EN 10143**; “continuously hot-dip coated steel sheet and strip-tolerances on dimensions and shape” for plate tolerance limits. The tolerance limits changes depending on the thickness of the plate, such as, the tolerance for a 0.40 mm. plate is 18 mm. Otherwise, the undulating panels especially when used on walls with “cast-in-situ” systems show the defects very clearly.

The polyurethane filled panels used for roof and wall system should have constant mechanical features. (in accordance with **TS EN 13165**, density tolerance limits: 40 kg/m³ ± 2 kg/m³). The polyurethane filling in the sandwich panels should have a homogeneous density and with no pores to change the porosity. While production, the amounts of polyol, isocyanate and pentane gas mixtures should be proportioned correctly. The effectiveness of polyurethane can be provided with only correct amounts of mixtures. Also, the temperatures of the upper and lower plates, raw materials and the kiln are important. If the amounts of polyol, isocyanate and pentan gas mixtures in the polyurethane filling are not well-proportioned, the defects are only seen after production as deformations on the panels. This problem can partially be solved with re-settling the polyurethane with some tools. The deformations usually occur on the sun-seeing façade, not the North façade. This problem can be reduced by considering the precautions stated above. When such a problem is faced, first, only the swollen part of the upper plate should be drilled with 1-2 mm bit, and so the swelling would be stopped. But if it is not drilled on time, the plate would have been deformed and drilling would only stop the progression, the physical deformation would still remain. As removing the sandwich panel and mounting another would be costy, another solution might be mounting a trapeze plate or some other material directly on the panel. On the extraordinary dark painted plates, a protective polyetilen folio should definetely be used to avoid scrathes or other damage.

In mineral wool filled sandwich panels, polyol and isocyanate mixture is used to adhere the wool to the metal. But the mixture used for mineral wool is different than the one for polyurethane. There occurs no deformation of damage on the mineral wool panels. Sometimes as a production defect, there might be insufficient adherence and for this reason the panels and the filling material might detach. The adherent mixture should be homogeneous and spread effectively.

Epoxy prime paint is smeared on the inner side of the aluminum or galvanized plate to adhere it to the filling material. If the outer side of the metal panel is not painted, prime paint is applied to the inside. Before the prime, a chemical process is applied on the plate. This chemical process and prime on the bottom may cause the upper part lose resistance to corosion and deformation and an unwanted appearance. For these reasons, the manufacturer to prevent these problems in short-term, produces the panels without the prime paint, which causes the the fillings to detach from the panels. As aluminum is a soft material, there appears stains on the plate if past from the pulley thick and unpainted. Before and after the production of the sandwich panels, the quality control department should control the dimensional stability, type and color of the paint, the convenience of the raw polyurethane material and the deformation risks.

2.3. The Effects of Storage and Transportation Defects on Durability

To adhere the metal panels to the mineral wool filling, polyol and isocyanate mixture, which is also used for polyurethane production, is sprayed on the mineral wool filling. So, the adherence is enstrengthened to let the sandwich panel carry, hold itself up and down while mounting without detaching. For mineral filling sandwich panels are flexible, if they are longer than 8-9 m., might break apart when carried by two people from both sides. So, even if the break on the plate is repaired, it never looks like before. It then might be used as a roof according to the will of the customer, but not on the walls. The weight should be considered when forming the dimensions of the mineral wool panels, as well as the transportation to the place and mounting it. These factors are not valid for the polyurethane panels as they are much lighter than the mineral panels. Moreover, polyurethane filling adheres to the panels much better than the mineral ones.

Mineral filling materials are easily affected from water and damp. Mineral panels for this reason, should definetely be covered before and after transportation. In the construction site, the panels should be stored in an inclined position so that the rain or snow would not stay on. If the mineral panels are damaged, they will not be recovered; within the visuality, it will also lose its thermal conductivity. So, they should not be piled on the others while kept waiting to be mounted. Usually panels are

transported by long vehicles. For the panels longer than the damper of the truck, the damper might be opened and 1,5 mt max might go out.

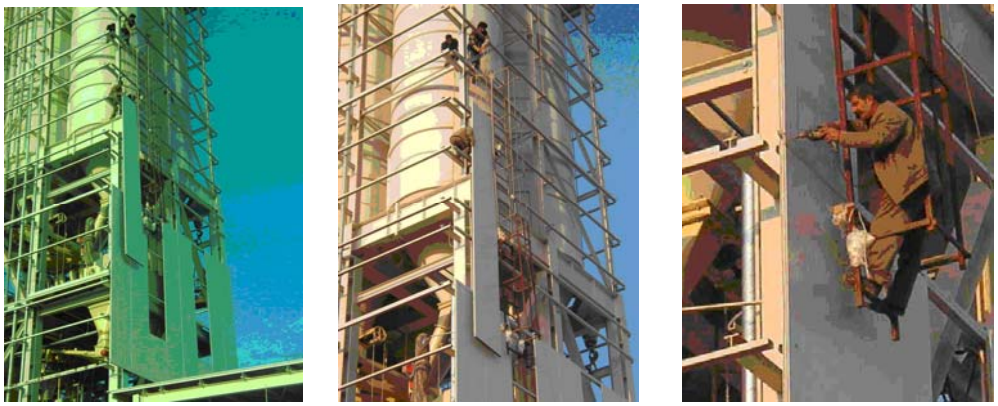

Figure 1 a, b, c Mountage of the panels.

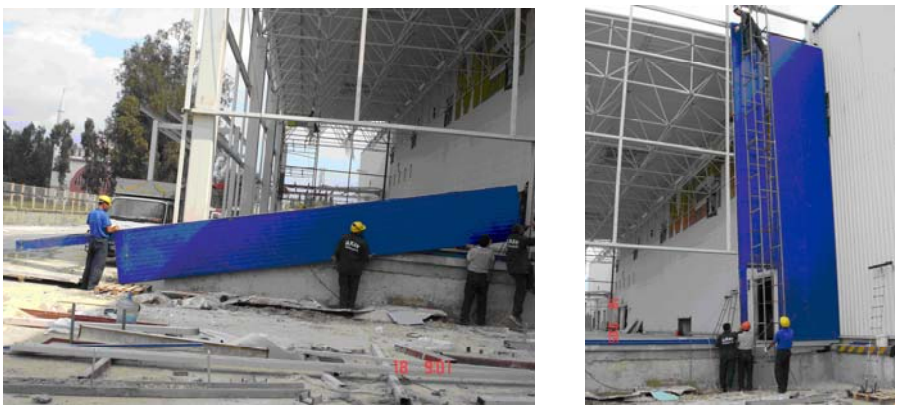

Figure 2 a and b. Transportation and mountage of the panels in the construction site

2.4. Effects of Application Errors on Durability

The main principle of the application is that the details should be mounted waterproof, airproof and not forming a cold bridge. The roof and wall panels cannot tolerate or cover the construction mistakes, but also causes the defects of the construction seem more clearly. So, before the mountage, the defects of the carcasse should be re-checked, and if there happens to be a problem, it should be corrected before mountage.

The folio adhered to protect the panels should be torn out before mountage because after being exposed to sunlights, it might be harder to tear it or might look unaesthetic.
The construction site should be cleaned after work hours every day. Otherwise, with rain, the small pieces of metals might cause corosion on the panels.

The panels should not be mounted in snowy or foggy weather, or when the wind speed is more than 9m/s. The mountage should start on the opposite direction to the wind, in order to prevent the joint surfaces be exposed to wind.

Panels should not be spread around randomly on the roof where they are being mounted, but be piled as a point load. The parts to remain under the panels like accessories for ridge, eaves, and valley should be mounted before the panels. And then, finishing accessories such as corner profil, ridge profile should be mounted.

The roof panels should be screwed from on the top of the undulating panel untill the construction. The screw should have an EPDM gasket. The gasket should be checked from time to time as long as the construction is used, because the damage of the gasket causes the risk to leak. The screw should be chosen as at least three threads longer.

Figure 3. Roof panel montage

Figure 4. Mineral wool filling wall panels

Mineral wool panels, if to be mounted on the concrete purlins on a reinforced concrete carcasse construction roof, the concrete screws should be used over the top of the undulating panel **(Figure 3)**. As the concrete screws don not have threads on their bottoms, upper panel plate and screw cannot join as strong as to bear the load, so, because of the thermal changes and the load on the flexible roof, there happens deformations on the bottoms of the screws, which may again cause the roof to leak. **(Url. 3)** For these reasons, the mountage of the mineral panels on the roofs should be on the concrete purlins with metal profiles, gaskets and screws with threads.

For the isolation filling not to get wet, on roofs, eaves and ridge profiles and on walls, wall coping profiles should be mounted on the same day with mineral wool filling panels **(Figure 4)**. Especially on wall panels, if isolation filling gets wet, it may yield because of gravity.

Sandvich panels which are used for valley on roofing, getting a 10 cm overlapping, before mountage, bottom metal plate should be cut 10 cm and fillings in it should be emptied and then, bottom plate should be twisted. Thus leak of water is prevented. This detail solution should be applied especially for mineral wool panels. Throughout ridge, between the panels which are come from two different surfaces of a roof exist uncovered gap.

Througout ridge, on the upper and bottom surfaces of panels, ridge profile should be mounted and isolation filling should be put in to between these two ridge profiles. In addition ısolation band should be used to prevent of condensation or cold bridge between ridge profile and panels. Frequency of mountage screw determined according to geographical conditions. Overlapping between the consecutive panels should be minimum 15 cm.

According to horizontal or vertical mountage of wall panels mountgage starts up to down or down to up. Choosing convenient screw for wall panels, it is consider, screw should be aable to transfer the loads, which are beared by panels, through carcasse.

In mineral wool panels with hidden screw **(Figure 5)**, excess driving of screw cause to deformation of metal plate of panel. To prevent this kind of deformation “screw inferior plate” should be used. Details for valley, lateral side profile, ridge, wall coping, dilatation, inner-outer corners, door, window and water drip, metal bending profile is used which is the same kind of metal with panels.

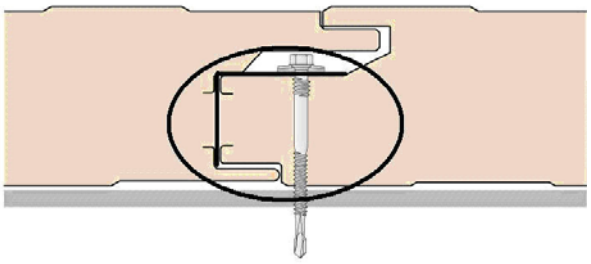

Figure 5. Hidden screw detail

3. CONCLUSION

Sandwich panels, having accelerated the construction speed, been a significant step in prefabrication. The durability of the sandwich panels depend on the production features, the correct combination of components, transportation on determined conditions, storage conditions and a detail design, as well as the performance features.

REFERENCES

TS EN 10142 Continously hot-dip zinc coated low carbon steel strip and sheet for cold forming-Technical delivery conditions

Eren C. 2005, "Çatıdaki Görünmeyen Tehlike İzoleli Sandviç Paneller ve Yangın Riski" Riziko Kontrol
ve Yönetim Departmanı, Koç Allianz, *End Risk Dergisi 3*, 3-5.

Url 1: "Endüstriyel Tesislerde Sandviç Panel Kullanımı ve Yangın Problemleri" Commercial Union Sigorta, www.aviva.com.tr/cus/docs/Risk_Yönetimin_TBI.pdf

Url 2: Bilal F., "Poliizosiyanurat Çekirdekli Sandviç Panel",
http://izoder.org.tr/pdfadmin/files71186988999.pdf

Karasu T. 2006, "Yalıtımlı Panellerin Özellikleri" *Dizayn Konstrüksiyon*, sayı:251.

TS EN 10143 Continuously hot-dip coated steel sheet and strip - Tolerances on dimensions and shape.

TS EN 13165: -Thermal insulation products for buildings - Factory made rigid polyurethane foam (PUR) products.

Url 3: Çınar H.,"Yangına Dayanıklı Sandviç Çatı ve Cephe Panelleri"
http://izoder.org.tr/pdfadmin/files/1154690640.pdf

Experimental Programme to Assess ETICS Cladding Durability

Bruno Daniotti [1]
Riccardo Paolini [2]

T 24

ABSTRACT

The paper reports on the experimental evaluation of the durability of ETICS cladding through accelerated laboratory ageing, which is now being developed by BEST – Polytechnic of Milan. The experimental programme as a whole includes accelerated laboratory ageing, long-term outdoor exposure, comparison and analysis of results. Four types of specimens have been built with masonry wall acting substrate EPS as insulation and polymeric additives incorporated in the base coat mortar. Of the additives included in the mortar, two were prepared with acrylic resin and two with vinyl resin. Additionally, for each type of specimen, one included a typical finishing coat and another one an acrylic painting. For each series of ETICS specimens, a one set will be aged and the other remains as the (cladding system reference set). There are also four pairs of sets of smaller scale samples on which disruptive tests are to be completed. The ageing cycle consists of 125 UV cycles, 125 summer thermal shock cycles and 50 winter thermal shock and freeze-thaw cycles. In order to assess performance decay on the reference specimen and on the aged specimens at the end of their service life, several disruptive tests will be carried out, including: water absorption, water vapour permeability, tensile bond strength of adhesive and of base coat to insulation, render strip tensile tests, and pull off tests. Non-disruptive tests (e.g. record of T [°C], RH [%] and heat flow) are being conducted throughout the ageing process and, at every end of test cycle, characterization tests are carried out to assess changes in thermal conductance, moisture transfer properties, dynamic effects and thermal inertia. Infrared thermography and capillarity tests are also being carried out and photos are taken in order to survey evolution of cladding degradation.

KEYWORDS

ETICS, Thermal shock, Polymer added mortar

[1] Politecnico di Milano, Building Environment Science and Technology Department (BEST), Milano, Italia 20133, Piazza Leonardo Da Vinci, 32, Phone +39 2 2399 6002, Fax +39 2 2399 6020, bruno.daniotti@polimi.it
[2] Politecnico di Milano, Building Environment Science and Technology Department (BEST), Milano, Italia, 20133, Piazza Leonardo Da Vinci, 32, Phone +39 02 2399 6015, Fax +39 2 2399 6020, riccardo.paolini@mail.polimi.it

1 INTRODUCTION

This paper portrays structure and methodology of ETICS experimental programme, which has been developed by Durability of building components group (BEST Department – Polytechnic of Milan) since November 2003. The research programme concerns the durability assessment of ETICS (External Thermal Insulation Composite Systems with rendering) also well known as EIFS (Exterior Insulation and Finish System). This building component has been chosen due to its widespread distribution across Europe and North America and the problems concerning its durability. The study has two types of objectives: general and specific ones. General objectives are methodological ones and include: the search for innovative tools useful for Service Life assessment test design, design of methods for estimating service life, design of methods for forecasting degradation and performances decay. On the other hand, specific objectives, more closely related to the performance assessment of ETICS cladding are also sought, and include: observation and measurement of performance decay, qualitative degradation models (for ETICS), and knowledge useful for technology improvement.

This work is linked to studies concerning durability of building components developed by other research units of the Italian Durability network and it's the development of methodologies set during the research activity brought on by BEST in collaboration with SUPSI (Italian Swiss Professional University School) about paintings durability. Main special features and innovations of ETICS experimental programme are:

- Usage of degradation factors and mechanisms analysis as a tool in designing accelerated ageing cycles (not only to find the agents to be reproduced and as preliminary analysis);
- Ageing cycles pre-design with climatic data analysis (not excluding re-scaling with outdoor specimens);
- Dynamic thermal performance decay measurement.

Future targets of research activity are outdoor exposure and time re-scaling got with degradation comparison of indoor and outdoor specimens, design of other specific tests suited for studying ETICS degradation mechanisms. First results are not to be considered as quantitative values, but as a first step in developing a method and a measurement technique suited for assess ETICS and building components durability generally. In particular, in results analysis should be considered errors and approximations due to:

- Ageing cycles not reproducing all agents (e.g. atmospheric pollution, wind and vibrations are not included);
- Limited dimensions and number of specimens;
- Limited number of sensors (iso-determined equation systems);
- Accuracy and measurement errors;
- Prototype research programme.

First results got with accelerated ageing tests concern degradation, water absorption and thermal insulation performance decay (related to water absorption).

2 SPECIMEN DESCRIPTIONS

Four kinds of specimen have been designed: two with acrylic additive in base coat (one with acrylic painting, one with finishing coat) and two with vinyl additive in base coat (one with acrylic painting, one with finishing coat). For each type one specimen to age and one not to (to test as reference for system characterization) are provided and for each type also are tested one big sample reproducing the complete wall (i.e. substrate and ETICS) and sets of small samples (only ETICS on polystyrene) suited for measuring single characteristics (thermophysical and mechanical ones). In order to study each

considered combination of ETICS, small samples are stored inside a climatic chamber and a big sample is used as door of the chamber.

Large-scale samples (100 x 100 x 22,45 cm) are comprised of three mechanically fixed and adhesively bound insulation panels (two panels 50 x 50 cm in the lower part, and one 100 x 50 cm in the upper part) are used in order to reproduce one T joint in the middle of the specimen. Polypropylene anchors are used are fixed in five positions (in four middle points and in coincidence with T joint) and aluminium profiles are used to reproduce boundary conditions and in coincidence with profiles there is a superposition for 10 cm of two sheets of glass fibre mesh. First ETICS kind tested is type A.1.

Table 1. Types of ETICS specimens and related components

Layer	s [m]	*Specimen type*			
INTERIOR		A. 1	A. 2	B. 1	B. 2
Interior finishing	0,005	Gypsum plaster			
Interior plaster	0,015	Lime cement plaster			
Masonry Substrate	0,12	Non load bearing aerated clay bricks 12x25x25 cm (holes percentage 64 [%]) laid with cement bed mortar			
Plaster	0,015	Lime cement plaster			
Adhesive	0,003	Vinyl additive	Acrylic additive	Vinyl additive	Acrylic additive
Insulation product	0,06	EPS 150 according to EN 13163 (density 25 kg/m^3)			
Base coat	0,005	Vinyl additive	Acrylic additive	Vinyl additive	Acrylic additive
Glass fibre mesh	-	155 g/m^2			
Finishing coat	0,0015	Acrylic binder		NO	NO
Painting	-	NO	NO	Acrylic	
EXTERIOR					

2.1 Bed Mortar and Plasters

The bed mortar for the masonry brick substrate is pure cement mortar designed, according to proportions suggested by the EMPA (of Dübendorf), whereas the mix design for the lime cement plaster was carried out according to Italian National specifications for masonry construction (D.M. 20/11/87). On the other hand as binder for the polystyrene and as base coat, a pure cement mortar with polymeric additive was used.

Table 2. Mix Characteristics of Bed mortar, Plasters and Base Coat. (w/b: water – binder mix proportion, V/V_{CEM}: volume on cement volume)

Mortar	Bed mortar: w/b = 0.56		Plasters: w/b = 0.67		Adhesive and base coat	
Material	*Type*	*V/V_{CEM}*	*Type*	*V/V_{CEM}*	*Type*	*V/V_{CEM}*
Water		0.83		1.33		0.5
Cement	CEM II/A-L 32.5	1.00	CEM II/A-L 32.5	1.00	CEM II/A-L 32.5	1.00
Sand	EN 196-1 normalized	2.84	EN 196-1 normalized	4.00	0/1 [mm] EN 13139	3.00
Lime	No	-	Hydraulic	0.50	No	-
Additive	No	-	No		Vinyl / acrylic	0.05

2.2 Finishings

Two kinds of finishing systems, characterized by PVC (Powder Volumetric Concentration), are compared: an acrylic painting with PVC 40 and a 1.5 mm thick finishing coat with PVC 80, that

consists of sand (0/1 mm) and an acrylic resin binder plus additives. Both finishings are red, with solar absorbance $\alpha = 0.6$. Surface emissivity is measured as $\varepsilon = 0.82$.

2.3 Construction and Curing Time

Specimens were fabricated inside the laboratory (spraying plaster and base coat to avoid shrinkage) and were allowed a minimum curing time of three months after the installation was completed (five months after construction of substrate) before ageing the first sample. This was done to ensure that the same initial water content for all specimens (reducing the construction water) was maintained.

Figure 1. Sample A.1, Base coat with vinyl additive and finishing coat with acrylic resin.

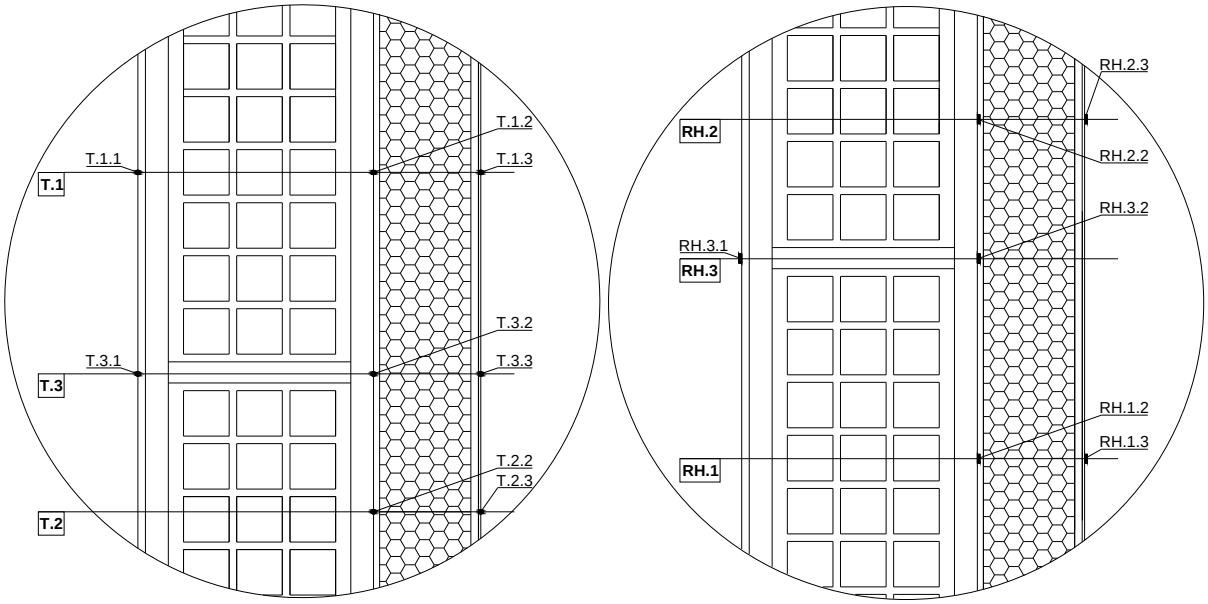

Figure 2. Location of sensors in section RH sensors are placed in the lower part of the sample.

2.3 Measurement Apparatus

For large-scale samples (100 x 100 cm) during the cladding fabrication process, relative humidity (RH) and temperature (T) sensors were placed in the assembly such that three T and RH data profiles could be obtained (one in section, one coincident with EPS panel joints, and one coincident with bed mortar joint). In each profile, sensors were positioned on the interior and exterior surface of the

specimen and between the insulation and the plaster. A heat flow meter was also placed on the interior surface of the main section.

The specimen to age is placed is binded as door of the climatic chamber with a steel frame (separated from it by XPS panels) and it is insulated at boundaries (in order to get a one-dimensional heat flow). Temperature and relative humidity are recorded on the inside of the climate chamber and in the laboratory.

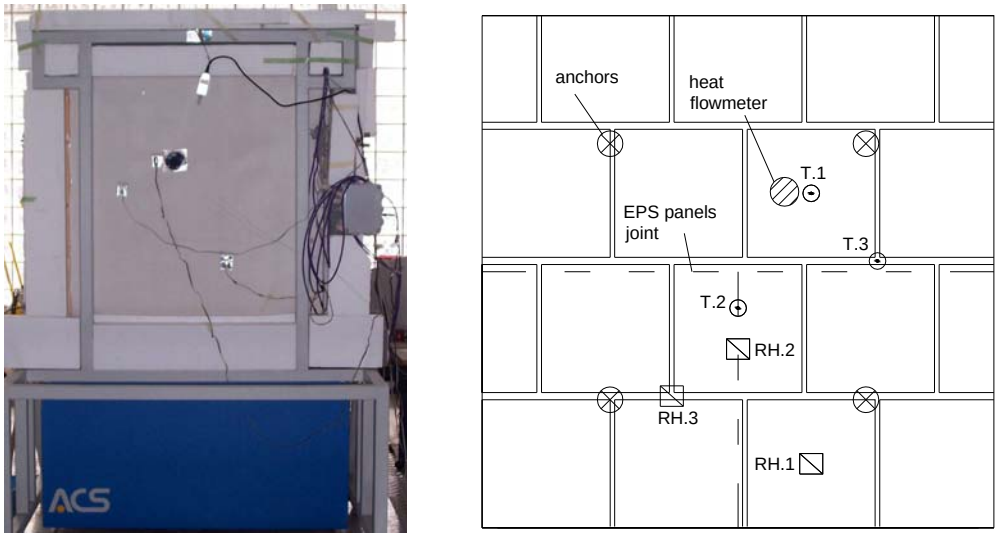

Figure 3. On the left the sample linked to the climatic chamber; on the right sensors profiles position.

3 PREPARATION PHASE

3.1 Degradation Factors

A wide analysis concerning degradation factors and mechanisms (see Daniotti & Paolini [2005]) has been brought on throughout the experimental programme in order to assess which environmental agents must be reproduced and their related intensity, and as well, on which characteristics of the building component are important, that means what to observe to identify the degradation and the performance decay evolution.

3.2 Ageing Cycle

In order to design the accelerated cycles and assess the proportion between its parts, two ways have been pursued: standard reference (ETAG 004) and analysis of climatic data of Milan context (Test Reference Year and UNI 10349). Thanks to this study, three ageing cycles (UV cycle, winter thermal shock + freeze-thaw cycle and summer cycle) have been planned and the proportion between the summer cycles and the winter one set to 2,5. However the correct proportion between summer and winter ones must be determined with time re-scaling, studying the comparison between the degradation of the outdoor exposition specimens and the indoor accelerated ones. The value here proposed has the only intent to be a pre-design value.

Ageing sub-cycles are repeated in order to maintain the proportion 2.5. So in each complete cycle CX there are 25 UV cycles, 10 winter cycles and 25 summer cycles. Complete ageing cycles CX therefore are assembled in groups of five so to get a macro-cycle TX (its overall duration is about one month).

Table 3. Agents included and not included in the ageing cycle. Agents not included cannot be reproduced in laboratory tests or can be reproduced, but not included into an accelerated cycle.

Agent – type of solicitation		*Layer / component of most interest*
Included in the ageing cycle	**Summer and winter thermal shock**	Base coat and finishing
	Freeze - thaw	Base coat and finishing
	Rain	Base coat and finishing
	UV radiation	Finishing
	Cyclic variations in T [°C] and RH [%]	Base coat and finishing, insulation
Not included in the ageing cycle	Pollution	Base coat and finishing
	Mould	Base coat and finishing
	Vibrations	Whole system
	Impacts	Base coat and finishing
	Wind	Anchors, whole system

Table 4. Basic Ageing or Ageing sub-cycles (Note: set point values in bold type).

Basic Cycle	Repeat	N°	Phase	Climatic chamber				Laboratory		
				T_{air} [°C]	T_{sup} [°C]	T_{H20} [°C]	RH [%]	$T_{op,i}$ [°C]	RH [%]	Duration [min]
UV	25	1.1	UV	***35***	-	-	15 ± 2	26 ± 3	60 ± 5	60
Winter	10	2.1	Rain: 1 [lt/m^2]	***5 ± 1***	-	5 ± 1	100	19 ± 2	60 ± 5	60
		2.2	Freeze	***-20 ± 2***	-	-	-	19 ± 2	60 ± 5	180
		2.3	Winter heat	***30 ± 2***	-	-	50 ± 2	19 ± 2	50 ± 5	60
Summer	25	3.1	Dry heat	***70 ± 5***	70 ± 5	-	15 ± 2	26 ± 3	60 ± 5	60
		3.2	Rain	*20*	-	20	100	26 ± 3	60 ± 5	60

4 DEGRADATION AND PERFORMANCE DECAY MEASUREMENTS

In order to observe the decay in performance and the evolution of degradation, two main types of tests are taken into account: disruptive and non-disruptive.

4.1 Non-disruptive Tests

Non-disruptive tests are brought on big specimens before the accelerated exposition (not aged sample) and throughout ageing time every macro-cycle TX (that means every 5 complete cycles = 5 x (25 UV cycles + 10 winter cycles + 25 summer cycles). Two kinds of non-disruptive tests are performed (in this order):

- Qualitative degradation evolution assessment:
- Photographic degradation survey in six fixed positions (one point in the centre, four points in the half of the half of diagonals and one under the centre in coincidence with vertical joint between insulation panels). Degradation evolution is checked according to ISO 4628;
- Non-disruptive capillary absorption test (Karsten's method according to NORMal 44-93) measurement of low-pressure absorption of water volume (in [ml]) by the surface of a porous material at fixed time steps. Results report absorption [lt/m^2] versus square root of time [s^{-1}]
- Hygrothermal performances characterization cycles (record of T [°C], RH [%] and heat flow):
- SINa – Summer dynamic conditions – low wave

Simulation of 21 July outdoor temperature variation in Milan context (according to UNI 10349) without solar radiation influence
Duration: 48 hours (2 sine curves with period of 24 h)
Conditions: T [°C] sine curve: max = 31.9 [°C], min = 20 [°C], amplitude = 12 [°C]

RH [%] = 50 constant

- SINb – Summer dynamic conditions – high wave

Simulation of 21 July outdoor temperature variation in Milan context (according to UNI 10349) with solar radiation influence: air – sun temperature with solar absorbance $\alpha = 0.6$

Duration: 48 hours (2 sine curves with period of 24 h)

Conditions: T [°C] sine curve: max = 65.5 [°C], min = 20 [°C], amplitude = 45.5 [°C]

RH [%] = 50 constant

- TI – Thermal Inertia

Assessment of time constants and thermal capacities.

Duration: 72 hours (3 sine phases of 24 h)

Conditions: T [°C] 24 h at 20 [°C], 24 h at 70 [°C], 24 h at 20 [°C]

RH [%] = 50 constant

- CON – Thermal Conductance in steady thermal state

Assessment of thermal insulation performance decay

Duration: 96 hours

Conditions: T [°C] = – 20 constant

RH [%] = 0 constant (inside the climatic chamber below 0°C must not be water or humid air for technical reasons)

- Infrared thermography

To capture the response of surface temperature gradients on the specimen surfaces during the CON cycle, an infrared thermographic camera is positioned for 24 hours outside the climate chamber, pointing towards the interior surface of the specimen (gypsum plaster),. At the end of ageing time (end of Service Life declared) the specimen is turned round of 180° and another thermography is executed for 24 hours (T = - 20 [°C] inside the climatic chamber) in order to assess the evolution of thermal bridges in coincidence with joints between insulation panels.

- RHst – Relative Humidity stabilization

Assessment of stabilization time of relative humidity (and so water content) only for the exterior layers (base coat and finishing).

Duration: 8 hours (4 phases of 2 hours each)

Conditions: T [°C] = 35 [°C] constant

RH [%]: 2 h at 20 [%], 2 h at 50 [%], 2 h at 80 [%], 2 h rain 1 [Lt/m^2]

A longer exposition (to assess moisture changes inside the whole sample) could influence the overall thermal capacity and alter ageing tests storing an excessive moisture amount.

4.2 Disruptive Tests

Disruptive tests are performed both on non-aged samples (characterization tests) and on aged samples when the end of Service Life is reached. Disruptive tests prepared for this experimental programme are: water absorption, water vapour permeability, tensile bond strength of adhesive and of base coat to insulation, render strip tensile test.

Other disruptive tests, such as resistance to hard body impact or resistance to perforation, could be executed, but the analysis of test methods highlighted that they do not offer numeric results and they are have to be evaluated without a precise scale.

Disruptive tests are so performed both on large samples (1m^2) and on sets of selected smaller scale samples (as prescribed by the specific standards), that incorporate only the ETICS cladding component and not the masonry substrate. A set of small specimens (for all disruptive tests) is stored inside the climatic chamber and a comparison between results obtained by tests on these small aged samples and the ones obtained by tests carried on cores taken from large-scale aged samples are compared in order to help understand the influence on degradation of different position inside the chamber, different dimensions of samples and of constraints given by substrate and plastic anchors.

Table 4. Disruptive tests, dimension and number of samples and standard test method chosen.

Test	*Sample dimensions*	*N°*	*Standard*
Water absorption (capillarity test)	200 x 200 mm	3	ETAG 004 - § 5.1.3.1
Water vapour permeability	Round samples: A > 5000 mm^2	5	EN 12086
Render strip tensile test	600 x 100 mm. Mesh length: 800 mm, (100 mm leaning out at boundaries)	3	ETAG 004 - § 5.5.4.1
Tensile bond strength of adhesive and base coat to insulation	200 x 200 mm	3	EN 13494

5 CONCLUDING REMARKS

Ageing tests are in progress on specimen Type A.1 that includes a vinyl resin base coat and finishing coat, the preliminary results being given in Daniotti & Paolini [2008]. Other tests related to improving knowledge of the evolution in performance decay and degradation are now being studied, whereas specific tests suited for understanding degradation mechanisms are now being designed. For example, tests methods are being devised for determining if capillary absorption properties vary more significantly in the base coat or finish coat and the phenomena that cause such variations). On the other hand, ageing tests on all specimen types in an on-going process and outdoor exposure tests will also be performed in the future.

REFERENCES

Daniotti, B. & Paolini, R. 2008, 'Evolution of Degradation and Decay in Performance of ETICS', 11th DBMC, Istanbul 11-14 May 2008

Daniotti, B. & Lupica Spagnolo, S. & Paolini, R. 2008, 'Climatic data analysis to define accelerated ageing for Reference Service Life evaluation', 11th DBMC, Istanbul 11-14 May 2008

Daniotti, B. & Paolini, R. 2006, 'La valutazione della durabilità di pareti perimetrali con isolamento esterno a cappotto', in *La valutazione della durabilità di pareti perimetrali verticali*, ediTecnica editrice, Palermo, pp. 37 - 74

Daniotti, B. & Paolini, R. 2005, 'Durability Design of External Thermal Insulation Composite Systems with Rendering', 10th DBMC, Lyon 17-20 April 2005

ETAG 004 – Edition March 2000. Guideline for European Technical Approval of external thermal insulation composite systems with rendering

EN 196-1: 1996 – Methods of testing cement. Determination of strength

ISO 4628: 2003 – Paints and varnishes – Evaluation of degradation of coatings – Designation of quantity and size of defects, and of intensity of uniform changes in appearance

UNI 10349: 1993 – Riscaldamento e raffrescamento degli edifici – Dati climatici.

EN 12086: 1997 – Thermal insulating products for building applications – Determination of water vapour transmission properties

EN 12524: 2001 - Building materials and products - Hygrothermal properties - Tabulated design values

EN 13139: 2003 – Aggregates for mortar

EN 13163: 2003 – Thermal insulation products for buildings – Factory made products of expanded polystyrene (EPS) – Specification

EN 13187: 2000 – Thermal performance of buildings – Qualitative detection of thermal irregularities in building envelopes – Infrared method

EN 13494: 2003 – Thermal insulation products for building applications – Determination of the tensile bond strength of the adhesive and of the base coat to the thermal insulation material

EN 13499: 2003 – Thermal insulation products for buildings – External thermal insulation composite systems (ETICS) based on expanded polystyrene – Specification

NORMal 44 – 93 – Assorbimento d'acqua a bassa pressione

Defacement of ETICS Cladding Due to Hygrothermal Behaviour

Eva Barreira [1]
Vasco Peixoto de Freitas [2]

T 24

ABSTRACT

External thermal insulation systems for walls (expanded polystyrene insulation faced with a thin rendering) – ETICS – have been used in Portugal since the nineties. Despite the thermal advantages, Portuguese buildings covered with ETICS are faced with a huge and yet unsolved problem: the system's defacement caused by microbiological growth.

In recent years, although several studies have been carried out to solve this problem, the practical conclusions are not very satisfactory: so far the only feasible solution is to use biocides. These chemical products are not environmentally friendly and are considerably expensive because of their short-term effectiveness.

To obtain a less expensive solution to this problem, it is essential to first understand the hygrothermal behaviour of façades covered with ETICS, namely, the dynamic heat exchange between the ETICS exterior layer and the atmosphere. It is also very important to study the influence of the surface's orientation and the local climate.

This paper presents the results of an experimental characterization of ETICS' hygrothermal behaviour performed by the Building Physics Laboratory (LFC) of the Faculty of Engineering of Porto University (FEUP). "In-situ" tests are being carried out on a building covered with ETICS located in Portugal's northwest region.

KEYWORDS

Cladding defacement, Hygrothermal behaviour, ETICS, Microbiological growth

[1] Building Physics Laboratory (LFC), Faculty of Engineering, University of Porto (FEUP), Portugal, barreira@fe.up.pt
[2] Building Physics Laboratory (LFC), Faculty of Engineering, University of Porto (FEUP), Portugal, vpfreita@fe.up.pt

1 INTRODUCTION

External thermal insulation composite systems (ETICS) have been applied on a somewhat regular basis in European buildings since the 70's. The systems' main advantages are guaranteed continued thermal insulation, thinner exterior walls, greater thermal comfort due to the higher interior thermal inertia and ease of application. The latter is particularly important in refurbishment since it may be applied without disturbing the building's dwellers [Freitas 2002].

However, past applications of ETICS have revealed some problems, particularly low impact resistance and diminished long-term durability. The scientific community has performed various studies to fully characterise these systems, to measure the properties of the respective materials, to identify the main problems and, in some cases, to develop solutions [Hens & Carmeliet 2002].

One of the problems not yet solved is the cladding defacement due to accumulated dirt and, in particular, microbiological growth (Fig. 1). Studies already performed in this field were not very satisfactory since, although the phenomenon is known, the only feasible solution is to use biocides which imply economic and, in particular, environmental drawbacks.

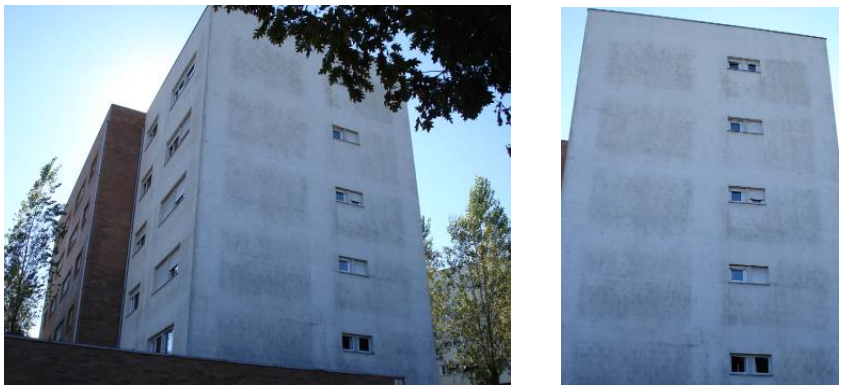

Figure 1. Building covered with ETICS showing microbiological growth.

During the last decade, studies have been performed about the physical phenomenon that promotes microbiological growth on the surface of ETICS [Kunzel & Sedlbauer 2001; Becker 2003]. It is known that the longwave radiation exchange between the exterior surface and the atmosphere during the night causes the ETICS' surface temperature to drop [Kunzel & Sedlbauer 2001; Zillig *et al.* 2003; Holm *et al.* 2004]. Condensation forms when the exterior surface temperature is lower than the dew point temperature. If the drying process is not sufficiently fast, the surface moisture content remains high for long periods and consequently increases the risk of microbiological growth [Krus *et al.* 2006].

Knowledge of this physical phenomenon made it possible to develop mathematical models simulating heat and moisture transfer between the system's exterior surface and the atmosphere [Kunzel *et al.* 2002; Becker 2003]. However, no simple process has yet been developed to foresee the degradation of exterior thermal insulation systems and which may be used by designers and by ETICS application companies.

It is therefore essential to study the causes underlying the degradation of ETICS. This is the only way to develop rules that will guarantee its durability.

2 DEFACEMENT OF ETICS CLADDING

ETICS cladding represent a substantial market share of external thermal insulation systems for façades. Its growing popularity was, however, undermined by some pathologies [Freitas 2002].

Although no statistical studies are available, we may presume that there are a relatively high percentage of cases where algae and fungi have grown on the façades of Portuguese buildings coated with ETICS, particularly when located in coastal zones. Portugal's climate aggravates the problem, particularly in the west coast, which has relatively mild temperatures and very high relative humidity year-round (Fig. 2).

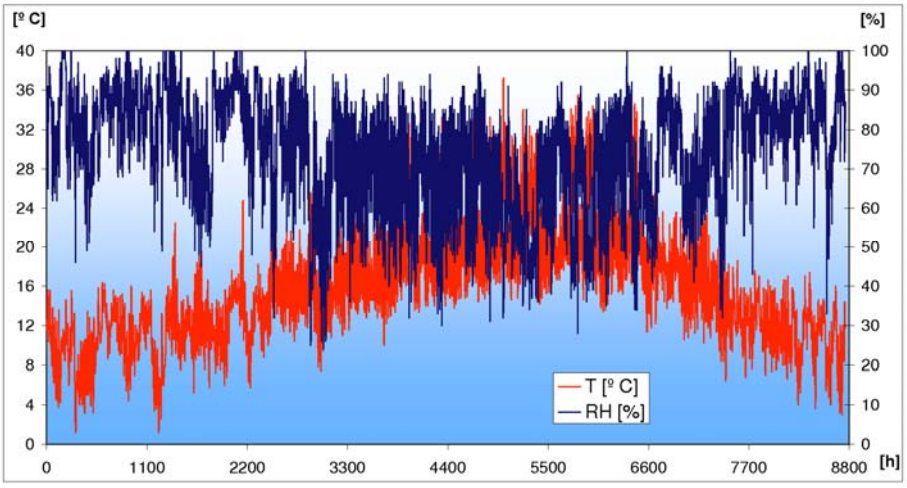

Figure 2. Annual outdoor temperature and relative humidity variations in Lisbon (TRY)

Degradation due to microbiological growth occurs, in particular, on façades facing north and west, since their coating's high surface moisture content is maintained for longer periods.

3 LONGWAVE RADIATION EXCHANGE

Superficial condensation, which takes place predominantly during the night, is caused by a longwave radiation exchange between the exterior surface and the atmosphere. Although radiant exchange occurs on all exterior surfaces, it has more serious consequences on components with substantial thermal insulation – which reduces the flow of heat through the construction element practically to zero – and on components whose thin exterior layer has a very low thermal inertia, as in the case of ETICS [Kunzel & Sedlbauer 2001].

The radiant balance of the building's façade is affected by three parameters: the building's radiation, the sky's radiation and radiation emitted by terrestrial surfaces located near the building (Fig. 3).

A building emits longwave radiation with a total intensity, E_b, calculated according to the Stefan--Boltzmann Law:

$$E_b = \varepsilon_b \cdot \sigma \cdot T_b^4 \qquad (1)$$

T_b Surface temperature

$\sigma = 5{,}6704 \cdot 10^{-8} \quad W \cdot m^{-2} \cdot K^{-4}$ Stefan-Boltzmann constant

ε_b Surface emissivity

On the other hand, the façade absorbs part of the longwave radiation emitted by surrounding objects (terrestrial radiation) and by the sky (atmospheric radiation) [Holm *et al.* 2004]. Terrestrial radiation is caused by the sum of longwave radiation emitted by the different terrestrial surfaces whose temperature is similar to the building's temperature. Since the temperatures are identical, the radiation exchanges between the building's surface and the surrounding surfaces are somewhat balanced.

Figure 3. Radiant balance of a building's façade.

Atmospheric radiation depends mostly on what comprises the atmosphere and may behave in two distinct manners. If the sky is cloudy, the atmosphere behaves like a grey body whose temperature is the same as the building's, and emits radiation in a continuous spectrum at an intensity similar to that of terrestrial surfaces. If the sky is clear, the atmosphere stops emitting continuously for all wavelengths. In wavelengths between 8 and 13 μm, the atmosphere's emitted radiation is decreased considerably mostly due to the influence of molecules of water, carbon dioxide and ozone. Since the maximum intensity emitted by all terrestrial surfaces occurs for 10 μm, there is a loss of radiation to the sky which is not compensated by atmospheric radiation.

This negative balance that is not compensated by solar radiation during the night causes the building's superficial temperature to decrease, which is maintained until heat transport by convection and by conduction compensate for the loss by radiation [Holm *et al.* 2004]. Condensation takes place whenever the superficial temperature is lower than the dew point temperature. The accumulation of condensed water creates favourable conditions for algae and fungi growth.

Algae is able to grow when the relative humidity on the façade's surface is greater than 70%-80%, within a temperature range between 0º and 40º C. Algae can withstand long dry periods and then begin to flourish again when enough humidity is available. Consequently, a dry surface during the day is not sufficient to prevent algae growth [Zillig *et al.* 2003]. Fungi require a minimum relative humidity of 80% to grow. However, and unlike algae, fungi need nutrients to grow, a factor which depends on the finishing layer's materials [Zillig *et al.* 2003].

4 EXPERIMENTAL STUDY

4.1 Setting Up the Test

To evaluate exterior superficial temperature variations on the ETICS, instruments were set up on the façades of a low building in the Northwest of Portugal whose walls face the four cardinal directions (Figs. 4 and 5).

While the system was being applied, in April 2007, T-type thermocouples (copper constantan) were placed inside the system on the four façades, at about 1 m from the ground, as shown in Fig. 5. Three thermocouples were placed on each façade wall (on the interior side of the thermal insulation, between the thermal insulation and the rendering and on the rendering's exterior surface). A second thermocouple was placed on the North and West façades, on the exterior surface of the rendering next to the North/East and West/South corners, respectively. Two temperature and relative humidity sensors were also installed, coupled to a data acquisition system, to monitor the hygrothermal conditions (temperature and relative humidity) inside and outside the building.

Figure 4. Building where the measurements are being taken.

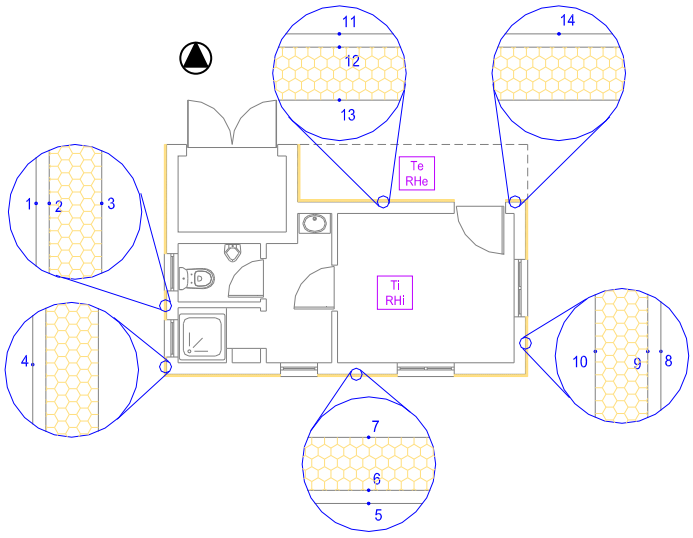

Figure 5. Layout showing thermocouple locations.

4.2 Results

The temperature and relative humidity measurements inside and outside the building (Fig. 6), between 17/05/2007 and 14//06/2007, reveal that:

- The exterior temperature varies from 11º C to 31º C;
- The exterior relative humidity is relatively high, on average about 76%;
- The interior temperature is somewhat constant and of about 24º C;
- The interior relative humidity is, on average, of about 64%.

In the same period, the temperature variation in the ETICS of the West façade's wall is indicated in Fig. 7 and 8. These graphs also indicate the dew point temperature (Tdp), witch is dependant on the exterior temperature and relative humidity. An analysis of the data measured in the façade wall reveals that:

- The temperatures measured by the T1 and T2 thermocouples are very similar: remain somewhat constant during the night, increase progressively at dawn and morning and reach their maximum at about 18:00 h;
- The maximum temperatures measured by the T1 and T2 thermocouples varied from 23º C to 52º C, and the temperatures measured during the night varied from 10º C to 18º C;
- The temperatures measured by thermocouple T3 ranged from 17º C to 29º C, and the maximum temperature occurred at about 19:00 h. Note that the temperature measured by the T3 thermocouple differed, on average, by about 2º C from the interior temperature.

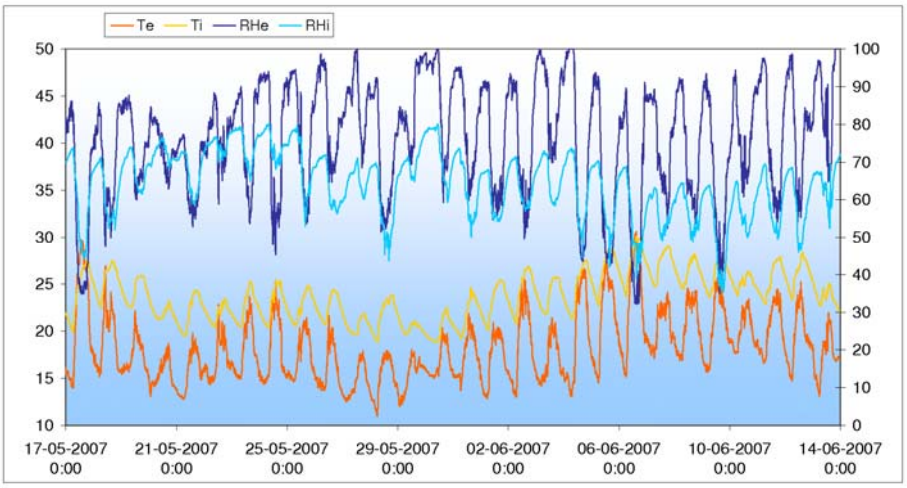

Figure 6. Interior and exterior temperature and relative humidity (17/05/2007 to 14/06/2007).

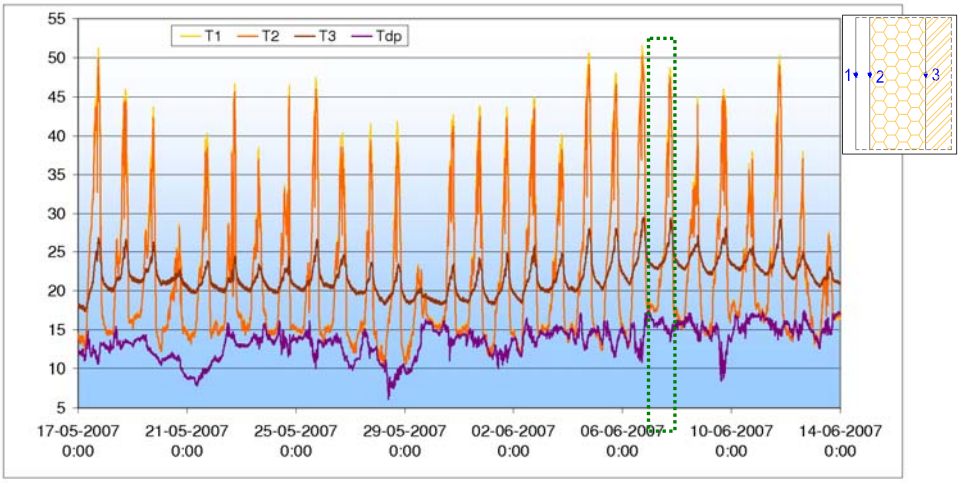

Figure 7. Temperature variation in the ETICS and of the dew point temperature (17/05/2007 to 14/06/2007).

By comparing the exterior superficial temperatures of the ETICS, obtained by the T1 thermocouple, with the dew point temperature (Tdp), we were able to determine the differences between the two temperatures. The graph in Fig. 9 shows only the negative temperature differences (superficial temperature lower than the dew point temperature), whereby the positive temperature differences were taken as equal to zero. The graph in Fig. 10 defines the total daily time during which superficial condensation takes place in the west façade's wall.

4.3 Review of Results

An analysis of the results obtained until now reveals that:

- The thermal resistance of the ETICS' exterior layer is practically nil, since the temperatures on the two sides are very similar. This result was foreseeable because of the thin exterior layer.
- The temperature on the inner side of the thermal insulation varied about 5º C during the day and is relatively similar to the temperature inside the building.
- Condensation takes place whenever the surface temperature is lower than the dew point temperature. In the period under analysis, surface condensation took place during less than 10% of the time.

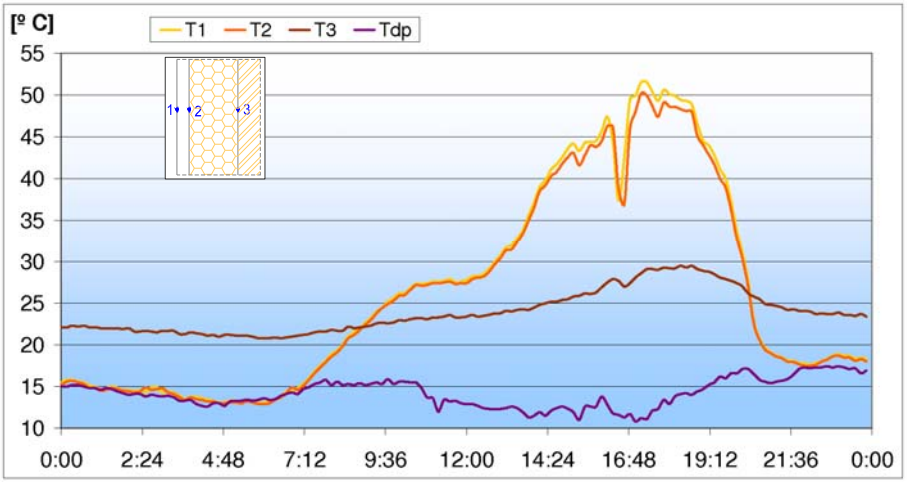

Figure 8. Temperature variation in the ETICS and of the dew point temperature on 06/06/2007.

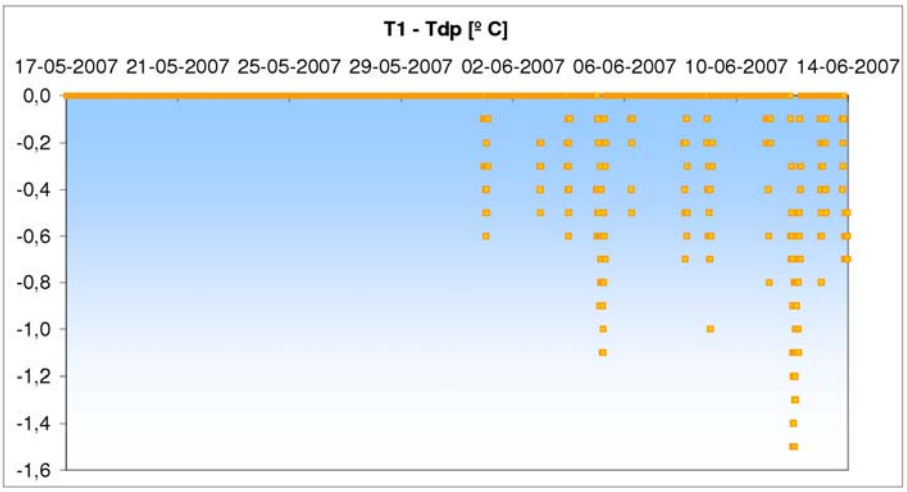

Figure 9. Difference between the superficial temperature of the ETICS and the dew point temperature (17/05/2007 to 14/06/2007). Positive temperature differences were taken as equal to zero.

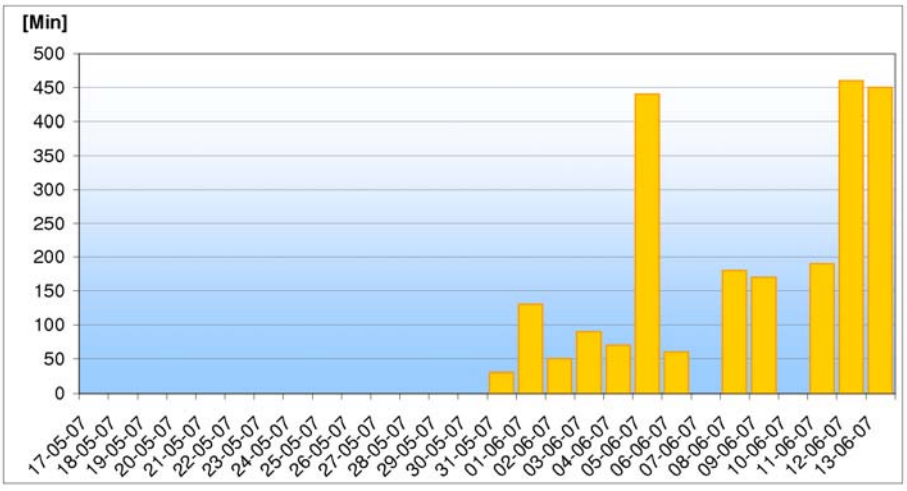

Figure 10. Period during which superficial condensation took place (17/05/2007 to 14/06/2007).

4 CONCLUSIONS

ETICS have been applied regularly in Portuguese buildings. However, despite their advantages, the cladding defacement is a very worrisome pathology. Increased suface moisture content, caused by nighttime condensation, is one of the factors that influence this aeshetical degradation. Superficial condensation is caused by radiative cooling of the surface, which is more detrimental during the night due to the lack of incident solar radiation. ETICS are highly susceptible to superficial condensation.

Instruments were placed on a small building in the Ovar zone to evaluate superficial temperature variations in ETICS. Measuredata is being collect since May 2007, making it possible to evaluate the period during which superficial condensation takes place and the difference between the superficial temperature and the dew point temperature.

In the future, the authors wish to maintain this experimental program by continuing to collect data during autumn and winter. Superficial temperature variations according to the orientation will also be evaluated.

ACKNOWLEDGMENTS

The authors would like to thank Iberfibran – Poliestireno Extrudido, SA for having created the necessary conditions to carry out this experimental campaign.

REFERENCES

Becker, R. 2003, 'Patterned staining of rendered facades: hygrothermal analysis as a means for diagnosis', *Journal of Thermal Envelope and Building Science*, **26**[4], 321-341.

Freitas, V. P. 2002, *Isolamento Térmico de Fachadas pelo Exterior – Reboco Delgado Armado Sobre Poliestireno Expandido (ETICS)*, HT 191A/02, Prof. Engº Vasco P. de Freitas, Lda, Porto, Dezembro.

Hens, H. & Carmeliet, J. 2002, 'Performance prediction for masonry walls with EIFS using calculation procedures and laboratory testing', *Journal of Thermal Env. & Bldg Sci*, **25**, 167-187.

Holm, A., Zillig, W. & Kunzel, H. 2004, 'Exterior surface temperature and humidity of walls – Comparison of experiment and numerical simulation', Proc. Performance of Exterior Envelopes of Whole Buildings IX, ASHRAE, Florida, USA, 5 10 December 2004.

Kunzel, H. & Sedlbauer, K. 2001, 'Biological growth on stucco', Proc. Perform. of Exterior Envelopes of Whole Buildings VIII: Integration of Building Envelopes, ASHRAE, Florida, 2 7 Dec. 2001.

Kunzel, H., Schmidt, Th. & Holm, A. 2002, 'Exterior surface temperature of different wall constructions – Comparison of numerical simulation and experiment', Proc. 11th Symposium of Building Physics, TUD, Dresden, Germany, 26 30 September 2002, Vol. 1, pp. 441-449.

Krus, M., Rosler, D., Sedlbauer, K. 2006, 'New model for the hygrothermal calculation of condensate on the external building surface', Proc. Third International Building Physics Conference – Research in Building Physics and Building Engineering, Montreal, 2006, pp. 329-333.

Zillig, W., Lenz, K. & Krus, M. 2003, 'Condensation on façades – influence of construction type and orientation', Proc. Research in Building Physics, Leuven, 14 18 September 2003, pp. 437-444.

11th International Conference on Durability of Building Materials and Components
Istanbul Turkey May 11-14, 2008

Durability of External Wall Insulation Systems with Extruded Polystyrene Insulation Boards

Durmus Topcu [1]
Holger Merkel [2]

T 24

ABSTRACT

External wall insulation systems (ETICS = External Thermal Insulation Composite Systems) are one of the most common insulation systems in Europe. The systems are designed to provide the appropriate thermal insulation of the wall.

An ETICS comprises the thermal insulation product and a reinforced render. The insulation boards are bonded onto the wall either by an adhesive or a mechanical fixation or a combination of both. External thermal insulation systems with extruded polystyrene boards (XPS) are widely used in Turkey and other European countries.

The paper shows results of durability tests done at laboratory scale as well as results and findings from building projects.

The durability tests were carried out using hygrothermal test facilities to simulate heat, rain and frost conditions. The results show the high tensile bond strength between the render system and the XPS insulation boards after simulated ageing of the ETICS. Due to very low water absorption of the XPS type used there is no risk of moisture accumulation within the system. This is of high importance for the durability of thermal performance of the whole construction.

The test results are in good correlation with practical experience. Examples of ETICS with XPS insulation will be provided.

KEYWORDS

Thermal insulation, Extruded polystyrene foam, Walls, ETICS

[1] Dow Turkey, Istanbul, Turkey 34469, Phone +90 216 463 7744, Fax 216 3806019, dtopcu@dow.com
[2] Dow Anlagenges.mbH, 65824 Schwalbach, Deutschland, Phone +49 6196 566 158, Fax +49 6196 566 426, hmerkel@dow.com

1 INTRODUCTION

Europe continues to waste at least 20% of its energy mainly due to thermal inefficiency of buildings [EC 2006].

The most cost and energy efficient measure to reduce energy consumption and CO_2-emmissions is thermal insulation of buildings, which in addition improves the indoor-air quality and the living comfort. It has a significant impact on the durability of a building by reduction of ageing of the building structure due to thermal and moisture impact.

The total ETICS (ETICS = External Thermal Insulation Composite System) market in Turkey has reached around 10MM m^2 in 2006 and expected to reach to 40MM m^2 in coming 5 years time. The average growth rate of ETICS market has been 35% in last 5 years. This growth is coming both from new buildings and also very strong renovation segment.

2 EXTRUDED POLYSTYRENE FOAM –XPS

XPS is produced by a continuous extrusion process which finally forms a homogenous closed cell foam structure.

Variations in the slot die allow board thicknesses between 20 mm and 200 mm. After passing through a cooling zone, the board edges are trimmed. The smooth foam skin resulting from the extrusion process remains on the boards or is removed mechanically (planed) for particular board types to achieve better adhesive strength in combination with e.g. concrete, mortar, or construction adhesives.

XPS foam is a standardized insulation product which complies with harmonized European Product Standard [EN 13164:2001] and the corresponding Turkish standard [TS 11989 EN 13164].

XPS insulation products have a closed-cell structure throughout the foam.

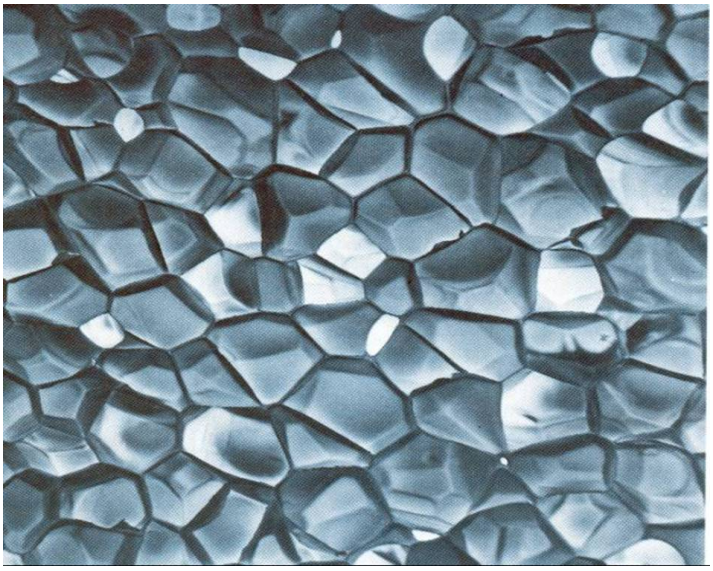

Figure 1. typical closed cell structure of XPS (Photo: Dow Building Solutions).

Extruded Polystyrene Boards, such as Styrofoam do not contain capillaries. This is important especially for exterior wall areas which are close to ground level. Liquid water cannot be transported within the foam behind plaster.

The typical water absorption characteristics are listed in Table 1.

Table 1. Requirements in terms of water absorption for XPS insulation products, in accordance with [EN 13164:2001].

Water absorption characteristics	Thickness [mm]	Limit value [Vol-%]	EN code (EN 13164)
by diffusion	50	≤ 3.0	WD(V)3
by diffusion	100	≤ 1.5	WD(V)3
by diffusion	200	≤ 0.5	WD(V)3
after freeze-thaw	40 – 200	≤ 1.0	FT2
by full immersion	40-200	≤ 0.7	WL(T)0.7

Extruded polystyrene is a thermoplastic material which demonstrates visco-elastic behaviour [Merkel 2004].

The homogeneous closed structure of XPS provides high mechanical resistance; e.g. tensile strength and shear strength [Strzepek 1990]. Additionally XPS exhibits a high resistance against forces pulling through mechanical fixations. These properties are important for the resistance of the ETICS against wind load. The robustness of an XPS product makes it ideal for handling under the tough conditions on a job-site.

The XPS products manufactured according EN 13164 are subjected to a continuous factory production control (FPC) of properties. In some European countries; e.g. France and Germany the application related product properties are certified by independent institutes (notified bodies). Thus quality and compliance of XPS products with the product standard is assured.

3 REQUIREMENTS FOR INSULATION PRODUCTS IN ETICS

The requirements for the insulation component of the system are specified in [ETAG004].
These are related to:

- Thermal resistance
- Water absorption
- Water vapour permeability
- Tensile strength
- Shear strength
- Reaction to fire

The XPS products are classified as reaction to fire class E according to the European Standard EN 13501-1. In Turkey, XPS products shall meet the requirements of German Fire Classification B1 [DIN 4102]; e.g. Styrofoam Shapemate IB.

The water absorption by partial immersion shall not exceed 1kg/m² after 24 hours.

The value has been established to cover also Mineral Wool and EPS products. For XPS the value is close to zero. Low water absorption means the performance is unaffected by moisture in this application.

The μ-value (water vapor diffusion resistance factor) shall be declared. There is however no requirement for a specific μ-value of the insulation. This is obvious, since the water vapour transport and the moisture behaviour of the wall is determined by the entire build-up with all layers and the internal and external climate conditions.
The minimum tensile strength shall not be lower than 80kPa. For XPS the declared tensile strength perpendicular to the surface is >100kPa. Actual values (provided by Dow Building Solutions) are

between 400kPa and 500kPa. The shear strength is well above the required value of ≥ 0,02 N/mm² (20kPa). Actual values are about 0,20 N/mm² (200kPa).

The shear strength is very important for the mechanical resistance of bonded systems to carry the permanent weight of the system.

The surface of XPS boards for ETICS application shall be planed which allows sufficient tensile bond strength between render and insulation. Products with a smooth skin type of surface are not appropriate.

The thermal conductivity of XPS boards is sufficiently low to meet the energy savings requirements. Typical values for XPS products; e.g. Styrofoam Shapemate IB are in the range of 0,030 W/(mK) up to 60mm thickness according to Turkish Standard.

4 TESTING OF ETIC-SYSTEMS WITH EXTRUDED POLYSTYRENE FOAM (XPS)

It is undisputable that the hygro-thermal wall-test is most important for the determination of the durability of an ETIC-System.

The results reported in this paper were obtained from tests performed in a test facility with two walls forming the envelop of a closed climatic chamber (see Fig. 3).The test conditions were more severe than required in [ETAG004].

The two completed test walls (after 28 days drying) were assembled into the test rig. The arrangement of the test rig is shown in Figs. 2 and 3.

Hot air at 70°C was circulated into the test chamber for a period of 3 hours. After this time, the supply of hot air was terminated and a water spray of at least, 1.0 liter per square meter of wall area per minute was applied to the rendered surface of the wall. The water spray was maintained for a period of 3 hours. These conditions were maintained over 140 cycles.

After the cycles, the walls were subjected to a series of twenty 24 hour cycles consisting of exposure to a temperature of 30°C for 8 hours and exposure to a temperature of minus 20°C for 16 hours.

The water flow rate to the spray head was calibrated before the test began, which confirmed a rate of 1.25 liter per square meter of wall area per minute. Measurements of the water temperature during the test indicated that the temperature varied between 15°C to 18°C.

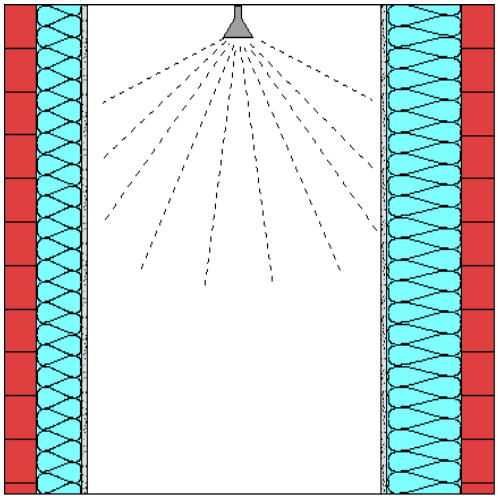

Figure 2. Schematic design of “two wall” test rig.

The test is halted briefly during the heating and moisture cycles for observation after 8, 20, 35, 49, 60, 81, 95, 107, 120 cycles.

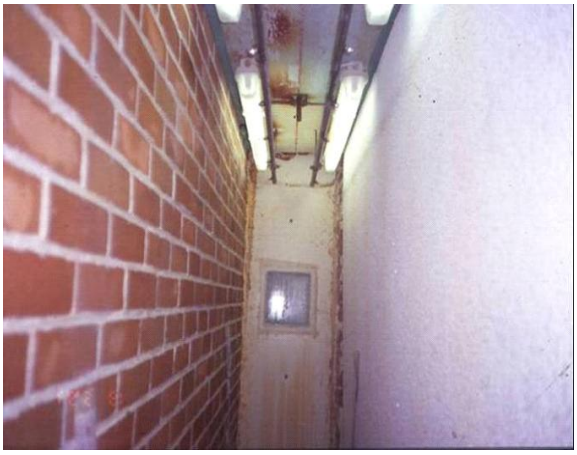

Figure 3. A look into the test chamber; two walls on the left and right side can be tested (Photo: Dow Building Solutions).

The durability of a system can be characterized by determining key parameters, e.g.

- Water absorption
- Tensile bond strength between base coat and insulation

after the hyrothermal test.

Figure 4 shows the water content of the insulation after hygro-thermal ageing of an ETIC-system under the above mentioned test conditions. In general the water content is rather low for the products tested. But it is obvious that the XPS insulation products contains only a negligible amount of water due to their high water resistance.

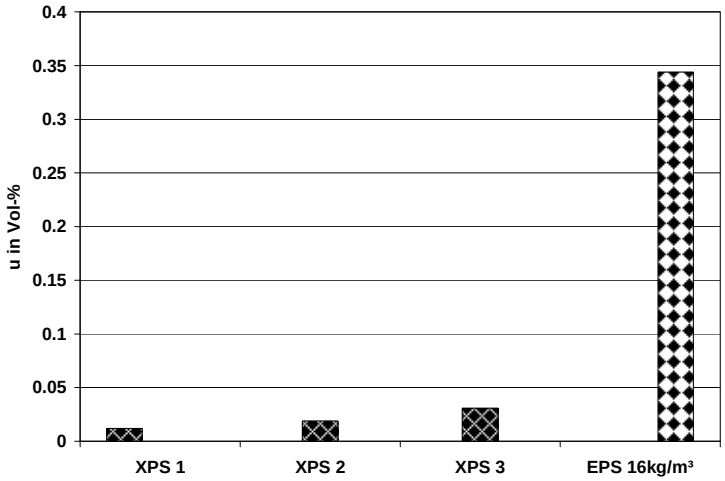

Figure. 4. water content of the insulation after hygro-thermal ageing for XPS and EPS products.

The water absorption by long-term fully immersion was tested separately according to [EN 120875]. Typical results are listed in table 2. Some values in the third column of this table were converted into kilogram water absorbed per square meter. This makes it possible to compare with water absorption values determined according EN 1609 [EN 1609]

Table 2. Water absorption (WA) after long-term (28 days) fully immersion for planed XPS.

Thickness in mm	WA in m³/m³ (Vol-%) acc.[EN 1609]	WA in kg/m²	WA in kg/m² acc. [ETAG004]
40	0,52	~ 0,07	~0,01
50	0,45		
50	0,58		
60	0,75	~0.14	
80	0,30		
80	0,61	~0,13	

When comparing the values it has to be taken into account that the test conditions of EN 12087 are much more severe than those of EN 1609. This is very important regarding the assessment of durability under moisture impact.

The tensile bond strength between the base coat and the XPS insulation depends on the composition of the base coat and the surface properties of the foam.

The durability of the tensile bond strength is exemplified by values given in Fig. 5. The test has been performed according to [ETAG004]. It is obvious that the adhesion between base coat and insulation significantly depends on the performance of the base coat itself, given that the surface of the insulation provides sufficient porosity.

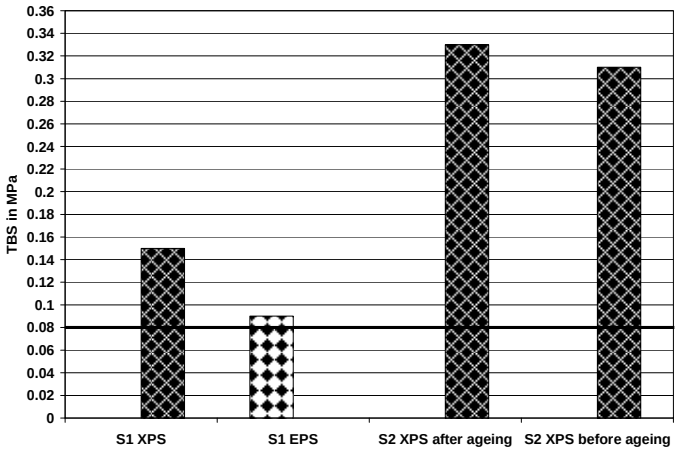

Figure 5. Tensile Bond Strength (TBS) after ageing between base coat and insulation for two different render Systems S1 and S2.

The impact of hygrothermal ageing on the tensile bond strength properties of systems with XPS is rather small as shown in Fig. 5. The required minimum tensile bond strength of 0,08 MPa [ETAG004] is sufficiently exceeded by both systems.

5 APPLICATION OF XPS IN ETICS

From a building physics point of view the external thermal insulation is the preferred solution for wall insulation. The problem of thermal bridges can be easily solved. There is no need for internal vapor retarder (barrier) like for internal thermal insulation solutions. The water vapor resistance is decreasing from inside to the outside of the construction. This means that the construction gets the more diffusion open the more externally the layer is located. Water vapor gets not blocked at the outer layer of the wall. There is no risk of interstitial condensation.

Extruded Polystyrene Foam does not contain capillaries due to the closed cell structure. Hence there is no capillary moisture transport through the foam. This prevents moisture absorbed by the render during a rain period from penetrating into the system. The moisture will dry out to the outside.

The improved moisture resistance of XPS over other insulation materials [Merkel 2002] is of great importance in areas where the ETICS is connected to other structural parts of the building, in particular to perimeter insulation. Moisture from the ground cannot penetrate behind the render via the insulation.

The durability of XPS makes the products applicable to wall construction of highly exposed multistory buildings as shown in Figs. 6 and 7. Even under warm climate conditions XPS based systems show good long-term performance [Concesion 189]

Figure 6. ETIC-system applied to multistory building in Istanbul/Turkey (Photo: MARDAV).

Figure 7. ETICS with XPS after ~15 years of service. No cracks nor blisters are detectable. (Photo: residential buildings in Guadalaraja/Spain).

6 SUMMARY

There is positive experience with XPS in external rendering applications for a long time. Millions of square meters were installed over the last 20 to 30 years in Europe.

The results of hygrothermal ageing tests and the practical experience demonstrate the durability of XPS based ETICS provided that the different building materials layers and their interaction were properly designed and tested.

Extruded Polystyrene Foam (XPS) is a standardized insulation product according EN 13164 and is widely and successfully used for external rendering applications in a number of countries for decades. The main advantages of XPS in ETIC-System are:

- high water resistance,
- closed cell structure of the entire foam, no capillaries, no gaps between cells,
- high shear strength, to carry the permanent load of the system,
- high tensile strength,
- high impact strength,
- appropriate vapor transport performance to avoid condensation risk in moderate and in warm climates.

Hence, extruded polystyrene foam manufactured according EN 13164 or TS 11989 EN 13164 is well suitable as insulation component in ETIC-Systems and meets the requirement of durability.

7 REFERENCES

EC 2006: Action Plan for Energy Efficiency, *Communication from the Commission, Brussels, Oct. 2006*

EN 13164:2001 : *Thermal Insulation Products for Buildings –Factory made products of extruded polystyrene foam (XPS) -Specification*

Merkel,H., 2004: 'Determination of Long-Term mechanical Properties for Thermal Insulation under Foundations. *BUILDINGS IX, Proc. International Conference Clearwater, Florida 2004, ASHRAE 2004*

Strzepek, W.R. 1990: Overview of physical properties of cellular thermal insulations, *Insulation Materials, Testing and Applications, ASTM STP 1030, American Society for Testing and materials, Philadelphia 1990*

DIN 4102-1 : Brandverhalten von Baustoffen und Bauteilen. *Teil 1 Baustoffe , Begriffe, Anforderungen und Prüfungen. Berlin, Beuth Verlag 1981*

TS 11989 EN 13164 *: Isı Yalıtım Mamulleri-Binalar İçin-Fabrikasyon Olarak Ekstrüzyonla İmal Edilen Polistiren Köpük (XPS)- Özellikler"*

ETAG004 : *Guideline for European Technical Approval of External Thermal Insulation Composite Systems with Rendering*, EOTA, Brussels March 2000

EN 12087: *Thermal insulating products for building application – Determination of long term water absorption by full immersion*

EN 1609: *Thermal insulating products for building application – Determination of short term water absorption by partial immersion*

Merkel, H. 2002*:* Wärmeschutz erdberührter Bauteile (Perimeterdämmung)- Dämmstoffe, Beanspruchungen, Konstruktionen*, Bauphysik-Kalender 2002, Verlag Ernst&Sohn, Berlin 2002*

Concesion 189: Sistema de aislamiento termico exterior COTETERM ET*, Instituto Eduardo Torroja Madrid 1989*

Durability of Repaired Concrete Facade Elements

Riccardo Nelva [1]
Roberto Vancetti [2]

T 24

ABSTRACT

This paper illustrates the major criteria for designing and performing repairs on reinforced concrete facade elements, as identified through experimental investigations of repair durability and work at a pilot site. A number of fundamental aspects of repair work are discussed, including the need to understand the causes of degradation and the condition and characteristics of the area to be repaired, the need to develop a correct design procedure that specifies each stage of repair, and the need to identify the methods for monitoring and inspecting repairs that are most appropriate from the standpoint of durability.

A series of experimental investigations have been carried out at the Politecnico di Torino Second School of Engineering in Vercelli, together with the LTS laboratory at DACD - SUPSI of Canobbio (CH), and with the cooperation of a number of manufacturers in the sector. Through this work, accelerated aging tests for repair mortars were developed, product behavior was analyzed, and comparative tests were carried out on the basis of recently issued European standards EN 13687-2 and 13687-4. The experience gained during work at the pilot site demonstrated the advisability of approaching repair projects case by case, analyzing the specific deterioration conditions, performing preliminary investigations, and planning repair work on an ad hoc basis for all stages, from selecting the products to be used to specifying application methods. To ensure durability, it is essential that the critical stages of repair work be monitored through on-site tests.

KEYWORDS

Building refurbishment, Concrete repair, Façade elements, Technologies and workmanship, Durability

[1] Politecnico di Torino, Dipartimento di Ingegneria dei Sistemi Edilizi e Territoriali, c.so Duca degli Abruzzi n°24 – 10129 Torino Italy - Phone +39 011 5645316, Fax +39 011 5645399, riccardo.nelva@polito.it
[2] Politecnico di Torino, Dipartimento di Ingegneria dei Sistemi Edilizi e Territoriali, c.so Duca degli Abruzzi n°24 – 10129 Torino Italy - Phone +39 011 5645323, Fax +39 011 5645399, roberto.vancetti@polito.it

1 INTRODUCTION

The large number of buildings with reinforced concrete elements and structural members, the fact that many of these buildings are several decades old and some are now approaching the hundred-year mark, recent environmental changes that expose concrete to extremely aggressive conditions, and the poor quality of the construction techniques prevailing in the latter half of the 20th century have all combined to draw attention to the problem of degradation in concrete masonry units and products, and to their protection, maintenance and repair.The economic issues that these problems raise thus affect all kinds of buildings, including residential and non-residential civil construction as well as industrial construction.

Concrete's durability is affected by a number of factors. Essentially, these factors can be classified as either chemical, resulting from aggressive environmental pollutants, physical or mechanical. For building structures exposed to air, one of the major factors contributing to degradation is the action of carbon dioxide and the resulting phenomenon of carbonation. As is known, in fact, the durability of reinforced concrete structures is heavily dependent on the protection which the concrete affords to the metal reinforcement: the concrete creates a highly alkaline environment which blocks the onset of oxidation reactions on the part of the rebars. Cured concrete is permeable to gases to some extent, which allows carbon dioxide and other atmospheric pollutants to convert alkaline hydrates into carbonates, thus lowering the initial high pH and making it possible for the reinforcing steel to oxidize, giving rise to further concrete degradation phenomena such as spalling, etc..

The problems associated with concrete's durability in this connection have received extensive attention since the 1960s, with studies; a number of technical guides have also been published, including those produced by the ACI (1996, 2003) together with the BRE and ICRI. Recent experimental studies have addressed the durability of mortar repair techniques and the accelerated aging tests developed to assess them. As regards European standardization, a number of recent UNI EN standards have been issued for "Products and systems for the protection and repair of concrete structures". These standards specify reference concretes for testing (UNI EN 1766 - 2001) and types of mortars and resins (UNI EN 1504.1 - 2000), general principles for the protection and repair of concrete structures and the requirements and properties of the products and systems used (UNI EN 1504.3 – 2006), and accelerated aging test methods (UNI EN 13687-2, 13687- 4).

2 PHENOMENA AFFECTING THE DURABILITY OF REPAIR WORK

This paper illustrates the major criteria for designing and performing repairs on reinforced concrete facade elements, as identified through a series of experimental investigations of repair durability and the experience gained through work at a pilot site. In particular, a number of fundamental aspects of repair work are discussed, viz.: the need to determine the condition and characteristics of the area to be repaired, and identify the causes of degradation; the need to develop correct design procedures that take each stage of repair work into account; the need to identify the methods for monitoring and inspecting repairs that are most appropriate from the standpoint of durability.

A number of correlated phenomena take place when a repair mortar is applied to an existing concrete substrate, many of which depend on the mortar's properties. After mortar is applied, it contracts as it dries. This *drying shrinkage* is counteracted by the mortar's *bond* with the existing substrate (which is assumed to be stable at any given temperature). A tensile stress is thus established in the mortar which will persist as long as the latter continues to adhere to the substrate. At the same time, the mortar's stress capacity will gradually increase as it sets and cures. The situation is thus governed by two phenomena that operate simultaneously: the increase in tensile stress resulting from shrinkage, and the increase in the mortar's mechanical strength. These phenomena can lead to cracking if the mortar's stress capacity is exceeded or to the mortar detachment if the bond between the substrate and the mortar at the interface between the two materials is not sufficient to counteract the tensile stress in the

mortar. *Creep* phenomena (fluage) help promote the system's stability because they reduce the tensile stresses in the applied repair mortar, keeping them below the breaking stresses. The thickness of the applied mortar layer is also a factor, as the tensile stresses set up in the mortar as its shrinkage is counteracted must be balanced by the tangential stresses at the mortar/substrate interface. If the bond strength is exceeded, mortar detachment may occur.

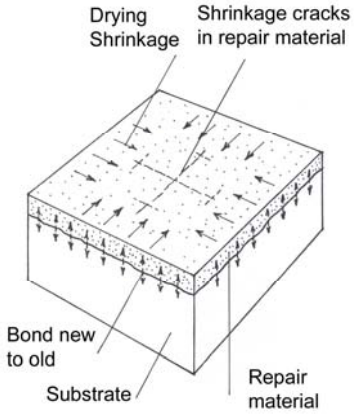

Figure 1. Schematization of the phenomena tied to the drying shrinkage of repair mortar applied to a support.

A further aspect that affects durability concerns the fact that the repair material's *modulus of elasticity* (E) must not be higher than that of the concrete substrate. If the system is subject to external stresses (e.g., compression at a pier or along a beam), the stiffer repair mortar would be required to absorb higher stresses, and could thus break off or detach from the substrate. In general, the *coefficient of thermal expansion* of repair mortars is similar to that of concrete. However, abrupt changes in temperature at the applied mortar layer can cause excessive stress to build up as a result of shrinkage, leading to cracking or detachment from the substrate. The repair mortar's *water transmission* must also be borne in mind, as it must be sufficiently high to reduce the likelihood that interstitial condensation will be formed in cold weather, when outdoor temperatures and water vapor levels are significantly lower than in the building's interior, thus causing water vapor to be transmitted from the interior to the exterior through the building envelope. Other properties that promote repair durability include a high *carbon dioxide diffusion resistance* and low *surface water absorption*. Repair mortars are thus formulated to provide an excellent bond with the substrate, a modulus of elasticity that does not exceed certain specified levels (depending on the properties of the substrate), modest drying shrinkage, a coefficient of thermal expansion similar to that of concrete, low water vapor transmission, high carbon dioxide diffusion resistance, and low surface water absorption.

3 RESULTS OF EXPERIMENTAL INVESTIGATIONS OF ACCELERATED AGING TESTS. STANDARD EUROPEAN TEST METHODS

A series of experimental investigations have been carried out at the Politecnico di Torino Second School of Engineering in Vercelli by R. Nelva and R. Vancetti. This work was performed together with the DACD – Department of Environment Construction and Design – Experimental Technical Laboratory (Prof. Tiziano Teruzzi, supervisor) at SUPSI – University of Applied Sciences of Southern Switzerland – Canobbio (CH), and with the cooperation of a number of manufacturers in the sector. The purpose of these investigations was to assess accelerated aging test methods for repair mortars, analyze the behavior of applied products, verify test significance and carry out comparative tests on the basis of recent European standards.
European standards covering repair products specify a number of tests for assessing the durability of repairs by evaluating the thermal compatibility of the materials involved, i.e., the mortar and the concrete substrate. These standards include EN 1504-3 (2006), which contemplates two test methods for exposed facade elements: carbonation resistance as per draft standard UNI EN 13295, and thermal

compatibility as determined by means of the thunder shower cycling test (EN 13687-2) and the dry thermal cycling test (EN 13687-4). In the latter two tests, concrete specimens measuring 30x30x10 cm to which repair mortars have been applied are subjected to thermal shock cycles, and the effects of aging are assessed by visually inspecting specimen surfaces and by means of pull-off bond strength tests. Bond strength tests are also carried out on control specimens which were not subjected to accelerated aging. Dry thermal cycling tests (temperature cycles in air at –25 °C/+55 °C) were carried out using an Angelantoni CH 250 environmental chamber. For the thunder shower cycling tests (cycles of water spray on a specimen heated to 60 °C), a special test rig was designed and constructed for the purpose.

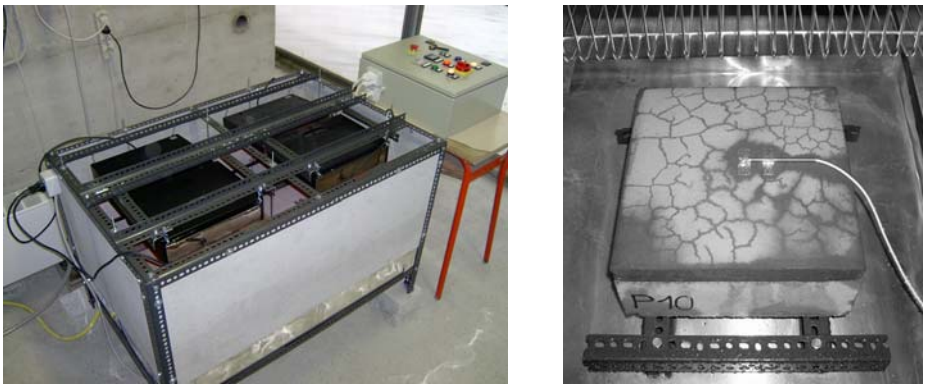

Figure 2-3. Apparatus for tests of quick aging "Thunder Shower cycling".

Findings of laboratory tests were as follows:

- Elastoplastic protective paint on the exterior surface significantly improves the system's performance as regards microcracking as well as water permeability, which was almost nil even after the artificial aging cycles. Performance as regards carbon dioxide permeability was also improved, with specimens coated with protective paint showing lower carbonation depth.
- In the pull-off bond strength tests, it was found that when failure does not take place in the finish layer, the values determined after aging are good, averaging between 1 and 2 N/mm^2 (with peaks up to 3 N/mm^2), as against bond strengths of 2 to 3 N/mm^2 (with peaks up to 4 N/mm^2) for unaged specimens. If failure occurs at the interface between the surface finish and the mortar (or within the finish layer), bond strengths are markedly lower, often falling below 1 N/mm^2 both before and after aging. This fact must be borne in mind when comparing results with specified performance requirements.
- In comparing the results of the thunder shower cycling and dry thermal cycling tests, it was found that the former would appear to be more stringent and leads to greater degradation, reducing pull-off bond strength, increasing water permeability, and causing cracks.
- In general, the tests demonstrated the mortars' high modulus of elasticity and good bond with the substrate, as well as their low vapor permeability. These properties must be borne in mind when designing repairs in order to ensure that they are compatible from the physical and static standpoints.
- Careful product application procedures were found to be crucial to the end result.

4 OPERATING SEQUENCES AND SPECIAL PRECAUTIONS

The intervention systems for the repair and the maintenance of the reinforced concrete elements can be summarized in two main typologies: conservative intervention (punctual and less impacting) and intervention of reparation. The first system has the purpose to protect the structures, when the deterioration is not still advanced, or to correct defects of concrete castings of new realization. A conservative typical intervention is the action of attenuation of the aesthetical defects which are present on a concrete façade and the consequent protection of the structure. A typical intervention is

the sealing of the "nests of gravel", that consists in the stretching of a thin layer of mortar and in the removing the part in excess, in order to close the superficial porosities. The intervention of reparation, instead, consists in the identification and elimination of the deteriorations through the substitution of the decayed material and in the protection against a further stadium of deterioration. In this case it is important to know the physical-mechanical characteristics of the original concrete and to identify its state of deterioration and its causes. Then it is necessary to conduct a series of cognitive investigations in order to determine, by tests in situ, the following characteristics (with these data it is possible to elaborate correctly the executive project of the intervention):

- depth of the carbonation (by a phenolphthalein indicator);
- state of corrosion of steel bars (by visual check and by measuring electric potential);
- modulus of elasticity (for the correct choice of the reparation mortars);
- compressive strenght (indicative of the mechanical properties);
- bond strenght by pull-off test (that furnishes a datum of reference for the subsequent phases of control and test);
- surface water absorption (indicative of the quality and of the state of deterioration of the concrete).

The main phases of these works of reparation are: the surface preparation of the concrete, the cleaning of the steel bars, the protection treatement of steel bars, the application of repair mortars, the application of finishing levelling mortar and of the elastoplastic superficial protective film. The work has to follow the instructions of the UNI EN 1504-1÷10, "Products and systems for the protection and repair of concrete structures".

Figure 3-4-5-6. Removal of decayed material and roughering of concrete substrate by mechanical demolition and by high-pressure water jets.

The choice of the products to apply is related to the causes of deterioration, to the properties of the existing concrete, to the local stresses and to the requested durability. On the basis of the modulus of the elasticity of the existing concrete it is necessary to require a mortar with a smaller modulus of elasticity than the one of the existing concrete. The phase of preparation of the concrete surface substrate is fundamental to get a suitable bond of the repair systems; this requires the removal of decayed material and the roughening of the concrete substrate. The removal of the decayed materials and the products of corrosion is obtained by the high-pressure water jets or by the mechanical demolition. The first technique employes an high pressure water jet and it is proper to the removal of superficial layers and to the demolition. The efficiency of the technique depends on the pressure of water jet and on the water-flow. For the choice of the technique of concrete preparation it is necessary to consider the impact of workmanship on the building site and on the environment (noise, dusts, etc.). The risks in the use of the high-pressure water jets are tied up to possible physical damages of workers and to the damages of structures and plants. The following phase consists in cleaning of the steel bars by abrasive blasting (the operation is not necessary if high-pressure water jets have been used).

Figure 7-8-9. Comparison of steel bars cleaning: by mechanical demolition, by high-pressure water jets, by abrasive blasting.

The degree of cleaning of the steel bars is indicated by the EN ISO 8501-1:2001 and by the UNI EN 1504-10:2005. The standard provides two different methods of cleaning: the abrasive blasting (the degree of cleaning is pointed out by the Sa code following by a numerical index among 0 and 3), or the brushing (the degree of cleaning is pointed out by the St code following by a numerical index among 0 and 3). Subsequently it is necessary to apply the protect treatment of the steel bars against the corrosion. The application of a cement alkaline mortar, with or without a polymeric modifier, allows to get an inhibition effect. The possible additional or substitutive steel bars may be fixed by mechanical connectors, welding, lapping on the existing steel bars or anchorage in the existing concrete (UNI EN 1504-10:2005).

Figure 10. Application of the protect treatment of the steel bars against the corrosion.

The application of the mortar may be mechanically by shotcrete machines in the case of large areas and substantial thicknesses. The equipment may be a dry-mix shotcrete (repair material is placed dry into shotcrete machine and mixed with compessed air; the mixture is transported to the exit nozzle where water is introduced) or a wet-mix shotcrete (pre-batched and thoroughly mixed repair material is transported via pumpline to an exit nozzle). The spray application of the mortar has to be made with an angling as near as possible to 90° related to the existing concrete surface. The applied mortars have to be protected with wet sheets to avoid a rapid drying in the first days after the application.

The finishing consists in the application of the levelling mortar in thin thickness (by hand with plastering trowel) and in the subsequent application of a superficial elastoplastic protection. The elastoplastic protective coating on the exterior surface improves significantly the system's

performance in regard to microcracking as well as water permeability; performances in regard to carbon dioxide permeability are also improved (film thickness about 400-500 μm).

Figure 11-12. Application of the mortar mechanically sprayed (by wet-mix shotcrete) and finishing by hand with plastering trowel.

Figure 13-14. Protection of repair mortar by wet sheets and finishing by elastoplastic superficial protection.

5 MONITORING REPAIR WORK – FINAL INSPECTION

A series of initial tests has to be done to have some data with which compares the tests during the execution and the final inspection. The trial sample has to be choised in a significant zone of the building that represents the main situations of the whole intervention in order to check the application of the complete cycle of restoration. The tests consist in the determination of bond strenght (Pull-off, UNI EN 1542:2000 after 7 days from the application of the layer of mortar of reparation and after 28 days). On the basis of the results at 7 days of the pull-off tests, the site engineer may require ameliorative measures concerning the materials or the cycles of preparation and application. In order to evaluate the test results at 7 days it's necessary to know the diagram of the resistance increase in time correlation of the repair mortars. These data should be furnished by the producers. At the beginning it is possible to refer approximatly to the Swiss Standard Sia 162/5-1997, "Conservation des structures en béton" witch shows that the resistance values of pull-off test at 7 days can reach 70% of those at 28 days. Recent experimentations showed that this value can be also lower. The test results at 28 days are useful to the setting of the tests for the final ispection. The tests that are performed for the final ispection are:
- bond strenght by pull-off test (UNI EN 1542:2000);
- surface water absorption (Karsten method, UNI EN 1504-10:2005);
- thickness of the superficial elastoplastic protection film.

The evaluation of the results of the pull-off tests needs particular attention: it is necessary to take into consideration the position of the plans of separation (it's necessary to examine the extracted cores).

The values to be fixed as minimum limit for the acceptance of results of the pull-off test are connected to the characteristics of the substrate concrete and of the repair mortars. The standard Sia 162/5 shows indicative values for the preliminary tests of the mortars (28 days resistance: structural mortars M3 r = 2,5 N/mm^2; for the building-site qualification tests r = 1,5 N/mm^2 for all types of repair mortars). The standard UNI 1504-3:2006 EN fixes resistance values in laboratory tests r = 2 MPa (R4 class) and r = 1, 5 MPa (R3 class); for the non structural materials r = 0,8 MPa. These values have even to be reached after accelerated aging tests for repair mortars ("dry thermal cycling" and "thunder-shower cycling"). Concerning the surface water absorption tests, the Sia standard 162/5 requires k≤ 0,5 kg m^{-2} h$^{-0,5}$.

Figure 15-16. Determination of bond strenght by pull-off test.

Figure 17-18: Two extracted cores of the pull-off test wich show different positions of the plans of separation.

6 REFERENCES

Nelva R., Vancetti R., Frigeri G., Teruzzi T., Durability evaluation for repair work on reinforced concrete, Management of Durability in the Building Process, Maggioli Ed., Milano, 2003.

Nelva R., Vancetti R., Durability of repaired concrete facade elements: design criteria, workmanship and testing, Construction in the XXI Century:Local and global challanges, CIB W065/W055/W086 Symposium Proceedings 2006, Edizioni Scientifiche Italiane.

ACI, BRE, Concrete Society, ICRI, Concrete Repair Manual, 2nd Edition, 2003.

Nelva R., Vancetti R., Frigeri G., Teruzzi T., Elementi di facciata in cls armato: La durabilità delle riparazioni, sperimentazioni di invecchiamento accelerato, in "Arkos", ottobre 2003, pp. 52-57.

Nelva R., Vancetti R., Frigeri G., Teruzzi T., Metodi di valutazione della durabilità di tecniche di reintegrazione con malte di elementi di facciata in conglomerato cementizio armato, in AA:VV (a cura di G. Biscontin e G. Driussi), Architettura e Materiali del Novecento, Conservazione, Restauro, Manutenzione, Edizioni Arcadia Ricerche, Marghera-Venezia 2004, pp. 719-728.

Enhanced Service Life of Coated Wooden Facades

Per Jostein Hovde [1]
Bjørn Jacobsen [2]
Bjørn Petter Jelle [3]
Erik Larnøy [4]
Geir Vestøl [5]

T 24

ABSTRACT

Coated wooden claddings are widely used in Norway and some other countries, and this is expected to endure due to environmental issues. However, discolouring fungi on outdoor coated wood are an increasing concern, both because of increased focus on aesthetic service life and due to ongoing climate changes. This paper presents an ongoing research project that is being carried out in cooperation between Norwegian universities, research institutes and industry. The main objective is to develop new methods for early prediction of durability and longer aesthetic service life of outdoor coated wooden claddings. Various test specimens from Norway spruce (*Picea abies)* are exposed to natural and artificial weathering. Two methods, qPCR and FTIR spectroscopy, are studied as tools for quantitative and qualitative identification and evaluation of early colonization by discolouring fungi on painted surfaces. These methods will be compared with other existing methods for evaluation of discolouring fungi. The wood materials used in the project are carefully selected and characterized, in order to find effects of wood quality on the performance of coatings. Wood materials, wood surface structure and treatment will be studied to find the optimal combinations that serve long maintenance intervals of painted claddings. Finally, studies will be performed of how the test results can be implemented into service life prediction procedures according to ISO standard 15686.

KEYWORDS

Wood, Cladding, Durability, Service life

[1] Norwegian University of Science and Technology, Dept. of Civil and Transport Engineering, N-7491 Trondheim, Norway, Phone +47 73594547, Fax +47 73597021, per.hovde@ntnu.no
[2] Norwegian Institute of Wood Technology, N-0314 Oslo, Norway, Phone +47 22965667, Fax +47 22604291, bjorn.jacobsen@treteknisk.no
[3] SINTEF Building Research, N-7465 Trondheim, Norway, Phone +47 73593377, Fax +47 73593380, bjorn.petter.jelle@sintef.no
[4] Norwegian Forest and Landscape Institute, N-1431 Ås, Norway, Phone +47 64949016, Fax +47 64948001, erik.larnoy@skogoglandskap.no
[5] Norwegian University of Life Sciences, Dept. of Ecology and Natural Resource Management, N-1432 Ås, Phone +47 64965736, Fax +47 64965001, geir.vestol@umb.no

1 INTRODUCTION

1.1 Project Description

The project presented in this paper started in 2007 and will run until the end of 2010. The main objective is defined as

"Develop new methods for early prediction of durability and longer aesthetic service life of coated outdoor wooden claddings related to consumer needs and new building and environmental regulations."

The project work is organised in 7 Work Packages (WP), and the titles should explain the content of the WPs and the overall work to be done in the project. The Work Packages are:

WP1: Method development for evaluation of fungi - qPCR
WP 2: Method development for evaluation of fungi - FTIR
WP 3: Comparison of evaluation methods
WP 4: Natural and artificial weathering of wooden claddings
WP 5: Characterization of wood materials - implications for fungal growth
WP 6: Characterization of coatings and wood performance
WP 7: Service life prediction of wooden claddings

1.2 Cooperation Partners

The project is carried out in a joint cooperation between the following research institutions:

- Norwegian University of Science and Technology (NTNU), project management
- Norwegian Forest and Landscape Institute
- Norwegian Institute of Wood Technology (NTI)
- Norwegian University of Life Sciences (UMB)
- SINTEF Building and Infrastructure

Two industry partners are involved in the project. Jotun AS and Kebony ASA are supplying surface treatment and modified wood materials (furfuryl alcohol treated), respectively.

1.3 Project Funding

The project work is mainly funded by the Research Council of Norway. In addition, funding is received from The Norwegian Sawmilling Industry, Viken Skog BA, and the Wood Research Fund at the Norwegian Institute of Wood Technology. The research institutions involved in the project are also contributing to the project work by various ways of funding and support.

2 PRODUCTS TO BE TESTED

2.1 Wood Materials

The performance of wood in outdoor applications depends on wood quality as well as surface treatment. Numerous studies have been performed on wooden cladding, and some have taken wood quality into consideration. Studies have been performed on the influence of surface roughness and porosity on coating adhesion [Williams & Feist 1994; Nussbaum et al. 1998], the influence of annual ring width on water sorption properties of wood [Flæte & Alfredsen 2004], and the influence of heartwood content on water sorption properties and fungal growth [Bergstrom & Blom 2005]. The influence of wood-coating interactions on the growth of discolouring fungi is still not well enough

known. In many studies of coated wood, the description of the wood is sparse and the variation between the wood specimens is seemingly of little interest.

Since wood is a heterogenous and non-isotropic material, some variation will always be present. This might influence the effects of the treatments if it is not taken into consideration. According to Kollmann & Côtè [1968], the properties that influence most on sorption behaviour are fibre angle, density and content of extractives, i.e. heartwood content. Williams et al. [2000] mentioned knots as an important factor for coating performance. In spruce, heartwood content has been found to influence growth of surface fungi and water affinity rather than water absorption [Bergstrom & Blom 2005].

In order to have different levels of annual ring width, materials of Norway spruce (*Picea abies*) were sampled from two fertile sites and two poor sites in South-eastern Norway. Sites were classified as poor if the site index, defined as dominant height at 40 years age, was 14 m or lower and as fertile if the site index was 20 m or higher. While the trees at the fertile sites were about 50 years old, had large annual ring width and small taper, the trees from the poor sites were about 150 years old, had small annual ring width and larger taper. Five trees with breast height diameter between 27 and 30 cm and five trees with breast height diameter between 32 and 35 cm were sampled from each site. This sampling also represents some difference in wood density since it is negatively correlated to annual ring width within a site index and a geographical area [Klem 1934].

Butt logs and second logs were processed to claddings with dimensions 19 x 98 mm^2. While butt logs contain wood with small and dry knots, second logs usually contain wood with larger and often sound knots. Since fibre deviations are related to knot size, these two positions also represent some of the variation in fibre angle. The claddings to be analyzed were chosen from both inner centreboards and outer centreboards. The sawing pattern is presented in Fig. 1. Inner centreboards are mainly heartwood and contain some proportion of juvenile wood. Juvenile wood is defined as a number of growth rings from the pith and is characterized by shorter fibres and larger variation in wood density than mature wood [Kucera 1994]. Outer centreboards contain mature wood with longer fibres and smaller variation in wood density, and they may have some proportion of sapwood.

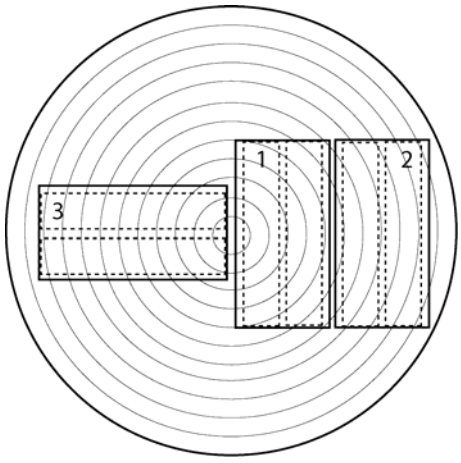

Figure 1. Claddings were produced from (1) inner centreboards, (2) outer centreboards, and from (3) radially sawn boards.

Moisture-induced deformations of wood might lead to cracks in coatings that are exposed to variations in temperature and relative humidity. Since shrinking in tangential direction is about twice as large as that in radial direction [Kollmann & Côtè 1968], one may expect more cracks and then a shorter lifetime for tangentially sawn claddings than radially sawn claddings. To test this difference some of the material was produced as radially sawn claddings as seen in Fig. 1, and those are compared to a corresponding part of tangentially sawn claddings. Moisture-induced deformations of tangentially sawn claddings may also lead to cupping. Cladding with the internal face exposed is recommended

since it is more stable on the wall. Since most sawmills also produce claddings where the external face is exposed, a sub-sample was painted on the external face to test if this has any effect on the coating.

The sample of claddings represents a wide range of wood properties. Since the number of specimens was limited, many properties were measured but not stratified in the sample. These variables, i.e. heartwood proportion, annual ring width, density, fibre angle and knot size will be treated as covariates. Heartwood content was measured from CT-images of the timber scanned before drying. Knots, reaction wood, and other defects were measured on the specimens before painting. Annual ring width and density were measured from small pieces of clear wood. Fibre angle will be measured later when the claddings have been exposed.

2.2 Wood Treatment

The claddings produced from the various trees as described in clause 2.1, were treated with an oil based primer and two exterior acrylic top coats by an industrial process at Moelven Langmoen AS, Brumunddal, Norway. This was done to avoid handmade differences and uncertainties of the various claddings. Red or white colour of the surface treatment was applied, respectively. The red colour was applied to achieve maximum temperature variations within the exposed specimens during testing, and the white colour was applied in order to see the discolouring fungi on the surface as early as possible. The surface treatment was carried out before cutting the specimens to be exposed to natural weathering or tested by artificial weathering in the laboratory.

The test programme also includes Norway spruce (*Picea abies*) treated with furfuryl alcohol. These materials were not prepared from the trees described in clause 2.1. The furfuryl alcohol is applied as an impregnation to the wood material, and is polymerized as a result of heat treatment. It is shown to improve the durability and service life of wood. This type of treatment is found to be more environmental friendly than metal based inorganic salts.

3 NATURAL AND ARTIFICIAL WEATHERING

3.1 Natural Weathering

Specimens to be tested are exposed at two outdoor test sites in Norway. One is situated in Sørkedalen outside Oslo, and the other is situated at Voll, Trondheim. Climate data for the two sites are given in table 1.

Table 1. Position and climate data for outdoor test sites at Sørkedalen, Oslo *) and Voll, Trondheim.

Test site	*Position*	*Monthly minimum temperature [^oC]*	*Monthly maximum temperature [^oC]*	*Annual average temperature [^oC]*	*Monthly minimum precipitation [mm]*	*Monthly maximum precipitation [mm]*	*Annual average precipitation [mm]*
Oslo	60^{o}10´ N 10^{o}20´ E	-5.6 (Jan)	13.6 (Jul)	3.5	60 (Feb)	138 (Oct)	1200
Trondheim	63^{o}25’ N 10^{o}27’ E	-3.0 (Jan)	13.0 (Jul)	4.8	45 (Apr)	110 (Sep)	855

*) The actual data are for Tryvasshøgda, close to Sørkedalen.

The specimens are mounted in racks positioned at an angle of 45^o, facing south. An example of mounting at Sørkedalen is shown in Fig. 2. The specimens will be checked regarding various degradation parameters on a regular basis during the project period.

Figure 2. Wood cladding specimens mounted at the outdoor test site at Sørkedalen, Oslo.

3.2 Artificial Weathering

Natural climate exposure and ageing of exterior materials require long time periods to achieve reliable results. Therefore, numerous laboratory test methods for artificial (accelerated) weathering of materials have been developed, and a number of them are standardized. In a standard for service life prediction of building materials and components [ISO 15686-2], the procedures are based on a combination of test results from both natural and artificial weathering. Most methods for artificial weathering have been developed for testing of various types of materials, and some of the methods include only one exposure parameter (temperature, moisture, UV radiation). In this project, the following standardized test methods will be applied: NT Build 495 [NT Build 495] including UV/light radiation, heat radiation, water spray and freeze exposure, and QUV cabinets for UV radiation and water spray. The QUV cabinets conform to numerous international standards, e.g. EN 927-6 [EN 927-6]. In addition, specimens will be exposed to UV/light radiation, heat and moisture in a commercial climate chamber.

4 METHODS FOR CHARACTERISATION OF DISCOLOURING FUNGI

4.1 Quantitative Polymerace Chain Reaction (qPCR)

Polymerase chain reaction (PCR) based techniques can be used for sensitive and specific monitoring of phytopathogenic microbes in their natural substrates. Real-time PCR is currently a promising PCR method for quantifying DNA. The measurements are performed during the exponential phase of the reaction, when PCR efficiency is not influenced by limiting reagents, small differences in reaction components, or cycling conditions. The incorporation of probes increases the specificity relative to traditional PCR and allows the monitoring of several DNA targets in the same reaction tube (multiplex real-time PCR). As a result, real-time PCR has been increasingly used for the quantification of infectious agents.

The development of DNA-based real-time PCR (polymerase chain reaction) and taxon-specific primers has provided new possibilities for specific detection and quantification of fungi in their natural substrates [Hietala et al. 2003]. In qPCR (quantitative real-time PCR), the accumulation of the PCR product is detected for each amplification cycle. These highly sensitive techniques have already been applied to quantify plant pathogens in a number of cases [Mumford et al. 2000; Weller et al. 2000; Hietala et al. 2003] and in wood materials [Eikenes et al. 2005].

4.2 Fourier Transform Infrared Spectroscopy (FTIR)

Performing a fourier transform infrared radiation (FTIR) analysis yields a fingerprint of the material specimen, and changes due to ageing processes, e.g. artificial climate ageing, may be studied. That is, decomposition and formation of chemical bonds and products can be investigated in a FTIR analysis. Both qualitative and quantitative FTIR measurements may be performed. Studies of different changes occuring within the material, ranging from chemical reactions to concentration changes, are possible. Both solids, liquids and gases, including fast reactions, may be studied. In addition, as in this project, biological growth, e.g. mould and fungi, may also be examined by FTIR analysis, as well as the impact on the attacked material. Several aspects may complicate an FTIR analysis, e.g. the FTIR signals from the degradation products in the surface might be hidden behind the signals from the substrate material. Further, several chemical reactions may be occurring simultaneously or at different times, making it difficult to differentiate between them. Inhomogenities in the fungus specimens, depending on the physical dimensions, will also complicate the FTIR measurements.

FTIR characterization is carried out by using an FTIR spectrometer with a horizontal attenuated total reflectance (HATR) accessory (single reflection) with a diamond crystal. The wavelength range is from 4000 cm^{-1} (2.5 μm) to 400 cm^{-1} (25 μm) in an atmosphere with minimalized CO_2 and H_2O content. Each FTIR spectrum presented is based on a recording of 32 scans at a resolution of 4 cm^{-1}. In order to ensure satisfactory contact between the HATR diamond crystal and the specimen, three or more FTIR spectra are recorded at various locations on the specimen.

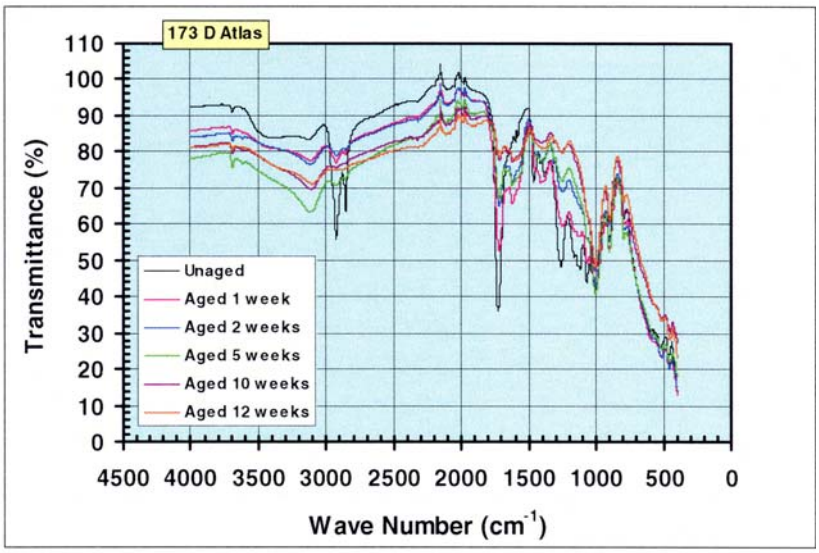

Figure 3. Example of an FTIR spectrum of paint on wood substrate [Olsen 2007].

5 TEST AND EVALUATION METHODS

In general, all the test results will be applied to study the durability of the surface treated and furfuryl treated wood materials, and the extent of discolouring fungi on these materials. Special attention will be paid to the effect of the wood characteristics on the various properties.

For the specimens exposed to natural weathering, visual inspections will be carried out once a year. In addition, specimens will be cut out for further analyses in the laboratory. For the specimens tested by artificial weathering in the laboratory, a number of standardized test and evaluation methods will be applied, e.g. methods to study water vapour permeability, liquid water permeability, cracking, blistering, flaking, chalking, adhesion and colour change. The test results from the artificial weathering exposures will be carefully studied and compared to the test results from natural

weathering. It will be important to establish a variety of degradation and durability data for the test materials, in order to see how these data can be applied as input to the service life prediction procedures as described in ISO 15686 [ISO 15686-2]. There is also a need for further studies of the relations between natural and artificial weathering of materials, and how specific climate parameters can be varied and combined in order to simulate various natural climate exposures artificially in a reliable manner.

6 SERVICE LIFE PREDICTION

Finally, in the last phase of the project, the test data from both the natural and the artificial weathering of the various materials will be applied as input to the service life prediction procedures as described in the international standard ISO 15686. This standard in fact comprises a series of specific standards, altogether describing different aspects of service life prediction. Two alternative procedures are described for a careful prediction or a more simple estimation of the service life, respectively. It will be important to study how the test data obtained during this project can be applied as input to the two procedures mentioned, and to what extent this type of data can be applied to predict or estimate the service life of various wooden claddings.

ACKNOWLEDGMENTS

The authors want to thank the Research Council of Norway and the following institutions for funding the project: The Norwegian Sawmilling Industry, Viken Skog BA and the Wood Research Fund at the Norwegian Institute of Wood Technology. Further, we thank Jotun AS and Kebony ASA for providing paint and treated wood materials to the project, respectively, and Moelven Langmoen AS for preparing the painted specimens by an industrial handling process. Finally, we want to express our thanks to our colleagues at the cooperating institutions.

REFERENCES

Bergstrom, M. & Blom, Å. 2005, *Above ground durability of Swedish softwood*, Doctoral Thesis, Växjö University, Växjö, pp. 1-105.

Eikenes, M., Hietala, A., Alfredsen, G., Fossdal, C.G. & Solheim, H. 2005, 'Comparison of chitin, ergosterol and real-time PCR based assays for monitoring colonization of *Trametes versicolor* in birch wood', *Holzforchung* **59,** 568–573.

EN 927-6 2006, *Paints and varnishes - Coating materials and coating systems for exterior wood - Part 6: Exposure of wood coatings to artificial weathering using fluorescent UV lamps and water,* EN 927-6:2006, European Committee for Standardization, Brussels, Belgium.

Flæte, P.O. & Alfredsen, G. 2004, *Gran som ubehandlet utvendig kledning,* Glimt fra skogforskningen 8. Skogforsk, Ås, Norway (In Norwegian).
Hietala, A.M., Eikenes, M., Kvaalen, H., Solheim, H. & Fossdal, C.G. 2003, 'Multiplex real-time PCR for monitoring *Heterobasidion annosum* in planta. Colonization in Norway spruce clones differing in disease resistance', *Applied Environmental Microbiology,* **69**, 4413-4420.

ISO 15686-2 2001, *Buildings and constructed assets – Service life planning – Part 2: Service life prediction procedures,* ISO 15686-2:2001, International Organization for Standardization, Geneve, Switzerland.

Klem, G.G. 1934, 'Undersøkelser av granvirkets kvalitet (Untersuchung über die Qualität des Fichtenholzes)'. *Meddelelser fra det Norske Skogforsøksvesen*, **5**:197-348. (In Norwegian)

Kollmann, F.F.P. & Cöté, W.A. 1968, *Principles of wood science and technology*. Springer-Verlag, Berlin, Heidelberg, New York, Tokyo, pp. 1-551.

Kucera, B. 1994, 'A hypothesis relating current annual height increment to juvenile wood formation in Norway spruce', *Wood and Fiber Science*, **26**[1], 152-167.

Mumford, R.A., Walsh, K., Barker, I. & Boonham, N. 2000, 'Detection of potato mop top virus and Tobacco rattle virus using a multiplex real-time fluorescent reverse-transcription polymerase chain reaction assay', *Phytopathology* 90: 448-453.

NT Build 495 2000, *Building materials and components in the vertical position: exposure to accelerated climatic strains*, Nordtest, Espoo, Finland.

Nussbaum, R.M., Sutcliffe, E.J. & Hellgren, A.C. 1998, 'Microautoradiographic studies of the penetration of alkyd, alkyd emulsion and linseed oil coatings into wood', *Journal of Coatings Technology*, **70**[878], 49-57.

Olsen, M. B. 2007, *Nano technology for surface treatment of wooden claddings. Examples of products, properties and possibilities*, Master thesis, Norwegian University of Science and Technology, Trondheim, Norway (In Norwegian).

Weller, S.A., Elphinstone, J.G., Smith, N.C., Boonham, N. & Stead, D.E. 2000, 'Detection of *Ralstonia solanacearum* strains with a quantitative multiplex, real-time, fluorogenic PCR (TaqMan) assay', *Appl Environ Microbiol* 66: 2853-2858.

Williams, R.S. & Feist, W.C. 1994, 'Effect of preweathering, surface-roughness, and wood species on the performance of paint and stains', *Journal of Coatings Technology*, **66**[828], 109-121.

Williams, R.S., Jourdain, C., Daisey, G.I. & Springate, R.E. 2000, 'Wood properties affecting finish service life', *Journal of Coatings Technology*, **72**[902], 35-42.

11DBMC International Conference on Durability of Building Materials and Components
ISTANBUL, Turkey 11-14 May 2008

Study on the Relation Between Mockup Test and Lifecycle of Curtain Wall Construction - Case Study in Taiwan

Chih-Min Chi [1]
Chun-Ta Tzeng [2]

T 24

ABSTRACT

The performance of curtain wall could be simply divided into two parts: one is performance of material and another is performance of system. When we think about the durability of curtain wall, we shall consider the life of curtain wall. Lifecycle theory is one of the important method for studying constructions and materials of sustainable building. Lifecycle of curtain wall construction has been divided into several parts, including plan, design, test, manufacture, installation, usage, maintaining, renew, and recycle.

Mockup performance test is common method to make sure of objective by phases of lifecycle. Development of Pre-fabricated curtain wall in Taiwan is over 30 years. In the meantime, the economy of Taiwan is on the decline. And the bidding of Construction changed from Best Value Contracting (BVC) to Lowest Price Contracting (LPC). Recently, the price of material has raised a lot. With factors mentioned above, some management problems were discovered, such as some contractors would never fabricate according to drawings, and they change the design by themselves.

Mockup test is one of the full-size performance tests of exterior wall and it is one of the macro methods to control quality of the construction. In this study, the results and applications of 30 test cases were investigated. Results of this study included wrong test attitude of constructor, workers of installation in test and in site were not the same, and the results of tests did not feeding back to designer and manufacturer, etc.

KEYWORDS

Mockup test, Curtain wall, Quality management, Lifecycle, Sustainable construction

[1] National Cheng Kung University, Department of Architecture, Tainan, Taiwan, ufna2320@ms9.hinet.net
[2] National Cheng Kung University, Department of Architecture, Tainan, Taiwan, z9108008@mail.ncku.edu.tw

1 INTRODUCTION

Curtain wall is one kind of Building exterior wall. Development of Pre-fabricated curtain wall in Taiwan is over 30 years. In the meantime, the economy of Taiwan changed from the highest to the lowest. And the bidding of construction changed from Best Value Contracting (BVC) to Lowest Price Contracting (LPC). Recently, the price of material has raised a lot. With above factors, some problems of management were discovered, such as some contractor never made according to drawing and changing the design by themselves. With all this problems, it direct affected the system performance of curtain wall. The relation between results of mockup test with initial performance of curtain wall will be discussed in this study.

2 METHOD

This study use two methods, literature review and case study. Method of literature review is used to search and collect data of curtain wall, including definition, category, performance, installation, test and lifecycle of curtain wall. Method of case study is use to collect cases of mockup test and their tracing data when the building finish constructing.

The cases shall conform to following:
a. Building located in Taiwan.
b. Completed Project.
c. Test items follow total laboratory procedure of CNS 14280 or AAMA 501.

3 LITERATURE REVIEW

3.1 Definition of Curtain Wall

According to Republic of China Building Construction Regulations [Government of TAIWAN, Republic of China 2007], the definition of curtain wall is “exterior wall of frame-construction building, which only bearing self weight, wind load and earthquake load, and un-bearing or no-passing other loads.” In another word, exterior wall which is not load-bearing wall is curtain wall.

A standard curtain wall contains 4 kinds of components: surface material, supporting frame, connector for stress passing, and filler. [Fig. 1]

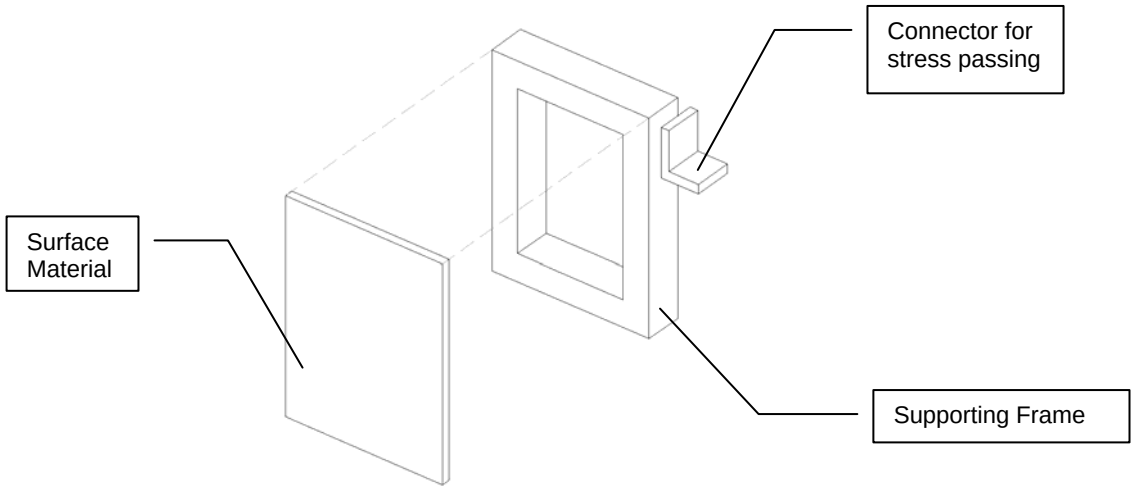

Figure 1. Components of a standard curtain wall [Chi & Chen 2003].

3.2 Lifecycle of Curtain Wall

Lifecycle of curtain wall has been divided into several parts, including plan, design, test, manufacture, installation, usage, maintaining, renew, and recycle. [Fig. 2]

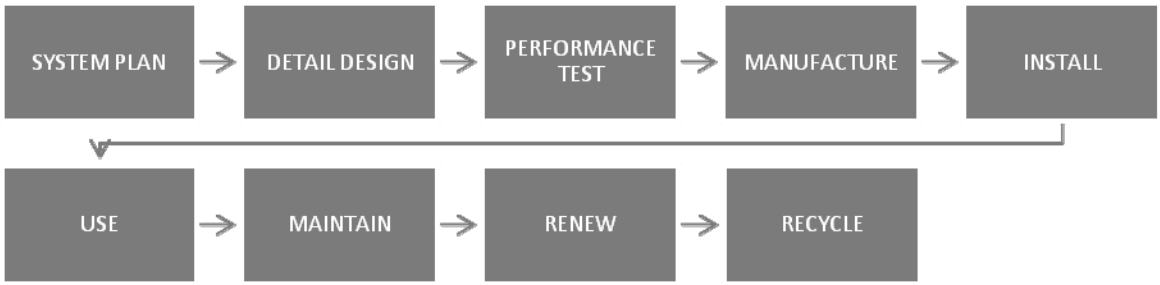

Figure 2. Lifecycle of Curtain wall.

In the area of sustainable curtain wall, 2 important control points shall be focused:

a. System plan:
In this phase, the total cost, construction and main materials, and lifecycle of curtain wall will be setting. Decisions in system plan phase have great effect upon the lifecycle of curtain wall.

b. Performance test:
Mockup test is one of the full-size performance tests of exterior wall and it is one of the macro methods to confirm the system function of the curtain wall. The result will determine the possible lifecycle setting.

3.3 Performance of Curtain Wall

Performance of curtain wall could be divided into two parts [Chi and Chen 2003], performance of materials and performance of physics (knows as system).

a. Performance of materials:
Including metals (e.g. aluminum, steel, stainless, etc.), precast concrete (e.g. concrete, rebar, aggregate, etc.), glass (e.g. plate glass, glass brick, etc.), sealant (e.g. fixed form sealing, non-fixed form sealing, etc.), and others (e.g. skirt, fire stopping, etc.).

b. Physical performance (system performance):
This performance include wind pressure resistance, watertight, storey deformation absorption, and airtight.

3.4 Classification of Curtain Wall

There are many types of curtain wall, and many kinds of sorting ways, in general it is classified according to Surface materials, Frame materials, Functional, Structural, System, Building appearance and etc. At present in Taiwan, Architects and owner prefer to classify by Cladding materials, but most of the curtain wall contractors classifies by system and frame materials. However, for students and researchers, system classification is the most common used. Chi and Chen [2003] offered a sounder definition of System classification: stick, unitized, semi-unitized (unit-and-mullion and column-cover-and-spandrel), panel, and structure glass. [Figs. 3 –8]

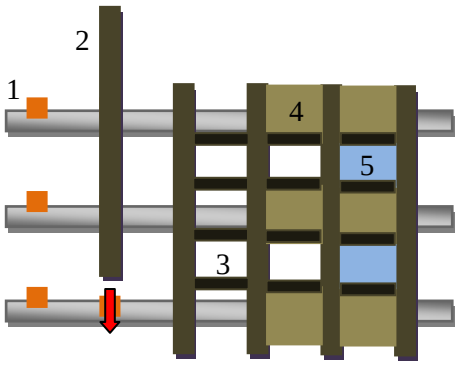

Figure 3. Stick Curtain wall.

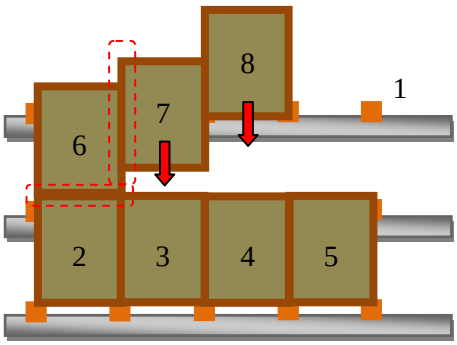

Figure 4. Unitized Curtain wall.

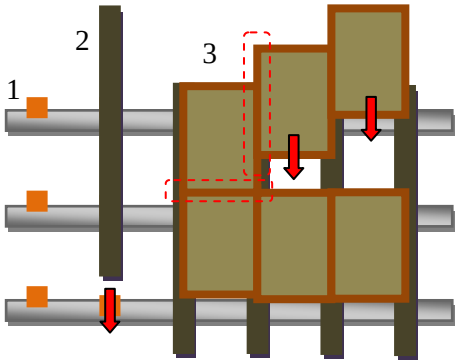

Figure 5. Unit-and-mullion Curtain wall.

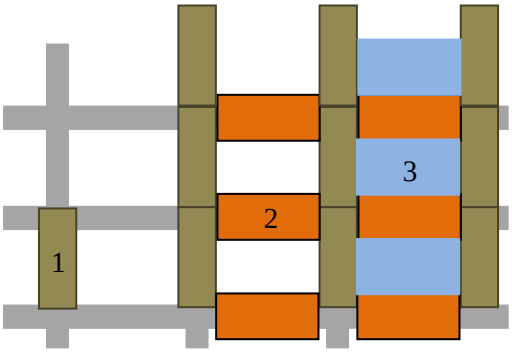

Figure 6. Column-cover-and-spandrel Curtain wall.

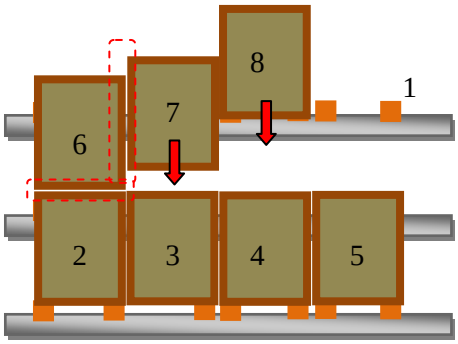

Figure 7. Panel Curtain wall.

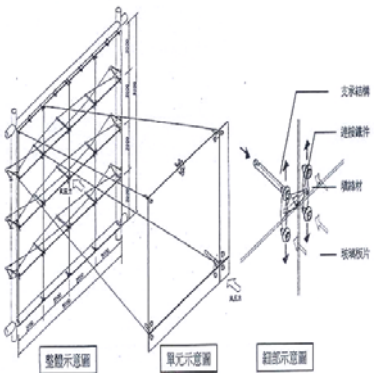

Figure 8. Structure glass Curtain wall [Hsueh & Huang 2002].

3.5 Mockup Test

The purpose of mockup test is to confirm whether the required performance of curtain walls is satisfied and thereby back up the safety and working function of the products. According to CNS14280 [Government of TAIWAN, Republic of China 2007] or AAMA 501[American Architectural Manufacturers Association 2007] requirement, the major test items include: test for air infiltration (CNS 13971, ASTM E 283), test for water penetration with static pressure (CNS 13974, ASTM E 331), test for water penetration with dynamic pressure (CNS 13973, AAMA 501.1), test for structure under static pressure (CNS 13972, ASTM E 330), and test for storey deformation (CNS 14281, AAMA 501.4). [Figs. 9 –13]

Figure 9. Test for air infiltration.

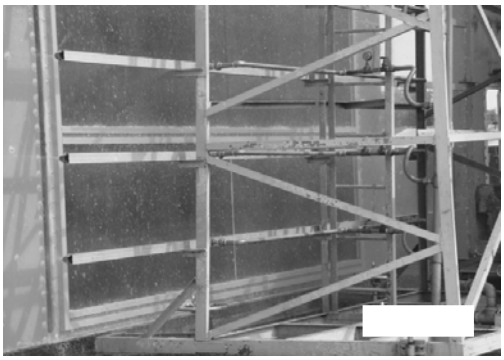

Figure 10. Test for water penetration with static pressure.

Figure 11. Test for water penetration with dynamic pressure.

Figure 12. Test for storey deformation.

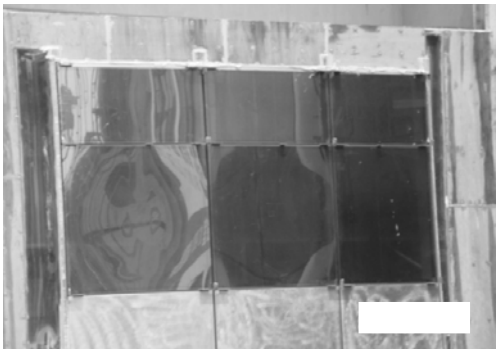

Figure 13. Test for structure under static pressure.

4. CASE SYUDY

4.1 Sample of Case

According to the limitation in this case study, we have selected 30 samples, from 2001 to 2006 [Fig. 14]. From the selected samples, the ratio of government buildings to private buildings is almost one to one [Fig.15].

Figure 16 showed the ratio of various curtain wall systems. Stick curtain wall is the most popular system in the market, because it is the ancient system that use in most building and lower price due to its simple component, which make it more competitive compare to the other system. Figure 17 showed

there are 8 cases of different workers use in laboratory and in the site. The reason of the first 2 samples is because the company laboratory is far apart from the construction site (i.e. different country). The reason for the remaining 6 samples is due to the misleading project time, where they have to test on time, but they had not found a sub-contractor at the same time.

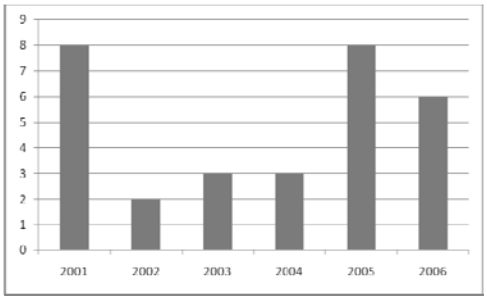

Figure 14. Year range of 30 samples.

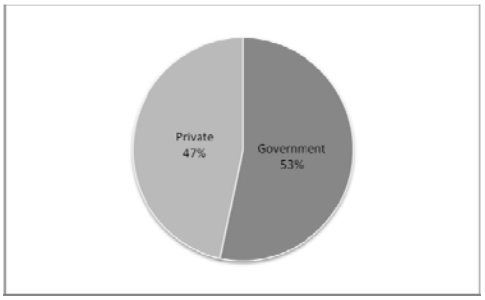

Figure 15. Ratio of government/private building.

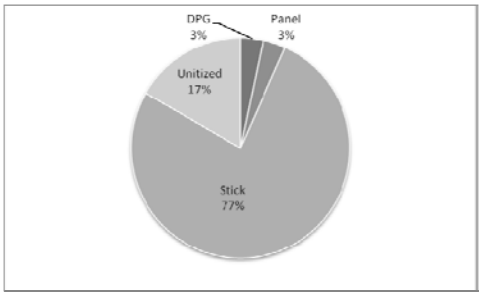

Figure 16. Ratio of curtain wall system from 30 samples.

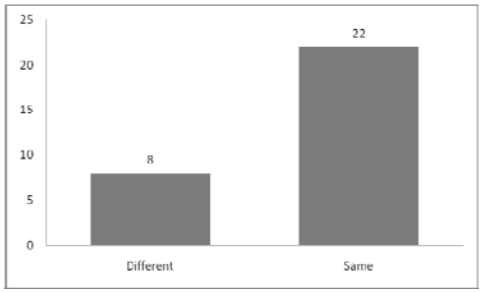

Figure 17. Workers in laboratory and in filed.

4.2 Data Analysis

Figure 18 showed only 30% of samples passed the prepare test for water penetration with static pressure when they finished mature time. In other words, these curtain walls might be unsuccessful in sites, if they did not conduct the test. This also shows that mockup test is important. 67% of samples passed all test items during one time [Fig. 19]. It means that there still 1/3 of the samples have problems during the mockup test. 90% of these problems are water penetration [Fig. 20]. It means that the biggest problem for curtain wall system design came from water penetration. 78% of water penetration samples failed in first time of test for water penetration with static pressure [Fig. 21]. 45% of prepare test failing samples failed in first time of test for water penetration with static pressure (Figure 22). Although CNS, AAMA, ASTM test standards allow curtain wall manufacturers to repair test specimens in site, the rate of success for repair is still too low.

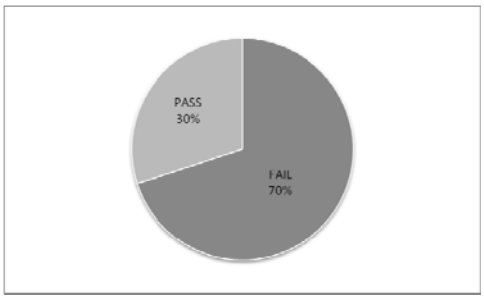

Figure 18. Ratio of passing the prepare test of 30 samples.

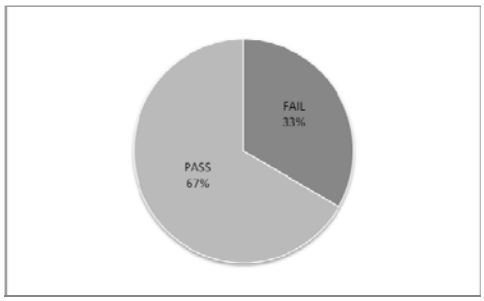

Figure 19. Ratio of passing all test items during one test of 30 samples.

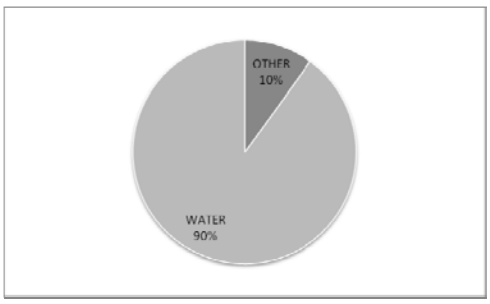

Figure 20. Ratio of problems during the test of test failing samples.

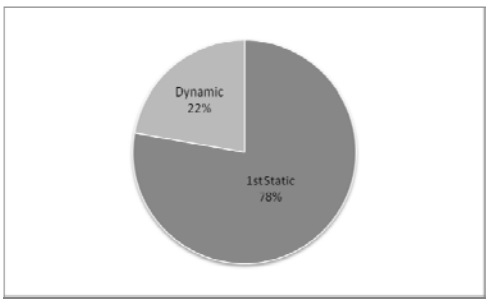

Figure 21. Ratio of water penetration problems.

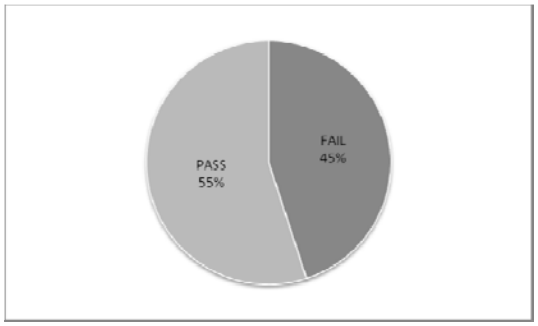

Figure 22. Ratio of 1st water penetration of prepare test failing samples.

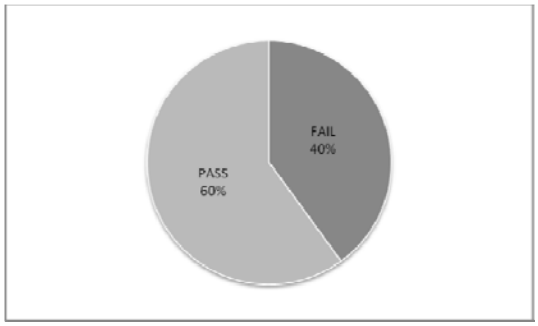

Figure 23. Ratio of watertight test in site of 30 samples.

4.3 Result of Samples Tracing

40% of 30 samples repeated water penetration at test area in the site [Fig. 23]. 80% of passing test samples (i.e. all test items) had not found water penetration in the site [Fig. 24]. This indicates that mockup test is helpful. Figure 25 showed 94% of 80% samples workers work in both laboratory and in the site. We have found 3 points:

a. The mockup test is helpful to check the performance of curtain wall.
b. It can help manufacturers to train their workers during the test before quantity installation in the site.
c. Same workers in the laboratory and in the site are easier to share experience. Different workers might let test become only paper work, the results of test are helpless to building.

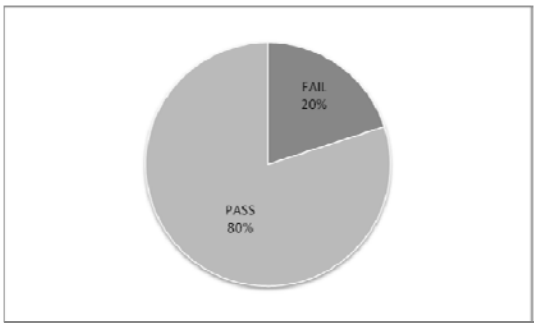

Figure 24. Ratio of water penetration in the site of passing test samples.

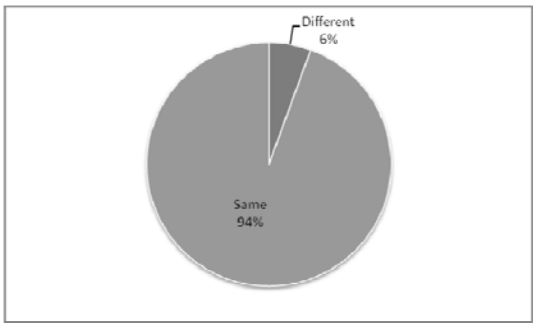

Figure 25. Ratio of workers work both in laboratory and in the site of no water penetration in site samples.

5. CONCLUSION

Setting of lifecycle is necessary for constructions and materials of sustainable building. The main points of control the lifecycle of curtain wall are the system plan phase and the performance test phase. We set the period of lifecycle of curtain wall in system plan phase, and we make sure the setting is correct in performance test phase.

Recently in Taiwan, almost all bidding of construction is Lowest Price Contracting (LPC). This make the lifecycle of curtain wall short, hence it is important to make sure the lifecycle of curtain wall will not be shorter for performance level down.

Mockup test is one of macro methods to control early day performance and quality of exterior wall. These performances directly influence life of every material, and these might shorten the whole life of curtain wall.

From the results of samples and their tracing data, we can conclude follow points:

a. Curtain wall manufacturer in Taiwan should pay more attention on preventing water penetration.
b. The attitude of curtain wall manufacturer can be seem from the way they selected the worker, and it effect the result of performance of curtain wall in both laboratory and the site.
c. The successful rate of passing prepare test for water penetration when finishing mature is too low. This shows that pre-education and training is very important before the installation work start.
d. During water penetrating, the success rate of repair/ reinforce is too low. It is better to check all over the system again rather than only repair the positions of penetrating.
e. If the mockup test is passed, 80% guaranty that the job is successful in the site. Thus, mockup tests certainly a good tool to check lifecycle of curtain wall.

REFERENCES

Government of TAIWAN, Republic of China 2007, *Republic of China Building Construction Regulations*

Chi, Chihmin & Chen, Tainon 2003, *A Research on the Interface Integration of Different Curtain Wall Construction- Main on Unitized Construction –*

Hsueh, ChengYao & Huang, Bin 2002, *A Research on the Tolerance Control on the Construction of Point Supported Glass Curtain Wall in Taiwan*

Government of TAIWAN, Republic of China 2007, *Chinese National Standards, 13971, 13972, 13973, 13974, 14280, 14281*

American Architectural Manufacturers Association 2007, *AAMA Standards*, 501, 501.1, 501.4, CW-DG-1

American Society for Testing and Materials 2007, *ASTM Standards*, E 283, E 330, E 331

11DBMC International Conference on Durability of Building Materials and Components
ISTANBUL, Turkey 11-14 May 2008

Decay Diagnosis of Goan Laterite Stone Monuments

Sutapa Das [1]

T 25

ABSTRACT

Heritage monuments in laterite stones have suffered from harmful intervention during restoration due to inadequate research done on laterite as masonry material based on its great regional variation and mixed property of stone, brick and soil. To preserve these structures, it is crucial to conduct monument investigation for defect analysis along with characterization of local laterite. This research was undertaken for decay diagnosis of Goan laterite monuments with the Basilica of Bom Jesus, India as a case study along with a combination of field and laboratory tests on freshly quarried stones.

During the monument investigation, a majority of the 20 visible defects indicated that efflorescence and biological growth due to water ingress were responsible for deterioration. An in-situ profile study of the quarry showed that though the stone was a matured variety of laterite, however presence of salt, clay-mineral, quartz, and iron patches were responsible for efflorescence, high water absorption, hard patch, and staining respectively. Hence a megascopic study was required for obtaining good quality masonry material. From laboratory tests on freshly quarried samples for geochemical-mineralogical, physical and engineering properties, again it was proved that durability of laterite masonry was attributed to water tightness rather than strength. Physical protection from water by design detailing or application of preservative treatment for water proofing can significantly enhance the lifespan of monuments.

KEYWORDS

Decay diagnosis, Laterite masonry, Monument investigation, Preservative treatment, Water ingress

[1] National University of Singapore, School of Design and Environment, Singapore 117566, Phone +65 8112 5061, Fax +65 6775 5502, sutapa@nus.edu.sg / sutapa.d@gmail.com

1 INTRODUCTION

Laterite is a weathered rock found in tropics and sub-tropics and is named after the Latin word 'Later' or brick [Buchanan, 1807]. Numerous monuments including prehistoric megaliths of Kerala and world heritage sites of churches of Goa, India, third generation Angkor temples or walls in Group G monuments of My Son, Vietnam are made of laterite. Laterite is neither soil nor does it belong to the triplet group of including igneous, metamorphic and sedimentary rocks [Aleva, 1994]. On the contrary, due to its mixed property of stone, brick and soil, laterite has remained as a subject of controversy among geologists and engineers over a century [Banerjee, 1998]. Perhaps this is the only stone that is soft during quarrying, hardens after atmospheric exposure [Gidigasu, 1976; Nichol, 2006], and yet requires a waterproofing plaster and a dense damp proof course [Das, 2007].

Great regional variations has hindered in depth research to characterize laterite as masonry material. It has lead to harmful interventions during restoration of monuments [Bhandari, 1995; Engelhardt, 2005]. To preserve these heritage structures, it is of paramount importance to conduct a comprehensive decay diagnosis comprising of: (1) monument investigation for identification of defects and their analysis; and (2) characterization the local laterite as masonry material. To address this knowledge gap, the current study was undertaken to investigate Goan laterite block masonry with the Basilica of Bom Jesus as a case study. Old Goa on the west coast of India is known as 'The Vatican of East' for its group of beautiful Baroque churches. This 16th century basilica built by the Portuguese rulers is a world heritage monument and is one of the best examples of fine ashlars masonry in Goan laterite [Rajagopalan, 1987].

2 RESEARCH METHODOLOGY

For any natural stone, its composition and microstructure determine its engineering properties and durability [Fitzner, 2000]. The properties of laterite vary widely with location and depth of the quarry [Kasthurba, Santhanam & Mathews, 2007]. Moreover its hardness depends on: (1) degree of weathering of parent rock [Gidigasu, 1976]; (2) quantity, nature and distribution of iron [Alexander & Cady, 1962] and (3) homogeneity, structure and age [Maignien, 1966]. Hence for a thorough understanding of the decay mechanism of laterite, a three pronged approach had been adopted in this study:

- Monument investigation to identify the signs and causes of decay.
- Profile study at a local quarry to study depth-wise variation of laterite of that region.
- Laboratory experiments on freshly quarried stones to determine its engineering properties.

2.1 Monument Investigation

A detailed field study at the basilica was conducted just after the rainy season for easy identification of defects. Only non-destructive tests were allowed at this protected site, hence the investigation was limited to expert walkthrough, photo documentation of the defects, discussion with the personnels of Archaeological Survey of India (ASI) and review of past restoration records.

2.2 Field Survey

The in-situ testing was carried out at Patradevi quarry at north Goa for a profile study and qualitative strength tests. Patradevi was selected for this research due to the fact that stones from this active quarry have similar characteristics as that of the original stones used in the monument and is highly recommended by ASI, for restoration of Goan monuments [Architectural Conservation Cell, 1999]. A detailed profile study of the exposed vertical face of matured laterite layer was conducted. A depth-wise variation of surface hardness as a qualitative indicator of strength was measured for a particular

profile using Type P pendulum hammer [Proceq, 2003]. About three tons of samples were collected from various depths, marked, sealed in wooden crates and transported to the laboratory.

2.3 Laboratory Experiments

As mentioned earlier the engineering property and durability of laterite is a function of its chemical composition and microstructure, hence the following test programme was developed to study the engineering properties of laterite:

- Chemical or wet analysis: gravimetric method for impure silica and volumetric method for Fe2O3, Al2O3 [IS 2720: Part 25]
- Atomic absorption spectrometry for trace alkali metals [Varma, 1985]
- Petrography thin section study for maffic [dark] and felsic [light] mineral [DIN EN 12407]
- X-Ray diffraction [XRD] analysis for altered clay minerals [Moore & Reynolds, 1997]
- Test for water absorption, specific gravity and porosity [DIN 52103]
- Test for water absorption coefficient through capillary action [DIN EN 1925]
- Test for compressive strength [DIN 52105] and flexural strength [DIN 52112]
- Salt crystallization test [DIN 52111]

3 RESULTS AND SISCUSSION

3.1 Findings from Monument Investigation

From the internal reports of ASI [1964-1999], it was noted that majority of the problems started in 1930s after de-plastering of 2m thick walls to solve the problem of water seepage through them. As it was difficult to introduce a damp proof course, external lime plaster was peeled off to apply paper poultice for removal of efflorescence. Since that date various restoration activities have taken place. Most of these interventions were irreversible in nature and had shown detrimental effect in the long run. For example, walls lost breathability due to the application of acrylic paint on inner surface, stronger cement mortar used for re-pointing was incompatible with soft stone, pruning effect of pulling and plucking to prevent vegetation growth in reality resulted in abundance of vegetation etc.

Most of the decay features were found to be associated with the external walls only, except very few surface cracks in floor and ceiling. Twenty visible defects were identified and grouped into 5 major categories [Weathering Research Gr., 2003], namely: (1) mechanical weathering; (2) efflorescence; (3) material and methods of construction; (4) human intervention and (5) biological decay (Table 1).

3.2 Findings from Field Study

Patradevi is an active quarry. Hence, the strata such as duricrust, lithomerge and parent rock were not observed. The visible laterite zone was about 9m deep appeared as a uniform brick wall without any significant variation. However, a close inspection revealed patches of salt, clay, quartz and iron which may lead to efflorescence, water absorption, hardness and staining respectively (Figure 1).

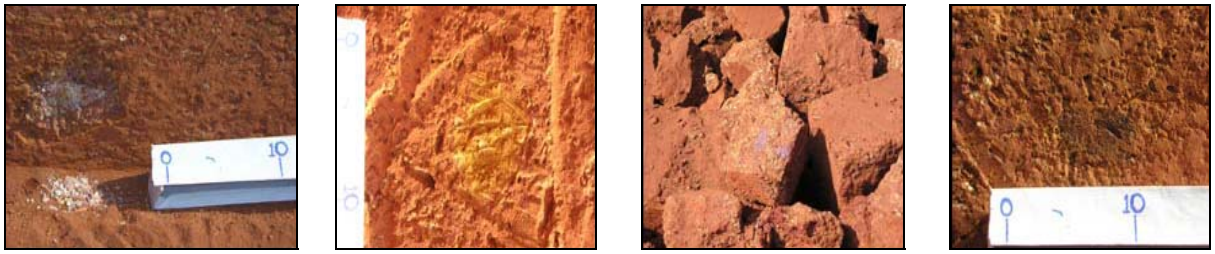

Figure 1. Defects found by visual inspections (L to R: patches of salt, clay, quartz and iron)

Table 1. Summary of decay features.

Category	*Description of defects*	*Probable cause*
Mechanical weathering	Granular disintegration	Cement holding the grains together is weakened by water and washed away.
	Flaking (depth <5mm)	Salt weathering and wetting-drying cycle
	Scaling (depth >5mm)	Accumulation of salt at a frequent wetting depth within the stone and the eventual lifting away of the outer layer
	Honeycombing	Merging of adjacent depressions due to multiple flaking, granular disintegration and salt accumulation
	Caverns	Severe honeycombing
Efflorescence	Salt patch / stain	Lashing rain and rising moisture
Materials and methods of construction	Inadequate plinth protection	The conventional practice of a nonporous granite damp proof course is absent
	Loss of mortar	Poor workmanship at pointing leaves the mortar joints weak and susceptible to rainwater ingress.
	Cracks by corrosion	Volume increase of iron fixing due to corrosion
	Heterogeneity	Inferior quality blocks placed along with good ones become weak point for a wall
	Widening of joints	Due to absence of drip course, the water follows the mouldings and gets absorbed through mortar joints.
Human intervention	Incompatible mortar	Stronger cement mortar used for re-pointing of soft stone
	Peg mark	Use of pegs to maintain uniform plaster thickness
	De-plastering	Repair work
Biological decay	Biological colonization & fern growth	High silica content and presence of moisture
	Bio-chemical weathering	Formation of dark crust due to leaching of iron at the places of root penetration
	Cracks	Root penetration through soft and porous stone
	Deformation	Thick roots causing dislodgement of stone blocks

3.3 Findings from Laboratory Experiments

3.3.1 Geochemical and Mineralogical Analysis

Laterite samples from upper, middle and bottom level of quarry was tested for major oxides and trace elements (Table 2). As the depth-wise variation in both field investigation and chemical composition was found insignificant, in later studies depth of quarrying was no more considered as a criteria. High silica content implied a high amount of clay responsible for water absorption.

Table 2. Quantity of major oxides and trace elements

Sample No	*Major oxides [%]*				*Trace elements [ppm.]*			*Total*
	SiO_2	Fe_2O_3	Al_2O_3	*LOI*	Na^+	Ca^{++}	Pb^{++}	[%]
GA1 (upper)	52.34	21.79	9.22	14.23	150.09	8.34	332.60	97.58
GA2 (middle)	57.73	16.34	8.93	16.23	162.83	15.23	310.50	99.23
GA3 (bottom)	54.54	18.86	10.45	15.05	170.47	22.69	277.50	98.90
Average	54.87	19.00	9.53	15.17	161.13	15.42	306.87	98.57

XRD analysis detected abundance of clay minerals namely, kaolinite, biotite and chlorite (Figure 2). According to Schelmann's [1981] definition the high content of secondary silica indicated matured variety of laterite. Petrographic analysis of thin sections (Figure 3) revealed presence of both: (1) maffic mineral (haematite and red iron oxide) and (2) felsic minerals (feldspar and quartz).

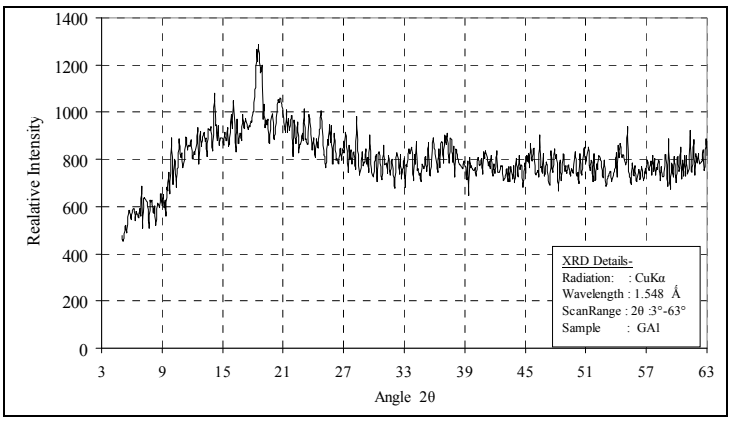

Figure 2. Result of X-Ray difractogram

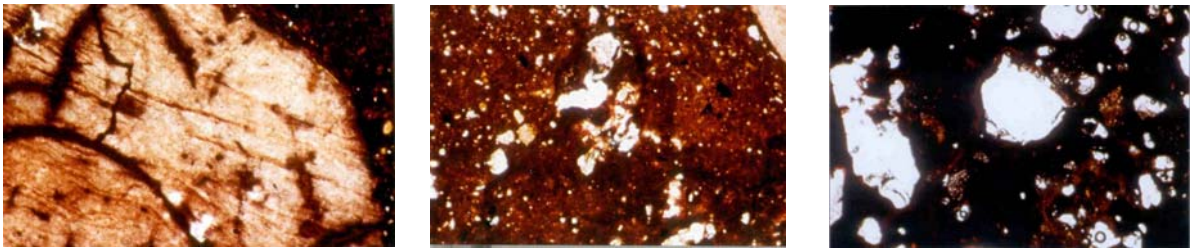

Figure 3. Result of thin section study

3.3.2 Physico-mechanical Analysis

Results of the physico-mechanical analysis is presented in Table 3.In spite of the difference between apparent and true specific gravities, the apparent and true porosities had similar values. Although the high porosity of laterite was reaffirmed in this result, it is difficult to explain the difference in the specific gravities or in other words, it is not easy to suggest that all pores in the system were interconnected. This anomaly might be a result of the fact that while measuring the actual saturated surface dry (SSD) mass of the specimen, it is almost impossible to keep the near-surface pores fully saturated. Average value of water absorption was found as 11.45%. Both porosity and water absorption were fairly low while compared to range of standard values [IS 2720: Part 25] indicating a matured variety of laterite. The value of 1641 g/m² / $min^{0.5}$ for coefficient of absorption through capillarity was found to be lesser than that of sandstones [Jäger & Burkert, 2002]. Hence it can be concluded that though laterite is porous, numbers of micro-pores are less and not susceptible to capillary action.

Table 3. Results of physico-mechanical tests

Properties	*Sub-properties*	*Values*	*Unit*
Capillarity	---	1641	g/m² / $min^{0.5}$
Water absorption	---	11.45	%
Specific gravity	Bulk	1.79	---
	SSD	1.99	---
	Apparent	2.25	---
	True	3.06	---
Porosity	Apparent	25.75	%
	True	26.48	%
Compressive Strength	---	5.05	MPa
Flexural strength	---	1.23	MPa

The average values of compressive and flexural strength of the sample were found to be 5.06 MPa, and 1.28 MPa respectively (Table 3). This indicates that laterite is a weak stone, even weaker than good quality brick [IS 1077]. This value is much lower than the calculated average strength of 10.3MPa found from rebound hammer test. Such a large difference in values occurred because in quarry a continuous surface was tested while the manufacturer's conversion graph was meant for 20 cm cubes.

3.3.3 Salt Crystallization Test

In the salt crystallization test of 15 weathering cycles, there was sharp weight gain of 5.07% on the first day but the rate of weight gain became steady up to 8-th cycle with a marginal difference within 3%. The large surface-pores accumulated salt crystals to a great extent on the very first day. As more salt solution seeped in, there was a slow but steady weight gain. Between 6th and 8th weathering cycles, specimens showed rapid weight loss of 4.7%. But during next three cycles, though there was again weight gain, but in later cycles the specimens started losing integrity and finally almost crumbled down (Figure 4). Probably during 6th to 8th cycles, resistance of samples was lost by a considerable extent such that pressure exerted by volume increase of salt crystals dislodged a few grains. Assuming most of these grains were internal, it can be concluded that some previously inaccessible pores might have got exposed to salt solution allowing more salt to enter, crystallize and cause weight gain. But in later stages, the excessive amount of salt had a splitting effect on week laterite and hence caused total disintegration of the specimens.

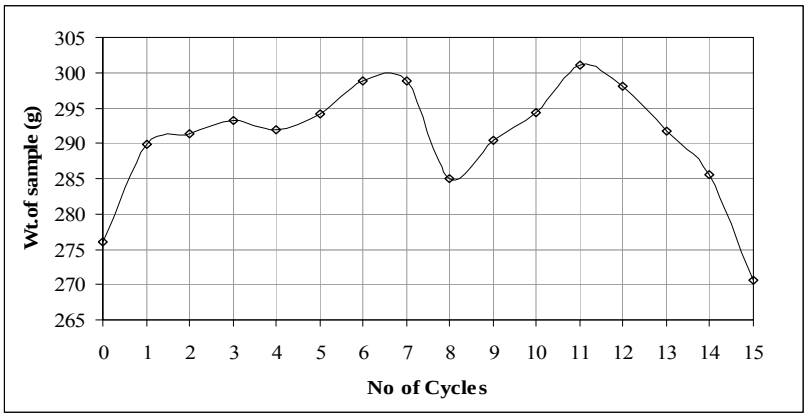

Figure 4. Result of salt crystallisation test

3.4 Discussion

From the monument investigation, the root cause of most of the defects was identified as water ingress either from lashing rain or from rising moisture leading to salt efflorescence and vegetation growth. Until1930, application of lime plaster before each monsoon prevented the harmful weathering actions to a great extent. Structural failure was not visible, hence a preliminary conclusion can be drawn that durability of laterite is more dependent on water tightness rather than strength. At local quarry, no significant depth-wise variation was found, but presence of clay minerals affirmed that though Goan laterite is a matured and stronger variety of laterite, it is susceptible to water ingress. Laboratory testing affirmed these facts. It was also found that though the stone has high porosity, the pores might not be interconnected and large enough to resist capillary action.

4. CONCLUSION

Goan laterite was tested at a world heritage monument, at local quarry and in laboratory using chemical analysis, petrographic microscopy, and physical tests to determine the decay mechanism. Most of the defects were as a result of water ingress. At quarry a matured type of laterite with less variance with depth was observed. Hence through megascopic analysis, good quality masonry material

can be selected to achieve the first line of defence against weathering. In spite of high content of strength-giving iron oxide, Goan laterite is weak in compression and flexure even compared to standard brick. Hence the durability of masonry was attributed to water tightness rather than strength. It can also be concluded that water repellence in the form of design detailing or water proofing agent can significantly improve the life span of monuments built in Goan laterite. The facts obtained from this study can contribute to an integrated database of laterite research and can be applied in the development of stone preservatives enhancing the pore structure and water tightness.

ACKNOWLEDGMENTS

This research was conducted under the supervision of Prof. Manu Santhanam of Indian Inst. of Technology, Madras. Additional research support from Prof Wolfram Jäger and Dr. Toralf Burkert of Chair of Load Bearing Structures, Technical University of Dresden, Germany and financial support from the Ministry of Human Resource Development of India are gratefully acknowledged.

REFERENCES

Aleva, G.J.J. (Compiler). 1994, *Laterite–Concepts, Geology, Morphology & Chemistry*, ISRIC, Wageningen, Netherlands.

Alexander, L.T. & Cady, J.G. 1962, 'Genesis and hardening of laterite in soils', *U.S. Dept. of Agriculture Technical Bulletin*, **1281**, 1-10.

Architectural Conservation Cell, 1999, *Methodology and Actual works of Restoration of The Chapel of Our Lady of Mount, Old Goa*, Associated Cement Company Ltd. Thane.

Archaeological Survey of India (ASI). 1964-1999, *Internal Reports*. Author, New Delhi, India.

Banerjee, P.K. 1998, 'Basic research on laterites in tropical countries', *Quaternary Int.*, **51/52**, 69-72.

Bhandari, C.M. 1995, *Saving Angkor*, White Orchid Press, Bangkok.

Buchanan, F. 1807, *A Journey from Madras Through the Countries of Mysore, Canara and Malabar*, T. Cadell & W. Davies, London, (Reprint, 1988, Asia Educational Services, New Delhi).

Das, S. 2007, 'Laterite monuments of India', *Const. History Society Newsletter*, UK, 15-19, May.

DIN 52103. 1988, *Testing of Natural Stone and Mineral Aggregates - Determination of Water Absorption and Saturation Coefficient*, Deutsches Institut für Normungm (DIN), Berlin.

DIN 52105. 1988, *Testing of Natural Stone – Determination of Compressive Strength*, DIN, Berlin.

DIN 52111. 1990, *Testing of Natural Stone and Mineral Aggregates - Crystallization Test with Sodium Sulphate*, DIN, Berlin.

DIN 52112. 1988, *Testing of Natural Stone – Determination of Flexural Strength*, DIN, Berlin.

DIN EN 1925. 1999, *Natural Stone Test Methods - Determination of Water Absorption Coefficient Capillarity*, DIN, Berlin.

DIN EN 12407. *Natural Stone Test Methods - Petrographic Examination*, DIN, Berlin.

Engelhardt, R. 2005, *Safeguarding My Son World Heritage – Demonstration and Training in the Application of International World Heritage Standards of Conservation at My Son Group G Monuments*, UNESCO Project Terminal Report, UNESCO, Bangkok

Fitzner, B. 2000, 'Damage index for stone monuments: protection and conservation of the cultural heritage of Mediterranean cities', Proc. of the 5th International Symposium on Conservation of Monuments in the Mediterranean Basin, Sevilla, Spain, pp. 677-689.

Gidigasu, M. D. 1976, *Laterite Soil Engineering – Autogenesis and Engineering Principles*. Elsevier Scientific Publishing Company, Amsterdam.

IS 1077. 1992, Common *Burnt Clay Bldg. Bricks – Specification*, Bur. Indian Standards, New Delhi.

IS 2720: Part 25. 1982, *Standard Method of Test for Soils: Determination of Silica Sesquioxide Ratio*. Bureau of Indian Standards, New Delhi, India.

Jäger, W. & Burkert, T. 2002, *Verwendung Modifizierter Siliciumdioxid-Nanosole zum Schutz und zur Konsolidierung von Umweltgeschädigten Kulturgütern aus Sächsischem Elbsandstein am Beispiel der Skulpturen der Fasanerie Moritzburg*, TISA Research report, TU-Dresden, Germany.

Kasthurba, A.K., Santhanam, M., & Mathews, M.S. 2007, 'Investigation of laterite stones for building purpose from Malabar region, Kerala state, SW India – part 1: field studies and profile characterisation', *Construction and Building Materials,* **21**[1], 73–82.

Maignien, R. 1966, 'Review of research on laterites', *Natural Resources Research IV*, UNESCO, Paris

Moore, D.M. & Reynolds, R.C. 1997, *X-Ray Diffraction and the Identification and Analysis of Clay Minerals (2 Ed)*, Oxford University Press, USA.

Nichol, D. 2006, 'The geo-engineering significance of laterite construction in Goa, SW India', *Quarterly Journal of Engineering Geology and Hydrogeology*, **33**[3], 181 – 185.

Proceq. 2003, '*Portable concrete testing instruments for non-destructive. site investigations'*, http://www.procequsa.com/documents/Proceq_Concrete_Line_Catalog_72.pdf (retrieved Oct 19, '03).

Rajagopalan, S. 1987, *Old Goa*, Archaeological Survey of India, New Delhi.

Schellmann W. 1981, 'Considerations on the definition and classification of laterites', Proc. the Int. Seminar on Laterisation Process, Trivandrum, India, pp. 1–10.

Varma, A. 1985, *Handbook of Atomic Absorption Analysis Vol. 1*, CRC Press, Boca Raton.

Weathering Research Group 2003, '*Weathering features tutorial'*, http://www.qub.ac.uk/geomaterials/weathering/weatheringfeatures.html (retrieved Sept., 22, 2003).

11DBMC International Conference on Durability of Building Materials and Components
ISTANBUL, Turkey 11-14 May 2008

Faults and Repairs in House of Bagheri: A Cultural Heritage Construction in Gorgan (North of Iran) – A Case Study

Mehrab Madhoshi [1]
Javid Eimanian [2]

T 25

ABSTRACT

This papers aims to show some features of one of the most important old constructions of Gorgan (North of Iran), called House of Bagheri, which, was built approximately 150 years ago with a built up area of 3000 m^2. Solid wood was utilized in large amounts as a construction material in structural elements like beams, columns, rafters, roofing and flooring system. Bricks and cob (a mixture of clay and straw) were used for walls. Doors and windows are completely wooden and look intact. The building is now considered as a Cultural Heritage Construction and its maintenance is important for Iranian Cultural Heritage Organization because of its history and tourism potential. In this paper, some important architectural and structural characteristics are considered with particular emphasis on wood as a construction material; study was conducted on existing faults and their reasons, including biological and environmental factors. The adopted repair methods are explained, and further comments on those methods are considered. The wooden species are identified in laboratory at macroscopic and microscopic levels and their existing mechanical strength were investigated, mainly compression parallel to grain and flexural strength. The results indicated that the domestic hardwood such as oak, elm, maple and imported softwood such as pine were used in construction of House of Bagheri. Some structural elements possessed acceptable strength in spite of their decayed appearance.

KEYWORDS

Faults, Heritage constructions, Repair, Wood

[1] Department of Wood and Paper Sciences and Industries, Gorgan University of Agricultural Sciences and Natural Resources, Gorgan 49138-15739, Golestan, Iran, mmadhoushi@hotmail.com
[2] Iranian Cultural Heritage Organization, Gloestan Head Office, Golestan, Gorgan, Iran.

1 INTRODUCTION

Gorgan is located in North of Iran between Caspian sea and Alborz mountains where the climate is mostly mediterranean (with average rain fall of 432.1 mm and RH = 62.5% to 74%). It is considered a heritage city because of its history and historical buildings. Solid wood has been utilized as structural elements in some of them .

This papers aims to show some features of one of the most important old constructions of Gorgan (North of Iran), called House of Bagheri. This was built approximately 150 years ago with a built up area approximately 3000 m^2 (Eimanian, 2001). This building is now under repair. Solid wood was utilized in large amounts as a construction material in structural elements like beams, columns, rafters, roofing and flooring system. However, brick and cob (a mixture of clay and straw) were used for walls. Doors and windows are also completely of wood finish and are in a good condition. Nowadays, it is known as a Cultural Heritage Construction and its maintenance is important for Iranian Cultural Heritage Organization because of its history and tourism attractions.

Today, repair and restoration of historic buildings is a major challenge in societies (Lourenco *et al.* 2007). Previous studies conducted on wooden historical buildings showed that moisture and fungal decay could be considered as the main source of damge (Ronca & Gubana 1998, Pasanen *et al.* 2000). In this study of fungal decay, insects and and weathering are investigated as the source of damage (Wilkinson, 1979).

2 MATERIALS AND METHODS

A visual study was conducted of existing faults and their reasons, including biological and environmental factors. The adopted repair methods are explained and some comments on those methods are considered. Furthermore, the wooden species are identified in the laboratory at macroscopic and microscopic levels (Parsapajouh, 1988) and their existing mechanical strength investigated, mainly compression parallel to grain and flexural strength (Bodig & Jane, 1984).

3 RESULTS

3.1 Architectural and Structural Characteristics

The House of Bagheri is a collection of several main buildigs ad compounds and yards. A small pool is located in a central area of each yard and the buildings have been built around them. Although there is a one-storey building in this complex, it is mainly known as two-stories with a few steps between floors (Figure 1). The buildings have nearly identical architectural characteristics and the plan of one building is shown in Figure 2. The influance of Islamic art can be seen as the dome shaped window designs (Fig 3d).

Figure 1. Some views from House of Bagheri**.**

Thanks to its special design, air circulates easily providing good ventalation, which in turns provides a lower damp enviroment inside the building. The structure is rectangular and constructed essentially with brick and cob in shear walls and solid wood for load bearing elements. Figure 3 shows some areas where solid wood has been used as a construction material.

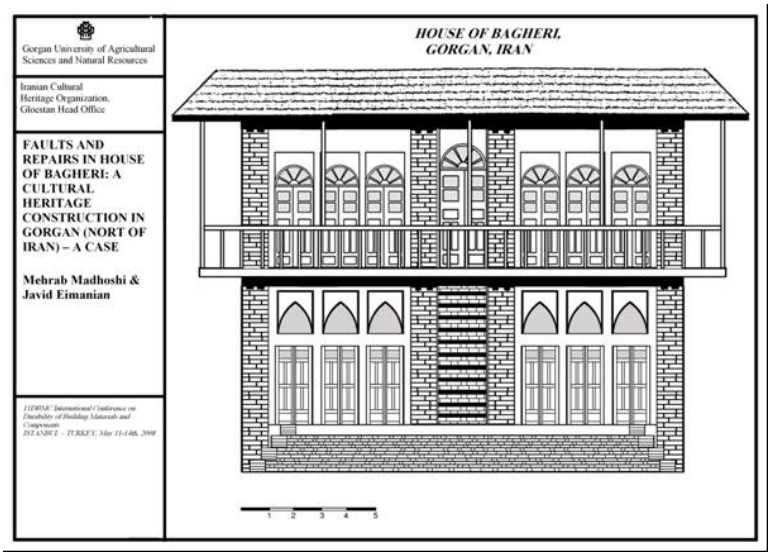

Figure 2. An Elevation of A Building in House of Bagheri**.**

Figure 3. The main construction materials used in House of Bagheri, (a) brick and cob, (b) solid wood beneath the door, (c) solid wood up the door and (d) solid wood as main beam and rafters.

3.2 Faults and Repairs

Although studies have been carried on the whole structure and other material, in this paper only the main faults/ and their reasons related to timber members are reported. The main faults can be considered in three groups as follows: 1. corrosion / by weathering, 2. decay/ by fungi attack and 3. internal holes/ by insects. These faults (or defects) are more or less common in North of Iran because of the climate. However, their distribution depends on area and species. Hence, the investigation on the type of faults existing in each building is necessary. It should be noted that faults due to dimensional variation related to swelling and shrinkage of wood were also found, but their effects were ignored in this study.

Corrosion caused by weathering (due to sunshine and rainwater splashing) was found in opening frames and balconies. In some parts, it was very intensive and combination with fungal decay, the wooden elements ad significant detemoration and could not be used again (Fig 4a). These elements have now been substituted by new members. In other elements the weathering was just a surface phenomena with the elements having nearly their primary strength (Fig. 4b). These elements could have been used again by surface intervention. Unfortunately, this method was ignored and the new members were utilized.

Figure 4. (a) Intensive weathering and (b) surface weathering, existing in House of Bagheri.

With regarding to the fungi and insect attack, the defects were disperesed over the buildings. The fungal growth and decayed parts were found mainly on rafters and internal beams exposed to moisture flows. Decay, like the weathering, depends on its severity and two conditions were noted. One recelting in colour change the other very intensive resulting in strength loss.The lullar was seen in an area with inadequate sun exposure and ventilation such as internal beams.
These elements (about 85%) have been substituted by new ones (Fig. 5b). However, they were ignored in a few areas where the elements were inside of walls. It should be noted that the moisture-related problem still remains in the replaced parts (Fig 6) leading to new stains and fungal decays.

Internal holes due to insects were also found in some parts especially where the hardwood was used (Fig. 7). It is obvious that the insects are not living anymore in wooden members, however, their effects on mechanical properties is very considerable. Although the members affected by this fault were renewed they were not considered in some areas and were ignored diving restoration.

3.3 Wood Specie

The wood members used in buildings can be considered in two main groups: domestic wood and imported woods. Domestic wood contains hardwood provided from the northern forests of Iran. Imported woods are softwood which have been probably imported from Russia. Although their identification was possible in field at a macroscopic level, a more detailed macroscopic (especially soft wood) was also considered in the lab. The species were identified: *Pinus sylvestris* (scots pine),

Figure 5. (a) Intensive decay and (b) new substituted rafters.

Figure 6. Existing moisture-related problem in new member

Figure 7. Holes due to insects attack

3.4 Mechanical Properties

Table 1 shows the measeared mechanical properties of some old members. It can be seen that the old members (except the last one which was decayed overall) possessed acceptable mechanical strength. It shows that the members should be conservatively changed because despite their appearance they were still structurally sound.

Table 1. The mechanical properties of old wood members measured in laboratory

The area of sample	MOR (MPa)	MOE (MPa)	E in C_{ll} * (MPa)
Rafter (nearly sound)	79.12	10465.95	3116.48
Rafter (sound)	88.73	8901.518	3429.06
Coulmn (sound)	-	-	2436.92
Up of door (nearly sound)	79.77	9099.37	1007.74
Up of door (decayed oveall)	12.67	2124.28	2148.97

- Modulus of elasticity in compression parallel to grain

CONCLUSION

1. The House of Bagheri is a heritage construction building in Gorgan in which the timber members have some damages and building required to repair and restoration.
2. The main faults considered in the builidng are corrosion, fungal decay and insect attack.
3. Some adpoted repair methods should be changed.
4. Domestic and imported wood was used in construction of building.
5. The mechanical propeties of wood showed that the old members possessed still acceptable strength.

REFERENCES

Bodig, J. & Jane, B. 1993, *'Mechanics of wood and wood composites'*, Krieger Publishing Company,

Eimanian, J. 2001, *'Restoration suggestions on House of Bagheri'*, MSc, Thesis, Islamic Azad University.

Lourenco, P. B., E. Luso and M. G. Almeida. 2006. *Defects and moisture problems in buildings from historical city centres: a case study in Portugal.* Building and Environment 41 (2): 223-234.

Parsapajouh, 1988. *'Atlas of wood grown in North of Iran'* .Tehran University Publication.

Pasanen, A. L., J. P. Kasanena, S. Rautialaa, M. Ikaheimoa, J. Rantamakib, H. Kaariainenb and P. Kalliokoskia. 2000. *Fungal growth and survival in building materials under fluctuating moisture and temperature conditions.* International Biodeterioration & Biodegradation 46 (2000) 117 – 127.

Ronca, P., A. Gubana. 1998. *Mechanical characterisation of wooden structures by means of an in situ penetration test*. Construction and Building Materials, 12 (4): 233-243

Wilkinson, J. G., 1979, *'Industrial Timber Preservation'*, Associated Business Press.

11DBMC International Conference on Durability of Building Materials and Components
ISTANBUL, Turkey 11-14 May 2008

Issues in the Identification and Monitoring of Historical Structures – Monuments

Yasemin Didem Aktaş [1]
Ahmet Türer [2]

T 25

ABSTRACT

This paper aims to introduce a general methodology for the structural identification and monitoring of historical monuments. The identification and monitoring procedure was discussed within four main frameworks: (1) visual inspection, (2) finite element modeling, analysis, updating, validation and simulation, (3) short term measurements, and (4) long term monitoring. The defined approach targets to determine the current state (material data, structural behavior, and existence/extend of damage) of structure as well as monitor changes and extrapolate them over time or event basis (e.g. environmental deterioration and earthquakes). The mentioned steps were presented in the form of a detailed and hierarchical schema regarding both methodology and instrumentation. The methods proposed for the structural identification and material characterization of monuments were mainly non-destructive. In addition, the eminent monuments of the Mount Nemrud in Adıyaman, Turkey were chosen as a case study, briefly explaining the preparation studies carried out so far.

KEYWORDS

Structural monitoring, Historical structures, Non-destructive methods, Finite element modeling and analysis, Structural identification

[1] Middle East Technical University, Restoration Program, Ankara, Turkey 06531, Phone +90 312 2105424, Fax 312 2107991, yasemindidem@yahoo.com
[2] Middle East Technical University, Civil Engrg. Department, Ankara, Turkey 06531, Phone +90 312 2105419, Fax 312 2107991

1 INTRODUCTION

The identification, monitoring, and evaluation of historical structures / monuments have some additional difficulties in comparison with that of modern structures. These difficulties were mentioned before by many scholars [i.e. Lourenço 2002 and Binda & Anzani 1997]. The most important of them can be briefly listed as follows:

1. There are no standards applicable for monitoring and system identification (St-Id) of historical structures,
2. The physical, mechanical, chemical, and compositional characterization of materials are difficult, expensive and sometimes too destructive to be accepted in the case of historical structures,
3. Masonry walls are generally composite structures. While the material properties of each individual building material (e.g., brick, mortar, stone etc.) can be successfully obtained, it is still a problem to determine the overall effective material properties of composite masonry walls,
4. Masonry is a heterogeneous material both in terms of constitution (rubble stone masonry, multi-leaf walls, or those having inclusions and/or voids) and material properties (historical brick and mortars not produced according to some common standards and therefore having different characteristics throughout the structure). Therefore, it is difficult to obtain meaningful representative values by considering just a few reference locations; however, taking many samples from a historical structure is not preferred due to nondestructivity principle,
5. The damage to a historical structure by taking material samples may be minimized by taking micro samples; but, samples taken under these circumstances are not in standard test size and shapes,
6. Structure's inner and outer walls are normally covered with plaster and like, so it is not possible to see the masonry surface to evaluate the external texture parameters such as mortar joint thickness, distribution and size of building blocks, etc.,
7. Since the original material properties of a historical structure are not well known, it is usually not possible to evaluate the material damage caused by environmental conditions over time, except for the original material can be found from nearby quarries or other resources,
8. The experimental data to be used for calibration of analytical models are usually not available or not adequate,
9. History of structural modifications (e.g. removing load carrying walls, opening windows, adding floors etc.), functional modifications (house, library, museum), structural damages (e.g. seismic), repairs, or restoration works on the monument may not always be available.

Facing up to these matters necessitates unique approaches for each case to collect needed data, processing, evaluation, and management of them. For these purposes, the authors developed a hierarchical schema regarding both methodology and instrumentation, which is described in the following section.

2 A GENERAL METHODOLOGY FOR THE STRUCTURAL MONITORING

Structural monitoring is more than arbitrarily attaching a few sensors and collecting data for a selected period of time. The general approach to structural monitoring may be considered to be a three dimensional matrix where the width can be defined as (1) visual inspection, (2) finite element analysis, (3) short term measurements, and (4) long term monitoring. The depth can be defined as different parameters to be monitored/evaluated and methods used for this purpose. The height of the defined three dimensional methodology matrix is formed by the type, number, and location information; however, these parameters show great variation and are highly case dependent. Therefore, the methodology matrix developed in this study was limited to only two dimensions, which are the width and depth. It is important to note that this study was aimed to present a general framework for the structural monitoring and evaluation of the historical structures; however, each individual case may have specific requirements and conditions. Each individual item of the presented matrix is described under each heading below.

2.1 Visual Inspection

Visual inspection step is the most direct and economical step of the condition assessment and structural monitoring of historical structures. The qualitative evaluation of the state of conservation is mainly based on visual inspection which can detect:

- Structural anomalies (structural cracks, deformations, tilted columns and walls, sagged slabs etc.) which gives idea on load transfer mechanisms and possible foundation problems,
- Mechanisms of material deterioration, degradation, and decohesion (visible in the form of efflorescence, biodeterioration, color changes, non-structural cracks, flaking, detachments etc.), their potential causes (unhealthy drainage, large temperature changes, wetting-drying cycles, damping problems, freeze and thaw, previous restorative interventions performed with incompatible material such as concrete), level of deterioration (in a relative manner), and their distribution in the structure,
- Some basic features of structure in terms of construction materials, structural technology (different construction materials and techniques used, mural and structural typology etc.), possible plan or elevation irregularities in geometry,
- Perceptible structural changes and adaptations performed throughout the life of a structure (an added bell tower, a divided room etc.) and the traces of previous repairs and restorations.

Visual inspection method obviously cannot be performed to detect invisible features or to obtain quantitative data and yet it is a very basic part of structural investigation of a historical structure / monument. As a matter of fact, visual inspection methods are frequently referred during short and long term measurements for structural monitoring, as a strong complementary support.

Visual inspection can be additionally used for on-site environmental survey, to evaluate close range water sources, topographical features such as slopes, soil conditions (clay, sand, rock), potential construction material resources, similar structures in the vicinity (from structural, material, and exposed conditions' points of view). Thereby, a regional catalogue of mural morphology can also be developed using open cross sections.

2.2 Finite Element Analysis

Finite element analysis is defined to have five stages: modeling, analysis, updating, validation, and simulation. Modeling stage would include preliminary, original, and calibrated analytical models. The preliminary model approximately reflects the geometrical and material characteristics of the structure, and used to give an idea about the structural system and behavior. The original model uses basic dimensions taken during on-site measurements or from available plans. The calibrated model would form the last modeling step and mostly uses short-term test results; the static loading and dynamic measurement results (mode shapes, modal frequencies) are tried to be replicated by the analytical model and the structural parameters (such as effective elastic modulus, poisons ratio, density, support-boundary conditions) are iteratively modified until the simulated and measured responses are closely matching. The calibrated analytical model would closely reflect the actual structural behavior/response and be used for structural identification (St-Id). The calibrated models are especially important in the case of historical structures, since there are many uncertainties associated with the material, boundary, and geometrical features.

The field tests conducted for calibration of analytical models and related structural identification studies need to be in the linear range to prevent any damage to the structure. The constructed model is analyzed under certain loading cases defining the normal service conditions as well as those thought to be critical. Response of historical structures should often times be evaluated for extreme loading cases such as earthquakes, where demand on the structure is in the non-linear range and material and geometric nonlinearities should be considered. Therefore, the choice of the analysis type to perform is a function of the level of loading and forms another crucial point [Lourenço 2002].

The available modeling types, such as smeared (macro) modeling or micro modeling, would also play an important role for the simulation studies. The overall modeling of a structure would usually be not feasible using micro modeling, since large number of members and related degrees of freedom would require extensive amount of computer time. The global behavior of a structure in the linear range may be well simulated using elements that would reflect the average properties of composite structural members; on the other hand, non-linear range modeling and simulation using smeared (macro) modeling may only give a rough idea. Although exact nonlinear behavior of a historical structure can never be fully modeled, modeling carefully each detail of composite geometry and material characteristics of the whole structure (micro modeling on a global scale) would give the closest results to actual response.

2.3 Short Term Measurements

Short term measurements may include parameters related to structural morphology such as
- geometrical features (member size and dimensions, type and distribution of load carrying members, crack width, differential settlement, tilt, section loss, georadar, etc. measurements)
- technological characteristics of structural members defining the material type and distribution (material variation across the thickness of a masonry multi-leaf wall, physical, chemical, mechanical, and compositional characterization of building materials, connection of members, ultrasonic pulse velocity, elasticity etc. measurements)

Furthermore, dynamic and static test results constitute the products of form and structure of a system and would also be collected during short term measurements. The static tests generally include loading the structure with a known magnitude of force which would remain in the linear range of the system. Dynamic tests are conducted using either ambient vibration or forced vibration excitation. The structural parameters are obtained in the form of structural stiffness-flexibility and mode shapes, frequencies, damping ratios. All these parameters should be evaluated and used to update the original finite element model.

2.4 Long Term Monitoring

At the long term monitoring step, the parameters exhibiting change over time are investigated; these parameters would include environmental factors like temperature, humidity, wind and rain, and other factors related to structural changes over time such as crack width variation, dynamic characteristic changes etc. Long term measurements might as well include short term static and/or dynamic measurements which are repetitively conducted over time (mostly with equal time intervals such as once every three months). Long term static measurements mostly consider measurements of temperature, humidity, change in crack width, strain, tilt etc. and these are repeated with frequent intervals in a quasi-continuous manner (such as one measurement at every 30 minutes). On the other hand, the continuous measurement of dynamic characteristics of a structure generates large size data packets which are not possible to store as raw data. Therefore, all dynamic data are not recorded; instead, the data are processed online and only relevant dynamic characteristics (such as periods) are stored. In the case of repetitive loading – such as vehicles passing over a historical bridge – statistical methods are utilized to generate histograms.

As seen, the four steps mentioned above are interrelated. The correct management of the collected data requires a multi-level comprehension. In the given schema, the potential methods and instruments that

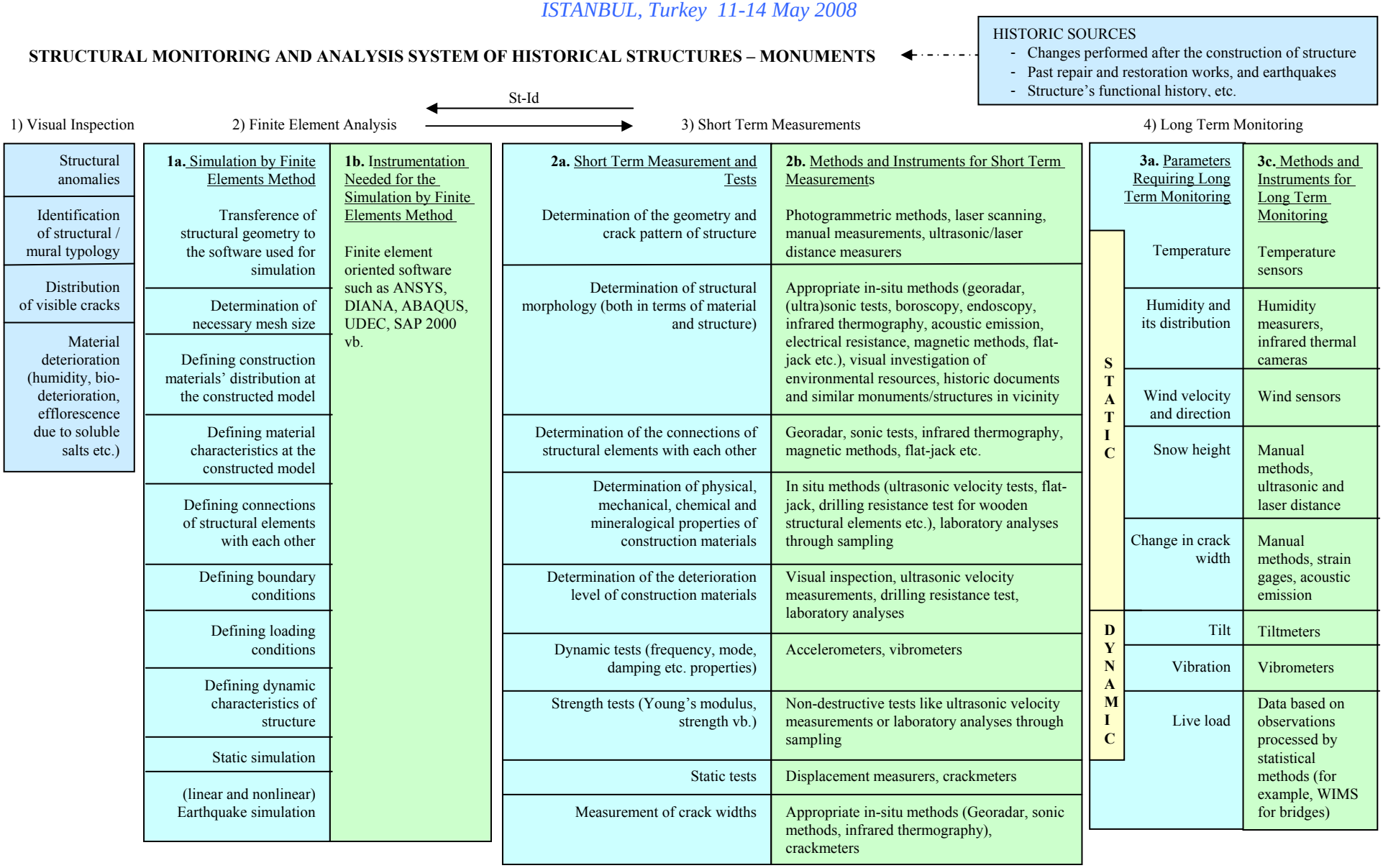

Figure 1: Schema for the structural monitoring of historical monuments

are related to measurements are also listed in the second column of Fig 1. The examples presented in Fig 1 are general; therefore, each unique application case should be evaluated individually for the method and instrument selection. The needed level of accuracy and information, available human resources, and budget also play an important role in the choice of instrument, which points out the significance of planning in such studies. In the case of historical structures, the selected methods are expected to be as non-destructive as possible. Since non-destructive methods give generally indirect results, one method should always be supported with one of its complementary methods (in the relevant literature, there are many studies on NDE and complementary techniques [i.e. Binda *et al.* 2004 and Binda *et al.* 2003]). It should also be noted that some indirect non-destructive investigation techniques on historical structures may be lacking calibration (e.g., ultrasonic pulse velocity, georadar) for different types of heterogeneous and aged materials used in historical structures. Similarly, standards may not be applicable for some specific NDT techniques (such as forced infrared thermography) applied on historical structures. The ongoing studies are promising for their reliability when each technique is used within its specific applicability limitations. Another problem of common NDE methods is that the raw data obtained are mostly difficult to evaluate, requires post-processing, and therefore depends on expertise causing possible increase of the evaluation costs.

In addition to all of these, historical sources may also be put to use if present. These historic sources can be inscriptions, visual and/or written archive documents, travel books, etc. The use of available documents can constitute a tool for anamnesis, informing us on the changes, adaptations, additions / cancellations performed on the structure, repair and restoration works carried out, the seismic and functional history of the structure.

3 NEMRUD MONUMENTS

Nemrud is an archaeological site in Adiyaman, in the eastern part of Turkey. The site, which was discovered in 1835, is famous with the big monumental statues (8 to 10 meters in height) more than two thousand years old, lined up in the form of two rows on two sides (east and west terraces) of a centered tumulus. The site belongs to an ancient kingdom called ‘Commagene’ and is located at the top of Mount Nemrut (2150 m). Each statue, except that of the king building the site, represents a Greek god / goddess corresponding at the same time to a Persian sacred figure, which is sitting on a throne. At the backsides of the thrones there are some inscriptions which render the site also valuable in terms of the presence of written documents [Cimok 1995].

The bodies of the statues are composed of big stone blocks. They are probably simply put on top of each other without any physical binder or mechanical connection like mortar or metal clamps. The heads are made of a single piece of stone. The statues are made of limestone which is a readily available material of the region. Moreover, the statues on the east and west terraces are almost identical. In spite of these similarities, those in the east terrace are in relatively good structural condition in comparison with those located on the west terrace. The west terrace statues were torn down towards west, while the statues on the east side have a better physical integrity and yet, all of the statue heads were detached from their bodies and fallen down. The site is located at a highly seismic zone; therefore, the detachments are thought to have happened during a previous strong earthquake or series of earthquakes. Furthermore, the difference between the two terraces in terms of physical integrity is thought to be caused by non homogeneous distribution and accumulation of snow load due to high winds. The accumulated snow might be pushing down the slope, slowly moving segments of stones over hundreds of years causing a progressive failure.

There are different material deterioration phenomena observed in Nemrud Monuments. Material is further abraded due to physical and mechanical inducements of environment such as wind, serious seasonal and daily temperature variations, precipitations, sun exposure etc. For all these reasons, an international Nemrud project was funded by the Turkish Ministry of Culture, World Monument Fund, and TUBITAK (104I011). The aim of the project is to execute a more structured and proper damage assessment and diagnosis of the monuments in a multi-disciplinary, integrated manner from structural

and materialistic assessment, conservation, site presentation, restoration points of view. The preliminary site and material investigations have begun in 2006 within the framework of current project and some in-situ studies, such as ultrasonic velocity measurements and stone deterioration maps were obtained. Two temperature and humidity sensors as well as a sensor to meaure the direction and velocity of wind were installed on site which would continuously collect data and can be remotely connected via GSM modem (Fig 2). Meanwhile, the preliminary FEM of a typical Nemrud monument was constructed and a modal analysis was carried out to have an idea about the range of natural frequencies and mode shapes. The initially obtained mode shapes indicate that the heads may have fallen because of an earthquake (Fig 3-4). Moreover, dynamic tests were conducted to obtain the natural vibration frequencies of the standing statues.

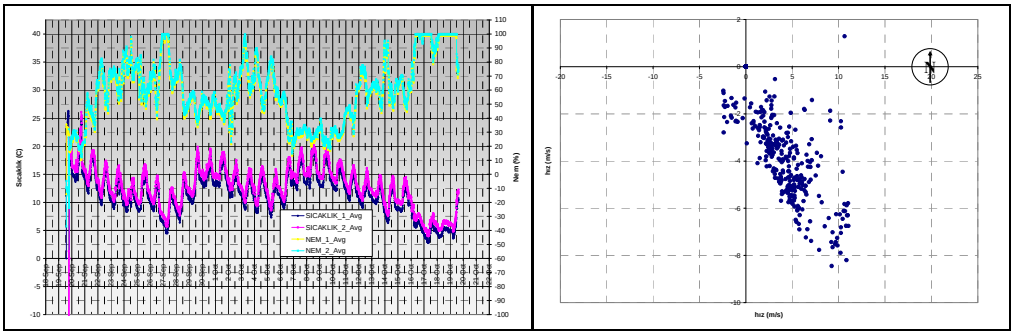

Figure 2. An example data reading obtained for temperature and humidity, and for wind velocity and direction, respectively.

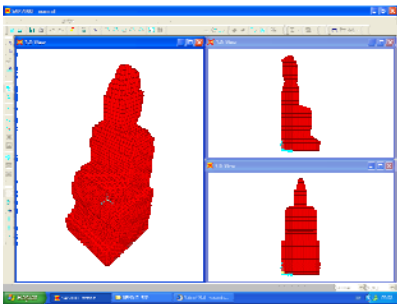

Figure 3. 3D FEM of a typical Nemrut monument

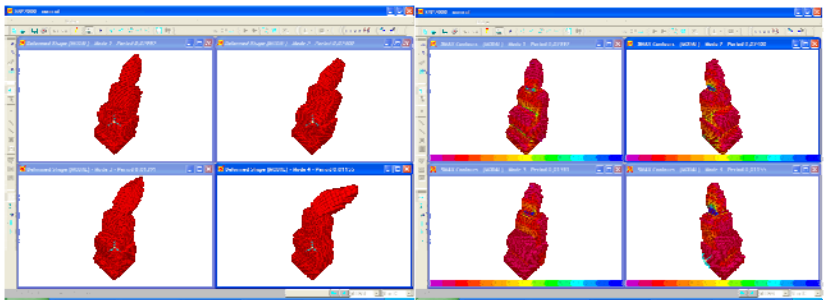

Figure 4. The obtained modal shapes and the corresponding maximum stress distributions

In 2007, the sensors to monitor the snow height will be installed. Moreover, the stone location map of collapsed statues will be obtained by photogrammetric methods. The structural investigations are planned to be continued with more detailed calibrated linear and non-linear FE models, synthetic and recorded earthquake simulations, and the formation of retrospective damage scenarios. The 3D-FE model will be updated using field measured dynamic data to conduct St-Id. The short term dynamic measurements and long term monitoring results will be combined to understand the behavior and

deterioration mechanisms. The calibrated analytical model will be used to simulate possible earthquake loading and pertinent damage scenarios. These investigations will be fed by the data regarding the materials, obtained by more in-situ measurements and laboratory analyses. Finding sensors functioning at extremely harsh environmental conditions is another challenging task in the Nemrud project. In addition, the site is at the top of a mountain, far from settling areas, which brings in additional difficulties e.g. easy access, accommodation, lack of electricity, and security concerns.

3 CONCLUSIONS

- This paper aims to introduce a four-step framework for structural monitoring of historical / archaeological structures regarding both methodology and instrumentation. According to this framework, a structural monitoring study can be handled as (1) visual inspection, (2) finite element modelling, analysis, updating, validation and simulation, (3) short term measurements, and (4) long term monitoring. These four steps form the general approach of identification and monitoring of historical structures – monuments,

- The structural monitoring of historical / archaeological structures entails some extra difficulties in comparison with that of modern structures. These difficulties should be tackled within the constraints recognized for cultural heritage investigations (e.g., non-destructivity),

- As the Nemrud example indicates, each case of historical / archaeological structure / monument / site exhibits particular problems that should be specially considered. The information and accuracy needed, available human resources and budget etc. are other factors playing role in the constitution of monitoring approach. Therefore, each case is unique within itself.

REFERENCES

Lourenço, P.B., 'Guidelines for the Analysis of Historical Masonry Structures', Finite Elements in Engineering and Science, Proc. 2nd International DIANA Conference, , A.A. Balkema, Rotterdam, The Netherlands, 2002, pp. 241-247.

Binda,L., Anzani, A. 1997, 'Structural Behavior and Durability of Stone Masonry' in *Saving Our Architectural Heritage: The Conservation of Historic Stone Structures*, eds N.S. Baer & R. Snethlage, John Wiley & Sons Ltd., pp. 113-149.

Lourenço, P.B. 2002, 'Computations on Historic Masonry Structures', *Progress in Structural Engineering and Materials*, 4, 301-319.

Binda, L., Cantini, L., Fernandes, F., Saisi, A., Tedeschi, C. & Zanzi, L. 2004, 'Diagnostic Investigation on the Historical Masonry Structures of a Castle by the Complementary Use of Non Destructive Techniques', Proc. 13th International Brick and Block Masonry Conference, Amsterdam.

Binda, L., Saisi, A. & Zanzi, L. 2003, 'Sonic Tomography and Flat-Jack Tests as Complementary Investigation Procedures for the Stone Pillars of the Temple of S.Nicolo' L'Arena (Italy)', *NDT&E International*, 36, pp. 215-227.

Cimok, F. 1995, *Commagene Nemrut*, Aturizm Publications, Istanbul.

The Durability of Materials and Treatments for The Operation on the External Curtains of The Historical Buildings

Rosa Caponetto [1]
Giuseppe Luciano [2]
Umberto Rodonò [3]
Salvatore Secondo [4]

T 25

ABSTRACT

The operation on the existing estate demands the employement of compatible solutions (from the material and technological, as well as environmental and typological point of view), which are suitable to satisfy new requirements (by reason of the evolution of the required performig levels, but also with regard to the possible changes of in-use destination and/or variation of intensity of the straining context) and mostly durable or rather capable to maintain over time the required performing levels.
The proposed research activity enters in this field and aims at identifying innovative materials and components to employ in the operations on existing building, evaluating their performances over time.
In the specific case, the carried out study aims at putting into practice an experimental evaluation of the durability of materials to employ in the operations on building curtains and, in particular, in the coverings (both traditional and innovative) to apply to the stone facade equipment (limestone) typical of "iblea" area.
The results of this kind of investigation may contribute to represent the basis for setting up an abacus containing all the operitive possibilities of operation on each noticed finishing category, as well as the procedures in order to proceed to a correct employement of the external finishing materials, plaster, stone parameters, and finally the superficial treatments to employ.

KEYWORDS

Historical estate, Building curtains, Cognitive investigation, Experimantal investigation, Operation criteria.

[1] University of Catania, Department of Engineering, Catania, Italia 95125, telephone +39 095 7382538, Fax +39095330309, rosa@dau.unict.it
[2] University of Catania, Department of Engineering, Catania, Italia 95125, telephone +39 095 7382538, Fax +39095330309, ing.giuseppeluciano@tele2.it
[3] University of Catania, Department of Engineering, Catania, Italia 95125, telephone +39 095 7382508, Fax +39095330309, urodono@dau.unict.it
[4] University of Catania, Department of Engineering, Catania, Italia 95125, telephone +39 095 7382508, Fax +39095330309, ssecondo@dau.unict.it

1 THE OPERATION ON EXISTING BUILDING

The operation on existing estate requires, as everybody knows, a marked sensitivity, a deep technical competence and a cosiderable respect for the history of the building. The line of material, technological and environmental compatibility is already consolidate, but often it must be faced the problem to intervene on the manufactures that, on account of the renewed in-use destination and mostly of the changed environmental conditions, are at present submitted to new straining conditions. It follows that it is necessary to know which choice allows, in the respect of the building and tradition, to obtain durable solutions over time. Moreover, it is necessary to explain the opportunity to re-propose traditional materials or rather to decide for innovative solutions (in part or on the whole), that are suitable to answer to the current performing requirements. What is just explained is referred to every kind of operation on the historical building estate and in a particular to the operations concerning the external covering of building; in fact, as the covering is in direct contact with the external environment particularly agressive, it requires continuous maintenances.
The work which is presented below is a part of a study that the research unit is carrying out in order to define preliminary methodologies and tools to the redaction of the Colour Plan of the town of Ragusa. Colour plan intended as a real operative plan of operation, which is not limited to face the problem of the hypothetical "colour" of the facades but rarher is aimed at going into the theme both in terms of modality of approach and of real operations.

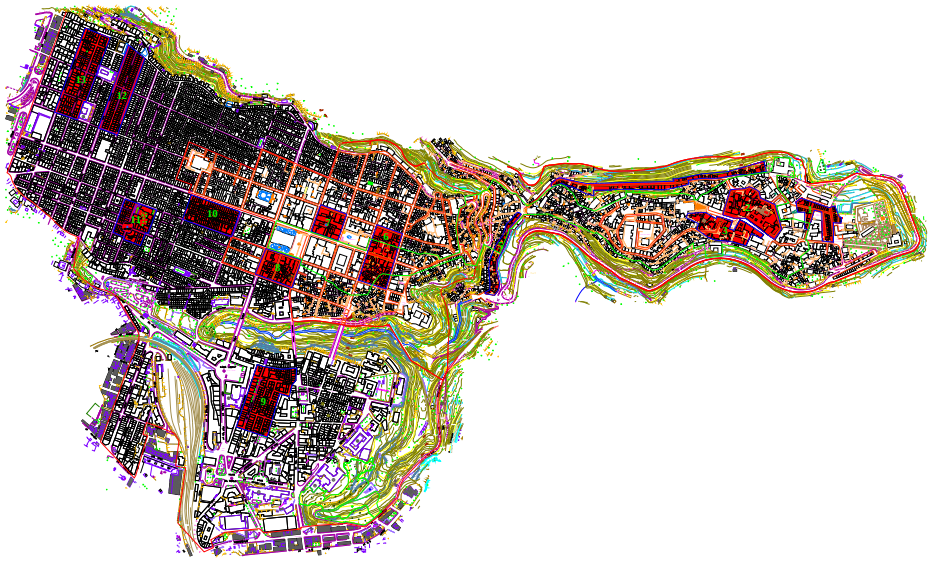

Figure 1. City plan of the historical centres of Ragusa

The town of Ragusa is developed in two historical units, the former more ancient, "Ragusa Ibla", closed between two deep valleys, and the latter more recent, "Ragusa Superiore". The first unit represents a medival area on which eighteenth-century reconstruction has been superimposed (post-earthquake of 1693). The result is both a curious and charming effect of internal contrast characterized by narrow and winding alleys, picturesque stairs and sumptuous facades of baroque churches and buildings. The second unit, "Ragusa Superiore", planned after the earthquake of 1693, follows a chequered scheme with long parallel roads characterized by majestic late baroque fronts of buildings and culminating in theatrical perspectives. Since 2002 Ragusa is part of Unesco humanity estate.

2 THE CARRIED OUT INVESTIGATION

In order to produce a preliminary study to the redaction of the colour plan, the research group has pursued the following stages:

1. bibliographical and archival investigation to identify typical building material and finishes of "iblea" area; the aim of this section is to gather all the information to know the modalities and techniques of execution of building finishes, with great attention to the gathering of news obtained directly by technicians and local workers.
2. cognitive investigation of the buildings that belong to a pilot area made up of 13 sections (figure1). Such a section has been carried out through filling in synoptic cards of survey (filled in situ) containing information about characteristics and conditions of: plasters, stone facade equipement, covering and metallic elements;
3. geometrical, material (instrumental) and chromatic[1] survey of the building curtains that belong to the pilot area;
4. experimental investigation for evaluating the duration of traditional and innovative treatments in order to protect stone surfaces. This last phase is coming up in this paper.

3 THE TYPICAL MATERALS OF IBLEA CURTAINS

Bibliographical and archival investigation, together with technicians information and local workers, as well as inspections carried out on pilot areas have made it possible to identify the materials that characterize the historical town centre of Ragusa. The main characteristics of plasters, stone facade elements and employed finish products are explained briefly as follows.

3.1 The Plasters

The carried out studies made it clear that the plasters of the town of Ragusa were usually manufactured by lime mortar and lime sand (sometimes pounded terra-cotta). Generally, they were spread on two layers: the first, nearly 3 cm, of rough inert materials, and the second of di 5-10 mm, of thinner granulometry. The proportions between inert material and limestone were of 1:2. To protect the plaster was generally added a further finish (cf. 3.3).

3.2 The Stone Facade Equipment

The employed stones to decorate building facades of Ragusa were essentially white limestone (hard, for the elements of skirting board, basement, external paving, corners, steps; or soft, for stone frames, capitals and every kind of decoration, cf. figure 2A) and the asphaltic grey-black rock, that is a swinestone, the material of which iblea plateau is rich.[2] The swinestone presents two varieties distinguished in the level of bitumen impregnation, so in consistency, so in workability, so in employement:

- **pietra pece (pitchstone)**, at high bitumen impregnation, darker, softer, (employed for decorative elements, figure 2B.) but also more wear-proof (this characteristic has made it suitable for the flagstones of balconies and for pavement;
- **pietra zoccolo**, harder, because of at low bitumen impregnation. It was employed for the basement, steps and brackets of balconies (figure 2C).
-

Figure 2. A: white limestone; B: pietra pece; C: pietra zoccolo.

As the asphaltic stone tend to whiten over time, because of the atmospheric agents, it was (if left at the sight) covered by linseed oil and carbon black.

3.3 The Finishes

Plasters as well as stone decorations were generally protected by:

- light coverings with linseed oil and coloured earths (sometimes when added albumin), figure 3A;
- whitewashings with fast coloured lime water (when added oxides) or light coloured (when added natural earths), figure 3B;
- "lime paint", always made up of lime dissolved in water and combined with colouring earths, but of a consistency more mellow than the whitewashing, figure 3C.[3]

Figure 3. A: Samples of light coverings with linseed oil and natural earths.; B: Plastering with lime water and natural earths.; C: "Lime paint" on plaster (lime milk and oxides).

4. THE EXPERIMENTATION

The aims that are being persued in laboratory exposing the samples to artificial ageing cycles are those to identify and study phisical and performing decays primed by strainings artificially produced by the cycle and to compare these decays with those examined on samples exposed to a natural ageing. Regulation (ISO 15686, UNI11156, etc.) has developed some protocols for the evaluation of the durability of the building components, but some points of the procedure are still to define in a sole way. More precisely, the formulation of the standard of the accelerated ageing cycle is not well defined yet. This has great importance in the experimentation. It must be suitable to reproduce strainings artificially that are referable, in type, intensity and duration to the strainings to which the technical solution, which is the object of the investigation, is exposed during the course of its life.
In relation to what is explained above and to the experiences that have been carried out on further building components by the research unit until now, (Caponetto R., 2006) it has been considered right

to set up the experimental investigation in such a way as to perfect the sizing of the accelerated ageing cycle compared to what have been done by our team until today.

4.1 Object of The Experimentation

The experiment which is presented below has carried out the evaluation of the durability of covering systems of the stone facades equipment of Ragusa. More precisely, tests of durability on two kinds of more recurrent stone material (limestone and swinestone) have been carried out in laboratory and outdoors examing different kinds of coverings (traditionals and not). The set up of the accelerated ageing cycle is shown in paragraph 4.1.2. The results of this test will be, as it is provided for by regulation, compared with those resulting from the natural ageing, so as to evaluate the trend of the performances in time and thus to determine the service life of the investigated component under certain straining conditions.

4.1.1 Definition of The Solution and Samples

The choice has been that of testing, for the two stone materials, the following solutions of superficial covering:

Table 1. Testing solutions

PITCHSTONE		*WHITESTONE*	
A1	Covering with linseed oil	**B1**	Covering with linseed oil
A2	Covering with linseed oil and carbon black	**B2**	Covering with lime milk with natural pigments
A3	Covering with linseed oil plus carbon black with compound a basis of siloxanes	**B3**	Covering with lime milk and acrylic resin (Acrylic 33) with natural pigments
A4	Covering with compound a basis of siloxanes in organic solvent	**B4**	Covering with compound a basis of siloxanes in organic solvent

For each solution 6 cylinder-shaped samples three of which of diameter and height 5 cm and three of diameter 8 cm and height 3 cm have been realized.

4.1.2 Definition of Accelerated Ageing Cycle

The accelerated ageing procedure to set in climatic room checks a cycle characterized by a structure that re-proposes the natural sequence of the four climatic seasons: Winter, Spring, Summer and Autumn. The cycle is made up of four under-cycles which are divided into four phases, each of them representing a climatic condition simulating by the engine: Cold climate (Phase I), Rain (Phase II), Wet warm climate (Phase III), Dry warm climate by sun radiation (Phase IV).

Table 2. Structure of the cycle

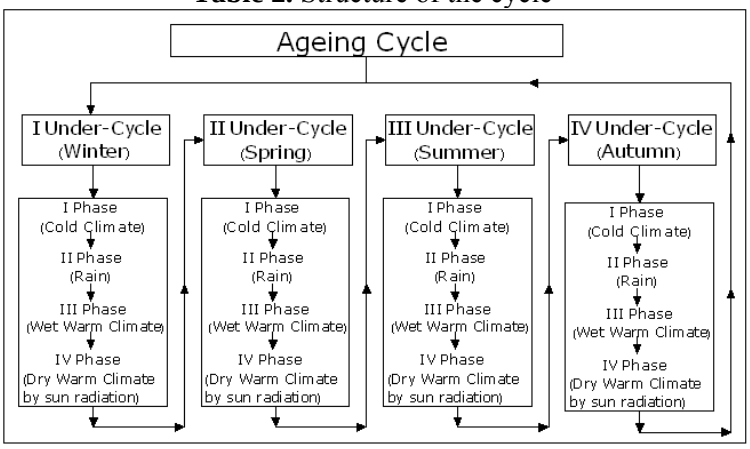

In order to determine the values of the climatic parameters of the single phases of each under-cycle, data characterizing the climate of the town of Ragusa[4] have been employed, making reference to a

period of time which goes from 1968 to 1994. Thanks to simple mathematical formulas[5], the values of the climatic parameters for each season have been characterized (Table 3).

Table 3. Values of climatic parameters characterizing each season

Season	*Temperature min (°C)*		*Temperature max (°C)*		*Relative humidity*	*Mean Precipitation*	*Dealy mean sun radiation*
	Mean	*Peack*	*Mean*	*Peak*	*(%)*	*mm*	*hours*
Winter	+01.47	-03.16	+09.25	+11.31	78.3	77.97	10.46
Spring	+07.28	+02.66	+29.43	+36.41	45.8	27.48	13.54
Summer	+13.07	+08.31	+34.25	+39.51	58.2	18.13	13.55
Autumn	+06.32	+01.79	+13.77	+18.60	88.1	79.22	10.39

The characteristic values of each individual phase, for each under-cycle, to assign to the climatic cell have been determined according to the standards described by the following Table 4:

Table 4. Standards of Choice of the Intensity of the Degrading Agents

PHASE	*PARAMETER*	*SEASON (UNDERCYCLE)*			
		WINTER (I°)	*SPRING (II°)*	*SUMMER (III°)*	*AUTUMN (IV°)*
I	T	Minimum of peak	Mean	Mean	Minimum of peak
COLD	R.U.	no	no	no	no
CLIMATE	SUN RAD.	no	no	no	no
	RAIN	no	no	no	no
II	T	no	no	no	no
RAIN	R.U.	no	no	no	no
	SUN RAD.	no	no	no	no
	RAIN	Firing[6]	Firing	Firing	Firing
III	T	Mean	Maximum of peak	Maximum of peak	Mean
WET	R.U.	Mean	Mean	Maximum of peak	Mean
WARM	SUN RAD.	no	no	no	no
CLIMATE	RAIN	no	no	no	no
IV	T	Mean	Maximum of peak	Maximum of peak	Mean
DRY	U.R.	no	no	no	no
WARM	SUN RAD.	Firing	Firing	Firing	Firing
CLIMATE	RAIN	no	no	no	no

For what concerns the definition of the time of actions of such agents, the first step has been to impose that the cycle lasts 40 hours[7]. Time T of each idividual under-cycle is determined by simple proportion starting from no. of days characterizing each individual climatic season (respectively 90, 92, 94, 89, Table 5).

Table 5. Time T of Each Under-Cycle

Under-cycle - Season	*Proportion*	*Time T*
I Winter	40:365 = T:90	T = 9h and 50min
II Spring	40:365 = T:92	T = 10h and 04min
III Summer	40:365 = T:94	T = 10h and 18min
IV Autumn	40:365 = T:89	T = 9h and 48min
Total		T = 40 hours

Obtained time T of each individual under-cycle, times of each single phase, of each under-cycle, are determined assigning some weights P (Table 6):

Table 6. Weights of Each Phase for Each Under-Cycle

Under-cycle - Season	*Time T*	*PHASE I*	*PHASE II*	*PHASE III*	*PHASE IV*
I Winter	9h and 50min	P_{11} x T	P_{12} x T	P_{13} x T	P_{14} x T
II Spring	10h and 04min	P_{21} x T	P_{22} x T	P_{23} x T	P_{24} x T
III Summer	10h and 18min	P_{31} x T	P_{32} x T	P_{33} x T	P_{34} x T
IV Autumn	9h and 48min	P_{41} x T	P_{42} x T	P_{43} x T	P_{44} x T

The weights P of phases I, III e IV depend on daily hours of seasonal exposure to the sun while the weights of phases II on the mm seasonal rain (Table 3) and they are obtained by the following formulas:

- Data P_{x1}, P_{x3}, P_{x4} (where x represents the season or the under-cycle), the sum of the three weights must be equal to 1(phase 2 of rain do not have sun radiation), that is: $P_{x1} + P_{x3} + P_{x4} = 1$
  The propotion that must be considered to obtain the weight of the phases of wet warm climate and dry warm climate is the following:

  $(P_{x3} + P_{x4})$: (hours of mean exposure to the sun of x) = 1 : 24 h

  $P_{x3} = P_{x4}$

  For the cold phase:

  $P_{x1} = 1 - (P_{x3} + P_{x4})$

  Datum P_{x2}, the sum of the weights of phases II must be equal to a 1, that is:

  $P_{12} + P_{22} + P_{32} + P_{42} = 1$

- The propotion that must be considered for each weight is the following:

  $P_{x2} : 1 =$ (mm of rain of x) : (annual mm of rain)

In the light of what is said above the result is the following:

Table 7. Weights

Undercycle - Season	*Time T*	*PHASE I*	*PHASE II*	*PHASE III*	*PHASE IV*
I Winter	9h and 50min	0,58 x T	0,38 x T	0,21 x T	0,21 x T
II Spring	10h and 04min	0,42 x T	0,13 x T	0,29 x T	0,29 x T
III Summer	10h and 18min	0,42 x T	0,09 x T	0,29 x T	0,29 x T
IV Autumn	9h and 48min	0,58 x T	0,40 x T	0,21 x T	0,21 x T

In conclusion, times of each under-cycle and those of each individual phase are expressed in the following table[8]:

Table 8. Times

Under-cycle - Season	*PHASE I*	*PHASE II*	*PHASE III*	*PHASE IV*	*TOTAL time*[9]
I Winter	5h and 42min	1h and 52 min	2h and 03 min	2h and 03 min	11h and 40 min
II Spring	4h and 13min	0h and 39 min	2h and 55 min	2h and 55 min	10h and 42 min
III Summer	4h and 20min	0h and 28 min	3h and 00 min	3h and 00 min	10h and 48 min
IV Autumn	5h and 41min	1h and 58 min	2h and 03 min	2h and 03 min	11h and 45 min

The trend of the cycle is represented by Figure 4.

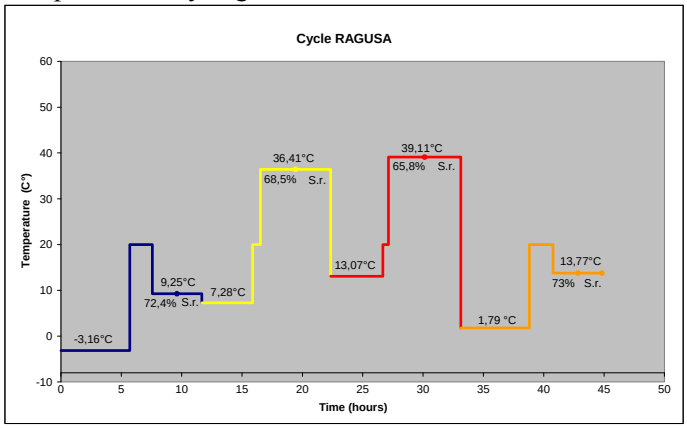

Figure 4. Characterization of Ageing Cycle

4.1.3 Definition of The Characterizing Test Program

Tests of characterization to evaluate the decay of the performing characteristics of material over time are carried out on the bases of the definition of ageing cycle as well as of the recurrence, formality and execution time provided for by regulation. Such tests are performed at zero time and at the end of each accelerated ageing cycle.
The performing characteristics noticed during the tests are:
- Weight P (kg);
- Capillary absorption coefficient A (kg/(m$^2 \cdot$ h0,5));
- Water vapor permeability ω (kg/(m$^2 \cdot$ Pa));

By means of photographic relief also the chromatic alterations of the surface of the samples are noticed.

What is explained above represents the structure of the investigation that has been carried out. It has been useful to present it because it is a step forward in the improvement of the accelerated ageing. The results of the tests that requires two more months will be exposed during the congress.

REFERENCES

Bell, D. 1973, The Coming of Post-Industrial Society, Basic Books, New York.

Caponetto, R. 2006, *La valutazione del decadimento prestazionale di componenti edilizi tipici del contesto mediterraneo*, Editecnica, Palermo.

ISO 15686-1, 1999, *Building and constructed assets. Service Life planning. General Principles*.

ISO 15686-2, 1999, *Building and constructed assets. Service Life planning. Service life prediction principles*.

UNI 11156-1, 2006, *Valutazione della durabilità dei componenti edilizi – Terminologia e definizione dei parametri di valutazione*.

UNI 11156-3, 2006, *Valutazione della durabilità dei componenti edilizi – Metodo per la valutazione della durata*.

[1] The material and chromatic survey of the facades has been carried out by the group Boero Bortolomeo S.p.a. of Genova.
[2] Sedimentary cenozoic limestone rock, constituted of alternate calcarenites and calcirudites, impregnated of bitumen. Bitumen impregnation goes from 4% to 10%. Is not submitted to the crumbling phenomenon. Scanty external chromatic gelation. Excellent internal chromatis gelation. Good external physical durability. Excellent internal physical durability. The presence of bitumen make it suitable in wet climate.
[3] The difference between "whitewashing" and "lime paint" is suggested by the will of reproposing the local lexicon. Actually, the kinds of finish could be gather together in two cathegories: light coverings and whitewashing (the latter more or less thick).
[4] Data extracted from SIAS regional centre.
[5] The values of the climatic parameters of each season have been obtained considering the values characterizing each individual month belonging to that season, as regards to the number of the total days of the same season.. Es. In order to obtain the value of the minimun peack of temperature of the winter season (I Under-cycle) it has been solved in the following ratio:

$$\frac{\left[(10(\text{g. December})\times(-2.5)+31(\text{g.January})\times(-3.5)+28(\text{g.February})\times(-3.4)+21(\text{g.March})\times(-2.5))\right]}{90(\text{g.winter season})}=-3.16°\text{C}$$

[6] As for the parametrs Rain and Sun Radiation is concerned, which characterizes Phases II and IV of each under-cycle, it is not possibile to determine the intensity as it happen for the temperature and humidity parameters as the climatic cell does not have the possibility to modify in an automatic way the Capacity of rain and the Thermic Power.
[7] In 40 hours times of transition are excepted (that is technical times of the engine to pass from defined climatic conditions to other) and times of phase II (Rain).
[8] It could be noticed that times of actions of rain obtained through the proportion in relation to the mm of seasonal rain have been all halved because they have been considered excessive for the samples.
[9] Transition times excepted.

11DBMC International Conference on Durability of Building Materials and Components
ISTANBUL, Turkey 11-14 May 2008

Durability Properties of Innovative Plasters for Renovation of Historical Buildings

Radka Pernicová [1]
Milena Pavlíková [2]
Robert Černý [3]

T 25

ABSTRACT

The current practice of the solution of the problem of historical buildings surface layers damage is based more or less on the method of analogy. At a reconstruction, usually such material and method of its application is used which is according to the meaning of supervisory authorities compatible with the original treatments and which already was found to be suitable at an application on some other building before. The durability of new surface layers is mostly estimated on the basis of experience because too few parameters are known for a reliable durability estimate. The choice of a material for reconstruction is then often less suitable regarding to the moisture and salt content in the masonry which leads to low durability and short service life of surface layers. In this paper, main durability properties of innovative lime plasters with metakaolin admixture, namely water sorptivity, moisture diffusivity, water vapor diffusion coefficient, thermal conductivity and specific heat capacity are determined, together with the main mechanical parameters such as compressive and bending strengths. Comparative measurements with common lime plaster are done as well. On the basis of the experiments performed, it can be concluded that the analyzed lime-metakaolin plasters are suitable for an application in reconstruction of historical buildings. While their mechanical properties are significantly better compared to the reference lime plaster, their thermal and hygric properties are mostly similar or slightly improved.

KEYWORDS

Plasters, Historical buildings, Renovation

[1] Czech Technical University in Prague, Faculty of Civil Engineering, Department of Materials Engineering and Chemistry, Thákurova 7, 166 29 Prague 6, Czech Republic, Phone +420224354688, Fax: +420224354446, radka.pernicova@fsv.cvut.cz

[2] Czech Technical University in Prague, Faculty of Civil Engineering, Department of Materials Engineering and Chemistry, Thákurova 7, 166 29 Prague 6, Czech Republic, Phone +420224354688, Fax: +420224354446, milena.pavlikova@fsv.cvut.cz

[3] Czech Technical University in Prague, Faculty of Civil Engineering, Department of Materials Engineering and Chemistry, Thákurova 7, 166 29 Prague 6, Czech Republic, Phone +420224354429, Fax: +420224354446, cernyr@fsv.cvut.cz

1 INTRODUCTION

In many historical buildings parts of the original mortars, which have been deteriotated by natural weathering, need replacement. From the point of view of a historian, it is not acceptable to use lime-cement plasters in Romanesque, Gothic, Renaissance and Baroque buildings. The demands of conservators who take care of historical monuments are, that the materials for repair or innovation of plasters must have the most similar composition as the historical materials and they have to be applicable by the original methods [Hošek & Losos 2007]. This concerns especially the number and the structure of coated layers, the way of plaster surface treatment by striking, indentation or making it smooth. In most cases, inventions had employed cement and polymer based materials, which resulted in advancing the destruction, since harmful by-products have induced severe damage to the background stone blocks or bricks [Maravelaki-Kalaitzaki *et al.* 2005]. In addition, the polymer-based materials are incompatible to the existing materials of the original masonries, thus exhibiting different behaviour in the environmental conditions.

Plaster can play its function, ie architecturally and as a protection against negative environmental conditions, only if it creates a compact cover with surface treatment. Contemporary plasters meet these requirements due to their proper raw materials, technological processing, suitable storing and final application. Historical facade restoration brings not just new plaster creation but also protection of existing one. It is difficult and mainly unsuitable to produce plasters with the same composition and behaviour as historical plasters. The current solution of the problem of surface layers damage of historical building is based more or less on the improvement of technology and properties of each input raw material with preservation of visual and physico-chemical compatibility to original plaster.

As the chemical analyses of many plasters from historical buildings show, the past centuries external plasters that are preserved until today contain products formed by lime reaction with pozzolanic or hydraulic admixtures. Pozzolanic admixtures appeared to have positive effect on properties of lime binder in the past [Rojas and Cabrera, 2002]. According to the composition of the applied pozzolana, compounds similar to Portland cement products were formed but even compounds of zeolite character were found, such as phillipsite $3CaO.3Al_2O_3.10SiO_2.12H_2O$ and analcime $Na_2O.Al_2O_3.4SiO_2.2H_2O$, in connection with microcrystalline calcite. These compounds are the cause of the plaster resistance against environmental conditions and in this way of the durability of these plasters [Cabrera & Rojas 2001].

The lime plasters are known to have high values of liquid water transport parameters. This is not a very convenient feature from the point of view of their exposure to the external environment as any intensive rain can lead to water penetration deep into the material. Therefore, an application of hydrophobization admixtures seems to be a logical solution for achievement of the increase of service life of lime-based plasters. In this paper, we used zinc stearate as the hydrophobization admixture for lime-pozzolana plaster and investigated its effect on mechanical and hygric properties.

The main reason was construction materials deterioration are salt crystalization, water and salt solutions movement through the walls by capillarity and harsh environmental conditions. Therefore, in this paper, we are focused on the basic material characteristics and water vapour and liquid water transport parameters of basic lime plaster in the comparison with innovative plasters.

2 EXPERIMENTAL

Several different types of innovative lime plasters for renovation of historical buildings were tested to compare their durability properties to pure lime plaster (denoted as VO) with the same composition. Metakaolin as a pozzolanic admixture was used in the case of mixture denoted as VOM as binder increment, in the case of other two mixtures, denoted as VOM II and VOM H as replacement of lime. To improve high values of liquid water transport parameters we used zinc stearate as the

hydrophobization admixture for the lime-pozzolana plaster VOM H. The water/binder ratio was modified according to mixture workability. The composition of mixtures for sample preparation is presented in Table 1.

Table 1. Composition of tested plaster mixtures.

Type of mixture	*Amount* [kg]				
	Lime	*Sand 0/2mm*	*Metakaolin*	*Hydrophobization admixture*	*Water*
VO	4.80	14.40	-	-	4.80
VOM	4.80	14.40	0.80	-	5.50
VOM II	4.00	14.40	0.80	-	4.80
VOM H	4.00	14.40	0.80	0.02	4.20

2.1 Materials

Plaster mixtures were prepared using laboratory mixing machine with forced rotation for 3 minutes and then compacted using vibrating machine. Each mixture was cast into a standard prism form, after two days all prisms were taken out of forms and then cured for 28 days in high relative humidity environment.

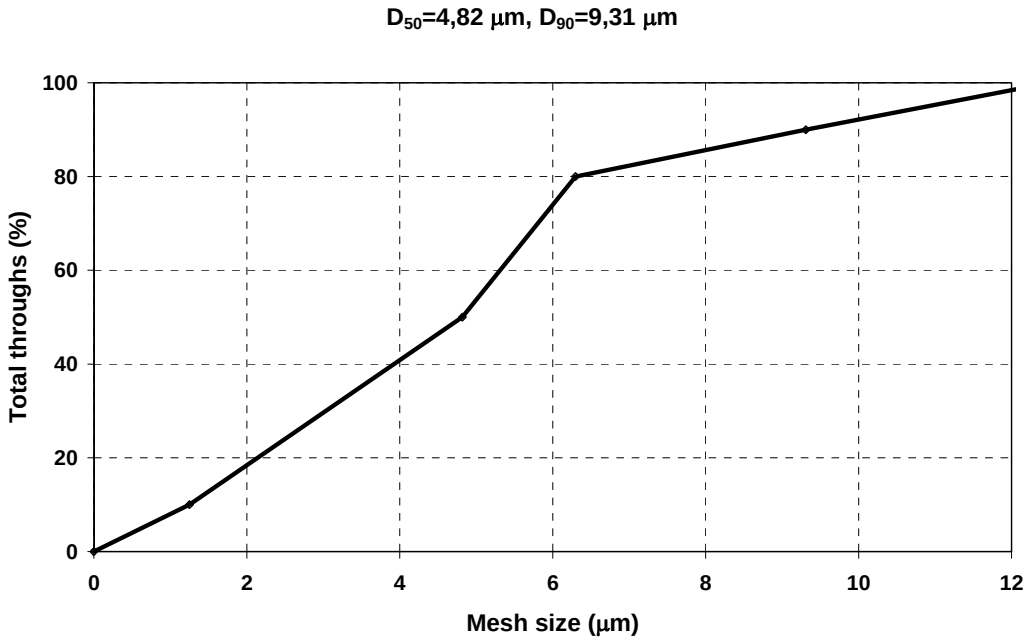

Figure 1. Granularity of used metakaolin.

The lime CL 90 was produced by limekiln Morká, Czech Republic. Metakaolin MEFISTO K05 was a product of České lupkové závody Inc., Nové Strašecí. It is a highly active pozzolanic material on metakaolinite basis. MEFISTO is supposed to be used first of all as an alternative silicate binder. It can replace 5-15% of cement by weight at concrete production where it can be used instead of microsilica. It can also be utilized in the production of geopolymers. The reason for using MEFISTO in the mentioned applications is the supposed increase of compressive and flexural strength and frost resistance, decrease of water absorption and reduction of the occurrence of efflorescence. Dominant compounds of metakaolin MEFISTO represent SiO_2 (55%) and Al_2O_3 (41%). Fe_2O_3, TiO_2, CaO,

MgO, and Na_2O are present in minor amounts. Average particle size of metakaolin is in the interval of 3 to 5 μm, see Fig. 1.

Hydrophobization admixtures have to reduce pore walls wettability and replace capillary suction by capillary depression. Addition of hydrophobization admixture to lime plaster leads to lower sorptivity and better resistance to water and aggressive solution penetration. Fatty acid salts are often used as a hydrophobizator, namely calcium or zinc stearate. One end of the carbon chain is hydrophilous and it is connected to mineral structure while the other end which is formed of hydrophobic group is oriented outside the structure and can repulse water.

Sand 0/2 mm fraction was delivered by Heidelberg Cement Group, Brněnské písky Inc., affiliate Bratčice, normalized according to EN 196-1. The grain-size distribution curve of applied sand is shown in Fig. 2.

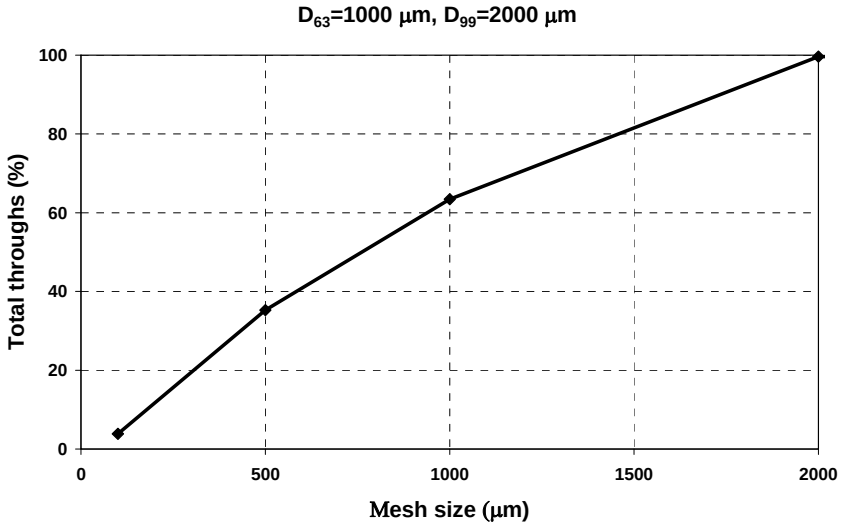

Figure 2. Granularity of used sand.

2.2 Experimental Methods

At first, basic material properties of all tested lime plasters were determined. As fundamental physical material characteristics, bulk density ρ_b [kg m^{-3}], matrix density ρ_m [kg m^{-3}], and open porosity ψ [%] were determined. Bulk density was measured using gravimetric methods. Matrix density was obtained using Pycnomatic ATC, automatic helium pycnometer with fully integrated temperature control with precision of ± 0.01 °C and real multi volume density analyzer. The samples for the basic material parameters determination were cut from cubic prisms with the size of 40 x 40 x 40 mm and their dimensions were 40 x 40 x 20 mm.

Investigation of mechanical parameters was carried out according to the norm [ČSN EN 196-1, 2005]. The compressive and flexural strengths were determined as the most important mechanical parameters for lime-based plasters. For each measurement standard prisms 40 x 40 x 160 mm were tested with DSM 2500 hydraulic testing device, Inova Praha. The flexural strength was measured using standard three-point bending test. The compressive strength was determined using the same test device on the remainder of the specimens after bending test. The measurements were done after 7, 14, 28, 90 and 180 days of hardening period.

The thermal conductivity as the main parameter of heat transport and the specific heat capacity as the main parameter of heat storage were determined using the commercial device ISOMET 104 (Applied Precision, Ltd.). ISOMET 104 is a multifunctional instrument for measuring thermal conductivity, thermal diffusivity, and volumetric heat capacity. It is equipped with various types of optional probes, needle probes are for porous, fibrous or soft materials, and surface probes are suitable for hard

materials. The measurement is based on the analysis of the temperature response of the analyzed material to heat flow impulses. The heat flow is induced by electrical heating using a resistor heater having a direct thermal contact with the surface of the sample.

The cup method was used for determination of water vapour transmission properties. The measurement performed in this work was based on the standard [ČSN 72 7031]. The measurement is carried out in steady state under isothermal conditions. It is based on one-dimensional water vapour diffusion and measuring the water vapour flux through the specimen and partial water vapour pressure in the air under and above specific specimen surface. Water vapour transmission properties of a material are obtained by placing a specimen of the material on the top of a cup and sealing it. Two versions of the common cup method were employed in the measurements of the water vapour diffusion coefficient. In the first one, the sealed cup containing burnt $CaCl_2$ (0% relative humidity) was placed in a controlled climatic chamber at 25±0.5°C and 45% relative humidity and it was weighed periodically. In the second one, the cup containing saturated K_2SO_4 solution (97% relative humidity) was placed at 25±0.5°C and 45% relative humidity environment. Firstly, samples sizes of 95 mm in diameter x 20 mm were cut from the standard prism 100 x 100 x 100 mm and water vapour-proof insulated with epoxy resin. Then, the sealed cups with samples were weighed periodically. The steady state values of mass gain or mass loss were utilized for the determination of the water vapour transfer properties. In the practical calculations of water vapour transport parameters in porous buildings materials, the diffusion coefficient of water vapour D [m^2s^{-1}] and water vapour diffusion resistance factor μ [-] were determined.

The simplest way, how to describe liquid water transport through a porous material is realization of a one-dimensional free imbibition experiment [Roels *et al.* 2004]. Specimens sizes of 40 x 40 x 20 mm were cut from the original prisms and then water and vapour-proof insulated with epoxy resin on four lateral sides, and after that dried in an oven. The face side of each sample was immersed 1-2 mm into water on top of a saturated sponge. The sample mass was measured continuously. The water absorption coefficient, A [$kgm^{-2}s^{-1/2}$], was calculated from the linear part of the dependence of the increase of tested sample's mass on the square root of time. Then, the apparent moisture diffusivity κ [m^2s^{-1}] was calculated using the vacuum saturation moisture content w_{sat} [kg m^{-3}] and water absorption coefficient [Kumaran 1994].

3 RESULTS AND DISCUSSION

Basic properties of all materials are summarized in Table 2. Each result represents the average of five measured values. The open porosity was found not to be distinctly affected by the metakaolin and zinc stearate addition. The observed differences were between 3-5 % in the case of lime-metakaolin plasters, and 8% in the case of hydrophobized plaster which is clearly due to the lower water/binder ratio. So, the addition of fine grained metakaolin MEFISTO did not change the basic material properties as bulk density, matrix density and total open porosity in a significant way. The observed differences were within the range of the accuracy of applied measuring methods. All studied materials have proven high porosity, which is a very positive factor from the point of view for application on historical buildings. The high porosity of plaster guarantees fast water vapour transport, and so its fast removal from the load bearing structures of reconstructed historical buildings.

Table 2. Basic properties of studied mixtures.

Type of mixture	ρ_b [kg m^{-3}]	ρ_{mat}	Ψ [%]
VO	1 650	2 575	36.0
VOM	1 670	2 570	35.0
VOM II	1 695	2 580	34.0
VOM H	1 745	2 625	33.0

The survey of mechanical properties of studied plasters is presented in Figs. 3 and 4. Each result represents the average value of six or three values in the case of compressive and flexural strength measurement, respectively.

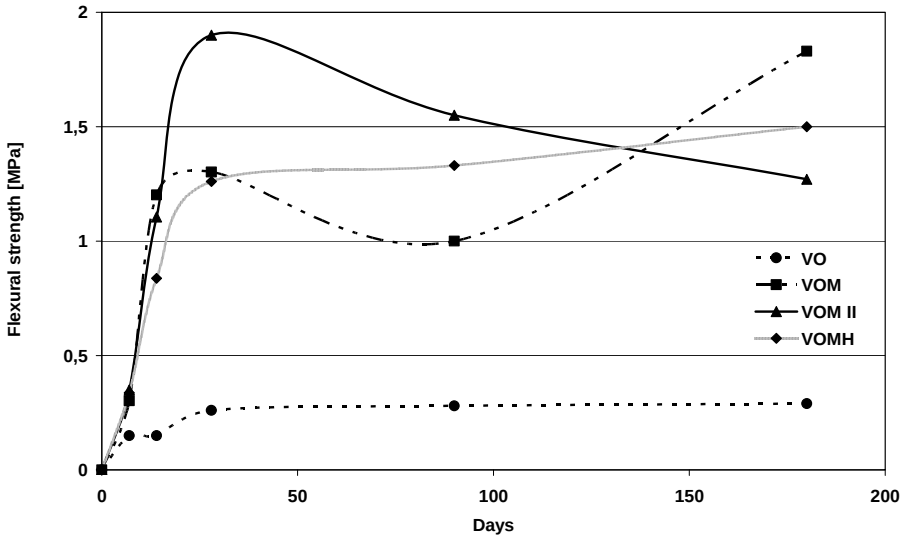

Figure 3. Flexural Strength of Tested Plasters.

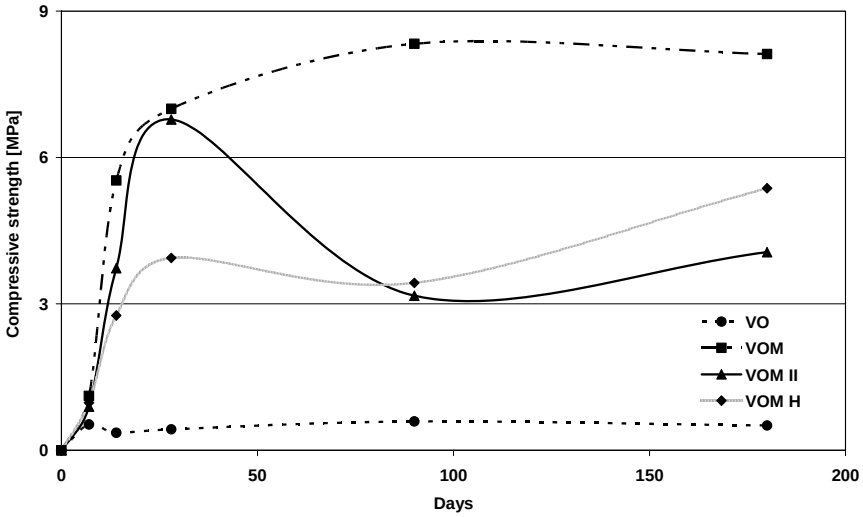

Figure 4. Compressive strength of tested plasters.

The flexural strength of pure lime plaster reached its maximum after 28 days and then it had almost the same value even after 180 days hardening period. Its compressive strength, on the other hand, had somewhat fluctuating character. Lime plasters with metakaolin addition have proved two times higher both flexural and compression strength than pure lime plaster already after 7 days of hardening. In the case of incremetal metakaolin addition (VOM mixture) the flexural strength exhibited certain decrease after 28 days of hardening but after 180 days it was the highest among all tested plasters, six times higher than for the pure lime plaster. The compressive strength of the same mixture increased more continuously. Its maximum was achieved after 90 days of hardening, where it was eight times higher than after 7 days and even fourteen times higher than the compressive strength of pure lime plaster at the same time. In the case of metakaolin replacement mixture (VOM II) the flexural strength increased until 28 days of hardening then it slowly decreased. The maximum was nearly five times higher in the comparison with flexural strength of pure lime plaster. The VOM II mixture reached fourteen times higher value of compressive strength than pure lime plaster after 28 days but then a substantial decrease was observed. The hydrophobization admixture addition caused reduction of both flexural

and compressive strengths at the same time in comparison with other lime plasters with metakaolin addition, but both compressive and flexural strength development had ascending trend.

Thermal properties of the studied plasters are presented in Table 3. The lime-pozzolana plasters exhibited slightly higher thermal conductivity than the reference lime plaster. This is in accordance with their higher bulk density and lower porosity (Table 2). The values of specific heat capacity were very similar for all the studied mixtures, the differences being within the error range of the applied method.

Table 3. Thermal properties of studied mixtures.

Type of mixture	λ [W/mK]	c [J/kgK]
VO	0.67	580
VOM	0.71	590
VOM II	0.88	620
VOM H	0.85	610

The results of water vapour and liquid water transport parameters determination are presented in Table 4, each result represents the average value from five measurements.

Table 4. Water vapour and liquid water transport parameters.

Type of mixture	D [m^2s^{-1}]		μ [-]		A	w_{sat}	κ
	97-45% RH	0-45% RH	97-45% RH	0-45% RH	[kg $m^{-2}s^{-1/2}$]	[kgm^{-3}]	[m^2s^{-1}]
VO	2.90E-6	4.50E-6	9.0	5.0	2.20E-1	359.0	4.40E-7
VOM	2.50E-6	5.10E-6	10.0	4.5	2.70E-1	350.0	5.70E-7
VOM II	1.80E-6	5.70E-6	13.0	4.0	2.20E-1	343.0	4.30E-7
VOM H	1.60E-6	4.40E-6	15.0	5.0	6.50E-2	332.0	3.90E-8

The water vapour transport parameters were not very different for all studied plasters. Lime-metakaolin plasters had higher water vapor diffusion resistance factor than the reference lime plaster but the differences were not very significant. From the quantitative point of view, the obtained values of water vapour diffusion parameters of innovative plasters are very promising for application in restoration of historical buildings and renewal of the old materials. The values of liquid water transport parameters were in case of lime-metakaolin plasters without hydrophobization similar or slightly higher than for pure lime plaster. This may be considered as a negative finding in general because the rain water could be transported either the same fast or even faster into the load bearing structure. However, from the quantitative point of view the differences were not very high so that this is only a minor flaw on otherwise significantly improved material. In the case of zinc stearate addition the liquid water transport parameters decresed in a significant way, the moisture diffusivity by about one order of magnitude, which is a very positive feature.

4 CONCLUSIONS

Main durability properties of innovative lime plasters with metakaolin admixture were determined in the paper and compared with the reference lime plaster. The modified plasters showed significant improvement of mechanical properties. Another good point with the studied lime-metakaolin plasters was that the hygric and thermal properties were basically unaffected by the metakaolin addition. The

material retained the good water vapour transmission properties which are characteristic for the lime plasters and exhibited also acceptable thermal properties. The application of hydrophobization admixtures in lime-pozzolana plasters was proved successful. It resulted in an order of magnitude decrease of moisture diffusivity which means a significant reduction of liquid water transport in the plaster.

ACKNOWLEDGMENTS

This research has been supported by the Czech Science Foundation, under project No. 103/06/0031.

REFERENCES

Cabrera, J. & Rojas, M. F., 2001, 'Mechanism of hydration of the metakalolin-lime water system', *Cement and Concrete Research*, **31**, 177-182.

ČSN EN 196-1, 2005. Metody zkoušení cementu. Stanovení pevnosti.

ČSN 72 7031. Měření součinitele difúze vodní páry stavebních materiálů metodou bez teplotního spádu.

Hošek, J. & Losos, L. 2007, *Historické omítky*, Grada Publishing, Praha.

Kumaran M.K., 1994, 'Report on Measurements to Determine Moisture Diffusivity of Eastern White Pine', *IEA Annex XXIV Report T3-CA-92/04*.

Maravelaki-Kalaitzaki, P., Bakolas, A., Karatasios, I. & Kilikoglou, V. 2005, 'Hydraulic lime mortars for the restoration of historic masonry in Crete', *Cement and Concrete Research*, 35**,** 1577-1586.

Roels S., Carmeliet J., Hens H., Adan O., Brocken H., Černý R., Pavlík Z., Hall C., Kumaran K., Pel L., Plagge R., 2004, 'Interlaboratory Comparison of Hygric Properties of Porous Building Materials', *Journal of Thermal Envelope and Building Science*, **27**, 307-325.

Decision Making about Cleaning Interventions on Marble Surfaces Using a Fuzzy Logic Approach

Antonia Moropoulou [1]
Ekaterini T. Delegou [2]
Myrto Konstandinidou [3]
Chris Kiranoudis [4]

T 25

ABSTRACT

In this work, a fuzzy classification system is presented for the assessment of cleaning interventions on sulphated marble surfaces. The acquired data by Scanning Electron Microscopy with energy dispersion by X-ray analysis (SEM-EDS), Digital Processing of SEM Images, Laser Profilometry (LP) and Colorimetry, determine the (a) chemical and mineralogical composition of marble surfaces, (b) texture roughness and fracturing of the surface and (c) color parameters. These results comprise the input variables which under the process of decomposing produce the necessary fuzzy sets. In parallel, the fuzzification process includes the formation of fuzzy sets for the output variable, which in this case is cleaning performance index (CPI) for sulphated marble surfaces. The knowledge base of the fuzzy system is completed when a set of fuzzy if-then-else rules is used to process the inputs and produce a fuzzy output. Finally, an effective knowledge based expert system is produced in order to make decisions concerning cleaning interventions performance on sulphated marble surfaces. The designed fuzzy logic system is demonstrated in practice on marble surfaces of a historic building in Athens, Greece.

KEYWORDS

Fuzzy logic, Cleaning, Marble, Decision making

[1] National Technical University of Athens, School of Chemical Engrg, Lab. of Materials Science and Engineering, 157 80 Zografou, Athens, Greece, tel:+302107723276, fax:+302107723215, amoropul@central.ntua.gr
[2] National Technical University of Athens, School of Chemical Engrg, Lab. of Materials Science and Engineering, 157 80 Zografou, Athens Greece. tel:+302107721432, fax:+302107723215, edelegou@central.ntua.gr
[3] National Technical University of Athens, School of Chemical Engrg, Computational Fluid Mechanics Lab. 157 80 Zografou, Athens Greece. tel:+302107721503 fax:+302107723228 myrto@ipta.demokritos.gr
[4] National Technical University of Athens, School of Chemical Engrg, Computational Fluid Mechanics Lab. 157 80 Zografou, Athens Greece. tel:+302107721503 fax:+302107723228, kyr@chemeng.ntua.gr

1 INTRODUCTION

Sulphated marble surfaces are commonly found on historic buildings located in polluted urban atmospheres. Sulphur dioxide (SO_2) attacks calcite ($CaCO_3$) of marble and after reaction produces gypsum ($CaSO_4 \cdot 2H_2O$). Gypsum along with black particles, soot, iron oxides and alumino-silicates forms black-grey crusts at rain sheltered areas, [Moropoulou *et al.* 1998]. Black crusts greatly affect not only, the physico-chemical condition of the historical monuments, but also their aesthetic view. Discontinuities detected in the crusts functions as areas, where the deteriorative factors are concentrated. The presence of deteriorated areas on marble surfaces not only alters the visual appearance of the stonework due to the discoloration development, but also leads to further decay. Gypsum layers and black-grey crusts absorb a great amount of humidity resulting in the development of a lamellar texture and subsequently to the abruption of the crust and loss of the stone material, [Maravelaki – Kalaitzaki *et al.* 1999]. Furthermore, apart from discoloration, the accumulation of black depositions in black-grey crusts acts as catalyst for the sulphation processes, accelerating further decay. Therefore, the employment of cleaning becomes essential not only for the conservation of the deteriorated areas, but also for preventing further erosion phenomena. Moreover, apart from physicochemical reasons, esthetical ones are important as well for the employment of cleaning, in order to reveal and preserve monuments' artistic value. The most objective parameters for the assessment of cleaning interventions are those concerning physicochemical characteristics of materials, surface morphology, as well as aesthetic characteristics like color, [Biscontin *et al.* 1995]. Threshold values of these parameters have not been established yet and therefore their combinations for decision making on the evaluation of a cleaning method is a complex procedure. Thus, the need of using a modeling tool that can resemble the way experts make decisions based on their knowledge and experience is great.
In this work, a knowledge based expert system that can assess cleaning interventions, applied on sulphated marble surfaces (black-grey crusts) is developed. This system uses as a modeling tool Fuzzy Logic which can resemble the way humans think; make inferences and decisions, [Vakalis *et al.* 2004]. Fuzzy logic theory has emerged over the last years as a useful tool for modeling processes which are too complex for conventional quantitative techniques, or when the available information from the process is qualitative, inexact or uncertain. Fuzzy inference systems have been successfully applied in fields such as automatic control, data classification, decision analysis, expert systems, and computer vision. The most popular fuzzy model suggested in the literature, is the Mamdani's method, proposed in 1975 by Ebrahim Mamdani [Mamdani & Assilian [1975] as an attempt to control a steam engine and boiler combination by synthesizing a set of linguistic control rules obtained from experienced human operators. In this work, the Mamdani type of fuzzy model, was developed under Visual Studio using the C++ programming, in order to design a decision – making system on marble cleaning.

2 RESULTS & DISCUSSION

2.1 Experimental Procedures and Techniques Used for Cleaning Assessment

The evaluation of cleaning interventions is fundamental during pilot cleaning applications or final cleaning treatment works, for the determination of the cleaning efficacy of each applied method (for particular material and particular decay pattern). Cleaning interventions assessment is focused on the modifications that cleaned surfaces are sustained concerning chemical and mineralogical composition, texture roughness, fracturing and color. In this work, Scanning Electron Microscopy with energy dispersion by X-ray analysis (SEM-EDS) is used for the chemical and mineralogical composition of the cleaned surfaces, Laser Profilometry (LP) is used for the texture roughness assessment, Digital Image Processing (DIP) of SEM images is utilized for the measurement of surface fracturing and colorimetry evaluates color modifications of the cleaned surfaces. More information on the techniques used for the presented case study and the selection of fuzzy system input parameters are given bellow:
(SEM-EDS) is applied on collected monument samples, (a) before cleaning, for the identification of mineralogical and chemical composition of the substrate, the presented patinas and decay patterns

(which in this case were gypsum layer and black depositions) their stratifcation and thickness; whereas (b) after cleaning, study of the surface morphology regarding patina, the remaining decay products, their stratifcation and thickness, the possible by-products/side effects of the cleaning method, are recorded. The core samples analyses in the presented case study, that is stone specimens cut in cross-section, were carried out using JEOL JSM-5600, OXFORD LINKTM ISISTM 300 with Energy Dispersive X-ray Microanalysis system, Accelerating Voltage 20 KV, Beam current: 0.5nA, Livetime: 50 sec, Beam diameter <2μm. All the collected images were back-scattered electron-micrograph images.

DIP of SEM images using the EDGE program which was developed by the US Geological Survey [Mossotti & Eldeeb 2000], [Mossotti *et. al.* 2002]. EDGE program was developed for the analysis of back-scattered electron-micrograph images stored in a binary file format that represents images with lateral resolution of 1.7μm/pixel. However, the images presented in this work had a lateral resolution of 2μm/pixel [Moropoulou *et al.* 2007]. EDGE measurements have to be made by computer analysis of 100x SEM images of core cross sections, consisting of 512 rows with 512 pixels per row, where each pixel is encoded with 8 bits on a 256-shade gray-scale palette. The fractal dimension of the exposed surfaces of stone specimens cut in cross-section are measured. More information on EDGE program can be found in [Mossotti & Eldeeb 2000], [Mossotti *et. al.* 2002] and [Moropoulou *et al.* 2007]. Three indexes of the marble micro-structure can be assessed, based on the fractal dimension determination and the special image calibration procedure. One of these marble micro-structural indexes is the near-surface fracture density (FD) of the stone which is a measure of the fraction of the stone volume filled by fractures, crevices, and pore space. The FD results are reported as the percentage of pixels identified as components of the fractures calculated until 100μm under the surface area. FD value was used as evaluation index of the marble fracturing after cleaning which can be ascribed as cleaning side-effect as well as susceptibility deegre of marble surface to further decay.

(LP), is one of the most recently developed non destructive testing approaches for the description of surface topography, surface roughness and surface area measurements. Surface texture includes roughness and waviness, while many surfaces may have lay, that is, directional striations across the surface. Roughness generally results from a particular production process or material condition [Avdelidis *et al.* 2004], [Stout & Blunt [1995]. The roughness parameter Rq is defined as the mean root square of the values of all points of a given surface profile and is commonly used in the fields of tribology and materials engineering, [BS EN ISO 4288:1998].

$$Rq = \sqrt{\frac{1}{l}\int_0^l z^2(x)dx}$$

In the presented case study, 3-D micro-topography plots of the monument collected core samples were attained using the Proscan 2000 with a laser triangulation sensor of 1μm resolution. The software within the instrument calculates, amongst others, the Rq parameter on a specific length scale via a two-dimensional line profile. This is important since Rq is a length scale dependant property, and therefore in order to compare Rq values they have to be evaluated over the same measurement length. According to BS EN ISO 4288:1988, the Rq values were calculated in an evaluation length of 1.25mm, with a step size of 1μm and a cut-off filter of 0.25mm. The application of cut-off filter is obligatory in order to dispatch the unnecessary frequencies (waviness information) and keep only the roughness data which include the finest (shortest wavelength) irregularities of a surface [BS EN ISO 4288:1988]. Following the above mentioned specifications, 50 line profiles across the X-axis and 50 line profiles across the Y-axis were acquired with the intention of determining the average of Rq for X-axis (Rqx) and the average of Rq for Y-axis (Rqy) for each tested stone sample. The higher mean value between Rqx and Rqy is the representative one for each sample [BS EN ISO 4288:1988]. In parallel, the ratio of actual to projected surface area was measured at each micro-topography. This ratio is a geometrical descriptor of a surface and has a very close relation with some functional properties of surfaces like wear, [Stout *et al.* 1993]. The values of these characteristics (Rq and ratio) function as assessment indexes of the surface morphology regarding to the susceptibility of the surface to further decay, that is slow reactivation of sulphation process and slow adsorption of black particles.

Colorimetry The Dr Lange color-pen LMG159/160 colorimeter, was applied in situ on the investigated marble surfaces, for measuring the L*, a*, b*, according to CIELab Uniform Colour Space. Using this non destructive testing and evaluation technique, an average of twenty five values of L*, a*, b* components was calculated per cleaning area. Hereafter, the total colour difference ΔE, the luminosity difference ΔL*, the red-green difference Δa*, and the yellow-blue difference Δb*, were calculated, taking as reference the primary values, that is before cleaning. Total colour difference ΔE, was estimated according the ASTM D2244-93, by the following formula:

$$\Delta E = \sqrt{\Delta L^2 + \Delta a^2 + \Delta b^2}$$

Therefore, colorimetry was used to assess the aesthetical modifications that the architectural surfaces undergone due to cleaning interventions, reflecting as well the degree of black depositions removal.

2.2 Short overview of Fuzzy Modeling

Fuzzy logic starts with the concept of a fuzzy set. A fuzzy set is a set without a crisp, clearly defined boundary. The fundamental difference of fuzzy logic compared to conventional modeling techniques is on the definition of sets. Traditional set theory is based on bivalent logic where an object is either a member of a set or it is not. Contrary to that, fuzzy logic allows a number or object to be a member of more that one sets and most importantly it introduces the notion of partial membership, [Klir & Yuan 1995]. Information flow through a fuzzy model requires that the input variables go through three major transformations before exiting the system as output information, which are known as fuzzification, fuzzy inference, and defuzzification. The three steps are depicted in Fig.1, which shows the structure of a fuzzy logic system and are explained in brief:
Fuzzification: It is the process of decomposing a system input variables into one or more fuzzy sets, thus producing a number of fuzzy perceptions of the input.

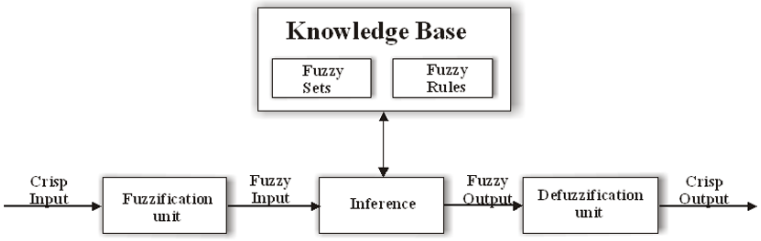

Figure 1. The structure of a typical fuzzy logic system

Fuzzy Inference: After the inputs have been decomposed into fuzzy sets, a set of fuzzy if-then-else rules is used to process the inputs and produce a fuzzy output. Each rule consists of a condition and an action where the condition is interpreted from the input fuzzy set and the output is determined from the output fuzzy set. In other words fuzzy inference is a method that interprets the values in the input vector and, based on some set of rules, assigns values to the output vector.
Defuzzification: It is the process of weighting and averaging the outputs from all the individual fuzzy rules into one single output decision or signal. The output signal eventually exiting the system is a precise, defuzzified, crisp value.
Fuzzy modeling methodologies are procedures for developing the knowledge base of the system, i.e. the set of fuzzy rules. The natural way to develop such a system is to use human experts who build the system based on their intuition, knowledge and experience. In this case the fuzzy sets and the membership functions are defined by the experts, usually based on a trial and error approach. The rule structure is then determined based on how the designers interpret the characteristics of the variables of the system.
The most popular fuzzy model suggested in the literature, also used in this work, is the one proposed by Mamdani [Mamdani 1974] that has the following formulation with respect to its fuzzy rules:

$$\forall r \in R:\ if \ \underset{1\le i\le n}{\wedge}(x_i \in A_i^r) \ \ then \ \underset{1\le j\le m}{\wedge}(y_j \in B_j^r)$$

Where; n: number of input variables,
m: number of output variables,
$x_i, 1 \le i \le n$: input variables,
$A_i^r, 1 \le i \le n$: fuzzy sets defined on the respective universes of discourse,
$y_j, 1 \le j \le m$: output variables and $B_j^r, 1 \le j \le m$ are fuzzy sets defined for the output variables.

2.3 Development of a Fuzzy Classifier for the Estimation of the Cleaning Performance Index of Cleaning Interventions on Sulphated Marble Surfaces

The fuzzy logic modeling architecture that was used to build a model for the estimation of the performance index of cleaning interventions was based on important influencing factors. In order to develop the database and the rule base of the system, human experts were employed. The experts used (a) their knowledge and experience on matters of decay of materials, as well as marble cleaning and (b) a database of measurements concerning physicochemical and aesthetical characteristics of marbles before and after cleaning. The Mamdani type of fuzzy model was selected and the development of the system was completed in three steps.

Step 1 – Selection of Input Parameters & Output Parameter: According to the cleaning assessment methods analytically described in 2.1 paragraph, the characteristics that are measured for the assessment of cleaning interventions constitute the input parameters of our fuzzy system. These characteristics concern the (a) chemical and mineralogical composition of marble surfaces, (b) texture roughness and fracturing of the surface and (c) color parameters. Therefore, the chosen input variables are:

(a) Patina preservation index (%), (SEM-EDS results)
(b) Thickness of gypsum layer (μm), (SEM-EDS results),
(c) Fracture density, (%), (DIP of SEM images results),
(d) Actual/Projected area ratio, (LP results),
(e) Roughness (μm), (measured parameter: Rq; LP results)
(f) Total color difference, ΔE, (Colorimetry results).

The output variable is the Cleaning Performance Index of cleaning interventions (CPI).

Step 2 – Development of the Fuzzy Sets: In this step, fuzzy sets were defined for all the input and output parameters. More specifically, three fuzzy sets were defined for all the input variables except for the patina preservation index for which two fuzzy sets were appointed, and the fracture density where four fuzzy sets were defined. The output variable was classified by four fuzzy sets as well. A more detailed description of the fuzzy sets appointed to each input or the output variable follows next:

Patina preservation: Two fuzzy sets, were defined on the input space, named as "Non preservation of patina" and "preservation of patina". Values belonging to the "preservation of patina" are the accepted ones, as cleaning methods which cause patina removal are totally unaccepted even by Venice Charter since 1964. Therefore, the patina preservation is a prerequisite for an effective and successful cleaning intervention.

Thickness of gypsum layer: Three fuzzy sets, namely "Low", "Medium" and "High" were proposed on the input space which measures the thickness of gypsum layer (Fig. 2). Acceptable values are those belonging to the "Medium" fuzzy set, since in this case the resulting surface holds the microcrystalline gypsum layer, which is acceptable and desirable [Moropoulou *et al.* 2007]. Microcrystalline gypsum is

the first and compact part of marble sulphation process, [Elfving *et al.* 1994] and the desirable remaining part of the black-grey crust during cleaning, since it preserves the details of carved and plane surfaces, [Skoulikidis & Charalambous 1981], [Moropoulou *et al.* 2007]. Values belonging to the "Low" set show that cleaning intervention probably has caused loss of authentic material (that is calcite and/or microcrystalline gypsum); while values of the "High" set show that cleaning intervention was ineffective, that is didn't manage to remove the crust.

Fracture Density: Four fuzzy sets, "Low", "Medium", "High" and "Extra High" were defined on the input space. In this case the acceptable values belong to the "Low" fuzzy set. Values belonging to the rest sets show that cleaning intervention has caused micro-cracking and fracturing on the marble surface, that is the resulting surface will display higher susceptibility to further decay.

Ratio of Actual to Projected Area: Three fuzzy sets were defined in this case, namely "Low", "Medium" and "High". Accepted values are considered those of the "Low" fuzzy set, that is slow reactivation of sulphation process and slow adsorption of black particles. Higher values are unaccepted, because higher ratio values indicate higher susceptibility to further decay.

Roughness: Again three fuzzy sets were defined, "Low", "Medium" and "High". Accepted values are those belonging to the "Low" fuzzy set, that is slow reactivation of sulphation process and slow adsorption of black particles. Higher values are unacceptable, because higher roughness values indicate higher susceptibility to further decay.

Total color difference (ΔE): Three fuzzy sets were defined, as "Low", "Medium" and "High". Accepted values are those belonging to the "Medium" fuzzy set. Values belonging to the "High" set show that cleaning intervention caused high difference in the aesthetics of the surface after cleaning, whereas values of the "Low" set show that cleaning intervention was ineffective, that is remaining of black depositions.

Cleaning Performance Index (CPI): The only output variable is CPI of an intervention and its range of values extends from 0 to 10. For this variable, four triangular fuzzy sets were defined as, "Not acceptable cleaning", "Medium cleaning", "Acceptable cleaning" and "Recommended cleaning-Optimum", (Fig. 3).

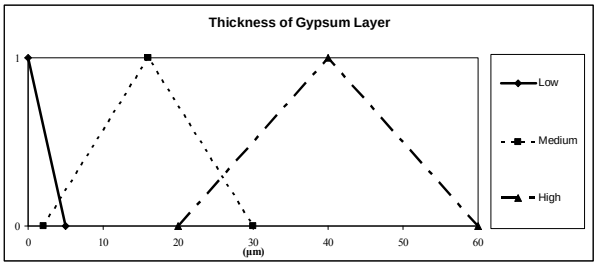

Figure 2. Fuzzy Sets of the "Thickness of Gypsum Layer" input parameter

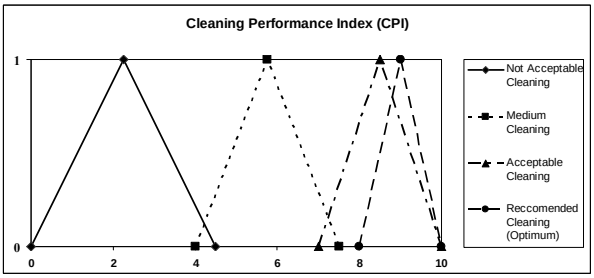

Figure 3. Fuzzy Sets of the "Cleaning Performance Index" output parameter

Step 3 – Development of the rule base: During this step, the experts were employed to develop a number of fuzzy rules, based on their intuition and experience on decay as well as on cleaning matters. The fuzzy rules were developed, so that they could relate successfully all the input conditions. At the same time these rules resulted in specific and repeatable (same inputs gives same output) results. The experts developed 648 rules, one for each combination of fuzzy rules of the input parameters. All the rules use the logical *AND* operation. An example of a fuzzy rule is shown below:

*"**IF** the patina is preserved, **AND** the thickness of gypsum layer is Medium, **AND** the fracture density is Low, **AND** the actual/projected area ratio is Low, **AND** the roughness is Low, **AND** the total color difference is Medium, **THEN** CPI is High (that is recommended cleaning-Optimum)"*

Fuzzy Model Operations: The above three-step procedure defines the knowledge base of the fuzzy system. When the fuzzy model is to be applied to a set of input parameter values, the information flows through the fuzzification – inference - defuzzification processes which are depicted in Fig. 1, in order to generate the fuzzy estimation of the degree of a cleaning intervention. For this particular fuzzy system, the three above processes are executed as follows: *Fuzzification:* During the fuzzification process, the triangular membership functions (fuzzy sets) defined on each input variables are applied to their actual values, to determine the degree of truth for the application of each rule. *Inference*: During the inference process, the real value (degree of truth) for the application and activation of each rule is computed, and applied to the conclusion part ("then" part) of the rule. This procedure results in the assignment of one output fuzzy set for each rule. The "min-max" inferencing technique has been used [Zadeh, 1973], where the output membership function of each rule is clipped off at a height corresponding to the rule activation (degree of truth). If a part of the rule is not activated (zero degree of truth) then the rule is not activated either, as the inference technique considers the minimum degrees of activation for each rule. The combined fuzzy output membership function is constructed by combining the results of all the fuzzy rules. If an output fuzzy set is activated by more than one rule, the maximum of all activations is considered in the construction of the combined output membership function. *Defuzzification*: The final output of the fuzzy system for the degree of suitability should be a crisp number, so the fuzzy output needs to be defuzzified. The centroid defuzzification method [Driakov *et al.* 1993] was used, where the crisp value of the output variable is computed by finding analytically and not numerically the (meta)center of area that is covered by the combined membership function.

2.4 The case study of National Library of Greece Historic Building – Results of test runs

The investigation area (a black-grey crust area) was an architectural surface of the historic building of the National Library of Greece (NLG), consisted of Pentelic marble (Fig. 5a-5b), [Moropoulou *et al.* 2000]. The building was constructed at the beginning of 20th century and is situated in the center of Athens. Fig. 6 presents the investigation area after cleaning, while Table 1 lists the applied cleaning methods of the pilot interventions on the investigated surface. The application of Colorimetry occurred before and after the pilot cleaning interventions in field, while core samples were collected before and after the pilot cleaning interventions for the LP and SEM-EDS examination in lab. DIP of the SEM images using EDGE programme occurred in lab, (see 2.1 paragraph for further details on all used techniques).

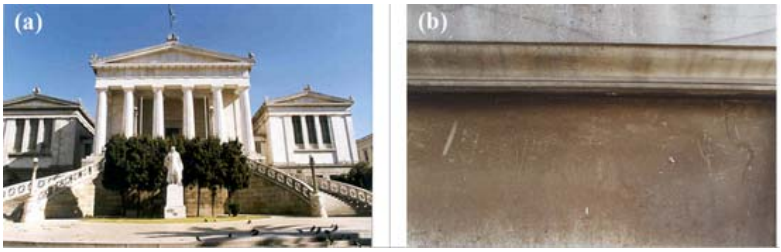

Figure 5. (a) main façade of the NLG Historic Building, (b) investigation area before pilot cleaning.

When the fuzzy model was applied with the 7 sets of input parameter values, it generated the fuzzy estimation of the Cleaning Performance Index for each cleaning intervention. Table 1 presents the results of the used experimental techniques which also represent the values of the system crisp inputs, and the fuzzy system output CPI. Figures 7 and 8 display representative SEM and LP results respectively. The input parameter of "Patina preservation index" was not included in the presented test runs, since no patina was found at the investigated surface during decay diagnosis [Moropoulou *et al.* 2000]. Therefore, the rest five input parameters were used for the test runs, while the number of the used rules were reduced to 324. It is obvious, after running the tests, that the pilot cleaning intervention which could be recommended for the removal of the black-grey crust was the application of AB57 poultice for 1h, since this technique mainly corresponds to the accepted cleaning set and marginally to the recommended cleaning-optimum (CPI value 8.05).

Table 1. Applied cleaning methods-Values of crisp inputs (results of experimental techniques)-Results of the fuzzy system (CPI)

		Values of Crisp Inputs-Results of experimental techniques					*Output*
A/A	*Applied Cleaning Methods*	*Thickness of Gypsum layer (μm)*	*Fracture Density (%)*	*Actual to Projected area ratio*	*Roughness (Rq) (μm)*	*Total Color Difference (ΔE)*	*CPI*
1	Mora Poultice* 2 hours	0	11.4	1.385	7	31.44	4.22
2	AB57 Poultice*, 2 hours	0	13.8	1.625	13	31.20	4.62
3	Poultice of $(NH_4)_2CO_3$, 10% w/v with deionized water, 2 hours	0	16.3	1.427	7	38.40	4.82
4	Poultice of Sepiolite with deionized water, 3.5 hours	50	10.0	1.350	6	5.52	5.17
5	AB57 Poultice*, 1 hour	12	10.4	1.428	7	14.70	8.05
6	Poultice of $(NH_4)_2CO_3$, 10% w/v with deionized water, 1 hour	0	10.5	1.351	6	37.70	4.58
7	Poultice of bi-sodium E.D.T.A., 3% w/v with deionized water, 1 hour	55	12.1	1.324	5	7.38	6.25

* Where, Mora Poultice is consisting of 1lt deionized water, 60gr NH_4HCO_3, 60 gr $NaHCO_3$, 25 gr of bi-sodium E.D.T.A., 10ml Desogen, 800gr sepiolite, and AB57 Poultice of 1lt deionized water, 30gr NH_4HCO_3, 50 gr $NaHCO_3$, 25 gr of bi-sodium E.D.T.A., 10ml Desogen, 800gr sepiolite.

Fuzzy system outputs (CPI) agrees with human experts considerations on the presented case study. In particular, the presented crust, as SEM results indicated (fig. 7a), consisted mostly of gypsum grains mixed with dust fall (mainly aluminosilicates and Fe), whereas the lower part of the crust was made of microcrystalline gypsum (diameter <10μm). The layer seemed cohesive, retained an intense relief and a mean width of 40μm [Moropoulou et al. 2007]. After cleaning, the surface of NLG presented the following characteristics; at the surface cleaned with poultice of $(NH4)_2CO_3$ for 2h, gypsum was entirely removed, (fig. 7c), an unaccepted fact as already described in 3.2 paragraph. Even though the marble surface presented a low to medium Rq and ratio values, many micro-cracks and fractures appeared, as a result of the effect of the cleaning, (medium to high FD value). Moreover, the high ΔE value indicated the desirable removal of black depositions, but unaccepted color modification of the surface. Therefore, the low CPI value resulted from the fuzzy system, is indeed a not acceptable cleaning. Cleaning with Mora poultice, AB57 poultice for 2h and poultice of $(NH4)_2CO_3$ for 1h

presented analogous surface characteristics to the poultice of $(NH4)_2CO_3$ for 2h. Thus, these techniques were also classified as not accepted cleaning methods, both in fuzzy system output and experts considerations. After the treatment with AB57 poultice for 1h, the width of the gypsum surface layer had been reduced (mean width of 12μm), preserving most of the desirable gypsum micro-crystals layer, (fig. 7b). The displayed low values of fracturing, Rq and ratio, as well as the medium ΔE value resulted in high CPI which is in accordance with experts opinion to classify this method as accepted cleaning and possible recommended. On the contrary, cleaning with the sepiolite poultice for 3.5h, did not reduce the gypsum layer, resulting in the retention of the black-grey crust, (fig. 7d). In parallel, the low presented values of fracturing, Rq, ratio and ΔE, classified this cleaning method as medium, both in fuzzy system results and experts estimations. A similar to the above interpretation can be given for the EDTA cleaning as well.

Figure 6. The investigation area after the application of the pilot cleaning interventions.

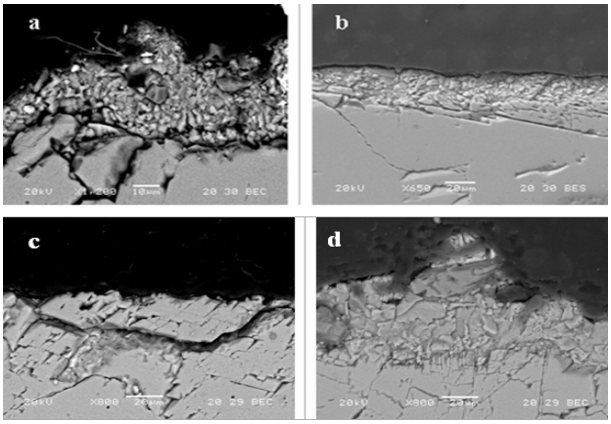

Figure 7. Representative SEM images of surface (a) before cleaning, (b) after cleaning with AB57 poultice for 1h, (c) after cleaning with $(NH_4)_2CO_3$, poultice for 2 hours and (d) after cleaning with sepiolite poultice for 3.5h.

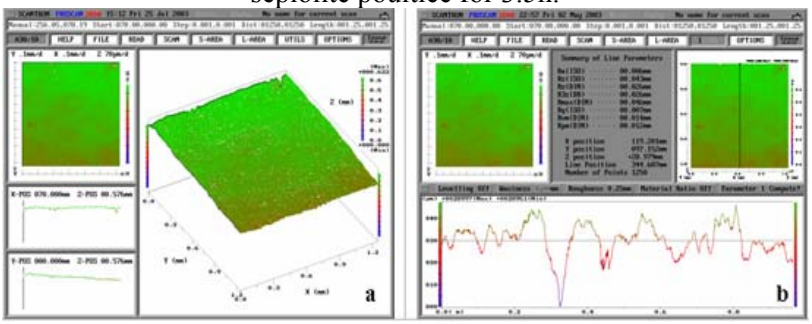

Figure 8. Representative LP results of the area cleaned by AB57 1h, (a) image of 3D micro-topography plot, (b) image of line profile acquisition.

3. CONCLUSIONS

The developed knowledge based expert system using fuzzy logic is a powerful decision making tool, as far as it concerns the assessment of cleaning interventions applied on sulphated marble surfaces. This knowledge based expert system included the following five input variables: Patina preservation index, Thickness of gypsum layer, Fracture density, Actual/Projected area ratio, Roughness, Total color difference, while the output parameter was the cleaning performance index (CPI). These input variables resulted from four different techniques: Scanning Electron Microscopy with energy dispersion by X-ray analysis (SEM-EDS), Digital Image Processing (DIP) of SEM images, Laser Profilometry (LP) and Colorimetry. The developed system was build based on the results that the above mentioned experimental techniques give when measurements in situ and/or in lab are performed according to the given specifications. The suggested decision making tool has operated with 29 different and real scenarios of cleaned sulphated marble surfaces, 7 of which are presented in this work. The results were very satisfactory and in the range of expectations, since cleaning performance classification was in aggreement with the human experts considerations. Moreover, authors have developed a similar tool for the assessment of cleaning interventions applied on washed out marble surfaces, as well as on inter-granular fractured and marble surfaces.

REFERENCES

Moropoulou, A. Bisbikou, K. Torfs, K. Van Grieken, R. Zezza, F. Macri, F. 1998, 'Origin and growth of weathering crusts on ancient marbles in industrial atmosphere', *Atmospheric Environment*, **32**[6], 967-982.

Maravelaki-Kalaitzaki, P. Zafiropoulos, V. Fotakis, C. 1999, 'Excimer laser cleaning of encrustation on Pentelic marble: procedure and evaluation of the effects', *Applied Surface Science*,**148**, 92-104.
Biscontin, G. Zendri, E. Bakolas, A. Longega, G. Driussi, G. Moropoulou, A. 1995, 'Alcune considerazioni sullapulitura delle superfici architettoniche', Proc. of Symb. Scienza e Beni Culturali XI on Pulitura, Bressanone, Italy, 1995, pp.625-631.

Vakalis, D. Sarimveis, H. Kiranoudis, C.T. Alexandridis, A. Bafas, G.V. 2004, 'A GIS based operational system for wild-land fire crisis management I. Mathematical Modeling and Simulation', *Applied Mathematical Modelling*, **28**, 389- 410.

Mamdani, E.H. Assilian, S. 1975, 'An experiment in linguistic synthesis with a fuzzy logic controller', *International Journal of Man-Machine Studies*, **7**[1], 1-13.

Mossotti, V.G. Eldeeb, A.R. 2000, *MORPH-2, A software package for the analysis of scanning electron micrograph (binary formatted) images for the assessment of the fractal dimension of exposed stone surfaces,* Open file report: 00-013, U.S. Geological Survey, Virginia, U.S.A..

Mossotti, V.G. Eldeeb, A.R. Fries, T.L. Coombs, M.J. Naude, V. N. Soderberg, L. Wheeler, G. S. 2002, *The effect of selected cleaning techniques on Berkshire Lee marble; A scientific study at Philadelphia City Hall*, Professional Paper 1635, U.S. Geological Survey, Virginia, U.S.A.

Moropoulou, A. Delegou, E.T. Vlahakis, V. Karaviti, E. 2007, 'Digital processing of SEM images for the assessment of evaluation indexes of cleaning interventions on pentelic marble surfaces', *Materials Characterization*, **58**[11-12], 1063-1069.

Avdelidis, N.P. Delegou, E.T. Almond, D.P. Moropoulou, A. 2004, 'Surface roughness evaluation of marble by 3-D laser profilometry and pulsed thermography', *J. NDT & E Int.,* **37**[7], 571-575.

Stout, K.J. Blunt, L.A. 1995, 'Application of 3-D topography to bio-engineering', *J. International Machine Tools Manufacturing*, **35**, 219-229.

BS EN ISO 4288:1998, Geometrical product specification-surface texture (1998).

Stout, K.J. Sullivan, P.J. Dong, W.P. Mainsah, E. Luo, N. Mathia, T. Zahouani, H., 1993, *The development of methods for the characterization of roughness in three dimensions*, Research Working Paper EUR 15178 EN, Programme for Applied Metrology and Chemical Analysis (BCR), Uni. of Birmingham.

ASTM D2244-93. Standard Test Method for Calculation of Color Differences from Instrumentally Measured Color Coordinates (1993).

Klir, J.G. Yuan, B. 1995, *Fuzzy Sets & Fuzzy Logic: Theory and Applications*, Prentice Hall, New Jersey.

Mamdani, E.H. 1974, 'Application of fuzzy Algorithms for Simple dynamic Plants', Proc. IEE, 121(12), 1585-1588.

Zadeh, L.A. 1973, 'Outline of a new approach to the analysis of complex systems and decision processes,' *IEEE Trans. Syst., Man, Cybern*, **3**, 28-44.

Driankov, D. Hellendoorn, H. Reinfrank, M. 1993, *An introduction to Fuzzy Control*, Springer-Verlag, Berlin.

Skoulikidis, Th. & Charalambous, D. 1981, 'Mechanism of sulphation by atmospheric SO2 of the limestone and marbles in the ancient monuments and statues, II. Hypothesis concerning the rate determining step in the process of sulphation, and its experimental confirmation', *British Corrosion J.,* **16**, 70-76.

Elfving, P. Panas, I. Lindqvist, O. 1994, 'Model study of the first steps in the deterioration of calcareous stone: I. Initial surface sulphite formation on calcite' Applied Surface Science, **74**, 91-98.
Moropoulou, A. Koui, M. Delegou, E.T. Avdelidis, N.P. Bakolas, A. Giabanis, D. Kouris, S. Stefanou, J. Fotoniata, E. Tzamalis, A. 2000, *Decay Diagnosis and Conservation Interventions Planning for the facades of the National Library of Greece Historic Building,* Lab of Materials Science and Engineering, Final Research Working Paper, National Technical University of Athens, December.

The Assessment of Roof Drainage System of a Historical Turkish Bath: Sengul Hammam

Gulsen Disli [1]
Ayse Tavukcuoglu [2]
Levent Tosun [3]
Ermanno Grinzato [4]

T 25

ABSTRACT

A well-designed roof drainage system is of vital importance for the survival of historical buildings over the centuries. In order to maintain these systems in good performance, comprehensive studies are necessary in terms of their drainage system characteristics, discharge capacities and faults. These studies should ideally be done by using non-destructive methods.

In the study, the roof drainage system of a 15th century Ottoman bath, the Sengul Hammam, located in the province of Ankara, Turkey, was examined in terms of its surface slopes, discharge capacity, faults and its potential for taking corrective action. The study consisted of the mapping of decay forms, levelling survey, infrared thermography (IRT) and roof drainage calculations together with some supportive laboratory analyses. The method used for the roof drainage calculations was based on a contemporary method modified and developed according to the characteristics of the roof at hand.

Serious dampness problems arising from certain roof drainage faults were identified in the Sengul Hammam. Its roof was configured to provide a peripheral drainage system and this system was found to have failed at present due to earlier incorrect interventions by mesh-reinforced concrete and subsequent lack of maintenance. The ideal case for the improvement of the roof drainage system was discussed together with some suggestions on the urgent remedial interventions, preventive measures and future improvements. The joint interpretation of non-destructive analyses provided a good combination for the assessment of the roof drainage system of a historical building on a quantitative basis.

KEYWORDS

Non-destructive testing, Roof drainage calculations, Levelling survey, Infrared thermography, Turkish baths

[1] Middle East Technical University, Department of Architecture, Graduate Programs in Building Science, Inonu Bulvari, 06531, Ankara, Turkey; Phone: +90 312 3098910-247,Fax: 312 3098902-16, disligulsen@yahoo.com;
[2] Middle East Technical University, Department of Architecture, Graduate Programs in Building Science, 06531, Ankara, Turkey; Phone: +90 312 2106214,Fax: 312 2107966, tayse@metu.edu.tr;
[3] Middle East Technical University, Department of Architecture, Graduate Programs in Building Science, Inonu Bulvari, 06531, Ankara, Turkey, Phone: +90 312 4171919,Fax: 312 2107966, ltosun@metu.edu.tr
[4] Consiglio Nazionale delle Ricerche, CNR-ITC Padova, Italy, Phone: +39 049 8295722,Fax: +39 0498295728, ermanno.grinzato@itc.cnr.it

1 INTRODUCTION

It is essential to better understand the original roof drainage system of historical baths (hammams) in terms of their performance, capacity and adequacy in order to keep their proper functioning for long periods of time. Extensive studies are, therefore, needed to discover those technologies and to define appropriate conservation programs for their survival.

This study was focused on the investigation of roof drainage system for a 15th century Ottoman bath, the Sengul Hammam, located in the province of Ankara, Turkey. Some non-destructive methods, such as levelling survey, mapping of decay forms, infrared thermography and roof drainage calculations, were used in the study. Its roof drainage system was examined in terms of its discharge capacity, adequacy and faults. Some urgent and long-term maintenance programs were suggested for the improvement of the roof drainage as well as for contributing to the overall rainwater drainage system.

2 MATERIALS AND METHODS

The Sengul Hammam is a typical Ottoman double bath consisting of two separate parts for men and women. It was constructed with stone masonry walls with brick transitions and a brick upper structure [Disli *et al.* June 2007], [Disli *et al.* September 2007]. The roofs above the tepidarium and caldarium sections, hot water storage and firewood storage rooms of the hammam, including the dome surfaces, were repaired with an addition of 8 cm thick mesh-reinforced concrete layer (Fig. 1). The roofs of the frigidarium sections at the north and south are timber pitched roofs covered with fired-clay roof tiles (Fig. 2). The immediate periphery of the structure was totally surfaced with asphalt pavement.

Figure 1. (a) The general view of the mesh-reinforced concrete roof above the caldarium and tepidarium sections (at left) [Disli *et al.* June 2007], [Disli *et al.* September 2007], (b) The pitched roof, A1, over the frigidarium of women's part with its discharge components: gutter and downpipes (at right)

The roof areas under study were presented in 'Fig. 3'. These areas were composed of four roof areas; A1, A2, B1 and B2, having different geometry and drainage systems (Fig. 3) [Disli *et al.* June 2007]. The roofs A1 and A2 were pitched roofs similar with each other, consisted of two parts; the four-sided pitched roof covering the square area and the lantern roof at its top. A peripheral drainage system was provided by means of zinc eaves gutters and fourteen downpipes, some of which discharge water directly onto the concrete-clad roof, B1 (Fig. 4a). The roof B1 was a low-slope roof including domes, configured to provide peripheral drainage, with flows from elevated interior edges to lower exterior ones, and then, to waterspouts located at the eaves level along the west side of the roof (Figs.4b and 4c). There were nine spouts, with similar dimensions, serving this roof area. The roof B2 was a flat roof configured to provide an internal drainage, with flows towards an internal gutter located at the middle of the roof area (Fig.4d). The water collected in the gutter was discharged through a grilled outlet located at its north end, and then, carried by a drain line (buried in the garden) to the rainwater drainage network (buried under the street).

These roof areas were examined by using some non-destructive methods. The maps of visual decay forms observed on the building facades were produced for the analysis of the problem areas in the structure, their distribution as well as the probable sources of these problems. Following this

preliminary on-site visual survey, a planimetric survey was conducted to record the topographical features of the roof. Readings were then converted into a detailed map indicating overall slopes and local falls in reference to roof drainage components (waterspouts and downspouts). This made it possible to locate problem areas with a potential risk of ponding on the map. Dimensions of all spout outlets, eaves gutter and downspouts were also taken to facilitate capacity calculations. These areas under study, together with the lower and upper parts of the exterior walls, were scanned by a thermal camera to define damp zones. Special attention was given to the lower parts of the walls at points where a roof drainage component existed overhead. Damp zones were compared with the risky areas for ponding. Drainage calculations were made to assess the discharge capacity of the roof discharge components and their adequacy whether they provide acceptable rates of water evacuation from roof surfaces. The ideal situations were also examined to achieve a proper roof slope arrangement providing evenly-distributed roof areas feeding each discharge component and to determine satisfactory flow dimensions for these components. The roof drainage calculations was based on the methods explained in the literature [Disli *et al.* June 2007], [Disli *et al.* September 2007], [Tavukçuoğlu *et al.* 2007], [Hall 1996], [Griffin and Fricklas 1995] [TSE 826, 1988], [BRE Part 1, 1976], [BRE Part 2, 1976], and adapted to the characteristics of the roof at hand.

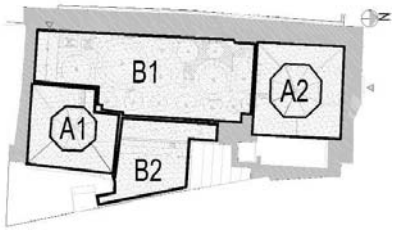

Figure 3. Plan of the building, showing the roof areas under study and immediate grounds [Disli *et al.* June 2007], [Disli *et al.* September 2007]. **A1**–timber pitched roof covered with roof tiles above the women's frigidarium section; **A2**-timber pitched roof covered with roof tiles above the men's frigidarium section; **B1**–mesh-reinforced concrete roof above the caldarium and tepidarium sections; **B2**–mesh-reinforced concrete roof above the hot water storage room and the fire wood storage room; **Grey-shaded areas**–immediate grounds of the building.

Figure 4. Views of the building, showing the roof areas under study[Disli *et al.* June 2007], [Disli *et al.* September 2007].

The results were interpreted together to examine the roof characteristics of the structure in terms of surface slopes, discharge capacity and faults and its potential for taking corrective action. The recent interventions done with incompatible materials were also discussed.

3 RESULTS AND DISCUSSIONS

The combined interpretation of the results were done in terms of the faults of the roof drainage system, adequacy of the roof drainage system and suggestions for the improvements of the roof drainage system. The results are summarized below under respective headings.

3.1 Faults of the Roof Drainage System

The present condition of the roof was determined to be unsatisfactory due to unconscious interventions and poor maintenance. In particular, the repair with mesh reinforced concrete layer added on the roof was unacceptable since it was an incompatible intervention introducing the salt problems to the structure and triggering the deterioration mechanisms in presence of dampness. This heavy concrete layer also increased the dead load of the structure and weakened it against lateral stresses. Most faults observed on the roof surfaces were inevitably the result of this concrete layer.

The map of decay forms and infrared images showed the problem areas of continuous rainwater penetration and their location in the structure. The severe material loss on masonry surfaces together with staining and salt deposits were found to correspond with the damp zones (Figs.5 and 6). Those surfaces were exposed to rainwater, overflowing from the eaves gutter, downpipes and waterspouts. Hence, the lower parts of the walls on the axis of downpipes and waterspouts were found to be damp and cold in the infrared images (Figs.7 and 8). The height of cold areas were detected to extend towards the discharge components above (Fig.8). The periodical wetting and drying at those damp zones must have caused such severe deterioration on wall surfaces. The recent repairs with cement mortar also introduced salt problems accelerating the deterioration mechanisms at the presence of dampness.

Figure 5. The maps showing the distribution of material loss (at top) and the distribution of discoloration and deposits on surfaces of the north façade (at bottom). The severe loss and detachment on surfaces was observed together with white staining and salt deposits, especially at the lower parts of the rainwater pipes at both sides of the façade and stone courses at the top, underneath the eaves gutter[Disli *et al.* June 2007].

Figure 6. The infrared image of the selected region at the north façade, showing the severe material loss as warmer areas and the detachments which were not observed visually as colder areas, both suffering from the roof drainage faults [Disli *et al.* June 2007], [Disli *et al.* September 2007].

The faults of the roof drainage system, preventing its proper functioning, were summarized as follows:

– All discharge components serving the roof areas had, in one way or another, become disfunctional (Fig. 9): All spouts were observed to suffer from the accumulation of soil deposits and plant growth, obstructing the free discharge of rainwater from the roof. In addition, all spouts, zinc gutters and downpipes were observed to be severely-deteriorated due to the wrong restoration

practices, such as repairs with cement-based mortars as shown in 'Fig.10'. Almost all metal components were observed to have corroded and lost their functions.

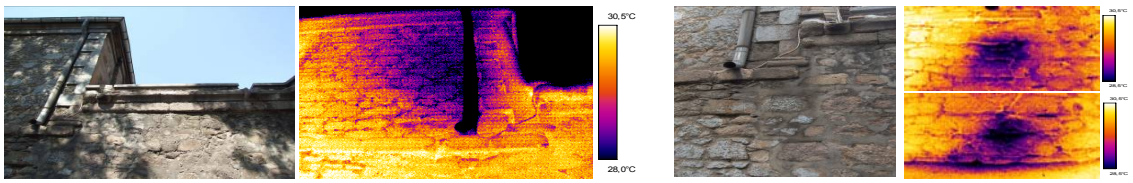

Figure 7. (a) The detached areas close to the rainwater downpipes were detected as colder areas [Disli *et al.* June 2007], [Disli *et al.* September 2007]., (b) The lower parts of the wall corresponding to the axes of the downpipe and the waterspout were found to be cold and damp [Disli *et al.* June 2007], [Disli *et al.* September 2007

- The reverse or nil falls were found to cause local ponded areas on the concrete-clad roofs, B1 and B2 (Fig. 9). Some waterspouts, particularly the spouts WS5, WS6 and WS7, were determined to be overloaded due to the improper surface slopes and direct discharge of rainwater from the timber pitched roofs to the conctere-clad roof B1 and then causing discrete roof areas feeding each spout unevenly (Fig.11). The overloaded spouts could also be detected in their IR images (Fig.12).
- A later addition of parapets on the roofs B1 and B2 were observed to cut the water flow of the rainwater towards the discharge components, causing ponding and soil/dirt accumulation in their fronts (Figs.9 and 13).
- The regions at the south of the roof B1 and at the north of the roof B2 were also the risky areas due to the lack of discharge components (Fig.9). Overflowing and/or ponding from the eaves level, therefore, were inevitable for these regions.
- The rainwater collected on the neighbouring building at the east, was observed to be discharged directly on to the roof B2, above the firewood storage of Sengul Hammam (Fig.14). This added a considerable drainage load to the interior gutter, IG and outlet, O1 [Table 1].
- As a recent unconscious addition, a green garden with 22m^2 area, was observed to exist on the roof B1 (Fig.9). This garden was attached for growing some vegetables by taking advantage of the heat and rainwater of the roof. This garden area was surrounded by a concrete parapet of 40cm height without any discharge component, acting like a pool entrapping the rainwater and, without doubt, causing serious dampness problems at both interiors and exteriors.
- Some cracks were also observed on the mesh-reinforced concrete surfaces following the slopes, inevitably causing water leakages into the sublayers and heat loss from the interiors.

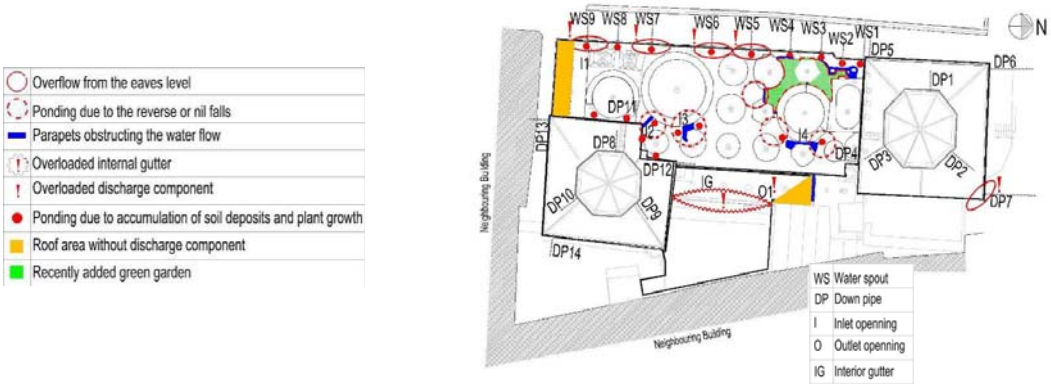

Figure 9. The map showing the faults of the roof drainage system and their location.

Figure 10. The spouts, WS1, WS4, WS5 and WS7 (from left to right, respectively) showing the severely-deteriorated sluiceways due to cement-based mortar repairs [Disli *et al.* June 2007].

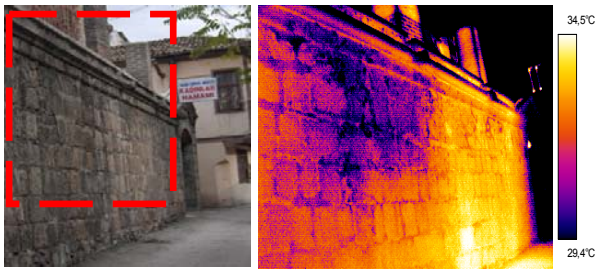

Figure 11. The roof map of the as-is case, prepared according to the results of levelling survey, showed that the discrete effective areas feeding the individual discharge components were not evenly distributed [Disli *et al.* June 2007], [Disli *et al.* September 2007].

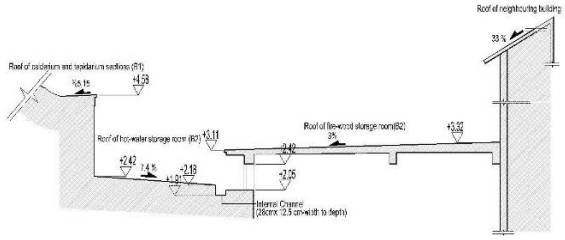

Figure 12. Darker areas in the IR image of the selected region indicated the damp zones at the upper parts of the wall due to the overflowing from the roof eaves level between the spouts WS6 and WS7. Severe material loss together with salt deposits and biological growth overlap with the colder areas [Disli *et al.* June 2007], [Disli *et al.* September 2007].

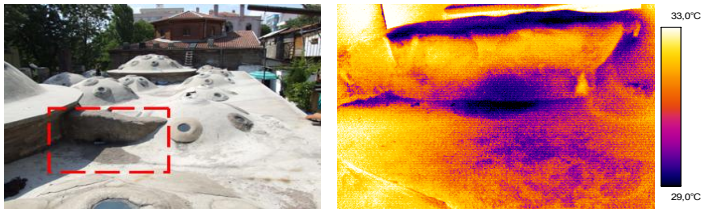

Figure 13. The IR image of the parapet cutting the water flow and causing soil/dirt accumulation in front of its outlet. The gradual decrease of surface temperatures towards the outlet exhibited the potential for absorbing and retaining rainwater [Disli *et al.* June 2007], [Disli *et al.* September 2007].

Figure 14. The cross section A-A from the roof B2 showing the roof slope arrangement towards the interior gutter and additional rainwater loading from the neighbouring building at the east [Disli *et al.* June 2007].

3.2 Adequacy of the Roof Drainage System

The roof drainage system of Sengul Hammam was evaluated in terms of its surface grading, discharge capacity and adequacy. The map showing the surface slopes, their directions and extents on roof surfaces in reference to roof drainage components were given in 'Fig. 15'.

The slopes of the pitched roofs, A1 and A2, were found to be in the range of 32% and 42%. For the roof B1, the primary slopes from east to west were in the range of 3% and 6% while the secondary slopes towards the spouts along the west side (eaves level) of the roof were, similarly, in the range of 3%-5%. The roof B2 was found to have slopes in the range of 3% and 10%, towards the interior gutter located in the middle (Fig. 15). Although it seemed to have some surface slopes providing water flow, the slope arrangement was observed to be far away from a satisfactory removal of rainwater from the concrete-clad roof surfaces. The as-is case of the roof drainage system was inadequate that not allowing a free discharge of rainwater due to the unconscious interventions of mesh-reinforced concrete layer with improper surface grading, parapets and green garden, as mentioned in the previous section.

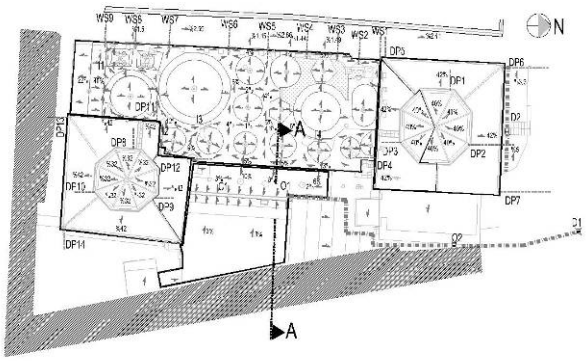

Figure 15. The map showing the direction and extent of surface slopes on the roofs of Sengul Hammam and its immediate periphery [Disli *et al.* June 2007], [Disli *et al.* September 2007].

The drainage calculations clearly exhibited the inadequacy of the roof drainage system in as-is case on quantitative basis (Table 1). For instance, the overall roof runoff rate of the concrete-clad roof B1, 18.2l/s, was almost the twice of the total discharge capacity of the waterspouts, 10.2l/s. Similarly, the total roof runoff rate of the concrete-clad roof B2, 9.7l/s, was calculated to be considerably higher than the discharge capacity of the drain O1, 5.4l/s. This drain O1 was the only discharge component of the roof B2 and in case of its partially or completely blockage, the roof B2 seemed to suffer from rainwater accumulation in considerable amounts.

The calculations also presented the uneven distribution of rainwater loading for each discharge components. For instance, the spouts WS5, WS6, WS7, WS9 and the downpipe DP7, were found to be overloaded considerably while the spouts WS1, WS2, WS3 and WS8 were found to work undercapacity [Table 1] (Fig.11). This corresponds with the results of the map showing the discrete roof areas feeding each waterspouts (Fig.11). According to the calculations, the spouts WS5, WS6 and WS7 were extremely-loaded with the roof run off rates of 5.8l/s, 4.6l/s and 3.6l/s, respectively, even reaching to the four times of their as-is discharge capacities [Table 1].

Table 1. The results of roof drainage calculations for the as-is case: The lines in red show the as-is flow capacities of the discharge components (Q_O) not enough to cope up with the individual roof runoff rate (Q_R).

Roof Spouts	A_R	A_T	Sizes width x height	Qo	Q_{TO}	Q_R	O_{RT}
	(m²)	(m²)	(cm)	(l/s)	(l/s)	(l/s)	(l/s)
WS1	24	657	8.5 x 7.5	1,18	**10,20**	0,68	**18,22**
WS2	17		9.0 x 7.0	1,13		0,42	
WS3	26		8.5 x 5.5	0,74		0,62	
WS4	35		9.5 x 6.5	1,06		0,82	
WS5	206		6.0 x 11.0	**1,48**	<	**5,79**	
WS6	162		10.0 x 7.0	**1,25**	<	**4,56**	
WS7	124		12.0 x 6.5	**1,34**	<	**3,55**	
WS8	14		9.0 x 6.5	1,01		0,38	
WS9	49		9.0 x 6.5	**1,01**	<	**1,4**	
DP7	62		Φ=10	**1,79**	<	**1,85**	1,85
IG1	325	325	28 X 12.5	**8,35**	8,35	**9,74**	9,74
O1	325	325	18 X 12.5	**5,37**	5,37	**9,74**	9,74

Q_O: the flow capacity of an outlet;
Q_{TO}: the total discharge capacity of the spouts serving each roof area;
A_I: the discrete effective areas feeding individual spouts;
A_T: the total effective area of each roof under study;
Q_R: the rate of runoff from each effective area feeding individual spouts;
Q_{TR}: the total runoff from each roof under study.

The discharge coefficient for the low-sloped surfaces of the roof B1, was also discussed according to the results of drainage calculations. The discharge coefficient of the dome surfaces was accepted as '1.0' because of their high slope [Hall, 1996; TSE, 1988]. Considering the ideal roof fall arrangement which is explained in the next section and the original spout dimensions, 10x9cm in width and depth, the surface conditions for the low-sloped surfaces at the past could be calculated. This was found to be in the range of 0.2-0.3 for the low-sloped surfaces signalling the a considerably-high water absorption capability of the surface, such as earth [Hall 1996], [TSE 1988]. Further studies are needed to discover the drainage characteristics of original roof materials.

3.3. Suggestions for the Improvement of the Roof Drainage

The study has shown up the priorities for the improvement of the roof drainage system and maintenance program particular to the building. It appeared that the roof drainage system is not possible to funcion properly anymore due to the presence of unacceptable mesh-reinforced concrete layer. This incompatible layer definitely accelerates the soluble salts and dampness problems and destroys the functioning of roof drainage system. The recent studies also showed that the concrete/reinforced-concrete repairs destroy the structural stability of the historic masonry structures [Aktas, 2006] and weaken the structures against the lateral stresses. It is essential to correct the surface grading of the roof surfaces but it is not possible to repair these surfaces with additional concrete layers. Considering all, the present roof drainage system of the mesh-reinforced concrete roofs could not be improved by usual remedial measures. The mesh-reinforced concrete layer, therefore, should definitely be removed from the structure and then the roof should be covered with the layers of compatible roof plasters in the context of a well-planned conservation program developed by the structural engineers and conservation experts. The ideal case for the improvement of the roof drainage system was suggested as follows:

(a) as much as the present surface geometry allowed, an even distribution of rainwater loading for each discharge component should be achieved as suggested in 'Fig. 16'. The arrangement of roof

slopes should be corrected accordingly for a pond-free drainage system. Special care should be given to level the reverse falls in front of spout openings properly for a fast water runoff;
(b) the extreme loading from the roof of neigbouring building at the east of the roof B2 should be prevented, without doubt, by a separate roof drainage of the neighbouring building.
(c) The discharge capacities of the waterspouts should be improved by increasing their flow dimensions. For a rainwater discharge in acceptable ranges, the ideal flow dimensions for the spouts, WS1, WS2, WS3, WS4, WS5, WS8 and WS9 were calculated to be 10cm x 9cm in width and depth, having the discharge capacity of 1.8l/s. A larger discharge capacity of 2.7l/s were needed for the spouts WS6 and WS7 with the flow dimensions of at least 11 x 11 cm in order to cope up with the roof runoff 2.5l/s and 2.8l/s [Table 2a]. The as-is dimensions of O1, 12.5 x 18.0cm in width and depth, needed to be increased to 12.5 x 28.0cm to cope up with the free discharge of the rainwater from the roof area.
(d) The internal gutter IG1 should be extended to cover the whole length of the roof B2, 17.40 m, where it suffers from the lack of drainage component (Fig.16). An alternative drain is suggested which may act as an overflow drain in case of any partial/complete blockage of O1;
(e) There is a necessity of a discharge component at the south of B1, suffering from the uncontrolled overflow and severe dampness problems on the wall surfaces. Here, the water discharge should be provided by means of an additional waterspout WS10 together with a collecting channel at the eaves level as shown in 'Figs. 16 and 17'.

Some urgent interventions related to the timber pitched roofs were also recommended to improve their existing conditions:-
(f) The timber pitched roofs should be repaired to let it properly function as a four-sided pitched roof/hipped roof as suggested in 'Fig.16'. The eaves gutter and downpipes forming the peripheral drainage system for these pitched roofs should be replaced with the properly-sized ones. The drainage systems for the pitched roofs and low-sloped roofs should be seperated. The direct discharge from the pitched roofs onto the roofs B1 and B2 should definitely be prevented by the addition of downspouts diverting rainwater to the surface-water drainage system at the immediate periphery of the structure. The placement of these downpipes were shown in 'Fig.17' and the ideal sizes for each downpipe and eaves gutter were listed in [Table 2b]. The 23 downpipes located at four sides of the roofs were recommended with diameters of 70mm for the downpipes and of 250mm for the eaves gutters while smaller diameters could be enough for the lantern part of the pitched roofs as listed in [Table 2b].

Such improvements summarized above are essential for a pond-free drainage system and the survival of the structure. In addition, some preventive measures were also suggested, such as the regular cleaning of discharge components from soil and plant deposits. For future improvements, any subsequent intervention and its effect on the discharge system should be checked by means of roof drainage calculations used in this study.

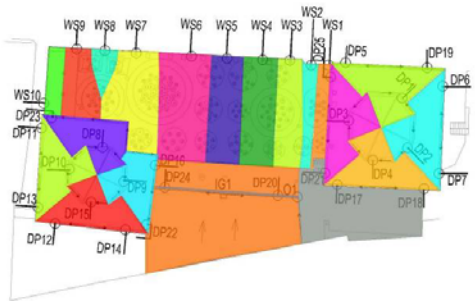

Figure 16. The ideal roof map showing the discrete effective areas feeding individual discharge component which provides an even rainwater loading for each component.

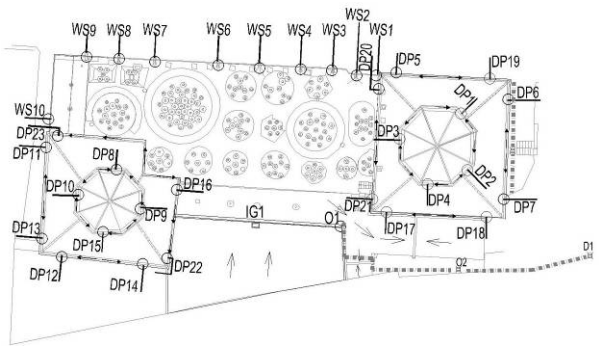

Figure 17. The roof map of the ideal case showing the location of each individual discharge component.

Table 2: The results of roof drainage calculations for the ideal-case of **(a)** the roofs B1 and B2 (at the left); and **(b)** the roofs A1 and A2.

Roof Spouts	A_R	A_T	Sizes width x height	Qo	Q_{TO}	Q_R	O_{RT}
	(m²)	(m²)	(cm)	(l/s)	(l/s)	(l/s)	(l/s)
WS1	35	501	10.0 X 9.0	1,82	19,96	0,99	13,77
WS2	19		10.0 X 9.0	1,82		0,49	
WS3	51		10.0 X 9.0	1,82		1,36	
WS4	65		10.0 X 9.0	1,82		1,76	
WS5	58		10.0 X 9.0	1,82		1,58	
WS6	93		**11.0 X 11.0**	2,7		2,54	
WS7	101		**11.0 X 11.0**	2,7		2,79	
WS8	14		10.0 X 9.0	1,82		0,38	
WS9	47		10.0 X 9.0	1,82		1,34	
WS10	18		10.0 X 9.0	1,82		0,54	
IG1	288	288	28 X 12,5	8,35	8,35	8,25	8,25
O1	288	288	28 X 12,5	8,35	8,35	8,25	8,25

Roof downpipes and gutters	A_R	A_T	Sizes Downpipe	Sizes Gutter	Qo	Q_{TO}	Q_R	O_{RT}
	(m²)	(m²)	(cm)	(cm)	(l/s)	(l/s)	(l/s)	(l/s)
DP1	14,9	460,5	Φ=6	Φ=20	1,1	34,3	0,51	15,9
DP2	13,58		Φ=6	Φ=20	1,1		0,47	
DP3	14,24		Φ=6	Φ=20	1,1		0,49	
DP4	13,63		Φ=6	Φ=20	1,1		0,47	
DP5	16,47		Φ=7	Φ=25	1,7		0,57	
DP6	19,54		Φ=7	Φ=25	1,7		0,67	
DP7	32,49		Φ=7	Φ=25	1,7		1,12	
DP8	10,23		Φ=6	Φ=20	1,1		0,35	
DP9	10,24		Φ=6	Φ=20	1,1		0,35	
DP10	10,75		Φ=6	Φ=20	1,1		0,37	
DP11	25,6		Φ=7	Φ=25	1,7		0,88	
DP12	27,77		Φ=7	Φ=25	1,7		0,96	
DP13	15,98		Φ=7	Φ=25	1,7		0,55	
DP14	17,75		Φ=7	Φ=25	1,7		0,61	
DP15	10,56		Φ=6	Φ=20	1,1		0,36	
DP16	5,51		Φ=7	Φ=25	1,7		0,19	
DP17	30,27		Φ=7	Φ=25	1,7		1,04	
DP18	17,86		Φ=7	Φ=25	1,7		0,62	
DP19	31,7		Φ=7	Φ=25	1,7		1,09	
DP20	32,35		Φ=7	Φ=25	1,7		1,12	
DP21	15,96		Φ=7	Φ=25	1,7		0,55	
DP22	30,55		Φ=7	Φ=25	1,7		1,05	
DP23	42,61		Φ=7	Φ=25	1,7		1,47	

4 CONCLUSION

In order to have survived under the effects of the prevailing harsh climatic conditions over the centuries, Sengul Hammam must originally have had quite a well-designed roof drainage system. However, the study showed that the roof of this structure has not been able to withstand the test of time due to the inappropriate interventions and a lack of maintenance. At present, there are serious dampness problems arising from the presence of an imcompatible mesh-concrete layer above the roof structure together with certain roof drainage faults.

For a satisfactory-functioning of the roof drainage system and the survival of the stucture it is essential to remove this concrete layer from the roof structure and then cover it with the layers of compatible roof plasters. These works should be well-planned in the context of a comprehensive conservation program. The ideal case for the improvement of the roof drainage system was suggested and preventive measures have been pointed out,herewith.

The joint interpretation of non-destructive analyses, including mapping of the decay forms, IRT analyses, leveling survey and drainage capacity calculations, provided a good combination for the assessment of the roof drainage system of a historical building. The roof drainage calculations used in the case of Sengul Hammam can also be applied to the roof of historical buildings in a similar condition for the assessment of their adequacy on a quantitative basis.

REFERENCES

Archives of the General Administration of Pious Foundations, File on Sengul Hammam.

Dişli, G., Tavukcuoğlu, A., Tosun, L., Grinzato, E., Caner-Saltık, E. N., (in press). Rainwater Drainage System Investigation Of An Historical Hammam By Using Non-Destructive Methods, *Water And Cultural Heritage, Proceedings - 7th International Symposium on the Conservation of the Monuments in the Mediterranean Basin*, June 6-9, 2007, Orleans , France.

Dişli, G., Tavukcuoğlu, A., Tosun, L., Grinzato, E., Caner-Saltık, E. N., (2007). Assessment of Water Supply And Drainage Systems For An Historical Hammam By Using Non- Destructive Methods, *33rd International Symposium, CIB W062 2007 on Water Supply and Drainage For Buildings*, September19-21, 2007, Brno , Czech Republic, pp. 281-294.

Tavukcuoğlu, A., Düzgüneş, A., Demirci, Ş., Caner-Saltık, E. N. 2007, 'The assessment of a roof drainage system for an historical building', Building and Environment, 42, 2699–2709.

Hall F. 1996, 'Rainwater pipes and gutters, flow over weirs. In: Building services and equipment', vol. 3. 3rd ed. UK: Longman Scientific & Technical, pp. 33–41.

Griffin CW, Fricklas RL. 1995, 'Draining the roof. In: Manual of low-slope roof systems', 3rd ed. New York: McGraw Hill.

Turk Standartları Enstitüsü (TSE) 1988, 'TS 826/Aralık 1988-Binalarda Pis Su Tesisatı Hesaplama Kuraları—Rules for the calculation of waste water, installations in buildings' Ankara, TSE.

BRE. 1976, 'Roof Drainage: Part 1. BRE Digest 188', April. Watford: BRE.

BRE. 1976, 'Roof drainage: Part 2. BRE digest 189', May. Watford: BRE.

Aktaş Y. 2006, Technological characteristics of a brick masonry structure and their relationship with the structural behaviour. Unpublished Master Thesis. METU, Department of Civil Engineering.

The Restoration and Upgrading of The 100 Year Old Victoria Institution: the Adaptive Reuse of a School into an Auditorium

Kribanandan Gurusamy Naidu

T 25

ABSTRACT

The former Victoria Institution is located in the center of Kuala Lumpur and was year marked to be upgraded and extended in 2005 in an adaptive reuse of a cultural heritage building. The main structure was built in 1893 and was in ruins having deteriorated over time due to physical impact of human activity as well as weathering over time and the impact of a fire in 1999.

A detailed investigation, sampling and materials testing of the building and the surrounding ground conditions was undertaken to provide a basis for the redesign and upgrading works. The change of use necessitated major design changes associated with the Roof Structure to cater for long open spans required for the auditorium seating. In keeping with the Heritage guidelines a church designed by the same Architect during the same period was investigated and used as the basis to achieve historical authenticity in design.

This paper contains an overview of the award winning project including the materials intervention and the structural engineering undertaken including an innovative intervention to restore the masonry arches to achieve the adaptive reuse objectives.

KEYWORDS

Adaptive Reuse, Masonry strengthening and pinning, Building pathology, Redesign, Materials investigation.

1 PROJECT SUMMARY

1.1 Project Brief

The former Victoria Institution (V.I) now called the Kompleks Taman Budaya, Wilayah Persekutuan located in the center of Kuala Lumpur was originally built in 1893. The structure had been abandoned for several years and was in ruins having deteriorated over time due to physical, environmental and fire impacts (See Figure 1). Following the gazetment of the building under the Monument Act 1976, a contract was let to rebuild the structure in an adaptive reuse of a cultural heritage building to a modern auditorium for the Arts. Besides the upgrading and conservation works, a new Annex building with a basement was included as part of the development of the site. Prior to any intervention associated with the upgrading / rectification works, a detailed condition survey was undertaken covering the external and internal building elements as well as the infrastructure services. This was followed by an in depth sampling and testing program which formed the basis on which to develop a remedial intervention program keeping the compatibility of new and old materials in view and as far as possible minimizing the extent of physical intervention.

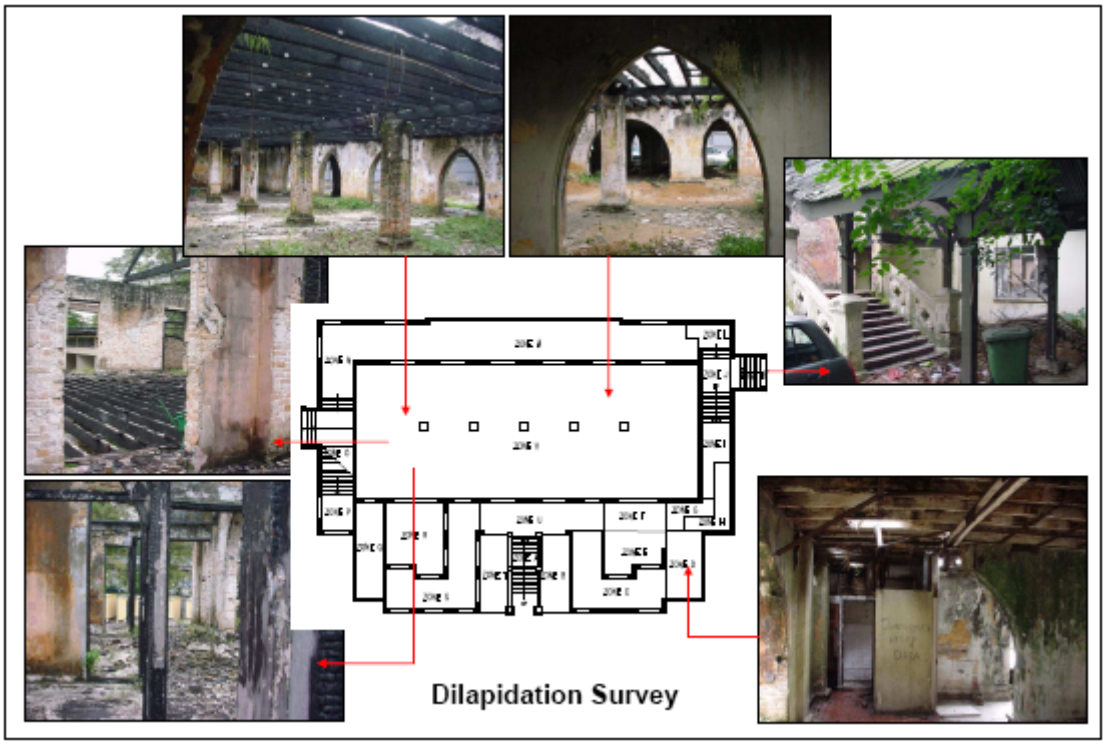

Figure 1. Photographic Record of Dilapidation Survey

1.2 Project Background

The site of the old V.I. building is in a historically significant part of Kuala Lumpur. It is located at the southern end of Jalan Tun H.S. Lee (also named Jalan Bandar) and adjacent to other buildings of historic relevance. The project consisted of:

a) Conservation and upgrading works for adaptive reuse of the former Victoria Institution.
b) An additional adjoining new annex building (3 storeys) with 1 level basement.
c) Infrastructure, facilities and services upgrading.

The overall size of the site is approximately 0.8 acres. The original size of the Conservation building was 6650m² and this was increased to 7710m² with the additional floor. The plinth area for the Annex building is 8850m².The construction programme spanned from Oct 2002 to Nov 2004

The structure was one of the icons of the colonial era and very much part of Kuala Lumpur history. By reinstating the structure to its original historical context and at the same time adapting it to an auditorium, a new and significant venue for the Arts at the heart of the old city has been established. This has also helped boost tourism by adding a new historical landmark and new places of interest for local and foreign visitors.

1.3 Client Brief and Requirements

The conservation building was reconstructed to house an Auditorium, while the Annex building complemented this development by providing the space for cultural performance studios and an administrative office. The requirement was one of a re-adaptation of an existing building which required a high level of conservation knowledge and approach. The new annex building was to be constructed with modern construction methods with minimal disturbance to the existing original façade as well as the floor of the conservation building.

2 ENGINEERING FEATURES

2.1 Scope of Works

The scope of works included :

a) Condition and Dilapidation Survey undertaken in relation to the Department of Museum and Antiquities HABS requirements.
b) Structural Evaluation and Assessment.
c) Underpinning and masonry arch strengthening by a novel pinning method to minimize intervention.
d) Structural design to recreate the structure (see Figures 2 & 3) including a new roof design in keeping with the Architectural Accent of the time to fit in with the adaptive reuse requirements.
e) Construction methodology with strong emphasis on the basement area and methods to mitigate against impact of the new Annex building construction on the historical building.
f) Providing proposed remedial treatment for defects identified.
g) Supervision of civil and structural works.
h) Supervision of upgrading and reinstatement works.

2.2 Complexity of Design

There were several critical issues associated with the upgrading works which required careful engineering judgement. This included:

a) The building was badly decayed due to human, physical, environmental and fire impacts and therefore carefully planned construction methodologies for the upgrading work sequence was required.
b) Detailed monitoring and testing were required to confirm the structural strength, stability and insitu condition of the structure and the potential impact of new loads acting on the structure.
c) Ground settlement problems associated with the adjacent basement excavation works and ground water movement and its potential impact on the adjacent walls of the heritage structure was undertaken.
d) The need for a rigorous monitoring system for the heritage building and alternative design approaches were considered.
e) The need to integrate the existing structural elements with new elements while complying with the historical building and conservation guidelines.

f) In keeping with the adaptive reuse and the need to minimize external impact on the original structural elements an internal steel frame was designed to support the new roof structure. This not only eased the construction approach, it also allowed structural works to proceed as the upgrading works were ongoing.

2.3 Design Approaches

2.3.1 Design Philosophy

The approach to the conservation building upgrading was to restore where possible all elements of the structure to its original intent coupled with the introduction of a new load bearing internal steel frame structure within the inner auditorium. The latter was thought necessary for the following reasons:

a) Fire damage had weakened the masonry elements particularly at the upper levels.
b) Several years of weathering due to complete exposure of the masonry elements had accelerated deterioration.
c) Change of use of the structure requiring large spans and increased loading due to the auditorium seating.
d) Re-establishment of the Chinese roof tiles which were significantly heavier than the sheet elements previously in place.

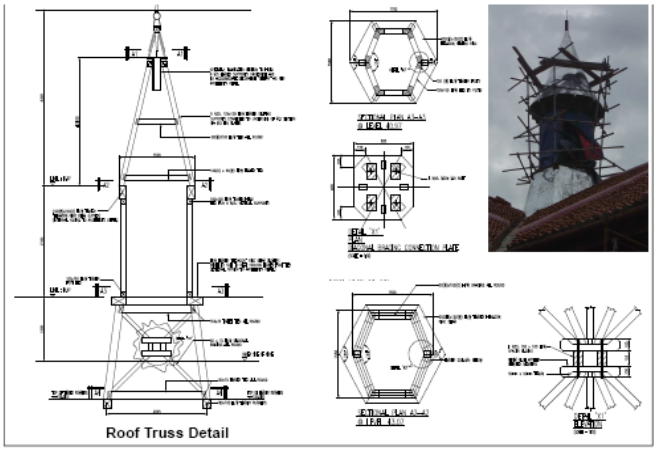

Figure 2. Roof Truss details reestablishing the original Bell Tower.

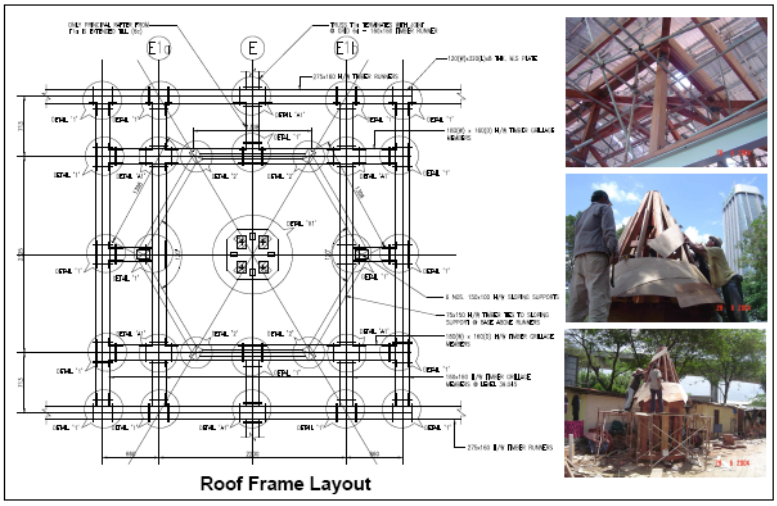

Figure 3. Roof truss Details- Timber roof to cater for new long spans for the adaptive reuse.

2.3.2 Key Design Considerations

The reinstatement of the existing structure needed to consider not only the problems of fire damage, water ingress, erosion and mould growth but also the structural strengthening needs particularly of arches and masonry elements.

Key design considerations included structural assessment and redesign, and the development of options for reinstatement, material consultancy including rising damp, timber retention and/or replacement, overall site drainage, redesign of the roofing system and conservation of ruins. The scope for the new structure involved a complete redesign. From the outset one of the parameters the team embarked upon was to introduce the timber truss system. This was deemed necessary as this constituted a primary component of the conservation building.

2.3.3 Conservation Building

Based on a detailed assessment the existing masonry walls, these were considered inappropriate as the primary structural member as outlined in Section 2.3.1.

A secondary inner steel fame was therefore recommended to be specially designed in order to take the structural loads. This required careful planning to avoid encroachment onto the existing structure with particular considerations at foundation level. This frame was also used to support the temporary roof cover during the upgrading works. To minimize the influence of the foundation works on the main structure, a cantilever strap beam arrangement was designed allowing the footing placement at > 600m away from the existing wall (see Figure 4). The footings and strap beams were designed to minimize any excavation requirements adjacent to the masonry wall foundations. A temporary support system was designed to shore the walls during construction which was also used as an access platform for the investigation and upgrading works.

2.3.4 Annex Building

The structure was designed as a conventional 3-storey concrete frame structure with a one level basement. Special attention was given to the basement works and foundation design such that any impact to the existing Conservation Building would be minimized. Of particular concern was the excavation works for the basement which required dewatering and potentially a draw down on the water table. The other was the potential uplift forces during the temporary construction phase which required anchoring of the basement.

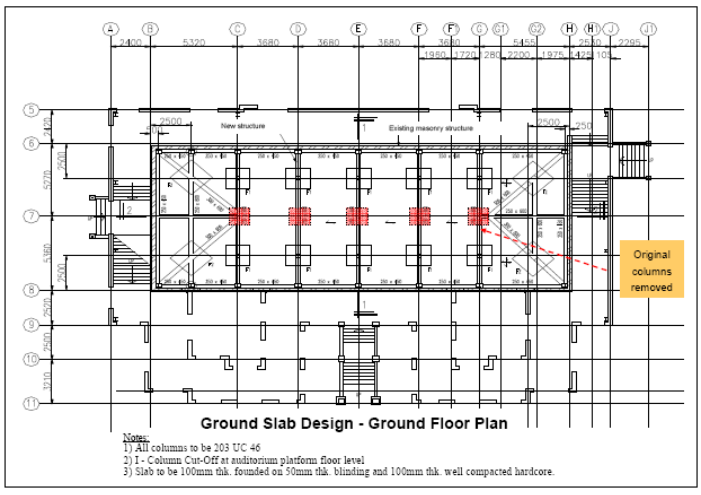

Figure 4. Ground Floor plan, central columns removed and new steel Frame structure in place

2.4 Design Solutions / Engineering Merit

2.4.1 Overview

The strategy and methodology adapted for this project consisted of the following:

a) The construction approach clearly required dividing the works into two distinct parcels. The conservation building was treated as a separate construction entity with a team of workers who were under strict guidance with skills training as deemed necessary to the conservation standards. The new Annex building was handled by a separate team of sub contractors.
b) Priority in terms of safety and stability of the existing Conservation Building was established while the construction of the new Annex Building was carried out. Adequate means and relevant procedures were observed.
c) Civil and structural works carried out positively addressed the issues of rainwater, impact and dewatering in safeguarding the Conservation Building during upgrading works.
d) All temporary works including scaffolding works and shoring works to the existing remains were handled very sensitively and in accordance to the norms of the standard practice where conservation is concerned.
e) The quality of workmanship and materials used were strictly adhered to as per specification requirements and the rigorous investigations undertaken on the conservation structure to confirm compatibility of approach.
f) The infrastructure works complemented the conservation works and where necessary conservation was given priority.

2.4.2 Conservation Building

a) Overview

Based on the historical significance of the structure and its deteriorated state due to the physical impact of the environment, the upgrading works undertaken required special attention and care. Of particular importance was the minimization of the potential impact of the adjacent annex building basement works and the new foundation and ground beam works within the auditorium which was required to house the new structural frame within the Conservation Building. Prior to any works starting the protection of the structure by temporary roof cover, bracing and shoring proceeded immediately and was fully in place. The shoring of the adjacent basement excavation against any soil collapse and the minimization of ground water seepage was established prior to the start of the works.

Ground engineering studies were undertaken to measure ground water fluctuations. In all cases permeability measurements were also taken to obtain accurate information about the soil properties and form a basis to predict ground water flow characteristics. Testing results were used to confirm suitability of the basement design and construction approach. This identified a clear danger to the conservation structure and required in-depth presentation to the client to change the original size and extent of the Annex Building basement and the introduction of a physical barrier between the Annex and Conservation buildings to minimize water flows.

b) Temporary Protection of the Structure

Footings of the conservation structure were much shallower than originally thought based on the information provided during the tender exercise. These were confirmed by measurement following excavation of the footings and were found to be only at 1m below ground level. The requirement for temporary shoring of the structure and additional protection of the masonry foundations prior to any excavations or work beginning was therefore imperative. A combination of methods was undertaken:

- the introduction of a secant pile wall and Jet Grouting as a physical barrier between the basement excavation and the conservation building.

- protection bracing of the structure using timber and/or steel elements.

c) Protection of the excavation

Following the basement excavation the sides of the basement embankments adjacent to the existing conservation building were shored by approved means. The secant pile wall socketed to rock was considered an adequate solution. The provision of a capping beam and strutting at corners provided additional measures required for stability during construction.

d) Monitoring and Instrumentation of adjacent structures

A rigorous monitoring regime was set up. This included monitoring points on the structural masonry elements closest to the basement excavation, temporary benchmarks, tilt monitoring and monitoring of building and ground settlements. The measurements were used as a basis to increase the shoring requirements as appropriate.

e) Mitigation of differential settlement

The monitoring results provided an indication of actual movement potential. A combination of construction sequencing and programming and measures to minimise ground water movement was undertaken as the mitigation approach. The adoption of secant pile provided a barrier against water flows and this minimised the risk of the associated settlement. This coupled with the reduced basement size and depth requirements as suggested by us was accepted and considered a workable solution.

f) Specialist Remedial Requirements

There were several issues concerning the upgrading of the fabric of the structure which required careful planning. This included plaster restoration, brickwork reinstatement, timber replacement (See Table 1) and the need to undertake trials, all of which impacted the overall programming of the structural framing requirements. Proposals from other specialists and contractors were incorporated into detailed method statements for the remedial treatment works.

g) Retention of Main Structure

The outer corridor structure was retained as its original design and layout with the masonry walls acting as the main structural members. In this case the actual loading on the structure could be maintained as there was no indication of any fire damage at the masonry wall levels. Random testing of the brickwork undertaken prior to contract award suggested that the strength of the bricks (See Table 2) were well above requirements and had not deteriorated despite the exposure to the environment.

Further testing of the bricks and mortar was commissioned to confirm the adequacy of the bricks for this purpose. Calculations based on the typical footing details obtained following the excavations and the expected structural loads indicated that the compressive strength required for the bricks was up to an order of magnitude below that reported following testing earlier undertaken. Steel frame trusses were used to allow the corresponding structural loads to be reduced accordingly.

A good proportion of the main masonry arches were pinned using a novel approach developed for this project and was found to be very cost effective.

3 PROJECT ACCOMPLISHMENT

3.1 Client Needs

The client needs can be outlined as follows:
a) Upgrading, conservation and preservation works need to be true to the authenticity and originality of the former design style, type and physical outlook.
b) Replacement of building materials should follow the Conservation requirements as imposed by the Museum and Antiquities Department.
c) Requirements compliance for adaptive reuse of the building to suit the new function, purpose and objectives.

3.2 Budget and Project Time Line

The project was successfully controlled due to the implementation of proper documentation in the forms of proformas and checklists undertaken at all stages of construction, i.e. pre-construction, during construction and post-construction periods. The difficulty in budget controls for conservation projects is well known due to unforeseen circumstances at the time of project procurement leading to intervention not originally considered necessary. In this case cost control was exercised, as the main issues of concern had been raised during the tender submission and the increased budget was related primarily to the need to establish protection measures against ground water movement and possible settlement of the Conservation Building. This was also one of the reasons for the delays in the original programme. The other was related to the procurement of Chinese tiles and special timber for the roof structure.

Table 1. Summary results of timber

No	Sampling Ref	Sample No	Zone	Type of Timber	Mean Compressive Strength (Across Grain) (Mpa)	Mean Compressive Strength (Along Grain) (Mpa)	Moisture Content (%)	Density Board at Test (kg/m3)
1	FJ/E1/23	F14	U	Merbau	6.22	48.15	16.45	743.69
2	FJ/M1/02	F2	N	Merbau	7.58	50.97	17.99	780.63
3	FJ/D1/18	F12	S	Merbau	8.52	59.68	15.43	748.61
4	FJ/M1/36	F5	M	Merbau	9.22	59.86	15.87	800.71
5	FJ/M3/01	F8	M	Merbau	9.7	59.38	14.86	794.33
6	FJ/M1/25	F4	M	Balau	10.5	55.7	15.1	886.77

Table 2. Summary results of bricks

Sample No.	Zone	Dimension			Moisture Content (%)	Water Absorption (%)	Compressive Strength (MN/m²)	Mineral	Major Components
		Length (mm)	Width (mm)	Thickness (mm)					
C1	N (O)	215	105	54	14.57	22.70	15.0	Quartz & Muscovite	Silica & Aluminum
C2	P (O)	216	107	55	9.24	21.00	14.0	Quartz & Muscovite	Silica & Aluminum
C3	M (O)	215	110	57	13.82	20.70	23.0	Quartz	Silica & Aluminium
C4	V (I)	217	105	54	2.46	22.60	27.0	Quartz & Muscovite	Silica & Aluminium
C5	S (I)	213	100	52	3.78	15.20	24.0	Quartz & Muscovite	Silica & Aluminium
C6	V (I)	191	90	52	1.94	14.80	20.5	Quartz & Muscovite	Silica & Aluminium
C7	B (I)	-	-	-	-	-	13.5	-	-
C8	M (O)	-	-	-	-	-	21.5	-	-
C9	C (I)	-	-	-	-	-	19.5	-	-
C10	H (O)	-	-	-	-	-	18.5	-	-

Table 3. Mortar & plaster compositions

No	Component	Range of Composition Ratio
	Mortar	
1	Sand	38-45
2	Lime	6-11
3	Water	5-9
4	Clay	1
	Plaster	
1	Sand	41- 47
2	Lime	7 – 11
3	Water	5 – 9
4	Clay	1

3.3 Overview

The ultimate client for the project was the Department of Museum and Antiquities of the Ministry of Tourism, Culture and Arts who controlled the budget allocation. A key Client requirement was the conservation and upgrading of the badly decayed building to suit the new function while at the same time maintaining the originality and authenticity of the building design and style. The project was completed with constraints on budget and design alternatives were constantly reviewed to achieve the most feasible and cost-effective solutions. Following engineering feedback, overall concept changes were made after award of the contract. This resulted in an improved overall development, minimization of risk to the Conservation Building and matched the client's overall objectives closely (see Figure 5).

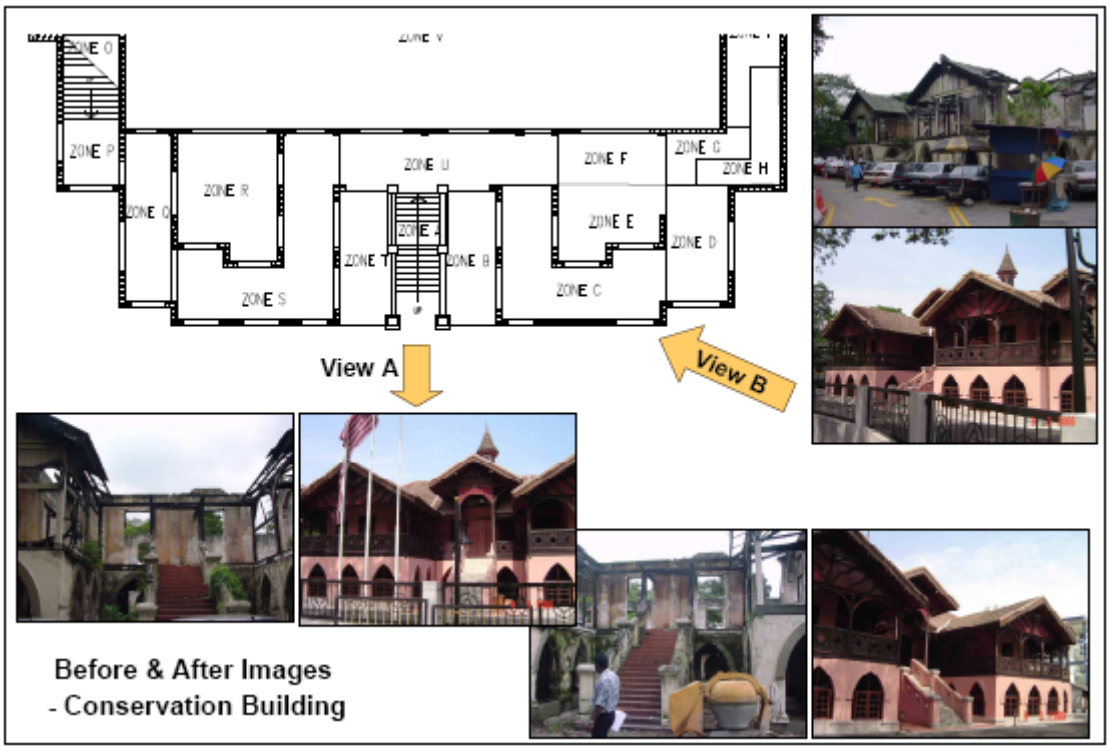

Figure 5. Before and after views of the front of the building.

Classification of Restoration Mortars by Principal Component Analysis and Correlation Between Their Properties and Synthesis

Antonia Moropoulou [1]
Kyriaki Polikreti [2]
Petros Moundoulas [3]
Eleni Aggelakopoulou [4]

T 25

ABSTRACT

During historic building restoration works, one of the most critical factors in planning syntheses for durable restoration mortars is to understand the correlation between mortar properties and raw materials.

Towards this direction, the present work aims to prove that multivariate statistics and especially Principal Component Analysis (PCA) is an invaluable tool for classifying restoration mortars in separate groups, depending on their synthesis and physicochemical characteristics. Different syntheses of restoration mortars were prepared using traditional techniques and materials such as binders (aerial and natural hydraulic lime), pozzolanic additives (natural and artificial pozzolanas) and aggregates (sand and crushed brick).

Thirty five samples in total were analysed by thermal analyses (differential thermal analysis [DTA] and thermogravimetric analysis [TGA]), mercury intrusion porosimetry and mechanical strength tests. The results give us a very useful and illustrative tool in and planning syntheses for restoration purposes.

KEYWORDS

Restoration mortars, Principal Component Analysis, Historic buildings, Thermal analysis, Mercury intrusion porosimetry, Mechanical strength test

[1] National Technical University of Athens, Department of Chemical Engineering, Zografou Campus, 9 Iroon Polytechniou Street, Athens 157 73, Greece, Phone +30 210 7721429, Fax 210 7723215, amoropul@central.ntua.gr
[2] Hellenic Ministry of Culture, Directorate of Conservation of Ancient and Modern Monuments, Department of Applied Research, Peiraios 81, 105 53, Greece, +30 210 3218475, +30 210 3310342, kpolikre@ucy.ac.cy
[3] National Technical University of Athens, Department of Chemical Engineering, Zografou Campus, 9 Iroon Polytechniou Street, Athens 157 73, Greece, Phone, Phone +30 210 7721429, Fax 210 7723215, pmoun@central.ntua.gr
[4] National Technical University of Athens, Department of Chemical Engineering, Zografou Campus, 9 Iroon Polytechniou Street, Athens 157 73, Greece, Phone +30 210 7721429, Fax 210 7723215, lagela@central.ntua.gr

1. INTRODUCTION

It is well known that historic building restoration interventions may cause significant failures and accelerate degradation of the building elements, if the restoration materials are not compatible to the original ones. Especially in the case of mortar restoration, cement-based materials have been proved improper for major or minor restoration works [Fassina & Borsela 1993; Moropoulou 2000]. However, the term "compatibility" is vague and not clearly defined and guidelines for compatible mortars do not yet exist [von Konow 1997].

Towards this direction, the present work aims to prove that multivariate statistics and especially Principal Component Analysis (PCA) is an invaluable tool for classifying restoration mortars in separate groups, depending on their synthesis and physicochemical characteristics. PCA is a technique for simplifying a data set, by reducing the number of variables [Davies 1986]. Due to its effectiveness in 'summarizing' data, PCA reveals similarities and differences and is usually the first step to search for groups in large data sets.

The technique has previously been used by Moropoulou *et al.* [2003] to classify historical mortars. A similar approach will be presented in here for restoration mortars. The restoration mortars presented herein belong to two different series. First is a series of sixteen (16) laboratory syntheses, made for research purposes and second a series of twenty seven (27) restoration mortars, which have been prepared for real application on historic buildings. The first series includes pastes with different pozzolans, that is natural, artificial and highly reactive pozzolans [Moropoulou *et al.* 2004). The second series includes pastes, which have been prepared for restoring the Basilica of Aghia Sophia (Istanbul, Turkey), a water-mill at Veroia (Greece) and an orphanage at Aigina (Greece).

2. MATERIALS AND TECHNIQUES

The first series of pastes includes syntheses which were prepared by mixing a commercial lime with three types of pozzolans (Table 1): a natural pozzolan (earth of Melos island, Greece - EM), an artificial pozzolan (ceramic powder of ground, handmade bricks fired at low temperatures - CP) — and an artificial highly reactive pozzolan (metakaolin - Metastar 501 of IMERYS Minerals Ltd. – MK). Mortars indicated by L and LPu are referred to lime powder and lime putty mortars. All syntheses are produced by quartz sand except the LCal and LPuCal syntheses where a calcite sand was used. The exact chemical composition of the pozzolans is given in Moropoulou *et al.* [2004]. The metakaolin is the finest pozzolan with cumulative passing percentage (CPP) at 64 μm of 100% and at 16 μm up to 95.6%, the earth of Milos shows a CPP from 64 μm up to 95.9% and the corresponding percentage for the ceramic powder is up to 88.1%. The second series of syntheses is given in Table 2. Lime putty, lime powder and natural hydraulic lime were used as binding materials. Lime putty is generally encountered in historic mortars, while lime powder was used as an alternative binding material for the substitution of lime putty due to the higher and quasi-stable percentage of $Ca(OH)_2$ content. The aggregate materials were mainly siliceous sand and crushed brick. The former has already been detected in historic mortar samples with the effect of producing lightweight mortars, due to its lower bulk density in respect to the sand aggregates, along with lower modulus of elasticity that it provides. In some of the mixtures natural and artificial pozzolanic additions (Melos earth, Ceramic Powder respectively) were used.

Samples from the pastes were analysed by Mercury Intrusion Porosimetry, Differential Thermal Analysis (DTA), Thermogravimetric Analysis (TGA) and tested by mechanical strength tests. DTA and TGA were carried out (DTA/TG, Netzsch 409EP), in a static air atmosphere with heating rate of 10 ^{0}C/min from 25–1000 ^{0}C. Measurements were done on the total sample and on the fraction smaller than 63 μm, which constitutes the binding materials [Bakolas *et al.* 1998]. A Carlo Erba 4000 mercury porosimeter was used for porosimetry measurements and the cylindrical mathematical model was employed to elaborate the results. Tests on compressive and flexural strengths were carried out at 12

months (Toni-Technik DKD-K-23301 compressive tester/load rate: 0.01 kN/s, ToniTechnik-D-70804 flexural tester/load rate: 0.05 kN/s). The results for the two series of data are given in Tables 3 and 4.

Table 1. Syntheses for the first series of restoration mortars.

Sample	*Pozzolan type*	*Lime/Pozzolan*	*Sample*	*Pozzolan type*	*Lime/Pozzolan*
L	-	-	EM1	Melos earth	1/1
Lpu	-	-	EM2	"	1/2
LCal	-	-	EM3	"	1/3
LPuCal	-	-	EM4	"	1/4
MK1	Metakaoline	1/1	CP1	Ceramic powder	1/1
MK05	"	1/0.5	CP2	"	1/2
MK5	"	1/5	CP3	"	1/3
MK2.5	"	1/2.5	CP4	"	1/4

Table 2. Syntheses for the second series of restoration mortars: AS = Aghia Sophia, Istanbul, Turkey, BE = Water-mill at Veroia, Greece, EG = Orphanage, Aigina, Greece, REF = Reference samples.

	LP	*LPo*	*NHL*	*CS*	*FS*	*CB*	*NP*	*AP*	*A*	*C*
AS1	30	0	0	70	0.0	0.0	0	0	0	0
BE1	35	0	0	65	0.0	0.0	0	0	0	0
AS2	37	0	0	0	63.0	0.0	0	0	0	0
BE2	35	0	0	0	65.0	0.0	0	0	0	0
AS3	30	0	0	0	31.5	38.5	0	0	0	0
ASA3	40	0	0	0	30.0	30.0	0	0	0	0
AS4	0	0	25	75	0.0	0.0	0	0	0	0
BE4	0	0	25	75	0.0	0.0	0	0	0	0
AS5	0	0	25	0	75.0	0.0	0	0	0	0
EG5	0	0	27	0	7.0	0.0	66	0	0	0
AS6	0	0	29	0	0.0	70.0	0	0	1	0
AS7	0	0	25	0	32.0	43.0	0	0	0	0
ASA7	0	0	30	0	35.0	35.0	0	0	0	0
AS8	20	0	0	70	0.0	0.0	10	0	0	0
BE8	20	0	0	65	0.0	0.0	15	0	0	0
AS9	20	0	0	70	0.0	10.0	0	0	0	0
AS10	20	0	0	0	31.5	38.5	0	10	0	0
ASA10	25	0	0	0	25.0	25.0	0	25	0	0
EG10	25	0	0	0	25.0	25.0	0	25	0	0
AS11	20	0	0	0	31.5	38.5	10	0	0	0
ASA11	25	0	0	0	25.0	25.0	25	0	0	0
REF1	25	0	0	0	70.0	0.0	0	0	0	5
REF2	25	0	0	0	31.5	38.5	0	0	0	5
ASA12	0	35	0	0	30.0	35.0	0	0	0	0
EG12	0	17	0	0	66.0	0.0	17	0	0	0
EG12a	0	17	0	0	66.0	0.0	17	0	0	0
EG12a1	0	11	0	0	66.0	0.0	22	0	0	0

LP=Lime Putty, LPo=Powder of lime, NHL=Natural Hydraulic Lime, CS=Coarse Sand, FS=Fine Sand, CB=Crushed Brick, NP=Natural Pozzolan, AP=Artificial Pozzolan, A=Aluminum powder, C=Cement

Table 3. Results of Mercury Intrusion Porosimetry, Thermal Analysis and Strength Tests for the mortars of Table 1.

Sample	*SSA* (mm^2/g)	*PR* (μm)	*Db* (g/cm^3)	*Por* (%)	*H*	*H-CH*	*CH*	*CH* (%)	CO_2 (%)	*Ff* (MPa)	*Fc* (MPa)	*Fc/Ff*
L	3.37	0.59	1.67	34.53	0.32	2.37	9.74	57	9.49	1.33	3.67	2.8
Lpu	3.52	14.01	1.75	32.85	0.13	2.42	9.95	53	7.32	0.90	2.17	2.4
LCal	3.33	0.53	1.65	37.81	0.12	1.81	7.44	65	39.75	1.43	4.68	3.3
LPuCal	3.09	15.64	1.75	33.91	0.14	2.52	10.35	54	34.88	1.12	2.18	1.9
MK1	18.06	0.03	1.63	36.22	5.27	0.00	0.00	100	2.14	1.59	8.95	5.6
MK05	10.41	0.04	1.60	37.46	5.38	0.00	0.00	100	4.85	1.54	7.76	5.0
MK5	5.56	0.29	1.75	33.57	3.60	0.00	0.00	100	10.70	1.51	5.88	3.9
MK2.5	4.15	0.32	1.73	34.30	1.91	0.00	0.00	100	12.38	1.59	3.92	2.5
EM1	2.76	0.64	1.79	31.85	2.87	0.00	0.00	100	6.65	0.70	1.78	2.5
EM2	3.39	0.70	1.86	31.71	2.54	0.00	0.00	100	4.70	0.26	1.25	4.8
EM3	3.96	0.86	1.82	30.41	1.97	0.00	0.00	100	3.19	0.27	1.67	6.2
EM4	3.37	0.73	1.82	31.30	2.39	0.00	0.00	100	2.68	0.20	1.25	6.3
CP1	3.20	0.45	1.78	34.39	0.58	0.53	1.93	86	6.49	0.61	2.07	3.4
CP2	3.46	0.50	1.84	32.19	0.72	0.19	0.76	91	4.86	0.67	1.88	2.8
CP3	3.04	0.49	1.84	31.96	0.92	0.00	0.00	100	4.23	0.35	1.63	4.7
CP4	3.74	0.55	1.83	31.54	0.53	0.00	0.00	100	3.37	0.40	1.65	4.1

SSA = Specific Surface Area, PR = Pore Radius, Db = Bulk density, Por = Total Porosity, H = Mass loss attributed to hygroscopic water (%) for lime mortars and to water of CSH for pozzolanic ones, H-HC = Mass loss attributed to water of Ca(OH)2, CH = $Ca(OH)_2$, CH = consumed $Ca(OH)_2$, CO_2 = Mass loss attributed to CaCO3 (%), Fc = Compressive strength, Ff = Flexural strength.

3. RESULTS AND DISCUSSION

The application of PCA on the two data series gave a number of Principal Components (PCs), the two first of which are given in Figures 1a and 2a. These figures show the projection of the original variables on the PCs plane. Figures 1a and 2a are very useful because they help us understand the contribution of the original variables to each PC.

Three well defined and distinct groups are formed in Figure 1b. The lime mortars are very well separated from all the other samples. The critical variables for this separation are H, H-CH, CO_2 and Pore Radius, Porosity. Lime mortars present larger values of pore radius average attributed to the nature of binder and larger values of H-CH and H-CH since there is no addition of pozzolan in their pastes.

The group of pastes with the artificial pozzolan (metakaoline, MK) is also very compact and easily discriminated by the others. The critical variables are Specific Surface Area, Fc and H. Metakaolin is a high reactive pozzolan, leading to high values of chemical bound water, dense microstructure and high values of compressive and flexural strength.

As for the mortars with crushed brick, they are grouped very close to those with Melos earth. Altogether form another well defined group, separated from the others, with density being the critical variable. Both pozzolanic additions did not exhibit a high pozzolanic activity therefore their characteristics are analogous.

As it is shown from the plots of Figure 2b, there is a strong relation between the presence of pozzolanic additives and the high values of chemically bound water, but also the high values of compressive and flexural strength. At the same time the rates of carbonation remain high allowing the quick setting and hardening. We have also to note the development of a microstructure with greater values of specific surface area and lower values of average pore radious and total porosity.

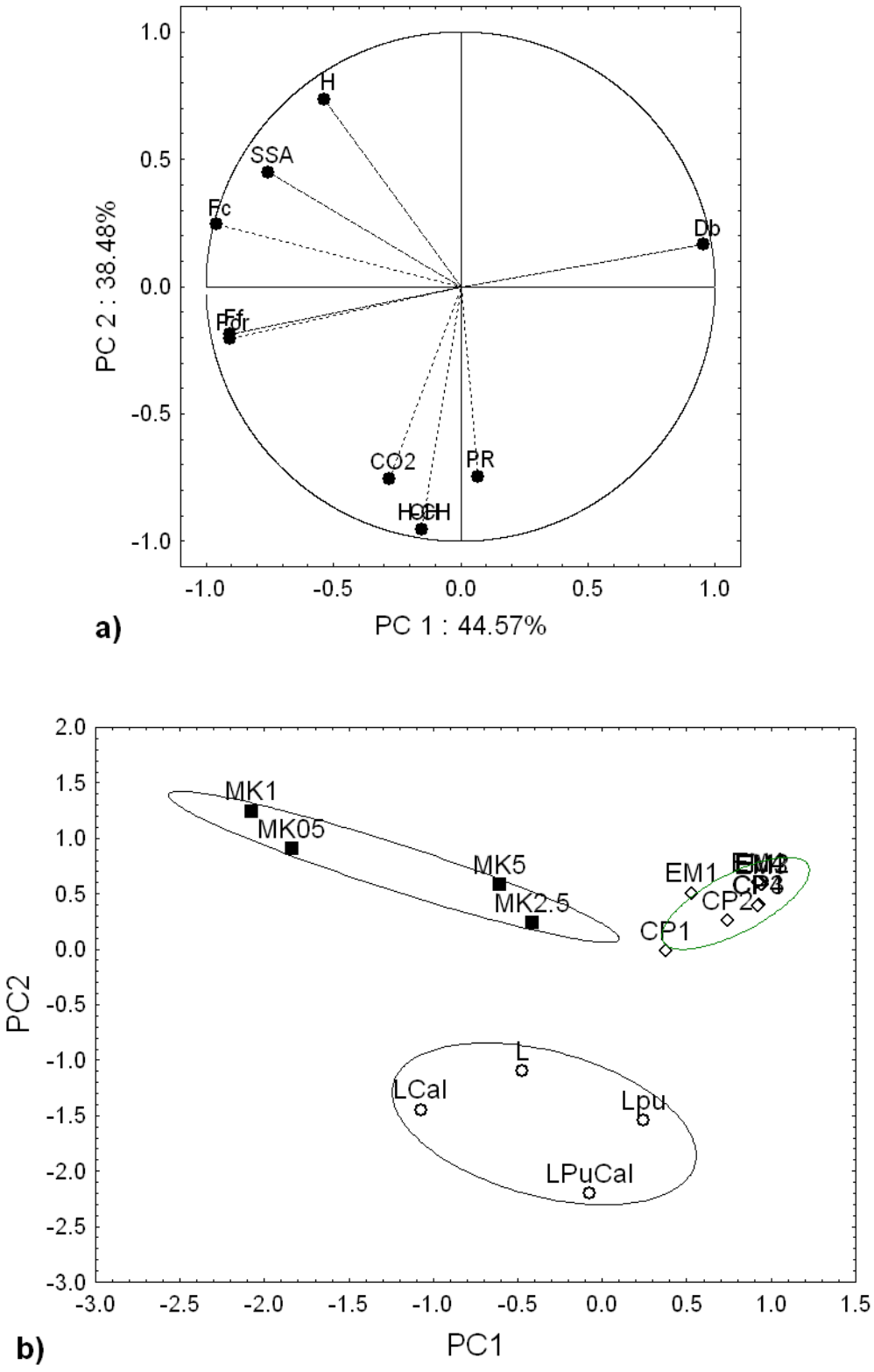

Figure 1. First series of samples: a) Projection of the variables on the plane of the Principal Components 1 and 2 and b) The PCA scores of the first series of the mortar samples

Table 4. Results of Mercury Intrusion Porosimetry, Thermal Analysis and Strength Tests for the mortars of Table 2

Sample	SSA (mm^2/g)	PR (μm)	Db (g/cm^3)	Por (%)	CBW (%)	$CaOH_2$	CO_2 (%)	Ff (MPa)	Fc (MPa)	Fx (MPa)
AS1	2.37	0.40	2.01	28.40	0.75	0.24	19.02	0.50	1.60	0.30
AS2	2.99	7.52	1.88	35.80	0.50	1.07	11.28	0.70	1.90	0.50
AS3	4.75	0.42	1.72	40.80	0.62	0.68	9.98	0.40	1.30	0.30
AS4	4.24	0.28	1.90	28.70	1.90	0.00	16.47	1.00	4.50	0.70
AS5	3.59	0.27	1.75	33.10	2.03	0.00	11.12	0.80	2.90	0.50
AS6	5.80	1.16	1.54	42.20	1.29	0.39	30.75	1.90	5.40	1.30
AS7	4.57	0.32	1.74	38.90	2.22	0.00	11.09	0.80	3.50	0.50
AS8	1.85	0.43	2.06	31.60	0.85	0.39	11.14	0.40	1.50	0.30
AS9	2.22	0.41	2.00	29.60	1.01	0.24	11.15	0.50	1.90	0.30
AS10	3.57	0.50	1.77	41.10	0.61	0.19	7.23	0.60	2.50	0.40
AS11	2.02	0.58	1.71	44.50	0.95	0.25	7.41	0.50	0.60	0.30
REF1	2.62	0.42	1.90	29.00	0.91	0.36	14.03	0.30	1.70	0.20
REF2	4.34	0.57	1.60	41.70	1.14	0.40	10.23	0.40	0.70	0.30
ASA7	5.24	1.43	1.70	36.77	2.52	0.00	12.07	2.53	0.62	0.41
ASA3	5.91	0.45	1.75	39.51	0.73	0.82	11.30	1.34	0.52	0.35
ASA12	5.90	0.38	1.61	39.96	0.82	0.91	10.60	2.40	0.76	0.51
ASA11	4.24	2.14	1.53	39.43	1.54	0.47	8.74	1.12	0.40	0.27
ASA10	5.64	0.68	1.58	39.85	0.76	0.25	8.62	1.23	0.46	0.31
EG10	6.47	0.41	1.64	37.53	0.82	0.31	7.93	4.36	1.03	0.69
BE4	8.91	0.38	1.64	34.00	4.69	0.75	19.49	0.90	4.40	0.60
BE8	5.97	0.73	1.69	35.90	3.55	0.89	20.62	0.35	1.85	0.23
BE1	3.47	0.77	1.72	36.20	1.66	1.01	24.69	0.30	1.50	0.20
BE2	3.09	0.75	1.66	36.20	1.72	1.21	24.88	0.30	1.45	0.20
EG5	7.50	0.37	1.72	35.50	4.28	0.15	20.46	0.72	3.86	0.48
EG12	2.93	0.76	1.75	33.20	3.44	0.76	18.50	0.30	0.75	0.20
EG12a	2.88	0.98	1.70	34.20	2.62	1.02	19.45	0.30	0.68	0.20
EG12a1	5.12	0.67	1.68	33.80	4.68	0.24	13.47	0.36	1.62	0.24

SSA = Specific Surface Area, PR = Pore Radius, Db = Bulk Density, Por = Total Porosity, CBW= Chemically Bound Water, CO_2 = Mass loss attributed to CaCO3 (%) , Fc = Compressive strength, Ff = Flexural strength.

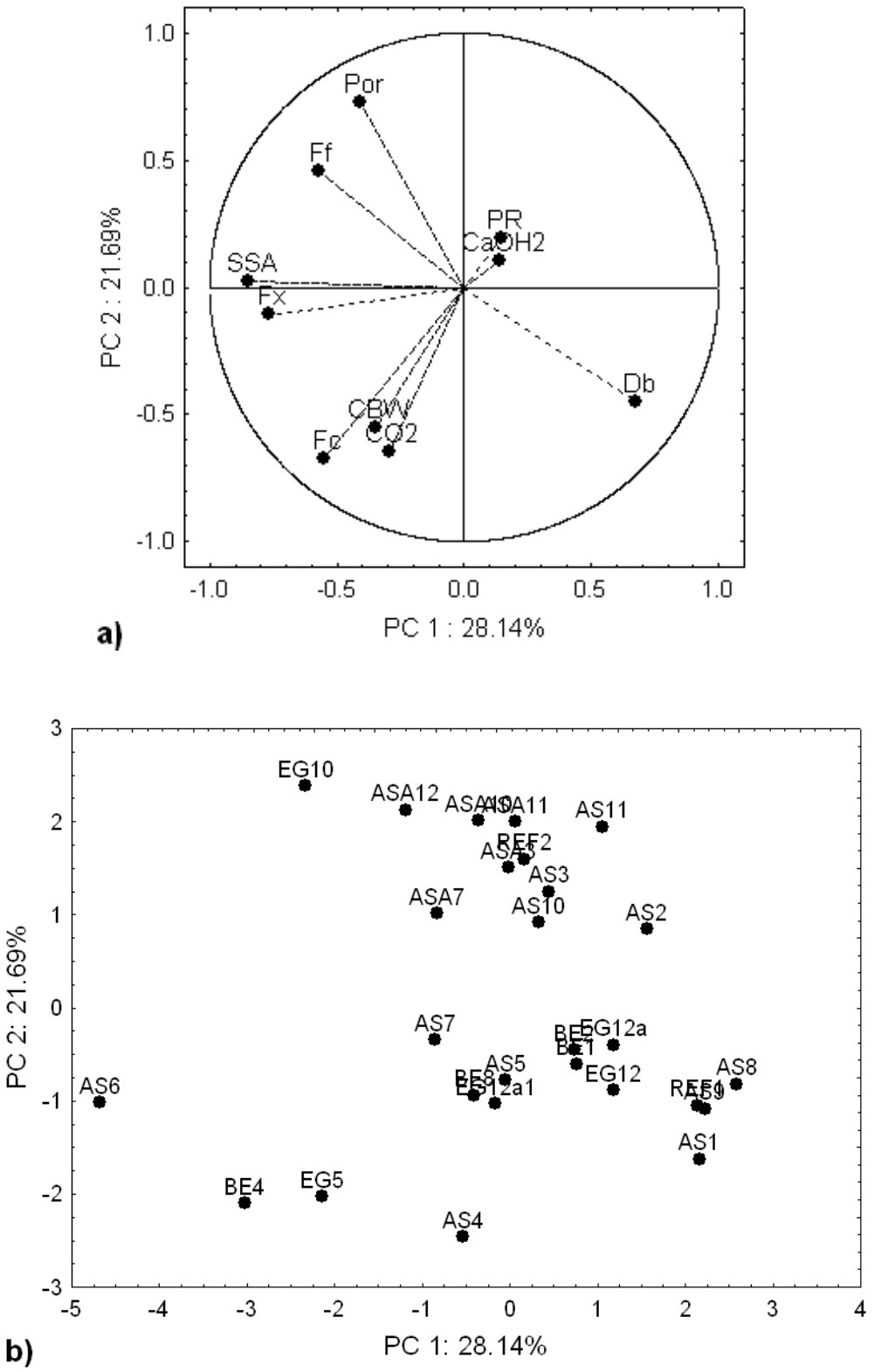

Figure 2. Second series of samples: a) Projection of the variables on the plane of the Principal Components 1 and 2 and b) The PCA scores of the second series of the mortar samples

These are the main characteristics of the restoration mortars for the orphanage at Aigina and the water-mill at Veroia. The mortars with active aggregates (crushed brick) show a different behavior, mainly because the specific microstructure of the ceramics influence the results of the microstructure reported. On the other hand and in the cases where pozzolanic additives or active aggregates were not used the main aim was the compatibility with the historic compounds. In these cases the development of high values of strength was not the main issue. In these cases there is a strong relation between the lower carbonation rate with the development of a certain microstructure (greater average pore radious, higher values of total porosity) and lower values of strength.

4. CONCLUSIONS

In order to ensure compatibility of restoration mortars the present work used PCA for classifying restoration mortars, depending on their synthesis and physicochemical characteristics. The results of Mercury Intrusion Porosimetry, Thermal Analysis and Strength Tests for thirty five mortar samples were treated with PCA. The results may contribute in the future, in developing guidelines for compatible restoration mortars.

REFERENCES

Bakolas, A., Biscontin, G., Moropoulou, A. & Zendri, E. 1998, 'Characterization of structural Byzantine mortars by Thermogravimetric analysis', *Thermochimica Acta*, **321**[1–2], 151–160.

Davies, J.C. 1986, *Statistics and data analysis in geology*, John Wiley and Sons, New York.

Fassina, V. & Borsela, S. 1993, 'The effects of past treatments on the acceleration of weathering processes in the statues of Prato Delle Valle', Proc. UNESCO-RILEM Congr. on the Conservation of Stone and Other Materials, Paris, 1993. p. 129.

Moropoulou, A. 2000, 'Reverse engineering to discover traditional technologies: a proper approach for compatible restoration mortars', Proc. PACT 58 - Compatible Materials for the Protection of European Cultural Heritage Conf., Athens: Technical Chamber of Greece, pp. 81–107.

Moropoulou, A., Bakolas, A. & Aggelakopoulou, E. 2004, 'Evaluation of pozzolanic activity of natural and artificial pozzolans by thermal analysis', *Thermochimica Acta*, **420**, 135–140.

Moropoulou, A., Polikreti, K., Bakolas, A. & Michaelides, P. 2003, 'Correlation of physicochemical and mechanical properties of historical mortars and classification by multivariate statistics', *Cement and Concrete Research*, **33**[6], 891-898.

Von Konow, T. 1997, 'Reliable restoration mortars—requirements and composition', Proc. 4th Int. Symp. on Conservation of Monuments in the Mediterranean Basin, Technical Chamber of Greece, Rhodes, 1997, vol. 4, pp. 415–425.

Technological Features and Decay Processes of A "New" Building Type at The Beginning of XX Century

Fabio Fatiguso [1]
Giambattista De Tommasi [2]

T 25

ABSTRACT

Building at the beginning of the 20th century results from a "transitional" architectural knowledge, where the traditional culture (connected to Best Practice Codes) and the modern one (resulting from the Industrial Revolution), join together. From a constructional and technological point of view, a new building "type" is defined, *mixed structure building*, characterised by the combination and/or the substitution of traditional building elements with other ones made out of "new" materials and techniques. Experience shows that such buildings were subjected, during the years, to ageing due to a material and "technological" decay that was increased and not prevented at all. This study gives an overview of mixed structure buildings, as a result of a progressive transformation. Moreover, it highlights potential critical aspects and specific decay processes. The research defines material, technical, technological features of the "new" building type and it analyzes physical, technological, functional and normative decay. It classifies the material and technological decay processes and it localizes potential lacking points where decay can generate. The research aims at systematizing all the information about this heritage in order to define specific methodologies and guidelines for maintenance and renovation of performance quality.

KEYWORDS

Refurbishment; Maintenance; Mixed-structure-buildings; Construction technologies; Decay processes

[1] DAU – Department of Architecture and Town Planning, Technical University of Bari, Via Orabona, 4 70125 Bari Italy Tel. (+39) 080/5963789-5963347 Fax (+39) 080/5963348, f.fatiguso@poliba.it
[2] DAU - Department of Architecture and Town Planning, Technical University of Bari, Via Orabona, 4 70125 Bari ItalyTel. (+39) 080/5963342-5963347 Fax (+39) 080/5963348, g.detommasi@ poliba.it

1 INTRODUCTION

Between the end of the 19th century and the beginning of the 20th century, buildings are characterized by a progressive combination and/or substitution of traditional materials and constructional techniques with modern ones. This process is referred to a general transformation within the historical, social, economic and cultural context. The co-presence of traditional and modern elements caused evident and peculiar decay effects. This study explains the most significant results of a research funded by the Italian Ministry of University on knowledge and conservation of mixed structure buildings at the beginning of the 20th century, in terms of materials, techniques and technologies. The aim is to define maintenance guidelines and tools for recovering the lost qualities and adapting to new performance requirements [De Tommasi 2007].

2 A "NEW" BUILDING TYPE AT THE BEGINNING OF 20th CENTURY

Buildings in the first decades of the 20th century result from a "transitional" architectural knowledge, where the traditional culture (connected to Best Practice Codes) and the modern one (resulting from the experimental activities during the Industrial Revolution), join together. In that period, great trust is given to innovative materials and techniques, their possible uses and their durability. In fact, there is the progressive introduction of "modern" materials and elements in "traditional" techniques and technologies for buildings [Curioni, 1873]. The result is a new building type, *the mixed structure construction*, that shows the co-presence of materials and elements from pre-modern construction tradition – vertical bearing walls made of stone and/or bricks – and of "new" materials and elements – iron and cement, wooden and iron floors, iron and bricks floors, reinforced concrete floors and vertical elements realised with iron columns, concrete beams and pillars -. At the beginning, floors with I-shape iron beams as bearing element are widely used; they are finished with little vaults in natural or artificial blocks, with "volterrane" and "hollow flat blocks". Technical and technological solutions become more and more complex after the evolution of scientific studies and components [Formenti 1893]. Such innovation, in a construction process which was unchanged for centuries, doesn't change the constructional, technological and functional conception of the building. Progressive introduction of reinforced concrete structures, as a result of experimentations and application of static calculation theory [Morsch 1930], doesn't modify the described situation. By the way, in the reality, structural and constructional conception of building is changing. Some new building features are: increased loads and strengthening of horizontal floors, more efficient connections between horizontal and vertical elements, decreased capacity of masonry to undergo light differential assessments. The evolution of studies and technological solutions, as well as of functional requirements determines the diffusion of frame structures (beams and pillars), first only for substitution of main wall of the buildings. Only after a long time the use of frame structure concerns the building as a whole system with the consequent advantages from the function and distribution point of view.

3 THE CONSERVATION OF MIXED STRUCTURE BUILDINGS

Experience has shown that such buildings – combining very different techniques and materials - were subjected, throughout the years (and they are still subjected), to ageing caused by an increasing and unpredictable material and "technological" decay. The consequent reduction of the service life and the presence of elements with decreased performances are due to the concomitant actions of physiological and pathological factors. This is mostly evident in some specific "critical points", and often determined by the overlap (and supposed integration) between traditional and modern materials and techniques or by the employment of technologies under experimentation that were not jet durable and reliable enough.
During the time the mixed structure heritage has also undergone a constant adaptation to new requirements concerning function and safety issues, as well as compliance to new codes. These adaptations and maintenance interventions were often carried out without supervision and by unskilled

operators. As a consequence, they frequently have caused a further significant decrease of the performance qualities to the technical elements/subsystems and to the whole building. Some maintenance works often underestimated decay processes and causes, so that pathologies appeared again after a short time. Moreover, the short term of transition from the traditional structure to the modern one (30- 40 years) caused a low attention towards the mixed structure building typology, which has been not too much explored. It was just seen as an extension of the masonry building tradition or as an anticipation of the modern constructional techniques and of the reinforced concrete buildings.

4 A METHODOLOGICAL APPROACH TO MAINTENANCE AND REFURBISHMENT

Then, a methodological approach is necessary that considers the specific material, technical and constructional features and the more frequent pathologies of mixed structure buildings. The approach should define appropriate and congruent activities for recovering the lost performances and meeting the actual quality standards. Nevertheless, a mature historical and architectural sensibility has recognized the relevant interest of buildings of the first years of the 20th century as a heritage to preserve through specific interventions. Certainly, it doesn't make sense the obstinate conservation and/or the re-proposition of unrecoverable materials and constructional technologies, because they did not show durability during the time, they are replaced by new and more efficient products and their production is not sustainable anymore. As a consequence, the methodological approach comes from the identification of pathologies and performance losses and from the analysis of well known intervention typologies, related to the single technical elements. This approach refers to a well established procedure of survey, analysis and design. It is specifically developed for mixed structure buildings, by the typology recognition of technical elements. It identifies frequent pathologies and performance losses, relative causes and correlated diagnostic surveys. Finally it defines possible maintenance and refurbishment works.

Table 1. Scheme of approach of analysis and refurbishment process.

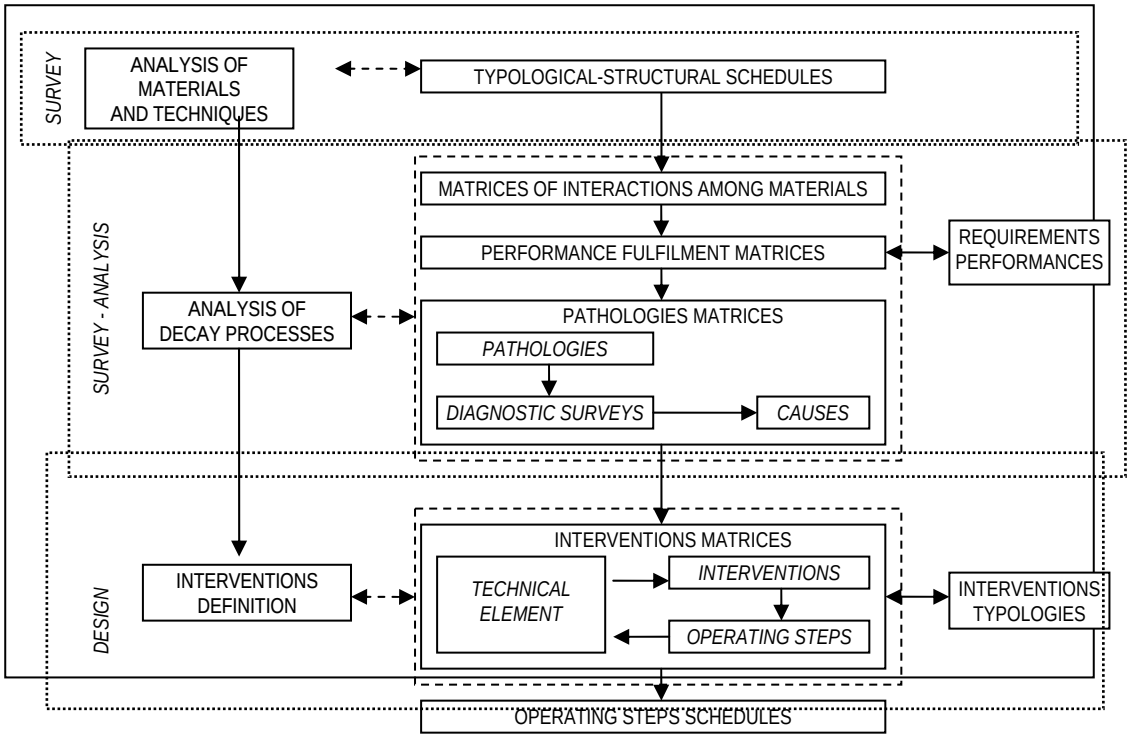

The approach, whose scheme is shown in the Tab.1, is structured as an ordered multilevel sequence of schedules and synthesis matrixes, guide and control tools of the whole design path.
The initial procedural step is the typological analysis and the identification of the material, technical and constructional features. It allows, through typological and constructional schedules (par. 4.1), the recognition of the technical elements according to a taxonomic systematization from the technological point of view. The following phase is the analysis of obsolescence and decay processes. Since that, for each technical element, residual performances and pathological alterations are recognized, through the crossed exam of the matrixes, referred to the interaction of materials, the performance behaviour and the pathologies (par. 4.2).
The previous elements define the relations between the performances losses, the verifiable pathologies, the possible causes and the relative diagnostic surveys. As a consequence the diagnosis can be carried out with an acceptable level of reliability. As far as the refurbishment and maintenance works are concerned, an intervention matrix (par. 4.3) correlates the possible intervention solutions to the single technical elements, also by describing the operating phases of each intervention. The planner can choose the interventions among several typologies in the matrix, also correlating to the context specificity. Once defined the intervention and its consequent articulation, the operative phases schedules provide with the specific techniques that are congruent and appropriate.

4.1 Building Technologies

The initial research step is focused on the knowledge systematisation of buildings of first decades of the 20th century, through the analysis of the historical and technical evolution and the definition of the new building type features. Such step results from the comparison between technical information related to constructional elements in handbook literature (1850-1940), as well as from some “case studies” which, for typology, extension, morphological and constructional features, can be considered representative.
These case studies refer to the public residential state built in Apulia and Basilicata Regions between 1900 e 1940. Specifically, the research considered 23 existing building complexes (totally 110 dwellings). For all the buildings, cataloguing, technical and constructional survey and analysis of material-typological-structural features of technological units have been carried out.
The study has allowed a taxonomical systematisation of technological units, sub-systems and technical element classes as well as the definition of their typological construction, technological and structural features. The results are shown in analysis schedules (fig. 1). Analysis schedules point out some example schemes of possible basic typologies (eventually with some variants), geometry and dimensions of single elements, employed materials and techniques, technological solutions, connections with vertical bearing structures.
The research was focused on technical elements of floors, staircases and balconies, for which major variety of types, materials and solutions does exist. For instance, as far as the floors are concerned, they are characterized by different materials and techniques, even if they are in the same building. There should be traditional vaults, as well as more modern floors, realized by several technological solutions. Case studies in Basilicata Region and in Foggia city show some floors with iron beams, connected with typical lateritious elements like “tavelloni”, “pignatte”, volterrane” and “voltine”. In some building complexes in Matera city lateritious elements are replaced by tuff block, certainly less expensive and more available on the territory. Nevertheless, in Bari there are many floors made out of reinforced concrete slabs or reinforced concrete beams and light hollow flat blocks.

4.2 Decay Processes and Pathologies

The research allowed to define, for each technical element within the mixed structure system, as previously scheduled, potential critical points for decay. It also allowed characterize obsolescence processes by verifying performance requirements, coming from the actual dispositions and the survey of alterations and pathologies.

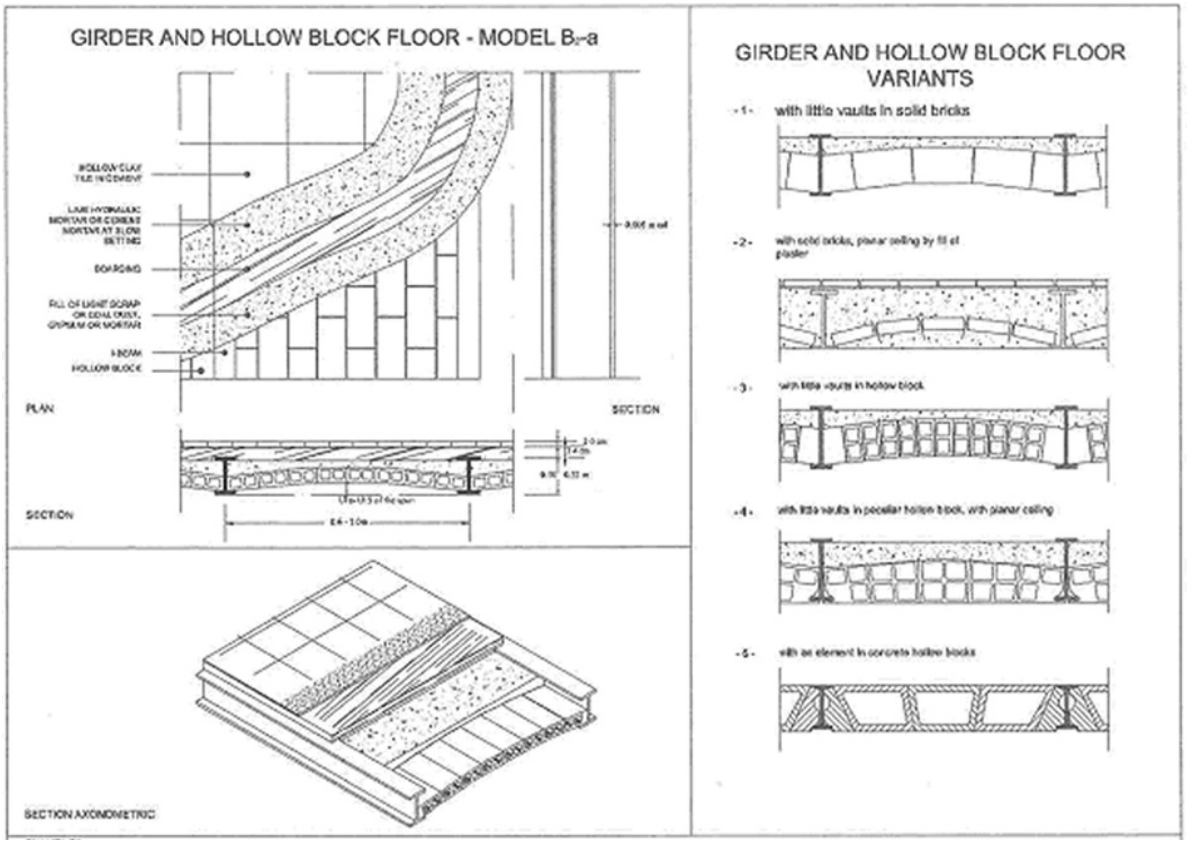

Figure 1. Example of typological-structural Schedule referred to B2b type floor.

Figure 2. B2 type floor: plaster detachment and impost brick breaking; C1 type floor: concrete elements detachment and bricks breaking.

In particular, the study has examined the processes of physical, technological, functional and normative obsolescence. Specifically, physical decay appears like a natural phenomenon in the "contact points" between different techniques and technologies. As a consequence, this decay is due to the juxtaposition of different materials, natural and artificial ones, that are not ever compatible, and it is worsen by the "ignorance", at the their construction, about the performance characteristics of the "new" materials.

Most of the decay phenomena seem to be originated from the concomitant action of physiological and pathological factors, that has reduced the service life of the buildings and/or perturbed the functionality of subsystems and components. Furthermore, natural and pathological obsolescence causes are often overlapped, whose origin is often hard to identify.

The study has assessed the quality levels of the technical elements connected to the general requirement classes from the UNI8289 and to the specific technical requirements (UNI 8290, ISO 6241, Directive 89/106 CEE). For each technical requirement, the performance levels and the minimum performance threshold of the technical element have been individuated.
Moreover, for each constructional element an analysis of the possible alterations and pathological manifestations has been conducted, by the results from the 23 existing building complexes considered as "case studies".

The general picture point out similar pathologies occurring for similar technological elements and solutions. For instance, slabs with iron bearing beams show often plaster detachment, namely surface stains and deteriorations, cracks and detachments between iron beams and filling ("voltine", "tavelloni", "pignatte/volterranee"). Possible causes are high deformability and surface corrosion of iron beams. There are cracks and detachments on the floors, as well, due to the poor mechanical compatibility between the different materials and elements. Breaking of lateritious elements, as well as section reduction and inflection/deformation of iron beams (due to the corrosion) are less frequent. Fig. 2 show some common observed pathologies on the technical element "floor", related to the plaster detachment, the breaking of tiles, the decay of bar cover and the lesions/fractures/separations of concrete elements.
Due to the presence of several anomalies and pathologies, different performance requirements and complex compatibility issues for the used materials, analysis has been summarized in order to define the relations between residual performances, failures, causes and diagnostic surveys. Such relation have been expressed under matrix form.

An example of the matrix is given in Table 2 for the technical element "floor". Such matrix is also a summarizing abacus of performance fulfilment of each element in comparison with the required performances. The matrix highlights three different levels of performance of the technical element types and explains the improvement possibility of performance levels by different intervention methods.

Table 2. Performance fulfilment matrix of floors: abstract referred to requirements E1 Safety, E2 Comfort, E3 Fruition, E4 Aesthetic value.

PERFORMANCE FULFILMENT MATRIX										
			TYPE FLOOR							
REQUIREMENTS		PERFORMANCES	B1	B2a	B2b	B2c	B3	B4	C1	C2
E1	RS1a	PS1a	◘ ●	◘ ●	◘ ●	◘ ●	◘ ●	◘ ●	◘ ●	◘ ●
	RS1b	PS1b	□ o	□ o	◘ o	□ o	□ o	◘ o	◘ o	◘ o
	RS1c	PS1c	□ o	□ o	◘ o	□ o	■	◘ o	■	■
E2	RS2a	PS2a	◘ ●	◘ ●	◘ ●	◘ ●	◘ ●	◘ ●	◘ ●	◘ ●
	RS2b	PS2b	□ o	□ o	◘ o	◘ o	□ o	□ o	□ o	◘ o
	RS2c	PS2c	□ o	◘ ●	◘ ●	◘ ●	◘ ●	■	■	◘
	RS2d	PS2d	□ o	□ ●	◘ ●	□ ●	□ ●	□ ●	◘ ●	□ ●
E3	RS3a	PS3a	□ ●	□ ●	□ ●	□ ●	◘ ●	◘ ●	◘ ●	◘ ●
E4	RS4a	PS4a	✖ o	✖ o	✖ o	✖ o	✖ o	✖ o	✖ o	✖ o
	RS4b	PS4b	◘ o	□ o	◘ o	◘ o	□ o	◘ o	□ o	◘ o

PERFORMANCE STANDARDS
□ LOW ◘ MEDIUM ■ HIGH

✖ EVALUATION STANDARDS ARE UNRELATEDS TO TYPE FLOOR

PERFORMANCE IMPROVEMENTS
o Ordinary maintenance interventions
o Protection interventions
● Integration/substitution interventions

Table 3 shows, still as an example and referred to technical element of floor, an abstract of the matrix that specifies pathologies, failures and losses, possible causes and related diagnostic surveys.

4.3 Maintenance and refurbishment interventions

The proposed approach indicates, in general terms, that mixed structure buildings should require recovery works for the existing damage and degradation. They should require performance improvements, with the revision/rectification/removal of the incongruities determined by the union of traditional and modern constructional techniques.

Table 3. Pathologies matrix: abstract referred to B2 type floors**.**

PATHOLOGIES MATRIX															
TYPE FLOOR					FAILURES LOSS	CAUSES						DIAGNOSTIC SURVEYS			
CATEGORY		TYPE		SUBTYPE											
B	IRON	2	NATURAL OR ARTIFICIAL ELEMENTS	a LITTLE VAULTS	AS1	C1	C3	C6	C9			V1	V2		
					AS2	C1	C3	C7	C8	C9		V1			
					AS3	C1	C3	C6	C9			V1	V2		
				b HOLLOW FLAT BLOCKS	AS4	C1	C6	C8	C9			V1	V7		
					AS5	C1	C6	C8	C9			V1	V3	V15	
					AS6	C1	C6	C8	C9			V1	V3	V15	
				c HOLLOW FLOOR BLOCKS	AS7	C3	C7					V1			
					AS8	C7	C11	C12				V1	V6	V8	V16
					AS9	C4	C7	C8	C9			V1	V2		

The analysis of the obsolescence and degradation processes points out that, with reference to the considered technical elements, the maintenance and refurbishment intervention typologies are the superficial protection (of structural elements and not), the improvement/reconstruction of the connections and of the old/new interfaces (between traditional and modern materials), the reconstruction/remaking of decayed parts (of structural elements and not), the structural reinforcement and the compliance to actual dispositions.

The intervention typologies in the intervention matrix come from this general structure that is detailed in the research for every considered technical element. These typologies, even if they are not exhaustive of the possible different technical possibilities, resume the main technological solutions feasible for the performance losses and the existing pathologies. Once defined the intervention typology, within a decision process based on the pathology analysis and diagnosis, the interventions matrix (tab. 4) allows the individuation of the different operating phases in which the intervention is articulated. The interventions matrix synthesizes the structured relations among technical element, congruent solutions and consequent operating phases, in a practical guide tool for the project.

For each operating phase, monographic schedules have been defined, containing technical specifications. The monographic schedules are structured in informative blocks with aims (objectives and efficacy of phase in relation with the general intervention typology), preconditions (preliminary conditions that have to be verified to realize the operating phase and to guarantee the predicted efficacy), specific requirements (characteristics and prerogatives of the phase related to the mixed structure buildings specificity), techniques (detailed execution procedures), tools (instruments, utensils, implements) and materials (raw materials and products).

Table 4. Interventions matrix: abstract referred to principal interventions on floors

Phases \ Interventions		I1	I2	I5		I7	I9	I10	I11	I12	I14	I15
F1	Plaster removal											
F2	Cover bar removal											
F5	Tiled floor removal											
F6	Decayed concrete removal											
F8	Iron elements paint-stripping		F8-1/3		F8-1/3							
F9	Iron elements cleaning	F9-1/2	F9-1/2	F9-1/2	F9-1/2	F9-1/2/3	F9-1/2		F9-1/2	F9-1/2/3	F9-1/2/3	F9-1/2/3
F10	Iron elements passivation	F10-1	F10-1	F10-1	F10-1	F10-1	F10-1		F10-1	F10-1	F10-1	F10-1
F11	Beam ending reconstruction		F11-1/2/3									
F15	Cracks repair	F15-1/2							F15-2			
F17	Ties laying											F17-1/2
F18	Iron rod anchorage						F18-2		F18-1/2			
F20	Steel bar protection	F20-1				F20-1	F20-1		F20-1			
F22	Iron elements painting		F22-1/2		F22-1/2							
F25	Connectors fixing							F25-1/2			F25-3/4	
F26	Welded net laying							F26-1		F26-1	F26-1	
F27	Slab-wall connection							F27-1/2/3		F27-1/2/3	F27-1/2/3	
F28	U-bolts laying									F28-1/2		
F29	Concrete laying							F29-1		F29-1	F29-1	F29-1
F30	Concrete cover bar reconstruction	F30-1/2		F30-1/2		F30-1/2	F30-1		F30-1			
F32	FRP application						F32-1					
F33	Plaster laying	F33-1	F33-1	F33-1		F33-1	F33-1		F33-1			

Interventions
I1 Concrete reconstruction
I2 Iron beam ending refurbishment
I5 Surface protectiont of iron beams
I7 Surface protection of reinfocerd concrete structures
I9 Structural reinforcement by FRP
I10 Reinforcement by light concrete slab integration
I11 Reinforcement by lower bars integration
I12 Reinforcement by upper bars integration
I14 Reinforcement by light concrete slab
I15 Reinforcement by iron ties

5 CONCLUSIONS

The research has demonstrated that the mixed structure heritage realized at the beginning of the 20th century is much more common - both in terms of "new" constructions and refurbishment of existing buildings in the historical centres – than what it was supposed to be. It is moreover characterized by "values" - historical, social, architectural, material and technological ones – that were not so much examined till now. This undervaluation was probably due to their presumed "spontaneous" origin. The study has permitted the characterization, in general terms, of the mixed structure buildings, with reference to the material, technical, technological and typological aspects, and the individuation, of the different obsolescence phenomena and consequent conservation issues. The suggested methodological approach allows the conservation, the maintenance and the refurbishment of the performances through congruent and adequate interventions. The procedural model can be considered as an intervention protocol, since it is aimed at the achievement of the expected result without the rigid imposition of a univocal possibility of satisfaction. It can be used as a tool of guide and control of the project qualities, by keeping a predefined framework of compatibilities and congruencies.
Finally, in general terms and even if further research developments are necessary, the application on real cases shows that the method is correct and offers several possibilities: the solutions seem consistent with the effective situations and, as a consequence, adaptable to different necessities. This approach also enhances rediscovery and refurbishment of materials and technologies that were

abandoned too soon, but that today can be partially reused after assessing their residual performances: this does make sense not for a simple and "romantic" re-proposition of materials and past stylistic elements, but for the execution of a "correct" refurbishment in addition to a possible contemporary reinterpretation of technological solutions that are still valid.

REFERENCES

De Tommasi G. (2007 - in stampa) *L'edilizia a struttura mista dei primi del '900: codice di pratica per la conservazione e manutenzione*. Adda Editore Bari.

Curioni G. (1873) *L'arte di fabbricare*, Tipografia A.F.Negro, Torino

Formenti C. (1893) *La pratica del fabbricare*, Hoepli, Milano.

Morsch E. (1930) *Teoria e pratica del cemento armato*, Hoepli, Milano.

Offenstein F. (1995) *Compatibilità dei materiali*, UTET, Torino.

11DBMC International Conference on Durability of Building Materials and Components
ISTANBUL, Turkey 11-14 May 2008

Evaluation of Environmental Degradation Factors for Service Life Prediction

Johann Mc Duling [1]
Emile Horak Pr [2]
Chris Cloete [3]

T 32

ABSTRACT

Evaluation of environmental degradation factors forms an integral part of Service Life Prediction. External climate contribute to degradation of building components through mechanical, electromagnetic, thermal, chemical and biological agents. Although the combined effect of the macro- meso- and micro- climate should be taken into consideration, this paper illustrates how macroclimate zones can be classified, based on work by Weinert [1980] on rainfall, evaporation and the weathering of Karoo dolerite, commonly used throughout South Africa in road construction and as aggregate in concrete. Water only contributes to the degradation process if present on the surface of components or microclimate. Evaporation of surface water is determined by humidity and temperature of the surface and surrounding air. Weinert calculated an N-value based on a factored ratio between evaporation and precipitation, where $N < 5$ represents wet and $N > 5$ dry regions. Although Weinert's N-values can be used to categorise the macroclimate for degradation of building components, other degradation factors such as pollution should also be taken into consideration. Chemical and biological degradation agents are dominant in wet regions, while mechanical, electromagnetic and thermal degradation agents occur mainly in dry regions. The same macroclimate might be aggressive towards one component, but favourable for another. An evaluation of the macroclimate should therefore be based on an impact analysis of the prevailing degradation agents applicable to the climatic region and component under consideration.

KEYWORDS

Environmental degradation, Macroclimate, Service life prediction

[1] Asset Management, Architectural Sciences, Built Environment, Council for Scientific and Industrial Research, Pretoria, South Africa, Phone +27 83 700 4027, Fax +27 12 349 9700, mcduling.johann@builtcare.co.za
[2] Civil and Biosystems Engrg, Faculty of Engrg, Built Environment and Information Technology, University of Pretoria, South Africa, Phone +27 12 420 2429, Fax +27 12 362 5218, emile.horak@up.ac.za
[3] Department Construction Economics, Faculty of Engineering, Built Environment and Information Technology, University of Pretoria, South Africa, Phone +27 12 420 4545, Fax +27 12 420 3598, chris.cloete@up.ac.za

1 INTRODUCTION

Exposure of buildings and components to the external, internal and operational environment contributes to degradation and effects durability and service life. [Jernberg et al, 2004]. Evaluation of environmental degradation factors therefore forms an integral part of Service Life Prediction. However, according to Eurin et al [1985] cited by Jernberg et al [2004] "every attempt in practice to measure and describe the degradation environment is an approximation and simplification."

Three of the seven factors considered in the Factor Method for Estimation of Service Life of Components and Assemblies as presented in ISO 15686 Part 1 [ISO 2000] can be classified as environmental degradation factors, namely:

- factor D: indoor environment
- factor E: outdoor environment
- factor F: in-use conditions

This paper illustrates how the outdoor or external environment (factor E) can be evaluated, based on work by Weinert [1980] on rainfall, evaporation and the weathering of Karoo dolerite, commonly used throughout South Africa in road construction and as aggregate in concrete.

2 EXTERNAL ENVIRONMENTAL DEGRADATION FACTORS

The external environment comprises of a macroclimate, mesoclimate and microclimate. The macroclimate describes the gross meteorological conditions "in terms like polar climate, subtropical climate and tropical climate. The descriptions are based on measurement of meteorological agents such as air temperature, precipitation etc." The meso climate takes "the effects of the terrain and of the built environment" into account, while "the climatological description is still based on the standard meteorological measurements." The local scale describes "The local conditions in the building proximity, such as for example in the streets around the building." The meteorological variables in the absolute proximity of a material surface are described by the microclimate, which "is crucial to understanding and estimating material degradation. The most important variables describing microclimate include relative humidity, surface moisture, surface temperature, irradiation and deposition of air pollutants. ... The actual in-use condition relevant to materials degradation is the microclimate, i.e. the prevailing environmental condition in a layer adjacent to a component surface. ... As weather does not repeat itself — i.e. every year is not a standard year — one has to be cautious in drawing conclusions from one exposure period to another." [Jernberg et al, 2004]

2.1 Weinert's Climatic N-values

According to Weinert [1980] the influence of the environment on the life and performance of a road is often greater than realized. Observed variations in the performance of weathered dolerite used in road construction in different parts of the South Africa eventually culminated into the development of Weinert's climatic N-value, which is expressed by the following formula:

$$N = \frac{12E_J}{P_a}$$

where E_J is the computed evaporation from a shallow free water surface during January (warmest month), and P_a is the total annual precipitation

There was a marked difference in the performance of dolerite when used in road pavements to the east and west of an imaginary north-south line running through the middle of South Africa. This line has an N-value of 5 as shown in Figure 1 below. To the east of this line where $N < 5$ and chemical decomposition predominates the performance was unsatisfactory, while to the west where $N > 5$ and mechanical disintegration is the predominant mode of rock weathering the performance was satisfactory.

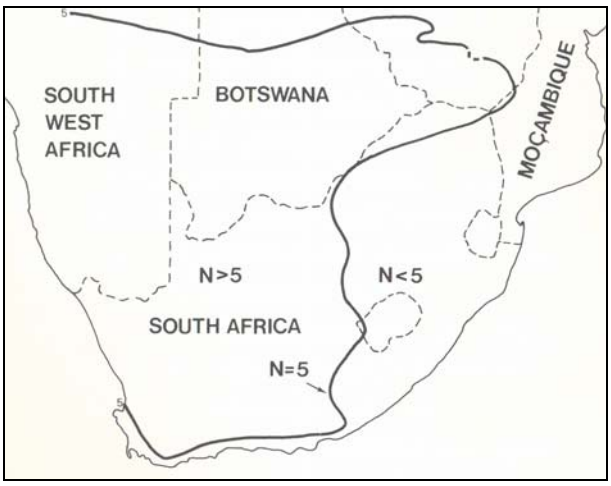

Figure 1: Weinert's Climatic N-values [Source: Brink, 1978]
[* South West Africa = pre-independence name of Namibia]

In Figure 2 below the three macroclimatic regions of Southern Africa is shown. In the western region, which has a dry climate with N > 5, mechanical degradation is dominant. The southern and central region is smaller and a transitional zone with a moderate climate, where both mechanical and chemical degradation take place. The eastern region has a wet climate with an N-value < 5, where chemical degradation is dominant. This demarcation is based on the weathering of natural road materials such as dolerite, which is a natural rock occurring throughout South Africa. Some of the materials used in the built environment are also natural materials and these three macroclimates could therefore also apply to these natural materials.

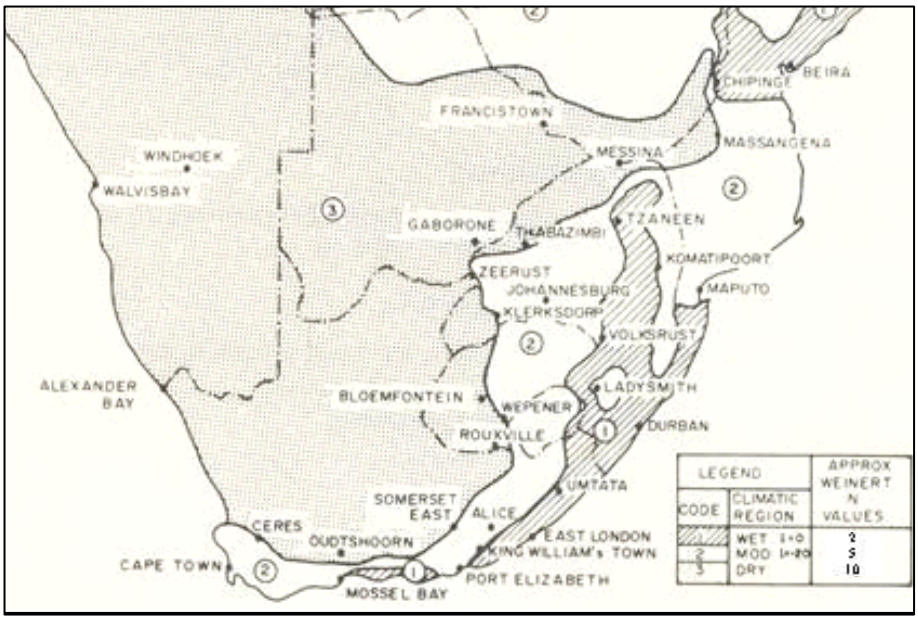

Figure 2: Macroclimatic Regions of Southern Africa [Source: CSIR, 1985]

2.3 Marco Climate Zones

The mean annual rainfall, evaporation and temperatures for South Africa are shown in Figures 3 to 5 below. It is interesting to note the correlation with the three macroclimatic zones shown in Figure 2 above.

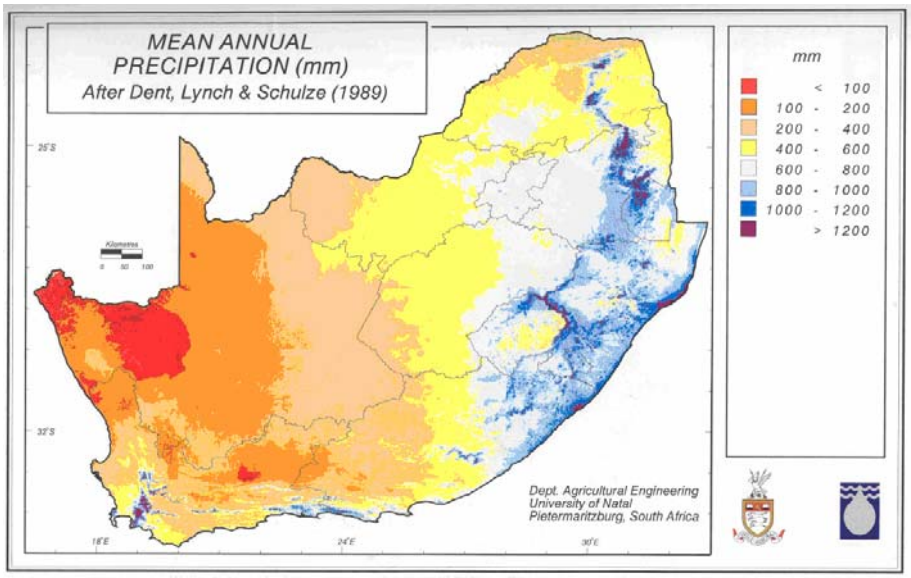

Figure 3: Mean Annual Precipitation for South Africa [source: University of Natal]

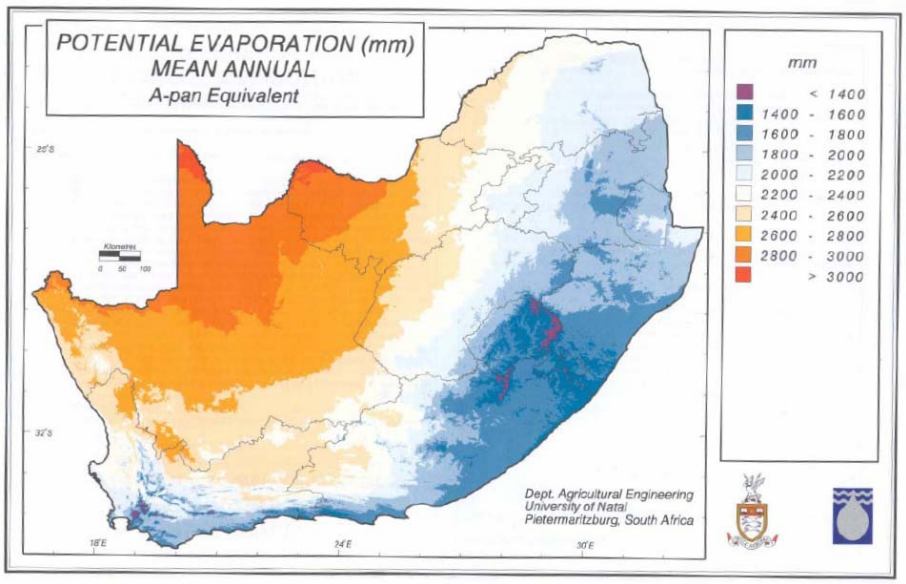

Figure 4: Mean Annual Potential Evaporation for South Africa [source: University of Natal]

The macroclimate in the South African context plays a major role in degradation, as can be seen from Weinert [1980], Brink [1978] and CSIR [1985]. Weinert's work was based on the weathering of Karoo dolerite, commonly found throughout South Africa and besides road construction, also used as aggregate in concrete. Just like dolerite most of the materials used in building construction are natural materials. Some of the materials are used in their natural state while others are processed or combined with other materials. The addition of bonding materials and chemicals during the processing of these materials could change the characteristics of the natural material to some extend (e.g. galvanising of steel, anodising of aluminium), but the base material will remain the same.

Weinert's N-values are based on rainfall and evaporation. Water can only contribute to the degradation process if it is present on the surface of material (the microclimate). The evaporation of surface water is determined by the humidity of the surrounding air and the temperature of the surface and the surrounding air.

On the wetter eastern coastline of South Africa (Weinert's N-value < 2) corrosion of metal is a major problem, while in regions with an N-value > 5, corrosion is less problematic. Mould growth is another scourge of the coastal regions, which is almost unknown in the drier regions. In regions with an N-value < 5 special attention should be given to the impact of water on the degradation process.

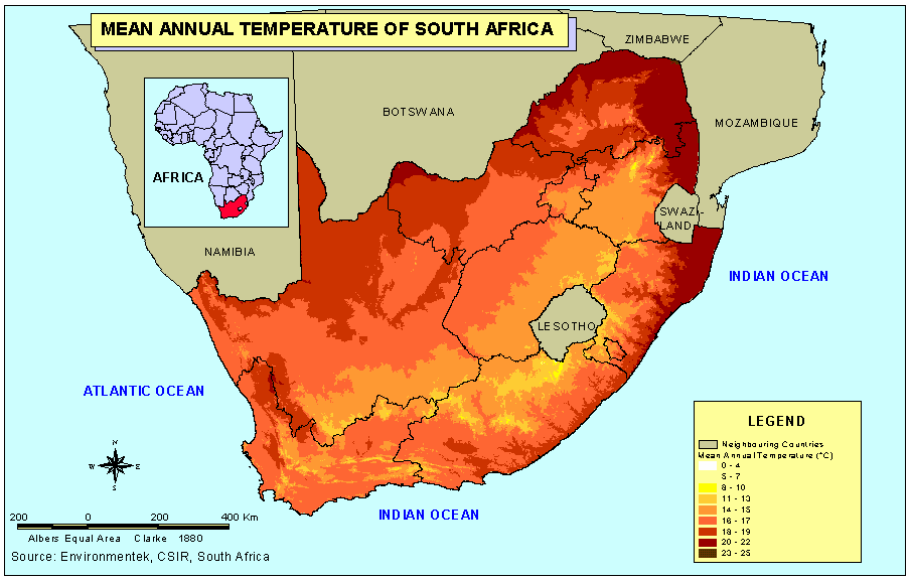

Figure 5: Mean Annual Temperatures [Source: CSIR]

There is an interesting difference between the eastern coastal areas and the Western Cape, both with an N-value < 5. In KwaZulu Natal, a summer rainfall region, there are lots of moisture (rainfall season) and heat (hot summer months), but because of the high humidity of the air, evaporation is low, resulting in an aggressive environment for buildings. In the Western Cape, a winter rainfall region, the temperatures are low during the rainfall season resulting in low evaporation of surface water; again an aggressive environment in terms of degradation processes less dependent on temperature.

Although Weinert's N-values can be used, with circumspection, to categorise the macroclimate for degradation of building components, water is not the only degradation agent found in the external climate and other degradation factors such as pollution should also be taken into consideration. Chemical and biological degradation agents are dominant in wet regions, while mechanical, electromagnetic and thermal degradation agents occur mainly in dry regions.. Electromagnetic processes, especially in the drier and hotter parts of the country (N-value > 5), could in combination with high temperatures have a very negative impact on the degradation patterns of building materials. Ultra-violet radiation is harmful not only to humans, but also to building materials, and its effect should not be underestimated.

The mesoclimate should also be considered, especially in major industrial and surrounding areas, where air and water pollution could be a problem. Acid rain, caused when fossil fuels are burnt (e.g. coal-fired power stations) and sulphur is released into the air, has a major impact on degradation of building materials and should be taken into consideration where applicable.

2.2 Rating of external environment

In general the classification of the CSIR [1985] as shown in Figure 2, could be quite useful, if the applicable degradation processes are taken into consideration. The dry regions (N-value > 5) could in general be classified as 'favourable', the moderate areas (2 < N-value < 5) as 'less favourable', and the wet areas (N-value < 2) as 'slightly aggressive'. Again, this should not be applied blindly as certain materials could be more vulnerable to degradation in dry and hot conditions.

The proposed zones for chemical and biological degradation agents in Figure 6 above correspond with the TRH4 [CSIR, 1985] zones for roads. There are three macroclimate zones (mean annual evaporation > 2600 mm, < 2600 mm and > 2000 mm, and < 2000mm), with a fourth zone along the narrow eastern and southern coastal belt, where corrosion is a problem. The broken line indicates an area where the macroclimate could be classified as 'aggressive' in the case of biological degradation.

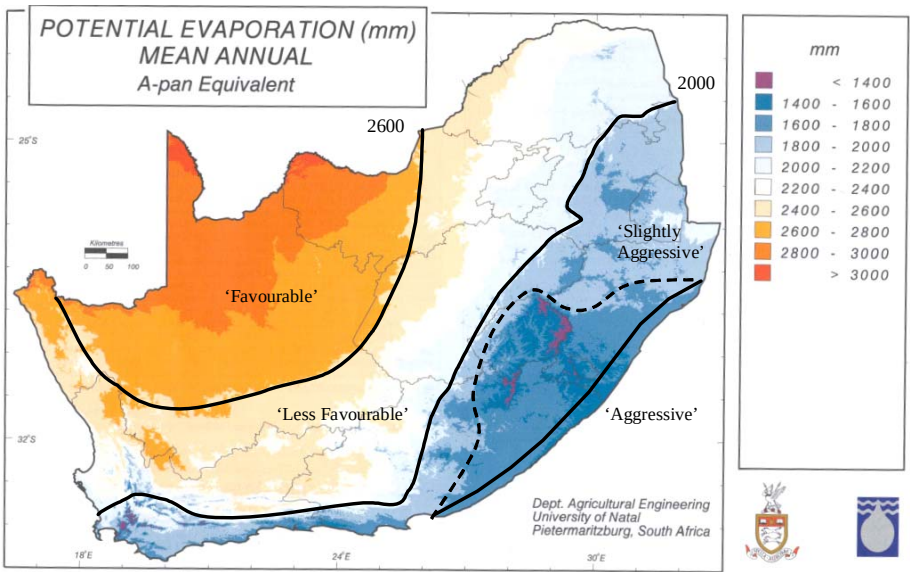

Figure 6: Proposed Macroclimate Zone Classification for Chemical and Biological Degradation Agents [Base map: University of Natal]

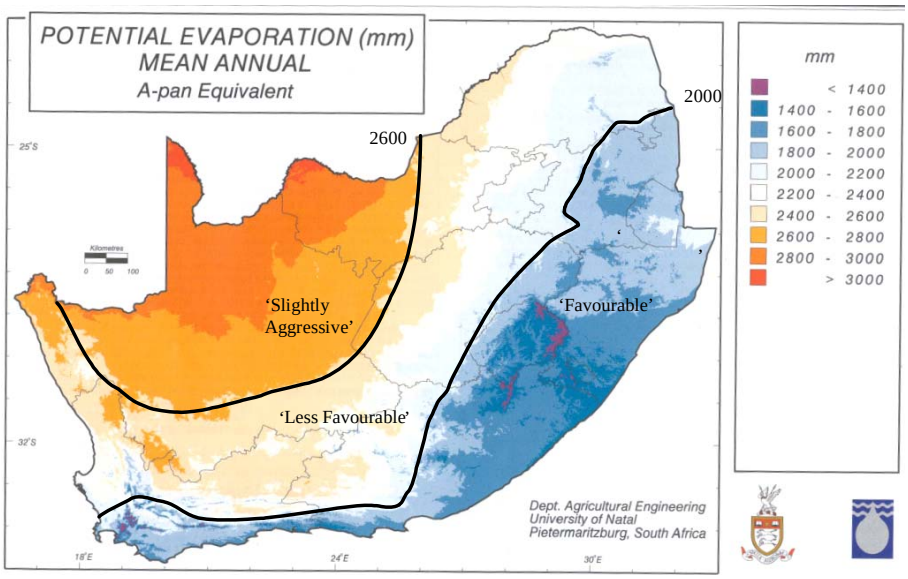

Figure 7: Proposed Macroclimate Zone Classification for Mechanical, Electro-magnetic and Thermal Degradation Agents [Base map: University of Natal]

The same macroclimate might be aggressive towards one component, but favourable for another. An evaluation of the macroclimate should therefore be based on an impact analysis of the prevailing degradation agents applicable to the climatic region and component under consideration. In the western regions mechanical, electromagnetic and thermal degradation agents are more dominant and the classifications are as shown in Figure 7 above should apply.

The external environment can be classified as 'aggressive' to 'slightly aggressive' if buildings are in or down-wind from heavily polluted industrial areas'. Should the macroclimate have a classification of 'slightly aggressive' and the mesoclimate is 'aggressive', the external environment could become 'aggressive' to 'very aggressive' depending on the microclimate or space in the absolute proximity of a material surface. Here the design level should also be considered to determine the level of protection offered by the design and installation of the component. The combined effect of all three external environmental levels (macro, meso and micro) should be taken into consideration, with microclimate being the decisive factor.

In the analysis of building degradation the opinion of domain experts and inconsistent field data are often the only sources of information. Mc Duling [2006] used a five point rating system to evaluate condition and degradation and durability factors, similar to the factors used in the Factor Method, in a Service Life Prediction model based on the Markov Chain and Neuro-Fuzzy Artificial Inteligence to translate "IF-THEN" rules based on domain expert knowledge and reasoning into crisp probability values to populate the Markovian transitional probability matrices. The following ratings are used to evaluate the external environment:

- 5 – 'Favourable': External environment has very little or no effect on the building or component.
- 4 – 'Less Favourable': The building or component is exposed to external environmental degradation agents from time to time. The dosages are relatively low and of short duration.
- 3 – 'Slightly Aggressive': The building or component is exposed to external environmental degradation agents for longer periods. Areas where large temperature variations, strong winds, heavy driving rain, hail and snow, earth tremors (mining areas) occur.
- 2 – 'Aggressive': The building or component is exposed to high doses of external environmental degradation agents (e.g. industrial areas where pollution is problematic), where a combination of degradation agents are present (e.g. moisture and heat) on the surface of the component (microclimate) most of the time.
- 1 – 'Very Aggressive': The building or component is constantly and directly exposed to very aggressive external environmental degradation agents (e.g. unprotected steel exposed to salt-spray or within 50 meters from the high water mark on the east coast)

Although this is different to the factor values between 0.8 and 1.2 proposed in the Factor Method, the above ratings can be used to minimise subjectivity in evaluating the outdoor or external environment (factor E), as shown below:

- 1.2 – 'Favourable'
- 1.1 – 'Less Favourable'.
- 1.0 – 'Slightly Aggressive' ("normal" environment)
- 0.9 – 'Aggressive'
- 0.8 – 'Very Aggressive':

3 CONCLUSION

Although Weinert's N-values can be used to categorise the macroclimate for degradation of building components, other degradation factors such as pollution should also be taken into consideration. Chemical and biological degradation agents are dominant in wet regions, while mechanical, electromagnetic and thermal degradation agents occur mainly in dry regions. The same macroclimate might be aggressive towards one component, but favourable for another. An evaluation of the

macroclimate should therefore be based on an impact analysis of the prevailing degradation agents applicable to the climatic region and component under consideration.

Until such time when a more scientific based method can be developed the proposed process can be used to evaluate the effect of external environmental degradation agents for service life prediction purposes. Figures 6 and 7 are however only indicative of macroclimate zoning and need further investigation, development and refinement.

REFERENCES

Brink, A.B.A., 1979. *Engineering Geology of Southern Africa, Volume 1*, Pretoria: Building Publications.

Council for Scientific and Industrial Research, 1985. *Technical Recommendations for Highways, TRH4:1985, Structural Design of Interurban and Rural Road Pavements.* Pretoria: Council for Scientific and Industrial Research.

Hövde, P.J., and Moser, K., 2004. State of the Art Reports, CIB W080 / RILEM 175-SLM Service Life Methodologies Prediction of Service Life for Buildings and Components, *CIB Report, Publication 294, March 2004.*

Jernberg, P., Lacasse, M. A., Haagenrud, S. E., and Sjöström, C., 2004. *Guide and Bibliography to Service Life and Durability Research for Building Materials and Components*, Joint CIB W80 / RILEM TC 140 – TSL Committee on Service Life of Building Materials and Components, CIB Report, Publication 295. March 2004.

Mc Duling, J.J., 2006. *Towards the Development of Transition Probability Matrices in the Markovian Model for the Predicted Service Life of Buildings*, PhD Thesis, Department of Civil and Biosystems Engineering, University of Pretoria, South Africa.

Weinert, H.H., 1980. *The Natural Road Construction Materials of Southern Africa*. Pretoria: Academica.

Climatic Comparison to Analyse Different Degradation Levels in External Walls' Outdoor Exposure

Bruno Daniotti [1]
Sonia Lupica Spagnolo [2]

T 32

ABSTRACT

In the last few years the Durability of Building Components Group is carring out an experimental programme to evaluate Reference Service Life of self supporting external walls made of a double masonry with thermal insulation inside. In parallel with the accelerated ageing tests it was planned an outdoor exposure in order to evaluate the existing time re-scaling factor between the two kind of ageings.
Analysing the different agents' stresses which characterize the specific outdoor environment the importance to compare different degradation and performance levels on different reference outdoor exposure sites brought to realize a coupled outdoor exposure in different climatic contests.
The paper deals in particular with the results obtained in exposing some specimens, analogous to the ones tested under accelerated ageing, in two cities: Milano (Italy) and Lugano (Switzerland). The two weathering conditions lead to different degradation levels.
The analysis of the different climatic loads allows to relate the degradation effects with the actions. This is useful to define different Service Lives related to different outdoor weathering conditions and looking toward a better definition of accelerated ageing cycles, selecting the relevant loads, determining durability differences. To simplify and make the comparison more immediate, degradation levels have been classified using an evaluating dimensional scale from 0 (no visible damages) to 3 (presence of relevant damages such as detaches).

KEYWORDS

Natural ageing , Climatic conditions, External walls, Degradation level, Reference Service Life

[1] Politecnico di Milano, BEST Department, Milan, Italy, 20133, piazza Leonardo Da Vinci, 32, Phone +39 0223996002, bruno.daniotti@polimi.it
[2] Politecnico di Milano, BEST Department, Milan, Italy, 20133, piazza Leonardo Da Vinci, 32, Phone +39 0223996002, sonia.lupica@polimi.it

1 INTRODUCTION

The chief objective of the experimental programme on self supporting external walls, undertaken since 1999, has been to define the Reference Service Life of some double masonries with thermal insulation inside protected by different kind of paints (acrylic and vinylversatic) prepared with different concentration of resin (PVC40 and PVC60), following the methodology proposed in ISO 15686-2:2001 "Building and constructed assets – Service life planning: Service life prediction procedures". According to the ISO standard the comparison between long – term and short – term exposure results should be used in the assessment of building components' service life, once it has been verified that there is the same degradation level in each one of the samples: the experimental programme needed on one side laboratory accelerated tests and on the other side natural outdoor exposure because it was then necessary to understand the existing correspondence between the two studied ageing conditions [Daniotti *et al.* 1999]. It was, therefore, necessary to realize some specimens, analogous to the ones tested under accelerated ageing, to expose to natural environment. Starting from the monitoring results related to outdoor samples this paper reports about the climatic comparison between the two exposure contexts: Milano (Italy) and Lugano (Switzerland).

2 THE OUTDOOR EXPOSURE FOR NATURAL AGEING

In the experimental phase of natural ageing, 8 partial samples for each site (Milano and Lugano) have been tested; they are composed of, perforated brickwork coated by a layer of plaster and then a protective film of paint. These specimens are totally analogous to the one used in accelerated proofs, in order to permit the comparison between the two ageing conditions, obtaining the so-called time-rescaling factor.

The following variables have been adopted, in order to gain as more information as possible:

- *Different kind of painting protection (Acrylic paints, Vinylversatic paints)*: in order to study both the degree of waterproofing and the degradation's mechanisms;
- *Different resin ratio (PVC 40, PVC 60)*: Powder Volume Concentration (PVC), which measures the powders' percentage inside the paint, so that the resin ratio in the paint is given by the complement to 100 of the PVC-value;
- *Double exposure (Milano – I, Lugano – CH)*, to evaluate the effects due to different weathering and pollution conditions (in both sites they were exposed toward South);
- *Different slope (90°, 45°)*: the 45° configuration should accelerate the degradation and make the effects on the masonry more evident.

Figure 1. Natural ageing asset in Lugano (picture on the left) and Milano (picture on the right).

The comparative analysis between the two contexts is related most of all to the pollution level, and to temperatures and radiation levels.

2.1 Pollution Comparison Between Exposure Sites

An important information to take into consideration for a durability prevision is the pollution level of the site with particular attention to the concentration of pollutants such as SO_2, PM10 and NO_2 which are considered the most damaging agents for external walls. A time course of 6 years (from 1999 to 2005) has been studied. Three graphics underlining the course of concentration of polluting agents in Milan, where the pollution is higher, are here reported.

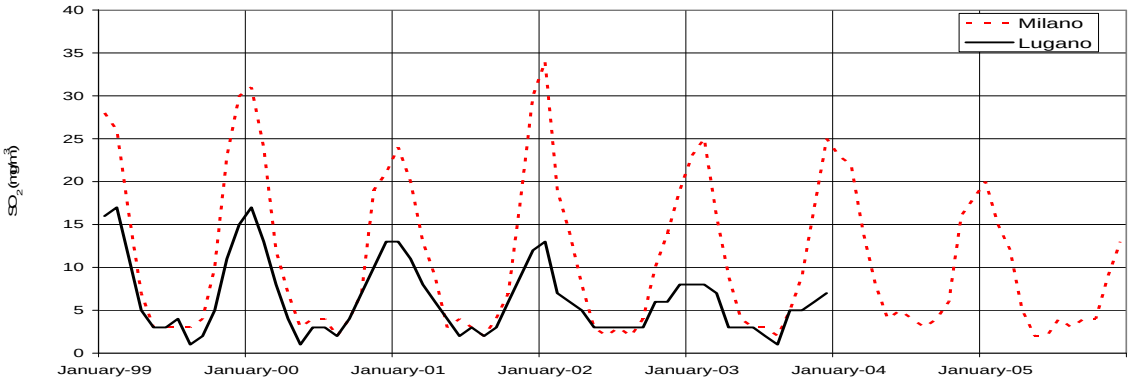

Figure 2. SO_2 concentration course in Milano (Italy).

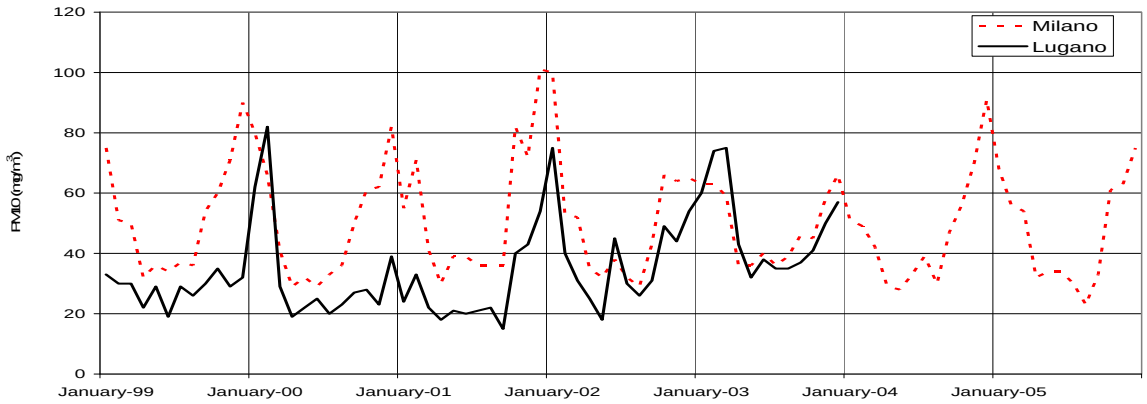

Figure 3. PM10 concentration course in Milano (Italy)

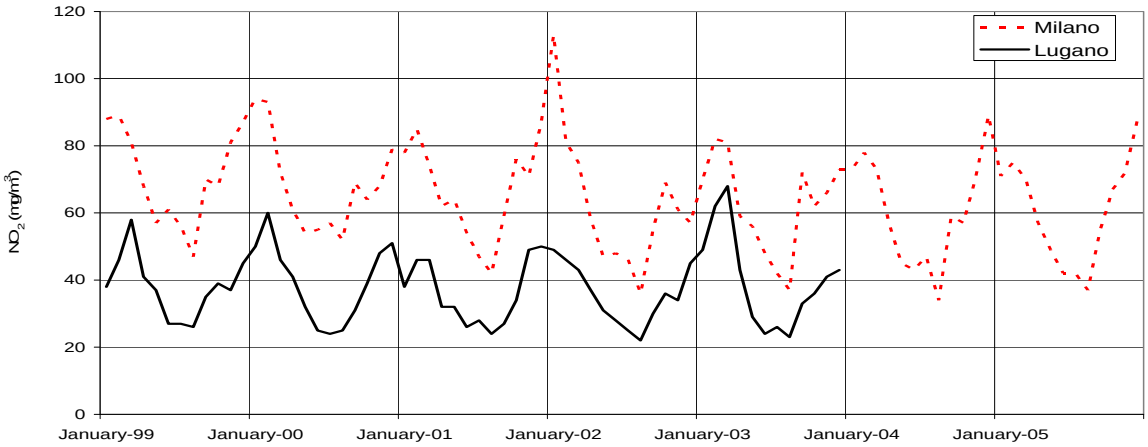

Figure 4. NO_2 concentration course in Milano (Italy)

In particular, the graphic about SO_2 concentration shows a swinging course with an important increase in winter and an evident decrease in the summertime. An Italian standard imposes that the concentration of SO_2 cannot exceed the value 125 µg/m³ for more than three times in the year. In Milan it is possible to notice that the highest registered values never exceed 34 µg/m³, widely below

the limit. In Lugano SO_2 concentration remains below the admissible thresholds too. Moreover, the concentration of SO_2 in the considered period has notably decreased in Lugano and it shows a swinging course in Milan with a light decreasing in the last two years (2004 and 2005).

Considering PM10 it is possible to notice the same swinging course found out with SO_2 concentrations, but in this case PM10 concentration is often near the admitted level, overcoming it most of the times, especially in winter. The admissible thresholds for PM10's concentration are, in fact, overcome in both the climate contexts: in Lugano there is an increase in the considered last year, while in Milan there is a light diminution.

An identical behavior is showed by NO_2 concentration course during the year, with an overcoming of the admitted levels in both the climates: in particular in Milan a light decrease can be noticed while in Lugano there was a progressive increasing of their concentration.
The annual mean values for the considered range of time and for the three polluting agents can be eventually compared with the admitted thresholds: the synthesis of such comparison is shown in the table below.

Table 1. Syntesis of the annual mean values for the considered polluting agents compared with the legal maximum values for both the climatic contexts

	SO_2		**PM10**		**NO_2**	
	Annual mean value [μg/m^3]		**Annual mean value [μg/m^3]**		**Annual mean value [μg/m^3]**	
	Measured	**Legal Maximum**	**Measured**	**Legal Maximum**	**Measured**	**Legal Maximum**
Milan	11,72	80	51,03	40+1,6	65,32	40+12
Lugano	6,23	30	35,35	20	37,71	30

2.2 Temperatures Comparison

Therefore, to better define the climatic differences between the two context it is necessary to analyze daily values of temperatures (maximum, minimum and mean ones) and of solar radiation.

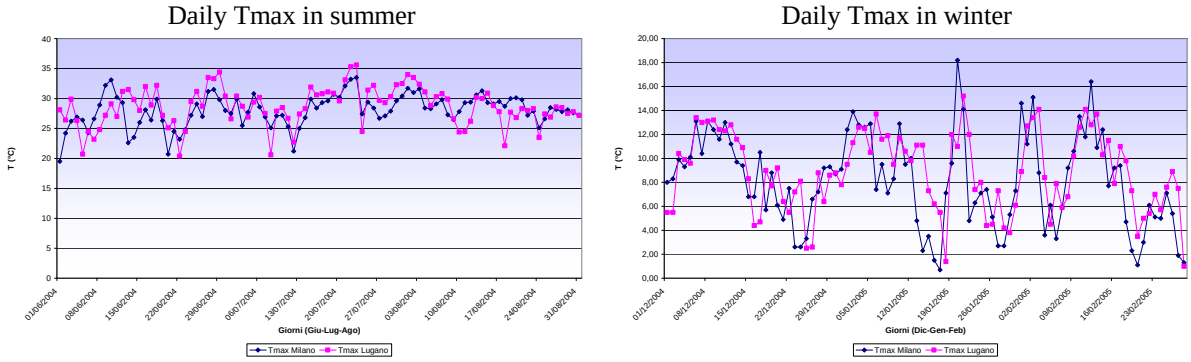

Figure 5. Comparison between daily maximum temperatures in summer and in winter.

Maximum temperatures are reached more frequently and with higher values in Lugano. In particular, the difference between the two localities is more evident in June and in July. Looking at the hourly course for the most significant days in summer it is possible to notice this difference.

Figure 6 shows in particular that daily maximum temperatures are nearly always reached in Lugano and not in Milan.

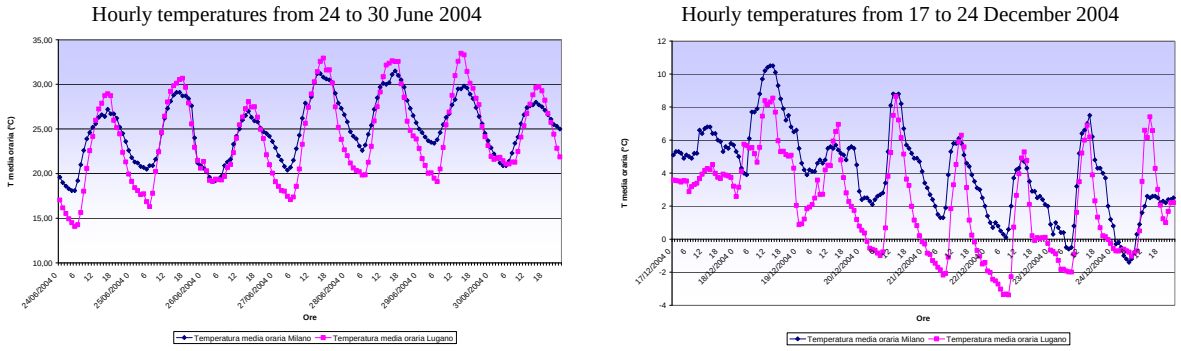

Figure 6. Comparison between hourly temperatures in relevant days in summer and in winter.

Taking into consideration the course of minimum temperatures, it is possible to notice that they are higher in Milan than in Lugano: in the Swiss city there are frequently temperatures under zero, while in Milan it seldom happens.

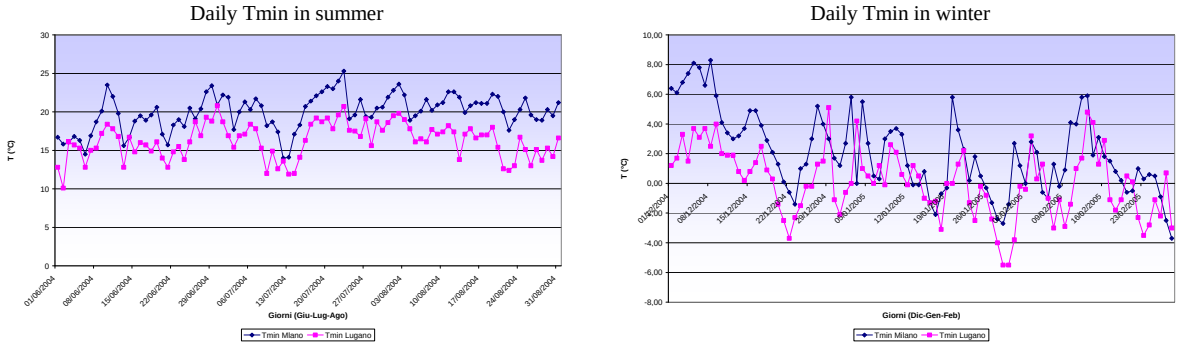

Figure 7. Comparison between daily minimum temperatures in summer and in winter.

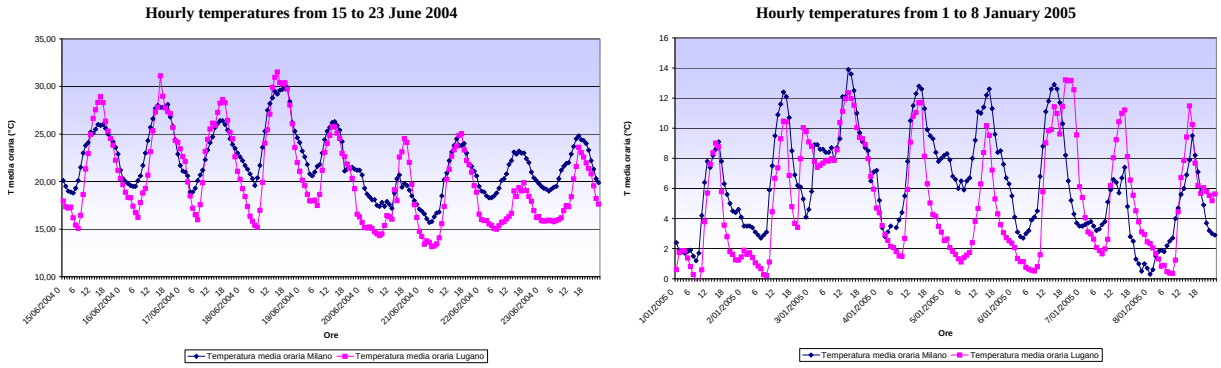

Figure 8. Comparison between hourly temperatures in significant days in summer and in winter.

Climatic conditions in Lugano are characterized by high daily ΔT values: in fact in Milan maximum temperatures are lower while mean ones are higher than in Lugano.

2.3 Solar Radiation Comparison

In Milan the daily course of solar radiation is characterized by a higher number of hours of exposure and a higher intensity of these values. The maximum value registered in Milan is 1000 W/m^2, while in Lugano it is 894,2 W/m^2, with a maximum daily solar energy received equal to 8223 Wh/m^2 in the Italian city and 7442 Wh/m^2 in the Swiss one.

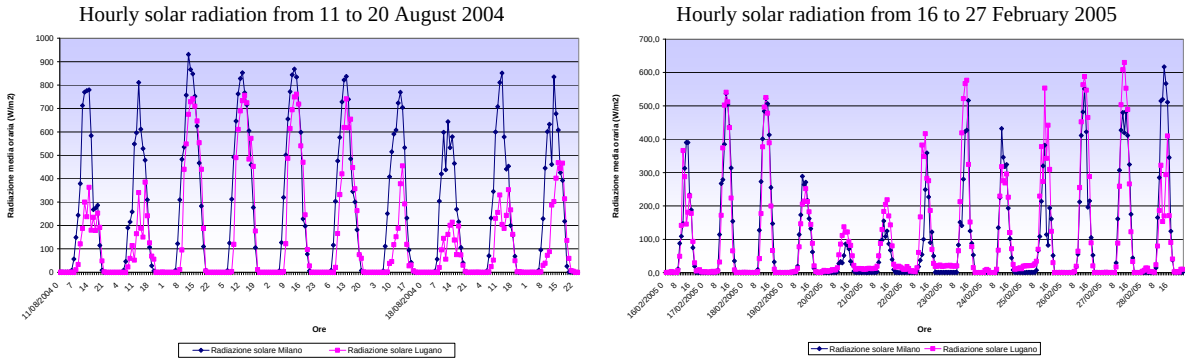

Figure 9. Comparison between hourly solar radiations in significant days in summer and in winter.

2.4 Degradation Comparison

To evaluate the decay during time for the different specimens, a classification of degradation levels through a dimensional scale (from 0 to 3), based on a photographical analysis, has been defined:

- **DL0**: undamaged protecting layer, there can be microcracks due to the presence of air during the applying step and following drying of the paint, but there are not cracks or swellings;

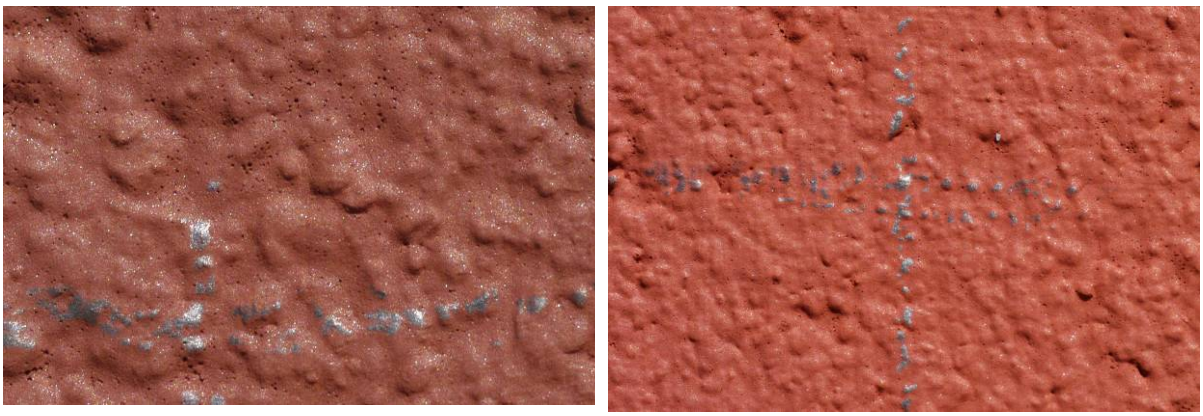

Figure 10. Photographs which show two examples of degradation level 0.

- **DL1**: broken swellings or local cracks;

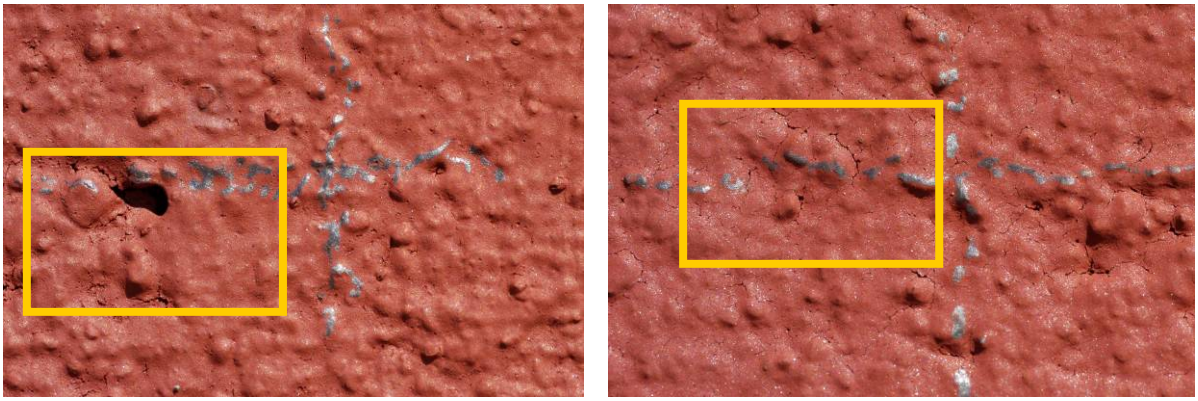

Figure 11. Photographs which show two examples of degradation level 1 (broken swelling on the left, local cracks on the right one).

- **DL2**: many microcrackles and cracks;

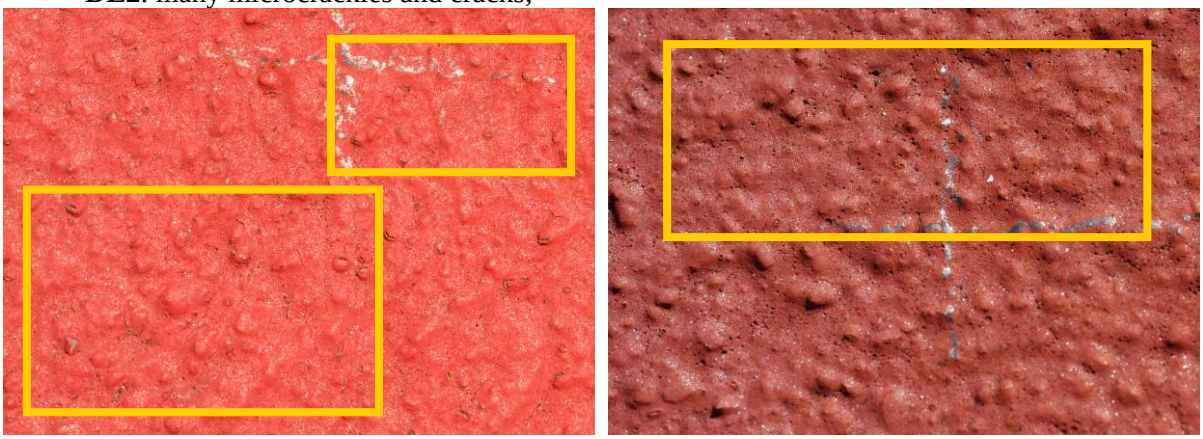

Figure 12. Photographs which show two examples of degradation level 2 (broken swelling on the left, local cracks on the right one).

- **DL3**: torn bubbles, detaching and saline crystallisation of surface.

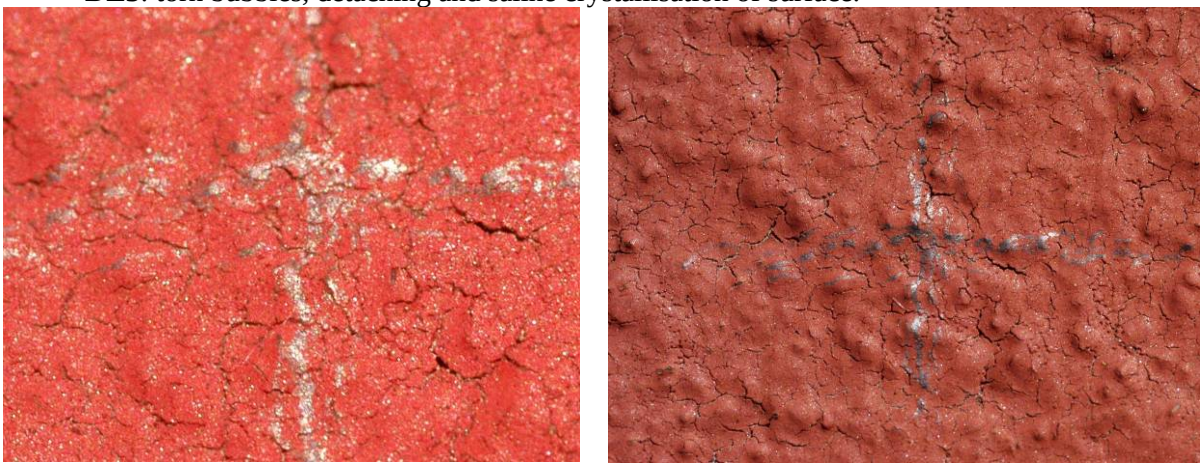

Figure 13. Photographs which show two examples of degradation level 3.

This kind of classification allowed the behaviour comparisons during time and will be used in developpng diagnostic cards in order to define inspection procedures; thanks to the comparison among degradation levels found in Milano and in Lugano for the two slopes it is possible to sum up the following considerations:

- ageing of 90° sloped specimens is quite similar for the two exposure sites; the only important difference is for VL90 specimens (V= vinylversatic resin, L=low concentration of resin) because they are more damaged in Milan than in Lugano;
- ageing of 45° sloped specimens is faster than for 90° sloped ones.

Table 2. Synthesis of Degradation Levels for 90° sloped specimens in Milano

	VH 90	***VL 90***	***AH 90***	***AL 90***
2001	DL 0	DL 1	DL 0	DL 0
2003	DL 0	DL 2	DL 0	DL 0
2004	**DL 1**	DL 2	DL 0	DL 1
2005	DL 1	DL 3	DL 0	DL 1
2006	DL 1	DL 3	DL 0	DL 1
2007	DL 2	DL 3	DL 0	DL 2

Table 3. Synthesis of Degradation Levels for 90° sloped specimens in Lugano

	VH 90	***VL 90***	***AH 90***	***AL 90***
2001	DL 0	DL 0	DL 0	DL 0
2003	DL 0	DL 0	DL 0	DL 0
2004	DL 0	DL 1	DL 0	DL 1
2005	DL 1	DL 1	DL 0	DL 1
2006	DL 1	DL 2	DL 0	DL 1
2007	DL 2	DL 3	DL 1	DL 2

Table 4. Synthesis of Degradation Levels for 45° sloped specimens in Milano

	VH 45	***VL 45***	***AH 45***	***AL 45***
2001	DL 0	DL 1	DL 0	DL 0
2003	DL 0	DL 1	DL 0	DL 0
2004	DL 1	DL 2	DL 0	DL 1
2005	DL 1	DL 3	DL 1	DL 2
2006	DL 2	DL 3	DL 1	DL 2
2007	DL 3	DL 3	DL 1	DL 2

3 CONCLUSIONS

Comparison between accelerated ageing results and outdoor ageing ones (analysed on the surface through optical microscope) has given the possibility to define Reference Service Life for considered paints: after 4 years of outdoor exposure and 150 cycle of artificial one; specimens covered by acrylic paint show a relevant level of water protection, while specimens covered by vinylversatic paints have lost their performance levels , then reaching the end of their service life.
In particular, acrylic paints show a better protection than vinylversatic ones, high concentration of resin increases the protection and vinylversatic paints with low concentration of resin end their service life after 4 years of outdoor exposure. In order to correctly interpret the results obtained, an analysis of the climatic conditions and pollution concentrations in the two cities (Milano and Lugano) was carried out during the exposure period, with such results:

- In Lugano the quantity of rain and daily thermal difference are higher;
- In Milano values of pollution (PM10, SO_2 and NO_2), solar radiation and medium temperature are higher than in Lugano.

As a first hypothesis based on materials' information, vinylversatic paints degrade themselves more quickly in Milano than in Lugano due to solar radiation stresses: this hypothesis will be verified with specific tests. The paper underlines the importance to study climatic data, and pollution levels focusing on agents which can provoke degradations on the studied building component, while analysing the results from outdoor exposure experimental programmes.

REFERENCES

B. Daniotti, P.N. Maggi, M.G. Rejna, F.Re Cecconi, G. Rigamonti A. Jornet, T. Teruzzi. "Experimental program to evaluate building elements service life: first results on brickwork." Proceedings of 8th DBMC Vancouver (Canada), 1999

Daniotti, B. & Iacono, P. 2005, Evaluating the Service Life of External Walls: a Comparison between Long-Term and Short-Term Exposure, in papers of the conference "10th DBMC", Lyon, France.
Daniotti, B. & Lupica Spagnolo, S. 2007, *Service life prediction for buildings' design to plan a sustainable building maintenance*, in papers of the conference "Sustainable construction, materials and practices", Lisbon, Portugal.

11DBMC International Conference on Durability of Building Materials and Components
ISTANBUL, Turkey 11-14 May 2008

Climatic Data Analysis to Define Accelerated Ageing for Reference Service Life Evaluation

Bruno Daniotti [1]
Sonia Lupica Spagnolo [2]
Riccardo Paolini [3]

T 32

ABSTRACT

In order to define accelerated ageing cycles useful to evaluate reference service life is very important to analyse the "reference" climatic conditions to be simulated. In this paper we will report the activities developed by Durability of Building Components Group of Politecnico di Milano to set up the accelerated ageing cycle for ETICS, based on a national agreement within the Italian Network of Durability Evaluation laboratories. Statistical climatic data as Test Reference Year and standardized data have been considered to determine the most severe climatic conditions relevant for ETICS durability aspects. The considered agents have been selected taking into account the degradation and failure modes for the specific ETICS component. The most severe thermal shock events in summer and winter conditions have been analysed to define the temperatures during sub-cycles. Rain ,freeze and UV conditions have been defined taking into account their statistical occurrence and the ratio between summer and winter cycling have been defined on the base of statistical probability of such events. This analysis allowed to obtain lab ageing cycles calculated on the base of statistical data for the considered Reference climatic and geographical conditions. This will be useful to compare results based on lab accelerated ageing and outdoor exposure results.

KEYWORDS

Accelerated ageing , Climatic conditions, ETICS, Thermal shock, Reference service life

[1] Politecnico di Milano, BEST Department, Milan, Italy, 20133, piazza Leonardo Da Vinci, 32, Phone +39 0223996002, bruno.daniotti@polimi.it
[2] Politecnico di Milano, BEST Department, Milan, Italy, 20133, piazza Leonardo Da Vinci, 32, Phone +39 0223996002, sonia.lupica@polimi.it
[3] Politecnico di Milano, BEST Department, Milan, Italy, 20133, piazza Leonardo Da Vinci, 32, Phone +39 0223996017, riccardo.paolini@mail.polimi.it

1 INTRODUCTION

One of the most important issues concerning laboratory durability evaluation is the choice of ageing cycles and so the main goal of this study is to set a procedure appropriate for pre-design accelerated ageing. First of all it's important to remember that different kinds of accelerated cycles exist, which have different aims:

- torture cycles – their purpose is to get a first evaluation of durability of the component in extreme conditions, much harsher than those ever encountered in use. These kind of tests couldn't be considered as proper durability tests;
- "standard" cycles – their aim is to test a building component and release an approval (such as in case of cycles of ETAGs) or a certificate (such as in case of cycles in specific standards). In both cases the result of the test should be valid over all the territory where the standard or the technical guide is applied. For this reason only one cycle is designed to reproduce ageing conditions in a very wide area: it's an envelop cycle of the extreme durability conditions all over Europe. That's why they cannot be considered service life prediction tests;
- real ageing accelerated cycles – their aim is to assess the durability of a building component in order to get a value of Reference Service Life and assess the overall performance decay and degradation evolution.

The aim of pre-designing ageing cycles is to avoid a large number of trials (up to convergence of degradation got with long-term and with short-term exposure) and to get an ageing cycle suited for the climatic context.

1.1 Avoiding a Large Number of Trial Tests

ISO 15686-2 sets a procedure for service life prediction of building components where a milestone is the comparison between degradation got with artificial accelerated ageing (i.e. laboratory tests and, only for walls, natural exposure with inclined surface) and degradation got with long-term exposure. If there is a great difference in degradation levels, pre-testing cycles must be re-designed and the procedure repeated. That means that a bad pre-design could cost a large number of trials. On the other hand, in the experimental programme about accelerated ageing tests on paintings carried on by Politecnico di Milano in collaboration with SUPSI, the methodology of time re-scaling has been proposed. This means that when the same degradation level is got, a comparison is set between long-term ageing time (field exposure with specimens of the same size of the ones used in short-term ageing) and the ageing cycles reproduced in laboratory tests, in order to gain the rate of ageing cycles per year. This kind of comparison could be implemented only if there is not a big initial error in pre-designing the cycle (the ageing cycle reproduces the climatic ageing phases in a similar proportion and, by means of time re-scaling, the correct proportion will be achieved) or the transport error will produce misleading results.

1.2 Ageing Cycle Suited for The Climatic Context

Ageing in different contexts cannot be assessed with the same ageing cycle. EOTA Guidance Document 3, in Annex A, individualizes four climatic conditions for Europe, different meso-climatic conditions (orientation and position of the building) and several internal environment conditions. This means that only one ageing cycle is not obviously sufficient in order to assess the behaviour in all Europe, but a large number of agents combinations should be taken into account. All combinations couldn't be reproduced and so the most representative and diffuse conditions may be chosen.

The need for more ageing cycles for the same building component is highlighted by the need for evaluating the Estimated Service Life. In ISO 15686-8 is suggested that data concerning RSL should be rejected "when the degradation agents deemed to be significant for the expected degradation process(es) are not all encompassed" and it is also recommended that "data based on reference in-use

conditions similar to the object-specific in-use conditions should always be sought", in order to "keep the modifying factors as unified as possible, thus minimizing the probability of error in the ESL due to uncertainty in the way mechanisms of degradation are affected by the modifications; and minimize the probability that a critical property not encompassed by data becomes the terminal critical property".

This involves that not only one value of RSL for a building component should be sought, but a set of Reference Service Lives may be taken into account and the nearest RSL to in-use conditions should be chosen as starting value for calculating ESL. In particular, in order to get different RSL values, different ageing cycles should be designed and so reduce the transport error from RSL to ESL.

2 AGEING CYCLE PRE-DESIGN

In this paragraph a first overview of different possibilities in ageing cycles pre-design is portrayed, while in the third paragraph examples cases are given.

2.1 Ageing Cycle Pre-designing Tools

Both determining the intensity of agents and determining the rate between ageing phases is fundamental in planning accelerated ageing tests and, in order to do this, three main different ways (at different analysis level) of pre-designing ageing cycles could be set:

- standard reference - if a standard for hygrothermal tests exists (even if not suited for durability assessment) it could be assumed as first hypothesis (e.g. see point 3.1);
- environmental data analysis - pure statistic analysis or analysis of environmental data beyond a critical threshold, got with the degradation factors and failure mechanisms analysis;
- preliminary degradation model - the weight of every ageing event (every event over the critical threshold) is determined thanks to a preliminary degradation simulation model (it doesn't simulate the whole ageing cycle, but only the first cycle).

2.2 Environmental Data Analysis

The aim of an environmental analysis is both to set the intensity of agents to be reproduced and their frequency in one year, in order to get a basic cycle corresponding just to one year. In case of several ageing phases (or sub-cycles) included in the ageing cycle, the aim of this analysis is to get their rate too, in order to design the cycle as close as possible to the environmental and stress context that has to be reproduced (e.g. the rate of UV phase on freeze – thaw phase will be different in assessing the service life of the same component in Norway or in Greece).

2.2.1 Basic climatic data analysis

No information is available concerning neither critical thresholds values nor frequency of critical events. In this case studying the environmental conditions in order to reproduce a "typical" ageing condition could be a first analysis tool.

2.2.2 Analysis of conditions of probability for critical events happening

No complete data are available that could allow to assess the real happening of critical events. In this case it's possible to assess when there is the probability (i.e. suitable conditions for happening) of a critical event. In order to operate this analysis preliminary data concerning critical values are needed. Critical thresholds could be defined by means of two different methods:

- standard reference for that specific degradation mechanism;
- preliminary tests suited for determining the critical value (e.g. trough the repetition of only one phase of whole ageing cycle).

2.2.3 Critical events counting

The aim of an accelerated ageing cycle is to "compress" ageing time and so reproduce only critical events. This criterion consists in searching for critical intensities of ageing factors, beyond which the studied material or building component is subject to fatigue or ageing. This method needs suited data. For instance, in case of assessing ageing due to summer thermal shock the occurrence of high external surface temperatures values and followed by a storm should be recorded. On the other hand in case of winter thermal shock the cloud index value should be measured in order to take into account different conditions that can cause low surface temperatures.

Different methods of collecting environmental data suited for durability analysis – and their importance – are discussed in Haagenrud *et al.* [2005]. The most important part of available data on demand for durability concerns agents relevant in corrosion process (both for steel and reinforced concrete structures), for wood and for paintings, while for several other building components, among those ETICS, there is a lack of information.

Another point is that even the statistic analysis method of climatic data in terms of energy approach and in terms of durability is different: mean data in the first case, while the complex of data (over a period of time corresponding to the foreseen RSL of that class of building component) in the second case. This means that in counting the number of critical events a mean year (as TRY) is an approximation that excludes peak values.

2.3 Degradation Model

Thanks to an environmental data analysis only the frequency of events over the critical threshold can be taken into account. In fact critical events (i.e. events beyond the critical threshold) have not the same intensity (see Fig. 1) and so produce not the same effect. Due to this fact their influence in ageing the material should be weighed by use of a model which simulates the real behaviour of the material under defined conditions (e.g. real stress - strain curve). In case of materials or building components with a low critical threshold (in comparison with average environmental conditions), this kind of study is relevant. In order to use this analysis tool a large amount of data is required.

2.3.1 Preliminary degradation model

A preliminary degradation model could assess only the first event of the degradation chain and only the mutual weight of critical events (it could be a basic dose-response function).

2.3.2 Complete degradation model

A complete degradation model is able to build up a degradation hypothesis by cycling the phenomenon and up-dating the material properties after each degradation events. This kind of complex analysis is very useful in case of non stochastic distribution of critical events, in order to assess the influence of different distributions of ageing events.

In case of ETICS, for instance, a degradation analysis tool could be a time-variant nonlinear stress – strain model of base coat (the thin exterior plaster applied on insulator) and its failure process (considering the degradation of the whole system linked to the failure of base coat). A complete degradation model would need both a proper description of the element and proper input data concerning material properties and actions applied.

A description of the geometry of the problem could be a finite element discretization of a plate of indefinite width with in of plane loading due both to temperature and moisture change and to the contribute to prevented deformation, even if small, given the insulator material (that could be reproduced considering a continuous elastic constraint parallel to the plate). On the other hand, several properties of the mortar should be obtained by preliminary tests: the real stress – strain curve both in dry and in wet conditions, the Poisson's coefficient, thermal and moisture expansion coefficients, the rigidity of the constraint given by the insulator, etc.

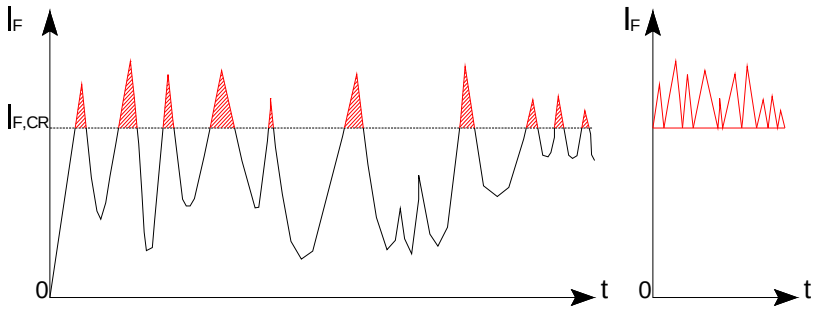

Figure 1. Acceleration of ageing time is based on the idea of excluding not ageing parts of one year.

3 A CASE OF AGEING CYCLE PRE-DESIGN: ETICS EXPERIMENTAL PROGRAMME

Since 2004, a research activity concerning durability of ETICS has been carried on by Durability of Building Components Group (DBCG) at Politecnico di Milano. This research programme involves accelerated ageing of specimens in order to survey the behaviour over time of the most external layer: base coat (a cement mortar with acrylic or vynilic resin as additive) and finishing layer (1.5 mm finishing coat with sand and acrylic resin as binder or acrylic painting).

In defining the cycle to submit the specimens to, both information from standard reference and statistic elaborations based on Milan's TRY (Test Reference Year) input data have been carried out.

3.1 Standard Reference: ETAG 004

As first reference value, the rate between the number of summer cycles and the number of winter ones designed in ETAG 004 (see Tab. 1) has been studied. This proportion corresponds to 2,29.

3.2 TRY Input Data Elaboration

3.2.1 About TRY

Efficient heating and cooling is largely dependent on building design and on the design of the heating and cooling system. Comparison of heating and air-conditioning systems in a locale needs a consideration of the effects of the weather. This weather information must be in great detail. With this aim, American Society of Heating, Refrigeration and Air-conditioning Engineers, (ASHRAE) established a task group on energy requirements for heating and cooling large structures.

Simultaneously, in the interest of energy conservation, the National Bureau of Standards (NBS) and the National Oceanic and Atmospheric (NOAA) were attempting to develop climatic data packaging most useful for building design applications. Joining forces, the three groups established a working group to develop the concept of a TRY. TRY consists of hourly weather data values (dry temperature, for global, diffuse and direct normal solar radiation, and for wind velocity) typical for the location for a selected reference year to be used by engineers in a given area to compare different heating and air-conditioning systems in the same building or in different buildings and, in general, to study thermal behaviour of technological and technical building's components. At the same time, the Federal Energy Administration (FEA) - as a member of the Steering Group on Climatic Conditions and Reference Year of the NATO Committee on Challenges of Modern Society - was also working on the problem. A consolidation of both efforts resulted in the development of a selection process for the Test Reference Year, an international format for presentation of the TRY data, and TRY calculations for 60 cities within the U.S. The ASHRAE approved procedure was chosen for selecting a TRY. The principle of selection is to eliminate years in the period of record containing months with extremely high or low mean temperature until only one year remains.

Table 1. ETAG 004 – Hygrothermal behaviour and freeze – thaw tests

Heat - rain cycles [80 cycles]
1. heating to 70°C (rise for 1 hour) and maintaining at (70 ± 5)°C and 10 to 15 % RH for 2 hours (total of 3 hours);
2. spraying for 1 hour (water temperature (+ 15 ± 5)°C, amount of water 1 l/m^2 min);
3. leave for 2 hours (drainage).
After at least 48 hours of subsequent conditioning at temperatures between 10 and 25°C and a minimum relative humidity of 50 %.
Heat-cold cycles [5 cycles]
1. exposure to (50 ± 5)°C (rise for 1 hour) and maximum 10 % RH for 7 hours (total of 8 hours),
2. exposure to (- 20 ± 5)°C (fall for 2 hours) for 14 hours (total of 16 hours).
Freeze – thaw [30 cycles]
1. Exposure to water for 8 hours at (+ 20 ± 2)°C by immersion of the samples, render face downwards, in a water bath, by the method described in 5.1.3.1 Capillarity test.
2. Freezing to (- 20 ± 2)°C (fall for 2 hours) for 14 hours (total of 16 hours).

3.2.1 Analysis on TRY for defining ageing cycles for ETICS

Starting from the TRY store for Milan Linate, the elaboration of climatic input data was conducted by DBCG in order to individuate the most stressing actions for the chosen building component and calculating how many times these stressing conditions happen in the Test Reference Year. Thanks then to a statistical elaboration of these data, it was possible to give an analytical validation to the defined cycle and, in particular, to the chosen ratio between summer cycles and winter ones.

The following tables show the results of elaborations developed using Milan Linate's TRY and taking into consideration, above all, the highest probability of stressing conditions both in winter and in summer, according to the "agents-actions-effects" analysis previously undertaken for ETICS.

In particular, in winter season, has been considered as ageing event the contemporary presence of low (under zero) temperatures and high relative humidity percentage, assessing the highest risk of superficial condensation that can provide water to be absorbed by the finishing coat and then, due to freezing, it can create cracks in the layer. In summer season, instead, it has been assessed the probability of thermal shocks, considering the occurrence of high air temperatures (or high air sun temperatures) and contemporary high relative humidity percentage (in order to take into account the probability of summer storms, in lack of precise data concerning it).

Despite this, it must be underlined that TRY is a collection of mean values of hourly mean data: it doesn't take into account peaks which can be relevant critical actions.

According to this statistical analysis it was then possible to observe the distribution of the ratio between summer and winter cycles: this rate is always higher than the one proposed by EOTA (equal to 2,29, as indicated at point 3.1).

In order to assume a more realistic rate value, without getting too far from the value suggested by EOTA, it was decided to repeat ageing sub-cycles maintaining the proportion 2.5: in each complete cycle CX there are 25 UV cycles, 10 winter cycles and 25 summer cycles. Complete ageing cycles CX therefore are assembled in groups of five so to get a macro-cycle TX. The overall duration of a macro-cycle is more or less one month.

Table 2. Daily elaborations for winter and summer seasons

Cycle	*t daily*		*RH max daily*	*Number of days in one year*	*Percentage in one year (%)*
WINTER	$T_{AIR\ MIN}$	≤ 0°C	≥ 80%	85	23,29
		≤ 0°C	≥ 90%	77	21,10
		≤ -5°C	≥ 80%	13	3,56
		≤ -5°C	≥ 90%	10	2,74
SUMMER	$T_{AIR\ MAX}$	≥ 25°C	≥ 80%	85	23,29
		≥ 25°C	≥ 90%	39	10,68
	$T_{AIR\ SUN\ MAX}$	≥ 50°C	≥ 90%	33	9,04
		≥ 55°C	≥ 90%	11	3,01

Table 3. Hourly elaborations for winter season

Cycle	*t hourly*	*RH hourly*	*v wind*	*Number of hours in one year*	*Percentage in one year (%)*
WINTER	≤ 0°C	≥ 80%	---	600	6,85
	≤ 0°C	≥ 90%	---	354	4,04
	≤ 0°C	≥ 80%	> 4 m/s	43	0,49
	≤ 0°C	≥ 90%	> 4 m/s	32	0,37

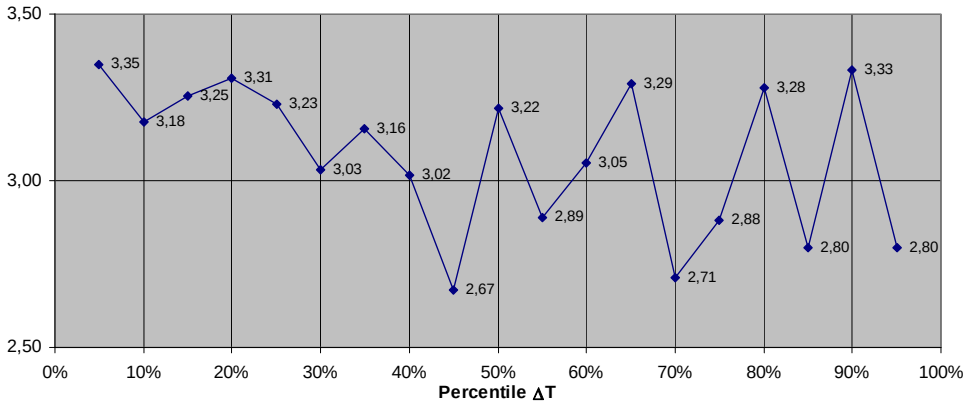

Figure 2. Ratio between summer and winter cycles, according to different percentiles

Table 4. Ageing sub-cycles or basic cycles (in bold set point values).

Basic cycle	Repeat	n°	Phase	Climatic chamber				Laboratory		
				T_{air} [°C]	T_{sup} [°C]	T_{H20} [°C]	RH [%]	$T_{op,i}$ [°C]	RH [%]	Duration [min]
UV	25	1.1	UV	***35***	-	-	15 ± 2	26 ± 3	60 ± 5	60
Winter	10	2.1	Rain: 1 [lt/m^2]	***5 ± 1***	-	5 ± 1	100	19 ± 2	60 ± 5	60
		2.2	Freeze	***-20 ± 2***	-	-	-	19 ± 2	60 ± 5	180
		2.3	Winter heat	***30 ± 2***	-	-	50 ± 2	19 ± 2	50 ± 5	60
Summer	25	3.1	Dry heat	***70 ± 5***	70 ± 5	-	15 ± 2	26 ± 3	60 ± 5	60
		3.2	Rain	*20*	-	20	100	26 ± 3	60 ± 5	60

4 CONCLUDING REMARKS

Lack of knowledge of environmental exposure data and models is an important barrier for further progress towards Service Life prediction.

The methodology for defining accelerated ageing cycles adopted by DBCG and applied to the ETICS experimental programme could be considered a first step in establishing a procedure for choosing the most proper ageing cycle for the studied building component: this is a topic emerged as a methodological problematic in particular during the last Italian national meeting in Favignana (TP). The necessity underlined is to adopt a common proceeding methodology for defining ageing cycle which better simulate the real climatic context to which they are associated.

REFERENCES

Daniotti, B. 2005, *La durabilità in edilizia*, CUSL, Milan, Italy.

Daniotti, B. 2007, *La valutazione della durabilità dei componenti dell'involucro edilizio*, 3rd International congress Ar.Tec, Ancona, Italy.

Daniotti, B. & Lupica Spagnolo, S. 2007, *La gestione del ciclo di vita dei componenti e degli organismi edilizi,* ed. ISTeA, Favignana (TP), Italy.

Daniotti, B. & Lupica Spagnolo, S. 2007, *Service life prediction for buildings' design to plan a sustainable building maintenance,* in papers of the conference "Sustainable construction, materials and practices", Lisbon, Portugal.

Daniotti, B. & Paolini, R. 2008, 'ETICS experimental programme', 11th DBMC, Istanbul 11-14 May 2008

Daniotti, B. & Paolini, R. 2008, 'ETICS end of Service Live', 11th DBMC, Istanbul 11-14 May 2008

Daniotti, B. & Paolini, R. 2006, 'La valutazione della durabilità di pareti perimetrali con isolamento esterno a cappotto', in *La valutazione della durabilità di pareti perimetrali verticali*, ediTecnica editrice, Palermo, pp. 37 - 74

Daniotti, B. & Paolini, R. 2005, 'Durability Design of External Thermal Insulation Composite Systems with Rendering', 10th DBMC, Lyon 17-20 April 2005

Haagenrud, S.E., Krigsvoll, G., Lisø, K.R., Thiis, T. & Sjöström, C. 2005, 'Environmental characterization and mapping with respect to Durability', 10th DBMC, Lyon 17-20 April 2005

European Organisation for Techinal Approvals (EOTA). Assessment of Working Life of Products (EOTA GD 003). Edition December 1999.

ETAG 004 – Edition March 2000. Guideline for European Technical Approval of external thermal insulation composite systems with rendering

ISO 15686:2000 – Building and constructed assets – Service life planning – Part 8 – Reference service life and service-life estimation

11DBMC International Conference on Durability of Building Materials and Components
ISTANBUL, Turkey 11-14 May 2008

Hail Impact Resistance of Building Materials Testing, Evaluation and Classification

Peter Flüeler [1]
Maja Stucki[2]
Fabio Guastala[3]
Thomas Egli [4]

T 32

ABSTRACT

Results are presented from an extensive research project on the hail impact resistance of various building materials and components including tiles, metal sheets, skylights, wood, glass, flexible sheets, exernal thermal insulation and finished systems, window shutters. The data established by impacting specimens with simulated hailstones made of plastic balls and ice spheres are correlated to each other. The results are discussed and recommendations are given for a new testing practice which will be implemented in Switzerland. In the project, it became evident that high speed hail tests can not be replaced by a dart impact test using falling steel balls to achieve the same kinetic energy. The values of hail impact resistance (HIR) show a marked difference between high modulus and low modulus materials, and their structural stiffness and surface properties.

A new classification system for the hail impact resistance of building materials is proposed. This system considers the five predominant damage categories experienced during impact; specifically, loss of functionality, deformation, fracture, aesthetics, and damage affecting aging. The results also show that requirements of certain standards such as that for solar modules do not comply with the hail size observations made during naturally-occurring hail storms.

KEYWORDS

Hail impact resistance, Testing, Correlation ice spheres vs. plastic ball impact, Classification

[1] Swiss Federal Laboratories for Materials Testing and Research EMPA, dept. civil and mechanical engineering, CH-8600 Dübendorf Switzerland, Phone +41 44 823 55 11, Fax 823 4026, peter.flueler@empa.ch and
FPC Flüeler Polymer Consulting GmbH, CH-8607 Aathal Switzerland, p.flueler@hispeed.ch

[2] Swiss Federal Laboratories for Materials Testing and Research EMPA, dept. civil and mechanical engineering, CH-8600 Dübendorf, Switzerland, internship at EMPA as trainee

[3] Egli Naturgefahren, CH-3001 Bern Switzerland Phone +41 31381 52 90, Fax+41 31 381 5291, stucki@naturgefahr.ch

[4] Egli Naturgefahren, CH-9001 St. Gallen Switzerland, Phone +41 71 274 7148 , Fax +41 71 274 7149, egli@naturgefahr.ch

1 INTRODUCTION

In Switzerland, each year hailstorms cause substantial damage to building envelopes and over time, total losses show an upward trend. The use of a plastic ball to simulate hail impact started in Switzerland in 1970 when roofing membranes were competing against traditional roofing materials like roof tiles. Standards such as SN 564 280 [1], recommendations of building authorities and insurance companies referred to such procedures. In determining hail impact resistance (HIR), a 40 mm plastic ball is shot at a specified speed at the test specimen. Temperature sensitive materials are cooled at the surface to 5° C and positioned on a rigid and/or flexible support. Facade elements are fastened at an angle of 45° or 90° with regular fasteners, and jointed to each other. The resultant damage is assessed for leakage and /or visual deficiencies.
Constant projectile properties, reproducibility, instant damage assessment, time and costs savings are the advantages of the current test procedures. There are, however, various disadvantages in this procedure in regard to the natural weather influences. In general, the density of plastic balls is higher than that of natural hailstones and the fracture behaviour is brittle for ice, elasto-plastic for plastic balls. This means that a plastic ball exerts higher energy than that occurring with a natural hail stone.

2 HIGH MASS - LOW SPEED VERSUS LOW MASS - HIGH SPEED

The approach to this problem with reference to natural environmental condition demands knowledge of the impact speed of a hailstone. It can be calculated from analytical evaluation or – as in recent times – from the use of measuring devices during a hail storm. If a high speed camera is available, the impact speed can be indirectly established by video-recording the impact.

2.1 Evaluation of Impact Velocity

At impact on the ground, hail appears to be of white colour. This fact leads to the conclusion that the amount of trapped air in the ice is apparently rather high. With increasing size, however, sliced hailstones often show a shell-like structure. Within this structure, clear ice alternates with porous ice resulting from many ups and downs in the turbulent air circulation within a storm super cell. Size of hailstone and aerodynamic drag c_w as determined by the hailstone shape has the strongest influence on impact velocity.

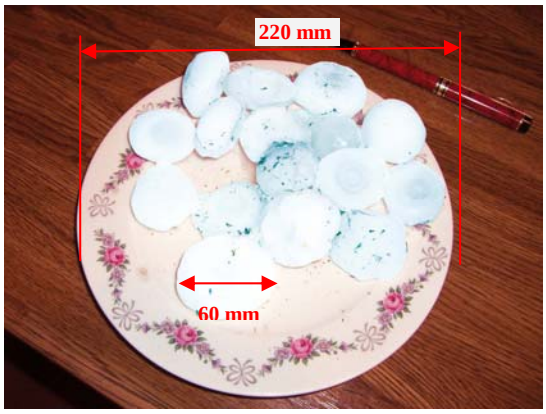

Figure 1. Shapes and dimensions of collected hailstones that fell from a super cell near Lugano on June 21, 2007 (photo by F. Terrasi)

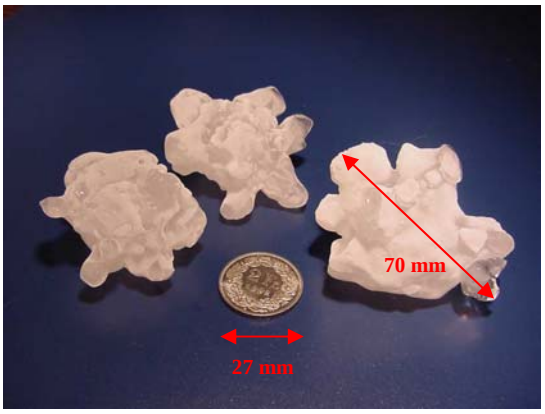

Figure 2. Shapes and dimensions of collected hailstones that fell from a super cell in the city area of Zurich on June 24, 2002 (photo by U. Spreiter; the diameter of the 2-Swiss Francs coin is 27 mm.)

These shapes vary from round, egg-shaped, disk-like, smooth, warty, bulgy, and even extremely jagged surfaced. Recently, bulgy, pointed forms were detected also in smaller-sized hailstones (Figure 1 and 2). Therefore the aerodynamic drag coefficient, c_w, can range from 0.45 for a smooth surface to 0.8 for a rough surface. In turn, the density, ρ_{ice}, may range from 0.60 to 0.91 kg/dm^3.

In the past, various scientists have reported on the hail impact velocity and its destructiveness. As an example: In 1937, Bilham and Relf [2] studied differences between small (< 10 mm) and large hailstones. Motz [3], Kawashita/Flüeler [4], and others evaluated the most cited equations for terminal velocity. Figure 3 shows the range of the calculated terminal velocity, v_{tH}, for hailstone diameters ranging from 20 to 100 mm. As a rule, factors in the calculation include the sphere diameter, d_H, the density of the ice, $\rho_{ice,}$ the density of the air, ρ_{air}, and the coefficient of aerodynamic drag in air, c_w. The following formula is most frequently used:

$$v_{tH} = \sqrt[2]{\frac{4 \cdot d_H \cdot g \cdot \rho_{ice}}{3 \cdot c_w \cdot \rho_{air}}} \qquad (1)$$

$$E_{kin} = m \cdot v^2/2 \qquad (2)$$

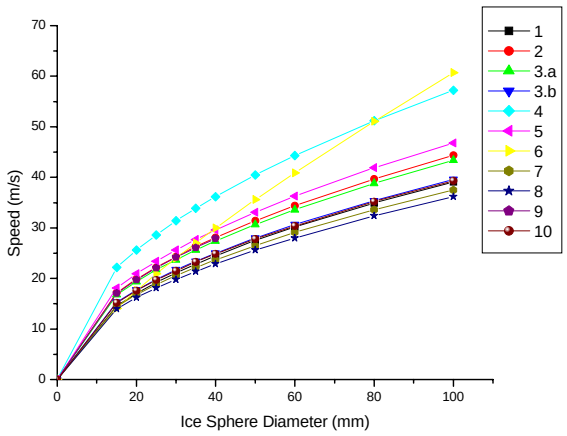

Figure 3. Calculated terminal velocity for round hailstones from different authors: 1. Bohm, 2. ASTM 1038-05, 3a. EMPA with c_w 0.5, 3b. EMPA c_w 0.6, 4. Motz ρ_{air} 0.9,kg/m^3, 5. Motz ρ_{air} 1.23,kg/m^3, 6. Heymsfield, 7. Pflaum, 8. and 9. Matson, 10. Lozowski, Guastala and Flüeler

In this present study, the following constants are used (Figure 2, curve 3a): Ice density, ρ_{ice} : 875 kg/m^3, air density at 20 ° C, ρ_{air} : 1.226 kg/m^3, and coefficient of aerodynamic drag, c_w: 0.5 kg/m^2.

2.2 Test Practices of Common Standards

Since the beginning of recorded history, Australia, South America, the United States, and Central Europe have known the effects of hailstorms. To toughen materials against hail impact, test procedures were first established in South Africa in the 1950s and in the United States at NIST in the 1960s. In Switzerland, the plastics industry provided evidence in the early 1970s that polymer roofing membranes are equal or even superior to classic roofing materials such as clay tiles. Initial impact testing was conducted using ice spheres. Nevertheless, for practical and economical reasons, a 40 mm polyamide (PA) sphere was chosen. Comparisons of in-service hailstone damage on polymer roofing membranes to that obtained with the PA spheres showed similar damage patterns. Due to this fact, SIA established a test protocol in 1977 [1] with the requirement of a velocity of 17 m/s when shooting at a chilled waterproofing membrane supported by a steel plate and soft thermal insulation board (EPS).

This velocity equates to a kinetic energy of 5.6 J. In comparison, good classic clay tiles become damaged at a velocity of 9 m/s which is equal to 1.6 J.

3 TEST PROGRAM

To simulate the conditions of natural hail and its impact on the building envelope, an extensive experimental investigation was performed. A comparative study was carried out on 50 types of materials originating from 11 fields of application using laboratory-made ice spheres and plastic balls.

3.1 Test Apparatus and Parameters

The test apparatus consisted of a pneumatic gun positioned vertically (Figure 4). This apparatus was originally designed for use with plastic balls only. In the course of expanding our technical investigations, the apparatus was modified to launch 15 to 50 mm ice spheres. By using a light beam, the projectile velocity is instantaneously measured at the end of the gun barrel in a distance of 30 cm. Target and distance are exactly aimed at by two focussing lasers (Figure 5). The velocity is set by the pneumatic pressure corresponding to calibration values enabling a repeatability of < 1 m/s.

Figure 4. Test apparatus and tilted steel frame with mounting for a wood framed window glass

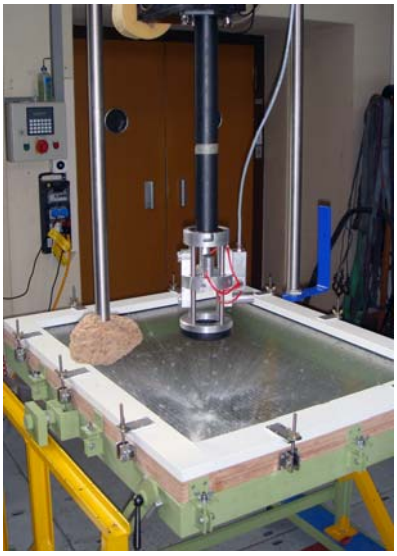

Figure 5. Edge impact of a 50 mm ice sphere on a 6 mm thick wire glass window

For the project, the following parameters were chosen:

Set-up of test specimen:	Condition new, as installed in building, custom-designed
Size of test specimen:	0.8 to 1.1 m^2 with jointing, possible overlaps, original fasteners
Surface treatment:	Temperature sensitive materials: chilled with ice granules for 3 min.
Test temperature:	Room temperature and humidity, approx 23° C/50 % r. h.
Impact angle:	Roofing 90°, façade 45°, both applications 45° and 90°
Type of impact:	Single shot mode
Impact speed:	Appropriate speed for size of projectile

3.2 Projectiles and Properties

For projectiles, precision balls made from PA 66 (density of 1.16 kg/dm^3) and laboratory ice spheres (density 0.875 g/cm^3) were used. The ice spheres were made in silicon moulds using demineralised water. The production of crack-free and essentially pore-free ice spheres required approx. 17 hours at -20° C in a freezer. Freezing of the water was induced by a freezer plate at the bottom of the mould, thus facilitating slow growth of the ice core from bottom to top. Due to time-dependent changes of ice,

a shelf time of less than 3 weeks was observed for the newly made ice spheres. The important properties of both types of projectiles are listed in Table 1:

Table 1. Mass of ice spheres and plastic balls for various diameters.

Type of sphere	Unit	Diameter (mm)				Failure behaviour
		20	30	40	50	
Mass of ice	(g)	3.8	12.3	30.2	58.3	brittle
Mass of Polyamide	(g)	4.8	16.1	38.8	74.9	tough

3.3 Procedure

To investigate the damage mechanism and weak points, test specimens were first impacted using PA-balls fired within the velocity range observed for real hailstones at impact. At a damage velocity considerably higher or lower than natural velocities, test specimens were impacted by sphere sizes 10 mm higher or lower. Then, the procedure was applied by using ice spheres.

4 DAMAGE ASSESSMENT AND EVALUATION

Assessment of damage in regard to insurance codes of practice was the most challenging task. The diversity of materials, supports, substrates, and fastenings along with the wide-ranging damage characteristics at impact demanded very close examination of each application. Therefore, the damage characteristics due to impact were grouped within the following general categories:

a) Loss of a main function: such as water tightness, breakdown of mechanical/electrical properties, loss of load bearing property etc,
b) Deformation: indentation, dent formation, deformation of defined depth,
c) Cracking and fracture: visible cracks, spontaneous fracture, delamination,
d) Aesthetics: change of appearance, loss of light transmission, change of aesthetical appearance, view in back light from a distance of 5 m, and
e) Damage affecting aging: inherent cracking, face separation, de-bonding, damage of surface layers.

After impact, the damage category was assigned based on the lowest velocity (i.e., kinetic energy according to Eq. 2) that resulted in damage. For ductile materials such as metallic sheets, the formation of a dent was judged to be aesthetic damage. In general, aesthetic damage was not observable until the depth of the indent reached about 0.5 mm.

5 RESULTS

The diversity of the investigated materials and their uses generated a wide range of results. Nevertheless, these results could be classified into three material categories according to load bearing behaviour, i.e. stiffness (Tables 2.1 – 2.3). A condensed report is provided by [6], also in French.

Figure 6 is a plot relating depth of indentation to projectile kinetic energy for the case of a 0.7 mm zinc-plated, corrugated steel sheet impacted using 40 mm PA balls and 40 mm ice spheres. Figure 7 shows a photo of the indentations at projectile velocities of 26, 30, and 36 m/s. At a 90° impact angle, both projectile types caused circular indentations that increased in size with increasing velocity. At an angle of 45° mainly ellipsoidal indents resulted. Upon impact, PA balls remained intact and showed no cracking. In contrast, ice spheres tended to split - even at a velocity as low as 10 m/s - depending on the nature, mass and surface topology of the specimen. A clear observation from the testing was that, for heavy mass specimens such as clay tiles, the ice fragmentation pattern was distinct and more diverse changing with increasing velocity in comparison to the fragmentation of compliant specimens. A heavy mass specimen is one for which the ratio of the test specimen mass to the projectile mass is

greater than 50. Another observation was that low HIR values (i.e., < 3 J) were in general found for specimens where the damage was categorized as aesthetic rather than functional.

Table 2.1. High stiffness, tough materials

Material/Component	Element stiffness	E·I (kN·mm²/mm)	Angle (°)	E_{kin} (J)	HIR-class	Lowest values for Product	Ø (mm)	E_{kin} (J)
Tiles	high	2330-2635	90	13.7 - 27.3	4	clay tiles	50	13.75
Glass	high	370 - 3000	45	5.5 - 46.7	3 - 5	wire glass 7	40	5.5
Fibre cement	high	140-252	45/90	17.6 - 38.2	4 - 5	corrug. plate 5.5	40	17.6
Polymer plates	high	0.3-9.6	90	6.4 - 38.8	3 - 5	PMMA 4	30	6.4
Skylights	high	5.3 - 7.4	90	0.8 – 3.1	2 - 3	PMMA 2.5	30	0.8
GRP boards	high	6-88	45	1.4 - 20.5	2 - 4	GRP-UP struct.	30	1.4

Table 2.2. Low stiffness materials, non load bearing

Material/Component	Element stiffness	E·I (kN·mm²/mm)	Angle (°)	E_{kin} (J)	HIR-class	Lowest values for Product	Ø (mm)	E_{kin} (J)
Shutters	very low	0.1-4.2	45/90	0.05 – 1.75	1 - 2	profile, foam 0.25	20	0.05
Roller blinds	very low	0.5-1.2	45/90	0.2 – 0.7	1 - 2	folded 0.45	20	0.2
GRP: corrug., trapez.	low	1.95	90	0.4 – 0.5	1	GRP-UP trp. 1.4	20	0.4
Metal sheets, facade	low	1.9-2.6	45	0.6 – 1.7	1 - 2	alu 0.7	30	0.6
Membrane: stiff*	medium	0.001-0.6	90	39 - 90	5	SBS 3.7 sand coat	50	> 80
Membrane: soft*	medium	0.001-0.6	90	12.9 - 53.3	4 - 5	SBS 3.7 sand coat	40	12.9

Table 2.3. Medium stiffness materials

Material/Component	Stiffness	E·I (kN·mm²/mm)	Angle (°)	E_{kin} (J)	HIR-class	Lowest values for Product	Ø (mm)	E_{kin} (J)
Larch wood	medium	1.7	45	0.6 - 1.8	1 - 2	coated	30	0.6
Spruce wood	medium	1.5	45	0.8 - 3.1	2	planed	30	0.8
EIFS**	medium	1.7 – 2.8	45	5.7 - 17.0	3 - 4	EPS 20, 4	30	5.7
Metal sheets, roof	medium	2.1 - 6.0	90	0.6 - 2.0	1 - 2	cupper, 0.6	30	0.6

*membrane placed on stiff / soft substrates, respectively **External Insulation and Finished System

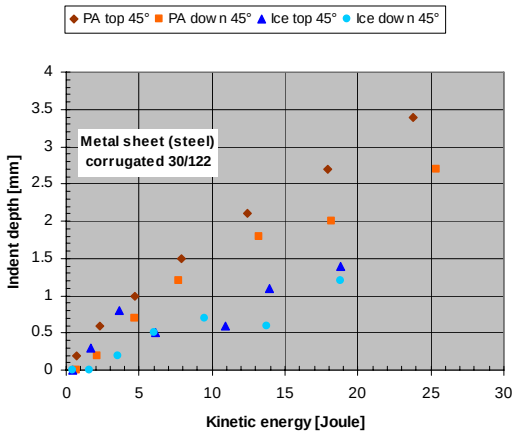

Figure 6: Indentation versus kinetic energy (J) of a corrugated 0.7 mm steel sheet tested using 40 mm PA balls and 40 mm ice spheres

Figure 7: Indentations caused by 40 mm projectiles; impact using PA balls (left) and ice spheres (right) at velocities of 26, 30 and 36 m/s

6 CORRELATION OF DATA FROM POLYAMID AND ICE SPHERES

Test data from two projectile materials - ice versus Polyamide - allow a correlation of the tested materials. A ratio (I/P) can be calculated between the values of velocity (and also kinetic energy) of ice (I) spheres and Polyamide (P) balls sphere. Figure 8 shows the relationship between the primary kinetic energy data for various specimens tested using 40 mm PA balls and 40 mm ice spheres.

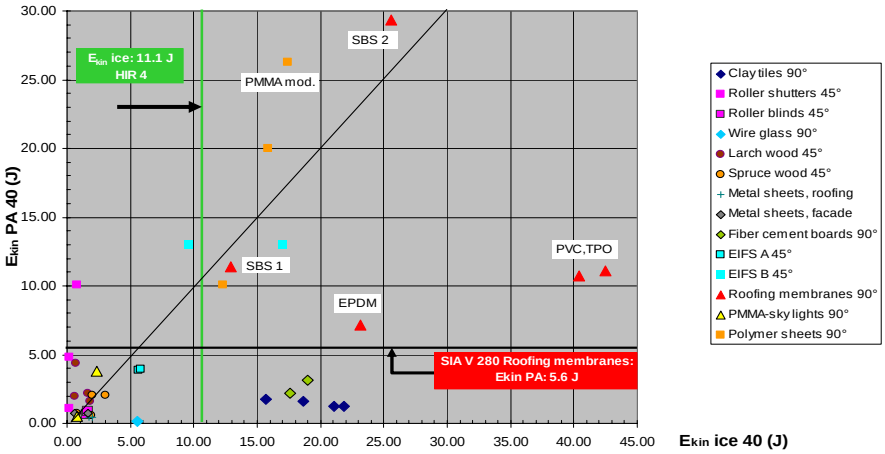

Figure 8. Kinetic energy in J for ice spheres and PA balls causing damage. Actual reqirement (red) for roofing membranes in Switzerland

This figure confirms clearly that many specimens experienced damage at very low kinetic energies. It is noted that hailstones having diameters less than 30 mm generally have kinetic energies of less than 3.5 J. Most important from Figure 8, it is evident that the data points for many specimens fell well below or above the correlation line indicating for these cases that testing needs to be conducted with ice spheres and not with PA balls. This is especially the case for roofing membranes tested on rigid substrates and for clay tiles.

7 CLASSIFICATION AND DESCRIPTION

A classification of building materials should be understood not only by material scientists and professionals in the building business but also by users. So, it should be ease to understand and related to the observed weather phenomena. In a 1991 publication, Flüeler [5] made an attempt to define a classification system including 5 levels of hail impact resistance. It is now stated to classify hail impact resistance into classes 1 to 5 (Table 3) that corresponds to hailstone diameters of 10 to 50 mm at which the building materials remain damage-free. It includes the corresponding terminal velocity of an impacting hailstone, as calculated using equation 1, curve 3a of the plot in figure 2 and calculated kinetic energy using equation 2. An examination of Table 3 shows that for each HIR class, the range of kinetic energy corresponding to that given HIR Class is rather large, for example, ranging from 11.1 J to < 27.0 J for HIR Class 4. This realization dictates that, for a more precise description differences in kinetic energy sustained without damage must be taken into account in the proposed classification system. The classification thus signifies not only the HIR class designation, but also the highest kinetic energy achieved without damage for the given sized ice sphere. Table 4 provides HIR Class designations (without kinetic energy) for the specimens in this study.

Table 3: Classification of hail impact resistance (HIR) and calculated kinetic energy

HIR-Class	Ice Sphere diameter (mm)	Mass (g)	Terminal velocity (m/s)	Kinetic energy (J)
1	10	0.5	13.8	***0.04***
2	20	3.6	19.5	***0.7***
3	30	12.3	23.9	***3.5***
4	40	29.2	27.5	***11.1***
5	50	56.9	30.8	***27.0***

Table 4: HIR-guide values of tested building materials and predominant damage category

HIR Class	Material/Component	Type	Thickness (mm)	Predominant Damage Category
1	Roller shutters, roller blinds	aluminium, folded	< 0.5	Deformation, aesthetics
	Metal sheets	cupper, tin	< 0.6	Deformation, aesthetics
	GRP-panels	light, shaped	> 2	Fibre matrix defect
2	Metal sheets façade and roofing	Fe, Cu-Fe, Ti plated	>0.5 - 0.7	Deformation, aesthetics
	Roller shutter reinforced	aluminium profile	0.9	Deformation, aesthetics
	Wood panels	planed, coated	25	Indent, cracked paint
3	Skylights	PMMA	2.5	Fracture, leakage, transparency
	GRP-double face panels	structural	20	
	EIFS (EPS and rock wool)	reinforced glass web	>3	Fibre matrix defect
	Wire glass	wire net 10 mm	7	Cracking, de-bonding Fracture
4	Roofing membranes	EPDM, SBS	4	Leakage
	Polymer sheets	PMMA modified	4	Transparency, defect
	Roof tiles	clay, structured surface	15	Internal fissure (sound check)
	Fibre cement boards/roofing	flat, undulated	6	Indent, surface crack, fissure
5	Roofing membranes	TPO, PVC-P	>1.5	Leakage
	Polymer sheets, skylights	PC, plain + structured	4	Deformation
	Safety glasses	single, laminated	6	Splitting, fracture
	Window glasses	insulated, alum. framed	4/16/4	Splitting, fracture

Note: HIR Classes in this table are examples achieved in the study and should not be taken as requirements or guide values.

8. CONCLUSIONS

1. This study confirmed field observations particularly from insurance companies that indicate that considerable hail damage payment (> 80 %) is made for the materials that fall within the HIR Class 1 and 2. They experience damage at kinetic energies of 0.7 J or less.

2. Impact of stiff, high-mass construction materials by a PA ball provokes considerably higher kinetic energy than that of an ice sphere of the same size. The fragmentation energy is not available for the damage process. For very stiff and high-mass materials, ice spheres have a kinetic energy up to 15 to 20 times greater than that of a PA ball to inflict damage.

3. With the exception of mass difference, lightweight elastic materials behave almost similarly with the two types of projectiles because of low fracture/deformation energy absorption.

4. For materials with structured cross sections with thin faces (e.g., double face plate, < 1 mm), a smaller projectile diameter might provoke damage while a larger diameter causes no damage.

5. Very often, hail damage resulting in loss of functionality or other physical characteristics is not as disconcerting as aesthetic damage. As an example, car bodies dented by hail are still roadworthy.

6. The effect of hail impact on the aging behaviour must be sufficiently taken into consideration.

7. Due to the diversity of materials and systems used for building envelopes, HIR evaluations have to be performed using ice spheres impacting at natural terminal velocity. Moreover, the kinetic enegy sustained during these evaluations has to be taken into account in an HIR classification system.

ACKNOWLEDGMENTS

The research was funded by the prevention fund of the Swiss association of cantonal building insurance companies. The authors wish to acknowledge the various contributions from the building material industries and the support of the EMPA laboratories, mainly polymer and composites.

REFERENCES

SIA, '*Polymer waterproofing membranes/Kunststoff-Dichtungsbahnen'*, Swiss Assoc. of Engineers and Architects, standard SN 584 280, editions 1977, 1988, 1996.

Bilham, E.G., Relf, E.F. 1937, '*The dynamics of large hailstones'*, Symon's Meteorogical Magazine, pp.149-162

Motz, H.D. 1986, '*Hagelrisiko- eine sicherheitswissenschaftliche Studie von Kausalität und Effekt'*, PhD-Thesis Univ. Gesamthochschule Wuppertal, D 468, Wuppertal, Germany.

Kawashita, L., Flüeler, P. 2002, Simulated Hail impact tests with ice and polyamid spheres, internal research report Empa no 860'091/2 (not public), August 20, 2002

Flüeler, P., Rupp, F. 1988, 'The *Hail Impact Resistance of Plastic Components of the Building Shell'*, Proceedings 3dbmc int. conference on durability of building materials, Bournemouth England.

Swiss Assoc. of Fire Insurance Companies VKF Bern, 7/2007, *Elementarschutzregister Hagel, Synthesebericht*, Untersuchungen zur Hagelgefahr und zum Widerstand der Gebäudehülle, 32 pages

Prediction of Atmospheric Corrosion Rate Using An Artificial Neural Network

Gülşah Doğan [1]
Emrah Gökaltun [2]

T32

ABSTRACT

Atmosphere is the environment to which the building materials are naturally exposed. Air pollution which is formed due to polluting this environment in an uncontrolled way causes undeniable negative results for both living beings and building materials. One of these unfavorable results is the atmospheric corrosion damage to the metal building materials. The weight loss as a consequence of the atmospheric corrosion significantly affects the performance and lifetime of the metal building materials and it results in big economical and social costs.

In order to quantify the impact of the corrosion on the metal building materials, the corrosion rate is often measured, if possible, or predicted using a mathematical model or an artificial neural network (ANN). Motivated from the proven performance of the ANNs in modeling the corrosion dynamics, in this study, an artificial neural network (DYSA) was developed to predict the atmospheric corrosion rate. When compared to the ANNs proposed in the literature for the corrosion rate estimation, the DYSA distinguishes itself from the rest by its unique data clustering technique together with Levenberg-Marquardt training algorithm using Bayesian regularization. The prediction performance of the DYSA was compared against the well-known MICAT network presented in the literature. The fact that the DYSA can predict the corrosion rate better than the MICAT network in the statistical sense was based on the following encouraging simulation results: DYSA decreased the mean square error by 84% and 54% for the training and test data sets, respectively; increased the correlation coefficient by 10% for the training data set as compared to the MICAT network.

KEYWORDS

Metal building materials, Atmospheric corrosion, Corrosion rate, Artificial neural network, MICAT

[1] Anadolu Univesity, Faculty of Engineering and Architecture, Eskişehir, Turkey 26470, Phone + 90 222 3223662, Fax222 3239501, gulsahdogan@anadolu.edu.tr

[2] Anadolu Univesity, Faculty of Engineering and Architecture, Eskişehir, Turkey 26470, Phone + 90 222 3223662, Fax 222 323 9501, egokaltun@anadolu.edu.tr

1 INTRODUCTION

The sustainability of life for all living beings on the world is only possible provided that there is synergy between them and their environment. This is because the environment is composed of living and nonliving elements and there are sophisticated relations and interactions between these elements. Human being, which depends on its environment like all other living beings for maintaining its life, is affected by its environment and affects it as well. The multi-faceted and uninterrupted interaction between human and its environment lasting throughout has started to impair in time due to the fact that humans have exploited the environment in an unconscious way for meeting their unbounded needs. Human originated effects like developing technology, population growth and its accompanying result of unplanned urbanization have started to damage the environment balance. As a result, the environment has been used for the consumer society's needs. Ignoring the environment in the production and consumer operations has caused many environmental problems. One of these problems is the air pollution which is due to the combustion of fossil fuels for supplying increasing energy demand from day to day. The air pollution, which has become a global environmental issue due to the transportation and dispersion processes, damages living as well as nonliving environment.

Buildings, depending on their ambient conditions, are exposed to a variety of effects in their life. These effects, in time, cause deterioration of and damage to the inner structure or surface of the building materials. The deterioration of materials forming the building affects the comfort and health of its users and decreases the lifetime of the building. Thus, it is required that effects and factors that can cause a damage to the building materials be understood in order to take the proper protective measures, that is, maintaining the health of the building, increasing the service lifetime of the building structure, avoiding the economical and social costs due to the damages/deteriorations. The air pollution among these factors plays an important role in forming a variety of damage mechanisms or speeding up the damage mechanisms. Thus, the air pollution has become a research topic in the field of architecture in which the possible impact of the air pollution on monuments, historical buildings and nowadays buildings is investigated [Atkinson 1970].

In this study, the impact of the atmospheric corrosion, which is one of the results of the air pollution, on the building materials is addressed. Atmosphere is the environment to which metal building materials are often exposed, and it is quite corrosive due to its nature. However, in the existence of pollutants like SO_2 and NO_2 which are released into atmosphere as the combustion wastes of fossil fuels used in production, heating and transportation and which play an important role in forming the air pollution, the corrosivity of the atmosphere highly increases. These pollutants, combined with other factors (temperature and humidity), affect the metals as well as all other materials by means of *Dry and Wet Deposition Mechanisms* [Dehri 1994].

In order to quantify the impact of the corrosion on the metal building materials, the *corrosion rate* is measured or predicted where the corrosion rate can be defined as the amount of substance dissolved per unit time at a specified surface. Determining the corrosion rate is important for understanding the durability of the metals and alloys to the corrosion. Furthermore, knowing the aptness of the material to the corrosion depending on the corrosivity of the ambient is very important for selecting the most suitable materials to be used in the building and taking the required protective measures for them. In the literature, a variety of methods has been developed to find out the corrosion rate: artificial neural networks [Pintos *et al.* 2000], power function and linear regression [Hou & Liang 2004], and D/R (Dose/Response) equation [Knotkova 2005]. In particularly, artificial neural network's proven success in modeling the nonlinear and complex systems and its ability of producing results even for the unseen examples based on its past experience make it an ideal choice for predicting the corrosion rate as compared to the linear regression techniques. Some of the studies which used the artificial neural network for predicting the corrosion rate in the literature are as follows: [Cai *et al*. [1999]; Cottis *et al*. [1999]; Pintos *et al*. [2000]; Parthiban *et al*. [2005]].
Based on the success achieved by the artificial neural networks for predicting the corrosion rate in the literature, an artificial neural network (DYSA) was developed to predict the corrosion rate in this study

as well. The DYSA's distinguishing features include its unique data clustering technique together with Levenberg-Marquardt training algorithm using Bayesian regularization. The prediction performance of the DYSA was compared against the well-known MICAT network (Pintos *et al.* [2000]) presented in the literature. The fact that the DYSA can predict the corrosion rate better than the MICAT network in the statistical sense was based on the following encouraging simulation results: DYSA decreased the mean square error by 84% and 54% for the training and test data sets, respectively; increased the correlation coefficient by 10% for the training data set as compared to the MICAT network.

The rest of the paper is organized as follows. Section 2 presents the MICAT network model proposed by Pintos *et al.* [2000]; Section 3 introduces DYSA network developed in this study; Section 4 compares the prediction performance of MICAT and DYSA networks; Section 5 concludes the paper.

2 MICAT ANN MODEL

The Mapa Iberoamericano de Corrosión Atmosférica (MICAT) project includes seventy-two test sites exposed to the atmosphere in fourteen countries throughout Iberoamerica. These countries are Argentina, Brasil, Chile, Colombia, Costa Rica, Cuba, Ecuador, Portugal, Peru, Mexico, Venezuela, Panama, Spain, and Uruguay. The MICAT project has three main objectives: (i) construct the corrosion map for Iberoamerica, (ii) provide a better understanding of atmospheric corrosion phenomena, (iii) identify mathematical models that could predict the corrosion rate of metals in the atmosphere as a function of meteorological and pollution variables for Iberoamerica [Pintos *et al.* 2000].

According to Pintos *et al.* [2000], the third objective of the MICAT project can be attained by means of an artificial neural network (ANN). Thus, a database, which will be used for training and testing the ANN to be developed, was established by collecting data from seventy-two test sites in fourteen countries during the MICAT project. Based on this database, Pintos *et al.* [2000] predicted the corrosion rate of carbon steel (Fe, μm/year) as a function of six different metereochemical variables using a three layer ANN. The metereochemical variables constituting the database are temperature (T in ^{o}C), relative humidity (RH in %), time of wetness (TOW), precipitation (P in mm), sulfate deposition rate (SO_2 in mg/m^2/day), and chloride deposition rate (Cl^- in mg/m^2/day). Technical features of the ANN model developed by Pintos *et al.* [2000] are presented in Table 1.

Table 1. Technical features of MICAT artificial neural network developed by Pintos *et al.* [2000].

ANN model	Multi-layer perceptron (one hidden layer)
Number of input/hidden/output layer neurons	6/6/1
Activation function	Sigmoid
Training algorithm	Gradient descent
Method for avoiding over-training	Early stopping

3 DYSA ANN MODEL

In this section, DYSA ANN, which was developed to predict the corrosion rate better in the statistical sense than the MICAT ANN, and its design process will be presented.

3.1 DYSA Network Model

In order to define an ANN with multi-layer perceptron network topology, it is required that the number of layers and the number of neurons together with an activation function for each layer in the

network be determined. DYSA, similar to MICAT network, has three layers: input layer, hidden layer, and output layer. The rationale behind three layer network topology can be explained as follows. Predicting the corrosion rate as a function of some variables is truly a *function estimation problem*. According to Demuth *et al.* [2006], for the function estimation problems, a three layer perceptron network topology is enough to predict any function with an arbitrary accuracy provided that the number of hidden layer neurons, the activation functions of the hidden and output layer, and the weights are determined appropriately.

After the specification of the DYSA network topology, the number of neurons in each layer and the related activation functions are determined as follows. The number of input layer neurons is six, which is equal to the number of metereochemical variables in the database; the number of output layer neurons is one, since only corrosion rate will be predicted. In the literature, there is no known method that can be used to set the number of hidden layer neurons as well as the hidden layer and output layer activation functions. Thus, the trail-and-error approach was followed for setting them so that the prediction performance of the DYSA is maximized. As a result, the number of hidden layer neurons was fixed to be eight; both hidden and output layer activation function was determined to be the hyperbolic tangent [Doğan 2006].

3.2 DYSA Training Algorithm

Various training algorithms have been proposed for multi-layer perceptron ANNs. These algorithms can be classified into four groups: Gradient descent, conjugate gradient descent, Newton, and Levenberg-Marquardt [Haykin [1994]; Demuth *et al*. [2006]]. It is a fact that the training time and prediction performance vary from algorithm to algorithm. For the function estimation problems, Levenberg-Marquardt algorithm, as compared to the other ones, takes less time to complete training and shows better estimation performance [Demuth *et al*. 2006]. Thus, the training algorithm of the DYSA was chosen to be Levenberg-Marquardt algorithm.

Table 2. Technical features of DYSA artificial neural network.

ANN model	Multi-layer perceptron (one hidden layer)
Number of input/hidden/output layer neurons	6/8/1
Activation function	Hyperbolic tangent
Training algorithm	Levenberg-Marquardt
Method for avoding over-training	Bayesian regularization

During the training of an ANN using any training algorithm, it is possible to experience some common disadvantages of ANNs which may lead an ANN to producing unacceptable results. One of these disadvantages is the *loss of generalization due to over-training* [Danaher 2004]. There are a few techniques that can be applied to alleviate this disadvantage. One of them is *early stopping* used by the MICAT ANN. In the early stopping, database is split into three groups, namely: training, validation, and test. A down side of the early stopping is that it is unknown how to form the validation group, which is used to check for the over-training during the training. Another technique is *Bayesian regularization*, which does not need a validation group. Thus, DYSA has adopted Bayesian regularization. Technical features of the DYSA are presented in Table 2.

3.3 Preprocessing Data For DYSA

In the training and test of the DYSA, the MICAT database of Pintos *et al.* [2000] was exploited. The database needs to be split into two as training and test group. However, in the literature, there is no method proposed for creating training and test groups for a multi-layer perceptron ANN from a

database. Furthermore, the training group affects the training time as well as the training and test performances of an ANN. Thus, how the database is partitioned is a crucial to the performance of any ANN. One of the important and distinguishing contributions of this study is the method developed to partition a database into training group and test group. This method is explained below.

- There are 130 observations in the MICAT database. Each observation is a 1 × 7 vector of measurements, where six of them correspond to the metereochemical variables (T, RH , TOW, P, SO_2, Cl^-) and the last one is the corrosion rate (Fe). It was decided for the DYSA that the training group includes 105, and the test group contains 25 observations. Thus, the training group is a matrix of 105 × 7 and the test group is a matrix of 25 × 7. It should be noted that the MICAT ANN has a training group of 105 observations and a test group of 9 observations. Thus, the size of the training group is the same for the DYSA and MICAT; yet, DYSA will be challenged with a greater test group.
- The observations in the database were split into 20 disjoint groups using MATLAB's clusterdata function so that each group has at least one observation. Clusterdata function, first, computes the distance between any two observation pair by means of Mahalanobis distance function and then, groups the observations using based on these distances. Specifically, each observation is included in the group with the minimum average distance among twenty groups, where the average distance is the average of distances between the observation at hand and the observations in a group. As a result, Clusterdata function groups observations close to each other into the same group.
- After the grouping, the number of observations in the groups can be arbitrary. It is possible that a group includes just one observation, while another one has 20 observations. Thus, in order to make it possible to represent each group in the training data set, a maximum number of 130/20 ≈ 6 observations from each group is randomly selected. In this way, 68 observations were chosen in the first round. Remember that the training group should have 105 observations. Thus, the remaining 105 – 68 = 37 observations were randomly selected among 62 observations. Finally, the test group is formed using the rest of the observations.

Following the procedure explained above, the training and test groups were determined. In order to use the training group for training the DYSA, the training group must be scaled. This scaling is accomplished in two steps as follows:

- The training group is a matrix of 105 × 7. Each row of this matrix corresponds to an observation and each column to a variable. For example, the fourth column includes only precipitation data. When this column is studied, it is seen that the precipitation data varies in a highly wide range (between 13.0 and 4656.0 mm). Thus, when this column is scaled down into the range [-1,1] in the next step, there will be a great loss of accuracy. In order to avoid this situation, the fourth column is logarithmically scaled between 2.56 and 8.44. In the MICAT ANN, the fourth column is not logarithmically scaled.

- Demuth *et al*. [2000] stated that Levenberg-Marquardt algorithm using Bayesian regularization gives the best results if the training group is scaled in the range [-1,1]. Thus, each column of the training group is separately scaled in the range [-1,1]. In the MICAT ANN, each column is separately scaled so that the column mean is zero and the column standard deviation is one.

4 RESULTS

As stated above, the training group is a matrix of 105 × 7. The first six columns of this matrix correspond to metereochemical variables and the last column to the corrosion rate. In the framework of the *supervised learning*, the scaled training group is split into two as *training input matrix* and *training target vector*. The training input matrix (105 × 6) is composed of the first six columns of the training group; the training target vector (105 × 1) is the last column of the training group. In a similar way, the

test group of 25 × 7 is first scaled as described above and then, it is split into two as the *test input matrix* (25 × 6) and the *test target matrix* (25 × 1).

The performance of the DYSA for both the training and test input matrices was measured by using two different metrics, namely, mean square error (*mse*) and correlation coefficient (*R*). These metrics are defined below:

$$mse = \frac{1}{N}\sum_{k=1}^{N}(y_k - \hat{y}_k)^2 \tag{1}$$

$$R = \frac{\sum_{k=1}^{N}(\hat{y}_k - \bar{y})(y_k - \bar{y})}{\sqrt{\sum_{k=1}^{N}(\hat{y}_k - \bar{y})^2 \sum_{k=1}^{N}(y_k - \bar{y})^2}} \tag{2}$$

In these two equations: N denotes the number of elements in the training/test target vector; y_k is the kth element of the training/test target vector; $\hat{y}_k$ represents the kth element of the corrosion rate vector predicted by the DYSA; $\bar{y}$ is the average value of the training/test target vector. Based on these metrics, the DYSA has the following goals: (i) the difference between the predicted corrosion rate vector by the DYSA and the target vector must be minimized by minimizing the mean square error. (ii) The correlation coefficient must be maximized in order for the DYSA to account for the variations in the target vector.

The training and test of the DYSA was accomplished by a program written in MATLAB language. The training process of the DYSA can be summarized as follows: The training input matrix is applied to the DYSA whose weights are randomly determined for the first iteration. The prediction error vector is computed by subtracting the training target vector from the DYSA's output for the training input matrix. If the computed error is smaller than an acceptable error value, the training is stopped. Otherwise, the training algorithm computes a new set of weights so that the prediction error gets smaller, and then it starts over. The test process of the DYSA includes the computing DYSA's performance based on the output vector obtained after applying the test input vector to the DYSA and the test target vector. In the MATLAB program, in order to minimize the probability of converging a local solution, the training process was repeated for 500 times with different initial weights at each time and then, the ANN showing the best performance in terms of the mean square error and correlation coefficient is determined to be DYSA. The DYSA's weights can be found in [Doğan 2006].

The training and test performances of the DYSA and MICAT networks are presented in Table 3. Note that the training and test input matrices used for the DYSA are different from the ones used by MICAT. Thus, the performance of the DYSA was measured for the DYSA input matrices obtained by the procedure developed in this study as well as the MICAT input matrices in Pintos *et al.* [2000]. According to Table 3, the DYSA shows much better performance for both its input matrices and the MICAT input matrices than the MICAT. The DYSA decreases the mean square error as much as 84% for the DYSA training input matrix and 54 % for the DYSA test input matrix, while it increases the correlation coefficient by 10 % for the DYSA training input matrix. Furthermore, the DYSA decreases the mean square error as much as 73% for the MICAT training input matrix and 89 % for the MICAT test input matrix, while it increases the correlation coefficient by 9 % for the MICAT training input matrix. According to these encouraging results, the DYSA developed in this study is capable of predicting the corrosion rate better than the DYSA in the statistical sense.

Table 3. Performance comparison of DYSA and MICAT networks.

	DYSA				MICAT	
	DYSA input matrices		MICAT input matrices			
	mse	***R***	***mse***	***R***	***mse***	***R***
Training	21.15	0.99	37.31	0.98	140.0	0.90
Test	100.28	0.75	23.65	0.99	220.0	□

The performance of the DYSA in predicting the corrosion rate is studied by means of sensitivity analysis for each metereochemical variable as well. This analysis consists of two steps: (i) Forming a test input matrix for each metereochemical variable, (ii) Observing the output of the DYSA while applying these input matrices one by one to the DYSA. For the sensitivity analysis, the test input matrix was formed as follows. The minimum and maximum values of the variable for which the sensitivity analysis will be made are found in the database. In the test input matrix, this variable takes values between it minimum and maximum values with equal intervals. For the other variables, in the test input matrix, their average values computed from the database are used. In this way, six different test input matrices are prepared and the output of the DYSA for each of these matrices is determined. In this study, because of the space limitations, the sensitivity analysis for the temperature and the relative humidity are only presented for the DYSA in Fig. 1.

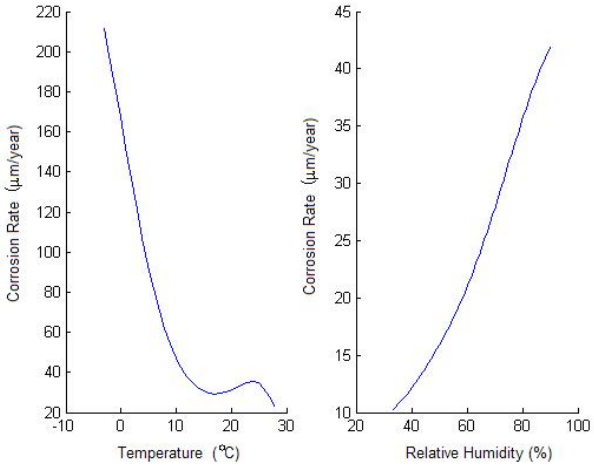

Figure 1. The sensitivity analysis of the DYSA for the temperature and relative humidity.

According to Fig. 1, while the temperature is rising, the corrosion rate is decreasing. The impact of the temperature on the corrosion rate can be in two different ways: (i) Rising of the temperature increases the reaction rate, thereby increasing the corrosion rate as well. (ii) Rising of the temperature decreases the time of wetness of the metal due to the increased vaporization, thereby decreasing the corrosion rate [Dehri, 1994]. As a result, the DYSA reacts to the rising of the temperature in the framework of (ii). As far as the relative humidity-corrosion rate relation is concerned, increasing the humidity results in more amount of electrolyte layer on the metal, thereby increasing the corrosion rate. This relation is clearly shown in Fig. 1.

5 CONCLUSIONS

As an essential building material, metals are affected the most by the destroying effects of the atmospheric pollution and the most important damage mechanism due to the interaction with the atmosphere is the atmospheric corrosion. The atmospheric corrosion with high economical losses is a

very complex matter due to the fact that many factors including environmental and atmospheric ones affect the corrosion reactions. Thus, the determination of the atmospheric corrosion rate of metals is a sophisticated and intriguing problem as well. In this study, an artificial neural network, DYSA, was developed for the solution of the problem, and it was shown that it can be used to predict the atmospheric corrosion rate with higher accuracy than the MICAT network.

REFERENCES

Atkinson, B. 1970, 'Weathering and performance' in *The Weathering And Performance Of Building Materials*, eds J.W. Simpson, & P. J. Horrobin, John Wiley & Sons, Great Britain.

Cai, J., Cottis, R.A. & Lyon, S.B. 1999, 'Phenomenological modelling of atmospheric corrosion using an artificial neural network', *Corrosion Science*, **41**, 2001-2030.

Cottis, R.A., Qing, L., Owen, G., Gartland, S.J., Helliwell, I.A. & Turega, M. 1999, 'Neural network methods for corrosion data reduction', *Materials&Design*, **20**, 169-178.

Danaher, S., Datta, S., Waddle, I. & Hackney, P. 2004, 'Erosion modeling using bayesian regulated artificial neural networks', *Wear*, **256**, 879-888.

Dehri, İ. 1994, *Corrosive Impact of Athmospheric Pollutants to Building Materials*, Ph.D. Dissertation, Çukurova University, Graduate School of Science, Adana.

Demuth, H., Beale, M. & Hagan, M. 2006, *Neural Network Toolbox User's Guide*, The Mathworks, Natick, Massachusetts.

Doğan, G. 2006, *An Experimental Study On The İmpact Of The Atmospheric Corrosion On The Metal Building Meterials And Prediction Of The Corrosıon Rate Via Artificial Neural Network*, M.Sc. Thesis, Anadolu University, Graduate School of Science, Eskişehir.

Haykin, S. 1994, *Neural Networks A Comprehensive Foundation*, Prentice-Hall, Inc., New Jersey.

Hou, W. & Liang, C. 2004, 'Atmospheric Corrosion Prediction of Steels,' *Corrosion*, **60**[3], 313-322.

Knotkova, D. 2005, 'Atmospheric corrosion-research, testing, and standardization', *Corrosion*, **61**[8], 723-738.

Parthiban, T., Ravi, R., Parthiban, G.T., Srinivasan, S., Ramakrishnan & K.R., Raghavan, M. 2005, 'Neural network analysis for corrosion of steel in concrete', *Corrosion Science*, **47**, 1625-1642.

Pintos, S., Queipo, N.V., Rincon, O.T. & Morcillo, M. 2000, 'Artificial neural network modelling of atmospheric corrosion in the MICAT project', *Corrosion Science*, **42**, 35-52.

11DBMC International Conference on Durability of Building Materials and Components
ISTANBUL, Turkey 11-14 May 2008

Predicting The Initial Rate of Water Absorption in Clay Bricks

Mariarosa Raimondo [1]
Michele Dondi [2]
Davide Gardini [3]
Guia Guarini [4]

T 33

ABSTRACT

In this work the capillary suction behaviour of fifteen clay bricks was investigated (UNI 10859) in order to assess the effect of product characteristics and processing conditions and to verify the reliability of the available models. The suction behaviour of bricks, in terms of both total amount of liquid absorbed and kinetics of the process, can basically be brought back to the models of Gummerson et co-workers and Hoffman and Niesel; these latter, however, do not make provision for the effect of product microstructure and water physical properties on the liquid-porous solid interactions. Even if experimentally the liquid suction presents a first dependence on the amount of porosity - a less dense ceramic body is undoubtedly able to absorb a larger liquid amount - other characteristics of the porous structure (size, tortuosity and internal specific surface of the capillary system, as well as the presence of mineralogical phases) request to be more deeply investigated since they could affect the process kinetics.
According with the Beltran's model, which revealed to be sufficiently reliable, the values of capillary coefficient K_s were calculated and their correlation with the experimental ones has been provided. The results obtained indicate that, for a given liquid and in the same experimental conditions, varying in a controlled way the product microstructure (i.e. decreasing the pore size, increasing the pore tortuosity and/or controlling the amorphous/new formed phases ratio) should allow to design materials having a more suitable behaviour.

KEYWORDS

Clay brick, Capillary absorption, Porosity, Microstructure, Phase composition

[1] Institute of Science and Technology for Ceramics, ISTEC-CNR, Faenza, Italy 48018, Phone +39 0546 699718, Fax 0546 46381, mrosa@istec.cnr.it
[2] Institute of Science and Technology for Ceramics, ISTEC-CNR, Faenza, Italy 48018, Phone +39 0546 699728, Fax 0546 46381, dondi@istec.cnr.it
[3] Institute of Science and Technology for Ceramics, ISTEC-CNR, Faenza, Italy 48018, Phone +39 0546 699749, Fax 0546 46381, davide@istec.cnr.it
[4] Institute of Science and Technology for Ceramics, ISTEC-CNR, Faenza, Italy 48018, Phone +39 0546 699718, Fax 0546 46381, guiagrn@istec.cnr.it

1 INTRODUCTION

In the structural design of masonry, the suction behaviour of clay bricks has to be strictly controlled in order to optimize the mechanical performances and to prevent deterioration processes. Clay bricks capacity of absorbing liquids and moisture, from both the immediate surrounding and the other building materials, can be referred as their "capillarity". Since clay bricks have to satisfy many requirements (i.e. thermal and acoustic properties, load-bearing capacity and ecological impact), the relationship between these properties and capillarity phenomenon goes through their microstructural characteristics and, in particular, amount, size and shape of pores.

In the literature, a time dependent law of fluid absorption by porous materials, taking the form:

$$m = K_s \cdot t^{1/2} \tag{1}$$

has been proposed [Gummerson *et al.*, [1981]]: the water absorbed by a porous solid per surface unit area (m) increases as the square root of the elapsed time (t), with K_s being defined as the capillary coefficient. In the last years, other mathematical functions were empirically derived [Hoffman *et al.* [1985, 1990]] and the simple relation (1) was replaced by an exponential one:

$$m = a\,[1-\exp(-bt^{1/2})] \tag{2}$$

where a is the maximum moisture content and b a factor influencing the suction kinetics; multiplying a per b, the liquid absorption coefficient is obtained. Equation (1) was furtherly developed [Beltrán *et al.* [1988]] considering that the capillary coefficient K_s must depend on both properties of liquid and of porous solid. Accordingly, the capillary coefficient can be expressed by the formula:

$$K_s = \rho\left(\frac{\gamma}{\mu}\right)^{1/2} \frac{OP}{\lambda}\, r_0^{1/2} \left[\cos\vartheta/2\right]^{1/2} \tag{3}$$

where ρ, γ and μ are, respectively, the density, the surface tension and the viscosity of the liquid, while OP represents the open porosity accessible by the liquid, r_0 the median pore size and λ the pore tortuosity of the solid; θ is the liquid-brick contact angle.
For a given temperature, grouping the liquid properties and the contact angle term into a constant C, the equation (3) is reduced to:

$$K_s = C \cdot \frac{OP}{\lambda} \cdot r_0^{1/2} \tag{4}$$

while equation (1) can be written in the form:

$$m = \left[C \cdot \frac{OP}{\lambda} \cdot r_0^{1/2}\right] \cdot t^{1/2} \tag{5}$$

When the experimental results are represented graphically in the form of m versus $t^{1/2}$, a straight line with a slope K_s should be observed.

The aims of this work are: i) giving a representative survey of the suction behaviour of clay bricks and ii) assessing the influence of the main microstructural and compositional parameters of clay bricks on the absorption process. The results pursued could allow to improve the evaluation of the effects of product and processing conditions on the capillary suction of porous bodies, thus representing an important starting point in the structural design of masonry components.

2 MATERIALS AND METHODS

Fifteen samples of clay bricks were collected in different brickworks, representing the Italian production. Products were characterized by the determination of phase composition, open and total porosity, bulk density, pore size distribution and pore specific surface. Phase composition was quantitatively determined by X-ray powder diffraction (Rigaku Miniflex, CuKα radiation) with the Reference Intensity Ratio method (Al_2O_3 as internal standard, experimental error is within 5% relative). Open porosity (OP) and bulk density (BD) were quantified according to ASTM C373. Specific weight (SW) was measured by He pycnometry (Micromeritics MVP 1305, ASTM C329), while total porosity (TP) was calculated by the equation: TP = (1-BD/SW) ·100.
Pore size distribution (in the 0.01 – 100 μm range) was determined by MIP (Thermo Finnigan Pascal 140/240) with an experimental uncertainty of about 1% relative. Porosimetric data are expressed as r_0 (median pore radius), amount of micropores (P50) having a diameter < 0.05 μm (i.e. < 50 nm) and amount of macropores (P3) having diameter > 3 μm. Pore specific surface (SS) analyses were performed by nitrogen absorption (Micromeritics FlowSorb II 2300) following the B.E.T. single point method.

The capillary absorption of samples was determined according to UNI 10859 on circular disks (20.0 ± 0.1 cm diameter, thickness between 1.5 and 2.0 cm). Samples were dried in an electric oven at 60 ± 2°C for 7 days and, after cooling, their weight (m_0) was measured. A basal face of each disk was put into direct contact with a 1 cm layer of paper, filled with distilled water at 20°C, in a closed vessel. The mass of specimens (m_i) was recorded after 10, 20, 30 minutes and 1, 4, 6, 24, 48 and 72 hours and the liquid mass absorbed per surface unit area (m) was calculated by the formula:
$m = (m_i - m_0)\, A^{-1}$ (6) where A is the area of the specimen in contact with the paper layer.
The capillary absorption of each sample was described plotting m versus the square root of the elapsed time (Fig.1). The graph obtained presents an initial straight line, whose slope is the experimental capillary coefficient K_s, and a final stage characterized by an asymptotic trend.

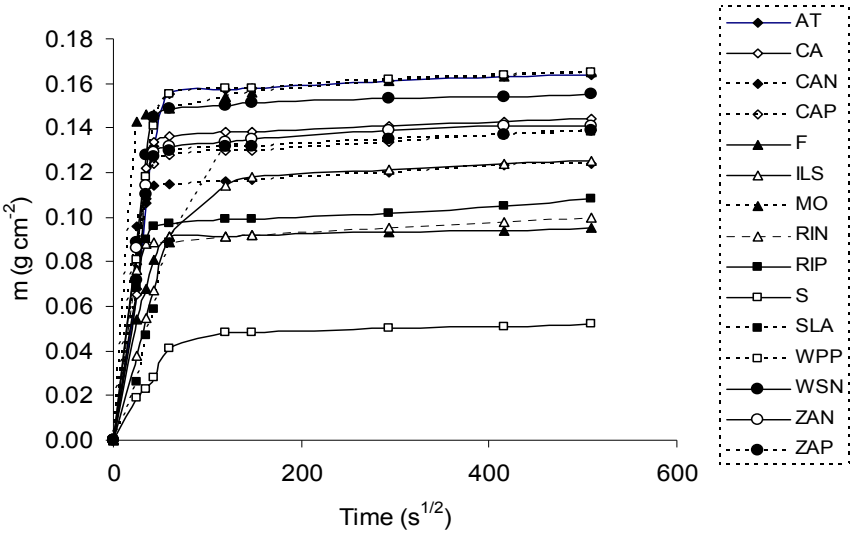

Figure 1. Suction behaviour of clay bricks.

In order to verify equation (3), the following physical properties of water at 20°C were utilized (3): density ρ = 0.998 g cm^{-3}; surface tension γ = 72.7 mN m^{-1}; viscosity μ = 1.0 mPa s. The capillary tortuosity factor λ, which is an empirical dimensionless parameter, was calculated as the ratio:

$$\lambda = \frac{r_0 \cdot SS \cdot BD}{2 \cdot OP} \qquad (7)$$

The water-brick contact angle was measured on the brick surface (DataPhysics Instrument OCA15) obtaining an average value of θ = 87± 3°. A statistical elaboration of data was performed by linear binary correlation and multivariate analysis techniques (factor analysis, scree test for eigenvalues) using the StatSoft Statistica 6.0 software.

3 RESULTS AND DISCUSSION

3.1 Physical Properties

Samples show a great variability of their physical and microstructural parameters [Table 1]: total porosity is in the 19-43 %vol. range, mostly represented by open porosity (19-40 %vol). The median pore size r_0 is between 0.1 and 1.0 μm, while specific surface varies in the 0.6-2.4 $m^2\ g^{-1}$ range. An exception is represented by the sample SLA, which has the smallest pores (r_0 = 0.09 μm) developing a high specific surface (12.3 $m^2\ g^{-1}$). The fraction of pores having dimensions under 50 nm (P50) is quite significant in sample S (13.4 %vol), despite being the less porous material. On the other hand, the amount of the larger pores (P3) is maximum in samples RIN, MO and WPP.

Table 1. Open (OP) and total (TP) porosity, bulk density (BD), median pore radius (r_0), specific surface (SS), amount of pores having a diameter smaller than 0.05 μm (P50) and greater than 3 μm (P3), pore tortuosity (λ) and thickness of clay bricks.

Samples	*OP* (%vol)	*TP* (%vol)	*BD* (g cm^{-3})	r_0 (μm)	*SS* ($m^2\ g^{-1}$)	*P50* (%vol)	*P3* (%vol)	λ (adim.)	*Thickness* (cm)
AT	39.0	42.6	1.605	0.48	2.40	2.7	1.2	2.4	1.83
CA	33.3	34.9	1.763	0.66	2.00	0.9	1.1	3.6	1.95
CAN	36.0	39.3	1.696	0.61	2.02	0.8	0.8	2.9	1.49
CAP	36.7	38.4	1.684	0.61	1.87	0.1	0.6	2.6	1.65
F	24.4	27.3	1.870	0.42	1.00	0.6	0.5	1.6	1.55
ILS	27.7	37.5	1.716	0.38	1.90	1.5	1.1	2.2	1.84
MO	36.3	36.5	1.766	0.43	1.20	0.7	4.5	1.3	2.02
RIN	33.3	36.2	1.712	0.99	2.11	4.2	4.8	5.4	1.47
RIP	32.7	34.0	1.715	1.00	1.47	5.8	4.2	3.9	1.63
S	18.8	18.8	2.121	0.61	0.60	13.4	1.6	2.1	1.62
SLA	28.9	28.9	1.896	0.09	12.30	0.8	1.2	3.5	2.02
WPP	36.5	38.6	1.657	1.00	1.61	3.1	6.1	3.7	2.15
WSN	35.2	38.1	1.673	0.84	1.40	0.8	2.7	2.8	2.07
ZAN	38.5	41.0	1.632	0.54	2.30	0.8	1.2	2.6	1.62
ZAP	38.4	41.4	1.627	0.56	2.36	0.6	2.2	2.8	1.58

As far as phase composition, samples are mainly made up of quartz (17-45%), with residual K-feldspar and plagioclase up to 25 and 17%, respectively. Illite/mica is also present in most samples, with AT and SLA showing a content as high as 20%. The amorphous phase ranges from 6% (samples CAP and ZAP) to 45% (sample S), while the total amount of pyroxene, wollastonite and melilite fluctuates between 2 and 46%.

3.2 Initial Rate of Water Absorption

The suction behaviour of samples is illustrated in Fig.1. Most of them reach saturation conditions after less than 3 hours, showing then an asymptotic trend involving very small variations of the liquid mass absorbed; nevertheless, the total amount of water absorbed varies from 0.05 g cm^{-2} of sample S to about 0.16-0.17 g cm^{-2} of samples AT, MO, WPP and WSN [Table 2]. On the whole, samples seem to follow two main trends; most present an initial water uptake characterized by a steep slope (K_s values

between 0.6 and 5.9 $\cdot 10^{-3}$ g $cm^{-2}s^{-1/2}$, Fig. 1 and Table 2) that suddenly develops towards the asymptote, while samples S, ILS and SLA exhibit a more gradual behaviour (K_s between 0.6 $\cdot 10^{-3}$ and 1.5 $\cdot 10^{-3}$ g $cm^{-2}s^{-1/2}$, Fig. 1 and Table 2). These different trends can be brought back, respectively, to the models proposed by Gummerson and co-workers [1981] or Hoffmann and Niesel [1988]. In particular, the resistance (in terms of both m and K_s) offered by S, ILS and SLA to capillary suction has a first correspondence with their pore size and amount: the very low porosity and the significant percentage of micropores of sample S, as well as the smaller pores, when compared to the mean pore size of the other products, present in both ILS and SLA, confirm somehow the conclusions of the literature [Latridou and Ozouf [1978] [Vos and Tammes [1969]].

3.3 Capillary Suction vs Microstructural Properties

Since physical parameters of water can be considered constant in the experimental conditions, liquid absorption and K_s should depend only on the solid characteristics.
A positive correlation of both OP (Fig. 2A) and TP (Fig. 2B) with K_s seems to exist though with a quite low statistical significance (r^2 = 0.524 and 0.347, respectively) mainly due to the sample MO, which presents a "capillary capacity" much higher than expected on the basis of its porosity. Hence, if it is true that a less dense ceramic body is able to absorb a higher liquid amount, for the same porosity the influence of other parameters characterizing the capillary structure is not obvious.

Table 2. Total amount of absorbed water (m), experimental (K_s) and predicted (K_s*) values of capillary coefficient.

Samples	m (g cm^{-2})	$K_s \cdot 10^3$ (g $cm^{-2}s^{-1/2}$)	$K_s^* \cdot 10^3$ (g $cm^{-2}s^{-1/2}$)
AT	0.164	3.1	15.4
CA	0.144	3.3	10.4
CAN	0.124	2.8	13.2
CAP	0.139	3.0	15.2
F	0.095	1.9	13.3
ILS	0.125	1.5	10.8
MO	0.165	5.9	25.1
RIN	0.100	2.2	8.4
RIP	0.108	2.3	11.7
S	0.052	0.6	9.7
SLA	0.138	1.5	3.4
WPP	0.165	3.4	13.4
WSN	0.155	3.5	15.7
ZAN	0.121	3.1	15.2
ZAP	0.139	3.1	13.9

Concerning the relationships of K_s with r_0 (Fig. 2C) and P50 (Fig. 2D), the following conclusions can be drawn: i) the suction kinetics is not dependent on the pore size (r^2 = 0.015) since, for most samples, very different pore dimensions correspond to quite similar values of K_s; ii) the correlation of K_s with P50 gives rise to a cloudy distribution of data (r^2 = 0.269) also because, among the samples, there are not big differences in the relative amount of micropores; at all events, the behaviour of sample S (P50 as high as 13.4%) suggests that such micropores could represent an effective restriction to the liquid uptake. In addition, when K_s is plotted against P3, a correlation with low statistical significance is obtained, so that the statement that larger pores should be the most involved in the suction phenomenon [Beltrán *et al.* [1988]] was proved to be not completely reliable.

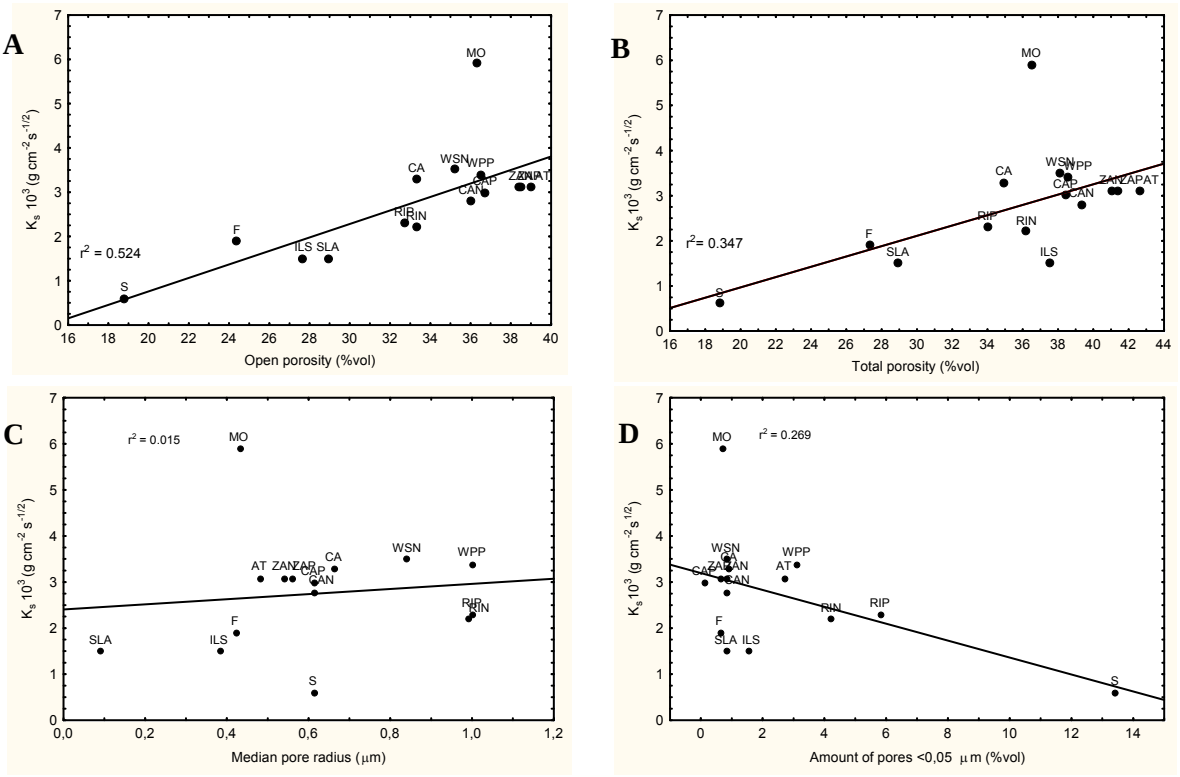

Figure 2. Experimental capillary coefficient K_s vs. (A) open porosity, (B) total porosity, (C) mean pore size and (D) amount of pores < 0.05 μm of clay bricks.

3.4 Predicting the Capillary Coefficient K_s

The reliability of the model proposed by Beltràn and co-workers [1988-1999] was checked introducing into the equation (3) the physical data of water at 20°C and, for each sample, the experimental values of open porosity, median pore size, water-brick contact angle (θ = 87°) and tortuosity factor as calculated in the present work. The predicted K_s values obtained range from 3.4 $\cdot 10^{-3}$ (g cm^{-2}s$^{-1/2}$) of sample SLA to 25.1 $\cdot 10^{-3}$ (g cm^{-2}s$^{-1/2}$) of sample MO (K_s*, Table 2) and their correlation with the experimental ones being illustrated in Figs. 3A and B; fitting the results by linear regression, the straight line going through the origin (r^2 = 0.692) provides the following relationship: the value of the capillary coefficient K_s^* predicted on the basis of equation (3) has to be multiplied by 0.212 to obtain the experimental one so that the real suction kinetics of all samples is proved to be lower than expected on the basis of model.

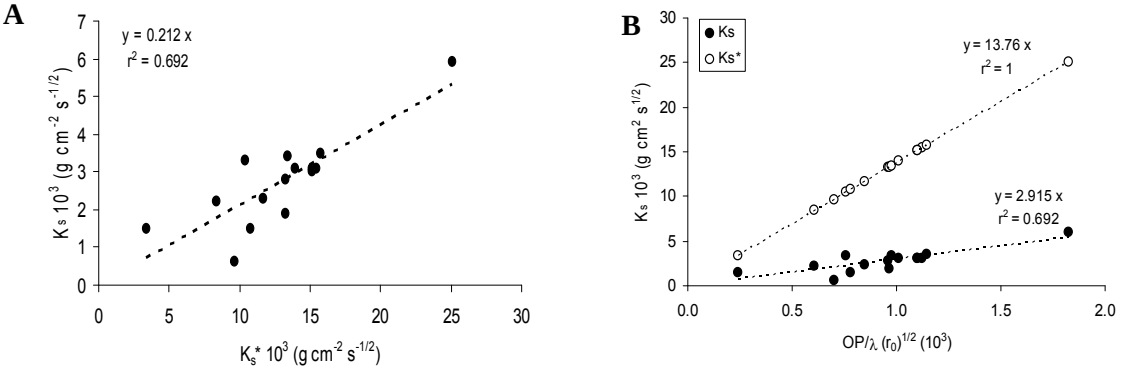

Figure 3. (A) The experimental K_s vs. the predicted K_s* values of capillarity coefficient and (B) the capillary coefficients vs. the term OP/λ□$(r_0)^{1/2}$.

Focusing our attention on these aspects, both predicted and experimental values of the capillary coefficient were plotted as function of the term OP/λ $(r_0)^{1/2}$ (Fig. 3B); the linear fitting provides straight lines having, respectively, the form:

$$K_s = 2.915 \frac{OP}{\lambda} (r_o)^{1/2} \qquad (r^2 = 0.692) \tag{8}$$

and

$$K_s^* = 13.760 \frac{OP}{\lambda} (r_o)^{1/2} \qquad (r^2 = 1) \tag{9}$$

The ratio between the slope values (2.915/13.760 = 0.212) coincides with the slope of the straight line fitting the experimental/predicted K_s relationship. Moreover, the slope value of equation (8) must correspond to the term: $\rho(\frac{\gamma}{\mu})^{1/2}[\cos\vartheta/2]^{1/2}$ which, considering constant the physical data of water at 20°C, provides the value of the water-brick contact angle fitting the experimental results: θ = 89°, very similar to the experimental average value (θ = 87°) utilized in the present work.
Looking back at equation (8) and Fig.3B, it is reliable to conclude that, besides some exceptions, the Beltràn's model is sufficiently satisfied: for the same value of open porosity, decreasing the pore size and/or increasing the pore tortuosity means to limit the suction rate and, hence, the capacity of clay bricks of absorbing moisture. At any event, this also means that, varying in a controlled way the product $OP/\lambda\ (r_0)^{1/2}$, it could be possible to design clay bricks having a more suitable suction behaviour and, at least, to bound the structural deterioration of masonry optimizing the performance of its components.

3.5 Capillary Suction vs Phase Composition

During firing, the decomposition of $CaCO_3$, with the formation of Ca-silicates by reaction with the clay minerals and release of CO_2, promotes a greater amount of porosity; theoretically, this circumstance it is expected to cause higher values of K_s as it is somehow confirmed (Fig. 4A). On the other hand, the amount of amorphous phase, together with the low sintering degree achieved at the brick firing temperature (900-1000°C), involve the presence of a smaller porosity, which, in turn, seems to be a restriction to the liquid suction phenomenon (Fig.4B).

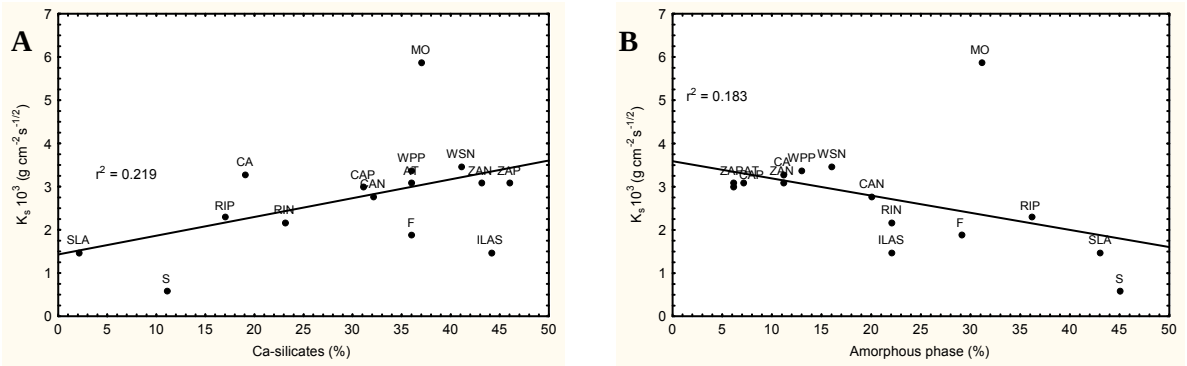

Figure 4. Experimental capillary coefficient K_s vs. amount of (A) Ca-silicates and (B) amorphous phase of clay bricks.

A statistical treatment of data was also undertaken through the extraction of the principal components: in the procedure, the amount of Ca-silicates and amorphous phase, other than K_s, were also considered as variables in addition to the microstructural ones (OP, TP, r_0, P50, P3, SS, λ). The positive or negative influence of each variables on K_s clearly stands out when the factorial weights are plotted grafically (Fig. 5): a higher porosity, in terms of both open and total values, makes the liquid uptake faster. The restrictive role played by the amount of micropores and the amorphous phase on the water

suction rate is also underlined by the statistical procedure, as well as the opposite role played by the new formed Ca-silicates.

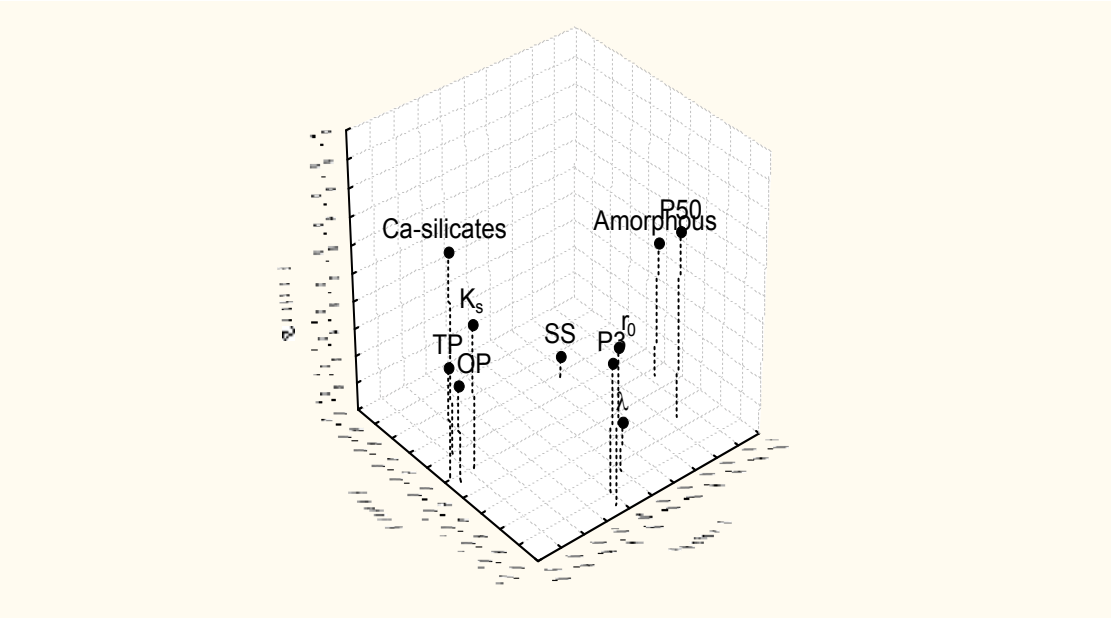

Figure 5. Principal components analysis: factors extracted.

4 CONCLUSIONS

On he whole, the suction behaviour of clay bricks follows the models of Gummerson et al. [1981] and Hoffmann et al. [1988]; however, they do not provide any information about the liquid-solid interactions, so that no prediction of the material behaviour in working conditions can be done. The suction capacity of bricks, in fact, is expected to depend on their microstructural characteristics, in particular, amount, size and shape of pores. Besides some exceptions, the linear relationships between the capillary coefficient K_s and these microstructural variables substantially confirm the role played by open porosity in increasing the absorption capacities of clay bricks, while the influence of pore characteristics on the suction kinetics does not clearly stand out.
The values of the capillary coefficient K_s were also calculated on the basis of Beltrán model [1988], whose effectiveness in predicting K_s values proved to be quite good. This means that, varying in a controlled way the term $OP/\lambda\ (r_0)^{1/2}$, it is possible to design materials having a predictable suction behaviour, hence to bound the damages in terms of structural deterioration. The capillary coefficient K_s, together with the microstructural variables and phase composition, finally underwent a statistical procedure that confirmed the influence of porosity, as well as of a coarser pore dimension (in terms of both radius and percentage of pores greater than 3 μm) in increasing the liquid adsorbing rate with the highest statistical significance. In addition, the sintering pattern of products, leading to a different amorphous/crystalline phases ratio, proved to be relevant on the definition of the most suitable microstructure: the higher porosity, promoted by the complete $CaCO_3$ decomposition, and the smaller pore size, connected with the low sintering degree of clay bricks, work in the opposite way.

REFERENCES

Gummerson, RJ, Hall, C. & Hoff, WD. 1981, 'The suction rate and the sorptivity of bricks', Brit. *Ceram. Trans. J.*, **80**, 150-152.

Hoffmann, D. & Niesel, K. 1988, 'Quantifying capillary rise in columns of porous material', *Am. Ceram. Soc. Bull.*, **67**[8], 1418.

Hoffmann, D., Niesel, K & Wagner, A. 1990, 'Capillary rise and the subsequent evaporation process measured on columns of porous material', *Am. Ceram. Soc. Bull,* **69**[3]392-396.

Beltrán, V., Escardino, A., Feliu, C., & Rodrigo, MD. 1988, 'Liquid suction by porous ceramic materials', *Br. Ceram. Trans. J.,* **87**, 64-69.

Beltrán, V., Barba, A., Rodrigo, MD & Escardino, A. 1989, 'Liquid suction by porous ceramic materials: 2. – Influence of pressing conditions', *Br. Ceram. Trans. J.*, **88**, 219-222.

Beltrán, V., Barba, A., Jarque, JC. & Escardino, A. 1991, 'Liquid suction by porous ceramic materials: 3. – Influence of the nature of the composition and the preparation method of the pressing powder', B*r. Ceram. Trans. J,.***90**, 77-80.

Escardino, A., Beltrán, V., Barba, A. & Sánchez, E. 1999, 'Liquid suction by porous ceramic materials: 4. – Influence of firing conditions, *Br. Ceram. Trans. J***. 98**[5)], 225-229.

Lautridou, JP. & Ozouf , JC. 1978, 'Relations entre la gelivité et les propriétés (porosité, ascensión capillaire) des roches calcaires' in *Colloque int. UNESCO-RILEM. Alteration et protection des monuments en pierre*, Paris 5 June.

Vos, BH.& Tammes, E. 1969, 'Moisture and moisture transfer in porous materials', Report no BI-69-96. Institute TNO for building materials and building structures, Delft, Holland.

11DBMC International Conference on Durability of Building Materials and Components
ISTANBUL Turkey 11-14 May 2008

Simulating Water Leaks in External Walls to Check the Moisture Tolerance of Building Assemblies in Different Climates

Hartwig M. Künzel [1]
Daniel Zirkelbach [2]
Achilles Karagiozis [3]
Andreas Holm [4]
Klaus Sedlbauer [5]

T33

ABSTRACT

The moisture tolerance of building assemblies is becoming a major durability issue worldwide because it is almost impossible to create perfectly tight building assemblies. Alerted by numerous cases of severe moisture damage caused by rain water penetration through stucco clad walls in North-America, the American Society of Heat Refrigeration and Air-conditioning Engineers (ASHRAE) has recently put out a standard on moisture design criteria for public review. This new standard forms the basis for hygrothermal performance evaluations by numerical simulation that should ultimately lead to better moisture control in buildings. In this paper the moisture behaviour of stud walls with leaks in the exterior thermal insulation system (EIFS or ETICS) is simulated by applying the procedure described in the ASHRAE standard. In a parametric study the different assembly modifications and outdoor climate conditions in North America and Europe are considered. The results show severe problems dealing with exterior insulation systems based on polystyrene insulation. Only in some cases increasing the drying potential toward the interior by replacing the vapour barrier by a smart retarder helps to solve the problem. However, when the polystyrene insulation is exchanged by mineral wool the penetrating rainwater rapidly dries out through the exterior insulation system and the humidity conditions in the wall always remain below the critical threshold.

KEYWORDS

Exterior insulation, Hygrothermal simulation, Drying potential, Water penetration

[1] Fraunhofer Institute for Building Physics, Department of Hygrothermics, Fraunhoferstr. 10, 83626 Valley, Germany
Phone +49 8024 643 245, Fax +49 8024 643 366, hartwig.kuenzel@ibp.fraunhofer.de
[2] Fraunhofer Institute for Building Physics, Department of Hygrothermics, Fraunhoferstr. 10, 83626 Valley, Germany
Phone +49 8024 643 229, Fax +49 8024 643 366, daniel.zirkelbach@ibp.fraunhofer.de
[3] Oak Ridge National Laboratory, Building Technology Center, 1 Bethel Valley Rd, Oak Ridge, TN 37831-6070
Phone +1 865 576 3924, Fax +1 865 576 9331, karagiozisan@ornl.gov
[4] Fraunhofer Institute for Building Physics, Department of Indoor Climate, Fraunhoferstr. 10, 83626 Valley, Germany
Phone +49 8024 643 226, Fax +49 8024 643 366, andreas.holm@ibp.fraunhofer.de
[5] Fraunhofer Institute for Building Physics, Board of Directors, Nobelstr. 12 , 70504 Stuttgart, Germany
Phone +49 711 9703300, Fax +49 8024 643 366, klaus.sedlbauer@ibp.fraunhofer.de

1 INTRODUCTION

Approximately 50 years ago, the first exterior wall insulation systems – nowadays called **E**xternal **T**hermal **I**nsulation **C**omposite **S**ystems (ETICS) in Europe and **E**xterior **I**nsulation **F**inish **S**ystems (EIFS) in North America – were installed on buildings. Despite being exposed to higher hygrothermal loads than most façade systems, EIFS on concrete or masonry have a satisfactory track record in Europe. They seem to be at least as durable as conventional façades with render or stucco [Künzel et al. 2006]. However, there is only little long-term experience concerning the application of EIFS on wood frame structures in Europe where these systems are increasingly installed to alleviate thermal bridging caused by the framework or to retrofit existing buildings. Therefore, it makes sense to analyze the situation in North America where EIFS on wooden structures have a mixed track record due to numerous failures related to elevated moisture in the construction. Since it is unlikely that the reported damage cases will remain confined to North America, this paper focuses on investigating the hygrothermal behaviour of EIFS on wooden structures under selected climate conditions in America, and Europe.

2 INTERNATIONAL EXPERIENCES

2.1 Composition of EIFS (ETICS)

EIFS in North America usually closely resemble those in Europe. The original composition – recent versions may also include a drainage layer – of an EIFS is shown in Figure 1. The EIFS is glued or mechanically fastened to the exterior sheathing that might consist of OSB, plywood, gypsum sheathing or wood fibreboard. Expanded Polystyrene (EPS) normally serves as insulation material. The use of mineral fibre insulation, also quite common in Europe, is practically unknown in North America. On top of the insulation a polymer modified base coat including a reinforcing glass fibre mesh are applied, followed by a finish coat. The reinforced base coat together with the finish or top coat is called lamina which is usually approximately 5 mm thick.

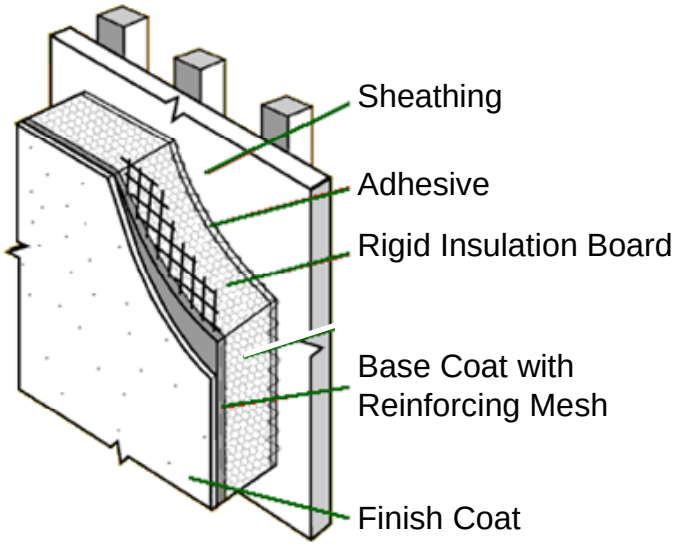

Figure 1. Composition of a typical **E**xterior **I**nsulation **F**inish **S**ystem

2.2 Damage Cases in North America and Lessons Learned

In the middle of the 90s the first substantial damage cases associated with EIFS were reported from North Carolina [Crandell & Kenney 1996] and similar reports from other regions with high precipitation intensities (e.g. Seattle, Vancouver) followed [Desjarlais et al. 2001]. Usually moisture

problems occurred mostly at the exterior sheathing boards that served as substrate for the EIFS. Pictures of rotten OSB or disintegrated gypsum board quickly spread among the building community and forced manufactures to react [Nisson & Best 1999]. A comprehensive literature review of Cheple & Huelman [2000] analysing more than 10 investigations carried out on several objects each, comes to the following conclusions: The main reasons for moisture damage are leaks around windows and joints where rainwater penetrates beneath the insulation layer. However, problems due to air convection or diffusion of indoor air may also have caused elevated moisture in some cases. An aggravating factor is the low drying potential of the construction. Moisture can neither dry-out quickly to the exterior because of the vapour retarding foam insulation nor to the interior due to the usual presence of a polyethylene vapour barrier. The solutions proposed by Cheple & Huelman [2000] are limited to managing rain water penetration by proper sloping and flashing of joints and wall openings and by applying drainable insulation systems. Sheathing materials such as untreated gypsum board, are very sensitive to moisture uptake and hence are considered inappropriate as EIFS substrates. Other work has shown that enhancing the drying potential towards the interior spaces by an innovative vapour control strategy may also alleviate the problem [Karagiozis & Kumaran 1997].

The moisture problems that occurred on North American constructions in the 90s were not limited to walls having EIFS. Buildings with normal stucco façades (render applied on building paper over OSB or plywood) were also affected [Lawton 1999]. This resulted in a new design approach that aimed at better detailing to reduce rainwater penetration and at increasing the drying potential of the whole assembly. It has been realized that it is difficult to set-up a perfect building that will never leak. Therefore the building envelope should be designed in such a way that small leaks can be handled. Consequently the ASHARE Standard 160 [2006] on criteria for moisture design states that in the absence of performance proofs it should be assumed that 1% of the wind driven rain hitting the façade is deposited on the weather resistive barrier (WRB) behind the cladding. If there is no WRB, another layer should be selected where the penetrating rainwater is likely to go (e.g. the sheathing beneath the EIFS in Figure 1).

2.3 Experiences with EIFS (ETICS) in Europe

EIFS (ETICS) in Europe have a track record of about 50 years. More than 40 million square meters of EIFS are installed on new and existing buildings every year in Germany and severe problems or damage cases have been rare [Künzel et al. 2006]. In contrast to North America where EIFS are mainly considered as a finish system, the purpose of EIFS in Europe is to provide adequate thermal performance of external walls that usually consist of masonry or poured concrete. Therefore the average insulation thickness is higher in Europe (approx. 100 mm in 2006) than in the U.S. (25-50 mm). EIFS in Europe require a Technical Approval as a system that ensures harmonized system components and trained installers. However, it is doubtful that better quality control and workmanship alone can explain the huge difference in past performance of EIFS between Europe and North America. An important reason is probably the sensitivity of the substrate. While concrete and masonry readily absorb and redistribute small quantities of leakage water without any signs of degradation, the same amount of water may severely damage typical sheathing materials such as OSB or gypsum board that are used in wood frame walls in North-America. Since EIFS have more recently been applied to wooden wall structures in Europe as well, there may also be an increase in moisture problems such as those described by Schulze & Radovic [1992] and by Schumacher [2006]. Therefore it makes sense to investigate the moisture tolerance of wooden structures with EIFS for European construction types and climate conditions in order to prevent moisture-related problems.

3 HYGROTHERMAL SIMULATIONS

The transient temperature and moisture distributions in external wall assemblies with EIFS are calculated using version 4.1 of the hygrothermal simulation model WUFI® [Künzel 1995] which has been validated many times by comparison with experimental building envelope investigations

including measurements on wall structures with EIFS (e.g. [Künzel 1998a]). In order to cover North American and European building practice the following wall assembly has been selected.

- EIFS: 10 mm lamina (exterior rendering) on 60 mm EPS
- Sheathing: 15 mm OSB
- Cavity insulation: 160 mm glass fibre batts
- Vapour retarder: polyethylene film (s_d = 20 m) or polyamide film (0.1 m < s_d < 5 m)
- Interior panelling: 12 mm gypsum board (installation gap 40 mm)

The material properties are taken from the WUFI® database. The polyethylene (PE) film represents a standard vapour retarder with a diffusion resistance (s_d) of 20 m which is equivalent to 0.16 U.S. perm. The polyamide (PA) film is a humidity controlled vapour retarder whose diffusion resistance varies with ambient humidity conditions [Künzel 1998b]. It has been developed to enhance the drying potential of building assemblies [Künzel 2005]. The colour of the exterior stucco is assumed to be bright (solar absorptivity 0.4).

3.1 Selected Locations and Loads

The first location considered is North Carolina where the EIFS problems started. As representative weather conditions the meteorological data for a cold year in Wilmington are selected from the WUFI® climate database. For Europe a sample of four locations is chosen: Hannover in the middle of Germany's Northern plain, Lisbon at the Atlantic South-West Coast of Europe, Locarno in the Southern part of the Swiss Alps and Vienna at the edge of the East-European plain. The average temperatures and humidities as well as the annual sum of wind driven rain hitting the middle of a low-rise building at the most exposed orientation are displayed in Table 1 for all selected locations. While the average relative humidity does not differ much from one location to the other, the average temperatures range from approximately 17°C to 25°C in summer and from 0°C to 10°C in winter. Hannover is the coldest place and Wilmington and Lisbon, which are the warmest locations, experience the highest wind driven rain loads.

Table 1. Driving rain load at the surface of the most exposed façade orientation and average hygrothermal conditions at the selected locations in North America and Europe.

Location	Driving rain load (façade orientation)	Rel. Humidity	Temperature (annual/monthly mean)		
		(Annual mean)	Year	January	July
Wilmington	186 l/m²a (S)	73%	16,1 °C	5.7 °C	24,9 °C
Hannover	160 l/m²a (W)	80%	8,6 °C	-0,1 °C	17,1 °C
Lisbon	193 l/m²a (W)	75%	15,6 °C	9,8 °C	20,7 °C
Locarno	133 l/m²a (E)	72%	11,5 °C	2,1 °C	22,2 °C
Vienna	112 l/m²a (W)	73%	10,4 °C	0,1 °C	20,6 °C

The hygrothermal simulations which begin in October of the representative year are continued over a period of three years by repeatedly running through the same meteorological data-set. The initial conditions in all material layers of the building assembly are set to EMC_{80} (equilibrium moisture content at 80% RH). If rainwater penetration through imperfections cannot be ruled out, 1% of the wind driven rain load from Table 1 is deposited on the exterior surface of the OSB sheathing. In practice rain water will penetrate at joints or windows. Leaks will therefore be concentrated at these locations. However for the purpose of a one-dimensional analysis it is assumed that penetrating rainwater will be evenly distributed over the entire surface of the wall's OSB sheathing.

4 SIMULATION RESULTS

The North American damage cases have shown that the substrate layer, to which the EIFS is applied, experiences the most critical moisture conditions in the assembly. Therefore the moisture content of the OSB sheathing is monitored in the present study. Moisture contents below 20 M-% are considered to be safe, i.e. the OSB will not face any moisture-related durability problems. Figure 2 displays the temporal changes in OSB moisture content (average over the thickness of the OSB) under three different scenarios. Assuming perfect workmanship (no leaks) results in permanently dry conditions (MC < 13 M-%) no matter what vapour retarder is applied to the interior side of the stud wall. If rainwater leaks are present the OSB moisture content will rise in wintertime with extended drying spells in summer. However, when there is only very little vapour diffusion towards the interior because of the rather impermeable vapour retarder (PE-film), the drying potential is limited and long-term moisture accumulation may occur (MC > 25 M-% after 3 years). By replacing the PE-film with the humidity controlled PA-film the drying potential is enhanced enough to assure long-term OSB moisture conditions below 18 M-%.

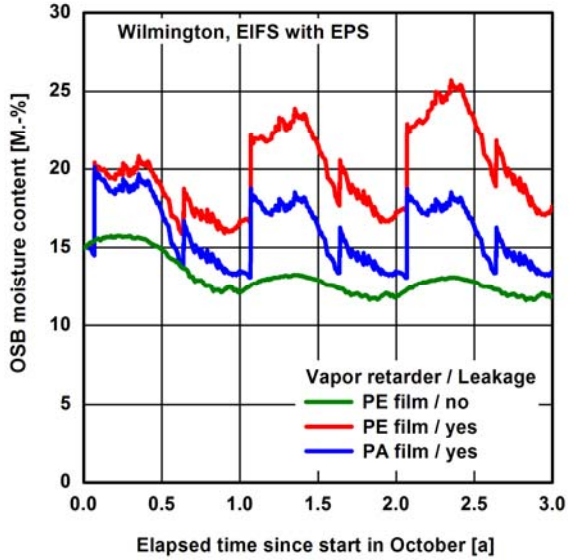

Figure 2. Temporal changes in simulated moisture content of the OSB sheathing beneath the EIFS in Wilmington for the standard case with and without rainwater leakage and with a PA-film replacing the PE-film as vapour retarder of the stud wall.

When the simulations are repeated for the coldest location considered (Hannover), a different picture develops (Figure 3). As was shown in the previous case for Wilmington, when there is no leak there is no problem. However, when there is a leak the OSB moisture content will repeatedly exceed 20 M. -% even if the dying potential to the interior is enhanced by the PA-film. An explanation for the different behaviours obtained from building assemblies investigated under different climate conditions lies in the divergence in vapour gradients. The high summer time temperatures in Wilmington result in a considerable inward vapour drive making efficient use of the drying potential provided by the humidity controlled vapour retarder. Without such a strong inverse vapour pressure gradient the drying rate towards the interior cannot compensate the rainwater leakage and damage may occur.

A good indicator of potential problems is the maximum OSB moisture content attained during the 3rd year of the simulation period. In order to be on the safe side, it should not exceed 20 M. -%. That means if rainwater penetration through imperfections is assumed, enhancing the drying potential towards the interior is no solution for Hannover. However it may help to enhance the drying potential towards the exterior by replacing the EPS insulation of the EIFS with high-density mineral wool slabs (MW). This kind of insulation material, largely unknown in North America, is widely used for EIFS in

Europe. Its thermal conductivity is very similar to that of EPS but its vapour permeability is very high. When such a system is applied to a stud wall in Hannover, the OSB moisture content remains well below 20 M.-%, even if the predefined rain water penetration occurs. The simulation results of all European locations are summarized in Figure 4 by comparing the maximum moisture content in the OSB sheathing during the third year. The best solution with the lowest OSB moisture content at all locations provides the choice of mineral wool (MW) as EIFS insulation material. However, all variants seem to work in Locarno and Vienna where the annual wind driven rain load is less than 140 l/m²a. In Lisbon the situation is comparable to Wilmington, i.e. enhancing the drying potential towards the interior by employing a humidity controlled vapour retarder appears to be sufficient.

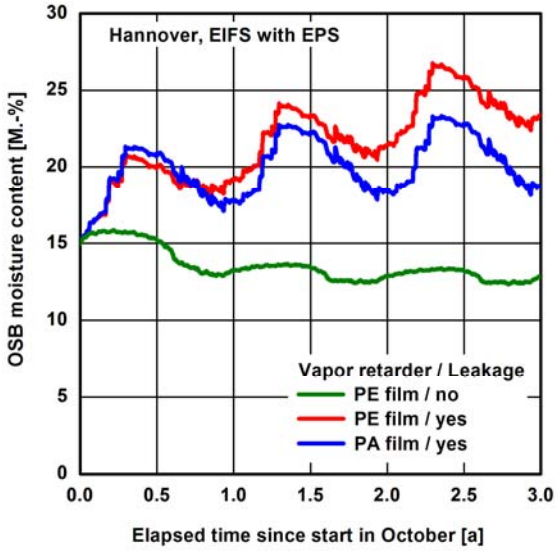

Figure 3. Temporal changes in simulated moisture content of the OSB sheathing beneath the EIFS in Hannover for the standard case with and without rainwater leakage and with a PA-film replacing the PE-film as vapour retarder of the stud wall.

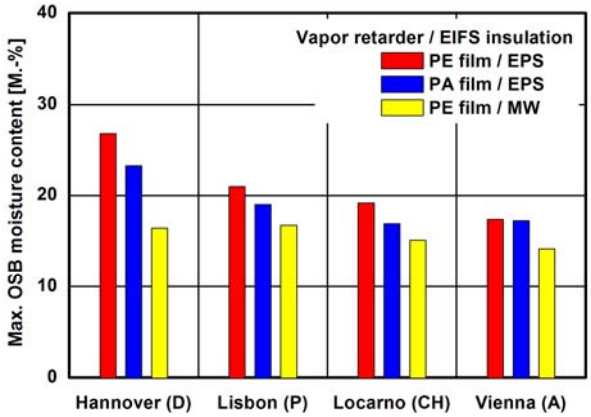

Figure 4. Maximum moisture content of the OSB sheathing during the simulated 3-year period at different European locations depending on the vapour retarder of the stud wall and the insulation material of the EIFS.

4 SUMMARY AND CONCLUSIONS

The results show that EIFS on lightweight structures pose no moisture problem when the detailing of joints and openings is well done, i.e. there is no rainwater leakage. This holds for all locations investigated. However, if water leakage cannot be completely excluded and therefore the North-American Standard assumptions - penetration of 1% of the driving rain load - are applied this picture

changes. Now, the drying potential of such wall assemblies becomes an essential feature to consider in the design process of the wall. Normal EIFS composed of vapour retarding EPS insulation slabs cannot provide much drying towards the exterior and may therefore be responsible in part for increasing the risk to moisture damage for the underlying substrate.

The application of a humidity controlled vapour retarder (PA-film) instead of a conventional polyethylene film at the interior side of the building assembly enhances the overall drying potential of the construction by allowing some vapour diffusion towards the interior spaces. However the use of such a vapour retarder should only be considered as a solution for warmer locations, such as Wilmington, North Carolina, or Lisbon where the enhancement of the drying potential may be sufficient to compensate the water leakage. Colder climates require additional measures or other solutions. The best, but also most expensive, solution for reducing the risk to moisture related problems in EIFS wall assemblies would be to replace the expanded polystyrene (EPS) by high-density mineral wool insulation slabs.

Alternative ways of solving the rainwater penetration problem are currently being developed and tested in North America. Some systems provide a drainage plane between the substrate and the EIFS as well as special devices to force out the water at the bottom. Initial tests of these drainable EIFS have shown encouraging results [Onysko & Thivierge 2007]. Other systems keep the face seal approach and rely on sophisticated detailing with improved sloping and flashing of openings and joints. In both cases the long-term performance is still unknown. In order to avoid a repetition of the North American problems with EIFS applied to wood frame structures, it is important to communicate this issue and possible solutions to the European construction trades. Hygrothermal simulations may help to raise the awareness to the risks of damage and the importance of qualified workmanship involved in the application of EIFS especially for locations with high wind driven rain loads.

5 REFERENCES

BSR/ASHRAE Standard 160P Sept. 2006. Design Criteria for Moisture Control in Buildings. Public review draft.

Cheple, M. & Huelman, P. 2000. Literature Review of Exterior Insulation Finish Systems and Stucco Finishes. Report MNDC/RP B80-0130, University of Minnesota.

Crandell, J.; Kenney, T. 1996. Investigation of moisture damage in single-family detached houses sided with exterior insulation finish systems in Wilmington, NC. 2nd ed. Upper Marlboro, MD: NAHB Research Center. 9 p.

Desjarlais, AO.; Karagiozis, A.N.; Aoki-Kramer, M. 2001. Wall moisture problems in Seattle. Prodeedings, performance of exterior envelopes of whole buildings VIII, Atlanta, GA: ASHRAE. 8 p.

Karagiozis, A. & Kumaran, K. 1997. Drying Potential of EIFS Walls: Innovative Vapor Control Strategies. STP 1339, American Society for Testing and Materials (ASTM), West Conshohocken.

Künzel H.M. 1995. Simultaneous Heat and Moisture Transport in Building Components. - One- and two-dimensional calculation using simple parameters. Fraunhofer IRB Stuttgart. .

Künzel, H.M. 1998a. Drying of Masonry with Exterior Insulation. Proceedings of the Fifth International Masonry Conference. British Masonry Society, No. 8, Stoke-on-Trent 1, pp 245-250.

Künzel, H.M.1998b. The Smart Vapor Retarder: An Innovation Inspired by Computer Simulations. ASHRAE Transactions 1998, V. 104, Pt. 2, pp 903-907.

Künzel, H.M. 2005. Adapted vapour control for durable building enclosures. Proceedings 10dbmc (10th Int. Conf. on Durability of Building Materials and Components), Lyon April, TT2-86.

Künzel, H, Künzel, H.M. & Sedlbauer, K. 2006. Long-term Performance of External Thermal Insulation Systems (ETICS). ACTA Architectura 5, vol.1, pp. 11-24.

Lawton, M. 1999. Vancouver's Rotting Condominium Problem – How Did We Get into This Mess? Journal of Thermal Envelope & Building Science vol. 22, pp 356-363.

Nisson, N. & Best, D. 1999. Exterior Insulation and Finish Systems. Compilation of articles from EDU-Newsletter, Cutter Information Corp., Arlington.

Onysko, D. & Thivierge, C. 2007. Darinage and Retention of Water by Cladding Systems, Part 3 Drainage Testing of EIFS Wall Systems. CMHC research report, 71 p.

Schulze, H. & Radovic, B. 1992. Zweigeschossiges Holzhaus mit Wäremedämm-Verbundsystem; Putzschäden im Bereich der Geschossdecke. Deutsches Archiktektenblatt H. 1, S. 123.

Schumacher, R. 2006. Außenwand aus Holztafeln mit Wärmedämmverbundsystem – Feuchteschaden wegen fehlerhaftem Sohlbankeinbau. Der Bausachverständige H. 6, S. 14-16.

11DBMC International Conference on Durability of Building Materials and Components
ISTANBUL, Turkey 11-14 May 2008

Daily Hygroscopic Inertia Classes: Application in a Design Method for the Prevention of Mould Growth in Buildings

Nuno M. M. Ramos [1]
Vasco P. de Freitas [2]

T 33

ABSTRACT

The persistence of high relative humidity values inside buildings favours mould growth on material surfaces, causing their degradation and bringing about social and economical problems for the users. Heating and ventilating are fundamental actions for the control of humidity in the indoor environment, but the hygroscopic inertia provided by the materials that contact the inside air can be a complement for that control.
As the hygroscopic inertia concept can be very difficult to approach for building designers, a definition of daily hygroscopic inertia classes is presented, based on numerical and laboratory work on this subject.
An outline of a simple method, using those classes, that allows for the evaluation of the reduction of mould growth potential associated to a configuration of inside finishes is proposed.
The method is then used in several hygrothermal scenarios to illustrate how different values of hygroscopic inertia can contribute to the prevention of mould growth in buildings. The analysed scenarios also contribute to a sensitivity analysis of the influence in relative humidity of several parameters such as outside climate, ventilation, vapour production, heating, solar gains and envelope quality combined with hygroscopic inertia.

KEYWORDS

Relative humidity, Hygroscopic inertia, Surface finishings, Mould growth

[1] Building Physics Laboratory (LFC), Faculty of Engineering, University of Porto (FEUP), Portugal, Phone +351 22 508 1770, Fax +351 22 508 1940, nuno.ramos@fe.up.pt
[2] Building Physics Laboratory (LFC), Faculty of Engineering, University of Porto (FEUP), Portugal, Phone +351 22 508 1932, Fax +351 22 508 1940, vpfreita@fe.up.pt

1 INTRODUCTION

Relative humidity (RH) inside buildings can influence thermal comfort, the perceived air quality (PAQ), users' health, building materials durability and energy consumption. This dependency has been established by science but the common user will not always recognize it. Mould growth on building element's surfaces, on the other hand, is easily associated with the persistence of high RH levels even by users and can be tied not only to durability but also to PAQ and health. The relevance of this pathology is one of the motivations for the heat and mass transfer research reported in this article.

The prevention of mould growth in building elements will greatly depend on the control of RH conditions. These are a function of exterior vapour pressure, ventilation, vapour production, hygroscopic inertia and inside temperature. Most of these factors can be easily combined and analysed to predict RH variation in time. Hygroscopic inertia, on the contrary, is a poorly defined concept and, as a consequence, usually ignored by building designers. The recent IEA Annex 41 research project (http://www.kuleuven.ac.be/bwf/projects/annex41/), which included the authors' participation, tried to enhance the knowledge on this subject.

This text defines daily hygroscopic inertia classes and proposes their implementation as an easy way of including the building materials moisture storage capacity influence on RH variation and mould growth risk analysis. A proper selection of interior finishes can obviously benefit from that inclusion. In the next sections a description of daily hygroscopic inertia classes can be found, followed by the selected method of mould growth risk assessment. A set of numerical simulations of a room's hygrothermal behaviour is developed in order to illustrate an evaluation method of the influence of inside finishes configuration in mould growth risk.

2 HYGROSCOPIC INERTIA CLASSES

2.1 Principle

A method of bringing the hygroscopic inertia concept closer to practitioners has been developed and experimentally evaluated by Ramos [2007]. The basic idea, illustrated in Fig. 1, is to have a prediction tool that can establish a relation between the moderation of the RH variation in a room and its hygroscopicity level, which is mainly dependant on the surface finishing materials.

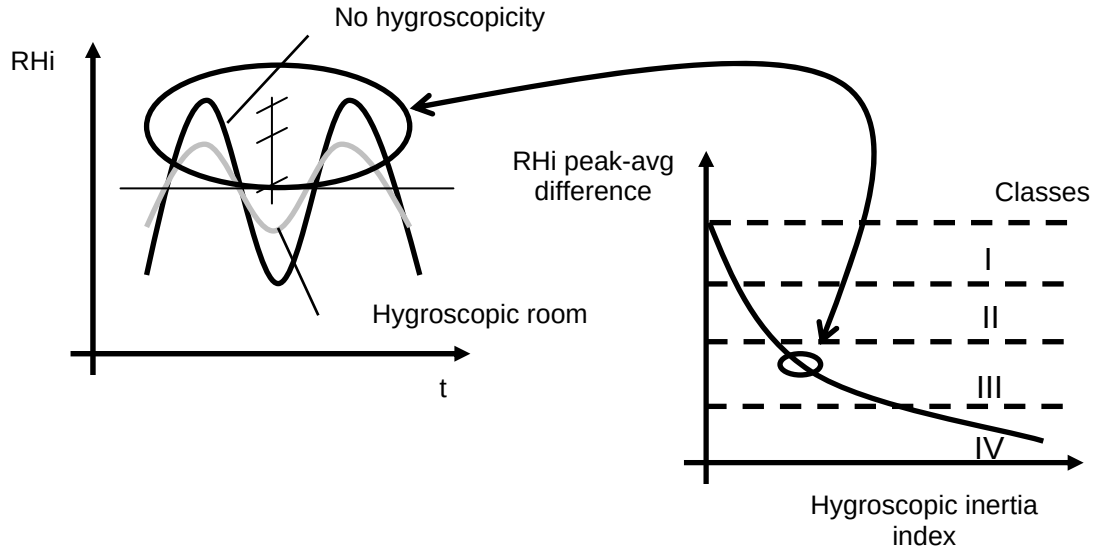

Figure 1. Hygroscopic inertia class's definition principle

2.2 Daily Hygroscopic Inertia Index

According to the principle established in the last section, a hygroscopic inertia index was defined as a single number, representing the hygroscopic inertia of a room and that can correlate to the expected reduction of the RH fluctuation. It was decided that this index should concentrate only on daily cycles and it should be derived from room configuration and known material properties.

The MBV – Moisture Buffer Value was the selected material/element property thus acting as a base for that index definition. MBV is a recently developed property [Rode et al, 2005] and it represents the amount of moisture buffered by a specimen with only one open surface exposed to a square RH variation. Cyclic climatic exposures should consist of 8h of high relative humidity, followed by 16h of low relative humidity. This test tries to replicate the cycle seen in bedrooms. The low relative humidity can be 33% and the high relative humidity 75%, for a constant temperature of 23ºC. The cycles are repeated until the specimen weight over the cycle varies less than 5% from day to day. A numerical example of MBV assessment, mocking the experimental procedure, is presented in the section 3.2 of this paper.

MBV can be obtained as a material or element property. For the purpose of this paper, it's always considered as an element property. This means that, for example, a 2 cm thick gypsum render, painted with a primer and an acrylic coating can be characterized with its MBV.

The proposed daily hygroscopic inertia index, $I_{h,d}$, is defined by Ramos [2007] as a function of MBV, according to expression (1), where MBV_i = Moisture buffer value of element i (g/(m^2.%RH)); S_i = surface of element i; MBV_{obj} = Moisture buffer value of complex element j (g/%RH); C_r = Imperfect mixing reduction coefficient (-); N = air exchange rate (h^{-1}); V = room volume (m^3); TG = Vapour production period (h). The $I_{h,d}$ can be understood as the room MBV, homogenized to air renovation conditions and vapour production period variations.

$$I_{h,d} = \frac{\sum_{i}^{n} C_{r,i} \cdot MBV_i \cdot S_i + \sum_{j}^{m} C_{r,j} \cdot MBV_{obj,j}}{N \cdot V \cdot TG} \rightarrow \left[\frac{g}{m^3 \cdot \%HR}\right] \quad (1)$$

2.2 RH Variation Evaluation

The evaluation of a RH variation curve in time should be based on a single number, keeping in mind the principle described in section 2.1.

The AMDR parameter was defined according to expression (2), where HR_m is the average relative humidity variation and $\overline{HR_{90}}$ stands for the daily average of the 90th percentile of the relative humidity variation. The index *ref* refers to the base scenario of a room without hygroscopicity and *sim* identifies a scenario under study for that same room. The AMDR parameter can therefore be interpreted as relative daily average amplitude of a RH variation of a room hygroscopic configuration. This parameter is interesting since the average RH variation in long-term analysis will not be affected by daily hygroscopic inertia.

$$AMDR = \frac{\left(\overline{HR_{90}} - HR_m\right)_{sim}}{\left(\overline{HR_{90}} - HR_m\right)_{ref}} \quad (2)$$

2.3 Classes Definition

The selected parameters were proven by Ramos [2007] to be connected by expression (3). The resulting curve supports the definition of daily hygroscopic inertia classes, according to Fig. 2, and the limits defined in Table 1.

$$AMDR = \frac{1}{0{,}00998 + 0{,}0793 \cdot I_{h,d}^{1{,}16}} \% \tag{3}$$

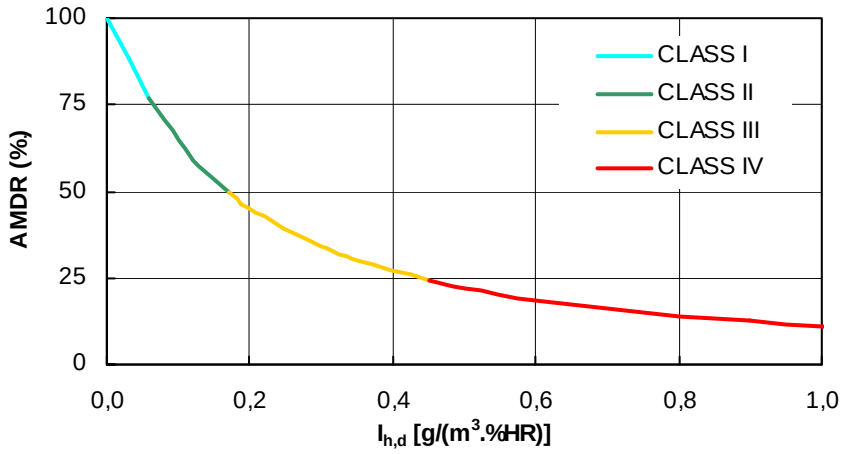

Figure 2. Graphic relation between AMDR and $I_{h,d}$

Table 1. Daily hygroscopic inertia classes limits

CLASS I	$0 \leq I_{h,d} < 0.06$	$100\% \geq AMDR > \sim 75\%$
CLASS II	$0.06 \leq I_{h,d} < 0.17$	$\sim 75\% \geq AMDR > \sim 50\%$
CLASS III	$0.17 \leq I_{h,d} < 0.45$	$\sim 50\% \geq AMDR > \sim 25\%$
CLASS IV	$0.45 \leq I_{h,d}$	$\sim 25\% \geq AMDR$

3 NUMERICAL SIMULATION

3.1 Purpose

A decision was made to numerically simulate the behaviour of a room and the moisture buffer capacity of the materials used in the room simulation. This provided data that can illustrate the desired relation between hygroscopic inertia and room configuration.

3.2 Numerical Model

The authors chose to use for these simulations the software program HAM-Tools [Kalagasidis 2004]. The International Building Physics Toolbox, is a software library specially constructed for HAM system analysis in building physics.
As part of IBPT, HAM-Tools is open source and publicly available on the Internet. The library contains blocks for 1-D calculation of Heat, Air and Moisture transfer through building materials. The toolbox is constructed as a modular structure of the standard building elements using the graphical programming language Simulink. All models are made as block diagrams and are easily assembled in a complex system through the well-defined communication signals and ports.

3.2 MBV Simulations

An assembly of HAM-Tools modules was used for simulating the MBV experiment. The simulations were performed using the virtual specimens listed in Table 2. The data for the chosen materials used in the simulations was retrieved from Kumaran [1996]. The different β (convective water vapour transfer coefficient) values used represent the possibility of coatings with different additional vapour resistances applied in the gypsum board specimens.

Table 2. Virtual specimen's characteristics

Specimen	Material	β (s/m)	Thickness (m)
1	Gypsum board	2e-8	0.01
2	Gypsum board	2e-9	0.01
3	Gypsum board	2e-10	0.01
4	Spruce	2e-8	0.01

In Figure 3, the mass variation of all the specimens in the steady cycle is presented. The MBV for each specimen is also presented in Table 3. As we can see, this number, when associated to the tested elements, provides the means to compare them. But as it was said before, this number is used ahead for hygroscopic inertia analysis.

Table 3. MBV for the four specimens tested

Specimen	1	2	3	4
MBV(kg/m^2)	0.0971	0.0366	0.0045	0.0832

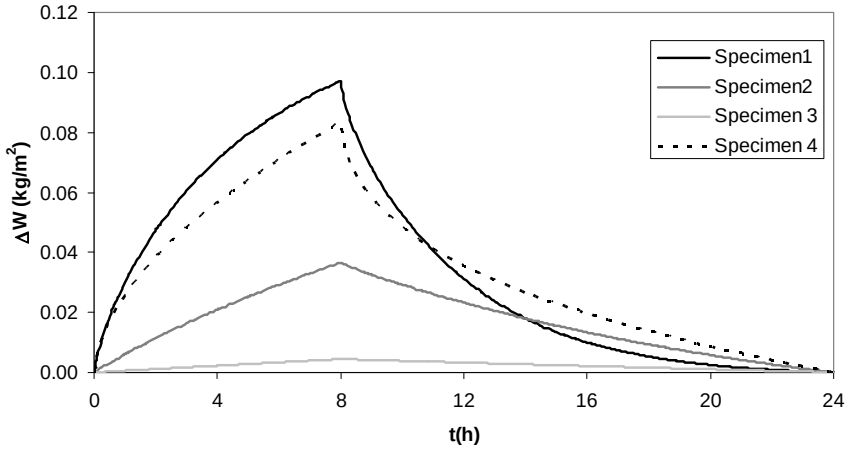

Figure 3. Moisture content variation of all the specimens in a stable cycle

3.3 Room Simulations

A different HAM-Tools modules association allowed for the simulation of a room's hygrothermal behaviour in yearly cycles. The virtual room is 3.5x3.5x2.5 m^3, with one exterior wall, containing a 1 m^2 window, facing south. The surrounding rooms are assumed to have similar conditions of temperature and relative humidity as the simulated room. The climate conditions were defined for Lisbon, using Meteonorm software. The inside temperature was allowed to float between Tmin and 28 ºC, and RH was allowed to float below 90%. The ventilation rate is constant and the vapour production takes place between 0h and 8h, with a constant value. On walls and ceiling the admitted material was gypsum board and on the floor spruce. Tables 4 and 5 describe the conditions that were changed for each simulation. It can be easily inferred that the room configuration in the first line of Table 5 stands for the room with no hygroscopic inertia, the reference room.

Table 4. Hygrothermal parameters adopted in simulations

Simulations	Tmin (ºC)	G (g/h)	N (h^{-1})
SG1-SG2	18	100	1.0
SG11-SG12	18	150	1.0
SG15-SG16	15	100	1.0
SG19-SG20	21	100	1.0
SG23-SG24	18	100	0.67
SG27-SG28	18	100	0.33

Table 5. Room configurations

Simulations	Walls		Ceiling		Floor	
	Area (m^2)	β (s/m)	Area (m^2)	β (s/m)	Area (m^2)	β (s/m)
SG: 1-11-15-19-23-27	34	2e-12	12.25	2e-12	12.25	2e-12
SG: 2-12-16-20-24-28	34	2e-8	12.25	2e-8	12.25	2e-12

Partial results from simulations SG1 and SG2 are presented in Fig. 4, illustrating the tested scenarios.

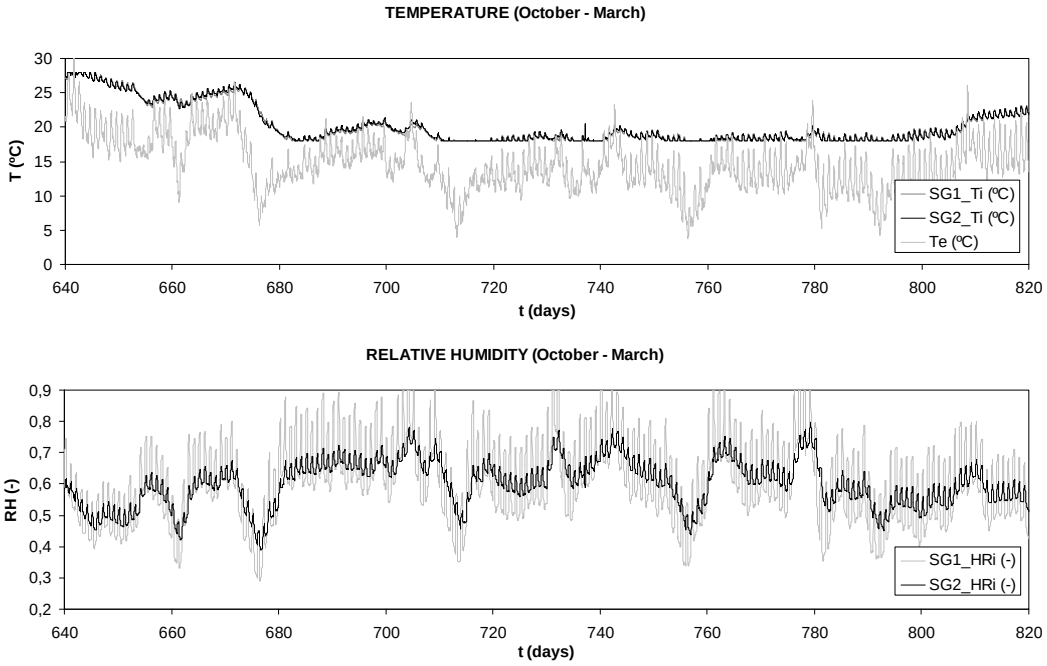

Figure 4. Results from simulations SG1 and SG2

3.3 Hygroscopic Inertia Analysis

The application of the method from section 2 allows for the definition of parameters AMDR and $I_{h,d}$ corresponding to the simulation scenarios. The values obtained are presented in Table 6, and reveal that the scenarios hygroscopicaly active would be placed in class III-IV

Table 6. Parameters for hygroscopic inertia analysis

Simulations	$I_{h,d}$ (g/(m^3.%RH)	AMDR (%)
SG: 1-11-15-19-23-27	0	1.0
SG2	0.438	0.23
SG12	0.438	0.24
SG16	0.438	0.24
SG20	0.438	0.23
SG24	0.653	0.18
SG28	1.326	0.12

4 MOULD GROWTH RISK ASSESSMENT

Several authors have studied the relationship between water activity in a substrate and the development of mould on its surface [e.g. Adan [1994], Sedlbauer [2001]]. The mould development under transient conditions of temperature and humidity is highly complex. Adan [1994] proposed a model based on the TOW (time of wetness) concept to solve this problem. TOW is the quotient between the time period where the surface RH is above 80% and the total duration of the period under analysis. Using that model in several laboratory tests, there was evidence that for TOW<0,5 the risk for mould growth is very low. Using the TOW concept when simulating a room's hygrothermal behaviour it is possible to define the number of days with TOW>0,5, $nd_{tow>0,5}$, as a simplistic indicator of the mould growth risk. This approach loses accuracy if the simulations indicate actual surface condensation and the analysis tool is unable to treat that process with high precision.

Additionally, the authors use another parameter, nd_{cond}, representing the number of days when surface condensation was detected. The objective of these indicators is not to accurately estimate mould growth risk, but rather to compare hygrothermal scenarios. Using these parameters in the above simulated scenarios and imposing an additional condition of the existence of a rather extreme thermal bridge, defined by $f_{Rsi} = \frac{T_{surf,i} - T_e}{T_i - Te} = 0.5$, the results for each scenario are as presented in Fig. 4.

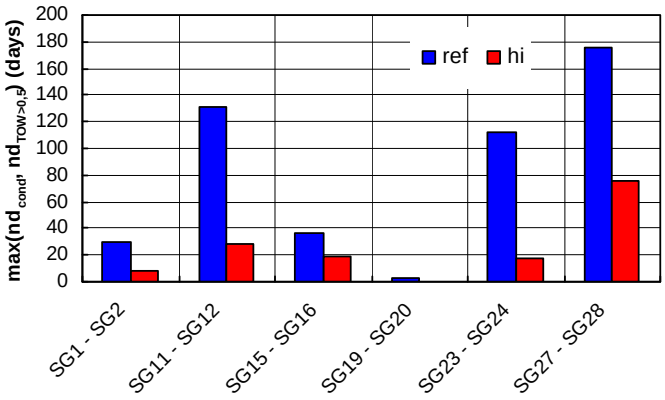

Figure 4. Mould growth risk analysis

This result shows the importance of hygroscopic inertia and the benefits that can derive from a stable RH variation with important peak reduction. A design method for the prevention of mould growth can be derived from this analysis. The method itself can have different levels of complexity. The basic idea is:

- define the risk associated with the room's RH variation for the four classes of hygroscopic inertia;
- select the adequate $I_{h,d}$ value and define the room's renderings to provide that value.

5 CONCLUSIONS

This paper presents research that allows for the following conclusions:

- The definition of daily hygroscopic inertia classes based on a room's index allows for the prediction of the RH variation amplitude;
- The MBV property can be used as an indicator of an element's contribution to the room's hygroscopic inertia;
- Mould growth risk is lower for higher values of hygroscopic inertia, admitting the same composition of the surface's final rendering;
- The design and selection of interior finishes in practice can benefit from the proposed approach to the hygroscopic inertia concept.

ACKNOWLEDGMENTS

The authors would like to thank the FCT - Fundação para a Ciência e Tecnologia for supporting this research in the frame of "POCI/ECM/57722/2004 – Humidade na construção", co-financed by FEDER.

REFERENCES

Adan, O., 1994, *On the fungal defacement of interior finishes*, PhD Thesis, Eindhoven University of Technology

Kalagasidis, A., 2004, *HAM-Tools: An Integrated Simulation Tool for Heat, Air and Moisture Transfer Analyses in Building Physics*, Department of Building Technology, Building Physics Division, Chalmers University of Technology, Gothemburg, Sweden.

Kumaran, M., 1996 IEA ANNEX 24: Heat, Air and Moisture Transfer Through New and Retrofitted Insulated Envelope Parts (Hamtie).

Ramos, N., 2007, *The importance of hygroscopic inertia in the hygrothermal behaviour of buildings* (in Portuguese), PhD Thesis, Department of Civil Engineering, FEUP, Porto, Portugal.

Rode, C., Peukhuri, R., Mortensen, L., Hansen, K., Time, B., Gustavsen, A., Svennberg, K., Arfvidsson, J., Harderup, L., Ojanen, T. & Ahonnen, J., 2005, Moisture Buffering Materials, Report BYG-DTU R-126, Department of Civil Engineering, DTU, Lyngby, Denmark.

Sedlbauer, K., 2001, *Prediction of mould fungus formation on the surface of and inside building components*, PhD Thesis – report, Fraunhofer Institute for Building Physics, Germany.

11DBMC International Conference on Durability of Building Materials and Components
ISTANBUL, Turkey 11-14 May 2008

Modelling for Development of Wood Rot Decay with Simultaneous Heat and Moisture Transfer for Building Envelopes

Hiroaki Saito [1]
Kiyoharu Fukuda [2]
Takao Sawachi [3]
Akira Oshima [4]

T 33

ABSTRACT

In this study, a durability assessment model for building envelopes design based on hygrothermal and wood rot decay analysis is presented. The durability assessment model can quantitatively predict hygrothermal conditions within the building envelopes, and progress of wood rot decay of timber frame under variable conditions. The followings are characteristics of the durability assessment models in this study. One is that development of wood rot decay is represented by a differential equation with a variable of mass loss; the other is that moisture production by wood rot decay is added into moisture balance equations. Hence, the model can assess long term performance regarding both durability and drying potential for building envelopes. Rate constants of the wood rot decay and a coefficient of the moisture production for the model are determined by the mass loss data of small wood samples in decay tests with a brown rot fungus *Fomitopsis palustris*. Additionally, progress of the wood rot decay within an external wooden wall is demonstrated.

KEYWORDS

Heat and moisture transfer, Service life prediction, Durability assessment, Wood decay, Wooden wall

[1] Building Research Institute, Department of Environmental Engineering, 1 Tachihara, Tsukuba, Japan 305-0802, Phone +81 29 879 0609, Fax 29 864 6654, hi-saito@kenken.go.jp
[2] Tokyo University of Agriculture and Technology, Faculty of Agriculture, 3-5-8 Saiwai-cho, Fuchu, Tokyo, Japan 183-8509, Phone + 81 42 367 5723, Fax 42 334 5700, kfukuda@cc.tuat.ac.jp
[3] National Institute for Land and Infrastructure Management, Housing Department, 1 Tachihara, Tsukuba, Japan 305-0802, Phone +81 29 864 4356, Fax 29 864 6774, sawachi-t92ta@nilim.go.jp
[4] Japan Testing Centre for Construction Materials, Material Group, 5-21-20 Inari, Soka, Saitama, Japan 340-0003, Phone +81 489 35 1992, Fax +81 489 31 9137, oshima@jtccm.or.jp

1 INTRODUCTION

Moisture accumulation within building envelops of wood frame constructions significantly affects problems related to durability, such as wood decay, mould and termite. To avoid these moisture-related damages, various building components and wood preservatives have been developed and applied to actual constructions until recently. However, health issue for occupants, e.g. the indoor air quality, has potential to remove the chemical wood preservatives from the lumber in the building components, and energy issue such as the Kyoto Protocol has made the wood frame constructions airtight. The drying capability related to the durability of the building envelopes has consequently decreased. Therefore proper design for moisture control within the building envelopes is necessary to achieve both durable structure and healthy environment.

On the other hands, advanced hygrothermal analysis models can accurately predict temperature and moisture behavior within building assemblies under various climate conditions. The calculation results by these models [e.g. Hens 1996] are useful in design and assessment for the moisture control. Mostafa and Kumran [1999] presented an approach to develop durability assessment system that links the hygrothermal analysis model with the moisture related damages. As well Krus [2001] tried similar approach regarding the mould growth, and implemented damage analysis that integrates the hygrothermal model with the biological damage predictions. In these models, the calculated temperature and moisture profiles are applied to prediction for progression of the biological damages. However these challenges did not completely simulate decay process regarding degradation of wood substance in terms of moisture balance. Wood rot fungi that can degrade cellulose, e.g. *Sepula lacrymans* and *Coniophora puteana*, produce non-negligible moisture through the decay process. Consequently, this mechanism makes the decay process continue even though relative humidity of the surrounding air is below saturation point [e.g.Viitanen 1997]. Impacts of the moisture production on the biological prediction need to be verified in terms of safety evaluation for the wood constructions.

With these points as background, this study proposes a wood decay model to which the moisture production due to the decay process is introduced. Coefficients for the proposed model are determined by experimental data of decay tests with small wood samples. Furthermore progress of the wood rot decay in exterior wall assemblies is demonstrated to better understand the impact of the moisture production.

2 MODELING FOR WOOD DECAY CONSIDERING MOISTURE BALANCE

2.1 Hypothesis of Proposed Model

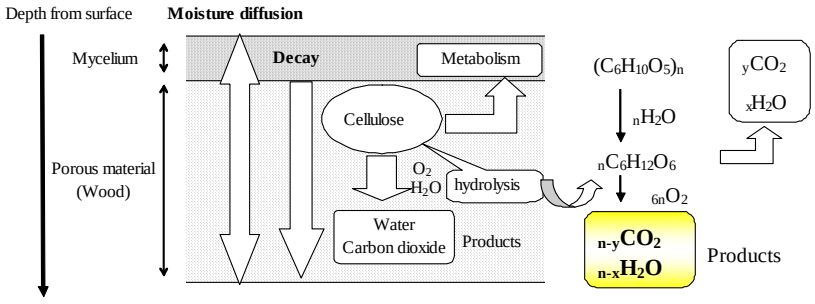

Figure 1. Scheme for wood decay and moisture transfer within the wood substance

Wood rot fungi degrade mainly cellulose within the wood substance by enzymatic reactions, and consequently produce both H_2O and CO_2 through this degradation. This wood brake down mechanism consists of two step biochemical reactions, which are hydrolysis and aerobic degradation. Both the biochemical reactions and moisture transfer occur simultaneously within the decayed wood, shown in

Figure 1. In this study, these phenomena are expressed as a numerical simulation model regarding the mass loss and the moisture content. Additionally, we define a rate constant that is determined by experiments to predict the mass loss, on the basis of deterministic un-structural model. The followings are hypothesis for the simulation model.

(1) Material properties for hygrothermal analysis are stable before and after the wood decay.
(2) Quantity of the mass loss has a single correlation with that of the moisture production by the biochemical reactions.
(3) Impacts of both O_2 and CO_2 concentrations to the wood decay can be neglected.
(4) Impacts of diversity of wood and fungus species are presented by experimental coefficients.

2.2 Progression of Wood Decay

The proposed wood decay model supposed that the progression of the mass loss is determined by hygrothermal conditions, such as temperature and relative humidity, at a control volume for finite difference analysis. The mass loss by the wood decay is defined as:

$$L = \frac{m_n - m_d}{m_n} \tag{1}$$

where L is the mass loss by the wood decay (-), m_n is the mass of the wood material before the decay, and m_d is the mass of the wood material after the decay respectively.
The wood rot fungi need liquid water to progress the mass loss based on the biochemical reactions. Thus the mass loss on the surface node of wood material progresses when the relative humidity within micro-pore is above the critical relative humidity φ_c (%RH) in Equation (2). As well, Equation (3) is applied to the progression of the mass loss at the inner node, because grown hypha of the wood rot fungi needs to reach this node for the decay progression.

$$\left.\frac{dL}{dt}\right|_{x=0} = k_m(\theta) \qquad (\varphi_i \geq \varphi_c) \tag{2}$$

$$\left.\frac{dL}{dt}\right|_{x>0} = k_m(\theta) \qquad (L_{i-1} or L_{i+1} > 0, \varphi_i \geq \varphi_c) \tag{3}$$

where t is the time (s), φ_i is the relative humidity (%RH) at the node i, φ_c is the critical relative humidity for the beginning of the wood decay (%RH), $k_m(\theta)$ is the rate constant that corresponds to a time factor for decay development by the wood rot fungus, as a function of temperature θ (^{o}C). The rate constant needs to be determined experimentally, because various conditions (e.g. wood species and hygrothermal conditions) affect development of the wood decay.
Concentration of the hypha in the each node may affect the rate constant. Gooding [1966] pointed out that growth rate of the hypha within the wood material is several millimeter per day. Thus this model assumes that the hypha concentration has already been uniformed within the node i, at the stage of beginning of the mass loss of the node $i+1$ or $i-1$.

2.3 Heat and Moisture Balance in Decayed Wood Material

Heat and moisture balance coupling the moisture production by the biochemical reactions is presented by Equation (4) and (5). The reaction fever with the biochemical reactions is neglected in Equation (4), and the third term of right side of Equation (5) corresponds to the moisture product.

$$\rho_m c \frac{\partial T}{\partial t} = \nabla\left\{\left(\lambda + r\lambda'_{Tg}\right)\nabla T + r\lambda_{\mu g}\nabla\mu\right\} \tag{4}$$

$$\rho_w \frac{\partial \phi}{\partial \mu}\frac{\partial \mu}{\partial t} = \nabla\left(\lambda'_\mu \nabla\mu + \lambda'_T \nabla T\right) + W_L \tag{5}$$

where ρ_m is the material density (kg/m^3), T is the Kelvin temperature (K), c is the material specific heat (J/kg), λ is the thermal conductivity (W/mK), r is the latent heat of moisture (J/kg), λ_{Tg} is the moisture conductivity in gaseous phase related to temperature gradient (kg/msK), $\lambda_{\mu g}$ is the moisture conductivity in gaseous phase related to water chemical potential gradient (kg/ms[J/kg]), ρ_w is the density of liquid water (kg/m^3), ϕ is the moisture content per volume of material (m^3/ m^3), μ is the water chemical potential (J/kg), and W_L is the the moisture product quantity (kg/sm^3).
Since this model assumes that quantity of the mass loss has a single correlation with the moisture product, moisture product ratio h (-) that corresponds to relation between them in a closed moisture system regarding moisture balance can be defined as:

$$h = \frac{d\phi}{dL} \tag{6}$$

The moisture product ratio h can not be determined from reaction formulae regarding the biochemical reactions for the decay process, because quantitative details of the metabolism regarding wood rot fungi within the wood substance is uncertain. However the moisture product quantity is expressed as Equation (7), where the moisture product ratio can be determined experimentally.

$$W_L = h\rho_w \frac{dL}{dt} \tag{7}$$

3 DETERMINATION OF COEFFICIENTS FOR THE MODEL

Wood decay tests under sterile condition in a laboratory were conducted to determine the rate constants and the moisture product ratio. Test samples of general standardized wood decay tests such as EN113 [1991] and JIS K 1571 [2004] are exposed on the surface of active agar colony of a fungus. Estimation of the moisture balance in the test samples is however difficult employing these standardized test methods, because the mycelium of the fungus keeps supplying moisture and nutrition to them through the agar medium. Therefore, the decay tests in this study were conducted in plastic dish without agar medium. Also the relative humidity levels in the plastic dish were adjusted by saturated salt solutions.

3.1 Outline of Experiments

The test samples for the decay tests (dimensions 40x20x5mm) were cut from the outer part of the sapwood of *Pinus densiflora* (wood species: Japanese red pine), which is classified as a un-durable species against fungus attack. A brown rot fungus *Fomitopsis palustris* was used as a test fungus, because this fungus showed less dispersion in the decay tests and is also employed as a test fungus in JIS K 1571 [2004]. Before the start of the decay tests, dry weights of the test samples were measured (at 105^{o}C). After the test fungus was grown on the agar medium for 2 weeks, inoculations of the test fungus were made through resin mesh on the mycelium (Figure 2). The resin mesh was employed to not contact directly between the test samples and the agar medium. The inoculated test samples were transferred to the plastic dish after the mycelium on the surface of the samples was observed by a microscope. Furthermore the plastic dish with the test samples were incubated at temperature between 5 and 40^{o}C.

In the incubation, the relative humidity in the plastic dish was controlled by the saturated salt solutions without the agar medium (Figure 3). These inoculation processes were performed under sterile condition.Exposure conditions for the decay tests are shown in Table 1. The mass loss and the moisture contents of the test samples were determined by weighting and drying after the exposure time in Table 1.

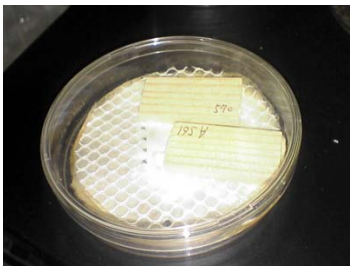

Figure 2 Inoculation of fungus to test samples on mycelium

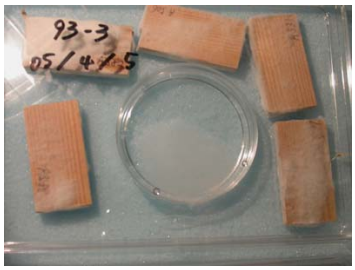

Figure 3 Test samples in plastic dish in which relative humidity levels were adjusted by saturated salt solutions

Table 1. The exposure conditions and details regarding the decay tests

Temperature (^oC)	5、10、20、30、40
Humidity (%RH)	93[KNO_3], 97[K_2SO_4], 100[distilled water]
Exposure time (months)	1, 2, 3, 6, 9, 12month (12month is only 100%RH)
Number of replications	5 (Summation of samples:475)
Initial moisture contents(kg/kg)	0.25 (Average of 10 replications after inoculation)

*[ ] means employed saturated salt solutions

3.2 Time-dependent Change of Mass Loss and Moisture Content

According to the results of the decay tests at 100%RH in Figure 4, the mass loss approximately reached to 0.4 by 12 months at 20 and 30 ^oC. Although progress of the mass loss at 5 and 15 ^oC were lower than 20^oC, the activity of the fungus and the mass loss could be clearly detected after 6 months. On the other hands, no decay was detected below 97%RH at any temperature conditions. Initial moisture contents of the test samples after the inoculation were approximately 0.25kg/kg. These results consequently indicate that the wood decay never progress without liquid water within micro-pore (i.e. under fiber saturation point).

Figure 5 shows the comparison of temperature dependence of the mass loss after 2 months' exposure. Although the temperature dependence in this experiment is similar to references at 28 ^oC [Fukuda 1980, Suzuki 1994], Suzuki's results that test samples were exposed on agar medium are approximately threefold compared to our values. It is conceivable that these impacts were caused by the agar medium supplying nutrition to the test samples. However the mycelium on building components is difficult to get such sufficient nutrition, if it can't reach soil around the foundation. Hence our results without the agar medium can be postulated as suitable for the time-dependent wood decay model on the actual exposure conditions within the building envelopes.

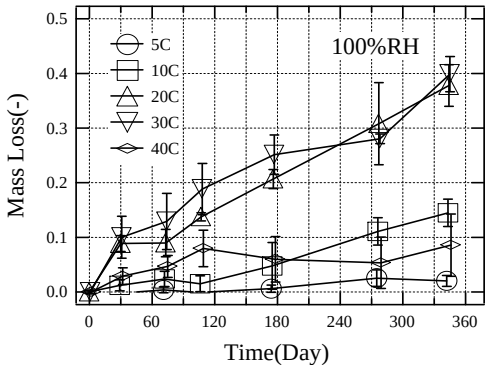

Figure 4 Time-dependent change of mass loss of test samples in 100%RH (Average and Standard deviation)

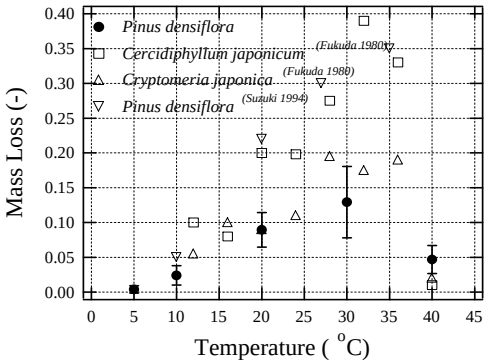

Figure 5 Comparison of temperature dependence of the mass loss after 2 months exposure in 100%RH (White dots are the quoted

3.3 Determination of Moisture Product Ratio

The moisture product ratio was determined by relation between the mass loss and the moisture contents of the test samples. Figure 6 shows the time dependent change of moisture contents at 100%RH. The gradients of the moisture contents in Figure 6 are similar to those of the mass loss in Figure 4. The differences of the gradients can be regarded as the impact of the reaction product related to the wood decay, where the moisture evaporation from the test samples is neglected in 100%RH. Consequently, the moisture product ratio h (-) could be determined as 0.319 by the relationship between the mass loss and the moisture content by volume in Figure 7. The coefficient of determination of regression analysis (R^2) was larger than 0.7.

3.4 Determination of Rate Constant

The rate constant was determined by linear regression analysis for the time dependent change of the mass loss in each temperature conditions shown in Figure 4. A regression curve in Figure 8 presents relation between the determined rate constants and temperature. The empirical formula regarding the rate constants is given by Equation (8). The mass loss were predicted using this equation and experimental conditions. Figure 9 shows good correlation between the predicted value and the measured values of the mass loss against all the test samples. The coefficient of determination of the regression analysis (R^2) was larger than 0.85.

$$k_m(\theta) = 2.77 - 3.23\theta + 0.865\theta^2 - 0.0189\theta^3 \quad (8)$$

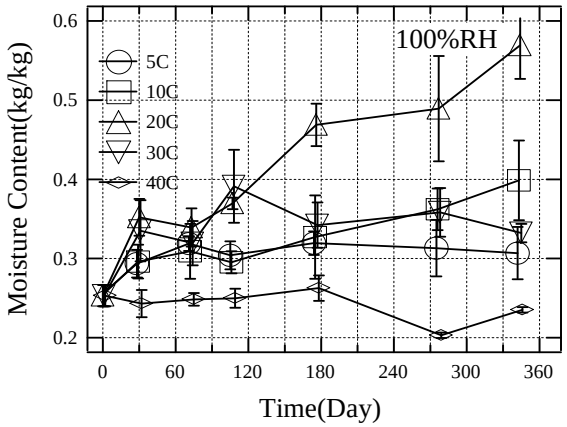

Figure 6 Time dependent change of moisture contents of test samples in 100%RH (Average and Standard deviation)

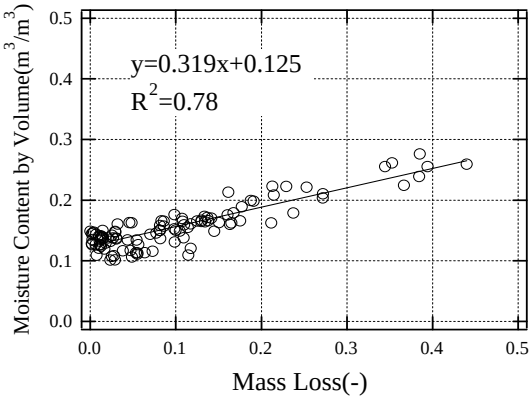

Figure 7 Relation between mass loss and moisture contents for all test samples in 100%RH

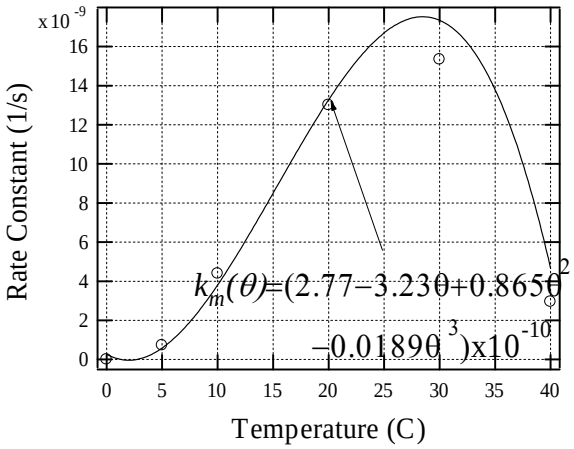

Figure 8 Relation between the determined rate constants and temperature

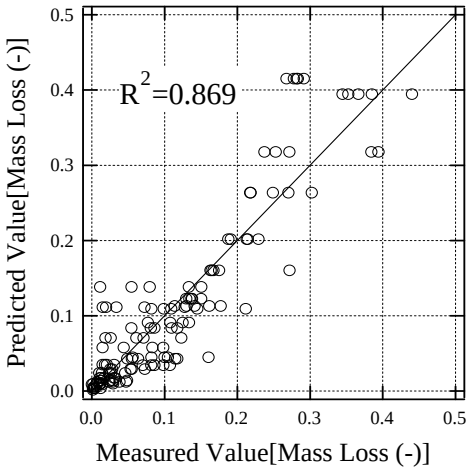

Figure 9 Relation between measured and predicted value in 100%RH

4 APPLICATION FOR BUILDING ENVELOPES

4.1 Outline for the Analysis

To better understand progress of the wood decay in building envelopes, the wood decay model was applied to an exterior wall using the determined coefficients. The numerical simulations for the wood decay that employed Equation (2) – (7) assumed one-dimensional heat and moisture flow in finite differential approximations. The critical relative humidity φ_c (%RH) for the beginning of the wood rot was set on 98%RH, on the basis of the experimental results in this study. Initial response time that is period to start the wood decay after reaching the critical relative humidity proposed by Mostafa and Kumaran [1999] was neglected.
Figure 10 shows the wall assembly for the analyses. Vapor retarder for the wall was removed intentionally, because the wood rot never progresses less than the critical relative humidity in this simulation. For the similar reason, the initial moisture content of the structural wood board (*Pinus densiflora*) was set 0.66 kg/kg. While the calculations regarding heat and moisture transfer were performed against all the layer of the building components, the wood decay analyses were implemented against only the structural wood board on the outside of the glass wool. The moisture properties of the building components are shown in Figure 11, and Table 2 shows calculation conditions.

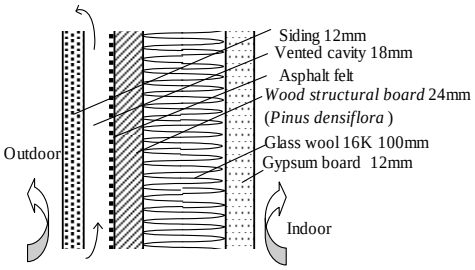

Figure 10 Wall assembly for analysis

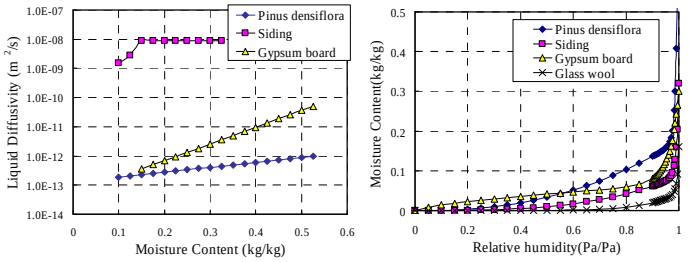

Figure 11 Moisture diffusivity and sorption curve

Table 2. Calculation conditions

Indoor conditions	Temperature: $\theta_r = 25.0 + 5.0\cos[2\pi(DAY^* - 212)/365]$(°C)
	Relative humidity: 60(%RH)
Outdoor conditions	Climate data in Osaka (Mild climate region in Japan)
Calculation period	One year (From October 1st to September 30th)
Initial moisture content	0.66 (kg/kg) [Equivalent to 99%RH]

**DAY* means the number of days from January 1st.

4.2 Results and Discussion

In order to understand long-term progress of the wood decay, annual variation of the mass loss and the moisture contents are presented in Figure 12 and Figure 13 respectively. The mass loss at the surface node of the structural wood board (i.e. 0mm) increased mainly in the spring rather than the mid winter because of the temperature dependence regarding the rate constant. As well the moisture product that is attribute to increase of the mass loss was observed in this period in Figure 13. Monthly increase of the mass loss on the January and February was smaller than the value of spring according to Figure 12 (approximately 0.01). Hence, significant point in terms of the prevention of the moisture damage is that the moisture contents of wood products should be controlled below the critical relative humidity by the early spring in this climate region.

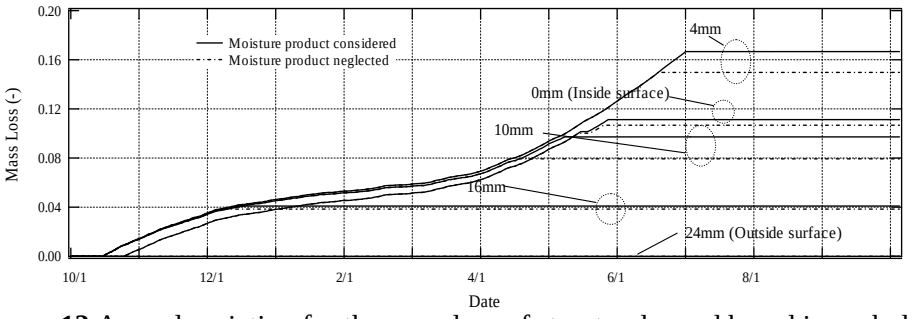

Figure 12 Annual variation for the mass loss of structural wood board in each depth

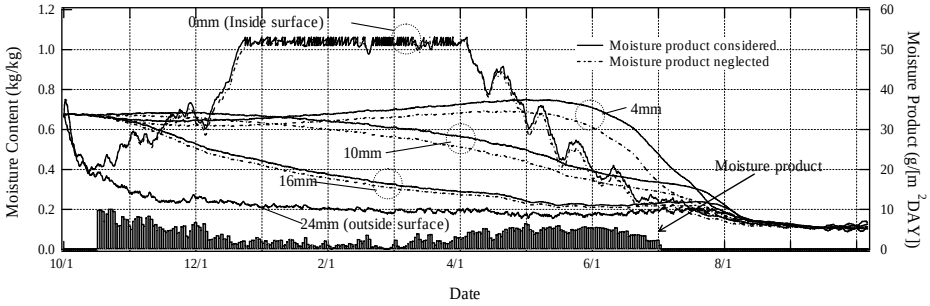

Figure 13 Annual variation of the moisture contents of structural wood board in each depth (lines) and daily summation of moisture product (Bar)

As for impact of the moisture production to the mass loss and the moisture contents, the differences in the calculation condition against the moisture product appeared at the internal node of the structural wood board (e.g. 4mm or 10mm) rather than the surface node in Figure 12 and Figure 13. This result suggests that quantity of the moisture product at the internal layer is larger than that removed by the moisture diffusion. Therefore, addition of the moisture product term to the moisture balance equations is significant in terms of assessment of the wood decay, where the moisture content at the internal layer is kept above the critical relative humidity.

5 CONCLUSION

The wood decay model considering the moisture balance due to the decay process has been presented. The decay tests using small wood samples were conducted under sterile conditions. Results of the decay tests were used to determine the coefficients for the wood decay model. Furthermore the wood decay analysis due to the moisture accumulation within a building assembly was implemented to better understand the impact of the moisture product on the decay progression. The analysis results suggested that the moisture product significantly affects the increase of the mass loss and the moisture contents at the internal layer of the wood substance. These consequences should be verified under various conditions experimentally to enhance reliability of this model. However, significance of this study from viewpoint of the building simulation is that the integration of biochemical reactions into hygrothermal analysis was presented as an advanced model.

REFERENCES

Hens, H., 1996, 'Heat, air, and moisture transfer in insulated envelope parts. Task 1; modeling.' Final report, International Energy Agency, Energy Conservation in Buildings and Community System. Annex24: - Heat, air, and moisture transfer in new and retrofitted building envelope parts.

Nofal, M., Kumaran, M.K., 1999, 'Durability assessments of wood-frame construction using the concept of damage-functions.', 8th International Conference Durability of Building Materials and Components., Vancouver, Canada, pp.766-799

Krus, M., Sedlbauer, K., 2005, 'MOULD GROWTH PREDICTION BY COMPUTATIONAL SIMULATION', Annex41 report 'A1-T4-D-5-1.pdf' in *Trondheim meeting*, Trondheim, Norway, 8p.

Hannu A. Viitanen, 1997, 'Modelling the Time Factor in the Development of Brown Rot Decay in Pine and Spruce Sapwood –The Effect of Critical Humidity and Temperature Conditions', Holzforschung Vol.51, pp.96-106

Gooding et.al, 1966, ' Effect of temperature on growth and survival of Fomes annosus', Forest Science. Vol12, pp.325-333

EN 133, 1991, 'Determination of toxic value of wood preservatives against wood destroying basidiomycetes cultured on agar medium', European committee for standardization, Brussel, 24p.

JIS K 1571, 2004, 'Test methods for determining the effectiveness of wood preservatives and their performance requirements', Japanese standard association, Japan, 42p.

Kentaro Suzuki, 1994, 'Effect of Cyclic Change of Temperature on Fungal Growth and Mass Loss' , The International Research Group on Wood Preservation, Document No.IRG/WP 94-10065, Bali, Indonesia, pp.1-11

Kiyoharu Fukuda, Yuji Okayasu, Takafusa Haraguchi, 1981, 'Influence of Temperature on the Growth and Wood-decomposing Ability of Wood-rotting Fungi', Bulletin Experiment Forests Tokyo University of Agriculture and Technology No.17, pp.49-55

Influence of Thermal Properties of Materials in Condensation and Microorganism Growth on Building Facades

Neide Matiko Nakata Sato [1]
Marcia Aiko Shirakawa [2]
Kai Loh [3]
Vanderley Moacyr John [4]

T 33

ABSTRACT

This paper presents the results of a study conducted to investigate the causes of microorganism growth on several buildings' facades, in São Paulo, Brazil. Those buildings presented several rounded stains distributed along the facades. In order to investigate the occurrence of condensation mainly over the stains, measurements of surface temperatures in different areas of the facade and of temperature and relative humidity of the air next to these areas were made. Based on the values of dry bulb temperatures and relative humidity of the air, the dew point temperatures were calculated. The external surface temperatures of the wall were compared to the dew point temperatures. The comparison showed that the temperatures over the rounded stains, during long periods of the night, were lower than the dew point temperatures and condensation took place during those periods. At the same time, surface temperatures of other areas of the facades were higher than the dew point temperatures and on those areas condensation did not take place. The differences in surface temperatures along the facade were due to the fact that the wall material behind stained areas had higher thermal resistance than the materials behind unstained parts of the facades. In facade zones with higher thermal resistance the effect of night cooling of the surface is more pronounced leading to the occurrence of condensation problems and microorganism growth.

KEYWORDS

Microorganism on facade, Condensation, Humidity, Thermal resistance of wall.

[1] Nove de Julho University, Civil Engrg. Dept, São Paulo, Brazil, Phone +55 11 3665 9000, Fax 11 3743 6917, neide.sato@uninove.br
[2] São Paulo University, Escola Politécnica, Dept. Construction Eng., São Paulo, Brazil, Phone +55 11 3091 5248, Fax 11 3091 5544, shirakaw@usp.br
[3] São Paulo University, Escola Politécnica, Dept. Construction Eng, São Paulo, Brazil, Phone +55 11 3091 5789, Fax 11 3091 5544 , kai.loh@poli.usp.br
[4] São Paulo University, Escola Politécnica, Dept. Construction Eng,, São Paulo, Brazil, Phone +55 11 3091 5784 Fax 11 3091 5544, john@poli.usp.br

1 INTRODUCTION

The environmental conditions in hot and humid climates - such as those that occur in many areas of Brazil - can promote the growth of a great variety of micro-organisms. In São Paulo, Brazil, the largest metropolitan area in South America, disfigurement of paint by microbial growth on wall surface is a common scene in many buildings. Building design, thermal properties of the construction materials, climatic conditions and location are decisive factors in this process.

The object of investigation of this work are the causes of occurrence of patterned staining on facades of rendered walls, as a consequence of selective growth of microorganisms on their surfaces. It was verified that fouling patterns that were found were associated to the time of wetness of parts of the facade. Frequent repainting was therefore necessary to hide the affected areas and short repainting cycles meant high maintenance cost.

2 DEVELOPMENTS OF MICROORGANISMS

Fungi are heterotrophic organisms, in other words, they need pre-elaborated organic matter as nutrient source. These compounds can be found in several materials used as building coatings. Some coating systems can serve as a source of nutrients for fungi or just as a substratum allowing its development. Phototrophic organisms such as algae and cyanobacteria need light as energy source and CO_2 as carbon source. Both groups of microorganisms are found on external walls of buildings [Allsopp *et al.* 2004], [Gaylarde & Gaylarde 2005], [Shirakawa *et al.* 2002].

For the fungal growth to happen, relative humidity on the surface area should be above a critical value and the surface temperature should also be favorable to the growth of these microorganisms [Pasanen et al. 2000]. The longer the period in which the relative humidity stays above the critical value, the higher is the proliferation level and therefore more visible is the problem. The higher the relative humidity or the temperature, the shorter is the necessary period of time for the establishment of the colonies. The relative humidity of the surface depends on the humidity content of the material, on its properties and on the humidity conditions and temperature of the atmosphere [ASHRAE 1997], [BRE 1972]. The dependence of the relative humidity on the surface on these several factors makes it difficult to establish the relationship between this parameter and the proliferation of the microorganisms.

Beside the humidity and the nutrients in the coating, temperature, pH and the amount of oxygen are other factors that interfere in the occurrence of this pathology [GILLAT 1991].

Models to predict theoretically the germination and growth potentials or rates of microorganisms in buildings were developed [Sedlbauer 2002], [Moon & Augenbroue 2005], [Krus *at al.* 2001] considering the complexity of the biological or mycological mechanisms involved and the hygrothermal conditions of the surface. The results of the models may be used to indicate potentials or for comparisons but more data are still needed for the variety of building materials and available microorganisms.

3 PATTERNED STAINING OF FACADES

The patterned staining of rendered facades as a consequence of selective growth of microorganisms can be explained by differences in moisture content at various locations with different substrates. The more infected areas present larger moisture contents [Becker 2002].

Temperature and moisture content on external surfaces of walls can be predicted through simulation of heat and mass transfer through facades. With simulations Becker [2002] and Johansson at al.

[2005] found that the external surface temperature for an outgoing heat flux will always decrease with the increase in wall insulation and when radiation to sky is included, surface temperatures of insulated walls drop even further. Becker [2005] investigated areas of facades with different substrates including concrete column and lightweight aerated concrete block. He concluded that, due to the dynamic nature of the simultaneous heat and mass transfer phenomena and the phase lags associated with them, the lowest temperature of the external surface of the walls was above ambient dew point temperature and condensation did not take place. The results of simulation showed that the combination of surface temperature, ambient relative humidity and moisture transport phenomena leads to substrate-dependent evolutions of moisture contents in the rendering layer, observing that the moisture content of the rendering over thermal insulation was higher than over concrete.

Johansson *at al.* [2005] simulated the temperature over a rendered building facade with regularly spaced dots with less microbial growth on the facade otherwise covered with microorganisms. They found that a fastener of steel was placed behind every dot. The computer simulations showed that the fasteners are heat bridges that lead to 1-2 K higher temperature of rendering over the fastener than the rest of the facade. They concluded that this difference can promote a high enough difference in relative humidity to almost prevent the development of microorganisms.

This paper aims to evaluate the influence of facade details on condensation and microorganism growth on a residential condominium in São Paulo.

4 STUDIED BUILDINGS

The problem of microorganisms development in facades was investigated in a residential condominium located in the city of São Paulo (Figure1). The building is supported by a reticulated cast-in-place reinforced concrete structure. The external walls were composed of precast sandwich panels, constituted of expanded polystyrene boards with both faces covered with reinforced micro-concrete. Each polystyrene board has cylindrical holes filled with micro-concrete and a concrete border which constitutes thermal bridges and facade areas with higher thermal capacity (Fig. 2). All panels had been painted with a water-based paint. As it can be seen on Fig.1 the panels were covered with microorganisms, except on areas located just above the insulation holes and reinforced borders of the precast panels. In other areas – such as the reinforced concrete structures – of the facade, microorganism growth was less intense.

Figure 1. Building facade with microorganism development

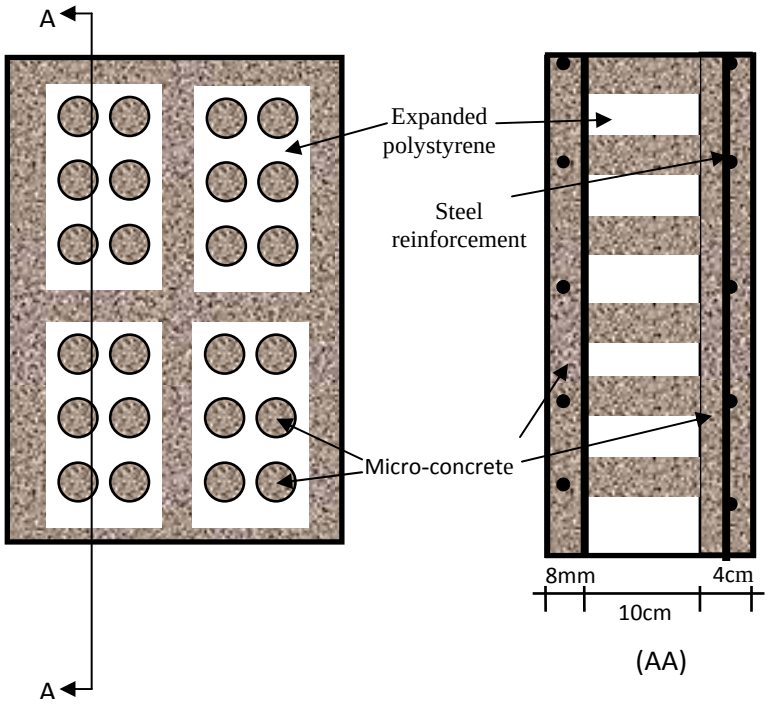

Figure 2. Schematic details of the precast panel facade.

5 MATERIALS AND METHODS

In order to indentify microorganisms that appeared in the darkened areas, microbiological evaluations of material collected from the surface were made. Samples were collected with sterilized carpet for the assesment of surface fungal colonization [Shirakawa et. al. 2002]. The culture was carried out in Agar Sabouraud Dextrose at 25 ^{o}C for 72 hours and identification was defined according Lacaz et. al. [2002]. Adhesive tape was used to collect samples for analysis of phototrophic organisms [Gaylarde 2005].

An investigation was conducted in order to see if there was humidity on the facade. A hypothesis was made that the humidity was due to water condensation. To determine the occurrence of condensation over the facade, measurements of dry bulb temperature and of wet bulb temperature of the air and surface temperature of the facade were made. From the values of dry bulb temperatures and wet bulb temperatures of the air, the dew point temperatures were calculated. The surface temperatures were compared with the dew point temperature of the air to see if condensation occurred.

The temperatures were measured with copper-constantan thermocouples connected to a Datataker Acquisition System every 5 minutes for several days.

6 RESULTS

6.1 Kinds of Microorganisms Present in the Darkened Areas of the Facade

Predominant genera of fungi found on the dark discoloration of facades were *Cladosporium*, followed by *Aureobasidium*. Other genera were also found in minor concentrations: *Alternaria*, *Arthrinium*, *Epicoccum*, *Monascus*, *Nigrospora*, *Penicillium* and *Pestalotia/Pestalopis*. *Mycelia sterilia*, a non sporulating group was found as well. Among the phototrophic microrganisms the predominant genus found was *Gloecapsa* (cyanobacteria). These results are in agreement with studies carried out by Shirakawa et al [2004] in others building in the same city.

6.2 Condensation

The results of the measurements are presented on the following figures. The caption for the following figures is:

- External air: dry bulb temperature of the external air;
- Concrete: temperature of the external surface of the facade in the area that had concrete as substratum;
- Thermal insulation: temperature of the surface of the facade in the area that had the expanded polystyrene as substratum;
- Dew point: dew point temperature.

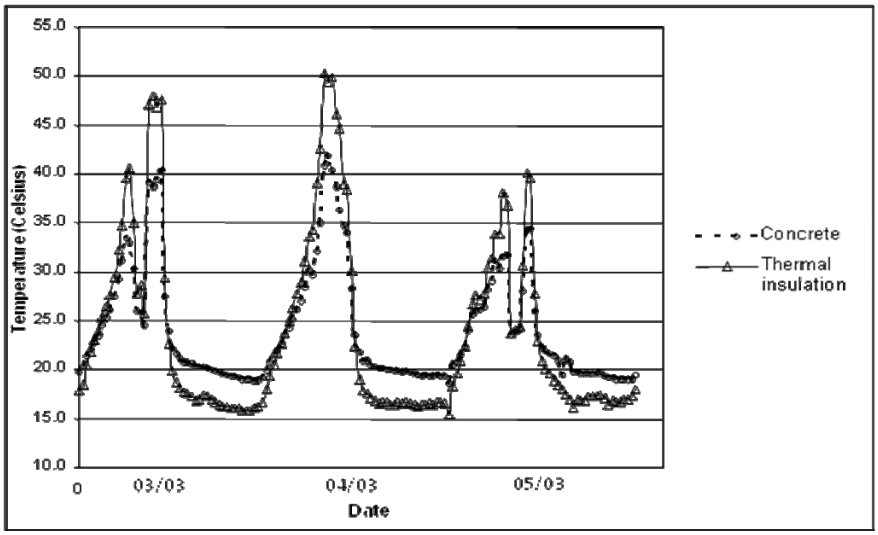

Figure 3. Surface temperatures of the facade during three consecutive days

Figure 3 shows that during the measurement period, the amplitude of oscillation of the surface-temperature in the area with thermal insulation as substratum is always higher than the one over the area with micro-concrete that fills the insulation holes. The amplitude of the temperature at the insulated area was about 35ºC whereas the temperature on surfaces that lied above concrete had amplitude of about 23ºC.

Assuming that the heat transfer is one-dimensional, during the day the incident solar radiation on the facade is absorbed by the external covering and transferred to the internal surface of the wall. Due to the lower thermal conductivity of the thermal insulation, the absorbed solar energy is transferred to the internal surface at a lower rate than in the area with concrete only, resulting in a higher temperature over the insulation during this period. At night the temperature on facade in the area over thermal insulation is lower than in the area over concrete only because the amount of heat accumulated internally during the day in this part of the wall is lower than in the area with concrete. This means that the relative humidity on the surface over thermal insulation will be higher and increase the risk of microorganism growth.

At dawn the temperature in the area of the facade over the thermal insulation becomes lower than the dew point temperature. During this period condensation takes place on the surface. This phenomenon occur in facades of buildings because, even if the atmospheric air is not saturated, the temperature of external surfaces of the buildings during the night is lower than the temperature of the external air, due to the loss of thermal energy by radiation of long waves to the sky.

Depending on the material of the facade, night cooling can be more or less intense. In facade areas with low thermal resistance and of large thermal capacity, night cooling is weaker than in façade areas

with high thermal resistance and lower thermal capacity, because the heat accumulated during the day in the material and in the internal environment of the building is transmitted on a larger scale to the outdoor, reducing the effect of the external night cooling.

The condensed water stays on the surface for a period of time that can be longer or shorter depending on – among other factors – the solar orientation of the facade, air temperature and humidity and on the speed and direction of the wind. In the southern hemisphere the time of wetness in facades with south orientation is longer than ones with north orientation. Due to the fact that they receive a smaller amount of solar radiation, the rate of evaporation of the condensed water is lower, favoring the development of microorganisms.

During visits to the site early in the morning (around 6:00 a.m.) it was observed that the amount of condensed water was enough to be clearly visible on the surface of the facade.

As condensation occurred only during the night, measurements made overnight are presented on figures 4, 5 and 6. In the area of the facade with only concrete as substratum, the surface temperature was always higher than the dew point temperature and therefore over this part of the facade the water did not condense. However, in insulated areas of the panels, even on a summer night, the temperature can be close to or even bellow dew point temperature, making condensation possible.

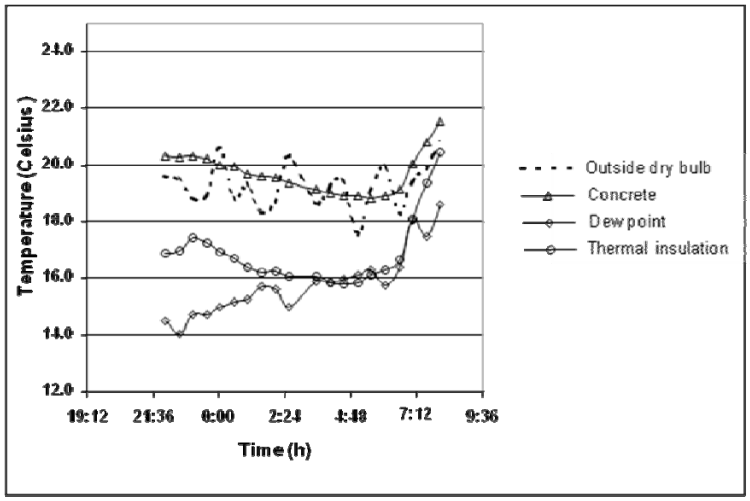

Figure 4. Condensation on facade over thermal insulation substratum from approximately 3:00 to 6:00 a.m.

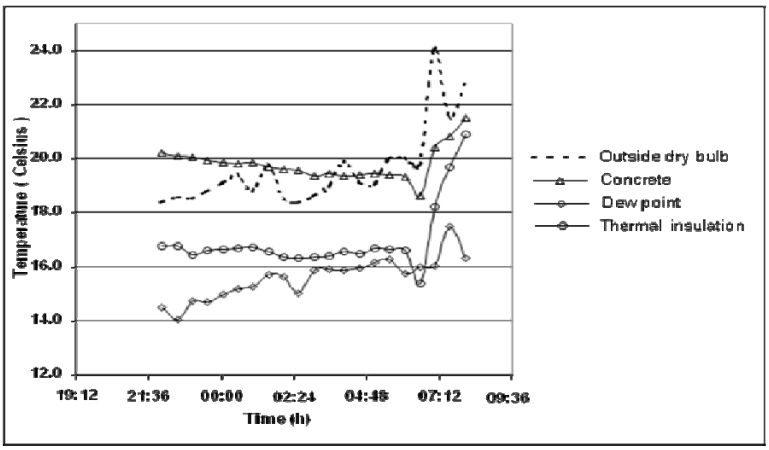

Figure 5. Condensation on facade over thermal insulation substratum from approximately 5:00 to 6:00 a.m.

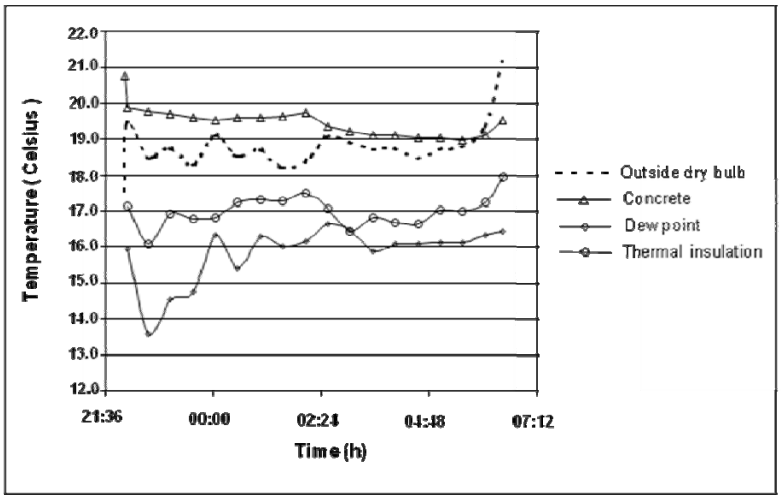

Figure 6. Condensation on facade over thermal insulation substratum at certain moments

7 CONCLUSIONS

The fouling pattern of the facades is a result of selective growth of microorganisms on the facade mainly on the rendered area over thermal insulation. No significant difference was observed among the humidity content inside of the concrete or of inside of expanded polystyrene substrate, indicating that the humidity was essentially on the surface and that the painting system protected the facade against water penetration.

Unlike the other study by Becker [2002], from the measured data it was possible to conclude that the necessary water for the development of microorganisms originated mainly from the condensation of the humidity of the air.

ACKNOWLEDGEMENTS

The authors acknowledge the support of FAPESP (Research Support Foundation of the State of São Paulo) for the development of research projects in biodeterioration of building materials and mass transfer areas that had supplied subsidies for the development of this work.

REFERENCES

Allsopp, D., Seal, K.J & Gaylarde, C.C. 2004, *Introduction to Biodeterioration*, Cambridge University Press, Cambridge, pp. 79-85.

Building Research Establishment. 1972. *Condensation*. BRE Digest 110. Watford.

Becker, R, Putterman, M. 2002. 'Patterned mold growth on renderede facades in Israel – a consequence of substrate thermal insulation', Proc. Building Physics 2002 – 6th Nordic Symposium, Trondheim, Norway 17 19 june 2002, Section 15, pp. 667-674.

Gaylarde P.M. & Gaylarde C.C. 2005, 'A comparative study of the major microbial biomass of biofilms on exteriors of buildings in Europe and Latin America', *International Biodeterioration & Biodegradation*, 55:131–139.

Gillatt, J. 1991. 'The need for antifungal and antialgal additives in high performance surface coatings', *Surface Coatings International*, 74: 6-12.

Johansson, S., Wadsö, L. & Sandin, K. 2005. 'Microbial growth on buildings facades with thin rendering on thermal insulation', Proc. 7 th Nordic Building Physics Symposium, Reykjavik, 13 15 June.

Krus, M., Sedlbauer, K., Zillig, W. & Kunzel, H. M. 2001. 'A new model for mould prediction and its application on a test roof', The Second Internal Scientific Conference on The Current Problems of Building Physics in the Rural Building, Cracow, Poland, Nov.

Lacaz, C.L., Porto, E.; Martins, J.E.; Heins-Vaccari, E & Mello, N.T., 2002, *Tratado de micologia médica*, Sarvier, São Paulo.

Moon, H. J., Augenbroue, G. 2005. 'A mixed simulation approach to analyze mold growth under uncertainty'. Proc. Ninth International IBPSA Conference. Montreal, Canada, 15 18 August, pp. 785-792.

Pasanen, A-L., Kasanen, J-P., Rautiala, S., Ikäheimo, M., Rantamäki, J., Kääriäinen, H & Kaliokoski, P. 2000, 'Fungal growth and survival in building materials under fluctuating moisture and temperature condictions', *International Biodeterioration & Biodegradation*, 46: 117-127.

Sedlbauer, K. 2002. 'Prediction of mould growth by hygrothermal calculation, *Journal of Thermal Env. & Bld. Sci.*, **25** [4], 321-336.

Shirakawa, M.A., Gaylarde, C.C, Gaylarde, P.M, John,V.& Gambale, W. 2002, 'Fungi Colonization and sucession on newly painted building', *FEMS Microbiology Ecology*, 39 [2], 165-173.

Shirakawa, M.A., John, V. M; Gaylarde, CC, Gaylarde, P.M, & Gambale, W. 2004, 'Mould and phototroph on mansory facades after repainting', *Materials and Structure*, 37, [271]: 472-79.

11DBMC International Conference on Durability of Building Materials and Components
ISTANBUL, Turkey 11-14 May 2008

Development and Benchmarking of a New Hygrothermal Model

Fitsum Tariku [1]
Kumar Kumaran [1]
Paul Fazio [2]

T 33

ABSTRACT

Building enclosures are subjected to a random climatic loading on the exterior surface and a relatively stable indoor condition on the interior. These loadings result in a transport of Heat, Air and Moisture (HAM) across the structure. Depending on the boundary conditions, a building envelope component may experience wetting or drying as it is exposed to real weather conditions that change by hours and seasons. In addition to the time varying external loading, the thermal and moisture storage characteristics of the layers, which constitute the enclosure component, make the HAM transport a complex non-linear process. HAM models, which take these complex interactions, have a significant benefit for evaluation of building envelope performance as they can provide detailed spatial and temporal conditions of the component.

In this paper, the development and benchmarking of a new hygrothermal model (HAMFit) are presented. First, a set of partial differential equations (PDEs) that govern the heat, air, and moisture transfer across building envelopes are formulated based on building physics. Then, these nonlinear and coupled PDEs are solved simultaneously for air velocity, temperature, and moisture distributions in the computational domain for a given outside environmental condition (weather data) and prescribed indoor conditions. The PDEs are solved using finite-element based commercial software called COMSOL Multiphysics and MatLab. The model is benchmarked using internationally published numerical model test cases. The good agreements obtained with the respective test cases suggest that the model can be used for products development and evaluations as well as hygrothermal performance assessment of different building envelope components.

KEYWORDS

HAMFit, HAM, hygrothermal modeling, Building envelope model

[1] Institute for Research in Construction, Ottawa, Canada
[2] Department of building, Civil and Environmental Engineering, Concordia University, Montreal, Canada

1 INTRODUCTION

Building enclosures are subjected to a random climatic loading on the exterior surface and a relatively stable indoor condition on the interior. These loadings result in a transport of Heat, Air and Moisture (HAM) across the structure. The direction of flow of these entities depends on the gradient of the driving potential of the respective entity. In addition to the time varying external loading due to time varying weather conditions, the thermal and moisture storage characteristics of the layers, which constitute the enclosure component, make the heat and moisture transport in the building envelope a transient and complex process. The complex phenomena including the dynamic wetting and drying processes of the building envelope component can be captured using computer models. In various research projects, hygrothermal models are used to assess the performance of a wall system as it is exposed to climatic conditions of different geographical locations, or to select an appropriate building envelope system for a given geographic locations (Tariku et al. 2007; Tariku and Kumaran, 2006, 1999). The model presented here (HAMFit) is part of the recently emerging class of HAM models that use commercial software to solve building physics problems (Kalagasidis, 2004; van Schijndel, 2007). These models are more transparent and flexible for futures upgrades (for example to 2D or 3D), addition of new features and integration with other models.

2 MATHEMATICAL MODELS IMPLEMENTED IN HAMFit MODEL

2.1 Moisture transfer

The general equation for moisture transfer through a porous media is given by Equation [1]. This governing equation is based on conservation of mass, and accounts for moisture transfer by vapor diffusion, convection and liquid water conduction. The vapor diffusion and liquid conduction fluxes are given by Fick's and Darcy's law, respectively.

$$\frac{\partial w}{\partial t} + div\left(\rho_a V \omega\right) + div\left(-\delta_v \frac{\partial P_v}{\partial x_i}\right) + div\left(D_l\left(\frac{\partial P_s}{\partial x_i} + \rho_w g\right)\right) = 0 \qquad (1)$$

Where w is moisture content (kg/m^3), ρ_a is air density (kg/m^3), V is air velocity (m/s) and ω absolute humidity (kg/kg-air), P_v and P_s are vapor and suction pressures (Pa), respectively, ρ_w is density of water (kg/m^3), g is the acceleration due to gravity (m/s^2), δ_v and D_l are the vapor permeability and liquid conductivity of the material (s). The moisture balance equation, Equation [1], comprises of various moisture driving potentials, P_v, P_s, w and ω. In the numerical method adapted here it is important to express the driving forces and flow variables with a single flow potential. The chosen flow potential in this work is relative humidity (ϕ) since it is continuous at interface of two layers of materials with different moisture storage properties (sorption and moisture retention), in the contrary to moisture content, which is discontinuous. Thus, the mathematical model implemented in HAMFit for moisture transfer through building envelope component is presented as shown in Equation [2], The full mathematical derivation of the moisture and heat transfer equations are given in Tariku's Ph.D. thesis (to be published in early 2008). In Equation [2] Θ is sorption capacity (kg/m^3), T is temperature (^{o}C), $C_c = \frac{0.622}{P_{atm}}$, $\hat{P}$ and P_{atm} are saturated vapor and atmospheric pressure (Pa), respectively, R and M are the universal gas constant (8.314 J.mol^{-1}) and molecular weight of water molecule (0.01806 kg.mol^{-1}), respectively

$$\Theta\frac{\partial\phi}{\partial t}=\frac{\partial}{\partial x_i}\left(D_\phi\frac{\partial\phi}{\partial x_i}+D_T\frac{\partial T}{\partial x_i}\right)-\frac{\partial}{\partial x_i}\left(D_l\rho_w\vec{g}+\rho V_i C_c\hat{P}\cdot\phi\right) \tag{2}$$

where: $D_\phi=\left(\delta_v\hat{P}+D_l\frac{\rho_w R}{M}\frac{T}{\phi}\right)$ $D_T=\left(\delta_v\phi\frac{\partial\hat{P}}{\partial T}+D_l\frac{\rho_w R}{M}\ln(\phi)\right)$

2.2 Heat transfer

After some mathematical manipulations, the conservation equation for the total energy (sum of internal, kinetic and potential energy) can be expressed in terms of enthalpy, *h*, Equation [3] (Kuo, 1986).

$$\frac{\partial(\rho h)}{\partial t}+div(\rho Vh)=-div(j_q)+\dot{Q}_s \tag{3}$$

Where j_q is a diffusion term, which comprises heat transfer by conduction and enthalpy transport due to moisture transfer. Q_s is a heat source (or sink) term. The mathematical model that is implemented in the HAMFit model for heat transfer through building envelope component is obtained (Equation [4]) after substituting the transient, convection and diffusion terms with the corresponding mixture enthalpy (moisture, air and solid matrix), and carried out some mathematical manipulations.

$$\rho_m Cp_{eff}\frac{\partial T}{\partial t}+\rho_a(Cp_a+\omega Cp_v)div(VT)+div(-\lambda_{eff}grad(T))=\dot{m}_c h_{fg}+\dot{m}_c T(Cp_v-Cp_l)+\dot{Q}_s \tag{4}$$

Where ρ_m is density of material (kg/m^3), ρ_a is density of air (kg/m^3), Cp_a, Cp_v and Cp_l are the specific heat capacity of air, vapor and liquid water (J/(K.kg)), respectively. Cp_{eff} and λ_{eff} are the effective specific heat capacity and thermal conductivity (which take moisture effect into account), respectively. h_{fg} is the latent heat of condensation/evaporation (J/kg). $\dot{m}_c=div\left(\delta_v\frac{\partial P_v}{\partial x_i}\right)-\rho_a div(V\omega)$ is the amount of moisture condensation/evaporation (kg/s)

2.3 Airflow through porous media

Airflow through a porous media can be expressed by using Poiseuille's law of proportionality (Hens, 2007), which relates pressure gradient and flow velocity (Equation [5]).

$$V=-\frac{k_a}{\mu}div(P) \tag{5}$$

Where k_a and μ are the airflow coefficient and dynamic viscosity, respectively. Combing the mass conservation equation for incompressible flow (in building physics applications, the air is considered as incompressible due to very low airflow speed, and low pressure and temperature changes) with Equation [5], gives the governing equation for airflow through porous media.

$$div\left(\delta_a div\left(P\right)\right)=0 \tag{6}$$

Where $\delta_a = \rho_a \frac{k_a}{\mu}$ is the air permeability of the porous media.

3 DEVELOPMENT OF A NUMERICAL TOOL FOR HAM ANALYSIS (HAMFit)

3.1 Numerical tool

The governing equations implemented in the building envelope model (HAMFit) are Equation [2], [4], and [6] for moisture, heat and air transport, respectively. To obtain the airflow velocity, temperature and relative humidity fields across the computational domain (building envelop component), the coupled and nonlinear partial differential equations (PDEs) need to be solved simultaneously. Here, a finite-element based computational tool called COMSOL Multiphysics and MatLab (Mathworks) are used to solve these three equations. COMSOL Multiphysics has a library of predefined models to solve familiar engineering problems such as convection diffusion problems, fluid dynamics, heat transfer and other similar problems. Also it has a provision to create and solve user-developed models, which may not be solved by the standard modules. In fact, HAMFit model is developed using this equation based modeling technique "PDE Modes", where the formulated HAM governing PDEs are directly implement it in the COMSOL Multiphysics working environment. The solver is based on an explicit scheme with variable time stepping. The user can predefine the maximum time step so that it will match with the boundary condition change period. It is possible to solve any one of the three or all equations simultaneously. In addition to its efficient solver it has a graphical user interface (GUI) to create computational domain geometry, automatic and user controlled mesh generator, and also has an integrated post processing capability for plotting, interpolating and integrating simulation results.

3.2 HAMFit model

The newly developed building envelope model, HAMFit, has two versions, HAMFit-1D and HAMFit-2D. HAMFit-1D is used for one-dimensional heat, air and moisture analysis of building envelope components. And HAMFit-2D is used to solve two-dimensional HAM problems that are caused by the geometry of the region of interest such as wall-floor junction, two-dimensional corner section, and also in cases where the physical process itself has three-dimensional nature but can be approximated in two-dimension (for example airflow and gravitational moisture flow in the structure). The models take advantage of the smooth interfaces of COMSOL Multiphysics, MatLab and SimuLink computational tools, which all are from the same development environment. In fact COMSOL Multiphysics is one of the blocks in the SimuLink model library, and it is also possible to call MatLab functions from COMSOL Multiphysics working environment. Making use of these flexible simulation environments, HAMFit model is developed in such a way that a number of functions are created in MatLab; and these functions are called by COMSOL MultiPhysics multiple times during solving the HAM equations, which are caste in COMSOL MultiPhysics "PDE Modes". The "PDE Modes" data structure of the problem including the geometry, mesh, PDEs and boundary conditions are embedded in the SimuLink S-function. Finally, the hygrothermal simulation (S-function) is run in the SimuLink simulation environment where the overall simulation parameters including outputs of the simulation results are controlled. S-function is a user-developed SimuLink block written in MatLab or C programming language, and where the developer sets the block's tasks, inputs and outputs. One of the advantages of this modeling technique is that it allows simulation of HAM transfer in any building envelope detail with no geometric (shape) restriction.

4 BENCHMARKING OF HAMFit

In this section, the newly developed building envelope model, HAMFit, is benchmarked against published test cases. The complete benchmarking exercises that are undertaken to test the model are presented in Tariku Ph.D. Thesis (to be published in early 2008). Here, two of the five benchmarking exercises that are designed in the European HAMSTAD (Hat, Air and Moisture Standards Development) project are used for assessing the accuracy of the model through inter model comparison. The objective of the HAMSTAD project was to develop test cases by which the accuracy of the existing and newly developed hygrothermal models will be evaluated (Hagentoft, 2002).

4.1 Comparative Analysis 1—HAMSTAD Benchmark Exercise #3

In benchmark #3, the effect of airflow (exfiltration and infiltration) on the wetting (accumulation of moisture) and drying of a lightweight structure of 200 mm thickness is analyzed. Although the main moisture transfer mechanism in this exercise is by airflow, moisture transports due to temperature and moisture gradient across the monolithic wall layer. The pressure gradients across the wall, which causes heat and moisture transfer by convection, in both infiltration and exfiltration periods are 30 Pa, Figure 1. The exterior surface of the structure is vapor tight (painted), where as the interior surface is open. Accordingly the mass transfer coefficients of the exterior and interior surfaces are 7.38E-12 and 2E-7 s/m, respectively. The heat transfer coefficients for both surfaces are 10 W/(m^2K).

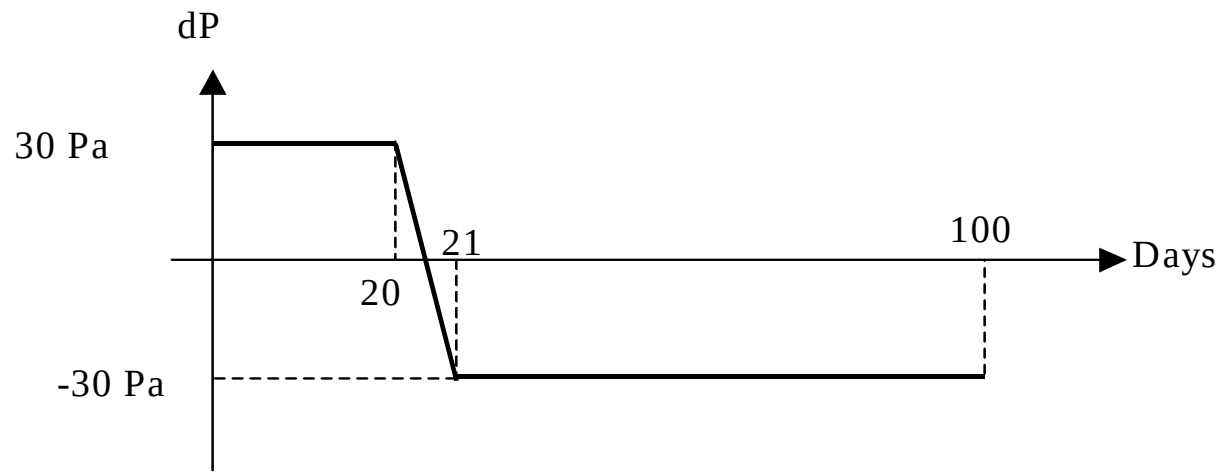

Figure 1. Pressure gradient across the wall.

The initial hygrothermal conditions of the structure are 20^{o}C and 95% temperature and relative humidity, respectively. In the first 20 days the airflow is from inside to outside (exfiltration) and the airflow is reversed in the next 80 days (infiltration). The interior temperature and relative humidity conditions are 20^{o}C and 70%, respectively. Where as the exterior temperature and relative humidity conditions are 2^{o}C and 80%, respectively. These boundary conditions are maintained constant for the 100 days of simulation period. The density and specific heat capacity of the monolithic layer are 212 kg/m^3 and 1000 J/(kg.K), respectively. The full description of this benchmark exercise is given in Hagentoft (2002). Here, the temperature and moisture content time history of the left and right section of the wall, 0.05 and 0.19 m respectively, are presented in Figure 2 below. For comparison purpose, the HAMFit simulation results are superimposed on the solutions provided by the HAMSTAD participants. The top two figures are the temperature and the bottom two figures are the moisture content profiles of the left and right sections of the walls. As can be seen in these figures, the HAMFit simulation results agree very well with the other models solutions (labeled 1 to 4).

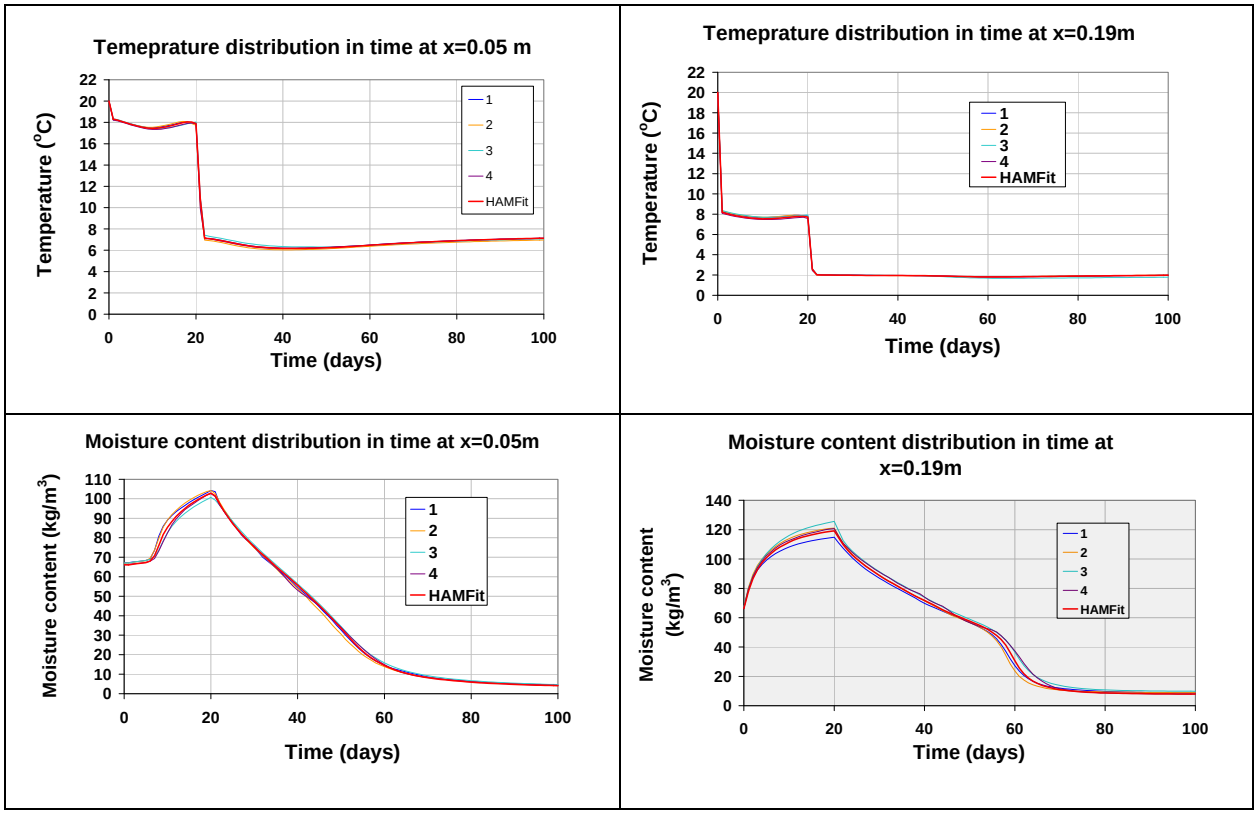

Figure 2. Temperature and moisture content time history of the wall at 0.05 and 0.19 m depth.

4.2 Comparative analysis 3—HAMSTAD Benchmark Exercise #4

The second comparative analysis deals with heat and moisture transfer in a two-layer wall system exposed to realistic internal and external boundary conditions. The wall system is composed of a load-bearing layer on the exterior and finishing layer on the interior. The load-bearing is 100 mm thick and has a density of 2050 kg/m^3, and specific heat capacity of 840 J/(K.kg), where as the finishing layer has a thickness of 20 mm, density 790 kg/m^3 and specific heat capacity of 870 J/(K.kg). The full description of this benchmark exercise is given in Hagentoft (2002). The test case is more challenging (Hagentoft et al., 2004) as it involves severe climatic load that causes surface condensation on the exterior surface due to nighttime cooling (low equivalent temperature), and frequent occurrences of wetting and drying of the wall due to the alternating rain and solar radiation loads. Moreover, the problem involves rapid rainwater absorption at the interfaces and fast moisture movement within the layers due to the extremely high liquid water absorption property of the load-bearing layer. For comparison purpose, the simulation results of HAMFit are superimposed on the corresponding HAMSTAD project participants' solutions. In Figure 3 the surface moisture content and temperature, as well as the moisture and temperature profiles across the wall sections at 96 hours are presented. As can be seen in these typical results presented here, the simulation results of HAMFit agree very well with the other six models solutions (labeled 1 to 6).

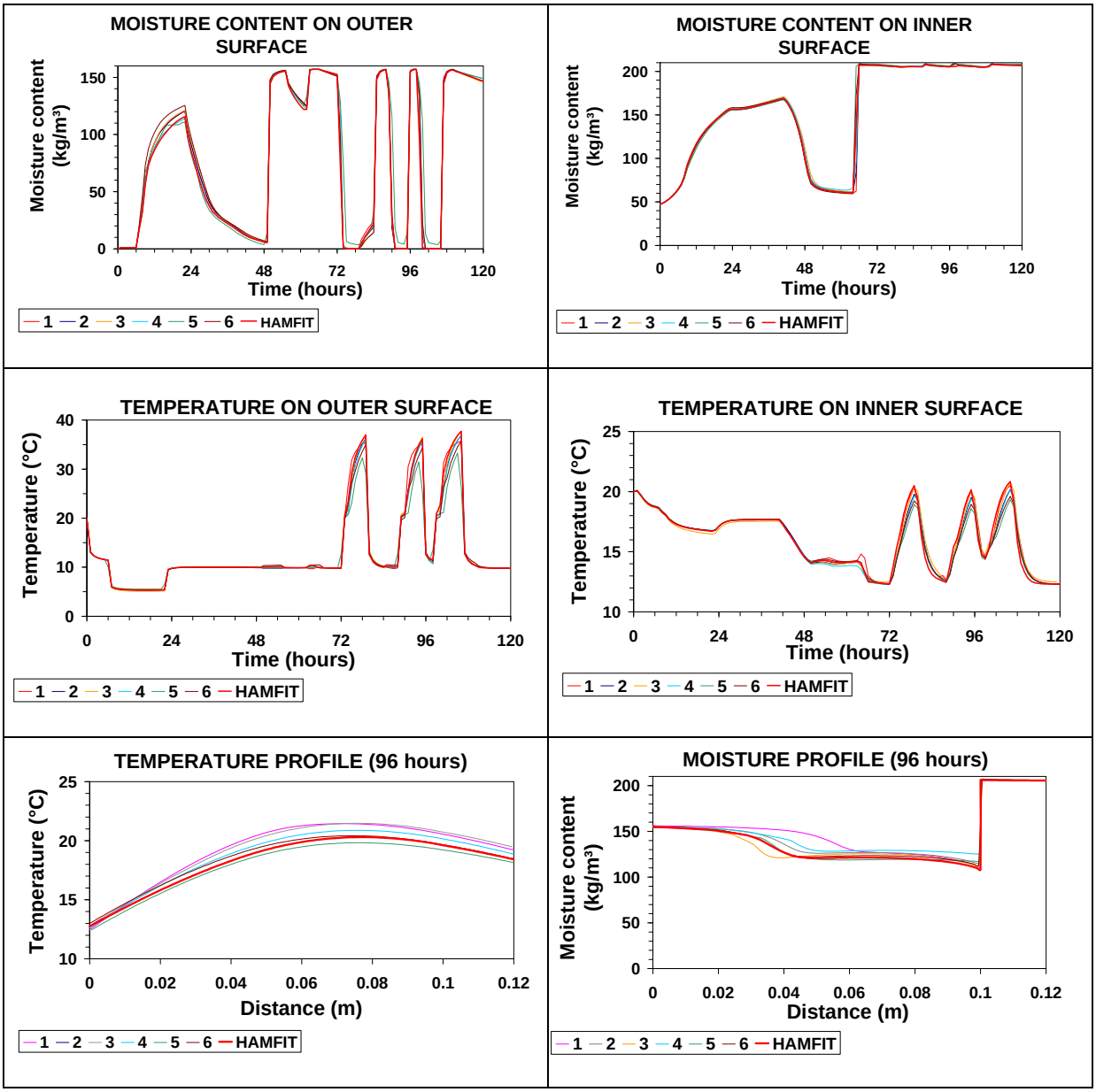

Figure 3 The moisture and temperature conditions of the surfaces and the wall at 96 hours

5 CONCLUSION

Heat, Air and Moisture (HAM) models are useful for hygrothermal performance assessment of building envelope components, new building materials and systems. In this paper, a new hygrothermal model, which utilizes equation based modeling technique, is developed. The model takes advantage of the smooth interfaces of commercial software of the same family, namely COMSOL Multiphysics, MatLab and SimuLink. The equation based modeling technique provides high transparency and flexibility of modeling HAM problems. Moreover, with this modeling technique addition of new feature and maintaining the software are relatively easy and less time consuming. The accuracy of HAMFit model is tested by carrying out two internationally accepted test cases. In both benchmarking exercises, the HAMFit

simulation results are in very good agreement with other models' respective solutions, and consequently the model can be used with great confidence. In general, the model can solve airflow through a building component and the associated heat and moisture transfer, and accounts for simultaneous vapor and liquid capillary flow, and also has a capability of solving multi-dimensional HAM problems.

REFERENCE

COMSOL Multiphysics: http://www.comsol.com/

Hagentoft, C-E. (2002). HAMSTAD – Final report: Methodology of HAM-modeling, *Report R-02:8*. Gothenburg, Department of Building Physics, Chalmers University of Technology.

Hagentoft, C-E.; Kalagasidis, A.; Adl-Zarrabi, B.; Roels, S.; Carmeliet, J.; Hens, H; Grunewald, J.; Funk, M.; Becker, R.; Shamir, D.; Adan, O.; Brocken, H.; Kumaran, K.; Djebbar, R. (2004). Assessment Method of Numerical Prediction Models for Combined Heat, Air and Moisture Transfer in Building Components: Benchmarks for One-dimensional Cases. *Journal of Thermal Envelope and Building Science*. Vol. 27 (4), pp. 327-352

Kalagasidis, A. (2004). HAM-Tools: An Integrated Simulation Tool for Heat, Air and Moisture Transfer Analysis in Building Physics. *Ph.D. Thesis*, Chalmers University of Technology, Sweden
Kuo, K. (1986). Principles of Combustion, *Published by John Wiley & Sons Inc*. ISBN 0-471-09852-3

Mathworks http://www.mathworks.com

Schijndel, A.W.M. van (2007). Integrated Heat Air and Moisture Modeling and Simulation. *Ph.D. Thesis*, Eindhoven University, Eindhoven, The Netherlands.

Tariku, F. *PhD. Thesis* (to be published in 2008), Concordia University, Montreal, Canada

Tariku, F.; Kumaran, M.K. (1999). Application of IRC's Advanced Hygrothermal Model to Assess the Role of an Air Cavity in a Drying Process, *MEWS Consortium: Technical Report T7-02*, (NRCC-44269)

Tariku, F.; Kumaran, M. K. (2006). Hygrothermal Modeling of Aerated Concrete Wall and Comparison With Field Experiment. *Proceeding of the 3rd International Building Physics /Engineering Conference*, August 26-31, Montreal, Canada, pp 321-328
Tariku, F.; Cornick, S.; Lacasse, M. (2007). Simulation of Wind-Driven Rain Effects on the Performance of a Stucco-Clad Wall. *Proceedings of Thermal Performance of the Exterior Envelopes of Whole Buildings X International Conference.* Dec. 2-7, Clearwater, FL

11DBMC International Conference on Durability of Building Materials and Components
ISTANBUL, Turkey 11-14 May 2008

The Impact of the Indoor Climate on the Hygrothermal Behaviour and the durability of External Components – Standard Boundary Conditions vs. Hygrothermal Indoor Climate Simulation

Andreas Holm [1]
Hartwig M. Künze [2]
Klaus Sedlbauer [3]

T33

ABSTRACT

In civil engineering there is an increasing demand for calculation methods to assess the moisture behaviour of building components. Intensive work has been done over the past few years on the development of mathematical approaches and procedures to evaluate real thermal and moisture transfer processes. The boundary conditions have, beside the correct material properties, a very significant influence on the simulated hygrothermal performance.

In this paper the moisture behaviour of the different construction assemblies of a house are simulated with a well validated one dimensional model using the internal boundary conditions according to the European standard EN 13788 and EN 15026. But it is well known, that the hygrothermal behavior of the building envelope affects the overall performance of a building as well. Therefore in this paper such a combined model, that takes into account moisture sources and sinks inside a room, input from the envelope due to capillary action, diffusion and vapor ab- and desorption as a response to the exterior and interior climate conditions as well as the well-known thermal parameters will be applied. In influence of different scenarios (usage of the building, loads, ventilation strategies,…) will be compared to the simplified approaches described in the standards.

KEYWORDS

Hygrothermal simulation, WUFI, WUFI Plus, EN 13788, EN 15026

[1] Fraunhofer Institute for Building Physics, Department of Indoor Climate, Fraunhoferstr. 10, 83626 Valley, Germany Phone +49 8024 643 226, Fax +49 8024 643 366, andreas.holm@ibp.fraunhofer.de
[2] Fraunhofer Institute for Building Physics, Department of Hygrothermics, Fraunhoferstr. 10, 83626 Valley,Germany Phone +49 8024 643 245, Fax +49 8024 643 366, hartwig.kuenzel@ibp.fraunhofer.de
[3] Fraunhofer Institute for Building Physics, Board of Directors, Nobelstr. 12 , 70504 Stuttgart, Germany Phone +49 711 9703300, Fax +49 8024 643 366, klaus.sedlbauer@ibp.fraunhofer.de

1 INTRODUCTION

The hygrothermal behaviour of building components is very important, due to the effects of weathering and ground moisture as well as increased airtight construction and higher indoor relative humidity. Thus, it is significant to assess this behaviour as concerns the construction of new buildings or in case of renovation measures. The indoor air temperature and relative humidity must be known parameters besides outdoor climate boundary conditions to carry out hygrothermal computation of building components. The indoor climate is determined by the behaviour of the users in contrast to the outdoor climate. The thermal capacity and water vapour sorption capacity of the internal components and furniture, however, provide a slightly dampened progress of air temperature and relative humidity. Hourly measurement values are therefore only necessary, if special problems occur. More exact values for the real conditions of indoor environments, especially for relative humidity, have not always been measured. Indoor boundary conditions according to DIN 4108-3 [1] for the dew period (20 °C and 50 % r. h.) and the evaporation period (12 °C and 70 % r. h.) can only be „generally“ applied for simple steady-state methods, e.g. the method of Glaser, and comprise security aspects. But it is impossible to calculate the real behaviour of building components in this way. This shortcoming became obvious in the past few years and resulted in extensive data acquisition of occupied and unoccupied rooms, aimed at determining the representative annual progressions of indoor air conditions [see 2, 3, 4, 5, 6, 7, 8, ,9].

More exact predictions on the indoor environment, occurring in interiors, especially relative humidity, can be achieved by means of hygrothermal indoor climate simulations under the condition that all non-stationary influencing factors are taken into consideration [10, 11]. Numerous models were developed in the past few years to compute the thermal behaviour of buildings, which have become a routine application in building design in the meantime. Besides the energetic assessment of the indoor environment, the combination with humidity processes in the enclosure surfaces is required. But so far, previous computation models offer only relatively simple approaches on humidity behaviour [12, 13]. The combined effects of non-stationary sorption, diffusion and capillary duct processes in the enclosure surfaces are not at all or only insufficiently considered. Yet the latter play an important role [14, 15].

The objective is to investigate the impact of standard boundary conditions or hourly measured indoor climate simulation values on the behaviour of the building components of a wall or roof construction. For this purpose, hourly measured weather data of a typical year for the Holzkirchen location served as climate outdoor boundary conditions.

Indoor boundary conditions for hygrothermal building component simulations are differently handled at present. The standard EN-ISO 13788 [16] has been especially developed for steady computations according to Glaser, and the standard EN-ISO 15026 [17] for non-stationary building component simulations. In addition, a data sheet for hygrothermal building component simulations was established by the International Association for Science and Technology of Building Maintenance and Monument Preservation (WTA) [18], which is valid especially for Central European countries.

2 STANDARD AND BOUNDARY CONDITIONS

The results of these investigations show that there is a correlation of outdoor air temperature, indoor relative humidity and moisture load in buildings with natural ventilation. Various standard boundary conditions for hygrothermal simulations are described in the following text and differences are discussed.

2.1 EN-ISO 13788

Indoor air humidity in buildings with natural ventilation is calculated from the monthly average value of outdoor air temperature, indoor air humidity and moisture load according to the European standard

EN-ISO 13788. The correlation of outdoor air temperature and indoor moisture load, as well as the resulting relative humidities are indicated in Figure 1 for a building in Holzkirchen with varying utilisation. Humidities are defined in 5 different classes according to utilisation.

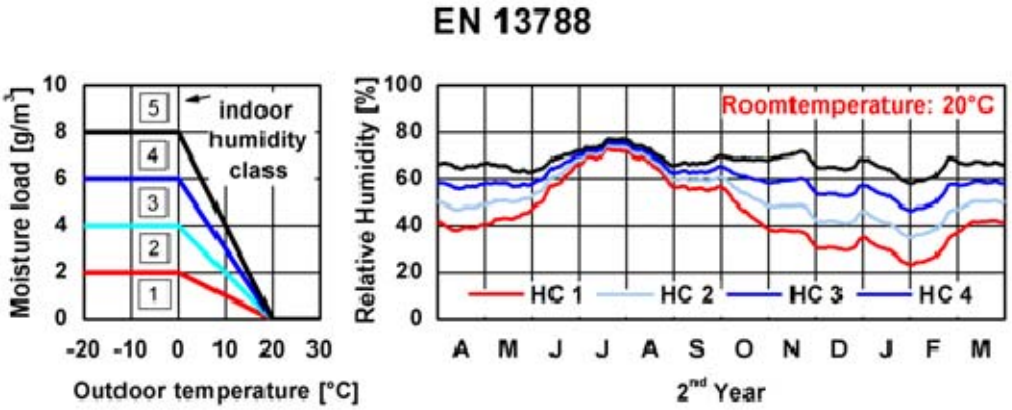

Figure 1. left: moisture load ranges in heated rooms without air-conditioning in dependence of the monthly average outdoor air temperature. Utilisation is defined as a class:
1: storehouse
2: offices, shops
3: apartments with low occupation
4: apartments with high occupation, sports halls, kitchens, staff canteens, buildings with gas thermes
5: specific buildings, i.e. breweries, indoor swimming pools, etc.
right: progression of calculated relative indoor air humidity for the Holzkirchen location according to 5 moisture classes.

Relative indoor humidity is determined by the absolute humidity of indoor air at the constant annual indoor air temperature of 20° C. The result for the absolute humidity ci is ci= ce + □c, with ce as outdoor absolute humidity and □c as moisture load, resulting from the monthly outdoor air temperature and the respective classification in 1 to 5.

The approach to compute indoor environment conditions described in this standard is based primarily on Scandinavian findings. The transformation of this approach to non-stationary conditions is highly dependent on the type of building and ventilation conditions. Another question is, whether this approach can be transformed to other European climate regions, especially southern European countries. The progression of moisture generation at temperatures below 0° C and classification in moisture classes is still problematic.

2.2 EN-ISO 15026

The method described in EN-ISO 15026 is based on measurements, carried out in different buildings in Germany. The progression of indoor temperature and relative humidity can be determined by means of transfer functions from outdoor air temperature. In this case and in contrast to EN-ISO 13788 a 24-hour variable average value is used for outdoor temperature with the intention to simulate daily variations. The transfer functions for indoor air temperature and relative humidity in dependence of the 24-hour variable average value of outdoor air temperature as well as the respective indoor environment conditions for the Holzkirchen location are indicated in Fig. 2.

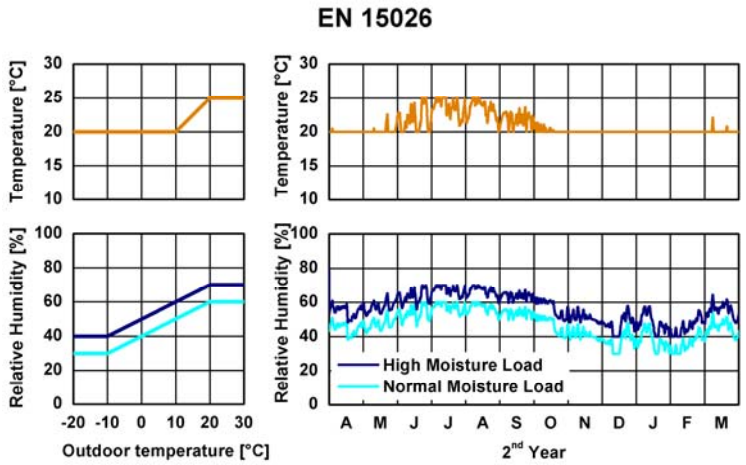

Figure 2. left: Transfer functions for indoor air temperature and relative humidity in dependence of the 24-hour variable average value of outdoor air temperature
right: progression of the computed relative indoor air humidity for the Holzkirchen location according to 2 moisture classes.

The progression of temperature seems to be more realistic in this standard in comparison to EN-ISO 13788, especially as concerns the fact that indoor temperatures in summer rise to values between 20° C and 25° C. There is generally a differentiation between only two moisture classes, a high and a low moisture load.

International Association for Science and Technology of Building Maintenance and Monument Preservation – Directive 6-2-01

Indoor environment conditions are reproduced in a simplified way by a sinusoidal smoothed annual progression in the German WTA-Directive 6-2-01. This approach is exclusively suited for Central European climate conditions. In contrast to EN-ISO 13788, however, there are only three moisture classes. If we compute the respective moisture load for a room, we learn that the limits of the respective classes intensely diverge in both standards. For example, the maximum moisture load for a living room with usual occupation at a monthly average outdoor air temperature of 10 °C results in 2 g/m3, and according to DIN EN ISO 13788 in 3 g/m3 (corresponds to a high moisture load in the WTA Directive). A possible explanation for this fact may be the differences in construction and climate-related ventilation behaviour, and could be justified as future approach on the basis of a secure interpretation of the moisture computation (higher indoor air humidity generally means higher humidity in the construction).

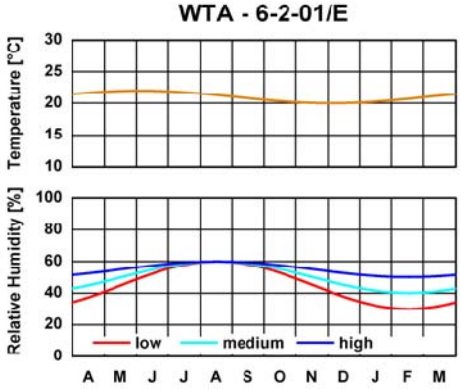

Figure 3. top: Transfer functions for indoor air temperature and relative humidity in dependence of the 24-hour variable average value of outdoor air temperature
bottom: progression of the computed relative indoor air humidity for the Holzkirchen location of 2 moisture classes.

Figure 3 clearly shows that the days with maximum values for relative humidity and temperature diverge. The maximum value is already reached in June in contrast to the observed progression of indoor air humidity.

3 HYGROTHERMAL BEHAVIOUR OF THE ENTIRE BUILING

The hygrothermal behaviour of the surfaces influences the behaviour of the entire building. The programme WUFI-Plus offers the possibility to simulate indoor climate conditions in buildings. The new hygrothermal computation tool can compute the temperature and humidity conditions of the ambient surfaces and of indoor air as well as the energy requirements or energy consumption.

3.1 Description of the Building

The hygrothermal behaviour of a 1½-storey building with a total living space of 160 m2 and a net spatial volume of 422 m3 was investigated for the study. The building is ideally constructed without basement. The roof has an inclination of 50 degrees and an orientation to the north and south. In case of the investigated roof, the 160 mm high clearance between the rafters is filled with cellulose fibres (assumed bulk density of 60 kg/m3). The wooden formwork is covered with a vapour-tight bitumen sheet. The insulation material has a thermal conductivity of 0.04 W/mK and a µ-value of 1.5. In contrast to mineral fibre materials, cellulose fibres have certain humidity storage capacities, which may have an influence on the hygrothermal behaviour. The vapour barrier is taken into account by a 1 mm thick layer with adequate µ-values. The limiting gypsum plasterboard, which is installed inside, has a respective sd-value of 0.15 m. The total u-value of the construction is 0.226 W/m2K. All façade elements have the following structure from the outside to the inside: 1cm mineral plaster (short-wave absorption 0.4), 5 cm wood wool lightweight construction sheet, OSB boards, 20 cm hydrophobic mineral wool. A wooden panel construction serves as internal shell. Two-pane windows are installed in each façade. All material data come from the WUFI database.

The hygrothermal computations started in April with an initial water content equivalent to 80 % relative humidity. The computations were carried out over a period of 2 years. Hourly climate boundary conditions for the Holzkirchen location are applied. Impacts of driving rain are only considered for façades and according to orientation. The external heat transmission resistance is 0.0526 for the roof and 0.0588 m2K/W for the façades. The heat transmission resistance for all internal surfaces is 0.0125m2K/W. The minimum indoor temperature of 20° C should be maintained by means of a heating system of 15 KW.

3.2 Description of the Investigated Variations

Fig. 4 gives a survey of the different simulated scenarios. The daily profile of ventilation and internal thermal and moisture loads is varied in the process. First of all, the pure hygrothermal behaviour of an empty building is simulated in the cases 1 and 2. The building is only ventilated by infiltration air exchange in case 1. Due to the airtight windows, the hourly air exchange rate amounts to 0.2 h-1. In the following cases, air exchange is varied in a way that the daily average air exchange is 0.5 h-1. In the cases 3 and 5, the building is occupied by 4 persons over a period of 24 hours a day. Two short-term ventilation strategies are investigated to simulate the impact of user behaviour. In case 4, the window is left ajar over a period of 1 hour, at 8 a.m. and 6 p.m. (n = 4 h-1). In the cases 5 to 7 ventilation is shorter (30 minutes), but more intensive (n = 8 h-1). To simulate the impact of irregular user behaviour, the building is occupied by 4 persons only between 6 p.m. and 8 a.m. in the cases 6 and 7. Thermal and moisture loads vary hourly during the day. In the process, special attention was paid to the fact that the moisture load was kept constant at 12 kg/day in all cases.

3.3 Simulated Indoor Climatic Conditions

The results for indoor air temperature and relative humidity computed for the cases 1 to 7 by means of WUFI-Plus are indicated in Fig. 5. These clearly demonstrate the impact of the internal thermal and moisture load as well as the non-stationary ventilation behaviour. If there are no additional thermal and moisture loads in the building, relative humidity varies between 15 % in winter and 70 % in summer. The difference of an air exchange of 0.2 and 0.5 is almost negligible. In an occupied building with a constant air exchange rate of 0.5 relative humidity varies between 40 % and 70 %. The minimum temperature of 20° C can be maintained. The temperature in summer rises to maximum values of almost 30° C. The reason is that no additional ventilation was assumed in summer and no additional measures for solar control were adopted. Most obvious is the impact of ventilation behaviour. In contrast to continuously constant ventilation short-term ventilation by opening the window modifies daily variations of relative humidity by almost -10 %. Moreover, it is impossible to maintain the indoor air temperature of 20° C in winter because of the insufficient heating systems during the ventilation phase. This corresponds to the measurements.

The resulting indoor air temperatures and humidities must be statistically analysed. The direct comparison of standard boundary conditions and progressions computed by WUFI-Plus shows clear-cut differences. This may be demonstrated by the example of an apartment with low and normal occupation. In this case and in accordance to EN 13788 the humidity class HC 3 is to be applied. The average value of relative humidity is approx. 60 % with fluctuations of approx. ± 10 %. The usual moisture load can be applied for such a building according to EN 15026. In this case, the average value of the relative humidity is approx. 45 % with fluctuations of approx. ± 10 %. A similar progression of the relative humidity is achieved by applying the standard boundary conditions according to the WTA Directive with an average value of approx. 50 % with fluctuations of approx. ± 10 %. If we compute the progression of relative humidity by means of WUFI-Plus, the result for the two first cases without any additional thermal and moisture sources is a relative humidity of a value slightly below 40 % with fluctuations of slightly below 20 % to 60 %. The impact of the users (cases 3 to 7) is clear-cut. The average relative humidity is increased by 45 % to 50 % for the respective case only by the real utilisation of the building simulated by thermal and moisture load. Indoor relative humidity is increased by a further 5 % by short-term ventilation by opening the window despite the same amount of thermal and moisture load.

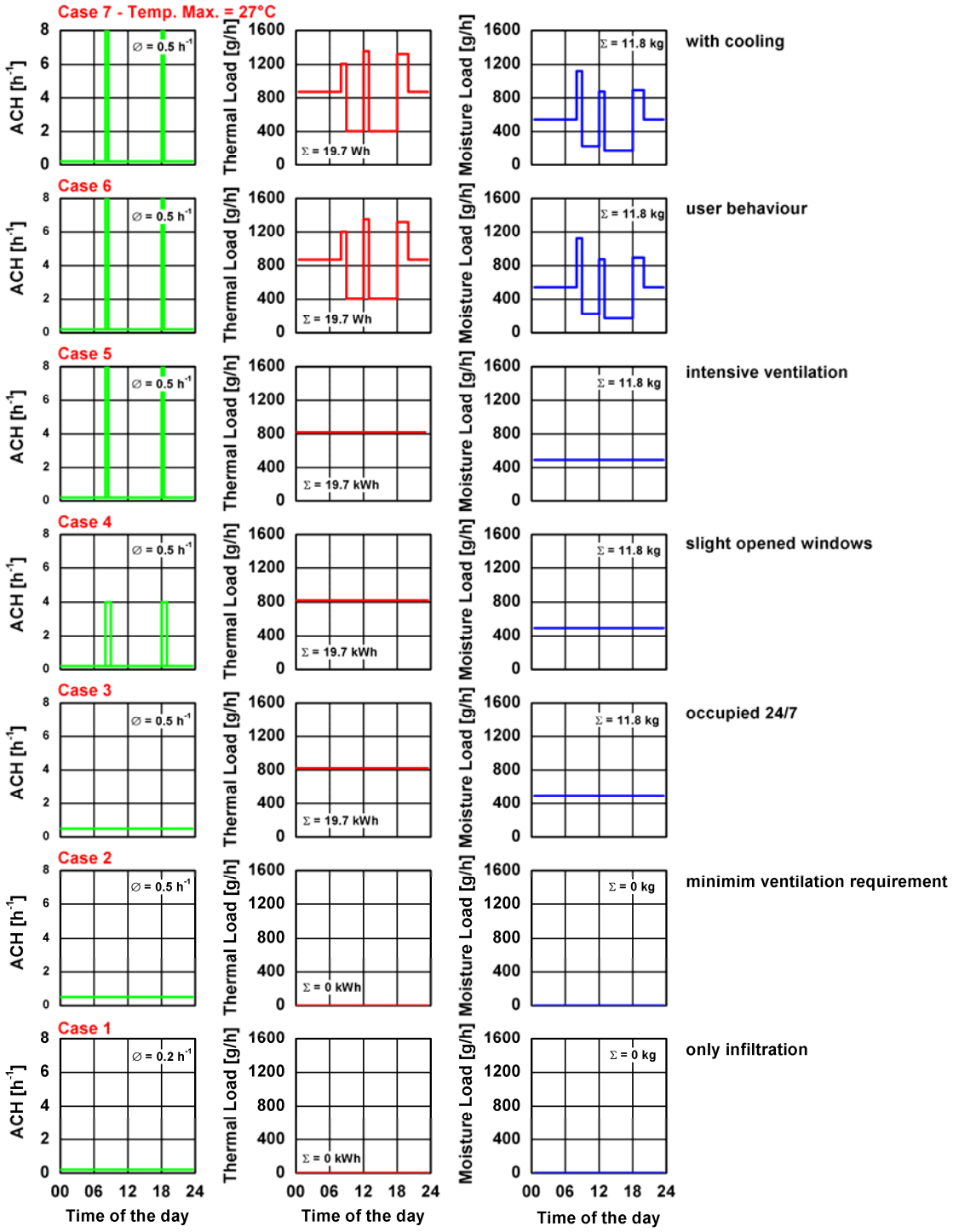

Figure 4. Daily profile for the estimated air exchange as well as internal thermal and moisture loads in seven cases.

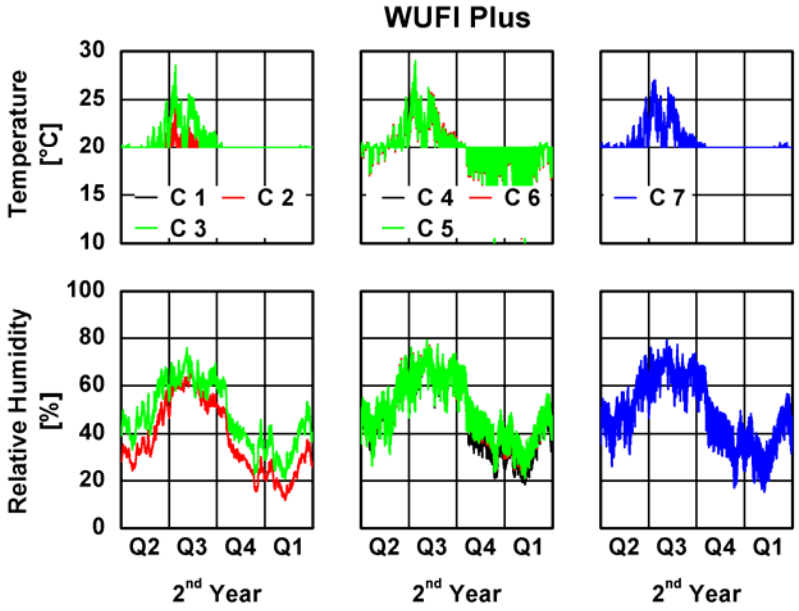

Figure 5. Resulting relative humidity and temperature of seven variations.

4 IMPACT ON THE HYGROTHERMAL BEHAVIOUR OF BUILDING COMPONENTS

It is investigated in the following, how the various standard boundary conditions according to the 3 standards and different user behaviour computed by means of WUFI-Plus influence the hygrothermal behaviour of a roof orientated to the north, or of a façade orientated to the west. For comparison, the water contents in the timber shell of a roof with a 50-degree inclination to the north was investigated as well as the total water contents in the construction.

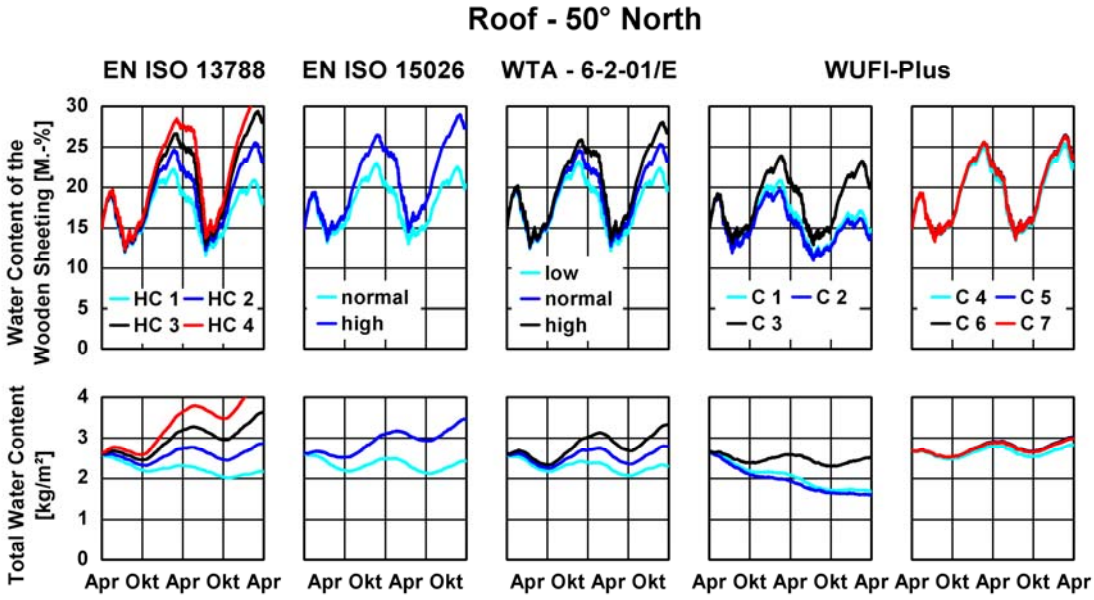

Figure 6. Computed progression of the water content in the timber shell (above) and of the total water content (below) based on various indoor climate data.

Figure 6 shows the results for the investigated roof in a diagram. Computations by means of WUFI of the hygrothermal behaviour according to the boundary conditions of EN 13788 show that this roof is no longer hygrothermally "secure" from moisture class 2. The assessment of this construction

according to EN 15026, however, rates it as hygrothermally harmless according to the respective usual boundary conditions. According to WTA, a slight increase in the total water content occurs in the course of the year at a standard moisture load. Computations by means of WUFI-Plus also provide clear-cut differences in the hygrothermal behaviour. Whereas the construction is rated to be hygrothermally harmless for the cases C1 and C2, it is assessed to be just hygrothermally harmless for case C3 (continuous occupation, constant ventilation). In case of non-stationary ventilation or non-stationary user behaviour with the same thermal and moisture load, however, the total water content as well as the water content in the timber shell clearly increase. If the results are compared to the respective standard boundary conditions, it is obvious that the moisture class is modified by one category by non-stationary behaviour alone. This means that the computations according to EN 15026 in case of non-stationary behaviour provide more realistic values for the moisture class. Similar results are achieved for the west façade (Fig. 7). If we compare the computed results by means of WUFI-Plus with those of the standard boundary conditions, we see that the standard boundary conditions have various effects on the hygrothermal behaviour, and that there is a clear impact of the user behaviour.

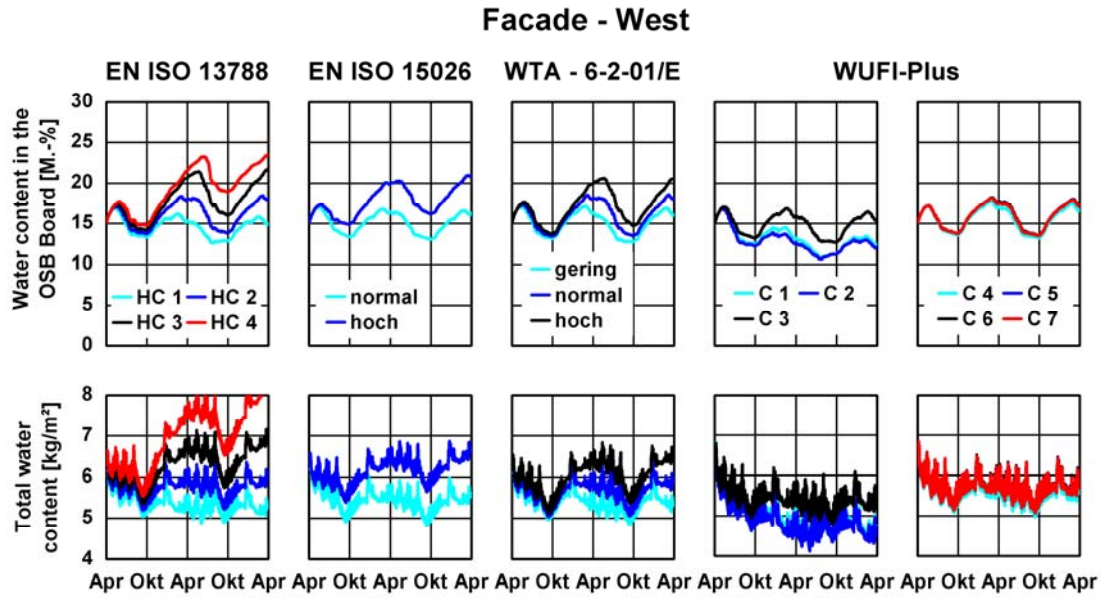

Figure 7. Computed progression of the water content in the timber shell (above) and the total water content (below) based on various indoor climate data.

5 SUMMARY

Average relative humidity in residential buildings is characterised by the seasons in Central European climate conditions. At outdoor air temperatures around the freezing point it is usually around 30 % r. h., during in-between seasons it is between 40 % and 50 % r. h., and in mid-summer it may rise to 60 % r. h. Since the hygrothermal measurement or assessment of building components strive for a result "on the safe side", excessive boundary conditions are applied for the most part instead of average indoor climate conditions.

As the effects of boundary conditions in case of simulation computations are manifold (e. g. impacts on the humidity- and temperature-dependent material parameters), it is recommended to apply climate conditions as realistic as possible. Supported by new standards and directives, the hygrothermal building component simulation continuously replaces the stationary calculation of Glaser as hygrothermal assessment method for building structures. Adequate boundary conditions must be selected accordingly, whereby indoor relative humidity is especially important.

The comparisons of the results from indoor climate simulation show that WTA boundary conditions for a standard moisture load should be usually applied for residential buildings or the respective

boundary conditions according to EN ISO 15026. Applying these boundary conditions means the choice for the safe side. It seems to be reasonable to apply high moisture loads in buildings, where particularly unfavourable indoor humidity conditions must be expected.
The moisture classes according to EN ISO 13788 provide too high values in any case, and must thus be selected with caution.

REFERENCES

1 DIN 4108-3: Klimabedingter Feuchteschutz. Juli 2001.

2 Cunnigham, M.J,: Inferring ventilation and moisture release rates from field psychrometric data only using system identification techniques. Building and Environment, Vol. 36 (Januar 2001) H. 1, S. 129-138.

3 Freitas, V. P.: The indoor climate and moisture problems in the building envelope. International Symposium on indoor quality in practice, Oslo 1995.

4 Gertis, K. und Erhorn, H.: Wohnfeuchte und Wärmebrücken. HLH 36 (1985), H. 3, S. 130-135.

5 Gertis, K. und Erhorn, H.: Neue Überlegungen zum Mindestwärmeschutz. WKSB-Sonderausgabe (1985), S. 39-42.

6 Künzel, H.M.: Raumluftfeuchteverhältnisse in Wohnräumen. IBP Mitteilungen 24 (1997) Nr. 314.

7 Sandberg, P.I.: Building components and building elements – Calculation of surface temperature to avoid critical surface humidity and calculation of interstitial condensation. Draft European Standard CEN/TC 89 W10 N107.

8 Sanders, C.: Report IEA Annex 24, Task 2: Environmental Conditions, International Energy Agency Annex 24 on Heat, Air and Moisture Transport in New and Retrofitted Building Envelope Parts, Leuven (1996).

9 Künzel, H.M., Holm, A. und Kaufmann, A.: Raumluftbedingungene für die Feuchteschutzbeurteilung von Wohngebäuden. IBP Mitteilung 30 (2003), Nr. 427.

10 Erhorn, H. et al: Stimmen Computerberechnungen des wärmetechnischen Verhaltens von Gebäuden mit praktischen Messungen überein? Bauphysik 10 (1988), H. 4, S. 97-104.

11 Stricker, R.; Erhorn, H.; Szerman, M.: Gütesiegel für Rechenergebnisse zum thermischen Gebäudeverhalten? Genauigkeitsanalyse von Programmen und Anwendereinflüsse. Bauphysik 11 (1989), H. 6, S. 205-210.

12 Woloszyn, M.: Modelisation hygro-thermo-aeraulique des batiments multizones. Proposition d'une strategie de resolution du systeme couple. Dissertation L'Institute National des Sciences Appliquees de Lyon (1999).

13 Preschk, A.: Gebäude-Anlagen-Simulation unter Berücksichtigung der hygrischen Prozesse in den Gebäudewänden. Dissertation Technische Universität Berlin (2000).

14 Holm, A.; Lengsfeld, K.; Künzel, H.M.; Sedlbauer, K.: Raumklima-Simulation - Methoden, Validierung, Anwendung : Dr. Helmut Künzel zum 80. Geburtstag gewidmet. In: WKSB 51 (2006), Nr.57, S. 37-44

15 Lengsfeld, K; Holm, A., Entwicklung und Validierung einer hygrothermischen Raumklima-Simulationssoftware WUFI®-Plus Development and validation of the hygrothermal indoor climate simulation software WUFI®-Plus, Bauphysik 29 (2007), Nr.3, S.178-186

16 EN ISO 13788: Wärme- und feuchtetechnisches Verhalten von Bauteilen - Oberflächentemperatur zur Vermeidung kritischer Oberflächenfeuchte und Tauwasserbildung im Bauteilinneren – Berechnungsverfahren, April 2000.

17 EN ISO 15026: Hygrothermal performance of building components and building elements - Assessment of moisture transfer by numerical simulation; German version EN 15026, July 2007.

18 WTA-6-2-01: Simulation of Heat and Mass Transfer.

Influences of the Indoor Environment on Heat, Air and Moisture Conditions in The Building Component: Boundary Conditions Modeling

Paul Steskens [1]
Carsten Rode [2]
Hans Janssen [3]

T 33

ABSTRACT

Current models to predict heat, air and moisture (HAM) conditions in building components assume uniform boundary conditions, both for the temperature and relative humidity of the air in an indoor space as well as for the surface transfer coefficients. Such models cannot accurately predict the HAM conditions in the component and on the surface of the component with non-uniform air temperature or relative humidity distributions in an indoor space. Moreover, the heat and moisture surface transfer coefficients strongly depend on the local air velocity, local temperature, water-material interactions and water content at the material surface and surface texture of the material. The objective of the present paper is to analyze the influence of the non-uniform local air velocity near the surface of a building component on the HAM conditions in the component. A case study and sensitivity study have been used to investigate this influence. The research showed that the indoor environmental conditions and local airflow velocity have a relatively large influence on the predicted HAM conditions in a building component. The influence of the convective surface heat transfer coefficient on the HAM performance of the component is relatively large compared to the influence of the convective surface mass transfer coefficient. With respect to the analyzed building component, the investigations showed that assuming an average value for the surface mass transfer coefficient is acceptable, while assuming an average value is not acceptable for the convective surface heat transfer coefficient. The study showed that the influence on the surface relative humidity is limited.

KEYWORDS

HAM component modelling, Boundary conditions

[1] Technical University of Denmark, Department of Civil Engineering, Kgs. Lyngby, Denmark, Phone +45 4525 1927, Fax 212 2856587, pas@byg.dtu.dk
[2] Technical University of Denmark, Department of Civil Engineering, Kgs. Lyngby, Denmark, Phone +45 4525 1852, car@byg.dtu.dk
[3] Technical University of Denmark, Department of Civil Engineering, Kgs. Lyngby, Denmark, Phone +45 4525 1861, haj@byg.dtu.dk

1 INTRODUCTION

The durability of building components is strongly dependent of the heat, air and moisture (HAM) conditions in the component. Current models to predict heat, air and moisture conditions in building components commonly assume uniform indoor boundary conditions, both for the temperature and relative humidity of the neighbouring interior air as well as for the interior surface heat and mass transfer coefficients. Due to local heat and moisture sources, imperfect mixing and microclimatic effects, temperature and relative humidity in the neighbouring air are seldom uniform. Similarly, the convective surface heat and moisture transfer coefficients strongly depend on the local air velocity, local temperature, water-material interactions and water content at the material surface and surface texture of the material. The HAM conditions on or in building components resulting from such non-uniform boundary conditions cannot be accurately predicted by current HAM models. This article investigates how the variability of the surface heat and mass transfer coefficients may affect the HAM performance of building components.

Currently, researchers assume average, uniform and constant values for the convective surface heat and mass transfer coefficients when performing a HAM component analysis. The convective surface transfer coefficients are obtained from fundamental theory or experimental work, in [Hens, 2007] for example, values of 3.5 W/m^2K and $3 \cdot 10^{-8}$ s/m for the interior convective heat and mass transfer coefficients respectively are recommended.

Previous research [Worch 2004] [Novoselac 2005] have shown that different relationships for the surface heat transfer coefficient for mixed convection near a building component have been reported. Similar experimental investigations of the relationship between the surface mass transfer coefficient and the local airflow velocity have been described in [Bednar & Dreyer 2003], [Mortensen *et al*. 2006] and [Iskra & Simonson 2007]. Other researchers, for example [Steeman *et al*. 2007], tried to determine the surface heat and mass transfer coefficients by using Computational Fluid Dynamics (CFD).

The literature study showed that a considerable number of relationships between the indoor environmental conditions and the surface heat transfer coefficients have been developed, all having their specific limitations and applications. When performing a HAM building component analysis, often, researchers arbitrarily use these relationships for a HAM component simulation, without considering these limitations. The use of these correlations may introduce errors in the predicted HAM conditions. The objective of the present paper is to analyze the influence of the non-uniform distribution of the transfer coefficients caused by variations in the air velocity near the surface of a building component on the HAM conditions on and in the component. A parameter study has been used to investigate this influence.

2 CASE STUDY

A building detail has been selected for the analysis. Two rooms (on top of each other) are connected by a lightweight concrete floor. Both rooms are connected to the outdoor climate by a wall, consisting of a layer of brick, interior mineral wool insulation and a gypsum board finishing layer. Air circulates in the room from the ceiling along the wall to the floor. The construction is presented in Fig. 1. Due to inertia effects, the air velocity near the corners (indicated by 1 and 2, Fig. 1) is relatively low compared to the average air velocity in the room. Lower air velocities result in relatively low convective surface heat and mass transfer coefficients near the corner compared to the surface transfer coefficients in the centre of the components.

First of all, lower and upper limits for the surface transfer coefficients have been determined based on the literature study. Second, the HAM performance of the component Fig. 1 has been investigated using several indoor environmental conditions and different values for the convective surface heat and

mass transfer coefficients. The specific conditions which have been analyzed are described in Section 2.1. Section 2.2 presents the climatic conditions, which have been applied.

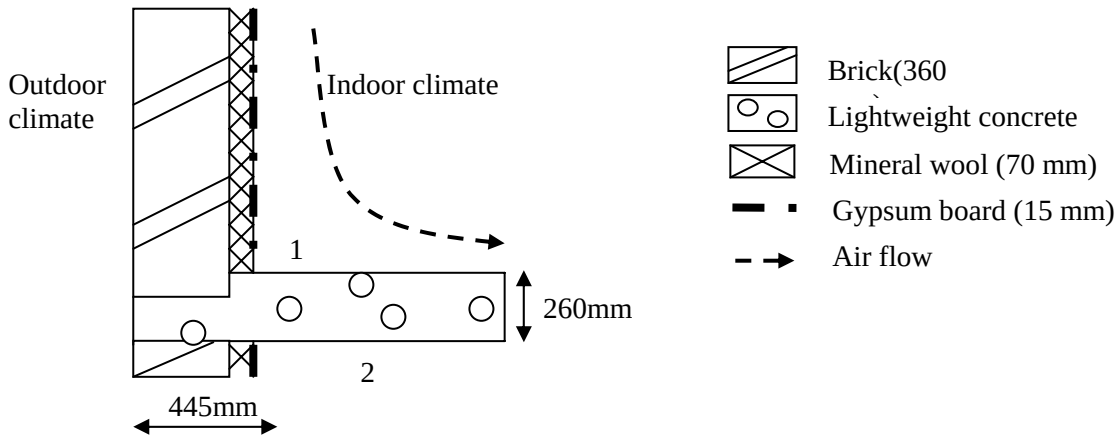

Figure 1. Building detail that has been selected for analysis. Two rooms, connected to the outdoor climate by a wall, consisting of a layer of brick, interior mineral wool insulation and a gypsum board finishing layer. Air circulates in the room from the ceiling along the wall to the floor. The surface heat and mass transfer coefficients near the corners are relatively low compared to the surface transfer coefficients in the centre of the components.

2.1 Parameter Analysis

Based on the literature study, lower and upper limits for the surface heat and mass transfer coefficients have been determined. For 'still' air conditions, where the local air velocity near the component is relatively low, the surface heat and mass transfer coefficient are assumed to be respectively 1 W/m^{2}K and $1 \cdot 10^{-8}$ s/m. For 'moving' air conditions, where the local velocity near the component is relatively high, values of 8 W/m^{2}K and $1 \cdot 10^{-7}$ s/m for the convective surface heat transfer coefficient ($_c$) and the convective surface mass transfer coefficient ($_c$) respectively.

Several indoor environmental conditions have been investigated:
Lower limits: A HAM component analysis assuming lower limits for the convective surface transfer coefficients has been performed.
Upper limits: A HAM component investigation applying upper limits for the convective surface transfer coefficients has been carried out.
Lower limits and average heat transfer coefficients: A HAM component analysis assuming lower limits for the surface moisture transfer coefficients and an average value for the convective surface heat transfer coefficient ($_c$) has been applied.
Upper limits and average heat transfer coefficients: An average value for the convective surface heat transfer coefficient ($_c$) has been applied, while the higher limit for the convective moisture transfer coefficient is applied.
Lower limit region: A (more realistic) situation was analyzed using a combination of a lower limit for the surface transfer coefficients in the region near the corner and upper limits outside of this layer. The size of the region has been varied between a distance of 30 cm (5a) and 10 cm (5b) from the corner of the building component

Typical values for the convective heat and moisture transfer coefficients, which have been applied for the different indoor environmental conditions, are presented in Table 1. The objective of the investigations (1 and 2) is to determine minimum and maximum HAM conditions, which are likely to

occur in the building component. The objective of studying the conditions using an average value for the convective surface heat transfer coefficient (conditions 3 and 4) is to compare the influences of the convective heat transfer coefficient and the moisture transfer coefficient separately. With respect to the lower limit region, this investigation intends to determine the influence of the size of the still air region on the predicted HAM conditions.

Table 1. Convective heat and moisture transfer coefficients, which have been applied for the different indoor environmental conditions.

Conditions	$_c$ [W/m^{2}K]	$_c$ [10^{-7} s/m]
1 Lower limits	1	10
2 Upper limits	8	1
3 Lower limit $_c$ and average $_c$	3.5	10
4 Higher limit $_c$ and average $_c$	3.5	1
5a 30 cm region	1 and 8	10 and 1
5b 10 cm region	1 and 8	10 and 1

2.2 Boundary conditions

The parameter analysis has been performed using the Test Reference Year (TRY) for Danish (Copenhagen) outdoor climatic conditions. With respect to the indoor environment, hourly values for the indoor air temperature and relative humidity have been obtained using a whole building performance simulation of the building from the IEA & ECBCS programme, Annex 41, Subtask 1 [Rode & Woloszyn 2006]. The document [Rode & Woloszyn 2006] presents Common Exercise 1 which expands on Common Exercise 0 by adding an analysis of the indoor and building envelope moisture conditions for the BESTEST building used in Common Exercise 0 (from IEA SHC Task 21 & ECBCS Annex 21). The building has been simulated in HAMBASE [Wit, de 2006] using set points of 20^{o}C (during office hours) and 12^{o}C (outside office hours) for heating and 27^{o}C for cooling (during office hours). With respect to the moisture production in the building, an average vapour production of 10 litres per day is spread out over the day. The indoor environmental conditions resulting from the simulation are applied as boundary conditions on the surfaces at the internal sides.

3 RESULTS

The HAM performance of the building component (Fig. 1) has been simulated using the CHAMPS-BES Program for Coupled Heat, Air, Moisture and Pollutant Simulations in Building Envelope Systems [Nicolai & Grunewald 2006]. Outdoor and indoor climate conditions (Section 2.2) have been applied at the boundaries. With respect to the initial conditions, an initial temperature and relative humidity of 20^{o}C and 50 % RH respectively have been applied throughout the entire component. The simulation time is one year. The simulation results for 70 days are presented in Fig. 2.

Figure 2 shows that a relatively large difference is present between the lower limit (1) and the higher limit (2). Considering the average difference between both limits over the entire year, an average temperature difference of 2.5^{o}C and an average difference in relative humidity of 16.8 %RH have been observed. A difference in partial vapour pressure of approximately 77 Pa between the lower limit and higher limit condition has been observed. For temperatures around 15-20 °C and saturation pressures around 1500-2000 Pa, this is less than 4 % RH difference and may be negligible. Moreover, the partial vapour pressure resulting from both conditions (1) and (2) follow a similar trend. The influence of the convective surface heat transfer coefficient on the HAM performance is thus relatively large compared to the influence of the convective surface mass transfer coefficient. Figure 3 presents the heat and

moisture fluxes to the indoor environment. Comparing conditions with lower (1) and higher limits (2), a significant difference between the size and the direction of the heat fluxes has been observed.

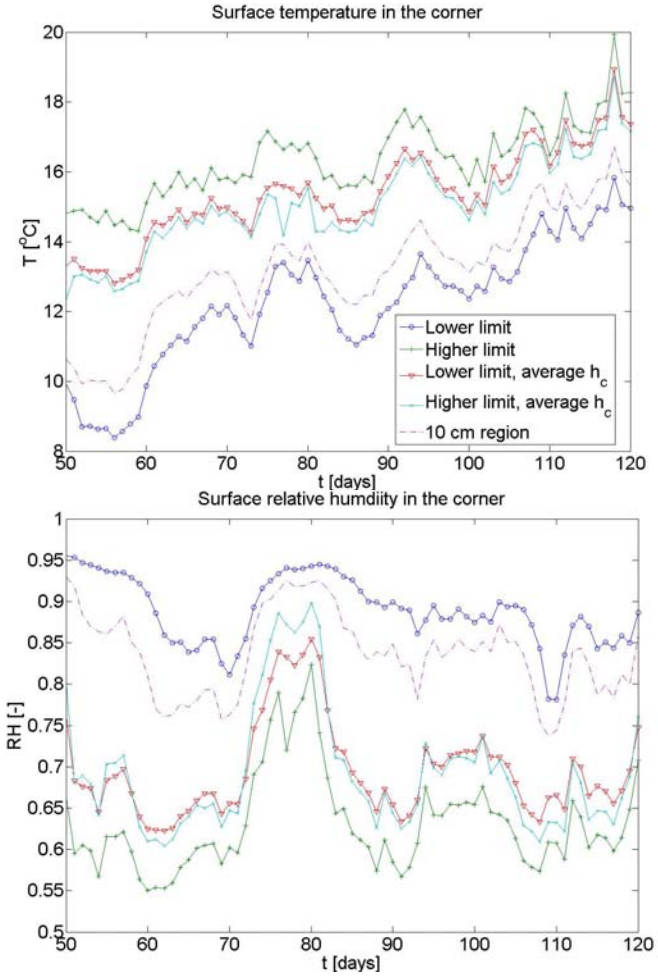

Figure 2. Surface temperature (left) and relative humidity (right) in the corner of the building component. The different conditions (Section 2.1), i.e. lower limits, higher limits and average values for the surface transfer coefficients corresponding.

Figure 2 shows that the predicted HAM conditions for the conditions with an average surface heat transfer coefficient (conditions 3 and 4) are comparable. The average temperature and relative humidity deviation over the year between conditions 3 and 4 is approximately 0.33°C and 0.26 % RH respectively. The simulation results show that the influence of the surface heat transfer coefficient on the predicted HAM conditions is relatively large compared to the influence of the surface moisture transfer coefficient. In addition, the moisture fluxes (Fig.3) for both conditions (3 and 4) are relatively comparable.

Regarding the size of the still air region (condition 5), the difference in average surface temperature and relative humidity in the corner is 0.5°C and 2.5 % RH respectively. Figure 2 presents relatively comparable HAM conditions even when the size of the still air region is varied by a factor 3. In summary, the investigations show that the local airflow conditions near the component (especially in the corner) should be taken into account. The size of the lower limit region, which is assumed, is less important for the conditions in the corner. However, the size of the low coefficient region will of course determine the size of the region with potential durability problems.

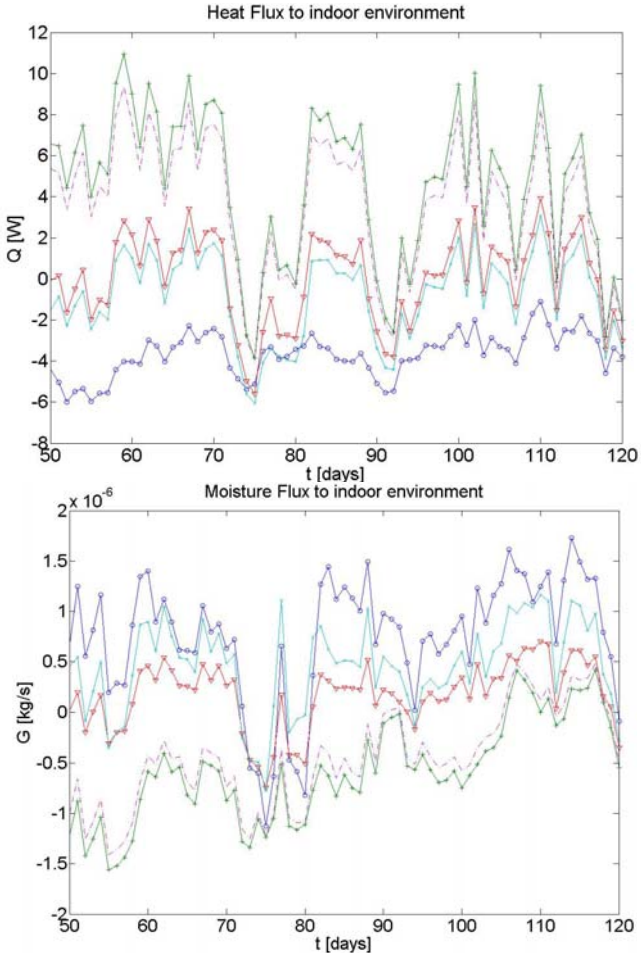

Figure 3. Heat fluxes (left) and Moisture (right) to the indoor environment. The different conditions (Section 2.1), i.e. lower limits, higher limits and average values for the surface transfer coefficients corresponding. The corresponding legend is presented in Fig. 2.

The simulation results show that a relatively large deviation is observed between the lower limit and higher limit conditions. Assuming 'moving' air conditions near the component, the average temperature and relative humidity in the corner are approximately 17.7°C and 70 %RH. These conditions may develop moisture problems, for example mould growth. However, the risk for moisture problems is relatively small compared to the predicted lower limit conditions, i.e. an average temperature of 15.2°C and a relative humidity of 87.8 %RH in the corner. Focussing on the (more realistic) case with a 'still' air region near the corner, these results also show that moisture problems are likely to occur. It is concluded that the application of the appropriate airflow conditions near the component has a relatively large influence on the predicted HAM performance of the component.

4 CONCLUSION and DISCUSSION

This section presents the conclusions from the parameter study and the consequences of the investigations for HAM component performance analysis. The influence of the non-uniform surface heat and mass transfer coefficients on the HAM conditions in the building component has been analyzed. A parameter study has been used to investigate this influence. Lower and upper limits for the convective surface transfer coefficients ($_c$ and $_c$), assuming respectively 'still' air and 'moving' air conditions, have been assigned. The simulated conditions resulted in minimum and maximum HAM conditions in the building component. Moreover, the combination of a 'still' air region near the building component has been investigated.

It is concluded that:

- The non-uniform distribution of the transfer coefficients caused by variations in the air velocity near the surface of a building component have a relatively large influence on the predicted HAM conditions in a building component. Different surface temperature, relative humidity and vapour pressures are predicted, when different airflow conditions near the component, resulting in different convective surface transfer coefficients, are applied. When performing a HAM performance analysis and simulation, it is important to take the local airflow velocity near the component into account.
- The influence of the convective surface heat transfer coefficient on the HAM performance is relatively large compared to the influence of the convective surface mass transfer coefficient. With respect to the analyzed building component, the investigations showed that assuming an average value for the surface mass transfer coefficient is acceptable, while assuming an average value is not acceptable for the convective surface heat transfer coefficient. The study showed that the influence on the surface relative humidity is limited. However, an influence on the fluxes is still present.
- Local indoor environmental conditions and deviations in local air velocities, for example due to corners, should be taken into account. A possible approach is to assume a still air region. The size of the still air region, which is assumed, showed to be less important for the quality of the predicted conditions in the corner, but will determine the possibly mould affected region's size.

Building researchers and designers should be aware that the appropriate indoor environmental conditions are applied, when performing a HAM component simulation and analysis. The local airflow conditions near the component have a relatively large influence on the predicted HAM performance of the component. It is recommended that, for example in a design stage, different local airflow conditions are investigated to predict the influence of these conditions on the HAM performance of the specific component.

Future research should focus on the analysis and determination of the relationship between the local air velocity near the component and the convective surface heat transfer coefficient. A more detailed description and prediction of the interaction between the indoor environment and the HAM conditions in the building component is desired. The quality of such an analysis could be improved by providing guidelines and relationships between the convective surface heat transfer coefficient and the local air velocity near the building component. With respect to the convective surface mass transfer coefficient, it is acceptable to assume an average coefficient.

REFERENCES

Bednar, T. & Dreyer, J. 2003, 'Determination of moisture surface transfer coefficients under transient conditions', Proc. Int. Building Physics Conference II, Research in Building Physics, Leuven, Belgium, 14 18 September 2003.

Hens, H. S. L. C. 2007, *Building Physics - Heat, Air and Moisture - Fundamentals and Engineering Methods with Examples and Exercises*, Ernst und Sohn, Berlin

Iskra, C.R. & Simonson, C.J. 2007, 'Convective mass transfer coefficient for a hydrodynamically developed airflow in a short rectangular duct', *International Journal of Heat and Mass Transfer*, **50**[11], 2376-2393.

Mortensen, L.H., Rode, C. & Peuhkuri, R. 2006, 'Effect of airflow velocity on moisture exchange at surfaces of building materials', Proc. Int. Building Physics Conference III, Research in Building Physics and Building Engineering, Montreal, Canada, 27 31 August 2006.

T 33, Influences of the Indoor Environment on Heat, Air and Moisture Conditions in The Building Component: Boundary Conditions Modeling, P. Steskens et al.

Nicolai, A. & Grunewald, J. 2006, *CHAMPS-BES Program for Coupled Heat, Air, Moisture and Pollutatant Simulations in Building Envelope Systems (User Manual)*, BEESL - Building Energy and Environmental Systems Laboratory, Department of Mechanical and Aerospace Engineering, Syracuse University, NY.

Novoselac, A. 2005, Combined *airflow and energy simulation program for building mechanical system design*, Ph.D. thesis, Pennsylvania State University; The Graduate School; College of Engineering.

Rode, C. & Woloszyn, M. 2006, "Simulation tests in whole building heat and moisture transfer", Proc. Int. Building Physics Conference III, Research in Building Physics and Building Engineering, Montreal, Canada, 27 31 August 2006.

Steeman, H.J., Janssens, A. & De Paepe, M. 2007, 'About the use of the heat and mass analogy in building simulation', Proc. 12th Symposium for Building Physics, Dresden, Germany, 27 31 March 2007, pp. 455-461.

Wit, M.H. de 2006, *HAMBASE - Heat Air and Moisture model for Buildings And Systems Evaluation*, Eindhoven University Press, Eindhoven, the Netherlands.

Worch, A. 2004, 'The behaviour of vapour transfer on building material surfaces: The vapour transfer resistance', *Journal of Thermal Envelope and Building Science*, **28**[2], pp. 187-200.

Feedback System for Determination and Elimination the Effects of Durability Problems

Gamze Özkaptan Alptekin [1]

T 41

ABSTRACT

Depending on the innovation in material engineering and technology, a great many building materials and building components have been served to the construction market. Entering these newly developed materials and components to the building system, without finding sufficient opportunity for experimentation, may cause quality problems named as building failure. Selection of inappropriate materials/components and detailing errors in design phase (design failure), construction errors in construction phase, insufficient maintenance and misusage in occupation phase results in building failure, some of stemming from durability problems in life cycle of the building.

In order to improve building quality, multi-disciplinary and multi-phased building production process should be integrated by using the means of communication technology. Tracking of durability problems in occupation phase and feed-back of information to the design and construction organizations should prevent these organizations from repeating similar failures in further projects. Some models were developed in the context of Customer Relationship Management (CRM) in order to collect information from occupation phase, but a model which is focused especially on durability problems and their effects is needed. It is possible to use an information model in order to record building failure information systematically for eliminating losses and improve building quality. In this paper, conceptual structure of an information model developed for organizing building failure is presented.

KEYWORDS

Building failure, Durability, Information management, Guality management, Customer relationship management

[1] Istanbul Kültür University, Faculty of Engineering and Architecture, Istanbul, Turkey 34156, Phone +90 212 4984289, g.alptekin@iku.edu.tr

1 INTRODUCTION

Building production process is a multi-disciplinary and multi-phased activity. Usually independent organizations collaborate in the scope of a project for a limited time and scattered when their contract finished. Each organization has its own characteristics with their organizational culture such as organizational structure, type of working, information system and procedures. These organizations join to the project team for a limited time, in whatever time needed and leave whenever they finish their work. This situation constitutes a fragmented structure that obstructs the continuity in the building production process and results with some quality problems.

Some vital information which can be used in programming, design and constuction phases can be obtained in occupation phase in life cycle of the building. Lack of information flow between these phases and especially lack of feed-back information to the design organization causes quality problems stemming from coordination problems in the process as well as integration problems in the product.

Construction is a project type production and quality of a construction project can be evaluated with its process (production phases) and product (building) as a whole. Quality problems in a construction project can be resulted as cost overruns, time overruns and performance problems. Building failures constitute the main reason in quality problems. Reasons of building failure may differ, but durability problems are the major factor of building failure that can be determined in occupation phase. Enabling integration among the the poject phases and disciplines, feed-back of information from occupation phase to the design phase may increase project quality by eliminating durability problems.

Design phase and design product is core of the quality problems because the most critical decisions, according to the scope of the project, construction system, technical subsystems, materials and components, that are determinant on building quality, are taken on this phase. As the volume of information flow in design phase is very large, an information system is needed for keeping and tracking of this information to secure the quality of design phase and design documents in project level. When we look from design organization's point of view, more than one complex projects may be undertaken which are in different phases simultaneously. Information in a design organization is constituted from the information produced in the design organization and information gathered from outer resources. Design organization uses and integrates the information that is gathered from outer resources in order to produce design products. Some of this information is related with the materials selected, codes, standards, specifications and information taken from material suppliers which is directly related with the scope of this paper. Information flow in a design organization is so complex and must be put in order by using a systematically structured information system. Such a system may have a sub-module for enabling feedback information according to performances of building materials and components determined in occupation phase.

2 RELATED WORKS

In a literature review, it can be seen that there are some resarch studies about integration of building production process. Conceptual models by Baldwin *et al.* [1999], Tan & Lu [1995], Matta *et al*. [1998] and Chan & Chan [1999], Erdener [2003] were proposed to serve as interfaces of information management, design management, facility management and quality management.

Some of the application models which were developed by Kanoglu [2001], to serve integration of design and construction management; by Mokhtar *et al.* [1998], Hegazy *et al.* [2001], Zaneldin *et al.* [2001], to serve design change management, can be found in literature.

Some studies realized by Marques *et al.* [2006], Ugwu *et al.* [2005], Richard [2007] according to durabilities of materails in particular can be found in literature.

There are some commercial softwares as SAP, InfoExchange, Barracuda, etc. Serving to FM (Facility Management) and CRM (Customer Relationship Managment) [http://solutions.iinet.org].

These models and studies bring out some partial solutions to the quality problems in building production. However, it has not been possible to locate a model to record and feedback building failures determined in occupation phase in order to increase building quality.

3 PROBLEM STATEMENT

Depending on the innovation in material engineering and technology, a grate many building materials and building components have been served to the construction market. By the enforcement of economical or technical requirements, or design preferences, these new materials take part in designs. Entering these newly developed materials and components to the building system, without finding sufficient opportunity for experimentation, may cause quality problems named as building failure. Selection of inappropriate materials/components and detailing errors in design phase (design failure), construction errors in construction phase, insufficient maintenance and misusage in occupation phase results in building failure, some of stemming from durability problems in life cycle of the building.

Information according to the materials and components supposed to be used in a design project is taking a significant place, in the large volume of information flow in design phase. Catalogues, codes and standards are some of the guiding documents that are to be used in preparing design documents and especially specifications. Nevertheless, many factors may have impact on the behaviour of the materials' or components' life cycle. Besides selecting the materials and components by the help of their testing results, appropriateness to the codes and standards, considering their warranty conditions, the risk caused by unexpected conditions may lead to problems on building quality. An information system is needed in order to record, organize and deliver project information in all the phases of building production process for tracking the performance of building components and materials in life cycle of the building.

Facility managers developed tools and guidelines to ensure occupants' comfort, building energy efficiency, environmental sustainability, building security, workplace flexibility, and other work environment requirements. The economic execution of the organizational, financial and operational processes as well as the continous fulfillment of the quality, security and environmental requirements, constitute the principal elements of facilities management [Ashuri, B. *et al.,* 2007]. There are some information models developed in the context of CRM, and FM, considering especially sales, service (operation and maintanence) and marketing, but there is a gap in feedback of information between design and FM organizations in order to determin and eleminate the effects of durability problems.

Feedback information is needed to be structured systematically as a part of the information system, because when it is not, relevant decisions often get lost or are ignored by busy specialists. Fisher [1995] emphasized some problems about feedback information in preconstruction phase as 'feedback loops are random, feedback is unmanaged, feedback is slow, significant feedback is very late, there are no inherent criteria for defining design versions, organizational control may lead to unstable designs, errors and omissions may occur in moving data from one discipline to another'. Potential benefits of successful integration include increased efficiency, reduced time, and improved quality for clients. Early, structured, precise, and rapid feedback will help specalists to recognise the effects of their choises on other specialties. Complete feedback from the viewpoint of all relevant disciplines is a major benefit of technical integration and will assist discipline experts in their understanding of the impact of their decisions and of the requirements of other disciplines [Fisher, 1995].

4 AIM OF THE STUDY

Building failures which constitute the main group in quality problems, may appear in construction and occupation phases. Building failures determined in construction phase generally may be solved preferably by a change order system or in situ. However, building failures determined in occupation phase are solved in the context of facility management, apart from the design or construction organization. Information according to technical details of building failures such as, reasons and effects of them are needed to be recorded and used by project participants, especially by design organizations. Reasons and effects of building failures determined in abovementioned phases differ, so separate information feedback models, as seen in 'Fig. 1' should be designed for each of them, as being the sub-modules of an integrated information system.

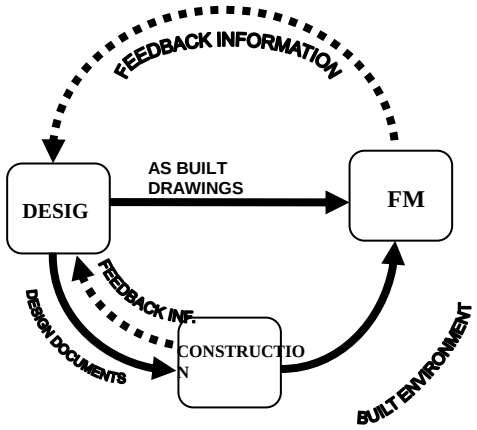

Figure 1. Information flow in Building Production Process

An information model in order to record and analyse the effects of building failure determined in construction phase 'IDEA' (Integrated Design Automation For Design/Build Organizations) was developed in an other research study made by the author [Alptekin 2006]. This model then integrated into MITOS-Multi Phased Integrated Automation System for Construction Industry, which has been developed for design/build organizations [Kanoğlu 1999]. A similar information model regarding building failures determined in occupation phase should be developed as a complementary module in order to be integrated into MITOS. By this way, it should be possible to determine the effects of building failure in general, and durability problems in particular serving to increase building quality.

A conceptual model, emphasizing the basic points that must be considered in the background of a practical model according to identify building failures determined in occupation phase will be put forward in this study.

5 A MODEL FOR DETERMINING AND ELEMINATING THE EFFECTS OF DURABILITY PROBLEMS

5.1 Reasons Of Durability Problems

Durability is defined as 'staying in good condition for a long time, even if used a lot' [Longman Dictionary of Contemporary English Online]. Peris Mora [2007] defined durability as 'the characteristic of those objects or materials that maintain their properties over time'. It can be understood that durability is directly related with the performances of materials or components in their lifecycle. Each material or component has a life span. Durability problem occurs when the material or component fails to accomplish its function before its intended life time. Because of this, durability problem is a type of building failure that can be detected in occupation phase. There are some factors

affecting the life span of the materials and components. Chew [2005] grouped these factors as design, material, construction and maintanence. Ugwu *et al.* [2005], added 'quality systems in use at the construction stages and environmental exposure of the building elements' as the factors affecting durability.

It can be seen from literature study that, mostly environmental factors are investigated as reasons of durability problems. Ransom [1987] defined the agencies causing deterioration as; solar radiation, moisture, biological agencies, gaseous constituents and pollutents of air, ground salts and waters, manufactured products and juxtaposition of materials and components. Addleson [1992] explained the causes of mechanisms of failure as; condensation,entrapped moisture, rain penetration, rising damp, movement, loss of adhesion, corrosion and timber decay. Although environmental factors are playing the main role on durability problems, design failure resulting from inadequate information about the materials or the interaction between the materials, and design defects in details have also a significant impact on them. Mitropoulos and Tatum [2000] emphasized the risk and liability involved in trying something new, difficulty in giving approval from third parties and resistance to change. Despite these barriers to innovation, nowadays designers are willing to take the risk and liability of using innovative materials, components and technologies in the competitive positions, for being different or for being cost-effective or for technical reasons. Neverthless, lack of information according to longterm behaviour of materials and lack of experince in applicaation on site may result with building failures.

Another problem may arise from the construction methods and workmanship on site. Construction is still a workman-based activity despite the efforts through industrialisation. Innovation in materials, components and procedures may require qualified site skills. Application of new materials and components by incompetent workmanship may affect durability of the materials and components.

Another reason of durability problems is related with the requirements of maintanance in occupation phase. Almost every building material or component has maintenance periods. Neglecting maintanance work or repair when needed, should have a negative impact on durability of building materials or components. Maintenance and repair activities are achieved in the context of facility management. An information model can be used in order to track maintenance periods and performances of building materials and components.

5.2 Effects Of Durability Problems

Durability problems cause the occupants feel unsatisfactory. If quality is explained as 'client satisaction', it is obvious that durability problems are one of the reasons of building quality problems. Durability problems have negative affect on performance of materials or components, as well as life cycle cost of the building. For a sustainable design, beginning from design stage to facility management, future maintenance, repair and replacement requirements are taken into account in life cycle cost planning. Durability problems causes revisions on cost plans because of unplanned repair or replacement costs. Durability problems may appear in a critical building element or component that is very difficult to reach, or may be in a close interaction with the other parts, so it may be a complex and costly work, to repair or replacement. Sometimes repair or replacement work may affect different subsystems or components. Under these sircumstances, durability problems may cause additional consequential costs including additional workmanship. Peris Mora [2007] suggested to use the advantage of certain building technologies as a solution for this problem. Modular construction would facilitate partial replacement of defective materials in engineering works enhancing the durability of the construction. But still durability problems can be considered as a risk for life cycle cost planning of the building.

5.3 Basic Elements Of Conceptual Model

There are some conseptual and practical models developed in literature and in practice according to both FM and CRM. These models are generally focused on sales, service (operation and maintanence)

and marketing. There are also some models serving to increase building quality by enabling integration between the phases of building production. There is a gap between facility management and design phase from the feedback of building failure information point of view. Information gathered in the context of facility management should be used in a structured feedback mechanism by the design organization in order to prevent repeating similar defects in further projects.

A model should be designed to function as a part of an integrated information system of Design/Build/FM organizations, in order to record building failure information determined in occupation phase. The model aims to maintain a feedback mechanism between facility management and design organizations. The proposed model should be built on the following dimensions:

- Integration in physical dimension: Organizations taking place in a project should be integrated by an appropriate organizational model as D/B/FM.
- Integration in conceptual dimension: New philosophical approaches should be considered such as Supply Chain, Just In Time, Lean Production, Total Quality Management should be used.
- Integration in virtual dimension: An information model should be designed by the existing possibilities and means of information technology.

A conceptual model should be developed considering the above dimensions. Such a model should be open to every organization taking part in the project. The reliability and functionality of the proposed model depends on mutual confidence. D/B/FM type project procurement system is the appropriate model for both the integration of project organizations and running of the proposed model. New philosophical approaches must be considered in order to supply integration in conseptual dimension. The conceptual model then should be converted to an information model as a further study.

Building failures determined in occupation phase should be collected, kept and fedback to the design organization in order to increase building quality. Durability problems as a type of building failure can be captured by using this proposed model. Design organizations may use this information to constitute an archieve of construction materials, components and details for tracking their long term performances. Building failures determined in occupation phase should be recorded and fedback with their technical details according to the type of failure, related dicipline, corrective actions, cost, duration and technics needed for corrective action and preventive actions. The model allows to filter the past projects and making analysis according to the types of failures, reasons of failures, cost losses etc. These analysis constitute a tool for eleminating the losses and prevents from further failures. Analysis of the data collected in occupation phase allows designers identifying the important risk factors affecting the level of maintainability and frequency of the occurrence of defects.

6 CONCLUSION

Integration of the project phases and project stakeholders may decrease quality problems in building production process. D/B/FM contracts combine Design, Build and Facility Management activities under a single company or by a joint venture structure. Organizational integration is a necessary, but not an enough attempt for enabling integration problems. Integration should be realised in philosophical and virtual dimensions as complementary tools.

Feedback of building failure information from both construction and occupation phases is vital for increasing building quality in general. Durability problems, which appear in occupation phase may be captured by such a feedback mechanism, in particular. Recording the building failure information in a systematically structured information system, with its technical details, will allow determination the reasons and effects of durability problems. Such an information system will also be a useful tool for eleminating durability problems and not repeating similar failures in future projects.

REFERENCES

Addleson, L., 1992, *Building Failures A Guide To Diagnosi, Remedy and Prevention,* Butterworth Heinemann, Oxford.

Alptekin, G., 2006, *Yapı Üretiminde Tasarım Kalitesinin Yükseltilmesine Yönelik Bir Model,* PhD Thesis, İTÜ Science Institute, Istanbul.

Ashuri, B., Rouse, W.B., Augenbroe, G., 2007, Different model of work in the modern services enterprise, *Information Knowledge Systems Management ,* 6, 29-59.

Baldwin, A.N., Austin, S.A., Hassan T.M., Thorpe, A., 1999, Modeling information flow during the conceptual and schematic stages of building design, *Construction Management and Economics,*17, 155-167.

Chan E.H., Chan A.T.S., 1999, Imposing ISO 9000 quality assurance system on statutory agents in Hong Kong, *Journal of Construction Engineering and Management,* 125 (4), 285-291.

Chew, M.Y.L., 2005, Defect analysis in wet areas of buildings, *Construction and Building Materials,* 19, 165-173.

Erdener, E., Linking programming and design with facilities management, 2003, *Journal of Performance of Constructed Facilities,* February, 4-8.

Fisher, M., Kunz, J., 1995, The circle: Architecture for integrating software, *Journal Of Cmputing In Civil Engineering,* Vol.9, No.2, April, 122-133.

Hegazy, T. Zaneldin, E., Grierson, D., 2001, Improving design coordination for building projects I: Information Model, *Journal of Construction Enginering and Management,* 127 (4), 322-329.

Kanoğlu, A., 1999, *Yüklenici Firmalar İçin Şantiye Düzeyinde Kompüter Tabanlı Enformasyon Sistemi Tasarımı,* Proje No: INTAG-912: Tübitak Destekli Araştırma Projesi, İstanbul.

Kanoğlu, 2001, MITOS: Multi-phased integrated automation system for building production process, Information and communication technology in the practice of building and civil engineering, *Proceeding of 2nd worldwide ECCE symposium organised by VTT and RIL,* Helsinki, Finland, 6-8 June, 183-188.

Longman Dictionary of Contemporary English Online, http://dictionary.cambridge.org, September, 2007

Marques, S.F., Ribeiro, R.A., Silva, L.M., Ferreira, V.M., Labrincha, J.A., 2006, Study of rehabilitation mortars: Construction of a knowledge correlation matrix, *Cement and Concrete Research*, 36, 1894-1902.

Matta, K., Chen, H., Tama, J., 1998, The information requirements of total quality management, *Total Quality Management*, 9 (6), 445-461.

Mitropoulos, P., Tatum, C.B., 2000, Forces driving adoption of new information technologies, *Journal Of Construction Engineering And Management*, September/October, 340-348.
Mokhtar, A., Bedard C., Fazio, P., 1998, Information model for managing design changes in a collaborative environment, *Journal of Computing in Civil Engineering,* 12 (2), 82-92.

Peris Mora, E., 2007, Life cycle, sustainability and the transcendent quality of building materials, *Building and Environment,* 42, 1329-1334.

Ransom, W.H., 1987, *Building Failure Diagnosis and Avoidance*, E&FN Spon, UK.

Richard, D., Hong, T., Hastak, M., Mirmiran, A., Salem, O., 2007, Life-cycle performance model for composites in construction, *Composites Part B 38,* 2007, 236-246.

Tan, R.R., Lu, Y.G., 1995, On the quality of construction engineering design projects: Criteria and impacting factors, *International Journal of Quality & Reliability Management,* 12 (5), 18-37.

Ugwu, O.O., Kumaraswamy, M.M., Kung, F., Ng, S.T., 2005, Object-oriented framework for durability assessment and life cycle costing of highway bridges, *Automaion in Construction,* 14, 611-632.

Zaneldin, E., Hegazy, T., Grierson, D., 2001, Improving esign coordination for building projects II: A collaborative system, *Journal of Construction Engineering and Management,* 127 (4), 330-336.

11DBMC International Conference on Durability of Building Materials and Components
ISTANBUL, Turkey 11-14 May 2008

Factor Method Application Using Factors' Grids

Bruno Daniotti [1]
Sonia Lupica Spagnolo [2]
Riccardo Paolini [3]

T 41

ABSTRACT

Among Estimating Service Life methods, Factor method is considered one of the main international references within ISO for the evaluation of building components' Service Life in the specific conditions of use; it gives an easy contextualization of Reference Service Life values of building components outside the system and the specific design context: the biggest advantage in choosing this method is, in fact, its great simplicity, which becomes itself its highest limit because it doesn't avoid possible errors in assigning factors' values according to user's own experience and point of view.
In order to avoid, or at least limit as more as possible, such subjectivity, Durability of Building Components Group of Politecnico di Milano suggests for this method some criteria to make more objective and scientifically validated values attributed to each single factor: the report deals with the development of an Enhanced Factor method ruled with grids which drive users in correctly assigning values to each factor, keeping the simplicity of the method, but making it more objective.
The paper reports about the definition of such Factor Grids, focusing on the methodological approach followed to individualize the main degradation actions, characterizing each factor, which has to be expressed through the use of specific sub factors. Once found these sub factors, it's then necessary to determine in which way and, above all, how much they can influence Service Life.
Eventually, an example of factors' grid for ETICS is showed, built using the proposed procedural iter.
This enhanced Factor method represents an important tool, scientifically validated but contemporarly easy to use: as a consequence, it can contribute to a more diffused application of Service Life planning.

KEYWORDS

Grid, factor method, Tools, Prediction, Sub factors

[1] Politecnico di Milano, BEST Department, Milan, Italy, 20133, piazza Leonardo Da Vinci, 32, Phone +39 2 23996002, bruno.daniotti@polimi.it
[2] Politecnico di Milano, BEST Department, Milan, Italy, 20133, piazza Leonardo Da Vinci, 32, Phone +39 2 23996002, sonia.lupica@polimi.it
[3] Politecnico di Milano, BEST Department, Milan, Italy, 20133, piazza Leonardo Da Vinci, 32, Phone +39 0223996017, riccardo.paolini@mail.polimi.it

1 INTRODUCTION

The evaluation of Service Life, according to international ISO 15686 and national UNI 11156 standards, can be made following some different methods proposed: it can be individualized a sort of reliable hierarchy among the three main families to which these methods belong:

1. probabilistic methods;
2. engineering methods;
3. deterministic methods.

The Factor method described in cited standards is proposed with a deterministic approach, but keeping its simplicity it can be developed using an engineering way to proceed: Politecnico di Milano is enhancing Factor method in order to standardize ESL's calculation, limiting users' subjectivity, thanks on one side to Montecarlo semi-deterministic method and on the other side to the use of ad hoc grids which can drive the user in choosing each factor.

As underlined by Bourke and Davies [1997] a Service Life Prediction system should desirably include the following important features:

- easy to learn, to update and to communicate;
- easy and quick to use;
- accurate;
- adaptable;
- supported by data;
- links with existing design methods and tools;
- free of excessive bureaucracy;
- recognises the importance of innovation;
- relevant to diverse environments;
- acceptable to practitioners and clients alike;
- reflects current knowledge;
- a flexible level of sophistication for either outline or detailed planning.

The evolution of Factor method based on driving grids perfectly answer to these requests. Moreover the structure of French Italian Data Base for collecting Reference Service Lives is based on grids: the enhanced method proposed by Politecnico di Milano can be easily implemented in the data base itself, exploiting its easy accessibility by internet.

2 ENHANCING THE FACTOR METHOD USING FACTORS' GRIDS

The application of factors' grids can be used with two different approaches:

1. in a static way: they can give a sort of photograph of the referring conditions in order to easily individualize the configuration associated to the given value of Referenfe Service Life;
2. in a dynamic way: they can allow to calculate the ESL by driving the user in giving the correct value to each sub-factor and then to factors themselves just selecting the real conditions associated to the considered building component.

The creation of evaluating grids should be done by experts: preferably, manufacturers themselves should provide such evaluation grids within the product's technical documentation. Evaluation grids are just functions, receiving as input data the performance classes found in the standards and returning particular values [Re Cecconi & Iacono 2005]. As the Factor Method is based on the comparison between reference and in-use conditions, and as the evaluation grids are built starting from the reference conditions of the building component, user has just to put the performance specification

inside the grid: in such a way, the comparison between two components will be automatically obtained.

Once defined the "n" sub-factors, it is possible to evaluate the relative importance of each characteristic compared to the others. Attention should be paid to the fact that comparisons among performance, in this step, represent precise design choices; the predominance of a sub-factor on another one is determined every single time by the designer, after considerations about:

- the final destination of the environment in which the building component will work;
- the final user;
- environmental loads and in-use conditions;
- etc.

All the evaluation grids are characterized by the fact that the neutral value is associated to the performance class in reference conditions; adopting and combining increasing or decreasing values is then possible to obtain the Estimated Service Life by the use of Factor method.

Hovde [1998] stated that there is a strong need for further evaluation of this method. He underlined the necessity of input data both for the quantification of Reference Service Life (RSL) as well as for the different factors in the equation. He pointed out the need of a more comprehensive evaluation of Factor method, including possibilities of quantitative description of the RSL and the factors, according to the general requirements for Service Life prediction methods, such as the requirements given in the introduction of this report. Moreover he gave a brief discussion of the following items that ought to be further evaluated:

- Estimation of the reference Service Life (RSL);
- Important factors;
- Necessary number and type of factors;
- Use of the factors in an equation;
- Reasonable span of the values of the different factors;
- Relative importance of the factors;
- Uncertainty of the factors;
- Factor dependency on material or component to be evaluated;
- Important considerations for practical use.

2.1 A Methodological Procedure Proposal for Defining a Grid

The system of equations that rules the Service Life Estimation is both a second order mathematic problem (the result at time t depends on the result at time t-1) and a bad conditioned system (which means that for little variations in input data there could be relevant variations in output) and so reliability and accuracy cannot be both achieved with the same entity.

In designing a factor method is important, as stated above, to avoid subjectivity and get an acceptable reliability and precision needed in results for the specific application. This means that for maintenance programming or for LCA and LCC evaluations a precision of one or two months over a Working Life of 25 years is not necessary. The consequence of this need is the development line of the method: it should be strong and reliable, despite of an extreme precision.

Another important issue for designing a factor method is to keep it easy to use and free of excessive bureaucracy. In order to achieve this target, a factor method should be designed needing input data already available and used in the design process. This could be done thanks to a basic research programme which gets the RSL value of the building component in a defined context, studying the degradation causes and finding the relationship between degradation – performance decay and basic

aspects (concerning factors from A to F) already known (used by designers, contractors, public administration, maintenance planners, real estate, etc.).

In the paragraphs below, guidelines in finding factors, sub-factors and their values are proposed.

2.1.1 Factor A – Quality of Component

Factor A could be assessed with simple tests on properties of basic material or of the whole building component that portray the sensibility of the material or of the building component in relation to the agent or aspect, which has been found as the most influent for the studied component's Service Life thanks to a basic experimental research programme.
For instance, in case of reinforced concrete structures two simple parameters concerning the material are used to characterize and study their durability: water – cement rate and compression resistance.
Basic research focuses on finding the relationship between w/c and freeze – thaw resistance, CO_2 penetration resistance, Cl^- penetration resistance or other chemical agents that lead the degradation evolution in the specific context.

2.1.2 Factor B – Design Level

Design level could be assessed considering three main aspects:

- cross section's dimensioning and designing (that could be assessed with simple tests on single characteristics):
  - thickness of layers (e.g. cover's thickness in reinforced concrete structures or painting's thickness in steel structures or base coat's thickness in ETICS);
  - dimensioning of joints, number of fixings (e.g. in ETICS), etc.;
  - different configurations of constraints (in cross section);
- design of building details (some could be assessed with simple specific tests, some thanks to interviews of panels of experts, some others with reference to database collecting data from inspections on existing buildings and information from maintenance managers):
  - risk of non-continuous protection against agents in critical points (e.g. structural joints);
  - use of special components and elements (e.g. profiles, components for connections, etc.);
  - increase in ageing and agents intensity due to specific configuration;
  - different configurations of constraints (at boundaries);
- influence of design of building details of other components on the durability of the studied building component (again simple specific tests, interviews of panels of experts, reference to database):
  - modification of microclimate (e.g. modification of driving rain on the façade, modification of shadows, etc.);
  - modification of stresses due to un-designed constraints.

2.1.3 Factor C – Work Execution Level

Work execution level could be assessed considering the respect of the construction plan relative to four main aspects:

- storage of materials in construction site;
- curing time and conditions;
- laying method;
- environmental conditions during construction.

2.1.4 Factor D – Indoor Environment

Indoor environment conditions critic for durability usually concern:

- condensation aspects and so relative humidity (for all kind of buildings): in this case the factor D could be assessed with a small set of parameters got with simulation by use of HMT (heat and moisture transfer) calculation methods with input data (moisture storage functions, thermal conductivity water content dependent, liquid water absorption and diffusion coefficients, etc.) get by characterizing the different materials in the building component; mold growth risk too could be assessed with specific tests on the finishing materials;

- storage of chemical products in industrial buildings: this aspect could be assessed with specific tests considering resistance and reaction to the chemical agent in the context;

- stress due to strain or vibrations of the structure: this aspect could be evaluated with suited fatigue cycles for internal partition kits too (not only for load bearing walls).

2.1.5 Factor E – Outdoor Environment

The influence of an outdoor environment different from the one reproduced by the experimental exposure could be taken into account analyzing the environmental data (climatic, concerning chemical pollution, or other agents too) and their "distance" from the experimental conditions. First of all a climatic context completely different from the tested one cannot be assessed modifying the experimentally determined RSL with factor E, but another experimental exposure should be set. The climatic data analysis should so consider the ageing phases in context in comparison to the ageing cycles reproduced in accelerated tests and set a proportion (number of cycles in real context per year on number of cycles per year in reference context reproduced with accelerated tests) and so define a scale in ageing conditions.

The same comparison method could be used in analyzing components subjected to degradation due to chemical agents, but in this case accelerated cycles cannot be set: suited test useful for measuring the sensitivity to that chemical agent could be used to build up a scale.

2.1.6 Factor F – In-use Conditions

In-use conditions usually concern impacts, perforations, vibrations of the structure due to the users and vandalism; a direct assessment of in-use conditions so is not possible and Reference condition (see ISO 15686-8) is absence of impacts, perforation, etc.

In order to correct the value of RSL, the factor F could be so determined according to the following procedure: a suited number of specimens is subject to a number of hard body impacts sufficient for providing a performance decay (measured with other tests suited for surveying performances) which overcomes the performance limit (end of Service Life). Then the decrease in Service Life due to in-use conditions different from reference ones is taken into account assessing the risk of the critical event in a defined context thanks to a stochastic evaluation on frequency of that critical event in a set of buildings collected in a durability database. The database should divide the study cases into classes of risk of critical event – frequency of critical event and each class could be assessd by one factor.

2.1.7 Factor G – Maintenance Level

The extension of Service Life provided by maintenance could be determined by tests too, depending on maintenance strategy programmed for the building component. In determining the values of other factors, the reference conditions should be chosen "as medium as possible", in order to reduce the transport error in transforming the RSL into ESL. In case of Factor G instead, considering absence of maintenance work as reference condition could be useful due to the fact that:

- the typology of maintenance is not known and fixed for a defined kind or class of building component and so deciding the frequency of maintenance (for each strategy) to be considered as reference is hard;

- expressing maintenance in terms of extension of Service Life could be useful in assessing the maintenance costs and convenience;

- accelerated tests without maintenance have to be performed in order to gain the complete degradation and performance decay curve.

2.1.7.1 Maintenance after failure (components with very high reliability at life time - for not bistable components, that doesn't pass suddenly from a working to a not working situation): on the aged sample, when the limit performance has been overcome, a maintenance work is executed and the ageing cycles go on until end of Service Life (overcoming of limit performances) is reached again. The rate expressed by the value in years of the extended Service Life after maintenance (multiplied for the foreseen number of economical acceptable maintenance works) over the value of RSL without maintenance determines the value of Factor G for this maintenance strategy.

2.1.7.2 Threshold preventive maintenance typologies (for the substitution at a constant age or at constant time steps during Service Life period – can be used for components with high reliability at life time i.e. for bistable components, that pass suddenly from functioning to not functioning situation): this type of maintenance could be studied with accelerated tests only if the exact value of years for accelerated ageing cycle has been determined with a previous exposure. Then a maintenance work can be performed at a fixed number of cycles and so the Factor G can be determined through the proportion between the Service Life of component with maintenance and the Reference Service Life without maintenance. The influence on durability of this kind of maintenance could be assessed thanks to databases too (but if data concerning costs and type of maintenance works is available, data concerning performances levels is more difficult to be collected).

2.1.7.3 Maintenance under condition (reparation and substitution maintenance works after inspections, with planned frequency, with the partial or total failure observation for components with low reliability at life time i.e. for not bistable components): during accelerated tests a maintenance work is performed each time that the performance limit is overcome and the value of Factor G is determined as the rate between Service Life with maintenance (considering an economically acceptable and sustainable number of maintenance works) and Reference Service Life without maintenance.

2.2 An example of Creating a Factors' Grid: The Application on ETICS

In the table below an example of the structure of a factors' grid specific for a building component is presented. The studied case is ETICS in environmental context of Milan.

The presented grid is only a first step in defining sub-factors classes. Future work will concern assigning the exact value to each sub-factor and the weight, in each context, of each factor on the whole ESL. This means that for ETICS several contexts of use and solicitation (i.e. maximum four classes according to ISO 15686-7 and EOTA Guidance Document 003) will bet set and a collection of Reference Service Lives and suited grids will be provided.

Table 1. Grid for a Factor method suited for ETICS in Milan context (or similar climates)

A	CE marking of products	Yes				No			
	ETA	Yes				No			
	Water absorption over 24h [kg/m^2] [ETAG 004]	known				unknown			
		W< 0,5	0,5 ≤ W ≤ 1	W > 1					
	Kind of base coat	Resin added 95% ≤ PVC ≤ 98 %		Resin added PVC > 98 %		Only cement mortar			
	Insulator material	EPS 100	EPS 120	XPS		Min. Wool		Wood Fiber	Other
	Fixing accessories	Yes				No			
	Finishing kind	Acrylic paint PVC 45 2 cycles	Acrylic paint PVC 60 2 cycles	Acrylic paint PVC 45 1 cycle	Acrylic paint PVC 60 1 cycle	Vynilic paint PVC 45 2 cycles	Vynilic paint PVC 60 2 cycles	Finishing coat acrylic binder	Finishing coat vynilic binder
B	**Base coat thickness**	t < 3 mm		3 mm ≤ t ≤ 4 mm		t > 4 mm			
	Mechanical fixings	Dimensioned considering wind load				Not dimensioned (1 for insulator panel)			
	Dilatation joints	No				Max every 200 m^2			
	Insulator storage time in construction site	Limited				Long			
	T[°C] during laying	T < 5 C°		5 C° ≤ T ≤ 30 C°		T > 30 C°			
	Substrate kind	New one				Old one			
	RH of substrate	RH ≤ 80%				RH > 80%			
	Substrate planarity	Yes (Δ ≤ 7 mm)				No (Δ > 7 mm)			
	Mechanical fixing scheme	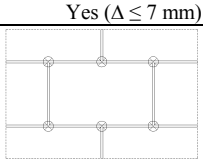 Type A				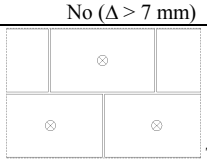 Type B			
	Laying team	Specialized				Not specialized			
	Laying according to construction plan	Yes				No			
D	**Indoor RH**	RH ≤ 65 %				RH > 65%			
E	**Climatic zone (Guidance Document 003 EOTA)**	A		B		C		Special conditions	
	Finishing color	Bright (α = 0,3)		Medium (α = 0,5)		Dark (α = 0,9)			
	Rain class	High		Medium		Low			
	Wind load zone	Zone 9	Zone 8	Zone 7	Zone 6	Zone 5	Zone 4	Zone 3	Zone 2	Zone 1
	Ground rugosity	Class A		Class B		Class C		Class D	
	Pollution	High		Medium		Low			
F	**Foreseen impacts**	Yes				No			
G	**Access for maintenance**	Yes				No			
	Maintenance level	High		Medium		Low			

3 CONCLUDING REMARKS

As reported in the general comments of ISO 15686 standards, Factor method brings together consideration of each of the variables that is likely to affect Service Life. It can be used to make a systematic assessment even when reference conditions do not fully match the anticipated conditions of use. Its use can bring together the experience of designers, observations, intentions of managers, and manufacturers' assurances as well as data from test houses.

Factor method does not provide an assurance of a Service Life: it merely gives an empirical esteem based on the available information. It is different from a fully developed prediction of Service Life, which will ideally provide the Reference Service Life for a factored estimate.

The activity undertaken by Durability of Building Component Group at Politecnico of Milano is finalized to improve Factor method proposed by ISO 15686, in order to control its great limit: the subjectivity. This can be done by the use of evaluating grids which can drive the user in obtaining the correct value of each factor.

The methodological procedure described has been applied to the experimental programme for defining Reference Service Life of External Thermal Insulation Composite Systems: thank to the analysis of

the state of the art, the experimental durability tests undertaken in the last two years and different simulation by using a specific software it was then possible to build the factors' grid presented (which has still to be implemented and eventually validated).
The report, starting from a general analysis approach, wants to give an idea of the work necessary to develop (making it more objective and reliable) the methodology proposed by ISO 15686, presenting a contribute to the work itself.

This evaluation grid, together with all the other ones built for other building components, will be inserted inside the Reference Service Life data base, so that the information about durability can be easily shared exploiting the use of internet.

REFERENCES

Bourke, K. & Davies, H. 1997, *Factors affecting Service Life predictions of buildings: a discussion paper,* Laboratory Report - Building Research Establishment, Garston, Watford, UK.

Daniotti, B. & Lupica Spagnolo, S. 2008, *Service Life Prediction Tools for buildings' design and management*, in papers of the conference "11DBMC International Conference on Durability of Building Materials and Components", Istanbul, Turkey.

Daniotti, B. & Lupica Spagnolo, S. & Hans, J. & Chorier, J. 2008, *Service Life Estimation using Reference Service Life Databases and Enhanced Factor Method,* in papers of the conference "11DBMC International Conference on Durability of Building Materials and Components", Istanbul, Turkey.

Daniotti, B. & Paolini, R. 2008, *ETICS experimental programme*, in papers of the conference "11th DBMC", Istanbul, Turkey.

Daniotti, B. & Paolini, R. 2008, *ETICS Performance decay and degradation evolution: laboratory tests results*, in papers of the conference "11th DBMC", Istanbul, Turkey.

Daniotti, B. 2007, *La valutazione della durabilità dei componenti dell'involucro edilizio*, 3rd International congress Ar.Tec, Ancona, Italy.

Daniotti, B. & Lupica Spagnolo, S. 2007, *La gestione del ciclo di vita dei componenti e degli organismi edilizi,* ed. ISTeA, Favignana (TP), Italy.

Daniotti, B. & Lupica Spagnolo, S. 2007, *Service Life prediction for buildings' design to plan a sustainable building maintenance,* in papers of the conference "Sustainable construction, materials and practices", Lisbon, Portugal.

Daniotti, B. 2006, *La valutazione della durabilità di pareti perimetrali verticali non portanti*, Ed. Editecnica, Palermo, Italy.

Daniotti, B. & Paolini, R. 2005, *Durability Design of External Thermal Insulation Composite Systems with Rendering*, in papers of the conference "10th DBMC", Lyon, France.

Daniotti, B. 2005, *La durabilità in edilizia*, CUSL, Milano, Italy.

Hovde, P. J. 1998, *Evaluation of the Factor Method to estimate the Service Life of building components, Materials and Technologies for Sustainable Construction*, CIB World Building Congress, Gävle, Sweden.

Hovde, P.J. & Moser, K. 2004, *Performance Based Methods for Service Life Prediction - State of the Art Reports*, CIB Report - Publication 294.

Maggi, P. N. 2002, *Building Components' Durability, Maintenance Planning and Sustainability*, 9th DBMC, Brisbane, Australia.

Re Cecconi, F. 2004, *Engineering method for Service Life planning: the evolved factor method*, in papers of the conference "CIB World Buiding Congress", Toronto, Canada.

Re Cecconi, F. & Iacono, P. 2005, *Enhancing the Factor Method – Suggestions to Avoid Subjectivity*, in papers of the conference "10th DBMC", Lyon, France.

ETAG 004 – Edition March 2000. *Guideline for European Technical Approval of external thermal insulation composite systems with rendering.*

ISO 15686-1:2000, *Building and constructed assets – Service Life planning: General principles*.

ISO 15686-2:2001, *Building and constructed assets – Service Life planning: Service Life prediction procedures*.
ISO/WD 15686-7:2003, *Building and constructed assets – Service Life planning: Performance Evaluation for Feed-back of Service Life data from practice.*

ISO/WD 15686-8.2:2003, *Building and constructed assets – Service Life planning: Reference Service Life and Service Life estimation.*
UNI 11156:06, *La valutazione della durabilità dei componenti edilizi*.

Service Life Estimation using Reference Service Life Databases and Enhanced Factor Method

Bruno Daniotti [1]
Sonia Lupica Spagnolo [2]

T 41

ABSTRACT

Service Life Prediction to plan optimized maintenance involves the necessity for designers to handle with tools which can allow the definition of Estimated Service Lives of single buildings' components and moreover of buildings themselves: ICT tools to manage service life prediction need Reference Service Life Data Bases. The report deals with the development of tools for the application of enhanced Factor Method through grids to guide users in assigning the values to the factors, avoiding subjectivity. Application of Factorial Method needs the knowledge of Reference Service Lives of building components, starting point of the calculation. That's the reason why, it is fundamental to provide a data collection of reference Service Lives which can help and drive the designer in obtaining the value of Extimated Service Life in each context of application. In collaboration with the C.S.T.B., Research Group on Durability of Building Components of Politecnico di Milano is collecting data coming from researches at Politecnico's itself and from the Italian durability network. The work wants to provide an open database which can be constantly implemented through the auxilium of researchers, owners, designers, manifactures, insurance companies, property asset managers from all over Europe, leaking and driving the insertion thanks to grids of control purposely prepared. Service life management systems are, therefore, analysed from the point of view of the information due to allow designers to manage service life prediction and maintenance planning. Databases will supply the input datas to predict Service Life of each single building component and will be available on internet in order to be a valid tool for designers. The paper reports on methods and tools developed to produce data and information in an easy-to-use form, on the durability of building components about both the quality of the manufacturing processes and the service life of products.

KEYWORDS

Database, tools, prediction, design, management.

[1] Politecnico di Milano, BEST Department, Milan, Italy, 20133, piazza Leonardo Da Vinci, 32, Phone +39 02 23996002, bruno.daniotti@polimi.it
[2] Politecnico di Milano, BEST Department, Milan, Italy, 20133, piazza Leonardo Da Vinci, 32, Phone +39 0223996002, sonia.lupica@polimi.it

1 INTRODUCTION

The Reference service life data is the information that includes the reference service life and any qualitative or quantitative data describing the validity of the reference service life.

As reported on the standard proposal ISO 15686-8, which provides guidance on the provision, selection and formatting of reference service life data and on the application of this data for the purposes of calculating estimated service life using the Factor method, a RSL and the appurtenant reference in-use conditions, together with additional required or useful information concerning the RSL, form a set of RSL data. A set of RSL data should be formatted into a RSL data record.

This International Standard provides guidance on RSL issues and a means of determining the ESL through application of the Factor method. The guidance for reference service life is structured into discussions regarding:
- provision of RSL data utilizing existing general data (see 4.2);
- selection of RSL data or general data (see 4.3);
- formatting of general data into RSL data records (see 4.4).

Manufacturers of building and construction products are usually in possession of considerable knowledge concerning the service life and durability of their products. However, such information is only occasionally made public, typically in product declarations, other documents, company websites and/or databases. Use of this International Standard is expected to motivate manufacturers to compile their knowledge and provide service life data following the guidelines and requirements stated in the proposal itself [ISO-DIS 15686-8: 2007].

The evaluation of service life, according to international ISO and national UNI standards, can be made following some different methods porposed. Politecnico di Milano is developing these methods, looking in particular an implementation of the Performance Based Approach in the construction industry, specifically in the design and management stages.

Analysing service life management systems form the point of view of the information due to allow designers to manage service life prediction and maintenance planning, Politecnico di Milano is structuring a Reference Service Life Data Bases thanks also to the Italian research durability network; that's the input needed by ICT tools to manage service life prediction in order to plan a sustainable building maintenance.

2 THE COLLABORATION WITH CSTB: THE FRENCH-ITALIAN DATABASE FOR RSL

In collaboration with the CSTB – Scientific and Technical Centre for the Building Industry, Durability of Building Components Group of Politecnico di Milano is going to collect data coming from all researches untertaken in the last 10 years in order to create a French-Italian database of reference Service Lives of building components. in order.

The aim is to to make available to designers, real estate and manifactures all data collected, giving them the possibility to apply methods described in ISO 15686 standards, and in particular the Factor one, for calculating Estimated Service Life.

To minimize the subjectivity of Factor method, ad hoc grids will be created which will drive users in choosing the right values of each factor according to the context conditions in which building components are placed.

These grids, obviously, can't avoid the subjectivity in calculating Service Life, but they move it in the moment of grid creation: that' why grids should be built by building sector experienced people, such as manufacturers themselves.

2.1 The French database

Currently, CSTB has already predisposed a Reference Service Life database, which is available on the web (see www.duree-de-vie-batiment.fr) and which becomes a very important tool to:
- exchage and collect data deriving from different providers of data, such as manufacturers of building and construction products, researchers, national assessment bodies and technical approval organizations, database holders;
- elaboration of evaluating and driving grids to determine each the seven factors needed by the Factor method (see table below).

Table 1. Factors used applying the Factor method.

AGENTS	REMARKABLE FACTORS		
Agent related to the inherent quality characteristics	A	Quality of components	Manufacture, storage, transport, materials, protective coatings (factory-applied)
	B	Design level	Incorporation, sheltering by rest of structure
	C	Work execution level	Site management, level of workmanship, climatic conditions during execution of the work
Environment	D	Indoor environment	Aggressiveness of environment, ventilation, condensation
	E	Outdoor environment	Elevation of the building, microenvironment conditions, traffic emissions, weathering factors
Operation conditions	F	In-use conditions	Mechanical impact, category of users, wear and tear
	G	Maintenance level	Quality and frequency of maintenance, accessibility for maintenance

An example of the layout provided by French database is given below and it shows how with a user-friendly grid it is possible to select the context conditions of designing for determining Estimated Service Life.

Caractéristiques de la Grille Couverture en petits élements terre cuite
Famille : Superstructure, Catégorie : Toitures, Sous Catégorie : Couvertures

Modes de défaillance: [Liste des modes de défaillances associés à la grille]

	Facteurs	Niveaux des facteurs respectif				
A	Géométrie	Emboitement		Glissement	Plate	Canal
	masse surfacique	ms [kg/m²]< 25	25 < ms [kg/m²] < 35	35 < ms [kg/m²] < 45		ms [kg/m²] > 45
B	Hauteur de l'ouvrage	Bâtiment très haut		Bâtiment haut		Bâtiment bas
	Complexité de la toiture	Toiture complexe			Toiture simple	
	Ecran sous toiture	absence d'écran			présence d'écran	
	Orientation de la toiture	Nord		Est - Ouest		Sud
	Valeur de la pente	p < 0,30	0,70 < p < 0,90	0,30 < p < 0,50	0,50 < p < 0,70	p > 0,90
	Type de fixation de tuiles	Aucune fixation		Fixation par clou	Fixation par crochet	
	Densité de fixation	1/6		1/3	1/2	
C	respect des pentes prescrites DTU	NON			OUI	
D	Non Applicable	Non Applicable				
E	Zone de vent considérée	Zone 4	Zone 3	Zone 2	Zone 1	
	Rugosité du terrain	Catégorie de terrain 0	Catégorie de terrain II	Catégorie de terrain III a	Catégorie de terrain III b	Catégorie de terrain IV
	Effet de site	Avec effet de site		Sans effet de site particulier		
F	Impact des accès successifs	Présence d'équipements en toiture			Pas d'équipement en toiture	
G	Fréquence des nettoyages	Jamais			Régulière	

Figure 1. Example of the grid for assigning factors.

Complétez la grille pour votre donnée
Grille de référence : Superstructure>Toitures>Couvertures>Couverture en petits élements terre cuite

	Facteurs	Niveaux des facteurs respectif				
A	Géométrie	Emboitement		Glissement	Plate	Canal
	masse surfacique	ms [kg/m²]< 25	25 < ms [kg/m²] < 35	35 < ms [kg/m²] < 45	ms [kg/m²] > 45	
B	Hauteur de l'ouvrage	Bâtiment très haut		Bâtiment haut	Bâtiment bas	
	Complexité de la toiture	Toiture complexe		Toiture simple		
	Ecran sous toiture	absence d'écran		présence d'écran		
	Orientation de la toiture	Nord	Est - Ouest		Sud	
	Valeur de la pente	p < 0,30	0,70 < p < 0,90	0,30 < p < 0,50	0,50 < p < 0,70	p > 0,90
	Type de fixation de tuiles	Aucune fixation		Fixation par clou	Fixation par crochet	
	Densité de fixation	1/6		1/3	1/2	
C	respect des pentes prescrites DTU	NON		OUI		
D	Non Applicable	Non Applicable				
E	Zone de vent considérée	Zone 4	Zone 3	Zone 2	Zone 1	
	Rugosité du terrain	Catégorie de terrain 0	Catégorie de terrain II	Catégorie de terrain III a	Catégorie de terrain III b	Catégorie de terrain IV
	Effet de site	Avec effet de site		Sans effet de site particulier		
F	Impact des accès successifs	Présence d'équipements en toiture		Pas d'équipement en toiture		
G	Fréquence des nettoyages	Jamais		Régulière		

Figure 2. Example of the selection for assigning factors.

2.2 The Italian contribution

Thanks to the cooperation among six Italian research units, Service Life prediction tools will take the input data from a set of the national regionalized information sources, a Reference Service Life Database, contemplating also a performance evaluation for feedback of Service Life data from practice, with an agreed European international structure (in conformity with ISO 15686).

The six research units of as many Italian university centres involved are Politecnico di Milano, Politecnico di Torino, University of Naples, University of Palermo, University of Brescia and University of Catania.

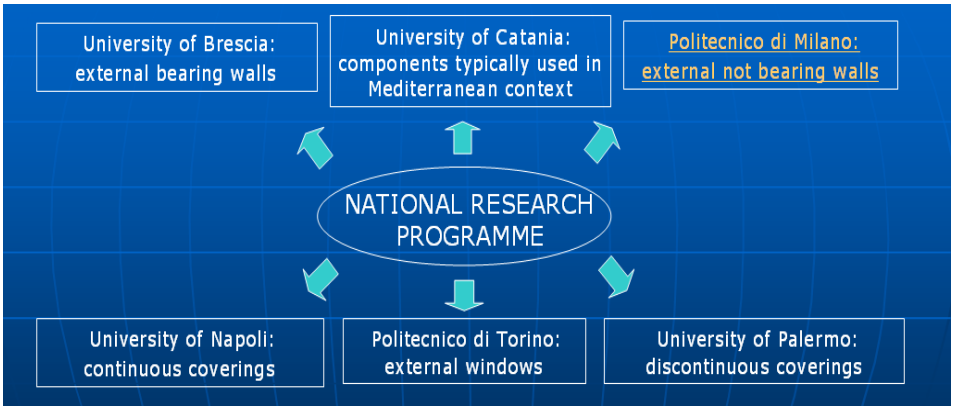

Figure 3. Italian research network for durability.

Using Factor method Politecnico di Milano is structuring a service life data collection of opaque vertical and horizontal enclosures taking into consideration different climatic contests; it is a collection of Reference Service Life values for different technical solutions among opaque vertical and horizontal enclosures, such as:

- traditional walls (double boarding of hollow and semi-hollow bricks with heat insulation interposed);
- externally thermal insulated walls;
- ceilings;
- enclosures typical of the Mediterranean contest.

Initially, the problem to solve is to defined the range of the study established, including identification or specification of essential data, depending on the aim and ambition of the SLP and on the level of existing knowledge of the component.

Two extreme ranges are as follows:
a) specific study: this is intended to focus on a rather specific application of the component tested in terms of service environment and usage with a specified set of performance requirements;
b) general study: this is intended to cover a broad application of the component tested in terms of service environment and usage with an unspecified or a loosely specified set of performance requirements. The aim is to establish performance-over-time functions for the performance characteristics chosen in the whole range of applications.

2.3 Ways of providing and selecting Reference Service Life data

The standard proposal ISO 15686-8 provides also a guidance to the providers of data on how to structure and format general data into RSL data, which have to be selected in order to be correctly applied for the evaluation of Estimated Service Life using Factor method.

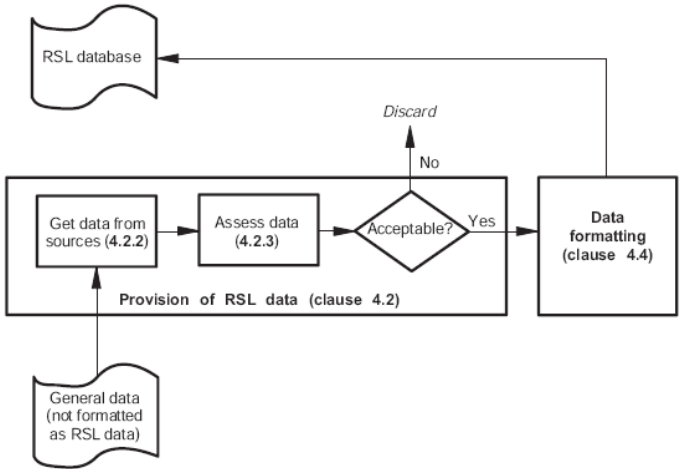

Figure 4. The process of providing RSL data.

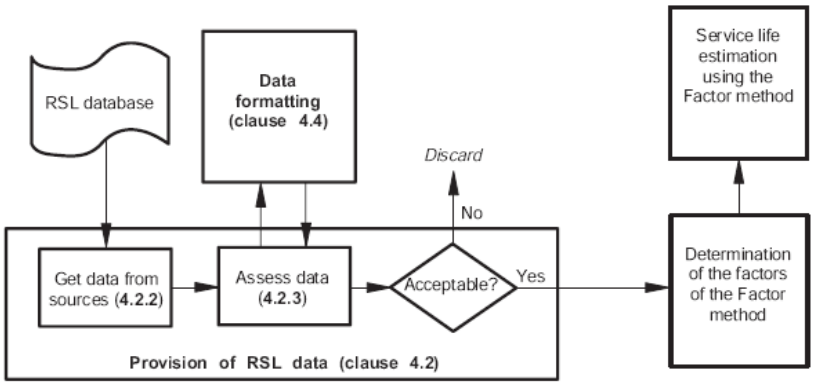

Figure 5. The process of selecting RSL data.

2.4 Enhanced Factor method

Durabity of Building Components Group has also developed the Factor method defining some criteria in order to make as more objective and scientifically validated as possible values given to each single factor. In fact, the Factor method provided by ISO 15686 is a very simple method for evaluating service life: thanks to seven deterministic factors, this method tries to model aleatory phenomena, such as climatic agents. That's the reason why the scientific community has showed the necessity to improve the method, through two ways to proceed.
As a consequence, DBCG suggests a probabilistic approach and uses the same equation proposed by ISO standard, but treating factors as aleatory variables. The proposal is based on the use of triangular distributions of ISO factors, adopting Montecarlo method for solving the equation. Aleatory variables' use describes better the complexity of decay and provides both the Service Life and an estreem of data's reliability: it is possible to obtain a evaluation of duration with precise probabilistic guarantees.

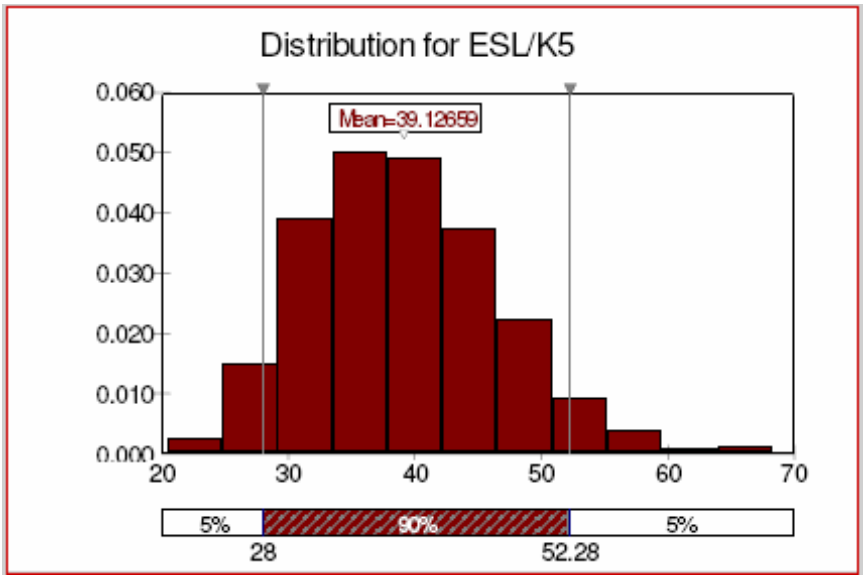

Figure 5. Enhanced Factor method: probabilistic (triangular) input for factors.

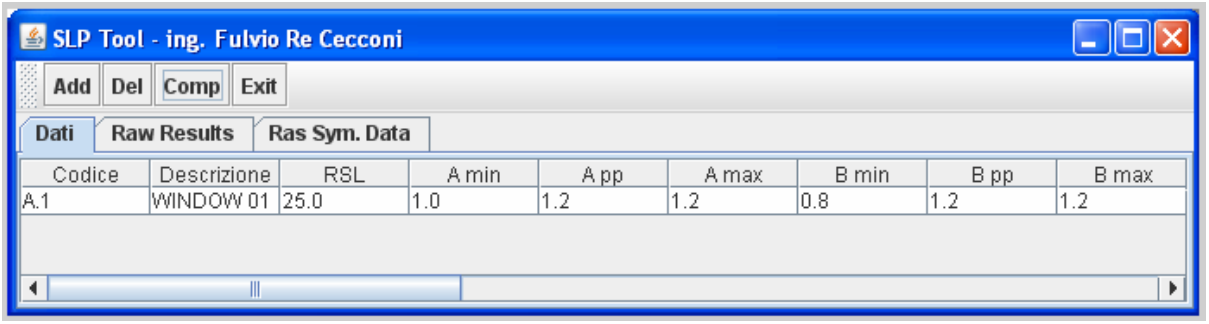

Figure 6. Software SLP Tool to apply Enhanced Factor method.

REFERENCES

Alaimo, G. & Accurso, F. 2006, *La stima dell'affidabilità del coperture discontinue*, Ed. Ediltecnica, Palermo.

Alaimo, G. 2006, *Valutazione sperimentale della durabilità di coperture discontinue. Un'applicazione al pannello sandwich*, Ed. Ediltecnica, Palermo.

Caponetto, R. 2006, *La valutazione del decadimento prestazionale di componenti tipici del contesto mediterraneo*, Ed. Ediltecnica, Palermo.

Daniotti, B. 2005, *La durabilità in edilizia*, CUSL, Milano.

Daniotti, B. 2006, *La valutazione della durabilità di pareti perimetrali verticali non portanti*, Ed. Editecnica, Palermo.

Daniotti, B. 2007, La valutazione della durabilità dei compoenti dell'involucro edilizio, 3rd International congress Ar.Tec, Ancona.

Daniotti, B. & Lupica Spagnolo, S. 2007, *La gestione del ciclo di vita dei componenti e degli organismi edilizi*, ed. ISTeA, Favignana (TP).

Daniotti, B. & Lupica Spagnolo, S. 2007, *Service life prediction for buildings' design to plan a sustainable building maintenance*, in papers of the conference "Sustainable construction, materials and practices", Lisbon.

Morra, L. 2006, *La valutazione di durabilità degli infissi esterni e delle pitture murali in esterno*, Ed. Ediltecnica, Palermo.

Nicolella, M. 2006, *La durabilità delle coperture continue*, Ed. Ediltecnica, Palermo.

Re Cecconi, F. 2004, *Engineering method for service life planning: the evolved factor method*, in papers of the conference "CIB World Buiding Congress", Toronto.

Re Cecconi, F. & Iacono, P. 2005, *Enhancing the Factor Method – Suggestions to Avoid Subjectivity*", in papers of the conference "10th DBMC", Lyon.

ISO 15686-1:2000, *Building and constructed assets – Service life planning: General principles*.

ISO 15686-2:2001, *Building and constructed assets – Service life planning: Service life prediction procedures*.
ISO-DIS 15686-8:2007**,** *Buildings and constructed assets - Service life planning: Reference service life and service life estimation.*

UNI 11156:06, *La valutazione della durabilità dei componenti edilizi*.

French National Service Life Information Platform

Julien Hans [1]
Julien Chorier [1]
Jean-Luc Chevalier [1]
Sonia Lupica [2]

T 41

ABSTRACT

At the beginning of the 20th century, about 90% of the cost of a building was attributable to the structure and the enveloppe. According to the good durability of the component contributing to the structure, it is understandable that we were designing building for 70 or 100 years without the same need of knowing the service life of the components as knowing its mechanical resistance.
New performances are today measured and taken into account during the design to fullfill among others, acoustic, fire safety or thermal insulation requirement.
But new requirements have to be thinked ahead. Today, up to 75% of the cost of a building is allocated to equipments and indoor fittings. Most of the time these components have to be replaced during the service life of the building, and the economical impact on the life cycle cost are significant: for 1 euros spent in the construction phase of an office building, 5 can be spend to maintain and manage it during 30 years! [Tupamaki, 2005]
The Environmental assessment of a building using Environmental Product Declaration is also required to estimate the service life of the components.
Thus, service life is on the point to become a very usefull data for building design and facility management according to the sustainable development principles [ISO SC17, 2007]. The aim of this paper is to present a platform for service life planning. www.durée-de-vie-batiement.fr . It's a french tool for the moment, but we intend to propose it at an international level to optimize its interest.
A collaboration between contracting authorities, architects, research offices, manufacturers and entrepreneurs has been established to develop this collaborative tool, a plateform to collect Reference Service Life (compatible with the ISO series of standard 15686). It proposes an organization of knowledge in grids in which are stored and indexed the essential informations, to estimate the service life of construction components and to evaluate the factors impacting building durability (quality of materials, quality of the implementation, environment, users, maintenance…).

KEYWORDS

Reference Service life, Service life planning, database, Factor method, ISO 15686

[1] CSTB / Scientific and Technical Centre for the Building Industry, Energy Health Environment Department, Grenoble, France, Phone +334.76.76.25.89, Fax +334.76.76.25.60, julien.hans@cstb.fr
[2] Politecnico di Milano, BEST Department, Milan, Italy, 20133, piazza Leonardo Da Vinci, 32, Phone +39 0223996002, sonia.lupica@polimi.it

1 INTRODUCTION

Buildings have always been built to last "for a long time". Houses have a patrimonial value, while office buildingsmay acquire, sometimes, an historic value. Since actors have diversified, the building action has become the result of a relatively prompt transaction: an owner orders a work to a contractor in order to obtain function more or less precisely defined. The building's owner is interested in its exploitation and therefore in the future stages of its history. The need addresses the perenity of the performances, materialized through the setting up of legal guarantees (decennial in France). A way to match the requirements related to these guarantees, can be to produce results of accelerated ageing tests applied to building materials and components. Moreover, the European Construction Product Directive underlines that the essential requirements which products must confer to the work must be satisfied "for an economically reasonable Working Life".

In the last few years, the need to respect the principles of this development, as well as the new economic models (life cycle cost, **Private Finance Initiative** (PFI) "Public-Private Partnerships" (PPP)) have changed the expectation related to the "durability" of construction works, and introduces the "service life planning" process. The whole life cycle of the building becomes a trading object, while protocols and consensual assessment ans decision aid tools (references, methodologies, databases, technical and economic guarantees) become essential.

Some more focused demands for service life data appear in different practical procedures.: typical service life are required in the environmental product declarations (EPD). The service life data of the components can be asked for in the contract in the frame of a private public partnership (PPP), which generally goes beyond legal decennial guarantee. Service life data should be attached to a performance in the energy diagnosis that will soon become compulsory for real estate transactions. In the energy saving certificates as well such data are needed These certificates allow validation of energy savings due to additional actions, such as reinforcement of insulation, change of energy supply product, …The energy unit used in the certificates is the kWh of final energy needed summed up and updated on the entire product's service life.

2 PRESENTATION

This plateform allows to organize and to share in a dynamic manner the knowledge concerning building components' Service Life.

The web address is: http://www.duree-de-vie.batiment.fr

First of all, the aim of the platform is to established a bridge between durability specialist and final users of service life data. For this reason, it first gives the possibility to create specific grids for each family of building components:

The specific grids for every family of building components will be established in accordance with the ISO 15686-8 [ISO SC14, 2007], to associate a "script" of ageing to every defined service life data for each component.. The following factors will be taken into consideration :

- A- Quality of materials and components
- B- Design level
- C- Work execution level
- D- Indoor environment
- E- Outdoor environment
- F- in-user conditions
- G- Maintenance level

For every grid created, reference service life data can be stored, by using the range of parameters which is provided by the corresponding grid.
Of course all the gathered data can the be read by all the user of the platform.

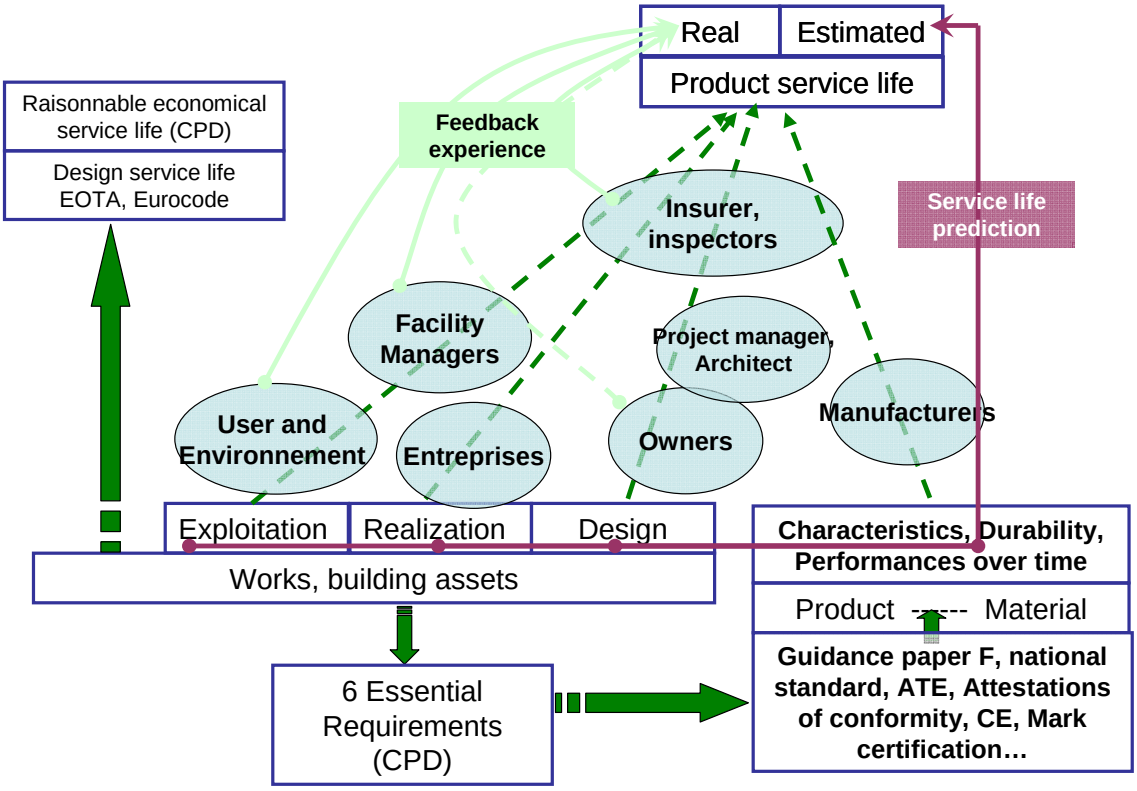

Figure 1. Impact of stakeholders on service life of building products, ability of each stakeholders to capitalize Reference service life. [HANS, 2006]

2.1 Creation of grids for factors conditioning Service Life

The first database's function is to allow the creation of grid for any building components, In these grids it is possible to take into consideration all factors impacting on building components' Service Life (materials, design level, inside and outside environment, in use condition, mechanical, thermal loading, etc.). The ISO 15686 part 8 standard developped within the ISO TC 59-SC14"Building and constructed assets – Service life planning" [ISO SC17, 2007] suggests to use seven factors (from A to G), as listed in [Table 1].

The creation of grids takes place in the following way:

- The first step consists in defining the component to study and the materials it is made of (generic window, or more specifically window wood, PVC window, window Aluminium);
- The second stage consists in identifying the possible damaging scenarios for this kind of component which the grid must permit to characterize. That's why it is necessary to lead a functional analysis and/or an analysis of the failure scenario of the component;
- The third stage has for object to define the grid of building component's service life and to create the different influencing factors and the level of this influence.

Table 1. Conditions to take into consideration for evaluating Service Life.

AGENTS	REMARKABLE FACTORS		
Agent related to the inherent quality characteristics	A	Quality of components	Manufacture, storage, transport, materials, protective coatings (factory-applied)
	B	Design level	Incorporation, sheltering by rest of structure
	C	Work execution level	Site management, level of workmanship, climatic conditions during execution of the work
Environment	D	Indoor environment	Aggressiveness of environment, ventilation, condensation
	E	Outdoor environment	Elevation of the building, microenvironment conditions, traffic emissions, weathering factors
Operation conditions	F	In-use conditions	Mechanical impact, category of users, wear and tear
	G	Maintenance level	Quality and frequency of maintenance, accessibility for maintenance

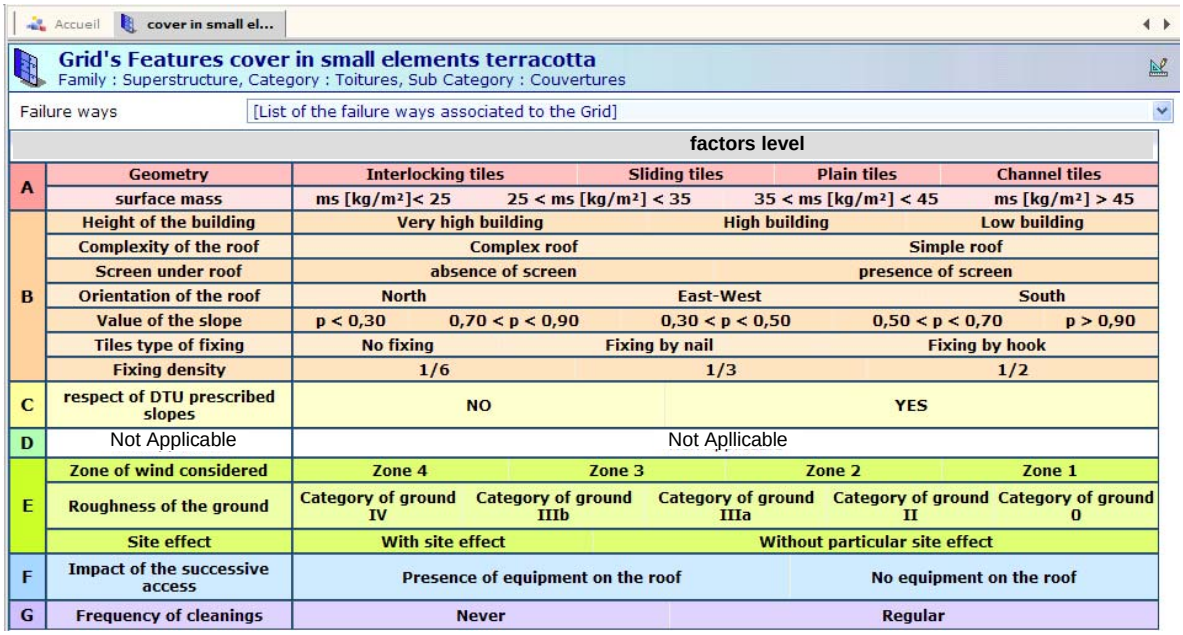

Figure 2. Illustration of possible grid for building components' Service Life (ex: roof covered with small clay tiles)

2.2 Collection of building components' Service Life data

Every Service Life data stored for a building component can be referenced while assigning it a range of values for determining each factors in the corresponding grid and for characterizing its specificities 'Fig. 3'.

Other information are associated to Service Life data:

- The format of Service Life value distribution (deterministic, range, asymmetric range, Gaussian distribution, etc.), see'Fig. 4'.

- The quality of the data: this information allow to determine data's reliability, important especially for merging all data. The quality of the data is related to the data source. If it acts of a test it is related to the type of test on which it is based, see 'Tab.2'

- Further information, such as :

- Year
- Place
- Bibliographic references
- Reason of the damaging
- Further observations

A	Geometry	Interlocking tiles	Sliding tiles	Plain tiles	Channel tiles
	surface mass	ms [kg/m²]< 25	25 < ms [kg/m²] < 35	35 < ms [kg/m²] < 45	ms [kg/m²] > 45
B	Height of the building	Very high building	High building	Low building	
	Complexity of the roof	Complex roof	Simple roof		
	Screen under roof	absence of screen	presence of screen		
	Orientation of the roof	North	East-West	South	
	Value of the slope	p < 0,30	0,70 < p < 0,90	0,30 < p < 0,50	0,50 < p < 0,70	p > 0,90
	Tiles type of fixing	No fixing	Fixing by nail	Fixing by hook	
	Fixing density	1/6	1/3	1/2	
C	respect of DTU prescribed slopes	NO	YES		
D	Not Applicable	Not Apllicable			
E	Zone of wind considered	Zone 4	Zone 3	Zone 2	Zone 1
	Roughness of the ground	Category of ground IV	Category of ground IIIb	Category of ground IIIa	Category of ground II	Category of ground 0
	Site effect	With site effect	Without particular site effect		
F	Impact of the successive access	Presence of equipment on the roof	No equipment on the roof		
G	Frequency of cleanings	Never	Regular		

Figure 3. Selection of factors level characterizing the ageing scenario of one reference service life

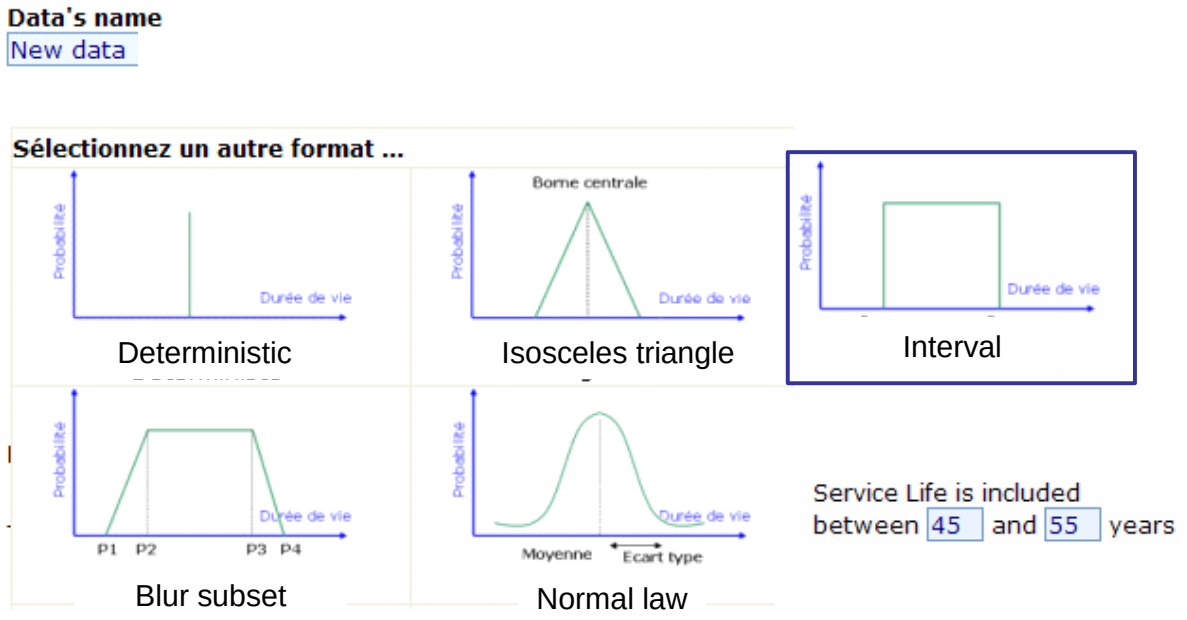

Figure 4. Formats of Service Life data value

It is important to define the data benchmark.

The capitalized data will have to enable us to limit the component Service Life. It is indeed necessary to born Service Life boundary and to know that it lies between 20 years (the most unfavourable case)

and 50 years (the most favorable case) for a failure mode. Intermediate data we will allow us to approximate our case of study. For example to reduce the interval at 25-35 years.

Table 2. A life tests comparison of the constructive entities. [Talon, 2006]

Tests	Scale	Interests	Limits
Exposure on the ground (long duration)	Material Products	real climatic Conditions	**(1)** Uncertainties on the climatic conditions (nature, intensity, frequency). **(2)** Extrapolation with other products or other sites difficult.
Inspection of the buildings (long duration)	Materials products buildings	**(1)** Material /Produces /real Building **(2)** Weaker experimentation cost	**(1)** climatic conditions and of use not measured . **(2)** Problems of censure. **(3)** Extrapolation with other constructive entities or other sites difficult. **(4)** Conditions of maintenance sometimes badly known.
Exposition in experimental buildings (long duration)	Materials products buildings	**(1)** real climatic conditions. **(2)** Knowledge of the total behavior.	**(1)** Uncertainties on the climatic conditions. **(2)** Extrapolation with other constructive entities or other sites difficult.
Exposure in service (long duration)	products buildings	**(1)** Produced / real Building. **(2)** climatic conditions and of use real **(3)** Knowledge of the total behavior. **(4)** weaker experimentation cost.	**(1)** Many uncertainties on the climatic conditions and of use. **(2)** Extrapolation with other constructive entities or other sites difficult.
Exposure of short accelerated duration	Materials products	**(1)** Control of the climatic conditions. **(2)** Time and reduced cost of experimentation.	Possible inaccuracy at the time of the passage to the real time.
Exposure in service of short duration	Products	**(1)** climatic Conditions and of use real. **(2)** Time and reduced cost of experimentation.	**(1)** Many uncertainties on the climatic conditions and of use. **(2)** Extrapolation with other constructive entities or other sites difficult.

For that it is necessary to determine :

- a number of relevant data per failure mode,

The number of data capitalized by failure mode will be related two parameters:

- homogeneity of the Service Life to reach the failure. More they will be near, less there will need data to obtain our kit of reference;
- More the failure mode is frequent more we will retain data.

It is necessary to study the impact of the various factors over the Service Life per failure mode. Indeed, if the impact of the factor is weak it will not be essential to vary the factor in the benchark data. On the contrary if the impact of the factor is important over the Service Life it will be necessary to vary the factor.

- a relevant choice of factors level selection to identify the representative extreme cases, see 'Fig. 5'.

The representative extreme cases are not case where all the factors are at the maximum or the least. Indeed, these extreme cases do not represent reality (red line on the 'Fig. 5'). It is necessary to make a small preliminary study to determine which case would be most unfavourable while remaining possible. This case is represented in green on the 'Fig. 5'.

- an identification of available data sources.

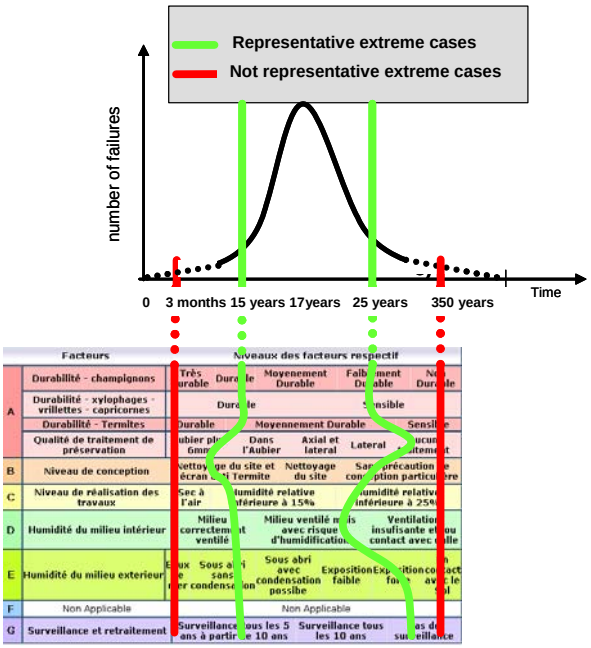

Figure 5. Identification of the representative extreme cases

To help us to make this study it can be interesting to set up an experimental plan.

2.3 Consultation of reference Service Life

Once these data capitalized in the platform, the originators will find there the Service Life which the investors could ask them. The managers of works will be able to draw information relating to maintenance there. The platform will be able for example to make it possible to check that the foreseeable Service Life of a constructive solution is adapted to the destination of the work, with its economic model.
The database allows the consultation of Service Life stored, in order to estimate Service Life of a component in similar conditions.
Three types of possible studies:

- Systems of prediction starting from the play of factors of the study;
- Decision-making aid starting from the play of some factors and the DDV concerned;
- Information starting from the play of factors of the study.

CONCLUSION

Components Service Life is an essential data to conceive and manage buildings. Creating a tool to capitalize and share information is needed for the knowledge of construction products Service Life. It

is required by the "French national service life information platform", financed by the French ministry for housing and carried out by the CSTB.
To go further in the capitalization of the data, an international extension of the platform is in project. It is carried out by Politecnico di Milano which works on Service Life Estimation using Reference Service Life Databases and Enhanced Factor Method [DANIOTTI, 2008].

REFERENCES

ISO/TC 59/SC 17 , 2007, *Sustainability in Building Construction — General Principles*

ISO TC 59/SC 14 N 315, 2007, *Buildings and constructed assets — Service life planning — Part 8: Reference service life and service life estimation*

Foliente G., Wang X., Wang C.H., 2005 'Reliability-based asset management of timber utility poles', CSIRO, 10 DBMC conference LYON.

Hans J., 2006, *French Guide for taking into account of service life in building industry*, FFB report

Bell, D. 1973, *The Coming of Post-Industrial Society*, Basic Books, New York.

Tupamaki O. , 2005, '*Total LCC and Probabilistics*', 11th Joint CIB International Symposium 13-16 June, Helsinki FI.

Talon A., 2006, *Évaluation des scénarii de dégradation des produits de construction*, UNIVERSITE BLAISE PASCAL – CLERMONT II - CSTB

Daniotti, B. & Lupica, S. 2008, *Service Life Estimation using Reference Service Life Databases and Enhanced Factor Method*, in papers of the conference "11 DBMC International Conference on Durability of Building Materials and Components", Istanbul, Turkey.

11DBMC International Conference on Durability of Building Materials and Components
ISTANBUL, Turkey 11-14 May 2008

Quantification of Façade Defects Using Photogrammetry within the *BuildingsLife* System

Pedro Vaz Paulo [1]
F. A. Branco [2]
Jorge de Brito [3]

T 41

ABSTRACT

In several studies on buildings pathology, the main objective is to define and characterize the observed defects and its quantification. However, in major cases, the success of these actions depends upon the observer's procedures and subjective interpretation. To establish a regular and unique information database, independent of the inspector's experience, it is important to focus on the treatment of this non-homogenous data collection in order to be able to make universal comparisons. This paper shows a study related to Buildings Management, which is a part of a PhD research project at Instituto Superior Técnico, Technical University of Lisbon - Portugal. The investigation defines a methodology to quantify the different existent defects (with independent parameters, such as area, length, location and orientation) in a building façade such as cracks in mortar, cracks in paint, paint flaking and mortar spalling, using photogrammetry images to avoid inspection errors based on personal interpretations or estimations. The photogrammetric process has the capability to use manual, semi-automatic and automatic measurement techniques, which were applied in more than 300 Portuguese buildings with an average age of 70 / 80 years. The orthophoto image is used in the web system *Buildings Life* (www.buildingslife.com) and it is being developed according to ISO 15686 which allows the characterization of the different phases such as analysis of the building, inspection, register and samples information, as well as validation model and results. This paper also describes the different types of defects and their quantification in façade buildings that occurred along the service life time related with maintenance interventions.

KEYWORDS

Photogrammetry, Service life, Building defects, Buildings management.

[1] Instituto Superior Técnico, Technical University of Lisbon, Civil Engineering. Research Assistant, Lisbon, Portugal, Phone +351 218 418 444, ppaulo@civil.ist.utl.pt
[2] Instituto Superior Técnico, Technical University of Lisbon, Civil Engineering. Head Professor, Lisbon, Portugal, Phone +351 218 418 444, fbranco@civil.ist.utl.pt
[3] Instituto Superior Técnico, Technical University of Lisbon, Civil Engineering. Associate Professor, Lisbon, Portugal, Phone +351 218 418 444, jb@civil.ist.utl.pt

1 INTRODUCTION

In the last years the principal intent of the investigators had been to predict the service life and durability of materials or constructive elements applied in buildings, railways, bridges, etc to optimize all the existing costs *Life Cycle Assessment (LCA)* before, during and after the construction [ISO 1997]. It will also give important information to the contractor, owner and designer, and will assure a better construction and durability. Due to this, the PhD thesis "Building management - BuildingsLife" was developed at Instituto Superior Técnico, Technical University of Lisbon - Portugal.

2 BULDINGSLIFE SYSTEM

The BuildingsLife architecture is based on ISO 15686 Buildings and Constructed Assets – Service Life Planning with different packs: desktop, external loads, building, survey checklist, defects, surveying, maintenance, prototype applications, settings, reports and degradation models. The BuildingsLife system can be accessed by internet, after login and password. The principal goals are:

- to help the owner on the management of his buildings indicating the best choice (temporal instant and appropriate technique) for maintenance;
- to help the designer defining the better constructive solutions and materials for the owner needs applied in known exterior load, such as, ambiental and environmental conditions;
- to establish a database of defects, building information and the best techniques to repair them and the costs involved;
- to classify the degradation states of different constructive elements;
- to estimate degradation probabilities of different constructive elements applied in different exterior loads;
- to define estimated degradation models (EDM) for buildings [Jernberg et al. 2004];
- to establish procedures to buildings survey;
- to predict the building maintenance with the parameters defined by the owner and according to Multi-Criteria Decision-Making (MCDM) in order to support their decisions.

To reach these objectives, different methods have been developed to assure that information surveys, done by different professionals, were uniform and produced equal results. This paper presents the PhotoMeasure prototype application to quantify any measurable defect over an orthoimage façade.

3 DESCRIPTON OF THE METHOD

The photogrammetric modelling technique is an interactive tool that allows the user to build a geometric model of an architectural façade based on a set of photographs. The technique is convenient, efficient, and robust and it allows the exploitation of the geometric structures common in architecture. The prototype implementation of this modelling technique is called *PhotoMeasure* (Fig.1).

The technique is powerful because it solves directly the architectural dimensions of the façade: the length of the walls, the width of the doors and windows, areas of mortar defects and the lengths of cracks.

As a result, the quantification defects problem becomes simpler through some orders of computational complexity and, more important: in the criteria analysis it's the only way to avoid surveying errors. This method had a field work and a laboratory phases that will be describe in the following paragraphs.

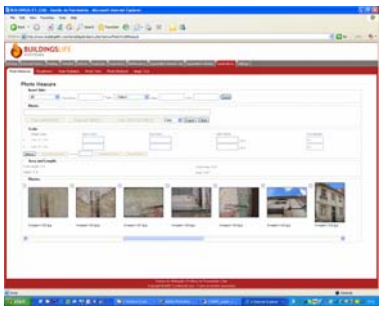

Figure 1. Application *PhotoMeasure* in www.buildingslife.com

4 GEOMETRIC DOCUMENTATION METHODS FOR BUILDINGS

According to Scherer [2002a] there are four principal methods used to compile metric data: traditional manual methods, topography, photogrammetry, and scanning. The choice of one method or another will depend on several factors: end use, accuracy required, budget available, characteristics of the structure to be documented, etc.:

- manual measurements methods determine dimensions by measuring angles and distances. The equipment used is very simple, for example, training. The fieldwork and data collection stages are inevitably time-consuming. Accuracy in locating points is above 8 cm [Scherer 2002 a];
- tacheometric (topographical) methods, which require specialized equipment, are based on three-dimensional (X,Y,Z) determination and coordination of specific points of an object in order to establish its geometry. Accuracy in locating points using the total station is generally above one centimetre [Scherer 2002 a];
- photogrammetric methods apply the classical techniques and methods of close-range photogrammetry. One of the great advantages of photogrammetry, compared to other techniques, is the short period of time spent measuring the object. Another feature is that it is performed without being in contact with the object. The accuracy of these methods goes from 1 mm (highly accurate methods) to 5 cm (simple photogrammetric methods) [Gardiol 2002];
- scanning methods have become popular recently due to the commercial availability of laser scanners, which automatically and very rapidly (1000 points/second) measure the angles and the distances from point to point. Accuracy in the locations of the points is between 5 mm and 5 m. The main disadvantage of these methods is the high cost of the equipments [Scherer 2002 a].

The choose method is influence by the precision need. For documentation for analysis of buildings and surveying artefacts (materials defects) 3 mm to 1 cm, for preservation of historic buildings and monuments, archaeology 1 cm to 2 cm, for architectural surveying, as built documentation 2 cm to 5 cm and for facility management 3 cm to 10 cm [Scherer 2002 b]. Thus, the photogrammetric method was choice to obtain the orthophoto façades images.

5 FIELD WORK

The fieldwork phase is further divided into orientation and scaling stage and photography stage. Close range photogrammetry is a technique for obtaining geometric information, e.g. position, size and shape of any object. There are two different strategies for image processing [Grussenmeyer 2002]:

- Single images, when the shape, the attitude of the façade surface in space (digital surface model – DSM) is known but the details on this surface, such as, blistering paint, cracking paint, cracking mortar, spalling mortar, etc. are not.

- Stereographic processing, when the building's geometry can't be defined with one image 2D. In this case the best way to characterize the façade is a 3D view with at least 2 images, a pair of "stereo images" with a stereo base (distance between the cameras).
- Bundle restitution, in cases that one single stereo pair is insufficient to reconstruct a façade building (frequently is a complex geometry building).

In this study all the façades images were processed in single method. The point of taking photos is that each point to be determined can be intersected by at least two rays with horizontal, vertical or oblique photos. The camera has fixed one point in the middle and at the far end of the façade (Fig.2). Approximately 45.5% of the building samples analysed had a maximum distance (street width) of object (façade) about 5 and 10 meters which result a difficult work to obtain correct photographs.

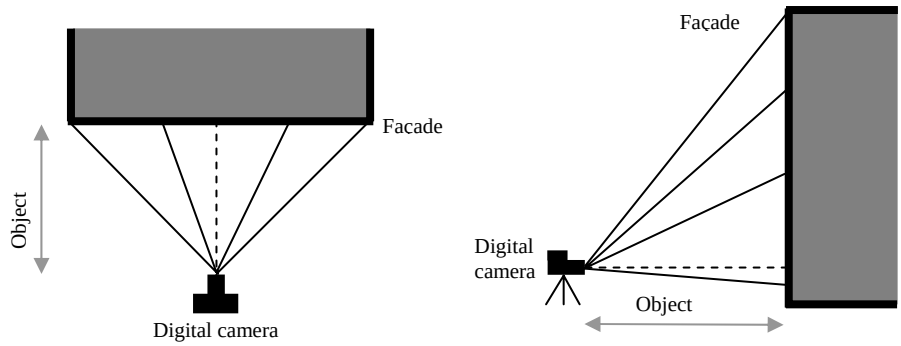

Figure 2. Position of digital camera.

Façade Alignment and Geometry
True position in space (alignment) and the scale of the models are performed as follows:

- to define vertical lines. If the building doesn't have any vertical elements (normally windows and sills are crucial in this work) it is necessary to use the plumb lines in order to define the direction of the Z axis in the absolute orientation process. The plumb lines should be suspended from any projecting element on the walls of the building. The length of the plumb lines will depend on the height of the construction to be surveyed, but should be as long as possible;
- to measure distances. Marks are made in the plumb lines at known distances. These should be visible enough to avoid confusion while photographing the building. The precise distance between marks should be known (for example, height and width building), as this is essential to obtain the scale of the model in the absolute orientation phase. Lengths should be proportional to the size of the construction, i.e. they should increase in line with building size [Valontová & Dolansky 2002].

Photographs Capture
Images can be taken with analogical or conventional low-cost digital cameras. If digital cameras are used, they should have focal length constant, they should be sufficiently stable internally, and resolution should be set at the maximum to obtain a good quality photograph on final process. Shots should be taken applying the principals of photography and photogrammetry, taking into account that restitution is carried out by using monoscopic equipment (Fig3.) and more important that,

- photographs should be taken in one single position and should be aligned with the half of the façade;
- overlaps between photographs should be at least 20%;
- the shots should be taken in a way that the photographed object covers most of the photogram surface;
- a large number of photographs should be taken, including general shots and close-range shots of items of interest (blistering or peeling paint), given that the redundancy of images facilitates the detection and elimination of error;

- it is important to eliminate the error caused by the sun light in the photographs of façade and sky.

The equipment used was a Canon G7 digital camera offering SLR-like functionality and high-end features such as fast lenses and external flash capabilities, with 10.0 Megapixels, 6x optical zoom lens with optical Image Stabilizer and SR coating, and DIGIC III and iSAPS with Advanced Noise Reduction and Face Detection AF/AE. The distances were measured using a Laser Distance Measurer – Stanley with an accuracy: ± 6mm at 30m, a range of 0.6m - 30m, and a laser: 650 nm, class IIIA. It was registered the height and the width of each building.

Figure 3. Six photographs, with overlap, of a façade building.

6 LABORATORY WORK

The laboratory phase involves analysing and processing the photographs taken (several commercial software can be used to reconstruct and create the orthophoto façade image). Processing the information requires the execution of two sequential processes:

- alignment photographs: The perspective rays are reconstructed in conditions similar to their formation within the camera. In this phase it is important that there are between the images, at least, 20% overlapping in order to analyse similar points in different photographs (Fig.4);

Figure 4. Interior photograph orientation.

- exterior photograph orientation: In this stage the rays generated in the inner orientation process are positioned, in relation to the ground, in the very same position adopted at the moment of exposure of the photographs. Each photograph is marked with a minimum of 4 points (depends of image complexity) to orientate the image horizontally (2 points) and vertically (2 points) with respective corrections (Fig.5). Exterior orientation includes two operations arranged in sequence known as relative and absolute orientation.

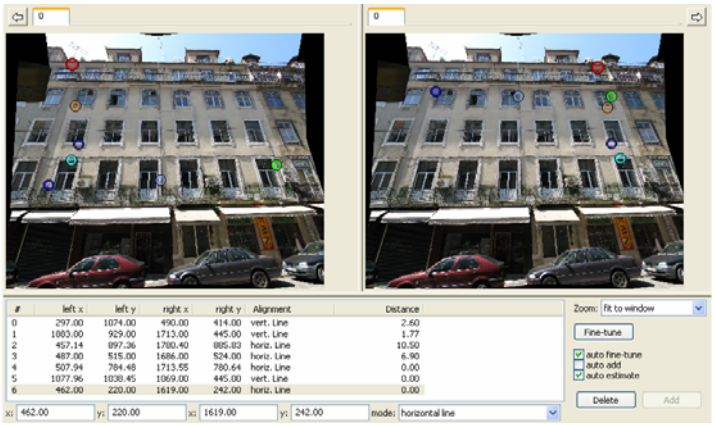

Figure 5. Exterior photograph orientation.

In the end of process the orthophoto image is processed and is necessary verify his quality by the doors, windows or balconies alignment (Fig.6).

Figure 6. At left the façade image reconstructed, at right the orthophoto façade image.

7 BUILDING SAMPLES

The proposed methodology was applied (until this moment) to 302 residential buildings in Lisbon, Portugal. In general, these buildings were constructed in the beginning of 1900, the façade wall is in stone and solid clay bricks with lime or cement mortar and with one or more paint layers of different quimical binders and resins. Although, to analyse the different degradation levels it is important to know and to distinguish the different characteristics of the materials but, this paper will not focus on this important systematization. When the façade orthoimage is placed at www.buildingslife.com server, on PhotoMeasure it's possible to define a horizontal and a vertical scale into image and then, measure any intended area or length. The analysed buildings had an average façade area of 127.2 m^2 and the distribution of buildings according to their area of façade is defined in table1.

Also, it is important to guarantee a high quality image to analyse any detail on it (Fig.7). Normally, these orthophoto images have 2600 x 3000 pixels that are enough to detect spalling mortar area, dirt collection area, fungal area, cracking mortar and paint length. This method has an accuracy of 3 % on any measure.

Table 1. Distribution of façade area.

Level	*Façade area [m2]*	*Percentage of buildings* [%]
1	[0;50]	11.8 %
2	[51;100]	41.8 %
3	[101;150]	25.7 %
4	[151;200]	11.2 %
5	[201;1000]	9.5 %
Average	113.9	

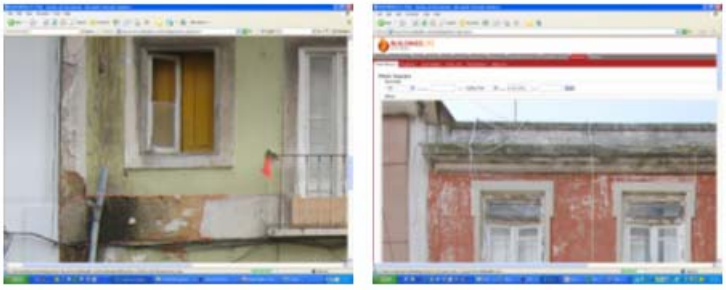

Figure 7. The measured area in PhotoMeasure is defined by a red line.

It is important too, to analyse table 2 and to verify that the average building height is about 12.6 meters, which represents a 4-floor building, and there are few buildings (1.7%) whose height is lower than 6 meters.

Table 2. Distribution of building height.

Level	*Building height [m]*	*Percentage of buildings* [%]
1	[0;6]	1.7 %
2	[6.1;9]	17.2 %
3	[9.1;12]	30.1 %
4	[12.1;15]	20.6 %
5	[15.1;1000]	30.4 %
Average	12.8	

8 RESULTS

The proposed methodology allows us to establish homogeneous orthophoto images and, more important, to quantify façades defects independently of surveyor analysis and interpretation. One of the defects is mortar spalling that was measured in 302 buildings and that obtained an average value of 6.86 m². For all these buildings the average maintenance (the intervention consists of applying the necessary action to bring back the original conditions) is about 28.6 years (Table 3).

To generate the degradation curve for the defect “mortar spalling”, the different values obtained in Photo Measure were aggregated in different degradation levels (Table 4) and the BuldingsLife system calculates the average maintenance for each level. These results are very important to understand the behaviour of buildings along their service life years, defined by the degradation curve in Fig 8.

Table 3. Distribution of maintenance period.

Level	*Maintenance period [years]*	*Percentage of buildings* [%]
1	[0;5]	11.2 %
2	[5.1;15]	32.2 %
3	[15.1;25]	17.4 %
4	[25.1;50]	33.9 %
5	[50.1;1000]	5.3 %
Average	28.6	

Table 4. Distribution of buildings in degradation levels for mortar spalling.

Degradation Level	*No. of buildings*	*Percentage of buildings* [%]	*Average maintenance buildings [years]*
0	151	50 %	9.9
1	62	21 %	27.2
2	57	11 %	36.1
3	11	4 %	45.3
4	15	5 %	48.7
5	6	2 %	56.7

Analysing this curve, we could define two distinct phases [Paulo *et al.* 2008]:

- Phase 1: before 27.2 years the degradation is more slow (end of state 1)
- Phase 2: after 27.2 years the degradation rate increases and between states 3 and 4 shows the maximum value.

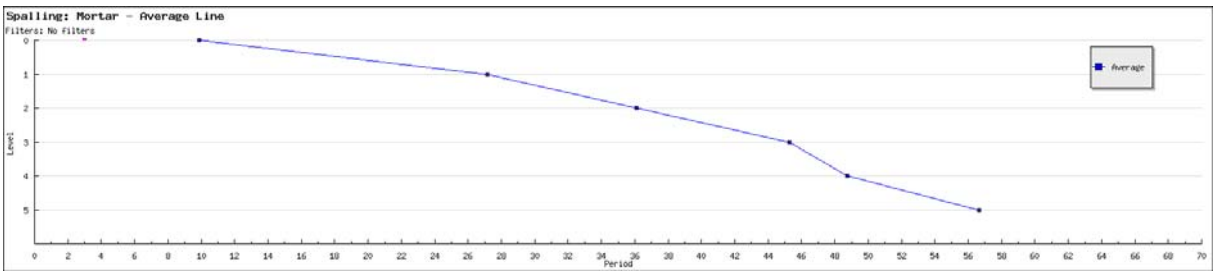

Figure 8. Degradation curve for defect: mortar spalling [Paulo *et al.* 2008].

Thus, at the end of this research project the buldingslife system has to be able to establish several correlations between materials characteristics, environmental and ambient loads and defects quantified on PhotoMeasure, and present degradation model curves and obviously analysed in detail each obtained degradation curve.

REFERENCES

ISO (International Organization for Standardization). 1997. *Environmental management - Life cycle assessment - Principles and framework (ISO 14040)*. Geneve: ISO.

Jernberg, P. *et al.* 2004. *Guide and Bibliography to service Life and Durability Research for Building and Components Part I*, CIB W080 / RILEM TC 140.

Grussenmeyer, P., Hanke, K., Streilein, A. 2002. *Architectural photogrammetry*. Chapter in « *Digital Photogrammetry* », edited by M. KASSER and Y. EGELS, *Taylor & Francis*, pp. 300-339.

M. Scherer, 2002 a. About the synthesis of different methods in surveying, Proceedings of XVIII International Symposium of CIPA, Potsdam, Germany, (pp. 423–429).

M. Scherer, 2002 b. Advantages of the integration of image processing and direct coordinate measurement surveying – development of the system TOTAL, FIIGXXII International Congress, Washington, D.C., U.S.A., April.

Paulo, Pedro Vaz; Branco, F.A.; Brito, Jorge de; 2008. Quantification of Façade Defects Using Photogrammetry within the *BuildingsLife* System, *11DBMC International Conference on Durability of Building Materials and Components, ISTANBUL, Turkey.*

Gardiol, Philips, 2002. External and internal surveying of a construction using low-cost equipment, Proceedings of XVIII International Symposium of CIPA. Postdam, Germany, (pp. 173–176).

M. Valentová, T. Dolanský, 2002. Data collecting for project of Czech historical monuments documentation, Proceedings of XVIII International Symposium of CIPA. Potsdam, Germany, (pp. 55–60).

11DBMC International Conference on Durability of Building Materials and Components
ISTANBUL, Turkey 11-14 May 2008

Homes in Iceland--Flexibility and Service Life Fulfilment of Functional Needs

Björn Marteinsson [1, 2]

T 41

ABSTRACT

The main requirement of any structure, apart from requirements of safety and health aspects, is fulfilling functional needs at an economical cost to the owner/user. As the structure grows older it is required to satisfy other needs than may have been foreseen at the start. The adaptability of the structure and its surroundings to changing requirements, while still satisfying the user's wishes, will largely determine the market price. The interest and willingness of the owner to invest in maintenance and refurbishments is, thus, dependent on this flexibility and may easily be the determining factor for effective service life of the structure. This paper presents the answers from about 250 owners of houses of different ages, located in two different cities in Iceland. The owners were asked to estimate the quality of houses and surroundings, together with maintenance and refurbishment needed to keep the standard desired.

KEYWORDS

Flexibility, Service life, Refurbishment needs

[1] University of Iceland, Faculty of Civil Engineering, Reykjavik, Iceland, Phone +354 xxxxx, Fax xxxx, bjomar@hi.is
[2] Innovation Center of Iceland, 112 Reykjavik, Iceland, Phone +354 522 9000, Fax 522 9111, bjorn.m@nmi.is

1 INTRODUCTION

The economical value of the built environment is very great, and monetary and environmental impact accompanying rebuilding this environment would be a heavy burden for the future. Therefore, it is of general interest to assess if the widely assumed economic service life of buildings, of at least 50 to 60 years, is at risk of being shortened due to obsolesce. This will be the case if the functionality of the buildings does not fulfil the requirements of generations to come, and has earlier been discussed by Aikivuori (1999).

It has sometimes been stated that "design for the future is not a problem as the future takes what it gets" (Deplazes, 2005). However, this will not necessarily be the case, as needs have certainly been changing for some time at a faster rate than often before. People have more possessions or "stuff" than ever, requirements for personal space are increasing, wishes for more spare time are always increasing, and automobiles are no longer a luxury. Even work tends to be done more at home, than has been customary for a long time. All of these changes put extra demands on the functionality of homes and environments of these buildings. For existing houses to be of any value in the future, it may easily be the case that generations to come will wish to modify them to their own requirements, and then in turn have to adapt themselves to the result.

It is therefore considered of interest to evaluate how adaptable the houses already built have been, regarding changes in requirements, and this can be most naturally measured as the performance of these houses, according to the owners'/users' opinions.

2 THE HOUSING INVENTORY AND SAMPLE OF HOUSES IN THE STUDY

This study is a part of a larger research project where the effect of various parameters on degradation and need for maintenance will be considered. The main parameters studied are: climate, age of buildings, type of building materials and earlier maintenance actions.

Information was gathered from two different municipalities: Reykjavik, the capital city of Iceland, and Akureyri, the main city on the north coast of Iceland. Reykjavík has about 110,000 inhabitants and Akureyri, a little more than 15,000. Due to the very different size of the municipalities, the level of strain on inhabitants is different (and even culture varies to some extent, though this is not a research question to be addressed by this paper). The two communities have considerably different climates. Reykjavik has a shore climate, typical of islands: wet, windy and temperate, whereas Akureyri has a more continental climate, with a greater difference between summer and winter temperatures, as well as being drier and less windy. The two places were chosen exactly for this reason, that is, to get a comparison between two different climatic locations.

The research is largely based on a questionnaire. The recipients of the survey where chosen by statistical methods from all house owners in the two municipalities, such that the chosen lot would be statistically representative for the houses in general, regarding type, age, owners and location. It was realised from the beginning, that the response ratio would be low, and the results, therefore, would not be statistically representative for all houses in the municipalities. In total, 1,850 houses were chosen from houses built after 1950 and having a maximum of three flats in each house. The restriction on the sample regarding building period was made because the average age of houses in Iceland is less than 30 years, and it was seen as necessary that at least 10 houses be in each age group of ten years in order to get comparable data amounts between age groups. In earlier works of similar nature it was difficult to get reliable information on refurbishment and maintenance for bigger houses, since no specific person had the responsibility of gathering the necessary information.

It is most customary for Icelanders to own their own homes, and at least until now, it is customary for the owner to personally participate in the maintenance and refurbishment work. The direct cost for

such works is therefore lower than if all workmanship was professionally contracted for, this then resulting in that maintenance in Iceland is often more or less a continuous process.

Homes in Iceland are mainly made of concrete, pored in-situ. Houses built until 1960 are often more than one storey high, and the floor slabs are usually made of concrete. In the period 1960-1990, a single-family home was typically only one storey, but later houses of two or more floor levels increased in popularity. Multi-family houses are always two storeys high or higher. Houses built in the 1950s and 1960s usually all have inner walls of concrete, and these have a load-bearing function. Later, only selected parts of the inner walls are load-bearing, the rest often being made of wood or light, ballast concrete stones. Room size differs somewhat between age groups, but especially in the 1960s and 1970s children's bedrooms are often rather small. At present, residents often wish for an open house plan; the spaces for kitchen, living room and dining room often flowing into each. Indoor-outdoor spaces or openings are also popular, as are glazed-in areas.

2.1 Research Questions and Questionnaire

In the study, the house owners/users were asked to answer a questionnaire with 48 questions regarding their houses and earlier maintenance and refurbishment.
The questions of interest to the paper presented are as follows:

- The building period and type of house
- How long the present owner/user has been living in the house
- What refurbishment actions have been taken to the knowledge of present owner/user
- How does the owner/user classify the performance of the house and its environment, on a scale from 1 (poor) to 5 (excellent)

The questionnaire was posted early spring 2006 and answers have been arriving until recently, although the bulk of them came early winter 2006. So far, 279 answers have arrived, and have been analysed regarding specific parts of the main study. However, this analysis is far from finished. For example, it is not currently known if houses in the two municipalities are comparable, age group for age group, or if the effect of some local traditions makes such comparison difficult. The number of answers is rather limited considering the size of the initial, randomly selected housings sample. The results are, therefore, not necessarily representative for all buildings in the two municipalities, but should give a reasonably good idea about the general situation.

3 RESULTS AND DISCUSSION

A total of 258 house owners gave answers to the questionnaire, which were useful to the study presented. The answers are not equally distributed by age groups or between the two municipalities, and therefore, comparison of results between groups must be done with care.

For more reliable results, it is important to get answers from inhabitants with diverse experiences, that is, both long-term residents and short-term residents. The information on occupation duration, Table 1, shows that the answers represent opinion of both long-term and short-term residents, and the distribution in occupation time spans a very broad range, or often almost the entire service time of each building age category. The average occupation time is near the middle of each span, and it can be said there is a considerable change of users, as the buyers on the market are clearly willing to consider houses in all age groups for residency. Information from real estate agents (not presented here) generally shows that prices of homes in Iceland are less affected by age of the houses, than by condition and location.

The home-owners' answers regarding previously done refurbishment of their homes, or planned actions, are shown in Table 2. The information in the table regards only refurbishment or changes in

layout of the houses or flats. Changes in fixtures and furnishings of kitchens or bathrooms, for example, are not included.

Table 1. Occupation time of present owners in houses from different building periods

Building period	No. of answers	Occupation time (years)			
		Max. possible occupation in buildings	shortest	average	longest
Reykjavik					
1950-59	10	56	2	8.1	14
1960-69	32	46	1	13.9	44
1970-79	20	36	2	19.5	35
1980-89	21	26	1	13.8	25
1990-99	17	16	1	7.8	14
2000-	10	6	1	3.4	6
Akureyri					
1950-59	12	56	7	27.7	50
1960-69	34	46	1	16.4	44
1970-79	28	36	1	15.8	34
1980-89	23	26	2	16.8	26
1990-99	27	16	1	8.2	16
2000-	24	6	1	2.5	6

Table 2. Refurbishment of houses in different age categories: already done or planned

Building period	Refurbishment		
	Already done (%)	Most frequent actions	Planned (%)
Reykjavik			
1950-59	70.0	Inner walls moved or removed	20.0
1960-69	46.9	Inner walls moved or removed	21.9
1970-79	40.0	Inner walls moved or removed	15.0
1980-89	23.8	Inner walls moved and/or house enlarged	23.8
1990-99	11.8	Inner walls moved or removed	11.8
2000-	10.0	Access for handicapped persons	10.0
Akureyri			
1950-59	66.7	Inner walls moved or removed + added insulation	25.0
1960-69	61.8	Inner walls moved or removed	11.8
1970-79	39.3	Inner walls moved and/or house enlarged	14.3
1980-89	26.1	Inner walls moved or removed	13.0
1990-99	22.2	Inner walls moved and/or house enlarged	11.1
2000-	0		4.2

As can be seen from Table 2, extensive refurbishment has already been done on a considerable number of the houses in the oldest age groups, and even more actions are planned. In the newer age groups, a much lower fraction of the houses have been refurbished, which may naturally be taken as an indication that the newer the houses are, the better they fulfil owners' needs. The most frequent refurbishment done is to move or even remove some inner walls. As these walls are often load-bearing, this often means considerable changes to the structural system, and the action is thus often

expensive. The amount of changes made, independent of age of houses, shows how willing owners, both short-term and long-term, are ready to invest in their houses. The houses are, therefore, seen as an economically sound investment by the market. Furthermore, the owner usually highly praises the performance of their house; see Table 3, where usually more than 70 % of houses get a very high mark on both indoor and outdoor performance. It is interesting to note that more houses generally get highest mark on performance in Reykjavik than in Akureyri, but the reason for this is currently unknown.

It may be seen as likely that the greater involvement in refurbishing of the older houses is at least partly responsible for the generally high opinion of performance of older houses. Even outdoor performance of older houses is highly praised, although less than is the case for new houses.
The location of older houses is often regarded by the general public as better, and these are usually more centrally located than newer houses. However, residents have a different insight towards location. Their view may be influenced by difficulties in parking of autos, which are more apparent in older quarters, built when private cars were not so numerous.

Table 3. Performance of buildings and environment, percentages of total in each age group
Performance marks: 1- poor … 5- excellent

Building period	Indoor performance					Outdoor performance				
	1	2	3	4	5	1	2	3	4	5
Reykjavik										
1950-59	0	0	30.0	10.0	60.0	0	0	30.0	30.0	40.0
1960-69	3.2	0	16.1	38.7	41.9	3.2	6.5	19.4	29.0	41.9
1970-79	0	0	15.8	36.8	47.4	0	5.3	10.5	42.1	42.1
1980-89	0	0	23.8	23.8	52.4	0	0	9.5	33.3	57.1
1990-99	0	0	5.9	70.6	23.5	0	0	17.6	35.3	47.1
2000-	0	10.0	0	20.0	70.0	0	0	20.0	30.0	50.0
Akureyri										
1950-59	0	0	33.3	33.3	33.3	0	0	16.7	66.7	16.7
1960-69	0	0	11.8	64.7	23.5	0	0	11.8	67.6	20.6
1970-79	0	0	10.7	57.1	32.1	0	7.1	7.1	53.6	32.1
1980-89	0	0	17.4	47.8	34.8	4.3	4.3	17.4	34.8	39.1
1990-99	0	3.7	7.4	40.7	48.1	0	7.4	11.1	29.6	51.9
2000-	0	0	0	33.3	66.7	0	0	4.2	37.5	58.3

4 CONCLUSIONS

There will always be an interaction between the inhabitants and their houses, as so wittingly said by W. Churchill (1943): “We shape our buildings and afterwards the buildings shape us”.

Requirements for personal space have been, and possibly still are, increasing. However, at the same time, family size has been diminishing, so the total space in older living houses is clearly often sufficient for the modern family. However, the inhabitants have a strong desire to shape their houses to their own needs and are clearly willing to invest in the houses to meet these needs, regardless of how old the house is. The houses perform rather well according to residents and they are also pleased with the outdoor space around the houses. Thus, there are no signs of the houses becoming obsolete with age, and service life will therefore, mostly be decided by technical – economical reasons.

The willingness of the average resident to continuously shape his environment according to his or her needs must be duly regarded in the design of new buildings, and flexibility of buildings must be ensured, so that new buildings will be of value for the future.

ACKNOWLEDGMENTS

The research project presented is funded in part by RANNÍS – the Icelandic Centre for Research and also Íbúðalánasjóður- The State Housing Board, whose financial support is gratefully acknowledged.

REFERENCES

A. M. Aikivuori , A.M. 1999, Critical loss of performance - what fails before durability, *Durability of Building Materials and Components 8*. Edited by M.A. Lacasse and D.J. Vanier, Institute for Research in Construction, Ottawa ON. K1A 0R6, Canada, pp.1369-1376, Vancouver, Canada

Deplazes, A. (editor) 2005, *Constructing architecture: materials processes structures – a handbook*, Birkhäuser, Germany, ISBN-10:3-7643-7189-7

Churchill, W. 1943, House of Commons on 28. October 1943, see The Churchill Centre; http://www.winstonchurchill.org

Information System and Interworking for a Durable Inheritance

Boulekbache Mazouz Hafida [1]

T 41

ABSTRACT

Important problems affect the management of the territory. This one relates in particular to management of the activities and specific information to this management and with human and material resources affected there. In this context, the article suggested aims to describe and to set up a methodology to accordingly improve management of the territories we present two principal parts :
A) a part of methodology, namely the use of systemic to describe and analyze a territory
B) a proposal of tool support to be also left a study of the existing Information Systems ; we apply that to a territory in the north of France (valenciennes with project SIGL) making of a tool of decision-making aid as regards management of the inheritance aims to manage and develop existing space built and not frames in a development prospect durable relates to the whole of the territory. SIGL is thus a conceived Information system in a generic way, in order to facilitate an unquestionable capacity for a transposition on other territories. In addition, the step is based on a participative approach associating the professional partners of the sector. The analysis, the evaluation and the confrontation of the existing approaches made it possible to work out a methodology to manage the territory in a "durable" way

KEYWORDS

Information system, Durability, Decision-making

[1] Valenciennes Technical University, Civil Engrg. Faculty, Valenciennes, France 59370, Phone +00 333 27511865, Fax 333 27511856, Hafida.Boulekbache@univ-valenciennes.fr

1 INTRODUCTION

The managers of the inheritance are confronted with problems which do not cease being important with the increase in housing stock. They must thus manage several related aspects with the good performance of the buildings and equipment of company or community (large surface, hospital, school, town hall, stage…).
To contribute to answer these problems, our work aims the definition of an effective information system. This system includes/understands a structured human organization and tools of assistance to the definition, the exchange and the information management suitable for real management.
In this article, we treat in particular the installation of this communication system dedicated to a durable management of the inheritance, by the professionals of the real estate and its users.

2 MISSIONS AND DESCRIPTIONS OF THE ROLE OF THE MANAGER OF THE REAL INHERITANCE

The managers of the inheritance must play a crucial role for the comfort and the safety of the occupants whose they take care not to disturb the activity. They carry out the maintenance of first level: control and repairing of lighting, plumbing, air-conditioning, doors and windows, furniture… But they are also brought to follow the intervention of outside firms for more specialized work.
Their missions consist with:

2.1 To Take Note:

- to prepare work to be carried out using documents (plane buildings, programs of maintenance…) ;
- to create these documents if they do not exist, on the basis of of the observation and regulation;
- to count the equipment and installations regulated (apparatuses with pressure, production of heat, elevators, hoists, extinguishers, circuits sets fire to, etc) and their instructions of maintenance

- to take note of the instructions of hygiene and safety suitable for the intervention: to make sure of the consignment of the installation (electricity, compressed air, warm water…), to identify the risks related to the maintenance products and tools used, to use the protective gears envisaged (helmet, safety shoes, gloves, glasses, helmet antibruit, respiratory protection…), in particular in the presence of certain substances such as asbestos in the buildings.

2.2 To Control and Diagnose:

- to visually control the state of the walls, ceilings, grounds, doors, windows, roof…
- to carry out operational tests of the equipment: telephone electrical communications and, materials of lighting (socket-outlet, fuses, lamps, switches, engines), equipment of kitchen, plumbing (taps, joints, piping), furniture, etc
- to include/understand the origin of a breakdown and to determine work which you will be able to carry out yourself or which you will have to entrust to a specialized outside firm

2.3 To Give in State: To Make and Do

- essentially to replace the worn or defective parts (fusible, bulbs, joints, taps, locks…), disassembling/reassembly of equipment being generally entrusted to a specialized speaker;
- to manage a store of spare parts and the consumable ones allowing to avoid any stock shortage;
- to follow the intervention of specialized outside firms from a technical point of view.

2.4 To Audit and Return Account:

- to make sure that the equipment given in state functions suitably;

- to fill and sign the card with intervention of the outside firm which attests result of the Service;
- to constitute the file of maintenance allowing to find the whole of the interventions carried out;
- to inform the GMAO (Management of the maintenance computer-assisted) if necessary to give an account of the progress of the work to its department head.

3 PROBLEMS AROUND THE REQUIREMENTS OF THE TRADE OF THE MANAGER OF THE REAL INHERITANCE:

A survey carried out near a certain number of managers of real inheritances (local government agencies, administrations, large companies, airports,…), the description of the principal problems allowed with which they are confronted. We present below the difficulties which affect, directly or indirectly, the organization and the communication related to the actions of maintenance and maintenance of the inheritance Indeed, the manager of the real inheritance must be able of:

- to plan activities very different from/to each other
- to control the diversity of the equipment;
- to supply at the appropriate time and with the need spare parts and consumable;
- to communicate as well with the users of the buildings as with the outside contributors

4 DURABLE MANAGEMENT OF REAL MAINTENANCE

To contribute to answer the problems exposed previously, our objective of treatment and follow-up, by the qualified technical structure, of the estimate and applications for a job carried out by the users of an inheritance, the communication system that we propose makes it possible to ensure an optimal and durable reflexion of the management of the real inheritance. It is elaborate starting from the three following concepts:

- the concept of actor, with which one associates a role and a right of access with information,
- the concept of process of data processing, which describes the successive interventions of the various actors, each one of them enriching information suitable for the treatment and the follow-up by the request,
- the concept of document which gathers in a centralized way information which will be successively indicated.

This system must in addition be supported by a simple and powerful tool for information management, and we propose an application Intranet with this intention.

5 WHAT IS WHAT A DURABLE APPROACH FOR THE MANAGEMENT OF THE REAL INHERITANCE ?

Real technical management is an optimized organization of the elements necessary for the operation and the maintenance of an inheritance, within the framework of definite orientations [PERRET-[1995].

On another plan, concerning the buildings to be built, in particular the problem of the bad definition of the requirements locally, often too fast remains, sometimes neglected. This is reflected on later maintenance, because these users modify their buildings and their envisaged use initially, or maintain them badly. The use of the buildings is also modified in production run, to meet new needs. It is the case for example at the time of the decision to use a room given like a room of files, catch at the end of a certain duration of occupation of the building, and which consequently is not always integrated in the program. This modification satisfies the users, but it is not very probable that this room fulfills the lawful requirements of the safety-fire.

This being, of the tools exist at the present time to help the managers in the achievement of their tasks, in particular of the computer tools.

6 COMPUTER TOOLS : A DURABLE ANSWER

The main aims of the computer tools for the management of the urban inheritance are:
- to provide a decision-making aid exploitation maintenance of the buildings, equipment and networks,
- The software of assistance to the managers of real inheritances is mainly of four different types:
- geographical Information systems (SIG) for the decision-making aid starting from data charted, for a total sight on the scale multisite or a site scale, district, city where of a vaster zone, and for a help with the management and the maintenance of external spaces and elements which compose them (green areas, networks,….),
- management software of the Maintenance Computer-assisted (GMAO) for the assistance with the management and the organization
- the management software Technique of Inheritance Computer-assisted (GTPAO) for the management and/or the assignment of surfaces, the diagnosis of the works,…,
- The tools available on the market integrate several of the functions described above and propose high level graphic functionalities, in particular for the seizure of plans, the calculation of surfaces or the representation in three dimensions.
- Nevertheless, a certain number of managers use yet at the present time only worksheets drawn up on spreadsheet, for the assistance with the management of their receipts and expenditure.

The difficulty for the managers who wish to acquire software tools is to carry out a wise choice, and to carry out a good analysis of their needs as regards patrimonial management, with the possible assistance of a consulting expert. The acquisition of these tools requires investments out of computer material, the recruitment and/or the training of the potential users. In addition, it is necessary to seize the database patrimonial, this long and generating stage being of costs. Thus, a certain number of experiments failed, in particular for lack of investments or organization. This irrefutable fact is all the more regrettable as these investments represent a tiny part of the costs of maintenance and maintenance of a real inheritance.
One will note that the most powerful systems at the present time combine SIG and GTPAO, via “gates Intranet” (or Internet) for the users (users, decision makers) wishing to reach the database patrimonial from their work station.

6.1 System for The Durable Management of The Real Inheritance

Within the framework of this study, we stick to the requests carried out by the users of the buildings near the persons in charge of the engineering services. These requests relate to estimates which the technical structure can establish or make establish by qualified companies, or of the interventions of corrective or preventive maintenance.

Lastly, according to the state of the document (three states: “request carried out by a user”; “request treated by a technical manager”; “completed and filed request”) and its type (three standards: “action of corrective maintenance”; “action of preventive maintenance”; “estimate”), the application classifies it in different and clearly identifiable repertories by the users: “new not yet examined requests”; “estimate in progress”; “actions of corrective maintenance in progress”; “actions of preventive maintenance in progress”; “requests for filed actions of corrective maintenance”, “requests for filed actions of preventive maintenance”, “requests for estimate filed”.

6.2 Protocol of Application

The objective of the "communication System for current real maintenance" being to be able to re-use without having to redefine them each time, of generic information.
He proposes to simplified cards, the access to the various actors of the process of maintenance:

- identification of work to be carried out on a card specifying the name of the applicant and his administrative or geographical membership as well as the date and the type of intervention.
- after validation by the person in charge of the engineering services, work of maintenance is carried out and filed after an update to facilitate the later consultation on the whole of work and the costs that those generated.

7 CONCLUSION

At the present time, important problems affect the management of the real inheritance and the information management which is attached there. In this context, our work aims to define and set up methods and tools for a powerful management of the real inheritances built and not built.
Within the particular framework of this article, we propose an effective communication system based on the one hand on a simple and robust human organization, on the other hand on an application Intranet dedicated to the treatment and the follow-up of the applications for a job and estimates carried out by the users of an inheritance.
This application is reinforced by others, of comparable nature, but dedicated to different uses, such as for example the document management of construction projects new, or with descriptive of a real unit.

REFERENCES

Meier, R.L. & Shen, Q. 1987, *Efficient, Ecologically Balanced Settlement on Estuaries*, Centre for Environmental Design, Research Working Paper No. 2, Uni. of California, Berkely, February.

Ascher F., (1995), « Métapolis ou l'avenir des villes », Editions Odile Jacob, Paris. 278p.

Authier, J.Y., *Réhabilitation et embourgeoisement des quartiers anciens centraux*, éd. Plan Construction et Architecture, 1999.

Dupagne A., Jadin M., Teller J., (1997) « L'espace public de la modernité », Région Wallone DGATLP, col. Etudes et Documents, 141p.

Elliot, A.., (2001) « INDEX, Software for Community Indicators », Criterion Planners/Engineers Inc., www.crit.com

Koolhaas, R., *Une machine qui devient bâtiment*, éd. Lucan Jacques, 1991.

Marcel, O., *Composer le paysage ; constructions et crises de l'espace (1789-1992)*, éd. Champ Vallon, Seyssel, 1989.

Roncayolo, M., *La ville et ses territoires*, éd. Gallimard, Paris, 1999.

Leleu-Merviel,S., *La conception en communication- Méthodologie qualité*, éd. Hermès, Paris, 1997.

Walliser, B., Systèmes et modèles : introduction critique à l'analyse de systèmes, éd. Seuil, Paris, 1977.

11DBMC International Conference on Durability of Building Materials and Components
ISTANBUL, Turkey 11-14 May 2008

Service Life of a Building in Environmental Assessment of Buildings

Appu Haapio [1]
Pertti Viitaniemi [2]

T41

ABSTRACT

The aim of this study is to analyse how the service life of a building should be taken into account in the environmental assessment of buildings. Over the past decade, various building environmental assessment tools have been developed for different needs and purposes. Many of these tools require an estimation of the building's lifetime. However, the service life of a building has not been emphasised within the tools. Therefore, the research results of the service life of a building need to be combined closely with the development process of the building environmental assessment tools.

KEYWORDS

Service life, Environmental assessment, Building

[1] Helsinki University of Technology, Department of Forest Products Technology, P.O.Box 6400, FI-02015 TKK; Finland, Phone: +358 9 4514264, Fax: +358 9 4514259, appu.haapio@tkk.fi
[2] Helsinki University of Technology, Department of Forest Products Technology, P.O.Box 6400, FI-02015 TKK; Finland, Phone: +358 9 4514261, Fax: +358 9 4514259, pertti.viitaniemi@tkk.fi

1 INTRODUCTION

The field of environmental assessment tools, developed for the building sectors, has become a popular research area over the past decade [e.g. Haapio & Viitaniemi 2008a; Peuportier & Putzeys 2005; Todd *et al.* 2001]. Numerous tools have been developed by various institutes and for different purposes. A variety of different tools exist for building products and components, whole buildings, and whole building frameworks. [e.g. Edwards & Bennett 2003; IEA Annex 31 2001]

In addition, the building environmental assessment tools cover different phases of the building's life cycle and take different environmental issues into account [Haapio & Viitaniemi 2008a]. Building environmental assessment tools are not all commensurable. Consequently, the comparison of the results calculated with different tools is difficult, if not impossible. [Haapio & Viitaniemi 2007] The building environmental assessment tools often require an estimation of a building's lifetime. However, the service life of a building has not been emphasised within the tools [Haapio & Viitaniemi 2008a]. And yet, a building may comprise over hundreds of different materials and products, all with different service lives [Kohler & Moffatt 2003].

1.1 Standardisation

The International Organization for Standardization (ISO) and the European Committee for Standardization (CEN) have been active in defining standardised requirements for the environmental assessment of buildings [see Haapio & Viitaniemi 2007]. ISO Technical Committee (TC) 59 *Building construction* and its Subcommittee (SC) 17 *Sustainability in building construction* have prepared standardised requirements for the environmental assessment of buildings. The standardised requirements concerning service life planning are also prepared by the same Technical Committee (TC 59), but by a different Subcommittee (SC 14 *Design life*). The principles for the service life planning of buildings are published in ISO 15686 series *Building and constructed assets – Service life planning* and it consists of the following parts:

- Part 1 (ISO 15686-1:2000): *General principles* [ISO 2000]
- Part 2 (ISO 15686-2:2001): *Service life prediction procedures* [ISO 2001]
- Part 3 (ISO 15686-3:2002): *Performance audits and reviews* [ISO 2007]
- Part 4 (ISO 15686-4): *Data requirements* [ISO 2004] under preparation
- Part 5 (ISO/DIS 15686-5.2): *Life cycle costing* [ISO 2007] under development
- Part 6 (ISO 15686-6:2004): Procedures for considering environmental impacts [ISO 2004]
- Part 7 (ISO 15686-7:2006): Performance evaluation for feedback of service life data from practice [ISO 2007]
- Part 8 (ISO/DIS 15686-8:2006): *Reference service life and service-life estimation* [ISO 2007] under development
- Part 9 (ISO/NP 15686-9): Guide on the inclusion of requirements of service life assessment and service life declaration in product standards [ISO 2007] under development
- Part 10 (ISO/WD 15686-10): *Levels of functional requirements and levels of serviceability – Principles, measurement and use* [ISO 2007] under development.

1.2 Aim of The Study

The aim of this study is to analyse how the service life of a building should be taken into account in the environmental assessment of buildings. Over the past decade, various building environmental assessment tools have been developed for different needs and purposes. Many of these tools require an estimation of the building's lifetime. However, the service life of a building has not been emphasised within the tools.

1.3 Content of The Study

In the first section, the research area, the standards are briefly introduced, the aim of the study is stated, and the content of this study is listed. The second section focuses on forecasting service life. The third section focuses on service life planning in the environmental assessment of buildings, and how it should be taken into account. In the fourth section, the future of service life planning and the environmental assessment of buildings is speculated.

2 FORECASTING SERVICE LIFE

The length of the service life is not precisely known in advance. Due to this, the objective becomes to make '*an appropriately reliable forecast of the service life using available data*'. The forecasting of the service life of a building (or a component) is to assure whether it can be expected to exceed the required design life with adequate reliability. [ISO 2000] Standard ISO 15686-1 gives the following definitions regarding forecasting service life [ISO 2000]:

- **Service life** is 'a period of time after installation during which a building or its parts meets or exceeds the performance requirements'
- **Reference service life** is 'service life that a building or parts of a building would expect (or is predicted to have) in a certain set (reference set) of in-use condition'
- **Predicted service life** is 'service life predicted from recorded performance over time'
- **Estimated service life** is '*service life that a building or parts of a building would be expected to have in a set of specific in-use conditions, calculated by adjusting the reference in-use conditions in terms of materials, design, environment, use and maintenance*'

Forecast service life is based on either predicted service life or estimated service life. The service life prediction procedure is described in ISO 15686-1 clause 8, and detailed in ISO 15686-2. ISO 15686-1 clause 9 provides a method, a factor method, for estimating service life. [ISO 2000, ISO 2001] According to Davies and Wyatt [2004], ideally service life should be predicted according to ISO 15686-1 clause 8, and ISO 15686-2. Where the ideal cannot be achieved, estimations using the factor method, described in ISO 15686-1 clause 9, might be required. A clear distinction between predicted and estimated service life should be made when forecasting service life. [ISO 2000]

2.1 Predicted Service Life

In the predictions of service lives, the evidence from previous use, the knowledge of service lives of similar components, the tests of degradation in specific conditions, and combinations of these, are utilised. In an ideal prediction, service life is expressed as a function of the in-use condition (environmental condition under normal use). There are two methods of testing degradation; long-term exposures and short-term exposure, and normally they are used in combination [ISO 2000, 2001]. Ideally, a service life prediction based on exposure tests provides the reference service life for a factored estimation. [ISO 2000]

2.2 Estimated Service Life

The purpose of the factor approach, according to Davies and Wyatt [2004], is to provide a rough-and-ready means of estimating service life. As stated in ISO 15686-1 [ISO 2000], '*the factor method does not provide an assurance of a service life: it merely gives an empirical estimate based on what information is available*'. The factor method is based on a reference service life and a series of modifying factors. [ISO 2000] These factors are:

- Factor A: Quality of components

- Factor B: Design level
- Factor C: Work execution level
- Factor D: Indoor environment
- Factor E: Outdoor environment
- Factor F: In-use conditions
- Factor G: Maintenance level

The estimated service life of a component can be expressed as a formula, where the reliability of the reference service life figure is critical:

*ESLC = RSLC * factor A * factor B * factor C * factor D * factor E * factor F * factor G*

where ESLC is the estimated service life of a component and RSLC is the reference service life of a component [ISO 2000].

3 CONSIDERING SERVICE LIFE PLANNING IN ENVIRONMENTAL ASSESSMENT OF BUILDINGS

Numerous tools have been developed for the building sector to help decision making and improve the environmental performance of buildings and building stocks. The variety of the tools is wide; LCA based tools, rating systems, technical guidelines, assessment frameworks, checklists and certificates. [e.g. Boonstra & Pettersen 2003; IEA Annex 31 2001] Many of these building environmental assessment tools require an estimation of the building's lifetime. The service life of a building, however, has not been emphasised within the tools. Rather, the service life is taken as given without further analysis [Haapio & Viitaniemi 2008a]. And yet, a single building may comprise over 60 basic materials and circa 2000 separate products, all with different service lives and unique production / repair/ disposal processes. [Kohler & Moffatt 2003]

3.1 Environmental issues within service life planning

Service life planning can be performed for several reasons. The economical and the technical aspects, including safety related issues, are quite obvious reasons. The economical viewpoint has been pointed out quite strongly in ISO 15686-1; General parts: *'Service life planning is a design process which seeks to ensure, as far as possible, that the service life of a building will equal or exceed its design life, while taking into account (and preferably optimizing) the life cycle costs of the building.'* [ISO 2000]

The environmental viewpoint has been taken into consideration in the standards ISO 15686-6 *Procedures for considering environmental impacts*. The standard defines how to assess relative environmental impacts of design options, and furthermore, it identifies the interface between environmental life cycle analysis and service life planning. [ISO 2004] However, the standard does not take a position on the balance between environmental and other aspects. It is suggested in ISO 15686-6 that the environmental assessment of design option should be done parallel with the technical and economical assessments. According to the standard, the environmental assessment allows the design team to include environmental aspects into decision making. [ISO 2004] However, the standard does not make it mandatory to include the environmental aspect into service life planning.

The field of building environmental assessment tools is vast, as mentioned earlier. These tools are specifically for the environmental assessment of buildings. Different tools use different criteria and different indicators to correspond to these criteria in the assessments. Furthermore, the tools take different phases of the building's life cycle into account. [Haapio & Viitaniemi 2007, 2008a]If the tool does not include all the phases of the life cycle, it is difficult to consider the effect of the service life on the results. On the other hand, life cycle assessment (LCA) is highlighted as a technique for assessing environmental aspects and potential impacts of a product in ISO 15686-6 [ISO 2004].

3.2 Maintenance of A Building

During the building's service life, the building needs to be maintained, and some components need to be replaced. The service lives of the components are different. The service life of inaccessible parts should be the same as the service life of a building, but the service life of accessible parts may be shorter [ISO 2000]. If the service life of accessible parts is shorter than the service life of the building, these parts need replacements. As an example, if the design life (intended service life) of a building is 150 years, the suggested design lives are [ISO 2000]:

- 150 years for inaccessible or structural components
- 100 years for components where replacement is expensive or difficult
- 40 years for major replaceable components
- 25 years for building services
- (easy-to-replace components may have design lives of 3 or 6 years)

Maintenance and replacements have environmental impacts. In proactive maintenance, the action is taken in advance – before the damage occurs. In reactive maintenance, the action is taken afterwards – after the damage has occurred. There is a possibility the remaining service life of the components is lost if the replacement is done proactively. If the replacement of the component is done reactively, the component may have damaged its surroundings. The maintenance of these damaged surroundings has economical and environmental consequences.

The time between the needed maintenances and replacements differs between different components, and also, the demands for the maintenances are different. In addition, the quality of the maintenance, i.e. the workmanship, influences the forthcoming maintenances and may reduce the remaining service life. Poor maintenance, or disregarded maintenance, may cause damage elsewhere, and thus influence the whole building. For example, as a consequence of missing out the oil change of a car, the engine of the car may seize up. The repair of the engine is far more expensive than the oil change would have been. Also, wide repair is always more challenging and exposed to further damages.

3.3 Obsolescence

Obsolescence is a condition of being antiquated, or out-of-date. What was modern ten years ago is probably old fashioned today. An obsolete item simply does not meet a condition of the current requirements or expectations. [ISO 2000; Lemer 1996] However, this does not indicate the item is broken or dysfunctional. In other words, the service life of the item is not necessarily over, even if the item is obsolete. Currently, the number of renovations caused by obsolescence is increasing, as the requirements and needs of tenants grow. These renovations have environmental impacts; if the component is replaced before its service life is finished, the remaining service life is wasted. [Haapio & Viitaniemi 2008b] It seems a waste, especially if the replaced building materials and components are not recycled. In a case like this, the environmental viewpoint is often forgotten.

The service life of a building is usually long – decades or even centuries. The service lives of the components vary from a few years up to the service life of the whole building [ISO 2000]. But during the building's long service life, manufacturing processes and products are developed. This causes problems in the maintenance; matching old and new techniques and products does not always go smoothly. Often at least some applications or compromises have to be made. For example, in the older buildings in Finland, the pipes are laid in concrete. If the pipes need renovations, the traditional renovation of the pipes is possible, or the service life of the pipes can be extended by lining the inside of the pipes with a newish technique.

The development of the techniques, processes and products has been overemphasised, and the importance of the implementation of the techniques has been underestimated. The requirements of the occupants have increased tremendously in recent decades, and there is no end in sight. In addition to

these factors, the development of information technology and HPAC set requirements for buildings. It is challenging to adjust these requirements in a sustainable way. These issues need to be taken into consideration in the design process. The focus should be on the development of easily replaceable components since the needs and requirements of the tenants grow and change constantly. The accessibility to the components during the maintenance and the replacement should be considered already in the design phase, in order to minimise the possible damages to the surroundings.

3.4 Experimental Building

To develop the construction processes, the buildings and the maintenance of the buildings, new designs, new products and new techniques are used occasionally. New designs and developments can be tested and studied in experimental buildings. These experimental buildings are important, since sometimes the experience from real construction sites is essential for the development process. Karjalainen [2002], for example, studied multi-story timber apartment buildings as pioneers in the development of timber construction. However, from time to time experimental building is regarded as a financing method. In these projects, nothing is necessarily experimented. These projects detract the reputation of the idea of experimental building.

The knowledge gathered during and after these on-site experiments is not utilised as well as it could be. Most of the knowledge stays with the people working in that particular project – it is not shared with others. The same mistakes might be made more than once. The knowledge gathered from experimental building should be taken to the next level. In order to be able to analyse building processes, solutions and components more thoroughly, at least some of the experimental buildings should be demolished before the end of their service life. Demolition, however, seldom takes place, even though it would provide more intimate knowledge of environmental performance and service life, and their interaction. How building solutions and components perform as part of a building should be studied by analysing them from demountable or demolished buildings.

4 DISCUSSION

Currently, most of the building environmental assessment tools are used towards the end of the design process to evaluate the environmental results. However, the assessment tools are not used simultaneously with the design tools. The later the evaluation of the results in the design process is made, the fewer possibilities it has to influence the design itself. In addition, optimising one structural solution may not be the ideal solution for the building. [Haapio & Viitaniemi 2008b] If the assessment tools and design tools are integrated, the task would be facilitated. Lützkendorf and Lorenz [2006] are expecting it to happen in the future.

The surroundings and the other components affect the component and its service life. The width of the ventilating slot between the wooden cladding and the exterior wall structure, for example, affects the maintenance and the service life of the cladding. When the distance between the wooden cladding and the exterior wall structure is adequate (i.e. the width of the ventilating slot is maximised), the situation can be compared to a fence in the field. On the other hand, when the width of the ventilating slot is miniscule, the wooden cladding acts as part of the exterior wall structure. Another example is the remarkable difference in the condition of the old and new wooden buildings in the town of Porvoo, in Finland. The cladding of the new buildings had to be renovated a few years after the completion. The cladding of the old buildings is in much better condition, even though the buildings are decades old. A controlled thermal leakage through the exterior wall structures could be one of the explanations for the better condition of the old wooden houses. In the new buildings, the thermal leakage through the exterior wall structures is much lower, but the cladding needs renovations more often. Which alternative is better from the economical viewpoint, and which is better from the environmental viewpoint? Which alternative is the best considering health related issues? If the observation time changes from 50 to 100 years, how does it affect the choice?

The service lives of building components, their effect on a building and its service life should be analysed in-depth. Currently, the effect of the service life has not been analysed thoroughly in the environmental assessment of buildings. [Haapio & Viitaniemi 2008b] The building environmental assessment tools often take the service life as given – no further analysis is made. It is not fully recognised how the service lives of the components and a building affect the results of the environmental assessment. Different building environmental assessment tools take different phases of the building's life cycle into account. If the tool does not include all the phases of the life cycle, it is difficult to consider the effect of the service life on the results. There is a need to properly include the service life into the environmental assessment of buildings. Only then, will the integration of the assessment and design tools (suggested by Lützkendorf & Lorenz 2006) maximise the benefits.

ACKNOWLEDGMENTS

The authors wish to thank the Finnish Cultural Foundation and the National Graduate School of Timber Construction and Design (coordinated by University of Oulu) for funding this research.

REFERENCES

Boonstra, C. & Pettersen, TD. 2003, 'Tools for environmental assessment of existing building'. *UNEP Industry and Environment*, **26**[2-3], 80-83.

Davies, H. and Wyatt, D. 2004, 'Forum: Appropriate use of the ISO 15686-1 factor method for durability and service life prediction'. *Building Research & Information*, **32**[6], 552-553.

Edwards, S. & Bennett, P. 2003, 'Construction products and life cycle thinking'. *UNEP Industry and Environment*, **26**[2-3], 57-61.

Haapio, A. & Viitaniemi, P. 2007, 'Environmental criteria and indicators used in environmental assessment of buildings'. Proc. CIB World Building Congress 2007, Cape Town, South Africa, 14-17th May 2007.

Haapio, A. & Viitaniemi, P. 2008a, 'A critical review of building environmental assessment tools'. *Environmental Impact Assessment Review*, Article in Press, doi: 10.1016/j.eiar.2008.01.002

Haapio, A. & Viitaniemi, P. 2008b, 'Environmental effect of structural solutions and building materials to a building'. *Environmental Impact Assessment Review*, Article accepted for publication.

IEA Annex 31, 2001, 'Energy related environmental impact of buildings'. [web page] Accessed Aug, 2007. http://www.annex31.com/.

ISO. 2000, *Buildings and constructed assets – Service life planning – Part 1: General principles.* ISO 15686-1:2000(E).

ISO. 2001, *Buildings and constructed assets – Service life planning – Part 2: Service life prediction procedures.* ISO 15686-2:2001(E).

ISO. 2004, *Buildings and constructed assets – Service life planning – Part 6: Procedures for considering environmental impact.* ISO 15686-6:2004(E).

ISO. 2007, TC 59, SC 14 'Design life, List of standards/projects'. [web page] Accessed Aug 2007. http://www.iso.org/iso/en/CatalogueListPage.CatalogueList?COMMID=1968&scopelist=ALL;

Karjalainen, M. 2002, 'The Finnish multi-story timber apartment buildings as a pioneer in the development of timber construction'. Doctoral Thesis, University of Oulu. [web page] http://herkules.oulu.fi/isbn9514266188/isbn9514266188.pdf. *(In Finnish, summary in English).*

Kohler, N. & Moffatt, S. 2003, 'Life-cycle analysis of the built environment'. *UNEP Industry and Environment*, **26**[2-3], 17-21.

Lemer, AC. 1996, 'Infrastructure obsolescence and design service life'. *Journal of Infrastructure Systems*, **2**[4], 153-161.

Lützkendorf, T. & Lorenz, DP. 2006, 'Using an integrated performance approach in building assessment tools'. *Building Research & Information*, **34**[4], 334-356.

Peuportier, B. & Putzeys, K. 2005, 'PRESCO, WP2 Inter-comparison and Benchmarking of LCA-based Environmental Assessment and Design Tools for Buildings', Final Report. [web page] Accessed Feb 2006. http://www.etn-presco.net/generalinfo/index.html]

Todd, J.A., Crawley, D., Geissle, S. & Lindsey, G. 2001, 'Comparative assessment of environmental performance tools and the role of the Green Building Challenge'. *Building Research & Information*, **29**[5], 324-335.

11DBMC International Conference on Durability of Building Materials and Components
ISTANBUL, Turkey 11-14 May 2008

Whole Life Cycle Costing as a Decision Tool for Use in French Healthcare Facilities

Samer Sliteen [1]
Orlando Catarina [2]

T 41

ABSTRACT

Whole Life Cycle Costing is increasingly becoming an important decision making tool for managers of French Healthcare Facilities. The life cycle of hospitals, analysed in this study, covers the period from construction to deconstruction and as well, the operation and maintenance phase. Over the course of the study on French healthcare facilities, several questions arose: e.g., what does the investment cost of health care facilities represent; in the management of health's building, what does the operation cost of health care facilities represent; which items are important to optimize future operational costs of health care facilities? The data necessary for this study was collected from 5 cases studies of 4 public hospitals and one private hospital. To reduce partially disparities among the cases studied and provide uniform information necessary to a transversal analysis, the investment costs were updated on the basis of the index BT01 to conduct in November 2004. To identify the relationship between operation costs and investment cost/activities an innovation methodology was developed. Some limitations of this research included the fact that the hospitals included in the study were recently constructed and there has not been any additional investment since construction. The study has yielded information on healthcare facility investment costs, and operation-maintenance cost as well as provides key performance indicators and information on benchmarking.

KEYWORDS

Healthcare facilities, Investment cost, Operation and maintenance costs, Whole Life Cycle Costing, Benchmarking

[1] Centre Scientifique et Technique du Bâtiment, University Paris-Est, France, samer.sliteen@cstb.fr , Phone 0033140502950
[2] Centre Scientifique et Technique du Bâtiment, France, orlando.catarina@cstb.fr, Phone 0033140502830

1 INTRODUCTION

The principal aim of the construction of hospitals is to provide healthcare to patients; the Hospital Plans (2007 to 2012) initiated by the French government, consists of a set of measures intended to in offer a new dynamic to the operation of hospital facilities. The principal objectives of this plan of investment are to allow the modernization and the reorganization of healthcare facilities as a means of improving the operation and management of these facilities and rationalising resources to obtain better efficiencies within the healthcare system. The modernization of the hospital sector is not only intended to decrease the overall consumption of energy of these facilities, but also provide changes to every construction related element of such projects such as accruing savings in the design, construction and operation of the facilities.

The complexity of healthcare construction projects requires a systematic planning to carry out heterogeneity (room of patient, cuisine, operating rooms, offices, etc.) and a flexibility of the operation. Indeed, the planning team has to provide the client not only with answers to architectural problems, but also a response to the requirements for technical and economic programs. This requires many different competencies such as those of architects, doctors, nurses, specialized engineers and representatives of the administration. For the project to be successful, these groups must work together during the duration of the project and indeed from the design phase to its commissioning and eventual exploitation ass a healthcare facility.

In France there are 6500 public and private healthcare facilities. Apart from receiving patients, they also accommodate healthcare professionals (persons in charge, frameworks of health, techniques and medico-techniques, biomedical engineers, heads of department and medical teams, etc.) and as well the administrative staff (e.g. hospital director). For this reason, it is important to study the life cycle of these establishments.

As suggested by Boussabaine and Kirkham [2001], 'Whole Life Cycle Costing' (WLCC) is a dynamic and ongoing process that enables the stochastic assessment of the performance of constructed facilities from feasibility to disposal. The WLCC assessment process takes into account the characteristics of the constructed facility, re-usability, sustainability, maintainability and obsolescence as well as the capital, maintenance, operational, finance, residual and disposal costs. The result of this stochastic assessment forms the basis for a series of economic and non-economic performance indicators relating to the various stakeholders interests and objectives.

2 METHODOLOGY

This study deals with the variation in the operation and investment costs to French healthcare facilities. The ISO standard FDIS 15686-5 had been applied to calculate the different costs. It provides techniques and methodologies that facilitate the practical implementation of whole life cycle costing as applied to healthcare facilities in France. Based on the WLCC data, one can estimate the operational costs for the building for each year of its expected life. 'The estimated yearly costs must be discounted to make proper allowance for the time value of money thus enabling comparison of alternatives on a common basis [Flanagan et al. 1989]'. As indicated by Ashworth [1999], the most common measure used to compare alternatives in Life Cycle Costing is the Net Present Value (NPV), although other measures, such as the Equivalent Annual Cost, Payback Period, Return on Investment, and Saving to Investment Ratio, could be also used.

Historically, hospitals have focused on increasing bed capacity and the number of patients treated per day by providing better services and advanced medical technology. But they have not considered strategies related to the building operations nor reflected on the importance of operating non-medical equipment in accruing savings and performance enhancements. The cost of hospital services or their impact on the overall profitability of the healthcare facility has not been widely considered. For

example, factors such as the number of occupied beds in relation to the age of the building, equipment capacity, period of maintenance and replacement has not typically been of importance.

The WLCC has now been applied to the development of healthcare facilities to help make investment decisions at the pre-construction phase of proposed new hospital projects, and to help in the organisation of building maintenance.

A two-step analysis was employed in this study:

1. The collecting data for the year 2004 (French Health Ministry does not hold a database; required information was obtained from the hospitals).
2. The data was then clustered by building maintenance, grounds maintenance, engineering maintenance and utilities.

The input data is representative of the principal operational and maintenance costs incurred in French healthcare facilities, it does not however include cleaning costs.

3 RESEARCH DATA

Certain costs such as water, energy, salaries, occur every year, whereas the level of replacement and maintenance costs depend on the quality of the facility. The research data used in this study are the costs and characteristics that are common to all French healthcare facilities. MAINH [2006] has shown the components that relate to the total service charge and illustrates that the average space of patient rooms in public hospital is more important than the plate form technique but on the contrary in private hospital.

Table 1. Basic Data on hospital size, capacity and related investment, operational and maintenance costs

Establishment	**Public**				**Private**
	Hospital 1	**Hospital 2**	**Hospital 3**	**Hospital 4**	**Hospital 5**
Gross internal floor area (m²) (GIA)	39083	31825	61300	63567	35312
Bed capacity or equivalent	395	320	635	469	271
Gross internal floor area /capacity (m²/ bed)	99	99	97	136	129
Year of construction	1994	1997	1991	2000	1990
% individual room	35%	83%	30%	73%	50%
Investment budget (K€ Net of taxes)	53458	38548	62527	76693	45559
Operation and maintenance budget(k€ net of taxes)	2267	1685	3433	2562	1072

3.1 Investment Costs

The investment cost in this study includes costs for: site and grounds works, structure and substructures, sewerage, water and gas systems, ventilation systems, heating installation, automated transport, medical supply system for medical fluids. It does not take into account such items as biomedical equipment, penalties for delay of execution of construction, replacement costs, or the funding of grand works and causes supporting the future development of the hospital.

The WLCC approach identifies all costs benefits and reduces them to the present value by using typical discounting methods. The appropriate discount rate varies according to the organisation and its choice largely depends on past experience. In this study, investment costs were discounted to a value dated to February 2004 and reported in k€, net of taxes by using index BT01 (i.e. in France, price factor index covering all building activities - base 100 in 1974):

Table 2. Descriptive statistics of the investment cost (€ / m²)

Descriptive	External works/m²GIA	Engineering works/m²GIA	Building/m²GIA	Total Investment/m² GIA (€/m²)
Mean	62.1	444.7	694.6	1201
Standard Deviation	15.5	30.9	92.6	123.2
Sample Variance	320.4	1273.6	11446.	20239
Minimum	43.5	394.7	581.7	1020
Maximum	82.3	478.9	839.7	1368

The following results include outputs from the Excel based WLCC tool. The pie chart shows the distribution of investment costs. It shows that the percentage of costs varies from 5% to 37% and illustrates the importance of both the finishing works and engineering works in respect to overall investment costs. Figures 2 and 3 illustrate that there is no clear relationship between investment costs and the number of beds or the GIA. Furthermore, investment costs relate more closely to the GIA than the equivalent number of beds.

3.2 Operation and Maintenance Costs

The operation-maintenance costs in this study are costs net of taxes for the year 2004 and include the exploitation budget, salaries of personal working on operation and maintenance of the hospital, operation-maintenance contract provided externally, the energy and fluids contract. Items not taken into account include costs of biomedical equipment, cleaning, some works of the parking area, fire safety services, waste removal, medical fluids, the major portion of linen services, and replacement costs.

From the following figures, it is very noticeable that the relationship between the operation-maintenance cost and the number of beds is more evident from that of the GIA. Hence, it may be easier to estimate future operation-maintenance costs based on the number of patient beds. The distribution shows that the engineering and building maintenance costs form more than 50% of the overall operation and maintenance costs; the actual proportion would depend on the kind of technical equipment used at the hospital and the quality of its construction.

3.3 Relationship Between Investment and Operation-Maintenance Costs

The consequence of investment choices made during the planning and design phases will be of great importance to the total future costs of the facility. As suggested by Bjorberg [1996], the calculation of annual costs is a way of evaluating investments versus the consequences of operating and maintaining buildings. All hospitals in the sample set have been in service from less than eleven years. These buildings have not yet begun their replacement cycle for components and equipment as these typically take place primarily between the fifteenth (15-yr) and sixtieth (60-yr) year of the building's life. From Figure 7 it is evident that the correlation between investment costs and operation-maintenance costs of these five cases is not entirely satisfactory, as the linear correlation coefficient is less than 0.5 indicating perhaps only an intermediate degree of correlation.

4 EXAMPLE

The following example of WLCC of Hospital 4 are based on [The Whitestone Building Maintenance and Repair Cost 1999, Facilities Maintenance and Repair Cost Data 13th annual edition 2006] to complete the data, in application of Excel based WLCC and ISO 15686, the hospital has been analysed. The assumed life is 60 years. According to Woodward [1997], errors of five or ten years in the predicted life will not make very much difference to the predicted equivalent costs when the life is fifty to sixty years.

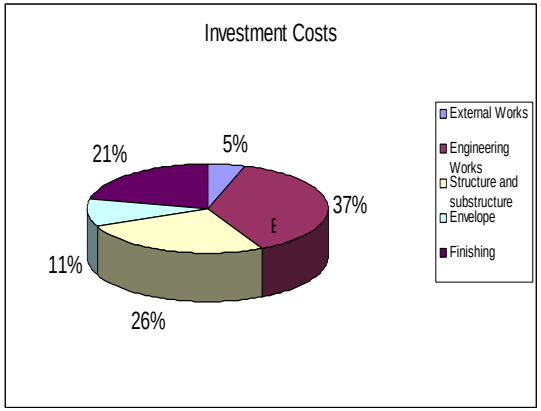

Figure 1. Distribution of the investment costs

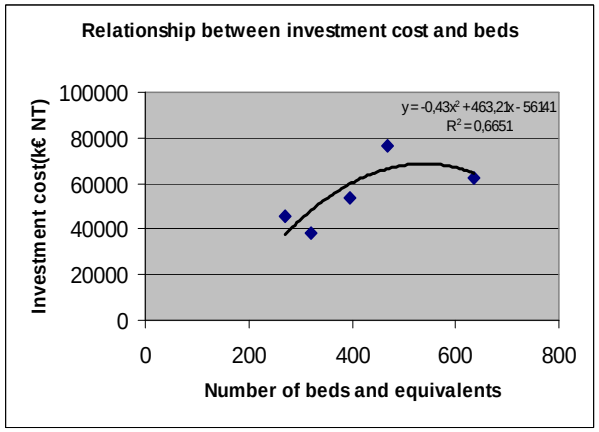

Figure 2. Relationship between investment cost and beds

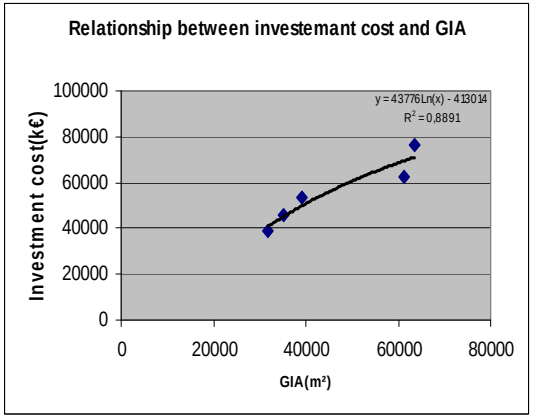

Figure 3. Investment cost and GIA

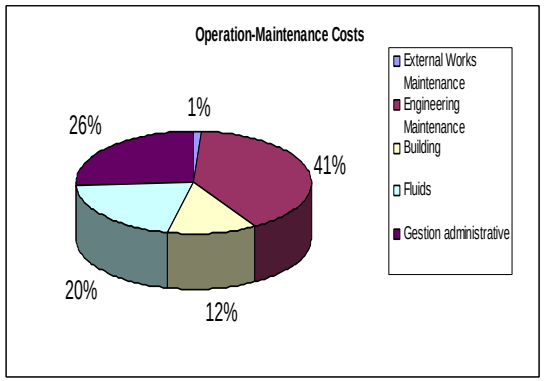

Figure 4 Allocation: operation-maintenance costs

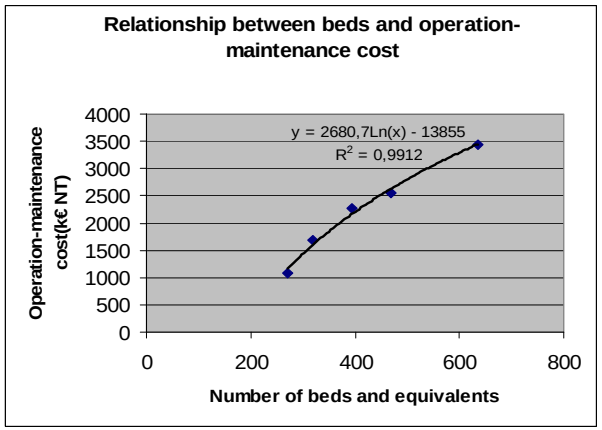

Figure 5 Operation maintenance cost vs. number of beds

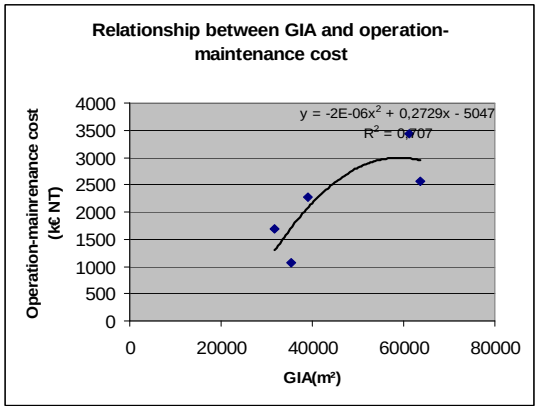

Figure 6. Operation maintenance cost and GIA

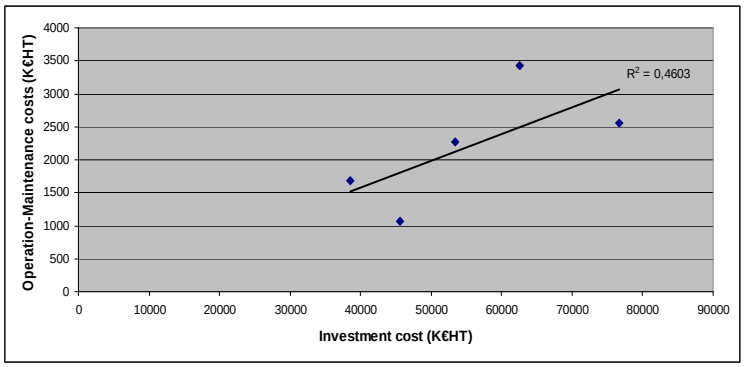

Figure 7. Relationship between investment and operation–maintenance costs (without replacement and cleaning)

The errors in the predicted costs, and hence design decisions, are likely to be greater when the life of the asset is taken substantially shorter than conditions warrant than when longer than justified. The WLCC plan provides a year by year the budget for the hospital and highlights the pattern of expenditure and works to be carried out and allows the directors to make tactical decisions to organize the flow of work and the expenditure form every year. It will also help to highlight where work can be grouped or delayed for the special situations of hospital. It also shows where planned replacement occurs, that helps in the strategic planning of the hospital (the budget, the capacity of the hospital during the period of works and the model of distribution work sites). For each year it will be easier to prepare the plan of detailed required works the budget for each item which will help in the planning and ordering of the work. The analysis shows that the distribution of costs for Hospital 4 over its life cycle are as follows: design, 2%; construction, 24%; operation and maintenance, 39%; replacement, 19%; utilities, 15%; demolition, 1%

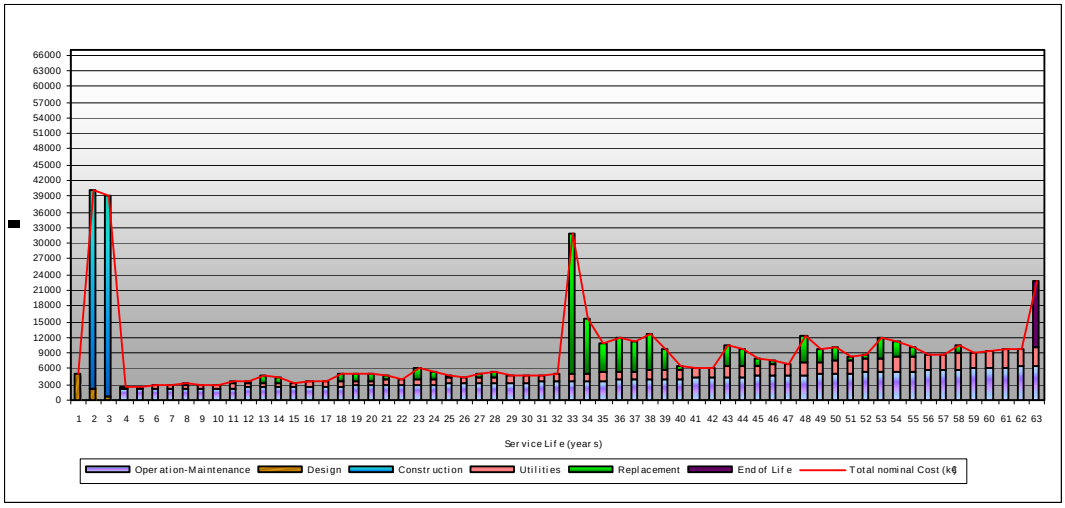

Figure 8. Total nominal cost per square metre

5 BENCHMARKING

Given diversity and complexity of hospitals and their related activities, it is unlikely that the mean values obtained from such type of studies accurately estimate the costs for the majority of development projects. By contrast, average values obtained in this study appear to be quite consistent with those presented in different observatories. Therefore, a methodology is proposed that gives hospital directors the principle

items required for estimating investment costs and operation-maintenance costs for their project or property. The approach takes the average value as input and then to estimate the existing hospital costs following the criteria listed in the benchmarking table (Table 3). The allocation of targets between the lower and upper ranges allows evaluating the cost compared with the average. Benchmarking for investment, maintenance and for the consumption of utilities has been carried out to help reduce operational costs.

Table 3. Benchmarking to estimate real estate investment costs

	Factor	Low bracket	High bracket	Wt.
Ground Works				
Ground Works	Rate of occupation of area	High, outdoor space limited	Low, outdoor space larger than floor area of building	5%
	Garden	Flat, mostly natural and grass	Little grass, various types of cover, fences	
	Roads and outdoor amenities	Normal materials	Materials/ high quality	
	Parking	Exterior	Garage	
Building				
Structure and substructures	Compactness	High	Low	26%
	Foundations	Normal	Special	
	Seismicity	Zone 0	Zone >0	
Envelope	Insulation	Regulatory	Better thermal and acoustic	11%
	Solar orientation	Favourable	Unfavourable	
	Roof	Terrace	Traditional	
	Materials	Coatings, Painting	Stapled, Glued, glazed	
	Density	High	Low	
	Automatic door exterior	No	Yes	
	Windows double glazing	No	Yes	
Internal finishing	Hospital activity	A low risk of infection	A high risk of infection	21%
	Quality of materials	Standard	High	
	Interior volume	limited	vaste	
Equipment				37%
	Hospital's activity	Ordinary technical of building	Special technical of building	
Heating, Ventilation and Air Conditioning	Capacity	Standard	More than needs	
	Building compactness	High	Low	
	Cooling	Partial	Total	
	Heating	central heating system of city	Boiler	
	Insulate cooling & heating syst.	Low	High	
	Cogeneration	None	Optimized	
	Ventilation	Simple flow	Double flow	
	Building technical control	Limited	Generalized	
	Hospital's activity	A low risk of infection	A high-risk of infection	
Electricity, high voltage and low voltage	Capacity	Standard	> Needs	
	Building technical control	Limited	Generalized	
	Fire safety	Low safety	High safety	
	Electricity generator	Limited	Generalized	
	Access control system	Limited	Generalized	
Plumbing	% Room individual	< 70%	100%	
	Quality of materials	Standard	High	
Automatic Transport	Number	None	Several	
Elevator	Capacity	Low	High	
	Number	None	Several	
Dimensioning	Surface GIA	From 30000 m² to 70000 m²	< 30000 m² or >70000 m²	
	Inpatient bed/GIA	>100 m² GIA per bed	*<100 m² GIA per bed*	

Table 4. Benchmarking to estimate the operation-maintenance costs for hospital 4

Hospital 4	Factor	Min €NT/bed	Average	Max €NT/bed	Correction Factor	Weight	Estimated OM cost
		4000	**5200**	**6400**			
Characteristics of Building and its equipments	**Compactness**	<0,4		>0,4	1,25	4	
	Density	<4		>4	0,95	4	
	Ratio GIA/capacity	<110		>110	1,25	4	
	Energy efficiency	High		Standard	0,9	4	
	Ratio Building Area	High		Low	1	1	
	Capacity of technical installations	Standard		Insufficient	0,95	2	
	Automated transport	Light		Heavy	0,95	4	
	Cooling	Partial		Total	0,95	2	
Activity	**Risk of infection**	Low		High	0,9	4	
	Room individual	<70%		>70%	1,1	3	
	Number of beds	300-600		>300, 600<	0,9	2	
site	**Climate**	Oceanic		Continental	1,2	4	
	Exposure aux risks exterior	Low		High	0,9	2	5200X1.032=5366

6 CONCLUSION AND PERSPECTIVES

This work concerns the whole life cycle costing of hospitals without cleaning and without specifying more elaborate operational elements. As an extension to this study on healthcare facility-wide costs, it may be useful to carry out research on other more reliable indicators. Additionally, risk assessment tools could provide a more thorough comparison of alternatives.

From another point of view, the development of this work raises four important issues perhaps worth further investigation. The first issue concerns collecting enough data to develop a model that can relate to such variables as the cost of time as might be carried out in a Monte Carlo analysis. The second issue concerns the relationship between building components and operation-maintenance costs. The third issue concerns the relationship between operation-maintenance cost and hospital's activity. The forth issue concerns the personnel who work in the hospital. One of the problems encountered over the course of this study was that there is insufficient amount of similar data. As well, there is always the problem of the misinterpretation of data. As well, it is acknowledged that the changing external economic environment may in certain instances invalidate much of the usefulness of past experience.

Finally, based on the results obtained in this work, it is clearly apparent that the relationship between investment cost and operation-maintenance costs is not evident. As such, additional work is required to establish the relationship between operation-maintenance costs and relevant hospital activities or other indicators.

ACKNOWLEDGEMENTS
The authors would like to thank Mr. Sylvain Zeghni, Mr. Marc Colombard-Prout and Mr. Jean Carassus for their support of this work.

REFERENCES
Ashworth, A. (1999), *Cost Studies of Buildings*, 3rd Edition, Longman Scientific, London, UK

Backis, N., Aouad, G., Amaratunga, D., Kish, M., Al-hajj, A. (2003), 'An integrated environment for life cycle costing in construction', *Construction Informatics Digital Library*

Bjorberg, S. (1996), *Annual cost, calculation methods of buildings*, the research council of Norway, Research Working Paper, Association of Consulting Engineers, Norway

Boussabaine, H. and Kirkham, R. (2006), Whole life cycle performance measurement re-engineering for the UK National Health Service estate (www.emeraldinsight.com/0263-2772.htm)

Boussabaine, H. and Kirkham, R. (2001), 'Useful Websites for Surveyors in Chartered Surveyor Monthly', *Journal of the Royal Institution of Chartered Surveyors (RICS)*

Boussabaine, H. (2007), *Cost Planning of PFI and PPP Building Projects*, Taylor & Francis, New York
Catarina, O. and Colombard-Brout, M. (2006), 'Les coûts d'exploitation des bâtiments hospitaliers et la relation à l'investissement et à l'activité hospitalière', CSTB, Paris

Drees (La Direction de la recherche, des études, de l'évaluation et des statistiques) (2006), Les Etablissements de Santé 2004, rapport N° 522, Paris, France

Flanagan, R., Norman, G., Meadows, J. and Robinson, G. 1989, *Life cycle costing - theory and practice*, BSP Professional Books

Holmes, R. 1994, CIOB Handbook of Facilities Management, Spedding, A., Ed., Longman, London, UK

Indice National du Bâtiment BT01, France 2006.

Kirkham, R. (2002), *A stochastic WLCC model for a National Health Service acute care hospital building*, unpublished Ph.D. Thesis, The University of Liverpool, UK

Langdon, D. (2007), 'Life Cycle Costing (LCC) as a contribution to sustainable construction: a common methodology', Final Report, Brussels Workshop, 16 March 2007

Lufkin, P. and Silsbee, R. (1999), *The Whitestone Building Maintenance and Repair Cost*, 5th Annual Ed., Whitestone research, Santa Barbara, CA

Lennerts, K. (2003), 'Reducing healthcare costs through optimised facility management-related processes', *Journal of Facility Management* Vol. 2, No. 2: pp. 192-206

Macedo, M. C. Dobrow P.V. and O'Rourke, J.J. (1978), *Value Management for Construction*, John Wiley & Sons, Toronto, Canada

MAINH (Mission National d'Appui à l'investissement Hospitalier) 2006, *Observatoire des Coûts de la Construction Hospitalière*, Rapport n°4, Paris

Melville, M. 2006, *Facilities Maintenance and Repair Cost Data*, 13th Annual Edition, R. S. Means, USA

NEUFERT, E. (2002), Les éléments des projets de construction

Newton, S. (1991), 'An agenda for cost modelling research', *Construction Management and Economics*, Vol. 2 : pp. 97-112

Woodward, D. (1997), 'Life cycle costing-theory, information acquisition and application', *International Journal of project management*, pp. 335 – 344

Service Life Prediction Beyond the 'Factor Method'

Johann Mc Duling [1]
Emile Horak [2]
Chris Cloete [3]

T 42

ABSTRACT

The ability to quantify changes in condition over time is important to ensure sustainable development in the built environment.The current 'state of the art' Factor Method [ISO 15686-1:2000] for service life prediction calculates an estimated service life, but not changes in condition.The application of the stochastic Markov Chain is restricted by limited availability of historic performance data on degradation of building materials required to populate transition probability matrices.This paper, based on a PhD thesis, looks at the application of neuro-fuzzy artificial intelligence to translate expert knowledge into probability values to supplement historic performance data for the development of Markovian transitional probability matrices, towards prediction of service life, condition changes over time, and effects of maintenance levels on service life of buildings. Expert knowledge is used to express durability and degradation factors in "IF-THEN" rules, which are translated into crisp probability values with neuro-fuzzy artificial intelligence to populate the Markovian transitional probability matrices.A case study is presented to proof that the limited availability of historic performance data on degradation of building materials can be supplemented with expert knowledge, translated into probability values through the application of Fuzzy Logic Artificial Intelligence, to develop transition probability matrices for the Markov Chain towards calculating the estimated service life of a building or component, quantifying changes in condition over time and determining the effects of maintenance levels on service life.

KEYWORDS

Condition changes, Markov Chain, Neuro-fuzzy artificial intelligence, Service life prediction, Maintenance levels.

1 Senior Researcher: Asset Management, Architectural Sciences, Built Environment, Council for Scientific and Industrial Research, Pretoria, South Africa, Phone +27 83 700 4027, Fax +27 12 349 9700, mcduling.johann@builtcare.co.za

2 Head of Dept, Civil and Biosystems Engrg, Faculty of Engrg, Built Environment and Information Technology, University of Pretoria, South Africa, Phone +27 12 420 2429, Fax +27 12 362 5218, emile.horak@up.ac.za

3 Professor, Department Construction Economics, Faculty of Engineering, Built Environment and Information Technology, University of Pretoria, South Africa, Phone +27 12 420 4545, Fax +27 12 420 3598, chris.cloete@up.ac.za

1 INTRODUCTION

The global importance of and need for sustainable socio-economic development demand an informed decision-making process from the built environment. Resources and non-renewable resources in particular, should be used as responsible and best possible to ensure optimum service life and life cycle costs, which depend on the ability to quantify the changes in condition of building fabric and components over time in any given physical and operational environment. If the change in condition over time can be defined mathematically, it will be possible to calculate the service life and remaining service life of buildings and components, and the consequences and risks of maintenance budget allocations and decisions to defer maintenance. The ability to predict changes in the condition profile of buildings or components is essential for cost-effective maintenance and rehabilitation decisions.

The current state of the art method for building service life prediction, the Factor Method [ISO 15686-1:2000], applies seven factors to a reference service life to estimate an empirical service life. Although the Factor Method calculates the estimated service life, it does not provide information on the degradation process, change in condition or condition profile.

A number of studies [Lounis et al, 1998a, p.1; Madanat et al, 1995, p.120; Morcous et al, 2003, p.353; Rudbeck, 1999 cited by Hövde and Moser, 2004, p.40] identified the Markov Chain, a stochastic approach used for simulating the transition from one state [condition] to another over time, as the preferred method for predicting service life and calculating changes in condition. The population of the Markov transitional probability matrix is a problem due to the lack of reliable and consistent historical performance data on the actual degradation rate of materials and components. Lounis et al [1998] cited by Moser [Hövde and Moser, 2004, p.66] stated: "The Markov model considers steadily degrading systems, where for each property, during each time period, a probability of deterioration is defined. This method thus requires sophisticated inputs in the form of probabilities, which are not easily estimated, as they cannot be read directly off the real behaviour of the structure in the field. The Markov model requires an in depth knowledge of the system dealt with or on the other hand has to rely on significant simplifications."

The development of a reliable and consistent database through regular field assessments is however a very slow process. In general, the best available source of information on degradation is the knowledge and reasoning of experts on material degradation in the built environment. However, as Negnevisky [2002, p.15] stated, "A major drawback is that human experts cannot always express their knowledge in terms of rules or explain the line of their reasoning. … experts do not usually think in probability values, but in terms as often, generally, sometimes, occasionally and rarely." On the interim, a system is needed to translate the verbally expressed knowledge and reasoning of experts into probability values, while using the assessment database as it grows to calibrate, learn and improve the system's reliability and ability to simulate the degradation process, providing for various combinations of the factors effecting degradation.

2 DEGRADATION PROCESS

A building is a complicated three-dimensional human-made configuration of a diverse range of fabrics, materials and components, each with its own characteristics, which interacts differently to the influences of its environment, could be old or brand new, raw or processed, come in different forms, shapes, sizes and finishes, and its applications could vary considerably. The environment acts on a building or component through mechanical, electromagnetic, thermal, chemical and biological agents causing degradation over time. The degradation process, as illustrated in Fig. 1 below, is a continuous interaction between durability factors, which counters degradation, and degradation factors, which promotes or cause degradation. These factors are the same as used in the 'state of the art' Factor Method.

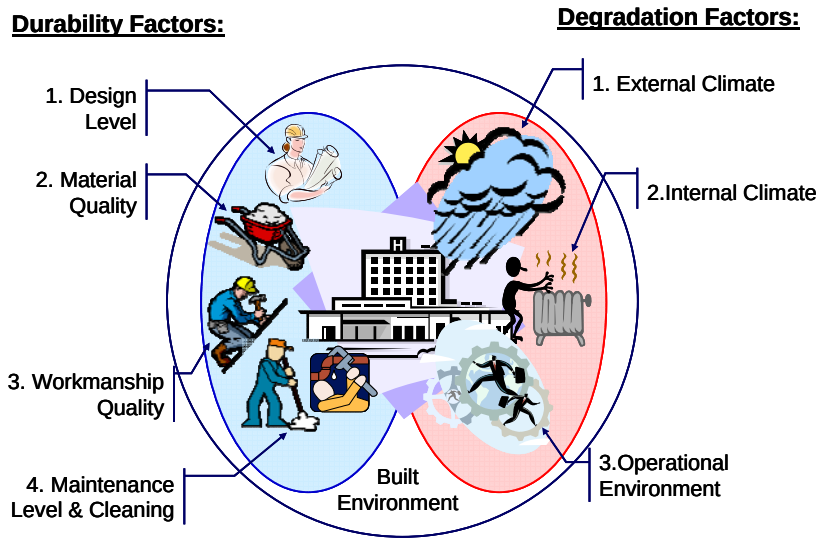

Figure 1: Degradation and Durability Factors [Mc Duling, 2006]

Durability is the ability of a building or component to resist the adverse effects of exposure to its environment. Degradation is determined by the environment, which can be divided into a physical and operational environment. The physical environment in and around the building or component comprises of a macroclimate [gross meteorological conditions], mesoclimate [terrain and local built environment] and microclimate [absolute proximity of a material surface]. The operational environment or 'user culture' is determined by the level and extent of the utilisation of the building by the occupants. Mechanical processes play a major role in the operational environment. The level of maintenance and cleaning is sometimes also taken into consideration with utilisation to determine the operational environment of a building. In the case of the 'Factor Method' this approach could result in 'double counting', because maintenance level is a factor in its own right.

3 NEURO-FUZZY ARTIFICIAL INTELLIGENCE

According to Negnevisky [2002, p.1-21] "Fuzzy logic is concerned with the use of fuzzy values that capture the meaning of words, human reasoning and decision making". It encodes and applies "human knowledge in a form that accurately reflects an expert's understanding of difficult, complex problems." An integrated neuro-fuzzy system has been selected to translate expert knowledge and reasoning into probability values because it "can combine the parallel computation and learning abilities of neural networks with the human-like knowledge representation and explanation abilities of fuzzy systems. … It can be trained to develop IF-THEN fuzzy rules and determine membership functions for input and output variables of the system. Expert knowledge can be easily incorporated into the structure of the neuro-fuzzy system." [Negnevisky, 2002, p.266-267]. The Mamdani-style fuzzy inference technique is used and performed in four steps: fuzzification of the input variables, rule evaluation, aggregation of the rule outputs, and finally defuzzification.

3.1 Structure of the Fuzzy Logic System

The system structure in Fig. 2 below identifies the fuzzy logic inference flow from the input variables to the output variables. The fuzzification in the input interfaces translates analogue inputs into fuzzy values. The fuzzy inference takes place in IF-THEN rule blocks, which contain the linguistic control rules. The output of these rule blocks is linguistic variables, which are translated into analogue variables through defuzzification in the output interfaces.

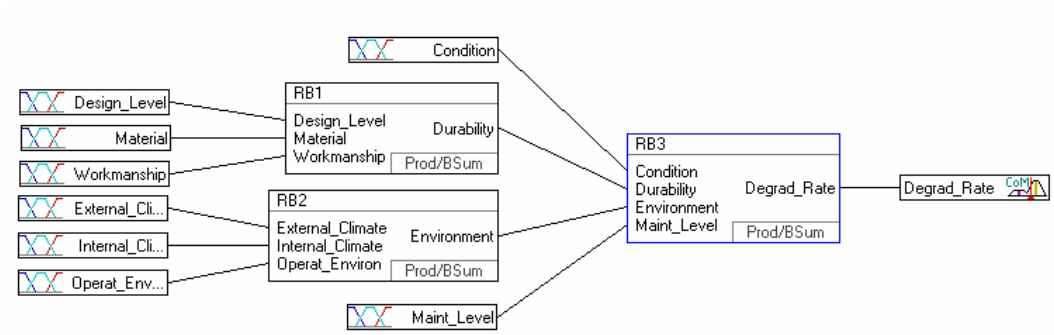

Figure 2: Structure of the Fuzzy Logic System [Mc Duling, 2006]

The input variables are the durability and degradation factors influencing the degradation of the material or component, defined in linguistic or fuzzy terms. These factors are similar to the factors used in the Factor Method, except for the valuation or rating of the factors. A five point colour-coded rating system is used based on a similar rating system used for condition assessments.

The input, intermediate and output variables are defined in Tables 1, 2 and 3 below:

Table 1: Input Variables for Fuzzy Logic Model [Mc Duling, 2006].

No	Variable Name	Rating	Term Names	No	Variable Name	Rating	Term Names
1	Condition	1 2 3 4 5	Very Bad Bad Fair Good Very Good	5	Maintenance Level	1 2 3 4 5	Very Low Low Normal High Very High
2	Design Level	1 2 3 4 5	Very Low Low Medium High Very High	6	Material Quality	1 2 3 4 5	Very Low Low Medium High Very High
3	External Climate	0 1 2 3 4 5	Internal Element Very Aggressive Aggressive Slightly Aggressive Less Favourable Favourable	7	Operational Environment	1 2 3 4 5	Very Aggressive Aggressive Slightly Aggressive Less Favourable Favourable
4	Internal Climate	0 1 2 3 4 5	External Element Very Aggressive Aggressive Slightly Aggressive Less Favourable Favourable	8	Workmanship Quality	1 2 3 4 5	Very Low Low Medium High Very High

Table 2: Intermediate Variables for Fuzzy Logic Model [Mc Duling, 2006].

No	Variable Name	Term Names
9	Durability	Very Low Low Medium High Very High
10	Environment	Very Aggressive Aggressive Slightly Aggressive Less Favourable Favourable

Table 3: Output Variable for Fuzzy Logic Model [Mc Duling, 2006].

No	Variable Name	Defuzzification method	Unit	Rating	Term Names
11	Degradation Rate	Centre of Moment	Percentage	0 25 50 75 100	Very Slow Slow Medium Fast Very Fast

The output variable, degradation rate, is expressed as the percentage of the material or component that changes from one condition to the next worst condition during one time interval. This interval, which could vary from material to material, is determined by the time required for the material to change from one condition to the next worst condition without jumping more than one-step at a time in order to keep the model as simple as possible and dictates the assessment frequency. The degradation rate is the transition probability required for the Markov process.

There are three rule blocks in the proposed system; an extract from Rule Block 3 [Fig. 2] is shown in Table 4 below as an example of a typical rule block.

Table 4: Extract from 'IF-THEN" Rule Block 3 [Mc Duling, 2006].

IF				THEN	
Condition	Durability	Environment	Maintenance Level	Degree of Support	Degradation Rate
Fair	Medium	Slightly Aggressive	Very Low	0.50	Very Fast
Fair	Medium	Slightly Aggressive	Very Low	0.50	Medium
Fair	Medium	Slightly Aggressive	Low	0.25	Very Fast
Fair	Medium	Slightly Aggressive	Low	0.25	Fast
Fair	Medium	Slightly Aggressive	Low	0.50	Medium
Fair	Medium	Slightly Aggressive	Normal	0.25	Very Fast
Fair	Medium	Slightly Aggressive	Normal	0.75	Medium
Fair	Medium	Slightly Aggressive	High	0.25	Very Fast
Fair	Medium	Slightly Aggressive	High	0.50	Medium
Fair	Medium	Slightly Aggressive	High	0.25	Slow
Fair	Medium	Slightly Aggressive	Very High	0.25	Very Fast
Fair	Medium	Slightly Aggressive	Very High	0.50	Medium
Fair	Medium	Slightly Aggressive	Very High	0.25	Very Slow

While the other variables were kept constant during the simulation, the maintenance level and condition ratings were adjusted to obtain degradation rates for various scenarios. The motivation for this is that design level, material, workmanship, and external and internal climate are largely predetermined during planning, design and construction, while operational environment could vary slightly but mostly stay relatively constant over the service life of the building or component.

Subsequent to completion of construction, the degradation rate is controlled mainly by the maintenance level. There is also an increase in the rate of degradation as the condition deteriorates.

3.2 Transition from Artificial Intelligence to Markov Chain

Degradation rate is defined as that percentage of the building or component that will 'transit' or change to a condition of worse degradation in one time interval. In the case of buildings, this time interval is normally one year, but could be months, weeks or even days, depending on the reference service life of the component under consideration. Due to the influence of the degradation and durability factors on the building, the transition to a condition of worse degradation is probabilistic with the transitional probabilities depending on the current condition of the building. Therefore, degradation rate is defined as the transition from condition i to the next worse condition j in one time interval:

Degradation rate = transitional probability P(ij)

A five-point condition rating system is used, with Condition 5 the initial condition, progressively worsening towards Condition 1, where the material or component has failed and needs to be replaced.

Based on the assumptions that under normal circumstances the condition will only deteriorate and not improve and a one year interval is short enough to ensure the change in condition will not jump more than one condition rating, or P(ij) = 0 when i < j and j < i - 1, the transitional probability matrix is defined as:

$$P = \begin{array}{c|ccccc|l} & [5] & [4] & [3] & [2] & [1] & \\ (5) & P(55) & P(54) & 0 & 0 & 0 & \sum P(5j) = 1 \\ (4) & 0 & P(44) & P(43) & 0 & 0 & \sum P(4j) = 1 \\ (3) & 0 & 0 & P(33) & P(32) & 0 & \sum P(3j) = 1 \\ (2) & 0 & 0 & 0 & P(22) & P(21) & \sum P(2j) = 1 \\ (1) & 0 & 0 & 0 & 0 & 1 & \sum P(1j) = 1 \end{array}$$

The transition probabilities P(54), P(43), P(32), and P(21) are obtained from the Neuro-fuzzy simulation, while P(55), P(44), P(33), and P(22) are obtained from ∑P(ij) = 1. These transition probabilities are then used to populate the Markov Transitional Probability Matrix.

Table 5: Markov Transition Probability Matrix for 'base-line' Model [Mc Duling, 2006].

Markov Transition Probability Matrix		Condition at time t = 1				
		5	4	3	2	1
Condition at time: t = 0	5	0.578	0.422	0	0	0
	4	0	0.516	0.484	0	0
	3	0	0	0.391	0.609	0
	2	0	0	0	0.453	0.547
	1	0	0	0	0	1

In the 'base-line' Neuro-fuzzy model, it was assumed that the variables in each rule block carried the same weight, and this resulted in deterioration rates being too high, as shown in Table 5 above. After evaluating the results and adjusting the weights based on expert knowledge and reasoning, more realistic values were obtained as shown in Table 6 below:

Table 6: Markov Transition Probability Matrix for revised Model [Mc Duling, 2006].

Markov Transition Probability Matrix		Condition at time t = 1				
		5	4	3	2	1
Condition at time t = 0	5	0.950	0.050	0	0	0
	4	0	0.915	0.085	0	0
	3	0	0	0.900	0.100	0
	2	0	0	0	0.875	0.125
	1	0	0	0	0	1

3.3 Calibration of the Neuro-Fuzzy Model

Although there are currently approximately 27 tertiary hospitals and 380 other government hospitals in South Africa, only six academic hospitals were chosen as pilot and control sites to calibrate the model because they are of similar age, were all built within a seven year period during the 1970's, have similar construction types, design, material and workmanship levels and operational environments, and their condition have been assessed at least twice since 1995. In Fig. 3 below the average assessed condition of the six hospitals are shown on performance over time curves for five levels of maintenance:

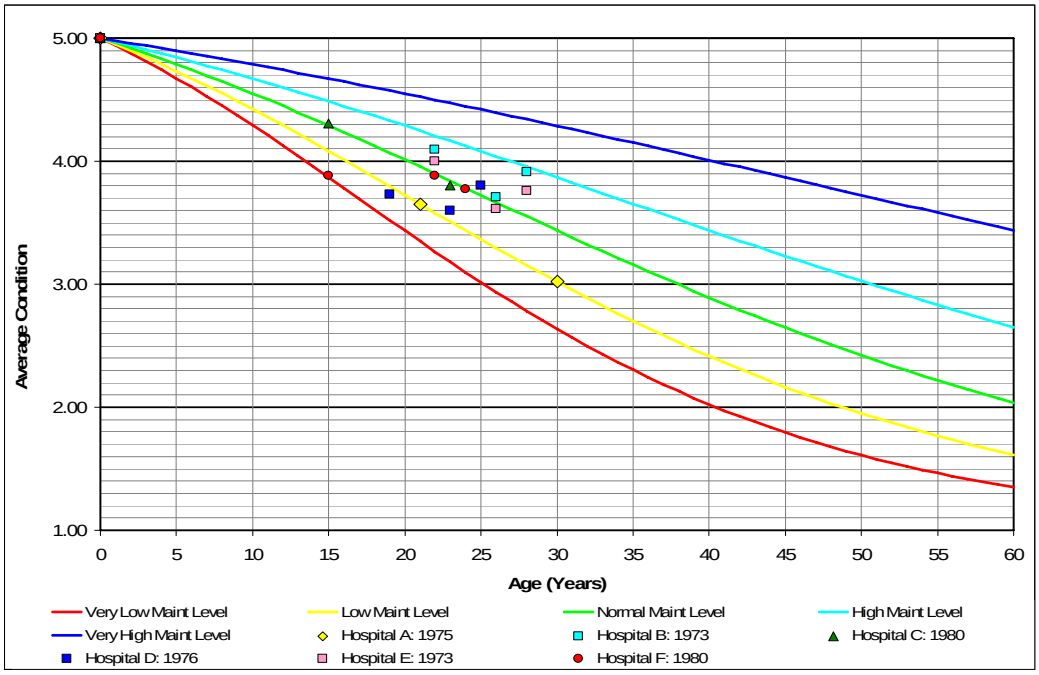

Figure 3: Performance over Time Curves [Mc Duling, 2006]

4 SERVICE LIFE PREDICTION

For service life prediction, the condition of a building or component is a relatively easy to assess and ideal to use performance indicator. The minimum performance requirement for academic hospitals should be Condition 3. Below a level 3 the building or component is simply not able to provide an environment supportive of proper health care. There are areas in hospitals where the performance requirements are higher [e.g. operating theatres and intensive care units]. For other building types, this performance standard may be different. The performance requirements for buildings and components should be determined by clearly defined and appropriate policies and codes.

5 CONCLUSION

The proposed model, based on the Markov Chain approach, translates expert knowledge and reasoning into probability values through the application of Neuro-Fuzzy Artificial Intelligence to supplement limited historical performance data on degradation of building materials for the development of Markov Chain transitional probability matrices to predict service life, condition changes over time, and consequences of maintenance levels on service life of buildings. Due to the limited availability of reliable historic performance data, expert knowledge and reasoning were used to develop initial transition probability matrices for the proposed model. However, the initial model produced unrealistic results and available historic performance data was used to calibrate the model. After calibration, the model produced realistic results, which compared well with historic performance data for other hospitals.

According to Lounis et al [1998b, p.5] "The development of the Markovian model requires a relatively limited amount of historical performance data at two or more points in time." This statement is supported by the results of the proposed model. But, instead of using the limited available historic performance data to develop the Markovian transition probability matrices, the proposed model reverses the process by using expert knowledge and reasoning, and supplements it with available historic performance data to calibrate the model. Historic performance data should however not be used indiscriminately. The degradation and durability factors could vary considerably between assessments and these potential variations should be taken into consideration.

REFERENCES

Hövde, P.J., and Moser, K., 2004. State of the Art Reports, CIB W080 / RILEM 175-SLM *Service Life Methodologies Prediction of Service Life for Buildings and Components*, CIB Report, Publication 294, March 2004.

Lounis, Z., Lacasse, M.A., Vanier, D.J., and Kyle, B.R., 1998a. *Towards Standardization of Service Life Prediction of Roofing Membranes*. In: Wallace, T. J., and Rossiter, W.J. Jr., eds, Roofing Research and Standards Development, 4th Volume, ASTM STP 1349. American Society for Testing and Materials.

Madanat, S., Mishalani, R., and Wan Ibrahim, W.H., 1995. Estimation of Infrastructure Transition Probabilities from Condition Rating Data. *Journal of Infrastructure Systems*, Vol. 1, No. 2, June 1995, p.120–125.

Mc Duling, J.J., 2006. Towards the Development of Transition Probability Matrices in the Markovian Model for the Predicted Service Life of Buildings, PhD Thesis, Department of Civil and Biosystems Engineering, University of Pretoria, South Africa.

Morcous, G., Lounis, Z., and Mirza, M.S., Nov 2003. *"Identification of environmental categories for Markovian Deterioration Models for Bridge Decks."* Journal of Bridge Engineering. Vol 8, p.353-361.

Negnevitsky, M., 2002. Artificial Intelligence, A Guide to Intelligent Systems. Essex, England, Addison-Wesley.

Evolution of Degradation and Decay in Performance of ETICS

Bruno Daniotti [1]
Riccardo Paolini [2]

T 42

ABSTRACT

This paper provides initial results from experimental work on laboratory accelerated ageing of external thermal insulation composite systems with rendering (ETICS) undertaken at the Building Environment Science and Technology department of the Polytechnic of Milan. The work forms part of a broader experimental programme seeking to develop knowledge on the relationship between critical properties affecting long-term performance and test parameters that reveal the process of degradation.
The performance evaluation of ETICS specimens consisted of several different types of tests conducted on non-aged specimens and specimens subjected to accelerated environmental ageing. The ageing procedure consisted of exposing specimens to different environmental macro-cycles comprised of ageing under ultraviolet radiation and warm and cold temperature cycling that replicated temperature cycling occurring in winter or summer in Italy. Non-destructive tests were carried out that included obtaining photos to characterise the evolution of surface degradation of specimens and conducting absorption tests to determine the degree of moisture uptake in the specimens. Other tests were used for assessing hygrothermal performances including dynamic thermal response, thermal inertia, thermal resistance and dynamic response to variations in moisture content of base and finish coat. In this paper the tests methods are described and initial results analysed following two ageing macro-cycles used to discern the process of degradation of the specimen, in terms of monitoring changes in capillary water absorption, thermal resistance and rendering degradation (photo survey). The long-term aim of this study is to develop a method to evaluate the Serviceability Limit State of building components based on understanding relationships between performance attributes and physical properties of building components.

KEYWORDS

ETICS, End of service life, Limit state, Performance decay, Degradation evolution

[1] Politecnico di Milano, Building Environment Science and Technology Department (BEST), Milano, Italia 20133, Piazza Leonardo Da Vinci, 32, Phone +39 2 2399 6002, Fax +39 2 2399 6020, bruno.daniotti@polimi.it
[2] Politecnico di Milano, Building Environment Science and Technology Department (BEST), Milano, Italia, 20133, Piazza Leonardo Da Vinci, 32, Phone +39 02 2399 6015, Fax +39 2 2399 6020, riccardo.paolini@mail.polimi.it

1 INTRODUCTION

The aim of this paper is to portray the initial results of an experimental programme to evaluate the thermal performance of ETICS, introduced by Daniotti & Paolini [2008]. The specimen being evaluated has a vinyl resin-based base coat and an acrylic resin-based finish coat. Performances have been surveyed on the non-aged specimens and every ageing macrocycle (i.e. 5 x (25 UV cycles + 10 winter cycles + 25 summer cycles) with non-destructive tests: i.e., photos of the evolution in surface degradation, capillary absorption tests and cycles suited for assessing hygrothermal performances (dynamic thermal response, thermal inertia, thermal resistance and dynamic response to variation in moisture content of base and finish coat). In this paper the tests methods are described and initial results analysed following two ageing macrocycles used to discern the process of degradation in the specimen, in terms of monitoring changes in capillary water absorption and thermal resistance. The long-term aim of this study is to search for a relationship between single performances and properties in order to develop a method to evaluate the Serviceability Limit State of building components.

2 PERFORMANCE LOSS IN THERMAL RESISTANCE

2.1 Preliminary Analysis of System Performance

As an initial step, the thermal performance of the building component being studied was evaluated in accordance with different reference standards, namely: EN 12524 for specimen type A.1; steady state properties calculated according to EN 6946; and, dynamic properties calculated according to EN 13786. These values are provided in Table 1.

Table 1. Physical and related hygrothermal properties of specimens

n°	*Layer*	*s [m]*	*ρ [kg/m^3]*	*λ_d [W/mK]*	*$c_{p\,d}$ [kJ/Kkg]*	*R [m^{2}K/W]*	*μ [adim]*	*M* [kg/m^2]*
1	Gypsum	0.005	900	0.300	1	0.017	10	4.500
2	Cement Lime Plaster	0.015	1600	0.902	1	0.017	10	24.000
3	Masonry wall	0.12	650	0.385	0.84	0.312	7	78.000
4	Cement Lime Plaster	0.015	1600	0.902	1	0.017	10	24.000
5	Adhesive	0.003	1800	1.001	0.84	0.003	15	5.400
6	EPS insulator	0.06	25	0.034	1.25	1.765	35	1.500
7	Base coat	0.005	1800	1.001	0.84	0.005	15	9.000
8	Finishing coat	0.0015	1100	1.000	0.84	0.001	7	1.650

Total thickness	s	0.2245	[m]
External surface coefficient of heat transfer	h_e	25	[W/(m^{2}K)]
Internal surface coefficient of heat transfer	h_i	7.7	[W/(m^{2}K)]
Conductive thermal resistance nodes 12	$R_{cd\,12}$	0.362	[m^{2}K/W]
Conductive thermal resistance nodes 23	$R_{cd\,23}$	1.774	[m^{2}K/W]
Total conductive thermal resistance	$R_{cd\,TOT}$	2.136	[m^{2}K/W]
Thermal conductance	Λ	0.468	[W/(m^{2}K)]
Total thermal resistance	R_{TOT}	2.306	[m^{2}K/W]
Thermal transmittance	U	0.434	[W/(m^{2}K)]
Thermal capacity nodes 12	C_{12}	118.02	[kJ / (m^{2}K)]
Thermal capacity nodes 23	C_{23}	15.36	[kJ / (m^{2}K)]
Total thermal capacity	C_{TOT}	133.38	[kJ / (m^{2}K)]
Decrement factor	f	0.3219	[-]
Shift (on internal side)	ϕ	6h 46’	[h]

2.2 Test Description

Before being exposed to ageing cycles and after every ageing macrocycle, the thermal insulation performance was evaluated with a steady state test (referred to as CON, i.e. thermal conductance measurement). Data provided in this paper relate to: (i) initial conditions determined according to EN 12524, (ii) non-aged specimens (ageing time, T0), (iii) aged specimens, following two macrocycles (i.e. ageing time T1, T2 and T2+); and, (iv) data (ageing time T2+) concerns loss in thermal performance after a rain cycle (last part of RHst cycle), while the other measuring cycles have been performed after three cycles suited for evaluating thermal dynamic properties in summer conditions (SINa, SINb and TI cycles). This was to ensure that the loss in thermal performance was not influenced by an excessive amount of water gained during the ageing cycles that included rain.

The CON measurement cycle consisted of exposure of the specimen for 96 hours to the following conditions:

Climatic chamber	T [°C] = – 20 constant; RH [%] = 0 constant
Laboratory	ΔT_{MAX} [°C] = 2; RH [%] = 40 ÷ 60 [acceptance intervals during test]
Recording	180 [s] between readings

Laboratory conditions are not fixed, however tests are considered valid because:
- temperature and relative humidity oscillations are not large;
- tests having high T [°C] or RH [%] oscillations (beyond acceptance intervals) were rejected;
- dynamic calculation to filter the contribution due to small oscillations in environmental conditions was adopted.

In order to observe the loss in thermal insulation, only the conductive portion of the thermal resistance of the wall assembly was determined (total values – thermal transmittance and total thermal resistance – are reported only with the aim towards completeness and for comparison purposes), because of the fact that surface heat transfer coefficients:
- are different in laboratory and outdoor and are different for a one square meter specimen;
- show great variations due to different conditions during the same test and different tests and are strongly influenced by radiative boundary conditions;
- are not obviously influenced by degradation.

The calculation of conductive thermal resistance of the substrate, of the ETICS and of the entire specimen has been performed according to ISO 9869, using the average and storage effect methods. The data that was analyzed was that of the main section profile, whereas the loss in thermal performance coincidence with thermal bridges located at joints between insulation panels and bed mortar joints were evaluated with IR thermography that permitted assessing the changes in thermal gradient across the face of the specimens.

An analysis using the average method (av in figures) provides a value of thermal resistance assessed over a period of 24 hours, when steady state thermal conditions are reached and as well, conditions specified in the standard are met. On the other hand, using the storage effect method, a correction to the mean heat flow rate was introduced that takes into account dynamic effects (using a resistance-capacity method). In this study, the correction to heat flow due to storage effects was performed by considering both the thermal capacity of the dry layer and the total thermal capacity of the layer, including the contribution of water present in the pores. EPS has been divided into six layers of 1 cm (referring to the outer section as EPS 6) and the thermal resistance of each layer and respective water contents were obtained from a numerical solution starting from an estimate of the moisture distribution and thermal gradient in the building component from the interior side of the assembly. It is important to highlight that the aim of this test was not to obtain a deterministic measurement of the physical properties of the specimen, but to evaluate the loss in thermal performance.

2.3 Discussion of İnitial Results of Loss in Performance of Thermal İnsulation

The initial results are useful to highlight the difference between the values for thermal resistance calculated with the standard reference and those measured that show an evident loss in insulation performance. At the same ageing conditions, and after a rain cycle, a significant loss in thermal resistance was observed.

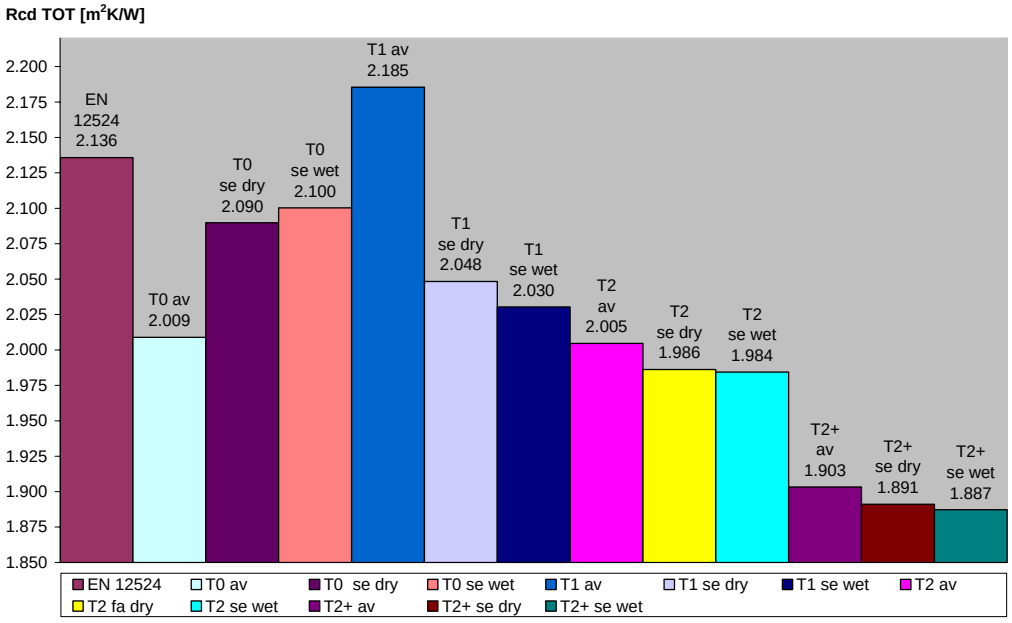

Figure 1. Loss in total conductive thermal resistance.

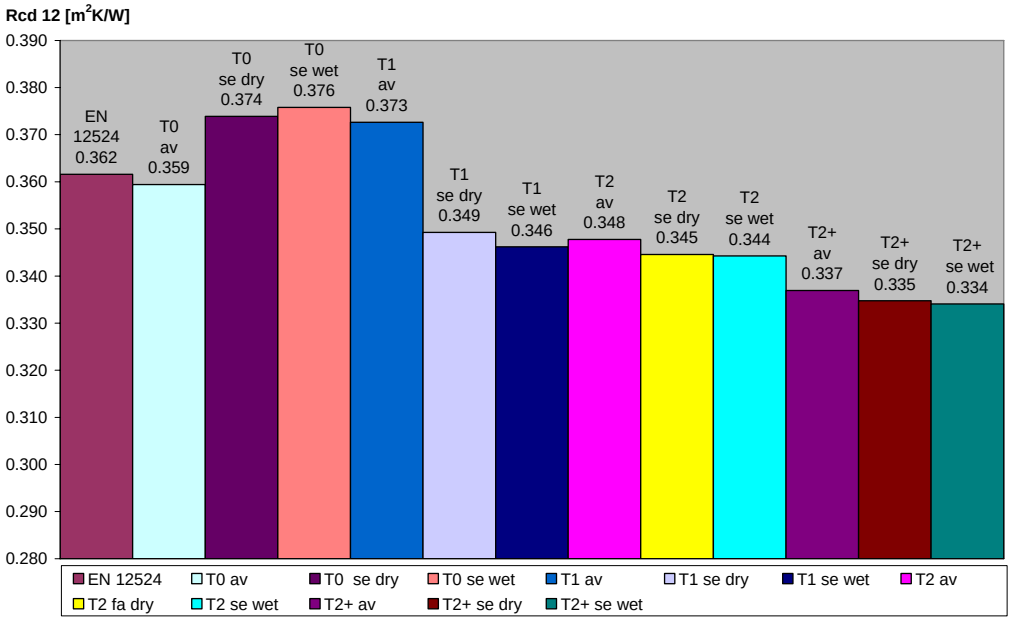

Figure 2. Loss in thermal resistance of masonry wall and plaster substrate.

In Figure 2 a limited reduction in thermal resistance of the substrate is noticed, that is due to an increase in moisture content; this increase in moisture was brought about by water that permeated the ETICS. It is estimated that construction water would be taken up prior to initiating tests (6 months later than fabrication of the substrate). On the other hand (see Figure 3), the thermal resistance of the ETICS suffers a pronounced loss, that could be explained by the increase in moisture content in the

outer layers of the EPS where water is in the solid phase at most exterior portion of EPS, and in a physical transition phase in the middle section of the EPS. Even if the thermal resistance of the base and finish coat are set to zero, the loss in thermal could not be reached.

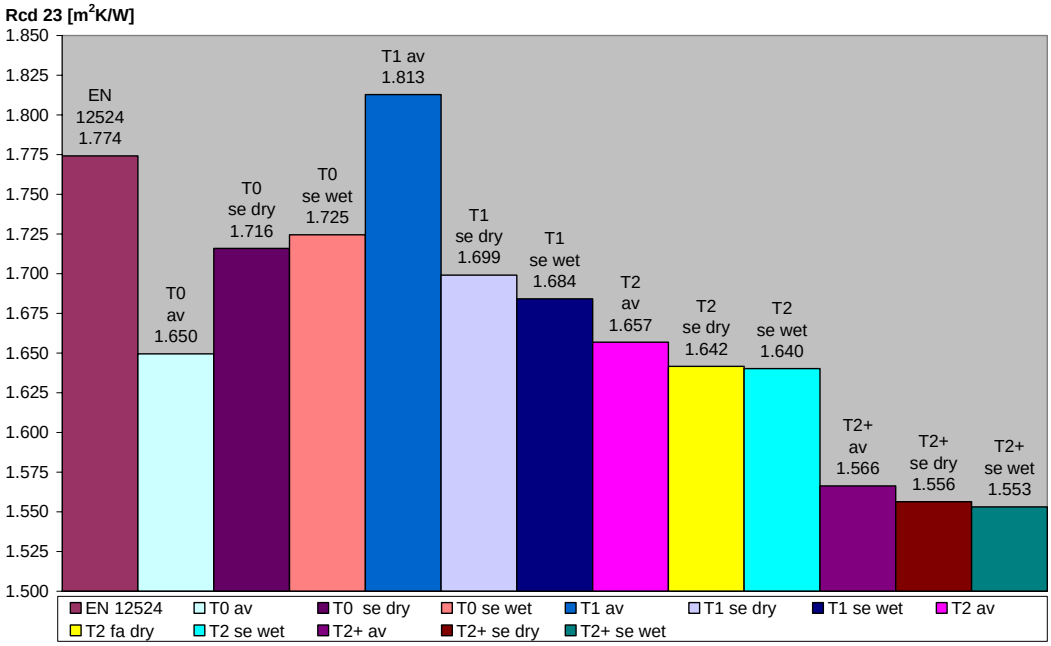

Figure 3. Loss in thermal resistance of ETICS (EPS, base and finishing coat).

Table 2. Values from standard and values measured at T0 and after two ageing macro-cycles.

Thermal property		*EN 12524*	*T0 dry*	*T0 wet*	*T1 dry*	*T1 wet*	*T2 dry*	*T2 wet*	*T2+ dry*	*T2+ wet*	*u.m.*
Substrate resistance	$R_{cd\ 12}$	0.362	0.374	0.376	0.349	0.346	0.345	0.344	0.335	0.334	$\left[\frac{m^2K}{W}\right]$
ETICS resistance	$R_{cd\ 23}$	1.774	1.716	1.725	1.699	1.684	1.642	1.640	1.556	1.553	$\left[\frac{m^2K}{W}\right]$
Tot conductive resistance	$R_{cd\ TOT}$	2.136	2.090	2.100	2.048	2.030	1.986	1.984	1.891	1.887	$\left[\frac{m^2K}{W}\right]$
Conductance	Λ	0.468	0.479	0.476	0.488	0.493	0.503	0.504	0.529	0.530	$\left[\frac{W}{m^2K}\right]$
Tot resistance	R_{TOT}	2.306	2.260	2.270	2.218	2.200	2.156	2.154	2.061	2.057	$\left[\frac{m^2K}{W}\right]$
Transmittance	U	0.434	0.443	0.440	0.451	0.455	0.464	0.464	0.485	0.486	$\left[\frac{W}{m^2K}\right]$
Substrate capacity	C_{12}	145.0	145.0	162.9	145.0	165.4	145.0	168.0	145.0	177.5	$\left[\frac{kJ}{m^2K}\right]$
ETICS capacity	C_{23}	15.7	15.7	18.7	15.7	19.0	15.7	19.9	15.7	21.3	$\left[\frac{kJ}{m^2K}\right]$
Tot capacity	C_{TOT}	160.6	160.6	181.6	160.6	184.5	160.6	187.8	160.6	198.8	$\left[\frac{kJ}{m^2K}\right]$

Performing a test with ice water or water in a transition phase does not introduce a useless complication in the analysis of data, but allows determining a more evident loss in thermal performance. Without the use of ice presence, it would be difficult to separate the loss in thermal resistance from measurement errors and other experimental uncertainties.

2.4 Infrared Thermography

The development of a thermal bridge coincidence with joints between insulation panels, in particular horizontal joints, is noticed from analysing the data provided by the infrared thermography performed at ageing time T2+. At the vertical joints the accumulation of water tends to spread at the base of the joint and not remain close to the joint line.

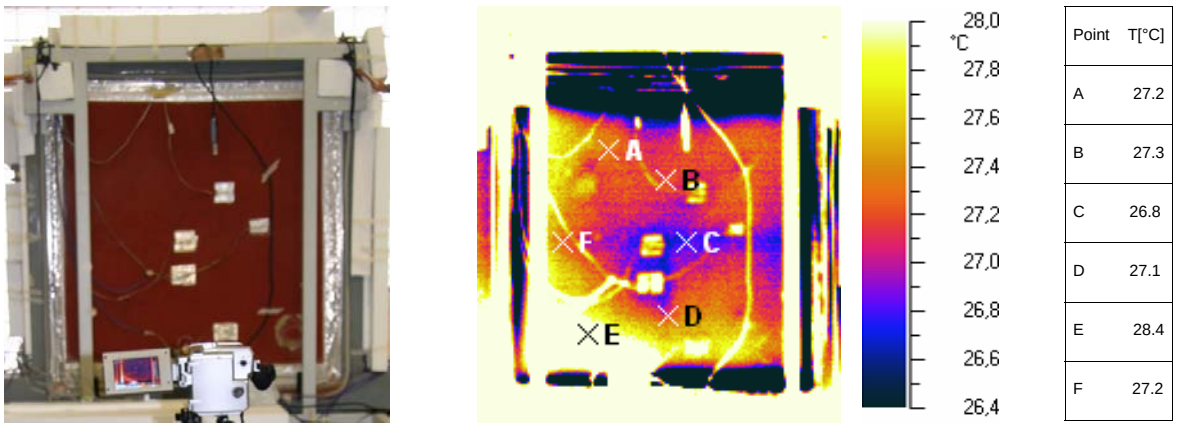

Point	T[°C]
A	27.2
B	27.3
C	26.8
D	27.1
E	28.4
F	27.2

Figure 4. Infrared thermography at ageing time T2+; Laboratory air temperature $T_{A.LAB}$ = 29.0 °C. Surface emissivity ε = 0.92. IR-camera distance from specimen: 4 [m].

3 CAPILLARY WATER ABSORPTION

In order to survey the water absorption evolution at different ageing times, the test on the same specimen was repeated a specified times using Karsten's method that is given in NORMaL 44-93. This method is a non-destructive test for water absorption using low water pressure. During the test, the volume of water [mL] absorbed by the exterior surface of the complete specimen was recorded at different times. The degree of water absorption [L/m^2] is expressed as a function of the square root of time [s$^{1/2}$].

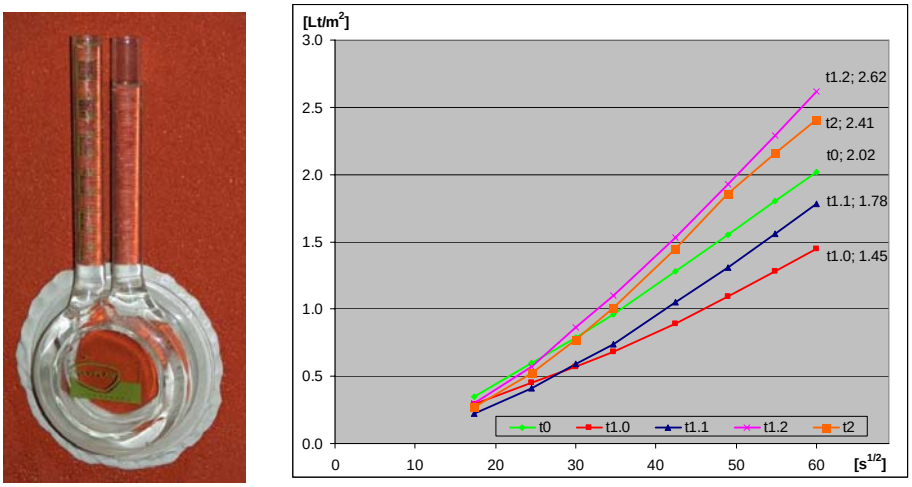

Figure 5. Measurement apparatus and initial results showing water absorption as a function of absorption time.

At ageing time T1.0 a relevant loss in absorption was noticed, that could have two possible causes: water saturation conditions and increase in cross-linking of polymeric binder of finish coat and curing of cement matrix of base coat. At ageing times T1.2 and T2 an increase in water absorption was measured. It is important to stress that this kind of test is useful because it is non-destructive; however, a significant standard deviation of results is obtained in this test. As such, it would require validation with other tests, in particular, tests such as the capillary absorption test, which is a disruptive test.

4 PHOTO-SURVEY OF SURFACE DEGRADATION

A photographic survey of the degradation of the surfaces of ETICS has shown that the most significant evolution in degradation at ageing time T1 is evident by the development of blisters on the surface of the finishing coat. As well, at all ageing times it has been observed that there is an increase in the dimension of pores of the finish coat.

Figure 6. (Left side) Photograph of ETICS finish coat at ageing time T1; blisters (larger ones: 10 cm diameter circa) are evident on the surface of the sample; (Right-side) dimension of pores and surface appearance are changed (aggregate dimension 0/1 mm); Localized fading due to rain-wash is shown.

5 CONCLUSIONS

5.1 Initial Results

Following on the analysis that was implemented and initial hypothesis for causes of degradation , decay in thermal performance is mainly due to an increase in water content of the EPS; hence an apparent rise in thermal conductivity of the EPS layer is evident. A first hypothesis for the evolution of ageing could be the following:

- UV cycles: UV degradation (i.e. progressive chain scission), of the polymeric binder of the finishing coat brings about an increase in cracking of capillary size and likewise an increase in the depth of penetration of UV rays;
- Winter cycles: the base coat and finishing coat are both subject to tensile forces that result in increases in the width of capillary cracks that in turn during rain events allow water penetration; such penetration also causes rain-wash. As well, wet rendering, having a reduced tensile strength, is susceptible to freeze-thaw cycling; this deteriorative effect contributes to the degradation of the cementitious matrix;
- Summer thermal shock cycles: base coat and finish coat are subjected to compression and adhesion stresses resulting in deformation of the finish coat that can lead to the formation of voids between layers that potentially can fill with moisture and cause blistering as water vapour intrudes the voids during a heating phase.

The cycle of degradation can be summarized as:

- Increase in capillary crack width; followed by,
- Water absorption; thereafter,
- Reduction in tensile strength; from which ensues,
- Reduction in thermal resistance; thereby bringing about an,

- Additional increase in capillary crack width
- Continued cycling of the degradation phenomena

5.2 Future Development of Research Programme

Future activities of this research programme that focuses on ETICS will be the evaluation of dynamic tests, performing destructive tests and exposure of specimens to exterior conditions to establish re-scaling factors useful for relating results derived from accelerated and long-term exposure tests. On the other hand the Performance Limit Method developed by the BEST will be used to experimentally assess ETICS such that the basic functional properties of ETICS and their respective performances can be linked to one another. This will permit moving towards an initial draft of a generic Serviceability Limit State Method suitable for assessing building components.

ACKNOWLEDGMENTS

Special thanks to Hartwig M. Künzel, of the Fraunhofer Institute of Building Physics, for providing WUFI software to assess the simultaneous heat and moisture transport of specimens.

REFERENCES

Daniotti, B. & Paolini, R. 2008, 'ETICS Experimental Programme to Assess ETICS Cladding Durability', 11th DBMC, Istanbul 11-14 May 2008

Daniotti, B. & Paolini, R. 2006, 'La valutazione della durabilità di pareti perimetrali con isolamento esterno a cappotto', in *La valutazione della durabilità di pareti perimetrali verticali*, ediTecnica editrice, Palermo, pp. 37-74

EN 12524: 2001, Building materials and products – Hygrothermal properties, Tabulated design values

EN 13187: 2000 – Thermal performance of buildings – Qualitative detection of thermal irregularities in building envelopes – Infrared method

International Energy Agency1991, Condensation and Energy, Catalogue of Material Properties, Report Annex XIV, Volume 3,

ISO 4628: 2003 – Paints and varnishes – Evaluation of degradation of coatings – Designation of quantity and size of defects, and of intensity of uniform changes in appearance

Künzel, H. M 1995., Simultaneous Heat and Moisture Transport in Building Components (One- and two-dimensional calculation using simple parameters), Fraunhofer Institute of Building Physics,
NORMal 44 – 93 – Assorbimento d'acqua a bassa pressione

Rotella, F. 2007 The Durability of Buildings – ETICS Cladding: An Analysis of the Degradation Caused by Water Absorption and Review of Related Standards (*La durabilità in edilizia. Pareti a cappotto: analisi dei degradi dovuti all'assorbimento d'acqua e analisi delle normative che ne regolamentano l'utilizzo)*, Degree Thesis (in Italian), Politecnico di Milano, 120 p.

A Multi-Performance Approach for Service Life Prediction

Aurélie Talon [1]
Daniel Boissier [2]
Julien Hans [3]

T 42

ABSTRACT

The service life is defined in the ISO 15686 standard as "the period of time after installation during which a building or its parts meets or exceeds the performance requirements" and a performance requirement is "the minimum acceptable level of a critical property (property of a building or a building part that has an acceptable value if its required function is to be fulfilled)".
In this context, a methodology to evaluate the service life of building components is proposed. It is based on the knowledge of evolution of their multi-performance profiles (representation of performance levels of their required functions and combinations of their required functions).

The methodology compounds four parts: (1) a qualitative analysis that reviews in an exhaustive way the possible degradation scenarios of a building component, (2) a quantitative analysis applied temporally that evaluates the service life and the probability of occurrence of the scenarios, based on unification and aggregation approaches, (3) a quantitative analysis of criticality that orders by degree of criticality the scenarios, this phase allowing to reduce the application of the fourth phase to the most critical scenarios, (4) a quantitative analysis of performance that permits to obtain multi-performance profiles of the building component based on the knowledge of the relation between degradation states of phenomena and performance levels of required functions.

This communication will focus on the fourth part of this methodology and will be applied to the case of a brick wall covered by an isolation complex.

KEYWORDS

Building components, Data unification, Degradation scenarios, Multi-performance profiles, Occurrence probability

[1] Polytech'Clermont-Ferrand / LGC, Civil Engineering, Clermont-Ferrand, France 63174, Phone +33 473407525, Fax +33 473407494, atalon@cus.univ-bpclermont.fr
[2] Polytech'Clermont-Ferrand / LGC, Civil Engineering, Clermont-Ferrand, France 63174, Phone +33 473407520, Fax +33 473407494, daniel.boissie@cust.univ-bpclermont.fr
[3] CSTB, Sustainable Development, Grenoble, FRANCE 38400, Phone +33 476762589, Fax +33 476762560, julien.hans@cstb.fr

1 INTRODUCTION

The continuous maintenance of acceptable performance levels of buildings and their components represents primary economical, political and sociological importance. Maintaining performance at an acceptable level requires an on-going evaluation throughout the service life; this corresponds to the global approach of "Performance-based building" as conveyed by the PeBBu network since 2001 [Lee & Barrett 2003] where "the basis of all building activities may be the building performance in service rather than the prescription of the manner that the building will be built".

Several methods and methodologies can aid evaluating the performance of materials, building components and buildings. At the material level, developed methods aim to define the performance criteria that *a priori* seem to best characterize the behaviour of the studied material; then these criteria are measured via experimentation in order to propose models of ageing mechanisms. The formalisation of this method is presented by Jernberg *et al.* [2004]. At the building component level, two typical approaches are identified. The first approach consists of testing the building component's ability to mechanically, physically and chemically resist predefined actions during a given period. This is the approach taken for building component certification. The testing protocols are standardized, such as the NF EN 1365-1 standard [AFN, 00] that specifies the fire resistance of load bearing walls. The second approach consists of evaluating the performance level of the critical function overtime, that is to say the function that is first to reach its threshold, such as the Performance Limits Method proposed by the BEST of the Polytechnic of Milan [Iacono 2005]. At the building level, the performance assessment regards the capacity of ensuring the six essential requirements as defined by the Construction Products Directive (1. mechanical resistance and stability, 2. fire safety, 3. hygiene, health and the environment, 4. safety in use, 5. noise protection, 6. energy efficiency and heat retention). This approach essentially aims to study on the one part the structural resistance under exceptional actions or accidental actions, such as fires, earthquakes, explosions, etc. and on the other part the capacity of buildings to ensure a defined level of comfort, such as acoustical comfort, thermal comfort, etc. The research in this domain consist of developing models, generally numerical ones, that aim to be as representative as possible of reality, bringing the building design to be as compliant as possible with master-building and users expectations, such as the method of ventilation control of buildings proposed by Jreijiry et al. [2004].

Existing methods and methodologies of performance assessment, at the material level, at the building component level and at the building level, have the same limitation: they try to study one or several performance criteria relevant to the same concern as, for example, the resistance to exceptional actions or accidental action, thermal comfort, etc.

In this context, we propose a methodology applicable to all building components and that, at each moment of the service life, provides a global vision of all the performance criteria relevant to the users expectations with regard to the building components.

The proposed methodology is presented in Section 2. Section 3 provides a detailled description of the fourth phase of this methodology: the quantitative analysis of performance that enables an examination of the degradation phenomena upon the functional performance levels, to obtain the multi-performance profile of all building components in service, that is to say the representation at a given date of all the performance levels of the functions and the function combinations of the considered building component. Section 4 provides an illustrative application of the methodology, more precisely of phase four; the case study being a brick wall covered by an insulation compound.

2 GLOBAL METHODOLOGY

The proposed assessment methodology of the multi-performance profile of all in-service building components is comprised of four phases as schematised in Fig. 1.

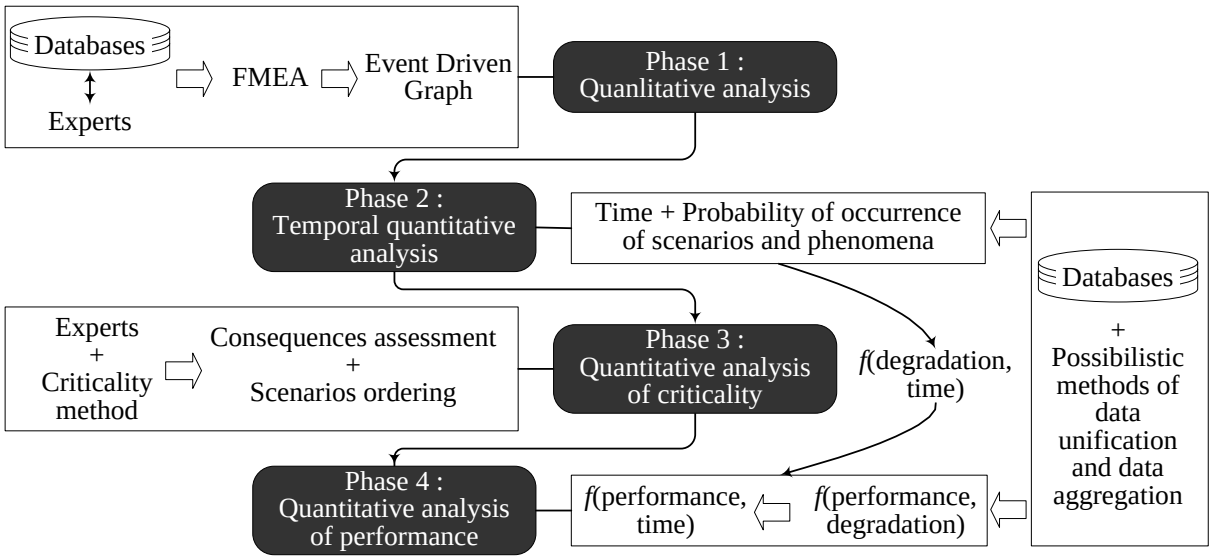

Figure 1. Assessment of the multi-performance profile of all in-service building components.

In the first phase, the qualitative analysis allows for the identification of all degradation scenarios (chains of degradation phenomena) that may damage the building component during its service life, potentially affecting its performance level. For each phenomenon involved in the scenarios, we identify: (1) the causes of this phenomenon, that may be climatic or usage conditions (rain, wind, temperature, impact, etc.) human mistakes (design error) or material incompatibilities (e.g. premature ageing of the silicone in contact with silver oxide), (2) the consequences of this phenomenon, (3) the elements of the building component that may be damaged by this phenomenon and, (4) the functions that may be affected by this phenomenon. This qualitative analysis is based on a structural analysis, a functional analysis and a failure mode and effects analysis (FMEA); these analyses are detailled and illustrated in a case study of a solar panel by Talon *et al.* [2004].

The second phase, the temporal quantitative analysis, consists of assessing the duration and occurrence probability of all identified degradation scenarios (from phase one) as well as the duration and occurrence probabilities for all the phenomena involved in these scenarios. This analysis is based on the use of all available multi-source data (expert opinion, diagnosis, probabilities, statistics, and experimentations).

In the third phase, the quantitative analysis of criticality, the aim is to assess the consequences of the degradation scenarios on the basis of three criteria: (1) the duration, (2) the occurrence probability and (3) the gravity of these consequences on the performance of the studied building component. The aggregation of these three criteria provides a means to order all the identified degradation scenarios by criticality importance in order to select only the most critical scenario, those having a significant impact on the studied building component.

Phase four, the quantitative analysis of performance, consists of assessing, for each triplet {function, phenomenon, element}, the relations between degradation states and performance levels; when combining the formula that link degradation states to time (defined in phase two) the evolution of performance levels overtime can be obtained. On the basis of these results and taking into account all

the phenomena, the functions and the elements at stake, the multi-performance profile of the considered building component can be obtained for any point in its service life.

These four phases of analysis are based upon: developed databases (database of environmental agents, database of functions, database of phenomena [Talon *et al.* 2003]); methods of data treatment based on theory of possibility (data quality assessment [Talon *et al.* 2007] based on NUSAP method [Funtowicz and Ravetz, 1990], data unification and data aggregation [Talon 2006] based on the data fusion method [Shafer 1976], [Lair 2000]); and, representation tools, such as the temporal event driven graph that schematises the most critical degradation scenarios, their common phenomena and their causes; an example of a temporal event driven graph is provided in Section 4.

3 PHASE OF PERFORMANCE ASSESSMENT

The objective of the quantitative analysis of performance (phase 4) is to obtain, at a fixed date during the service life of the building component, the performance levels associated to each of its functions and combinations of functions. This analysis is comprised of four sub-phases: (1) obtaining the mathematical function of performance level μ_i^k of a function F_k (e.g. mechanical resistance, transparency, etc.) associated with the phenomenon Ph_i (e.g. cracking, corrosion, etc.); (2) determination, for each pair {F_k, fixed date}, the corresponding performance level μ^k; (3) definition of the combinations between functions; and (4) obtaining of multi-performance profile.

3.1 Obtaining the Performance Level Function μ_i^k of a Pair {F_k, Ph_i}

The objective of this sub-phase is to model the relationship between mechanical, physical and chemical degradations of an element to its loss of functional performance. The proposed method is based on both the "classical" process of the evolution of the material degradation indicator and on the use of multi-source data. The "classical" process, as explained by Jernberg *et al.* [2004], consists of: (*i*) identifying the degradation indicator to be studied, via an analysis of the environmental actions and the known degradation mechanisms of the material; (*ii*) measuring, by experimentations (accelerated ageing test and natural ageing test), the evolution of this degradation indicator overtime; and (*iii*) determining the relations between the results obtained by the two kinds of tests in order to assess the service life of the material. Our process consists of: (*i*) identifying the degradation indicators associated to all functions, (*ii*) collecting all the available data from various sources (experimental results, theoretical results, such as modelling and numerical simulations, expert opinions, etc.); (*iii*) determining the relationship between these degradation indicators and the performance level of the considered function; and (*iv*) unifying this data in order to obtain a consensual mathematical function of performance level μ_i^k and quality indicators of this result.

Experts in material durability lead the first three items of our process. The fourth item is based on a fusion method detailled by Talon [2006]; the underlying principle is that when data has been collected from different heterogeneous sources , a belief mass that is reflective of the confidence in the data may be attributed to each dataset. Then, all collected data is combined in order to obtain a consensual dataset, regrouping the maximum of consensus and that best represents the available knowledge. The significance of our approach is the capability to base new evaluations upon previous studies that are quite similar and thereby take into account all the triplets {phenomena; functions; elements}; this cannot be done within the classical approaches.

3.2 Determination for Each Pair {F_k, fixed date} the Performance Level μ^k

The first step in determining the performance level is to select all the phenomena affecting the considered function F_k by a fixed date. For example, if one considers the function F_1 in Fig. 2, the function is affected by the selected phenomenon Ph_1, Ph_2 *and* Ph_9 (in black) prior to the "fixed date". Ph_7 is not selected as it starts at t_6, later than the "fixed date". Figure 2 contains three scenarios Sc_i that are respectively compounded actions of 4, 3 and 2 phenomena represented by rectangles; the associated function and the degradation state of this phenomenon at the considered date, as an example the date t_1 for the phenomenon Ph_1 are contained in these rectangles. Next, the degradation states for all phenomena at the fixed date on the basis of the results of the temporal quantitative analysis (second phase of the methodology) are determined. Then the performance levels that correspond to the degradation states on the basis of the mathematical functions of performance levels assess during the first sub phase are deduced. As the third step, the performance level of the considered function is inferred; as being equal to the minimum of the performance levels obtained for all the selected phenomena.

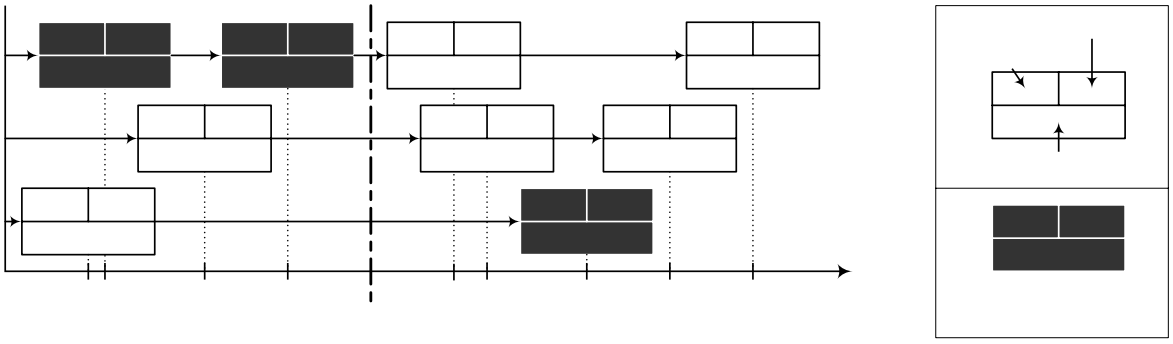

Figure 2. Illustration of the phenomena selection that affect the function F_1 at a fixed date

3.3 Definition of the Combinations of Functions

The objective here is to model the combination between all the functions in order to obtain an assessment that represents the global and realistic behaviour of the considered building component overtime. As an example, the visibility function through a double glass unit may be the combination of the transparency function and of the resistance function against environmental agents. We define the combinations between functions in order to take into account the fact that two functions independently may have an acceptable performance level but globally may lead to the failure of the building component. The functions of the relationship are identified and then that relationship is typically expressed by the following generalised formula:

$$\alpha_1 \times \mu^1 + \alpha_2 \times \mu^2 + ... + \alpha_n \times \mu^n \geq \mu_{threshold} \quad \text{and} \quad \sum_i \alpha_i = 1 \quad [1]$$

where $\mu_{threshold}$ represents a threshold performance level and the α_i represent coefficients.

3.4 Obtaining of the Multi-Performance Profile

In the proceeding steps the performance levels of the functions were considered independently. Now, we want to assess the performance level of each combination of functions; it is obtained by replacing the performance levels of the functions that were independently considered in the combination equations, such as the equation [1]. As an example, considering $\mu^1 = 0{,}6$ and $\mu^2 = 0{,}4$ at a fixed date and in a combination of F_1 and F_2 formalised by the equation $0{,}8 \times \mu^1 + 0{,}2 \times \mu^2$, the performance level of this combination at the fixed date is equal to 0.56.

We represent the performance levels of the functions and the combination of functions, at a fixed date, with radar representation, such as those in Fig. 5.

4 BRICK WALL CASE STUDY

It is to be noticed that the numerical data collected and used in order to perform this application has an heterogeneous reliability. In consequence, the numerical results presented here have only an illustrative value.

The structure of the studied brick wall is presented in Fig. 3 and the materials of the elements of this wall are included in the Table 1. This brick wall fulfils five functions: (1) F_1 – to stop the flow of environmental agents, (2) F_2 – to absorb the infrared radiation, the temperatures and the noises, (3) F_3 – to mechanically resist, (4) F_4 –to resist damaged by the contact of environmental agents, (5) F_5 – to be in accordance with the standards and requirements.

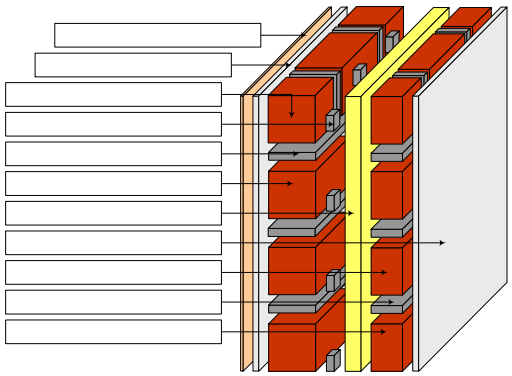

Figure 3. Schematisation of the brick wall structure

Table 1. Materials of the brick wall

N°	Material
1	Acrylic paint
2	Lime, cement, sand
3a-b	Terracotta
4	Mortar
5	Cement, sand, epoxy resin
6	Glass wool
7a-b	Terracotta
8	Mortar
9	Lime, cement, sand

The results of the qualitative analysis and of the temporal quantitative analysis of this wall are presented on the temporal Event Driven Graph of the Fig. 4. The names of the phenomena from Fig. 4 are regrouped in the Table 2 and the legend of each block is as defined in Fig. 2.

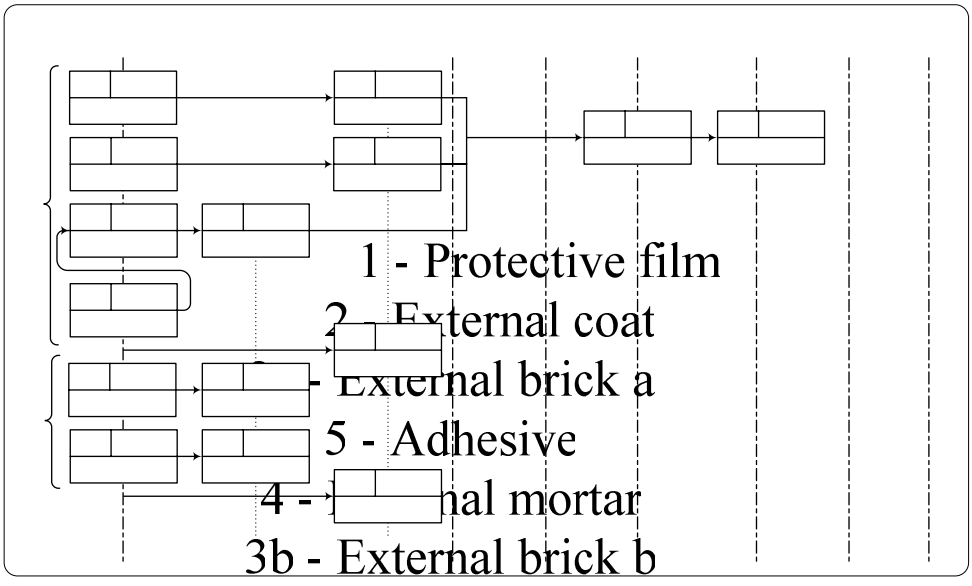

Figure 4. Temporal Event Driven Graph of the brick wall

Table 2. Names of the phenomena of the Fig. 4

N°	Phenomena
Ph_1	Uniform leaching of protective film
Ph_2	Erosion and chalking of protective film
Ph_3	Insufficient resistance of external brick a
Ph_4	Insufficient resistance of external brick b
Ph_5	Drying of external coat
Ph_6	Cracking of external brick a
Ph_7	Cracking of external brick a
Ph_8	Cracking of external coat
Ph_9	Cracking of protective film

N°	Phenomena
Ph_{10}	Unsticking of adhesive
Ph_{11}	Settling of insulation
Ph_{12}	Leaching of external coat
Ph_{13}	Alkali-reaction of external mortar
Ph_{14}	Non planarity of external layer
Ph_{15}	Non planarity of internal layer
Ph_{16}	Breakdown of external layer
Ph_{17}	Breakdown of internal layer

The multi-performance profiles of the brick wall obtained by conducting the quantitative analysis of performances at different points during the service life are presented in Fig. 5.

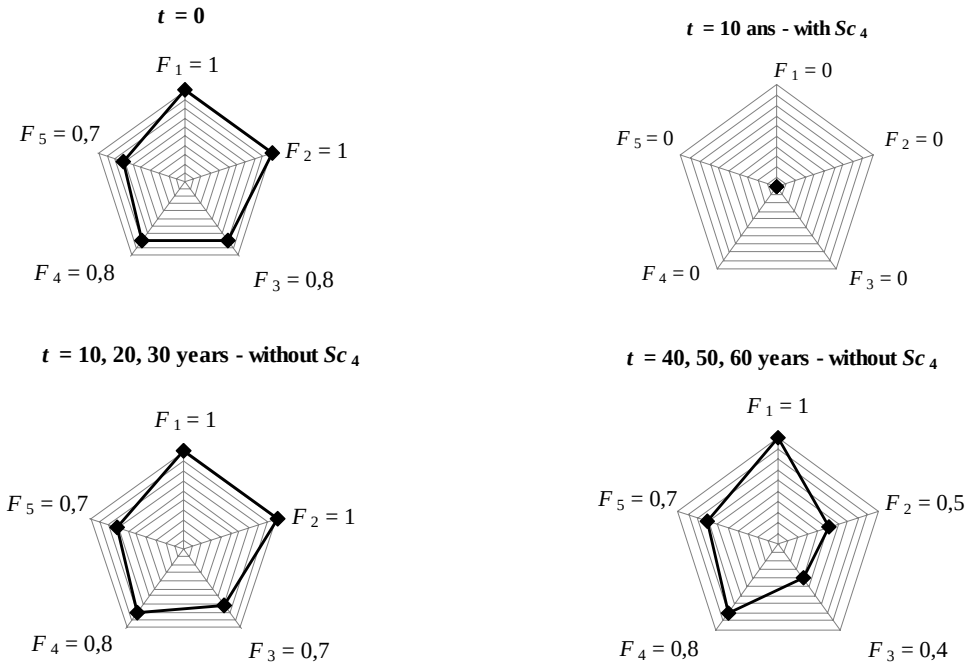

Figure 5. Multi-performance profiles of the brick wall at different moments of its service life

By considering the Sc_4 scenario of breakdown of the brick layers (external bricks with external mortar and internal bricks with internal mortar), a complete failure is obtained before 10 years, that is to say for all the functions of this wall.

This breakdown scenario can begin and end in the observation period of the study if the support of brick layers is significantly out-of-plane while the wall is subjected to a very strong impact. If this phenomenon and cause are not considered to occur, the multi-performance profiles obtained at different dates of the service life of this brick wall are the ones in Fig. 5 named "without Sc_4".

By formulating this hypothesis, one can note that the kinetics of the functions "F_2 – to absorb" and "F_3 – to mechanically resist" increase significantly between 30 and 40 years and that this is due to the complete achievement of the phenomena "Ph_{10} – unsticking of adhesive" and "Ph_{11} – Settling of insulation"; these phenomena may lead to an horizontal mechanical action on the bottoms of the brick layers that may result in crushing.

5 CONCLUSION

We present a methodology of assessment of the multi-performance profiles of all building components at a moment of their service life. This methodology is based on: (1) the identification of the degradation scenarios that affect the considered building component, (2) the quantification of the duration and the occurrence probability of these scenarios and the compound phenomena, (3) the quantification of the consequences of these scenarios and their ordering by criticality importance and, (4) the determination of the relation between degradation states and performance levels of the functions and the combinations of functions of the building component considered for obtaining its multi-performance profile. The main advantages of this methodology are: (1) to take into account all the degradation phenomena and all the functions at stake in the performance assessment, (2) to consider all the available and multi-source duration data, occurrence probability data and performance data, (3) to take into account all the interactions between elements that have a major influence on the performance assessment. The application of this methodology on the case study of a brick wall covered by an insulation compound has proved it is operational. The essential perspectives of this research work are: (1) to apply this methodology to other case studies in order to pursuit the implementation of the phenomena database with duration data, occurrence probability data and performance data in order to develop a knowledge base that allows the characterization of all building components in all environment types and, (2) to conduct a sensitivity analysis of the proposed methodology.

REFERENCES

AFNOR 2000, *Essais de résistance au feu des éléments porteur -Partie : murs*, NF EN 1365-1, Paris.

Funtowicz, S.O. & Ravetz, J.R. 1990, *Uncertainty and Quality in Science for Policy*, Kluwer Academic Publishers, Dordrecht.

Iacono, P. 2005, *Proposizione di un percorso metodologico applicabile alla valutazione della durabilità di elementi tecnici edilizi e degli elementi funzionali costituenti*, Thesis (PhD) of Polytechnic of Milan.

Jernberg, P. Lacasse, M.A. Haagenrud & S.E. Sjöström, C. 2004, *Guide and Bibliography to Service Life and Durability Research for Building Materials and Components*, Publication CIB n°295, Rotterdam.

Jreijiry, D., Husaunndee, A. Inard, C. & Villenave, J.G. 2004, 'Ventilation control based on indoor air quality using SIMBAD building and HVAC toolbox', Proc. CIB World Building Congress 2004, Toronto, 3 7 May 2004.

Lair, J. 2000, *Evaluation de la durabilité des systèmes constructifs du bâtiment*. Thesis (PhD) of Clermont-Ferrand Univeristy, CSTB and Lermes.

Lee, A. & Barrett, P. 2003, *Performance Based Building: First International State-of-the-Art Report*, International Council for Research and Innovation in Building and Construction, Rotterdam.

Shafer, G. 1976, *A mathematical Theory of evidence*, Princeton University Press, Chichester.

Talon, A. Boissier, D. & Hans, J. 2007, 'Durée de vie des produits de construction – Evaluation de la qualité des données', Proc. XXV^{èmes} Rencontres Universitaires de Génie Civil, Bordeaux, 23 25 May 2007.

Talon, A. 2006, *Evaluation des scénarii de dégradation des produits de construction*, Thesis (PhD) of Clermont-Ferrand University, CSTB and LGC.

Talon, A. Boissier, D. Chevalier, J-L. & Hans, J. 2004, 'A methodological and graphical decision tool for evaluating building component failure', Proc. CIB World Building Congress 2004, Toronto, 3 7 May 2004.

Talon, A. Boissier, D. & Chevalier, J-L. 2003, 'Capitalization and use of experience and knowledge on building products degradation', Proc. 2nd International Symposium on Building Pathology, Durability and Rehabilitation, Lisbonne, 6 8 November 2003.

Fuzzy Lifetime Prediction Of RC Structures Subject To Chlorides

Giuseppe Carlo Marano [1]
Giuseppe Quaranta [2]
Sara Sgobba[3]
Simona Sasso[4]
Michele Notarnicola[5]

T 42

ABSTRACT

Pitting corrosion of the steel bars is a process that strongly jeopardizes the durability of reinforced concrete structures exposed to chlorides. This is a problem widely studied in order to evaluate structural lifetime. Nevertheless, the proper treatment of the noteworthy sources of uncertainty, that affect the numerical values of geometrical and mechanical structural parameters, is still an open question. Such properties, in fact, cannot be considered as deterministic quantities. In many real problems, very few uncertain data are available and new non-probabilistic procedures need to be defined to perform lifetime estimation. In the present study, parameters are modelled using fuzzy set theory and a time-dependent fuzzy safety factor is defined in order to indicate how the critical chloride front is distant from the bars. Moreover, the study provides a more proper mathematical analysis of chloride penetration into concrete and an improved calibrating procedure to estimate sampling model parameters, also accounting of time variability. The analysis confirms that the application of oversimplified Fick's solutions leads to substantial conceptual errors in service lifetime estimation.

KEYWORDS

Chloride penetration model, Fuzzy Safety factor, Genetic Algorithms, Pitting corrosion, Service Life prediction.

[1] *Department of Environmental Engineering and Sustainable Development, Technical University of Bari, viale del Turismo 10 - 74100 Taranto (Italy)* gmarano@poliba.it
[2] *Department of Environmental Engineering and Sustainable Development, Technical University of Bari, viale del Turismo 10 - 74100 Taranto (Italy)* quaranta@aliceposta.it
[3] *Department of Environmental Engineering and Sustainable Development, Technical University of Bari, viale del Turismo 10 - 74100 Taranto (Italy)* s.sgobba@poliba.it
[4] *Department of Environmental Engineering and Sustainable Development, Technical University of Bari, viale del Turismo 10 - 74100 Taranto (Italy)* simona.sasso@poliba.it
[5] *Department of Environmental Engineering and Sustainable Development, Technical University of Bari, viale del Turismo 10 - 74100 Taranto (Italy)* notarnicola@poliba.it

1 INTRODUCTION

Economic consequences due to deterioration of reinforced concrete (RC) structural elements are one of the most pressing problems, especially in industrialized nations where maintenance and reparation of these types of constructions are an impelling necessitate. In most cases, it has been established that reinforcement corrosion is the foremost cause of deterioration [Apostolopoulos and Koutsoukos., 2007]. The corrosion process of reinforcing bars is a well known phenomenon as it is also known that the consequences of a pitting corrosion process on structural safety are more serious than that due to general corrosion. For this reason, lifetime estimation of RC subject to chloride exposure deserves particular design attention. The main difficulties that researchers face in the investigation of these problems are due to the noteworthy lack of precise information. For this reason, the service life design methodology should take into account uncertainties. In last years, probabilistic approaches have been used with the aim of conducting a time-dependent analysis of RC structures subject to corrosion under conditions of uncertainty, but it should be observed that not all the uncertainty variables can be treated following this approach. Probabilistic description is not the most adequate way to describe uncertainty for a great part of realistic conditions and sometimes its use may be inadequate for some real problems. This is particularly true when only few data about one or more models and structural parameters are available or when investigating mechanical and geometrical system properties, as well as load conditions, are economically inconvenient or practically impossible. This happens, for example, in historical constructions. In the field of non-probabilistic approaches, different methodologies have been proposed: particularly, the approach based on the concept of fuzzy sets [Zadeh 1965] also for estimating service life of RC structures [Anoop *et al.*, 2002], seems appropriate because it is able to take in account the so-called lexical and informal uncertainties that affect both data and models. In this paper, a fuzzy service lifetime estimation of RC elements subject to chloride ingress is performed considering uncertainty on problem parameters that are modelled by using a fuzzy criterion. It should be noted that the concept of corrosion initiation time is done to coincide with the general service lifetime of the structure which ends when pitting corrosion process starts. Preliminary to this kind of investigation, it has been necessary to examine the state-of-the-art in order to recognize the potential typologies of uncertainties, in chlorides penetration process. The analysis of the bibliography on this theme, have confirmed the high uncertainty in model parameters definition. This substantially depends on the intrinsic variability of some parameters, on the insufficient or inadequate availability of data, but also on the high number of oversimplifications and neglected factors that during the years have been applied on chloride penetration model. Today, a great number of mathematical models have been developed and the application of each of them leads to different values of the main parameters. It is thus clear that sampling parameters are estimated with different confidence level of knowledge. In detail, some geometrical and mechanical parameters are well defined as deterministic or at least probabilistic, because a wide number of experimental data can be available. Other parameters instead are not well defined and therefore affected by different level of uncertainty, because for example few experimental data are available or because the assumed physical model is empirically extrapolated or is oversimplified and therefore less representative of the real process. For these reasons, all the parameters are treated under non-probabilistic assumptions. In this case, the fuzzy approach represents a more suited theory to perform other kind of analysis, properly taking into account of uncertainties. Therefore, another important preliminary point of investigation of the present work, concerns the chosen of the best deterministic sampling parameters by using a more proper calibrating procedure and then use these variable for the fuzzy treatment. With this aim, a more accurate solution of Fick's law have to incorporate the time-dependence of the diffusion coefficient and some researchers have also integrated the diffusion law taking into account time-dependent surface concentration [Mejlbro, 1996]. Two of these improved models [Mangat and Molloy, 1994; Mejlbro, 1996] have been chosen by the authors to be tested with experimental data by mean of a genetic algorithm (GA), in order to obtain the deterministic calibration parameters of model. In the second section of the paper, some of these variables are modelled as fuzzy ones and finally, time-dependent fuzzy safety factor is obtained in order to assess the service life of RC elements in terms of

the critical chloride front closeness to the bars during the time. This tool may be useful in order to support the decision maker (DM) in the planning of the maintenance interventions.

2 CHLORIDE PENETRATION MODELS

2.1 Conventional Model

A simplified model for the chloride penetration procedure is based on the assumption that the chlorides diffusion process can be modelled by means of the Fick's second law, as firstly realised by Collepardi *et al.* [1972]. Having only results available from short time experiments, and probably also due to mathematical difficulties, they only considered the case of constant diffusion coefficient and constant surface chloride concentration. This is a diffused supposition (i.e. it is adopted by Stewart and Rosowsky [1998]). According to this law, the chloride ion content is given by:

$$C(x,t) = C_s\left[1 - erf\left(\frac{x}{2\sqrt{D_a t}}\right)\right] \tag{1}$$

where $C(x,t)$ is the chloride content (in kg/m^3) at a distance x (in m) in a generic time instant t (in s); C_s is the surface chloride concentration (in kg/m^3); D_a is the apparent diffusion coefficient (in m^2/s). Using eq. **Hata! Başvuru kaynağı bulunamadı.**, it is possible to define the corrosion initiation time with reference to an assigned critical threshold chloride concentration on steel bars (denoted as C_{lim}). The chloride diffusion coefficient D_a is assumed a constant value even if it is time dependent. It will typically decrease as time passes since the capillary pore system will be altered as hydration products continue to form [Mangat and Molloy, 1994]. This meant that the diffusion coefficient could be written as a power function [Tang, 1996]:

$$D(t) = D_{ref}\left(\frac{t_{ref}}{t}\right)^m = K_0 t^{-m} \tag{2}$$

where D(t) is the diffusion coefficient at time t; D_{ref}, the diffusion coefficient at some reference time t_{ref} and *m* is a constant that depends on mix proportions. K_0 incorporates all constants and is defined as the effective diffusion coefficient at time t of reference. The application of equation (1) is very common in literature and also in different documents that provide guidelines for the durability design of concrete structures, as for example in documents developed by the EU DuraCrete project [1998]. The *DuraCrete Model* is an empirical model, which also has Fick's second law of diffusion as a theoretical background that has the following form:

$$C(x,t) = C_s\left[1 - erf\left(x \Big/ \left[2\sqrt{\left(k_c k_e D_{ref}\left(\frac{t_{ref}}{t}\right)^m\right)t}\right]\right)\right] \tag{3}$$

It is clear that the presence of the two multiplication factors k_c and k_e, that are two constants introduced in order to take into account the probabilistic nature of the environmental aggressiveness (k_e –environmental factor) and the material properties (k_c – curing factor), does not change the mathematical characteristic of the chloride profile. Indeed, the DuraCrete model has been developed on the simplification that the diffusion coefficient is a constant value and doesn't vary with time.

Nevertheless, in order to take into account also time-dependence effects, it has been suggested to replace the constant value of D_a that appears in equation (1) with the relationship (2).

2.2 Evolutionary Models With Time-Dependent Parameters

Already in the 1980's it was realised that the standard oversimplified model, on which is based equation (1), gave unrealistic rapid transport of chloride ions, especially when long term predictions are based on results from short term tests [Cairns and Law, 2003]. For the accurate prediction of chloride-diffusion in concrete, the time-dependence of diffusion rates needs to be incorporated in the analysis procedure, properly deriving the Fick's second law. This model was developed by [Mangat and Molloy, 1994], leading to the following equation:

$$C(x,t) = C_s \left[1 - erf \left(\frac{x}{2\sqrt{\frac{K_0}{1-m} t^{1-m}}} \right) \right] \tag{4}$$

Other solutions of Fick's second law exist with varying surface concentration. Some researchers observed that the chloride concentration of the exposed concrete surface of a marine structure was time-dependent. Mejlbro [1996] proposes that the chloride penetration model ought to be described by the following function:

$$C(x,t) = \left(\frac{T}{T_0} \right)^p \psi_p(z) \tag{5}$$

where T is the transformed time variable $T = \left(t - t_{ref}\right) D_a(t) \quad for\, t \geq t_{ref}$, with $D_a(t)$, that is equivalent to $D(t)$ as defined in equation (2), and T_0 is introduced in order to to make the ratio dimensionless. The exponent p depends on how fast C_s increases with time, i.e. mainly on the type of binder and the environment and the function $\psi_p(z)$, where $z = x/\sqrt{4T}$, satisfy an ordinary differential equation of second order which can be solved by means of a series expansion.

3 ANALYSIS OF THE BEST DETERMINISTIC MODEL

Modelling the chloride ingress is an important basis for designing reinforced concrete structures and for assessing the service life of structures. Even if the present paper uses a fuzzy approach for the lifetime estimation problem, the authors firstly consider very important to overcome some conceptual limitations and also errors that may occur considering standard oversimplified models as those defined in Eq. (1) and (3) or other functions derived by using equivalent mathematical procedures and assumptions. Indeed, even if in the past years the models used in Eq. (1) and (3) have been applied in a wide number of important construction projects, some authors [Luping and Gulikers, 2007] have observed that it is necessary to evaluate the errors computed in lifetime estimation and therefore in durability design due to these mathematical oversimplifications assumed in simplified models. Several authors in fact (for example, [Maage *et al.*, 1995; Choe *et al.*, 2007]), seem to have simply substituite the constant diffusion coefficient in the error function solution to the Fick's second law by the time-dependent D, without adequate clarifying the mathematical basis of the diffusion. The mathematical mistake so committed results in a significant difference between the diffusion coefficient K_0 that appears in equation (4) and the same coefficient D_a that appears in equation (3), as demonstrated by

Luping and Gulikers [2007]. For the before described reasons and for the great variability whereby the diffusion law has been solved in literature, different values of the main model parameters have been obtained. Starting from this consideration about uncertainty in problem parameters definition, in the present paper an improving in service life assessment goes by two main steps. The first one regards the chosen of the best fit model in order to consider the most refined model to represent the physical process and deterministically determine the main parameters. At this stage, therefore, it tries to avoid some oversimplifications conceptually wrong in model definition, like the most common assumption of the time-independence of the diffusion coefficient. Nevertheless, parameters, which define the occurrence properties of variables, are non deterministic in nature and very often no information is available on their fluctuation. Therefore in the second part of the present paper, uncertainties have been introduced in the model parameters and a fuzzy modelization has been applied as useful tool to perform the lifetime assessment. Final results are obtained for a realistic example.

3.1 GA-Based Comparison Analysis Between Predicted And Measured Chloride Profiles

The model fitting analysis is based on the fundamental experimentation by Thomas and Bamforth [1999], applied to three concrete mixes: Portland cement concrete (PC), fly ash concrete (PFA) and slag concrete (GBS). Even if the proposed procedure followed by the authors used to determine the chloride profile, shows a very good correlation with the experimental data, it suffers of a significant conceptual limitation. This is due to the fact that firstly they assume the standard solution as written in equation (1), founding the values of C_s and D_a as best fit calibration parameters, by iteration. At the same time they assume the relationship (2) that describes the diffusion coefficient with time, in order to take into account time-dependence effects, not accounted in the previous used model. From this last equation, they obtain D_{28} and m values that best fit the data [Thomas and Bamforth, 1999]. Starting from this data, in order to determine the sampling parameters to adopt in the afterwards fuzzy analysis, a new genetic algorithm (GA) based procedure is applied. In the following, adopting the two time-dependence models of equations (4) and (5) and calibrating them also in function of the time variable, it tries to mathematically improve the deterministic estimation of the parameters, so that it is given a meaningful significance to their fuzzy treatment, later discussed. Once assumed these "evolutionary" models, the succeeding improvement in the estimation of the parameters consists in calibrating these one as time function. In this way, the chloride profile is no more defined in a bi-dimensional space that describes the chloride concentration with depth at a fixed time, but has to be dependent also on time. Therefore, the adjustment technique is developed in a three-dimensional depth-time space. Only in this manner, it is possible to rigorously estimate the diffusion coefficient and accounting for its changing with time. In order to simplify the notation, the model at the base of Eq. (4) will be called '*Model A*' and the profile of equation (5) will be called '*Model B*'. For each of these models, the chloride profile that best fit the experimental data is plotted. For the sake of argument, the three-dimensional profile Fig.1(a) and the contour graph Fig.1(b), in function of time and depth is reported with reference to the *Model A*, in case of Portland cement. Results show a good agreement between the model prediction and the experimental data of Thomas and Bamforth. In Tab.1 are also indicated the calibrating parameters values, for the Model A and the Model B. In order to compare these one with the other approaches, also the values of the same parameters referred to Thomas and Bamforth's model application are reported. For all mentioned reasons, the parameters successively treated as fuzzy variables are those obtained by the before described calibrating GA-based procedure, with reference to the mathematically improved model A, because as seen, more rigorously determined by an analytical and conceptual point of view.

Table 1. Main calibrating parameters of Models

Concrete Mix		C_s (%)	*Diffusion coefficient* $\left(cm^2/yr\right)$	m
PC	Model A	0.3775	K_0 = 1.864	0.2528

	Model B	0.3770	D_a = 6.988	0.3459
	Thomas and Bamforth [1999]	0.35	-	0.1
PFA	Model A	0.5259	K_0 = 0.283	0.5807
	Model B	0.3804	D_a = 5.317	0.7017
	Thomas and Bamforth [1999]	0.5	-	0.7
GBS	Model A	0.5267	K_0 = 0.076	0.9941
	Model B	0.5399	D_a = 9.999	0.8624
	Thomas and Bamforth [1999]	0.5	-	1.2

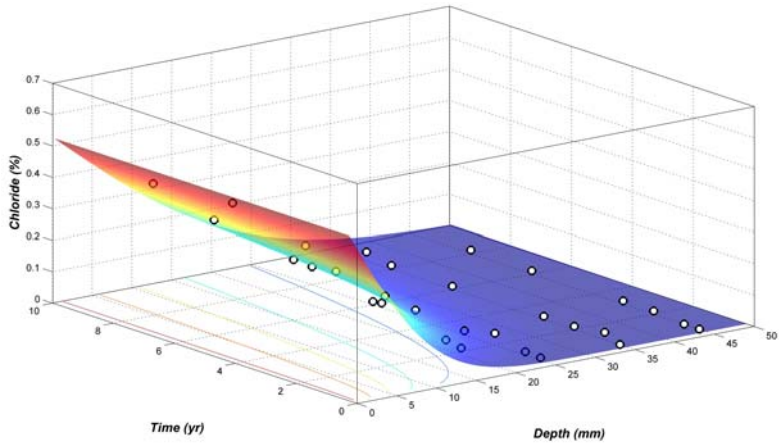

(a)

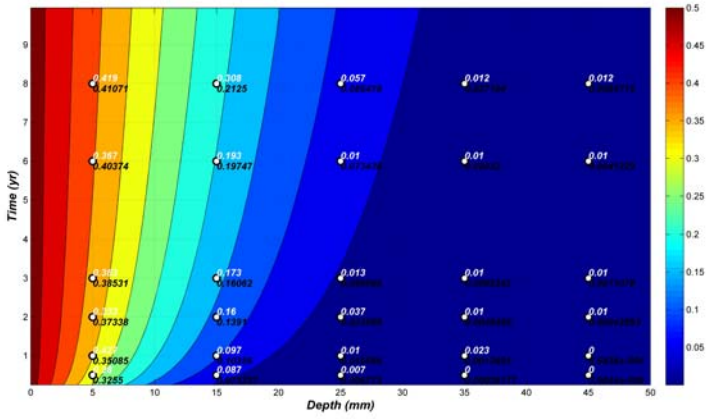

(b)

Figure 1. Correlation of Chloride profile with experimental data (Model A, PFA case)

4 FUZZY ANALYSIS OF STRUCTURAL SERVICE LIFE

The following treatment of lifetime prediction is conduct on the base that fuzzy sets are applied on the model variables. These variables, due to their conjectured informal or lexical uncertainties, can be treated by means of fuzzy sets theory [Zadeh, 1965].This can be considered an acceptable assumption due to the considerable semplifications that affect the model and the large variability whereby it is defined. Moreover, it is also necessary to observe that even model parameters may suffer of variations not always capable of being assimilated to specific probabilistic distributions which are tipically obtained on the basis of other models. Indeed, very often in literature is not possible to find probabilistic univocal approachs in order to represent the variables. On the basis of all these

considerations in the following it assumes that surface chloride concentration C_S and critical chloride concentration $C_{\lim}$ are non deterministic variables. Besides, for the before explained reasons, in addition to these parameters, also the age factor *m* and diffusion coefficient k_0 are assumed uncertain. The application of the fuzzy set theory, on the just cited variables, offers the possibility to consider a gradual assessment of the membership grade of an element in relation to the defined set. This degree of membership is described by a so-called membership function (MF). The MF acquisition of every fuzzy variable is one of the problems of structural analysis based on the fuzzy set theory. This is a "knowledge acquisition" problem [Klir and Yuan, 1995]. Generally, it is possible to assert that an unitary approach does'nt exist for the so-called fuzzification, but different procedures can be adopted for each situation. These methods for constructing MF can be either direct or indirect with a single expert or multiple experts [Klir and Yuan, 1995; Klir, 1996]. This work assumes that the MF is known for each fuzzy variable. In other words, we suppose that a knowledge acquisition procedure has been performed preliminary. Standard probabilistic approaches of reliability cannot be used in the presence of fuzziness and so different fuzzy reliability measures have been proposed, for instance by Shrestha and Duckstein [1998], Elishakoff and Ferracuti [2006(a), 2006(b)]. Finally, it is possible to define the central time-dependent fuzzy safety factor as follows [2006(a)]:

$$\beta(t) = \frac{C_{\tilde{c}}(t)}{C_{\tilde{f}}(t)} \tag{6}$$

where $C_{(\square)}(t)$ denotes the abscissa of the center of gravity of the MF (centroide). $\tilde{c}$ and $\tilde{f}$ respectively denote the fuzzy cover and the position of the chloride critical front.

4.1 Numerical Application

The central time-dependent fuzzy safety factor in (6) can be assumed as a valid tool to support the DM in planning maintenance works. Geometrical, mechanical and environmental data are reported in Table 2. In order to show the effectiveness of the proposed procedure, the fuzzy lifetime analysis of a RC column with section 0.3x0.3 m of PFA concrete mix, subject chloride ingress at one side, is performed considering uncertainties. In order for it to assume an unique value, the abscissa of the center of gravity of its MF has been considered.

Table 2. Parameters adopted in the numerical applications

Parameter	*Type of uncertainty*	*Values*
k_0	Fuzzy	$\langle 15,\ 25,\ 35 \rangle$
m	Fuzzy	$\langle 0.45,\ 0.50,\ 0.65 \rangle$
C_S	Fuzzy	$\langle 0.40,\ 0.45,\ 0.65 \rangle$
$C_{\lim}$	Fuzzy	$\langle 0.15,\ 0.20,\ 0.25 \rangle$
cover	Fuzzy	$\langle 15,\ 25,\ 30 \rangle$

In Fig. 2 is plotted the fuzzy safety factor as before defined. In the upper right corner of the figure, the MF (adopted of triangular shape) for the chloride critical front distance from side d_{cr} in five different years is reported with a continuous line. The corresponding safety factors and years are indicated in the principle diagram with the same symbols. The MF of the cover is also indicated with a dashed line for the purpose of comparison. For the same years the fuzzy critical front trend with time is plotted in Fig. 3 (in gray graduation from blank, for null degree of membership, to black, for unitary degree of

membership). The red indicator in figure the shows the centroide of the MF of cover. From the analysis of Figure 2 it is possible to observe that the safety factor reaches a unitary value after about 55 years. First of all, it is possible to observe that, in time, the support of the MF tends to increase. The analysis have been extended beyond the limit state (β <1), in order to prove that the centroide of the critical front MF changes position, during the course of time, depending on the low or high values of the fuzzy safety factor in comparison with the core. The centroide is positioned to the right, with respect to the core, in the safety region ($\beta \geq 1$). This is clearly shown with the circle and the upward-pointing triangle. This trend is not particularly visible in the safety region but becomes more appreciable in the unsafety one. This observation leads to conclude that the uncertainties are such that the deterministic analysis fournishes a more advanced fuzzy position of the chloride critical concentration front (the deterministic value is assumed in correspondance of the MF core), tending to overderestimate the critical front distance d_{cr} from the side, in comparison to a fuzzy approach, therefore it provides a conservative value of the lifetime estimation. Besides, this specific example shows that the effects of uncertainty, over a given time, tend to become more stable, as can be deduced by the approaching of the MF cores with time increasing and also by the stabilization of the centride-core distance.

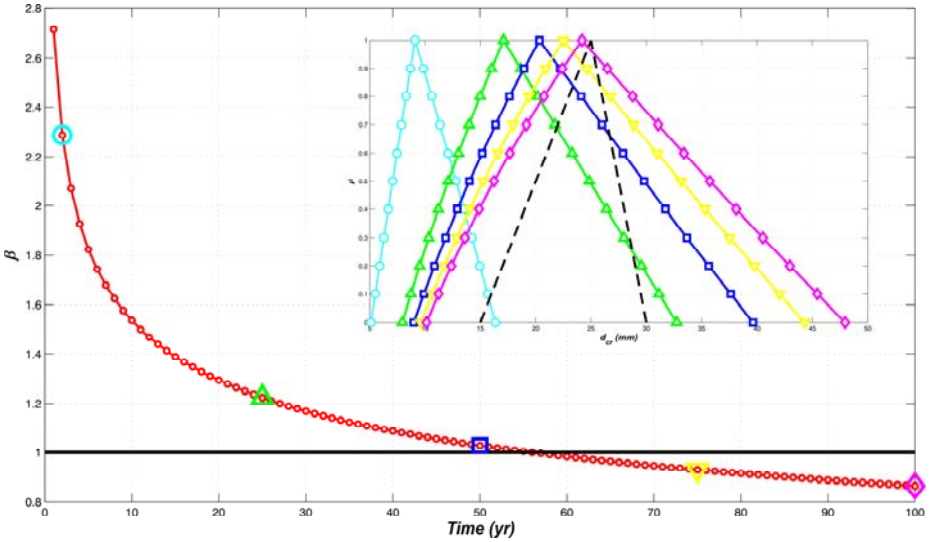

Figure 2. Illustrative example for PFA mix concrete

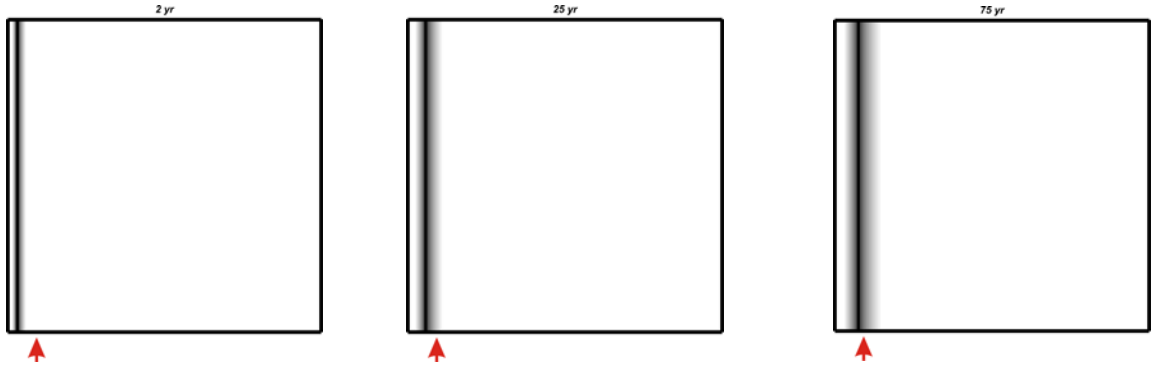

Figure 3. Trend of the chloride critical front at 5 (a), 25 (b) and 75 (c) years.

5 CONCLUSIONS

Service life of RC structural elements subject to chloride ingress has been estimated considering uncertainties in problem parameters. The analysis of the state-of-the-art conditions has shown that geometrical, mechanical and environmental parameters cannot be taken into account neglecting the different sources of uncertainty. Therefore, traditional probabilistic approaches cannot be performed.

This work develops a general procedure in which firstly the most refined deterministic models are selected and then, a calibration procedure GA algorithm-based is used in order to estimate the main parameters that are successively assumed as uncertain and treated as fuzzy variables. The fuzzy safety factor is obtained considering fuzzy variables for both the chloride front and the cover. A numerical example shows the effectiveness of the approach as useful tool to support the DM in economic analysis and planning of interventions, showing that the simple deterministic analysis, not properly accounting of intrinsic uncertainty of model parameters, cannot gather important aspects of lifetime prediction.The present approach is a very robust methodology, because it allows to overcome the notable difficulties that designers may face in real circumstances when non-statistical information, technical judgments and points-of-view have to be considered.

AKNOWLEDGMENT

The authors wish to express their gratitude to ***Prof. Lorenzo Liberti*** for his cultural and economical support to the development of the present work. The authors also wish to thank **Regione Puglia's** Funds, in the field of Progetto Esplorativo PE_017; research project "Valorizzazione di residui del processo di cottura del clinker per la produzione di cementi di miscela" (Det.Dir. Sett. progr. Politiche Com. Regione Puglia 23/0/06 n.13) for their economical support.

REFERENCES

Anoop, M.B. Rao, K.B. Rao, T.V.S.R.A. 2002, 'Application of fuzzy sets for estimating service life of reinforced concrete structural members in corrosive environments' *Engineering Structures* 24 1229–1242.

Apostolopoulos, C. A. Koutsoukos, P. G. 2007, 'Study of the corrosion of reinforcement in concrete elements used for the repair of monuments', *Construction and Building Materials* (2007, article in press).

Cairns, J. D.; Law, D. 2003, Prediction of the ultimate state of degradation of concrete structures. Proceeding of ILCDES 2003, Kuopio, pp169-174.

Choe, D-F *et al.* 2007, 'Probabilistic capacity models and seismic fragility estimates for RC columns subject to corrosion'. Reliab. *Eng Syst Safety* doi:10.1016/j.ress.2006.12.015 (2007, article in press).

Collepardi, C M. Marcialis, A. Turriziani, R. 1972, 'Penetration of chloride ions into cement pastes and concrete', *J. Am. Ceram. Soc*. 55 (10) 534–535.

Duprat, F. 2007, 'Reliability of RC beams under chloride-ingress', *Construction and Building Materials* 21, 1605-1616.

DuraCrete 1998, Modelling of Degradation, EU-Project (Brite EuRam III) No.BE95-1347, Probabilistic Performance based Durability Design of Concrete Structures, Report, vol. 4–5.

Elishakoff, I. Ferracuti, B. 2006(a), 'Fuzzy sets based interpretation of the safety factor', *Fuzzy sets and systems* 157, 2495-2512.

Elishakoff, I. Ferracuti, B. 2006(b), 'Four alternative definitions of the fuzzy safety factor', *Journal of aerospace engineering*, 19 (4), 281-287.

EN 1992-1-1:2004, Eurocode 2, Design of concrete structures-Part 1.1: General rules and rules for buildings.

Klir, G. J. 2006, *Uncertainty and information*, John Wiley & Sons.

Klir, G. J. Yuan, B. 1995, *Fuzzy sets and fuzzy logic*, Prentice Hall.

Luping, T. Gulikers, J. 2007, 'On the mathematics of time-dependent apparent chloride diffusion coefficient in concrete', *Cement and Concrete Research* 37, 589-595.

Maage, M. Helland, S. Carlsen, J. 1995, *Practical non-steady state chloride transport as a part of a model for predicting the initiation period*, in: L.-O. Nilsson, J. Ollivier (Eds.), Chloride Penetration into Concrete, RILEM, pp. 398–406.

Mangat, P.S. Molloy, B.T. 1994, 'Prediction of long-term chloride concentration in concrete', *Mat. Struct.* 27, 338– 346.

Mejlbro, L. 1996, *The complete solution to Fick's second law of diffusion with time dependant diffusion coefficient and surface concentration.* Proceeding of CEMENTA's workshop on Durability of Concrete in Saline Environments". Danderyd, Sweden.

Shrestha, B. Duckstein, L. 1998, 'A fuzzy reliability measure for engineering applications', *Uncertainty modelling and analysis in civil engineering,* CRC press LLC, 120-135.

Stanish, K. Thomas, M.D.A. 2003, 'The use of bulk diffusion tests to establish time-dependent concrete chloride diffusion coefficients', *Cem. Concr. Res.* 33 (1) 55–62.

Stewart, M. G. Rosowsky, D. 1998, "Time-dependent reliability of deteriorating reinforced concrete bridge decks", *Structural Safety* 20, 91-109.

Tang, L. 1996, *Chloride Transport in Concrete — Measurement and prediction*, PhD thesis, Publication P-96:6, Dept. of Building Materials, Chalmers Univ. of Tech., Gothenburg, Sweden.

Thomas, M.D.A. Bamforth, P.B. 1999, 'Modelling chloride diffusion in concrete—effect of fly ash and slag', *Cem. Concr. Compos.* 29 487– 495.

Zadeh, L.A. 1965, 'Fuzzy sets', *Information and control*, 8, 338-353.

Timber Structures Service Life Modelling

Jan-Willem van de Kuilen[1,2]
Nadine Edi Montaruli[1]

T 42

ABSTRACT

Timber has been used throughout the world in structural application from pile foundations to roof structures. As an example, old dutch cities are founded on wooden piles of up to 22 meters long, wheras roof spans in ancient Italian structures may reach more than 20 metres. These structures are slowly decaying, mainly caused by mechanical, physical and biological loads. Different inspection techniques are used to estimate the remaining sound cross sections, to classify the wood quality and to determine the activity level of the (biological) decay. Infrared spectroscopy is used to determine different types of biological decay (brown rot, soft rot, white rot) and in conjunction with the decay, the expected amount strength loss. Very often, questions arise about the remaining service life of such structures. In the paper an overview is given on different degradation mechanisms and the assesment procedure. Then, using an exponential damage accumulation model that takes into account influences of biological degradation, crack formation and mechanical stresses, estimations are given on the remaining service life in relation to current required safety levels. The exponential damage model was verified on long term strength tests for sawn timber and timber connections at diiferent load levels and climates. In the paper, special attention is given to large cracks that are often found in ancient floor and roof beams. Practical examples from existing building structures and hydraulic works will be given both with cracks and with biological decay.

KEYWORDS

Timber structures, Service Life, Damage modelling, IR-spectroscopy, Cracks

[1] Delft University of Technology, Fac. of Civil Engrineering and Geosciences, Delft, the Netherlands, Phone +31152782322, Fax +31152783713 , j.w.g.vandekuilen@tudelft.nl, Phone +31152784073, Fax +31152783713 n.e.montaruli@tudelft.nl;
[2] CNR-Ivalsa, San Michele all'Adige, Italy, vandekuilen@ivalsa.cnr.it

1 INTRODUCTION

Timber as a structural material may be found in many buildings and structures around Europe, with a current age of sometimes more than 500 years. Already in the Roman era the foundations were made with timber both in form of horizontal beams under brick walls and as vertical piles for deeper foundations. The use of timber is widely spread: timber can be found in foundations of famous heritage buildings such as the Royal Palace in Amsterdam, the Netherlands and bridges in Venice [Siviero and Murat, 1993]. Timber foundations are in these cases true foundations of cultural heritage and therefore their economic and technical importance is large. A complication in the assessment is that pile foundations are difficult to inspect and maintain, and yet many thousands of buildings and structures depend on them. The historic centres of many Dutch cities were all built during the Middle Ages and the golden age from about 1400 until recently. Timber with age of up to 500 years can also be found in many floor and roof structures. The Palazzo Vecchio in Florence, Italy is a fine example. Irrespectively of the applications, the assessment of these structures for their safety and serviceability requires models that take into account the history of the structure. Timber species and quality, the loads on the structure over history and the expected future loads are important in the assessment procedure. It will be shown that damage accumulation models, which take into account age, load history and current state of the material properties including decay of biological or physical nature, can be used in such an assessment procedure of timber structures.

2 DEGRADATION MECHANISMS

2.1 Introduction

Timber degradation can be distinguished in four different forms: mechanical, physical, chemical and biological. Mechanical degradation occurs in the form of long term stresses that deform the structure and slowly reduce the strength. This is generally called a duration of load effect and is accounted for in design standards such as Eurocode 5. For long term strength, loads must be classified in a load duration class, which can be either instantaneous, short term, medium term, long term or permanent. It has been shown in Van de Kuilen [1999] that mechanical loads only cause damage when they are short term and very high. Permanent loads are too low to cause serious damage and do hardly influence the service life of the structure, except for pile foundations. Physical degradation occurs either in case of fire (temperature), wind, UV radiation or drying. Especially in older structures, drying cracks may be visible. Depending on the size of these cracks, the structural safety may be at risk. The depth of these cracks depends on factors such as initial moisture content, climate after installation, sawing pattern of the beam and whether the heart of the tree is present or not. Although the stiffness is decreased, the bending strength is hardly affected since the amount of wood material is not changed in the highly stressed zones. For shear however, these cracks are important and the residual cross section has to be taken into account. The by far most important parameter for service life modelling is biological degradation, in combination with mechanical loads. Due to biological attack, structures are affected and cross section may be changed as a result. Examples are piles and poles that are attacked by fungi at ground-air level or at groundwater level, beams with supports in stone walls that are degraded due to high moisture content levels and hydraulic structures in general. Infrared spectroscopy is used to determine different types of biological decay (brown rot, soft rot, white rot) and in conjunction with the decay, the expected amount strength loss.

2.2 Assessment Techniques

Traditional inspection methods combine visual assessment and (sharp) tools, but NDT techniques such as ultrasound and stress waves are becoming more used. Also, techniques with small penetrating elements(Pilodyn hammer , drills) may also be used. The latter are favoured for dry conditions in buildings and are less applicable for wet circumstances. Furthermore, these types of drills must be

operated with great care since they are not always optimised for the wood species under investigation and require an experienced user. Drilling and strength testing of bore cores is also possible or full cross sections from parts of structures also allows for worthwhile information, but is more costly and not always possible. Newer technologies such as (near)infrared spectroscopy allow for a relative fast insight in a possible decay of a structure. In figure 2.1 the molecular degradation is shown of two pieces of basralocus, a sound one and one with decay. The decay becomes clear around 1400 cm-1, indicating a decrease in the amount of lignin. This in itself could be in indication that the type of decay is 'softrot' known to attack lignin.

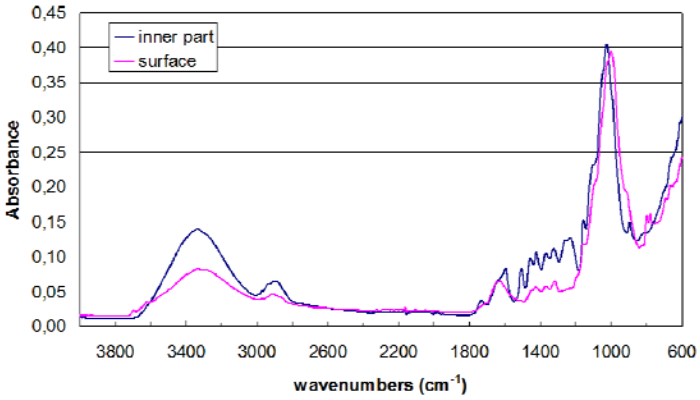

Figure 1. IR Spectrum of Basralocus pile used in hydraulic structure. Changes in molecular structure especially around 1400 cm^{-1}.

2.3 Fungi Growth and Fungi Recognition

Mid and Near Infrared Microscopy are relatively young techniques used to detect and analyse fungi decay in wood. They can give insight in how much decay is present and what is the extent of the decay in terms of molecular changes and consequently changes in mechanical resistance. In order to evaluate the service life of a structure affected by fungi decay, it is important to estimate, besides the strength loss, the rate of decay (or speed) of the process. Experimental data for the activity, expressed as weight loss in time, of different fungi species on different wood species are reported in studies focused on testing effectiveness of wood preservatives against wood decay according to standards such as EN 113. However, those methods have limitations when used for service life prediction of structures. The main limits are concerned with the restricted exposure time (generally up to 16 weeks) and the relatively small size respectively volume of the specimen (max 10x25x250 mm^3). The relation between volume of the wood specimen and the rate of degradation has not been reported in the literature so far. Previous research (Curling et al., 2002) showed that chemical alternations of the cell wall caused by fungi can be related with strength changes. Previous research (Curling et al., 2002) showed that chemical alternations of the cell wall caused by fungi can be related with strength changes. The present study deals with two aspects:
Develop a new protocol for laboratory decay test considering decay value by volume/time relations, together with CATAS Spa Testing Laboratory (Italy). The Attenuated Total Reflection (ATR) IR spectroscopy was used to characterize wood decay. NIR spectra of the samples were acquired after different exposure times and spectral differences were analysed by Multivariate analysis (MVA).

2.4 Materials and Methods

The timber species used was Norwegian Spruce (*Picea abies*) and Japanese Larch (*Larix kaempferi*) grown in The Netherlands. For each species two sets of 20 specimens differing in dimensions were prepared. The dimension of one set of sample was 10x10x100 mm^3 (ministakes) and for the other 44x44x200 mm^3 (stakes). The edges of each sample were sealed with a waterproof coating in order to prevent the fungi attack starting from the cross sections and proceeding along the longitudinal axis. The samples were oven-dried at 103±2˚C and weighed prior to inoculation.
The test fungi used was the brown rot Coniophora puteana (Schumacher ex Fries) Karsten. The inocula was obtained from cultures grown on a malt-agar culture medium.

As culture vessels (incubators) for the ministakes, five sterilized Petri dishes per wood species were used. Each dish was equipped with a basis of moist vermiculite, a plastic mesh and four wood samples, all previously autoclave sterilized. Per sample three inocula were introduced aseptically, so that the mycelium got in contact with the sample surface (Fig. 2.2). The incubators used for the stakes were autoclavable transparent bags. Sterilized moist vermiculite, plastic mesh and two wood samples were put into each bag. Each sample was inoculated with six inolcula (Fig. 2.3).

Figure 2. Inoculated ministakes
(10 x 10 x 100 mm)

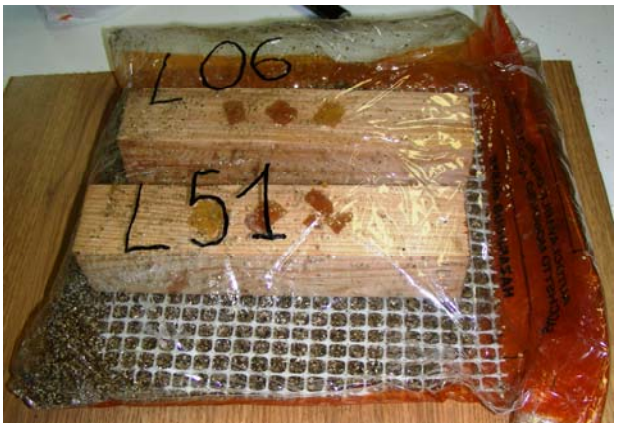

Figure 3. Inoculated stakes
(44 x 44 x 200 mm)

The samples preparation and the inoculation method used in this research aim to simulate fungi attack of timber in reality above ground. In fact, decay problems in buildings are often caused by moisture accumulation, water leakage and water condensation. These generally start from some spots on the surfaces of timber in the structure, and not as a uniform phenomenon of degradation of the whole member. The exposure time intervals for the ministakes were 2, 4, 8, 12, 16 weeks. The degradation of the stakes is still ongoing at CATAS Spa. The planned exposure times for them are longer than for the ministakes, up to 12 month. After each exposure time interval, four samples per species have been oven-dried in order to calculate the weight loss percentage relative to the initial oven-dried weight. For the stakes, compression tests will be performed at Delft University laboratory. For the ministakes, weight loss and NIR spectra were acquired after each exposure time.
Ten NIR spectra were collected from each ministake, so that more than 75% of the whole sample volume was scanned. The mean spectrum for each decayed sample was calculated and Principal Component Analysis (PCA) was performed on the resulting spectral matrix. PCA is a multivariate analysis method that projects the original variables onto a smaller set called Principal Components or PC (Martens et al, 1993). PC scores are the projected locations of each sample onto each PC. Scores can indicate latent structures and clusters of samples.

2.5 Preliminary Results

Weight loss
In the considered period of four months for the ministakes and six month for the stakes, the biodegradiation process by brown rot took place successfully. Figure 2.4 and 2.5 show the average of the weight loss percentage ($\Delta W\%$) for groups of four samples after each exposure time, for the ministakes and the stakes respectively. The weight loss is expressed as the ratio between the difference of the initial weight and the weight after decay over the initial weight, in oven-dry conditions. The data demonstrate that Norwegian spruce undertakes a stronger degradation than Japanese larch after the same exposure period, as the weight loss is more than 2 times higher for the spruce ministakes and almost 3 times higher for the stakes. According to the standard EN 350-2 that result was expected since the natural durability class for spruce is 4 (slightly durable) and for Japanese larch is 3-4 (moderately durable). A more interesting result comes from the comparison between decay process of small and big samples. As expected, the results show that the sample's volume strongly affects the rate of biodegradation. The speed of decay ($\Delta W\%$/days) decreases of a factor 2.3 for spruce and a factor 3 for larch, by increasing the volume of 40 times.

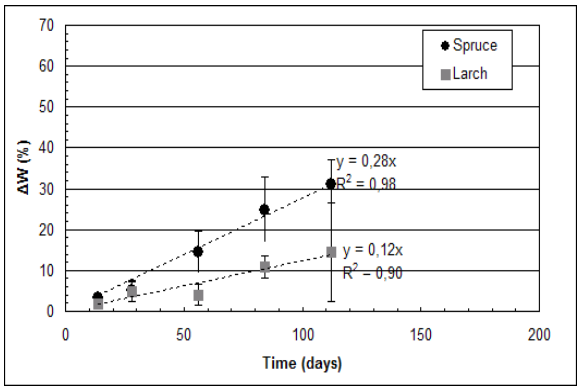

Figure 4. Weight loss in time for ministakes

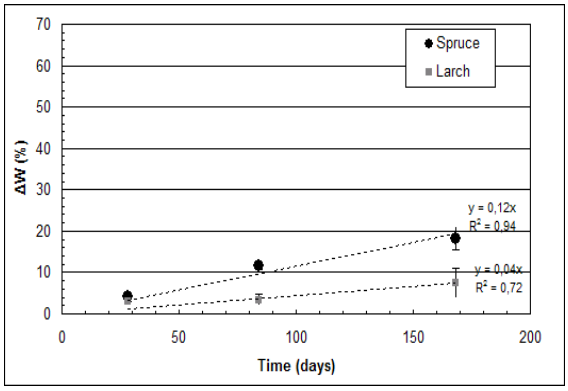

Figure 5. Weight loss in time for stakes

NIR analyses

After different exposure times decayed samples showed considerable differences in chemical composition observed by infrared spectroscopy. Figure 2.6 shows the NIR spectra of spruce ministakes decayed after different incubation time intervals, as well as the reference (sound) sample. Although it is hard to detect differences by visual inspection, it is possible to notice that the absorbance at 4780 cm^{-1} decreases as the incubation time increases. This peak is associated to the cellulose degradation (Kelley et al, 2002). Figure 2.7 shows the score plot for the two first principal components which describe the 96% of the total variance of the spectral data. Each score represents a sample, based on its chemical (spectral) constituents. The samples in the score plot are "labelled" with their measured weight losses. The graph shows clearly three clusters, representing sound samples (ΔW=0), low (ΔW<10%) and high (ΔW>10%) decayed samples (from the right to the left side of the PC1 axis). When the samples are labelled by their exposure time t, the three clusters in Figure 2.7 represent sound samples (t=0), low (t<1 month) and high (t >1 month) decayed samples. Some outliers are present in the score plot as well. These are situated in the upper left part of the plot. Although the outliers are characterized by high weight loss, their chemical changes are different from the other highly decayed samples. They will be further investigated. It seems to be possible that those samples will show a stronger link with clusters in terms of strength losses.

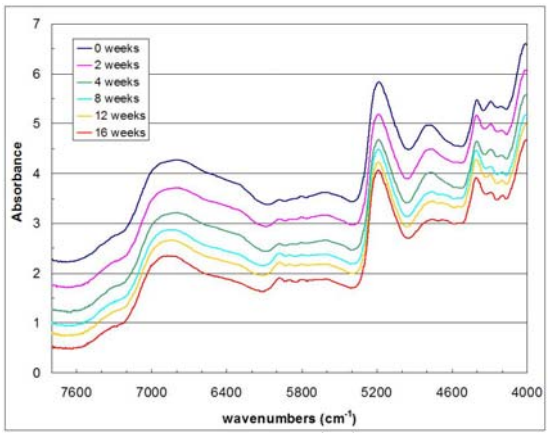

Figure 6. NIR spectra of decayed spruce

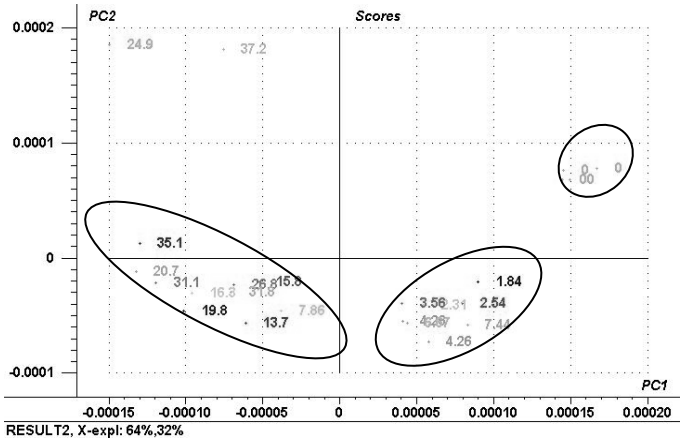

Figure 7. PC analysis discriminating decayed spruce

3 SERVICE LIFE AND DAMAGE MODELLING

3.1 Structural Assessment and Basis for Service Life Predictions

Flow charts for structural assesment have been developed by a number of researchers and institutes have been developed in order to be able to make a reliable assessment [Bonamini, 1995], [Görlacher, 1999]. Generally, these flow charts require analysis of the original structure, its uses, localization of defects/degradation and classification. On the basis of an analysis of the (historical) situation, the results of the inspection and the planned future use of the structure, an estimate is made on the residual lifetime and the necessity of repair or replacement. Since timber has a load and time dependent strength, the full short term resistance based on modern design principles may no longer be fully available, especially in the case of foundations, where the ratio between dead and live load is quite different from floors and roofs. In this respect, timber from floor and roof structures can be expected to have 100% strength capacity [Kuipers, 1986]. However, biological decay may affect the load carrying capacity. Decay may be both active or non-active, the effects on the resistance of the structure have to be examinated. The expected future loads can be determined from the new building plans or from current design codes. Depending on the situation and legal requirements, deviations from loads specified in design codes could be accepted in certain cases. The information obtained from the expected loads and the state of the structure allows for calculations of the residual strength of the structure and in conjunction with that the expected 'remaining' service life.
After an assessment of the structure, the final step is to predict the load carrying capacity and the residual lifetime. A new approach for this is the assessment of the strength using a modified damage accumulation model. Damage accumulated models have been used in timber research describing the strength development of timber under long term loads. Several models can be found in literature [Foschi et al. 1989],[Nielsen [1992], [Krausz & Eyring, 1975], Van der Put [1986] but the one from Gerhards [1987] will be used here as an example. Since these models only describe the strength development in time they have to be modified to include the influence of deterioration on the material properties, for instance biological degradation decay of the cross section and this may have considerable effect on the strength capacity of members. By combining durability models with strength models, it becomes possible to model the 'residual lifetime' of structures. Different approaches are possible using probabilistic calculations [Leicester et al., 2002], of kinetic based models [Winandy et al., 2002], but here the exponential damage accumulation model of Gerhards is modified. The limit state function is generally written as:

$$Z = R - S \qquad (1)$$

with Z = the limit state, R = the resistance and S = the solicitation or load. In reality, both the resistance and the solicitation are varying in time and the limit state function can be written as:

$$Z(t) = R(t) - S(t) \qquad (2)$$

A structure is assumed not to have failed while Z(t)>0. In figure 3.1 this is shown schematically. The probability of failure increases, since the resistance of members generally decreases with age. In case of timber, the resistance R(t) depends on the load and the load history. Mositure content and temperature also have an influence, but these are neglected here. Equation (2) can thus be written as:

$$Z(t) = R(s(\tau),t) - S(t) \qquad (3)$$

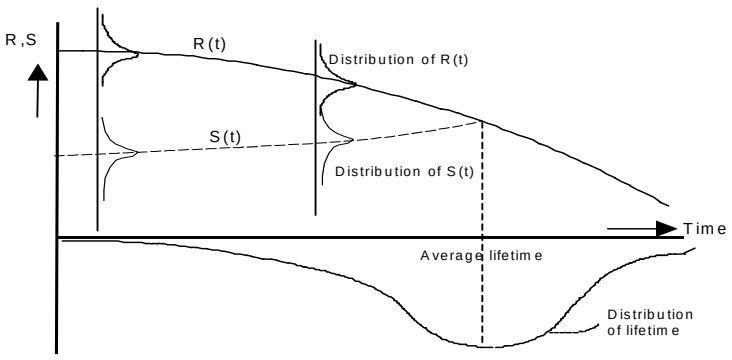

Figure 8. Schematic representation of the distribution of lifetimes of structures [Siemes, T, personal communication]

For the resistance function R(s(τ),t), the Gerhards damage function is used here, which is easy and straightforward to use [Gerhards and Link, 1987], but now the material strength is modified depending on the amount of

decay and residual strength of decayed timber. Thus, a time dependent resistance $f_s(t)$ is introduced in the model:

$$\frac{d\alpha}{dt} = \exp\left(-C_1 + C_2 \frac{\sigma(\tau)}{f_s(t)}\right) \tag{4}$$

The damage α takes a value: $0 \le \alpha \le 1$. By definition, failure occurs when $\alpha = 1$. This means that while $1- \alpha > 0$ the structure is still able to carry the load at that point in time and $Z(t) = 1 - \alpha$. The parameters C_1 and C_2 in the damage model are determined on the basis of time to failure tests on timber [Foschi and Yao, 1986], [Gerhards and Link, 1987] or joints [VandeKuilen, 1999]. The damage function can be used to estimate residual lifetimes of structures when the stress function $\sigma(\tau)$ representing the load path from the time of erection of the structure until the end of the time span under consideration is known as well the strength $f_s(t)$ representing the time dependent load carrying capacity of the material. For example in pile foundations the normal force has to be checked against the load carrying capacity [Van de Kuilen, 2006]. When the cross section is denoted A_{tot}, the value of the normal resistance F_u is determined $F_u = f_{c,0} A_{tot}$. When it is assumed that the pile is decaying, after a number of years the non-decayed cross section will be reduced to A_{rem} (remaining cross section). Denoting $f_{c,0,dec}$ the strength of the decayed timber and A_{dec} the cross section of the decayed area, the pile resistance can be written as:

$$F_u = f_{c,0} A_{rem} + f_{c,0,dec} A_{dec} \tag{5}$$

Equation 5 can be further modified into a more general form, using the rate of decay determined from the ministake and stake decay rates as a function of the volume. When the ratio between the remaining non-decayed cross section and the total cross section is defined as:

$$\delta = \frac{A_{rem}}{A_{tot}} \tag{6}$$

and when the strength ratio between the decayed timber and the non-decayed timber is defined as:

$$\beta = \frac{f_{c,0,dec}}{f_{c;0}} \tag{7}$$

equation 5 becomes:

$$F_u = f_{c,0} A_{tot} \left(\delta(1-\beta) + \beta\right) \tag{8}$$

The value of $f_s(t)$ in equation 4 can be replaced by F_u when the stress function $\sigma(\tau)$ is replaced by the load. Both β and δ are functions of time and wood volume as has been shown in paragraph 2, since the decay rate can be estimated.

3.2 Assessment of Drying Cracks

A similar derivation can be made for shear stresses in a governing cross section. Without drying cracks, the shear capacity can be written as:

$$F_{s,\max} = \frac{2}{3} f_{s,d} bh \tag{9}$$

Figure 9. Drying cracks in timber beam affecting shear capacity

However, when drying cracks occur at the neutral axis, the actual beam width becomes $b-2c_d$ with c_d the crack depth on one side of the beam. Especially in ancient structures, beams are large and generally cracked on both sides. An example is shown in figure 3.2. Vertical cracks in a cross section are not considered to have an influence on the remaining shear capacity. Consequently, the remaining load carrying capacity in shear is:

$$F_{s,\max} = \frac{2}{3} f_{s,d} (b - 2d_c) h \tag{10}$$

4 CONCLUSIONS

Timber structures service life can be estimated combining damage accumulation models with fungi growth models and drying crack growth models. Using such modified damage models, residual lifetimes can be predicted using different scenarios for rate of decay, the remaining strength of partly decayed timber or physical loads such as drying cracks. To adjust for fungi growth, a new test decay procedure has been developed in order to induce decay in two sets of samples differing in volume sizes. It was proven that the rate of degradation is strongly influenced by the volume of the samples: decreasing up to one third when increasing specimen's volume from 10^4 mm^3 to 40 times bigger for larch samples. FT-NIR technique and multivariate analysis were applied to characterize wood decay. The spectral analysis showed that it is possible to discriminate sound and decayed samples by infrared spectroscopy. Within the decayed samples, it was possible to discriminate between "low" and "high" decay.

ACKNOWLEDGMENTS

CATAS is greatly acknowledged for their aid and support in developing the new test procedure.

REFERENCES

Curling, S., C. A. Clausen, et al. 2002: Experimental method to quantify progressive stages of decay of wood by basidiomycete fungi. International Biodeterioratian & Biodegradation 49: 13-19.

Martens, H. and T. Næs 1993: Multivariate Calibration. Chichester, John Wiley & Sons.

Kelley, S. S., J. Jellison, et al. 2002: Use of NIR and pyrolysis-MBMS coupled with multivariate analysis for detecting the chemical changes associated with brown-rot biodegradation of spruce wood. FEMS Microbiology Letters 209: 107-111.

Bonamini, G, Restoring timber structures - Inspection and evaluation, STEP Lecture D3, Centrum Hout, The Netherlands, ISBN 90-5645-002-6

Foschi RO, Yao RC, Another look at three duration of load models. CIB/W18 Timber Structures, Paper 19-9-1, Meeting 19, September 1986, Florence, Italy.

Gerhards CC, Link CL, A cumulative damage model to predict load duration characteristics of lumber. Wood and Fibre Science, 19(2), 1987, pp. 147-164

Görlacher, R., 1999, Historische Holztragwerke. Untersuchen, Berechnen und Instandsetzen, Karlsruhe: Universität Karlsruhe (TH),

Kuipers J, Effect of age and/or load on timber strength. CIB/W18 Timber Structures, Paper 19-6-1, Meeting 19, September 1986, Florence, Italy,

Leicester RH, Foliente GC, Cole IS, Wang C-H, Mackenzie C, Prediction models for engineered durability of timber in Australia, 9th Int. Conf. on DBMC, March 2002, Brisbane, Australia.

Siviero E, Murat D, Preservation of the Venetian Bridges, Structural Preservation of the Architectural Heritage, IABSE symposium, pp. 581-588, Rome, Italy, 1994

Van de Kuilen JWG, 1999, The residual load carrying capacity of timber joints, HERON Vol. 44-3, pp. 187-214, ISSN 0046-7316,.

Van de Kuilen JWG, 1999, .Duration of load effects in timber joints, Ph.D. thesis, Delft University of Technology, ISBN: 90-407-1980-2,

Van de Kuilen JWG, Service life modelling of timber structures, RILEM, Materials and Structures, DOI 10.1617/s11527-006-9158-0.

Van der Put TACM, 1986.A model of deformation and damage processes based on the reaction kinetics of bond exchange. IUFRO S5.02/CIB-W18/19-9-3, Meeting 19 Florence, Italy,

Winandy JF, Lebow PK, Murphy JF, 2002, Predicting current serviceability and residual service life of plywood roof sheathing using kinetics-based models. 9th Int. Conf. on DBMC, Brisbane, Australia.

Performance-based Design for Anticorrosion of Reinforced Concretes under Air-borne Salt Attack

Kai-Lin Hsu [1]

T 43

ABSTRACT

The performance-based design leads the trend recently in the modt of the developed countries, instead of the specification-based design. How to design the structure based on the required performance is dependent on the importance, service level and service life of the design structures. For different performance level, the design structure must be verified to satisfy all the required performance.

In this study, based on the understanding of the trend of performance-based design(abbr. as PBD), by applying the technique of Monte-Carlo Simulation (MCS) on Fick's second diffusion law with the consideration of stochastic behavior of cementitious material as well as the microclimate around the concrete structures like temperature, air-borne salt, etc., one proposal for developing the performance-based design of anticorrosion of RC structures under air-borne salt attack is considered. Through the examples illustrated in this paper, the availability of the proposed performance-based design method can be verified even with different mixing proportion and mixing material for the required service life under various air-borne salt attack environment.

KEYWORDS

Performance-based design, Rebar corrosion, Air-borne salt, Vulnerability curve

[1] National Kaohsiung First University of Science and Technology, Construction Engrg. Assistant Prof., Kaohsiung 800, Phone +886 7 6011000 ext2151, Fax +886 7 601 1017, vichsu@ccms.nkfust.edu.tw

1 INTRODUCTION

At present, RC structures are still the representative construction works at practice. Especially, for the marine RC structures with the threat of the all-year-round sea wind, the rebar corrosion due to salt attack is commonly observed within the sea-island countries, e.g. Taiwan,etc. Thus, how to prevent in the design stage or early stage of corrosion is the key to effectively solve the corrosion problem of RC structures.

As for the investigation of background meterological data related to RC corrosion, some developed countries, e.g. Japan ,etc. has launched some pioneer researches since decades ago. Besides, lots of research results related to how to measure the chloride diffusivity within concrete have been speculated, such as AASHTO T227, ASTM C1202, AASHTO T259, NT Build 449-94,etc[Patrick, F. et al. 1999]. However, even for the so-called known specifications, the uncertainties with the measured chloride diffusivity cannot be fully avoided due to the stochastic behavior of the cementitious material as well as the microclimate around the concrete structures like temperature, air-borne salt, etc [Japan Soc. Civ. Eng. 1997]. Although there already exist several indoor accelerated tests for measuring chloride diffusivities[Friedmann, H. et al. 2004, Wu, L. et al.2006, Yang, C. & Wang, L. 2004], it is still hard to say if the true value of the chloride diffusivities within concrete be measured. Generally speaking, only the rough distribution of the chloride ions can be estimated. With the understanding on this intrinsic problem, one PBD method was proposed on the basis of reliability for designing RC structures under air-borne salt attack. What attempted in this paper is to control the corrosion probability of the rebar in RC structures for the various requried service life.

2 DESCRIPTION FOR PROPOSED PBD METHOD

Based on the trend of PBD, it is indispensible to describe the limit state of the required performance at first, for either safety or serviceability. For simplifying the design issue of RC structures under marine environment, the limit state is preliminarily considered as the occurrence of rebar corrosion. In order to apply Fick's second diffusion law with the consideration of uncertain behavior of material and environmental parameters, the stochastic determination of chloride diffusion coefficient and the surface chloride content are essential [Akiyama,M. *et al.* 2005, Ferreira, R. & Jalali, S. 2004]. In this paper, the diffusion coefficient of chloride ions for the assigned cementitious material is decided by statistically analyzing the published data in the literature within 10 years [Aoyama, M. *et al.* 2003, Japan Soc. Civ. Eng. 2000, Maruya, T. *et al.*1998]. After statistical analysis on the literature data, the mean-value, standard deviation and test for the "goodness to fit" will be set for the designated cementitious material. In addition, as for the surface chloride content, it is obtained by referring to the exiting experimental relationship converted from the surrounding air-borne salt [Maeda, T. *et al.* 2002] while ,for air-borne salt, it is experimentally decided in accordance with the proposed air-borne salt collecting procedure [SBRG of PWRI 1993]. Followed by the development of hazard curve and vulnerability curve according to the assumed structural, material and microclimate details of being-designed RC structures as well as the recognized limit state for rebar, the reliability index of the being-designed RC structure can be calculated by adopting the technique of Monte-Carlo Simulation (MCS). The schematic flow of the proposed PBD method is illustrated in **Fig. 1**. As for the details of the proposed PBD method, it will be described in the following context.

In this paper, Fick's second diffusion law is adopted for describing the migration of chloride ions within concrete, which was formulated by Crank, J. [1980] as eq.(1).

$$\frac{\partial c}{\partial t} = D\frac{\partial^2 c}{\partial x^2} \tag{1}$$

Where D is the diffusion coefficient (cm^2/year); c is the concentration of transport mass at certain location; x is the depth of diffusion(cm); t is the duration of diffusion(year). With the assumption of

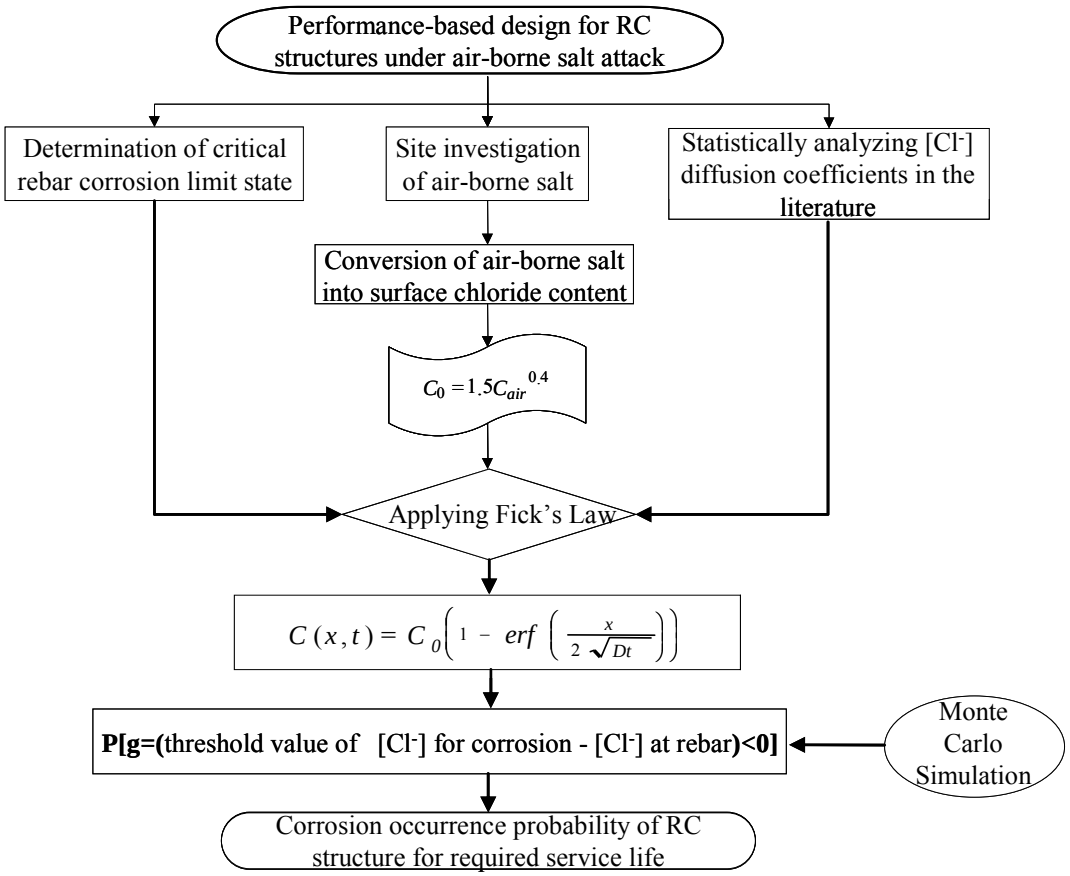

Figure 1. proposed PBD flow for RC structures under air-borne salt attack

initial and boundary conditions, i.e. c = 0 for x = ∞ and t ≥ 0 as well as c = 0 for x > 0 and t = 0, the solution of Eq.(1) can be given in the form of Eq.(2) as follows.

$$C(x,t) = C_0\left(1 - erf\left(\frac{x}{2\sqrt{Dt}}\right)\right) \quad (2)$$

Where C(x,t) is the concentration of chloride at depth x（㎝）and time t (year) (kg/m^3) ;Co is the surface chloride content（kg of Cl^-/m^3）; *erf* means error function. After statistical analysis on the literature data for chloride diffusion coefficients, the mean-value and standard deviation for the designated cementitious material can be used in Eq.(2) while the site-collected air-borne salt is regressed as the empirical function of the distance from seashore in Eq.(3a) and the surface chloride content is converted from the site-collected air-borne salt according to Eq.(3b). [Hsu, K. & Lin,Y. 2007]. Because **Fig.2** shows the uncertainty of the regression analysis for site-collected air-borne salt, one uncertainty factor U_r with lognormal distribution(1.029,1.22) is considered in Eq.(3c)

$$C_{air\ at\ location\ x} = 0.94 * e^{-0.9758d} \quad (\text{with } R^2{:}0.266) \quad (3a)$$

$$C_0 = 1.5C_{air}^{0.4} \quad (3b)$$

$$C_{air\ at\ location\ x} = U_r * e^{-0.9758d} \quad (3c)$$

Where $C_{air\ at\ location\ x}$: the site-collected air-borne salt(mdd of Cl^-);d:the distance from seashore (km). In order to obtain the hazard curve (i.e.exceeding probability for different airborne salt:$q_s(C_{air})$) , it is formulated in Eq. (4).

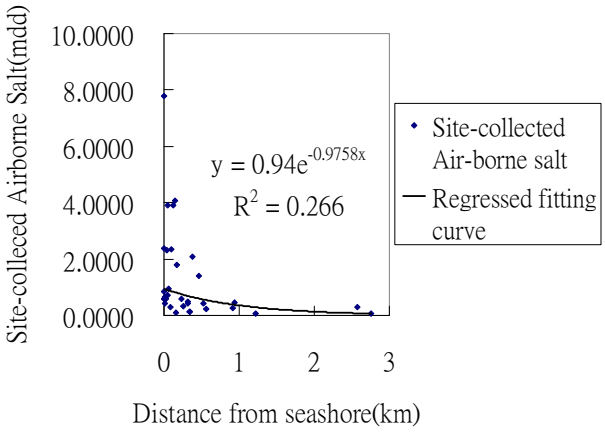

Figure 2. Regression Analysis on Site-collected Airborne Salt

$$q_s(C_{air}) = P(C_{air} > c_{air}) \quad (4)$$

Where c_{air} is the assumed air-borne salt (mdd of Cl^-).Once all the material and structural parameters for the being-designed RC structures can be decided as expressed in Eq.(2), the time-dependent chloride concentraion at rebar surface can be predicted. The fragility curve for assumed air-borne salt $F_r(c_{air})$ is calculated as follows:

$$F_r(c_{air}) = P(C(d_c,t_d) > c_{threshold}) \quad (5)$$

Where $C(d_c,t_d)$ is the chloride concentraion at rebar surface (kg/m^3 of Cl^-); d_c is the cover depth(cm); t_d is the design service life (years) ; $c_{threshold}$ is threshold value of chloride concentration for corrosion occurence (kg/m^3 of Cl^-). After the time-dependent chloride concentraion at rebar surface is available, the probability of Eq.(4) will be calculated by the utilization of MCS, which means the probability of threshold value of chloride concentration for corrosion occurence smaller than the chloride concentration at rebar surface.

***P*$_f$[g=[**threshold value of [Cl^-] for corrosion - [Cl^-] at rebar**) < 0]**

$$= \int_0^\infty \left(- \frac{\partial q_s(c_{air})}{\partial c_{air}} \right) \cdot F_r(c_{air}) \cdot \partial c_{air} \quad (6)$$

Where g means the equation of required limit state. As for the range of the threshold value of chloride concentraion, it differs nation by nations ,ranged from 0.4~1.2 kg/m3. For considering the locality of the proposed PBD method, it is considered as 0.3 kg/m3 due to the requirement in Chinese National Standards 12891 [1998]. After the failure probability is available, the reliability index (β) can be converted from P_f according to Eq.(7).

$$\text{Reliability Index } (\beta) = -\Phi^{-1}(P_f) \quad (7)$$

3 NUMERICAL VERIFICATION

In order to assure the availability of the proposed PBD method, some numerical tests were carried out by virtual design. This design problem under consideration is to build up one RC structure with required service life(50 years) for City A and City B, the air-borne salt at which was collected and

analyzed as shown in **Table 1** [Hsu, K. & Lin,Y. 2007]. The design issue for this problem is to find out the optimum of material type and structural layout.

Besides setting the threshold value of chloride concentration at corrosion occurrence as 0.3 kg/m^3, the surface chloride content was converted from the experimentally decided air-borne salt according to Eq.(3), which was calculated as 1.5kg/m^3,arround 5 times of threshold value of chloride concentration at corrosion occurrence. As for the chloride diffusion coefficients of the designated cementitious material, the mean-value, standard deviation and the distribution type of them are partially summarized in **Table 2** according to the literature review results. According to the settings in **Table** 1 and 2, the exceeding probabilities for City A and B are comparatively illustrated in **Fig. 3** while the fragility curve for different cover depth are calculated in **Fig.4**.

Table 1. Air-borne salt data at City A and B

City	Distribution type	Mean	Standard Deviation
A	Lognormal Distribution	3.1172（mdd）	0.355523
B	Lognormal Distribution	1.0053（mdd）	0.535587

Table 2. chloride diffusion coefficient for ordinary concrete

W/C / Value	0.3	0.35	0.4	0.45	0.5	0.55	0.6	0.65
Mean	0.93683	1.14686	1.52877	1.85708	2.1781	2.4732	2.61722	3.24936
Standard Deviation	0.48083	0.50829	0.73725	0.72908	1.2730	1.0004	0.83826	0.99650
Distribution type	Lognormal Distribution（cm^2/year）							

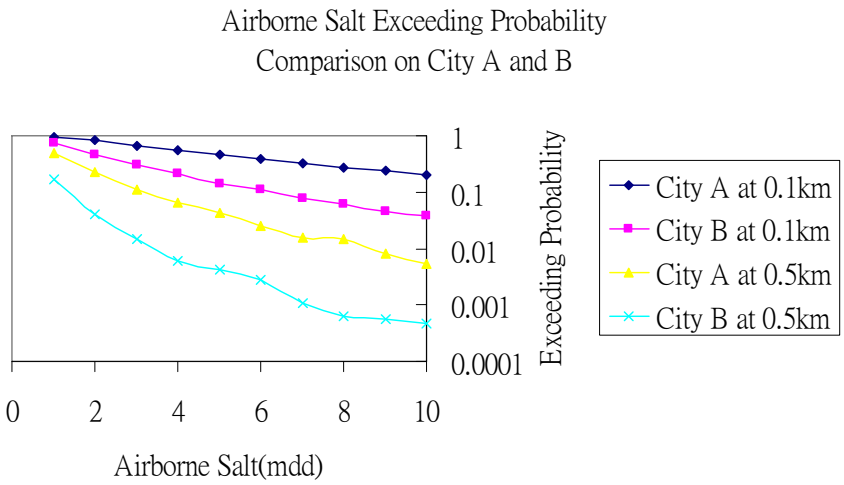

Figure 3. Compariosn of hazard curve on City A and B

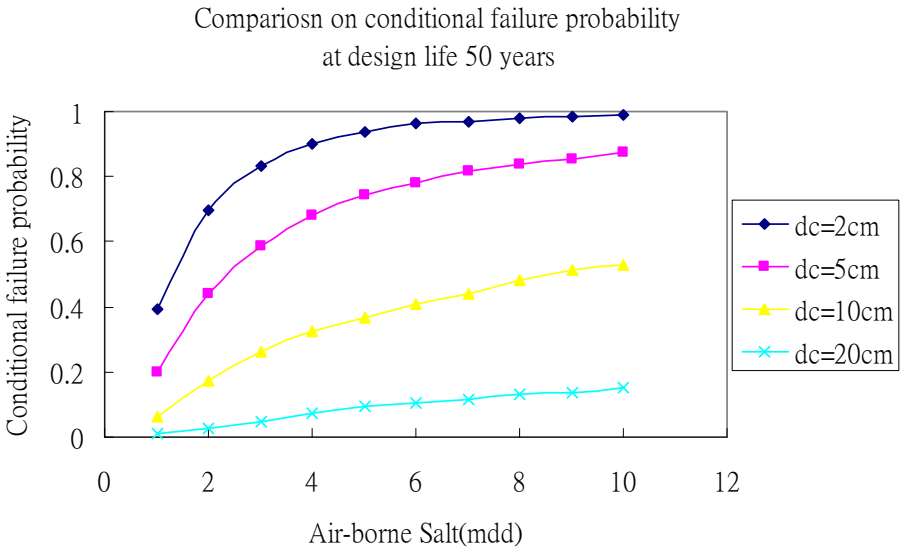

Figure 4. Compariosn on fragility curve for different cover depth at design life 50 years

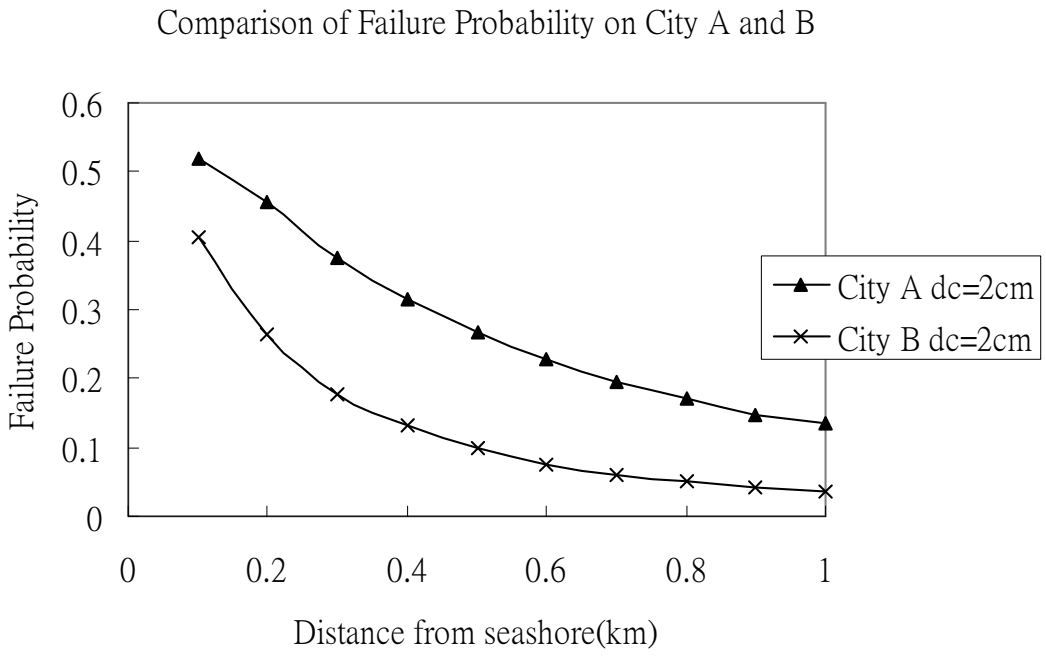

Figure 5. Compariosn of failure probability on City A and B at design life 50 years

Table 3. PBD settings for ordinary concrete on City B

Design Iter. No.	W/C	Cover Depth (cm)	Design Iter. No.	W/C	Cover Depth (cm)
1	0.45	2	4	0.35	2
2	0.45	5	5	0.35	8
3	0.45	10	SLS $\beta = 1.5$		

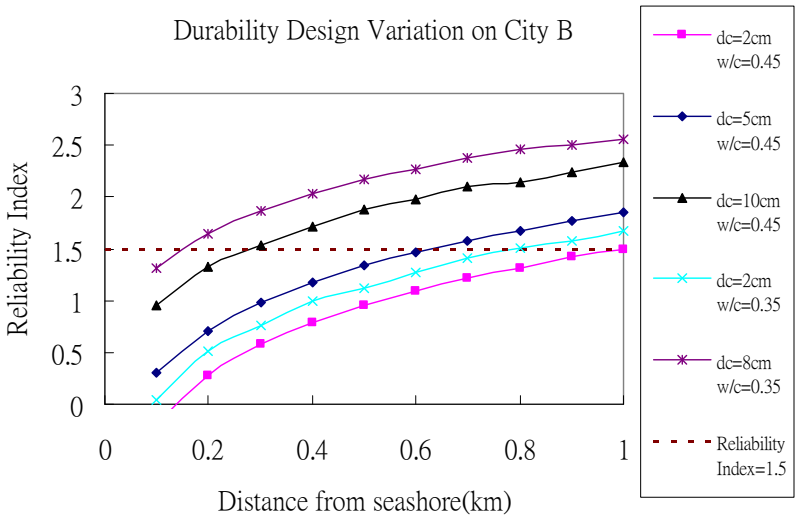

Figure 6. Iterative Process of PBD on City B at design life 50 years

Based on the calculated exceeding probability and fragility curve, the failure probability can be simulated in accordance with Eq.(6). As the threaten from air-borne salt on City A is more severe than that on City B from the site-collected airborne salt data in Table 1, it is expected that the failure probability on City A be larger than that on City B with the same material and structural parameters, as shown in **Fig.5**. Through **Fig.3-Fig.5**, the feasibility of the proposed PBD can be conceptually accepted. In order to illustrate the performance design process with the help of the proposed method, the PBD settings for ordinary concrete are illustrated in **Table 3,** which the acceptable service limit state index β is considered as 1.5 based on the work of Schiessl,P.[2005]. As it can be observed from Fig.6, the difference of location ,even with the same material and structural parameters, not all the design results can be accepted. For example, for the distance from the seashore as 0.1km, because the air-borne salt on City B is around 1 mdd (from **Table 1**), the results given in **Fig.6** indicate that almost all the design results based on the settings for ordinary concrete cannot reach the required service life (50 years) while ,for distance from the seashore as 1km , almost all the design results can reach the required serve life. This comparison re-emphasizes the importance of air-borne salt mapping for all the marine structures. On the other hand, it can also be found that the design result by changing the material and structural parameters simultaneously is the most effective improvement for this design case. How to find this best result without troublesome search process is the another issure for improving the prosposed PBD method.

4 CONCLUDING REMARKS

Through the above discussions, the concluding remarks of this paper can be summarized as follows:

1. the limit state for RC serviceability in this paper is set as the occurrence of rebar corrosion expressed in Eq(4). From the above results, not only the availability of the proposed PBD method was verified but also the extensibility of the proposed method on different definition of the limit state including the start of corrosion crack or loss of the loading capacity.

2. although the availability of the proposed PBD method is verified, it is still necessary to find out the stochastic behavior of the diffusion process for salt attack, for example, the temperature-dependence, time-dependence or material-dependence, etc. In addition, the site investigation at longer timescale for air-borne salt is also essential for the following researches. Based on the further clarified relationship

on these material parameters, the accuracy of the life-span simulation can be improved and the results of the design process can be accepted.

ACKNOWLEDGMENTS

The authors of this paper would like to acknowledge the support of the National Science Council of Taiwan by Grant NSC95-2221-E-327-047.

REFERENCES

Akiyama, M., Itoh, Y. & Suzuki, M. 2005, 'Durability design methodology of reinforced concrete structures against the chloride attack based on reliability design', Pro. 60th annual conference of the *Japan Soc. Civ. Eng.*, vol. 5, pp. 46–47. (in Japanese).

Aoyama, M., Torii , K. & Matsuda, T. 2003, 'A study on the chloride ion penetrability into concrete in concrete structures in a severe saline environment', *J. Materials, Concrete Structures and Pavements, Japan Soc. Civ. Eng.*, **746**[5-61], 251-264, (in Japanese).

Chinese National Standards 12891 1998, 'Mix design criteria of portland cement concrete'. http://www.cnsonline.com.tw/en/ (in Chinese).

Crank, J. 1980, *The Mathematics of Diffusion,* Oxford University Press, USA; 2nd edition.

Ferreira, R. & Jalali, S. 2004, 'Probability-based durability design of concrete structures in marine environment in *Concrete repair, rehabilitation and retrofittin*g, eds Alexander, M. et al., Taylor & Francis, London, pp. 321-326.

Friedmann, H., Amiri, O., Aït-Mokhtar, A. & Dumargue, P. 2004, 'A direct method for determining chloride diffusion coefficient by using migration test' ,*Cement and Concrete Research*, **34**[11], 1967-1973.

Hsu, K., Lin, Y. 2007, 'Site investigation of air-borne salt as well as discussion on salt limit of anticorrosion specification', Taiwan Concrete Institute 1st annual conference.(in Chinese)

Japan Soc. Civ. Eng. 1997, *The-state-of-the-art and Trend of The Research for Rebar Corrosion, Anticorrosion And Repair Technology*, edited by Corrosion and Anticorrosion Subcommittee of Concrete Committee, (in Japanese).

Japan Soc. Civ. Eng. 2000, *The-state-of-the-art and Trend of The Research for Rebar Corrosion, Anticorrosion And Repair Technology (2nd report)*, edited by Corrosion and Anticorrosion Subcommittee of Concrete Committee, (in Japanese).

Maeda, T., Takewaka, K. & Yamaguchi, T. 2002, 'Database for surface chloride content as well as the chloride diffusion coeffient within concrete',*CONCRETE ENGINEERING SERIES*, **46**, *Japan Soc. Civ. Eng.* (in Japanese).

Maruya, T., Tangtermsirikul, S. & Matsuoka, Y. 1998, 'Modeling of Chloride Ion Movement in The Surface Layer of Hardened Concrete, " *Concrete Library of Japan Soc. Civ. Eng.*, **32**, 69-84. (in Japanese).

Patrick, F., McGrath, R. & Hooton, D. 1999, 'Re-evaluation of the AASHTO T259 90-day salt ponding test',*Cement and Concrete Research*, **29**[8], 1239–1248.

T 43, Performance-based Design for Anticorrosion of Reinforced Concretes under Air-borne Salt Attack, Kai-Lin Hsu

Structual Bridge Research Group(SBRG) of Public Work Research Institute(PWRI) 1993, *Nationwide invesitgation on air-borne salt (IV) - relationship between distribution of air-borne salt and wind features*, Public Work Research Institute publication No.3175. (in Japanese).

Schiessl, P., 2005, 'New Approach to Service Life Design of Concrete Structures', *Asian Journal of Civil Engineering(Building and Housing)*, **6**[5], 393-407.

Tanaka, Y., Kawano, H., Watanabe, H. & Nakajo, T. 2006, 'Study on Cover Depth for Prestressed Concrete Bridges in Airborne-Chloride Environments', *PCI journal*, **51**[2], 42-53. (in Japanese).

Wu, L., Deng, D., Zeng, Z. & Yuan, T. 2006, 'RCM testing the penetration and diffusion of chloride ion in concrete',*Concrete-the core journal of China*, **1**, 100-103. (in simplified Chinese).

Yang, C. & Wang, L. 2004, 'The diffusion characteristic of concrete with mineral admixtures between salt ponding test and accelerated chloride migration test', *Materials Chemistry and Physics*, **85**, 266-272.

Application of the Reliability Theory to the Assessment of the Corrosion Risk due to Carbonation

Thiery Mickael [1]
Crémona Christian [2]

T 43

ABSTRACT

Atmospheric carbonation is one of the most significant degradation factors in the durability of reinforced concrete structures, since its consequences on the corrosion of steel rebars are disastrous. Due to the random nature of physically- and chemically-based properties of concrete (concerning the carbonation phenomenon) and given the uncertainties involved with the cover thickness and environmental factors, it is necessary to match deterministic carbonation models with probabilistic approaches in order to make a relevant prediction. The reliability theory provides interesting features as a decision-making framework for the optimization (serviceability limit state design) of concrete structures.

The Papadakis' and Bakker's carbonation models are studied in this paper through a reliability analysis. The first model predicts the formation of a sharp carbonation front which evolves as a square root of time law. The Bakker's model improves the Papadakis' approach by taking into account the influence of wetting and drying cycles. A performance function is introduced to express the margin between the carbonation depth and the concrete cover. The serviceability limit state is reached when this margin vanishes. The result of the durability assessment is a limit state-based failure probability which is assessed with the Hasofer-Lind reliability index determined using the Rackwitz-Fiessler algorithm.

In a first stage, a sensitivity analysis is performed in order to identify and quantify the most sensitive variables to be considered as probabilistic while some others can be treated as deterministic. In a second stage, a reliability analysis is carried out, as an illustration, to assess the residual service life of a 16-year old reinforced concrete structure. Finally, this study focuses on the use of field data (e.g. a depth of carbonation at a given time) for updating the reliability analysis according to a Bayesian approach.

KEYWORDS

Carbonation, Corrosion risk, Concrete, Modelling, Probabilistic approach

[1] Université Paris-Est, LCPC, Paris, France, Phone +33 140435241, Fax +33 140435498, thiery@lcpc.fr
[2] Université Paris-Est, Paris, France, Phone +33 140435344, Fax +33 140435498, cremona@lcpc.fr

1 INTRODUCTION

Long-term durability of reinforced concrete (RC) structures has become of major concern in view of the vast amounts of money required to maintain these infrastructures in a serviceable state. Regarding the steel RC-corrosion resulting from chloride ingress and/or atmospheric carbonation, the traditional approach has been to follow deem-to-satisfy rules which set requirements on mix-parameters, thickness of the cover concrete, crack width limitations, etc. However, these requirements are no longer appropriate and adequate, and even stifle the designer who has nowadays numerous possibilities in terms of material's mix-design parameters (use of admixtures like superplasticizers, air-entraining agents, etc., and use of cement blended with fly ashes, slag, etc.). That is why, a need is currently appearing for a performance-based approach [Baroghel-Bouny 2007], in which the rules basically concern the performance to be achieved in terms of concrete properties, the so-called durability indicators (porosity, water permeability, diffusion coefficients, etc.) and ambient exposure conditions (carbon dioxide concentration, external relative humidity, etc.).

Corrosion of the embedded reinforcement steel, resulting from atmospheric carbonation, is a matter of considerable concern which affects the serviceability of the RC-structures during their service life. Most concrete structures are actually exposed to the atmosphere, and thus to the action of carbon dioxide CO_2 which diffuses into the concrete cover, dissolves in the pore water, and reacts with the hydration products, causing a strong reduction of the pH-value from 12.5-13.5 to a level below 9 which makes the corrosion of the reinforcements possible. The simplest, and most effective way of enhancing the service life of RC-structures, is to increase the length of the induction period which is defined as the time required for the steels to be passivated [Tuuti 1982]. To make the prediction of this induction period possible, models are used, ranging from simple to very complex ones. Most of the time, a deterministic approach, where each parameter of the model is characterized by a mean value, is adopted. However, because of the random nature of the physical and chemical properties of the concrete cover, and owing to the uncertainties in the geometry of the structure and in the environmental conditions, it is necessary to resort to a probabilistic approach, in which each parameter is represented by a type of statistical distribution, a mean value, and a standard deviation. The outcome of such a probabilistic approach is a probability that a performance function, which corresponds to the margin between the carbonation depth and the concrete cover, vanishes. This probability value is related to a reliability index β_{HL}.

In this article two simple models of carbonation (the Papadakis and Bakker models) are studied in the framework of a time-dependent reliability approach. A sensitivity analysis is performed in order to identify and quantify the most sensitive variables. In a second stage, a reliability analysis is carried out to assess the service life of a concrete exposed to *in situ* conditions. Finally, this study focuses on the use of field data (e.g. a depth of carbonation at a given time) to update the reliability analysis.

2 CARBONATION MODELLING

2.1 The Papadakis Model

The Papadakis model [Papadakis *et al.* 1991] makes the assumption that carbonation is controlled by a steady-state regime of CO_2-diffusion, meaning that the chemical reactions involved are instantaneous. Under these conditions, it is possible to demonstrate that the carbonation front is sharp and separate a fully carbonated zone from an intact one. The carbonation depth X_C follows a square root of time law (see Eq. 1), involving the external CO_2-concentration C_0, the water liquid saturation S, the porosity ϕ, and the initial $Ca(OH)_2$ content of the material n_i.

$$X_C(t) = \sqrt{\frac{2C_0D}{n_i}}\sqrt{t} \qquad (1)$$

where D is the CO_2-diffusion coefficient which has been adjusted *vs.* ϕ and S [Thiery *et al.* 2007]: $D=D_0\phi^a(1-S)^b$ with a=2.74 and b=4.20.
The Papadakis model is based on two main assumptions:

a- An initially uniform medium: the model does not take into account the so-called skin-effects near the surface layer of the concrete, where wall-effects, sedimentation and segregation (as a result of gravity), permeation and evaporation of free water out of concrete lead to variations in cement-, aggregates- and water content, and so in porosity. Nevertheless, any microstructural changes due to carbonation, such as a decrease in porosity, are included in the model, since ϕ corresponds in Eq. (1) to the porosity of the completely carbonated area.
b- The liquid water saturation S is uniform and steady in time. S is at equilibrium with the external relative humidity RH, regardless the amount of H_2O which is produced by the chemical reactions. The link between S and RH is inferred from the desorption-adsorption isotherms which are experimentally determined by Baroghel-Bouny for a wide range of cement-based materials [Baroghel-Bouny 2007]. A good fit of the experimental desorption-adsorption curves S(HR) is obtained through the van Genuchten's functions (see Eq. 2) where α and β are two parameters which can be adjusted for the desorption and adsorption isotherms. Note that the capillary pressure p_C can also be written with respect to S (see Eq. 3) by taken the Kelvin equation into account (ρ_l is the water density, R is the gas constant, T is the absolute temperature, and M_v is the molar mass of water).

$$S = [1 + (-\alpha \ln HR)^{1/(1-\beta)}]^{-\beta} \quad (2)$$

$$p_C = \frac{\rho_l RT}{M_v}[S^{-1/\beta} - 1]^{1-\beta} \quad (3)$$

The second assumption (b) denotes that the Papadakis model is not able to take into account the variations of the external RH, and thus the wetting-drying cycles ocurring in the cover thickness of the concrete during rain period or dry intervals.

2.2 The Bakker's Model

Drying-wetting cycles have a dominating influence on the carbonation process of RC-structures, since the CO_2-diffusion coefficient in the concrete cover and the reaction rate of the CO_2-dissolution in the pores strongly depend on the moisture content. A minimum amount of water in which CO_2 has to be dissolved is needed for the reaction, while if the relative humidity is too high the liquid water inside the pores inhibits the CO_2-diffusion in the gaseous phase. Generally, it is considered that the carbonation ideally occurs for a relative humidity in the concrete pores between 50% and 70% [Wierig 1984].

At the present time, most of complex numerical models of carbonation are likely to take into account realistic drying-wetting cycles [Thiery *et al.* 2005]. However, there are currently very few simple engineering approaches existing which can tackle this problem. The physically- and chemically-based Bakker's model [Bakker 1993] was among the first ones. It is based on the assumption that the carbonation progress is negligible as long as the concrete is wet. To describe the carbonation progress, the Papadakis theory is used as a first approximation. Interactions between carbonation and drying-wetting cycles are taken into account by considering that the carbonation progress is stopped when the relative humidity in the pores is higher than a limit value HR_{lim}=80%.

During drying, the depth at which RH is equal to 80% follows a square root of time law ($X_d=d\sqrt{t}$). The coefficient d is assessed by a model of moisture transport [Thiery *et al.* 2007] where the porosity, the liquid water permeability (K_l), the capillary curve (desorption regime), and external and initial relative humidity intervene as input data. This model distinguishes the water vapor diffusion under gradients of partial vapor pressure from the liquid water permeation under gradients of capillary pressure. The following relationship illustrates the evolution of d according to small variations of the porosity ϕ, the

liquid water permeability K_l, the van Genuchten's coefficients α and β, and the external relative humidity around their mean value (symbolized by a 0 subscript or exponent):

$$d = d_0 \left(\frac{Kl}{K_l^0}\right)^{0.61} \left(\frac{\phi}{\phi_0}\right)^{-0.61} \left(\frac{\alpha}{\alpha_0}\right)^{-0.61} \left(\frac{\beta}{\beta_0}\right)^{0.95} \left(\frac{HR_{ext}}{HR_{ext}^0}\right)^{0.51} \quad (3)$$

During the drying step, the external RH_{ext} is lower than RH_{lim}, otherwise the carbonation cannot go ahead. Thus, the carbonation depth will in practice not proceed further than the maximum drying depth which can be reached. This drying depth depends not only on the concrete quality, but also on the environmental conditions. During wetting, the kinetic of water absorption (imbibition) is described in the same manner as the drying kinetic by a square root of time law ($X_w=w\sqrt{t}$), except that the capillary curve characterizes a phenomenon of water imbibition. t_w denotes the length of the wetting period and t_d the duration of the drying one. It is generally recognized that the wetting period is much shorter than the drying one. It is even possible to make the assumption that $t_w<<t_d$ (t_w tends towards zero).

The evolution of the carbonation front with time is given by a simple algorithm which depends on:

- The carbonation properties: an effective diffusion coefficient of CO_2 in the carbonated area (with respect to the liquid water saturation and the porosity of the material), the environmental CO_2 concentration C_0 and the initial content of $Ca(OH)_2$ n_i.
- The moisture properties: the kinetics coefficients (d and w), the drying t_d and wetting t_w periods determined by an environmental humidity monitoring, and the external RH_{ext}.

It appears that the carbonation depth predicted with this model deviates from an usual square root of time law (see Eq. 1) since the succession of wetting-drying cycles hinders the progress of carbonation.

2.3 Numrical Models

The Bakker's model is based on simplified approach concerning the modelling of carbonation, drying and wetting. Like the Papadakis model, the Bakker's one takes into account neither the build-up of water during carbonation (release of free water from the hydration products), nor the microstructure evolution caused by carbonation. Furthermore, these two models are based on an instantaneous mechanism of carbonation which is limited, given that it is usually recognized that the carbonation front is not sharp (Thiery *et al*, 2007). More accurate and comprehensive models have been recently elaborated. Most of them are based on numerical solving of the transport equations of CO_2 and moisture together with the chemical reactions of carbonation which are at stake. Saetta *et al.* (1993), Bary & Sellier (2004) and Thiery (2005) have proposed such sophisticated approaches. These models are suitable and efficient as long as the input data are available. Although possible in laboratory within the framework of accelerated carbonation tests, obtaining such properties for existing concrete structures is very difficult. In such conditions, the use of simplified models appears justified, provided that the input data are accompanied by statistical information (mean value, standard deviation, type of statistical distribution).

3 PROBABILISTIC APPROACH

3.1 The performance Function

The probability of corrosion being initiated by carbonation P_f is the propability of the carbonation front exceeding the concrete cover e. It can be expressed as:

$$P_f = \Pr ob(G(\mathbf{X}) < 0) = \int_{G(\mathbf{X})<0} f(\mathbf{X}) d\mathbf{X} \quad (4)$$

where $G(\mathbf{X})=e-X_C$ is the performance function and $f(\mathbf{X})$ is the joint probability function of the random vector $\mathbf{X}$ whose coordinates are the concrete parameters (ϕ, K_l, α, and β), the concrete cover (e), the environmental parameters (HR_{lim}, HR_{ext}, and C_0), and even some model's parameters like a and b (see the definition of the CO_2-diffusion coefficient). The probability of corrosion initiation may be assessed from the Hasofer-Lind reliability index β_{HL}. This is defined in the standard space as the minimum distance from the origin to the failure surface, which is the frontier between the safe set where $G(\mathbf{X})<0$ and the failure set where $G(\mathbf{X})>0$. Here, the Rackwitz-Fiessler is used to calculate β_{HL}.

3.2 A Practical Example: Concrete B25 Exposed to *in Situ* Carbonation Conditions

A low-grade concrete (B25, W/C=0.84, cement CEM I 52,5) has been studied under *in situ* conditions in Melun, an urban exposure site in France [Baroghel-Bouny *et al.* 2004]. Cores have been drilled out from RC structural elements exposed for 4 years to this natural urban environment. Note that RC-elements are not sheltered from rain.

Table 1. Statistical distribution of the input data of the model (concrete, envrionmental, and model properties).

Variable	Units	**Distribution**	**Mean**	**Standard deviation or**
W/C	(-)	-	0,84	-
C	($kg.m^{-3}$)	-	230	-
28-day comp. strength	(MPa)	-	24.0 ± 3.6	-
Cover e	(cm)	Lognormal	3	*20%*
ϕ	(%)	Lognormal	16.0	*10 %*
log(K_l)	(m^2)	Lognormal (Bakker)	-19	0.5
n_i	($mol.L^{-1}$)	Lognormal	1.3	*10 %*
α (desorption)	(-)	Normal (Bakker)	9.9	*10 %*
β (desorption)	(-)	Normal (Bakker)	0.44	*10 %*
α (adsorption)	(-)	Normal (Bakker)	121.4	*10 %*
β (adsorption)	(-)	Normal (Bakker)	0.32	*10 %*
α	(-)	Normal (Papadakis)	$(\alpha_{ad}+\alpha_{de})/2$	$(\alpha_{de}-\alpha_{ad})^2/12$
β	(-)	Normal (Papadakis)	$(\beta_{ad}+\beta_{de})/2$	$(\beta_{de}-\beta_{ad})^2/12$
C_0	($mol.L^{-1}$)	Normal	$2.0x10^{-5}$	*10%*
HR_{lim}	(%)	Normal (Bakker)	80	10%
HR_{ext}	(%)	Normal (Bakker) Uniform (Papadakis)	68 $(HR_{max}+HR_{min})/2$	10% $(HR_{max}-HR_{min})^2/12$
t_d	(days)	Normal (Bakker)	230	*10 %*
t_w	(days)	Normal (Bakker)	130	*10 %*
a (-)	(-)	Normal	2.74	*10 %*
b (-)	(-)	Normal	4.20	*10 %*

3.3 Concrete Parameters

Table 1 shows the characteristic parameters relating to the concrete B25 adopted in the Papadakis and Bakker's models. Note that some parameters are specific to the Bakker's model. The concrete porosity ϕ has been measured by gammadensitometry on drilled cores extracted from the RC-elements after a 4-year exposure. An average porosity is calculated by integrating the entire profile of porosity over 3 cm depth from the exposed surface. The initial $Ca(OH)_2$ content n_i is assessed by a thermogravimetric analysis (associated with a chemical analysis) carried out on a sample extracted at core, in the intact zone of the drilled specimen. The liquid water permeability K_l (used to assess the drying coefficient d in the Bakker'model) is determined by the Katz-Thompson [Thompson & Katz 1987] theory which involves the pore size distribution measured by mercury-intrusion porosimetry.

The near-surface properties of the concrete are affected over the first 3 cm by wall-effects, cement sedimentation, aggregates segregation, and evaporation of liquid water which hinders the hydration reactions if the curing step is too short and/or not efficient enough. Furthermore, some mix-parameters, like the water-cement ratio, show a random behavior, mainly as a result of the batching variability. As well as measurement inaccuracies, all these uncertainties sources lead to strong variations of the concrete parameters which are used as input data in durability models of carbonation (ϕ, n_i, K_l, α, and β).

In the framework of the Bakker's model, the van Genuchten's parameters α and β are fitted for desorption or adsorption conditions (see Table 1). Due to a lack of information about the type of probability density which should be chosen for these random variables, a normal distribution (matched with a coefficient of variation equal to 10%) is retained. In the framework of the Papadakis model, the wetting-drying cycles are not taken into account. Therefore, the van Genuchten's parameters α and β are considered to follow a uniform distribution whose boundaries are the coefficients which are fitted for adsorption or desorption.

The concrete cover e is a key parameter of the carbonation models which is required to define the performance function G (see equation 4). Its value strongly depends on the batching variability. This geometrical variable is considered as a random lognormal parameter which can be defined from data available in the literature. The coefficient of variation is generally high and can reach 20%-30%.

3.4 Environmental Parameters

The CO_2-concentration is assumed to follow a normal distribution (see Table 1). The average relative humidity data (given by *in situ* measurements) can be approximated as a cosine function (see figure 1) involving maximum and minimum relative humidity values (HR_{min} and HR_{max}). Regarding the Papadakis model, an uniform distribution is chosen for the external relative humidity between the two boundaries values HR_{min} and HR_{max}. Concerning the Bakkers' model, the limit relative humidity HR_{lim}, above which carbonation is stopped, is assumed to follow a normal distribution with a standard deviation of 10%. The external relative humidity RH_{ext}, which is used as input data in the Bakker's model, is the average value over the days whose daily RH is below RH_{lim} (assessed around 65%, see figure 1). RH_{ext} is considered to follow a normal distribution of standard deviation equal to 10%. In the framework of the Bakker's model, the drying and wetting times, t_d and t_w, are assumed to be described by a normal distribution associated with a coefficient of variation around 10%.

3.5 Model Parameters

The CO_2-diffusion coefficient is calculated with two parameters a and b (see Eq. 1) which are considered to follow a normal distribution with a coefficient of variation equal to 10% (see Table 1).

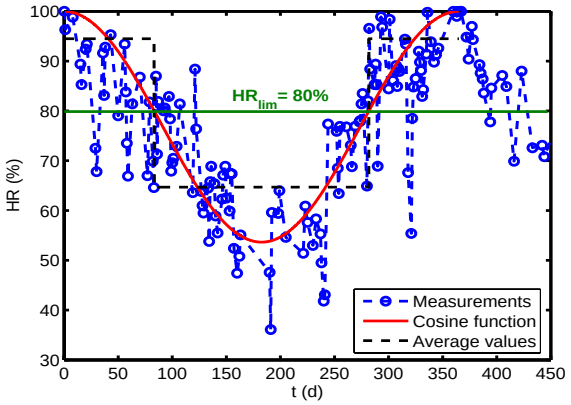

Figure 1. Relative humidity variations during one year.

T 43., Application of the reliability theory to the assessment of the corrosion risk due to carbonation, Thiery M. & Cremona C

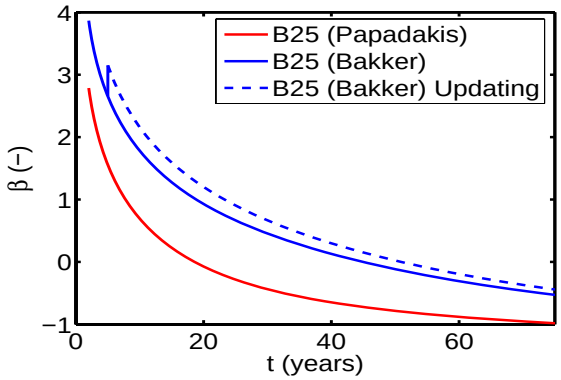

Figure 2. Reliability index *vs*. time for the two proposed models. For the Bakker's model: with and without updating.

4 RESULTS AND DISCUSSIONS

Fig. 2 illustrates the variation of the reliability index *vs.* the exposure time for the two models. Remember that this index is relevant to the occurrence of reinforcing depassivation due to carbonation and the subsequent risk of corrosion initiation. It can be seen that a significant decrease of the reliability arises with time: the starting value of the reliability index is close to 3 (in fact the first point is calculated for two years of exposure), but passes under the threshold value 1.5 recommended by the Eurocode for Serviceability Limit States after 6 years of exposure for the Papadakis model and 12 years for the Bakker's one. Note that the deterministic value is obtained for a reliability index which is 0 (after 18 years of exposure for the Papadakis model and 50 years for the Bakker's one).

The Papadakis model overestimates the carbonation depth (and so underestimates the reliability index) in opposition to the Bakker's model. Besides, the carbonation depth has been measured around 1 cm after a 5-year exposure, whereas the Papadakis model predicts a carbonation depth around 2 cm at the same date. Actually, the Papadakis approach is inappropriate if the external relative humidity varies with time. Concerning this last point, it is especially the case when the concrete is subject to drying-wetting cycles, since the effective diffusion coefficient of CO_2 is slower through the moisture-filled pores of the wetted concrete cover. Therefore, the use of the Papadakis model in the framework of a design strategy would offer a too high level of safety. The carbonation-depth measured after a 5-year exposure is used to revise the prediction given by the Bakkers's model. This updating is based on a Bayesian approach. The updated reliability index is shown in Fig. 2. The updating effect is modest pointing out that the Bakker's approach is rather efficient.

An useful measure for the importance of the uncertainty of the input variables is the normal unit vector $\boldsymbol{\alpha}$ to the limit-state surface at the design point (in the standardized space). When the α_i-coordinate is close to 0, the relative error on the reliability index is low. In practical situations, it is possible to identify if the random variable X_i may be replaced by a fixed value. Fig. 3 shows the α_i-coordinates *vs*. time if the Bakker's model is used. The less influential parameters are the initial $Ca(OH)_2$ content (n_i), the wetting time (t_w), the limit relative humidity (HR_{lim}), the external CO_2-concentration, and the model parameter b.

Fig. 4 illustrates the sensitivities with respect to the mean value for each random variable used in the Papadakis or Bakker's models. It appears that the influence of the concrete cover e, the porosity ϕ, the van Genuchten's parameter β is clear in every case of model. Among the variables which are specific to the Bakker's model, the most sensitive is the liquid water permeability K_l showing thus the importance of the drying-wetting cycles. Fig. 5 reports the sensitivities with respect to the standard deviations. This figure points out that standard deviations of the cover concrete e, the external relative

humidity HR_{ext}, the two van Genuchten's parameters, and the model parameter a need to be assessed with precision, so as to counteract the lack of reliability with respect to the serviceability limit states revealed for the present B25 concrete design.

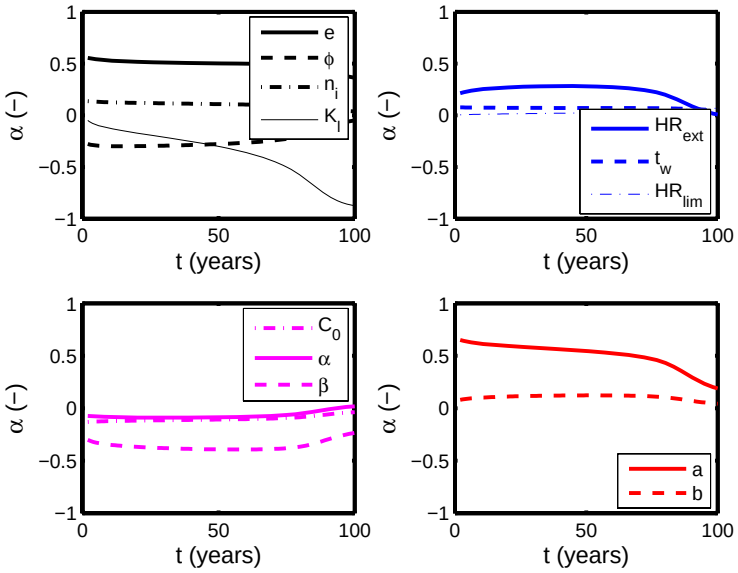

Figure 3. Direction cosines (towards the failure domain) with the exposure time (Bakker's model).

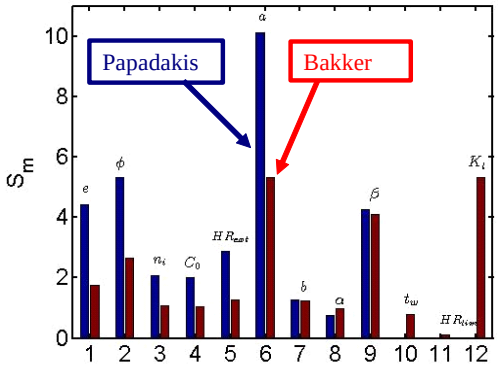

.

Figure 4. Normalized sensitivities with respect to the mean value of each random variable

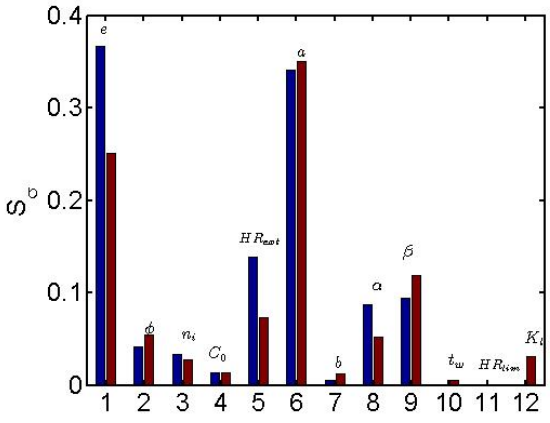

Figure 5. Normalized sensitivities with respect to the standard deviation of each random variable.

REFERENCES

Baroghel-Bouny, V. 2004, *Concrete design for a given structure service life*, Association Française du Génie Civil, Paris.

Baroghel-Bouny, V., *et al.* 2004. 'Ageing of concretes in natural environments: an experiment for the 21st century. iv - Results on cores extracted from field-exposed test specimens of various sites at the first times of measurement', *Bull. Lab. Ponts Chaussées*, **249**, 49-100.

Baroghel-Bouny, V. 2007. 'Water vapour sorption experiments on hardened cementitious materials (Part I)', *Cem. Concr. Res*., **37**, 414-427.

Bary, B. & Sellier, A. 2004. 'Coupled moisture-carbon dioxide-calcium transfer model for carbonation of concrete', *Cem. Concr. Res*., **34**[10], 1859-1872.

Papadakis, V.G., Vayenas, C.G. & Fardis, M.N. 1991, 'Physical and chemical characteristics affecting the durability of concrete', *ACI Materials Journal*, **88**[2], 186-196.

Saetta, A.V., Schrefler, B.A. & Vitaliani R. 1993. 'The carbonation of concrete and the mechanism of moisture, heat and carbon dioxide flow through porous materials', *Cem. Concr. Res*., **23[**4], 761-772.

Thiery, M., Dangla, P., Villain, G. & Platret, G. 2005, 'A prediction model for concrete carbonation based on coupled CO_2-H_2O-ions transfers and chemical reactions', in *10th DBMC, Conference on Durability of Building Materials and Components*, edt. Burn, S., Lyon (France), CSTB, 1-8.

Thiery, M., Villain, G., Dangla, P. & Platret, G. 2007, 'Investigation of the carbonation front shape on cementitious materials : effects of the chemical kinetics', *Cem. Conc. Res.*, **37**, 1047-1058.

Thiery, M., Baroghel-Bouny, V., Bourneton, N., Villain, G. & Stefani, C. 2007 , 'Modelling of the drying of concrete - Analysis of the different moisture transfer modes', *REGC*, **11**[5], 541-577.

Thompson, A.H., Katz, A.J. & Krohn, C.E. 1987, 'The microgeometry and transport properties of sedimentary rocks', *Adv. Phys.*, **36**[5], 625-693.

Tuuti, K. 1982, *Corrosion of steel in concrete*, CBI, Report Fo 4.82, Stockholm.

Wierig, H. 1984, 'Long time studies on the carbonation of concrete under normal outdoor exposure', in *RILEM Seminar Hannover*, 239-249.

Durability Limit States of Concrete Structures: Probabilistic Modeling

Dita Matesová [1]
Markéta Chromá [2]
Břetislav Teplý [3]

T 43

ABSTRACT

In the context of performance-based approaches, sustainability and whole life costing, the concrete structures durability issue has recently gained considerable attention. In the present paper a list and explanation of durability limit states (DLS) specialized for concrete structures and a combination of initiation and propagation durability states are introduced. The assessment of such limit states is based on degradation modeling and a probabilistic approach, enabling the assessment of service life and the relevant reliability level.

In this paper the durability limit states specialized for concrete structures are discussed and the review of some available analytical models for reinforced concrete degradation assessment, their randomization and the use of simulation techniques are provided. Some numerical examples using a special software tool are presented.

KEYWORDS

Durability limit states, Probabilistic modeling, Carbonation, Chloride ingress, Corrosion

[1] Brno University of Technology, Faculty of Civil Engineering, Institute of Structural Mechanics, Brno, Czech Republic 602 00, Phone +420 5 4114 7368, Fax +420 5 4124 0994, matesova.d@fce.vutbr.cz
[2] Brno University of Technology, Faculty of Civil Engineering, Institute of chemistry, Brno, Czech Republic 602 00, Phone +420 5 4114 7639, Fax +420 5 4124 7667, chroma.m@fce.vutbr.cz
[3] Brno University of Technology, Faculty of Civil Engineering, Institute of chemistry, Brno, Czech Republic 602 00, Phone +420 5 4114 7642, Fax +420 5 4124 7667, teply.b@fce.vutbr.cz

1 INTRODUCTION

During the last twenty years the concrete structures service life issue has been given considerable attention. This is clearly reflected also in standardization activities: the ISO/WD 13823 and fib-Model Code [2006] which are based on probabilistic approaches and will introduce the design of structures for durability – i.e. a time-dependent limit state approach with service life consideration.

2 DURABILITY LIMIT STATES FOR REINFORCED CONCRETE

When considering the degradation of reinforced concrete structures, the corrosion of reinforcement is the dominant effect. Usually the initiation and propagation periods are assessed. The former is the time from concrete casting to the moment when the reinforcement is no longer passivated. The latter includes the period since corrosion initiation. Generally, the limit state condition may be written as:

$$P_f(t_D) = P\left\{B(t_D) - A(t_D) \le 0\right\} \le P_d \qquad (1)$$

where $\boldsymbol{A}$ is the action effect, $\boldsymbol{B}$ is the barrier at time t_D = design service life and P_d is the design (acceptable, target) probability value. More about the limit states for durability (DLS) see e.g. in Teplý et al. [2008] or in fib-Model Code [2006]. Let us list possible actions and barriers usable for DLS:

Carbonation: $\boldsymbol{B} = a$ is a concrete cover and $\boldsymbol{A} = x_c$ is the depth of carbonation at time t_D.
Chloride ingress: $\boldsymbol{B} = C_{cr}$ is a critical concentration of dissolved Cl^- leading to steel depassivation and $\boldsymbol{A} = C_a$ is a concentration of Cl^- at the reinforcement at time t_D.
Concrete cracking due to corrosion: $\boldsymbol{B} = \sigma_{cr}$ is a critical tensile stress that initiates a crack in concrete (on the interface with a reinforcing bar) and $\boldsymbol{A} = \sigma$ is a tensile stress in concrete or $\boldsymbol{B} = w_{cr}$ is a critical crack width on the concrete surface and $\boldsymbol{A} = w_a$ is a crack width on the concrete surface generated by reinforcement corrosion.
A decrease of the effective reinforcement cross-section due to corrosion: $\boldsymbol{B} = A_t$ is the reinforcement cross-sectional area at time t_D and $\boldsymbol{A} = A_{min}$ is the minimum acceptable reinforcement cross-sectional area with regard to either serviceability limit state (SLS) or ultimate limit state (ULS).

As stated in the basic design code EN 1990 [2002], the recommended value of the reliability index for SLS (irreversible state) is 1.5, which is relevant to a 50-year design service life. It should be noted that the values of $0.8 < \beta_d \le 1.6$ for the DLS are currently under discussion (e.g. the recommendation of the fib Model Code reads $\beta_d = 1.3$). The level of reliability in the context of durability should be left to the client's decision together with the target service life - as indicated in both future documents ISO/WD 13823 and fib-Model Code.

3 ANALYTICAL MODELS

Several models were selected on the basis of the authors´ literature survey and are briefly mentioned within the next paragraphs. Most of the models were primarily published as deterministic ones; for our purposes all of them were randomized and included in the probabilistic software FReET [Novák et al. 2003], creating a special degradation module FReET-D [Teplý et al. 2007] – see section 4.1.

3.1 Initiation Period

The mathematical models of processes relevant for the initiation periode concern the concrete carbonation and chloride ions ingress.

(i) Carbonation models introduced herein are based on the diffusion of CO_2 in the pore system of concrete and have been discussed in [Teplý et al. 2005, 2008]. Both, the carbonation of concretes from

Portland Cement (OPC) and from blended cements (where the suplementary cementing materials – SCMs – are used) have been incorporated; more details about the latter case see in [Chromá et al. 2007], including the discussion of *k*-value concept. Model from *fib* Model Code [2006] is also included.

(ii) Chloride ingress models are also encompassed in FReET-D software module starting with the models utilizing the widely used Crank's solution to Fick's 2nd law for diffusion of chlorides through concrete, taking into account the fact that the transport of chlorides in concrete is mainly diffusion controlled, and the convection zone is relatively small [Hunkeler 2005].

The simplest models usually involve a diffusion coefficient D of chloride through concrete as a time and space independent input parameter. It is according to Tang & Gulikers [2007] too conservative due to the fact that D is naturally decreasing in time resulting from chloride binding. Therefore the value of D may be calculated e.g. on the basis of the formula proposed by Thomas & Bamforth [1999]. They have derived a formula for the diffusion coefficient as a function of time for (a) a control mix made of OPC only, (b) concretes with 30 % of fly ash and (c) with 70 % of slag as a partial replacement for OPC. Unfortunately, this mathematical simplification where parameter D is simply substitued by time-dependent $D(t)$ without adequate clarifying the mathematical basis of diffusion may not be quite correct [Tang & Gulikers 2007]. In such case the apparent diffusion coefficient is underestimated and it will cause errors in durability design and redesign of reinforced concrete structures. Also the mathematical expression adopted by *fib* Model Code [2006] does not fulfill the correct differential equation. The proper mathematical derivation of time-dependent diffusion coefficient was published by Nilsson & Carcasses [2004] and comparison of possible errors caused by some oversimplified mathematical expressions were presented by Tang & Gulikers [2007].

Although those models based on simple Fick's 2nd law are used by engineers in practical applications due to their relatively simple mathematical expressions, however models based on the actual physical or chemical processes would be more adequate. They are often used only for research purposes owing to necessities of more sophisticated calculations and only some models were simplified into a more engineer-friendly form [Papadakis et al. 1996, Tang 2007].

3.2 Propagation Period

The key factor for the modeling of steel corrosion as a time dependent process is the corrosion rate which is usually expressed through current density, i_{corr}. This variable is strongly affected by ambient conditions such as humidity and temperature, moisture and oxygen availability at steel level, the degree of concrete carbonation and amount of chlorides; thus depending on the diffusion characteristics of concrete. The presented models are sorted into three basic groups (i) - (iii) according to their output information and are also implemented in FReET-D.

(i) The loss of reinforcement in time may be expressed by formulas proposed by Andrade et al. [1996] and Gonzales et al. [1995] for uniform and pitting type of corrosion, respectively.Those formulas are based on current density and parameter R_{corr} that expresses the type of corrosion. The residual reinforcement cross section in the case of pits can be predicted by the simplification into a hemispherical form as proposed by Val & Melchers [1998].

(ii) Time to cracks initiation in concrete: Complex models that describe the entire process of stress and crack development in concrete due to corrosion are rather rare; more extensively published are models predicting only the time of cracking initiation in concrete. The model for calculation of the time to crack initiation in concrete cover proposed by Morinaga [1988] is an empirical equation based on experimental data. This model takes into account only the initial bar diameter, concrete cover thickness and rate of corrosion. It does not include any mechanical parameters of concrete. Bažant [1979] has proposed a physical-mathematical model for calculation of initiation time to corrosion cracking taking into account concrete cover depth, reinforcing bar diameter and spacing, mechanical

properties of concrete, etc. Concrete is considered to be a homogeneous elastic material shaped as a thick-wall cylinder. This model also solves the time of steel depassivation due to critical chloride concentration. Bažant´s model [1979] was extended by Liu & Weyers [1998] who proposed a model for time of crack initiation based on a comparison of the minimum stress required to cause cracking (which equals to the tensile strength of concrete cover) with the expansive pressure in concrete developed over time due to the growth of corrosion products. Another improvement was proposed by Maaddawy & Soudki [2007]. The authors have developed a relationship between steel mass loss and the internal radial pressure caused by rust growth. The time to corrosion cracking is estimated on the basis of Faraday´s law.

(iii) Stresses and cracks development in concrete: Bhargava et al. [2005] have developed a model describing the entire cracking process after crack initiation. Five modifications of the model are proposed to reproduce various experimental trends. Li et al. [2006] have also proposed a model describing the whole cracking process in concrete due to corrosion with the possibility of calculating the width of a crack on a concrete surface.

4 NUMERICAL EXAMPLE

In the following some of the above mentioned models are used to illustrate possible practical applications. Firstly, a software tool developed by the authors for the probabilistic assessment of different DLSs is introduced.

4.1 Software Tool

The multipurpose probabilistic software FReET, for general statistical, sensitivity and reliability analysis of engineering problems, has been used for randomization of the analytical models [Novák et al. 2003]. It enables the feasible and user friendly utilization of stochastic approaches (a combination of analytical models and simulation techniques) to form the specialized software FReET-D for assessing the potential degradation of newly designed as well as existing concrete structures [Teplý et al. 2007]. Implemented degradation models may serve directly for the durability assessment of structures in the form of a simple limit state (Eq. 1), i.e. the assessment of service life and the level of relevant reliability measure. The user may create different limit conditions. For the statistical analysis of the following examples the Latin Hypercube Sampling method was applied. For the output quantities the best fit of probabilistic distribution function (PDF) was found using the Kolmogorov Smirnov goodness-of-fit test.

4.2 Loss of Reinforcement Due to Corrosion Initiated by Chloride Ingress

Let us assume the critical loss of the reinforcement area to be 10 % (such a loss may e.g. lead to the exceeding of the reliability level for the ULS or SLS – depending on the structure and loading configuration). For the calculation of steel loss in time a deterministic model proposed by Andrade et al. [1996] was applied. Time to corrosion initiation t_i was calculated on the basis of model proposed in [Papadakis et al. 1996]: t_i = LN (47.4; 11.5) years. The full description of all input parameters is given in Tables 1 and 2. The decrease in rebar diameter over time is plotted in Fig. 1 The mean values of t_i and $t_{d,crit}$ = the time of a critical drop in rebar diameter are marked in this figure.

Table 1. Input parameters for the calculation of time to reinforcement depassivation.

Reflection of	*Variable*	*Unit*	*Mean value*	*COV*	*PDF*
Models	Uncertainty factor of model	-	1	0.15	Lognormal (2par)
Environment	CO_2 content in the atmosphere	mg/m^3	820	0.12	Normal
	Relative humidity	%	70	0.07	Beta (a = 0, b = 100)
Concrete mix	Unit content of OPC cement	kg/m^3	313	0.03	Normal
	Unit content of water	kg/m^3	185	0.03	Normal
	Unit content of aggregate (0-4 mm)	kg/m^3	847	0.03	Normal
	Unit content of aggregate (4-8 mm)	kg/m^3	386	0.03	Normal
	Unit content of aggregate (8-16 mm)	kg/m^3	625	0.03	Normal
	Specific gravity of cement	kg/m^3	3100	0.02	Normal
	Specific gravity of aggregate (0-4 mm)	kg/m^3	2590	0.02	Normal
	Specific gravity of aggregate (4-8 mm)	kg/m^3	2540	0.02	Normal
	Specific gravity of aggregate (8-16 mm)	kg/m^3	2660	0.02	Normal
Other	Concrete cover	mm	25 - 75	-	Deterministic
	Concentration of Cl^- on nearest concrete surface	mol/m^3	50	-	Deterministic
	Saturation concentration of Cl^- in solid phase	mol/m^3	140	-	Deterministic
	Threshold concentration of Cl^- in liquid phase	mol/m^3	13.4	-	Deterministic
	Diffusion coefficient of Cl^- in infinite solution	m^2/s	$1.6 \cdot 10^{-9}$	-	Deterministic

Table 2. Input parameters for calculation of loss of reinforcement due to corrosion.

Input parameter	*Unit*	*Mean value*	*COV*	*PDF*
Initial bar diameter	mm	30	0.025	Lognormal (2 par)
Time to corrosion initiation	years	47.4	0.244	Lognormal (2 par)
Current density	$\mu A/cm^2$	1	0.2	Normal
Coefficient of corrosion type	-	2	-	Deterministic
Uncertainty factor of model	-	1	0.15	Lognormal (2 par)

The best-fitted PDFs for output net rebar diameters are LN (2 par) for 0, 10 and 20 years, Student t for 30 years, Laplace for 40 and 50 years, LN (2 par) for 60, 70, 80, 90 and 100 years, LN (3 par) for 110 and 120 years and LN (2 par) for 130, 140 and 150 years. Chosen histograms of output parameter together with fitted PDFs are depicted in Fig. 2 showing the complexity of a statistical description of the problem solved. Note that lognormal PDFs appear for time intervals of 0-20 and 60-150 years. In the first interval the steel is not yet depassivated, while in the second time interval the steel is already depassivated in the majority of stochastic realizations. Therefore, the standard deviation (std) of output net rebar diameter in the time interval of 0 to 20 years is given by std of the input initial bar diameter

while the std in the time interval of 60-150 years is affected by all input variables and is much greater. In the intermediate part (i.e. 40-100 years) the standard deviation gradually increases (see Fig. 1).

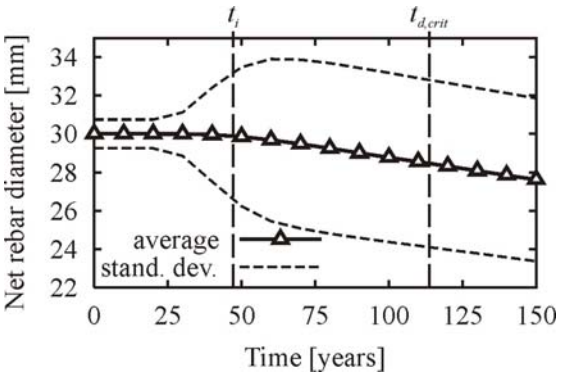

Figure1. Net rebar diameter (± standard deviation) vs. time.

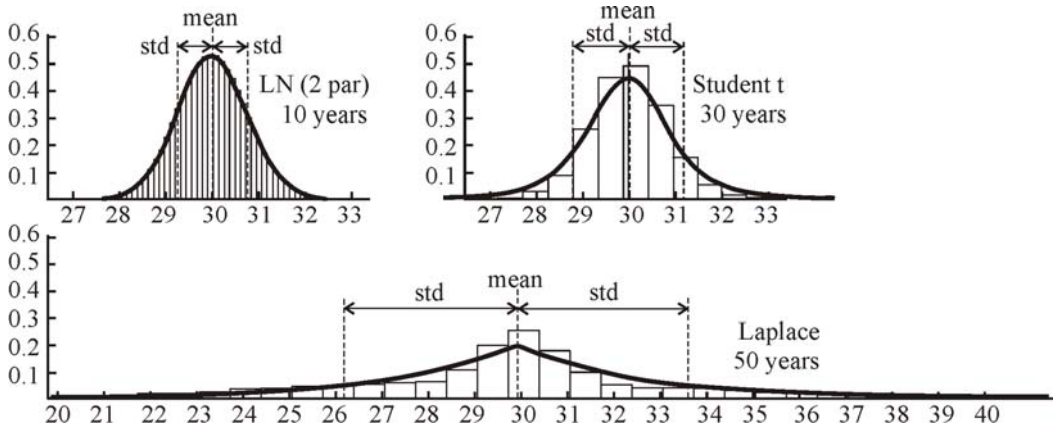

Figure 2. Histograms of output net rebar diameter plotted in figure1 (decreased due to corrosion) together with the best-fitted PDFs in chosen time steps.

5 FINAL REMARKS

The probabilistic durability design approach is discussed in this paper, focused on the initiation and propagation period. Appropriate limit states are explained and suitable models are briefly described. Finally, a numerical example is shown.

Concurrently, the presented approach lacks certain considerations, e.g.: (i) the spatial randomness of material and/or environmental characteristics are not considered (random fields could be a remedy), (ii) the spatial distribution of deterioration is not distinguished while assessing limit states, and (iii) combination with mechanical stress is not taken into account. The authors' ongoing research is focused in this direction partially; the effect of chloride concentration on reinforcement corrosion is also currently being studied utilizing the celullar automata technique.

ACKNOWLEDGMENTS

This outcome has been achieved with the financial support of the Czech Ministry of Education, project No. 1M0579, within the activities of the CIDEAS research centre.

REFERENCES

Andrade, C., Sarria, J. & Alonso, C. 1996, 'Corrosion rate field monitoring of post-tensioned tendons in contact with chlorides', Proc. Int. Conf. on Durability of Building Materials and Components 7 Stockholm, Sweden, vol. 2, pp. 959-967.

Bažant, Z.P. 1979, 'Physical model for steel corrosion in concrete sea structures-theory', *Journal of the structural division*, ASCE, 105 (ST6), 1137-1153. Proc. Paper 14651.

Bažant, Z.P. & Planas, J. 1998, *Fracture and size effect in concrete and other quasibrittle materials*, CRC Press, Boca Raton and London.

Bhargava, K., Ghosh, A.K., Mori, Y. & Ramanujam, S. 2005, 'Modeling of time to corrosion induced cover cracking in reinforced concrete structures', *Cement and Concrete Research*, **35**[11], 2203-2218.

Chromá, M., Rovnaník, P. & Teplý, B. 2007, 'Carbonation modelling and reliability analysis of RC structures made from blended cements', Proc. of International RILEM Workshop on Performance Based Evaluation and Indicators for Concrete Durability, 19-21 March 2006, Madrid, Spain, pp. 319-325.

Collepardi, M., Marcialis, A. & Turrizuani R. 1972, 'Penetration of chloride ions into cement pastes and concrete', *J. Am. Ceram. Soc.*, **55**[10], 534-535.

EN 1990, 2002, *Basis of Structural Design* (European Standard).

fib Bulletin 2006 *Service Life Design*, No. 34 (Part of the future fib Model Code).

Hunkeler, F. 2005, 'Corrosion in reinforced concrete: processes and mechanisms', Proc. of Corrosion in reinforced concrete structures, ed. H. Bőhni, Woodhead Publishing Limited, Cambridge.

Gonzales, J.A., Andrade, C., Alonso, C. & Feliu, S. 1995, 'Comparison of rates of general corrosion and maximum pitting penetration on concrete embedded steel reinforcement', *Cement and Concrete Research*, **25**[2], 257-264.

ISO/WD 13823, *General Principles on the Design of Structures for Durability* (currently under development). ISO TC 98/SC2/WG10.

Li, C.Q., Melchers, R.E. & Zheng, J.J. 2006, 'An analytical model for corrosion induced crack width in reinforced concrete structures', *ACI Structural Journal*, **103**[4], 479-482.

Liu, Y. & Weyers, R.E. 1998, 'Modeling the time-to-corrosion cracking in chloride contamined reinforced concrete structures', *ACI Material Journal*, **95**[6], 675-681.

Maaddawy, T. & Soudki, K.A. 2007, 'A model for prediction of time from corrosion initiation to corrosion cracking', *Cement and Concrete Composites*, **29**[3], 168-175.

Morigana, S. 1988, *Prediction of service lives of reinforced concrete buildings based on the corrosion rate of reinforcing steel*, Special Report No. 23, Institute of Technology, Shimizu Corporation, Tokyo, Japan.

Nilsson, L.-O. & Carcasses, M. 2004, *Models for Chloride Ingress into Concrete - A Critical Analysis*, Report of Task 4.1 in EU-Project G6RD-CT-2002-00855, ChlorTest.

Novák, D., Vořechovský, M. & Rusina, R. 2003, 'Small-sample probabilistic assessment - FREET software' Proc. of International Conference on Applications of Statistics and Probability in Civil Engineering (ICASP 9), eds. Der Kiureghian et al., San Francisco, USA, pp. 91-96.

Papadakis, V.G., Roumeliotis, A.P., Fardis, C.G. & Vagenas, C.G. 1996, 'Mathematical modeling of chloride effect on concrete durability and protection measures', Proc. of International Conference on Concrete in the Service of Mankind (Concrete Repair, Rehabilitation and Protection).Eds. R.K. Dhir & M.R. Jones, Dundee, Scotland, UK, pp. 165-174.

Tang, L. & Gulikers, J. 2007, 'On the mathematics of time-dependent apparent chloride diffusion coefficient in concrete', *Cement and Concrete Research*, **37**[4], 589-595.

Tang, L. 2007, 'Service-life prediction based on the rapid migration test and the ClinConc model', Proc. of International RILEM Workshop on Performance Based Evaluation and Indicators for Concrete Durability, 19-21 March 2006, Madrid, Spain, pp. 157-164.

Teplý, B., Keršner, Z., Rovnaník, P. & Chromá, M. 2005, 'Durability vs. Reliability of RC Structures', Proc. of the 10th International Conference on Durability of Building Materials and Components 10DBMC, 6 pages.

Teplý, B., Matesová, D., Chromá, M. & Rovnaník, P. 2007, 'Stochastic degradation models for durability limit state evaluation: SARA – Part VI.', Proc. of 3rd International Conference on Structural Health Monitoring of Intelligent Infrastructure (SHMII-3 2007), Vancouver, Canada, in press.

Teplý, B., Chromá, M. & P. Rovnaník 2008, Durability assessment of concrete structures: Reinforcement depassivation due to carbonation, *Structure and Infrastructure Engineering* (in press).

Thomas, M.D.A. & Bamforth, P.B. 1999, 'Modeling chloride diffusion in concrete: Effect of fly ash and slag', *Cement and Concrete Research*, **29**[4], 487-495.

Tuutti, K. 1982, *Corrosion of steel in concrete*, Swedish Cement and Concrete Research Institute, Stockholm, Sweden.

Val, D. & Melchers, R.E. 1998, 'Reliability analysis of deteriorating reinforced concrete frame structures', Proc. of Structural Safety and Reliability, eds. N Shiraishi et al., Balkema, Rotterdam, pp. 105-112.

11DBMC International Conference on Durability of Building Materials and Components
ISTANBUL, Turkey 11-14 May 2008

Development of a Simulation Tool for Insulated Glass Durability

Russell Pylkki [1]
Michael Doll [2]

T 43

ABSTRACT

Efforts to increase the energy performance of windows has been an ongoing effort that has seen fenestration progress from windows with storm windows to sealed double pane insulated glass (IG) to IGs with glass coatings which moderate the light and heat transfer through the glass. As time has progressed, the cost of glass failure has increased significantly. The United States Department of Energy is concerned that a lack of durability could lead to slow adoption.

In order to address the advancements that are needed to meet current and future building envelope energy performance goals, a project to deliver the foundation for a comprehensive IG durability simulation tool was undertaken. This need is based upon the lack of IG field failure data and the lengthy field observation time necessary for data collection. Ultimately, the simulation program is intended to be used by designers throughout the current and future fenestration industry supply chain. Its use is intended to advance IG durability as expectations grow and designs evolve around the impact a window has on energy conservation..

Included in the simulation model presentation are elements and / or methods to address IG materials, design, process, quality, induced stress (environmental and other factors), validation, etc. In addition, acquired data is presented in support of project and model assumptions.

KEYWORDS

Windows, Insulated glass units, Durability simulation

[1] Aspen Research Corporation, 1700 Buerkle Rd., St. Paul, MN 55110, USA, Phone +1 651 2646000, Fax 651 2646270, Russell.Pylkki@AspenResearch.com
[2] Pando Technology, Bloomington, MN, USA, Phone +1.952.2403171

1 INTRODUCTION

The Window Industry Technology Roadmap, sponsored the U. S. Department of Energy's Office of Building, State and Community Programs, identified durability of windows as a barrier to their advancement. This is of concern because of the pivotal role that insulating glass (IG) is expected to play in meeting the US Department of Energy (DOE) performance goals for current and future building envelopes. Although data is lacking regarding IG unit durability, there is a growing perception of costly IG unit failure rates that creates a barrier to new technology implementation and associated costs.

To address this concern, the DOE funded a project, "An Insulating Glass Knowledge Base," [Hage *et al.*, 2002; Doll, M. L. *et al.*, 2005] that included the development of a software model to evaluate the durability of IG units. This paper discusses the development of a software program that was to provide a mechanism by which durability characteristics of IGUs could be captured in a useful and practical manner.

2 APPROACH

2.1 FMEA/Fault Trees

General research efforts addressing IG unit durability have been and continue to be focused at the understanding IG unit seal systems and their materials. Although, as an example, permeation of moisture vapor and gasses through the sealant materials is an important aspect of IG unit durability, this project was defined and brings focus to identifying and evaluating all modes of root cause IG unit failure. This process requires that each IG unit be considered as a unique system with respect to its design, materials and assembly process. A Failure Modes and Effects Analysis (FMEA) was completed to document the possible root cause failure modes of the IG system. The FMEA was then used to develop an Event Tree Diagram, shown below for a box spacer in Fig. 1.

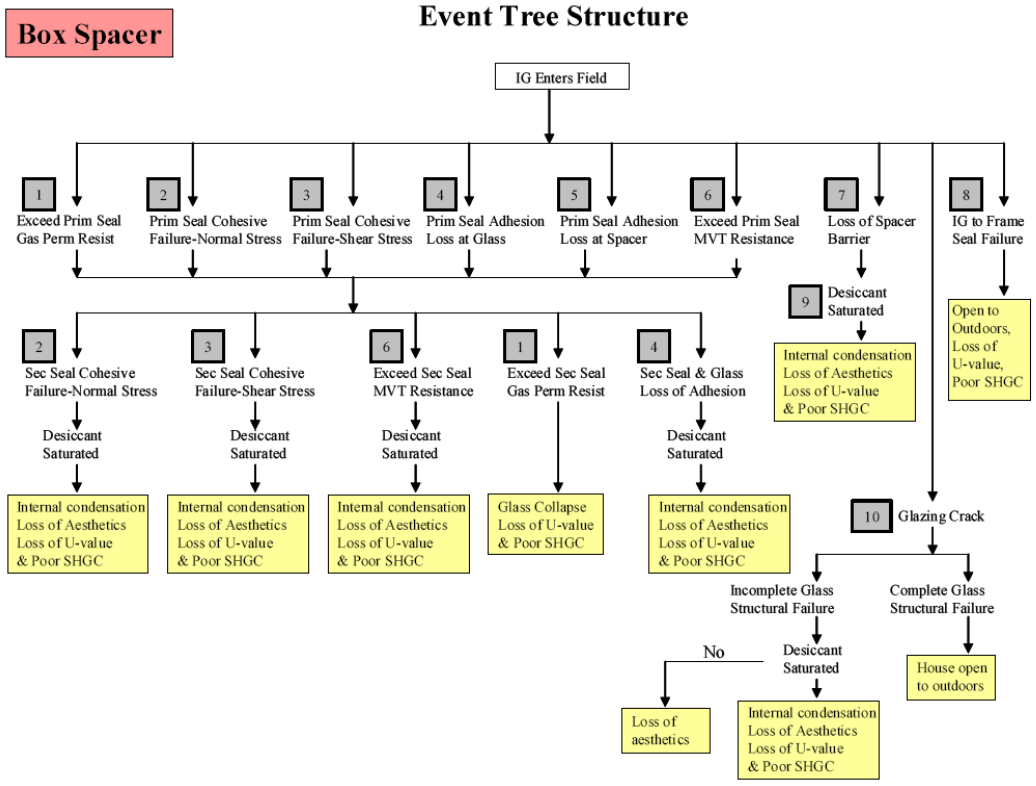

Figure 1. Example of an Event Tree for an IGU with a box spacer.

Understanding of failure mechanisms was also an input reference for the event trees. Specifically, understanding of the sequential chain of events leading to a system failure was captured from failure mechanism knowledge. The event tree differs from the FMEA in that it captures with more detail the sequence of events which must occur for a given system failure to be realized. This more thorough graphical representation of the failure chain allows greater qualitative understanding of the cause-failure effect chain. Such event trees were used the development of the model and were used to determine the model's failure criteria.

3 SIMULATION DESIGN

3.1 Simulation Schematic

A representation of an IG unit (box spacer) and the forces that act upon it are shown below in Figure 2. Stressors that act upon the IG unit include temperature, pressure (barometric and wind), solar radiation, which differ between the exterior and the interior environments, and gravity. The IG unit has multiple glass surface temperatures, gas pressure, gas composition and gas temperature.

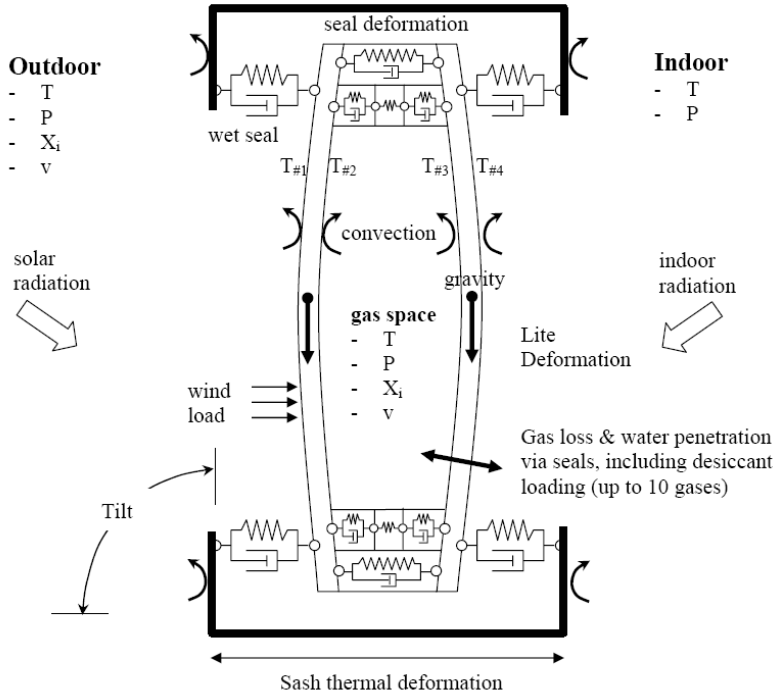

Figure 2. Schematic of the representation of in the model of and IG (Box Spacer) and indication of the physical effects modeled on an IG unit (T = temperature, P = pressure, X = gas composition, v = velocity

As a function of time, the durability design tool simulates the behavior of an IG unit exposed to realistic climate conditions. As the environment acts upon the IG unit, stresses and strains in the IG unit are calculated together with temperature distributions, gas permeation effects (i.e. gas loss and desiccant moisture loading), and dew point temperature in the IG unit air space, and changes in the heat transfer through the IG unit. The effects of the environmental exposure on the IG unit are compared against the strength of the window assembly to determine the durability of the design.

3.2 Simulation Components

In order to carry out the simulation, the IG unit's response to the environmental stressors is separated into three models (thermal, permeation, and stress) which are described briefly as follows.

3.2.1 Thermal Model

The thermal model, using meteorological data 1) calculates the incident angle of the sun on the window; 2) determines the optical properties of the glass at that angle; 3) calculates the optical properties of the IG unit; 4) calculates a center-of-glass temperature (using the average lite separation and IG gas fill) and 5) calculates a one dimensional temperature distribution in the sash.

3.2.2 Permeation Model

The permeation model calculates the movement of gasses (including water) with time through the IG unit's polymer seals and the loading of the desiccant with water. The model is also designed to work with sealant systems where the sealant is formulated with desiccant. This allows both a box spacer and a 'thermoplastic spacer' type designs to be modeled.

3.2.3 Stress Model

The stress model calculated the physical stresses that act upon the IG unit with time. These stresses include the movement of the IG unit components relative to each other that can take place due to the effects of thermal expansion or contraction, bending of the glass lites due to differences in pressure between the atmosphere and the IG unit gas space and wind loads.

3.3 Coupled Model Calculations

The coupling of the structural model with the thermal model and the model for gas permeation is the program is shown in the calculation sequence shown below in Fig. 3. At each time increment, the temperature model is solved (based on the most recent solutions for the permeation and structural models. The second model considered in Fig. 3 is the permeation model, in which the most recently determined temperature and structural data are used. The last model is the structural response, which uses the most recent solutions for the temperature and gas permeation. Since a sequence of calculations may not result in a balanced solution, convergence is tested. When

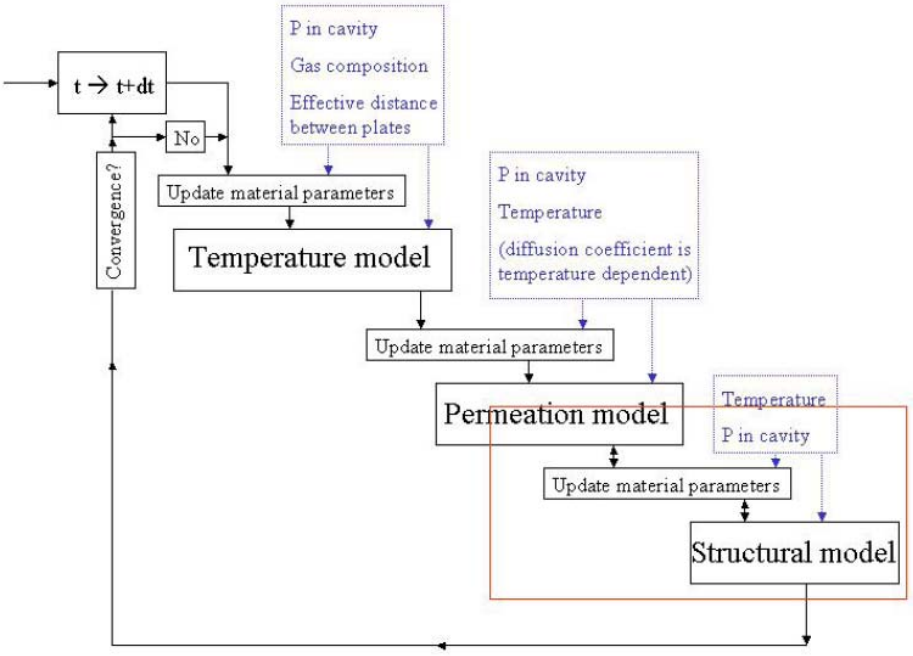

Figure 3. Sequence of coupled model calculations

3.4. Durability Tool – User Interface

The user interface is used to control the simulation. The user 'assembles' an IG unit to be tested, defining all aspects of its design: dimensions, glass thickness and coatings, spacer system, sealant materials and dimensions. Material properties for glass, spacer materials, and sealants are selected from their respective data bases. A standard deviation of material properties can be defined for use in Monte Carlo simulations. The International Glazing Data Base is used for the glass optical properties. Meteorological data (TMY2 format) are used to define the outdoor environmental conditions for the simulation. The user also defines the indoor environment. A total of 44 failure criteria can be selected and the user also sets the failure threshold. The interface program is also used to control the simulations parameters, launch the simulation and evaluate its results. An example of the input for sealants dimensions for a box spacer system is shown below in Fig 4.

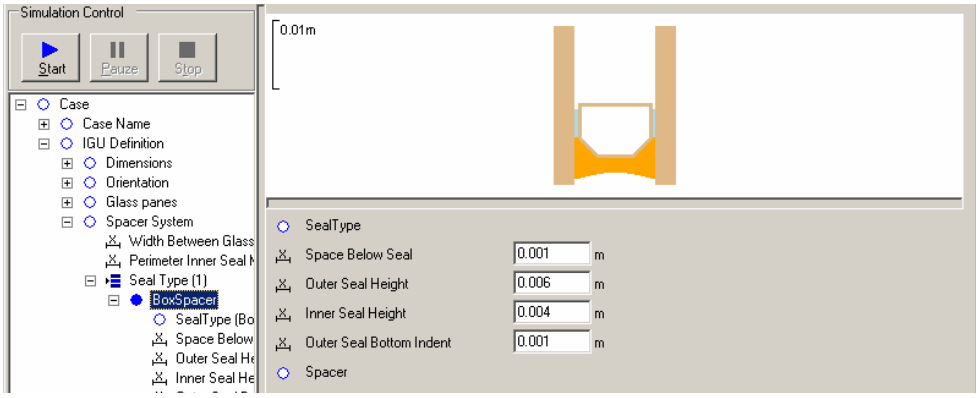

Figure 4. Seal dimension input screen (partial view)

When simulation is completed, the results are shown in a summary screen. In this example (Fig. 5), a simulation consisting of 50 Monte Carlo runs was made. The pie chart identifies the distribution of failure modes, while the details of the simulation are displayed below. The left axis shows the number of runs that were performed in the simulation while the time to failure is shown on the right axis. The frequency of failure modes are shown in a histogram format. The average time to failure and standard deviation are shown as a whisker plot for each failure mode encountered.

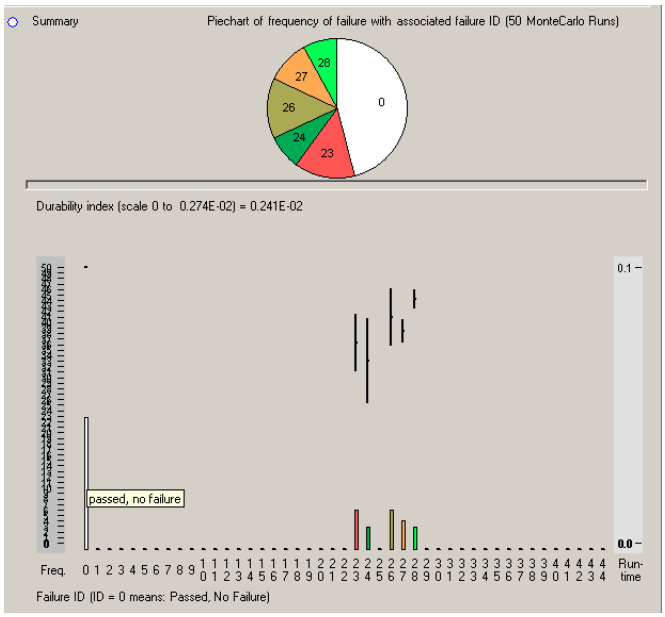

Figure 5. Results Summary Screen (parial view)

4 Simulation Tool Validation

Validation of the simulation tool will be an important aspect of continuing the tool development process. We know that the model is built upon an understanding of the physical forces that are acting upon an IG unit and the IG unit's response to those stressors. Assumptions were made with respect to the boundary conditions for the model. For example, the current release of the durability model leverages code from other modeling tools (WINDOW, THERM, etc.) widely used in the US in support of energy certification. Yet, to evaluate root cause failure, the durability model must extend analysis beyond the current tools and include, for example, direct and indirect radiant solar adsorption on the seal components. Thus, the program must model all the components during all environmental cycles and expected applications. As an example, the current tools output validated temperature gradients from a simulated winter night. The seal temperature which might be expected from these simulations differs greatly from the seal temperatures which will be achieved during a sunny late winter day.

Figure 6 presents the temperature along the bottom seal materials of an IG unit of a brown south-facing window, showing that the seal materials reach temperatures of *ca*. 50 °C. The glass surfaces on the same day were 32 °C, nearly 20 °C cooler than the temperature of the lower seal. Accurate estimation of temperatures is important in estimating the service life on an IG unit because the permeation properties of the sealants change with temperature and stresses that can be induced by thermal expansion of the IG unit's components. This effect of this temperature error on permeation can be compensated by providing the simulation tool with a file of seal temperatures as a function of time to use with the simulation.

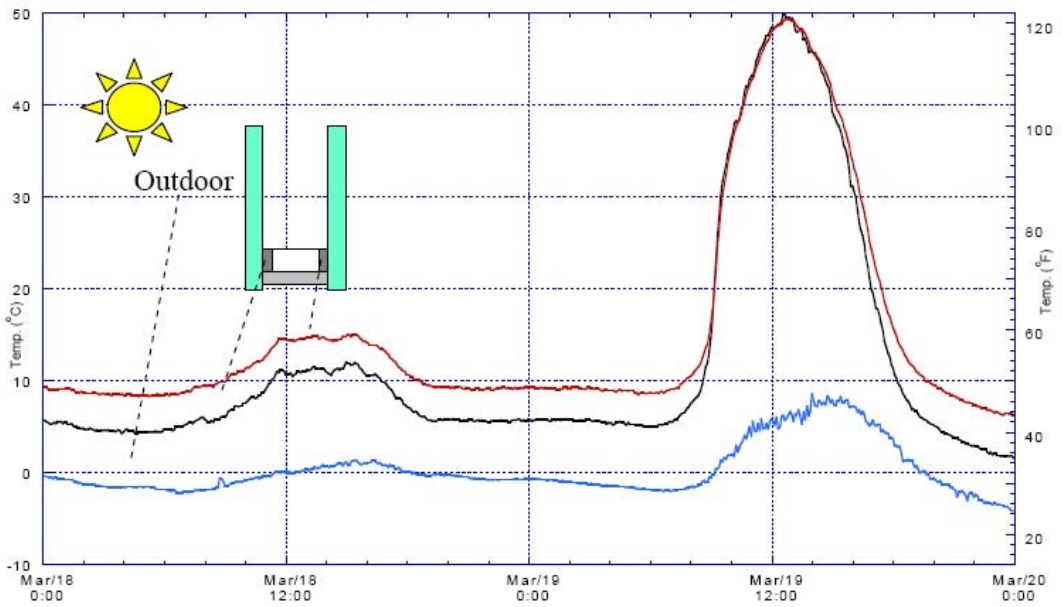

Figure 6. Effect of a cloudy vs. sunny day on the seal temperature of an IGU. The IGU is in a brown, south-facing window. The exterior temperature near the window is also shown.

5 SUMMARY

We have presented an overview of the development of a simulation tool for determination of IG unit durability. The development began with a Failure Mode and Effect Analysis of IG units and led to the definition of an Event Tree Structure for the IG unit's failure. This was used in the development of the simulation tool, which consists of coupled thermal, permeation and structural models of the IG unit's response to a user defined environment.

This simulation tool is envisioned to ultimately be a predictive model, utilizing Monte Carlo methods to statistically choose and compare stress and strength distributions of the IG unit. The current release is the foundation of that vision.

ACKNOWLEDGMENTS

We would like to acknowledge those outside of Aspen Research that were involved in the DOE project: Dr. Charlie C. Curcija (Carli, Inc., USA), and Han Velthuis, Dries Hagen, and Titus Riemersma (TNO, The Netherlands).

REFERENCES

Hage, R., Anderson, J., Bender, T., Eastep, M., Fairman, J., Hendrickson, G., Lagos, G., Pylkki, R., Rozynov, B., Scripter, C., Slough, W., and Wilken, D. 2002, *An Insulating Glass Knowledge Base, Phase I Final Report*, U. S. Department of Energy, DE-FC26-01NT41258, December.

Doll, M. L., Pylkki, R. J., Hendrickson, G., Lagos, G. Christensen, C and Curcija, C, 2005, *An Insulating Glass Knowledge Base, Phase II Final Report*, U. S. Department of Energy, DE-FC26-01NT41258, August.

Critical Considerations on the Assessment of the Durability (Serviceability) Limit State of Reinforced Concrete Structures

Rui Miguel Ferreira [1]
Joost Gulikers [2]

T 43

ABSTRACT

Until recently, reinforced concrete structures were not designed specifically for durability but this issue was incorporated indirectly in the prevailing codes without any type of mathematical or scientific verification. Traditionally, design for durability has been based on a deem-to-satisfy approach. However, this approach has been shown, in some situations, not to guarantee the required concrete quality necessary to achieve the specified service life. The lack of reliable information on the durability of the concrete makes it difficult to evaluate its quality and performance. The deem-to-satisfy approach does not quantify the durability of the concrete, and therefore also not the performance. Consequently, for a specific exposure environment, without prior knowledge of performance, design solutions can not be optimized for durability and costs.

However, and largely thanks to European projects like *Lifecon* and *DuraCrete*, a different approach has been developed based on that commonly used for structural design in which limit state (LS) equations define the acceptance or the rejection of design solutions. LS can be assessed deterministically, semi-probabilistically (use of factors that can reduce resistance and increase loads, alter time periods, etc.) and probabilistically. The probabilistic approach can allow for optimization but requires much more information, which is not always available. The LS equations are sometimes rewritten so as to focus either on the resistance of the material, the accumulation of damage, or even the development of the degradation process over time. A different formulation of the same LS equation can be adversely influenced by the type of variables and their sensitivities.

The objective of this paper is to critically analyze the assessment of the LS with probabilistic and semi-probabilistic approaches. The probabilistic assessment is based on the Monte Carlo simulation method. A critical overview of the assessment of the durability limit states shall be presented. A thorough comprehension of the underlining conditions for the use of these approaches is vital for the correct durability design of reinforced concrete structures.

KEYWORDS

Durability design, limit state, probabilistic, reliability, concrete structures, chloride

[1] University of Minho, Civil Engineering Department, 4800-058 Guimarães, Portugal. rmf@civil.uminho.pt
[2] Centre for Public Works, Ministry of Transport, Public Works and Water Management, NL-3502 LA, Utrecht, The Netherlands. joost.gulikers@rws.nl

1 INTRODUCTION

Until recently, reinforced concrete structures were not specifically designed for durability, but this aspect was incorporated indirectly in the prevailing codes without any type of mathematical or scientific verification. Traditionally, design for durability has been based on a deem-to-satisfy approach. The lack of reliable information on the durability properties of the concrete makes it difficult to evaluate its quality and performance. Such a deem-to-satisfy approach does not quantify the durability of the concrete, and therefore, also not it's performance. However, a different approach has been developed based on a LS equation that defines the acceptance or the rejection of design solutions. Limit states can be assessed deterministically, semi-probabilistically and probabilistically. The probabilistic approach can allow for optimization but requires much more information, which is not always available.

There are different ways of defining a serviceability limit state (SLS) according to the degree of deterioration, such as corrosion initiation, cracking, spalling, etc. For all these limit states, however, it is very difficult to define the associated criteria. Since corrosion initiation is considered a critical and well defined point of the degradation process, it is the most commonly used SLS.

The objective of this paper is to analyze critically the assessment of the limit states with a probabilistic approach based on the Monte Carlo simulation method. A critical overview of the assessment of the durability limit states shall be presented. A thorough comprehension of the underlining conditions for the use of these approaches is vital for the correct durability design of RCS.

2 CONSIDERATIONS ON THE VERIFICATION OF THE SLS

2.1 Definition of Probability of Failure and Degree of Reliability

The SLS defines the conditions beyond which a specified service requirements for a structure (or component) are no longer met for a certain degree of reliability (DR). The probability of failure (PF) is defined as the probability that a structure (or component) no longer satisfy the design performance requirements (i.e. SLS), where as the reliability index is defined as the fractile of a normalised normal probability function corresponding to the ability of the structure (or component) to perform its requirements without failure during a specific interval of time.The PF and DR are not easily understood by both the consultant and owner as it provides no information on the actual condition of the structure in terms of damage. It appears that an unambiguous definition of probability cannot be given and consequently the DR is based on arbitrary grounds [Gulikers 2007]. The DR is usualy indicated by the reliability index, β.

For the SLS of corrosion initiation, the physical phenomenon is a relatively well defined moment. What remains to be defined is the acceptable value of PF and the required value of the reliability index. Does the PF represent a physical degree of deterioration of the structure, or is it only a mathematical/ statistical value agreed on as being acceptable? For the SLS of corrosion initiation, the PF can be described as the mathematical likelihood that corrosion has been initiated. There is no indication as to the extent of corrosion initiation, however, it is usually assumed that the higher the PF the wider spread the phenomenon. Therefore, a 10 % or 90 % PF only indicates the likelihood that corrosion has been initiated, but not the extent or the severity of the corrosion. An extreme situation would be a PF of 0%. This level would logically correspond to a situation with complete absence of steel reinforcement corrosion. Another extreme situation is the PF of 100 %. It is a mathematical guarantee that corrosion has initiated, in some part of the structure, but it does not indicate that 100 % of the structure has initiated corrosion, i.e., all the reinforcement. According to LNEC E-465 [2005] the acceptable level of PF for the SLS of corrosion initiation, varies from approximately 2 % up to 12 %. However, in Germany probability levels up to 30% are suggested in order to arrive at reasonable cover depths.

How should the DR be quantified? Should it represent an economical optimum? The DR should depend on the type of structure, accessibility, the consequences of degradation and failure, maintenance, among other factors. In certain publications, the reliability index depends on the Reliability Classe (RC) of the structure, which in turn is associated with the Consequence Class (CC) of structural failure. In general, for SLS, a reliability index ranging from 1.3 to 1.8 is considered appropriate. These β-values correspond to probabilities of approximately 10 % and 3 %, respectively. Service life calculations have demonstrated that in most cases the adoption of β = 1.7 to 1.8 will result in an excessive cover depth, and for that reason β = 1.3 will generally be advocated. In the fib Model Code for Service Life Design, β = 1.3 is presented as a "recommended minimum value" for exposure class XS independent of the RC of the structure [Gulikers 2007]. According to the LNEC E-465 [2005], the reliability index varies according to the RC from 1.2 to 2.0 for the RC1 and RC3 class, respectively. These β-values correspond to probabilities of approximately 12 % and 2 %, respectively. It is apparent that there is no consensus as to what should be the appropriate values for the reliability index. As it remains unclear what is the acceptable value of PF (what physical phenomena is represents), and therefore what the appropriate DR or acceptable reliability index, then it seems unlikely that probabilistic calculations for the corrosion initiation can be conclusive. This issue has to be urgently addressed, and in the extreme, by convention it should be defined what the interpretation should be and what values are to be considered.

3 CHLORIDE INGRESS MODELING: ASSUMPTIONS AND PARAMETER ANALYSIS

With respect to chloride ingress service life calculations for reinforced concrete structures are commonly based on the mathematical solution to Fick's second law of diffusion, expressed by:

$$C(x,t) = C_i + (C_s - C_i)\cdot\left(1 - \mathrm{erf}\left[\frac{x}{2\sqrt{D_a \cdot t}}\right]\right) \qquad [1]$$

in which C_s - surface chloride content (%m/m cement); C_i - initial chloride content (%m/m cement); D_a - apparent diffusion coefficient (m^2/s); t - duration of exposure to chloride (s); erf - error function.

In practice, both the surface chloride content, C_s, and the apparent diffusion coefficient, D_a, are derived from chloride profiles measured on cores retrieved from existing concrete structures. Most often, the surface layer is discarded as in this region the chloride profile shows a distinct deviation from the profile as suggested by Eq. (1). Consequently, the value of C_s reflects a more or less fictitious chloride content which is quantified by extrapolation of the chloride profile at greater depths. Based on the results obtained over a longer period it has been concluded that the apparent diffusion coefficient gradually decreases over time according to the empirical relationship:

$$D_a = D_{a,o}\cdot\left(\frac{t_0}{t}\right)^a \qquad [2]$$

in which a - ageing factor (-); $D_{a,o}$ - apparent chloride diffusion coefficient at reference age t_0 (m^2/s); t_0 - reference concrete age (s); t - actual concrete age (s).

However, in order to allow for service life calculations of new concrete structures in the design stage the use of measured apparent diffusion coefficients derived from existing structures is considered less appropriate. Consequently, in DuraCrete [1999] and later in the fib Model Code [2006] mathematical expressions for D_a have been introduced which take into account the concrete quality aimed at. This has been accomplished by using a migration coefficient, $D_{RCM,0}$, determined on the target concrete by a laboratory test at age t_0 (usually 28 days), which is thereupon translated into a practical level, i.e. the $D_{a,o}$ level, by multiplication with one or more correction factors.

In contrast to DuraCrete, in the fib Model Code only a temperature factor, k_e, is employed whereas curing, type of cement and environmental exposure conditions are not considered to be of any relevance anymore. In order to account for chloride transport by capillary suction in the surface layer, in the fib Model Code a substitute exposure surface is suggested at a depth Δx from the exposed concrete surface. Consequently, chloride contents can only be calculated for $x > \Delta x$.

Taking into account the presence of a convection zone yields the overall expression employed in the fib Model Code:

$$C(x,t) = C_i + \left(C_{s,\Delta x} - C_i\right)\left(1 - erf\left[\frac{x - \Delta x}{2\sqrt{D_{a,o} \cdot t}}\right]\right) \quad [3]$$

in which $C_{s,\Delta x}$ - chloride content at substitute exposure surface (%m/m cement)

$$D_{a,o} = k_e \cdot D_{RCM,0}\left(\frac{t_0}{t}\right)^a \quad [4]$$

and

$$k_e = \exp\left(b_e\left[\frac{1}{T_{ref}} - \frac{1}{T_{real}}\right]\right) \quad [5]$$

in which k_e - environmental transfer variable (-); b_e - regression variable (K); T_{ref} - standard test temperature (K); T_{real} - temperature of the structural element or the ambient air (K).

In fact, Eq. (3) does not describe the underlying transport processes but rather gives an estimate of the resulting chloride profile after a considerable period of exposure time. In addition, Eq.(3) is applicable for 1-D situations only and thus is less suitable for columns and beams, especially in the regions near the edges. These situations would require a 2- or even a 3-D approach.

It should be noted that this expression includes a number of implicit assumptions. Amongst others, these involve the start of exposure to chloride at t = 0, i.e. immediately after casting, the continuous presence and fixed level of the exposure conditions as evidenced by a constant value of $C_{s,\Delta x}$, the overall dependence of D_a on time and temperature only, and the gradual decrease of the diffusion coefficient over time until infinity according to Eq.(4).

3.1 Considerations on the Age Factor and Critical Chloride Parameters

One of the most practical concerns in durability design is the pronounced influence of the age factor on the outcome whether this is expressed in terms of service life, t_{sl}, thickness of concrete cover, or migration coefficient. The empirically derived age factor *a* expresses the time-dependent development of the chloride diffusion coefffciencient over time according to Eq.(2). In practice, the value of *a* may range from 0.3 to 0.7, dependent on the type of cement and environmental humidity conditions. The influence of *a* is illustrated in Fig. 1 regarding thickness of concrete cover and migration coefficient, for a reference situation of t_{sl} = 100yr, C_s = 3.0%, C_i = 0.1%, C_{crit} = 0.6%, Δx = 0.0mm, whereas in Fig. 2 the effect of *a* on calculated service life is demonstrated (deterministic approach). An increase of the age factor from 0.5 to 0.6 would result in an increase of predicted service life by one order of magnitude, i.e. from 100 to 1000 years (c = 45mm). It can be concluded that in most situations the age factor is far more dominating than any other model parameter. Consequently, considerable care should be exercised in it's quantification. In the literature a wide range of values for *a* is suggested depending of the type of cement and exposure conditions. In order to allow for a reliable quantification of *a* a significant amount of chloride profiles obtained from concrete structures with the same type of cement and exposed to comparable conditions over a prolonged period of time, i.e. more than 50 years, should

be available. Regarding the time-dependency it should be noted that results obtained from laboratory tests may demonstrate a completely different time-dependency. For concretes produced with CEMIII/B an age factor of 0.36 has been derived for $D_{RCM,0}$, whereas the age factor based on chloride profiles of real structures suggested a value in excess of 0.60 [Gulikers, 2006].

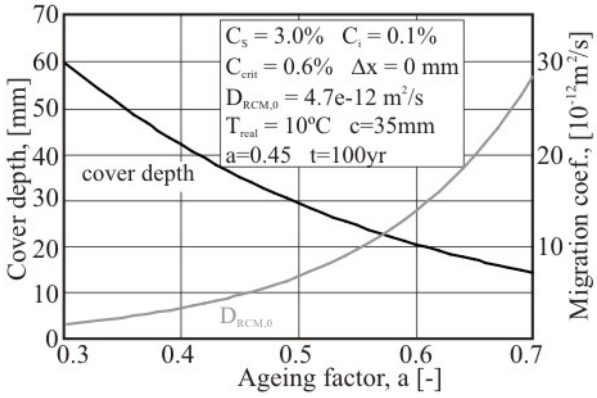

Figure 1. Influence of ageing factor on cover depth and migration coefficient.

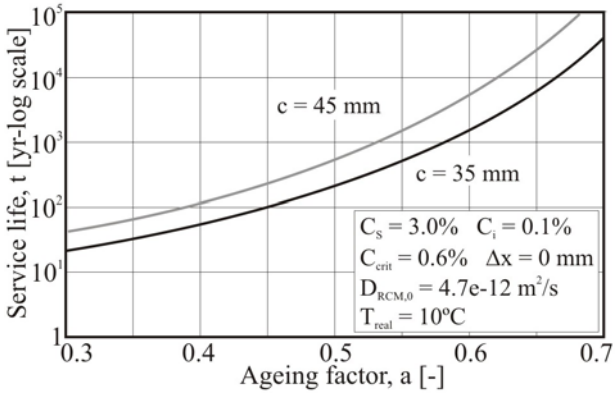

Figure 2. Influence of the ageing factor on predicted service life.

A matter of considerable debate also concerns the so-called critical chloride content. Firstly, a clear and practical definition of C_{crit} should be employed in order to be used in service life models. However, the amount of data obtained from real structures is rather scarce and poorly supplied with essential background information. Consequently, most of the data used is based on short-term laboratory tests performed on small, young, crack-free, well-cured concrete or mortar specimens using an accelerated electrical method. However, such laboratory results have proven to be less suitable to evaluate real structures. Thus a more thorough research is urgently needed on C_{crit} covering aspects like type of cement, humidity conditions, micro-cracking etc.

4 CONSIDERATIONS ON THE PROBABILISTIC IMPLEMENTATION OF THE SLS

One of the most practical ways to perform a probabilistic analysis is by Monte Carlo (MC) simulation. The PF is determined by the number of times the outcome of the simulation falls within the failure region defined by the limit state equation. Each simulation represents the verification of the same LS equation. The LS equation is defined by a model equation which, in this particular case, is the calculation of the time to reinforcement depassivation due to the presence of chlorides such as presented in the DuraCrete or in the fib Model Code, among others.

Typically $1x10^6$ simulations are used for this type of analysis. To perform a simulation, it is necessary to randomly generate values for the parameters of the limit state equation. Each model parameter is randomly sampled from its probability distribution function (PDF), using the inverse transform method, to generate the sample (or simulation) value. Once the PDF's of the various parameters are known, the PF is based on the evaluation of the limit state function for a large number of simulations. The PF is estimated by the following expression:

$$p_f = \frac{1}{N} \cdot \sum_{j=1}^{N} I[g(x)] \qquad [6]$$

in which I [g(x)] - indicator function; g(x) - limit state equation.

The reliability index β can be calculated from the PF by using the inverse of the standard normal distribution function, Φ( ), assuming that the outcome of the simulations is a normally random variable based on the Central Limit Theorem.

$$\beta = -\Phi^{-1}\left(p_f\right) \qquad [7]$$

However, it should be noted that if the reliability index is calculated based on the actual PDF of the outcomes of the LS equation, the values when compared are not exact, but very similar. This results from the inherent randomness associated with the creation of the PDF of the LS equation .

The MC simulation is a popular method as it is easy to implement, being both intuitive and relatively simple to use. The use of the MC simulation requires some knowledge of statistics and probability calculations. Many of the problems and errors that occur result from the incorrect use of the simulation method, or the lack of comprehension for the physical meaning of the model equation and its parameters. As the parameters are mostly stochastic, this is a potential source of error in the simulation.

4.1 Considerations on Parameter Definition

The outcome of the simulation is dependent on the correct choice of PDF to represent the parameter and on the sensitivity to a change of the PDF parameters (e.g.: average and standard deviation). The PDF should fit the available parameter data accordingly, not only in the neighborhood of the average value, but in some cases also in the distribution tails. The PDF of the parameter should take into account the physical limitation of the parameter. Negative values for concrete cover and migration coefficient will have no physical meaning. As another example, parameters such as the age factor have upper and lower boundaries. Howver, these parameters are often modeled with PDFs that do not take this into account. Figure 3 presents a normal and lognormal PDF for concrete cover, with μ = 45 mm and σ = 15 mm. From Fig. 3 it can be seen that by using the lognormal distribution to define the parameter, negative values for concrete cover do not occur. The distribution is skewed towards the constraint. This also has an effect on the outcome of the simulation. Figure 4 presents two PF vs. time curves where the PDF of the concrete cover has been changed according to Fig. 3. By observing the performance curve in Fig. 4, a difference in performance can be observed. For early ages, the use of a lognormal PDF for concrete cover has resulted in an increase of the time to limit state failure. The calculation of the PF was based on $1x10^6$ simulations. When concrete cover was simulated with a normal PDF, 866 negative values were detected.

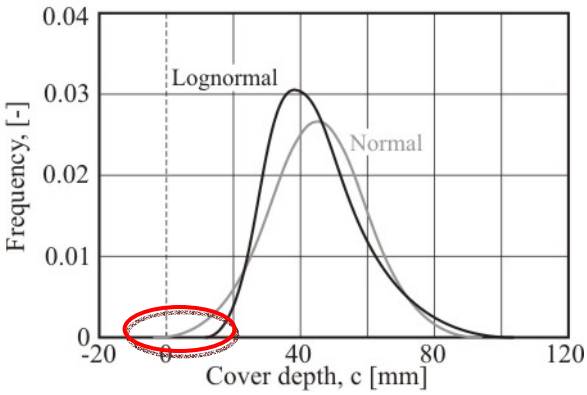

Figure 3. Comparison of the PDF for concrete cover (m = 45 mm, s = 15 mm)

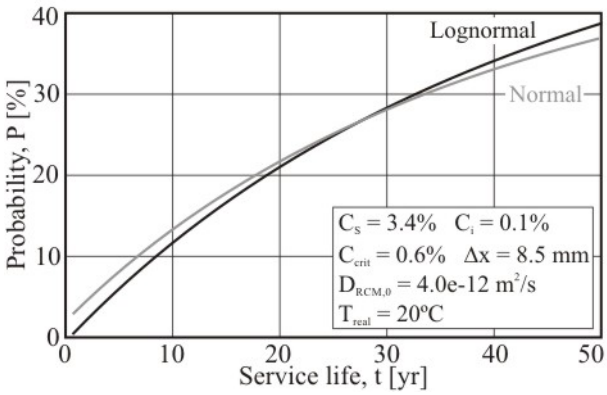

Figure 4. PF vs. time for simulation with different PDF for concrete cover.

As mentioned before, the outcome of the simulation is also dependent on the sensitivity to a change of the PDF parameters. In addition, some limit state equation parameters have a greater influence on the outcome than others. The most influential parameters are concrete cover, age factor and the migration coefficient, and to a lesser degree, the critical chloride content [Ferreira 2007]. The sensitivity of the limit state equation parameters can be seen by the influence on the simulation outcome introduced by changes in the PDF parameters. To demonstrate this further, two examples are given: the first in which the average value of the concrete cover is increased successively whilst the standard deviation is

maintained constant (see Fig. 5); and, the second where the coefficient of variation (CV) is varied from 10 % to 30 % whilst maintaining the average constant (see Fig. 6).

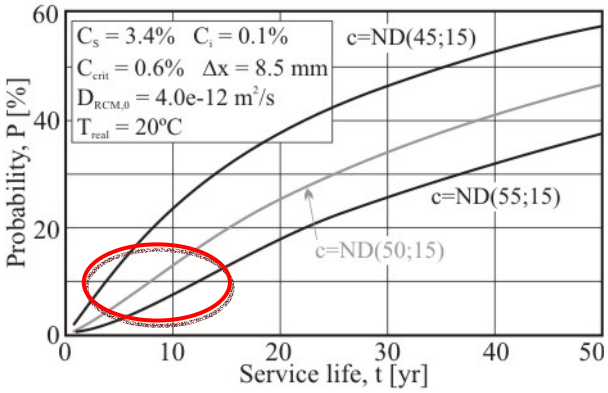

Figure 5. Influence of average value of concrete cover on the PF.

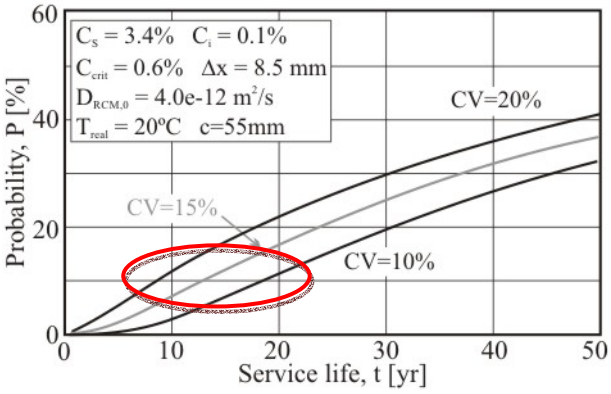

Figure 6. Influence of standard deviation value of concrete cover on the PF.

In Fig. 5, the effect of change of the average of the concrete cover on PF is shown. As the concrete cover is an influential parameter, the changes in PF are clearly visible. In Fig. 6, the same influence is observed, with respect to the influence of the standard deviation of the concrete cover.

Previously, the importance of the physical meaning of the limit state equation parameters in their stochastic characterization was shown. For some parameters, the stochastic nature describes the inherent variability (e.g.: temperature, chloride surface concentration), and the quality of the construction and the materials used (e.g.: concrete cover, migration coefficient). On the other hand, the age factor, a, depends on the type of cement used and the prevailing exposure conditions. The variation of these parameters implies a change in the material used, i.e. concrete or cement. As an example, by maintaining the average value of the age factor constant and by varying the CV between 10 % and 30 %, different PDF's are obtained, as shown in Fig. 7.

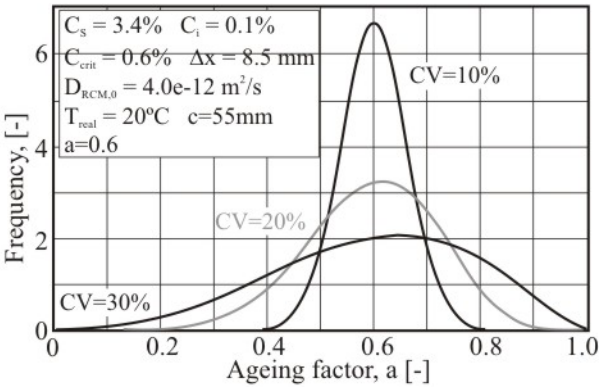

Figure 7. Effect in change of the age factor PDF on the simulation outcome.

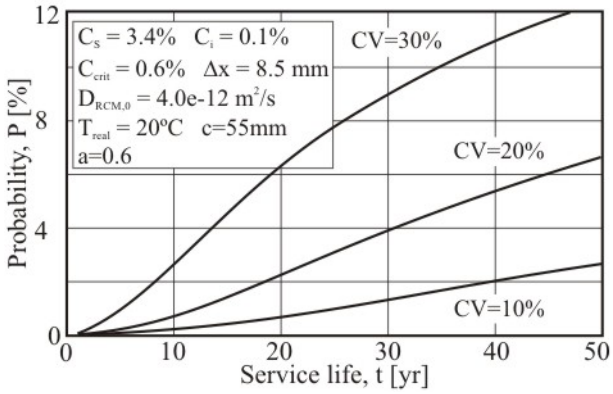

Figure 8. Comparison of the beta PDF for the age factor: a = 0.6, COV = 10%, 20% and 30%.

The age factor may vary between 0 (there is no influence with time) and 1 (the influence is the greatest). The values between these two limits represent the influence of different cements (among other factors) on the development of the migration coefficient over time. In Fig. 7, the different PDF's obtained as a result of using different CV's show how wider spread values are considered for the age factor. For a CV of 10%, the age factor varies between 0.4 and 0.8. For a CV of 30%, the age factor varies between 0.1 and 1.0. This implies that several different cement types are considered simultaneously to characterize the performance of the concrete. There is no consensus as to the appropriate values for the age factor for a given cement. As an example, in a marine environment values for a CEM I can vary from, for example, 0.3 [fib Model Code 2006] to 0.55 [E-465 2005]. As a

result, the effect on the performance is apparent, as shown in Fig. 8. The larger the CV, the more concrete (or cement) types are apparently being considered.

5 CONCLUSIONS

At present a probabilistic approach appears not to be suitable for durability design of real structures. Clear and concise definitions of probability of failure and reliability index are needed, even if by convention, so that that in all durability design (modelling) the same performance criteria have to be fulfilled. In addition, input values of model parameters may vary considerably and values are still under discussion. As an example, a more practical definition of the ageing factor is required. The material characteristic is often overlooked which seriously influences the outcome. A determinisitic use of this parameter should be considered.
As a result, durability design appears to be volatile, mainly due to parameter sensitivity. Models should consider more stable outcomes. In addition, probabilistic simulation is prone to user manipulation. Models should be accompanied by limitations to parameter values as well as recommended PDF.
Both Deem-to-satisfy and probabilistic approach should be evaluated and advantages should be combined as to result in an improved but still practical approach.

REFERENCES

DuraCrete, 2000, "Statistical quantification of the variables in the limit state function", The European Union - Brite EuRam III, Project No. BE95-137, Document R9.

Ferreira, R.M. 2007, "Sensitivity analysis of medel parameters for corrosion initiation and implications on design" in *International RILEM Workshop on Integral Service Life Modelling of Concrete Structures*. Eds Ferreira, R.M., Gulikers, J., Andrade, C., University of Minho, Guimarães, Portugal, ISBN 972-99179-2-2, pp 205-214.

fib Model Code, 2006, "fib Model Code for Service Life Design", bulletin 34.

Gulikers, J. 2007, "Critical issues in the interpretation of results of probabilistic servie life calculations" in *International RILEM Workshop on Integral Service Life Modelling of Concrete Structures*. Eds Ferreira, R.M., Gulikers, J., Andrade, C., University of Minho, Guimarães, Portugal, ISBN 972-99179-2-2, pp 195-204.

Gulikers, J. 2006, "A critical review of mathematical modelling of chloride ingress into concrete and the derivation of input data" in *International RILEM Workshop on Performance based evaluation and indicators for concrete durability*. Eds Andrade, C., Baroghel-Bouny, V., Torrent, R., Scrivener, K. Madrid, Spain, ISBN 978-2-912143-95-2, pp 165-175.

LNEC E-465 2005, "LNEC E-465: Concrete-Methodology for estimating the performance properties of the concrete", Laboratório Nacional de Engenharia Civil, Lisboa (*in Portuguese*).

International Standards on Durability and Sustainability of Construction Works

Christer Sjöström [1]
Wolfram Trinius [2]
Hywel Davies [3]
Jacques Lair [4]

T 45

ABSTRACT

The European Directive on Construction Products (CPD) establishes a set of essential requirements on construction products to be fulfilled throughout the "working life" of the construction works. The demands expressed in the directive is one significant driver, international attention another. Both CEN through a "task force on durability" and ISO through TC59/SC14 "Design Life" are addressing the subject. The work of ISO has led to the establishment of a suite of procedural standards on service life planning, including service life declaration and service life assessment methodologies, useful to be applied in the declaration and the application of service life information.

The political agendas related to sustainable development and the understanding that building and construction is a key industrial sector to implement sustainability principles have led to the establishment of ISO TC59/SC17 "Sustainability in building construction". Being the first ISO subcommittee expressly dealing with sustainability in relation to an industrial sector, the work focuses on economic, environmental and social aspects of sustainability relative to buildings and construction works.

Together with the established standards on service life and the concept of performance-based building, all the three provide a procedural reference point for the consideration of sustainability aspects. They all benefit when applied in common context, and can provide each other with necessary information. On a European scale this common context is elaborated with the work of CEN TC350. The status of development, key drivers and key success factors are elaborated in this paper.

KEYWORDS

Service life, Service life declaration, Service life assessment, Performance Based Building, Sustainability

[1] KTH Research School, Centre for Built Environment, Materials Technology, University of Gävle, SE-801 76 Gävle, Sweden, Phone +46 70 546 59 16, Fax +46 26 64 81 81, christer.sjostrom@hig.se
[2] Ingenieurbüro Trinius, Hamburg, Germany, Phone +49 179 501 9382, trinius@trinius.de
[3] Hywel Davies Consultancy, UK, Phone +44 (0) 779 261 1350, hywel@hyweldc.co.uk
[4] FFB, France, lairj@national.ffbatiment.fr

1 INTRODUCTION

There is a pronounced momentum and progress internationally and in Europe to provide the building and construction sector market with standard approaches and methodologies for service life planning and sustainable construction issues. These standards published or in different stages of preparation, are all performance based and give procedural guidance to actors in the building and construction sector.

The ISO set of standards on Service Life Planning developed by ISO TC59/SC14 and on Sustainability in Building Construction prepared by ISO TC59/SC17 form the basis for the emerging European standards by CEN TC350 on Sustainability of Construction Works.

2 PERFORMANCE OVER TIME, DIRECTIVES AND REQUIREMENTS

The performance concept in building is receiving a renewed interest. After having been very much in focus and discussed during the 1960 – 70:ies there is today a revitalisation. The performance concept is crystal clear as to its basic idea, and application is common practice in most industrial sectors. However, in construction this is yet far from the situation. The strive towards sustainable construction, increased international trade within construction, with building products and construction services, and a general call for improving the innovation climate in the construction industry may well speed up the performance approach in building. Where earlier the green focus in building was solely about environmental impact assessment, a move towards a sustainable construction concept incorporates economic, social, and cultural aspects, i.e. a move from assessment of impacts to an assessment of performance. Environmental performance can, however, not be described without a well-defined performance (over time) of the constructed asset as a reference point [Trinius & Sjöström 2005].

2.1 The European Construction Products Directive, CPD

The CPD [Council of the European Communities 1988], adopted in December 1988 by the EU Council, is a good example of a performance directive. Created with the aim of removing barriers to trade in this specific area, following the white paper on the internal market approved by the Council in June 1985, it does per se have little direct reference to sustainability. However, the CPD has a clear bearing on the view on performance over time of buildings (construction works) and has as such provided an important direction for international, European, and national work on standards and codes. The CPD fixes the essential requirements for construction works (both buildings and civil engineering works). There are six essential requirements which apply to the works as set out in annex I of the directive:

- Mechanical resistance and stability;
- Safety in case of fire;
- Hygiene, health and the environment;
- Safety in use;
- Protection against noise;
- Energy economy and heat retention,

These requirements must, subject to normal maintenance, be satisfied for an economically reasonable working life. The CPD has, however, not the aim of harmonising the regulations on works of the Member States but rather of bridging the "works" and the construction products put on the European market and used in these works. It therefore specifies the level of performances of these products: the products "have such characteristics that the works in which they are to be incorporated, assembled, applied or installed, can, if properly designed and built, satisfy the essential requirements...". This is the notion of "fitness for the intended use" of a construction product. The link between the essential requirements of the works and the product characteristics to be assessed is fixed in Interpretative Documents [CEC 1994; CEC 2004]. The Interpretative Documents, IDs, have been drafted on the basis of existing regulatory requirements of the Member States, each ID containing necessarily one chapter on the requirements of the works and one on the characteristics of the products, in principle

allowing to accommodate the requirements for the works.

The CPD specifies further that a construction product is fit for its intended use if it conforms to a, 1. harmonised European standard (drafted by CEN/CENELEC), 2. European Technical Approval (issued by an EOTA[1] member) or, 3. non-harmonised technical specification (e.g. a national technical specification) recognised at Community level, the three being denoted technical specifications. According to the CPD: "The products must be suitable for construction works which (as a whole and in their separate parts) are fit for their intended use, account being taken of economy, and in this connection satisfy the following essential requirements where the works are subject to regulations containing such requirements. Such requirements must, subject to normal maintenance, be satisfied for an economically reasonable working life". Furthermore, the IDs provide that product standards and Guidelines for European Technical Approval (ETAGs) "should include indications concerning the working life of the products in relation to the intended uses and the methods for its assessment".

3 STANDARDS ON SERVICE LIFE PLANNING AND SUSTAINABILITY

3.1 ISO TC59/SC14 Design Life

The ISO 15686 standards, produced by TC59/SC14, are:

• ISO 15686-1 General principles
Part 1 gives the general principles and procedures that apply to design, when planning the service life of buildings and constructed assets.

• ISO 15686-2 Service life prediction procedures
It describes a procedure that facilitates service life predictions of building components. The general framework, principles, and requirements for conducting and reporting such studies are given.

• ISO 15686-3 Performance audits and reviews
This part is concerned with ensuring the effective implementation of service life planning. It describes the approach and procedures to be applied to pre-briefing, briefing, design, construction and, where required, the life care management and disposal of buildings and constructed assets.

• ISO/WD 15686-4 Data requirements/data formats
This technical specification will describe the data requirements needed to carry out service life planning considering various service environments and other in-use conditions. In co-operation with the International Alliance for Interoperability, IAI, the aim is also to describe IFC[2]compliance for the ISO 15686 series.

• ISO/DIS 15686-5 Life cycle costing
Provides guidance on developing a model of the capital and running costs of the project, so that the overall costs can be assessed, and how this data can be used for financial appraisal.

• ISO 15686-6 Procedure for considering environmental impacts
The standard provides guidance on assessing the relative environmental impacts of alternate service life designs, and to identify the interface between environmental LCA and service life planning.

• ISO 15686-7 Performance evaluation for feedback of service life data from practice
Provides a generic basis for performance evaluation and feedback of service life data from existing buildings and constructed works.

• ISO 15686-8 Reference service life and service life estimation
The standard describes how to provide, format and extract Reference Service Lives of components, e t c, to establish the service life of the same in a particular usage. It also provides the Factor Method to carry out such estimations.

[1] European Organisation for Technical Approvals
2 IFC = Industrial Foundation Classes

• ISO/AWI 15686-9 Service life declarations
Aims at giving guidance to construction products manufacturers and standard writers on addressing durability and service life declarations in product standards. The work is performed in close co-operation with a CEN Task Force on Durability, which was set up to support European product standard committees (see below).

• ISO/CD 15686-10 Using requirements for functionality and ratings of serviceability during the service life
The standard provides process guidance for managing the capability of a building or other constructed asset through the service life of that asset to meet the stated levels of requirements.

At the end of 2007 all standard documents included in ISO 15686, except Parts 4 and 10, are published or in a stage near to final publication. Maintenance is at the moment discussed as new area of standardisation.

3.2 The CEN Task Force on Durability

The CEN Task Group on Durability was established in 2003 as a result of that year's CEN Construction Sector Network Workshop, held in Malta.

The Group was given two tasks within the scope of support to product standards committees. Firstly, to produce a short-term guiding document on durability and service life assessment and declaration for those standards committees still working on a 1st generation of harmonised product standards. This resulted in an up-date of the CEC Guidance Paper F on Durability [CEC 2004]. Secondly, to produce a long-term guiding document on durability and service life for 2nd generation product standards. Both guiding documents should be as far as possible harmonised with the approaches and concepts of the ISO 15686 standards. The ISO 15686-9 is the result.

3.3 ISO TC59/SC17 Sustainability in Building Construction

The technical committee on building construction (TC59) addresses sustainability in its subcommittee 17 "sustainability in building construction". A suite of standards is under development, aiming to set a broadly agreed basis for the establishment, communication and application of sustainability information relative to buildings and construction works.

The work program addresses the three pillars of sustainability (economic, environmental and social aspects). The documents on "General principles", "Terminology" and "Sustainability indicators" address the full scope of sustainability aspects, while the documents on "Environmental declaration of building products" and "Framework for methods for assessment of environmental performance of buildings" are clearly restricted to environmental aspects and environmental impacts.

The suite of standards addresses the general concept of sustainable development in the building and construction sector through the document on general principles (ISO FDIS 15392). This document provides the conceptual basis for the other documents in the suite of standards. The report on terminology (ISO 21932) fulfils two core functions, primarily – to the standard developers - it provides the subcommittee as well as other related subcommittees of TC59 with an engine to harmonise its terms and definitions, and secondly – to the reader of the standards - it provides a collated list of terms and definitions related to buildings and sustainability.

Sustainability indicators are useful for the simplification and communication of sustainability information. The ISO standard on a framework for sustainability indicators (ISO 21929) provides the conceptual basis for such sustainability indicators. With the latest adaptations of the SC17 work

program, the standard in sustainability indicators will be complemented with established lists of indicators, bringing the concept closer to application.

The following documents are more restricted in their scope, as they relate essentially to environmental aspects.

The document on environmental declaration of building products (ISO 21930) has been developed at the same time and in close harmonisation with the development of ISO 14025. It brings the concepts from ISO 14025 to the specific considerations to be tackled when addressing construction sector products.

A framework for the assessment of environmental performance of buildings is provided in ISO 21931-1. A new work item proposal is under preparation in order to address also other construction works than buildings. The newly established working group on construction works will identify the needs to complete or amend existing work items and will establish ISO 21931-2 on the assessment of environmental performance of construction works other than buildings.

3.4 CEN TC350

CEN TC350 was born out of the Commissions Mandate 350, aiming to harmonise European approaches for environmental declaration of building products. The variety and the conceptual differences between existing declaration programs were understood as a potential source of market confusion. The initial discussions in CEN rapidly clarified that this mandate could be addressed, but also clarified that the standardisation task would need to embed the environmental declaration of products both within the application context of the products – read that products are to be addressed at hand of their functional application in a building – and that the environmental declaration becomes more meaningful when relating to performance of the product and the building as well as to other sustainability aspects. Consequently, the concept of "Integrated building performance" became subject of CEN TC350. It was also early decided that the work by CEN TC350 should build on the ISO 15686 standards on Service Life Planning, and the standards developed by ISO TC59/SC17.

The work program of CEN TC350 contains:

- the establishment of a framework document containing the overall concept of assessing integrated building performance, including environmental performance, life cycle cost performance and quantifiable health and comfort aspects.
- the establishment of a report on the description of the building life cycle, indicating the route from a building description to a life cycle description, including concepts such as performance-based building and service life planning
- the establishment of product category rules for the environmental declaration of building products
- the indication of the application of generic data sets as back-ground information for the establishment of environmental product declarations
- communication formats for environmental product declarations
- guidance on the application of environmental product declarations as information source for a building assessment
- calculation methods for the assessment of environmental performance of buildings.

The work program is currently established to address all sustainability aspects in terms of environmental, life cycle cost and health and comfort performance on a conceptual level (framework and life cycle description), but is focussed on environmental declaration and environmental assessment on the more detailed level. Work items addressing economic and social performance in more detail will be pre-established, also to indicate the clear ambition of TC350 to cover these fields of work.

CEN TC350 has not yet published standard documents, the work is underway and intended to be concluded by 2010.

4 DISCUSSION AND FUTURE PERSPECTIVES

Figure 1 shows the service life planning process, and the vital role played by the client. The design and construction process is only a brief part of a building life, but is the period during which the essential conditions for its life performance are established.

Refurbishment, repair and maintenance constitute a major part of all building and construction activities, in fact in most societies some 35% of the total. Maintenance and maintenance management has scarcely at all been mentioned in this article, only as a possible up-coming area for standardisation within ISO TC59/SC14. The area is very important and presently in focus by CEN TC319. It should e.g. be noted that the CPD view on the working lives of construction works builds on declared working lives of products under the assumption of a normal maintenance. What is then a normal maintenance? The normal maintenance of a product or building part must be declared for a reference in-use situation, and this could be of vital importance for future standardisation.

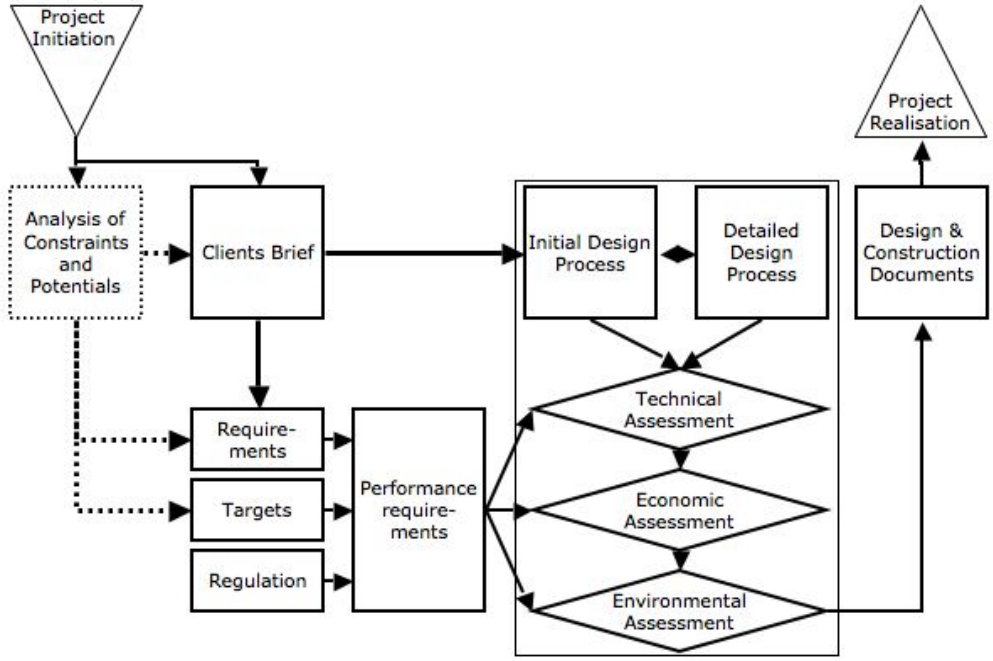

Figure 1. The service life planning process. The figure also highlights the important role of the client in the process.

The building and construction sector worldwide focuses pronounced challenges. These challenges are well encompassed and described by the three CIB Priority Themes, Sustainable Construction, Performance Based Building, and Re-valuing Construction, and also in essence identified and integrated in similar action plans or RTD-policies for the sector by e.g. the UN, WTO and EU.

Sustainable Construction contains the well-known identification of the building and construction sector to be the single most important industrial focus area if sustainable development in our societies is to be reached. The sector contributes some 40% of the green house gas emissions, consumes more than 40% of all energy and material resources, and is responsible for some 40% of all waste produced. The theme, well described by Agenda 21 for Sustainable Construction [CIB 1999], is since more than a decade a focus and priority area in international and European RTD-priorities, and a driving force in innovation and market development. How this is addressed by international standardisation is e.g. described by Sjöström and Davies [Sjöström & Davies 2005] and Sjöström et al [Sjöström et al 2006].

There is since many years a development towards performance concepts in building and construction, i.e. to via performance requirements on the constructed works describe and market the expectations on the functionality and serviceability of the works. The reasons for performance based building concepts are easily understood. Performance is closely connected to end customer values, it is in essentially neutral as to the technical solutions to meet the performance requirements, it is supposed to stimulate innovation, and contrary to deemed-to-satisfy technical specifications it does not so easily under-pin trade barriers. Directives, codes, regulations in e.g. the EU shall be performance based, and this is also a mandatory requirement on ISO standards. CPD is a very early example of a performance based (new approach) directive. Performance Based Building and Sustainable Construction are complementary. It can be argued that Sustainable Construction will necessitate the building and construction sector to follow the Performance Based route.

Re-valuing Construction focuses the apparent and pronounced potential for change and improvement in the building and construction sector. This includes not the least renewed and improved processes (business, and other) in construction and management, improved up-take of R&D-results, broader and more efficient use of ICT, industrialisation, profitability on invested capital, and value for money for end-users.

The standards earlier described, produced or in process, are all performance based and addresses the life cycle aspects of building and construction with focus on service life planning and sustainability. These instruments on the market will help define the business environment and the market. The opportunities offered are identified and addressed by an ongoing European funded RTD-project, STAND-INN [Europe Innova 2006]. The STAND-INN project addresses new manufacturing processes based on IFC standards and the performance based standards for sustainable development with the objectives of creating new and more efficient business processes in the construction sector. The idea is that new manufacturing processes based on IFC standards will facilitate the construction sector great potential for cost reduction and productivity increase and thereby improving the competitiveness of the building and construction industry. An ultimate goal will be to allow designers and other actors in the design process preceding new construction, planning of facility management or refurbishment, to integrate long-term performance aspects, life-cycle costing and environmental Life Cycle Analysis (LCA) into their decision making.

Another recently started EU project, Smart-ECO, (www.smart-eco.eu), [Trinius et al 2008], addresses questions related to the extent to which innovation, both technical and non-technical, can contribute to promoting sustainability in the building sector. The project embraces the EU concept “Eco-buildings” and relates to both the ISO TC59/SC17 and SC14 standards, as well as the CEN work, to an overall “vision of sustainable building”.

These projects and the earlier described standardisation depict a future perspective, based on only a few of the manifold activities to reach a sustainability conscious building and construction sector.

ACKNOWLEDGEMENTS

The authors gratefully acknowledge all the international and European experts co-operating in and contributing to the ISO and CEN work on standardisation on life cycle performance of constructed works.

REFERENCES

Trinius, W & Sjöström, Ch 2005, 'Service life planning and performance requirements' Building Research & Information, **33**(2), 173-181

Council of the European Communities 1988, 'Council directive of 21 December 1988 on the approximation of laws, regulations and administrative provisions of the Member States relating to construction products', 89/106/EEC

CEC 1994, 'Communication of the Commission with regard to the Interpretative Documents', EC OJ 28/2/1994, series C62

CEC 2004, 'Guidance Paper F - Durability and the Construction Products Directive', Revision December 2004

CIB 1999, 'Agenda 21 for Sustainable Construction', CIB Publication Report 237, International Council for Research and Innovation in Building and Construction, ISBN 90-6363-015-8

Europe Innova 2006, http://standards.eu-innova.org/stand-inn

Sjöström, Ch. & Davies, H. 2005 'Built to last – Service life planning', ISO Focus; 'Sustainable building', The Magazine of the International Organization for Standardization, vol. 2, No 12, December 2005, ISSN 1729-8709, 13 – 15

Sjöström, Ch., Trinius, W. & Davies, H. 2006 'Lifetime performance of buildings', ISO Focus; 'Fuelling the future', The Magazine of the International Organization for Standardization, Vol. 4, No 12 December 2006/No 1 January 2007, ISSN 1729-8709, 29 – 31

Trinius, W., Sjöström, Ch., Virk, G. S., Chevalier, J.-L., ' Smart-ECO – Developing a construction sector vision and related requirements for sustainable ECO-buildings' Proc. of the 11th Int. Conf. On the Durability of Building Materials and Components, Istanbul, Turkey

A Durability Assessment Tool for the New Zealand Building Code

Neil Lee[1]
Jessica Bennett[2]
Mark Jones[2]
Nicholas Marston[2]
Gareth Kear[3]

T 45

ABSTRACT

Materials and construction methods continue to evolve. The empirical knowledge derived from traditional building practice is often insufficient for predicting durability problems with emerging materials and construction techniques. Consequently the capability for robust durability assessment of new products and techniques is an essential platform for supporting an innovative, dynamic building industry.

The New Zealand Building Code (NZBC) is primarily performance-based: only for a few classes of materials, such as timber and concrete, do prescriptive 'deemed-to-satisfy' solutions exist. For other situations, the Code offers only the advice that suitable durability performance may be demonstrated through laboratory testing, a documented history of use, or by analogy with the behaviour of similar building components. Little further guidance is provided concerning how these criteria might be satisfied in practice.

In response, this paper describes the development of an overarching durability verification framework for assessing building materials, components and systems under the NZBC. The aims of the project include systematising existing durability knowledge and verification methods, identifying critical knowledge gaps to guide future research, and making this information available in a convenient manner to a wide range of potential users. The latter goal is achieved through the development of an interactive web-based interface to the underlying information.

KEYWORDS

Durability, Verification, Knowledge, Database.

[1] BRANZ Ltd, Private Bag 50-908, Judgeford, Porirua, New Zealand. Phone +64 4 238 1359, Fax +64 4 237 1171, neillee@branz.co.nz
[2] BRANZ Ltd, Private Bag 50-908, Judgeford, Porirua, New Zealand. Phone +64 4 237 1170, Fax +64 4 237 1171.
[3] Quest Reliability, PO Box 38-096, Lower Hutt, Wellington 5045, New Zealand, Phone +64 4 978 6630.

1 INTRODUCTION

It is hardly surprising that a strong demand for robust durability research and information has featured repeatedly on building industry needs surveys. Functional and durable construction is essential both for the health and well-being of owners and occupiers and the credibility of the industry. Consequently, the consideration of materials performance is critical over the entire building life-cycle, from initial construction to in-service maintenance, and finally renovation, alteration or retrofitting.

Furthermore, while operation normally accounts for the largest proportion of environmental costs over the life-cycle of a building, the intrinsic service life of the structure lies at the core of the concept of sustainable construction. Until durability performance can be predicted accurately, the feasibility of assessing the sustainability merits of alternative construction styles at the design stage remains doubtful.

2 DURABILITY UNDER THE NZBC

Ensuring that buildings have an appropriate durability has always been an important aspect of building regulations. This is emphasised by the current NZBC, which includes the functional requirement that: "*Building materials, components and construction methods shall be sufficiently durable to ensure that the building, without reconstruction or major renovation, satisfies the other functional requirements of this code throughout the life of the building*" [Building Industry Authority 1992].

The NZBC is a performance-based rather than prescriptive code, intended to permit innovative solutions and minimise the constraints placed on building design or choice of materials and techniques, providing the mandated minimum performance levels are achieved. The Code's B2 Durability clause is the single exception to this philosophy, setting default lifetimes for building elements depending on their criticality of function and ease of replacement (Table 1). These durability provisions apply to any part of the building which is fulfilling another Code requirement (e.g. structural stability or fire performance) but do not extend to aesthetic considerations.

Table 1. A summary of the performance requirements for building elements specified by the NZBC B2 Durability clause. Note that the mandated service life allows for routine maintenance, but not reconstruction or major renovation.

	Nature of Building Element	*Required Service Life*	*Typical Examples*
(i)	Provides structural stability, *or*	50 years	▪ Load-bearing walls
(ii)	Difficult to replace, *or*		▪ Buried electrical wiring
(iii)	Failure undetectable thorough normal maintenance regimes		▪ Building wraps behind masonry veneer walls
(i)	Moderately difficult to replace, *or*	15 years	▪ Building envelope cladding
(ii)	Failure undetectable during everyday occupancy of building		▪ Sealants and flashings
(i)	Easily replaced, *and*	5 years	▪ Architectural coatings
(ii)	Failure readily apparent		▪ External gutters

The reason for retaining this prescriptive aspect in an otherwise performance-based code is essentially one of consumer protection: it was considered inappropriate to allow the service life of buildings to be

effectively set by market forces, particularly given that a significant proportion of owners would have little expertise in evaluating the relative benefit of construction styles and materials [Bennett 1998]. Note that despite this prescription, the choice of materials for producing building elements of the required durability is left unregulated.

2.1 Industry Reaction

Specifying durability in terms of building element service life has a number of drawbacks. These include the issues of perception involved in judging difficulty of replacement and the potential mismatch between Code requirements and the expectation of owners who, for example, are often surprised to discover the roof of their house only needs to last 15 years. Chown and Oleszkiewicz [1997] offer some of the most telling criticism of this approach, noting that it may only be truly practical where the building element in question is essentially inaccessible (so that service life is independent of maintenance) and the rate of deterioration under the in-service environment is known. Otherwise, building designers, certifiers and owners assume a significant burden in determining and documenting material and component service life in various environments, based on an assumed level of maintenance. Often the information necessary to do this rigorously is not readily available.

This contention is supported by a survey of construction industry perspectives on the issue of durability and the B2 clause in particular [Clark and Bennett 2001]. As shown in Fig. 1, lack of reliable information was widely cited by survey respondents across all sectors of the industry as a primary barrier to the achievement of durability design.

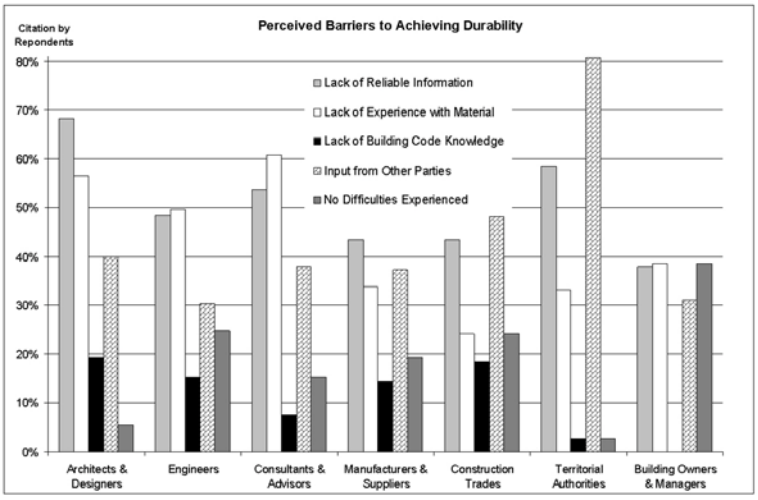

Figure 1. Perceived barriers to achieving the NZBC durability requirements, as identified by surveying the New Zealand construction industry. Data from Clark and Bennett [2001].

Perhaps the perception of an absence of reliable information is unsurprising, given that the same respondents identified ‘trade literature’, ‘industry information’ and ‘past experience’ as the most important sources of information concerning the durability of building materials (Fig. 2). It is also notable that the industry places a good deal of reliance on fitness-for-purpose systems appraisals similar to the European Agrément system.

One particular disappointment, given the reliance on trade literature, is that manufacturers have proven reluctant to invest the time and money necessary to establish reliable service life; formal declarations of Reference Service Life and the tabulation of modification factors, as described in ISO 15686-1 [ISO 2000], are almost unknown despite the usefulness of the concept.

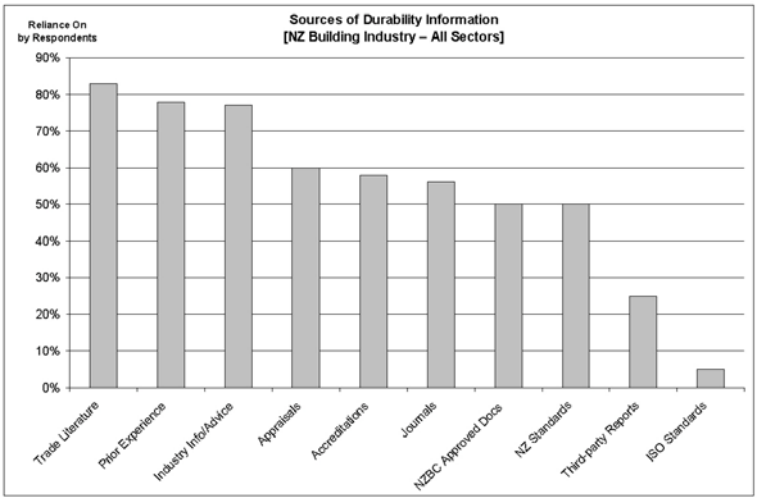

Figure 2. Importance of durability information sources, ranked from survey respondents in the New Zealand construction industry. Data from Clark and Bennett [2001].

2.2 Establishing Compliance

Part of this difficulty arises because, despite the unquestioned importance of the subject, there is no broadly applicable methodology available to verify that building materials, components and construction methods will meet the performance requirements of the NZBC B2 Durability clause. Manufacturers and, especially, the statutory bodies responsible for certifying buildings as compliant with the Code, frequently wish to rapidly assess the expected service life of a new material, or even a conventional one in a new environment. The absence of a list of specific test methods that will generate a 5, 15 or 50 year durability rating is consequently a source of frustration.

For a restricted range of building materials and techniques, the NZBC incorporates the concept of 'Acceptable Solutions'; prescriptive construction methodologies that, followed to the letter, will ensure Code compliance. Acceptable Solutions primarily exist for time-honoured construction methods (e.g. timber-framed or concrete construction, earth buildings) that draw on a background of many years' actual service history and development under New Zealand conditions. Even where an Acceptable Solution ordinarily covers durability compliance, the situation becomes complex when new materials with uncertain capability and interactions are introduced. A topical example in New Zealand is the marketing of copper azole (CuAz) and alkaline copper quaternary (ACQ)-based preservatives as a replacement for the environmentally less favourable copper-chrome-arsenic (CCA) treatment traditionally used to improve the durability of *Pinus radiata* timber. Recent research [Kear et al 2007] has demonstrated a significantly enhanced risk of zinc corrosion with these newer treatments, placing into question the established specifications for galvanised fastenings. When such developments occur, there is a pressing need both to effectively disseminate the research findings to practitioners and to provide robust guidelines for assessing the durability of the new materials.

In cases where an explicit durability evaluation is required, the NZBC documents an approved verification methodology, known as B2/VM1. Unfortunately B2/VM1 offers only the generic guidance that proof of performance should be demonstrated by in-service history, laboratory testing, or analogy with similar products/situations. Anyone involved with materials testing will appreciate that this advice is both valid and a profound over-simplification of the process required. In practice, there is no shortage of durability-related test methods for a vast variety of materials and potential applications. However, a considerable amount of skill is necessary to collate and synthesise this information in a reliable and appropriate fashion. Examples of the need for expert judgement include: considering whether the degradation methods in accelerated tests (heat, moisture cycling, freeze-thaw, UV exposure etc) are appropriately matched to real-world causes of deterioration; assigning quantitative service life predictions on the basis of qualitative rankings of observed durability; and

assessing likely variation in performance due the different macro- and micro-climates, materials interactions, intensity of use and maintenance that come with a specific instance of use on a particular building.

The provision of additional information is an obvious next step to ameliorating these difficulties and removing the barriers to durability design identified in Clark and Bennett [2001]. The standards published, and in preparation, for the ISO 15686 series on 'Design Life' provide valuable guidance and a uniform approach to the assessment of durability. However, whether this knowledge can easily be assimilated into future Code revisions remains unresolved. Also, the intent of these documents is not to provide details on the durability of specific materials, or even prescriptive methodologies for the determination of durability. Consequently, to solve the practical and immediate challenges faced by the New Zealand construction industry, there is a demand for more specific guidance documents that will take into account the properties of construction materials, their potential uses, and their performance in the environments within which they are likely to be used. The BRANZ Durability Assessment Tool is a response to this need.

3 BRANZ DURABILITY ASSESSMENT TOOL

BRANZ is an independent provider of information, research, materials testing and consultancy services to the building and construction industry, with a predominant focus on the needs of New Zealand clients. The Durability Assessment Tool is an initiative to improve the breadth, completeness and cogency of durability information available to the local industry. In essence, it involves the compilation of a database of authoritative and independent durability and compatibility information that covers the building components and materials commonly used in residential construction. Ultimately it is anticipated that this will be delivered as an interactive web-based tool, with the potential to generate an audit trail for verification of compliance with the service life requirements of the NZBC. To succeed in this role, the database will serve both as a convenient 'roadmap' to existing Acceptable Solutions and as an actively evolving repository of new information and research, generated both at BRANZ and elsewhere.

The delivered tool is intended to be helpful to people with a wide range of knowledge and experience. Envisaged users include designers, statutory bodies, manufacturers and wholesalers, in addition to building science researchers.

3.1 Expected Outcomes

The Durability Assessment Tool is explicitly expected to provide the following benefits:

- A catalogue of existing durability information, including précis of, and references to, current Acceptable Solutions.
- A resource for the development of compliance methods for novel building materials and a means of exposing these ideas to the wider industry for critique.
- An explicit mapping of gaps in durability knowledge for current building materials and environments of use, serving to focus the direction of future research.
- A potential method to demonstrate the compliance of a building with the B2 Durability clause of the NZBC.

On a broader theme, the hope is to provide the industry with the appropriate knowledge, tools and confidence to produce durable buildings that meet or exceed their owner's expectations of

performance. Research by Nana [2003] has also demonstrated the potential for a substantial economic benefit from efficiency gains in building and construction due to a knowledge-rich construction sector.

The choice of a computer-driven database over printed material for delivery reflects both the need to manage the complexity of the collected information and the increased use of online resources for information seeking due to time scarcity. The integrated and commercially-neutral nature of the web tool is intended to counter two of the principal drawbacks of online research: sophisticated search engines such as Google are domain independent, which can lead to information overload – 1.4 million hits for 'building durability' – while portals specifically targeted to the construction industry are often compromised by their marketing focus.

3.2 Design

The current framework for communication with the database, shown in Fig. 3, has a modular structure designed to provide answers to three basic questions:

1. *What are the **Performance Requirements** of the NZBC for a nominated building component?* To begin, the user selects the building components of interest, either by keyword search or point & clicking on interactive graphical models of a house. The database returns the corresponding required service life. The durability demand for the component is a function of location and purpose, not composition, so this information can be easily updated with future revisions to the Code.

2. *Which **Verification Methods** are suitable to demonstrate the requisite performance?* At this point the user defines the composition of the component and the environment under which it has to perform. From this, the database returns an existing ***Acceptable Solution*** (typically existing national standards containing durability test methods), an appropriate ***in-house BRANZ verification method***, or the answer that ***no reliable service life prediction*** method is presently available. Fig. 4 shows an example screenshot. These two modules together (*Performance* and *Verification*) will determine B2 Durability clause compliance for the NZBC, and may be all some users (e.g. statutory authorities) are likely to be interested in.

3. *What **Specialist Advice** underlies this information?* This module provides the justification for the earlier material and a compendium of durability information organised under uniform tabbed subject headings, as shown in Fig. 5, which will grow and develop as new information such as research results become available. Gap analysis of this collection of information also generates the roadmap for future research.

The purpose of this structure is to provide a clear division between normative and informative material (i.e. Code requirements vs advice) and it simplifies modification in case of changes to mandated durable life. The structure also allows a single model to be maintained for multiple classes of user.

3.3 Project Status

With the preliminary design concept developed, current effort at BRANZ is focussed on populating the database with sufficient information to allow the most pressing gaps in current durability knowledge to be identified and prioritised. A working prototype of the interactive web tool is currently in development for distribution to interested parties to provide the feedback necessary to evolve improvements in the interface and functionality.

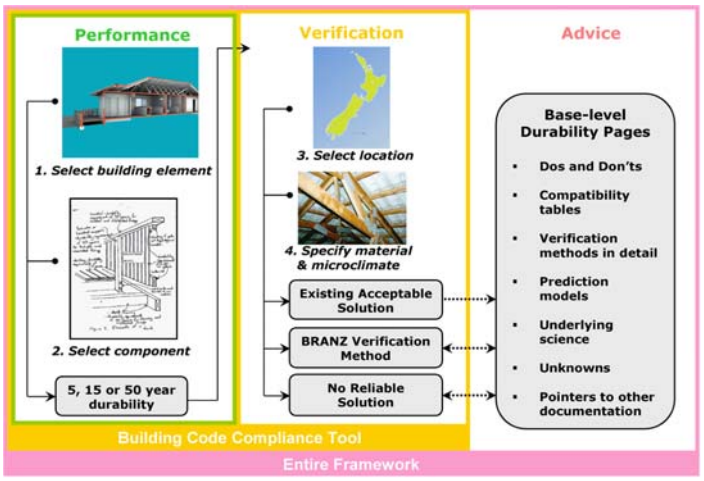

Figure 3. Conceptual framework of the Durability Assessment Tool.

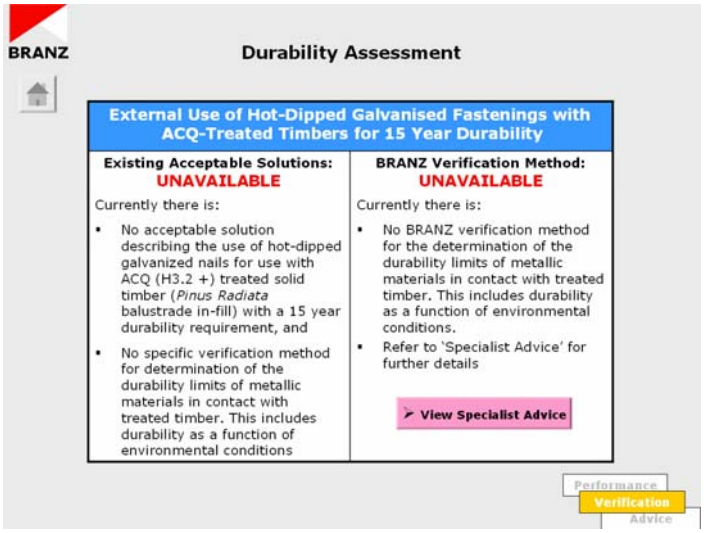

Figure 4. Example results from 'Verification' module use of for hot-dipped galvanised fastenings.

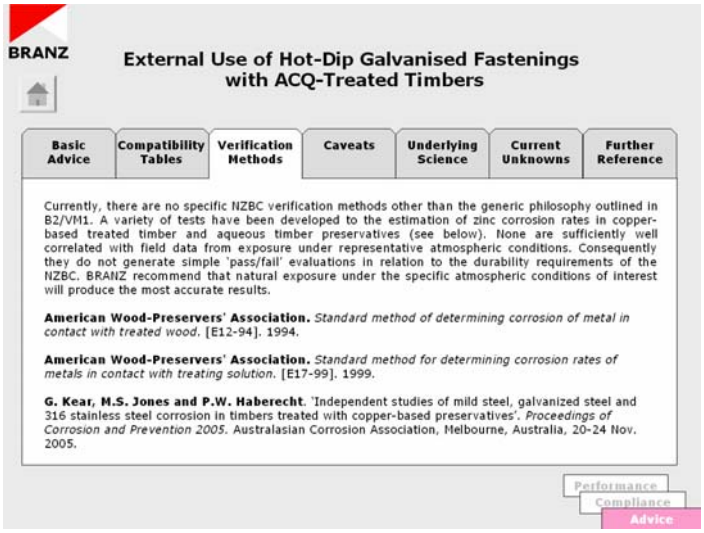

Figure 5. Example guidance from 'Advice' module for ascertaining durability of hot-dipped galvanised fastenings when used with ACQ-treated timber.

4 CONCLUSIONS

New Zealand has had a mandatory requirement for durability in its national Building Code since 1992. In theory this should have stimulated industry awareness of the issues behind achieving appropriate service life of building materials and foster an active interest in the development of standards and methodologies that could facilitate good durability design.

In practice, the transition from prescriptive to performance-based solutions has not been without its difficulties and the potential innovative and economic benefits have yet to be fully realised. New Zealand is a small country and there are few independent organisations with the technical resources and breadth of expertise to carry out rigorous assessments of materials durability. This is particularly evident when new, or composite, building systems are introduced to the market.

While based on sound scientific and engineering precepts, durability assessment remains as much art as science. This should change as the adoption of uniform assessment philosophies facilitates reliability-based service life prediction techniques. However, from a pragmatic perspective it is still essential that researchers, manufacturers and standards bodies continue to develop and refine predictive test methods for individual materials and their applications. It is hoped that the Durability Assessment Tool will prove a compelling initiative to collect these methods in a convenient and user-friendly form, promulgate them through the construction industry and stimulate the development of new ideas and techniques.

ACKNOWLEDGMENTS

The work described is supported by the New Zealand Building Research Levy.

REFERENCES

Bennett A.F. 1998, ‘Prediction of durability for performance-based codes’. Proceedings of the CIB World Building Congress, Gävle, Sweden, 7–12 June 1998, Symposium A, Vol 1, pp 85–92.

Building Industry Authority. 1992. *The New Zealand Building Code Handbook and Approved Documents*. Standards New Zealand, Wellington, New Zealand.

Chown G.A. and Oleszkiewicz I. 1997. ‘The national building code: durability requirements and their incorporation into an objective-based structure’. Proceedings of the Seventh Conference on Building Science and Technology, Toronto, Canada, 20–21 March 1997, pp 185–200.

Clark S.J. and Bennett A.F. 2001. ‘Design for durability: a review of NZ practice’. BRANZ *Study Report 99*. BRANZ Ltd, Judgeford, Wellington, New Zealand.

Kear G., Wu H.-Z., Bruce E.W., Kane C. and Jones M.S. 2007. ‘Metallic materials selection for timbers treated with non-CCA-based, copper-rich preservatives: implications for Australasia’. *Corrosion and Materials* 32 (1): 16–21.

International Organisation for Standards. 2000. *ISO 15686-1 Buildings and constructed assets – Service life planning – Part 1: General principles*. ISO Geneva, Switzerland.

Nana G. 2003. *Assessment of the economic impact of efficiency improvements in building and construction*. BERL Report 4219a, Building and Economic Research Ltd, Wellington, New Zealand.

EU-project STAND-INN –Integration of Standards for Sustainable Construction into Business Processes Using IFC Standards

Svein E. Haagenrud [1]
Jeffrey Wix [2]
Lars Bjørkhaug [3]
Wolfram Trinius [4]
Pekka Huovila [5]

T 45

ABSTRACT

The strategically very important building and construction (B&C) industry is now facing a paradigm shift, from where the buildings and building products are no longer considered only as physical objects, but are rather seen as service arenas designed to facilitate management of life cycle performance and value adding services to meet changing end user needs. This paradigm shift, coupled with the drive for customer orientation, sustainability and ICT deployment is regarded as the key driver for change and improvement in the B&C sector. New manufacturing processes based on the IFC standards will create new and more efficient business processes, thus facilitating the construction sector's great potential for cost reduction and increased productivity and competitiveness. Focus on improving the integration of open IFC- and performance based standards for sustainable construction into business processes (A2) is thus the main objective of the project, addressing also the role of standards in developing sustainable building products and services, including sustainable housing (A1), as well as standards in public procurement processes.

The suite of IFC standards for shared information exchange has the potential to change the entire B&C industry. These standards form the foundation and structure for effective e-collaboration practices, B2B and B2C exchanges, and B2A/building permit and public tendering procedures.

KEYWORDS

Building Information Modelling (BIM), BuildingSmart, IFC standards, Sustainability standards, Public procurement.

[1] SINTEF Building and Infrastructure, Oslo, Norway, Phone +47 91143791, svein.haagenrud@sintef.no
[2] AEC3 Ltd / AEC3 Ltd, Thatcham, Berkshire, United Kingdom, Phone +44 1635 864590, jeffrey.wix@aec3.com
[3] SINTEF Building and Infrastructure, Oslo, Norway, Phone +47 95156905, lars.bjorkhaug@sintef.no
[4] Ingenieurbüro Trinius, Dorotheenstr. 21, 22301 Hamburg, Germany, Phone +49 40 2275 9430, trinius@trinius.de
[5] VTT, Life cycle Technology, Espoo, Finland, Phone +358 20 722 5903, pekka.huovila@vtt.fi.

1 INTRODUCTION

The "STAND-INN" project (integration of performance based building standards into business processes using IFC standards to enhance innovation and sustainable development) was developed for the Coordination Action call "Standards in support of innovative business solutions" FP6-2005-INNOV-8, 15/04/2005. STAND-INN addresses the "Action 1.2.1.7 - Standards in support of innovative business solutions". It focuses on its objective 2: "*To facilitate the integration of open standards into business processes", h*owever, addressing also the two other objectives of the call: "*To facilitate the integration of open standards into the design of new products and services*", and "*To stimulate innovation through reference to standards in public procurement*".

STAND-INN, which is scheduled for 26 months to end late 2008, addresses new manufacturing processes based on IFC standards and performance based standards for sustainable construction with objectives of creating new and more efficient business processes in the construction sector. This will facilitate the sector's great potential for cost reduction and increased productivity and competitiveness, furthering sustainable development.
The Consortium comprises 28 members from 11 European countries (Norway, Finland, France, UK, Sweden, Italy, Lithuania, Spain, Portugal, Germany, Belgium, and with 5 European– wide networks (IAI, CIB, ECCREDI, ENBRI, CEN), entailing major stakeholders from industry including SMEs, users, R&D and standardization as well as 2 partners from China.

The work plan entails developing guidance material for improved innovation with respect to the IFC based design of business processes (WP1-Action 1, with links to design and performance of building products (WP2 -Action 2), -to sustainable housing (WP3-Action 1 and 2), and public procurement (WP4-Action3), as well as carrying out a series of work-shops on the themes (WP5) and developing handbooks on "best –practice" and pilots (WP6), and policy recommendations to enhance innovation (WP7). Some results will be exhibited in this paper.

2 STATE OF THE ART AND DRIVERS FOR CHANGE

The construction sector is strategically important for Europe, providing the buildings and infrastructure on which all other industries, and public bodies, depend. The sector employs more people than any other industrial sector, but because most firms in the sector are small and medium-sized enterprises (SMEs), its contribution to European GDP and its importance for the overall economic performance is often not fully recognized. In all it has been estimated that 26 million workers in the EU-15 depend on the construction sector, comprising 2,5 million enterprises (97% SMEs) and an investment of € 910 billion (10%of GDP) (ECTP 2005a).

This sector is now facing a paradigm shift, moving from a situation where the building and building products are considered as physical objects to one where the built assets are service arenas designed to supply and manage a set of environmental and other functional performance services throughout its total life-cycle with changing end user needs. It shifts attention from the traditional focus on hand-over and the defects period, to the years beyond-whether or not the supplier has (e.g. through a public private partnership) a commercial interest in that performance. This paradigm shift, coupled with the drive for customer orientation, sustainability and ICT deployment is regarded as the key drivers for change and improvement in the B&C sector. (ECTP 2005b, c)

2.1 An Inconvenient Truth-an Unsustainable Construction Sector

Global mean temperature coincides with CO2 content in atmosphere. The CO2 content is way above any former level, and it is skyrocketing, causing climate change with disastrous consequences for mankind (IPCC 2007).
The construction sector has a key influence on sustainability (ECTP 2005a). Its environmental impact is high because

- Buildings and the built environment uses 50% of the materials taken from the Earth's crust.
- During their life cycles buildings comprise the largest energy consuming sector with the almost half of the primary energy used and generating about 40 % of all greenhouse gas emissions in Europe.
- Waste produced from building materials are the source of 25 % of all waste generated.
- The building sector also has a major economic impact (10 % of the GDP of the EU).
- People spend almost 90 % of their time inside buildings.

This is why the industry - led ECTP so firmly and consistently states "becoming sustainable" as part of their vision (ECTP 2005a) and key targets for their Strategic Research Agenda (ECTP 2005b).

A key success factor towards the adoption of sustainability-related innovative foundations (i.e., standards, concepts, products, and process) in the Construction sector is that the knowledge and information is made available for decision makers and other stakeholders involved in the value and supply chain. It is necessary to provide new information-intensive services in order to successfully bring the knowledge produced (along the process) into its intended application.

Here is where the IFC model comes into play, since it targets the information used (in theory by all actors involved in the building process) to represent a construction product during its entire life cycle.

2.2 Customer Orientation And ICT Driven Interoperability Of The Building Process

The inefficiency and lack of information interoperability of the building process is a major cause for high production cost, building damages, etc. A NIST US report (2004) states "Inadequate interoperability in the US Capital Facilities industry costs approximately $ 15.8 billion annually, representing 2% of industry revenue".

Thus the construction process needs to decrease production costs and increase productivity. It must also change from a supply to demand/user driven focus across the building life cycle (ECTP 2005a,b). To achieve these goals requires business process innovation and a realisation that ICT based building standards provide the ' glue ' which can dramatically improve the performance of the value chains.

The process for change is driven by the International Alliance for Interoperability (IAI), which has more than 600 members across the world (www.iai-international.org). The IAI, supports, or oversees the *whole life cycle of developing and deploying integrated project working using interoperable solutions* (Liebich 2007). This has been IAI's reason for establishing the new branding buildingSmart, with the broad scope to support the whole adaptation process:
"buildingSMART is integrated project working and value-based life cycle management using Building Information Modelling and IFCs"

3 BUILDINGSMART-DEVELOPMENT AND IMPLEMENTATION OF IFC COMPATIBLE BIM

buildingSMART is the principal standard for information exchange and sharing across the whole construction life cycle, which is now being incorporated into major software products and the use of which is now being required by an increasing number of major clients throughout the world. It covers all the international specifications (BIM, IFC,IFD,IDM,etc) and technologies developed to meet the vision of IAI. Its adoption can bring about major changes/improvements in business processes for the

whole value chain. By providing a facility for shared information, it can provide a catalyst for the change from a contractor/supply driven industry to a more user/demand driven industry, Fig. 1

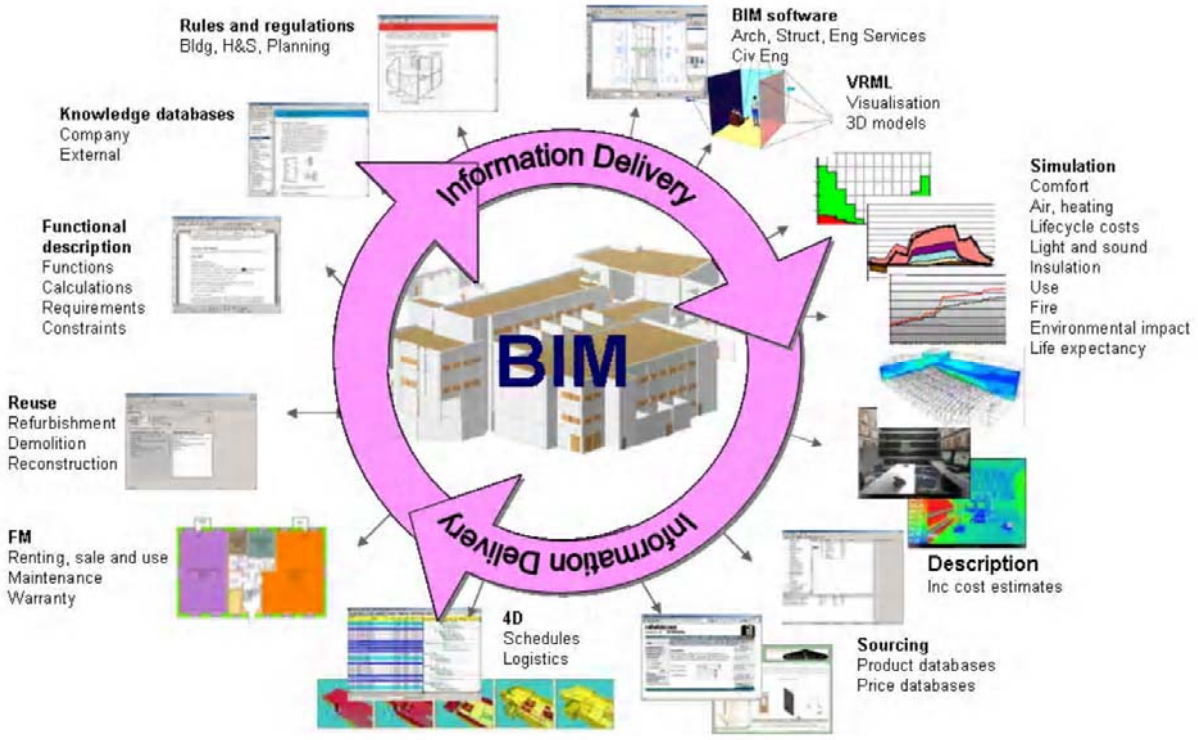

Figure 1. The information delivery over the building life-cycle.

3.1 BIM

Building Information Modelling (BIM) is a new and promising building design and documentation methodology. BIM is the term applied to the creation and use of coordinated, consistent, computable information about a building project in design, in construction and in building operation and management. The term has been adopted recently to replace ‘ Computer Aided Design ’ (CAD) so that the emphasis is placed on ‘ information ’ and ‘ modelling ’ . BIM is sometimes referred to as a ‘ virtual building ’ because it can be used as a simulation of the real building.

A ‘ BIM ’ is the collection of objects that describe a building. BIM software applications have been developed using ‘ object oriented ’ methods. This means that they work with ‘ objects ’ . An object represents an instance of ‘ things ’ used in building construction, that can include:

- - physical components (e.g. doors, windows, pipes, valves, beams, light fittings etc.),
- - spaces (including rooms, building storeys, buildings, sites and other external spaces),
- - processes undertaken during design, construction and operation/maintenance,
- - people and organizations involved,
- - relationships that exist between objects.

Within BIM, the geometric representation of an object is an attribute. This differs from CAD which works with geometry items like lines, arcs and circles from which geometric representations of objects can be created and stored.

BIM covers geometry, spatial relationships, geographic information, quantities and properties of building components (for example manufacturers' details). It can be used to store the results of

analysis and modeling of engineering requirements. BIM can be used to demonstrate the entire building lifecycle including the processes of construction and facility operation. Quantities and shared properties of materials can easily be extracted. Scopes of work can be isolated and defined. Systems, assemblies, and sequences are able to be shown in a relative scale with the entire facility or group of facilities.

Increasingly, BIM can also be used to support knowledge rich applications including:

- Sustainability analyses including building assessment (such as LEED, BREEAM), energy performance declaration, life cycle costing,etc
- Requirements checking through ensuring that requirements expressed by a client are met by the design or that design requirements are met by construction.
- Checking designs against statutory requirements like building codes and regulation.

A BIM is a repository for digital, three-dimensional information and data generated by the design process and simulations—it ' s the design, fabrication information, erection instructions, and project management logistics in one database. The BIM will exist for the life of a building and can be used to manage the client ' s asset.

An integrated BIM stores all the building relevant information during the total life-cycle of the building and provides access to that information for participating members.

A recent study by EraBuild shows that industry is gradually starting to use the concept of BIM, and that architects are the most adaptive to the new technology (Kiviniemi et al 2007). The major construction companies in the Nordic countries have all adopted BIM technology, but so far to a lesser extent the IFC compatible BIM.

3.2 IFC, IFD and IDM

In general, to enable interoperable flow and sharing of information contributing to the creation of a Product Model, three specifications/standardisations must be in place. These are;

- An exchange format, defining HOW to share the information. IFC (Industry Foundation Classes) (an ISO standard in development) is such a specification.
- A reference library, to define WHAT information we are sharing. The IFD Library (International Framework for Dictionaries) (an implementation of ISO 12006-3) serves this purpose.
- Information requirements, defining WHICH information to share WHEN. The IDM (Information Delivery Maual) approach (also an ISO standard in development) forms that specification.

This is the triangle of standards forming the basis for the product modelling that has been developed and implemented in other major industries, see Fig. 2. Now the AEC industry is at the core of change, and this change will facilitate the needed compliance with sustainability, user requirements etc

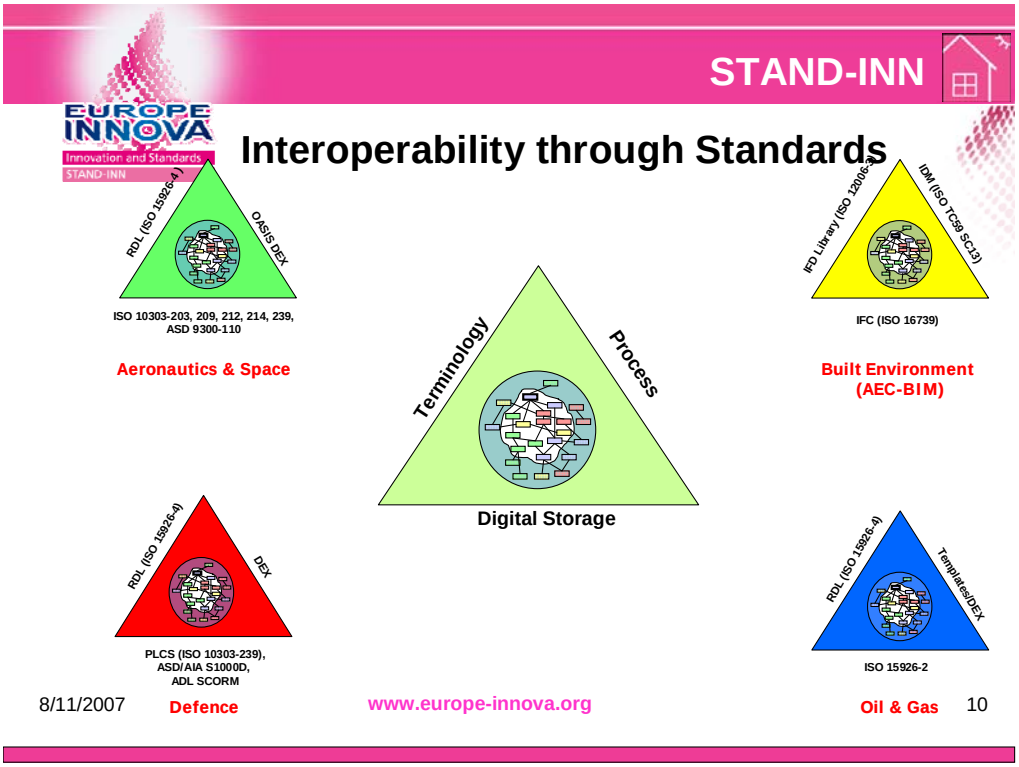

Figure 2. The interoperability triangle of standards for major industries

The development, maintenace, implementation and dissemination of IFC and IFC enabled products is part of the buildingSmart initiative of the IAI. IFCs are the result of an industry consensus building process. They contain common agreements on the content, structure and constrains of information to be used and exchanged by several participants in construction and FM projects using different software applications. The result is a single, integrated schema (or data model [1]) representing the common exchange requirements among software applications used in construction and FM specific processes.

The term IFC is used for the underlying schema and for data content structured according to the schema. The IFC schema is an open, publicly available and industry-wide standard for structuring and exchanging construction and FM specific information among software applications. The latest IFC extension release, IFC2x3, was published in year 2006.

In its simplest form IFD is a mechanism that allows for creation of multilingual dictionaries or ontologies, and would probably better have been named International framework for Ontologies. The name is used both for the IFD library and for the organization running and maintaining it. The model itself is pretty simple seen from a implementers view but it is proven to be very flexible and can therefore result in several different implementations. The structure of IFD is given in ISO 12006-3, that was formally published in April, 2007, and is a result of many years of standardization work by the ISO TC59/SC 13/WG 6 work group. Populating the IFD library is now a core activity. More info available at http://dev.IFD-library.org

The purpose of IDM is to define the information that one AEC/FM industry user needs to provide to one (or more) other AEC/FM industry users to support their work. This means that IDM delivers information at specific points in the business process. As well as defining the information that is needed, IDM also includes the idea of a 'Manual'. That is, it gives guidance to users on providing the information both at a general level and specifically for individual software applications. The aim is to

1 The term "schema" is used in order to avoid the confusion between data model and project model.

capture all of the information for all business requirements for the whole building lifecycle and for all building project participants. More info is avaialble at http://idm.buildingsmart.com .

Basic information and state of the arts reports about BIM, IFC; IFD and IDM's have been developed by the STAND-INN project (Wix et al 2007)

4 SUSTAINABILITY ASPECTS AND IFC SUPPORT

In order to assess the integrated performance of buildings it is necessary to regard a building as a whole with required performance and functions to fulfill. One of the objectives of STAND-INN is to integrate environmental indicators with BIM/IFC following the scheme of things presented in international standards dealing with environmental aspects of buildings.

Recently, CEN has established the standardisation work 'Sustainability of construction works' under the mandate 350 (CEN 2005), building also on the key features of all relevant ISO standards in their drafting. The standards will describe a harmonized methodology for assessment of environmental performance of buildings and life cycle cost performance of buildings, as well as the quantifiable performance aspects of health and comfort of buildings.

The primary standards and aspects of sustainability are considered in WP2, (Trinius 2007), and the aspects cover Economic, Environmental, and Social impacts as well as the Long Term Performance (related to Reusability of buildings, Adaptability to changes, and Service Life Planning), see Fig. 3.

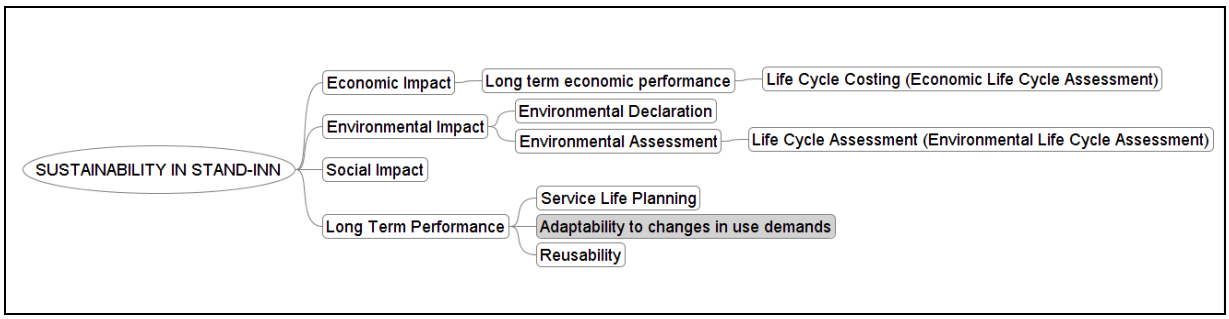

Figure 3. STAND-INN taxonomy for sustainability

The information needed for sustainable building design and construction is not only data in the form of 'environmental indicators' but also data about building site, local environmental conditions, technical performance of building components and systems etc., knowledge about the behaviour of building components in alternative conditions, information about needed measures of care and maintenance etc.

All these areas are important. The aspects and some of their contents is presented in different phases of the building process, as shown in Fig. 4. Even though the BIMs are presented here as separate models, it must be noted that the information exchange standard ensures the interoperability between different information models. In practice, some of these models may be as one model.

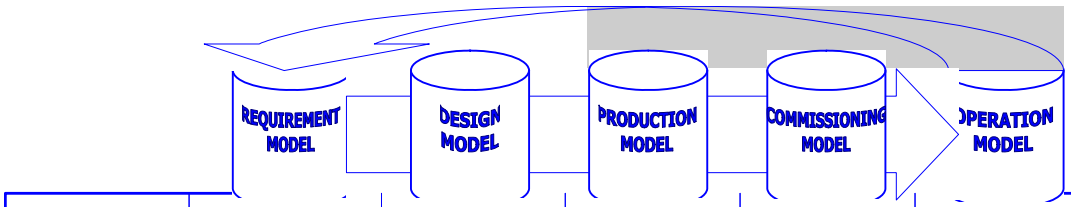

	REQUIRED	DESIGNED	CONSTRUCTED	DELIVERED	ACHIEVED
PERFORMANCE IN USE	• user requirements • desired performance in use	• designed technical solutions • estimated performance	• constructed building	• validated conformity	• user satisfaction • performance in use
ENVIRONMENTAL IMPACTS	• targeted environmental impacts over the life cycle	• estimated environmental impacts over the life cycle	• environmental impacts during construction	• estimated environmental impacts in use	• environmental impacts of building and its use
ECONOMIC IMPACTS	• targeted whole life costs • targeted business benefits and value of the facility	• estimated life cycle costs	• construction costs	• estimated running costs	• running, maintenance and refurbishment costs, recycling, reuse, demolition and waste disposal costs • value of facility
OTHER	• targeted social, cultural and institutional impacts		• construction safety • construction ethics		• social impacts in the neighbourhood • impacts to the cultural heritage

Figure 4. Innovative sustainable building and building information models.

Wix et al (2007) collected instances on the usage of BIM/CAD and application software for sustainability on projects to determine the extent of use, successes obtained and possible potentials. Sustainability applications fell into two groups. The first group includes those applications that are easily amenable to BIM integration whilst the second group includes those applications whose benefit has yet to be fully realized.

Energy performance declaration and life cycle costing fall into the first category as these can be more easily understood in the context of current software use. Environmental impact, service life and other applications fall into the second category. But this second group of applications can offer major benefit as is shown by the best practice examples.

6 CONCLUSIONS AND RECOMMENDATIONS

Some STAND-INN conclusions so far

1. The IFC and use of BIM have great potential for value creation during the whole life of buildings at least in the following areas
   - Focus on customer and end-user requirements and sustainability within the building process and life cycle phases
   - Increasing transparency in the decision-making process and re-engineering the building process with new business opportunities for new and existing actors
   - Cost saving to all actors and a better project economy
   - Improved possibilities for early stage analysis about: best practice design, construction cost, energy consumptions, environmental impacts, lifecycle cost, performance in use, flexibility, adaptability, indoor climate, usability and maintainability
   - A comprehensive and common international knowledge model database with standardized ICT tools, objects and communication rules and available best practices examples.
2. Standards act as catalyst for innovation and the integration of sustainability standards onto the suite of open IFC standards facilitating BIM, will greatly enhance the construction sector's need towards sustainable development.

3. Government (public procurement) plays an essential and decisive part in this tranformation of the construction sector, acting as the policy maker, regulator and by far the biggest customer, thus as the key player driving innovation and sustainable development.

ACKNOWLEDGMENTS

The authors are indebted to EU DG Enterprise for sponsoring the STAND-INN project.

REFERENCES

ECTPa, Challenging and Changing Europe's Built Environment. *A vision for a sustainable and competitive construction sector by 2030*. February 25th, 2005, available at: http://www.ectp.org

ECTPb, Strategic Research Agenda for the European Construction Sector. *Achieving a sustainable and competitive construction sector by 2030*. December 23rd, 2005, available at: http://www.ectp.org

ECTPc, Strategic Research Agenda for the European Construction Sector. *Implementation Action Plan*. Version 1, July 20th, 2007, available at: http://www.ectp.org

Huovila, P., Hyvärinen, J., Häkkinen,T., 2007, *Guidance on IFC/IFD for innovative sustainable housing*, STAND-INN Deliverable no 16, Research Report , Oslo, August 2007.

International Alliance for Interoperability, 2006, IFC 2x Edition 3 Model (IFC 2x3) Release, available at http://www.iai-international.org

IPCC, Climate Change, 2007, *Impacts, adaptation and vulnerability*, London, Sept. 2007

Kiviniemi, A., Tarandi, V., Karlshøj, J., Bell, H., Karud, O.J, 2007, *Review of the development and Implementation of IFC compatible BIM*.

Liebich, T. 2007, *IFC development Process-Quick guide*, STAND-INN White paper report, Oslo, October 2007

Gallaher, M. P:, O'Connor, A. C:, Dettbarn, J. L., Gilday, L. T., 2004, *Cost Analysis of Inadequate Interoperability in the U. S: Capital facilities Industry*, NIST contract report GCR 04-867, Gaithersburg, Maryland, U.S:

Trinius, W. 2007, *Guidance Report on the Integration of Modules and Information Exchange*, STAND-INN Deliverable no 14, Research Report , Oslo, July 2007.

Wix, J., 2007, *IFC and sustainable projects*, STAND-INN Deliverable no 6, Research Report , Oslo, May 2007.

Wix, J., 2007, *IFC support for sustainability*, STAND-INN Deliverable no 13, Research Report , Oslo, May 2007.

A Review of the European Commission Construction Products Directive Reaction-to-fire and Fire Resistance Classification of Building Materials and Components

Nuri Serteser [1]
Mustafa Özgünler [2]

T 45

ABSTRACT

Fire is one of the most important dangers both buildings and its users. All the livable buildings have to be resistant to fire at some degree and have to provide evacuation of the people safely till the fire brigade intervention. It needs to be stand along with the fire as a whole with all the parts constituting it. At the same time the materials of the building have to be selected amongst non-flammables or if not it have to be not releasing smoke and poisoning gases.

Each country evaluates the fire performance of materials and construction products according to their own standards and regulations. This diversity creates different standards and evaluation criteria of materials amongst the members of European Community endeavoring like a unique state in Europe. The Construction Products Directive (CPD-89/106/EEC) that has been applied in accordance with the approximation of laws and has been accepted for free trade of the construction products amongst the member states of European Union deals with the essential provisions must be satisfied by the construction products and the related matters. The classification of the reaction-to-fire performance of construction products as explained in Commission Decision 2003/632/EC and classification of the resistance-to-fire performance of construction products, construction works and parts as explained in Commission Decision 2003/629/EC has become operative by issuing a notification of Turkish Ministry of Public Works. The same classification system has also adopted by Institute of Turkish Standards (TSE) and has been issued as TS EN 13501-1.

KEYWORDS

Fire, fire standard, European directives, Classification of materials

[1] Istanbul Technical University, Faculty of Architecture, Istanbul, Turkey 34437, Phone +90 212 2931300-2313, Fax 212 2514895, serteser@itu.edu.tr
[2] Istanbul Technical University, Faculty of Architecture, Istanbul, Turkey 34437, Phone +90 212 2931300-2361, Fax 212 2514895, ozgunlerm@itu.edu.tr

1 INTRODUCTION

New building materials and elements that have a great interrelationship with construction industry are discovered in everyday. By the developing technology new materials are widely used in design and construction of nowadays buildings by designers. Lots of the sectors have an interconnection with construction sector and depending on the investment activity and the economic stabilization of the governments these are affected in a good or bad proportion. According to the economical data of some new members of EU, Poland, Czech Republic and Hungary alone, the turnover was 38 billion Euro in 2003 and the market is estimated to be growing at an average rate of +4.2% per year as explained official web site of EU [EC 2008].

Although the quality and performances of the building materials in production and in application are taken under guarantee by the legislations of the each EU member countries individually, each country has different standards and test procedures for the building materials. This has also affected free trade of the materials amongst EU members. In order to eliminate the legal differences like customs taxes, restriction of amounts and the technical differences like standards and classification systems of materials European Free Trade Association (EFTA) has attempted and new arrangements has been constituted enclosing the member countries [Demirel & Altındaş 2007], [Demirel & Altındaş 2006]. The importance of harmonization on the technical arrangements, standards and conformity assessment has been emphasized and common arrangements in 23 sectors have been adopted for the free trade of reliable matters amongst the member countries [Diz 2007].

CEN has issued Council Directive 89/106/EEC of December 21'st 1988 on the approximation of laws, regulations and administrative provisions of the member states relating to construction products [EC 2008]. As a candidate member of EU this directive has been accepted by our country's Ministry of Public Works and related to the execution of Commission decision of 2003/632/EEC amending decision 2000/147/EC as regards the classification of the reaction-to-fire performance of construction products and Commission decision of 2003/629/EC amending decision 2000/367/EC as regards the classification of the resistance-to-fire performance of construction products, construction works and parts has been published in the official gazette of Turkish Republic [TÜYAK 2005].

2 COUNCIL DIRECTIVE 89/106/EEC

The materials produced have to satisfy the procedures of the harmonized standards of European Commission. In the absence of harmonized standards, European Technical Approval (ETA) is used for the conformity procedures of the materials. In the absence of both of them the local standards have to be obeyed to answer the basic requirements [TMPW 2008].

The basic requirements are explained in interpretative documents. The interpretative documents explain the basic requirements of the directive. These are mentioned in turn as follows: mechanical resistance and stability; safety in case of fire; hygiene, health and the environment; safety in use; protection against noise; energy economy and heat retention.

According to the sub group of the directive "safety in case of fire" a construction works must be design and built such as:

- the load-bearing capacity of the construction lasts for a pre-determined time,
- the production of smoke and spread of fire is limited along with working,
- the spread of fire to the neighboring buildings is limited,
- occupants or the users of the construction can leave alone or can be evacuated securely,
- the safety team is in secure when they are working inside the construction [EC 2008].

The behavior of the material against fire is very important and sometimes has a vital effect when it's used in building construction. The features of a building material in a fire like heat contribution, combustibility, flame spread, smoke and poisoning gases and droplet formation has to be known

before using it on the design. Under certain temperature and pressure conditions the building materials are tested in an accredited laboratory and according to the behavior on the fire the materials classified. The purpose of reaction to fire testing is to determine whether a material fuels a fire. The EU reaction to fire evaluation criteria are the material's ignitability, rate of heat release, rate of spread of flame, rate of smoke production, toxic gases, flaming droplets/particles and/or a combination of these safety aspects.

DIN 4102 standard for the classification of the building and isolation materials has been widely used in the Fire Protection Regulation of Turkey, 2002. The materials has been divided mainly two main groups (A [non combustible] and B [inflammable]), the group A materials has been divided into two sub-groups (A1 [non-combustible building materials without portions of inflammable building materials] and A2 [non-combustible building materials with portions of inflammable building materials]) and the group B materials has been divided into three sub-groups (B1 [flame resistant building materials], B2 [normal inflammable building materials] and B3 [light inflammable building materials]) according to the fire test results [TÜYAK 2005].

3 NEW CLASSIFICATION OF BUILDING MATERIALS

The new building material standards and test procedures that will be valid throughout EU members against fire have been constituted by taking the local fire regulations into account. The new building material classification has been issued in Commission decision of 2003/632/EEC amending decision 2000/147/EC as regards the classification of the reaction-to-fire performance of construction products and has been accepted as a Turkish Standard, TS EN 13501-1. EN 13501-1 provides the reaction to fire classification procedure for all construction products, including products incorporated within building elements. Products are considered in relation to their end use application. This document applies to three categories, which are treated separately in this standard: construction products, excluding floorings and linear pipe thermal insulation products; floorings; linear pipe thermal insulation products. The symbols and classes of reaction to fire performance for construction products excluding floorings can be seen in Table 1 below [CONSLEG 2003], [TSE 2007]. The only building materials can carry CE mark if it is appropriate for the classification conditions of reaction-to-fire for the materials. In another words CE marking on a product indicates to all authorities that the product is in compliance with the essential health and safety requirements of all directives that apply to the product.

Symbols

ΔT	temperature rise
Δm	mass loss
t_f	duration of flaming
PCS	gross calorific potential
FIGRA	fire growth rate
THR_{600s}	total heat release
LFS	lateral flame spread
SMOGRA	smoke growth rate
TSP_{600s}	total smoke production
Fs	flame spread

Table 1. Classes of reaction to fire performance for construction products excluding floorings [CONSLEG 2003], [TSE 2007]

Class	Test method(s)	Classification criteria	Additional classification
A1	EN ISO 1182 ([1]) and	$\Delta T \leq 30$ ºC; and $\Delta m \leq 50$ %; and $t_f = 0$ (i.e. no sustained flaming)	—
	EN ISO 1716	PCS $\leq$ 2,0 MJ.kg^{-1} ([1]) and PCS $\leq$ 2,0 MJ.kg^{-1} ([2]) ([2a]) and PCS $\leq$ 1,4 MJ.m^{-2} ([3]) and PCS $\leq$ 2,0 MJ.kg^{-1} ([4])	—
A2	EN ISO 1182 ([1]) or	$\Delta T \leq 50$ ºC and $\Delta m \leq 50$ % and $t_f \leq 20$s	—
	EN ISO 1716 and	PCS $\leq$ 3,0 MJ.kg^{-1} ([1]) and PCS $\leq$ 4,0 MJ.m^{-2} ([2]) and PCS $\leq$ 4,0 MJ.m^{-2} ([3]) and PCS $\leq$ 3,0 MJ.kg^{-1} ([4])	—
	EN 13823 (SBI)	FIGRA $\leq$ 120 W.s^{-1} and LFS < edge of specimen and $THR_{600s} \leq$ 7,5 MJ	Smoke production ([5]), and flaming droplets/ particles ([6])
B	EN 13823 (SBI) and	FIGRA $\leq$ 120 W.s^{-1} and LFS < edge of specimen and $THR_{600s} \leq$ 7,5 MJ	Smoke production ([5]), and flaming droplets/ particles ([6])
	EN ISO 11925-2 ([8]) *Exposure =30s*	Fs $\leq$ 150 mm within 60s	
C	EN 13823 (SBI) and	FIGRA $\leq$ 250 W.s^{-1} and LFS < edge of specimen and $THR_{600s} \leq$ 15 MJ	Smoke production ([5]), and flaming droplets/ particles ([6])
	EN ISO 11925-2 ([8]): *Exposure =30s*	Fs $\leq$ 150 mm within 60s	
D	EN 13823 (SBI) and	FIGRA $\leq$ 750 W.s^{-1}	Smoke production ([5]), and flaming droplets/ particles ([6])
	EN ISO 11925-2 ([8]): *Exposure =30s*	Fs $\leq$ 150 mm within 60s	
E	EN ISO 11925-2 ([8]) *Exposure =15s*	Fs $\leq$ 150 mm within 20s	Flaming droplets/particles ([7])
F	No performance determined		

(*) The treatment of some families of products, e.g. linear products (pipes, ducts, cables, etc.), is still under review and may necessitate an amendment to this decision.
(1) For homogeneous products and substantial components of non-homogeneous products.
(2) For any external non-substantial component of non-homogeneous products.
(2a) Alternatively, any external non-substantial component having a PCS $\leq$ 2,0 MJ.m^{-2}, provided that the product satisfies the following criteria of EN 13823 (SBI): FIGRA $\leq$ 20 W.s^{-1}; and LFS < edge of specimen, and ►**C1** THR_{600s} ◄ $\leq$ 4,0 MJ and s1 and d0.
(3) For any internal non-substantial component of non-homogeneous products.
(4) For the product asa whole.
(5) s1 = SMOGRA $\leq$ 30m^2.s^{-2} and ►**C1** TSP_{600s} ◄ $\leq$ 50m^2; s^2 = SMOGRA $\leq$ 180m^2.s^{-2} and $TSP_{600s} \leq$ 200m^2; s3 = not s1 or s2.
(6) d0 = No flaming droplets/particles in EN 13823 (SBI) within 600s; d1 = no flaming droplets/particles persisting longer than 10s in EN 13823 (SBI) within 600s; d2 = not d0 not d1; ignition of the paper in EN ISO 11925-2 results in a d2 classification. 2000D0147 — EN — 03.09.2003 — 001.001 — 5
▼**B**
(7) Pass = no ignition of the paper (no classification); fail = ignition of the paper (d2 classification).
(8) Under conditions of surface flame attack and, if appropriate to the end-use application of the product, edge flame attack.

In the European standardization system, building products are divided to seven classes on the basis of their reaction-to-fire properties. There among other things additionally the measure for the smoke development and burning dripping off enter classification also. The description of building products classifications excluding floorings can be seen in Table 2 [Innofirewood 2008].

Table 2. The classification of building products description excluding floorings [Innofirewood 2008]

Class	Performance description	Examples of products
A1	No contribution to fire	Product of natural stone, concrete, bricks, ceramics, glass steel and many metallic product
A2	"	Products similar to those of class A1, including small amounts of organic compounds
B	Very limited contribution to fire	Gypsum boards with different (thin) surface linings, fire retardant wood product
C	Limited contribution to fire	Phenolic foam, gypsum boards with different surface linings (thicker than Class B)
D	Acceptable contribution to fire	Wood product with thickness ≥ about 10 mm and density ≥ about 400 kg/m^3 (depending on end use)
E	"	Low density fireboard, plastic based insulation products
F	No performance requirements	Product not tested (no requirements)

The smoke development features of the products are represented with s1 (very limited smoke production), s2 (limited smoke production) and s3 (not satisfy the demands of s1 and s2) and dripping features of the products are symbolized with d0 (no flaming droplets or particles), d1 (no flaming droplets or particles persist) and d2 (not satisfy the demands of d0 and d1) according to the amount of production. The classification of floorings and linear pipe thermal insulation products are represented almost the same like Table 1 with the exception; the flooring products are named with subscript "fl" and the others are named with subscript "L" by the name of the class (like C_{fl}, B_L). So the building products are called with the additional symbols like B-s2, d1, D-s1, d2. The additional symbols are restricted with s1 and s2 just in the floorings product classification for fire.

The roof materials and its coverings are also classified according to the reaction-to-fire by CEN. Commission decision of 2005/823/EC amending decision 2001/671/EC as regards the classification of the external fire performances of roofs and roof coverings has been printed and according to the four test methods, four product classes have been constituted. The description of each class can be seen in Table 3 below [CD 2001], [CD 2005].

Table 3. Description of roof product classes for external fire performances [CD 2001], [CD 2005]

Class	Performance description
B_{ROOF} (t1)	Burning brand alone
F_{ROOF} (t1)	
B_{ROOF} (t2)	Burning brand + wind
F_{ROOF} (t2)	
B_{ROOF} (t3)	Burning brand + wind + radiation
C_{ROOF} (t3)	
D_{ROOF} (t3)	
F_{ROOF} (t3)	
B_{ROOF} (t4)	Burning brand + wind + supplementary radiant heat
C_{ROOF} (t4)	
D_{ROOF} (t4)	
E_{ROOF} (t4)	
F_{ROOF} (t4)	

4 NEW CLASSIFICATION OF BUILDING ELEMENTS

The building elements have to be resistant to fire. This is important for evacuating the building users safely and also important to give enough time for intervention of fire brigade. A fire resistant building element or product must have the features of stability, integrity and isolation. These features of a

building element are examined in accredited laboratories under certain heat and pressure conditions. The test procedures of TS 1263, TS 4065 and DIN 4102 are obeyed in our country and the building elements regarding fire resistance are classified into five categories according to the test results. The fire resistance categories of building elements can be viewed in Table 4 [TÜYAK 2005].

Table 4. Fire resistance categories of building elements [TÜYAK 2005]

Class	Fire resistance (min)
F30	30-59
F60	60-89
F90	90-119
F120	120-179
F180	above 180

Commission decision of 2003/629/EC amending decision 2000/367/EC as regards the classification of the resistance-to-fire performance of construction products has been issued in official journal of the European Union. The classifications are expressed in tables for the separating, load bearing building elements and the related materials, materials used in ventilation systems, services, materials used for controlling smoke and heat. A sample table of the building element resistant-to-fire classification and the symbols used can be seen in Table 5 below [CD 2000], [CD 2003].

Symbols

R	Load-bearing capacity
E	Integrity
I	Insulation
W	Radiation
M	Mechanical action
C	Self-closing
S	Smoke leakage
P or PH	Continuity of power and/ or signal supply
G	Soot fire resistance
K	Fire protection ability
D	Stability duration under constant temperature
DH	Stability duration under the standard time-temperature curve
F	Functionality of powered smoke and heat ventilators
B	Functionality of natural smoke and heat ventilators

Table 5. Load-bearing elements without a fire separating function [CD 2000], [CD 2003]

Applies to	walls, floors, roofs, beams, columns, balconies, stairs, walkways									
Standard(s)	EN 13501-2; EN 1365-1,2,3,4,5,6; EN 1992-1.2; EN 1993-1.2; EN 1994- 1.2; EN 1995-1.2; EN 1996-1.2; EN 1999-1.2									
Classification : -										
R	15	20	30	45	60	90	120	180	240	360
Notes	-									

The symbols are used alone or two, three of together with the time in minutes according to the building element type. Time intervals must be 15, 20, 30, 45, 60, 90, 120, 180, 240 or 360 minutes. This represents the total or each criterion's minimum need for fire resistance (EI60, REI 90 etc).

5 CONCLUSION

Council Directive 89/106/EEC of December 21'st 1988 on the approximation of laws, regulations and administrative provisions of the member states relating to construction products has brought new arrangements in many sectors. Especially newly classification of building materials and products related to reaction-to-fire has changed radically by the desicion. After issuing the standard of EN13501-1 that has been adopted and issued as a local standard named TS EN 13501-1.

Although DIN 4102 standards and test methods has been adopted for the classification of building materials reaction-to-fire and fire resistive building elements in Fire Protection Regulation of Turkey 2002, the new classifications and test methods of CEN have been accepted in the latest version of fire regulation and has been announced in December 19'th 2007. The new reaction-to-fire classification of building materials has been arranged again according to the TS EN 13501-1 and has been shown in a table in annex part of the regulation. The new building material classification for reaction-to-fire except floorings can be seen in Table 6 below [TYKY 2007].

Table 6. The classification of building materials for reaction-to-fire except floorings according to TS EN 13501-1 [TYKY 2007]

Class	**TS EN 13501-1**
Non-combustible	A1
Non-combustible building materials with portions of inflammable building materials	A2-s1,d0
Flame resistant	B, C-s1, d0
	A2-s2, d0 A2, B, C-s3, d0
	A2, B, C-s1, d1 A2, B, C-s1, d2
(at least)	A2, B, C-s3, d2
Normal flammable	D, s1, d0 D, s2, d0 D, s3, d0 E
	D, s1, d2 D, s2, d2 D, s3, d2
(at least)	E-d2
Light flammable	F

Our country moving along to being a "real" member country of EU has performed very important development for harmonization of laws, standards and conformity assessment procedures yet. But the most development can be achieved by the execution and implementation of this rules and standards in our daily lifes.

REFERENCES

European Commission Home Page. 1995. Directorates General and Services of the Commission. 24 January 2008 <http://ec.europa.eu/enterprise/construction/index_en.htm>

Demirel, F., Altındaş, S. 2007, 'Yapı elemanlarının yangına dayanım performansları', *Yangın ve Güvenlik*, 95, 142-149.

Demirel, F., Altındaş, S. 2006, 'Yapı malzemelerinin Avrupa yangına tepki sınıfları, konunun Türkiye-Avrupa genelinde irdelenmesi ve ulusal sınıfların yeni Avrupa sınıflarına uyarlanması', *Gazi Üniversitesi Müh. Mim. Fak. Dergisi*, 21[1], 39-54.

Diz, T. 2007, 'Yeni Yangına Dayanıklılık ve Yanıcılık Sınıfları', *Yangın ve Güvenlik*, 98, 118-124.

European Commission Home Page. 1995. Directorates General and Services of the Commission. 24 January 2008 <http://ec.europa.eu/enterprise/construction/internal/cpd/cpd_en.htm>

TÜYAK 2005, *Türkiye Yangından Korunma Yönetmeliği 2002 (ikinci baskı)*, Önsöz basım yayıncılık, İstanbul.

Turkish Ministry of Public Works Home Page. 29 April 1997. Taşkın Nar. 23 January 2008 <http://64.233.183.104/search?q=cache:Q04WTAcHOnYJ:www.bayindirlik.gov.tr/turkce/yapideneti m/html/pgdegitimi.pdf+89/106/EEC&hl=tr&ct=clnk&cd=5>

European Commission Home Page. 1995. Directorates General and Services of the Commission. 24 January 2008 <http://ec.europa.eu/enterprise/construction/internal/intdoc/id2/scopeid2.htm>

CONSLEG: 2000D0147 2003, Official Journal, L220, 5.

TSE, TS EN 13501-1 2007, Yapı mamulleri ve yapı elemanları, yangın sınıflandırması bölüm 1: yangın karşısındaki davranış deneylerinden elde edilen veriler kullanılarak sınıflandırma.

InnoFire Wood, February 2000, Innofire Wood 18 January 2008<http://ananas.vtt.fi/virtual/innofirewood/stateoftheart/database/euroclass/euroclass.html>

2001/671/EC 2001, Commission Decision, Official Journal of The European Communities, L235/21.

2005/823/EC 2005, Commission Decision, Official Journal of The European Union, L307/54.

2000/367/EC 2000, Commission Decision, Official Journal of The European Union, OJ L133.

2003/629/EC 2003, Commission Decision, Official Journal of The European Union, OJ L218.

Türkiye Yangından Korunma Yönetmeliği 2007, *Resmi Gazete (19 Aralık 2007)*, Ek-2/Ç.

How Workmanship Should Be Taken Into Account in Service Life Planning

Appu Haapio [1]
Pertti Viitaniemi [2]

T45

ABSTRACT

The aim of this study is to analyse how workmanship should be included and taken into account in service life planning. In service life prediction, buildings and building components are assumed to meet certain quality requirements. According to the standard ISO 15686-1, if the skills and levels of workmanship do not meet the manufacturer's recommendation or the codes' workmanship standards, their effect on service life should be considered. However, the standard does not say how.

The quality of the construction influences the maintenance of the building, the life cycle cost, and also the environmental impact. Therefore, the skills and levels of workmanship should be emphasised more in service life planning.

KEYWORDS

Service life, Workmanship, Quality

[1] Helsinki University of Technology, Department of Forest Products Technology, P.O.Box 6400, FI-02015 TKK; Finland, Phone: +358 9 4514264, Fax: +358 9 4514259, appu.haapio@tkk.fi
[2] Helsinki University of Technology, Department of Forest Products Technology, P.O.Box 6400, FI-02015 TKK; Finland, Phone: +358 9 4514261, Fax: +358 9 4514259, pertti.viitaniemi@tkk.fi

1 INTRODUCTION

The service lives of different building products and components are different. According to the standard ISO 15686-1 [2000], the service life of the inaccessible parts should be the same as the service life of the building. In another words, the service life of the accessible parts can be shorter than the service life of the building. If the service life of a component is shorter than the building's service life, the component needs replacement. As an example, if the design life (intended service life) of a building is 150 years, the suggested design lives are [ISO 2000]:

- 150 years for inaccessible or structural components
- 100 years for components where replacement is expensive or difficult
- 40 years for major replaceable components
- 25 years for building services
- (easy-to-replace components may have design lives of 3 or 6 years)

In service life prediction, building materials and components are assumed to meet certain requirements. If the skills and levels of workmanship do not meet the manufacturer's recommendation or the codes' workmanship standards, their effect on service life should be considered, according to the standard ISO 15686-1. However, the standard does not say how.

1.1 Aim of the Study

The aim of this study is to analyse how workmanship should be included and taken into account in service life planning. The skills and levels of workmanship should be emphasised more, since the quality of the construction influences the maintenance of the construction, the life cycle costs, and also the environmental impact. Legal responsibilities have occasionally been referred to in this study only to give a wider prospect. However, they are not the focus of this study.

1.2 Content of the Study

In the first section, the research area is briefly introduced, the aim of the study is stated, and the content of this study is listed. In the second section, the focus is on the agents affecting the service life. In the third section, the skills and levels of workmanship are discussed. In the fourth section, the future of the assessment of the skills and levels of the workmanship is speculated.

2 AGENTS AFFECTING THE SERVICE LIFE

Service life is '*the period of time after installation during which a building or its part meet or exceed the performance requirements*' [ISO 2000, ISO 2004]. In forecasting the service life of a building (or a component), the objective is to establish whether it can be expected to exceed the required design life with adequate reliability. [ISO 2000] In forecasting the service life, there are critical issues which need to be taken into consideration:

- Agents of degradation
- Dose and intensity
- Combination of agents

2.1 Agents of Degradation

There are several agents, which affect the service life of building materials and components during their lifetime. In the standard ISO 15686-1 Annex C (taken from ISO 6241), these agents of degradation are classified by their nature:

- Mechanical agents (i.e. snow loads, vibration from traffic)
- Electromagnetic agents (i.e. solar / UV)
- Thermal agents (i.e. heat, fire)
- Chemical agents (i.e. air humidity, ground water, bird droppings)
- Biological agents (i.e. bacteria, moulds, termites) [ISO 2000]

After identifying the agents, it is important to assess the dose and the intensity of the agents. They are often evaluated over a reference period of time, e.g. a year. Westberg *et al.* [2001] point out the degradation agents can be considered one by one, but also the combination has to be taken into consideration. One agent may create a favourable environment for another agent. Therefore, the recognition of the combination is vital.

The durability of building materials relates closely to the service life of building materials. There are several studies on the durability of building materials. Van Acker *et al*. [2003], for example, tested the biological durability of wood in relation to end-use. Kamdem *et al*. [2006] studied the durability of heat-treated wood, and Saraswathy & Song [2007] studied the durability of concrete. However, as Brischke *et al.* [2006] point out, durability and service life are not synonyms. Service life is '*the period of time after installation during which a building or its part meet or exceed the performance requirements'*, and performance is '*the qualitative level of a critical property at any point of time considered'* [ISO 2000]. Durability is a property leading to a certain service life, but it is influenced by different agents in service. [Brischke *et al.* 2006]

2.2 Pre-İnstallation Factors İnfluencing the Service Life

There are several factors, which may affect the service life of building materials, or components, even before their service life begins, before they become a part of the building. This important subject area has been less addressed in research. In this study, these factors are called pre-installation factors. The window is used as an example here.

- The design of a window might be faulty. For example, a vertically low and horizontally wide window is challenging for the hinges if they are on the vertical side of the window frame. Or there might be mistakes in the measurement – the window frame is too small for the window opening.
- The quality of the raw materials might not meet the requirements. The moisture content of the wood might be too high, or there might be too many knots in the wood material.
- The manufacturing processes might cause damage to the window frames. The hinges and the fasteners might not be installed properly. The insulating tape might be tightened too much in the corners.
- The components are not stored properly during the manufacturing processes or at the construction site. For example, an excessive moisture content of wooden frames during the manufacturing and installation may cause cracking of the frames later on. Furthermore, rough handling of the products may damage them; i.e. cracks on the window frames can expose them to moisture.

- The installation of the window might not meet the requirements. The moisture content of the surroundings of the window opening might be too high during the installation. Later on, the wooden window frames may crack. Also, the installation instruction may have been neglected.

The pre-installation factors reducing the service life of the window, mentioned above, are similar to the pre-installation of other building materials and components. The different phases; design, raw material production, manufacturing, storage, and installation, influence the service life of the building material or component greatly. All these pre-installation factors cause the reduction of the service life of the building material or component, even before it begins. However, sometimes the damage appears later, during the use of the building. The faulty design of the window does not necessarily appear immediately after installation. Heavy rain, for example, may emphasise oversights in the installations of the window. Problems occur if rain water stays on the horizontal surface. A faulty product might have to be replaced with a new one. Due to this, the environmental load of production is already doubled. Also, there are environmental loads from the disposal of the faulty product. Furthermore, the faulty product and its replacement might have caused damage to the surrounding products, or even to the structure of the building, and reduced their service lives as well.

There is no point predicting or assessing the service life of building materials or components, if the pre-installation factors are not taken into consideration as they greatly affect the service life of a building. Due to these factors, the building materials or components may never reach the predicted service life. The possibility was lost somewhere in the phases of design, raw material production, manufacturing, storage, or installation. If the pre-installation factors are not taken into consideration, the significance of the service life planning is minor.

Considering the influence of the pre-installation factors on the service life of the building components, the comparison of the different raw materials becomes less significant. If the component does not reach the predicted service life due to the pre-installation factors, there is no point in comparing the service lives of components with different raw materials. The focus should be on assessing the pre-installation processes, and on how to avoid, or at least minimise, the possible damages to the building components during the pre-installation processes.

ISO 15686-3 [2002] focuses on describing the approach and procedures of service life performance audits. Audits are undertaken to provide a reasonable assurance that the required service life performance will be achieved. ISO 15686-3 [2002] provides a choice between formal independent audits and less formal internal review procedures. Both service life performance audits and reviews emphasise the pre-briefing, briefing and design stages of the construction projects. The emphasis of the construction, operation, refurbishment and disposal stages is secondary. The distinction between core and secondary audits is not intended to be definitive. However, this distinction does not seem justified. For example, the purpose of an audit at the construction stage is '*to assess whether correct or intended materials / components have been used and installation instructions have been properly implemented*' [ISO 2002]. If these two aspects are not assessed, it lessens the credibility of the service life performance audits. The use of incorrect materials or unqualified installation may reduce the predicted service life as well as cause damage to the surroundings.

3 SKILLS AND LEVELS OF WORKMANSHIP

The service life of a building varies from decades to even centuries. As mentioned earlier, the service life of the inaccessible parts of the building should be the same as the service life of the building, but the service life of the accessible parts can be shorter. When the service life of accessible parts is shorter than the service life of a building, they need maintenance and replacement during the building's service life. The maintenance and the replacements can be proactive or reactive [see Haapio & Viitaniemi 2008]. The maintenance and the refurbishment of the existing buildings are critical issues for sustainable building, especially in Europe. In Europe, the building stock is older than in

North America, where the urban areas grow rapidly [Kohler & Moffatt 2003]. Furthermore, the number of renovations caused by obsolescence is increasing, as the requirements and needs of the tenants grow [see Haapio & Viitaniemi 2008].

3.1 Examination Procedure for Approval

Before a new building is handed over to the building contractee (the owner) in Finland, the contractor convenes the constructor, and possibly the authorities, to the examination procedure for approval. The aim of the examination procedure for approval is to check that the building meets the requirements agreed in the contract. After one year, there is warranty repair by the contractor. However, there are damages, and faults which take more than one year to appear. The warranty period varies depending on the type of damage or fault. In these situations, the legal responsibilities have to be clarified. The clarification of the legal responsibilities becomes more problematic when sub-contractors are used.

The number of sub-contractors has been growing during the last decades. The sub-contractors work for the (main) contractor, but the constructor has made the contract with the (main) contractor. Basically, the sub-contractors are responsible to the (main) contractor, and the (main) contractor is responsible to the constructor. The more sub-contractors there are, the more difficult the project is to manage, and the project becomes logistically challenging. Also, supervising the level of workmanship becomes more difficult as the number of the sub-contactors increase.

Recently, schedules on the construction site have tightened even more. If one phase of the project is late, in the worst case the whole project will be late. If the building is not ready at the time agreed on in the contract, there will be fines. Unfortunately, when the schedule is tight, and the process is falling behind, sometimes a few steps are rushed, or even disregarded to save time.

3.2 Condition İnspection of the Buildings

When an old single family house is sold in Finland, the condition of the house is normally inspected by a professional, specialised in condition inspection. The aim of the condition inspection is to check the quality of the building, and survey possible faults and damages, for example, possible moisture damage. In addition, recommendations for future maintenance can be given, for example, an estimation of the renovation of the pipes. At some level, the condition inspection could be introduced to the new / newish buildings. For new buildings, the assessment of the installation damages could be useful.

Condition inspection is an excellent way to assess the quality of the building. If it is done regularly, maybe every 10 years, it could act as a plan for maintenance and refurbishment, and later on as a register of the maintenance actions. Even though the service lives of products and components are presented, they are only predictions. The building products and components might be exposed to agents of degradation which are not taken into account in service life prediction, or the maintenance of the building has been neglected. There is also a possibility that the pre-installation factors have damaged the products, but the damage appears only after several years.

3.3 Follow-up of the Building Defects

As an example, four sets of row houses were built in the end of 1970s on the coastal area in Finland. In the buildings red tiles were used as cladding. In total, three lots of red tiles were used. Unfortunately, one of the lots was faulty; the temperature of the burning process had been too low, and also some of the tiles were heterogeneous. During the winter time on the coastal area, the weather is often windy. The wind itself did not damage the tiles, but the rain which came with the wind did. During the rain, the tiles got too wet. Later, the weather got colder and the water in the tiles froze. During the warmer weather, the frozen water in the tiles melted. When this happened several times,

bits of the tiles (circa 3-4 mm thick) cracked from the surface, especially from the tiles in the south and west side of the buildings.

Westberg *et al*. [2001] have described the degradation process of a material in terms of: Agents → Mechanism → Effect. The façade was attacked by low temperature and moisture (agents), and frost expansion (mechanism) probably caused the cracking (effect). The tiles had to be changed. If the tile lots had been tested by the manufacturer before the brickwork, most probably the faulty tiles would have been found. However, considering the amount of produced tiles, testing all the tile lots would be very expensive, and time consuming. In this example, the changing of the tiles was difficult; only one of the tile lots was faulty, but which tiles belonged to that lot? The three lots had been mixed in the construction site. Otherwise, it would have been easy to trace back the faulty tiles. Furthermore, there was another factor, which may have contributed to the damage; the design of the buildings. There were no eaves to protect the walls from the direct rain. If there had been eaves, maybe the faultiness of the tiles would have been revealed much later, or maybe never.

At some level, an open data base for building defects would be an improvement. Probably, the data base would operate best on a national level as the collection of data and the maintenance of the data base would probably be easier to organise on a national level. Also, there are local building codes, local building traditions, and climate differences in different countries. However, the national data bases should be organised in a way which enable the exchange of the information between different countries. For example, a couple of big hall buildings have fallen apart in recent years in north and central Europe. Research groups, some international, have been established to analyse to the causes of the crashes. The gathered knowledge from these groups is utilised in the development process of the standardisation.

4 DISCUSSIONS

The EU has eased the mobility of labour within its member countries. There is a keen competition on building contracts and professional workmen. The lack of professional workers is currently a big concern within the construction sector, at least in Finland. Unfortunately, grey markets are boost in these kinds of circumstances. The number of sub-contractors has been growing over the past decades. Supervising the level of the workmanship becomes challenging as the numbers of the sub-contractors increase. Due to the mobility of labour, there are often several different nationalities in a construction site. In different countries, the building culture, the working methods, and the code of building regulations is different. This complicates the circumstances even more. At worst, it may be a matter of industrial safety. Moreover, professional pride is often not what it used to be. Before a construction worker used to show his work and say, *'This is what I built'*. Today, he shows his wallet, and says, *'This is what I earned'*.

The maintenance and the renovations of existing buildings are critical issues for sustainable building, especially in Europe. The service life of a building can be decades or even centuries. The service lives of the components vary from a few years up to the service life of a whole building [ISO 2000]. But during the building's long service life, manufacturing processes and products are developed. Matching old and new techniques and products is challenging, especially considering the lack of professional workers.

There are several factors, which may affect the service life of building materials or components, even before their service life begins, before they become a part of a building. These pre-installation factors cause financial loss and environmental damage. A component damaged by the pre-installation factors may damage the surroundings as well, and thereby increase the financial loss and environmental damage. Unfortunately, this important subject area has been less addressed in research. Therefore, a thorough analysis on the pre-installation factors and their impact on the components and their surroundings is vital. It is essential to analyse the pre-installation processes in order to pinpoint the

black spots of the processes. The focus should be on how to avoid, or at least minimise, the possible damages to the building components during the pre-installation processes. Development of the processes might also be required.

Special attention should be paid to the control phase. All the faulty components should be excluded already at the production plant; they should never reach the construction site. If the pre-installation factors have damaged the component, it will not meet the predicted service life. In addition, it may cause damage to the surrounding components. Control at the construction site should also be emphasised. For example, the storage of the components and the installation of the components are extremely important phases. Furthermore, the traceability of the components should be assured. Tracing back the manufacturer and the production lot of the faulty component is essential. The other components of the same production lot could be checked for possible damages before they cause damage to the surroundings.

The distribution of the liability could improve the quality of the building components, and installation. There could be certificates for every work phase for the contracting parties (e.g. producers, manufacturers, assemblers, and installers). By signing the certificate, they would guarantee that they have done their part according to the building code and the certificate. The signature would make the person responsible. However, this would increase bureaucracy. Naturally there are legal responsibilities for faulty materials and components. This could help to trace the responsible person, because in some cases it is very difficult to prove who is responsible. If the names of architects, designers, constructors, and inspectors were engraved on a plate on the front wall of the buildings, would the quality of the building be any better?

ACKNOWLEDGMENTS

The authors wish to thank the Finnish Cultural Foundation and the National Graduate School of Timber Construction and Design (coordinated by University of Oulu) for funding this research.

REFERENCES

Brischke, C., Bayerbach, R. & Rapp, A.O. 2006, 'Decay-influencing factors: A basis for service life prediction of wood and wood-based products'. *Wood Material Science and Engineering*, **1**[3&4], 91-107.

Haapio, A. & Viitaniemi, P. 2008, 'Service life of a building in environmental assessment of buildings'. Proc. 11th DBMC International Conference on Durability of Building Materials and Components, Istanbul, Turkey, 11-14th May 2008.

ISO. 2000, *Buildings and constructed assets – Service life planning – Part 1: General principles.* ISO 15686-1:2000(E).

ISO. 2002, *Buildings and constructed assets – Service life planning – Part 3: Performance audits and reviews.* ISO 15686-3:2002(E).

ISO. 2004, *Buildings and civil engineering – Vocabulary, Part 1: General terms.* ISO 6707-1:2004(E).

Kamden, D.P., Pizzi, A. & Jermannaud, A. 2002, 'Durability of heat-treated wood'. *Holz als Roh- und Werkstoff*, **60**[1], 1-6.

Kohler, N., & Moffatt, S. 2003, Life-cycle analysis of the built environment. *UNEP Industry and Environment*, **26**[2-3], 17-21.

Saraswathy, V. & Song, H-W. 2007, 'Improving the durability of concrete by using inhibitors'. *Building and Environment*, **42**[1], 464-472.

Van Acker, J., Stevens, M., Carey, J., Sierra-Alvarez, R., Militz, H., Le Bayon, I., Kleist, G. & Peek, R.D. 2003, 'Biological durability of wood in relation to end-use, Part 1: Towards a European standard for laboratory testing of the biological durability of wood'. *Holz als Roh- und Werkatoff*, **61**[1], 35-45.

Westberg, K., Norén, J. & Kus, H. 2001, 'On using available environmental data in service life estimations'. *Building Research & Information*, **29**[6], 428-439.

The Importance of LCA and Service Life Prediction in Sustainable Design

A. Berrin Çakmaklı [1]

T 51

ABSTRACT

The building sector has a greater impact on the global environment or faces a greater obligation to improve its environmental performance. In buildings that have really long life cycles; renovation and refurbishment contribute more significantly in their life cycle assessment (LCA) that is a methodology for assessing the environmental performance of a product over its full life cycle. At that point, accurate service life prediction plays important role in LCAs. Estimated service life of components, which is a function of reference service life in conjunction with other factors, is generally considered in usage phases of their life. For building components, the occupants decide to make replacements taking into consideration their functional service life.

In light of sustainable principles and policies it makes more sense to renovate or refurbish old buildings. Energy consumption in hotels is one of the highest compared to other building types. These refurbishments are really important because the hotels should follow the fashion in order to offer best services. Many of the services to hotel guests are highly resource intensive, whether it concerns energy, water or raw materials. To assess the life cycle of hotels and their components is really useful to understand the importance of LCA from the point of view of sustainability.

This study was about to assess the life cycle of the refurbishment project of the five star hotel in Ankara. The estimated service life of changing materials especially the finishing ones is really shorter than their reference service life. A LCA tool, ATHENA is used for analyzing this refurbishment project. According to the results of software analysis, a material matrix was proposed.

KEYWORDS

Life Cycle Assessment, Service Life, Sustainable Design, Hotel Buildings.

[1] Başkent University, Faculty of Fine Arts, Design and Architecture, Ankara, Turkey 06530, Phone +90 312 2341010-2056, Fax 312 2341152, zeytunberrin@gmail.com

1 INTRODUCTION

As the world's population continues to expand, environmental management should include environmental quality and extend it in time over the long-term on a sustainable basis. Implementation of resource-efficient measures in all areas of human activity is imperative. Industrialization is necessary for any real development and also it can be achieved in an environmentally sound manner. In sustainable economy, materials use will be guided by a hierarchy of options: firstly, to avoid using any nonessential item; secondly, to reuse a product; and thirdly, to recycle the materials to form a new product. Growing universal awareness of protecting the living and non-living environment leads to more enlightened decisions to achieve a sustainable development. Sustainable development is "the challenge of meeting growing human needs for natural resources, industrial products, energy, food, transportation shelter and effective waste management while conserving and protecting environmental quality and the natural resource base essential for future life" [Bartelmus, 1994].

Buildings should benefit humans, the community, and the environment. However, nowadays buildings are one of the biggest threats to environment; they consume significant quantities of energy at all stages of their life cycle and this causes short and long term environmental and economic problems on local and global scales. According to Edwards [1998], the building sector, including housing, comprises 30-40% of the world's total energy demand and approximately 44% of the total material use. Building professionals are increasingly becoming involved in dealing with these problems and as a result of this a new approach has been adopted. Designing for sustainability is an approach to the design, construction and operation of buildings and their surroundings to improve the relationship between the buildings, environment and occupants. Sustainable or "green" buildings include appropriate use of land and landscaping, the use of environmentally friendly materials that have closed loops, and attention to the life cycle effects of the building's design and operation.

2 SUSTAINABLE DESIGN PRINCIPLES

2.1 Life Cycle Assessment

The entire building process in its relation to the environment in terms of energy use and emission, between taking from environment and bringing back into the environment should be assessed. Life Cycle Costing (LCC) and Life Cycle Assessment (LCA) are two complementary methodologies, which measure the performances of products or systems in the units appropriate to each emission type or effect category. As defined by IS0 14040 [1997: iii, withdrawn and revised as ISO 14040: 2006] ,
"LCA is a technique for assessing the environmental aspects and potential impacts associated with a product, by:

- compiling an inventory of environmentally relevant inputs and outputs of a system.
- evaluating the potential environmental impact associated with those inputs and outputs.
- interpreting the results of the inventory and impact phases in relation to the objectives of the study.".

LCA has been identified as a strong tool that can be considered as a scientifically established method for generation of the necessary decision support system. Defining sustainable materials and encouraging their use seems to be one of the biggest challenges for the developers of green building rating systems. That challenge must be met by a better integration of LCA techniques and LCA based decision support tools in whole building rating and certification systems.

One of the great difficulties in assessing the environmental effects of resource extraction is that so many of the environmental effects that concern people — for example, the effects on biodiversity, water quality, soil stability and so on — are very site specific and not easily measured. For that reason they are often left out of life cycle inventory studies or given only passing mention.

LCA is a dynamic and iterative assessment process, which assesses the environmental impacts of products and services from a cradle -the place or moment where the raw materials or resources are taken from nature into the technical system- to grave perspective -the place and time when the products or used resources are returned to nature. Society of Environmental Toxicology and Chemistry is the first international organization that has studied the LCA principle systematically. ISO then proposed a framework that involves four interrelated phases; goal and scope definition phase, inventory analysis phase, impact assessment phase and interpretation phase; seen in Figure 1.

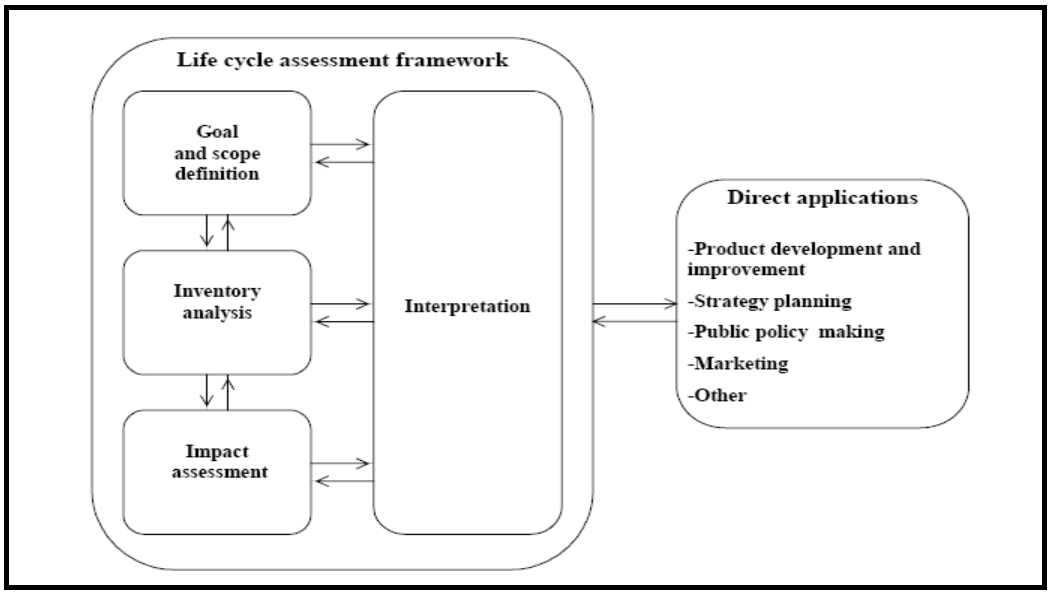

Figure 1. The four phases of an LCA [ISO 14040 Standard, 1997: 4].

2.2 Service Life Prediction

When the LCA methodology is applied to a building product, it is seen that an important parameter in LCA of buildings and building materials is the prediction of service life because the environmental loads per year is inversely proportional to the service life. According to Nunen et al. [2004], "The role of service life in LCA is underestimated which results in inconclusive assessment values". Understanding its role is really important to make accurate prediction about the environmental impact. The concept of Reference Service Life of Component (RSLC) was firstly introduced in ISO 15686-1 [2000, under development as ISO 15686-8], and defined as the "service life that a building or parts of a building would be expected or predicted to have in a certain set of reference in-use conditions". The objective of the service life planning was also stated as "to assure, as far as possible, that the service life of the component will be at least as long as its design life" [ISO 15686-1, 2000, under development as ISO 15686-1]. Not only long total service life of building but the service life of components is really important to decide the replacements. Most assessment methods that are carried out regard the service life as a fixed item. However, the buildings specific data are needed for types of maintenance and service life estimation. The fixed service life within the current assessments, the different phases within service life and the rate of replacement of components are important issues in LCA. Variation in materials or design solutions causes a calculated comparison between the various environmental burdens, and an optimization can be made.

2.2.1 Factor Method

In ISO 15686-1 [2000, under development as ISO 15686-8], the "Factor Method" was described as a means for addressing this problem. This method was used to modify a RSLC to obtain an estimated service life of the components (ESLC) of a design object, by taking account of the difference between the project-specific and the reference conditions. This was carried out by adjusting the RSLC by a function with a number of factors, each being from a particular factor class and reflecting a difference between the two sets of in-use conditions in the factor class. If the ESLC is known, the exact amount of material used throughout the overall service life is known as well. In its simplest form, the function was the product of the factors, as summarized below:

ESLC = RSLC * factor A* factor B * factor C * factor D * factor E * factor F * factor G

Where:

A = Material / Component factor B = Design factor C = Workmanship factor
D = Internal environment factor E = External environment factor F = In-use factor
G = Maintenance factor

Table 1. Examples of factors, relevant to building services plant (Saville & Moss; 2002: 4)

Factor	Examples
A Quality of components	Manufacture, storage, transport, materials, protective coatings
B Design / detailing	Incorporation into the building, detailing, system design
C Installation / workmanship	Site management, standard of workmanship, climatic conditions during installation
D Indoor environment	Aggressiveness of environment, ventilation, condensation
E Outdoor environment	Location of building, micro and macro environment, sheltering, pollution levels, weathering factors
F In-use conditions	Commissioning, hours/frequency of use, mechanical impact, category of users, wear, tear
G Maintenance	Quality and frequency of inspection and maintenance, accessibility for maintenance

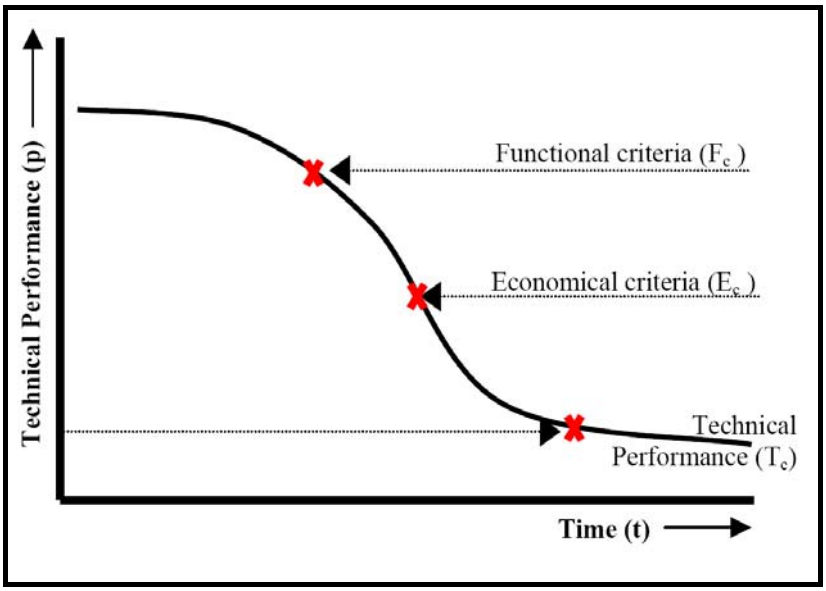

Figure 2. Different types of end of life [Nunen et al., 2004: 5].

In the ISO Standards, three kinds of end of life; technical, economical, and functional end of life; are seen in the building sector. The reference service life of components is the technical service life. The technical service life is over when the component can no longer sustain its performance. Economical end of life occurs when another component can be switched with lesser costs. The functional end of

life occurs first and the component's service life is over, when the component does not carry out the function people demand of the component.

Nunen et al. [2004] mentioned that Trend and Related factors should be added while calculating the ESLC because the sensitivity to fashion trends could decrease the functional service life of any component due to fashion changing. The other factor, Related factor comprised of two features: first one was the ease of the accessibility of a product that is replaced and the ease of replacing the combination of different components. For example, the replacement of a complete building part, like window frame, was easier than any component, frame without glass.

3 REFURBISHMENTS OF HOTEL BUILDINGS

It is obvious that most options in the design process to reach the best available environmental performance are available for new buildings only. However, the rebuilding of existing buildings presents opportunities to improve the buildings' environmental performance. Renovating an existing building can save money, time and resources with existing infrastructure and public transportation, enhancing convenience and reducing sprawl. Adaptable buildings are likely to use the same amount of space and materials more efficiently on average over their entire life. The annualized reduction in embodied and replacement energy, and the annualized reduction in solid waste generation from renovation and demolition are the successes of adaptability. It is noticed that rebuilding, including maintenance; activities represent almost half of the environmental impact in the residential and commercial sector. Among commercial buildings, accommodation facilities were unique with regard to operational schemes, the type of services offered, as well as the resulting patterns of natural resource consumption. Many of the services to hotel guests were highly resource intensive, whether it concerned energy, water or raw materials [Erlandsson, Levin, 2004].

Hotels should follow the technological improvements and apply them to their design processes. To maintain to highest standards to customers is really significant for hotels to remain competitive.
If a hotel was to be environmentally friendly, it should be constructed using environmentally sensitive materials. These materials should generally be less toxic, more durable and stronger, made of recycled materials, or environmentally certified. They should also have low embodied energy and be produced and available locally, in order to avoid transport-related impacts. An environmentally responsible design generated a number of benefits including considerably lower resource consumption and operational costs, as well as improved comfort and productivity for the occupants. The corporate image was also improved, thereby attracting new customers, as people came to prefer the "green" alternative. Hotels designed according to sustainability principles were called as "sustainable hotels".

Stipanuk & Roffman [1992] classifies renovations for hotels in three categories:

- Minor renovation (6 year cycle): the scope of a minor renovation is to replace or renew the non-durable furnishings and finishes within a space without changing the space's use or physical layout such as replacing carpets, wall coverings, drapery, and bedspreads; minor painting; and touching up the furniture.
- Major renovation (12 to 15 year cycle): the scope of a major renovation is to replace or renew all furnishings and finishes within a space, and may include extensive modifications to the use and physical layout of the space itself like replacement of all furniture, bedding, lighting, replacing floor finishing and artwork.
- Restoration (25 to 50 year cycle): the scope of a restoration is to completely gut a space and replace systems that are technically and functionally obsolete, while restoring furnishing and systems that can still be used, given current needs of the facility such as interior demolition of entire guestroom floors to reconfigure the mix of rooms and placement of bathrooms.

Making lifetime estimation in preliminary design stage is advantageous in refurbishing programming. The user activities, deterioration agents, and mostly visual obsolescence define the life expectancy of finishes in relation to the maintenance policy concerning renewal cycles. For example, long life

expectancy is one of the main criteria in selecting doors, windows and their components because frequent replacement of them is an expensive and time taking work in a refurbishment project. Special designs for carpeting, wallpapers, upholstery and curtains could limit the future replacements so it was not preferable. And gave examples to this by indicating the lifetime expectancy for carpets in guestrooms as 6 years, for drapes and spreads as 5 years, for beds 15 years, for mattresses 12 years, Venetian blinds 8 years and furniture 10 to 12 years due to Hilton International Engineering Manual.

4 REFURBISHMENT OF CASE STUDY BUILDING

Although Ankara is not a coastal city, nor a mountain resort, it is the capital city and therefore hosts many delegations, which is why it has many hotels. This being the case it needs to have world-class hotels to accommodate the official guests. This in turn means that the hotels in Ankara have to be kept up to date and must be renovated every how and then to meet the high standards of equivalent hotels elsewhere. According to data taken from Ankara Chamber of Architects, the percentage of hotels renovated in the six year period 2000-2006 is almost 53%.

Renovation works in hotels were undertaken mostly from the point of view of customer satisfaction. The guests were asked to fill up a questionnaire to assess their satisfaction. Some of the questions were posed to determine those aspects which impressed the guests most. The aim was also to find out whether the guests were bored with the decor or not. Unless there was a sudden change in fashion trends, this was one of the reasons of refurbishment. For example, in the case hotel for this paper, there were light-colored marble tiles and vanity basin with matching faucet fittings in the bathroom of the guestrooms before refurbishment. Although these fittings and fixtures were in good condition, they were replaced with darker new marble cladding and fittings only because of the changing fashion trends; as seen below in Figure 3 and Figure 4.

Figure 3. Fittings before refurbishment

Figure 4. Fittings after refurbishment.

Data pertaining to refurbishment/renovation project of five star hotel in Ankara was gathered in 2005 and photographs of the refurbished rooms were taken in 2007. This hotel belongs to an international chain which operates 2,700 hotels in 70 countries. Although, major renovations included such public areas as the lobby, conference-meeting rooms, ballroom, restaurants etc, only data for guestrooms has been analyzed in this paper, as the design decisions for one room is repeated hundreds of times over.

In order to assess the environmental impacts of the materials most commonly replaced during this refurbishment project, a life cycle assessment tool (ATHENA) is used. After entering the bill of quantity (BOQ) of guestrooms as the input to the software, the summary tables were obtained as the output and common materials that were used in all case guestrooms could be evaluated.
As an output of this software, the projects were evaluated according to six indicators. These were:

- Primary Energy Consumption: Absolute primary energy consumption by fuel type for each life cycle stage as well as annual operating energy.
- Solid Waste: Recovered matter resulting from the production and delivery process.
- Air Pollution Index: Inflows and outflows that contribute pollutants to the air.

- Water Pollution Index: Inflows and outflows that contribute pollutants to the water.
- Global Warming Potential: How much a given mass of greenhouse gas is estimated to contribute to global warming over a specific time interval.
- Weighted Resource Use: The quantities of raw materials or intermediary products consumed.

Table 2. BOQ of guestroom floors of the case hotel included common materials.

Material	**Unit**	**CASE HOTEL**
Levelling Conc. - Screed	m3	1576.7357
1/2" Fire-Rated TypeX Suspended	m2	4854.608
5/8" Fire-Rated TypeX Gypsum Board	m2	3051.488
Paper Tape	tones	13.5629
Water Based Latex Paint	l	1719.1080
Hardwood Skirting	m2	424.8825
(Modular) Brick Wall	m2	228.48
Plaster, gypsum spackling	m2	76199.024

Table 3. The impacts of seven common materials according to six indicators derived from software.

MATERIALS		**Primary Energy Consumption (MJ)**	**Solid Waste (KG)**	**API**	**WPI**	**GWP (KG)**	**Weighted Resource Use (KG)**
CASE HOTEL	**Levelling Conc.**	3244607	102758	48898	2	350177	4332806
	Gypsum Board	647917	22922	10324	1	24763	106365
	Paper	402919	6210	6223	0	14914	41270
	Water-Based Paint	50739	53	497	0	944	3343
	Hardwood	21128	89	199	0	610	12495
	Brick	246331	1263	3304	0	8933	26757
	Plaster	433034	4	139	0	781	1223392

5 CONCLUSION

The choice of materials and components has an important role in determining energy performance. Environmentally responsible specification of building materials and components includes the consideration of embodied energy, reusing, recycling, resource efficiency and local and global environmental impacts. As a result, the proposed matrix was devised and ecological scores were given to seven materials used, as shown in Table 4. Points were given to them according to their LCA. For primary energy consumption, solid waste, air pollution index, water pollution index, global warming potential and weighted resource use; the highest point, seven, was given to the material, which has the maximum impact; and the lowest point, zero, was given to the material, which has no impact.

According to Table 4, the maximum score, which is forty-two and being the most damaging material in this refurbishment work, belongs to levelling concrete mostly depended on the cement manufacture; the minimum score, which is 9, belongs to hardwood which is the least damaging material. As a result of this, use of levelling concrete and gypsum board should be minimized in refurbishment projects or alternative energy sources and processes should be found during manufacturing cement in order reduce the damage to the ecosystem. For these two materials, the recycling, reducing and reusing strategies are most significant. Filtering methods should be used while manufacturing in order to reduce the air and water pollution. Hardwood has the minimum ecological score so wooden materials mostly should be preferred while refurbishing.

Table 4. Proposed matrix

MATERIALS	Primary Energy Consumption	Solid Waste	API	WPI	GWP	Weighted Resource Use	Ecological Scores
Levelling Concrete	7	7	7	7	7	7	42
Gypsum Board	6	6	6	6	6	5	35
Paper	4	5	5	0	5	4	23
Water Based Paint	2	2	3	0	3	1	11
Hardwood	1	3	2	0	1	2	9
Brick	3	4	4	0	4	3	18
Plaster	5	1	1	0	2	6	15
7 points = Most damaging 0 point = No damaging							

In this case hotel while refurbishing, wooden suspended ceiling was replaced by gypsum board ceilings, which are not as durable as wood. Even the wooden pelmets were replaced with gypsum ones. From these examples it can be seen that sometimes good quality and durable materials are replaced with those of poorer quality and strength and also have worse impacts to nature. Additionally, the structures with permanent joints, anchors and glues should be avoided, since the hotel maintenance and renovation guideline offer a shorter useful life than their expected life. It would be prudent to use replaceable material and components with de-mountable joints. Since furniture is changed after every 8 to 10 years, it is advisable not to use fixed furniture or parts, such as wall mounted headboards or night stands. It would also be more economical and healthy if floors were covered with wooden parquet or marble tiles depending on the climatic region, and rugs were used instead of wall to wall carpeting, which attracts dust and stains easily. These rugs can be washed or replaced at considerably lesser costs.

REFERENCES

Bartelmus, P. 1994, *Environment, Growth and Development: The Concepts and Strategies of Sustainability*, Routledge Press, London.

Edwards, B. 1998. *Sustainable Architecture: European Directives and Building Design*, Architectural Press, Oxford.

ISO International Standard 14040. 1997E. *Environmental management – Life Cycle Assessment Principles and framework*, International Organization for Standardization (ISO), Geneva; revised as

ISO International Standard 14040. 2006. *Environmental management – Life Cycle Assessment Principles and framework*.

Nunen, N., Hendriks A. & Erkelens, P. 2004. 'Service Life as Main Aspect in Environmental Assessment', in: *CIB World Building Congress 2004*, Toronto, Canada.

ISO/DIS International Standard 15686-1. 2000. *Buildings & Constructed Assets – Service Life Planning, Part 1: General Principles,* International Organization for Standardization (ISO), Geneva, under development as ISO/DIS International Standard 15686-1. *Buildings & Constructed Assets – Service Life Planning, Part 1: General Principles* and ISO/DIS International Standard 15686-8. *Buildings & Constructed Assets – Service Life Planning, Part 8: Reference Service Life and Service-Life Estimation* .

Saville, A. & Moss, G. 2000. *Design for Life – Meeting the Industry's Needs for Robust Data on the Whole Life Performance of Building Services Plant,* Building Performance Group Project, 2000.

Erlandsson, M. & Levin, P. 2005. Environmental Assessment of Rebuilding and Possible Performance Improvements Effect on a National Scale', in: *Building and Environment* 39 (pp. 1453-65).Els. Ltd.

Stipanuk, D. & Roffman, H. 1992. *Hospitality facilities management and design.* The Educational Institute of the American Hotel and Motel Association.

Life Cycle Management Tool For Buildings

Erkki Vesikari [1]

T 51

ABSTRACT

Uncertainty in future needs of maintenance, repair and rehabilitation (MR&R) of buildings and new real estate management requirements have led to the need for special life cycle management systems and tools. The programme “MaintenanceMan” was aimed to be a new kind of life cycle management tool which fulfils the requirements of many stakeholders such as owners, contractors, designers and maintainers. The program “MaintenanceMan” can be characterised as predictive, optimising, integrated, life-cycle based and probabilistic.

The life cycle management tool “MaintenanceMan” was meant to be a prototype of a later commercial program. The preliminary version of the tool was programmed as a Visual Basic Application on Microsoft Excel. Only the building envelope, i.e. the facades, balconies and roof coverings were included in the system but the system can be extended to cover any parts of buildings. Several optional materials are available. By the help of the program it is possible to plan the future MR&R actions for modules (building parts) and to find the optimal maintenance strategy with regard to financial, functional and ecological aims. The functional condition analysis is probabilistic and based on the Markov Chain method.

The design process includes three stages: MR&R action design, project design and annual resources design. The MR&R action design is specific to each module of a building and results in MR&R action profiles with action specifications and timings. In the project design single actions are combined into groups of actions which are planned to be executed in the same project. At the last stage of design the annual project programs are prepared taking into account the annual budget.

KEYWORDS

life cycle management, Life cycle design, Sustainable design

[1] VTT Technical Research Centre of Finland, P.O.Box 1000, 02044 VTT, Finland. Phone +358 20 722 6922, Fax +358 20 722 7002, erkki.vesikari@vtt.fi

1 INTRODUCTION

Uncertainty in future needs of maintenance, repair and rehabilitation (MR&R) of buildings, and new real estate management requirements have led to the need for special life cycle management systems and tools [Vanier 2001]. In response to this need a new life cycle management tool called "MaintenanceMan", was developed.

The existing version of the tool was programmed as a Visual Basic Application on Microsoft Excel and was not as such meant for commercial use. Rather it was planned to serve as a prototype of a later commercial application. It covers the building envelope, i.e. the facades, balconies and roof coverings. Several material groups are incorporated: concrete, steel plate, wood, masonry and rendering for facades, concrete for balconies and concrete tile, steel plate and bitumen membrane for roof coverings. For each product group several options with varying materials and details are reserved. The system allows later complementation of both building parts and material groups.

The life cycle management system can be described with the following terms /1,2/: predictive, optimising, life cycle based, integrated and probabilistic. It is “predictive” as it uses service life models by which it is possible to predict the service life of the modules (building parts). It is “optimising” as it is possible to use the programme for optimising the maintenance strategy. It is “integrated” and “life cycle based” as it includes life cycle analyses for functional performance (condition), MR&R costs and environmental impacts. It is also “probabilistic” as the degradation analysis is probablistic allowing studies at different risk levels [Söderqvist & Vesikari 2006].

The programme MaintenaceMan works on modular basis. It means that the buildings are divided into structural parts which are called “modules”. The modules serve as the units for inspection, analysis, design and execution of actions. A module can be a part of a structural element or consist of several structural elements. The essential thing is that the materials and the environmental stresses are the same within a module. Examples of modules would be “steel roof” or “masonry façade to the west”, “balconies to the south” etc.

2 FEATURES OF MAINTENANCEMAN

2.1 General Process

Figure 1 shows the general process of life cycle management by MaintenanceMan. The process starts from the inspection of structures and ends in the execution of projects. Between the start and the end of the process, the programme MaintenanceMan produces project execution plans in three phases:
1. Action planning
2. Project planning and
3. Annual resources planning

The action planning is a combination of manual and automatic processes. The specification of MR&R actions is performed manually for each module using the displays of programme MaintenanceMan. The timing of these actions is, however, performed automatically by the life cycle based condition analysis of the system (ref. Chapter 2.3). The automatically produced lists of actions with timings (life cycle action profiles) can be later altered manually. The life cycle costs and environmental impacts of MR&R actions are calculated concurrently.

Project planning means combination of single MR&R actions into a group of actions which is planned to be executed at the same time and by the same contractor. In the project design the level of design is changed from the module level into the building level and the optimisation of the repair strategy is considered from a wider perspective. The module level actions are grouped into projects so that

synergy profit could be gained. The programme MaintenanceMan automatically combines the actions assuming tentatively that all actions scheduled for the same year are performed in that year as a single project. However, the designer can manually share the actions ascribed to a year into several projects and specify an action to be implemented in any year and in any project.

From project design the designer proceeds to annual resources design. The annual resources design means giving the final timing for projects so that the annual project costs are in harmony with the annual budget. For balancing the project costs with the budget the designer can rearrange the timings of projects and, if that is not enough, the designer can skip to the "project design" or even to the "action design" to make altorations to the planned actions and projects so that when returning back to the "annual resources design" the costs and resources can be balanced.

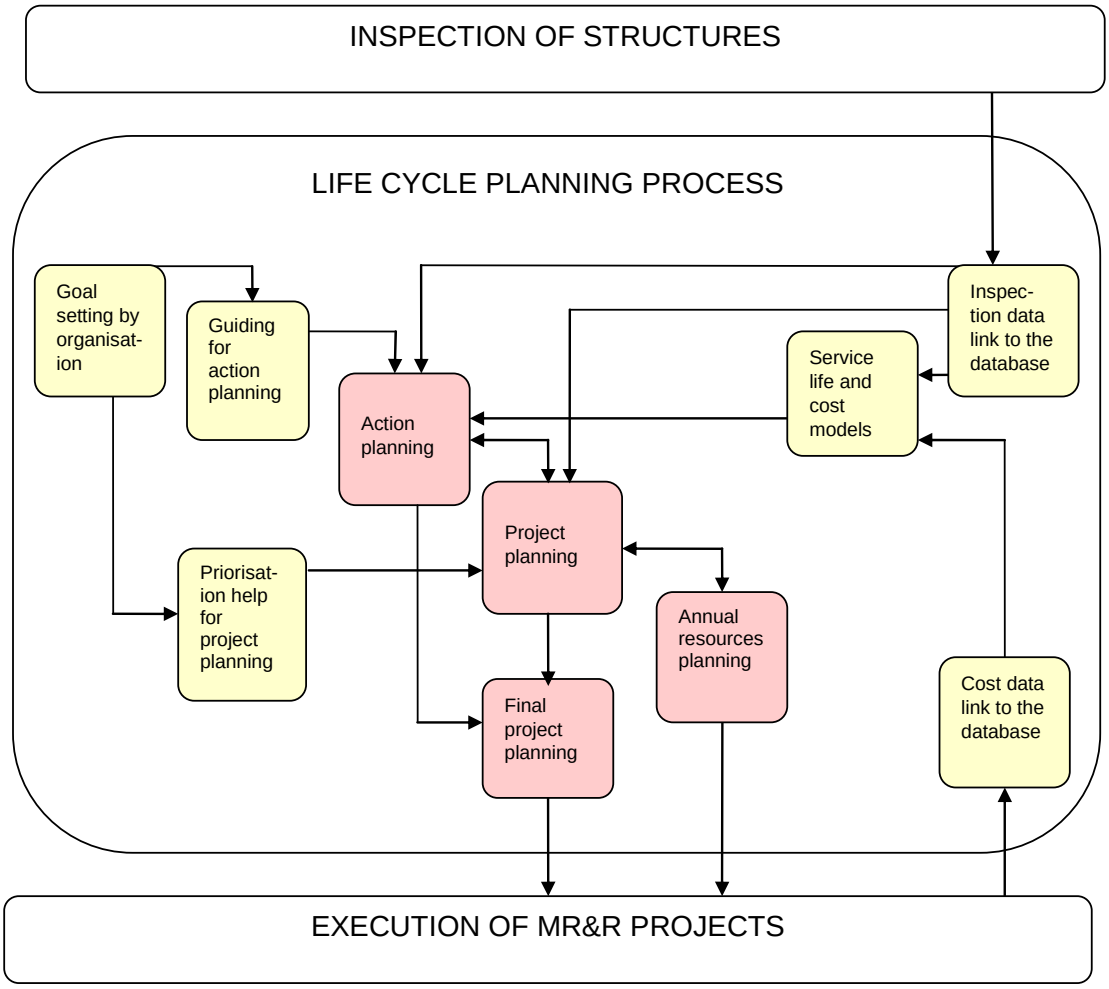

Figure 1. Life cycle management process of MaintenanceMan.

2.2 Data Flow

In the course of all three design phases, data for the buildings, modules and MR&R actions are needed. These data come from a set of databases representing buildings, modules, and repair systems.

The databases of buildings and modules can be produced by the user through the displays of MaintenanceMan. These databases include data concerning identification, materials, structures, exposure, fabrication, maintenance history and condition. The condition data consists of module specific degradation and damage data gathered by inspections.

The database of modules contains also the data of MR&R action specifications to be applied during the life of the module. The user of the program is supposed to specify these actions before entering into the analysis process. However, in case the user omits to do this default specifications are used.

Databases of repair systems contain data of MR&R systems used in the management system. They are not directly revisable by the user. However, the databases of repair systems contain many selective data items that the user can choose from through the displays. As the assortment of repair systems is different for each product group a separate repair system database is reserved for each of them.

The life cycle analysis process is organised so that the same process can be used irrespective of module, material or repair system at hand. Only the initial data, which are gathered in the "Data table of the active module", change when operating with sequential modules.

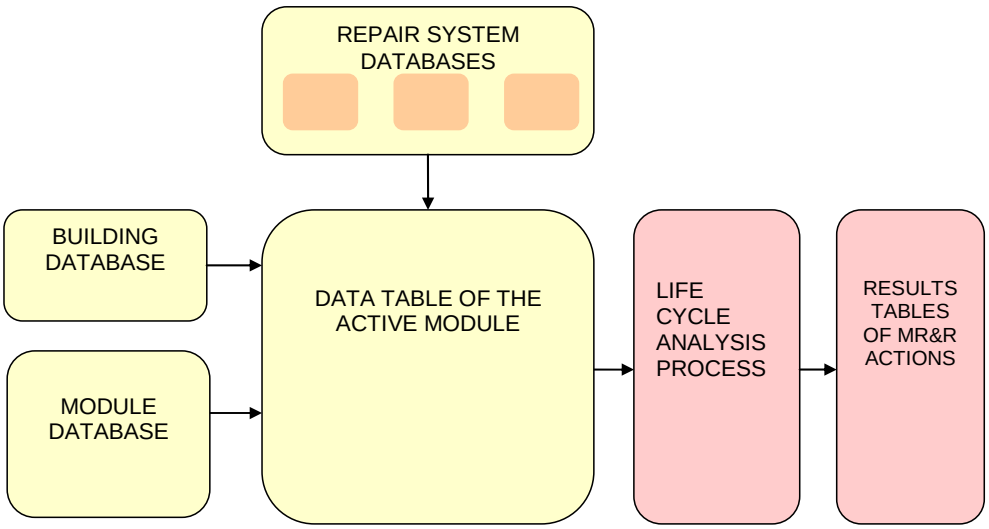

Figure 2. Data flow in the programme MaintenanceMan.

2.3 Life Cycle Analysis Process

The core of the programme MaintenanceMan is the combined condition, cost, and environmental impact analysis (Fig. 3). The condition analysis is based on the service life models and the Markov Chain method by which the annual condition state distributions of modules are evaluated through the whole design period. By the Markov Chain method the condition prediction of modules is changed from a deterministic condition analysis to a stochastic one. Specifically, an automatic condition guarding system is established on the Markov Chain based condition analysis. Every time the condition limit state is exceeded with the maximum allowable probability the defined repair action is triggered. The triggering of repair action in a certain year causes automatically application of the action effect matrix (of transition probabilities) instead of degradation matrix which is normally used in the Markov Chain analysis. Also the costs and environmental effects resulting from the MR&R actions are automatically added to the cost and environmental impact counters by the side of the condition analysis. The process is described in more detail elsewhere [Söderqvist & Vesikari 2006; Vesikari 2003].

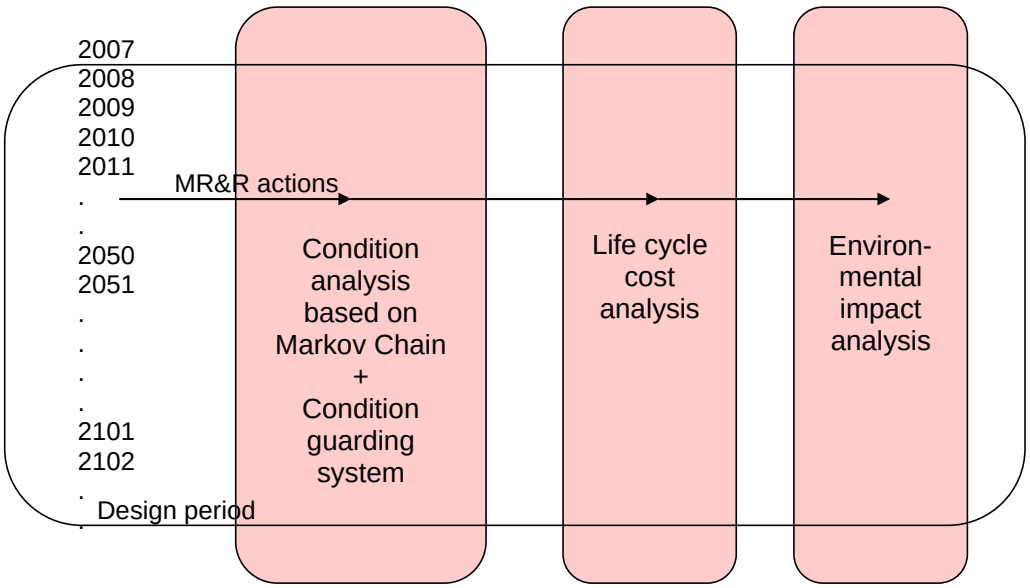

Figure 3. Combined condition, cost, and environmental impact analysis.

3 OPERATION WITH MAINTENANCEMAN

3.1 Establishing Databases of Buildings and Modules

If the building has not been analysed before by the programme MaintenanceMan the first thing that the user is supposed to do is to establish the databases of buildings and modules. In this the user operates with the input data displays of MaintenanceMan. Figure 4 shows the dataform of the module database. When adding condition data (resulting from inspections) or defining future MR&R actions other data forms are used.

3.2 Life Cycle Planning

The “action planning” is performed automatically by the programme MaintenanceMan. The timings of MR&R actions are defined by the service life models, Markov Chain based condition analysis, and the condition guarding system. The results of the design are shown for each module in three displays: (1) Results of MR&R actions, (2) Results of costs, and (3) Results of environmental impacts. Figure 5 shows the results display of MR&R actions.

In Figure 5 the results can be seen in two tables: Actions resulting from unpredictable damages (above), and actions resulting from predictable degradation (below). The tables contain data on identification of module, year of action, specification of action and volume of action. The costs and environmental impacts of actions are presented in other displays. If the designer is not satisfied with the automatically performed plan he/she can make modifications in the plan by the buttons below the tables.

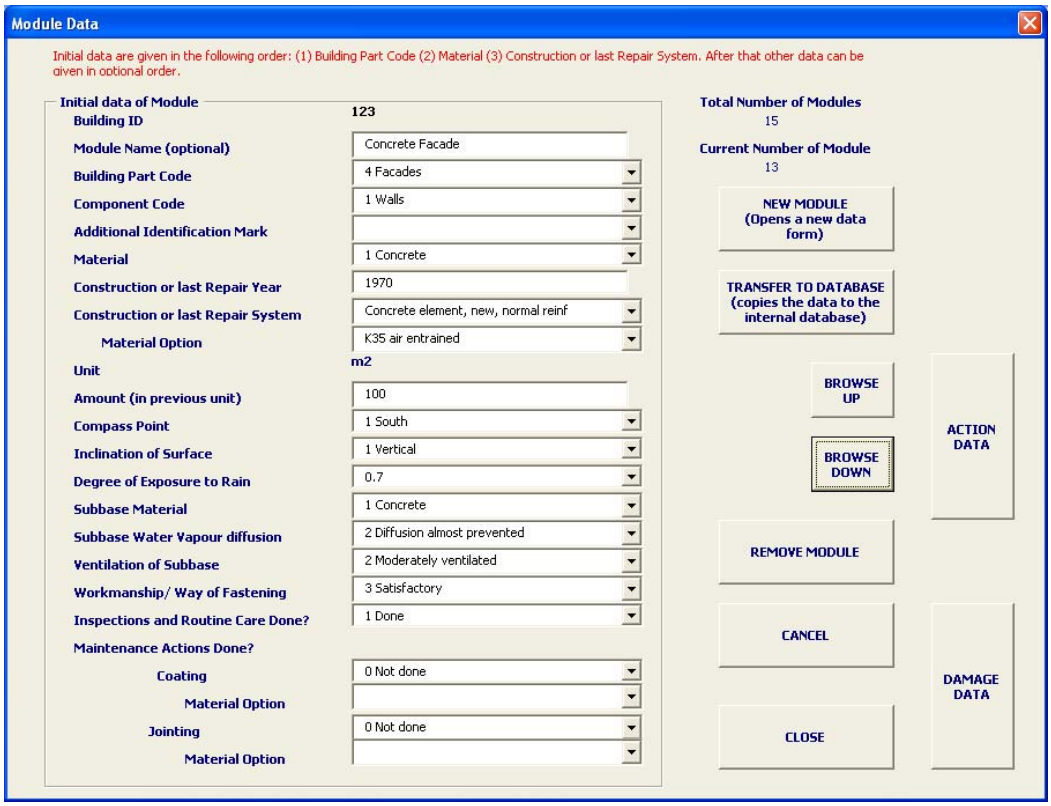

Figure 4. Dataform of the module database.

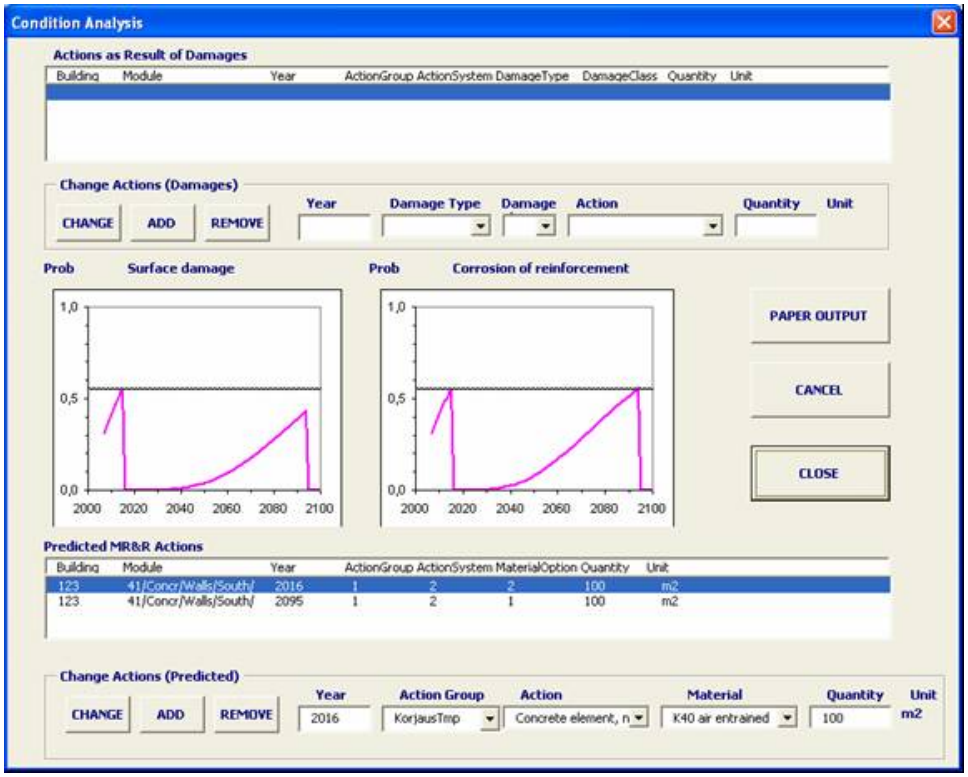

Figure 5. Display of the planning results.

Other displays are provided for summarised data for the whole building and for the whole design period. The display of life cycle costs is presented in Fig. 6.

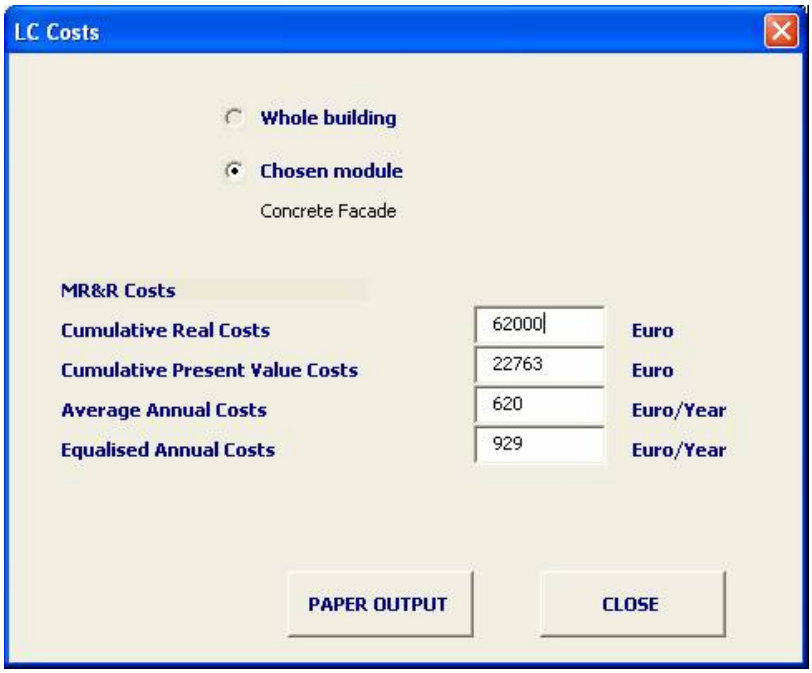

Figure 6.. Summerised data on Life Cycle Costs.

3.3 Optimisation with Maintenance Man

Comparative costs calculations can be conducted by the programme MaintenanceMan. A couple of examples are given in Tables 1 and 2. In Table 1 optional repair methods for concrete facades are compared. In Table 2 alternative repair methods of bitumen membrane roofs are compared. The time frame in these examples is 100 years and the discount rate is 4%. With the discount rate of 4% the discount factor after 50 years is 0.141 and after 100 years 0.020. It means that the relative contribution on MR&R costs for any action after 50 years is small and after 100 years insignificant. That is why the residual value after 100 years is omitted. In case several repears occur during the selected time frame the applied repair method is always the same.

Table 1. Repair methods of concrete facades. Present Value costs and equalised annual costs.

Repair method	*PV Cost Euro/m²*	*Equalised annual costs Euro/yr/m²*
Concrete element, new, normal reinforcement	228	9.29
Concrete element, new, rst reinforcement	253	10.32
Concrete element, tiled	271	11.09
Concrete outer slab, normal reinforcement.	169	6.89
Concrete outer slab, rst reinforcement.	168	6.88
Thermal isolation 45-50mm + fibercement sheet	160	6.51
Thermal isolation 45-50mm + polymerconcrete sheet	160	6.51
Thermal isolation 45-50mm + steel plate	131	5.35
Thermal isolation 45-50mm + rendering	151	6.17

Table 2. Repair methods of bitumen membrane roofs. Present Value costs and equalised annual costs.

Repair method	*PV Cost Euro/m²*	*Equalised annual costs Euro/yr/m²*
1-layer rubber bitumen membrane roof	21.0	0.86
2-layer rubber bitumen membrane roof	23.9	0.97
Renewal of whole roof structure	53.0	2.16
Additional rubber bitumen membrane on the old roof	13.2	0.54

4. CONCLUSIONS

A life cycle management tool "MaintenanceMan" was produced as a response to the obvious need in the area of life cycle planning and maintenance management. The programme MaintenanceMan was aimed to be a new kind of life cycle management tool which fulfils the requirements of many stakeholders such as owners, contractors, designers and maintainers. The management system of MaintenanceMan can be characterised as predictive, optimising, integrated, life-cycle based and probabilistic.

MaintenanceMan was meant to be a prototype of a later developed commercial application. The preliminary version of the tool was programmed as a Visual Basic Application on Microsoft Excel. For the time being only the "envelope" of the building, i.e. the facades, balconies and roof coverings are included in the system but the system can be extended to cover any parts of the buildings. Several optional materials are available. By the help of the program it is possible to plan the future MR&R actions, projects and resources and to find the optimal maintenance strategy with regard to financial, functional and ecological goals.

REFERENCES

Vanier, D.J. 2001. 'Why industry needs asset management tools'. *Journal of computing in civil engineering*. 1[15]2001, pp. 35 – 43

Söderqvist, M.-K. & Vesikari, E. 2006. 'Life cycle management process'. In: *Predictive and Optimised Life Cycle Management. Buildings and Infrastructure*. ed. A. Sarja, Taylor & Francis, London and New York, pp. 530 – 635.

Vesikari, E., 2003. 'Statistical Condition Management and Financial Optimisation in Lifetime Management of Structures.' Part 1: 'Markov Chain Based Life Cycle Cost Analysis' Part 2: 'Reference Structure Models for Prediction of Degradation', *Lifecon GIRD-CT-2000-00378 Deliverable D2.2*. 113 p. http://lifecon.vtt.fi/

Simulated Long-term Thermal Performance of a Building That Utilizes a Heat Pump System and Bore Hole

Jan Akander [1]
Bojan Stojanović [2]
Daniel Hallberg [3]

T51

ABSTRACT

Over the last decades, installation and use of heat pumps has grown rapidly in Sweden, to the extent that these mainly or partly heat roughly 25 % of the heated floor space in single-family houses. A majority are ground coupled where the heat exchanger is a borehole of 60-220 m depth. As the heat pump system operates, heat extraction will in time reduce borehole temperatures, rendering lowered efficiency of the heat pump system thus directly affecting its economical and environmental aspects.

Within the building sector, durability and life performance dynamics of energy systems is often not reflected upon. System performance and efficiency is assumed to be static over time, changing only due to different operation scenarios. This paper serves to quantify the long-term thermal performance degradation of a component, in this case the borehole, and how the degradation of this component affects performance-over-time of an entire system, in this case the heating system of the building. A dynamic thermal simulation model is used to assess the long-term thermal performance of the borehole. The building, which the heat pump serves, is assumed to be a typical Swedish house with normal energy consumption. Simulation results show that the depth of the borehole is of great importance to limit over-time temperature drops. The efficiency of the heat pump system is directly dependent of temperatures in the borehole. How the overall system performance is affected by component performance degradation, is highlighted.

KEYWORDS

Long-term thermal performance, Heat pump system, Borehole, Simulations.

[1] University of Gävle, KTH Research School, Centre for Built Environment, Gävle, Sweden, Phone +46 26 648118, Fax +46 26 648181, jpa@hig.se
[2] University of Gävle, KTH Research School, Centre for Built Environment, Gävle, Sweden, Phone +46 26 648137, Fax +46 26 648181, bsi@hig.se
[3] University of Gävle, KTH Research School, Centre for Built Environment, Gävle, Sweden, Phone +46 26 648108, Fax +46 26 648181, dhg@hig.se

1 INTRODUCTION

Installation and use of heat pumps has rapidly grown in Sweden during the last decades. Today, Sweden has the largest heat pump market in Europe, with more than 690 000 installed residential heat pump systems that heat approximately 25 % of the heated floor area of single family houses [Forsén 2007]; [Forsén *et al*. 2007]. A majority of the installed heat pumps are ground coupled where the heat exchanger is a borehole, while air-to-air, exhaust air and air-to-water heat pump systems are steadily increasing in popularity [Forsén *et al*. 2007]. During the 1980's, heat pump technologies were regarded as an "alternative energy technology" which reduced energy consumption and environmental impact. A recent investigation states that a residential electric heat pump with a **S**easonal **P**erformance **F**actor (SPF) of 2.5-3.0 will give an approximately equal CO_2-contibution to the atmosphere as a heating system based on burning fossil fuel [STEM 2002]. This, however, depends on how the electricity on a national basis is generated. In general, heat pumps are considered to reduce energy consumption, but it is important to increase the SPF to keep the environmental and economical arguments for installing residential heat pump systems.

When the heat pump coupled with a **B**orehole **H**eat **E**xchanger (BHE), the depth is 60-220 m. As the heat pump system operates, heat extraction from the BHE will in time reduce ground temperatures. Because of this effect, the efficiency of the heat pump system reduces, which directly affects its economic performance. These changes require a performance over time assessment for the BHE's due to their intended long-term usage as components in heat pump systems. By mathematical modelling, the long-term thermal performance of a BHE and its influence on the efficiency (SPF) of the heating system can be simulated.

2 OBJECTIVES

This paper presents the simulated long-term thermal performance of a heat pump system with a single heat extraction BHE equipped with an U-pipe. Since the performance of the heat pump is directly influenced by the temperatures at which heat is collected (the low temperature) and released (the high temperature), an over-time reduction of the lower temperature will have a negative influence on the over-all performance of the heating system: a greater temperature difference will require more driving electricity. By means of computational simulations, the order of magnitude of performance degradation is estimated. Since the simulations consider long-term runs, models are kept simple with monthly data input. Simulations cover a 50-year period in a case study where buildings are situated in Stockholm, Sweden. Energy requirements of two buildings are simulated: one which can be regarded as an average single-family dwelling in the Swedish stock and the other that is built in correspondence with the Swedish building regulation BBR12 [Boverket 2006]. The methodology presented in this paper is applied in the "LMS-ByggaVilla" project that is presented by Hallberg *et al.* [2007].

3 ESTIMATION OF THE HEATING REQUIREMENT

The primary reason for analysis of heating reqirement is to provide an annual load profile that renders realistic monthly heat extraction from the BHE. This profile may be obtained from measured or assumed data or from detailed simulations. A simple method degree-day method is presented below.

Two residential single-family houses are considered. A "new house" built in one storey according to the most recent Swedish building regulation BBR12 [2006] is simulated. The house has a heated floor space corresponding to the average size of houses completed in 2005, 124 m² [Statistics Sweden 2007], and has construction U-values that fulfil building regulation requirements (Tab. 1). It is assumed that 70 % of the heat in the exhaust ventilation air is recovered and transferred to the supply air. Air infiltration corresponding to 0.1 air changes per hour is also modelled.

Table 1. Building envelope components area and U-values applied to the modelled new house.

Construction	*Area* [m²]	*U-value* [W/(m²·K)]
Roof	124	0.13
Floor	124	0.15
Walls	92.7	0.18
Windows, doors	24.8	1.3

The other residence, "the old house," has a heating requirement that is set equal to the average single-family dwelling of the Swedish building stock. The space heating requirement is around 15 000 kWh/year and the heated space floor area is 144 m² [STEM 2007].

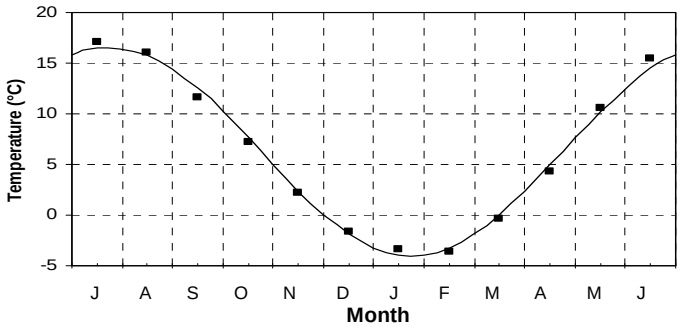

Figure 1. Monthly outdoor temperatures [Nevander *et al.* 1994] and a harmonic curve fit for Stockholm. Note that the x-axis starts at July.

The heating requirement is estimated by means of the degree-day method. A sinus curve is fit to monthly climate data (Fig. 1), in this case data for Stockholm. From estimations on when the heating season starts and ends, the degree-days are found by the integration of the difference between approximated outdoor temperature and the indoor base temperature. The indoor base temperature is dependent on heat gains in relation to heat loss coefficients of each building.

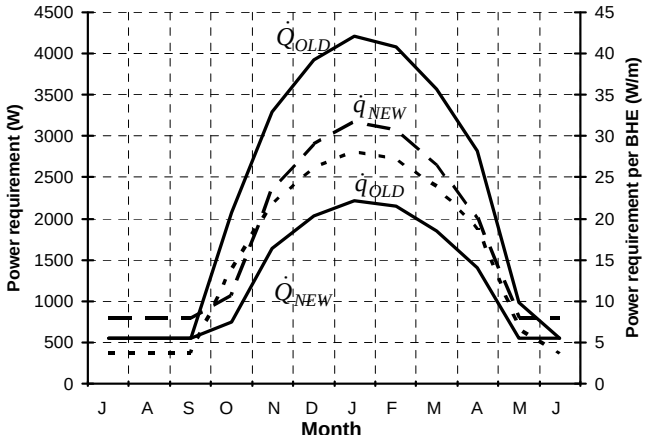

Figure 2. The plot starts with July. The y-axis to the left shows the heating requirement profile (filled curves $\dot{Q}_{NEW}$ and $\dot{Q}_{OLD}$) for each house. The y-axis to the right shows heating requirement per meter BHE (dashed), here **70 m BHE for the new house** ($\dot{q}_{NEW}$), **150 m BHE for the old house** ($\dot{q}_{OLD}$).

There is no space-heating requirement during the summer, but heat will be extracted from the BHE to provide the building with **D**omestic **H**ot **W**ater (DHW). Heat for DHW production is hypothetically constant every month. The annual DHW consumption usually corresponds to some 4 800 kWh [STEM

2007] for a family of four. Figure 2 shows the annual energy requirement profile. The estimated space heating requirement of the new house is 5 990 kWh/year, and for the old house 15 000 kWh/year.

4 MODELLING OF THE HEAT PUMP AND THE BHE

The simulations consider a BHE under the influence of a building that has a defined energy requirement – thereof the previous section. Given the energy requirement of the building, this method will automatically calculate heat extraction and efficiency of the system. The resolution of input data is on a monthly basis, power peaks will be lost when monthly data is utilized. This will affect output data for reasons discussed below.

4.1 Heat Pump Modelling

Heat pumps in Sweden commonly supply heat to spaces and to DHW. In practice, heat pumps deliver heat to DHW at temperatures of around 55 °C while space heating usually is supplied at variable (floating) condensation temperatures, which are dependent on outdoor temperatures. Efficiency is enhanced as the condensation temperature is reduced. For a house heated by radiators, as is assumed in this case, the maximum supply temperature of 55 °C is permitted when outdoor conditions have design values. It is assumed that the condensation temperature increases linearly as temperatures outdoor drop towards design conditions (so-called outdoor temperature compensation).

During peak power periods, the heat pump itself will not cover the heating requirement since these are commonly installed to embrace about 70 % of the power requirement, whilst providing the building with 90 % of the energy requirement [STEM 2006]; all this to enhance the efficiency of the heat pump system. Auxiliary systems, in most cases an electric coil in the heat pump, will provide the remaining energy (10 %) during the coldest outdoor conditions. In the present work, it is assumed that the heat pump fulfils 100 % of the heating requirement.

The efficiency of a heat pump is often characterized by the **C**oefficient **o**f **P**erformance (COP), Eq. 1, which indicates rate of heat flow delivered from the heat pump in relation to the rate of energy flow (electricity) supplied to the process. Another measure of efficiency is the **S**easonal **P**erformance **F**actor (SPF), Eq. 2, which for a given time period considers the amount of output heat in relation to how much energy has been utilized to fulfil the heating requirement. COP and SPF differ in the auxiliary energy, which represents heat from another heat source and/or electricity supplied to run other components in the heat pump system, such as pumps or control devices. In this work, the auxiliary energy is set to zero, which gives these two factors the same value.

$$COP = \frac{\dot{Q}}{\dot{W}_t} \quad , \quad SPF = \frac{Q}{W_t + E_{aux}} \qquad (1), (2)$$

where

$\dot{Q}$ is rate of output heat from the heat pump in operation, [W]

$\dot{W}_t$ is the rate of energy input to the heat pump (compressor work) in operation, [W]

Q is energy output during a considered period of time, [J] or [kWh]

W_t is energy supplied to the heat pump (electricity) during the period, [J] or [kWh]

E_{aux} is heat or electricity supplied to the heat pump system during the period, [J] or [kWh]

The relationship between COP (in this case also SPF) and temperatures at which the refrigerant in the heat pump evaporates and condensates is, with Carnot's efficiency η, expressed in Eq. 3 so that

$$COP = \eta \cdot \frac{T_{cond}}{T_{cond} - T_{evap}} \qquad (3)$$

with

T_{cond} denoting condensation temperature of the refrigerant of the heat pump, [K]
T_{evap} denoting evaporation temperature of the refrigerant of the heat pump, [K]
η denoting efficiency of a true process in relation to the Carnot process, [-]

Since temperatures within the heat pump process seldom are measured, these are within this work estimated on basis of statistics from products [Forsén 2007]. The refrigerants evaporation temperature is assumed to be ΔT_{evap} = 4 K less than the temperature of the cold carrier fluid in the evaporator of the heat pump. The refrigerants condensation temperature is in turn assumed to be ΔT_{cond} = 1 K higher than the temperature of the supply DHW or supply water for space heating. Carnot's efficiency, η, is assumed to be constant in time; here using the value 0.45.

By solving the set of equations above, Eq. 4 (here on a monthly basis) is obtained which gives the relationship between the heating requirement and the heat that is extracted from the BHE, such that

$$Q_{extracted} = \left[1 - \frac{1}{\eta}\right] \cdot (Q_{SH} + Q_{DHW}) + \frac{T_{cold} - \Delta T_{evap}}{\eta} \left[\frac{Q_{SH}}{T_{SH} + \Delta T_{cond}} + \frac{Q_{DHW}}{T_{DHW} + \Delta T_{cond}}\right] \quad (4)$$

where

Q_{SH} and Q_{DHW} are space- and DHW heating requirements, respectively, [kWh] or [J]
T_{cold} temperature of the cold carrier exiting the heat pump, [K]
T_{SH} and T_{DHW} are supply temperatures for space heating and DHW, respectively, [K]
ΔT_{evap} and ΔT_{cond} are temperature differences between the refrigerant and carrier in the heat exchangers of the evaporator and condenser, respectively, [K]

The difference between heating requirement and the extracted heat corresponds to energy that is supplied to the heat pump process. Note the role of the evaporation temperature, here represented by $T_{cold} - \Delta T_{evap}$. When the temperature in the BHE decreases over time, T_{cold} will also decrease and render reduced heat extraction. This, in turn, means that the heating requirement will be fulfilled by increased use of heat compressor energy and/or auxiliary energy.

4.2 Borehole Modelling

The modelling of a single BHE is described in detail by Stojanović *et al.* [2005] and here briefly summarized. The borehole, U-pipe and ground are modelled by means of a RC-network that simulates heat exchange and temperatures in the time domain. However, parameters of the RC-network are pre-processed and optimized on basis of the dynamic thermal response in the frequency domain. An advantage of this modelling method is that it establishes a simplified yet sufficiently accurate thermal BHE model, which requires less computing time and power compared with a traditional finite difference/element model. This facilitates system simulation over several decades.

In this work, the U-pipe of polyethylene has an inner and outer radius of 0.017 m and 0.02 m, respectively. It is filled with a 25 % ethanol-water mix. Ground properties are set to Swedish mean values: the thermal conductivity to 3.5 W/(m·K) and the volumetric heat capacity to $2.2*10^6$ J/(m^3·K). The filling material between the pipe and the ground is water. A minor change is done in the new model: The star network between pipes and the ground of the earlier model is replaced by a thermal resistance between the mean cold carrier fluid temperature and the ground. This thermal resistance is given the value 0.10 K/(W/m), which is the mean of a high value for filling water with low convection rate, 0.138 K/(W/m) [Gustavsson 2006], and measured values obtained from Hellström and Kjellsson [2000]. Initial temperatures of the undisturbed ground are dependent on site location. The temperature for Stockholm is estimated to be 7.5 °C at a depth of 100 m [Kjellsson 2004].

5 RESULTS AND DISCUSSION

Heat extraction from a BHE will in time reduce temperatures of the surrounding ground, as illustrated in Fig. 3. In order for the cold carrier fluid to absorb heat, its temperature must be lower than that of the ground and it is at this lower temperature that the heat pump will obtain heat. In time, the reduction in ground temperature will diminish as the BHE and its surroundings approach a state of equilibrium. Figure 4 illustrates monthly temperatures: after the tenth year, temperature reduction is negligible. A temperature that deserves attention is that of the cold carrier that exits the heat pump and enters the BHE. It is tolerated that this temperature occasionally is lower than 0 °C, but should not occur over for periods longer than a few weeks per heating season.

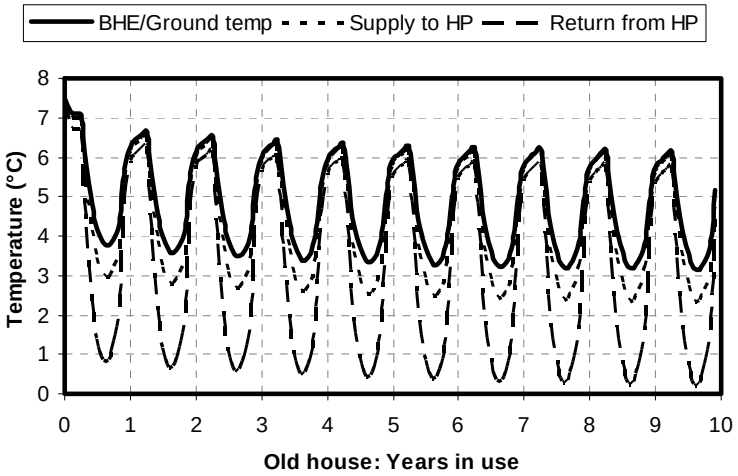

Figure 3. Fluctuation in the BHE/ground interface temperature and the temperatures of the cold carrier fluid of the old house during the first decade of use.

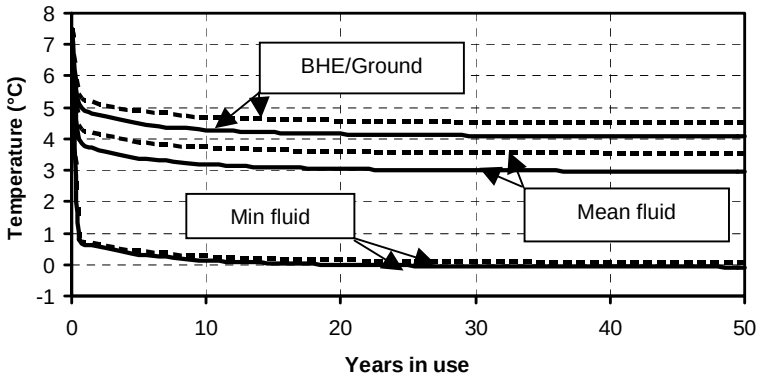

Figure 4. Annual mean values of the BHE/ground wall temperature and cold carrier fluid mean temperatures are plotted for 50 years of use. The minimum monthly average of each year is also plotted; in this case the fluid exiting from the heat pump which enters the BHE. Dashed curves for the old house; filled curves for the new house.

It is at the predicted equilibrium stage that the design of the energy system should be performed. In Sweden, the design of a BHE considers a 10-year heat extraction. This case study shows that the predicted equilibrium stage is reached after approximately 10 years.

The measure of efficiency of the heat pump system is SPF. The reduction in BHE temperatures decreases heat extraction, as can be seen in Eq. 4, and thereby SPF. For the two cases shown here, change in SPF is illustrated in Fig. 5. In the computational runs, the over-time SPF is compared with a SPF that would have been obtained if the cold carrier (thus BHE) constantly has the same temperature

as the undisturbed ground. Reduction of SPF is larger for the new house since more heat is extracted per meter of BHE. This is also seen in Fig. 4: the mean fluid temperature is lower.

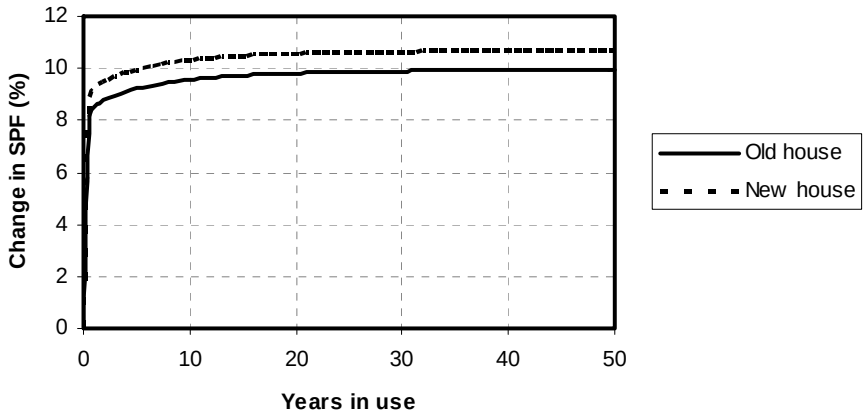

Figure 5. The change in SPF over time for the new and the old house in comparison to the maximal SPF that hypothetically can be obtained if the temperature of the BHE does not reduce.

Whereas Fig. 5 displays changes in relation to undisturbed ground temperatures, it is of interest to compare performances during the first and the last year: keeping in mind that greatest change occurs during the first year. Table 2 shows values, which conclude that the temperature reduction of a BHE has a minor influence on supplied energy. SPF is higher for the old house since the energy for DHW (high temperature heating) is a smaller part of the total heating requirement.

Table 2. Comparison between the 1st and the 50th year of operation. *El* depicts supplied electricity.

House	*SPF Year 1* [-]	*SPF Year 50* [-]	*SPF decrease* [%]	*El Year 1* [kWh]	*El Year 50* [kWh]	*El increase* [%]
New house	2.99	2.93	2.0	3609.5	3683.5	2.1
Old house	3.22	3.16	1.9	6155.3	6275.7	2.0

The assumptions made during the course of the modelling should be noted. The BHE delivers heat only by heat conduction in the ground (no flow of water etc) which gives “pessimistic values”. On the other hand, there are no other near-by heat sinks/sources, and the fact that the modelled heat pump delivers 100 % of the energy (no auxiliary sources or components) gives “optimistic values”. Future work will consider these aspects and an attempt will be made to introduce failure statistics where components within the heat pump itself fails to work.
This work has served to illustrate how a long-term temperature reduction in the BHE, influences the thermal performance of the entire system. After some 10 years, temperature reduction in the BHE is negligible. On basis of this study, the reduction in BHE temperature will after 50 years give an increase of the annual electricity consumption corresponding to 2 %, provided that the building and system continuously has been exposed to a “normalised” annual climate. Annual variations in real climate give larger discrepancies in energy consumption.

REFERENCES

Akander, J. (1999), *Värmetröghetens Inverkan på Energibehovet – Studier på ett Småhus*, Dept of Building Technology, Working Report 1999:2, Royal Institute of Technology (KTH).

Boverket 2006, *Regelsamling för Byggande - Boverkets Byggregler BBR*, BBR 2006:12, Sweden.

Claesson, J., Eftring, B., Eskilson, P. & Hellström, G. 1985, *Markvärme - En Handbok om Termiska Analyser*, Swedish Council of Building Research, Report T17: 1985, Sweden.

Forsén, M. 2007, President of SVEP, Swedish Heat Pump Association, *Personal communication*.

Forsén, M., Roots, P., & Bertenstam, A.L. 2007, *GROUND-REACH Market Status for Ground Source Heat Pumps within Europe*, EU-Project GROUND-REACH Deliv 2, SVEP, Sweden.

Gustavsson, A.M. 2006, *Thermal Response Test – Numerical Simulations and Analyses,* Dept of Civil and Environmental Engineering, Lic Dissertation 2006:14, Luleå University of Technology (LuTH).

Hallberg, D., Akander, J., Stojanović, B. & Kedbäck, M. 2008, 'Life cycle Mangagement System – A planning tool supporting long-term based design and maintenance planning', Proc. 11th Int. Conf. on Durability of Building Materials and Components, Istanbul, Turkey, 11-14th May 2008.

Hellström, G. & Kjellsson. E. 2000, 'Laboratory measurements of heat transfer properties of different types of borehole heat exchangers', Proc.8th Int. Conf. on Thermal Energy Storage, Stuttgart, Germany.

Kjellsson, E. 2004, *Solvärme i Bostäder med Analys av Kombinationen Solfångare och Bergvärmepump*, Div. of Building Physics, Report TVBH-3047, Lund Institute of Technology (LTH).

Nevander, L-E. & Elmarsson, B. 1994, *Fukthandboken*, AB Svensk Byggtjänst, Stockholm, Sweden.

Statistics Sweden 2007, *Yearbook of Housing and Building Statistics*, SCB-Tryck, Örebro, Sweden.

STEM 2006, *Villavärmepumpar – Energimyndighetens Sammanställning av Värmepumpar för Småhus*, Swedish Energy Authority, Report ET 2006:25, Eskilstuna, Sweden.

STEM 2002, *Marginal elproduktion och CO_2-utsläpp i Sverige*, Swedish Energy Authority, Report ER 14:2002, Eskilstuna, Sweden.

Stojanović, B. & Akander, J. 2005, 'Long-term thermal performance modelling and simulations of a borehole', Proc. 7th Symp. Build. Phys. in Nordic Countries, Reykjavik, Iceland, June 13-15, 2005.

Measuring Economical Risk in Life Cycle Management

Fulvio Re Cecconi [1]
Marco Pitzalis [2]

T 51

ABSTRACT

Life cycle base management of building and building assets is strictly bound to economical management in many cases: a company that owns its facilities and need to reduce maintenance costs or to get better building performance for the money spent; a private company that is involved in a PPP, PF Initiative, etc. This strong relationship brings the need for tools to measure and minimize economical risk in life cycle base management of building. A Life cycle management process can be divided in sub-processes (inventory registration, condition survey, service life performance analysis, maintenance analysis, maintenance optimization, maintenance planning). Some of these sub-processes are more relevant than other for economical risk and this paper shows first results of a research, conducted at the Polytechnic of Milan, aimed to identify and deal with risk related activities in building maintenance planning. Two points of the life cycle management process are analyzed with deep details: the identification of maintenance activities to be done on a building and the estimation of costs related with these activities. For the first point the paper shows an evolved approach to FMECA based on risk management techniques to measure the probability of not including a maintenance operation that will be necessary. For the second point the paper shows a methodology developed at the BEST – Polytechnic of Milan to estimate maintenance costs within a probabilistic approach.

KEYWORDS

Risk analysis, Maintenance planning, Service life.

[1] Politechnique of Milan, Building Environment Science & Technology, Milan, Italy 20133, Phone +39 02 2399 6052, Fax +39 02 2399 6020, fulvio.rececconi@polimi.it

[2] Politechnique of Milan, Building Environment Science & Technology, Milan, Italy 20133, Phone +39 02 2399 6033, Fax +39 02 2399 6020, marco.pitzalis@polimi.it

1 INTRODUCTION

In construction industry [Loosemore, 2006] “it is necessary for firms to strike a balance between the avoidance of all risk on the one hand and risk-seeking behavior on the other. The challenge is not to avoid risk but to take calculated risks by recognizing and managing them effectively”. The traditional approach to risk management, risks are offloaded to the weakest part in the supply chain, generally a sub-contractor, is now showing its limits with new form of building procurement like Built to Order (BOT), Private Public Partnership (PPP) or Private Finance Initiative (PFI). A new [Loosemore, 2006] “life cycle approach to risk, which emphasizes the collective responsibility and interdependence of all involved in each stage of the building procurement process” is indeed needed.

2 RISK IN LIFE CYCLE MANAGEMENT

2.1 Introduction to Life Cycle Management

In 1993 ISO TC59/SC14/WG9, Design Life of Building, was started with the purpose of documenting steps to be taken at various stage of the building cycle to ensure that the resulting building will last for its intended life without incurring large unexpected expenditures. Since then methods and tools for obtaining a systematic life cycle base management strategy on the European level have become major objective and focus of the European Union Action Plans and FW program.
The life cycle based management and maintenance planning approach includes condition assessment, predictive modelling of performance changes, maintenance analysis and maintenance, repair and refurbishment (MR&R) planning and decisions. Most of newly developed approaches aimed to turn today’s reactive and short-term design, management and maintenance planning towards an optimised and long-term technical approach. An example of this new approach can be found in LIFCON LMS [LIFECON 2004], where the life cycle management process is divided into six sub-processes: Inventory recording; Condition survey; Service life performance analysis; Maintenance analysis; Maintenance optimization; Maintenance planning.

2.2 Introduction to Risk Management

Introducing a risk assessment system applied to life cycle management is the way to obtain more reliable results about maintenance costs and time.
We talk about risk assessment because, according to the literature and the ISO guide 73, it includes both risk analysis (risk identification and risk estimation) and risk evaluation. All the phases of a typical risk assessment approach and their relationships are described in figure 1.

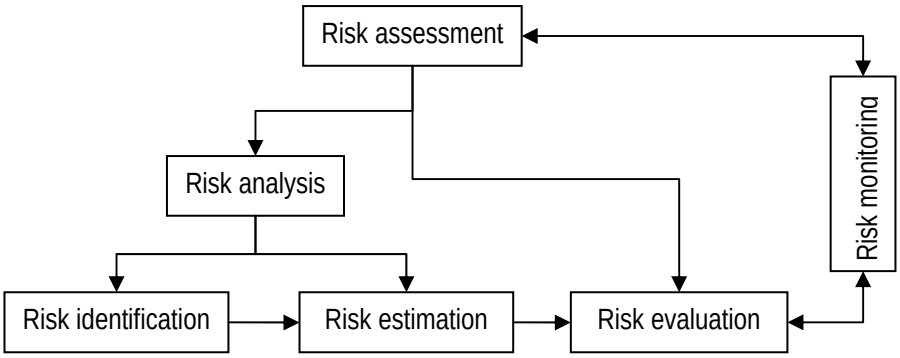

Figure 1. Risk management phases [ISO guide 73]

In this paper the three basic steps identification, estimation and evaluation of risks will be pointed. The aim of the first step, risk identification, is to find out and describe every possible failure for building components and their potential negative consequences. In order to do this FMEA (Failure Mode Effect Analysis) method is used.
During the risk estimation phase risks are measured, assigning a probability and a severity grade to the events and combining these data to achieve the risk dimension that is the fundamental parameter to determine risk response. This is of course a key point in risk analysis and the reliability of final results depends on various factors: the quality and quantity of available information about frequencies of the events; the presence of historical data about gravity of consequences; the accuracy of the technique used to measure the risks.
In many cases, because of the lack of statistical data in building sector, the risk estimation is based on qualitative approach [A.Ceric 2003]. In this research work a first qualitative risk estimation is implemented by a Montecarlo simulation forwarding a probabilistic approach, useful to measure which is the error in the estimations.
At the end, risk evaluation is the comparison process between risks exposure and the risk acceptability criteria to take decisions about the acceptability of risks and how to treat them to reduce the risk level. Of course, criteria are different based on the context and the strategy of the organization involved in the project.
Along all this process is important to consider just another phase that is the risk monitoring. It's very important to control the risk's tendencies and to make new choices about risk treatment.
Next chapter will present an integrated system of risk assessment applied to life cycle management, combining FMECA methodology and Montecarlo simulation.

2.3 Risk Analysis in Life Cycle Management

The studies presented in this paper show implementations of risk analysis tools to solve two different kinds of risks found in the life cycle management process:

- the first one is the risk associated to errors made using FMECA tool for prioritizing aging effects and their treatments (maintenance operations). So it will be possible to know and assess which is the retained risk also for unplanned maintenance operations (fig.2). To achieve this result it is necessary to implement a probability approach using Montecarlo simulations in risk analysis.
- the second one is the risk associated to errors made estimating time and costs of maintenance in maintenance schedule program. Also in this case a Montecarlo simulation is implemented to set up a maintenance plan with reliability information (fig.8)

The risk analysis method proposed to treat the first kind of errors comes out from collaboration between Polytechnic of Milan and CSTB (Centre Scientifique et Technique du Bâtiment – France) that in the last years have worked a lot on durability and life cycle management.

The common starting point of view is that FMEA and FMECA (Failure Mode Effect Analysis and Failure Mode Effect and Criticality Analysis) are the main tools to identify possible failures of building components and their effects during life cycle and to make a priority list of maintenance's operation to reduce the probability and the gravity of damns.

According to fig.2, the logical steps of risk identification using FMEA are:

- System analysis, divided in structural, functional and process analysis, in which the building components behaviour is studied;
- Qualitative failure modes analysis, in which are studied the components degradation modes, the causes of degradation and the consequences due to the degradation.
- Result presentation, that is the way to evaluate which are the most suitable maintenance operation to avoid the failure and so increase the durability of building components an the overall quality of life cycle (i.e. corrective maintenance, conditional maintenance, preventive maintenance)

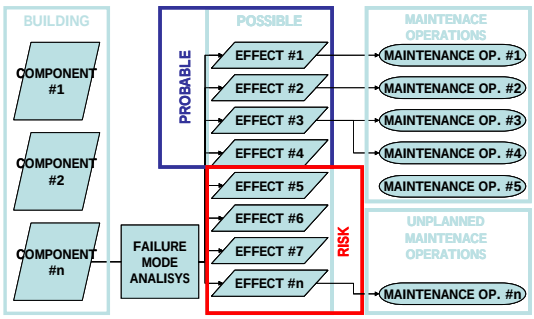

Figure 2. Risk identification using FMEA

The plain use of FMEA technique causes an important problem: every effect is measured estimating only the probability of the occurrences. This approach, in a risk analysis view, means to estimate only one of the two risk parameters necessary to calculate risk dimension. The negative effects of this procedure could be crucial. An

empirical law says that the less is the probability of an event the biggest is its gravity, and that the disasters are often the summarization of a lot of little probable events [Flanagan and Norman, 1993].
The aim is not to protect from all negative events, but to estimate related risk and control them during life cycle.

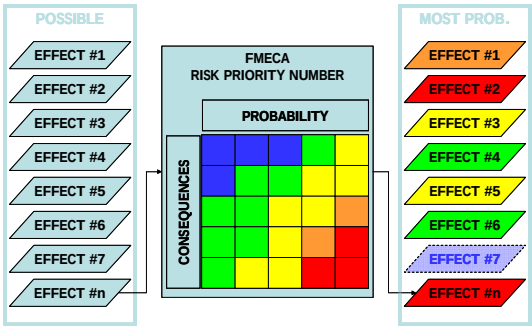

Figure 3. Risk analysis using FMECA

To solve this lack an implementation of FMEA tools was studied, named FMECA. The add value is represented by the implementation of a criticality analysis of the failure mode scenarios and their effects to obtain a risk list organized by priority based on risk dimension. So, both risk probability and risk gravity are measured and a risk priority value is attributed to the failure mode effect, simply multiplying the two previous parameters, as shown in fig.3.
In this way the list of possible effects becomes the list of most probable effects, and their treatments can be planned. In life cycle management it means to plan cost and time of maintenance operations.

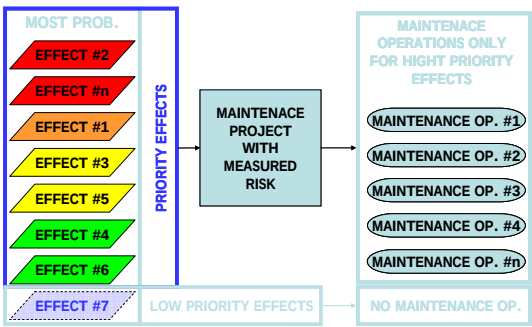

Figure 4. First level risk: errors in risk prioritization

As shown in fig.4 the output of criticality analysis implemented by FMECA is just a priority list of effects that should be treated in the life cycle, to guarantee the global durability of the building's components, but no measures of risk are presented: so, for example, risk 3 and risk 5 have the same priority and it means that is no possible to estimate the reliability of the risk estimation. Which one is better to consider as

first? Which is the error made during the estimation? How much is probable that a yellow risk will became a red one?
To improve the risk analysis, is important to measure each risk dimension considering the possibility of error made by the evaluator and improve a semi-probabilistic method.
The technique here proposed starts from a qualitative assessment of the probability and the gravity of events. In fact, for each dimension different classes that represent a different level of probability and gravity are proposed:

- Probability: form class 1 (very improbable) to class 5 (quite sure)
- Gravity: form class 1 (trifling) to class 5 (catastrophic)

For each class a standard numeric value is associated whose value is the same of the related class (from 1 to 5) and the evaluator, by a direct estimation, chooses the more suitable class for the two risk dimensions.
Though his decision can be supported by his own experience, historical data, and so on, it's always possible he is doing an error. So starting from the chosen class, a discrete distribution of probability is associated to all the dimension's classes (fig.5).

Probability	80.00%	10.00%	5.00%	2.50%	2.50%	100.00%
1	1	2	3	4	5	

Gravity	2.00%	8.00%	80.00%	8.00%	2.00%	100.00%
3	1	2	3	4	5	

Risk estimation
3

DISCRETE DISTRIBUTION

Figure 5. Discrete distribution of risk dimension assessment

%tile	Value
5%	2
10%	3
15%	3
20%	3
25%	3
30%	3
35%	3
40%	3
45%	3
50%	3
55%	3
60%	3
65%	3
70%	3
75%	4
80%	5
85%	6
90%	8
95%	10

In a typical risk analysis the result of the risk measurement presented in figure 5 would be a risk equal to 3 (Probability 1 x Gravity 3). Instead, using the Montecarlo simulation it's possible to calculate the probability of error related to risk estimation (fig.6).
Today implementing a Montecarlo simulation is very easy (a lot of simple software can help to do it) and the benefits coming out are very significant. For the example proposed in figure 5 and 6, it's clear that a risk equal or less than 3 will be possible at 70%, but in other words it means that there is a 30% of possibility that the risk is higher: this information could be critical and is very important for the stakeholders during the risk evaluation.
The advantage is not only to have a risk measured, but also to know which is the attention level that the organization has to pay during life cycle management.

Figure 6. Percentile calculated by Montecarlo simulation

Besides, the knowledge of the variability of the risk estimation makes possible to set up a better monitoring system, that is the way to prevent the negative events or in the worst case to reduce their impacts.
After estimating risk and choosing the treatments, the next step is to schedule the maintenance program to build the economical and financial plan of the life cycle.
To do that it is necessary to estimate time and costs of every operation (the number has been already defined within the risk evaluation).
The risks linked to this phase are of two kinds: first of all the cost could be higher than the estimated cost; then the real moment of maintenance could be different from the period supposed in the plan. The financial consequences of these risks can be dangerous for the organization and for the durability of the building.

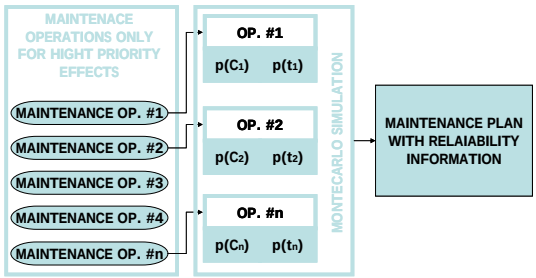

Figure 7. Semi-probabilistic approach for the maintenance time and cost scheduling

The idea is to move from a deterministic approach to a semi-probabilistic analysis and also in this case a Montecarlo simulation is the solution proposed.
First of all a deterministic assessment is made to estimate which is the most probable cost and time for the identified maintenance operation. Then other two values are defined both for cost and time: one that is the optimistic assessment and one that is the pessimistic value.
At the and by Montecarlo Simulation the uncertainty of time and cost is calculated for each maintenance operation planned. In this way a probabilistic relevance is

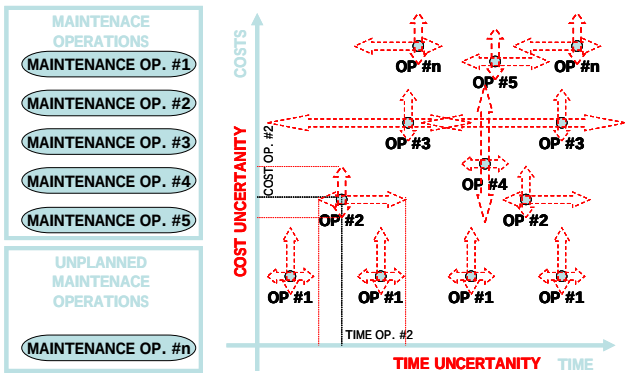

Figure 8. Cost and Time uncertainty in maintenance plan

given to the data loaded into the maintenance plan and the knowledge of the variability of time and cost let the organization to prepare the necessary financial resources for the maintenance operations avoiding ad surprises.

2.4 Case Study

A hotel building in the suburbs of Milan has been selected as the case study for this research. In particular, risk identification, estimation and evaluation has been made for the costs and time uncertainty in the maintenance plan made in the design stage of the building. Figure 9 shows results obtained in terms of reliability of costs forecast for the maintenance plan.
The information obtained by Montecarlo simulation can be use to take decision with a level of risk that is agreed by maintenance planner and the client.

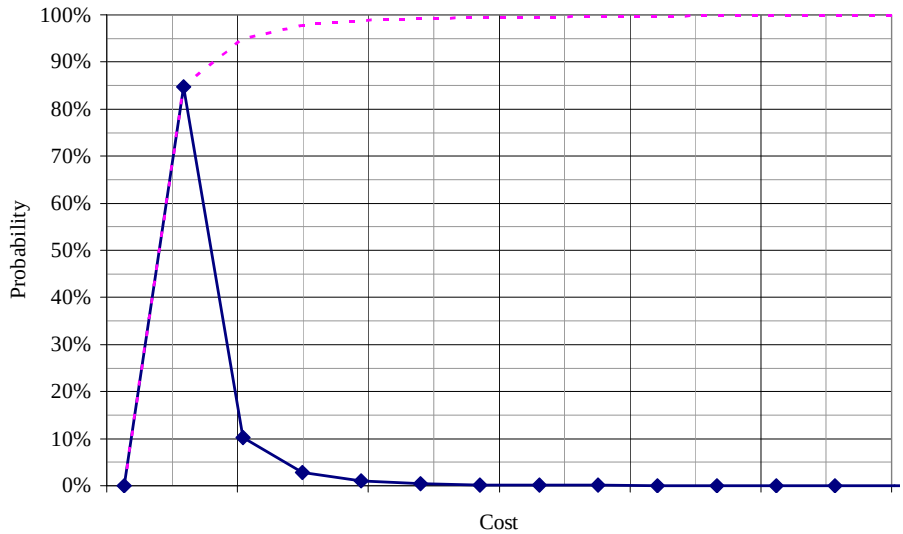

Figure 9. Costs probability of a maintenance plan calculated using Montecarlo simulation

3 CONCLUSIONS

Life cycle management is a risk business. Errors are likely to be done in the whole process and the presented research shows how to deal with to of the most likely. The questions are

- what if an unplanned maintenance operation is to be done? [i.e. what if an error is made in the FMECA process of prioritising effects?]
- what if time or/and costs forecast of a maintenance operation are wrong?

The paper shows how statistic can help practitioner to measure these errors and take more conscious decisions.

4 REFERENCES

Ceric A., 2003, a framework for process-driven risk management in construction projects, Phd thesis.

Flanagan R., Norman G., 1993, *Risk management and Construction*, Blacwell Science

Loosemore, M., Raftery, J., Reilly, C., Higgon, D., 2006, *Risk Management in projects 2nd Edition*, Taylor & Francis, Great Britain.

LIFECOM, 2004, *Validation of LIFECON LMS and recommendations for further development*, Deliverable D 6.1 of EU Competitive and Sustainable Growth Programme

Service Life and Sustainable Design Methods: A Case Study

Johann Mc Duling [1]
Geoff Abbott [2]

T 51

ABSTRACT

The design life of hospitals normally varies between 50 to 60 years. This paper presents a case study of a major academic hospital that reached the end of its service life only 30 years after commissioning due to a combination of unsustainable design methods and inappropriate maintenance levels. Unsustainable design methods, such as long narrow multi-floor structures resulting in excessive walking distances and ineffective flow of patients and visitors, and insufficient structural depth and height, impaired the ability of the existing structure to accommodate changing demands of a modern health care environment, and the maintainability of services, such as sanitation, steam, ventilation and air-conditioning.

According to Ashworth [1996] building materials, components and technology may last for 100 years or more depending upon quality and standards, while engineering services have a life expectancy of about 15 years, and finishes and fittings frequently less than 10 years. Information technology hardware systems "are becoming outdated even after a period of only 3 years." This raises the question of a realistic design life for health care facilities. Should we not rather use a shorter design life to accommodate changing needs in modern healthcare technology and differences in life expectancy?

Inappropriate maintenance levels in addition to impaired maintainability of services due to unsustainable design methods caused premature deterioration to the extent that the facility's condition could no longer support a healing environment, resulting in a need to replace the hospital.

KEYWORDS

Service life, Design life, Sustainable design methods, Maintainability, Maintenance levels.

[1] Senior Researcher: Asset Management, Architectural Sciences, Built Environment, Council for Scientific and Industrial Research, Pretoria, South Africa, Phone +27 83 700 4027, Fax +27 12 349 9700, mcduling.johann@builtcare.co.za

[2] Specialist Research Architect: Health Facility and Asset Management, Architectural Sciences, Built Environment, Council for Scientific and Industrial Research, Pretoria, South Africa, Phone +27 12 841 2542, Fax +27 12 841 3504, gabbott@csir.co.za

1 INTRODUCTION

This paper presents a case study of Tygerberg Hospital, a major academic hospital near Cape Town in South Africa, that reached the end of its service life only 30 years after commissioning due to a combination of unsustainable design methods and inappropriate maintenance levels. Tygerberg Hospital was conceptualised nearly 50 years ago and has been in operation for 32 years. During this time the community served and service required have changed as have health service delivery and medical training philosophy and practice, medical technology has developed substantially, and new technologies such as ICT have evolved. Unsustainable design methods, such as long narrow multi-floor structures resulting in excessive walking distances and ineffective flow of patients and visitors, and insufficient structural depth and height, impaired the ability of the existing structure to accommodate changing demands of a modern health care environment, and the maintainability of services, such as sanitation, steam, ventilation and air-conditioning. At the same time maintenance has been wholly inadequate and the condition of the buildings has deteriorated significantly. Many of the technical and engineering systems have also reached the end of their design life.

Tygerberg currently operates as an academic institution with 1 290 commissioned beds, some 600 fewer than the original design provided for when built in the early 1970's. The facility has some 74 buildings totalling some 312 000 m^2. Not all the buildings are currently used as hospital buildings. The main block is some 218 000m^2 and is 15 storeys high.

2 FACILITY ASSESSMENT

During 2005 the Council for Scientific and Industrial Research [CSIR] was commisioned to undertake a high level options review of Tygerberg Hospital aimed at identifying and quantifying the implications of redeveloping the facility from its current service to its planned use in terms of the 2010 Health Service Plan for the Western Cape. The study was confined to the administration block, the main hospital block, mortuary, oncology unit, boiler house, pump house and main electricity substation as well as the interlinking site engineering services reticulation.

The provision of health services at Tygerberg Hospital is influenced by the physical design of the facility, the current condition of the buildings and services infrastructure and the way in which the facility is currently being operated and maintained. The review covered, therefore, both an assessment of the existing structure in terms of its current use, condition, functionality and suitability as well as of the potential of the existing shell for redevelopment. As such the study provided the platform for the development of options for redevelopment.

A wide range of issues were identified in the study pertinent both to the development of options for the redevelopment of Tygerberg as well as important for the ongoing operation of the facility in the interim period while the selected strategy is being implemented. Should the existing facility be retained, the location of some departments will need to change as existing relationships between departments are not always ideal and many departments would need to be remodelled to a greater or lesser extent to accommodate more efficient planning, new service requirements and general upgrading.

A range of condition and non-compliance issues were highlighted by the assessment team as needing either critical or urgent attention. Critical issues included soil water discharge pipes and stacks and fire systems, while urgent issues included theatre air-conditioning, vacuum, potable water, lifts, cleaning and various hospital maintenance issues. Measures have been introduced by the Department to address these issues in the short to medium term during the redevelopment process. Some of these will impact on the redevelopment strategy and investment required.

2.1 Physical Assessment

The overall condition of the facility was found to have deteriorated further from the average 3,65 condition established in the 1995/96 National Health Facilities Audit to 3,02 on a 5 point condition assessment scale [5 being very good and 1 very bad] representing an increase in the maintenance backlog over the 10 year period of some ZAR335m [ZAR7 = US$1±]. This average figure hides a range of elements where the condition was found to be substantially worse while in a few areas the condition had improved due to limited recent repairs and upgrading [as in some wards]. While the overall shell of the building, with the exception of the roof, appeared to be in relatively good condition, of primary concern are a number of core systems and elements identified such as the soil water [sewage] system in the building, various mechanical systems including air-conditioning, medical gases and steam systems and some electrical systems such as lifts. The level of maintenance was found to be very low with a lack of planned or preventive maintenance.

The poor condition of key systems and components in the facility coupled to physical design constraints and ad-hoc changes made to the building in use, have led to the situation where the facility, in many respects, no longer meets required service delivery standards or legislated performance safety standards and has reached the end of its service life 20 years prematurely.

2.2 Functional Assessment

The current utilisation of Tygerberg Hospital, at 1 290 beds, is more than 35% below the original design capacity. With the planned utilisation expected to remain at about 1 300 beds, the existing facility measures nearly twice the area per bed than currently accepted as the norm, with significant negative functional and operational implications. There is no clear entrance or point of arrival, and the dual corridor legacy of the original functionally separated design and current scattered location of departments [such as the poor relationship between theatres and ICU's] lead to poor functioning, operating inefficiencies and pressure on staff and risk to patients. The functional layout of wards and ICU's are particularly poor, being constrained by the physical shape of the building and circulation. The design and current use does not allow good operational practice to be adhered to, resulting in high infection risk to patients and staff alike. Of particular concern is the use of the ICU's as thoroughfares from one side of the hospital to the other and various compromises in good theatre practice.

A number of issues were also identified in the assessment where there was concern regarding patient and staff safety through non-compliance with provisions of the Occupational Health and Safety Act [OHS] and the National Building Regulations [NBR]. Areas highlighted in the operational risk and regulatory compliance assessments include fire risk, materials handling, air-conditioning and ventilation systems, finishes, water supply and sanitising equipment and medical gases. Action, identified during the assessment, has been initiated to bring aspects of the facility into line with most requirements of the OHS Act and NBR. Some are being addressed at a management level but many more are fundamental in nature, such as fire compartmentation and shallow buildings unsuitable for modern hospital layouts, and will require major remodelling of the shell to resolve.

2.3 Financial Performance

It is estimated that the current equivalent cost to rebuild the hospital as it now stands is some ZAR1,92bn [including Value Added Tax and professional fees], more than 50% above the current benchmark cost of R1,24bn for a new facility. The estimated budget to reinstate the facility to an acceptable condition is ZAR788m or over 60% of the cost of a new facility. The actual annual current maintenance expenditure of ZAR35m is only 4,6% of the estimated current requirement.

The total hospital [including salaries, administration and medicine] and facility operating costs

[including utilities, steam, security, cleaning, building and equipment maintenance] are 32,5% and 4,8% respectively of the current equivalent construction cost. Facility operating costs are well below benchmark levels as building maintenance, cleaning and security are all well below estimated funding requirements. The balance between facility and service operating costs will change for those options where the total building area is reduced to actual requirements.

2.4 Transient, Alterable and Fundamental Issues

Issues identified during the assessment can be classed into one of three broad categories: transient, alterable or fundamental issues. Transient issues can generally be addressed through management intervention alone and include housekeeping, and some legislative compliance and safety issues, such as blocking of escape routes by stored equipment. Alterable issues generally require minor or major capital work and include issues that can be undertaken without significant, long term disruption to services and include issues such as redecorating or repair of finishes, and repair or replacement of engineering plant or equipment [e.g. air-conditioning, lifts and standby generators].

Fundamental issues affect the basic structure and systems and require major intervention and disruption to normal operation, usually involving major building work at high cost. These include issues such as layout, structure, and replacement of major engineering systems and networks. All three levels are evident at Tygerberg. Many of the problems, such as the shallow buildings and the physical spread of the overall structure [24 km of passages] are fundamental and intractable and can only be addressed through extensive demolition and remodelling of the shell at very high cost.

2.4.1 Design and Layout

Most new wards in modern hospitals have a far more compact layout than those at Tygerberg, see Figure 1 below. There are significant advantages to a compact design including shorter walking distances between patient beds and key work areas [nurses station, clean and dirty utility, etc], better observation of patients by staff, less overall area, better external wall to area ratios and therefore lower cost. A compact ward with a central nurses' station also allows more effective air-conditioning air flow with supply flow from the nurses' station outwards through patient and service rooms.

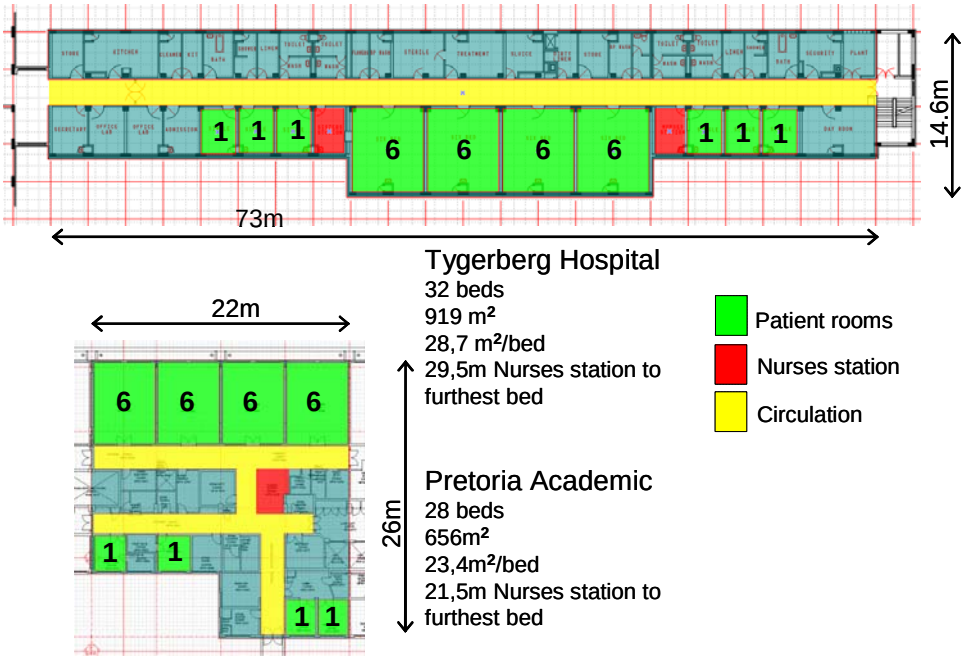

Figure 1: Ward shape comparison

The current elongated layout was designed originally for natural ventilation. Air-conditioning was added but is not working. The location of the plant rooms [at the furthest point from the entrance near the escape stair] is problematic as all maintenance and moving of soiled filters have to go along the length of the ward. The elongated ward required the separation and duplication of some support spaces including two nursing stations [ward secretary at entrance, sister's station and nurse's station along the length of the ward], two sluice rooms [including duplication of equipment], two linen rooms, and main kitchen and sub-kitchen. Control of the ward and observation of patients is problematic and security is a concern. Patients in single rooms towards the end of the wards can easily be forgotten. Many of the wards have their escape doors leading to the fire escape stairs locked for security reasons or open but not alarmed.

2.4.2 Replacement of Major Engineering Systems and Networks

The access to service ducts is from inside the building as shown in Figure 2 below. This makes maintenance and repairs extremely difficult. Removing blockages from sewer pipes is difficult resulting in spillages of waste, sometimes into wards, as shown in Figure 3 below. Replacing sewer pipes can only be addressed through extensive demolition and remodelling of the shell at very high cost. The same applied to the steam and airconditioning installations.

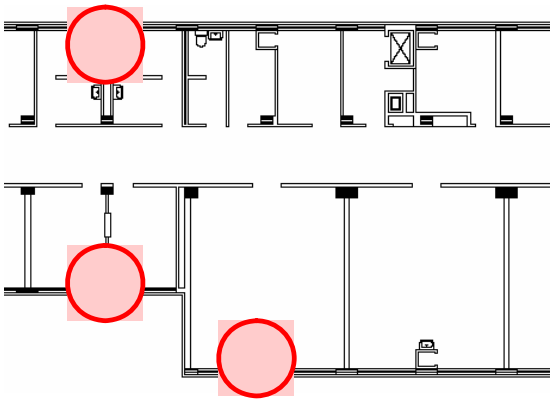

Figure 2: Location of Service Ducts

Figure 3: Duct to Service Duct, Inside Service Duct and External Wall outside Service Duct

2.4.3 Maintenance Levels

In Figure 4 below, the actual average condition of Tygerberg Hospital as assessed during the NHFA and 2005 CSIR assessment is compared to the anticipated change in average condition over time for various levels of maintenance, ranging from no maintenance to a very high level of maintenance. For a health care facility, such as Tygerberg Hospital, a high level of maintenance [the curve second from

the top] would be appropriate. From the graph it can be seen that the 1996 NHFA and 2005 CSIR Assessment average condition of Tygerberg Hospital falls on the low maintenance curve.

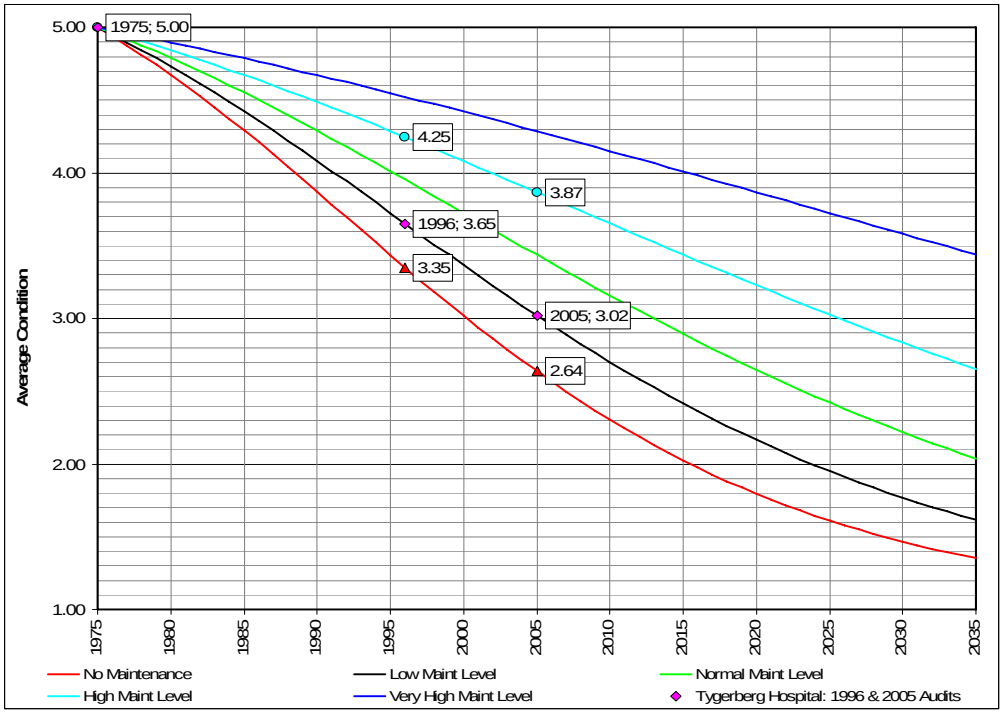

Figure 4. Anticipated Average Condition over Time vs Level of Maintenance [Mc Duling, 2006]

The anticipated average condition of Tygerberg Hospital should have been around 3.87 for a high level of maintenance and 2.64 for no maintenance. The consequences of the inappropriate level of maintenance amount to R428 million more required now than what should have been the case if the facility was properly maintained [high level of maintenance].

3 OPTIONS DEVELOPMENT AND APPRAISAL

In order to address the primary concerns identified in the assessment study, three broad redevelopment options, outlined below, were identified for further development, costing and evaluation. The results of the assessment and the options development study were presented at a workshop of key role players from the Hospital, the Medical Faculty and the Departments of Health and Public Works. The advantages and disadvantages of each option were reviewed and a high level of consensus reached that Option C, for a new facility, would provide the best solution.

3.1 Option A – Rehabilitation

This option involved the reuse of the existing hospital buildings with minimal alterations and upgrading, sufficient only to address areas of critical interventions identified in the assessment and to create separate level 2 and 3 management units. This option was not supported as, while the capital costs and relative speed of delivery are lower than other options, most of the inherent constraints, costs and inefficiencies of the existing shell would remain and, as the area will still be far more than required, operational costs would be far higher than other options, leading to substantially higher operational costs in total.

3.2 Option B – Remodelling

Option B involved the reuse of the existing shell with extensive remodelling to address key functional, condition and compliance constraints identified in the assessment. Entrances, circulation and layouts would be rationalised and many features of a modern hospital could be built into the design. While the solution would have offered a workable hospital within the existing shell and the net present value [consolidating capital and operating costs over a 10 year period] would be slightly less than for a new facility, the solution was not supported, as there was still a significant legacy cost to the remainder of the shell and the severe disruption to hospital operation, patients and academia during remodelling.

3.3 Option C - New Facility

Option C involves building an entirely new facility on the same site and either the demolition or reuse of the existing facility for a new function. While this solution has higher capital costs, operational costs will be the lowest of the three options and over a short period the solution will become far more economic than working with the existing facility. This solution was supported for further development as it offers the most effective financial and functional solution and has the major advantage in that all construction work will be separated from the running of the existing facility.

4 CONCLUSION

Tygerberg Hospital reached the end of its service life only 30 years after commissioning. The design life of hospitals normally varies between 50 to 60 years, which means between 40% and 50% of its design life has been lost.

Building materials, components and technology may last for 100 years or more depending upon quality and standards, while engineering services have a life expectancy of about 15 years, and finishes and fittings frequently less than 10 years.

This raises a number of questions around a realistic design life for health care facilities. Should a shorter design life not rather be used to accommodate changing needs in modern healthcare technology and differences in life expectancy? Can we really plan for 50 to 60 years when technology develops at a mind-boggling rate? Why plan and design for 50 to 60 years if after 30 years new healthcare needs render the facility unsuitable? Should we not rather use a shorter design life to accommodate changing needs in healthcare technology?

REFERENCES

Ashworth, A., 1996. Assessing the Life Expectancies of buildings and their Components in Life Cycle Costing. Cobra ’96, Royal Institution for Charted Surveyors.

Capital Investment Manual: Business Case Guide, 1995. London: HMSO

Design Brief Working Group, Richard Burton [Chairman], 2002. “Advice to trusts on the main components of the design brief for healthcare buildings.” NHS Estates, Department of Health, July 2002.

Mc Duling, J.J., 2006. Towards the Development of Transition Probability Matrices in the Markovian Model for the Predicted Service Life of Buildings, PhD Thesis, Department of Civil and Biosystems Engineering, University of Pretoria, South Africa.

Smart-ECO – Developing a Construction Sector Vision and Related Requirements for Sustainable Eco-buildings

Jean-Luc Chevalier[1]
Hywel Davies [2]
Christer Sjöström [3]
Wolfram Trinius [3,4]
Gurvinder Singh Virk [5,6]

T 51

ABSTRACT

The EU project Smart-ECO brings together experienced organizations spanning the full range of stakeholders covering the area of sustainable building. These include universities, R&D organizations, companies developing, supplying and using innovative technologies, consultants, users, government and policy makers. Smart-ECO uses this core partnership together with a wider stakeholder group community to focus on global issues of sustainable building to identify and evaluate priorities for current and future RTD activities. Activities and policies are due to be mapped to identify gaps and to focus future efforts. Innovative technologies, as well as improvements of the construction process, and their introduction into the building sector will be considered in relation to sustainable development, life performance, ambient intelligence, and other relevant stakeholder concerns.

The project focuses on routes and means to enable the uptake of efficient technological and non-technological innovation that in turn enable the building and construction sector to meet the requirement for sustainable building. The current situation and the vision of a more sustainable built environment sets the frame for the appreciation of the long term effectiveness of Eco-buildings and innovative technologies, especially renewable energy systems. Together, the vision and relevant EC policies will serve as a reference framework for the analysis of life performance aspects of innovative technologies applied to realise more energy efficient and more sustainable buildings.

This paper presents and discusses the process of establishing a reliable vision for sustainable buildings and related performance requirements.

KEYWORDS

sustainable building, vision, Performance requirements, Stakeholder involvement

[1] CSTB, 24 Rue de Fourier, 38400 St-Martin-d'Hères, France, jean-luc.chevalier@cstb.fr
[2] Hywel Davies Consultancy, 2, The Furlong, Bedford MK41 8EE, UK, hywel@hyweldc.co.uk
[3] Centre for Built Environment, Materials Technology, University of Gävle, SE-801 76 Gävle, Sweden, Phone +46 70 546 59 16, Fax +46 26 64 81 81, christer.sjostrom@hig.se
[4] Ingenieurbüro Trinius, Dorotheenstr. 21, 22301 Hamburg, Germany, Phone +49 40 2275 9430, trinius@trinius.de
[5] Endoenergy Systems Ltd, Sheffield, South Yorkshire, UK. gsvirk@endoenergy.com
[6] School of Engineering and Advanced Technology, Massey University, Private Box 756, Wellington, New Zealand, g.s.virk@massey.ac.nz

1 INTRODUCTION

Smart-ECO is the acronym for the EU-FP6-project "Sustainable Smart Eco-Buildings in the EU". The project started in October 2007 and is conducted by a project consortium consisting of 12 partners, led by the Center for Built Environment at Gävle University in Sweden.

Smart-ECO aims to evaluate technical and non-technical innovations relative to their contribution to a vision for sustainable building. Such innovations will only be successful if the potential to implement and apply the new solutions will be sufficiently promising. Consequently, combining these criteria, we will deem any innovation to have promise if it is satisfies the following:

- It contributes to the development that is in-line with the vision for sustainable building
- It fulfils the desired performance requirements that arise from such a vision
- It is perceived as being feasible by a wide range of stakeholders.

To start with, the vision for sustainable building needs to be identified, discussed and anchored with a relevant panel of stakeholders that is wide enough to represent all legitimate views on sustainable development in the building sector. As the building sector is so strongly interlinked with other sectors of the economy (i.e. the energy sector, transport, and labour development and deployment), the perspective applied when establishing the vision needs to be extensive and all-inclusive. The project vision aims to use the current status of sustainable construction within the EU (including the major outputs of previous related EU projects and thematic networks) as the starting point and to set out an ambitious yet realistic roadmap of development.

An extensive stakeholder group has been formed to contribute to the establishment of the vision and to serve as an anchor providing legitimacy to the reference points of the project. The starting point is represented by the current position and described by established practice, current policies, existing standards and EU-directives. An analysis of completed and ongoing research and development projects may provide an indication of the short- and mid-term drivers for development. Strategies and policies addressing other sectors, especially energy and transport, need to be considered as well, as they often address aspects that are relevant to the building sector.

A vision is usually a rather descriptive and qualitative presentation of the ambition. However, specific, measurable requirements and metrics are needed to quantify progress towards successful development of movement towards realising goals in the vision. The potential of technical and non-technical innovations to contribute to such developments can then be discussed and assessed against the requirements.

The later evaluation of innovation will necessarily apply these metrics, after discussion and agreement with the stakeholder group. The evaluation should not only consider the requirements derived from the vision, but should also address other stakeholder concerns. The stakeholder perspective is the core novelty of this approach, based on the project group's conviction that it is essential to successfully bring innovation into application. The implementation of such an evaluation routine itself can be interpreted as a non-technical innovation aiming at enhanced sustainability in the building sector. Likewise the application of assessment methodologies as part of the evaluation of building sector products and services can be perceived as innovative. The project therefore applies a cycle of self-evaluation involving assessment methodologies such as Environmental Life Cycle Assessment (LCA), Economic Life Cycle Assessment (Life Cycle Costing LCC), Service Life Planning (SLP), Life Cycle Management Systems (LMS) or the concept of Performance-Based Building (PBB).

2 THE INTERNATIONAL PLAYING FIELD

The recent United Nations Climate Change Conference in Bali, 3-14 December 2007 clearly brings the international discussions on climate change to the mind and its relevance to sustainability. While ongoing, the expected short term outcomes range to be somewhere between no agreement, continued discussions, or agreement to a reduction target for industrialized countries somewhere between 25 and 40% by 2020. The Kyoto conference and all subsequent conferences and protocols are an excellent example for the international process of policy setting, when international concerns need to be balanced with national and regional interests. However, it seems very likely that the political consensus is moving to embrace significant, concerted international action to address the challenge of a changing climate.

Sustainable Development is a much broader thematic complex, and an EU-project vision for sustainable building must necessarily be embedded in the interpretation of the concept of sustainable development to "sustainability in building construction" and to the regional situation and the regional potentials of the building and construction section in Europe. As an internationally harmonized background, a set of ISO standards is well advanced, and a further series of CEN standards is also under development; with its core content published and available to serve as a reference point (*see "International Standards on Durability and Sustainability of Buildings and Construction Works" by Sjöström, Trinius, Davies and Lair in these proceedings*). The ISO standards discussed in that paper are those directly applicable to the vision-requirements-innovation-evaluation process of the Smart-ECO project presented here, using the ISO standards presented in the companion paper.

Finally, addressing the building and construction sector also results in considering various international Agendas being of relevance, like for instance the Habitat Agenda, and the older but still very relevant CIB Agenda 21 on Sustainable construction.

3 THE EUROPEAN PLAYING FIELD

Giving itself the task to develop a vision for sustainable building in the EU, and to measure the contribution of innovation to that vision requires:

- The expression of the vision and the identification of clearly described measures expressing that vision (requirements)
- The identification of the current state as the "starting point", and the goal status against which we can measure progress towards the vision
- The identification of technical and non-technical innovations that need to be considered, discussed and evaluated in contributing to realising the vision.

Consequently, the current status of the construction sector and the business environment in terms of policies, directives, standards and legislation needs to be scrutinized and expressed to provide a initial starting basis for the Smart-ECO project. At the same time, it is clear that conditions vary throughout the European regions and countries, so that innovation with a promising potential in one region may fail in other regions. Applying what is common practice in one region may be perceived as highly innovative in another. Applying a "national" approach is not the aim of Smart-ECO, as it does not focus on policy setting. However, Smart-ECO is part of a "project cluster" together with other R&D projects, one of which, ECOBUILD, focuses on innovation and policies supporting innovation. Instead, Smart-ECO can adapt to regional differences and commonalities by relating the evaluation of potential impacts of innovation to clearly described characteristics of the built environment, the social environment and the economic environment within which the innovation needs to perform.

The European Construction Technology Platform (ECTP) aims to increase the sector's performance and competitiveness, by analysing the major challenges in terms of society, sustainability and

technological development. Concerning sustainability, the platform's first ambition was to raise awareness among stakeholders and to promote R&D activities bringing human concerns to the forefront (ECTP 2007). Again, these sector ambitions, put together in the Strategic Research Agenda (SRA) are a highly important existing driver, to which the Smart-ECO project should connect.

4 EU POLICIES AND DIRECTIVES

The European Commission communicates white papers, green papers and prepares policies, communications and guidelines, as well as Directives and Regulations in fields that are crucial to the building and construction sector. Besides Directives and Regulations directly aiming at the sector and its products, such as the Construction Products Directive CPD (Council Directive 89/106/EEC) and the Energy Performance of Buildings Directive EPBD (Directive 2002/91/EC), other Directives address sectors that are significant to the building sector, or address cross-sectorial concerns, such as the Council Directive to limit carbon dioxide emissions by improving energy efficiency (Council Directive 93/76/EEC). Specific functional components, such as e.g. boilers, may also be subject to product specific Directives (Council Directive 92/42/EEC), and to the Framework Directive for energy using products.

Following EC policies and Directives, various initiatives and projects may follow, the R&D Framework Programmes are aligned, and standardization and harmonization tasks may be initiated. These overall initiatives set the frames for business development and aim to create the means needed for the industries to develop into the desired direction.

5 TOWARDS A STAKEHOLDER SUPPORTED VISION

In order to apply a sustainability perspective to the appreciation of innovative technologies for the building and construction sector, a vision for sustainable development in construction needs to be established and anchored with requirements from the stakeholders. Determining the vision consists of three components:

- Analysis of the current European status for guiding principles and reference points, which can be drawn from EU policies and Directives, and from RTD and TN projects performed under FP5, FP6 and other initiatives.
- To determine the requirements of the stakeholders that support EU policies on sustainable building together with the indicators to assess the impact of the innovations
- To plan a development pathway for the EU building sector, to meet the vision of sustainable development and address parallel European interests concerning innovation, technology, quality of life, etc.

This vision needs to be developed and "owned" by the stakeholder community. Then it can be adopted to serve as the "guiding light" for the consideration of life performance aspects of adopting innovative technologies and process improvements to be more energy efficient and more sustainable. Ultimately, such a vision will be vital in enabling the assessment, promotion and dissemination of all the new concepts proposed by Smart-ECO as well as other FP5 and FP6 projects.

Elements that can contribute towards achieving a more sustainable construction sector, and their potential impact if successfully adopted, need to be identified. Smart-ECO will investigate the approaches and results of completed and ongoing international research projects, thematic networks, various EU and international policies and international standardisation activities (in ISO and CEN).

The vision developed for sustainable buildings and the associated metrics developed will form a reference point against which to estimate the potential contribution of the various technical and non

technical innovations which may contribute to it. Research and development projects usually contain an evaluation as well as a dissemination and implementation part, however the criteria for the evaluation is to be set from within the project's own frame. Without disregard to the validity of such evaluations, Smart-ECO will perform new wide-ranging evaluations using the developed and accepted vision as the setting to assess the contributions of the projects and their potential impact.

"Elements" considered can be technological innovations (e.g. PV systems, bio-mass, wind energy generators, solar thermal technologies, smart decision making, etc), methodologies for analysis and assessment (e.g. Life Cycle Assessment (LCA) and Life Cycle Costing (LCC), management concepts (e.g. Life Management Systems), standards (e.g. General Principles of Sustainability in Building Construction), recommendations (e.g. those gathered within the EC thematic network on Practical Recommendations for Sustainable Construction (PRESCO)) and tools (e.g. systems of indicators as proposed by the EC Thematic Network on Construction and City Related Sustainability Indicators (CRISP)).

For the vision to be useful it must be able to be used to determine "useable metrics" based on the requirements to estimate the impact potential of successful adoption of eco-building innovations. The metrics established for the various elements under consideration need to be able to objectively assess vastly differing innovations so that proper comparisons are possible. When it comes to the process aspects and the new approach for designing and planning a project, the same ambition applies, and for instance the results of the EC Thematic Network on Performance Based Building (PeBBu, 2005), and of the European Construction Research Network (e-Core, 2005) will be investigated in terms of assessment indicators identification.

Hence the innovations must be investigated, the metrics to be used in assessing their contribution to the vision defined, and a methodology to estimate the likely impact of the innovation formulated.

Smart-ECO will illustrate how technological and non-technological innovations that have the potential to contribute to the vision can be promoted in order to become successfully integrated into the construction sector. The project will show where and how existing elements can measurably support the vision, how far the building sector can develop towards the vision based on these elements, and indicate what further innovation is needed to meet the aims of the vision. Relevant stakeholders and multipliers (including education and training organisations) will be key targets to whom the project's results will be disseminated. This is a bidirectional dialogue rather than a dissemination of project results.

6 DISCUSSION AND PERSPECTIVES

The building and construction sector is facing significant challenges. Sustainability, Performance-based Building and Performance-based design and facility management processes are key items and strong priority themes describing international trends and drivers for research and development as well as for standardisation, policy setting and market initiatives.

International Standardisation as well as European Standardization develops standards addressing sustainability in building construction. The conceptual anchor is the concept of sustainable development, as laid out in the Brundtland report to the United Nations. With respect to further work of, for example, UNEP, the WTO, etc, the concerns of sustainable development have matured and now not only policies are being set in relation to sustainable development, but also businesses address these concerns. Indeed, it is arguable that the primary driver of the sustainability agenda is now the business community. Consequently, businesses need to, and want to, adopt and communicate sustainability-related issues. International standards aim to define a common basis against which information can be

communicated. With the first sets of standards available, the communication of information between businesses but also between businesses and consumers is being made easier.

Another, even more important, step is the creation of a market for information relating to sustainability. When market actors generate information about their environmental, economic and social "sustainability performance", they do not only want to be able to communicate such information externally, but to use such information in their decision-making within their business.

Building designers, investors, facility managers and users rely on information that is provided from the product chain, from product manufacturers and from service providers. Whenever a building is the object of for example, an environmental assessment, information about all its constituent parts, plus information about the building itself and its context is needed. At the same time, manufacturers and providers will often only generate the information where they see a larger scale of application.

Any decision-making that takes account of sustainability information will usually rely on the capability to express targets or goals for sustainability aspects of a service, product or building. Decision takers need to be able to express goals, to relate information to these goals and to make balanced judgments of decision alternatives. Such decision-making necessarily involves the consideration of the functionality and the performance of the object. ISO/FDIS 15392 states "sustainable development of buildings and other construction works brings about the required performance and functionality with minimum adverse environmental impact, while encouraging improvements in economic, social (and cultural) aspects at local, regional and global levels". With this, the concept of performance-based building and performance-based facility management becomes an integral part of sustainable building. The concept is open to involve the anticipated business-model move from cost-based construction through service-based construction to value-based construction (Haagenrud 2007), all depending on the concerns for which performance requirements can be expressed and handled in the decision making processes.

The management of sustainability-related information as well as the management of performance requirements gains a significant role when striving to bring the construction sector towards sustainability. The current habit of re-entering more or less the same information up to seven times (Haagenrud 2007) provides for errors and causes cost. The information communicated to decisions makers relative to sustainability aspects is substantial in quantity and complexity. Databases fed from relevant and reliable data sources, on the basis of an agreed data set, paired with communication formats and interpretation aids are elements of the route currently being pursued in R&D and standardisation activities. Object-based generation of information, related to the decision alternatives as well as to the decision context of decision takers is suggested to be a powerful support on the route from "required sustainability", through designed and constructed to "delivered sustainability". The challenge for ICT structures facilitating the information, is naturally the content and the knowledge provision, where the implementation of performance based standards for sustainable construction are the key to pursue a sustainable value-based construction sector (Haagenrud 2007 and *EU-project STAND-INN –Integration of standards for sustainable construction into business processes using IFC standards* in these proceedings).

The ultimate and again very significant milestone on the route to achieving a more sustainable built environment is to enable the building user to operate the building in a way that it can actually achieve its intended performance in practice. For the Smart-ECO project, we entitled this last milestone as "smartness" – claiming that a high performance building may still be a failure if the users, whether professionals or private, do not have the capability or the information required to operate the building as intended, or as foreseen when designed. Bordass and Leaman have published extensively on the problems of user interactions with buildings, most recently in Leaman and Bordass (2007) but also in Derbyshire et al (2001).

At this point, let us redirect our attention to the Smart-ECO project presented here. Reflecting the above, Smart-ECO aims to

- establish a vision for sustainable building
- translate that vision into requirements
- apply the requirements in terms of indicators in the evaluation of innovation
- communicate the potential contribution of innovation to towards the vision

Throughout this process, stakeholders representing the various demands and interests of the building and construction sector, including the users and policy makers, are given not only a significant influence as a reference panel, but are given an active role in the establishment of the reference terms, requirements and indicators of the project.

REFERENCES

CIB *Agenda 21 on Sustainable Construction*, Report publication 237 July 1999

ECTP *Strategic Research Agenda for the European Construction Sector. Implementation Action Plan*. July 2007, www.ectp.org

E-Core (European Construction Research Network) *E-Core strategy for Construction RTD* May 2005
PeBBu (Performance Based Building – thematic network) *Performance Based Building: Conceptual Framework*, October 2005

Council Directive 89/106/EEC, *Council Directive of 21 December 1988 on the approximation of laws, regulations and administrative provisions of the Member States relating to construction products* (89/106/EEC)(OJ L 40, 11.2.1989, p.12)

Directive 2002/91/EC, *Directive of the European Parliament and of the Council of 16 December 2002 on the energy performance of buildings*

Council Directive 92/42/EEC, *Council Directive of 21 May 2992 on efficiency requirements for new hot-water boilers fired with liquid or gaseous fuel*

Council Directive 93/76/EEC, *Council Directive of 13 September 1993 to limit carbon dioxide emissions by improving energy efficiency*

Haagenruud 2007, workshop presentation "*Getting the construction sector lined up for sustainability*", US – EU Experts Exchange on Innovation, Brussels, December 2007

ISO/FDIS 15392:2008, *Sustainability in building construction – General principles*, Geneva 2008
Leaman and Bordass "*Are users more tolerant of 'green' buildings?*" Building Research and Information, Vol 35(6) November/December 2007

Derbyshire et al "*Post Occupancy Evaluation*" Building Research and Information, Vol 29(2) March/April 2001

Durability in Technology Design

Jacopo Gaspari [1]

T 51

ABSTRACT

The achievement of a sustainable dimension in contemporary architecture is a challenge that engages both its design and materials, components, systems the building is made of. Nevertheless durability is, nowadays, more than a requirement in the design phases. As a consequence the concept on which the building is based is deeply connected with the expected lifespan. No sustainable requirements can be correctly evaluated without using an Extended Life Cycle Cost (ELCC) approach.

This research is based on the idea that part of a sustainable approach is aimed at a building lifetime in which its quality could be preserved. Starting from this point of view durability is intended as the skill of a building to maintain efficient and functional its features in the time.

Lifespan can be influenced by the technology used, the maintenance and rehabilitation activity, the random events. The problem has been examined from a technological point of view. Masonry, concrete, steel, wood technologies present different expected lifetime. The growing complexity of the contemporary project leads to new requirements related to durability and performances.

The design activity plays a central role in the contemporary building process. Some case studies are used to analyse a new possible trend in building conception. This trend identifies some “permanent” and “reversible” elements in the building. The first ones are those, like the primary structure, the service core, the technical spaces, whose role and performance in the construction can be considered the same for all the lifetime. The second ones are those, like a cladding system or a climate control device, that can be changed in order to obtain an higher level of performance. Consequently the design activity has to foresee two different levels of durability which correspond to a more adaptable and sustainable use of technologies and materials.

KEYWORDS

Lifespan, Design, Permanent, Reversible, Adaptable.

[1] IUAV University of Venice, Architecture Faculty, Venice, Department of Construction of Architecture, c/o prof. G. Zannoni, Dorsoduro 2206, Convento delle Terese, Venice, Italy, Phone +39 349 4534457, gaspari@iuav.it

1 INTRODUCTION

Durability is a concept that has deeply changed its meaning during the time. Not really in its inner meaning that is still connected with a long period of time, but rather in defining the span of this time. In ancient times buildings were supposed to last for centuries, nowadays we design our buildings with a different approach. They have to reach their higher durability in relationship with the performance they've been built for. So durability is a matter of materials and components, but also of a design approach and of a technological choice. A cultural change is occurring in the world of building construction. Achieving a sustainable dimension in architecture, as part of a suitable sustainable future, has become a need, no more a desire of a limited part of the society. A sustainable construction is a challenge that is not only connected with the idea of an energy conscious building or a reduction of environmental costs during its realization, but also with the idea that the impact of building process conception would deeply influence both the design phases and the management ones.

In this topic, innovation technology, translated either in new concepts or applications, plays an important rule. A theoretical analysis of innovative contributions in building process using the Extended Life Cycle Cost (ELCC) method has been developed. This study aims to define new sustainable requirements and, basing on a comparative process of design methods and technologies used, to upgrade the assessment action with tasks related to design phases and management, maintenance and rehabilitation ones[1]

2 BUILDING PROCESS AND SERVICE LIFE

2.1 Durability and Quality in Technological Choice

When innovation is associated with the world of constructions its meaning is often linked with new materials or new systems.As Martin Pawley reminds [Pawley, 1990] some new materials and techniques have led to epochal changes in building construction, nevertheless another kind of innovation silently feeds evolution of buildings' world. It has been defined "the invisible technology" [Sinopoli, 1997] and it concerns both design and construction process. It has been called invisible because it isn't linked to the use of new materials or components, but it is the result of the relationship between the different "actors" involved in the building process. Their contributions start with the building conception, pass through its construction, management, use and end when the building has expired his time.

Durability involves all these phases and must be considered not only for what concerns the behaviour of materials and components during the lifetime of a building, but also when the building as a whole ends to work. A growing sensibility in contemporary building design is leading to foresee what it'd happen at the end of its lifetime, with the so called "deconstruction activity". This new task is strictly connected with the time a construction system is expected to preserve his quality. Quality is a concept which has been evolving during the time with the introduction of new requirements and functionalities involving sustainable strategies. For a technological system, durability can be intended as the skill of a building to maintain efficiently its quality, features and functions during the time [Manfron, 1995]. This can be deeply influenced by the materials used and by the construction methods.

To analyse the quality of a building as a whole means essentially to verify the technological solutions adopted in relationship with the expected lifespan [Manfron, 2005]. Technological choice is one of the most important elements which can influence lifespan. Masonry constructions, like most of historical buildings, may have an Expected Life Cycle ($E_{xp}LC$) of about 500 years, concrete and steel structures an $E_{xp}LC$ of about 300 years, balloon frame an $E_{xp}LC$ of 50-100 years, Hi-Tech is supposed to have an

[1] For this reason a research program that joints innovation technology, sustainable construction and assessment methods has been activated at IUAV University of Architecture in Venice. Part of this research is led in partnership with the PHD Technology School involving IUAV, Ferrara University of Architecture and Cesena University of Architecture.

E_{xp}LC of 50 years. These elements suggest how deep is the link between technological choice and durability and how the concept of durability can be different.

As an higher level of durability is not a direct consequence of an implementation of technological complexity, most part of this research concerns the assessment of recent technologies application, like assembled construction or Hi-Tech, trying to understand how they can influence the behaviour of the building with the passing of time. As a consequence the attention to the design activity has grown and the conception of the building has become the central point of the analysis.

2.2 Cost and Requirements in the Extended Life Cycle

The conception and the design weight strictly depend from the point of view the building process is examined. In preliminary phases, we are used to assess a project through costs evaluation which often involve only economic reasons. Otherwise, evaluating a project, environmental, social, cultural and energy costs, etc., must be considered too [Odum, 1997]. The Generalized Cost Equation (GCE) [Manfron, Siviero, 1998] summerizes costs as follows: $C_{gen}= C_c+C_m+C_{ma}+C_{re.}$ Where C_{gen} is generalized costs, C_c is construction costs, C_m is management costs, C_{ma} is maintenance costs, C_{re} is random events costs. All these factors can be specified in other sub-cost factors. Construction costs, for example, can be expressed as the addition of planning costs, site costs, design costs, building costs, etc.

These factors, typical of the preliminary phase of building process, involve mainly the promoter, the general contractor, the design team and the builder. All these "actors" share the interest to minimize, from an economic point of view, the so called Initial Costs (IC) which can be synthesized as follows:
IC = PC + FC + DC + BSC + CC + … Where PC are the planning costs, FC are the financing costs, DC are the design costs, BSC are the building site costs, CC are the construction costs. For all the actions connected to these cost factors a list of sustainable requirements can be set [Table1].

Table1. List of sustainable requirements set for the "actors" involved in the construction process.

Planned measures to minimize construction accidents
Planned measures to minimize construction time
Prefabrication/industrialization
Fast transport and packing
Reduction of the waste production during the construction and deconstruction phases
Reduction of the use of energy and raw materials
Simple and fast construction/deconstruction
Waste management on site

The above list represents only a part of sustainable requirements which can be associated with a building process. Many other elements can be added analysing the project from different points of view [De Capua, 2002]. A specific list of sustainable requirements concerning durability can be set up [Table2].

Table2. List of sustainable requirements concerning durability.

Reliability
Controllability
Maintenance
Reparability
Replaceability

To satisfy durability requirements is a matter of technological choice, material and components quality and use. As a consequence the design team has the responsibility to increase the quality of the project to reach a sustainable dimension of the building as a whole, but all the other "actors" involved have to share the additional costs (not only economic ones) that derive. Unfortunately the decisional power of

the different "actors" involved in the process is very different. Investors operate following economical goals which, for example, may be far from social interest. For this reason a cultural change in building design is occurring.

To have a sustainable vision of the process, the building behaviour must be analysed in its extended life cycle. When the building is completed, Lifespan Costs (LSC) involve owner, administrators and users, but some Long Term Costs (LTC) still have to be borne by society. To achieve a sustainable process means to minimize the Extended Life Cycle Cost equation [ELCC]. To reduce LTC means the growth of other factors, like design costs, in the Generalized Cost Equation (GCE).

3 DURABILITY AND INNOVATION TECHNOLOGY

3.1 Sustainable Design Methods

The reduction of LSC and LTC is strictly connected with the way the building has been thought. This probably means a more complex design activity (aimed to provide a higher level of performance to the building) rather than the use of a high level of technological solutions. LSC and LTC are expressions of how quality and durability have been considered at the moment of the building conception. A sustainable design is a project in which conscious choices are taken foreseeing a specific level of quality and durability for the building. These performances must be evaluated with an Extended Life Cycle Cost Analysis (ELCCA).

The choice of a specific technology or of a particular construction method can influence lifespan modifying the expected lifetime from 50 to 500 years. Nevertheless, when a technology has been chosen, some other factors can influence lifespan. Lifespan can be influenced by:

- Maintenance – which is not only connected to reliability, but also to the design concept, to the durability of materials and components and the way their joins have been done. In Hi-Tech and complex assembled buildings, maintenance costs include also the scheduled check activity on the components and the system behaviour.
- Rehabilitation – which allows, with the necessary transformation, to adapt the building to host new functions and to reach a longer lifespan.
- Random events – which represent all those catastrophic events like fires, earthquakes, collisions that can involve a building and modify its expected lifetime.

All these factors are closely linked to durability and each of them can also bring a level of transformation in the features of a building with a different corresponding influence in the Generalized Cost Equation. For these reasons the design phases are increasing their complexity and importance in establishing the durability of components, materials and technologies [Campioli, 1993]. When the Centre Pompidou was built, Hi-Tech solutions were considered innovative for the flexibility in the use of the inside spaces and also for the structural and technical choices, but the building wasn't supposed to bear a so deep change in energy consumption. The increasing of oil cost has brought to a different approach in thinking building conception and process.

Nowadays, in many international competitions design teams are asked to guarantee to their project a durability of, at least, 100 years without any extraordinary intervention. A new sensibility towards a sustainable approach is growing also in promoters and owners who ask to associate environmental features to architectural characters.

Contemporary buildings, e.g. the Swiss Re Tower in London by N. Foster, are thought to minimize energy loss, maintenance costs and especially running costs. This has led to another kind of innovation which regards, as in the Buckminster Fuller's projects, the idea of a synthesis between building design and technological performance.

In the Swiss Re Tower example, the reduction of running costs concerning climate control is obtained by a design conception which allows natural ventilation. Each floor-plate is rotated respect the one below, this allows to the space between the rating fingers of each floor to combine forming a spiral which help the climate control through a natural ventilation. This is reflected by the spiral design of the outside glass skin of the building [Fig.1]. The outside form is derived from a circular, radial plan which generates a profile that widens as it rises and then tapers towards its apex. The aerodynamic form has been explored in the wind-tunnel to test its behaviour in site conditions [Fig.2].

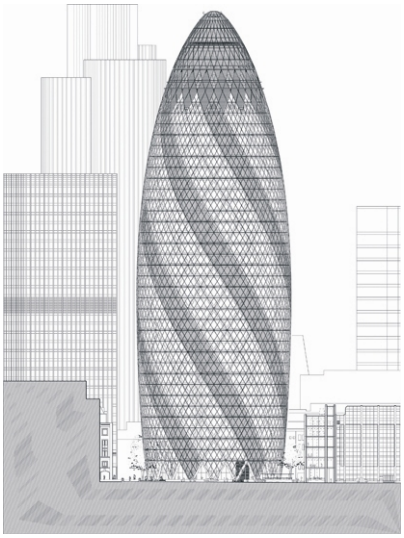

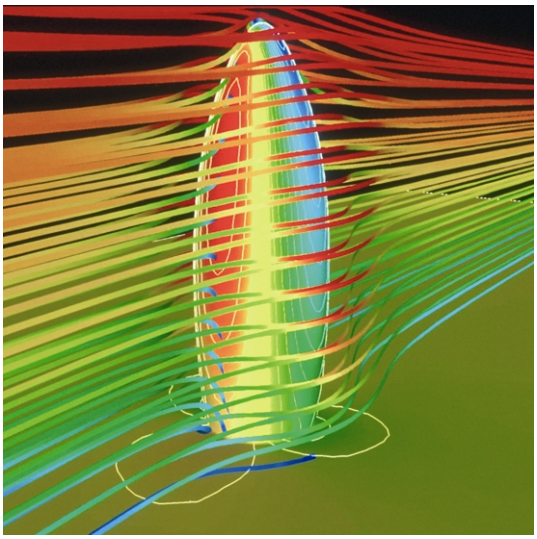

Figure 1. left: Swiss Re Tower, London, N. Foster – Schematic drawings of the spiral elements in the outside glass skin.
Figure 2. right: Swiss Re Tower, London, N. Foster – Diagram of aerodynamic behaviour explored with 3D models to simulate site conditions.

Many other important examples present a similar attention to sustainability and all of them are characterized by a high level of complexity in design phases. In contemporary design activity, part of assessment methods concern not only physical durability of materials (certification of components), but also durability as the skill of a building to survive to its original conception.

3.2 Layer of Durability

The achievement of a sustainable technology in the choice of a construction system is often associated with assembled structures or Hi-Tech solutions. This is connected with the reversible character of this technology and with the idea that the materials and the components used can be disassembled and recycled. Lifespan of this kind of buildings is expected in 100 years both for the deterioration of materials and the loss of performance in the technological system. In this case durability can be increased with a maintenance activity or a rehabilitation action with unavoidable consequences in the balance of Generalized Cost Equation.

On the other side the use of irreversible technologies brings to a negative balance of environmental factors in the same equation. For this reason a great attention is given to adaptable and transformable solutions. A new design approach can be identified working on separate layers of durability in building conception. A hierarchical organization of structural, technical and functional elements can be set as an answer to some specific sustainable requirements. This analysis brings to two different kinds of durability.

A first group of elements belongs to a *layer*, that can be called *permanent*, which is thought to have a long life cycle period (about 500 years) without any meaningful change.

A second group of elements belongs to a *layer*, that can be called *reversible*, which is thought to have a shorter life cycle period (about 100 years) without any meaningful change but also thought to be transformed during the *permanent layer* life cycle.

The use of irreversible technologies to realize permanent elements that last for centuries allows to spread their environmental costs in the long period and to minimize energy consumption connected with these activities. In the meanwhile the use of reversible technologies in the same building allows to foresee an answer to the evolution in terms of functional and technical requirements. Agbar tower in Barcelona for example is characterized by a permanent structure and a reversible skin [Fig.3]. The outside skin seems to envelope the bearing elements.

The tower has been built with an external concrete structure and an internal core [Fig.4]. The steel substructure and the glass brise-soleil [Fig.5] which provide natural ventilation to all the façade, need a scheduled maintenance activity which will bring in the future to a substitution of the skin. At that moment environmental conditions might have had some changes and the technological solution for the skin will need to be updated.

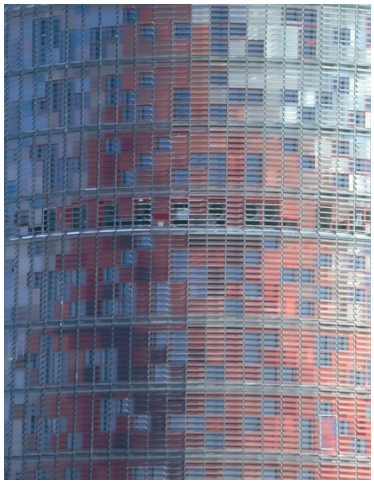

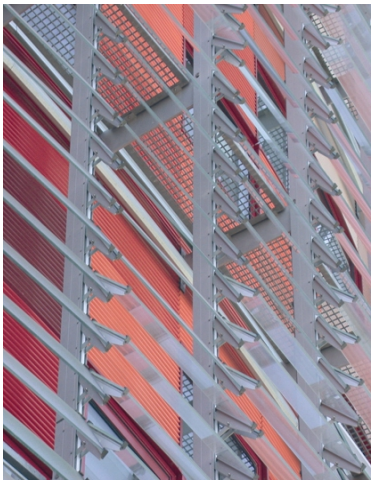

Figure 3. left: Agbar tower, Barcelona, J. Nouvel – View of the outside skin of the tower.
Figure 4. center: Agbar tower, Barcelona, J. Nouvel – A construction phase of the external concrete structure of the tower.
Figure 5. right: Agbar tower, Barcelona, J. Nouvel – Particular of the glass brise-soleil of the outside skin.

In the Agbar Tower example, the choice to have an external concrete structure guarantees to have a great degree of adaptability on each floor, but in the meanwhile forbids any change in terms of relationship with the outside environment. In the case of NET Center Tower in Padua, built with a central core and external steel structure [Fig.6], it's possible to image a different solution for the outside skin.
The glass façade with horizontal brise-soleil supported by a steel substructure [Fig.7-8] can be modified to create a different set of openings and voids in all the height of the tower.



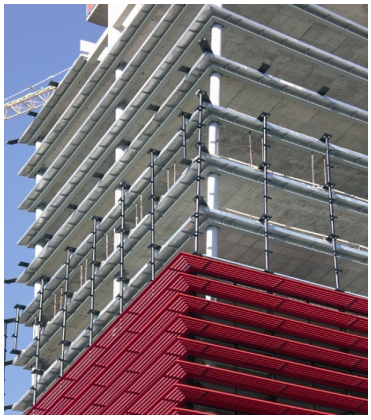

Figure 6. left: NET Center Tower, Padua, A. Galfetti – View of the central concrete core of the tower.
Figure 7. center: NET Center Tower, Padua, A. Galfetti – Detail of the steel supporting substructure.
Figure 8. right: NET Center Tower, Padua, A. Galfetti – The main steel structure, the substructure and the horizontal brise-soleil façade during a construction phase.

Adaptability is improving its importance and the chance to modify the section of different floors is considered as a new requirement in the design conception. In the NET Center case the concrete slabs don't allow a vertical adaptability which, on the contrary, a steel floor would have provided, but match a specific structural answer. As a matter of fact different layers of durability bring to different levels of transformation too. The chance to replace a reversible structure with another can increase the performance of the system, but it can also bring to a deep morphological change of the original conception of architecture. In this case too, the design of the building plays an essential role defining the degree of transformation and giving an architectural identity that can't be changed.

4 CONCLUSIONS

A design activity based on different layers of durability brings to a deep change in the behaviour of a building during the time. The typical behaviour of a traditional building can be represented by a graph [see figure 9] in which there is a progressive loss of performance during lifetime. This loss, represented by a split line ["A"], can be reduced by ordinary and extraordinary maintenance which can be translated in a vertical segment in the split line.

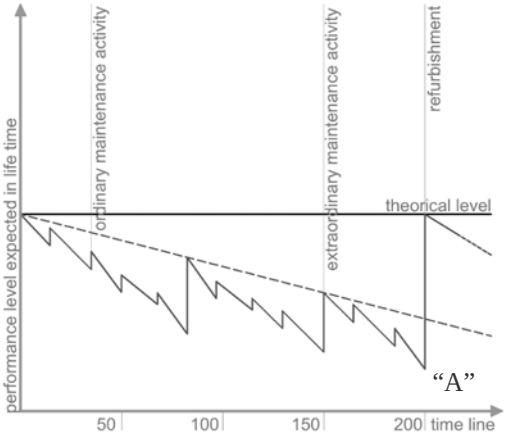

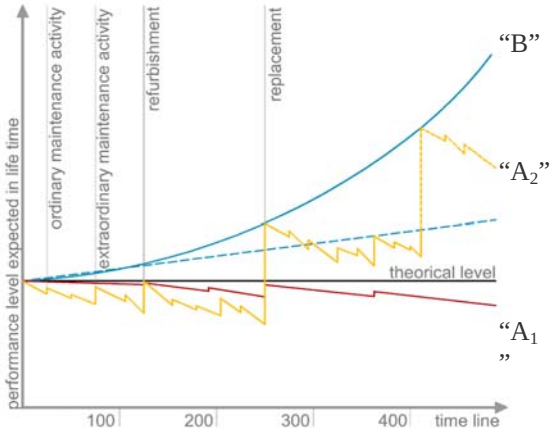

Figure 10.

Each action aims to increase the technological performances of the building, but it's unable to bring it back to its starting condition. This can only be obtained by a refurbishment action when the technological performance level is near to the end of expected lifetime. This action brings to a deep change in the building with costs that can be compared to a new building construction. This graph represents only the physiological obsolescence of the building not the obsolescence deriving from an increasing level of functional or technological requirements.

Nowadays this must be considered a strategic factor. In fact, the growth of requirements linked to energy reduction, adaptable spaces, environmental solutions, etc., cannot be represented by a linear trend, but rather by an exponential one [see figure 10, line "B"]. The design activity has to answer to a really different kind of requirements in the expected behaviour of the building during its lifetime. Building with a *permanent layer* [line "A_1"] and a *reversible layer* [line "A_2"] means to have two different split lines whose trend is really different. The first one is supposed to have a loss of performance during time interval of 150-200 years, the second one during time interval of 50-75 years. This brings to reduce costs of ordinary and extraordinary maintenance concerning the *permanent layer* while allows to invest in modyfing the *reversible layer* to match rising requirements. For what concerns the *reversible layer* ordinary and extraordinary maintenance actions are aimed to preserve technological efficiency not really to increase the performances of the building which can only be reached with a refurbishment action. When the starting technological choice is unable to answer to the growth of requirements, the reversible character of the layer allows to replace some technological solutions with more suitable other ones.

This method gives the chance to extend the expected lifetime of a building and to spread some costs in a longer period of time. Moreover it allows to answer to the contemporary question about adaptable and transformable spaces, but it can also bring to an unrecognizable architecture. When the distance between line "A_1" and "A_2" is high it means that a deep morphological change is occurring and the architectural identity of the building can be lost. For this reason any new design method has to aim at the preservation of architectural identity which represents the highest philosophical meaning of durability.

REFERENCES

Campioli A., 1993, *Il contesto del progetto. Il costruire contemporaneo tra sperimentalismo high tech e diffusione delle tecnologie industriali*, Franco Angeli, Milano,

De Capua A., 2002. *Nuovi paradigmi per il progetto sostenibile. Contestualità, Adattabilità, Durata, Dismissione*, Gangemi, Roma

Manfron V., 1995. *Qualità e affidabilità in edilizia*, Franco Angeli, Milano,

Manfron V., Siviero E., 1998. *Manutenzione delle costruzioni: Progetto e gestione*, UTET, Torino

Manfron V., 'A 2005. Brief About Extended Life Cycle Cost', in *Strategie di architettura per la sostenibilità*, DVD, Brixia Expo-IUAV,

Odum E.P., 1997. *Ecology: a bridge between science and society*, Sinauer Associates,

Pawley M., 1990. *Theory and design in the second machine age*, BlackWell, Oxford, Cambridge,

Sinopoli N., 1997. *La tecnologia invisibile. Il processo di produzione dell'architettura e le sue regie*, Franco Angeli, Milano,

Technological Characterization of the Envelope in Multi Purpose High Rise Buildings

Dario Trabucco[1]

T 51

ABSTRACT

Tall buildings have always been built as totem: in fact, the skyscrapers acted a central role in the city of the early twentieth century and therefore they had to be fully recognizable from all the parts of the city. Their role changed along the last decades becoming in some cities of the world the only viable solution to face the growing price of the land. Skyscrapers are now spread almost everywhere and they are integrating a number of functions at the same time: offices, residences, hotels and public spaces; according to some studies, they seem to be one of the challenges for the sustainable city of the next century. In order to achieve this goal some mistakes have to be avoided. Today's skyscrapers are built as mere glass-boxes where the internal environment is only controlled by air conditioning. Often, they seem to be built without taking into account the constraints given by the setting: sunlight, wind, solar radiation, surroundings (other buildings, views, etc). Moreover, the needs of the users differ according to the purpose of their presence within the building: offices, hotels, residential floors or touristy places are placed one over the other "wrapped" within the same enclosure. Each typology of user requires very particular characteristic by the places he is living in: i.e. the need of light of a worker doesn't match with the light requirement of a person sleeping one story higher; also, the façade facing South doesn't have the same stressors than the one facing North, and so on. The actual way of producing building's enclosures creates discomforts in the users and increase the energy requirements of an high rise building.
This paper analyze the opportunities given by architecture and building technology to characterize the enclosure of a skyscraper in order to improve its performances and meet the requirements of sustainability needed by our culture. An example of regional setting of a skyscraper is provided.

KEYWORDS

Tall building, Envelope, Energy saving, Multi purpose, İnternal comfort.

[1] Iuav University of Venice, Italy, Architect, PhD Student, +39 041 2571287, trabucco@iuav.it

1 INTRODUCTION

In modern cities, tall buildings have the role of pivots, around which the urban shape seems to be developed. Their capacity of marking the land and of declaring from far away the presence of a city makes skyscrapers icons of urban modernity and landmarks for the surrounding areas. The economical and cultural background of the American society of early '900 has to be analyzed in order to understand the role that skyscrapers had within a city.
When they firstly appeared, more than 100 years ago, tall buildings defined a brand new building typology. They were asked to declare, using the language of architecture, the power and the richness of the developer, who had reached that social position through his work and skills; this was the main force that influenced the design of a tall building. Nowadays the design process is still governed by this idea; according to the concept used for decades in the U.S., the skyscrapers are built as an urban uniqueness showing out proudness and sometimes event a brazen behavior. This idea creates figures that stand up over the surrounding areas as totem or obelisk. Since they become the target of everyone's sight they have to be fully recognizable from everywhere; thus, their fronts have an homogeneous design and it's hard to recognize a main façade or a back front.
Tall buildings are now changing their role; it's more and more common that universities, hotels, public administrations or residential enterprises become the tenants of a tall building. Despite the change of tenancies this building typology keeps on representing a landmark for the cities; thus, the symmetric silhouette is preserved in order to allow a full recognizability from every point of the city it is seen.

2 IMPORTANCE OF ARCHITECTURAL AND TECHNOLOGICAL CHARACTERIZATION OF THE ENVELOPE.

Since ever, the rules of the thumb of building practice teach to design a building taking into account the constraints and the advantages given by the site where it will be set. Vitruvio suggested the featuring that a building was supposed to have if it had to be build in the northern regions of the roman empire as well as the characteristics for building an house in the warmer climates. He also gave suggestions on the most suitable disposition of the internal spaces and "technological" advices for building the walls according to the characteristic of the outside weather. Those rules, that characterized 2000 years of building practice across the World, were forgotten when skyscrapers born.
As previously stated, the skyscraper is on obelisk; exactly like Egyptian obelisks are now in the capital cities of many Countries, the unbuilt projects of some skyscrapers can be relocated somewhere else and built in places that have sometimes urban and climatic characteristics very different from the site where they were firstly developed.
The symmetrical aspect of tall buildings often doesn't take into account:
- The sun path: it changes according to seasons and latitude.
- Dominant winds: each place often has a dominant wind that should influence the design.
- Urban context: the existence of other buildings can create problems as: shadows, air turbulence, privacy, outlook.

For instance, considering just the positive and negative effects of the sun, a symmetrical envelope is justified only nearby the Equator line: here the sun position at noon shines the North façade in June and the South one in December, while the East and West fronts are lighted every day at sunset and sunrise. At higher latitudes, this condition doesn't exist and one façade is never lit by the sun all the year long.

3 A NEW URBAN OPPORTUNITY: MULTI PURPOSE TALL BUILDING.

Tall buildings seem to be the main tool to fight the growth of metropolis in several regions of the world and they can provide a real opportunity for building more sustainable cities and conquer better living conditions. In order to fit the urban regulations and to fulfill the requirements of urban zoning, tall buildings are often having multiple uses proposed at a time. All the major cities in the world are experiencing a constant rise of land price that pushes more and more citizens to leave the internal

zones and to look for lower prices and better living conditions in suburbs and satellite cities. The separation of residential places from the working areas of the city has negative consequences both on the individual (the increase in time and cost to reach the office) and on collectivity (traffic, pollution, crashes). With the aim of limiting those stressors on the population several urban interventions are proposing various tenancy typologies included in the same building; sometimes the same building also hosts public functions or leisure areas. The presence of a multiplicity of uses within the same tall building should give the chance to define three-dimensional urban regulations: the surfaces available at height will be adopted as those at street level to provide the space required by the urban zoning policy. The urgency of new urban regulations is particularly clear in some cities of Asia, where the speculative market and the objective need of built spaces makes non-remunerative areas to desappear: gardens, leisure and sport areas, cultural and associative areas should then be placed on the upper floors.

4 PERFORMANCES REQUIRED BY USERS ACCORDING TO THE BUILDING'S PURPOSE OF USE.

As previously seen, it is more and more common to have two or more typologies of users within the same building. Each typology is characterized by some specific aspects that can be seen in table 1:

Table 1: Characteristics of use of the various typologies of users

Typology	Residential	Office	Hotel	Public
Day occupancy	Low	High	None	High
Night occupancy	Medium	None	Medium	None
Human activity	Low	High	Low	Medium
Human heat gains	Low	Medium/high	Low	High
Equipment h. g.	Low with except.	High	Low with except.	High
Moisture	Low with except.	Medium	Low with except	Medium

The requirements and expectations of those typologies of users are often different or sometimes even opposite. The architect can control those aspects since the very beginning of the design process. This is particularly true if one considers the characteristics of lighting, ventilation and shading expected from the envelope of the building, as shown in table 2:

Table 2: Performance required by users. Public spaces are omitted due to the variability of final use.

Typology	Residential	Office	Hotel
Light required	Medium	High	Low
Natural light	Everywhere	As much as possible	In every room
Size transparent surf.	Medium	High	Low
Darkening possibility	Necessary	Optional	Necessary
Operable windows	Necessary	Preferable	Preferable
Openings to outside	Everywhere	As much as possible	View from each room

5 LIMITS OF NOWADAYS DESIGN OF TALL BUILDINGS

The analysis of the characteristics of use and of the user's performance requirements clearly shows that is a nonsense to "wrap" within the same enclosure expectations and requirements that are so different. The architectonic uniformity (or even worse, the technological uniformity) of the envelope causes that each user typology suffers discomfort alternatively: particular attention should be paid at the environmental features of places occupied by people.
In table 3 are listed the main typologies of envelop adopted in tall building construction, and the benefits or disadvantages created in each typology of users.

Table 3: Pros and Cons of several envelope featuring according to user's requirements.

Envelope typology	Pros & Cons for: All	Residential	Office	Hotel
Fully glazed curtain wall	Cons: low thermal insulation. Low thermal inertia .	Cons: low privacy. Low furnishing possibilities. Bad darkening possibilities	Pros: high natural lighting.	Cons: bad darkening possibilities.
Double skin	Pros: improved energy efficiency. Cons: high cost.	Cons: low operability of windows. Difficult management of interspace both for right to use and for cleaning.		
Use of opaque materials	Pros: improved thermal inertia if heavy materials are adopted	Pros: internal ambient similar with traditional housing .	Cons: Lower lighting.	Pros: more comfortable ambient in the rooms.
Absence of operable windows	Pros: lower thermal loss due at leaking . Cons: Claustrophobia, sick building syndrome .	Cons: total discomfort.	Cons: Lower possibilities of controlling the micro environment.	
Permanent brise soleil or shading	Pros: better energy efficiency. Cons: possible noise when windy.	Cons: discomfort due to jail-feeling.	Pros: Better diffusion of light within the internal spaces.	Pros: Better diffusion of light within the internal spaces.
Existence of external balconies or backspaces of the façade	Pros: Better energy efficiency given by the shading effect	Pros: better comfort and improved quality of the built spaces.	Cons: lower penetration of natural light.	Cons: uselessness of the spaces.
Existence of terraces and courts in the sky	Pros: improved quality and value of the building. Cons: high cost for maintenance.	Pros: possibility of use for kid's play and leisure whenever those areas are not available at ground level.	Pros: creation of lobbies and leisure spaces that don't require climatic control.	Pros: creation of lobbies and leisure spaces that don't require climatic control.

6 TECHNOLOGICAL AND ARCHITECTONIC POSSIBILITIES TO MEET THE ENERGETIC PERFORMANCES EXPECTED FROM THE ENVELOPE.

The most effective answer for the issue of the energetic behavior of tall buildings is provided by the choices that can be taken from the very first step of the design process. There are three different approaches:
- "hidden" technological characterization: it is achieved through a technological differentiation of the building envelope conforming it to the performances required and using only invisible features like: selective glazing, different thickness of insulation layers, ventilated façades that have the external appearance of the other parts of the building and so on;
- "visible" technological characterization: it may include some external apparatus like brise soleils, balconies, recessed façades, double skin façades and so on. At European latitude the main issue is to avoid excessive solar heat gain: the best solution is to shade it before the rays enter the envelope. Controlling the size or typology of windows and the presence of balconies is one of the easiest way to protect the south façade from excessive light and solar gain. Also, in order to delay the heat transmission, it is important to provide the walls with a good thermal inertia.

- architectural features: Several buildings have been recently built with shapes that differ significantly from the glazed box we are used to. The goal is to enhance the natural ventilation and the solar shading by the design of the building's silhouette. Braking its volume into smaller parts improves the energy behavior of the building; the chances are: greater light penetration and improved natural ventilation, self-shading of the building, terraces and naturally chilled public places and so on.

7 MULTI PURPOSE TALL BUILDINGS: SUITABLE ENVELOPE CHARACTERIZATION

The design of a multi purpose tall buildings is always an hard task for the team involved, because it requires an enhanced coordination and a very complex decision-making process. Placing three different purpose of use within the same building requires to meet needs and requirements that can totally differ one from eachother. In fact, an office building requires an open plan design with wide spam beams (12 meters or more) in order to provide the maximum flexibility for the offices. Otherwise a residential building will have a thinner shape, in order to provide natural light and ventilation in all the areas of the apartments: the structure will have therefore shorter spams. The same is for hotels; furthermore it has to be considered that all the bedrooms of the hotel must have a view; therefore, the inner areas of the core will be used for public amenities, and a lot of the gross floor area will be non remunerative. Matching all these features in the same building requires to take choices that may vary from case to case. Generally, an horizontal subdivision of the functions is adopted:
- the lower floors will be used for offices, as they require high performances from the vertical circulation system and because they allow the use of wider floor areas;
- the middle floors will be used for residential units, therefore placed away from noise and air pollution coming from the street;
- on the higher floors (which can have a smaller floor surface) there are the hotels that can benefit a better view and a more efficient plan layout;
- the top floors are often used for public amenities (restaurants, sightseeing, etc) or extra-luxury apartments.

Considering the climatic stressors that affect a building, another subdivision of the functions seems to be more suitable: a vertical partition of the building. If we consider the benefits arising from a technological and architectonic characterization of the building's envelope we will understand that those match with the user's requirements of each purpose of use.

Considering those aspects we can find out that the most suitable orientation for residential units is the south façade: here they will benefit from balconies and have normal size windows shaded by the terraces of the upper floors. The act as a thermal buffer for the whole building. The office areas will be disposed with a "c" shape around the central service core and the residential units; therefore they are oriented East, North and West. The North side, entirely glazed, provides natural lighting but it preserves the heat loss using a double skin façade. The East and West sides, quite similar, are distinguished for the presence of terraces on the west side. Eventually, the hotel will be located on the East side; in fact, during the hot season, it can cool down in the evening before guest come for sleeping.
Table 4 shows the possibilities of such a different characterization of the envelope of a tall building. For each direction some environmental constraints are analyzed and a suitable technological solution for the envelop is provided.

Table 4: general principles for the technological featuring of the envelope for a proposed tall building in Paris, La Defence.

	North	East	South	West
Lighting	Soft, it is suggested to foster its penetration in the building.	Medium, early in the morning. It should be diffused within the building.	Strong. Its penetration should be avoided.	Medium, in the evening. It should be diffused within the building.
Solar Radiation	Low. In winter it is suggested to preserve the heat loss with appropriate technologies.	Medium, in the morning. At summer-time it has to be shaded in order to prevent the over-heating of the building. In winter it has to be used for pre-heating the spaces.	Hight. It has to be shaded. Also during the winter it can cause an overheating of the internal areas.	Hight, in the evening. It has to be shaded or its effect has to be delayed through thermal inertia of the enclosure. In winter it can help pre-heating the spaces to avoid excessive night cooling.
Wind	Low, cold in winter. To be controlled and kept out	Low, brings pollution from the city. It has to be kept out.	Low.	Strong. It is cold and humid in winter and therefore it has to be kept out. Cool and clean in summer, it should be used for natural ventilation.
Suitable envelope technology	Glazed Double skin with heat recovery system.	Glazed, with brisesoleil which control and diffuse the natural light. They have to be operable in order to let the solar radiation in the building in winter and avoid it in summer.	Opaque envelope, with an improved thermal inertia. It should include balconies and brisesoleil in order to shade the solar radiation. Small openings must be shaded or regressed from the perimeter.	Glazed envelope with brisesoleil. It is the most suitable side for green terraces and "courts in the sky". It should have wide operable windows to benefit the summer ventilation, It should have a good thermal inertia to delay the summer heating.

8 CONCLUSIONS

Multi purpose tall building represent an opportunity for creating more sustainable and livable cities. Limiting the energy requirements is becoming a prerogative for the feasibility of every human activity: buildings have to be designed keeping this in mind. Therefore it is required to design them, and every part of them, with the idea that the energy consumption is no more just an economic issue but is becoming a social and marketing discriminant. Tall buildings have experienced, since their first appearance, a multitude of major technological and stylistic improvements but they kept on conserving their totemic external symmetry. Giving up with this design anomaly will help in creating more comfortable skyscrapers that will more suitably match the user's requirements and will achieve major energy savings, especially in the summer months.
Multi purpose tall buildings, that are progressively taking a dominant role, especially in the group of super-tall towers, are a viable proposal to solve many problems of nowadays cities. Reducing the spread of the city and augmenting its density and social variability are among the most positive factors in favor of tall buildings and of multi purpose tall building particularly. However, architecture have to

start considering the tall building as a place to live or work in, not (or not only) as a sculptural totemic object. By considering the needs of the users that live within the building the design team could achieve a more differentiated and performing envelope, improving the energetic behavior as well.

REFERENCES

Depecker, P., Menezo, C., Virgone, J., Lepers, S., 2000 '*Design of building shape and energetic consumption*'. In Building and Environment n°36, Pergamon, London,

Pank, W., Girardet, H., Cox, G., 2002 '*Tall Buildings and sustainability*' Faber Maunsell, London,

Raman, M., 2001 '*Aspects of energy consumption in Tall Office Building*', in CTBUH Vol 1 n°3, Lehigh University Press, Bethlehem, Pennsylvania

Yeang, K,. 1996 '*The skyscraper bioclimatically considered'*, Academy Editions, London,

Yeang, K., 1991 '*Designing the green skyscraper*', in Habitat intl vol 15, Pergamon Press, London

Wood, A., '*Mixed use high rise in the uk: an urban renaissance*?', 6th international conference on tall buildings 6th-8th December 2005, Hong Kong

Towards a Framework for Durability Design & Life Cycle Costing of Infrastructure Projects

O. O. Ugwu [1]
S. T . Ng [2]

T 52

ABSTRACT

This paper discusses a study that investigated organizational issues and requirements for improved durability design and life cycle assessment/costing as part of integrated sustainability audit in delivering infrastructure projects. The Hong Kong based study was conducted between 2003 and 2006. The research methods include; questionnaire survey of a cross section of Hong Kong construction professionals (consultants, contractors, clients, and other suppliers), analysis of the responses from the survey to elicit current state-of-practice and identify areas that require improvements, development of framework for durability design and life cycle costing within the broader context of improved sustainability audit, and case study project investigations. The study highlights significant issues that cumulatively impinge on durability design and life cycle costing at the proect level. Conclusions are drawn and recommendations given for the delivery of sustainable infrastructure projects, trugh integarted sustainability audit that subsumee durability and life cycle assessment.

KEYWORDS

Durability design, Life cycle analysis, İnfrastructure whole life costing, Sustainbility audit, Hong Kong

[1] JU Consulting & Research Services Limited, Hong Kong,, Phone +852 95701612, Fax +852 28585104, ougwu@acm.org ; oougwu@yahoo.co.uk
[2] Dept of Civil Engineering. The University of Hong Kong, Pokfulam Road, Hong Kong, Phone +852 28578556, Fax +852 25595337, tstng@hkucc.hku.khk

1. INTRODUCTION & BCKGROUND TO STUDY

Both pubic and private sector clients are now placing increasing emphasis on the need to "design for durability". In this context the underlying objective is to ensure that construction defects and life cycle maintenance requirements are kept to minimum. Consequently designers are increasingly being charged with the responsibility to ensure that a design is durable. Achieving this design goal demands attention to construction process and other critical factors such as the interaction between a structure and its environment, which cumulatively impinge on quality and durability of the structure in use. For example in Hong Kong SAR, the government requires consultants to specify design life for all structures (HKSAR Highways Department 1997). Also in 2001, the HKSAR Construction Industry Review Committee gave several recommendations to improve the construction sector. Some of the recommendations focused on durability aspects of infrastructure delivery. The Tang Report recommendations include (CIRC 2001): (i) (giving) more considerations on the life cycle cost of a building, (ii) developing costing models and tools for the calculations of life cycle costs, (iii) developing a database on the life cycle costs and performance of materials and components, and (iv) developing a common set of accepted performance-based specifications for materials and components.

The main motivation for this paper is to understand current practice in *durability design* and life cycle costing, identify the issues that need to be addressed for improvement, and make contributions that address the identified based on the research findings.

The outline of the paper is as follows: Section 2 discusses the ontological diemension of durability design problem, while section 2 discusses the research objectives and methodology. The findings from indsutry survey are discussed in section 3. A framework for durability assessment and life cycle costing in the context infrastructure delivery, is dicussed in section 4. Finally section 5 draws concluons and gives recommedations based on the reserch findings.

2. RESEARCH OBJECTVES & METHODOLOGY

The main driving research question is: *how do various stakeholders and construction professionals perceive, define and address durability in infrastructure projext life cycle - design, construction, operation and maintenance?* The research questions enacpasulate the objectives. The objectives were: (i) to investigate current practice in durability design and assessment, and (ii) identify the duarability design knowledge sources as well as the the associated problems and difficulties in current practice, and (iii) propose a solution (e.g. a framework) based on (i) and (ii).

2.1 . Questionnaire Design & Emperical Survey

The study began with an extensive review of literature and desiging a quationaire surevy instrument that captured various aspecsts of durability and life cycle costing investigated. The questionaire had 5 main constructs that captured several details including: (i) demogarphic data of the respondnet and organisation, (ii) current approaches to durability design and process-related issues including clients briefing process, assessment in various project phases; and (iii) scope of the assessment. The questionnaire was sent to 60 industry profesionals working in different constructio organisations in HKSAR. A total of 37 completed questionnaires were returned after follow-up commincations with the organsiations and professionals the questionnaires were addressed to. This gives a response rate of **62%**. The next section gives analysis of the results. Table 1 shows the size of repsonding construction organsistions and the scope of porjects they undertake, while table 2 givs a summary of various responses to the constructs in the quationnaire.

2.2 . Analysis of Results

Table 1: Size of, and Scale of Projects undertaken by, responding organisations

		Average cost of projects (HK$)					
Organisation Size (Number of Employees)	**Total Number of Organisations**	**<$10m**	**$10m - $50m**	**$50m - $100m**	**$100m - $200m**	**$200m - $300m**	**>$300m**
<50	5	20.0% (1)	0.0% (0)	20.0% (1)	0.0% (0)	40.0%n (2)	20.0% (1)
51-250	3	0.0% (0)	0.0% (0)	0.0% (0)	33.3% (1)	33.3% (1)	33.3% (1)
251-500	6	0.0% (0)	16.7% (1)	0.0% (0)	50.0% (3)	0.0% (0)	33.3% (2)
>500	23	4.2% (1)	4.2% (1)	0.0% (0)	8.3% (2)	29.2% (7)	54.2% 13)

Note: HK$ is pegged to US$ @ HK$7.8 to US$1.00

Table 2: Summary of Responses (source: analysis of survey data)

Table 2a: Type of organisation

Client (Public & Private sector)	4 (10.81%)
Consultants	20 (50.05%)
Contractors	13 (35.14%)

Table 2b: Organisation uses a system (e.g. guidance) to identify and/or include specific service life requirements in project briefs

Yes	3 (8.33%)
No	33 (91.67%)

Table 2c: Type of Construction Organisations Use

Traditional (Design-bid-build)	27 (72.97%)
Design and Build	17 (45.97%)
Prime Contracting	0 (0.00%)
Design Operate and Transfer (BOT)	1 (2.7%)
Build Own Operate Transfer (BOOT)	1 (2.7%)
Private Finance Initiative (PFI)	4 (10.81%)
Private Public Partnership (PPP)	3 (8.11%)
In-House	1 (2.7%)
Two stage tender	1 (2.7%)

Table 2d: Organisation's Definition of "end" of Service Life

End of economic life	7 (17.9%)
Client definition	4 (10.3%)
Obsolescence of use	10 (25.6%)
Design life	16 (41.0%)
Others	2 (5.1%)

Table 2e: Organisation's Potential Benefits from Clearer Definition of Durability at Briefing Stage

Improved design process	13 (35.14%)
Improved material specification	4 (10.8%)
Planned maintenance scheduling	9 (24.32%)
Improved building regulations	0 (0.00%)
Clearer understanding of project priorities	3 (8.11%)
Improved clarity of client's understanding	15 (40.54%)
Reduced costs of over-specification	13 (35.14%)
Improved quality of execution	1 (2.70%)
Reduced disruption associated with repairs	4 (10.8%)
Clear guidance and allocation of responsibilities	9 (24.32%)
Reduced costs associated with durability failure	7 (18.92%)
Marketing opportunities	2 (5.41%)

Table 2f: Respondents Preferred Sope of Durability Assessement

The whole construction project	11 (29.73%)
Only components whose durability is critical to the performance of the whole system	11 (29.73%)
Those components for which your organization had some contractual responsibility	11 (29.73%)
All components whose durability is critical or important to the performance of the whole construction	5 (13.51%)

Table2g: Organisation's Approach to Service Life in Constrution

Organisation normally decide, or receive, specific details of the required service life of a project	Yes (18;48.65%) No (19; 51.35%)
Organisation use details to differentiate different component types within a project i.e. **localised** (e.g. structural elements, services, facades) or are more **distributed** across the project	Differentiate: **Localised** Components (14) & **Distributed** Components (19)
Organisation use details to differentiate components based on the consequences of	Differentiate: **Localised**

premature failure	Components (14) & **Distributed** Components (19)		
		Optimization between capital and operational expenditure	3 (8.11%)
		Improved risk management	5 (13.51%)
		Speed up decision making	7 (18.92%)

Table 2h: organization would consider paying for durability assessment if it is known to deliver significant savings once the building is in use

Yes	
No	

Table 2i: Respondents' Awareness of Mtools, Guidelines and Methods (i.e Knowledge sources) for Durability Design

Tool/Guidelines etc	***Use***	***Aware but don't' use***	***Not Aware***
BS 5400	23 (62.16%)	3 (8.11%)	11 (29.73%)
BS 5950	22 (59.46%)	2 (5.41%)	12 (32.43%)
BS 8110	23 (62.16%)	3 (8.11%)	10 (27.03%)
Structural Design Manual for Highways and Railways (HKSAR Specific)	21 (56.77%)	4 (10.81%)	12 (32.43%)
In-house service life definition and design procedures	11 (29.73%)	4 (10.81%)	21 (56.77%)

Table 2j: Current Prcatice- Organization assess designs against the service life requirements of the client

Yes	3 (8.33%)
No	33 (91.67%)

Table 2k: Respondents opinion on whether design service life should be checked against the requirements of the brief

Yes	35 (97.22%)
No	1 (2.78%)

Table 2 l: Respondents opinion on whether Organization would accept, or advocate acceptance of increased briefing and design cost if offset by savings in operation and maintenance cost

Yes	6 (16.67%)
No	30 (83.33%)

Table 2m: Respondents opinion on whether Organization would accept, or advocate acceptance of increased briefing and design cost if offset by savings in operation and maintenance cost

Yes	6 (16.67%)
No	30 (83.33%)

3. DISCUSSION OF FINDINGS FROM INDUSTRY SURVEY

3.1 Types of Contractual Arrangements

Table 2c shows that 17 responding organizations (approx 46%) are involved in design and build projects. This is significant as it indicates that they have the necessary flexibility to design for durability providing there exist appropriate incentives and enabling environment that instills the culture of whole life costing in project design and construction, amongst others. The table also shows that the majority of the responding organizations (about 73%) are involved in the traditional Design-Bid-Build contractual arrangements.

3.2: Current State-of- Industry- Practice in HKSAR

3.2.1.Organizations' Identification and Definition of Service Life

However, it is observed from table 2b that only 8.33% of the responding organizations (3 out of 36) use a system such as documented guidelines to identify and/or include service life requirements in the project brief stage. This gap is also very significant considering that identification and inclusion of service life requirement at the briefing stage is a precursor to effective planning and designing for durability of the respective functional components of the infrastructure system. Furthermore table 2d cleary shows different definitions of *end of serive life*. 17.9% see the definition as 'end of economic life" while 25.6% and 41.0% respectively define it as 'obsolescene of use' and d'desgin life'. 10.3% (4 out of 37) look upon the cleint for definition. The result suggests that the concept of whole life costing or life cycle assessment is not well understood and commonly adopted.

3.2.2.Durability Assessment of Design and Construction

Table 2g summarizes the results on the scope of durability and life cycle assessment suggested by the respondents are shown below. The results do not indicate a clear a preference on the scope of durability and life cycle assessment. Almost allthe respondents (35 out of 36) agreed that the design service life should be checked against the requirements of the brief (Table 2k). However, only 3 (8.33%) of them use a system for specifying service life requirements in project briefs and then review whether the design is capable of meeting those requirement (Table 2b). In considering who bears the extra cost assocaited with durabiliy assessment, most respondents (30 out of 36) indicated that their organizations will accept increased briefing costs if its is offset by savings in operation and maintenance cost. Also a 30 out of 36 respondents agreed that their organizations will accept increased briefing and design cost if offset by savings in operation and maintenance cost (Tables 2l & 2m). The results suggest that clear demonstration of the benefits of life cycle assessment will increase industry awareness. This would facilitate the incorporation of durability and life cycle assessment in the the project briefing stage.

3.2.3.Current Approaches to Service Life in Construction & Design Knowledge Sources

Regarding the knowledge sources for durability design (Table 2i), more than half of the respondents used the British Standard design codes (BS5400, BS5950, and BS8110) and Structural Design Manual for Highways and Railways (published for use in HKSAR) in durability design. However, only 30% indicate that they use their in-house service life definition and design procedure and that 60% are not ware if there is in-house service life definition and design procedure in their organizations.

3.3 Benefit of Durability / Service Life Requirement

Despite the conflicting definitions of end-of service life (Table 2d), and the apparent absence of systems to identify and/or include service life requirements in 91.67% of the responding organizations (table 2b), the benefits of clear and unambiguous definition are quite obvious from the responses. The respondents identified the following top 5 benefits: (i) improved clarity o client's understanding (40.54%), (ii) Improved design process (35.14%), (iii) Reduced costs of over-specification (35.14%), (iv) planned maintenance scheduling (24.32%), and (v) Clear guidance and allocation of responsibilities (24.32%). Other high ranked benefits include Reduced costs associated with durability failure (18.92%), speed up decision making (18.92%) and improved risk management (13.51%).

Table 2k shows that, where durability is specified in the project brief, designs are (or more appropriately should be) checked against this specification. Hence to increase the uptake of durability assessment and life cycle assessment it must be led by the client through the briefing process. Finally there is a clear understanding of the benefits of inclusion of durability specification in the project brief and durability assessment of the construction. This shows that the drivers for uptake of durability and life cycle assessment methodologies are present. The next section discusses a framework that addresses the identified process-oriented (methodological) issues.

4. A FRAMEWORK FOR DURABILITY DESIGN & LIFE CYCLE ASSESSMENT

This section discusses a framework that addresses the issues and problems identified in the study as they impact durability design and whole life costing of infrastructure projects.

The framework incorporates different process-level activities. It begins with the Client's Project Briefing and requirements specification. At this stage durability issues related to durability should be clearly identified and outlined in very clear terms. At both the prelimnary and detailed design stages, references should made to appropraie knowledg soiurces inclding design standards, Element audist are perfoenr for the variopus functional elemsnt fop the projetc, and lifec cycle assessment is acrried out. The construction stage considers aspects related to (i) material such as sourcing and storage, (ii) construction process sequence inclusing worksmanship and (iii) quality related aspects of the construction. The operation and maintanance stage (O &M) considers inspection regime and the

frequency of inspectiuo to encure prooer maintainance. Figure 1 delineates the variois costings involved troughout the project life cycle.

In a broder context, the framwork shown in Figure 1, encapsulate the following methodological process steps for durability design and life cycle costing (Ugwu et al 2003):

i. Estimate the construction costs based on each of the possible design configuration options;
ii. Identify recurrent costs. These include relevant analyses of each structural element, along with the cost implications with respect to maintenance, inspection and repair;
iii. Assess risks throughout the life-cycle, including probabilities and potential impacts of each applicable risk factor; and project potential costs accordingly;
iv. Determine the operation cost and recurrent cost relationships;
v. Assess durability: which includes for example, establishing existing environmental parameters, evaluating their effects on concrete design and corrosion maintenance requirements and taking appropriate design decisions; and
vi. Compute the life cycle cost (in terms of the *net present values*) based on above design configurations, and the operation and maintenance requirements.

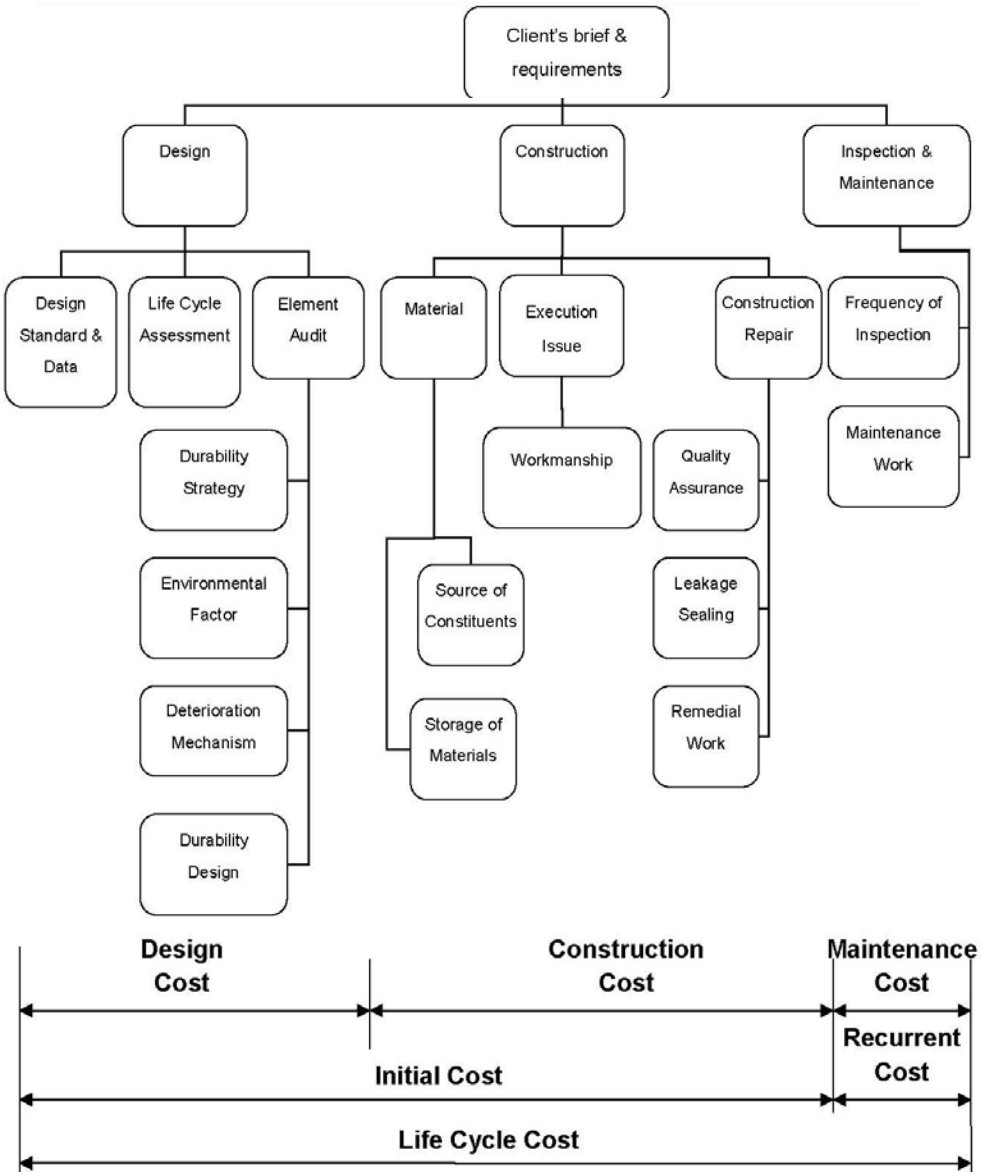

Figure 1: A Framework for Durability Assessment & Life Cycle Costing of Infrastructure Projects

(Ref: Source: Lam 2006 – Framework Adapted from *Ugwu et al 2003 & 2005* and modified for the study scope)

5. CONCLUSIONS & RECOMMENDATIONS

The study highlights significant issues that cumulatively impinge on durability design and life cycle costing at the proect level. The research discussed in the paper shows that some of these issues have *epistemological, process-oriented* and *pedagogical* dimensions. The epistemological dimensions relate to varying understanding and perceptions of durability and life cycle analysis concepts such as *design life* and *service life*. The aspects of ontology dimension investigated in this durbality design problem research focus on the basic level of human understanding, concept definition, and communication. A proper understanding of the contextual definition. interpretation and process-level implementation of durability is critical in achieving the objectives of designing for durability at the appropriate project interfaces (conceptual & detailed design stages). The importance and significance of this ontological dimension to the problem becomes more pronounced in the wider goal of delivering sustainable infrastructure projects. From a philosophical perspective, the ontology question has taken on epistemological dimension. In recent times the scope of ontological and epistemologcal arguement has expanded to the definition of sustainability and all its strategic-level abstract connotations that need deconstruction to design decision-making variables at project levels. Moreover, sustainability is very significantly impinged upon by the durability of constructed physical artifacts, and the impact of durabiity covers several aspects of the internationally accepted *tipple bottom line substantiality envelope*- economy, environment and society. As an illustration, durability addresses **economic** dimension (from point of view of initial cost as well as operation and maintenance – *Life Cycle Cost*), **environment** - *resource utilization* (from the conserved natural resources that are saved through adopting optimal designs that maximize use of resources including innovative materials, and material re-use during construction, as well as designing for de-construction), and **society** - *health and safety* (through the delivery of durable infrastructure systems that are safe while in use).

The process-oriented issues include client-designer communications and interactions during the project briefing process in order to delineate durability requirements in unambiguous terms. The paper propsed and discussed a framework that addresses the identified user requirements from the study. It is oberved that that an effective implementation of integrated *sustainability audit*, requires a paradim shift in educational curriculum to incoprate such a holistic approach at various interfaces in infrastructure delivery – conceptualisation, design, construction, operation & maintenance (a *pedagogical dimension*). The main educational challenge is to incorperate sustainbaility design and audit in the education of future constructyion professionals. So far this is not properly articulated in engineering and construction/project management courses although several professional organisations such as the ameerican sociery for Civil engineers (ASCE) and the Institution of Civil Engineers (ICE) UK, have started to address this in recent years. The findings and recommendations constitue useful lessons to construction researchers, educators and design professionals.

REFERENCES

Construction Industry Review Committee – CIRC 2001, *Construct for Excellence*. *Report of the Construction Industry Review Committee,* Hong Kong,

HKSAR Highways Department 1997: *Structural Design Manual for Highway and Railways*, Highways Department, The Government of the Hong Kong Special Administrative Region. Hong Kong, 1997.

Lam T. K 2006 : "Durability and Life Cycle Assessment of Infrastructure Projects" MSc (Eng) Thesis Submitted in Partial Fulfillment of the Requirements of the Department of Civil Engineering, HKU.

Ugwu O. O, Kumaraswamy M. M, and Kung F; 2003: "Understanding the Economics of Durability Design for Highway Bridges", Proceedings *of the 3rd International Conference on Current and Future Trends in Bridge Design, Construction and Maintenance,* (Barr B. I. G, Shaopei L, et al Eds.) China, Shanghai, China, 29 Sept. – 1 October 2003, pp 150-158, Institution of Civil Engineers (ICE), UK

Ugwu O. O., Kumaraswamy M. M, Kung F, Ng S .T 2005: "Object-Oriented Framework for Durability Assessment and Life Cycle Costing of Highway Bridges", *Automation in Construction,* **14** (5), pp 611-632 Elsevier Science Ltd

Acknowledgements:
The authors acknowledge the contribution of Lam Tsz Kong, Ernest in collecting field data as part of MSc (Eng) Project work submitted in partial requirement of the Department of Civil of Engineering HKU.

The Role of Using Durable Building Materials and Components in Reducing the Environmental Load of Buildings

Tülay Esin [1]
Nilay Coşgun [2]

T 52

ABSTRACT

Natural resource and energy consumption resulting from construction activities, emissions, construction and demolition wastes cause a great load on environmental values. The ecological characteristics of building materials and copmponents determine the ecological characteristics of the buildings, and accordingly their environmental loads. Durability is an important ecological characteristic for the building materials and components. In this study, the effects of the durable building materials and cpmponents towards reducing the environmental effects/loads of buildings are emphasized. In the scope of the study, durability and the potential for re-use possibilities is explicated in the context of the reasons for renewal of building materials and components by means of conducting a survey related to modifications done to existing houses. As a result of this study; it was discovered that modifications were done frequently mainly due to ageing and deterioration reasens, followed by modifications done due to aesthetic concerns. Only 25% of the modifications were done due to the ageing and deterioration of the buildings. Therefore the building material and components that not yet completed their usage life turn into waste. However, after checking the durability of such materials and components and making the necessary maintenance and repair, the possibility of re-use is considered as being quite high.

KEYWORDS

Durability, Building material, Building component, Environmental load , Reuse.

[1] Gebze Institute of Technology, Faculty of Architecture, Gebze-Kocaeli, Turkey 41400, Phone +90 262 6051606, Fax 262 6538495, tesin@gyte.edu.tr
[2] Gebze Institute of Technology, Faculty of Architecture, Gebze-Kocaeli, Turkey 41400, Phone +90 262 6051610, Fax 262 6538495, nilaycosgun@gyte.edu.tr

1 INTRODUCTION

Throughout their life cycle, buildings have negative effects on the environment due to many reasons. Natural resource and energy consumption resulting from construction activities, emissions, construction and demolition (C&D) wastes cause a great load on environmental values. The level of this load is related to the sustainable characteristics of the buildings.

Methods adopted towards the protection of natural resources and energy, and reducing waste, which all compose the base for sustainable development can also be implemented in the construction sector. The ecological characteristics of building materials and copmponents determine the ecological characteristics of the buildings, and accordingly their environmental loads. Durability is an important ecological characteristic for the building materials and components.

The reusability of building materials and components significantly reduces the environmental load of the buildings in which they are used. In this way natural resources and energy can be protected and pollution can be reduced. Building materials and components that are excluded from the scope of reuse and recycle are released to the environment as waste. This leads to environmental pollution which is amongst one of the most important environmental problems today. However, while reuse and recycling of materials prevents the formation of waste and pollution, it also allows for gaining new resources and reducing the environmental load. Reusability is related to the durability and usage life of the building materials and components against several effects.

In this study it is aimed to discuss the effects of the durability of building materials and components on reducing the environmental load of buildings. In this scope, the effects of the durability of building materials/components on reducing production of C&D waste and pollution is emphasized. It is known that buildings cause an important intensity of C&D waste during their life cycle. It is seen that a large quantity of C&D waste evolves particularly when modifications are done during usage phase. For this reason, in line with the aim specified, C&D waste that evolves the usage of buildings was chosen as the subject of the study.

2 DURABILITY OF BUILDINGS

Durability is one of the most important characteristic which defines the building materials and components and is expected to be permanent during the usage life of the building. Durability of building materials and components directly affects the durability of the building they are used in. The durability of building materials and components is related to their internal structure and their physical, chemical and mechanical characteristics. Durability can be reduced according to the faults and/or deficits done during the production and/or construction processes of the building and building materials. The building materials and components can be damaged due to the reasons such as detailing defects during the design phase , application defects and defects due to workmanship during the construction of the building. Accordingly the usage life of building can be shortened. External environmental conditions such as climatic factors and atmospheric emissions affect the durability of building materials negatively as well.

The durability performance expected from the building is directly related with the use of appropriate material. The selection of materials should be made according to the factors which affect the building materials on the basis of their usage position. Besides, it is important to state that different materials that are used together can interact and cause a reduction in durability. Using material with appropriate characteristic and standard at the construction is strongly associated with the material knowledge of the designer. The prevention of defects due to workmanship which effect the durability of the building and building materials negatively is possible by esuring detailing of design and efficient auditing. Providing sufficient attention to maintenance and repair during usage of the building is important in terms of the durability of building materials and the building's expansion of existence. Building

materials also have a definite life time and it is possible to expand this period via maintenance of building components at intervals changing according to building materials. The structure would be designed for the longest life +50 years. Exterior surfaces change about every 20 years. Wiring, plumbing, and other surfaces tend to wear out or go obsolete every 7 to 15 years. Interior walls and other components of the floor plan tend to change every few years in some buildings [Milani 2001].

3 ENVIRONMENTAL LOAD OF BUILDINGS – CONSTRUCTION AND DEMOLITION WASTE

Building life cycle is closely related to environmental impact. Buildings create a great burden on the environment during their existence because they utilize energy and natural resources and as a result of this, generate emissions and wastes. According to the data from Worldwatch Institute [Ngowi 2001]**;** building activities consume up to 40% of stone, gravel and sand, 25% of natural wood, 16% of water and 40% of energy used worlwide. Approximately 78% of carbon emissions come from fossil fuels that are burnt to make cement, and 60% of the water that runs through pipelines is consumed in cities [Eduardo 2007]. This situation causes some pollution and increases the deterioration of the environmental values. Waste production is accepted as one of the most important environmental problems of the 21st century. C&D wastes are defined as priority wastes in many countries due to their large volumes, quantities and complexities. Construction & demolition waste generates from:

- Building related waste; Construction, Demolition, Renovation,
- Roadway related waste,
- Bridge related waste,
- Landclearing & inert debris waste.

EPA (U.S.Environmental Protection Agency) estimates that in America 136 million tons of construction waste was generated in 1996 [EPA 1998]**.** It is stated that in Hong Kong 65% of the waste area was covered with C&D waste in 1994-95 [Stokoe *et al*. 1999]. This value is 35% in Canada [Cedar 2007]. According to EPA of Australia, 21% of all waste generated in Sydney is C&D waste [Gutovic *et al*. 2005].

There is no clear data in terms of C&D waste amounts in Turkey. It is stated that the average urban solid waste generation is 1.04 kg per capita/day or ~380 kg per capita/year in Turkey [Çevre ve Orman Bakanlığı 2006]. This value includes both the domestic waste and the C&D waste. According to the data from ISTAC (İstanbul Çevre Koruma ve Atık Maddeleri Değerlendirme San.ve Tic.A.Ş.), approximately one kilogram solid waste including C&D waste is generated per capita/day in Istanbul [ISTAÇ 2006].

As construction waste's have a larger volume than residential waste's, wide waste areas are essential since they put pressure on the existent landfill areas. When these wastes are released to the forests, rivers, streams or empty areas in an uncontrolled manner, they cause for erosion, the contamination of ground and surface water resources and the deterioration of natural areas [Construction Recycling Directory 2003]. The characteristics of solid changes and habitats are destroyed. Destructive contaminators spread out to the atmosphere by means of uncontrolled burning of paint, isolation materials and flammable materials. When these wastes are released to the environment uncontrollably they need to be cleaned and this is very costly both environmentally and cost economically.

4 THE ROLE OF USING DURABLE OF BUILDING MATERIALS AND COMPONENTS IN REDUCING THE ENVIRONMENTAL LOAD

C&D waste which causes economical and environmental load can be reduced through a rationalist management. However, the best method is to initially prevent waste generation. In this respect the

designer hold great responsibility. It is necessary that right decisions are taken towards preventing or reducing waste generation at the very beginning of design.

The selection of appropriate building materials and components is very important decision. It is also important to consider the durability and characteristics of reuse in the selection of building materials and components during the design phase. Because, the durability of building materials and components against variable factors is an important ecological characteristic which ensures the protection of resources and prevents waste generation. Such materials make important contributions to the reduction of environmental load as a result of their performances stated as follows;

- Building materials and components which have a high level of durability don't require much maintenance and repair during usage. This way, the reduction in the use of new materials ensures the protection of resources and pollution doesn't occur because waste that could be generated during maintenance and repair is prevented.
- Materials which have a high level of durability have a long life. For this reason, they don't need to be replaced for a long time and this detains the need for new raw materials and thus, the protection of the resource is ensured.
- Building materials and components that have a high level of durability can be reused after the building completes its life cycle or is changed before the building completes its life cycle. Thus, the need for new resources disappears or is delayed and therefore the protection of natural resources is ensured. As the materials are reused, there is no waste to throw away and therefore waste generation is prevented and pollution is reduced through reuse of them as new raw materials or sources.
- As such materials reduce the use of new resources and materials, the environmental effects (consumption of resources and water, emission etc.) that they have during their life cycle also disappears.
- Because they have long usage time, their total environmental effects gradually diminish since these effects are separated into long time periods.

5 SURVEY STUDY/ DETERMINATION OF DURABILITY AND REUSE POTENTIAL OF BUILDING MATERIALS AND COMPONENTS GENERATED AFTER MODIFICATIONS

Waste generation appears during various phases of the building's life cycle. It is observed that an important quantity of C&D waste is generated during various modifications done in the usage phase [Esin, Cosgun 2005]. EPA has reported that nearly 44% of the C&D waste results from the modifications activities in the buildings [EPA, 1998]. The long utilization time of the buildings effects in increasing this amount. In order to prevent waste generation it is important -in terms of environmental and economic aspects- to recover these C&D wastes generated in this process.

In the scope of this study, a survey conducted to determine the possible potential for re-using or re-cycling construction wastes generated by the modifications on the basis of their durability. Knowledge in regard to the reasons for modifications is important in terms of determining potential for the reuse of building materials and components. For this purpose, the modifications done in buildings, the reasons for modifications, which building materials and components are focused on during modification and how they are evaluated was researched.

A survey was conducted face to face with 90 building owners in Istanbul, the city chosen as a research area. According to the survey data results; Buildings varying from 60-200 m^2 are 1-20 years old. 80% of the survey participants are the building owners with middle income. 77% of the participants have done modifications in their buildings. 74% of them stated that they had modifications done (generally 5-6 years) after they moved into building.

It is seen that in the majority of the buildings various types of modifications have been done. The mostly preferred modification is the floor covering (61%). Followed by exterior door (43%), kitchen components (sink, counter, kitchen cupboard, etc.) (39%), window frames (36%), wall covering (33%), bath/WC components (bath-tub, wash-bowl, closet, bath cupboard) (31%), debris of wall demolish (23%), interior door (16%), ceiling covering (carton pierre, wainscot, etc.) (14%), heating system (13%), plumbing systems (11%) and electricity systems (10%) modifications [Figure 1].

It is found out that after the modifications, high percentage of building materials and components are thrown away. Accordingly, 58% of the material generated during the modification of floor covering is thrown away. 63% of exterior door, 59% of kitchen components, 60% of window frames, 70% of wall covering, 59% of bath/WC components, 82% of debris of wall demolish, 64% of interior door, 50% of plumbing systems, 55% of heating system materials are thrown away after modifications. 100% of the material generated during the replacement of ceiling covering and electricity systems are thrown away [Figure 1].

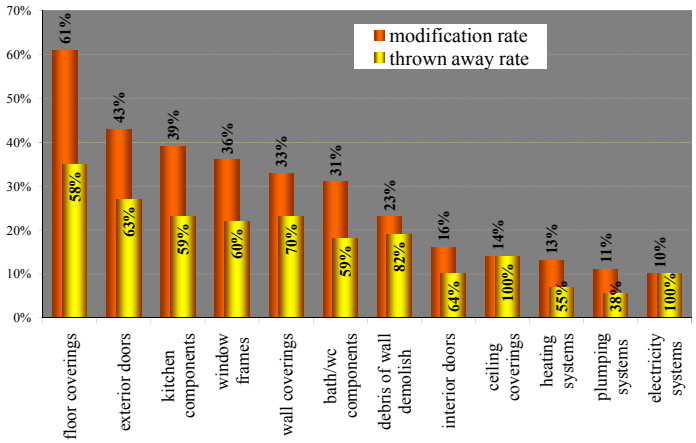

Figure 1. The rate of modifications done in buildings and the rate of materials thrown away after the modifications.

In regard to the modifications made, the participants of the survey ticked one or more reasons listed in the survey form as reasons for making modifications. Accordingly, modifications are done mainly due to ageing and deterioration (%25). Then it is followed by reasons of aesthetic (%19), amelioration in the material quality (%16), difficulty of usage (%10), insufficient space (%9), security (%8), amelioration in the workmanship quality (%6), demand of using fashionable material (%4) and respectively health reasons (%3). It is found out that the rate of modifications done due to the reasons excluding ageing and deterioration is much more (75%) [Figure 2].

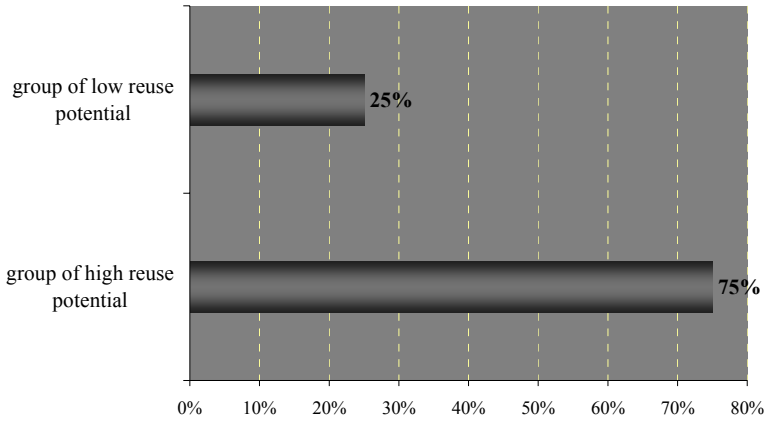

Figure 2- The rates of reuse potentials of modified building materials and components.

As a result of the cross-examination on how the building materials and components are utilized (thrown away, reused or not re-used) in the context of the alteration reasons are given in Figure 3. According to this, it is obseved that a majority of the generated materials for each modification reason are thrown away. It is determined that 65% of the building materials and components which changed due to reasons excluding ageing and deterioration and can be defined as "the group which have include high reuse potential" are thrown away [Figure 3]. Building materials and components which fit into the reuse group (sold, given to the modifier, given to somebody in need, kept in warehouse) are generally exterior and interior doors, kitchen cupboards and sanitary fixtures. The group defined as "stayed onsite" after modification are the wall, flooring and ceiling coverings that can not be removed.

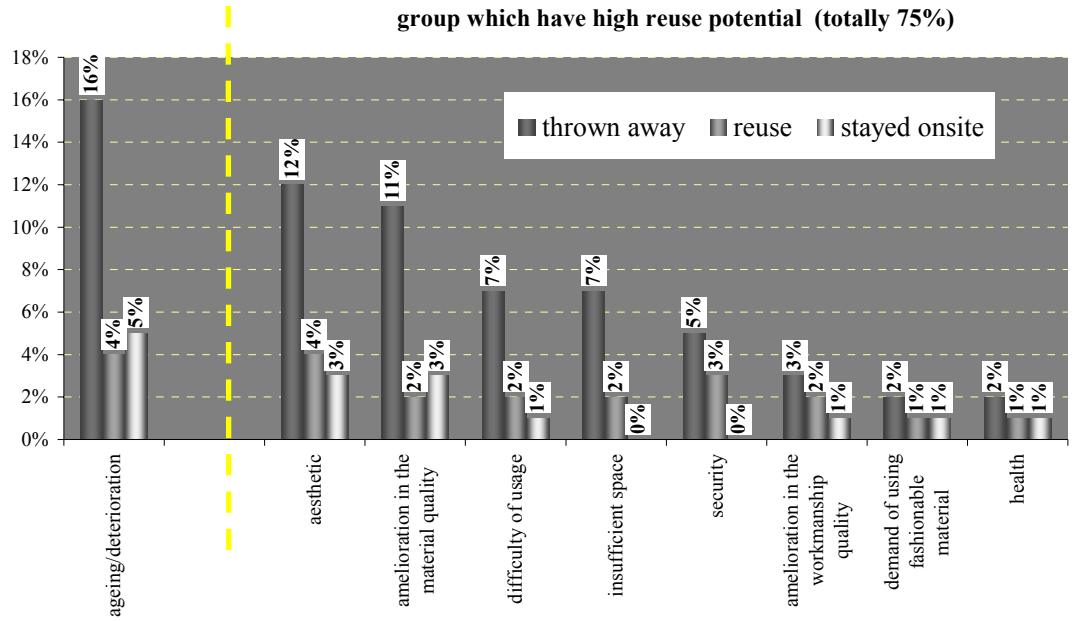

Figure 3- Reuse potentials of building materials and components in context of the reasons for modifications done in houses.

In the survey, a question was asked towards determining the environmental sensibilityof the participants which was related to "the issues in regard to giving importance to the selection of building

materials and components during modification". Figure 4 shows the results given by the participants to this question. According to this, while making modifications to their houses; it is observed that the users generally give importance to the durability and aesthetic outlook in the selection of building materials and components. Als it is observed that they don't give significance to the issue of using material that is non-harmful to the environment [Figure 4].

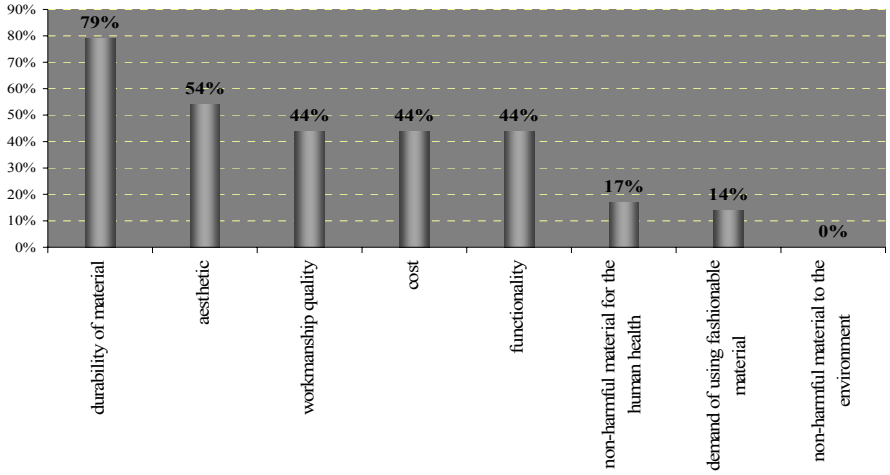

Figure 4- Issues given significance in the selection of building material and component during the modification

6 DISCUSSION AND CONCLUSION

Modification activities are done generaly due to ageing and deterioration. The second reason for modifications is due to the concerns of esthetic outlook. It is observed that the rate of building materials and components that are generated after modifications and that are thrown away is quite high [Figures 1, 3]. While the modification reasons are mainly due to ageing and deterioration, the materials and components which are replaced with new ones can hardly be reused. Thus they turn into waste materials. Some materials generated during modifications done due to the other reasons are modified before they complete their life cycle. Therefore their reuse potential is relatively high. 75% of the modifications are done due to reasons that exclude ageing and deterioration [Figures 2, 3]. Building materials and components that are modified due to reasons that exclude aging and deterioration can be reused (if they are durable) as they haven't completed their usage life. In particular it is understood that the majority of exterior and interior doors, kitchen components, sanitary fixtures and heating systems (radiators) are thrown away [Figure 1]. However, it is possible that such materials and components can be reused after their durability is controlled and the necessary maintenance and repair is done. As can be seen in 'Fig. 3', the majority of materials generated during modifications is due to the reasons that exclude ageing/deterioration are thrown away (~65%) and a very low rate of reuse possibilities (~23%).

The situation of the users in not giving signficance to using and selecting building materials that are "non-harmful to the environment" can be acknowledged as an indictor of the lack of environmental sensibility and awareness. However, the situation of the users' in giving importance to the "durability" characteristics in the selection of building materials is positive since it contributes to the reduction of environmental load [Figure 4].

In Turkey there are many modifications done due to aesthetic outlook concerns and thus building materials and components become waste before they complete their usage life. If these materials are durable they have the high potential for reuse. For this reason, by designing buildings according to the users' demands and expectations in a more satisfactory way, the modifications done before materials

complete their usage life and their turning into waste can be prevented. In meeting the users' expectation for long usage, the materials that have the characteristics of durability and reuse should be seleced. It is important to realize the necessary studies in order to inform and raise the awareness of the users.

The designers must have knowledge and awareness in regard to the selection and implementation of building materials that have the characteristic of durability. This is an important issue which should be stressed in training programs. The production of building materials and components which don't have durability and don't meet the standard should be prevented with the corporation of universities, industries and government. An efficient auditing system should be established by preparing laws and regulations on this issue. It is a fact that the environmental load of buildings will increase as building activities continues to rise. Giving importance to the durability in the selection of building materials and components for the sustainability of environmental values will contribute to the reduction of the environmental load of buildings.

REFERENCES

Cedar Corner Construction, http://www.cedarcorner.com/construction.htm

Construction Recycling Directory Seattle/King County, Prepared by King County, 2003–2004.

Çevre ve Orman Bakanlığı, Çevre Yönetimi Genel Müdürlüğü, Atık Yönetimi Daire Başkanlığı, "Katı Atık Ana Planı Nihai Rapor", Cilt I, İSTANBUL, 2006, www.cevreorman.gov.tr.

Eduardo, P.M., 'Life cycle, sustainability and the transcendent quality of building materials', *Building and Environment*, 42 (3), 2007, PP. 1329–1334.

EPA530-R-98-010, 'Characterization of Building-Related Construction and Demolition Debris in The United States', 1998, http://www.epa.gov/epaoswer/hazwaste/sqg/c&d-rpt.pdf.

Esin, T., Coşgun, N., 'Ecological Analysis of Reusability and Recyclability of Modified Building Materials and Components at Use Phase of Residential Buildings in Istanbul', *UIA 2005 ISTANBUL XXII World Congress of Architecture - Cities: Grand Bazaar of Architectures*, 3-10 July 2005, Istanbul

Gutovic, M., Klimesch, D.S. and Ray,A., **'**Strength Development in Autoclaved Blends Made with OPC and Clay-brick Waste', Construction and Building Materials
19 (5), 2005, pp. 353-358.

İstanbul Çevre Koruma ve Atık Maddeleri Değerlendirme San.ve Tic.A.Ş. www.istac.com.tr, 2006.

Milani, B., 'Building Materials in a Green Economy Community-based Strategies for Dematerialization', Paper delivered to the biennial conference of the Canadian Society for Ecological Economics (CANSEE), McGill University, Montreal, August 25, 2001.

Ngowi, A.B., 'Creating Competitive Advantage by Using Environment-Friendly Building Processes', *Building and Environment* 36, 291-298, 2001.

Stokoe, M.J., Kwong,P.Y., Lau, M.M., 'Waste Reduction: A Tool for Sustainable Waste Management for Hong Kong', In: Barrage, A., Edelmann, Y., editors. *Proceedings of R'99 World Congress*, vol. 5, Geneva, Switzerland, 1999, pp. 165–170.

Analysing Building Construction in Time, the ABC Research Matrix

Hielkje Zijlstra [1]

T 52

ABSTRACT

It is necessary to analyse the existing before changing it. That is the only way to regenerate buildings, parts of cities and urban landscapes with conscience. New applied research methods are needed to develop a sustainable environment including our heritage. In my research I concluded: Continuity + Changeability = Durability. Apart from studying relevant literature and other sources I studied seven buildings to develop a method for analysing these buildings.
Past, present and future are all relevant to the buildings. Three levels of analysis have been used to cover these phases. The objective of my research was to identify the qualities of buildings which are relevant when trying to shift from decay to preservation. The influence of construction engineering, the way we can learn from it now, and the way in which a building is able to accommodate change determine the chances of a building's long term survival – the outcome of the interaction of continuity and change.
My research method starts with the contextual aspects: commission; location; architect; typology and design process. The information obtained in the observation stage is reduced to the contextual information which affected the design, creation, existence and preservation/decay of the building. The later sections, which consider the building(s) itself in greater detail, are initially ordered by time: creation, existence, and preservation/decay. Within these, the elements of the building(s) are analysed at three levels: space (interior and exterior); structure (load-bearing elements and elements which determine the structure); matter (shaping the space through materials which affect light, colour, texture, surface, sound, impression, smell, size and weight); building services (climate control, comfort, maintenance and communications). In this way the ABC Research Matrix was created.
The ABC research method will be illustraded by the case study of the Rijksverzekeringsbank ((National Insurance Bank) in Amsterdam.

KEYWORDS

Regenrate, Durability, Analysing, Buildings, Time.

[1] Delft Technical University, Faculty of Architecture ®MIT, Delft, Netherlands, POX 5043, 2614 TM, Phone +31 152782982, Mobile +31 6 10013649, h.zijlstra@tudelft.nl

1 INTRODUCTION

In 2006 I finished my dissertation named: Building Construction in the Netherlands 1940-1970, Continuity + Changeability = Durability. This resulted in the research method: Analysing Building Construction in Time. This method was guided by the following themes: Observation - with an engineer's eye, Research analysis and Regenerative conclusions. It is a method to analyse the existing before changing it. That is the only way to regenerated buildings, parts of cities and urban landscapes with conscience. The main result of my research was this new research method. Also one of the conclusions of this research maintains that a new building typology will be needed to develop a sustainable environment including our heritage.

2 RESEARCH THEMES

Architecture is about more than just constructing buildings. Architecture adds meaning to buildings created by technology. In principle, buildings should be durable (in terms of time as well as finance) objects and therefore changeable, flexible. The lifespan of buildings, i.e. architectural objects, is inextricably linked with their ability to accommodate change. Being aware of this, learning from this, considering this when working on completely new design commissions or commissions concerning existing buildings (where technology will always be needed to implement the design) are all challenges associated with modern building practices which take a long-term view.

2.1 Observation - with an Engineer's Eye

I considered engineering and technology and the views of both architectural critics and practising architects about technology by studying the relevant literature and sources. Technology evolved after the Second World War as a result of the use of new materials, changes in legislation and standards, and the industrialisation of the construction process. Comments about the contribution, or lack thereof, of technical progress to a higher architectural quality were always personal visions primarily shaped by personal taste and habits. Architects developed from supervisors to architect-managers of the entire construction process. Time schedules became an important instrument and working together with structural engineering and building services consultants became steadily more important. The best results were developed on the basis of synergy between the different disciplines.

2.2 Research Analysis

When designing either completely new objects or objects to be incorporated into an existing structure it is important to learn from the past. Not to copy it, but to analyse it and apply the lessons learned while respecting the present context. We have to evaluate knowledge and methods and develop our own design method. This learning aspect is emphasised when a design commission concerns an existing building, but even a new build project always has a context. When dealing with an existing building that building provides the primary context and immediately becomes an element of the key points of the architect's brief. In my view, studying criticism, experiences and interviews, and thoroughly analysing the work of others is not adequately included in the education and training of architects as designers yet.

2.3 Regenerative Conclusions

Regeneration concerns changes which add a new period, a new generation, to the lifecycle of a building. Life means change and the past means that we progress in a spirit of tradition and memory. Furthermore, change cannot happen without continuity. Changes to buildings are affected by both financial and technical considerations. The existing adds a layer of history which can never be created in a true new build project. During the design and construction of the Trade Union Museum in

Amsterdam, housed in the building of the former Dutch Diamond Workers' Union (ANDB), I was introduced to issues related to National Monuments and making changes to such buildings. Fig. 1.
The examples by architects such as Piano, Foster and Herzog & de Meuron demonstrate that leading architects can produce excellent results when regenerating buildings [Powell 1999]. Figs 2 and 3.
The opinions aired by the original architects whose buildings are being changed make it eminently clear that some of them object to any changes to their buildings. Around 1950, architecture critics still felt that architecture amounted to an inviolable work of art. Optional changes were therefore considered an anathema. Architects also resisted changes to their work and event went to court to defend their copyright - it appeared that demolition was not prevented by this copyright but that changes to a building were.
Views about changes also changed themselves. In some cases the original architects are engaged to regenerate their own work. This requires them to take enough distance from "their building" to be able to accept it as a new commission. Of course, this is more likely to happen under legislation which allows listing after 30 years, than under the Dutch system where the period is 50 years.
'Refurbishment is the hard-headed business of making use of what is usable in the ageing building stock; the skilful adaptation of a building shell (which is valuable in its own right and not due to any historic mystique) to a new, or an updated, version of its existing use. The existing building, once refurbished, should be equally as efficient in its new role as a purpose-designed building would be, given the usual number of restraints which always impede the designer realising the ideal in new or refurbished merit and will, by its preservation, improve the amenity of the environment, so much the better.'[Marsh 1983].
To give regeneration a real opportunity, it is particularly important that those initiating projects are prepared to consider regeneration and do not automatically choose demolition. Bringing about this change in attitude is particularly relevant with respect to buildings dating from after 1940. There are definitely opportunities for such buildings in both the near and distant future.
Demolition amounts to a waste of energy and is neither durable nor sustainable, while reuse, changes in use and regeneration of buildings are.
Without a past there can be no future, and changes can only occur if there is continuity. The "creative re-use" advocated by Latham can produce a built environment stratified in time and therefore rich in appearance and the way it is experienced [Latham 2000]. Demolition is sometimes the best option and there is no need to preserve everything. However, a careful assessment which gives serious consideration to repurposing, reuse and regeneration provides many opportunities for creating a rich spectrum of buildings.

Figure 1. The ANDB building in Amsterdam from erected in 1900 by architect Hendrik Petrus Berlage. Regenerated in 1988 by the author at the office of Atelier PRO The Hague.

Figures 2. and 3. The Tate Modern in London, erected in 1963 by Sir Giles Gilbert Scott. Regenerated in 2000 by Herzog & de Meuron.

3 ANALYSING BUILDING CONSTRUCTION IN TIME

Past, present and future are all relevant to buildings. Three levels of analysis have been used to cover these phases. Where buildings are concerned, we have to look at creation, existence and preservation/decay. The objective of my research was to identify the qualities of a building which are relevant when trying to shift from decay to preservation. Main issues for redevelopment are: space and structure. The influence of construction engineering, the way we can learn from it now, and the way in which a building is able to accommodate change determine the chances of a building's long term survival – the outcome of the interaction of continuity and change. Research can provide data for careful and imaginative observation and analysis. The conclusions which can be drawn in this way may help us make discoveries to understand a building when either designing or redesigning it. Fig. 4. My research didn't only result in relevant conclusions, but also in a research method which will be applied to the subjects covered by the Faculty of Architecture of Delft University of Technology and could be used on international scale. It is a method to analyse the existing before changing it. That is the only way to regenerated buildings, parts of cities and urban landscapes with conscience. Analysing Building Construction in Time aims to discover the qualities of a building, rather than its value. Observation, the first stage of the research, aims to obtain information from the literature, the building

itself, archives and interviews with stakeholders. The second stage, analysis, includes structuring, analysing and interpreting the information. In the third stage, conclusions can then be drawn on the basis of the research themes discussed above. The information is structured in accordance with the research brief. In the long term, it will be possible to identify connections (concerning both buildings and building construction) between the results of Analysing Building Construction in Time, using the research themes defined by me. The information obtained in the observation stage is reduced to the contextual information which affected the design, creation, existence and preservation/decay of the building. Context is the title of the first section in which the contextual aspects are discussed: commission; location; architect; typology and design process. The later sections, which consider the building itself in greater detail, are initially ordered by time: arising, continuing and expiring. Within these, the elements of the building are analysed at three levels: space (interior and exterior); structure (load-bearing elements and elements which determine the structure); material (shaping the space through materials which affect light, colour, texture, surface, sound, impression, smell, size and weight); building services (climate control, comfort, maintenance and communications). In this way the actual research ABC Research Matrix was created. Fig. 5.

Figure 4. Palace of Justice in Arnhem. Renovated and extended with an extra floor in 1996.

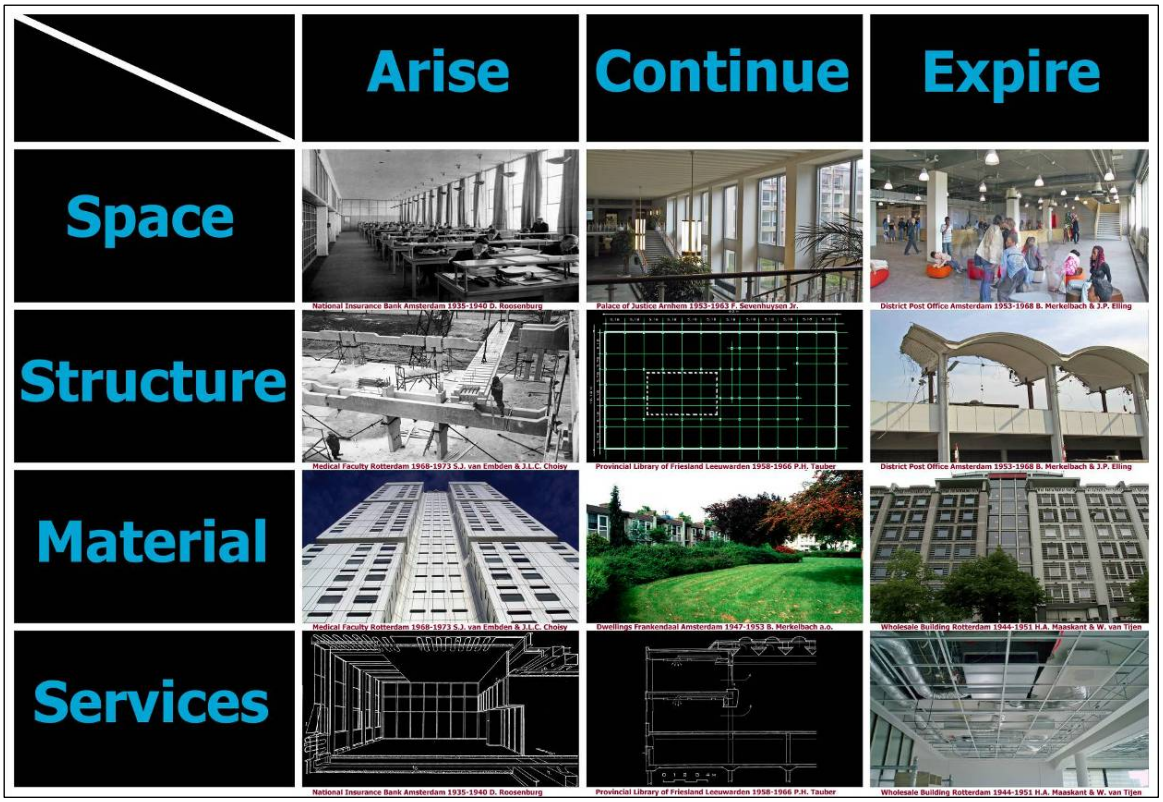

Figure 5. The Analysing Building Construction in Time Research Matrix.

4 CASE STUDY: RIJKSVERZEKERINGSBANK AMSTERDAM 1935 – 1940

Architect D. (Dirk) Roosenburg (1887-1962) designed the Rijksverzekeringsbank (National Insurance Bank) building for the Plan Zuid (South Plan) in Amsterdam drawn up by H.P. (Hendrik) Berlage (1856-1934) who also made the first sketch design for the building in 1925.
The premises of the Rijksverzekeringsbank, the body responsible for the implementation of social security legislation in the Netherlands since 1901, were to be built at the site of the Kunstenaarshuis. At the time the commission for this building was being defined, Roosenburg worked at Berlage's office where he worked on Holland House in London which has some similarities with the later Rijksverzekeringsbank. In 1916 Roosenburg set up his own practice in The Hague, which now operates under the name LIAG.
The high-rise section of the Rijksverzekeringsbank intersects the site diagonally and was placed on top of a round building housing the archives. The ring shape was imposed by the 'adressograeph', the machine transporting the filing cards. The shipping department and plant rooms (accessible by truck) were located in the basements. Fig. 6.
The above-ground part had a prefabricated steel structure. The entrance to the office block was placed in the middle, the section at the front was wider than that at the back and the floor-to-floor height was 4.95 metres. The hydronic heating system installed in the ceilings could also be used for cooling. There was an innovative ventilation system installed, all in accordance with the overall design. Fig. 8.
Originally, the building was clad with ceramic tiles, in 1968 LIAG architects replaced these with smooth travertine cladding. Unfortunately this meant that the original texture and relief effect were lost. Based on insufficient research the decisions were made. All the architectural drawings, including those of the ceramic facade tiles, are archived at the NAi. Similarly, the roof terrace was replaced by a large plant room.
The building was extensively modified in 1993. The ring was demolished and then rebuilt with a car park underneath it. The ring also gained a floor level and was used as offices. The steel window frames were replaced by a reasonable alternative in aluminium. In the office section, a floor was

inserted in the double-height space at the front of the building and a new stairwell was built, intersecting the structure. The interior was furnished with precious woods, dark colours, suspended ceiling and high-pile carpet for a law firm which left the building after only five years. The service systems have been removed completely. They functioned very well, but described as 'out of date'. Ceilings were covered by suspended tiles, creating a space for new ducts of one and a half meter height. The next refurbishment was undertaken in 2002. However, the sense of light and openness of the past would never return. Fig. 7.
The technical options are those of just before the Second World War; the steel structure was partly prefabricated; the plant engineering was innovative; part of Berlage's Plan Zuid for Amsterdam. For this study, the building of the Rijksverzekeringsbank was analysed as offices and archives.
The Rijksverzekeringsbank was a technically impressive and beautiful building. It was an example for the technical possibilities just before the Second World War started. Its exterior was seriously affected by the 1968 refurbishment. If a more serious research should have made the reasons for the problems and the qualities should have been recognised. Later, too much money was thrown at it to remove the internal structure and it was pretentiously furnished, resulting in a complete negation of the building's original lightness and neutrality. In 2008 the building will be left again from the nowadays tenant, maybe an opportunity to get back to some of its original ideas that were an example of durable use of materials and services. The unique techniques could be analyzed by the ABC research method. Some of the conclusions out of the research are:
The height of the floors to 4.95 m, is one of the most important factors for possibilities in future change of buildings. As a starting point of the design of new buildings, in consideration of the regeneration of buildings, it is necessary to create an excess of measure in length, depth, height, tolerable load and infrastructure. The future is always unknown so it is better not to waste money on options for future modification as change is always unpredictable, but instead invest in space, dimensions, permissible loads and avoid the unnecessary use of elements which are specific to the building and difficult to reproduce. Examples to support this include the envisaged expansion of the Rijksverzekeringsbank with two floors which never happened, however the roof was fully occupied and the floor loads throughout the building allowed its use as archives.
The results of the ABC research of the facade of the Rijksverzekeringsbank proved that mistakes were made during refurbishments because the technical aspects of these buildings had not been studied in sufficient detail. Construction engineering research is an instrument to show what changes have been made so far and how the building was originally intended to look. Identifying these essences requires a study of the design history of the building. Decisions should not be taken lightly just because generous funding is available. [Zijlstra 2006].


Figures 6. and 7. The Rijksverzekeringsbank in Amsterdam the exterior still under construction in 1939 and the original interior in 1941.

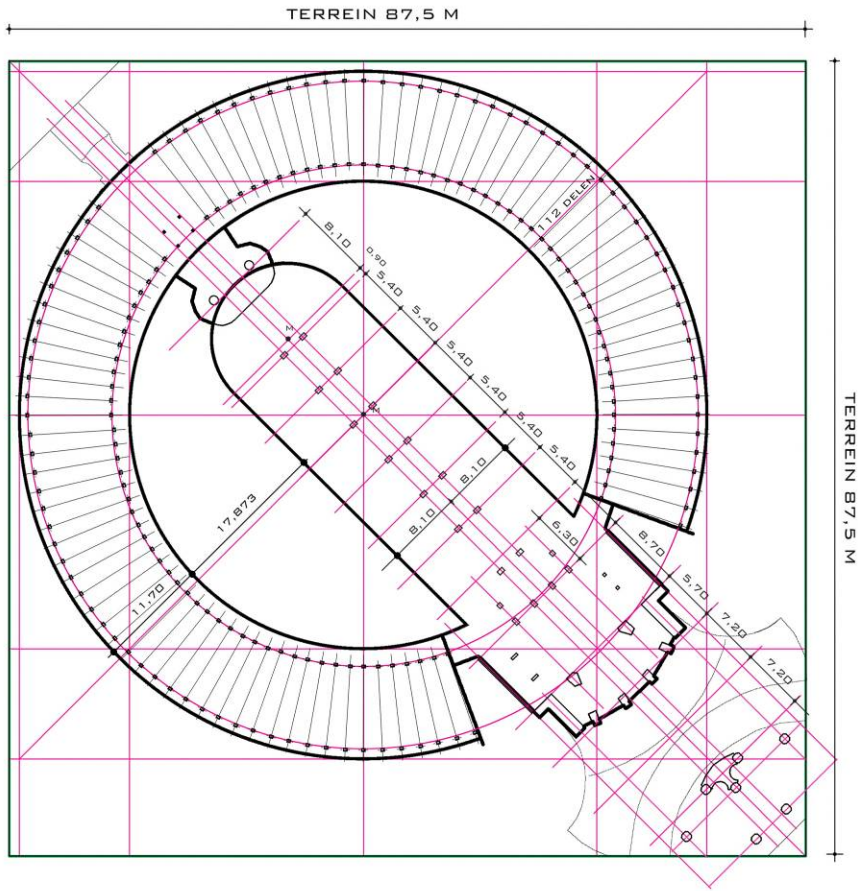

Figure7. The Rijksverzekeringsbank in Amsterdam reduction drawing of the floor plan.

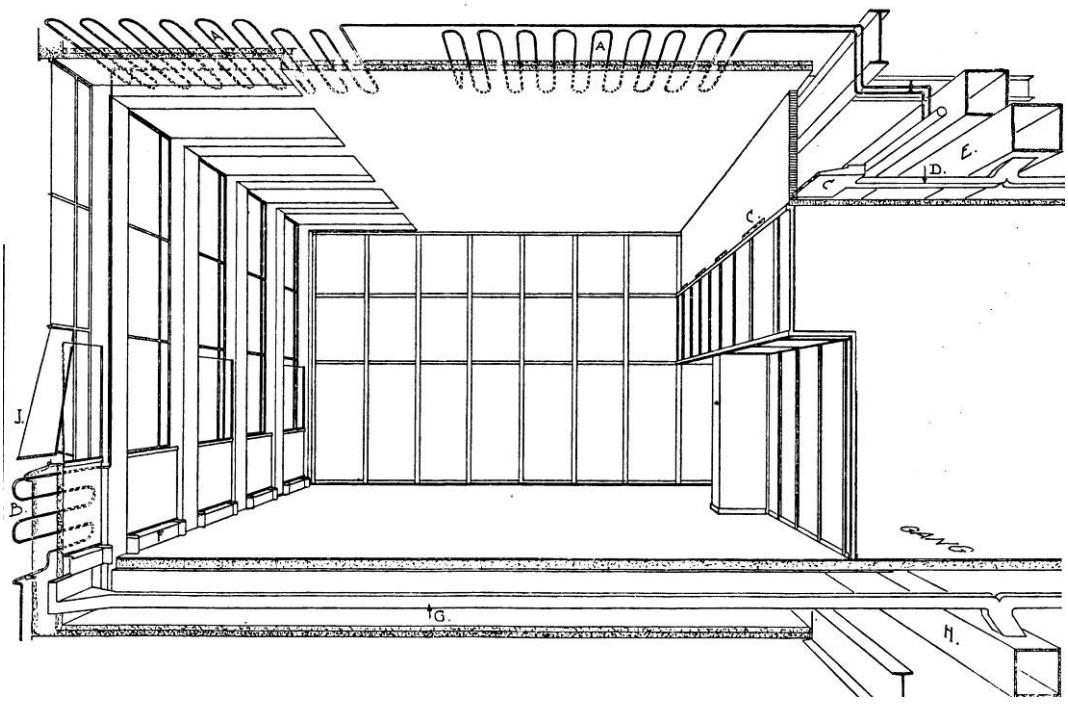

Figure 8. Section of the Rijksverzekeringsbank Amsterdam with the concept of services for heating and ventilation.

5 CONCLUSIONS

The influence of Analyzing Building Construction in Time, the way we can learn from it now, and the way in which a building is able to accommodate change determine the chances of a building's long term survival – the outcome of the interaction of continuity and change. Research can provide data for careful and imaginative observation and analysis. The conclusions which can be drawn in this way may help us make discoveries to understand a building when either designing or redesigning it. A careful assessment which gives serious consideration to repurposing, reuse and regeneration provides many opportunities for creating a rich spectrum of buildings.
Past, present and future are all relevant to the buildings I have investigated so far and those which I will be investigating in future. I use three levels of analysis to cover these phases. Where buildings are concerned, we have to look at creation, existence and preservation/decay. The objective of my research is to identify the qualities of a building which are relevant when trying to shift from decay to preservation. Change and durability appear to be intimately linked to guarantee a degree of continuity of our built environment:

CONTINUITY + CHANGEABILITY = DURABILITY

Engineer-architects should not only be familiar with architecture (as the art and science of designing and constructing buildings) but also with building engineering (as the science of what is needed to construct buildings). However, architecture is about more than just constructing buildings. Like the case study of the Rijksverzekeringsbank in Amsterdam proved. Architecture adds meaning to buildings created by technology. In principle, buildings should be durable (= able to exist for a long time without significant deterioration in terms of time as well as finance) objects and therefore changeable, flexible. The lifespan of buildings, i.e. architectural objects, is inextricably linked with their ability to accommodate change. Being aware of this, learning from this, considering this when working on completely new design commissions or commissions concerning existing buildings (where technology will always be needed to implement the design) are all challenges associated with modern building practices which desires a long-term view to produce real durable buildings.

ACKNOWLEDGMENTS

Figures 1-5 and 7 by the author.
Figure 6 from: Liag Architects.
Figure 8 from: Geneeskundig tijdschrift der Rijksverzekeringsbank, (1940) 3.

REFERENCES

Latham, D. 2000, 'Creative Re-use of Buildings. Vol.1. Principles and Practice', Donhead Shaftesbury.

Macdonald, S. 1996, 'Modern Matters', Donhead Shaftesbury.

Marsh, P. 1983, 'The Refurbishment of Commercial and Industrial Buildings', London.

Powell, K. 1999, 'Architecture Reborn', Rizzoli New York, pp. 223–231.

Zijlstra, H. 2006, 'Building in the Netherlands 1940-1970. Continuity + Changaebility = Durability', Publication Office Faculty of Architecture Delft Technical University.

Life-Cycle Cost Analysis For The Residentıal Buildings

Esra Bostancıoğlu [1]

T52

ABSTRACT

Decreasing the housing cost – decreasing the life cycle costs that include initial investment costs along with the operating and maintenance & repair costs – will yield beneficial results both for the owners and/or users of the housing facility, and also for the economy of the country. If we consider the big share of housing sector within energy related expenditures, it becomes obvious that ensuring a decrease in the housing energy expenses will also substantially contribute in decreasing energy related expenditures of the country. Such studies and right decisions taken in the course of architectural design will lead to healthy, comfortable and sustainable buildings that consume less and less of limited and scarce resources and thus prevent environmental pollution. Upon understanding in which ratios the materials of building components affecting the initial investment, operating, maintenance & repair costs of the residential buildings would affect the costs as such; there will be preference to have quality and low cost residential buildings in the design phase. From investor's perspective, it will be possible to identify any cost-change rate or items that might be changed within a limited budget depending on the materials of a given building construction. From user's perspective, it will be possible to identify the rate of any potential decrease in the annual operating and maintenance & repair costs depending on the changing materials of building components. From the perspective of domestic economy, it will be possible to witness the potential rates of energy saving and less pollution of the environment thanks to the changing materials of building components.

This study aims at identifying the extent of any changes to occur in initial investment costs, operating costs and life-cycle costs as a result of a change made in the building envelope properties, which is also a factor affecting initial investment cost and operating cost of a building. Life cycle costs of two residential buildings have different structural systems (load bearing and reinforced concrete systems) are analyzed. To this end, building initial investment costs, operating costs and life-cycle costs have been identified and evaluated in line with the changes made in the materials used in the building components forming the building envelope including wall, roof and ground flooring.

KEYWORDS

Life cycle cost, İnitial investment cost, Operating cost, Energy saving.

[1] İstanbul Kultur University, Faculty of Engineering and Architecture, Istanbul, Turkey, 34156, Phone +90 212 4984284, Fax 212 6618563, ebostancioglu@iku.edu.tr

INTRODUCTION

Housing construction in Turkey enjoys large shares within the construction sector and domestic investments. On the other hand, the housing need in our country prevails considerably in line with the increase of population. It is necessary to meet the **"quality and low-cost"** housing need of Turkey. Apart from addressing to the sheltering need of people, residential buildings should also offer comfort conditions to the users within their life-cycle. In connection with the increase in energy consumed by artificial subsystems, problems such as decline in energy resources in place, dependency on foreign countries for these resources, hazardous effects of gases emitted for energy consumption on the human health, increase in the air pollution and accordingly global warming have become significant in terms of providing comfort conditions. In the light of this information, it's necessary to construct and operate buildings, which meet required comfort conditions and ensures minimum energy consumption.

Decreasing the housing cost – decreasing the life cycle costs that include initial investment costs along with the operating and maintenance & repair costs – will yield beneficial results both for the owners and/or users of the housing facility, and also for the economy of the country. If we consider the big share of housing sector within energy related expenditures, it becomes obvious that ensuring a decrease in the housing energy expenses will also substantially contribute in decreasing energy related expenditures of the country. Such studies and right decisions taken in the course of architectural design will lead to healthy, comfortable and sustainable buildings that consume less and less of limited and scarce resources and thus prevent environmental pollution. Upon understanding in which ratios the factors affecting the initial investment, operating, maintenance & repair costs of the residential buildings would affect the costs as such; there will be preference to have quality and low cost residential buildings in the design phase. From investor's perspective, it will be possible to identify any cost-change rate or items that might be changed within a limited budget depending on the characteristics of a given building construction. From user's perspective, it will be possible to identify the rate of any potential decrease in the annual operating and maintenance & repair costs depending on the changing characteristics of building construction. From the perspective of domestic economy, it will be possible to witness the potential rates of energy saving and less pollution of the environment thanks to the changing characteristics of building construction.

This study aims at identifying the extent of any changes to occur in initial investment costs, operating costs and life-cycle costs as a result of a change made in the building envelope properties, which is also a factor affecting initial investment cost and operating cost of a building. To this end, building initial investment costs, operating costs and life-cycle costs have been identified and evaluated in line with the changes made in the materials used in the building components forming the building envelope including wall, roof and ground flooring.

2. COST CONCEPT AND LIFE-CYCLE COST

Building cost emerges in different phases of building construction process. Life-cycle cost of buildings is as much necessary as their initial investment costs. Buildings will also have costs during their utilization. Maintenance, repair and operating costs arising within the utility period amount to a significant line in the budget of house owners.

In terms of energy efficiency, an assessment of life-cycle costs to be conducted during the design, implementation, utilization or renovation phases of a building will contribute in taking right decisions about the design. With their acknowledged nature of continuity, the operating costs have a significant impact on the emergence of life-cycle costs along with the initial investment costs. Energy costs, which are also considered to be a part of the real operating costs, are the most important parameters to be controlled within the building life-cycle so as to ensure energy efficiency. The energy needed for heating and cooling, a major part of overall energy expenditures, can be controlled by means of building location, distance between buildings, building position, building form and building envelope

that provide climatic comfort conditions with a minimum heat loss. Similarly, the lightning energy can also be controlled. Since life-span of buildings is targeted to be reduced; initial investment costs, operating, maintenance-repair costs and renovation costs should be tackled altogether in the design phase.

By means of life-cycle cost, one can identify whether or not a project is going to be more cost-effective than its initial investment cost and under which circumstances maximum cost-effectiveness will be in place. Various projects can be compared for this purpose. Whenever a decision is to be made amongst various investment options, then the option having the minimum life-cycle cost is accepted as the most appropriate option. (Manioğlu, 16-17) (NBS Handbook 132, 14-20)

Design parameters affecting energy conservation are as follows: location, direction, building form, building envelope, thermophysical and optical properties, volume dimensions, settlement type, distance between buildings, natural ventilation system. (Berköz, Küçükdoğu v.d., 1995) The design parameters affecting the heating energy conservation in a given building are building form, building envelope, optical and thermophysical properties. Building envelope optical properties include absorption, conductivity and reflection coefficients against solar radiation; whereas thermophysical properties amount to total thermal conductivity coefficient (U (k)) and transparency ratio. All these properties are the determining factors for the heat quantity coming from the building envelope unit space, which is gained or lost by the effects of outside air temperature and solar radiation.

3. TWO DIFFERENT TYPES OF CONSTRUCTION SYSTEMS - LOAD BEARING AND REINFORCED CONCRETE FRAME SYSTEMS

Load bearing system is the one where various and relatively smaller construction materials including stone, brick, briquet blocks, wood, sun-dried brick and gasbeton are piled up one on the other to build a load-bearing wall by either standing on their own weight and or by using binder/adhesive materials. In such systems, it is allowed to leave spaces on load-bearing slot and exterior walls for doors and windows in line with the ratio and locations specified by the corresponding regulations. In those systems, walls are connecting to horizontal and vertical elements called bond beams and columns, which are based on pulling force.

In accordance with the provisions of "Regulation on the Buildings to be Constructed in Earthquake Zones" in effect in Turkey, the following unreinforced materials might be used on load-bearing walls: natural stone, solid brick in compliance with the Turkish Standards; bricks and block bricks having a void ratio not exceeding the maximum allowed void ratio for load-bearing wall material as specified by the Turkish Standards TS-2510 and TS EN 711-1, gasbeton construction materials and elements, lime - sandstone, solid concrete briquet block, sun-dried bricks or other similar masonry units. Natural stone bearing walls can only be built at the basement and ground floors of unreinforced buildings. Reinforced concrete bearing walls can only be built at the basement of load bearing buildings.

The minimum wall thickness rates -excluding plaster thickness- of bearing walls are illustrated in the Table 1 in relation to the number of building storeys. If there is no basement in place, then the minimum wall thickness rates of ground floor and upper floors will apply as indicated in the Table 1. Wall thickness rate of a permitted additional attic storey will be the wall thickness rate of its lower floor. (Resmi Gazete No:26100)

Table 1. Minimum thickness rates for bearing walls (Resmi Gazete No:26100)

Earthquake Zone	Permitted Storeys	Natural Stone (mm)	Concrete (mm)	Brick and gasbeton	Other (mm)
1, 2, 3 and 4	Basement	500	250	1	200
	Ground Floor	500	-	1	200
1, 2, 3 and 4	Basement	500	250	1,5	300
	Ground Floor	500	-	1	200
	First Floor	-	-	1	200

Reinforced Concrete Frame systems; are the ones where carrying elements such as columns and beams withstand the dynamic and static loads affecting buildings and where vertical loads are transferred to main system by means of columns. In such systems, all walls do only bear their own loads and impose the load to their underlying floor in any storey; floors then transfer their assumed loads to columns either by means of beams or directly. Not having a bearing character, walls in this system (except for the curtain walls) can be relocated or lifted in any storey; thus making space management flexible.

4. METHOD AND ACCEPTED CONCLUSIONS

- This study tackles building envelope properties, one of the efficient design parameters required for an energy efficient environment and for heating energy conservation in buildings. Building components forming a building envelope are walls, roof and the ground flooring. If materials used in walls, roof and flooring are to be changed, the initial investment costs and operating costs of a building will be different. This study is based on the existing standards and regulations in our country; therefore the unit prices of the Ministry of Public Works (Akçalı, Ü., 2007) and the materials that can be used in walls, floorings and roofs as specified in TS 825 (TS 825, 1998) have been identified in the first place. Since ground flooring is linked to the construction system and since wood rafter framing roof is approved, insulation materials and their thickness rates have been differentiated in those building components. It is determined that 4 cm of extrude polystyrene foam may be used in ground floor furnishing systems, and that fiberglass (6, 8, 10 cm fiberglass) of different thicknesses may be used on the roof as insulator. It is assumed that carrier brick and gasbeton shall be used in reinforced concrete system; and brick with vertical holes and gasbeton shall be used in concrete skeleton system as wall body material. For both systems, it is assumed that materials with identical thickness values are used in exterior walls. (19 cm brick, 19 cm aerated concrete) Different alternatives are created with the use of extrude polystyrene foam and rock wool in different thicknesses as wall insulator. Since it is a more convenient system in places that are used for a prolonged period, such as housings, and condensation possibility is less as a result of steam diffusion, it is assumed that insulators are applied externally on walls. Project alternatives generated by differentiating body and insulation materials in construction compounds are displayed in Table 2.
- Life-cycle cost consists of initial investment costs, operating costs and maintenance-repair costs. However, initial investment costs along with heating costs - having the largest share within the costs incurred in a building life-cycle - have been considered as operating costs in this study when identifying the life-cycle costs. Other costs have not been taken into scope.
- Initial investment costs of residential buildings - stand-alone buildings with two storeys covering a total of 148 m2- to be constructed by means of load bearing and reinforced concrete frame systems are calculated. The Ministry of Public Works unit price rates, a measurement standard adopted and used in Turkey, have been used in the calculation of initial investment costs (Akçalı, Ü., 2007). Unit Price Analysis has been conducted for the wall insulation materials with different thickness ratio, which are not covered by the Ministry of Public Works unit price list. The initial investments costs calculated also cover the costs

relating to civil works.

- It is aimed that projects also provide required climatic comfort conditions for users. Therefore, it is investigated whether the shell design conducted in all of the evaluated projects conform to specifications of TS 825, and whether it is less than restricted heat energy requirement. Also, it is checked whether there is any condensation in wall alternatives in the projects conducted. all project alternatives evaluated in Table 2 provide the required thermal comfort as per TS 825, and no condensation occurs in wall alternatives. Determination of operating costs of project alternatives is based on annual heating cost calculation. In order to be able to calculate annual heating costs, "TS 825 Heat Requirement Calculations" computer program is used. (www.izoder.org) Through this computer program, annual heat requirement values ($Q_{yıl}$) are calculated for all of the project alternatives. Annual fuel quantity is calculated through the following formula:

  $$By = \frac{Q_{yıl}\,(kWh) \times 1{,}3}{2 \times H_u\,(kWh/m^3) \times \eta_k} \quad (m^3/yıl)$$

  By: Annual fuel quantity (m^3/yıl)
  $Q_{yıl}$: Annual heat requirement of building (kWh)
  H_u: Fuel heating value (kWh/m^3) = 10,38 (kWh/m^3) for natural gas.
  η_k: Boiler efficiency= 0,85-0,92 for natural gas. (Anon., 2002)

  It is assumed that natural gas is consumed in all project alternatives, and annual heating expenditures of project alternatives are determined in accordance with natural gas prices in Istanbul in 2007.
- And when determining lifecycle cost, initial investment costs and operating costs are taken as basis. Buildings are evaluated considering their lifecycle as 60 years.

5. ASSESSMENT

As illustrated by the Table 2, when the initial investment costs of residential buildings - constructed through load bearing system having different building envelope alternatives - are assessed; the alternative in which a wall body material of 19 cm vertical perforated brick is jacketed with exterior 4 cm XPS and in which a 10 cm fiberglass is used in attic has been identified as the most cost-effective alternative in terms of initial investment costs. When it comes to annual heating energy quantities; the alternative in which a wall body material of gasbeton is jacketed with an XPS having maximum thickness and in which a 10 cm fiberglass is used in attic is considered to be the best alternative having the minimum annual heating energy quantity. When alternatives in which 19 cm gasbeton is jacketed with 8 cm XPS and with 8 cm rock wool are to be compared, extruded polystyrene foam alternative has proved to cause less heat loss. As regards the initial investment costs; the alternative in which gasbeton wall is jacketed with 2,5 cm XPS and in which 10 cm fiberglass is used for attic has turned out to have the lowest initial investment cost as compared to the other alternatives using gasbeton body material.

As illustrated by the Table 2, when the initial investment costs of residential buildings - to be constructed through reinforced concrete frame system having different building envelope alternatives - are assessed ; the alternative in which a wall body material of 19 cm horizontal perforated brick is jacketed with exterior 5 cm XPS and in which a 8 cm fiberglass is used in attic has been identified as the most cost-effective alternative in terms of initial investment costs. When it comes to annual heating energy quantities; the alternative in which a wall body material of gasbeton is jacketed with an rock wool having maximum thickness and in which a 10 cm fiberglass is used in attic is considered to be the best alternative with the lowest annual heating energy quantity.

The alternative in which a wall body material of 19 cm brick is jacketed with exterior 8 cm XPS and in which 10 cm fiberglass is used for attic, is the most cost-effective alternative in terms of the life-cycle

cost as compared to the alternatives to be constructed through load bearing system. The alternative in which a body wall material of 19 cm brick is jacketed with external 8 cm XPS and in which 10 cm fiberglass is used for attic, is the most cost-effective alternative as compared to the other alternatives to be constructed through reinforced concrete frame system.

Table 2. Initial investment, operating and life cycle costs of the residential buildings which are with constructed with load bearing system and reinforced concrete frame system.

MATERIAL OF WALL BODY-19 CM BRICK, GROUND FLOOR INSULATION 4 CM XPS														
		REINFORCED CONCRETE FRAME SYSTEM					LOAD BEARING SYSTEM					COMPARISON (REINFORCED CONC.FR. SYS/ LOAD BEARING SYSTEM)*100		
ROOF INSULATION	WALL INSULATION	(Qyıl) (kWh / yıl)	ANNUAL HEATING ENERGY (M3)	ANNUAL OPERATING COST (YTL)	INITIAL INVEST. COST (YTL)	LIFE CYCLE COST (YTL)	(Qyıl) (kWh / yıl)	ANNUAL HEATING ENERGY (M3)	ANNUAL OPERATING COST (YTL)	INITIAL INVEST. COST (YTL)	LIFE CYCLE COST (YTL)	INITIAL INVEST. COST	ANNUAL OPERATING COST	LIFE CYCLE COST
10 cm fiberglass	4 cm XPS	-	-	-	-	-	11.758,00	866,22	522,40	57.318,62	88.662,80	-	-	-
6 cm fiberglass	5 cm XPS	-	-	-	-	-	11.692,00	861,36	519,47	57.544,13	88.712,37	-	-	-
8 cm fiberglass	5 cm XPS	11.505,00	847,59	511,16	62.880,54	93.550,28	11.317,00	833,74	502,81	57.774,69	87.943,26	91,88	98,37	94,01
10 cm fiberglass	5 cm XPS	11.264,00	829,83	500,45	63.011,47	93.038,75	11.092,00	817,16	492,81	57.905,62	87.474,39	91,90	98,47	94,02
8 cm fiberglass	6 cm rockwool	11.739,00	864,82	521,56	64.722,18	96.015,71	11.540,00	850,16	512,72	59.616,33	90.379,37	92,11	98,30	94,13
10 cm fiberglass	6 cm rockwool	11.497,00	847,00	510,81	64.853,12	95.501,53	11.298,00	832,34	501,97	59.747,26	89.865,18	92,13	98,27	94,10
6 cm fiberglass	7 cm rockwool	11.626,00	856,50	516,54	65.104,88	96.097,17	11.454,00	843,83	508,90	59.999,03	90.532,81	92,16	98,52	94,21
8 cm fiberglass	7 cm rockwool	11.258,00	829,39	500,19	65.335,44	95.346,73	11.095,00	817,38	492,95	60.229,58	89.806,35	92,19	98,55	94,19
10 cm fiberglass	7 cm rockwool	11.024,00	812,15	489,79	65.466,37	94.853,87	10.867,00	800,58	482,82	60.360,52	89.329,49	92,20	98,58	94,18
6 cm fiberglass	8 cm rockwool	11.233,00	827,55	499,08	65.832,53	95.777,18	11.100,00	817,75	493,17	60.726,68	90.316,78	92,24	98,82	94,30
8 cm fiberglass	8 cm rockwool	10.880,00	801,54	483,39	66.063,09	95.066,72	10.746,00	791,67	477,44	60.957,24	89.603,65	92,27	98,77	94,25
10 cm fiberglass	8 cm rockwool	10.640,00	783,86	472,73	66.194,03	94.557,87	10.496,00	773,25	466,33	61.088,17	89.068,14	92,29	98,65	94,19
6 cm fiberglass	6 cm XPS	11.529,00	849,35	512,23	63.235,10	93.968,81	11.293,00	831,97	501,74	57.868,10	87.972,69	91,51	97,95	93,62
6 cm fiberglass	8 cm XPS	11.041,00	813,40	490,55	64.407,23	93.840,05	10.755,00	792,33	477,84	59.040,23	87.710,64	91,67	97,41	93,47
8 cm fiberglass	6 cm XPS	11.162,00	822,32	495,92	63.465,66	93.221,04	10.940,00	805,96	486,06	58.359,81	87.523,38	91,95	98,01	93,89
8 cm fiberglass	8 cm XPS	10.681,00	786,88	474,55	64.637,79	93.110,93	10.388,00	765,30	461,53	59.531,94	87.224,01	92,10	97,26	93,68
10 cm fiberglass	6 cm XPS	10.933,00	805,45	485,75	63.596,60	92.741,51	10.707,00	788,80	475,71	58.490,75	87.033,20	91,97	97,93	93,84
10 cm fiberglass	8 cm XPS	10.439,00	769,05	463,80	64.768,72	92.596,74	10.147,00	747,54	450,83	59.662,87	86.712,48	92,12	97,20	93,65
MATERIAL OF WALL BODY-19 CM GASBETON, GROUND FLOOR INSULATION 4 CM XPS														
10 cm fiberglass	2,5 cm XPS	-	-	-	-	-	11.636,00	857,24	516,98	61.408,69	92.427,64	-	-	-
8 cm fiberglass	4 cm XPS	-	-	-	-	-	11.502,00	847,36	511,03	61.570,32	92.232,06	-	-	-
10 cm fiberglass	4 cm XPS	-	-	-	-	-	11.262,00	829,68	500,37	61.701,25	91.723,20	-	-	-
6 cm fiberglass	5 cm XPS	11.121,00	819,30	494,10	65.430,38	95.076,46	10.876,00	801,25	483,22	62.511,89	91.504,85	95,54	97,80	96,24

8 cm fiberglass	5 cm XPS	10.768,00	793,29	478,42	65.660,94	94.366,00	10.502,00	773,69	466,60	62.742,44	90.738,40	95,56	97,53	96,16
10 cm fiberglass	5 cm XPS	10.518,00	774,87	467,31	65.791,87	93.830,49	10.277,00	757,12	456,60	62.873,38	90.269,54	95,56	97,71	96,20
6 cm fiberglass	4 cm XPS	11.631,00	856,87	516,76	64.843,38	95.849,00	11.287,00	831,53	501,48	61.924,89	92.013,49	95,50	97,04	96,00
8 cm fiberglass	4 cm XPS	11.262,00	829,68	500,37	65.073,94	95.095,89	10.933,00	805,45	485,75	62.155,44	91.300,35	95,52	97,08	96,01
10 cm fiberglass	4 cm XPS	11.029,00	812,52	490,01	65.204,87	94.605,70	10.701,00	788,35	475,44	62.286,38	90.812,83	95,52	97,03	95,99
10 cm fiberglass	3 cm XPS	11.727,00	863,94	521,03	64.619,74	95.881,28	11.262,00	829,68	500,37	61.701,25	91.723,20	95,48	96,03	95,66
10 cm fiberglass	3 cm rockwool	-	-	-	-	-	11.779,00	867,77	523,34	62.657,71	94.057,87	-	-	-
6 cm fiberglass	4 cm rockwool	-	-	-	-	-	11.809,00	869,98	524,67	63.023,87	94.504,00	-	-	-
8 cm fiberglass	4 cm rockwool	-	-	-	-	-	11.432,00	842,21	507,92	63.254,43	93.729,56	-	-	-
10 cm fiberglass	4 cm rockwool	11.651,00	858,34	517,65	66.303,85	97.362,79	11.199,00	825,04	497,57	63.385,36	93.239,37	95,60	96,12	95,76
6 cm fiberglass	5 cm rockwool	11.704,00	862,25	520,00	66.630,63	97.830,86	11.345,00	835,80	504,05	63.712,14	93.955,35	95,62	96,93	96,04
8 cm fiberglass	5 cm rockwool	11.328,00	834,55	503,30	66.861,19	97.059,08	10.994,00	809,94	488,46	63.942,70	93.250,23	95,64	97,05	96,08
10 cm fiberglass	5 cm rockwool	11.104,00	818,04	493,35	66.992,13	96.592,89	10.768,00	793,29	478,42	64.073,63	92.778,69	95,64	96,97	96,05
6 cm fiberglass	6 cm rockwool	11.275,00	830,64	500,94	67.272,02	97.328,63	11.004,00	810,68	488,90	64.353,53	93.687,71	95,66	97,60	96,26
8 cm fiberglass	6 cm rockwool	10.922,00	804,64	485,26	67.502,58	96.618,17	10.645,00	784,23	472,95	64.584,09	92.961,26	95,68	97,46	96,22
10 cm fiberglass	6 cm rockwool	10.687,00	787,32	474,82	67.633,51	96.122,64	10.411,00	766,99	462,56	64.715,02	92.468,40	95,68	97,42	96,20
6 cm fiberglass	7 cm rockwool	10.938,00	805,81	485,97	67.885,28	97.043,52	10.719,00	789,68	476,24	64.966,78	93.541,22	95,70	98,00	96,39
8 cm fiberglass	7 cm rockwool	10.577,00	779,22	469,93	68.115,83	96.311,73	10.353,00	762,72	459,98	65.197,34	92.796,10	95,72	97,88	96,35
10 cm fiberglass	7 cm rockwool	10.344,00	762,05	459,58	68.246,77	95.821,54	10.142,00	747,17	450,60	65.328,28	92.364,57	95,72	98,05	96,39
6 cm fiberglass	8 cm rockwool	10.660,00	785,33	473,62	68.612,93	97.030,09	10.466,00	771,04	465,00	65.694,44	93.594,44	95,75	98,18	96,46
8 cm fiberglass	8 cm rockwool	10.300,00	758,81	457,62	68.843,49	96.300,97	10.128,00	746,14	449,98	65.925,00	92.923,96	95,76	98,33	96,49
10 cm fiberglass	8 cm rockwool	10.080,00	742,60	447,85	68.974,42	95.845,43	9.887,00	728,39	439,28	66.055,93	92.412,44	95,77	98,09	96,42
6 cm fiberglass	6 cm XPS	11.194,00	824,67	497,34	66.015,50	95.856,18	10.779,00	794,10	478,91	63.097,01	91.831,39	95,58	96,29	95,80
6 cm fiberglass	8 cm XPS	10.905,00	803,38	484,50	67.187,63	96.257,90	10.415,00	767,28	462,73	64.269,14	92.033,18	95,66	95,51	95,61
8 cm fiberglass	6 cm XPS	10.849,00	799,26	482,02	66.246,06	95.167,05	10.411,00	766,99	462,56	63.327,57	91.080,95	95,59	95,96	95,71
8 cm fiberglass	8 cm XPS	10.537,00	776,27	468,15	67.418,19	95.507,46	10.070,00	741,87	447,41	64.499,69	91.344,04	95,67	95,57	95,64
10 cm fiberglass	6 cm XPS	10.598,00	780,77	470,86	66.376,99	94.628,87	10.171,00	749,31	451,89	63.458,50	90.572,09	95,60	95,97	95,71
10 cm fiberglass	8 cm XPS	10.303,00	759,03	457,76	67.549,12	95.014,60	9.829,00	724,11	436,70	64.630,63	90.832,53	95,68	95,40	95,60

6. CONCLUSIONS

As a result even though brick is the most cost-effective wall body material in terms of initial investment costs; gasbeton is the most cost-effective alternative in terms of annual operating costs for reinforced concrete frame and load bearing systems. Brick is also the most cost-effective alternative in terms of life-cycle costs for both systems.

When two residential buildings to be constructed through load bearing system and reinforced concrete frame system with the same features and same envelope properties (wall, roof and ground flooring) are to be compared, residential building to be constructed with load bearing system will found to be more cost-effective when compared to the residential building to be constructed with reinforced concrete frame system both in terms of initial investment and of operating costs, thus being more effective option in terms of life-cycle costs. As illustrated by the Tables 2, alternatives to be constructed with load bearing system has 4,23- 8,49% lower initial investment costs, 1,18- 4,60% lower operating costs and 3,51- 6,53% lower life-cycle costs as compared to the alternatives to be built with reinforced concrete frame system.

REFERENCES

Manioğlu, G. 2002, 'Isıtma Enerjisi Ekonomisi ve Yaşam Dönemi Maliyeti', Yayınlanmamış Doktora Tezi, İstanbul Teknik Üniversitesi, Fen Bilimleri Enstitüsü, pp. 16-17.

NBS Handbook 132, 1980, *'Energy Conservation in Building: An Economics Guidebook for Investment Decisions'*, U.S. Departement of Commerce, pp. 14-20.

Berköz E., Küçükdoğu M., Yılmaz Z., Kocaaslan G. ve diğerleri, 1995. 'Enerji Etkin Konut ve Yerleşme Tasarımı', TÜBİTAK-INTAG 201, Araştırma Raporu.

Resmi Gazete No: 26100, Tarih: 6 Mart 2006, 'Deprem Bölgelerinde Yapılacak Binalar Hakkında Yönetmelik'.

Akçalı, Ü. 2007, '2007 Yılı İnşaat Birim Fiyat Analizleri', Şafak Matbaacılık San.Tic.Ltd.Şti., Ankara.
Anon., 'Binalarda Isı Yalıtım Kuralları', Türk Standartları 825, 1998, TSE, Ankara.

www.izoder.org

Anon., 2002. 'Kalorifer Tesisatı Proje Hazırlama Esasları', Makine Mühendisleri Odası Yayın No: MMO/ 2002/259/3, pp. 75-76.

Prioritizing Timber Defects – A Study of Telapak Naning, Malacca, Malaysia

Adi Irfan Che Ani [1]
Nor Haniza Ishak [2]
Nur Azfahani Ahmad [3]
Ahmad Ramly [4]
Yacob Omar [5]

T71

ABSTRACT

Timber traditional houses can pose a significant image of Malaysian built environment heritage. It is then crucial for professional to undertake the responsibility in ensuring the timber houses still in a fair condition. In judging the building condition, it is good to have a more concrete evaluation, so that the reliable recommendation can be made within short period of time. The Prioritize Ranking System which is still in the process of developing is deem fit for this purpose. The streamline methodology of the system is using the numerical coding for the survey pro forma. From the prioritize ranking, the data is then used as to foresee the condition of the house; either dilapidated, fair or good. For the pilot project, the system is tested to the small-scale timber traditional house namely Telapak Naning. The finding of the survey is found true in reflecting the current state of the house. The limitation of the research is regarding the reliability of the system; how does it suit in measuring the timber defects of traditional houses. Since then, the future research suggested is more concern on the reliability aspect, with more and more timber traditional houses should be surveyed using this proposed system.

KEYWORDS

Fungal Infestation, Insects Attack, Prioritise Ranking System, Timber Defects

[1] Department of Architecture, Faculty of Engineering, Universiti Kebangsaan Malaysia, Malaysia. Phone +06 0192033551, Fax +06 0389216841, adiirfan@gmail.com
[2] Department of Building Surveying, Faculty of The Built Environment, University of Malaya, Malaysia. Phone +06 0133657331, Fax +06 0379675713, niza_alambina@um.edu.my
[3] Department of Building Surveying, Faculty of Architecture, Planning & Surveying, University Technology MARA, Perak Branch, Malaysia. Phone +06 0196165652, Fax +06 053742244, nuraz020@perak.uitm.edu.my
[4] Department of Building Surveying, Faculty of The Built Environment, University of Malaya, Malaysia. Phone +06 0133711098, Fax +06 0379675713 , drabr@msn.com
[5] Department of Architecture, Faculty of Architecture, Planning & Surveying, University Technology MARA Malaysia. Phone +06 0193795425, Fax +06 0355444724, yacob_omar@yahoo.com.sg

1 INTRODUCTION

Malaysia, in aiming towards Vision 2020 as a develop country; still have large numbers of timber traditional houses which scattered in the suburban and rural area throughout the country. Some of them age, perhaps a few decades; and a number of them have reached a century. Become old and 'antique' across time, it is indeed requires the evaluation of maintenance, for the purpose of repair and replacement, could be; as to function up to the standard as well as providing safety for the occupants. In addition to that, these traditional houses also have a very significant potential in being gazetted as national heritage. Therefore we have to put an effort in realising this potential, or otherwise it will just be a conservation paradigm.

Moving forward the direction, this research gives focus in establishing the certain criteria to be used in evaluating the timber defects for traditional houses. To date, there is very little in number of published research focusing specifically on rating these traditional houses. Syed Zainal [1995] through Badan Warisan Malaysia provides some valuable criteria in assessing the building that should be classify as national heritage. But then, it is more to town building as well as colonial types. With the intention to link the said gap, this research concentrates on the idea of providing the criteria to be used when evaluating the timber defects via a building condition survey work. Apart from descriptive survey, this research tries to develop the Priority Ranking System, with the use of more numerical data for coding and analysing purposes.

Therefore, this paper discussed the said numerical-building-condition-survey based namely 'Timber Defects Prioritizing Ranking System'. The central approach of the system is to rank the timber defects that are found in one particular building. This will provide some guidance for the owner/care-taker in planning their repair (or replacement) work to be undertaken. After all, it will contemplate the current condition of the house, whether it is fit for occupancy or not. The discussion starts with the brief introduction of the timber house, literary discussion of the system as well as research approach, plus the survey pro forma adapted. It will then follow by the data analysis and discussion of finding, before end up with concluding remarks and future research to be done.

2.BRIEF DESCRIPTON OF TELAPAK NANING

Telapak Naning located at Kampung Sungai Jerneh, Brisu, Malacca, Malaysia, being among the oldest house within the vicinity. Telapak Naning has its own historical significance value. It takes about one hour and half by driving from the capital city of Kuala Lumpur, with estimated travel distance around 170 kilometres. Fig. 1(a) shows an image of Telapak Naning and background information in brief respectively. Telapak Naning was built in the year of 1800 as an arrogance of traditional Malay residential building by the great ancestors of Tuan Haji Nayan Karin. This 206 years house comprises many spaces for resting and welcoming guests (verandah), family occasion (huge main hall) and sleeping (bedroom).

(a) The exterior of Telapak Naning **(b)** The original portion of Telapak Naning

Figure 1(a) & 1(b): The house of Telapak Naning *Source*: Fieldwork (2007).

In 1967, the custodian of the house built an annex building to provide shelter for his younger sister. He had also made some replacement to the few building materials. The original portion of Telapak Naning can be seen in Fig. 1(b). Now, the house is not occupied at most of the time. The younger sister of Haji Nayan has been responsible to look after the house since her house is built as an annex to Telapak Naning. The house is raised on stilt which built from timber. According to Hj Nayan, only one big tree was used during the construction. This tree is cut into pieces to adapt the traditional structure of the house, namely column, raised floor, wall framing and roof truss. The joining of the structure is majority based on the type of tongue-and-groof and mortise-and-tenon.

In term of heritage or legacy setting, the special features of Telapak Naning predominantly affects by the historical value (as claimed by the custodian) of the house, which had been used by the Naning warrior named Dol Said as a place to rest, somewhere around 200 years back. This manifestation claimed to be true as it had been mentioned by national digest magazine in Malaysia, Mastika [2006] which stated that this house is a symbol of bravery and independence. As for further clarification, it should be confirmed by the Department of Museum, State of Malacca regarding the historical story line of the house. Until now, the house is proclaim to have some sort of supernatural element, in which it is said to give some sign if there will be anything likely to be happened to the family, or even to the area or *kampong*.

3.THE SYSTEM AND RESEARCH APPROACH

Remarks : October 2006 / Clear weather / Visual and Preliminary Inspection/ Detail Examination			
Scope of Condition Survey (Telapak Naning)	Covers: Exterior Public and Semi-private • Verandah • Living Rooms	Limitations	Excluded: Private Area (Bedroom) Attic Space Annex Building

Figure 2: Scope and limitations of condition surveys on site.

This survey used two (2) power tools, namely Protimeter SurveyMaster MM and Ventilation Meter and the scope of survey as per Fig. 2. The Protimeter is used for identifying the surface and internal moisture content of the timber element. Ventilation Meter is to identify the surrounding temperature and air velocity inside the house. The data from Protimeter is then refer to the simple diagnosis chart as depicted in Table 1, to determine whether the timber member have either condensation defect, rising dampness or no defect at all. For Velocity Meter, data gathered is for recording purpose only.

Figure of Condition Survey Checklist For Timber Defects

No.	Const. Element	Design & Construction	Building Survey: Defect Diagnosis – Causes	Building Survey: Defect Diagnosis – Types	Building Survey: Defect Prognosis	Building Survey: Proposed Remedial	Prioritise Ranking (Refer TOR) a	b	c	d	e	P.SM: Measure Mode	P.SM: Search Mode	Remarks

Guidelines:

1 "Causes" code: 1 Insects; 2 Fungal; 3 Weathering; 4 Mechanical Failure

2 "Types" code: 1 Termites-Subterranean; 2 Termites-Drywood; 3 Termites-Others; 4 Beetles; 5 Other insect; 6 Wet rot (brown); 7 Wet rot (white); 8 Dry rot; 9 Soft rot; 10 Blue stain; 11 Other rot

3 Prioritise Ranking: a Physical Condition; b Fabric Effect; c User Effect; d Potential Risk; e Risk Effect

4 P.SM (Protimeter SurveyMaster SM) [Measure=Surface; Search=Below] L = Low ; H = High

Figure 3: Condition Survey Checklist for Timber Defects
Source : This research (2007).

Table 1: Simple Diagnosis Chart for Protimeter SurveyMaster MM
Source : Protimeter (---)

Measure Mode	Search Mode	Interpretation and Comment
Low Reading	Low Reading	Dry surface, dry below the surface – safe
Low Reading	High Reading	Dry surface, damp below the surface. Investigate further using Deep Wall Probes in Measure Mode
High Reading	Low Reading	Damp surface, dry below the surface – probable condensation
High Reading	High Reading	Damp surface, damp below the surface. Trouble. Investigate further with Deep Wall Probes.

Data collection is mostly in the form of numerical coding. By referring to Fig. 3, the latter section of survey pro forma indicates the information required for calculating the sum of timber defects in determining its priority. Two types of data have to be collected, which are the physical data and risk data as per Fig. 4.

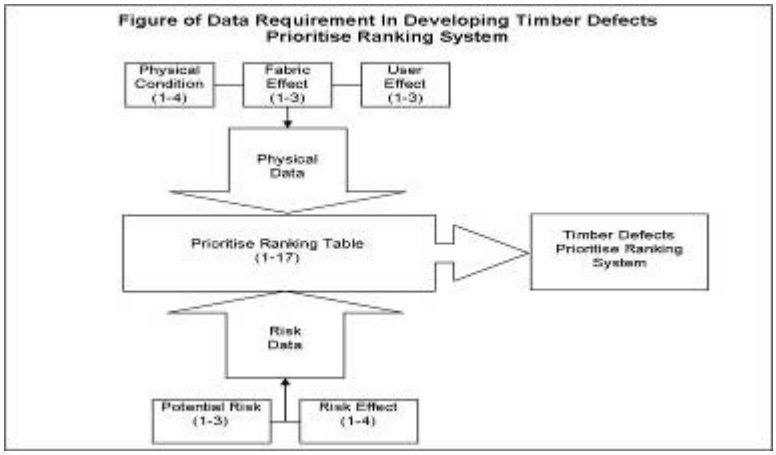

Physical data:
Current condition of the building at the time survey conducted.

Risk data:
The potential hazard that might be occurred to the building

The physical data and risk data is sub-divide into 5 categories, with 3 types and 2 types respectively

Figure 4: Data Requirement In Developing Timber Defects Prioritise Ranking System
Source : Modified from Pitt (1997).

Data is sum-up as to get the ranking of defects priority. Towards the end, one particular building that being surveyed is rated out of 3 conditions in term of structural stability, namely Condition 1: Dilapidated; Condition 2: Fair and Condition 3: Good. The linguistic value and average marks of these 3 conditions is given in Table 3.

Table 2: Term of Reference For Timber Defects Prioritise Ranking System
Source : This research (2007)

No.	Type of Data	Scale Value	Chronology Value	Linguistic Value
a	Physical Condition	0	Repair or replacement is needed within the period of 1 month	Element/structure not function at all
		1	Repair or replacement is needed within the period of 1-6 month(s)	Serious defect, can not function to an acceptable standard
		2	Repair or replacement is needed within the period of 6-12 months	Functional sound, but need an urgency repair or replacement
		3	Repair or replacement is needed within the period of 1-2 year(s)	Structurally function, only minor defects
		4	No need for repair or replacement	Free from any visible defects
b	Fabric Effect	1	Significant effect	If one particular element/structure is malfunction, what is the possible effect to the other element/structure member
		2	Have effect	
		3	Minor or no effect at all	
c	User Effect	1	Significant effect	If one particular element/structure is malfunction, what is the possible effect to the other element/structure member
		2	Have effect	
		3	Minor or no effect at all	
d	Potential Risk	1	Most possible	Risk particularly to structural damage, which in turn lead to death or injury (if the scale value is 3, the "risk effect" should have the score value of "4")
		2	Possible	
		3	Not possible	
e	Risk Effect	1	Death or serious injury	Risk particularly to structural damage, which in turn lead to death or injury
		2	Injury	
		3	Minor injury	
		4	No risk associated	

Table 3: Condition Assessment of the Building
Source : This research (2007)

Condition	Linguistic Value	Average Total Marks
Condition 1: Dilapidated	✓ Not safe for occupancy	04-05
Condition 2: Fair	✓ Sign of defect in secondary structural member (not give effect to the building stability) ✓ Need repair or replacement	06-10
Condition 3: Good	✓ Main structural member is strong and stable ✓ Defects which influence aesthetic value only	11-17

4.ANALYSIS AND DISCUSSION OF FINDINGS

By the time survey is conducted, the ventilation meter indicates the surrounding temperature is 27 degree Celsius, with the air velocity of 2.5 m/s. This shows the possibility of low moisture content and providing the dry surface for the whole site. Proceed with the analysis, the result of condition survey is shown in Table 4. According to the number of appearances, rotting is the highest number of occurrence, followed by termites attack and beetles. Therefore, insect attacks and fungal infestation remain as the main causes of timber defects, since more than half of the number of defects recorded fall within these two categories of causes. The location of defects is mostly found in the exterior part of the house. The defects can be seen in Fig. 5.

(a) **(b)** **(c)** **(d)**

Figure 5 (a), (b), (c) and **(d):** Defects which occurred at the surface of the timber at the site.

For the analysis of timber defect prioritise ranking, the lowest total marks is 5, whereas the highest score recorded is 16. The indication for marking system is the priority should be given to the lowest score. In this condition survey, the element of roof beam at staircase area is found to have the serious defects cause by fungal infestation, with the type of defect is dry rot. The score for this defected roof beam is 5 with the occurrence number is 1. The second serious defect with total mark of 10 is still cause by the fungal infestation, and located behind the area of defected roof beam. Total mark of 16 is recorded as the highest with prioritise ranking number 6; and 4 number of defects occurrence. The defects which classified as the least priority defects are caused mostly by the insect attacks.

The result of moisture content for defected timber element is depicted in Table 4, which shown under column of P.SM. A particular attention should be given to H (high) score, regardless whether the score is under measure mode or surface mode. Based on the survey result, the dampness defects could be raising dampness, since the characteristic of the reading is dry at the surface and damp below the surface. Thus eliminates the possibility of condensation defects. The roof beam which is the serious defects among 12 has the reading of low and high for the surface and below surface measurement

respectively. As to confirm whether raising dampness is occur, a further testing should be done using Deep Wall Probes, which is not carried out since the custodian did not allow for any destructive testing.

After prioritising each and every single timber defects found, it is important to deliberate about the overall condition assessment of the house; whether it is dilapidated, fair or good. Furthermore, this finding is much more useful for the occupants of the house for the sake of safety. According to the rated score of 5 types of data in determining timber defects prioritise ranking system; this research has extended the calculation in getting the total average marks for rating of condition assessment. The analysis reveals the average score is 13, thus indicates the condition of good (as refer to classification in Table 3). The level of severity for each timber defects is determined by the calculation of severity index.

Two types of data is required, namely the frequency and the average score of risk effect for each particular defect. The frequency is determined when the survey completed by referring to the number of defects occurrence in "defect diagnosis-types section" (as per Table 4). At first, the frequency is translated into percentage form. Then, the average score of risk effect is matched with the cross-reference table to get the accumulate multiplier. The accumulate multiplier is used as weight-age for average score of risk effect, with 0.25 is assign for each score. The formulation of severity index is shown below. In interpreting the result, the highest percentage indicates the most severe defect.

Severity Index *= Frequency (%) x Accumulate Multiplier of Risk Effect*

Table 4 : Analysis of Building Survey and Timber Defects Prioritising For Telapak Naning, Malacca, Malaysia
Source : This research (2007)

No.	Construction Element	Design and/or Construction	Building Survey		Timber Defects Prioritise Ranking System							P.SM		References	Remarks
			Defect Diagnosis		a	b	c	d	e	Total Marks	Prioritise Ranking	Measure Mode	Search Mode	Photo/ Drawing no.	
			Causes	Types											
1	Beam	Tongue & groove	1	4	3	3	3	3	4	16	6	L	L	(As Fig.5)	External
2	Window frame	Double leave window with green glass door, side hung	1	4	3	3	3	3	4	16	6	L	L		External
3	Floor	Timber joist	2	6	2	2	3	2	4	13	4	L	L	A	External
4	Floor	Timber joist	2	6	2	2	3	2	4	13	4	L	L	A	External
5	Column (under house)	Square in shape	1	4	3	3	3	3	4	16	6	L	H	B	External
6	Fascia board (at both sides)	Decorative with air Space	3	2	2	1	2	3	4	12	3	L	L		External
7	Floor joist (header)	Square in shape	1	1	3	2	3	3	4	15	5	L	L	C	External
8	Roof beam	Lean-to-roof	2	8	0	1	1	1	2	5	1	L	H	D	Staircase
9	Ceiling joist	Lean-to-roof	2	8	2	1	2	2	3	10	2	L	H	D	Staircase
10	Ceiling board	Lean-to-roof	2	8	2	1	3	3	4	13	4	L	H	D	Staircase
11	Wall board	Plywood	4	3	3	3	3	3	4	16	6	L	L		*Serambi*
12	Ceiling board	Plywood	2	6	1	2	3	3	4	13	4	L	L		Living room
								Total		158					

Condition Assessment

Average Total Marks = 158/12

13 (Condition 3: Good)

(continued from Table 4)

Guidelines:

1 "Causes" code
- 1 Insects
- 2 Fungal
- 3 Weathering
- 4 Mechanical Failure

2 "Types" code
- 1 Termites-Subterranean
- 2 Termites-Drywood
- 3 Termites-Others
- 4 Beetles
- 5 Other insect
- 6 Wet rot (brown)
- 7 Wet rot (white)
- 8 Dry rot
- 9 Soft rot
- 10 Blue stain
- 11 Other rot

3 Prioritise Ranking
- a Physical Condition
- b Fabric Effect
- c User Effect
- d Potential Risk
- e Risk Effect

4 P.SM (Protimeter SurveyMaster SM)
[Measure=Surface; Search=Below]
L = Low ; H=High

Table 5: Analysis of Severity Index For Telapak Naning, Malacca, Malaysia
Source : This research (2007)

Types of Defects	"Types" Code	Frequency	Frequency (%)	Average Score of Risk Effect	Accumulate Multiplier*	Severity Index	Severity Index (%)
Termites-subterranean	1	1	8.33	4	0.25	2.08	4.76
Termites-drywood	2	1	8.33	4	0.25	2.08	4.76
Termites-other	3	1	8.33	4	0.25	2.08	4.76
Beetles	4	3	25.00	4	0.25	6.25	14.29
Wet rot (brown)	6	3	25.00	2	0.75	18.75	42.86
Dry rot	8	3	25.00	3	0.50	12.50	28.57
TOTAL		12	100.00			43.75	100.00

* cross-reference

Risk Effect	Score	Multiplier	Accumulate Multiplier
	1	0.25	1.00
	2	0.25	0.75
	3	0.25	0.50
	4	0.25	0.25

From this finding, suffice to mention that all timber defects found in Telapak Naning is classified as not very much severe, since no severity index above 50% is recorded. Termites attack found to be the lowest index (below 10%) and considered not severe to the house. The finding of severity index is then confirmed and supported the score of condition assessment, which good with no severe defects found. From the research conducted, the main finding can be drawn as below:-

a. Element to be repaired (in order of priority) – details to be refer from Table 4 and 5

1) Roof beam;
2) Ceiling joist
3) Fascia board;
4) Either floor (timber joist) or ceiling board;
5) Floor joist (header); and
6) Either beam, window, column or wall board

b. Overall Condition Assessment – Condition 3: Good

c. Severity Index – Wet rot (brown) with almost 43%

5 CONCLUSION

Telapak Naning gives significant remarks to Kampong Sungai Brisu, Malacca, Malaysia. This small-scale house at one time ago is used by the Naning warrior and its team as a rest house during Naning War. Now, the house is left unoccupied (except for special occasion) since the annex building is build by the custodian siblings. The special feature of this house is regarding its historical value. Major renovation which carried out around 1967 gives quite a lot of changes, especially for finishing materials. This is found to be the main cause in which the occurrence of timber defects in term of numbers is very minimal to the house nowadays.

Building condition survey reveals that the house is still in a good condition and classified as good. For maintenance purpose, the custodian should give priority for replacement of the roof beam element at the staircase area (the lean-to-roof structure). In term of severity level, frankly to quote that no element had seriously damaged. This is because all the timber defects are recorded to be below of 50% severity index. Keep in mind that only one portion of the house namely roof beam at the staircase area that need to be replace urgently, otherwise the severity level reflects the number of defects occurrence for the whole structure. The limitation of the research is the reliability of the system developed for the purpose of rating criterion namely Timber Defects Prioritise Ranking System. Telapak Naning form as pilot project for the system and it is likely to be found that the findings reflect the current state of the house. More and more building should be surveyed using this system in evaluating the system reliability. Therefore further research to be done is to carry out a building condition survey work, particularly to the timber traditional houses.

ACKNOWLEDGEMENT

The authors would like to acknowledge the parties that help in preparing the paper, in one way or another, especially to Tuan Haji Nayan Karin, the custodian of Telapak Naning and University Malaya, Malaysia for funding this research under fundamental research grant no. FP058/2005D. Last but not least, to all families members whom had give endlessly supports and encouragements.

REFEENCES

Mastika 2006. *Petanda Itu Semakin Jelas*. An article about Telapak Naning witten by Shamran Sarahan. Ogos 2006. pp. 80-84. Kuala Lumpur: Utusan Karya Sdn. Bhd.

Pitt, T. J. 1997. Data Requirements For The Prioritization of Predictive Building Maintenance. *Journal of Facilities*. Volume 15 Number 3/4. pp. 97-104. MCB University Press Limited.

Protimeter (---). *Protimeter "Compleat" Dampness Kit MK II: Detailed Instructions For All The Instruments & Accessories Included In The Kit.* pp. 11. England: PROTIMETER plc.

Syed Zainal A. I. 1995. *Pemeliharaan Warisan Rupa Bandar*. Kuala Lumpur: Badan Warisan Malaysia.

Condition Assessment of Façade Rendering through in-Situ Testing

Inês Flores-Colen[1]
Jorge de Brito[2]
Vasco P. de Freitas[3]

T 71

ABSTRACT

Condition assessment of rendering façades should compare required performance level with supplied performance level, on a practical and unambiguous basis, in order to help the serviceability assessment and maintenance planning of rendering during the post-occupancy stage. The application of rendering on-site performance assessment has been difficult due to several reasons: design solutions are mostly prescriptive instead of based on performance assessment criteria; technical data provided by the manufacturers is insufficient or descriptive; and legal requirements (EN 998-1) are not enough to evaluate its global performance. Therefore, condition assessments have been restricted to visual inspections, without quantitative parameters through testing techniques.

This paper presents a methodology that can be used in condition assessment (supplied in-service performance) of rendering façades through in-situ testing. This ongoing research (within the PhD study of the first author) intends to identify some rendering properties (related to surface condition, mechanical strength and water resistance) that can be measured through on-site suitable and expedient techniques, and compared with standard hardened rendering properties or integrated into reference in-service performance profiles (IPP). Finally, performance criteria of mechanical strength is discussed through an experimental campaign that compares open porosity, apparent dry bulk density, compressive strength, adhesion strength, apparent ultrasonic pulse velocity and dynamic elastic modulus for different types of mainly cement-based renders (sound samples), used in common Portuguese buildings.

KEYWORDS
Rendering, Performance, In-situ, Testing, Condition assessment.

[1] DECivil-IST, Technical University of Lisbon, Av. Rovisco Pais, 1049-001, Lisboa, Portugal, Phone +351 21 8418372, Fax +351 21 8497650, ines@civil.ist.utl.pt

[2] DECivil-IST, Technical University of Lisbon, Av. Rovisco Pais, 1049-001, Lisboa, Portugal, Phone +351 21 8419709, Fax +351 21 8497650, jb@civil.ist.utl.pt

[3] DEC-FEUP, University of Porto, Faculty of Engineering, Rua Dr. Roberto Frias, 4200-465, Porto, Portugal, Phone +351 22 5081932, Fax +351 22 5081940, vpfreita@fe.up.pt

1 INTRODUCTION

Façade rendering is a common cladding system in Portugal. According to 2001 national statistics, rendering represents 61.6% of 2,561,227 Portuguese buildings built between 1946 and 2001 (81% of all Portuguese buildings), followed by architectural concrete (21.3%), stone (11.3%), ceramics (5.5%), and others (0.8%). Render mortars used in Portuguese recent buildings are of two types: cement and sand mortars in two or three layers, mixed in-situ (current renders), and factory-made mortars, made of cement, sand, admixtures and additives in a single layer (ready-mixed renders), in which the finishing layer is either the render itself ("one-coat mortars") or other materials (e.g. a paint). The use of ready-mixed mortars started in the 90's in Portugal and it has increased. In 2005, about 30 manufacturers produced 1.2 million tons of ready-mixed mortars, with a total amount about 90 million euros. In 2006-2015, the reduction of mortars made on site is expected to increase the production of ready-mixed mortars until around 2.5 million tons.

Condition Assessments are required throughout the life cycle of the building façade, and are an important tool to improve the knowledge of in-service conditions and helping the inspectors in maintenance planning. A condition survey is defined by RCIS [1997] as "the collection of data about the condition of a building, estate or portfolio; assessing how that condition compares to a pre-determined standard, to identify any actions necessary to achieve that standard now, and maintain it there over a specific time horizon, the purpose being to support management decision making". Conditioned-based maintenance by performing inspection assessments has been for some time a useful tool for reducing life cycle costs and finding more efficient ways of using maintenance budgets [Hertlein 1999], and it is also an appropriate maintenance strategy for elements whose condition can be suitably monitored.

In this context, condition assessment of rendering façades should compare the required performance level (properties that have been specified at the design stage) with the supplied performance level, in order to help the serviceability assessment. The application of rendering on-site performance assessment has been difficult. The lack of performance information provided by the manufacturers, the complexity of the building process, and the difficult relationship between users and products requirements, have led, in the majority of the cases, to in-field assessment based only on visual observation of defects / anomalies, instead of quantitative performance requirements analysis.

2 RENDERING CONDITION ASSESSMENT

Rendering condition assessment, based on technical in-service assessment, must define the problem, collect available data, characterize existing anomalies [Flores-Colen *et al* 2008] and their probable causes, evaluate in-service performance (fulfilment of the functions established at design), check whether user's demands are being fulfilled and, finally, define corrective, preventive or monitoring maintenance actions. The comparison of required performance level (the minimum performance level that must be provided at a certain moment in time) with supplied performance level (the maximum performance which can be provided by a building component at a certain moment in time) over time can be made if both supply and demand for components are expressed in the same way. Fig. 1 shows the proposed relationship between demand and supply sides, when a rendered façade condition assessment is made through visual observations, in-situ and lab testing. The relationship of these two conceptual languages is based on the context of Conceptual Framework for the Whole Life Cycle of Facilities [Szigeti & Davis 2005].

The required hardened properties rendering mortar (required performance criteria) are established by European standard EN 998-1 [CEN 2003] (rendering mortars based on inorganic binders use on walls with different fields of use and exposure conditions), and complemented by other technical issues (see Fig. 1). These properties are assessed through laboratory tests using standard apparatus and specimens.

According to Hermans [1995], the supplied performance level has to be determined on-site (it is affected not only by design decisions, but also by construction process, material characteristics, its shape and location in façade) and contains a set of performance levels belonging to various performance categories at a certain moment. This author also compares deterioration with performance "the term deterioration is connected to the change of the characteristics, instead of to the change of the performance level itself". Therefore, it is important to recognize that some cases of reduction of properties do not affect critical aspects of performance.

In-situ assessment of rendering in-service performance has been usually restricted to a visual appraisal without systematic methodologies in the majority the cases, which has led to a deficient diagnosis and consequent implementation of inadequate maintenance interventions. The usual absence of records of intervention (historic of the building) and means of access in the buildings aggravate this situation through an accumulation of errors.

Most field inspections of buildings that include an assessment of the performance of materials and components are descriptive. From literature, recent empirical studies have been developed to assess mainly degradation of common rendering façades through visual observation (symptomatic analysis) such as the application of a physical and visual five ranking (each level describes visual or functional loss of performance) for claddings [Shohet *et al* 2002] or a single deterioration indicator for render façade (OLD - overall degradation level) that is obtained through the average weighted sum of all defects, according to their condition level [Gaspar & de Brito 2005].

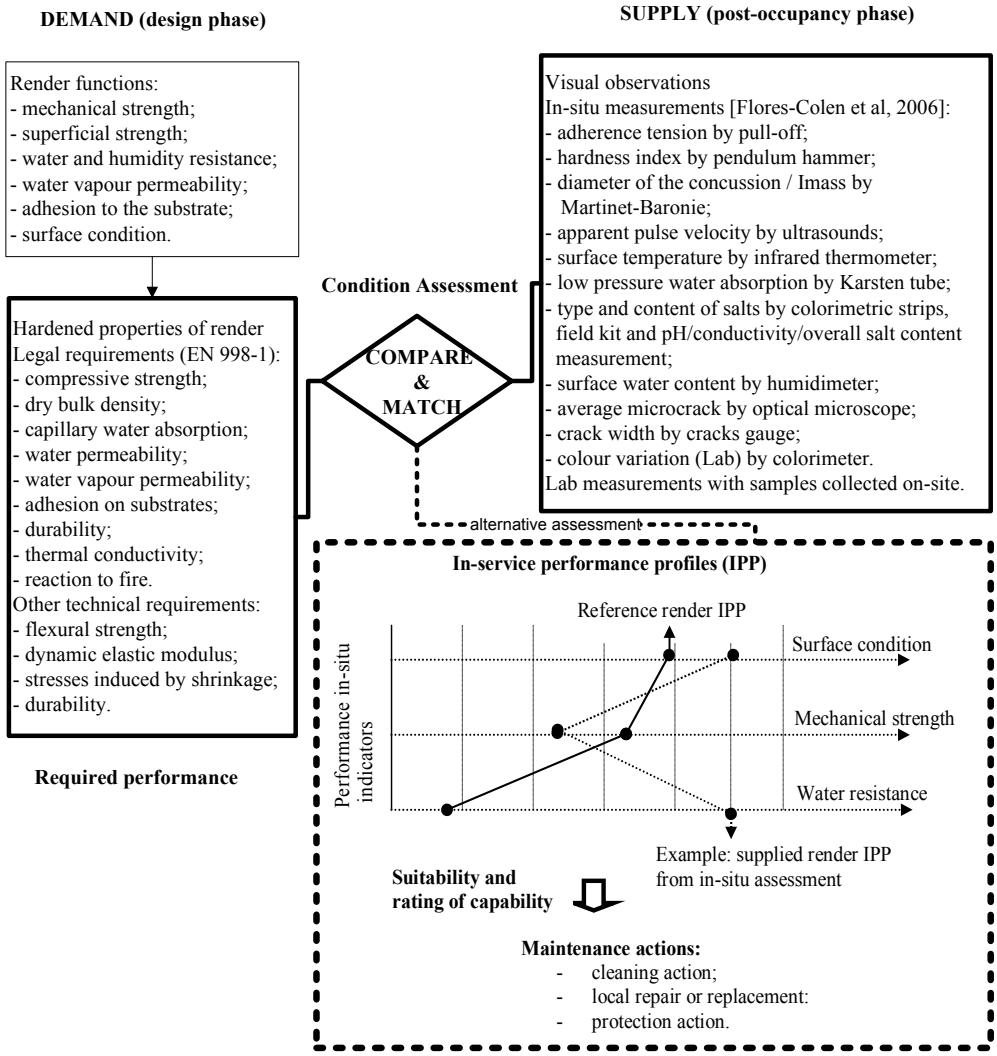

Figure 1. The methodology for rendering condition assessment.

Figure 1 shows in the supply column the in-situ techniques that have been used in field assessment [Flores-Colen *et al* 2006]. It can be concluded that these in-situ techniques (except for adherence tension by pull-off test) do not provide a direct correlation with the performance requirements for rendering in European standard EN 998-1 or other technical documents; most of these criteria result from laboratory tests. Therefore, it is important for conditioned-maintenance planning that in-situ characterization of each render includes relevant properties that are measurable on-site, complementing (or correlating with) standard performance requirements.

An alternative assessment is proposed (see Fig.1) using in-service performance profiles (IPP) that include in-service performance indicators and reference values of properties measured on-site (reference IPP). Three performance categories are proposed: surface condition, mechanical strength and water resistance. Conditioned maintenance should be applied when the supplied in-service performance level (at least in one of the three previous categories) is not acceptable, through cleaning, repair, replacement and protection actions.

3 INDICATORS OF MECHANICAL STRENGHT - EXPERIMENTAL CAMPAIGN

3.1 Testing Program and Results

In this paper, some indicators of mechanical strength are discussed in terms of in-service performance assessment. Therefore, an initial set of laboratory tests was performed in order to help the interpretation of in-situ technique results. This experimental campaign included the production of standard samples (3 samples for each property to be studied, with dimensions of 4 x 4 x 16 cm^3 or 2.5 x 2.5 x 28.5 cm^3 in the dynamic elastic modulus determination), and also of 9 small-scale models (1.5 cm of render + brick substrate, with dimensions of 49 x 19 cm^2), as shown in Fig. 2. These models were produced with different render mortars, taking into account the types that are currently used in rendering of brick cavity-wall façades:

- pre-mixed mortars (compositions specified by the manufacturer), that are applied in a single coat, without finishing (designated by one-coat renders - PM), with heavy finishing - PP (e.g. ceramic tilling) or light finishing (e.g. paint - PL);
- made on-site mortars (with cement and/or lime binders) that normally applied as multi-coat systems (but not in these tests), PC with cement binder and PB with lime and cement binders.

Figure 2. Standard prisms of rendering mortar (left), and small-scale models (centre and right).

Table 1 shows the average of three or five values for the following hardened rendering properties: apparent dry bulk density (ρ_A), compressive strength (R_C), dynamic elastic modulus (E_d), open porosity (P_{open}), adhesion strength (f_A) and apparent ultrasonic pulse velocity ($V_{apparent}$). The first three were determined by standard testing (see Table 1). The remaining properties were obtained by techniques that can be applied on-site (in this testing program those tests occurred on the surface of small-scale models or on small samples collected from those models).

The adhesion strength (f_A) is determined by the tensile extraction test (pull-off), Fig. 3, on the left, according to the EN 10 155-12 [CEN 2000], taking into account the recommendation MDT.D.3 of RILEM [2004] to evaluate in-situ adherence. The test program included five tensile extraction tests on the small-scale models for each product, using square metallic test piece with dimensions 5 x 5 cm^2.

The device that was used measured the force necessary to extract the disk. The pulling-off resistance was calculated by the equation 1.1. The types of the rupture (cohesive or adhesive) were also observed.

After pull-off test and adequate preparation (remove the metallic piece and remaining glue), three samples were submitted a compressive tests (Fig. 3, at the center). The other samples were used on open porosity determination (Fig. 3, on the right).

$$f_A\left(N/mm^2\right)=\frac{F_u}{A_{square}} \quad \text{.....Eq.1.1}$$

where: F_u (rupture force, in N), A_{square} (area of a square test piece, in mm^2).

Table 1. Results of testing program for hardened rendering properties in renders, at 28 days.

Render type	*w/c*	*Mixing proportions in mass**	*Tests on standard prisms*			*Tests on small-scale models*		
			ρ_A (kg/m³) EN 1015-10	R_C (N/mm²) EN 1015-11	E_d (N/mm²) NF B 10-511	P_{open} (%)	f_A (N/mm²)	$V_{apparent}$ (km/s) ASTM C597
PM	1.40	1: 0.2: 6	1320	2.83	5250	23.38	0.31	2.76
PP	1.07	1: 0.2: 5	1660	12.56	16150	9.86	0.54	3.79
PL	1.5	1: 0.25: 7	1340	1.32	4825	33.64	0.38	3.06
PC	1.0	1:__: 5.5	1660	5.92	11220	15.53	0.44	3.69
PB	1.0	1: 0.3: 4	1720	5.96	13275	15.18	0.40	**

Legend: *mixing proportions in mass = cement: lime: sand; **the measurement was impossible to perform because the render cracked and detached from the support during the impact tests (tests not included in this paper but which occurred before ultra-sound tests).

Figure 3. Pull-off test (left), compressive strength test with small samples (centre), and samples for open porosity determination (right).

The open or apparent porosity (P_{open}) expresses the percentage of the relationship of the volume of open pores in the test specimen to its exterior volume, and can be measured by microscopy and intrusion techniques. The simplest indirect porosity measurement is total pore volume determination by vacuum saturation, where only pores that are interconnected are measured. This technique does not give any information about size and shape of the pores [Thomson *et al* 2004].

In this testing program the open porosity (P_{open}) was measured by immersion in water (Archimedes' principle), according to the equation 1.2 from ASTM C 830 [2006], but with the following adaptations: four samples with dimensions 2.5 x 2.5 x 2.5 cm^3 (cut from the samples that were obtained in the adhesion tests on the models) and process of saturation (samples were measured after having been subjected for 2 days to a correspondent pressure of 10 cm water column followed by a higher pressure of 88 cm water column for at least 7 days), using a pressure pump (Fig. 4, on the left). This procedure was set to guarantee that water penetrates in all open pores, even the ones that could be partially occluded, giving probably values close to the absolute porosity [Fernandes *et al* 2005].

Figure 4. Pressure pump (left), determination of suspended weight (centre), and transit time measurement on the surface of the model (right).

$$P_{open}(\%) = \frac{W - D}{W - S} * 100 \quad \text{.....Eq.1.2}$$

where: W (saturated weight, when two consecutive weightings do not differ by more than ±0.05 g), D (dry weight, in the oven at a temperature of 70 ºC), and S (suspended weight, after saturation and while suspended in water, Fig. 4 at the centre).

The apparent ultrasonic pulse velocity ($V_{apparent}$) was calculated by using ultra-sound equipment PUNDIT that generates low frequency ultrasonic pulses and measures the time taken for them to travel from one transducer to the other through the material tested (Fig. 4 on the right). The transducers were placed on five points on the surface of the render (indirect or surface transmission) with a distance between them of 100 mm. The apparent ultrasonic pulse velocity was determined from equation 1.3.

$$V_{apparent}(km/s) = \frac{d}{T} \quad \text{.....Eq.1.3}$$

where: d (path length between transducers, in mm) and T (transit time, in μs).

3.2 Discussion of Tests Results

The results have shown that the open porosity of small samples (using Archimedes principle technique and higher pressure in saturation process) can be used as an on-site indicator of render type, and of hardened standard properties (compressive strength $R_{exp}^2 = 0.9808$ and dynamic elastic modulus, $R_{log}^2 = 0.9174$, see Fig. 5). With these results, rendering façade of common buildings (mainly cement-based renders) should be divided into two groups. The first one includes the majority of pre-mixed mortars (one-coat renders without finishing or to receive light finishing), like PM and PL mortars. In this group of mortars it is to be expected (in small samples collected on site) values of open porosity higher than 20%, compressive strength lower than 5 MPa (categories CSI, CSII or CSIII according to EN 998-1), and dynamic elastic modulus lower than 10 000 MPa (according to LNEC 427/05 [Veiga 2005], ready-mixed mortars should have $E_d \leq 10\,000$ MPa to limit the cracking susceptibility). The second group includes all made on-site renders and some ready-mixed mortars (mostly to receive heavy finishing), and the expected values are open porosity lower than 20%, compressive strength (CSIII or CSIV according to EN 998-1) higher than 5 MPa, and dynamic elastic modulus higher than 10 000 MPa (for example, wall with high exposure to impact loads).

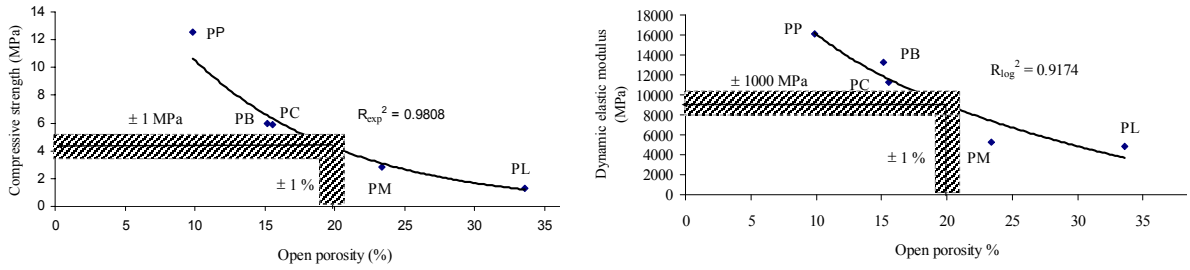

Figure 5. Relationship between open porosity and compressive strength (left) and dynamic elastic modulus (right) from test results.

According to other authors the porosity of cement-based mortars is low when compared with lime-based mortars, with reference values of 20 to 25% [Begonha 2001]. Another study has obtained a wide range of porosity from 10 to 35% in cement-based mortars and using water saturation [Goueygou *et al* 2003]. Also that compressive strength is a function of the porosity and the type of binder [Thomson *et al*, 2004], however the study of pore size distribution is important to understand in detailed mechanical properties of air-entrained cement-based mortars, like PM type; in general, only voids of diameters smaller than 50 nm enhance both compressive and flexural strength [Wieloch & Klemm, 2005].

The porosity is related with the compacity of render. The results have also shown the relationship between open porosity and apparent dry bulk density with $R_{linear}^2 = 0.7247$, with for example for first group: $P_{open} < 20\% \Rightarrow \rho_A < 1500$ kg/m^3. The results have also shown that the pull-off test can be an useful on-site technique, because its results can be compared with standard values (according to EN 998-1 and LNEC 427/05, it should be $f_A \geq 0.3$ MPa or a cohesive fracture pattern); it also can be used as an indicator of compressive strength of the render (the increase of compressive strength of in-situ samples when compared with standard samples can be due to application procedure changes, Fig. 6, on the left).

The results have also shown a good correlation between apparent ultrasonic pulse velocity and dynamic elastic modulus ($R^2 = 0.8804$, with $V_{apparent} < 3.5$ km/s $\Rightarrow E_d < 10\,000$ MPa for the first group of mortars, see Fig. 6 on the right), despite using indirect method (surface transmission). From literature, the ultrasonic waves are directly influenced by its elastic parameters (relation of shear velocities and Young's modulus for homogeneous material), and elastic modulus depend on porosity, therefore pulse velocity decreases with porosity increase [Goueygou *et al* 2003]; this tendency was observed with relation $R^2 = 0.6759$ between $V_{apparent}$ and P_{open}.

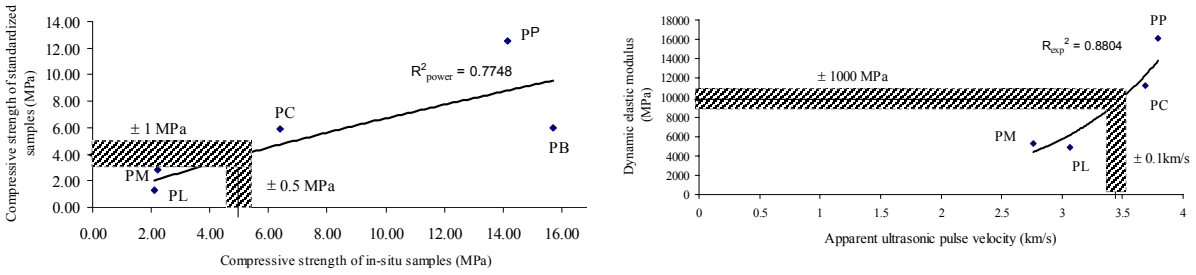

Figure 6. Relationship between compressive strength of in-situ and standardized samples (left), and apparent ultrasonic pulse velocity and dynamic elastic modulus (right) from test results.

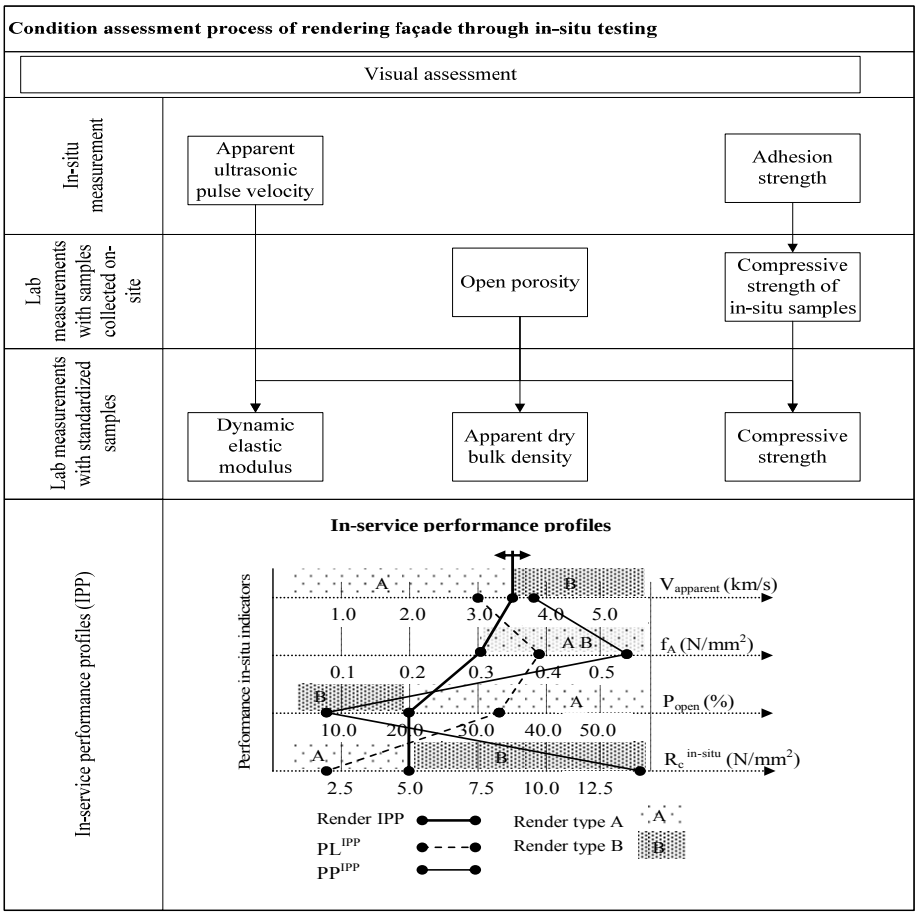

Figure 7. Condition assessment of rendering through hierarchy on-site mechanical strength indicators.

5 CONCLUSIONS

This paper is focused on in-service performance assessment within rendering condition assessment, in order to help conditioned-maintenance during its service life. The experimental campaign on sound samples allowed the specification of mechanical strength indicators that are measurable through in-situ expedient techniques or in laboratory with samples collected on-site, in terms of apparent ultrasonic pulse velocity, adhesion strength, open porosity and compressive strength (see Fig.7), despite the high variability of the material under study. Results have also shown that the extrapolation of standard hardened properties (dynamic elastic modulus, apparent dry bulk density and compressive strength) from previous on-site properties, and their comparison with required performance can be made. It can also be concluded that the use of an in-service performance profile (IPP) in serviceability assessment is possible with the identification of a reference IPP that considers two groups of renders (A and B), taking reference values (as shown in Fig. 7, in this example, the ready-mixed mortars PL belongs to group A and PP to group B). This profile allows the integrated study of more than one on-site property and therefore it can increase the reliability of the assessment. Finally, it is concluded that there is a potential to follow this methodology (with expedient techniques instead of more advanced techniques that can increase costs and time consuming of inspections) of rendering condition assessment, even though its reliability can only be acquired through wider and longer experimental campaigns. The actual performance in-situ during early age of rendering façade is yet to be fully understood (an important step to maintenance planning), therefore, more studies and further research should be conducted in sound and damaged samples.

ACKNOWLEDGMENTS

Acknowledgements are given to FCT (Foundation for Science and Technology), to ICIST Research Institute of IST, Building Physics Laboratory of FEUP, and to Luís Silva of Weber Cimenfix.

REFERENCES

ASTM 2006, 'C 830 - Test methods for apparent porosity, liquid absorption, apparent specific gravity and bulk density of refractory shapes by vacuum pressure', American Society for Testing and Materials, 4 p.

Begonha, A. J. 2001 *Meteorization of granite and deterioration of stone in monuments and buildings in the city of Oporto*. Doctoral thesis, Faculty Engineering of Oporto, 438 p.

CEN 2003, 'EN 998-1 - Methods of test for mortar for masonry - Part 1: Rendering and plastering mortar', European Committee for Standardization, Brussels.

CEN 2000, 'EN 1015-12 - Methods of test for mortar for masonry - Part 12: Determination of adhesive strength of hardened rendering and plastering mortars on substrates', European Committee for Standardization, Brussels, February, 10 p.

Fernandes, V., Silva, L., Ferreira, V. M. & Labrincha, J.A. 2005, 'Influence of the kneading water content in the behaviour of single-coat mortars', *Cement and Concrete Research*, 35, pp. 1900-1908.

Flores-Colen, I. de Brito. J. & Freitas, V.P. 2008, 'Stains in facades' rendering - Diagnosis and maintenance techniques' classification', *Construction and Building Materials*, 22 [3], pp. 211-221.

Flores-Colen, I., de Brito, J. & Freitas, V. P. 2006, 'Expedient in situ test techniques for predictive maintenance of rendered façades´, *Journal of Building Appraisal*, 2[2], pp. 142-156 (15).

Gaspar P. L. & de Brito J. 2005, 'Assessment of the overall degradation level of an element, based on field data', Proc. 10th Int. Conference on the Durability of Building Materials & Components, Lyon, France, 17-20 April, pp. 1043-1050.

Goueygou, M., Lafhaj, Z. and Kaczmarek, M. 2003, 'Relationship between porosity, permeability and ultrasonic parameters in sound and damaged mortar'. Proc. Int. Symposium Non-Destructive Testing in Civil Engineering, Berlin, September.

Hermans, M. 1995, *Deterioration of building components. A data collecting model to support performance management*, Ph.D. Thesis, Faculty of Architecture and Building Science, Eindhoven, University of Technology.

Hertlein, B. 1999, 'Predictive maintenance - What should be in a condition database? ', Proc. 8th International Conf. on Durability of Building Materials and Components, Institute for Research in Construction, Ottawa, Canada, pp. 1203-1212.

RCIS 1997, *Stock condition survey - a guidance note*, Royal Institution of Chartered Surveyors, UK.
RILEM 2004 'Recommendation MDT D.3. Determination "in situ" of the Adhesive Strength of Rendering and Plastering Mortars to their Substrate', *Materials and Structures*, 37, August-September, pp. 488-490.

Shohet, I. M., Puterman, M. & Gilboa, E. 2002, 'Deterioration Patterns of Building Cladding Components for Maintenance Management', *Construction Management and Economics*, 20, 305-314.

Szigeti, F. & Davis, G. 2005, ´ASTM Standards methods: concept and case study´, International Centre for Facilities, AIA Centre for Building Performance Symposium, October 27.

Thomson, M. L., Lindqvist J. E., Elsen, J. & Groot, C.J.W.P. 2004 'Porosity of historic mortars', Proc. 13th International Brick and Block Masonry Conference, Amsterdam, July 4-7.

Veiga, M. 2005, *Rules for conceding application documents for pre-dosed mineral renderings based on cement*, Report 427/05 NRI, National Laboratory of Civil Engineering, Lisbon, December, 30 p.

Wieloch, M. & Klemm, A. J. 2005, 'The effects of pore structure of air-entrained cement-based mortars on freezing and thawing deterioration', Proc. PRoBE conf., Glasgow Caledonian University, Glasgow, 16-17 November, pp. 517-526.

Durability Evaluation of a Realkalisation Treatment Using Impressed Current

Yun Yun Tong [1]
Véronique Bouteiller [2]
E. Marie-Victoire [3]
Suzanne Joiret [4]

T 71

ABSTRACT

The aim of this paper is to explore the durability aspect of a realkalisation treatment using impressed current. To that purpose, a series of small slabs of poor quality reinforced concrete were cast and artificially carbonated. A first set of electrochemical experiments were then performed, including rest potential, linear polarization and impedance measurements. Afterwards, carbonated slabs were realkalised using an impressed current of 1 A/m² of steel following the CEN/TS 14038-1 specification [1]. The efficiency of the treatment was determined 15 days, 10 weeks, 6 months and 12 months after realkalisation through different electrochemical measurements and analytical characterizations.
The rest potentials and corrosion currents results indicate a slight decrease of the corrosion activity after treatment although the passive state of the reinforcement encountered in uncarbonated concrete was not recovered. The efficiency of the treatment is clearly demonstrated with the phenolphthalein test just after treatment with the pink coloration around the rebars, but, the colour is not so obvious after 12 months. SEM and Micro-Raman analysis indicate an evolution of the rust products from active to passive, thus confirming the decrease of corrosion activity. Concerning the impact of the treatment on the cement matrix, a noticeable enrichment in potassium concentration was encountered on the treated surface. But the mechanical performances of the concrete do not seem to be affected.

KEYWORDS

Carbonation, Corrosion, Electrochemical method, Realkalisation, Impressed current

[1] Laboratoire Central des Ponts et Chaussées, 58 bd Lefebvre, 75732 Paris Cedex 15, FRANCE, Phone +33 1 40 43 53 09, Fax +33 1 40 43 65 15, yunyun.tong@lcpc.fr
[2] Laboratoire Central des Ponts et Chaussées, 58 bd Lefebvre, 75732 Paris Cedex 15, FRANCE, Phone +33 1 40 43 65 39, Fax +33 1 40 43 65 15, veronique.bouteiller@lcpc.fr
[3] Laboratoire de Recherche des Monuments Historiques, 29 rue de Paris, 77420 Champs sur Marne, FRANCE, Phone +33 1 60 37 77 80, Fax +33 1 60 37 77 99, elisabeth.marie-victoire@culture.gouv.fr
[4] Laboratoire Interfaces et Systèmes Electrochimiques, UPR 15 CNRS, Case 133, Tour 22, Université Pierre et Marie Curie, 4, place Jussieu, 75252 Paris Cedex 05, FRANCE, Phone +33 1 44 27 40 51 Fax +33 1 44 27 40 74, sjoiret@ccr.jussieu.fr

1 INTRODUCTION

Good quality concrete protects steel reinforcement. Chemical protection is provided by the concrete's high alkalinity and physical protection by the concrete cover acting as a barrier which impedes the access of aggressive species. Nevertheless, the corrosion of steel in concrete is becoming the most common cause of failure in concrete structures. The corrosion can be due either to the presence of chlorides at the steel level or by the carbonation of the concrete cover. Concerning the latter, the natural ageing carbonation process leads to a consumption of portlandite inducing a decrease of the pH. Then, the concrete cover is no longer protective and active corrosion can take place [1-3]. Since the rust products as a result of corrosion have a 2-4 times bigger volume than that of steel, it causes volume expansion developing tensile stresses in concrete, which ultimately result in cracking and spalling of the concrete cover. Before its spalling, reinforced concrete structures affected by carbonation may be cured by two realkalisation techniques using either impressed current or sacrificial anodes [3]. In these techniques, rebars play the role of cathodes and an anode is temporarily applied onto the concrete surface. Electrical conductivity is assessed by an alkaline electrolyte contained in a cellulose pad. Realkalisation treatments are supposed to both generate hydroxyl ions around the rebars by hydrolysis and induce a migration of alkaline ions from the electrolyte to the concrete cover. A few studies [5-16] deal with the efficiency of the realkalisation treatment but very few explored the durability aspect [16-17].
The aim of this paper is to evaluate the efficiency and the durability performances of a realkalisation technique using impressed current applied to carbonated reinforced using electrochemical measurements (rest potential, linear polarization and impedance) and analytical characterizations (phenolphthalein, Micro-Raman Spectroscopy, Scanning Electron Microscopy combined with EDS, alkaline concentration profiles and mechanical tests).

2 EXPERIMENTAL

2.1.Specimens

Seven 300x300x50 mm reinforced concrete slabs were cast using Portland cement (CEM I, 275 kg/m^3) and a 0.7 water to cement ratio according to the EN 1766 Standard. The reinforcement consisted in three parallel steel rebars (Fe235, 6 mm in diameter and 400 mm in length) embedded in a 22 mm concrete cover. On these rebars, a 200 mm zone was delimited in the centre using epoxy resin (Fig. 1).

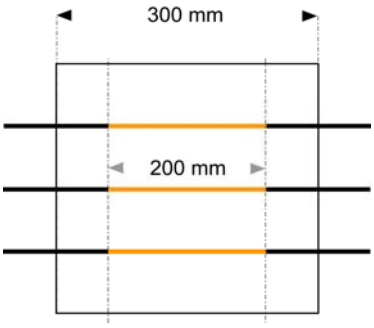

Figure 1. Diagram of the reinforced concrete slabs

After curing, one slab was conserved as a sound reference specimen and the other six were preconditioned for a month (45 °C, 60 %RH) and then carbonated for two months (22 °C, 50 %CO_2, 60 %RH). Prior to the study, all the slabs were stored in water in order to prevent the carbonation of the sound concrete slab.

2.2.Treatment Realkalisation Using Impressed Current

The realkalisation treatment using impressed current was applied on 4 reinforced concrete slabs (Table 1). The three rebars of each slab were connected together as the cathode. An anode (steel, grid of 5x5 mm meshing, 2 mm diameter) was placed on the top surface of each slab, embedded in a cellulose pad impregnated with a potassium carbonate-based (Ka_2CO_3) electrolyte. The pad was kept wet by spraying electrolyte during the treatment, on a daily basis. The four slabs were put in series, with the anode and the cathode connected to an electrical supplier with an imposed current density of 1A/m² of steel. The temperature and the current generated by the electrical supplier were monitored with a Sefram datalogger during the treatment. In order to reach the 200 A.h/m² efficiency threshold given in the European Specification [1], a current density of 1 A/m^2 of steel was imposed for 8.5 days. At the beginning of the treatment, the necessary voltage to deliver the correct current was about 18 V for the four slabs.

Table 1. Slab references

Slab references	Treatments
1-S	None (sound concrete reference slab)
2-C	Carbonation (carbonated concrete reference slab)
3-C	Carbonation
4-R, 5-R, 6-R and 7-R	Carbonation and realkalisation

2.3.Characterizations

2.3.1 Electrochemical measurements

Non-destructive electrochemical measurements were used to estimate the corrosion state of the steel rebars embedded in concrete. As such measurements depend so much on temperature and humidity, a specific preparation of the slabs was required in order to obtain reproducible data : thus, the measurements were performed at 20°C, on a slab that had been totally immersed in water for 24 hours the day before.

The electrochemical system was composed of three electrodes, the working electrode being the steel rebar, the reference electrode being a calomel saturated with KCl ($E°_{(NHE)}$=242mV), the counter electrode being a titanium/platinum based grid and the chosen electrolyte being water. The measurements were conducted with a portable potentiostat PARSTAT PAR2263 on 9 sites (sites 1, 2 and 3 for rebar 1 ; 4, 5, and 6 for rebar 2 and 7, 8 and 9 for rebar 3) of the slab surface as illustrated in Fig.2.

Figure 2. The electrochemical system

Three types of electrochemical measurements were performed. First of all, the potential monitoring gave the rest potential value after 10 minutes. Second of all, the slope (1/(Re+Rp)) of the linear polarization resistance measurement (± 10 mV around the rest potential and a sweep rate of 2.5 mV/min) was determined. Third of all, the impedance technique (± 10 mV around the rest potential, 39 mHz < frequency < 100 kHz) was used to assess the concrete cover and the electrolyte resistance (Re). Finally, corrosion currents (taking into account the ohmic drop and the polarised surface; and expressed in µA/cm²) were calculated according to equation (1).

$i_{corr}=26.10^{-3}/(Rp.S)$ (1)
with Rp the polarisation resistance and S the considered steel surface.

2.3.2 Analytical characterizations

Complementary analytical characterizations (Table 2) were performed, mainly on the carbonated concrete reference slab 3-C and on the treated slab 7-R, in order to both evaluate the efficiency of the realkalisation treatment and detect eventual side effects such as transformations of the cement matrix. The sampling locations are given in Fig. 3.

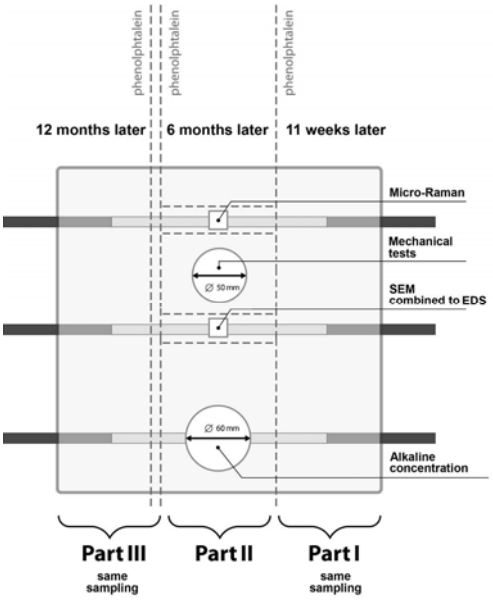

Figure 3. Sampling locations for analytical characterizations

Table 2. List of analytical characterizations

Analytical characterizations	Samples	Expected information
Phenolphthalein test *(Colour indicator)*	Freshly sawed surface	pH evolution
Micro-Raman Spectroscopy	Freshly broken surface	Rust identification
SEM combined to EDS *(JEOL JSM-5600)*	Freshly broken surface	Transformations of cement matrix and rust
Alkaline concentration profiles *(Atomic absorption spectroscopy)*	Powders at different depths	Penetration of alkaline ions in concrete
Elastic modulus (E_{dyn}) *(Ultrasonic measurement)*	Cores (50 mm in diameter and 50 mm in height)	Evolution of mechanical properties
Compressive strength (Rc)	Cores (50 mm in diameter and 50 mm in height)	Evolution of mechanical properties

3.RESULTS AND DISCUSSION

3.1.Electrochemical Measurements

A set of electrochemical measurements was performed before, 15 days, 10 weeks, 6 months and 12 months after the realkalisation treatment in order to evaluate its efficiency and durability.

3.1.1.Rest Potentials

Before the realkalisation treatment (Fig. 4), the rest potentials are respectively around -100 mV for the sound concrete slab (slab 1-S) and mainly between –300 and -550 mV for the five carbonated slabs (2, 4, 5, 6 and 7). ASTM C876 [19] indicates that the corrosion probability of rebars embedded in concrete is less than 10% when the rest potential is above -120 mV (SCE) and it is more than 90% when the rest potential is below -276 mV (SCE). This standard has been quite discussed lately, due to a discrepancy between the thresholds above mentioned and the real state of corrosion encountered for steel reinforcement embedded for example in chloride contaminated concrete (where very low potential values can be measured due to the salinity of the concrete more than to a real corrosion of the rebars). Therefore, the results are more commonly interpreted considering potential gradients instead of absolute values. Nevertheless, as far as the slab were cast using ordinary Portland cement and carbonated, the thresholds can still be considered as relevant.

Thus, the rebars in the sound concrete are probably passive whereas an active corrosion probably takes place on the rebars in the carbonated concrete. It is to be noticed that although the fabrication, the curing, the accelerated carbonation and the measurement protocol were strictly the same for the five carbonated slabs, their electrochemical rest potential response showed a variation of about 250 mV.

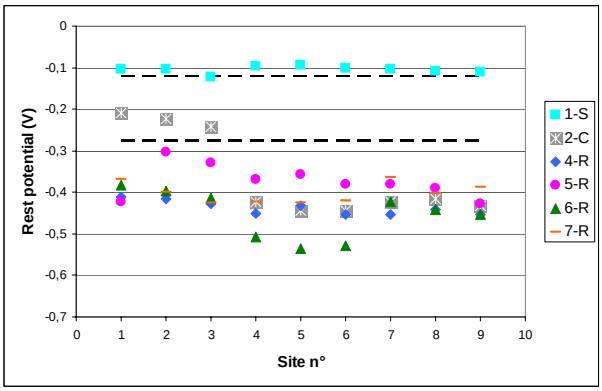

Figure 4: Rest potentials for the sound, carbonated references and the carbonated slabs before the realkalisation treatment

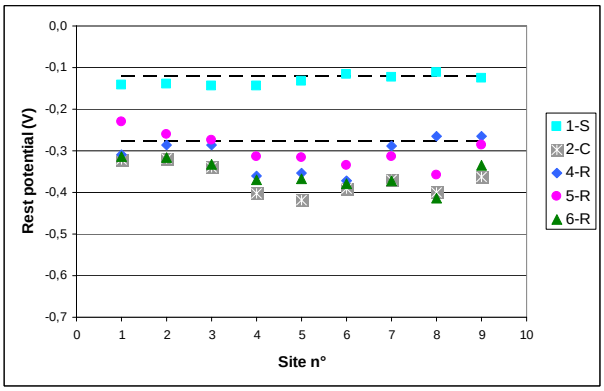

Figure 5: Rest potentials for the sound carbonated references and the carbonated slabs 10 weeks after the realkalisation treatment.

Just after treatment, the rest potentials have shifted to values of about –1.2 V indicating that the rebars have been polarized. This polarization effect has to be monitored to confirm that the treatment has been done correctly. After about 2 weeks, the polarisation effect is no longer observed except maybe for rebar 3 of the four treated slabs.

Ten weeks after treatment (Fig. 5), the rest potentials of the non treated slabs are respectively between –150 and –100 mV for the sound concrete reference (slab 1-S) and between –400 and –300 mV for the carbonated concrete reference (slab 2-C). These rest potentials shifted slightly towards more negative values. On the contrary, the rest potentials for treated slabs 4, 5 and 6 shifted towards more positive values and are more homogeneous

(-300 mV ± 100 mV) than the initial ones. This rather indicates a slowdown of the corrosion probability after the realkalisation treatment.

Twelve months after treatment (Fig. 6), the rest potentials of the untreated slabs are respectively between –200 and –100 mV for the sound concrete reference (slab 1-S) and almost equal to –450 mV for the carbonated concrete reference (slab 2-C). Thus, these rest potentials continue to decrease slightly. Concerning the treated slabs, the rest potential values are almost the same as those obtained after 10 weeks (more or less 50 mV).

As an example, the evolution of the rest potential measurements for treated slab 6-R, versus time (before treatment, 15 days, 10 weeks, 6 months and 12 months after treatment) is illustrated in Fig. 7. After treatment, the rest potential values are always higher than the initial ones indicating an efficiency of the realkalisation treatment (except for rebar 3, 15 days after treatment which can be due to a non depolarisation of the steel). The rest potentials increase with time starting from before treatment to 15

days after, to 10 weeks after and to 6 months after but then slightly decrease for those obtained after 12 months.
More electrochemical measurements are needed to verify the durability of the realkalisation treatment for a longer time.

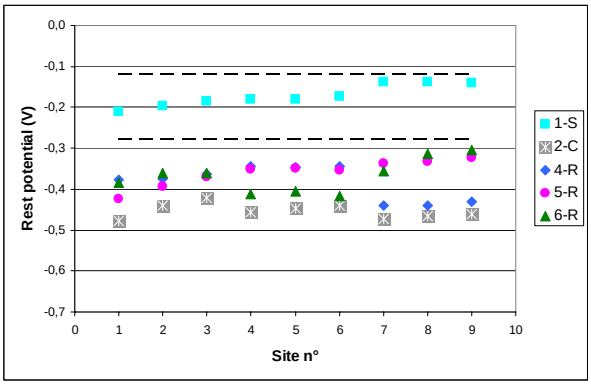

Figure 6: Rest potentials for the sound carbonated references and the carbonated slabs 12 months after the realkalisation treatment.

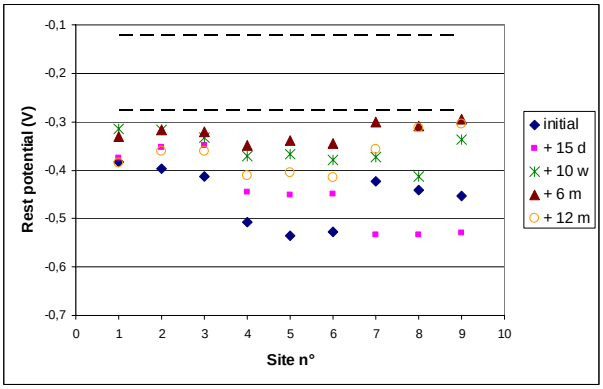

Figure 7: Evolution of the rest potentials for treated slab 6-R.

3.1.2 Corrosion currents

The corrosion currents of the sound concrete reference (slab 1-S), the carbonated concrete reference (slab 2-C) and the treated slabs (4-R, 5-R, 6-R and 7-R) are illustrated in Fig. 8 (before treatment), Fig. 9 (10 weeks after treatment) and Fig. 10 (12 months after treatment).
According to RILEM studies [21], 4 ranges of corrosion activity can be distinguished from negligible, to weak, to moderate and up to high, the corresponding thresholds being 0.1, 0.5 and 1 µA/cm².

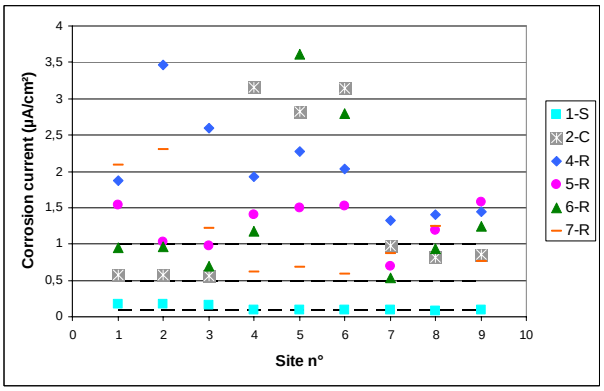

Figure 8: Corrosion currents for the sound carbonated references and the carbonated slabs before the realkalisation treatment.

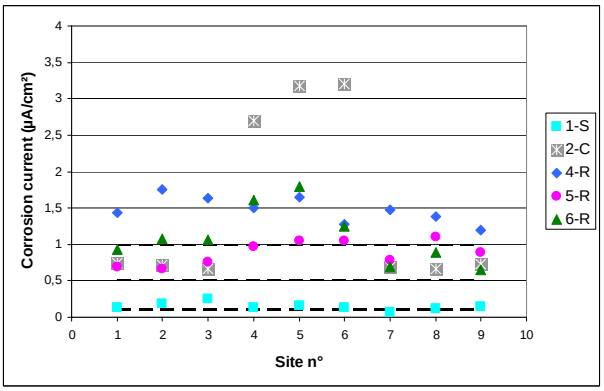

Figure 9: Corrosion currents for the sound carbonated references and the carbonated slabs 10 weeks after the realkalisation treatment.

Before the realkalisation treatment, the corrosion activity of the rebars in the sound concrete reference (slab 1-S) is negligible to weak as the average corrosion current value for the slab is equal to 0.12 (± 0.04) µA/cm². But the five carbonated slabs show a corrosion current ranging from 0.5 to 3.6 µA/cm², indicating a moderate to high corrosion activity of the rebars. Here again, the corrosion current response is quite large although the fabrication, the curing, the accelerated carbonation and the measurement protocol have been exactly the same for the five slabs. With time, the corrosion currents for the sound concrete reference slab 1-S remain low (0.15 ± 0.05 µA/cm², 0.18 ± 0.06 µA/cm² and 0.12 ± 0.05 µA/cm² respectively for 10 weeks, 6 months and 12 months after treatment).
Concerning the carbonated concrete reference slab 2-C, the corrosion currents of rebars 1 and 3 remain almost constant with time while those for rebar 2 decrease (the average value for rebar 2 is 3.02 ± 0.23

µA/cm², 2.11 ± 0.21 µA/cm² and 1.55 ± 0.12 µA/cm² respectively for 10 weeks, 6 months and 12 months after treatment).

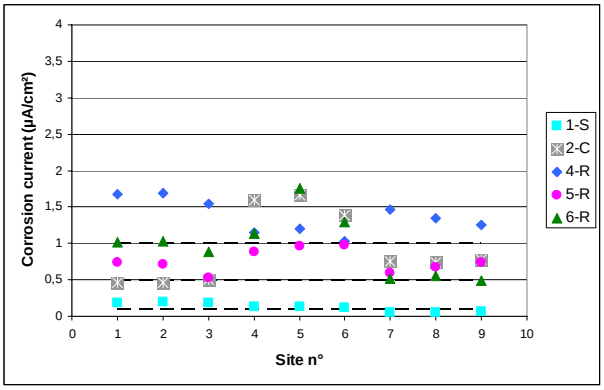

Figure 10: Corrosion currents for the sound carbonated references and the carbonated slabs 12 months after the realkalisation treatment.

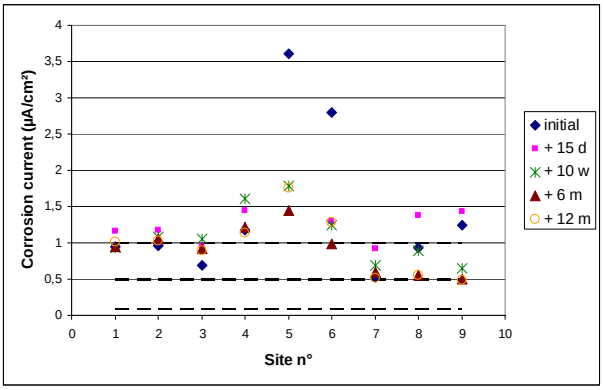

Figure 11: Evolution of the corrosion currents for treated slab 6-R.

After treatment, the realkalised slabs show lower corrosion currents with time and 12 months after treatment the corrosion current range is from 0.49 to 1.76 µA/cm².
As an example, the evolution of the corrosion current measurements for treated slab 6-R, versus time (before treatment, 15 days, 10 weeks, 6 months and 12 months after treatment) is illustrated in Fig. 11. For rebar 1, there is no clear tendency of the corrosion currents. For rebar 2, the corrosion currents drastically decrease after treatment. Finally, for rebar 3, where the corrosion currents before treatment were in the range moderate to high, they are in the range of weak corrosion activity 12 months after treatment. The values obtained 15 days after treatment are higher than the initial ones and can be explained as rebar 3 is not completely depolarized.
It is to be noticed that this corrosion current decrease tendency, which could be considered as an efficiency indicator for the realkalisation treatment, is more noticeable for rebars showing a high initial corrosion activity. In some cases, the corrosion activity decreased to a lower range but the negligible range encountered for the sound concrete slab was never reached. So the corrosion process is probably slowed down but not stopped.

3.1.3 Comments on electrochemical characterizations

The increase tendency of potentials and the decrease tendency of corrosion currents for the treated slabs seem to indicate that the realkalisation treatment reduces corrosion activity with time.
Concerning the durability aspect of the realkalisation treatment, no conclusion can be drawn from these results. Therefore, all the slabs are now ageing naturally and a complementary set of electrochemical characterizations is scheduled in order to explore this last issue.

3.2.Analytical Characterizations

3.2.1 Phenolphthalein test

Phenolphthalein is a colour indicator that turns pink when pH is above 9 and remains colourless for lower pH values. It was sprayed on freshly broken concrete surface before the realkalisation treatment, 15 days, 6 months and 12 months after the treatment (Fig. 12).
Before treatment, the phenolphthalein test revealed a complete carbonation of the concrete which remained colourless (as expected after the artificial carbonation ageing).
Just after realkalisation, the efficiency of the treatment is demonstrated by the presence of a pink zone, around the rebars, indicating a pH increase above 9. Nevertheless, the durability of the realkalisation is questionable as the change in colour is less and less obvious after 6 months and 12 months. The same type of results was obtained, on reinforced concrete containing either slag or sulphates [8, 14, 16]. Moreover, the phenolphthalein indicator only indicates if the pH value is higher or lower than 9-10.

Some authors such as, Yeih suggest that 9 is not enough to ensure the repassivation of the rebars and recommend a pH value of 11 that can be evaluated either with rainbow indicator [15] or thymolphthalein [8].

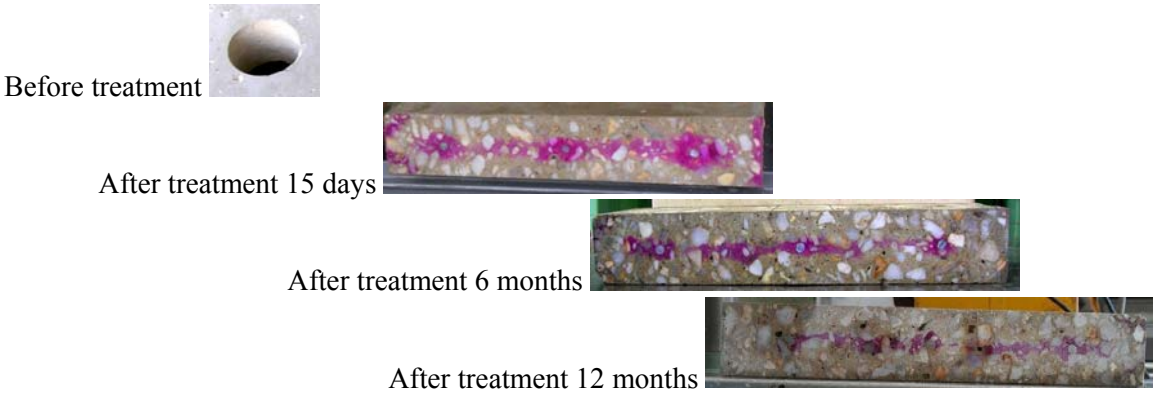

Figure 12: The phenolphthalein tests before, 15 days, 6 months and 12 months after the realkalisation treatment.

3.2.2 Micro-Raman Spectroscopy

Rebars embedded in concrete were also observed using Micro-Raman Spectroscopy to assess the nature of the rust. The presence of green rust and goethite (α-FeOOH) was detected on the carbonated control specimen indicating an active corrosion of the rebars. Six months after treatment, stable ferric products (magnetite and hematite) were detected. It could be supposed that green rust and goethite were transformed to a dense magnetite layer after the treatment (as shown in Equation 2).

$$6FeOOH + 2e^- \rightarrow 2Fe_3O_4 + 2H_2O + 2OH^- \quad (2)$$

This equation highlights the FeOOH reduction at the magnetite-oxyhydroxide interfaces, as suggested by Stratmann [22].

3.2.3 SEM combined to EDS

Both treated and untreated samples were observed with SEM combined to EDS 6 months and 12 months after the realkalisation treatment.

The SEM observation of the carbonated concrete control first corroborates the carbonation of the matrix, portlandite being replaced by calcium carbonate (Fig. 13a). In addition, a large presence of rust crystals (Fig. 13b) was observed on the concrete around the rebars which indicates an active corrosion process. Finally, alkali-silica gels were identified close to the rebars (Fig. 13c). This latter observation is rather unexpected as the aggregates were chosen as non alkali-silica reactive (unless the long storage time in water before the study could have favoured such a phenomenon).

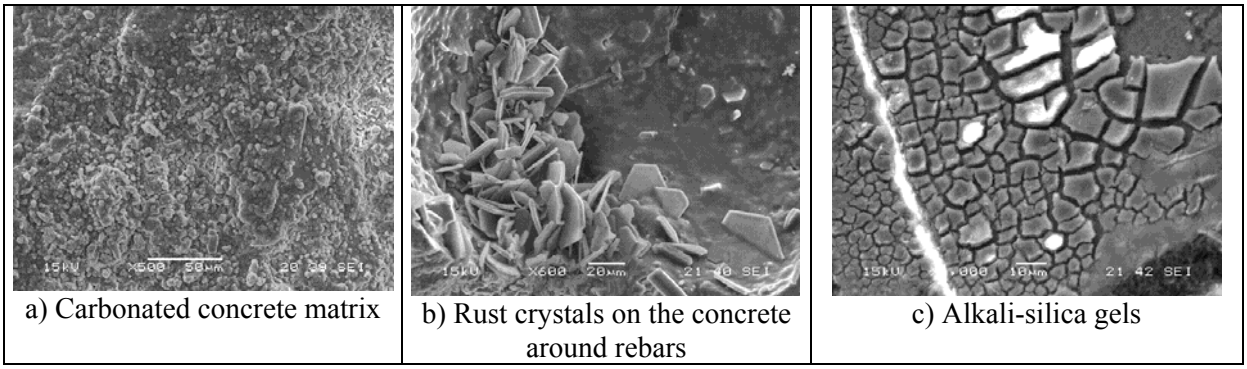

a) Carbonated concrete matrix

b) Rust crystals on the concrete around rebars

c) Alkali-silica gels

Figure 13. SEM observations of the carbonated concrete control slab (3).

Six months after treatment, no obvious transformation of the cement matrix was observed. Though a few rust crystals were still visible scattered in the concrete, a compact and dense rust layer was

observed (Fig. 14a) that could be a magnetite layer as previously seen through Micro-Raman Spectroscopy.
Alkali-silica gels were also observed on the realkalised concrete 12 months after treatment (Fig. 14b). As the nature of the gels in carbonated or realkalised concrete is almost identical (potassium-silica species), these gels can hardly be attributed to the realkalisation treatment. Complementary observations are ongoing to better understand this gel formation.

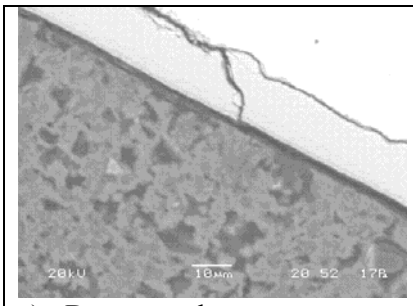

a) Dense and compact rust layer observed between rebars and concrete after 12 months

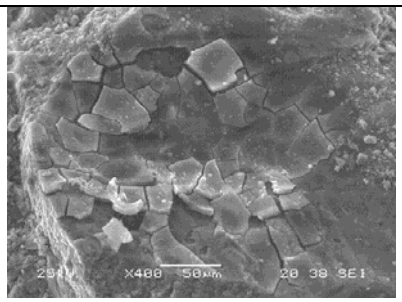

b) Alkali-silica gels

Figure 14. SEM observations of the realkalised concrete slab (7).

3.2.4 Alkaline concentration profiles

In order to obtain a potassium concentration profile, the cores were sliced in 10 pieces (5 mm thick), half of which were titrated by atomic absorption spectroscopy (Fig. 15).
For the carbonated concrete reference slab, a constant potassium concentration (about 0.13 %) was detected whatever the depth (at the 20mm-rebar depth, no powder was collected but it can be assumed that the potassium content is equivalent).
Eleven weeks after treatment, a great increase in potassium ion concentrations was detected. On the top surface of the slab, the potassium concentration (0.38%) was 3 times higher than that of the control specimen. On the rebar level (depth 25 mm), it was the same as that of the control specimen. Finally, on the bottom surface of the slab, the potassium concentration (0.32%) was 2.5 times higher than that of the control specimen.
During the realkalisation treatment, the potassium ions contained in the electrolyte placed on the top surface of the slab are supposed to penetrate into the concrete to the rebar level through two processes : capillary absorption and electrical migration. The results are in agreement with this assumption. However, the capillary contribution seems the most important as can be seen on the slab bottom surface (the electrolyte ran down the slab) where there is no electrical field.
But, it has to be noted that the potassium content does not provide direct indication on steel repassivation nor on the pH value around the rebars.

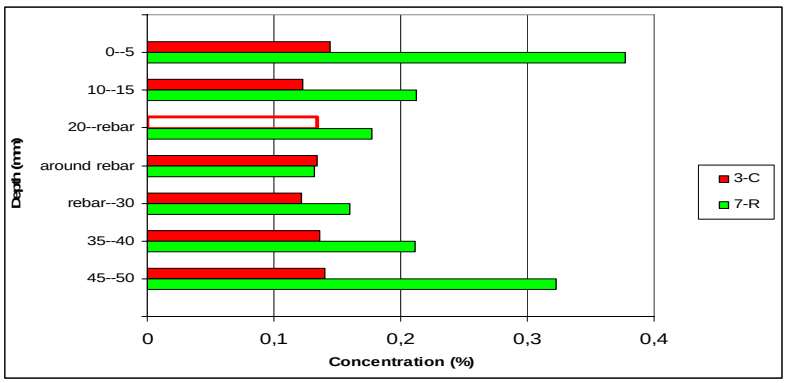

Figure 15. Potassium concentration profile before and 11 weeks after treatment.

In order to assess the durability of the treatment, complementary alkaline concentrations are scheduled. A diffusion process leading to a re-distribution of the potassium ions might be encountered.

3.2.5 Mechanical tests

Mechanical measurements (dynamic modulus of elasticity and compressive strength) were conducted on cylinders (diameter 50 mm, height 50 mm) respectively cored in the carbonated concrete control slab 3-C and in the realkalised slab 7-R.
The results are summarized in Table 3. Compared to the control specimen, there is no clear evolution either of dynamic modulus of elasticity or of compressive strength in time.

Table 3. Evolution of dynamic modulus of elasticity and compressive strength

	Slab 3-C (Carbonated control)	Slab 7-R
		After 11 weeks
E_{dyn} (GPa)	34.2	34.8
Compressive strength (MPa)	60.8	58.4

5. CONCLUSIONS AND OUTLOOK

The purpose of this study was to evaluate both the efficiency and the durability of realkalisation using impressed current. Therefore, a series of tests was performed on poor quality concrete slabs artificially carbonated, before and after an 8.5-day realkalisation treatment.
Concerning the efficiency just after treatment, promising results were obtained : alkaline titration revealed a significant penetration of potassium ions, and phenolphthalein tests just after treatment showed a clear pink coloration around the rebars indicative of a pH recovery induced by the realkalisation treatment.
Electrochemical characterizations, even if the results were difficult to analyse, showed an increase tendency of potential and a decrease tendency of corrosion currents, indicating a slowdown of the corrosion activity. The evolution of the nature of the corrosion products observed by Micro-Raman spectroscopy confirmed this phenomenon.
Regarding potential side effects, no evolution of the mechanical properties was noticed, and SEM combined with EDS did not reveal any significant transformation of the cement matrix.
Finally, dealing with durability, 12 months after treatment phenolphthalein tests and electrochemical characterizations still seem to indicate an efficiency. However, as the change in colour observed in the phenolphthalein tests concerned smaller areas with time, further work on pH evaluation is necessary and durability needs to be confirmed after longer periods. Therefore, the slabs are now exposed to natural ageing and characterizations will be continued.

ACKNOWLEDGEMENTS

The authors wish to thank the Renofors Company for their technical contribution to this study, supported by the Ministry of Sustainable Development and the Ministry of Culture in France.

REFERENCES

FD CEN/TS 14038-1, 2005,Electrochemical realkalisation and chloride extraction treatments for reinforced concrete – Part I Realkalisation

J. P. Broomfield, 1997, Corrosion of steel in concrete, understanding, investigation and repair, E&FN SPON, , ISBN 0-419-19630-7.

A. Raharinaïvo , G. Arliguie, T. Chaussadent & Al. 1998, La Corrosion et la protection des aciers dans le béton, Presses de l'école nationale des Ponts et chaussées, Paris, France, 167 p. ISBN 2-85978-300-8.

J. Jacob & G. Taché, 2003,Réhabilitation du béton armé dégradé par la corrosion, Association Française de Génie Civil & CEntre FRAnçais de la CORrosion, Bagneux, France,

L. Odden, 1994,,The repassivating effect of electro-chemical realkalisation and chloride extraction, Corrosion and corrosion protection of steel in concrete, edited by Naryan Swamy, Sheffield Academic Press. Vol. II, p. 1473-1488.

J. Mietz, 1995, Electrochemical realkalisation for rehabilitation of reinforced concrete structures, Materials and corrosion, Vol.46, 527-533.

G. Sergi, R.J. Walker and C.L. Page, Mechanisms and criteria for the realkalisation of concrete, Proceedings of the fourth international symposium on corrosion of reinforcement in concrete constructions, Cambridge, United Kingdom, 1996, pp. 491-500, ISSN 1466-5026.

8. V. Pollet, R. Guerin, C. Tourneur, H. Mahouche and A. Raharinaivo, 1997, Concrete realkalisation using sacrificial anodes, Eurocorr'97, Trondheim, Norway, pp523-528.

PFG. Banfill, 1997, Re-alkalisation of carbonated concrete-effect on concrete properties, Construction and Building Materials, Vol. 11, p 255-258.

B. Elsener, L. Zimmermann, D. Bürchler and H. Böhni, 1998, Repair of reinforced concrete structures by electrochemical techniques – field experience, Eurocorr'97, Trondheim, Norway, edited by J. Mietz, B. Elsener and R. Polder. - European federation of corrosion publications, n° 25, pp.125-140.

C. Andrade, M. Castellote, J. Sarria and C. Alonso, 1999, Evolution of pore solution chemistry, electro-osmosis and rebar corrosion rate induced by realkalisation, Materials and Structures, Vol. 32, pp.427-436.

J.A. Gonzalez, A. Cobo, M.N. Gonzalez & Al., 2000, On the effectiveness of realkalisation as a rehabilitation method for corroded reinforced concrete structures, Materials and corrosion, Vol. 51, pp.97-103.

A. Raharinaivo, G. Grimaldi and E. Marie-Victoire, 2001, Effectiveness of re-alkalisation and chloride removal, Corrosion of steel in reinforced concrete structures : Cost 521 : proceedings of the 2001 Workshop, Tampere, Finland, p. 257. ISBN 952-15-0634-2.
E. Cailleux, E. Marie-Victoire, A. Texier & Al., 2003, Experimental investigation of realkalisation treatments used for restoration of historical monuments made of reinforced concrete, Concrete solutions : proceedings of the first international conference on concrete repair, Saint-Malo, France, pp. 527-534. ISBN 0-9545502-1-8.

W. Yeih, J.J. Chang, 2005, A study on the efficiency of electrochemical realkalisation of carbonated concrete, Construction and Building Materials, Vol. 19, pp516-524.

E. Cailleux and E. Marie-Victoire, 2006, Influence of the concrete composition on the efficiency and the durability of realkalisation treatment, Concrete solutions : proceedings of the second international conference on concrete repair, Saint-Malo, France, pp. 271-279. ISBN 1-86081-915-X.

J.S. Mattila, M.J. Pentti and T.A. Raiski, 1996, Durability of electrochemically realkalised concrete structures, Corrosion of reinforcement in concrete construction : proceedings of the Fourth

international symposium, Robinson college, Cambridge, United Kingdom, pp. 481-490. ISBN 0-85404-731-X.

J.M. Miranda, J.A. Gonzalez, A. Cobo, E. Otero, 2006, Several questions about electrochemical rehabilitation methods for reinforced concrete structures, Corrosion Science, Vol.48, pp2172-2188.

ASTM standards, 04.02 concrete and aggregates, C876, Standard test method for half cell potentials of uncoated reinforcing steel in concrete. .

B. Elsener & Al., 2003, Half-cell potential measurements – Potential mapping on reinforced concrete structures, RILEM TC 154-EMC : Electrochemical Techniques for Measuring Metallic Corrosion - Recommendations, Materials and Structures, Vol. 36, pp.461-471.

C. Andrade, A. Alonso & Al., 2004, Test method for on-site corrosion rate measurement of steel reinforcement in concrete by means of the polarization resistance method. RILEM TC 154-EMC : Electrochemical Techniques for Measuring Metallic Corrosion - Recommendations, Materials and Structures, Vol. 37, pp.623-643.

M. Stratmann and K. Hoffmann, 1989, In situ Mössbauer spectroscopic study of reactions within rust layers, Corrosion Science, Vol. 29, pp. 1329-1352. ISSN 0010-938X.

Use of Information Technology in the Diagnosis of Concrete Deterioration

Hisham Qasrawi [1]
Lama Da'as [2]
Aram Serpekian [3]
Husam Qasrawi [4]

T 71

ABSTRACT

During its service life, concrete undergoes several deteriorating mechanisms which affect its performance and strength. Diagnosis of the cause(s) of deterioration is(are) important in order to arrive at the correct repair and rehabilitation method. The first step in the diagnosis of concrete deterioration is visual inspection. In this paper, diagnosis of concrete deterioration by the use of an interactive software is introduced. This software can be a useful guide for engineers during their inspection of deteriorated and cracked concrete. As a first step in the preparation of the software, five different deterioration factors (corrosion of steel reinforcement, sulphate attack, alkali silicate reaction, freeze and thaw and plastic shrinkage) have been studied in detail. The symptoms of deterioration of these factors have been studied and later have been incorporated in a computer program. The user can arrive at the cause of deterioration by responding to direct simple questions which appears on the screen. Furthermore, the program can provide photos of similar cases to those introduced by the user. By simple comparison of the actual case and the photo provided, the user can assure the diagnosis of the case under consideration.

KEYWORDS

Concrete, Deterioration, Diagnosis, Information technology, Software.

[1] Civil Engineering, The Hashemite Univ, Zarqa 13115, Jodan, Phone +962 5 3903333 ext 4582, qasrawi2@yahoo.com
[2] Lama Da'as, Civil Engineering, The Hashemite Univ, Zarqa 13115
[3] Aram Serpekian, Private Sector, Amman
[4] Husam Qasrawi, Head of Planning and Development Department, PTU Kadoorie University, Toulkarim.

1 INTRODUCTION

Cracks in concrete, which have many causes, can affect appearance only or may also indicate significant structural distress or a lack of durability [ACI 224.1R]. Also, cracks may represent the total extent of the damage, or they may point to problems of greater magnitude. Their significance depends on the type of structure, as well as the nature of the cracking.

The cracks that appear in concrete structures are either structural (which usually occur due to excessive loads) or nonstructural, which are due to the presence of concrete in certain environments. Nonstructural cracks occur due to physical, chemical, mechanical or biological effects on plain or reinforced concrete. While the specific causes of cracking are manifold, cracks are normally caused by stresses that develop in concrete due to the restraint of volumetric change or to loads which are applied to the structure [ACI 224R]. Cracks can expose reinforcing steel to oxygen and moisture and make the steel more susceptible to corrosion.

The main physical factors that cause concrete cracking are freeze and thaw effect, shrinkage of concrete (plastic and drying shrinkage), movement of concrete against restraints and temperature effects (uniform or differential). The main chemical effects are alkali-silicate reaction, sulfate attack, seawater effect, acid attack and corrosion of reinforcing steel. The main mechanical factors are wear and abrasion. Biodeterioration occurs when concrete is in an environment suitable for the growth of microorganisms, such as the sulfate reducing bacteria, the sulfur oxidizing bacteria and the iron oxidizing bacteria [Qasrawi 2006, Qasrawi 2005]. Each type of deterioration is characterized by its cracks and symptoms which reveilles its identity. For example, alkali-silicate reaction is characterized by its map cracking which appear after more than five years of construction only in damp areas and extends throughout the whole body of affected concrete [Neville and Brooks 2004]. Hence, diagnosis of concrete deterioration starts with the study of cracks. The study should include shape, length, width, direction, extent and distribution of the crack. Furthermore, other factors, such as the time of occurrence of cracks and the presence of colored chemicals on the surface of concrete, are considered critical in the diagnosis.

Since repair of structures is critical in maintaining the integrity and durability of concrete structures, proper repair of cracks depends on correct diagnosis and later on selecting the repair procedures. Of course, incorrect diagnosis will result in improper repair and hence further cracking and deterioration. According to [ACI 224.1R] successful long-term repair procedures must attack the causes of the cracks as well as the cracks themselves. Only expert engineers are able to diagnose correctly the cause of cracking. Therefore, it is important to guide engineers and help them diagnose correctly the main cause.

According to Moodi and Knapton [2003], the use of information technology in construction is becoming increasingly sophisticated, with virtual reality, knowledge-based systems, database management systems, objected-oriented approaches, and neural networks among the latest technological advances now available for performing condition surveys, consistent and quantitative condition assessment, and database management. Database management systems are important in those engineering computing applications where the volume of data is very large and where several users and programs must share the same data. Engineering computing applications are making increasing use of database management systems to provide these capabilities [Ullman 1988; REMR 1996; Betts and Smith 1999].

Several attempts have been used in order to use the information technology and the computer capabilities in the diagnosis of concrete deterioration. Some of the attempts are described in the following paragraphs.

Kaetzel and Clifton [1991] presented a survey of thirteen expert/knowledge based systems applications and development methods related to concrete pavements and structures. These systems can be considered as initial steps in the development of expert systems diagnosis of concrete.
Chan [1996] presented a study in order to develop a prototype knowledge based expert system (called RCDES) for civil engineering applications in the knowledge domain of diagnosis of deterioration and other problems in reinforced concrete structures. The research emphasized on providing a broad view of diagnosis of reinforced concrete structures by capturing the knowledge of human experts and using a modular approach. Traditionally, the process of diagnosis is carried out by human experts/specialists and the use of computerized systems exhibiting artificial intelligence to provide a systematic and efficient diagnosis process.

Jepsen [2002] designed and used a neural network to investigate the influence of different parameters on the salt frost resistance of concrete.

Iyoda et al [2003] presented a study where they made a concept of a database of deteriorated concrete bridges in metropolitan area of Japan. They included database, which includes some information such as locations of bridges, year of construction and degree of deterioration. They also included many photos and the results of non-destructive tests such as digital still camera and thermal camera. In order to inspect the deteriorated concrete bridges, they used “the inspection software for deteriorated concrete structures” which has been produced by IIS, Japan. By the use of this software, they could recognize the cause and degree of deterioration to a certain degree of accuracy

Moodi and Knapton [2003] have developed a repair of concrete database which has been introduced as REPCON that deals with the diagnosis, evaluation, maintenance, and repair of concrete structures. The REPCON Management System has been designed to be an effective support tool for experts whose data can be evaluated and tested to ensure that the evolving database retains its integrity. The work explains how a computerized database management system can allow an initial database to evolve and become a forum for exchanging ideas in the field of concrete repair, and how the new methodology of data/user evaluation could have wide implication in many knowledge-rich areas of expertise.

Lücken and Stangenberg [2003] developed an expert system for an assessment strategy for deteriorating concrete bridges, which included in-situ inspections, evaluation of inspection results and condition assessment of the bridges.

Kanada et al [2003] developed an inspection software for maintenance of concrete bridges. It has been based on the concept that inexperienced engineers can easily diagnose and indicate necessities for the detailed inspections through a visual check. The described software should also enable user to refer to many samples of deterioration patterns and to the structure types when clear diagnosis cannot be made. The causes and levels of deterioration are determined by the software, based on the data collected during the visual inspection. In this process, the inspection methods related to the causes already listed in the database are deduced automatically. Finally, the current condition and the result of diagnosis are stored part-by-part for each inspected structure so the history of inspection can also be traced

Parthiban et al [2005] presented a systematic study to predict the corrosion of steel in concrete (based on neural network) in order to develop a suitable method that can accept, analyze and evaluate experimental data that are at random and/or influenced by external, unpredictable variables using the back propagation method.

Papadakis [2005] and Papadakis and Efstathiou [2006] introduced and presented field studies for a computer software based on proven predictive models, for estimation of concrete service life, strength and cost. The software offers the possibility of investigating the efficiency of various protection measures, such as waterproof sealants, cement-lime mortar coatings, inhibitors, etc. Comparing the

software results with field measurements from various real structures, a satisfactory general agreement is observed.

Ferreira and Jalali [2006] and Ferreira [2004] presented a model and developed a software for probability based durability analysis of concrete structures in marine environment which was based on a special simulation - called Monte Carlo simulation.

2 GOALS OF THE RESEARCH

All previous studies are either limited to specific applications or require specialists to be available in the diagnosis of concrete defects. Moreover, none of them considers and differentiates between structural and nonstructural cracking. Therefore it was important to develop a computer software which can (a) differentiate between structural and nonstructural cracks, (b) diagnose with a high degree of accuracy the cause of the cracks, (c) be used by engineers of only limited experience in the diagnosis of concrete cracking and (d) be developed by user when further data is available.

3 METHODOLOGY

In order to arrive at the goals described earlier, the following steps have been followed:

1. Collection of data: This includes the collection of data available for all possible cracking in concrete structures. Specialists, experts, available literature (such as ACI manuals of concrete practice and RILEM publications) and the data provided by the internet, are all useful tools in this respects. These will form a data management system for the software.
2. The cracks data is then grouped according to the time of occurrence, spacing, geometry, depth location, width, length, extension and presence of colored material on the surface.
3. The data is incorporated in a computer software (named as **C**oncrete **C**rack **D**iagnosis **CCD** software) that can be easily applied by engineers.
4. Provide photos that can direct the engineer in the diagnosis.
5. Allow the user to add his own photos to the program, and hence be able to develop his own experience and compare similar cases.

4 THE "CCD SOFTWARE"

As a first step in the preparation of the software, cracks five different deterioration factors (corrosion of steel reinforcement, sulphate attack, alkali silicate reaction, freeze and thaw and plastic shrinkage) have been studied in detail.

In order to use the software, the user must first identify the crack if it is structural (due to excessive loads) or due to other factors (named here nonstructural), as shown in Fig.1.

Then the user can respond to some of the information given directly. Once the information is input in the computer, and depending on the information available, the possible cause(s) will appear on the screen. The user can then be able to view photos showing similar cracks. Fig. 2 shows the application and response to nonstructural cracking. The user can then continue previewing the photos offered by the program in order to assure the diagnosis offered by the software.

If structural cracking is chosen, the engineer has, first, to choose the member subjected to cracking (column, beam, foundation, wall, slab or beam-column). Once the member is chosen, the engineer can choose similar crack patterns; a double click on the chosen pattern will produce further information and photos, which guide the engineer in the final diagnosis. Fig. 3 shows an example of the application.

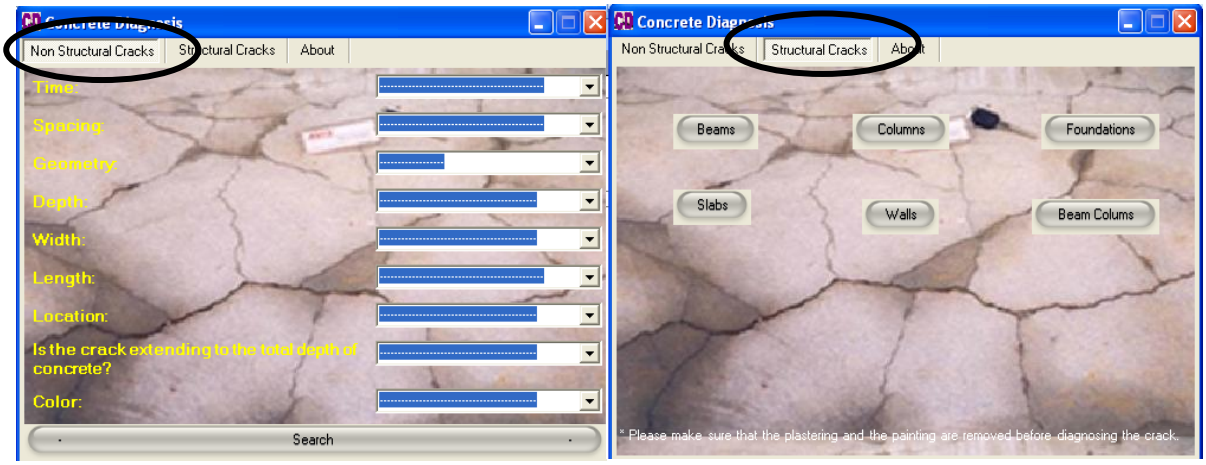

Figure 1: Start of the software (Structural or Nonstructural Cracks)

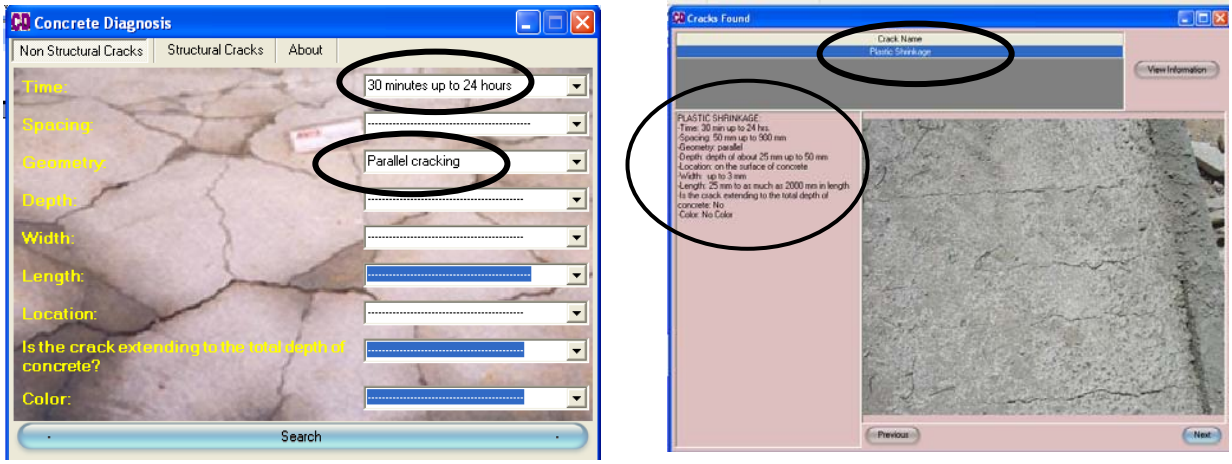

(a) Choice of crack properties (b) Additional information and photos

Figure 2: Response of the user to simple inquiries for nonstructural cracks.

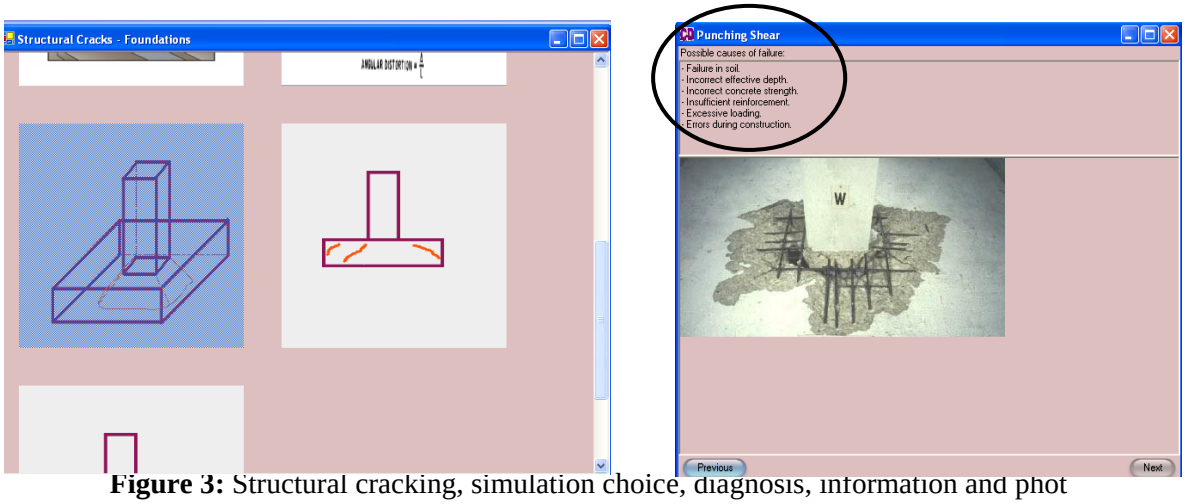

Figure 3: Structural cracking, simulation choice, diagnosis, information and phot

ACKNOWLEDGMENTS

The authors appreciate the help provided by Nadia Al-Nsour**,** Talin Enkababian and Jamil Dababneh in the data collection and preparation during the first stages of the study.

REFERENCES

ACI 224.1R-93,*'Causes, Evaluation and Repair of Cracks in Concrete Structures'*, Manual of Concrete Practice 2000, ACI, USA.

ACI 224R-90, *'Control of Cracking in Concrete Structures'* Manual of Concrete Practice 2000, ACI, USA.

Betts, M. & Smith, D. 1999. '*Strategic Management of IT in Construction*', Blackwell Science, Oxford, U.K.

Ferreira, R. M. 2004, '*Probability Based Durability Analysis of Concrete Structures in Marine Environment* University of Minho, Portogal, 339 pp.

Ferreira, R.M., & Jalali, S. 2006, 'Software for probability-based durability analysis of concrete structures *Concrete Repair, Rehabilitation and Retrofitting* – Alexander (eds.) Taylor & Francis Group, London, pp 321-326.

Jepsen, M. T. 2002 'Predicting concrete durability by using artificial neural network' *Featured at the proceedings "Durability of Exposed Concrete containing Secondary Cementitious Materials, Hirtshals*, Danish Technological Institute, 12pp.

Iyoda, T., Kato, Y.., and Uomoto, T. 2003 'A study of making a database for the deteriorated concrete bridges', in *New Technologies for Urban Safety of Mega Cities in Asia*, October, Tokyo, pp 141-148.

Kaetzel L. J, & Clifton, J. R. 1991, *'Expert/Knowledge-Based Systems for Cement and Concrete: State-of-the-Art Report'* National Institute of Standards and Technology, Gaithersburg, Maryland, USA, SHRP-C/UWP-91-527, 36pp.

Kanada, H., Yamashita, H., Shimizu, T., Uomoto T. 2003, 'Development of inspection software For deteriorated concrete structures' *in International Symposium (NDT-CE 2003) Non-Destructive Testing in Civil Engineering* pp.547-558.

Lücken, T., & Stangenberg, F. 2003, Analysis and assessment of deteriorating concrete bridges using fuzzy set theory' *in International Symposium (NDT-CE 2003) Non-Destructive Testing in Civil Engineering* pp 175-181.

Moodi, F. & Knapton, J. 2003, 'Research into a management system for diagnosis, maintenance, and repair of concrete structures, *Journal of Construction Engineering and Management ASCE* / September/October, pp 555-561.

Nevill, A. M., & Brooks, J. J. 2004 *'Concrete Technology'*, Prentice Hall, UK.

Papadakis, VG. , 2005, *'Estimation of concrete service life – The Theoretical Backgroun'* Patras Science Park, Patras.

Papadakis, V.G., Efstathiou, M.P. 2006, 'Field validation of a computer-based prediction for concrete service life' *in 2nd International fib Congress, June 5-8, Naples, Italy*

Parthiban, T., Ravi, R., Parthiban, G.T., Srinivasan, S., Ramakrishnan, K.R., Raghavan, M. 2005, 'Neural network analysis for corrosion of steel in concrete' *Corrosion Science* 47, pp1625–1642

Chan, P.P F., 1996, *'An Expert System for Diagnosis of Problems in Reinforced Concrete Structures'* Thesis submitted in partial fulfillment of the requirements for the Degree of Master of Applied Science in Information Technology, Department of Computer Science Royal Melbourne Institute of Technology City Campus, Melbourne Vic 3001, Australia December, 93pp.

Qasrawi, H. 2005, 'Corrosion of steel reinforcement in concrete by bacteria', *in Proceedings of 12th Conference for Building & construction*, Cairo, pp 190 – 124.

Qasrawi, H. 2006 'Deterioration of concrete sewers by bacteria: A combined approach", presented in the 4th Jordanian Civil Engineering Conference, Jordan.

REMR. 1996, *'REMR Management System for Concrete Navigation Lock Monoliths'*, REMR Technical Note OM-MS-1.2, U.S. Army Construction Engineering Research Laboratories, Champaign, Ill.

RILEM Draft Recommendation.1994. 'Draft recommendation for damage classification of concrete structures.' *J. Mater. Struct.*, 27, pp 362–369.

Ullman, J. D., 1988 '*Principles of database and knowledge-based systems, Vol. 1'*, Computer Science Press, Rockville, Md.

A Diagnostic System Created for Evaulation the Quality of Building Constructions

Attila Koppány[1]

T 71

ABSTRACT

The successful diagnostic activity has an important role in the changes of the repair costs and the efficient elimination of the damages. The aim of the general building diagnostics is to determine the various visible or instrumentally observable alterations, to qualify the constructions from the suitability and personal safety (accidence) points of view.

Our diagnostic system is primarily based on a visual examination on the spot, its method is suitable for the examination of almost all important structures and structure changes of the buildings. During the operation of the diagnostic system a large number of data – valuable for the professional practice – was collected and will be collected also in the future, the analysis of which data set is specially suitable for revaluing construction and the practical application of the experiences later during the building maintenance and reconstruction work. For using the system a so-called "morphological box" has been created, that contains the hierarchic system of constructions, which is connected with the construction components' thesaurus appointed by the correct structure codes of these constructions' place in the hierarchy. The thesaurus was not only necessary because of the easy surveillance of the system, but to exclude the usage of structure-name synonyms in the interest of unified handling.

The analysis of which data set is specially suitable for revaluing earlier built constructions and can help to create knowledge based new constructions for the future.

KEYWORDS

Building diagnostic, Morphological box, Thesaurus of components

[1] Széchenyi István University, Győr, Hungary, Phone +36 96 503 454, koppany@sze.hu

1. INTRODUCTION

It is important, that people in architecture science give a useful guide – especially concerning questions raised by new trends of the changing, transforming building activities and construction development – to people in the professional practice. Seeing that in the aspect of adequacy the appearance of new constructions and building materials always raises new problems to be solved, and the experts in practice busy with the daily tasks of the profession 'according to Möller [1945] cannot always pay enough attention to them'. The efficient diagnostic activity as it has been explained before plays a very important part in the formation of maintenance costs and elimination of damage. It has an equally important part in the preparation of a decision, as having a clear picture of the technological conditions of buildings or group of buildings can be of service at the preparation before making financial decisions of great significance.

2. DIAGNOSTIC SYSTEM

A faulty diagnosis can lead to incorrect decisions causing financial loss. The research group of the Széchenyi István University (Győr) worked out such a comprehensive diagnostic system (see Fig. 1.) which contains a common inspection method 'according to Molnárka [2000.] for the vast majority of constructional components (for traditional and actually used constructions in Hungary), and can be used for computer data registration and analysis.

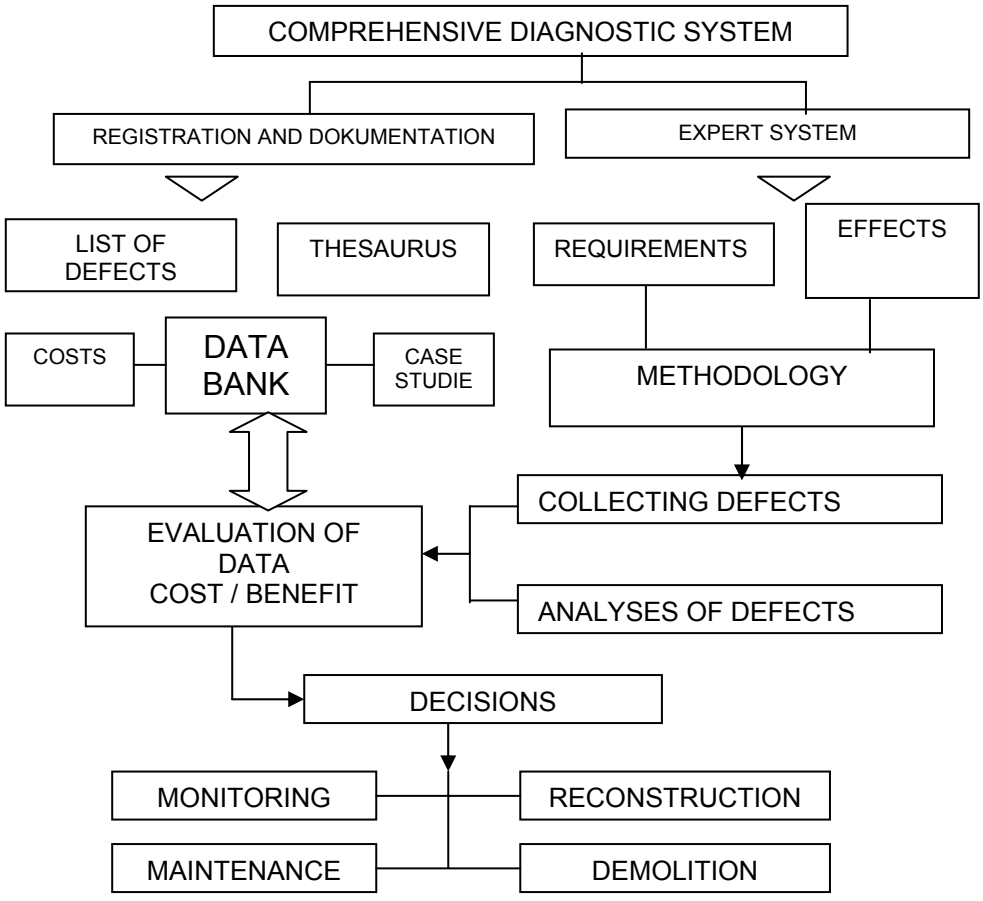

Figure 1.

The morphological box theory created by Prof. Zwicky [1966] is connected with the construction components' thesaurus denoted by the correct structure codes of these constructions' place in the

hierarchy. The theory of using morphological box for data registration in the process of building diagnostic that was published in Hungary eleven years ago [Koppány 1977]. The "matrix" construction of our morphological box fits to the methodology of the visual examination and to the hierarchy of the common building constructions in Hungary [Koppány 2002] (see Fig. 2.).

MAIN CONSTRUCTIONS	CONSTRUCTIONS AND THEIR SUPPLEMENTARY CONSTRUCTIONS			
CODE ⇒ A.	A.X	A.0X	A.00X	A.00X
1. FOUNDATIONS	1.1 Shallow foundations 1.2 Deep foundations		1.001 Insulations against ground-water	
2. VERTICAL LOAD BEARING CONSTRUCTIONS, NON LOAD BEARING CONSTRUCTIONS AND THEIR SUPPLEMENTARY STRUCTURES	2.1 Load bearing walls 2.2 Frames	2.01 Non load bearing walls 2.02 Partition walls 2.03 Doors and windows in internal walls	2.001 Wall-insulations 2.002 Plasters on facades 2.003 Plasters inside 2.004 Claddings inside	2.0001 Grates, balustrades, parapets
3. HORIZONTAL LOAD BEARING CONSTRUCTIONS, NON LOAD BEARING CONSTRUCTIONS AND THEIR SUPPLEMENTARY STRUCTURES	3.1 Ring beams 3.2 Arches, lintels 3.3 Floors, vaults	3.01 Suspended ceilings	3.001 Water-proofings to floors 3.002 Floorings	
4. STAIRCASES, BALCONIES, OPEN CORRIDORS, LOFTS AND THEIR SUPPLEMENTARY STRUCTURES	4.1 Staircases 4.2 Balconies, open corridors,lofts		4.001 Stair-tread covering 4.002 Balconies flooring 4.003 Open corridors flooring 4.004 Lofts flooring	4.0001 Balustrades, parapets, handrails to stairs 4.0002 Balustrades, parapets, handrails to balconies 4.0003 Balustrades, parapets, handrails to open corridors 4.0004 Balustrades, parapets, handrails to lofts
5. ROOFS, ROOF ACCESSORIES, CHIMNEIS, VENTILATION	5.1 Pitched roofs 5.2 Flat roofs 5.3 Roof superstructures 5.4 Chimneis 5.5 Air shafts 5.6 Vent pipes	5.01 Roofings	5.001 Water-proofing 5.002 Thermal insulation 5.003 Vapour-proofing 5.004 Flat roofs tiles and other functional layers 5.005 Roof edges and joining accessories	5.0001 Roof accessories
6. FACADES		6.01 Skirting board	6.001 Surfacings	6.0001 Grates, balustrades, parapets on the facades

Figure 2.

The main task of our thesaurus (graph-version) is to help the visual survey. It can be very useful to understand the hierarchy and the connections in the field of building constructions (see Fig. 3.). The thesaurus is not only necessary the easy surveillance of the system, but to exclude the usage of

structure-name synonyms in the interest of unified handling. We have another tool too for the quick survey of the results of the visual examination, it is the hexagonal morphological box (see Fig.4.). The box shows the actual checked constructions or all constructions of the building.
The various conditions of the building constructions can be marked with corresponding colours in the box-fields (see Fig. 5.and Fig. 6.).

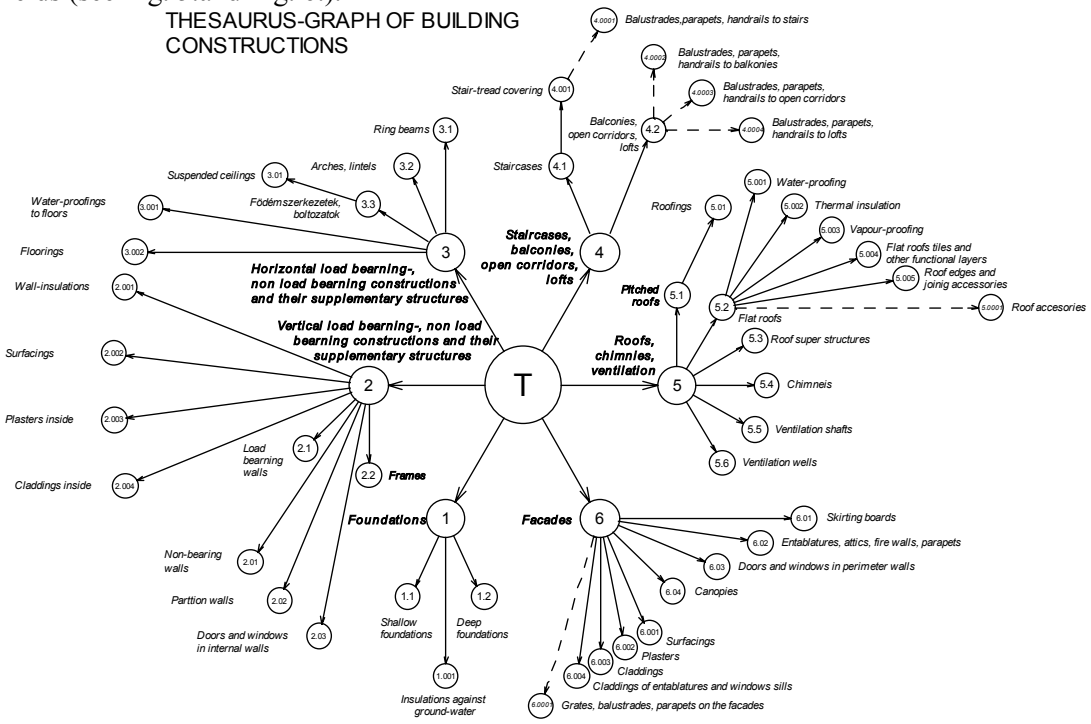

Figure 3.

Figure 4.

The results of an examination are shown on Fig. 5., Fig. 6. and Fig.7. The diagnostic system has been successfully checked in the course of a course of an examination involving 60 buildings.

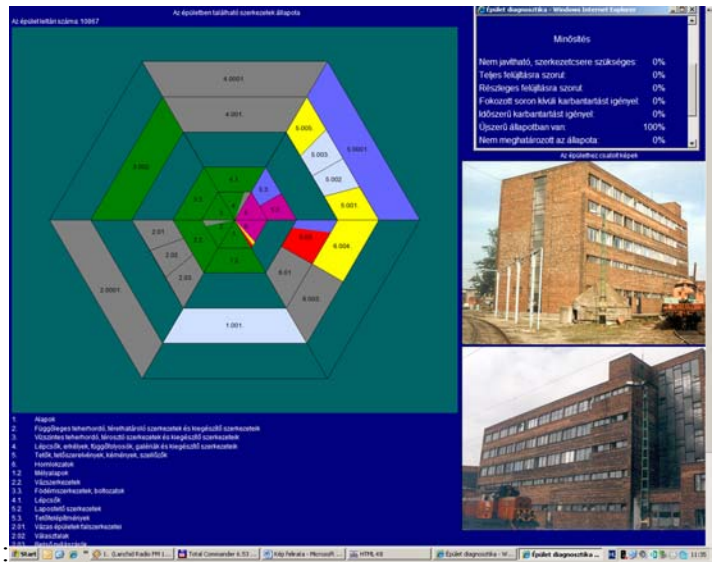

Colour	Rating
red	failed
yellow	very poor
violet	poor
grey	fair
green	good

Figure 5.

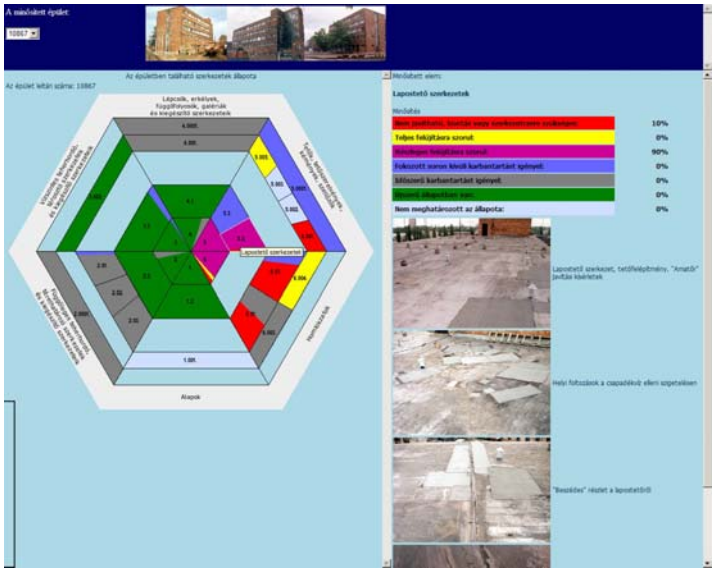

Figure 6.

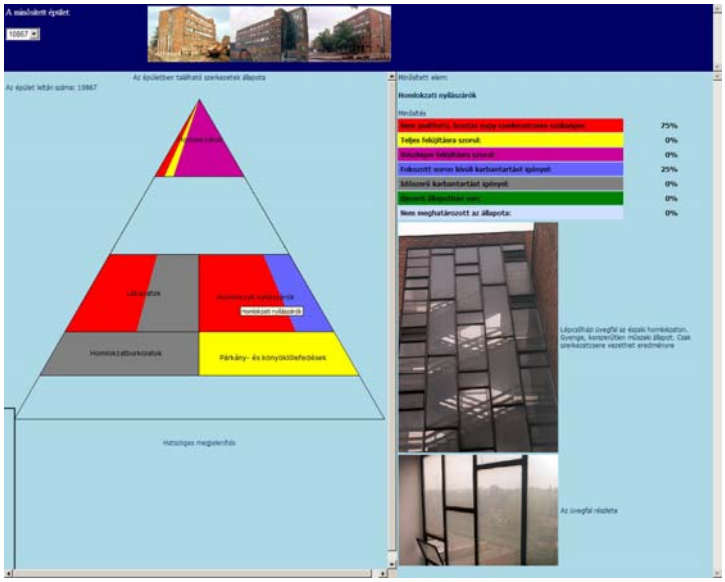

Figure 7. Qualification of the façade-details.

3. EXPERIENCES OF FLAT ROOFS EXAMINATION

The majority of the defects forming on *the flat roof water-proofing and heat insulation* can be observed on the conventional insulated roof. From the point of view of the protection of substance and providing of the proper application of the building it is very important to explore and repair professionally the failures as soon as possible. Concerning the costs it is very important to explore the failures in the beginning stage because the failures which can be repaired with relatively low costs at the beginning can be repaired only with much more expenditures and together with many other structures after the extension of the damage. It should be noted for example, that the water proofing should be checked by experts at least yearly because several extended and expensive damages can be prevented with this care. The typical failures of the roof can be systematised according to various points of view. The analysis can be performed by the layers of the layer construction of the roof insulation and water-proofing or according to the contribution to the creation of the roof insulation (e.g. material manufacturing, planning, execution, operation), but it can be carried out according the so called weak points, details of the structural nodes.

Before introducing the diagnostic procedures and testing methods applied for the flat roof construction it is reasonable to determine some principles [Koppány & Graf 1985] in connection with the examinations as follows:

- the examination mustn't inhibit the proper use of the building;
- the examination should be quickly performable with easily usable tools;
- during the whole process of the examination the least possible damage can come out in the flat roof water-proofing;
- if the destructing examination is unavoidable it can cover the least possible area and the place of sampling should be immediately repairable (in a waterproof way).

The diagnostic work can consist of several phases - which are important from the end point of view. At first before the examination on the spot it is reasonable to inform on the basic data, structures and building conditions of the building to be examined. In case of old roof it is not always possible since the plans and other documents could get lost and they cannot be often reconstructed. In a significant part of the cases the structural character, layer construction, the used materials and the technologies should be identified during the examination on the spot.

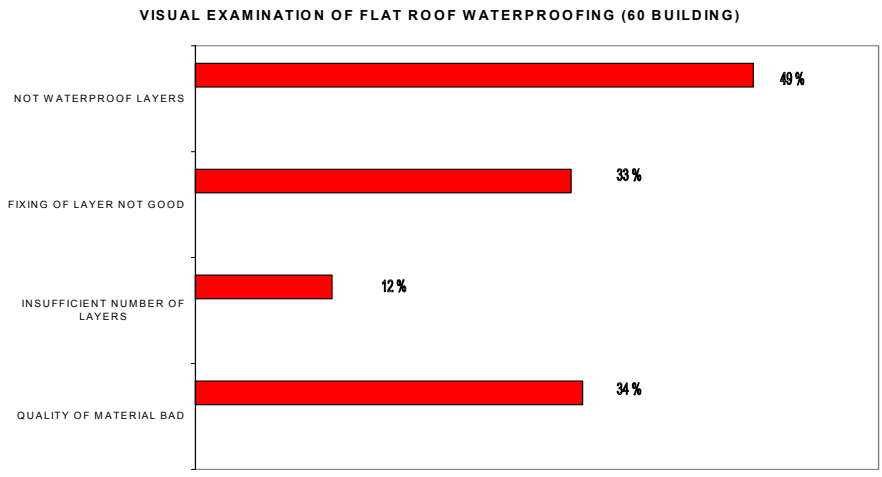

Figure 8.

During the visual examination the visual failures should be discovered then the analysis of the operation of the structure can lead to the determination of the more complex causes of the failures. During the visual examination the identification of the place of leak for large discontinuities (damages) on the water proofing of direct layer order has generally no difficulty. In case of quick examination the condition of the roof

water-proofing is determined basically with visual examination, completed with a deteriorate free instrumental measurement if necessary (see Fig. 8.).

For comprehensive examinations the procedure covers the all structural and complementary elements of the roof. The condition, load capacity, deformation of the bare floor should be examined, the building physical properties of the floor structure, etc. should be evaluated.

There are a lot of interesting data from the examination of 60 flat roof constructions (see Fig.9.) This figure shows the characteristics of frequency of the typical defects at the examined old flat roofs. The greatest number of defects were in the expansion joints area, nearly fifty percentage. The age of the examinnated roofs was on average 20 years. The roofs of the older industrial building had the worst condition, most of them were in bad repair.

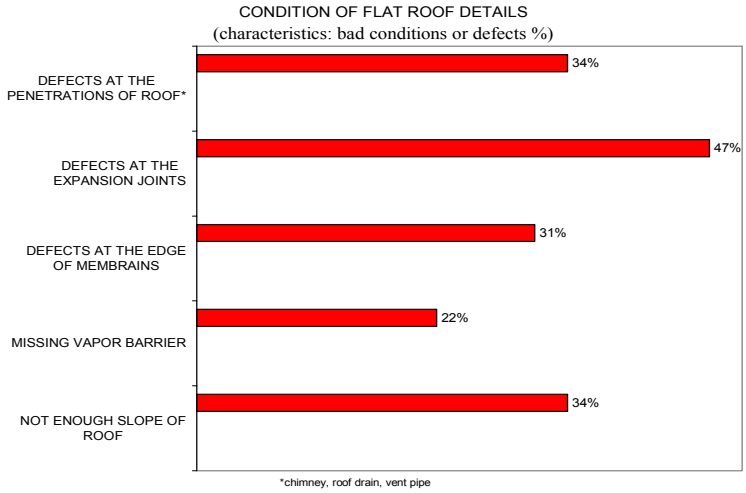

Figure 9.

So in order to maintain the condition, safe and durability of the flat roof water-proofing and insulation all significant factors should be examined even with a deterioration examination if necessary. It can happen that the diagnostics are started with a visual examination performed within the frame of a quick examination and to determine exactly the causes of the abnormalities, defects observed during the examination a complex examination is required.

4. **CONCLUSION**

The paper reported on the development and structure of a field based survey methodology by the research group at the Széchenyi István University. The methodology offers practical diagnostic decision support tools. The new system was developed for the one of the biggest building holder-operator organisation in Hungary. The diagnostic system is firstly based on a visual examination on the spot.
At the beginning of the developing work an important requirement was the visual demonstration of the examinations' results. It was expected from the system tools to be able to show the general condition of the buildings or the condition of the selected constructions. In the process of visual examination the experts have a big amount of data. For the effective handling and using the data the research group of the university created a registration subsystem with tools:
• morphological box for building constructions and
• thesaurus of building construction (connections with the morphological box).

The morphological box as a diagnostic tool had not been used earlier in Hungary. The first probation of this tool was successfully completed and our client, the building holder-operator has installed this tool in his data registration subsystem.

Using these tools the experts can survey the connections of the examined constructions and can use also a clear visual survey the different durability's of the existing constructions. Some details from the results of the visual examination of 60 different flat roofs can illustrate the efficiency the new subsystem.

It would be proper if the results of the constructional diagnostics, the experiences of the pathologic analyses make easier the work of experts using our registration subsystem. The practikal diagnostic decision support tool can help choose the appropriate correctiv maintenance procedures, and identify which remedy to the real causes of the failure.

REFERENCES:

Möller, K.1945, Építési hibák és elkerülésük. (Building defects and prevention of defects), Egyetemi Nyomda, Budapest, pp.32

Molnárka, G.2000, The methodology in visual examination in building pathology. Hungarian Electronic Journal of Science, 2000. (www.sze.hu) pp. 10

Zwicky, F. ,1966, Entdecken, Erfinden, Forschen im Morphologischen Weltbild, Droemer/Knaur, München/Zürich pp. 174

Koppány, A. 1997, Épületszerkezetek morfológiai rendszere.(Morphological System of Building Constructions), Research Working Paper, p.40, SZIF, Győr

Koppány, A. 2002, Building Diagnostics. Construction and City Related Sustainability Indicators (CRISP). EU 5. Framework. CRISP Working Committee Conference, Budapest. ÉMI. p. 8 (summary on: http://crisp.cstb.fr /Database-Hungary)

Koppány, A. and Graf, H. 1985, Mängel an Flachdacheindeckungen und ihreUntersuchungs- methoden, Bauzeitung, Berlin, pp. 135-137

11th International Conference on Durability of Building Materials and Components
Istanbul Turkey May 11-14, 2008

'Comparative' Diagnostic: an Instrument for the Durability of Interventions

Antonella Guida [1]
Antonello Pagliuca [2]

T 71

ABSTRACT

An intervention for preserving a historical building, whatever its architectural or artistic value might be, is in general as much appropriate as deeper the knowledge of its following elements is manufacture, up-to-now evolution, materials, building techniques and carrying structure.

Therefore, considering a monument as expression of belonging to a defined environment, it is necessary to wonder how to act on it in order to preserve it from any deterioration.

The importance of the diagnostic stage cannot be ignored, for both interventions (and not only single procedures) control and global system behaviour, in particular within a long-term building maintenance program aimed to guarantee the durability of intervention itself.

Research focuses attention on the necessity of crossing results obtainable from different kinds of test (destructive and not destructive), in order to get data that may be qualitatively and quantitatively correct and extended to the whole building system.

The analysis and qualification of monuments building structures points out how much useful this approach is, in order to classify interesting pathological events and implement innovative solutions that could guarantee the durability of the recovery intervention on the building.

KEYWORDS

Diagnostic, Durability's intervention, Comparative analysis.

[1] Associate Professor, Department of Architecture, Planning and Infrastructures for Transport – School of Engineering, University of Basilicata, Viale dell'Ateneo Lucano – 85100 Potenza (Italy), antonella.guida@unibas.it o architetto.guida@virgilio.it

[2] PhD Student - D.A.U. School of Engineering – Politecnico di Bari (Italy) - Via Orabona, 4 70125 Bari a.pagliuca@poliba.it

1 INTRODUCTION

The monumental building's reinforcement and restoration is strongly constructed both for the complexity of the built heritage and, sometimes, for the short availability of suitable means.
In fact, the monumental heritage's conservation issue has always been several researcher' object of attention. In 1931, the Athens Charter declared that "the question of the conservation of the artistic and archaeological property of mankind involves the community of the States, which stands surety for civilisation, […] hoping that the States will manifest their interest in the safeguard of masterpieces in which the civilisation has been expressed to the highest degree".
Assuming that the monument is an expression of belonging to a definite place, the problem is to define the right way to operate an intervention in order to protect the monuments from deterioration. In fact, prof. J. Kerisel, a famous researcher, recently has stated that if some artists had been necessary to construct old buildings, nowadays artists have still been necessary to their safeguard.
These are the assumptions of the present research:pointing out a methodology for the approach to the restoration interventions respecting every aspect which makes the architecturale heritage as a monumental work. In this way, diagnostic surveys have a great importance, because they became the condition to carry out an appropriate restoration intervention.The methodology used to develop this research is based on the direct survey on site through the use of destructive tests and not destructive tests and following processing of the results. And through the analysis and comparison of the results, it is possible to get quantitative and qualitative informations that can be considered as representative of the whole architectonic structure.

2 FROM SURVEY TO THE TESTS PROJECT

Nowadays, monumental heritage's safeguard and conservation shows various - sometimes alarming - aspects, which help us to identify the so-called "architectonic emergencies". This is linked to the great number and to the urgency of the cases to solve and, at the same time, to the short availability of time and of economic resources.
Observing a deteriorated monument, the restoration planner should reply essentially to three questions: "if" to carry out a restoration, "where" to carry out a restoration and "how" to carry out a restoration. It is possible to add the fourth question, where the economic aspect is strongly present: "when" to carry out a restoration. In order to suitably answer to these questions, it is necessary to proceed with following specifications, finding out the deterioration's cause, the assessment of the residual safety, the assessment of the restoration's necessity and suitability and, finally, the choice of the suitable intervention and the definition of its carrying out procedures. In the first step of data acquisition, the direct analysis of the building's characteristics and conditions and the checked deterioration' survey, must be accompanied by the research of the planning documents and the events which have affected the structure during its construction and its life. Transformation, changes, partial rebuilding and demolitions are quite frequent in the monumental buildings history. Since the reasons which have caused them are not always respectful of building static balance, the monument's efficiency is failing, that is sometimes difficult to find out for contemporary observers. A very high percentage of damages and settlements in monumental buildings is attributable to these not well thought-out changes, which have not respected of balances growed steady in time and have led into new stresses, not suitably distributed and/or controlled, [Togliatti 1973].
In the survey's step, an important element is checking and analysing the material's features. This information is essential in order to make a suitable model of the building, useful to a safety test of the current conditions. Now, several methods are available and they can be assembled in two different but complementary categories: destructive tests and non destructive tests, both carried out on site.
Non destructive tests on taking from walls samples represent the easiest approach in order to define deformability and resistance parameters, which characterize a building's masonry. It is important to point out that the taking samples must be undisturbed and really representative of the material's characteristics. The samples are also enough to guarantee reliability of results, considering the wide scattering of experimental data. Non destructive material's characterization tests are more indirect, but

more suitable for the restoration, even though they provide mostly qualitative data [Carabelli 1980]. Therefore it is necessary to combine the two kinds of tests in order to provide quantitative indications (deriving from destructive tests) which are qualitatively extensible to the whole structure (by means of non destructive tests). This comparison can draw a better and more complete knowledge of the building's condition in order to define suitable interventions and to guarantee their durability.

3 DIAGNOSIS AND NEED FOR A MODEL

After the analysis of the monumental building and the quantification of its deterioration, the most important and most charming part of the whole restoration process is the definition of its deterioration's causes.
The incapability of catching the real deterioration' causes, leads to wrong diagnosis: this leads to look after only the deterioration' symptoms, but it leads to negative interventions for the structure [Bonaldi *et al* 1980]. The constant progresses led to the structures' numerical modelling and the decrease of the analysis' costs allow a greater employment of these tools. Structural restoration interventions can be simulated realistically through a numerical or experimental model and their effectiveness can be assessed by the light of the achieved results. When it is not possible to assess the structure stress' state, the assessment of the safety factor can be only global and it points out the existing margin between current and limit collapse' conditions. Recently a theory, the so-called "theory of limit analysis" has been systematized. It allows to establish what is the margin which divides the building from the collapse, even though this theory is cautiously applicable to the masonries. In fact the material's conditions, required by the "theory of the limit analysis", are fulfilled only as a first approximation by the masonry [Binda 1982]. This topic represent an object of different studies and scientific researches. Recently some interesting results have been achieved. If the analysis on the numerical model provides uncertain results about safety, due to the lack of data or the assumption of too simplifying hypothesis, the use of reduced scale physical models and loading tests led on site, skilfully and carefully can provide the sought answer.

4 THE "SUITABLE" INTERVENTION CHOICE

This step goes from the choice of the intervention techniques to their implementation, to the planning of periodic checks until the restoration testing. The two steps which characterize the choice of the intervention can be summarized in the possible technical choices' analysis compared with the deterioration's level.
The economic factor is an important element in the intervention' choice, even in a monumental work; it represents an ambitious attitude, which is incompatible with the need for a positive use of the available resources. In order to increase the safety factor of a structure, it is possible to operate in two ways: removing the causes or opposing the effects.The first kind of intervention involves a reduction of the loads which burden on the structure. Typical examples are the chaining the vaulted structure, the shielding of the vibrations induced by traffic through a layers of soundproofing, the use of underpinning or grouting in case of structural settlements, etc. [AA.VV. 2003].
Furthermore, particular interventions on the structure's geometry - such as the creation of joints between adjacent blocks affected by differential settlements or the gradual correction of the juttings – are able to reduce drastically the imposed stresses.
The second kind of intervention, which tends to oppose the effects more than to remove the causes, involves integrations or additions to the material or to the structures, keeping geometries and loads unchanged. Where it is selected the restoration' intervention, it is suitable to carry out with a unit-methodology which involves interventions not differentiated in time. It is also fundamental that the technician of the structural restoration decides not only according to the materials' durability, but also to the changed parts' rigidity, in comparison with the adjacent ones. Putting too hard materials into the monument means to draw the most of loads on these areas. As a consequence, there is the possibility of fragile and localized breakings which can trigger a mechanism of chaining collapse in their turn.

For this reason, it is often advisable to replace deteriorated elements with materials which are more similar to the original ones or which have similar straining behaviours.
Among the interventions' specific techniques, which tend to oppose the effects of deterioration, two main groups can be considered: the first one concerns the interventions which tend to restore or improve the deteriorated materials' features; the second one, instead, concerns the interventions which place new supporting structures to the old ones even replacing completely their functions.
So, analysing in outline the problem of monument's structural restoration, it is clear how ethics and personal culture have to coexist in the technician in charge of the intervention. In fact, prof. J. Kerisel [Kerisel 1981], a famous researcher, has recently stated that if some artists had been necessary to construct old buildings, nowadays artists have still been necessary to their safeguard. This inevitably emphasizes the problem of the workers' training who worked upon the structural restoration. This promotional effort, supported by indispensable financing, legal and administrative means, could paradoxically build in the next future a "therapeutic intervention", which could be more successful for our monumental heritage [A.Guida *et al* 2005].

5 THE STUDY CASE: MATERA'S CATHEDRAL

This research focus upon the Matera's Cathedral, a massive architectural structure, built at the end of the XIII century. In Apulian Romanesque style, it keeps its formal and architectonic connotations almost unchanged outside, even though some interventions have substantially changed the style of the inside. It does not show any plain deterioration signs of its static structure, but it is plain a pathology outside.

Figure 1. The big dark spot on the external wall of Cathedral

It is a big dark spot 'Fig.1' which affects the whole building, along its perimeter. It seems to be caused by a deep phreatic rise which could have given birth to a humidity ascending pathology to the whole building, even though the spot's height is strongly doubtful, because it is difficult that ascending humidity reaches those heights. This kind of humidity, that raising from the subsoil, can be fed either by dispersed water or by an underground ground water table [Croce S. 1994]. The first one has been generated by local - and anyway limited - causes, such as the insufficient collecting of rain-waters, the leakage from wells or water pipes; all these causes have produced a local imbibition of the soil touching the foundations. They can often affect just one side of the building. They can be anyway shut off through suitable means and can be easily abolished. On the contrary, the underground ground water table is neither eliminable nor controlled. It attacks uniformly the building from the basis; it shows maximum rise height towards North North-East and minimum rise height towards the sunniest areas; it is widely spread to every buildings in the same area and it does not show any changes in the reascending height.
Analysing superficially the outer walls of Matera's Cathedral [Esposti W. *et al* 1983], the presence of ascending humidity could be observed as the result of the ground water table, since there are neither wells nor hollows which could allow the underground backwater. However, some hydrogeologic surveys carried out in this area, have shown that there has never been any underground ground water

table both nowadays and in the past. So, after verifying the ground water table lacking, it has been led a thermographic analysis 'Fig.2' of the whole building, in order to understand this big dark spot's nature.

Figure 2. The thermographic survey on Cathedral's façade

The thermographic survey [Eads L.G. *et al* 2000] is a non destructive test, which is based on the physical principle of the energy transmission by radiancy, through the electromagnetic radiation. The wave length of the radiation emitted by an object depends on its temperature, according to the Wien' s law Φ= A/ T. The wave lengths emitted from the objects usually belong to the band spectrum, which is situated into the infrared area (Φ included between 0.78 mm and 0.3 mm). Only at about 6000 K (sun's surface's temperature), the emission is at the centre of the visible spectrum. If you move on an object's surface from a higher temperature point to a lower temperature point, the quantity of radiant energy emitted in the two different areas will change (due to the Stefan's law) and the wave length of the emitted radiation will also change [Rosina E., 1997].
Thermovision scanner's explores the analysed surface using some wave lengths' band and point out the change of radiant energy's strength, according to standards UNI 10824. As this radiant energy is linked to the object's temperature only through emissivity, it is possible to evaluate the object's temperature knowing its emissivity coefficient and, opposite, it is possible to evaluate its emissivity knowing the object's temperature [Volpini S. *et al* 1990]. A suitable optical scanner system analyses the whole area of the camera shooting in details and then it generates an electric sign in a sequence according to the picture's thermal information and proportional to its strength, which is reproduced on the kinescope. To every change in surface' temperature will correspond a similar change in the radiant strength. The kinescope gives a particular colour to this changes.
The analysis was carried out in March 9th 2007. The outer temperature is 8°C and the air's relative humidity is 53%. An unusual result has been come out by the analysis of the achieved thermographic pictures: the lighter areas, corresponding to the dark spot on the façade, are hotter rather than colder, as it would have been expected if there had been rise humidity [Massa S., 1987]. This result would show that the masonry is actually dry and therefore the circumstances that masonry is hotter in the whole building's lower areas - even though at different heights - it would probably be justified as a different behaviour of the stone absorbing solar radiations and therefore the probable variation in the material's emission capacity. The big dark spot would seem to absorb more sunlight than the rest of the building, which has a light colour of the typical local stone, called "*tufa*". The physical mechanism that supervise this process is the irradiation that transfers the heat in the form of electromagnetic waves, in the specific case, directly from masonry irradiated by sunlight. For this reason, the spot is hotter than the rest of the building. However further tests on physico-chemical properties of the material and more detailed petrographic analysis are today being implemented to determine the exact nature of the phenomenon.
This kind of survey provides results, which are qualitatively acceptable, but it does not provide any information as for the quantity. This research aims to examine the possibility of comparing these qualitative results (deriving from the photograms analysis), with the quantitative results which can be derived from a destructive test such as the determination of the humid section's diagram.

In order to carry out this test, three cores have been taken out of the southern wall of the Cathedral, corresponding to S. Eustachio's altar 'Fig.3'.

Figure 3. The HIUTI DD-250E coring machine dry

It has reached 80 cm in depths inside the wall and got to the outer hewn stone. The 6 cm of diameter cores have been carried out using a HIUTI DD-250E coring machine dry. They have been taken out of walls along the same lines, 50 cm one from the other, starting from 2,70 m height from the floor. The samples have been wrapped up in the plastic film 'Fig.4', covered with paraffin and then catalogued in order to be analysed afterwards.

Figure 4. The samples have been wrapped up in the plastic film, covered with paraffin

The analysis has led to the definition of the water's content in the taken samples. In fact the material has been weighed when it was taken, then it has been dried in an oven and therefore it has been weighed again. The difference between the two weighings has defined the value of the water's content in the tested samples. It is necessary that every weighing operation has been carried out with the same scales in order to reduce instrumental mistakes. After weighing every container and sample have been put at 110°C in the oven for at least 16 hours and not more than 24 hours, according to the ASTM D 2216-80, D 2974-87 and CNR-UNI 10008 directions. When they have been dried, the samples have been weighed again: subtracting this value to the one collected before the drying process and comparing it to the dry weight, has been achieved the value of the water's content in every sample [Table]. So, analysing the data, it is clear that the masonry is dry and the water's content of the samples is the material's physiological content.

Table 1. The value of the water's content in every sample

CAMPIONE	NOME CONTENITORE	PESO DEL CONTENITORE	PESO CONT +CAMPIONE UMIDO	PESO CONT +CAMPIONE SECCO	CONTENUTO UMIDITA	PERCENTUALE
1/A	J	60,01	208,88	207,21	0,011345109	1,13451087
2/A	K	71,88	149,73	148,87	0,011430056	1,14300558
3/A	X	67,84	219,73	218,53	0,007963369	0,79633685
4/A	9	100	349,45	344,22	0,021415118	2,14151175
5/A	XX	66,93	249,84	246,4	0,019167549	1,91675488
6/A	Y	72,57	224,76	223,24	0,010088272	1,00882723
7/A	T	59,23	148,41	147,69	0,008139272	0,81392719
8/A	S	72,27	136,18	135,31	0,013800761	1,38007614
9/A	I	58,14	207,5	205,52	0,013434659	1,34346587

CAMPIONE	NOME CONTENITORE	PESO DEL CONTENITORE	PESO CONT +CAMPIONE UMIDO	PESO CONT +CAMPIONE SECCO	CONTENUTO UMIDITA	PERCENTUALE
1/B	AA	100,44	267,2	265,88	0,007978723	0,79787234
2/B	BB	99,16	203,47	202,14	0,012915129	1,29151291
3/B	CC	98,75	159,39	158,05	0,022596965	2,25969645
4/B	DD	101,25	218,91	215,42	0,038568451	3,85684505
5/B	EE	101,82	330,78	326,64	0,018414732	1,84147317
6/B	FF	97,33	311,01	309,06	0,009209843	0,92098427
7/B	GG	99,05	265,02	262,29	0,016723842	1,67238422
8/B	HH	99,05	236,65	235,46	0,008723701	0,87237006
9/B	II	100,49	155,43	154,8	0,011600074	1,16000736

CAMPIONE	NOME CONTENITORE	PESO DEL CONTENITORE	PESO CONT +CAMPIONE UMIDO	PESO CONT +CAMPIONE SECCO	CONTENUTO UMIDITA	PERCENTUALE
1/C	S	72,27	192,96	192,27	0,00575	0,575
2/C	J	60,01	242,62	241,23	0,007670235	0,76702350
3/C	T	59,23	254,14	246,78	0,039242869	3,92428657
3/C	XX	66,94	219,22	214,55	0,031637423	3,16374229
4/C	K	71,88	225,82	222,03	0,025241425	2,52414252
5/C	9	100	334,01	326,17	0,034664191	3,46641906
6/C	X	67,84	171,41	170,56	0,008274922	0,82749221
7/C	Y	72,57	237,43	236,36	0,006532755	0,65327553

CONCLUSIONS

This research shows how it is possible to compare the results achieved from different kinds of tests. To do this, it is necessary to correlate the results, in order to give systematized information on the conservation state of every monument, reducing the damage and the endangering of each structure.
The study aims to realize an applicative methodology more respectful of the built heritage, in order to avoid a simple acritical transposition of the calculation models in the recovery interventions.
The proposed methodology is based on a fundamental aspect of the refurbishment and/or restoration project which is the cognitive aspect, through tests on site and in laboratory. The following step is the realization - and then the validation - of the intervention and a periodical monitoring.
Technological tests were executed to determine the physical chemical and mechanical characteristics of the materials used in the realization of the buildings in the Sassi (tufa, mortar, plaster) and to evaluate the compatibility (chemical, physical, mechanical) with eventual new materials used in restoration's interventions and even to validate the choices made during some interventions.
This accurately projected surveys' plan presents oneself as a further knowledge instrument and as a mean to programme a recovery's intervention, respecting the ancient heritage and without compromising the requisites of durability and safety.
This research can also contribute to increment the typology of the tests to carry out on the masonry; in fact, in relation to all the problems of tests and investigations, it is not necessary to have only one kind of survey, but an organic plan to compare the results, to have a more possible complete cognitive frame. Often only comparing the analysis of more data, coming from different surveys, it is possible to interpret the real phenomena and give the necessary parameters to realize a correct intervention.

Chapters 1, 4 and 6 by both the writers.
Chapters 2 and 3 by Prof. A. Guida
Chapters 5 by Eng. A. Pagliuca

REFERENCES

Togliatti G., 1973, *Fotogrammetria e rilievo fotogrammetrico* in Enciclopedia Scienze e Tecnica, Milano.

Carabelli E., 1980, *I metodi geofisici nelle indagini su vecchie murature* in Corso di restauro edilizio e monumentale, Bergamo.

Bonaldi P., Rossi P.P., Jurina L., 1980, *Osservazioni sulle vicende statiche e geotecniche del Palazzo della Regione di Milano*, in XIV Convegno Nazionale di Geotecnica, Firenze.

Binda L., 1982, *Metodi statici di stima della capacità portante di strutture murarie*, in "Comportamento statico e sismico delle strutture murarie", Roma.

AA.VV., 2003, *'Chiesa di S. Maria della Pietà. Irsina (MT)"* in "Trattato sul consolidamento', Ed. Mancosu, ISBN 88-87017-06-9, pp. C526-C535, Roma

Kerisel J., 1981, *La città e gli edifici antichi* in 'Relazione generale presentata al X Convegno Internazionale SMFE', Stoccolma.

A.Guida, F. Fatiguso, F. Guida, C. De Fino 2005, *'Il Castello di Cancellara, castrum seu fortilitium. Una proposta metodologica per la tutela e la valorizzazione'*, ISBN 88-87687-47-1, Ed.Ermes PZ.

Eads L. G., Epperly R.A., Snell J.R, 2000, *Thermografhy*, ASHRAE Journal, n. 42, (3).

Esposti W., Tottoni S., 1983, *Analisi sperimentale delle irregolarità costruttive di strati superficiali di muratura portante e di opere d'arte tramite termografia infrarossa e metodi non distruttivi complementari*, Monografia CNR – ICITE.

Rosina E., 1997, *La termografia all'infrarosso* in Recupero e conservazione, n. 18, Roma.

Massa S., 1987, *I metodi non distruttivi per le misure di umidità: bilancio e prospettive*, Bologna.

Volpini S., Bertoncello R., 1990, *Tecniche chimico fisiche di analisi di superfici* in Superfici dell'Architettura: le finiture, Padova.

Croce S., 1994, *Patologia edilizia: prevenzione e recupero*, in Manuale di progettazione edilizia, Milano;

Survey of the State of Degradation of the School Buildings of the Lisbon Region

Sónia Raposo [1]
Manuel Fonseca [2]
Jorge de Brito [3]

T 71

ABSTRACT

The network of elementary public schools within the city of Lisbon, managed by the Lisbon Municipal Council, consists of around 95 buildings with an average age of 50 years. The lack of preventive and planned maintenance activities throughout the years has led to various cases of major degradation, with an estimate value for repair of the building school stock near 30 Million Euros.

These buildings can be classified in four major groups according to the technology and date of construction: those until 1930, those between the 30's and the 70's, the ones between the 70's and the 80's and those from then on. In the first group the majority were not designed to fulfill the function of school equipment (originally they were dwellings) and belong to the oldest Lisbon districts. In the second group buildings were designed as schools and were built during the so-called Estado Novo (the non-democratic regime before 1974). The buildings of the third group were based on a standard school project (P3 type) resorting to prefabrication for the structure and the outer and inner walls. Finally, the schools built after the 80´s, even though the youngest, present a worrying degraded condition.

In the present paper, the results obtained through a survey of the condition of 6 schools built in Lisbon after the 80's are presented. The aim was to infer the degree of degradation achieved and the main anomalies resulting from it.

KEYWORDS

Building Condition, Elementary public schools, Survey

[1] LNEC, Laboratório Nacional de Engenharia Civil, Buildings Department, Av. Brasil 101, 1700-066 Lisboa, Portugal Phone +351 21 844 37 98, Fax +351 21 844 30 28, sonia.raposo@lnec.pt
[2] LNEC, Laboratório Nacional de Engenharia Civil, Buildings Department, Av. Brasil 101, 1700-066 Lisboa, Portugal Phone +351 21 844 36 66, Fax +351 21 844 30 28, mfonseca@lnec.pt
[3] UTL, Instituto Superior Técnico, Civil Engineering and Architecture Department, Av. Rovisco Pais, 1049-001 Lisboa, Portugal, Phone +351 218 419 709, Fax +351 218 497 650, jb@civil.ist.utl.pt

1 INTRODUCTION

The elementary school building stock of the public network of the city of Lisbon is, in its great majority, the property of the municipality of Lisbon which also ensures its maintenance and conservation. This network, which is constituted of 95 buildings and frequented by close to 15800 students, presents construction characteristics which can be divided into four distinct periods: before 1930, between 1930 and 1970, between the 70's and 80's, and after the 1980's. The global state of conservation of this building stock is presently considered rather worrying, resulting from not only the average age of construction being approximately 50 years, but also from the absence of preventive maintenance practices and the delays in the execution of the maintenance work already identified as necessary by the municipality of Lisbon. On the other hand, there are indications that the group of buildings constructed after the 1980's is degrading faster than was predicted [Raposo *et al.* 2007]. This paper presents and analyses the results obtained through the observation of six schools of recent construction. They are schools where, in an integrated form or not (different buildings), kindergartens and elementary schools (EB1) function. One of the schools visited is Vasco da Gama School where four grades of education function in an integrated form, and is considered a model school.

2 RESEARCH METHODOLOGY

During August 2007, research work was done of the existing data in the municipality for each of the selected buildings, ehere it was possible to obtain, essentially, project data and information resulting from the utilization of the different buildings on the part of their users.

The fieldwork was undertaken at the end of 2007. The principal objectives of this work were: the verification of conformity of the project with the actual building and the identification of existing discrepancies, identification of any alteration that had taken place in the utilization of the building and a preliminary analysis of the buildings performance. A visual inspection of the buildings was undertaken and photographic and written records were made of the principal discrepancies and anomalies detected. In each visit it was possible to speak informally with the teachers and support staff which served to complement and verify the information collected from the municipality and the observation carried out.

3 BUILDING CHARACTERISTICS

Prista Monteiro School (PM) came into function in the 1997/1998 school year and is comprised of two distinct blocks of buildings, where building A is used for the kindergarten and building B for the EB1 students. Block B, with approximately 2200 m^2 of built-up area, is made of two floors laid out in a U shape, surrounding the exposed playground and recreation area (fig.1). The direction, management, and support staff premises are located on the ground floor as well as a gymnasium and six classrooms. On the first floor, there are eight classrooms, a library, and an IT room.

The structure of PM building B is a system of slabs, colums and beams in reinforced concrete. The involving exterior consists of 0.30 m thick walls, a sloping roof coated with ceramic tile, openings with metal framing and single-pane glass with a venetian system of exterior protection. In the interior, the wall thicknesses vary between 0.15 and 0.20 m, in general having been plastered and painted, along with the ceilings. The floor covering materials are predominantly ceramic and vinyl.

The Vasco da Gama School (VG) came into function in the 1999/2000 school year. The building where the kindergarten and the three first grades of elementary school function, present a gross area of 8800 m^2 distributed over three floors and a basement, where the parking is located. The kindergarten and elementary school (EB1), the common areas, the pedagogic and administrative support staff, the

cafeteria and kitchen, and the gymnasium and locker rooms are located on the ground floor. The resource centre premises (library, auditorium with 200 seats), the management and the teaching support staff offices are on the first floor and the classrooms for elementary school grades 2 and 3 (EB2 and EB3) on the second floor. The building has non-traditional roof covering of ceramic material (Fig. 1).

Figure 1. View of the interior patio of the PM school (left); model and building of the VG school (center; right)

The Vale de Alcântara School (VA) came into function in the 2001/2002 school year. The building, where the kindergarten and primary school function, has a gross area of approximately 1700 m^2 distributed over two floors. On the ground floor there are three kindergarten rooms, the administrative areas, the gymnasium/multi-purpose room, and the cafeteria and kitchen. On the first floor there are eight classrooms for the elementary school, and the areas for pedagogic and personnel support staff.

The building has a reinforced concrete structure and the envelope is made of double walls coated on the exterior by one coat render and porcelain mosaic, a flat roof and openings with aluminum framing and double-paned glass. The partition walls are 0.20 m thick and are stuccoed and painted, and in the wet areas there is a wainscot of ceramic material up to 2.00 m in height. The predominant floor coverings (classrooms, management and teaching support areas) are in wood.

The Alto da Faia School (AF) came into function in the 2001/2002 school year and has twelve classrooms for elementary school (EB1) and four activity rooms for the kindergarten. The school spaces are organized into seven interconnected blocks (Fig. 2): A block - elementary school classrooms, B block - central atrium, C block - resource centre, D block - kindergarten activity rooms, E block - kitchen and cafeteria, F block - gymnasium, G block - covered recreation area of the primary school, and H block - interior patio.

Block A is made of a building of 2400 m^2 distributed over two floors where the classrooms are located. On the ground floor, the building is articulated by a central atrium (block B) where the administration services, teacher and auxiliary educators' rooms are. The structure of block A is in reinforced concrete with an envelope made of a waterproofed type of flat covering, plastered and painted exterior double walls, and openings with metal framing and single-pane glass.

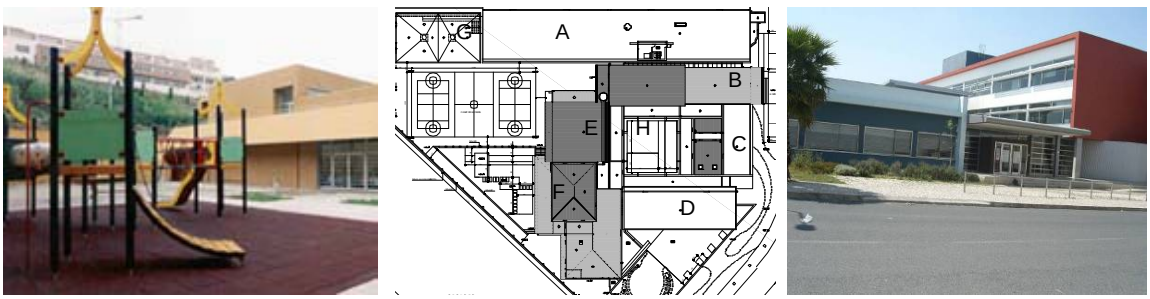

Figure 2. Posterior view of the VA school (left); campus plan of AF (center) view of the two floor block A building of the elementary school, B - central atrium and C - human resources (right)

School 34 came into function in the 2002/2003 school year. The building, where the kindergarten and elementary school function, has a gross area of 3000 m^2 distributed over two floors that are laid out in

plan in the shape of an L. For the kindergarten, there are four classrooms situated on the ground floor, and for the elementary school, there are twelve classrooms (four on the ground floor and eight on the first floor) linked by a corridor of 60 m in length (Fig. 3). The gymnasium, kitchen and cafeteria are located in the base of the L shape (the smallest area of the school), with ceilings twice the normal height.

Figure 3. View of school 34 (left); SB entrance and ground floor plan (center; right)

The structure of the classroom building is in reinforced concrete and the support services area is in metal. The envelope is made of double walls 0.30 m thick, a flat covering, and openings with aluminum framing and single-pane glass. The exterior walls present water-based paint on plaster finishing, exposed varnished concrete, and in the area of the metallic structure there are wooden formica panels. In the interior, the walls are 0.20m thick with a water-based paint finish, also used on the ceilings. The predominant pavement coatings are linoleum.

The São Bartolomeu School (SB) came into function in the 2003/2004 school year. The building where the kindergarten and elementary school function has a gross area of 3500 m^2 and is implanted on a landfill site which is very steep along the longitudinal and transversal development of the building. The building is made of two blocks: block A, a two floor building where the classrooms, administrative nucleus and teaching support staff function, and block B, of only one floor where the cafeteria and kitchen, gymnasium and locker rooms are located. The access between these two blocks is made through the use of a ramp and staircase beginning at the main atrium.

The structure is in reinforced concrete and the envelope is made of exterior double walls with perforated brick masonry, a flat cover, and exterior openings with aluminum framing and colourless double-paned glass. The exterior wall coatings are paint and ceramic material. The predominant coating of the partition walls is paint with a coating of ceramics wainscot and the flooring is a vinyl material with wooden baseboards.

4 RESULTS

4.1 Foundation and Structure

No significant structural anomalies were found, with the exception of the SB school where the opening of cracks of some dimension was noticed between block A and block B which seem to indicate the occurrence of diferential movements between the two structures.

In the case of school 34 and the AF school buildings, deteriorated expancion joints without grout were observed.

4.2 Building Envelope

4.2.1 Roofs

Three of the schools presented infiltration problems directly related with the roof: PM, AF, and VG. In the PM school, infiltrations were observed in the area of the gymnasium affecting the ceiling and the covering of the gymn floor, which already had been replaced in the area affected. The existence of broken ceramic tiles was subsequently aggravated by the fall of a drain pipe which, being damaged, led rain water to this area of the lining which was already fragile. The AF school presented infiltration problems in the roof areas of the elementary school building block with the building block of the main atrium, and in the gymnasium area with the curling staircase that gives access to the upper gallery of the gymn. (Fig.4). Lastly, the VG school presented infiltrations through the large skylight above the main atrium and in some areas of the roof.

In the SB school, the existence of a roof without the slope defined in the project, with uneven constituent elements, was identified. There were alterations to the project, with the introduction of a chimney originating from the boiler, cutting a hole in the roof without caution to the finishing necessary for the good function of the waterprofing system at this sensitive point (Fig. 4).

Figure 4. AF school - view of the gymnasium roof and the roof of the curling staircase which gives access to the upper observation gallery of the gymn where infiltrations were noted (left); VG school - infiltrations in the skylight (center); SB school - bad execution of the coating of the roof (right)

4.2.2 Exterior walls and windows

In the SB school, infiltration problems were identified in the bearing exterior walls, in the ramp linking the two floors, which has resulted in visible degradation of the interior coating of these walls (Fig. 5). The degradation of the coating of an interior lateral wall of a classroom located on the ground floor indicating a probable moistening of the wall by cappilary ascension of the ground water and waterproofing deficiencies (Fig. 5).

In school 34, the coating of the wooden formica panels presents signs of degradation due to acts of vandalism (scratches and *graffiti*) and presents the absence of a filling in the joints between the panels. In the AF school, accentuated degradation of an exterior wooden panel was observed located next to the interior patio (block H) (Fig. 5).

Figure 5. SB school: degradation of the interior coating of the bearing wall and the lower area of the classroom wall (left, center); AF school : very serious degradation of the exterior panel (right)

In relation to framing, no significant anomalies were observed in their function. Discrepancies were observed between the project and the construction: in school 34 and SB, polystyrene blinds were planned which do not exist. This situation stops the students from sitting next to the window due to the sun exposure, and also hinders visibility of the board. Curtains were placed, but now there are complaints about the thermal performance of the spaces with high temperatures in the summer.

4.3 Building Interior

4.3.1 Floors

The main anomalies detected in the coatings are directly related to the infiltration problems already referred to, caused by the roofs and the walls in contact with the soil causing localized degradation in the surface of the coatings, detachments and rotting. In the case of the gymnasium of the PM school, it was necessary to proceed with a partial replacement of the flooring.

In school 34, detachment problems were observed as well as lack of material at the level of the baseboards of the vinyl covering (Fig. 6). In the AF school, it was noticed that the flooring of the entrance area showed scratches and localized absence of material (Fig. 6), and in the VA school, some of the classrooms had loose floorboards with open joints.

The PM, AF and VA schools referred to problems related with the difficulty in maintaining the good appearance of the flooring because these demanded cleaning care and impractical maintenance (expensive materials, staff hours, poor durability of the appearance) namely of the floor coverings in wooden floorboards (Fig. 6) and clear-coloured vinyl floors.

Figure 6. School 34 - absence of a baseboard due to loss of adherence (left); AF school - detail of the wear and tear of the central atrium's floor covering (center); VA school - deficient maintenance of the floors of the rooms (right)

4.3.2 Walls and doors

In the SB, PM and VA schools, diverse fissures in the partition walls were observed, with the greatest incidence in the first building and probably related to the detected settling in its structure (Fig. 7). The most frequent anomalies are tied up with the deficient protection of the wall corners and the lack of adoption of wainscot in areas of great use causing aesthetical degradation.

All the schools referred to in-use problems of the interior doors with bad functioning of the locks (broken and jammed) and the deficient attachment of the handles. With less frequency, cases of degradation to the door coatings were observed which, in the more serious cases, has led to the visible appearance of the nucleus of the door (school 34 and VA). Some cases were observed of deficient attachment of the frame of the doors to the door itself (broken and loose hinges) as well as the frame to the masonry (school 34).

The model of the sliding doors used in the separation of the classrooms from the arts and crafts areas (school 34 and PM) showed functional problems related to maneuverability, vertical planing, deficient fixation, and loose runners. The most serious case was observed in school 34 (fig.7) where the doors were removed from one of the openings for safety reasons.

Figure 7. SB school - detail of the cracking of the walls of the ground floor (left); VA school - detail of a door deterioration (center); school 34 - removed sliding doors (right)

4.3.4 Sanitary services

One of the biggest worries referred to by the coordinators of the schools is connected with the maintenance of operability of the sanitary installations. Their ill-treatment by the users is associated with the breakdown of the equipment of the water and sewer networks, and has resulted, in the most serious cases, in floods. At the level of use, it is frequent for the faucets to be left open and/or the clogging of drains and toilets. The most frequent anomalies in the systems are: the breakdown of the toilet flow controllers, problems with the attachment of the faucets, problems in the enclosures of the washbasins and toilets, and problems at the level of draining capacity of residual waters.

In school 34, it was noticed that in the arts and crafts areas, next to the classrooms, there were signs of frequent water leaks from the washbasin siphons with constant ponding on the floor covering. The results of this anomaly are easily visible in Fig. 8 where three steps of the degradation process of the floor covering are presented.

Figure 8. School 34 - effect of the permanent water leaks on the floor covering

4 DISCUSSION OF THE RESULTS

The SB school, with five years of existence, is the one that causes the greatest worry due to the presence of three factors which, according to the CSA (1995), may lead to an acceleration of the degradation of the building: structural problems, a badly executed waterproofing system of the cover and buried elements with infiltrations. The observations show that it is necessary to make an analysis of the structure and of its eventual stabilization, perform reparation work of the cover (to replicate the project condition) and to the drainage system of the buried wall.

In the VG school, the non-traditional solution of the cover, in ceramic material, is not performing satisfactorily, with areas without a coating and others which are damaged. More studies are necessary, but the worrying signs of the impact of this anomaly on the interior of the building have already been felt with the rotting of the wood next to the door frames of the classrooms and with the repainting and substitution of part of the floor covering in the library. In the AF school, the existence of unevenness between building blocks, with the different types of covers, and the existence of infiltration problems in the interface leads to the establishment of a link between the two facts. It is unknown to what extent a detailed global study was done of the drainage of rain water in these sensitive areas, or if it is a question of bad project execution.

School 34 presents a worrying panorama due to the low quality of finishings used which, associated with a problematic population, is leading the building to high degrees of deterioration. Acts of vandalism have degraded the envelope of the building with walls showing marks and scratches, as well as in the wooden panels. In the interior, there is a worrying number of damaged doors (80% of the openings), detached floor coverings, unprotected white coloured walls without wainscot and with broken corners and serious problems in the function of the water system. It is thought that the doors specifications were not the correct ones in the face of their predicted use. In general this problem exists in all the finishing materials.

5 CONCLUSIONS

The principal observations of the visits to the six schools of very recent construction were presented in this paper. Although it deals with preliminary results, to be treated in greater depth in the PhD work in progress, this study seems to confirm the existence of problems originating from either the design phase or the execution phase, with consequences and important impacts in the maintenance phases and the use of the buildings.

In the envelope, problems can be detected in the roofs and in the bearing walls, areas where the repair could prove difficult to access and/or be onerous. A greater detailing of these construction elements in the projects, and a higher standard of quality control in the execution phase may become important in the reduction in the frequency of the anomalies. In the interior, problems with the doors, in the water systems and in the quality of the materials and finishings used can be detected. The managing entity should organize and improve its database in the sense of providing relevant information to the planners resulting from the utilization of the existing buildings, thus avoiding the repetition of errors and demanding better and more durable solutions in the future.

ACKNOWLEDGMENTS

The authors would like to thank João Semedo and his department of the CCL for aiding in the research on school building project design and available information exploitation. The authors also wish to express their thanks to all the school board management directorates for their time and views about their building.

REFERENCES

CSA 1995, *Guideline on durability in buildings*. Canadian Standards Association, Etobicoke, Ontario, Canada, S478-95 (Reaffirmed 2001).

Chong, W. K., Low, S. P. 2006. ‘Latent building defects: causes and design strategies to prevent them.’ *Journal of Performance of Constructed Facilities*, 213-221.

Pedro, J., Paiva, J., Raposo, S. & Vilhena, A. 2006, *Proposal for an evaluation method of buildings’ maintenance state. Discussion and experimental application*, Buildings Department, Report No 185/2006, Laboratório Nacional de Engenharia Civil, Lisboa, June.

Raposo, S., Fonseca, M. & Brito, J. 2007, ‘Characterization of the Lisbon elementary public school building stock’, Proc. Portugal SB07. Sustainable Construction, Materials and Practices. Challenge of the industry for the New Millenium, Lisboa, Portugal, 12-14 September 2007, vol. 1, pp. 109-115.

Pathologies of the Industrialized Systems: 192 Flats Built in Avellino (Italy) at *Quattrograna West* District.

Francesco Paolo R. Marino [1]

T 71

ABSTRACT

This study is referred to 192 flats in *Quattrograna West* District at Avellino, completed in 1986, now object of building recovery and heavy restructured.

The 14 buildings have foundations realized with grade beams in reinforced concrete on drilled piles, and elevation structure in steel, constituted by HEB pillars, IPE beams and Z steel section folded up by pressure used as edge for the floors made by *prédalle*. The façades are constituted by non carrying infill prefabricated panels of the *solidale sandwich* type.

Of particular interest are: 1) the study of the pathologies of the system of façade, above all the penetration of water from the joints "head to head", interstitial condensations, cracking and putting out of concrete protecting the steel rods in correspondence of the pivots of anchorage of the non carrying prefabricated panels and the floors; and 2) the idea that is not necessary to make interventions of maintenance and building recovery, but that it is preferable to demolish and to reconstruct.

KEYWORDS

Pathology, Industrialized systems, Durability of steel components.

[1] University of Study of Basilicata, Faculty of Engineering, Potenza 85100, Italy, Phone +39 971 205176, Fax +39 971 205185, francesco.marino@unibas.it

1 INTRODUCTION

The 192 flats of 14 buildings realized in *Quattrograna West* District, are part of an important intervention (1.023 flats) of financed building [Marino 2006] that was necessary after the '80s earthquake and was in the program of rebuilding and development of ruined zones of Campania and Basilicata, thanks to law 219/81.

The district is now object of a re-qualification program started in 1997 with *District Contract* that establishes the recover of residential districts with spread buildings degradation, urban surrounding and shortage services in context of lacking social cohesion and with living discomfort. This has been realized involving in projects inhabitants and local contractors.

Because of social reasons and inherent inadequacy of flats, even if without a careful analysis of existing pathologies and of recovering interventions, the municipal government has decided to demolish the originals 14 bodies of factory and the construction of a building "to open court" to the district, the realization of 3 experimental buildings too and the inner reconstruction of other flats with different dimensional cuts to adjust the dimension of the flats to the one of the family nucleus and to respond to users need.

In this study, it is paid the adequate attention to the evaluation of technical faults (such as general degrade of plastic plaster, water penetration in façades and from coverings, superficial and interstitial condensation, expulsion of the layer protecting the steel rods in correspondence of the walls of the sitecast stairwell and the precast infill panels of the façades, the elevation and the breaking of floors, condensation risk of steel elements), that is necessary to realize any recovering intervention or adaptation of buildings to guarantee the preservation of the same buildings and a good comfort for users.

2 THE PREFABRICATED FLATS IN *QUATTROGRANA WEST* DISTRICT

The "heavy" prefabrication in *Quattrograna West* District, is object of General Town Planning Scheme approved with deliberation of Town council executed in '91 and of Recovering Plane for *Mazzini* District and *QuattrogranaEst and West* Districts, according to the Law 457 of the '78 and according to the *Contract of District* as established by the Ministery of the LL.PPs. in 1997.

At the moment, the residential buildings have typological and the morphological characters very simple, that clearly denounce a standard and serial building process. The 192 flats are distributed in 14 bodies of factory, 8 of this form a "cross", while another group of 4 mark 2 opposed "L", 2 further buildings lined up form another body (Fig. 1). Every building has its typology in line, with two stairs, without elevator, that serve 2 flats by floor. The social centre, near the 4 buildings, is isolated from the first areas analyzed.

The bearing structure is realized with IPE beams and steel pillars HEA 140 that constitute the frameworks in longitudinal direction; the site cast stairwell have prefabricated flight and on the perimetrical pluggings are realized modulated *predalle* with base in reinforced concrete made in situ, to which the resistance is submitted to entirely the horizontal seismic resistance. The metallic frameworks instead are realized to resist to vertical actions for its own part. (Fig. 2)

In elevation, the buildings are developed on 3 floors plus the covering: the complete height is 13,61 meters. The groundfloor has a partial arrangement to "pilotis". In every buildings, on the groundfloor, there is a flat of 95 square meters, except to the building n° 11, smaller than the others, where there is a flat of 70 square meters; in this level, in every flats, there are the cellars. Inside there is a strong division between day and night zone. Furthermore the bathrooms are in surroundings without direct

aeration and solar light because of openings lack. Every living flat has 2 loggias.

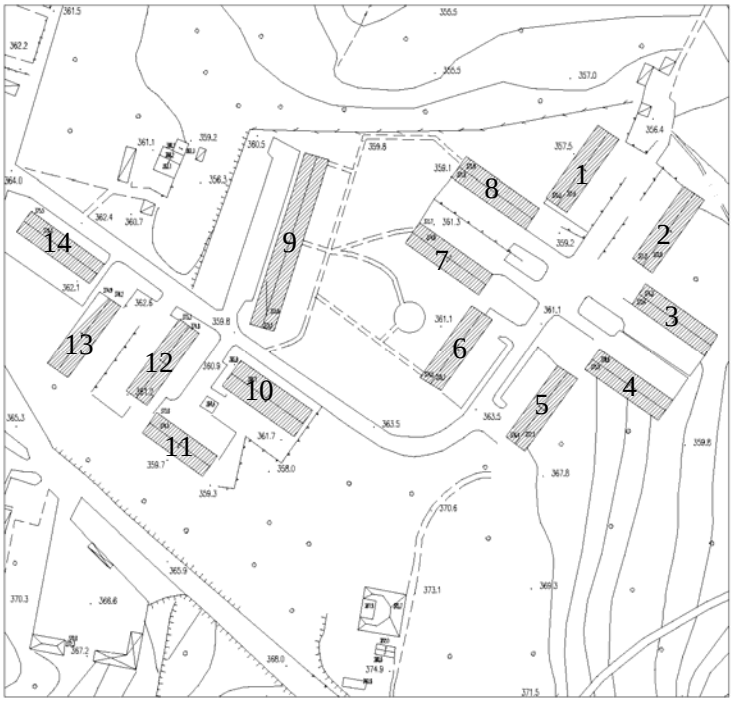

Figure 1. Aerophotografhy with location of the 14 buildings in the *Quattrograna West* District.

Figure 2. Bearing structures of buildings and non carrying infill prefabricated panels of façades

2.1 The Building Technique

The foundations are type indirect to upside-down beams corresponding to the steel pillars, and type grade slabe for stiffened cores, put on drilled caissons of diameter mm 500 and 800 and length m 17, fixtures in the carrying layer of the clays of base for around 5+7 m. The pillars are linked to foundation thought a base plate and hanger bolts in concrete. As said, the floors are “predalle” thick cm 25 lighted with panels of polystyrene (thick cm 5) and completed with laying of concrete in situ.

The external infill panels are realized with prefabricated concrete panels with electrowelded net, “*solidale sandwich*” type hight 300 cm and thick 20 cm, in these ones the external layer thick 7 cm and linked, through connectors that cross the central polystyrene stratus of 6 cm, to the inner one thick 7 cm. The link between panel and panel is obtained by smooth joints, type “head to head”, suture in concrete and sealed with polyurethane foam with closed cells. The structural scheme used is m 3,60 x 3,00.

The covering is realized with an auto bearing structure, with structural steels that form a truss fixed to the floor, completed with corrugated slabs made of eternit-cement-asbeat.

The external fixtures of the flats are realized in structural aluminium anodized with shutter opening, "coordinated block" type with PVC roller blinders. In the stairs, the frames are in structural aluminium anodized with *vasistas* opening. This materials are deeply degradated, so they are not suitable and functional anymore. The low ability to give a right isolation from atmospheric factors is proved by the fact that in most of estates, the users, on their own initiative, have installed a second series of external frames to improve the thermic isolation.

All the metallic parts are protected from corrosion with synthetic alkyl rustproof paint, 70 microns thickness, performed in the establishment previous SA2 abrasive blasting and following application, for the only parts at sight, of layers of oleo-synthetic paint.

Inside the pluggings are covered with stabs in plasterboard and insulating with a coat of glass fibre thick 4 cm. The inside division walls are realized with panels of plasterboard thick 13 mm built on metallic structure put on interaxis of cm 60. The complessive thickness of the separating is 10 cm with an air space thick 7,5 cm. For the separatings between flats, and for inner courts have been used 4 plasterboard panels thick 18 mm, alterned and insulated by glass fibre thick cm 4, built on frame bearing structure structured with plate zinc coated. The stairweel walls are made in reinforced concrete, isolated with polystirene thick cm 3 and whitewashed, the cellars ones in cement blocks of 14 cm thickness. In the loggias the pluggings are in hollow cement blocks, thick cm8, completed externally with plaster.

2.2 The Flats Typologies

There are 2 typologies of flats, each ones has on 2 sides of the buildings: flat type "F" (Fig. 3), with a net surface of 95 square meters; flat type "C" with a net surface of 70 square meters.

The author's analysis was restricted to the restructured buildings, so the typologies of buildings "A" and "B" are illustrated below. The "A" type are composed by one raised plan and 3 levels out ground for residential use. Every ground floor is composed by a flat "F" type with same height access; every residential level is composed by 2 flats "F" type. The buildings is composed by two flats per ground floor and 4 for level each ones linked to stair that serves 2 flats for level in total of six apartments. Every apartment has two loggias. The "B" type is composed by one raised plan and 3 levels out ground for residential use. Every ground floor is composed by a flat "F" type and by flat "C" type. The building has two flats per ground floor and four for type plane each linked by a stair that serves two floors on a total of flats. The "C" type has one loggia.

The flats have been dimensioned following the techniques indicated by the Execution Rule for Building Public Interventions for Municipalities of Campania Region.

3 MAIN CHECKED DEFECTS

The main defects checked and attributed to the building in object, are imputable to twos categories: typological-spatial deficit, or rather typological and dimensional inadequacy of flats; deficit of technical character.

As regards the typological-spatial aspects, deficiencies are translated in: lack of differentiation in the dimensional cuts of the lodgings, potentially too much great in comparison to the dimension of the family nucleuses; monotony of the façades and lack of recognition and articulation of the blocks; absence of elements of mediation between the inside space and the outside one; lack of quality of the external spaces and definition of the green spaces.

The technical faults are in the envelope of buildings (considering the cracks of the plaster coat of

façades, water infiltrations through joints head-to-head not sealed by panels and linked to frames, the degrade of frames, degrade of coverings, panels breached, inadequacy of the layer protecting the steel road) and in the bearing steel elements without zinc coating and not pre-painted, except to the pillars element where there is a too thin oleo-synthetic paint that has detached (high risk of condensation and presence of corrosion for differential aeration).

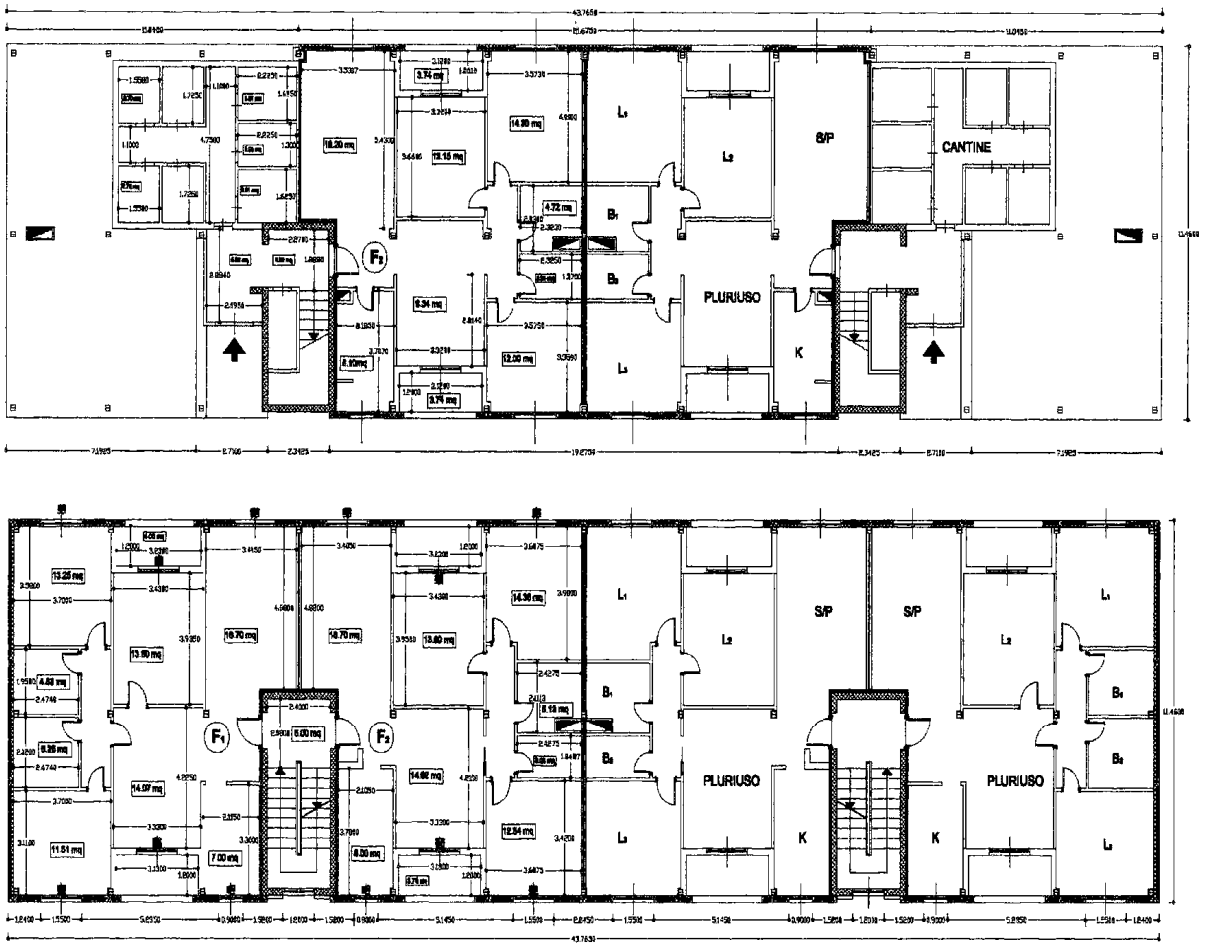

Figure 3. Example of the adopted typologies that are for the large part constituted by flats type "F" of m^2 95,00 of clear surface

3.1 The Pathologies Checked

The pathologies checked in the flats under examination, are attributable to a series of factors, among which there are errors of planning, errors of execution, lack of maintenance, lack of rules to control the quality of building product, particularly in the tendering for contract. In fact, the only considered parameter was the "cost", when is well known that this factor has no meaning when the aim is the quality, that is the "added value" on the final product.

For generally evaluating the state of the Quattrograna's buildings, investigations has been realized "in loco" to define the current conditions and performance evaluation sheets has been filled, before the building was divided in subsystems.

Main pathologies are: - corrosion of the steel elements; - expulsion of the layer protecting the steel road, above all recurrent in correspondence of the walls of the site cast stairwell, and on the façade panels; - water infiltrations along the window-sills; - interstitial and superficial condensations; - floors raising.

Very important is the status of the steel elements, that are protected (for the pillars) with anticorrosive paints applied during the realizations, but since the treatment subsequently has not refreshed and because of the lack of zinc coating, have been corroded by atmospheric agents and, in particular, above all by rainwater, that not only normally acts “by wind” (with West façades more exposed, otherwise in wind direction), but comes from by covering too, along the façade because is not efficiently protected by the overhang of a pitches.

The corrosion is diffused by differential aeration of steel structural elements, in particular in junction zones of the pillars to stairwell walls and in the arcades (Fig.4), as well as on the reinforcing rods and on the hooks of lifting and connection of the infill panels and on the hooking systems of the same floors panels (Fig.5).

Figure 4. Corrosion of the steel elements, beams and pillars

Figure 5. Corrosion of the hooks of lifting and connection of the infill panels and on the hooking systems of the same floors panels

The precast infill panels of façades are *solidale sandwich* type. They are in more parts breached and cracked: has been diagnosed the use of concrete of low quality, very porous and not very compact. The break up and the detaching of the layer protecting the steel rod (less than 20mm) causes the reinforcing rods corrosion (Fig. 6). The same causes are the origin of the corrosion of the reinforcing rods of the stairwell’s walls realized in sitecast reinforced concrete. Now they show the irons reinforcing rods, because the expulsion of the layer protecting the steel rod.

It must be added the disconnection of joints between panels and the low quality of the sealing realized with polyurethane foam. The swelling and the cracking of the plastic plaster (Fig. 6) of the external façades can be seen exactly in correspondence to joints and with horizontal orientation, in wide fronts zones. Corresponding to last floors panels, there are washing away of the arcade because of absence of roofing with drip to protect the cover element not very jutting, and humidity stains because of thermal bridges corresponding to horizontal roofing perimeter and because of condensation inside the stratification of the same package of covering.

Figure 6. Expulsion of the layer protecting the steel road on the façade panels.
Swelling and cracking of the plastic plaster

As regards the humidity pathologies, the research, realized on a sample of representative flats arranged to several floors, showed that the presence of problems connected to the formation of interstitial and superficial condensation and to relative apparition of humidity stains and moulds on the living walls, that comes again after every colour-wash painting, especially in the points where there is pour ventilation. There are humidity stains and moulds in the walls (inside walls and parts of ceiling), and this in spite of the general complaint of users for the low air quality of fixtures and for the inefficiency of heating systems. The mould presence in the rooms is not only an aesthetical problem, but a very hygienically one that gives no ambient wellness.

Humidity stains, superficial condensation, moulds are visible: - in bathrooms (without windows and with the ventilation system that in most cases does not work at all and is not used because of noise) at the intrados of the floor corresponding to the steel structural joint beam-pillar: corresponding to steel bear structure, the floor temperature, because of insulating lack, goes down referred to the inner air, because of the conductibility of the steel on the concrete; - in the corners of the bedrooms exposed to North-East, with moulds corresponding to thermal bridges between perimetral walls, floors and joints with the external wall; - in the kitchens on the inner surface of the panels of façade on the plasterboard layer in the low part of the window where the mould is caused by the condensation corresponding to thermal bridge; - in the loggias at the intrados next to steel bears.

Corresponding to box shutters and along the fixtures there are stains and moulds because of infiltration of meteoric water. Because of different acting of elements, humidity stains are checkable on the plasterboard slabs that cover the steel pillars inside the flats next to the joint between partition wall and floors.

The rising and the break-up of the floors in ceramics, even if they could derive from the lack of splitting up joints, united to the dimensional increase of the tiles caused by slow resumption of humidity from the environment and to the reduction of the available space caused by *fluage* of the floors, is in this case the consequence of low mortar quality, as checked in the users floors related to the floor damages on the durface because of massive solicitations and strokes (object fall, draging of heavy elements).

4 CONCLUSIONS

Is one more time clear how in the building prefabricated techniques, to a not careful project is usually followed by a bad execution, as demonstrated by the faults available so far. In fact very often the use of this building technique is required in case of unusual facts as calamitous events, and even in the project there is not the right attention to reliability, durability and maintenance.

Added to this, there is the lack of laws to control the quality of building product, in the tender for contract, in the project and in the realization, to obtain a "*finish product*" with a high control quality standard.

This research brings a contribution to Italy's researches to knowlwdge of buildings, creating a "data bank" [Lembo F. & Marino F.P.R. 2002] on pathologies and its causes, where study to "*feed the project with the memory of faults*".

REFERENCES

Marino, F.P.R. 2006, *The pathologies of the industrialized systems:1.023 flats realized in Avellino (Italy) in the '80s.*, Proc. Construction in the XXI Century: Local and Global Challenges, joint 2006 CIB W065/W055/W086 International Symposium, Rome, Italy, 18-20 October 2006

Lembo, F. & Marino F.P.R. 2002, *Il comportamento nel tempo dei sistemi edilizi 'tradizionali' ed 'industrializzati' – Cause di degrado e soluzioni progettuali attraverso alcuni casi di studio*, EPC Libri, Roma.

An Example of Good Durability of Building Systems: Survey on 303 Flats Built in *Alvanite District* at Atripalda (Avellino,Italy), Made in *Coffrage Tunnel* and Precast Sandwich Panels for Facades

Filiberto Lembo [1]

T 71

ABSTRACT

The survey presents a study on a public residential intervention, realized after the destroying earthquake of 1980 (between 1983 and 1991) using industrialized building systems (reinforced concrete structure cast in situ in *coffrage tunnel* and precast sandwich panels for façades).

During construction, before the dwellings were accomplished, it were found humidity problems related with water penetration from facades and moisture condensation, and therefore were introduced many upgrade in design and in quality of constructional details, as an external insulation.

The result today is a conservational state many times better than similar and co-eval buildings - evidence that durability is the result of very critical factors, design and building stage.

In the report are showed results of this study, and is highlighted how some inhabitability problems existing in dwelling. They are related too, to design faults in passive ventilation of the rooms, related to the particular climatic conditions.

KEYWORDS

Durability, Pathology, Industrialized Building systems, External insulation, Ventilation/moisture control.

[1] University of Study of Basilicata, Faculty of Engineering, Potenza 85100, Italy, Phone +39 971 205177, Fax +39 971 205185, filiberto.lembo@unibas.it

1 INTRODUCTION

In Italy, in the range of housing scheme, the use of industrialized buildings technique, that in '60 and '70 was typical of big public interventions of subsidized and conventioned building, at least the "10 years Plane" ones aimed to solve the problems of low cost flats in suburbs of big cities, such as Turin, Milan, Boulogne, Rome; in the following years has been and it's now bordered in particular occasions, in which is requested the production of big volumes built in short time, in confined areas and with typologies of "*mass housing*"; the natural diseases, in particular, improved this use, such the case of Pozzuoli's bradyseism, next to Naples, that caused the realization of a new city, Monterusciello, or the earthquake that hit Campania e Basilicata in 1980. In such emergency situations, the contract award procedures "*in concessione*" (with project and supervision of works assigned from the same working executor enterprise) have rendered ineffective the usual controls over quality projects an over execution, with the result of heavy pathologies, above all related to impermeability and to thermo-hygrometric type [Lembo F. & Marino F.P.R. 2002], [Lembo F. 2005], [Marino F.P.R. 2005], [Marino F.P.R. 2006], such as happened in England 10 years before [Lembo F. 1988].

It is surprising recognize that in some cases such as the object of this study, even a long time ago from the finishing, the flats built with industrialized buildings techniques "*by risk*", and especially with the Italian systems of awarding of contract "*in concessione*", after the earthquake of 1980, are in good conditions, except the following case. So, can be seen, for this case, an exception that proves the general rule.

2 DESCRIPTION OF ANALYZED DISTRICT

After the 23/11/80's earthquake, the historical centre buildings' of Atripalda, (with 7.000 inhabitants, in province of Avellino, situated at 50 Km east from Naples) were almost entirely damaged or collapsed, so they were demolished. The government commissioner for earthquake emergency decided, with order 16/06/81 n°323, to built n° 303 new flats, with 4 typologies, from m^2 45, 55, 65 and 85, with residential technique to improve their realization (with a strong "*acceleration prize*": 0,1% of the amount under contract for each day in advance in the fulfillment of the works, as the penalty for each day of delay).

The intervention was located on an area individuated out of urban perimeter, in Alvanite district, on a hill Nord West side along the motorway Avellino-Salerno (fig. 1) and the expected sum, with expropriation area and urbanization, was 20 milliards of Italian lires (i.e. about € 10,3 millions).

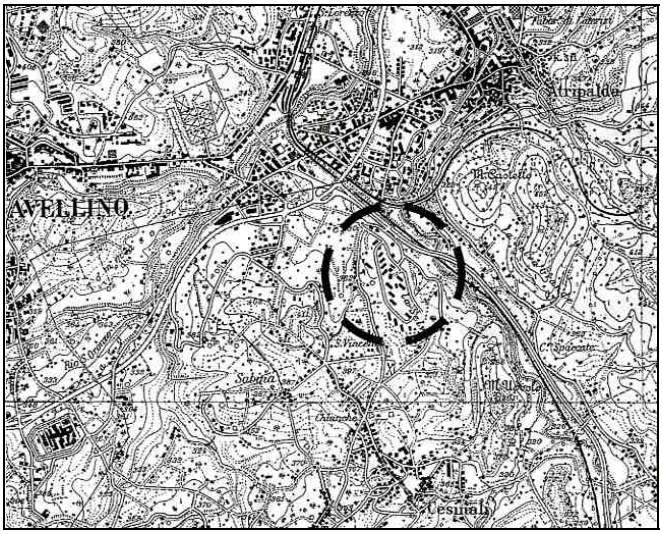

Figure 1. Chorography with location of the 303 flats in the Alvanite District at Atripalda.

The contractor offer tendering for "concession" (including the activities for the expropriation of the area, the design, the direction of the work, and the construction of housing and urbanization works) was the one submitted by the A.LO.SA. S.p.a. of Rome which provided the use of *coffrage* tunnel and precast sandwich panels for façade. The concession contract was signed on 13.12.1982. The draft drawn up by the dealer has provided 17 buildings in 3 or 4 floors above the ground. The dwellings have generally double facing, except the m^2 45 ones, and are characterized by constant span of m 3.60 interaxis, with a depth of m 11,10 (Fig. 2).

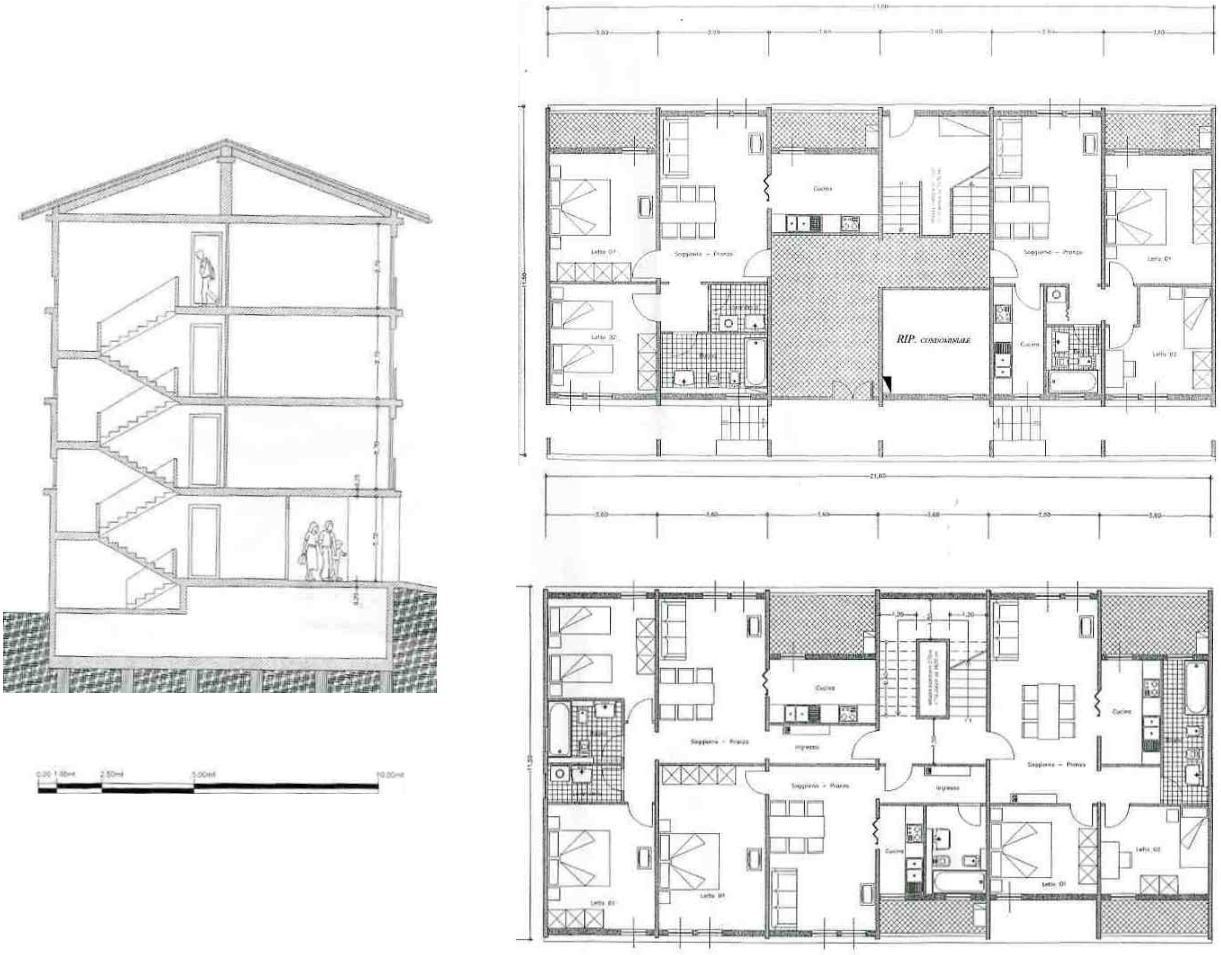

Figure 2. Typical plans and section of dwellings of various typologies.

The grant construction was issued on 10.11.1983, and the time available for the implementation of the work was 16 months (productivity: 227 flats/year). In reality, the residential buildings were completed only after more than double the time contractually agreed (September 1986) (real productivity: 106.3 flats/year). Main work parts has been finished after 2 years more (October 1988), while another part, with linking bridge to Atripalda's centre, has been finished after 3 years more (October 1991).

3 BUILDING CHARACTERISTS AND PROJECT FAULTS, CAUSE OF PATHOLOGIES AND DURABILITY REDUCTION

The buildings has been realized and projected according to *"tunnel builder's dream"*: equal spans, even the staircases ones, with transversal bearing walls (thick cm 14, interaxis m 3,60, to let the advantancing on longitudinal direction of castings, without (or minimal) deposits equipment exchanging. The head walls were isolated from the inside by pilaster slabs, with obvious problems of interstitial condensation (fig 3).

T71, An example of good durability of building systems: survey on 303 flats built in Alvanite district at Atripalda (Avellino, Italy), made in coffrage tunnel and precast sandwich panels for facades, Filiberto Lembo

The plugging of the façades was realized with sandwich panels made of light concrete (cm 4 inside and cm 6 outside) and middle expanded polystyrene from cm 6: useful only for the type section, but full of thermic links corresponding to ribbings, and linked to bearing walls and to floors to realize the formation of thermal bridges along the outline (figg. from 4 to 5) and the windows perimeter. There wasn't the isolations to the overlooking stairwell walls, not warmed.

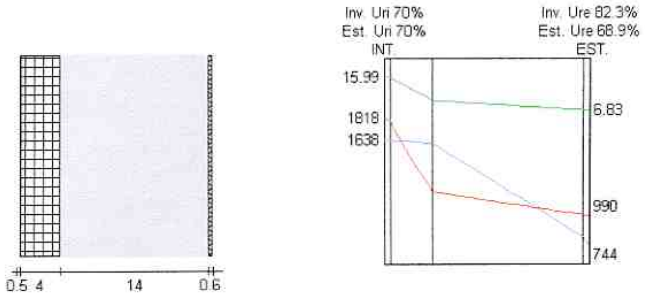

Coeff. liminare interno hi (W/m²°C): 8.10 - Coeff. liminare esterno he (W/m²°C): 24.50

Tipo materiale (descrizione)	Cond. (W/m°C)	C.Spec. (J/kg°C)	Massa vol. (kg/m³)	δ·10-¹² (kg/msPa)	Spess. (cm)
rasatura pronta per interni	0.840	837	1800.0	9.60000	0.50
Cartongesso in lastre	0.210	1090	900.0	23.00000	4.00
cls rbk250	1.768	879	2200.0	2.74285	14.00
intonaco plastico al quarzo	0.900	837	1400.0	1.28000	0.60

Figure 3. Glaser diagram of the external wall made by tunnel 14 cm and insulated by gypsum 4 cm – as built, before thermal retrofitting with 3 cm expanded polystyrene and plastic plaster.

Figure 4. On the left: vertical section trough external wall and intermediate floor - as built; on the right: horizontal section trough bearing wall made by tunnel and two sandwich lightweight concrete panel – as built.

Analytically, the project (so the unrealized work) didn't respected the following rules: Law 373/76 and Decree connected to the dispersions, Ministerial Circular LL.PP. n° 1351 of 22/05/67 and Ministry of Health Decree 05/07/75 connected to condensation control.

The design faults mentioned, have immediately determined, as soon as delivered the flats, at the end of 1986, water infiltrations in singular points, (in particular the joints between panels and tunnels related to the thermic dilatations and to the inefficiency of the join solution) and condensation phenomena, in particular where the flats were arranged according to particular orientations. For this, must be specified that here wasn't respected the project in consideration of particular climatic conditions, a peculiar of the valley where Atripalda and Avellino are; in literature this is well know because here the rain fall with a west wind that hit the façades in a horizontal way, causing a violent psychometric evaporation cooling [Massari G. & I. 1985, pp. 297-301].

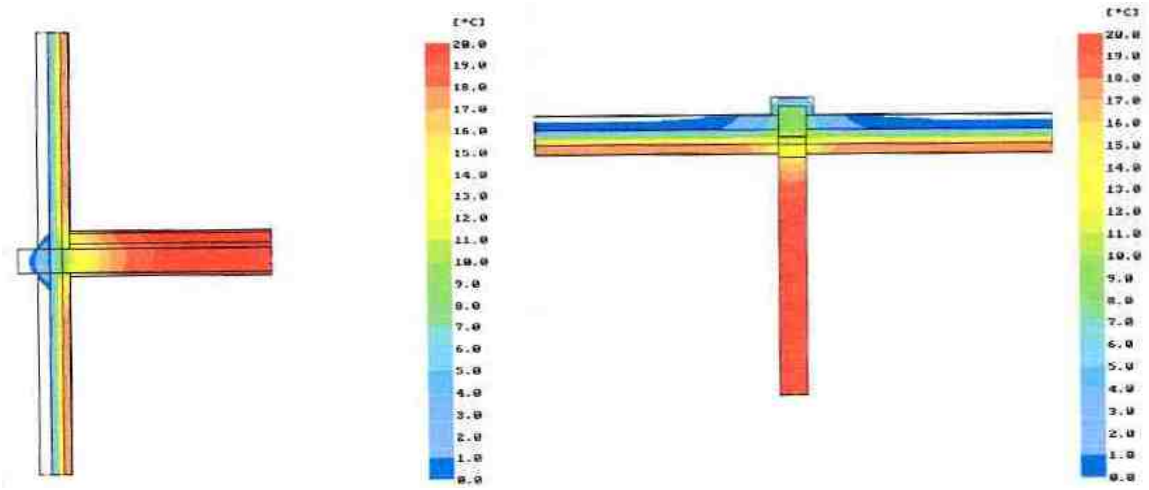

Figure 5. Temperature diagram, showing thermal bridges of Figure 4.

4 THE THERMIC RETROFITTING INTERVENTION REALIZED

The clever Municipal Government has programmed for "*correction*" of given buildings, a *thermic retrofitting* interventions of buildings facades, asking to Campania Region further financial supports that in 1993 (7 years after the finishing and the occupation) applying an isolation system from the outside with plaster thin on insulating (thick cm 3) and various sealing operations, tinsmith ryes and belt courses, on 13 of 17 flats, of € 516.000, and then, 3 years after, in 1996, on remained 4 flats (€ 697.300). In this way, the external walls has been improved for the impermeabilization (passing, according to French D.T.U, from type I – *mono-layer with hydrophilic insulating contact*, to type IIa - *with vertical capillarity cut, formed by an an-hydrophilic insulating*), and for the transmittance.

5 BUILDINGS STATUS AFTER 13/10 YEARS FROM RETROFITTING AND 20 FROM CONSTRUCTION

The research realized in 2004/2005 by Angela Laurino e Marco Moscati for their thesis in Engineering, showed that the thermic retrofitting realized was important for many problems. By an estimate check of calculation, the dispersion has been reduced to 19%, although the intervention wasn't referred to wall's of the stairs (if the intervention were realized here to, it would be verified a further reduction of 12%). The thermal bridges has been removed by every intervention on the walls, and with these the consequent condensation (these remains only corresponding to stairwell's walls, where there wasn't intervention).

Now there are:

- a massive humidity level in ground floor flats (many of these are not occupied), that comes from an insufficient drainage of superficial waters, that when it rains flood the sanitary interspaces under the ground floor floors, with relatives strong phenomena of capillarity rising and humidity saturation on sanitary vacuum walls and to the superior floor intrados, that absorbs humidity and transmits it to the upper flat (with consequence of fast degrade of reinforcings – fig. 6);
- execution defects of external insulating finishing, plus ground floors damages (because there isn't a specific and additional reinforcing against vandalism acts - fig. 7);
- allergy and pulmonary pathologies between inhabitants of the district.

Figure 6. Hollow space under first floor, with signs of flood and great humidity ratio. On the top, right-hand, steel bars spelling concrete cover.

Figure 7. Vandalic damages, made easier for the lack further of specific reinforcing.

6 LONG TERM RESULT OF INSUFFICIENT NATURAL VENTILATION OF FLATS

Without a specific epidemiological research, through the interviews realized with inhabitants, has been found a considerable diffusion of allergy and pulmonary pathologies, that comes from the insufficient natural ventilation of flats; in a flat with condensation on the stairwell's wall, that provokes the spread of moulds and pollens, can be defined the bad inner air quality, that can be the origin of pathologies.

After a careful study about the wind dynamics that hit the buildings (fig 8), that helped to understand the spots distribution for thermophoresis on facades, has been verified the renewing air rate in the flats

thought the apply of Italian rule UNI 10344 "*Warming of buildings calculus of requirement of energy system*", and resulted the renewal rate of 0,05 renewals/hour, while the rules gives a rate 10 times superior, 0,5 vol/h. For a flat of m^2 65 of surface, is m^3/h 84, it would be necessary obtain with a specific natural system of ventilation. There is a foreseeable consequence of use a building system not traditional, with characteristics different from the used ones: it is for itself watertight to steam, and has steel frames (and, for many flats, aluminium dead fixtures too), and has been sealed by addiction of insulation from outside. The flats in particular are the 45 m^2 ones, exposed by one side, that have the biggest problems for a natural ventilation.

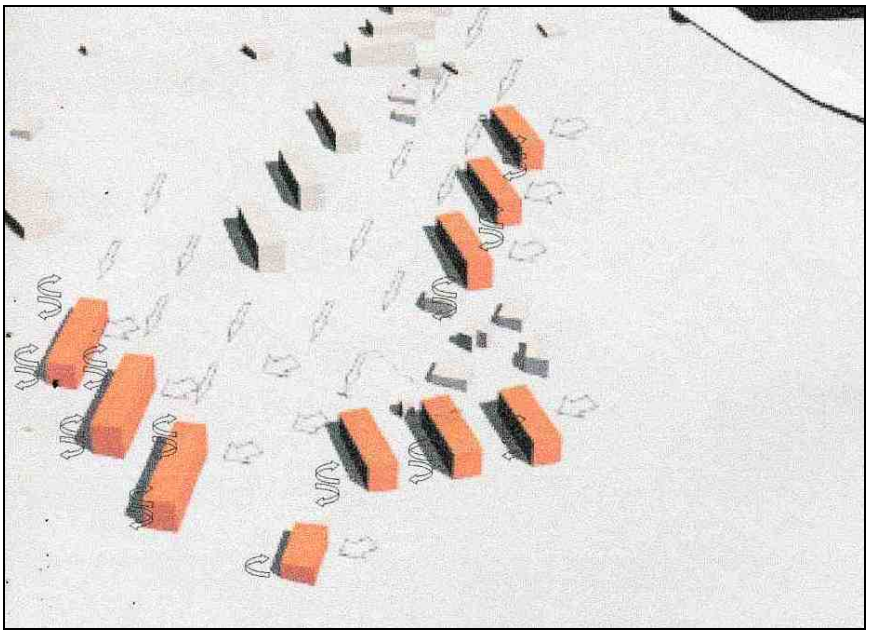

Figure 8. Tri-dimensional study of the winds and their effects on pathologies of buildings and on natural ventilation of dwellings.

It would been necessary realize (but is necessary now) specific air inlet and air outlet, for example equipped with polyamide filters (braids hygro-adjustable) that improve porosity, so the capacity to be passed by air, when the inner humidity level is high, and decrease on the contrary; disposed to let the perfect mixing of incoming air with the surrounding one (fig 9).

Figure 9. Study of specific devices for optimizing natural ventilation in dwellings.

T71, An example of good durability of building systems: survey on 303 flats built in Alvanite district at Atripalda (Avellino, Italy), made in coffrage tunnel and precast sandwich panels for facades, Filiberto Lembo

This system must born with the project and must follow it until the execution, when is decided the use of building systems impermeable to vapour.

7 CONCLUSIONS

The good durability performance of building industrialized intervention in Atripalda is not referred to the original project, but to the *thermic retrofitting* applied after the finishing; anyway there are many improvements that can be realized, to enlarge its life and improve the performances; and is necessary work on durability of the persons that live inside, introducing as fundamental element of project the quality of indoor air, and so a careful ventilation project, natural if possible.

ACKNOWLEDGMENTS

Thanks to Eng. Marco Moscati for his particual contribution given to this research and for the illustrations, that comes from his work.

REFERENCES

Massari, G. & I. 1985, *Risanamento dei locali umidi*, Ulrico Hoepli, Milano.

Lembo, F. 1988, "Qualità e conservazione nel tempo delle costruzioni industrializzate – l'esperienza inglese", *Recuperare – edilizia, design, impianti*, **33**, 90-99.

Lembo, F. & Marino F.P.R. 2002, *Il comportamento nel tempo dei sistemi edilizi "tradizionali" ed "industrializzati" – Cause di degrado e soluzioni progettuali attraverso alcuni casi di studio*, EPC Libri, Roma.

Lembo, F. 2005, "Industrialized building typologies in public residential building and durability of materials and components. Research on some important interventions in Middle-South Italy", Proc. 10th DBMC International Conference on Durability of Building Materials and Components, Lyon, France, 17-20 April 2005, CSTB Press.

Marino, F.P.R. 2005, "Building typologies of public residential building and durability of materials and components. Research on 12.500 flats of E.P.E.R. of Potenza", Proc. 10th DBMC International Conference on Durability of Building Materials and Components, Lyon, France, 17-20 April 2005, CSTB Press.

Marino, F.P.R. 2006, "Pathologies of the industrialized systems: 1.023 flats realized in Avellino (Italy) in the years '80", Proc. International Symposium 'Construction in the XXI Century: local and global challenges', Rome, Italy, 18-20 October.

11th International Conference on Durability of Building Materials and Components
Istanbul Turkey May 11-14, 2008

Corrosion of Rebars Embedded in Ancient Concrete : Correlation between on Site Testing and Corrosion Products Identification

E. Marie Victoire [1]
E. Cailleux [2]
D. Neff [3]
V. L'Hostis [4]
L. Vincent [4]
A. Texier [1]
L. Bellot-Gurlet [5]
P. Dillmann [6]

T 71

ABSTRACT

Several hundreds of buildings made of reinforced concrete are now classified as historical in France. Their major pathology is carbonation induced corrosion. The cracking and spalling decays induced by this natural aging process cause loss of material incompatible with the deontology of historical monuments conservation. Therefore it is crucial to understand the corrosion process of embedded steel and to be able to evaluate precisely the corrosion activity on site, in order to predict and may-be to prevent such decays. Current on site non destructive tools for diagnosis operations are potential mapping or corrosion rate measurements. But, such electrochemical techniques are clearly season influenced. Moreover, corrosion rates induced by carbonation are often very low and therefore can be difficult to measure. As a consequence, in areas heavily affected by spalling phenomena, low corrosion activity is often evidenced, so that the interpretation of the results can be problematic. A last hypothesis could be that the oxide layer formed is so resistive that the conductivity necessary for the measurement is lost. In order to better understand the corrosion process of rebars embedded in carbonated concrete, and may be to improve the reliability of those diagnosis tools, it seemed interesting to try to correlate on site measurements with the identification of corrosion patterns. Therefore, on a 56 years old industrial building (Air Purifier of the Meudon Wind tunnel), several sets of potential mapping, resistivity and corrosion rate measurements were performed, respectively in winter time and in spring time, and after medium or heavy moistening. Then reinforced concrete cores were sampled both in supposed active and passive corrosion areas, in order to evaluate the carbonation depth and to identify the corrosion patterns.

KEYWORDS

Historical buildings, Concrete, Corrosion, Diagnosis tool, Corrosion patterns

[1] Laboratoire de Recherche des Monuments Historiques, Champs-sur-Marne, France, Phone 33 1 60 37 77 84, Fax 33 1 60 37 77 99, annick.texier@culture.gouv.fr
[2] Cercle des Partenaires du Patrimoine, Champs-sur-Marne, Fr, Ph 33 1 60 377786,emmanuel.cailleux@culture.gouv.fr
[3] Laboratoire Pierre Süe, CEA/CNRS UMR 9956, CEA Saclay, Gif-sur-Yvette, France, Phone 33 1 69 08 33 40, Delphine.neff@cea.fr
[4] LECBA, CEA Saclay, 91191 Gif/Yvette cedex, France, Phone, Fax, valerie.lhostis@cea.fr, laurent.vincent@cea.fr
[5] Laboratoire de Dynamique, Interaction et Réactivité (LADIR), UMR 7075 CNRS and Université Pierre et Marie Curie Paris 6, Thiais, France, Phone 33 1 49 78 11 14, Fax 33 1 49 78 11 18, Bellot-Gurlet@glvt-cnrs.fr
[6] I RAMAT LMC CNRS UMR5060 & Laboratoire Pierre Süe CEA/CNRS UMR9956, CEA Saclay, Gif-sur-Yvette, France, Phone 33 1 69 08 14 69, Fax 33 1 69 08 69 23, philippe.dillmann@cea.fr

1 INTRODUCTION

One of the major sources of decay of historical monuments made of reinforced concrete in France is carbonation. This phenomenon consists in a reaction between atmospheric carbon dioxide and the cement paste hydrates, inducing a decrease of pH from values up to 13 in a sound concrete, down to 9 in a carbonated concrete. At these lower pH values, concrete is no longer protective for the steel reinforcement and an active corrosion of the rebars can take place if enough water and oxygen are available. Nevertheless, this corrosion process, very influenced by atmospheric conditions, seems slow-acting, and therefore it is sometimes difficult to monitor on site through electrochemical measurements. Moreover, in heavily decayed areas, where thick oxide layers can be observed, sometimes very low corrosion activities are measured. As a consequence, interpretation of on site measurements can be tricky. So it seemed interesting on one hand to study the influence of atmospheric conditions but also of preliminary moistening on electrochemical on site tests ; and on the other hand to verify these measurements by identifying the corrosion patterns on points prior assessed either active or passive.

2 TESTING SITE AND PROTOCOLE

2.1. Description and Preliminary Characterization

Tests were performed on the extension of a wind tunnel, built in 1950 in the western suburb of Paris (Figs 1 and 2). On the eastern façade, of this ancient air purifier, numerous honeycombing and spalling areas were visible on the pillars, with locally very thick oxides layers (Fig. 3). Due to the age of the building, a carbonation induced corrosion was suspected.



Figures 1, 2 and 3 : The air purifier (on the left) is an extension of the Meudon wind tunnel (in the center). It is locally very decayed, with large spalling areas (on the right) often linked to honeycombing.

In a prior study [1] characterization by optical and SEM observations of both fractures and cross sections revealed a great heterogeneity of the concrete ; locally very compact areas, with good cement-aggregates contacts, cohabiting with numerous very porous zones. A carbonation phenomenon was observed, portlandite being gradually replaced by calcite, but the extent of the reaction was clearly linked to the compactness of the concrete. Finally, cement was identified as an Ordinary Portland Cement containing small amounts of slag, which can be compared to a current CEM II/A.

2.2. Testing Area

A 1m² testing area, with a large spalling zone and visible corroded rebars was selected (Fig.4).
In this testing zone, 5 vertical rebars (2 being visible) and 5 horizontal rebars were located (Fig.5) using an electromagnetic technique (pachometer rebar plus©).

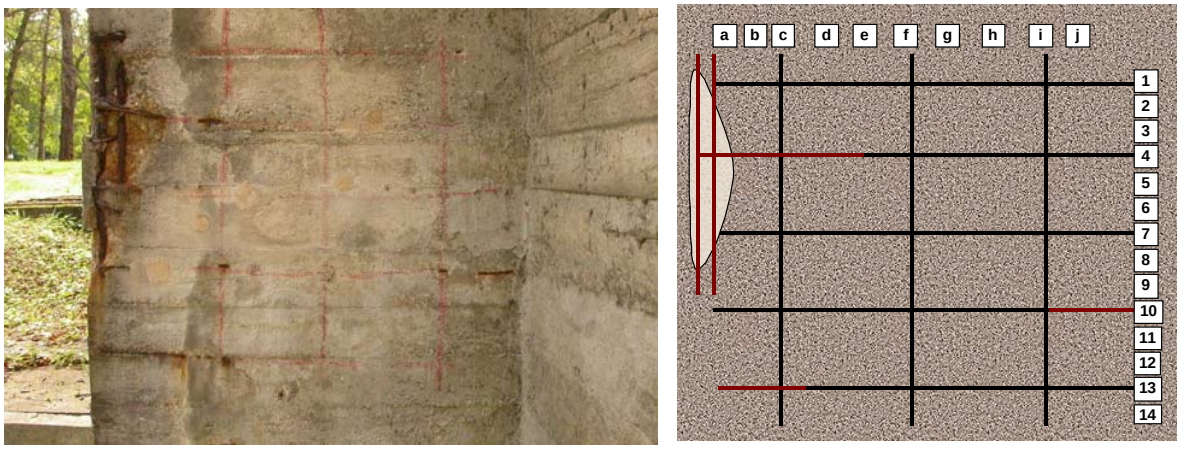

Figures 4 and 5 : In the selected testing area (left picture), 5 vertical and 5 horizontal rebars were located (right diagram).

2.3. Testing protocole

First in order to evaluate the influence of the climate on the corrosion activity, a series of electrochemical measurements (resistivity, potential mapping and corrosion rate) was carried out on site, both in winter and in spring time, after standard moistening of the examined surface. Then to study the impact of preconditioning, during the spring tests, 2 sets of measurements were performed respectively after heavy moistening or after heavy and repeated moistening.Then, as carbonation was the suspected source of corrosion of the rebars, the carbonation depth was evaluated through phenolphthalein tests, realized on cores.

Finally, cores containing a rebar were sampled on areas identified by the electrochemical measurements as active or passive. From those cores, in order to identify the corrosion species, cross sections were prepared and optical microscopy, Scanning Electron Microscopy (SEM) coupled to Energy Dispersive Spectroscopy (EDS), and Raman micro-spectrometry were carried out following the protocole described by Neff & al. [8].

3 ON SITE TESTING

3.1. Resistivity Measurements

Resistivity measurements were performed with a Gecor6© device, using a copper-copper sulfate electrode. Four thresholds of corrosion risk are indicated by the manufacturer, from nil (ρ>100 kΩ.cm) to low (50<ρ<100 kΩ.cm), moderate (10<ρ<50 kΩ.cm), up to high (ρ<10 kΩ.cm). But in practice, such measurements which are so dependent on the concrete dampness and salts contents, are more used as a relevance indicator for electrochemical measurements. Thus, it is commonly admitted that when resistivity is higher than 100, the concrete is too dry, and when it is lower than 5, it is too water saturated, to perform electrochemical measurements.

In winter time (12/01/06, 5.2°C, 70% RH), resistivity values ranging between 9 and 30 were measured (Fig. 6), indicating a suitable moisture content for electrochemical measurements, with a moderate corrosion risk.
The first measurements performed in springtime (02/05/06 AM, 15.4°C, 53.3% RH, Fig. 7) after “standard” preliminary moistening, lead to resistivity values between 273 and 521 kΩ.cm, indicating that the concrete was clearly too dry.

After heavy moistening, a new series of measurements was carried out (02/05/06 PM, 18.5°C, 43.8% RH, Fig. 8), and resistivity values between 19 and 144 kΩ.cm were collected, indicating that the concrete was then wet enough for electrochemical measurements, even if the corrosion risk stayed moderate to low.

The day after, a last set of resistivity measurement was performed (03/05/07 PM, 19.7°C, 54.3% RH, Fig. 9), after heavy and repeated wetting of the testing area. Values very close to the previous ones, ranging between 10 and 133 kΩ.cm, were measured.

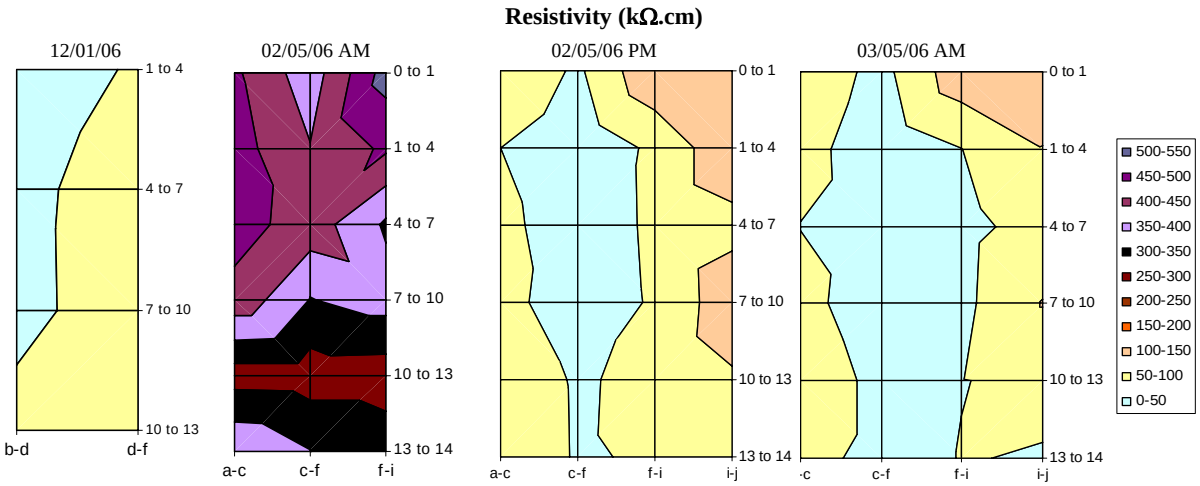

Figures 6, 7, 8 and 9 : Resistivity mapping realized in winter time (12/01/06) ; and in springtime after standard moistening (02/05/06 AM), after heavy moistening (02/05/06 PM), and after heavy and repeated moistening (03/05/06 AM).

3.2. Potential mapping

Potential mappings were carried out using a Canin© corrosimeter, equipped with a copper-copper sulfate reference electrode. If ASTM C876 standard defines thresholds of corrosion probability for potential measurements, it is commonly admitted that it is preferable to realize potential mapping and to identify potential gradients. Thus corrosion is considered as probable when potential differentials of at least 100 mV are encountered.

On the first mapping, realized in winter time (12/01/06, 5.2°C, 70% RH, Fig. 10), potential values quite high, ranging between –69mV and –275 mV were measured. According to the ASTM standard it would indicate a low corrosion probability, but clear potential gradients were observed on the top two horizontal rebars (lines 1 and 4), and on the bottom of the testing area, indicative of a probable corrosion.

Then on the second mapping, performed in springtime (02/05/06 AM, 15.4°C, 53.3%RH, Fig. 11), even higher potential values were obtained (between –292mV and +15mV), confirming the resistivity measurement, indicating that the concrete was very dry. But on the same time, evident potential gradients were observed at the same location as in the winter measurements (i.e., on the top two horizontal rebars = lines 1 and 4, and on the bottom of the two first vertical rebars = lines c and f).
Finally, the third and fourth potential maps respectively obtained after heavy wetting (02/05/06 PM, 18.5°C, 43.8% RH, Fig. 12) and heavy and repeated wetting (03/05/06 AM, 19.7°C, 54.3% RH, Fig. 13) were almost similar. The potential values drastically decreased (ranging between –20 and –367 mV) compared to the previous ones, but the same singular points were observed ; an additional one appearing more obviously on the fourth horizontal rebar (line 10).

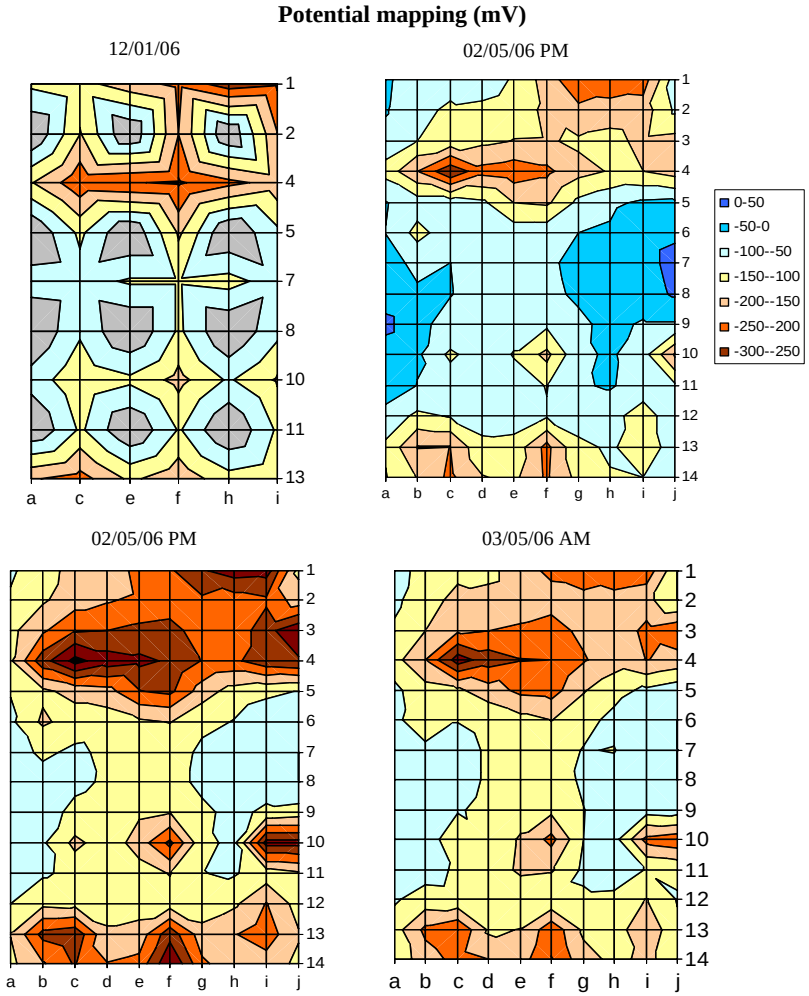

Figures 10, 11, 12 and 13 : Potential mapping realized in winter time (12/01/06) ; and in springtime after standard moistening (02/05/06 AM), after heavy moistening (02/05/06 PM), and after heavy and repeated moistening (03/05/06 AM).

3.3. Corrosion Rate Measurements

Corrosion rate measurements were realized with a Gecor6© device, equipped with copper-copper sulfate electrodes. For each point, the values presented in this paper correspond to the average of at least three measurements, standard deviations being very low (0.01 up to 0.028).

When possible, tests were carried out on areas where, according to the potential mapping, highly probable corrosion or on the contrary no corrosion were suspected (Figs 14 and 15).

In winter time (12/01/06, 5.2°C, 70% RH, Table 1), four points were monitored, but for only three of them, exploitable data were obtained. Thus in points B and C, about 0.4 µA/cm² corrosion rates were measured. According to the RILEM TC 124-EMC recommendation (Table 2), in those points corrosion activity can be considered as low. When, on point A, a negligible corrosion activity was encountered (0.118µA/cm²).In springtime, after “standard” pre-wetting (02/05/06 AM, 15.4°C, 53.3% RH), as expected with the high resistivity and potential values previously obtained, none exploitable corrosion rate could be measured, the concrete being too dry.

After heavy moistening (02/05/06 PM, 18.5°C, 43.8% RH) and heavy and repeated moistening (03/05/06 AM, 19.7°C, 54.3% RH), two corpus of results were obtained :
- in points G2 and G5, corrosion rates almost nil were measured,

- when on points G1, G3 and G4, corrosion rates close to the low corrosion activity threshold were found.

It is interesting to notice that for both winter and spring measurements, the highest values were obtained on the same point (B or G4), where relevant potential gradients were also observed.

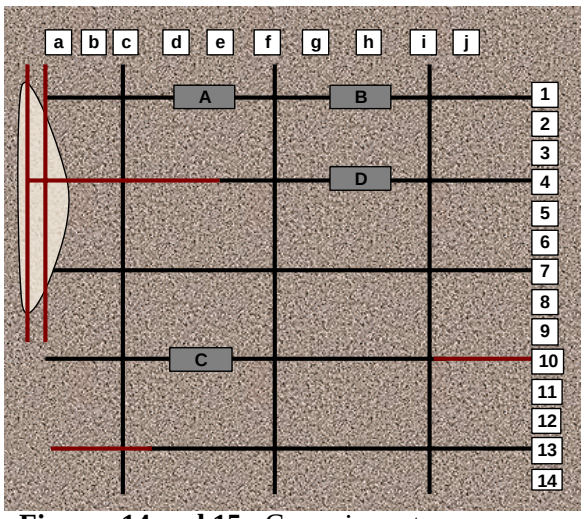

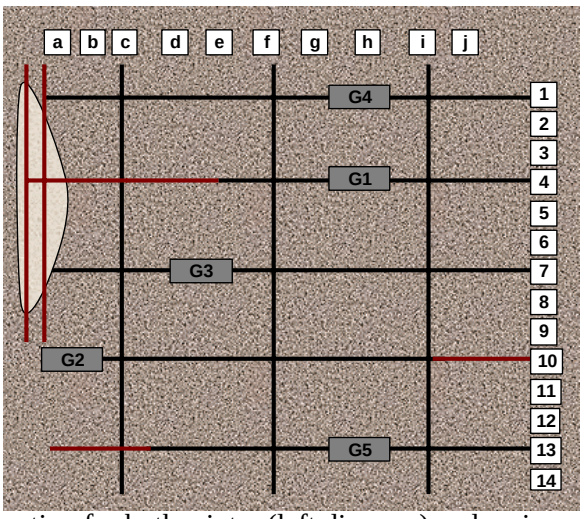

Figures 14 and 15 : Corrosion rate measurements location for both winter (left diagram) and spring (right diagram) measurements.

Table 1 : Corrosion rate measurements obtained in winter and spring.

Measurement Location	Icorr (µA/cm²)	Potential (mV)	Date
A	0,118	-197	12/01/2006
B	0,446	-276	12/01/2006
C	0,433	-144	12/01/2006
D	/	/	12/01/2006
G1	0,167	-261	02/05/06 PM
G1b	0,192	-231	03/05/06 PM
G2	0,011	-101	02/05/06 PM
G2b	0,007	-107	03/05/06 PM
G3	0,157	-158	02/05/06 PM
G3b	0,102	-192	03/05/06 PM
G4	0,237	-359	02/05/06 PM
G4b	0,108	-275	03/05/06 PM
G5	/	/	02/05/06 PM
G5b	0,042	-191	03/05/06 PM

Table 2 : Corrosion rate thresholds of the RILEM TC 154-EMC recommendation.

Corrosion rate (µA/cm²)	Corrosion activity
Icorr < 0.2	Negligible
0.2 ≤ Icorr ≤ 0.5	Low
0.5 < Icorr ≤ 1	Moderate
Icorr > 1	High

4 AUTOPSY

In order to validate the electrochemical measurements, six cores were sampled, notably in points prior identified as active or passive.

4.1. Phenolphthalein Test and Visual Observations

As expected, considering the visible concrete heterogeneity, confirmed by the SEM observations, wide-ranging carbonation depths (varying from none up to 4.2 cm) were measured by phenolphthalein tests (Table 3). As a consequence, as concrete covers varied from 0.7 cm, up to 1.5 cm, carbonation reached only part of the rebars.
Thus on sample O20, carbonation has reached the rebar which is visibly corroded. On the contrary, on sample O22, carbonation hardly reached the rebar which is not corroded.

Table 3 : Phenolphthalein tests and visual observations.

Core reference	Carbonation depth (cm)	Concrete cover (cm)	Rebars diameter (cm)	Visual observations
O19	2 to 4	1	0.8	Slightly corroded
O20	3 to 4,2	1.3	0.8	Corroded
O21	0.2 to 0.7	1.5	0.8	
O22	0.2 to 0.6	0.7	0.8	Non corroded
O23	0 to 0.7	x	no rebar	/
O24	0.5 to 1	x	no rebar	/

4.2. Oxide layers characterization

Two samples in which corrosion was assessed as either active (O20) or passive (O22) with the on site electrochemical measurements, were studied more in details.
Optical microscope observation of cross sections revealed an evident difference in oxide layers thickness between the two samples. Effectively, on sample O22 a quite homogeneously thin oxides layer was observed (average maximum thickness : 50 µm, but very locally up to 100 µm), whereas on sample O20 a very heterogeneous oxide layer was encountered (thickness varying from 10 µm, up to 600 µm).
Then SEM observations coupled with EDS and Raman microspectrometry were carried out, indicating first a complexity of the corrosion layouts but also an heterogeneity of the corrosion products formed on each rebar, on a given metal section. As shown in prior studies [7], corrosion patterns can be classified into three general types depending on the oxide layer thickness and on the corrosion products identified.
It is first to be noticed that on a given metal section several types were encountered. Thus, on sample O22, type 1 pattern, called the “orginal layer” was predominant. It was composed of wüstite (FeO), magnetite (Fe_3O_4) and hematite (α-Fe_2O_3). These phases are characteristic of hot working at temperature above 570°C, so that they were probably formed during the manufacturing process of the rebars. But in some localized zones, a type 2 pattern was observed, goethite (α-FeOOH) being detected between the “original layer” and the metal, which is characteristic of the beginning of an active corrosion (Fig.16). These layers were about 40 µm-thick, up to 100µm-thick in areas containing goethite.
On sample O20, two very different zones were also observed around the same rebar section. Thus type 1 was only locally detected. The major corrosion form identified was a type 3, which is very close to long-term corrosion layouts encountered on archeological samples [5]. It consisted in a thick oxide layer (up to 600 µm), mainly constituted of goethite, locally containing akaganeite (β-FeOOH), lepidocrocite (γ-FeOOH) on the external part of the corrosion layer ; and less crystallized phases appearing in lighter marblings inside the darker phases (ferrihydrite, $5Fe_2O_3.9H_2O$ and/or feroxyhite,

δ-FeOOH) (Fig.17). It is to be noted that at the end of a crack, a variant of this complex pattern was encountered, with traces of carbonates.

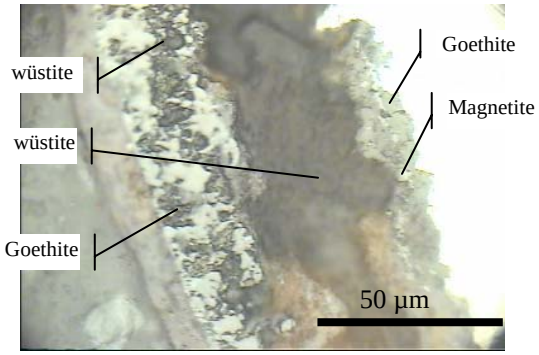

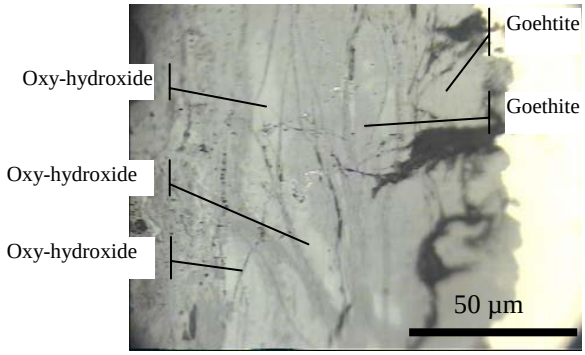

Figures 16 and 17 : Microphotographies of the corrosion layers observed on sample O22 (left picture), and on sample O20 (right picture).

5 DISCUSSION

As expected, due to the known influence of concrete moisture content on corrosion activity of the rebars, a noticeable season impact was observed on the on site electrochemical measurements, as on the same location, and after the same preconditioning, corrosion rate measurements indicated a low corrosion activity in wintertime and an absence of corrosion in springtime.
But preconditioning is also clearly of importance, as heavy preliminary moistening in springtime lead to results comparable to the wintertime ones. It is nevertheless to be noticed that heavy and repeated moistening did not improve the measurement, heavy preliminary moistening being sufficient.
Otherwise, among the electrochemical measurements performed in this study, potential mapping appeared to be the best corrosion indicator, as far as potential gradients and not absolute values were considered. Effectively, the corrosion phenomenon linked to carbonation doesn't seem to be very active, and therefore it is difficult to monitor it on site by polarization resistance measurements. Moreover, potential measurements could be performed even when the concrete was very dry, and potential gradients appeared on the same location whatever the season and the preconditioning.
Finally, an overall correct correlation was observed between the electrochemical measurements, the carbonation depths measured, and the corrosion layouts identified (Table 4). Nevertheless, quite complex patterns were observed, and as an example a noticeable impact of concrete defects such as cracks, was noticed on the nature of the corrosion products formed. This last phenomenon was already observed in prior studies [6] [7].

Table 4 : Results synthesis.

Core reference	Carbonation	Corrosion rate (µA/cm²)	Rebars observation
O20	Yes	G1b = 0.192	Corroded, thick oxides layers
O22	No	G2b = 0.007	Almost non corroded

6 CONCLUSION

In order to try to better monitor carbonation induced corrosion on site, a series of electrochemical measurements, coupled to detailed examination of the metallic reinforcement, was performed both in winter and in springtime, on the pillars of an air purifier built in the 1950ies with reinforced concrete.
On the basis of the tests performed on this specific concrete, on site electrochemical measurements appeared very seasonal variations sensible, potential mapping being the more reliable. Moreover, as carbonation was the main mechanism involved in the rebars corrosion process, very low corrosion rates were measured. As a consequence, a diagnosis based on polarization resistance performed after

standard preconditioning in springtime would have lead to contradictory conclusions compared to a diagnosis carried out in wintertime. Nevertheless, a clear influence of preconditioning was assessed, preliminary heavy moistening clearly improving the correlation between winter and spring measurements.
Finally, the examination of the corrosion layouts, generally corroborated the on site tests. But complex patterns were observed and a noticeable impact of the concrete local defects was noted. Therefore, complementary analyses are scheduled on the same building on areas where the interpretation of the electrochemical measurements was difficult, and a new series of tests will be performed on other types of concrete.

AKNOWLEGMENTS

The authors wish to thank the French Aerospace Lab (ONERA) team of the Meudon Center, for their kind help in this study, and the French Ministry of Culture for their financial support through the PNRC program.

REFERENCES

E. Marie-Victoire, E. Cailleux, A. Texier, November 2006, Carbonation and historical buildings made of concrete, Journal de physique IV, vol. 136, p. 305-318.

ASTM standards, 04.02 concrete and aggregates, C876, Standard test method for half cell potentials of uncoated reinforcing steel in concrete. .

B. Elsener & Al., 2003, Half-cell potential measurements – Potential mapping on reinforced concrete structures, RILEM TC 154-EMC : Electrochemical Techniques for Measuring Metallic Corrosion - Recommendations, Materials and Structures, Vol. 36, pp.461-471.

C. Andrade, A. Alonso & Al., 2004, Test method for on-site corrosion rate measurement of steel reinforcement in concrete by means of the polarization resistance method. RILEM TC 154-EMC : Electrochemical Techniques for Measuring Metallic Corrosion - Recommendations, Materials and Structures, Vol. 37, pp.623-643.

W-J. Chitty, P. Dillmann, V. L'Hostis, G. Béranger, 2005. Use of ferrous archaeological artefacts in binders to improve the knowledge on long term corrosion mechanisms of reinforced concrete, Eurocorr'05, Lisbon, Portugal, September

V. l'Hostis, L. Vincent, V. Praca, D. Neff, L. Bellot-Gurlet, P. Dillmann, 2007.Characterization of long-term corrosion of rebars embedded in concretes from French historical buildings aged from 50 to 80 years, Eurocorr'07, Freiburg im Breisgau, Germany, 9-13 September

D. Neff, E. Marie-Victoire, V. l'Hostis, E. Cailleux, L. Vincent, A., L. Bellot-Gurlet, P. Dillmann, 2007. Preservation of historical buildings : understanding of corrosion mechanisms of metallic rebars in concrete, Metal 07 : Study and conservation of composite artefacts, meeting of the ICOM-CC Metal WG, Amsterdam, 17-21 September

Neff, D., L. Bellot-Gurlet & al., 2006. Raman imaging of ancient rust scales on archaeological iron artefacts for long term atmospheric corrosion mechanisms study, Journal of Raman Spectroscopy 37, pp.1228-1237,

11DBMC International Conference on Durability of Building Materials and Components
ISTANBUL, Turkey, May 11-14th, 2008

Structural Health Monitoring of Historical Buildings Using Fibre Optic Sensors

Mariella De Fino [1]
Giambattista De Tommasi [2]

T 71

ABSTRACT

Structural health monitoring is widely used in engineering as a diagnostic tool for detecting the presence of defects, performance decreases or imminent failures, as well as for scheduling maintenance and repair operations. Among the different technologies for structural integrity control, fibre optic systems, FOSs, show some advantages over conventional devices, including immunity to electric fields and electromagnetic interferences, small dimension and light weight, durability in harsh environmental conditions and access to different measurands such as strain, vibration, temperature, humidity and chemicals. FOSs can be also multiplexed. More than a single sensor can be provided along an optical fibre, with interesting enhancement, in terms of flexibility and versatility.
Beside the wide interest to these technologies for monitoring composite and concrete structures, a lower attention has been given to masonry structures.
The paper is focused on the importance of integrated structural control for the historical heritage. It aims at proposing methodological guidelines and technical solutions in order to integrate FOSs into masonry structures, with particular attention to the conservation of the architectural, constructional and functional features of the buildings. Some laboratory tests with Fibre Bragg Grating sensor systems on a model wall have been also performed in order to assess the reliability of these technologies, by comparing their measurements with the results from traditional devices, namely strain gauges.

KEYWORDS

Structural Monitoring, Historical Buildings, Fibre Optic Sensors

[1] Polytechnic of Bari, Faculty of Engineering, Department of Architecture and Town Planning, Bari, Italy, Phone +39 0805963442, Fax +39 0805963348, m.defino@poliba.it
[2] Polytechnic of Bari, Faculty of Engineering, Department of Architecture and Town Planning, Bari, Italy, Phone +39 0805963342, Fax +39 0805963348, g.detommasi@poliba.it

1 INTRODUCTION

Non destructive diagnostics offers innovative techniques for qualification of masonries. These techniques don't interfere with the structural integrity. They allow the investigation of elements that are not accessible with visual and direct inspection. They provide with comprehensive qualitative information on materials and constructional systems, state of conservation and transformations over the time. Nevertheless, they show some drawbacks. They may require the correlation with destructive diagnostics techniques, the control by skilled operators, the interruption of operating activities, the mobility of heavy equipment. As a result, they may be not effective, in terms of cost, time and results. Moreover, these techniques are generally used to support a correct diagnosis after an alteration in the constructional and static conditions may produce a damage.
Since that, during the last years, the scientific research has focused on new technologies that are cheaper, simpler, safer and quicker. Structural health monitoring is based on the physical integration into materials and structures of complex systems, composed of sensors and microprocessors that are connected by communication networks to platforms for gathering and elaborating data. These systems are able to provide with information on the local and global conditions of structures, in terms of stresses, strains, temperature, chemicals, humidity, with following detection of anomalies and defects.
Beyond a technological innovation, these systems basically offer a new methodological approach. From the classical knowledge process, where an operator takes a direct measurement in order to analyse and interpret the results, we are going towards an integrated system where detection and analysis are carried out by the structure that is able to transmit to the operator some information about its configuration. The sensor integration allows the structure at performing the constant and continuous control of the state of conservation (sensor system), the analysis of structural and environmental parameters all over the service life (elaboration data system) and the identification of a critical condition (interpretation and valuation system). Nevertheless, these technologies offer many advantages. Sensors are light, small and durable. Management costs are low. Data are updating continuously, with possible immediate intervention. System control can be carried out from remote places by Internet. Moreover, these techniques can detect a critical constructional and static condition before it producing a damage or even the failure.

2 FIBER OPTIC TECHNOLOGIES

Optic fibres, classified as dielectric light carriers, are one of the most promising and challenging technologies for the structural monitoring. They can be mounted on the surface and integrated into the material. From an input electric signal, a light is emitted by a laser source, it passes through the fibre, it is detected by an optic receiver and it is converted in an output electric signal. The variation of the electric signal, namely the light properties, along the fibre connected to the structure, can be valuated in order to gather information about the state of the structure, in terms of strain, stress, vibration, temperature, humidity, chemicals and to detect anomalies and defects.
Fibres transmit electromagnetic waves, with low losses. They are made out of two concentric layers: a central cylindrical core and an external cladding. Total diameter is typically 125 μm. The external layer is realized with a lower refractive index than the internal core, so that, according to the total refraction principle (Snell Law) the light is kept inside if the fibre does not undergo a sharp bend.
These technologies show several advantages. They are small and light, so that they do not alter the structural integrity of materials. They are resistant in harsh environmental conditions. They can undergo production and manufacturing processes with very high pressures and temperatures. They are immune to electric and electromagnetic interferences. They are compatible with the ordinary telecommunication fibres. They don't show significant signal attenuation.
There are different technologies based on fibre optic sensors, according to the investigated light property and the exploited physical principle. Nevertheless, they can be all grouped into three categories, in relation with the pattern of sensors along a single fibre. There are:

- Local sensors, where the measure concerns a single area that is generally several centimetres long over the fibre (for instance, interferometer sensors).

- Semi distributed sensors, where the measure concerns several portions, generally one millimetre long each, over the fibre (for instance, Fabry-Perot sensors and Bragg grating sensors).
- Distributes sensors, where each point of the fibre is sensor active (for instance, Raman and Brillouin sensors).

Beyond specific description, it is important to underline that these patterns correspond to different methodological approaches and technical applications.
Local sensors aim at gathering specific information referred to a limited area. Nevertheless, their application, also for historical buildings, generally concerns the control of cracks and /or deformations after defects or an anomalies have appeared on the structure and they have produced a visible damage. In this sense, that allow a traditional monitoring with innovative technologies.
On the opposite, semi distributed and distributed sensors go toward a constant and diffuse monitoring, by mapping and controlling a set of points during the whole life cycle of the structure. As a consequence, they perform when the structure is under working conditions and they can detect, or even predict, defects and anomalies before they produce a damage. Applications of semi distributed and distributed technologies are basically referred to steel components, reinforced concrete and fibre composite structures, while experimentation on masonries are really isolated.

3 APPLICATION OF FIBRE OPTIC SYSTEMS TO MASONRY STRUCTURES

Although the applications to masonries were isolated, the potential advantages of fibre optic systems for existing structures are really interesting. Static and dynamic performances of masonry structures, as well as mechanical and physical properties of traditional materials, are often very difficult to characterize. In fact, an existing building is the result of a comprehensive background, in terms of project, construction, transformation and utilization, that make it unique. As a result, mathematic models and information systems, created on the basis of the material, constructional, technical and technological characteristics, as well as of the simulation of damage and decay processes, can lead to simplified and schematic valuations that are non consistent with the actual structure. In fact, they may not consider the intrinsic balance that a building may achieve for its capability, acquired over the time, to respond and adapt to different external effects, both natural and human. On the opposite, integrated monitoring technologies are non invasive systems to know the structural conditions for a wide set of points and they let qualify the real behaviour of the structure. This approach is really interesting for the structure over its life cycle under ordinary working conditions. But it is even more attractive for the structure during a repair or maintenance work. In fact, a constant control enables the operator to plan properly the intervention, to know the response of the structure in progress and to valuate the structural parameters corresponding to the final configuration over mid and long terms.
According to the previous remarks, the application of fibre optic systems to masonry structures can be carried out in two ways:

- Integration of sensors into the structure
- Application of sensors on the surface of the structure

From the methodological point of view, the former approach can be validated, by studying the transfer of the experimental results achieved for reinforced concrete and composite structures, as well as for steel elements, to the technical solutions commonly employed for the maintenance and the repair of masonry structures [Fig.1-2]. In fact, a wide range of restoration and conservation strategies exploit the integration of reinforced cement injections, reinforced concrete slabs and carbon/glass fibre composites to improve and upgrade the mechanical behaviour of masonry elements.
As far as the latter approach is concerned, the application of optic fibre technologies to existing surfaces can be validated by experimentally studying how these sensors perform when they are bonded on different materials. The assessment of their suitability concerns different issues. Some are referred to the functioning of the sensor system:

- Reliability and relevance of measures
- Physical, mechanical and chemical compatibility between sensors and materials

Other issues have to be taken into account involving conservation principles and referring to the historical and cultural value of the structure, in terms of:

- Formal, architectural and technical compatibility between system and structure

Figure 1. Optic fibres protected by carbon fibre cladding to be embedded into reinforced concrete and composite structures

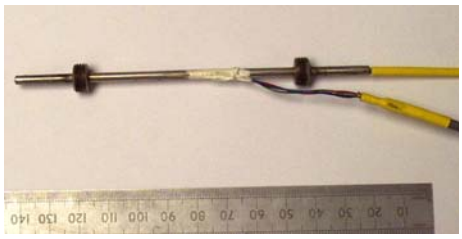

Figure 2. Optic fibres protected by stainless steel cladding to be embedded into reinforced concrete structures

4 LABORATORY TESTS

Some laboratory tests were carried out at the School of Construction Management and Engineering, University of Reading (UK), in order to assess the reliability and the compatibility of Bragg grating fibre systems applied on the surface of a model wall.
A Fibre Bragg Grating (FBG) is a longitudinal periodic variation of the refractive index of the optical fibre that can be induced by an intense ultraviolet source. This refractive index modulation allows the Bragg grating, which is about 10 mm long, at reflecting a specific wavelength of the incoming broadband spectrum. This wavelength, called Bragg wavelength, λ_b is expressed by the following equation:

$$\lambda_b = 2\, n_e\, \Lambda \qquad \textbf{(1)}$$

where n_e is the effective core refractive index and Λ is the period of the grating [Fig.3].

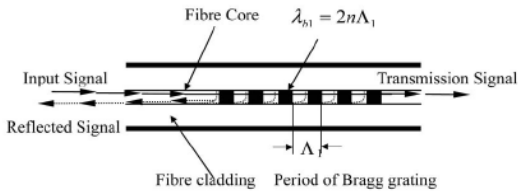

Figure 3. Configuration of a Bragg grating fibre

The Bragg wavelength can be shifted by parameters that can induce a change in the periodicity of the grating, as well as in the refractive index of the fibre. Such wavelength variations can be induced by changes, in terms of temperature and/or mechanical stress, in the structural area surrounding the grating. Specifically, the variation in the Bragg wavelength, $\Delta\lambda/\ \lambda_b$, can be expressed by the following linear relationship that combines the strain and temperature sensor response:

$$\Delta\lambda/\lambda_b = (1 - \rho_\varepsilon)\,\Delta\varepsilon + (\alpha + \xi)\,\Delta T \qquad \textbf{(2)}$$

where ΔT is the temperature variation, $\Delta\varepsilon$ is the strain variation, α is the coefficient of thermal expansion of the optical fibre, ξ is the thermo-optical coefficient and ρ_ε is the coefficient of photo-elasticity. α , ξ and ρ_ε can be determined experimentally.
According to (2), the wavelength variation results from a deformation, due to both temperature and mechanical stress variation. In order to know only $\Delta\varepsilon$, it is possible to measure ΔT with a second FBG sensor, coupled with the first FBG sensor. The FBG temperature sensor can be inserted in a metallic tube that allows at isolating the fibre from the mechanical stresses. As a result, the variation in the Bragg wavelength in the second FBG sensor, is due only to ΔT and the measure from the second FBG sensor can be used to compensate the measure from the first FBG sensor.
FBG can provide semi distributed measurements because a single fibre can be multiplexed. It can be up to hundreds metres long and it can contain up to 25 Bragg gratings. Each single grating is set on a specific Bragg wavelength, with a difference of 5 nm at least compared with all the other gratings on the same fibre.
An experimental validation of Bragg Grating Fibres were addressed.
Fibres were applied on a wall model in order to assess the reliability of these technologies, by comparing the measures with those ones coming from traditional devices, such as the strain gauges, during different compression tests. Wall was made out of light bricks, with a Young's modulus of 2200 MPa, maximum stress of 2.2 MPa and maximum strain of 1000 microstrains. Wall section was 880 x 260 mmq. Three fibres were applied. FBG1, placed on the back side of the model wall, had 1 temperature sensor and 1 deformation sensor. FBG2, placed on the left side of the front wall, had 5 deformation sensors, while FBG3, placed on the right side of the front wall, had 1 temperature sensor and 4 deformation sensors. Six strain gauges were mounted close to six fibre optic sensors [Fig. 4-5].

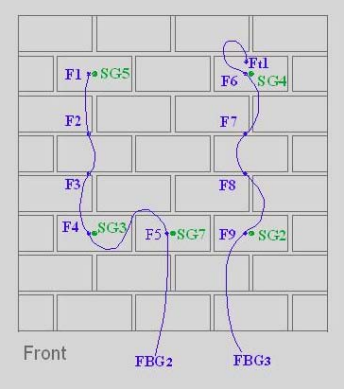

Figure 4. Sketch of the model wall. Front side

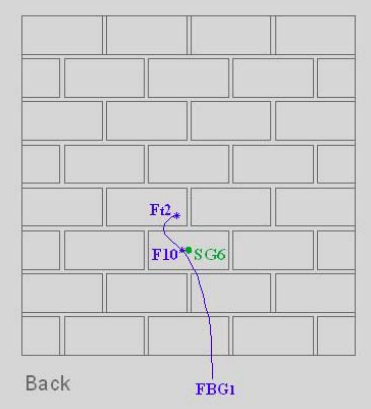

Figure 5. Sketch of the model wall. Back side

Deformation sensors [Fig.6] were bonded on the surface by using epossidic resin, while temperature sensors [Fig.7], protected by a plastic cladding in order to isolate the system from the mechanical stresses of the wall, were applied by using a simple adhesive tape, as the mechanical adhesion was not required. Since the passive elements on the fibres were short, they were not bonded on the wall. They were just applied by following smooth bends, in order to avoid signal attenuation due to sharp bends and break due to straight configuration.

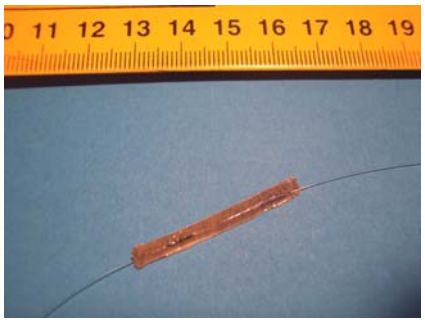

Figure 6. Deformation sensor

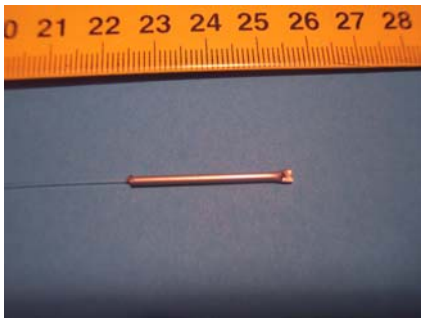

Figure 7. Temperature sensor

Tests were carried out by using Bragg Gratings written using an excimer laser (TuiLaser BraggStar 200) on 1550 nm optical fibres (Fibercore Ltd) that were provided by the University of Cranfield (UK).
In Table 1, the different wavelengths are listed.

Table. Wavelengths λb referred to each Bragg grating along the three optic fibres

Fibber	FBG1		FBG2					FBG3				
Sensor	T2	S10	S1	S2	S3	S4	S5	T1	S6	S7	S8	S9
λb (nm)	1538	1543	1538	1543	1548	1564	1559	1538	1543	1548	1564	1559

The Bragg grating interrogation system was IS7000 developed by Fiberpro (South Korea). The system was connected to a laptop via a USB cable where the sensor wavelengths were recorded using LabView (National Instruments).
Compression tests were carried out by putting on the wall a progressive load, with steps of 50 N, 100 N, 150 N, 200 N and 250 N. Loads were first centred, with maximum value of 600 (2/3 of the failure value). Then loads were 40 mm off-axis in order to achieve failure strains, with maximum value of 1000 microstrain, that was the calculated theoretical maximum value. Nevertheless, after the compression test with off-axis loads, the wall showed small cracks in some critical points.

RESULTS

In this application, the relation (2) can be expressed by:

$$\Delta\lambda/\lambda_b = (0.78 \times 10^{-6}\ \Delta\varepsilon) + (6.65 \times 10^{-6}\ \Delta T) \quad \textbf{(3)}$$

where $\Delta\varepsilon$ is 0.55 x 10^{-6} °C^{-1}, α is 6.1 x 10^{-6} °C^{-1} and ξ is 0.22.
In this application, the temperature sensors showed no temperature changes, as the surrounding thermal conditions were constant during the tests. As a result, the previous relation were simplified as:

$$\Delta\lambda/\lambda_b = 0.78 \times 10^{-6}\ \Delta\varepsilon \quad \textbf{(4)}$$

Results have demonstrated a good consistency between the measures, with an average error smaller than 15% [Fig.8 and Fig.9].

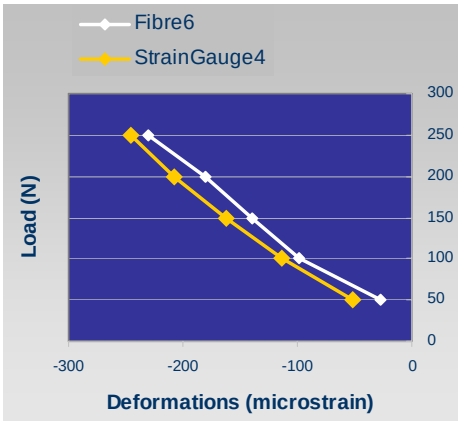

Figure 8. Comparison of results. Fibre sensor 6 and strain gauge 4

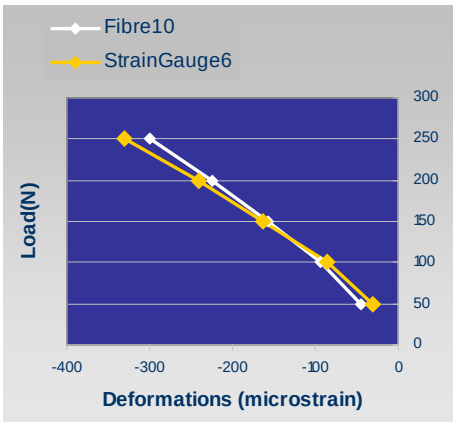

Figure 9. Comparison of results Fibre sensor 10 and strain gauge 6

CONCLUSIONS

Lab tests have suggested some operating remarks:

- Application of fibre optic systems on the surface of existing materials requires highly skilled operators in order to ensure a suitable adhesion and, as a consequence, a reliable mechanical transmission between sensor and structure.
- Fibres cannot undergo a bend with a ray smaller than 5 mm without any signal attenuation.
- Passive tracts of the fibres cannot be placed according to a straight line in order to avoid them to break for unpredictable tensions.
- Optic fibres can be covered by plaster without any alteration of measure.
- Fibres better perform if they are applied on the structure where it is unload in order to assess progressive, as well as further, deformations.

Nevertheless, from the methodological point of view experimentations have demonstrated that:

- Optic fibres show reliable and effective performances for monitoring strains on the surface of a structural element.
- Optic fibres represent a more practical and flexible technology compared with traditional devices. In order to gather information about a set of measurement points, a structure can be equipped by a single 0.125 mm width fibre, with different multiplexed sensors or by different strain gauges, each of them connected to the reading unit by a 0.5 cm width different cable.
- Optic fibres allow at detecting strain values until the failure of the structures. For the model wall, the off-axis compression test achieved 1000 microstrains, considered as the maximum theoretical value.

As a consequence, further developments will concern the experimentation of Bragg grating fibre systems on different materials that are typically present within the historical heritage, for instance stone and wood, both in not reinforced and reinforced conditions, in order to assess the effective signal transmission from the structure to the sensor and to analyse interface materials that can improve that transmission.

REFERENCES

AA.VV., 2004, *Handbook of Smart Systems and Materials*, IoP Publishing, London.

AA. VV., 2002, *Handbook of optical fibre sensing technology*, John Wiley & Sons, New York.

Addington, D.M., Schodeck, D.L., 2005, *Smart Materials and New Technologies*, Elsevier, Paris.

Gebremichael YM, Li W, Boyle WJO, Meggitt BT, Grattan KTV, McKinley B, et al., 2005, "Integration and assessment of fibre Bragg grating sensors in an all-fibre reinforced polymer composite road bridge", *Sensors and Actuators* A 118, 78–85.

Holnicki-Szulc, J., Rodellar, J., 1999, *Smart structures: requirements and potential applications in mechanical and civil engineering*, Kluwer Academic, Boston.

Hong-Nan Li, Dong-Sheng Li, Gang-Bing Song, 2004, *Recent applications of fibre optic sensors to health monitoring in civil engineering*, Engineering Structures, 26.

Inaudi, D., 2005, *Overview of fibre optic sensing to structural health monitoring applications*, Proceedings of ISISS'2005, International Symposium on Innovation & Sustainability of Structures in Civil Engineering, Nanjing, China.

Kister, G. et alii, "Methodology and integrity monitoring of foundation concrete piles using Bragg grating optical fibre sensors", *Engineering Structures*, article in press.

Leng, J.S. et alii, 2006, "Structural NDE of concrete structures using protected EFPI and FBG sensors", *Sensors and Actuators,* A 126, 340-347.

LinYB, Pan CL, Kuo YH, Chang KC, Chern JC., 2005, "Online monitoring of highway bridge construction using fiber Bragg grating sensors", *Smart Materials and Structures*, 14, 1075–82.

Lopez-Higuera JM, Misas CJ, Incera AQ, Cuenca JE., 2005, "Fiber optic civil structure monitoring system", *Optim Eng*, 44, 044401.

Measure, R.M., 2001, *Structural Monitoring with Fiber Optic Technology*, Academic Press.

Moyo, P., Brownjohn, J.M.W., Suresh, R., Tjin, S.C., 2005, *Development of fibre Bragg grating sensors for monitoring civil infrastructures*, in Engineering Structures.

Mufti, A.A., 2003, "FRPs and FOSs lead to innovation in Canadian civil engineering structures", *Construction and Building Materials*, 17, 379–387.

Suleman, A., 2001, *Smart Structures: applications and related technologies*, Springer, New York.

Zhang W, Gao JQ, Shi B, Cui HL, Zhu H., 2006, "Health monitoring of rehabilitated concrete bridges using distributed optical fiber sensing", Comput-Aided Civ Inf, 21, 411–24.

Artificial Stone at the Beginning of the XX Century: Materials, Technologies, Decay Processes and Refurbishment

Albina Scioti [1]
Fabio Fatiguso [2]

T 71

ABSTRACT

At the beginning of the XX century, the building area has been characterized by a significant interest towards innovative materials and techniques, whose feasibility and durability the planners have been completely relied on. A specific example is given by building elements realized with "artificial stone". This "artificial stone" was a "new" but nonetheless "basic" material, that allowed replacement of natural stone that was more expensive to procure and also more difficult to obtain. This study provides an in depth analyses of the use of artificial stone for façade. Previous research has aided illustrating both the positive effects, as well some potential critical points of this material. Furthermore, knowing that these elements can undergo specific material and technological decay require practitioners having the requisite knowledge or technological "culture" pertinent to the refurbishment of artificial stone, without which often leads to unsuitable maintenance and repair work. Particularly, the analysis of materials and technologies employed for the building envelope have been developed. Starting from the scientific knowledge of elements and typologies and from the taxonomical identification of potential decay processes and macroscopic alteration forms, that these handiworks could undergo, the study aims at investigating the possibility to produce an artificial stone to repair or replace the damaged material with particular attention to its composition and durability and the compatibility between ancient and new materials.

KEYWORDS

Artificial stone, Decay, Materials, Replacement

[1] Polytechnic of Bari, Dept. of Architecture and Urban Planning, Bari, Italy 70125, Phone +39 0805963442-5963347, Fax 0805963348, a.scioti@poliba.it
[2] Polytechnic of Bari, Dept. of Architecture and Urban Planning, Bari, Italy 70125, Phone +39 0805963789-5963347, Fax 0805963348, f.fatiguso@poliba.it

1 INTRODUCTION

Artificial stone is a building material that characterizes a large part of the architectural heritage built between the XIX and the XX centuries. The historical architectural value given to buildings rendered in artificial stone, seldom ascribed to the artificial stone as bearer of historical or technological value. As a consequence, one frequently has inadequate maintenance, refurbishment or restoration work that are typically oriented towards the replacement of elements rather than to their preservation.

The paper focuses on the definition of pathologies and decay processes for artificial stone used in the external façade of buildings in general, using the specific example of some Apulian buildings as a reference case. Hence the goal was to define suitable guidelines and operating criteria for maintenance and restoration of the artificial stone.

The study starts from the material-technical-technological evolution due to the introduction of a new material and to the development of a new technology within a process that took place, in great part, without the direct participation of academia, reconstructed also by the study of design patents lodged between 1870 and 1940 in Patent Office of the National Central Archive (of Italy) From the patent information, it is possible to draw extract information on mixtures and preparation techniques, and also defects and lack of performance that the new material demonstrated over time. Additionally, in certain instances the patent information provided empirically based diagnosis of the causes of defects or performance deficits and possible improvements in regard to both the selection of basic mix materials and the technology for maufacturing these products. The study made possible a direct comparison between mixtures and the manufacturing process through an analysis of appropriate case study of Apulia.

1.1 Artificial Stone Over Time

Research on the artificial stone manufacturing process has very ancient origins and represents a constant in the building history. Nevertheless, it is possible to outline a way characterized by testing and manufacturing aimed at obtaining materials that are both aesthetically like natural stone and guarantee of a greater durability for buildings.

Since Roman times, to obtain a stone that became hard when exposed to the air over time, a blend of one part crushed lime with two parts sand was used. Over the centuries, a good number of architects such as Bramante, Palladio and Bernini, have experimented with imitation stone with mixes that were basically based on lime.

During the Renaissance the use of plaster became common for covering building façades. Use of natural stone was limited to structures of civic or national importance, and as well to architectural decorations on these buildings. These elements were so limited that it was possible the low cost imitation by elements made out of common lime or water lime mortars. This employment is especially evident on the façades of residential buildings realized with ashlar stone: natural stone was used for the base of the façade whereas the upper part was realized using artificial stone and in an exact imitation of the course and pattern used for laying the natural stone in the base of the wall. During this period, rendering mixtures for artificial stone essentially included marble dust, lime and glue. [Cavallini & Chimenti, 1996]

There are several techniques developed in the XVIII and the XIX centuries to obtain a material that simulated cut stone. For example, mix of sand, hill and pigments applied on wood bases or plaster worked to simulate ashlars of stone, or cast iron worked for appearing as stone. Between the end of the XIX century and the first half of the XX century artificial stone has been achieved in large part due to the rapid growth of the use of Portland cement. The introduction of Portland cement, in the first decades of the XIX century and the consequent progress of the respective technologies made possible the production and the spreading of the new material with very low costs. The use of these techniques

to produce artificial stone permitted replacement of natural stone, a more expensive product and one that was difficult to procure given the distance to quarries and the cost and expenses of quarrying stone.

European and North American manufacturing centres started to produce artificial stones by earthenware or cement (Pulham stone, Haddon stone) and several mixes of modified gypsum plasters and were patented as artificial marbles [Proudfoot, 1996]. The use of the artificial stone became increasingly widespread and a symbol of progress obtained in the new industrial society. New production processes, industrial management methods, artisan traditions all found in the artificial stone building sector are illustrative of the close alliance between art and industry in this period of industrial development.

The imitation of natural stone, moreover, does not only concern aesthetical issues such as the choice of colours, grain or texture, as it was during the Renaissance, but also performance related issues such as flow, shrinkage and curing. As such, one has the development of a new technology that involves different parts of the building, particularly the external façade and those related to brick or stone masonry.
The new material seems to very well meet the requirements of the architectural culture at that time, which was connected to eclecticism and Art Decò; such type of architecture was characterized by extremely “plastic” elements that are easily produced using a cementitious mixture placed in moulds.

This evolution leads to the use of this material beyond that which was first proposed to replace natural stone, and from the 1930’s this product becomes an independent architectural subject, extensively used in the building industry and with shapes and element never before realized with natural stone.

1.2 Manufacturing and Patenting

First, we have some tests for the use of cement to simulate stone at the end of the XVIII century in France and England. The “Coade Stone” is one of the most widely used products first produced in England and used in European and American architecture until the end of the XIX century. However, from the second half of the XIX century, the largest number of patents is produced, in particular, those from America, England, France and Italy.

An early American patent, dating back to 1868, belongs to George A. Frear from Chicago for “Frear Stone”, a mixture of natural cement and sand with the addition of a shellac solution to enhance the strength in the curing first phase. This method is used and copied extensively with some differences in the choice of materials and methods; whatever is used however, today the specific typology of decay is evident.

"Coignet concrete" or "Coignet Stone" as developed by the pioneer of cement use in France, Francois Coignet, has a French patent that uses the cement as binder. This patent, dated 1869 and 1870, makes use of Portland cement, water, lime and sand as raw materials to manufacture prefabricated cement elements. These are immediately modified in the US manufacturing process with a mixture of sand and Rosendale cement. Hence, in the 1870 American patent awarded to Coignet, this modified formulation is sold to an American, John C. Goodrich Jr., who founded the New York and Long Island Coignet Stone Company. This company manufactured the artificial stone for the Cleft Ridge Span in Prospect Park, Brooklyn, New York, and consdered to be one of the earliest known use of this type of architectures in the USA.

The patent of Frederick Ransome is one of the most widespread English patents, in which is used a mixture of sodium silicate and calcium chloride to obtain calcium silicate blocks, whereby the removal of sodium chloride produced from the process is completed by means of washing with water during the cure. But for a great number of formulations we have soon the use of Portland as binding, that is a more reliable and less expensive product.

First the experimentations and the success of the new material are focused on a cheap artificial stone as a substitute for more expensive and less available natural stone. Then the manufacturing doesn't aim anymore at an imitation of the natural stone from an aesthetic point of view, but also and above all in regard of performances.

As evidence we have a large number of patents of the different kinds of mixture brought onto the market between the XIX and the XX century. There, we can see an advanced research aimed at improving the physical-mechanical feature and at developing a new technology, in a process mainly based upon products whose definition is the result of experiences made in artisan way but with proto-industrial developing for production.

The goal of the study of patents registered between 1870 and 1940 in Italy is the historical, technical and technological knowledge of this material. The research was carried out by means of a critical review of patents that allowed cataloguing these in accordance with essential mixtures and with regard to the binder used.

For each one of this typology declared defects and probably causes has been identified, and then, for each defect, improvement strategies suggested with regard to the mixture form, as wells as to technique and manufacturing procedures.

In the first manufacturing phases of these materials, during the XIX century, the main required performances are design, durability, cheapness and easy fitting. As a consequence, the manufacturing aims to guarantee and to improve these requirements for the market.

The main used bindings are lime, Portland cement and Sorel cement. The latter is largely used by the best producers of that period like the Union Stone Company in Boston that adds sand or crushed stone to the hydrate cement in order to obtain a variety of artificial stone.

Since the end of the XIX century many patents declare some defects of products on sale and suggest adding some additives that improve their performances. In specimens with lime and sand, we can have frequently change of geometry and cracks in the final products. The reason of this is the type of lime, the additives used to make easier the cohesion between ingredients and the content of water in the mixture.

When the caustic lime is used, the most common aim is to obtain crystallized masses by adding sulphuric or sulphurous acid in the mixture. But this doesn't produce the expected results, because reactions with sulphuric acid are too quick and they don't allow a good combination between lime and gypsum.

On the opposite, the mixture containing sulphurous acid slows down the natural process of cohesion and it doesn't permit to arrive at a strong and firm level of cohesion. So this type of mixture is modified using water lime (Patent No. 52901- 28/08/1899 Kiefer) to replace the caustic lime, and the production process is helped adding sulphuric acid that in this situation acts at the right velocity.
With regard to the content of water, it cannot be checked with accuracy, because often the sand used is not completely anhydrous but it shows variable and not measurable quantity of water. Then the indication is to make row materials totally anhydrous, by means of centrifugation for example (Patent No. 53024 - 25/09/1899 Schwartz), and to add the right quantity of water just after carefully mixing.
Further described defects concern the poor compactness of mixture after setting that can cause fragility and strength below expectation.

To face up to this inconvenience we have many indications. Some patents suggest to obtain a better cohesion in the mixture increasing grain size assortment by fine milling of sand (Patent No. 74288 - 15/11/1904 Kwiatkowski), or in other case to let the lime slake at the same time of lime and sand

milling and mixing.The slaking can happen in one or two subsequent steps. In the first case (Patent No. 72121 - 13/05/1904 Stoffler) the lime slaking is contemporary to the milling and the mixing of lime, sand and water. In the second case (Patent No. 74288 - 15/11/1904 Kwiatkowski) part of sand is milling with quicklime to obtain his partial slaking using the content of water of the sand. Then, the remaining sand is added with the water needed to end the slaking and to obtain the expected density.The success and the diffusion of the new material lead the manufacturing to correct the defects and to satisfy the increasing performance request. So, for example, a large number of additives are added at the main row material in order to obtain the same workability of stone, a good fire resistance, weatherproof, lightness and insulating capacity. It is suggest (Patent No. 71963 - 29/04/1904 Cordes) to add barium hydroxide or carbonate in the mixture of water, lime for cement and gypsum in order to manufacture an artificial stone that is workable with saw and chisel, light, with a good strength, fireproof, weatherproof, and insulating. Some shavings are put in the mixture in order to manufacture a quick and durable stone hardening, to help particles cohesion, and so to increase the strength of final mass wood. The use of coal ash guarantees a uniform distribution of wood shavings in the mass because the ash adheres to the shavings and prevents their floating into the mixture.In compounds with Sorel cement as binding agent it is often possible to have volume variations and cracks that make the artificial stone not much durable, sensitive to freeze-thaw cycles and to the presence of water. To obtain a better durability for the product with magnesia binding, the water absorption capacity, typical of Sorel cement is reduced, as well as the consequent variations of geometry and volume that cause cracks in the handmade, by adding phosphate of lime in the mixture (Patent No. 43116 - 22/03/1896 Preussner). The phosphate lime combined with the magnesia avoids the production of calcium chloride that is responsible for water absorption.To obtain a good strength to freeze-thaw cycles it is suggested (Patent No. 51473 - 20/04/1899 Ameloung) to add amorphous silica with inert like soil sand and sawing. In this way the additions react with cement to obtain magnesium silicate; the obtained stone is porous and it is necessary to use soluble glass or alkaline solution as a finishing surface.In compounds with Portland cement as binding it is often possible to assess vulnerability to atmospheric agents, to variation of temperature and to acid etchings. To improve the behaviour of the material it is suggested to insert many additives in the mixture like, for example, (Patent No. 69147 - 09/09/1903 Jurschina) a mixture of soda silicate and milled clay, that makes not alterable the traditional mix of Portland and sand or marble dust, after cooking at 1000-1400°C. In the same case, the Portland cement is totally replaced with the aim to increase the strength of the products. Substitutes are, for example, residual products of combustion of coal and of metal founding like the cast iron or the steel. These are milled and mixed with lime at a ratio of 83:17 or 66:34 (Patent No. 57293 - 15/10/1900 Martinelli).

Finally, there are many patents in which, a part of the binding typology, suggestions are given to improve specific features such as the impermeability, freeze-thaw cycles resistance, as well as fire resistance, atmospheric agents resistance and colour stability. Among the suggestions (Patent No. 71166 - 18/02/1904 Muller) there is the adding of vitriol, iron, copper or metal oxide in the mixture.

2 PATHOLOGIES AND DECAY PROCESSES

As it is clearly underlined within the patents, defects and pathologies are characteristic of artificial stone since the period of its greatest production. They are basically referred to some categories, shown in Table1.

They can be connected with the quality and the typology of the raw materials, as well as to the manufacturing techniques. Some pathologies have also been surveyed by an investigation on some samples of artificial stone buildings in Bari. In fact, in Bari, and more generally in Puglia, artificial stone was widespread, also due to the development of some firms, like Ditta Peluso and Ditta Ghilardi [Peluso, 1931], with national and international relevance.

Case studies were chosen according to some significant parameter, for instance functional destination (economic and popular building, middle class building, monumental building, public building)

because it is connected to the different quality of materials; exposition to natural and anthropical agents (e.g. proximity to the sea or a town centre having high traffic levels); location of samples on the façade (base, column) and their interaction with close elements. Figure 1 shows the form used to catalogue to building survey information and from which an analysis was based for each case study that was conducted. As was evident from the critical analysis of the available patent information, the durability of artificial stone depends on several factors: the quality of materials, care in execution of the work, and from the degree of exposure to environmental agents casing deterioration. In some cases, the resistance of this product may be comparable or superior to natural stone. Nevertheless, the survey on some artificial stone samples shows a decaying process that relates to several casual effects.

First, the dirt depositing with the action of atmospheric and polluting agents, above all on the elements in relief as capitals, pilasters and trabeations, decorations and friezes, often subjected to break-up of mortars and erosion of surfaces. Then, the grain size composition, making the surface more or less rugged, significantly influences the capability of pathogenic agents to adhere to its surface, such as the incapability of materials, and particularly of binding, to resist to the breaking action of water.

Table 1. Pathologies verified during the period of greatest production

Binding Agent	Defect	Pathology	Causes
Lime	Loss of geometry	early strength to temperature variations early strength to moisture variations early strength to atmospheric agents	typology/quality of raw materials quantity of water content
	Cracking	early strength to temperature variations early strength to moisture variations early cohesion of particles	typology/quality of raw materials quantity of water content manufacturing process
	Fragility	early cohesion of particles	grain size variety inadequate typology/quality of raw materials manufacturing process
Sorel Cement	Variation of volume	high capacity of water absorption sensitivity to freeze-thaw cycles	typology of raw materials
	Cracking	high capacity of water absorption sensitivity to freeze-thaw cycles	typology of raw materials
Portland Cement	Variation of volume	early strength to temperature variations early strength to atmospheric agents	typology/quality of raw materials quantity of water content
	Cracking	early strength to atmospheric agents early strength to temperature variations sensitivity to freeze-thaw cycles	typology/quality of raw materials quantity of water content manufacturing process
	Superficial crumbling	early strength to temperature variations early strength to acid etchings early strength to atmospheric agents	typology/quality of raw materials quantity of water content

Variations of temperature and humidity cause a loss in dimensional stability and loss in mass of the stone; cracking is evident due to the expansion and the shrinkage that these stresses cause to building materials. With regard to the realisation of elements in artificial stone we have often too thick elements without any reinforcement or clamping elements. This condition produces the separation of parts that are more or less significant in relation with the grain size and the binding.

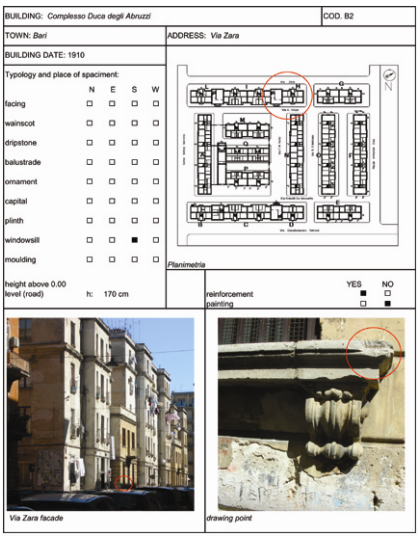

Figure 1. Specimen taken from a windowsill

Poor connections between adjacent elements made in factory and subsequently placed in work determine wide cracks, as well as scarce protection of clamping and clinging elements that causes their corrosion. Again the efficacy of protection depends to the quality of material forming the mixture that envelopes vulnerable parts by corrosion. Bad maintenance interventions, commonly performed during years: superficial treatments through covering paintings, often preceded by impregnation of the supports with irreversible fixatives, besides altering chromatic values of the material, compete to bait phenomenon of decay, even of notable entity. The start points of the described decay can be located in edges and relief parts, in surfaces of portions reinforced with metallic elements subjected to oxidation, in connections among different elements, in the zones of lifting and separation of following paintings, where deposit of particles and/or meteoric waters is possible.

Specimens were submitted to diffractometry and spectrographic tests to characterize the physical chemical petrographic. Results are not yet complete, however, no substantial differences in the composition of the mixtures are evident at this stage. Further tests are necessary to further understand the phenomena of decay of these materials

From an analysis of case studies and patents, and also with reference to a taxonomic systematization [De Tommasi & Fatiguso, 2005], a matrix of pathologies for artificial stone facades was defined that summarizes and classifies the main decay processes related to the mixture as provided in Table 2.

Table 2 - Pathologies for artificial stone facades summarizing the primary decay processes

DECAY		POINT OF CRISIS				CAUSES						PATHOLOGIES
A6	Crumbling	PI4	PI5	PI16		C3	C4	C5	C6	C8	C14	P1 P3 P4 P5 P6 P7
		PI2				C2						
A7	Detachment	PI7	PI8			C2	C9	C10				P1 P2 P3 P4 P5 P6 P7
		PI8	PI9			C10						
		PI1	PI4			C11	C12					
		PI11				C8	C14					
A8	Efflorescence	PI12				C15						P5 P6
A9	Erosion	PI4				C4	C16					P3 P4
A10	Exfoliation	PI1	PI4			C15						P3 P4 P6 P7
A11	Cracking	PI1	PI12			C8	C14					P1 P2 P3 P4 P5 P6
		PI1	PI2	PI10		C17						
		PI2				C2	C9	C19				
		PI13				C18						
A17	Swelling	PI1	PI2	PI12		C2	C11	C14	C19			P1 P3 P5 P6
A18	Presence of chips	PI1	PI2	PI12		C5	C12	C19				P1 P3 P7

POINT OF CRISIS	
PI1	Entire surfaces
PI2	Steel reinforced surfaces
PI4	Decorations
PI5	Rough surfaces
PI7	Arris
PI8	Basements
PI9	Passing zone
PI10	Single parts
PI11	Core-outside division surface
PI12	Small thickness covering
PI13	Connections between elements realized out of side
PI16	Contact zone (different materials)

CAUSES	
C2	Corrosion of reinforcement
C3	Air pollutions dregs
C4	Rain action
C5	Chemical etching
C6	Washing away
C8	Wrong mixture composition
C9	Scarce protection of steel reinforcement
C10	External mechanical stress
C11	Large thickness without reinforcement
C12	Different features of layers
C14	Manufacturing mistakes
C15	Moisture of bearing
C16	Wind action
C17	Shrinkage
C18	Ineffectiveness of connection
C19	Mechanical stress

PATHOLOGIES	
P1	early strength to temperature variations
P2	early strength to moisture variations
P3	early strength to atmospheric agents
P4	early cohesion of particles
P5	high capacity of water absorption
P6	sensitivity to freeze-thaw cycles
P7	early strength to acid etchings

3 CONCLUSIONS

The Second World War, as well as the definitive affirmation of a "modern" architectural and technical-technological culture in which the assumptions that favoured birth and diffusion of artificial stone don't find place anymore, decrees the end of the brief success season of such technologies. They quickly disappear with the men that produced them and with the knowledge mainly derived from their experience. As a consequence, actual lack of a "culture" of artificial stone is the cause of a frequent difficulty of action that leads to wrong maintenance and/or restoration interventions, or even worse, to the removal of such elements. According to what has been said, the research has to be oriented toward the definition of specific operational procedures for maintenance, refurbishment and integration of manufactured articles in the artificial stone.

A preventive phase of knowledge of building is fundamental therefore, referred to chemical-physical characterization of materials and their components, to measurement and survey of environmental parameters, to study of previous refurbishments and use conditions, to recognition and description of macroscopic alterations, to be followed by a phase of diagnostic of decay and individualization of relative causes. Such phase of knowledge, will be the object of further researches, must be structured in order to allow definition of types of intervention and operative guidelines.

Particularly it is necessary to define specific techniques and technological solutions for interventions, referred to both the integration and/or remaking of lacking parts and the maintenance of coverings of façade. For the former, research aims at the individualization of re-proposition modalities of technologies and original materials. For the latter the objective is the definition of typologies of intervention in relation to the required performances, of specific executive methodologies and of fittest materials for conservation of elements.

REFERENCES

AA.VV. 1993. *Building Pathology: a State of the Art Report*. Rotterdam: CIB W86

Cavallini, M. Chimenti, C. 1996, *La pietra artificiale*, Alinea, Firenze.

De Tommasi, G. and Fatiguso, F. 2003, 'The refurbishment of the "coade stone" building external surfaces for the residential housing at beginning of xx century', Proc. XXXI IAHS World Congress on Housing - Housing Process & Product, Montreal (CA) , June 23-27, 2003.

F. Fatiguso and G. De Tommasi, 'The artificial stone for the building at beginning of XX century: the decay processes of an "innovative" material', Proc. International Seminar "Theory and Practice about construction: knowledge, instruments, models", Ravenna, Italy, 27-29 October 2005.

Freestone, I.C., Binson, M., Tite, M.S. 1984, "The Constitution of Coade Stone", Ancient Technology to Modern Science, Proc. 86th Annual Meeting, American Ceramic Society Pittsburgh PA, Kingery W.D. Vol. 1.

Offenstein, F. 1995, *Compatibilità dei materiali*, UTET, Torino.

Peluso, F.lli. 1931, Arte del cemento. Cromofibrolite, Tipografia Editrice Salentina, Lecce.

Pieper, R., 1996, The maintenance, repair and replacement of historic cast stone, New York.

Proudfoot, T. 1996, *"Artificial Stone", The Dictionary of Art*, Grove's Dictionaries Inc, New York.

11DBMC International Conference on Durability of Building Materials and Components
ISTANBUL, Turkey 11-14 May 2008

Energy-Based Damage Measure for Reinforced Concrete Frames

Nilay Celik [1]
Yuri S. Petryna [2]

T 71

ABSTRACT

In the most seismically active zones, such as exist in Turkey, it is often necessary to estimate the damage level of existing buildings that have already experienced one or more earthquakes and may face another in the near future. A reliable and rapid classification of the building environment according to its damage level is a challenging task when assessing and managing risk of structural failure in such areas. Additional difficulties usually arise, for example due to the poor quality of structural components or the lack of documentation. For that purpose, there exist several empirical approaches based on visual inspections and other descriptive assessment procedures. Unfortunately, these do not provide sufficiently reliable results to resolve the requirement for damage appraisal and related risk assessment.

The present work focuses on the dominant structural type in the Istanbul area, namely reinforced concrete frame structures. Starting from the moment-curvature relationship of rectangular cross-sections, the secant bending stiffness of the members is derived with damage related to the concrete cracking and yielding of the reinforcement. This local damage information helps define a global damage index based on the virtual work associated with the damaged stiffness. The proposed damage measure is thoroughly tested by both simulation and experiment on a two-storey structural frame fabricated in a laboratory setting. The results obtained show that it is suitable for the in-situ assessment of reinforced concrete frames. It provides a reliable measure of the overall reduction of the bearing capacity even without finite element analysis. Therefore, it can be used, in combination with straightforward non-destructive techniques, to provide a rapid classification of damaged structures following the occurrence of an earthquake.

KEYWORDS

Damage measure, Concrete frames, Nonlinear simulation, Experiment

[1] Istanbul Technical University, Faculty of Civil Engng., Department of Civil Engng., Division of Structures, Theory of Structures Workgroup, Istanbul, Turkey 34469, Phone +90 212 2853085, celikni@itu.edu.tr,
Technische Universität Berlin, Department of Civil Engrg., Chair of Structural Mechanics, 13355 Berlin, Germany, Phone +49 30 314 72322, statik@tu-berlin.de

[2] Technische Universität Berlin, Department of Civil Engineering, Chair of Structural Mechanics, 13355 Berlin, Germany, Phone +49 30 314 72320, Fax +49 30 314 72321, statik@tu-berlin.de

1 INTRODUCTION

The durability of structural components and systems generally implies their continued reliability with respect to failure, serviceability and functionality. In earthquake areas, additional requirements must be fulfilled with respect to the seismic safety of structures. In the most seismically active zones, such as Turkey, it is often necessary to estimate the damage level of existing buildings, which have already experienced one or more earthquakes and will certainly face the next one in the near future. A reliable and rapid classification of the building environment according to its damage level or seismic capacity is a challenge for the risk assessment and management in such areas. Additional difficulties usually arise due to a poor quality of structural components and the lack of documentation.

Several damage measures for seismic damage assessment have previously been described and are reasonably well known. A comprehensive overview of these can be found, for example, in [Yao et al. 1986; Kratzig & Meskouris 1998]. Although some of these reflect purely empiric approaches, such as the inter-storey drift, others refer to the use of the cross-section level, such as the ductility index, stiffness index or the energy index, the latter approach defined based on moment-curvature relationships. Thus, they are generally not suitable for the entire structure. Some damage measures are empirical in nature and mechanically inconsistent, such as the combined index derived from relative displacement and relative energy as devised by Park & Ang [1985]. The damage index proposed by Krätzig & Meskouris [1998] accounts for the hysteretic energy dissipation during cyclic loading in beam and frame members. It requires, however, an explicit modelling or recording of response history. Several general damage indices have been proposed in [Krätzig & Petryna 2001; Petryna & Krätzig 2005] basing on the simulated or recovered structural stiffness under damage. In addition, such approaches presume the knowledge of the original, undamaged, i.e. the reference stiffness, which is generally unknown for many already existing structures.

Although the state-of-the-art nowadays offers several suitable approaches, they are nonetheless, not readily applicable to the above mentioned problem that requires a specific damage assessment for use in seismic areas. There exist several alternative empiric approaches based on visual inspections and a rather descriptive assessment procedure accounting for the number of storeys, the existence and the kind of balconies, or similar linguistic information.

Obviously, it is hardly possible to develop a simple, unified and reliable measure for all structural types. Therefore, the present work focuses on the dominant structures in the Istanbul area, namely on reinforced concrete frames that are also typical of most buildings located in the Mediterranean area. Starting from the moment-curvature relationship, the secant stiffness of the member at different critical sections in the damaged state is first derived. In order to use this local information for a global damage measure, each local stiffness is superimposed to a virtual displacement field, this field being typical of local earthquake activity. From a comparison of the virtual work, associated with both the original and damaged stiffness and along the same virtual displacement field, a scalar energy-based damage index is ultimately defined. Based on the nonlinear finite element analysis, useful results in combination with “realistic” displacement fields are obtained, but also with almost arbitrary virtual displacements, which simply look affine to the latter. The damage assessment, proposed in the present work, does not require any calculations with the exception of the moment-curvature relationships for various cross-sections, the corresponding secant stiffness and related virtual displacements. It can therefore be applied with the use of standard computers and office tools, and without any special software for structural analysis.

2 DAMAGE MEASURE

The damage in material may generally be defined as softening of its stiffness that can be easily illustrated using the one-dimensional damage-affected elastic material law:

$$\sigma = E \times \varepsilon = (1 - D) E_0 \times \varepsilon \,. \tag{1}$$

The extent of damage in the material can be properly quantified through a reduction of its current modulus of elasticity (E_x) with respect to an initial value in the non-damaged state (E_0) and the critical value (E_f) at failure:

$$D = \frac{E_0 - E_x}{E_0 - E_f} \,. \tag{2}$$

The obvious advantage of this definition is: a scalar damage variable, D, ranges exactly from 0 (no damage) to 1 (failure).

A similar definition can be applied to structural members by use of proper stiffness values. For example, the reduction of the bending stiffness EI of the beam elements can serve as damage measure defined on the cross-sectional level:

$$D = \frac{(EI)_0 - (EI)_x}{(EI)_0 - (EI)_f} \,. \tag{3}$$

In steel structures, the Young's modulus, E, can decrease due to the plasticity or damage of steel. In reinforced concrete structures, EI can decrease due to yielding of reinforcement as well as cracking of concrete. Both cases are usually taken into account during structural design, and thus are entirely acceptable as structural states with damage.

For the risk assessment in seismic areas, it is however necessary to quantify damage on the structural level. Due to the high degree of uniqueness of civil engineering structures, the development of general damage measures, suitable for diverse structures and damage mechanisms, is still a challenge [Yao et al. 1986]. In the case of structures, a proper way is to associate the current degree of damage to the current structural stiffness or capacity, similar to the material or the cross-sectional measures proposed by Krätzig & Petryna [2001], specifically:

$$D = \frac{\lambda_0 - \lambda_x}{\lambda_0 - \lambda_f} \,. \tag{4}$$

Unfortunately, structural stiffness is a multi-dimensional function, not a scalar. In structural simulations using the finite element method, one deals, for instance, with the global stiffness matrix K, containing thousands of individual stiffness values. The choice of the proper scalar values λ in equation (4), that correlate well with the overall reduction of the structural stiffness, is a challenge.

Hanganu et al. [2002] proposed to deduce damage measure from the relation of the actual free energy, Ψ , of the damaged material and the elastic free energy, Ψ_o , of a fictitious undamaged material as follows:

$$\Psi = (1 - d) \times \Psi_0 \,. \tag{5}$$

By integrating the free energy over the entire structure one can relate its total deformation energy to that of a fictitious structure without damage as follows:

$$W_p = \int_{V_o} \Psi dV = \int_{V_o} (1 - d) \rho_o \Psi_o dV = (1 - D) W_p^o \,, \tag{6}$$

Where from the global damage measure, D, can be successfully derived:

$$D = 1 - \frac{W_p}{W_p^o} = 1 - \frac{\int_{V_o} (1 - d) \rho_o \Psi_o dV}{\int_{V_o} \rho_o \Psi_o dV} \,. \tag{7}$$

Herein, W_p^o, is the fictitious ever-elastic potential energy due to the actual strains and W_p is the actual potential energy. By use of the finite element simulation, this energy-based global damage index can be calculated for the actual displacement field as follows:

$$D = 1 - \frac{W_p}{W_p^0} = 1 - \frac{\sum_e \mathbf{a}^T \int_{V_e} \mathbf{B}^T \boldsymbol{\sigma}\, dV_e}{\sum_e \mathbf{a}^T \int_{V_e} \mathbf{B}^T \boldsymbol{\sigma}_0 dV_e}, \tag{8}$$

where **a** stands for the nodal displacement vector, **B** for the strain shape matrix and V_e for the volume of each finite element e. Further, **σ** denotes the actual stress vector and $\boldsymbol{\sigma}_0$ the stress vector calculated for the undamaged material and the same global displacement **a**. Herein, the total potential energy W_p as well as W_p^0 is accumulated over all finite elements.

In order to apply such an energy-based scalar damage measure to experimental damage assessment, we propose to transform (8) by use of the element stiffness matrices of the damaged ($\boldsymbol{K}_d$) or non-damaged ($\boldsymbol{K}_0$) structure respectively and to use a suitable virtual displacement field $\mathbf{a}_V$ instead of **a**, which originates from the finite element calculation. Finally, the proposed virtual energy-based damage index reads:

$$D_V = 1 - \frac{\sum_e \mathbf{a}_V^{(e)T} \times \mathbf{K}_d^{(e)} \times \mathbf{a}_V^{(e)}}{\sum_e \mathbf{a}_V^{(e)T} \times \mathbf{K}_0^{(e)} \times \mathbf{a}_V^{(e)}}. \tag{9}$$

3 TEST FRAME

The above damage measure has been tested on the nonlinear response and damage evolution of a two-storey reinforced concrete frame (Fig.1). The 2.30-m high and 1.2-m long plane frame consists of columns with a 10 by 15-cm cross-section and storey beams with a 15 by 15-cm cross-section. The bottom beam containing a hole serves to clamp the frame to the test floor. The variation of the reinforcement in the columns and the beams leads to totally 8 cross-sectional types with different stiffness. The basic six cross-sections are presented in Fig. 1; the remaining two cross-sections differ only by the position of the non-symmetric reinforcement. The applied material properties are given in Table1.

Table 1. Material properties of the reinforced concrete frame under consideration.

Concrete		Reinforcing steel	
Young's modulus	E_c = 35400 N/mm²	Young's modulus	E = 200000 N/mm²
Poisson's ratio	ν = 0.15	Poisson's ratio	ν = 0.3
compressive strength	f_c = 53 N/mm²	yielding strength	σ_y = 550 N/mm²
tensile strength	f_{ct} = 3.8 N/mm²	ultimate strength	σ_u = 580 N/mm²
ultimate compressive strain	ε_{c1u} = -0.0035		

The frame is subjected to a single horizontal force at the top corner and experiences a quasi-static load history with several loading-unloading loops until failure. The stresses and strains as well as the damage states during the entire load history are continuously monitored for comparison with computer

simulations. The failure of the frame is accompanied by a rapid growth of displacements at the almost constant force of about F = 12 KN.

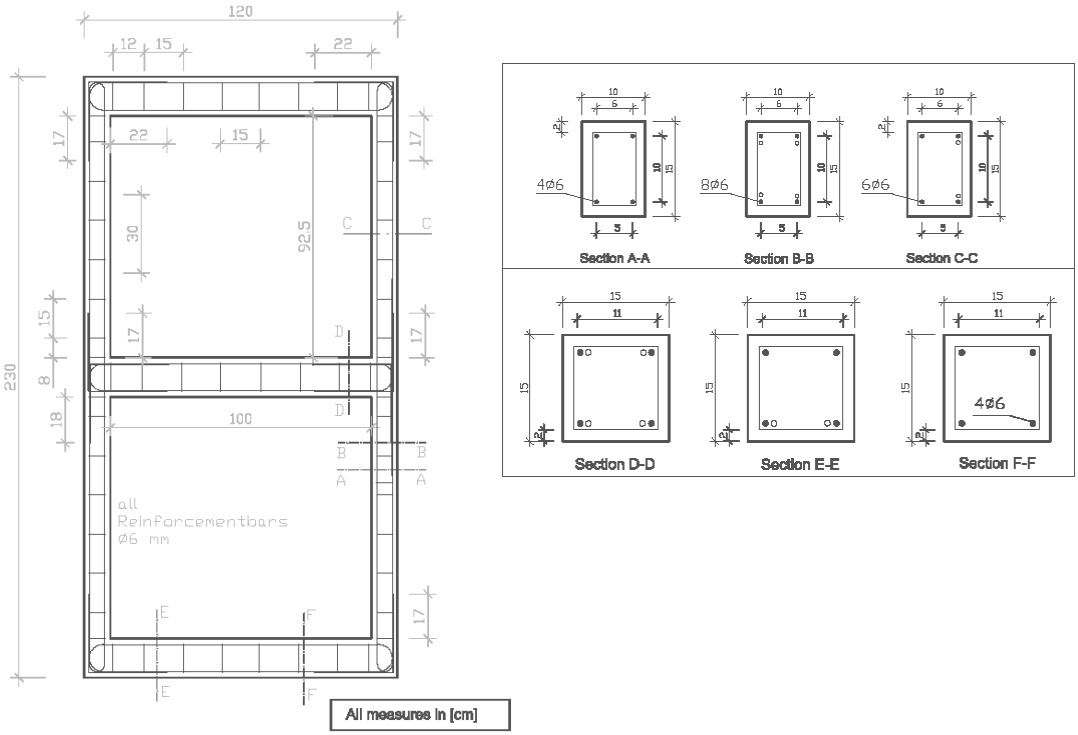

Figure 1. Geometry, cross-sections and reinforcement of the test frame.

4 DAMAGE ASSESSMENT BY SIMULATION AND EXPERIMENT

The frame response under static loading and damage are first simulated with a finite element program (FRAME) developed in-house and within the Matlab environment [2006] using classical beam elements. The nonlinear constitutive equations are implemented in the form of moment-curvature relationships for rectangular cross-sections taking into account cracks in the concrete and yielding of the reinforcing steel. The calculated load-displacement diagram for the horizontal displacement of the top corner (load application point) shows an excellent agreement with the experimental results (Fig.2). The damage state is characterized by progressive cracking of the concrete at multiple locations. The location and depth of the cracks observed in the experiment correlate well with the extent of damage computed by FRAME, as can be seen in Fig. 3 that illustrates the state of the frame at failure.

The FRAME program was then extended to calculate the damage indices according to equation (9). In the present study, damage is associated only with the change in bending stiffness, EI, of each cross-section due to cracks in the concrete and yielding of the reinforcement. The global non-damaged stiffness of the frame, $\boldsymbol{K}_0$, is calculated by use of the original EI_0, whereas the damaged one, $\boldsymbol{K}_d$, originates from the secant stiffness, EI_d, of the current damage state. Both values EI_0 and EI_d can be determined from the moment-curvature diagram for each cross-section of the frame.

Thus, the damage index D can be calculated according to equation (9) at each step of the loading path by taking the damage state, $\boldsymbol{K}_d$, and the displacement state, $\boldsymbol{a}$, from the current finite element solution. Figure 4 shows such an evolution of the damage index D during the monotonic loading of the frame until failure.

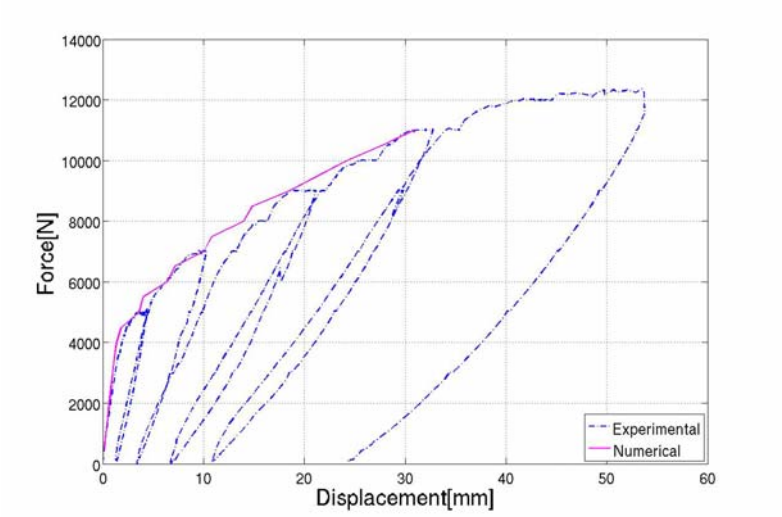

Figure 2. Experimental and numerical load-displacement diagram.

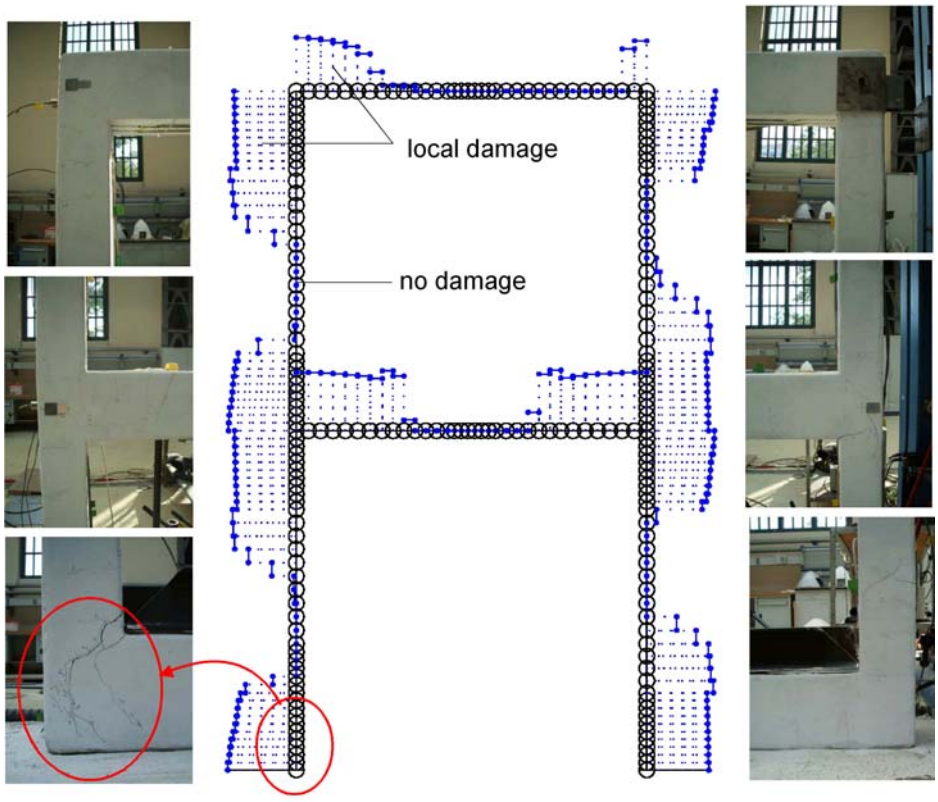

Figure 3. Experimental and numerical damage state at failure.

The first damage increments appear at F = 4 KN due to the first concrete cracks. Then, the damage grows rapidly up to D = 0.8 due to extensive cracking at multiple locations. One can see the corresponding plateau in Fig. 4. After that, the damage growth decelerates significantly resulting in the change of the slope in Fig. 4 above of F = 6 KN. It can be associated with the opening of existing cracks and the yielding of the reinforcement. The damage index D = 0.92 at failure is quite close to the theoretical value of D = 1.0. The difference can be explained by the fact, that the frame loading has been stopped before the real failure occurs in order to study the corresponding damage state. Moreover, the experimental failure load of F = 12 KN could not be reached in the finite element

simulation due to the loss of the convergence. The achieved level of damage must be objectively smaller than that at failure (D = 1).

The damage evolution curve in Fig. 4 was obtained by use of the complete stiffness matrix and all degrees-of-freedom. However, very similar results have also been computed by use of a relatively coarse mesh; in this instance, it is assumed that all really damaged areas are in fact captured.

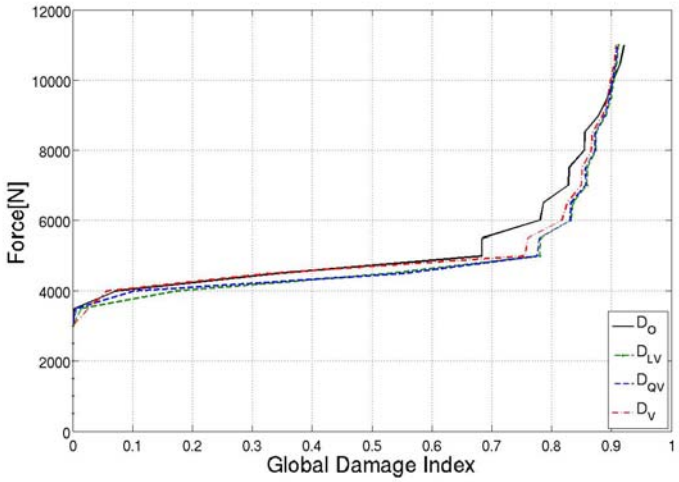

Figure 4. Load-damage diagram of the frame.

4 IN-SITU DAMAGE ESTIMATION FOR SEISMIC RISK

The approach presented above by use of simulation and experiment is less suitable for the classification of structures in earthquake areas. The primary reasons for this include: the lack of time, of material and structural data, as well as of appropriate measurement instruments and computer tools available on-site. In order to apply the proposed damage measure for this purpose, we presume solely the damaged areas Ω_i in concrete frames to be approximately known with respect to their length L_i and depth δ_i , as depicted in Fig. 5. By interpreting these areas as damaged beam elements of length L_i and with a crack depth δ_i we can calculate their original, non-damaged bending stiffness EI_0 as well as the damaged stiffness EI_d using the moment-curvature relationship. If no information on the reinforcement is available, we assume a symmetric one with a certain cross-section area. The boundaries of the damaged areas can be taken as reference nodes. We further apply a virtual displacement field $\mathbf{a}_V$ on these nodes to compute the virtual energy-based damage index D_V according to equation (9). Although the virtual displacement $\mathbf{a}_V$ can, in principle be arbitrarily chosen, it is an advantage if this conforms to the loading type. For instance, we can assume a linear $\mathbf{a}_{LV}$, a quadratic $\mathbf{a}_{QV}$ or a stepwise linear $\mathbf{a}_{SV}$ virtual displacement field for the test frame, as depicted in Fig. 5. The only necessary condition is that all damage areas are accounted for by means of the reference nodes. Thus, finite element analysis is no longer required to estimate the extent of damage of the framed structure.

As can be seen from Fig. 4, the proposed approach provides very good results. Three curves for the evolution of the damage index have been calculated at each step with the actual damaged stiffness and a virtual displacement field: D_{LV} for linear, D_{QV} for quadratic and D_{SV} for stepwise linear displacements. The fourth curve is obtained by use of the direct finite element solution. All curves correlate very well, thus, confirming the applicability of the virtual displacement approach. Finally, we consider a coarse mesh of only selected reference points, which correspond to the boundaries of the damaged areas (Fig.5). The local crack depths and the length of the cracked areas have been estimated from the visual

inspection of the frame after finishing the experimental program described above. These input data should be similar to those of the in-situ inspections of real concrete frames.

Although the values obtained for the damage index ($D_{LV} = 0.75$; $D_{QV} = 0.75$; $D_{SV} = 0.84$) differ from the critical ones at failure that were presented in Fig. 4 for the finite element mesh, they still provide acceptable estimates of the damage state of the frame shortly before collapse.

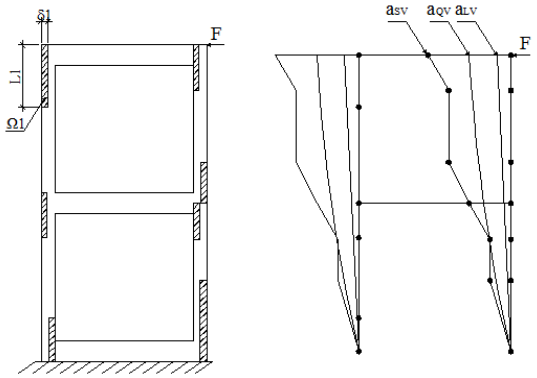

Figure 5. Damage areas Ω_i and applied virtual displacements.

5 CONCLUSION

A virtual energy-based damage measure suitable for in-situ estimation of the overall damage of reinforced concrete frames has been proposed and tested. It provides a reliable and appropriate measure of the residual structural capacity without any finite element analysis. Therefore, it can be applied for the rapid classification of frame structures subjected to earthquake loads.

ACKNOWLEDGEMENTS

The authors gratefully acknowledge the financial support of the Technical University Berlin for the PhD Fellowship of the first author. A valuable contribution of Krassimire Karabeliov, Andreas Künzel and Andre Brendike for the execution of experiments and nonlinear computer simulations is also gratefully acknowledged.

REFERENCES

Hanganu, A.D., Onate, E. & Barbat, A.H., 2002, 'A finite element methodology for local/global evaluation in civil engineering structures', *Computers & Structures*, **80**[20-21], 1667-1687.

Krätzig, W.B. & Meskouris, K., 1998, 'Assessment of seismic structural vulnerability as a low-cycle fatigue process', In: Bisch Ph, editor. *Proc. 11th European Conf. on Earthquake Engineering, Paris, France, Balkema, Rotterdam, 6-11 September 1998*, pp. 161–178.

Krätzig, W.B., & Petryna, Y.S., 2001, 'Assessment of structural damage and failure', *Archive of Applied Mechanics*, **71**, 1–15.

Matlab Release R2006b –User Manual. Massachusetts, The MathWorks Inc., 2006.

Park, Y.J., & Ang, A.H.S., 1985, 'Mechanistic seismic damage model for reinforced concrete', *J. Struct. Eng.*, **111**[4], 722-739.

Petryna, Y.S., & Krätzig, W.B., 2005, 'Compliance-based structural damage measure and its sensitivity to uncertainties', *Computers & Structures*, **83**[14], 1113-1133.

Yao, J.T.P., Kozin, F., Wen, Y.K., Yang, J.N., Schueller, G.I., & Ditlevsen, O., 1986, 'Stochastic fatigue, fracture and damage analysis', *Structural Safety*, **3**, 231–267.

Facility Management In Stratified Housing: Satisfaction Survey In Malaysia

Adi Irfan Che Ani [1]
Norngainy Mohd. Tawil [2]
Nur Azfahani Ahmad [3]
Ahmad Ramly [4]
Nor Haniza Ishak [5]

T 72

ABSTRACT

Stratified housing is now becoming a trend of living style among the urban professional community in Malaysia. The main difference as compared to a landed property is the need for residents to set-up a Management Corporation (MC), as a body to regulate and manage all the amenities provided by the developer, as stipulated in the Strata Title Act 1985. To a certain extent, the idea seems to work successfully for about a few years after the housing schemes are granted with the final title. Subsequently, being so long with the facilities provided, coupled with ineffective management, a gap is identified between the residents as stakeholders and the council members of the Management Corporation, which also comprised of members of the same housing scheme. This research looked into the matter, with particular focus on the facility management construct. The satisfaction level formed the primary measurement criteria in identifying and measuring the gap between the residence and the Management Corporation. The findings of this research revealed that there were significant difference in terms of satisfaction between the Management Corporation and the residents, where the Management Corporation reported a higher level of satisfaction compared to the residents in every criterion. The sample selected for this study was non low-cost stratified housing only, thus making the results limited within this particular focus group. Further research is suggested to find ways to minimize the gap identified as well as to develop an effectiveness model as a tool to measure the performance of the management body.

KEYWORDS
Facility Management, Management Gap, Stratified Housing

[1] Department of Architecture, Faculty of Engineering, Universiti Kebangsaan Malaysia, Malaysia. Phone +06 0192033551, Fax +06 0389216841, adiirfan@gmail.com
[2] Department of Architecture, Faculty of Engineering, Universiti Kebangsaan Malaysia, Malaysia. Phone +06 0196841934, Fax +06 0389216841, aniemz72@yahoo.com
[3] Department of Building Surveying, Faculty of Architecture, Planning & Surveying, University Technology MARA, Perak Branch, Malaysia. Phone +06 0196165652, Fax +06 053742244, nuraz020@perak.uitm.edu.my
[4] Department of Building Surveying, Faculty of The Built Environment, University of Malaya, Malaysia. Phone +06 0133711098, Fax +06 0379675713 , drabr@msn.com
[5] Department of Building Surveying, Faculty of The Built Environment, University of Malaya, Malaysia. Phone +06 0133657331, Fax +06 0379675713, niza_alambina@um.edu.my

1 INTRODUCTION

Living in stratified property has become the trend in Malaysia today especially among the town dwellers. One of the reason people prefer to stay in a stratified property is the facilities provided within the housing area. The residents have to pay a fee for the facilities provided. The MC is the responsible party to manage all the facilities.

The management of stratified housing in Malaysia can be categorised into three periods namely, before the establishment of Management Corporation (MC), during the initial period and after the developer had handed over the management responsibilities to the residents [DBKL 1999; HBA 2003; Sapian 2003]. The stratified housing is governed by the Strata Title Act 1985 (herein after is called STA, unless otherwise specified). The concept of STA in Malaysia is inherited from the New South Wales Conveyancing (Strata Title) Act 1961 [Alinah 2004].

This paper focused on stratified housing managed by the residents through the MC. The former two periods are not included in this study because the management is temporary in nature and the residents have no say at all in managing their own property. Theoretically, in managing stratified property, both parties, i.e. MC and the residents have to achieve a consensus in all management-related matters. This is to ensure an effective management for stratified housing schemes. Unfortunately, this study found that there was some pattern of management gap between MC and residents, who are the beneficiary of the facility management services. In discussing this matter, the paper starts briefly on several key issues that led to a management gap. It is then followed by the methodology in identifying the management gap and the prominent findings from this study.

2 ISSUES REGARDING FACILITY MANAGEMENT IN STRATIFIED HOUSING

Stratified housing is a unique property and it differs from landed property, such as bungalows and terrace houses. Its uniqueness presents itself during the management era after the properties have been occupied, where facilities management became an issue [Linariza and Ashok 2003]. To handle the issues pertaining to the management and maintenance activities, STA was implemented in 1985, to accommodate the insufficiency of the National Land Code that was ineffective in handling the issues that arose in stratified housing schemes [Tiun 2006]. According to STA, the MC is accountable for all the management and maintenance aspects of the properties and common facilities in the building [Teo 1993; Jamila 1994]. Unfortunately most of the housing schemes found were not effectively managed. Residents complained through the mass media and the issues were always about incompetent facility management i.e. dysfunctional lifts, rubbish not collected according to schedule, vandalism, misuse of sinking funds; as well as disputes among resident. In short, all the issues raised were centred around the 3 aspects in providing effective facility managements, namely financial, maintenance and people, i.e., the residents themselves.

On the management side, the most challenging issues faced by them in managing a stratified housing scheme was collecting monthly maintenance charge and to run facility management activities [Liias 1998; Jamila 1994; Malaysia Government 1999; Sapian 2003; Tiun 2006; Eddy 2004a]. Maintenance charge is a fee imposed on all the residents to maintain the facilities [Malaysia Government 2003d]. For stratified property, the amount charged is based on the share unit for every parcel [Malaysia Government 2003d]. Unfortunately, there are some residents who believe that the amount charged is higher than what they expected and refused to pay.

Illogical excuses were created, for example, they claimed that they did not fully use the facilities provided [Jamila 1994] and the charge was not reasonable as compared to the service quality [Malaysia Government 1999; Tiun 2006]. According to Teo [1993], although the MC can prosecute through a court of law in collecting the arrears as stipulated in Sect. 52(2), Sect 53A, Sect 53(2) and Sect 55A of the STA, it is rarely enforced due to its impracticality [Tiun 2006] and it might affect the overall housing complex occupants' pride and image [Sapian 2003]. When most occupants neglect to pay the charge, consequently, the fund was insufficient. As a result, most of the facility management activities cannot be carried out on time and thus affect the facility management effectiveness for the building as a whole [Malaysia Government 1999; Tiun 2006].

These issues led to the management gap in managing facilities of stratified housing. The management gap occurred when the expected services by the residents cannot be delivered by the MC. The residents were paying on a monthly basis and expected the facility management to be effective. Under STA, there is a legal provision for the MC to engage the services of a Management Agent as the party responsible for running the facility management activities. In practice, most MC functions in that way because they do not have the expertise to run and maintain the housing complex. If the MC fails to function well as stipulated in STA, the residents of the particular housing complex have the right to summon the said MC. Therefore in order to avoid this case, the MC normally engages a Management Agent in order to transfer their liability towards the housing complex.

Even so, the management gap continued to exist as referred to the on-going issues reported in mass media [Tiun 2006]. Residents continued to complain about the low service quality of facility management provided by the Management Agent, as well as the responsibility of MC in ensuring effective facility management. In discussing this matter, this paper looked into the Malaysian case study to identify the management gap in stratified housing. The framework of the study that was used as a measurement basis is presented below.

3 THE FRAMEWORK OF EFFECTIVE FACILITY MANAGEMENT IN IDENTIFYING MANAGEMENT GAP

The framework as depicted in Fig. 1 shows the linkage of 12 variables in measuring the management gap via effective facility management for stratified housing. It is categorized under 3 constructs namely financial, maintenance and resident; which is then supported by its own dimensions. In between construct and dimension, there is respondents' category namely Members of MC, Management Agent and Resident.

The financial construct has 3 dimensions namely financial resources, financial allocation and financial expenses. In running the day-to-day activity, the MC needed resources, otherwise little can be done. In medium and high cost stratified housing, the problem of monthly collection was not threatening since the collection of maintenance charges was just fair enough to run the activity. On top of this, the financial aspect needed to be planned via allocation and monitoring of its expenses. As an example, allocation for cosmetic recovery should be the last agenda in housing maintenance activity [Amarilla *et al.*, 2002]. An effective facility management is not merely based on the collection of fund itself, the management of the limited resources by the MC need to first be looked into [Hui, 2005].

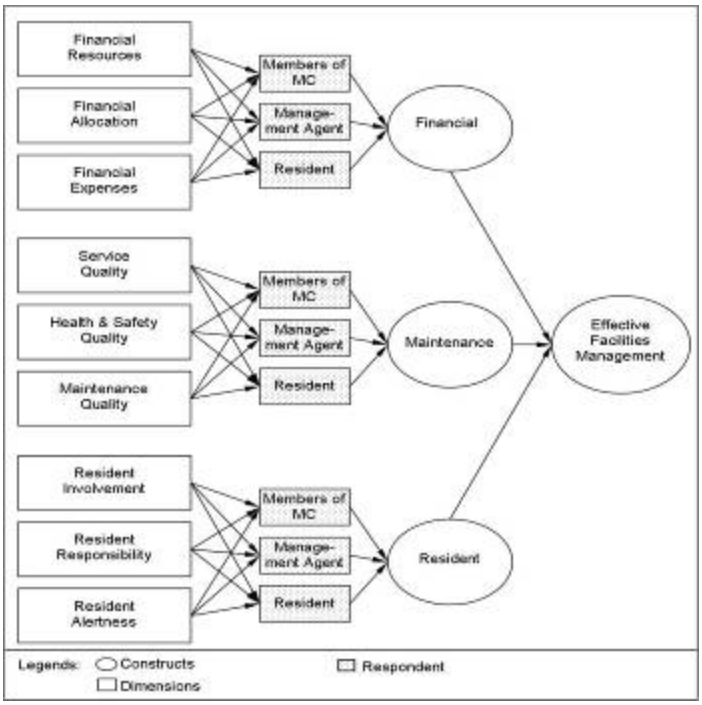

Figure 1. The Research Framework

The second construct, maintenance, also had 3 dimensions namely service quality, health and safety quality, and maintenance quality. The aspect of building maintenance was one of the crucial tasks in facility management [Thompson 1994]. It also played the main role in providing sustainable housing. Theoretically maintenance can be seen from a 'hard' and 'soft' perspective. The 'hard' perspective referred to the maintenance output or product, which the resident can see and feel the impact of maintenance work. As an example, landscaping provided good scenery and a tidy environment, in which the resident can view and enjoy. The 'soft' perspective looked into the service quality demonstrated on the process of carrying out the particular work and more to human respond i.e. counter service. For the safety and health, it was also put under the maintenance consideration to safeguard the resident's health interest, so that they felt secure and comfortable living within their compounds.

The third looked at the resident construct, which also had 3 dimensions, namely resident involvement, resident responsibility and resident alertness. In providing effective facility management, the end-user had to respond accordingly to the management. The participation of residents was crucial since all the facility management activities were designed for and dedicated to them. In addition, the residents were paying the maintenance charges. The involvement of residents was really needed during the Annual General Meeting to set-up the MC, to determine the amount of monthly fee and to agree upon a few things as stipulated in the STA. Other than involvement, the residents had to understand their responsibilities as those living in a community i.e. having neighborhood spirit and avoiding selfishness; which were largely dependent on the residents' background and status (owner or tenant). The residents' alertness were towards the on-going changes i.e. housing rules and community activities within their stratified scheme, environmental condition as well as maintenance service standard (especially routine maintenance work).

4 RESEARCH METHODOLOGY

The research strategy adopted was quantitative in nature and data collection technique was through a personally assisted questionnaire. The questionnaire was formulated based on the described facility management variables above which consisted of financial, maintenance and resident constructs. The respondents had to respond accordingly to a Likert scale of 1 to 5, which expressed the respondents' satisfaction level. The range of the scale were 1=not satisfied, 2= less satisfied, 3= neutral (neither satisfied nor dissatisfied), 4= quite satisfied and 5= very satisfied. The software for data analysis was Statistical Package for Social Sciences (SPSS) version 12.

Based on the statistics provided by the Land Office, there were only 495 non low-cost housing complexes which fulfilled the samples' main criterion, namely the non low-cost stratified housing that had conducted their First Annual General Meeting. Out of 495, this research had drawn approximately 30% or 150 housing schemes as its sample, in order to get a 96% confidence level (sampling calculation via www.custominsight.com). The selection of sample was done using the SPSS software. Each non low-cost housing complex was represented by 5 respondents namely 3 members of MC, 1 Management Agent and 1 resident (who had experienced being the MC's member). Therefore, the total number of respondents interviewed was 750 people.

In identifying the management gap, this study looked into the differences in satisfaction level via the analysis of MANOVA and ANOVA. Before proceeding with the MANOVA, the statistical pre-test had to be conducted via Levene and Box's M test to determine the equality of variance assumption and the variance-covariance matrix. In order to proceed, both pre-test should get the result of non-significance i.e. p *value* > 0.05. It was only then that the MANOVA and/or ANOVA can be conducted. To further study the differences between respondent categories, this study proceeded with the Bonferonni test. The gap existed when there was a significant difference in levels of satisfaction between respondents.

5 ANALYSIS OF DATA AND DISCUSSION OF FINDINGS

Before proceeding with the final field work survey, a pilot study was carried out involving 150 respondents (30 housing schemes) which was selected randomly from the total respondents to justify the reliability of the measurement scale of each variable. The result of the reliability test was that all the variables achieved internal consistency and was considered to have a high reliability with the value of Cronbach's Alpha above 0.8 for each variable. To determine whether a parametric or non-parametric test was to be used, the normality test using Kolmogorov-Smirnov (because the respondents were more than 100) was carried out. In short, the p-value was less than 0.05, but the skewness value was between -1 and 1. Therefore the data could be categorized as normal and the parametric test was used for the statistical analysis.

The unit analysis was the satisfaction level among the 3 categories of respondents, namely members of MC, Management Agent and resident. According to the research framework (as per Fig. 1), this study only concentrated on the analysis of satisfaction level on the central concept (effective facilities management) and among the 3 constructs only. This showed the pattern of management gap in providing effective facility management. The result of the study is presented below.

Table 1. Levene Test For Constructs

Constructs	F statistic	P value
Financial	0.224	0.799
Maintenance	0.039	0.961
Residents	1.095	0.335

Table 2. Box's M Test For Constructs

Value	F statistic	P value
4.574	0.378	0.972

Table 1 and 2 shows that there were no significant difference in both Levene and Box's M test. Therefore the MANOVA and ANOVA were valid to be adopted in measuring relationship between the constructs and respondents category.

Table 3. Result of MANOVA & ANOVA For Constructs

Multivariat Test					**F statistic**	**P value**
Wilks' Lambda					7.717 (0.941)	0.000*
Constructs	**Respondent**	**N**	**Mean Score**	**Standard deviation**	**F statistic**	**P value**
Financial	MC	450	3.2737	1.0355	3.377	0.035*
	Mgt. Agent	150	3.1408	1.0060		
	Resident	150	3.0353	0.9916		
Maintenance	MC	450	3.2747	0.7139	9.163	0.000*
	Mgt. Agent	150	3.4227	0.6993		
	Resident	150	3.0754	0.6939		
Residents	MC	450	3.1082	0.7809	3.750	0.024*
	Mgt. Agent	150	3.0727	0.7325		
	Resident	150	2.9107	0.7579		

*Significant at 0.05

Based on the result in Table 3, the MANOVA found that collectively, there was a significant difference among the constructs and the respondents' category. The ANOVA also showed that there was significant difference in satisfaction level of respondents for every single construct. Looking at the mean score, the resident reported the lowest satisfaction level for all constructs as compared to MC and Management Agent.

Table 4. Result of Bonferonni Test For Constructs

Constructs	**Respondent**	**Respondent**	**Difference of mean score**	**P value**
Financial	MC	Mgt. Agent	0.1329	0.503
	MC	Resident	0.2384	0.040*
	Mgt. Agent	Resident	0.1055	1.000
Maintenance	MC	Mgt. Agent	-0.1480	0.080
	MC	Resident	0.1992	0.009*
	Mgt. Agent	Resident	0.3472	0.000*
Residents	MC	Mgt. Agent	0.0355	1.000
	MC	Resident	0.1975	0.019*
	Mgt. Agent	Resident	0.1620	0.203

* Difference of mean score was significant at 0.05

Table 4 shows further differences in each respondent's category. It also depicts a pattern of significant difference, especially between MC and resident for each construct. Other than that, there was a significant difference between Management Agent and resident for maintenance construct, whereby resident was less satisfied in the maintenance construct as compared with Management Agent. After looking in detail into the 3 constructs, it seemed that the resident was always less satisfied than the other respondents. In other words, it showed the existence of a management gap in managing facility management of stratified housing. To achieve confirmation in a bigger perspective, this study discussed the central concept of effectiveness of facility management as follows:

Table 5. Levene Test For Concept

Concept	F statistic	P value
Effectiveness	0.916	0.400

Table 6. Result of ANOVA For Concept

Concept	Respondent	N	Mean score	Standard deviation	F statistic	P value
Effectiveness	MC	450	3.4015	1.0774	3.851	0.022*
	Mgt. Agent	150	3.2222	1.0105		
	Resident	150	3.1489	1.0981		

*Significant at 0.05

The pre-test as in Table 5 (where P value was not significant) showed that it was valid to conduct an ANOVA to measure the relationship of respondent's category towards the effectiveness of facility management. Based on Table 6, there was a significant difference in satisfaction level among respondents for effectiveness concept. Also, the satisfaction level of residents was lower than the others.

Table 7. Result of Bonferonni Test For Concept

Concept	Respondent	Respondent	Difference of mean score	P value
Effectiveness	MC	Mgt. Agent	0.1792	0.227
	MC	Resident	0.2525	0.037*
	Mgt. Agent	Resident	0.0733	1.000

* Difference of mean score was significant at 0.05

Table 7 shows the only significant difference in satisfaction level towards effectiveness of facility management was between the MC and residents, where the residents were found to be less satisfied. This finding further confirmed the existence of management gap in facility management of stratified housing.

From the analysis above, the main reason behind all the issues that arose in facility management of stratified housing in Malaysia is now clear. The management gap which existed, in turn formed a barrier in providing effective facility management. The residents were always found to be less satisfied than the MC. The management gap is termed 'in-house' since in almost all cases; there was no significant difference in all constructs and effectiveness concept between Management Agent and the MC, as well as the resident. Based on the findings, the management gap was still in its infancy and considered not serious since the difference in mean score was not more than 1.

Therefore there is room for improvement for both parties i.e. MC and resident to rectify their relationship via minimizing the gap to provide better scenario of effective facility management.

6 CONCLUSION

This paper discussed the identification of management gap in stratified housing in Malaysia. Management gap exist when there is significant difference in satisfaction level among respondents towards the concept of effectiveness and the constructs behind it i.e. financial, maintenance and resident. The issues of facility management in stratified housing is reported quite extensively through the mass media, thus giving some clue about the gap in stratified housing management. This study has confirmed the existence of management gap, which is the answer to why the issues arose. It also had been a barrier for both parties namely the Management Corporation and resident to cooperate in creating effective facility management. In relation to the literary discussion, the identified management gap also contributed to the 'chicken and egg' scenario. What is heartening is that the management gap is still not in the serious stage, thus giving an opportunity for parties involved to minimize the gap. It is feared that the condition might worsen in the near future. It is thus necessary to identify the exact needs and expectations of both parties towards each other. Since there was no significant difference in the perspective of Management Agent (except for maintenance construct), it is suggested that they play the role of mediators in bridging the management gap.

ACKNOWLEDGEMENT

The authors would like to acknowledge the parties that helped in preparing the paper, in one way or another, especially the Public Service Department (JPA) Malaysia, Universiti Kebangsaan Malaysia and University of Malaya. Last but not least, to all family members who had given their endless support and encouragement.

REFERENCES

Alinah, A. 2004. *Taklimat Penubuhan PraPerbadanan Pengurusan*. LPH Selangor.

Amarilla, B.; Dunowicz, R.; Hasse, R. 2002. Social Housing Maintenance. *Proceedings of The XXX IAHS World Congress on Housing*. 9-13 September 2002. Edited By: Oktay Ural, Vitor Abrantes, Antonio Tadeu. Portugal: Pedro Batista – Artes Graficas, Lda. pp. 1951-1957.

DBKL 1999. *Hak Milik Strata & Perbadanan Pengurusan*. JPPH; JPP, Kuala Lumpur City Council (DBKL).

Eddy, C. L. L. 2004a. *Affordable Housing Development: Coming Together For The Benefit of The Nation*. The National Housing & Property Summit. 12-13 August 2004. Kuala Lumpur.

HBA 2003. *Recommendations on Stratified Property Presented To YB Dr Tan Kee Kwong, Deputy Minister of Land & Cooperative Development on 12 June 2003 during the 'Mesyuarat Pendidikan Untuk Bangunan Bil. 3/2003'*. House Buyers Association of Malaysia (HBA).

Hui, E. Y. Y. 2005. Key Success Factors of Building Management In Large & Dense Residential Estates. *Journal of Facilities*. Volume 23 Number 1/2. pp. 47-62. MCB University Press.

Jamila, H. 1994. *Strata Title In Malaysia*. Selangor: Pelanduk Publications (M) Sdn. Bhd.

Liias, R. 1998. Housing Stock: The Facilities For Future Development. *Journal of Facilities*. Volume 16 Number 11. pp. 288-294. MCB University Press.

Linariza, H.; Ashok, V. 2003. Facility Management: An Introduction. *Journal of The Malaysian Surveyor*. 1st Quarter 2003 (38.1). pp. 13-19.

Malaysia Government 1999. *Housing In The New Millenium – Malaysian Perspective*. Alamat: http://www.kpkt.gov.my/jabatan/jpn/artikel3.htm [Dilawati: 7 Sept 2004]. Kemas kini: Julai 2003.

Malaysia Government 2003d. *Panduan Kehidupan Bersama Dalam Bangunan Bertingkat (Pra-Strata)*. Jilid 1. Jabatan Ketua Pengarah Tanah & Galian, Kementerian Sumber Asli & Alam Sekitar.

Sapian, I. 2003. *Pengurusan Penyenggaraan Bangunan & Kualiti Kehidupan Di Kondominium Di Malaysia*. Seminar Pengurusan & Penyenggaraan Bangunan Ke-2, 22-23 Disember 2003, Kuala Lumpur.

Teo, K. S. (terjemahan) 1993. *Hak Milik Strata Di Malaysia*. Kuala Lumpur: Dewan Bahasa & Pustaka.

Thompson, P. 1994. The Maintenance Factor In Facilities Management. *Journal of Facilities*. Volume 12 Number 6. pp. 13-16. MCB University Press.

Tiun, L. T. 2006. *Managing High-Rise Residential Building In Malaysia: Where Are We?*. Persatuan Sains Sosial, Universiti Putra Malaysia. 8-10 Ogos 2006. Fakulti Ekologi, Universiti Putra Malaysia.

Maintenance and Rehabilitation Program for Algerian Bridges

Mouloud Abdessemed [1]
Said Kenai [2]
Ahmed Attar [3]
Abderrahmane Kibboua [4]

T 72

ABSTRACT

Algeria launched in 2004 a vast construction program which envisages the realisation of more than 450 infrastructure assets, of which 80% are bridges. In addition to this program, there are more than 8000 existing bridges that require maintenance and monitoring in both the short and medium terms to prevent structural deterioration due to environmental effects and traffic loads. For this reason, the Ministry of Public Works launched few years ago a rehabilitation program to monitor, repair and strengthen more than 80 bridge structures. This paper presents a research and development program established to generate information related to various deterioration phenomena using new techniques. Such information will be used to improve the planning of repair and rehabilitation programs for existing infrastructure and also, for the design of future projects. Information is provided on a preliminary study of a Road Bridge located on the west coast of Algeria, a concrete structure first built 80 years ago. An evaluation has been conducted based on ultrasonic pulse velocity testing; as well as ambient vibration tests before and after rehabilitation.

KEYWORDS

Bridges, Repair and rehabilitation, Concrete durability, Non-destructive testing

[1] Ministry of Public Works, Ben Aknoun, 2 Rue Mustapha Khalef, Algiers, Algeria, Phone (213) 72731750, Fax (213) 21913585/95, abdesmoul@yahoo.fr
[2] University of Blida, Civil Engineering Department, Blida, Algeria, Phone/fax: (213) 25433939,
[4] National Earthquake Engineering Center 'CGS', Rue Kaddour Rahim, B.P. N° 252, Hussein Dey, Algiers, Algeria, 16040, Phone (213) 21495547, Fax (213) 21 495536

1 INTRODUCTION

Algeria, by its geographical situation, is exposed to natural disasters like earthquakes and floods, which affect various structures. Statistical studies showed that there are a lot of reinforced concrete structures which need repair or strengthening [MTP 2005]. These structures present cracks and spalling due to concrete degradation, reinforcement corrosion or insufficient steel reinforcement to cater for high modern load traffic. These disorders are also induced by errors in the design phase, materials properties or lack of good quality control during the construction phase. Lack of preventive periodic maintenance also accelerates deterioration mechanism. Before strengthening or repairing these structures, a detailed investigation campaign should be conducted to decide on immediate preventive action to limit the propagation of degradations. This will be followed by a detailed investigation using suitable monitoring techniques and conducting non destructive and laboratory testing. Reinforcement and repair works are usually conducted to reinstate the original rigidity and strength to the deteriorated elements and if possible improving their performances and their durability.

The Ministry of public works in Algeria has undertaken a monitoring program of bridges exceeding fifty years of age. The existing structures are composed of more than 40% of structures over 50 years of age and hence need rehabilitation [MTP 2006]. The techniques of non destructive tests can be local, that means those that give reduced information and only in the controlled zone, as the ultrasonic tests, and those that are general and give global answers of the structure tested as the dynamic tests to ambient vibrations, forced vibrations or to optic fibres. These methods along with the infrared thermography and radar have been used successfully to detect the location and the size of deterioration, delamination, voids and other structural damages.

The aim of this paper is to present a case study of an 80 years old reinforced concrete bridge monitored before and after strengthening using non destructive tests and ambient vibration method.

2 ALGERIAN BRIDGES INHERITANCE

The inventory established by the Algerian Ministry of Public work in 2006, showed the existence of about 8000 bridges of which 4808 are road bridges and 4000 railway bridges, with 80% highways and national roads bridges, and 20% small rural road bridges (Fig. 1). It is noted that 1032 bridges are in either bad or medium conditions.

Moreover, the analysis of the level of the rate of deterioration of the various bridges components shows that over 2308 bridges need to be rehabilitated. These bridges are mainly those over 50 years of age. They are masonry, reinforced concrete, prestressed concrete, steel or composite structures. The rehabilitation program aimed to optimize the use of materials, products and repair techniques. It aims also to analyse the information generated from the diagnosis, repair and rehabilitation of these structures to learn some lessons for the design of new projects. In 2003, the Ministry launched an international tender for the diagnosis and rehabilitation of 25 bridges. In 2006, two other tenders were launched for the diagnosis and evaluation of 50 other damaged bridges all over the Algerian territory [MTP, DEER 2006].

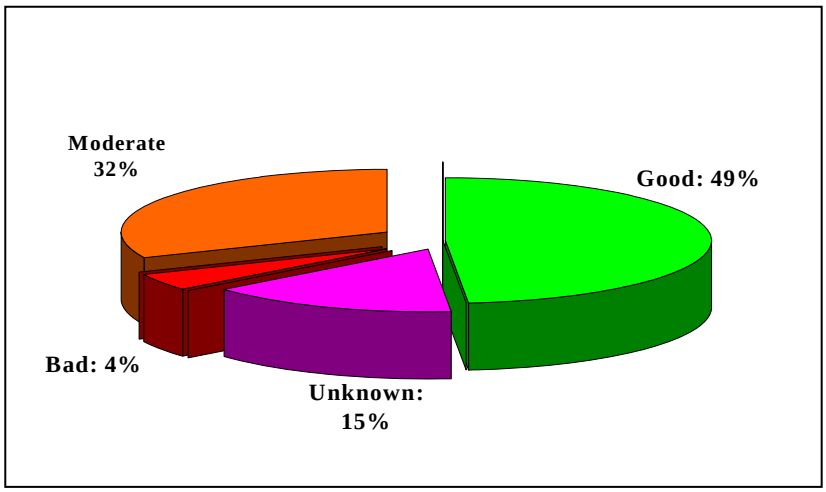

Figure 1. State of road bridges in Algeria

3. DETERIORATION DIAGNOSIS

Concrete bridges are required to maintain their serviceability over long periods of time, hopefully 100 years or more [Mallett, 1994]. The life of any bridge depends on the preservation of the physical integrity of both the superstructure and the substructure. Before deciding on a repair, it is necessary to check the cause of the damage and the degradation mechanisms. The main objective of the proposed program is to develop a rational integrated procedure for condition assessment of concrete bridges components involving existing test methods. Radar and Impact echo methods [EDG 2007] to detect steel corrosion of steel bars in reinforced concrete and prestressed cables in prestresed concrete structures or to evaluate the mechanical characteristics of concrete (propagation velocity, possible cracking, honeycombing, voids, etc) are widely used. Other testing methods based on global structural behaviour such as ambient or forced vibrations tests and optical fibres tests have been recently introduced.

The introduction on the Algerian market of new rehabilitation and repair techniques and materials requires some care and a good quality control as for their practical use and suitability for the local hot and aggressive environment. Indeed, quality of workmanship and quality control of materials is always a major concern of the Ministry of public works in construction of infrastructures and rehabilitation works.

For more than fifteen years [SAPTA 2004], the public work sector has undertaken repair and strengthening work on some strategic infrastructures, such as Sidi Rached Constantine cable stay Bridge, El Harrach white bridge in Algiers, Laghouat Road Bridge and Tipaza Oumazer River Bridge. The choice of repair materials and techniques is guided mainly by the nature and magnitude of the damage, the availability of the materials and local expertise. In Algeria, carbon fibres composite materials are the most used rehabilitation technique in bridges due to their ease and speed of application where repair work could be done without closing the bridge to traffic. Other advantages include their corrosion resistance, high tensile strength and low weight [Ferrar 1999; Djellal 1998 and Abdessemed 2003].

4. A CASE STUDY: OUMAZER BRIDGE

Oumazer Road Bridge was constructed in 1920 and is located few meters from the Mediterranean Sea coast in a high seismic activity region. It is a reinforced concrete bridge with three spans composed of four reinforced concrete beams with variable inertia, and two piles each one composed of four

Figure 2. Oumazer river Road Bridge

Some degradations were visible on its structural elements. Concrete delamination, steel corrosion and cracks were observed on its columns and girders (Fig. 4). This is due probably to the high aggressive marine environment. The diagnosis reveals also diagonal cracks with 45° on main beams which is primarily due to the increase in shear stresses due to traffic increase (SAPTA, 2004). The repair consisted mainly of reinforced concrete jacketing of piles, epoxydic resin injection of the cracks, ready mixed repair mortar application for spalled concrete and the strengthening of beams by carbon fibre composite sheets.

Figure 3. State of degradation of the bridge piles

5. REPAIR EVALUATION

5.1 Cracks Repair and Ultrasonic Tests

Epoxy resins were used to fill and repair the cracks of the damaged beams. In order to assess concrete quality of the bridge and to check the filling operation of the cracks, ultrasonic tests were performed before and after cracks repair (Fig. 4).

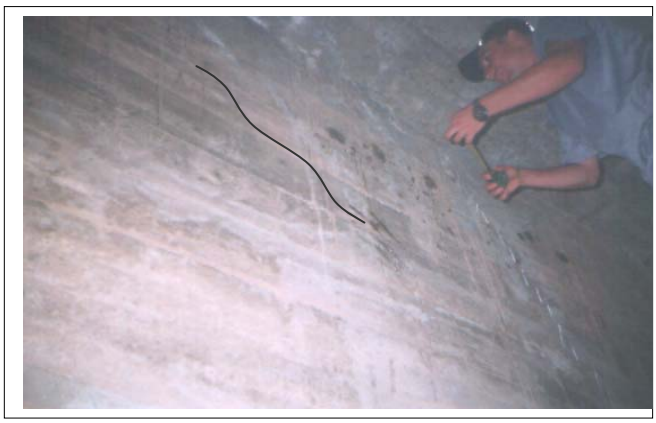

Figure 4. *Ultrasonic assessment of cracks* repair

The principle consists in measuring pulse velocity in concrete over a crack. Velocity increases with modulus of elasticity and therefore with concrete strength and density. In case of unfilled cracks or voids, velocity is decreased and hence the efficiency of the repair could be evaluated. Table 1 summarizes pulse velocities values measured on cracked beams: two tests were performed, on the top and the bottom of the crack.

Table 1. Ultrasonic velocity on a cracked beam

Distance (m)	0.25	0.45	0.70	0.92
Speed before resin injection (m/s)	2523	2335	940	1034
Speed after resin injection (m/s)	2604	2444	2818	30213

As shown in table 1, an increase in velocity is observed after the injection of the resin. Crack injection by resin improves concrete homogeneity up to 70 % and contributes to the enhancement of its durability. However, it should be noted that measured velocities remain low because of the low concrete quality. Consequently, it was necessary to reinforce the bridge structural elements (beams and columns) by carbon fibre composite materials.

5.2 Applied Repair Materials

To restore to the deteriorated elements their initial performances, it is important to choose adequate repair materials for the structural elements to support new high traffic loads. In fact, strengthening of the bridge consisted of piles jacketing, application of an unidirectional wrap fabric for beams sides and a laminate carbon fibres on beams lower faces. Table 2 summarizes the used materials properties.

Table 2. Repair Materials properties

Repair Materials	Modulus E (GPa)	Density	f_t (MPa)	f_c (MPa)	Elongation (%)	Thickness (mm)
Resin	12.8	1.8	30	55	-	-
Wrap fabric	230	-	3500	-	1.5	0.13
Laminate	165	1.5	2800	-	1.7	1.2

5 .3 Non Destructive Tests on the Bridge

Ambient vibrations tests were conducted on the bridge before and after repair and strengthening. The test is considered to carry out recordings of basic noise using a CityShark II-6 recording station, and four Lennartz seismometers. The CityShark station can simultaneously record six sensors signals. For this study, only four sensors were used (Fig. 5). These sensors are equipped with three components: a vertical component, and two perpendicular horizontal components between them. Recording duration is 15 minutes. Measurements of the natural frequencies were taken on the bridge before and after application of carbon fibres composite sheets. The main aim of this test is to determine the most dominating modes of vibration and see the influence of the composites on the bridge behaviour. The seismometers positions (Fig. 6) were selected based on numerical modelling using SAP2000 finite element software. Seismometers C1 and C2 are placed on the two pavements and at the transverse axis of the bridge, and C3 and C4 are placed six meters away from C1 and C2. After achieving the measurements, the seismometers are moved along the bridge until covering the total length. Two other measurements were taken on the two piles. The obtained measurements are illustrated in tables 3 to 5.

Tables 3 to 5 synthesize the results obtained for each phase of measurements of the frequencies of vibration of the bridge. The reference case is the test done before the application of composite materials on the main beams of the bridge. Measurements were made according to three directions' of the bridge, namely the vertical direction (table 3), the transversal direction (table 4), and on the bottom of the piles (table 5). The obtained values show a little effect of composite materials on the ambient frequencies of vibration corresponding to 0.02 Hz accounting for only 0.05% for the vertical natural mode, 0% for the horizontal mode, and 1.6% for the piles.

Figure 5. City Shark station and Lennartz seismometer

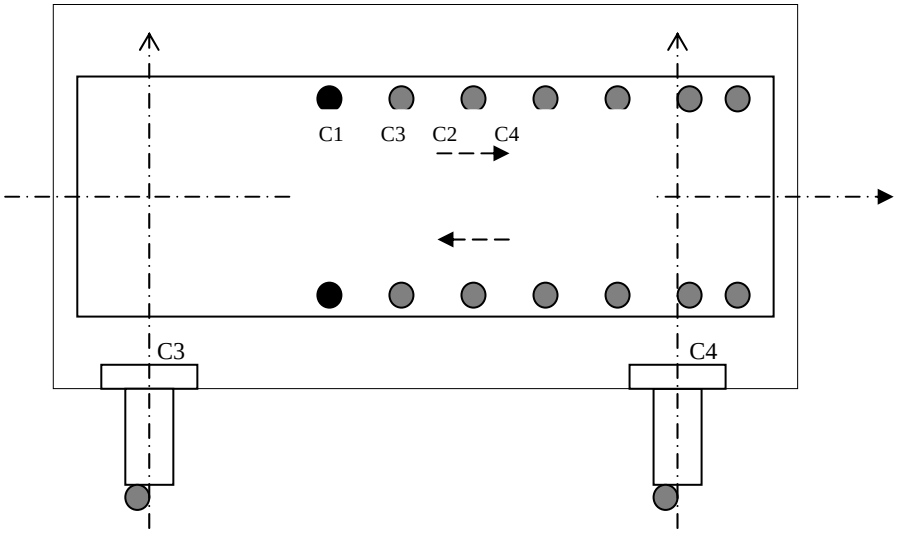

Figure 6. Seismometers position on the bridge

Table 3. Frequency values before and after repair of beams (Vertical peaks)

	Frequency (Hz)	Frequency (Hz)	Frequency (Hz)	Frequency(Hz)
Measurements	C 1	C2	C 3	C 4
Before repair	5 .01	4.60	4.90	4.58
After repair	5.00	4.58	4.92	4.56

Table 4. Frequency values before and after repair of beams (Transversal peaks)

Measurements	Frequency (Hz)	Frequency (Hz)	Frequency (Hz)	Frequency(Hz)
	C 1	C2	C 3	C 4
Before repair	3.97 – 5.01	3.97 – 5.01	3.97 – 5.01	3.96 – 5.01
After repair	3.97 – 5.01	3.97 – 5.01	4.00 – 5.00	4.01 – 5.01

Table 5. Frequency values on piles

Position	f_0 (Hz) transversal	f_0 (Hz) longitudinal	f_0 (Hz) vertical
Left pile	4.50	3.91	10.5
Right pile	4.46	3.85	10.5

One can note the following dominating frequencies modes:

- Natural frequency of the transversal mode of vibration of the slab is 4.51 Hz ;
- Natural frequency of the vertical mode of vibration of the slab is 4.90Hz ;
- Natural frequency of the longitudinal mode of vibration of the piles is 3.88 Hz ;
- Natural frequency of the transversal mode of vibration of the piles 4.48 Hz
- Natural frequency of the vertical mode of vibration of the pile 10.5 Hz.

These tests have shown that ambient vibration test, comparatively with forced vibration or dynamic test by vehicle or traffic can not be very significant for the determination of dynamic evaluation for bridges of small or average length. The mass variation due to the composite addition is low comparing to its effect on the rigidity K of the structure which differs before and after the application of the composite. The composite materials addition affect the vibrations amplitude of the structure, while the natural frequency is not affected (absorption of the vibrations by the composites) [CSTB, 2001 and Freyssinet International, 2004].Thus, it is recommended to carry out other dynamic tests on other existing bridges to help in the establishment a consistent database to evaluate the current state of the Algerian infrastructure.

6. CONCLUSION

A maintenance program has been established by the Algerian Ministry of public works for monitoring, repair and strengthening of existing bridge. In fact, repair and rehabilitation of existing structures for durability makes it possible to enhance the remaining service life and the actual field performances. Development of a rational integrated procedure for condition assessment of concrete bridge components, involving existing and newly developed diagnostic tests contribute to detection and location of structural damages. In our study, ultrasonic tests enabled us to ensure successful cracks injection in a reinforced concrete beam bridge, while ambient vibrations test allowed us to evaluate the performance of strengthening by fibre reinforced composite sheets.

REFERENCES

Abdessemed, M, 2003, "*Comportement des poutres renforcées par des matériaux composites à base de fibres de carbone*", Master Thesis, University of Blida, Blida, Algeria.

CSTB, 2001"*Avis technique 3/01/345 TFC*", Freyssinet France, Paris, France.

Djelal, C , David, E ,Buyle-Bodin, F and Y. Gicquel, 1998, "*Renforcement des poutres en béton armé à l'aide de lamelle composites*", Annales du bâtiment et des travaux publics, pp. 39-47.

Européenne de Géophysique (EDG), 2007, "*Domaine et méthodes d'intervention*", Paris, France.

Ferrar, C.R, Duffey T.A, Conwell P.J and. Doebling S.W., 1999, "*Excitation methods for bridge structures*", in Proceedings of the 17th international Analysis Conference on Kissimmee, FL, USA.

Freyssinet International, 2004, "Fiche technique, Renforcement structurel avec du TFC", Paris, France.

Mallett, G.P., 1994, "State of the Art Review. "*Repair of concrete bridges*", Thomas Telford, London.

Ministère des Travaux Publics (MTP), 2005, "*Entretien et expertise des ouvrages d'art*", Algiers.

Ministère des Travaux Publics (MTP), 2006, "'*Saisi des données de 4808 ouvrages d'art en Algérie"*, Algiers, Algeria.

Ministère Algérien des travaux publics (MTP, DEER), 2006, "*Internal report"*, Algiers, Algeria

Société Algérienne des Ponts et Travaux d'art (SAPTA), 2004, "*Rapport d'expertise des ponts*", Algiers, Algeria.

11DBMC International Conference on Durability of Building Materials and Components
ISTANBUL – TURKEY May 11-14th, 2008

Life Cycle Management System – A Planning Tool Supporting Long-Term Based Design and Maintenance Planning

Daniel Hallberg [1]
Jan Akander [2]
Bojan Stojanović [3]
Mikael Kedbäck [4]

T 72

ABSTRACT

Construction projects include large amounts of information that has to be communicated to a number of actors, such as authorities, companies, clients and end users. Information exchange is complex, involving various players on different levels and phases of the construction process. For private clients, who generally have little experience and knowledge of this process, the on-going "Bygga Villa"-project has developed a web-portal, which offers them relevant information about the process and a number of services to facilitate realisation of their projects. One of the services provides a tool for supporting long-term strategy planning. The tool is based on the Life cycle Management System (LMS) that is a predictive and generic life cycle-based management system, aimed to support decision-making and planning of optimal design and maintenance of any construction works. The LMS-Bygga Villa tool estimates service life and maintenance intervals of different building parts and systems based on environmental-dependent degradation models. Simulated scenarios can give optimised solutions by applying life cycle cost analysis. This paper presents two case studies within LMS-Bygga Villa. The first case focuses on service life performance analysis of exterior parts of buildings. The second focuses on service life performance analysis of energy systems; here specifically a borehole assisted heat pump system used for heating a Swedish single-family residence.

KEYWORDS

Life cycle Management System, Design, Maintenance, Service life, Heat pump system

[1] University of Gävle, Centre for Built Environment, Gävle, SE-801 76, Phone +46 26 648108, Fax +46 26 648181, daniel.hallberg@hig.se
[2] University of Gävle, Centre for Built Environment, Gävle, SE-801 76, Phone +46 26 648118, Fax +46 26 648181, jan.akander@hig.se
[3] University of Gävle, Centre for Built Environment, Gävle, SE-801 76, Phone +46 26 648137, Fax +46 26 648181, bojan.stojanovic@hig.se
[4] Future Position X, Gävle, Sweden SE-802 69, Phone +46 26 614400, micke.kedback@fpx.se

1 INTRODUCTION

A construction project includes large amounts of information that has to be communicated to a number of parties, such as authorities, municipalities, companies, clients and end users. The information exchange is complex, involving various players on different levels and phases of the construction process. Private clients, who generally have little or no experience and knowledge of construction projects, often see this process as complicated and time-consuming. Authorities, municipalities, county councils and companies offer a number of electronic services (e-services) that are intended to support the private client in the construction process. However, there is no common "entrance" to these services. The Swedish Administrative Development Agency (VERVA) has been commissioned by the Swedish Government to promote the development of electronic public administration and promote the development of services that will improve the access to public information [Finance Ministry 2007]. As a part of this mission, VERVA has published a handbook with guidance on development of websites and e-services in the public sector [VERVA 2006]. On basis of this guidance, the Swedish Governmental Agency for Innovation Systems (VINNOVA), has granted 6.5 million SEK to the "Bygga Villa"-project in order to develop a website where a number of e-services, supporting private clients in the construction process, are gathered [Ottosson 2005]. This paper will present an e-service that provides a tool that support long-term strategy planing and decision-making of design and maintenance of buildings and heating systems. The aim of the service is to give the private client an aid to and understanding of the long-term performance and future need of maintenance of buildings.

2 LIFE CYCLE MANAGEMENT SYSTEM

Promoted by an increased European focus on research and development on sustainable construction, several EU-projects [Haagenrud et al 1999, Haagenrud 2001, Sarja 2004] have developed methods, systems and tools for predictive maintenance management in order to meet the demand on sustainability during the whole service life of the construction works. A result of the projects is a predictive and generic Life cycle Management System (LMS), which aims at supporting all types of decision making and planning of optimal design, maintenance, repair and refurbishment (MR&R) activities of any construction works and systems therein. Due to its predictability function, it is possible to adopt short-term as well as long-term planning in which decisions may be based on economical, environmental, safety, cultural and social values etc. The LMS is a system by which the complete system or parts thereof, works in co-operation or as a complement to existing business support systems. The system is module-based, where each module represents a sub-process within the maintenance management process. Figure 1 shows the structure of LMS (6 modules) and its connection to other business support systems. The first module, i.e. the *Inventory Registration Module*, contains systematic registration, classification and description of technical and administrative data of the objects/systems. The *Condition Survey Module* includes systematic recording of condition data. This includes guidelines and protocols for condition assessment and survey in order to obtain consistent and reliable inspection/observation results on the items and their environment. The "heart" of the system is the *Service Life Performance Analysis* (SLPA) module. This module contains applicable degradation models and simulates the loss of performance over time of a material, component item or a system. The *Maintenance Analysis Module* includes systematic analysis of different MR&R alternatives by utilising the predictive functions of the SLPA module in order to evaluate the efficiency of the MR&R alternatives. The *Maintenance Optimisation Module* contains models for optimisation of those MR&R actions suggested in the Maintenance Analysis Module. It takes into account a number of aspects such as Life Cycle Cost (LCC) and Life Cycle Ecology (LCE). The final module within the LMS is the *Maintenance-Planning Module.* This module serves to establish optimised long-term plans of MR&R actions.

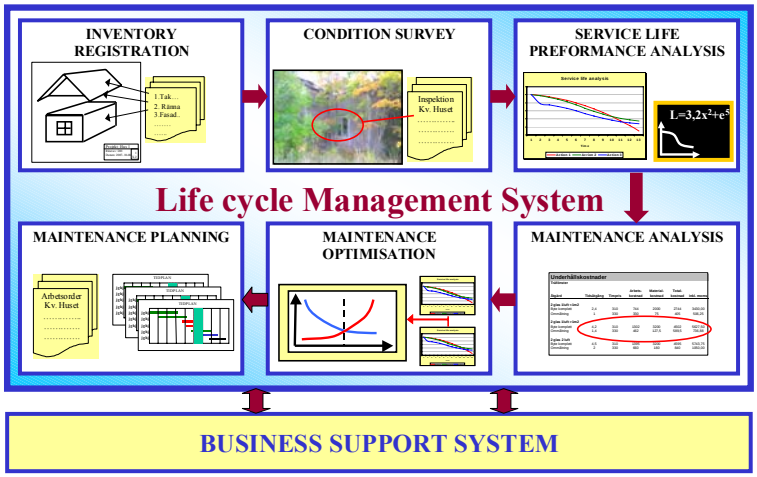

Figure 1. Structure of the module based LMS

3 THE LMS-BYGGA VILLA TOOL

User friendliness, simplicity and consistency have been keywords in the development of the LMS-Bygga Villa tool. The tool is not intended to be an advanced simulation tool for experts of design and maintenance management, rather a simple tool that will give the private client a hint of future need of maintenance and long term performance of the building and its heating system. The LMS-Bygga Villa tool is built on database technique and is divided into two interfaces; an administrative interface and a user interface. The administrative interface is restricted to those who are responsible for maintaining and upgrading the tool. This part of the tool consists of a catalogue of building types, building components and different heating systems, building materials and corresponding damage functions. The administrative part is linked to the user interface in which the user will be able to define a building, its location and calculate the service life for each building component/system. The location of the building is selected from a list of cities or from a Geographic Information System (GIS) map (the latter will be developed in the near future). Each location (city) has a defined environment, based on data from meteorological and environmental institutions as well as from the cities themselves. This data is coupled to the city and stored in the administrative part of the database. The building is composed piece by piece, in a hierarchical order, where each building component and system is selected from the building type catalogue. This will guarantee a consistent definition of the building. Figure 2 shows the calculation process in the LMS-Bygga Villa tool.

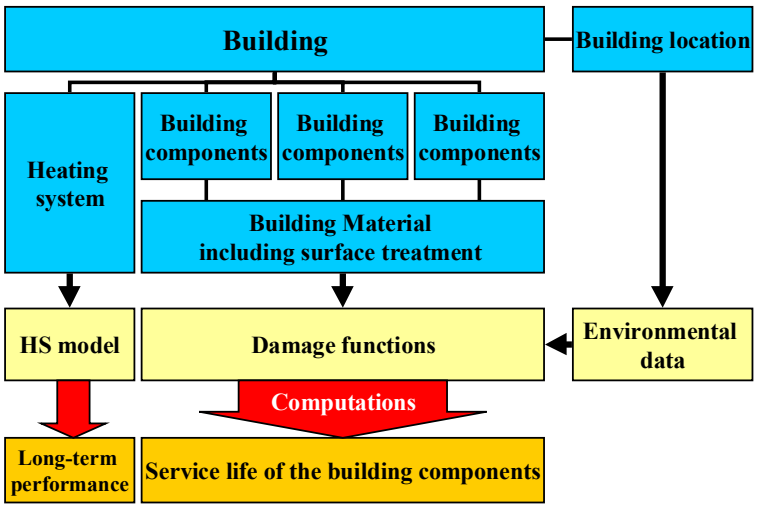

Figure 2. The calculation process in the LMS-Bygga Villa tool.

The computation is done directly in the database manager and the result is presented for all defined building components/systems. On the basis of the service life calculation/ long-term performance analysis results, it will be possible estimate the life cycle cost of each building component. A life cycle cost module adapted for the LMS-Bygga Villa tool is under development. In the following sections, two case studies will show some examples of service life calculations and long-term performance analysis and how the results may be used in the LMS-Bygga Villa life cycle cost module. The first case illustrates the LMS-application on windows and roof for a building situated in Gävle, Sweden. The second case shows performance degradation of a heat pump system with a borehole heat exchanger.

4 CASE STUDY 1

4.1 Exterior Part - Windows and Roofs

The service life of a building is expected to be at least 50 year on condition of normal maintenance [EOTA 1999]. Roofs and the windows are two examples of important parts of the building. The roof protects the rest of the building from being exposed to above all, rain and snow. A leak in the roof will soon lead to heavy damages on the rest of the building. It is therefor important to maintain the roof properly. The window is a complex component of the external wall construction with additional number of functional requirements to meet, such as inlet of daylight, visibility and aesthetics. Windows are also quite expensive since the replacement cost varies from a couple of hundreds to over thousand of Euros, depending on size, type and quality. Replacement of windows in Sweden is normally done after 30-70 years in service, often in combination with major building maintenance/repair actions [SBT 1984]. The following case will compare calculations of service life of windows made of wood and tin roofs of coil coated galvanised steel.

4.2 Service Life Calculations

A number of damage- and lifetime functions derived from the ICP Material program [UNECE 2004] and from the MOBAK study are included in the LMS-Bygga Villa tool. The MOBAK project, accomplished during the second half of the 1980's by initiative of the Nordic Council of Ministers, was a comprehensive study aimed to develop a methodology for data inventory of building materials and damages [Tolstoy *et al.* 1990]. The study encompassed damage inventory and condition assessments for a number of building components. By using extrapolation techniques, Andersson [1994] developed a number of lifetime functions based on the results from the MOBAK study. These functions are basically damage functions derived indirectly from inventories of maintenance intervals and therefore suitable in calculations of maintenance intervals. Following damage-/lifetime functions are used in this case study.

Service life (L) of painted wood [Andersson 1994]:

$$L = \frac{1000}{1{,}03 \cdot [SO_2] + 87{,}5 + 260 \cdot [H^+] \cdot rain} \quad (1)$$

Service life (L) of coil coated painted galvanised steel [Andersson 1994]:

$$L = \frac{1000}{0{,}37 \cdot [SO_2] + 62{,}9 + 95 \cdot [H^+] \cdot rain} \quad (2)$$

Service life (L) of coil coated galvanised steel [UNECE 2004]:

$$L = \left(\frac{10 - ASTM}{(0.0084 \cdot [SO_2] + 0.015 \cdot Rh + f(T)) + 0.00082 \cdot Rain} \right)^{\frac{1}{0.43}} \quad (3)$$

f(T) = 0.040(T-10) when T<10°C, otherwise -0.064(T-10). Equation 3 referes to the ASTM scale, 1 to 10, where 10 is good condition. The limit for maintenance actions is set to 5.

Environmental data on SO_2 (μg/m^3), H^+ (mg/l), Rain (mm/y), RH (%) and T (°C) is obtained from The Swedish Environmental Research Institute (IVL), Centre for Built Environment (BMG) and Gävle Municipality. Inserting the environmental data into the damage- and lifetime functions gives the results presented in Table 1. The result considers a 50-year planning period.

Table 1. Calculated service life for different coating materials in Gävle, Sweden.

	Painted wood (eq. 1)	Painted coil coated galvanised steel (eq. 2)	Coil coated galvanised steel (eq. 3)
Service life	8	13	18

It is assumed that the maintenance action on the roof is to repaint the roof. Thus, the following maintenance intervals will refer to painted coil coated galvanised steel, which will be necessary every 13 years. The total number of maintenance action on windows, i.e. repainting, is 7. The total number of action on the roofing is 4. This information, in combination with action cost data will be then input to total cost calculations. Man hour- and material costs data are estimated values. The result is presented in Table 2 and considers a 50-year planning period.

Table 2. Calculated action costs for wooden windows and tin roofs (1 Euro ≅ 9.20 SEK).

Building part	Type of action	Action cost	Number of actions per period	Periodic action cost
2 light window, 2 glass	Replacement	5740 SEK	1	5740 SEK
	Repainting	1050 SEK	7	7350 SEK
Tin roof, coil coated galvanised steel	Repainting	120 SEK/m^2	4	480 SEK/m^2

5 CASE STUDY 2

5.1 Borehole Assisted Heat Pump System

The use of borehole assisted heat pump system in Sweden has grown remarkable fast during the last decades, where half of the European heat pump market is in Sweden. The heat pump technology has been seen as an "environmental friendly" energy alternative which reduces the electricity consumption and thus the environmental impact. However, the Seasonal Performance Factor (SPF) of electrical heat pumps is about 2.5 – 3.0, which gives a similar CO_2 contribution to the atmosphere as heating system based on fossil fuel. To preserve the "environmental stamp" and the environmental arguments for installing heat pump systems, it is important to increase the SPF. Borehole assisted heat pump systems consists of a heat pump coupled to a Borehole Heat Exchanger (BHE), where the depth of the BHE varies from 60 to 170 m depending on the heating requirements [Akander *et al*. 2007]. During operation of the heat pump system heat will be extracted from the BHE, which reduces the ground temperature. When the ground temperature decreases, the heat pump system has to operate for a

longer period to meet the heating requirements. This reduces the SPF. A model for simulation of this effect is presented by Akander *et al*. [2007].

$$SPF = \frac{Q}{W_t + E_{aux}} \tag{7}$$

where Q is heat output during a considered period of time, [J] or [kWh], W_t is energy supplied to the heat pump (electricity) during the period, [J] or [kWh], E_{aux} is heat or electricity (auxiliary energy) supplied to the heat pump system during the period, [J] or [kWh] [Akander *et al*. 2007]. The energy (electricity) supplied to the heat pump i.e. the required energy to extract energy from the BHE is given in eq. 8 [Akander *et al.* 2007].

$$Q_{extracted} = \left[1 - \frac{1}{\eta}\right] \cdot (Q_{SH} + Q_{DHW}) + \frac{T_{cold} - \Delta T_{evap}}{\eta} \left[\frac{Q_{SH}}{T_{SH} + \Delta T_{cond}} + \frac{Q_{DHW}}{T_{DHW} + \Delta T_{cond}}\right] \tag{8}$$

where Q_{SH} and Q_{DHW} are space- and DHW heating requirements, respectively, [kWh] or [J], T_{cold} temperature of the cold carrier exiting the heat pump, [K], T_{SH} and T_{DHW} are supply temperatures for space heating and DHW, respectively, [K], ΔT_{evap} and ΔT_{cond} are temperature differences between the refrigerant and carrier in the heat exchangers of the evaporator and condenser, respectively, [K]. When the BHE temperature decreases, the temperature of the cold carrier T_{cold} will do the same. A BHE model describing this temperature decrease is presented by Stojanović *et al*. [2005]. The model takes into account factors such as borehole depth, ground conditions and initial ground temperature. The result, given in Table 3 and Fig. 3 is derived from a calculation of SPF reduction over time for a new residence located in Bromma/Stockholm. The borehole depth is considered to be 70 m. A more detailed description of the calculations and data is presented by Akander *et al.* [2007].

Table 3. A comparison of SPF and supplied electricity between year 1 and year 50.

	Year 1	Year 50	Change (%)
SPF	2.99	2.93	2.0
Supplied electricity	3609.5 (kWh)	3683.5 (kWh)	2.1

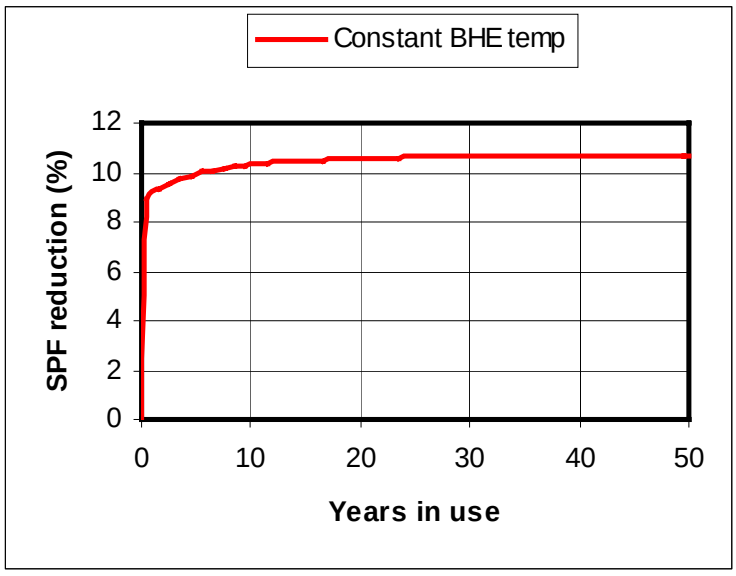

Figure 3. SPF reduction over time.

The complex BHE model is not yet applicable for the LMS Bygga Villa tool. However, the complex BHE model will be "simplified" by using regression analysis for various locations and borehole depths.

6 DISCUSSION AND CONCLUSIONS

In the first case, a number of different damage-/lifetime functions have been used for service life calculations. These are partly developed in Sweden, partly in an environment close to the conditions in Sweden, which justify the use of the functions in this application. This statement is strengthening by the fact that the results of the service life analysis are close to the common assessments of service life on the building component in question. Nevertheless, in general damage-/lifetime functions are developed in different research projects with different prerequisites, so one must be cautious when adopting these functions in service life performance analysis. Some of these are based on dose-response functions, which are functions that are not convenient for service life calculations since there is no direct link between the response and the loss of performance [Haagenrud 1997]. This is solved by adding a performance requirement to the dose-response function, which then will be valid as a damage function and thus, suitable in service life calculations. The tricky part is to define the performance requirements. Another difficult part is to collect and unify environmental data, appropriate for the use in service life calculations. A problem is that the various data is collected by different institutions for different purposes. Data is also presented in different formats, not always manageable. One example is transformation of environmental data from one "geographical level" to another. Another example is whether point sources of pollution should be included or not in an application such as LMS-Bygga Villa.

There is an ongoing discussion about the cooling effect in boreholes. The discussion is on, whether recharging is economical justified or not. This case shows nevertheless that the cooling effect is almost negligible for a single borehole of correct depth. It is true that the SPF of the heat pump system is heavily reduced during the first year in operation. But the fact that this effect is taken into account in the design of the system and that the performance loss is only 2.0 % the next 50 years in operation does not motivate recharging of the borehole. Transformed into economic terms the magnitude of the reduced performance during the 50 years in operation corresponds to 1-year operation cost. During this time the heat pump is probably replaced by a new and more effective one or by a complete different heating system.

7 FUTURE WORK

The development of LMS-Bygga Villa tool will continue. The main focus in the near future will be on development of a user-friendly interface and development of an economy module in which the user will be able to compare different maintenance actions in terms of life cycle costing. Along with the development of a user friendly application follows development of a GIS module in which mainly environmental data such as meteorological data, geological data, pollution data, etc. can be stored and presented. Another part of the near future work will be on development of a simplified borehole model applicable for LMS-Bygga Villa in which different heating distribution system and borehole depth is taken into consideration.

REFERENCES

Finance Ministry. 2007, 'Regleringsbrev för budgetåret 2007 avseende Verket för förvaltningsutveckling' (In Swedish) Swedish Government - Finance Ministry, Fi 2007/1638

VERVA. 2006, 'Vägledningen 24-timmarswebben - Effektivare och bättre service på webbplatser i offentlig sektor' (In Swedish) Swedish Administrative Development Agency, Report 2006:5

Ottosson, P. 2005, 'Bygga Villa; Projektbeskrivning', (in Swedish), Lantmäteriverket, Gävle, Sweden

Haagenrud, S., Stordahl, P., Eriksson, B., Riks, E., Krigsvoll, G. and Garofolo, I. 2001, 'System for Maintenance Management of Historic (Wooden) Buildings' (acronym: MMWood), Final report, EU-Project ENV4-CT98-0796

Haagenrud, S., Veit, J., Eriksson, B., Henriksen, J. F. and Krigsvoll, G. 1999, 'System and Methods for Assessing Conservation State and Environmental Risks for Outer Wooden Parts of Cultural Buildings' (acronym: Wood-Assess), Final Report, EU-project ENV4-CT95-0110

Sarja, A. 2004, 'Life Cycle Management System – LIFECON LMS, Technical summary', Lifecon G1RD-CT-2000-00378, Public usage

EOTA. 1999, 'Assumption of working life of construction products in Guidelines for European Technical Approval', European Technical Approvals and Harmonised Standards, Guidance Document 002, European Organisation for Technical Approvals

SBT. 1984, 'Fönster –Projektering, Byggand, Underhåll' (In Swedish) ed. Maurin, G. AB Svensk Byggtjänst, Stockholm, Sweden

UNECE. 2004, 'International Co-operative Programme on Effects on Materials, including Historic and Cultural Monuments' ed. Kucera, V., Mapping manual 2004, UNECE Convention on Long-range Transboundary Air Pollution

Tolstoy, N., Andersson, G., Sjöström, C. and Kucera, V., (1990), 'External building materials – quantities and degradation', Research report TN:19, The National Swedish Institute for Building Research, Gävle, Sweden

Andersson, B. 1994, 'Korrosionsskadekostnaden orsakad av SO_2-emissioner – en beräkning för Sverige 1991' (In Swedish) National Institute of Economic Research

Akander, J., Stojanović, B. and Hallberg, D. 2007, 'Simulated Long-term Thermal Performance of a Building That Utilizes a Heat Pump System and a Bore Hole' submitted for *The 11th International Conference on Durability of Building Materials and Components*, Istanbul, Turkey, 11-14th May 2008.

Stojanović, B. & Akander, J. 2005, 'Long-term Thermal Performance Modelling and Simulations of a Borehole', *Proceedings of the 7th Symposium on Building Physics in the Nordic Countries*, Reykjavik, Iceland, June 13-15, 2005.

Haagenrud, S. E. 1997, 'Environmental Characterisation including Equipment for Monitoring', CIB W80/RILEM 140-PSL, Norwegian Institute for Air Research – NILU, Kjeller, 1997

Quantifying Maintainability Parameters for Vertical Transport System

Chew M.Y.L.[1]
Sutapa Das [2]
Nur H.B. Sulaiman [3]

T 72

ABSTRACT

Elevators or lifts form the vertical transportation spine of modern high rise buildings. Safety and convenience being two critical issues, it is important to identify the associated risk factors. To complement the technological advancements of system design and greater users' expectation, there is a noted absence of maintainability aspect which not only ensures efficient system performance but also lowers the total life cycle cost through smooth operation and minimal maintenance. To address this knowledge gap, this research was undertaken to identify, analyse and quantify serious defects prevalent in the vertical transport system of commercial buildings of Singapore.

From detailed case study at five commercial buildings, total 114 types of common defects were identified for five main components including machine room, car, hoistway, landing and pit. Out of them, 28 were graded as significant by 40 experienced facility managers in a five pomt Likert scale in terms of frequency of occurrence, and adverse effect on: economy, system performance and safety & comfort. Comprehensive defect analysis established that inadequate or careless maintenance was the main cause for most of them. This study provides foresight of the long term effect of the decisions made during design, construction and operation-maintenance stage and forms the basis of good practices for efficient and safe functioning of highly maintainable vertical transport system. This generic method is applicable for any other building services.

KEYWORDS

Defect Analysis, Life Cycle Cost, Maintainability, System Performance, Vertical Transport

[1] National University of Singapore, School of Design and Environment, Singapore 117566, Phone +65 6516 3496, Fax +65 6775 5502, bdgchewm@nus.edu.sg
[2] National University of Singapore, School of Design and Environment, Singapore 117566, Phone +65 8112 5061, Fax +65 6775 5502, sutapa@nus.edu.sg / sutapa.d@gmail.com
[3] National University of Singapore, School of Design and Environment, Singapore 117566, Phone +65 9644 4215, Fax +65 6775 5502, nhsulaiman@gmail.com

1 INTRODUCTION

Elevators or lifts form the vertical transportation spine of modern high rise buildings. Since the invention of safety gear by Elisha Otis in 1953, elevators have undergone significant improvement especially in related areas such as: traffic handling, control systems, traction systems and vibration dampers. As modern elevators are complex equipment designed, produced and installed under stringent regulations, they are inherently safe. However in spite of a safety factor as high as 16, ISO certification of most of the manufacturers / installers, elevators and escalators related accidents kill about 30 and seriously injure about 17,100 people each year alone in the United States and 50% of the victims are trained elevator mechanics [McCann 2004].

Safety rules [ISO 2004] are focused at various types of accidents with lifts: shearing, crushing, falling, impact, trapping, fire, electric shock, damaged material, accidents due to wear or corrosion (Staal & Quackenbush 1998). Among the prevalent problems such as over speeding of car, uncontrolled low speed, car moving before door is closed etc, the most common hazard is fatal fall through elevator shaft due to opening of lobby door on pressing of call button before the car arrives [Vlahovic 1990]. Moreover equipment shutdown incurs in expensive over time 'callbacks' and inconvenience to the users. Such malfunctioning can be prevented by efficient maintenance practices [NEII 2007].

In spite of regular inspection according to elevator maintenance checklists [Schloss 1998], defects are prevalent. From extensive literature review it was established that to complement the technological advancements of system design and greater users' expectation, there is clear need for a better understanding of maintainability aspect to ensures efficient system performance and lower total life cycle cost through smooth operation and minimal break-down. Causes and long term effects of defects need to be addressed explicitly in design guidelines and maintenance handbooks. This research was undertaken to identify the defects common in the vertical transport system in commercial buildings of Singapore and to rank the significant one based on the scientific quantification of their seriousness. This study focuses on traction type passenger elevators generally found in high-rise commercial buildings.

2 RESEARCH METHODOLOGY

2.1 Data Collection

In order to obtain a preliminary idea of common maintenance problems in vertical transport system, major components were listed from available literature for a systematic site investigation. In the first phase of data collection, an in-depth field survey was conducted in five commercial towers. Discussion with facility managers (FM) and maintenance personnel was followed by expert walk-through and photo documentation of all permissible areas to investigate elements such as the machine room, car interior etc. The defects were analyzed with the help of information provided by FMs, past maintenance records of the buildings under study and the knowledge gained through the literature review [McKain 1999; O'Donoghue & Jarboe 2007; SAC 2000; Strakosch 1986] were elicited.

From preliminary analysis, a defect was observed to have adverse effect on (1) economy, (2) system performance; and (3) safety & comfort. These factors contribute to the level of seriousness of a defect and were considered to establish the significance of a defect. A frequent defect might have insignificant effect, while a very serious defect may occur rarely. For example, closing of car door while user are getting in and out of the car is common but the force exerted causes only nudging effect, while false opening of a lobby door when there was no elevator car is rare but can cause fatal fall through hoistway. The three major impacts were defined as:

- Economic loss: considerable financial damages sustained as a result of the defect, e.g. call back if users are caught in a stalled car due to deactivated safety switches or faulty circuits.

- System performance loss: here the system performs significantly below normal operating efficiency due to the defect, e.g. repeated opening and closing of car door.
- Safety & comfort loss: affected safety of the users and maintenance personnel as a result of the defect, e.g. opening of fire lift car door in fire floor if the lobby smoke detector is faulty.

The defect data related to major components and sub-components of vertical transportation system was collated in a detailed survey questionnaire. In a face to face interview, 40 experienced facility managers (FM) were asked to indicate the frequency of the defect in a five point Likert scale, where, 1 = 'rare', 2 = 'sometimes', 3 = 'quite often', 4 = 'very often' and 5 = 'always'. In order to estimate the impact of each defect, the respondents were asked to indicate the significance of the defects in terms three consequences also in a five point Likert scale, where, 1 = 'Nil', 2= 'Slight', 3 = 'Moderate', 4 = 'Serious' and 5= 'Very serious / fatal'. Among five major components, the questionnaire for elevator hoistway is shown in Appendix A as an example.

2.2 Data Analysis

Mean ratings for determining the level of seriousness of the defects were calculated from the feedback received. Mean rating for frequency was defined as $\overline{X}_{FR}$, while the same for impacts on four aspects, namely, economy, system performance, and safety & comfort were denoted by $\overline{X}_{EC}$, $\overline{X}_{SP}$ and $\overline{X}_{SC}$ respectively. For each defect, the mean rating was calculated by a general formula (Equation 1). Using statistical tool SPSS 12 (Statistical Package for the Social Sciences), T-test was carried out to identify the significance of each mean. The midpoint test value of 3 (by definition) was assigned to measure whether the defects have a significantly large enough mean with $p<0.005$.

$$\text{Mean frequency of occurrence } \overline{X} = \sum_{i=1}^{5} i \times n_i \Big/ \sum_{i=1}^{5} n_i \qquad (1)$$

Where, i = frequency rating and n_i = number of responses for i-th rating

3 RESULTS AND DISCUSSION

3.1 General Observation

Most of the commercial buildings in Singapore are accessible by elevator.. Geared traction elevators are used generally up to 20 storeys, while gearless express type is common for taller buildings. Misuse and vandalism such as banging on door, repeated pressing of buttons, littering and forceful opening of lobby door were observed, in lift lobby and car interior. These are accessible to users. Most of the system related defects were attributed to poor installation quality or mishandling during maintenance which could have been prevented by cleaning and proper lubrication of machinery.. Causes of defects were grouped into: (1) design-specification (D); (2) construction-installation (C) and (3) maintenance (M).

3.2 Survey Results

The summary of survey results illustrating the prevalent defects and their significance is presented in Tables 1 – 5. A total of 114 defects related to five major components of vertical transportation system were identified, out of which 28 were found serious and among those 11 were referred by FMs as frequent and 14 occurs in two or more categories. Economy, system performance, and safety & comfort were affected by 14, 14 and 9 defects respectively. Few defects which are not significant but contribute to overall maintainability were captured by three generic categories, namely, design, construction and maintenance. As an example, defects in hoistway are discussed in details

Table 1. Significance of defects in machine room

Sub-comp.	*Defects in machine room*	*Cause*			$\overline{X}_{FR}$	$\overline{X}_{EC}$	$\overline{X}_{SP}$	$\overline{X}_{SC}$
Significant defects (7 nos.)								
Controller	(1) Lift jam (stalled car)			M		2.62	3.10	3.15
	(2) Uncomfortable motion / jerky landing		C	M	2.29		2.80	3.15
	(3) Long waiting time (>30sec)	D		M	2.28			
Governor Machine	(4) Vibration during travel due to governor rope worn/ uneven tension/ not strong	D		M			2.90	
	(5) Intermittent fault difficult to detect`	D	C	M		2.65		
---	(6) Poor workmanship. E.g. Brake rod not secured to plate / uneven		C		2.51			
---	(7) Mishandling. E.g. under / over lubrication			M		3.08		
Other defects (30 nos.)								
Machine Room	(1) Dirty with rubbish, carbon dust, lubricant; (2) Insufficient lighting (<200 lux at floor level); (3) Water seepage through wall / ceiling; (4) Overheated (>38°C) machines in stuffy room; (5) Inadequate clearance around machines & control panel							
Controller	(6) Transformer noisy / dirty; Inverter cooling fan dirty / dusty, (7) Intermittent faults/ fire from overused/ burnt resistor, (8) Noisy bearing; (9) Dirty machine with leaking cover/ oil seal							
Traction machine	(10) Oil level is too low or high; (11) Oil level gauge blurred / faulty; (12) Faulty brake; (13) Noise and vibration by worn out, dry secondary sheave bearing/ groove; (14) Machine bed isolation rubber worn; (15) Main rope worn; (16) Carbon brush holder loose/ damaged							
Tractn. motor	(17) Bearing noisy; (18) Overheated motor, (19) Cooling fan dirty / noisy							
Brake assembly	(20) Vibration and jerky emergency stops; (21) Brake drum scratched, burnt lining; (22) Incorrect clearance of plunger stroke; (23) Brake rod is not secured to plate; (24) Brake lever uneven; (25) Brake slips excessively for emergency stop; (26) Brake shaft collar clearance out/ screw loose; (27) Levers jammed/ slippery							
Governor Machine	(28) Noisy operation; (29) Oily / dirty machine							
---	(30 Faulty design. E.g. less clearance, long waiting							

Table 2. Significance of defects in lift hoistway

Sub-comp.	*Defects in hoistway*	*Cause*			$\overline{X}_{FR}$	$\overline{X}_{EC}$	$\overline{X}_{SP}$	$\overline{X}_{SC}$
Significant defects (7 nos.)								
Guide rail	(1) Noisy vibration due to excess movement in guide / roller shoe over slippery rail			M	2.00			
Wire rope	(2) Wrong tension in rope causes wear & tear		C	M				1.82
	(3) High vibration. car hitting at top or bottom	D			1.84	2.71		2.59
	(4) Corrosion of rope	D	C				2.60	
---	(5) Faulty design. E.g. Limit switch v. close to governor rope (over conservative design)	D						2.06
---	(6) Poor workmanship. E.g. Rope socket is slanted or with bullock-clip in the wrong position causes wrong tension in wire rope		C		2.52	2.44	2.75	
---	(7) Mishandling. E.g. Oil spillage			M		3.08	2.74	
Other defects (6 nos.)								
Governor	(1) Updown switch roller jammed/ misaligned; (2) Limit switch & gov. rope too close							
Guide rail	(3) Separator beam, rail bracket dirty with rubbish; (4) Slippery by oil spillage							
Shaft	(5) Not covered by hatch; (6) Water seepage							

Table 3. Significance of defects in lift car

Sub-comp.	*Defects in lift car*	*Cause*		$\overline{X}_{FR}$	$\overline{X}_{EC}$	$\overline{X}_{SP}$	$\overline{X}_{SC}$
Significant defects (6 nos.)							
Car Interior	(1) Wear and tear with time: discolouration, dents, , worn flooring, worn off buttons, missing / blurred message /certificate plate	D	M	4.73	3.23		
Car Door	(2) Door jam/ stuck		M		3.55	4.08	
	(3) Repeated opening and closing		M			4.17	
	(4) Incomplete opening and closing		M		3.51	3.74	
	(5) Door closing on moving users as PE eyes or multi beams not aligned to detect movement	C	M				3.93
---	(6) Design specification sensitive to vandalism. E.g. Car operating panel (COP) dirty/ delaminated/ with buttons which are loose / jammed / without light / unable to register call. Easy opening of emergency exit at top	D		4.46			
Other defects (34 nos.)							
Car Top	(1) car top rope socket wrongly placed/ slanted / hitting; (2) Misfit rope wedge; (3) Excessive movement in car guide roller shoe; (4) Safety gear/linkage oily& dirty or dry & noisy; (5) Low overhead without warning sign; (6) Dirty with debris, lubricant						
Car Bottom	(7) Overload switch / cell jammed; (9) Compensation cable not firmly secured; (10) Safety gear jammed/ missing parts/ inadequate clearance; (11) Travelling cable not firmly secured; (12) Lower surface is dirty with cobwebs; (13) Excessive movement of guide shoes / roller						
Car Interior	(14) Dirty / damaged light diffuser; (15) loose /noisy false ceiling, noisy fan; 16) Architectural finishes hindering maintenance.						
Car Door	(17) Banging; (18) Linkages worn; (19) Door shoe is worn/ inaccurate clearance / loose; (20) Door sill is bulging; (21) Speed mismatch with lobby door (time lag); (23) Door jamb loose / rusty / stopper missing; (24) Car safety shoes hitting / noisy						
Door operator	(25) Door motor is slanted or causing vibration; (26) Door motor belt tension loose / worn; (27) Door motor chain/ sprocket/ wheel is loose / worn out and dry; (28) Faulty micro switch is unable to prevent door opening within unlocking zone; (29) Faulty mechanical lock; (30) Car door bar / hanger roller is dirty/ worn / rusty						
Travelling	(31) Lift levelling with landing > 5mm; (32) Jerk, vibration, noise						
---	(33) Poor workmanship. E.g. Loosely fitted false ceiling						
---	(34) Mishandling. E.g. damaged micro switch.						

Table 4. Significance of defects in lift pit

Sub-comp.	*Defects in pit*	*Cause*		$\overline{X}_{FR}$	$\overline{X}_{EC}$	$\overline{X}_{SP}$	$\overline{X}_{SC}$
Significant defects (3 nos.)							
----	(1) Dirty with rubbish or lubricant		M	3.42		3.10	3.40
	(2) Compensation cable/ sheaves misaligned	D	C		2.84		3.43
	(3) Noisy compensation cable		M	1.62	2.75	2.79	
Other defects (1 no.)							
----	(1) Damaged switch / light						

Table 5. Significance of defects in lift landing

Sub-comp.	*Defects in landing*	*Cause*	$\overline{X}_{FR}$	$\overline{X}_{EC}$	$\overline{X}_{SP}$	$\overline{X}_{SC}$
Significant defects (5 nos.)						
Landing door	(1) Rubbing/ large gap (> 10mm) in panel	D C M			3.28	3.68
	(2) Catch device roller worn/ hitting/clearance out	D M		2.78		
Lift Landing	(3) Hall button damaged/ no light/ loose/ jam	D M	4.18	3.08		
---	(4) Poor workmanship. E.g. misaligned door roller wears easily	C			2.75	
---	(5) Mishandling. E.g. jammed mechanic's access switch by forceful use of other key	M		3.08	2.74	
Other defects (8 nos.)						
Landing door	(1) Closing on moving users / no self-closing; (2) Door roller worn/ rusty/ clearance out/jammed; (3) Weight wire pipe damaged/ missing/ loose; (4) Lock contact worn / clearance out; (5) Shoe worn / clearance out; (6) Missing /damaged rubber stopper					
Smoke detector	(7) Missing/ damaged detector unable to stop lift reaching the fire floor					
---	(8) Faulty design. E.g. Sensitive finishes used in lobby with heavy use, inferior make of lock, clutch shoe wear off easily					

3.3 Discussion

For four sub-components of hoistway, a total of 13 common defects were identified from the first phase of data collection, among which seven were found to be significant for their impacts (Table 2). Excessive noise and vibration in guide rail during lift travel was found to be a frequent issue due to excess movement in guide or roller shoe. Careless maintenance is not only responsible for oil spillage during lubrication but also for wrong size of roller shoe. As mentioned earlier, elevators are manufactured under stringent ISO certification, it can be realized that misfit shoe is a result of replacement, not a manufacturing defect. This same logic is equally applicable to misaligned socket or improper wedge size causing wrong tension in rope. Overloading can be considered as an example of misuse rather than inadequate design consideration in this case. Vibration in hoisting rope was reported to occur quite often, but more than being frequent it has major implication on economy and comfort. The distress caused to users actually results in complaints and costly callbacks. Ropes get corroded due to undue stress and water seepage through hoistway. Both have the root cause of poor workmanship either during installation of lift or construction of lift shaft. All of these four significant defects mentioned had poor workmanship as common cause. This fact was further illustrated by the fact that it was graded as the most frequent defect. It is in agreement with the general understanding that quality control at site is not as strict as of factory. As a result the systems performance is highly affected since commissioning incurring higher maintenance cost. Limit switch too close to governor rope was an example of over conservative design. It creates uncomfortable emergency stops. Wrong maintenance practices such as oil spillage during lubrication or misalignment of machine parts was observed to affect system performance seriously, and have highest impact on cost.

From the present study, it was established that among many defects in vertical transport system, most of the defects can be prevented by considering three major maintainability criteria, namely, design and specification, construction or installation, and operation & maintenance (O&M). Few defects may have more than one cause. It is important to know at which stage what are the defects arise so that the appropriate preventive measures can be taken to improve the maintainability. It was found that among 28 significant defects, 12 were design related, 10 were due to faulty installation or poor construction quality and inadequate O&M practises were responsible for 19 defects. The maintenance quality was largely subjective with regard to cleanliness and lubrication.

3 CONCLUSIONS

The study had identified 28 persistent defects out of total 114 defects commonly occurring in five major components of vertical transportation system. Mishandling of components during regular maintenance including improper lubrication and inadequate cleaning was detected as the most common cause for majority of the defects. From the analysis based on feedback provided by 40 experienced FMs regarding: (1) frequency of occurrence of various defects and (2) seriousness of the defects in terms of their adverse effect on economy, system performance and users' safety & comfort, it was established that the most important contributing factors for maintainability is good maintenance, next comes good design and material specification, followed by workmanship during construction or installation. This comprehensive defect analysis was aimed to help the designers, contractors and facility managers to realize the long term effect of their decisions made and form the basis of an enhanced maintainability to promote good practices for efficient and safe functioning of highly maintainable vertical transportation system. Further, this may provide a simple guideline for FM to achieve and as well as owner to enjoy lower life cycle maintenance cost of building services. This generic research method can be applicable for any other building services.

REFERENCES

Barney, G.C. (ed). 1986, *Elevator Technology*, Ellis Horwood, NY.

Heerwagen, D. 2004, *Passive and Active Environmental Controls: Informing the Schematic Designing of Buildings*. The McGraw-Hill Companies, NY.

McCann, M. 2004, *Deaths and Injuries Involving Elevators or Escalators*, The Center to Protect Workers' Rights, Research Paper, Silver Spring, March.

McKain, J. 1999, *Elevator Maintenance Manual*, Elevator World Inc., Mobile, AL.

NEII: National Elevator Industry, Inc. 2007, *Building Transportation Standards and Guidelines*, Part 7: Maintenance guidelines, Author, Salem, NY.

O'Donoghue, J. & Jarboe, T. 2007, *Elevator & Escalator Rescue: A Comp. Guide*, Penwell, Tulsa.

SAC: Singapore Accreditation Council. 2000, *CP 2: 2000*: Code of practice for installation, operation and maintenance of electric passenger and goods lift, SPRING, Singapore.

Schloss, R.D. 1998, 'Elevator & escalator equipment & systems maintenance and repair services", in *Facility Manager's Operatn. & Maintenance Handbook*, ed B. Lewis, McGraw-Hill, NY, pp.15.1-41.

Staal, J, & Quackenbush, J. 1998, 'Elevators, escalators and hoists', in *Encyclopaedia of Occupational Health and Safety, 4th Edition*, eds J.M. Stellman, International Labour Office, Geneva, Volume III, chapter 93, pp. 40-44.

Strakosch, G.R. 1998, *The Vertical Transportation Handbook, 3rd Edition*. Wiley, NY.

Vlahovic, C.E. 1990, 'Rationale for New Rules in CSA-B44 Safety Code for Elevators', in *Elevator World Educational Package and Reference Library*, eds Elevator World Educational Division, Elevator World Inc., Mobile, AL, Volume III, pp. 66-72.

APPENDIX A: Sample questionnaire for defects in hoistway

DEFECTS FOR ELEVATOR HOISTWAY			**Grading for Frequency**	**Grading for Impacts**		
Sub-component	**Description of defect**	**Probable Causes of the Defect**	**1= Rare 2= Sometimes 3= Quite often 4= Very often 5= Always**	**1=Nil 2= Slight 3=Moderate 4=Serious 5=Very serious**		
				Econ	**Sys**	**Sfty.**
Governor	Up-down switch roller jammed/ worn/ misaligned [M]	−Intermittent fault due to circuit breaks −Dust / dirt deposit into the hoist way				
	Limit switch too close to governor rope [D]	−Wrong selection of design factor				
Guide rail	Noisy vibration due to excess movement in guide / roller shoe [M]	−Guide / roller shoe of the wrong size −Slippery rail due to oil spillage during lubrication				
	Separator beam, rail bracket dirty with rubbish [M]	−Vandalism (rubbish thrown by users) −No cleaning after regular maintenance				
	Slippery by oil spillage [M]	−Careless lubrication				
Shaft	Not covered by hatch [M]	−Removal of cover during careless maintenance				
	Water seepage [C]	−Poor workmanship of building structure				
Hoisting rope	Excessive vibration / car hitting at top or bottom [D]	−Overloading of car −Wrong tension in rope if 3-fold instead of 4-folds				
	Wrong tension in wire rope causes wear & tear [C, M]	−Overloading of car −Rope socket is slanted / hitting / socket bullock-clip is in the wrong position −Wedge of wrong size				
	Corrosion of rope [D, C]	−Stress corrosion, hoistway not dry,				
-----	Design defects [D]	−Faulty design or poor specification				
-----	Construction defects [C]	−Poor workmanship during installation				
-----	Maintenance defects [M]	−Mishandling during careless maintenance				

[D] Defect caused by poor design or material specification
[C] Defect caused by poor workmanship during construction / installation
[M] Defect caused by inadequate or careless maintenance

Optimal Maintenance Plan by Minimizing Life-cycle Cost Including Deterioration Risk

Chien-Kuo Chiu [1]
Takafumi Noguchi [2]
Manabu Kanematsu [3]
Hironori Nagai [4]

T 72

ABSTRACT

This paper shows deterioration models due to carbonation in consideration of uncertainty to estimate the initiation and the rate of corrosion, and to analyze the structural capacity and serviceability of RC members, i.e. shear capacity, bending strength and width of severe spalling/cracking of columns or beams with corroded reinforcing bars based on simple formulas formed through the past experiments.

Then, the failure and severe spalling/cracking probability during earthquakes and the deterioration risk of members in specified years from construction could be evaluated by this method proposed in this paper.

In addition, by applying immune algorithm to minimization of life-cycle cost including the deterioration risk, the optimal maintenance plan and semi-optimal solutions with high diversity of reinforced concrete members could also be found in a single analysis and a case study is finally conducted to prove the effectiveness of this system.

KEYWORDS

Deterioration Risk, Immune Algorithm, Life-cycle Cost, Failure, Spalling/cracking

[1] The University of Tokyo, Department of Architecture, Graduate School of Engineering, Tokyo, Japan 113-8656, Phone +81 3 5841-6202, Fax +81 3 5841-6202, ckchiu@bme.arch.t.u-tokyo.ac.jp
[2] The University of Tokyo, Department of Architecture, Graduate School of Engineering, Tokyo, Japan 113-8656, Phone +81 3 5841-6202, Fax +81 3 5841-6202, noguchi@bme.arch.t.u-tokyo.ac.jp
[3] Tokyo University of Science, Department of Architecture, Faculty of Science and Technology, Chiba, Japan 278-8501, Phone +81 4 7122-9470, Fax +81 4 7124-1669, manabu@rs.noda.tus.ac.jp
[4] The University of Tokyo, Department of Architecture, Graduate School of Engineering, Tokyo, Japan 113-8656, Phone +81 3 5841-6202, Fax +81 3 5841-6202, nagai@bme.arch.t.u-tokyo.ac.jp

1 INTRODUCTION

Generally, structural members, beams, or columns whose reinforcing steel components are corroded by carbonation or chloride attack are appropriately repaired/retrofitted after investigating the cause of corrosion. However, few studies discuss how an optimal maintenance plan can be envisaged beforehand to minimize the life-cycle cost (LCC) of a structure, including the deterioration risk caused by earthquakes. Therefore, there is a need for a system that can be used to determine a maintenance strategy to minimize the LCC in terms of structural capacity and serviceability. In this paper, we describe a system that can estimate the LCC, including the deterioration risk (induced by carbonation), of an RC beam or column resulting from failure and severe spalling/cracking during earthquakes (Fig.1). In addition, we analyze the ability of an immune algorithm (IA) capable of searching for semi-optimal solutions with high diversity to find the optimal maintenance plan.

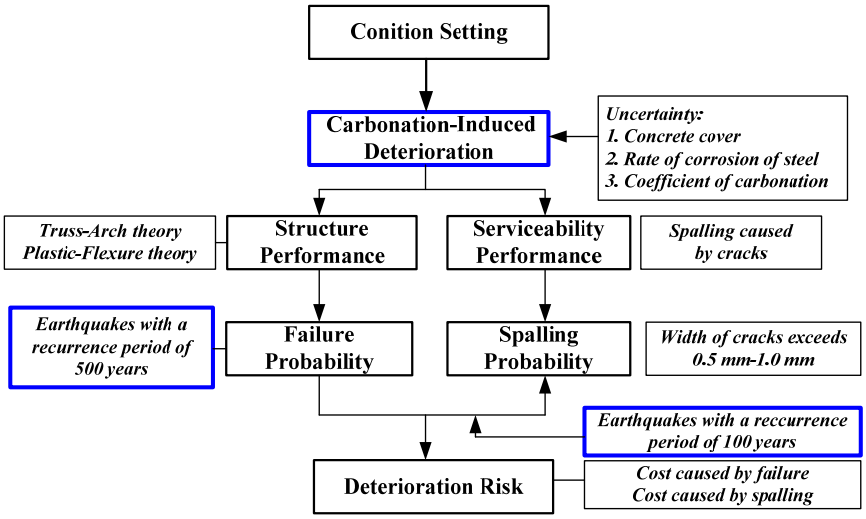

Figure 1. Flowchart depicting how deterioration risk induced by carbonation is evaluated

2 EVALUATION OF DETERIORATION RISK AND LCC

2.1 Deterioration Model

2.1.1 Carbonation

In this paper, the process of corrosion of the reinforcing steel due to carbonation is modeled on the basis of a previous research [Seiichi & Toyoaki 2004].

2.1.1.1 Initiation stage. This stage is defined as the time period required for corrosion to begin. Under steady hygrometric conditions, the depth of carbonation increases in proportion to the square root of time; therefore, the depth of carbonation, C, can be expressed in millimeters as follows:

$$C = A\sqrt{t} \quad \text{.....(1)}$$

where A = carbonation coefficient in mm/year$^{0.5}$, and t = time of exposure in years.

Based on previous investigations, when the carbonation front reaches the surface of the steel, it can be assumed that corrosion has been initiated [AIJ 2004]. This paper considers the uncertainties with regard to the carbonation coefficient and concrete cover induced by the environment or construction conditions to calculate by using Monte Carlo simulation the probability that the corrosion of the outermost reinforcing steel layer has been initiated. In the simulation, corrosion is considered to have occurred when the probability of corrosion initiation exceeds 10%. In the probabilistic analysis, the carbonation coefficient and concrete cover are treated as lognormal random variables with coefficients of variation of 45% [Taichiro *et al.* 2006] and 20% [Yoshitaka & Taketo 2005], respectively.

2.1.1.2 Propagation stage and former period of acceleration stage. The propagation stage is defined as the period from corrosion initiation to cracking initiation of the concrete surface. The former period of the acceleration stage is defined as the period from crack initiation to spalling initiation of the concrete surface. Based on a model developed previously [Seiichi & Toyoaki 2004], the rate of corrosion in these two stages is assumed to be same, and this rate is treated as a lognormal random variable with a mean equal to 0.06%/year (percentage weight loss) [Seiichi & Toyoaki 2004] and a coefficient of variation of 50% [Toshiaki et al. 2005].

2.1.1.3 Latter period of acceleration stage. In the latter period of the acceleration stage, the concrete surface spalls severely so that the concrete cover is almost unable to prevent the steel from corroding. In this paper, the latter period is characterized by severe spalling, which is regarded as an increase in the crack width in excess of 1.0 mm; the corrosion in a 1.0 mm crack can be quantified as follows:

$$w_c = 0.141 \exp(1.078d/\varphi) \times x \quad \ldots\ldots(2)$$

$$r = \frac{400 w_c}{\rho_s \varphi_o} \quad \ldots\ldots(3)$$

where w_c = corrosion of steel in mg/mm^2; x = crack width in millimeters; d = concrete cover in millimeters; φ = diameter of steel in millimeters; φ_o = diameter of steel without corrosion in millimeters; ρ_s = density of steel in mg/mm^3 (7.85 mg/mm^3); and r = corrosion of steel in percentage weight loss (%).

Based on previous researches [Seiichi & Toyoaki 2004, Toshiaki *et al.* 2005], the rate of corrosion at this stage is equal to the rate of corrosion of steel without any concrete cover and is treated as a lognormal random variable with a mean equal to 0.14%/year (percentage weight loss) and coefficient of variation of 50%.

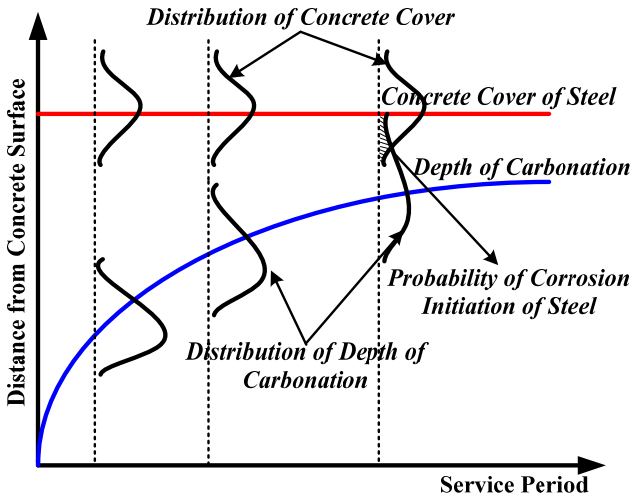

Figure 2. Evaluation of the probabilityof corrosion initiation

2.1.1.4 Carbonation suppressive effect of finishing. Because finishing can prevent the concrete surface from coming into contact with CO_2, it could also suppress carbonation. In this paper, if the material of finishing is composed of cement, the depth of carbonation can be estimated as shown in Eq.4 based on the concept of an equivalent concrete cover [AIJ 2004].

$$C = A\sqrt{t} - M_{eq} \quad \ldots\ldots(4)$$

where M_{eq} = equivalent concrete cover in relation to the thickness of finishing in millimeters.

If the material of finishing is made up of a polymer mixture, we must use Eq.5, which includes a material aging factor dependant on ultraviolet radiation, rain, and wind, to estimate the depth of carbonation [AIJ 2004].

$$C = A(\sqrt{t + R^2} - R) \quad \ldots\ldots(5)$$

where R = resistance of carbonation in relation to year and the coating thickness in year$^{0.5}$.

2.2 Probability of Failure and Spalling

2.2.1 Capacity degradation of beam and column

2.2.1.1 Shear and flexure capacity. In this paper, two major causes of the reduction in capacity due to corrosion are considered. The first cause is the degradation of the yield stress of the reinforcing steel. In the case of general corrosion, the yield stress of reinforcing steel can be estimated as [JCI 1998]

$$\sigma_y = \sigma_{yo}(1 - 2.17r / 100) \quad \ldots\ldots(6)$$

where σ_{yo} = yield stress of reinforcing steel without corrosion and r = corrosion of steel in percentage weight loss (%).

The second cause is the degradation of the ultimate bond stress of the reinforcing steel and concrete, and it can be estimated as [JCI 1998]

$$\tau_{bu} = \tau_{bo} \times exp(-0.0607r) \quad \ldots\ldots(7)$$

where τ_{bo} = ultimate bond stress without corrosion.

The shear capacity of an RC beam or column in the case of bonding failure or stirrup yielding induced by corrosion can be estimated by a previously developed model [Chien-Kuo *et al.* 2007], which in turn is based on the truss-arch theory associated with Eq.(6) and Eq.(7). The flexure capacity can be estimated by the plastic flexure theory associated with Euler-Bernoulli beam theory and Eq.(6) [Chien-Kuo *et al.* 2007].

2.2.1.2 Shear demand. The shear demand of an earthquake with a recurrence period of 500 years is defined as the shear force caused by an earthquake and the vertical loading , Q_{DS}.

$$Q_{DS} = Q_L + \alpha \times Q_E \quad \ldots\ldots(8)$$

where Q_L = shear force caused by vertical loading; Q_E = shear force caused by the earthquake; and α = an additional factor.

2.2.2 Structure performance and failure probability

Using the capacity and the shear demand of an RC beam or column obtained based on 2.2.1, the shear performance index, D_V , and the flexure performance index, D_M, are defined as follows:

$$D_V = \frac{min(V_{bu}, V_u)}{Q_{DS}} \quad \ldots\ldots(9)$$

$$D_M = \frac{2M_u / L}{Q_{DS}} \quad \ldots\ldots(10)$$

where L = length of beam or column. If $D_V \leq 1.0$, shear failure is implied. If $D_M \leq 1.0$, flexure failure is implied.

Clearly, D_V and D_M decrease and approach the value of the limit (equal to 1.0) with the passage of time, as illustrated in Fig.4. In this paper, the rate of corrosion of reinforcing steel is treated as a random variable and Monte Carlo simulation is used to calculate the distributions of D_V and D_M. Then, the area of the distribution below the limit value can be evaluated and defined in terms of the shear failure probability, P_V, and flexure failure probability, P_M, respectively.

2.2.3 Serviceability performance and spalling probability

It is generally perceived that the serviceability performance of RC structures is affected when spalling is caused with the formation of a crack with a width in excess of 0.5–1.0 mm [Dimitri V. & Mark G. 2003]. The limit quantity of corrosion resulting in spalling can be estimated by Eq.(2) and Eq.(3). Therefore, when the quantity of corrosion of the outermost reinforcing steel component in the RC beam or column exceeds the limit quantity, spalling can be assumed to occur on the surface of the concrete. Monte Carlo simulation is used to evaluate the spalling probability, P_S, similar to how it was used in the case explained in 2.2.2. When an earthquake with a recurrence period of 100 years occurs, it is reasonable to expect that a higher spalling probability caused by carbonation would lead to a higher expected cost of serviceability failure.

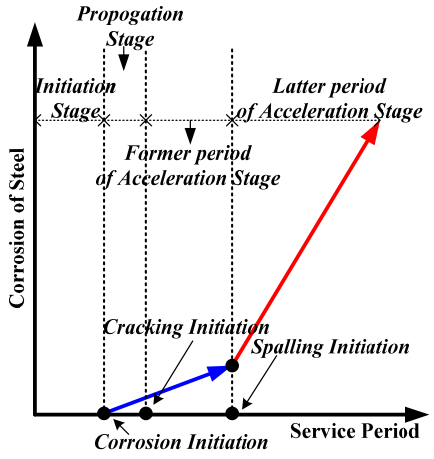

Figure 3. Stages of deterioration caused by carbonation

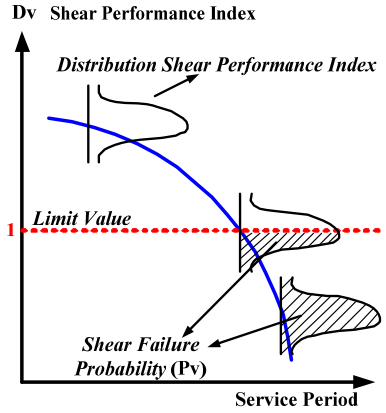

Figure 4. Definition of shear failure probability

2.3 Deterioration Risk and Life-cycle Cost

2.3.1 Deterioration risk of service period

In this paper, the deterioration risk of a specified service period, E, is estimated as

$$E = \int_0^T \frac{1}{(1+k)^t} \times (C_f \times (P_M + P_V) \times v_f + C_s \times P_s \times v_s) dt \quad \ldots\ldots (11)$$

where C_f = cost of failure; C_s = cost of severe spalling/cracking; v_f = annual probability of an earthquake with a recurrence period of 500 years (if a Poisson distribution is assumed, 0.2%); v_s = annual probability of an earthquake with a recurrence period of 100 years (if a Poisson distribution assumed, 1%); T = specified service period; k = discount rate.

2.3.2 Life-cycle cost

Besides the deterioration risk stated in 2.3.1, the construction cost, retrofitting cost, and repair cost must also be considered. Therefore, the LCC, C_T, is defined as

$$C_T = C_I + \Sigma(C_{Rep} \times \frac{1}{(1+k)^{t_{Rep}}}) + \Sigma(C_{Ret} \times \frac{1}{(1+k)^{t_{Ret}}}) + E \quad (12)$$

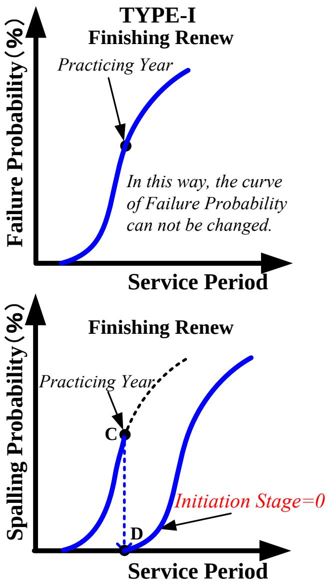

Figure 5. Setting of repair/retrofit

where C_I = construction cost; C_{Rep} = repair cost; C_{Ret} = retrofitting cost; t_{Rep} = year of repair; t_{Ret} = year of retrofitting.

2.4 Maintenance Strategy

The selection of repair/retrofit techniques significantly affects the lifetime performance of an RC beam or column. In this paper, three repair/retrofit techniques are considered. Moreover, in order to improve the computing efficiency of the immune algorithm to find the optimal maintenance plan, the model illustrated in Fig.5 is used to directly reflect the effect of the maintenance strategy on the failure probability and spalling probability.

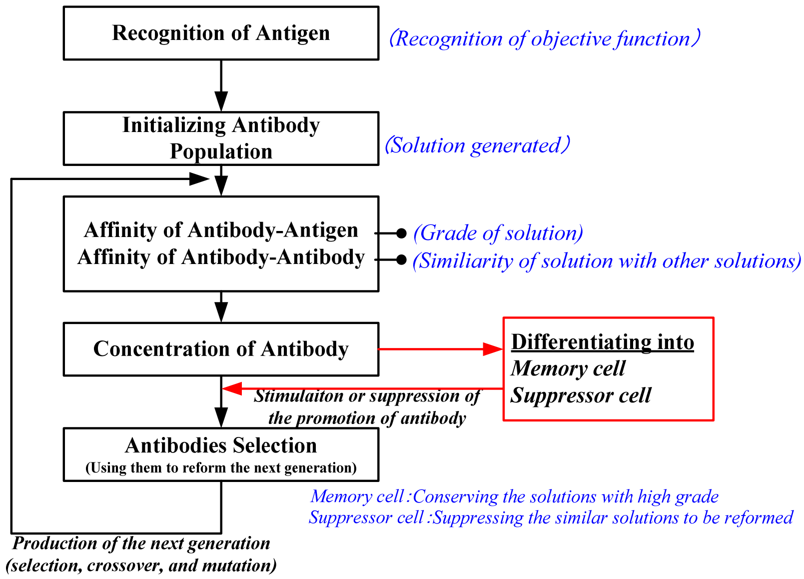

Figure 6. Flowchart showing computing procedure in IA

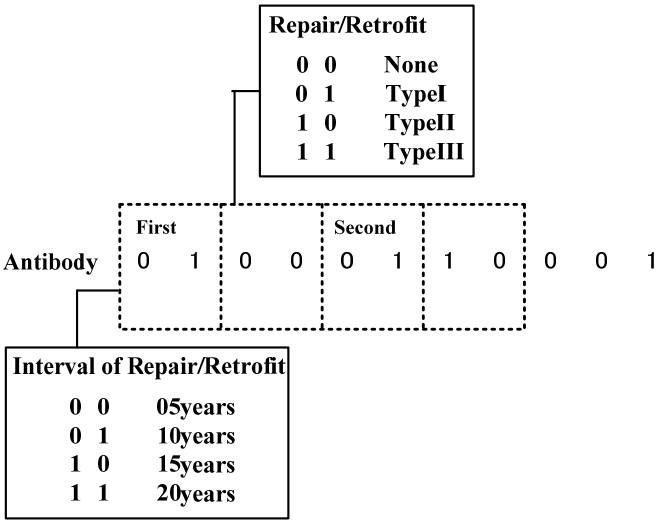

Figure 7. Code of an antibody

3 IMMUNE ALGORITHM

The immune algorithm [Toshio *et al.* 2005], which emulates the biological immune system, is mainly composed of the genetic algorithm (GA), which is used to reform solutions/antibodies of the next generation, memory cells, which are used to conserve higher-affinity solutions/antibodies, and suppressor cells (T-cells), which are used to suppress the re-seeking of higher-affinity solutions conserved in memory cells, and proposed to solve optimization problems.

3.1 Computing Procedure

[Step 1] Recognition of antigen. Antigens and antibodies correspond to objective functions and associated feasible solutions. In this algorithm, memory cells are used to conserve higher-affinity solutions/antibodies, which can be regarded as a set of feasible solutions. In addition, objective/antigen and solutions/antibodies are defined as LCC (C_T) and maintenance plans of an RC beam or column in this research, respectively.

[Step 2] Randomly initialized antibody population. Similar to the GA developed by Manabu [Manabu & Takafumi 2001], the initial population of antibodies utilizing a multi-variable binary-code string is generated randomly. In this paper, four bits are used to express one repair/retrofit work including the method (2 bits, 2^2 kinds) and time (2 bits, 2^2 kinds) this method was planned, as illustrated in Fig.7. Further, each maintenance plan has a maximum of ten repair/retrofit works; therefore, 40 bits are built in one antibody.

[Step 3] Calculating affinity of antibody-antigen or antibody-antibody. In this paper, the inverse of the LCC is used to express the affinity of the antibody v and the antigen, as shown in Eq.(13). Clearly, the greater the affinity, the lower is the LCC caused by the antibody v and its higher grade.

$$\Phi_v = \frac{1}{C_T} \quad \text{.....(13)}$$

The affinity Ψ_{vw} between antibodies v and w is defined as the ratio of the similarity of binary code strings in them. Note that $0 \le \Psi_{vw} \le 1$, and when $\Psi_{vw} = 1$, the antibodies v and w are identical.

[Step 4] Calculating concentration of antibody. The concentration Θ_v is used to express the similarity of the antibody v with other antibodies, as shown in Eq.(14)

$$\Theta_v = \frac{1}{N}\sum_{\omega=1}^{N}\pi_{v\omega} \quad \text{.....(14)}$$

where N = the number of antibodies. If $\Psi_{vw} \geq T_{\pi 1}$, $\pi_{vw} = 1$; otherwise, $\pi_{vw} = 0$; $T_{\pi 1}$ = user-defined threshold value that illustrates the allowable difference between two antibodies.

In this algorithm, as the concentration increases, the higher probability is selected as the memory cell and suppressor cell.

[Step 5] Antibody differentiation into memory and suppressor cells. If the concentration Θ_v of the antibody v exceeds the user-defined threshold value T_{II}, the antibody v becomes a candidate memory cell. Then, candidate memory cells are chosen for differentiation into a pool of memory cells in the order of the affinity of antibody-antigen and into a pool of suppressor cells in the order of the concentration.

[Step 6] Stimulation or suppression of antibody promotion. In this paper, we use the affinity of the antibody-suppressor cell, Ψ_{sv}, to suppress the creation of similar antibodies. Therefore, if Ψ_{sv} exceeds the user-defined threshold value T_S, the antibody will be eliminated. In addition, in order to add and maintain the diversity of the next generation of antibodies, those antibodies that have a high expected value based on Eq.(15) are chosen to create the next generation by the GA method (including selection, crossover, and mutation).

$$E_v = \Phi_v \prod_{s=1}^{S}(1-\Xi_{vs}) \quad \text{.....(15)}$$

where S = number of suppressor cells. If $\Psi_{vw} \geq T_{\pi 2}$, $\Xi_{vw} = \Psi_{vw}$; otherwise, $\Xi_{vw} = 0$.

3.2 Diversity of Solution/Antibody [Toshio *et al.* 2005]

In this paper, we use the concept of entropy to estimate the diversity of a solution/antibody. First, the diversity of the locus j of an antibody in the same generation $H_j(N)$ can be expressed as shown in Eq.(16). Then, the average value of $H_j(N)$ is estimated by Eq.(17) to represent the diversity of the generation. It could be said that the higher the $H(N)$, the higher is the diversity.

$$H_j(N) = -\sum_{i=1}^{L} p_{ij} \log p_{ij} \quad \text{.....(16)}$$

$$H(N) = \frac{1}{G}\sum_{j=1}^{G} H_j(N) \quad \text{.....(17)}$$

where N = number of antibodies in one generation; G = number of loci in one antibody; L = number of symbols in one locus; p_{ij} = probability of the symbol i appearing in the locus j.

4 CASE STUDY

The optimal maintenance plan for the columns (outside column) [details in Chien-Kuo *et al.* 2007] coated with mortar (Coating-1) and those coated with resin (Coating-2) on the first and sixth floors of a twelve-story RC building are analyzed by the method proposed in this research to prove its suitability. The parameters required for the analysis are listed in Table 1, Table 2 [June & Haresh 1997, Mark G. & Dimitri V. 2003], and Table 3.

The LCC, failure probability, and spalling probability of the columns without maintenance are illustrated in Fig.8. According to the results, when the same finishing material is used, the spalling probability curve of the column does not change with the floor considered. However, because a higher floor has a lower shear demand, the failure probability of the column on the sixth floor is smaller than

that on the first floor. Moreover, we observe the same phenomenon with regard to the LCC. The optimal maintenance plans for columns coated with resin are found by this system and illustrated in Table 4 and Fig.9. When compared with the LCC without maintenance, the optimal maintenance plans yield a definite and effective improvement, irrespective of which floor the column belongs to.

Furthermore, the diversity of the solution/antibody is used to prove the effectiveness of this system and is shown in Fig.10. In the figure, besides the diversity of the memory cell (if in GA, the best 10 are chosen) (SAH), the diversity of each generation is also expressed. With reference to the diversity of solution/antibody in one generation (SH), IA shows more intense variation than GA. Due to the high intensity variation of diversity, IA can suppress similar solutions and does not easily resort to local-solution searching. In other words, IA does not converge to one solution by the original adjustment mechanism (suppressor cells). In addition, the diversity of the memory cell increases with the generation and lasts until the end of the analysis. It also can be said that IA has the ability to research semi-optimal solutions with a high diversity in a single analysis.

Table 1. Parameters for the estimation of deterioration

Compression strength of concrete (kN/mm^2)	25
Thickness of mortar (Coating-1,mm)	20
Thickness of resin coating (Coating-2, mm)	0.05
Carbonation coefficient ($mm/year^{0.5}$)	7.57

Table 2. Parameters for the estimation of LCC

Construction cost (C_I)	1.00
Cost of failure (C_f)[Jun 1997]	20.0
Cost of severe spalling/cracking (C_s)[Mark 2003]	2.00
Finishing renewal	0.20
Finishing renewal and patch repair	0.40
Finishing renewal, patch repair, and steel supplement	0.60
Discount rate (k)	0.00

Table 3. Parameters for GA and IA

Number of antibodies	100
Number of generations	400
Selection method	Roulette and elite conservation
Crossover method	Crossover of one point with probability of 75%
Probability of mutation	0.5%
Number of memory cells (IA)	10
$T_{\pi 1}$, $T_{\pi 2}$, T_S *(IA)*	0.90
T_{Π} *(IA)*	0.65

Table 4. The optimal maintenance plan

First floor (1F)	C_T	*Maintenance plan (Year-TYPE)*
GA (Optimal)	2.30	25-II, 45-II, 70-II (minimal LCC)
IA (Optimal)	2.30	25-II, 45-II, 70-II (minimal LCC)
IA	2.34	25-II, 50-II, 70-II
IA	2.36	30-II, 55-II, 75-II
Sixth floor (6F)	C_T	*Maintenance plan (Year-TYPE)*
GA (Optimal)	2.26	35-II, 65-II (minimal LCC)
IA (Optimal)	2.26	35-II, 65-II (minimal LCC)
IA	2.34	35-II, 65-I, 75-II
IA	2.36	35-II, 65-I, 70-I

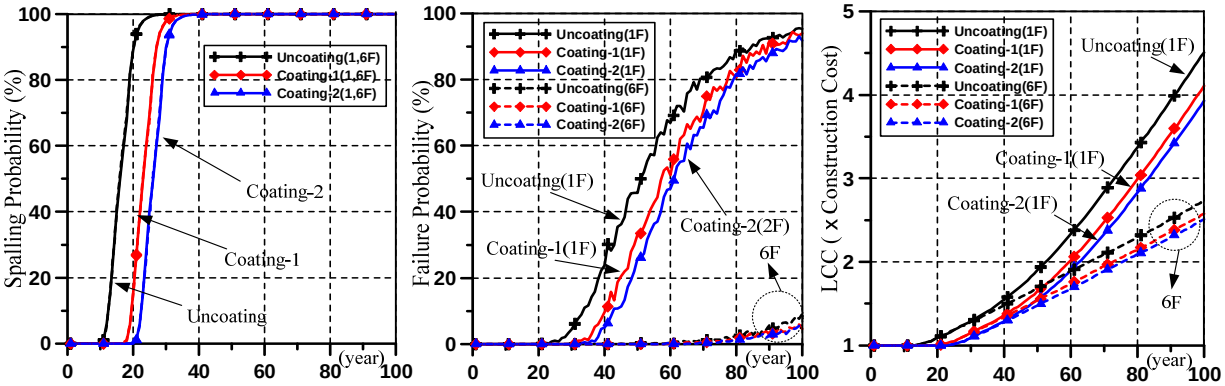

Figure 8. Spalling probability, failure probability, and LCC of the columns without maintenance

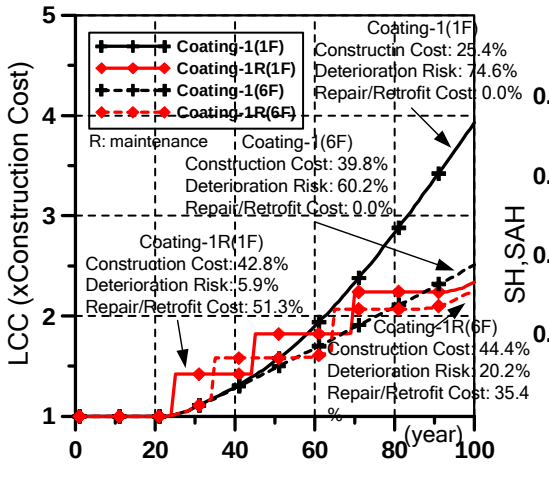

Figure 9. LCC of the columns without the optimal maintenance plan

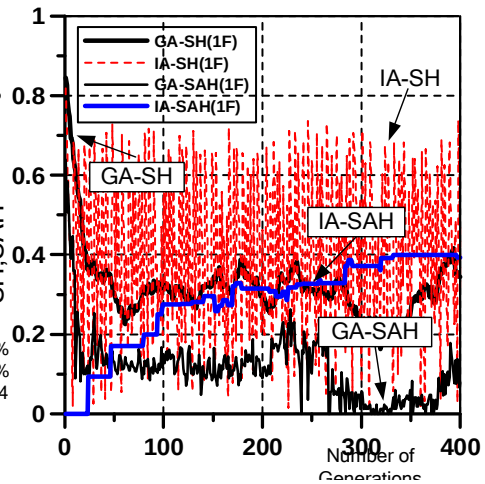

Figure 10. Diversity of generation and memory cell

5 CONCLUSIONS

In this paper, we described a system that can estimate the deterioration risk of carbonation caused by earthquakes. We also applied the immune algorithm to minimize the LCC, including the deterioration risk, and find the optimal maintenance plan for an RC beam or column. According to the results of the case study, besides the optimal maintenance plan, semi-optimal solutions with high diversity are also provided in a single analysis. In other words, the system can obtain multiple maintenance plans with high diversity, thereby allowing a user to select the suggestion he/she finds most appropriate.

REFERENCES

Seiichi T. & Toyoaki M. 2004, 'Deterioration prediction of concrete structures concerning rebar corrosion due to carbonation', *Journal of the Japan Society of Civil Engineers*, No.767, V-64, pp.35–46.

AIJ 2004, Recommendations for Durability Design and Construction Practice of Reinforced Concrete, Tokyo.

Taichiro K. & Hitoshi H. & Yoshihiro M. 2006, 'Analysis of the carbonation of concrete based on investigation of existing buildings', *Journal of Structural and Construction Engineering (AIJ)*, No.608, pp.9–14.

Yoshitaka K. & Taketo U. 2005, 'Proposal of method of selecting structure that should be inspected by priority based on repair-risk', *Concrete Research and Technology (JCI)*, Vol.16, No.2, pp.101–107.

Toshiaki T. & Michitaka S. & Hiroshi S. & Manabu M. 2005, 'Calculation of LCC and selection system of repairing method for reinforced concrete members exposed to sea environments', *Concrete Research and Technology (JCI)*, Vol.16, No.3, pp.21–29.

JCI 1998, Committee report of study on the Rehabilitation of concrete structures, Tokyo.

Chien-Kuo C. & Manabu K. & Takafumi N. & Hironori N. 2007, 'Optimization maintenance plan by minimizing life-cycle cost including deterioration risk due to chloride attack', *Journal of Structural and Construction Engineering (AIJ)*, No.616, pp.41–47.

Dimitri V. V. & Mark G. S. 2003, 'Life-cycle cost analysis of reinforced concrete structures in marine environments', *Structure Safety*, Vol.25, pp.343–362.

Toshio H. & Hiroyuki K. & Nobuyoshi T. 2005, 'Optimization of structure system by using an immune algorithm and diversity of its solution', *Journal of Structural and Construction Engineering (AIJ)*, No.588, pp.103–110.

Manabu K. & Takafumi N. 2001, 'Study on optimization method of maintenance and repair scheme by applying a genetic algorithm', *Proceedings of JCI Symposium on Evaluation and Maintenance Planning for Combined Deterioration of Concrete Structures*, pp.51–54.

Jun K. & Haresh S. 1997, 'Engineering role in failure cost evaluation for buildings', *Structure Safety*, Vol.19, No.1, pp.79–90.

Mark G. S. & Dimitri V. V. 2003, 'Multiple limit states and expected failure costs for deteriorating reinforced concrete bridges', *Journal of Bridge Engineering (ASCE)*, Vol.8, No.6, pp.405–415.

Deterioration of Reinforced Concrete Buildings and Rehabilitation Process

Nilay Coşgun [1]
E.Özlem Aydın [2]

T 72

ABSTRACT

Reinforced concrete buildings which for various reasons have completed or are about to complete their life cycle have become one of the most important issues of the decade. To demolish these buildings and to rebuild new ones that meet new requirements is one option to solve the issue. However construction and demolition waste to be generated during this process cause environmental loads. Another option is to lengthen life cycle of these buildings by appropriate repair and maintenance techniques.

For the long period re-use of the existing building stock and especially for some particular reinforced concrete buildings which reflect architectural characteristic of modern time, it is essential to achieve repair and maintenance techniques without faults and problems. In order to succeed in doing this process, identifying the nature and cause of the damage is a precondition. In this study, the deteriorations formed in reinforced concrete buildings and their causes have been explicated systematically. Current repair and maintenance techniques developed for rehabilitation have been emphasized. In this context, the stages conducted during the rehabilitation process of reinforced concrete buildings/monuments have been presented in a scheme format. The efficiency of the architects and conservators has been tried to determine during the process. The conservation of modern architectural heritage will be ensured by application of this process without fault. At the same time, reassessment of existing building stock and prevention of demolition waste will be an environmental approach.

KEYWORDS

Reinforced Concrete Buildings, Deterioration, Repair, Maintenance Techniques, Rehabilitation Process

[1] Gebze Institute of Technology, Faculty of Architecture, Gebze-Kocaeli, Turkey 41400, Phone +90 262 6051610, Fax 262 6538495, nilaycosgun@gyte.edu.tr
[2] Gebze Institute of Technology, Faculty of Architecture, Gebze-Kocaeli, Turkey 41400, Phone +90 262 6051615, Fax 262 6538495, ozlemoral@gyte.edu.tr

1 INTRODUCTION

Reinforced concrete buildings which for various reasons have completed or are about to complete their life cycle have become one of the most important issues of the decade. To demolish these buildings and to rebuild new ones that meet new requirements is one option to solve the issue. However construction and demolition waste to be generated during this process cause environmental loads. In many countries, the large volumes of construction waste strain landfill capacities and leads to environmental concerns. Another option is to lengthen life cycle of these buildings by appropriate techniques. For the long period re-use of the existing building stock and especially for some particular reinforced concrete buildings which reflect architectural characteristic of modern time, it is essential to achieve repair and maintenance techniques without faults and problems. In this context, there is a lack of methodology for the rehabilitation process of reinforced concrete buildings/monuments, which requires interdisciplinary studies (engineering, architecture, conservation).

In this study, the deteriorations formed in reinforced concrete buildings and their causes have been explicated systematically. Current repair and maintenance techniques developed for rehabilitation have been emphasized. In this context, the stages conducted during the rehabilitation process of reinforced concrete buildings/monuments have been presented in a scheme format. The efficiency of the architects and conservators has been tried to determine during the process.

2 REASONS AND DAMAGES WHICH REQUIRE THE REHABILITATION OF REINFORCED CONCRETE BUILDINGS

The term of “rehabilitation” is used in architectural field as “adaptive-reuse” and “re-functioning”. The term is also used in engineering field as a comprehensive term to include all the concepts of “repair”, “upgrading”, “retrofitting” and “strengthening” [Fukuyama & Sugano 2000]. Rehabilitation application is a more complex method both in terms of architecture and engineering compared to the construction of a new building. In order to succeed in doing the rehabilitation application without faults and problems, identifying the nature and cause of the damage is a precondition.

Apart from the human factors such as the designer, contractor and user faults manifesting through the design, decisions, selections and applications, there are various factors such as climatic, physical, chemical, biological, mechanical, and geological which directly or indirectly impact and cause damage to buildings [Gaudette *et al.* 1995; Ersoy 2004; Ekinci 2004; Ahunbay 1996; Cosgun *et al.* 2002] [Table 1].

Human factors which lead to the deterioration of buildings:

- Design failures: Disregarding user needs and environmental data during the planning and sizing of the space in the building, structural design failure caused by using the wrong or inappropriate system, and inadequate work on detail,
- Wrong material selection: Due to lack of knowledge by the designer, the contractor or the user in terms of building materials, the building materials were not of the appropriate type and standard,
- Workmanship and application faults: Inadequacy of the contractor in terms of project reading, knowledge of building materials and construction techniques,
- User faults: Ignoring the necessary maintenance and repairs, unconscious repairs,
- Lack of control: Failure to comply with the specifications, standards and regulations at the design, workmanship and application and lack of an effective audit system.

Environmental factors which lead to the deterioration of buildings:

- Climatic factors: Rain, wind, thermal differences, humidity, sun,
- Physical factors: Impact, Friction, UV rays, polluting impacts,

- Chemical factors: Oxide impact, air pollution, impact of chemical materials,
- Biological factors: Plants, insects and micro organisms,
- Mechanical factors: Vertical loads, horizontal loads such as wind and earthquake,
- Geological factors: Impact of underground water, soil structure.

Table 1. Types of deteriorations in reinforced concrete buildings and their factors

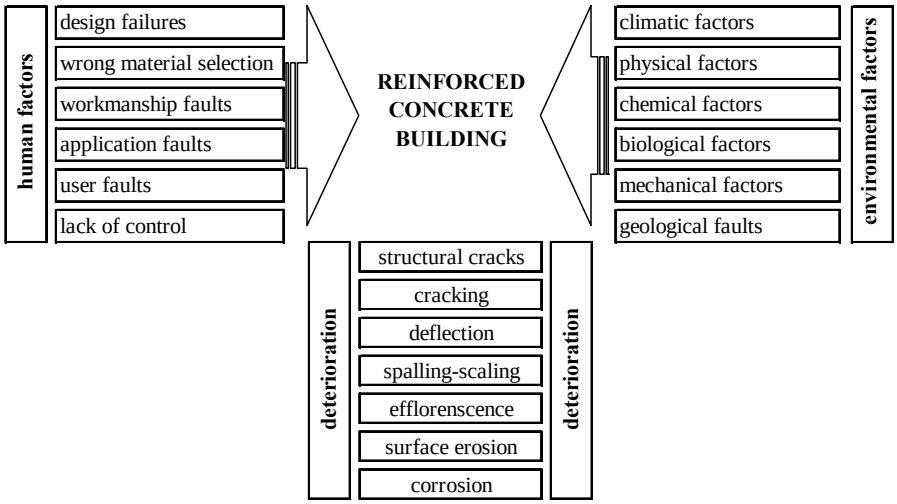

Types of damage seen in reinforced concrete buildings caused by human and environmental factors are as follows: Structural Cracks, Cracking, Deflection, Spalling, Efflorescence, Surface Erosion and Corrosion [Gaudette *et al.* 1995; Coney 2007]:

- Structural cracks can result from temporary or continued overloads, uneven foundation settling, temperature changes or design inadequacies.
- Cracking occurs over time in virtually all concrete. Sulphate attack which may come from the environment or from one or more of the concrete constituents also leads to the forces that eventually crack the concrete. Cracks vary in depth, width, direction, pattern, location.
- Deflection is the bending or sagging of concrete beams, columns, joists, or slabs, and can seriously affect both the strength and structural soundness of concrete. It can be produced by overloading, by corrosion, by inadequate construction techniques.
- Spalling is the loss of surface material in patches of varying size. It occurs when reinforcing bars corrode or water absorbed by porous aggregate freezes, thus creating high stresses within the concrete. As a result, chunks of concrete pop out from the surface. The surface weakness encourages scaling, which is spalling in thin layers.
- Efflorescence is a white, powdery stain produced by the leaching of lime from Portland cement, or by the practice of adding lime to whiten the concrete. Also stains can be produced by alkali-aggregate reaction, which forms a white gel exuding through cracks and hardening as a white stain on the surface.
- Erosion is the weathering of the concrete surface by wind, rain, snow, and salt air or spray. Erosion can also be caused by the mechanical action of water channelled over concrete.
- Corrosion, the rusting of reinforcing bars in concrete, can be a most serious problem. Normally, embedded reinforcing bars are protected against corrosion by being buried within the mass of the concrete and by the high alkalinity of the concrete itself. This protection, however, can be destroyed in two ways. First, by carbonation, which occurs when carbon dioxide in the air reacts chemically with cement paste at the surface and reduces the alkalinity of the concrete. Second, chloride ions from salts combine with moisture to produce an electrolyte that effectively corrodes the reinforcing bars. Cracking, spalling, deflection are frequent results of corrosion.

3 REPAIR AND MAINTENANCE TECHNIQUES OF REINFORCED CONCRETE BUILDINGS

The architectural significance of the building, its age, existing condition, structural system and whether it is located in an earthquake risk area, are priority factors in taking the decision for rehabilitation. In this context, evaluation studies of the current condition of reinforced concrete building are completed. After the preliminary examination consists of reviewing the current situation and building's documents the analysis study is carried out. This study includes, soil surveys, determining the quality of the reinforced concrete, statically evaluation of the building, and re-functioning studies. If the dimension of the building elements and the quality of the reinforced concrete is adequate, then it may be enough to do only repairs and conservation. However if the study shows the reinforced concrete not to be of adequate quality, then a comprehensive rehabilitation may be required. According to the determined strategy, the project and planning goes ahead using one or more of the available methods.

In the conservation of reinforced concrete, the key issue is whether the existing material can be repaired and conserved or whether it must be replaced. The concrete and the structure must be investigated to develop repair options and strategies. Laboratory analysis of the concrete to be repaired is an important part of the investigation. All repairs of existing concrete require proper preparations to provide a clean, sound surface to which the repair can adequately bond. During the repair existing reinforcement may be also required cleaning, priming, and painting with a rust-inhibitive coating. The repair area should be reinforced and mechanically attached to the existing concrete. Reinforcement materials can include regular steel, epoxy-coated steel, or stainless steel, depending on the conditions. Preparing trial repairs and mock-ups permit evaluation of the designs of the aesthetic acceptability [Gaudette *et al.* 1995].

Various repair methods, available today, reduce the rate of corrosion of embedded reinforcing and associated concrete deterioration. One method is cathodic protection. Cathodic protection is intended to reduce the rate of corrosion of embedded steel in concrete, which in turn reduces overall deterioration. Another technique to protect concrete is realkalization. Other methods include flooding with a corrosion inhibitor or, more aggressive, removing the concrete cleaning the exposed steel coating with a epoxy and covering the new concrete, and then sealing. Concrete deterioration is heavily influenced by moisture penetration; rehabilitation may also entail application of a decorative surface coating or a clear penetrating sealer, if appropriate. These water-resistant coatings and sealers should be breathable and alkali resistant. If specific components in reinforced concrete structures are beyond repair, replacement components can be cast in place to match historic ones. As with surface repairs, placement and finishing will dictate how well replacement concrete matches the historic concrete [Gaudette *et al.* 1995].

Especially in areas of high earthquake risk, comprehensive rehabilitation works are required for reinforced concrete buildings. Many rehabilitation techniques were investigated recent 20 or more years to apply to both pre-earthquake and post-earthquake rehabilitation. The expected performance level of the building following the earthquake (operational, immediate occupancy, life safety, collapse prevention) and the earthquake hazard levels impact the selection of the techniques [FEMA 356 2000];

- Operational level: Backup utility services maintain functions; very little damage.
- Immediate occupancy level: The building remains safe to occupy; any repairs are minor.
- Life safety level: Structure remains stable and has significant reserve capacity; hazardous non-structural damage is controlled.
- Collapse prevention level: The building remains standing, but only barely; any other damage or loss is acceptable.

Methods and elements used in the comprehensive rehabilitation of existing reinforced concrete buildings are as follows [Fukuyama & Sugano 2000]:

a. Infill existing frames
- Cast-in-situ reinforced concrete wall
- Precast concrete or steel panel
- Concrete blocks or brick infill

b. Brace existing frames
- Steel or reinforced concrete brace
- Post-tensioning cables

c. Place side walls
- Cast-in-situ reinforced concrete wall
- Precast concrete panel

d. Jacket existing members
- Steel encasement
- Steel straps
- Cast-in-situ reinforced concrete

e. Provide back-up structure
- Reinforced concrete or steel peripheral frames
- Reinforced concrete or steel buttresses

f. Wrapping existing members
- Fibber sheets
- FRP (Fibber Reinforced Plastic) sheets

Another concept to reduce seismic response is to use base isolation systems. For base isolation [Fukuyama & Sugano 2000]:
a. Rubber bearing systems
b. Friction pendulum systems are presently available.

4 REHABILITATION PROCESS PROPOSAL

Rehabilitation process of reinforced buildings/monuments which require contributions of conservators, architects and engineers has been proposed on the basis of above explications. Main stages and sub-stages of the rehabilitation process proposal and the methods and tools that will be used to reach the activities/results have been illustrated in scheme format [Table 2].

At the first column of the scheme seven main stages of the process; preliminary examination, analysis, determination of strategy decision, planning and preparation of project, control of project, application and control have been displayed. The sub-stages have been presented at the second column. Methods and tools that will be utilized during rehabilitation applications have been displayed at the third column. At the last column, activities and/or results of the stages have been presented. Sub-stages and methods/tools should be chosen according to the architectural significance of the building, its age, existing condition, structural system and whether it is located in an earthquake risk area within the framework of the proposed scheme.

During the implementation of the process -sub-stages, methods/tools and activities/results- the efficiency of the architects/conservators display differences. The efficiency of the architects/conservators during the rehabilitation process is highlighted in the proposed scheme in grey tones. Architects/conservators play most efficient role during -preliminary examination, determination of strategy decision, planning and preparation of project, control of project and control- main stages. Architects/conservators also play most efficient role during the re-use study and control sub-stages.

Table 2. Rehabilitation process proposal for buildings/monuments:

MAIN STAGES	SUB-STAGES	METHODS/TOOLS	ACTIVITIES AND/OR RESULTS	
PRELIMINARY EXAMINATION	**Pre-observation of existing condition**	Determination of visual construction damages		
	Determination of authentic architectural features			
	Investigation of original construction and repair documentations	**Archive research**	**1** Determination of structural damages (Determination of cracking and deflection causes, determination of building components that lost bearing capacity)	
ANALYSIS	Soil surveys (Inspection Hole)	Soil Profile , Ultimate strength , Allowable soil pressure , Settlement analysis , Unit weight of soil , Modulus of shear , Modulus of bulk, Poisson ratio, Modulus of elasticity , Soil fundamental period , Wave velocity P and S , Site Seismic Hazard	**2** Determination of non-structural damages (Determination of cracking caused by corrosion, Determination of shrinkage cracking, Determination of the segregated zone, concrete deteriorations)	
	Determination of material quality	Core sample, Ultrasonics and rebound hammer readings, Determination of rebars diameter and location with pachometer and cover meter, Petrographic evaluation, Chemical analysis		
	Evaluation of building structure	Preparation of structural survey, Determination of accordance with new requirements and regulations of structural system	**3 Determination of re-use alternatives** (continuity of original function, new function possibilities)	
	Re-use study	**Preparation of building survey, Determination of new functioning potential, Determination of conformation of new function to the project, Aboriginal cost analysis**		
DETERMINATION OF STRATEGY DECISION	**Strategy Decision**	**Analysis Result Report Determination of expected performance level of the building** (operational, immediate occupancy, life safety, collapse prevention)	**Repair & Conservation**	Comprehensive rehabilitation strategy: **1** Rehabilitation with seismic resistant techniques **2** Rehabilitation with seismic isolation techniques **3** Rehabilitation with mix techniques (seismic resistant &seismic isolation)
PLANNING AND PREPARATION OF PROJECT	**Selection of material & technique**	**Organization of specialists and technical team**	**1 The Re-Use (Architectural) project**	
	Preparation of necessary detailed drawings		**2** Retrofitting (Static) project	
	Preparation of work plan		**3** Mechanical project	
	Cost analysis		**4** Electrical project	
CONTROL OF PROJECT	**Determination of conformation to related regulations and specifications**	**Academic and professional organs Local and state organs**	**Approval for the application**	
APPLICATION	Taking measures for technical safety	**Organization of technical team**	**Rehabilitated building/monument**	
	Preparation of the building			
	Technical operations	**Conservation methods**		
		Addition of new footing Strengthening of existing footing Infill existing frames Brace existing frames Place side walls Jacket existing members Provide back-up structure Wrapping existing members Rubber bearing system Friction pendulum system		
	Control	**Organization of team**		
CONTROL	**Control of material**	**Academic and professional organs**	**Approval for the use of building**	
	Observation on site	**Local and state organs**		

Efficiency of architects :	**most efficient**	less efficient	non-efficient

CONCLUSION

The proposed scheme will contribute to regularize the rehabilitation process of reinforced concrete buildings/monuments if implemented under the supervision of experts (engineers, architects and conservators). Looking for new solutions and adding new components to the buildings/monuments during the rehabilitation process, in order to bring the buildings to contemporary up to the standards, is acceptable. However, rehabilitation techniques such as the jacketing of the structural system can cause a loss of space because of increased size. This may affect the functional performance of the building to be subjected to rehabilitation. This situation may lead to the decision to demolish these buildings. Because of these reasons optimum solutions should be chosen for sustainability of old reinforced concrete buildings.

The architectural significance of the building, its age, existing condition, structural system and whether it is located in an earthquake risk area are priority factors in taking the decision for their rehabilitation and repair/maintenance techniques. During the analysis non destructive evaluation (NDE) methods have to be preferred. In this context, after evaluation studies of the current condition of the building, if the load resisting system and concrete quality is adequate, then it may be enough to do only repairs and conservation. Otherwise, a comprehensive rehabilitation may be required which needs the contributions of engineers, architects and conservators. According to the determined strategy, the re-use project and planning goes ahead using one or more of determined available methods. It is expected that this proposed rehabilitation process will make available to re-use old reinforced concrete buildings/monuments and it will guide for their rehabilitation.

REFERENCES

Ahunbay, Z., 1996, Restoration and conservation of historic environments, YEM press, Istanbul;1996, pp. 38 - 58. (in Turkish)

Coney, W.B., ‘Preservation of Historic Concrete Problems and General Approaches’, Technical Preservation Services (Preservation Brief 15),
http://www.cr.nps.gov/hps/TPS/briefs/brief15.htm; 2007.

Cosgun, N., Ipekci, C., Yilmaz, Y., 2002, Analysis of construction defects, 1. National building materials congress book, Istanbul; 2002, pp.558-569. (in Turkish)

Ekinci, CE., 2004, Red book, construction hand book for building and designer, Universite press. Ankara; 2004, pp. 417-421. (in Turkish)

Ersoy, U., 2004, ‘A Discussion on the seismic performance reinforced concrete buildings’, Concrete 2004 congress book; 2004, pp.16–21.

FEMA 356, 2000, Pre-standard and commentary for the seismic rehabilitation of buildings. Prepared by the American Society of Civil Engineers (ASCE). Reston, VA, 2000.

Fukuyama, H., Sugano, S., 2000, ‘Japanese seismic rehabilitation of concrete buildings after the Hyogoken-Nanbu Earthquake’, *Cement and Concrete Composites* 2000; 22: pp.59-79.

Gaudette, P., Hime, WG. & Conolly, JD., 1995, Reinforced concrete, Twentieth century building materials: history and conservation. Ed. Jester TC., National Park Service. Mc Graw Hill Companies USA; 1995, pp. 94-101.

Service Life Prediction Tools for Buildings' Design and Management

Bruno Daniotti [1]
Sonia Lupica Spagnolo [2]

T 72

ABSTRACT

Service Life Prediction is necessary to evaluate Life Cycle Costs and Life Cycle Assessment for a sustainable construction process. In order to provide a specific time schedule for a sustainable building maintenance, Politecnico di Milano has developed a specific method for Service Life Prediction based on the correlation between users' requirements and measured decays of building components' performance characteristics.

The report deals specifically with the definition of tools and methods to control indoor quality with a performance based approach, which analyses the existing link between user's needs and technological requirements. The performance loads' distribution for functional-technological elements is defined through computational models which relate predicted indoor conditions to technological performance specifications. The stage of technological design has to be supported by methods for calculating and by laboratory or in-site tests. The time behaviour of building components is simulated using time dependant environmental models, thanks to the correlation between performance characteristics' decay (measured by lab programmes) and the conditions established by users' requirements.

The paper reports on the activities undertaken by the Research Group on Durability of Building Components, at Politecnico di Milano's, for the development of operative tools for Service Life Prediction, thanks also to the cooperation inside the Italian research network for durability, born in the framework of the international links with CIB and ISO.

KEYWORDS

Tools, Performance, Models, Design, Management.

[1] Politecnico di Milano, Building Environment Science and Technology Department (BEST), Milano, Italia 20133, Piazza Leonardo Da Vinci, 32, Phone +39 2 2399 6002, Fax +39 2 2399 6020, bruno.daniotti@polimi.it
[2] Politecnico di Milano, Building Environment Science and Technology Department (BEST), Milano, Italia 20133, Piazza Leonardo Da Vinci, 32, Phone +39 2 2399 6002, Fax +39 2 2399 6020, sonia.lupica@polimi.it

1 INTRODUCTION

A sustainable building process requires to control and to plan the use of material and economic resources necessary during its all life cycle. Designers' choices should be oriented towards building components and products characterised by an economically reasonable Working Life, i.e. which require sustainable maintenance activities, considering the predicted Service Life. In this optics Building Science is fundamental to furnish suitable information to designers to make such choices.

The Durability of Building Components Group of Politecnico di Milano is undertaking some researches to set up methods for building components' evaluation of durability, applying them to building materials and components for external walls. In particular, an experimental programme with a technical solution belonging to the external not load-bearing walls' family has been planned in collaboration with the Swiss technical experimental laboratory of the "Scuola Universitaria Professionale della Svizzera Italiana" (SUPSI) in Lugano. Both accelerated ageing proofs and real exposition ones have been conducted in two different climatic contexts: Milan and Lugano. Thanks then to the comparison between accelerated and natural ageing results it was then possible to evaluate the so called "time re-scaling factor" bringing to the definition of Reference Service Life, in particular, of the external protecting covering layer. Through, eventually, to this factor it is, in fact, possible to say that a certain number of accelerated cycles corresponds to a certain number of years of natural (real) ageing.

2 DEVELOPMENT OF METHODS FOR THE APPRAISAL OF BUILDING COMPONENTS' DURABILITY IN DESIGN PHASES

In 2003, with the co-financing of Ministry of Instruction, University and Research, in Italy a pluriannual research on "Methodologies of planning and evaluating durability of buildings components for sustainable production processes" started: the proposed research programme has developed methodologies for Service Life Prediction of some building components, belonging to the classes of external walls, external casings, continuous and discontinuous coverings.

In this programme, six research units of as many Italian university centres are involved: Politecnico di Milano, Politecnico di Torino, University of Naples, University of Palermo, University of Brescia and University of Catania. Thanks to this collaboration, it has been created a meaningful methodological-experimental reference for the developing of a national net of systematic experimentations on building components' durability both in technological laboratories (tests of accelerated ageing in standard conditions) and in outdoor environment (tests on out-exposed specimens in real conditions of use).

The chief objective of the Italian research network is to develop interoperable modular ICT tools (SW/ Web Services) focused on Service Life and maintenance issues and take into account the knowledge acquired on Service Life prediction methods to plan maintenance and inspection. Such tools have to allow to plan and manage works, responding to the demands and requirements of Designers, Maintenance Planners, Real Estate and Facility Managers and contributing to drive designing choices in civil application from a sustainable point of view.

Thanks to the cooperation among the six Italian research units, Service Life prediction tools will receive input data from a set of the national regionalized information sources, through an ad hoc structured (in conformity with ISO-DIS 15686-8) Reference Service Life Database [Daniotti & Lupica Spagnolo 2007], contemplating also a performance evaluation for feedback of Service Life data from practice.

A particularly meaningful and innovative aim of this research is also to determine conventional performance limits for each building's component in order to recognize the end of Service Life, providing, moreover, an method as suggested by ISO standards.

Moreover, the purpose is to provide a graduate acquaintance of durability, contributing to the international research of CIB and also developing ISO standards in this field through the Italian National Agency of Standardization (UNI). With this aim, in 2006 the Italian standard

That's why, deepening the evaluation methods indicated by ISO 15686 Durability of Building Components Group of Politecnico di Milano has contributed to the developing of methods for the appraisal of building components' durability, useful for the prevision of Service Life and of reliability propensity in the design step. As a first result, this activity carried to the emanation in 2006 of the Italian standard UNI 11156 "Valutazione della durabilità dei componenti edilizi (Appraisal of building components' durability)".

The studied methods are:

– Evaluating building component's reliability method, which can be applied starting from a careful examination of component's design through a functional and technical analysis of the design itself.

  This analysis is developed evaluating the four components of reliability (functional, executive, inherent and critical) and following precise procedural indications. The average of the four calculated reliabilities' values is then assumed as propensity to reliability of the building component's spontaneous duration [Daniotti et al. 1990].

  The evaluation of reliability propensity method can be applied to the technical designing of buildings, according to three opportunities of use.
  - The first opportunity concerns the conception and designing moment of a technical element, trough the optimisation of the four components of reliability, as a useful tool for the "design for durability" and in order to limit designing pathology risk.
  - The second one is about technical element's choosing criteria for its correct use inside a specific building intervention. The application of the esteeming reliability method proposed by DBCG allows the evaluation of reliability propensity at the time of building components' Service Life through this comparison with known components: esteems are the more reliable the more building components (belonging to that repertory) are examined.
  - The third opportunity is to act for buildings' retraining, suggesting design interventions for each functional building's part; this is possible only keeping into consideration evaluations about reliability propensity made on the existing, according to the proposed method.

– "Failure Modes and Effects Analysis (FMEA)": through a systematic analysis of the building organism decomposed in its fundamental components, this method concurs to give precious information in the perspective of a maintenance planning. Its application produces an exhaustive list of all the sceneries of degradations that could be possible in the various steps of building process [Daniotti 2006].

– evaluation of building components' Service Life method: it provides on one hand to obtain, through an experimental programme, Reference Service Life values and, on the other hand to adopt these values as input data for ESL's calculation in the considered context of exposition, of production, of use and of maintenance.

  Among this last family of methods, the Factor one gives an easy contextualization of Reference Service Life values of building components outside the system and the specific context of design. This method is considered one of the main international references within ISO for the valuation of building component's Service Life in the specific conditions of use.

  Politecnico di Milano's research suggests for this method some criteria in order to make more objective and scientifically validated the values attributed to each single factor [Re Cecconi & Iacono 2005]. In this optics, in structuring the Reference Service Life Database, it appears very

important to create grids for every introduced RSL value in order to describe precisely the reference condition and to help the user in calculating the ESL through the Factor method [Daniotti & Lupica Spagnolo 2008].

Eventually, the Performance Limits Method (PLM) has been developed because Service Life prevision must necessarily be based on a performance concept. The aim is to correlate directly building component's Service Life to environmental performances (thermal and hygrometrical comfort) of the space that the components themselves delimit; this allows accomplishing a durabilistic analysis on the capability to maintain during their Service Life the performances for which such components were thought, planned and realized.

2.1 The Factor Method

About the Factor Method, the research group has defined some criteria in order to make as more objective and scientifically validated as possible values given to each single factor. In fact, ISO 15686 has provided a very simple method for evaluating Service Life, the Factor method: thanks to seven deterministic factors, this method tries to model aleatory phenomena, such as climatic agents. That's the reason why the scientific community has showed the necessity to improve the method, through two ways to proceed:

- The first way is based on a probabilistic approach and uses the same equation proposed by ISO standard, but treating factors as aleatory variables. The DBCG's proposal is based on the use of triangular distributions of ISO factors, adopting Montecarlo method for solving the equation [Re Cecconi 2004]. Aleatory variables' use describes better the complexity of decay and provides both the Service Life and an esteem of data's reliability: it is possible to obtain an evaluation of duration with precise probabilistic guarantees. Despite this, the Factor method still remains too subjective.
- The second way to proceed is to adopt guiding grids, which can drive the designer in assigning values to each factor. These grids, obviously, cannot avoid the subjectivity in calculating Service Life, but they move it in the moment of grid creation: that's why grids should be built by experienced people belonging to the building sector, such as manufacturers themselves. In this way grids remove subjectivity during the esteeming factors phase, making it proper even for not experienced people [Re Cecconi & Iacono 2005].

2.2 The Performance Limits Method (PLM)

Durability of Building Components Group has, therefore, developed a method based on the evaluation of durability as the esteem of building component's performance decay till a limit of acceptability: the Performance Limits Method.

This method consists of the five following fundamental moments:
- definition of performance targets;
- individuation of requirements and specification of performances that the component must supply;
- translation of performance specifications into technical functional characteristics;
- individuation of the performance thresholds for Service Life;
- evaluation of Service Life.

The analysis of the performance and functional decay is fundamental to model the degradation phenomena through a linked chain relation: i.e. Agents-Actions-Effects-Degradation (see figure 1).

Once this functional decay relation has been developed for specific components of the assembly, these relations are useful for the designer to verify, for each component, the relevant agents and actions that can cause degradation and performance decay.

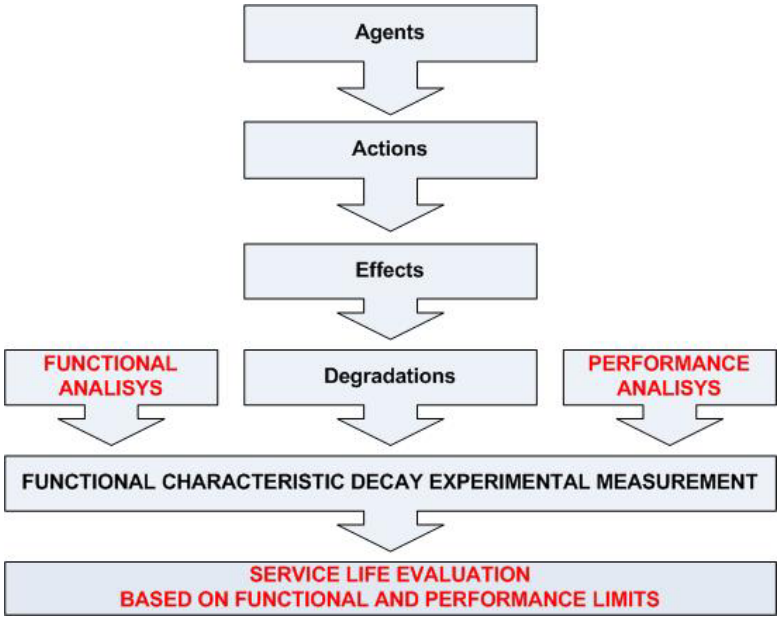

Figure 1. Analyses scheme for building components' durability evaluation.

The durability evaluation derived from results of experimental work gives information on products' Service Life related to environmental conditions, and is useful to help optimise designers' choices for components and component finishes.

The input data for modelling is based on the decay of functional characteristics measured through ageing tests. The experimental Service Life evaluation method reported in paragraph 3 is an application of this method: an analysis of trends for loss of performance characteristics between differently finished components was completed. This was specifically carried out for paint coatings based on acrylic and vinyl resins that are typically used to protect cementitious-based wall renderings.

The component's behaviour over time was measured in regard to the decay of their functional characteristics and degradation phenomena.

Currently, this method represents a valid help when it is necessary to evaluate Service Life in relationship with a precise performance decay.

2.3 Evaluation of the Gravity of Decays and Damages

As a result of the international collaboration between Politecnico di Milano and CSTB (Centre Scientifique et Technique du Bâtiment) a proposal for the evaluation of gravity (Criticality) and the risk consequent to decays and damages has been defined.

The proposed methodology introduces tools and guide lines in order to lead the designer across this investigation, individualizing a hierarchy of the innumerable sceneries returned from FMEA (Failure Modes Effects Analysis) method. These sceneries allow the designer to esteem the more or less gravity of determined sceneries, with temporal indications regarding the frequencies of these phenomena.

With this aim, two indexes were introduced:

a) IG_1 (functional index): to correlate the decay to the no more guaranteed function at the end of a series of events which lead to the not operation of functional elements (or of entire technical solutions);
b) IG_2 (maintenance index): to correlate the decay to the complexity of maintenance required to re-establish the correct initial working.

3 EXPERIMENTAL EVALUATION OF RSL: ONE CASE STUDY

The international standards ISO 15686 introduce a general evaluation methodology divided in two steps:

- the experimental evaluation of Reference Service Life (RSL);
- the prediction of Estimated Service Life (ESL) for the design stage.

The method to predict Reference Service Lives of building components, (i.e. the period of time, after installation, during which a building component meets or exceeds performance requirements in normal conditions of use and maintenance), has been divided into the following five main points:

- definition: of user requirements and of agents influencing building's behaviour (ageing agents, location, etc.), the characterization of building material, etc;
- preparation: identification of degradation agents, mechanisms and effects, choice of performance characteristics and evaluation techniques, feedback from other studies;
- pre-testing: session in order to check mechanisms and loads and to verify the choice of characteristics and techniques;
- exposure and evaluation phase: short term exposure and long term exposure degradations are compared;
- analysis and data elaboration.

Applying this procedure since 1996 a research programme has been developed at Politecnico di Milano: the aim of this research is to evaluate Reference Service Life of external not load-bearing walls with double masonry, thermal insulation inside and two different kinds of protecting covering layers. The criteria followed to choose this technical solution was to opt for a traditionally widespread solution in the building market so that results and considerations could have been more interesting and more immediate to be verified.

3.1 Accelerated Ageing in Laboratory Proofs

Accelerated proofs in laboratory started first of all with not protected masonries and then with protected by paints masonries: the aim was to study the behaviour of external layers of masonries subjected to artificially reproduced climatic stress. For this reason, four specimens at one time were fitted in the climate chamber, with external surface turned toward the centre of it, just in front of the origin of ageing agents stress.

The whole ageing cycle lasts 6 hours and 25 minutes (including transition phases) and is structured as in the following table.

Table 1. Accelarated ageing in laboratory: used cycle

Phase	*Temperature (°C)*	*Relative humidity (%)*	*Duration (minutes)*
Rain	20	95	60
Freeze	-20	95	90
Humid heat	55	95	60
Dry heat + UV	30	40	80

Masonries were then periodically subjected to not destructive characterization proofs: visual inspections of paint's aspect and, through weighting, measurement of residual water; moreover, at the end of ageing period some destructive proofs through core boring were conducted: determination of plaster's compressive strength, adhesion between external plaster and bricks, plaster's porosity, water absorption, vapour diffusion resistance and microstructure.

3.2 Natural Ageing Proofs in Outside

The same elements tested in accelerated proofs were reproduced and exposed toward South for a natural external ageing both in Milan and in Lugano, cities with similar climatic conditions but with different pollution levels [Daniotti & Lupica Spagnolo 2008]. In doing that, two different inclinations were used: the vertical one at 90° and the sloping at 45° one, which, according to ISO normative, should accelerate the natural ageing.

In order to evaluate the damaging during time for the different specimens has been defined a classification of decays through a dimensional scale (from 0 to 3), based on a photographical analysis:
DL0: intact protecting layer;
DL1: local cracks or broken swellings;
DL2: many microcracks and cracks;
DL3: torn bubbles, detaching and saline crystallisation of the surface.

This kind of classification allows analytical comparisons during time and can be then used in implementing diagnostic card in order to define inspection ways for these solutions. Thanks then to the comparison among damaging levels found both in Milan and in Lugano for the two slops, it is possible to sum up the following considerations:

- ageing of sloped at 90° specimens is quite similar for the two localities of exposition; the only important difference is for VL90 specimens (V= vinylversatic resin, L=low concentration of resin) because they are more damaged in Milan than in Lugano;
- ageing of sloped at 45° specimens is faster than ageing of sloped at 90° ones.

In order to correctly interpret the results obtained, climatic data of the two different cities during the exposition period were studied, noticing that in Lugano the quantity of rain is higher and that in Milan values of pollution (PM10, SO_2 and NO_2), solar radiation and medium temperature are higher than in Lugano [Daniotti & Lupica Spagnolo 2008]. As a consequence of these considerations, vinylversatic paints degrade themselves more quickly in Milan than in Lugano because of thermal stresses.

3.3 Comparison Between Accelerated Ageing Results and Outdoor Natural Ageing Ones for Reference Service Life's Evaluation

Comparison between accelerated ageing results and outdoor ageing ones (analysed on the surface through optical microscope) gave the possibility to define the time-rescaling factor and, eventually, the Reference Service Life for the considered paints. In fact, specimens covered by high concentration of vinylversatic resin paints show the same levels of damaging after 150 cycles in laboratory and 4 years of outdoor natural exposition: presence of many torn bubbles and detaches. It is then possible to quantify the time-rescaling factor: 150 of the accelerated used cycles correspond to 4 years of natural exposure. Moreover, considering the performance decay evaluation of the external water protecting layer, quantified through water absorption measurements, it was possible to state that the Reference Service Life for Vinylversatic paints with low concentration of resin is 4 years.

The experimental programme is still going on in order to quantify Reference Service Life also for the other tested paints, but, in summary, it can be already asserted that:

- acrylic paints show a better protection than vinylversatic ones;
- high concentration of resin increases the protection.

5 CONCLUDING REMARKS

Service Life evaluation methods described by ISO 15686 still need precise tools for their application and, most of all, for obtaining reliable predictions. Following this guiding principle, Politecnico di Milano has been working to develop new tools for durability's evaluation and to improve existing ones: on one hand Durability of Building Components Group has defined a method to determine

building components' reliability propensity while on the other hand it is developing Service Life planning thanks to RSL's definition based on a performance approach and ESL's evaluation applying enhanced Factor methods.

Eventually, to make the application of these methods possible and to share results coming out from undertaken researches, a Reference Service Life Database is going to be developed, chief tool for the actual use of such evaluating Service Life methods.

REFERENCES

Daniotti, B. & Lupica Spagnolo, S. 2008, *Climatic comparison to analyse different degradation levels in external walls' outdoor exposure*, in papers of the conference "11DBMC International Conference on Durability of Building Materials and Components ISTANBUL, Turkey.

Daniotti, B. & Lupica Spagnolo, S. 2008, *Service Life Estimation using Reference Service Life Databases and Enhanced Factor Method*, in papers of the conference "11DBMC International Conference on Durability of Building Materials and Components ISTANBUL, Turkey.

Daniotti, B. & Lupica Spagnolo, S. & Paolini, R. 2008, *Factor Method application using factors' grids*, in papers of the conference "11DBMC International Conference on Durability of Building Materials and Components ISTANBUL, Turkey.

Daniotti, B. & Lupica Spagnolo, S. 2007, *Service life prediction for buildings' design to plan a sustainable building maintenance,* in papers of the conference "Sustainable construction, materials and practices", Lisbon, Portugal.

Daniotti, B. 2006, *La valutazione della durabilità di pareti perimetrali verticali non portanti*, Ed. Editecnica, Palermo, Italy.

Daniotti, B. & Iacono, P. 2003, *Long–Term Degradation Under Outdoor Exposure Conditions*, Proceedings of MDBP2003 International Workshop "Management of Durability in the Building Process", Ed. Maggioli, Milan, Italy.

Daniotti, B., Maggi, P.N., Boltri, P., Croce, S., Gottfried, A., Lucchini, A., Morra, L. & Rejna, M.G. 1990. *Contribution to the design for durability of the building technological system: a methodology for the evaluation of the reliability of the functional models*, Proceedings of 5th International Conference on Durability of Building Materials and Components, Brighton, United Kingdom.

Re Cecconi, F. & Iacono, P. 2005, *Enhancing the Factor Method – Suggestions to Avoid Subjectivity*", in papers of the conference "10th DBMC", Lyon; France.

Re Cecconi, F. 2004, *Engineering method for service life planning: the evolved factor method*, in papers of the conference "CIB World Buiding Congress", Toronto, Canada.

ISO 15686-1:2000, *Building and constructed assets – Service life planning: General principles*.

ISO 15686-2:2001, *Building and constructed assets – Service life planning: Service life prediction procedures*.

ISO-DIS 15686-8:2007**,** *Buildings and constructed assets - Service life planning: Reference Service Life and service life estimation.*

UNI 11156:06, *La valutazione della durabilità dei componenti edilizi.*

11DBMC International Conference on Durability of Building Materials and Components

ISTANBUL – TURKEY May 11-14th, 2008

FMECA and Management of Building Components

Aurélie Talon [1]
Daniel Boissier [1]
Julien Hans [2]
Michael A. Lacasse [3]
Julien Chorier [2]

T 72

ABSTRACT

In accordance with the principles of "sustainable development" and "performance-based building", building components are expected to maintain their required performance levels over their service life. This is typically achieved through the use of planned maintenance interventions. However, providing relevant management of building components likely requires both the identification and evaluation of the most critical degradation scenarios. Failure Modes and Effects Analysis (FMEA), is a method developed in the 1970s in the industrial domain, and has more recently been adapted to the construction domain as a mean to identify all the possible degradation scenarios. From all the available results obtained from the FMEA, the most critical scenarios are established on the base of a further analysis of the criticality of these scenarios, so obtained through a FMECA ("C" for criticality). In this paper, two variations of methods are proposed to complete the criticality analysis. The first method is based on the formalisation with expert's system of the relation between elements, environment, functions and degradation in order to perform FMEA. The second one is based on unifying and aggregating relevant service life data in order to obtain the service of building component in a given environment. This paper provides: (1) An overview of the FMECA method; (2) A brief review of the state-of-the-art on FMECA research for and application to the construction domain; (3) Method based on expert's system to perform FMEA (4) Method of service life prediction of building components based on FMEA; (5) Application of the FMECA in a maintenance planning project of building facades.

KEYWORDS

Building components, Degradation scenarios, Maintenance management, Maintenance planning, Service life prediction

1 Polytech' Clermont-Ferrand / LGC, Civil Engineering, Clermont-Ferrand, France 63174, Phone +33 473407525, Fax +33 473407494, atalon@cust.univ-bpclermont.fr, daniel.boissier@cust.univ-bpclermont.fr

2 CSTB, Sustainable Development, Grenoble, FRANCE 38400, Phone +33 476762589, Fax +33 476762560, julien.hans@cstb.fr, julien.chorier@cstb.fr

3 Institute for Research in Construction, Building Envelope and Structure, Ottawa, Canada K1A 0R6, Phone +1 613 993 9715, Fax +1 613 954 5984, Michael.Lacasse@nrc-cnrc.gc.ca

1 INTRODUCTION

Building components are expected to maintain their required performance levels over their service life (SL). This notion is in accordance with the principles of sustainable development [Charlot-Valdieu & Outrequin 1999] and those of the "performance-based building" as espoused in the PeBBu project [Lee & Barrett 2003]. Over the life of a building component, its' performance levels depend, on the one hand, on the quality of the design and, on the other hand, on the quality of the maintenance affected during its SL. Research has evidently been completed in these both areas; however in this paper emphasis in placed on the SL of building components as it relates to the management and planning of maintenance.

The management and planning of maintenance of building components focuses on information, of two types: (qualitative and, quantitative information). Qualitative information regroups the knowledge of the structure and the function of the building component, as well as the phenomena that deteriorate the component, the causes of these phenomena and their possible consequences. Among all available methods of failure analysis (e.g. hazard and risk analysis, failure tree, butterfly knot, etc.), the failure modes, effects and criticality analysis (FMECA) seems to be the most appropriate for obtaining such type of qualitative information.

In this paper, a succinct presentation of the FMECA method is provided followed by a brief overview of the state of the art on FMECA research as applied to the construction domain. Given that different building components may be comprised of similar materials, functions and degradation scenarios, an evident idea is to formalise the commonality among components such that the process of conducting a FMEA can be automated; this approach is presented in a subsequent section of the paper. The quantitative information necessary for the management and the planning of maintenance are, on the one hand, information related to the SL of the building component and the duration of the respective degradation phenomena and, on the other hand, information on the cost of the maintenance or repair actions. A method that allows obtaining these durations is presented and the final section offers information on a project in which FMECA is used within a maintenance management model for building facades to help plan maintenance actions.

2 AN OVERVIEW OF THE FMECA METHOD

The FMECA is a method that is used to identify all possible degradation phenomena of a given building component in a specified in-use environment. The in-use environment relates to the specific context in which it is used, namely its function, performance requirements and environmental factors affecting its long-term performance. As well, it permits determining the series of degradation phenomena, referred to as degradation scenarios, associated to a particular component and environment. For each degradation phenomenon that is identified, the causes, consequences, and related damaged functions of the building components is determined; in this manner, the failure modes of the building component may be then determined.

Historically, the FMECA was developed in the 1970's in the development of nuclear arms domain and thereafter, in the aeronautical domain [Dyadem Press 2003]. This method has since been widely used in different industrial fields such as the aerospace, chemical, automotive fields as well as in the highly critical field of design of nuclear power plants. At the present time, this failure analysis method is one of the most universally used in the industrial domain.

Before undertaking an FMECA, it is essential to have in-depth knowledge of the building component being analysed; that is to say, have knowledge of the elements and materials of which the components is comprised, the functions ensured by this building component and its in-use environment. This may entail categorising several sub-environments (e.g. for a façade component, defining external and internal

environments) and the corresponding environmental agents (e.g. rain, temperature, thermal shock, etc.) associated to each of these situations. This knowledge may be obtained by first completing a component constituent analysis and thereafter, a functional analysis of the building component. To facilitate this first step in the analysis, certain databases have been developed [Talon 2006] that provide information on: (1) environmental agents (regroups all environmental agents that may compound the primary environments of building components); (2) function of building components (regroups all generic functions ensured by building components) and; (3) degradation phenomena (regroups 120 generic degradation phenomena).

The results of FMEA are quite often summarized in an FMEA table in which the information is typically provided in five columns: (1) functions identified during the functional analysis, (2) elements of the building components identified during the constituent analysis, (3) degradation phenomena appropriate to the component and function, (4) causes of these degradation phenomena and, (5) consequences arising from theses degradation phenomena as these relate to the function as provided in the first column. A same degradation phenomenon can cause damage to several different component functions and can also generate other degradation phenomena. For this reason: (1) there is as many lines in the FMEA table as there are {function, phenomenon} pairs and, (2) FMEA is necessarily an iterative process. Specifically, in an initial review all information "triplets" (i.e., environmental agents, functions, elements) are searched and subsequently, in a second review, the degradation phenomena generated in the first review likewise searched, and so on, until all degradation scenarios that lead to failures of the building component are identified.

Given that FMEA is a systematic process, it is capable of being exhaustive in identifying degradation phenomena; however, the quality of the result depends directly on the knowledge level of those expert seeking to use it for failure analysis of building components and their related degradation phenomena.

An example of FMEA carried out for a solar panel is provided by Talon *et al.* [2004]; it provides details of the different phases of analysis including constituent and functional analysis, and FMEA.

The "C" in FMECA corresponds to criticality analysis; this analysis is one that completes FMEA. The intent of carrying out such an analysis is to estimate the consequences of failure arsing from each degradation phenomenon or degradation scenario, as the case may be. This then permits classifying the consequences of failure by degree of criticality such that these can then be used to determine which maintenance actions are most important to complete.

Generally, the degree of criticality corresponds to the product of three criteria: (1) the likelihood of occurrence of the phenomena, (2) the level of significant related to the consequence of failure of the component and, (3) the degree of detectability of failure [Faucher 2004]. Each of these criteria is typically assessed with quotation grids that are scales varying from [0; 10]. Several variants of this formulation are used when two criteria [Sctrick & Goussy 2003] or five criteria [Department of Defence 1980] are considered, or when the criteria product is replaced by a weighted product [Sahraoui 2006] or by fuzzy inferences [Bowles & Pelaez 1995].

3 BRIEF STATE OF THE ART ON FMECA RESEARCH FOR AND APPLICATION TO THE CONSTRUCTION DOMAIN

A succinct review of different approaches in the construction domain that are based on FMECA is presented here in which information is provided on the use of FMECA in different international projects carried out in the past 9 years; a more detailed description of this state of the art is provided in [Talon *et al.* 2006].

The approach adopted by the Aspen Research Corporation [2002] is based on carrying out FMECA in order to qualitatively and quantitatively explain the degradation mechanisms of double-glazed

insulated glass (IG) units. This study corresponds to a Department of Energy (US) project entitled: "An Insulating Glass Knowledge Base". This knowledge base of the more critical failure modes of IG units provides behaviour models so as to determine the characteristics of accelerated short-term exposure tests to be used in validating these models.

At the Building Research Establishment [Barlett & Clift 1999] the use of FMECA is integrated in a global approach for the improvement of the supply chain of buildings during their whole SL cycle. In this context, FMECA is used as a method for identifying the more critical failures of the supply process. In this way, this approach allows supplying a "Reliability Centred Maintenance" program that aims to optimize the process reliability. As such, it provides descriptions of corrections actions or modifications required during either the management or during design phases.

In the context of a project led with cladding manufacturers, the Centre for Window and Cladding Technology [Layzell & Ledbetter 1998] applied FMECA to study cladding failures at the elemental, system, and building process level. The aim of this study was to improve cladding quality during the design phase and to facilitate the inspection and survey actions during the installation phase.

The SP Swedish National Testing and Research Institute [Carlsson *et al.* 2002] applies a method quite similar to FMEA, referred to as the Initial Risk Analysis (IRA). IRA is completed in order to determinate possible failure modes of solar panels. The aim of this study was to qualitatively define the parameters that influence the durability of the building component. These parameters were then studied by completing ageing tests on specific components of the assembly. The development of mathematic models and their correlation with experimental test results allowed assessing the SL of the solar panels. This study was completed in the framework of an international project entitled: "Durability assessment methodology development" (International Energy Agency Task 27 Proj. B1).

The approach undertaken by the Polytechnic of Turin [Pollo 2003] was improvement of the SL of building components from the design phase and consisted in combining three methods: FMEA, "Life Cycle Cost", and "Maintenance Cost Planning". This method aimed to: (1) foresee the degradation rates of components when taking into account their in-service use; (2) improve their maintenance, and; (3) optimise their global cost over their SL.

The approach proposed by Wyatt [Wyatt 2005] consisted in integrating FMEA and the fault tree method into the control and audit procedures for assessing building performance. The FMEA is used to identify any possible errors made during the building design phase.

In France, the Cemagref [Peyras 2002] integrates FMEA in a novel method for the management of dams; this method combines a knowledge base of ageing mechanisms and a database of ageing history of dams that facilitate the failure diagnosis for a specific dam. FMEA allows developing the knowledge base by, on the one hand, structuring expert opinions relevant to the ageing of dams and, on the other hand, by establishing the cause-effects relations and possible degradation scenarios.

4 METHOD BASED ON AN EXPERT SYSTEM PERFORMING FMEA

The objectives of an expert system are to assist FMEA by computer in order to:

- Accelerate the "time consuming" phases of the study;
- Obtain a better formalisation and reuse of existing information such as degradation phenomena, results of previously performed FMEA on other building components;
- Build and to feed the knowledge base on environmental agents, functions, materials, and degradation scenarios.

The use of an ontological approach, which is simply a formal model that allows expressing assertions in a structured manner, permits thereafter to render the model "computable". Ontology is a formal representation of a system from a certain point of view, a specific perspective. Such a representation

provides details of concepts of the system and the interactions or interrelations that exist between concepts [Gruber 1993]. For instance, one can study a low-emissive, double-glazed, insulated glass unit in its environment, from the point of view of its thermal properties or its thermal performance. Once the model is developed, it is then possible to capitalize on different aspects of knowledge of the unit as different "instances" of this model, and in so doing, ensure that this knowledge is completely structured and hence, computer accessible. These instances are expressed as for example:

My **component** Frame *is composed of* **material** "Aluminium". My **component** "Frame" *has as a* **function** to be watertight. My **Environment** External *contains* the **environmental agent** Humidity, Gas, UV, rain, etc.…

An example of providing information on the interrelation between concepts one may have:

The **Environment** External is in contact with the **component** Frame…

In the example, words in bold face are concepts of which the model is comprised, those in italic give the relation between concepts, and underlined words are specific instances of the model). Hence, the set of "instances" allows describing a building component on which one wants to perform the FMEA. Figure 1 provides an example of a generic building component model.

The various "instances" that together describe the product form the basis on which one identifies the possible set of degradation scenarios according to the information one can extract and thereafter, studies the consequences of these scenarios.

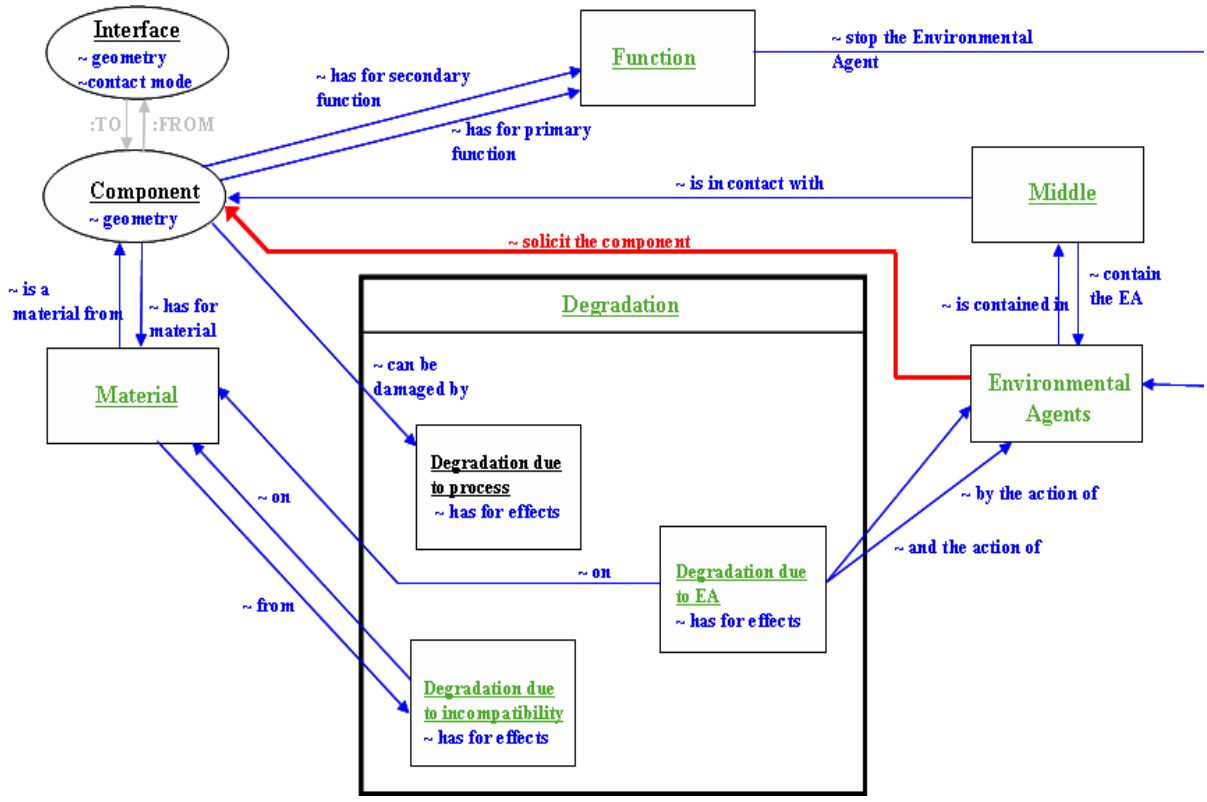

Figure 1. Description of the ontological-based product model from which FMEA can be performed on building components.

5 METHOD OF SERVICE LIFE PREDICTION

This paragraph provides a summary of a method based on FMECA that assesses the SL of building components; this SL estimate is essential information for the planning of maintenance of buildings.

This method uses all available data collected from several sources. The intent of the assessment process is to obtain the SL of a given building component in a given environment when all degradation phenomena and degradation scenarios implicated in the deterioration the functions of this building component during its SL are taken into account.

Two key practical elements must first be considered when retrieving SL data for a given building component and complimentary environment data. Data is: (i) not often available and, on the other hand, data does not necessarily have an acceptable level of quality. Given this situation, the following two-phased approach was proposed as a means to render the information useful: (i) the first phase is used to assesses the quality of each collected data set and; (ii) the second phase consists in combining all collected data of acceptable quality in order to obtain a harmonized data set that regroups those sets that together reflect the maximum consensus among the data sets, and an indicator of the quality of concurrence of the service life data.

The second phase may be formalised as a procedure. The process is initiated by carrying out research for all relevant SL data related to the given building component and its intended in-use environment. Thereafter, an assessment of the quality of each of the collected data sets is completed. Should the quality of the data be acceptable, then the entire collection of SL data is transformed into a plausibility format that allows categorising the different types of available data as being, e.g., derived from expert opinion, based on statistics, or extracted from a probabilistic method of SL estimation. Thereafter, the SL data set is harmonised using data fusion rules. From this process, the quality of concurrence of the SL data is obtained and related data quality indicators are provided (i.e., values for belief, Smets's probability, and plausibility functions respectively [Talon 2006]).

In the case where the quality of the SL data collected is not acceptable, research is then focused on the degradation phenomena identified during the FMEA and information on the duration of the phenomena is sought. Similar steps are then taken in this portion of the process: the quality of collected data is reviewed; data is transformed into a plausibility format, data is harmonised; the quality of the concurrence of the data is provided in terms of the data quality indicators. Finally, the results are aggregated at the phenomenon level in order to obtain the SL of the building component, thus taking into account all the degradation scenarios of the component. Specifically, for each degradation scenario identified from FMEA, the duration of each phenomenon of which the scenario is comprised is assessed. The duration of each scenario is then equal to the sum of the durations of its constitutive phenomena. The same assessment process is completed for all identified scenarios. Finally, the service life of the building component corresponds to the minimum value of durations extracted from these degradation scenarios. The proposed method for SL prediction is provided in more detail by Talon in [Talon 2006].

6 APPLICATION OF FMECA IN A MAINTENANCE PLANNING PROJECT FOR BUILDING FACADES

This project focuses on the development of a Markovian-based, building façade maintenance management (BMM) model that permits the optimization of maintenance planning, and introduces software that permits a user to initiate building maintenance actions. The intent was to provide building managers who are faced with having to maintain their buildings assets more efficiently, with a tool that could reduce the short and long-term costs of maintenance and rehabilitation. In essence, the BMM software can either optimize maintenance planning actions based on an expected maintenance budget or determine the budget required to maintain the façade to a minimum acceptable level of performance. An overview of the project is provided in [Kyle et al 2008] and a schematic of the primary components of the software is given in Fig. 2; details in respect to the Markovian approach to façade maintenance management is given in Lacasse et al. [2008]. The façade was first considered in development of the BMM software given that it is a significant element of the building envelope and of the building itself.

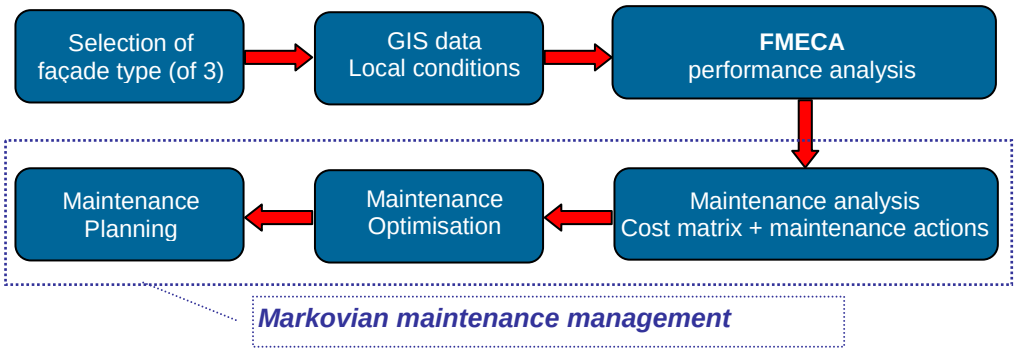

Figure 2. Schematic key project components of BMM model [Lacasse et al 2008].

The BMM model is built on several parts, however one of the key components is FMECA and performance analysis of the façade and related components; the several steps of this process are provided in Fig. 3 [Lacasse et al 2008]. The first step consists of developing a façade component criticality index. This is based on outcomes of a FMECA and permits determining the relative importance assigned amongst the different façade components, as proposed by [Talon 2006].

The basis for determining component criticality resides with understanding the criticality of the different degradation scenarios. Since the criticality of the different degradation scenarios is known and given that a degradation scenario may affect various components, the component criticality is equal to the maximum scenario criticality of the component, or simply:

$CC_j = \max (C_{r_{ij}})$ criticality of component *j*

where $C_{r_{ij}}$ represents the criticality of degradation scenario *i* affecting component *j*. Once the degree of criticality of the component is known, classifying components in respect to their relative degree of criticality is given by the ratio of the component criticality to the overall criticality of the façade system comprised of a number of components, i.e.:

$IC_j = CC_j / \Sigma CC_n$ degree of importance of component *j*

where, CC_j is the criticality of component *j* and ΣCC_n represents the sum total of criticality for *n* components of the system.

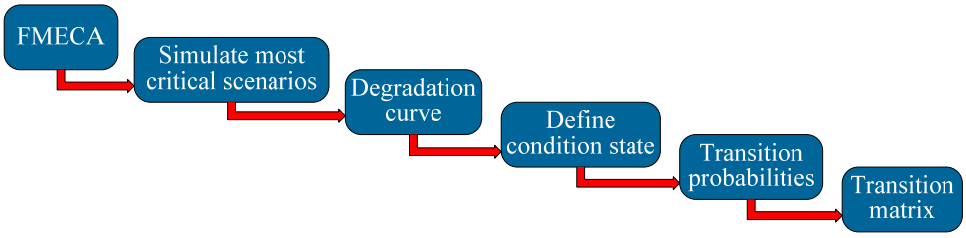

Figure 3. Description of performance analyses and development of Markov condition state matrices for service life estimation.

Given that building managers do not necessarily dispose of unlimited budgets for maintenance actions, only the most critical set of components are further analyzed by simulation of the deterioration process. These simulations provide degradation curves of the change in condition state of façade components as a function of time. The different condition states are then defined ensuring that it is possible to observe these conditions during an inspection. The condition state matrix provides information on the likelihood of a component remaining or changing state at given inspection intervals. Thereafter, the transition probabilities that correspond to the different sates are deduced that in turn permits obtaining the transition matrix. Such a matrix permits estimating the service life of components, or assembly of components, through an analysis using the Markovian model.

7 CONCLUSIONS

FMECA has been shown to be an essential method for failure analysis in the planning of maintenance and maintenance management of built assets. Indeed, this method allows obtaining a broad range of qualitative information (phenomena, causes, consequences) useful for planning maintenance. It provides a hierarchy of and direction for maintenance and repair actions to be undertaken by providing the real causes of degradation or failure. This method is also the basis, on the one hand, of an expert system for performing FMEA, representing a primary advantage for the efficient use of this method and, on the other hand, of quantitative methods for assessing the service life of building components, this latter item, essential information for planning maintenance. The wide range of different applications based on FMECA as well as its use in a maintenance planning project for building façades helps illustrates the relevance of this method in the construction domain.

REFERENCES

Aspen Research Corporation 2002, 'Deliverables for Phase I of the DOE project – An Insulating Glass Knowledge Base', Proc. IGMA Technical Division Meeting, Août 2002.

Barlett, E.V. & Clift, M. 1999, 'Reliability and Whole Life Performance : Integrating the supply chain', Proc. Durability of Building Materials and Components 8, Vancouver, 30 May – 3 June 1999, pp. 1916 - 1923.

Bowles, J.B. & Pelaez, C.F. 1995, 'Logic prioritization of failures in a system failure mode, effects and criticality analysis', *Reliability Engineering and System Safety*, **50**, 203-213.

Carlsson, Bo., Moller, K., Marechal, J-Ch., Kohl, M., Heck, M., Brunold, S. & Jorgensen, G. 2002, 'General Methodology Of Test Procedures For Assessment Of Durability And Service Life', Proc. 9th Durability of Building Materials and Components, Brisbane, 17-21 March 2002. Paper n°212.

Charlot-Valdieu, C. & Outrequin, P. 1999, 'La ville et le développement durable. Cahiers du CSTB', Livraison 397, Cahier 3106.

Department of Defence 1980, 'Military standard procedures for performing a failure mode, effects and criticality analysis' MIL-STD-1629A.

Dyadem Press 2003, *Guidelines for Failure Modes and Effects Analysis (FMEA), for Automotive, Aerospace, and General Manufacturing Industries*, CRC Press, Ontario.

Faucher, J. 2004, *Pratique de l'AMDEC*, DUNOD, Paris.

Kyle, B., Lacasse, M. A., Cornick, S. M., Hilly, T. and Abdulghani, K. 2008, 'A GIS-Based Framework for the Evaluation of Building Façade Performance and Maintenance Prioritization', Proc. 11th International Conference on Durability of Building Material and Components, Istanbul, 11-14 May 2008.

Lacasse, M. A., Kyle, B., Talon, A., Boissier, D., Hilly, T. and Abdulghani, K. 2008, 'Optimization of the Building Maintenance Management Process Using a Markovian Model', Proc. 11th International Conference on Durability of Building Material and Components, Istanbul, 11-14 May 2008.

Layzell, J. & Ledbetter, S. 1998, 'FMEA Applied to cladding systems – reducing the risk of failure', *Building Research and Information*, **26**(6), 351-357.

Lee, A. & Barrett, P. 2003, *Performance Based Building: First International State-of-the-Art Report*, CIB Publication, Rotterdam.

Peyras, L. 2002, 'Diagnostic et analyse de risques liés au vieillissement des barrages – Développement de méthodes d'aide à l'expertise', Thesis (PhD) of Clermont-Ferrand University, Lermes and Cemagref.

Pollo, R. 2003, 'Service Life and LCC Assessment. The Use Of FMEA As Design Tool', Proc. International Workshop on Management of Durability in the Building Process, Milan, 25 26 June 2003, ref n° 24.

Sahroui, A-E-K. 2006, 'Méthodes et techniques : AMDEC, RCM, MAC' ;Available **[on line]** <http://www.laas.fr/~kader/MI5.fr>.

Sctrick, L. & Goussy, B. 2003, 'Document unique concernant les risques biologiques – Risque d'accident exposant au sang (et autres liquides biologiques)'; Available **[on line]** <http://anmteph.chez-alice.fr/docuniqaes.pdf>.

Talon, A. 2006, 'Evaluation des scénarii de dégradation des produits de construction', Thesis (PhD) Clermont-Ferrand University, CSTB and LGC.

Talon, A., Chevalier, J-L. & Hans, J. 2006, *Failure Modes Effects and Criticality Analysis Research for and Application to the Building Domain*, CIB Publication n° 310, Rotterdam.

Talon, A., Boissier, D., Chevalier, J-L. and Hans, J. 2004, 'A methodological and graphical decision tool for evaluating building component failure', Proc. CIB World Building Congress 2004, Toronto, 2 7 May 2004, n°600.

Wyatt, D.P. 2005, 'The contribution of FMEA and FTA to performance review and auditing of service life design constructed asset' Proc. 10th Durability of Building Materials and Components, Lyon, 17 20 April 2005, 8p.

11DBMC International Conference on Durability of Building Materials and Components
ISTANBUL, TURKEY, May 11-14th, 2008

Condition Assessment of a 63-year Old Reinforced Concrete Structure Exposed to the North Sea

Robert E Melchers [1]
Chun-Qing Li [2]
Mark Davidson[3]
Shangtong Yang[4]

T 72

ABSTRACT

This paper describes the condition of a reinforced concrete balustrade consisting of some 1000 individual beam elements all exposed similarly to the hostile marine environment of the North Sea at Arbroath, Scotland since 1943. A comparison is made of the condition of the original construction with the condition of repairs carried out in 1968 and in 1993. It is shown that the 1943 construction shows very little corrosion-induced cracking and little rust staining even though it does not appear to be of high construction quality. Only a very low percentage of the balustrade beams have been replaced. In contrast the beam installed in 1968 and later in 1993 show very considerable and large concrete cracks directly attributable to the corrosion of the longitudinal reinforcement, even though the concrete is of a higher quality and density.

A detailed condition survey and statistics of crack sizes are presented in the paper. It is found that the higher corrosion resistance of the 1943 concrete is generally consistent with the concrete electrical resistivity measurements but the degree of corrosion of the reinforcing bars is inconsistent with chloride penetration measurements. The results are compared with the very few observations available in the literature for ageing concrete structures in marine environments. The results cast doubt on the conventional wisdom that chloride content at the reinforcement correlates well with reinforcement corrosion.

KEYWORDS

Reinforcement, Corrosion, Marine, Concrete, cracking.

[1] Centre for Infrastructure Performance and Reliability, the University of Newcastle, Australia, NSW 2308, Phone +61 2 4921 6044, Fax, 2 4921 6991, rob.melchers@newcastle.edu.au
[2] Department of Civil Engineering, the University of Greenwich at Medway, England, ME4 4TB, Phone +44 1634 883518, Fax, 1634 883153, c.q.li@greenwich.ac.uk
[3] Road Division, Angus Council, Scotland, DD8 3WR, Phone, +44 1307 473315, Fax, 1307 473388, davidsonma@angus.gov.uk
[4] Department of Civil Engineering, the University of Greenwich at Medway, England, ME4 4TB, Phone +44 1634 883031, Fax, 1634 883153, s.yang@greenwich.ac.uk

1 INTRODUCTION

It is well known that chloride is the predominant cause for the corrosion of reinforcing steel in marine concrete structures. What is less known however is to what extent the chloride (content) affects the corrosion, in particular the corrosion process. One measure widely used is the critical ratio of chloride to hydroxide ions for corrosion initiation with acceptance levels defined largely arbitrarily [Bentur et al. 1997]. However, the mechanisms involved in corrosion process including the propagation phase continue to be poorly understood [Melchers and Li 2006]. Although there are many structures with high degrees of reinforcement corrosion after only a few years service, there are also some isolated cases of no apparent occurrence of corrosion even after long exposure periods including in normally highly aggressive environments [Lukas 1985, Lau et al. 2007]. Relevant to these observations is that some laboratory experiments have shown that although corrosion initiation can occur quite early but that there may not be continued active corrosion until much later [Francois and Maso 1988, Li 2002].

Unfortunately, there are very few older reinforced concrete (RC) structures exposed to marine exposure conditions for which detailed investigation have been reported [Lau et al. 2007, Poupard et al. 2006, Liam et al. 1992, Weibenga 1980, Gjorv and Kashino 1986, Polder and de Rooi 2005]. This means that direct comparison to more recent concrete structures is difficult in general. One case that does allow such comparison is available at Arbroath, Scotland, where there is a 1.5 km long RC promenade railing exposed directly to the North Sea. Particularly during winter storms seawater washes over the railing. Importantly, the railing consists of 244 nominally identical sections each composed of 4 precast concrete railing beams set in cast-in-situ posts (Figure 1). There are therefore nearly 1000 nominally identical 'samples'.

Figure 1. Typical (part-)section of the RC promenade railing showing the four precast railing beams, the cast-in-situ central support and the left end-post.

Initial construction of the promenade railing was in 1943. It has been estimated that about 1% of 1943 the railings were replaced in. 1968 and about 10% in 1993. Unfortunately details of the original 1943 design and concrete and reinforcement properties and those of the replacements in 1968 are not available. recent sand laboratory observations show that the 1943 beams contain four 6 mm diameter bars with a nominal (but highly variable) cover of about 20-25 mm. The 1993 beams contain only two bars (16mm) on the vertical axis with 25mm cover. The 1968 beams are similar except that the bars were coated with a commercial zinc-rich primer. Also, the concrete used in the 1993 beams was air-entrained, apparently to counter problems with freeze-thaw behaviour.

These observations and details were considered to present a good opportunity to obtain some further insight regarding reinforcement corrosion of essentially similar concrete elements exposed to similar

marine environment conditions but for concretes with considerably different ages. The comparative study of these elements is the purpose of the present paper.

2 CONDITION SURVEY

The structure was surveyed in detail during the summers of 2003 and 2006. Matters recorded included overall condition, and rack size, length and depth, concrete blistering and spalling. The extent of exposed reinforcement and evidence of repairs (such as patching) were noted also. Table 1 presents an abbreviated summary of crack size.

Visual examination of the surface texture of the three types of beams revealed considerable differences. The 1943 beams all have a rough surface with some external wear and some deterioration of once sharp edges (Figure 2). Close examination showed that these beams were constructed using aggregates of widely varying size and the concrete also contains a significant amount of crushed seashells. These were identified both by their characteristic shapes and through testing with a very fine application of hydrochloric acid.

Table 1 Summary of crack sizes in 2003

Bay No.	Origin year	Crack Size (mm)			
		A	B	C	D
11-14	1993	3-7	3-7	3-8	3-7
16	1993				
21-24	1993	0-10	3-10	6-19	5-12
47	1993	8	8	3	12
48	1993	12	15	10	20
57	1968/93?	5	12	10 (11)	10
59	1993 ?		10		
60	1993	12	15	12	12
61	1993	5	5	6	10
62	1993	3	3	3	5
63	1993	10		5	
64	1993			5	
79	1993	10	7	2	2
87	1993	4	1	4	4
102	1993	10	2	3	
113	1968	5	7	3	10
118	1993	-	12	7	12
126	1968	8	7		
212	1943?			2	

Figure 2. Typical condition and surface roughness of 1943 (left) concrete railing beams.

Only about 2% of the 1943 railings still in existence in 2003 showed minor (hairline) cracking and minor local spalling. In contrast, most of the 1968 and 1993v replacement railings are badly cracked longitudinally. There is clear evidence within the cracks of very heavy corrosion of the reinforcement steel (Figure 3).

Figure 3. Typical crack pattern in 1993 railing beams

For the 1968 and the 1993 concrete beams the exterior surfaces generally show a smooth and dense surface texture. This suggests a well-graded concrete mix at the surfaces. They also show sharp edges. This suggests a good quality concrete. Rebound hammer tests were carried out at three locations (centre and towards the ends of each beam) on surfaces rubbed smooth using a carborundum stone for randomly selected samples of each beam type. Table 2 shows the results. These tend to be consistent with the superficial observation of surface density for the 1943 and 1968 beams. However, the 1993 beams appear to have rather lower than expected rebound results. This could be the result of the use of an air-entraining agent for the 1993 concrete.

Table 2. Rebound hammer results

	Construction		
Position	1943	1968	1993
1 (mean of 10 tests)	41.1	47.4	42.5
2 (mean of 10 tests)	38.4	47	41.4
3 (mean of 10 tests)	42.1	47.4	38.4
Average	40.5	47.2	40.7

Microscopy observations of the 1993 concrete showed a considerable number of voids (Figure 4). These are likely to be also the result of the use of an air-entrainment agent. The imposed grid is 10

mm. A resin was used to reveal more clearly the cracks, voids and aggregate. The image has been modified to give greater intensity and contrast. It shows a high degree of good cement bond.

The 1943 beams show some localized blistering and spalling of the concrete cover but no serious cracking. Hairline cracks offset from the centreline were observed. These are likely to be the result of the corrosion of the 6mm reinforcing bars relatively close to the exterior surface. The 1943 beams show about 5% of the with localized patch repairs. However, many exhibited some degree of minor rust staining on the exterior surfaces. These various observations suggest that very localized corrosion initiation had occurred for many of the 1943 beams but that by 2003/6 it had not yet progressed to the stage of inducing spalling of the concrete cover. Most the 1968 and 1993 replacement beams, on the other hand, showed severe longitudinal cracking with very large crack openings (Figure 3). Only some 25% of these beams remained uncracked in 2003/6. Moreover, nearly all of the longitudinal cracking was of considerable crack size, much more than would be expected according to the standard linear damage model. This suggests that damage and hence cracking increases gradually with age after corrosion initiation [Bentur et al.1997].

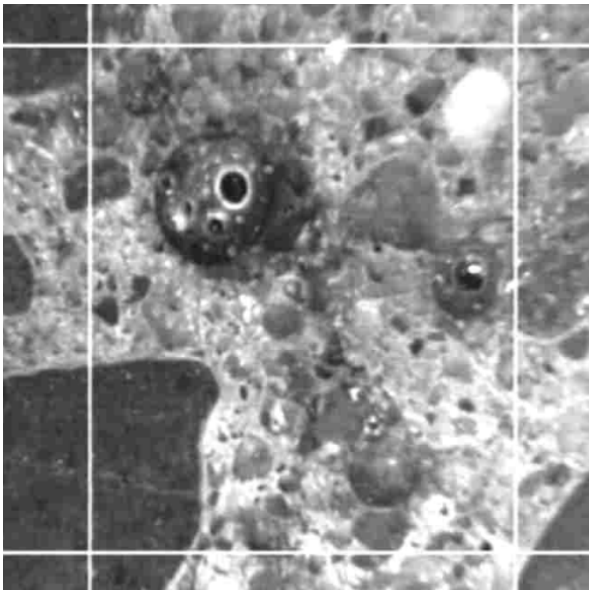

Figure 4 Micrograph of a typical section of concrete in the 1993 beams

3 CRACK STATISTICS

Maximum crack size as a function of period of exposure and year of construction are shown in Table 3 as at 2006. It is interesting to note that there is clearly some artificialness owing to to the usual preference in measurements for discrete sizes. Nevertheless, it is clear that the 1943 beams show much lower overall crack sizes also that many of these beams uncracked. In contrast, the 1968 and 1993 beams show a very substantial number of cracks and most of these are of large size. The considerable difference between the crack sizes indicates that it is highly unlikely that it is due to randomness in cracking, as has been suggested for reinforced concrete structures generally [Bamforth 1999]. Table 1 shows that of the 22 sections (i.e. 88 beams) reconstructed in 1993, only 22 beams have survived to 2006 without significant cracking. Moreover, the data from 2003 and the 2006 surveys shows that of the 1993 beams, about 9 beams failed during this time interval. This can be interpreted as an annual failure rate of about 0.5%. The failure of 66 beams from 1993 to 2006 suggests that the remaining 22 beams could be expected to fail in 3-5 years, that is 2010 or so.

Table 3. Frequency of maximum crack size

Maximum crack size (mm)	1943	1968	1993
0	222	0	0
1	4	0	1
2	18	1	5
3	2		10
4			7
5		3	9
6			5
7		1	6
8		2	2
9		1	2
10		2	11
11			
12		1	7
13			1

Similarly it is estimated that for the 2 beams still remaining from 1968 these can be expected to fail by about 2008 and by 2010 all the replacement beams are likely to have failed. The failure rate from then on will be that for the 1943 beams. This can be estimated from the period 1993-2006 if it is assumed (since as noted no records are available) that in 1993 all defective beams, both from 1943 and from 1968, were replaced. If this was done, there would then have been no defective beams left in 1993 and all failures evident in 2003/6 date from that time.

Chloride profiles and concrete resistivity are also being investigated as part of the present investigation and will be reported separately in due course. However, it is noteworthy that the chloride contents for the 1943 and the 1993 beams were similarly high at the reinforcement and that both were much higher than that for the 1968 beams, despite the considerable differences in exposure period for these three classes of beams.

4 DISCUSSION

Using the conventional the bi-linear damage model as a guide for the progression of corrosion with time in RC structures, it might have been expected that both the 1968 and the 1993 beams display a range of crack sizes since the model suggests that damage is a linear function of time after crack initiation and active corrosion has occurred, and cracking should be consistent with damage. Clearly, this expectation is not evident in the observations, even for the population of 1993 beams. This raises the possibility that the linear damage model is not quite correct - recently it has been proposed that the corrosion propagation stage of reinforcement corrosion is much more complex than indicated by the linear damage model [Melchers and Li 2006].

Table 4 gives a summary of the estimates of the corrosion rates, concrete densities and resistivity and chloride profile results. It shows that although the 1943 beams are surviving much longer than the beams constructed in 1968 and in 1993, this durability is not consistent with the lower or similar density and lower or similar permeability of the 1993 beams. Given their long exposure periods, the chloride concentrations at the surface of reinforcement could be expected to be greater for the 1943 beams than for the others, yet this is not the case. Moreover, the conventional thinking about the influence of chloride penetration on corrosion activation (e.g. Bentur et al. [1997]) suggests that the 1943 beams should have failed much earlier than their replacements. The statistics clearly indicate that this is not the case. One measure that is consistent with the loss rates of the 1943 and 1993 beams are the concrete resistivity readings. However, since the exposure conditions for all beams was and remains essentially similar, it might be expected that the concrete resistivity should reflect concrete density. It is surprising, therefore, that this is not the case.

Table 4 Overview of consistency between corrosion and physical properties.

	Corrosion loss rate*	Minimum cover (mm)	Superficial Concrete density	Rebound hammer	Chloride profile	Concrete resistivity
1943	≤ 0.16%	20-25	medium-good	medium	deep	very high
1968	~ 2.3%	20-25	good	higher	1/3 of others	medium-high
1993	~ 5.8%	20-25	good (a)	medium (a)	deep	low

* proportion of beams failed per unit time of exposure; ** from polarization resistance
(a) air-entrained concrete

Similar inconsistencies between chloride content, density and resistivity and durability have been reported by others. For example, Lukas [1985] reported long service lives for road bridges in Austria despite harsh exposure conditions and heavy use of de-icing salts. Lau et al. [2007] found little sign of reinforcement corrosion, despite around 40 years of exposure and only about 23-40mm concrete cover for more than 1000 reinforced concrete cylinder bridge piles exposed in the marine tidal zone in southern Florida. This was a 'striking' contrast with the performance of some other conventional reinforced concrete marine substructures in the same area. They noted high levels of chlorides at the reinforcing bars after 40 years exposure although this resulted only in minor rust staining and little evidence of preferential chloride penetration along cracks.

The above observations and comparisons show clearly there remain a number of issues for further exploration and research. This is despite the view in some quarters that the corrosion of reinforcing bars in concrete is reasonably well-understood and that its control involves mainly the achievement of good quality concrete and high resistance to chloride diffusion [Polder and de Rooi 2005]. The long-term field observations described herein, together with those reported by others [Lukas 1985, Lau et al. 2007], all indicate that in real structures chloride penetration to the reinforcing bars may not be very indicative of the initiation of reinforcement corrosion. It appears to be also not well-correlated with the rate of corrosion. The conventional view, that in order to achieve greater durability of reinforcing bars it is necessary to have greater and/or denser concrete cover is not fully supported by the present observations or those for the Florida piers. It follows that there are still important questions to be answered as to what influences are important and to what extent and duration in the initiation and progression of reinforcement corrosion. Evidently, more fundamental research into the precise mechanics and causes of reinforcement corrosion is required.

5 CONCLUSION

Many of the approximately 1000 reinforced concrete promenade railing elements constructed around 1943 and exposed to a harsh North Sea sea-spray environment for over 63 years show little evidence of reinforcement corrosion However the elements constructed more recently in 1968 and in 1993 show very serious reinforcement corrosion. As a reult they exhibit extensive considerable corrosion damage asuch as wide longitudinal cracking.

The 1943 concrete elements show remarkably good corrosion resistance for their concrete density and rebound hammer measurements, even though these are not consistent with concrete electrical resistivity measurements. Moreover, corrosion of the reinforcing bars was found to be inconsistent with chloride penetration measurements. Overall the observations are not consistent with the usual understanding of the role of chloride concentration and corrosion propagation. It is suggested that despoite decades of investigation of the problem, more detailed research is required to improve understanding of the role of chloride in the long-term corrosion of reinforcement bars.

ACKNOWLEDGEMENTS

The support of the EPSRC (EP/E00444X/01) and the Australian Research Council is appreciated. Mr McCoughlan performed the 2003 field survey and carried out some testing as part of a final year Honours project at the University of Dundee, Scotland.

REFERENCES

Bamforth, PB, 1999, 'An enduring problem', *Concrete Engineering International*, **3(8),** 28-31.

Bamforth, PB, Price, WF and Emerson, M, 1997, 'An international review of chloride ingress into structural concrete', *TRL Contractor Report 359*, TRL Scotland.

Bentur A, Diamond S and Berke NS, 1997, 'Steel corrosion in concrete: Fundamentals and civil engineering practice', E&FN Spon, London.

Francois, R and Maso, JC, 1988, 'Effect of damage in reinforced concrete on carbonation or chloride penetration', *Cement and Concrete Research*, **18,** 961-970.

Gjorv, OE and Kashino, N, 1986, 'Durability of a 60-year-old reinforced concrete pier in Oslo Harbor', *Materials Performance*, **25,(2),** 18-26

Lau, K, Sagues, AA, Yao, L and Powers, RG, 2007, 'Corrosion performance of concrete cylinder piles', *Corrosion*, **63,(4)**, 366-378.

Li, CQ, 2002, 'Initiation of chloride induced reinforcement corrosion in concrete structural members – Prediction', *ACI Structures Journal*, **99(2)**, 133-141.

Liam, KC, Roy, SK and Northwood, DO, 1992, 'Chloride Ingress Measurements and Corrosion Potential Mapping Study of a 24-year-old Reinforced Concrete Jetty Structure in a Tropical Marine Environment', *Magazine of Concrete Research*, **44(160)**, 205 – 215.

Lukas, W, 1985, 'Relationship between chloride content in concrete and corrosion in untensioned reinforcement on Austrian bridges and concrete road surfacings', *Betonwerk und Fertigteil-Technik*, **11,** 730-734.

Melchers, RE and Li, CQ, 2006, 'Phenomenological modelling of corrosion loss of steel reinforcement in marine environments', *ACI Materials Journal*, **103(1)**, 25-32.

Polder, RB and de Rooi, MR, 2005, 'Durability of marine concrete structures - field investigations and modelling', Heron**, 50(3),** 133-153.

Poupard, O, L'Hostis, V, Catinaud, S and Petre-Lazar, I, 2006 'Corrosion damage diagnosis of a reinforced concrete beam after 40 years natural exposure in marine environment', *Cement and Concrete Research*, **36 (3)**, 504-520.

Weibenga, JG, 1980, 'Durability of concrete structures along the North Sea coast of the Netherlands', Special Publication SP65, *American Concrete Institute*, Detroit, 437-452.

11th International Conference on Durability of Building Materials and Components
Istanbul Turkey May 11-14, 2008

A GIS-Based Framework for the Evaluation of Building Façade Performance and Maintenance Prioritization

Brian Kyle [1]
Michael A. Lacasse [2]
Steven M. Cornick [2]
Denis Richard [3],
Khaled Abdulghani [2]
Thibaut Hilly [2]

T 72

ABSTRACT

Maintenance of building façades should be an on-going process. However, maintenance prioritization issues are often neglected due to the lack of available tools to assess susceptibility to deterioration. Key components of the façade system most in need of maintenance interventions ought to be identified to prevent premature failure of façade components, to sustain the health and safety of the occupants, and to maintain the serviceability of the system over its service life. The effects of moisture and other climate effects on the deterioration of façade components are known. Likewise, water penetration of the façade from wind-driven rain to the interior causes damage, mould growth and degradation of thermal performance. Knowledge of the combined effects of wind, moisture and thermal loads permits determining the response of the wall, that in turn allows evaluating the hygrothermal performance, dilation at panel joints, susceptibility to water penetration, or the product of combined responses that act to deteriorate the façade system. The most severe combinations most likely to deteriorate the facade can then be determined and thus provide a basis for prioritizing maintenance programs for buildings. The process can be used to establish the risk of deterioration from climatic effects among different types of walls for a given building façade, between the level of risk among different buildings in a given climate, or for comparing the relative effects of similar facades located in different climate zones. This paper provides an overview of a project focused on developing a GIS-based framework for evaluating building façade performance and maintenance prioritization. Climate effects are discussed in relation to wall response and expected damage arising from the deterioration of façade components is given. Loss in functional performance of components is examined and the consequences of these losses are related to maintenance interventions.

KEYWORDS

Building façades, Building maintenance, Component deterioration, GIS-based maintenance, Maintenance prioritization

1. Public Works and Government Services Canada, Innovations and Solutions Directorate, Place du Portage Phase III, 11 Laurier, Gatineau, Canada K1A 0S5; Phone +1 819 956-3420; Fax +1 819 956-3400, Brian.Kyle@PWGSC.GC.CA
2. National Research Council Canada, Institute for Research in Construction, 1200 Montreal Road, Building M20, Ottawa, Canada K1A0R6, Phone +1 613 993 9715; Fax +1 613 954 5984; Michael.Lacasse@nrc-cnrc.gc.ca
3. Intempco Controls, 2511 Guenette, Saint-Laurent, Canada, H4R 2E9, Phone +1 514 337 7471; Fax +1 514 337 7475; denisr@intempco.ca

1 INTRODUCTION

1.1.Background

Maintenance of high and medium-rise building façades should be an on-going process. Maintenance prioritisation issues are often neglected due to the lack of available tools to assess vulnerability to climatic effects and susceptibility to deterioration. Key components of the façade system most in need of maintenance interventions ought to be identified to prevent premature catastrophic failure of any of the façade components, to sustain the health and safety of the occupants, and to maintain the serviceability of the system over its service life.

The effects of moisture and other climate parameters on the deterioration of façade components is well known; spalling of masonry caused by freeze-thaw action, spalling and degradation caused by salt migration, damage due to expansion of materials or components; loss of adhesion or rupture of jointing products from joint movement. Likewise, water penetration of the façade from wind-driven rain to the interior causes failure of interior finishes, damage to gypsum plasters, mould or mildew growth and degradation of the thermal performance of insulation.

Knowledge of the combined effects of wind, moisture and thermal loads on the façade system permits determining the response of the wall, be it metal-glass curtain walling, stone or brick masonry veneer, prefabricated concrete panel, or other types of wall assemblies. This in turn allows evaluating the response of the wall to climate loads, including the hygrothermal performance, dilation at the panel joints, susceptibility to water penetration or the product of combined responses that act to deteriorate the façade system. Hence evaluating climatic effects in combination with wall response permits establishing the most severe combinations most likely to deteriorate the facade and thus provides a basis for prioritising maintenance scenarios for high-rise buildings. It is proposed that this process can be used to establish risk of deterioration from climatic effects among the different walls for a given building façade, between the level of risk among different buildings in a given climate, or for comparing the relative effects of similar facades located in different climate zones.

Evaluating risks of deterioration of building components from climate effects on buildings in different geographical locations requires the integration of environmental loads to the location of the buildings; given the previous studies completed in this area, it was thought that this would best be achieved through the use of a Geographic Information System (GIS).

1.2.Related Studies

An overview of the use of GIS in the building domain is provided in Haagenrud [2005] and in which a select number of studies are identified that served as a basis for the development of the current project. These include:

Wood-Assess [*Haagenrud* 1999a] and *MMWood* [Haagenrud 1999b; Haagenrud 2001] – These EU-projects combined European resources to develop methods and technologies for the assessment of the conservation state of wooden heritage buildings and mapping of environmental risk factors to these built assets. A condition assessment protocol was first developed and methods for continuous measurements of moisture and temperature in the microenvironment of buildings established in *Wood assess*. Thereafter for the *MMWood* project, these methods were extended to whole buildings in which estimates of environmental exposure of wood components were determined; for example the effects driving rain were based on the European standard EN 13013-3 [*p*EN 1999]. A PC-based pilot version of the assessment protocol was implemented on a GIS platform that can store, integrate and further process text, pictures, maps and related data.

LIFECON [Haagenrud 2004, Hallberg 2005] – A Life cycle based Maintenance System (LMS) was developed as a generic software tool to aid the documentation, inspection and maintenance management of cultural buildings, infrastructures and the built environment. The GIS-based

technology is open, object oriented and modular, can be extended to any type of built asset and includes management of component functionality during the life cycle of the asset. The LIFECON project is a specific implementation of the LMS for concrete infrastructure assets. Validation of LMS system was demonstrated by application for environmental characterisation of and performance analysis on a concrete bridge located in Fäeltskärsleden, Norway. The technology was also adapted to a municipality in Norway responsible for administering 8800 rental objects in which the system was used to document buildings information, building condition, maintenance costs, and maintenance planning and optimization information.

This paper provides an overview of a project to develop a GIS-based framework for the evaluation of façade performance and maintenance prioritisation, for high and medium-rise buildings with consideration of the likely environmental loads. A brief review of related studies and project methodology is provided, as is information on key project components, including: a Geographical Information System (GIS) based MMS interactive database for climate information, and building data; a Markovian-based, building façade maintenance management (BMM) model.

2 APPROACH

A schematic providing an overview of the approach adopted for the GIS-based assessment method as applied to building cladding systems is provided in **Figure 1**. Emphasis has been placed on characterising key climate variables such as moisture, thermal, wind and other loads for any given location in Canada. Evaluating climatic effects in combination with wall response provides a basis for setting maintenance priorities given that damage and deterioration can bring about loss in performance of the functional elements of the wall system. The process is used to establish risk of deterioration among the different walls for a given building façade, between the level of risk among different buildings in a given climate, or for comparing the relative effects of similar facades located in different climate zones.

The schema for the proposed GIS-based implemenation of the building façade performance and maintenance prioritisation framework is given in Figure 2 and consists of a GIS-based interactive database for climate information and building data (described in following section), the climate response module, maintenance condition and forecast module, and the National Maintenance Management System (NMMS). The web accessible GIS provides access to building data, as derived from the NMMS, climate data, and climate loads that are derived from climate data, and the climate response and field data module. Additional information on the climate response module and the building façade maintenance condition and forecast module are provided in a subsequent section. The NMMS is administered by the Real Property Branch of Public Works and Government Services Canada and is responsible for managing over 300 buildings across Canada.

Development of the identified tools will permit building managers to rate the relative applicability of various façade systems to particular geographic locations. System and material selections that more closely tie to the expected climatic loadings will result in reduced deterioration rates and should produce heightened thermal efficiency and performance of envelope systems. The project will help designers avoid design choices that can cause adverse indoor environmental conditions by evaluating the likelihood of water penetration into facades and examining the potential for propagation of mould and mildew. The net result provides for location specific designs and selections of façade materials and insulation that result in reduced energy consumption and extend life expectations of the components and wall assemblies in service.

Façade types considered in the framework include:

- Metal-glass curtain wall;
- Brick masonry veneer (stone and); and
- Prefabricated masonry and concrete panel.

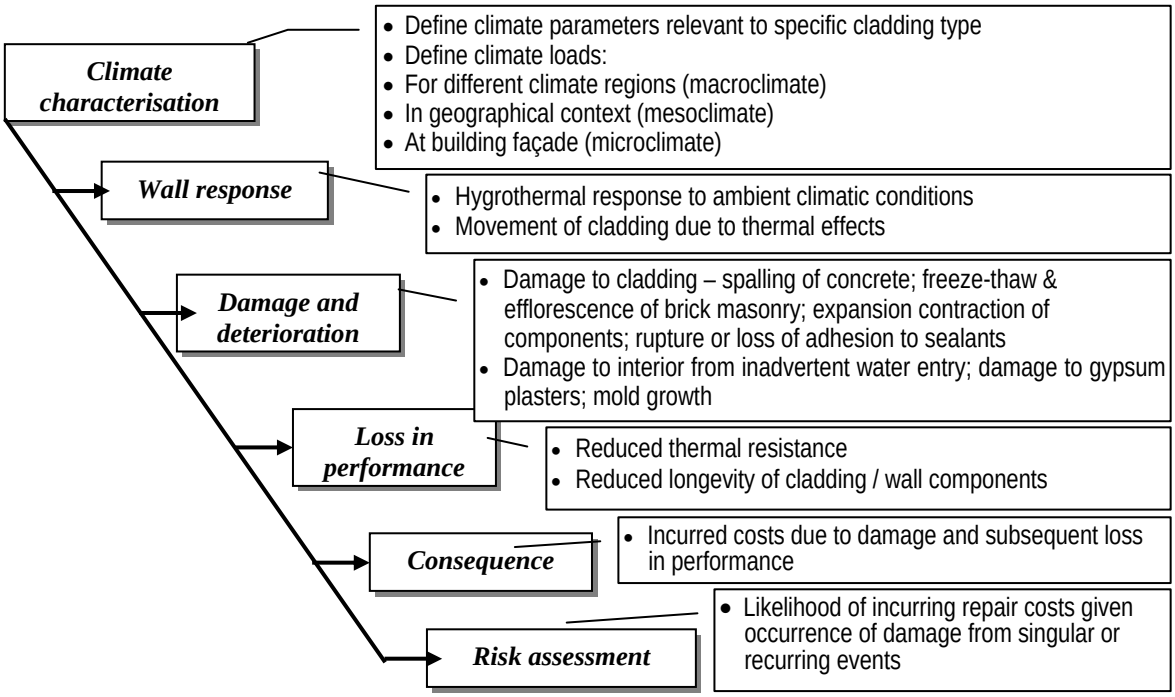

Figure 1. Schematic showing sequence of cause and effects on a wall assembly and the process of risk assessment method, from: (1) characterisation of climate effects; (2) wall response; (3) damage and deterioration; (4) performance reduction; (5) consequences; (6) risk assessment.

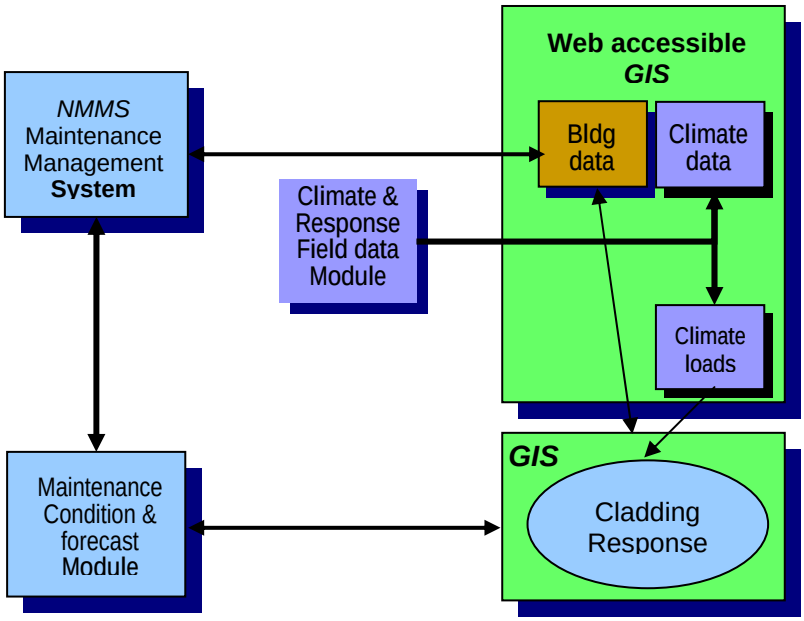

Figure 2 . Schema of proposed GIS-based implemenation of framework for evaluation of building façade performance and maintenance prioritisation

3 DEVELOPMENT OF GIS-BASED MMS INTERACTIVE DATABASE FOR CLIMATE INFORMATION, AND BUILDING DATA

The GIS-based MMS contains performance, damage, and durability models to make probabilistic predictions of changes in the state of the cladding or estimates of the service life due to prevailing conditions or some actual or planned event, such as an extreme climate event or maintenance interventions. These performance, damage, and durability models require information. A GIS approach was selected as the means of obtaining the necessary integration of climate- and building-related information in a geographical context. The GIS system comprises a national geographic base of

Canada and additional details for specific cities of interest. The system contains several databases including, but not limited to: a historical climate database, topographical data in the form of large scale topographic information for large parts of Canada and small scale data for urban areas, and database of built assets such as roads, bridges, and specifically buildings from real property databases. The web accessible GIS system integrates these several databases and provides the basic input to the cladding response models. These cladding response models feed input to the tools used for assessment and prioritization, discussed in subsequent sections. The basic architecture and relationship of the GIS portion to the rest of MMS system is illustrated in **Figure 2**.

The GIS data can be grouped under three general categories: climate-related data, building-related data, and physical data (e.g. topographic or hydrological data). These types of data are kept separately but the GIS is used to integrate the various databases. Only the climate-related data is discussed in this paper. The information incorporated into the GIS can be broadly categorized into two abstract types: gridded (mapped) data and point data. Point data can be essentially viewed as a tuple, the first two parts of the tuple locating the third part or element in two-dimensional space (and perhaps time). A latitude, longitude, and elevation can be considered to be a point whereas a table consisting of latitudes, longitudes, and elevations is a gridded data set. The distinction is arbitrary but useful since, for example, data regarding individual buildings or large amounts of historical weather data from a meteorological station can be considered as point data. Viewing the source of information as point data permits transforming, deriving, and exporting large of amounts of data to the cladding response models. Examples of gridded data, best viewed in a map form, are mean annual rainfall or mean wind speed.

As conceived the GIS system, shown in **Figure 3**, has the following capabilities:

Display a map — The primary purpose of this mode is to display gridded data. In this mode, a rough appreciation of the climate loads or risks can be obtained and measures of performance, risk, or condition state can be assigned to assets within the portfolio.

Display charts/graphs/roses/reports — In map mode, specific points can be selected, for example, a single building. Additionally, specific climate data can be attached to a particular building, such as hourly weather data from nearby meteorological stations. At this level more detailed climate loads can be determined, wind-driven rain on a particular façade for example.

Export data files — This mode of interaction is similar to the “Display” mode except that in this mode data files can be created from the database and exported for use in the performance and damage assessment models described below. The GIS data can be transformed or derived from the original data or used directly.

3.1.GIS Climate-Related Data

One of the objectives of this project is to render specific climate data in a form suitable for inclusion in either hygrothermal simulation models or damage index models. Hence, the climate is the primary information from which derivative climate parameters are developed. It also provides the basic information to determine the microclimate on a building façade. For example, given the geographical positioning of a site several scenarios are possible for determining the appropriate macro- or meso-scale data source or sources to obtain climate data that is most suited for the circumstances. i.e. use:

1. The nearest hourly meteorological station.
2. A nearby local weather station.
3. A very local station such as an instrumented building or a portable weather station.
4. A surrogate station with similar characteristics deemed appropriate.
5. Nearby stations extrapolating, interpolating or generating the required climatic information.
6. Long-term climate data (if the model can use long-term data) or interpolate, extrapolate from long-term climate data

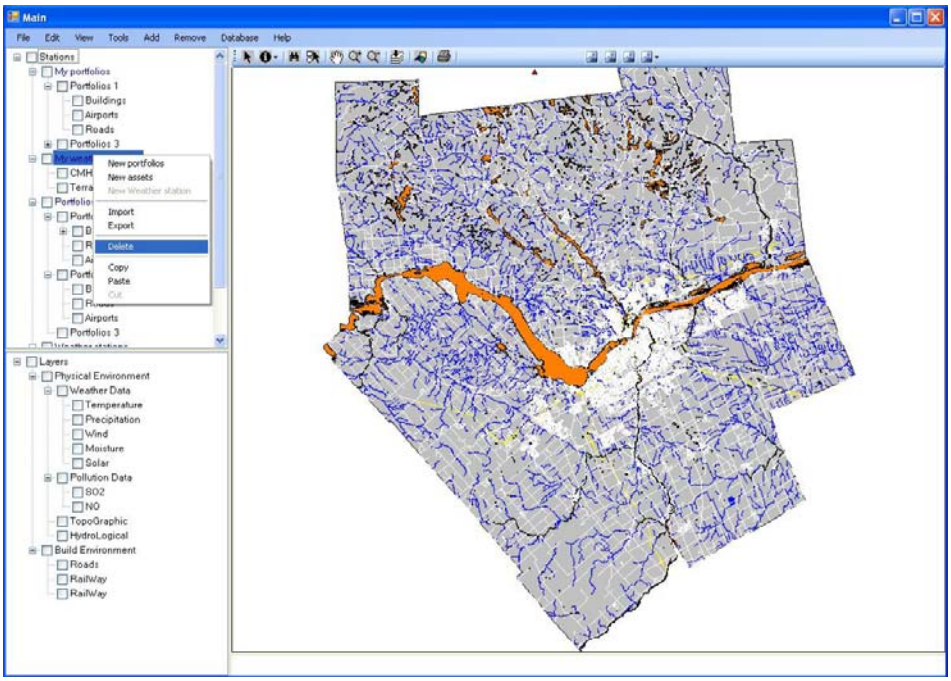

Figure 3. Basic GIS-MMS interface, display in map mode.

Thus after determining the appropriate source of information for a particular building asset the weather loads can be estimated. Various types of climatic information can be generated depending on the specific cladding response model utilised. For example, hygrothermal simulation models generally equire hourly weather data spanning over several months or years; energy simulation models, hourly data from either typical years (e.g. Weather Year For Energy Calculations or Typical Meteorological Year) or weather records from meteorological or local weather observation stations; a freeze-thaw model may only require the mean number of freeze-thaw cycles per year. Other models require information such as yearly, monthly, or daily data such as daily range, monthly averages. In all cases however the type of climatic information needed is historical. The GIS-MMS system provides a seamless method for determining the required climatic data for the appropriate models.

The GIS system allows the climate data to be accessed on a variety of time-scales, annual means, for example, to hourly data at the finest useable time-scale. Finally the required local or meso-scale climate data can be reduced through ancillary or helper applications to a micro-scale. These applications, through theoretical, empirical or numerical (e.g. computational fluid dynamics) models, make use of the building-related and physical data to reduce the scale of the climate-related data to the micro-scale: i.e. to bring the weather to the façade.

4 DEVELOPMENT OF RISK-BASED ASSESSMENT AND PRIORITISATION FRAMEWORK FOR FACADE BMM

The risk-based assessment and prioritisation framework for the facade BMM is based on two modules; the:

- Cladding response module that imparts information on the effect of environmental loads (climate or interior loads) on wall assemblies or specific components of the assembly; may also provide information on deterioration or damage of specified components over time.
- Building façade maintenance management (BMM) and forecast model.

Each of these is briefly described in turn.

4.1.Cladding Response Module

The cladding response module is comprised of several models that are either applications built on top of the GIS platform or stand-alone applications linked to the GIS. These models take input in the form of loads from the GIS and export the results to the maintenance management and forecast models. Some typical models that could be linked to the GIS include:

- Hygrothermal simulation (e.g. 1-D hygIRC [Cornick 2003])
- Energy simulation (e.g. DOE-2 Building energy analysis program [Mukhopadhyay 2006]
- Masonry freeze-thaw index [Mukhopadhyaya 2005]
- Scheffer's climate index for wood decay [Scheffer1971]
- Atmospheric corrosion models for metals [Roberge et al 2002]
- Masonry brick metal tie corrosion [Hegel and Lissel 2005]
- Jointing product (sealant) durability model [Lacasse et al. 2002]

4.2.Building Façade Maintenance Management (BMM) and Forecast Model

The Markovian-based, building façade maintenance management (BMM) model permits the optimization of maintenance planning, and introduces software that permits a user to initiate building maintenance actions. The intent was to provide building managers who are faced with having to maintain their buildings assets more efficiently, with a tool that could reduce the short and long-term costs of maintenance and rehabilitation. In essence, the BMM software can either optimize maintenance planning actions based on an expected maintenance budget or determine the budget required to maintain the façade to a minimum acceptable level of performance.

A schematic of the primary components of the software is given in **Figure 4**; details in respect to the Markovian approach to façade maintenance management are given in Lacasse et al. [2008]. The façade was first considered in development of the BMM software given that it is a significant element of the building envelope and of the building itself.

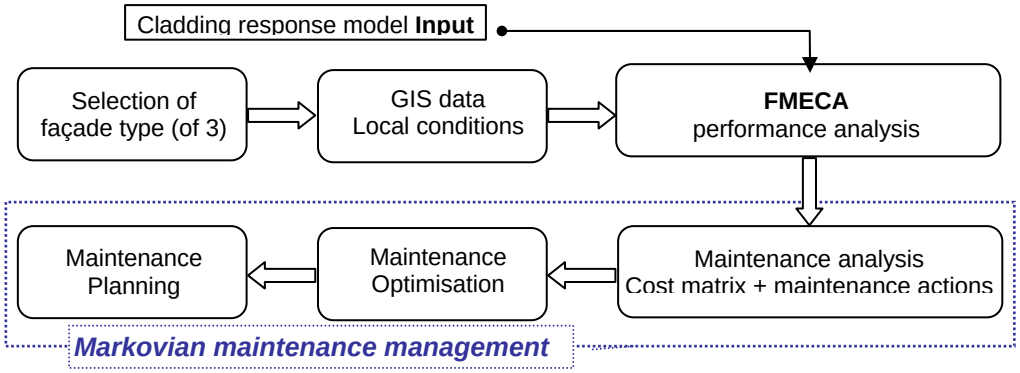

Figure 4. Schematic key project components of BMM model [Lacasse et al 2008].

The BMM model is built on several parts, however one of the key components is Failure Mode Effects and Criticality Analysis (FMECA) and performance analysis of the façade and related components; the several steps of this process are provided in **Figure 5** [Lacasse et al 2008]. The first step consists of developing a façade component criticality index that is based on outcomes of a FMECA. This permits determining the relative importance assigned amongst the different façade components, as proposed by [Talon 2006]. The basis for determining component criticality is described in more detail in Lacasse et al [2008].

Given that building managers do not necessarily dispose of unlimited budgets for maintenance actions, only the most critical set of components are further analyzed by simulation of the deterioration process. These simulations provide degradation curves of the change in condition state of façade components as a function of time. The different condition states are then defined ensuring that it is possible to observe these conditions during an inspection. The condition state matrix provides information on the likelihood of a component remaining or changing state at given inspection

intervals. Thereafter, the transition probabilities that correspond to the different sates are deduced that in turn permits obtaining the transition matrix. Such a matrix permits estimating the service life of components, or assembly of components, through an analysis using the Markovian model.

Figure 5. Description of performance analyses and development of

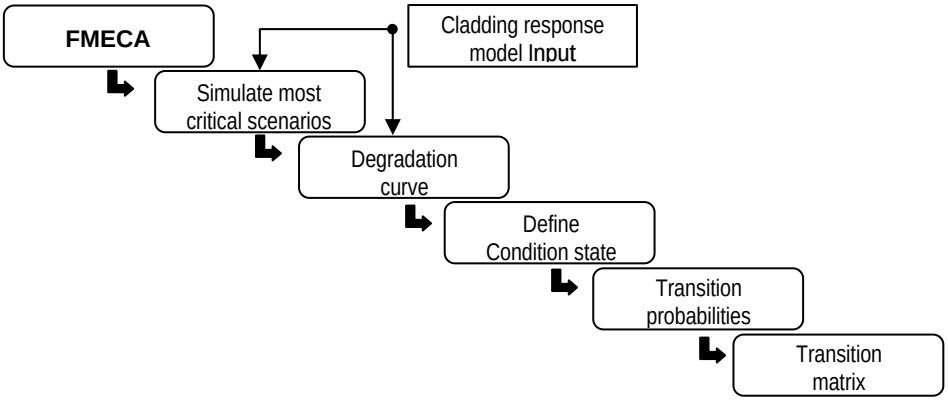

Markov condition state matrices for service life estimation.

5 SUMMARY

An overview is provided of a project focused on developing a GIS-based framework for the evaluation of building façade performance and maintenance prioritization. Climate effects are discussed in relation to wall response and expected damage arising from the deterioration of façade components is given. Loss in functional performance of components is examined and the consequences of these losses are related to risk as measured in terms of potential cost of maintenance interventions.

ACKNOWLEDGEMENTS

The authors are indebted to the Program of Energy Research and Development (PERD), part of the Office of Energy Research and Development, together with their respective organisations for funding of this project. Additionally, the authors would like to thank other contributors to this effort in particular, Mr. Denis Richard, Principal, Intempco Controls, and those from the GIS directorate of PWGSC, CMHC and NRCan who supported this project.

REFERENCES

Haagenrud, S.E., Cole, I.S., Sjöström, C. & Esposito, M.A. 2005, 'CIB W106 Geographical Information Systems - final report', Proc. 10DBMC: Int. Conf. on Durability of Building Materials & Components, Lyon, France, 17-20 April 2005, Paper TT9-194

Haagenrud, S., Veit, J., Eriksson, B., Henriksen, J. F. and Krigsvoll, G., 1999, 'System and Methods for Assessing Conservation State and Environmental Risks for Outer Wooden Parts of Cultural Buildings' (acronym: Wood-Assess), Final Report, EU-project ENV4-CT95-0110

Haagenrud, S. E.; Eriksson, B.; Sjöström, C.; Skancke, T. 1999, 'PC/GIS based system for maintenance management of wooden buildings – MMWOOD', Eighth International Conference on Durability of Building Materials and Components, 8dbmc; Vancouver; Canada; 30 May-3 June 1999. pp. 1602-1614. 1999

Maintenance Management of Historic (Wooden) Buildings' (acronym: MMWood), Final report, EU-Project ENV4-CT98-0796
prEN 13013-3 'Calculation of driving rain index for vertical surfaces from hourly wind and rain data'

Haagenrud, S.E., Krigsvoll, G., Gussiås, A., Sjöström C. and Hallberg, D. 2004, 'Life Cycle Management of built Environment-an ICT based concept and some cases, CIB world congress, Toronto, April 2004.

Hallberg, D. 2005 Development and Adaptation of a Life Cycle Management System for Constructed Works, Licentiate Thesis, Oct. 2005, KTH Research School – HIG, Centre for Built Environment, Univ. of Gävle, SE

Cornick, S.M.; Maref, W.; Abdulghani, K.; van Reenen, D. 2003, '1-D hygIRC: a simulation tool for modeling heat, air and moisture movement in exterior walls', Building Science Insight 2003 Seminar Series (15 Cities across Canada, October 07, 2003), pp. 1-10, October 01, 2003 (NRCC-46896)

Hegel, M.D. and Lissel S. L., 2005, 'Empirical Vs. Theoretical Service Life for Wall Ties in Brick Veneer Steel Stud Wall Systems', 10th Canadian Masonry Symposium, Banff, Alberta, June 8 – 12, 2005

Lacasse, M.A.; Cornick, S.M.; Shephard, N. 2002, 'Estimating the service life of jointing products and systems - application of a crack growth model to different climates,' 9th International Conference on Building Materials and Components (Brisbane, Australia, March 17, 2002), pp. 1-11, March 01, 2002 (NRCC-45362)

Lacasse, M. A., Kyle, B., Talon, A., Boissier, D., Hilly, T., Abdulghani, K. 2008, 'Optimization of the Building Maintenance Management Process Using a Markovian Model', in: Proceedings of the 11th International Conference on Durability of Building Material and Components, 11-14 May, Istanbul, Istanbul Technical University, Turkey.

Mukhopadhyay, J. and Haberl, J. S. 2006, 'Performance of High-Performance Glazing in IECC Compliant Building Simulation Model (DOE-2)' Energy Systems Laboratory (Texas Engineering Experiment Station, Texas A&M University), Proceedings of the SimBuild 2006 Conference (MIT, Cambridge, MA, August 2-4, 2006)

Mukhopadhyaya, P.; Kumaran, M.K.; Nofal, M.; Tariku, F.; van Reenen, D. 2005, 'Assessment of building retrofit options using hygrothermal analysis tool', 7th Symposium on Building Physics in the Nordic Countries (Reykjavik, Iceland, June 13, 2005), pp. 1139-1146, June 01, 2005 (NRCC-47742)

Roberge P.R., Klassen, R. D., Haberecht, P.W. 2002, 'Atmospheric corrosivity modeling - a review', Materials and Design Vol. 23: 321-330

Scheffer, T.C. 1971, 'A climate index for estimating potential for decay in wood structures above ground', Forest Products Journal Vol. 21(10): 25–31

A Methodology for Protection of Masonries against Rising Damp

Maria Karoglou [1]
Antonia Moropoulou [2]
Magdalyni K. Krokida[3]
Dimitris K. Konstantopoulos [4]
Vasilis Z. Maroulis [5]

T 72

ABSTRACT

The building envelope restoration and retrofitting suffering from rising moisture problems is one of key issues in sustainability of buildings, considering that moisture effects indoor air quality, energy consumption and durability of building materials and components. New tools are needed for the ability of building, its parts, components and materials to resist the degrading action of moisture over a period of time. In this work, an integrated methodology for the moisture protection of buildings against rising damp is proposed. This methodology includes real experimental data, phenomenological mathematical modelling and simulation. This methodology contributes to the prognosis of masonry moisture content, as well as to the decision-making on compatible restoration materials.

KEYWORDS

Capillary rise Kinetics, Drying kinetics, Plaster

[1] National Technical University of Athens, Chemical Engineering, Faculty, Athens, 15780, Phone +30 210 7721432, Fax 210 7723215, margo@central.ntua.gr
[2] National Technical University of Athens, Chemical Engineering, Faculty, Athens, 15780, Phone +30 210 7721432, Fax 210 7723215, margo@central.ntua.gr
[3] National Technical University of Athens, Chemical Engineering, Faculty, Athens, 15780, Phone +30 210 7723150, Fax 210 7723155, mkrok@central.ntua.gr
[4] National Technical University of Athens, Electrical and Computer Engineering, Faculty, Athens, 15780, Phone +30 210 7723151, Fax 210 7723155 el01154@central.ntua.gr
[5] National Technical University of Athens, Electrical and Computer Engineering, Faculty, Athens, 15780, Phone +30 210 7723151, Fax 210 7723155, el01206@mail.ntua.gr

1 INTRODUCTION

Moisture causes a number of structural and aesthetical problems in buildings. The effects of moisture can be combined with other deteriorating factors such as air pollution and/or environmental loads (such as frost) and create an even more aggressive condition. Apart from creating structural, aesthetical problems, moisture can cause degradation of indoor quality, since it enhances the development of mould, and mildew, and favourable conditions for biological attack of a building. It also increases the relative humidity of the indoor environment, and decreases the thermal insulation of the building, causing increase of buildings energy requirements.

There is a wide agreement that the management of moisture in its various forms is essential for buildings to be durable, safe and energy efficient. One of the main mechanisms of moisture transfer is capillary rise of ground moisture. The capillary rise kinetics is indicative of materials susceptibility to decay factors and can provide important information for the selection of compatible building materials. In addition the frontiers of moisture analysis for buildings involve the development of computer software tools and underlying methods capable of modelling all types of moisture flows through buildings. Indeed, there are many facets to the moisture issue and many approaches to modelling [PATH, 2004].In this work an integrated methodology for the protection of buildings against rising damp phenomenon is proposed. This methodology includes retrieval of experimental data, and thereafter, phenomenological mathematical modelling and simulation of moisture transport effects. With the aid of this methodology materials moisture content can be assessed. Moreover appropriate restoration materials for masonries suffering by rising damp phenomenon can be assessed before their real application, contributing to the maintenance of such structures.

2 DATA/ MODELLING

A first stage for the realisation of this methodology is carrying out a basic laboratory experimental study, focused on chemical, mineralogical, and microstructural characteristics of building materials, e.g. determining porosity, bulk density and average pore radius of porous moisture susceptible materials. Concerning the phenomena of water transport in porous materials, two processes are of importance: capillary rise and drying kinetics

For the study of the kinetics of capillary rise of moisture, variations of capillary height to time are recorded for each material. A first-order kinetics model is proposed, in which the equilibrium moisture height, derives from Jurin law, based on materials average pore radius [Karoglou et. al. 2005a]. The concept of capillary height time constant is introduced for the first time. The first order kinetic model is fitted to experimental data. The parameters of the proposed model result from an optimization technique to minimize the residual sum of squares between experimental and calculated values of capillary height. The model predicts successfully the capillary rise of water. The capillary height time constant is affected by the material characteristics. In Table 1 it is shown the capillary rise mathematical model.

Table 1. Capillary rise mathematical model

Properties	
H capillary rise height	(cm)
t_{cr} capillary rise constant time	(d)
Factors	
He capillary rise equilibrium height	(cm)
T air temperature	(^{o}C)
r average porous radius	(μm)
Equations	
$\frac{dH}{dt} = \frac{1}{t_{cr}}(H_e - H)$	
$H = H_e - (H_e - H_o)\exp(-\frac{t}{t_{cr}})$	
$H_e = \frac{2\sigma}{\rho g r}$	
Parameters	
H_0 correction factor	(cm)
ρ water density	(g/cm^3)
σ water surface tension	(dyn/cm)
Factors affecting parameters	
material→ H_0	
environment→ρ, σ	

For the study of drying kinetics an experimental air dryer of controlled drying air conditions can be used. Environmental factors, such as air temperature, relative humidity, and air velocity affect drying; hence these factors are monitored in the experimental study. A first order kinetic model is used to describe the drying process. The model predicts successfully the experimental data. The drying time constant is a function of drying conditions and materials characteristics [Karoglou et. al. 2005b]. In Table 2 it is shown the mathematical model for drying.

Table 2. Drying mathematical model

Properties	
X moisture	(kg/kg db %)
t_{cd} drying time constant	(h)
Factors	
Xe moisture equilibrium	(kg/kg db %)
T air temperature	(^{o}C)
α_w water activity	(-)
u air velocity	(m/s)
Equations	
$\frac{dX}{dt} = -\frac{1}{t_c}(X - X_e)$	
$t_{cd} = c_o\, T^{\,c_1}\ \alpha_w^{\,c_2} u^{\,c_3}$	
$t = -t_{cd} \ln(\frac{X - X_e}{X_o - X_e})$	
$t_{cd} = -\frac{1}{K}$	
Parameters	
c_0	(h)
c_1	(-)
c_2	(-)
c_3	(-)
Factors affecting parameters	
material→ c_0	
environment→ c_1, c_2, c_3	

In Figure 1 the effect of relative humidity and air velocity on the drying process of a plaster (PRL) is shown. As expected, there is an acceleration of the drying process due to the increase in air velocity from 1 to 8 m/sec. The effect of relative humidity is also very important as this decreases the drying rate as the relative humidity increases from 30 to 70%.

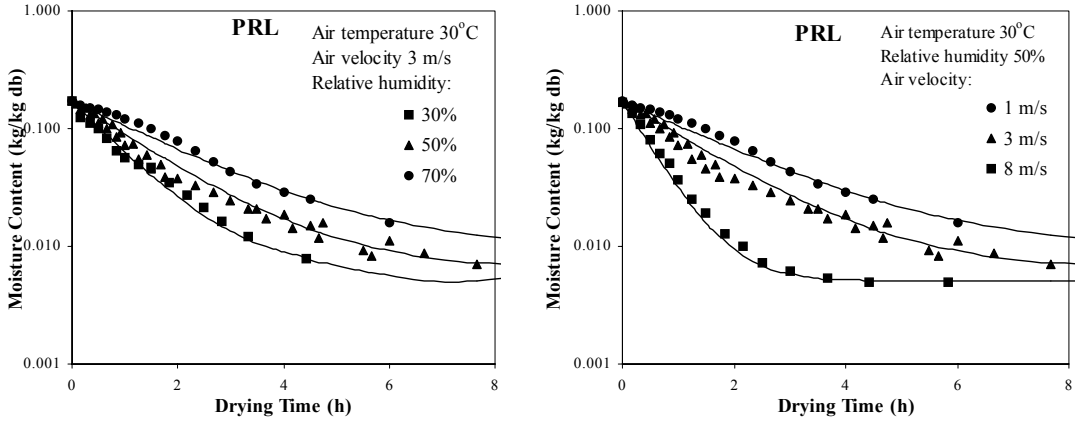

Figure 1. Effect of air relative humidity and air velocity at drying kinetics of a plaster

For the estimation of the moisture equilibrium of each material, moisture sorption (adsorption and desorption) isotherms, are defined. This is made using a water sorption analyser, obtaining materials sorption isotherms at three different temperatures. A modified Oswin equation is used to predict the

experimental data, for water activity in the range of 0-0.9 [Karoglou et. al. 2005c]. The governing equation for sorption, forming the basis for the mathematical model and definitions of the basic model parameters, is provided in Table 3.

Table 3. Water sorption mathematical model

Properties	
X_e moisture equilibrium	(kg/kg db %)
Factors	
T air temperature	(^{o}C)
α_w water activity	(-)
Equation	
$X_e = b_o \exp(\frac{b_1}{T})(\frac{a_w}{1-a_w})^{b_2}$	
Parameters	
b_0	(kg/kg db%)
b_1	(^{o}C)
b_2	(-)
Factors affecting parameters	
material→ b_0	
environment→ b_1 , b_2	

The equilibrium moisture content of the material is affected by temperature and humidity of the surrounding air. Thus, the equilibrium moisture content is higher at lower air temperature and at higher humidity levels. The equilibrium moisture content of various materials is presented at Fig. 2.

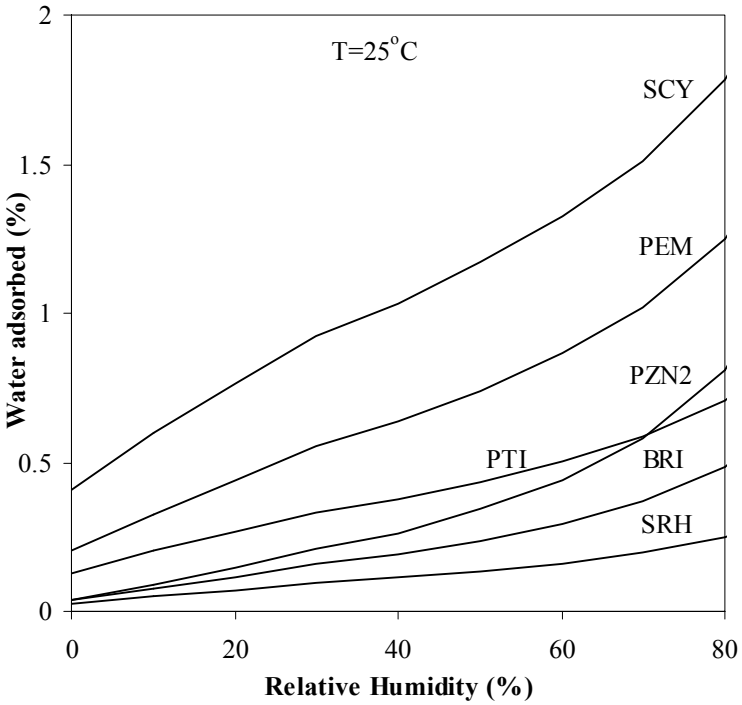

Figure 2. Isotherms of selected building materials at T = 25 ^{o}C (S: Stone, B: Brick; P: Plaster)

All the suggested phenomenological models predict the experimental data. A correlation between the parameters of the moisture transport model affected by materials characteristics and microstructural parameters is attempted. The primary objective of this work is the development of a general

phenomenological model that allows the prediction of all related hygroscopic properties, based on its microstructural characteristics. This approach is very significant, because permits the prediction of the hygroscopic properties of the material, when only experimental data related to the microstructure of the material is available or when there is no possibility to obtain experimental data [Moropoulou et. al. 2005].

3 SIMULATION

After data collection and modelling, a moisture transport simulator is developed (HygroScope). HygroScope is developed for a two-layer masonry wall, consisting of a wall substrate and a plaster layer of varying height and width. The masonry layer consists of one material (referred to as wall), either stone or brick, and the outer layer of a plaster with various compositions [Konstantopoulos et al. 2007]. Various plasters before their real application can be tested, like macro-porous plasters, which are suitable for the protection of masonry against rising damp. The simulator takes into account the: (i) moisture transfer mechanisms to and from the building (capillary rise, drying); (ii) wall configuration (materials and size); (iii) properties of the construction materials; (iv) seasonal regional meteorological data (air temperature, humidity and wind speed). It can calculate the: (i) seasonal wall moisture content along with the corresponding equilibrium moisture height; (ii) rate of capillary rise; (iii) rate of wall drying. The software application is developed using Visual Studio (2005) development software based on C+ programming language. The simulator is a combination of three basic components that include the: Database, Mathematical Model Library, and Graphical User Interface (GUI); each of these is briefly described below.

3.1 Database

Material and environmental data are stored in the database. The terms material and environmental data correspond to a collection of attributes that fully define a set of materials and a set of environmental conditions. For material data these attributes are: porosity, density, capillary saturation moisture, equilibrium moisture constant, drying constant, average pore radius, capillary time constant and the name of the material. For environmental conditions these attributes are the minimum and maximum temperature, moisture and air velocity values that appear in the specified environment, the date when the maximum for each of the above values is observed, daily observed temperature, moisture and air velocity conditions (365 values – one for each day) and the name of the location where these conditions dominate. Each material and environmental collection is stored in a separate XML file. The advantage of having a XML file format is that the user can change, if desired, the data files without necessarily running the application.

3.2 Mathematical Model Library

The second component is the mathematical model library embedded in the application. This library is the core of the simulator, since it brings into effect the methods and the principles previously described.

3.3 Graphical User Interface (GUI)

The third component, the Graphical User Interface (GUI), consists of four basic windows (screens) The GUI enables the user to interact with the database in various ways (create, delete and update information) and also create and manage simulation projects. It also permits the user to customize the application settings through the ‘settings’ window. The Simulation ‘project screen’ is given in Figure 3.

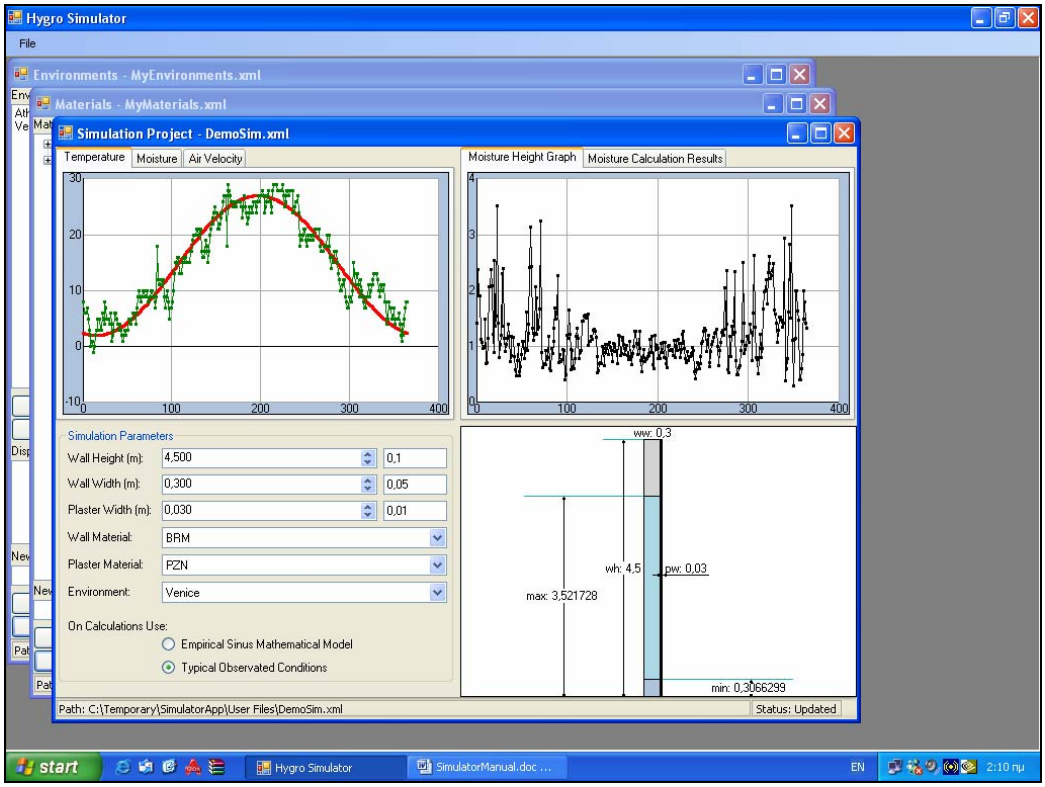

Figure 3. Simulation Project Screen

To initiate a new simulation project, the user has to select the File – New – Simulation Project menu. This starts a new blank simulation project and opens the relative window which will host the project. When the simulation project has been created or loaded the user will be able to see four different areas inside the window. In the bottom left area are located the controls with which the user can interact to manage the simulation project. After the desired values for these controls have been set, the simulator calculates the curve for the moisture height and presents it to the graphic area located in the upper right part of the window. This is the curve that depicts the height of the moisture (vertical axis) relative to time (horizontal axis) for all 365 days of the year. From this curve the user can also see the minimum and maximum heights of moisture during the whole year. On top of this graphic area are two tabs from which the user can switch between the curve view and the report view, where he can see the moisture height results of the calculations. In the lower right part of the window there is a graphic design of the wall with the plaster material attached.

This graphic design is in scale and shows the geometrical aspects of the wall – plaster. It also shows the minimum and maximum height of moisture during the year once the calculations have finished. In the upper left part of the window is another graphic area that shows the measurements curve and the proximal sinus curve of the selected environment. The user can select one of the three tabs on top of this graphic area to change among the temperature, moisture and air velocity curves. The current simulation project can be saved by accessing the File – Save (of Save As) menu. Each simulation project is saved in a separate XML file.

3.4 Case Study

With the aid of this methodology various restoration building materials can be assessed, with respect to properties related to their capability of retaining moisture, before their real application. The fundamental variable expressing the suitability of such materials is the variation of moisture height, which is the maximum height that moisture creeps on a vertical wall with respect to materials used for construction. A case study with respect to the ability of decision making on different restoration

plasters is stated below. It is considered masonry situated at Athens. The wall is constructed with a traditional hand-made clay brick, named as, BRM, has a height of 3.3 m and width 0.5 m. The plaster application width is equal to 0.03 m. The masonry suffers from rising damp. The question arising is what kind of restoration plaster should be used. Two different plasters are investigated. PZN, which is a traditional plaster and PEM, which is a macroporous plaster. The attributes for the afore-mentioned materials are shown in Table 4.

Table 4. Materials attributes

Properties	**BRM**	**PZN**	**PEM**
Porosity%	32.6	41.3	63.8
Average pore radius(μm)	2.02	0.52	33.2
Density (kg/m^3)	2.77	3.25	4.4
Capillary saturation moisture %	11.6	17	18.6
Equilibrium moisture content (%)	1.62	33.8	31.3
Drying constant (h)	2.62	2.77	3.13
Capillary rise constant (d)	1.39	3.54	0.04

With the aid of HygroScope (Figure 4), it is found that PEM reduces more moisture height in comparison to PZN. This can be justified comparing materials attributes. PEM presents higher porosity and very high average pore radius value. Moreover PEM contains hydrophobic substances, resulting at a very capillary rise rate and high drying rate due to the existence of macropores. Thus PEM is preferable to be applied, instead of PZN.

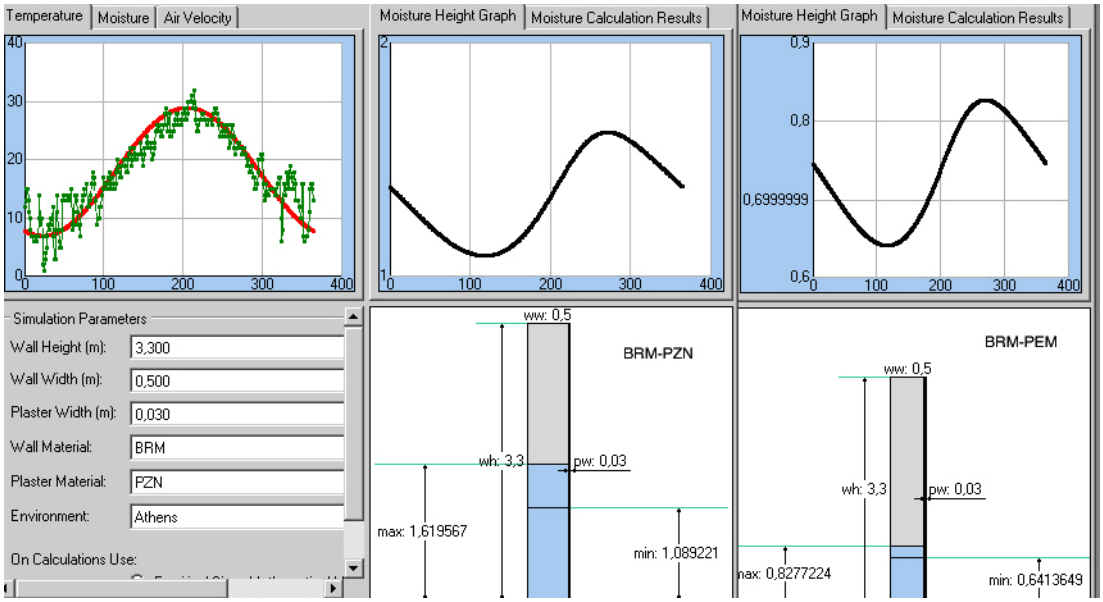

Figure 4. Simulation Project Screen for the two different plasters

4 CONCLUSIONS

Capillary rise of water is one of main moisture transfer mechanisms at buildings. In this work an integrated methodology to tackle rising damp problem is proposed. This methodology involves specific stages such as; conduction of basic experimental work, data modelling and simulating. The simulator supports satisfactory decision making concepts concerning the selection of the appropriate protecting strategy, e.g., plaster selection (material, size). With the use of this methodology, the

assessment of the effectiveness of restoration materials before their real application can be made, contributing to the maintenance of masonries suffering by rising damp.

REFERENCES

PATH, 2004, Building moisture and durability, report of U.S. Department of Housing and Urban Development, Office of Policy Development and Research ,Washington D.C.

Karoglou, M., Moropoulou, A., Giakoumaki, A., Krokida, M.K., 2005, 'Capillary rise kinetics of some building materials', J. of Colloid and Interface Science, **284** [1], pp. 260-264.

Karoglou, M., Moropoulou, A., Krokida, M.K., Maroulis, Z.B., 2005, 'Drying kinetics of some building materials', J. Drying Technology, **23** [1-2], pp. 305-315.

Karoglou, M., Moropoulou A., Krokida M.K., Maroulis, Z.B., 2005, 'Water sorption isotherms of some building materials', J. Drying Technology, **23** [1-2], pp. 289-303.

Moropoulou, A., Karoglou, M., Krokida, M.K., Maroulis, Z.B., Saravacos, G.D., 2005, 'Prediction of hygrometric properties of building materials based on the average pore radius', 7th World Congress of Chemical Engineering, Glasgow, United Kingdom,10-14 July 2005, (CD ROM).

Konstantopoulos D. K., Maroulis V. Z., Karoglou M., Moropoulou A., Mujumdar A. S., 2007, 'HygroScope: a moisture transfer simulator for buildings', Drying Technology, **25** [6], pp. 1119 – 1125.

11th International Conference on Durability of Building Materials and Components
Istanbul Turkey May 11-14, 2008

Optimization of the Building Maintenance Management Process Using A Markovian Model

Michael A. Lacasse [1]
Brian Kyle[2]
Aurélie Talon[3]
Daniel Boissier[4]
Thibaut Hilly[1]
Khaled Abdulghani[1]

T 72

ABSTRACT

Building managers are increasingly faced with having to maintain their building assets more efficiently whilst reducing the short and long-term cost of maintenance and rehabilitation. Several different systems employing a Markovian approach have been adapted to the bridge structure domain; fewer in the domain of buildings. The present paper describes a parallel approach to maintenance management used in bridge structures but adapted to the maintenance of building facades. The maintenance of several components of a concrete panel façade system is considered in the context of both yearly and longer-term maintenance planning. The significance of different components in relation to others in the system is determined by first conducting a Failure Mode Effect and Criticality Analysis (FMECA) on all façade components. The FMECA permits developing a component criticality index from which their relative importance is assigned amongst the different façade components. An optimization of different possible maintenance actions are considered in relation to the cost of specified actions to or replacement of components based on a multi-objective index. This index provides a means of relating competing maintenance objectives; that of controlling maintenance intervention costs and maintaining component condition ratings. It provides yearly maintenance costs of individual components for a given wall system over a long-term horizon that spans the life of the façade system.

KEYWORDS

Building facade, Building maintenance, Component deterioration, Failure mode analysis maintenance optimization

1. National Research Council Canada, Institute for Research in Construction, Ottawa, Canada K1A0R6, Phone +1 613 993 9715, Fax +1 613 954 5984, Michael.Lacasse@nrc-cnrc.gc.ca, Khaled.Abdulghani@nrc-cnrc.gc.ca
2. Public Works and Government Services Canada, 11 Laurier Street, Gatineau, Canada K1A 0S5, Phone: +1 819 956 3420; Fax: +1 819 956 3400, brian.kyle@pwgsc.gc.ca
3. CEMAGREF, *Unité Ouvrages Hydrauliques et Hydrologie*, 3275 route Cézanne - CS40061, 13182 Aix en Provence Cedex 5; Phone +33 4 42 66 99 80, Aurelie.Talon@cemagref.fr

4. Polytech' Clermont-Ferrand - Department of Civil Engineering, 24 Avenue des Landais, BP 206, Aubière, France 63174; Phone +33 473407525; Fax +33 473407494; daniel.boissier@cust.univ-bpclermont.fr

1 INTRODUCTION

Building managers are increasingly faced with having to maintain their building assets more efficiently whilst reducing the short and long-term cost of maintenance and rehabilitation. In the domain of construction infrastructure, there exist several examples of infrastructure maintenance that employ the Markovian approach; examples can be found in the domain of roadway pavements [Nesbitt et al 1993; Durango-Cohen and Mandanat 2006], storm water sewerage works [Micevski et al 2002] and several related to the bridge structure domain [Cesare et al. 1994; Morcous et al. 2003; Morcous and Lounis 2006; Robelin and Mandanat 2007]. However there are fewer examples of the Markovian approach used in the domain of buildings although some useful examples include the work of Van Winden and Dekker (1998), Lounis and Vanier [2000] and that of Augenbroe and Park [2002].

~~DETERIORATION~~ Approaches to Maintenance Management of Building Components:

The Markov-based decision model for rationalising building maintenance, developed by Van Winden and Dekker (1998) was used at the strategic level for the planning of maintenance for buildings owned by a building society. The value of the model as a management instrument in estimating and allocating maintenance budgets was demonstrated in a pilot case of four (4) building elements, namely: masonry, pointing, window frames and painting. Modelling the deterioration of these components permitted determining the maintenance policy that ensured a specified average quality level at minimal cost. The intent of the study was to provide some estimate of life cycle costs to the building and as such, the study provides useful information related to methods of establishing cost matrices. However, there appears to be some missing information related to the allocation of costs.

Lounis and Vanier [2000] describe the development of a roofing maintenance management system that integrates an existing condition assessment module (i.e. *Roofer;* [Bailey 1990]), and performance prediction based on a Markovian model, with a multi-objective optimization scheme. The maintenance optimization includes the determination of the optimal allocation of funds and prioritization of roofs for maintenance, repair and replacement that satisfy: (i) minimization of maintenance and repair costs; (ii) maximization roof performance; and (iii) minimization of risk of failure. Compromise programming is used to solve the optimization problem and the system purports to provide building managers an effective decision support system that identifies optimal projects for repair and replacement whilst achieving satisfactory trade-offs between conflicting maintenance objectives.

Augenbroe and Park [2002] suggest that the building maintenance problem can be formulated as a Markov decision process. They indicate that the discrete Markov chain model aptly describes both the time-dependence and randomness of building system performance and thus can be used for systematic decisions regarding replacements of building components that affect the scope of yearly maintenance activities. Such an approach permits comparison of various maintenance policies on resulting maintenance costs and building quality. The authors also suggest that this approach gives insight into the relation between yearly maintenance costs and the quality of the building, both on short as well as a long term.

The present paper describes a parallel approach to the maintenance management of bridge desks initially postulated by Lounis and Vanier [1998] and on which the work of Lounis and Vanier [2000] on roofing was developed, of which a broader overview of the roofing project is provided by Kyle et al. [2002]. In this instance, these approaches have been adapted to the maintenance management of buildings facades and have also drawn upon the more recent work of Morcous et al. [2003] and Morcous and Lounis [2006].

2 PROPOSED MARKOVIAN-BASED, BUILDING FAÇADE MAINTENANCE MANAGEMENT (BMM)

The Markovian-based, building façade maintenance management (BMM) model permits the optimization of maintenance planning, and introduces software that permits a user to initiate building maintenance actions. The intent was to provide building managers who are faced with having to maintain their buildings assets more efficiently, with a tool that could reduce the short and long-term costs of maintenance and rehabilitation. In essence, the BMM software can either optimize maintenance planning actions based on an expected maintenance budget or determine the budget required to maintain the façade to a minimum acceptable level of performance. A schematic of the primary components of the software is given in Figure 1. The façade was first considered in development of the BMM software given that it is a significant element of the building envelope and of the building itself.

Figure 1. Schematic key project components of BMM model.

Consider for example, the maintenance of several components of a concrete panel façade system in the

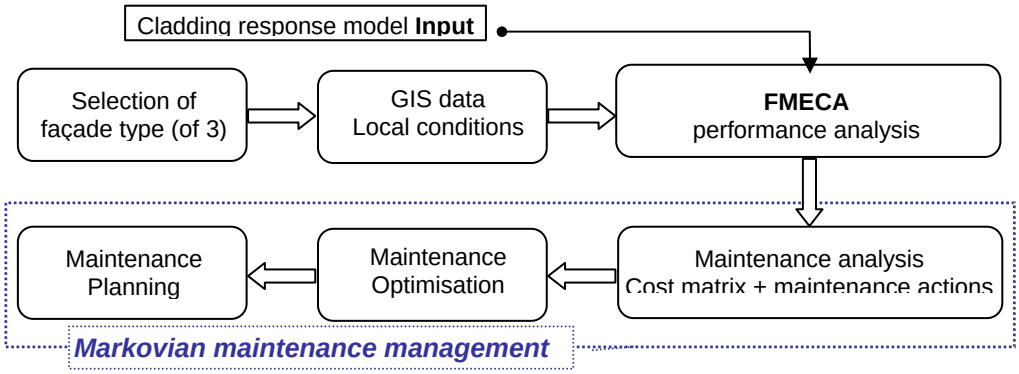

context of both yearly and longer-term maintenance planning. The significance of different components in relation to others in the system is determined by first conducting a Failure Mode Effect and Criticality Analysis (FMECA) on all façade components. This permits developing a component criticality index from which their relative importance is assigned amongst the different façade components. An optimization of different possible maintenance actions can then be considered in relation to the cost of specified actions to or replacement of components. However, a means of relating competing maintenance objectives is required that controls maintenance intervention costs whilst maintaining component condition ratings.

3 O~~VERVIEW~~~~UTLINE~~ OF FMECA IN THE CONTEXT OF MAINTENANCE MANAGEMENT

Of the several parts of which is comprised the BMM model, one of the key components is Failure Mode Effects and Criticality Analysis (FMECA) and performance analysis of the façade and related components; the several steps of this process are provided in Figure 2. The first step consists of developing a façade component criticality index that is based on outcomes of a FMECA. This permits determining the relative importance assigned amongst the different façade components, as proposed by Talon [2006].

Given that building managers do not necessarily dispose of unlimited budgets for maintenance actions, only the most critical set of components are further analyzed by simulation of the deterioration process. These simulations reflect the change in condition state of façade components and thus the degree of overall deterioration over time. The different condition states are necessarily defined thereby ensuring that it is possible to observe symptoms of these conditions during an inspection. The condition state vector ($\boldsymbol{D}_t$), given in Figure 2, provides information on current condition; each element in this vector having S condition states, represents the estimated percentage of all like components in a particular condition state after time t, for which t, is expressed in transition periods, or e.g., periods

between inspection. The likelihood of a component remaining or changing state at given inspection intervals provides the transition probabilities ($p^{i,j}$), that is, probability of changing (or not) condition from state *i* to a lower state *j*, and for which the corresponding transition probability matrix (**P**) is obtained. Such a matrix (*S* x *S*), shown in Figure 2, permits estimating the service life of components, or assembly of components, through an analysis using the Markovian model. Given the present condition vector of a component ($\boldsymbol{D_t}$), the future condition vector ($\boldsymbol{D_{t+n}}$) can be obtained as: $D_{t+n} = D_t \times \mathbf{P}^n$, where n, is the number transition periods in the future.

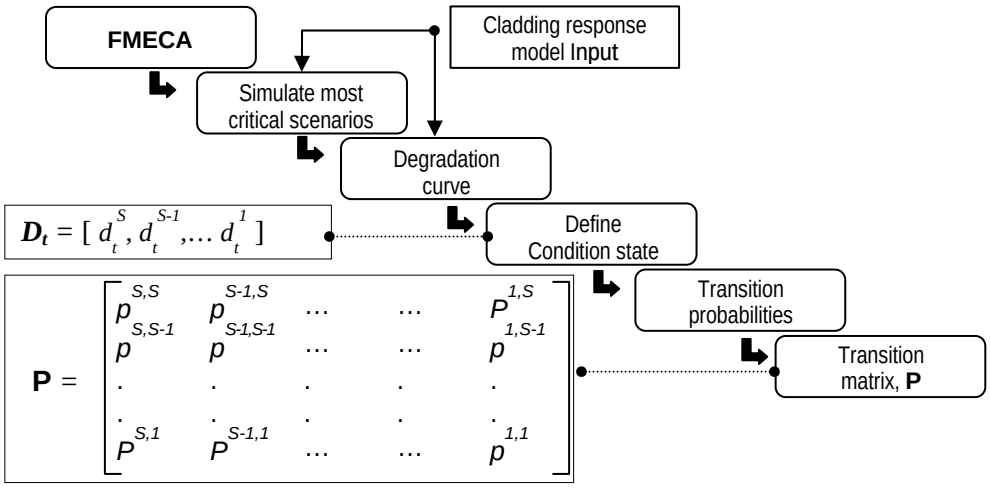

Figure 2. Description of performance analyses and development of Markov condition state matrices for service life estimation.

4 MANAGEMENT OF COMPONENT CONDITION STATE USING A MARKOVIAN METHOD

There are different maintenance actions that maintenance managers can take over the course of managing the façade component condition state. For example, the component might be repaired such that its condition can be maintained or it might be completely replaced. If repaired, consideration should be given to how amenable to repair the component. Can the component be repaired more than once? Then again, can the component be repaired indefinitely? Provided a component is readily accessible then repair is likely possible. However, it is unlikely that any building façade component can be repaired indefinitely so then repairs should be considered as actions capable of retarding the degradation process but ultimately not preventing the need for replacement at some time in the future. Hence a repair action undertaken on a component typically would not renew the component to its original condition state but the action would improve its condition to a stated higher level.

If, however, the component were replaced then its condition state would be renewed to that of a new component. A typical example of components in a building façade more likely replaced as opposed to repaired would be the insulated glass (IG) component of a window. The IG unit is either, functioning adequately (i.e. IG unit is transparent, and still holds an inert gas between glass lites), or its seal has failed and the unit is now clouded, as is evident by the presence of moisture on the interior glass lites.

As well, it may be decided that no maintenance action be taken, in which case the loss in performance over time would continue at the rate prescribed by the deterioration process.

For each of these actions (described as a maintenance vector, $\mathbf{M}_{ct}$), including the no maintenance action, there exist transition matrices that reflect the action taken (i.e. $\mathbf{P}_{ct}$) and associated with each of these a cost for repair or replacement, and perhaps in some cases, a cost for no action as well ($\mathbf{C}_{ct}$). The general stages in the maintenance action approach are provided schematically in Figure 3. Once the

consequences of maintenance actions are established, one can then consider optimization of maintenance actions.

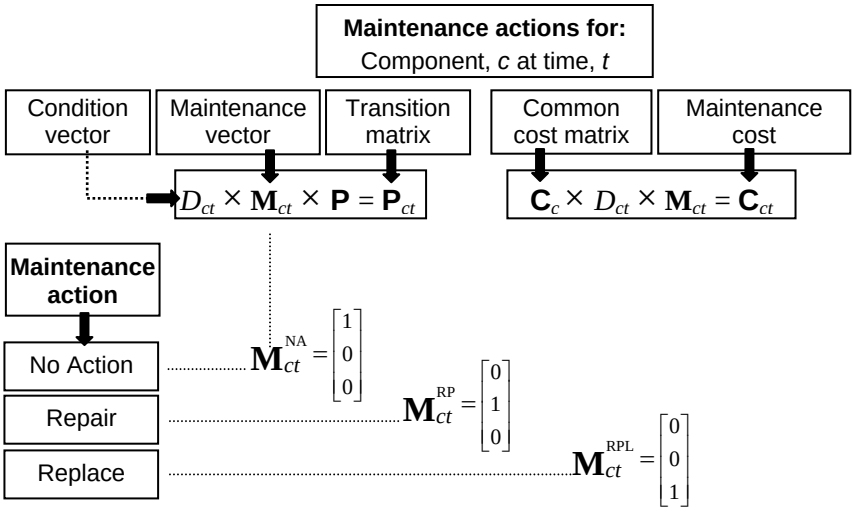

Figure 3. Description of maintenance analysis – possible choice of maintenance actions, associated maintenance vector, transition matrix and cost matrix.

5 OPTIMIZATION OF MAINTENANCE ACTIONS~~OF~~

An optimization of different possible maintenance actions considers three scenarios that relate aggregated component condition rating (ACCR) to a desired or available maintenance budget. These scenarios include:

- Maximization of component condition rating for a given annual maintenance budget.
- Minimizing the maintenance budget for a targeted condition state (aggregated condition state for all components)
- Use of multi-objective index when neither the budget is neither defined nor is the expected condition state – a compromise solution between maximisation of the budget and minimisation of the condition state over time.

The aggregated component condition rating (AACR) is derived from the a knowledge of the number of "sections" in any given condition state at a given time, a section being defined as a measurable part or portion of the entire set of sections that together form the representative "mass" for a given component type. As illustrated in Figure 4, at any given timer, *t*, component sections will be in their respective conditions state.

The multi-objective index (MOI), obtained from Morcous and Lounis [2006], with evaluation criteria, *i*, a set of criteria, *m*, and assuming the solution metric with $p = 1$, is given by:

$$MOI(x) = \left[\sum_{i=1}^{m} w_i \bullet \left| \frac{f_i(x) - \min f_i(x)}{\max f_i(x) - \min f_i(x)} \right| \right]$$

Where, w_i is the weight given to criteria *i*, $f_i(x)$ the value of objective function, and max $f_i(x)$ and min $f_i(x)$ the maximum and minimum values of the same function respectively. The choice of *(p)* indicates all deviations from the ideal solution are considered in direct proportion to their magnitudes Lounis and Vanier [2000]. If it is assumed that the competing objectives are budgeted maintenance cost and AACR (i.e. m = 2), then this index provides a means of relating competing maintenance objectives; that of controlling maintenance intervention costs and maintaining component condition ratings.

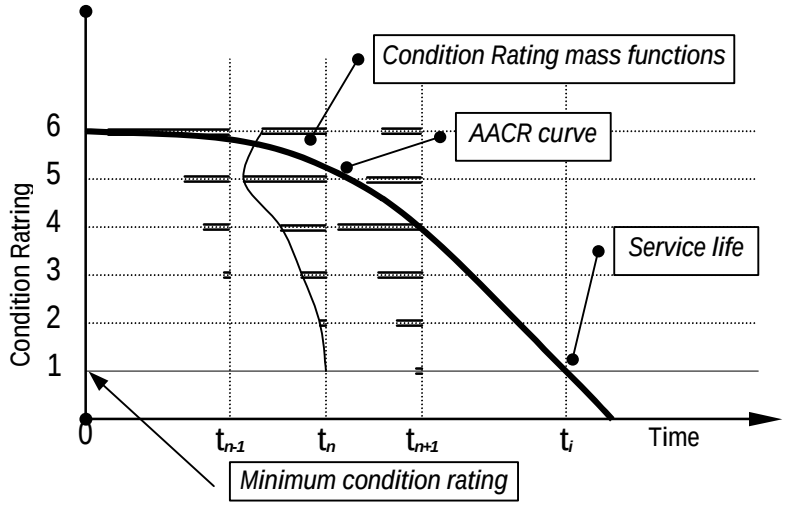

Figure 4. Condition state mass functions that define the aggregated component condition rating (AACR).

If a building maintenance manager is aware of the expected annual budget or has made the necessary provision for acquiring the requisite funds to conduct a proper maintenance program then in this case, the maintenance strategy is to maximize the overall component condition rating. Essentially, the manager has interest to maximise the gains afforded by a given annual maintenance budget allocation.

Another scenario is one where the building manger may know the overall component condition rating to attain, or maintain, but wishes to minimise the budgetary requirements. Whereas a more likely scenario, as in the third case, is one in which the manager may not as yet have defined budgetary requirements and as well, is not aware of the average aggregate condition state under which he should be operating the facility beyond minimum acceptable levels. Indeed, the building manager may require some insight into the most cost effective maintenance he can expect over a longer-term horizon and still operate the facility above a minimum acceptable condition state.

This is a case where a compromise is to be reached between two competing objectives: maintaining a minimum acceptable AACR in relation to the yearly maintenance budget. The intent is to determine the highest achievable AACR for any given yearly maintenance budget. As such, a multi-objective index (MOI) approach is used that is based on the: degree of criticality of amongst components; number of components being considered; condition state vector; relative importance brought to the budget in relation to the building condition state; and the AACR, and limiting values for ACCR (i.e. $ACCR_{min}$ and $ACCR_{max}$).

In respect to the limiting values for AACR, these values are selected by the building manager to better manage the maintenance process. For example, it is unlikely that a new window unit should require replacement in its initial years of use; likewise one would expect that a failed unit would be replaced. Hence, the manager can set limits on minimum and maximum values of ACCR for each façade component. For example, the building manager can determine that if the AACR of the components lies between “new condition” (e.g. state 6) and an “average” condition (e.g. state 4), then no action to consider replacing the unit should be taken. Whereas a repair could be requisitioned should the components be considered in the poor, urgent of critical states (e.g. condition states 3, 2, 1 resp.). The determination of such limits thus permits the building manager to establish a policy of when actions

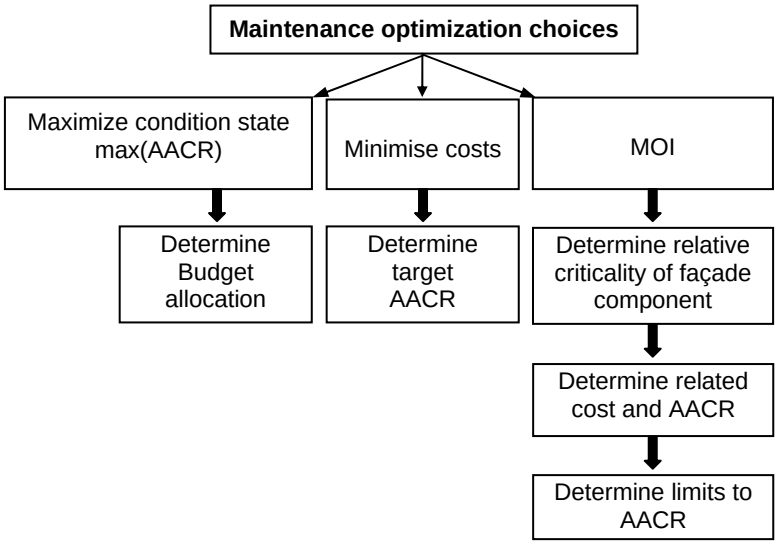

Figure 5. Maintenance optimisation choices: maximise condition rating; minimise maintenance budget; use of MOI – multi-objective index; AACR – average aggregate condition rating.

should be taken and indeed the system could be used to determine how such policies might affect overall maintenance costs. A summary of the three different maintenance scenarios is given in Figure 5. In essence, the façade BMM system provides yearly maintenance costs of individual components for a given wall system over a long-term horizon that spans the life of the façade system.

6 ~~CONCLUSION~~SUMMARY

A building façade maintenance management system is proposed that considers the effect of different maintenance options on the overall cost of maintenance over a yearly and longer time scale. Performance predictions in respect to component condition state are based on a one-step Markovian model. An optimization of different possible maintenance actions are considered in relation to the cost of specified actions to, or replacement of, components based on a multi-objective index. This index provides a means of relating competing maintenance objectives; that of controlling maintenance intervention costs and maintaining component condition ratings.

ACKNOWLEDGEMENTS

The authors acknowledge funding support from the Program of Energy Research and Development (PERD), the Publics Works and Government Service Canada, and the Institute for Research in Construction. As well, they would like to extend their gratitude for the support offered by the LGC, CUST, Clermont-Ferrand II, and University Blaise Pascal.

REFERENCES

Augenbroe, G.L.M. and Park, C.S., 2002, *Towards a Maintenance Performance Toolkit for GSA*, Interim Report submitted to GSA, Georgia Inst. of Tech. http://www.publicarchitecture.gatech.edu/Research/project/gsatoolkit.htm

Bailey, D.M, Brotherson, D.E., Tobiasson, W. & Knehans, A., 1990, ROOFER: An engineered management system (EMS) for bituminous built-up roofs, *USACERL Tech. Rept. M90/04.*

Cesare, M., Santamarina, J.C., et al. 1994, *Risk-Based bridge management: optimization and inspection scheduling*, Can. J. Civ. Engrg., Vol. 21(6), pp.897-902.

Durango-Cohen, P. L. and Madanat, S. M. (2006), *Optimization of inspection and Maintenance Decisions for Infrastructure Facilities under Performance Model Uncertainty: A quasi Bayesian Approach*, Transp. Res. Pt. A: Policy and Practice: to be published, 25 p.

Kyle, B.R.; Vanier, D.J.; Lounis, Z., 2002a, *The BELCAM Project: A Summary of Three Years of Research in Service Life Prediction and Information Technology*, 9 th Intl. Conf., Durability of Building Materials and Components, Brisbane, AU, Mar. 17-20, Paper 138, pp. 1-10.

Lounis, Z.; Vanier, D.J., 1998, "Optimization of bridge maintenance management using Markovian models", In: Developments in Short and Medium Span Bridge Engineering '98 (Calgary, Alberta, 13 July), pp. 1045-1053.

Lounis & Vanier 2000, *A Multi-Objective and Stochastic System for Building Maintenance Management*, Computer-Aided Civil and Infrastructure Engineering, Vol.15, pp.320-329.

Micevski, T., Kuczera, G. and Coombes, P., 2002, *Markov Model for Storm Water Pipe Deterioration*, J. Infrastructure Systems, Vol. 8(2), pp. 49-56.

Morcous, G., Lounis, Z. and Mirza, M.S., 2003, *Identification of Environmental Categories for Markovian Deterioration Models of Bridge Decks*, J. Bridge Engrg., Vol. 8(6), pp. 353-361.

Morcous, G. and Lounis, Z., 2006, Integration of Stochastic Deterioration Models with Multicriteria Decision Theory for Optimizing Maintenance of Bridge Decks, Can. J. Civ. Engrg., Vol. 33(6), pp.756-765.

Nesbitt, D. M., Sparks, G. A. & Neudorf, R. D., 1993, *A Semi-Markov Formulation of the Pavement Maintenance Optimization Problem*, Can. J. Civ. Engrg., Vol. 20(3), pp.436-447.

Robelin, C. A. and Madanat, S., 2007, *History-Dependent Bridge Deck Maintenance and Replacement Optimization with Markov Decision Process*, Journal of Infrastructure Systems, Vol. 13(3), pp.195-201.

Talon, A., 2006, Évaluation des scénarii de dégradation des produits de construction, Thèse préparée au Centre Scientifique et Technique du Bâtiment – Département Développement Durable – Division Environnement, Produits et Ouvrages Durables et au Laboratoire Génie Civil. Clermont Ferrand : Blaise Pascal Clermont II, 2006.

Van Winden, C. and Dekker, R., 1998, *Rationalisation of Building Maintenance by Markov Decision Models: A Pilot Case Study*, J. Operations Research Society, Vol. 49, pp. 928-935.

A Structural Condition Assessment;Environmental Agents versus Structural FailuresThe Case of Ataturk Culture Center AKM,Istanbul, Türkiye

Kemal Çayırlı [1]

T 72

ABSTRACT

A structural condition assessment is partially conducted in a specified method to reveal environmental agents that are causes of structural failures in the case of AKM. By suggesting a perceptually outlined assessment strategy, a structure of the case study is initiated to look closely structural partitions of the front foyer. Various site survey techniques, visual observation, measuring, interviewing and relate items are issued to collect rough data according to symptoms of the structural failures and these data are transformed into models of the symptoms. Furthermore, environmental agents, like wind, are identified that are stated as causes. Specific titles of the failures according to the symptoms, vibration of vertical member -louvers and canvas behavior of curtain wall -glass surface are named and related with corresponding environmental agents to conclude the case study that the front foyer of AKM partly has a sufficient service life.

KEYWORDS

Structural Condition Assessment, Environmental Agents, Wind, Façade, Failures,

[1] Eskişehir Osmangazi University, Faculty of Engineering & Architecture, Department of Architecture, Eskişehir, 26030 ,Phone +90 222 230 3972-120 kemalcayirli@gmail.com

1. INTRODUCTION

A building could be an object of cultural heritage in any country according to the certain way reading of its features no matter its construction date. Especially; when its features seem to be so identical, it becomes much more crucial to keep and improve its role not only in the position of the discipline but also in the atmosphere of the public realm by applying the concept of durability in overall building. Durability means to extent overall service life of a building, its components and materials. According to Feilden, [1982], "conservation" and "renovation" could be practically related with the concept of durability in the domain of historical buildings. This understanding fundamentally covers rejuvenating the building by preserving the image of the building in terms of its original systematic and main characteristics while applying current construction methods and materials for extending the service life of the building.

According to Modena, [2004], all conservations consist basically of actions taken to prevent decay, and within this objective it also includes management of change and presentation of the object so that intent of messages conveyed by the object are made comprehensible and without distortion. Furthermore, architectural conservation is more complex; first because a building must continue to stand up; secondly, economic factors usually dictate that it should remain in use; thirdly, it has to resist the effects of climate; and lastly, a whole team of 'professionals' have to collaborate.

When evaluating economic factors, the concepts of maintenance and renewal of the overall structure need to be challenged y considering all the pros and cons regarding maintenance issues. When the the concept of sustainability is considered in the case of AKM, then maintenance is a first priority, as in this instance sustainability of the AKM should be understood from a basis of cultural and social concern for this historical structure, given that the AKM is also central to its modern public image in Turkey.

Climatic effects are importance in this case study because of the geographical location of the building in Istanbul, which is located in proximity to Taksim Square. Taksim Square is a location subjected to considerable wind effects in particular on the west façade of the AKM. Although symptoms of failure are not clearly perceived at the first glance, the evidences of failure direct that vertical louver and glass curtain wall as partitions of the façade system should be issued as issues for the structural condition assessment. The partitions of the façade seem so critical not only in the concept of the facility management but also public appreciation of the building image.

The fourth notion of conservation actions as suggested by Modena [2004] relates to the requirement for collaboration among 'professionals'. This implies that for the process to be effective, it must obtain contributions from other disciplines needed to apply the proper procedures to bring about the necessary conservation measures. Specifically, when conducting this case study, precise information was needed regarding the wind speeds and direction and related behavior characteristics in the upper structure of the urban land in Istanbul.

The case study was conducted by applying a systematic process of structural condition assessment to distinguish critical symptoms on the structural system and its partitions that need to be revised to extent and improve the building service life and quality as much as possible in the example of the selected part, the front foyer and west façade of AKM. Beyond the process of the assessment, the concept of durability and sustainability could be extensively correlated as important partitions of design profession in nowadays as further applications of the study.

2. A CASE STUDY: The FRONT FOYER in AKM

In this section; specific data, information and a specific method of analysis about the front foyer of AKM are intend to provide a proper method and useful example for conducting a structural condition assessment methodology. Specifically detailed parts are determined to open up the topic in discussion

according to preliminary strategy of the case study such as site survey and available building specifications on the research issues; and static and dynamic loads.

The first part of this section provides an outline of the proposed assessment outline that reflects on an individual understanding and perception of the research process. The second part focuses on a physical definition and materialistic description of the front foyer of the AKM and gives a brief explanation of the space. Regarding symptoms of structural failure, basic graphics of visual observations obtained from an on-site survey are drafted and described. Building inspection data, in which the building movements have been monitored, form the basis for developing failure diagnosis evaluation models. Confronting possible environmental agents to symptoms of structural failure is a content of the report conclusion in that reason-result equations are established to clarify the environmental agents as causes.

2.1. A Proposed Condition Assessment Outline

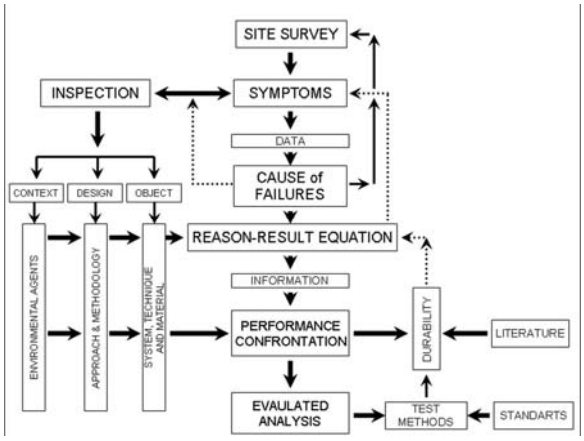

Fig. 1: A Chart of Proposed Assessment Outline

To propose a condition assessment outline is an individual outcome for understanding the process of the case study.

The proposed assessment outline becomes a priority for the researcher to limit the study to predefined expectations; it also serves as a useful guide. According to the outline, there is a hierarchal process suggestion in order to apply a directional approach while integrating supplementary components from test methods to concept of durability. Furthermore; "*Inspection*" that is divided into three interrelated partitions (context, design and object) directly supports the hierarchical process in two different steps.

By combining within the ready-made concrete knowledge as references –literature and test methods, it is expected to have a feedback process to reach a reliable end-result. In certain steps, there is a check point to help ensure a cross control of the process.

Although the assessment outline is a proposition to be a guide, it is not run effectively and accordingly as a result of lack of the local and referential resources. One of them is that even construction documents of AKM could not be institutionally revealed. For this reason, it becomes a conceptual statement that is not realized completely.

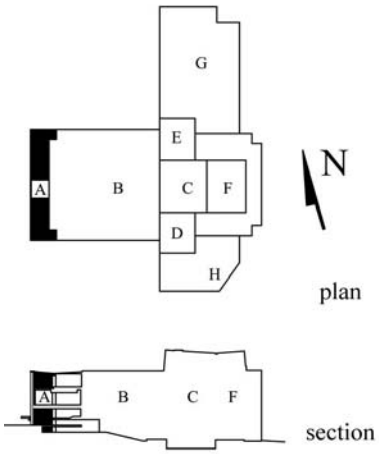

Fig 2: Schemes of AKM

2.2. Description of the Space

According to TMMOB, Branch of Istanbul publication about AKM, *As a Part of Cultural Life: Theatre and the Buildings,* and various site visits, the sections of **Description of the Space** and **Structural System & Material** are outlined. The Front Foyer of AKM, shown as **[A]** in the scheme is specifically chosen to apply structural condition assessment concept because of its fully exposed position to multi environmental agents and its visually accessible partitions. Because of that most of public access is on this side of the building and consequently, it becomes a hinge point. This possibly increases the effects of environmental agents on the components of this space.

Facing West, the front foyer outlines a dimensional space of 54.50x10.80x25.70 m dimensional space outline that covers whole façade, as an identical image of the building.

The vertical façade within a horizontally abstracted of a stage curtain defines the civic building image in the square of Taksim that is one of the most important public spaces of Istanbul.

The foyer also gives a unique baseline to the building circulation system. Major performance halls in the AKM are accessed from this foyer. Although, it gives a sense of a single volume from outside, it is divided into three non-uniform sub foyers in the building.

2.3. Structural System & Material

A close look to the front foyer reveals itself that multiple structural systems and materials are integrated into a unified space. It varies from reinforced concrete applications to structural metals; steel and aluminum. In addition to the specified and original structural detailing, nature of materialistic appearances are established in a way of realistic presentation.

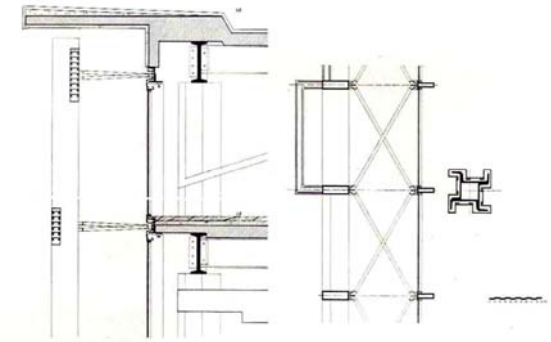

Fig 3: Section & Plan of West Façade System

In the general structural appearance, skeleton frame system is applied through out the building. Structural steel column-beam and reinforced concrete frame applications are unified into whole volume of the front foyer. Four (4) channels of structural steel are composed of being a single column of the façade and then it is connected to reinforced concrete portion of the building by I-beams. And, a reinforced concrete slab completes the main floors and roof enclosure. In the underground portion of the front foyer, structural steel columns are supported by single foot establishments and other reinforced columns transfer load by single foot and shear wall integration.

Two layers of the façade, louvers and a curtain wall, define an image of the West façade. While Grinatal Aluminum Louvers dominate the vertical portion of the west façade, a uniform glass curtain wall covers the inner side of the façade. A single louver, (8,2-20,3-2570cm), is made of a corrosion resistant grinatal which is an aluminum alloy (% 0,5-5 Si, % 0,7 Mg). With 7 segments and 3 pinpoint connections to the main floor slabs of the front foyer, it has a rigid connection to the ground. At the +22.20 level, there is a strip that connects all louvers to each other. The glass curtain wall is constructed by 4.5-10cm metal members without any vertical or horizontal differentiations. It is connected to structural steel column at three levels by edged connections and hinge type points.

2.4. Symptoms of Structural Failures

In the proposed condition assessment outline, the first stage of the assessment is site survey is pointed as process. In the content of 'Structural Condition Assessment', by Ratay R.T. [c2005], the site survey could be basically conducted by various steps: visual observation, measuring, photographing, interviewing, probing, record keeping, documentation, and report preparation, as a directional procedure. At this point, the visual observation step in the scope of the case study is initially directed to focus on main partitions of the space; floor, ceiling and walls. Among the various symptoms in the front foyer, the façade is specified to analyze deeply because of its vulnerability in terms of environmental agents and its openness characteristics to site survey. Two main symptoms were detected on the west façade of AKM. *Non-Axial Deformation of the Vertical Louver and Non Linearity of the Glass Curtain Wall.* Both these items were selected to carry out further stages of the proposed condition assessment outline.

2.4.1. Non-Axial Deformation of Vertical Louver

Because of its closely integrated vertical configuration within an image of gradually opened up stage curtain, it is pretty difficult to recognize with bare observation that every vertical louver segment of the façade has a defect. This defect is a non-axial deformation through its length of grinatal aluminum louver in various amounts and directions. Fifty six (56) vertical louvers within 7 segments at each louver have fragmental characteristics that are nature of the building elements.

Fig. 4.: Photographs of the Louvers

2.4.2. Non Linearity of Glass Curtain Wall

As a second layer of the façade, the glass curtain wall with almost 460 m^2 gross area is under risk of loosing its vertical linearity. The curtain wall that is composed of a uniform section of vertical and horizontal mullions and glass surfaces has rigid connections at the base and upper floor and it is attached to the main column of the foyer with a hinge type connection at three different levels. In particular, there is a limited hinge connection that looses its position at the + 0.65 level. When all these type of connections at the curtain wall are considered, at this level there is only a deformation on the hinge connections.

Fig 5: Photographs of the Curtain Wall

2.5. Evaluation Models of Object Inspections –The Building

As a result of visual observations from the site survey, simple models have been introduced to obtain basic data from the site. These models are based on measuring, photographing, record keeping, and documentation of physical substances that relate to with symptoms of structural failure in the foyer space. According to the symptoms' specifications, ground movement & settlement, vertical louver deformation and glass curtain wall deflection models are developed and presented.

2.5.1 Vertical Louver Deformation

It should be mentioned that there is a compact visual perception of the louver system at the west façade of AKM without perceiving any physical defect at the first glance. On the other hand, it should be an expectation that the louver system is under critical treat of various environmental agents; wind, temperature, and pollution, etc. since 1978.

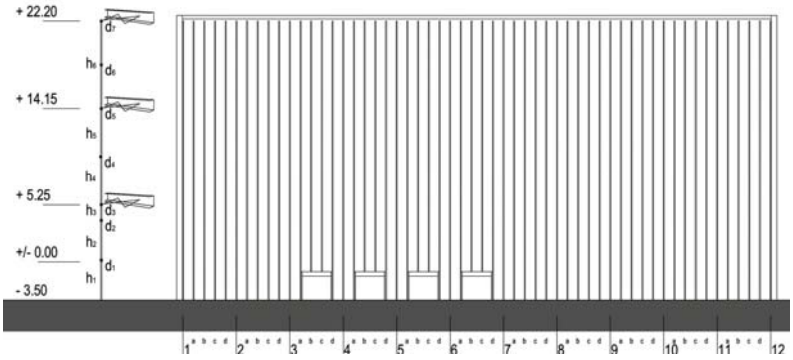

Fig. 6: The vertical louvers of West Façade

In Figure 6 one can identify whether the deformation is on or off of the vertical louver. For this reason, each louver is coded (i.e. 1a or 11d) and fragmented according to the number of portions (i.e. h1, h2) and joints (i.e. d1, d2) on the louver. Levels in elevation are pointed along the height of the louver to get numeric data of possible deformations.

In Figure 7, there is an end result drafting of the visual observation about the louvers' deformations. The main result in the visual observation is that most of the louvers have a defect of the deformation in various direction, position and degrees. Actually, there are two distinctive directions of the fragment movement, the north and south that are shown at the base of the figure (< >) within a colored line. And also, the deformation positions in terms of louvers' fragments and joints are presented in the format of the façade. This situation is more clearly understood by comparing with levels –fragments and joints– and connection type and the levels of the louver to the main building.

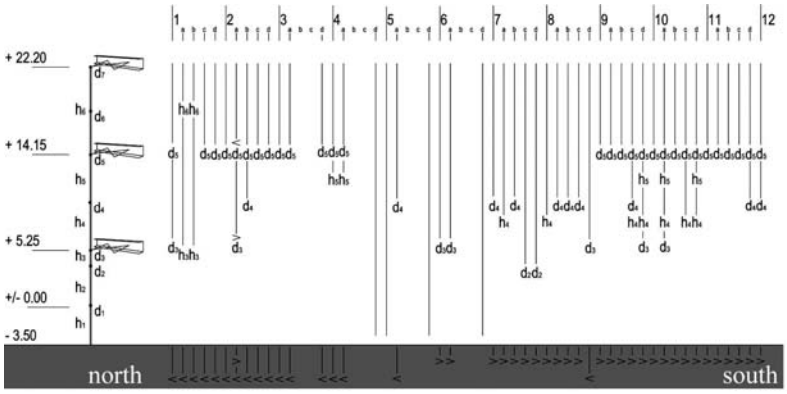

Fig. 7: Drafted Analysis of the Louver Deformation

Figure 8 contains measurement of the degree of deformation of the louvers. In this manner, there is only a degree that is stated in the direction of north to south. The data is only current for "*h1*" fragment of the louver. It is presented only a ratio of h1 deformation that is a result of a simple measuring. And it is expectation that a total deformation of h1 could be figured according to the full height of the h1 that is 3.65 m. That varies from 4,5 to 7,3cm.

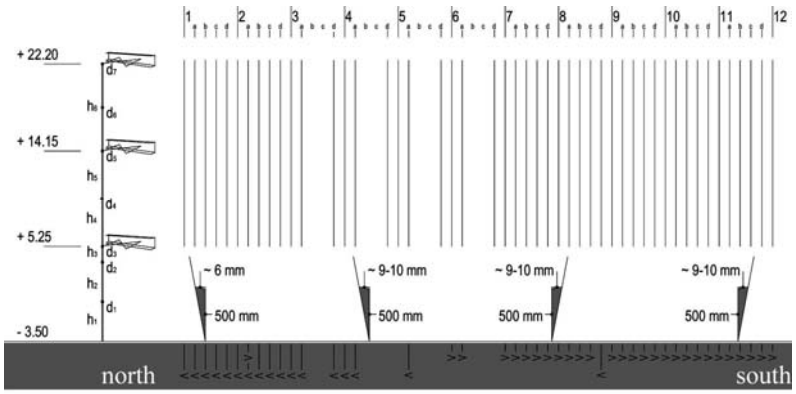

Fig. 8: Deformation Amounts in the partial level of the louvers

2.5.2 Glass Curtain Wall Deflection

In the model, the glass curtain wall system is defined by visual observation and measuring. It is stated that a uniform of the metal mullion with 4,5 / 10 cm rectangular section is applied along the every segment of the system without any differentiations in horizontal and vertical lines. On the other hand, it is noticed that horizontal segments of the lines have a continuum characteristic while vertical segments is fragmented according to the horizontal lines.

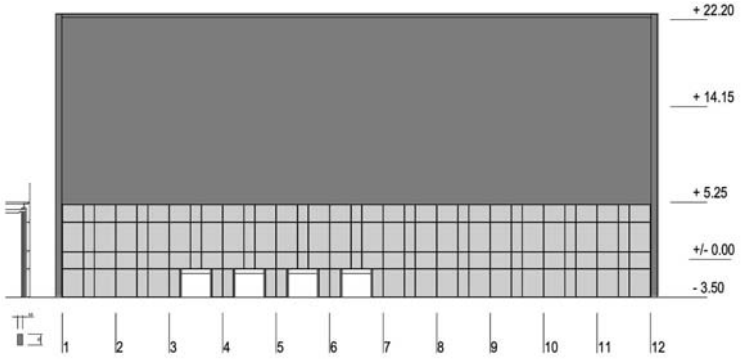

Fig. 9: Curtain Wall

The graphics explain the deflection's direction in the glass curtain wall and amount of the deformation in the system. Because of the movement at the middle hinge connection and the basics of measuring, the direction is observed towards to inside of the front foyer.

The measuring data reflects a ratio of the deformation in various points. The ratio should be evaluated and confirmed through whole façade.

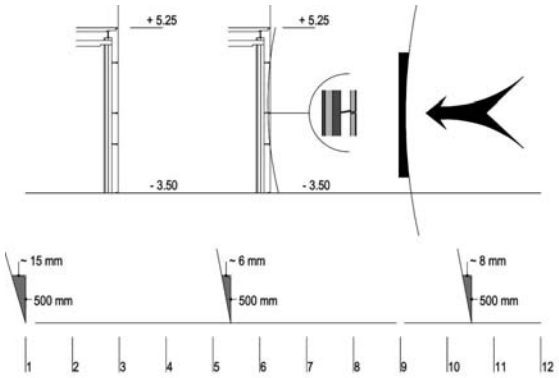

Fig. 10: Deflection Amounts in the Curtain Wall

2.6. Possible Environmental Agents to Symptoms of Structural Failure

In general understanding of performance requirement model, "safety" is defined as a social and psychological requirement of the building performance, and it has two fundamental environmental agents in its domain; static and dynamic loads. While static loads are classified by dead, live and impact load, dynamic loads are specified with earthquake and wind loads, thermal and moisture movements in the 'Structural Analysis of Historical Constructions' by Claudio Modena, P. B. [2004]. In this part of the study, a new perception towards structural loads is presented that is based on upper classified titles, named 'static' and 'dynamic'. This situation offer a transition point to relate the structural loads as environmental agents with the symptoms of structural failure in the front foyer of the AKM. Finally, this suggests a temporal reading of environmental agents that are specified in the example of the case study.

2.6.1. Static

- Eccentric Load

It is a type of a load imposed on a structural member at some point other than the center line of the section. In the case of an ideal column under an axial load, the column remains straight until the critical load is reached. However, the load is not always applied at the center line of the cross section, as is assumed in Euler buckling theory. In fact, misalignment of the structural member in the structural system could initiate and even multiple defects of the structural failure that are issued in the 'Design and Construction Failures' by Kaminetzky, D [c1991]. And also, dead load of the structural member becomes a reason of the eccentric load in itself. Within consideration of the symptom at the west façade of AKM, the eccentric load could be issued for the vertical louver. If certain construction

defects were in discussion like misalignment of linear elements, the eccentric load would be main causes of the defect; vertical louver deflections.

2.6.2. Dynamic

- Wind

Wind is the result of a number of factors such as atmospheric pressure differences, differential radiation of the sun, and the rotation, curvature & surface characteristics of the earth. Overall understanding and analyzing the wind are stated in the 'Wind Effects on Buildings', Lawson, T. V. [1980]. In the nature of wind characteristics, the behavior of the wind consists of two components: a steady flow; and a turbulent fluctuating system. The first has a mean of wind speed; the second, a fluctuating velocity due to turbulence or gusting. The dynamic component causes vibration & flutter of structures. In other words, wind load is a reason of turbulence at the side of the vertical object when it passes through by its vortex behavior. This consequence is a reason of vibration in the object. Vibrations are located at the perpendicular sides of the wind direction. When a flat surface reflects and redirects the wind, understanding the effects of the wind load on the vertical louver becomes more complicated analysis. In fact that a first effect of wind is to behave as a lateral load to turn over or relocate any structure in itself. But, if this is not possible by an existing sufficient structure, deformation effect is on scene in certain degrees. Especially, a flat surface becomes a dynamic object to see canvas behavior like a sail.

3. CONCLUSION

By comparing the symptoms as defects and agents as causes, three specific titles are listed as end result definitions of the specific structural condition assessment. *Vibration of Louvers and Canvas Behavior of Façade* are described with related defects and causes.

Vibration of Louvers

Wind is a natural event that occurs in any geographical location with variation in loads and intensities. As well, certain shapes common to nature naturally affect and shape, direct, deflect and perhaps increase the speed and effect of the wind on man-made structures. Besides the physical characteristics of a city, the layout of upper structure features within city could be important determinants of those effects. For example, a street could provide a channel to direct the wind in an intentional way or vice versa. In the same way, a building could be located in terms of getting positive wind effects or eliminating the negative circumstances of wind.

The AKM is located in one of the dominant hills in Istanbul. Although the dominant wind has not been monitored, it has been noticed that the center west façade could at times be under threat of prevailing winds, either from the direction of Gumussuyu and Macka Park to Tarlabası Avenue. Moreover, the openness characteristic of Taksim square could further raise the wind effects in an undetermined way.

A gradual graphic representation in Figure 11 is shown here to explore the expected outcome of wind effects on louvers. In the gradual sequences, the end point is seen as permanent deformation of a vertical object. However, the end point could also be a dynamic elastic deformation.

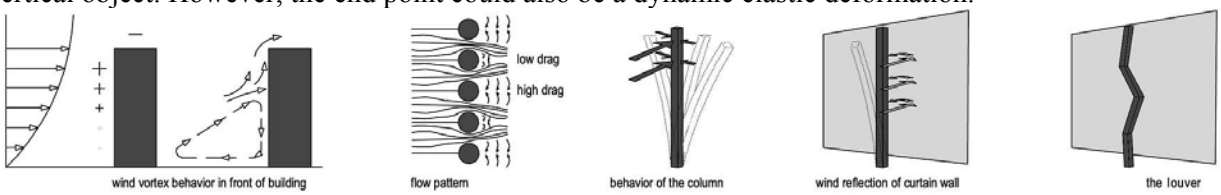

Fig. 11: Wind and its Circumstances

At the AKM, permanent deformation of the louvers and locations are presented according to a limited time based site survey. In the example of the louvers at the west façade of the AKM, extensive monitoring methodology that covers a long time based data should be applied to finalize determining the likelihood of deformations and their expected characteristics.

An eccentric load could be a main defect for a linear building element, if there is a failure to keep up the louvers' straightness during the construction phase. To investigate a misalignment of a louver is not possible in current database.

Canvas Behavior of Curtain Wall

Another negative effect of the wind could be mentioned on the curtain wall that could be called as a canvas behavior of the flat surface. In Figure 12, it is shown that this effect basically result from wind pressure in the direction of the wind. Uniformity and strength of the flat surface, while eliminating local failures, could become an initiative of the defect.

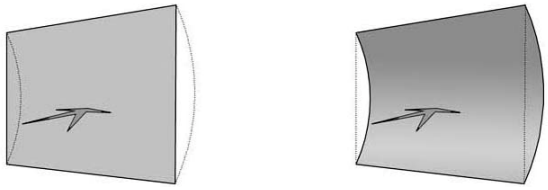

Fig. 12: Canvas Behavior of Curtain Wall

The west façade of the AKM is divided into three partial curtain walls having various dimensions. In this assessment, only the ground level curtain wall is considered in respect to deformation and this is estimated, based on interpolation, to range between 5 and 13cm. The interpolation method in various horizontal locations at the middle level of the curtain level, + 0,87 where it is already a deformed hinge connection line level. It could be possible to compare the amount of the deflection of the curtain wall with in relation to reference deflection data to state the amount that is in a critical level to determine whether total or partial collapse is in agenda.

As it is mentioned that the case study is to be a medium not only to offer further remediation outline but also to give a scientific perception to the public debate whether the AKM, in Istanbul, is well constructed and performed sufficiently without any fundamental renovation or it is necessary to design a new civic building. The outcomes given in the case study are accepted as an analytical data in the conclusion part to finalize the study. For this reason, there is a suggestive classification to outline as a next step after reviewing the failures. In the ISO 15686-1 [2002] standard relating to service life planning of buildings and constructed assets (i.e. Part 1) provides a method in which failure modes are classified into six levels according to safety and economic factors as shown in Table 1. In the table, three specific titles are perceptually ranked in terms of the classification strategy.

Table 1: Failure Modes versus Specific Titles

Failure Modes		Vibration of Louvers	Canvas Behavior of Curtain Wall
Danger to life	:		
Danger to health	:		
Costly repair	:	X	X
Frequent repair repeat	:	X	
Interruption of building use	:		X
No exceptional problems	:		

ACKNOWLEDGMENTS

The case study described in this paper that focused on the Atatürk Culture Center (AKM) in Istanbul, Turkey, formed part of a course taken in the fall session of 2007, entitled "Performance of Building Elements under Environmental Effects", conducted by Assoc. Prof. Hülya KUŞ in the Building Science Ph. D. program in the Faculty of Architecture, at ITU.

REFERENCES

Feilden, S. B., 2003, Conservation of Historic Buildings, 3rd Edition, Architectural Press, pp. 1–10.

Modena, C. , Lourenco, P. B., Roca, P. 2004, Structural Analysis of Historical Constructions, Taylor & Francis, UK, 1466 p.

TMMOB, Branch of Istanbul, As a Part of Cultural Life: Theatre and the Buildings, pp. 52–70.

Ratay R.T. 2005, Structural Condition Assessment, J. Wiley & Sons, N.J., pp. 4–18.

Kaminetzky, D 1991, Design and Construction Failures , McGraw-Hill, New York, pp. 1–54.

Lawson, T. V. 1980, Wind Effects on Buildings, Applied Science Publisher, Bristol, UK,

ISO 15686-1, Buildings and Constructed Assets -Service Life Planning -Part 1:General Principles First Edition, Article 6.8.1